RESCEU SYMPOSIUM ON

GENERAL RELATIVITY AND GRAVITATION

as JGRG22

November 12–16　2012

Koshiba Hall, The University of Tokyo, Hongo, Tokyo, Japan

Contents

Opening address

Jun'ichi Yokoyama JGRG22(2012)111200

The pre-inflationary dynamics of loop quantum cosmology: Confronting quantum gravity with observations

Abhey Ashtekar JGRG22(2012)111201

Nonlinear massive gravity and cosmology

Shinji Mukohyama JGRG22(2012)111202

The Standard Model and beyond after LHC at 8 TeV

Mihoko Nojiri JGRG22(2012)111203

Non-gaussian bubbles from tunneling in the inflationary era

Kazuyuki Sugimura JGRG22(2012)111204

Non-linear superhorizon perturbation and nonlinear gauge transformation

Yuichi Takamizu JGRG22(2012)111205

Curvature perturbation spectrum in two-field inflation with a turning trajectory

Shi Pi JGRG22(2012)111206

Effective field theory approach to quasi-single inflation

Toshifumi Noumi JGRG22(2012)111207

Revisiting perturbations of a scalar field in an anisotropic universe

Masato Minamitsuji JGRG22(2012)111208

Probing dark radiation with inflationary gravitational waves

Kazunori Nakayama JGRG22(2012)111209

Dynamics of oscillating scalar field in thermal environment

Kyohei Mukaida JGRG22(2012)111210

Higgs condensation in the inflationary universe

Taro Kunimitsu JGRG22(2012)111211

Forecast constraints on cosmic strings from future CMB, pulsar timing and gravitational wave direct detection experiments

Sachiko Kuroyanagi JGRG22(2012)111212

Effects of chameleon scalar field on rotation curves of the galaxies

Sirachak Panpanich JGRG22(2012)111213

Self-consistent initial conditions for primordial black hole

Tomohiro Nakama　JGRG22(2012)111214

On the vacua of maximal gauged supergravity

Masato Nozawa　JGRG22(2012)111215

Gravity as the origin of spontaneous symmetry breaking in an inflationary universe

Yuki Watanabe　JGRG22(2012)111216

Fuzzy objects in noncommutative geometry and their applications

Shinpei Kobayashi　JGRG22(2012)111217

Critical exponents of gravity with quantum perturbations

Hongsheng Zhang　JGRG22(2012)111218

Triangular solution to the general relativistic three-body problem

Kei Yamada　JGRG22(2012)111219

Research of the celestial objects by the gravitational lensing

Naoki Tsukamoto　JGRG22(2012)111220

Dark matter and dark energy as a single manifestation of a fundamental length scale

Ivan Arraut　JGRG22(2012)111221

Wave function in 2+1 dimensional causal dynamical triangulation

Takayuki Hikichi　JGRG22(2012)111222

Selfgravity effects of blackfold

Kentaro Tanabe　JGRG22(2012)111223

Analysis of Gregory-Laflamme mode in large D limit

Ryotaku Suzuki　JGRG22(2012)111224

Glocal properties of solutions to the Einstein-matter equation

Makoto Narita　JGRG22(2012)111225

Primordial non-gaussianity from preheating

Andrei Frolov　JGRG22(2012)111301

Towards more precise estimates of the primordial bispectrum

Jinn-Ouk Gong　JGRG22(2012)111302

Testing the origin of primordial perturbation: Use of bi- and tri-spectrum

Teruaki Suyama　JGRG22(2012)111303

Recent developments in gravitational lensing

Matthias Bartelmann　JGRG22(2012)111304

Measuring distance with gamma-ray bursts

Ryo Tsutsui　JGRG22(2012)111305

Stacking of cluster profiles

Yousuke Itoh　JGRG22(2012)111306

Black hole solution and binary gravitational waves in dynamical Chern-Simons gravity

Kent Yagi　JGRG22(2012)111307

Gauss-Bonnet braneworld redux: A novel scenario for the bouncing universe

Hideki Maeda　JGRG22(2012)111308

Instability of charged Lovelock black holes

Tomohiro Takahashi　JGRG22(2012)111311

Criterion for bound (or unbound) orbits in the Kottler spacetime

Naomasa Fushimi　JGRG22(2012)111313

Problems in nth-order extension of the gauge-invariant perturbation theory

Kouji Nakamura　JGRG22(2012)111315

Non-inertial effects on Landau levels

Kohkichi Konno　JGRG22(2012)111316

Quantum interferometer in Chern-Simons modified gravity

Hiroki Okawara　JGRG22(2012)111317

Excess power method with the Hilbert-Huang transfom in search for gravitational wave signals

Masato Kaneyama　JGRG22(2012)111318

Potential-driven Galileon inflation

Junko Ohashi　JGRG22(2012)111319

Evolution and thermalization of axion dark matter in the condensed regime

Ken'ichi Saikawa　JGRG22(2012)111321

Ghost in multimetric gravity

Kouichi Nomura　JGRG22(2012)111322

Scale-dependent bias with the higher order primordial non-gaussianity

Shuichiro Yokoyama　JGRG22(2012)111323

Gravitational lensing by modified lens gravity

Takao Kitamura　JGRG22(2012)111325

Gravitational field of a rotating ring around a Schwarzschild black hole

Yasumichi Sano　JGRG22(2012)111327

Effect of the comological constant on the bending of light and the cosmological lens equation

Hideyoshi Arakida　JGRG22(2012)111328

Graphical approach to the Lovelock black holes

Takashi Torii　JGRG22(2012)111329

Short-range gravity experiment searching for a large extra dimension

Haruna Murakami　JGRG22(2012)111330

Curvature perturbation in conformally related frames

Jonathan White　JGRG22(2012)111332

Features in the CMB spectrum as a probe of heavy physics during inflation

Ryo Saito　JGRG22(2012)111333

High frequency limit for gravitational perturbations of cosmological models in modified gravity theories

Keiki Saito　JGRG22(2012)111334

Wormhole dynamics in Gauss-Bonnet gravity

Hisaaki Shinkai　JGRG22(2012)111336

Numerical study of 5-dimensional gravitational collapses

Yuta Yamada　JGRG22(2012)111337

Effects of metric perturbations in vacuum 5D universe on material 4D universe

Takao Fukui　JGRG22(2012)111338

Search of strong gravitational field around nuclei using electron-nuclear scattering experiment by geodesic precession

Saki Tanaka　JGRG22(2012)111340

Theory for observational verification of black hole existence

Hiromi Saida　JGRG22(2012)111341

Equilibrium states of magnetized disc-central compact object systems

Kotaro Fujisawa　JGRG22(2012)111342

Gravitational collapse of the Einstein cluster in the Lovelock gravity

Seiju Ohashi　JGRG22(2012)111343

Einstein equation of state and its cosmological applications

Takuya Maki　JGRG22(2012)111344

Cosmic wiggly string in black hole spacetime

Hiromi Suzuki　JGRG22(2012)111346

Effect of dark matter halos around IMBHs on gravitational waves

Kazunari Eda　JGRG22(2012)111347

The effect of gauge fields on oscillating scalar fields at finite temperature

Yuhei Miyamoto　JGRG22(2012)111348

Search for gravitational wave events with KAGRA and the world-wide network of laser interferometers in the advanced detector era

Hideyuki Tagoshi　JGRG22(2012)111401

Status of KAGRA

Takaaki Kajita　JGRG22(2012)111402

Virgo: design, results and perspectives

Francesco Fidecaro　JGRG22(2012)111403

LIGO: Recent results, plans and prospects

David Reitze　JGRG22(2012)111404

Electromagnetic counterparts to binary neutron star mergers

Koutarou Kyutoku　JGRG22(2012)111405

General relativistic simulations of magnetized binary neutron star merger

Kenta Kiuchi　JGRG22(2012)111406

Shear oscillations in hadron-quark mixed phase

Hajime Sotani　JGRG22(2012)111407

Non-axisymmetric oscillations of rotating relativistic stars by conformally flat approximation

Shin'ichirou Yoshida　JGRG22(2012)111408

Nonlinear effect of r-mode instability in uniformly rotating stars

Motoyuki Saijo　JGRG22(2012)111409

Upper limits of particle emission from high-energy collision and reaction near a maximally rotating Kerr black hole

Tomohiro Harada　JGRG22(2012)111410

Stable null bound orbits around a black ring

Hideki Ishihara　JGRG22(2012)111411

Axion bosenova

Hirotaka Yoshino　JGRG22(2012)111412

Curvaton induced modulated reheating

Osamu Seto　JGRG22(2012)111413

Finite-time future singularities and rip cosmology in f(T) gravity

Kazuharu Bamba　JGRG22(2012)111414

Adiabatic evolution of resonant orbits in Kerr space time

Soichiro Isoyama　JGRG22(2012)111415

An improved method for CMB lensing reconstruction and its cosmological applications

Toshiya Namikawa　JGRG22(2012)111416

Cosmological constraints on sterile neutrino mass in f(R) gravity

Hayato Motohashi　JGRG22(2012)111417

Testing gravity with galaxy cluster

Tatsuya Narikawa　JGRG22(2012)111418

Constraints on general second-order scalar-tensor models from gravitational Cherenkov radiation

Rampei Kimura　JGRG22(2012)111419

Weak lensing generated by vector perturbations and detectability of cosmic strings

Daisuke Yamauchi　JGRG22(2012)111420

Higgs-inflation and the latest LHC results

Dmitry Gorbunov　JGRG22(2012)111421

Tunneling fields in non-linear massive gravity

Yingli Zhang　JGRG22(2012)111422

Probing for massive gravitational-wave background with a ground-based detector network

Atsushi Nishizawa　JGRG22(2012)111423

New cosmological solutions in massive gravity

Daisuke Yoshida　JGRG22(2012)111424

Inflation in bimetric gravity

Yuki Sakakihara　JGRG22(2012)111425

Parity violation in the CMB bispectrum

Maresuke Shiraishi　JGRG22(2012)111426

The cosmological constant problem

Jerome Martin　JGRG22(2012)111501

SuMIRe project: Hyper Suprime-Cam (HSC) and Prime Focus Spectrograph (PFS)

Masahiro Takada　JGRG22(2012)111502

The first law of binary black hole dynamics

Luc Blanchet　JGRG22(2012)111503

Charmed by spacetime physics – from four to higher dimensions

Hideo Kodama　JGRG22(2012)111504

A few thoughts on gravity and cosmology

Misao Sasaki　JGRG22(2012)111505

GR in the observational cosmology

Toshifumi Futamase　JGRG22(2012)111506

Gravitational-wave and neutrino emissions from black hole-neutron star binary merger

Yuichiro Sekiguchi　JGRG22(2012)111601

Stability of black holes: summary of some results for the past 10 years

Roman Konoplya　JGRG22(2012)111602

Vacuum transitions and the arrow of time

Jaume Garriga　JGRG22(2012)111603

Duration and decay branching ratios of stochastic inflation

Alexei Starobinsky　JGRG22(2012)111604

Conclusion

Kei-ichi Maeda　JGRG(2012)111605

Jun'ichi Yokoyama, JGRG 22(2012)111200

"Opening address"

RESCEU SYMPOSIUM ON

GENERAL RELATIVITY AND GRAVITATION

JGRG 22

November 12-16 2012

Koshiba Hall, The University of Tokyo, Hongo, Tokyo, Japan

RESCEU SYMPOSIUM ON GENERAL RELATIVITY AND GRAVITATION



also known as

JGRG22

which is

"The 22nd Workshop on General Relativity and Gravitation in Japan"

November 12 - 16 2012

Koshiba Hall, The University of Tokyo, Hongo, Tokyo, Japan

Welcome address by

Professor Hiroaki Aihara
Dean of School of Science

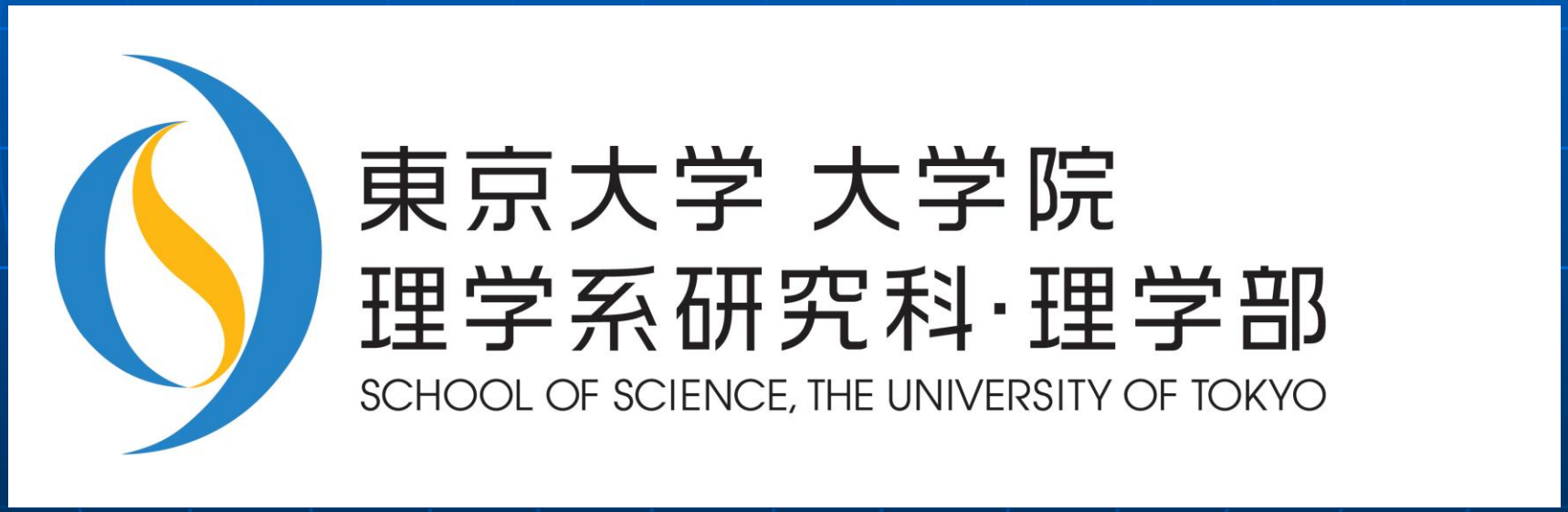

RESCEU Projects



PROJECT 1

Very Early Universe and Large-scale Structure

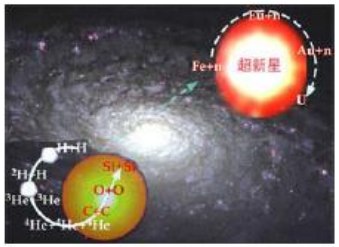

PROJECT 2

Theory of Galaxy Evolution



PROJECT 3

Formation and evolution of galaxies and clusters of galaxies



PROJECT 4

Submillimeter-wave Observation



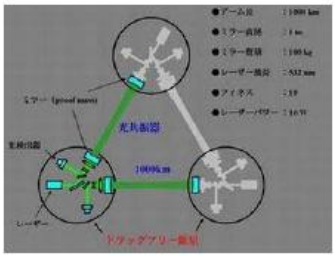

PROJECT 5

Search for Gravitational Waves



PROJECT 6

direct search for dark matter and solar axions



PROJECT 7

Researches using Space-Borne Instruments

RESCEU International Symposia



The 1st RESCEU International Symposium:
"The Cosmological Constant and the Evolution of the Universe" (11/7-10, 1995)
The 2nd RESCEU International Symposium:
"Dark Matter in the Universe and its Direct Detection" (11/26-28, 1996)
The 3rd RESCEU International Symposium:
"Particle Cosmology" (11/11-13, 1997)
The 4th RESCEU International Symposium:
"The Birth and Evolution of the Universe" (11/16-19, 1999)
The 5th RESCEU International Symposium:
"New Trends in Theoretical and Observational Cosmology" (11/13-16, 2001)
The 6th RESCEU International Symposium:
"Frontier in Astroparticle Physics and Cosmology" (11/4-7, 2003)
The 59th Yamada conference
"Inflating horizon of particle astrophysics and cosmology " (6/20-24, 2005)
The 7th RESCEU International Symposium:
"Astroparticle Physics and Cosmology" (11/11-14, 2008)
The 8th RESCEU International Symposium, Horiba international conference:
"COSMO/CosPA 2010" (9/27-10/1, 2010)

Construction of KAGRA started in January, 2012.

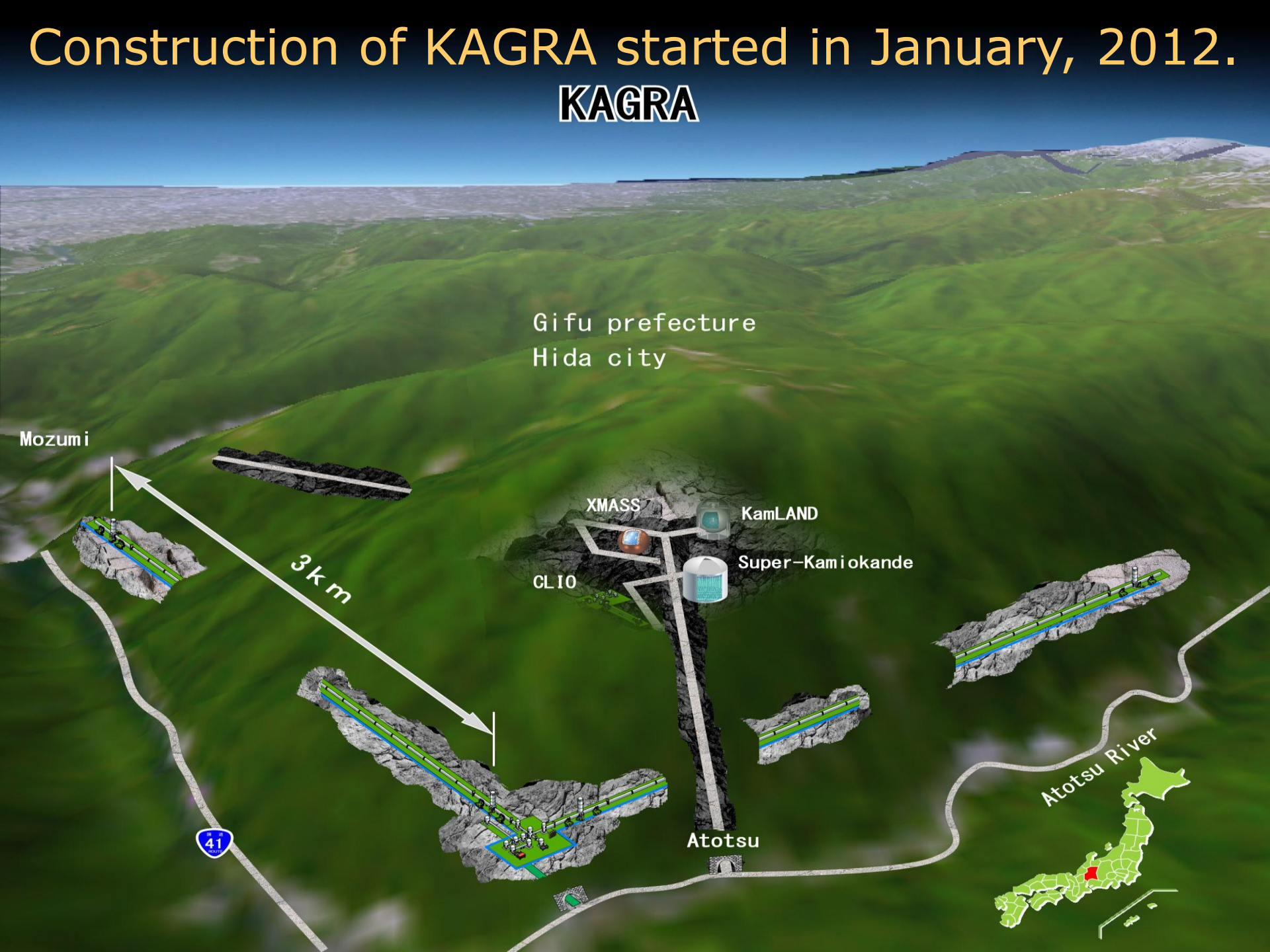

Construction of KAGRA started in January, 2012.









Construction of KAGRA started in January, 2012.







Takaaki Kajita “Status of KAGRA”

Francesco Fidecaro “Virgo: design, results and perspectives”

David Reitze “LIGO: Recent Results, Plans, and Prospects”

RESCEU Projects



PROJECT 1

Very Early Universe and Large-scale Structure

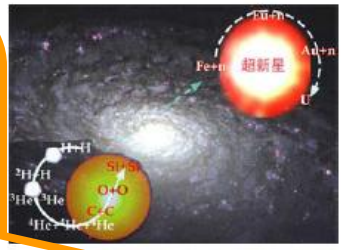

PROJECT 2

Theory of Galaxy Evolution



PROJECT 3

Formation and evolution of galaxies and clusters of galaxies



PROJECT 4

Submillimeter-wave Observation



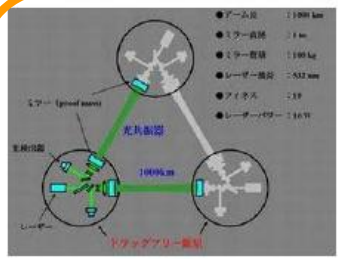

PROJECT 5

Search for Gravitational Waves



PROJECT 6

direct search for dark matter and solar axions



PROJECT 7

Researches using Space-Borne Instruments

jointly organized KAGRA data analysis school @RESCEU



Yousuke Itoh @RESCEU

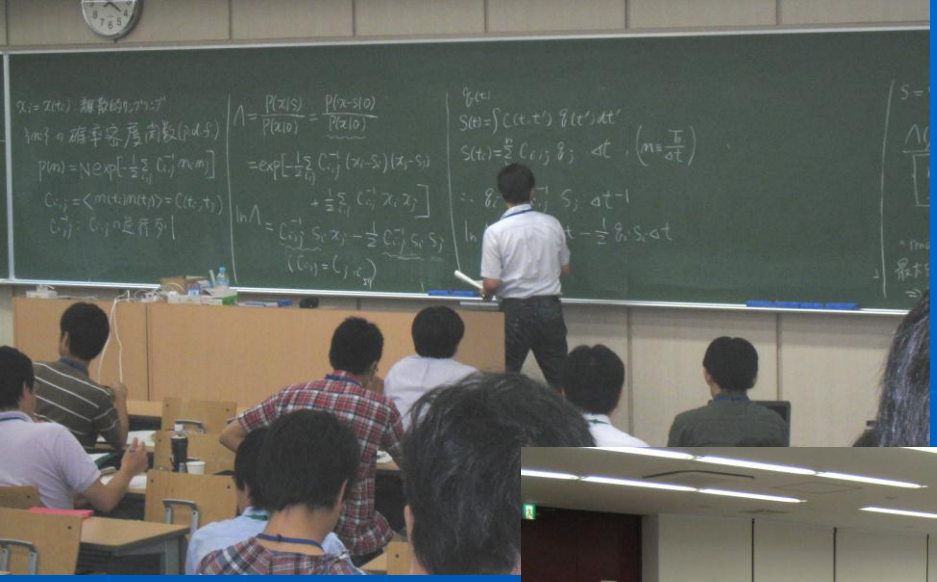

Lectures by Dr. H. Tagoshi



Programming Practice

Until very late at night!



History of JGRG

JGRG1 (Tokyo Metropolitan University, 12/4-6, 1991)
JGRG2 (Waseda University, 1/18-20, 1993)
JGRG3 (The University of Tokyo, 1/17-20, 1994)
JGRG4 (YITP, Kyoto University, 11/28-12/1, 1994)
JGRG5 (Nagoya University, 1/22-25, 1996)
JGRG6 (Tokyo Institute of Technology, 12/2-5, 1996)
JGRG7 (YITP, Kyoto University, 10/27-30, 1997)
JGRG8 (Niigata University, 10/19-22, 1998)
JGRG9 (Hiroshima University, 11/3-6, 1999)
JGRG10 (Osaka University, 9/11-14, 2000)
JGRG11 (Waseda University, 1/9-12, 2002)
JGRG12 (Komaba, The University of Tokyo, 11/25-28, 2002)
JGRG13 (Osaka City University, 12/1-4, 2003)
JGRG14 (YITP, Kyoto University, 11/29-12/3, 2004)
JGRG15 (Tokyo Institute of Technology, 11/28-12/2, 2005)
JGRG16 (Niigata Prefectural Center, 11/27-12/1, 2006)
JGRG17 (Nagoya University, 12/3-7, 2007)
JGRG18 (Hiroshima University, 11/17-21, 2008)
JGRG19 (Rikkyo University, 11/30-12/4, 2009)
JGRG20 (YITP, Kyoto University, 9/21-25, 2010)
JGRG21 (Tohoku University, 9/26-29, 2011)
JGRG22 (RESCEU, 11/12-16, 2012)

JGRG1 (Tokyo Metropolitan University, 12/4-6, 1991)
JGRG2 (Waseda University, 1/18-20, 1993)
JGRG3 (The University of Tokyo, 1/17-20, 1994)
JGRG4 (YITP, Kyoto University, 11/28-12/1, 1994)
JGRG5 (Nagoya University, 1/22-25, 1996)
JGRG6 (Tokyo Institute of Technology, 12/2-5, 1996)
JGRG7 (YITP, Kyoto University, 10/27-30, 1997)
JGRG8 (Niigata University, 10/19-22, 1998)
JGRG9 (Hiroshima University, 11/3-6, 1999)
JGRG10 (Osaka University, 9/11-14, 2000) → International (English)
JGRG11 (Waseda University, 1/9-12, 2002) Sasaki & JY
JGRG12 (Komaba, The University of Tokyo, 11/25-28, 2002)
JGRG13 (Osaka City University, 12/1-4, 2003)
JGRG14 (YITP, Kyoto University, 11/29-12/3, 2004)
JGRG15 (Tokyo Institute of Technology, 11/28-12/2, 2005)
JGRG16 (Niigata Prefectural Center, 11/27-12/1, 2006)
JGRG17 (Nagoya University, 12/3-7, 2007)
JGRG18 (Hiroshima University, 11/17-21, 2008)
JGRG19 (Rikkyo University, 11/30-12/4, 2009)
JGRG20 (YITP, Kyoto University, 9/21-25, 2010)
JGRG21 (Tohoku University, 9/26-29, 2011)
JGRG22 (RESCEU, 11/12-16, 2012)

JGRG1 (Tokyo Metropolitan University, 12/4-6, 1991)
JGRG2 (Waseda University, 1/18-20, 1993)
JGRG3 (The University of Tokyo, 1/17-20, 1994)
JGRG4 (YITP, Kyoto University, 11/28-12/1, 1994)
JGRG5 (Nagoya University, 1/22-25, 1996)
JGRG6 (Tokyo Institute of Technology, 12/2-5, 1996)
JGRG7 (YITP, Kyoto University, 10/27-30, 1997)
JGRG8 (Niigata University, 10/19-22, 1998)
JGRG9 (Hiroshima University, 11/3-6, 1999)
JGRG10 (Osaka University, 9/11-14, 2000)
JGRG11 (Waseda University, 1/9-12, 2002)
JGRG12 (Komaba, The University of Tokyo, 11/25-28, 2002)
JGRG13 (Osaka City University, 12/1-4, 2003)
JGRG14 (YITP, Kyoto University, 11/29-12/3, 2004)
JGRG15 (Tokyo Institute of Technology, 11/28-12/2, 2005)
JGRG16 (Niigata Prefectural Center, 11/27-12/1, 2006)
JGRG17 (Nagoya University, 12/3-7, 2007)
JGRG18 (Hiroshima University, 11/17-21, 2008)
JGRG19 (Rikkyo University, 11/30-12/4, 2009)
JGRG20 (YITP, Kyoto University, 9/21-25, 2010) 60th anniversary of
JGRG21 (Tohoku University, 9/26-29, 2011) Nakamura & Maeda
JGRG22 (RESCEU, 11/12-16, 2012)

JGRG1 (Tokyo Metropolitan University, 12/4-6, 1991)
JGRG2 (Waseda University, 1/18-20, 1993)
JGRG3 (The University of Tokyo, 1/17-20, 1994)
JGRG4 (YITP, Kyoto University, 11/28-12/1, 1994)
JGRG5 (Nagoya University, 1/22-25, 1996)
JGRG6 (Tokyo Institute of Technology, 12/2-5, 1996)
JGRG7 (YITP, Kyoto University, 10/27-30, 1997)
JGRG8 (Niigata University, 10/19-22, 1998)
JGRG9 (Hiroshima University, 11/3-6, 1999)
JGRG10 (Osaka University, 9/11-14, 2000)
JGRG11 (Waseda University, 1/9-12, 2002)
JGRG12 (Komaba, The University of Tokyo, 11/25-28, 2002)
JGRG13 (Osaka City University, 12/1-4, 2003)
JGRG14 (YITP, Kyoto University, 11/29-12/3, 2004)
JGRG15 (Tokyo Institute of Technology, 11/28-12/2, 2005)
JGRG16 (Niigata Prefectural Center, 11/27-12/1, 2006)
JGRG17 (Nagoya University, 12/3-7, 2007)
JGRG18 (Hiroshima University, 11/17-21, 2008)
JGRG19 (Rikkyo University, 11/30-12/4, 2009)
JGRG20 (YITP, Kyoto University, 9/21-25, 2010)
JGRG21 (Tohoku University, 9/26-29, 2011)
JGRG22 (RESCEU, 11/12-16, 2012) 60th anniversary of Kodama, Futamase, and Sasaki (special lectures on Thurs.)

JGRG1 (Tokyo Metropolitan University, 12/4-6, 1991)
JGRG2 (Waseda University, 1/18-20, 1993)
JGRG3 (The University of Tokyo, 1/17-20, 1994)
JGRG4 (YITP, Kyoto University, 11/28-12/1, 1994)
JGRG5 (Nagoya University, 1/22-25, 1996)
JGRG6 (Tokyo Institute of Technology, 12/2-5, 1996)
JGRG7 (YITP, Kyoto University, 10/27-30, 1997)
JGRG8 (Niigata University, 10/19-22, 1998)
JGRG9 (Hiroshima University, 11/3-6, 1999)
JGRG10 (Osaka University, 9/11-14, 2000)
JGRG11 (Waseda University, 1/9-12, 2002)
JGRG12 (Komaba, The University of Tokyo, 11/25-28, 2002)
JGRG13 (Osaka City University, 12/1-4, 2003)
JGRG14 (YITP, Kyoto University, 11/29-12/3, 2004)
JGRG15 (Tokyo Institute of Technology, 11/28-12/2, 2005)
JGRG16 (Niigata Prefectural Center, 11/27-12/1, 2006)
JGRG17 (Nagoya University, 12/3-7, 2007)
JGRG18 (Hiroshima University, 11/17-21, 2008)
JGRG19 (Rikkyo University, 11/30-12/4, 2009)
JGRG20 (YITP, Kyoto University, 9/21-25, 2010)
JGRG21 (Tohoku University, 9/26-29, 2011)
JGRG22 (RESCEU, 11/12-16, 2012)

JGRG33

Social Events

Reception: Today from 18:30 @ Sanjo Conference Hall

Poster & Beer: Tomorrow from 16:30 here
(Beer will be served after 17:00)

Self-service Excursion and Banquet: Thursday evening
@Ooedo Onsen Monogatari in Odaiba
(Hot springs with Edo-era(1603-1867) Style)

A free shuttle bus is available for non-Japanese speaking participants and invited speakers.

Japanese participants, please come by yourselves.
丸ノ内線本郷三丁目から新橋乗り換えゆりかもめでテレコムセンター下車徒歩2分。

Please show your name tag at the entrance

大江戸温泉物語 OOEDO ONSEN MONOGATARI

Welcome to Ooedo-Onsen-Monogatari







Dress code: Since you will be requested to wear a Edo-era style *Yukata* robe in the premise, please come in casual clothes. Wearing neckties and jackets is discouraged.

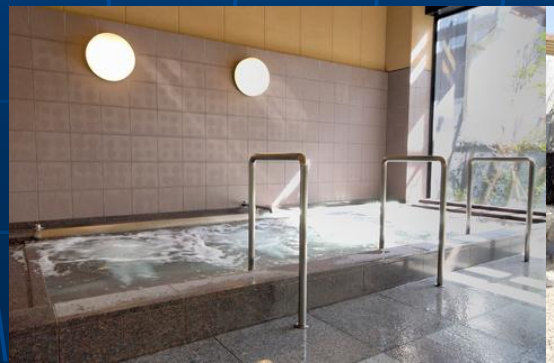



A New Attempt in the 22 years' history of JGRG

Launching JGRG Presentation Award

Participants who attended until the end of each parallel session have a right to vote for one talk in the session.

For the poster award, participants who participated in the discussion until 18:30 on Tuesday have a right to vote for one poster presentation.

Based on the results of the votes and recommendation by parallel session chairs, the selection committee consisting of the organizing committee members will decide who will be awarded.

In case you wish to move from one parallel room to the other? No problem, just vote for one of the talks you attended regardless of the room where you are at the end of the day.

Supported by

MEXT Grant-in-Aid for Scientific Research on Innovative Areas No. 21111006
“Quest for the Ultimate Theory on the Basis of Direct Observations of the Evolution of the Early Universe” (Kodama & JY)

MEXT Grant-in-Aid for Scientific Research on Innovative Areas, No. 24103006
"Theo ysics through multimessenger observations of gr s" (Nakamura & Tanaka)

JSPS fic Research (A) No. 21244033
“Cosm perturbative gravitational phenomena" (Sasaki)

JSPS fic Research No. 23540282
“Theo tional Waves from Fast Moving Sources, Strong Grav ly Universe” (Futamase)

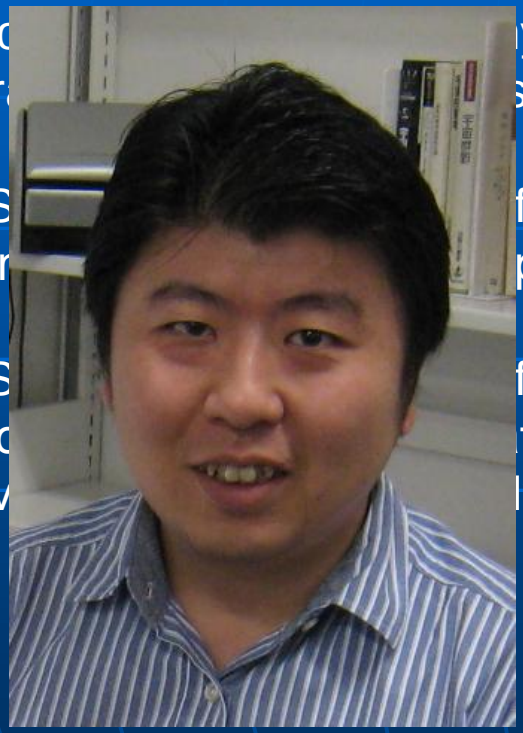

Our new assistant professor
Teruaki Suyama

Where to have lunch (A campus map is available.)



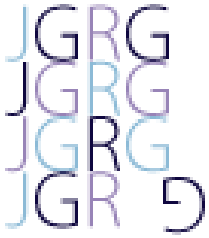

Abhey Ashtekar, JGRG 22(2012)111201

"The pre-inflationary dynamics of loop quantum cosmology:

Confronting quantum gravity with observations"

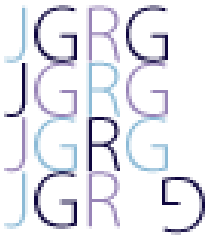

RESCEU SYMPOSIUM ON

GENERAL RELATIVITY AND GRAVITATION

JGRG 22



November 12-16 2012

Koshiba Hall, The University of Tokyo, Hongo, Tokyo, Japan



The pre-inflationary dynamics of LQC
Confronting quantum gravity with observations

Abhay Ashtekar

Institute for Gravitation and the Cosmos, Penn State

Dedicated with Pleasure to

Hideo Kodama, Misao Sasaki & Toshi Futamase

Friends, Colleagues and Creative Scientists,

Who Have Enriched us With So Many Insights!

RESCEU Symposium on GRG, 12-16 November, 2012

Organization

1. Introduction: Successes and Limitations of Inflation

Overcoming the limitations:

2. Singularity Resolution in Loop Quantum Cosmology
3. Cosmological Perturbations on quantum FLRW Space-times
4. Extracting Physics: Power Spectra & Non-Gaussiantity.
5. Summary and Discussion

Understanding emerged from the work of many researchers, especially:

Agullo, Barrau, Bojowald, Cailleatau, Campiglia, Corichi, Grain, Kaminski, Lewandowski, Mielczarek, Nelson, Pawlowski, Singh, Sloan, ...

For summary, see AA, Agullo & Nelson 1209.1609 PRL (at Press); More complete references: AA, Agullo & Nelson 1211:1354; AA Sloan GRG (2011), PLB (2009), GRG (2011); AA, Corichi & Singh PRD (2008); Pawlowski, Singh, PRL & PRD (2006).

Inflationary Paradigm

- Major success: Prediction of inhomogeneities in CMB which serve as seeds for structure formation. Observationally relevant wave numbers in the range $\sim (k_o, 2000k_o)$ (radius of the observable CMB surface $\sim \lambda_o$).

- Rather minimal assumptions:

1. Some time in its early history, the universe underwent a phase of accelerated expansion during which the Hubble parameter H was nearly constant.

2. Starting from this phase till the CMB era, the universe is well-described by a FLRW background with linear perturbations. Only matter: inflaton in a suitable potential.

3. At the onset of this 'slow roll inflationary phase' Fourier modes of quantum fields describing perturbations were in the Bunch-Davis vacuum (at least for co-moving wave numbers in the range $\sim (k_o, 2000k_o)$); and,

4. Soon after a mode exited the Hubble radius, its quantum fluctuation can be regarded as a classical perturbation and evolved via linearized Einstein's equations.

- Then QFT on FLRW space-times (and classical GR) implies the existence of tiny inhomogeneities in CMB seen by the 7 year WMAP data.

All large scale structure emerged from vacuum fluctuations!

Inflationary Paradigm: Incompleteness

Particle Physics Issues:

- Where from the inflaton? A single inflaton or multi-inflatons? Interactions between inflatons? How are particles/fields of the standard model created during 'reheating' at the end of inflation? ...

Quantum Gravity Issues:

- Big bang singularity also in the inflationary models (Borde, Guth & Vilenkin). Is it resolved by quantum gravity as has been hoped since the 1970's? What is the nature of the quantum space-time that replaces Einstein's continuum in the Planck regime?

- Does the slow-roll inflation used to explain the WMAP data naturally arise from natural initial conditions 'at the Beginning' that replaces the big bang in quantum gravity?

- In classical GR, if we evolve the modes of interest back in time, they become trans-Planckian. Is there a QFT on quantum cosmological space-times needed to adequately handle physics at that stage?

- Can one arrive at the Bunch-Davis vacuum (at the onset of the WMAP slow roll) from more fundamental considerations?

‘Standard’ View & its limitations

Why Planck scale physics could affect the scenario?

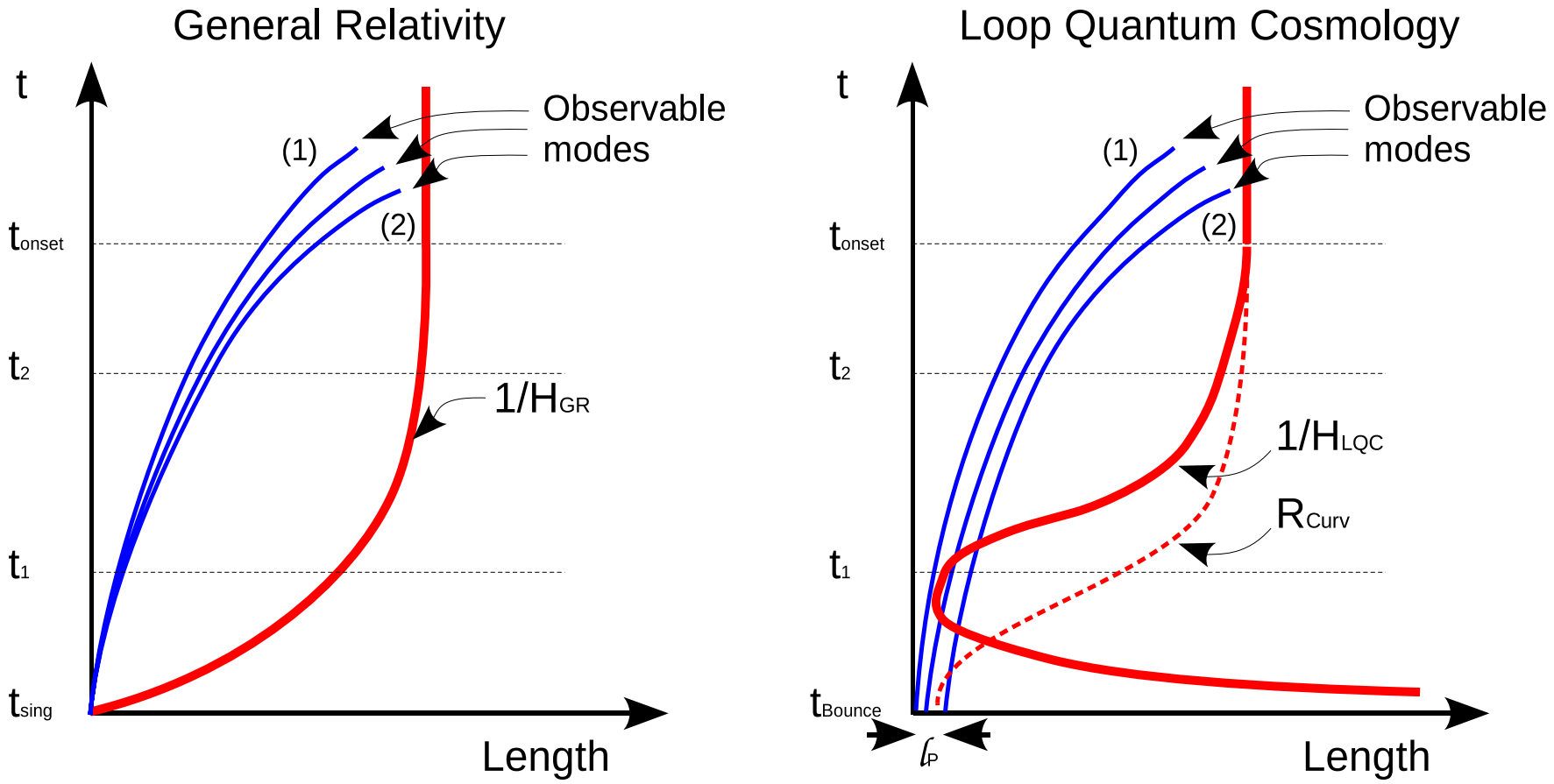

Inflationary Scenario: Incompleteness

Quantum Gravity Issues:

- Big bang singularity also in the inflationary models (Borde, Guth & Vilenkin).

Is it resolved by quantum gravity as has been hoped? Nature of the quantum space-time that replaces Einstein's continuum in the Planck regime?

> "One may not assume the validity of field equations at very high density of field and matter and one may not conclude that the beginning of the expansion should be a singularity in the mathematical sense." A. Einstein, 1945

- Does the slow-roll inflation used to explain the WMAP data naturally arise from natural initial conditions 'at the Beginning' that replaces the big bang in quantum gravity?
- In classical GR, if we evolve the modes of interest back in time, they become trans-Planckian. Is there a QFT on quantum cosmological space-times needed to adequately handle physics at that stage?
- Can one arrive at the Bunch-Davis vacuum (at the onset of the WMAP slow roll) from more fundamental considerations?

2. Singularity Resolution

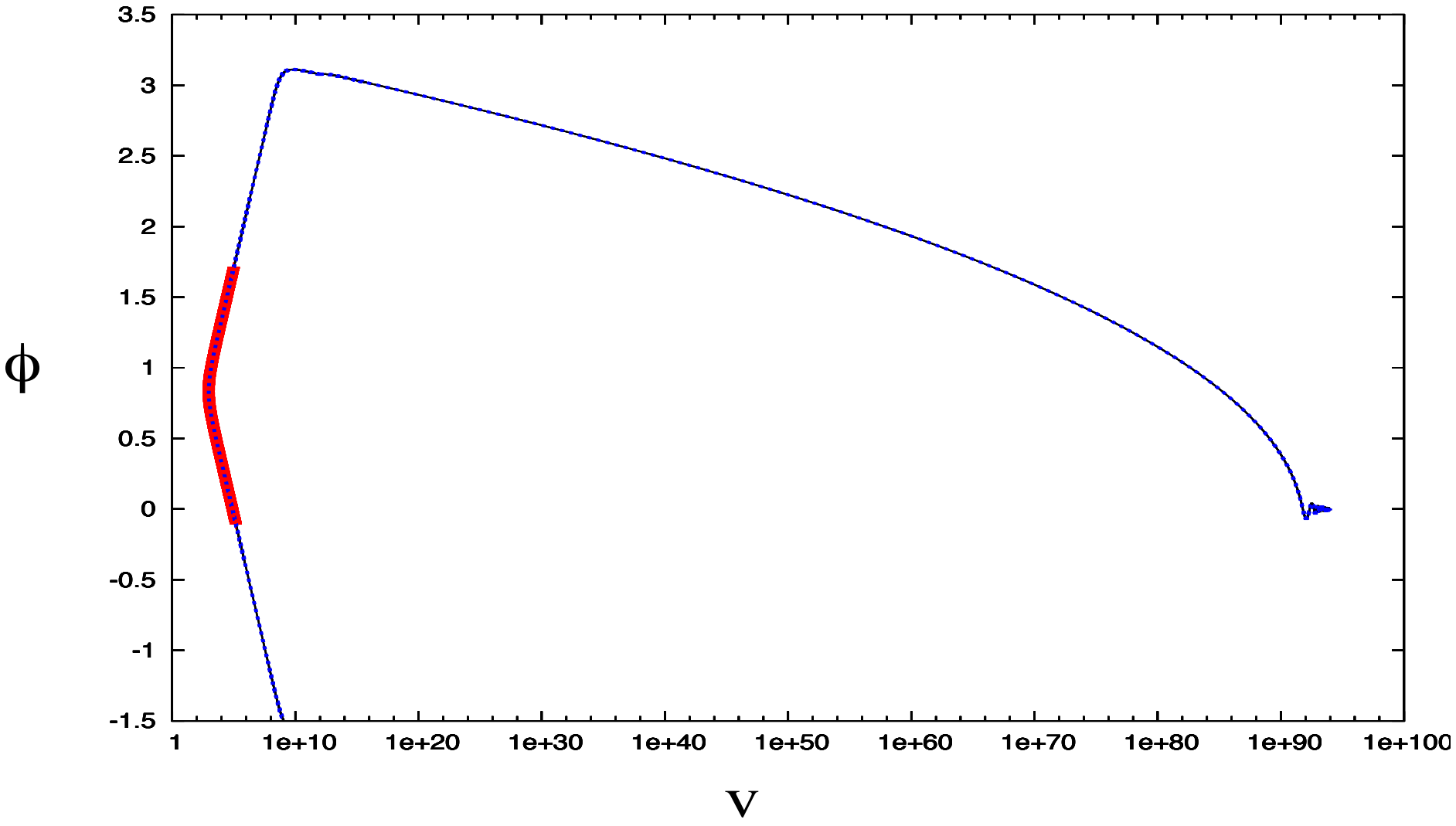

Expectations values and dispersions of $\hat{V}|_\phi$ for a massive inflaton ϕ with phenomenologically preferred parameters (AA, Pawlowski, Singh). The Big Bang is replaced by a Big Bounce. Similar resolution in a wide class of cosmological models.

What is behind singularity resolution?

• In full LQG, we have a mathematically rigorous kinematical framework uniquely selected by the requirement of background independence (Lewandowski, Okolow, Sahlmann, Thiemann; Fleishchhack). This descends to LQC in a well defined manner (AA, Campiglia).

• This kinematics is distinct from the Schrödinger representation used in the WDW theory. In particular, the differential operator of the WDW equation, $\partial^2\Psi_o(v,\phi)/\partial v^2 = \ell_P^2\hat{H}_\phi\Psi_o(v,\phi)$ fails to be well-defined on the LQC Hilbert space and is naturally replaced by a difference operator:

$$C^+(v)\,\Psi_o(v+4,\,\phi) + C^o(v)\,\Psi_o(v,\phi) + C^-(v)\Psi_o(v-4,\,\phi) \;=\; \ell_P^2\;\hat{H}_\phi\Psi_o(v,\phi)$$

(The Step size is determined by the area gap of Riemannian quantum geometry underlying LQG)

• Good agreement with the WDW equation at low curvatures but drastic departures in the Planck regime precisely because the WDW theory ignores quantum geometry (the area gap).

Singularity Resolution in LQC: k=0

- No unphysical matter. All energy conditions satisfied. But the left side of Einstein's equations modified because of quantum geometry effects (discreteness of eigenvalues of geometric operators.)

- Effective Equations: To compare with the standard Friedmann equation, convenient to do an algebraic manipulation and move the quantum geometry effect to the right side. Then:

$$(\dot{a}/a)^2 = (8\pi G\rho/3)[1 - \rho/\rho_{\rm crit}] \quad \text{where} \quad \rho_{\rm crit} \sim 0.41\rho_{\rm Pl}.$$

Big Bang replaced by a quantum bounce. *Effective equations are surprisingly effective even in the Planck regime.*

- Observables: The matter density operator $\hat{\rho}$ has an absolute upper bound on the physical Hilbert space (AA, Corichi, Singh):

$$\rho_{\rm sup} = \sqrt{3}/16\pi^2\gamma^3 G^2\hbar \approx 0.41\rho_{\rm Pl}!$$

Provides a precise sense in which the singularity is resolved.

- Mechanism: Quantum geometry creates a brand new repulsive force in the Planck regime, neatly encoded in the difference equation. Replaces the big-bang by a quantum bounce.

Inflationary Paradigm: Incompleteness

Quantum Gravity Issues:

- Big bang singularity also in the inflationary models (Borde, Guth & Vilenkin). Is it resolved by quantum gravity as had been long hoped? What is the nature of the quantum space-time that replaces Einstein's continuum in the Planck regime?

- Does the slow-roll inflation used to explain the WMAP data naturally arise from natural initial conditions 'at the Beginning' that replaces the big bang in quantum gravity?

- In classical GR, if we evolve the modes of interest back in time, they become trans-Planckian. Is there a QFT on quantum cosmological space-times needed to adequately handle physics at that stage?

- In the more complete theory, is the Bunch-Davis vacuum at the onset of the slow roll compatible with WMAP generic or does it need enormous fine tuning?

3. Cosmological Perturbations on Quantum Space-times

• **LQG Strategy:** Focus on the appropriate truncation/sector of classical GR and pass to quantum gravity using LQG techniques. Sector of interest for inflation: Linear Perturbations off FLRW background with an inflaton ϕ in a suitable potential as matter. Includes inhomogeneities, but as perturbations. In detailed calculations, $V(\phi) = (1/2)m^2\phi^2$.

Truncated Phase Space $\ni \{(v, \phi;\ \delta h_{ab}(x), \delta\phi(x))$ and their conjugate momenta$\}$
Quantum Theory: Start with $\mathbf{\Psi}(v, \phi;\ \delta h_{ab}(x), \delta\phi(x))$ and proceed to the quantum theory using LQG techniques.

• Test field approximation: $\mathbf{\Psi} = \Psi_o(v, \phi) \otimes \psi(\delta h_{ab}, \phi)$. Linearized constraints $\Rightarrow \psi(\delta h_{ab}, \phi) = \psi(T^{(1)}, T^{(2)}, \mathcal{R};\ \phi)$, where $T^{(1)}, T^{(2)}$ are the tensor modes and $\mathcal{R}$ the scalar mode. In the Planck regime of interest, ϕ serves as the 'internal/relational time'.

• Idea: Choose $\Psi_o(v, \phi)$ to be sharply peaked at an effective LQC solution g^o_{ab}. Such 'coherent states' exist. ψ propagates on the quantum geometry determined by Ψ_o: QFT on QST a la AA, Lewandowski, Kaminski.

Choice of the Cosmological Background Ψ_o

- Let us start with generic data at the bounce **in the effective theory** and evolve. Will the solution enter slow roll at energy scale $\rho \approx 7.32 \times 10^{-12} m_{\rm Pl}^4$ determined from the 7 year WMAP data ? Note: 11 orders of magnitude from the bounce to the onset of the desired slow roll!

- Answer: **YES**. In LQC, $|\phi_{\rm B}| \in (0, 7.47 \times 10^5)$. If $|\phi_{\rm B}| \geq 1.05 m_{\rm Pl}$, the data evolves to a solution that encounters the slow roll compatible with the 7 year WMAP data sometime in the future. In this sense, 'almost every' initial data at the bounce evolves to a solution that encounters the desired slow roll sometime in the future. (AA & Sloan, Corichi & Karami)

- Result much stronger than the 'attractor' idea because it refers to the slow roll compatible with WMAP.

- Hence, for the background quantum geometry, we can choose a 'coherent' state Ψ_o sharply peaked at a 'generic' effective trajectory at the bounce and evolve using LQC. Slow roll phase ensured!

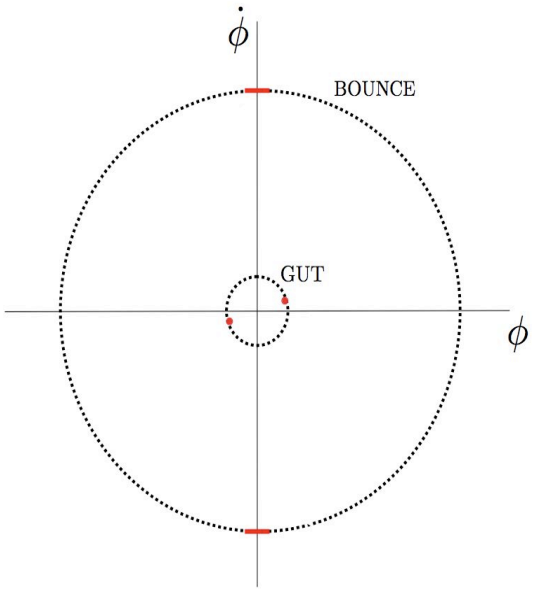

Inflationary Paradigm: Incompleteness

Quantum Gravity Issues:

- Big bang singularity also in the inflationary models (Borde, Guth & Vilenkin). Is it resolved by quantum gravity as had been long hoped? What is the nature of the quantum space-time that replaces Einstein's continuum in the Planck regime?

- In the systematic evolution from the Planck regime in the more complete theory, does a slow roll phase compatible with the WMAP data arise generically or is an enormous fine tuning needed?

- In classical GR, if we evolve the modes of interest back in time, they become trans-Planckian. Is there a QFT on quantum cosmological space-times needed to adequately handle physics at that stage? **Yes!** Can the basic ideas in AA, Lewandowski, Kaminski be developed to obtain well-defined stress energy operators in this new theory? Can one justify the truncation procedure even in the Planck regime?

- Can one arrive at the Bunch-Davis vacuum (at the onset of the WMAP slow roll) from more fundamental considerations?

4. Extracting Physics

First, thanks to the background quantum geometry, trans-Planckian modes pose no problem, provided the test field approximation holds: $\rho_{\rm Pert} \ll \rho_{\rm BG}$ all the way from the bounce to the onset of slow roll.

- Second, surprisingly, truncated dynamics of $\hat{T}^{(1)}, \hat{T}^{(2)}, \hat{\mathcal{R}}$ on the quantum geometry of Ψ_o is mathematically equivalent to that of $\hat{T}^{(1)}, \hat{T}^{(2)}$, $\hat{\mathcal{R}}$ as quantum fields on a smooth space-time with a 'dressed' effective, c-number metric $\bar{g}_{ab}$ (whose coefficients depend on $\hbar$):

$$\bar{g}_{ab} dx^a dx^b = \bar{a}^2(-d\bar{\eta}^2 + d\vec{x}^2)$$

with

$$d\bar{\eta} = \langle \hat{H}_o^{-1/2} \rangle \, [\langle \hat{H}_o^{-1/2} \hat{a}^4 \hat{H}_o^{-1/2} \rangle]^{1/2} \, d\phi; \qquad \bar{a}^4 = (\langle \hat{H}_o^{-1/2} \, \hat{a}^4 \hat{H}_o^{-1/2} \rangle)/\langle \hat{H}_o^{-1} \rangle$$

where H_o is the Hamiltonian governing dynamics of Ψ_o. Analogy with light propagating in a medium.

- Because of this, the mathematical machinery of adiabatic states, regularization and renormalization of the Hamiltonian can be lifted to the QFT on cosmological QSTs under consideration. Result: Mathematical control to compute the CMB power spectrum, and spectral indices starting from the bounce.

Initial conditions

- Hilbert space: $\mathcal{H}$ of perturbations ψ on the quantum geometry Ψ_o is spanned by 4th adiabatic order states on the smooth Friedmann metric $\bar{g}_{ab}$. Excellent control.

- Symmetries: Ψ_o (and hence $\bar{g}_{ab}$) homogeneous and isotropic. Preferred states: $\psi \in \mathcal{H}$ also invariant under translations and rotations. Far from unique. However, Can narrow it down by:

- Physical Considerations: State $\Psi_o \otimes \psi$ at the bounce $\Rightarrow$ **Initial quantum homogeneity!** Can be qualitatively justified as follows. Because of inflation, the observable universe has size of $\leq 10\ell_{\rm Pl}$ at the bounce. The repulsive force of quantum geometry dilutes all inhomogeneities at this scale. So universe is as homogeneous and isotropic as the uncertainty principle allows it to be!

- Renormalized energy density is well-defined on these states. For $\hat{T}^{(1)}$, $\hat{T}^{(2)}$, and $\hat{\mathcal{R}}$ to be test fields on the quantum geometry Ψ_o we also require that the stress energy in ψ be negligible compared that in Ψ_o at the bounce time.

Key Questions

1. Does the back-reaction remain negligible as ψ evolves all the way to the onset of the slow roll compatible with WMAP (so that our truncation strategy is justified by self-consistency)?
Answer: **YES**

2. At the end of the WMAP compatible slow roll, do we recover the observed power spectrum: $\Delta^2_{\mathcal{R}}(k, t_{k^\star}) \approx \frac{H^2(t_{k^\star})}{\pi m^2_{\rm Pl}\epsilon(t_{k^\star})}$? ($t_{k^\star}$ is the time the reference mode $k^\star \approx 8.58 k_o$ exits the Hubble horizon during slow roll)

Answer: **YES** provided $\phi_{\rm B} \geq 1.14 m_{\rm Pl}$. Thus, we have arrived at a quantum gravity completion of the inflationary paradigm.

3. Does $\psi(T^{(1)}_{\bar{k}}, T^{(2)}_{\bar{k}}, \mathcal{R}_{\bar{k}}; \phi_{\rm B})$ evolve to a state which is indistinguishable from the Bunch Davis vacuum at the onset of slow roll or are there deviations with observable consequences for more refined future observations (e.g. non-Gaussianitities in the bispectrum)?
(Agullo & Shandera; Ganc & Komatsu)

Answer: There **ARE** deviations if $\phi_{\rm B}$ lies in a small window just after $\phi_{\rm B} = 1.14 m_{\rm Pl}$.

Self-consistency of Truncation: $\rho_{\rm Pert}/\rho_{\rm BG}$ vs time

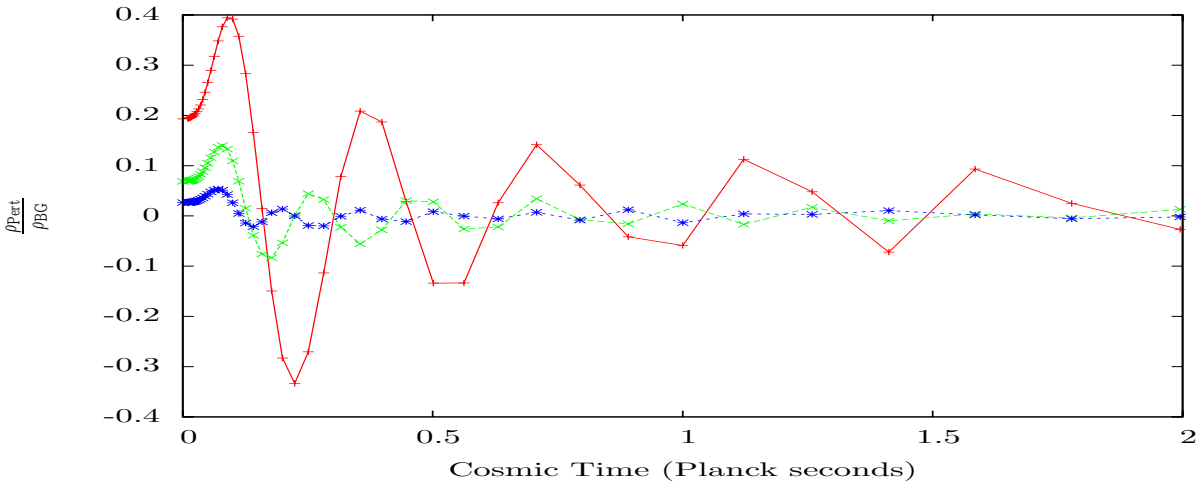

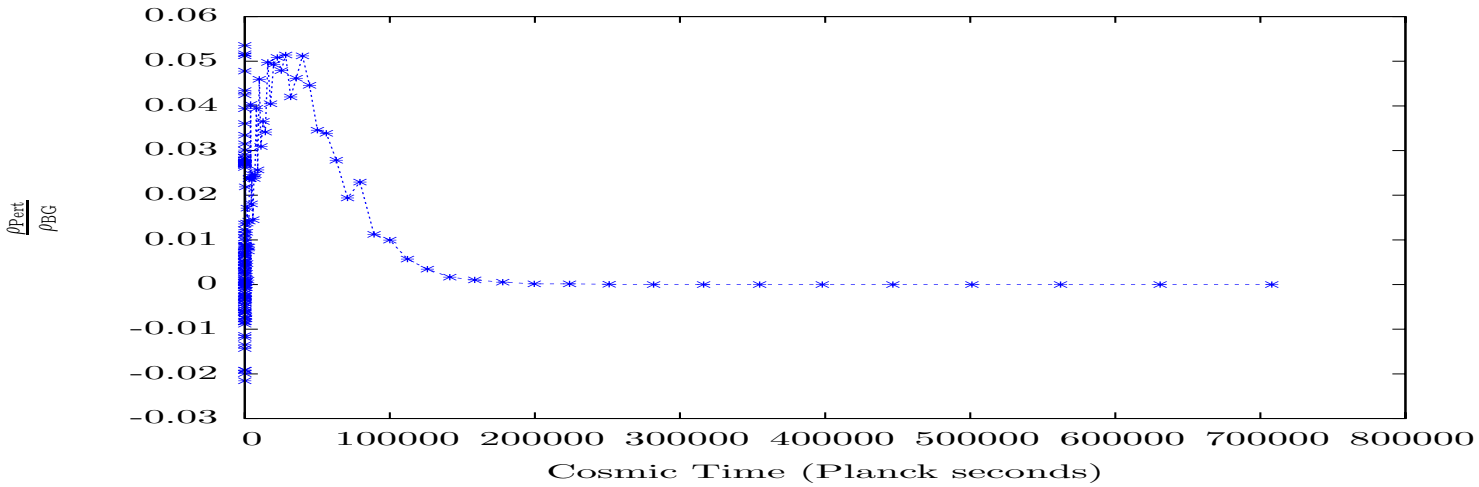

Renormalized energy density in ψ is negligible compared to that in Ψ_o all the way from the bounce to the onset of slow roll. Here $\phi_{\rm B} = 1.15 m_{\rm Pl}$.

Key Questions

1. Does the back-reaction remain negligible as ψ evolves all the way to the onset of the slow roll compatible with WMAP (so that our truncation strategy is justified by self-consistency)?
Answer: **YES**

2. At the end of the WMAP compatible slow roll, do we recover the observed power spectrum: $\Delta^2_{\mathcal{R}}(k, t_{k^\star}) \approx \frac{H^2(t_{k^\star})}{\pi m^2_{\rm Pl}\epsilon(t_{k^\star})}$? ($t_{k^\star}$ is the time the reference mode $k^\star \approx 8.58 k_o$ exits the Hubble horizon during slow roll)
Answer: **YES** provided $\phi_{\rm B} \geq 1.14 m_{\rm Pl}$. Thus, we have arrived at a quantum gravity completion of the inflationary paradigm.

3. Does $\psi(T^{(1)}_{\bar{k}}, T^{(2)}_{\bar{k}}, \mathcal{R}_{\bar{k}};\, \phi_{\rm B})$ evolve to a state which is indistinguishable from the Bunch Davis vacuum at the onset of slow roll or are there deviations with observable consequences for more refined future observations (e.g. non-Gaussianitities in the bispectrum)?
(Agullo & Shandera; Ganc & Komatsu)
Answer: There **ARE** deviations if $\phi_{\rm B}$ lies in a small window just after $\phi_{\rm B} = 1.14 m_{\rm Pl}$.

The Scalar Power spectrum: Ratio $(\mathcal{P}_{\rm LQG}/\mathcal{P}_{\rm BD})$

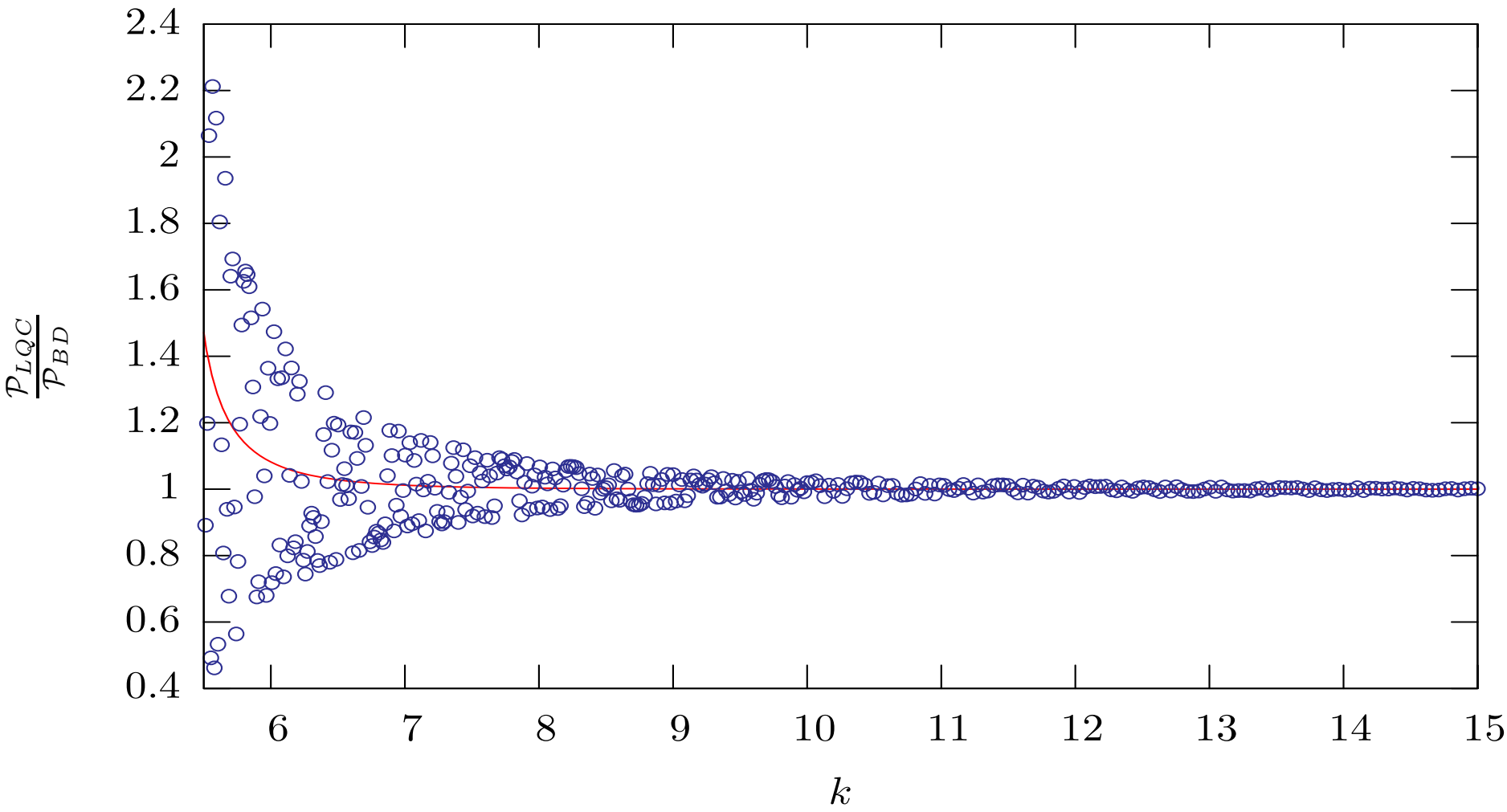

Ratio of the LQC and the standard BD power spectrum for the scalar mode. Blue: Raw data points. Red: Average. LQC prediction is within observational errors for $\phi_{\rm B} \geq 1.14 m_{\rm Pl}$.

For $\phi_{\rm B} = 1.2 m_{\rm Pl}$, WMAP $k_{\rm min} = 9 m_{\rm Pl}$. Complete agreement with BD vacuum for $\phi_{\rm B} \geq 1.2 m_{\rm Pl}$. For $\phi_{\rm B} < 1.2 m_{\rm Pl}$: Certain non-Gaussiainities for future observations.

The LQC Tensor Power spectrum

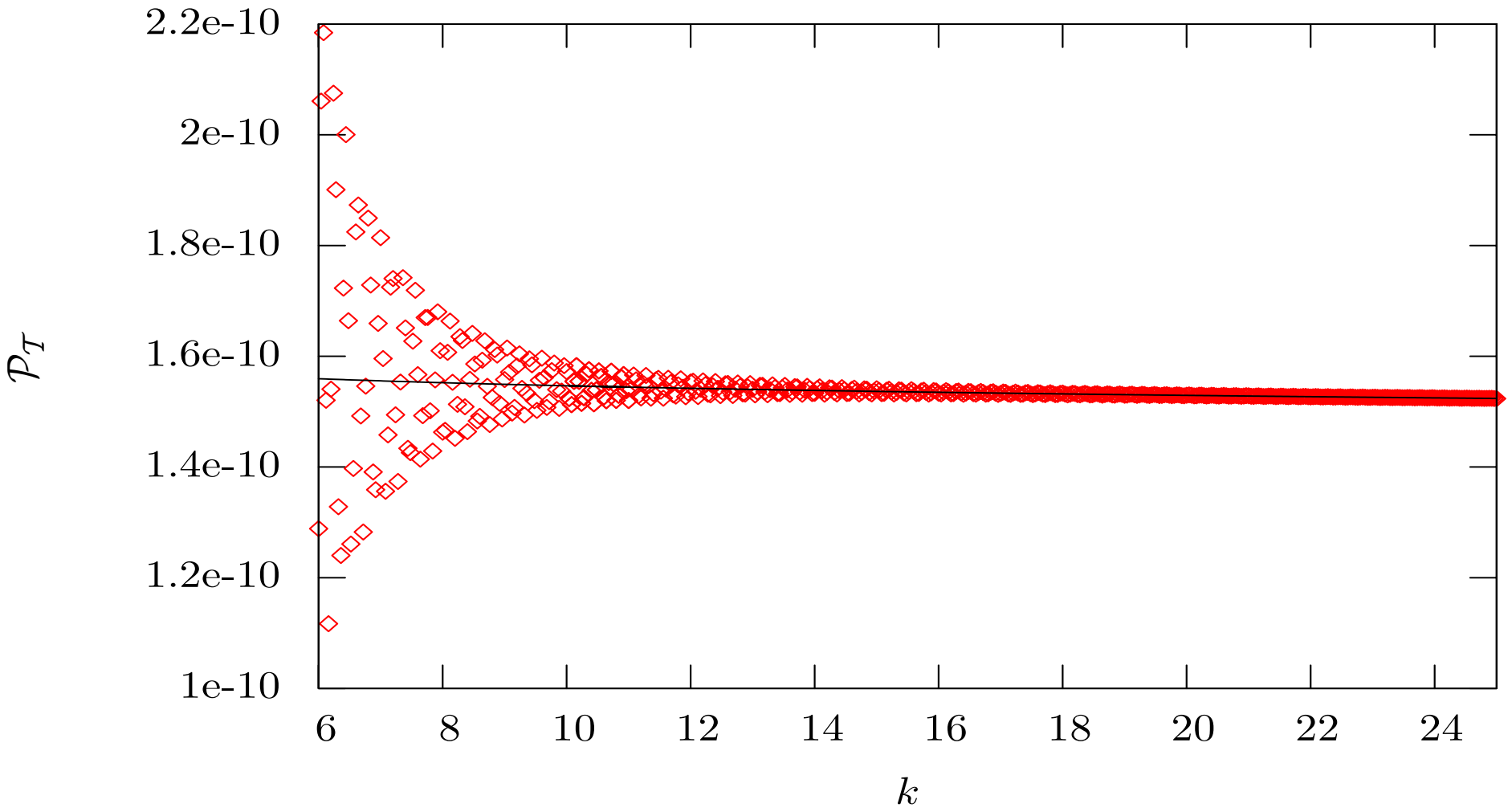

Predicted power spectra for the tensor mode. Black: Average. Red: Raw data points.

Understanding the Power Spectrum

Modes with $\lambda > R^{-1/2}$, the curvature radius, in the pre-inflationary era are excited and populated at the onset of inflation. Can occur in a narrow window for $\phi_{\rm B} \leq 1.2 m_{\rm Pl}$.

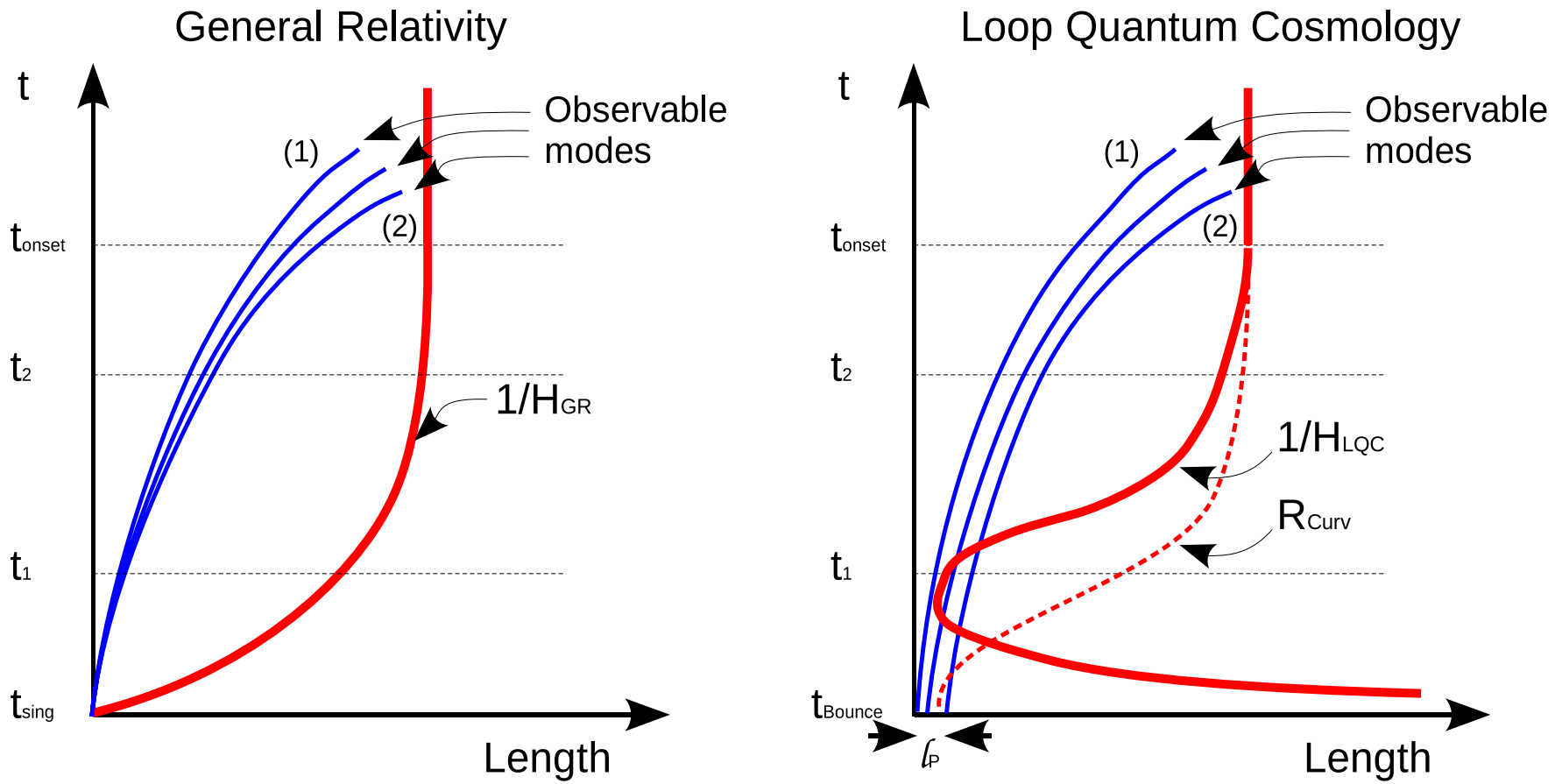

5. Summary: Framework

• The early universe provides an ideal setting to test quantum gravity ideas. The inflationary paradigm provides a telescope to peer into the Planck regime. Furthermore, it has been extremely successful with structure formation. Can one provide a quantum gravity completion of the inflationary paradigm thereby overcoming some of its limitations?

In LQG the answer is **YES** in the following precise sense:

• **Background geometry:** Singularity Resolution and precise quantum geometry for the Planck regime. $\surd$

• **Perturbations:** Since they propagate on quantum geometry, using QFT on cosmological quantum geometries (AA, Lewandowski, Kaminski), trans-Planckian issues can be handled systematically provided the test field approximation holds. Analyzed in detail using the renormalized stress-energy of $\hat{T}^{(1)}, \hat{T}^{(2)}, \hat{\mathcal{R}}$ on the quantum geometry of Ψ_o. Detailed numerics show that the approximation does hold if $\phi_B > 1.14 m_{\rm Pl}$. (Agullo, AA, Nelson)

Summary: Implications

• Extension: If $\Phi_{\rm B} > 1.14 m_{\rm Pl}$ & ψ is a 'permissible vacuum,' modes of observational interest are all in the Bunch Davis vacuum at the onset of the WMAP slow roll $\Rightarrow$ Predictions of the standard inflationary scenario for the power spectra, spectral indices & ratio of tensor to scalar modes are recovered starting from the deep Planck era. (Agullo, AA, Nelson)

• Non-Gaussianity: There is a small window in $\phi_{\rm B}$ for which at the onset of inflation ψ has excitations over the Bunch-Davis vacuum. These give rise to specific 3-point functions ('bi-spectrum') which are important for the 'halo bias'. Could be observed in principle: Link between observations and the initial state! A window to probe the Planck era around the LQC bounce. (Agullo, AA, Nelson, Shandera, Ganc, Komatsu)

• Note: LQG does not imply that inflation must have occurred because it does not address particle physics issues. The analysis simply assumes that there is an inflaton with a suitable potential. But it does show concretely that many of the standard criticisms (e.g. due to Brandenberger) of inflation can be addressed in LQG by facing the Planck regime squarely.

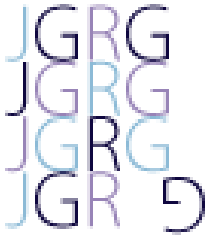

Shinji Mukohyama, JGRG 22(2012)111202

"Nonlinear massive gravity and cosmology"

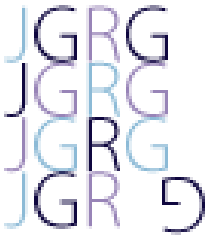

RESCEU SYMPOSIUM ON

GENERAL RELATIVITY AND GRAVITATION

JGRG 22



November 12-16 2012

Koshiba Hall, The University of Tokyo, Hongo, Tokyo, Japan



KAVLI IPMU INSTITUTE FOR THE PHYSICS AND MATHEMATICS OF THE UNIVERSE

Nonlinear massive gravity and Cosmology

Shinji Mukohyama
(Kavli IPMU, U of Tokyo)

Based on collaboration with
Antonio DeFelice, Emir Gumrukcuoglu, Chunshan Lin

Happy Birthdays!

- I would like to congratulate Kodama-san, Sasaki-san and Futamase-san on their 60th birthdays.







KAVLI IPMU INSTITUTE FOR THE PHYSICS AND MATHEMATICS OF THE UNIVERSE

Nonlinear massive gravity and Cosmology

Shinji Mukohyama
(Kavli IPMU, U of Tokyo)

Based on collaboration with
Antonio DeFelice, Emir Gumrukcuoglu, Chunshan Lin

Why alternative gravity theories?

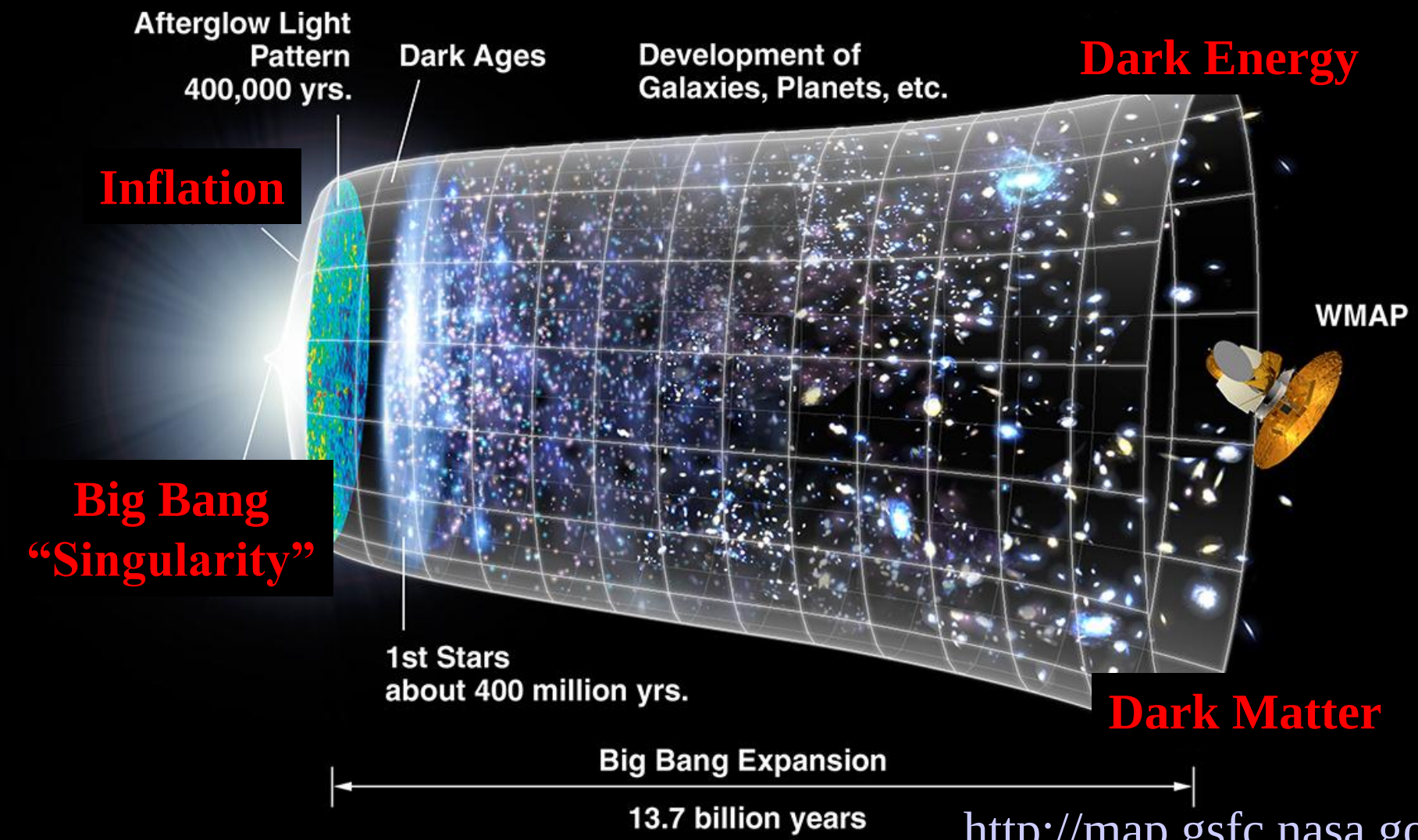

http://map.gsfc.nasa.gov/

Three conditions for good alternative theories of gravity (my personal viewpoint)

1. Theoretically consistent
   e.g. no ghost instability
2. Experimentally viable
   solar system / table top experiments
3. Predictable
   e.g. protected by symmetry

Some examples

I. Ghost condensation
   IR modification of gravity
   motivation: dark energy/matter

II. Nonlinear massive gravity
   IR modification of gravity
   motivation: “Can graviton have mass?”

III. Horava-Lifshitz gravity
   UV modification of gravity
   motivation: quantum gravity

IV. Superstring theory
   UV modification of gravity
   motivation: quantum gravity, unified theory

A motivation for IR modification

- Gravity at long distances
  Flattening galaxy rotation curves
  extra gravity
  Dimming supernovae
  accelerating universe

- Usual explanation: new forms of matter (DARK MATTER) and energy (DARK ENERGY).

Dark component in the solar system?

Precession of perihelion observed in 1800's…

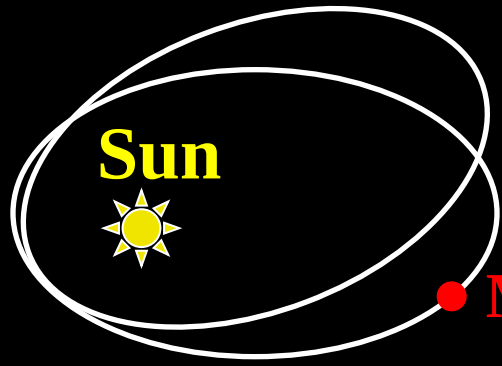

which people tried to explain with a "dark planet", Vulcan,

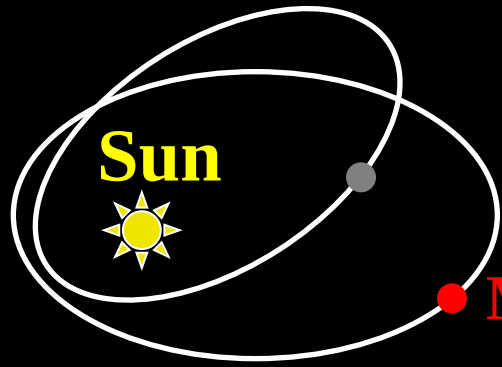

But the right answer wasn't "dark planet", it was "change gravity" from Newton to GR.

Can we change gravity in IR?

- **Change Theory?**
  Massive gravity **Fierz-Pauli 1939**
  DGP model **Dvali-Gabadadze-Porrati 2000**

- **Change State?**
  Higgs phase of gravity
  The simplest: Ghost condensation

  Arkani-Hamed, Cheng, Luty and Mukohyama, JHEP 0405:074,2004.

Massive gravity: history

Simple question: Can graviton have mass?

May lead to acceleration without dark energy

Yes?

No?

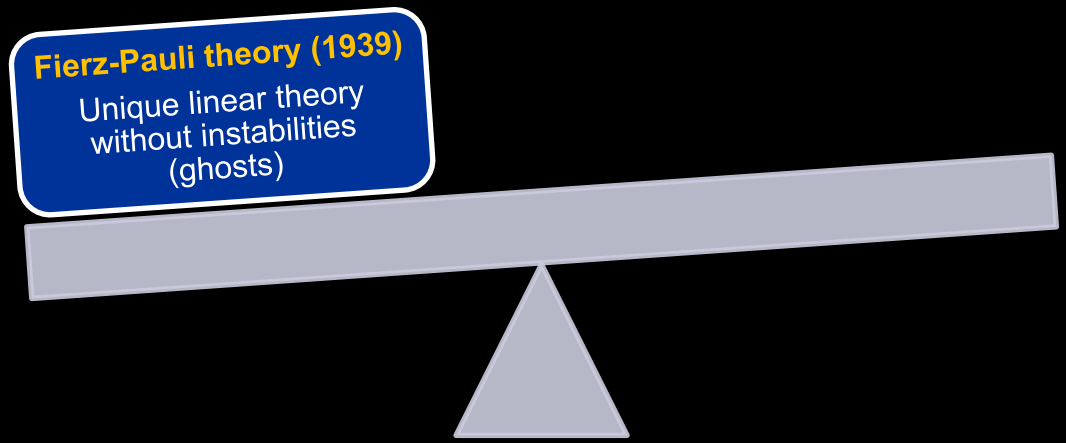

Massive gravity: history

Simple question: Can graviton have mass?

May lead to acceleration without dark energy

Yes?

No?

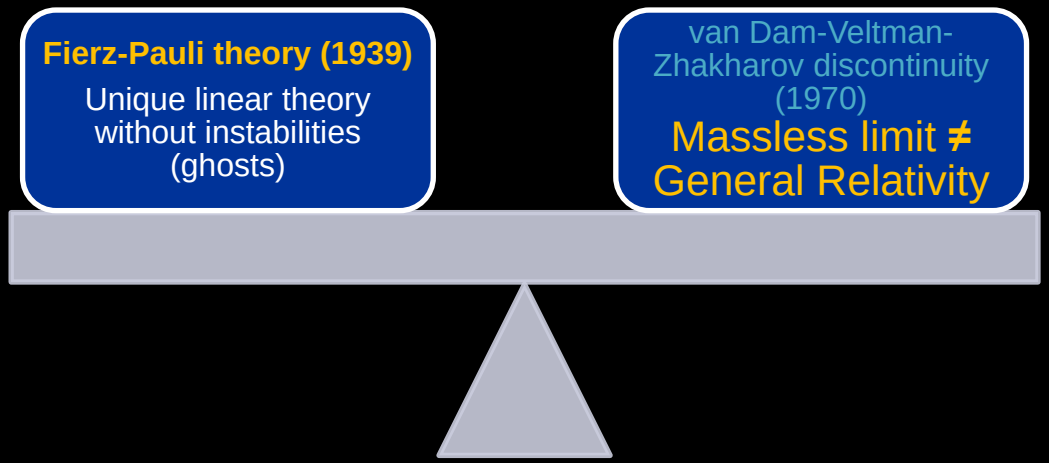

Massive gravity: history

Simple question: Can graviton have mass?
May lead to acceleration without dark energy

Yes?

No?

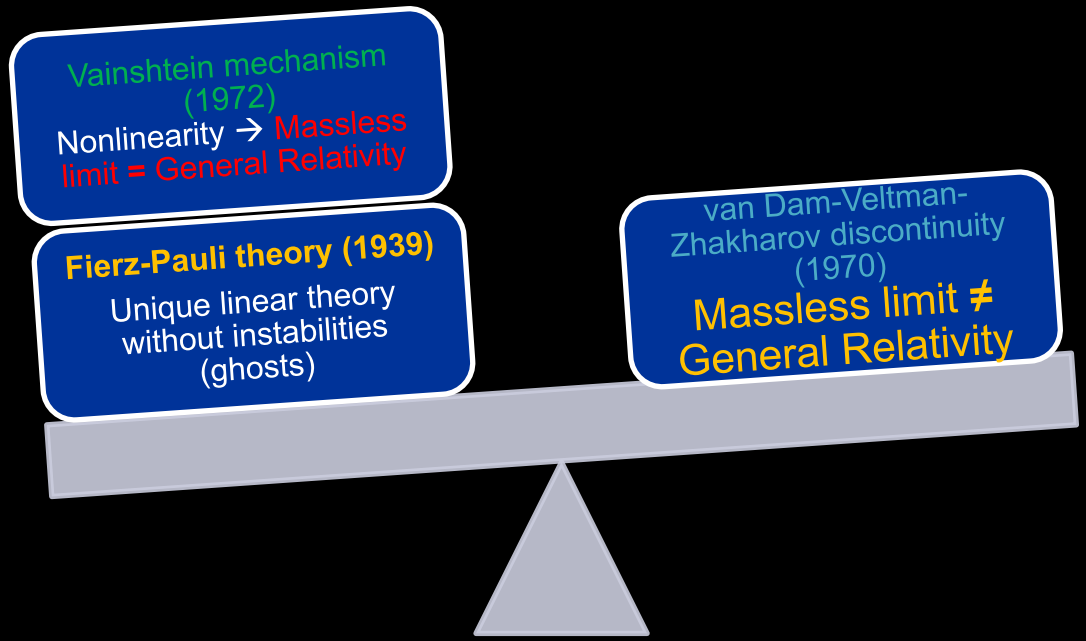

Massive gravity: history

Simple question: Can graviton have mass?
May lead to acceleration without dark energy

Yes?

No?

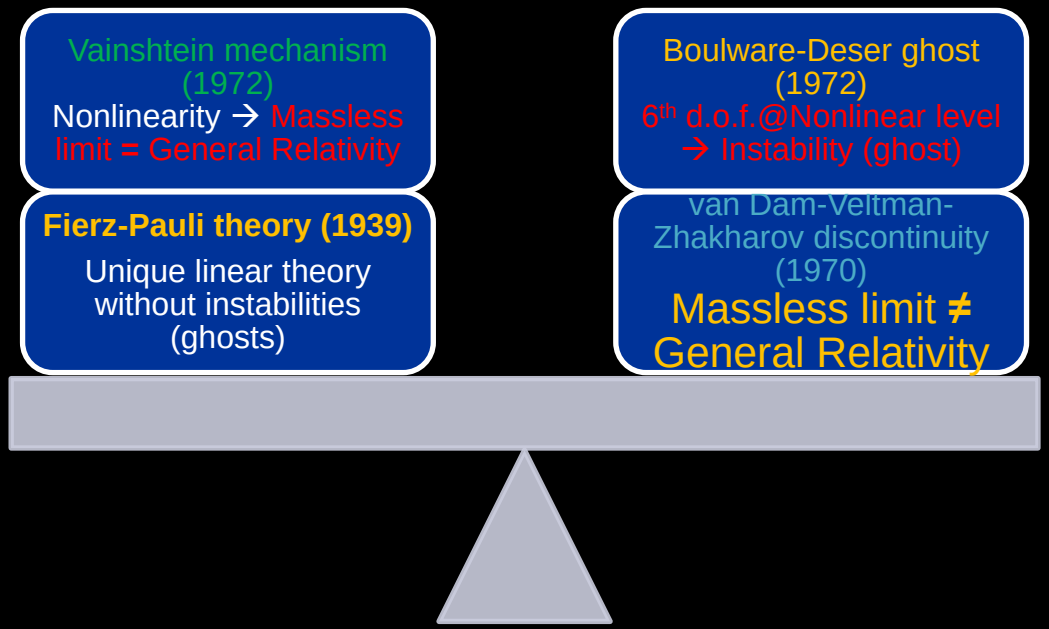

Nonlinear massive gravity

de Rham, Gabadadze 2010

- First example of fully nonlinear massive gravity without BD ghost since 1972!
- Purely classical
- Properties of 5 d.o.f. depend on background

- **4 scalar fields ϕ^a (a=0,1,2,3)**
- **Poincare symmetry in the field space:**

$$\phi^a \to \phi^a + c^a, \quad \phi^a \to \Lambda^a_b \phi^b$$

→ $$f_{\mu\nu} \equiv \eta_{ab} \partial_\mu \phi^a \partial_\nu \phi^b$$

Pullback of
Minkowski metric in field space
to spacetime

Systematic resummation

de Rham, Gabadadze & Tolley 2010

$$I_{mass}[g_{\mu\nu}, f_{\mu\nu}] = M_{Pl}^2 m_g^2 \int d^4x\sqrt{-g}\,(\mathcal{L}_2 + \alpha_3\mathcal{L}_3 + \alpha_4\mathcal{L}_4)$$

$$f_{\mu\nu} \equiv \eta_{ab}\partial_\mu\phi^a\partial_\nu\phi^b$$

$$\mathcal{K}^\mu_\nu = \delta^\mu_\nu - \left(\sqrt{g^{-1}f}\right)^\mu_{\ \nu}$$

$$\mathcal{L}_2 = \frac{1}{2}\left([\mathcal{K}]^2 - [\mathcal{K}^2]\right)$$

$$\mathcal{L}_3 = \frac{1}{6}\left([\mathcal{K}]^3 - 3[\mathcal{K}][\mathcal{K}^2] + 2[\mathcal{K}^3]\right)$$

$$[\mathcal{A}] \equiv Tr\mathcal{A}$$

$$\mathcal{L}_4 = \frac{1}{24}\left([\mathcal{K}]^4 - 6[\mathcal{K}]^2[\mathcal{K}^2] + 3[\mathcal{K}^2]^2 + 8[\mathcal{K}][\mathcal{K}^3] - 6[\mathcal{K}^4]\right)$$

No helicity-0 ghost, i.e. no BD ghost, in decoupling limit

$$\mathcal{K}_{\mu\nu} = \partial_\mu\partial_\nu\pi \Rightarrow \mathcal{L}_{2,3,4} = (\text{total derivative})$$

No BD ghost away from decoupling limit (Hassan&Rosen)

Massive gravity: history

Simple question: Can graviton have mass?

May lead to acceleration without dark energy

Yes?

No?

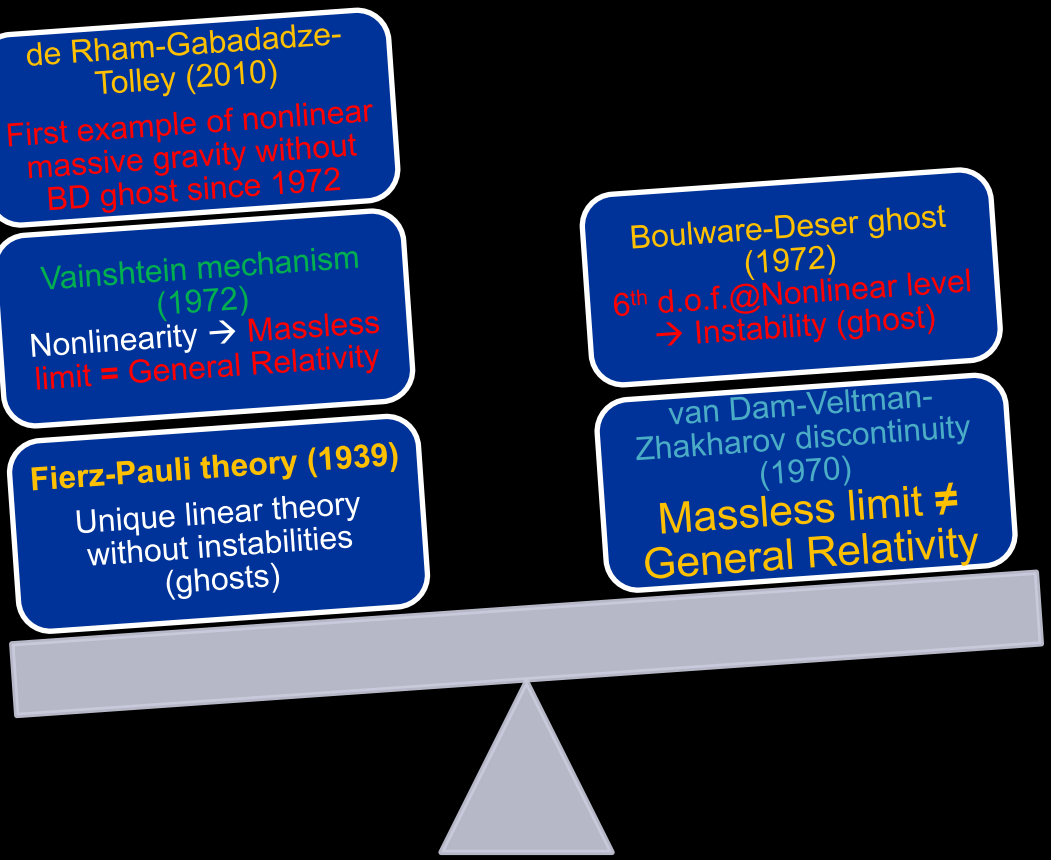

No FLRW universe?

D'Amico, de Rham, Dubovsky, Gabadadze, Pirtshalava, Tolley (2011)

- Flat FLRW ansatz in "Unitary gauge"

  $g_{\mu\nu}dx^\mu dx^\nu = -N^2(t)dt^2 + a^2(t)(dx^2+dy^2+dz^2)$

  $\phi^a = x^a$ ⇒ $f_{\mu\nu} = \eta_{\mu\nu}$

- Bianchi "identity" → a(t) = const.

  c.f. $\nabla^\mu \left(\frac{2}{\sqrt{-g}} \frac{\delta I}{\delta g^{\mu\nu}} \right) = \frac{1}{\sqrt{-g}} \frac{\delta I_g}{\delta \phi^a} \partial_\nu \phi^a$

  → no non-trivial flat FLRW cosmology

- "Our conclusions on the absence of the homogeneous and isotropic solutions do not change if we allow for a more general maximally symmetric 3-space"

Massive gravity: history

Simple question: Can graviton have mass?
May lead to acceleration without dark energy



Consistent Theory found in 2010 but

No Viable Cosmology?

Open FLRW solutions

Gumrukcuoglu, Lin, Mukohyama, arXiv: 1109.3845 [hep-th]

- $f_{\mu\upsilon}$ spontaneously breaks diffeo.
- Both $g_{\mu\upsilon}$ and $f_{\mu\upsilon}$ must respect FLRW symmetry
- Need FLRW coordinates of Minkowski $f_{\mu\upsilon}$
- No closed FLRW chart
- Open FLRW ansatz

$$\begin{aligned}
\phi^0 &= f(t)\sqrt{1+|K|(x^2+y^2+z^2)}, \\
\phi^1 &= \sqrt{|K|}f(t)x, \\
\phi^2 &= \sqrt{|K|}f(t)y, \\
\phi^3 &= \sqrt{|K|}f(t)z.
\end{aligned}$$

$$f_{\mu\nu}dx^\mu dx^\nu = -(\dot{f}(t))^2\,dt^2 + |K|\,(f(t))^2\,\Omega_{ij}(x^k)dx^i dx^j$$

$$\begin{aligned}
g_{\mu\nu}dx^\mu dx^\nu &= -N(t)^2dt^2 + a(t)^2\Omega_{ij}dx^i dx^j\,, \\
\Omega_{ij}dx^i dx^j &= dx^2+dy^2+dz^2 - \frac{|K|(xdx+ydy+zdz)^2}{1+|K|(x^2+y^2+z^2)}\,,
\end{aligned}$$

Open FLRW solutions

Gumrukcuoglu, Lin, Mukohyama, arXiv: 1109.3845 [hep-th]

- EOM for ϕ^a (a=0,1,2,3)

$$(\dot{a}-\sqrt{|K|}N)\left[\left(3-\frac{2\sqrt{|K|}f}{a}\right)+\alpha_3\left(3-\frac{\sqrt{|K|}f}{a}\right)\left(1-\frac{\sqrt{|K|}f}{a}\right)+\alpha_4\left(1-\frac{\sqrt{|K|}f}{a}\right)^2\right]=0$$

- The first sol $\dot{a}=\sqrt{|K|}N$ implies $g_{\mu\upsilon}$ is Minkowski

  → we consider other solutions

$$f=\frac{a}{\sqrt{|K|}}X_\pm,\quad X_\pm\equiv\frac{1+2\alpha_3+\alpha_4\pm\sqrt{1+\alpha_3+\alpha_3^2-\alpha_4}}{\alpha_3+\alpha_4}$$

- Latter solutions do not exist if K=0
- Metric EOM → self-acceleration

$$3\,H^2+\frac{3\,K}{a^2}\;=\;\Lambda_\pm+\frac{1}{M_{Pl}^2}\rho$$

$$\Lambda_\pm\equiv-\frac{m_g^2}{(\alpha_3+\alpha_4)^2}\left[(1+\alpha_3)\left(2+\alpha_3+2\,\alpha_3^2-3\,\alpha_4\right)\pm2\,\left(1+\alpha_3+\alpha_3^2-\alpha_4\right)^{3/2}\right]$$

Self-acceleration

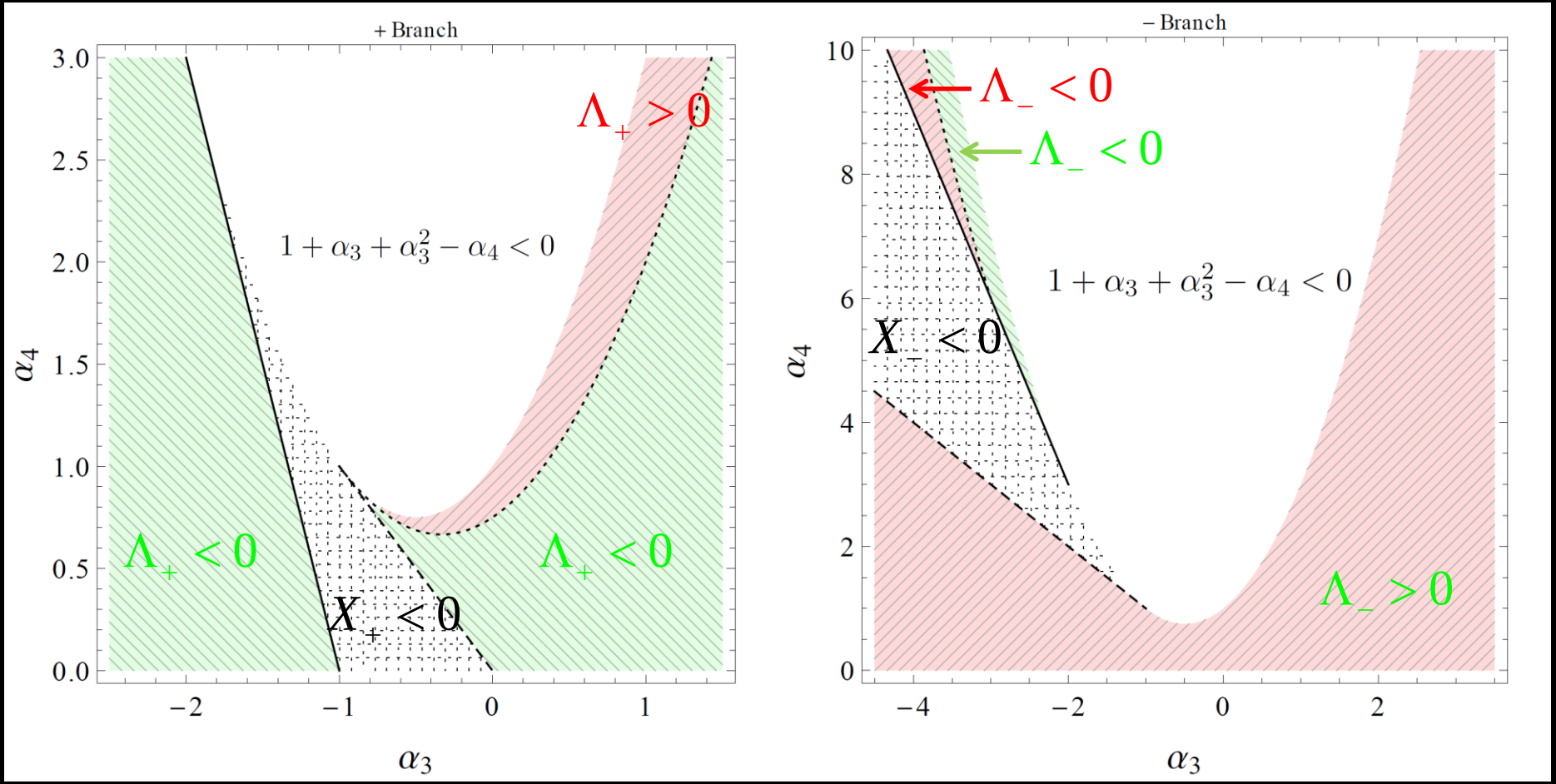

$$f = \frac{a}{\sqrt{|K|}} X_\pm, \quad X_\pm \equiv \frac{1 + 2\alpha_3 + \alpha_4 \pm \sqrt{1 + \alpha_3 + \alpha_3^2 - \alpha_4}}{\alpha_3 + \alpha_4}$$

General fiducial metric

Appendix of Gumrukcuoglu, Lin, Mukohyama, arXiv: 1111.4107 [hep-th]

- **Poincare symmetry in the field space**
  → $f_{\mu\nu} = (Minkowski)_{ab}\,\partial_\mu \phi^a \partial_\nu \phi^b$
- **de Sitter symmetry in the field space**
  → $f_{\mu\nu} = (deSitter)_{ab}\,\partial_\mu \phi^a \partial_\nu \phi^b$
- **FRW symmetry in the field space**
  → $f_{\mu\nu} = (FLRW)_{ab}\,\partial_\mu \phi^a \partial_\nu \phi^b$

Flat/closed/open FLRW cosmology allowed if "fiducial metric" $f_{\mu\nu}$ is de Sitter (or FRW)

→ **Friedmann equation with the same effective cc**

$$3\,H^2 + \frac{3\,K}{a^2} = \Lambda_\pm + \frac{1}{M_{Pl}^2}\rho$$

$$\Lambda_\pm \equiv -\frac{m_g^2}{(\alpha_3+\alpha_4)^2}\left[(1+\alpha_3)\left(2+\alpha_3+2\,\alpha_3^2-3\,\alpha_4\right) \pm 2\,\left(1+\alpha_3+\alpha_3^2-\alpha_4\right)^{3/2}\right]$$

Cosmological perturbation with any matter

Gumrukcuoglu, Lin, Mukohyama, arXiv: 1111.4107 [hep-th]

$$I^{(2)} = \tilde{I}^{(2)}[Q_I, \Phi, \Psi, B_i, \gamma_{ij}] + \tilde{I}^{(2)}_{mass}[\psi^\pi,\ E^\pi,\ F^\pi_i, \gamma_{ij}]$$

$$\tilde{I}[g_{\mu\nu}, \sigma_I] \equiv I_{EH,\tilde{\Lambda}}[g_{\mu\nu}] + I_{matter}[g_{\mu\nu}, \sigma_I] \qquad \tilde{\Lambda} \equiv \Lambda + \Lambda_\pm$$

$$\tilde{I}^{(2)}_{mass} = M_{Pl}^2 \int d^4x N a^3 \sqrt{\Omega}\, M^2_{GW}$$

$$M^2_{GW} \equiv \pm(r-1)m_g^2 X_\pm^2 \sqrt{1+\alpha_3+\alpha_3^2-\alpha_4},$$

$$r \equiv \frac{na}{N\alpha} = \frac{1}{X_\pm}\frac{H}{H_f}, \quad H \equiv \frac{\dot{a}}{Na}, \quad H_f \equiv \frac{\dot{\alpha}}{n\alpha}$$

$$\times \left[3(\psi^\pi)^2 - \frac{1}{12} E^\pi \triangle(\triangle + 3K) E^\pi + \frac{1}{16} F^i_\pi (\triangle + 2K) F^\pi_i - \frac{1}{8}\gamma^{ij}\gamma_{ij} \right]$$

- **GR&matter part + graviton mass term**
- Separately gauge-invariant
  Common ingredient is γ_{ij} only
- Integrate out ψ^π, E^π and F^π_i → $I^{(2)}_{s,v} = I^{(2)}_{GR\ s,v}$
- Difference from GR is in the tensor sector only

Summary so far

- Nonlinear massive gravity
  free from BD ghost
- FLRW background
  No closed/flat universe
  Open universes with self-acceleration!
- More general fiducial metric $f_{\mu\upsilon}$
  closed/flat/open FLRW universes allowed
  Friedmann eq does not depend on $f_{\mu\upsilon}$
- Cosmological linear perturbations
  Scalar/vector sectors → same as in GR
  Tensor sector → time-dependent mass

Nonlinear instability

DeFelice, Gumrukcuoglu, Mukohyama, arXiv: 1206.2080 [hep-th]

- de Sitter or FLRW fiducial metric
- Pure gravity + bare cc → FLRW sol = de Sitter
- Bianchi I universe with axisymmetry + linear perturbation (without decoupling limit)
- Small anisotropy expansion of Bianchi I + linear perturbation
  → nonlinear perturbation around flat FLRW
- Odd-sector:
  1 healthy mode + 1 healthy or ghosty mode
- Even-sector:
  2 healthy modes + 1 ghosty mode
- This is not BD ghost nor Higuchi ghost.

	Higgs mechanism	Ghost condensate
Order parameter	$\langle \Phi \rangle$ 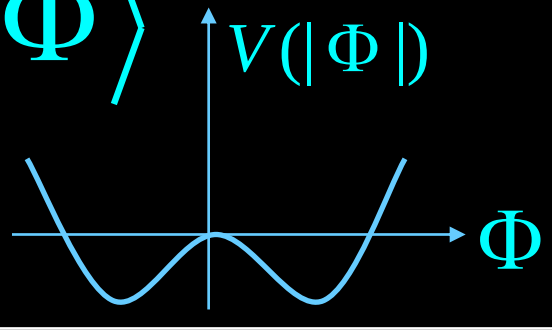	$\langle \partial_\mu \phi \rangle$ 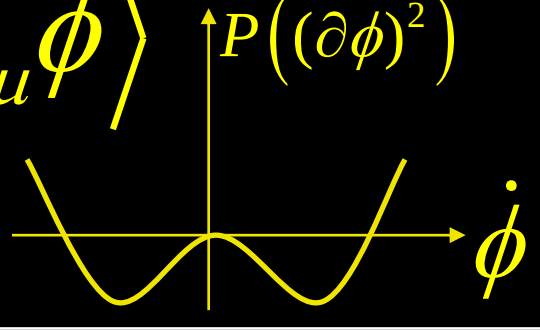
Instability	Tachyon $-\mu^2\Phi^2$	Ghost $-\dot{\phi}^2$
Condensate	V'=0, V''>0	P'=0, P''>0
Broken symmetry	Gauge symmetry	Time translational symmetry
Force to be modified	Gauge force	Gravity
New force law	Yukawa type	Newton+Oscillation

New class of cosmological solution

Gumrukcuoglu, Lin, Mukohyama, arXiv: 1206.2723 [hep-th]

- Healthy regions with (relatively) large anisotropy
- Are there attractors in healthy region?
- Classification of fixed points
- Local stability analysis
- Global stability analysis

At attractors, physical metric is isotropic but fiducial metric is anisotropic.

→ Anisotropic FLRW universe!

statistical anisotropy expected (suppressed by small m_g^2)

New class of cosmological solution

Gumrukcuoglu, Lin, Mukohyama, arXiv: 1206.2723 [hep-th]

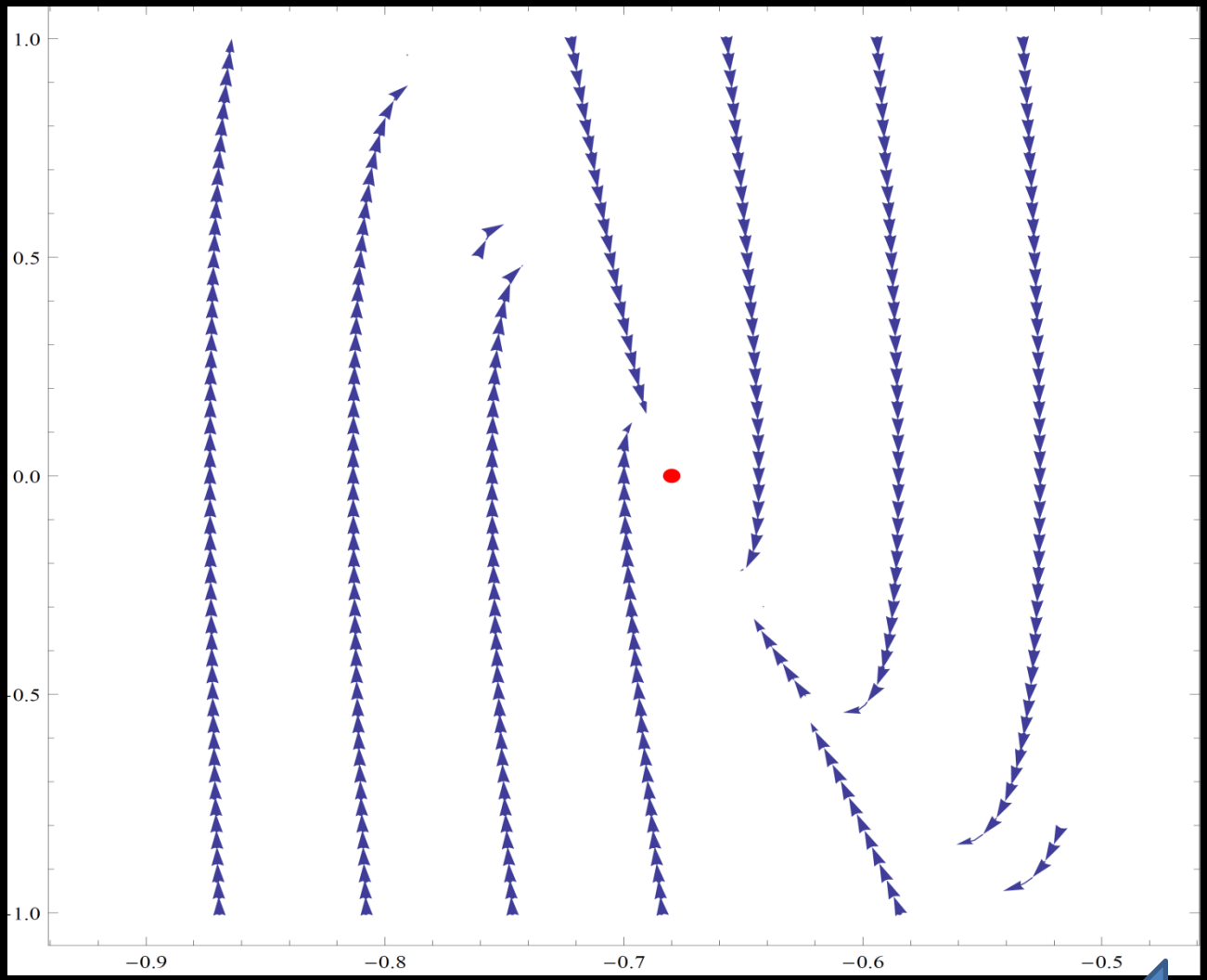

Anisotropy in Expansion

Anisotropy in fiducial metric

Summary

- Nonlinear massive gravity
  free from BD ghost
- FLRW background
  No closed/flat universe
  Open universes with self-acceleration!
- More general fiducial metric $f_{\mu\upsilon}$
  closed/flat/open FLRW universes allowed
  Friedmann eq does not depend on $f_{\mu\upsilon}$
- Cosmological linear perturbations
  Scalar/vector sectors → same as in GR
  Tensor sector → time-dependent mass
- All homogeneous and isotropic FLRW solutions have ghost
- New class of cosmological solution:
  anisotropic FLRW → statistical anisotropy (suppressed by small m_g^2)
- Analogue of Ghost Condensate!

Why alternative gravity theories?

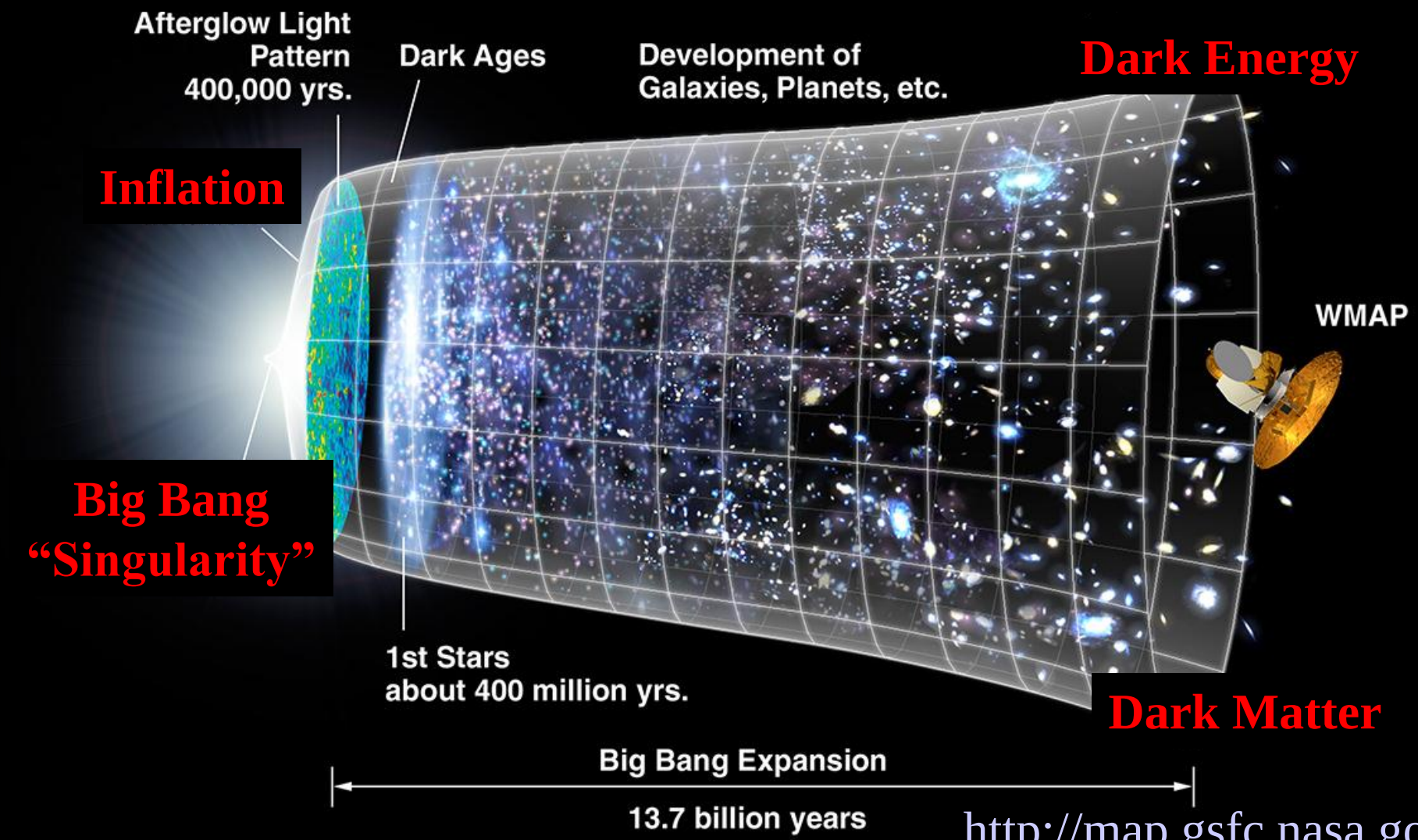

http://map.gsfc.nasa.gov/

BACKUP SLIDES

Linear massive gravity (Fierz-Pauli 1939)

- Simple question: Can spin-2 field have mass?
- $L = L_{EH}[h] + \mathbf{m_g^2[\eta^{\mu\rho}\eta^{\nu\sigma}h_{\mu\nu}h_{\rho\sigma}-(\eta^{\mu\nu}h_{\mu\nu})^2]}$
  $g_{\mu\nu} = \eta_{\mu\nu} + h_{\mu\nu}$
- Unique linear theory without ghosts
- Broken diffeomorphism
  → no momentum constraint
  → 5 d.o.f. (2 tensor + 2 vector + 1 scalar)

vDVZ vs Vainshtein

- van Dam-Veltman-Zhakharov (1970)
  Massless limit ≠ Massless theory = GR
  5 d.o.f remain → PPN parameter $\gamma = ½ \neq 1$
- Vainshtein (1972)
  Linear theory breaks down in the limit.
  Nonlinear analysis shows continuity and GR is recovered @ $r < r_V=(r_g/m_g^4)^{1/5}$.
  Continuity is not uniform w.r.t. distance.

Naïve nonlinear theory and BD ghost

- FP theory with $\eta^{\mu\nu} \rightarrow g^{\mu\nu}$
  $L = L_{EH}[h] + m_g^2[g^{\mu\rho}g^{\nu\sigma}h_{\mu\nu}h_{\rho\sigma} - (g^{\mu\nu}h_{\mu\nu})^2]$
  $g_{\mu\nu} = \eta_{\mu\nu} + h_{\mu\nu}$
- Vainshtein effect (1972)
- Boulware-Deser ghost (1972)
  No Hamiltonian constraint @ nonlinear level
  → 6 d.o.f. = 5 d.o.f. of massive spin-2 + 1 ghost

Stuckelberg fields & Decoupling limit

Arkani-Hamed, Georgi & Schwarz (2003)

- Stuckelberg scalar fields ϕ^a (a=0,1,2,3)

$$g_{\mu\nu} = \eta_{ab}\partial_\mu\phi^a\partial_\nu\phi^b + H_{\mu\nu} \qquad \phi^a = x^a + \pi^a$$

  $H_{\mu\upsilon}$: covariant version of $h_{\mu\upsilon} = g_{\mu\nu} - \eta_{\mu\nu}$

- Decoupling limit

  $m_g \to 0$, $M_{Pl} \to \infty$ with $\Lambda_5 = (m_g{}^4 M_{Pl})^{1/5}$ fixed

- Helicity-0 part π: $\eta_{ab}\pi^b = \partial_a\pi$

  sufficient for analysis of would-be BD ghost

Would-be BD ghost vs fine-tuning

Creminelli, Nicolis, Papucci & Trincherini 2005
de Rham, Gabadadze 2010

$$H_{\mu\nu} = -2\partial_\mu\partial_\nu\pi - \partial_\mu\partial^\rho\pi\partial_\rho\partial_\nu\pi \Leftarrow h_{\mu\nu} = 0, \eta_{ab}\pi^b = \partial_a\pi$$

Decoupling limit — Helicity-0 part

- Fierz-Pauli theory
  $H_{\mu\upsilon}{}^2 - H^2$
  no ghost
- 3rd order
  $c_1 H_{\mu\upsilon}{}^3 + c_2 H H_{\mu\upsilon}{}^2 + c_3 H^3$
  no ghost if fine-tuned
- …
- any order
  no ghost if fine-tuned

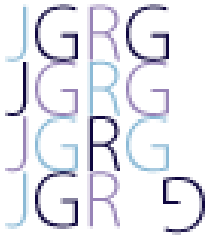

Mihoko Nojiri, JGRG 22(2012)111203

"The Standard model and beyond after LHC at 8 TeV"

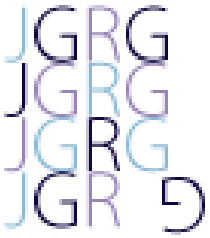

RESCEU SYMPOSIUM ON

GENERAL RELATIVITY AND GRAVITATION

JGRG 22



November 12-16 2012

Koshiba Hall, The University of Tokyo, Hongo, Tokyo, Japan



Higgs discovery and BSM

Mihoko M. Nojiri

Higgs discovery at the LHC

- Higgs boson: The Last missing particle of the SM particles

- Probably starting point of “the Beyond the stard model”

- why we think so, and how it conflicts with data

Standard model of particle physics history

- Discover the symmetry “SU(3)xSU(2)xU(1)” out from interactions involving mesons, leptons, and baryons

- finding “the three generation in the matter sector”

- The SM identify “universal forces” to the gauge symmetry, representation (charge) difference leads interaction difference.

- putting origin of the symmetry breaking (“mass”) to nature of the spin 0 sector (Higgs boson).

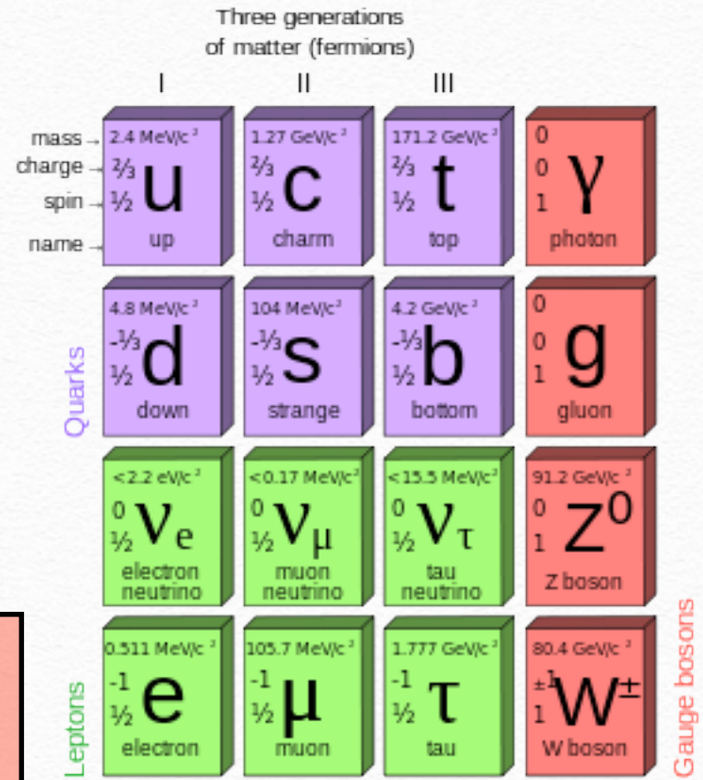

H ?

discovery summary

- Higgs couples to massive objects in the tree level, tt, bb, ZZ, WW...

- discovery in photon and lepton channel H→γγ H→ ZZ and H→ WW. We can only measure (procution) x (branching ratio) at LHC.

- production gg→ H dominant, subdominant WW, ZZ→ H contribution is seen. The two process overlap significantly.

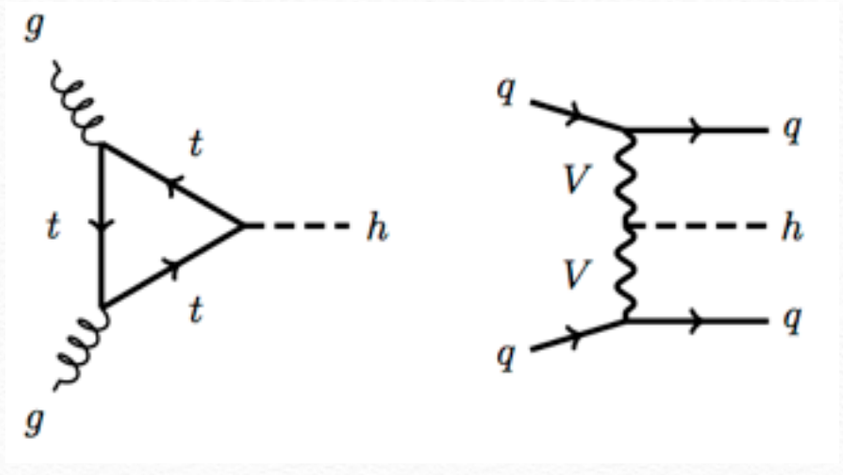

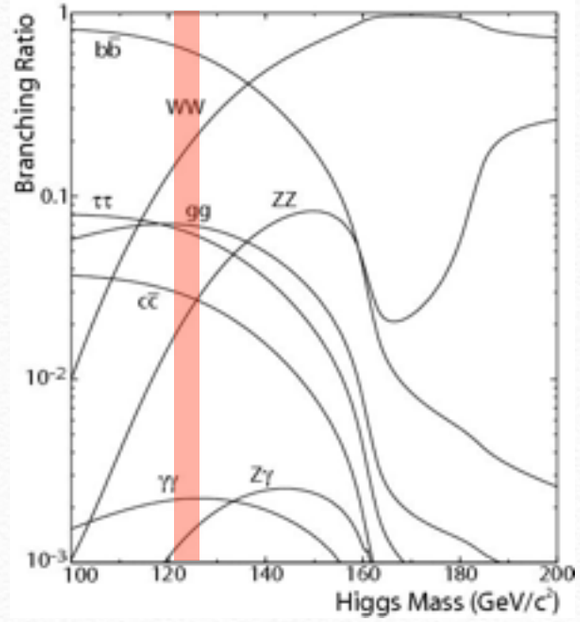

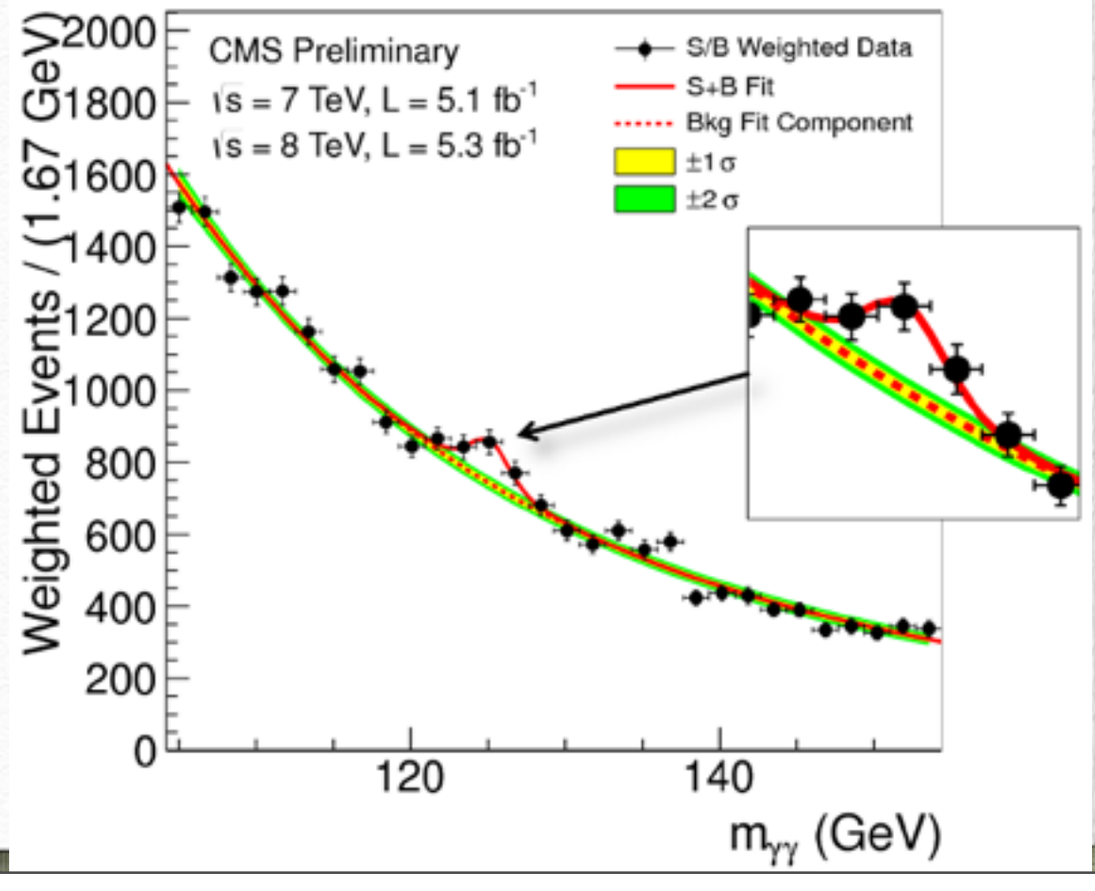

question on the mass value

Are we in meta stable vacuum or there are new physics in between? is this consistent with cosmology?

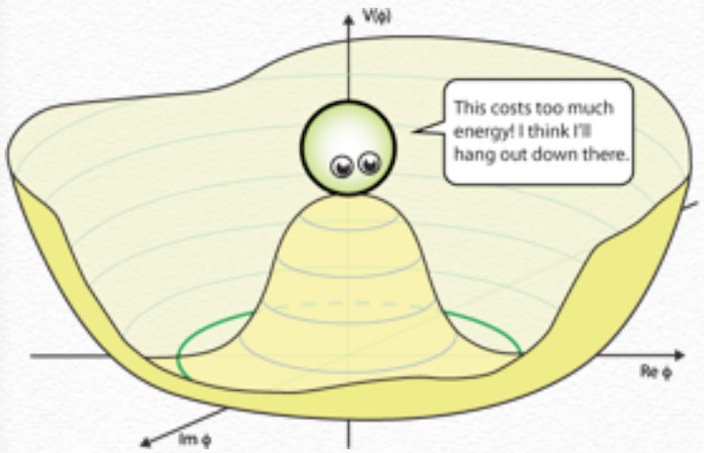

$V(\varphi)=-m^2\varphi^2+\lambda\varphi^4$

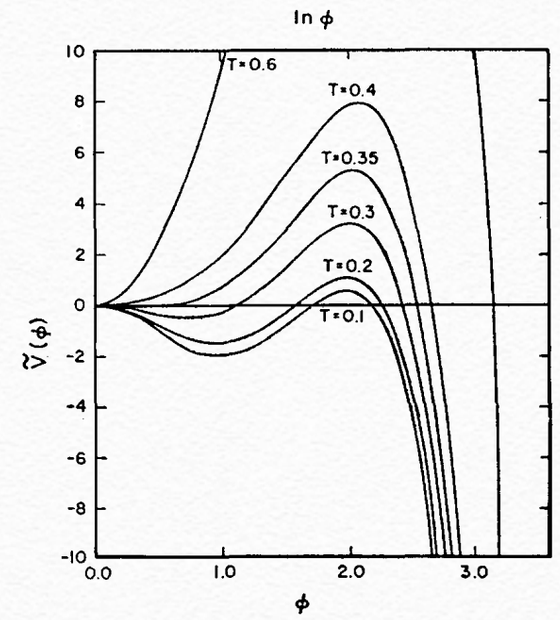

Fig. 18. The temperature dependent potential for $m_{Higgs} = 50$ GeV and for $m_t = 240$ GeV. Here, $\tilde{V} = 8V/m^2_{Higgs}$ and units of $\sigma = 1$ are used.

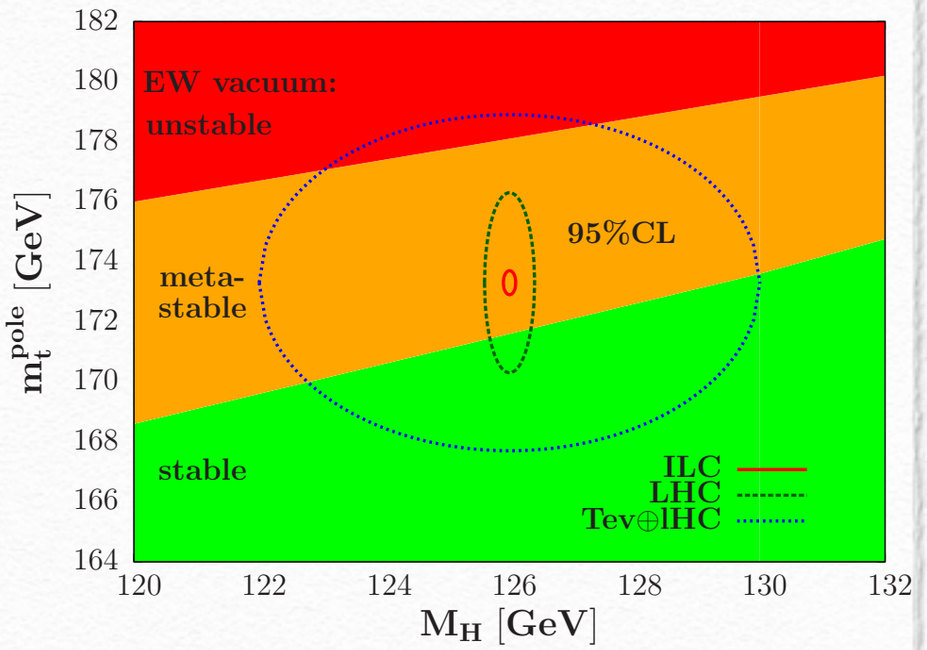

but λ get negative

correction at large φ

We are on the meta stable vacuum?

or there is something between 100GeV to 10^{19}GeV

question on the mass value

Are we in meta stable vacuum or there are new physics in between? is this consistent with cosmology?



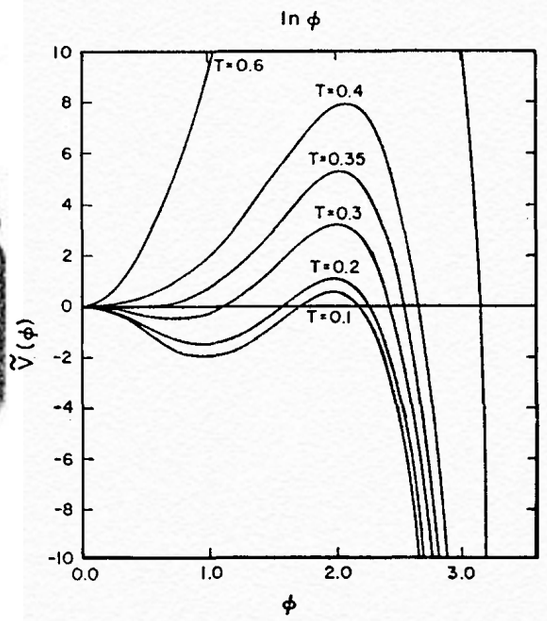

Fig. 18. The temperature dependent potential for $m_{\text{Higgs}} = 50$ GeV and for $m_t = 240$ GeV. Here, $\tilde{V} = 8V/m^2_{\text{Higgs}}$ and units of $\sigma = 1$ are used.

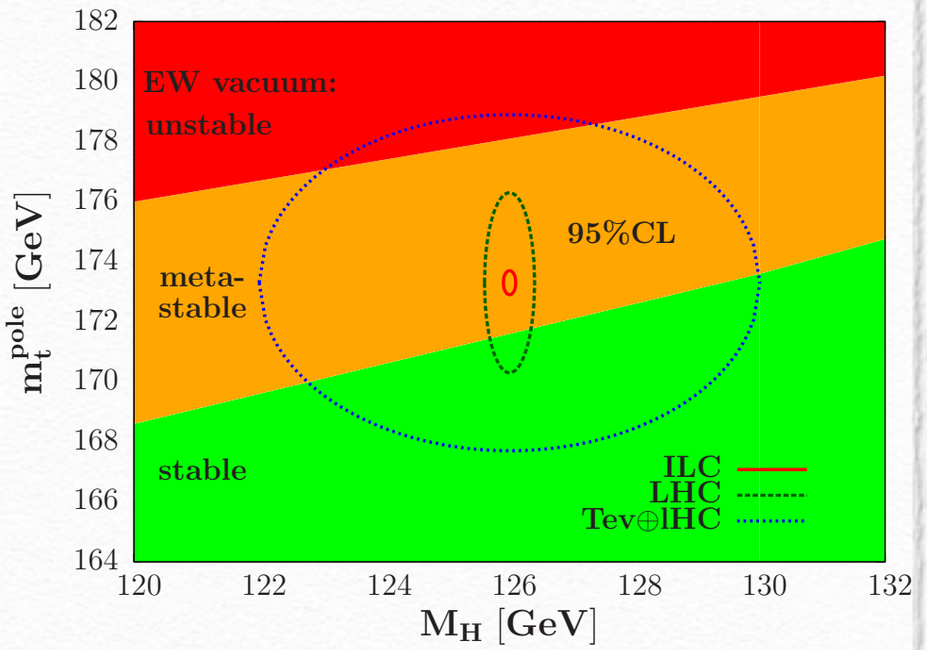

but λ get negative
correction at large φ
We are on the meta stable vacuum?
or there is something between 100GeV to 10^{19}GeV

New Physics, Clue

Fine tuning in the Higgs sector

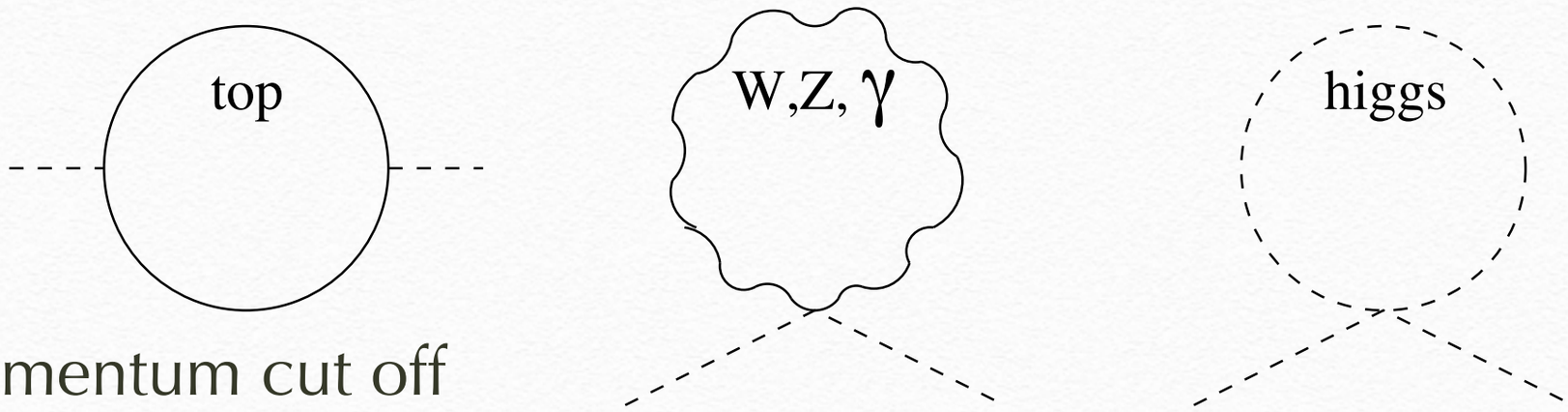

if scale of momentum cut off

Λ =5TeV

$$\begin{aligned}
\text{top loop} \qquad & -\tfrac{3}{8\pi^2}\lambda_t^2\Lambda^2 \quad \sim \quad -(2\ \text{TeV})^2 \\
SU(2)\ \text{gauge boson loops} \qquad & \tfrac{9}{64\pi^2}g^2\Lambda^2 \quad \sim \quad (700\ \text{GeV})^2 \\
\text{Higgs loop} \qquad & \tfrac{1}{16\pi^2}\lambda^2\Lambda^2 \quad \sim \quad (500\ \text{GeV})^2.
\end{aligned}$$

Others are reasonable

Why Higgs vev is O(200) GeV??

$m_f \log \Lambda$ fermion mass

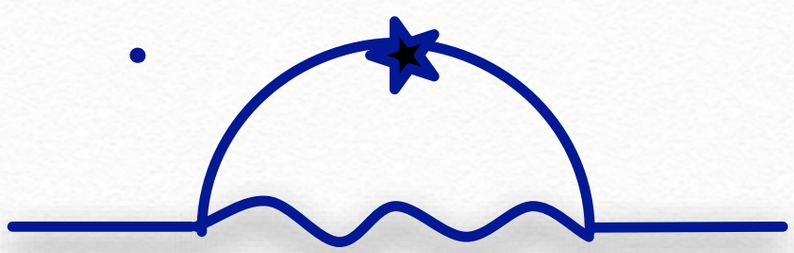

gauge two point function

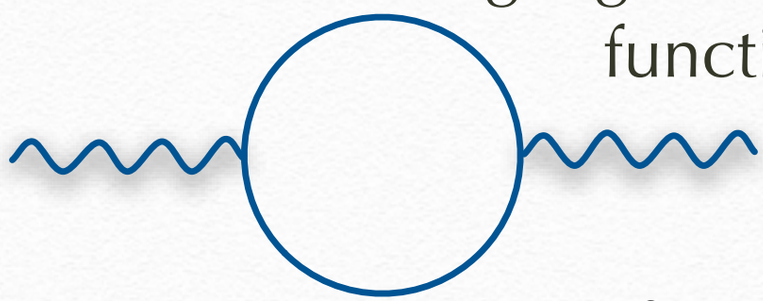

$$\Pi_{\mu\nu} = (g_{\mu\nu}p^2 - p_\mu p_\nu)\Pi$$

Classic Solution:Supersymmetry

- exchange boson and fermion. $\phi \leftrightarrow \psi$
  - sfermions(0), gaugino(1/2), higgsinos(1/2)
- boson and fermion are in the same multiplet; chiral symmetry extended to bosons. No quadratic divergence
- No new dimensionless coupling and no quadratic divergence
- Higgs 4 point coupling is written by gauge coupling. (no negative 4 point coupling.)
- gauge coupling unification
- R parity in MSSM . New stable particle→ DM candidate.

Higgs 4 point coupling at low energy

tree level Higgs mass < mZ + additional correction to from stop sector

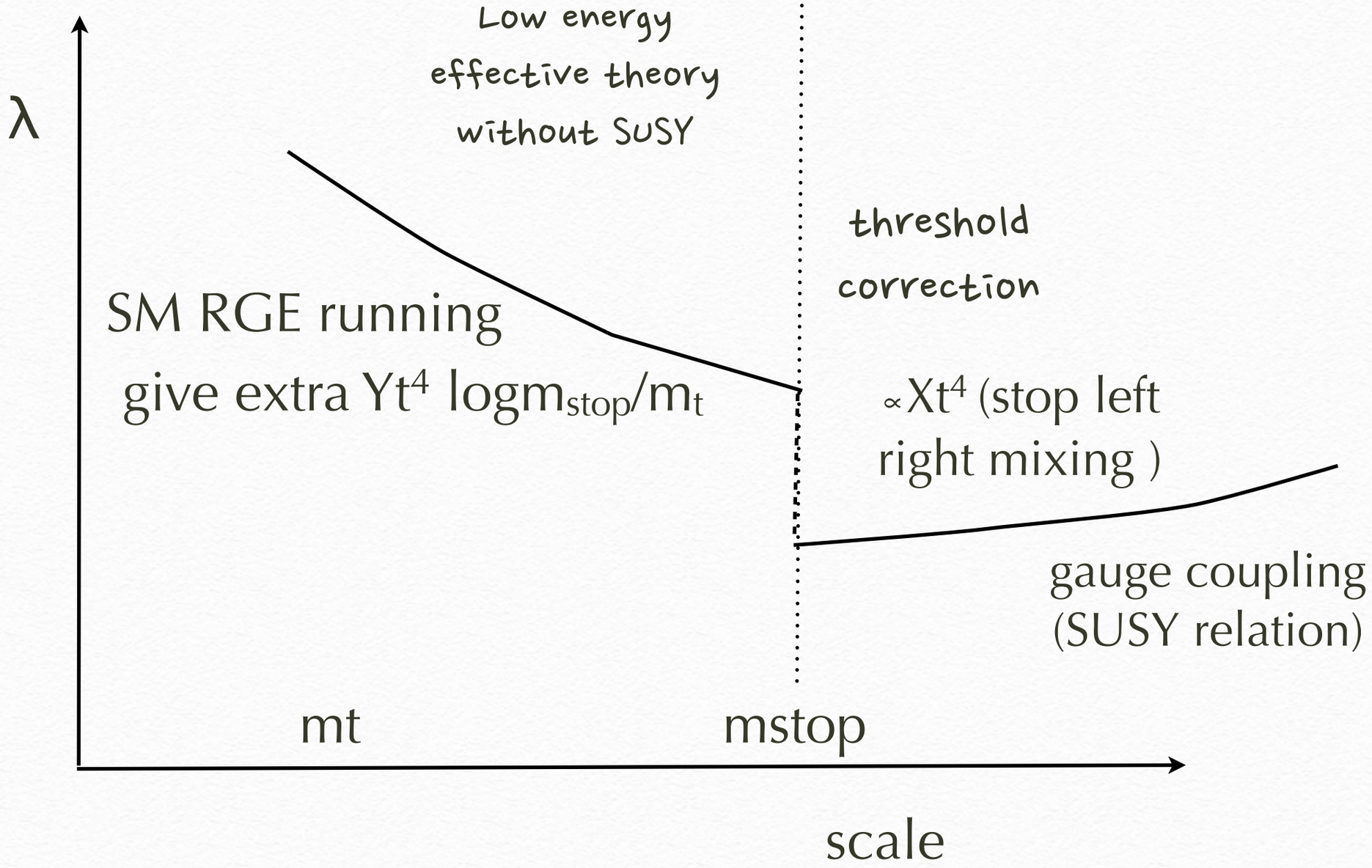

Higgs mass vs SUSY

off diagonal part

large stop mixing

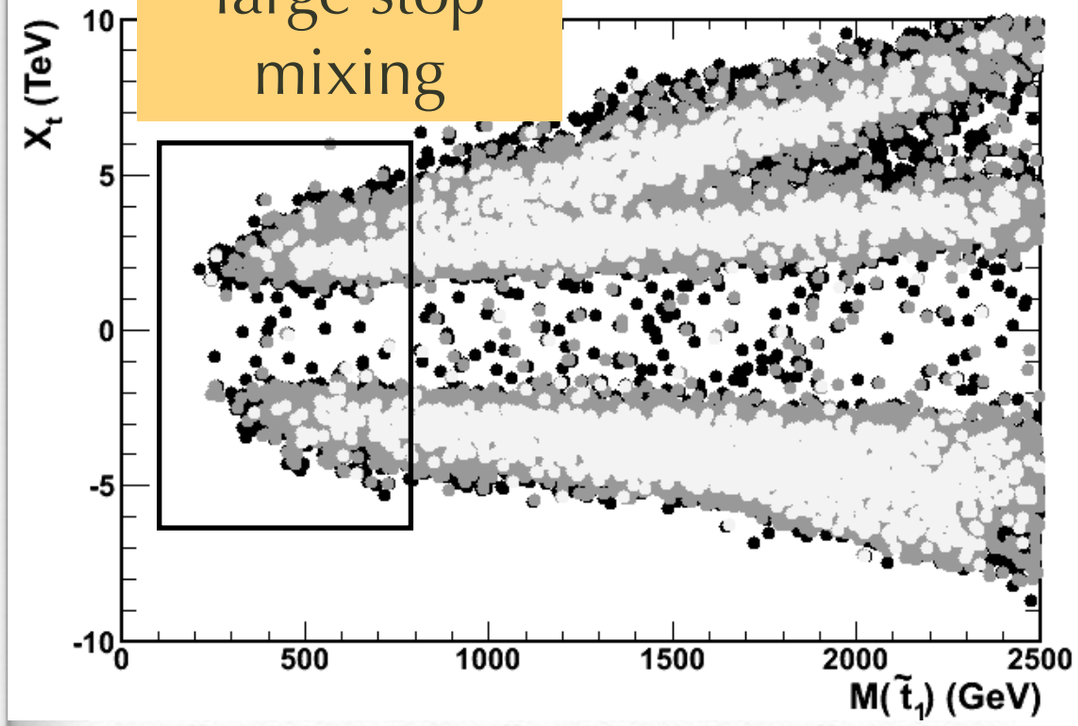

large SUSY scale required
in simple gauge and
anomaly mediation
=> Huge Tension

large stop mixing required for
light stop mass in model
independent approach

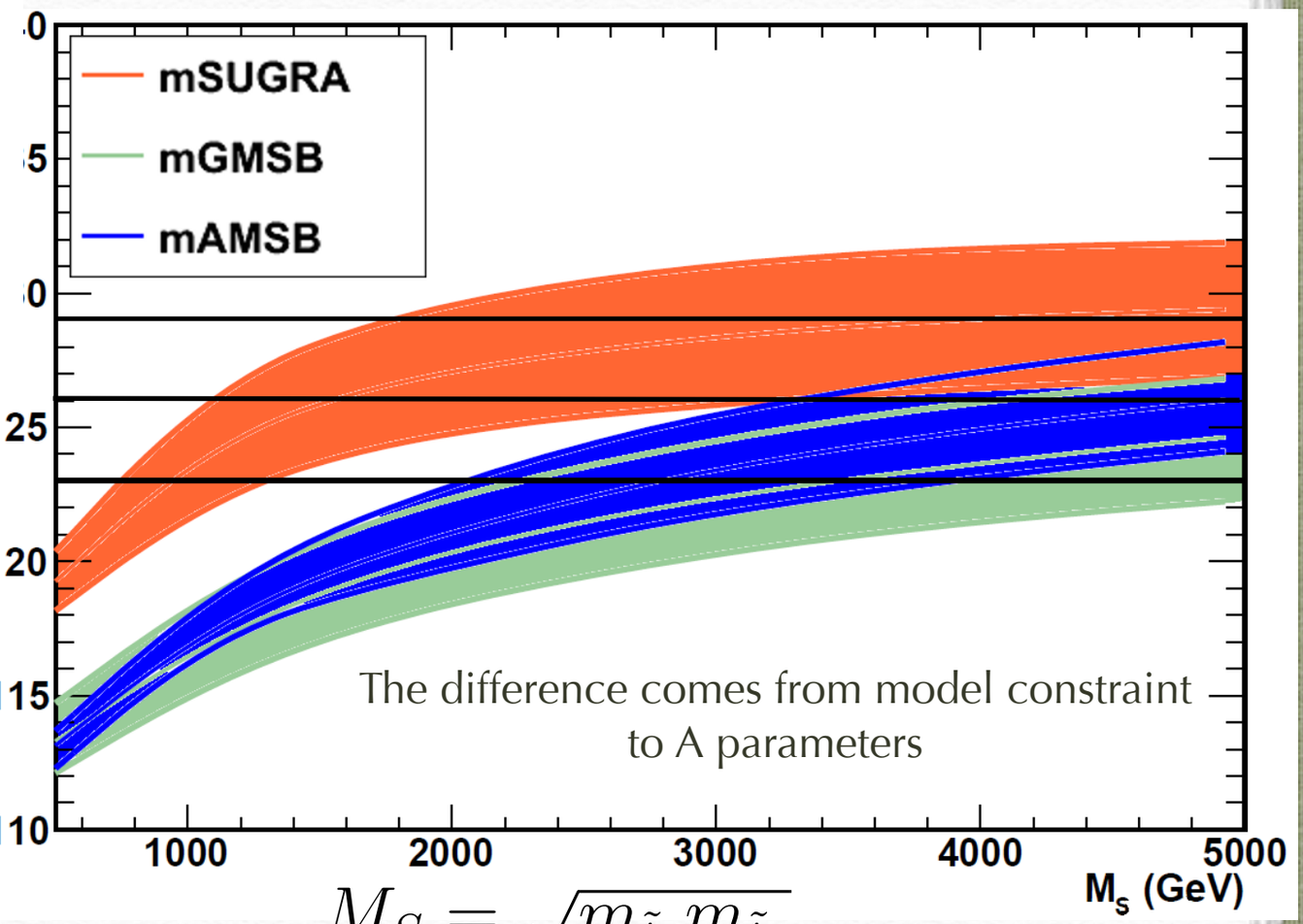

$$M_S = \sqrt{m_{\tilde{t}_1} m_{\tilde{t}_2}}$$

Higgs mass vs SUSY

off diagonal part

large stop mixing

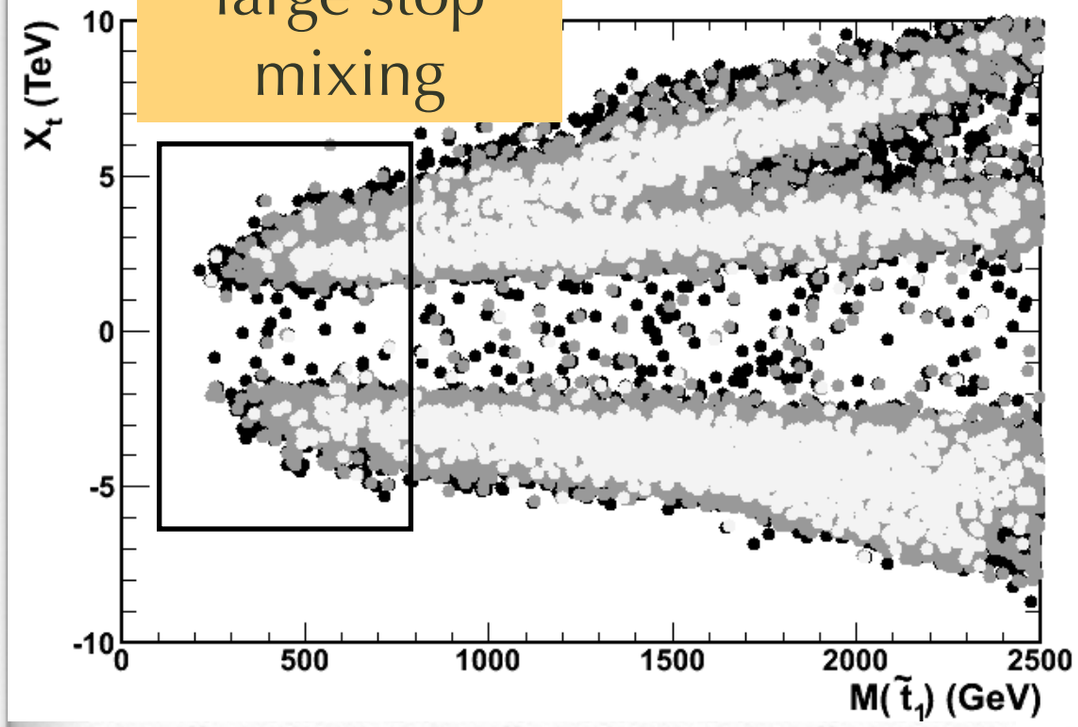

large SUSY scale required
in simple gauge and
anomaly mediation
=> Huge Tension

large stop mixing required for
light stop mass in model
independent approach

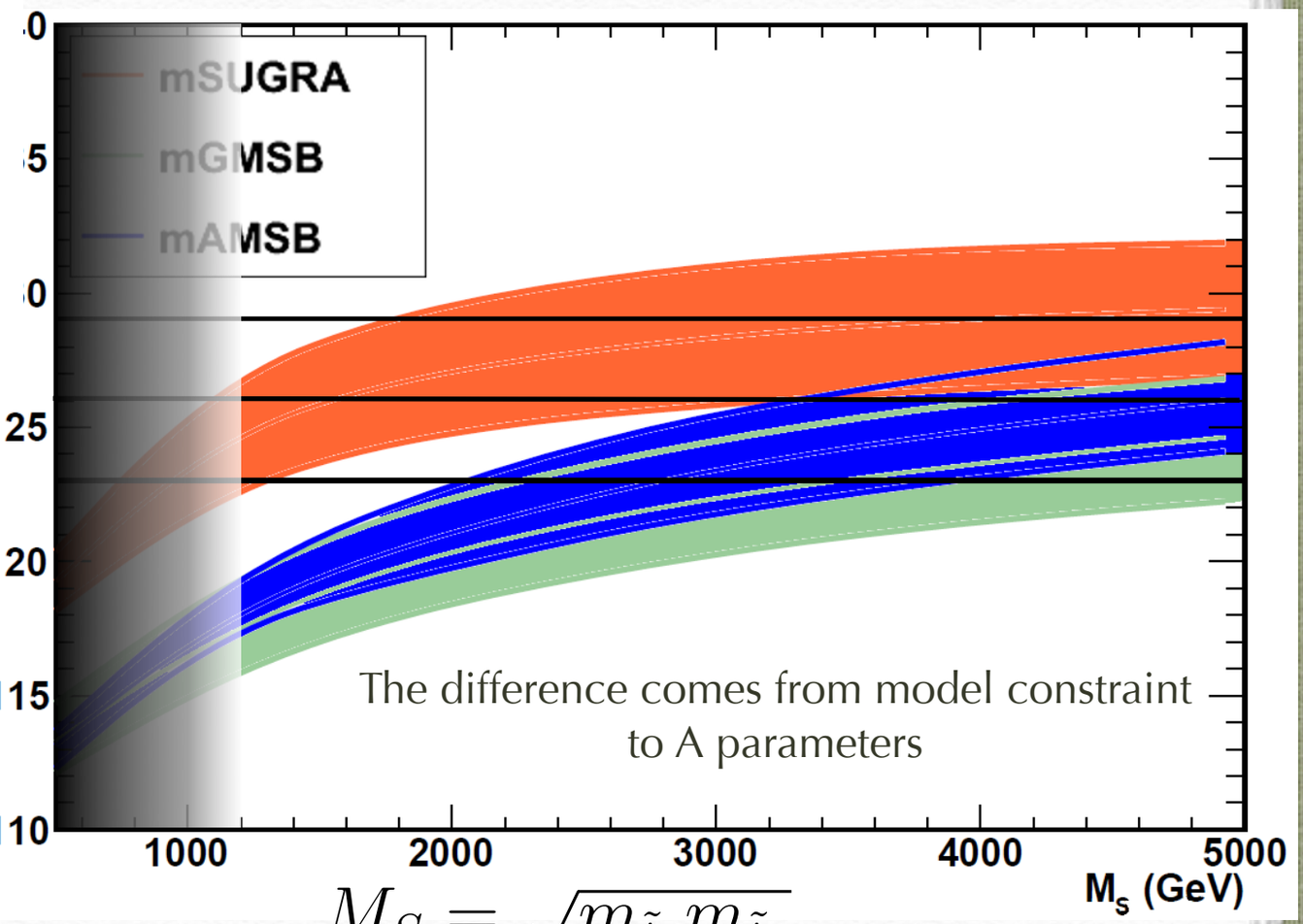

$$M_S = \sqrt{m_{\tilde{t}_1} m_{\tilde{t}_2}}$$

limit at 8TeV (from recent ATLAS)

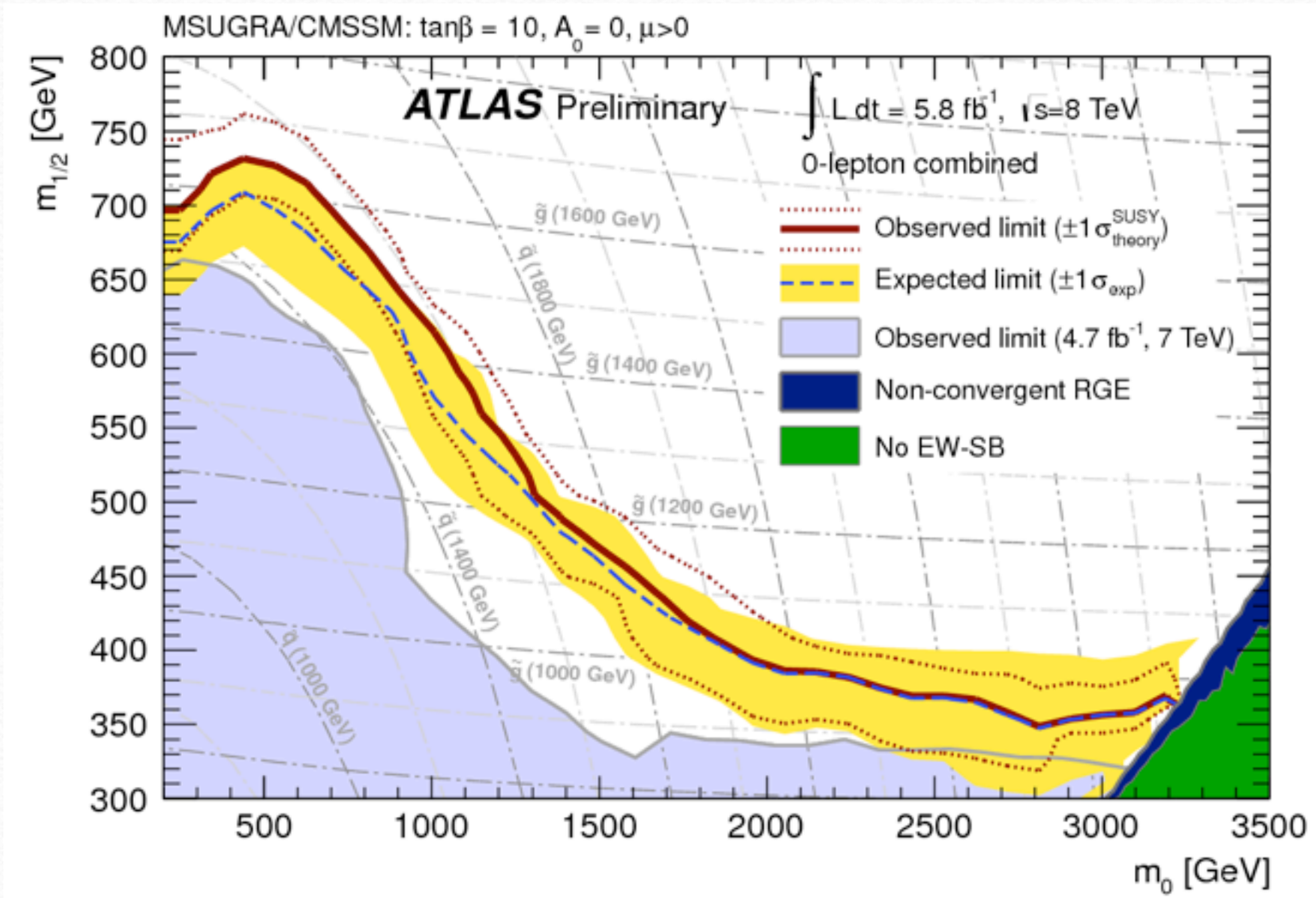

SUSY > (or maybe >>) 1TeV, Does this cause fine turning?

under the assumption of **universal SUSY breaking**(MSUGRA) ,
sleptons are much above 300 GeV

Basic collider objects and supersymmetry

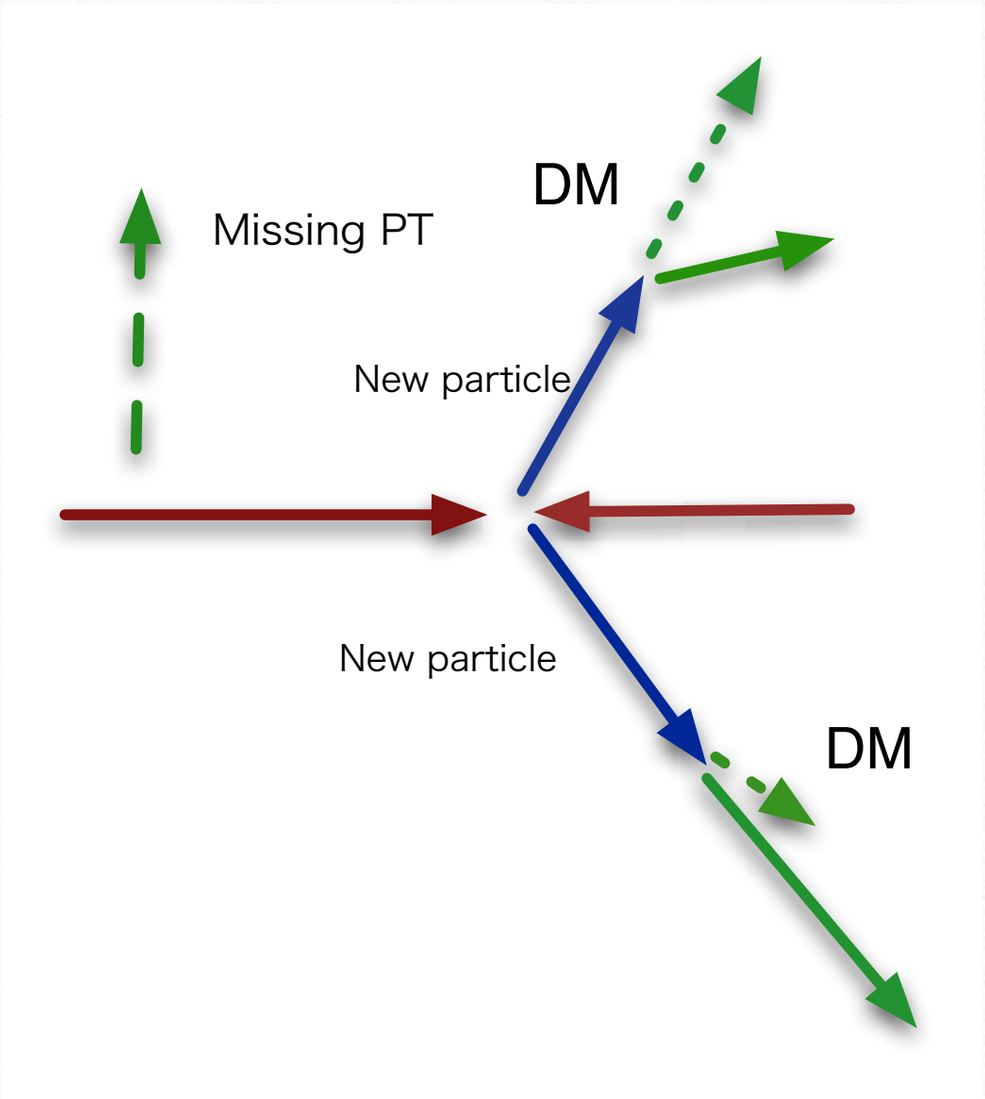

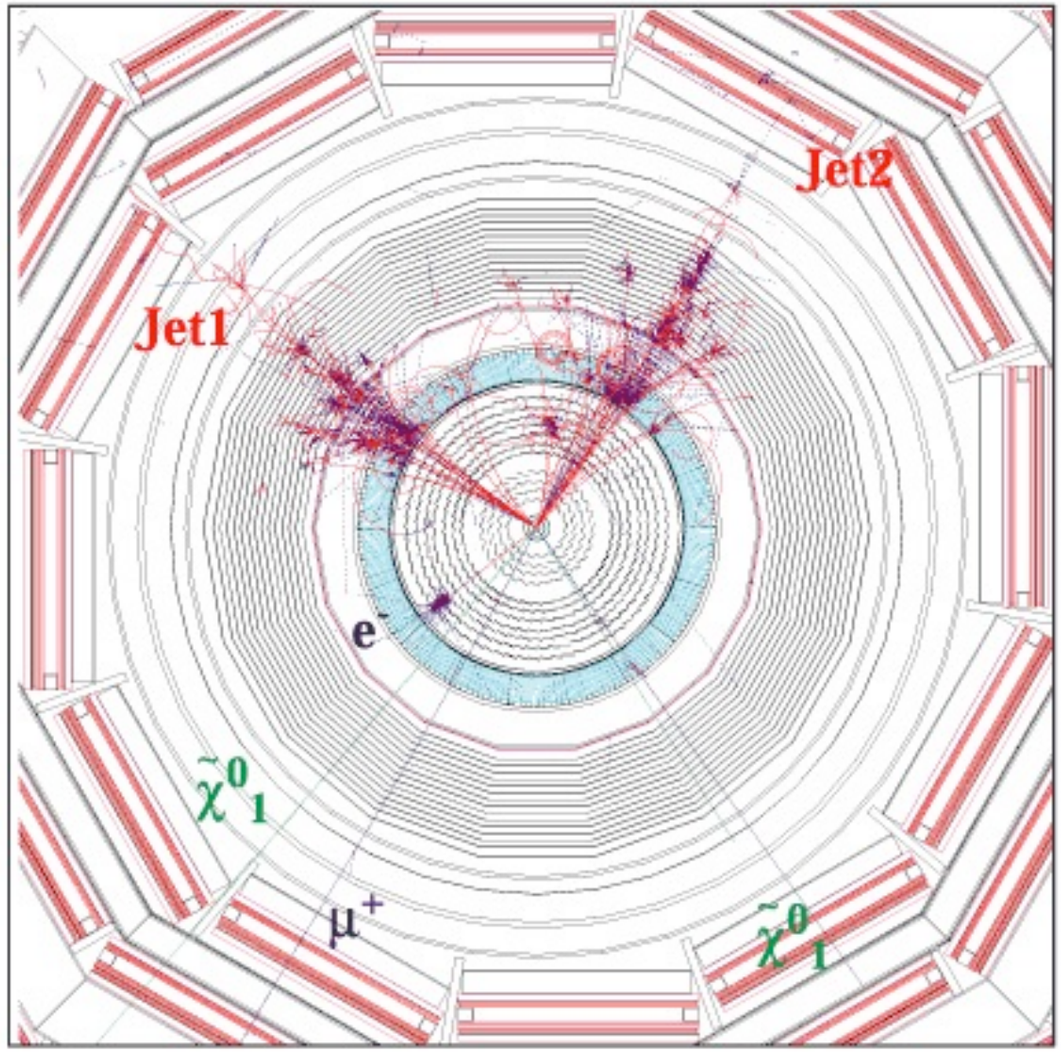

really SUSY particles are so heavy?

- Too large fine turning? Correction to the higgs mass exceed higgs mass
  - Is this such a big problem? GUT/weak scale fine turning has been solved. We have fine turning in vacuum energy anyway..
- By extending model to **Next Minimal SUSY**, higgs masses upper limit increase→ allowing light SUSY particles.
- contribution from 4th generation can also contribute

$$W = Y' H_u Q' U' + M'(Q'\bar{Q}' + U'\bar{U}')$$

$$\Delta m_h \simeq \frac{3v^2}{4\pi^2} Y'^4 \ln \frac{m_S^2}{m_F^2} + \ldots$$

$m_{S(F)}$: vector scalar(fermion) mass

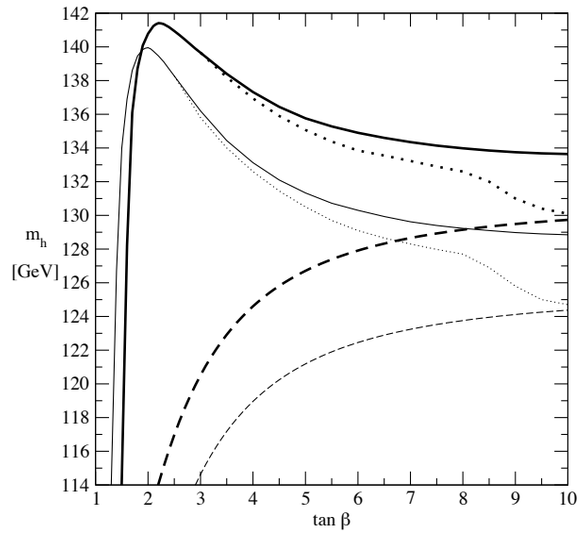

Figure 1: Upper bound on the lightest Higgs mass in the NMSSM for $m_{top} = 178$ GeV (thick full line: m_A arbitrary, thick dotted line: $m_A = 1$ TeV) and $m_{top} = 171.4$ GeV (thin full line: m_A arbitrary, thick dotted line: $m_A = 1$ TeV) and in the MSSM (with $m_A = 1$ TeV) for $m_{top} = 178$ GeV (thick dashed line) and $m_{top} = 171.4$ GeV (thin dashed line) as obtained with NMHDECAY as a function of tanβ. Squark and gluino masses are 1 TeV and $A_{top} = 2.5$ TeV.

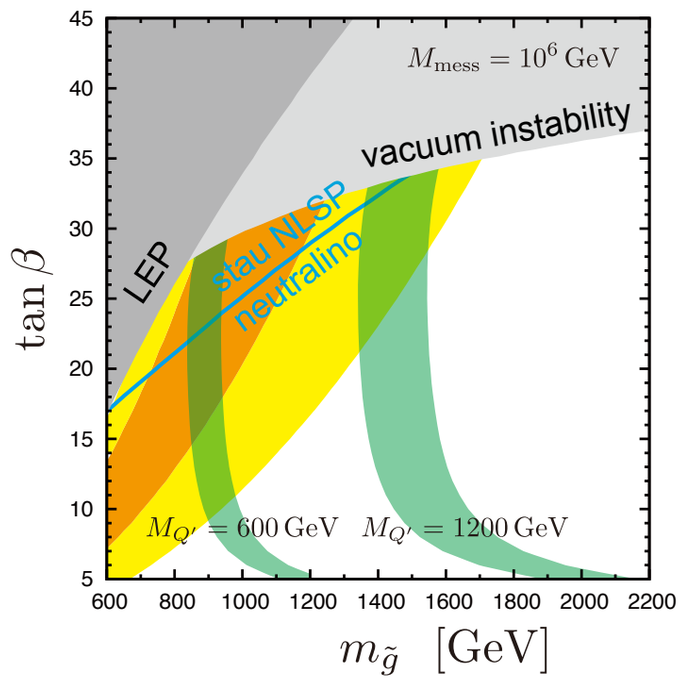

stop search

Direct search limit are actually not so strong
allows for relatively light stop for NMSSM

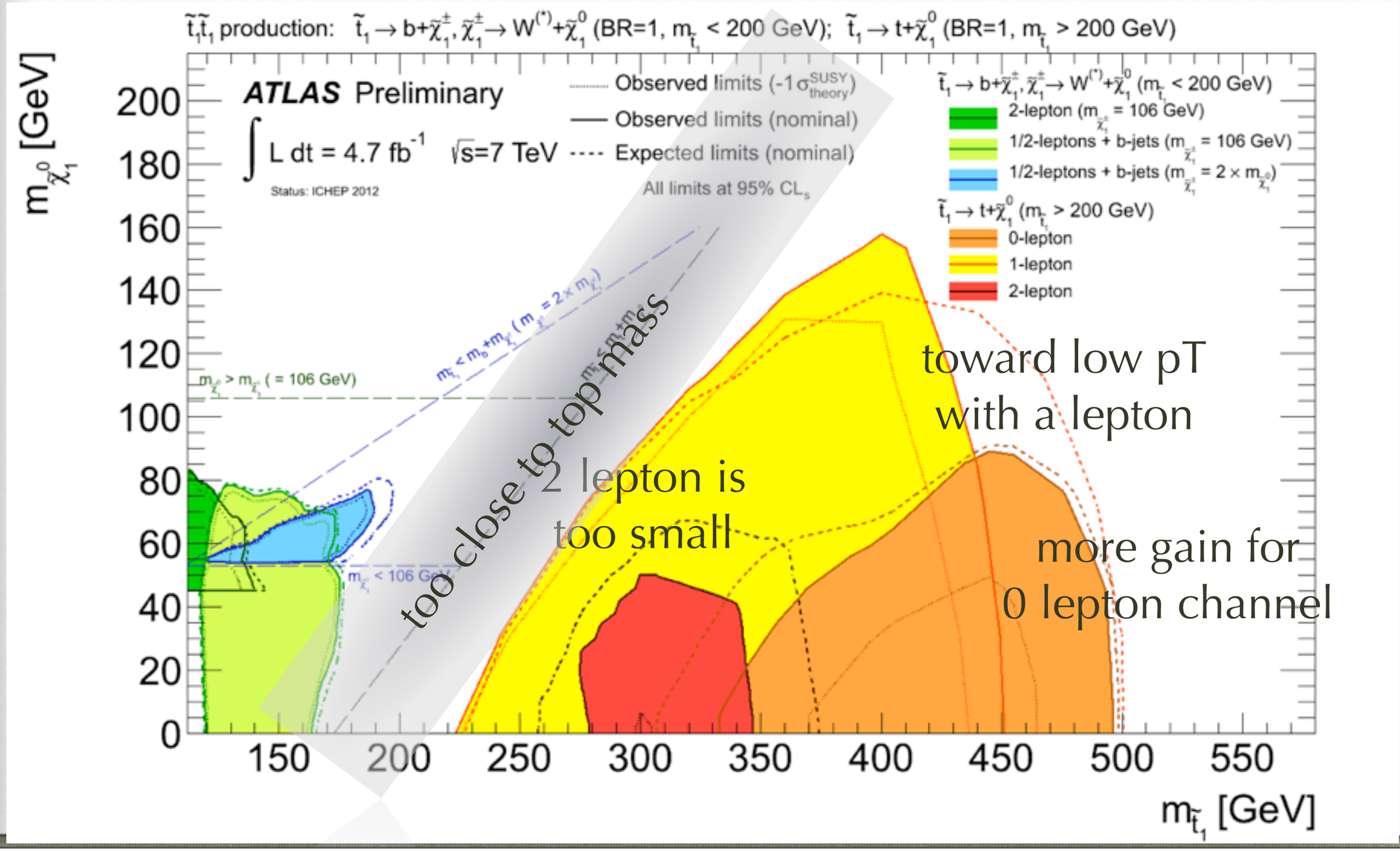

toward low pT
with a lepton

2 lepton is
too small

more gain for
0 lepton channel

if light stop is found

- stop mixing makes the lighter stop light
- model is NMSSM so that stop is need not to be light.
- stop mixing → top polarization from stop decay(visible at LHC)

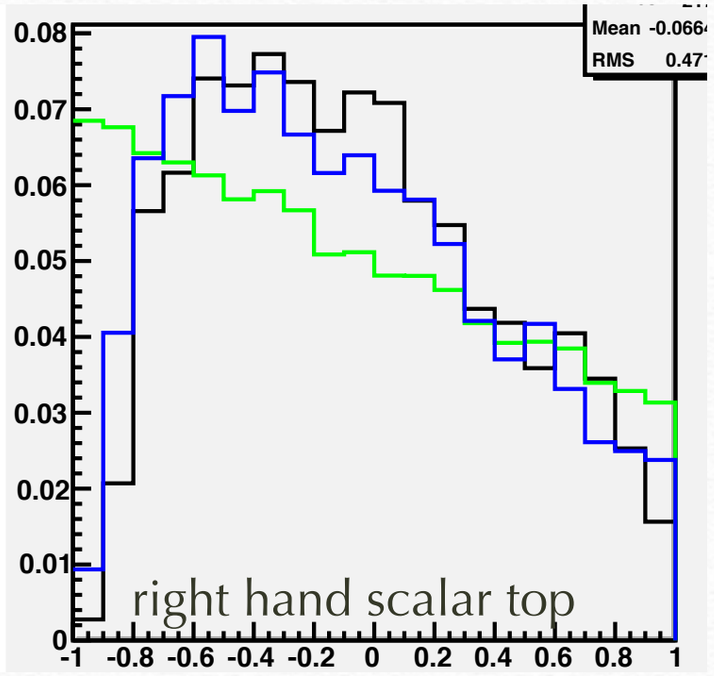

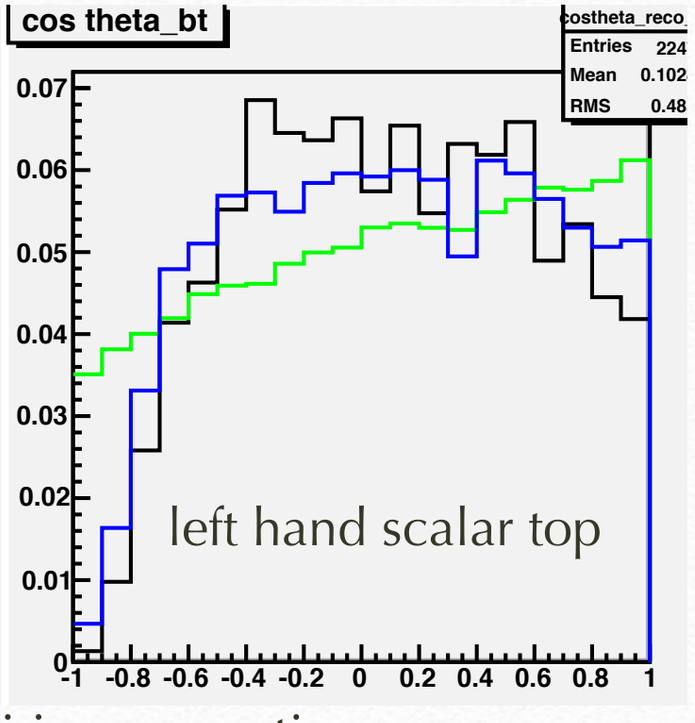

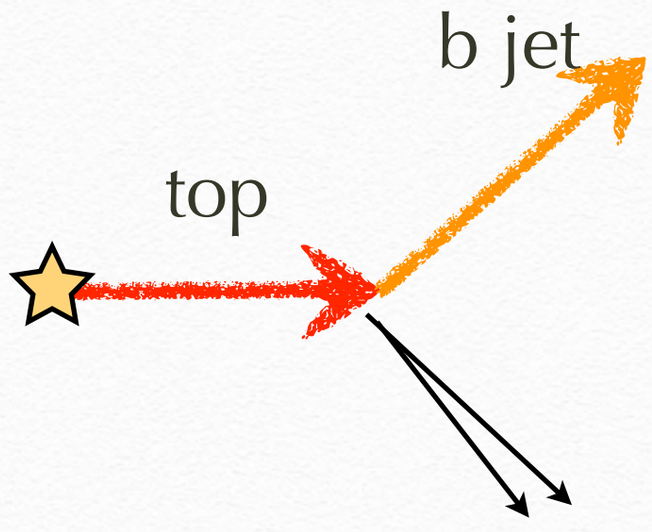

Biplob Bhattacherjee Sourav K Mandal Mihoko.M Nojiri in preparation

Limit for degenerate SUSY

The previous plot assumes universal
scalar and gaugino mass at GUT scale.
=> large mass splitting between QCD and EW SUSY particles

model independent gluino and squark mass could be
much lighter (stop still needs to be heavy in MSSM)

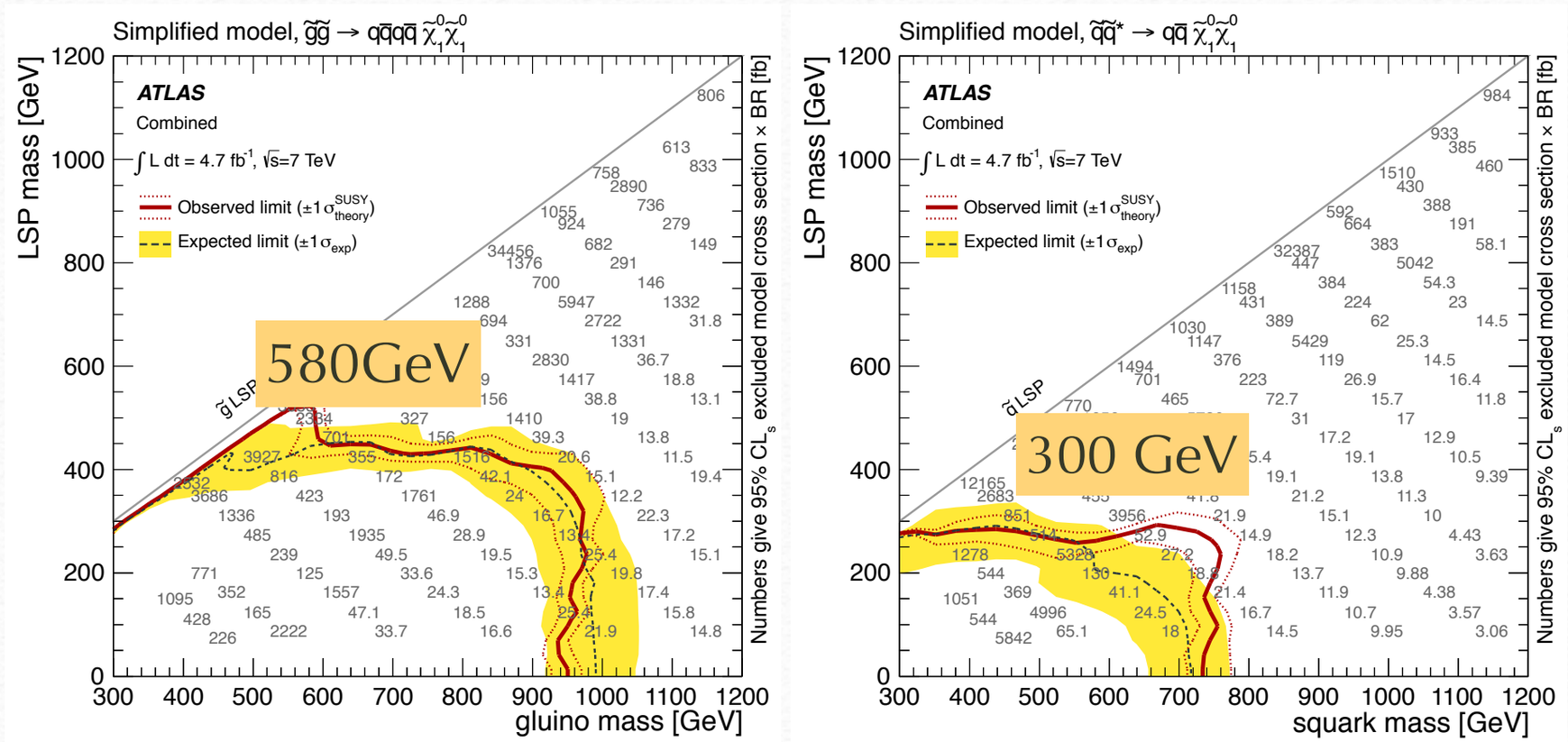

FIG. 12: The 95% CL_s exclusion limits on simplified models assuming direct production of (a) gluino pairs with decoupled

How about the EW SUSYparticle ?

this is a window to
new physics

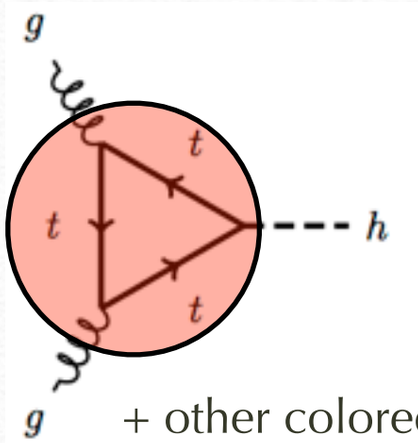

+ other colored
new particles

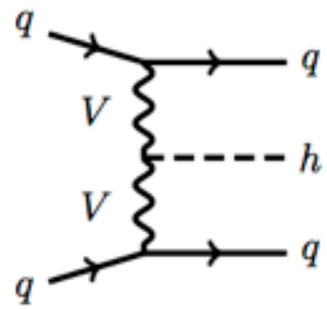

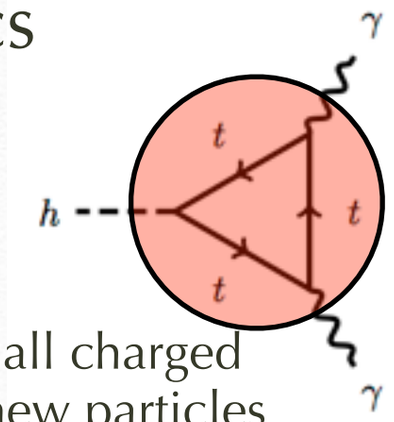

all charged
new particles

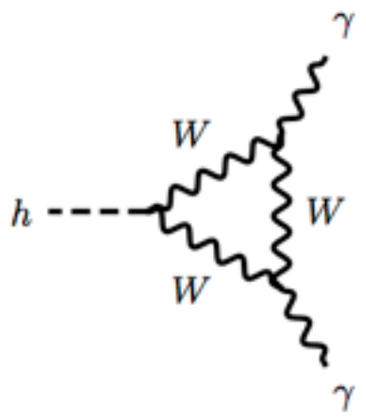

production of
Higgs boson

very light stau O(100GeV)
or scalar top generation may
change Higgs branches up
to 20%
NMSSM can account for
deviations from SM

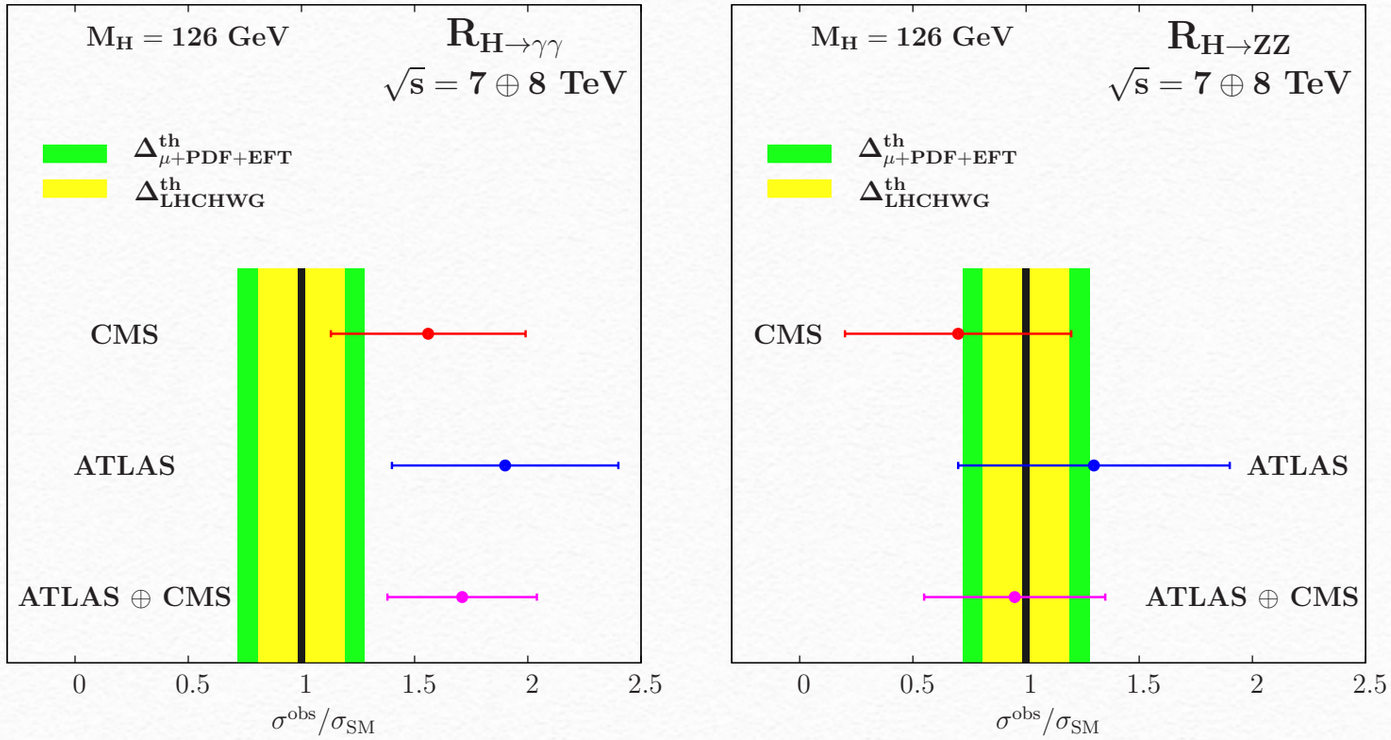

Figure 2: The value of R_{XX} for the $H \to \gamma\gamma$ and ZZ final states given by the ATLAS and CMS collaborations, as well as their combination, compared to the theoretical uncertainty bands.

How about the EW SUSYparticle ?

this is a window to
new physics

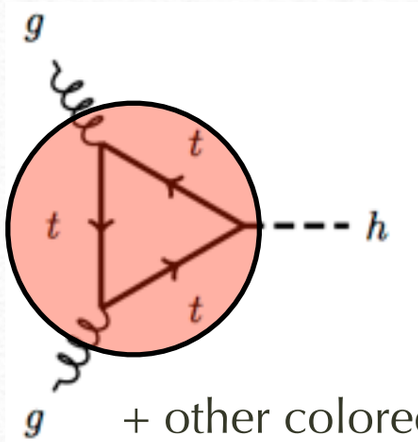

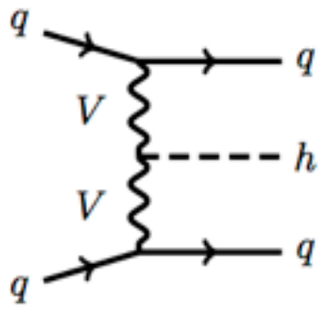

+ other colored
new particles

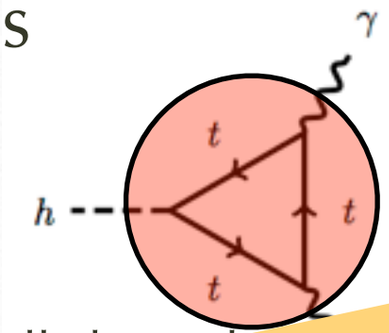

all charg

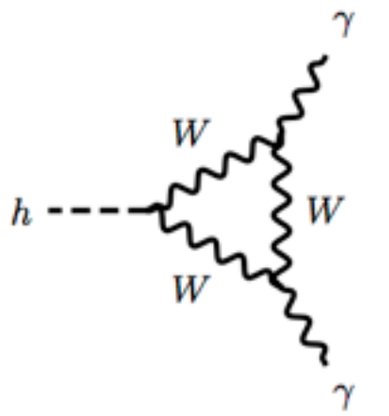

Need to wait until Thusday
this week

production
Higgs boson

very light stau O(100GeV)
or scalar top generation may
change Higgs branches up
to 20%
NMSSM can account for
deviations from SM

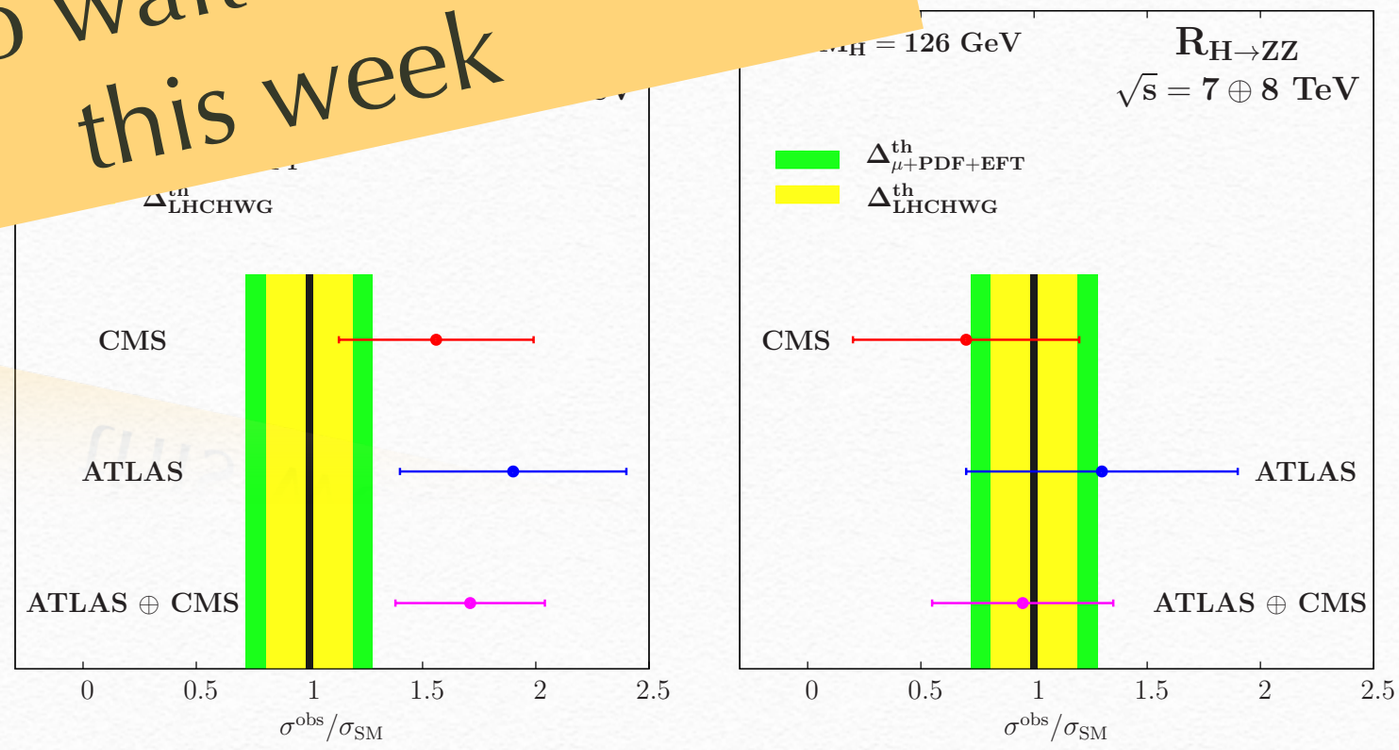

Figure 2: The value of R_{XX} for the $H \to \gamma\gamma$ and ZZ final states given by the ATLAS and CMS collaborations, as well as their combination, compared to the theoretical uncertainty bands.

Maybe sleptons are light at least?
muon g-2

$a_\mu^{\rm exp} =$ 116 592 089 (63) [10^{-11}]

$$a_\mu^{\rm exp} - a_\mu^{\rm SM} = (26.1 \pm 8.0) \cdot 10^{-10}$$ > 3σ deviation

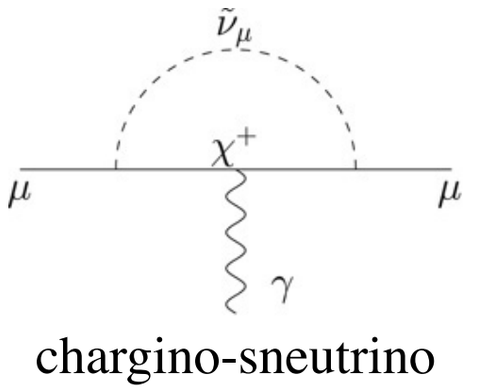

chargino-sneutrino

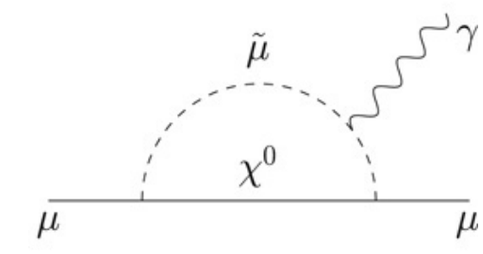

neutralino-smuon

need light EW SUSY particle

Endo, Hamaguchi, Iwamoto, Nakayama Yokozaki

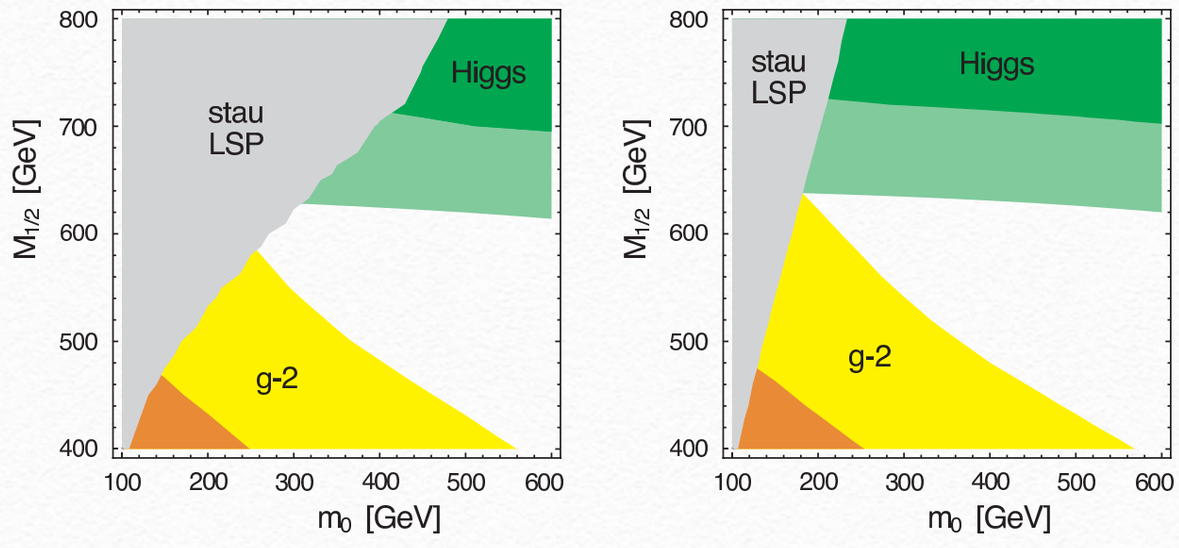

Figure 3: Contours of the Higgs mass and the muon $g-2$ are shown. The Higgs mass are maximized by choosing A_0 and A_u appropriately under the $\mathrm{Br}(\bar{B} \to X_s\gamma)$ constraint in the CMSSM models (left) and the extension (right), respectively ("m_h-max scenario"). In the dark green region, the Higgs mass is 124 – 126 GeV, and it becomes larger than 124 GeV in the light green region once the uncertainties are included. In the orange (yellow) regions, the muon $g-2$ is explained at the 1σ (2σ) level. The LSP is the (lighter) stau in the upper-left shaded region, while the lightest neutralino in the rest.

Other new physics?

- Ex Randall Sundrums model

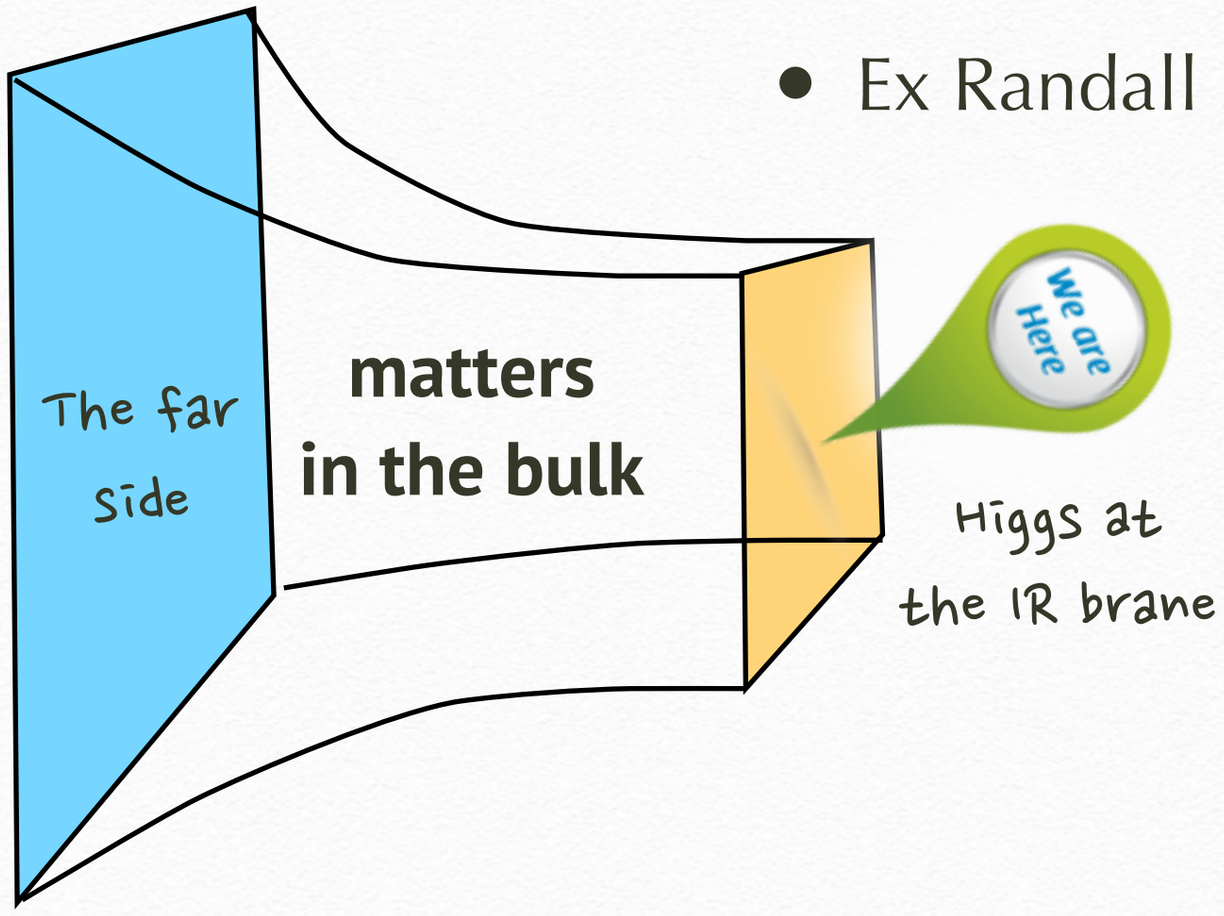

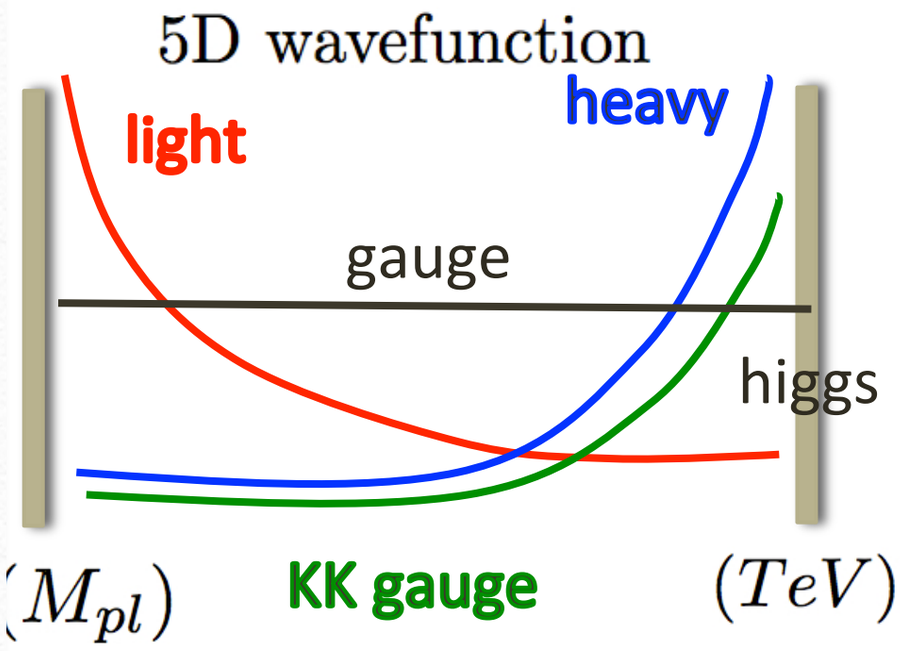

huge contribution to gg→h and h→γγ process

+mixing between radion(the 5th direction mode) and higgs boson

$$\mathcal{L}_\xi = \sqrt{g_{\rm ind}}\xi R(g_{\rm ind})H^\dagger H$$

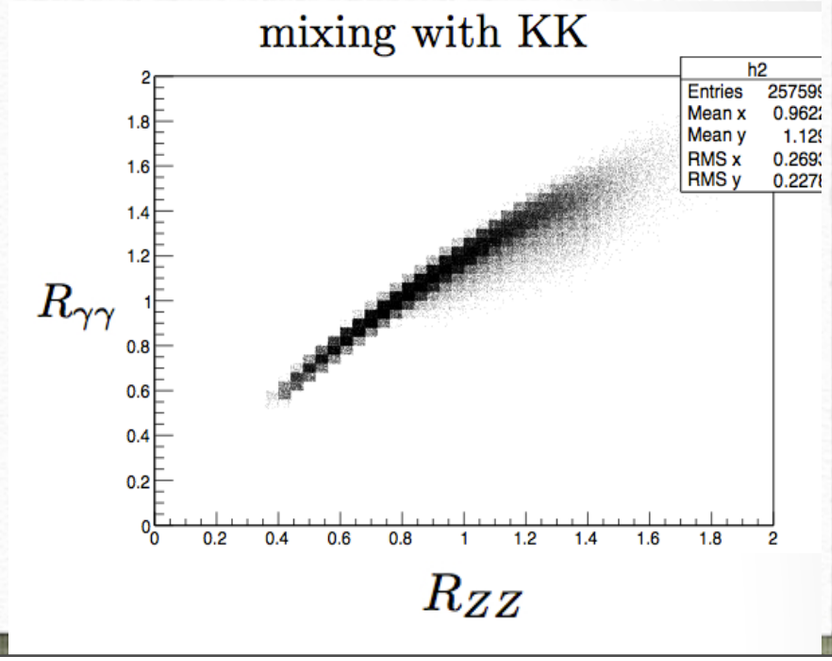

Mind of some theorists

Light Supersymmetry

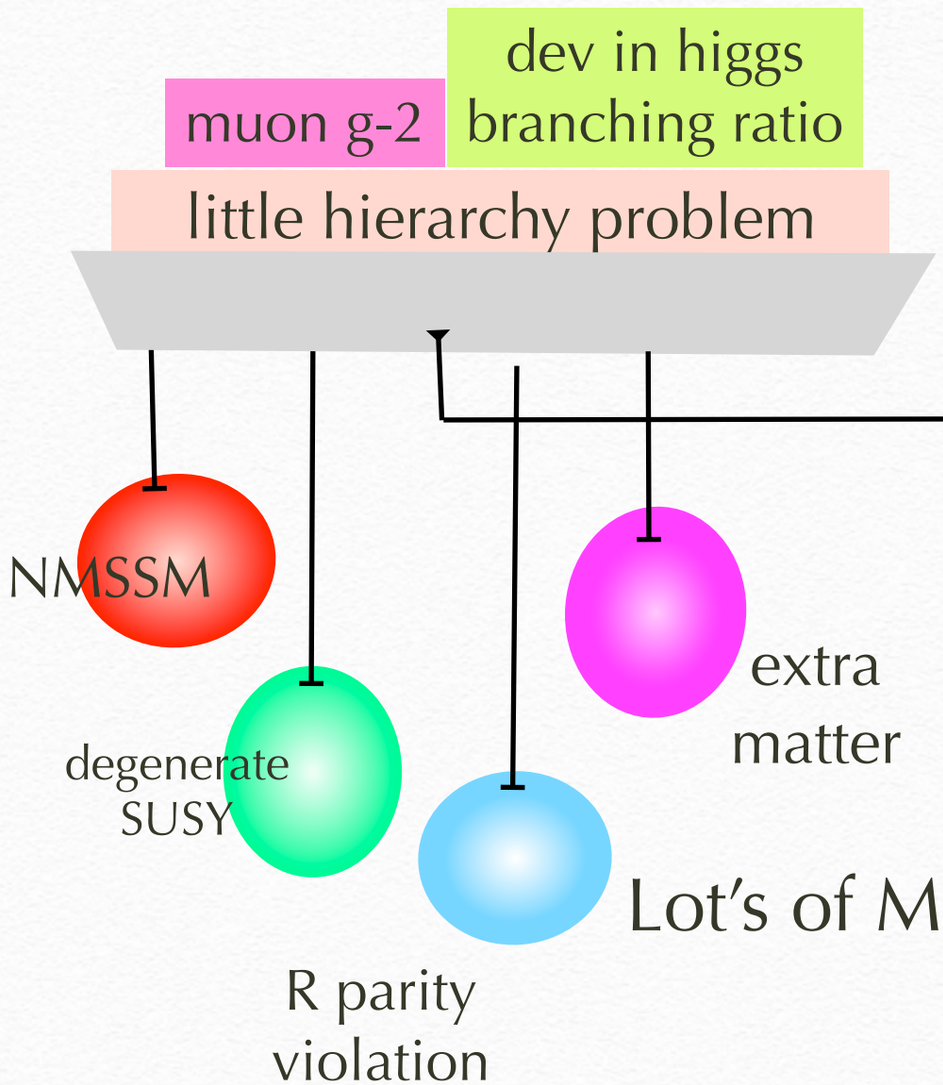

Heavy Supersymmery

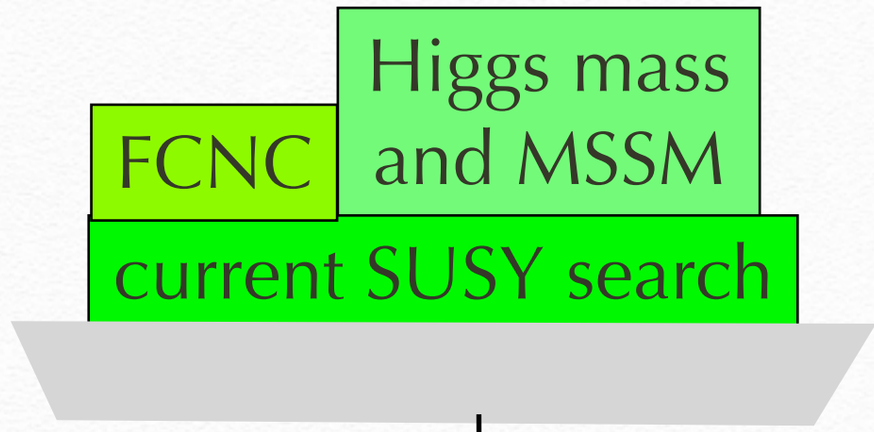

Lot's of Model building here..

“really nothing so far
(except the SM higgs boson) ”

“Is this a dead end of particle physics?”

My impression is different

Hadron collider searches:past and now

- To calculate SUSY background, we need to know W, t, Z with multiple jets in the final state. In 90's: we did not know how to calculate the processes appropriately for the hadron collider. "I do not trust hadron collider physics" was typical attitudes in e^+e^-collider funs.
  - It took very long time to get limit from hadron collider data, and there were fake discovery as well (famous SPS1a...)

photo 1972

- **Progress in "Matching" and NLO,** we have better background prediction now.
- We can "exclude" the model parameters rather convincingly , and we do not "discover" much unless we comes to **the point to discover**.



Parton shower and hard process

- MC simulation for hadron collider roughly divided into three parts

$$d\sigma_{n+1} = d\sigma_n \frac{dt}{t} dz \frac{\alpha_s}{2\pi} \widehat{P}_{ba}(z)$$

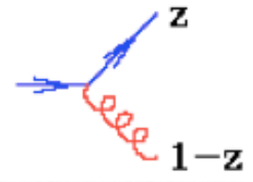

  - "hard process" gg→H, gg, qq→SUSY..

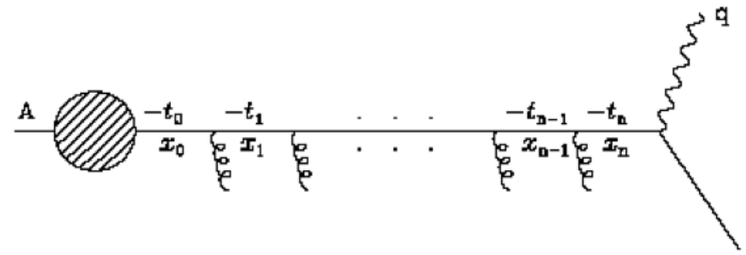

  - Initial/final state radiation: multiple emission of **collinear gluon and quarks**. often treated by parton shower approximation (multiple emission summed.

- Background: QCD process with multiple **hard jets**. ex: process of W+n hard parton: some of the hard partons overlap with parton showers. "double counting problem"

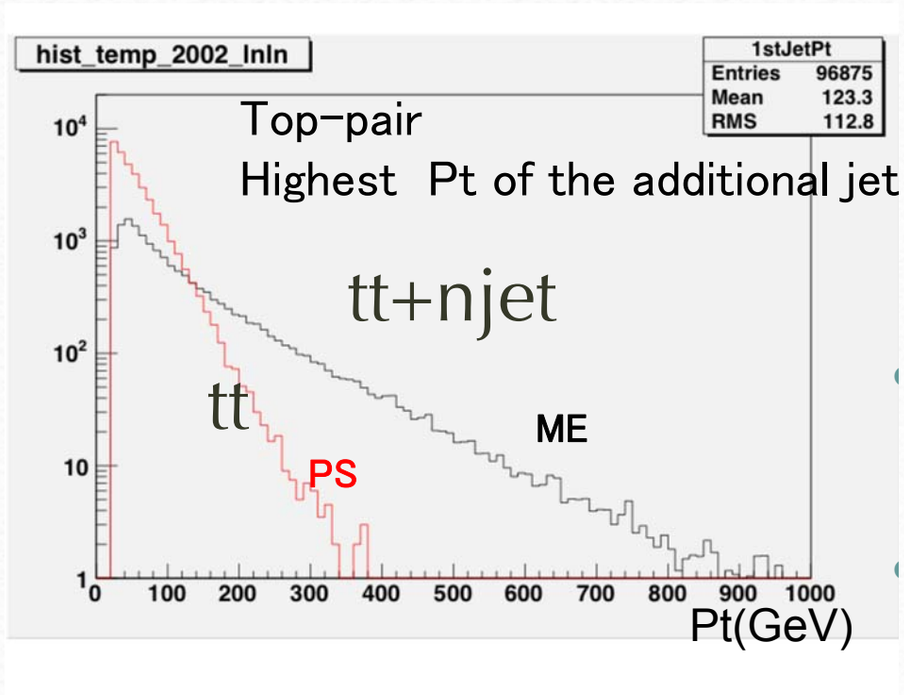

- "Maching" is a consitent treatment to veto the overlap between hard and soft process.

W+jets (leading SUSY BG at 7TeV)

Data vs Theory in 2003

Data vs Theory

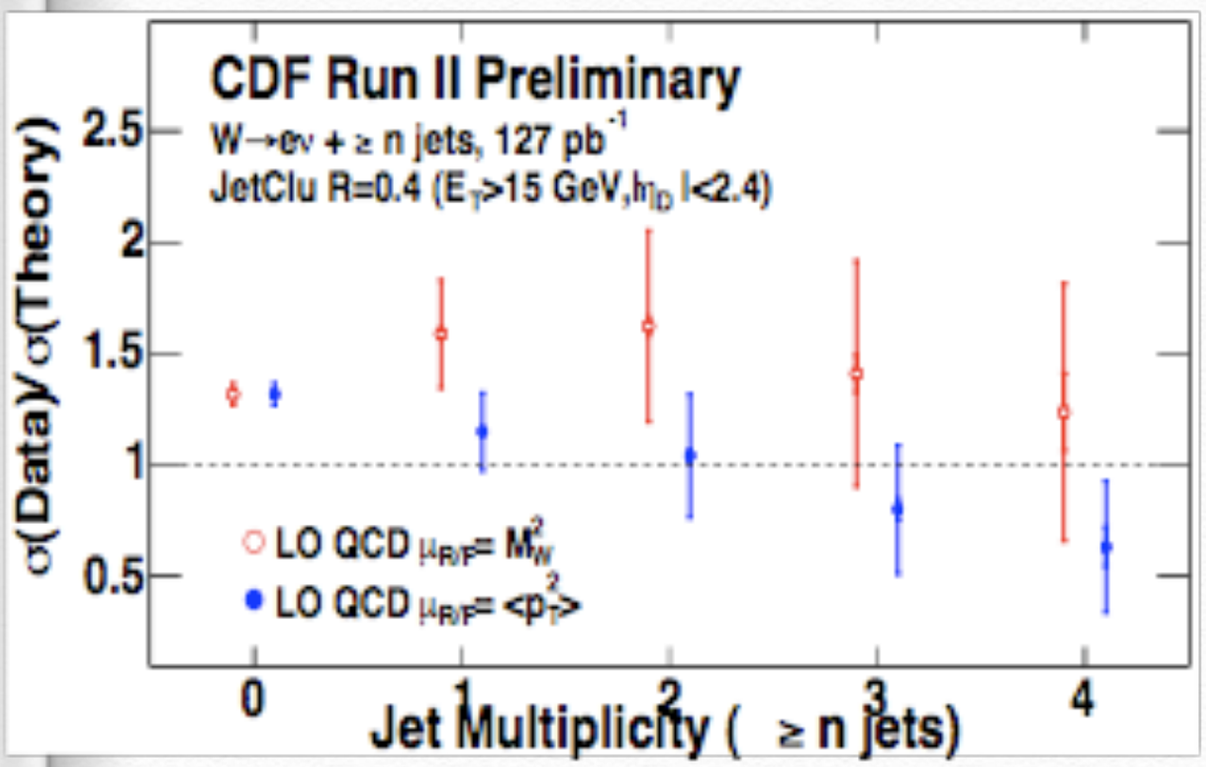

Ratio of Cross-sections

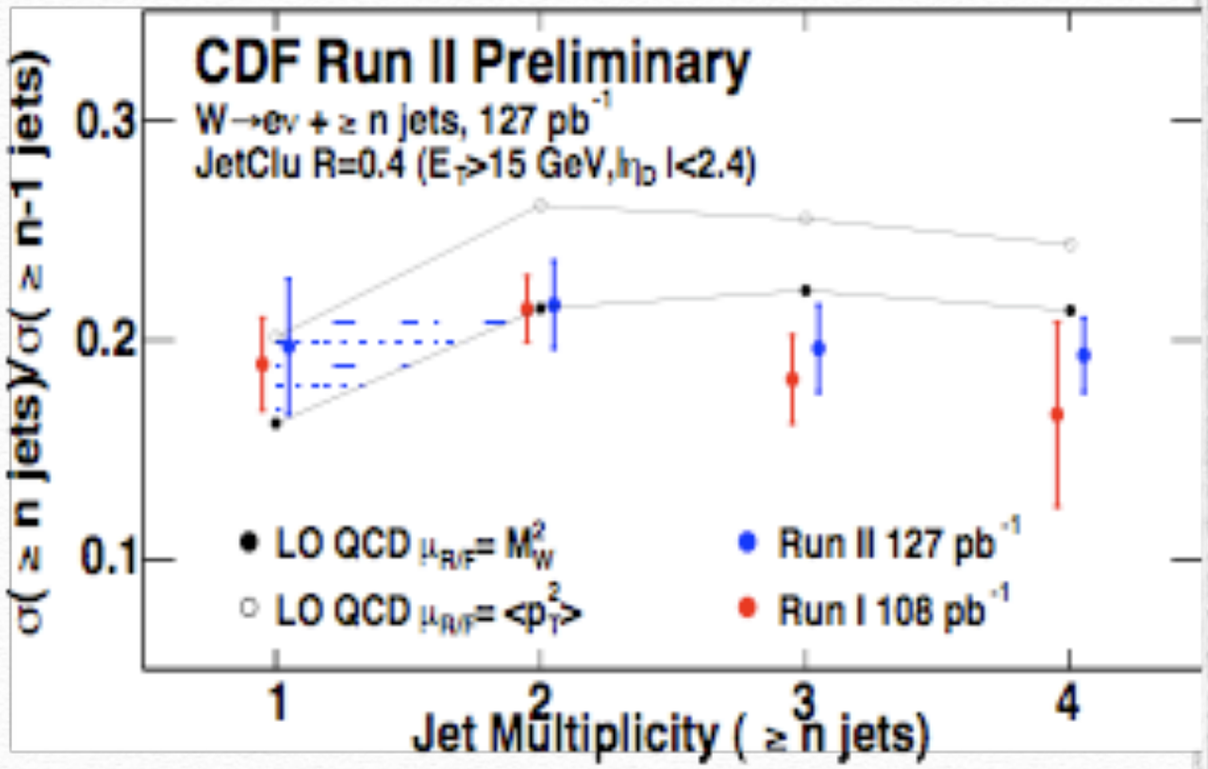

This allows estimate of background with “confidence “

W+jets (leading SUSY BG at 7TeV)

Data vs Theory in 2011

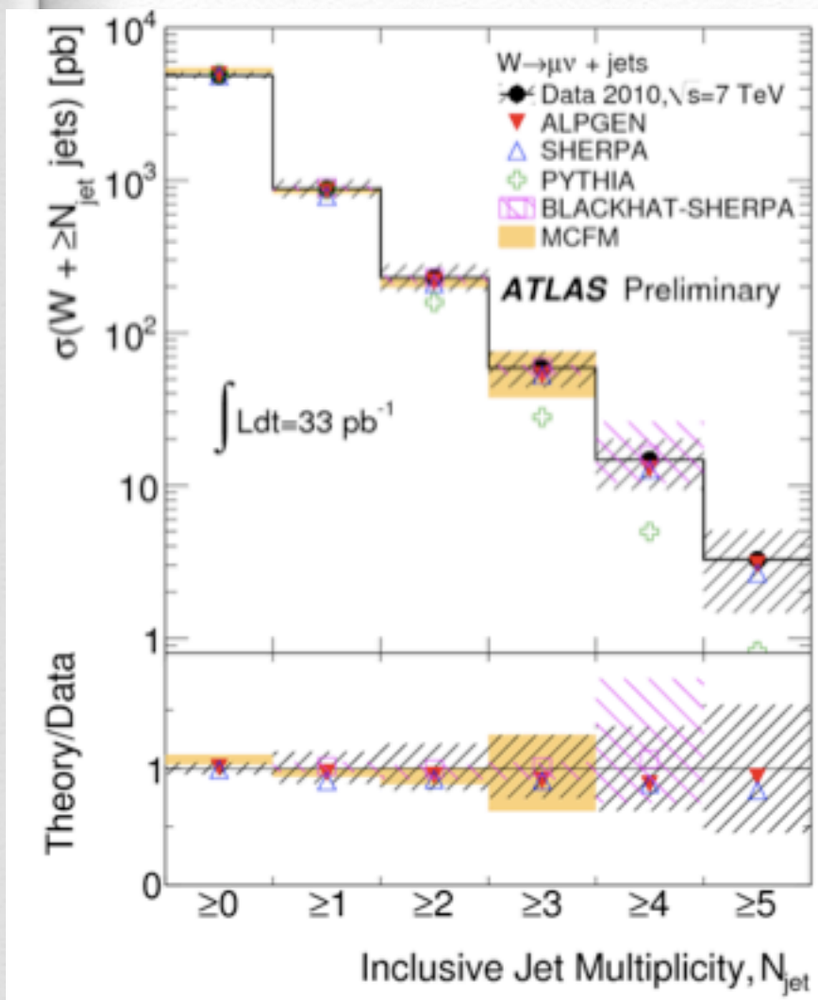

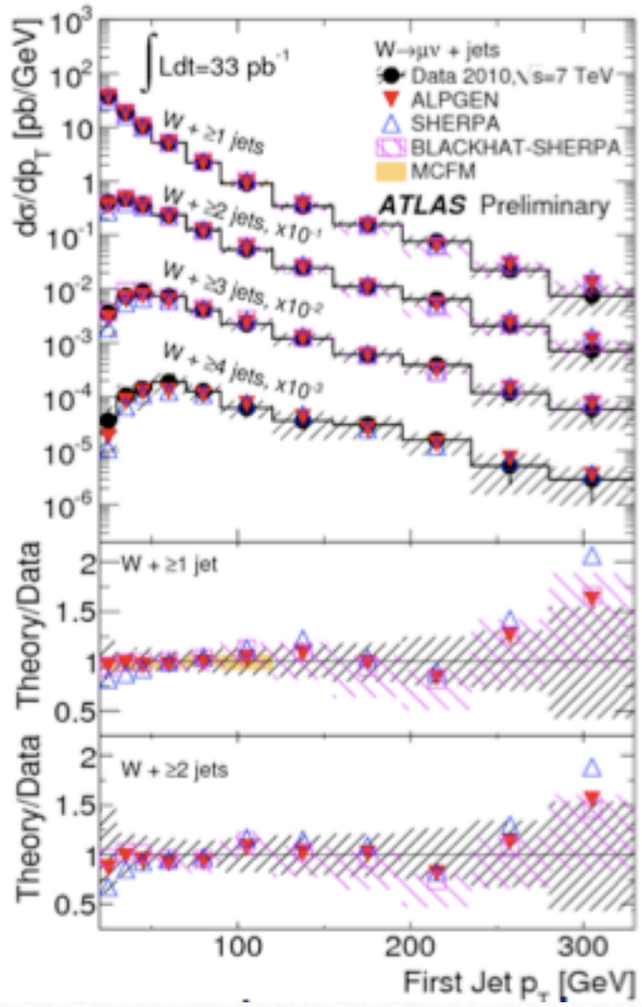

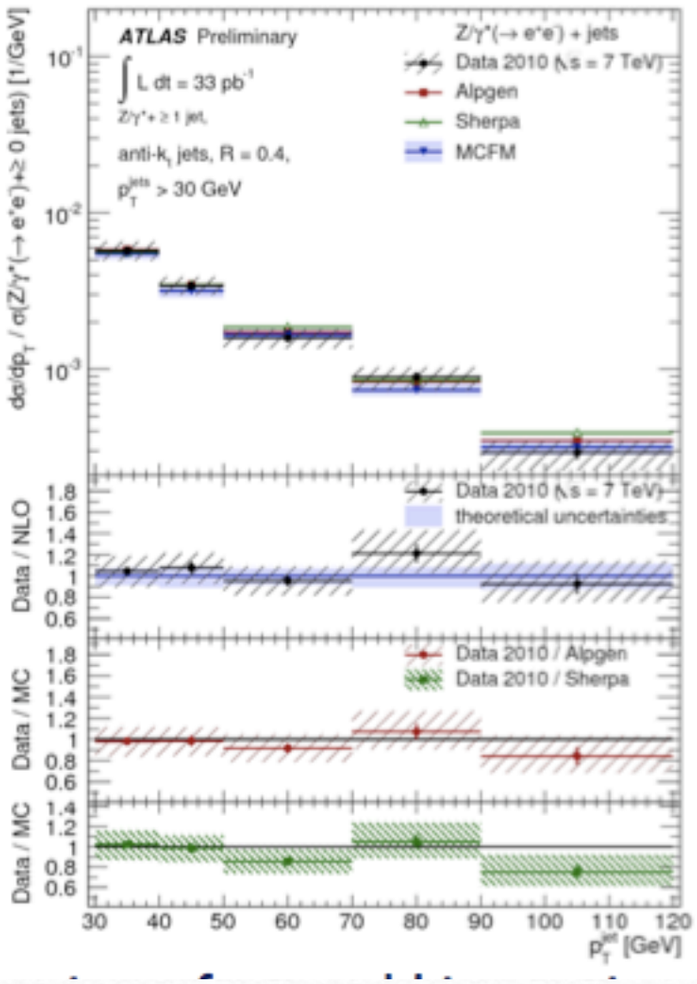

This allows estimate of background with “confidence “

cross section at 13TeV run

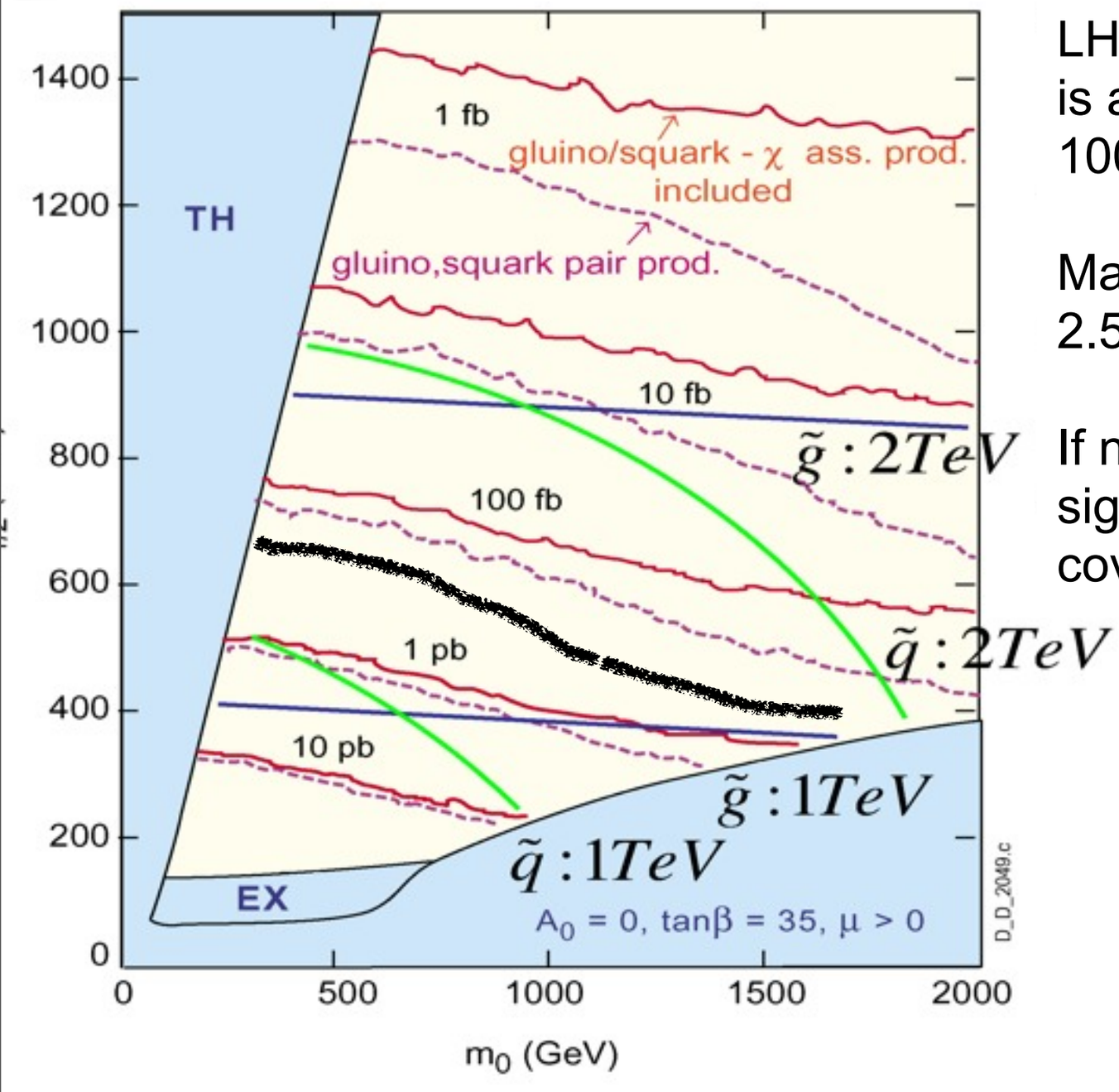

LHC at 13TeV max total cross section is around
100 fb-1→1000 events

Max reach will be around 10fb to 1fb 2.5TeV

If nature takes supersymmetry, significant parameter space will be covered by the 13TeV run

Study of Higgs sector is also very important O(10%) measurement of Branches
e+e- collider O(1%)

Direct search will be serious constraint this year

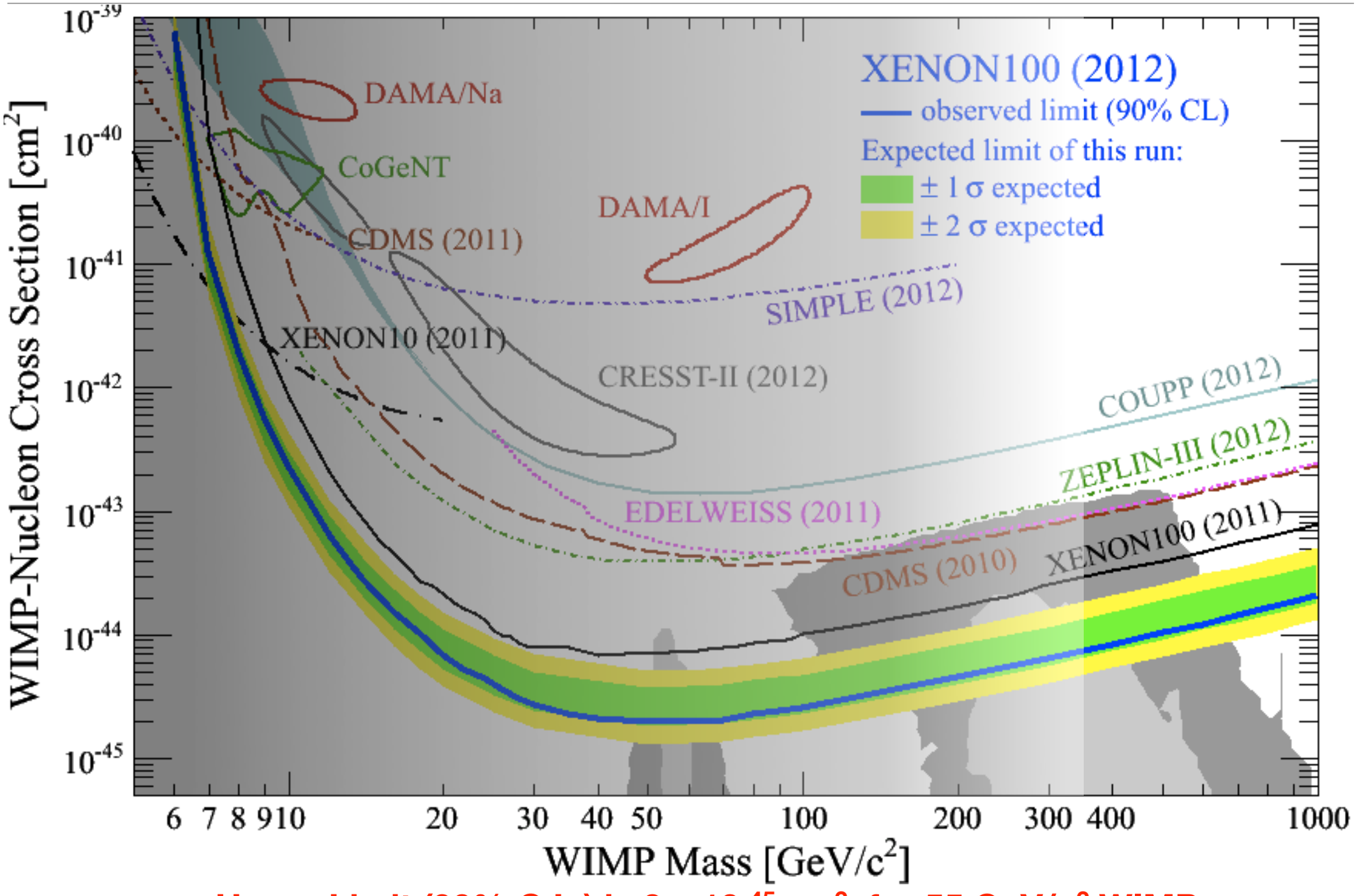

Upper Limit (90% C.L.) is 2 x 10^{-45} cm^2 for 55 GeV/c^2 WIMP

waiting for new data to decide the direction

with LHC at 13TeV, it will have a great fall ...

To where?

waiting for new data to decide the direction



with LHC at 13TeV, it will have a great fall ...

To where?

Kazuyuki Sugimura, JGRG 22(2012)111204

"Non-gaussian bubbles from tunneling in the inflationary era"

RESCEU SYMPOSIUM ON

GENERAL RELATIVITY AND GRAVITATION

JGRG 22

November 12-16 2012

Koshiba Hall, The University of Tokyo, Hongo, Tokyo, Japan

Non-Gaussian bubbles in the sky

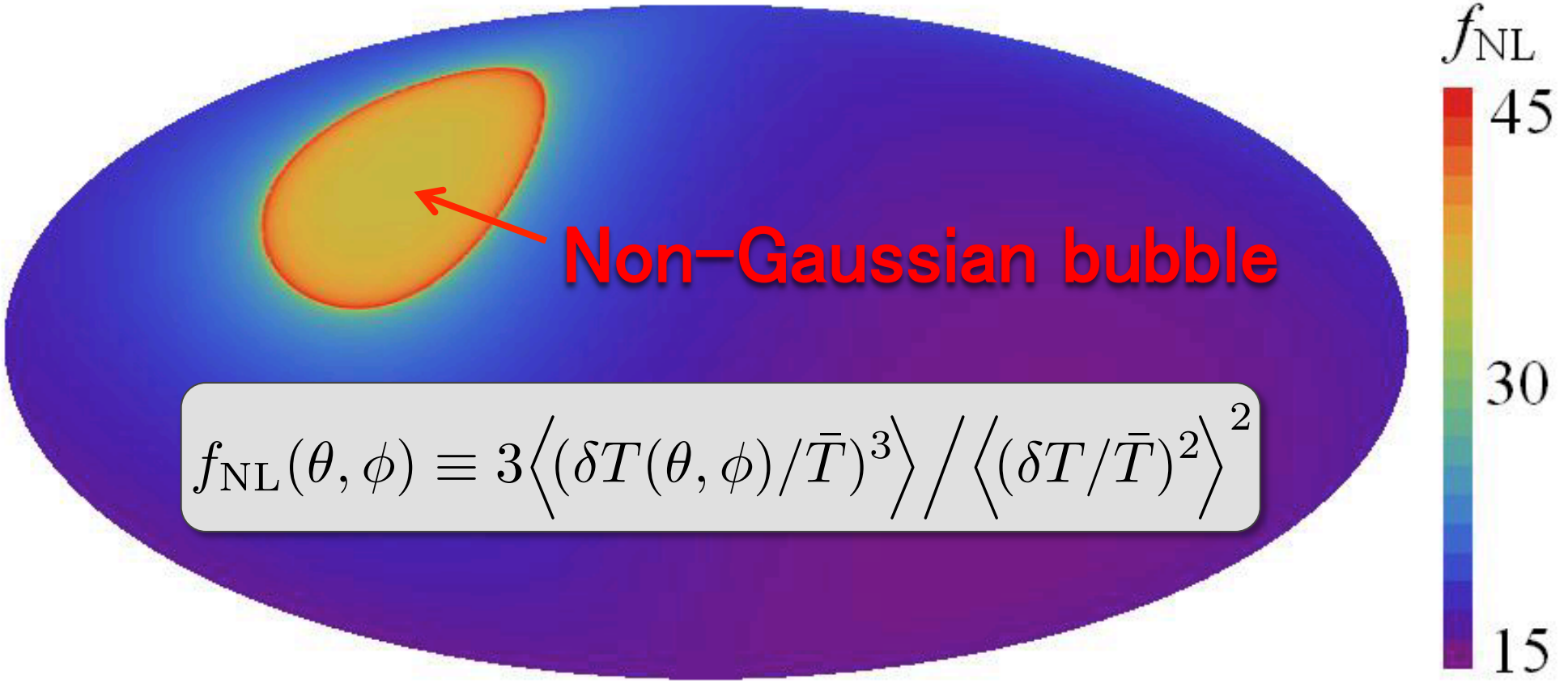

YITP YUKAWA INSTITUTE FOR THEORETICAL PHYSICS

Kazuyuki Sugimura (YITP, Kyoto University)

D. Yamauchi and M. Sasaki, (EPL 100 (2012) 29004)

Non-Gaussian bubbles in the sky

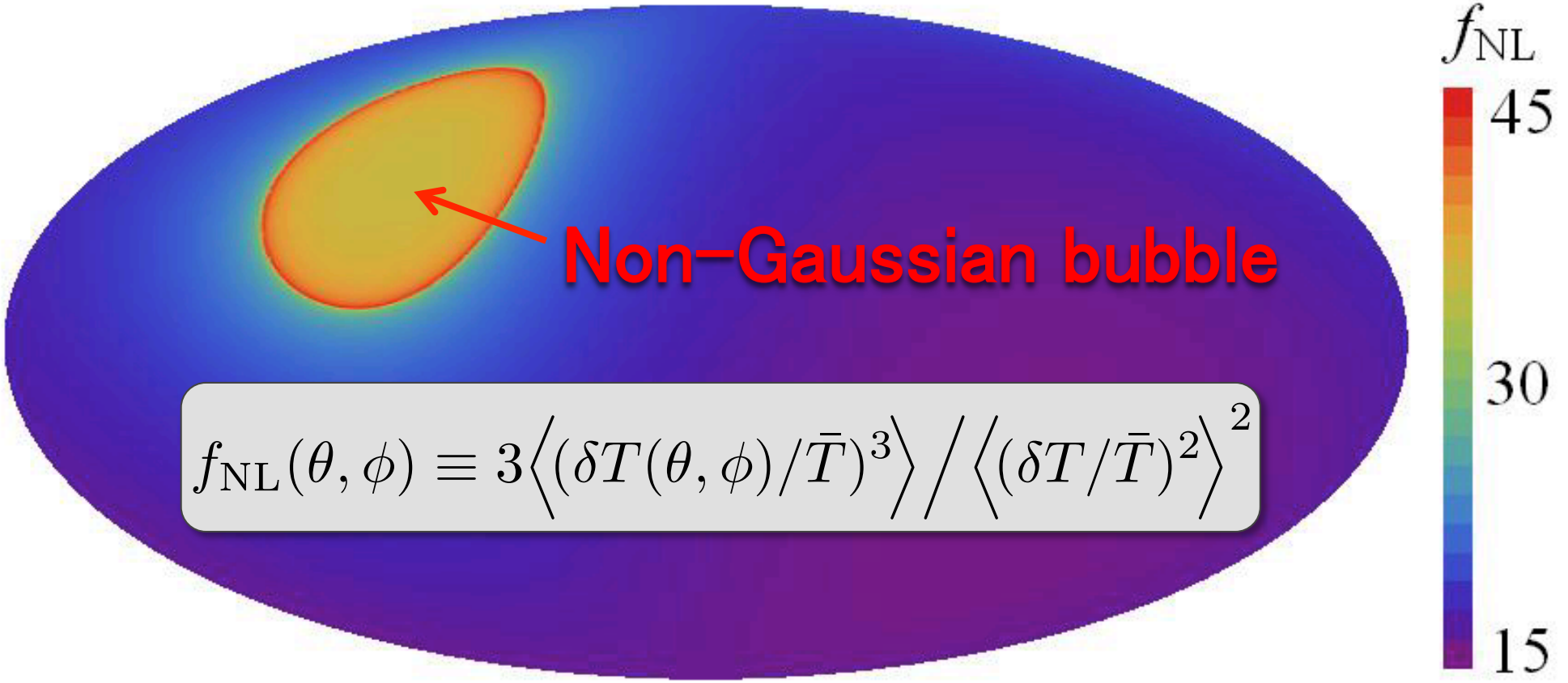

YITP YUKAWA INSTITUTE FOR THEORETICAL PHYSICS

Kazuyuki Sugimura (YITP, Kyoto University)

D. Yamauchi and M. Sasaki, (EPL 100 (2012) 29004)

60th celebration of the birthday, congratulations!!



Introductions

Motivation

- Inflation (flatness, homogeneity, power spectrum)
  - good consistency with observation
  - What is the physical origin of inflation?

- String landscape (Susskind, 2003)
  - attempt to explain the origin of inflation with string theory
  - many scalar fields & local potential minima

http://journalofcosmology.com

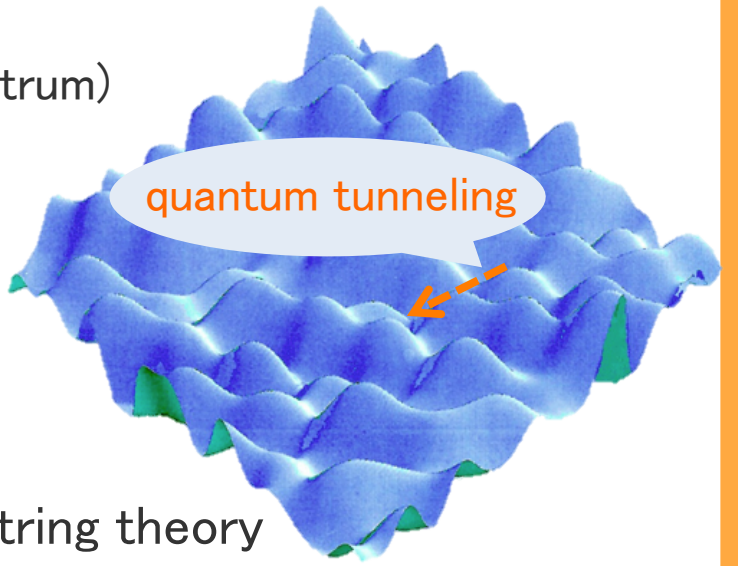

potential for scalar fields

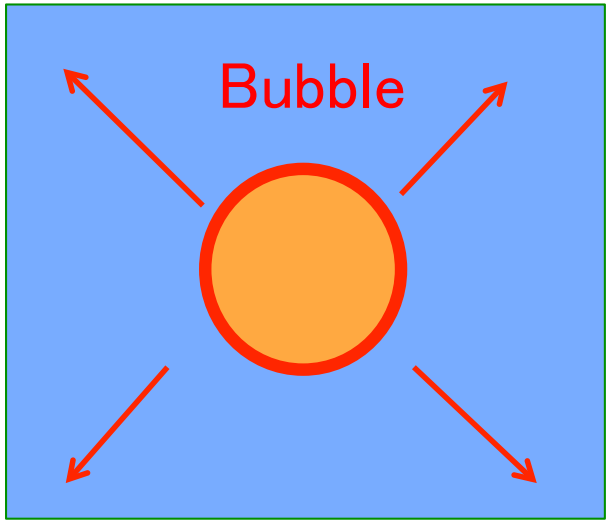

bubble nucleation

- Bubble nucleation (= quantum tunneling) (= 1st order phase trainsition)
  - tunneling between local minima
  - scalar-field bubble is nucleated during inflation

Bubbles in the sky

- After inflation
  - all scalar fields, including bubbles, decay
  - but, signature of bubbles may be seen as some bubble feature in the sky
- Non-Gaussianity f_{NL} (Komatsu and Spergel, 2001)

$$\phi(x) = \phi_{\rm L}(x) + f_{\rm NL}\left(\phi_{\rm L}^2(x) - \left\langle \phi_{\rm L}^2 \right\rangle\right)$$

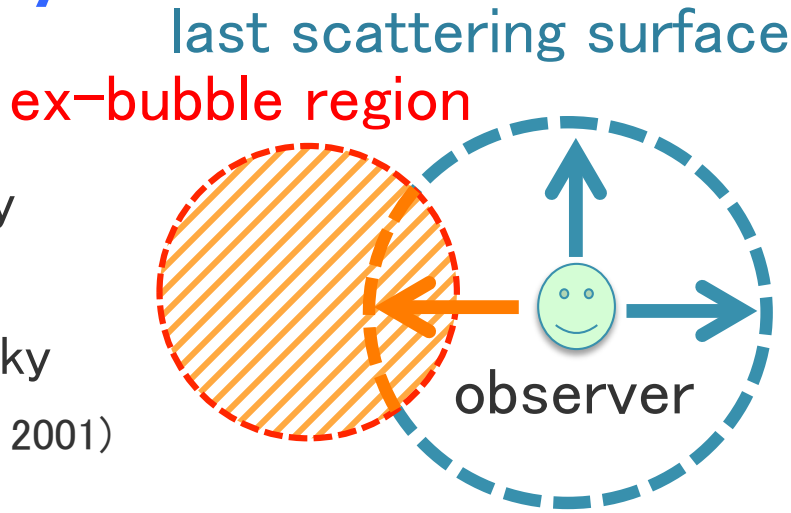

(in comoving coordinate)

  - f_{NL} is one way to parameterize deviation from Gaussian statistics (ϕ_L: Gaussian variable)
  - small for the simplest inflation model (Maldacena 2002)
  - suitable for detection of deviation from the simplest model
- Non-Gaussian bubbles
  - bubble signature may be seen in non-Gaissianity
  - f_{NL} can be different for each CMB sky patch
  - we show how it happens using a toy model

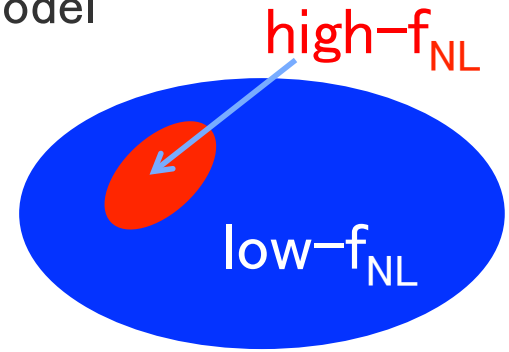

CMB sky map



Toy Model

Three scalar fields

Name	Role	Energy density/Hierarchy
Inflaton: Ψ	slow-roll inflation	high
Tunneling field: σ	bubble nucelation	middle
Curvaton: ϕ	curvature pert. generation	low

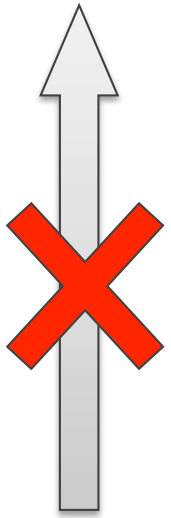

(Lyth, Ungarelli & Wands;
Enqvist & Sloth; Moroi & Takahashi)

no backreaction approximation

(Curvaton scenario: Curvaton affects neither slow-roll inflaiton nor bubble nucleation. But it decays later than inflaton and tunneling field. Then, its energy density becomes relatively higher and it creates curvature pert. when it decays.)

Bubble nucleation during slow-roll inflation

- Slow-roll inflation is not affected by bubble nucleation
- Bubble nucleates at one moment of slow roll inflation
  (for simplicity, we consider single nucleation case)

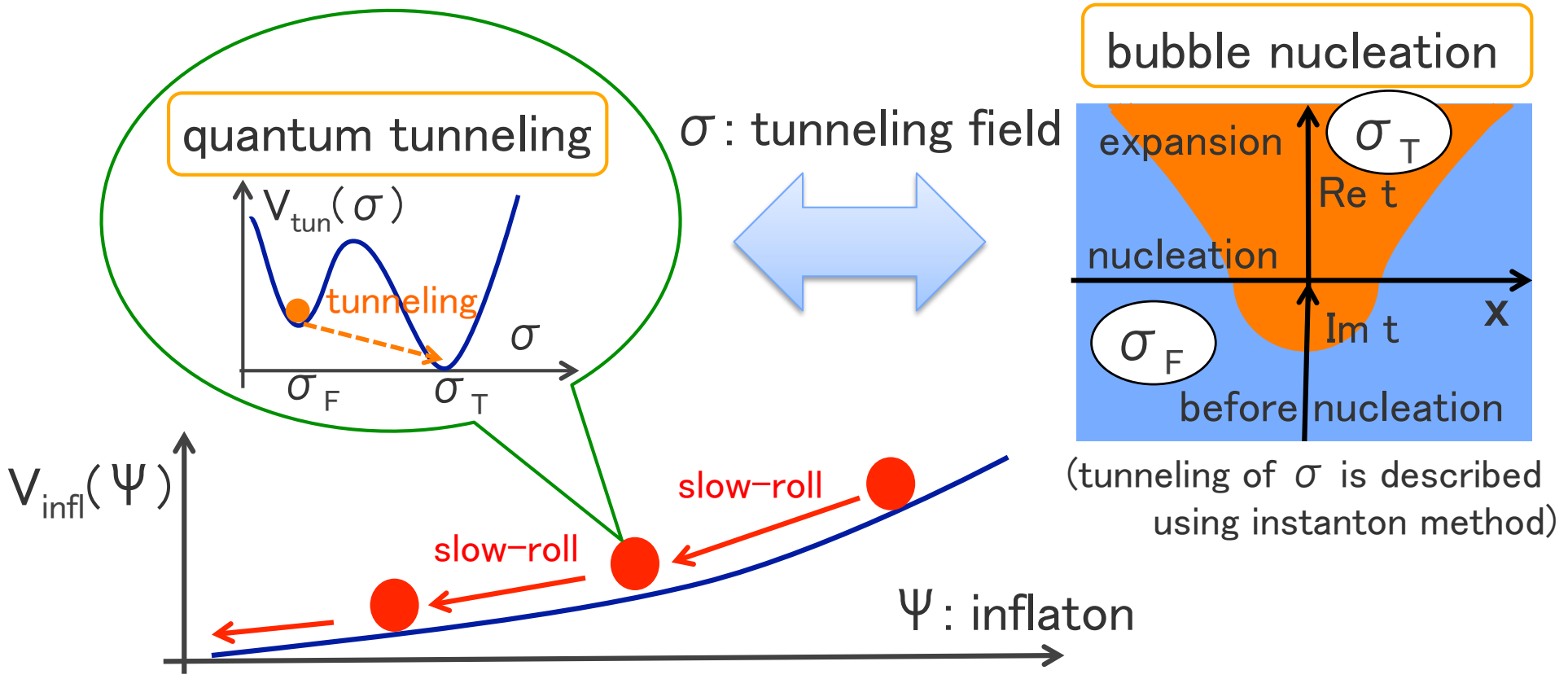

Curvaton evolution in the universe with a bubble

- Original potential for curvaton ϕ has interaction with tunneling field

$$V(\phi) = \frac{m^2}{2}\phi^2 + V_{\rm int}(\sigma, \phi)$$

- Effective potential for ϕ in the universe with bubble of σ

$$V_{\rm int}^{(\rm eff)}(\phi; x) := V_{\rm int}(\bar{\sigma}(x), \phi)$$

substituitng background bubble

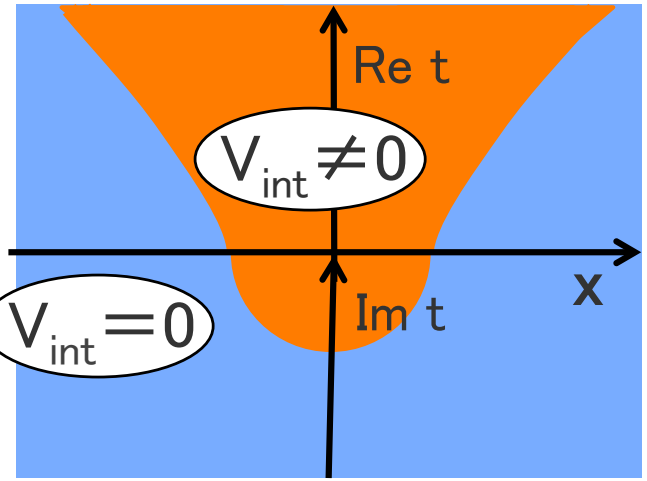

- Non-linear self interaction

is assumed to vanish at false vacuum

$$V_{\rm int}(\sigma, \phi) = \lambda(\sigma)\phi^3 \qquad (\lambda(\sigma_{\rm F}) = 0)$$

⇒ Non-Gaussianity is generated only inside bubble



Method

How to calculate 3pt function in the universe with a bubble

- Background bubble of σ is described by CDL instanton

  (Coleman and De Luccia(CDL), 1980)

  - imaginary time evolution describes nucleation process
  - real time evolution describes expansion afterwards

- skewness of ϕ on bubble background

$$\left\langle \phi^3(x) \right\rangle = \left\langle 0 \left| P\left(\phi^3(x) \exp\left[-\frac{i}{\hbar} \int_{C_1+C_2} dt \int d^3\mathbf{x}\sqrt{-g} V_{\rm int}^{(\rm eff)}(\phi(x);x) \right] \right) \right| 0 \right\rangle$$

  - extension of in-in formalism to the case with bubble
  - in-in time path consists of both imaginary and real time

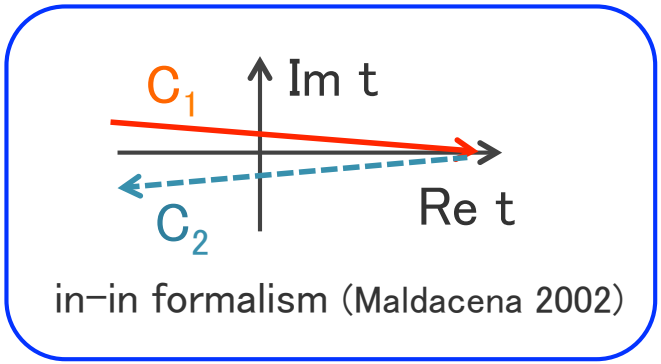



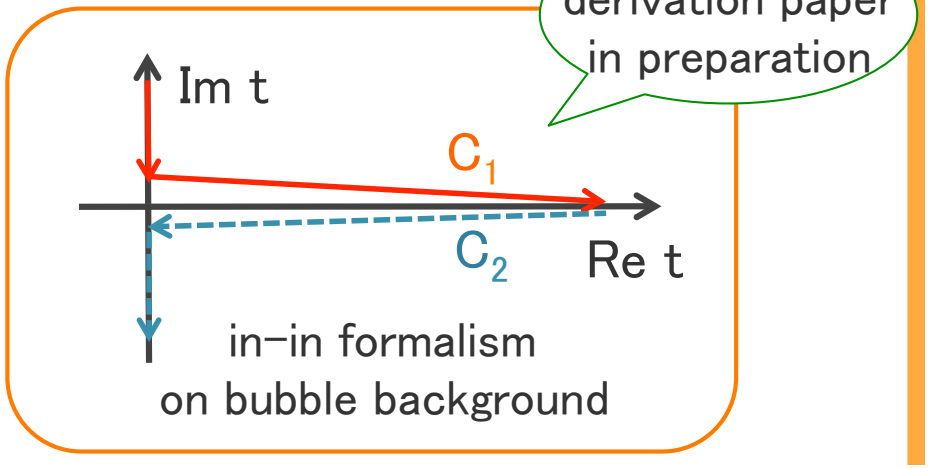

From curvaton fluctuation to δT

- How fluctuation evlolves

Curvaton mechanism　　Sachs–Wolfe effect

$\phi(x)$ → $\zeta(x)$ → $\delta T(\theta, \varphi)$

curvaton flucutuation　　curvature pert.　　CMB anisotropies

- CMB skewness: $\left\langle \delta T^3(\theta, \varphi) \right\rangle$
  - skewness of ϕ becomes skewness of δT
  - observer sees high skewness spot
    (= Non–Gaussian bubble)

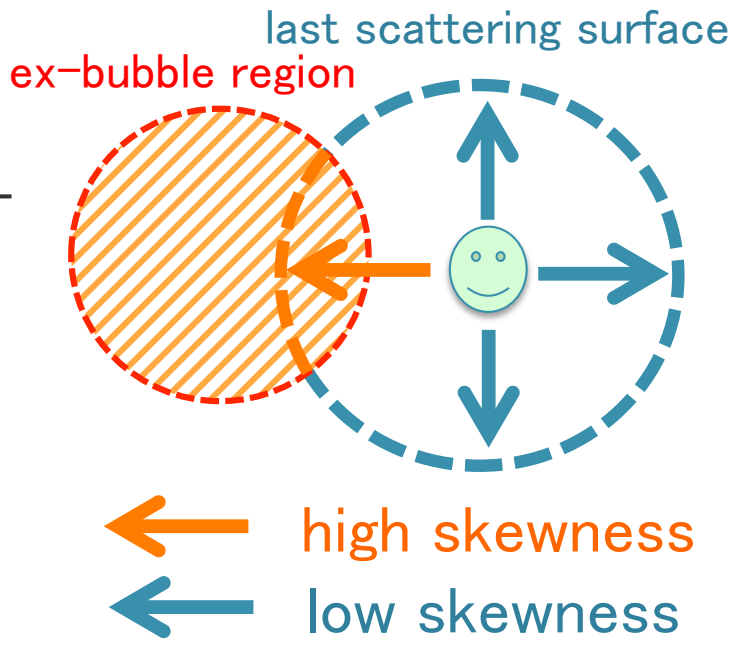



Result and Conclusion

Result

- calculated non-Gaussian bubble in the CMB sky

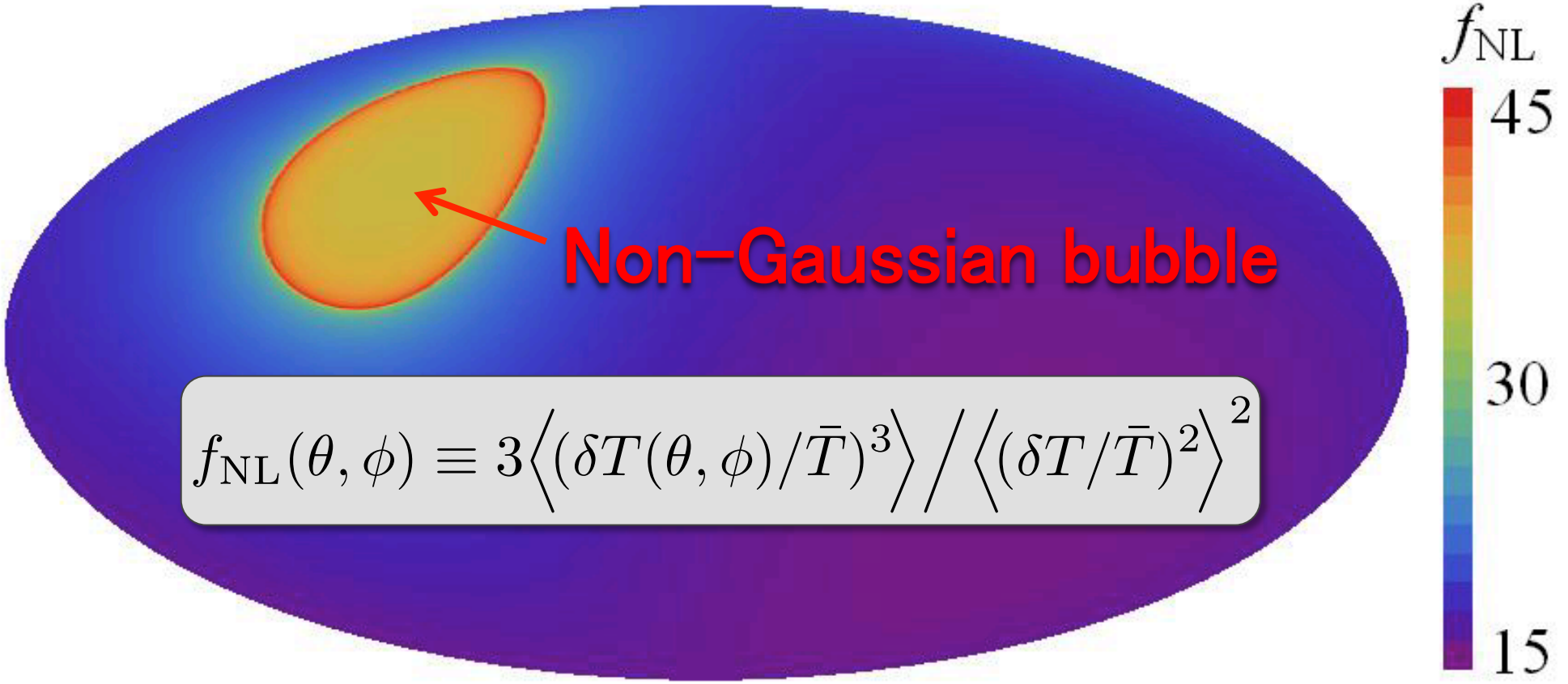

cf. PLANCK's expected precision(2013 March)
(for homogeneous non-Gaussianity)

$$|\Delta f_{\rm NL}| \sim \mathcal{O}(5)$$

Conclusions

non-Gaussian bubble

- We have shown that a bubble-shaped high-skewness spot in CMB anisotropies may be generated if a bubble is nucleated during inflationary era by using a toy model.

- Usual analysis using statistically homogeneous templates will miss non-Gaussian bubbles even if they exist. However, you may find them by making special analysis targeting them.
(future work)

- If you find non-Gaussian bubbles in near-future observations, it might be the first observational signature of string theory!

Appendix

Model parameters

- Thin-wall instanton

$$\bar{\sigma}(\chi) = \begin{cases} \sigma_{\rm T} & \text{for} \quad 0 \leqslant \chi < HR_{\rm W}, \\ \sigma_{\rm F} & \text{for} \quad HR_{\rm W} < \chi \leqslant \pi \end{cases}$$

(O(4) symmetric instanton
depends only on coordinate χ)

- Effective Lagrangian for $\phi = \phi_0 + \delta\phi$

$$\mathcal{L}_I = -\sqrt{-g}\,\lambda H \delta\left(\chi - HR_{\rm W}\right)\delta\phi^3$$

effective coupling const.

V_{int} is assumed to be large only around bubble wall

- Model parameters for the example

$$H/\phi_0 = 0.001 \;\; \lambda = 0.005, \quad m/H = 0.3, \quad HR_{\rm W} = 0.2\pi$$
$$r_\phi = 0.1, \;\; |\boldsymbol{x}_0| = r_* = 2, \;\; Ht_{\rm e} = 50$$

(parameters are chosen so that curvaton doesn't affect power spectrum, which is assumed to be generated by inflaton's fluctuation)

- Parameter dependence of f_{NL} at the center of bubble

$$f_{\rm NL}^{(\rm cen)} \approx \frac{3\times 10^{-4}\,\lambda\, r_\phi^3\, \sin^3(HR_{\rm W})}{A_\zeta^4\, \exp\left(\left(\frac{m}{H}\right)^2 Ht_{\rm e}\right)} \left(\frac{H}{m}\right)^6 \left(\frac{H}{\phi_0}\right)^3.$$

Graphical description of in-in formalism with bubble

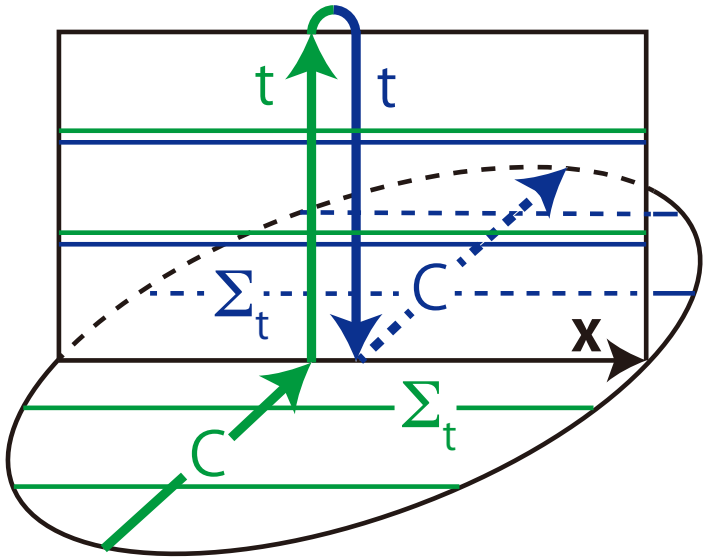

in-in time path for
in-in formalism with bubble

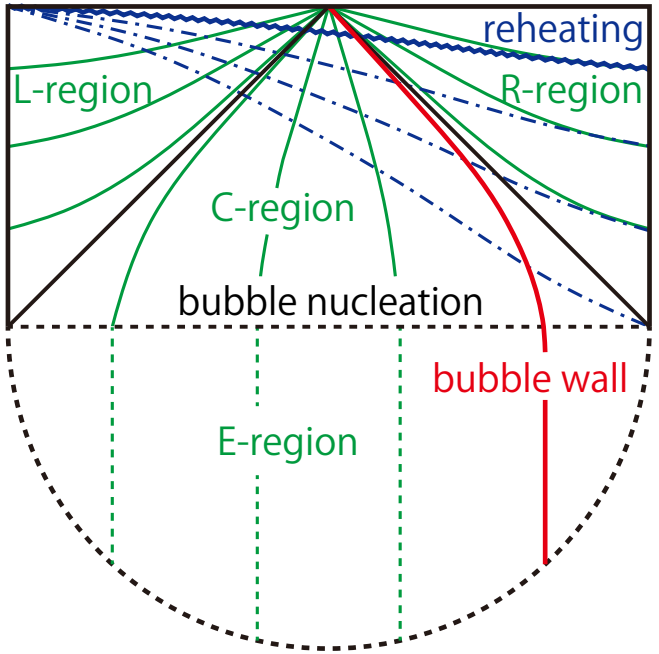

Penrose-like diagram of the
bubble nucleating universe

- N-point function

$$\left\langle \delta\phi(x_1)\delta\phi(x_2)\cdots\delta\phi(x_N)\right\rangle = \frac{\left\langle 0\left|P\delta\phi(x_1)\delta\phi(x_2)\cdots\delta\phi(x_N)e^{i\int_{C\times\Sigma_t}dtd^3\mathbf{x}\mathcal{L}_I}\right|0\right\rangle}{\left\langle 0\left|Pe^{i\int_{C\times\Sigma_t}dtd^3\mathbf{x}\mathcal{L}_I}\right|0\right\rangle}$$

curvaton mechanism and $\langle \delta\phi^3 \rangle$ to f_{NL}

(Lyth, Ungarelli & Wands; Enqvist & Sloth; Moroi & Takahashi)

- Curvature pert. at the decay of curvaton (conserves outside horizon after that)

$$\zeta = (1 - r_\phi)\zeta_r + r_\phi \zeta_\phi$$

- curvature pert. from inflaton
- ratio of curvaton contribution
- curvature pert. from curvaton

$$\zeta_\phi = \frac{1}{3}\frac{\delta\rho_\phi}{\rho_\phi}\bigg|_{t_e} = \frac{1}{3}\left(2\frac{\delta\phi}{\phi_0} + \frac{\delta\phi^2}{\phi_0^2}\right)\bigg|_{t_e}$$

t_e: inflation end

subdominant

- Sachs–Wolfe effect

$$(\delta T/T)(\hat{\boldsymbol{n}}) = (1/5)\,\zeta(\boldsymbol{x}_0 + r_*\hat{\boldsymbol{n}}, t_*)$$

- f_{NL} as a function of $\langle \delta\, \phi^3 \rangle$

$$f_{\rm NL}(\mathbf{n}) \equiv 3\Big\langle (\delta T(\mathbf{n})/\bar{T})^3 \Big\rangle \Big/ \Big\langle (\delta T/\bar{T})^2 \Big\rangle^2$$

$$\approx \frac{40 r_\phi^3}{81\langle\zeta^2\rangle^2}\frac{\langle \delta\phi^3(|\boldsymbol{x}_0 + r_*\hat{\boldsymbol{n}}|, t_e)\rangle}{\phi_0^3}$$

$\langle\zeta^2\rangle = A_\zeta^2 \equiv 6.25 \times 10^{-10}$ (obs.)

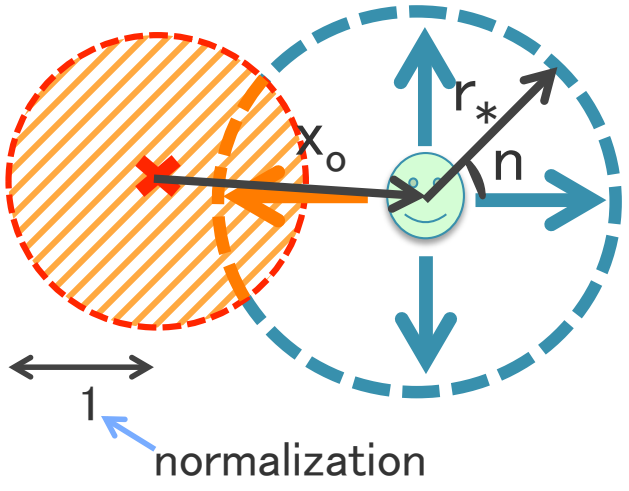

normalization

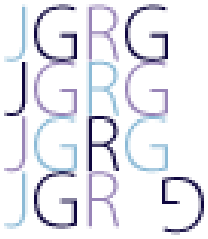

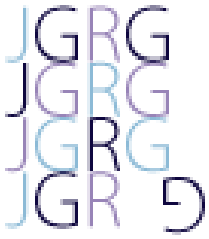

Yuichi Takamizu, JGRG 22(2012)111205

"Non-linear superhorizon perturbation and nonlinear gauge transformation"

RESCEU SYMPOSIUM ON

GENERAL RELATIVITY AND GRAVITATION

JGRG 22

November 12-16 2012

Koshiba Hall, The University of Tokyo, Hongo, Tokyo, Japan





Nonlinear superhorizon perturbation and nonlinear gauge transformation

Yuichi Takamizu [1] [(a)] , Atsushi Naruko [2] [(b)] , Misao Sasaki [3] [(a)]

[(a)] *Yukawa Institute for Theoretical Physics Kyoto University, Kyoto 606-8502, Japan*
[(b)] *APC (CNRS-Université Paris 7), 10 rue Alice Domon et Léonie Duquet, 75205 Paris Cedex 13, France*

Abstract

We develop a theory of nonlinear cosmological perturbations on superhorizon scales for a multi-component scalar field with a general kinetic term and a general form of the potential in the context of inflationary cosmology. We employ the ADM formalism and the spatial gradient expansion approach valid up to second-order in the expansion. We provide a formalism to obtain the solution in the multi-field case and also derive fully nonlinear gauge transformation rules valid through second-order. These fully nonlinear gauge transformation rules can be used to derive the solution in a desired gauge from the one in a gauge where computations are much simpler.

1 Introduction

Recent observations of the cosmic microwave background anisotropy show a very good agreement of the observational data with the predictions of conventional, single-field slow-roll models of inflation, that is, adiabatic Gaussian random primordial fluctuations with an almost scale-invariant spectrum. Nevertheless, possible non-Gaussianities from inflation has been a focus of much attention in recent years. To study possible origins of non-Gaussianity, one must go beyond the linear perturbation theory. In particular, in the classical production on superhorizon scales case, the δN formalism [1] turned out to be a powerful tool for computing non-Gaussianities thanks to its full non-linear nature, where one can employ the spatial gradient expansion approach. The length scale of the perturbation is longer than the Hubble radius. In the context of inflation, based on the leading order in gradient expansion, the δN formalism [1] was developed. This leading order in the expansion provides a general conclusion for the evolution on superhorizon scales that the adiabatic growing mode is conserved on the comoving hypersurface. In multi-field inflation, a non-slow-roll stage may appear when there is a change in the dominating component of the scalar field. The previous analyses are essentially based on the δN formalism and it is in general necessary to extend it to second-order in the expansion, that is, to the *beyond* δN formalism. As for a single scalar field, it has been developed in [2]. We focus on the case of a multi-component scalar field following recent our paper [3].

2 Basics

We develop a theory of nonlinear cosmological perturbations on superhorizon scales. For this purpose we employ the ADM formalism and the gradient expansion approach. In the ADM decomposition, the metric is expressed as $ds^2 = -\alpha^2 dt^2 + \hat{\gamma}_{ij}(dx^i + \beta^i dt)(dx^j + \beta^j dt)$, where α is the lapse function, β^i is the shift vector and Latin indices run over 1,2 and 3. We introduce the extrinsic curvature K_{ij} defined by $K_{ij} = (\partial_t \hat{\gamma}_{ij} - \hat{D}_i\beta_j - \hat{D}_j\beta_i)/2\alpha$, where $\hat{D}$ is the covariant derivative with respect to the spatial metric $\hat{\gamma}_{ij}$. In addition to the standard ADM decomposition, the spatial metric and the extrinsic curvature are further decomposed so as to separate trace and trace-free parts $\hat{\gamma}_{ij} = a^2(t)e^{2\psi}\gamma_{ij}$ and $K_{ij} = a^2(t)e^{2\psi}(K\gamma_{ij}/3 + A_{ij})$, where $a(t)$ is the scale factor of a fiducial homogeneous FLRW spacetime, the determinant of γ_{ij} is normalised to be unity and A_{ij} is trace free. As for a matter field, let us focus on a minimally-coupled multi-component scalar field, described by $S_m = \int d^4x\sqrt{-g}P(X^{IJ}, \phi^K)$, $X^{IJ} \equiv -g^{\mu\nu}\partial_\mu\phi^I\partial_\nu\phi^J$, with ϕ^K denoting the K-th component of the scalar field. Note that we do not assume a specific form of both the kinetic term and potential, which are arbitrary functions of X^{IJ} and ϕ^K. The

[1]Email address: takamizu@yukawa.kyoto-u.ac.jp
[2]Email address: naruko@apc.univ-paris7.fr
[3]Email address: misao@yukawa.kyoto-u.ac.jp

equation of motion for the scalar field is given by $\frac{2}{\sqrt{-g}}\partial_\mu\big(\sqrt{-g}P_{(IJ)}g^{\mu\nu}\partial_\nu\phi^J\big)+P_I=0$, where the subscript I in P_I represents a derivative with respect to ϕ^I and $P_{(IJ)}$ is defined as $P_{(IJ)}=(\frac{\partial P}{\partial X^{IJ}}+\frac{\partial P}{\partial X^{JI}})/2$. Now we write down the Einstein equations. In the ADM decomposition, the Einstein equations are separated into four constraints, the Hamiltonian constraint and three momentum constraints, and six dynamical equations for the spatial metric.

In the gradient expansion approach we suppose that the characteristic length scale L of a perturbation is longer than the Hubble length scale $1/H$ of the background, i.e. $HL\gg 1$. Therefore, $\epsilon\equiv 1/(HL)$ is regarded as a small parameter and we can systematically expand equations in the order of ϵ, identifying a spatial derivative is of order ϵ, $\partial_i Q=\mathcal{O}(\epsilon)Q$. To clarify the order of gradient expansion, we introduce the superscript (n). For example, ${}^{(2)}\alpha$ means the lapse function at second order in gradient expansion. As a background spacetime, we consider a FLRW universe. This leads to the following condition on the spatial metric: $\partial_t\gamma_{ij}=\mathcal{O}(\epsilon^2)$. Since we adopt this assumption, the spatial metric at leading order is given by an arbitrary spatial function of the spatial coordinates. Throughout this paper, in order to simplify the equations, we set the shift vector to zero up to second order in gradient expansion, $\beta^i=\mathcal{O}(\epsilon^3)$. Let us call this choice of the spatial coordinates as the *time-slice-orthogonal threading*.

2.1 Leading order in gradient expansion

In this subsection, we study the leading order gradient expansion and make clear the correspondence between the leading order equations and background equations. This correspondence can be used to construct the solution at leading order in gradient expansion in terms of the background solution. We will introduce the proper time τ by $\tau(t,x^i)\equiv\int_{x^i=const.}dt\ \alpha(t,x^i)$. In terms of τ, the expression of K is simplified under the time-slice-orthogonal threading condition $K=\frac{1}{\alpha}\frac{\partial_t(a^3e^{3\psi})}{a^3e^{3\psi}}=3\frac{\partial_\tau(ae^\psi)}{ae^\psi}$. Under the identification, $ae^\psi\Leftrightarrow a$ and $\tau\Leftrightarrow t$, one also has the correspondence, $K\Leftrightarrow 3H$. This means that the basic equations at leading order take exactly the same form as those in the background modulo above identifications. Namely, given a background solution, $\phi^I(t)\big|_{\rm background}=\phi^I_{\rm BG}\big[t,\,\phi^I_0(t_0)\big]$, one can construct the solution at leading order in gradient expansion as $\phi^I(t,x^i)\big|_{\rm gradient}=\phi^I_{\rm BG}\big[\tau,\,\phi^I_0(\tau_0)\big]$. All the information of inhomogeneities is contained in the initial condition as well as in the proper time τ. Thus it is sufficient to solve the background equations to obtain the solution at leading order in gradient expansion. In passing, we note that the e-folding number is often used as the time coordinate to describe the background evolution. For convenience, we define it as the number of e-folds counted backward in time from a fixed final time. That is, $N=\int_t^{t_0}dt'H(t')$. Accordingly, the scale factor is expressed as $a(N)=a_0e^{-(N-N_0)}$. By replacing t with τ and H with $K/3$ we can generalise the e-fold number to the one defined locally in space as $\mathcal{N}\equiv\int_t^{t_0}\alpha(t',x^i)dt'\,\frac{1}{3}K(t,x^i)\big|_{x^i=const.}$. Again one can check the validity of the above correspondence in terms of $\mathcal{N}$ as the time coordinate.

2.2 Towards the next-to-leading order in gradient expansion

One needs to specify the gauge condition to study perturbations in perturbation theory or in gradient expansion. Since spatial coordinates have been already fixed by the time-slice-orthogonal threading, one has to determine the time-slicing condition. Here, let us list various slicings and their definitions, Uniform expansion; $K(t,x^i)=3H(t)$, Uniform e-folding number; $\mathcal{N}(t,x^i)=N(t)$. Hereinafter, we call the uniform expansion and uniform e-folding number slicings as the uniform K and uniform $\mathcal{N}$ slicings, respectively. We mention that there is a remaining gauge degree of freedom in the synchronous or uniform $\mathcal{N}$ slicing, while the time slices are completely fixed in the uniform K slicing. As for the uniform $\mathcal{N}$ slicing, the gauge condition demands $\partial_t\psi$ to vanish. As we have seen in subsection 2.1, the leading order solutions are given by functions of τ in terms of the background solutions. At next-to-leading order in gradient expansion, terms with spatial derivatives of the leading order solution appear in the evolution equations. To evaluate those terms, one needs to calculate the spatial derivative of the lapse function, for example in $\partial_i\phi$, $\partial_i\phi_{BG}(\tau)=\partial_\tau\phi_{BG}(\tau)\,\partial_i\tau=\partial_\tau\phi_{BG}(\tau)\int dt\partial_i\alpha$. However the leading order ${}^{(0)}\alpha$ is in general given explicitly only after solving the following equation for α:

$$\alpha=f\Big[t,\,\phi(\tau)\Big]=f\Big[t,\,\phi\Big(\int\alpha dt\Big)\Big]. \tag{1}$$

It is clearly shown that it is almost impossible to solve this equation, at least in an analytical way. This problem did not appear in the single-field case. It is because one can show that various different slicings become identical at leading order in gradient expansion. It means that for all the slicings, we may set $\alpha = 1$ if desired. On the other hand, one has to face this problem in the case of multi-field inflation. We overcome this problem by uniform $\mathcal{N}$ slicing, which gives us a *homogeneous time* coordinate. On these slicings, one can evaluate the spatial derivatives of the leading order solution which appear as source terms and construct a solution to next-to-leading order in gradient expansion by integrating those terms.

3 Nonlinear gauge transformation

We derive the gauge transformation rules for the metric, its derivative (K and A_{ij}) and the scalar field. We consider a nonlinear gauge transformation from a coordinate system with vanishing shift vector $\beta^i = 0$, to another coordinate system in which the new shift vector also vanishes, $\tilde{\beta}^i = 0$. We note that once the time slicing is changed, the shift vector appears in the new slicing in general. So the spatial coordinates also need to be changed to eliminate thus appeared shift vector. We use the background e-folding number N as the time coordinate and define the temporal and spatial shift, n and L^i, respectively, $\tilde{N} + \tilde{n}(\tilde{N}, \tilde{x}^i) = N\,, \tilde{x}^i + \tilde{L}^i(\tilde{N}, \tilde{x}^i) = x^i$. Under the change of the coordinates, the line element should remain invariant, $ds^2 = -\frac{\alpha^2}{H^2(N)}dN^2 + a^2(N)e^{2\psi}\gamma_{ij}dx^i dx^j = -\frac{\tilde{\alpha}^2}{H^2(\tilde{N})}d\tilde{N}^2 + a^2(\tilde{N})e^{2\tilde{\psi}}\tilde{\gamma}_{ij}d\tilde{x}^i d\tilde{x}^j$. Equating the coefficients of $d\tilde{N}^2$, $d\tilde{N}d\tilde{x}^i$, and $d\tilde{x}^i d\tilde{x}^j$ on both sides of the above, we obtain the nonlinear gauge transformation rules. As a result, let us summarize the derived rules. The leading order transformation rules are

$$\tilde{\alpha}(\tilde{N}, \tilde{x}^i) = \frac{H(\tilde{N})}{H({}^{(0)}\tilde{N})}(1 + \partial_{\tilde{N}}{}^{(0)}\tilde{n})\ \alpha + \mathcal{O}(\epsilon^2)\,,\ \tilde{\psi}(\tilde{N}, \tilde{x}^i) = \psi - {}^{(0)}\tilde{n} + \mathcal{O}(\epsilon^2)\,, \tag{2}$$

$$\tilde{\gamma}_{ij}(\tilde{N}, \tilde{x}^i) = \gamma_{ij} + \mathcal{O}(\epsilon^2)\,,\ \tilde{K}(\tilde{N}, \tilde{x}^i) = K + \mathcal{O}(\epsilon^2)\,,\ \tilde{\phi}(\tilde{N}, \tilde{x}^i) = \phi + \mathcal{O}(\epsilon^2)\,. \tag{3}$$

The next-to-leading order transformation rules are

$$\begin{aligned}{}^{(2)}\tilde{\alpha}(\tilde{N}, \tilde{x}^i) = {}& \frac{\alpha H(\tilde{N})}{H({}^{(0)}\tilde{N})}(1 + \partial_{\tilde{N}}{}^{(0)}\tilde{n})\left(\frac{{}^{(2)}\alpha}{\alpha} + {}^{(2)}\tilde{n}\frac{\partial_N \alpha}{\alpha} - {}^{(2)}\tilde{n}\frac{\partial_N H({}^{(0)}\tilde{N})}{H({}^{(0)}\tilde{N})} + \frac{\partial_{\tilde{N}}{}^{(2)}\tilde{n}}{1 + \partial_{\tilde{N}}{}^{(0)}\tilde{n}}\right) \\ & - \frac{1}{2}\frac{\alpha^3 H(\tilde{N})(1 + \partial_{\tilde{N}}{}^{(0)}\tilde{n})}{a^2({}^{(0)}\tilde{N})e^{2\psi}H^3({}^{(0)}\tilde{N})}\gamma^{ij}\partial_{\tilde{i}}{}^{(0)}\tilde{n}\partial_{\tilde{j}}{}^{(0)}\tilde{n} + \tilde{L}^i(\partial_{\tilde{i}}\alpha)\frac{H(\tilde{N})}{H({}^{(0)}\tilde{N})}(1 + \partial_{\tilde{N}}{}^{(0)}\tilde{n}) + \mathcal{O}(\epsilon^4)\,,\end{aligned} \tag{4}$$

$${}^{(2)}\tilde{\psi}(\tilde{N}, \tilde{x}^i) = {}^{(2)}\psi - {}^{(2)}\tilde{n} + {}^{(2)}\tilde{n}\partial_N\psi + \tilde{L}^i\partial_{\tilde{i}}\psi + \frac{1}{3}\partial_{\tilde{i}}\tilde{L}^i - \frac{1}{6}\frac{\alpha^2\gamma^{ij}\partial_{\tilde{i}}{}^{(0)}\tilde{n}\partial_{\tilde{j}}{}^{(0)}\tilde{n}}{a^2({}^{(0)}\tilde{N})e^{2\psi}H^2({}^{(0)}\tilde{N})} + \mathcal{O}(\epsilon^4)\,, \tag{5}$$

$$\begin{aligned}{}^{(2)}\tilde{\gamma}_{ij}(\tilde{N}, \tilde{x}^i) = {}& {}^{(2)}\gamma_{ij} + {}^{(2)}\tilde{n}\partial_{\tilde{N}}\gamma_{ij} + \tilde{L}^k\partial_{\tilde{k}}\gamma_{ij} + \gamma_{jk}\partial_{\tilde{i}}\tilde{L}^k + \gamma_{ik}\partial_{\tilde{j}}\tilde{L}^k - \frac{2}{3}\partial_{\tilde{k}}\tilde{L}^k\gamma_{ij} \\ & - \frac{\alpha^2}{a^2({}^{(0)}\tilde{N})e^{2\psi}H^2({}^{(0)}\tilde{N})}\left(\partial_{\tilde{i}}{}^{(0)}\tilde{n}\partial_{\tilde{j}}{}^{(0)}\tilde{n} - \frac{1}{3}\gamma^{kl}\partial_{\tilde{k}}{}^{(0)}\tilde{n}\partial_{\tilde{l}}{}^{(0)}\tilde{n}\gamma_{ij}\right) + \mathcal{O}(\epsilon^4)\,,\end{aligned} \tag{6}$$

and

$$\begin{aligned}{}^{(2)}\tilde{K}(\tilde{N}, \tilde{x}^i) = {}& {}^{(2)}K + {}^{(2)}\tilde{n}\partial_N{}^{(0)}K + \tilde{L}^i\partial_{\tilde{i}}{}^{(0)}K + \frac{3H({}^{(0)}\tilde{N})}{(1 + \partial_{\tilde{N}}{}^{(0)}n)\alpha}\left(\partial_{\tilde{N}}{}^{(0)}\tilde{n}\frac{{}^{(2)}\alpha}{\alpha} - \frac{\partial_{\tilde{N}}{}^{(2)}\tilde{n}}{1 + \partial_{\tilde{N}}{}^{(0)}\tilde{n}}\right) \\ & + \frac{3\alpha\gamma^{ij}\partial_{\tilde{i}}{}^{(0)}\tilde{n}\partial_{\tilde{j}}{}^{(0)}\tilde{n}}{2(1 + \partial_{\tilde{N}}{}^{(0)}n)a^2({}^{(0)}\tilde{N})e^{2\psi}H({}^{(0)}\tilde{N})} + \frac{\partial_{\tilde{i}}{}^{(0)}\tilde{n}\partial_{\tilde{j}}{}^{(0)}\tilde{n}}{2\alpha a^2({}^{(0)}\tilde{N})H({}^{(0)}\tilde{N})}\partial_N\left(\frac{\alpha^2}{e^{2\psi}}\gamma^{ij}\right) \\ & + \frac{3H({}^{(0)}\tilde{N})}{(1 + \partial_{\tilde{N}}{}^{(0)}n)\alpha}\left[\partial_{\tilde{N}}{}^{(2)}\tilde{n}(1 - \partial_N\psi) - (\partial_{\tilde{N}}\tilde{L}^i)\partial_{\tilde{i}}\psi - \frac{1}{3}\partial_{\tilde{i}}\partial_{\tilde{N}}\tilde{L}^i\right] \\ & + \frac{H({}^{(0)}\tilde{N})\alpha\gamma^{ij}}{2(1 + \partial_{\tilde{N}}{}^{(0)}n)e^{2\psi}}\partial_{\tilde{N}}\left(\frac{\partial_{\tilde{i}}{}^{(0)}\tilde{n}\partial_{\tilde{j}}{}^{(0)}\tilde{n}}{a^2({}^{(0)}\tilde{N})H^2({}^{(0)}\tilde{N})}\right) + \mathcal{O}(\epsilon^4)\,,\end{aligned} \tag{7}$$

$$\begin{aligned}\tilde{A}_{ij}(\tilde{N}, \tilde{x}^i) = {}& A_{ij} - \frac{H({}^{(0)}\tilde{N})}{2(1 + \partial_{\tilde{N}}{}^{(0)}\tilde{n})\alpha}\left(\partial_{\tilde{N}}\tilde{L}^k\partial_{\tilde{k}}\gamma_{ij} + \gamma_{jk}\partial_{\tilde{i}}\partial_{\tilde{N}}\tilde{L}^k + \gamma_{ik}\partial_{\tilde{j}}\partial_{\tilde{N}}\tilde{L}^k\right)^{TF} \\ & - \frac{H({}^{(0)}\tilde{N})}{2(1 + \partial_{\tilde{N}}{}^{(0)}\tilde{n})\alpha}\partial_{\tilde{N}}\left[\frac{\alpha^2}{a^2({}^{(0)}\tilde{N})e^{2\psi}H^2({}^{(0)}\tilde{N})}\left(\partial_{\tilde{i}}{}^{(0)}\tilde{n}\partial_{\tilde{j}}{}^{(0)}\tilde{n}\right)^{TF}\right] + \mathcal{O}(\epsilon^4)\,,\end{aligned} \tag{8}$$

$${}^{(2)}\tilde{\phi}(\tilde{N}, \tilde{x}^i) = {}^{(2)}\phi + {}^{(2)}\tilde{n}\partial_N{}^{(0)}\phi + \tilde{L}^i\partial_{\tilde{i}}{}^{(0)}\phi + \mathcal{O}(\epsilon^2)\,, \tag{9}$$

where $\tilde{L}^i$ is given by

$$\tilde{L}^i = l^i(\tilde{x}^i) + \int_{\tilde{N}_0}^{\tilde{N}} d\hat{N} \frac{\alpha^2(1+\partial_{\hat{N}}\tilde{n})}{a^2({}^{(0)}\hat{N})e^{2\psi}H^2({}^{(0)}\hat{N})}\gamma^{ij}\partial_j\tilde{n} + \mathcal{O}(\epsilon^3)\,. \tag{10}$$

4 Beyond δN formalism

Let us briefly summarise the five steps in the *Beyond δN formalism*.

1. Write down the basic equations (the Einstein equations and scalar field equation) in the uniform $\mathcal{N}$ slicing with the time-slice-orthogonal threading. For convenience let us call the choice of the coordinates in which one adopts the uniform X slicing with the time-slice-orthogonal threading the X gauge. So the above choice is the $\mathcal{N}$ gauge. In this gauge the metric components at leading order are trivial since both ψ and γ_{ij} are independent of time.
2. First solve the leading order scalar field equation under an appropriate initial condition and then the next-to-leading order scalar field equation which involves spatial gradients of the leading order solution.
3. Solve the next-to-leading order Einstein equations for the metric components and their derivatives.
4. Determine the gauge transformation from the $\mathcal{N}$ gauge to the K gauge and apply the gauge transformation rules to obtained the solution the obtained solution in the K gauge.
5. Evaluate the curvature perturbation $\mathfrak{R} = \psi + \chi/3$ in the K gauge, where χ is to be extracted from γ_{ij}.

5 Summary and discussion

In this paper, we developed a theory of nonlinear cosmological perturbations on superhorizon scales in the context of inflationary cosmology. We considered a multi-component scalar field with a general kinetic term and a general form of the potential. To discuss the superhorizon dynamics, we employed the ADM formalism and the spatial gradient expansion approach.

Different from the single-field case, there is a difficulty in solving the equations in the multi-field case. At leading-order, the equations take the same form as those for the homogeneous and isotropic FLRW background with suitable identifications of variables. In cosmological perturbation theory, the most important quantity to be evaluated is the curvature perturbation on the comoving slices which is conserved on superhorizon scales after the universe has reached the adiabatic limit. This quantity accurate to next-to-leading order may be relatively easily obtained in the single-field case because of the above mentioned coincidence among several temporal slicings. On the other hand, in the multi-field case, such a coincidence between different slicings does not hold.

In this paper, we developed a formalism to go beyond the leading order which avoids the problem. Namely, we first solve the field equations in a slicing in which the lapse function is trivial. The synchronous slicing is one of such slicings, but we adopt the uniform e-folding number slicing in which the time slices are chosen in such a way that the number of e-folds along each orbit orthogonal to the time slices, $\mathcal{N}$, is spatially homogeneous on each time slice. In this slicing we can solve the equations to next-to-leading order without encountering the above mentioned problem. After the solution to next-to-leading order is obtained, we transform it to the one in the uniform expansion slicing which is known to be identical to the comoving slicing on superhorizon scales in the adiabatic limit. Thus the gauge transformation laws play an essential role in our formalism. We derived them which are accurate to next-to-leading order. Note that they are fully nonlinear in nature in the language of the standard perturbation approach.

References

[1] M. Sasaki and E. D. Stewart, Prog. Theor. Phys. **95**, 71 (1996).

[2] Y. Takamizu, S. Mukohyama, M. Sasaki, and Y. Tanaka, JCAP **1006**, 019 (2010).

[3] A. Naruko, Y. Takamizu and M. Sasaki, arXiv: 1210.6525, which has been determined to be published as PTEP (2013).

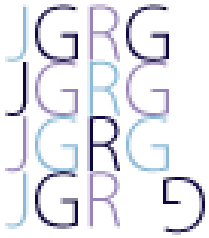

Shi Pi, JGRG 22(2012)111206

"Curvature perturbation spectrum in two-field inflation with a turning trajectory"

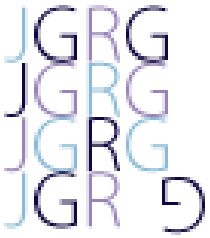

RESCEU SYMPOSIUM ON

GENERAL RELATIVITY AND GRAVITATION

JGRG 22



November 12-16 2012

Koshiba Hall, The University of Tokyo, Hongo, Tokyo, Japan



Curvature Perturbation Spectrum in Two-field Inflation with a Turning Trajectory

Shi Pi(皮石)

Physics Department,
Peking University

November 12th, 2012

Collaborate with Misao Sasaki,

based on arXiv:1205.0161,

JGRG 2012, RESCUE, University of Tokyo.

Outline

1 Introduction

2 Quasi-single Field Inflation with Large Isocurvaton Mass

3 Non-Gaussianity of Equilateral Shape

4 Conclusion

Primary Parameters

Define the parameters

- Slow-roll parameter along the trajectory ϵ and η.
- Angular speed of rotation in field space $\dot{\theta} \sim V_s$.
- Effective mass perpendicular to the trajectory $M_{\rm eff} = V_{ss} + 3\dot{\theta}$.

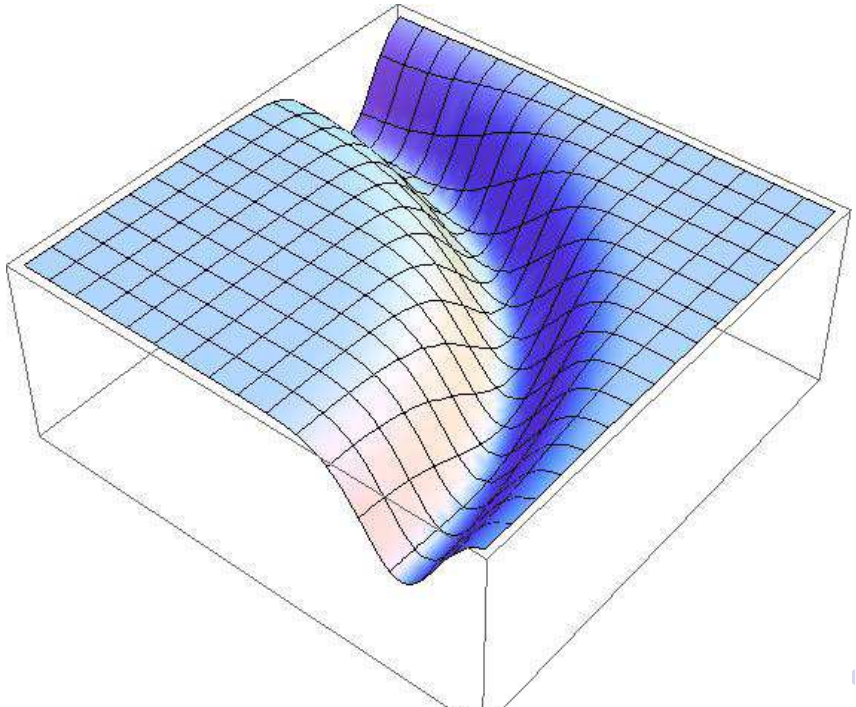

Classification

The ordinary 2-field inflation can be classified by these parameters in the slow-roll region as

1. $\dot{\theta} \ll H$, $M_{\text{eff}} \ll H$: 2-field inflation with a negligible coupling between adiabatic and curvature perturbations inside the horizon. Gordon 2001.
2. $\dot{\theta} \ll H$, $M_{\text{eff}} \sim H$: Quasi-single field inflation in the original form. Chen 2010.
3. $\dot{\theta} \ll H$, $M_{\text{eff}} \gg H$: After integrating the heavy field out, one can get an effective single field with a corrective speed of sound. Achucarro 2011,2012. Cespedes 2012.

Classification

The ordinary 2-field inflation can be classified by these parameters in the slow-roll region as

1. $\dot{\theta} \ll H$, $M_{\rm eff} \ll H$: 2-field inflation with a negligible coupling between adiabatic and curvature perturbations inside the horizon. Gordon 2001.
2. $\dot{\theta} \ll H$, $M_{\rm eff} \sim H$: Quasi-single field inflation in the original form. Chen 2010.
3. $\dot{\theta} \ll H$, $M_{\rm eff} \gg H$: After integrating the heavy field out, one can get an effective single field with a corrective speed of sound. Achucarro 2011,2012. Cespedes 2012.

We are suppose to connect 2 and 3.

“Massless” Slowball



Quasi-single Panda



Coaster with “Large Isocurvaton Mass”.



EFT result

In EFT, after integrating out the heavy field (σ in our case), one have an effective single field inflation with an effective speed of sound c_s which is

$$c_s^{-2} = 1 + \frac{4H^2}{\tilde{M}_{\rm eff}^2}\left(\frac{\dot{\theta}}{H}\right)^2, \tag{1}$$

Finally we got via EFT that

$$\delta\mathcal{P}_{\mathcal{R}} \propto c_s^{-1} - 1 \sim 2\left(\frac{\dot{\theta}}{\tilde{M}_{\rm eff}}\right)^2.$$

Our main task is to verify this relation by in-in formulism.

Outline

1 Introduction

2 Quasi-single Field Inflation with Large Isocurvaton Mass

3 Non-Gaussianity of Equilateral Shape

4 Conclusion

Lagrangian

The action for the fields can be decomposed into

$$S_m = \int d^4x\sqrt{-g}\left[-\frac{1}{2}(\tilde{R}+\sigma)^2 g^{\mu\nu}\partial_\mu\theta\partial_\nu\theta - \frac{1}{2}g^{\mu\nu}\partial_\mu\sigma\partial_\nu\sigma - V_{\rm sr}(\theta) - V(\sigma)\right],$$

where

- $R\theta$(tangent field) and σ(radial field),
- $V_{\rm sr}(\theta)$ is a slow-roll potential along the valley,
- $V(\sigma)$ is a potential that forms the valley and traps the isocurvaton at $\sigma = \sigma_0$,
- $\tilde{R}$ denotes the radius of the minima valley,
- $R = \tilde{R} + \sigma_0$ is the constant radius where the trajectory is trapped with the centripetal force under consideration.

EOM

The Hubble equations and equations of motion are

$$\begin{aligned} 3M_p^2H^2 &= \frac{1}{2}R^2\dot{\theta}_0^2 + V + V_{\rm sr}, \\ -2M_p^2\dot{H} &= R^2\dot{\theta}_0^2, \\ 0 &= R^2\ddot{\theta}_0 + 3R^2H\dot{\theta}_0 + V'_{\rm sr}, \\ 0 &= \ddot{\sigma}_0 + 3H\dot{\sigma}_0 + V' - R^2\dot{\theta}_0^2\,, \end{aligned}$$

We can see in the tangent direction of the trajectory, field $R\theta$ obeys the ordinary equation of motion for single-field inflation.

Perturbative Hamiltonian

Hamiltionian density in interaction picture (spatially flat gauge)

$$\begin{aligned}
\mathcal{H}_0 &= a^3\left[\frac{1}{2}R^2\dot{\delta\theta}^2+\frac{R^2}{2a^2}(\partial_i\delta\theta)^2+\frac{1}{2}\dot{\delta\sigma}^2+\frac{1}{2a^2}(\partial_i\delta\sigma)^2+\frac{1}{2}M_{\rm eff}^2\delta\sigma^2\right],\\
\mathcal{H}_2^I &= -c_2a^3\delta\sigma\dot{\delta\theta}, \qquad c_2=2R\dot{\theta},\\
\mathcal{H}_3^I &= -a^3R\delta\sigma\dot{\delta\theta}^2-a^3\dot{\theta}\dot{\delta\theta}\delta\sigma^2+aR\delta\sigma\left(\partial_i\delta\theta\right)^2+\frac{a^3}{6}V'''\delta\sigma^3,\\
M_{\rm eff}^2 &= V''+3\dot{\theta}^2,
\end{aligned}$$

Our method is valid when

$$\left(\frac{\dot{\theta}}{H}\right)^2\ll 1, \quad \frac{|V'''|}{H}\ll 1. \tag{2}$$

Perturbative Hamiltonian

Hamiltionian density in interaction picture (spatially flat gauge)

$$
\begin{aligned}
\mathcal{H}_0 &= a^3\left[\frac{1}{2}R^2\dot{\delta\theta}^2+\frac{R^2}{2a^2}(\partial_i\delta\theta)^2+\frac{1}{2}\dot{\delta\sigma}^2+\frac{1}{2a^2}(\partial_i\delta\sigma)^2+\frac{1}{2}M_{\rm eff}^2\delta\sigma^2\right],\\
\mathcal{H}_2^I &= -c_2a^3\delta\sigma\dot{\delta\theta}, \qquad c_2=2R\dot{\theta}\ =\text{constant},\\
\mathcal{H}_3^I &= -a^3R\delta\sigma\dot{\delta\theta}^2-a^3\dot{\theta}\dot{\delta\theta}\delta\sigma^2+aR\delta\sigma\left(\partial_i\delta\theta\right)^2+\frac{a^3}{6}V'''\delta\sigma^3,\\
M_{\rm eff}^2 &= V''+3\dot{\theta}^2\ =\text{constant},
\end{aligned}
$$

In a constant turn case!

Illustrative Explanation

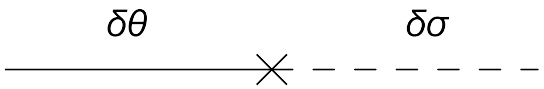

Figure: The second order interacting vertex $\mathcal{H}_2 = -c_2 a^3 \delta\sigma\dot{\theta}$, while $c_2 = 2R\dot{\theta}$.

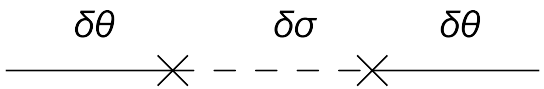

Figure: The 2-pt func with a heavy isocurvaton mediation.

And the curvature perturbation $\mathcal{R}$ is connected to θ via

$$\mathcal{R} = -\frac{H}{\dot{\theta}}\delta\theta.$$

Quantization

- Quantize the Fourier components

$$\begin{aligned}\delta\theta^I_{\mathbf{k}} &= u_{\mathbf{k}}a_{\mathbf{k}} + u^*_{-\mathbf{k}}a^\dagger_{-\mathbf{k}},\\ \delta\sigma^I_{\mathbf{k}} &= v_{\mathbf{k}}b_{\mathbf{k}} + v^*_{-\mathbf{k}}b^\dagger_{-\mathbf{k}}.\end{aligned}$$

- The commutators

$$[a_{\mathbf{k}}, a^\dagger_{-\mathbf{k}'}] = (2\pi)^3\delta^3(\mathbf{k}+\mathbf{k}'), \quad [b_{\mathbf{k}}, b^\dagger_{-\mathbf{k}'}] = (2\pi)^3\delta^3(\mathbf{k}+\mathbf{k}').$$

Quantization

The equation for mode functions,

$$\begin{aligned} u''_{\mathbf{k}} - \frac{2}{\tau}u'_{\mathbf{k}} + k^2 u_{\mathbf{k}} &= 0, \\ v''_{\mathbf{k}} - \frac{2}{\tau}v'_{\mathbf{k}} + k^2 v_{\mathbf{k}} + \frac{M^2_{\rm eff}}{H^2\tau^2}v_{\mathbf{k}} &= 0. \end{aligned}$$

Solve The EOMs by setting the initial conditions

$$Ru_{\mathbf{k}}\,, \quad v_{\mathbf{k}} \to i\frac{H}{\sqrt{2k}}\tau e^{-ik\tau},$$

when $k \gg Ha$.

Solution

The solution is

$$u_{\mathbf{k}} = \frac{H}{R\sqrt{2k^3}}(1+ik\tau)e^{-ik\tau},$$

and

$$v_{\mathbf{k}} = -ie^{i(\nu+\frac{1}{2})\frac{\pi}{2}}\frac{\sqrt{\pi}}{2}H(-\tau)^{3/2}H_{\nu}^{(1)}(-k\tau), \quad \text{for } M_{\text{eff}}^2/H^2 \leq 9/4,$$

where $\nu = \sqrt{9/4 - M_{\text{eff}}^2/H^2}$, or

$$v_{\mathbf{k}} = -ie^{-\frac{\pi}{2}\mu+i\frac{\pi}{4}}\frac{\sqrt{\pi}}{2}H(-\tau)^{3/2}H_{i\mu}^{(1)}(-k\tau), \quad \text{for } M_{\text{eff}}^2/H^2 > 9/4,$$

where $\mu = \sqrt{M_{\text{eff}}^2/H^2 - 9/4}$.

2-point function

We use in-in formulism to calculate the 2-point function of $\delta\theta^2$

$$\begin{aligned}\langle\delta\theta^2\rangle &\equiv \langle 0|\left[\bar{T}\exp\left(i\int_{t_0}^{t}dt'H_I(t')\right)\right]\delta\theta_I^2(t)\left[T\exp\left(-i\int_{t_0}^{t}dt'H_I(t')\right)\right]|0\rangle \\ &\sim \mathcal{P}_{\mathcal{R}}{}^{(0)}+\delta\mathcal{P}_{\mathcal{R}} \\ &= \frac{H^4}{4\pi^2R^2\dot{\theta}^2}\left[1+\frac{\delta\mathcal{P}_{\mathcal{R}}}{\mathcal{P}_{\mathcal{R}}{}^{(0)}}\right].\end{aligned}$$

Feynman Rules

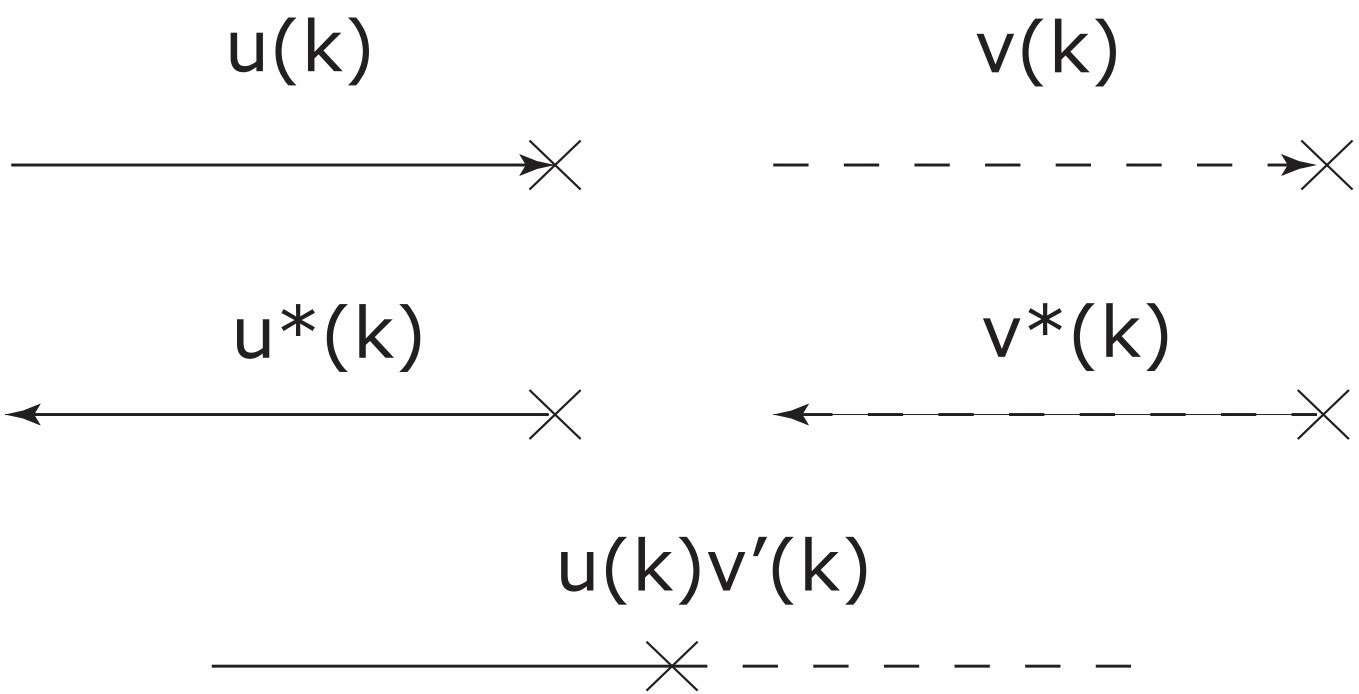

Correction to Power Spectrum

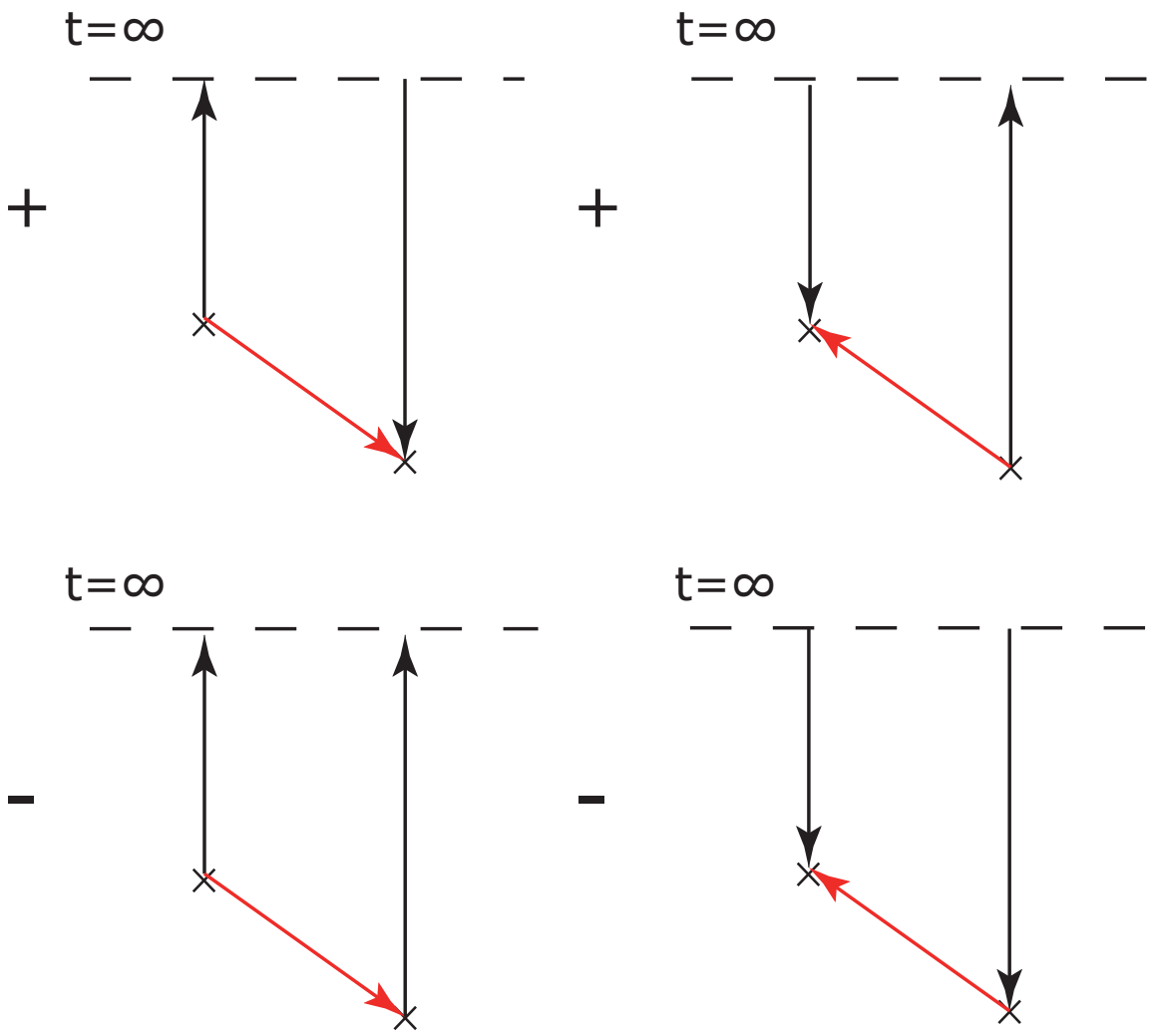

Calculating α

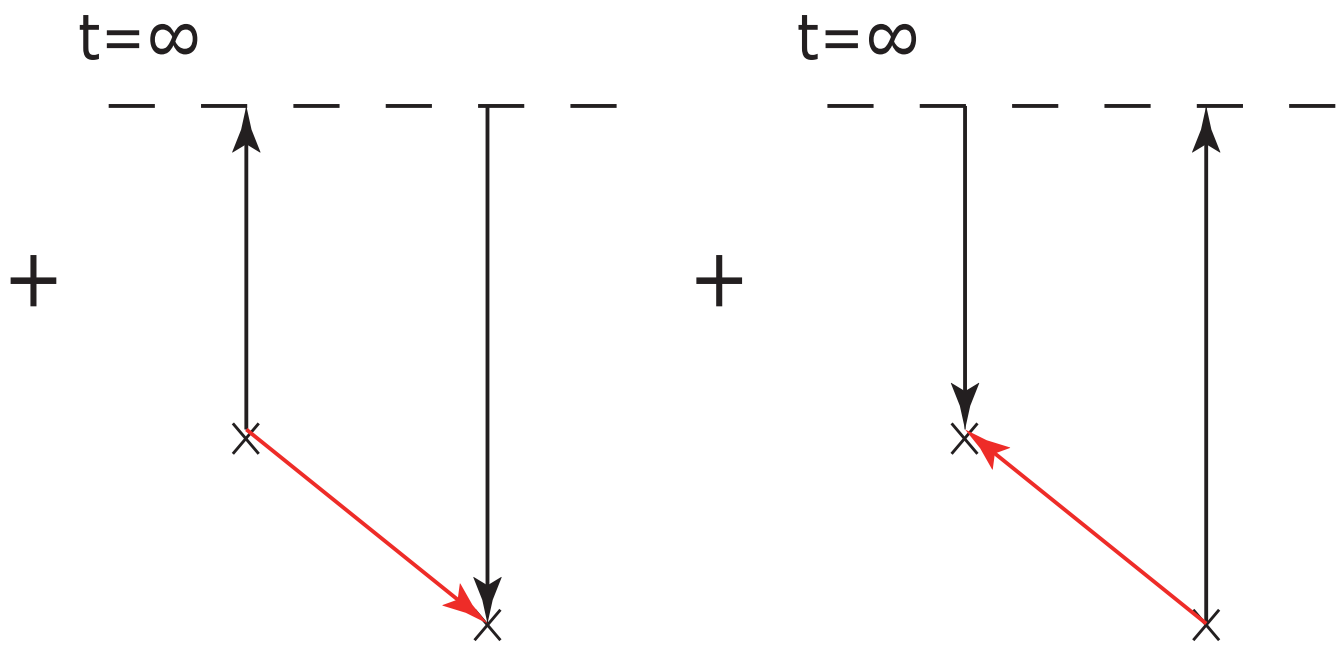

Interchange the momenta

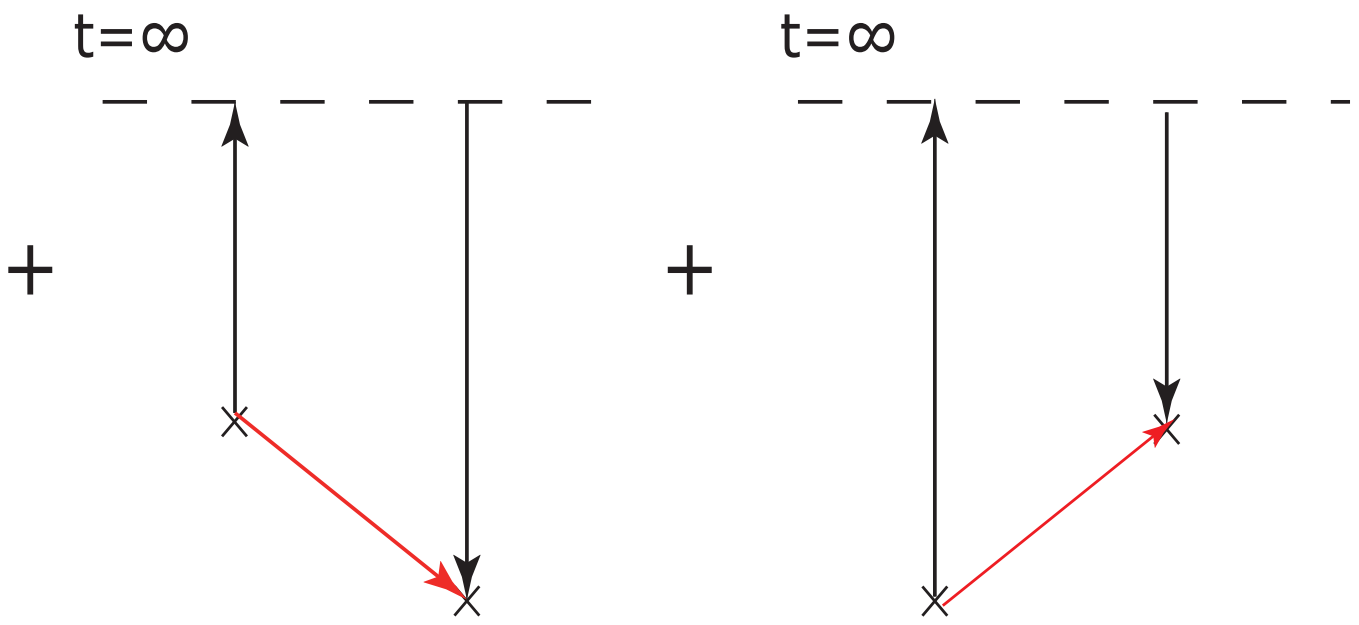

"Split" the integral

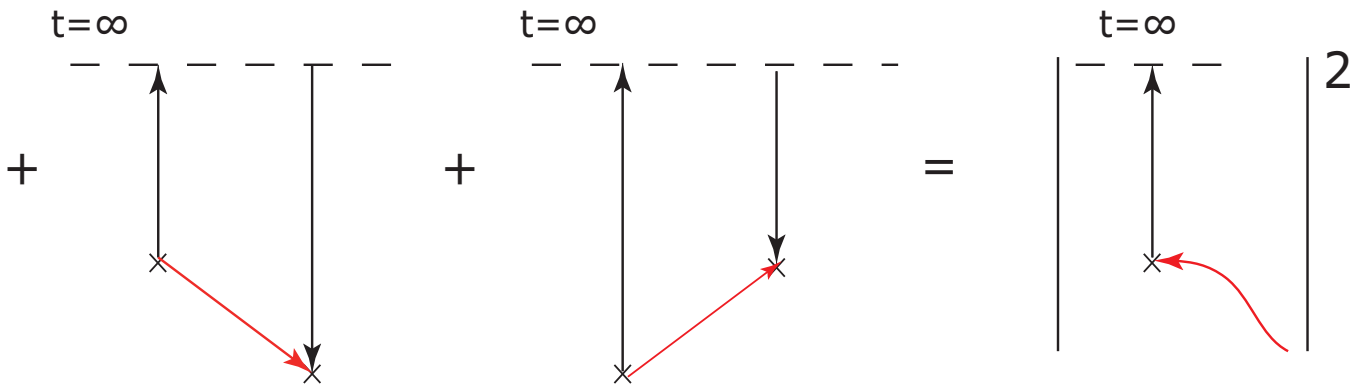

The Cut-in-the-Middle integral α is

$$\alpha = \left| \int_0^\infty dx\, x^{-1/2} H_{i\mu}^{(1)}(x) e^{ix} \right|^2 .$$

Calculating β

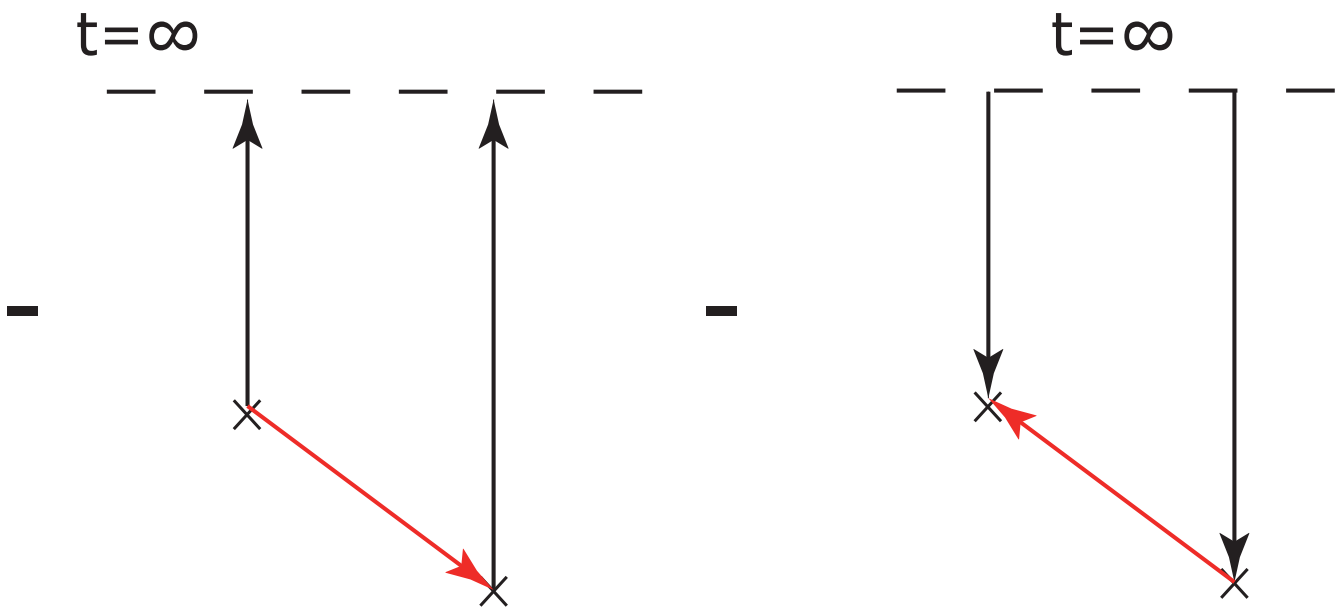

Take the Conjugate

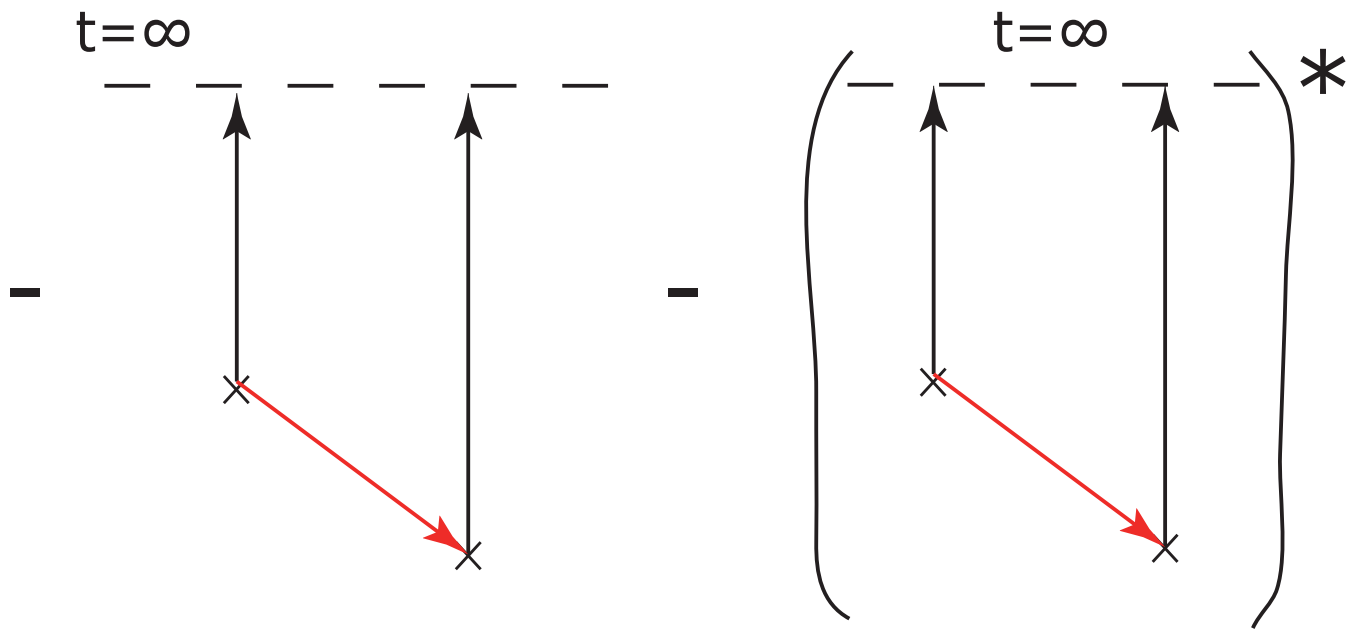

Sum the Integral

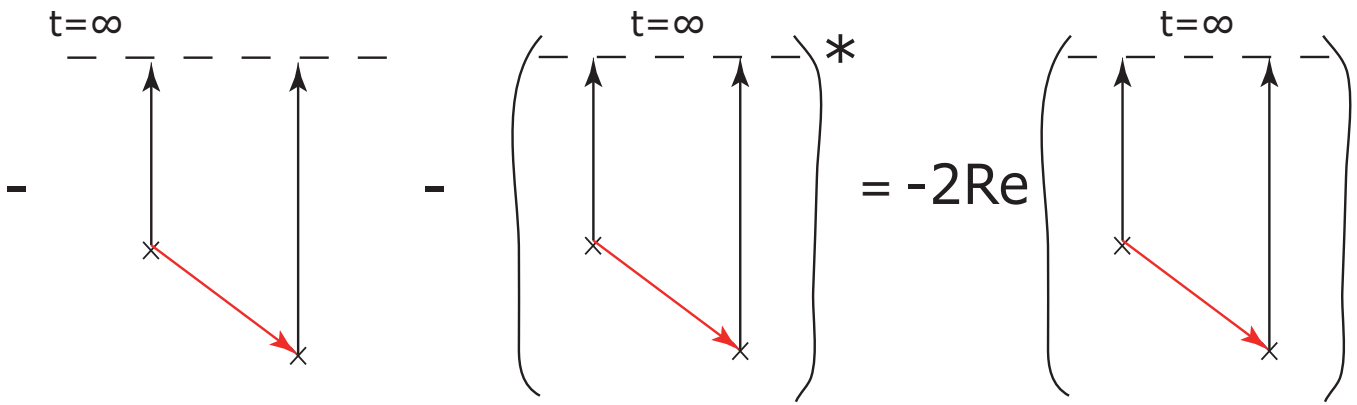

The Cut-in-the-Side integral β is

$$\beta = 2\mathrm{Re}\int_0^\infty dx_1\, x_1^{-1/2} H_{i\mu}^{(1)}(x_1) e^{-ix_1} \int_{x_1}^\infty dx_2\, x_2^{-1/2} (H_{i\mu}^{(1)}(x_2))^* e^{-ix_2}.$$

The Correction to Power Spectrum

$$\frac{\delta\mathcal{P}_{\mathcal{R}}}{\mathcal{P}_{\mathcal{R}}^{(0)}} = \pi\left(\frac{\dot{\theta}}{H}\right)^2 e^{-\mu\pi}(\alpha-\beta),$$

$$\alpha-\beta =$$

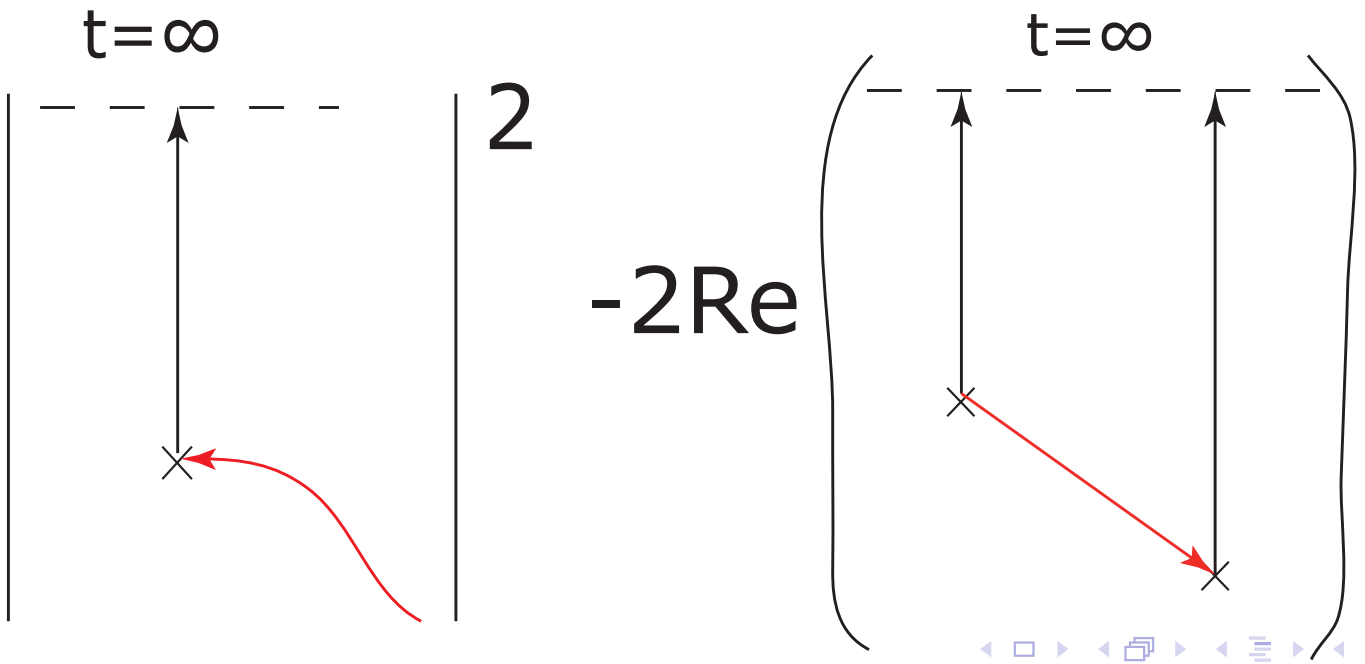

The Correction to Power Spectrum

$$\frac{\delta\mathcal{P}_{\mathcal{R}}}{\mathcal{P}_{\mathcal{R}}^{(0)}} = \pi\left(\frac{\dot{\theta}}{H}\right)^2 e^{-\mu\pi}(\alpha-\beta),$$

$$\alpha-\beta =$$

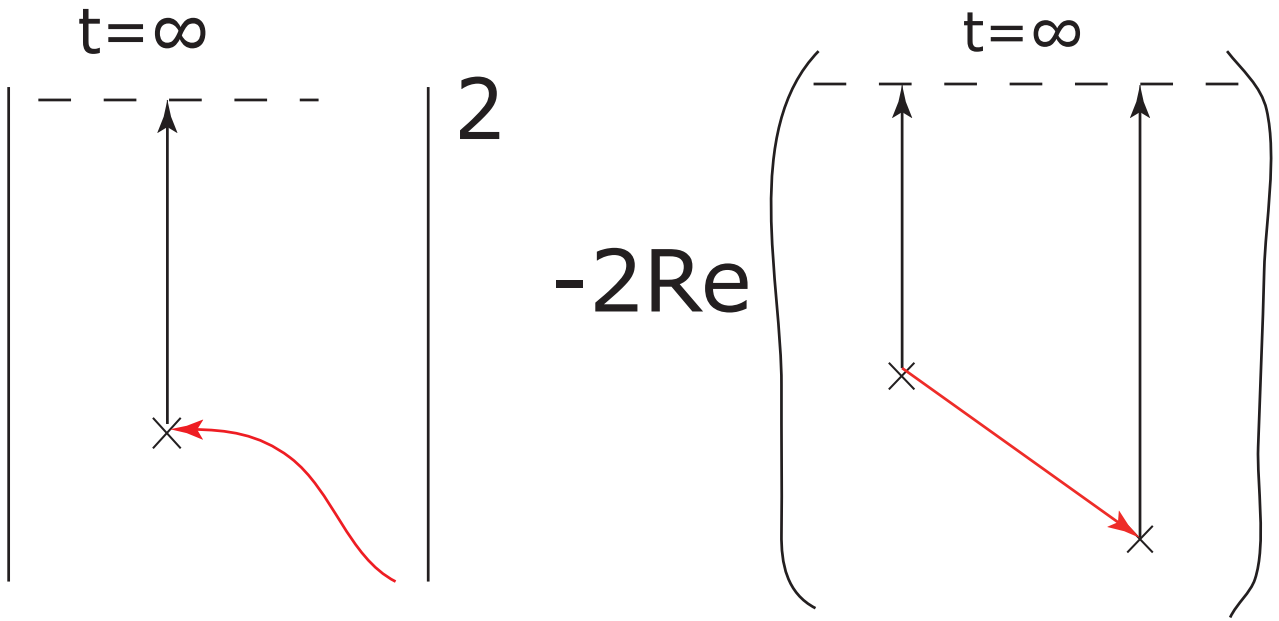

Calculating α

- α can be directly integrated,

$$\begin{aligned}\alpha &= \frac{1}{\pi}\left|\frac{e^{\mu\pi/2}}{2} - \frac{\sqrt{2}}{\sinh\mu\pi} + i\left(\frac{e^{-\mu\pi}}{2} + \sqrt{2}\coth\mu\pi\right)\right|^2 \\ &\to 1,\end{aligned}$$

  when $\mu \to \infty$.

- CIM is exponentially suppressed!

Calculating β

Use the asymptotic formula of Hankel function when $x \ll \mu$:

$$H_{i\mu}^{(1)} \to \frac{1}{e^{i\mu(\ln\mu - 1)}} \sqrt{2\frac{e^{\pi\mu}}{\mu}} \exp\left[-\frac{x^2}{4\mu} e^{-i\frac{\pi}{4}}\right] \left(\frac{x}{2}\right)^{i\mu}.$$

The main contribution to β comes from infrared $x \ll 1$. The result is

$$\beta = -2\frac{e^{\mu\pi}}{\pi\mu^2}\left[1 + \mathcal{O}\left(\frac{1}{\mu^2}\right)\right].$$

The Power Spectrum

- We have the final result (SP & Sasaki 2012, Chen & Wang 2012, Noumi et. al. 2012)

$$\begin{aligned} \mathcal{C}(\mu) &\approx \frac{1}{4\mu^2}, \\ \mathcal{P}_{\mathcal{R}} &\approx \mathcal{P}_{\mathcal{R}}^{(0)} \left[1 + 2\frac{H^2}{M_{\rm eff}^2} \left(\frac{\dot{\theta}}{H} \right)^2 \right] . \end{aligned}$$

- This result coincide with that from Effective Single Field Approach. (Tolley 2010, Achucarro 2011 & 2012, Sebastian 2012)

Outline

1 Introduction

2 Quasi-single Field Inflation with Large Isocurvaton Mass

3 Non-Gaussianity of Equilateral Shape

4 Conclusion

Bad News

- There are $\mathcal{O}(10)$ terms of 3-p vertices.
- There are 10 integrals for each vertex (with 6 momenta permutations).
- There is an integral of quadruple product of Hankel functions.

Good News

- There are $\mathcal{O}(10)$ terms of 3-p vertices. But the only vertex that is possible to generate large Non-Gaussianity is V'''.
- There are 10 integrals for each vertex (with 6 momenta permutations).
- There is an integral of quadruple product of Hankel functions.

Good News

- There are $\mathcal{O}(10)$ terms of 3-p vertices. But the only vertex that is possible to generate large Non-Gaussianity is V'''.
- There are 10 integrals for each vertex (with 6 momenta permutations). But the integrals have similar structures.
- There is an integral of quadruple product of Hankel functions.

Good News

- There are $\mathcal{O}(10)$ terms of 3-p vertices. But the only vertex that is possible to generate large Non-Gaussianity is V'''.
- There are 10 integrals for each vertex (with 6 momenta permutations). But the integrals have similar structures.
- There is an integral of quadruple product of Hankel functions. But we are free to use the asymptotic forms.

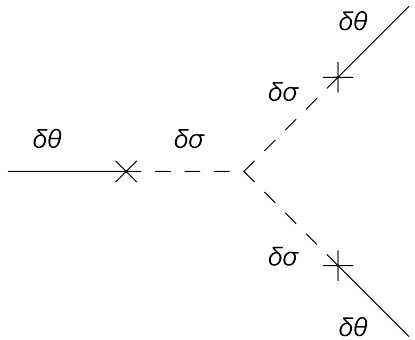

This is the only vertex that can generate large non-Gaussianity. And we calculate one integral

$$\begin{aligned}\langle\delta\theta^3\rangle \quad &\supseteq \quad -12u_{p_1}u_{p_2}u_{p_3}(0)c_2^3c_3 \\ &\times \quad \mathrm{Re}\left[\int_{-\infty}^{0}d\tau\ a^4v_{p_1}v_{p_2}v_{p_3}(\tau)\int_{-\infty}^{\tau}d\tau_1\ a^3v_{p_1}^*u_{p_1}'^*(\tau_1)\right. \\ &\qquad \left.\int_{-\infty}^{\tau_1}d\tau_2\ a^3v_{p_2}^*u_{p_2}'^*(\tau_2)\int_{-\infty}^{\tau_2}d\tau_3\ a^3v_{p_3}^*u_{p_3}'^*(\tau_3)\right] \\ &\times \quad (2\pi)^3\delta^3(\sum_i \mathbf{p}_i) + 5\ \mathrm{perms.}\end{aligned}$$

The result is

$$\langle \delta\theta^3 \rangle \supseteq -\frac{1}{\sqrt{2}} \frac{\dot{\theta}^3 V'''}{H R^3 \mu^4} \frac{k_1 + k_2 + k_3}{k_1 k_2 k_3 \left(k_1^2 + k_2^2 + k_3^2\right)^2}.$$

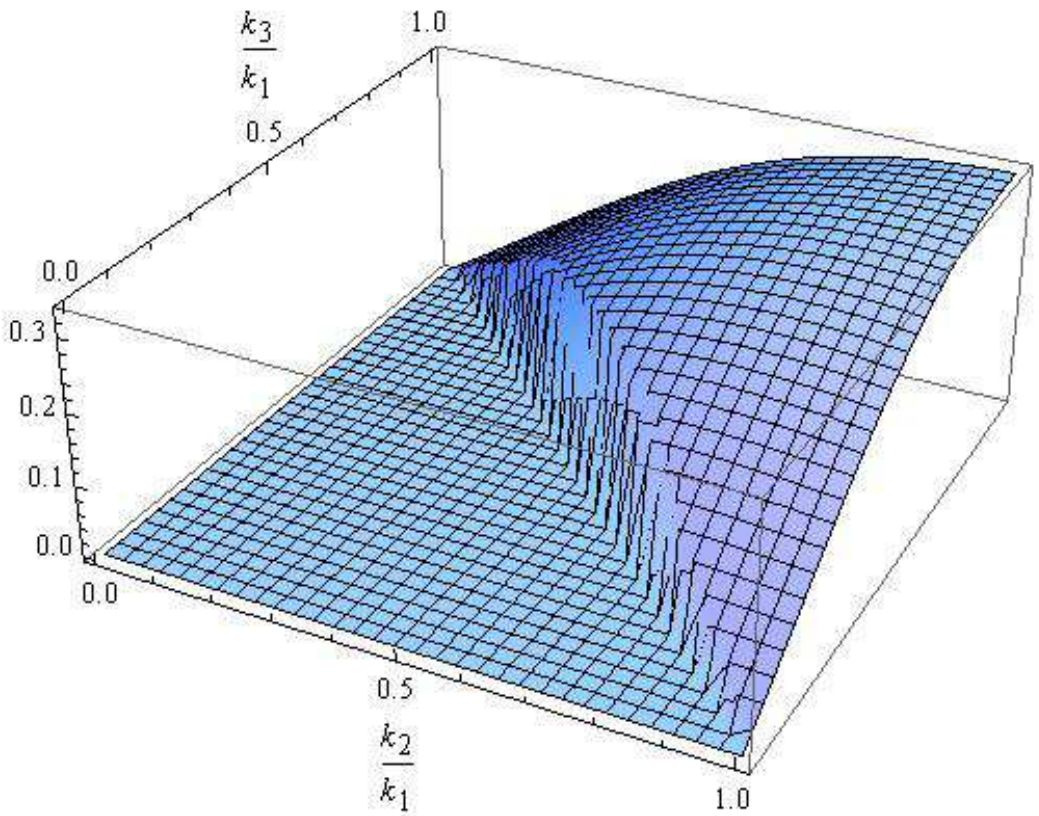

Outline

1 Introduction

2 Quasi-single Field Inflation with Large Isocurvaton Mass

3 Non-Gaussianity of Equilateral Shape

4 Conclusion

Our Conclusion

$$\boxed{\text{Effective Single Field Approach} \equiv \text{In-in Formulism}}$$

Our Conclusion

$$\boxed{\text{Effective Single Field Approach} \equiv \text{In-in Formulism}}$$

(But it seems only hold for 2-point function and at leading order...)

Comments

1. Non-constant turn case.
2. Non-adiabatic turn. Shiu 2011, Gao2012.
3. To embed the QSI into a segment of inflationary trajectory.
4. Loop corrections. Chen 2012.
5. Effective field theory of QSI. Noumi 2012.
6. Non-Gaussianities with (1)large mass limit and (2)small mass limit.



Figure: "New star near Antares", record of a possible supernova in Shang Dynasty, 1600-1046 B.C.

Thank you!

GBKsong

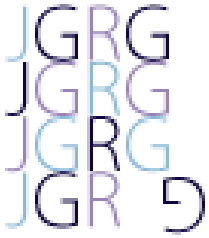

Toshifumi Noumi, JGRG 22(2012)111207

"Effective field theory approach to quasi-single inflation"

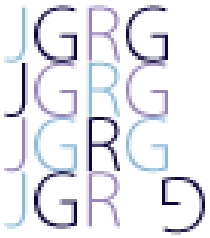

RESCEU SYMPOSIUM ON

GENERAL RELATIVITY AND GRAVITATION

JGRG 22



November 12-16 2012

Koshiba Hall, The University of Tokyo, Hongo, Tokyo, Japan



Effective field theory approach to quasi-single field inflation

Toshifumi Noumi

(The University of Tokyo, Komaba)

based on arXiv: 1211.1624

with Masahide Yamaguchi and Daisuke Yokoyama
(Tokyo Institute of Technology)

JGRG22 - RESCEU, 12th November 2012

Quasi-single field inflation

classification of inflation models w.r.t. relevant dof

	relevant dof
single field	adiabatic mode ζ (massless)
multiple field	adiabatic + isocurvatures

Quasi-single field inflation

classification of inflation models w.r.t. relevant dof

	relevant dof
single field	adiabatic mode ζ (massless)
multiple field	adiabatic + isocurvatures
"multi field"	light isocurvatures (m<<H)
quasi-single field	isocurvatures m $\sim$ H

Quasi-single field inflation

classification of inflation models w.r.t. relevant dof

	relevant dof
single field	adiabatic mode ζ (massless)
multiple field	adiabatic + isocurvatures
"multi field"	light isocurvatures (m<<H)
quasi-single field	isocurvatures m $\sim$ H

- well motivated by model building
(string inspired, supergravity based, ...)

Quasi-single field inflation

classification of inflation models w.r.t. relevant dof

	relevant dof
sing	adiabatic mode ζ (massless)
multiple field	adiabatic + isocurvatures
"multi field"	light isocurvatures (m<<H)
quasi-single field	isocurvatures m $\sim$ H

modulus in string theory (landscape)

- well motivated by model building
(string inspired, supergravity based, ...)

Quasi-single field inflation

classification of inflation models w.r.t. relevant dof

	relevant dof
sing	adiabatic mode ζ (massless)
multiple field	adiab
"multi field"	light isocurvatures (m<<H)
quasi-single field	isocurvatures m $\sim$ H

modulus in string theory (landscape)

curvature coupling in supergravity

- well motivated by model building
(string inspired, supergravity based, ...)

Quasi-single field inflation

classification of inflation models w.r.t. relevant dof

	relevant dof
sing	adiabatic mode ζ (massless)
multiple field	adiab
"multi field"	light isocurvatures (m<<H)
quasi-single field	isocurvatures m $\sim$ H

modulus in string theory (landscape)

curvature coupling in supergravity

- well motivated by model building
 (string inspired, supergravity based, ...)
- phenomenologically interesting
(characteristic signatures in primordial perturbations)

QSI & non-Gaussianities

quasi-single field inflation [Chen-Wang '09]

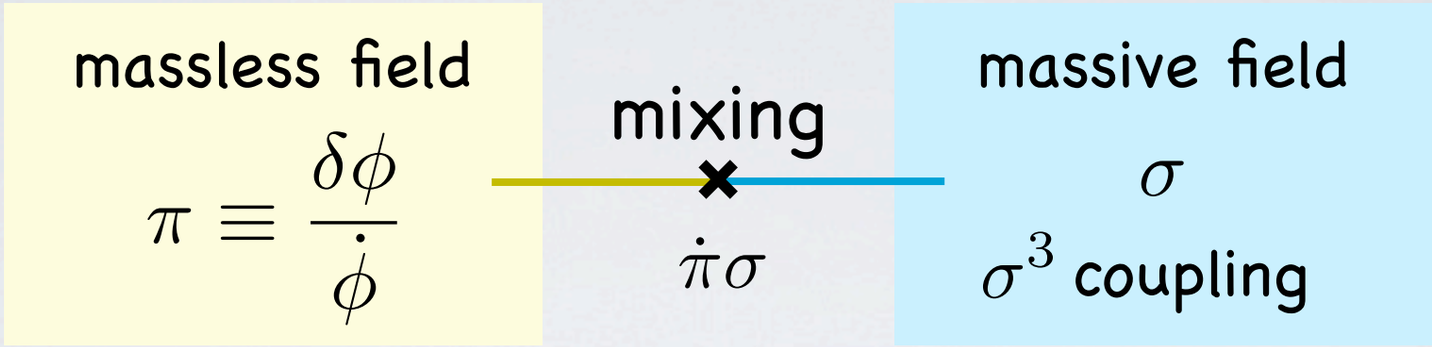

QSI & non-Gaussianities

quasi-single field inflation [Chen-Wang '09]

massless field	mixing	massive field
$\pi \equiv \frac{\delta\phi}{\dot{\phi}}$	$\dot{\pi}\sigma$	σ σ^3 coupling

- can potentially give large non-Gaussianities

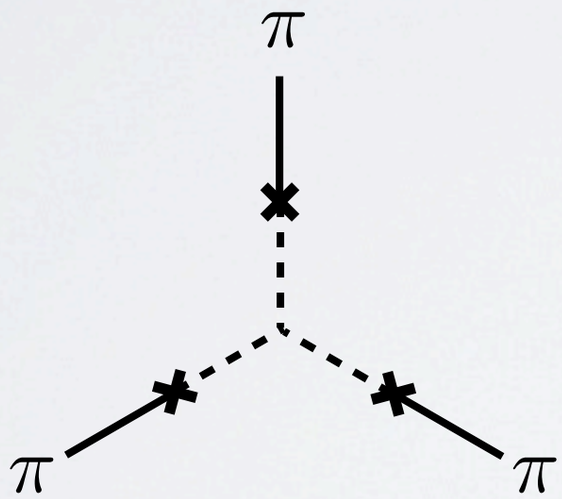

QSI & non-Gaussianities

quasi-single field inflation [Chen-Wang '09]

massless field	mixing	massive field
$\pi \equiv \frac{\delta\phi}{\dot{\phi}}$	$\dot{\pi}\sigma$	σ σ^3 coupling

- can potentially give large non-Gaussianities

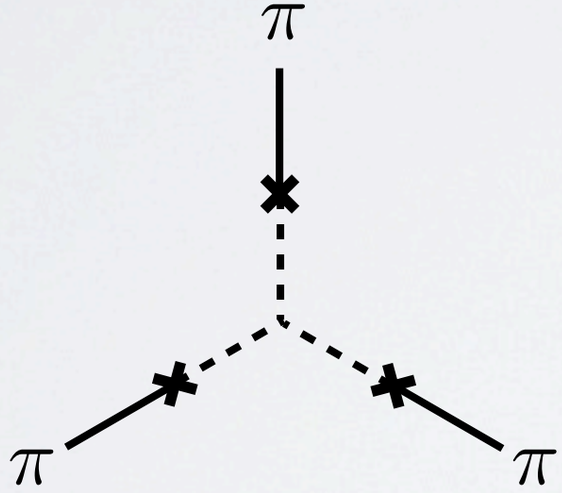

- intermediate shape between local and equilateral types

QSI & non-Gaussianities

quasi-single field inflation [Chen-Wang '09]

massless field	mixing	massive field
$\pi \equiv \dfrac{\delta\phi}{\dot\phi}$	$\dot\pi\sigma$	σ σ^3 coupling

- can potentially give large non-Gaussianities

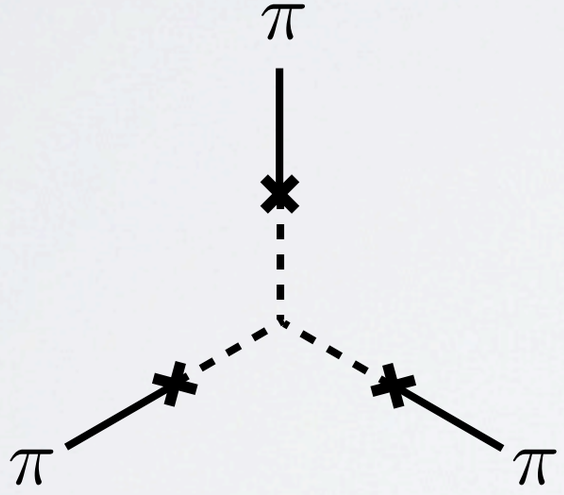

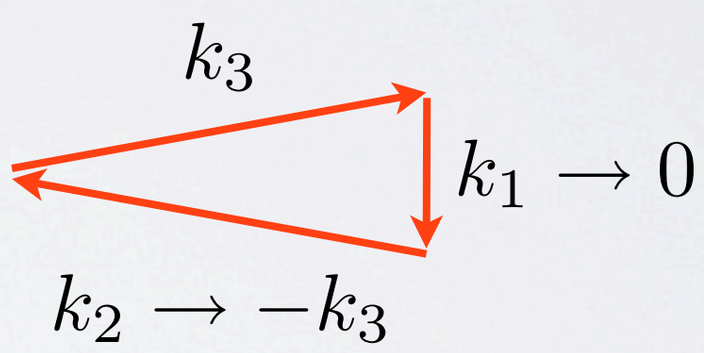

$$|k_2| = |k_3| = k,\ |k_1| = \kappa k$$

- intermediate shape between local and equilateral types
- characteristic scaling in squeezed limit

$$\langle \pi_{k_1} \pi_{k_2} \pi_{k_3} \rangle \propto \kappa^{-3/2-\nu} k^{-6} \qquad \nu = \sqrt{9/4 - m_\sigma^2/H^2}$$

QSI & non-Gaussianities

quasi-single field inflation [Chen-Wang '09]

massless field	mixing	massive field
$\pi \equiv \frac{\delta\phi}{\dot{\phi}}$	$\dot{\pi}\sigma$	σ
		σ^3 coupling

- can potentially give large non-Gaussianities

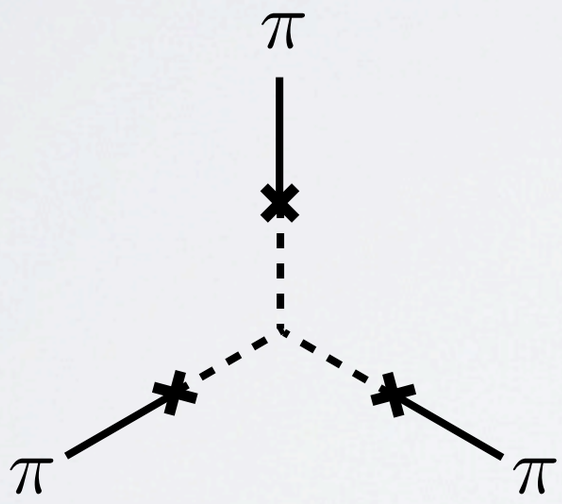

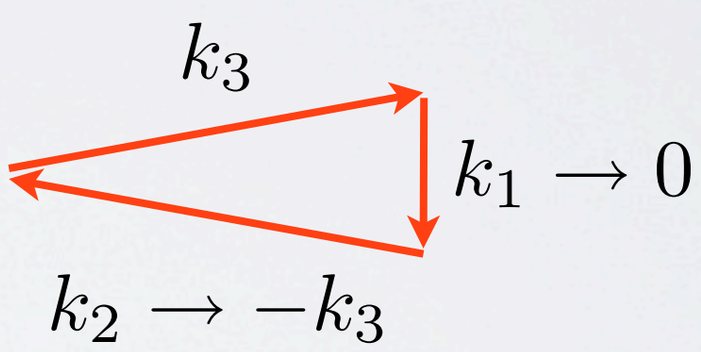

$$|k_2| = |k_3| = k,\ |k_1| = \kappa k$$

- intermediate shape between local and e
- characteristic scaling in squeezed limit

※ sensitive to the mass of σ

$$\langle \pi_{k_1} \pi_{k_2} \pi_{k_3} \rangle \propto \kappa^{-3/2-\nu} k^{-6} \qquad \nu = \sqrt{9/4 - m_\sigma^2/H^2}$$

Motivation

quasi-single field inflation:

- naturally realized in supergravity
- characteristic signatures in non-Gaussianities
  (between local & equilateral, scaling in squeezed limit)

Motivation

quasi-single field inflation:

- naturally realized in supergravity
- characteristic signatures in non-Gaussianities
  (between local & equilateral, scaling in squeezed limit)



would like to discuss QSI - in general settings

- in a systematic way

Motivation

quasi-single field inflation:

- naturally realized in supergravity
- characteristic signatures in non-Gaussianities
  (between local & equilateral, scaling in squeezed limit)



would like to discuss QSI - in general settings
- in a systematic way



effective field theory approach!

EFT approach

effective field theory approach [Cheung et al '07]

time dependent background evolution during inflation

(time-dependent vev: $R(t)$, $\phi_0(t)$)

EFT approach

effective field theory approach [Cheung et al '07]

time dependent background evolution during inflation

(time-dependent vev: $R(t)$, $\phi_0(t)$)

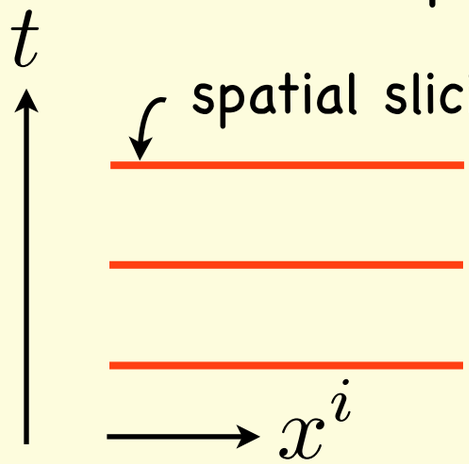

EFT approach

effective field theory approach [Cheung et al '07]

time dependent background evolution during inflation

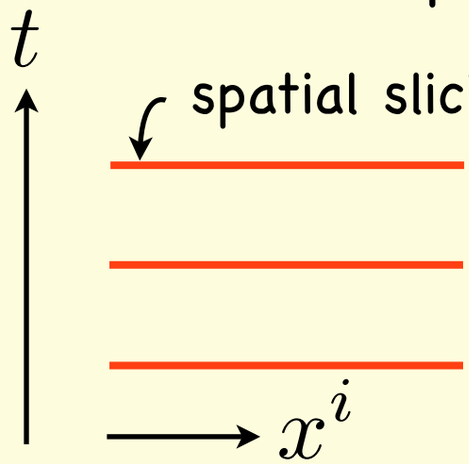

(time-dependent vev: $R(t)$, $\phi_0(t)$)

→ spontaneous breakdown of time diffeo

EFT approach

effective field theory approach [Cheung et al '07]

time dependent background evolution during inflation

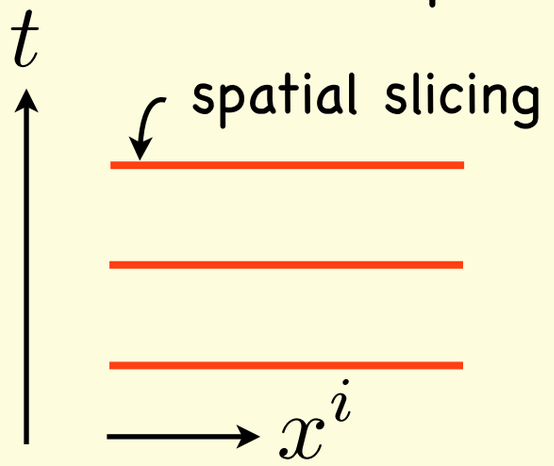

(time-dependent vev: $R(t)$, $\phi_0(t)$)

→ spontaneous breakdown of time diffeo

※ unbroken time-dep. spatial diffeo

$$\delta x^i = \epsilon^i(t, x^i)$$

EFT approach

effective field theory approach [Cheung et al '07]

time dependent background evolution during inflation

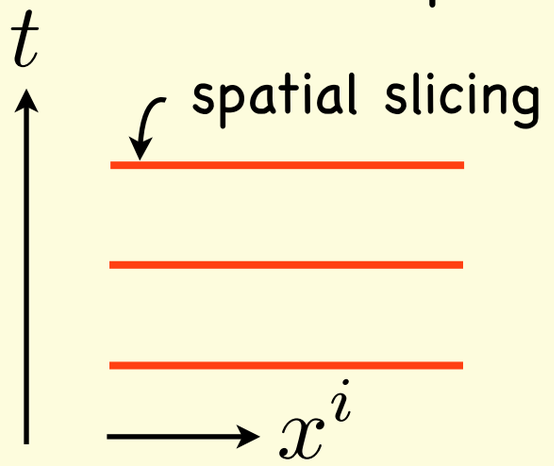

(time-dependent vev: $R(t)$, $\phi_0(t)$)

→ spontaneous breakdown of time diffeo

※ unbroken time-dep. spatial diffeo

$$\delta x^i = \epsilon^i(t, x^i)$$

assuming relevant dof. during inflation,
we would be able to construct effective action for inflation
based on the unbroken time-dependent diffeo

EFT approach

effective field theory approach [Cheung et al '07]

time dependent background evolution during inflation

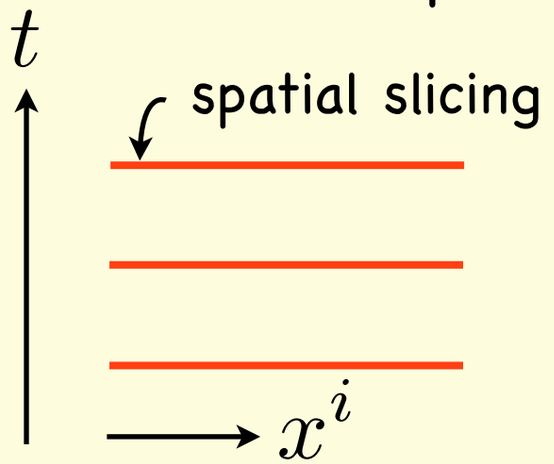

(time-dependent vev: $R(t)$, $\phi_0(t)$)

→ spontaneous breakdown of time diffeo

※ unbroken time-dep. spatial diffeo

$$\delta x^i = \epsilon^i(t, x^i)$$

assuming relevant dof. during inflation,
we would be able to construct effective action for inflation
based on the unbroken time-dependent diffeo

advantages:
- systematic expansions in fluctuations and derivatives

EFT approach

effective field theory approach [Cheung et al '07]

time dependent background evolution during inflation

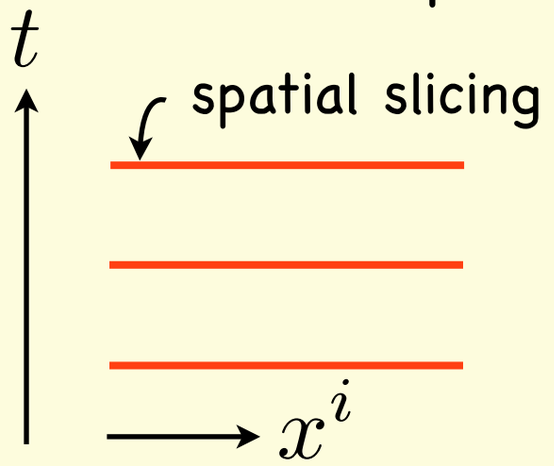

(time-dependent vev: $R(t)$, $\phi_0(t)$)

→ spontaneous breakdown of time diffeo

※ unbroken time-dep. spatial diffeo

$$\delta x^i = \epsilon^i(t, x^i)$$

assuming relevant dof. during inflation,
we would be able to construct effective action for inflation
based on the unbroken time-dependent diffeo

advantages:
- systematic expansions in fluctuations and derivatives
- simplification in the dynamics of Goldstone boson π

EFT approach

effective field theory approach [Cheung et al '07]

time dependent background evolution during inflation

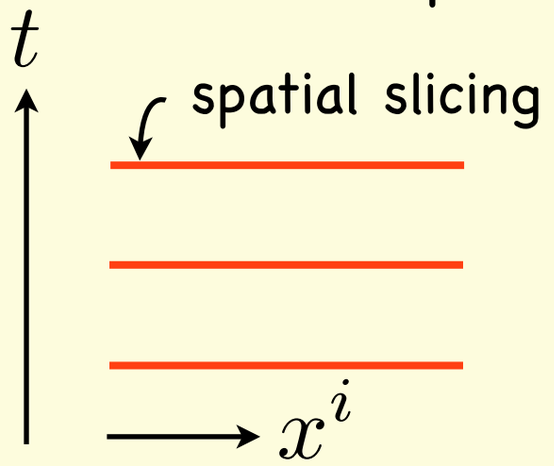

(time-dependent vev: $R(t)$, $\phi_0(t)$)

→ spontaneous breakdown of time diffeo

※ unbroken time-dep. spatial diffeo

$$\delta x^i = \epsilon^i(t, x^i)$$

assuming relevant dof. during inflation,
we would be able to construct effective action for inflation
based on the unbroken time-dependent diffeo

advantages:
- systematic expansions in fluctuations and derivatives
- simplification in the dynamics of Goldstone boson π
- relations between physics and non-Gaussianities are clear!

General action

general action of quasi-single field inflation

relevant dof = three physical modes of graviton
+ additional massive scalar field σ

General action

general action of quasi-single field inflation

relevant dof = three physical modes of graviton
+ additional massive scalar field σ

schematically written as $S = S_{\rm grav} + S_\sigma + S_{\rm mix}$

General action

general action of quasi-single field inflation

relevant dof = three physical modes of graviton
+ additional massive scalar field σ
schematically written as $S = S_{\rm grav} + S_\sigma + S_{\rm mix}$

ex. $$S_{\rm mix} = \int d^4x\sqrt{-g}\,\big[\beta_1(t)\delta g^{00}\sigma + \beta_2(t)\delta g^{00}\partial^0\sigma + \beta_3(t)\partial^0\sigma - (\dot\beta_3(t) + 3H\beta_3(t))\sigma\big]$$

General action

general action of quasi-single field inflation

relevant dof = three physical modes of graviton
+ additional massive scalar field σ
schematically written as $S = S_{\rm grav} + S_\sigma + S_{\rm mix}$

ex. $$S_{\rm mix} = \int d^4x\sqrt{-g}\,\big[\beta_1(t)\delta g^{00}\sigma + \beta_2(t)\delta g^{00}\partial^0\sigma + \beta_3(t)\partial^0\sigma - (\dot\beta_3(t) + 3H\beta_3(t))\sigma\big]$$

Stuckelberg method

$$S_{\rm mix} = \int d^4x\, a^3\left[-2\beta_1\dot\pi\sigma + (2\beta_2 - \beta_3)\dot\pi\dot\sigma + \beta_3\frac{\partial_i\pi\partial_i\sigma}{a^2} - \beta_1\left(\dot\pi^2 - \frac{(\partial_i\pi)^2}{a^2}\right)\sigma + 3\beta_2\dot\pi^2\dot\sigma - 2\beta_2\frac{\partial_i\pi\partial_i\sigma}{a^2}\dot\pi - \beta_2\frac{(\partial_i\pi)^2}{a^2}\dot\sigma + \dots\right]$$

General action

general action of quasi-single field inflation

relevant dof = three physical modes of graviton
+ additional massive scalar field σ
schematically written as $S = S_{\rm grav} + S_\sigma + S_{\rm mix}$

ex. $$S_{\rm mix} = \int d^4x\sqrt{-g}\,\big[\beta_1(t)\delta g^{00}\sigma + \beta_2(t)\delta g^{00}\partial^0\sigma + \beta_3(t)\partial^0\sigma - (\dot\beta_3(t) + 3H\beta_3(t))\sigma\big]$$

$$S_{\rm mix} = \int d^4x\, a^3\left[-2\beta_1\dot\pi\sigma + (2\beta_2 - \beta_3)\dot\pi\dot\sigma + \beta_3\frac{\partial_i\pi\partial_i\sigma}{a^2} - \beta_1\left(\dot\pi^2 - \frac{(\partial_i\pi)^2}{a^2}\right)\sigma + 3\beta_2\dot\pi^2\dot\sigma - 2\beta_2\frac{\partial_i\pi\partial_i\sigma}{a^2}\dot\pi - \beta_2\frac{(\partial_i\pi)^2}{a^2}\dot\sigma + \dots\right]$$

large non-Gaussianitis from mixings β_1 and β_2 — $\zeta \sim -H\pi$

Power spectrum

power spectrum

$$S_{\rm mix} = \int d^4x\, a^3 \left[\underbrace{-2\beta_1}_{\tilde{\beta}_1} \dot{\pi}\sigma + \underbrace{(2\beta_2 - \beta_3)}_{\tilde{\beta}_2} \dot{\pi}\dot{\sigma} + \underbrace{\beta_3}_{\tilde{\beta}_3} \frac{\partial_i \pi \partial_i \sigma}{a^2} \right]$$

Power spectrum

power spectrum

$$S_{\rm mix} = \int d^4x\, a^3 \left[\underbrace{-2\beta_1}_{\tilde{\beta}_1} \dot{\pi}\sigma + \underbrace{(2\beta_2 - \beta_3)}_{\tilde{\beta}_2} \dot{\pi}\dot{\sigma} + \underbrace{\beta_3}_{\tilde{\beta}_3} \frac{\partial_i \pi \partial_i \sigma}{a^2} \right]$$

$$\langle \zeta_{\mathbf{k}}\, \zeta_{\mathbf{k}'} \rangle = H^2 \langle \pi_{\mathbf{k}}\, \pi_{\mathbf{k}'} \rangle$$

Power spectrum

power spectrum

$$S_{\rm mix} = \int d^4x\, a^3 \left[\underbrace{-2\beta_1}_{\tilde\beta_1} \dot\pi\sigma + \underbrace{(2\beta_2-\beta_3)}_{\tilde\beta_2}\dot\pi\dot\sigma + \underbrace{\beta_3}_{\tilde\beta_3}\frac{\partial_i\pi\partial_i\sigma}{a^2}\right]$$

$$\langle \zeta_{\mathbf{k}}\,\zeta_{\mathbf{k}'}\rangle = H^2\,\langle \pi_{\mathbf{k}}\,\pi_{\mathbf{k}'}\rangle$$



$$\langle \zeta_{\mathbf{k}}\,\zeta_{\mathbf{k}'}\rangle = (2\pi)^3\delta^{(3)}(\mathbf{k}+\mathbf{k}')\frac{2\pi^2}{k^3}\mathcal{P}_\zeta(k)$$

deviation from single field

$$\mathcal{P}_\zeta(k) = \frac{H^2}{8\pi^2 M_{\rm Pl}^2\epsilon\, c_\pi}\left[1+\frac{\pi}{4\alpha_\sigma^2}\frac{c_\pi^2}{M_{\rm Pl}^2(-\dot H)}\left(\frac{\tilde\beta_1^2}{H^2}\mathcal{C}_{11}+\tilde\beta_2^2\,\mathcal{C}_{22}+\tilde\beta_3^2\,\mathcal{C}_{33}\right.\right.$$
$$\left.\left.+\frac{\tilde\beta_1}{H}\,\tilde\beta_2\,\mathcal{C}_{12}+\frac{\tilde\beta_1}{H}\,\tilde\beta_3\,\mathcal{C}_{13}+\tilde\beta_2\,\tilde\beta_3\,\mathcal{C}_{23}\right)\right]$$

Power spectrum

$\mathcal{C}_{ij}(m_\sigma/H, c_\sigma/c_\pi)$ for fixed $r_s = c_\sigma/c_\pi$

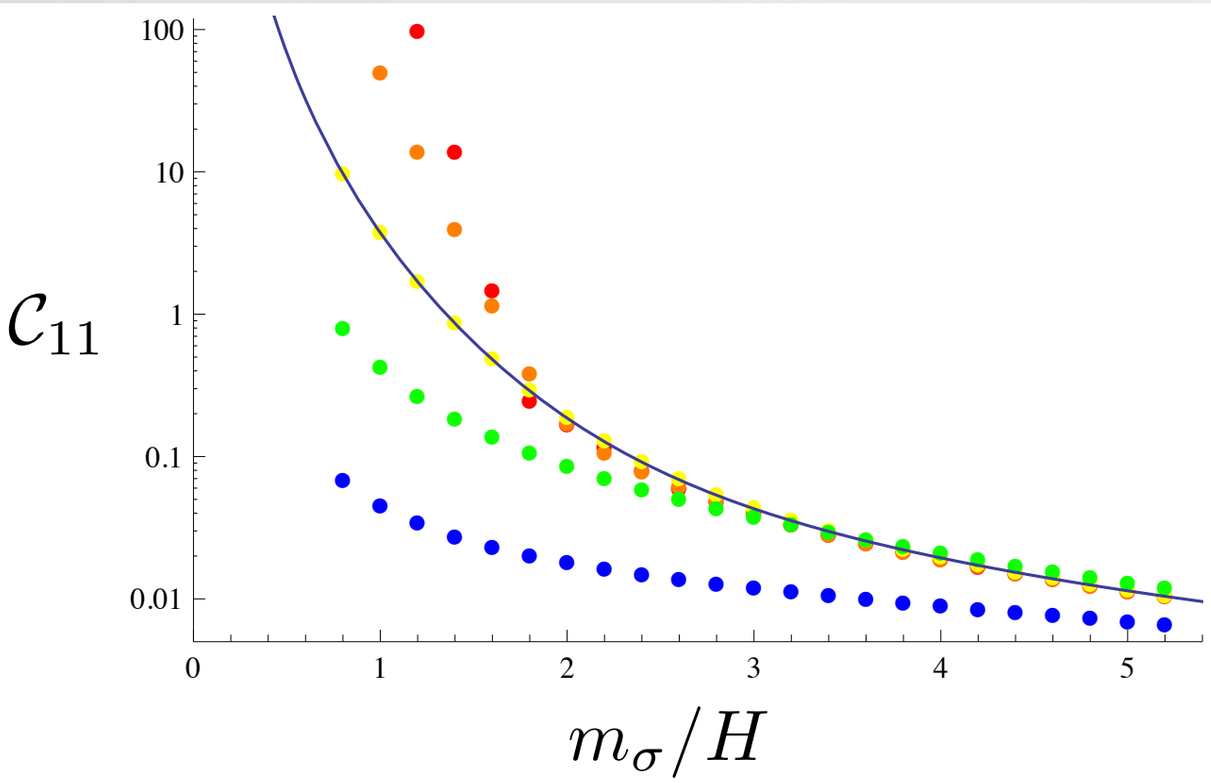

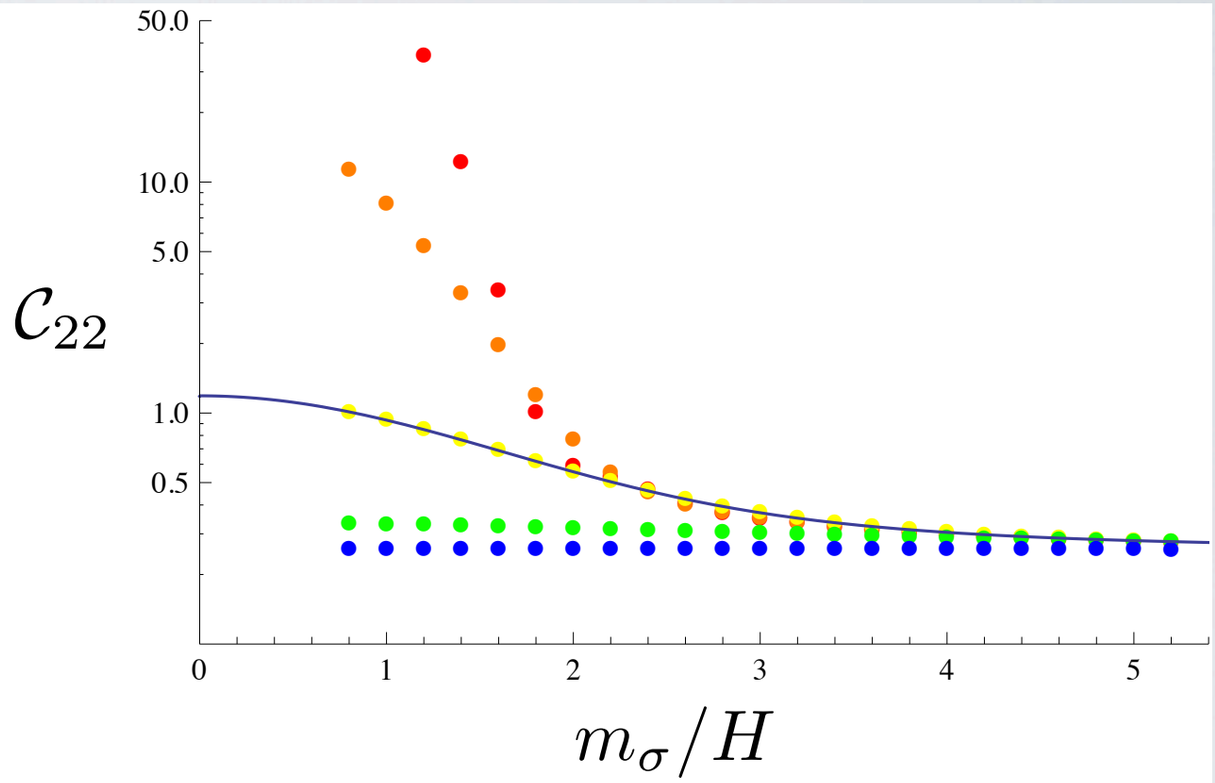

The dots are numerical results for $r_s = 0.1$ (red), 0.3 (orange), 1 (yellow), 3 (green), and 10 (blue).

The curve is an analytic result for $r_s = 1$.

※ $\mathcal{C}_{22}$ does not vanish even in the heavy mass limit

$\tilde{\beta}_2 \dot{\pi} \dot{\sigma}$

3pt functions

three point functions in the squeezed limit

- original models of quasi-single field inflation

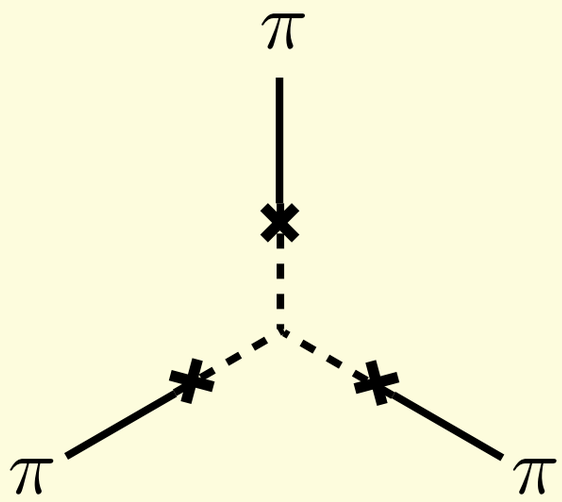

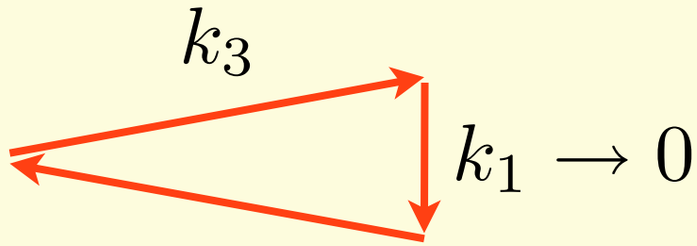

$k_2 \to -k_3$

$$|k_2| = |k_3| = k,\ |k_1| = \kappa k$$

$$\langle \pi_{k_1} \pi_{k_2} \pi_{k_3} \rangle \propto \kappa^{-3/2-\nu} k^{-6} \qquad \nu = \sqrt{9/4 - m_\sigma^2/H^2}$$

3pt functions

three point functions in the squeezed limit

- original models of quasi-single field inflation

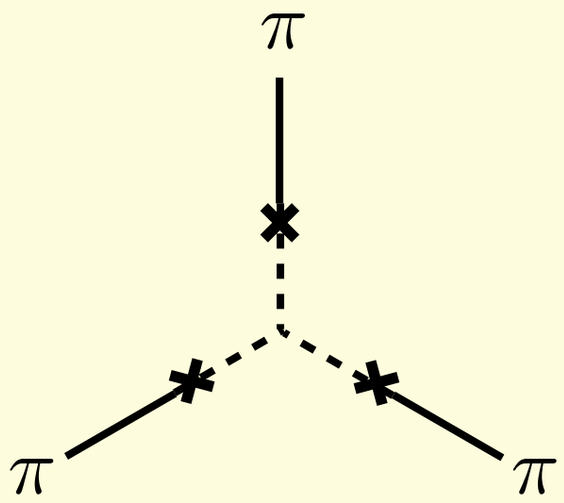

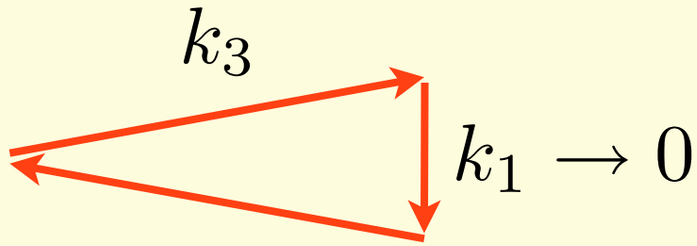

$k_2 \to -k_3$

$|k_2| = |k_3| = k,\ |k_1| = \kappa k$

$$\langle \pi_{k_1} \pi_{k_2} \pi_{k_3} \rangle \propto \kappa^{-3/2-\nu} k^{-6} \qquad \nu = \sqrt{9/4 - m_\sigma^2/H^2}$$

- for general mixing and cubic couplings

3pt functions

three point functions in the squeezed limit

- original models of quasi-single field inflation

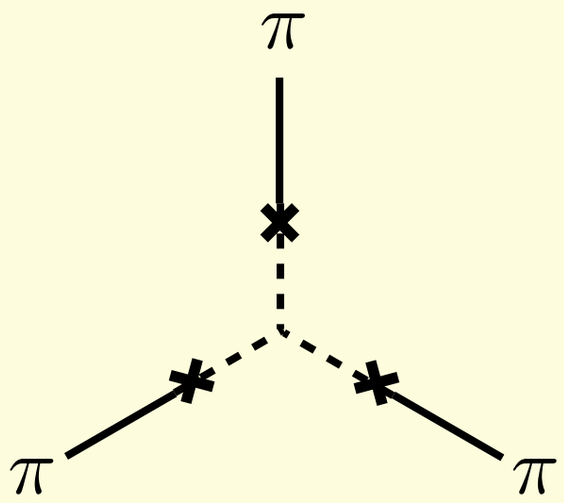

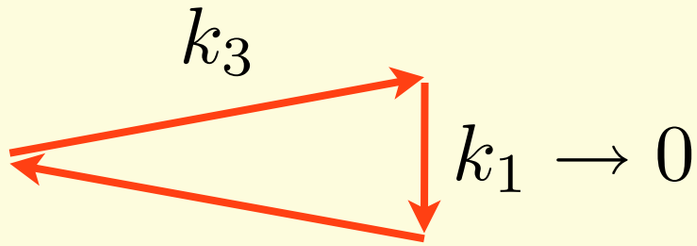

$k_2 \to -k_3$

$|k_2| = |k_3| = k,\ |k_1| = \kappa k$

$$\langle \pi_{k_1} \pi_{k_2} \pi_{k_3} \rangle \propto \kappa^{-3/2-\nu} k^{-6} \qquad \nu = \sqrt{9/4 - m_\sigma^2/H^2}$$

- for general mixing and cubic couplings

① scaling does not depend on details of mixing

3pt functions

three point functions in the squeezed limit

- original models of quasi-single field inflation

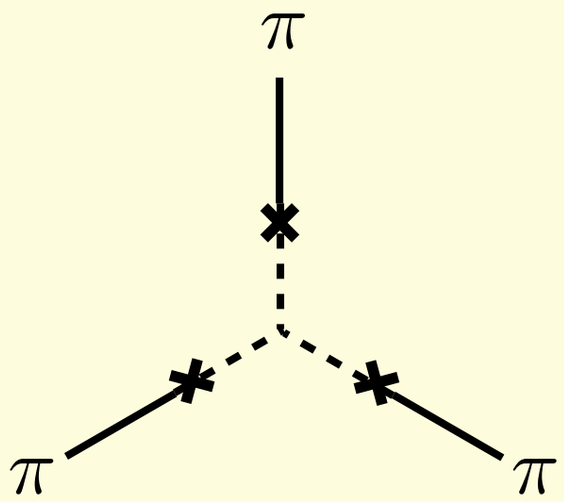

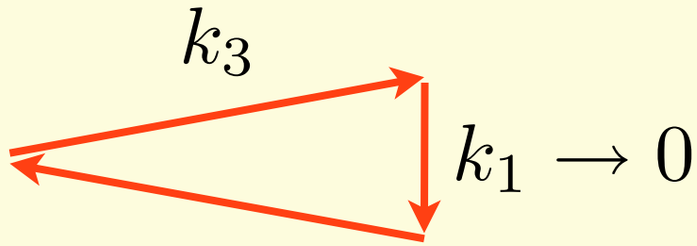

$k_2 \to -k_3$

$|k_2| = |k_3| = k,\ |k_1| = \kappa k$

$$\langle \pi_{k_1} \pi_{k_2} \pi_{k_3} \rangle \propto \kappa^{-3/2-\nu} k^{-6} \qquad \nu = \sqrt{9/4 - m_\sigma^2/H^2}$$

- for general mixing and cubic couplings

① scaling does not depend on details of mixing

② determined only from cubic interaction in the diagram

three point vertices	momentum dependence
$\dot\pi^3,\ \dot\pi\dfrac{(\partial_i\pi)^2}{a^2}$	$\kappa^{-1}k^{-6}$
$\dot\pi^2\sigma,\ \dot\pi\dot\sigma,\ \dot\pi\sigma^2,\ \dot\pi\sigma\dot\sigma,\ \dot\pi\dot\sigma^2,\ \ddot\pi\sigma\dot\sigma,$ $\sigma^3,\ \sigma^2\dot\sigma,\ \sigma\dot\sigma^2,\ \sigma\dfrac{(\partial_i\sigma)^2}{a^2},\ \dot\sigma^3,\ \dot\sigma\dfrac{(\partial_i\sigma)^2}{a^2}$	$\begin{cases}\kappa^{-3/2-\nu}k^{-6} & \text{for}\quad m_\sigma<\dfrac{3}{2}H\\ \kappa^{-3/2}k^{-6}\sin[i\nu\log\kappa+\delta_\nu] & \text{for}\quad m_\sigma>\dfrac{3}{2}H\end{cases}$
$\dot\pi\dfrac{\partial_i\pi\partial_i\sigma}{a^2}$	$\kappa^{-2}k^{-6}$
$\dfrac{(\partial_i\pi)^2}{a^2}\sigma,\ \dfrac{(\partial_i\pi)^2}{a^2}\dot\sigma,\ \dfrac{\partial_i\pi\partial_i\sigma}{a^2}\sigma,\ \dfrac{\partial_i\pi\partial_i\sigma}{a^2}\dot\sigma$	$\begin{cases}\kappa^{-3/2-\nu}k^{-6} & \text{for}\quad m_\sigma<\sqrt{2}H\\ \kappa^{-2}k^{-6} & \text{for}\quad m_\sigma>\sqrt{2}H\end{cases}$
$\dot\pi\dfrac{(\partial_i\sigma)^2}{a^2}$	$\begin{cases}\kappa^{-1/2-\nu}k^{-6} & \text{for}\quad m_\sigma<\sqrt{2}H\\ \kappa^{-1}k^{-6} & \text{for}\quad m_\sigma>\sqrt{2}H\end{cases}$

non-trivial scaling in the squeezed limit when mixing is relevant!

$$\nu=\sqrt{9/4-m_\sigma^2/H^2}\quad 0<\nu<3/2\quad\text{or}\quad \nu=\text{pure imaginary}$$

Summary and prospects

summary

applied EFT approach to QSI

- systematic expansions in fluctuations and derivatives
- simplification of action for π in decoupling regime
- relation between physics & non-Gaussianities is clear

calculated power spectrum for constant mixing

discussed scaling of 3-pt functions in squeezed limit

- sensitive to # of fields and their mass

also discussed effects of heavy particles, sharp turning

prospects

full non-Gaussianities, detectability, ...

EFT for sugra based inflation,

more on sharp turning, ...

THANK YOU!!

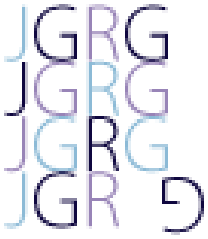

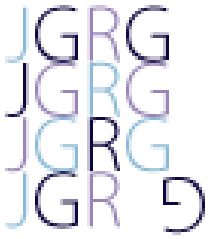

Masato Minamitsuji, JGRG 22(2012)111208

"Revisiting perturbations of a scalar field in an anisotropic universe"

RESCEU SYMPOSIUM ON

GENERAL RELATIVITY AND GRAVITATION

JGRG 22

November 12-16 2012

Koshiba Hall, The University of Tokyo, Hongo, Tokyo, Japan





Revisiting perturbations of a scalar field in an anisotropic universe

Hyeong-Chan Kim [1(a)] and Masato Minamitsuji [2(b)]

[(a)] *School of Liberal Arts and Sciences, Korea National University of Transportation, Chungju 380-702, Korea*

[(b)] *Yukawa Institute for Theoretical Physics, Kyoto University, Kyoto 606-8502, Japan*

Abstract

We revisit the issue on signatures of pre-inflationary background anisotropy by considering the quantization of a massless and minimally coupled scalar field in an axially symmetric Kasner background, mimicking cosmological perturbations. We show that the power spectrum of the scalar field fluctuation has a negligible difference from the standard inflation in the non-planar directions, but it has a sharp peak around the symmetry plane. For the non-planar high-momentum modes, we use the WKB approximation for the first period and the asymptotic approximation based on the de Sitter solution for the next period. At the boundary, two mode functions have the same accuracy with error of $O(H_i/k)$. We calculate the approximation up to the order of $(H_i/k)^6$ and show that the power spectrum of the scalar field fails to get corrections until we execute the approximation up to 6th order. This note is based on our recent paper [1].

1 Introduction

Inflation has become one of the paradigms of modern cosmology. First of all, inflation elegantly solves many problems which are present in the standard Big-Bang model such as the horizon and flatness problems. Second, it accounts for the origin of the large scale structure of the universe in terms of the quantum fluctuations originating from the adiabatic vacuum structure in early universe. Remarkably, the nature of the primordial fluctuations is understood in terms of symmetries of the de Sitter spacetime. In general, we need n-point correlation functions to characterize the statistical nature of primordial fluctuations. However, these symmetries lead the power spectrum of a scale invariant form. These predictions from symmetries are robust and universal in inflationary scenarios. In fact, the above predictions have been confirmed, e.g., by the measurements of cosmic microwave background (CMB). As the observational precision increases, we have to go beyond the power spectrum to look at fine structure of the primordial fluctuations. Since in the realistic inflationary universe the symmetries of the de Sitter spacetime do not hold exactly, violation of them provides a measurable effect. One possibility is introducing spatially homogeneous models violating the spatial isotropy [2–4], where the Copernican principle is kept since there is no privileged positions in the universe. The universe has a privileged direction. From the observational point of view, a lot of anomalies indicating the statistical anisotropy are reported although its statistical significance is uncertain.

We start from the discussion on the evolution of anisotropic universe in the Einstein gravity minimally coupled to a massive scalar field, where the scalar field plays the role of the inflaton. To obtain a sufficiently long period of inflation, one usually imposes the slow rolling condition, $\phi_0 \gg M_P$, where ϕ_0 is the initial value of the inflaton. Under the assumption, as discussed in Ref. [5], the background metric can be approximated by the Kasner spacetime with a positive cosmological constant, $\Lambda(=3{H_i}^2)$. Among all, we are mainly interested in the the regular Kasner spacetimes with two dimensional axial symmetry with metric,

$$ds^2 = -d\tau^2 + \sinh^{\frac{2}{3}}(3H_i\tau)\left[\tanh^{-\frac{2}{3}}\left(\frac{3H_i\tau}{2}\right)(dx_1^2+dx_2^2) + \tanh^{\frac{4}{3}}\left(\frac{3H_i\tau}{2}\right)dx_3^2\right]. \quad (1)$$

[1]Email address: hckim@ut.ac.kr

[2]Email address: masato@yukawa.kyoto-u.ac.jp

The spacetime has a privileged axis x_3 orthogonal to the symmetry plane. The spacetime has a Rindler-like event horizon at $\tau = 0$ since $g_{11}(= g_{22})$ approaches to a finite value and g_{33} goes to zero linearly. This spacetime is a good testing ground in analyzing the properties of anisotropic universes because of a couple of reasons. First, it bears various important features of the whole anisotropic universes including large anisotropy at $\tau = 0$. Second, only in this symmetric case of all anisotropic expansions, we can impose proper anisotropic vacuum state in terms of the zeroth order WKB approximation [6].

If one uses the Sasaki-Mukhanov variable, except for the complication due to the mixing of tensor-scalar modes, the evolutions of the metric perturbations are not much different from that of a massless scalar field [7]. In Ref. [5], it was also shown that the mode mixing modifies the power spectrum only by a proportionality factor with a small correction term of order m/H_i, where m is the mass of the inflaton. Therefore, as a formulation level, it is good to deal with the scalar field rather than the metric perturbation itself. Hence in this work, we are interested in the evolution of a massless, minimally coupled scalar field propagating on the background anisotropic universe (1) with action

$$S_\phi = -\frac{1}{2}\int d^4x\sqrt{-g}\Big(g^{\mu\nu}\partial_\mu\phi\partial_\nu\phi\Big). \tag{2}$$

This scalar field is not the inflaton but just a *mimic of metric perturbations*.

2 Quantization of the Scalar field on anisotropic vacuum

The canonical quantization of the minimally coupled massless scalar field with the action (2) in the anisotropic spacetime (1) is done in the standard manner:

$$\phi = \int d^3k\Big(u_{\mathbf{k}}a_{\mathbf{k}} + u^*_{\mathbf{k}}a^\dagger_{\mathbf{k}}\Big), \tag{3}$$

where the creation and annihilation operators satisfy the commutation relations $\left[a_{\mathbf{k_1}}, a^\dagger_{\mathbf{k_2}}\right] = \delta(\mathbf{k_1} - \mathbf{k_2})$ (others are zero) and $u_{\mathbf{k}} = e^{i\mathbf{kx}}\phi_{\mathbf{k}}/(2\pi)^{3/2}$. The details of the quantization process depend on the choice of the mode function $u_{\mathbf{k}}$. We normalize the mode function as $\phi_{\mathbf{k}}\partial_\tau\phi^*_{\mathbf{k}} - \big(\partial_\tau\phi_{\mathbf{k}}\big)\phi^*_{\mathbf{k}} = \frac{i}{e^{3\alpha}}$.

For the later convenience, we introduce a dimensionless time x by $\sinh(\varepsilon x) = \frac{1}{\sinh(3H_i\tau)} = e^{-3\alpha}$, where ε denotes a small expansion parameter which will be specified later. The arrow of time for x is inverted since it varies from ∞ to $0+$ as the comoving time τ increases from $0+$ to ∞.

The equation of motion for the scalar field is written in the form of a time-dependent oscillator

$$\Big(\frac{d^2}{dx^2} + \Omega_{\mathbf{k}}(x)^2\Big)\phi_{\mathbf{k}} = 0\,, \tag{4}$$

where the dimensionless frequency squared is

$$\Omega^2_{\mathbf{k}}(x) = \left(\frac{\varepsilon}{3H_i}\right)^2 \frac{2^{4/3}\big(k_\perp^2 e^{-2\varepsilon x} + k_3^2\big)}{(1-e^{-2\varepsilon x})^{4/3}} = \frac{2(\bar{k}\varepsilon^{2/3})^2}{9}\left(\frac{e^{\varepsilon x}}{\sinh\varepsilon x}\right)^{1/3}\left(\frac{1}{e^{2\varepsilon x}-1} + r^2\right). \tag{5}$$

Here we define a scaled wave-number and a measure of planarity of a given mode by $\bar{k} = \varepsilon^{1/3}\frac{k}{H_i}$, $\quad r = \frac{k_3}{k}$, where $k^2 := k_1^2 + k_2^2 + k_3^2 = k_\perp^2 + k_3^2$. Later in this paper, we omit $\mathbf{k}$ in the frequency squared $\Omega^2_{\mathbf{k}}$ for simplicity. The power spectrum is defined by

$$\langle 0|\phi^2|0\rangle := \int d\ln k \int \frac{d\theta_{\mathbf{k}}}{2}P, \quad P = \frac{k^3}{2\pi^2}\big|\phi_{\mathbf{k}}\big|^2. \tag{6}$$

In contrast to the case of the standard de Sitter universe the direction dependence would be included in the power spectrum. The vacuum is chosen at the initial anisotropic era: $\tau \to +0$ to satisfy $a_{\mathbf{k}}|0\rangle = 0$. For this purpose, we choose the solution to be purely positive frequency mode with respect to τ at the early stage.

3 Non-planar high-momentum modes

As mentioned in the introduction, we use the WKB solution at early times ($x > x_*$) and asymptotic solution at later times ($x < x_*$). At the matching time $x = x_*$, the accuracies of the two are equal. Later in this paper, we set $x_* = 1$ by choosing ε appropriately. We also assume that $\bar{k}$ is larger than one, which will be satisfied with the modes we are interested in at the present approximation.

The WKB approximation is if $\epsilon(x) := \left|\frac{\frac{d\Omega^2(x)}{dx}}{\Omega^3(x)}\right| \ll 1$. For the early times, the WKB wavefunction is expanded up to an enough adiabatic order, to validate our matching scheme with the solutions in the asymptotic region. The next order of the approximation will improve the accuracy by the order $E_{\rm WKB}(x) \sim \epsilon(x)^2 \simeq \frac{1}{\bar{k}^2\, x^{2/3}}$.

In the later time limit, the space-time approaches that of the de Sitter spacetime. Therefore, it is natural that the zeroth order solution is just the well-known scalar field mode solution in the de Sitter spacetime. The higher order corrections are based on the *asymptotic approximation* based on the limit $\varepsilon x \ll 1$. By series expanding the frequency squared, we approximate the equation of motion (4) to be

$$\left(\frac{d^2}{dx^2} + \sum_{n=0}^{\infty} \varepsilon^n V_n\right)\phi = 0\,, \tag{7}$$

where the order by order corrections of the frequency squared are the same order for $x \sim 1$. The general solution to the differential equation (7) is given by $\phi = A_+ u(x) + A_- v(x)$, where u and v are the positive and negative frequency modes, respectively. We get the approximate solution by series expanding the modes $u = u_0 + \varepsilon u_1 + \varepsilon^2 u_2 + \cdots$ and $v = v_0 + \varepsilon v_1 + \varepsilon^2 v_2 + \cdots$ and then solving the equation of motions order by order. To determine the time when the WKB and the asymptotic approximations will be matched, we need to know the size of the error of the zeroth order solution for a given x. The relative ratio of the correction term to the zeroth order solution gives the error, $E_{\rm asym}(x) \sim \varepsilon\bar{k}\, x^{4/3}$. The approximation will be best if we choose the intermediate time x_* so that the accuracies of the two solution match: $E_{\rm WKB} = E_{\rm asym}$, which gives $x_* = (\varepsilon\bar{k}^3)^{-1}$. For simplicity, we choose to set $x_* = 1$. Therefore, the small expansion parameter becomes $\varepsilon = \bar{k}^{-3} = \left(\frac{H_i}{k}\right)^{3/2}$. Now, the size of error at $x = x_*$ becomes $E_{\rm asym} = \bar{k}^{-2} = H_i/k$, which ensures that the present approximation works well for high momentum modes.

After the matching, we find that the power spectrum acquires corrections only when we calculate to the adiabatic order $O(\bar{k}^{-12})$. The power spectrum including the corrections becomes

$$P \;=\; \frac{{H_i}^2}{4\pi^2}\left\{1 + \frac{9(11 - 90r^2 + 99r^4)}{32}\left(\frac{H_i}{k}\right)^6 + O\left(\left(\frac{H_i}{k}\right)^7\right)\right\}. \tag{8}$$

For mode with $k \sim 10H_i$, the relative size of the correction term is of $O(10^{-6})$. The isotropy violation at initial stage of the universe is not small but its effects on the spectrum for the non-planar modes are suppressed by the long duration of inflation and high momentum effect. The correction $O((H_i/k)^6)$ is highly dependent on k to suppress the anisotropy effect.

4 Planar modes

For the planar modes $r^2 \sim 0$, there appears a region where the WKB approximation may not be valid during a period in $\varepsilon x \gg 1$. We divide the time into three separate regions divided by the times x_1 and x_* (See Fig. 1). In the region $x_1 > x > x_*$ the WKB approximation is valid. For other two regions, we may find approximate solutions. In the case of $r = 0$ exactly, the adiabaticity parameter diverges in the limit of $x \to \infty$ and there is no anisotropic vacuum state. The mode $r = 0$ would behave classically, not quantum mechanically, and will be out of scope.

The characteristic behavior of $\epsilon(x)$ is shown in Fig. 1.

Matching the solutions in the three regions yields the final amplitude and hence the power spectrum

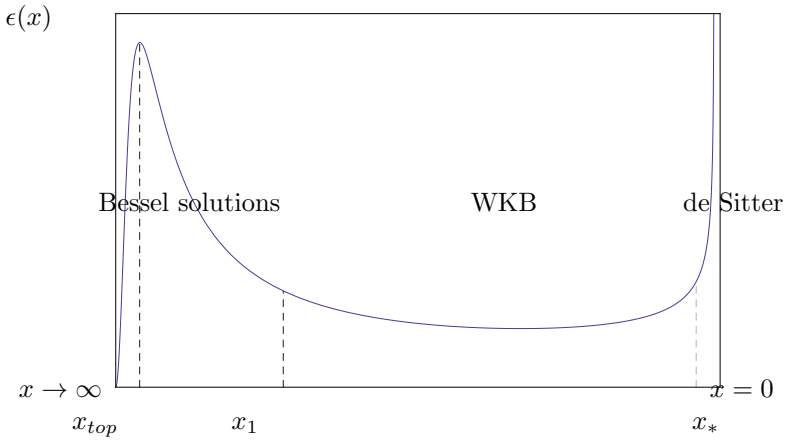

Figure 1: The behavior of the adiabatic parameter in the case of a planar mode. The left hand side ($x \to \infty$) corresponds to the past. The WKB approximation is temporary violated around $x \simeq x_{top}$.

obtained in the isotropic limit:

$$P = \left(\frac{H_i}{2\pi}\right)^2 \left(\coth \pi\bar{r} - \frac{\cos\left(2\Psi\right)}{\sinh \pi\bar{r}}\right), \tag{9}$$

where $\Psi(k) = \bar{k}x_*^{1/3} - \int_{x_1}^{x_*} \Omega(x)dx + \bar{q}e^{-\varepsilon x_1} - \frac{\pi}{4}$. The explicit value of the correction term becomes order of 10^{-3} for $\bar{r} \sim 3$. In the planar limit, the deviation of the power spectrum from the ansatz in Ref. [2] is quite clear.

5 Conclusion

We have reinvestigated the quantization of a massless and minimally coupled scalar field as a way to probe the signature of pre-inflationary background anisotropy in the spectrum of cosmological perturbations.

We first dealt the non-planar modes. We have shown that the power spectrum of the scalar field acquires non-vanishing corrections only when we execute the approximation up to 6th order. Hence, the direction dependence appears only at the order $O((H_i/k)^6)$.

For the planar mode, we have obtained essentially the same result as that in our previous analysis [5, 6], but was confirmed by a more accurate matching. For such a mode, the temporal breaking of the WKB approximation relatively enhances the effects of the primordial anisotropy in the power spectrum.

References

[1] H. -C. Kim and M. Minamitsuji, arXiv:1211.1132 [gr-qc].

[2] L. Ackerman, S. M. Carroll, and M. B. Wise, Phys. Rev. D **75**, 083502 (2007), Erratum-ibid. D **80**, 069901 (2009) [arXiv:astro-ph/0701357].

[3] C. Pitrou, T. S. Pereira and J. P. Uzan, JCAP **0804**, 004 (2008) [arXiv:0801.3596 [astro-ph]];

[4] A. E. Gümrükçüoğlu, L. Kofman and M. Peloso, Phys. Rev. D **78**, 103525 (2008) [arXiv:0807.1335 [astro-ph]].

[5] H.-C. Kim and M. Minamitsuji, JCAP 1103, 038 (2011), [arXiv:1101.0329[gr-qc]].

[6] H. C. Kim and M. Minamitsuji, Phys. Rev. D **81**, 083517 (2010) [arXiv:1002.1361[gr-qc]];

[7] A. E. Gumrukcuoglu, C. R. Contaldi, M. Peloso, JCAP **0711**, 005 (2007). [arXiv:0707.4179[astro-ph]].

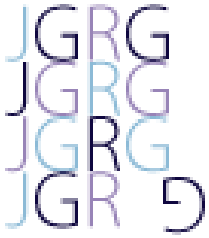

Kazunori Nakayama, JGRG 22(2012)111209

"Probing dark radiation with inflationary gravitational waves"

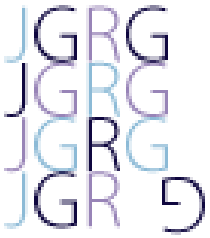

RESCEU SYMPOSIUM ON

GENERAL RELATIVITY AND GRAVITATION

JGRG 22



November 12-16 2012

Koshiba Hall, The University of Tokyo, Hongo, Tokyo, Japan



Probing dark radiation with inflationary gravitational waves

Kazunori Nakayama (The University of Tokyo)

R.Jinno, T.Moroi, KN, arXiv:1208.0184

JGRG22 @ University of Tokyo (2012/11/12)

Contents

- Observational evidence of dark radiation
- Effects of dark radiation on inflationary gravitational waves

Dark radiation

- Radiation energy density

$$\rho_{\rm rad} = \left[1 + N_{\rm eff}\frac{7}{8}\left(\frac{4}{11}\right)^{4/3}\right]\rho_\gamma$$

$N_{\rm eff} = 3.04$ in the standard model

- Helium abundance $N_{\rm eff} = 3.68^{+0.80}_{-0.70}\ (2\sigma)$

  Izotov, Thuan , 1001.4440

- WMAP+ACT+BAO $N_{\rm eff} = 4.56 \pm 0.75\ (68\%)$

  Dunkley et al., 1009.0866

- WMAP+SPT+BAO $N_{\rm eff} = 3.86 \pm 0.42\ (68\%)$

  Keiser et al., 1105.3182

- WMAP+ACT+SPT+BAO $N_{\rm eff} = 4.08^{+0.71}_{-0.68}\ (95\%)$

  Archidiacono, Calabrese, Melchiorri, 1109.2767

Dark radiation

$\Delta N_{\rm eff} \simeq 1$ → Dark radiation ?

- Dark radiation (X) should satisfy :
  - X interaction is negligibly small
  - X is relativistic at the CMB epoch
- Many models are proposed so far...

Ichikawa, Kawasaki, KN, Senami, Takahashi (2007), KN, Takahashi, Yanagida (2010),
Fischler, Meyers (2011), Kawasaki, Kitajima, KN (2011), Hasenkamp (2011)
Menestrina, Scherrer (2011), Jeong, Takahashi (2012), K.Choi et al (2012) and many others

What is unique signature of dark radiation ?

Inflationary GWs

- Inflation generates primordial GWs as quantum tensor fluctuations in de-Sitter spacetime

$$ds^2 = a^2(t)[-d\tau^2 + (\delta_{ij} + h_{ij})dx^i dx^j]$$

$$h_{ij} = \frac{1}{M_P} \sum_{\lambda=+,-} \int \frac{d^3k}{(2\pi)^{3/2}} h_k^\lambda(t) e^{i\mathbf{kx}} e_{ij}^\lambda$$

Quantization

$$\langle h_k^\lambda h_{k'}^{\lambda'} \rangle = \frac{H_{\rm inf}^2}{2k^3} \delta^3(k-k') \delta^{\lambda\lambda'}$$

- Dimensionless power spectrum almost scale invariant

$$\Delta_h^2(k) = \left(\frac{H_{\rm inf}}{2\pi M_P} \right)^2$$

Evolution of GW

- Eq.of.m of GW (without dark radiation)

$$\ddot{h}_\lambda + 3H\dot{h}_\lambda + (k/a)^2 h_\lambda = 0 \quad \Rightarrow \quad \begin{aligned} h_\lambda &\sim \text{const} \quad \text{for} \quad k \ll aH \\ h_\lambda &\propto a(t)^{-1} \quad \text{for} \quad k \gg aH \end{aligned}$$

- GW energy density at horizon entry

$$\rho_{\rm GW}(k) \sim M_P^2 \Delta_h^2(k)(k/a)^2 \sim M_P^2 H_{\rm in}(k)^2 \Delta_h^2(k)$$

$$\rho_{\rm tot} \sim M_P^2 H_{\rm in}(k)^2$$

$$\Rightarrow \quad \Omega_{\rm GW}(k) = \frac{\rho_{\rm GW}(k)}{\rho_{\rm tot}} \sim \Delta_h^2(k) \sim \text{const at horizon entry}$$

$$\Rightarrow \quad \boxed{\Omega^0_{\rm GW}(k) \sim \Omega^0_{\rm rad} \Delta_h^2(k) \quad \text{at present for } k \gg k_{\rm eq}}$$

KN, J.Yokoyama (2010)

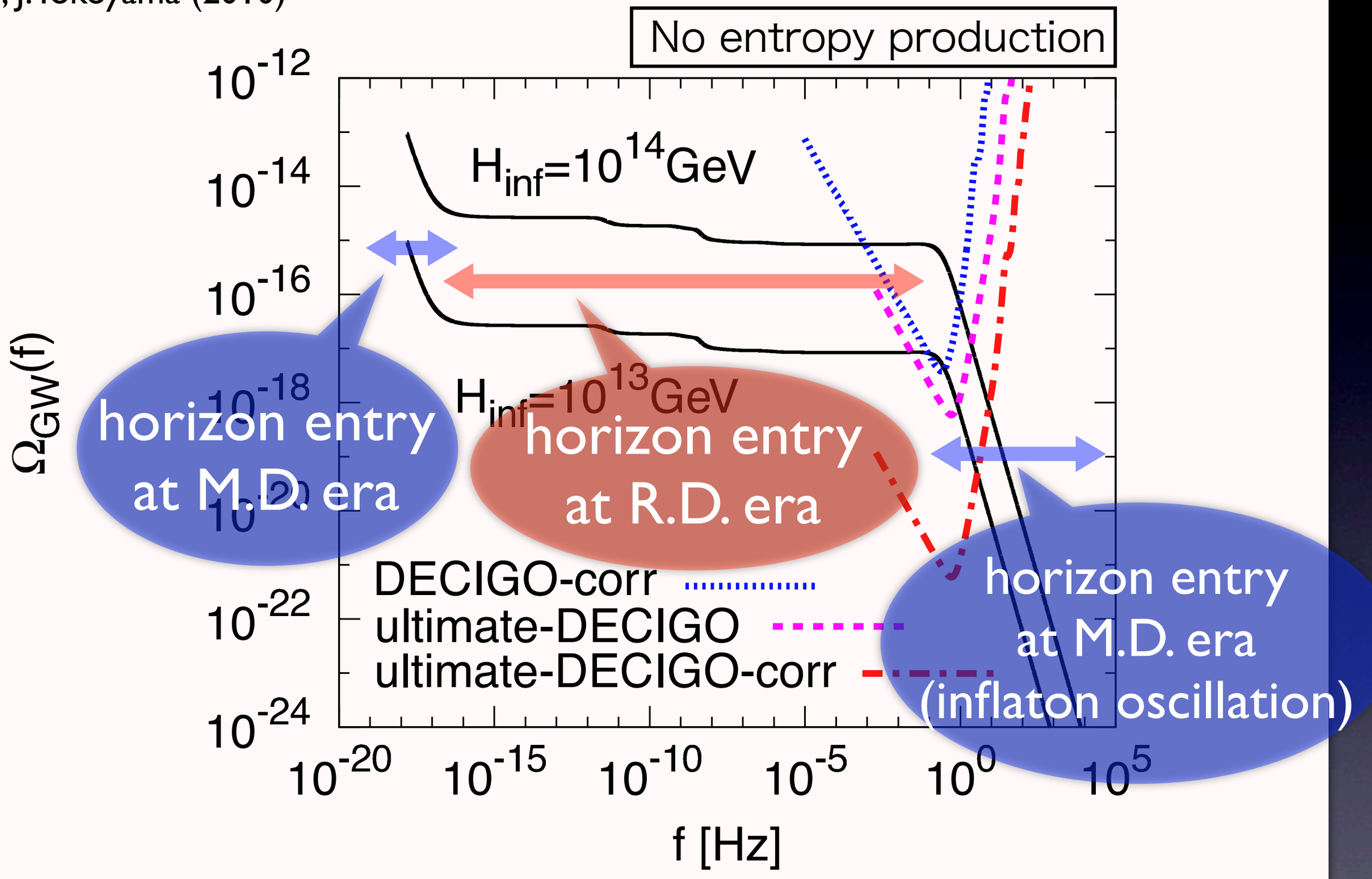

GW spectrum traces thermal history of the Universe !

N.Seto, J.Yokoyama (2003), Boyle, Steinhardt (2005), KN, Saito, Suwa, Yokoyama (2008)

Dark radiation and GW

- Dark radiation affects GW spectrum in two ways

$$\ddot{h}_{ij} + 3H\dot{h}_{ij} + (k/a)^2 h_{ij} = 16\pi G \Pi_{ij}$$

Modified expansion rate　　Anisotropic stress of X

cf) For standard neutinos, see

S.Weinberg (2003), Y.Watanabe, E.Komatsu (2005)

- Modified expansion rate by parent field of X
  → Modification on GW spectrum at high frequency
- Anisotropic stress is turned on after X production
  → Modification on GW spectrum at low frequency

A model

- A scalar field ϕ decays into X at $H \sim \Gamma_\phi$ with branching ratio B_X
- Background evolution :

$$\dot{\rho}_\phi + 3H\rho_\phi = -\Gamma_\phi \rho_\phi,$$
$$\dot{\rho}_{\rm rad} + 4H\rho_{\rm rad} = \Gamma_\phi (1 - B_X)\rho_\phi,$$
$$\dot{\rho}_X + 4H\rho_X = \Gamma_\phi B_X \rho_\phi,$$

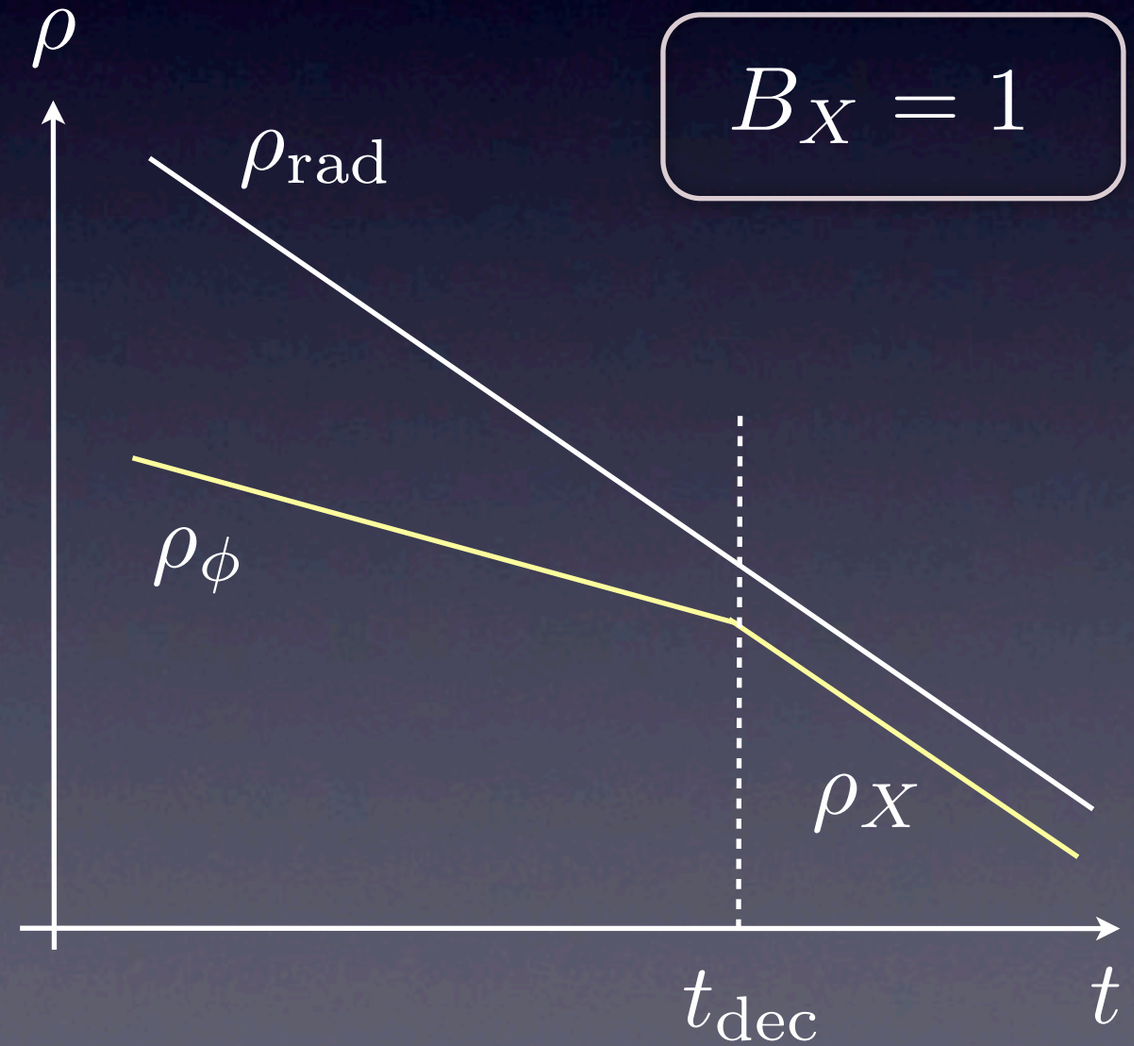

- ϕ nearly dominate at decay for $\Delta N_{\rm eff} \simeq 1$
- Example) ϕ : saxion
  X : axion

A model

- A scalar field ϕ decays into X at $H \sim \Gamma_\phi$ with branching ratio B_X
- Background evolution :

$$\dot{\rho}_\phi + 3H\rho_\phi = -\Gamma_\phi \rho_\phi,$$
$$\dot{\rho}_{\rm rad} + 4H\rho_{\rm rad} = \Gamma_\phi (1 - B_X)\rho_\phi,$$
$$\dot{\rho}_X + 4H\rho_X = \Gamma_\phi B_X \rho_\phi,$$

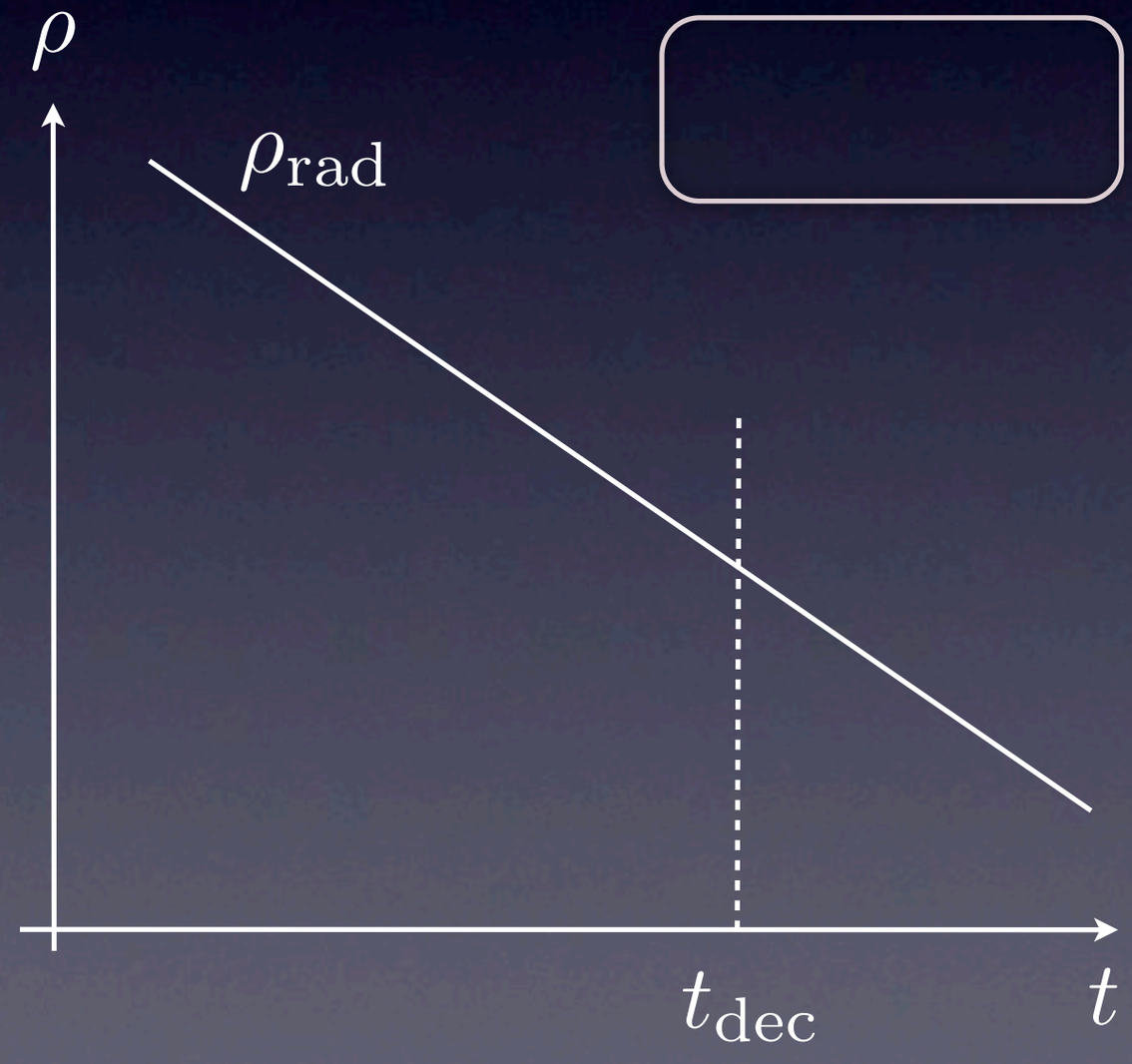

- ϕ nearly dominate at decay for $\Delta N_{\rm eff} \simeq 1$
- Example) ϕ : saxion
  X : axion

A model

- A scalar field ϕ decays into X at $H \sim \Gamma_\phi$ with branching ratio B_X
- Background evolution :

$$\dot{\rho}_\phi + 3H\rho_\phi = -\Gamma_\phi \rho_\phi,$$
$$\dot{\rho}_{\rm rad} + 4H\rho_{\rm rad} = \Gamma_\phi (1 - B_X)\rho_\phi,$$
$$\dot{\rho}_X + 4H\rho_X = \Gamma_\phi B_X \rho_\phi,$$

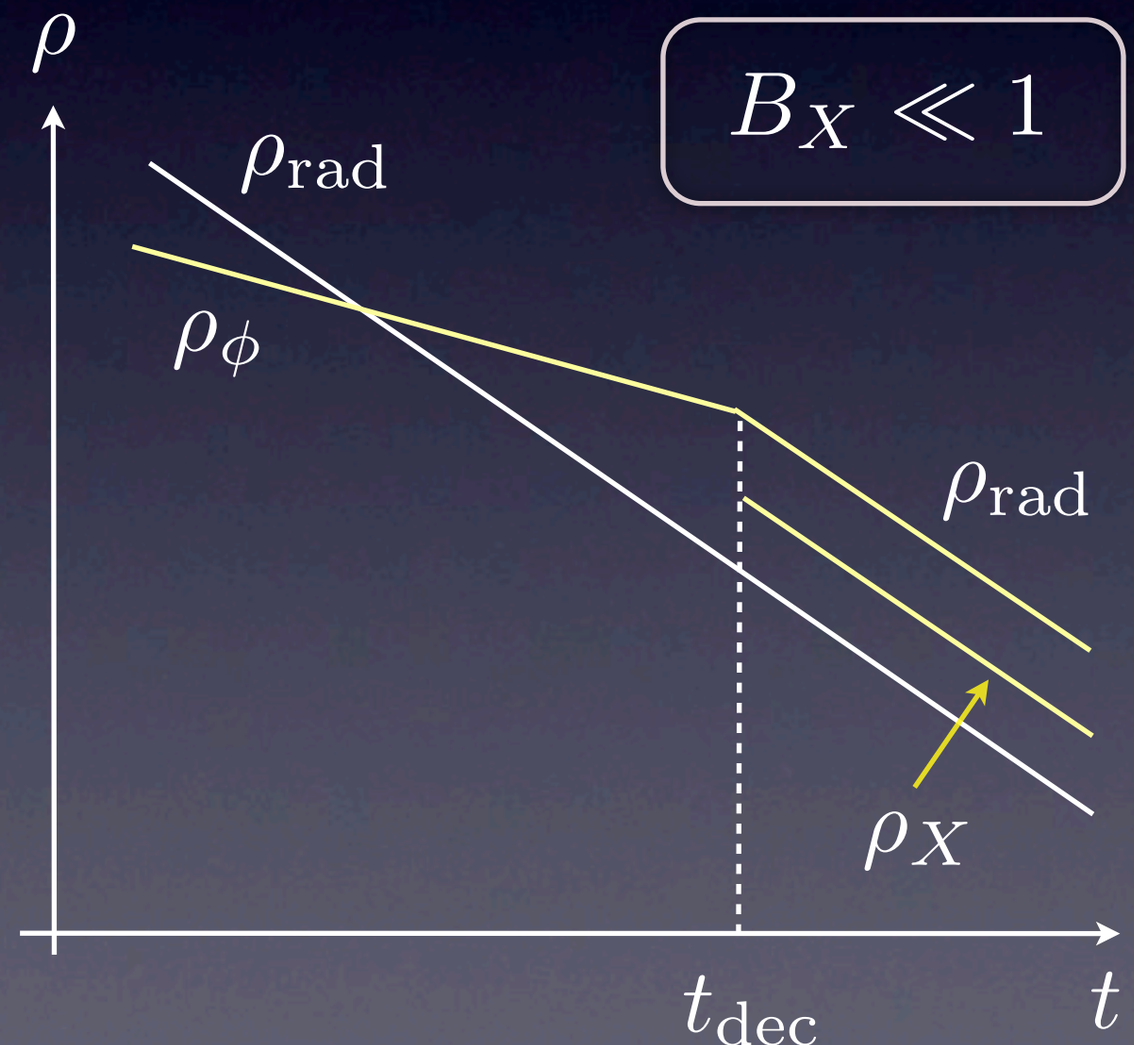

- ϕ nearly dominate at decay for $\Delta N_{\rm eff} \simeq 1$
- Example) ϕ : saxion
  X : axion

A model

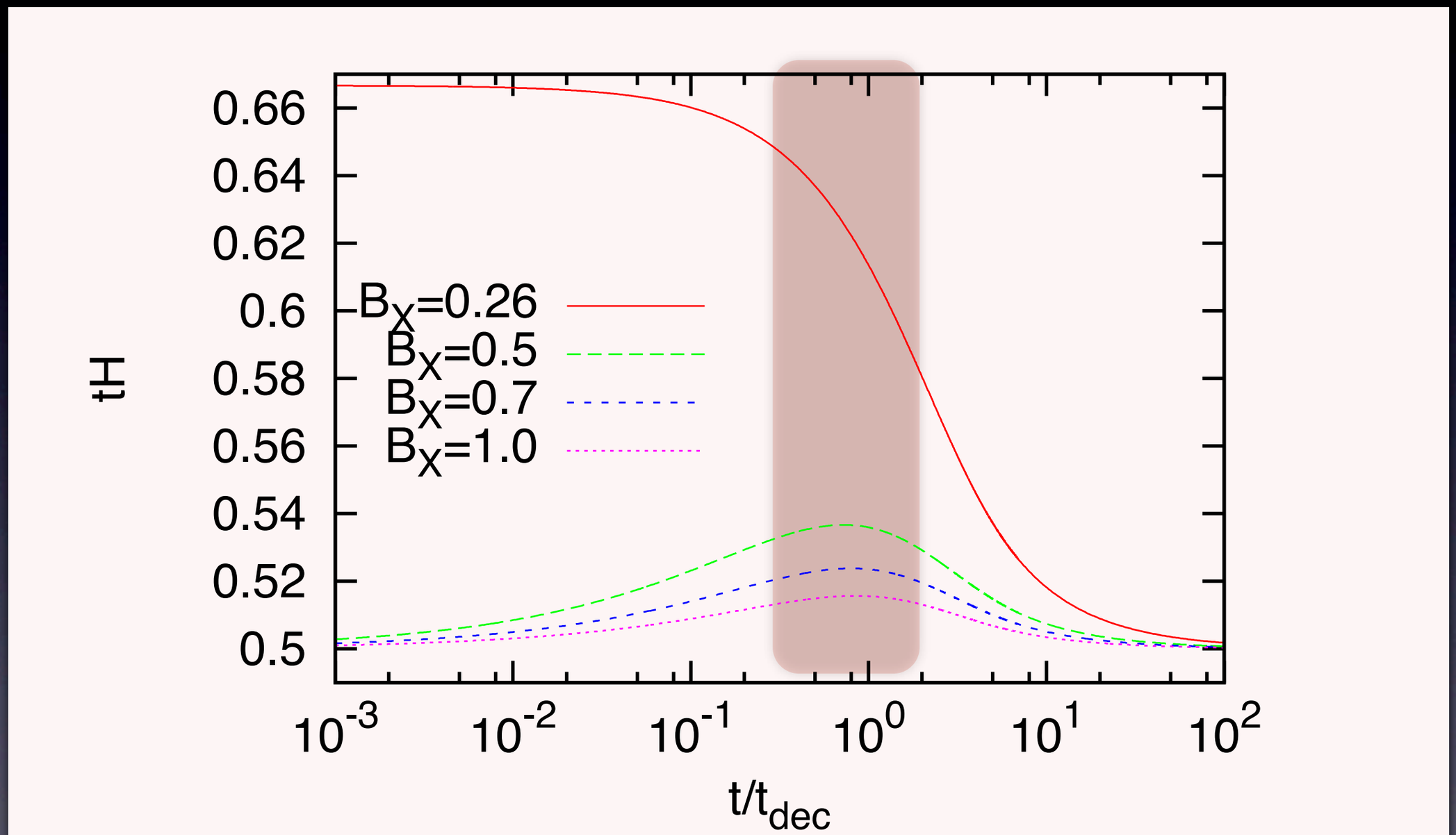

Deviation from R.D., tH=0.5, around Φdecay

Numerical result

$B_X = 1$

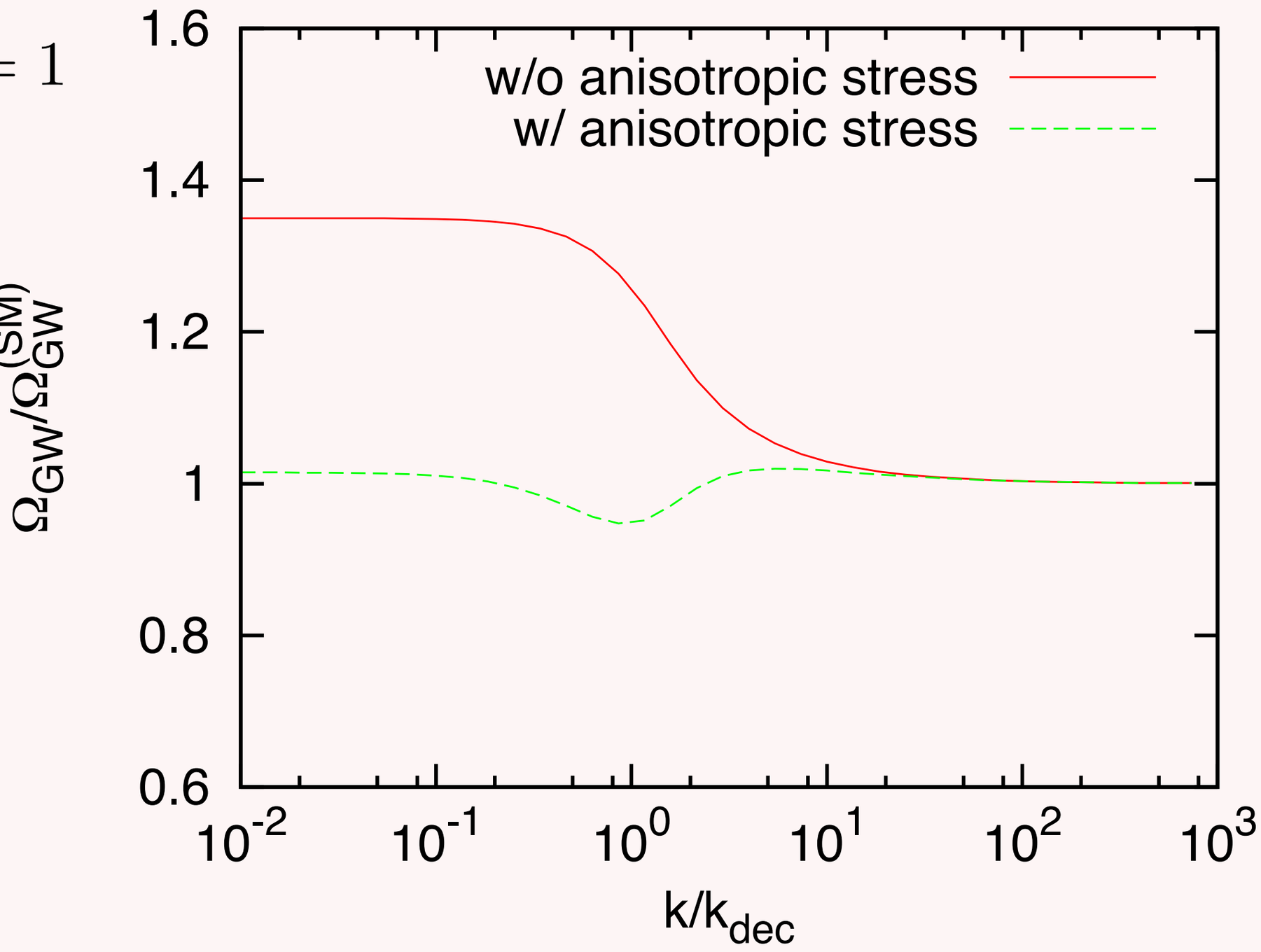

Numerical result

$B_X = 1$

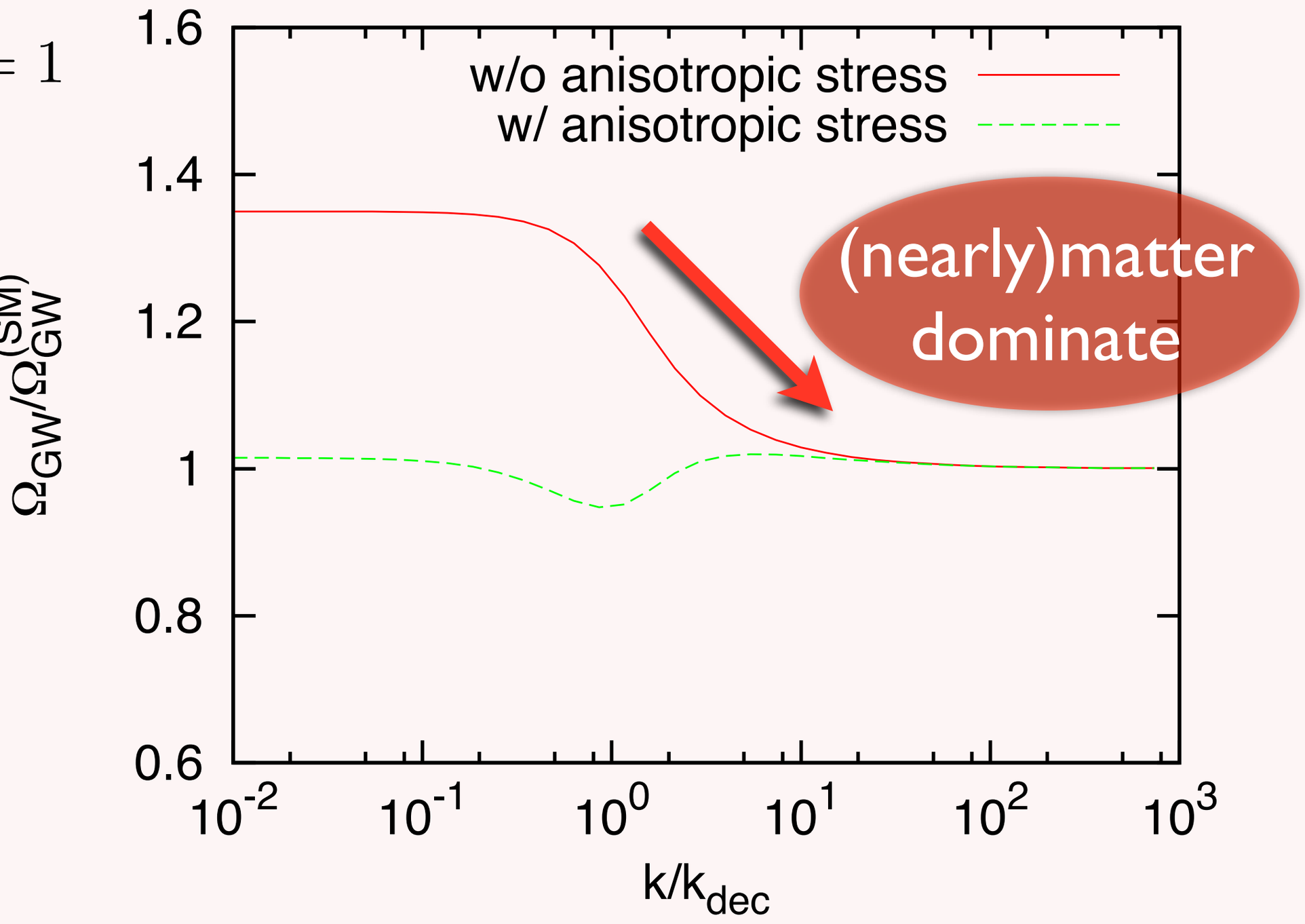

Numerical result

$B_X = 1$

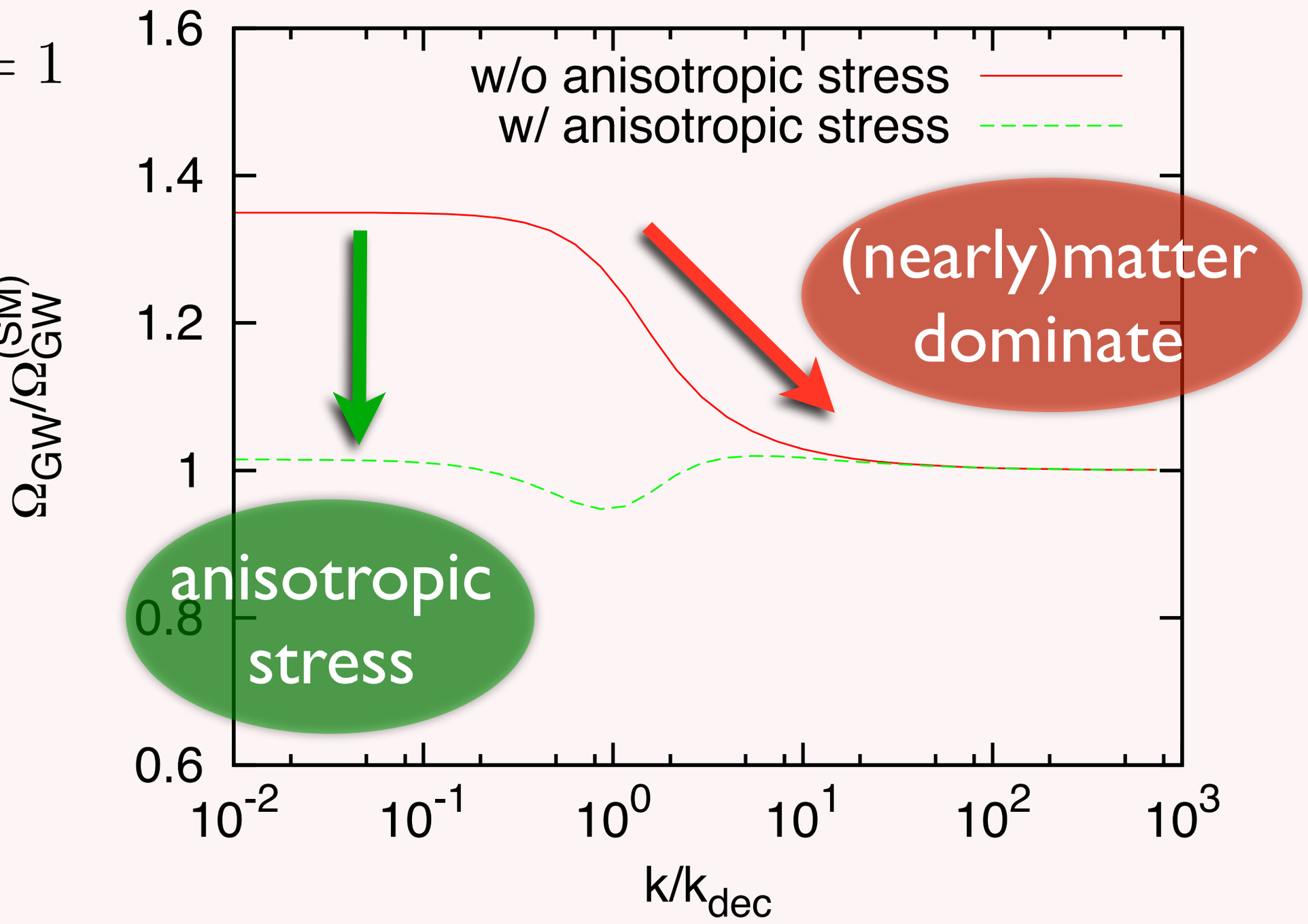

Numerical result

$B_X = 1$

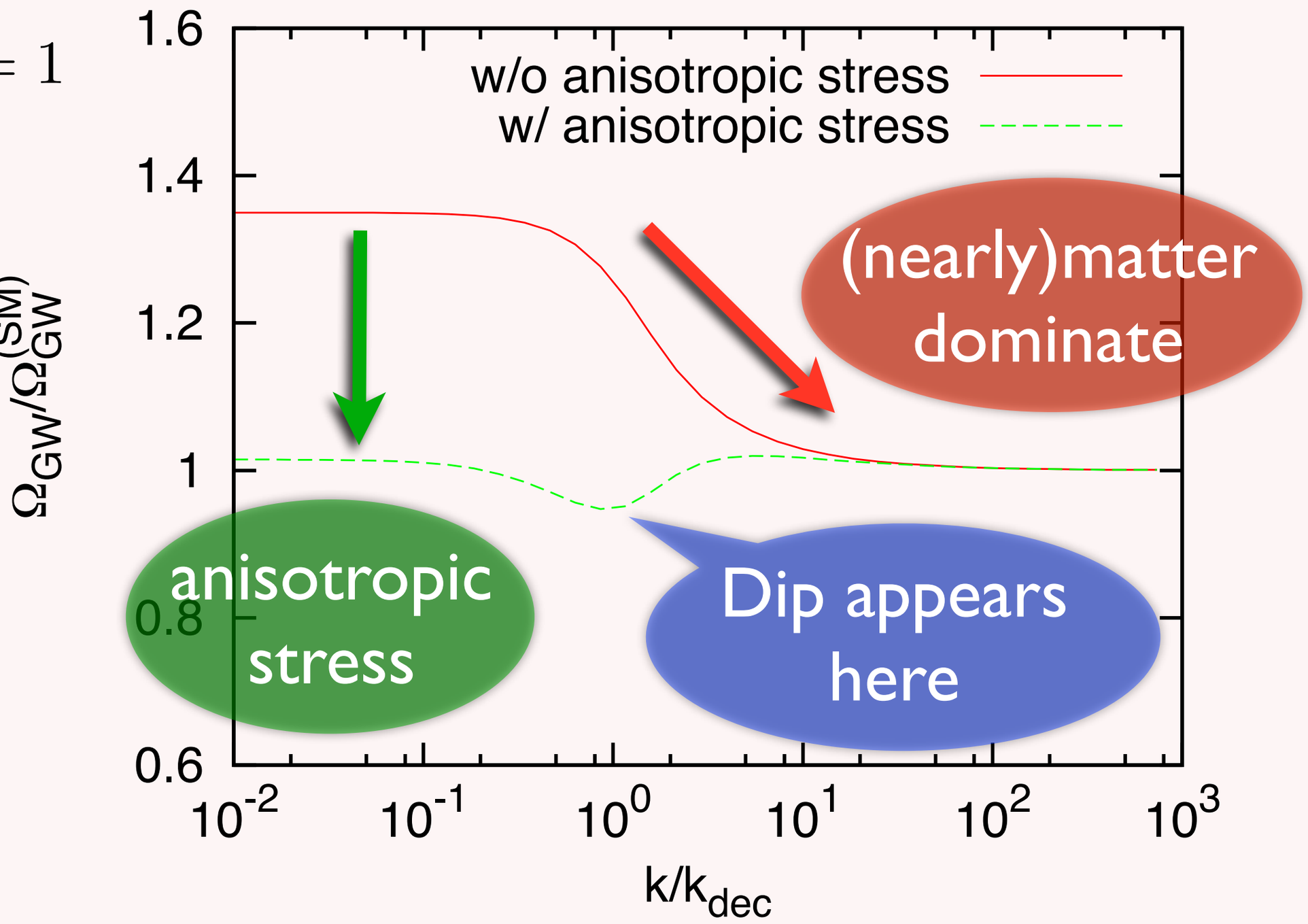

Numerical result

$B_X = 1$

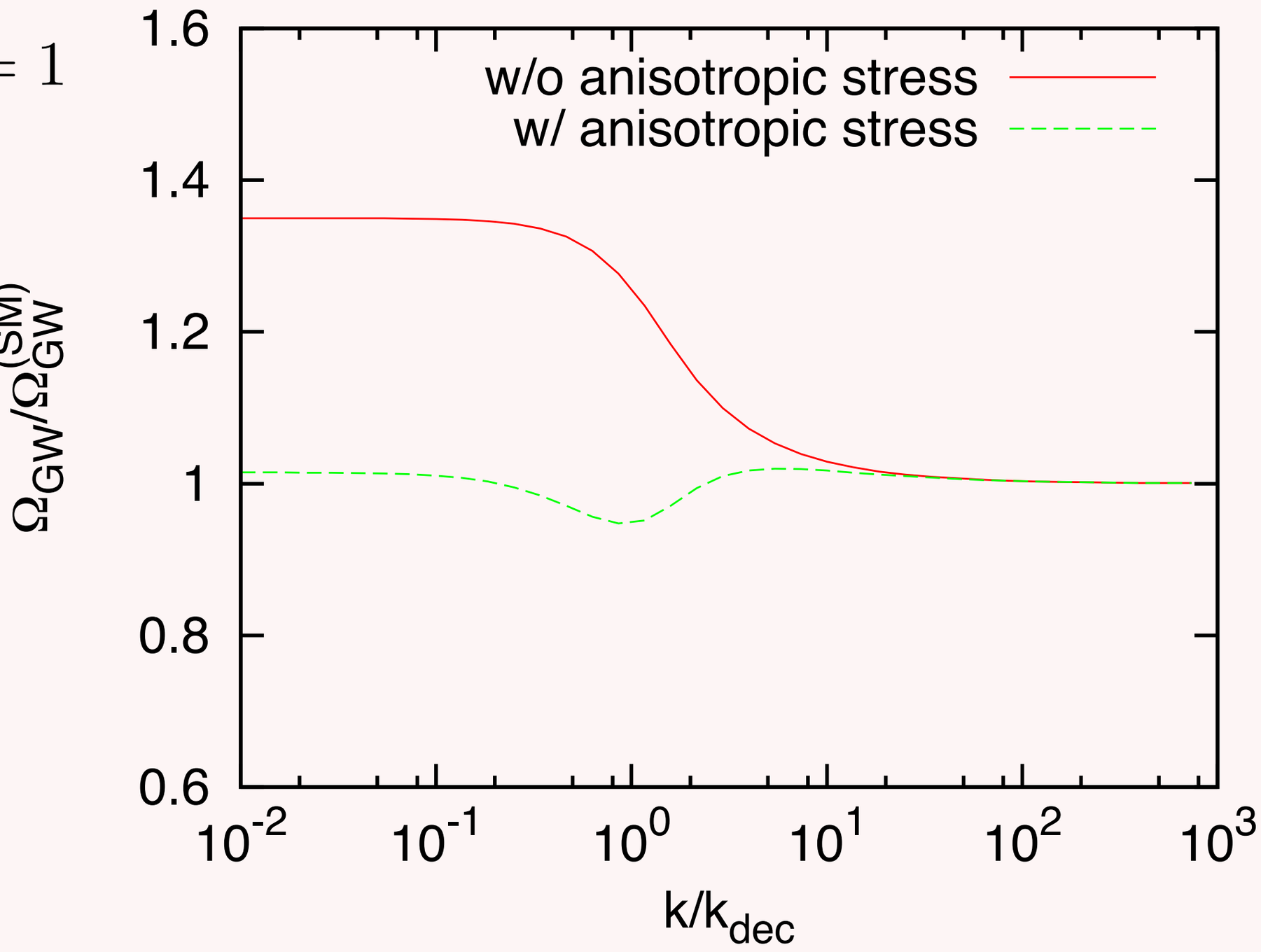

Numerical result

$B_X = 1$

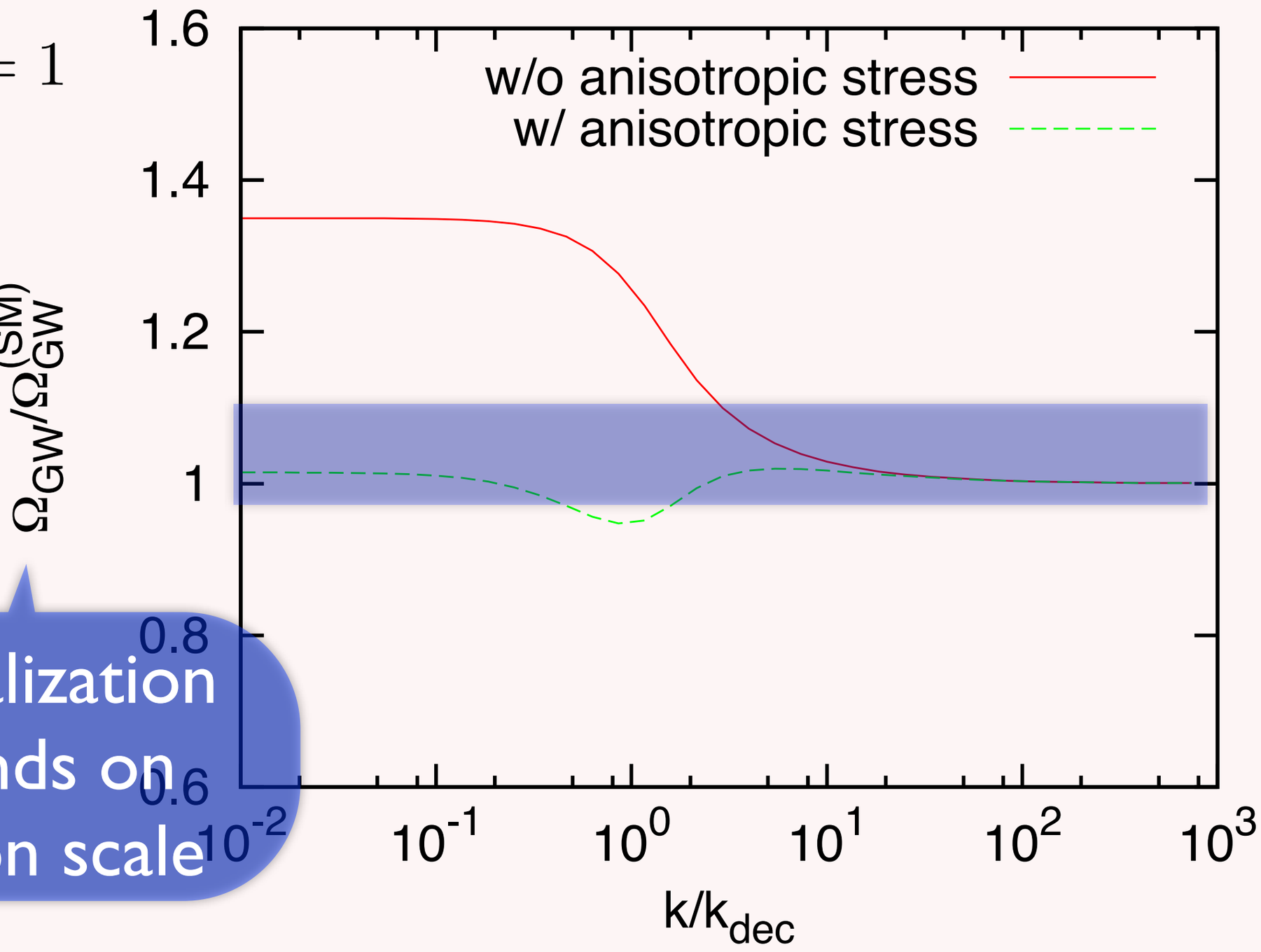

Normalization depends on inflation scale

Numerical result

$B_X = 1$

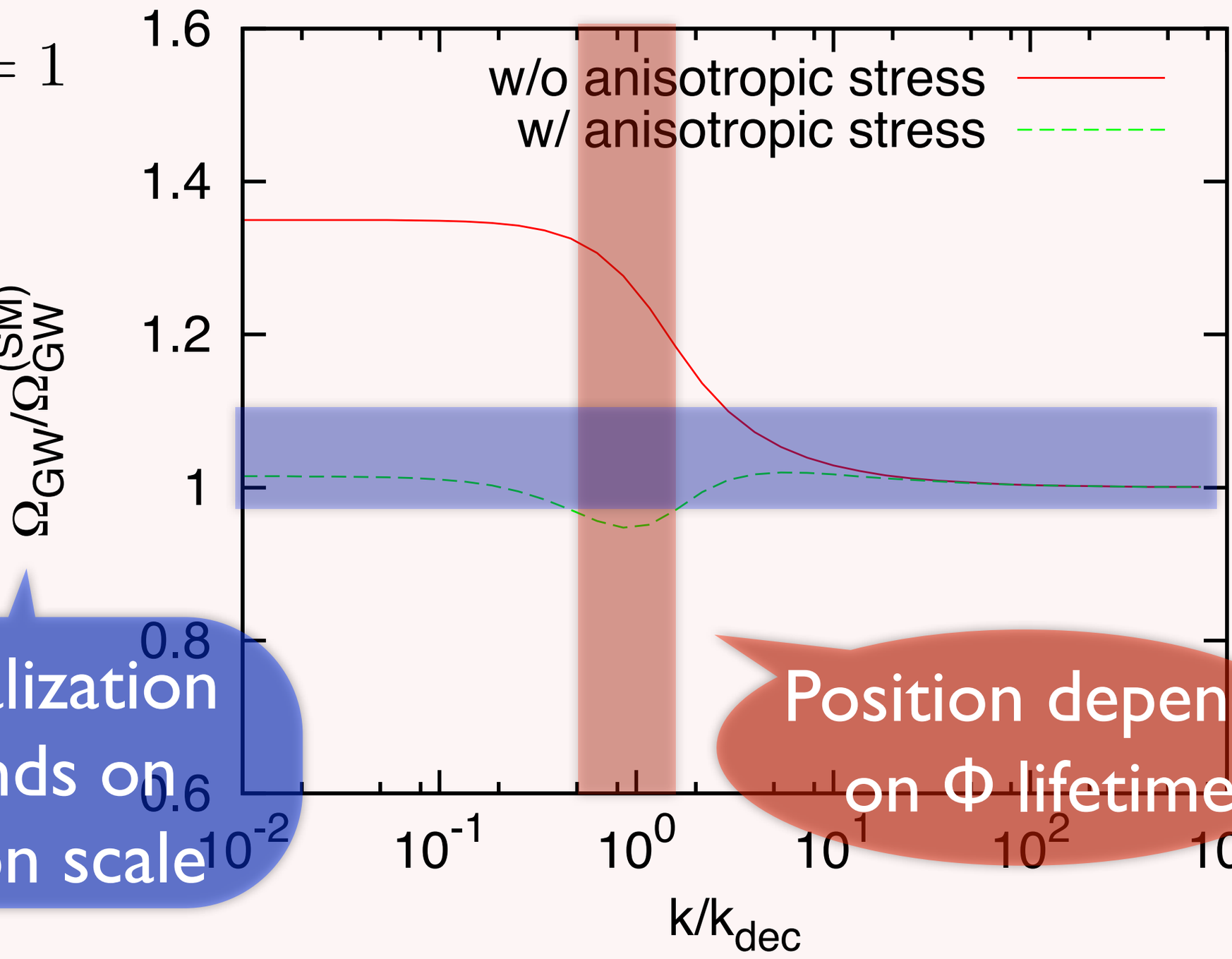

Normalization depends on inflation scale

Position depends on Φ lifetime

Numerical result

$B_X = 1$

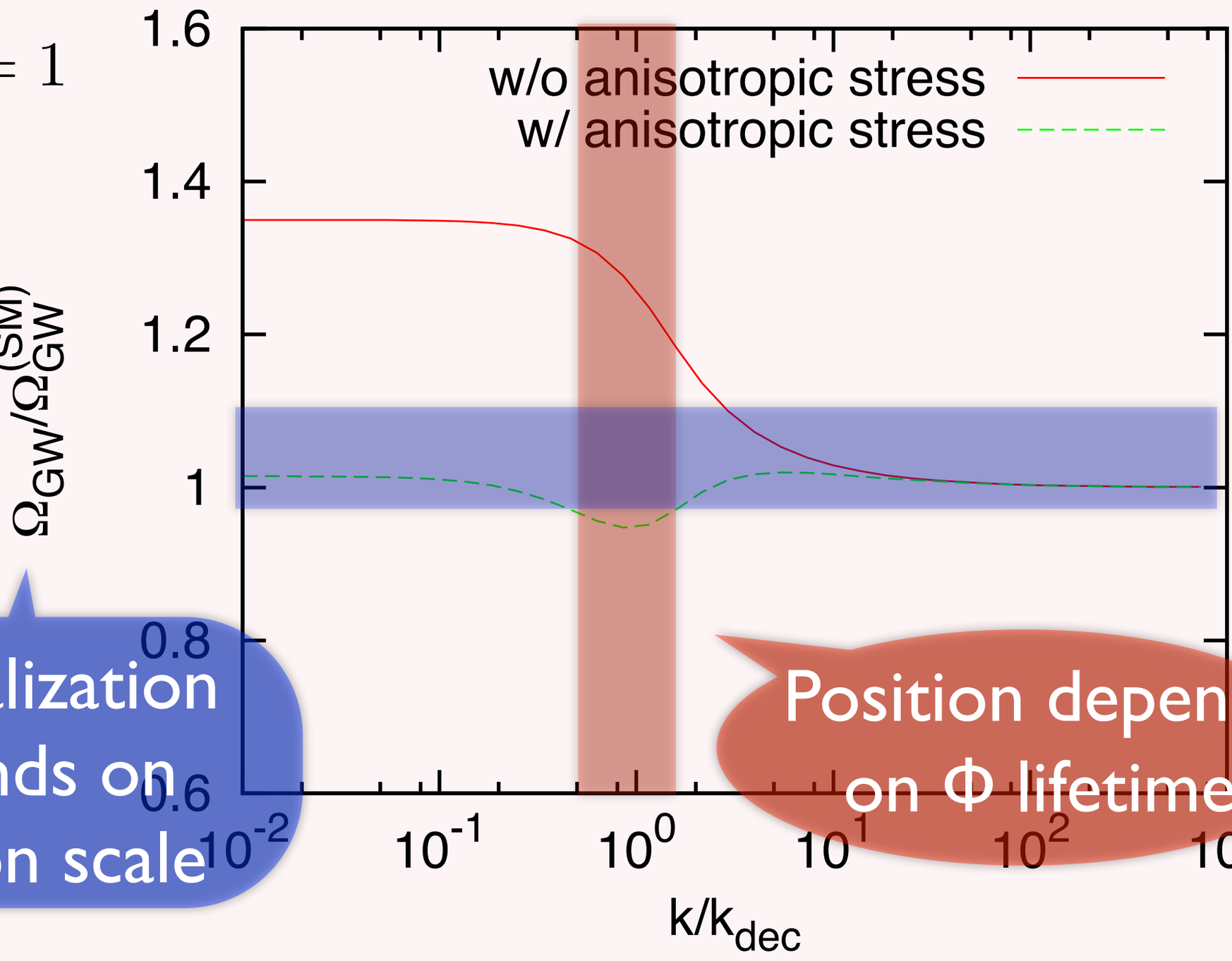

Normalization depends on inflation scale

Position depends on Φ lifetime

Detectable at DECIGO for $r \gtrsim 10^{-3}$ and $T_\phi \sim 10^7\,\mathrm{GeV}$

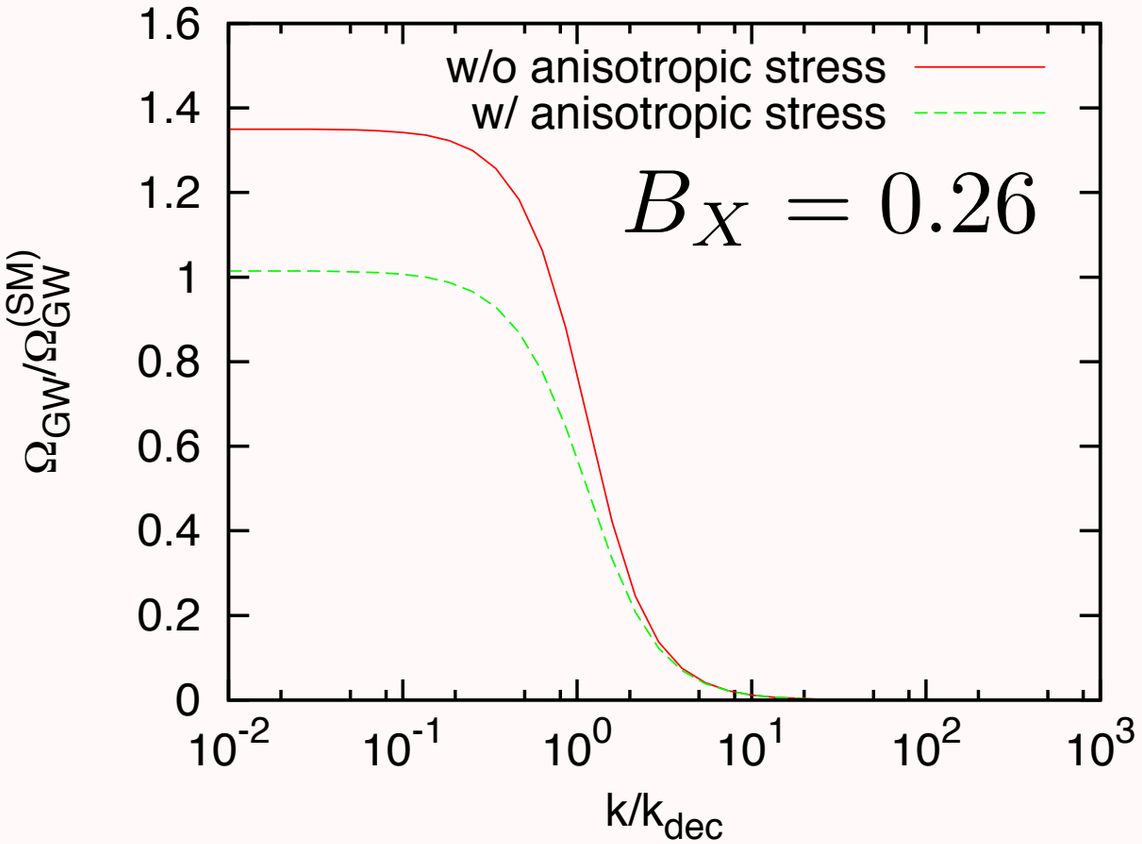
w/o anisotropic stress
w/ anisotropic stress
$B_X = 0.26$
$\Omega_{GW}/\Omega_{GW}^{(SM)}$
k/k_{dec}

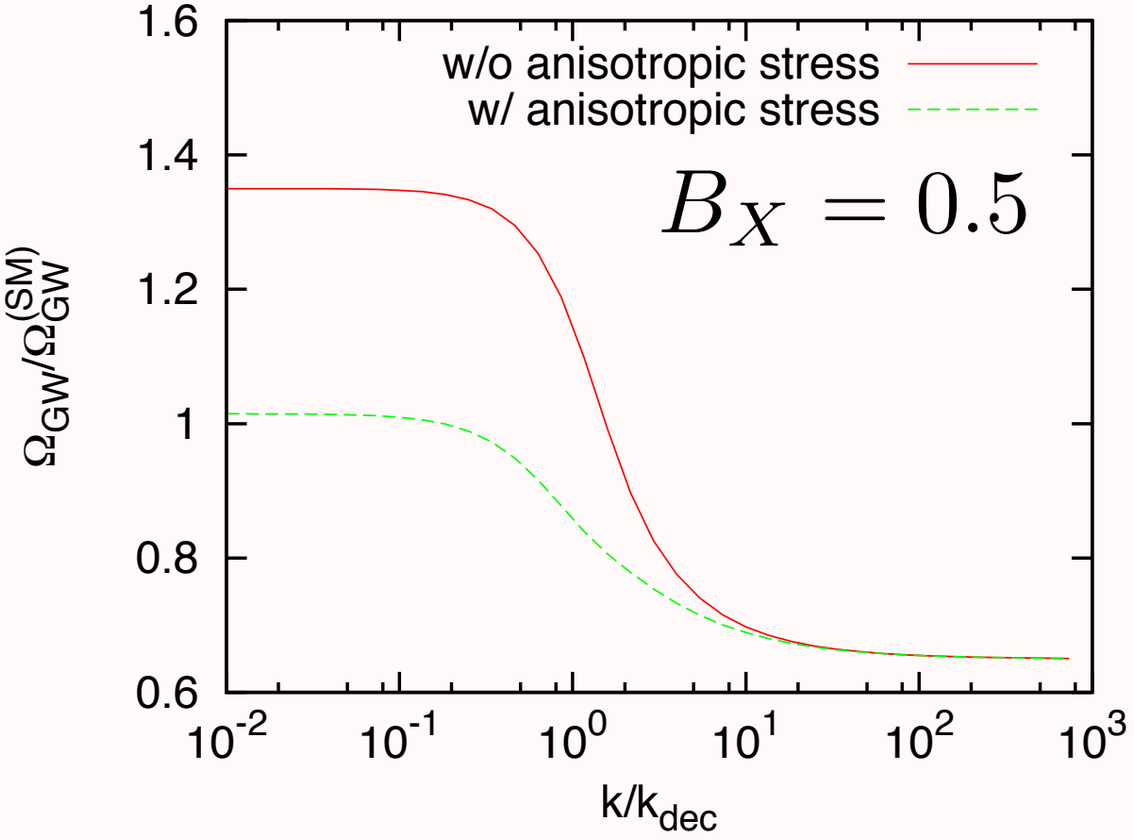
w/o anisotropic stress
w/ anisotropic stress
$B_X = 0.5$
$\Omega_{GW}/\Omega_{GW}^{(SM)}$
k/k_{dec}

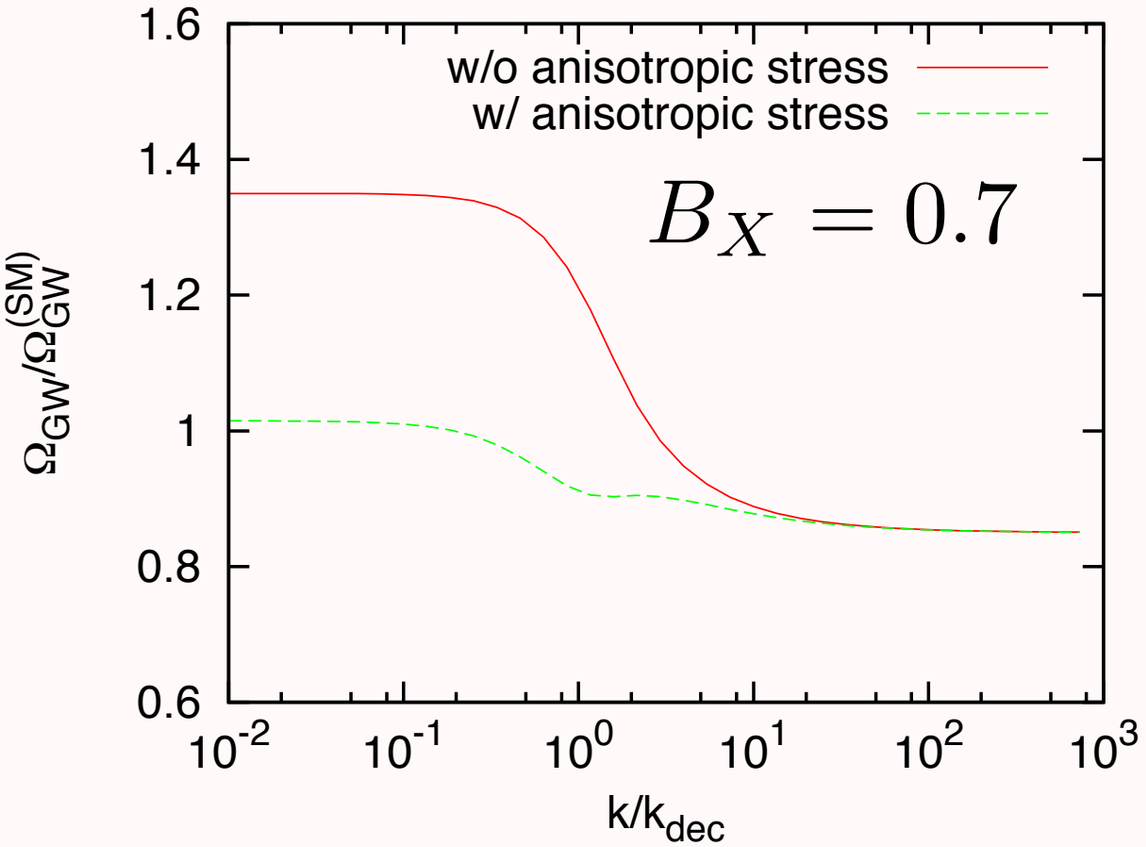
w/o anisotropic stress
w/ anisotropic stress
$B_X = 0.7$
$\Omega_{GW}/\Omega_{GW}^{(SM)}$
k/k_{dec}

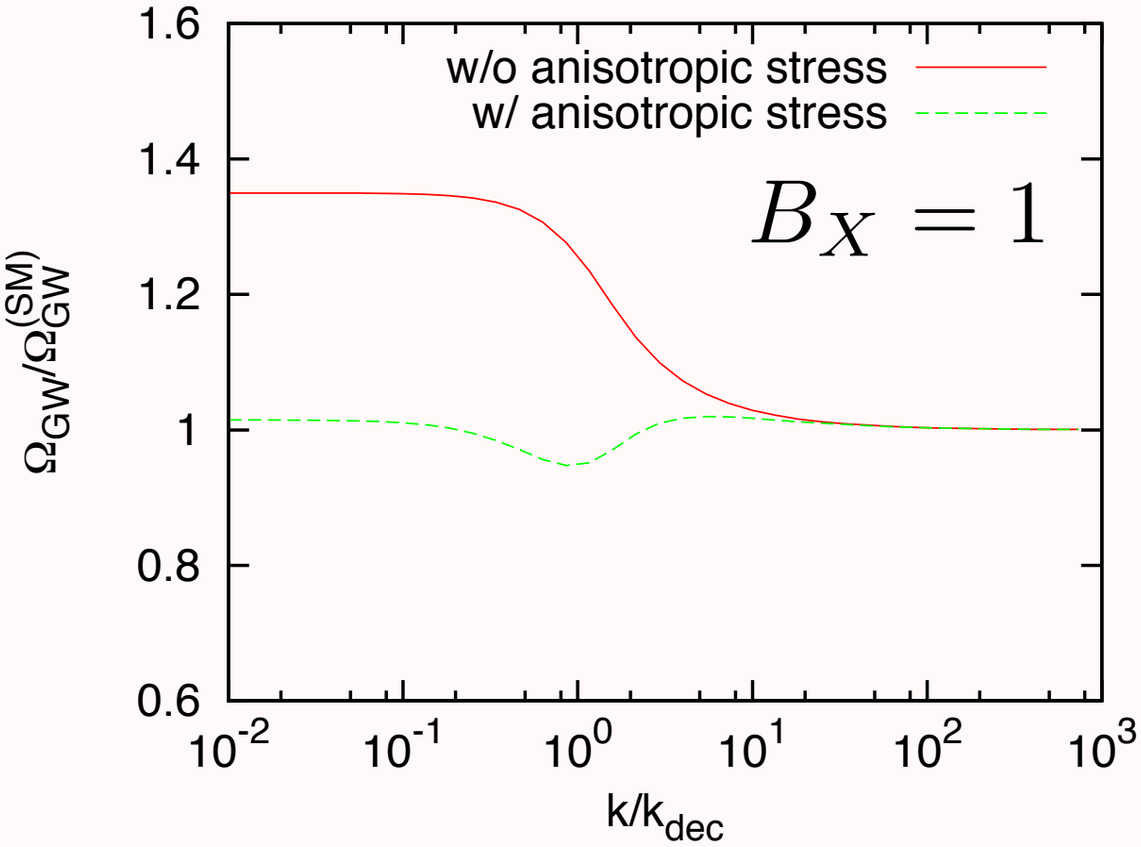
w/o anisotropic stress
w/ anisotropic stress
$B_X = 1$
$\Omega_{GW}/\Omega_{GW}^{(SM)}$
k/k_{dec}

Summary

- Recent observation suggest extra light species : dark radiation
- Dark radiation leaves characteristic signature in primordial GW spectrum
- It also contains information on the production mechanism of dark radiation.

Backup Slides

GW normalization

- Standard model
  - GW spectrum at horizon entry

$$\Omega_{\rm GW}(k=aH) = \frac{\Delta_h^2(k)}{24} \qquad \Delta_h^2(k) \equiv \frac{8}{M_P^2}\left(\frac{H_{\rm inf}}{2\pi}\right)^2\left(\frac{k}{k_0}\right)^{n_t}$$

- GW spectrum at present $(k \gg k_{\rm eq})$

$$\Omega_{\rm GW}^{\rm (SM)}(k) = \gamma^{\rm (SM)}\Omega_{\rm rad}^{\rm (SM)} \times \Omega_{\rm GW}(k=aH),$$

Expansion history :

$$\gamma^{\rm (SM)} = \left[\frac{g_*(T_{\rm in}(k))}{g_{*0}^{\rm (SM)}}\right]\left[\frac{g_{*s0}^{\rm (SM)}}{g_{*s}(T_{\rm in}(k))}\right]^{4/3},$$

GW normalization

- Standard model plus dark radiation
  - GW spectrum at present $(k \gg k_{\rm eq})$

$$\Omega_{\rm GW}(k) = \gamma \Omega_{\rm rad} \times \Omega_{\rm GW}(k = aH),$$

Expansion history modified by X :

$$\gamma = \frac{1 + \frac{7}{43}\left(\frac{g_{*s}(T_\phi)}{10.75}\right)^{1/3} \Delta N_{\rm eff}}{1/\gamma^{(\rm SM)} + \frac{7}{43}\left(\frac{g_{*s}(T_\phi)}{10.75}\right)^{1/3} \Delta N_{\rm eff}},$$

Radiation density :

$$\Omega_{\rm rad} = \Omega_{\rm rad}^{(\rm SM)} \times (g_{*0}/g_{*0}^{(\rm SM)}) \qquad g_{*0} = 2\left[1 + N_{\rm eff}\frac{7}{8}\left(\frac{4}{11}\right)^{4/3}\right]$$

Overall normalization is affected

GW normalization

- Parameterize normalization

$$\frac{\Omega_{\rm GW}(k)}{\Omega_{\rm GW}^{\rm (SM)}(k)} = C_1 \times C_2$$

Modified BG by X :

$$C_1 \equiv \frac{\gamma}{\gamma^{\rm (SM)}} \frac{g_{*0}}{g_{*0}^{\rm (SM)}}$$

Anisotropic stress X :

C_2 analytically derived in

Dicus, Repko (2004)

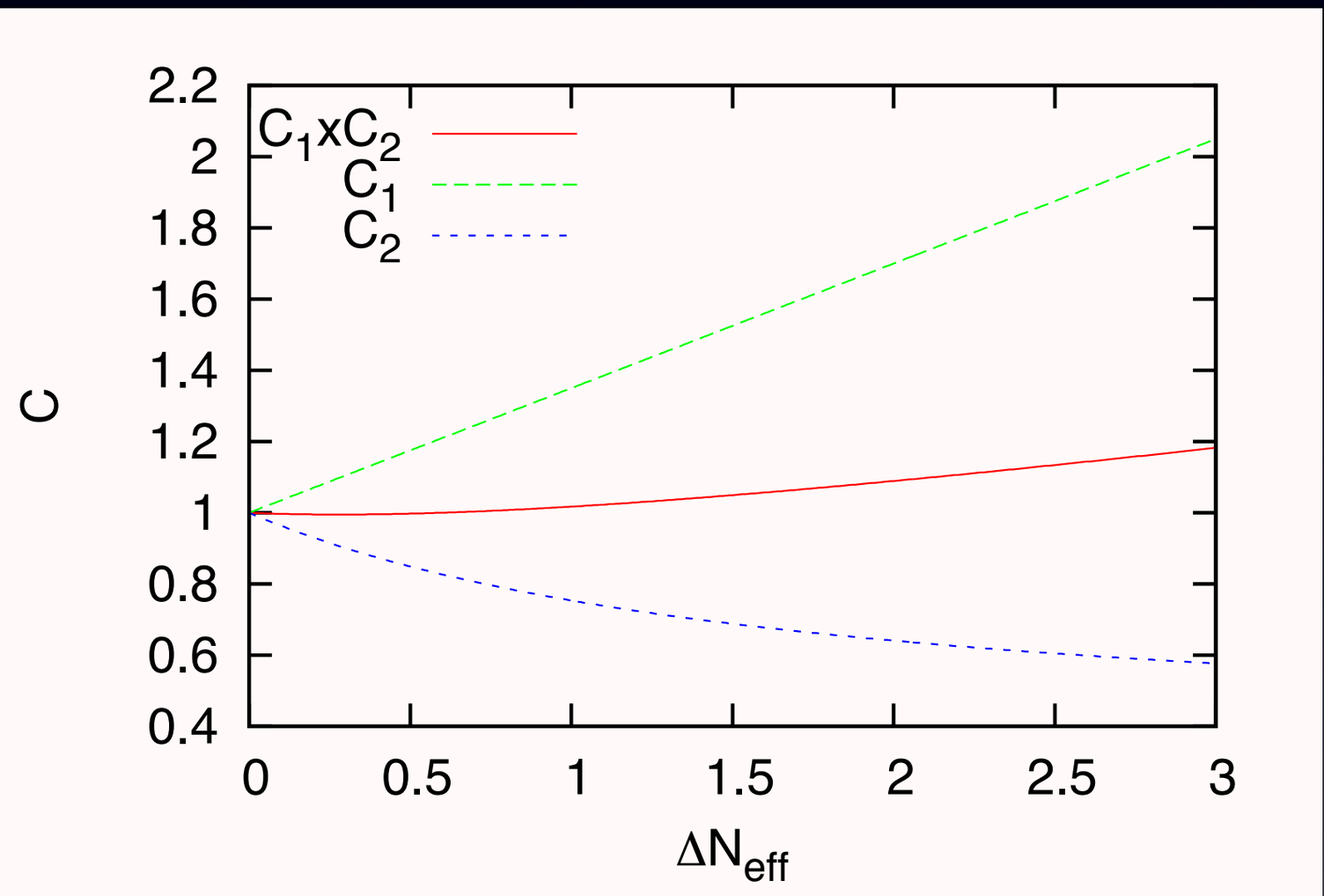

C1xC2 accidentally close to unity

Anisotropic stress

- Boltzmann eq. for X

$$\frac{dF}{dt} = \frac{B_X}{4\pi(p^0)^3}\Gamma_\phi \rho_\phi \delta\left(p^0 - \frac{m_\phi}{2}\right)$$

F : distribution function of X

$$\frac{dF}{dt} = \frac{\partial F}{\partial t} + \frac{p^i}{p^0}\frac{\partial F}{\partial x^i} + \frac{1}{2}g_{ij,k}\frac{p^i p^j}{p^0}\frac{\partial F}{\partial p_k}$$

GW effect here

cf) Geodesic eq.

$$\frac{dp_i}{dt} = \frac{1}{2}g_{jk,i}\frac{p^j p^k}{p^0}.$$

- Perturbed :

$$\frac{\partial(\delta F_1 + \delta F_2)}{\partial t} + \frac{\bar{p}^i}{\bar{p}^0}\frac{\partial(\delta F_1 + \delta F_2)}{\partial x^i} + \frac{1}{2}(\delta g_{jk})_{,i}\frac{\bar{p}^j \bar{p}^k}{\bar{p}^0}\frac{\partial \bar{F}}{\partial p_i} = a\frac{\partial^2 \bar{F}}{\partial p \partial t}\delta p^0$$

$$\delta F_1(t, x^i, p_i) \equiv \bar{F}(t, (g^{ij}p_i p_j)^{1/2}/a) - \bar{F}(t, p) \qquad \delta F_2(t, x^i, p_i) \equiv F - \bar{F} - \delta F_1.$$

$$\frac{\partial \delta F_2}{\partial t} + \frac{\hat{p}_i}{a}\frac{\partial \delta F_2}{\partial x^i} = \frac{1}{2}\frac{\partial h_{ij}}{\partial t}\frac{\partial \bar{F}}{\partial p}p\hat{p}_i\hat{p}_j.$$

Contributes to anisotropic stress

Anisotropic stress

- EM tensor of X

$$\delta T_{ij}^{(X)} = \frac{1}{a^3}\int d^3p\left[(\delta F_1+\delta F_2)\frac{p_ip_j}{\bar{p}^0}+\bar{F}p_ip_j\delta\left(\frac{1}{p^0}\right)\right] .= \frac{1}{a^2}\int d^3p\delta F_2 p\hat{p}_i\hat{p}_j+\frac{1}{3}a^2h_{ij}\rho_X$$

Anisotropic stress $a^2\Pi_{ij}$

- From Boltzmann eq :

$$\delta F_2 = \int_0^\tau d\tau'\frac{1}{2}\frac{\partial h_{ij}}{\partial\tau}(\tau')\frac{\partial\bar{F}}{\partial p}(\tau')p\hat{p}_i\hat{p}_j e^{-ik\mu(\tau-\tau')}$$

- Eq.of.m of GW (with dark radiation)

$$\ddot{h}^{(\lambda)}+3H\dot{h}^{(\lambda)}+\frac{k^2}{a^2}h^{(\lambda)} = -24H^2\frac{1}{a^4(t)\rho_{\rm tot}(t)}\times\int_0^t a^4(t')\rho_X(t')K\left(k\int_{t'}^t\frac{dt''}{a(t'')}\right)\dot{h}^{(\lambda)}(t',\mathbf{k})dt',$$

Anisotropic stress of X induced by GWs

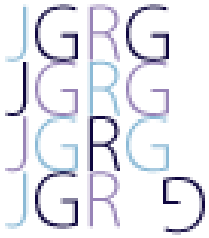

Kyohei Mukaida, JGRG 22(2012)111210

"Dynamics of oscillating scalar field in thermal environment"

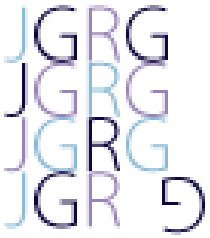

RESCEU SYMPOSIUM ON

GENERAL RELATIVITY AND GRAVITATION

JGRG 22



November 12-16 2012

Koshiba Hall, The University of Tokyo, Hongo, Tokyo, Japan



Dynamics of
Oscillating Scalar Field
in Thermal Environment

Kyohei Mukaida (Univ. of Tokyo)

Based on **1208.3399** with **Kazunori Nakayama**

Introduction

Introduction

- At the early universe, a scalar field may condensate homogeneously w/ a far from equilibrium value.
- It begins to oscillate coherently at H ~ m and behaves as “Matter”.
  - Examples: Inflaton, Moduli, Curvaton, Affleck-Dine field...
- To avoid the “overclosure”, the scalar condensate should decay to the “Radiation” sector at an appropriate epoch.

  ➡ **Interaction** btw the scalar and radiation

Introduction

- Such **interactions** btw scalar and radiation induce various effects that make the scalar dynamics complicated:

  - Thermal Effects
    - Thermally modified effective potential of the scalar field
    - Dissipation of scalar condensate into the radiation sector

    e.g., [J. Yokoyama; M. Drewes; A. Berera et al.]
  - Non-perturbative particle production

    e.g., [L. Kofman, A. Linde, A. Starobinsky]
  - (possible) non-topological soliton formation

    e.g., [E. Copeland et al.; S. Kasuya et al.]

➡ We included **these effects** simultaneously.

Set Up

- Let us consider the following simplest set up:

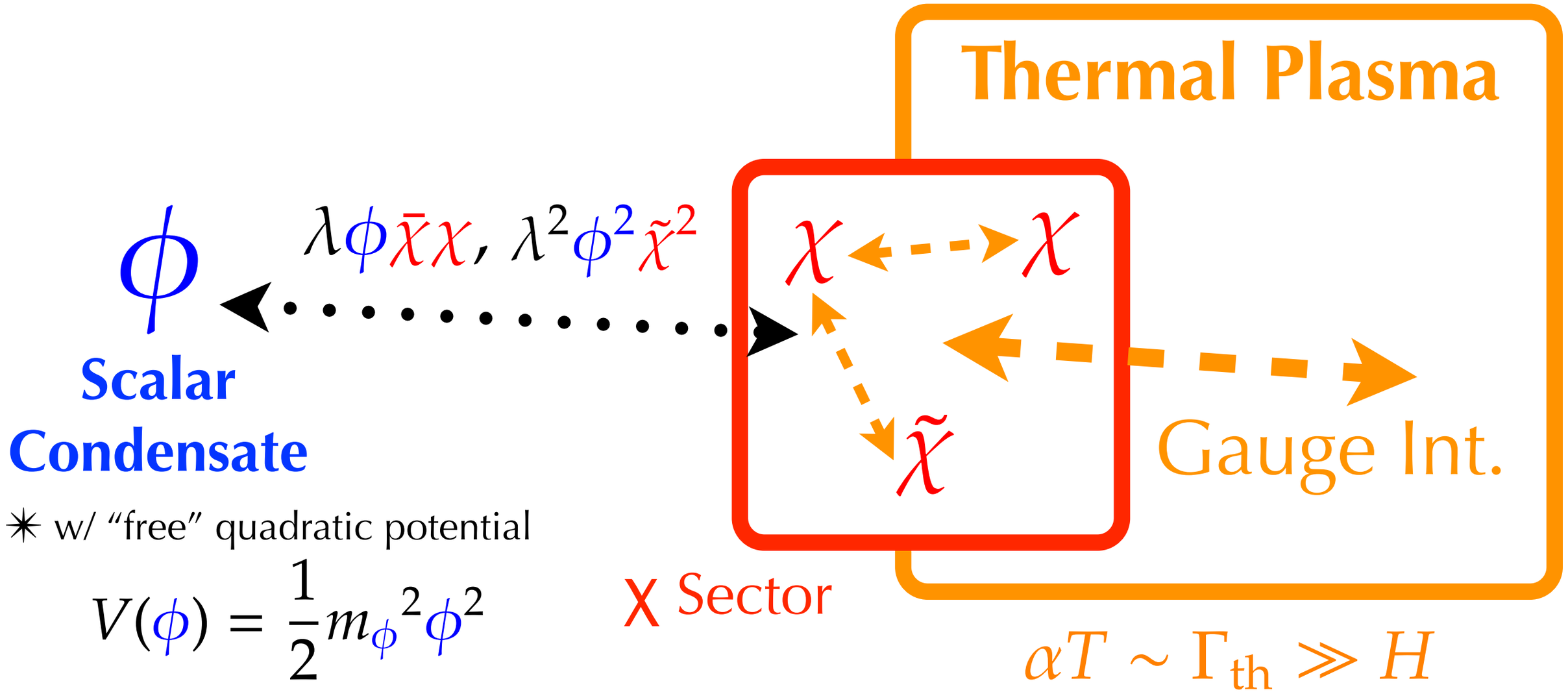

✳ w/ “free” quadratic potential

$$V(\phi) = \frac{1}{2} m_\phi{}^2 \phi^2$$

Outline

- Introduction
- Closed Time Path Formalism
- Thermal Effects
- Non-perturbative Particle Production
- Numerical Results

Thermal Effects

Thermal Effects

- Typically, there are two effects from thermal plasma.
  - Force from thermal plasma
  - Dissipation to thermal plasma

✳If the Bkg plasma remains in thermal equilibrium.

➡Reduced to Coarse-Grained EOM of **Φ**:

$$0 = \frac{\delta S}{\delta\phi} + \frac{\delta\tilde{\Gamma}}{\delta\phi} = \frac{\delta S}{\delta\phi} - \frac{\partial\mathcal{F}}{\partial\phi} - \Pi_{\rm ret} * \delta\phi + \cdots$$

$$\simeq \frac{\delta S}{\delta\phi} - \frac{\partial\mathcal{F}}{\partial\phi} - \Gamma_\phi\dot{\phi}; \quad \Gamma_\phi \simeq \lim_{\omega\to 0}\frac{\Pi_J(\omega,\mathbf{0})}{2\omega}.$$

e.g., [A. Berera et al., hep-ph/9803394]

Thermal Effects

- Typically, there are two effects from thermal plasma.
  - Force from thermal plasma:

$$\ddot{\phi} + (3H + \Gamma_\phi)\dot{\phi} + m_\phi^2 \phi = -\frac{\partial \mathcal{F}}{\partial \phi}$$

Free Energy of thermal plasma w/ the background ϕ.

Thermal Effects

- Typically, there are two effects from thermal plasma.
  - Force from thermal plasma:

$$\ddot{\phi} + (3H + \Gamma_\phi)\dot{\phi} + m_\phi^2 \phi = -\frac{\partial \mathcal{F}}{\partial \phi}$$

Free Energy of thermal plasma w/ the background ϕ.

-Small amplitude ⇒ Thermal mass

$$\mathcal{F} \propto \lambda^2 T^2 \phi^2; \;\; \lambda\phi \ll T$$

-Large amplitude ⇒ Thermal log

$$\mathcal{F} \propto \alpha^2 T^4 \ln(\lambda^2 \phi^2 / T^2); \;\; \lambda\phi \gg T$$

[A. Anisimov, M. Dine]

Thermal Effects

- Typically, there are two effects from thermal plasma.
  - Dissipation to thermal plasma:

$$\ddot{\phi} + (3H + \Gamma_\phi)\dot{\phi} + m_\phi^2 \phi = -\frac{\partial \mathcal{F}}{\partial \phi}$$

Friction coefficient from Kubo-formula $\Gamma_\phi \simeq \lim_{\omega \to 0} \frac{\Pi_J(\omega, \mathbf{0})}{2\omega}$.

Thermal Effects

- Typically, there are two effects from thermal plasma.
  - Dissipation to thermal plasma:

$$\ddot{\phi} + (3H + \Gamma_\phi)\dot{\phi} + m_\phi^2 \phi = -\frac{\partial \mathcal{F}}{\partial \phi}$$

Friction coefficient from Kubo-formula $\Gamma_\phi \simeq \lim_{\omega \to 0} \frac{\Pi_J(\omega, \mathbf{0})}{2\omega}$.

-Small amplitude: processes including X.

$$\Gamma_\phi \sim \lambda^2 \alpha T$$

-Large amplitude: multiple scattering by gauge bosons.

$$\Gamma_\phi \sim \frac{\alpha^2}{\ln \alpha^{-1}} \frac{T^3}{\phi^2}$$ [D. Bodeker; M. Laine]

Non-perturb. Particle Production

Non-perturb. Production

- The adiabaticity of χ particles can be broken down when the scalar passes through the origin.
  - Adiabaticity is broken if $\epsilon \gg 1$.

$$\epsilon := \left| \frac{\dot{\omega}_\chi}{\omega_\chi^2} \right| ; \quad \omega_\chi = \sqrt{\mathbf{k}^2 + m_{\rm eff}^\chi(T)^2 + \lambda^2 \phi^2(t)}$$

➡ Efficient χ production can occur at Φ~0.

[L. Kofman, A. Linde, A. Starobinsky, hep-ph/9704452]

Non-perturb. Production

- If Φ oscillates w/ the finite T potential (free-energy),

$$\begin{cases} \lambda \ll \alpha : \text{No efficient prod.} \\ \lambda \gg \alpha : \text{Complicated...} \end{cases}$$

- If Φ oscillates w/ the zero T potential, the efficient particle production occurs @ $|\phi| \lesssim \left[m_\phi \tilde{\phi}/\lambda\right]^{1/2}$.

$$n_\chi \sim \frac{k_*^3}{(2\pi)^3}; \quad k_* = \sqrt{\lambda \tilde{\phi} m_\phi}$$

[$\tilde{\phi}$: amplitude]

Non-perturb. Production

- The produced χ may decay @ $t_{\rm dec}\,\Gamma_\chi(\phi(t_{\rm dec})) \sim 1$.

[Otherwise the parametric resonance may occur]

- The Φ's energy is partially converted to the radiation, and it is estimated as

$$\frac{\delta\rho_\phi}{\rho_\phi} \sim \frac{\lambda^2}{4\pi^3\alpha^{1/2}};$$ @ every one oscillation.

Here we assumed that the decay rate of χ is given by

$$\Gamma_\chi \sim \alpha\, m_\chi(\phi).$$

[Felder, Kofman, Linde, "Instant preheating",hep-ph/9812289]

Numerical Results

Numerical Results

■ Contour plot of $\left.\dfrac{m_\phi^2 \tilde{\phi}^2/2}{\rho_{\rm rad}+\rho_{\rm inf}}\right|_{H=\Gamma_\phi}$. [$\tilde{\phi}$: amplitude]

$\alpha = 0.05$;
$T_R = 10^9$ GeV;
$m_\phi = 1$ TeV.

Coupling btw Φ & radiation: λ

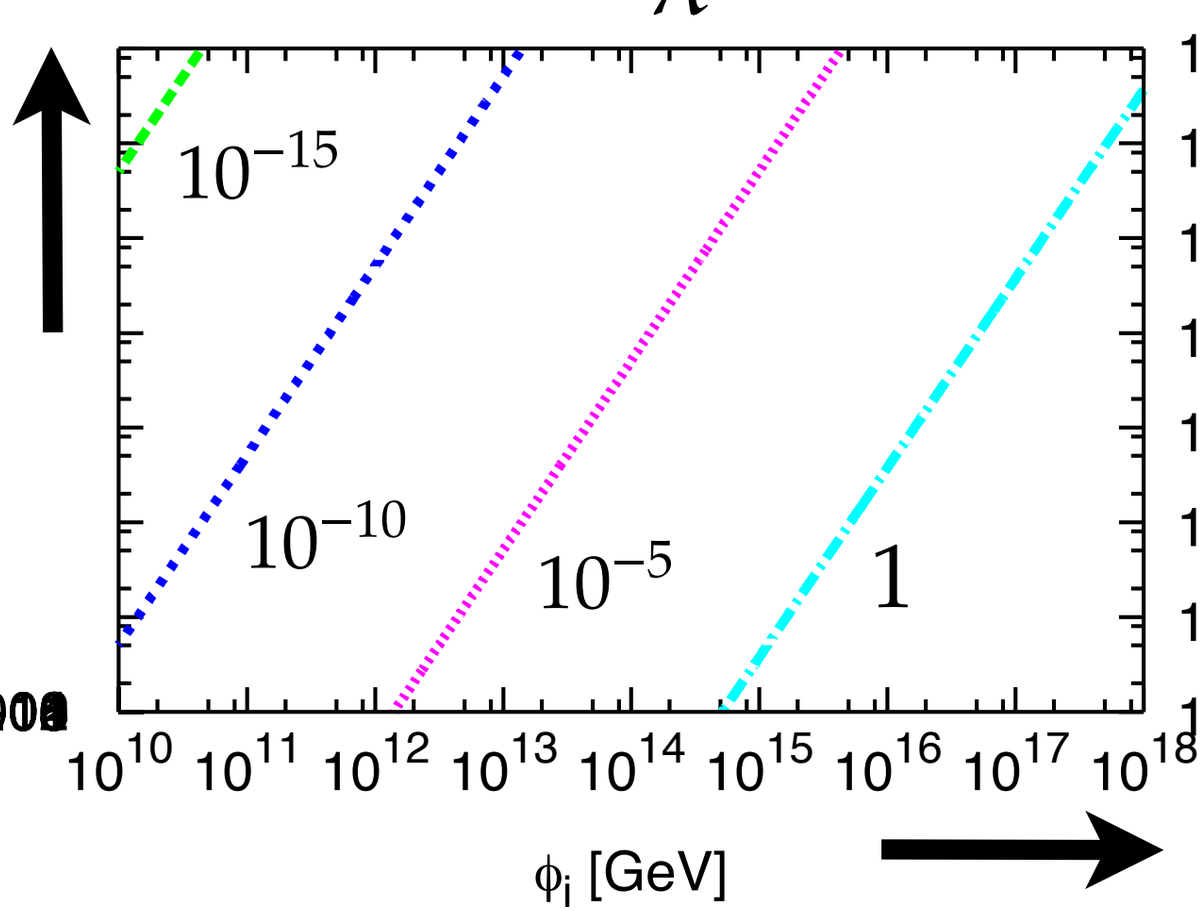

Initial amplitude: ϕ_i [GeV]

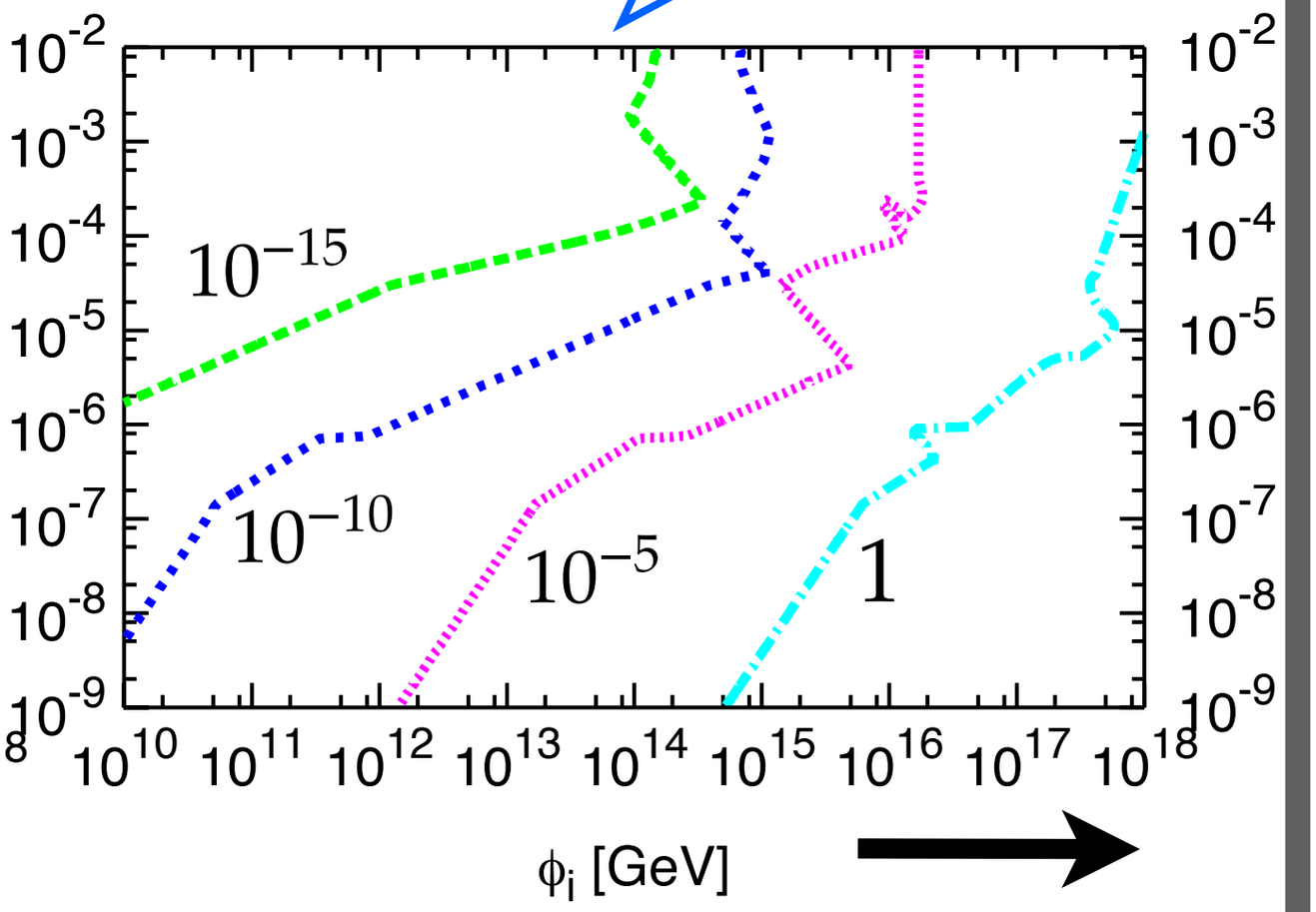

Initial amplitude: ϕ_i [GeV]

Summary

- **Interactions** btw scalar and radiation are often introduced to avoid overclosure.
- Such **interactions** induce various effects that make the dynamics of scalar condensate complicated.
- We take into account all these effects properly, and show that such effects can change the abundance of scalar condensate by orders in a broad range of parameters.

Back Up

CTP formalism

CTP Formalism

- Closed Time Path (CTP) formalism gives us useful tools to study an **evolution of expectation value**.

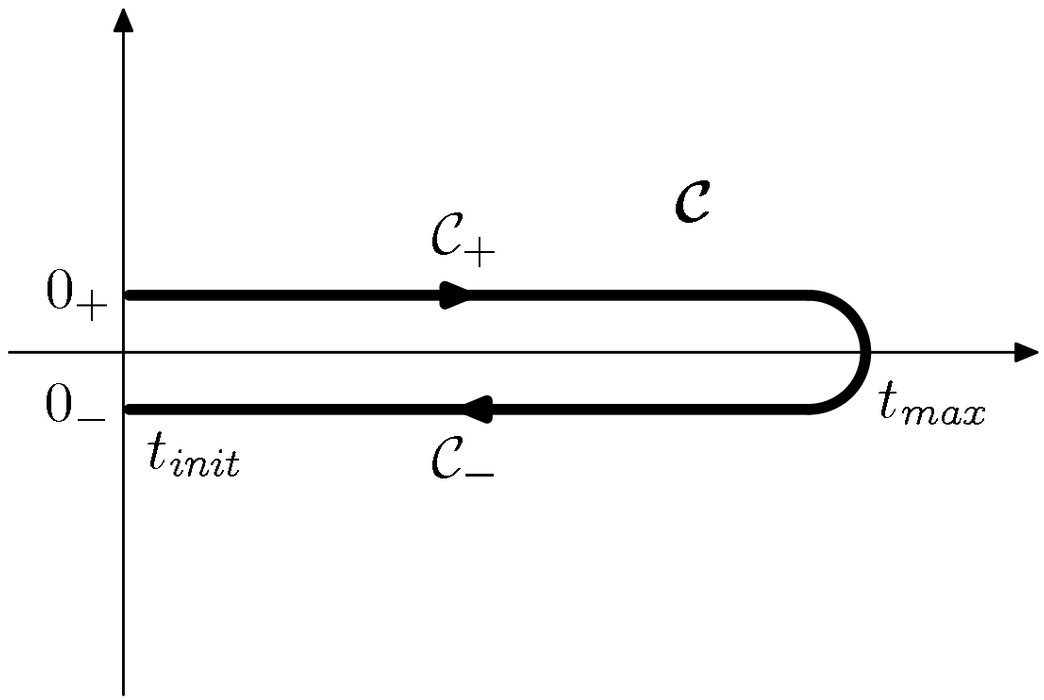

Fig. from M. Garny et al., 0904.3600

- An expectation value can be obtained from CTP integral:

$$\langle \hat{O}_H(t) \rangle = \mathrm{tr}\left[\hat{\rho}\, T_C \exp\left(-i \int_C dt' H_I(t') \right) \hat{O}_I(t) \right]$$

T_C : contour C ordering

ρ : density matrix

$\hat{O}_H(t)$: Heisenberg Picture

$\hat{O}_I(t)$: Interaction Picture

e.g., [J. Berges, hep-ph/0409233]

CTP Formalism

- It is useful to consider n-point functions on CTP.

$$\phi = \mathrm{tr}\left[\hat{\rho}\hat{\phi}\right]$$

$$G = \mathrm{tr}\left[\hat{\rho}\, T_C\, \hat{\phi}\hat{\phi}\right]^{\mathrm{con}}$$

$$V_n = \mathrm{tr}\left[\hat{\rho}\, T_C\, \hat{\phi}\cdots\hat{\phi}\right]^{\mathrm{con}}$$

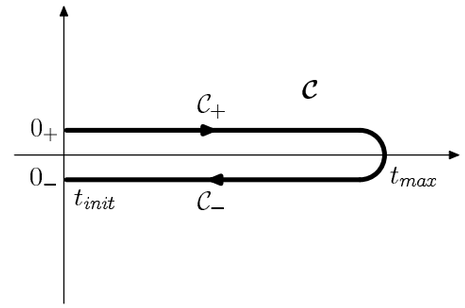

T_C : contour C ordering

[con. stands for connected part]

- **Kadanoff-Baym**: Follow the evolution of Φ and G self-consistently.

➡Schwinger Dyson equations on CTP [w/ skeleton diagram expansion]

$$G^{-1} = G_0^{-1} + \Pi[\phi, G]; \qquad \Pi = -2i\frac{\delta\tilde{\Gamma}[\phi, G]}{\delta G}$$

[Cornwall, Jackiw, Tomboulis,1974]

$$0 = \frac{\delta S}{\delta\phi} + \frac{\delta\tilde{\Gamma}[\phi, G]}{\delta\phi}$$

CTP Formalism

- Top-down approach:

Kadanoff-Baym eqs.

Thermal Plasma

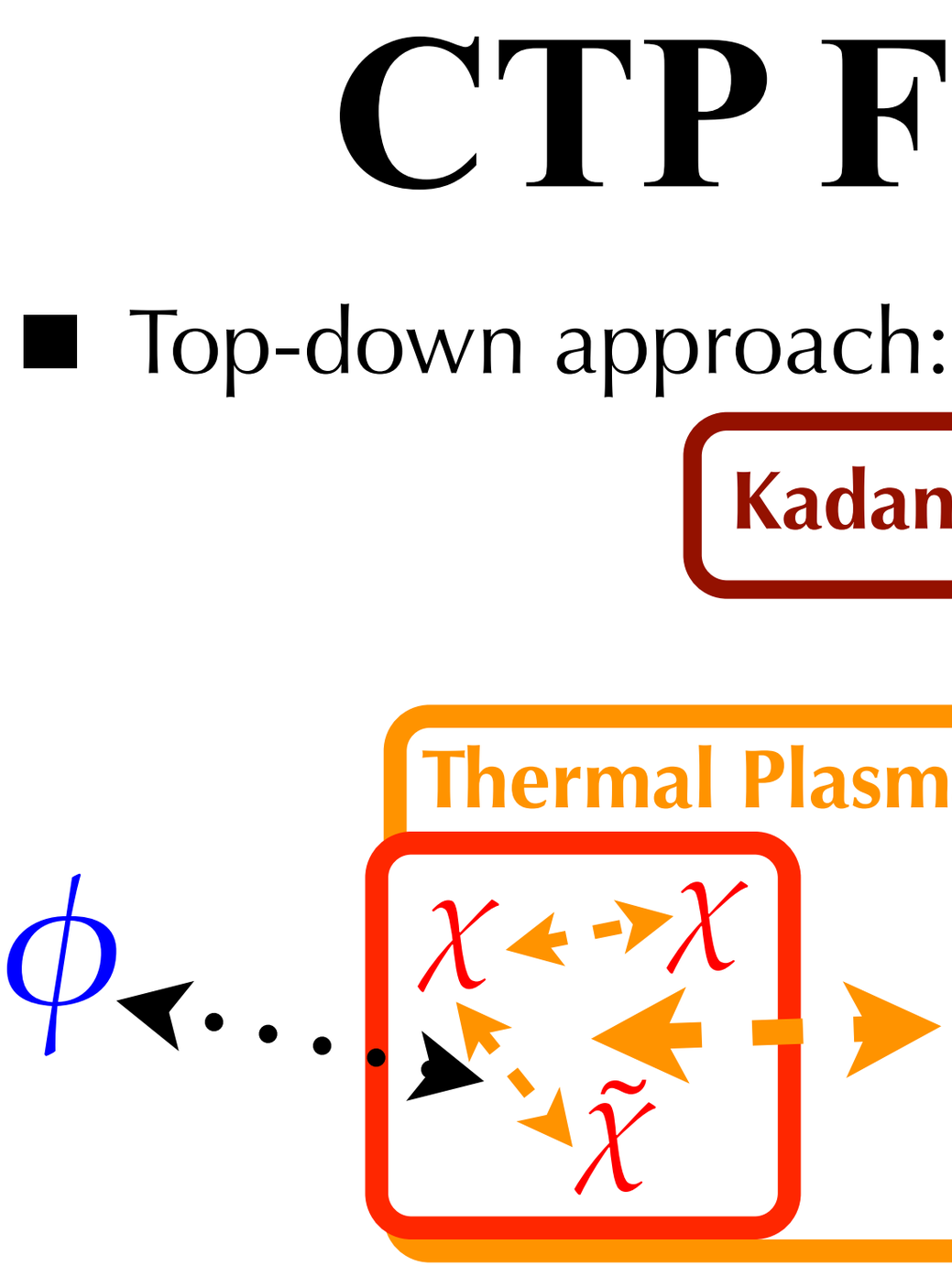

- Some fields may be kept in thermal equilibrium during the course of Φ's dynamics.
- Propagators of these fields

Thermal Propagators

-Thermal mass

-Thermal width

Reduce

Coarse-grained eq. for Φ

Coherent Oscillation

- Scalar condensate is obtained from one point func.
- If the scalar oscillates adiabatically w.r.t. thermal plasma...
  - Propagators in thermal bath → thermal ones

➡ Reduced to Coarse-Grained EOM of Φ:

$$0 = \frac{\delta S}{\delta\phi} + \frac{\delta\tilde{\Gamma}}{\delta\phi} = \frac{\delta S}{\delta\phi} - \frac{\partial\mathcal{F}}{\partial\phi} - \Pi_{\rm ret} * \delta\phi + \cdots$$

$$\simeq \frac{\delta S}{\delta\phi} - \frac{\partial\mathcal{F}}{\partial\phi} - \Gamma_\phi\dot{\phi}; \quad \Gamma_\phi \simeq \lim_{\omega\to 0}\frac{\Pi_J(\omega,\mathbf{0})}{2\omega}.$$

e.g., [A. Berera et al., hep-ph/9803394]

Coleman-Weinberg potential

CW potential

- In non-SUSY, there exists **Coleman Weinberg (CW) potential:**

$$\mathcal{V}_{\rm CW} = \sum_F \epsilon_F \frac{m_\chi^4(\phi)}{64\pi^2}\left[\ln\frac{m_\chi^2(\phi)}{\mu^2} - \frac{3}{2}\right]$$

$$\epsilon_F := \begin{cases} +1 & \text{for real scalar} \\ -2 & \text{for Weyl fermion} \end{cases} .$$

- In SUSY, such radiative corrections to flat directions are suppressed and remain only small logs due to the SUSY breaking effects.

Numerical Results

Numerical Results

■ The beginning of oscillation:

Coupling btw Φ & radiation: λ

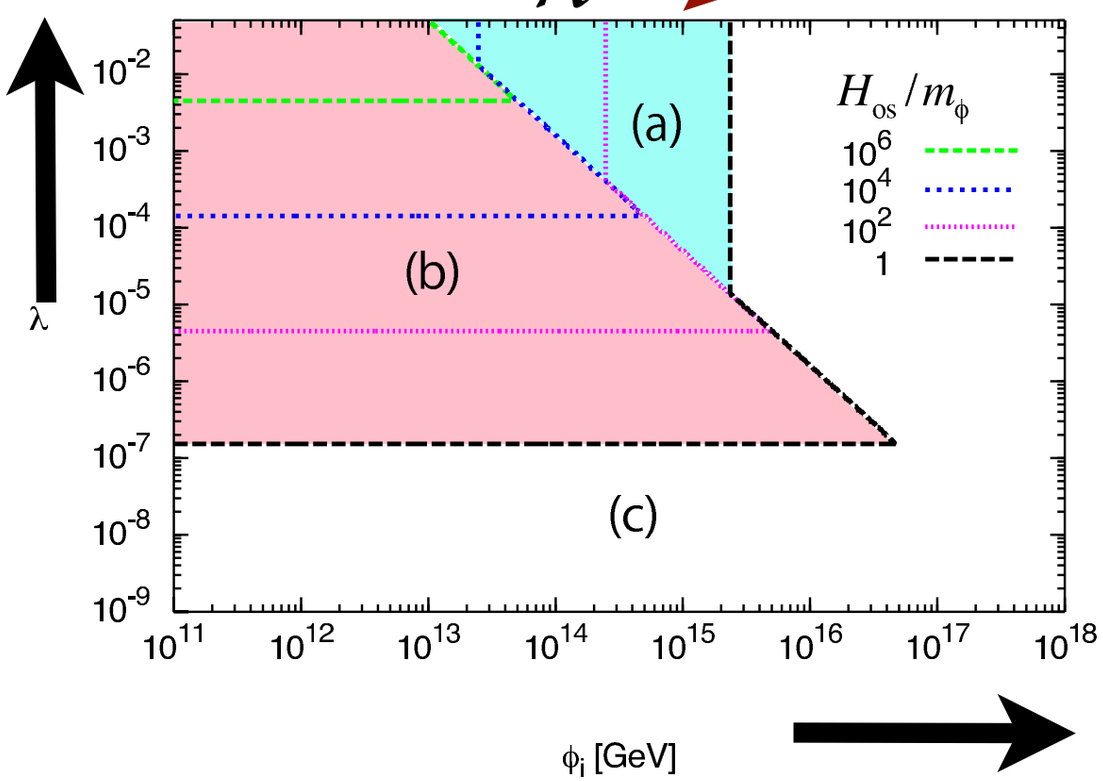

Initial amplitude: ϕ_i [GeV]

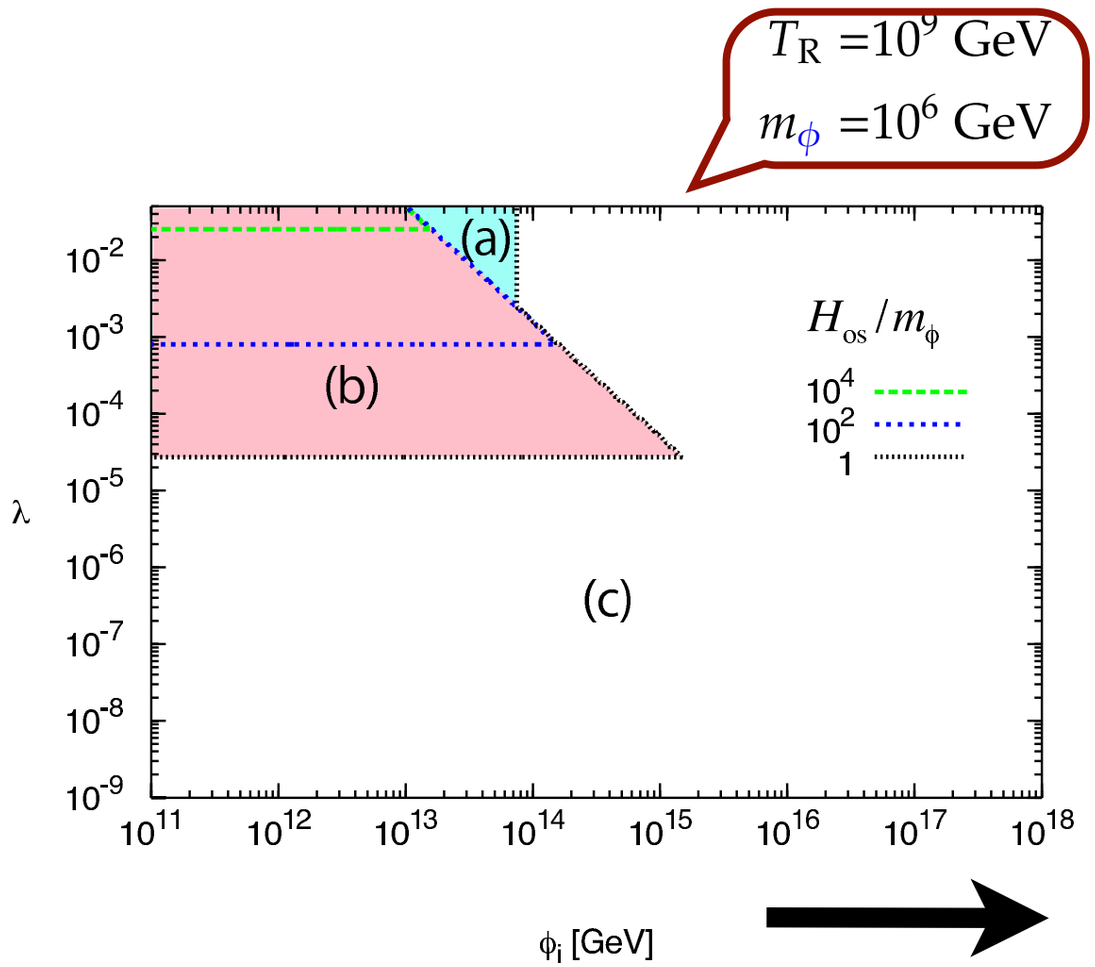

Initial amplitude: ϕ_i [GeV]

(a): thermal log, (b): thermal mass, (c): zero T mass

Numerical Results

- Oscillation w/ thermal log:

$m_\phi = 1\,\mathrm{TeV}$
$T_\mathrm{R} = 10^9\,\mathrm{GeV}$
$\lambda = 2\times10^{-3}$
$\phi_i = 10^{15}\,\mathrm{GeV}$

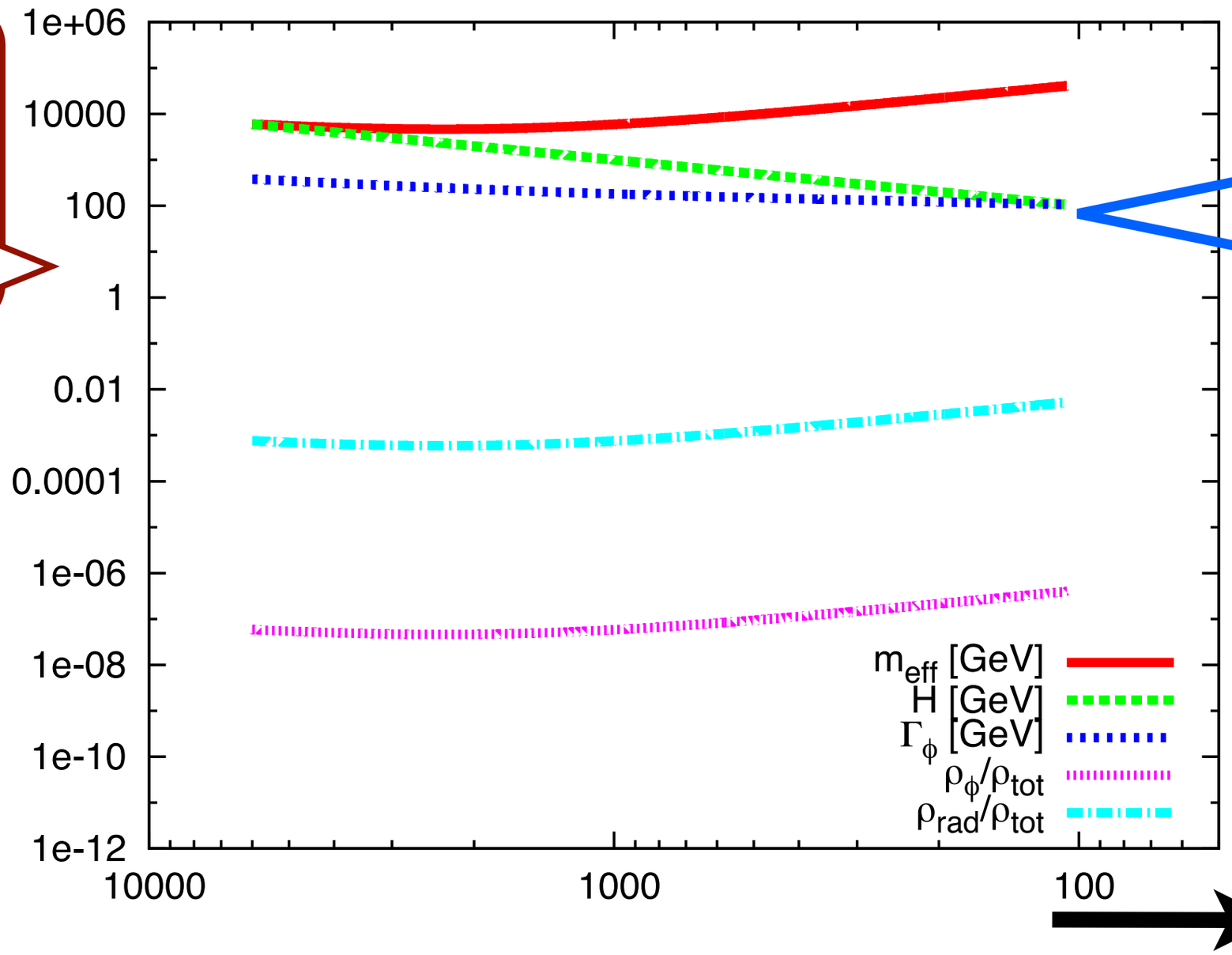

$\Gamma_\phi \sim \alpha^2 \dfrac{T^3}{\phi^2}$

Numerical Results

- Oscillation w/ thermal mass:

$m_\phi = 1\,\mathrm{TeV}$
$T_\mathrm{R} = 10^9\,\mathrm{GeV}$
$\lambda = 10^{-5}$
$\phi_i = 10^{14}\,\mathrm{GeV}$

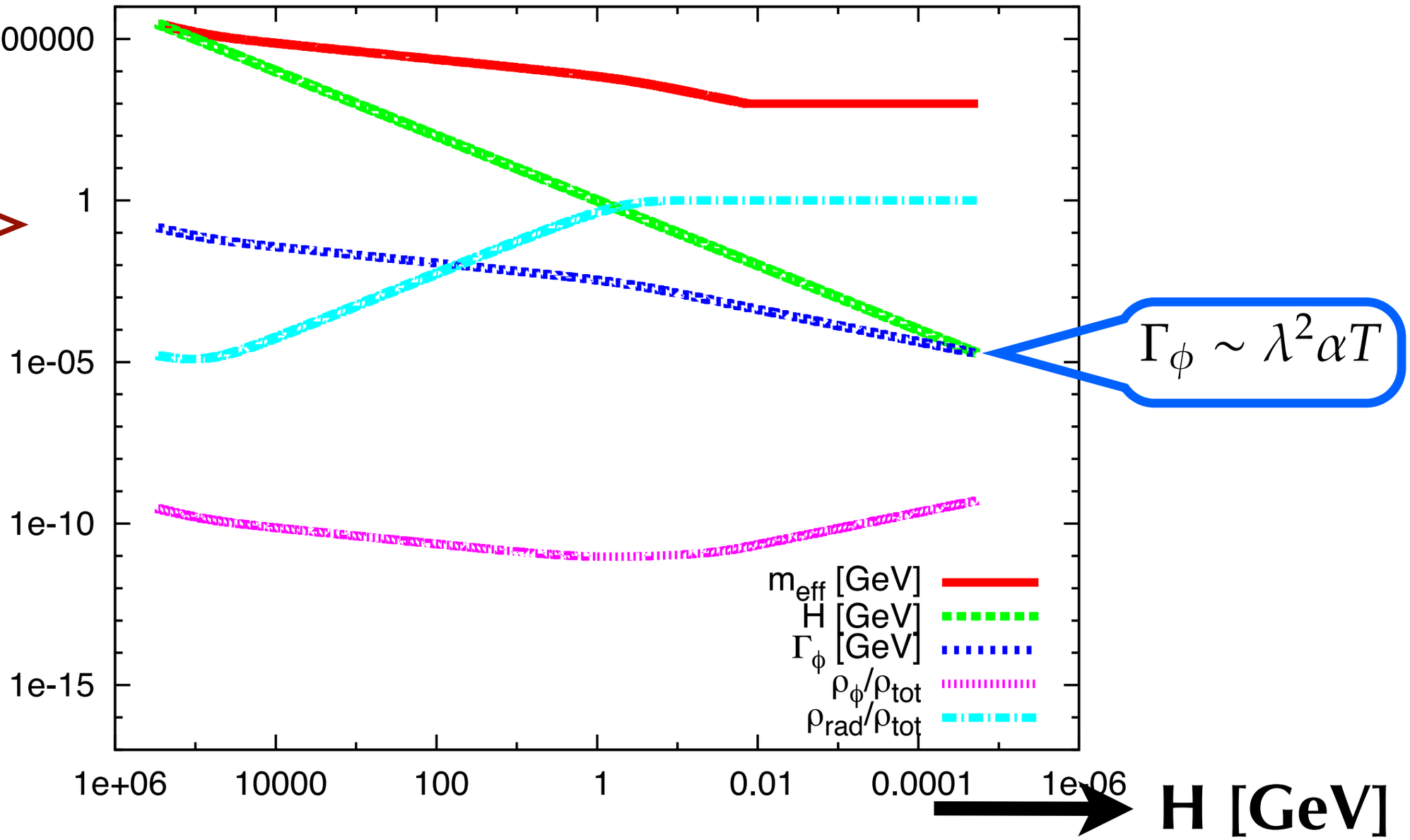

$\Gamma_\phi \sim \lambda^2 \alpha T$

Numerical Results

- Oscillation w/ zero T mass:

$m_\phi = 1\,\mathrm{TeV}$
$T_\mathrm{R} = 10^9\,\mathrm{GeV}$
$\lambda = 10^{-2}$
$\phi_i = 10^{18}\,\mathrm{GeV}$

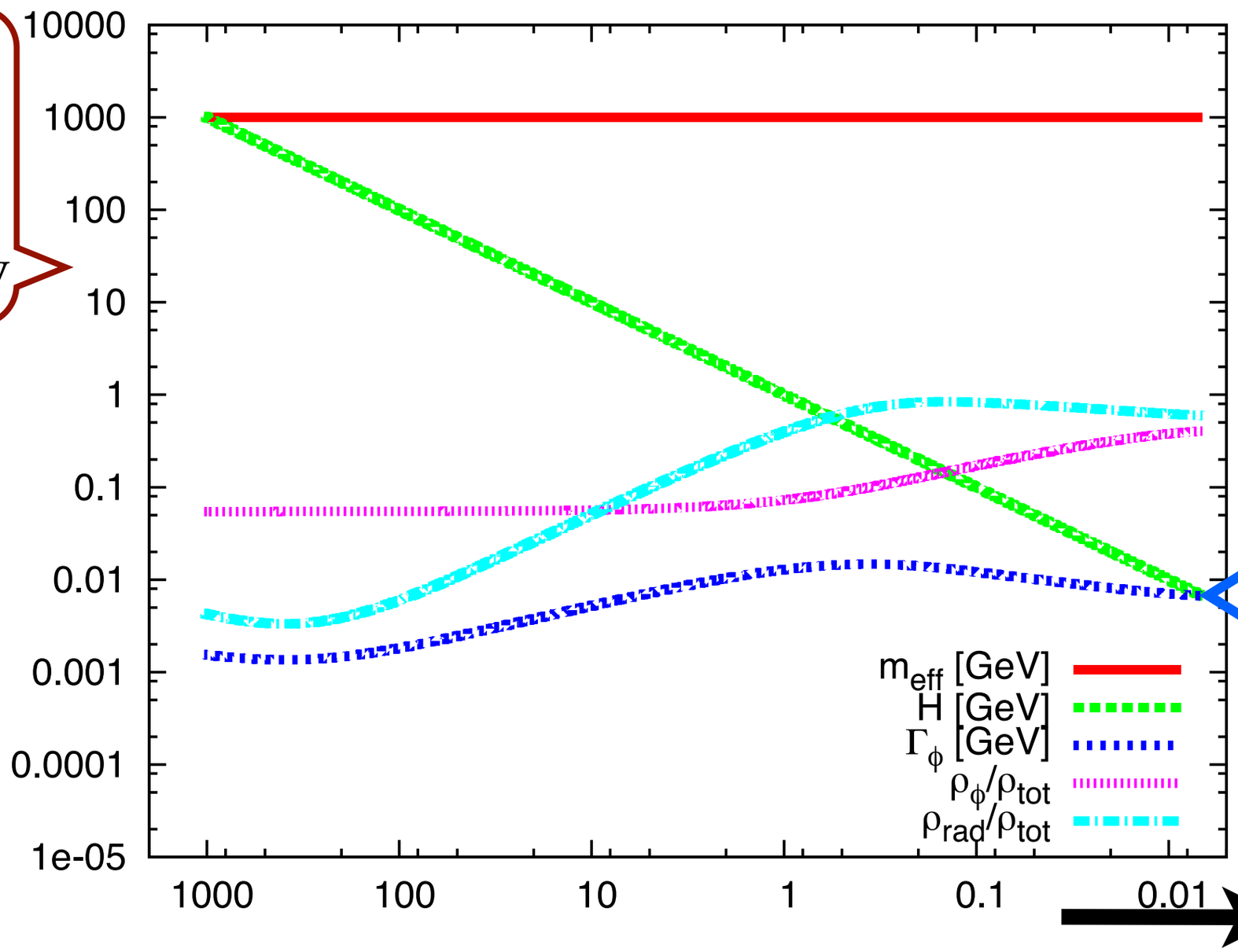

$\Gamma_\phi \sim \alpha^2 \dfrac{T^3}{\phi^2}$

Oscillon

Oscillon (I-ball)

- A coherently oscillating scalar with a potential flatter than the quadratic one has an instability and may fragment into classical lumps.
- Even if there is no conserved charge, their stability is guaranteed by the adiabatic invariant.

[Kasuya, Kawasaki, Takahashi, hep-ph/0209358]

- Such a non-topological soliton is dubbed as oscillon or I-ball.

e.g., [Copeland, Gleiser, Muller, hep-ph/9503217]
[Kasuya, Kawasaki, Takahashi, hep-ph/0209358]

Oscillon (I-ball)

■ The region where the I-ball may be formed.

Coupling
btw Φ & radiation: λ

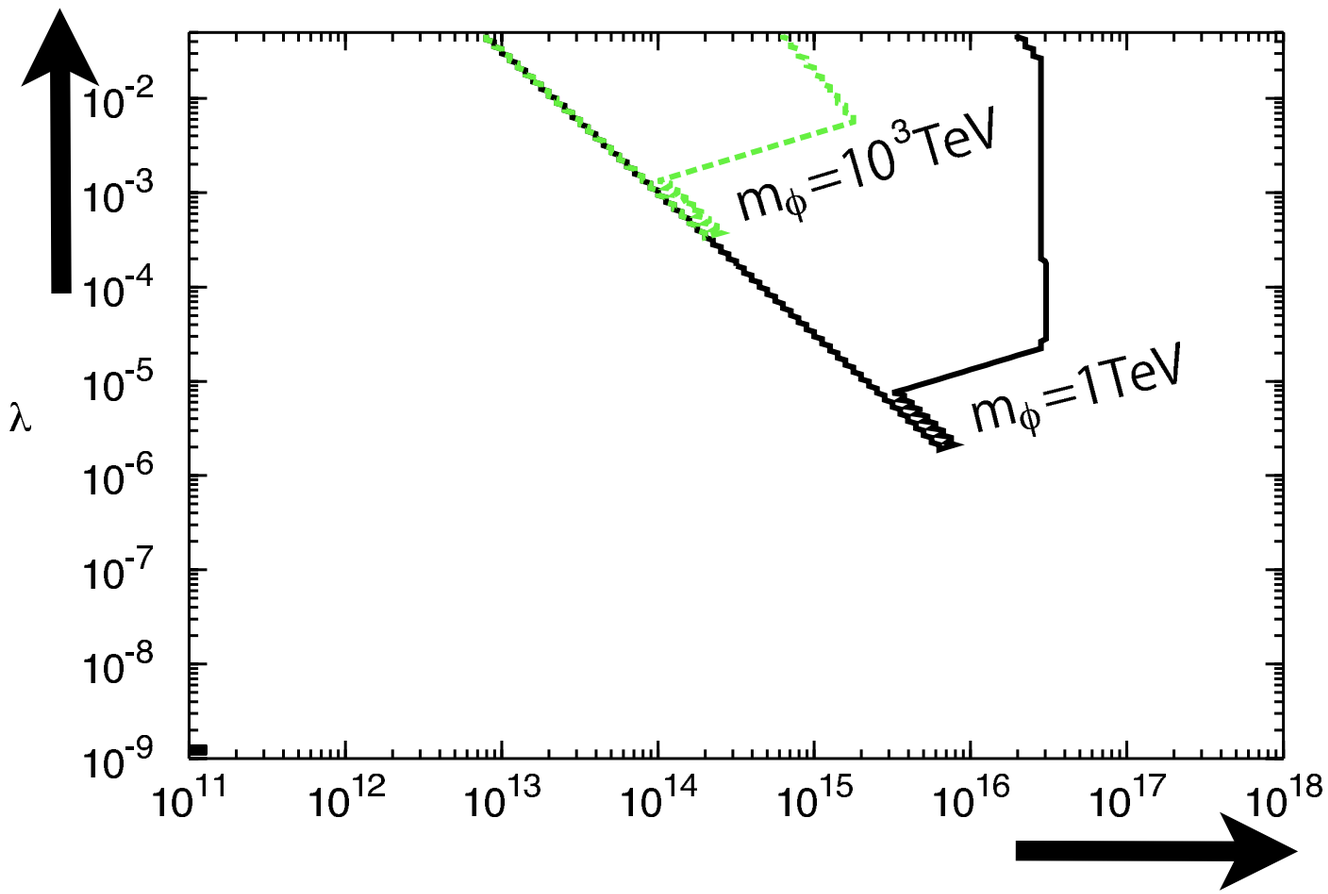

Initial amplitude: ϕ_i [GeV]

Oscillon (I-ball)

■ The region where the I-ball may be formed.

Coupling btw Φ & radiation: λ

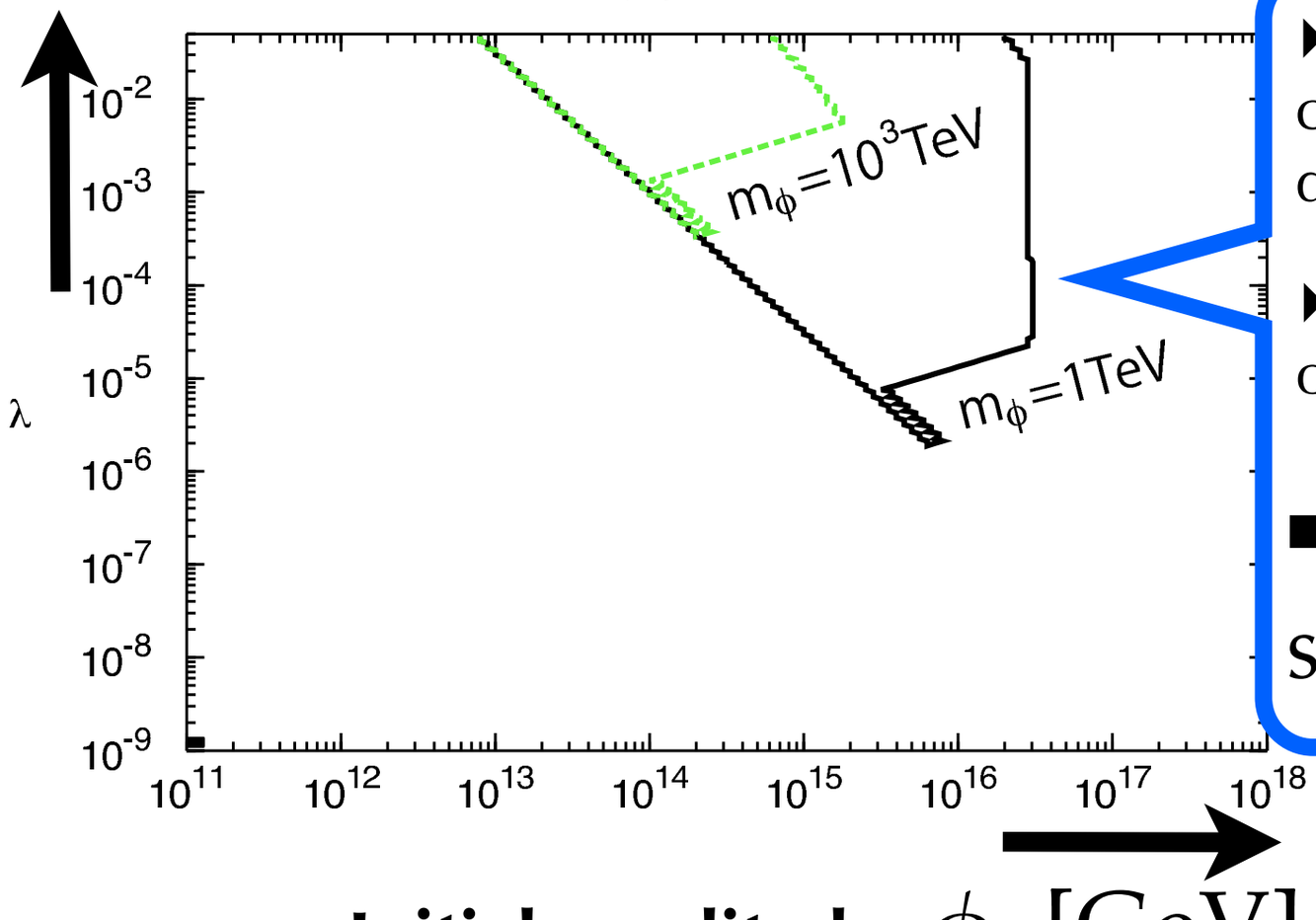

Initial amplitude: ϕ_i [GeV]

▸It is also possible that the scalar condensation evaporates due to the dissipation before the formation of oscillon.

▸Even if this is the case, the delayed type oscillon may be formed.

➡ Further study is needed to say something conclusively.

Bulk Viscosity

Bulk Viscosity

- The dissipation rate at large amplitude regime is directly related to the bulk viscosity of Yang-Mills plasma.

$$\Gamma_\phi = \lim_{\omega\to 0} \frac{\Pi_J(\omega, \mathbf{0})}{2\omega}$$

$$= \lim_{\omega\to 0} \frac{1}{2\omega} \int d^4x\, e^{-i\omega t} \langle [\hat{O}(t,\mathbf{x}), \hat{O}(0)] \rangle; \quad \hat{O}(x) = \frac{A}{8\pi^2\phi} F^{a\mu\nu}(x) F^a_{\mu\nu}(x)$$

[D. Bodeker; M. Laine]

$$\text{Bulk Viscosity: } \zeta = \frac{1}{9} \int d^4x\, e^{-i\omega t} \langle [T^\mu{}_\mu(t,\mathbf{x}), T^\nu{}_\nu(0,\mathbf{0})] \rangle$$

$$\zeta \sim \frac{\alpha^2 T^3}{\ln[1/\alpha]};\ @\ \text{weak coupling}$$

[Arnold, Dogan. Moore, hep-ph/0608012]

Taro Kunimitsu, JGRG 22(2012)111211

"Higgs Condensation in the inflationary universe"

RESCEU SYMPOSIUM ON

GENERAL RELATIVITY AND GRAVITATION

JGRG 22

November 12-16 2012

Koshiba Hall, The University of Tokyo, Hongo, Tokyo, Japan

Higgs Condensation in the Inflationary Universe

Research Center for the Early Universe (RESCEU)

Taro Kunimitsu

with Jun'ichi Yokoyama

PRD 86, 083541 (2012)

July 4, 2012



ATLAS Collaboration

$$m_H = 126.0 \pm 0.4 \pm 0.4 \mathrm{GeV}$$

Phys.Lett. B 716, 1 (2012)

CMS Collaboration

$$m_H = 125.3 \pm 0.4 \pm 0.5 \mathrm{GeV}$$

Phys.Lett. B 716, 30 (2012)

Could the Higgs field have dominated the Universe？

Could the Higgs field have dominated the Universe？

(within the SM + Inflaton framework)

Higgs Field during inflation

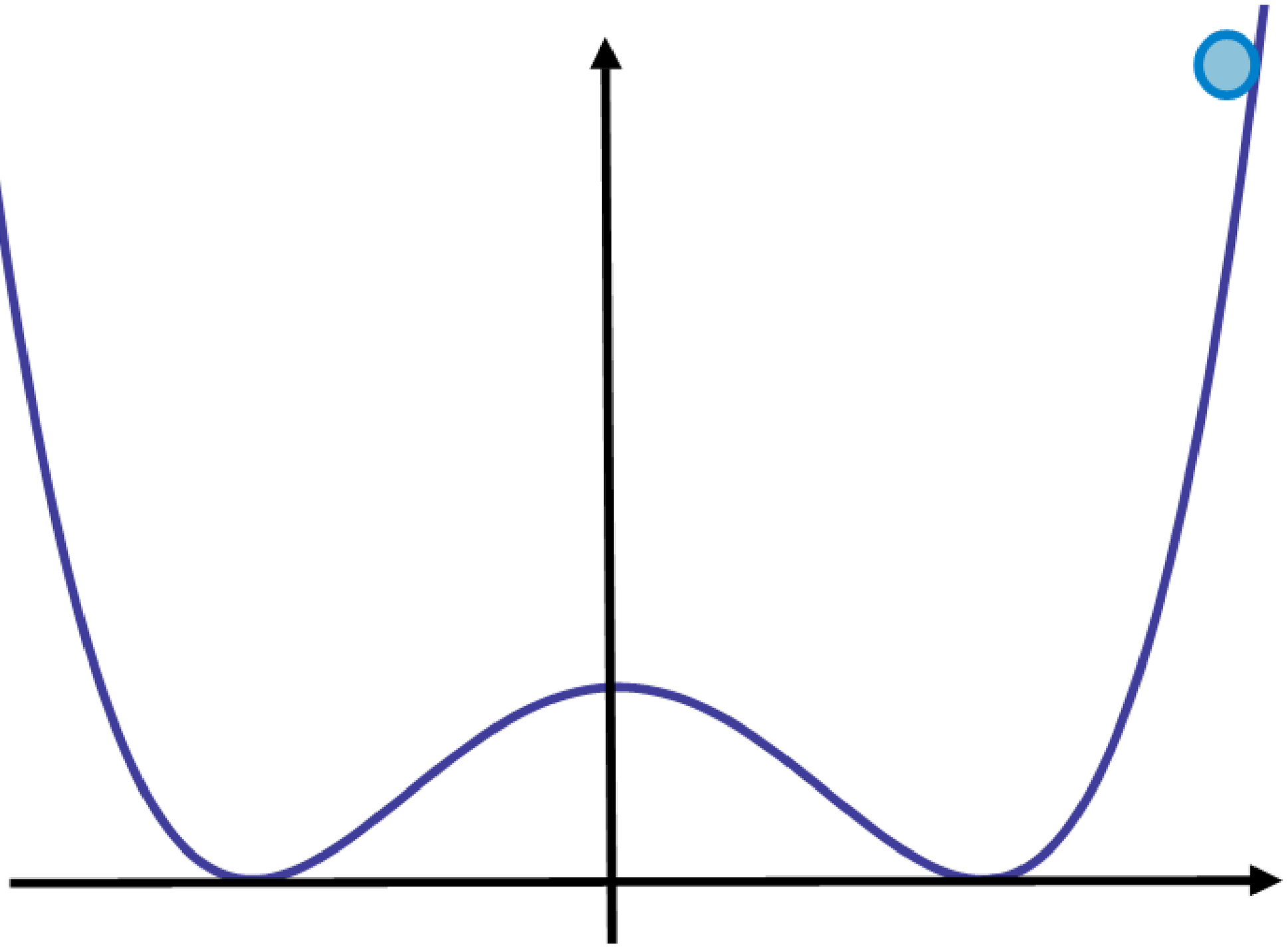

Higgs Field during inflation

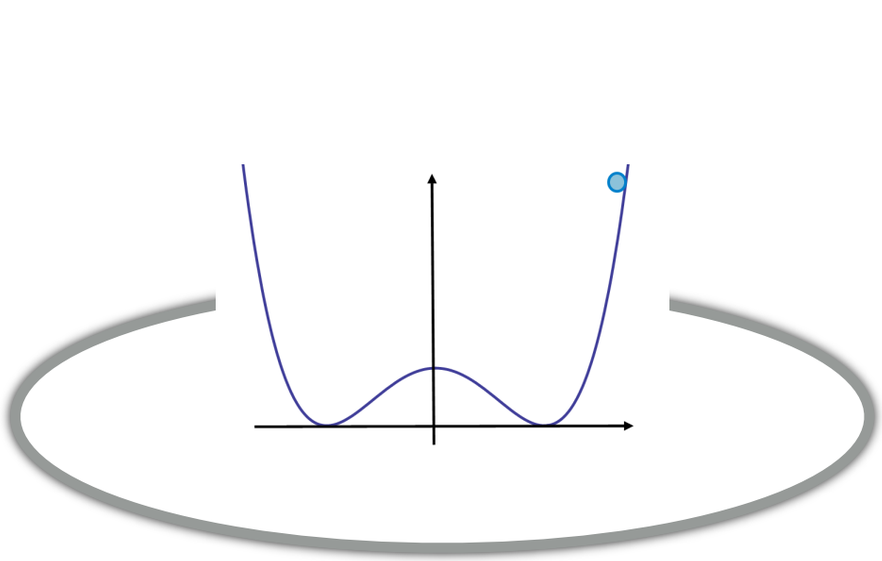

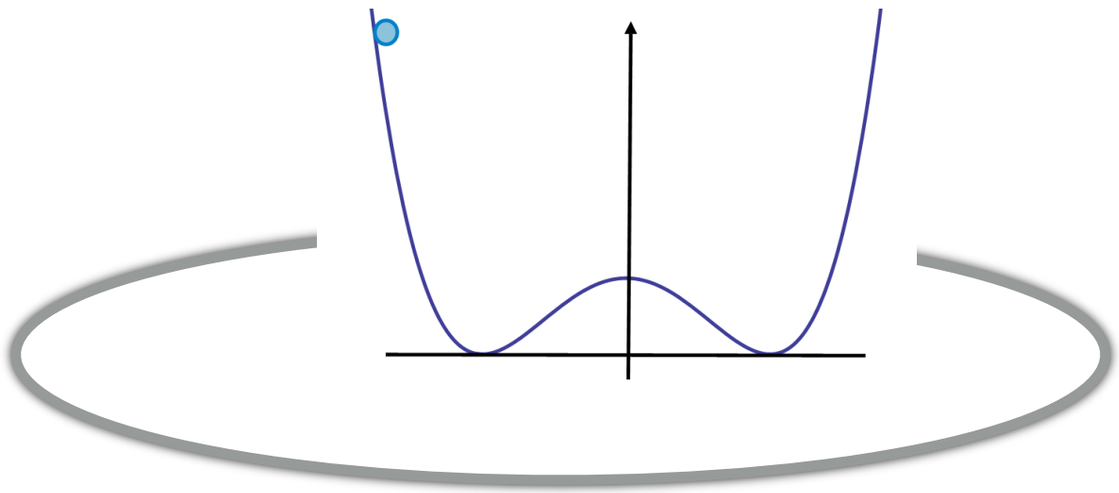



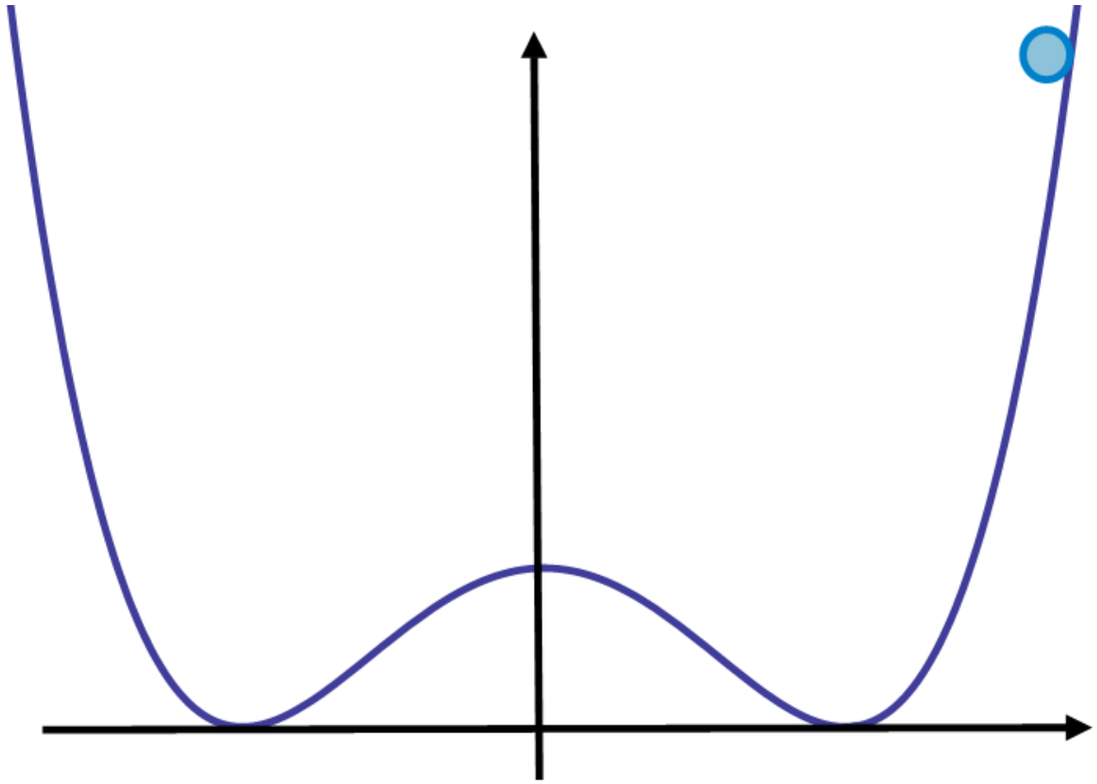

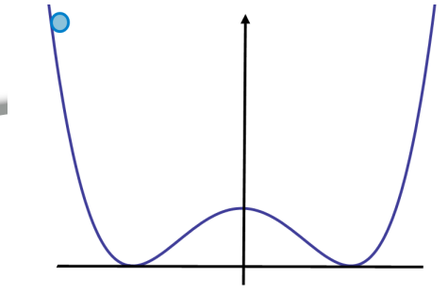

“Higgs Condensation"

Stochastic Inflation

Starobinsky (1984,1986)

long-wave part

$$\varphi(\mathbf{x},t) = \bar{\varphi}(\mathbf{x},t) + \int \frac{d^3k}{(2\pi)^{\frac{3}{2}}}\theta(k-\epsilon a(t)H) \times \left[a_{\mathbf{k}}\varphi_{\mathbf{k}}(t)e^{-i\mathbf{k}\cdot\mathbf{x}} + a^{\dagger}_{\mathbf{k}}\varphi^{*}_{\mathbf{k}}(t)e^{i\mathbf{k}\cdot\mathbf{x}}\right]$$

short-wave part

Stochastic Inflation

Starobinsky (1984,1986)

long-wave part

$$\varphi(\mathbf{x},t) = \bar{\varphi}(\mathbf{x},t) + \int \frac{d^3k}{(2\pi)^{\frac{3}{2}}}\theta(k-\epsilon a(t)H) \times \left[a_{\mathbf{k}}\varphi_{\mathbf{k}}(t)e^{-i\mathbf{k}\cdot\mathbf{x}} + a^{\dagger}_{\mathbf{k}}\varphi^{*}_{\mathbf{k}}(t)e^{i\mathbf{k}\cdot\mathbf{x}}\right]$$

short-wave part

Fokker-Planck equation

$$\frac{\partial \rho_1[\varphi(\mathbf{x},t)]}{\partial t} = \frac{1}{3H}\frac{\partial}{\partial \varphi}\{V'[\varphi(\mathbf{x},t)]\rho_1[\varphi(\mathbf{x},t)]\} + \frac{H^3}{8\pi^2}\frac{\partial^2 \rho_1[\varphi(\mathbf{x},t)]}{\partial \varphi^2}$$

Fokker-Planck equation

$$\frac{\partial \rho_1[\varphi(\mathbf{x},t)]}{\partial t} = \frac{1}{3H}\frac{\partial}{\partial \varphi}\{V'[\varphi(\mathbf{x},t)]\rho_1[\varphi(\mathbf{x},t)]\} + \frac{H^3}{8\pi^2}\frac{\partial^2 \rho_1[\varphi(\mathbf{x},t)]}{\partial \varphi^2}$$

$\rightarrow$ An equilibrium state exists

for $V[\varphi] = \dfrac{\lambda}{4}\varphi^4$

$$\rho_{1\mathrm{eq}}(\varphi) = \left(\frac{32\pi^2\lambda}{3}\right)^{\frac{1}{4}} \frac{1}{\Gamma(\frac{1}{4})H} \exp\left(-\frac{3\pi^2\lambda\varphi^4}{3H^4}\right)$$

Probability distribution

$$V[\varphi] = \frac{\lambda}{4}\varphi^4$$

$$\lambda \sim 0.01$$

$\rho_{1\mathrm{eq}}$

Probability distribution

$\langle \varphi^2 \rangle = 0.132 \lambda^{-\frac{1}{2}} H^2$

$\sqrt{\langle \varphi^2 \rangle} \sim H$

Inflation Model

Model : k-inflation

Armendariz-Picon, et al. (1999)

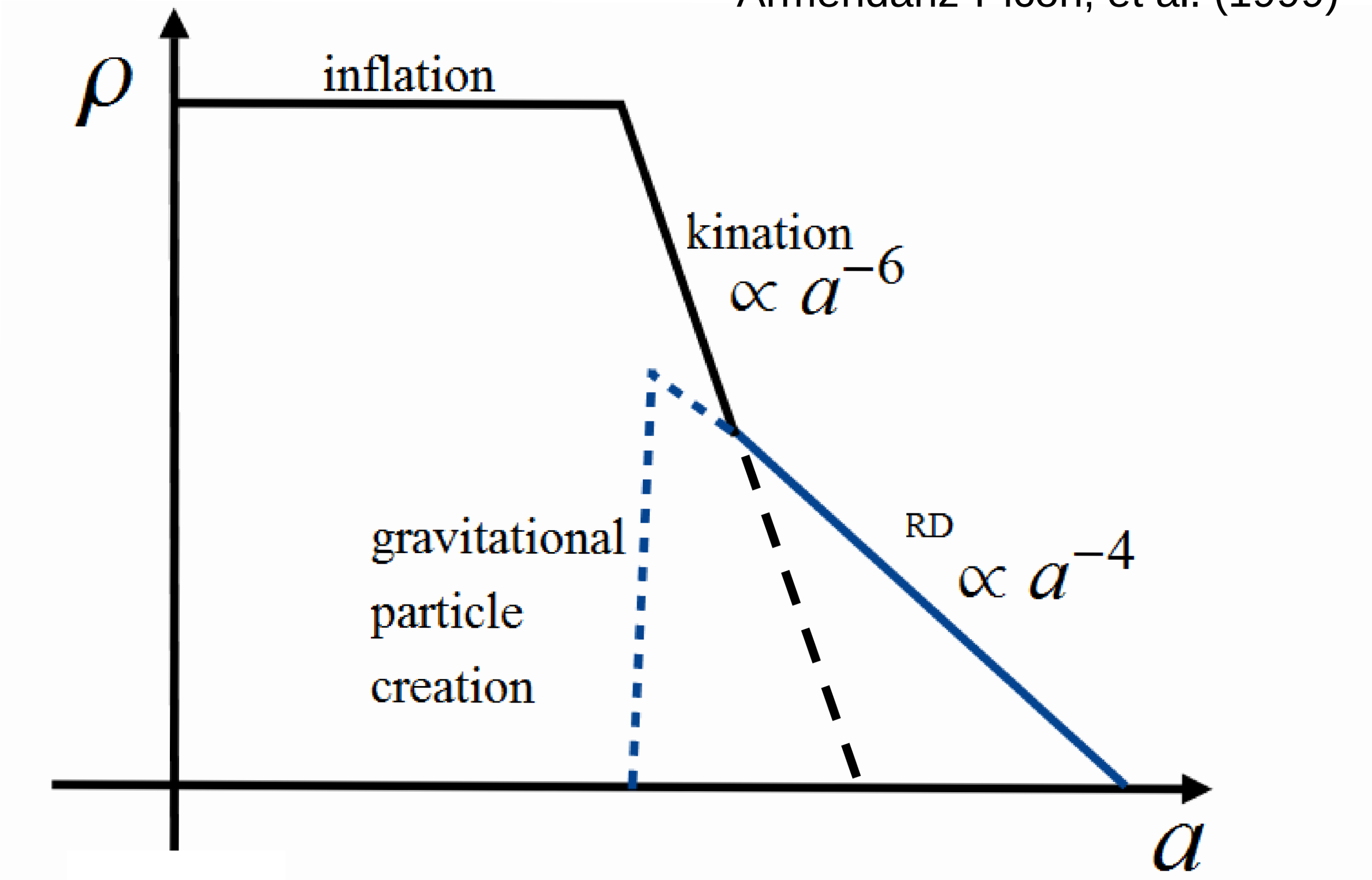

k-inflation with Higgs

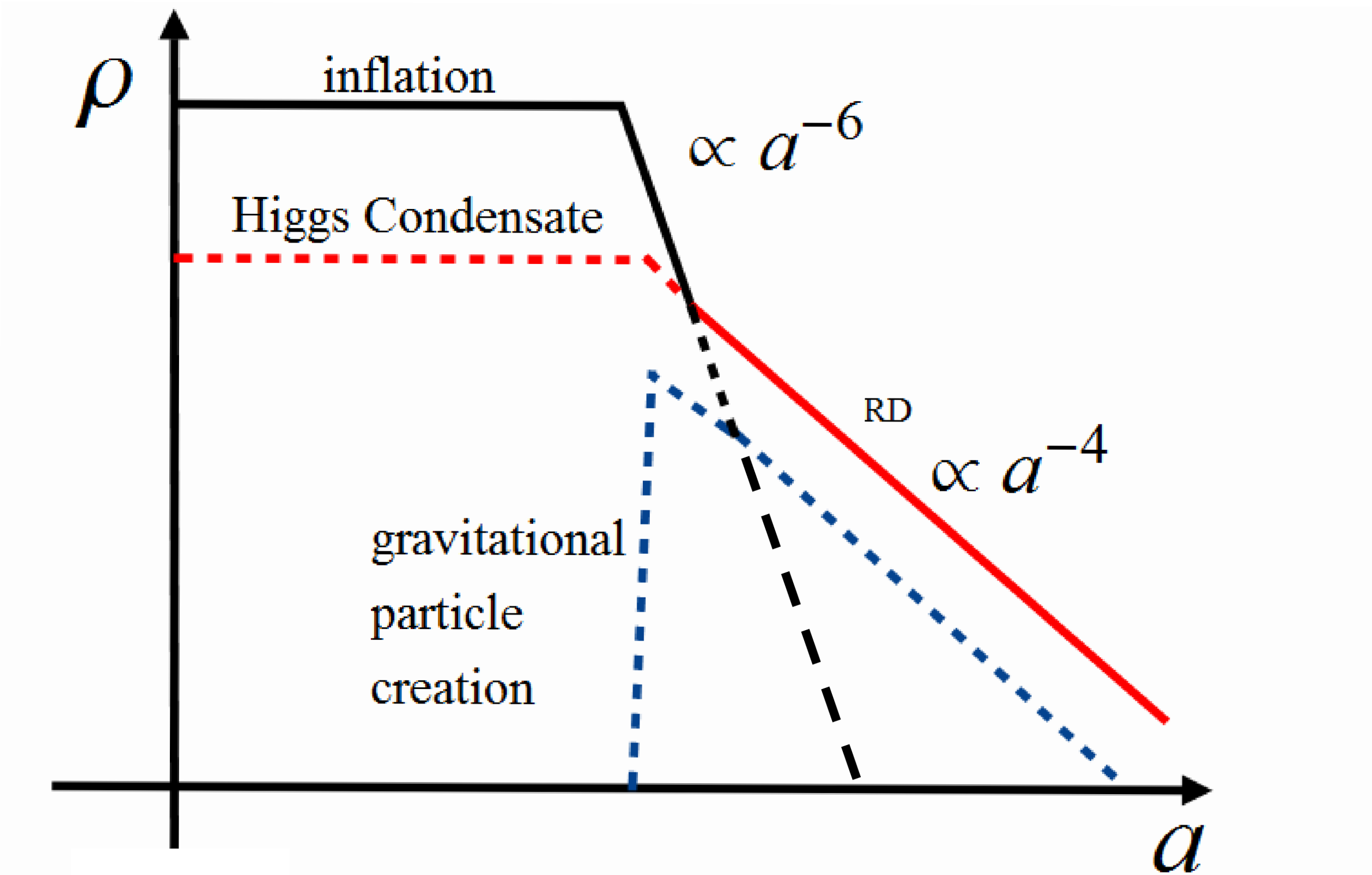

Primordial Fluctuations

Fluctuations

We want

$$\mathcal{P}(k) \sim 10^{-9}$$

Fluctuations

$$\Xi_{\Delta_h}(r) \equiv \left\langle \frac{\delta\rho_h(r)}{\rho_h} \frac{\delta\rho_h(0)}{\rho_h} \right\rangle$$

$$\simeq 4(Har)^{-0.178\sqrt{\lambda}}$$

Fluctuations

Fourier
Transform

$$P_V(k) \simeq 14\sqrt{\lambda}k^{-3}$$

$$\mathcal{P}_V(k) \equiv \frac{4\pi k^3}{(2\pi)^3} P_V(k) \sim \sqrt{\lambda} \sim 0.1$$

$\lambda \sim 0.01$

Fluctuations

We get

$$\mathcal{P}(k) \sim \mathcal{P}_V(k)$$

$$\sim 0.1$$

Too Large!

Summary

Higgs condensation

→Dominates the Universe in k-inflation

→We Showed that the fluctuations are too large

backups

Fokker-Planck equation

$$\frac{\partial \rho_1[\varphi(\mathbf{x},t)]}{\partial t}$$

$$= \frac{1}{3H}\frac{\partial}{\partial \varphi}\{V'[\varphi(\mathbf{x},t)]\rho_1[\varphi(\mathbf{x},t)]\}+\frac{H^3}{8\pi^2}\frac{\partial^2 \rho_1[\varphi(\mathbf{x},t)]}{\partial \varphi^2}$$

Probability Distribution Function

→ An equilibrium state exists

Starobinsky, Yokoyama (1994)

for $V[\varphi] = \dfrac{\lambda}{4}\varphi^4$

$$\rho_{1\mathrm{eq}}(\varphi) = \left(\frac{32\pi^2\lambda}{3}\right)^{\frac{1}{4}} \frac{1}{\Gamma(\frac{1}{4})H} \exp\left(-\frac{3\pi^2\lambda\varphi^4}{3H^4}\right)$$

Correlation time/length

$$t_c \simeq 76.2 H^{-1}$$

$$a(t) r_c \simeq e^{37.4} H^{-1}$$

During inflation

$$\varphi \sim H_{\rm inf}$$

$$\rho_{\rm inf} \sim H_{\rm inf}^2 M_P^2$$

$$\rho_h \sim \lambda H_{\rm inf}^4$$

When does Oscillation start?

$$\rho_h \sim \lambda H_{\rm inf}^4$$

$$\rho_{\rm inf} \sim H_*^2 M_P^2 \quad \leftarrow H_*^2 \sim \lambda H_{\rm inf}^2$$

$$\rightarrow \quad \frac{\rho_h}{\rho_{\rm inf}} \sim \frac{H_{\rm inf}^2}{M_P^2} \sim \mathcal{P}_t < 10^{-9}$$

Gravitational particle production

$$\rho_r = \frac{9H_{\rm inf}^4}{32\pi^2 a^4} \ln\left(\frac{1}{H_{\rm inf}\Delta t}\right)$$

$$\ln\left(\frac{1}{H_{\rm inf}\Delta t}\right) \sim 1$$

Energy density

$$\rho_r = \frac{9NH_{\rm inf}^4}{32\pi^2}\left(\frac{m_{\rm eff}}{H_{\rm inf}}\right)^{\frac{4}{3}} \simeq 1.59\times 10^{-3} NH_{\rm inf}^4$$

$$\rho_{\rm cond} = \frac{3H_{\rm inf}^4}{32\pi^2} \simeq 9.50\times 10^{-3} H_{\rm inf}^4$$

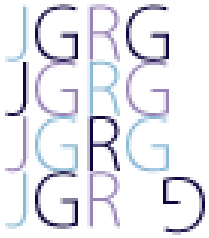

Sachiko Kuroyanagi, JGRG 22(2012)111212

"Forecast constraints on cosmic strings from future CMB, pulsar timing and gravitational wave direct detection experiments"

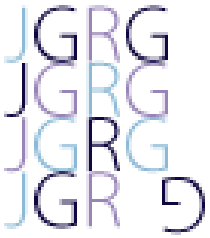

RESCEU SYMPOSIUM ON

GENERAL RELATIVITY AND GRAVITATION

JGRG 22



November 12-16 2012

Koshiba Hall, The University of Tokyo, Hongo, Tokyo, Japan



Forecast constraints on cosmic strings from future CMB, pulsar timing and gravitational wave direct detection experiments

Sachiko Kuroyanagi
Univ. of Tokyo
RESCEU
(RESearch Center for the Early Universe)

12 Nov 2012

Based on
S. Kuroyanagi, K. Miyamoto, T. Sekiguchi, K. Takahashi, J. Silk,
PRD 86, 023503 (2012) + arXiv:1210.2829 [astro-ph]

Cosmic string ?

One dimensional topological defect
generated in the early universe

Generation mechanism

1: Phase transition

spontaneous symmetry breaking

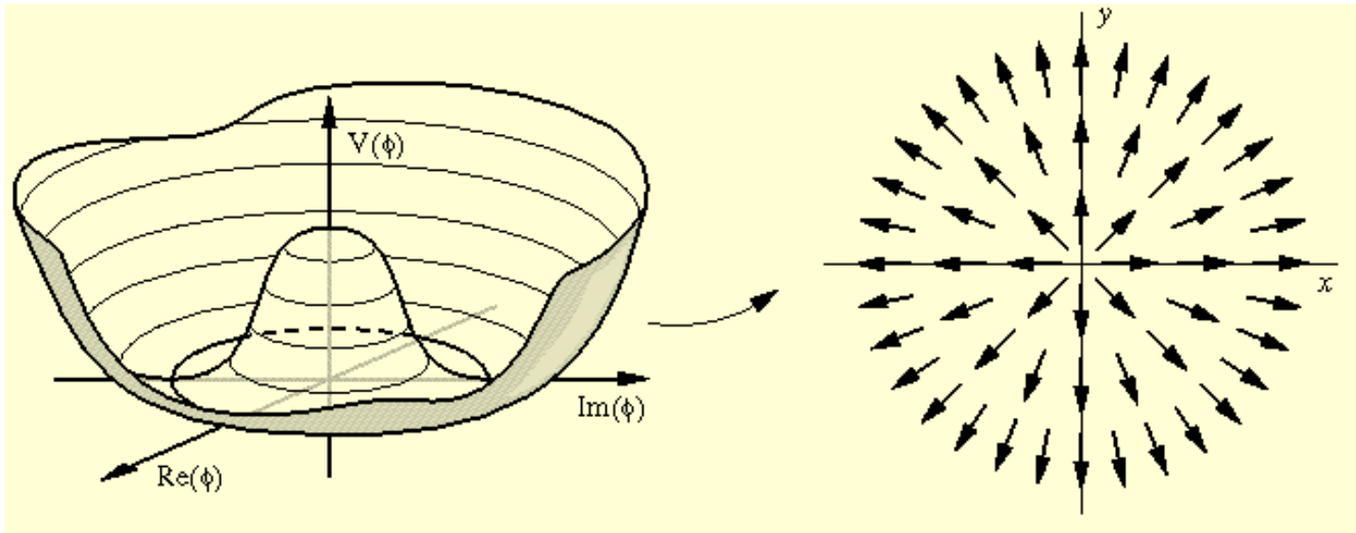

2: Cosmic superstrings

Cosmological size D-strings or F-strings remains after inflation

→ **could provide some insight into fundamental physics**

Evolution of cosmic strings

The energy density of cosmic strings $\propto a^{-2}$?

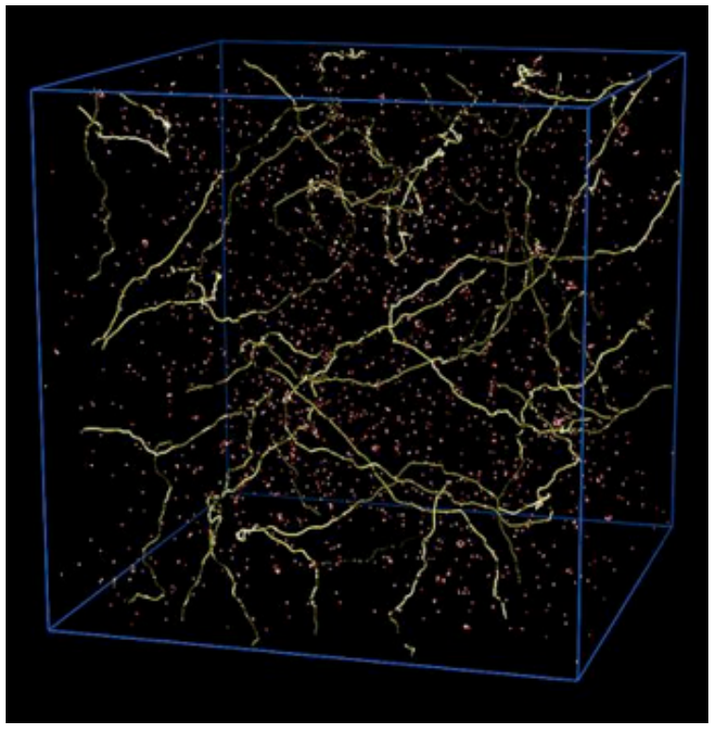

Scaling law

Cosmic String Networks approach a self-similar solution, which always looks same at the Hubble scale.

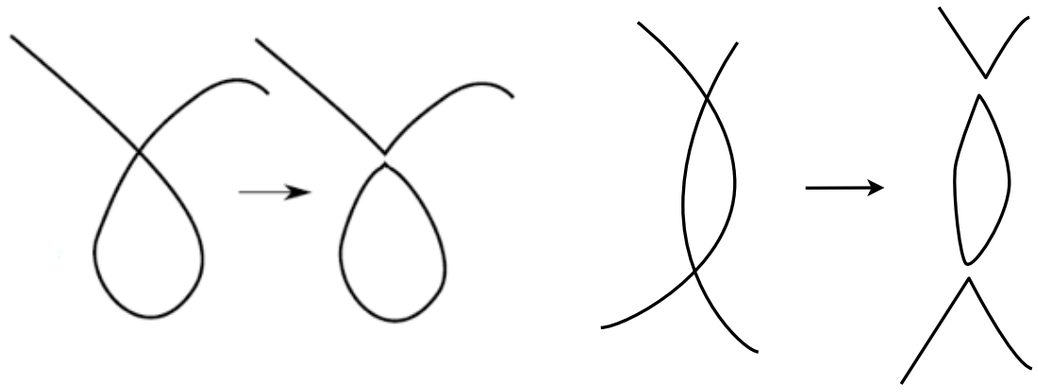

Cosmic strings become loops via **reconnection**.

Loops lose energy by emitting **gravitational waves.**

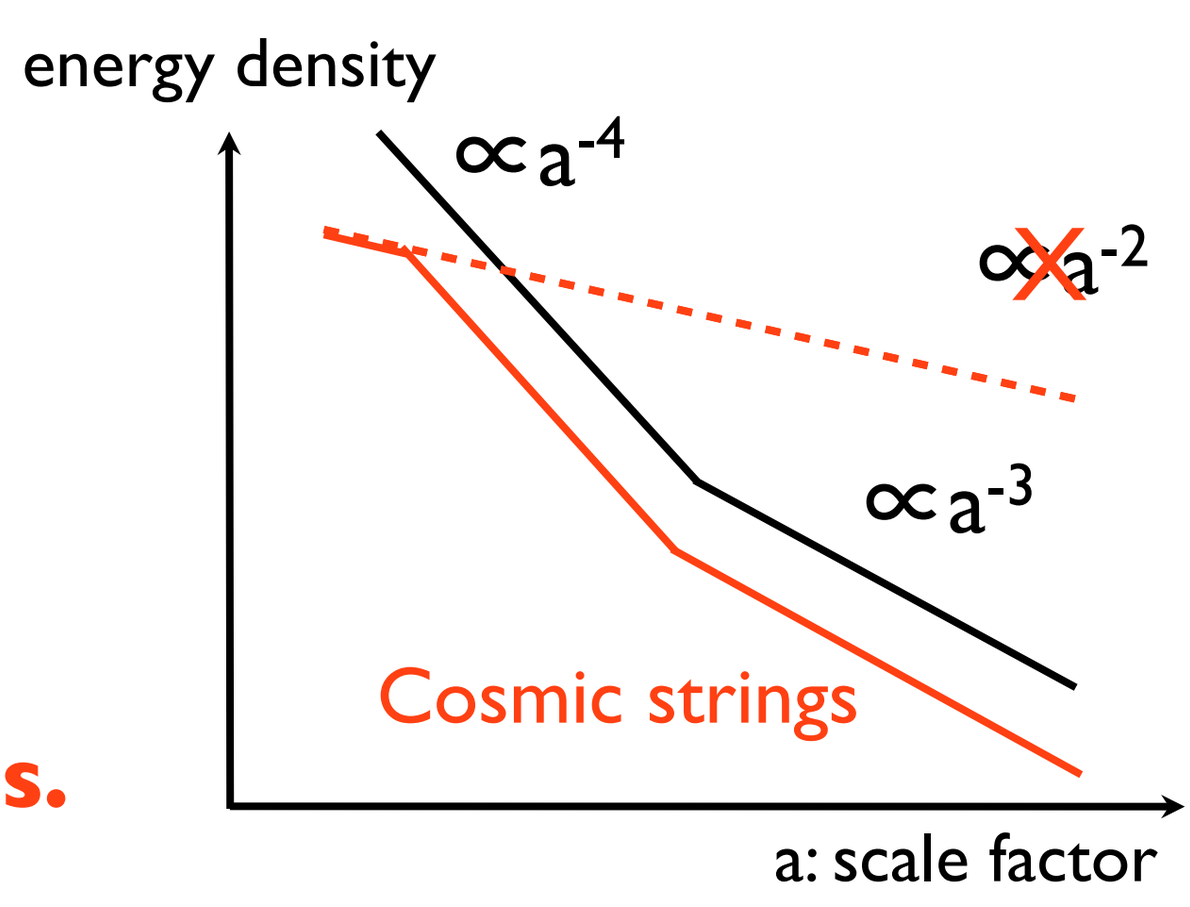

Observational Probe

1. Direct detection

Ground：Advanced-LIGO、KAGRA、

Virgo、IndIGO (2017-)

Space：eLISA/NGO (2022?)、DECIGO (2027)

2. Pulsar timing：SKA (2020)

3. CMB temperature fluctuation
+B-mode polarization：Planck, CMBpol

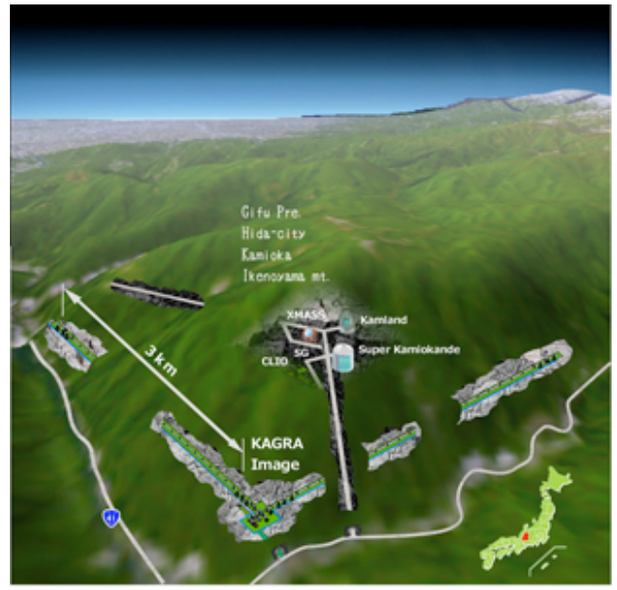

KAGRA image (http://gwcenter.icrr.u-tokyo.ac.jp/)

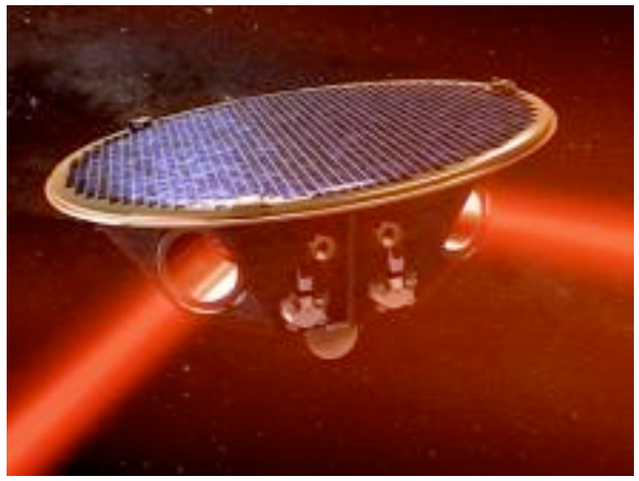

eLISA image (http://elisa-ngo.org/)

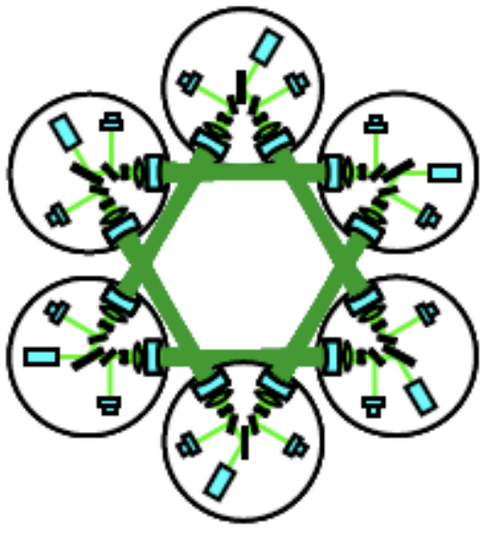

DECIGO image, S. Kawamura et al,
J. Phys.: Conf. Ser. 122, 012006 (2006)

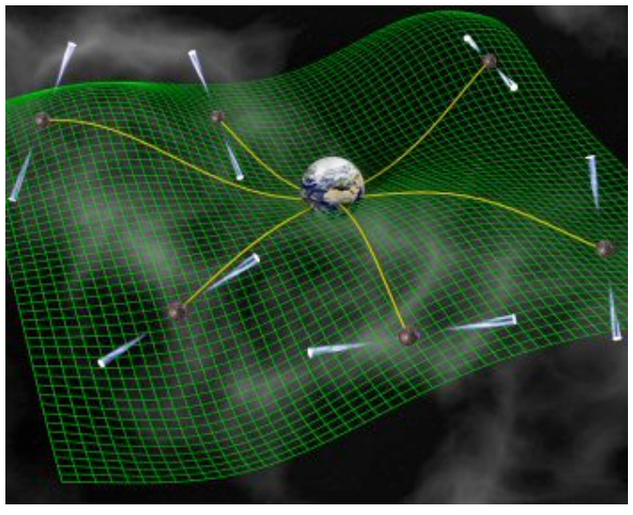

PTA image (NRAO)

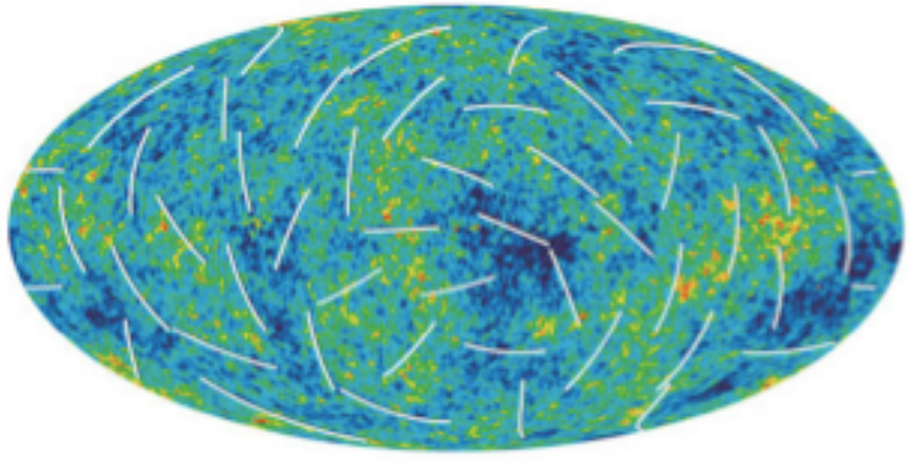

WMAP Three Year Polarized CMB Sky (http://wmap.gsfc.nasa.gov/)

Current constraints on cosmic string parameters

3 parameters to characterize cosmic string

- $G\mu$ (= μ / M_{pl}^2) : tension (line density)
- α : initial loop size $L \sim \alpha H^{-1}$
- p : reconnection probability → Phase transition origin: p=1, Cosmic superstring: p<<1

- CMB temperature fluctuation: $G\mu <\sim 10^{-7}$
- Gravitational lensing: $G\mu <\sim 10^{-6}$

for infinite strings

- Gravitational waves

  Pulsar timing: $G\mu <\sim 10^{-9}$

  Direct detection (LIGO GWB): $G\mu <\sim 10^{-6}$

for loops α =0.1, p=1

What about future constraints ?

Gravitational wave signals

Strong GW emission from singular points
called kinks and cusps

kink

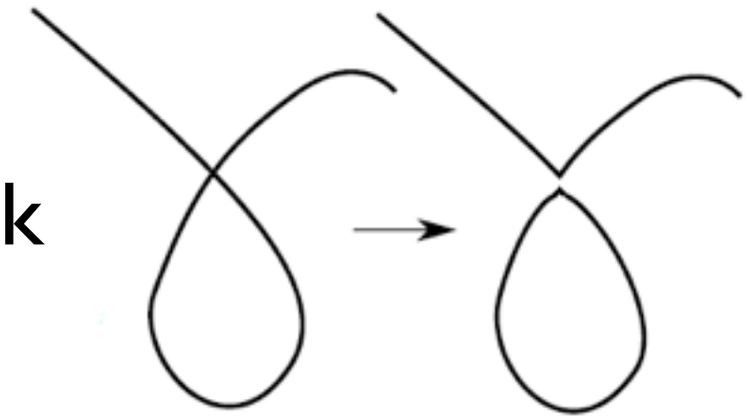

cusp

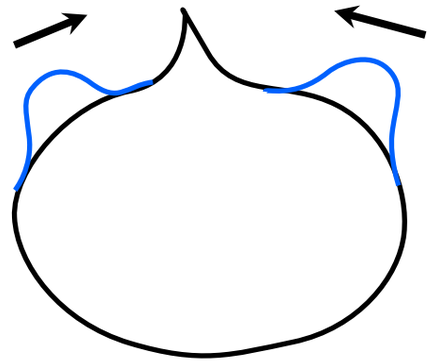

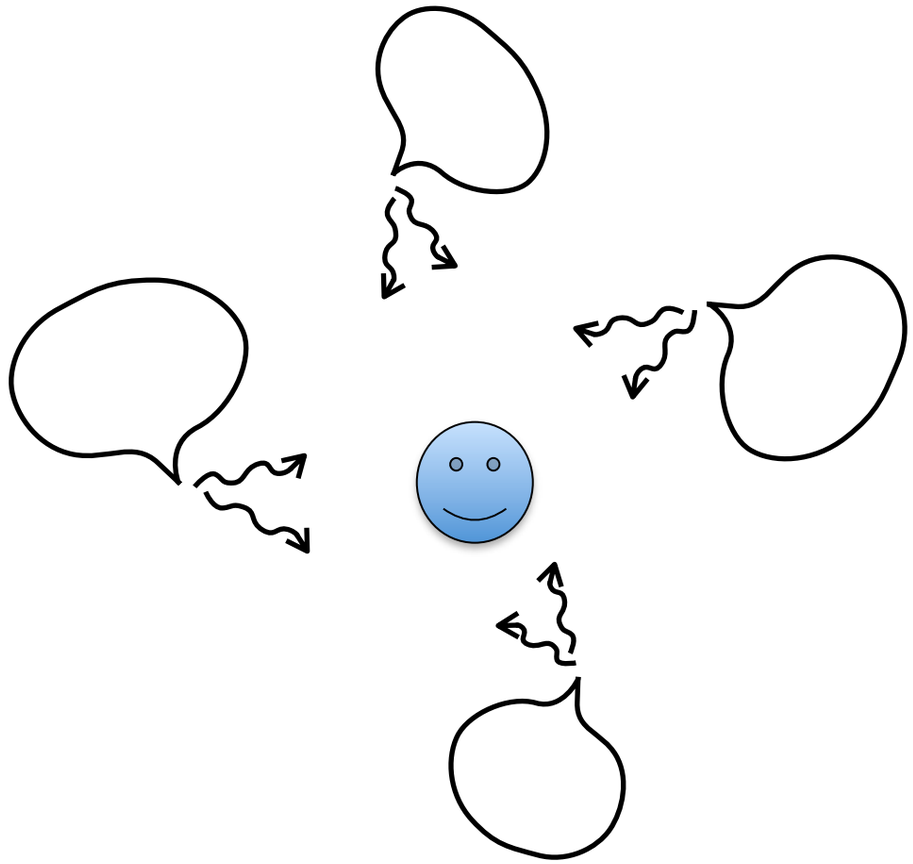

Rare Burst: GWs with large amplitude coming from close loops

→ direct detection

Gravitational wave background (GWB): superposition of small GWs coming from the early epoch

→ direct detection + pulsar timing

How many cosmic string bursts are coming to the earth per year?
(plotted as a function of the amplitude for the fixed frequency @220Hz)

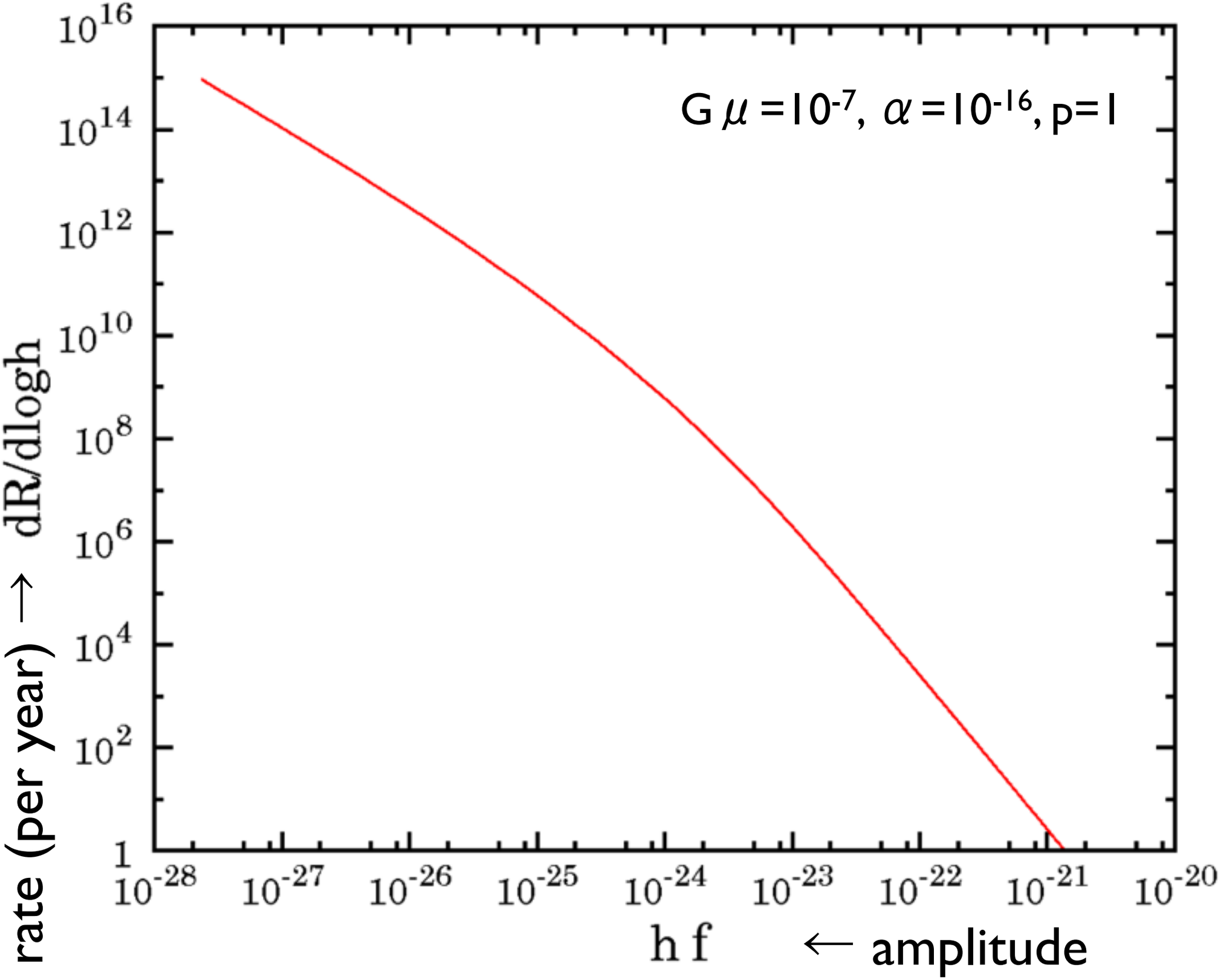

How many cosmic string bursts are coming to the earth per year?
(plotted as a function of the amplitude for the fixed frequency @220Hz)

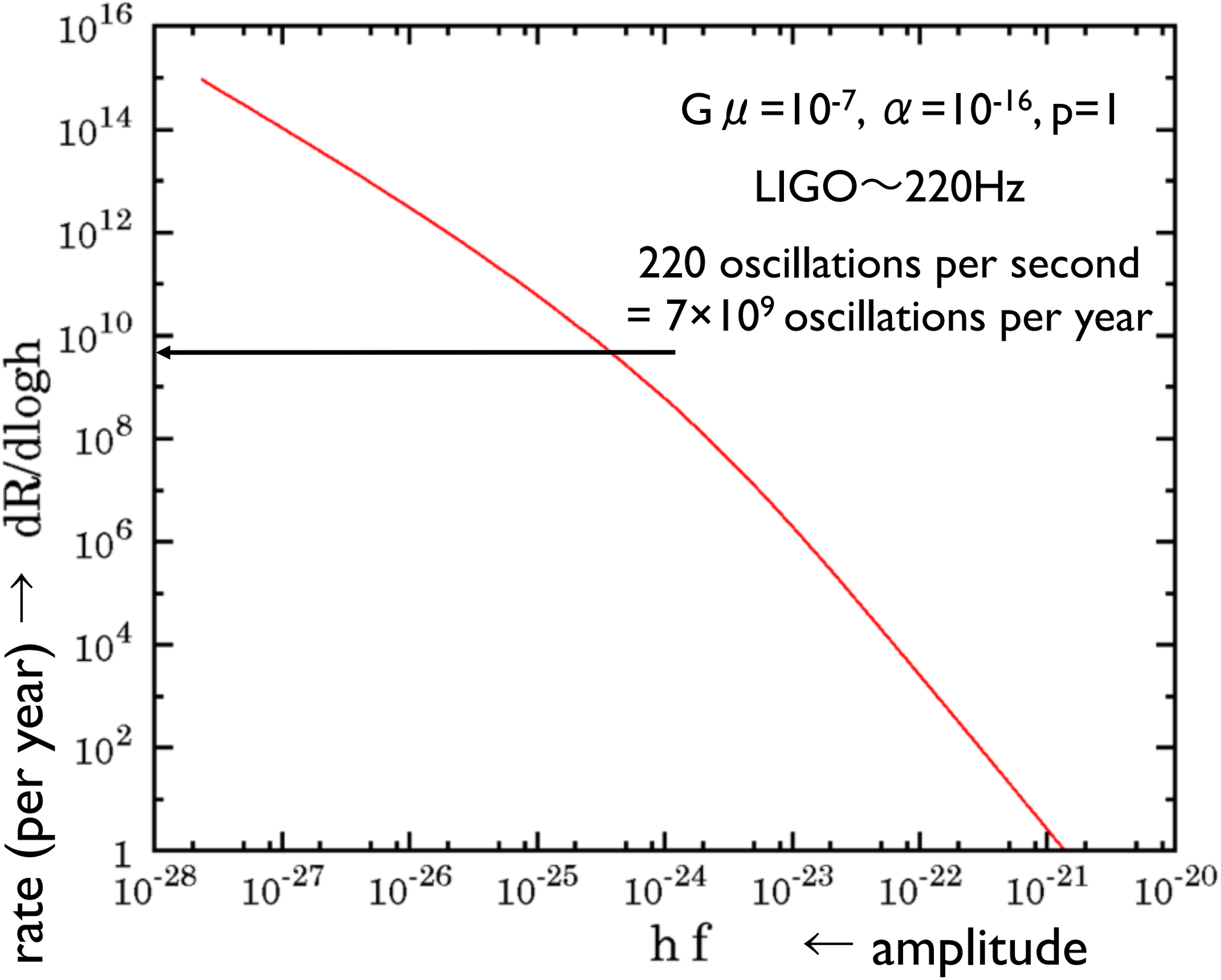

How many cosmic string bursts are coming to the earth per year?
(plotted as a function of the amplitude for the fixed frequency @220Hz)

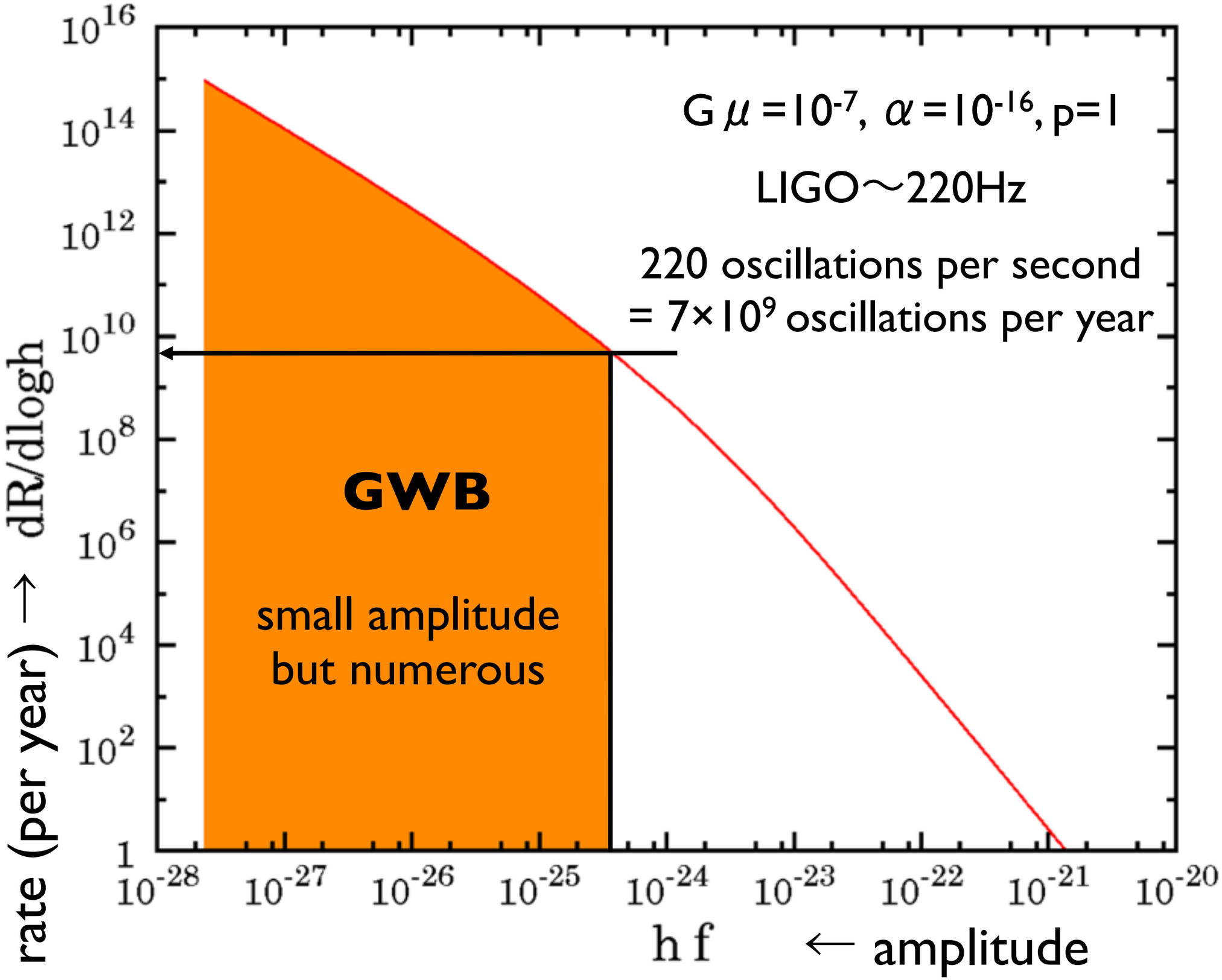

How many cosmic string bursts are coming to the earth per year?
(plotted as a function of the amplitude for the fixed frequency @220Hz)

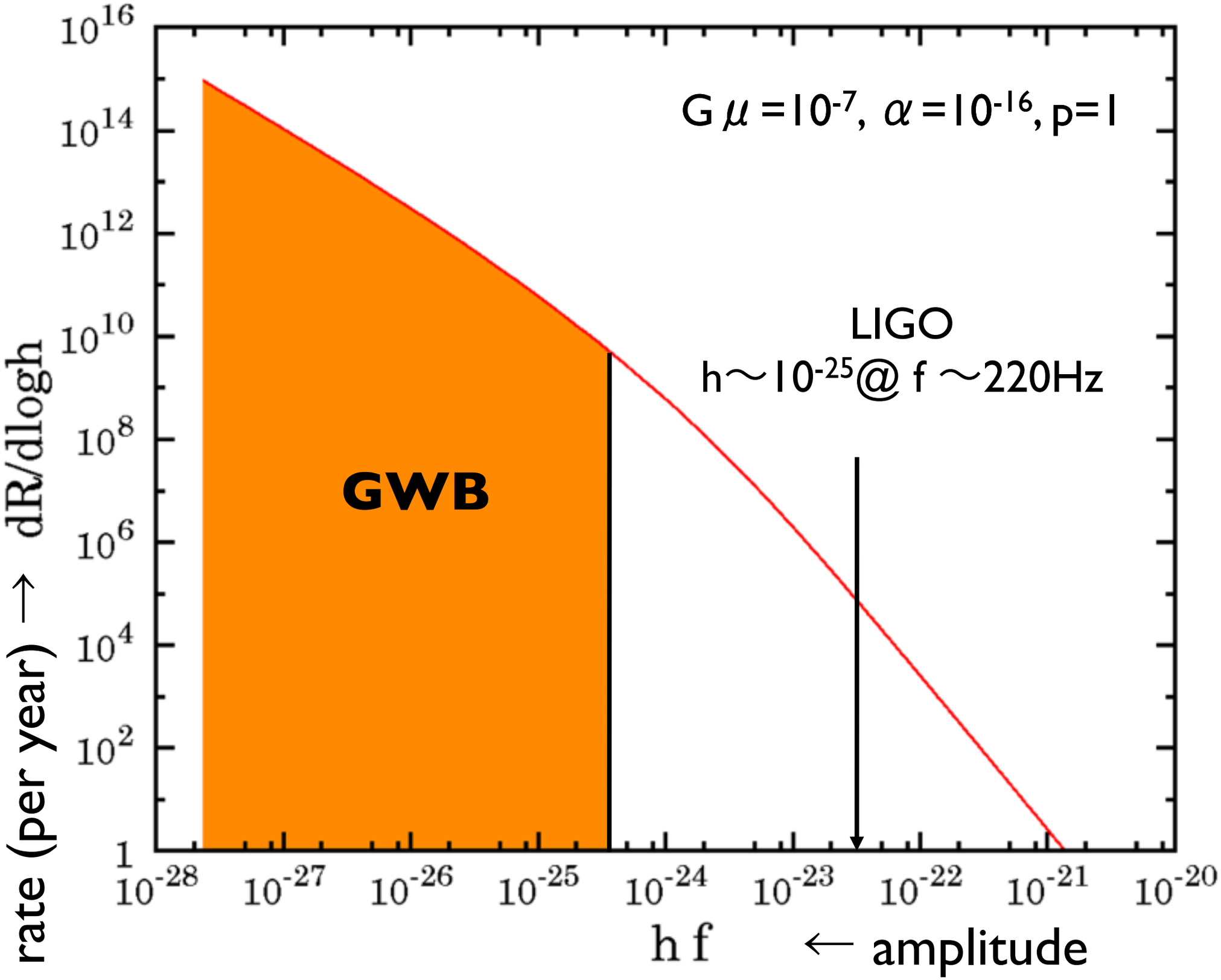

How many cosmic string bursts are coming to the earth per year?
(plotted as a function of the amplitude for the fixed frequency @220Hz)

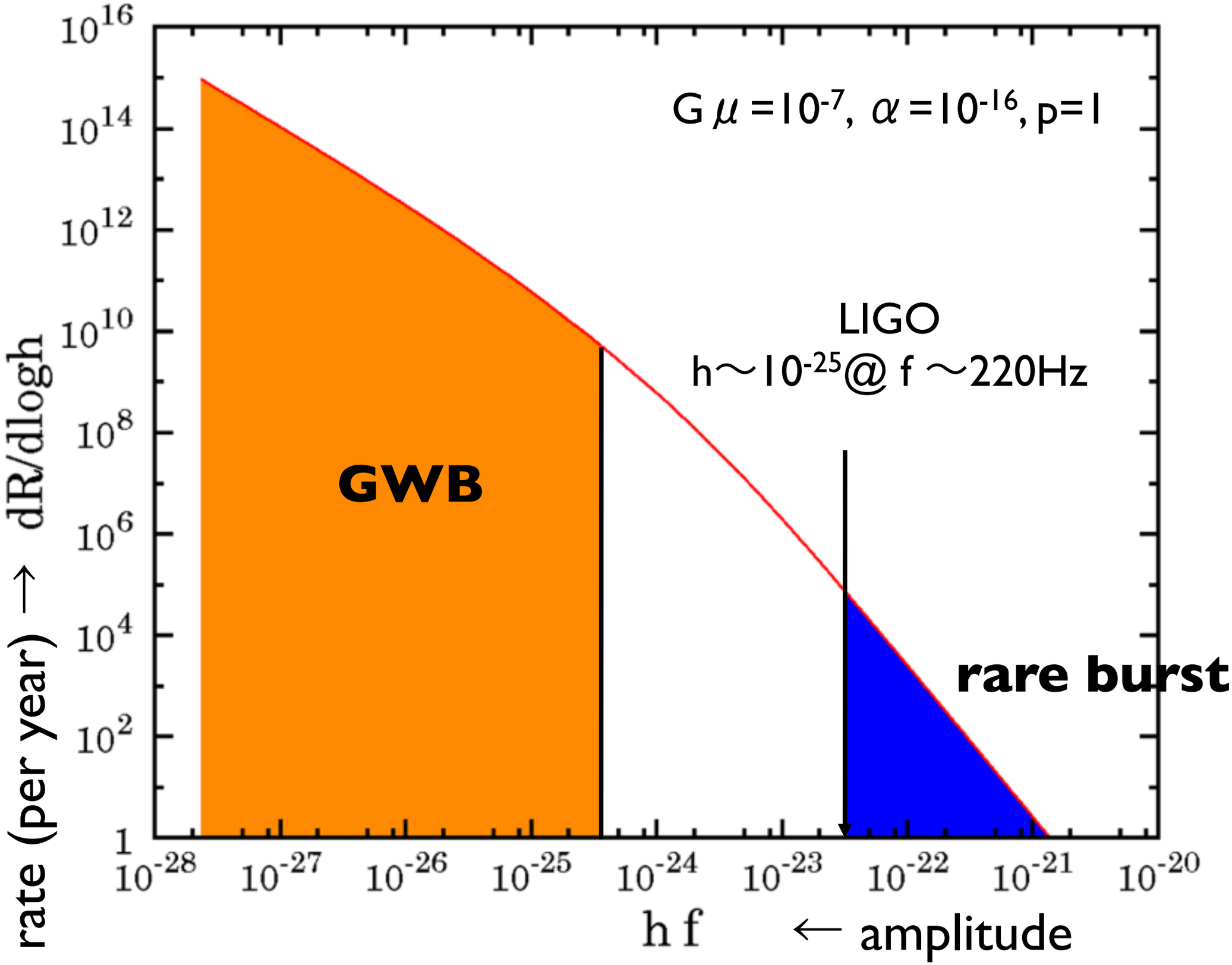

How many cosmic string bursts are coming to the earth per year?
(plotted as a function of the amplitude for the fixed frequency @220Hz)

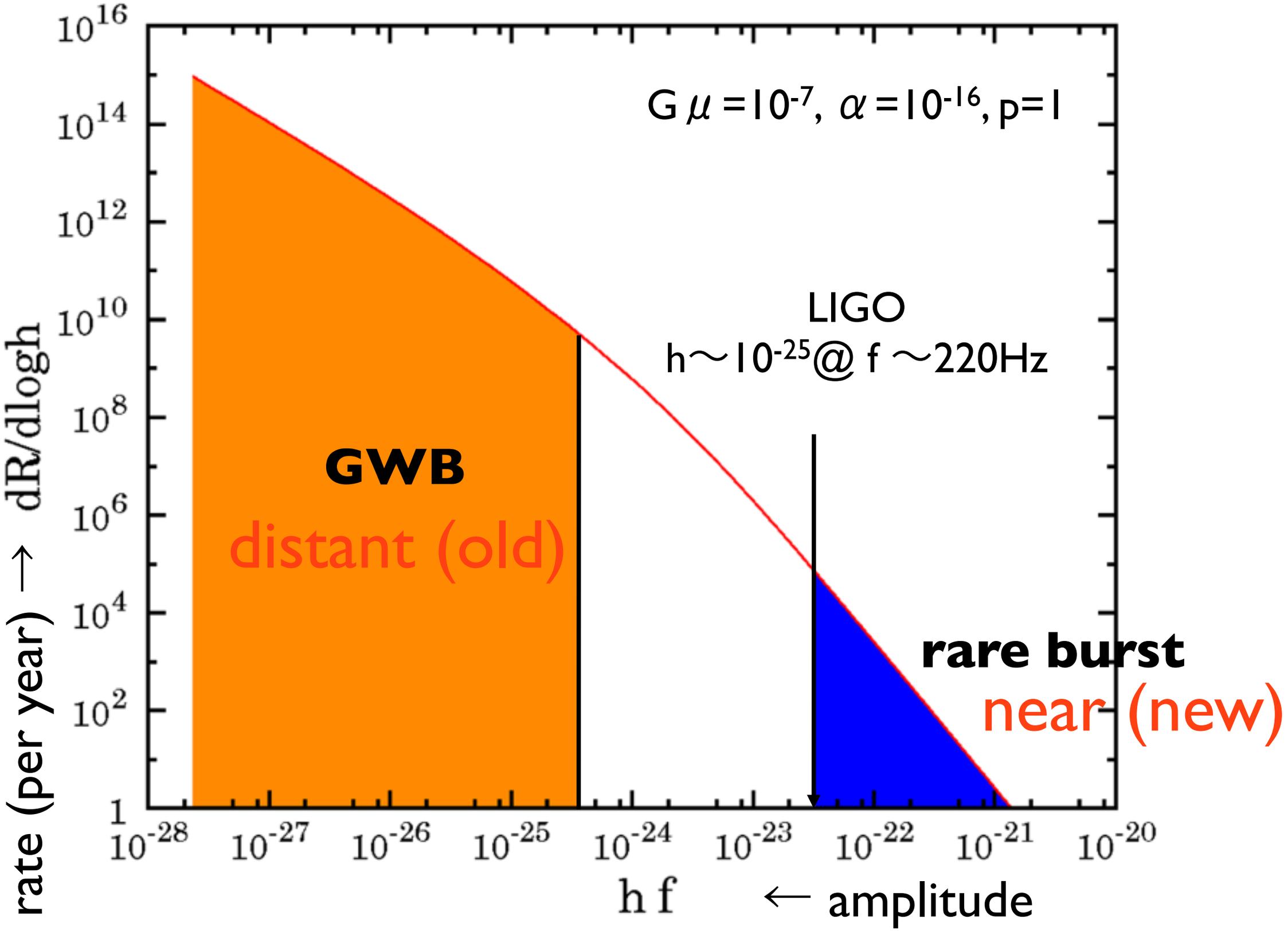

Parameter dependences of the rate

$G\mu$ ↑ **amplitude of GWs ↑**
lifetime↓ number density ↓

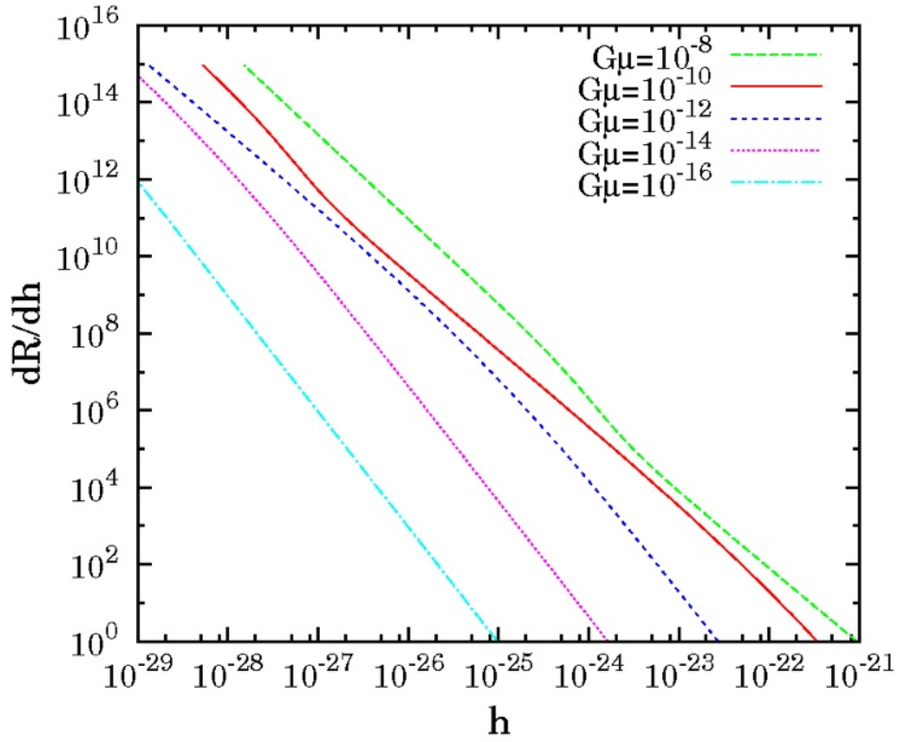

p ↓ **number density ↑**

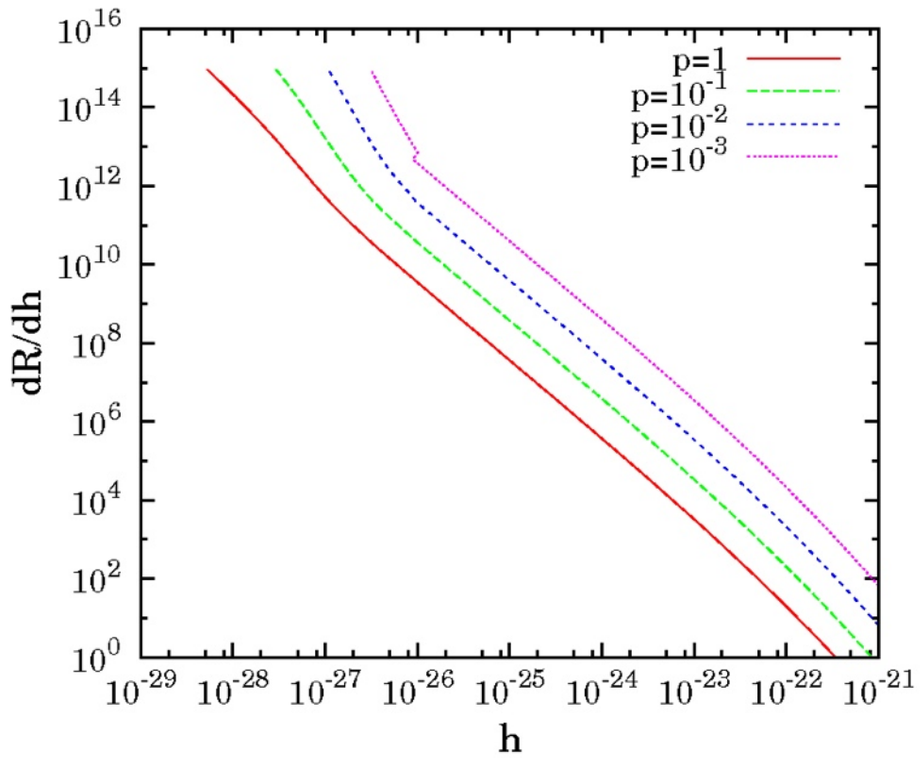

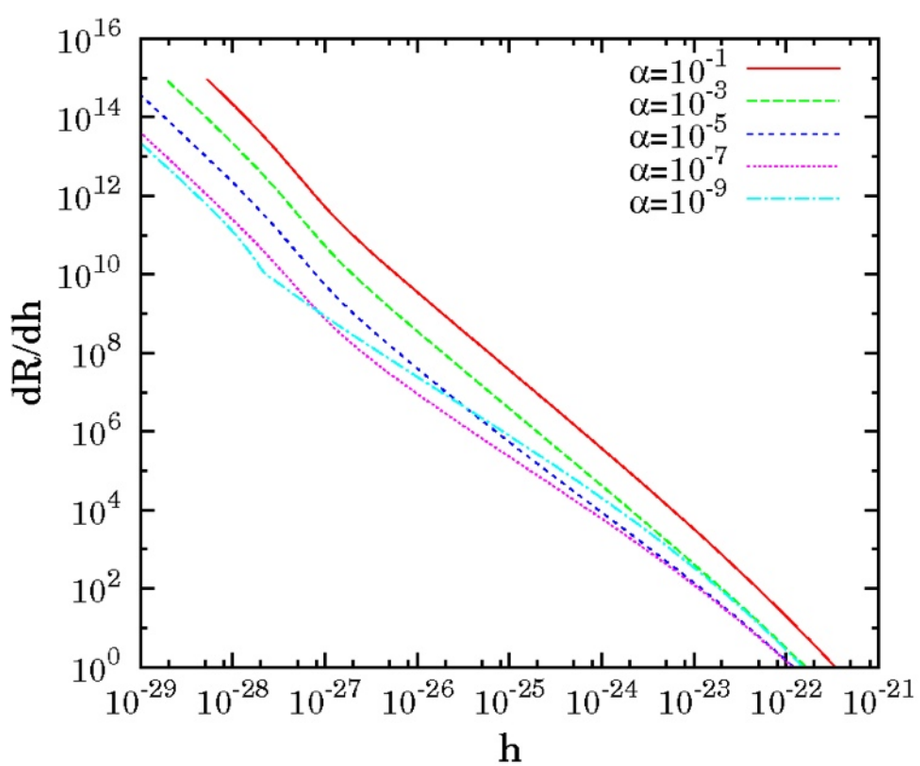

α ↓ **lifetime↓ number density ↓**

GW power $P = \Gamma G\mu^2$

Γ: numerical constant ~50-100

Lifetime of loops $= \dfrac{\text{(initial loop energy)}}{\text{(energy release rate per time)}}$

$= \dfrac{\mu\alpha t}{\Gamma G\mu^2} = \dfrac{\alpha t}{\Gamma G\mu}$

Parameter dependences of the rate

G μ

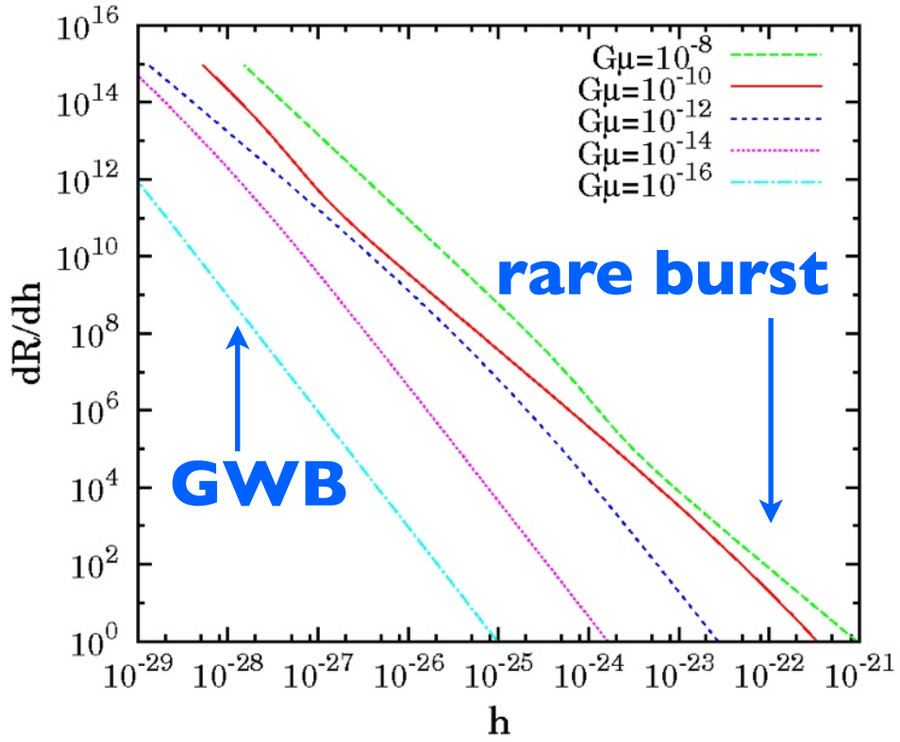

p

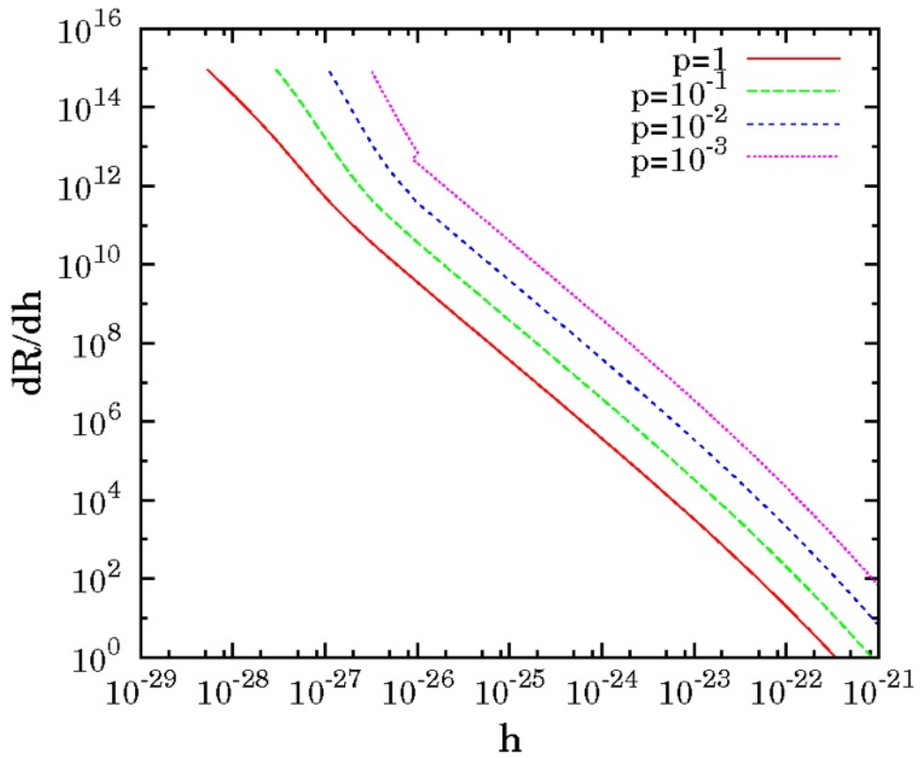

α

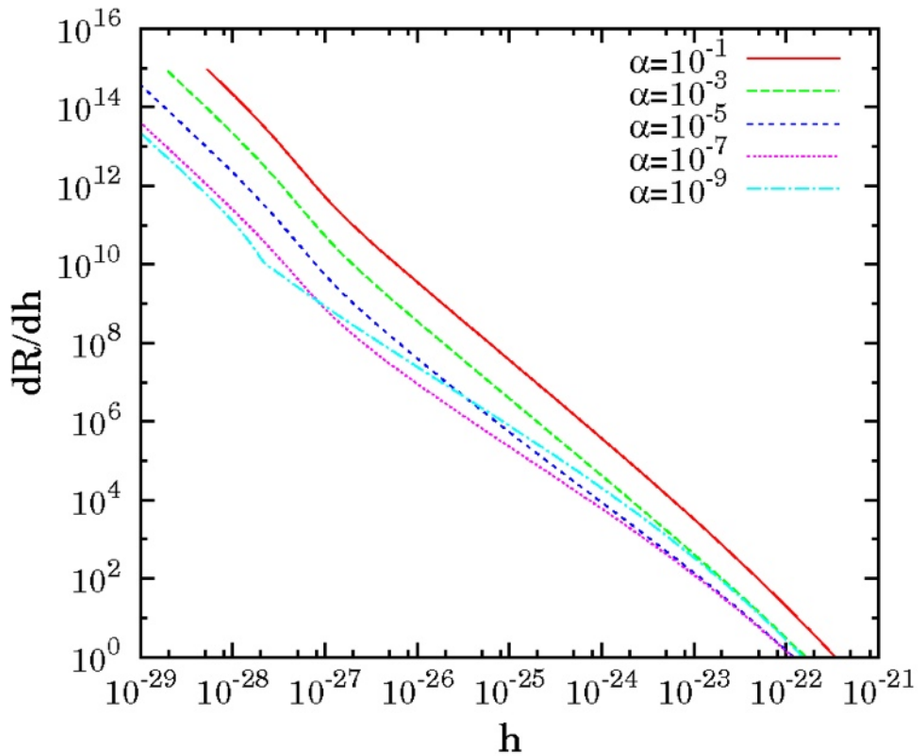

The parameter dependences of the large burst (rare burst) and small burst (GWB) are different because they are looking at different epoch of the Universe

→ **give different information on cosmic string parameters**

Spectrum of the GWB

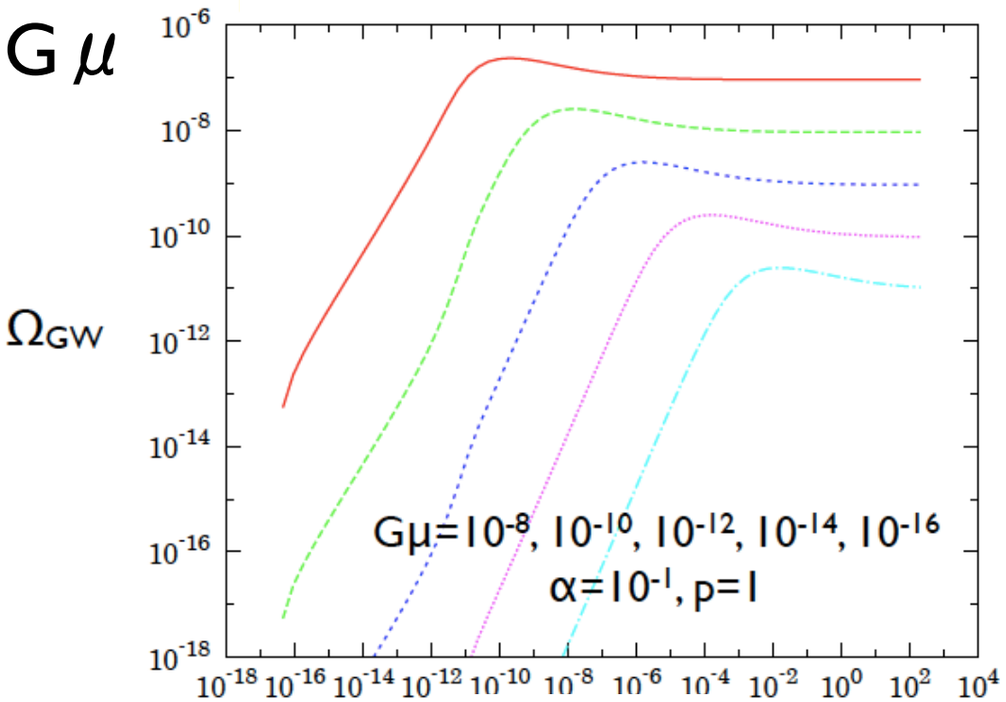

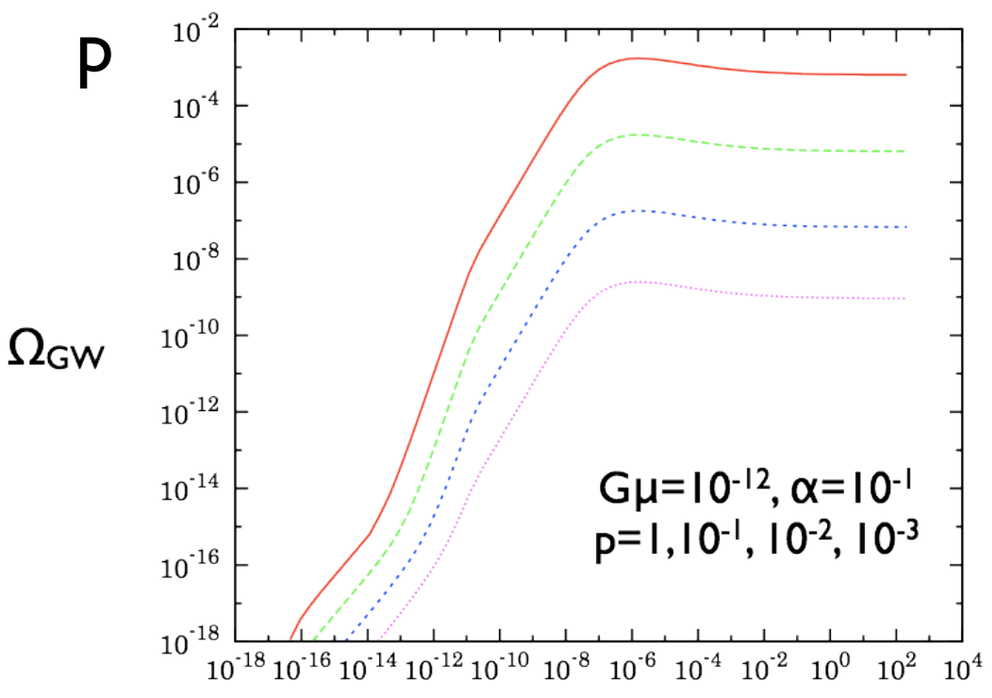

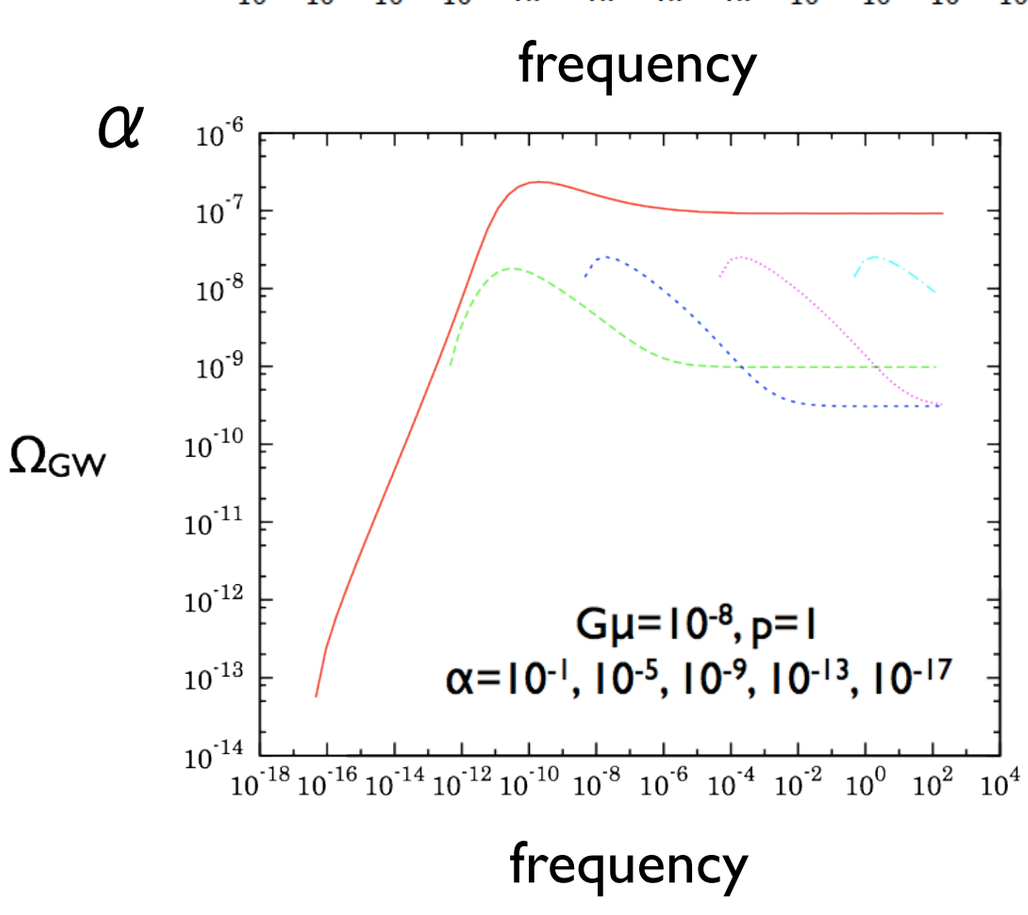

Accessible parameter region (for p=1)

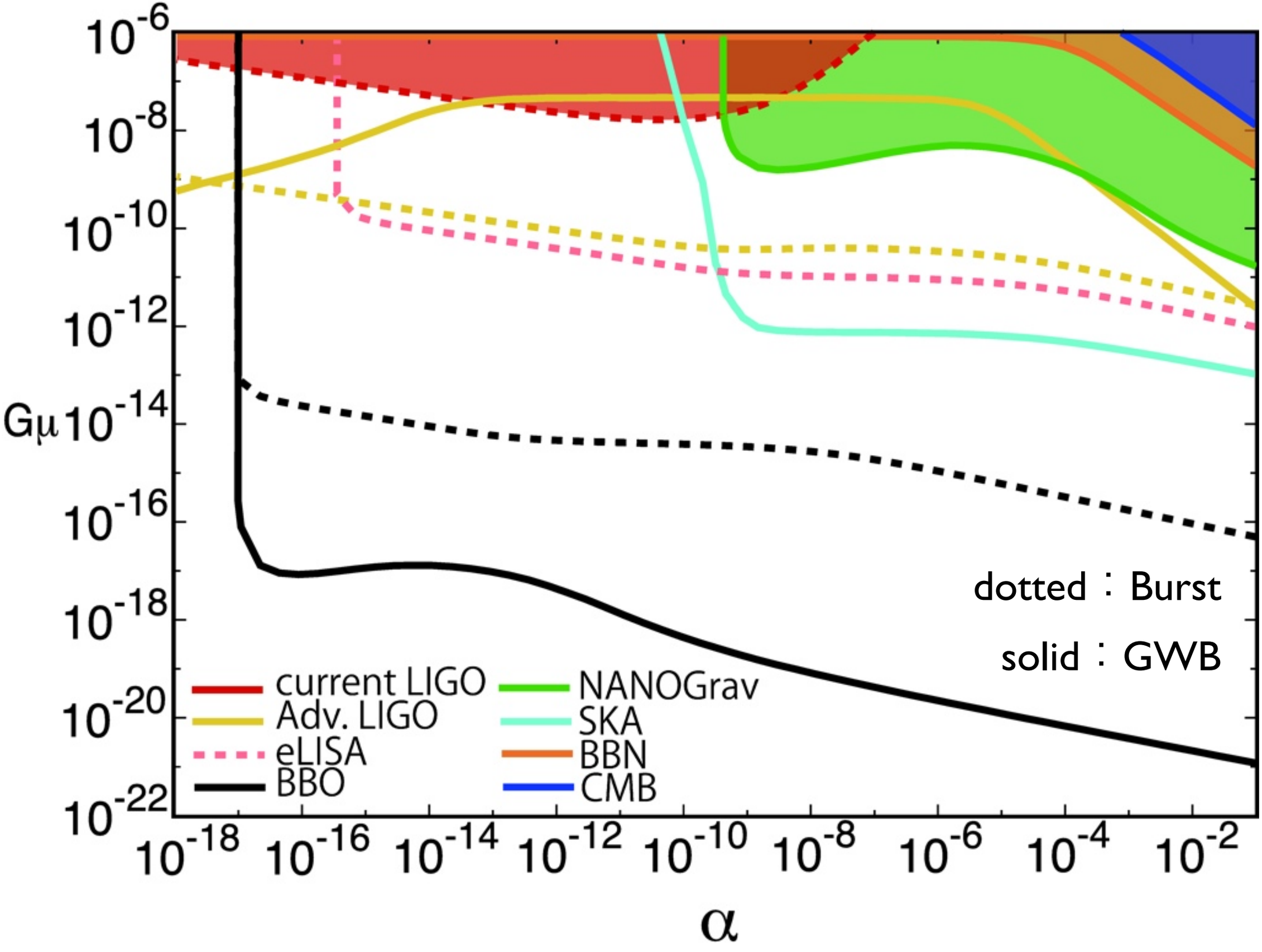

Advanced-LIGO can detect both rare bursts and GWB

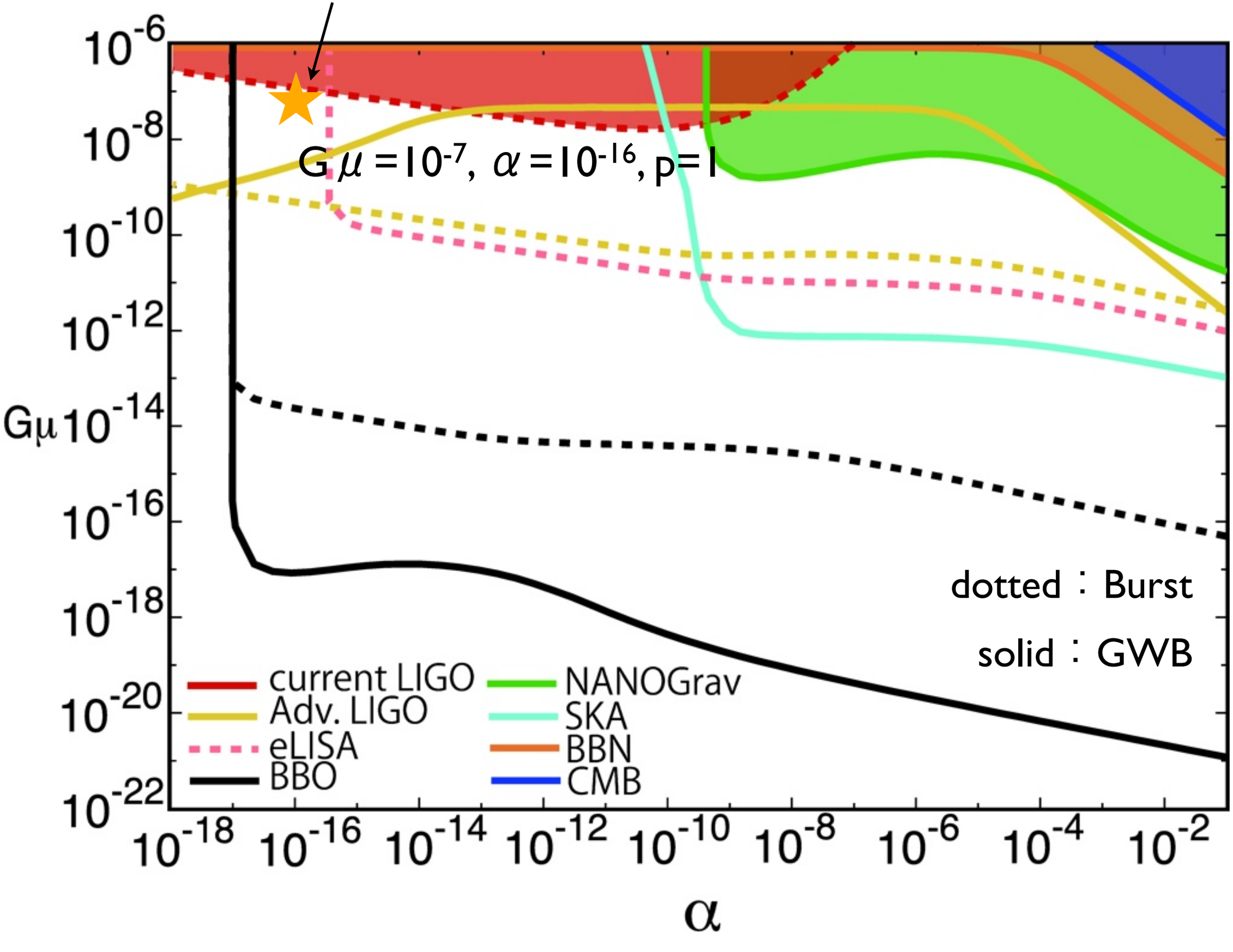

Constraint from direct detection experiments

Example: G μ =10^{-7}, α =10^{-16}, p=1
Adv-LIGO 3year

Kuroyanagi et. al. PRD 86, 023503 (2012)

different parameter dependence
= different constraints on parameters

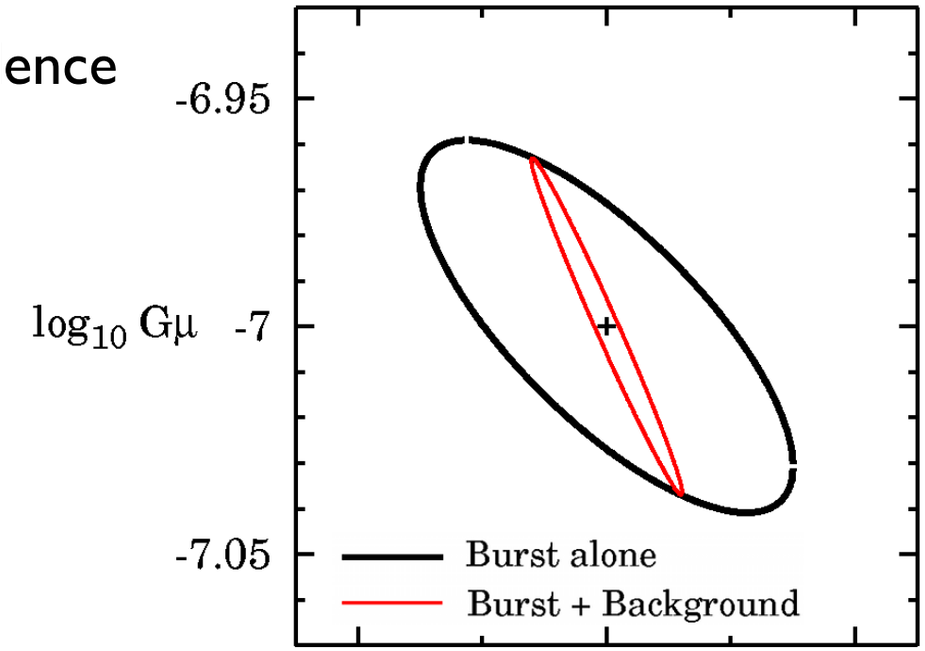

black ： Burst only

red ： Burst + GWB

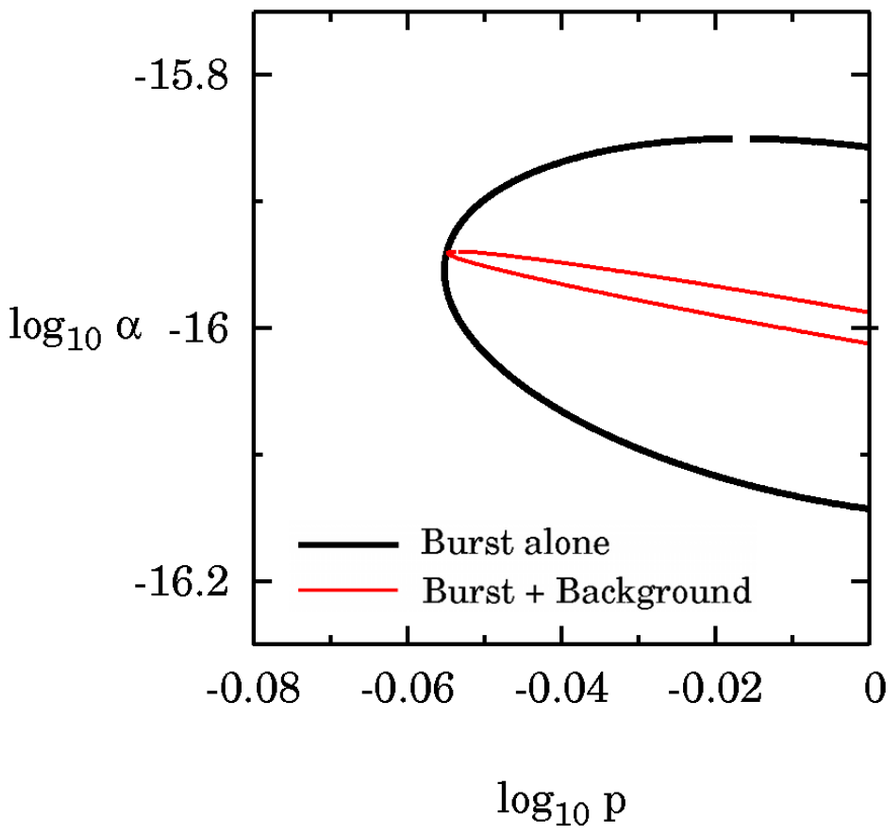

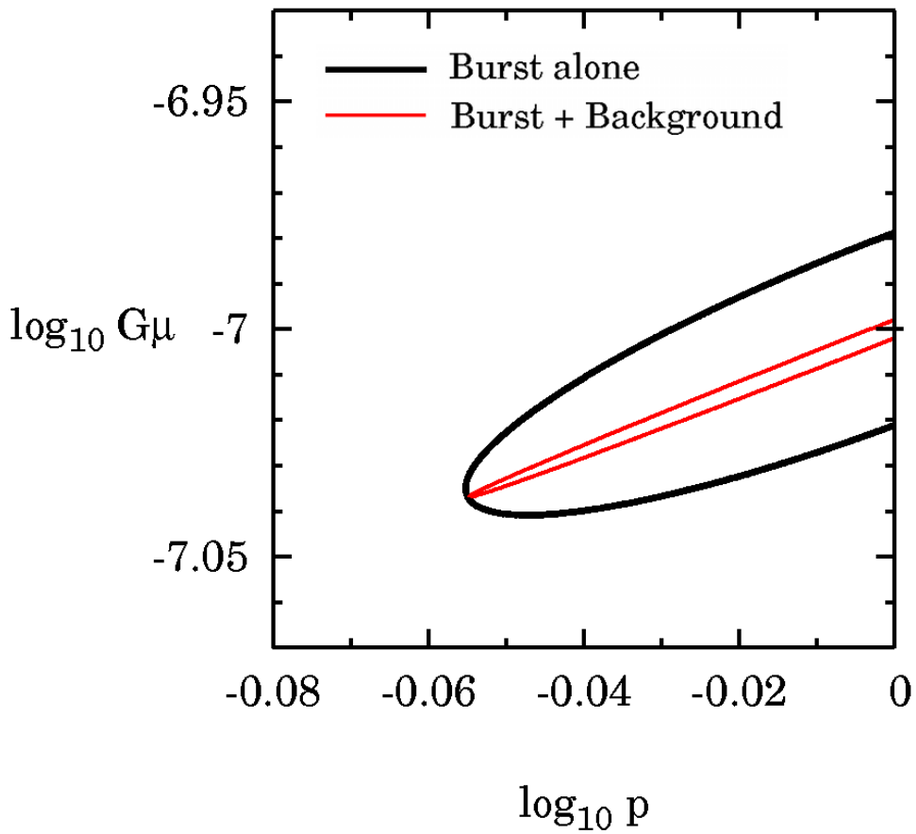

Constraint from direct detection experiments

Example: G μ =10^{-7}, α =10^{-16}, p=1
Adv-LIGO 3year

Kuroyanagi et. al. PRD 86, 023503 (2012)

black ： Burst only

dotted: GWB only

red ： Burst + GWB

Before marginalized over

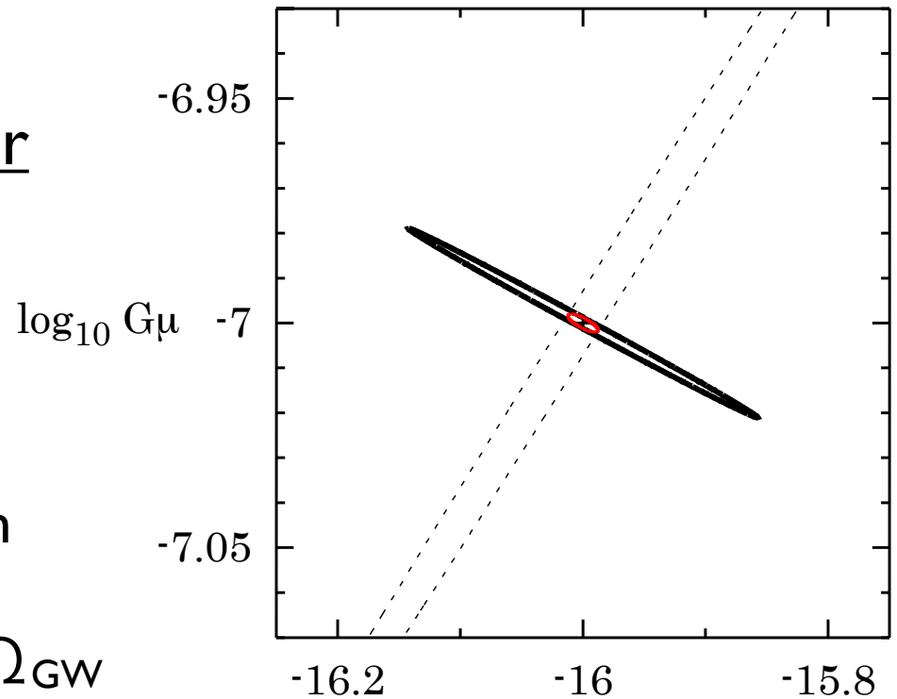

Strong degeneracy seen in constraint from GWB since the observable is only Ω_{GW}

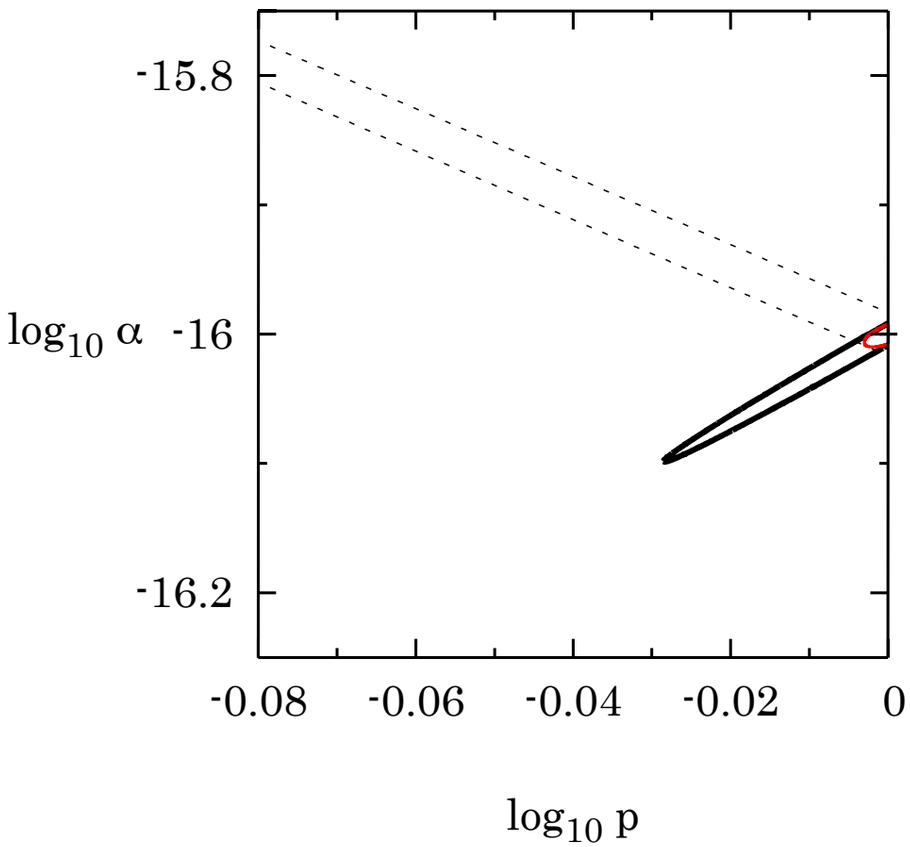

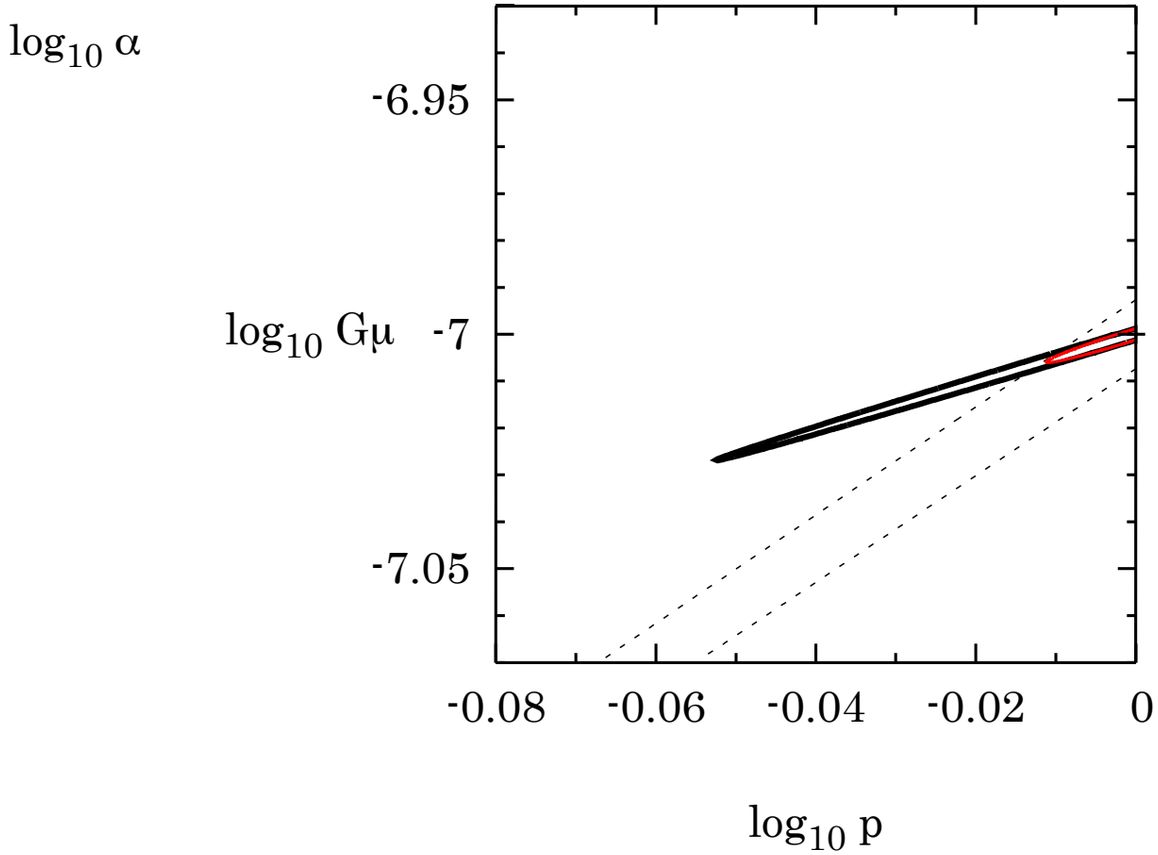

Signals in the CMB

temperature fluctuation

B-mode polarization

G μ

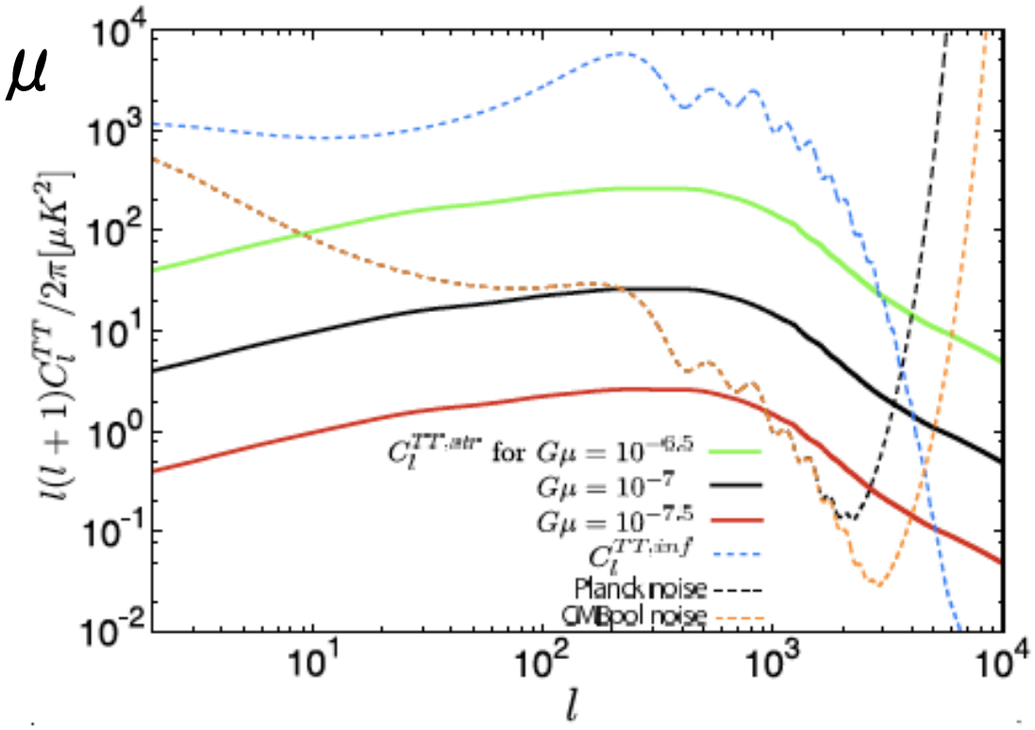

G μ

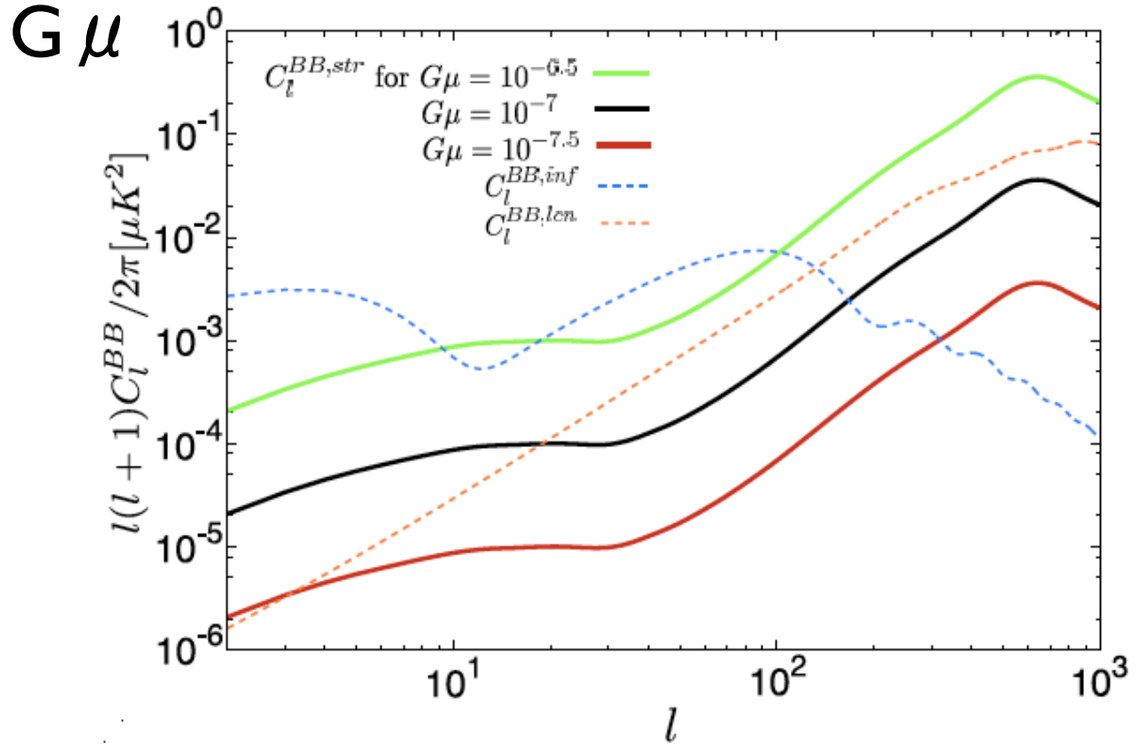

P

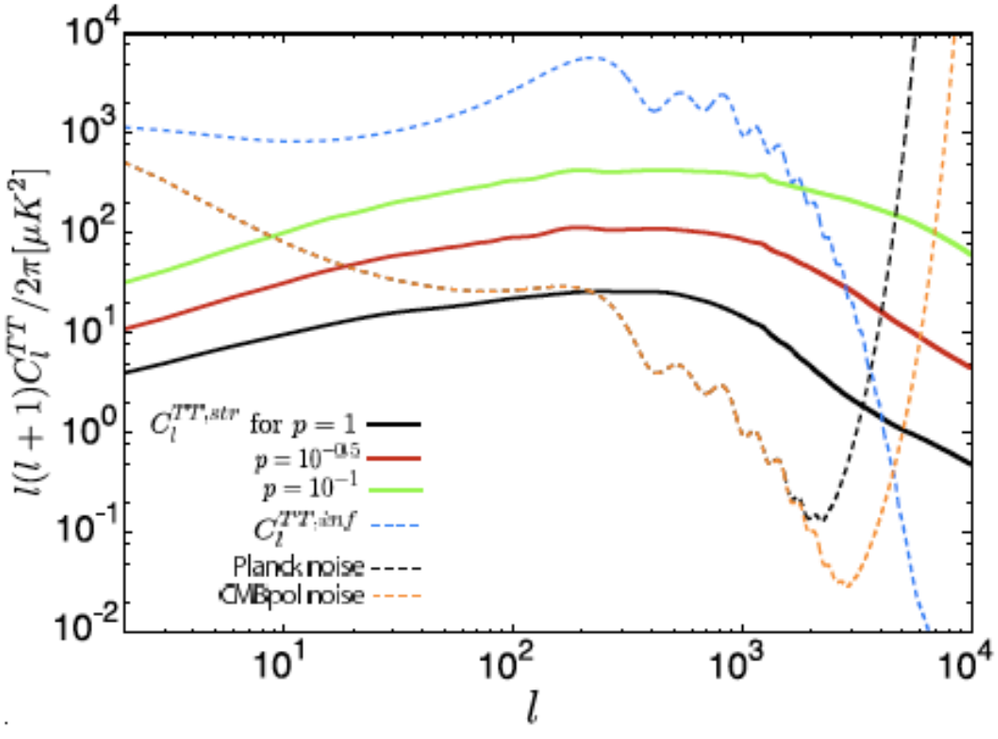

P

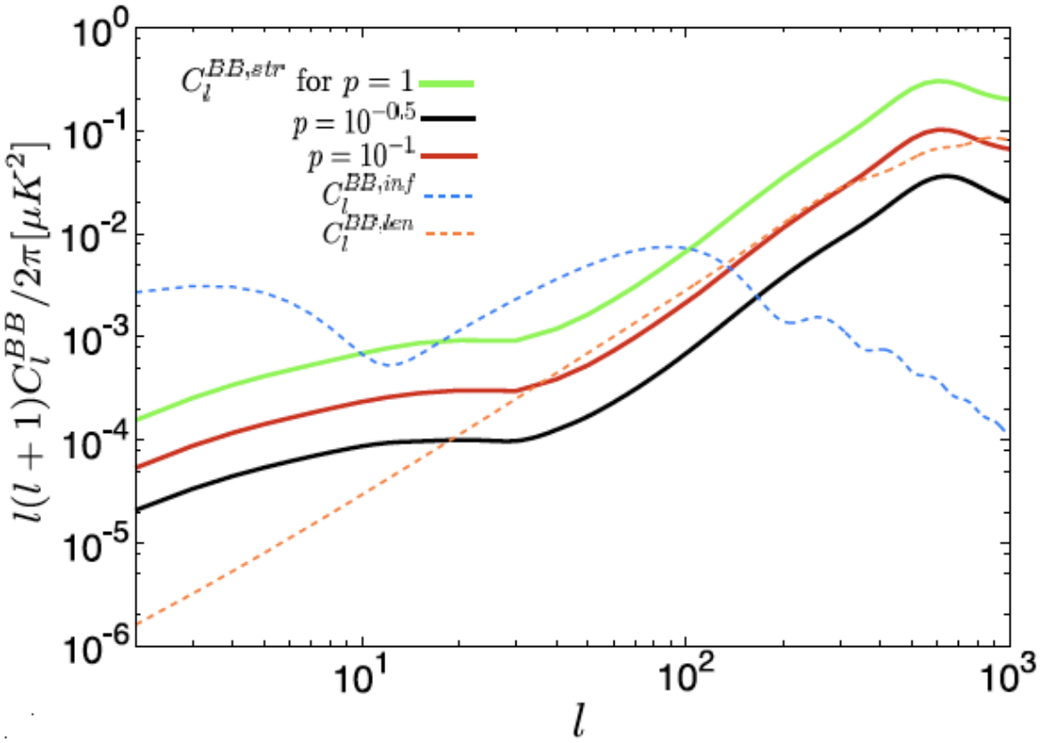

If we combine CMB constraints...

$G\mu = 10^{-7}$, $\alpha = 10^{-16}$, p=1
Adv-LIGO 3year
+ CMB B-mode

Kuroyanagi et al. arXiv:1210.2829

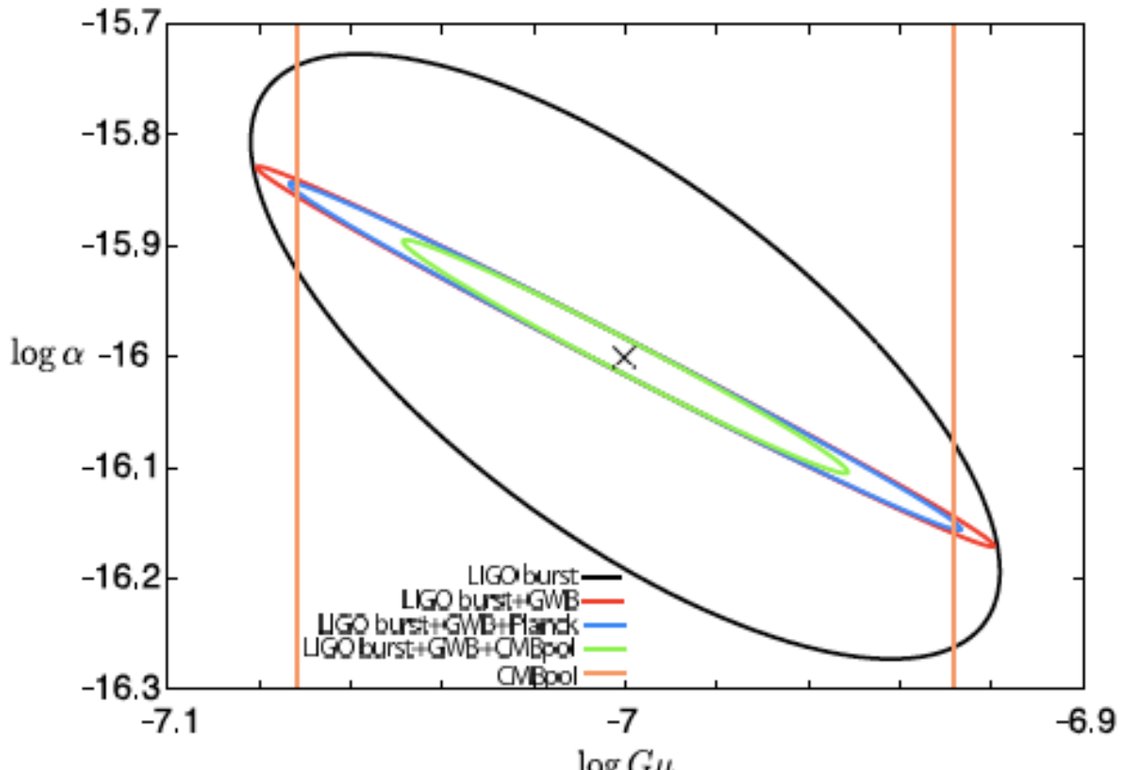

black : LIGO Burst only
red : LIGO Burst + GWB
blue: LIGO +Planck
green: LIGO+CMBpol
orange: CMB pol only

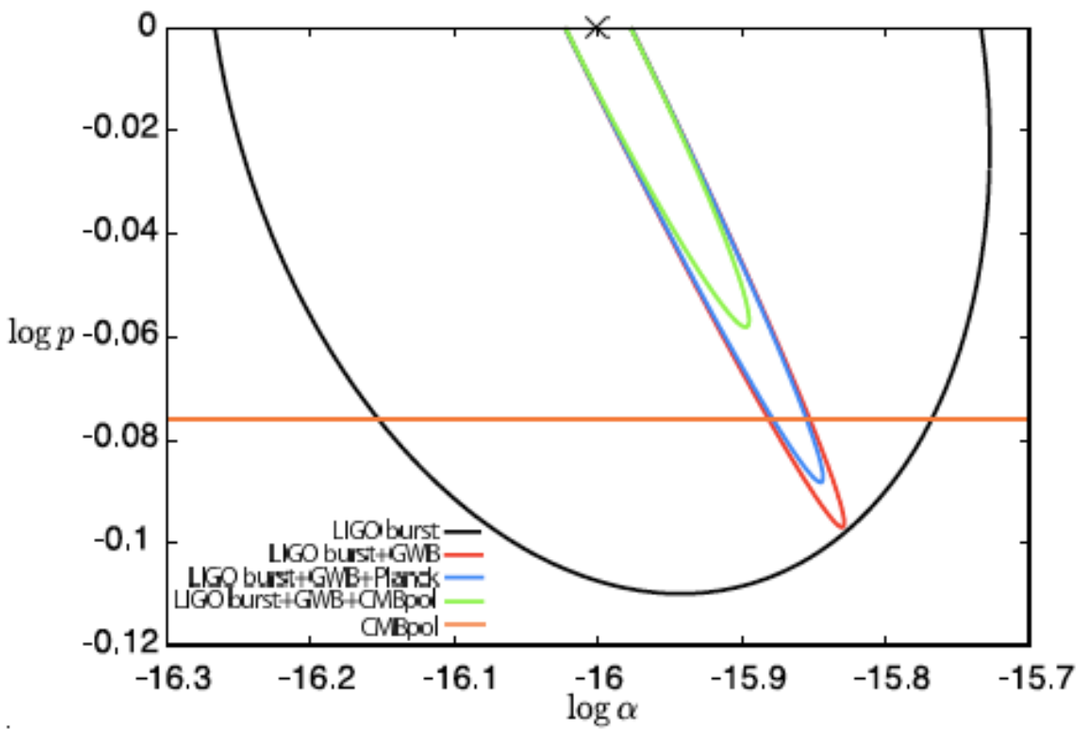

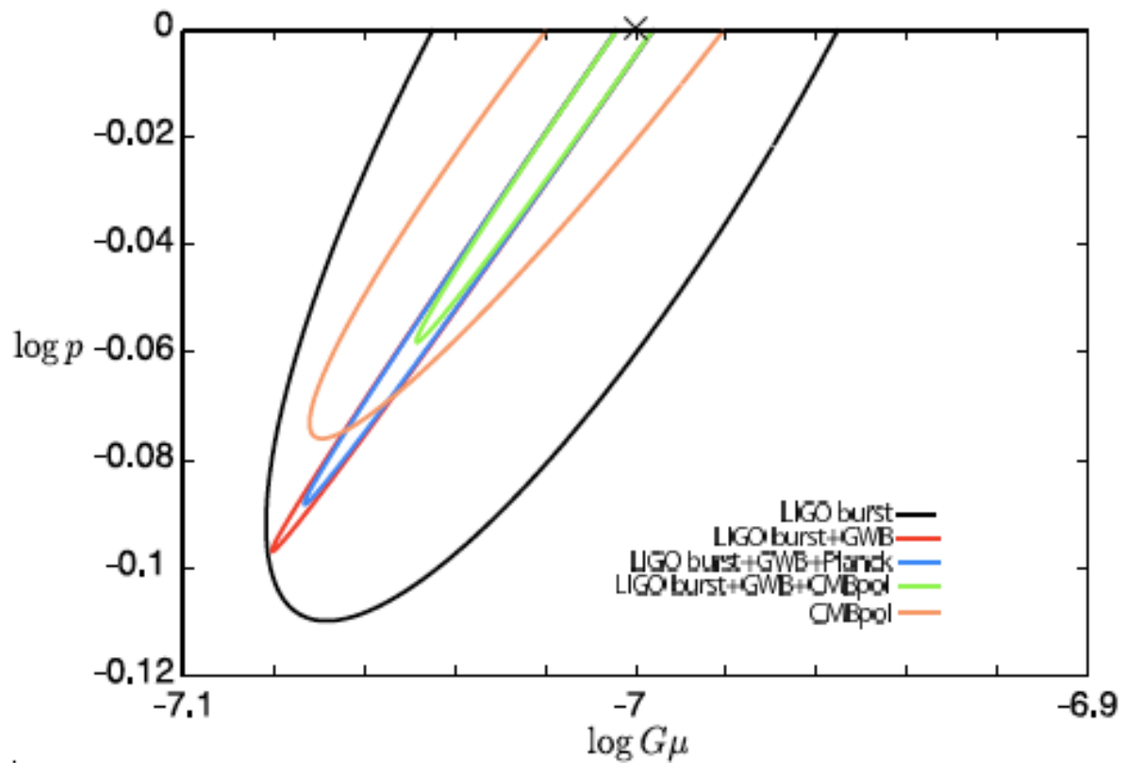

Constraints from pulsar timing and space direct detection mission

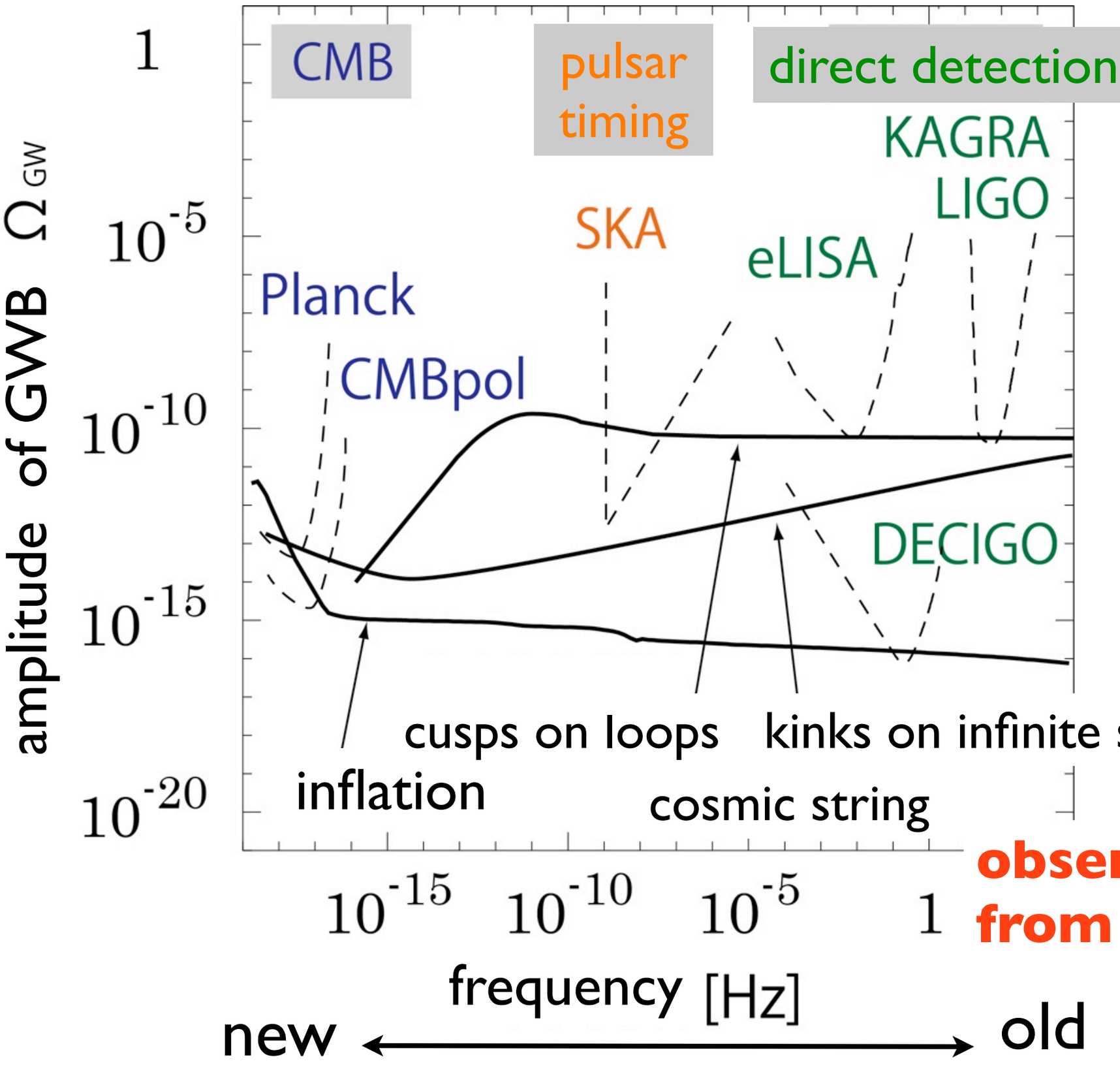

observing GWs from different epochs

Pulsar timing (SKA) + Advanced-LIGO burst search

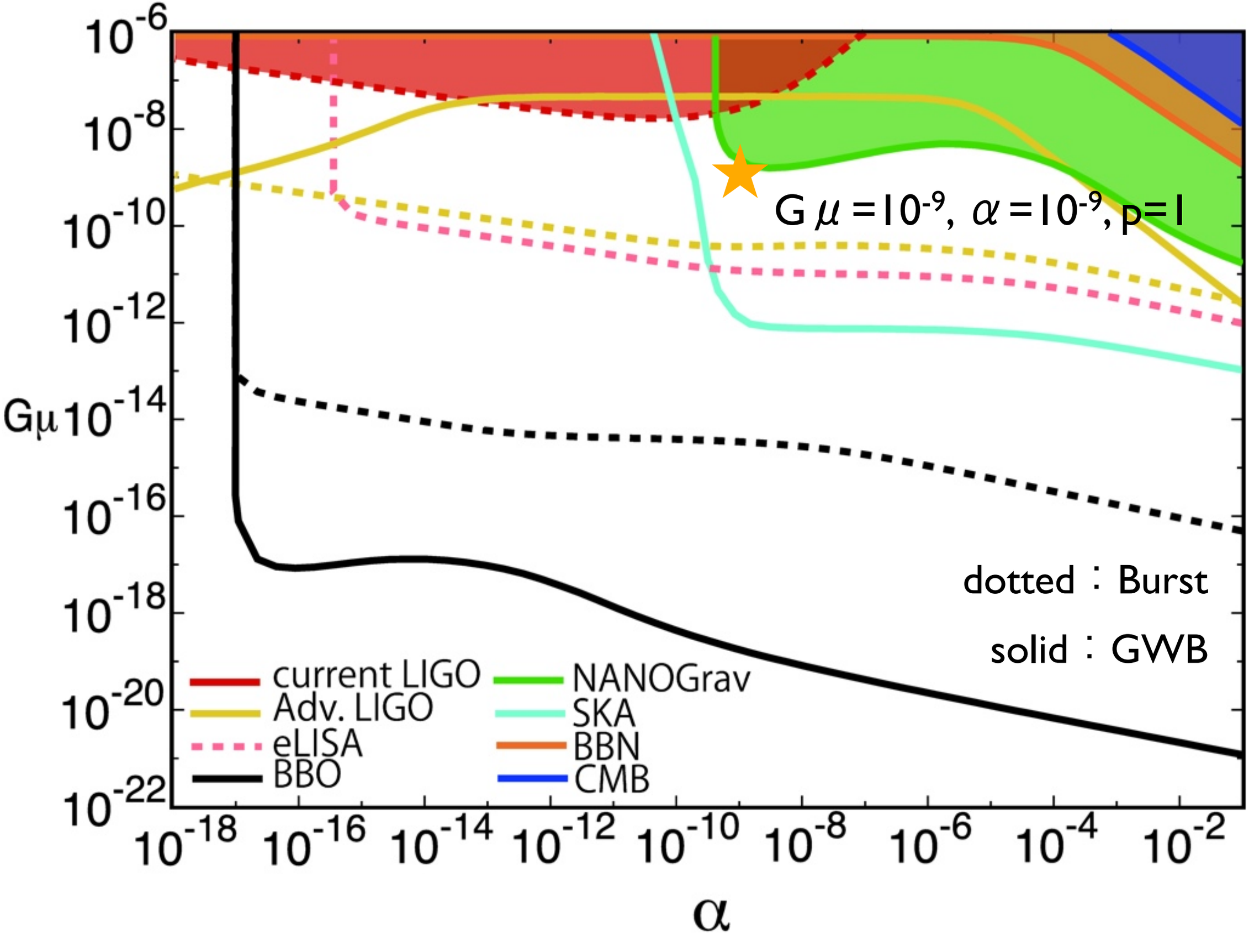

Direct detection + Pulsar timing

$G\mu = 10^{-9}$, $\alpha = 10^{-9}$, p=1
Adv-LIGO 3year (burst only)
+ SKA 10year

Kuroyanagi et al. arXiv:1210.2829

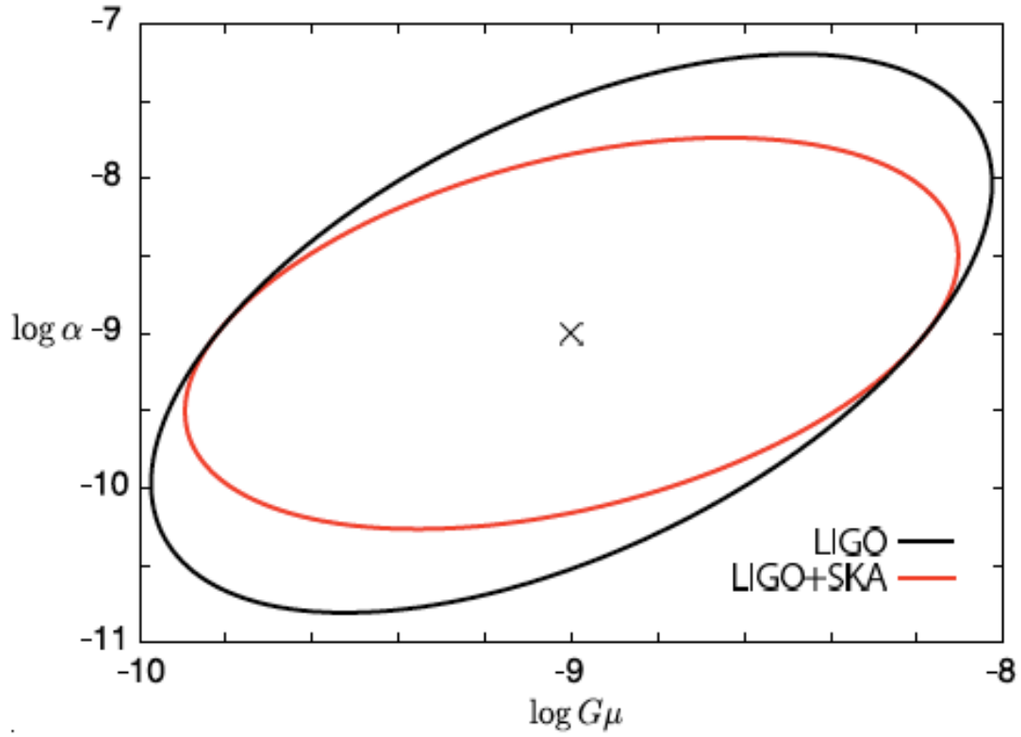

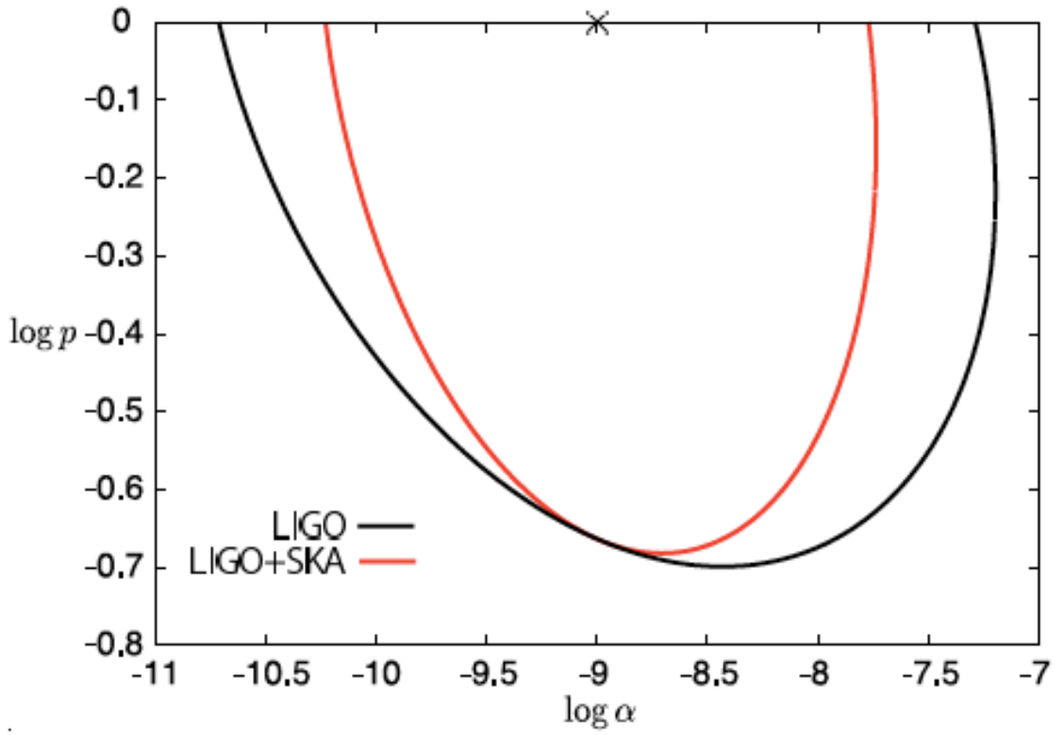

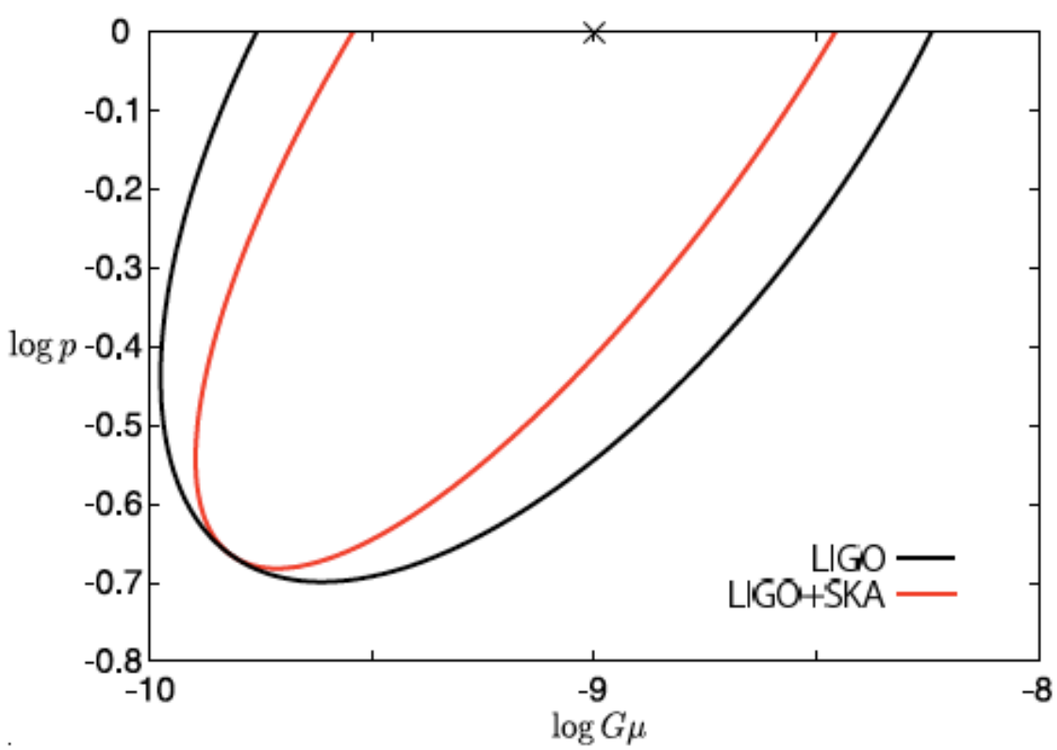

Parameter constraint by eLISA

G μ =10^{-9}, α =10^{-9}, p=1
eLISA 3year
(burst only)

Kuroyanagi et al. arXiv:1210.2829

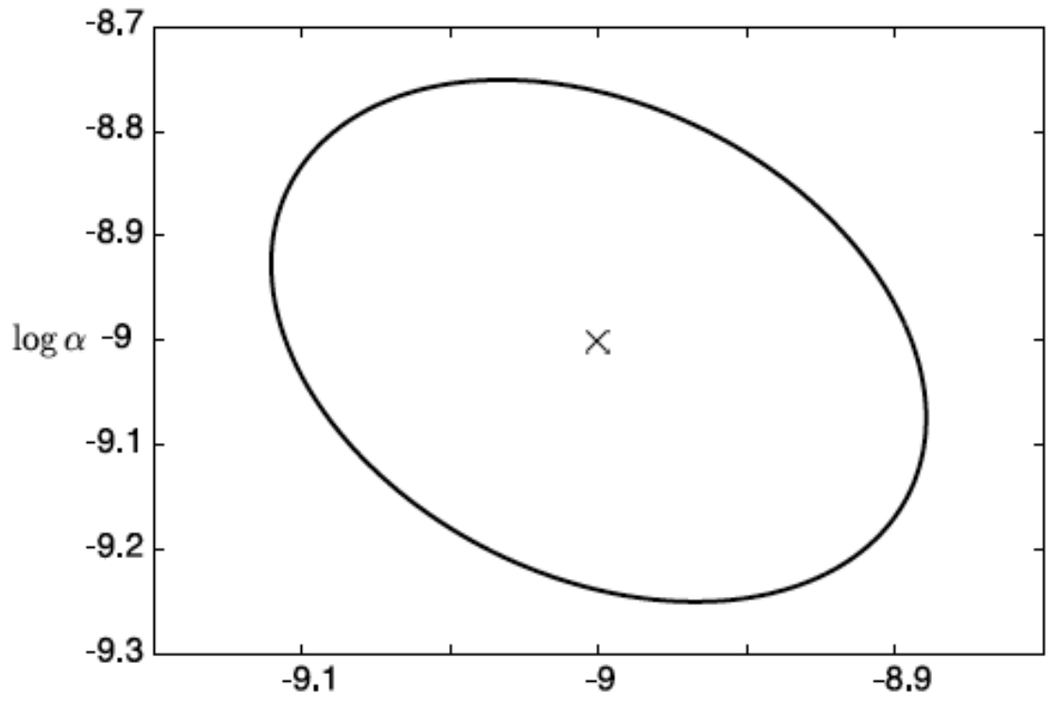

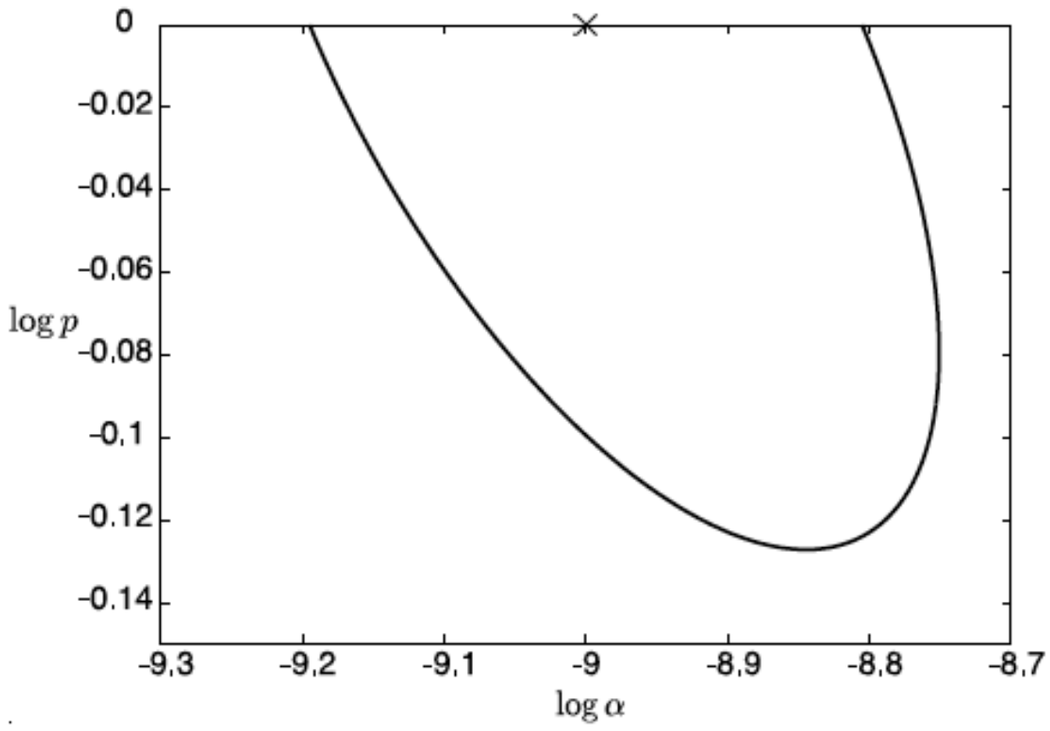

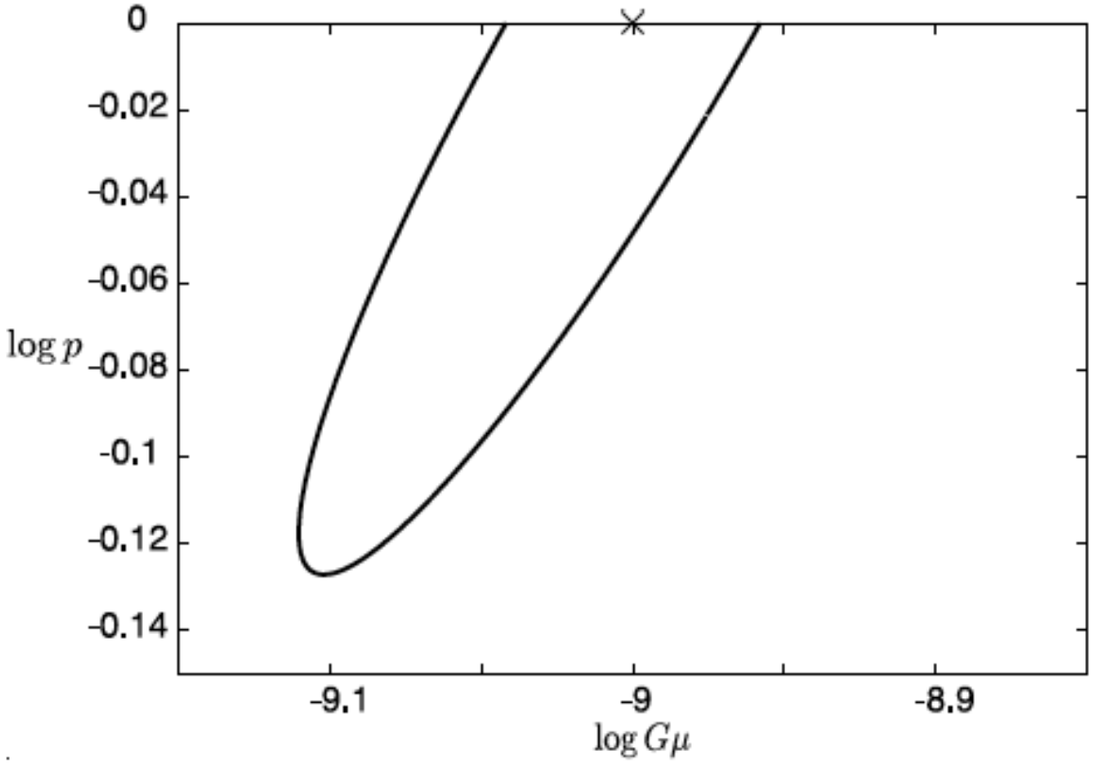

Summary

- Future CMB and GW experiments can be a powerful tool to probe cosmic strings.

- If signals are detected, it would determine cosmic string parameters, which can provide us with hints of fundamental physics such as particle physics or superstring theory.

- Two different kinds of GW observation (rare burst and GWB) provide different constraints on cosmic string parameters and lead to better accuracy in determining parameters.

- Combination of different experiments (CMB, Pulser timing, direct detection) also helps to get stronger constraints.

- Space GW missions are more powerful to prove cosmic strings.

Estimation of the GW burst rate

Initial number density of loops

depends on α and p

$$= \frac{\text{(length of infinite string discarded to loops)}}{\text{(initial length of loops} = \alpha t_i)}$$

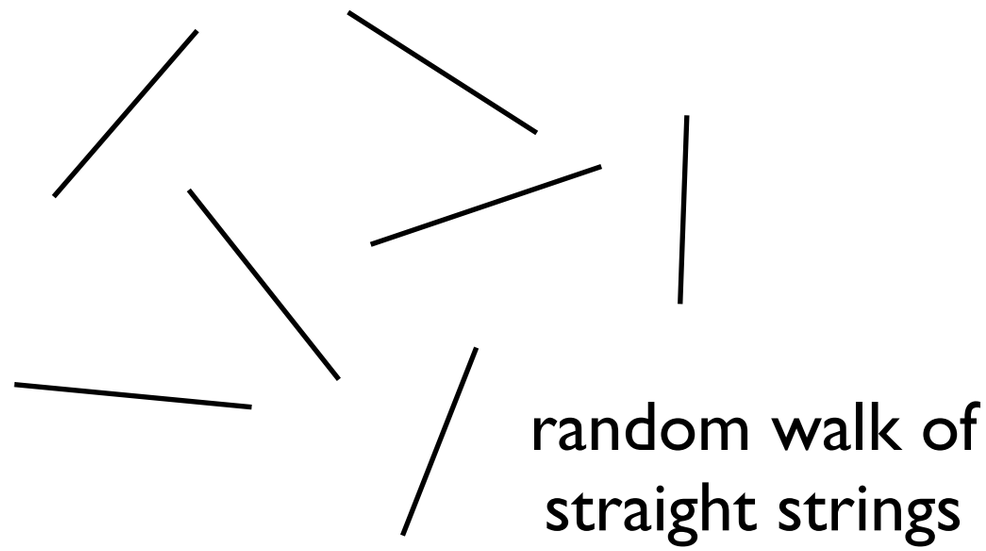

random walk of straight strings

length L, velocity v

Evolution of infinite strings

- velocity-dependent one-scale model

$$2\frac{dL}{dt} = 2HL(1+v^2) + cv$$

energy conservation

energy discarded to loops

$$\left.\frac{d\rho_{inf}}{dt}\right|_{loop} = cv\frac{\rho_{inf}}{L}$$

for small p: c → cp

$$\frac{dv}{dt} = (1-v^2)\left(\frac{k}{R} - 2Hv\right)$$

damping due to the expansion

acceleration due to the curvature of the strings

momentum parameter: $k = \frac{2\sqrt{2}}{\pi}\left(\frac{1-8v^6}{1+8v^6}\right)$

Estimation of the GW burst rate

<u>loop evolution</u> depends on Gμ and α

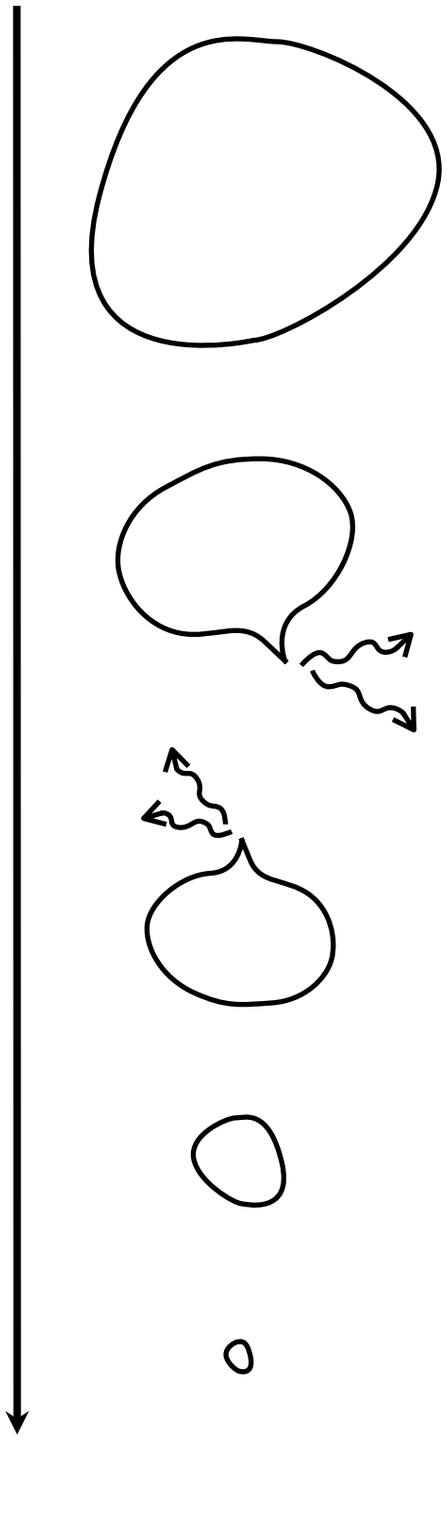

Initial loop length $= \alpha t_i$

t_i : time when the loop formed

GW power $P = \Gamma G\mu^2$ Γ: numerical constant ~50-100

From the energy conservation law

(energy of loop at time t =μl)

= (initial energy of the loop =μαt_i) − (enegry released to GWs =PΔt)

Loop length at time t $l(t, t_i) = \alpha t_i - \Gamma G\mu(t - t_i)$

Lifetime of the loop $=$ (initial loop energy) / (energy release rate per time)

$= \frac{\mu\alpha t_i}{\Gamma G\mu^2} = \frac{\alpha t_i}{\Gamma G\mu}$

Estimation of the GW burst rate

GW burst rate emitted at t∼t+dt from loops formed at t_i∼t_i+dt_i

$$\frac{dR}{dtdt_i}dtdt_i = \frac{1}{4}\theta_m(f,z,l)^2 \frac{2c}{(1+z)l(t,t_i)} \frac{dn}{dt_i}(t,t_i)\frac{dV}{dt}dtdt_i \times \Theta(1-\theta_m(f,z,l))$$

Beaming

Time interval of GW emission

Loop number

$\propto$ (loop length at t)$^{-1}$

$\theta_m \propto$ (loop length at t)$^{1/3}$

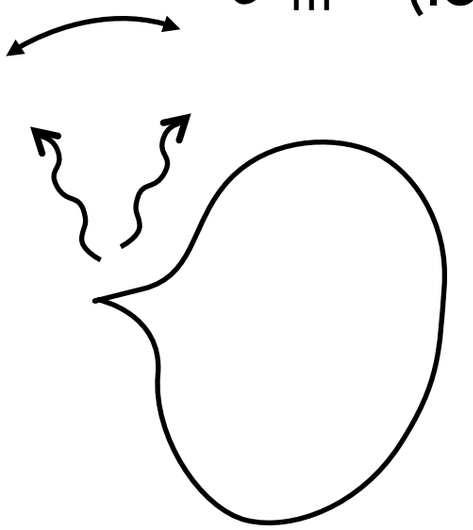

$$l(t,t_i) = \alpha t_i - \Gamma G\mu(t-t_i)$$

$$N = \frac{p^{-1}t}{\alpha t} = \frac{1}{p\alpha}$$

GW amplitude from loop of length l

$$h(f,z,l) \simeq 2.68 \frac{G\mu l}{((1+z)fl)^{1/3} r(z) f}$$

Generation mechanism 1: phase transition

The Universe has experienced symmetry breakings.

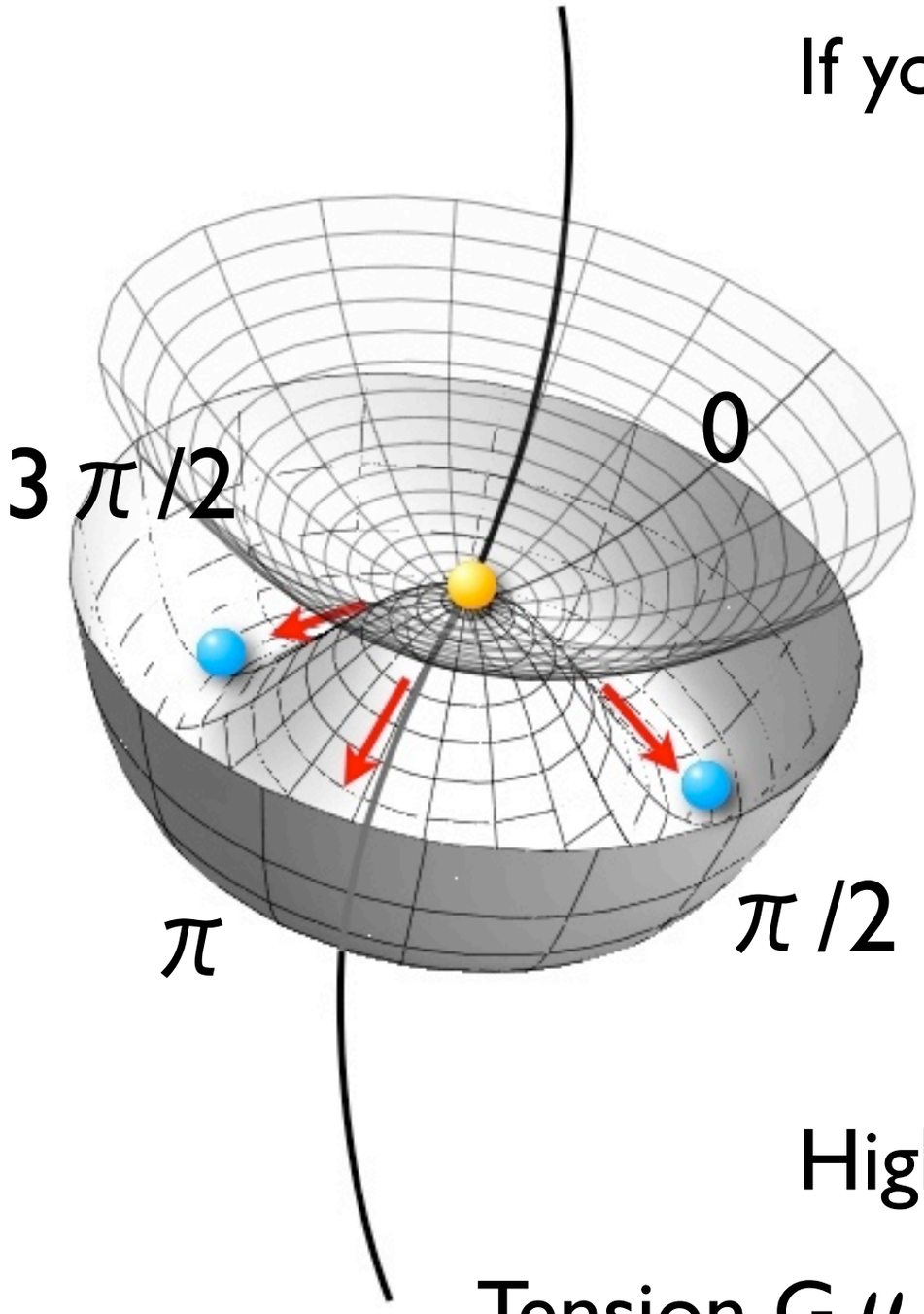

If you consider U(1) symmetry breaking...

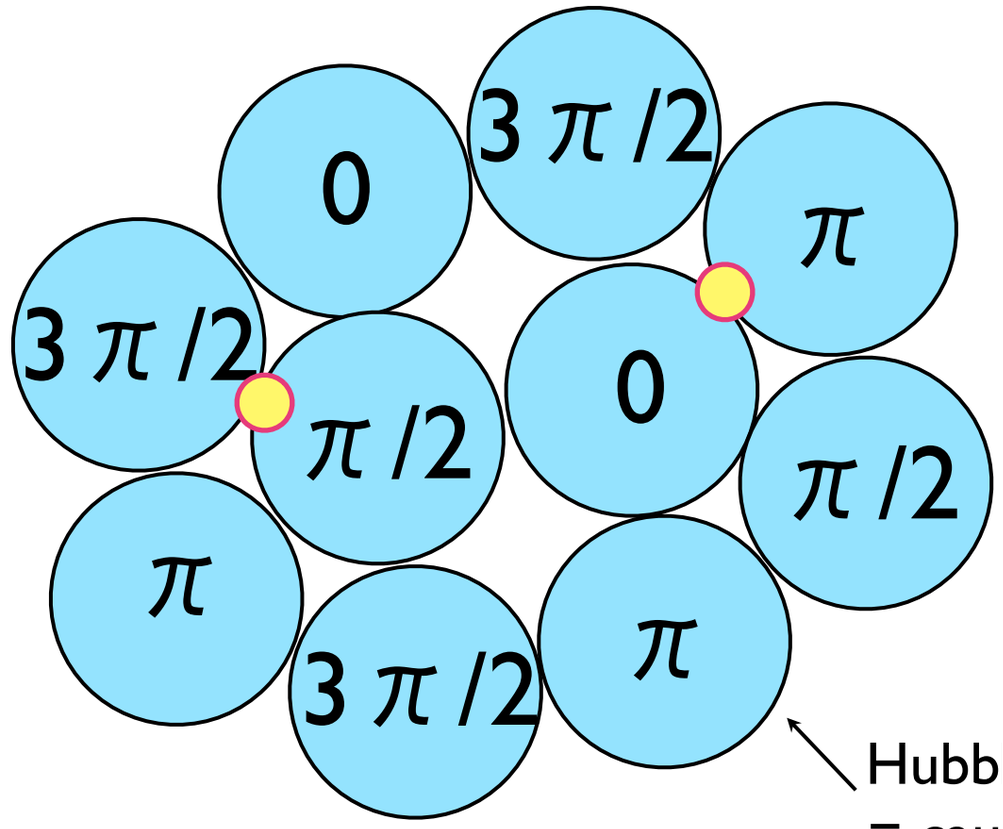

High energy vacuum remains at the center

Tension G μ ~ the energy scale of the phase transition

Generation mechanism 2: Cosmic superstrings

Cosmological size D-strings or F-strings remains after inflation in superstring theory

Difference from phase transition origin

・low reconnection probability (p) because of the extra dimension

Phase transition origin:	p=1	D-string:	p=0.1-1
		F-string:	$p=10^{-3}$-1

・broad values of $G\mu$ depending on the inflation scale and the extra internal degrees of freedom

(・Y-junction ・mixed strings with different $G\mu$)

→ Cosmic strings could give some insight into fundamental physics

Evolution of cosmic strings

Scaling law

Cosmic strings become loops when they collide and form a network composed by loops and infinite strings

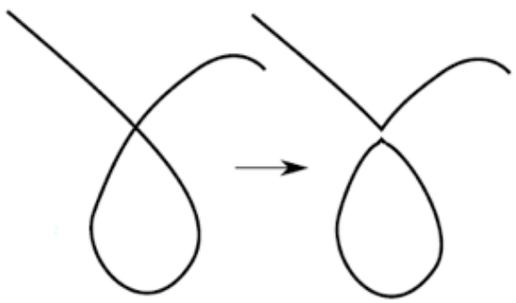

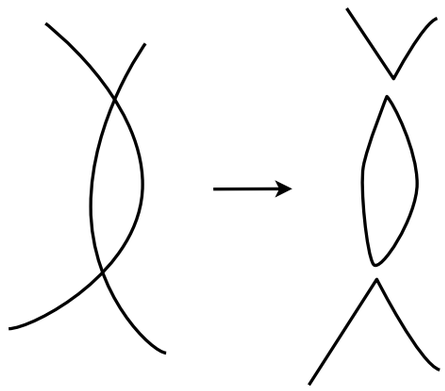

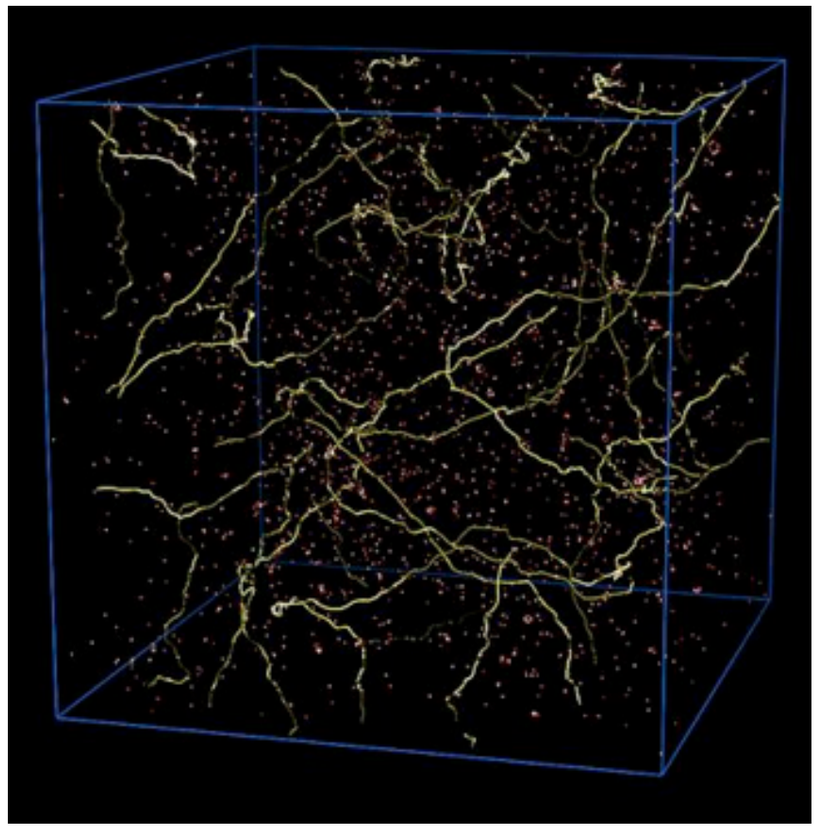

Loops lose energy by emitting gravitational waves and shrink

Increase of infinite string length by the Hubble expansion

⇔

Loss of infinite string length by generation of loops

Higher reconnection rate
more efficient generation of loops
more energy release by the emission of GWs

Evolution of cosmic strings

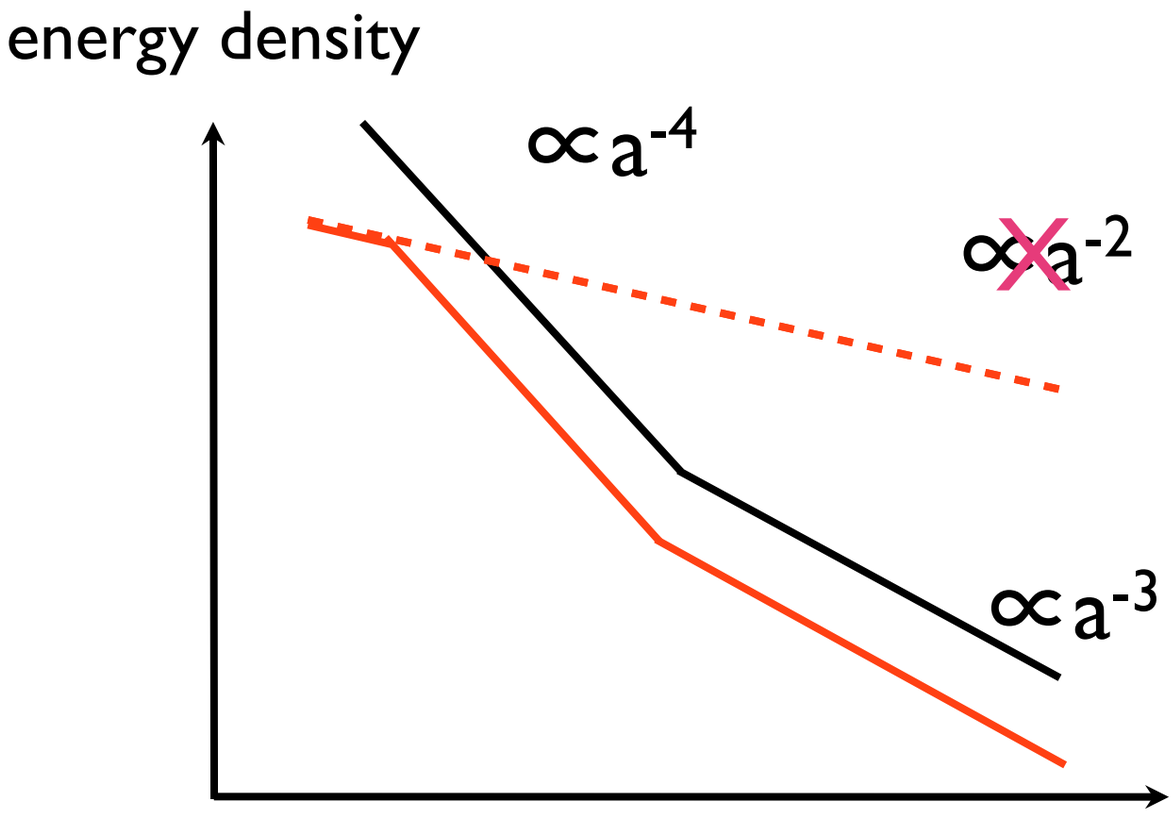

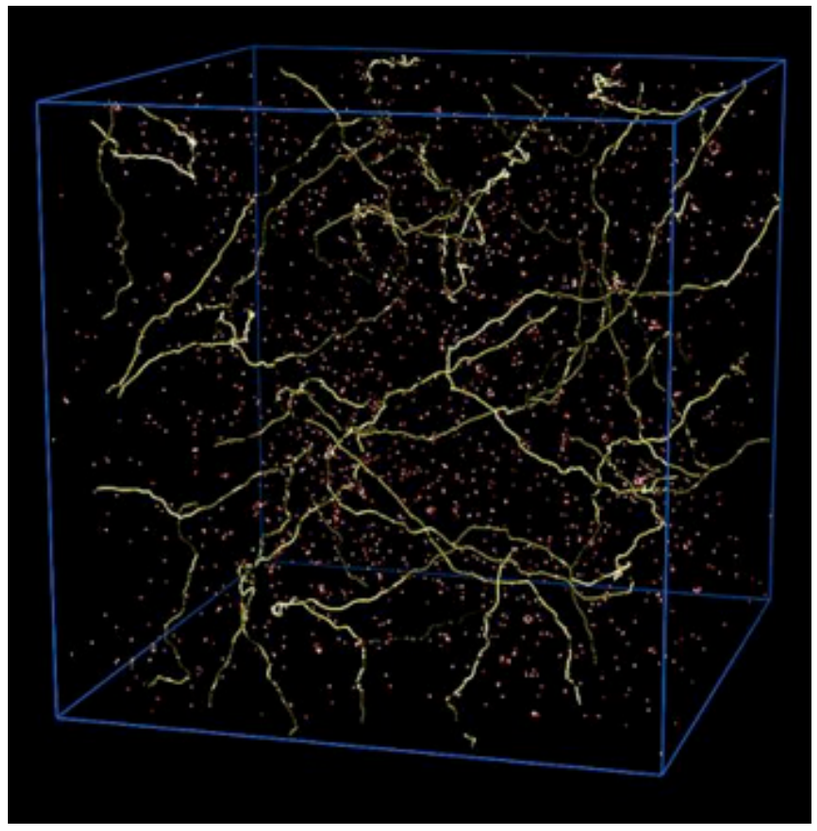

The network keeps O(1) number of infinite strings in the Hubble horizon

→ cosmic strings does not dominate the energy density of the Universe.

α ： initial loop size $L \sim \alpha H^{-1}$

p ： reconnection probability

Estimation of the GW burst rate

Initial number density of loops

Loop number generated per unit time

To satisfy the scaling law, infinite strings should lose O(1) Hubble length per 1 Hubble time. So they should reconnect O(1) times per Hubble time

To reconnect O(1) times per Hubble time, number of infinite strings per Hubble volume should be ~ p^{-1}

→total length of infinite strings ~$p^{-1}H^{-1}$~$p^{-1}t$

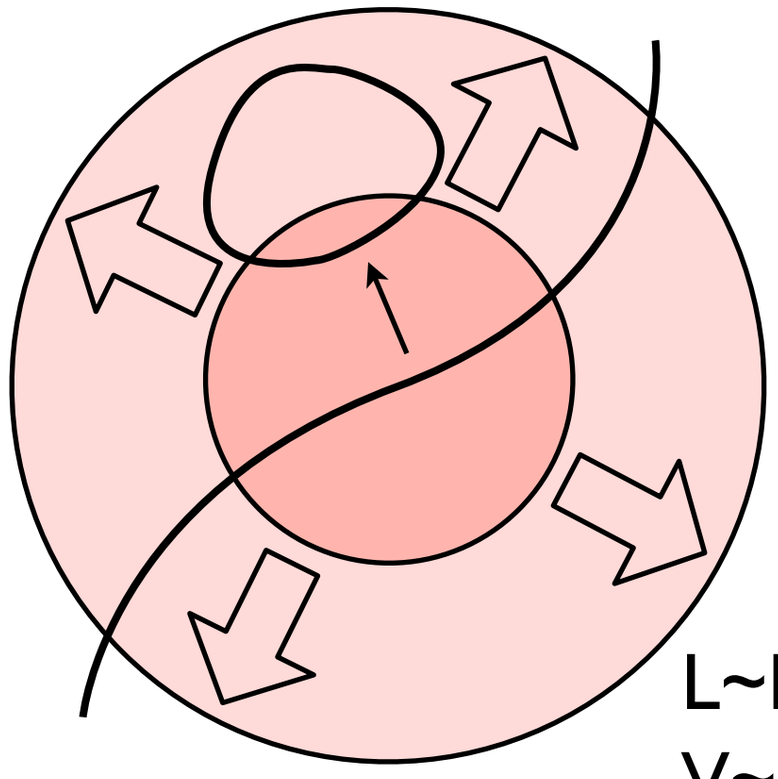

Number of loops = $\frac{\text{(length to lose)}}{\text{(initial length of loops)}}$

$$= \frac{p^{-1}t}{\alpha t} = \frac{1}{p\alpha}$$

Constraint on parameters

Fisher information matrix

$$\mathcal{F}_{ij} = -\left\langle \frac{\partial^2 \ln \mathcal{L}}{\partial p_i \partial p_j} \right\rangle$$

log(Likelihood)

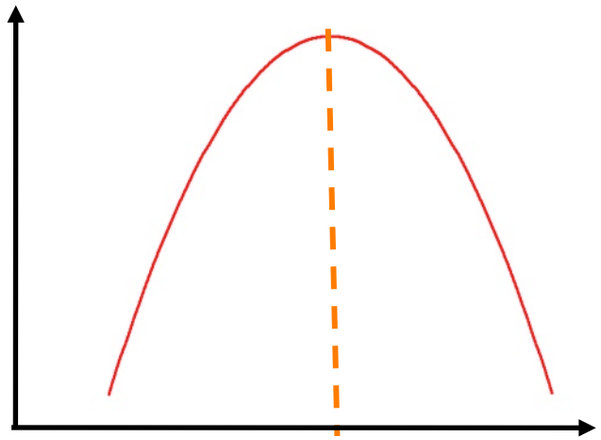

$\overline{\alpha}$

If the likelihood shape is sensitive to the parameter
= easy to estimate the parameter

Burst Observable : amplitude vs number

N is predictable by the rate dR/dh

$$\mathcal{F}_{ij} \propto \frac{\partial(dR/dh)}{\partial p_i} \frac{\partial(dR/dh)}{\partial p_j}$$

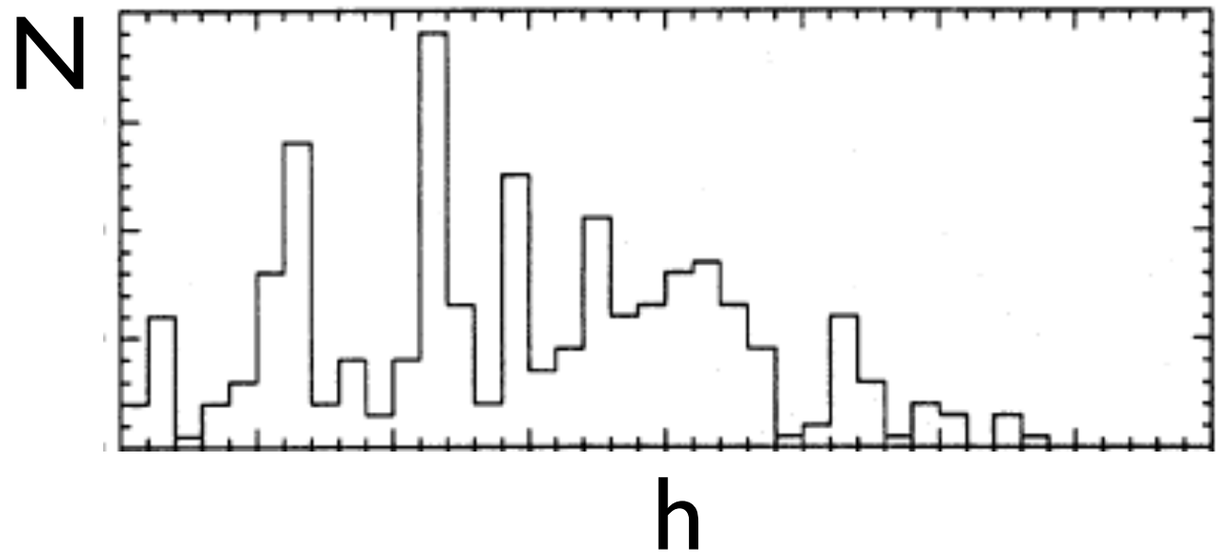

Constraint on parameters

Fisher information matrix

$$\mathcal{F}_{ij} = -\left\langle \frac{\partial^2 \ln \mathcal{L}}{\partial p_i \partial p_j} \right\rangle$$

log(Likelihood)

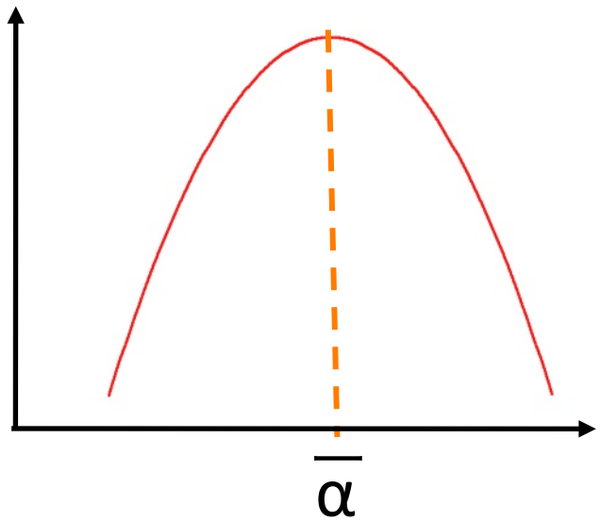

If the likelihood shape is sensitive to the parameter
= easy to estimate the parameter

GWB Observable : Ω_{GW}

$$\mathcal{F}_{ij} \propto \frac{\partial \Omega_{\rm GW}}{\partial p_i} \frac{\partial \Omega_{\rm GW}}{\partial p_j}$$

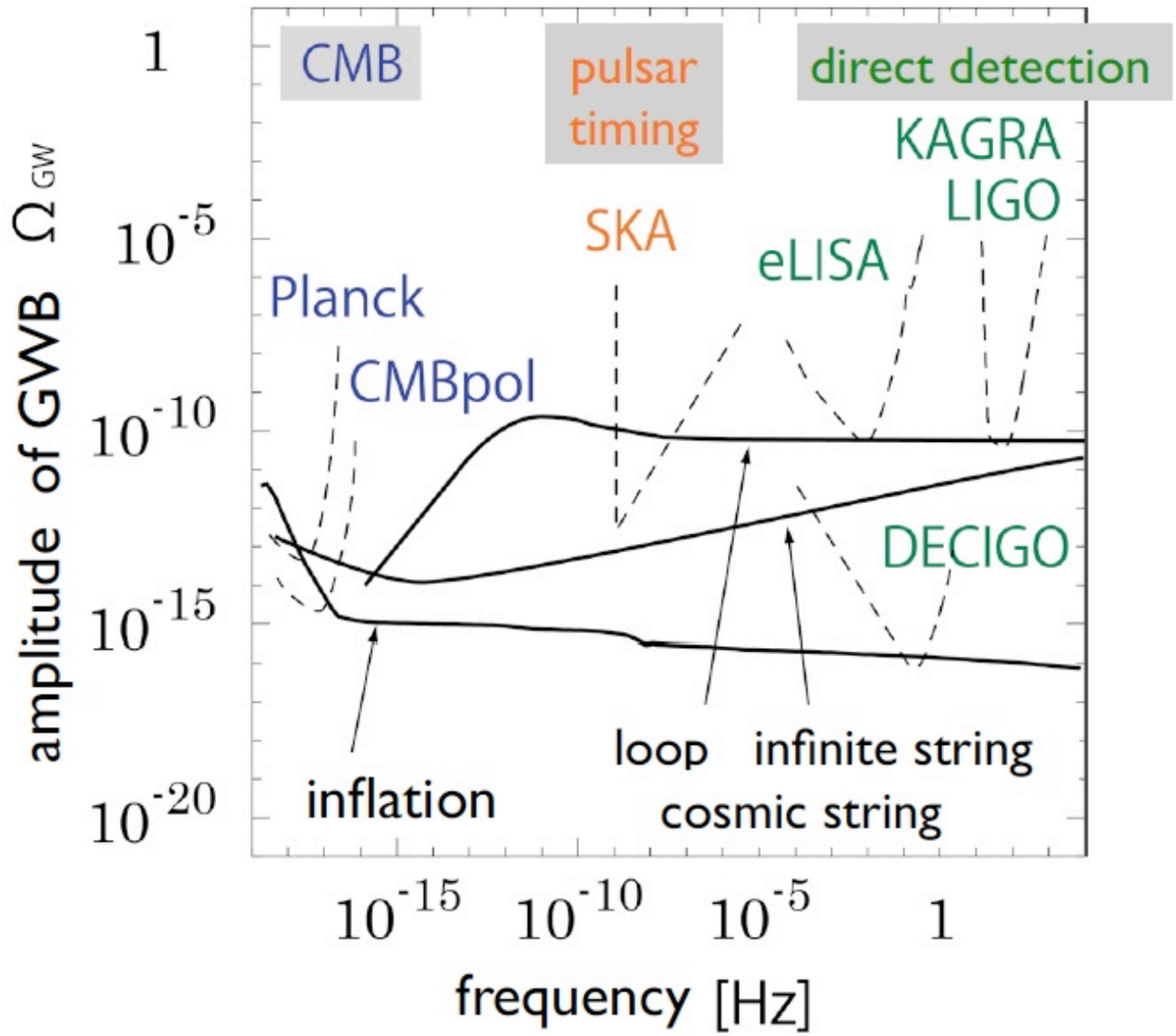

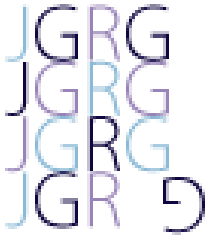

Sirachak Panpanich, JGRG 22(2012)111213

"Effects of chameleon scalar field on rotation curves of the galaxies"

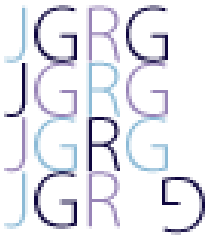

RESCEU SYMPOSIUM ON

GENERAL RELATIVITY AND GRAVITATION

JGRG 22



November 12-16 2012

Koshiba Hall, The University of Tokyo, Hongo, Tokyo, Japan



RESCEU Symposium on General Relativity and Gravitation
JGRG22 at University of Tokyo

Effects of Chameleon Scalar Field on Rotation Curves of the Galaxies

Sirachak Panpanich

Chulalongkorn University

Thailand

Int. J. Mod. Phys. D Vol. 21, No. 5 (2012) 1250041, arXiv:hep-ph/1103.1198v2

Outlines

- Introduction
- Chameleon Dark Energy Model
- Effects on a Rotation Curve
- Results
- Conclusions

Introduction

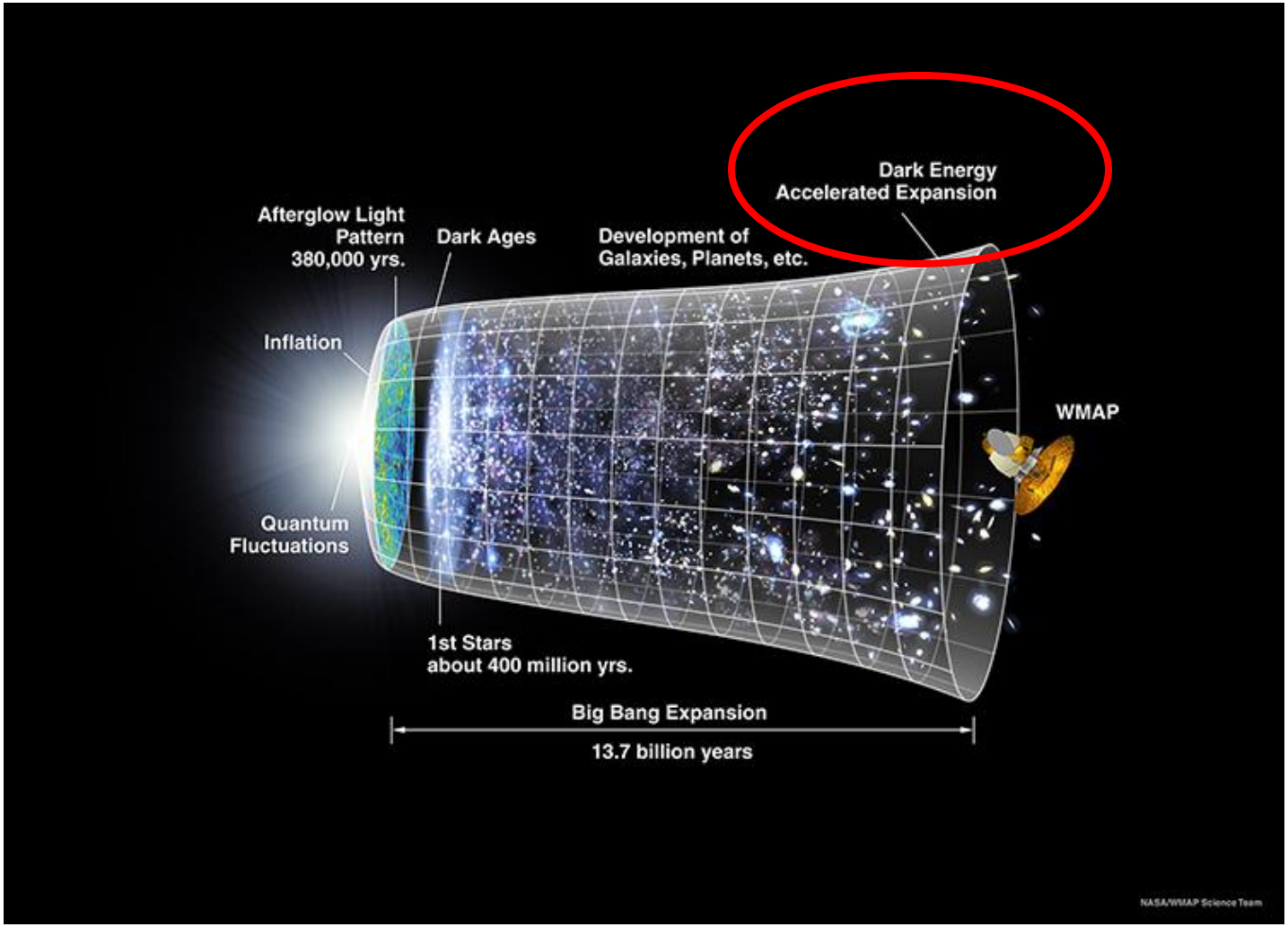

http://map.gsfc.nasa.gov/

Introduction

- From Equation of state $P = w\rho$

Matte
(non-relativi articles)

$$w_{matter} = 0$$

iation
(relativi articles and photons)

$$w_{radiation} = \frac{1}{3}$$

cannot be dark energy

- But, the accelerated expansion requires

$$w < -\frac{1}{3}$$

Introduction

- Quintessence

$$S=\int d^4x\sqrt{-g}\left[-\frac{1}{2}\partial^\mu\phi\partial_\mu\phi-V(\phi)\right]$$

Equation of motion

$$\ddot{\phi}+3H\dot{\phi}+\frac{\partial V}{\partial\phi}=0$$

Friction term

Driving term

Energy density and pressure density
+ Friedmann acceleration equation

$$\frac{\ddot{a}}{a}=-\frac{8\pi G}{3}\left[\dot{\phi}^2-V(\phi)\right]$$

Accelerated expansion requires

$$\dot{\phi}^2<V(\phi)$$

Flat potential
(in late time)

Introduction

- Quintessence

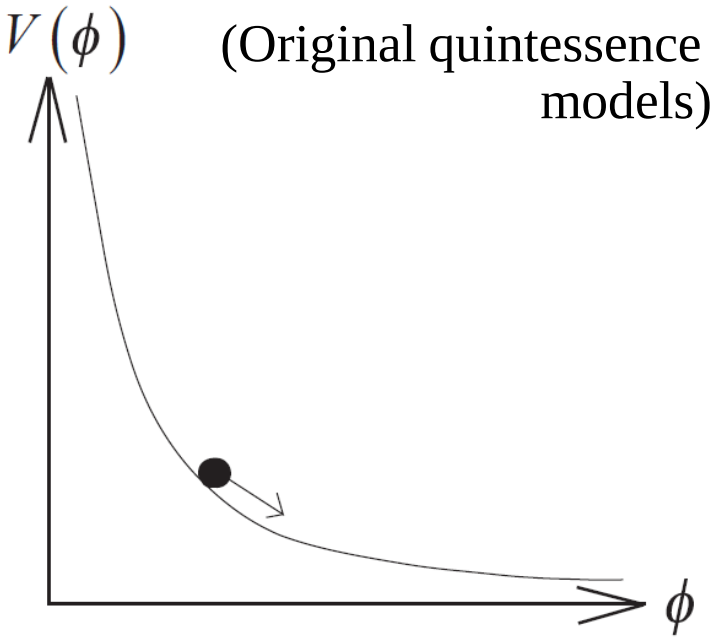

(Original quintessence models)

Power-law potential

$$V(\phi) = \frac{M^{4+n}}{\phi^n}$$

Equation of state

$$w_\phi = \frac{P_\phi}{\rho_\phi} = \frac{\dot{\phi}^2 - 2V(\phi)}{\dot{\phi}^2 + 2V(\phi)}$$

Slow-roll limit : $\frac{\dot{\phi}^2}{2} \ll V(\phi)$

$$w_\phi = -1$$

Introduction

- Quintessence

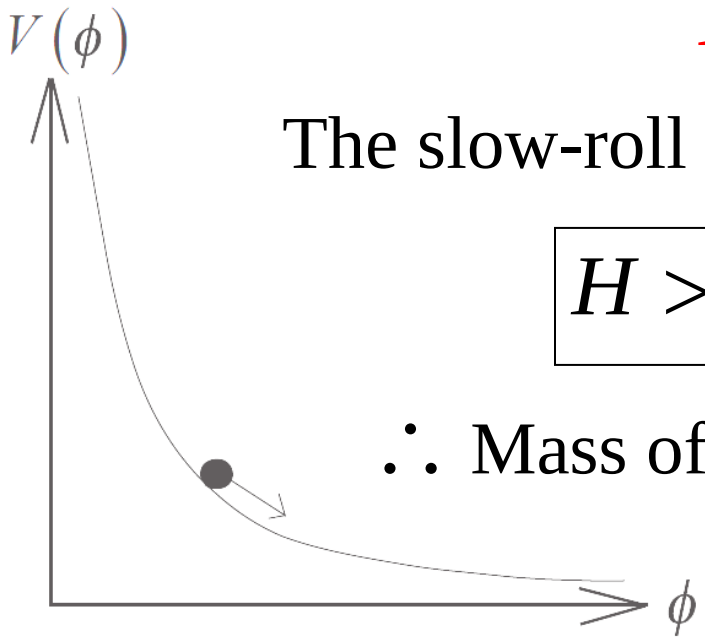

Problem

The slow-roll limit (overdamping) will occur if

$$\boxed{H > m_\phi} \quad \left(H_0 \approx 10^{-33} eV\right)$$

$\therefore$ Mass of scalar-field is very tiny

Long range force ?

(Why have we never detected it before?)

Chameleon Dark Energy Model

- Action in the Einstein frame

$$S=\int d^4x\sqrt{-g}\left(\frac{M_{Pl}^2}{2}R-\frac{(\partial\phi)^2}{2}-V(\phi)\right)-\int d^4x\mathrm{L}_m\left(\psi_m^{(i)},g_{\mu\nu}^{(i)}\right)$$

matter fields couple to a metric

Equation of motion

(Cosmological scale)

$$\ddot{\phi}+3H\dot{\phi}+\frac{\partial V_{eff}}{\partial\phi}=0$$

$$V_{eff}(\phi)=V(\phi)+\rho_m e^{\beta\phi/M_{Pl}}$$

Conformal rescaling

(Conformal transformation)

$$g_{\mu\nu}^{(i)}=e^{2\beta_i\phi/M_{Pl}}g_{\mu\nu}$$

Einstein frame metric

Chameleon Dark Energy Model

The effective potential

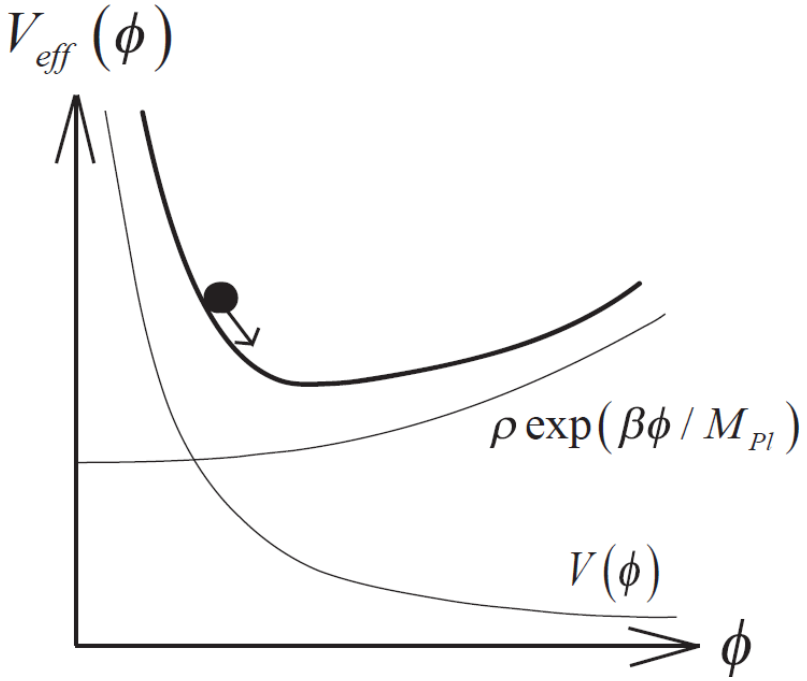

Minimum point

$$V_{,\phi}(\phi_{\min}) + \frac{\beta}{M_{Pl}} \rho_m e^{\beta\phi_{\min}/M_{Pl}} = 0$$

Mass of scalar field

(about the minimum)

$$m^2 = V_{,\phi\phi}(\phi_{\min}) + \frac{\beta^2}{M_{Pl}^2} \rho_m e^{\beta\phi_{\min}/M_{Pl}}$$

Large matter density ⇒ Huge m_ϕ

Small matter density ⇒ Tiny m_ϕ

Chameleon

Chameleon Dark Energy Model

Equation of motion (full-form)

$$\nabla^2\phi = V_{,\phi} + \frac{\beta}{M_{Pl}}\rho_m e^{\beta\phi/M_{Pl}}$$

In cosmological scale
(neglect the gradient term)

$$\ddot{\phi} + 3H\dot{\phi} + \frac{\partial V_{eff}}{\partial\phi} = 0$$

In the chameleon model

$$m \square H$$

But, the slow-roll limit still occurs
(arXiv:astro-ph/0408415v2)

On a spherically symmetric object
(neglect the time-dependent term)

$$\frac{d^2\phi}{dr^2} + \frac{2}{r}\frac{d\phi}{dr} = V_{,\phi} + \frac{\beta}{M_{Pl}}\rho(r)e^{\beta\phi/M_{Pl}}$$

Profile $\phi(r)$

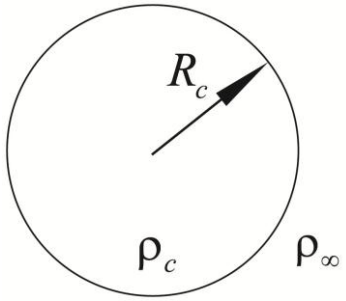

Chameleon Dark Energy Model

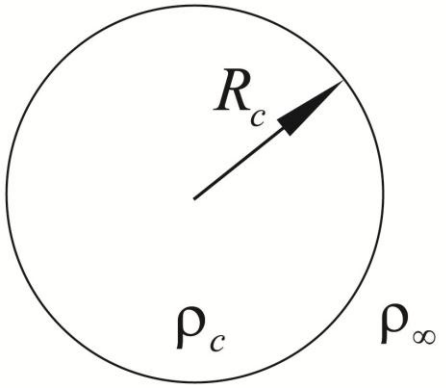

(Homogeneous density)

Since $\phi_{\min}$ and m_ϕ depend on local matter density

$\phi_{\min}$ and m_ϕ inside an object $\neq$ $\phi_{\min}$ and m_ϕ outside an object

The scalar field has to roll out minimum to satisfy continuous conditions (ϕ and $\frac{d\phi}{dr}$)

2 types of profile

(Divided by size of object)

- Thin-shell regime (large object)
- Thick-shell regime (small object)

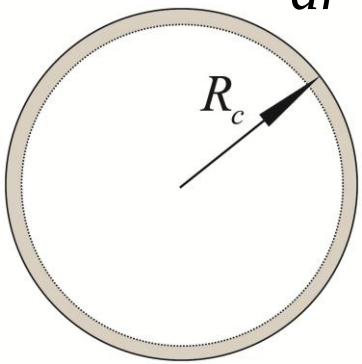

(Thin-shell regime)

Chameleon Dark Energy Model

Since scalar field couples to matter ➡ Fifth force

$$\vec{F}_\phi = -\frac{\beta}{M_{Pl}} M \vec{\nabla}\phi$$

Scalar field acts as a potential for the force

Proved by Conformal transformation + Geodesics equation

$$\ddot{x}^\mu + \Gamma^\mu_{\alpha\beta}\dot{x}^\alpha \dot{x}^\beta + \alpha_\phi \frac{\partial \phi}{\partial x_\mu} = 0$$

We have profile $\phi(r)$ from the thin-shell or thick-shell of an object.

Effects on Rotation Curves

Rotation curve

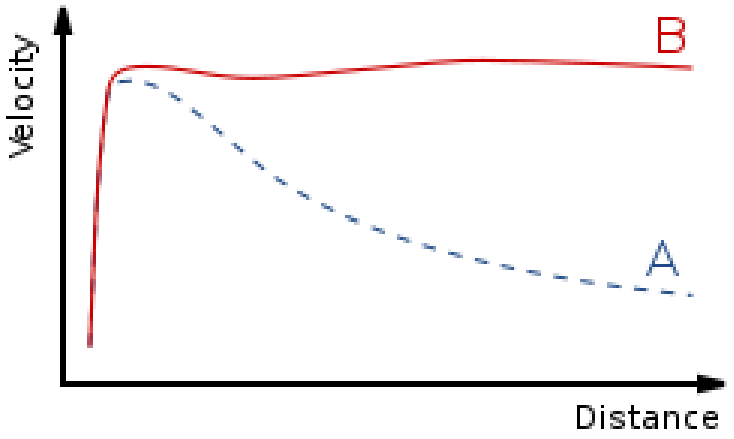

http://en.wikipedia.org/wiki/Galaxy_rotation_curve

Observational data (B)

$\neq$

Theoretical prediction (A)

We need dark matter

What will happen on a rotation curve if we have chameleon scalar field in our universe?

Effects on Rotation Curves

- Dark matter halo profiles for investigating are as the following

NFW profile	ISO profile	Parametrized model
$\rho(r)=\frac{\rho_0}{\frac{r}{a}\left(1+\frac{r}{a}\right)^2}$	$\rho(r)=\frac{\rho_0}{1+\left(\frac{r}{R_s}\right)^2}$	$\rho(r)=\frac{\rho_0}{\left(\frac{r}{r_s}\right)^{\alpha}\left(1+\frac{r}{r_s}\right)^{3-\alpha}}$

- We suppose that dark matter halo is a spherical symmetric object

Effects on Rotation Curves

- Chameleon profile inside a dark matter halo

$$\frac{d^2\phi}{dr^2}+\frac{2}{r}\frac{d\phi}{dr}=V_{,\phi}+\frac{\beta}{M_{Pl}}\rho(r)e^{\beta\phi/M_{Pl}}$$

Numerical solution

Analytic solution

  - Thick-shell regime : density of DM halo is a function of radius
  - Power-law potential : $V(\phi)=\frac{M^{4+n}}{\phi^n}$

Effects on Rotation Curves

- Numerical solution

$$\frac{d^2\phi}{dr^2}+\frac{2}{r}\frac{d\phi}{dr}=-n\frac{M^{4+n}}{\phi^{n+1}}+\frac{\beta}{M_{Pl}}\rho(r)e^{\beta\phi/M_{Pl}}$$

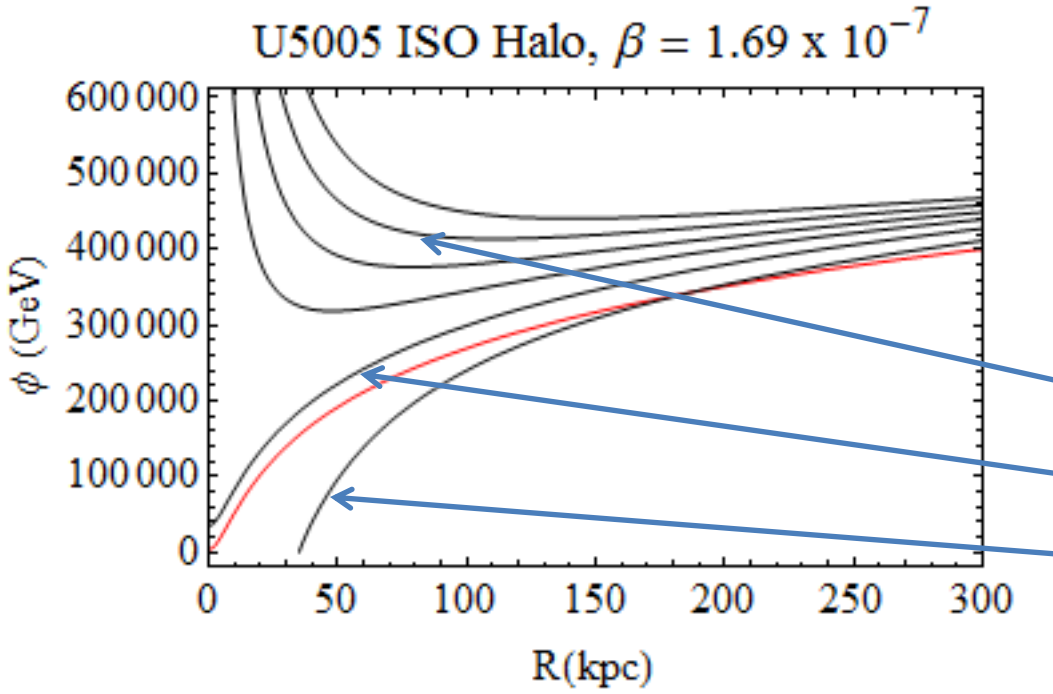

3 types of solution

- Diverge at origin
- Finite at origin
- Truncate before origin

Effects on Rotation Curves

- Analytic solution

$$\frac{d^2\phi}{dr^2}+\frac{2}{r}\frac{d\phi}{dr}\approx\frac{\beta}{M_{Pl}}\rho(r)$$

$e^{\beta\phi/M_{Pl}}\approx 1$

Neglect the power-law potential term

$$\phi'(r)=\frac{\beta}{4\pi M_{Pl}r^2}\left(M(r)-M_0+\gamma\right)$$

M_0 : Total mass
$\gamma \propto$ Slope

- Diverge at origin
- Finite at origin
- Truncate before origin

$\gamma < M_0$

$\gamma = M_0$

$\gamma > M_0$

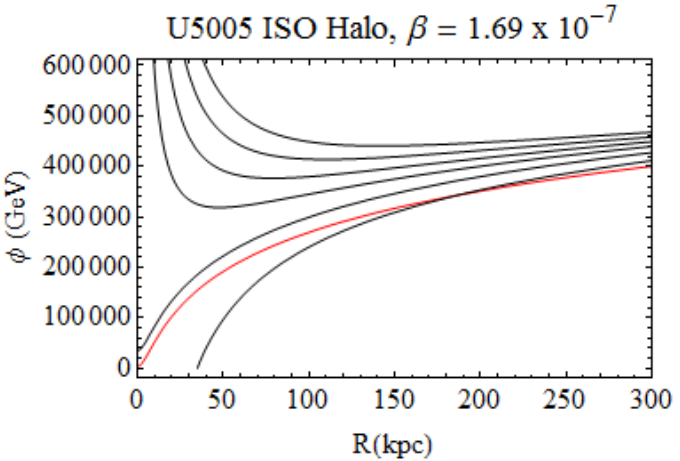

Effects on Rotation Curves

- Constraint on the matter-chameleon coupling

From EOM with approximation

$$\phi'(r) = \frac{\beta}{4\pi M_{Pl}}\left(\frac{M(r)}{r^2}\right) + \frac{1}{r^2}\left(\phi' r^2\Big|_{r=0}\right)$$

Boundary conditions
(original paper)

$$\frac{d\phi}{dr} = 0 \quad at \quad r = 0$$

$$\phi \to \phi_\infty \quad as \quad r \to \infty$$

$$\phi(r_{\max}) = \frac{\beta}{4\pi M_{Pl}} \int_0^{r_{\max}} dr \frac{M(r)}{r^2} + \phi(0)$$

$$\phi_\infty \geq \frac{\beta}{4\pi M_{Pl}} \int_0^{r_{\max}} dr \frac{M(r)}{r^2}$$

Minimum of effective pot.

$$\phi_\infty = \left(\frac{nM^{4+n}M_{Pl}}{\rho_\infty \beta}\right)^{\frac{1}{n+1}}$$

$$\beta_{\max} = \left(\frac{nM^{4+n}M_{Pl}}{\rho_\infty}\right)^{\frac{1}{n+2}} \left(\frac{4\pi M_{Pl}}{\int_0^{r_{\max}} dr \frac{M(r)}{r^2}}\right)^{\frac{n+1}{n+2}}$$

ISO U5005 1.69×10^{-7}

NFW U5005 1.76×10^{-7}

Effects on Rotation Curves

- Analytic solution (NFW profile)

$$\rho(r) = \frac{\rho_0}{\frac{r}{a}\left(1+\frac{r}{a}\right)^2}$$

$$\boxed{\phi(r) = \frac{a^3 \beta \rho_0}{M_{Pl}}\left(\frac{1}{a} - \frac{\ln(1+r/a)}{r}\right) + \phi(0)}$$

- Analytic solution (ISO profile)

$$\rho(r) = \frac{\rho_0}{1+\left(\frac{r}{R_s}\right)^2}$$

$$\boxed{\phi(r) = \frac{\beta R_s^3 \rho_0}{M_{Pl}}\left(\frac{\arctan(r/R_s)}{r} + \frac{\ln(1+r^2/R_s^2)}{2R_s} - \frac{1}{R_s}\right) + \phi(0)}$$

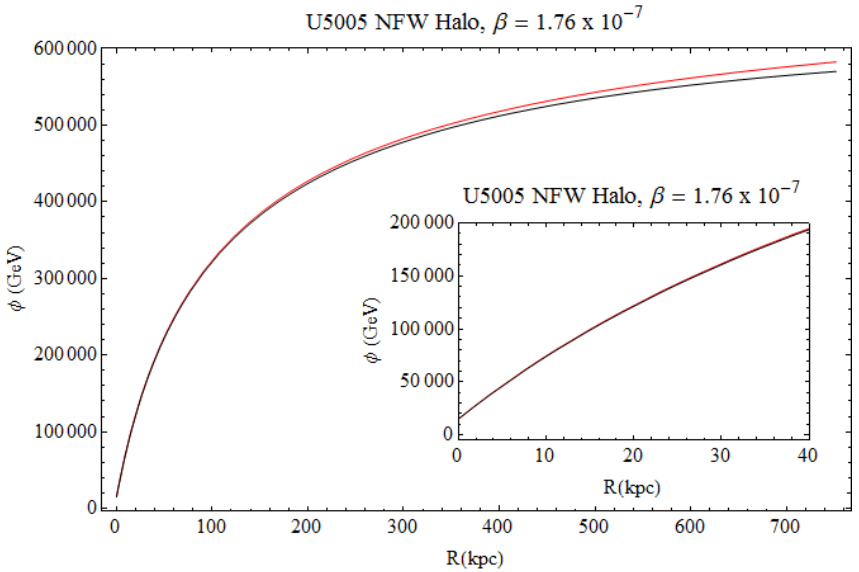

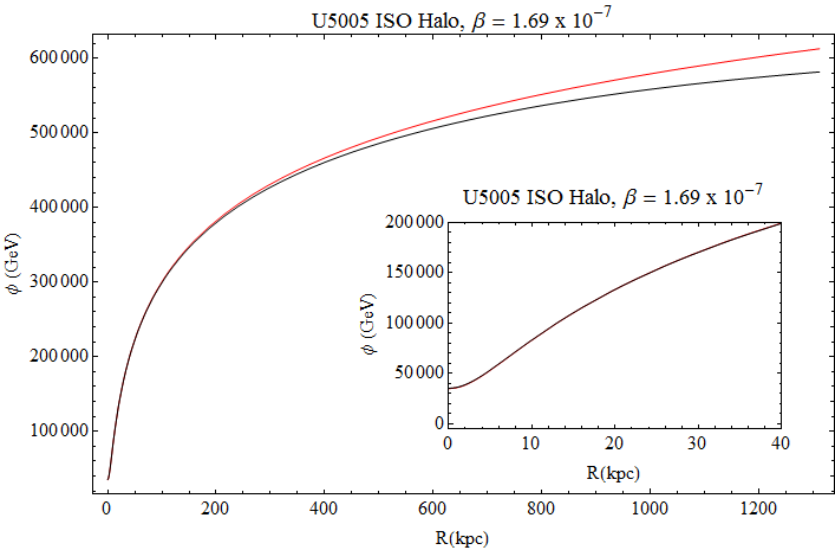

Effects on Rotation Curves

- Analytic solution (PM profile)

$$\rho(r) = \frac{\rho_0}{\left(\frac{r}{r_s}\right)^{\alpha}\left(1+\frac{r}{r_s}\right)^{3-\alpha}}$$

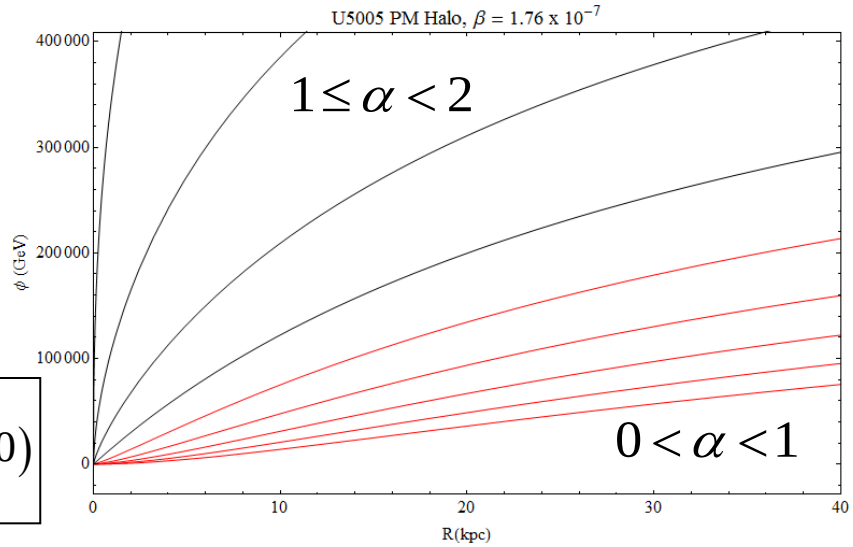

$$\phi(r) = \frac{\beta\rho_0}{M_{Pl}}\frac{r^{\alpha}}{3-\alpha}\left(\frac{r^{2-\alpha}}{2-\alpha}\,{}_2F_1\left(2-\alpha, 3-\alpha, 4-\alpha, -\frac{r}{r_s}\right)\right) + \phi(0)$$

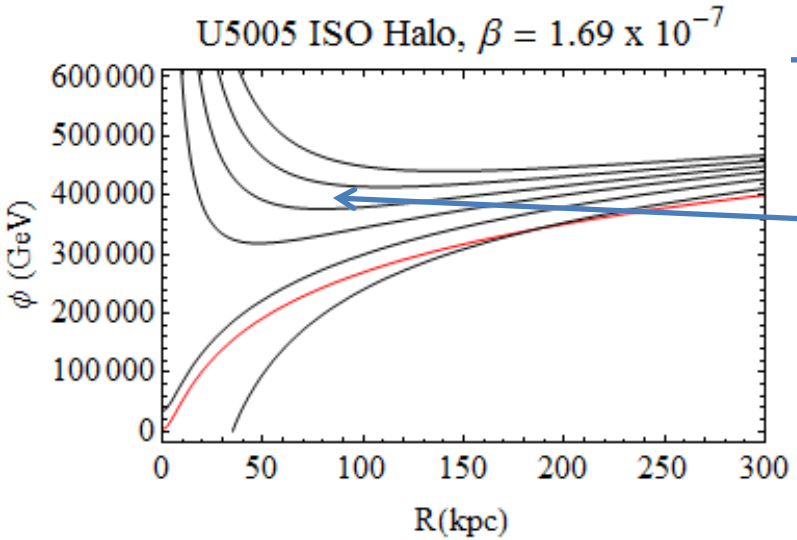

- Diverge at origin
- ~~Finite at origin~~
- ~~Truncate before origin~~

Effects on Rotation Curves

Circular velocity + Fifth force

$$v_c(r) = \sqrt{\frac{GM(r)}{r} + \frac{\beta r}{M_{Pl}}\frac{d\phi}{dr}}$$

Only DM halo profile

Numerical solution

Late-type low surface brightness (LSB) galaxies



Mainly effect on rotation curve comes from dark matter halo

Reference:

de Blok, W.J.G., and Bosma, A. High-resolution rotation curves of Low Surface Brightness galaxies. Astron. Astrophys. 385 (2002): 816

Results

- Rotation curves of U5005

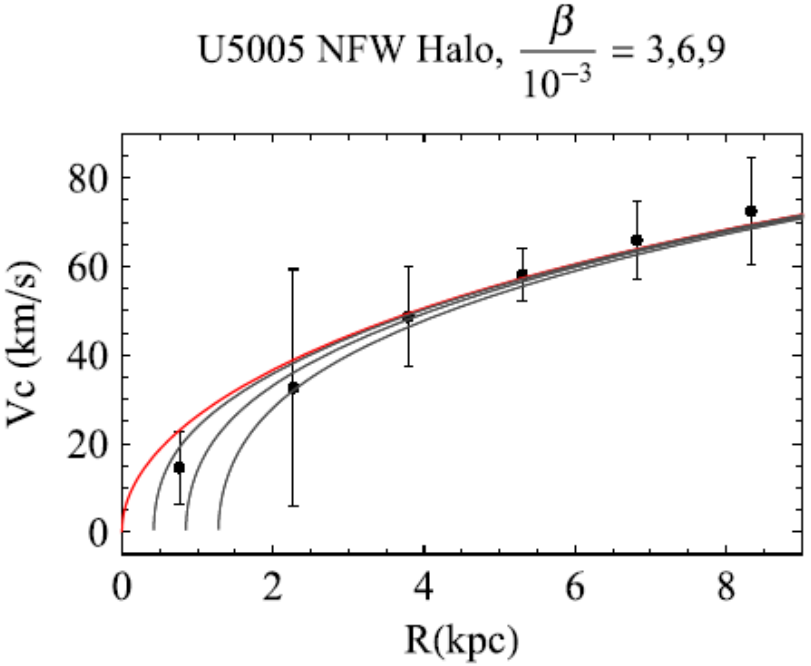

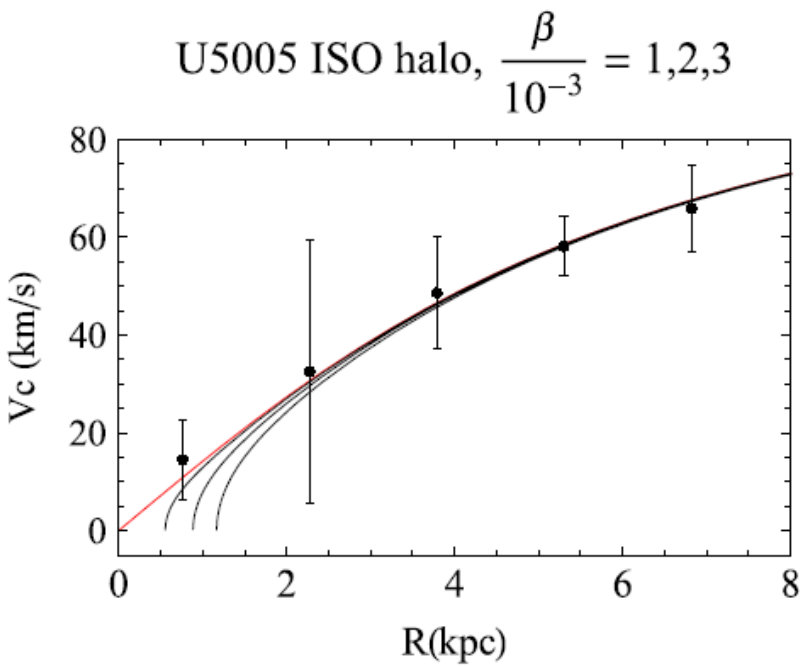

Red lines ➡ No chameleon effect

Error bar:
http://vizier.cfa.harvard.edu/viz-bin/VizieR?-source=J/A+A/385/816/

Results

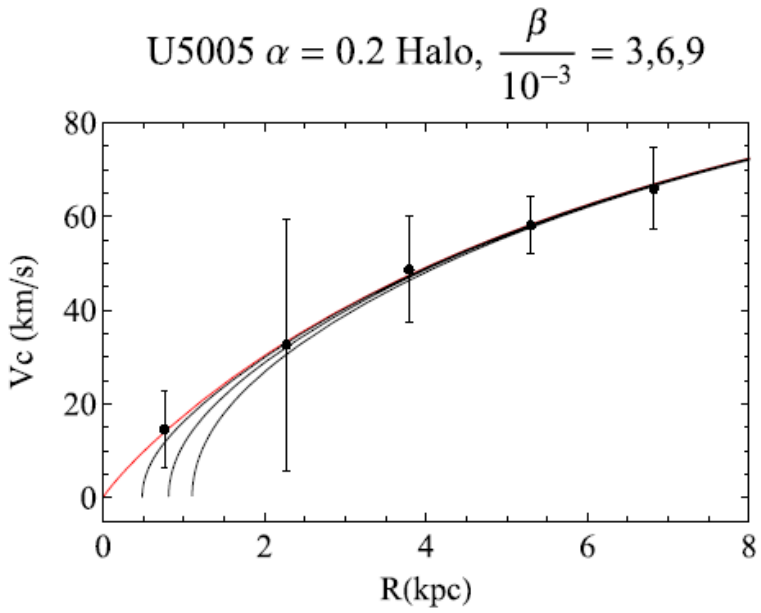

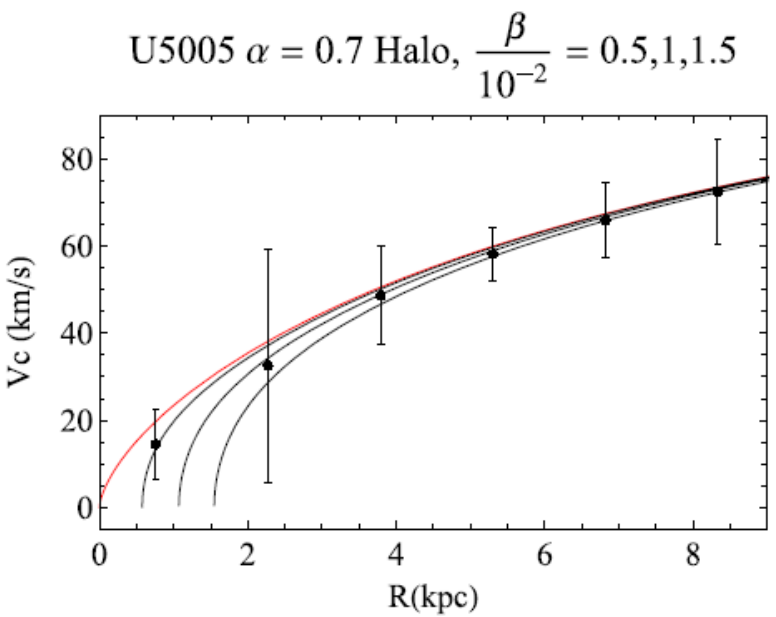

LSB galaxy	Upper bound on β at 95% C.L.
U5005 (NFW)	6×10^{-3}
U5005 (ISO)	2×10^{-3}
U5005 (PM $\alpha = 0.2$)	6×10^{-3}
U5005 (PM $\alpha = 0.7$)	9×10^{-3}

Conclusion

- We investigate effects of chameleon scalar field on rotation curves by **adding the fifth force**

- Analytic solution + Normal boundary conditions
  - ➡ Constraint on coupling constant
  - ➡ cannot occur in some DM halo profiles

- Divergent profile
  - ➡ Rotation curves are steeper around center of galaxy
  - ➡ Upper bound on coupling constant from observational data

Thank you for your attention

Int. J. Mod. Phys. D Vol. 21, No. 5 (2012) 1250041, arXiv:hep-ph/1103.1198v2

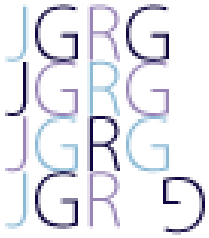

Tomohiro Nakama, JGRG 22(2012)111214

"Self-consistent initial conditions for primordial black hole"

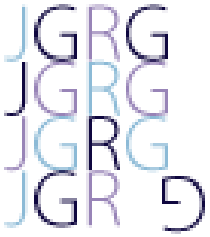

RESCEU SYMPOSIUM ON

GENERAL RELATIVITY AND GRAVITATION

JGRG 22



November 12-16 2012

Koshiba Hall, The University of Tokyo, Hongo, Tokyo, Japan



Self-consistent initial conditions for primordial black hole formation

Tomohiro Nakama (M2)
RESCEU, The University of Tokyo

JCAP09(2012)027

Collaboration with
Alexander Polnarev,
Jun'ichi Yokoyama

Introduction

- Large-amplitude inhomogeneities in the early universe collapse to form Primordial Black Holes.

- Some inflationary models predict large-amplitude curvature perturbation on small scales,

  leading to production of PBHs.

- CMB or LSS probes primordial perturbation on large scales, while information about that on small scales

  is scarce.

- Abundance of PBHs has been constrained by gravitational lensing, gravitational waves, etc…

- By investigating the condition for PBH formation in detail, PBH abundance can be correctly predicted assuming some inflationary model.

- Combined with observational data, the prediction can be used to probe primordial perturbation on small scales.

outline of PBH formation

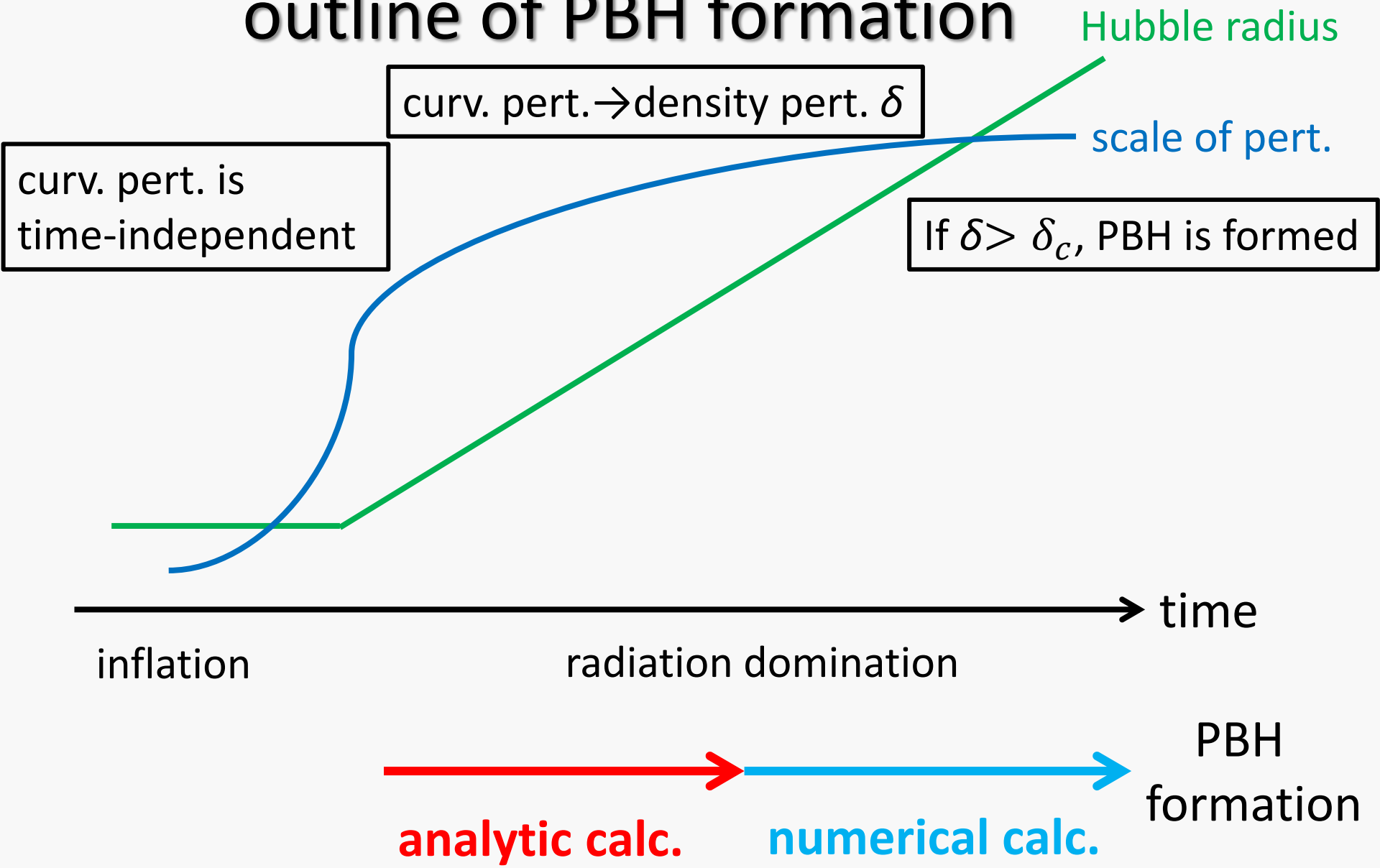

- When $\epsilon \equiv \frac{\text{Hubble radius}}{\text{scale of pert.}} \to 0$, pert. is time-independent.

So, initial curv. pert. profile is represented by $K_i(r)$.

When $\epsilon \ll 1$, the solution of the Einstein eqs.

can be obtained by asymptotic expansion over ϵ.

- first order asymptotic expansion: Polnarev, Musco 2007

- We have obtained higher order expansion.

Polnarev, Nakama, Yokoyama, JCAP09(2012)027

Benefits of higher order expansion

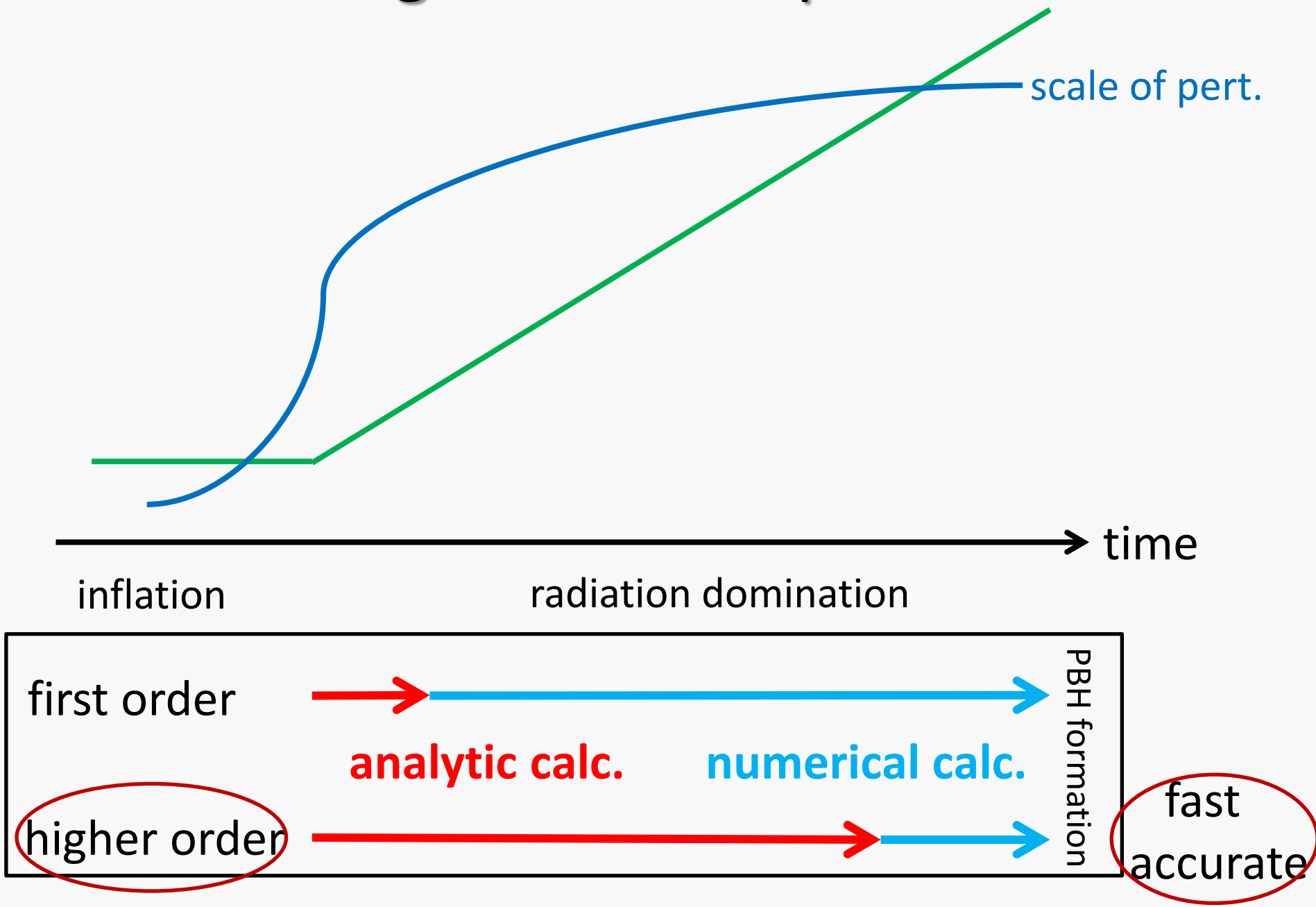

$$ds^2 = -a^2 dt^2 + b^2 dr^2 + R^2 (d\theta^2 + \sin^2\theta d\phi^2),$$

- $u \equiv \dfrac{\dot{R}}{a}$, (definition of u)

Einstein eqs. (Misner & Sharp, 1964)

$$\begin{cases} \dfrac{\dot{b}}{b} = \dfrac{a u'}{R'}, \\ \dfrac{a'}{a} = -\dfrac{\gamma}{1+\gamma}\dfrac{\rho'}{\rho}, \\ M' = 4\pi\rho R^2 R'. \\ \dot{M} = -4\pi p R^2 \dot{R}. \\ \dfrac{R'^2}{b^2} = 1 + u^2 - \dfrac{2GM}{R}. \end{cases}$$

- consider perturbed region surrounded by the flat FLRW univ.

$$ds^2 = -dt^2 + d(Sr)^2 + (Sr)^2(d\vartheta^2 + \sin^2\vartheta d\varphi^2)$$

- definition of curvature profile $K(t,r)$:

$$ds^2 = -a^2dt^2 + \frac{dR^2}{1-K(t,r)r^2} + R^2(d\vartheta^2 + \sin^2\vartheta d\varphi^2)$$

- initial curvature profile: $K(0,r) \equiv K_i(r) \left(< \frac{1}{r^2}\right)$

- boundary condition: $K(t,\infty) = 0$

The metric above coincides with the flat FLRW metric at spatial infinity.

example of initial curvature profile

central large curvature region

$$K_{\mathrm{i}}(r) = \left[1 + \frac{B}{2}\left(\frac{r}{\sigma}\right)^2\right] \exp\left[-\frac{1}{2}\left(\frac{r}{\sigma}\right)^2\right]$$

$$(B, \sigma) = (1, 0.7)$$

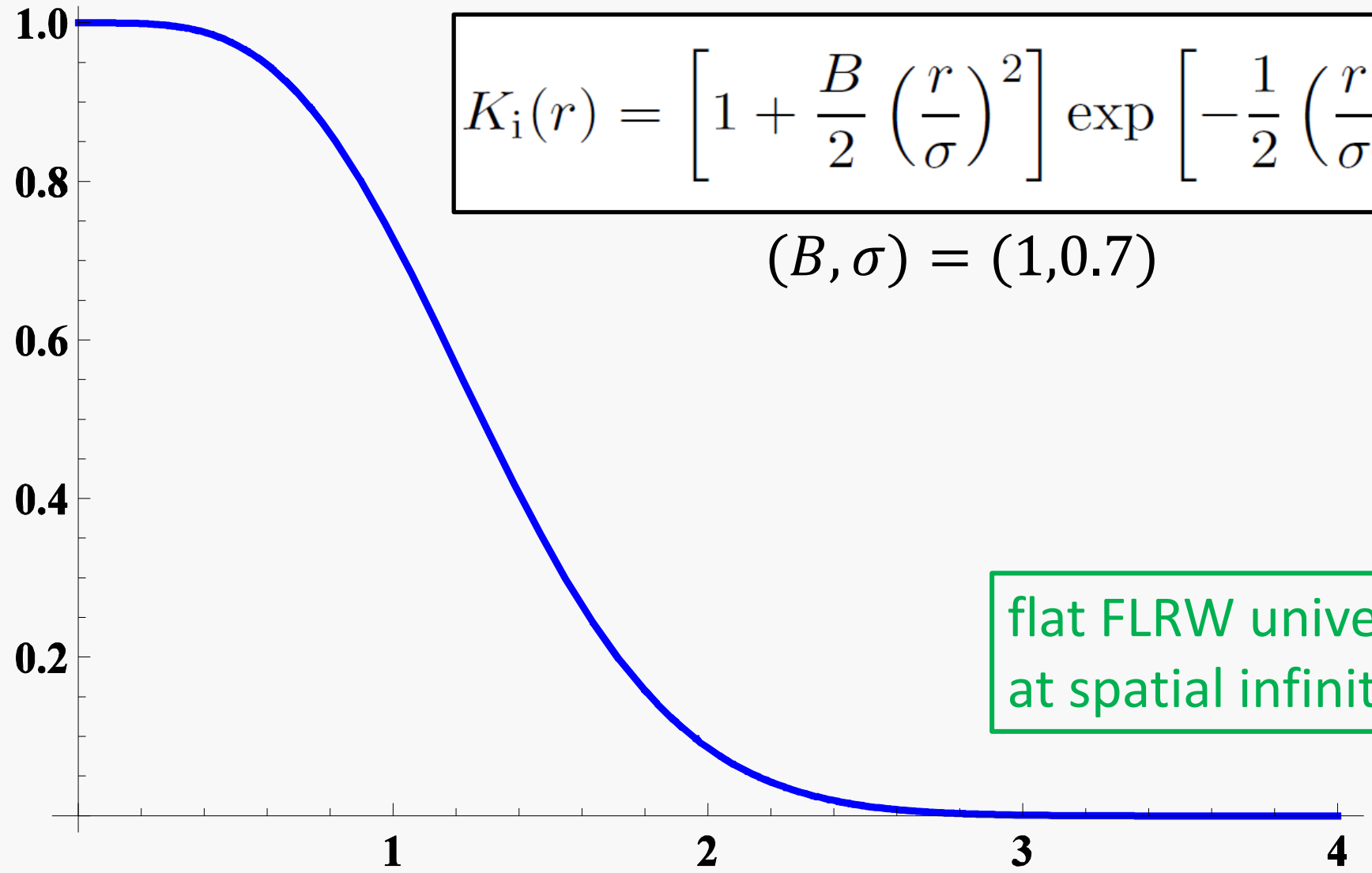

flat FLRW universe
at spatial infinity

・decompose all the quantities

$$X(t,r) = X_0(t,r)\tilde{X}(t,r)$$

FLRW solution

deviation from FLRW solution

・expansion parameter : $\epsilon \equiv \left(\frac{{H_0}^{-1}}{S(t)r_i}\right)^2 \propto t$ (R. D.)

comoving radius of perturbed region

・Rewriting the Einstein eqs. in terms of $\tilde{X}$ and plugging

$$\tilde{X}(t,r) = \sum_{n=0}^{\infty} \epsilon^n(t)\tilde{X}_{(n)}(r)$$

recurrence relations to calculate $\tilde{X}_{(n)}$ are obtained.

$\tilde{\rho}(t,r)$ up to second order in ϵ

$$1+\frac{2}{9}\,ri^2\,\epsilon\,(3\,K_i[r]+r\,K_i'[r])$$

← first order

$$-\frac{1}{540\,r}\,ri^4\,\epsilon^2\Big(-132\,r\,K_i[r]^2-8\,r^3\,K_i'[r]^2+2\,K_i'[r]\,\Big(-16+r^4\,K_i''[r]\Big)$$
$$-4\,r\,\Big(7\,K_i''[r]+r\,K_i^{(3)}[r]\Big)+2\,r^2\,K_i[r]\,\Big(-20\,K_i'[r]+2\,r\,\Big(8\,K_i''[r]+r\,K_i^{(3)}[r]\Big)\Big)\Big)$$

↑ second order

accuracy of asymptotic expansion

$$\mathrm{ERR}\left(\sum_{n=0}^{N}\epsilon^n\tilde{X}_{(n)}\right)\equiv\tilde{X}-\sum_{n=0}^{N}\epsilon^n\tilde{X}_{(n)}\sim O(\epsilon^{N+1}\tilde{X}_{(N+1)}).$$

- Letting Δ be the required accuracy,

$$\boxed{\epsilon^{N+1}M_{(N+1)}}<\Delta,$$

The maximum of $\epsilon^{N+1}\tilde{X}_{(N+1)}(r)$

Time dependence of errors

$(B, \sigma) = (1, 0.7)$

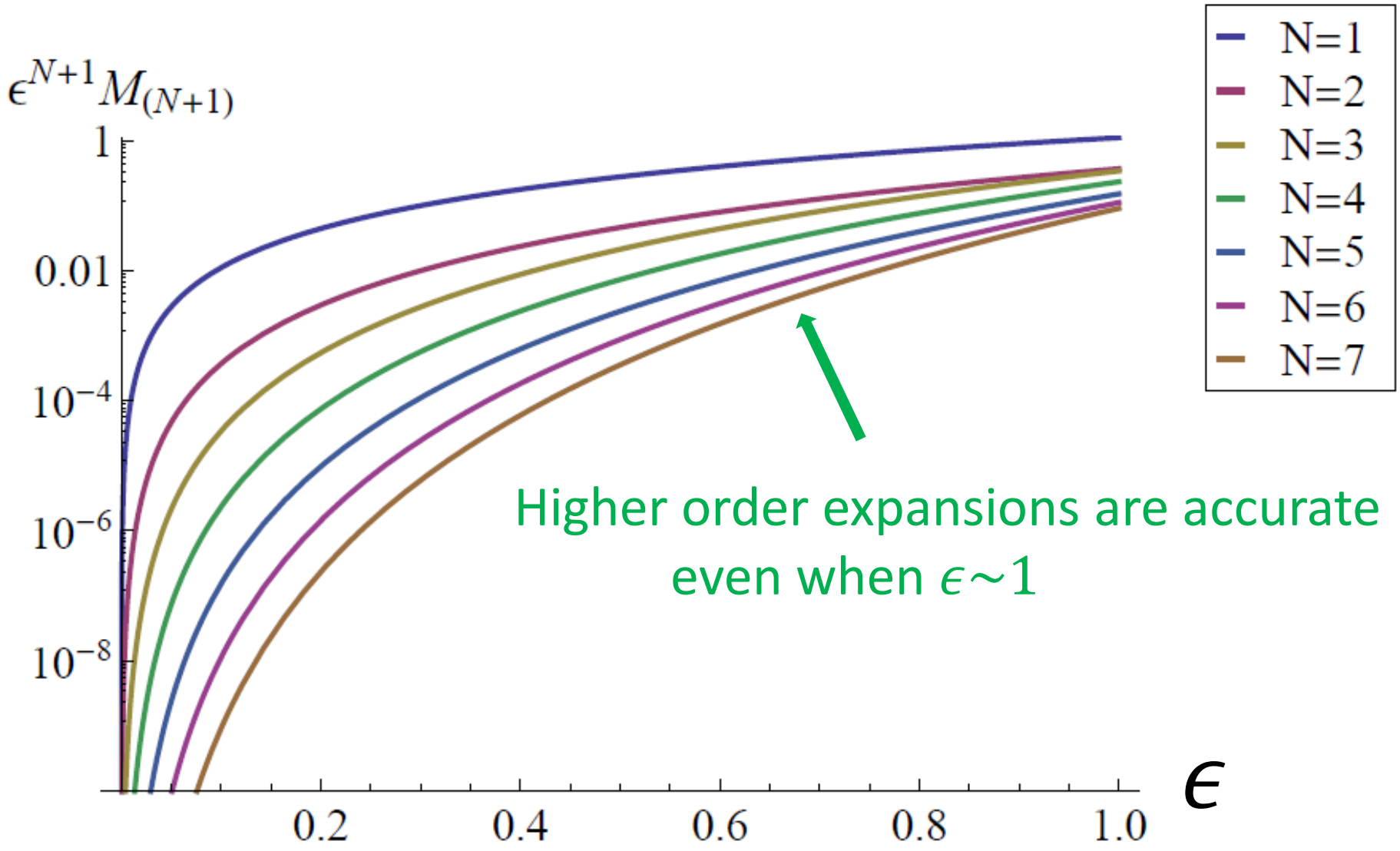

Letting Δ be the required accuracy,

$$\epsilon^{N+1} M_{(N+1)} < \Delta,$$

The maximum of $\epsilon^{N+1} \tilde{X}_{(N+1)}(r)$

The error is less than Δ if

$$\epsilon < \epsilon_{\max} \equiv \sqrt[N+1]{\frac{\Delta}{M_{(N+1)}}}.$$

When to start numerical computation

$((B, \sigma) = (0, 0.7))$

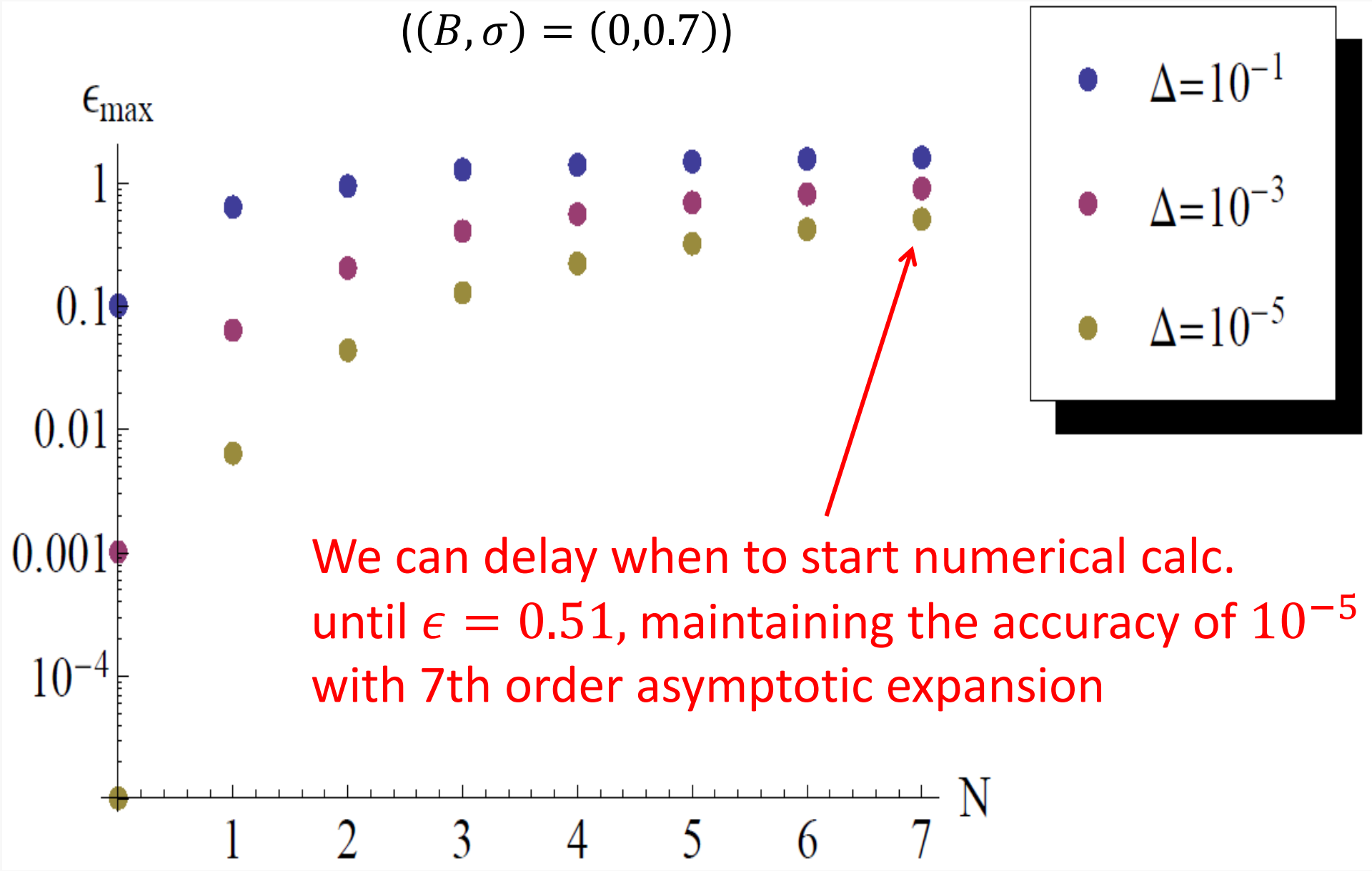

We can delay when to start numerical calc. until $\epsilon = 0.51$, maintaining the accuracy of 10^{-5} with 7th order asymptotic expansion

time evolution of density pert. profile

((*B*,*σ*)=(1,0.7),7th order expansion is used)

$$\delta(t,r) \equiv \frac{\rho(t,r)-\rho_0(t)}{\rho_0(t)} = \tilde{\rho}(t,r) - 1,$$

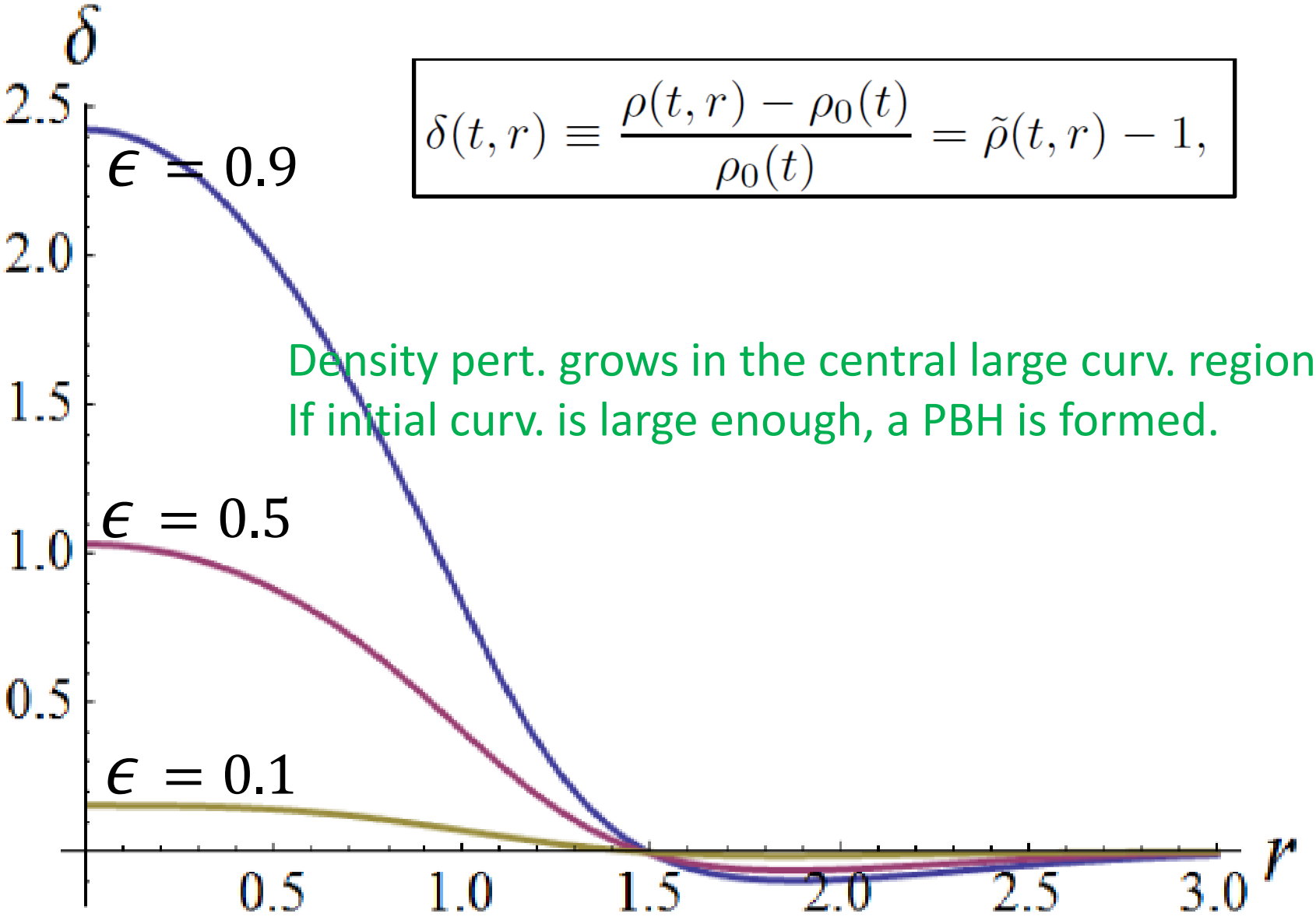

Density pert. grows in the central large curv. region.
If initial curv. is large enough, a PBH is formed.

summary

- Spherically symmetric large amplitude perturbation embedded in the flat FLRW universe is investigated.
- The solution of the Einstein eqs. is obtained

  by asymptotic expansion over ϵ.
- The solution is valid while the perturbed region is outside the horizon.
- Initial curvature profile, $K_i(r)$, generates the solution.
- Since the solution is accurate even when $\epsilon \sim 1$, we can delay the time when numerical computation is started.

work in progress

backups

- define $\widetilde{K}$, which describes time evolution of *K*

$$1 - K(t,r)r^2 = (1 - K_{\mathrm{i}}(r)r^2)\tilde{K}(t,r)$$

- $\widetilde{K}(t,\infty)$=1 since $K(t,\infty) = 0,\ K_i(\infty) = 0.$
- $\widetilde{K}(0,r)$=1 since $K(0,r) \equiv K_i(r).$
- $\widetilde{K} > 0$, so we can define $\widehat{K} \equiv \log\widetilde{K}$

The Einstein equations are rewitten in terms of $\tilde{X}$, $\hat{X}$.

$$\tilde{\mu} = \tilde{H}^2 + \epsilon \left[\frac{r_{\rm i}^2}{r^2} + e^{\hat{K}} \left(K_{\rm i} r_{\rm i}^2 - \frac{r_{\rm i}^2}{r^2} \right) \right] e^{-2\hat{R}}$$

$$\frac{\partial \tilde{\mu}}{\partial \xi} = 2(\tilde{\mu} - \tilde{\Phi} \tilde{f}),$$

$$\tilde{\rho} = \tilde{\mu} + \frac{1}{3} D_r \tilde{\mu},$$

$$\hat{a} = -\frac{\gamma}{1+\gamma} \hat{\rho},$$

$$\frac{\partial \hat{R}}{\partial \xi} = \frac{2}{3(1+\gamma)} (\tilde{\Phi} - 1),$$

$$\frac{\partial \hat{K}}{\partial \xi} = -\frac{4\gamma}{3(1+\gamma)^2} \tilde{\Phi} D_r \hat{\rho}$$

- construct solution by asymptotic expansion

$$\tilde{X}(t,r) = \sum_{n=0}^{\infty} \in^n (t)\tilde{X}_{(n)}(r)$$

$$\hat{X}(t,r) = \sum_{n=0}^{\infty} \in^n (t)\hat{X}_{(n)}(r)$$

- by definition, $\tilde{X}_{(0)} = 1,\ \hat{X}_{(0)} = 0.$

- By plugging the expansions into the Einstein eqs, recurrence relations to calculate the expansion coefficients $\widetilde{X}_{(n)}$ are obtained.

- example of recurrence relations

$$\boxed{\tilde{\rho}_{(n)} = \tilde{\mu}_{(n)} + \frac{r}{3}\tilde{\mu}'_{(n)} + W_{3(n)},}$$

$$W_{3(n)} \equiv S_{(n)}[(\tilde{\mu} - \tilde{\rho})(r\tilde{R})'] + \frac{r}{3}S_{(n)}[\tilde{\mu}'\tilde{R}],$$

$$S_{(n)}[\tilde{X}_1\tilde{X}_2] \equiv \sum_{i=1}^{n-1} \tilde{X}_{1(i)}\tilde{X}_{2(n-i)}.$$

- By plugging these expansions into the Einstein equations, we can obtain recursive relations to calculate $\tilde{X}_{(n)}$.
- We define

$$S_{(n)}[\tilde{X}_1\tilde{X}_2] \equiv \sum_{i=1}^{n-1} \tilde{X}_{1(i)}\tilde{X}_{2(n-i)}.$$

$$S^*_{(n)}[\tilde{X}F] = \sum_{m=1}^{n-1} m\tilde{X}_m F_{(n-m)}.$$

some function of $\tilde{X}$

- $S_{(n)}$, $S^*_{(n)}$ depend only on the expansion coefficients of up to n-1 order.

$$\tilde{\mu}_{(n)} = \frac{1}{1+A_n}(F_{(n)} + W_{1(n)} - W_{2(n)}),$$

$$A_n \equiv \frac{2}{1+\gamma}\left[\left(\gamma+\frac{1}{3}\right)n-\gamma\right],$$

$$F_{(n)} \equiv \delta^1_n r_i^2 K_i - 2r_{\rm i}^2 K_{\rm i}\hat{R}_{(n-1)} + r_{\rm i}^2\left(K_{\rm i}-\frac{1}{r^2}\right)\hat{K}_{(n-1)},$$

$$\begin{aligned} W_{1(n)} \equiv\ & S_{(n)}[\tilde{H}\tilde{H}] + r_{\rm i}^2\left(K_{\rm i}-\frac{1}{r^2}\right)S_{(n-1)}[e^{\hat{K}}e^{-2\hat{R}}] \\ & + \frac{1}{n-1}\left\{r_{\rm i}^2\left(K_{\rm i}-\frac{1}{r^2}\right)S^*_{(n-1)}[\hat{K}e^{\hat{K}}] - 2r_{\rm i}^2 K_{\rm i} S^*_{(n-1)}[\hat{R}e^{-2\hat{R}}]\right\}. \end{aligned}$$

$$W_{2(n)} \equiv 2\left(S_{(n)}[\tilde{a}\tilde{H}] + S_{(n)}[\tilde{\Phi}\tilde{f}] + \frac{\gamma}{n(1+\gamma)}S^*_{(n)}[\hat{\rho}(\tilde{\rho}-\tilde{a})]\right).$$

$$\tilde{\rho}_{(n)} = \tilde{\mu}_{(n)} + \frac{r}{3}\tilde{\mu}'_{(n)} + W_{3(n)},$$

$$\tilde{H}_{(n)} = -\frac{1}{2(1+A_n)}[A_n(F_{(n)} + W_{1(n)}) + W_{2(n)}],$$

$$\tilde{a}_{(n)} = -\frac{\gamma}{1+\gamma}\left(\tilde{\mu}_{(n)} + \frac{r}{3}\tilde{\mu}'_{(n)}\right) + W_{4(n)},$$

$$\hat{R}_{(n)} = \frac{1}{(1+3\gamma)n}(\tilde{a}_{(n)} + \tilde{H}_{(n)} + W_{5(n)}),$$

$$\hat{K}_{(n)} = -\frac{2\gamma}{(1+\gamma)(1+3\gamma)n}(r\hat{\rho}'_{(n)} + W_{6(n)}),$$

$$\tilde{R}_{(n)} = \hat{R}_{(n)} + \frac{1}{n}S^*_{(n)}[\hat{R}\tilde{R}],$$

$$\tilde{K}_{(n)} = \hat{K}_{(n)} + \frac{1}{n}S^*_{(n)}[\hat{K}\tilde{K}].$$

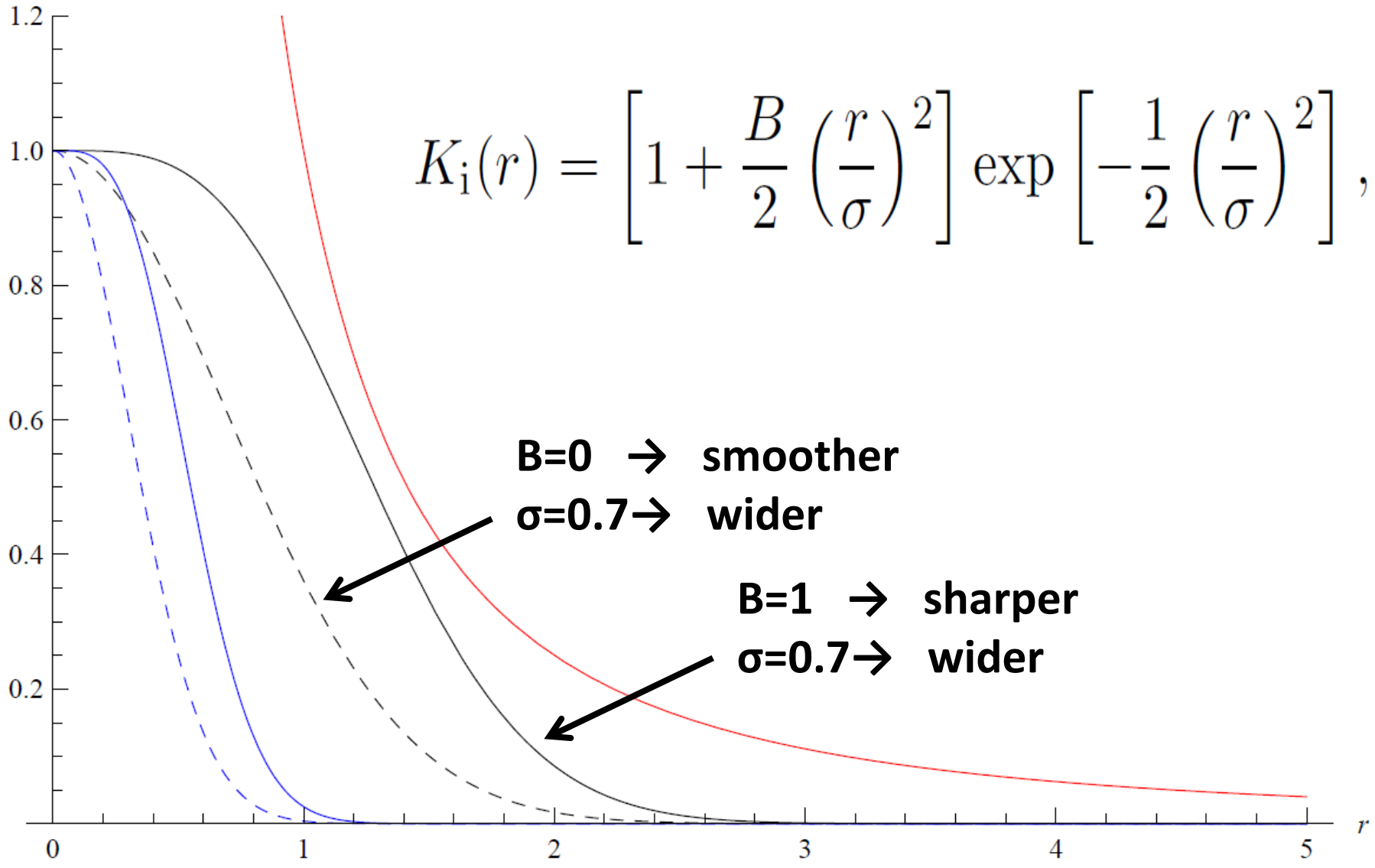
1.2
1.0
0.8
0.6
0.4
0.2
0
1
2
3
4
5
r
$K_i(r) = \left[1 + \frac{B}{2}\left(\frac{r}{\sigma}\right)^2\right] \exp\left[-\frac{1}{2}\left(\frac{r}{\sigma}\right)^2\right],$
B=0 → smoother
σ=0.7→ wider
B=1 → sharper
σ=0.7→ wider

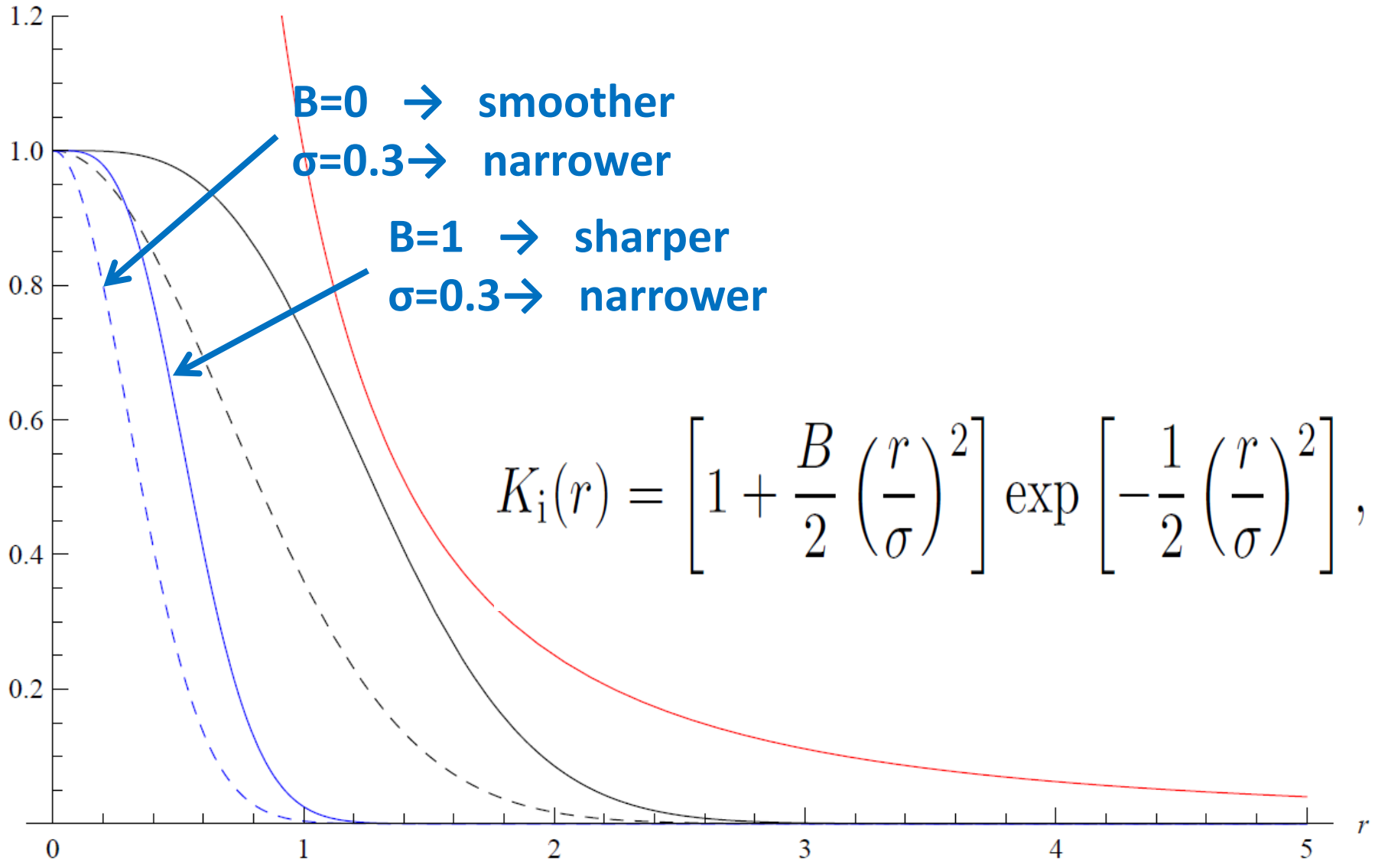

$$K_i(r) = \left[1 + \frac{B}{2}\left(\frac{r}{\sigma}\right)^2\right] \exp\left[-\frac{1}{2}\left(\frac{r}{\sigma}\right)^2\right],$$

$$\delta(t, r_{od})=0$$

r_i is defined as r_{od}
at an sufficiently early time.

$$\delta_{(1)}(t, r_i)=\frac{(1+\gamma){r_i}^2(3K_i(r)+rK_i'(r))}{5+3\gamma}\epsilon=0$$

time evolution of density pert. profile

((*B*,*σ*)=(1,0.7),7th order expansion is used)

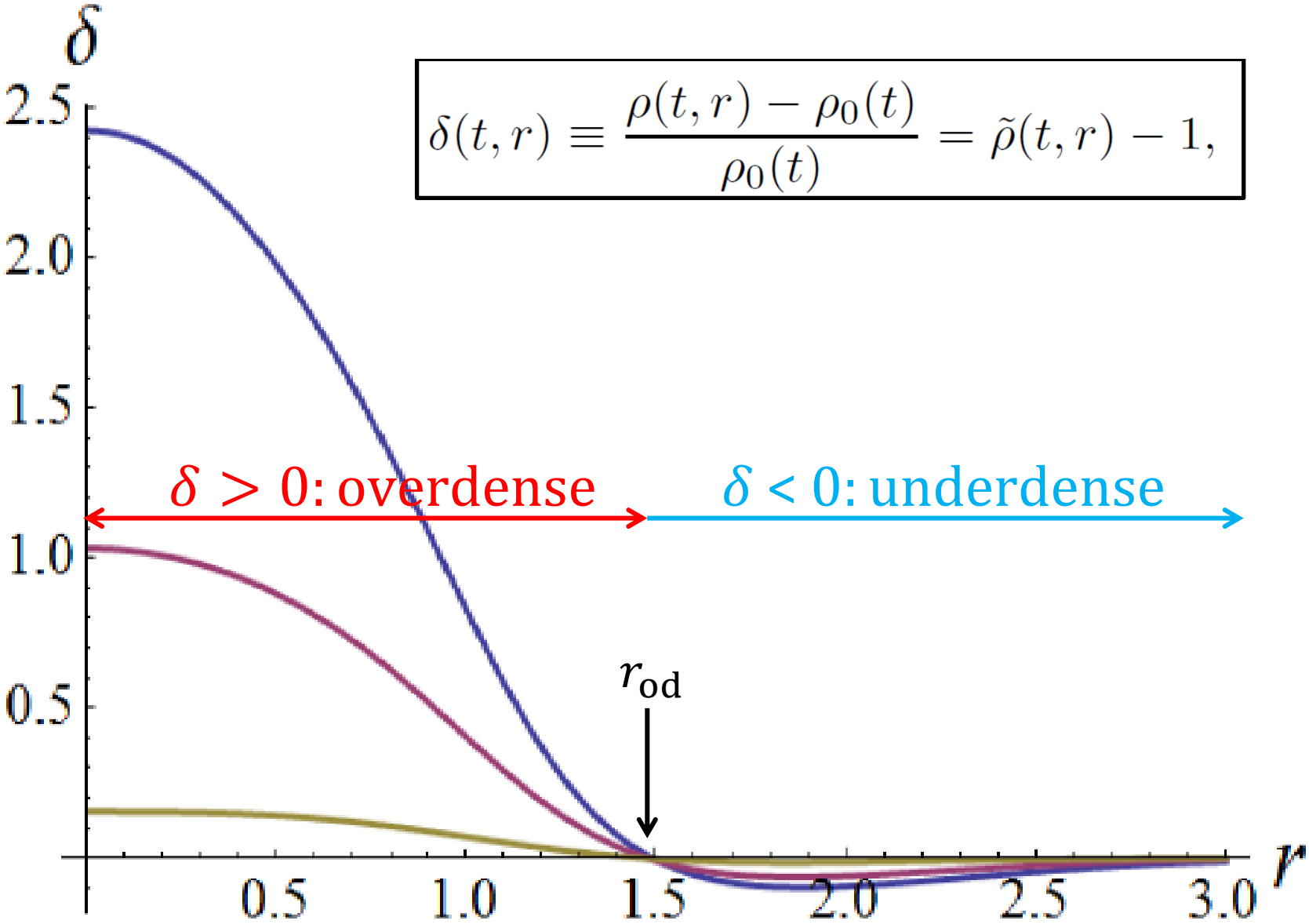

(B,σ)=(1,0.7)

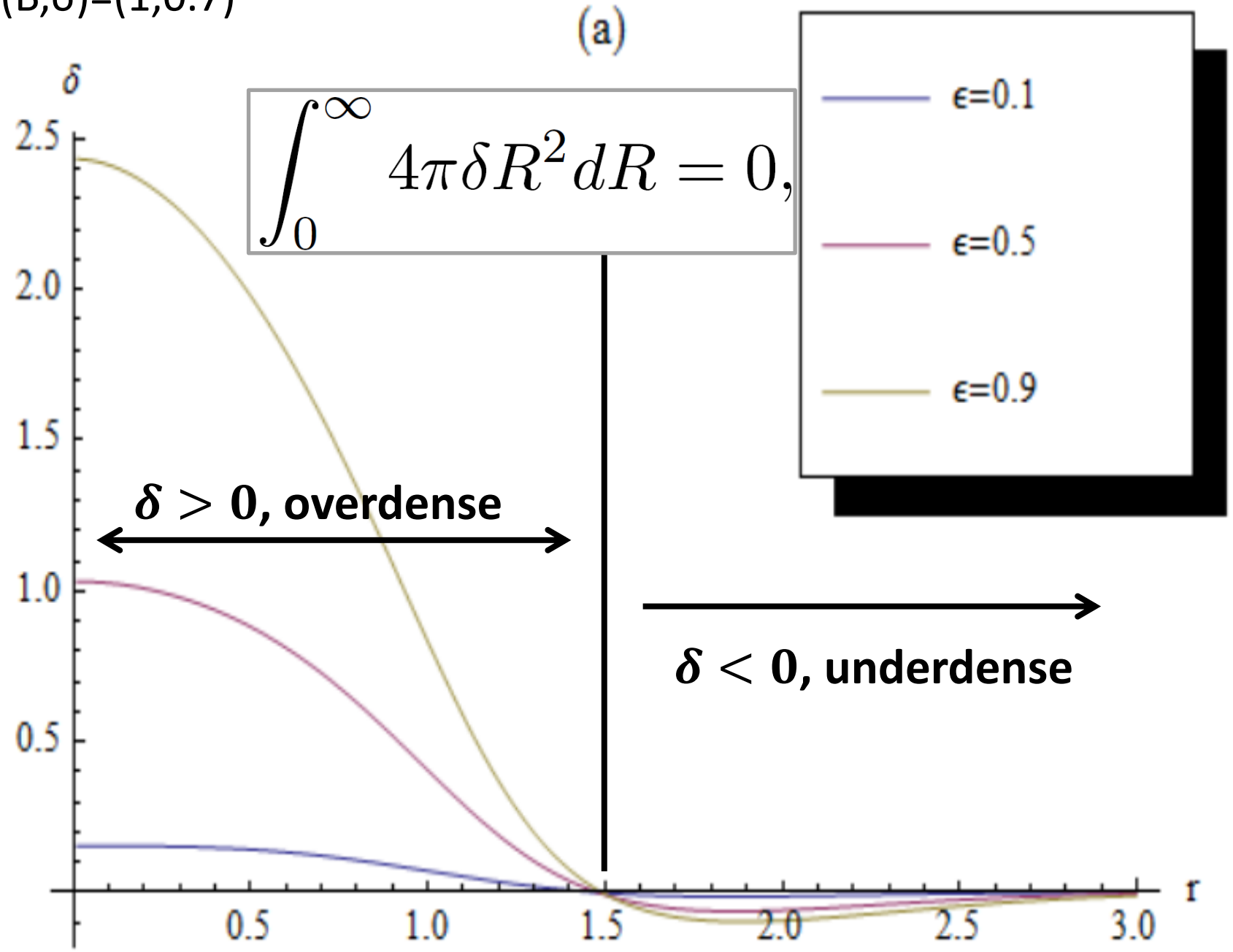
(a)
δ
2.5
2.0
1.5
1.0
0.5
0.5
1.0
1.5
2.0
2.5
3.0
r
$\int_0^\infty 4\pi\delta R^2 dR = 0,$
ϵ=0.1
ϵ=0.5
ϵ=0.9
$\delta > 0$, overdense
$\delta < 0$, underdense

Time evolution of averaged overdensity

$$\bar{\delta}(t) \equiv \left(\frac{4}{3}\pi R(t, r_{\rm od})^3\right)^{-1} \int_0^{R(t,r_{\rm od})} 4\pi\delta R^2 dR.$$

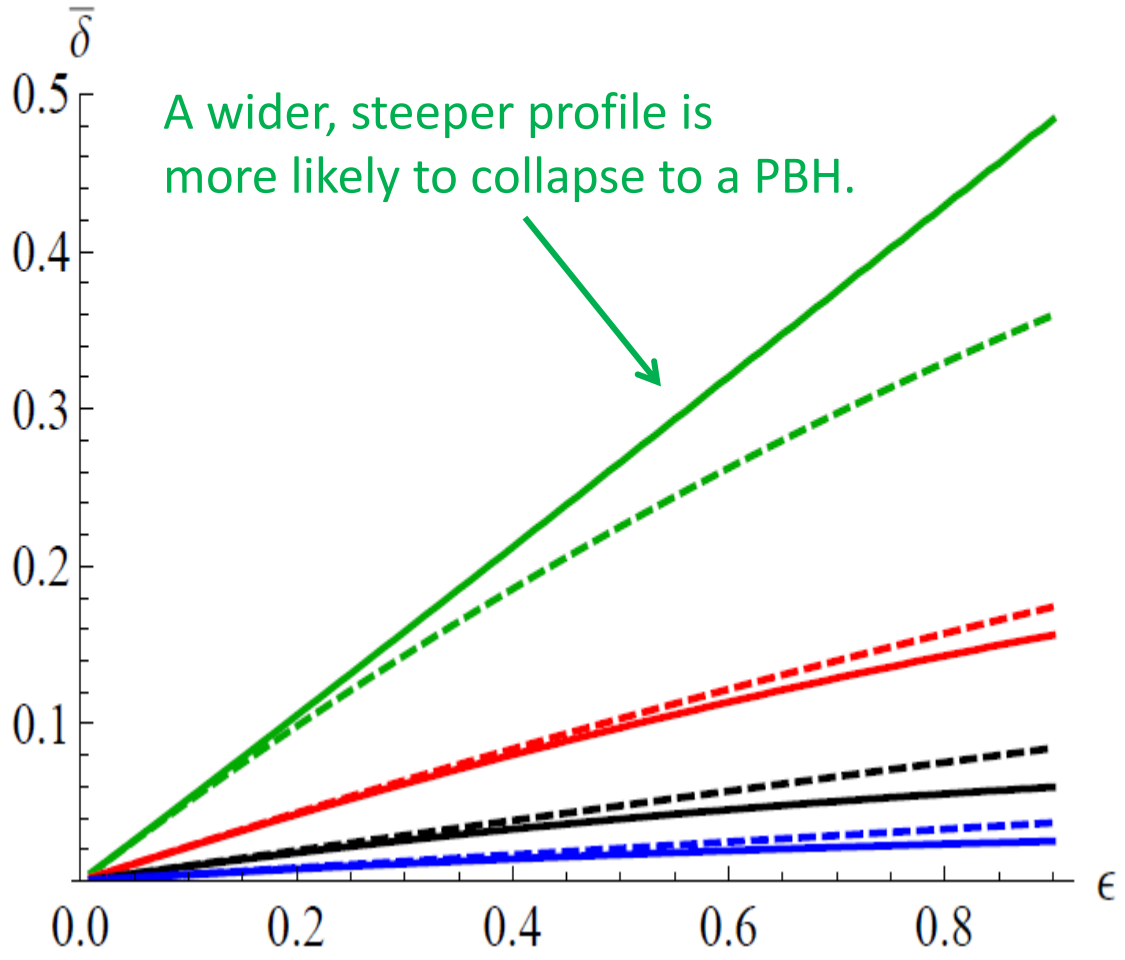

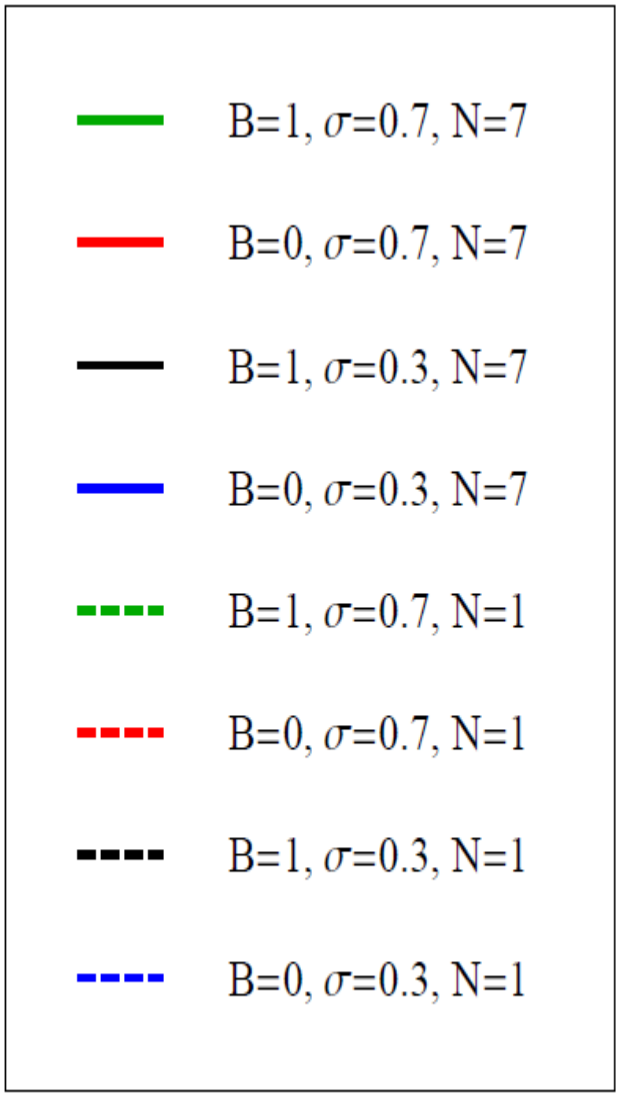

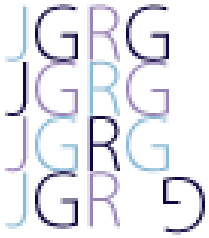

Masato Nozawa, JGRG 22(2012)111215

"On the vacua of maximal gauged supergravity"

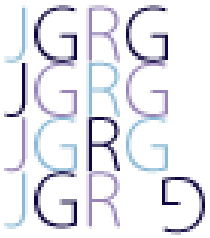

RESCEU SYMPOSIUM ON

GENERAL RELATIVITY AND GRAVITATION

JGRG 22



November 12-16 2012

Koshiba Hall, The University of Tokyo, Hongo, Tokyo, Japan



On the vacua of maximal gauged supergravity

Masato NOZAWA

(KEK)

Cowork with Hideo Kodama (KEK)

Based on

H.Kodama-M.N, arXiv:1210.4238

talk at JGRG22

Inflation in string theory

Precision Cosmology

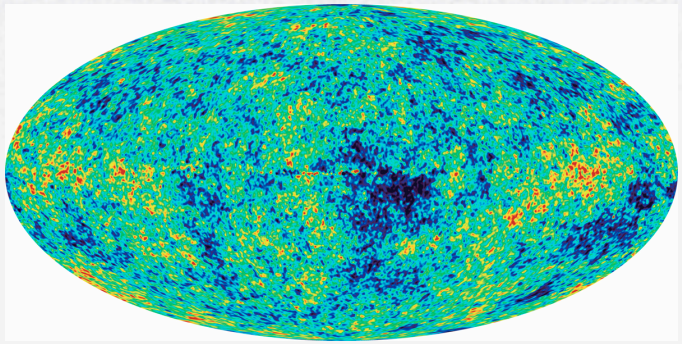

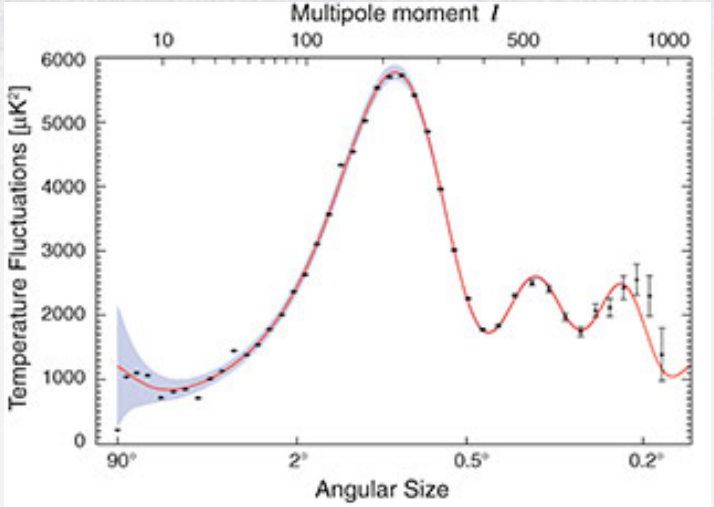

CMB data strongly implies **inflation**

Challenge: account for inflation from fundamental theories

String theory: candidate for unifying all gauge interactions

- based on supersymmetry
- formulated in 10/11 dimensions

not fully successful due to moduli stabilization, η problem...

KKLT, KKLMMT, axion monodromy,...

Why N=8 supergravity

N=8 supergravity *fails* to describe unified gauge interactions, but...

- *N*=8 SUGRA is the *restrictive* than *N*<8 theories
  - UV finite? (consensus: up to 7 loops)

    creditable guide toward quantum gravity

- direct relation to fundamental theories
  - IIA, IIB, M-theory : *N*=8

    ideal playground for exploring string theory dynamics independent of SUSY breaking objects

- Effective theory of M2branes
- AdS/CMP applications
- Landscape for string vacua

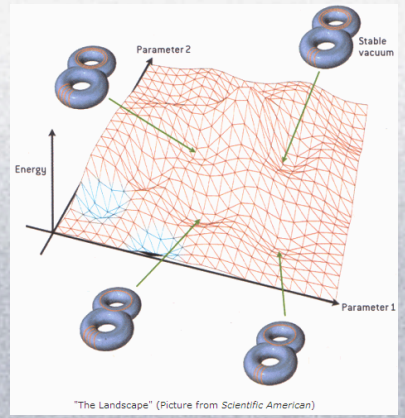

Our work

We want to reveal *full* moduli space structure of N=8 supergravity

- Focus:
  - classifying vacua (Mink/AdS/dS)
  - stability of vacua
- Motivations:
  - more realistic construction of string inflation
  - extract universal features of gravity sector of string theory
- Key:
  - embedding tensor formalism
  - homogeneous scalar manifold $E_{7(7)}$/SU(8)
- Abstract of our results:
  - an exhaustive list of SL(8,**R**)-type vacua
  - an analytic expression of full mass spectra

N=8 Supergravity

- gauged supergravity
- embedding tensor

N=8 ungauged supergravity

- Maximal (N=8) *ungauged* supergravity Cremmer & Julia 78

  - *N*=8 is the *maximal # of SUSYs* for spin≦2

  - unique multiplet: 2^8=128 bosons+128 fermions

	graviton	gravitino	vector	gaugino	scalar
# of fields	1	8	28	56	70
dof	2	2x8=16	2x28=56	2x56=112	1x70

  - 70 scalars parametrize $E_{7(7)}/SU(8)$

    coset representative: 56x56 matrix *i,j,...*= **8** of SU(8)

$$L(\phi)_{\underline{M}}{}^{\underline{N}} = \exp \begin{pmatrix} 0 & \phi_{ijkl} \\ \phi^{ijkl} & 0 \end{pmatrix} , \quad \phi_{ijkl} = \phi_{[ijkl]} = \eta(\star\bar{\phi})_{ijkl} , \quad \eta = \pm 1$$

  - obtained via T^7 compactification of M-theory

  - no scalar potential, no nonabelian gauge fields

Gauged supergravity

- N=8 *gauged* supergravity *a la* *embedding tensor formalism*

deWit-Samtleben-Trigiante 03

Gauging: enhances *global symmetry* $G \subset E_{7(7)}$ to *local symmetry*

$$\partial_\mu \;\rightarrow\; D_\mu = \partial_\mu - g A_\mu{}^M X_M \,.$$

g: gauge coupling

X_M: generators of G
t_α: generators of $E_{7(7)}$

$$X_M = \Theta_M{}^\alpha t_\alpha$$

α=1,..,133: adjoint of $E_{7(7)}$
M=1,..,56: fundamental of $E_{7(7)}$

- Consistency

Θ: embedding tensor

(i) Gauge group G satisfies dimG≦28

✓simplest ex: SO(8) gauging de Wit & Nicolai 81

(ii) G must form a closed subgroup

$$\Omega^{MN}\Theta_M{}^\alpha\Theta_N{}^\beta = 0$$

Ω: Sp(56,R)⊃$E_{7(7)}$ metric

(iii) SUSY $\quad \Theta_M{}^\alpha \in \mathbf{912} \subset \mathbf{56} \times \mathbf{133}$

✓$O(g)$: SUSY transformation rules for fermions

✓$O(g)$: *mass terms for fermions*

✓$O(g^2)$: *scalar potential*

Scalar potential

Mink/AdS/dS ⇒ Einstein-70scalar system $E_{7(7)}$/SU(8)

$$L = \frac{1}{2}R + \frac{1}{8}\mathrm{Tr}(\partial^\mu M \partial_\mu M^{-1}) - V(\phi)\,, \qquad M_{MN} = (L^T L)_{MN}$$

L=$L(\phi_{ijkl})$: coset rep. of $E_{7(7)}$/SU(8)

$$\boxed{V = \frac{g^2}{672}\left(X_{MN}{}^P X_{PQ}{}^S M^{MP} M^{NQ} M_{RS} + 7 X_{MN}{}^Q X_{PQ}{}^N M^{MP}\right)\,.}$$

- unbounded from below and above, and nonlinear fun. of ϕ_{ijkl}

- we can move critical pts to origin of scalar mfd Dall'Agata-Inverso'11
  - homogeneity of scalar mfd $E_{7(7)}$/SU(8)
  - V is invariant under $L(\phi') = U L(\phi) h^{-1}(\phi,\phi')$ + $\Theta' = U\Theta$

At the origin, ϕ_{ijkl}=0, $L(\phi)$=$\mathbf{1}_{56}$

$$\partial_\rho V \propto t_{\rho M}{}^N \Theta_M{}^\alpha \Theta_N{}^\beta (\delta_{\alpha\beta} + 7\eta_{\alpha\beta}) + \Theta_M{}^\alpha \Theta_M{}^\beta f_{\rho\beta}{}^\gamma \delta_{\alpha\gamma}$$

combined with closure condition $\Omega^{MN}\Theta_M{}^\alpha \Theta_N{}^\beta = 0$

→ just solve a set of quadratic eqs. for Θ

SL(8,R) vacua

Dall'Agata-Inverso considered gaugings $\subset$SL(8,**R**)$\subset E_{7(7)}$
for which $\Theta \in$ **912=36+36'+~~420~~+~~420'~~**

$$\Theta_{ab}{}^{c}{}_{d} = \delta_{[a}{}^{c}\theta_{b]d}\,, \qquad \Theta^{abc}{}_{d} = \delta^{[a}{}_{d}\xi^{b]c}\,, \qquad (\theta,\xi)\text{: 8x8 matrices}$$

- assumed ansatz on (θ,ξ) and found several vacua (Mink/AdS/dS)
- mass spectra coincide if residual gauge symmetries are equivalent

✓diagonalized 70x70 mass matrix by computers

gauging	residual sym.	V_c	$m^2/\lvert V_c\rvert$
SO(8) SO(7,1) SO(7) $\ltimes T^7$ SO(6)$\times$ SO(1,1) $\ltimes T^{12}$	SO(6)	AdS	$2^{(2)}, -1^{(20)}, -\frac{1}{4}^{(20)}, 0^{(28)}$
SO(7,1) SO(6)$\times$ SO(1,1) $\ltimes T^{12}$	SO(5)	AdS	$2^{(3)}, -\frac{4}{3}^{(14)}, \frac{2}{3}^{(5)}, 0^{(48)}$
SO(3,5)	SO(3) $\times$ SO(5)	dS	$-2^{(1)}, 4^{(5)}, 2^{(30)}, \frac{4}{3}^{(14)}, -\frac{2}{3}^{(5)}, 0^{(15)}$

Scanning Vacua

- all SL(8,R) type vacua
- stability of vacua

SL(8,R) vacua

We can list *all* possible SL(8,**R**) vacua by obtaining all 8x8 matrices (θ,ξ) satisfying

Kodama-MN '12

$$2(\theta^2-\xi^2)-(\theta\mathrm{Tr}\theta-\xi\mathrm{Tr}\xi)=2a\mathbb{I}_8\,,\qquad \theta\xi=c\mathbb{I}_8$$

a, c : constants

- SL(8,**R**) vacua are *exhausted* by list of Dall'agata-Inverso

Gauging	$G_{\rm reg}$	Λ
$\mathrm{SO}(4,4)$	$\mathrm{SO}(4)\times\mathrm{SO}(4)$	dS
$\mathrm{SO}(5,3)$	$\mathrm{SO}(5)\times\mathrm{SO}(3)$	dS
$\mathrm{SO}(8)$ $\mathrm{SO}(7,1)$ $\mathrm{SO}(7)\ltimes\mathbb{T}^7$	$\mathrm{SO}(7)$	AdS
$\mathrm{SO}(8)$ $\mathrm{SO}(7,1)$ $\mathrm{SO}(7)\ltimes\mathbb{T}^7$ $\mathrm{SO}(6)\times\mathrm{SO}(1,1)\ltimes\mathbb{T}^{12}$	$\mathrm{SO}(6)$	AdS
$\mathrm{SO}(7,1)$ $\mathrm{SO}(6)\times\mathrm{SO}(1,1)\ltimes\mathbb{T}^{12}$	$\mathrm{SO}(5)$	AdS
$\mathrm{SO}(6,2)$	$\mathrm{SO}(2)^4$	Mink.
$\mathrm{SO}(4)\times\mathrm{SO}(2,2)\ltimes\mathbb{T}^{16}$	$\mathrm{SO}(2)^4$	Mink.
$\mathrm{SO}(2)\times\mathrm{SO}(2)\ltimes\mathbb{T}^{20}$	$\mathrm{SO}(2)^2$	Mink.

SL(8,R) vacua

We can list *all* possible SL(8,**R**) vacua by obtaining all 8x8 matrices (θ,ξ) satisfying

Kodama-MN '12

$$2(\theta^2-\xi^2)-(\theta\mathrm{Tr}\theta-\xi\mathrm{Tr}\xi)=2a\mathbb{I}_8\,,\qquad \theta\xi=c\mathbb{I}_8$$

a, *c* : constants

- SL(8,**R**) vacua are *exhausted* by list of Dall'agata-Inverso
- Minkowski vacua are parametrized by continuous parameters
- For some vacua ($\Lambda\neq0$), a single parameter remains

  e.g., dS vacua with SO(4,4)→SO(4)xSO(4) gauging

$$\theta=\lambda\mathbb{I}_4\oplus(-\lambda)\mathbb{I}_4\,,\qquad \xi=\theta^{-1}\,,\qquad V=\frac{g^2}{4}\left(\lambda^2+\lambda^{-2}\right),$$

  implying 1parameter *deformation of the theory*

c.f. Dall'Agata-Inverso-Trigiante '12 for SO(8)

SL(8,R) vacua

Mass spectra are *analytically* determined Kodama-MN '12

$$(M^2)_{\rho\sigma} := \frac{g^2}{168}\left[(s_{(\rho}s_{\sigma)})_M{}^N \mathrm{Tr}(X_M{}^T X_N + 7X_M X_N) + 2(s_{(\rho})_M{}^N \mathrm{Tr}(s_{\sigma)}[X_{(M}, {}^T X_{N)}]) \right.$$
$$\left. -\mathrm{Tr}([s_{(\rho}, X_M][s_{\sigma)}, {}^T X_M])\right] .$$

$$s_\rho = \frac{1}{2}(t_\rho + {}^T t_\rho) = \begin{pmatrix} 2S_\rho \wedge \mathbb{I} & U_\rho \\ \star U_\rho & -2S_\rho \wedge \mathbb{I} \end{pmatrix}$$

$$\Theta_{ab}{}^c{}_d = \delta_{[a}{}^c \theta_{b]d} ,$$
$$\Theta^{abc}{}_d = \delta^{[a}{}_d \xi^{b]c} ,$$

decompose into SL(8,**R**) irrep ⟶

S_{ab}:**35** scalars $\quad S = {}^T S , \quad \mathrm{Tr}(S) = 0 ,$

U_{abcd}:**35** pseudoscalars $\quad U = \star U .$

⟶ kinetic term= $\frac{1}{2}\mathrm{Tr}((\partial S)^2) + \frac{1}{12}\partial U \cdot \partial U$

e.g. electric gaugings (ξ=0) & $V_c \neq 0$: cosmological constant

$$\theta = \begin{pmatrix} \lambda_1 \mathbb{I}_{n_1} & 0 \\ 0 & \lambda_2 \mathbb{I}_{n_2} \end{pmatrix} \qquad S = \begin{pmatrix} A_{11} & A_{12} \\ {}^T A_{12} & A_{22} \end{pmatrix} \qquad A_{11} = \frac{1}{n_1}\mathrm{Tr}(A_{11})\mathbb{I}_{n_1} + \hat{A}_1 ,$$

n_1+n_2(=8) split

SL(8,R) vacua

Mass spectra for $\Lambda \neq 0$ vacua

Kodama-MN '12

$$M^2_{(1)} = \frac{8}{n_1 n_2} m^2_{0(\mathbf{1},\mathbf{1})} \mathrm{Tr}(A_{11})^2 + m^2_{1(\mathbf{N}_1,\mathbf{1})} \mathrm{Tr}(\hat{A}_1^2) + m^2_{2(\mathbf{1},\mathbf{N}_2)} \mathrm{Tr}(\hat{A}_2^2) + 2 m^2_{*(\mathbf{n}_1,\mathbf{n}_2)} \mathrm{Tr}({}^T A_{12} A_{12}) \,,$$

SO(n_1,n_2)→ SO(n_1)xSO(n_2) $\qquad \theta = \begin{pmatrix} \lambda_1 \mathbb{I}_{n_1} & 0 \\ 0 & \lambda_2 \mathbb{I}_{n_2} \end{pmatrix}$

(n_1, n_2) correspond to the unbroken gauge symmetries

$$m^2_{0(\mathbf{1},\mathbf{1})} = -2V_c \,, \qquad m^2_{1(\mathbf{N}_1,\mathbf{1})} = \frac{4V_c}{n_1 - 2} \,,$$

m_*=0: NG directions

$m^2_{(\mathbf{p},\mathbf{q})}$: (**p**,**q**) irrp of SO(n_1)xSO(n_2) $\qquad N_1 = \frac{1}{2}(n_1 - 1)(n_1 + 2)$

Mass of pseudoscalars can be obtained similarly

$$m^2_{U[\ell]} = \frac{2[2\ell^2 - 2n_1\ell + (n_1 - 2)^2]}{(n_1 - 6)(n_1 - 2)} V_c \,.$$

l: labeling index

Mass spectra are dependent only on residual gauge symmetries

$\Rightarrow$ insensitive to original gaugings & deformation parameters

SL(8,R) vacua

Minkowski vacua

SO(6,2), SO(4)xSO(2,2)$\ltimes T^{16}$, SO(2)xSO(2)$\ltimes T^{20}$ admit Minkowski vacua

e.g., 35 scalar mass eigenvalues for SO(6,2)→SO(2)^4 gauging

$$\theta = r\mathbb{I}_2 \oplus s\mathbb{I}_2 \oplus t\mathbb{I}_2 \oplus \left(-\frac{1}{rst}\right)\mathbb{I}_2\,, \quad \text{:specified by 3 continuous parameters}$$

$$m^2_{(\mathbf{1},\mathbf{1},\mathbf{1})(\times 3)} = 0\,, \qquad m^2_{*(\times 24)} = 0 \quad : (\mathbf{2},\mathbf{2},\mathbf{1},\mathbf{1}) + \cdots\,,$$

$$m^2_{i(\times 8)} = \frac{g^2}{16r^2s^2t^2} \times \begin{cases} 4st(r-s)(r-t)(1+r^2st)\,, & : (\mathbf{2},\mathbf{1},\mathbf{1},\mathbf{1}) \\ 4rt(s-r)(s-t)(1+rs^2t)\,, & : (\mathbf{1},\mathbf{2},\mathbf{1},\mathbf{1}) \\ 4rs(r-t)(s-t)(1+rst^2)\,, & : (\mathbf{1},\mathbf{1},\mathbf{2},\mathbf{1}) \\ 4(1+r^2st)(1+rs^2t)(1+rst^2)\,, & : (\mathbf{1},\mathbf{1},\mathbf{1},\mathbf{2}) \end{cases}.$$

Unless (*r,s,t*) are pairwise equal, m^2 will be negative

→ generic Minkowski vacua are unstable

SL(8,R) vacua

Exhaustive list of SL(8,**R**) type vacua & mass spectra

Gauging	$G_{\rm reg}$	Λ	m_S^2	m_U^2
$\mathrm{SO}(4,4)$	$\mathrm{SO}(4)\times\mathrm{SO}(4)$	dS	$-2_{(\times 1)},\ 2_{(\times 18)},\ 0_{(\times 16)}$	$2_{(\times 18)}, 1_{(\times 16)}, -2_{(\times 1)}$
$\mathrm{SO}(5,3)$	$\mathrm{SO}(5)\times\mathrm{SO}(3)$	dS	$-2_{(\times 1)},\ \frac{4}{3}_{(\times 14)},\ 4_{(\times 5)},\ 0_{(\times 15)}$	$2_{(\times 30)},\ -\frac{2}{3}_{(\times 5)}$
$\mathrm{SO}(8)$ $\mathrm{SO}(7,1)$ $\mathrm{SO}(7)\ltimes\mathbb{T}^7$	$\mathrm{SO}(7)$	AdS	$2_{(\times 1)},\ -\frac{4}{5}_{(\times 27)},\ 0_{(\times 7)}$	$-\frac{2}{5}_{(\times 35)}$
$\mathrm{SO}(8)$ $\mathrm{SO}(7,1)$ $\mathrm{SO}(7)\ltimes\mathbb{T}^7$ $\mathrm{SO}(6)\times\mathrm{SO}(1,1)\ltimes\mathbb{T}^{12}$	$\mathrm{SO}(6)$	AdS	$-1_{(\times 20)},\ 2_{(\times 2)},\ 0_{(\times 13)}$	$0_{(\times 15)},\ -\frac{1}{4}_{(\times 20)}$
$\mathrm{SO}(7,1)$ $\mathrm{SO}(6)\times\mathrm{SO}(1,1)\ltimes\mathbb{T}^{12}$	$\mathrm{SO}(5)$	AdS	$-\frac{4}{3}_{(\times 14)},\ 2_{(\times 3)},\ 0_{(\times 18)}$	$\frac{2}{3}_{(\times 5)},\ 0_{(\times 30)}$
$\mathrm{SO}(6,2)$	$\mathrm{SO}(2)^4$	Mink.	Eq. (4.54)	Eq. (4.55)
$\mathrm{SO}(4)\times\mathrm{SO}(2,2)\ltimes\mathbb{T}^{16}$	$\mathrm{SO}(2)^4$	Mink.	Eq. (4.68)	Eq. (4.69)
$\mathrm{SO}(2)\times\mathrm{SO}(2)\ltimes\mathbb{T}^{20}$	$\mathrm{SO}(2)^2$	Mink.	Eq. (4.70)	Eq. (4.71)

- mass eigenvalues are insensitive to a deformation parameter
- all vacua break SUSY completely
- (A)dS vacua are always unstable

Summary

What we have done

- *complete classification* of vacua for gauge group contained in SL(8,**R**)
  - ✓many vacua ($\Lambda \neq 0$) contain deformation parameter
  - ✓except N=8 AdS vacua, all SUSYs are broken
- obtained *analytic expressions* of mass eigenvalues
  - ✓insensitive to underlying gaugings & deformation parameter
  - ✓all vacua are generically unstable

Future prospects

- explore other gaugings $\not\subset$ SL(8,**R**)
- construct inflationary models
- find higher dimensional flux vacua description

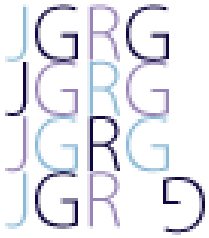

Yuki Watanabe, JGRG 22(2012)111216

"Gravity as the origin of spontaneous symmetry breaking in an inflationary universe"

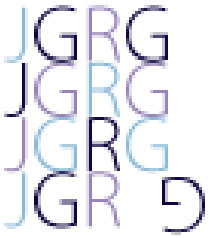

RESCEU SYMPOSIUM ON

GENERAL RELATIVITY AND GRAVITATION

JGRG 22



November 12-16 2012

Koshiba Hall, The University of Tokyo, Hongo, Tokyo, Japan



Gravity as the Origin of Spontaneous Symmetry Breaking in the Inflationary Universe

Research Center for the Early Universe (RESCEU), Univ. of Tokyo
Yuki Watanabe

arXiv: 12xx.xxxx
Work in progress with F. Bezrukov
PRD83, 043511 (2011)
PRD75, 061301(R) (2007) with E. Komatsu

The Inflationary Universe

- Inflation solves flatness, horizon, monopole problems of the big bang theory.
- At the same time, it provides the initial seed of density fluctuations that develop to cosmic structures like galaxies. Since the density fluctuations come from quantum vacuum fluctuations, they obey Gaussian statistics.
- From observations of CMB temperature anisotropy, the amplitude and tilt of the power-spectrum are given by $P_\zeta \sim 10^{-9}$, $n_s \sim 0.96$. It is consistent with Gaussian fluctuations: $-10 < f_{NL} < 74$.

The Standard Model Higgs

- The SM of elementary particles is composed of quarks, leptons, neutrinos, gauge bosons, and Higgs boson.
- The vev of Higgs gives rise to mass to all particles except photons, gluons, and neutrinos.
- From experiments of LHC, the SM Higgs seems to be detected. ATLAS: m ~ 126.5 GeV (5σ); CMS: m ~ 125.3 ± 0.6 GeV (4.9σ)

Is the inflaton Higgs?

- No, if gravity is minimally coupled to the Higgs.
  $P_\zeta \sim 10^4\,\lambda \sim 10^2$ too big!
- Yes, if gravity is *non-minimally* coupled to the Higgs.
  [Futamase & Maeda 89; Komatsu & Futamase 99; Bezrukov & Shaposhnikov 08; Barbinsky, Kamenshchik & Starobinsky 08; Germani & Kehagias 10; Germani & YW 11; Kamada, Kobayashi, Yamaguchi & Yokoyama 12; ...]
  $P_\zeta \sim \lambda/\xi^2 \sim 10^{-9}$ for $\xi \sim 5\times10^3$

$$\xi R h^2$$

- How to reheat the Universe? [YW & Komatsu 07; Bezrukov, Gorbunov & Shaposhnikov 09; Garcia-Bellido et al 09; YW 11]

Is the inflaton Higgs?

- No, if gravity is minimally coupled to the Higgs.
  $P_\zeta \sim 10^4 \lambda \sim 10^2$ too big!
- Yes, if gravity is *non-minimally* coupled to the Higgs.
  [Futamase & Maeda 89; Komatsu & Futamase 99; Bezrukov & Shaposhnikov 08; Barbinsky, Kamenshchik & Starobinsky 08; Germani & Kehagias 10; Germani & YW 11; Kamada, Kobayashi, Yamaguchi & Yokoyama 12; ...]
  $P_\zeta \sim 10^{-4} \lambda M^2/H^2 \sim 10^{-9}$ for $H/M \sim 50$

$$\frac{G^{\mu\nu}}{M^2}\partial_\mu h \partial_\nu h$$

- How to reheat the Universe? [YW & Komatsu 07; Bezrukov, Gorbunov & Shaposhnikov 09; Garcia-Bellido et al 09; YW 11]

Is the inflaton Higgs?

- No, if gravity is minimally coupled to the Higgs.
  $P_\zeta \sim 10^4\, \lambda \sim 10^2$ too big!
- Yes, if gravity is *non-minimally* coupled to the Higgs.
  [Futamase & Maeda 89; Komatsu & Futamase 99; Bezrukov & Shaposhnikov 08; Barbinsky, Kamenshchik & Starobinsky 08; Germani & Kehagias 10; Germani & YW 11; Kamada, Kobayashi, Yamaguchi & Yokoyama 12; ...]
  $P_\zeta \sim \lambda/\xi^2 \sim 10^{-9}$ for $\xi \sim 5\times10^3$

$$\xi R h^2$$

- How to reheat the Universe? → gravitational inflaton decay [YW & Komatsu 07; 08; Bezrukov, Gorbunov & Shaposhnikov 09; Garcia-Bellido et al 09; YW 11]

SM Higgs as the inflaton

$$\xi R h^2$$

- SM Higgs inflation [Bezrukov & Shaposhnikov 08; Barbinsky, Kamenshchik & Starobinsky 08; ...]
- *Minimalistic* to explain both CMB spectra and LHC data
- Higgs gives masses to gauge bosons and quarks. → Parametric resonance of W, Z happens during oscillations and reheats the Universe [Bezrukov, Gorbunov & Shaposhnikov 09; Garcia-Bellido et al 09]

Meta-stability of SM vacuum at high energy?

[J. Elias-Miro et al 12]

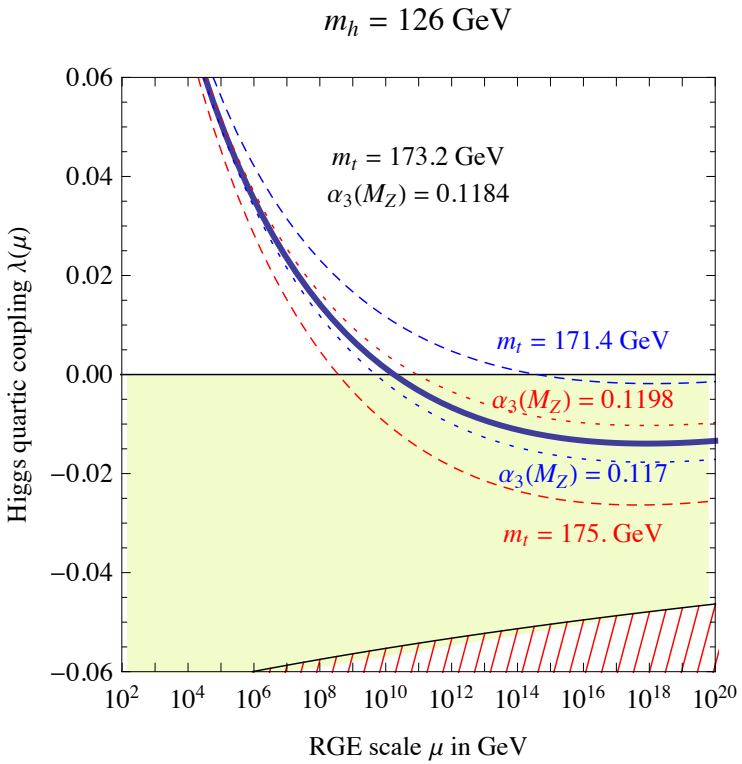

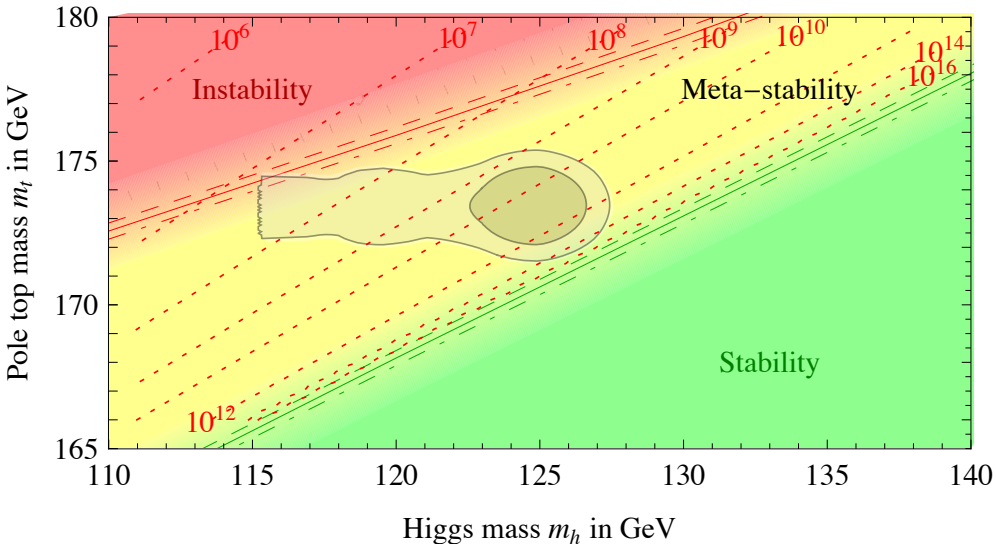

- RG running of λ is sensitive to top mass and strong coupling constant.
- Need additional d.o.f? Bosons change the running of λ positively while fermions do it negatively.

Any other classical condensates during Higgs inflation?

- Scalar condensate:
  - Heavy → integrated out; It may leave features on CMB spectra.
  - Light → frozen but affect inflationary dynamics later; It may become Dark Matter (if stable) after inflation.
- Vector condensate → anisotropy [M. Watanabe, Kanno & Soda 09; ...]
- Can they be curvatons?
- Do they change dynamics and reheating process?

"Spontaneous symmetry breakdown" due to gravity

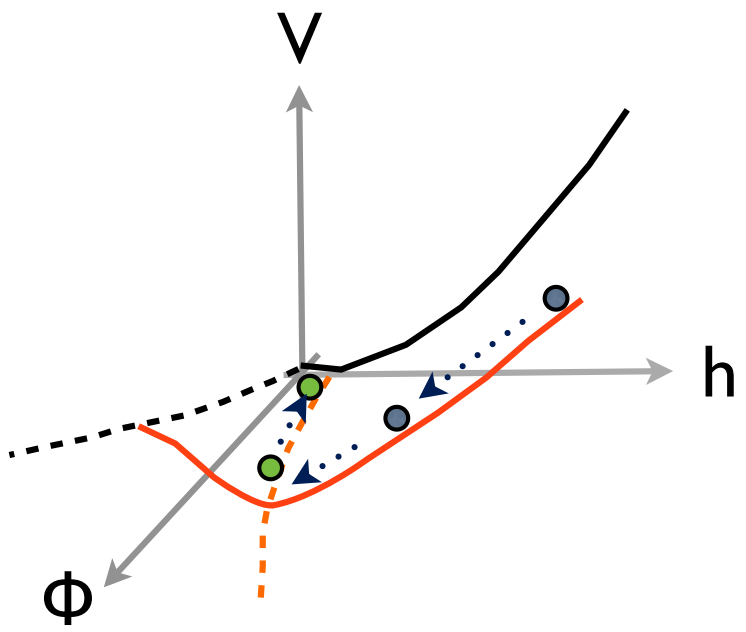

$$V \sim \lambda h^4 - \xi R h^2 + m^2\phi^2$$

$$v \sim \pm\sqrt{\frac{\xi R}{\lambda}} \sim \pm\sqrt{\frac{\xi}{\lambda}}\frac{m\phi_*}{M_p}$$

$$\sim 10^3 m \quad \text{for} \quad \phi_* \sim M_p$$

- Light scalar dominates energy density after inflation. → Higgs acquires non-trivial vev due to *negative mass term*. It diminishes the amplitude of Higgs oscillations, and reheating proceeds perturbatively.

Reheating with light scalar condensates

- Decay channels: Φ, W, Z, top → kinematically allowed? If not, Higgs decays mainly into Φ (tree), γ, gluon (loop) gravitationally. [YW 11]

$$\Gamma(h \to WW) \sim \Gamma(h \to ZZ) \sim g_2^2 m_W \qquad \Gamma(h \to \bar{t}t) \sim y_t^2 m_t$$

$$m_i \sim g_i \sqrt{|\hat{h}| M_p/\xi} \sim g_i v \qquad m_{\hat{h}} \sim \sqrt{\lambda} M_p/\xi$$

$$T_{\rm reh} \sim 0.1 \sqrt{\Gamma M_p}$$

- Light scalars become Dark Matter if they are stable. If unstable, they must decay before BBN.

Gravitational inflaton decay [YW 11]

$$g_{\mu\nu}(x) \to \hat{g}_{\mu\nu}(x) = \Omega^2(x) g_{\mu\nu}(x)$$
$$\approx g_{\mu\nu} + g_{\mu\nu}\frac{F(v)\sigma}{M_{Pl}^2}$$

$$T^{\mu}_{m\ \mu}[\hat{g}_{\mu\nu}] = -\frac{\Omega}{\sqrt{-\hat{g}}}\frac{\delta S_m[\hat{g}_{\mu\nu}]}{\delta\Omega}$$

Conformal invariance: local scale invariance
Mass term explicitly breaks scale invariance.

Conformal invariant field:
- Massless spin-½ fields
- Conformally coupled massless spin-0 fields
- Gauge fields (classical level)

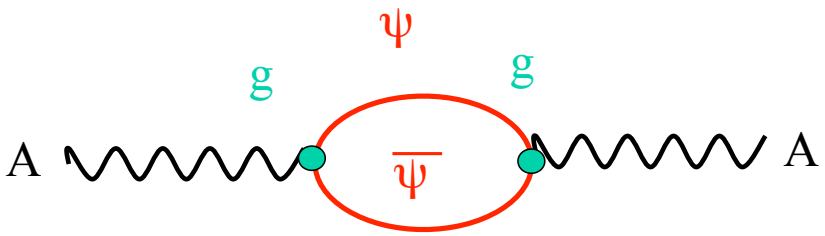

$$\mathcal{L}_{\rm int} = \sqrt{-g}\frac{F_1(v)\sigma}{2M_{Pl}^2}T^{\mu}_{{\rm m}\mu}$$

$$T^{\mu}_{{\rm m}\mu} = \sum_{s=1}^{N_\chi} 2\left[-(D_\mu\chi_s)^* D^\mu\chi_s + 2U(\chi_s^*\chi_s)\right] + \sum_{f=1}^{N_\psi} m_f\bar{\psi}_f\psi_f + \frac{\beta_h(g)}{2g}F_{\mu\nu}F^{\mu\nu}$$

at the classical level

Gauge trace anomaly: lowest order decay channel to photons

two-photon decay of the Higgs

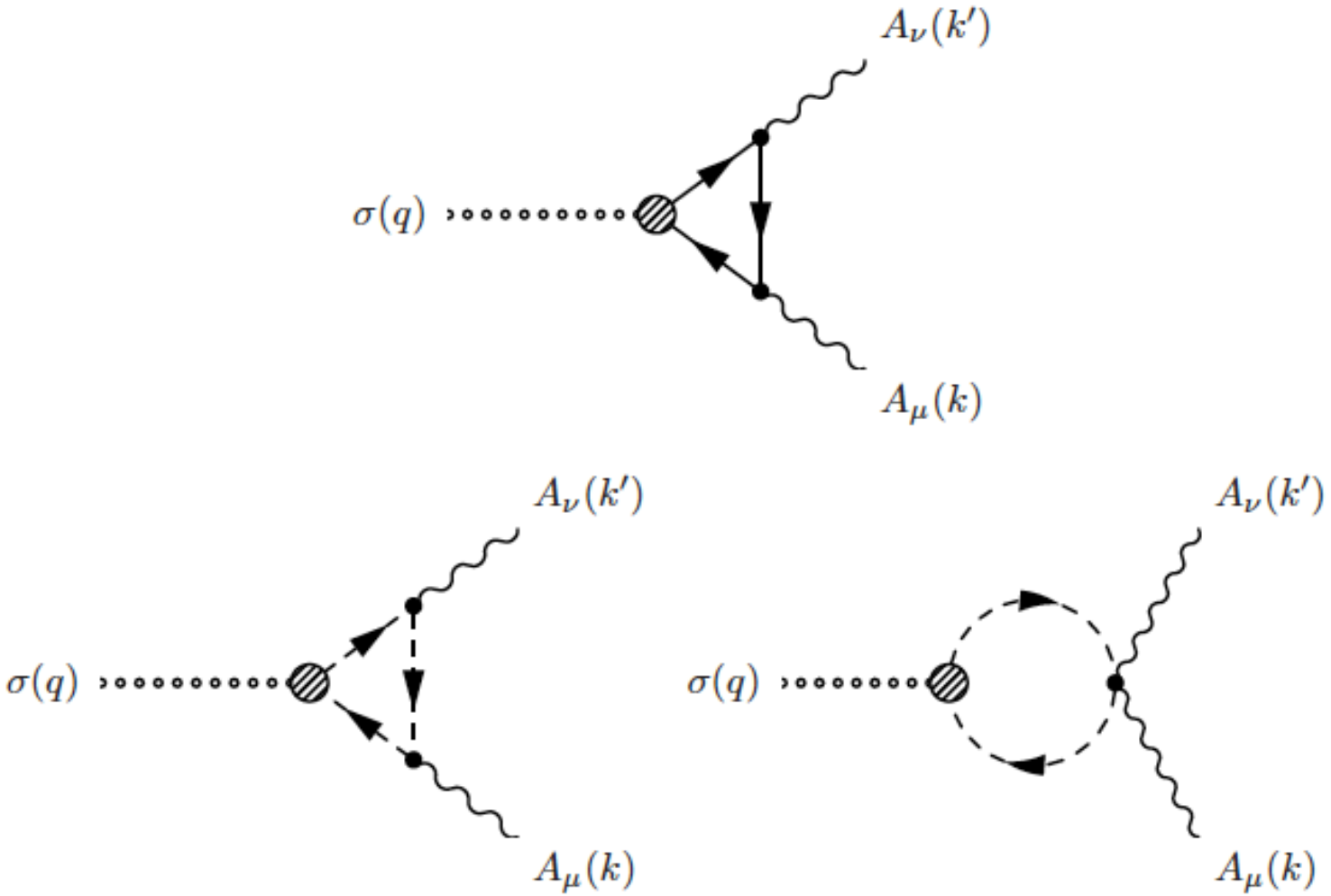

Summery of decay rates

Femions

$$\Gamma(\sigma \to \bar{\psi}\psi) \simeq \frac{N_\psi [F_1(v)]^2 m_\sigma m_\psi^2}{32\pi M_{Pl}^4}$$

Scalars

$$\Gamma(\sigma \to \chi_+\chi_-) \simeq \frac{N_\chi [F_1(v)]^2 m_\sigma^3}{64\pi M_{Pl}^4}$$

Probably most efficient.

Gauge fields

$$\Gamma(\sigma \to 2A_\mu) = \frac{\alpha^2 [F_1(v)]^2 m_\sigma^3}{1024\pi^3 M_{\rm Pl}^4} \left| \sum_{f=1}^{N_\psi} 2I_f\left(\frac{m_\sigma^2}{m_f^2}\right) + \sum_{s=1}^{N_\chi}\left(2+\frac{m_\sigma^2}{m_s^2}\right) I_s\left(\frac{m_\sigma^2}{m_s^2}\right)\right|^2$$

*Pre*heating with light scalar condensates?

- Gravitationally induced couplings cannot be so large since they are essentially Planck-suppressed.
- Direct couplings to the scalar are assumed to be small. Of course, yes in principle.

Conclusions and future work...

- SM Higgs inflation can be saved by additional scalars.
- However, *SSB due to gravity* may occur after inflation if the scalar dominates energy density.
- Reheating occurs naturally.
- Works left: Dark Matter abundance, Baryogenesis, ...

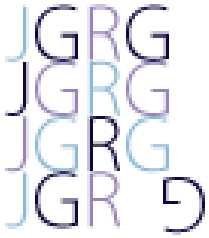

Shinpei Kobayashi, JGRG 22(2012)111217

"Fuzzy objects in noncommutative geometry and their applications"

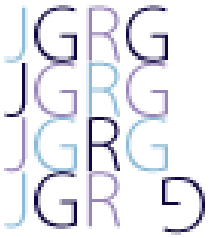

RESCEU SYMPOSIUM ON

GENERAL RELATIVITY AND GRAVITATION

JGRG 22



November 12-16 2012

Koshiba Hall, The University of Tokyo, Hongo, Tokyo, Japan



Fuzzy Objects in Noncommutative Geometry and Their Applications

Shinpei Kobayashi
(Gunma National College of Technology)

2012/11/12, JGRG22 @ RESCEU, University of Tokyo

Motivation

- Resolution of singularity
- String inspired
  - non-BPS D2/D0-system
  - 2-dimensional space with constant magnetic flux
- (an effective theory of) quantum gravity

Realization of Noncommutativity

- Noncommutativity between space coordinates

$$[x, y] = i\theta, \quad \theta \quad : \text{constant parameter}$$

- a realization: Wick-Voros product

$$(f \star g)(z, \bar{z}) = \exp\left(\frac{\partial}{\partial \bar{z}'}\frac{\partial}{\partial z''}\right) f(z', \bar{z}')g(z'', \bar{z}'')\Big|_{z'=z''=z}$$



$$[z, \bar{z}] = z \star \bar{z} - \bar{z} \star z = 1 \qquad \left(z = \frac{x + iy}{\sqrt{2\theta}}, \ \bar{z} = \frac{x - iy}{\sqrt{2\theta}}\right)$$

Field Theory on noncommutative space

commutative:

$$S = \int dt d^2x \left(\partial_z \phi \partial_{\bar{z}} \phi + \frac{m}{2} \phi^2 + \cdots \right)$$



noncommutative:

$$S = \int dt d^2x \left(\partial_z \phi \star \partial_{\bar{z}} \phi + \frac{m}{2} \phi \star \phi + \cdots \right)$$

Fuzzy Objects

Nontrivial Solutions
in Noncommutative Geometry

Noncommutative Solitons

- scalar field theory on NC plane: GMS solitons
  [Gopakumar- Minwalla- Strominger, Kraus-Larsen, …]

$$E = \int_D d^2 z V_\star(\Phi)$$

$$V_\star(\Phi) = \frac{b_2}{2}\Phi \star \Phi + \frac{b_3}{3}\Phi \star \Phi \star \Phi + \cdots$$

- circular symmetric, connection to D-branes

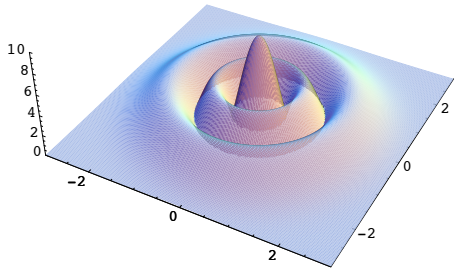

Weyl-Wigner Correspondence

function $f(\bar{z}, z) = \sum_{n=0}^{\infty} f_{mn}^{\mathrm{Tay}} \bar{z}^m z^n$

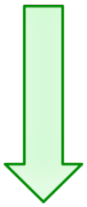

Weyl projection

operator $\hat{f}(\hat{a}^\dagger, \hat{a}) = \sum_{n=0}^{\infty} f_{mn}^{\mathrm{Tay}} \hat{a}^{\dagger m} \hat{a}^n$

Weyl-Wigner Correspondence

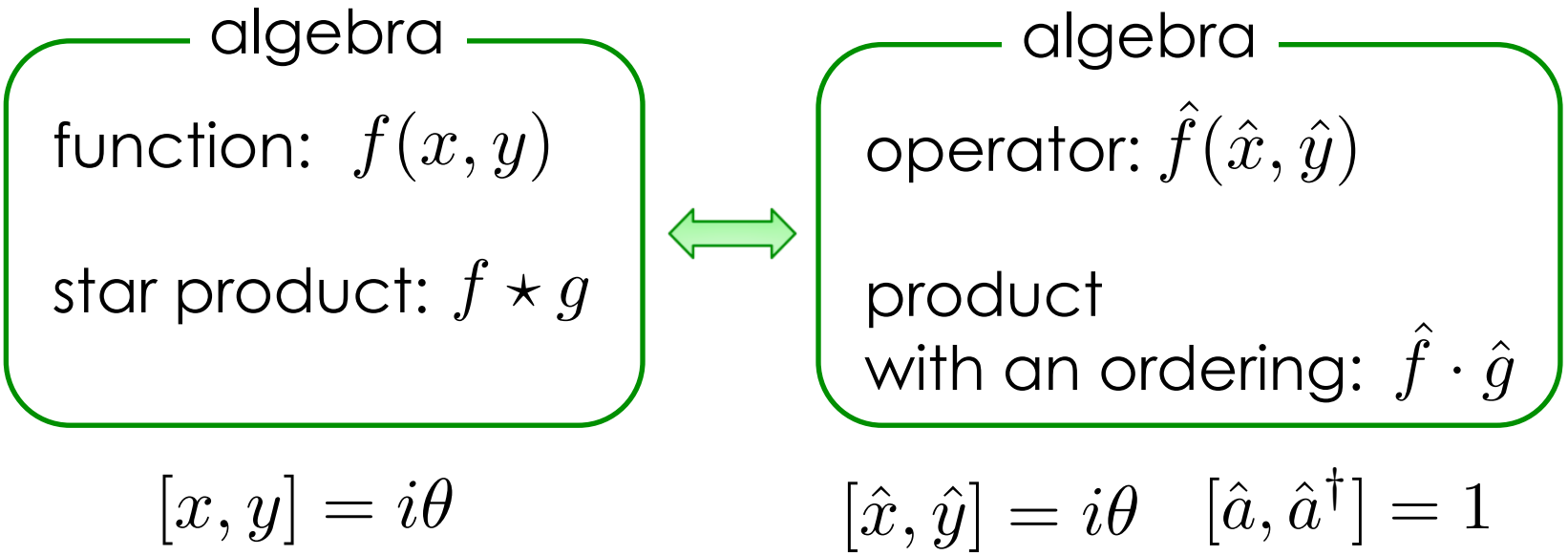

operators which act
on the Fock space
of a harmonic oscillator

Weyl-Wigner Correspondence

function $f(\bar{z}, z) = \sum_{n=0}^{\infty} f_{mn}^{\mathrm{Tay}} \bar{z}^m z^n$

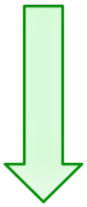

Weyl projection

operator $\hat{f}(\hat{a}^\dagger, \hat{a}) = \sum_{n=0}^{\infty} f_{mn}^{\mathrm{Tay}} \hat{a}^{\dagger m} \hat{a}^n$

Weyl-Wigner Correspondence

function $f(\bar{z}, z) = \langle z \,|\, \hat{f} \,|\, z \rangle$

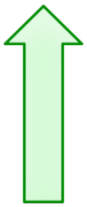

inverse Weyl projection

$\hat{a} \,|\, z \rangle = z \,|\, z \rangle$: coherent state

operator $\hat{f}(\hat{a}^\dagger, \hat{a}) = \sum_{n=0}^{\infty} f_{mn}^{\mathrm{Tay}} \hat{a}^{\dagger m} \hat{a}^n$

Weyl-Wigner Correspondence

In operator formalism:

$$\hat{N}\,|\,n\,\rangle = n\,|\,n\,\rangle$$

$$\hat{a} = \frac{\hat{x} + i\hat{y}}{\sqrt{2\theta}} \quad \hat{a}^\dagger = \frac{\hat{x} - i\hat{y}}{\sqrt{2\theta}} \quad \hat{N} = \hat{a}^\dagger \hat{a} = \frac{\hat{x}^2 + \hat{y}^2}{2\theta}$$

$$\mathcal{H} = \mathrm{span}\{|\,0\,\rangle, |\,1\,\rangle, |\,2\,\rangle, \cdots\}$$

Projection operators as NC solitons

[GMS (2000)]

- EOM: $0 = \dfrac{\partial V_\star}{\partial \Phi} = b_2 \Phi + b_3 \Phi \star \Phi + b_4 \Phi \star \Phi \star \Phi + \cdots$
- non-trivial sln: $\Phi = \lambda_* p_n(z, \bar{z})$ with $p_n^2(z, \bar{z}) = p_n(z, \bar{z})$



projection operator
$\hat{p}_n = |\, n \,\rangle \langle\, n \,|$



$$p_n(r) = \langle\, z \,|\, n \,\rangle \langle\, n \,|\, z \,\rangle = e^{-\frac{r^2}{2\theta}} \frac{r^{2n}}{n!(2\theta)^n}$$

:circular symmetric

Fuzzy Disc [Lizzi, Vitale, Zampini (2003)]

- Def.: finite dim. truncation of a noncommutative plane

$$\mathcal{H}_N = \mathrm{span}\{|\,0\,\rangle, |\,1\,\rangle, |\,2\,\rangle, \cdots, |\,N-1\,\rangle\}$$

- Two parameters:
  - noncommutativity: θ
  - fuzzyness : N
- applications:
  - matrix model
  - quantum Hall effect

A Fuzzy Disc
(*N=10, θ =1*)

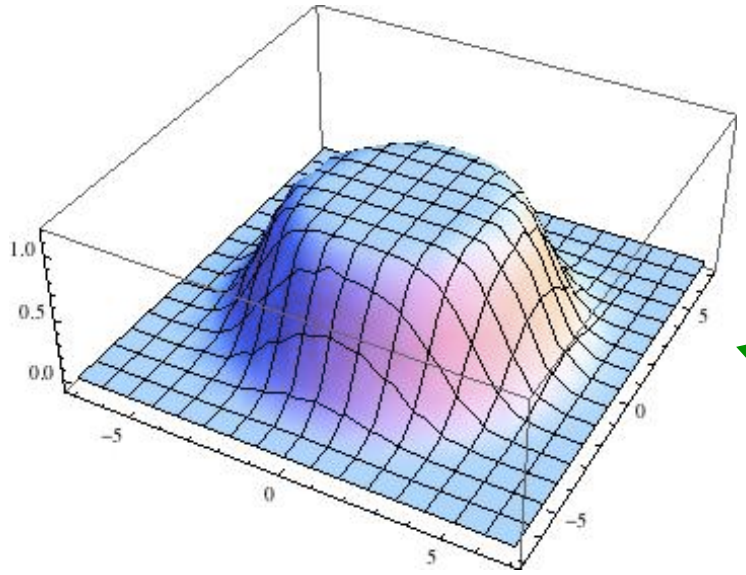

$$\hat{\mathcal{A}}_{10} = \hat{P}_{10}\hat{\mathcal{A}}\hat{P}_{10}$$

$$\hat{P}_{10} = \hat{p}_0 + \hat{p}_1 + \cdots + \hat{p}_9$$

$$p_0 + p_1 + \cdots + p_9 = \sum_{n=0}^{9} e^{-\frac{r^2}{2\theta}} \frac{r^{2n}}{n!(2\theta)^n}$$

GMS solitons and fuzzy disc

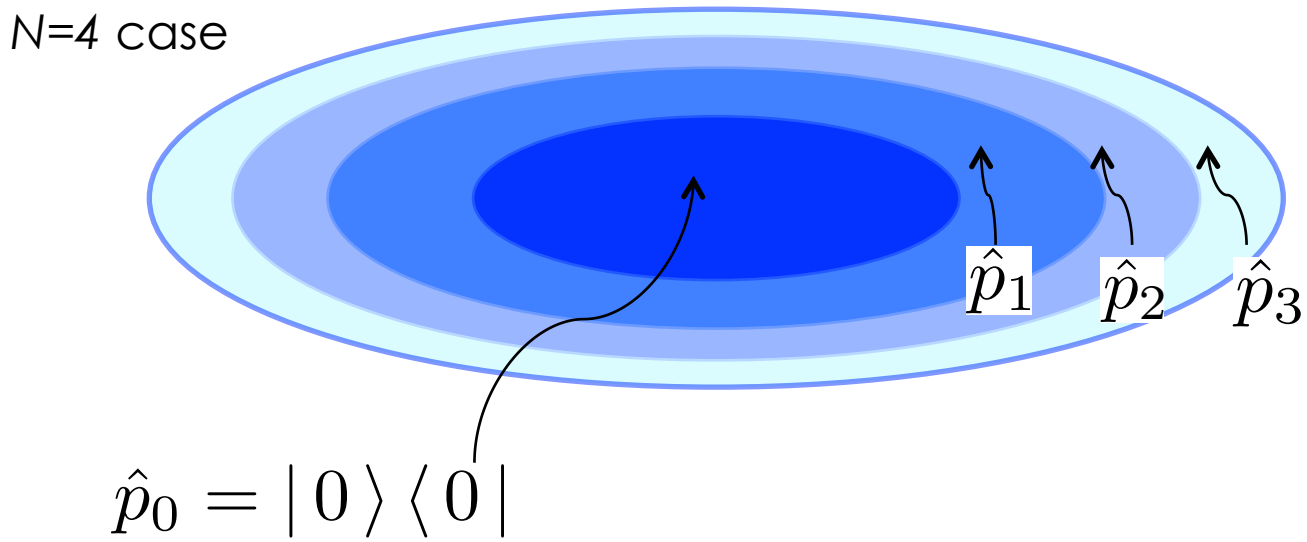

Another orthonormal basis : angle states?

- number basis: concentric cutting of space
  - $\hat{N}$ ~ radius $\quad (\hat{N} \sim \sqrt{\hat{x}^2 + \hat{y}^2})$

- another basis: radial cutting of space
  - $\hat{\varphi}$ ~ angle

Angles in the fuzzy disc

SK-Asakawa, arXiv:1206.6602

Angle Operator and States

- The angle operator: $\hat{\varphi} = \sum_{m=0}^{N-1} \varphi_m \, | \, \varphi_m \, \rangle \langle \, \varphi_m \, |$

with help of Pegg-Barnett phase operator

- Eigen states of the angle operator: $\hat{\varphi} \, | \, \varphi_m \, \rangle = \varphi_m \, | \, \varphi_m \, \rangle$
- Relation to the number state $| \, \varphi_m \, \rangle = \frac{1}{\sqrt{N}} \sum_{n=0}^{N-1} e^{in\varphi_m} \, | \, n \, \rangle$

- Orthonormality: $\langle \, \varphi_m \, | \, \varphi_n \, \rangle = \delta_{mn}$
- Angular projection operators:

$$\hat{\pi}_m = | \, \varphi_m \, \rangle \langle \, \varphi_m \, |$$

→ angular "delta function" peaked at $\varphi_m = \frac{2\pi}{N} m$

Two descriptions of fuzzy disc

- baum-kuchen vs shortcake

$$N = 4,\ \mathcal{H}_4 = \{|0\rangle, |1\rangle, |2\rangle, |3\rangle\}$$

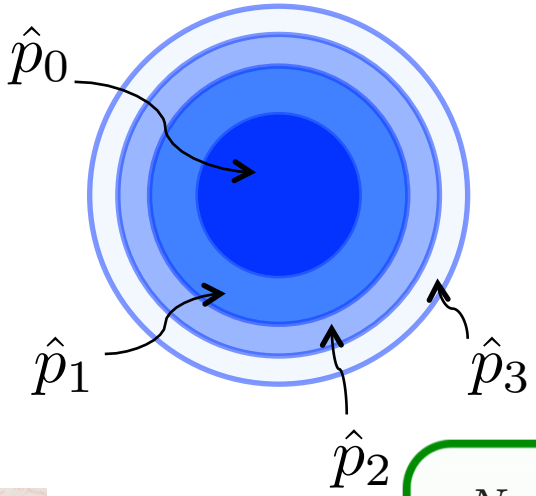

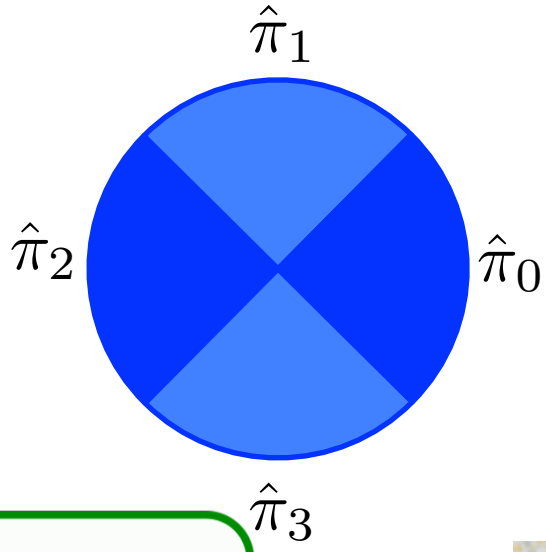

$$\sum_{n=0}^{N-1} \hat{p}_n = \sum_{m=0}^{N-1} \hat{\pi}_m$$





angular projection operators

$$\pi_k^{(N)}(r,\varphi) = \frac{1}{N}\sum_{m,n=0}^{N-1} e^{-\frac{r^2}{2\theta}} \frac{r^{m+n}}{\sqrt{m!n!(2\theta)^{m+n}}} e^{-i(m-n)(\varphi-\varphi_k)}$$

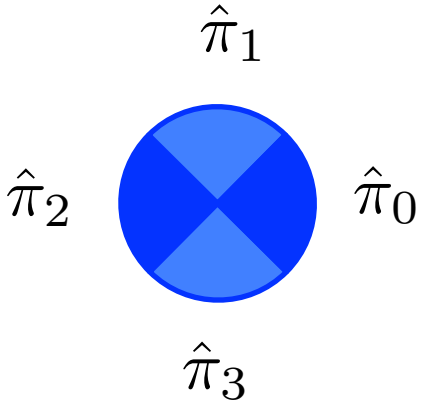

N=4 case

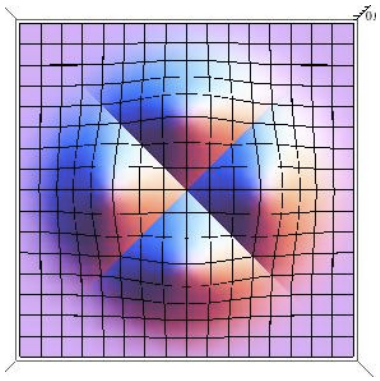

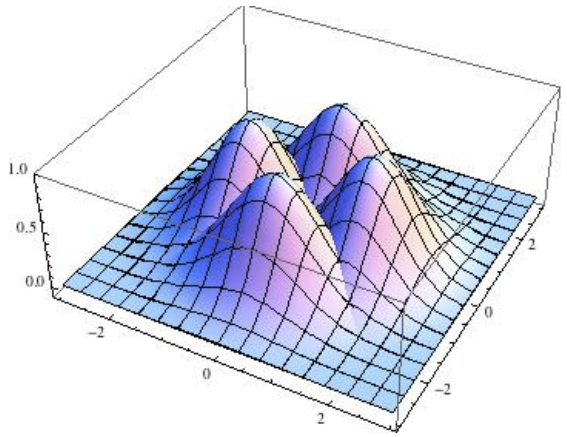

not concentric, but fan-shaped, like pieces of cake

Other fuzzy objects: e.g.) fuzzy Annulus



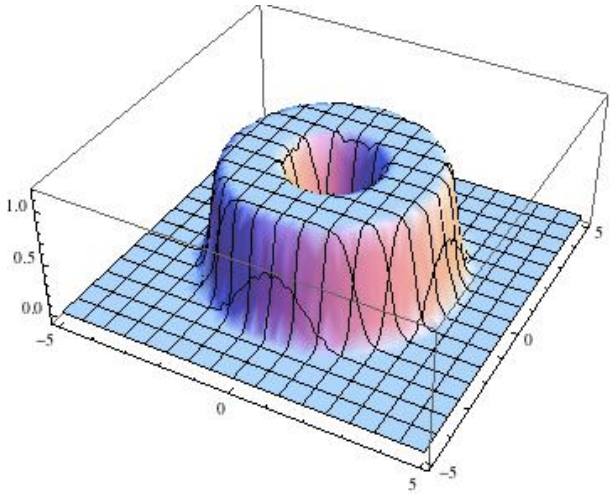

$$\hat{P}_N^M := \hat{p}_M + \hat{p}_{M+1} + \cdots + \hat{p}_{M+N-1}$$

any set of N orthonormal operators is allowed for truncation

Noncommutative Solitons as D0-branes

- scalar field on the NC plane
  = tachyon filed on a non-BPS D2-brane
- The solution $\Phi = \lambda_* \hat{p}_n$
  = a D0-brane (rank $\hat{p}_n = 1 \rightarrow$ same tension)

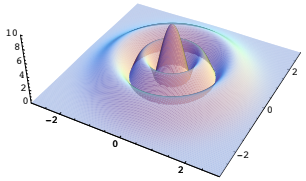

- Same thing can be said to our case:
  the solution $\Phi = \lambda_* \hat{\pi}_m$ also can be seen as a D0-brane with very different shape (fan-shaped)

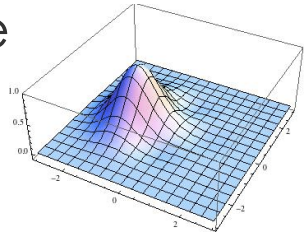

- Commutative limit (with Nθ fixed),
  angular NC soliton becomes thinner and thinner
  (A D0-brane is twisted into a string!)

Angular NC Solitons in Gravity

$$S = -\frac{\Lambda}{\kappa^2}\int dt d^2z\ E^\star \qquad E^\star = \det{}_\star E = \frac{1}{3!}\epsilon^{\mu\nu\rho}\epsilon_{abc}E^a_\mu \star E^b_\nu \star E^c_\rho$$

$$\epsilon^{\mu\nu\rho}\epsilon_{abc}\{E^b_\nu, E^c_\rho\}_\star = 0$$

$$E^a_\mu = \begin{pmatrix} E^0_0 & 0 & 0 \\ 0 & E^1_1 & 0 \\ 0 & 0 & E^2_2 \end{pmatrix} = \begin{pmatrix} \alpha_0\pi_0^{(N)} & 0 & 0 \\ 0 & \alpha_1\pi_1^{(N)} & 0 \\ 0 & 0 & \alpha_2\pi_2^{(N)} \end{pmatrix}$$

$$ds^2 = -\alpha_0^2\pi_0^{(3)}dt^2 + \alpha_1^2\pi_1^{(3)}dx^2 + \alpha_2^2\pi_2^{(3)}dy^2$$

$$\pi_k^{(3)}(r,\varphi) = \frac{1}{3}e^{-r^2/\theta}\left[1 + \frac{2r}{\theta^{1/2}}\cos(\varphi - \varphi_k^{(3)}) + \frac{r^2}{\theta}\left\{1 + \sqrt{2}\cos[2(\varphi - \varphi_k^{(3)})]\right\} + \frac{\sqrt{2}r^3}{\theta^{3/2}}\cos(\varphi - \varphi_k^{(3)}) + \frac{r^4}{\theta^2}\right]$$

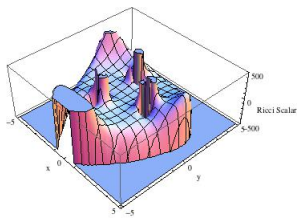

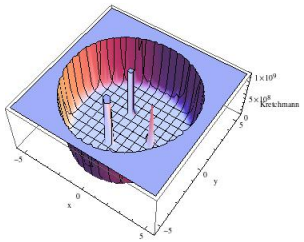

Experiment with laser

- Gaussian beam

$$I(r,z) = \frac{|E(r,z)|^2}{2\eta} = I_0 \left(\frac{w_0}{w(z)}\right)^2 \exp\left(\frac{-2r^2}{w^2(z)}\right) \quad ,$$

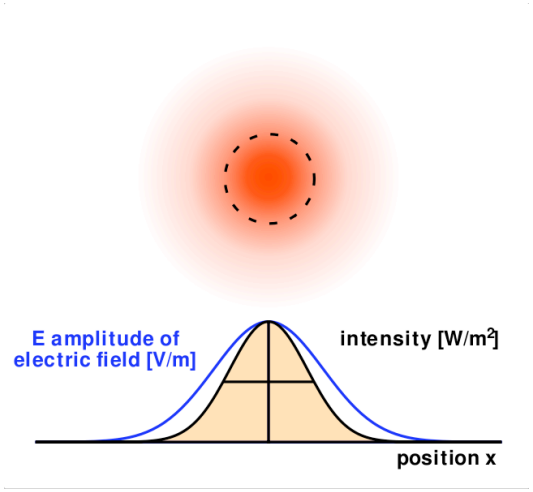

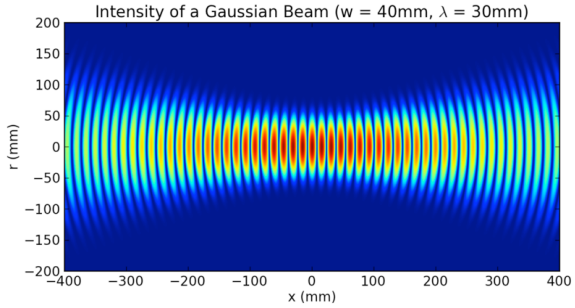

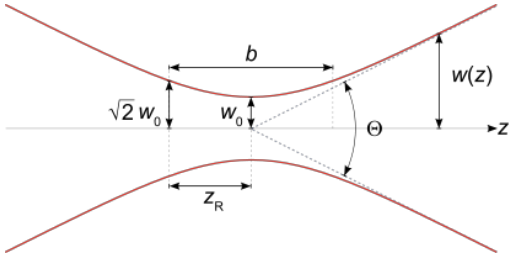

Experiment with laser

- Laguerre-Gaussian beam

$$u(r,\phi,z) = \frac{C_{lp}^{LG}}{w(z)}\left(\frac{r\sqrt{2}}{w(z)}\right)^{|l|}\exp\left(-\frac{r^2}{w^2(z)}\right)L_p^{|l|}\left(\frac{2r^2}{w^2(z)}\right)\exp\left(ik\frac{r^2}{2R(z)}\right)\exp(il\phi)\exp\left[-i(2p+|l|+1)\zeta(z)\right],$$

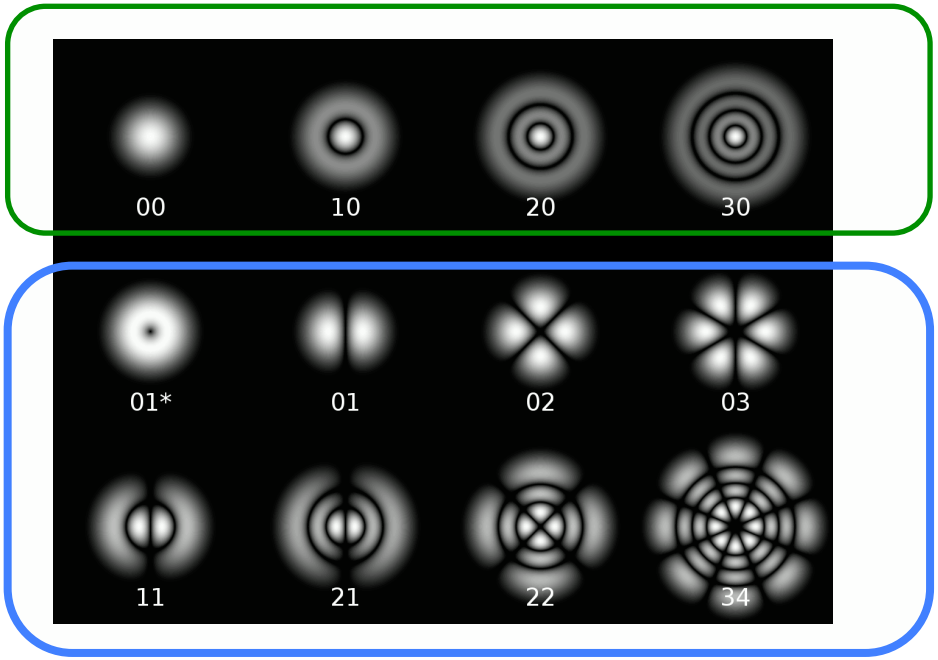

GMS solitons

angular NC solitons

Noncommutative Solitons with Time-Dependence

Weyl-Wigner Correspondence

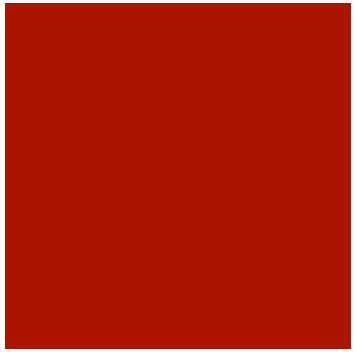

algebra

function: $f(x,y)$

star product: $f \star g$

$\Leftrightarrow$

algebra

operator: $\hat{f}(\hat{x},\hat{y})$

product
with an ordering: $\hat{f} \cdot \hat{g}$

$[x,y] = i\theta$

$[\hat{x},\hat{y}] = i\theta \;\; [\hat{a},\hat{a}^\dagger] = 1$

operators which act
on a harmonic oscillator

no restriction as long as $[\hat{x},\hat{y}] = i\theta$

Noncommutative Solitons with Time-Dependence

- Time-dependent Harmonic Oscillator

e.g.,

$$\hat{H}(x,p,t) = \frac{\hat{p}^2}{2m(t)} + \frac{1}{2}m(t)\omega^2(t)\hat{x}^2$$

$\rightarrow$ we can solve this system analytically by the LR method

Lewis-Reisenfeld Method

- Time-dependent Schroedinger equation

$$i\hbar\frac{\partial}{\partial t}\psi = \hat{H}\psi$$

- Invariant operator $\hat{I}$

$$\frac{d\hat{I}}{dt} = \frac{\partial\hat{I}}{\partial t} + \frac{1}{i\hbar}[\hat{I}, \hat{H}] = 0$$

- Eigenvalue problem

$$\hat{I}\phi_n(x,p,t) = \lambda_n\phi_n(x,p,t)$$

$$\begin{cases} \psi(x,p,t) = e^{i\epsilon(t)}\phi(x,p,t) \\ \hbar\dot{\epsilon} = \langle\, \phi_n(t) \,|\left(i\hbar\frac{\partial}{\partial t} - \hat{H}\right)|\, \phi_n(t)\,\rangle \end{cases}$$

Time-Dependent NC Solitons

- general, quadratic, time-dependent Hamiltonian

[Choi-Gweon (2004)]

→ apply to NC solitons

$$\hat{H}(\hat{x},\hat{y},t)$$
$$= A(t)\hat{x}^2 + B(t)(\hat{x}\hat{y}+\hat{y}\hat{x}) + C(t)\hat{y}^2 + D(t)\hat{x} + E(t)\hat{y} + F(t)$$

- creation and annihilation operator

$$\hat{a} = \sqrt{\frac{1}{\theta k^{1/2}}}\left\{\left[\frac{\sqrt{k}}{2\rho} + i\frac{2B\rho-\dot{\rho}}{2A}\right](\hat{x}-x_p(t)) + i\rho(\hat{y}-y_p(t))\right\}$$

$$\hat{a}^\dagger = \sqrt{\frac{1}{\theta k^{1/2}}}\left\{\left[\frac{\sqrt{k}}{2\rho} - i\frac{2B\rho-\dot{\rho}}{2A}\right](\hat{x}-x_p(t)) - i\rho(\hat{y}-y_p(t))\right\}$$

they satisfy $[\hat{a},\hat{a}^\dagger] = 1$

Time-Dependent NC Solitons

- time-dependent circular symmetric solitons [SK, in progress]

$$|\,\phi_n, t\,\rangle\,\langle\,\phi_n, t\,|$$

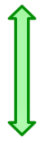

$$e^{-|\zeta(t)|^2}\,\frac{|\zeta(t)|^2}{n!}$$

$$|\zeta(t)|^2 = \frac{1}{\theta k^{1/2}}\left\{\frac{k}{4\rho^2}(x - x_p(t))^2 + \left[\left(\frac{2B\rho - \dot{\rho}}{2A}\right)(x - x_p(t)) + \rho\,(y - y_p(t))\right]^2\right\}$$

Time-Dependent NC Solitons

[SK, in progress]

e.g., Caldirola-Kanai oscillator

$$\hat{H} = e^{\gamma t}\hat{x}^2 + e^{-\gamma t}\hat{y}^2$$

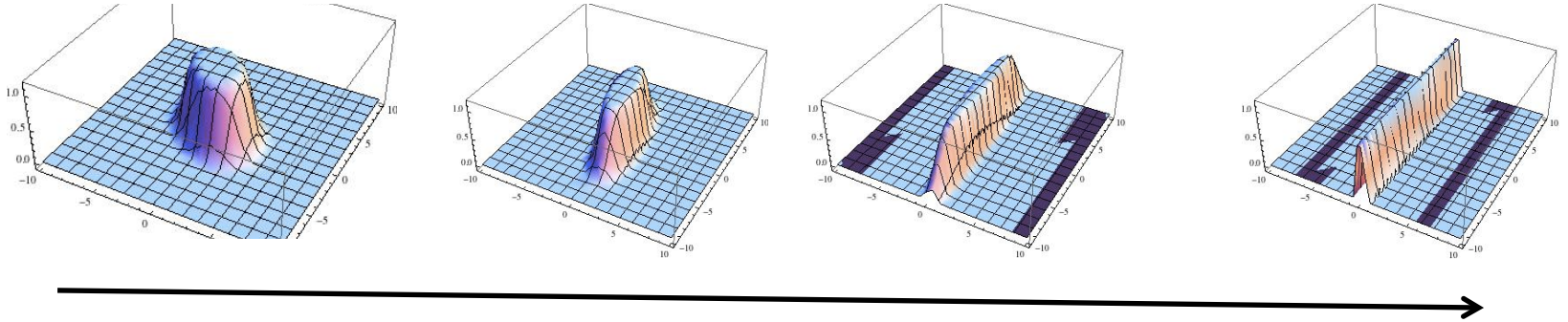

$$t = 1/\gamma$$

Summary

- The fuzzy disc:
  - a disc-shaped, finite region in the NC plane
  - a fuzzy approximation by θ
- Introduction of angles to the fuzzy disc
  - angle projection operator and angle states
  - directly relates the boundary to the bulk
- Application
  - angular NC scalar solitons & fan-shaped D-branes
  - angular NC gravitational solitons
  - laser physics
- Time-dependent noncommutative solitons exist

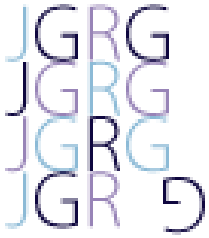

Hongsheng Zhang, JGRG 22(2012)111218

"Critical exponents of gravity with quantum perturbations"

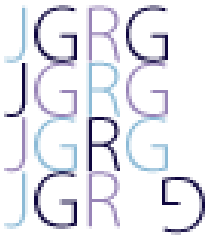

RESCEU SYMPOSIUM ON

GENERAL RELATIVITY AND GRAVITATION

JGRG 22



November 12-16 2012

Koshiba Hall, The University of Tokyo, Hongo, Tokyo, Japan



Critical exponents of gravity with quantum perturbations

张宏升

Center for Astrophysics,

Shanghai Normal University

Prime ref: H Zhang (张宏升), X Li, arXiv:1208.0106

Outline

- 1. Introduction to thermo dynamical gravity
- 2. Critical exponents of RN-AdS black hole
- 3. Quantum perturbations included

Introduction to thermo dynamical gravity

- Temperature: $1/(8\pi M)$
- Entropy: A/4
- Energy: M
- Event horizon: $r_+=2M$, $A=4\pi r_+$

Van der Waals-Maxwell gas-liquid system

Equation of state

$$p = \frac{RT}{v - b} - \frac{a}{v^2}$$

Critical point

$$\left(\frac{\partial p}{\partial v} \right)_T = 0,$$

$$\left(\frac{\partial^2 p}{\partial v^2} \right)_T = 0$$

Critical isotherm

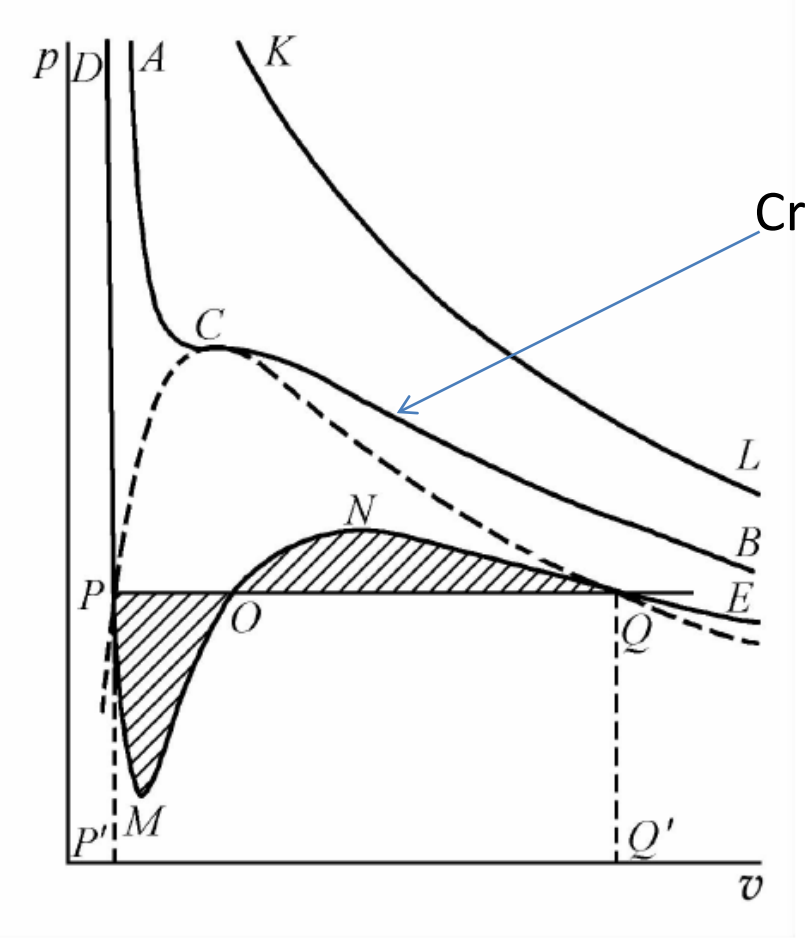

Critical isotherm

- Critical exponents of RN black hole

RN-AdS space time

$$ds^2 = -f(r)dt^2 + f(r)^{-1}dr^2 + r^2 d\Omega^2$$

$$f(r) = 1 - \frac{2M}{r} + \frac{q^2}{r^2} + \frac{r^2}{l^2}$$

$$2M = r_+ + r_- + \frac{r_+^4 - r_-^4}{l^2(r_+ - r_-)}$$

$$q^2 = r_+ r_- \left(1 + \frac{r_+^3 - r_-^3}{l^2(r_+ - r_-)}\right).$$

Entropy, temperature, and potential

$$S = \frac{1}{4}A = \pi r_+^2$$

$$T = \left(\frac{\partial M}{\partial S}\right)_q = \frac{(r_+ - r_-)(l^2 + 3r_+^2 + 2r_+r_- + r_-^2)}{4\pi l^2 r_+^2}$$

$$\phi = \left(\frac{\partial M}{\partial q}\right)_S = \frac{\sqrt{r_+r_-[1 + (r_+^2 + r_+r_- + r_-^2)/l^2]}}{r_+} = \frac{q}{r_+}$$

Equation of state of RN-AdS

$$4\pi T q\phi = \phi^2 - \phi^4 + \lambda q^2$$

$$\left(\frac{\partial q}{\partial \phi}\right)_T = 0$$

$$\left(\frac{\partial^2 q}{\partial \phi^2}\right)_T = 0$$

$$q \longleftrightarrow p(\text{pressure}), \qquad \phi \longleftrightarrow v(\text{volume})$$

Critical point

$$T_c = \frac{\sqrt{2\lambda}}{3\pi}, \qquad q_c = \frac{1}{\sqrt{12\lambda}}, \qquad \phi_c = \frac{1}{\sqrt{6}}.$$

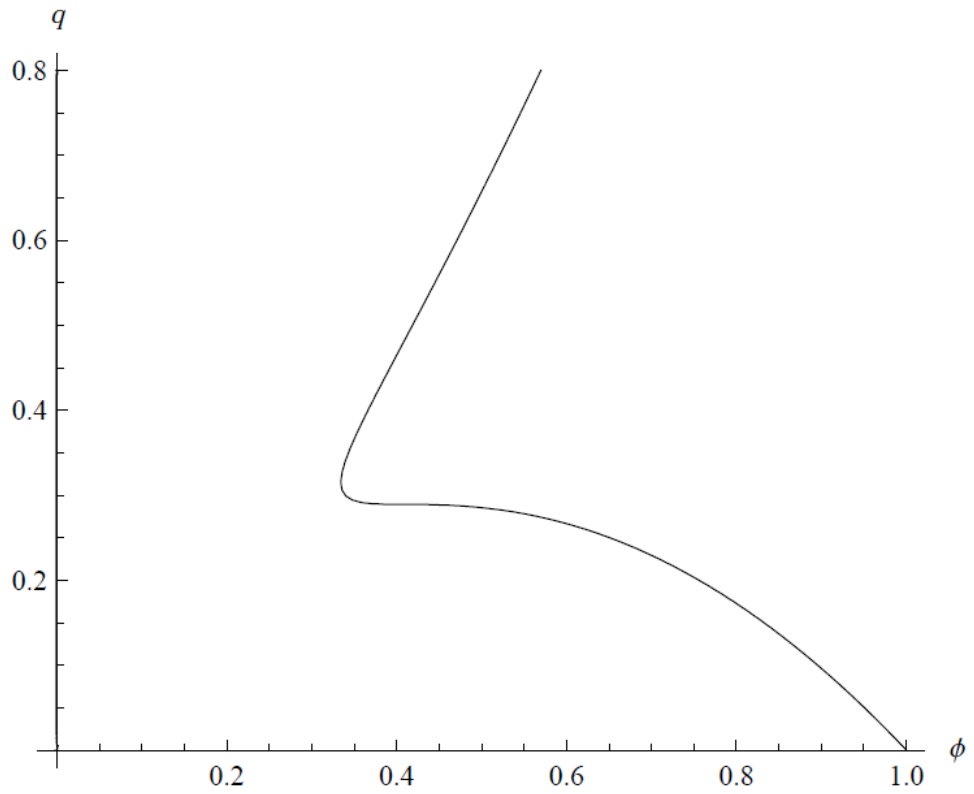

Critical exponents

Definition

$$
\begin{aligned}
&(1) \quad q - q_c \sim |\phi - \phi_c|^{\delta} \quad (T = T_c),\\
&(2) \quad \phi - \phi_c \sim |T - T_c|^{\beta} \quad (q = q_c),\\
&(3) \quad C_q \sim |T - T_c|^{-\alpha} \quad (q = q_c),\\
&(4) \quad \kappa_T \sim |T - T_c|^{-\gamma} \quad (q = q_c).
\end{aligned}
$$

$$
\delta = 3, \quad \beta = 1/3, \quad \alpha = 2/3, \quad \gamma = 2/3.
$$

N-dimensional case

- For n-dim RN-AdS black hole, the critical exponents take the same values as that of 4-dim case, ie,

$$\delta = 3, \quad \beta = 1/3, \quad \alpha = 2/3, \quad \gamma = 2/3.$$

C Niu, Y Tian, X Wu, Phys.Rev.D85:024017,2012

- This is a distinctive property of MFT(mean field theory).

- Quantum perturbations included

Temperature correction of Hawking radiation

$$T_{qu} = T\left(1 - \frac{k}{M^2}\right)$$

This equation includes the total effects of the quantum perturbations to all orders.

R. Banerjee and B. R. Majhi, JHEP 0806, 095 (2008)

$$T_{qu} = \left(1 - \frac{k}{M^2}\right)\left(\phi^2 - \phi^4 + \lambda q^2\right)$$

Critical point for corrected temperature

$$\left(\frac{\partial q}{\partial \phi}\right)_T = 0, \qquad \left(\frac{\partial^2 q}{\partial \phi^2}\right)_T = 0$$

$$\frac{q\left\{q^2\left(-\phi^2+3\phi^4+\lambda q^2\right)\left(3\phi^2+3\phi^4+\lambda q^2\right)^3-36k\phi^6\left[-6\phi^6+15\phi^8+14\lambda\phi^2q^2+7\lambda^2q^4+\phi^4\left(3-6\lambda q^2\right)\right]\right\}}{\phi q^2\left(-\phi^2+\phi^4+\lambda q^2\right)\left(3\phi^2+3\phi^4+\lambda q^2\right)^3+36k\phi^7\left[3\phi^8-14\lambda\phi^2q^2-7\lambda^2q^4-\phi^4\left(3+4\lambda q^2\right)\right]}=0$$

Values of critical quantities

- A special method to solve the above equation.
- The essential condition is that two roots of degenerates to one. Under this condition, and

$$\phi^2 \equiv x$$

$$(x - x_c)^2(c_0 + ... + c_5 x^5 + x^6) = 0$$

The simplified equation

$$c_0 x_c^2 - \frac{\lambda^4 q^8}{81} = 0,$$

$$(-2c_0 xc + c_1 x_c^2) - \frac{8}{81}\lambda^3 q^6 = 0,$$

$$\left(c_0 - 2c_1 x_c + c_2 x_c^2\right) - \frac{\left(18\lambda^2 q^6 + 12\lambda^3 q^8\right)}{81q^2} = 0,$$

$$(c_1 - 2c_2 x_c + c_3 x_c^2) - \frac{(180k\lambda^2 q^4 + 72\lambda^2 q^6)}{(81q^2)} = 0,$$

The simplified equation

$$(c_2 - 2c_3 x_c + c_4 x_c^2) - \frac{(-27q^2 + 360k\lambda q^2 + 108\lambda q^4 + 54\lambda^2 q^6)}{81q^2} = 0,$$

$$(c_3 - 2c_4 x_c + c_5 x_c^2) - \frac{(324k - 648k\lambda q^2 + 216\lambda q^4)}{81q^2} = 0,$$

$$(c_4 - 2c_5 x_c + x_c^2) - \frac{(-648k + 162q^2 + 108\lambda q^4)}{81q^2} = 0,$$

$$(c_5 - 2x_c) - \frac{(-108k + 216q^2)}{81q^2} = 0.$$

8 variables in the above set $x_c, q, \ c_0, \ c_1 \ldots, \ c_5$

The critical isotherm

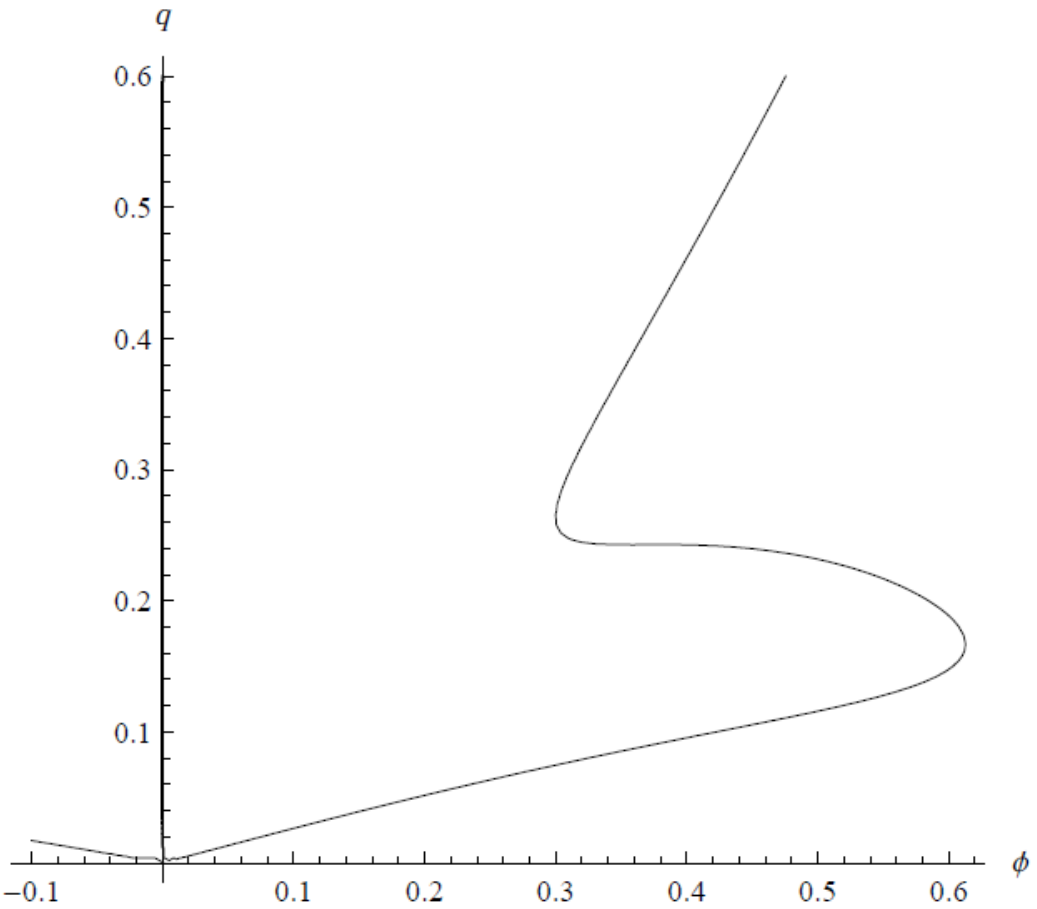

Result of critical exponents

$$\delta = 3, \quad \beta = 1/3, \quad \alpha = 2/3, \quad \gamma = 2/3.$$

Physical interpretations

- For ordinary matter, MFT and RGT present different critical exponents. Theoretically, MFT omits the perturbations around the critical point, while RGT carefully considers the perturbation effects at the critical point. In RGT, the whole system at the critical point is length scale free, that is, there is no special length scale in this system. In a gravity system, there is an inherent length scale *G^(-1/2), which* makes the RGT cannot do its work in a gravity system. A popular result is that the *G^(-1/2) with a length scale* hinders us to renormalize gravity. Here it hinders us to apply RGT in gravity, which makes the perturbed gravity and unperturbed gravity share the same critical exponents, though the perturbation shifts the critical point.

- *Thank you for your attention.*

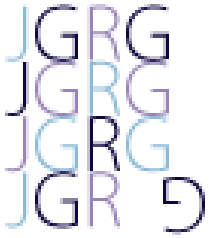

Kei Yamada, JGRG 22(2012)111219

"Triangular solution to the general relativistic three-body problem"

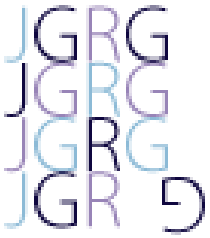

RESCEU SYMPOSIUM ON

GENERAL RELATIVITY AND GRAVITATION

JGRG 22



November 12-16 2012

Koshiba Hall, The University of Tokyo, Hongo, Tokyo, Japan



Triangular solution to the general relativistic three-body problem

Kei Yamada
Hirosaki University

with Ichita-san & Asada-san

Contents

- Introduction
- Equilateral triangular solution in GR
- Triangular solution in GR: general masses
- Summary

Contents

- Introduction
- Equilateral triangular solution in GR
- Triangular solution in GR: general masses
- Summary

Three-body problem

Particular solutions to the three-body problem

Euler's collinear solution (1765)

&

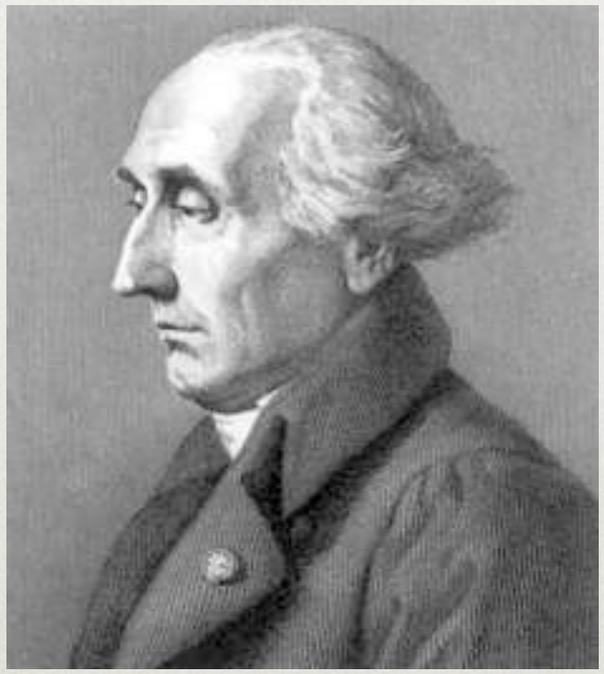

J. L. Lagrange

Lagrange's equilateral triangular solution (1772)

Equilateral triangular solution

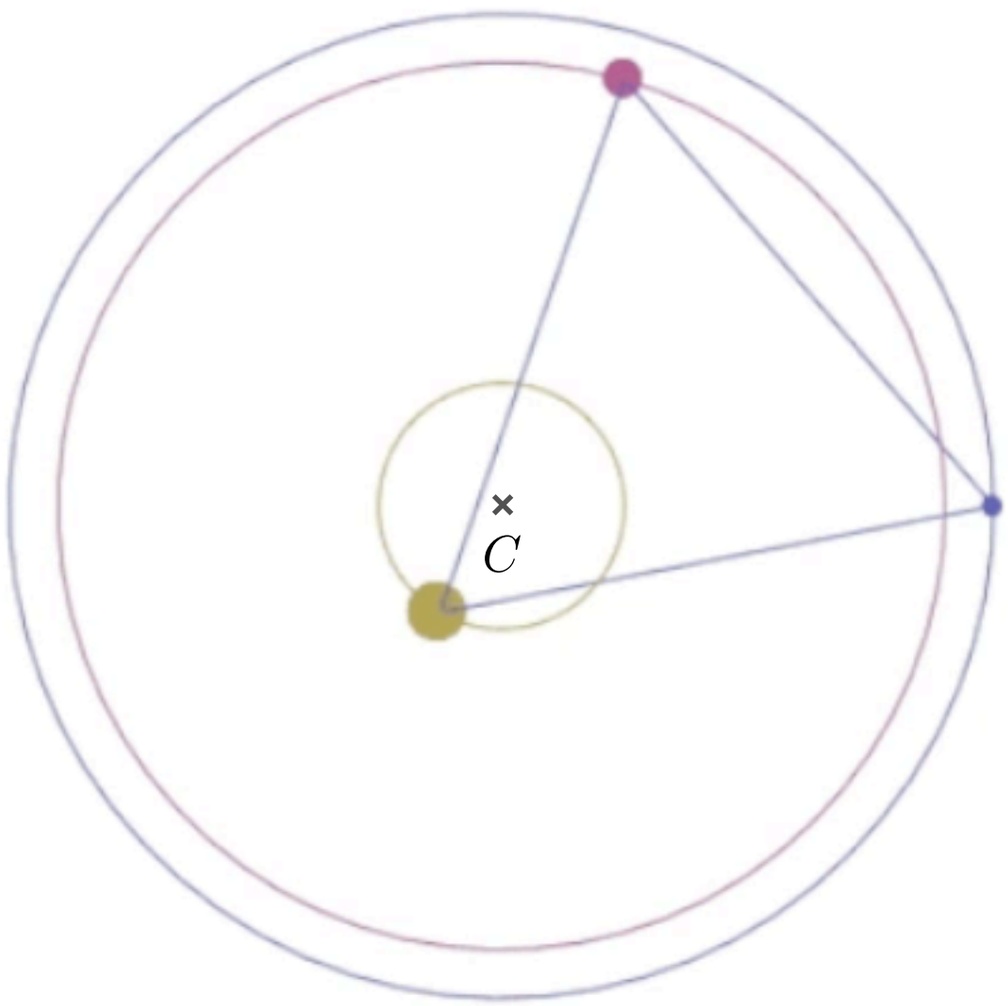

C : the center of mass

Lagrange points

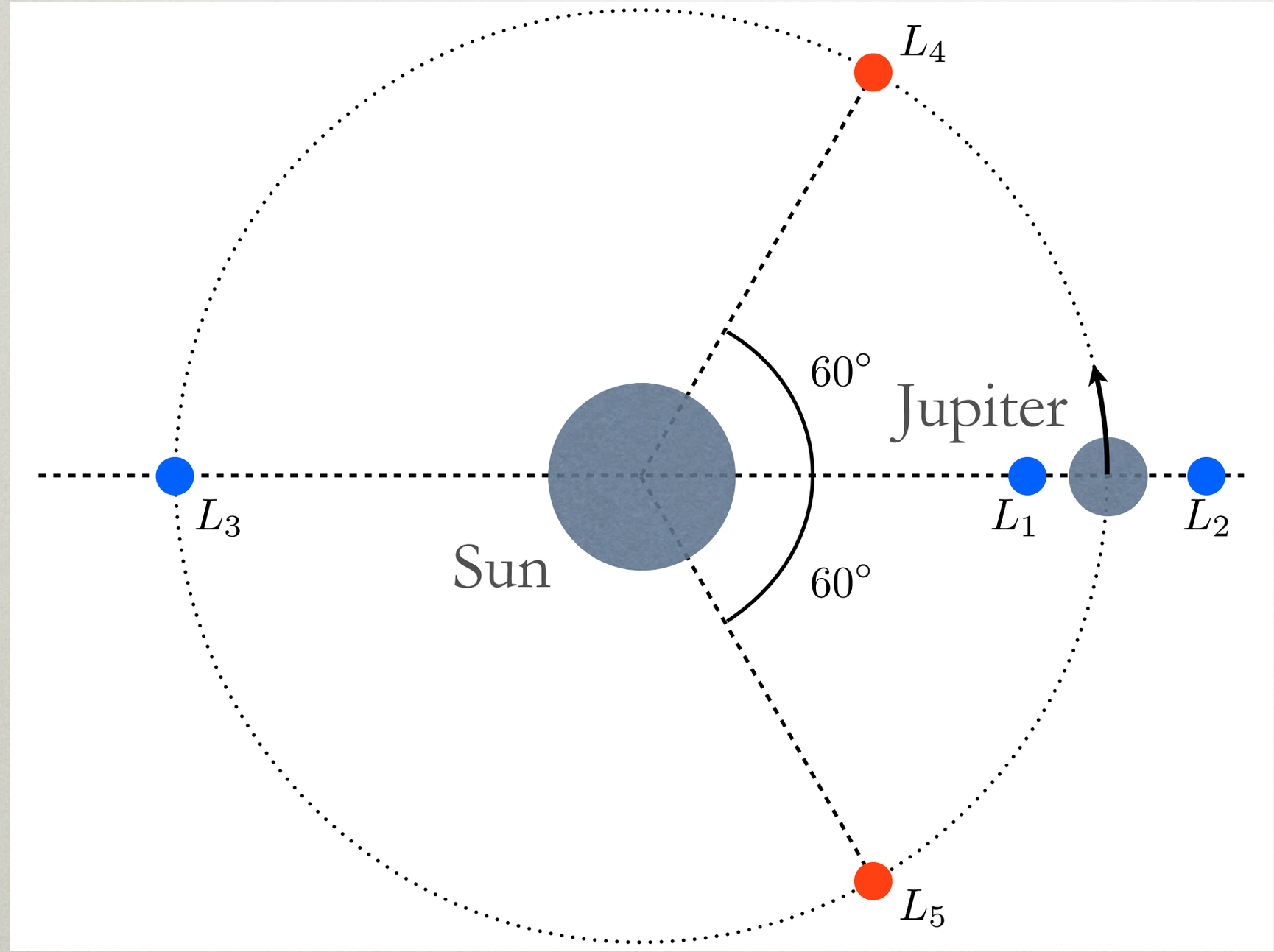

Lagrange points

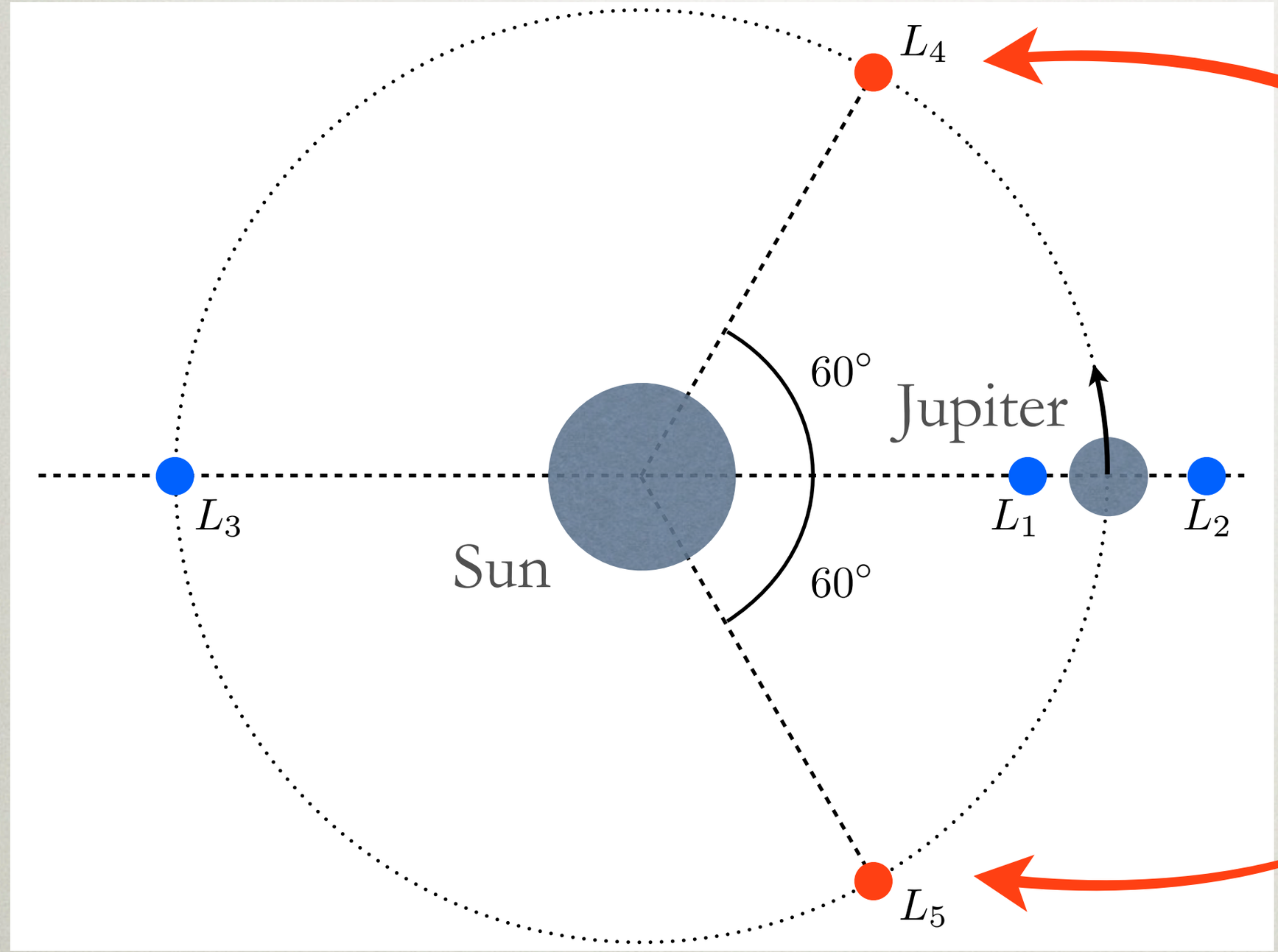

Lagrange points

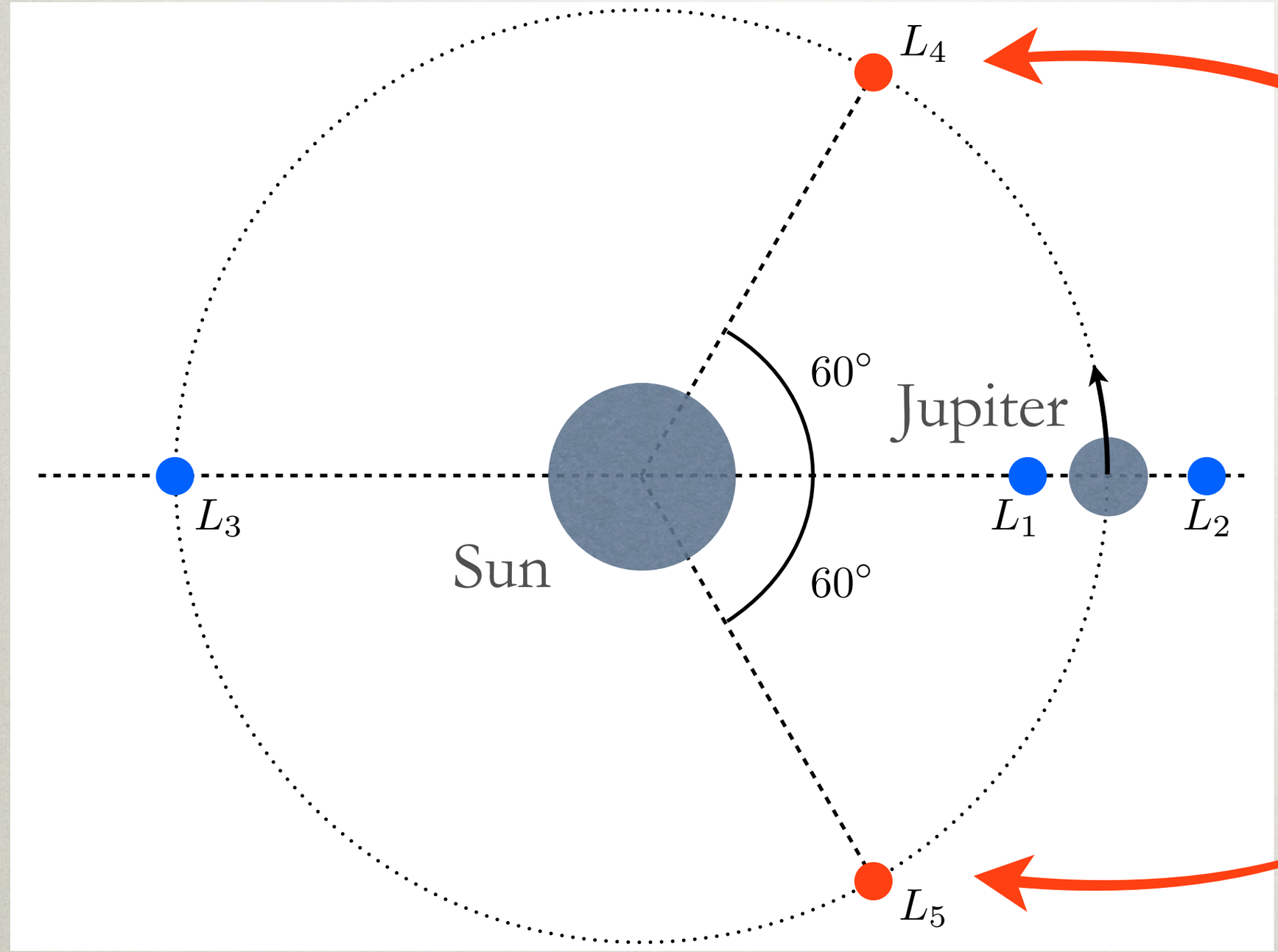

What happens in the general relativity (GR)?

GR effects of Solar system

Two-body systems: ○

(e.g. the perihelion precession of Mercury)

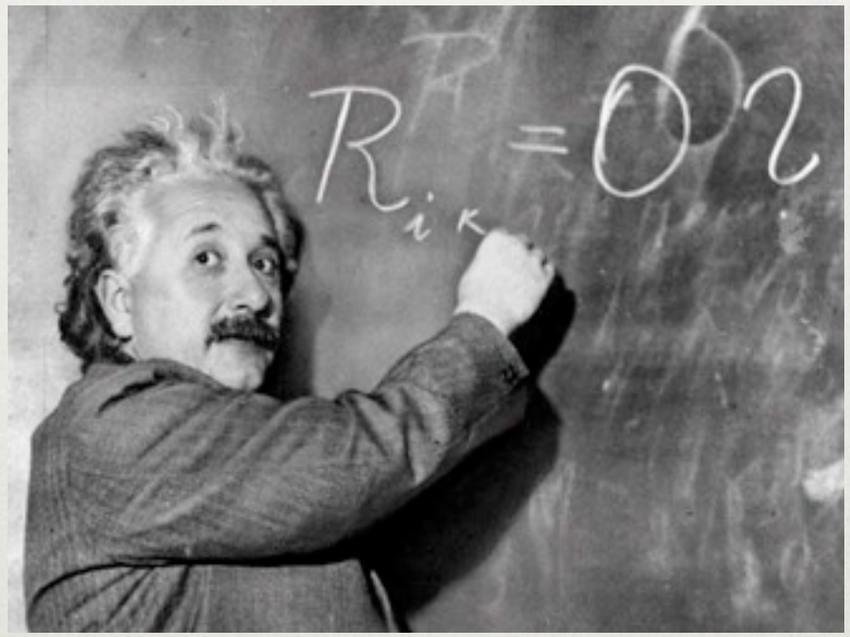

Three-body systems: ?

⇒ It is interesting as a new test of GR

EIH equation of motion

Einstein-Infeld-Hoffman (EIH) equation of motion for N bodies

Newtonian term

GR correction by mass

$$m_K \frac{d^2 \boldsymbol{r}_K}{dt^2} = \sum_{A \neq K} \boldsymbol{r}_{AK} \frac{G m_A m_K}{r_{AK}^3} \left[1 - 4 \sum_{B \neq K} \frac{G m_B}{c^2 r_{BK}} - \sum_{C \neq A} \frac{G m_C}{c^2 r_{CA}} \left(1 - \frac{\boldsymbol{r}_{AK} \cdot \boldsymbol{r}_{CA}}{2 r_{CA}^2} \right) \right.$$

GR correction by velocity

$$\left. + \left(\frac{\boldsymbol{v}_K}{c} \right)^2 + 2 \left(\frac{\boldsymbol{v}_A}{c} \right)^2 - 4 \left(\frac{\boldsymbol{v}_A}{c} \right) \cdot \left(\frac{\boldsymbol{v}_K}{c} \right) - \frac{3}{2} \left(\frac{\left(\frac{\boldsymbol{v}_A}{c} \right) \cdot \boldsymbol{r}_{AK}}{r_{AK}} \right)^2 \right]$$

$$- \sum_{A \neq K} \left[\left(\frac{\boldsymbol{v}_A}{c} \right) - \left(\frac{\boldsymbol{v}_K}{c} \right) \right] \frac{G m_A m_K}{r_{AK}^3} \boldsymbol{r}_{AK} \cdot \left[3 \left(\frac{\boldsymbol{v}_A}{c} \right) - 4 \left(\frac{\boldsymbol{v}_K}{c} \right) \right]$$

$$+ \frac{7}{2} \sum_{A \neq K} \sum_{C \neq A} \boldsymbol{r}_{CA} \frac{G m_C m_K}{r_{CA}^3} \frac{G m_A}{c^2 r_{AK}}$$

Triple product

We look for an equilibrium solution in a circular motion

Contents

- Introduction
- Equilateral triangular solution in GR
- Triangular solution in GR: general masses
- Summary

Equilateral triangular configuration

Equilateral triangle

$r_{IJ} = a \ (I, J = 1, 2, 3)$

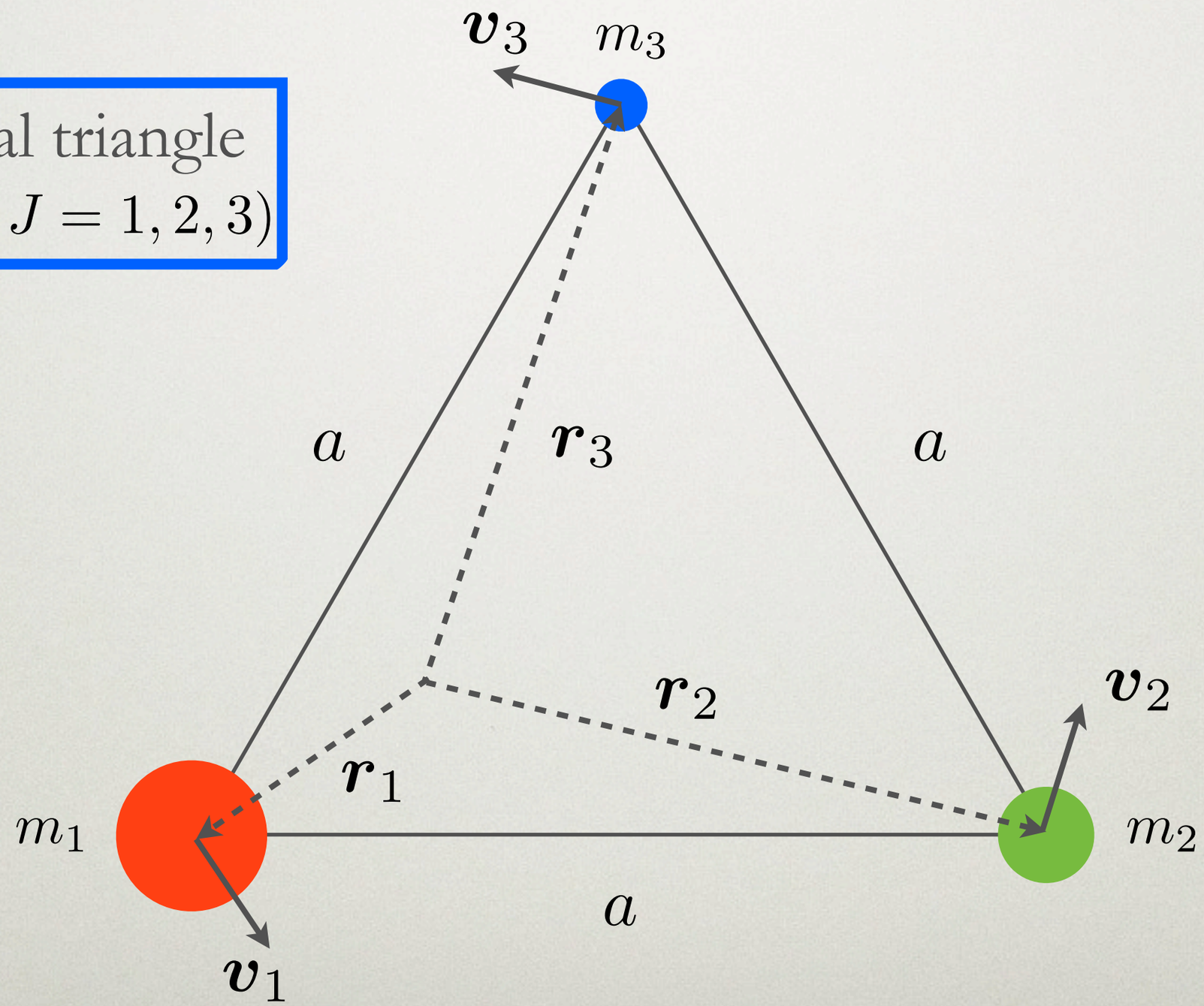

Center of mass at 1PN

$$\boxed{\boldsymbol{r}_G = \frac{\sum_A \nu_A \boldsymbol{r}_A \left[1 + \frac{1}{2}\left(\left(\frac{v_A}{c}\right)^2 - \sum_{B\neq A} \frac{Gm_B}{c^2 r_{AB}}\right)\lambda\right]}{\sum_C \nu_C \left[1 + \frac{1}{2}\left(\left(\frac{v_C}{c}\right)^2 - \sum_{D\neq C} \frac{Gm_D}{c^2 r_{CD}}\right)\lambda\right]}}, \quad \lambda \equiv \frac{GM}{c^2 a} \ll 1$$

In general, this is different from the Newtonian one

Center of mass at 1PN

$$\boxed{\boldsymbol{r}_G = \frac{\sum_A \nu_A \boldsymbol{r}_A \left[1 + \frac{1}{2}\left(\left(\frac{v_A}{c}\right)^2 - \sum_{B\neq A} \frac{Gm_B}{c^2 r_{AB}}\right)\lambda\right]}{\sum_C \nu_C \left[1 + \frac{1}{2}\left(\left(\frac{v_C}{c}\right)^2 - \sum_{D\neq C} \frac{Gm_D}{c^2 r_{CD}}\right)\lambda\right]}}, \quad \lambda \equiv \frac{GM}{c^2 a} \ll 1$$

In general, this is different from the Newtonian one

But

In this case, this agrees with the Newtonian case

Equilateral triangular solution at the 1PN

At 1PN order, EOM for m_1 becomes

$$-\omega^2 \boldsymbol{n}_1 = -\frac{M}{a^3}\boldsymbol{n}_1 + g_{PN1}\boldsymbol{n}_1 + \frac{\sqrt{3}}{16}\frac{M}{a^3}\frac{\nu_2\nu_3(\nu_2-\nu_3)}{\nu_2^2+\nu_2\nu_3+\nu_3^2}\left[6+9\left(\nu_2+\nu_3\right)\right]\lambda\boldsymbol{n}_{\perp 1}$$

$$g_{PN1} = \frac{\lambda}{16(\nu_2^2+\nu_2\nu_3+\nu_3^2)}\frac{M}{a^3} \times \Big[48(\nu_2^2+\nu_2\nu_3+\nu_3^2) - 2(8\nu_2^3+7\nu_2^2\nu_3+7\nu_2\nu_3^2+8\nu_3^3) + (16\nu_2^4+41\nu_2^3\nu_3+84\nu_2^2\nu_3^2+41\nu_2\nu_3^3+16\nu_3^4)\Big]$$

ω : angular velocity, $\nu_I \equiv m_I/M,\ M=\sum_I m_I\ (I=1,2,3)$

$\boldsymbol{n}_1 \equiv \boldsymbol{r}_1/|\boldsymbol{r}_1|,\ \boldsymbol{n}_{\perp 1} \equiv \boldsymbol{v}_1/|\boldsymbol{v}_1|,\ \boldsymbol{n}_{\perp 1}$ is normal to $\boldsymbol{n}_1$

Equilateral triangular solution at the 1PN

At 1PN order, EOM for m_1 becomes

$$-\omega^2 \boldsymbol{n}_1 = -\frac{M}{a^3}\boldsymbol{n}_1 + g_{PN1}\boldsymbol{n}_1$$
$$+\frac{\sqrt{3}}{16}\frac{M}{a^3}\frac{\nu_2\nu_3(\nu_2-\nu_3)}{\nu_2^2+\nu_2\nu_3+\nu_3^2}\left[6+9\left(\nu_2+\nu_3\right)\right]\lambda\boldsymbol{n}_{\perp 1}$$

$$g_{PN1} = \frac{\lambda}{16(\nu_2^2+\nu_2\nu_3+\nu_3^2)}\frac{M}{a^3}$$
$$\times\Big[48(\nu_2^2+\nu_2\nu_3+\nu_3^2) - 2(8\nu_2^3+7\nu_2^2\nu_3+7\nu_2\nu_3^2+8\nu_3^3)$$
$$+(16\nu_2^4+41\nu_2^3\nu_3+84\nu_2^2\nu_3^2+41\nu_2\nu_3^3+16\nu_3^4)\Big]$$

ω : angular velocity, $\nu_I \equiv m_I/M,\ M=\sum_I m_I\ (I=1,2,3)$

$\boldsymbol{n}_1 \equiv \boldsymbol{r}_1/|\boldsymbol{r}_1|,\ \boldsymbol{n}_{\perp 1} \equiv \boldsymbol{v}_1/|\boldsymbol{v}_1|,\ \boldsymbol{n}_{\perp 1}$ is normal to $\boldsymbol{n}_1$

Equilateral triangular solution at the 1PN

At 1PN order, EOM for m_1 becomes

$$-\omega^2 \boldsymbol{n}_1 = -\frac{M}{a^3}\boldsymbol{n}_1 + g_{PN1}\boldsymbol{n}_1 + \frac{\sqrt{3}}{16}\frac{M}{a^3}\frac{\nu_2\nu_3(\nu_2-\nu_3)}{\nu_2^2+\nu_2\nu_3+\nu_3^2}\left[6+9\left(\nu_2+\nu_3\right)\right]\lambda\boldsymbol{n}_{\perp 1}$$

$$g_{PN1} = \frac{\lambda}{16(\nu_2^2+\nu_2\nu_3+\nu_3^2)}\frac{M}{a^3} \times \Big[48(\nu_2^2+\nu_2\nu_3+\nu_3^2) - 2(8\nu_2^3+7\nu_2^2\nu_3+7\nu_2\nu_3^2+8\nu_3^3) + (16\nu_2^4+41\nu_2^3\nu_3+84\nu_2^2\nu_3^2+41\nu_2\nu_3^3+16\nu_3^4)\Big]$$

ω : angular velocity, $\nu_I \equiv m_I/M,\ M=\sum_I m_I\ (I=1,2,3)$

$\boldsymbol{n}_1 \equiv \boldsymbol{r}_1/|\boldsymbol{r}_1|,\ \boldsymbol{n}_{\perp 1} \equiv \boldsymbol{v}_1/|\boldsymbol{v}_1|,\ \boldsymbol{n}_{\perp 1}$ is normal to $\boldsymbol{n}_1$

Equilateral triangular solution at the 1PN

$$-\omega^2 \boldsymbol{n}_1 = -\frac{M}{a^3}\boldsymbol{n}_1 + g_{PN1}\boldsymbol{n}_1 + \frac{\sqrt{3}}{16}\frac{M}{a^3}\frac{\nu_2\nu_3(\nu_2-\nu_3)}{\nu_2^2+\nu_2\nu_3+\nu_3^2}\left[6+9\left(\nu_2+\nu_3\right)\right]\lambda\boldsymbol{n}_{\perp 1}$$

In only 2 cases, bodies satisfy EOM;

- mass ratio 1 : 1 : 1
- mass ratio 0 : 0 : 1

Equilateral triangular solution at the 1PN

$$-\omega^2 \boldsymbol{n}_1 = -\frac{M}{a^3}\boldsymbol{n}_1 + g_{PN1}\boldsymbol{n}_1 + \frac{\sqrt{3}}{16}\frac{M}{a^3}\frac{\nu_2\nu_3(\nu_2-\nu_3)}{\nu_2^2+\nu_2\nu_3+\nu_3^2}\left[6+9\left(\nu_2+\nu_3\right)\right]\lambda\boldsymbol{n}_{\perp 1}$$

In only 2 cases, bodies satisfy EOM;

- mass ratio 1 : 1 : 1
- mass ratio 0 : 0 : 1

This solution does not always exist in GR

[Ichita, KY & Asada, PRD **83**, 084026 (2011)]

Equilateral triangular solution at the 1PN

For the arbitrary mass ratio,
a solution exists?

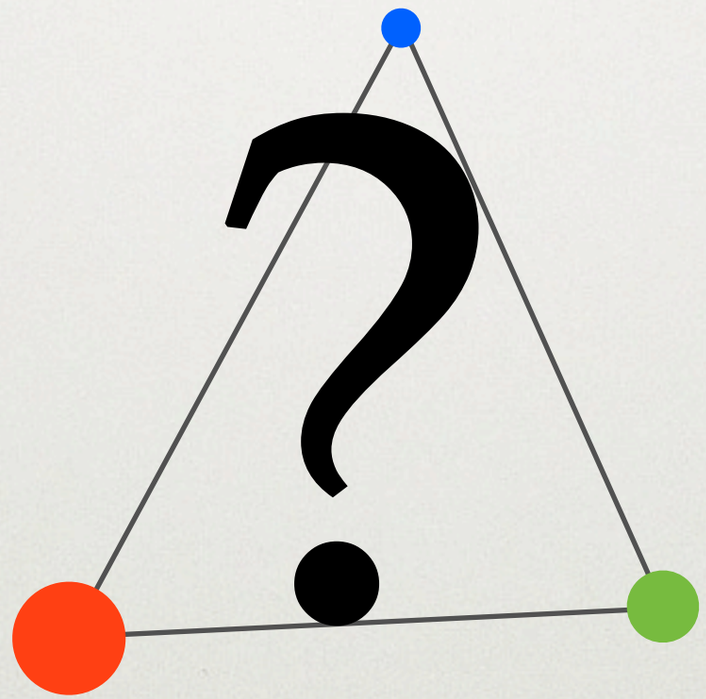

cf. [Krefetz, Astron. J. **72**, 471 (1967)]
for restricted 3-body problem,
used by [Seto & Muto, PRD **81**, 103004 (2010)]

Contents

- Introduction
- Equilateral triangular solution in GR
- Triangular solution in GR: general masses
- Summary

Corrections of distance

PN inequilateral triangle

$r_{IJ} = a(1 + \varepsilon_{IJ}),\ \varepsilon_{IJ} = \mathrm{O}(1\mathrm{PN})$

$\omega = \omega_N$

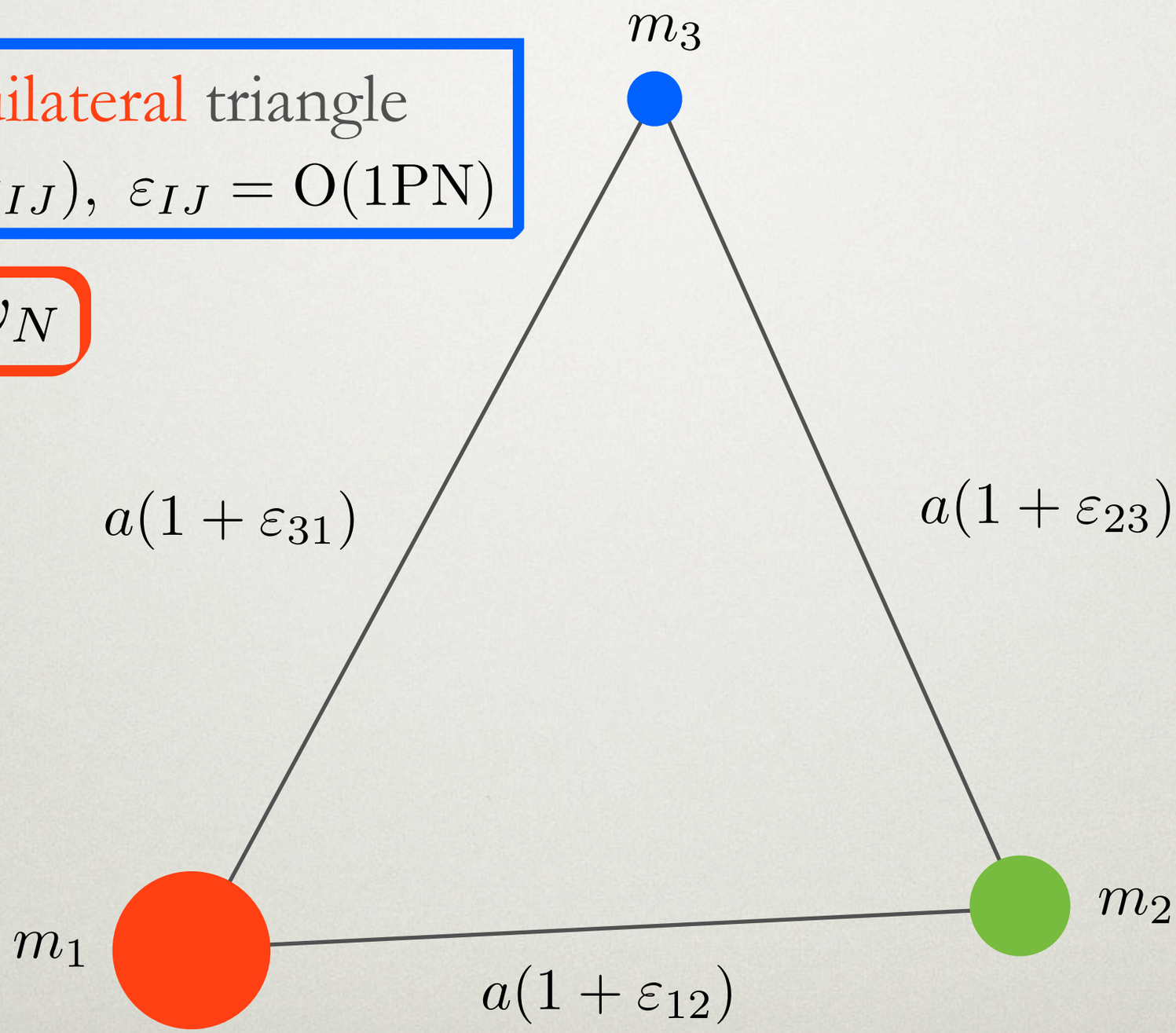

We can ignore the 1PN correction to the center of mass

Triangular solution at the 1PN

EOM for m_1 becomes

$$
\begin{aligned}
-\omega^2 \boldsymbol{r}_1 = & -\omega_N^2 \boldsymbol{r}_1 \\
& + \nu_2 \left(-3 + \nu_1\nu_2 + \nu_2\nu_3 + \nu_3\nu_1 - \frac{3}{8}\nu_3[5 - 3(\nu_1 + \nu_2)] \right) \lambda \boldsymbol{r}_{21} \\
& + \nu_3 \left(-3 + \nu_1\nu_2 + \nu_2\nu_3 + \nu_3\nu_1 - \frac{3}{8}\nu_2[5 - 3(\nu_3 + \nu_1)] \right) \lambda \boldsymbol{r}_{31} \\
& - 3(\nu_2 \varepsilon_{12} \boldsymbol{r}_{21} + \nu_3 \varepsilon_{31} \boldsymbol{r}_{31})
\end{aligned}
$$

$$\omega = \omega_N$$

Triangular solution at the 1PN

EOM for m_1 becomes

$$
\begin{aligned}
-\omega^2 \boldsymbol{r}_1 = &-\omega_N^2 \boldsymbol{r}_1 \\
&+\nu_2\left(-3+\nu_1\nu_2+\nu_2\nu_3+\nu_3\nu_1-\frac{3}{8}\nu_3[5-3(\nu_1+\nu_2)]\right)\lambda\boldsymbol{r}_{21} \\
&+\nu_3\left(-3+\nu_1\nu_2+\nu_2\nu_3+\nu_3\nu_1-\frac{3}{8}\nu_2[5-3(\nu_3+\nu_1)]\right)\lambda\boldsymbol{r}_{31} \\
&-3(\nu_2\varepsilon_{12}\boldsymbol{r}_{21}+\nu_3\varepsilon_{31}\boldsymbol{r}_{31})
\end{aligned}
$$

$\omega = \omega_N$ ⇒ $\square = 0$

Triangular solution at the 1PN

EOM for m_1 becomes

$$
\begin{aligned}
-\omega^2 \boldsymbol{r}_1 = & -\omega_N^2 \boldsymbol{r}_1 \\
& + \nu_2 \left(-3 + \nu_1\nu_2 + \nu_2\nu_3 + \nu_3\nu_1 - \frac{3}{8}\nu_3[5 - 3(\nu_1 + \nu_2)] \right) \lambda \boldsymbol{r}_{21} \\
& + \nu_3 \left(-3 + \nu_1\nu_2 + \nu_2\nu_3 + \nu_3\nu_1 - \frac{3}{8}\nu_2[5 - 3(\nu_3 + \nu_1)] \right) \lambda \boldsymbol{r}_{31} \\
& - 3(\nu_2 \varepsilon_{12} \boldsymbol{r}_{21} + \nu_3 \varepsilon_{31} \boldsymbol{r}_{31})
\end{aligned}
$$

$\omega = \omega_N$ ⇒ $\square = 0$

Triangular solution at the 1PN

As a result, we could uniquely express ε_{IJ}

$$\varepsilon_{12} = -\left[1 - \frac{1}{3}(\nu_1\nu_2 + \nu_2\nu_3 + \nu_3\nu_1) + \frac{1}{8}\nu_3[5 - 3(\nu_1 + \nu_2)]\right]\lambda,$$

$$\varepsilon_{23} = -\left[1 - \frac{1}{3}(\nu_1\nu_2 + \nu_2\nu_3 + \nu_3\nu_1) + \frac{1}{8}\nu_1[5 - 3(\nu_2 + \nu_3)]\right]\lambda,$$

$$\varepsilon_{31} = -\left[1 - \frac{1}{3}(\nu_1\nu_2 + \nu_2\nu_3 + \nu_3\nu_1) + \frac{1}{8}\nu_2[5 - 3(\nu_1 + \nu_3)]\right]\lambda.$$

Triangular solution for the arbitrary mass ratio at 1PN

[KY & Asada, submitted]

Application for Solar system

Corrections for L4 (L5) of Solar system [m]

Planet	Sun-Planet	Sun-L4 (L5)	Planet-L4 (L5)
Earth	-1477	-1477	-1477 -923
Jupiter	-1477	-1477	-1477 -922

The sign + denotes increase of distance

Contents

- Introduction
- Equilateral triangular solution in GR
- Triangular solution in GR: general masses
- Summary

Summary

- We found a triangular solution at the 1PN order
- The PN triangle is smaller than the Newtonian one (for same mass ratio), and changed from an equilateral triangle
- This solution may also be applied to near SMBHs and compact binaries
- Future observations are needed

Ongoing & Future works

- The Stability
- The Gravitational wave
- Higher order PN approximation
- An elliptical motion
- Four (or more) body systems



Thank you for your attention

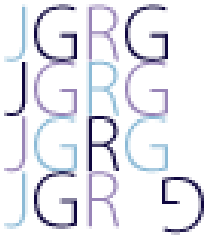

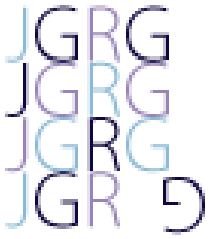

Naoki Tsukamoto, JGRG 22(2012)111220

"Research of the celestial objects by the gravitational lensing"

RESCEU SYMPOSIUM ON

GENERAL RELATIVITY AND GRAVITATION

JGRG 22

November 12-16 2012

Koshiba Hall, The University of Tokyo, Hongo, Tokyo, Japan





Research of the celestial objects by gravitational lensing

Naoki Tsukamoto,[1](a) Tomohiro Harada(a) and Kohji Yajima(a)

(a) *Department of Physics, Rikkyo University, Tokyo 171-8501, Japan*

Abstract

We will suggest two methods to detect Ellis wormholes which is an example of traversable wormholes of the Morris-Thorne class the with Einstein ring systems and with the double images. We show that, given the configuration of the gravitational lensing and the radii of the Einstein ring and relativistic Einstein rings, we can distinguish between a black hole and Ellis wormhole in principle. We also discuss the signed magnification sums of general spherical lens models including the singular isothermal sphere, the Schwarzschild lens and the Ellis wormhole. We show that the signed magnification sums are a very useful tool to distinguish exotic lens objects.

1 Comparison between wormholes and black holes with their Einstein ring and relativistic Einstein rings

The Ellis spacetime was investigated as a geodesically complete particle model by Ellis [1] and turned out to describe a wormhole connecting two Minkowski spacetimes. The Ellis wormhole spacetime is a static, spherically symmetric, asymptotically flat solution of the Einstein equation with a massless scalar field with a wrong sign as a matter field. Although such a matter field violates energy conditions, it could represent the negative energy density from the quantum effects, such as the Casimir effect. This spacetime is a typical and simplest example of wormholes proposed by Morris and Thorne [2, 3]. This is a traversable wormhole in the sense that an observer can cross this wormhole in both directions.

The deflection angle of light in the Ellis wormhole geometry was studied by Chetouani and Clement [4] and recently Nakajima and Asada [5]. The gravitational lensing on the Ellis geometry was studied by Dey and Sen [6], Abe [7] and Toki *et al.* [8] in the weak gravitational field and Perlick [9], Nandi *et al.* [10] and Tejeiro and Larranaga [11] in the strong gravitational field (see Virbhadra and Keeton [12], Virbhadra [13], Bozza [14], Bozza and Mancini [15] and references therein for the strong field limit).

Recently, Abe suggests to detect the Ellis wormholes with the light curves [7] and Toki *et al.* suggest a method to detect the Ellis wormholes with the astrometric image centroid displacements [8]. We will suggest two methods to detect them with Einstein ring systems [16] and with double images [17]. In this section, we consider the Einstein ring system.

The line element in the Ellis wormhole solution is given by

$$ds^2 = -dt^2 + dr^2 + (r^2 + a^2)(d\theta^2 + \sin^2\theta d\phi^2), \tag{1}$$

where a is a positive constant corresponding the radius of the wormhole throat at $r = 0$. The photon is scattered if $|b| > a$, while reaches the throat if $|b| \leq a$, where b is the impact parameter of the photon. Since we are interested in the scattering problem, we assume $|b| > a$. Chetouani and Clement [4] derived the exact deflection angle α of light on the Ellis wormhole geometry as follows:

$$\alpha = 2K\left(\frac{a}{b}\right) - \pi, \tag{2}$$

where K is the complete elliptic integral of the first kind. The deflection angle is diverging in the limit $|b| \to a$, while it is approximately given in the weak-field regime $|b| \gg a$ by $\alpha \approx \pm\frac{\pi}{4}\left(\frac{a}{b}\right)^2$.

Now we will consider the case that both the observer and the source object are far from the lensing object, or $D_l \gg b$ and $D_{ls} \gg b$, where D_l and D_{ls} are the separations between the observer and lens and between the lens and source, respectively. The configuration of the gravitational lensing is given in FIG 1.

[1]Email address: 11ra001t@rikkyo.ac.jp

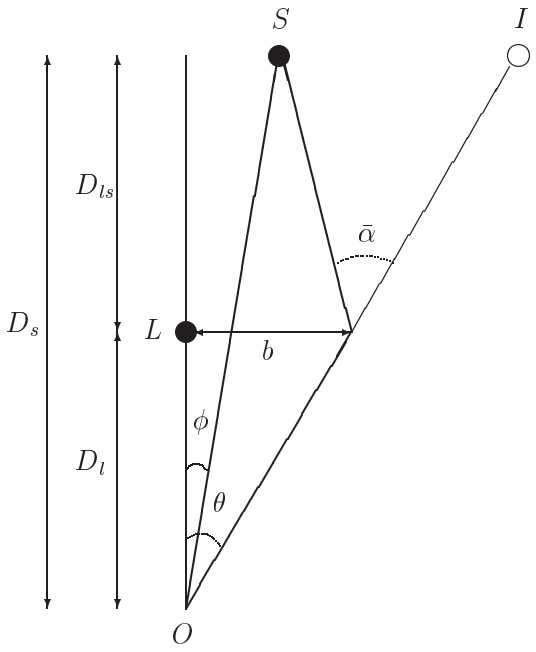

Figure 1: The configuration of the gravitational lensing. The light rays emitted by the source S are deflected by the lens L (a wormhole or a black hole) and reach the observer O with the angle of the lensed image θ, instead of the real angle ϕ. b and $\bar{\alpha}$ are the impact parameter and the effective deflection angle, respectively. D_l and D_{ls} are the separations between the observer and the lens and between the lens and the source, respectively.

The lens equation is given by

$$D_{ls}\bar{\alpha} = D_s(\theta - \phi), \tag{3}$$

where $\bar{\alpha} = (\alpha \bmod 2\pi)$ is the effective deflection angle, θ and ϕ are the angles of the lensed image and the real image from the observer, respectively, and $D_s = D_l + D_{ls}$ is the separation between the observer and source. Note that we have assumed $|\bar{\alpha}| \ll 1$, $|\theta| \ll 1$ and $|\phi| \ll 1$. The deflection angle can be expressed $\alpha = \bar{\alpha} + 2\pi N$, where N is a non-negative integer, denoting the winding number of the light ray. The ring image corresponds to the image angle θ for vanishing real angle $\phi = 0$. By the symmetry, the image is necessarily a ring with the diameter angle θ.

Since $b = D_l\theta$, we find that the ring image is given by $\theta_N = a/(D_l k_N)$, where $k_N \in (0, 1)$ is a unique root of the transcendental equation

$$2K(k) - \frac{\eta}{k} = (2n+1)\,\pi, \tag{4}$$

where $\eta = (D_s a)/(D_l D_{ls})$. We should note that $2K(k) - \eta/k$ is monotonically increasing with respect to k and changes from $-\infty$ to ∞ as k increases from 0 to 1. The uniqueness of the root follows from the monotonicity. Moreover, we can conclude that k_N monotonically increases and approaches 1 as $N \to \infty$ and hence the image angle θ_N monotonically decreases and approaches a/D_l.

In the weak-field regime $|b| \gg a$, the winding number N should be $N = 0$. Using the deflection angle $\alpha \approx \pm\frac{\pi}{4}\left(\frac{a}{b}\right)^2$, we can solve the equation (4) approximately and get the diameter angle of the Einstein ring

$$\theta_0 \simeq \left(\frac{\pi}{4}\frac{D_{ls}}{D_s D_l^2}a^2\right)^{\frac{1}{3}} \simeq 2.0\,\text{arcsecond}\left(\frac{D_{ls}}{10\text{Mpc}}\right)^{\frac{1}{3}}\left(\frac{20\text{Mpc}}{D_s}\right)^{\frac{1}{3}}\left(\frac{10\text{Mpc}}{D_l}\right)^{\frac{2}{3}}\left(\frac{a}{0.5\text{pc}}\right)^{\frac{2}{3}}. \tag{5}$$

This approximation is good for $D_l \gg a$ and $D_{ls} \gg a$. The relative error is $\sim 10^{-2}$ for $a = 0.5$pc and $D_l = D_{ls} = 10$ Mpc.

In the especially strong-field regime, where the winding number N becomes $N \geq 1$, we can easily check that $a \simeq b$ or $k_N \simeq 1$ satisfies the transcendental equation (4) in numerical calculations. Physically this means that the light rays which wind around the wormhole nearly on the photon sphere make the relativistic Einstein rings [9, 18]. Then the diameter angles of the relativistic Einstein rings are approximately given by

$$\theta_{N\geq 1} \simeq \frac{a}{D_l} \simeq 1.0 \times 10^{-2}\,\text{arcsecond} \left(\frac{10\text{Mpc}}{D_l}\right)\left(\frac{a}{0.5\text{pc}}\right). \tag{6}$$

If we are given the distance D_s to the source from the observer, the distance D_l to the lens from the observer and the radius θ_0 of the Einstein ring, we can determine the radius of the throat a from Eq. (5). Then, we can use $\theta_{N\geq 1}$ (6) to test the assumption that the lens object is a wormhole. From Eqs. (5) and (6) we obtain the relation between θ_0 and $\theta_{N\geq 1}$ by

$$\theta_{N\geq 1} \simeq \left(\frac{4}{\pi}\frac{D_s}{D_{ls}}\right)^{\frac{1}{2}} \theta_0^{\frac{3}{2}}. \tag{7}$$

This relation generally holds in astrophysical situations, as long as $a \ll D_l$ and $a \ll D_{ls}$ are satisfied.

The relation between θ_0 and $\theta_{N\geq 1}$ for the Schwarzschild spacetime (, see [19, 20, 21],)

$$\theta_{N\geq 1} \simeq \frac{3\sqrt{3}}{4}\frac{D_s}{D_{ls}}\theta_0^2 \tag{8}$$

is different from that on the Ellis spacetime (7). FIG. 2 shows the angle of the relativistic Einstein ring $\theta_{N\geq 1}$ versus the angle of the Einstein ring θ_0 for $D_l = D_{ls} = 10$Mpc. Thus, we can distinguish between black holes and wormholes in principle if we are given D_s/D_l, θ_0 and $\theta_{N\geq 1}$. We consider the experimental

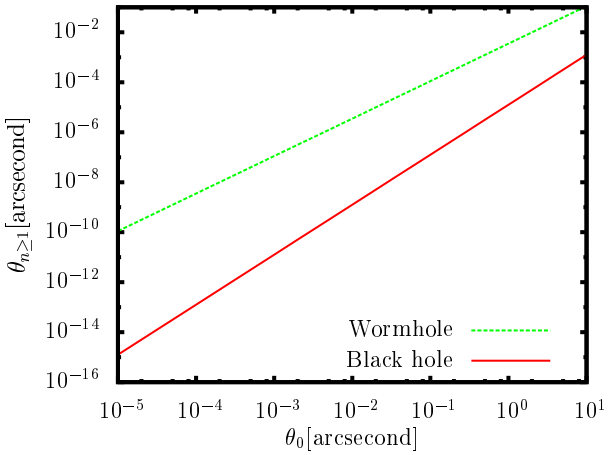

Figure 2: The angle of the relativistic Einstein ring $\theta_{N\geq 1}$ versus the angle of the Einstein ring θ_0 for $D_l = D_{ls} = 10$Mpc. The broken (green) and solid (red) lines plot the cases where the lens objects are a wormhole and a black hole, respectively.

situation where we know the separation D_s between the observer and the source and the separation D_l between the observer and the lens. We assume that we do not know whether the lens object is a black bole or a wormhole and do not its parameter, i.e., the mass M or the radius a of the throat in advance.

We need at least two observable quantities to determine whether the lens object is a black hole or wormhole since the lens system has one parameter in this situation. First, we observe an Einstein ring and determine the parameter for both possibilities. Second, we observe relativistic Einstein rings and tell the wormhole from the black hole. If the predicted relativistic ring angles by the black hole and by the wormhole were of similar size, we could not discern the difference. However, Eqs. (7), (8) and Fig. 2 show that we do not confuse them.

We conclude that we can detect the relativistic Einstein rings by wormholes which have $a \simeq 0.5$pc at a galactic center with the distance $D_l = D_{ls} = 10$Mpc and which have $a \simeq 10$AU in our galaxy with the distance $D_l = D_{ls} = 10$kpc using the most powerful modern instruments which have the resolution of 10^{-2}arcsecond such as a 10-meter optical-infrared telescope. Note that the corresponding black holes which have the Einstein rings of the same size are galactic supermassive black holes with $10^{10}M_\odot$ and $10^7 M_\odot$, respectively, and that the relativistic Einstein rings by these black holes are too small to measure with the current technology.

2 The signed magnification sums of the general spherical lens

In this section, we will show that the signed magnification sum would be a powerful tool to research the lens objects as well as the total magnification and the magnification ratio if we observe a multiple image. In particular, we will show that one can distinguish between the Ellis wormhole lens and the Schwarzschild lens with the signed magnification sums.

We consider the general spherical lens model with the deflection angle in the weak field approximation, parametrized by

$$\alpha = \pm C b^{-n} = \pm \frac{C}{D_l^n} \theta^{-n}, \tag{9}$$

where C is a positive constant and n is a non-negative integer and we have used the relation $b = D_l\theta$. If n is odd, then the sign is only the upper one, while if n is even, then the sign is the upper one for $\theta > 0$ and the lower one for $\theta < 0$. Thus, we have to treat two lens equations when n is even. This lens model describes the singular isothermal sphere, the Schwarzschild lens and the Ellis wormhole for $n = 0$, 1 and 2, respectively. The case where $n \geq 3$ would describe some exotic lens objects and the gravitational lens effect of modified gravitational theories. We do not consider the case $n = 0$ below for simplification. The following discussion does not depend on the value of C.

The lens equation is given by

$$\hat{\theta}^{n+1} - \hat{\phi}\hat{\theta}^n \mp 1 = 0, \tag{10}$$

where $\hat{\theta} \equiv \theta/\theta_0$ and $\hat{\phi} \equiv \phi/\theta_0$ and $\theta_0 \equiv \left(\frac{D_{ls}C}{D_s D_l^n}\right)^{\frac{1}{n+1}}$ is the Einstein ring angle. The lens equation (10) has symmetry with respect to the point $\hat{\phi} = \hat{\theta} = 0$, We can concentrate ourselves on the case where the source angle ϕ is positive for symmetry. The solutions $\hat{\theta}_1$, $\hat{\theta}_2$, $\cdots$, $\hat{\theta}_{n+1}$ of the lens equation (10) of $(n+1)$-th degree satisfy

$$\sum_{i=1}^{n+1} \frac{\hat{\theta}_i}{\hat{\phi}} \frac{d\hat{\theta}_i}{d\hat{\phi}} = 1. \tag{11}$$

Note that these solutions $\hat{\theta}_i$ may be complex and not all the magnifications are always physical and that Eq. (11) is satisfied regardless of the sign of Eq. (10). We realize the number of the real solutions ($\hat{\theta}_+ > 0$ and $\hat{\theta}_- < 0$) is always two , regardless of the value of n. Thus, the magnification invariant (11) is a observable quantity only when $n = 1$.

The signed magnifications of the images in the weak field limit are given by

$$\mu_{0\pm}(\hat{\phi}) \equiv \frac{\hat{\theta}_\pm(\hat{\phi})}{\hat{\phi}} \frac{d\hat{\theta}_\pm}{d\hat{\phi}}(\hat{\phi}). \tag{12}$$

Figure 3 shows that one can distinguish the general spherical lens models with their signed magnification sums $\mu_{0+} + \mu_{0-}$ which are less than unity. The lower bound of the total magnification $|\mu_{0+}| + |\mu_{0-}|$ is given by

$$\frac{2}{1+n} \leq \mu_{0+} + \mu_{0-} \leq |\mu_{0+}| + |\mu_{0-}|\,. \tag{13}$$

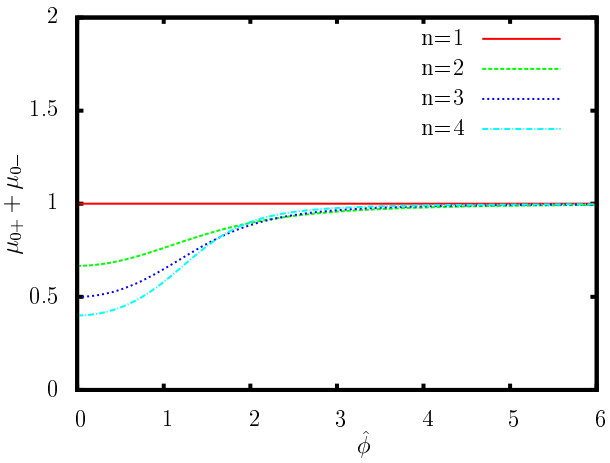

Figure 3: The singed magnification sums of some general spherical lens models. The solid, broken, dot and dot-dashed lines are the general spherical lens models for $n = 1$, 2, 3 and 4, respectively. This shows that we can distinguish each models from the others.

Therefore, gravitational lensing necessarily gives amplified light curves for $n = 1$, while it does not necessarily for $n > 1$. Recently, Kitamura *et al.* investigated the demagnified light curves [22].

The signed magnification sum is a powerful tool to find exotic lens objects because it only depends on the deduced source angle $\hat{\phi}$ and n and we just have to observe the images for $\hat{\phi} \lesssim 1$ and for $\hat{\phi} \gg 1$ to determine the signed magnification sum. However, we need a high resolution to observe the double images. We would also distinguish the lens objects with the ratio of magnifications of the double images and the total magnification. If we also measure the difference $\theta_+ - \theta_-$ of the image angles, one can determine the Einstein ring angle θ_0 and the source angle $\phi = \theta_0\hat{\phi}$.

Our method with the signed magnification sums is complementary to the methods to detect exotic lens objects with the light curves [7, 22] and the astrometric image centroid displacements [8]. To observe double images are much more feasible than to observe relativistic Einstein rings [16] because relativistic images are faint and small and because relativistic rings are rare sights.

References

[1] H. G. Ellis, J. Math. Phys. **14**, 104 (1973).

[2] M. S. Morris and K. S. Thorne, Am. J. Phys. **56**, 395 (1988).

[3] M. S. Morris, K. S. Thorne and U. Yurtsever, Phys. Rev. Lett. **61**, 1446 (1988).

[4] L. Chetouani and G. Clément, Gen. Relativ. Gravit. **16**, 111 (1984).

[5] K. Nakajima and H. Asada, Phys. Rev. D **85**, 107501 (2012).

[6] T. K. Dey and S. Sen, Mod. Phys. Lett. A, **23**, 953 (2008).

[7] F. Abe, Astrophys. J. **725**, 787 (2010).

[8] Y. Toki, T. Kitamura, H. Asada and F. Abe, Astrophys. J. **740**, 121 (2011).

[9] V. Perlick, Phys. Rev. D **69**, 064017 (2004).

[10] K. K. Nandi, Y. Z. Zhang and A. V. Zakharov, Phys. Rev. D **74**, 024020 (2006).

[11] J. M. Tejeiro and E. A. Larranaga, Rom. J. Phys. **57**, 736 (2012).

[12] K. S. Virbhadra and C. R. Keeton, Phys. Rev. D **77**, 124014 (2008).

[13] K. S. Virbhadra, Phys. Rev. D **79**, 083004 (2009).

[14] V. Bozza, Gen. Relativ. Gravit. **42**, 2269 (2010).

[15] V. Bozza and L. Mancini, Astrophys. J. **753**, 56 (2012).

[16] N. Tsukamoto, T. Harada and K. Yajima, Phys. Rev. D **86**, 104062 (2012).

[17] N. Tsukamoto and T. Harada, Phys. Rev. D **87**, 024024 (2013).

[18] V. Bozza, Phys. Rev. D **66**, 103001 (2002).

[19] S. Frittelli, T. P. Kling and E. T. Newman, Phys. Rev. D **61**, 064021 (2000).

[20] K. S. Virbhadra and G. F. R. Ellis, Phys. Rev. D **62**, 084003 (2000).

[21] V. Bozza, S. Capozziello, G. Iovane and G. Scarpetta, Gen. Relativ. Gravit. **33**, 1535 (2001).

[22] T. Kitamura, K. Nakajima and H. Asada, Phys. Rev. D **87**, 027501 (2013).

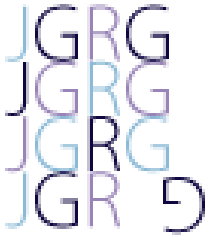

Ivan Arraut, JGRG 22(2012)111221

"Dark matter and dark energy as a single manifestation of a fundamental length scale"

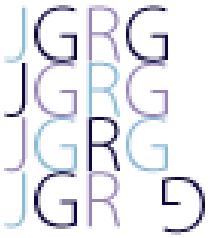

RESCEU SYMPOSIUM ON

GENERAL RELATIVITY AND GRAVITATION

JGRG 22



November 12-16 2012

Koshiba Hall, The University of Tokyo, Hongo, Tokyo, Japan





Dark Matter and Dark Energy as a possible manifestation of a fundamental scale.

Ivan Arraut

(Osaka University)

Motivation

Question in GR:
1). Why is the cosmological constant so small?
2). Why the velocity of rotation in galaxies is bigger than what is normally expected and what about the Gravitational Lenses?

→ **The project**

- Find some intermediate interesting scales.
- Analyze the importance of such scales.
- Find the Einstein's equations in a new formalism (in process, 3 different paths).
- For now the evolution of the parameters is not my bussiness.

Standard GR with Λ

- The Einstein's eqs. with a Cosmological Constant.

$$R_{\mu\nu} = -8\pi G S_{\mu\nu} - \Lambda g_{\mu\nu}$$

•The vacuum solution:

$$ds^2 = -e^{\nu(r)}dt^2 + e^{-\nu(r)}dr^2 + r^2 d\theta^2 + r^2 sin^2\theta d\phi^2$$

$$e^{\nu(r)} = 1 - \frac{2r_s}{r} - \frac{r^2}{3r_\Lambda^2}$$

•With an effective potential:

$$U_{eff}(r) = -\frac{r_s}{r} - \frac{1}{6}\frac{r^2}{r_\Lambda^2} + \frac{r_l^2}{2r^2} - \frac{r_s r_l^2}{r^3}$$

$$U_{eff}(r) \approx -\frac{r_s}{r} - \frac{r^2}{6r_\Lambda^2} + \frac{r_l^2}{2r^2}$$

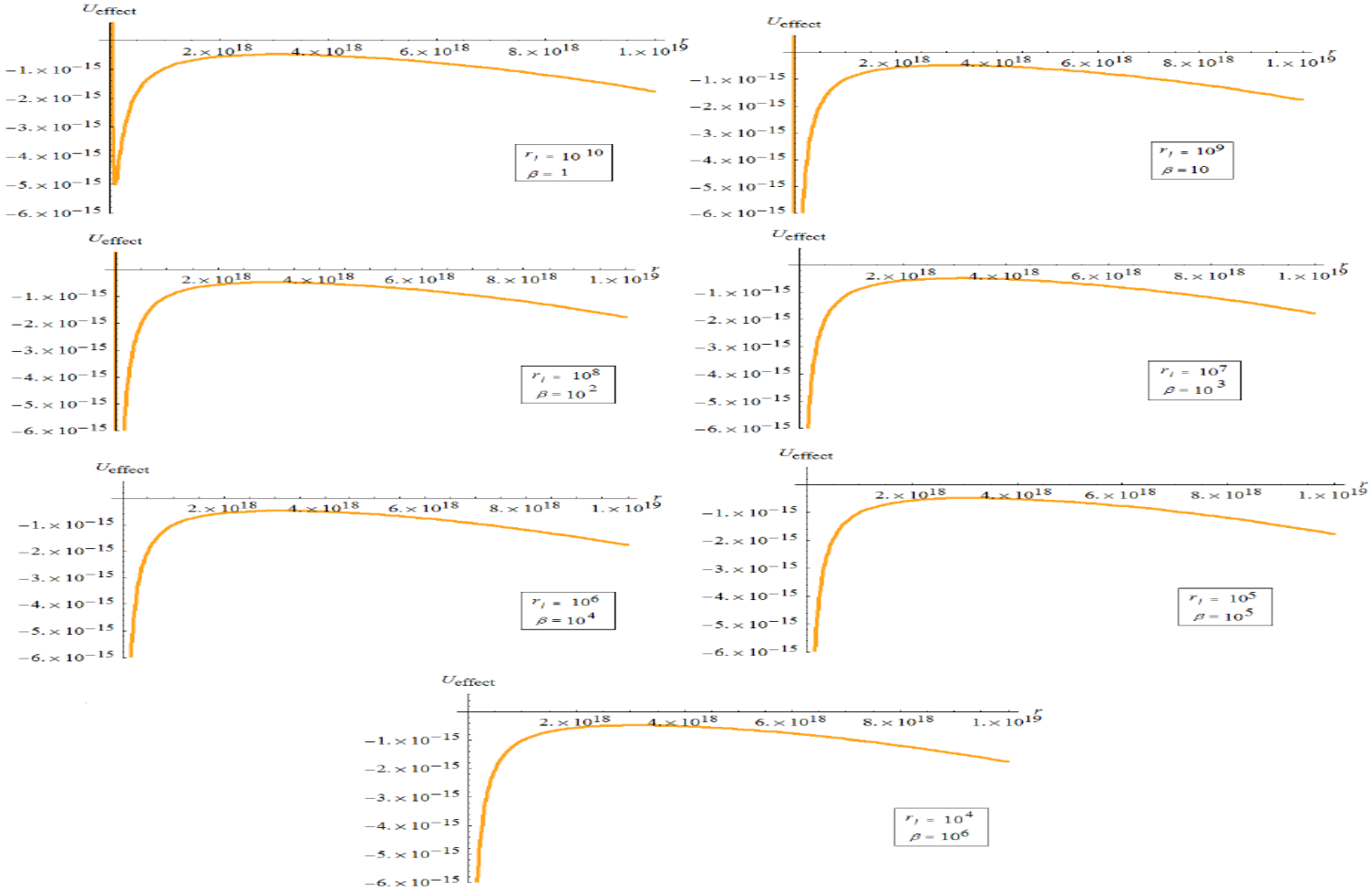

Figure 2.3: Effective potential for values of the distance near to the final critical point and $r_l >> r_s$.

•Special scale:

$$r_g = \left(\frac{3}{2} r_s r_\Lambda^2\right)^{1/3}$$

•The same scale used by Bousso and Hawking for the time-like Killing vector normalization (Hawking radiation). This is not a new scale at all!!!

•What about Dark Matter effects?
Absent until now. What can we do?

•MOND has something to tell us:
The fundamental scale in MOND is:

$$a_0^2 \sim \Lambda,$$

•Only one fit parameter.

•One interesting prediction of MOND:

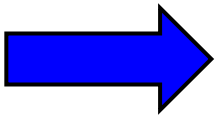

•Low surface brightness galaxies shows higher discrepancy in the mass content.

→ Problems with MOND

- Violation of energy-momentum conservation.
- It does not predict gravitational lenses effects.
- Problems with the cluster of galaxies.

•What can we do?

→ Possible Solution

- Relativistic version derivable from an action principle (many candidates).
- Among the possibilities we have:

A). Non-localities which can screen the Cosmological Constant but also can create Dark Matter effects. (Sasaki and colleagues. Mashoon).

B). But locality is relative in agreement with Amelino-Camelia, Lee Smolin, Freidel and Kowalzky. Should we pay attention to it?

C). But if there is Relative Locality, there should be Relative Co-locality which is a manifestation of the spacetime curvature (Arraut 2012, paper to be submitted soon).

D). Another path can be taken with gravity as a gauge theory (in process).

- The MOND formula is: $\tilde{\mu}(|\mathbf{a}|/a_0)\mathbf{a} = \mathbf{g}_N.$

$$\tilde{\mu}(x) = \frac{x}{1+x}.$$

- In the full MONDIAN regime, we have:

$$\frac{GM}{r^2} - \frac{1}{3}\frac{r}{r_\Lambda^2} = \sqrt{\frac{GM}{r_\Lambda}}\frac{1}{r}$$

•I am including the repulsive effect due to Λ in order to find the bound for the rotation curve.

•We can translate the problem. The MOND fit parameter is equivalent to say that the Dark matter scale is:

$$r_* \approx (GMr_\Lambda)^{1/2} = \left(\frac{r_s r_\Lambda}{2}\right)^{1/2}$$

•Additionally, it is equivalent to say that the Tully-Fisher law in its mass version is valid:

$$V_c^2 = \left(\frac{GM}{r_\Lambda}\right)^{1/2} - \frac{1}{3}\left(\frac{GM}{r_\Lambda}\right)$$

$$v^4 \sim M$$

$$r_{max} = \left(\frac{3}{2} r_s r_\Lambda^2\right)^{1/3}$$

•If: $r_s << r_\Lambda$

•What I propose: Is there any formalism where you can introduce at least 2 scales, one very large and another very small, such that those scales become dual? Rta: q-Bargmann Fock (Quantum groups).

•In the simplest case, the Bosonic algebra is deformed in agreement with:

$$\bar{\eta} := \frac{1}{2L}x - \frac{i}{2K}p \qquad \partial_{\bar{\eta}} := \frac{1}{2L}x + \frac{i}{2K}p$$

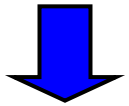

$$[x,p] = i\hbar + i\hbar(q^2-1)\left(\frac{x^2}{4L^2} + \frac{p^2}{4K^2}\right)$$

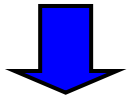

$$\Delta X \Delta P \geq \frac{\hbar}{2}\left(1 + (q^2-1)\left(\frac{(\Delta X)^2}{4L^2} + \frac{(\Delta P)^2}{4K^2}\right)\right)$$

•If we impose as an UV cut-off the Planck scale and as an IR cut-off the Cosmological Constant scale, then:

Minimum, maximum and mix scale

- The minimum scales in this model is: Kempf 1994.

$$\Delta X_{min} = L\sqrt{1-q^{-2}} \qquad \Delta P_{min} = K\sqrt{1-q^{-2}}$$

$$q \approx 1 + \frac{l_{pl}}{r_\Lambda} \qquad KL = \frac{(q^2+1)\hbar}{4}$$

$$f(\Delta X, \Delta P) := \Delta X \Delta P - \frac{\hbar}{2}\left(1 + (q^2-1)\left(\frac{(\Delta X)^2 + < X >^2}{4L^2} + \frac{(\Delta P)^2 + < P >^2}{4K^2}\right)\right)$$

- The total extremal condition is:

$$df(\Delta X, \Delta P) = 0 \qquad \Delta P \approx \frac{1}{(l_{pl} r_\Lambda)^{1/2}} = \frac{1}{l_0} \qquad \Delta X \approx (l_{pl} r_\Lambda)^{1/2} = l_0$$

- IR-UV mix scale.

The same but taking into account Relative Locality.

$$q \approx 1 + \frac{1}{r_\Lambda}\sqrt{\frac{\hbar|x|}{m_{pl}c}}$$

$$\Delta P_{mix} \approx \left(\frac{\hbar}{2}\right)^{1/2}\left(\frac{\hbar m_{pl}c}{|x|r_\Lambda^2}\right)^{1/4}$$

$$\Delta X_{mix} \approx \left(\frac{\hbar}{2}\right)^{1/2}\left(\frac{|x|r_\Lambda^2}{\hbar m_{pl}c}\right)^{1/4}$$

•Extending the relative locality to the momentum space (the fundamental scale in momentum space taken as Λ:

$$\Delta X_{min} = L\sqrt{\frac{q^2-1}{q^2}} \approx \sqrt{\frac{\hbar|x|}{m_{pl}c}} \Leftrightarrow \Delta P_{min} = K\sqrt{\frac{q^2-1}{q^2}} \approx \sqrt{\frac{\hbar|p|}{r_\Lambda}}$$

Relative Co-locality (extending the Majid ideas).

$$q \approx 1 + \sqrt{\frac{|p||x|}{r_\Lambda m_{pl} c}} + ...$$

$$\Delta P_{mix} \approx \left(\frac{\hbar}{2}\right)^{1/2} \left(\frac{|p| m_{pl} c}{|x| r_\Lambda}\right)^{1/4}$$

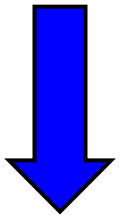

$$\Delta X_{mix} \approx \left(\frac{\hbar}{2}\right)^{1/2} \left(\frac{|x| r_\Lambda}{|p| m_{pl} c}\right)^{1/4}$$

•The correction to the observed momentum looks like the Tully Fisher law explained before. Can be Dark Matter only an UV-IR mix effect when we extend the Relativity principle to the phase space with a minimum scale in position and momentum?

Open problem and Conclusions.

- Still we have to verify if this is in reality a manifestation of the Tully-Fisher law and not a mere coincidence.
- Nex Step (in process). Derive the Einstein's equations inside this formalism. You should obtain: The standard GR with a Cosmological Constant + some contribution for DM due to UV-IR effect. For now it looks promising.

Acknowledgements

- 1). Lee Smolin for the bibliograpy suggestions and discussion.
- 2). Laurent Freidel for the discussion at the P.I about Relative Locality.
- 3). The friends of the Yukawa Institute, including Prof. Sasaki, Prof. Shiromizu for the kind weekly discussion about different topics.
- 4). Achim Kempf for his suggestions during the conference in Taipei “Quantum Horizons”.
- 5). Hagen Kleinert, for the additional submitted references. He has a different point of view.

Takayuki Hikichi, JGRG 22(2012)111222

"Wave function in 2+1 dimensional causal dynamical triangulation"

RESCEU SYMPOSIUM ON

GENERAL RELATIVITY AND GRAVITATION

JGRG 22

November 12-16 2012

Koshiba Hall, The University of Tokyo, Hongo, Tokyo, Japan

Wave function in 2+1 dimensional causal dynamical triangulation

JGRG22 (2012 11.12)

Takayuki HIKICHI (Nagoya Univ.)
collaborator
Yasusada NAMBU (Nagoya Univ.)
Hiromi SAIDA (Daido Univ)

Contents

3D Quantum Gravity defined by CDT
(Causal dynamical triangulation)

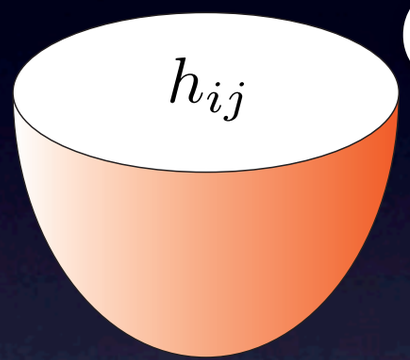

We consider
space-time with a spatial boundary.

We measure
the dynamics of spatial volume
and
whether spatial geometry is homogeneous.

Path integral and Wave function

trajectory（quantum mechanics）

→metric（quantum gravity）

path integral representation of a wave function

$$\Psi(h_{ij}) = \int \mathcal{D}g\, e^{iS^{\mathrm{EH}}[g_{\mu\nu}(x)]}$$

$$S^{\mathrm{EH}}[g_{\mu\nu}(x)] = \frac{1}{16\pi G}\int_{\mathcal{M}} d^3x\sqrt{-g}(R-2\Lambda) + \frac{1}{8\pi G}\int_{\partial\mathcal{M}} d^2x\sqrt{h}K$$

h_{ij} metric of a spatial boundary

The ground state wave function is given by a path integral over all compact Euclidean geometries which have a boundary.

Hartle&Hawking(1983)

Wick rotation

$$\tau_E := it,\ S_E^{\rm EH} := -iS^{\rm EH}|_{t=-i\tau_E}$$

Euclidean path integral

$$\Psi(h_{ij}) = \int \mathcal{D}g\, e^{-S_E^{\rm EH}[g_{\mu\nu}(x)]}$$

$= e^{-S_E^{\rm EH}}\{$ 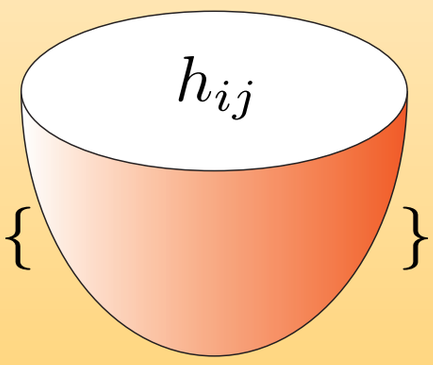

$\} + e^{-S_E^{\rm EH}}\{$ 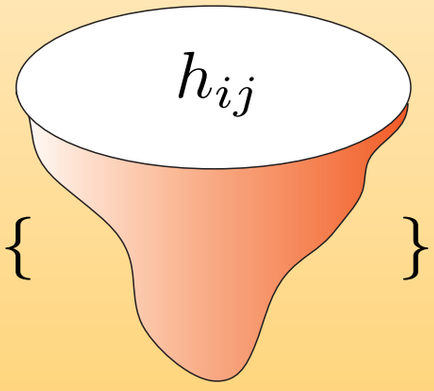

$\} + e^{-S_E^{\rm EH}}\{$ 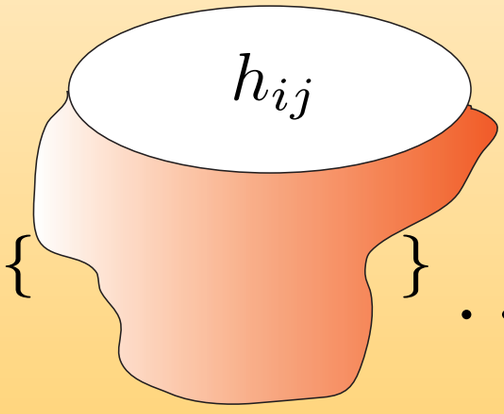

$\} \ldots$

Causal dynamical triangulation

→ a discrete **regularization method**
for gravitational path integral

The space-time is discretized by simplices.

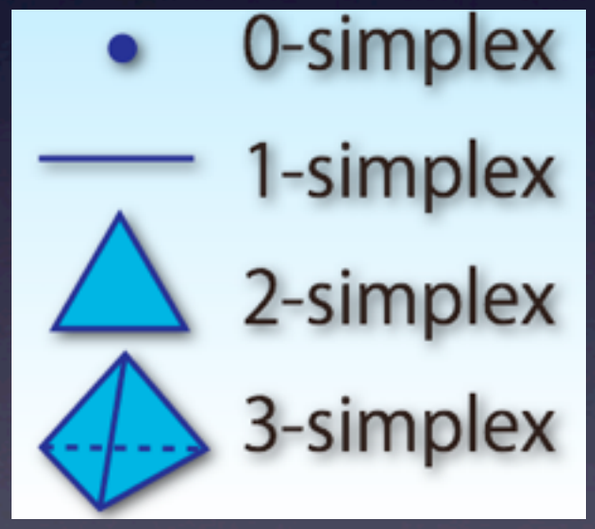

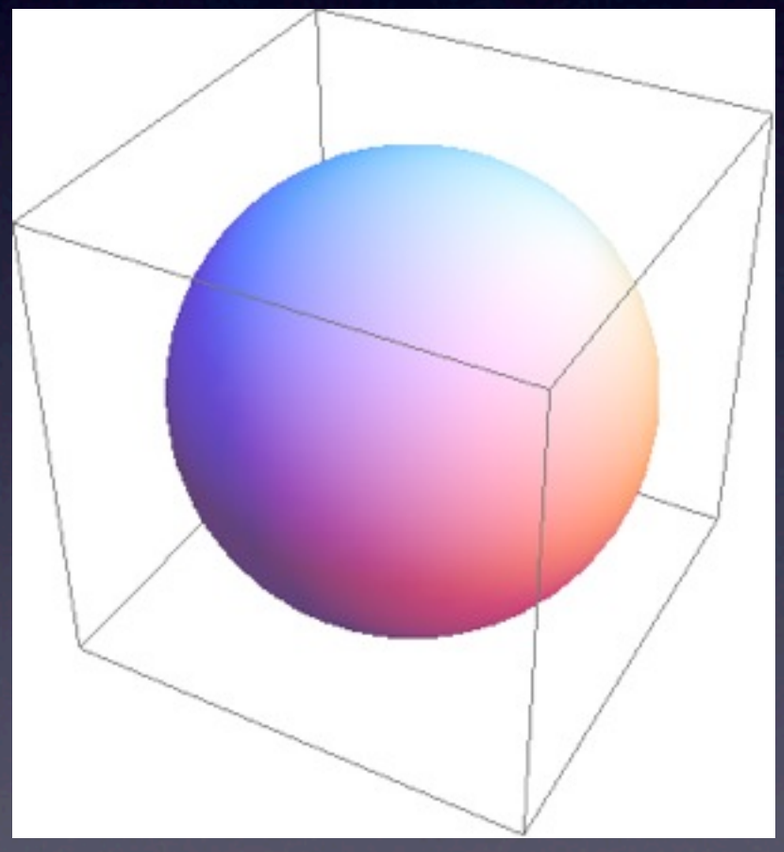

→

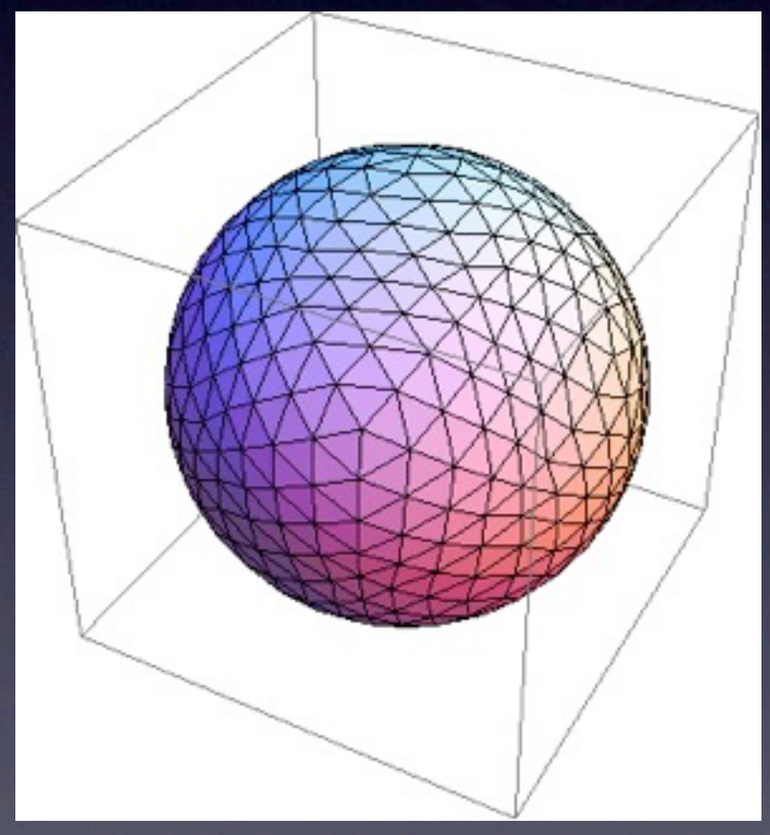

Advantage ・functional integral → **finite summation**

・avoid conformal divergence

Discretization of Lorentzian space-time & Wick rotation in CDT

discretized 3D Lorentzian space-time

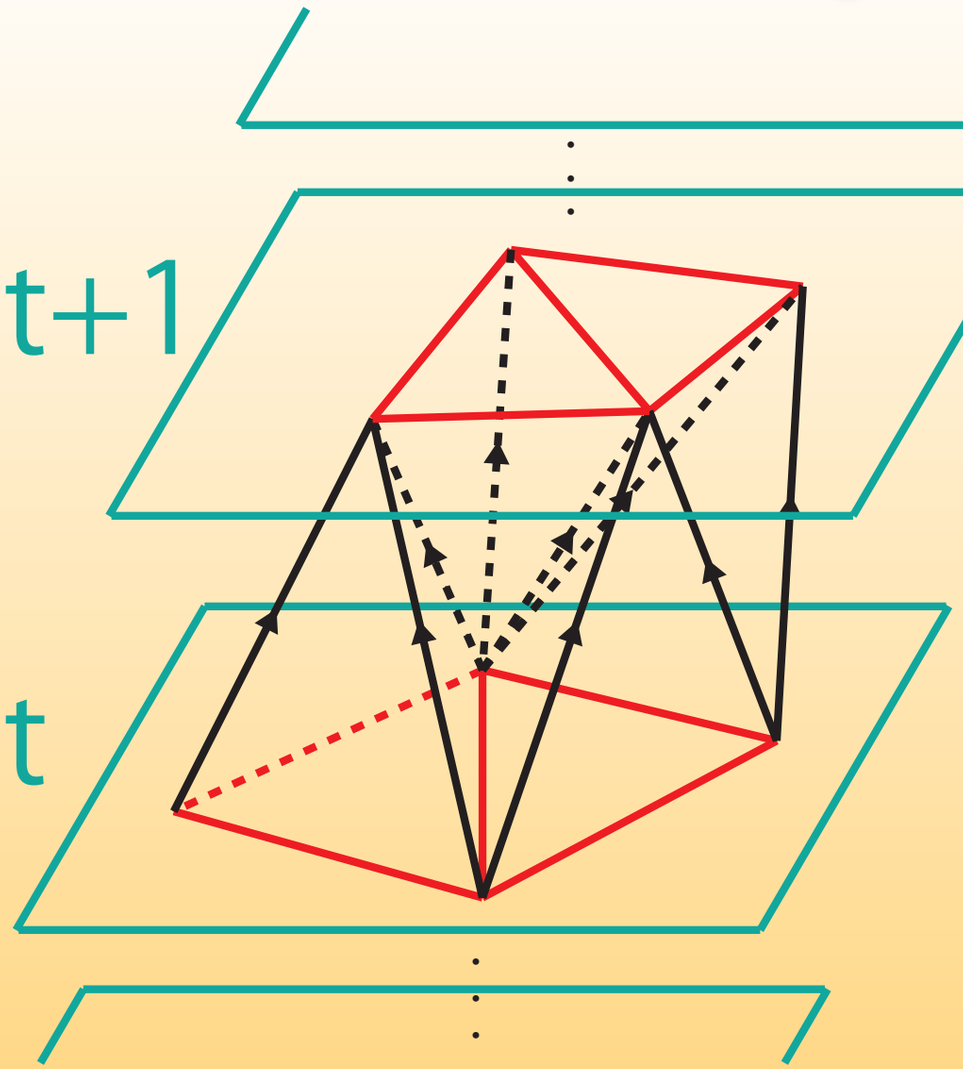

squared length of space-like links

$$l_{\mathrm{SL}}^2 = a^2$$

squared length of time-like links

$$l_{\mathrm{TL}}^2 = -\alpha a^2$$

$$\alpha > 0$$

Wick rotation

$$\alpha \to -\alpha$$

(We choose $\alpha = 1$ **)**

Curvature of discretized space-time

e. g. 2D

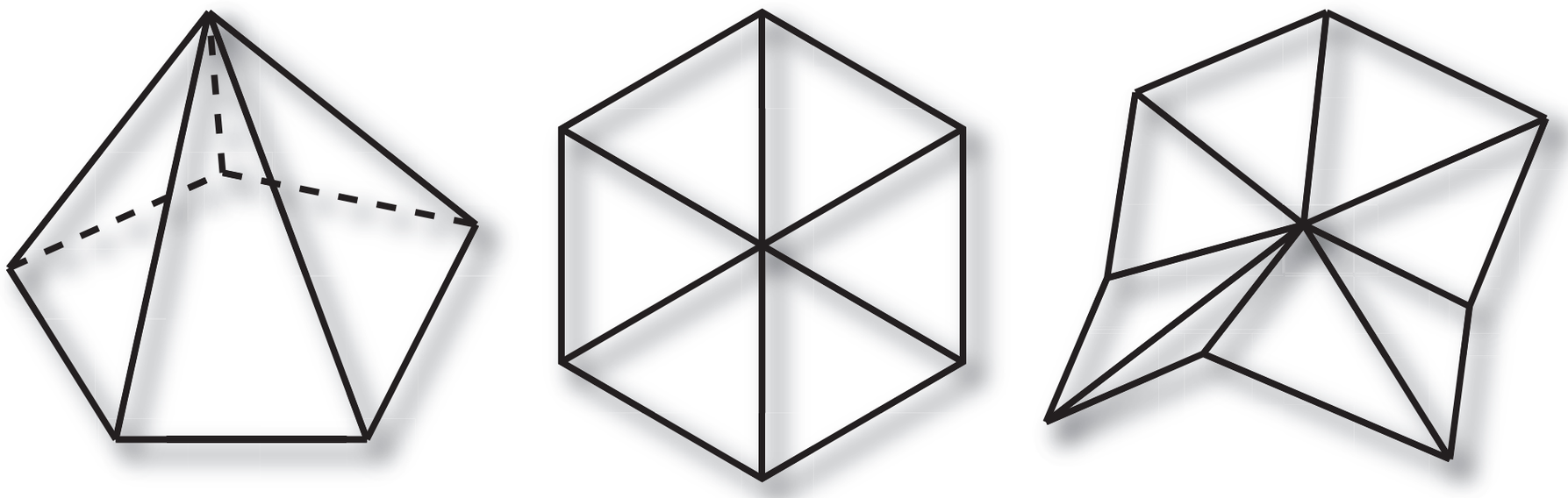

positive(5)　flat(6)　negative(8)

coordination number
(number of simplices around
a hinge(2d vertex, 3d link))
↔ curvature
flat space coordination number 6(2d), 5.104...(3d)

Wave function in CDT

discretized wave function

$$\Psi(h_{ij}) = \int \mathcal{D}g\, e^{-S_E^{\mathrm{EH}}[g_{\mu\nu}(x)]} \to \sum_{\mathcal{T}} e^{-S_E^{\mathrm{Regge}}[\mathcal{T}]}$$

$\sum_{\mathcal{T}}$ **sum over all discretized space-time**

$$S_E^{\mathrm{Regge}} = -\kappa_0 N_0 + \kappa_3 N_3 + \kappa_b N_2^b,$$

$\kappa_0 \cdots$	gravitational constant	$N_0 \cdots$	total number of vertices
$\kappa_3 \cdots$	cosmological constant	$N_3 \cdots$	total number of simplices
$\kappa_b \cdots$	coupling constant of a boundary term	$N_2^b \cdots$	total number of triangles on a boundary

Definition of boundary term in 3d DT: S. Warner, S. Catterall, R. Renken, Phase diagram of three-dimensional dynamical triangulations with a boundary, Phys. Lett. B 442 (1998) 266–272, hep-lat/9808006.

Simulation set-up

- **topology** $I \times S^2$

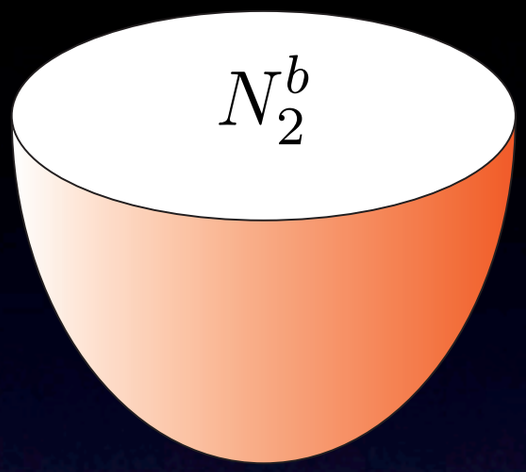

$I \times S^2$

spatial slice

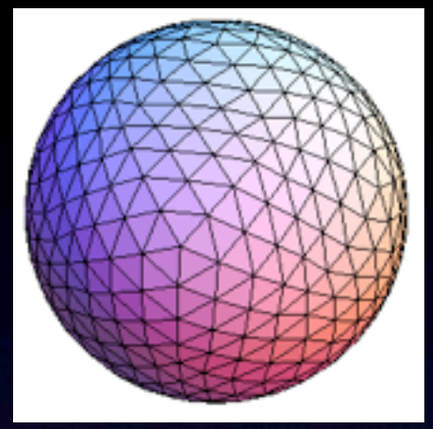

S^2

- **pure gravity**
- **fix volume of the spatial boundary**

$$N_2^b = 200, 600, 1000$$

- **fix space-time volume for technical reason**
- **We set** $N_3 = 10000$
- **We set gravitational constant** $\kappa_0 = 0.4,\ (3.0)$

We perform Markov chain Monte Carlo simulation.

Results

Typical configuration

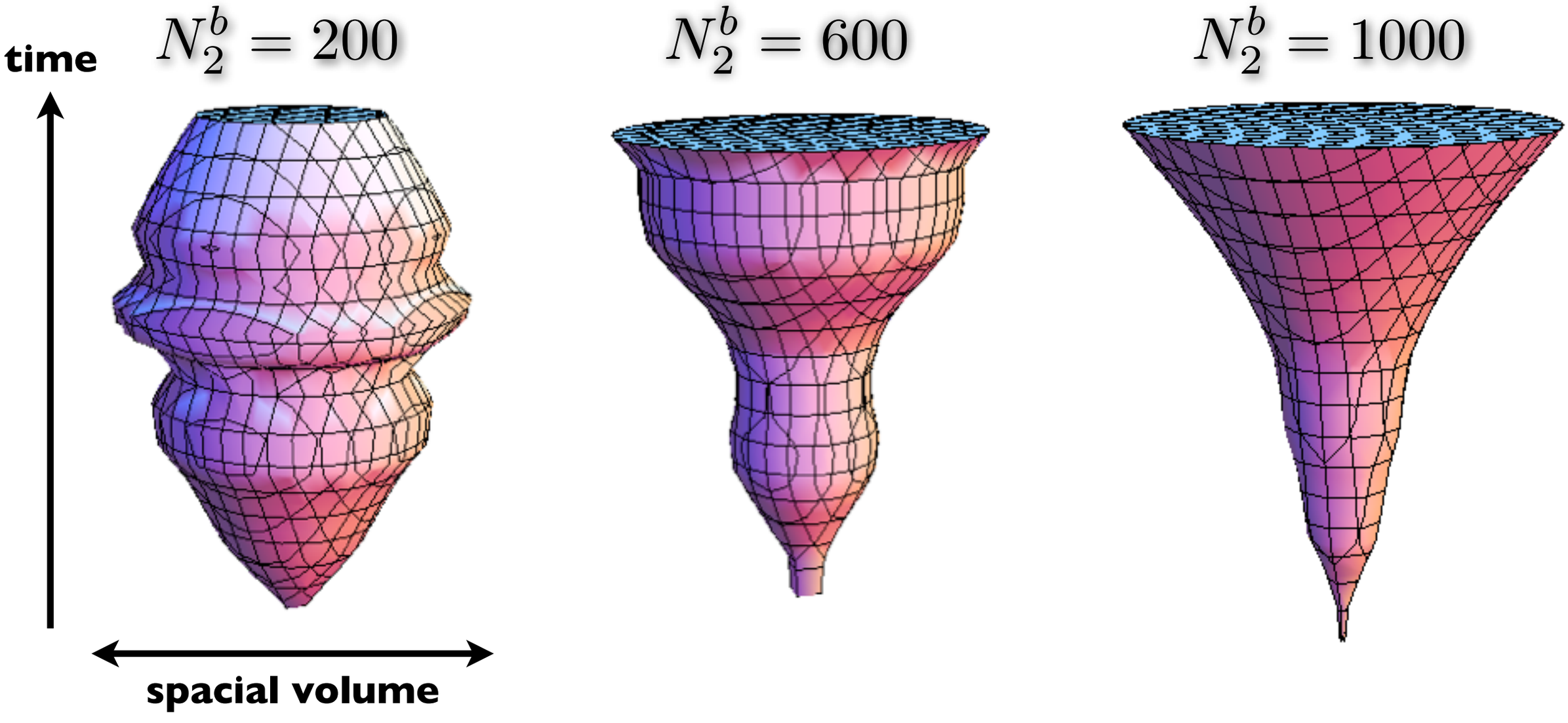

$$N_3 = 10000,\ \kappa_0 = 0.4$$

Spatial volume dynamics

In DT classical space-time didn't emerge.

In CDT the averaged spacial volume $\langle N_2(\tau)\rangle$ at Euclidean time τ can be described by de Sitter instanton.

$$\langle N_2(\tau)\rangle = A\cos^2(\frac{\tau}{B})$$

A, B constant

$$N_2^b = 600$$

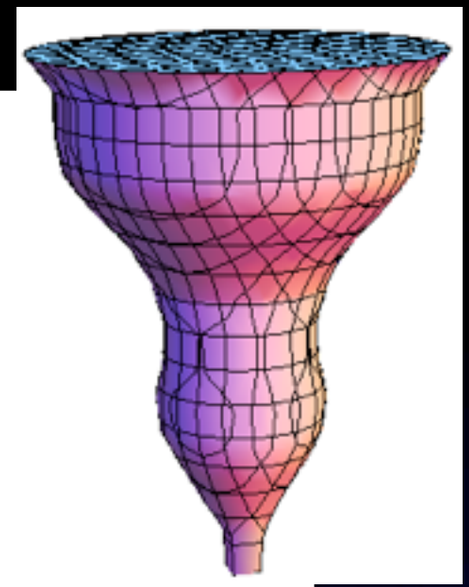

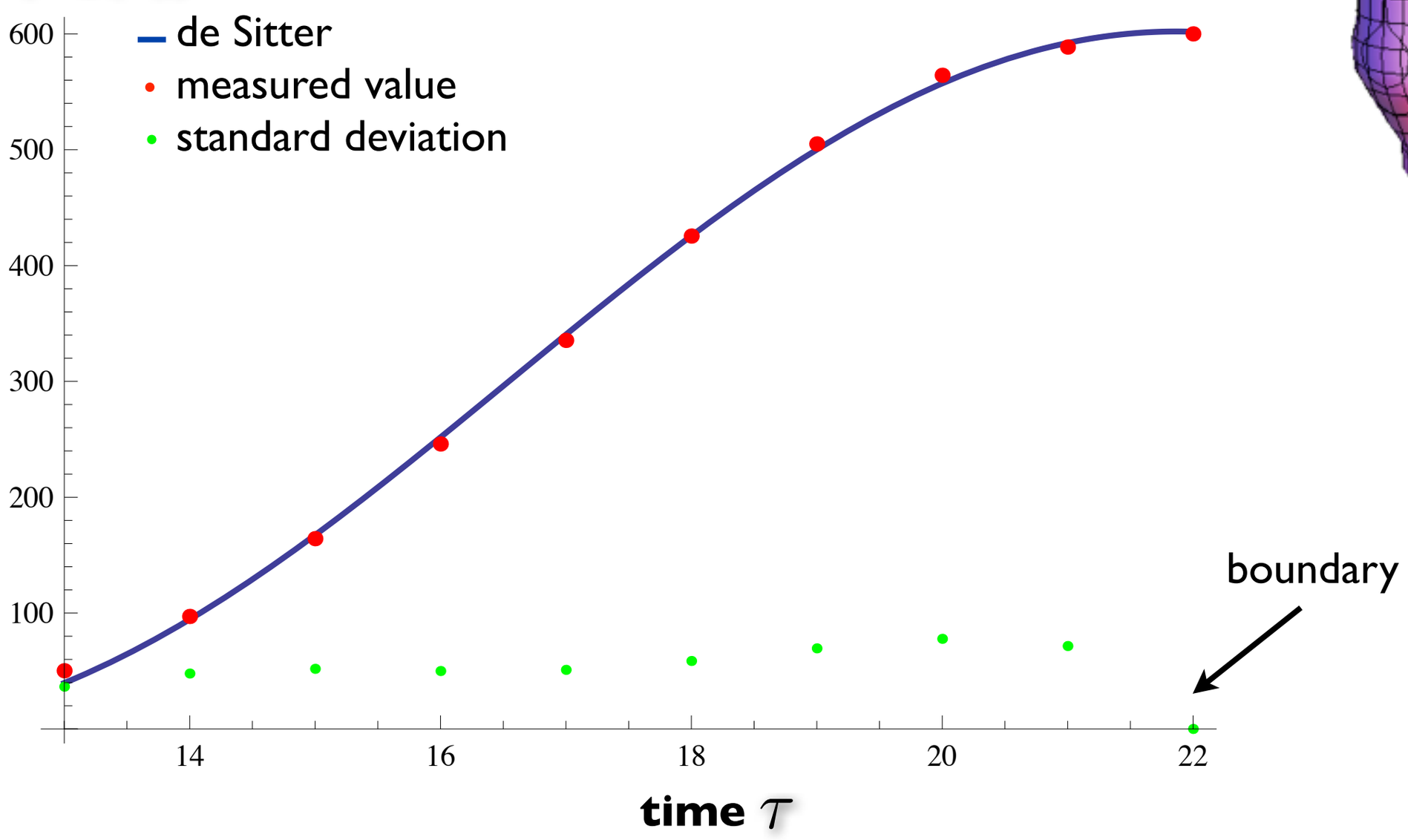
$\langle N_2(\tau) \rangle$
de Sitter
measured value
standard deviation
600
500
400
300
200
100
14
16
18
20
22
boundary
time τ

$N_2^b = 200$

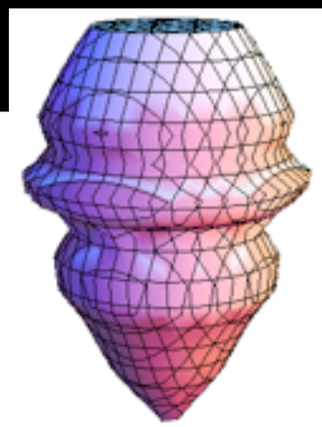

$\langle N_2(\tau) \rangle$

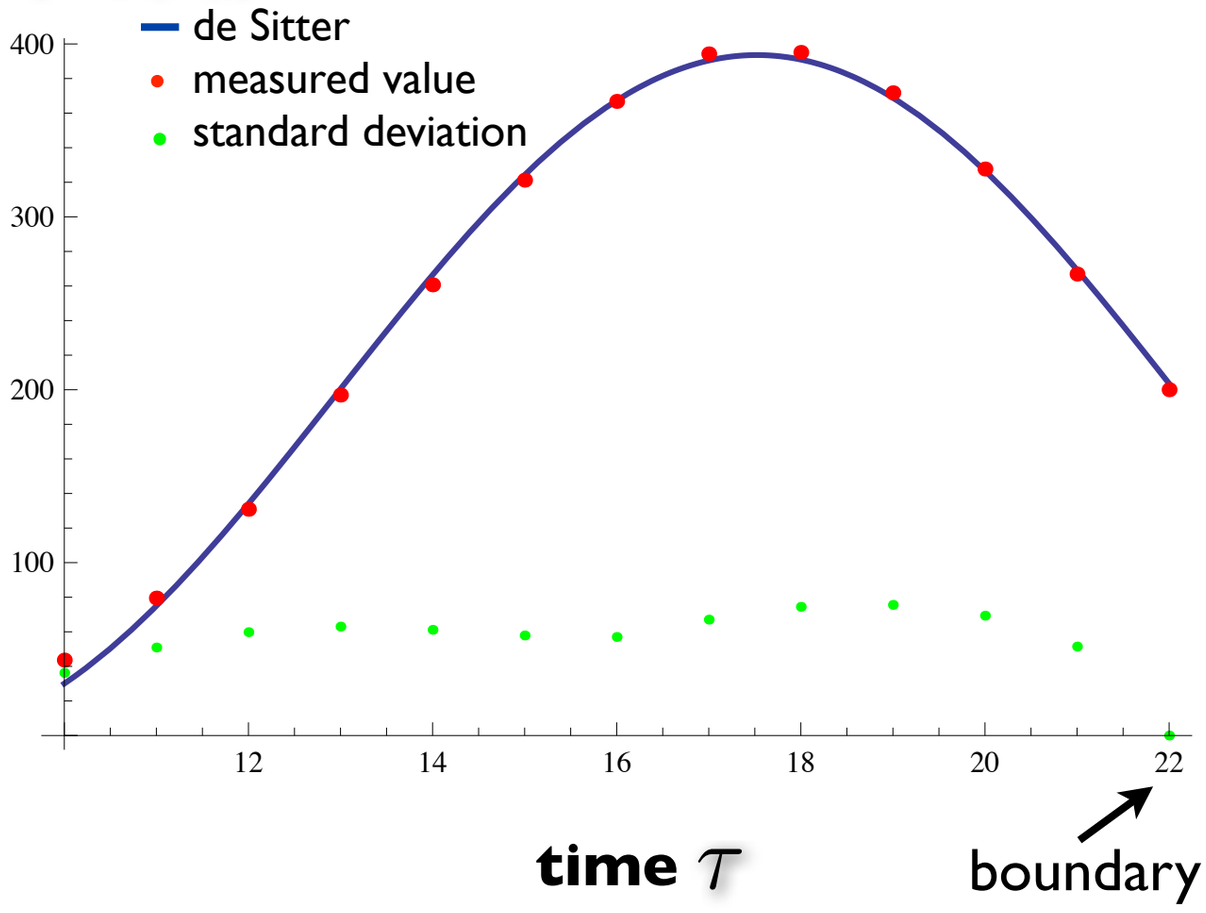

$N_2^b = 1000$

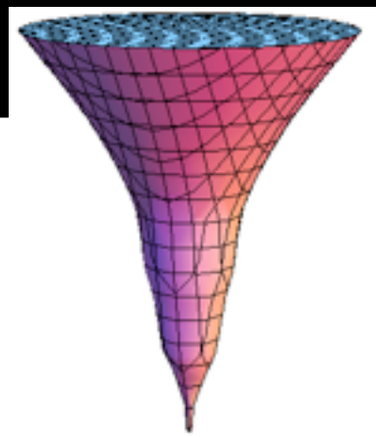

$\langle N_2(\tau) \rangle$

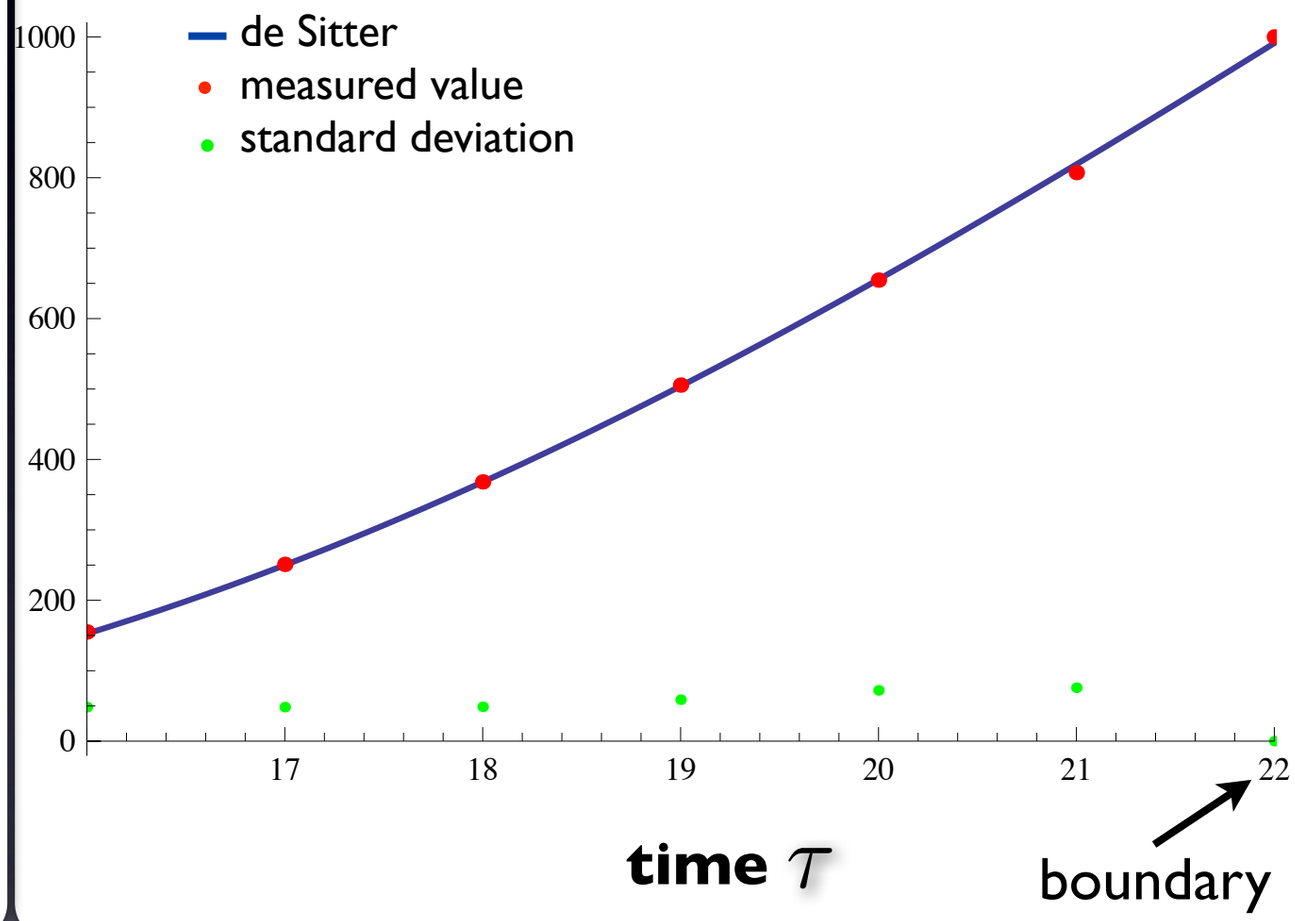

Homogeneity of spacial slice

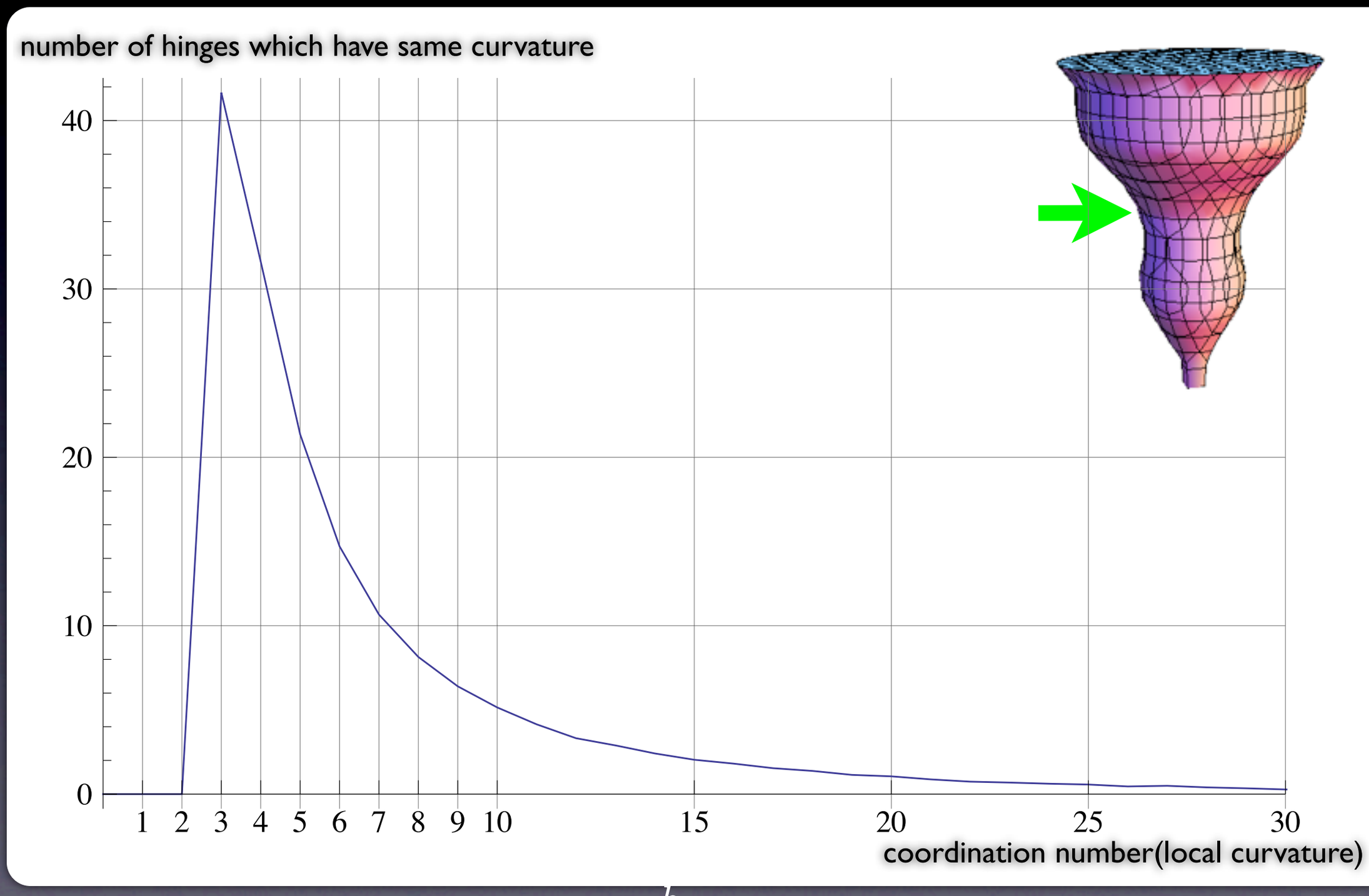

$$N_3 = 10000,\ N_2^b = 600,\ \kappa_0 = 0.4$$

Homogeneity of spacial slice

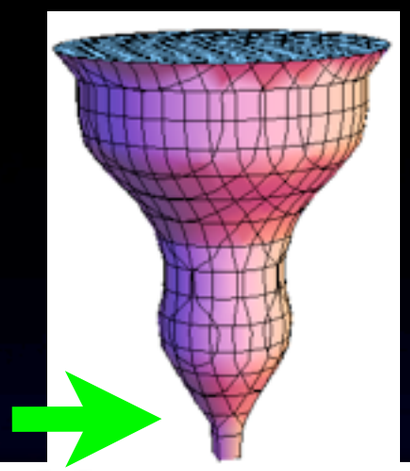

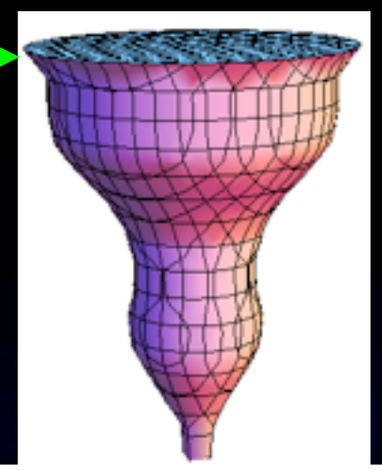

number of hinges which have same curvature

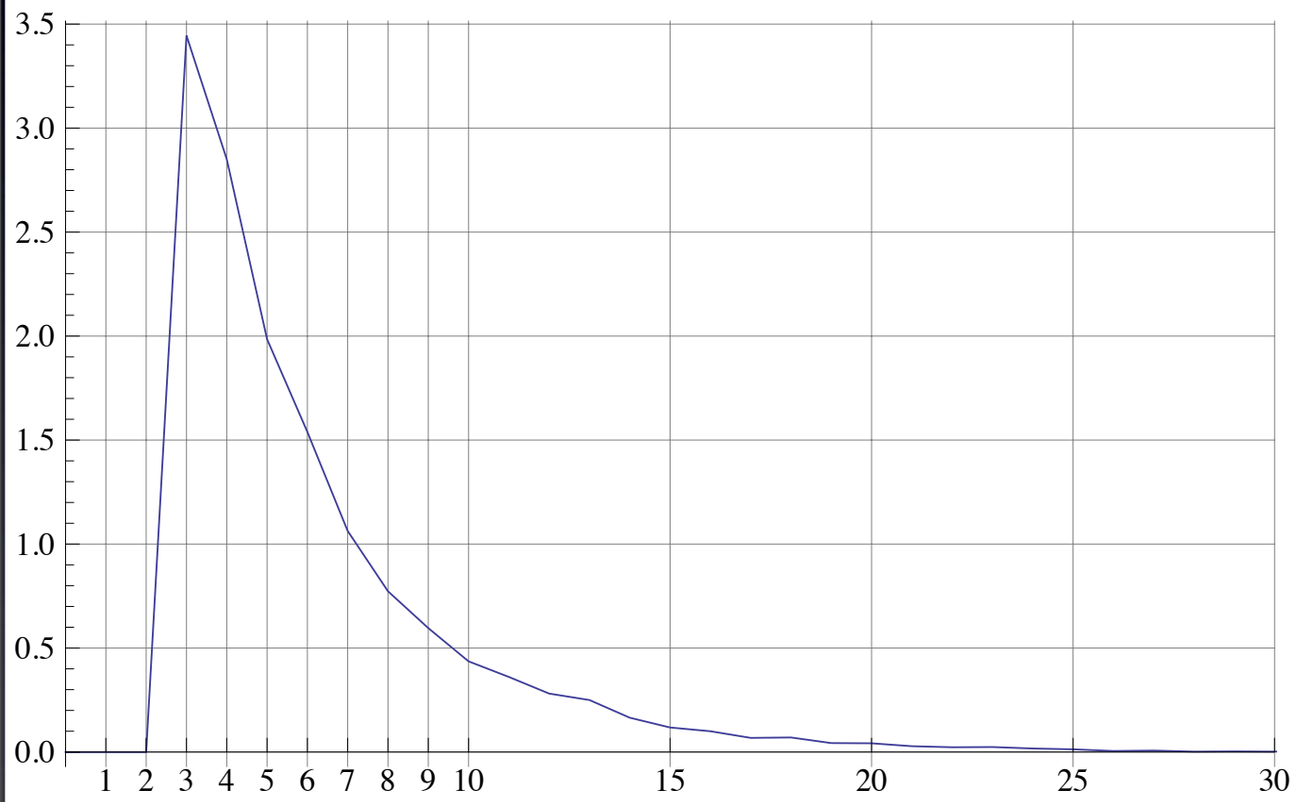

coordination number(local curvature)

number of hinges which have same curvature

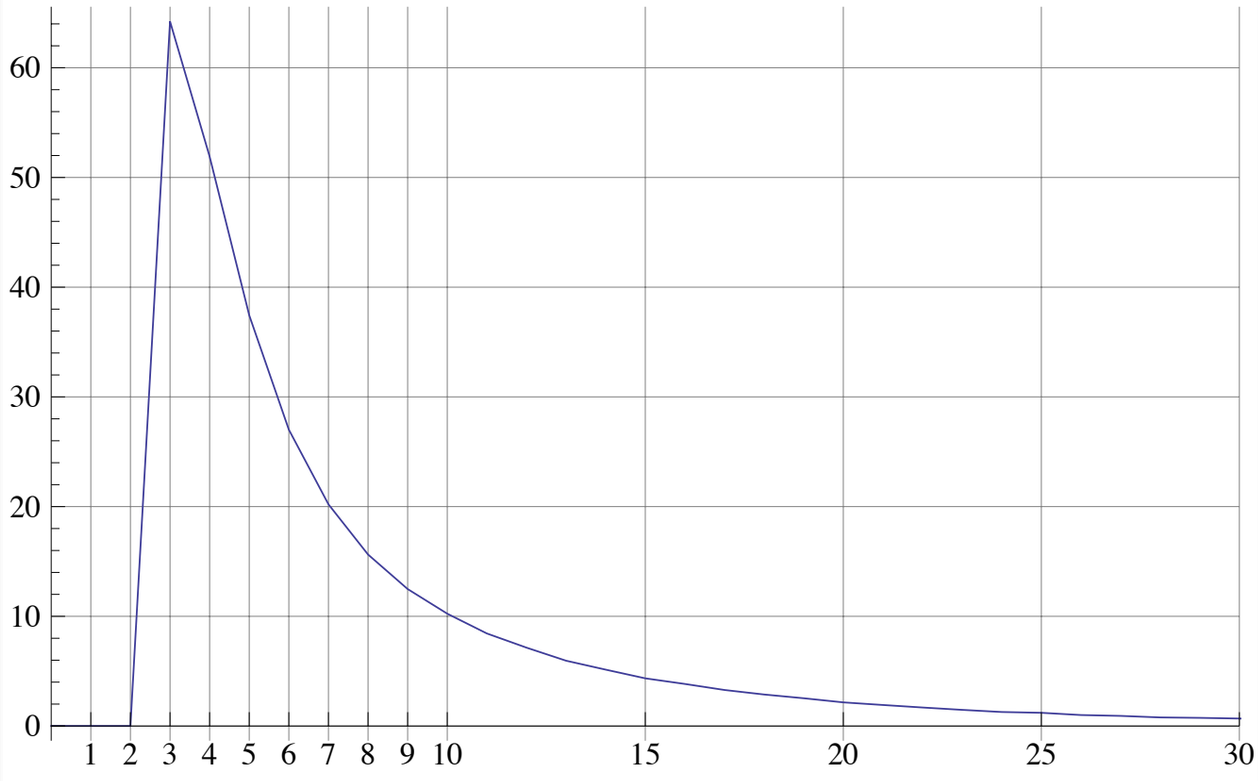

coordination number(local curvature)

$$N_3 = 10000,\ N_2^b = 600,\ \kappa_0 = 0.4$$

Summary

- **CDT is a discrete regularization method for gravitational path integral.**
- **The emergent space-time in $\kappa_0 = 0.4$ corresponds to de Sitter instanon and the spatial slices are homogenous.**

Typical configuration

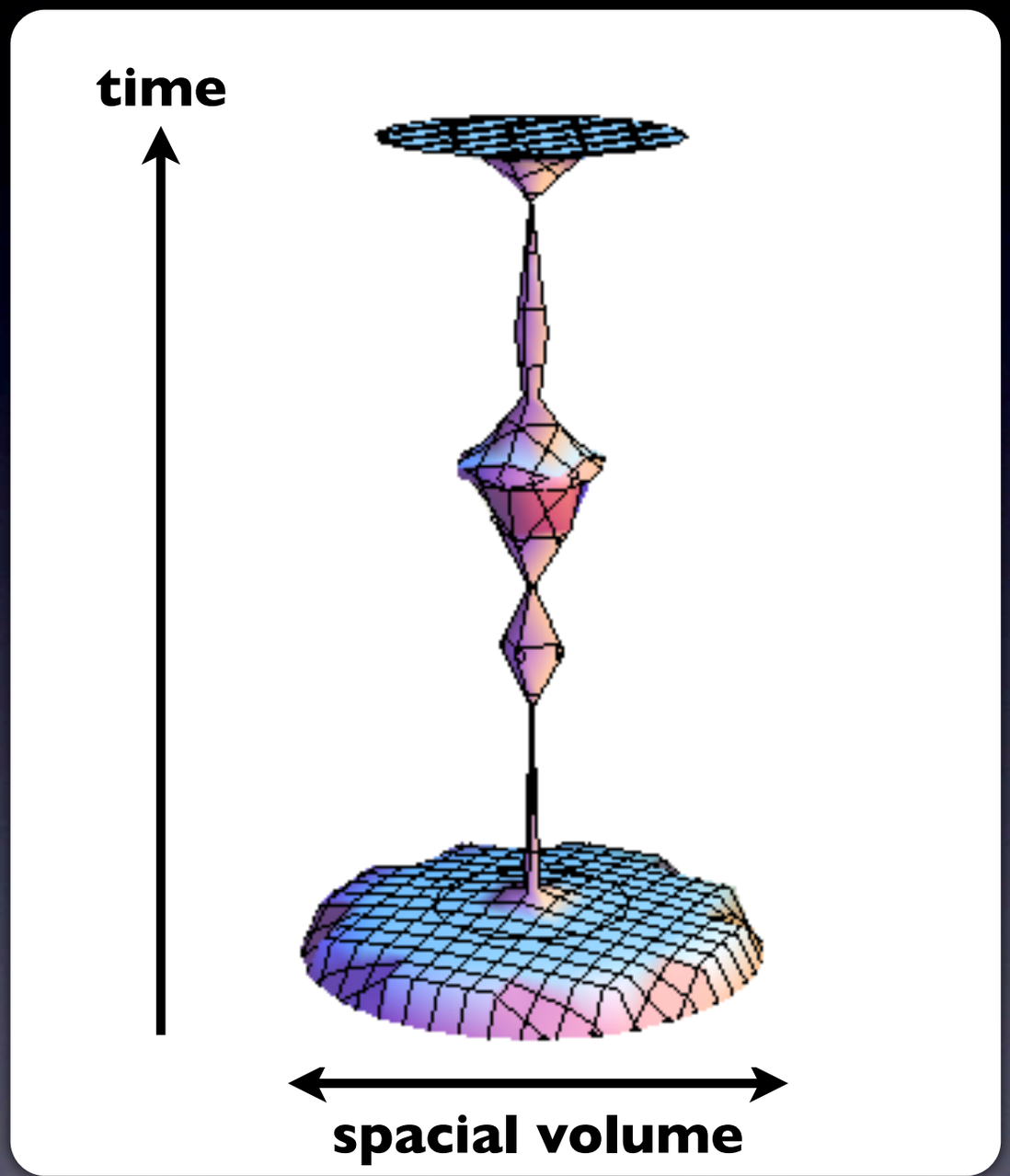

$$N_3 = 10000,\ N_2^b = 1000,\ \kappa_0 = 3.0$$

Homogeneity of space-time

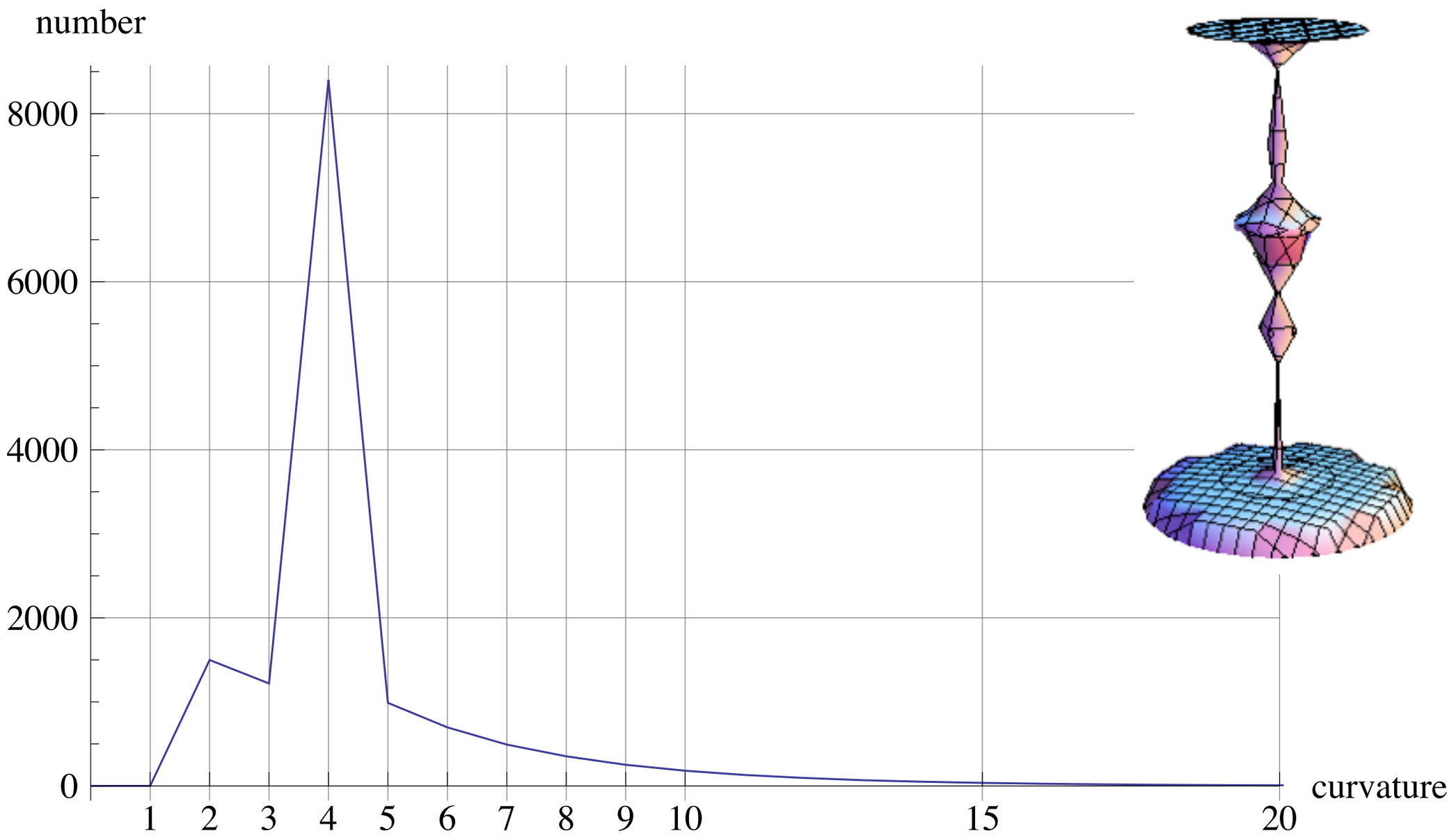

$$N_3 = 10000,\ N_2^b = 1000,\ \kappa_0 = 3.0$$

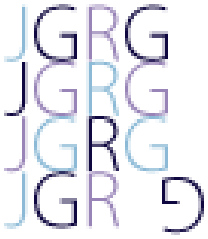

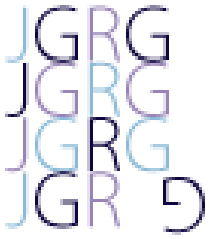

Kentaro Tanabe, JGRG 22(2012)111223

"Selfgravity effects of blackfold"

RESCEU SYMPOSIUM ON

GENERAL RELATIVITY AND GRAVITATION

JGRG 22

November 12-16 2012

Koshiba Hall, The University of Tokyo, Hongo, Tokyo, Japan





Self-gravity effects of blackfold

Kentaro Tanabe[1 (a)]

[(a)] *Departament de Física Fonamental and Institut de Ciències del Cosmos, Universitat de Barcelona, Martí i Franquès 1, E-08028 Barcelona, Spain*

Abstract

Blackfold approach can be used as a perturbative method to construct higher dimensional black hole solutions. We develop this blackfold approach to higher order and investigate the physical effects of higher order solutions such as self-gravity effects.

1 Introduction

The blackfold approach has been at first proposed as the worldvolume theory for the dynamical black branes by Emparan et. al [1], and it is supposed that the blackfold approach can be also used to construct the higher dimensional black hole solutions perturbatively. The construction of the higher dimensional black hole by the blackfold approach is based on the fact that the black hole solutions in $d \geq 6$ dimensions can have two different scales, $R \gg r_0$. Here R is the largest curvature scale of the black hole and r_0 is a thickness of the black holes. The black hole with the large angular momentum can have much bigger curvature R than its horizon thickness of r_0. Thus we can expect that the blackfold represents the black holes with large angular momentum in higher dimensions. From this speculation, Emparan et.al. constructed the higher dimensional black ring solutions with a large angular momentum perturbatively [2] and discussed phase diagrams of the various higher dimensional black holes [3]. To obtain further insight into the higher dimensional black holes, we should investigate the blackfold approach in detail and develop to higher order perturbation solutions.

In the blackfold approach, black hole solutions are constructed by matching two perturbation solutions in two different regions, far and near region. In Ref. [2], the Newtonian solutions corresponding to higher dimensional black ring was constructed and computed the first order correction to the metric in the near region by matching the Newtonian solution. In Ref [3], the Newtonian solutions corresponding to the various higher dimensional black holes were constructed and phase diagram of each solutions were proposed. In these researches, the properties of the blackfold were derived from the linear perturbation solutions. But, the effect of its backreaction has not been considered. In this sense it seems to be fair to say that we have not obtained the definite properties of higher dimensional black holes and not understood the essential property of them. In this paper we consider backreaction effects, that is, self-gravity effects, of the blackfold and investigate the properties of the higher dimensional black holes more accurately.

To study the self-gravity effects precisely, we must solve the higher order perturbation equation. The linear solution has the singular behavior on the source. The higher order perturbation equation contains the linear order solution in the source term. Thus, to solve the higher order perturbation equation, we should perform the appropriate regularization and specify the proper boundary conditions on the source. We use the technique of matched asymptotic expansion (MAE) to treat this problem. The MAE was used to compute the first correction to the metric around the near region in the original paper of the blackfold [2]. In the MAE method, we can calculate the self-gravity effects of the blackfold. The purpose of this paper is to clarify the matching ladder structure of the blackfold approach and compute the self-gravity effects.

2 Matching ladder structure

The blackfold has two separated scales $R \gg r_0$. Thus there are two different regimes of the geometry of the blackfold. In the far region $r \gg r_0$, the geometry of the blackfold can be well approximated with

[1] Email address: ktanabe@ffn.ub.edu

the perturbations by the energy-momentum tensor of the blackfold around the flat spacetimes. In the near region $R \gg r$, we can regard the geometry as the perturbation around the black p-branes. These two perturbation solutions are matched in the matching region $R \gg r \gg r_0$ and we obtain the geometry produced by the blackfold. In the MAE method, we can obtain the self-gravity corrections not only to the geometry in the far region, but also to the metric in the near region. Thus, we can check the regularity of the perturbative black hole solution including the self-gravity corrections. In this paper, we consider the blackfold which describes the d dimensional black ring solution. It is a simple task to extend our analysis to other blackfold solutions.

To clarify the matching ladder structure, we should study solutions in far and near region. In the far region, the geometry can be treated as the Newton theory and the corresponding Newton potential is produced by the energy-momentum tensor of the blackfold. In the black ring case, we find the solution at far region as

$$ds^2 = (-1+\Psi)dt^2 - 2Adtd\phi + \left(1+\frac{\Psi}{d-3}\right)ds_E^2, \tag{1}$$

where ds_E^2 is the ring coordinate as

$$ds_E^2 = dr_1^2 + r_1^2 d\Omega_{d-3}^2 + dr_2^2 + r_2^2 d\phi^2. \tag{2}$$

Ψ and A can be written as

$$\Psi = Rr_0^{d-4}\int_0^{2\pi}\frac{d\phi}{(r_1^2+(R\cos\phi - r_2)^2 + R^2\sin^2\phi)^{d-3/2}}, \tag{3}$$

and

$$A = \frac{Rr_0^{d-4}}{\sqrt{d-3}}\int_0^{2\pi}\frac{r_2\cos\phi d\phi}{(r_1^2+(R\cos\phi - r_2)^2 + R^2\sin^2\phi)^{d-3/2}}. \tag{4}$$

This Newton solution is produced by the following energy-momentum tensor

$$T_{tt} = \frac{d-2}{16\pi G}Rr_0^{d-4}\delta(r)\,,\; T_{t\phi} = \frac{\sqrt{d-3}}{16\pi G}R^2 r_0^{d-4}\delta(r). \tag{5}$$

$r=0$ represents the location of a blackfold. This energy-momentum tensor comes from Brown-York energy-momentum tensor of boosted black string. A boost parameter is determined by the blackfold equation.

This far region solution determines boundary conditions on the perturbation at near region. The geometry at near region is described by perturbations around $d-1$ dimensional boosted black string. The perturbation around this black string can be decomposed by spherical harmonics on S^{d-3}. By expanding te far region solution Eq. (1) at matching region $R \gg r \gg r_0$, we can see that the expansion parameter is r_0/R and the l mode perturbation with respect to spherical harmonics on S^{d-1} has $(r_0/R)^l$ order. Therefore the near region geometry $g_{\mu\nu}^{\rm near}$ can be represented as

$$g_{\mu\nu}^{\rm near} = g_{\mu\nu}^{\rm string} + h_{\mu\nu}, \tag{6}$$

where $g_{\mu\nu}^{\rm string}$ is a metric of boosted black string, background geometry. $h_{\mu\nu}$ is a perturbation metric which can be written as

$$h_{\mu\nu} = \sum_l \left(\frac{r_0}{R}\right)^l Y^l C_{\mu\nu}^l, \tag{7}$$

where Y^l is a spherical harmonics on S^{d-3}. The amplitude of the perturbation $C_{\mu\nu}^l$ is determined by the far region solution. Furthermore, using this corrected near region geometry as a boundary condition, we can compute the correction to the far region solution Eq. (1). This matching structure can be shown in Figure.1 up to self-gravity order. Here we call the correction to mass, angular momentum and area of black ring self-gravity effects. These corrections can be read from the corrections to Brown-York energy momentum tensor. As seen in Fig.1, there are two contribution to the self-gravity corrections. One is coming from $l=0$ mode perturbation on black string. Another is from the non linear contribution of $l>0$ mode perturbation. For instance, in $d=6$ dimensions case, self-gravity corrections have $(r_0/R)^2$ order. $l=1$ mode perturbation has r_0/R order and its quadratic contribution can be source of $l=0$ mode perturbation with $(r_0/R)^2$ order.

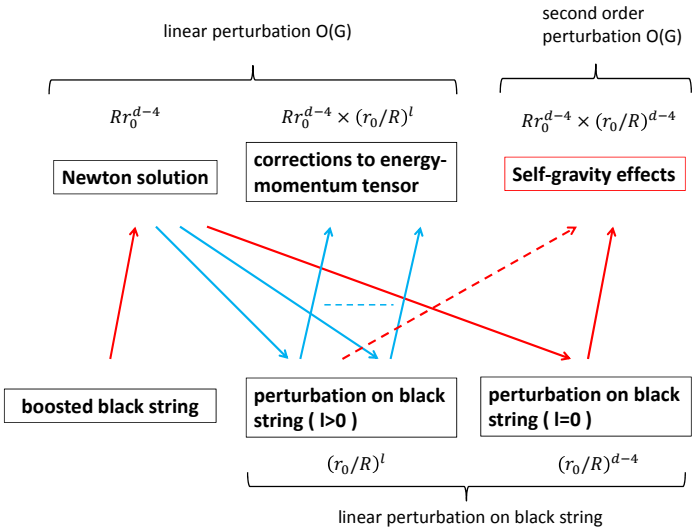

Figure 1: The matching ladder structure up to self-gravity order is shown. The red line represents the ladder of $l = 0$ mode perturbation. The blue line corresponds to $l > 0$ mode perturbation matching. The dashed red line describes the non linear contribution of $l > 0$ mode perturbation to $l = 0$ mode perturbation.

3 Self-gravity effects

To see self-gravity effects of blackfold, we study the second order solution at far region. The Newton solution Eq. (1) is the first order solution. The metric $g^{\rm far}_{\mu\nu}$ at far region can be written up to the second order as

$$g^{\rm far}_{\mu\nu} = \eta_{\mu\nu} + h^{(1)}_{\mu\nu} + h^{(2)}_{\mu\nu}, \tag{8}$$

where $\eta_{\mu\nu}$ is a flat metric and $h^{(1)}_{\mu\nu}$ is the first order solution. $\eta_{\mu\nu} + h^{(1)}_{\mu\nu}$ corresponds to the Newton solution Eq. (1). Then, the equation for the second order metric $h^{(2)}_{\mu\nu}$ can be derived from the Einstein equation as

$$\begin{aligned}\frac{1}{2}\Delta h^{(2)}_{\mu\nu} &= \frac{1}{2}h^{(1)\rho\sigma}\nabla_\mu\nabla_\nu h^{(1)}_{\rho\sigma} + \frac{1}{4}\nabla_\mu h^{(1)\rho\sigma}\nabla_\nu h^{(1)}_{\rho\sigma} + \frac{1}{2}(\nabla^\rho h^{(1)\sigma}{}_\mu - \nabla^\sigma h^{(1)\rho}{}_\mu)\nabla_\rho h^{(1)}_{\sigma\nu} \\ &\quad - \frac{1}{2}h^{(1)\rho\sigma}(\nabla_\rho\nabla_\mu h^{(1)}_{\sigma\nu} + \nabla_\rho\nabla_\nu h^{(1)}_{\sigma\mu} - \nabla_\rho\nabla_\sigma h^{(1)}_{\mu\nu}),\end{aligned} \tag{9}$$

where ∇_μ is a covariant derivative with respect to $\eta_{\mu\nu}$. Solving this second order equation, we can obtain the corrections to the mass, angular momentum and are of black ring solutions. The boundary conditions for the second order solutions can be read from the perturbed metric at near region (see Fig. 1). It is useful for understanding the physical meaning of corrections to draw the phase diagram of black ring solutions. To do this, we define the normalized area s and angular j momentum by the mass as

$$j^{d-3} = \frac{\Omega_{d-3}}{2^{d+1}}\frac{(d-2)^{d-2}}{(d-3)^{d-3/2}}\frac{J^{d-3}}{GM^{d-2}}, \tag{10}$$

$$s^{d-3} = \frac{\Omega_{d-3}}{2(16\pi)^{d-3}}(d-2)^{d-2}\left(\frac{d-4}{d-3}\right)^{d-3/2}\frac{S^{d-3}}{(GM)^{d-2}}. \tag{11}$$

Here M, J and S is a mass, angular momentum and are of black ring solution respectively.

In $d = 6$ dimensional case, the phase diagram of black ring up to the second order solutions is described in Fig. 2. Compared with the first order solutions, the area of the second order solutions is

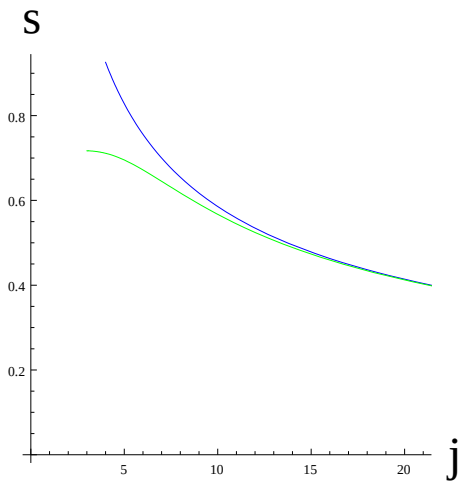

Figure 2: The blue line is the phase diagram up to first order, and the green line represents the phase diagram up to the second order solutions. This diagram shows the self-gravity effects of blackfold works attractively and its form is shrinking.

decreasing. This is because the self-gravity effects work attractively and the solutions becomes shrinking. This behavior does not depend on its dimensions, and in more higher dimensions $d > 6$, same behavior of the second order solutions can be confirmed.

4 Summary

The blackfold approach is very useful approach to investigate the physical properties of higher dimensional black holes. To develop the idea of blackfold, we should understand more precisely how black hole solutions can be constructed by this approach. In this paper, we clarify the matching ladder structure of the blackfold approach. Using this matching ladder, self-gravity effects of black ring solutions can be computed, and its attractiveness is shown explicitly.

References

[1] R. Emparan, T. Harmark, V. Niarchos and N. A. Obers, Phys. Rev. Lett. **102**, 191301 (2009)

[2] R. Emparan, T. Harmark, V. Niarchos, N. A. Obers and M. J. Rodriguez, JHEP **0710**, 110 (2007)

[3] R. Emparan, T. Harmark, V. Niarchos and N. A. Obers, JHEP **1004**, 046 (2010)

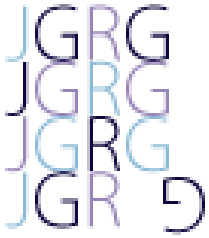

Ryotaku Suzuki, JGRG 22(2012)111224

"Analysis of Gregory-Laflamme mode in large D limit"

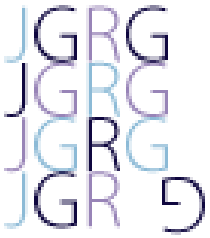

RESCEU SYMPOSIUM ON

GENERAL RELATIVITY AND GRAVITATION

JGRG 22



November 12-16 2012

Koshiba Hall, The University of Tokyo, Hongo, Tokyo, Japan



Analysis of Gregory-Laflamme mode in large D limit

Ryotaku Suzuki (Kyoto University)
with Roberto Emparan (University of Barcelona, ICREA)

JGRG22, November 12-16, 2012, RESCEU SYMPOSIUM

Outline

1. Introduction
2. Large D limit
3. Dispersion relation
4. Summary

Outline

1. Introduction
2. Large D limit
3. Dispersion relation
4. Summary

Gravity in Higher Dimension

Why higher dimension ?

String theory ➔ spacetime dimension > 4

- Various compactification
- Large extra dimension → higher dimensional gravity

Black hole in Higher Dimension

→ No uniqueness, No topology theorem

- Black String, Brane (KK spacetime)
- Black Ring, Black Saturn, etc…

Gregory-Laflamme Instability

Characteristic in extended black object (sting, brane,…)
Long wave length instability ~ hydrodynamic instability

Gregory-Laflamme Instability

- In 1993, Gregory and Laflamme found a long wave length instability of black string (brane)

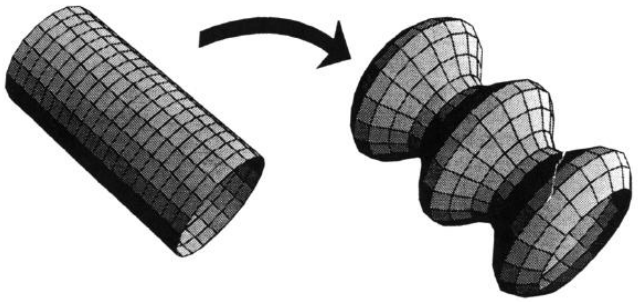

Gregory, Laflamme, 1994

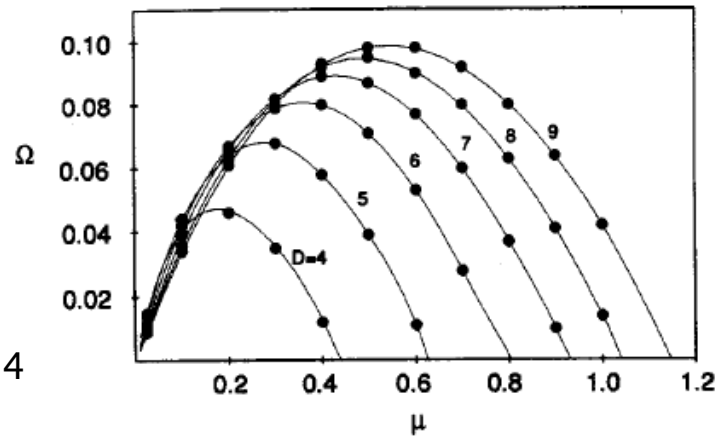

threshold : thickness ~ wave length

Importance

- Universal property for extended objects
- Determine Phase Diagram in KK spacetime

UniformBS – NUBS – (caged) Black hole

Outline

1. Introduction
2. Large D limit
3. Dispersion relation
4. Summary

Threshold mode k_GL in large D

Numerical Analysis

Sorkin (2004) studied the threshold mode numerically up to D=50

and observed $\mu_{GL} \propto \gamma^D \quad \gamma \approx 0.686$

$$\mu_{GL} = \frac{(d-2)\Omega_{d-2}}{16\pi}\left(\frac{r_0\, k_{GL}}{2\pi}\right)^{d-3}$$

dimensionless mass

$$\mu := G_D M / L^{D-3}$$

Large D limit

Kol, Sorkin(2004), Asnin, et.al.(2007)

solved analytically the threshold mode in large D limit

$$k_{GL} \to \sqrt{d} \;\Rightarrow\; \tilde{\gamma} = \sqrt{\frac{e}{2\pi}} \approx 0.658$$

agree with Sorkin(2004)

Matched asymptotic expansion

near horizon — new coordinate $X = r^n$ — expand with 1/n

asymptotic — expand with r_0^n / r^n

Hydrodynamical approximation

- Camps et.al(2010) studied the instability in long wave length limit ➔ Narvier-Stokes Eq. +viscosity

dispersion relation

$$\Omega = \frac{k}{\sqrt{n+1}}\left(1 - \frac{n+2}{n\sqrt{n+1}} k r_0\right)$$

valid up to k^3

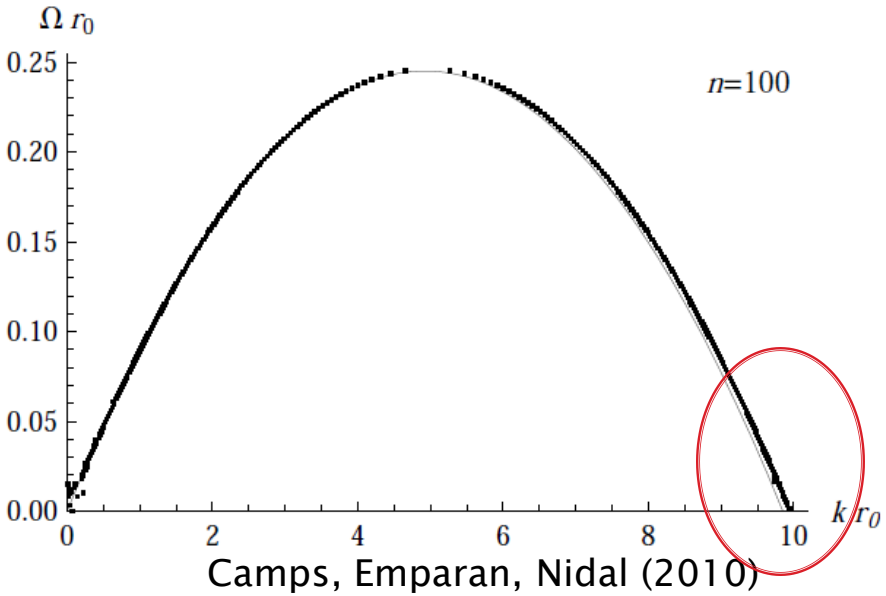

Camps, Emparan, Nidal (2010)

highly coincident with numerical data even k is large !

they proposed at large D

$$\Omega \to \frac{k}{\sqrt{n}}\left(1 - \frac{k}{\sqrt{n}}\right)$$

Question
Can we prove this dispersion relation analytically ?

Outline

1. Introduction
2. Large D limit
3. Dispersion relation
4. Summary

Set up and Master equation

Black String background

n = D – 4 Large D → Large n

$$ds_0^2 = -f(r)dt^2 + \frac{1}{f(r)}dr^2 + dz^2 + r^2 d\Omega_{n+1}^2 \qquad f(r) = 1 - r_0^n/r^n$$

Scalar Perturbation with Transverse-Traceless gauge

$$h_{\mu\nu} = \Re \exp\left[\left(\frac{\Omega t}{r_0} + \frac{ikz}{r_0}\right) P_{\mu\nu}\right]$$

$$P_{tt} = -f\psi(r), \quad P_{tr} = \eta(r), \quad P_{rr} f^{-1}\chi(r), \quad P_\Omega = r^2\kappa(r)\gamma_\Omega$$

Master equation for $\eta(r)$

➔ Same equation in GL94

Assumption

$$k = \sqrt{n}\hat{k}$$

$$\begin{aligned}
&(n^2 - 4r^2\Omega^2 - 2\left(n^2 + 2k^2r^2\right) f + n^2 f^2)\eta'' \\
&+\frac{1}{rf}(3\left(n^3 - 4nr^2\Omega^2\right) + \left(3n^2 - 6n^3 - 4r^2\Omega^2 + 8nr^2\left(-k^2 + \Omega^2\right)\right) f \\
&+ \left(-6n^2 + 3n^3 - 4k^2r^2 + 4k^2nr^2\right) f^2 + 3n^2 f^3)\eta' \\
&+\frac{1}{r^2 f^2}(n^4 - 5n^2r^2\Omega^2 + 4r^4\Omega^4 + \left(3n^3 - n^4 + 8k^2r^4\Omega^2 + n^2r^2\left(k^2 + 10\Omega^2\right)\right) f \\
&+ \left(-6n^3 - n^4 + 4nr^2(\Omega^2 - k^2) + 4r^2\left(k^4r^2 + \Omega^2\right) + n^2\left(1 - 2k^2r^2 - 5r^2\Omega^2\right)\right) f^2 \\
&+ \left(3n^3 + n^4 + 4k^2r^2 + 8k^2nr^2 + n^2\left(-2 + k^2r^2\right)\right) f^3 + n^2 f^4)\eta = 0
\end{aligned}$$

Near horizon in Large D

"Good" coordinate in Large D (used in Asnin et. al. (2007))

$X = r^n$ the effect of the horizon correctly incorporated at large D expansion

$$\eta(X)'' + P_X \eta(X)' + Q_X \eta(X) = 0$$

up to 1/n ➔ $X(X-1)^3\eta(X)'' + (X-1)^2(4X-1)\eta(X)' + (X-1)(2X-1)\eta(X) = S_1[\eta]$

$$S_1[\eta] = -\frac{1}{n}(2(X-1)^3(4\hat{k}^2X^2 - 2\hat{k}^2X + 1)\eta(X)' + (X-1)^2(\hat{k}^2(8X^2 - 4X + 1) + 3)\eta(X))$$

leading solution

$$U_1(X) = \frac{1}{X-1},\ U_2(X) = \frac{\ln(X-1) - \ln X}{X-1}$$

$U_1 \simeq X^{-1} + X^{-2}$ and $U_2 \simeq -1/X^2$ when $X \gg 1$,

➔ require up to $1/r^{2n}$ in asymptotic region

Asymptotic region in Large D

Leading order f(r) → 1

$$r^2\eta'' + (n+1)\eta' - (k^2+\Omega^2)\eta = 0.$$

Expansion with r_0^n/r^n

regularity at the infinity

→ $$\eta_{as}(r) = \frac{1}{r^{\frac{n}{2}}} K_\nu(k_\Omega r).$$

modified Bessel of 2nd kind

$$\nu = (n+2)/2 \text{ and } k_\Omega = \sqrt{k^2+\Omega^2}.$$

Next to Leading

modified Bessel Eq. with source term

$$u_1(r) = r^{\frac{n}{2}}\eta_1(r)$$

$$x = k_\Omega r$$

$$x u_{1,xx} + u_{1,x} - (x + \nu^2 x^{-1})u_1 - \mathcal{S}_1[u_0] = 0$$

$$\mathcal{S}_1[u] \equiv k_\Omega^{2\nu-2} x^{-2\nu+1}[(A_1 x^2 + A_2)u(x) + A_3 x u'(x)]$$

Using Green function

→ $$u_1(x) = C_1 K_\nu(x) - K_\nu(x)\int_{-}^{x} I_\nu(y)\mathcal{S}_1[u_0](y)dy - I_\nu(x)\int_x^\infty K_\nu(y)\mathcal{S}_1[u_0](y)dy$$

just contribute to ovarall scaling

$$\eta_{as,1} \simeq \left(1 - \frac{1}{2n} + \frac{\hat{k}^2}{2n} + \frac{\Omega^2}{2\hat{k}^2 n}\right)\frac{1}{r^n}\frac{K_\nu}{r^{\frac{n+2}{2}}}$$ (up to 1/n)

Intermediate region

Asymptotic solution

$X = r^n < n^k (k > 1 : \text{const.})$ so that $n^{-1} \ln X$ is subleading

$$\eta_{as} \propto \frac{1}{X} + \frac{1}{X^2} - \frac{1+\hat{k}^2}{n}\frac{\ln X}{X} + \left(\frac{\Omega^2}{2\hat{k}^2 n} - \frac{1}{2n} + \frac{\hat{k}^2}{2n}\right)\frac{1}{X^2} + \mathcal{O}(X^{-3}, n^{-2})$$

Leading at near horizon

$$\eta_0(X) = \frac{1}{X-1} \quad \rightarrow \quad S_1[U_1] = -\frac{\hat{k}^2+1}{n}(X-1)$$

$$\therefore \frac{K_\nu}{r^{\frac{n+2}{2}}} \propto \frac{1}{X}\left(1 - \frac{1+\hat{k}^2}{n}\ln X\right)$$

Sub-leading at near horizon

$$\begin{aligned}\eta_1(X) &= \frac{C_1}{X-1} + C_2\frac{\ln(X-1) - \ln X}{X-1} - \frac{1+\hat{k}^2}{n}\frac{\ln(X-1)}{X-1} \\ &\simeq \frac{C_1}{X} - \frac{1+\hat{k}^2}{n}\frac{\ln X}{X} + \frac{nC_1 - nC_2 + 1 + \hat{k}^2}{X^2}\end{aligned}$$

$$\rightarrow \quad C_1 = 0 \quad \text{and} \quad nC_2 - 1 - \hat{k}^2 = -\frac{\Omega^2}{2\hat{k}^2} + \frac{1}{2} - \frac{\hat{k}^2}{2}$$

Horizon regularity

At X -> 1, the regular solution is

large n limit

$$\eta(X) = (X-1)^{-1+\frac{\Omega}{n}}(1+\mathcal{O}(X-1)) \simeq \frac{1}{X-1}\left(1+\frac{\Omega}{n}\ln(X-1)+\dots\right)$$

matched solution

$$\eta(X) \simeq \frac{1}{X-1} + \frac{nC_2 - 1 - \hat{k}^2}{n}\frac{\ln(X-1)}{X-1}$$

$$nC_2 - 1 - \hat{k}^2 = -\frac{\Omega^2}{2\hat{k}^2} + \frac{1}{2} - \frac{\hat{k}^2}{2}$$

➔ $$\Omega = -\frac{\Omega^2}{2\hat{k}^2} + \frac{1}{2} - \frac{\hat{k}^2}{2}$$ **Leading order matching**

➔ $$\Omega = \hat{k} - \hat{k}^2,\ -\hat{k} - \hat{k}^2$$

Expected growing mode !!

Outline

1. Introduction
2. Large D limit
3. Dispersion relation
4. Summary

Summary

- We analytically solved the scalar perturbation on black brane in large D limit and obtained the expected dispersion relation.

- Our calculation shows that large D expansion should be useful analytic approximation
  in higher dimension.
  Application to another situation seems possible in the similar way.

Thank you !

Appendix

A. Matching at singular point

Master Eq has a singular point between horizon and the infinity

$$r_s^n = \frac{\sqrt{n}}{2\hat{k}} \exp\left(\frac{\hat{k}}{\sqrt{n}} - \frac{1}{2n} \ln \frac{n}{4\hat{k}^2} - \frac{\Omega^2}{2\hat{k}^2 n} + \frac{1}{2n^{\frac{3}{2}}} \left(-2\hat{k} - \frac{\hat{k}^3}{3} - \frac{\Omega^2}{\hat{k}} + \hat{k} \ln \frac{n}{4\hat{k}^2} \right) + \mathcal{O}(n^{-2}) \right)$$

We first attempted to do matching at the singular point as Kol, Sorkin (2004)

$$r_s = 1 + \frac{1}{2n} \ln \frac{n}{4\hat{k}^2} +$$

B.C $$\frac{r_s \eta'(r_s)}{\eta(r_s)} = -\frac{r_s Q_\eta}{P_\eta}\Big|_{r_s} = -n - 2\hat{k}\sqrt{n} - 1 - 3\hat{k}^2 - \frac{1}{\sqrt{n}}(2\hat{k}^3 + \hat{k} \ln \frac{n}{4\hat{k}^2} - \hat{k} + \frac{2\Omega^2}{\hat{k}}) + \mathcal{O}(n^{-1})$$

LO $r^{-n/2} K_\nu(k_\Omega r)$ ➔ $r_s \eta'_{as}(r_s)/\eta_{as}(r_s) = -n - \hat{k}^2 - 1 + \ldots$ trivial.

NLO $u_1(r) = r^{\frac{n}{2}} \eta_1(r)$ ➔ $\frac{r_s \eta_{as}(r_s)'}{\eta_{as}(r_s)} = -n - 2\hat{k}\sqrt{n} + \mathcal{O}(1)$ trivial…

$$u_1(x) = C_1 K_\nu(x) - K_\nu(x) \int_{x_s}^{x} I_\nu(y) \mathcal{S}_1[u_0](y) dy - I_\nu(x) \int_{x}^{\infty} K_\nu(y) \mathcal{S}_1[u_0](y) dy$$

NNLO

trivial…….

$$u_2(x) = -K_\nu(x) \int_{x_s}^{x} I_\nu(y) [\mathcal{S}_1[u_1](y) + \mathcal{S}_2[u_0](y) dy - I_\nu(x) \int_{x}^{\infty} K_\nu(y) [\mathcal{S}_1[u_1](y) + \mathcal{S}_2[u_0](y) dy$$

➔ $$\frac{r_s \eta'_{as}(r_s)}{\eta_{as}(r_s)} \sim -n - 2\hat{k}\sqrt{n} - 1 - 3\hat{k}^2$$

B. failure in KS04

As B.C. for asymptotic sols, Kol,Sorkin(2004) used

$$\chi'(r_s)/\chi(r_s) = -\frac{d}{r_s}$$

because master Eq. is singular at $r_s^{d-3} = \frac{d-1}{2}$

they say since $-d = \frac{r_s \chi'_{as}(r_s)}{\chi_{as}(r_s)} = -d + 1 - k^2/d$ ➔ $k_{GL} \to \sqrt{d}$

But, since 1/r^n ~ 1/n at r_s, NLO should affect the matching.

We calculated the next order and …

$$\frac{r_s \chi'_{as}(r_s)}{\chi_{as}(r_s)} = -d + 1 - k^2/d - (1 - k^2/d)$$

canceled

➔ Trivial matching !!

coincidence or
reflecting some physics ?

C. Asymptotic Perturbation

$$u_1(r) = r^{\frac{n}{2}}\eta_1(r)$$

$$xu_{1,xx} + u_{1,x} - (x + \nu^2 x^{-1})u_1 - \mathcal{S}_1[u_0] = 0$$

$$\mathcal{S}_1[u] \equiv \quad k_\Omega^{2\nu-2} x^{-2\nu+1}[(A_1 x^2 + A_2)u(x) + A_3 x u'(x)]$$

$$\begin{aligned}
A_1 &= k_\Omega^{-4}(k^4 + 3k^2\Omega^2 + 2\Omega^4) \simeq 1 \\
A_2 &= \frac{1}{2}k_\Omega^{-2}(3n^2\Omega^2 + 2n(n-1)k^2) \simeq n^2 \\
A_3 &= -k_\Omega^{-2} n(2k^2 + 3\Omega^2) \simeq -2n
\end{aligned}$$

$$\mathcal{S}_2[u] \equiv \quad \frac{k_\Omega^{4\nu-4}}{4x^{4\nu-1}}[(B_1 x^4 + B_2 x^2 + B_3)u(x) + (B_4 x^2 + B_5)xu'(x)]$$

$$\begin{aligned}
B_1 &= 4(k^2 + 3\Omega^2)k_\Omega^{-2} \simeq 4 \\
B_2 &= (2k^4(3n^2 - 2n) + 2n^2\Omega^4 + 10n^2k^2\Omega^2)k_\Omega^{-4} \simeq 6n^2 \\
B_3 &= n^4 + 3n^3 + 2n^2 \simeq n^4 \\
B_4 &= -2n(4k^4 + 12k^2\Omega^2 + 6\Omega^4)k_\Omega^{-4} \simeq -8n \\
B_5 &= 2n^2(n+1) \simeq 2n^3
\end{aligned}$$

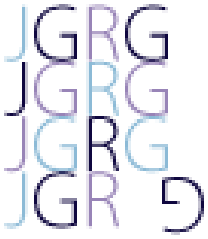

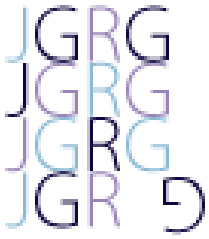

Makoto Narita, JGRG 22(2012)111225

"Global properties of solutions to the Einstein-matter equation"

RESCEU SYMPOSIUM ON

GENERAL RELATIVITY AND GRAVITATION

JGRG 22

November 12-16 2012

Koshiba Hall, The University of Tokyo, Hongo, Tokyo, Japan





Global properties of solutions to the Einstein-matter equations

Makoto Narita[1]

[1] *Department of Integrated Arts and Science, Okinawa National College of Technology, 905, Aza-Henoko, Nago, Okinawa 905-2192, Japan*

Abstract

We investigate global properties of magnetic Gowdy spacetimes. First, a global in time existence theorem for the Einstein-Maxwell equations with Gowdy symmetry. Second, for polarized magnetic Gowdy case, asymptotically velocity terms dominated singular solutions are constructed by using the Fuchsian technique.

1 Introduction

1.1 Singularity theorems and two conjectures

Singularity theorems are the most fundamental and important theorems in classical general relativity, which are proved by Penrose and Hawking in 1960's [6].

Theorem 1 (Penrose) *Suppose the following conditions hold: (1) a Cauchy surface Σ is noncompact, (2) the null convergence condition, (3) Σ contains a closed trapped surface. Then the corresponding maxmal future development $D^+(\Sigma)$ is incomplete.*

Theorem 2 (Hawking) *Suppose the following conditions hold: (1) a Cauchy surface Σ is compact, (2) the timelike convergence condition, (3) the generic condition. Then the corresponding maxmal Cauchy development $D(\Sigma)$ is incomplete.*

These theorems say physically reasonable spacetimes have singularities in general. However, (1) the theorems do not say us *nature of singularity* and (2) *predictability* is breakdown if singularity can be seen. For problem (1), a conjecture has been proposed:

Conjecture 1 (Belinskii-Khalatnikov-Lifshitz (BKL) conjecture) *Solutions to the Einstein(-matter) equations should be Kasner-like ones near spacetime singularity.*

For (2), there should not exist naked singularity physically, that is,

Conjecture 2 (Strong cosmic censorship (SCC) conjecture) *Generic Cauchy data sets have maximal Cauchy developments which are locally inextendible as Lorentzian manifolds.*

To prove these conjectures, we need to show

- *global existence theorems* of solutions to the Einstein(-matter) equations in suitable coordinates,
- existence of Kasner-like solutions near spacetime singularity *in generic*,
- and *inextendibility* of spacetimes.

There are some results for these problems (see [2, 5, 10, 11]). To solve global problems for the Einstein(-matter) equations, some assumptions will be needed, because the equations are very complicated nonlinear PDEs and then we have less mathematical tools to analyze such equations. In this work, we assume

- Existence of some spacelike Killing vectors will be assumed (so called *Gowdy spacetimes*, which are the most simplest inhomogeneous ones including dynamical degree of freedom of gravity) and
- Maxwell field as matter will be assumed.

[1] E-mail:narita@okinawa-ct.ac.jp

2 Einstein-Maxwell system in Gowdy symmetric spacetimes

2.1 Einstein equations in the areal coordinate

The action we will consider is

$$S = \int d^4x\sqrt{-g}\left[-R + F^2\right]. \tag{1}$$

Varying this action, we have the Einstein-Maxwell equations as follows:

$$R_{\mu\nu} = 2F_{\mu\rho}F^{\rho}_{\nu} - \frac{1}{2}g_{\mu\nu}F^2, \tag{2}$$

$$\nabla_\mu(\tilde{F}^{\mu\nu}) = 0, \tag{3}$$

$$\nabla_\mu F^{\mu\nu} = 0, \tag{4}$$

where $F_{\mu\nu} := 2\nabla_{[\mu}A_{\nu]}$, $\tilde{F}_{\mu\nu} := \frac{1}{2}\sqrt{-g}\epsilon_{\mu\nu\delta\rho}F^{\delta\rho}$. The metric for Gowdy symmetric spacetimes, whose spacial topology is T^3 is given by

$$g = -e^{2(\eta-U)}\alpha dt^2 + e^{2(\eta-U)}d\theta^2 + e^{2U}(dx + Ady)^2 + e^{-2U}t^2dy^2, \tag{5}$$

where η, α, U and A are functions of $t \in (0,\infty)$ and $\theta \in T^1$. We call this *areal coordinate*. We assume that the field strength of the Maxwell field is

$$F = Bdx \wedge dy.$$

From the Maxwell equations, B should be a constant. Under these conditions, Einstein equations are as follows:
Constraint equations

$$\frac{\dot{\eta}}{t} = \dot{U}^2 + \alpha U'^2 + \frac{e^{4U}}{4t^2}(\dot{A}^2 + \alpha A'^2) + \frac{\alpha e^{2(\eta-U)}B^2}{t^4}, \tag{6}$$

$$\frac{\eta'}{t} = 2\dot{U}U' + \frac{e^{4U}}{2t^2}\dot{A}A' - \frac{\alpha'}{2t\alpha}, \tag{7}$$

$$\dot{\alpha} = -\frac{4\alpha^2 e^{2(\eta-U)}B^2}{t^3}. \tag{8}$$

Dot and prime denote derivative with respect to t and θ, respectively.
Evolution equations

$$\ddot{U} - \alpha U'' = -\frac{\dot{U}}{t} + \frac{\dot{\alpha}\dot{U}}{2\alpha} + \frac{\alpha' U'}{2} + \frac{e^{4U}}{2t^2}(\dot{A}^2 - \alpha A'^2) + \frac{\alpha e^{2(\eta-U)}B^2}{t^4}, \tag{9}$$

$$\ddot{A} - \alpha A'' = \frac{\dot{A}}{t} + \frac{\dot{\alpha}\dot{A}}{2\alpha} + \frac{\alpha' A'}{2} - 4(\dot{A}\dot{U} - \alpha A' U'), \tag{10}$$

We also use the following auxiliary equation for P

$$\ddot{P} - \alpha P'' = \left(-\frac{1}{t} + \frac{\dot{\alpha}}{2\alpha}\right)\dot{U} + \frac{\alpha' P'}{2} + e^{2P}(\dot{A}^2 - \alpha A'^2), \tag{11}$$

where $P = 2U - \ln t$. We call this system **magnetic Gowdy system** [13].

2.2 Wave map

The system of the evolution equations is equivalent with the following system of nonlinear wave equations (wave map $u : (\mathcal{M}^{2+1}, G) \mapsto (\mathcal{N}^2, h)$):

$$S_{\rm MG} = \int_{S^1} dt d\theta \sqrt{-G} \left(G^{\alpha\beta} h_{AB} \partial_\alpha u^A \partial_\beta u^B + \frac{\alpha e^{2(\eta-U)} B^2}{t^4} \right), \tag{12}$$

where

$$G = -dt^2 + \frac{1}{\alpha} d\theta^2 + t^2 d\psi^2, \qquad 0 \le \theta, \psi \le 2\pi,$$

and

$$h = dU^2 + \frac{e^{4U}}{4t^2} dA^2.$$

Every functions depend on time t and θ. Note that the evolution parts in the Einstein equations is obtained by varying this action. The energy-momentum tensor $T_{\alpha\beta}$ for this system is given of the form:

$$T_{\alpha\beta} = h_{AB} \left(\partial_\alpha u^A \partial_\beta u^B - \frac{1}{2} G_{\alpha\beta} \partial_\lambda u^A \partial^\lambda u^B \right) - G_{\alpha\beta} \frac{\alpha e^{2(\eta-U)} B^2}{2t^4}. \tag{13}$$

Now, we can define the energy is defined as follows:

$$\begin{aligned} E(t) &= \int_{S^1} T_{tt} \frac{d\theta}{\sqrt{\alpha}} \\ &= \frac{1}{2} \int_{S^1} \left[h_{AB} \left(\partial_t u^A \partial_t u^B + \partial_\theta u^A \partial_\theta u^B \right) + \frac{\alpha e^{2(\eta-U)} B^2}{t^4} \right] \frac{d\theta}{\sqrt{\alpha}} \\ &= \int_{S^1} \left[\mathcal{E} + \frac{\alpha e^{2(\eta-U)} B^2}{2t^4} \right] \frac{d\theta}{\sqrt{\alpha}}. \end{aligned}$$

2.3 Global existence

Theorem 3 (N.[9]) *Let (M, g) be the maximal Cauchy development of C^∞ initial data for the magnetic Gowdy system. Then, M can be covered by compact Cauchy surfaces of constant areal time t with each value in the range $(0, \infty)$.* ◇

To prove this theorem, monotonicity for the energy is shown and the light cone estimate is used (see [3, 7, 8, 12]).

3 Existence of Kasner-like solutions near spacetime singularity

Recently, a new Fuchsian technique has been develoved by Ames-Beyer-Isenberg-LeFloch [1] (see also [4]). By using this technique, we can construct Kasner-like solutions to the Einstein equations. For our problem, the leading-order term for Kasner-like solution:

$$U = \frac{1}{2} \left(1 - k(\theta)\right) \ln t + U_{**}(\theta) + \cdots = U_0 + \cdots, \tag{14}$$

$$A = A_*(\theta) + t^{2k(\theta)} A_{**}(\theta) + \cdots = A_0 + \cdots, \tag{15}$$

$$\eta = \frac{1}{4} \left(1 - k(\theta)\right)^2 \ln t + \eta_*(\theta) + \cdots = \eta_0 + \cdots, \tag{16}$$

$$\alpha = \alpha_*(\theta) + \cdots = \alpha_0 + \cdots, \tag{17}$$

Then we have the following theorem, which means that there exists a Kasner-like solution to the Einstein-Maxwell equations in *polarized* magnetic Gowdy spacetimes.

Theorem 4 (N. [9]) *Suppose that an asymptotic data constant A_* and a set of asymptotic data functions $k, U_{**}, \alpha_*(>0), A_{**} \in C^\infty(T^1)$ which satisfy the integrability condition*

$$\int_0^{2\pi} \left((1-k(\theta))U'_{**}(\theta) - \frac{1}{2}(\ln \alpha_*)'(\theta) \right) d\theta = 0$$

with either

1. *$k(\theta) > 3$ for arbitrary $A_{**}(\theta)$, or*
2. *$k(\theta) > 3$ or $k(\theta) < -3$ for $A_{**}(\theta) \equiv 0$,*

at each point $\theta \in T^1$ Then, there is a $\delta > 0$, and a magnetic Gowdy solution U, A, η, α of the Einstein-maxwell equations of the form

$$(U, A, \eta, \alpha) = (U_0, A_0, \eta_0, \alpha_0) + W,$$

where the leading-order terms $(U_0, A_0, \eta_0, \alpha_0)$ is given by equations (16)-(15) and

$$\eta_*(\theta) := \eta_0 + \int_0^\theta \left((1-k(\theta))U'_{**}(\Theta) - \frac{1}{2}(\ln \alpha_*)'(\Theta) \right) d\Theta.$$

The remainder W is contained in $X_{\delta,\mu,\infty}$ for some exponent vector $\mu = (\mu_1, \mu_2, \mu_3, \mu_4)$ with $\mu_1, \mu_2 - 2k, \mu_3, \mu_4 > 0$. This solution is unique among all solutions with the same leading-order term and with the remainder $W \in X_{\delta,\mu,\infty}$.

3.1 Function spaces

In this section, we define some function spaces. Fix a smooth vector valued function $\mu : T^1 \to \mathrm{R}^\mathrm{d}$ with the corresponding diagonal matrix

$$\mathcal{R}[\mu](t, \theta) := diag(t^{-\mu_1(\theta)}, \cdots, t^{-\mu_d(\theta)}),$$

and then define the norm

$$\| w \|_{\delta,\mu,q} := \sup_{0<t\leq\delta} \| \mathcal{R}[\mu](t, \cdot) w(t, \cdot) \|_{H^q(T^1)},$$

for vecor-valued function $w(t, \theta) \in C^l((0, \delta], H^m(U))$. Here, $\| \cdot \|_{H^q(T^1)}$ denotes the standard q-order Sobolev norm on T^1. From this, we define the Banach space $X_{\delta,\mu,q}(T^1) = X_{\delta,\mu,q}$. We also define the space

$$X_{\delta,\mu,\infty} := \bigcap_{p=0}^{l} X_{\delta,\mu,q}.$$

References

[1] Ames, Ellery., Beyer, Florian., Isenberg, James. and LeFloch Philippe G., *Quasilinear hyperbolic Fuchsian systems and AVTD behavior in T^2 symmetric vacuum spacetimes*, gr-qc>arXiv:1205.1881.

[2] Andersson, Lars., *The global existence problem in general relativity*, in "50 years of the Cauchy problem in general relativity", (eds. Chrusciel and Friedrich, Birkhauser, Basel 2004), pp.71-120.

[3] Isenberg, James., Berger, Berverly K., Chrusciel, Piotr T. and Moncrief, Vincent., *Global foliations of vacuum spacetimes with T^2 isometry*, Ann. Physics, **260** (1997) 117-148.

[4] Beyer, Florian. and LeFloch, Philippe G., *Second-order hyperbolic Fuchsian systems. Gowdy spacetimes and the Fuchsian numerical algorithm*, Class. Quantum Grav. **27** (2010) 245012.

[5] Chrusciel, Piotr T., Galloway, Gregory J. and Pollack, Daniel., *Mathematical general relativity: A sampler*, Bull. Amer. Math. Soc. **47** (2010) 567-638.

[6] Hawking, S. W. and Ellis, G. F. R., *The Large Scale Structure of Space-Time*, (Cambridge Monographs on Mathematical Physics), Cambridge University Press, (1973).

[7] Isenberg, James. and Weaver, Marsha., *On the area of the symmetry orbits in T^2 symmetric spacetimes*, Class. Quant. Grav. **20** (2003) 3783-3796.

[8] Moncrief, Vincent., *Global properties of Gowdy spacetimes with $T^3 \times R$ topology*, Ann. Physics, **132** (1981), 87-107.

[9] Narita, Makoto., *Global solutions to the Einstein-Maxwell equations in magnetic Gowdy spacetimes*, in preperation.

[10] Rendall, Alan D., *Theorems on Existence and Global Dynamics for the Einstein Equations*, Living Rev. Relativity, **8** (2005) 6. URL:http://relativity.livingreviews.org/Articles/lrr-20105-6/

[11] Ringström, Hans., *Cosmic Censorship for Gowdy spacetimes*, Living Rev. Relativity, **13** (2010) 2. URL:http://relativity.livingreviews.org/Articles/lrr-2010-2/

[12] Smulevici, Jacques., *On the area of the symmetry orbits of cosmological spacetimes with toroidal or hyperbolic symmetry*, gr-qc>arXiv:0904.0806.

[13] Weaver, Marsha., Isenberg, James. and Berger, Berverly K., *Mixmaster Behavior in Inhomogeneous Cosmological Spacetimes*, Phys. Rev. Lett. **80** (1998) 2984-2987.

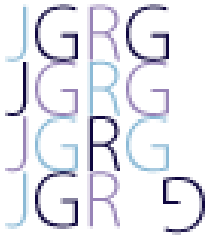

Andrei Frolov, JGRG 22(2012)111301

"Primordial non-gaussianity from preheating"

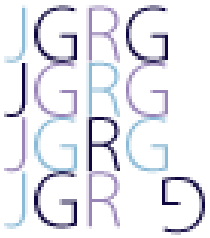

RESCEU SYMPOSIUM ON

GENERAL RELATIVITY AND GRAVITATION

JGRG 22



November 12-16 2012

Koshiba Hall, The University of Tokyo, Hongo, Tokyo, Japan



Primordial Non-Gaussianity from Preheating

arXiv:0903.3407 (BFHK); arXiv:1004.3559 (REVIEW)



Andrei Frolov

Department of Physics
Simon Fraser University

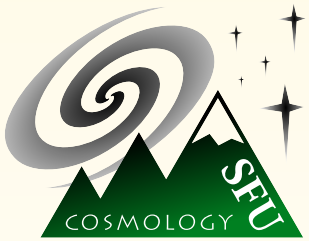

&

Lev Kofman, Dick Bond, Jonathan Braden, Zhiqi Huang (CITA)

RESCEU Symposium on General Relativity and Gravitation

University of Tokyo, Tokyo, Japan
13 November 2012

Brief History of the Universe

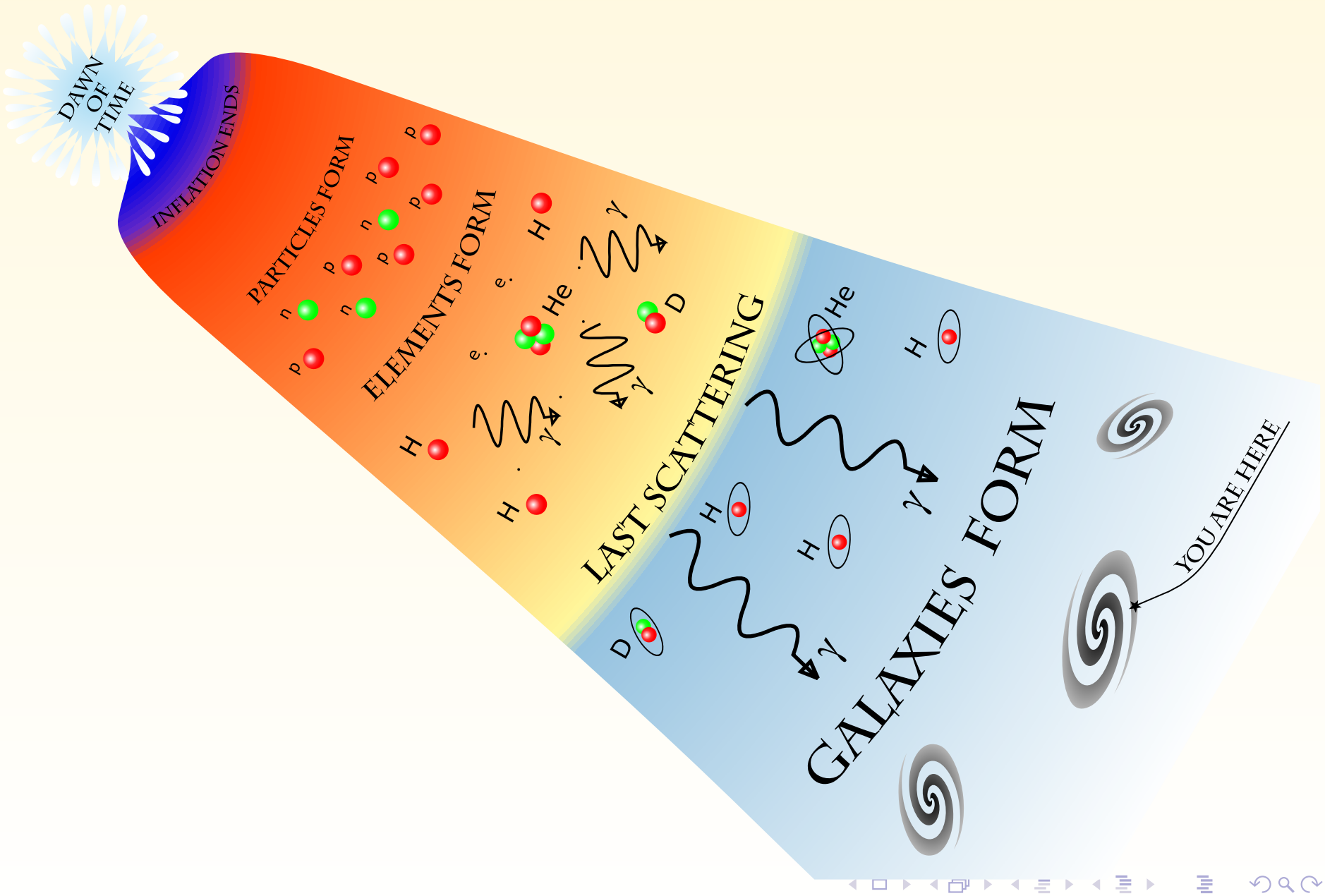

Brief History of the Universe

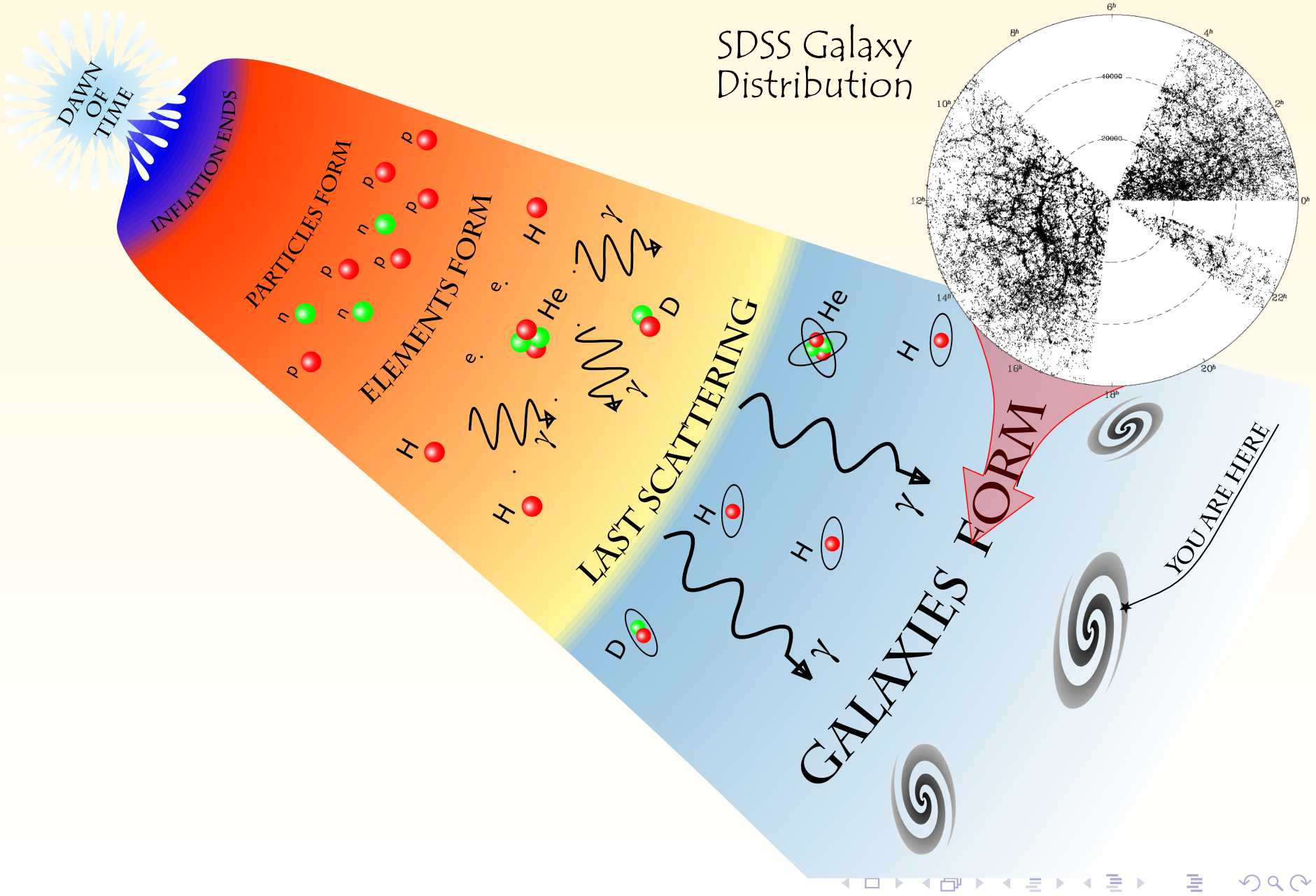

Brief History of the Universe

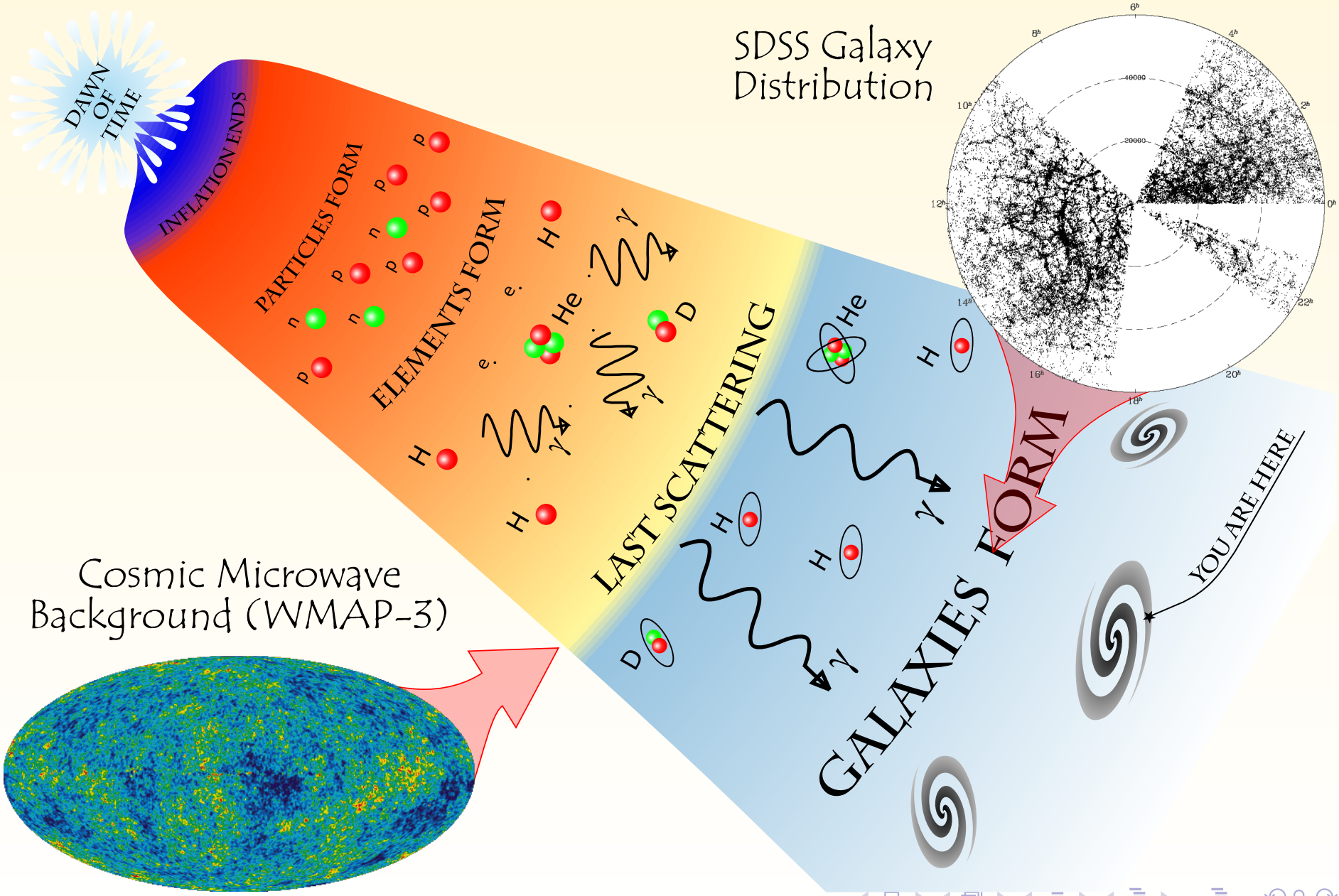

Brief History of the Universe

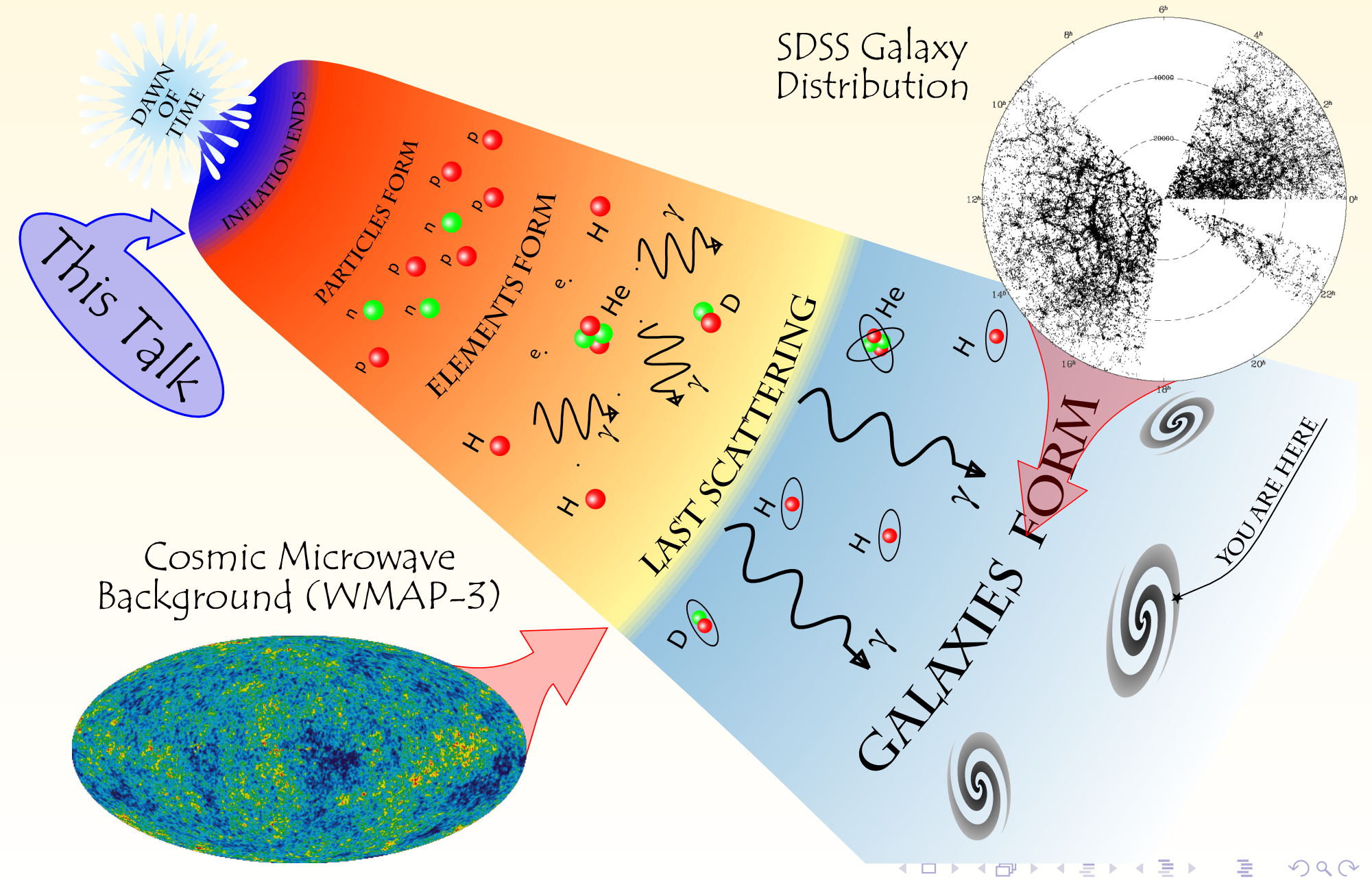

A Simple Model of Inflation...

Model with potential

$$V(\phi,\chi)=\frac{\lambda}{4}\phi^4+\frac{g^2}{2}\phi^2\chi^2$$

is invariant under

$$\begin{aligned} g_{\mu\nu} &\mapsto a^{-2}g_{\mu\nu}, \\ \phi &\mapsto a\phi, \\ \chi &\mapsto a\chi \end{aligned}$$

equation of state is $1/3$

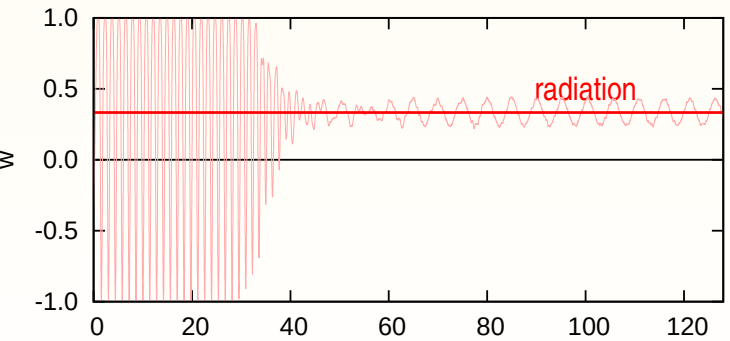

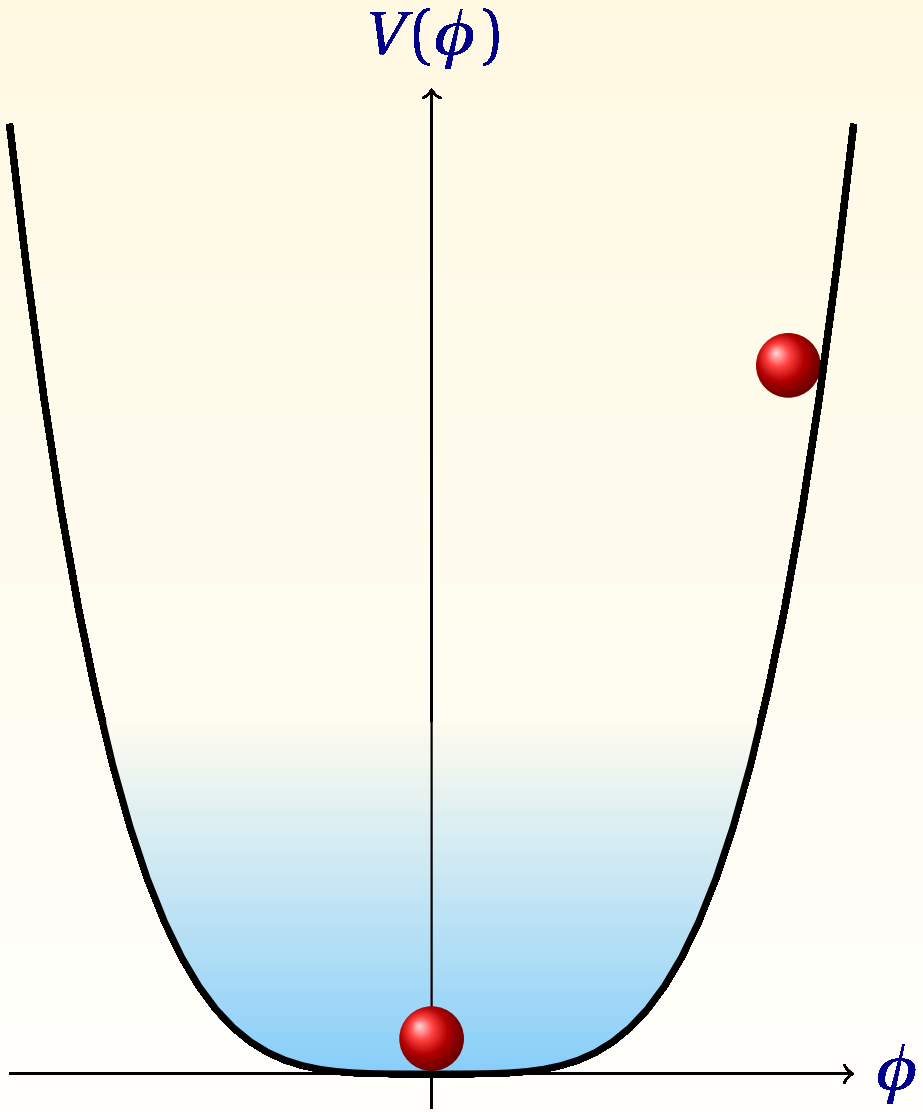

... Ending via Broad Parametric Resonance

Model with potential

$$V(\phi,\chi)=\frac{\lambda}{4}\phi^4+\frac{g^2}{2}\phi^2\chi^2$$

is invariant under

$$\begin{aligned} g_{\mu\nu} &\mapsto a^{-2}g_{\mu\nu}, \\ \phi &\mapsto a\phi, \\ \chi &\mapsto a\chi \end{aligned}$$

equation of state is $1/3$

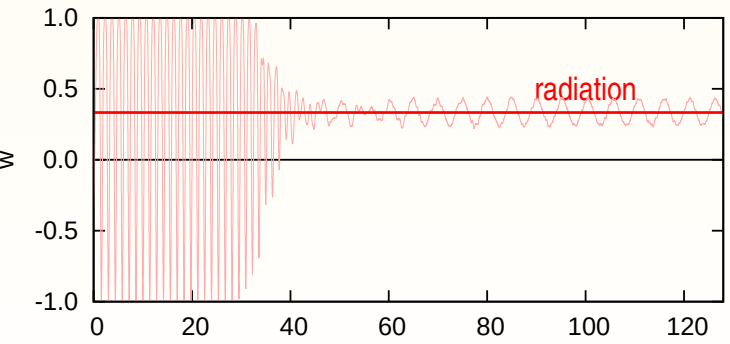

Stability of Lame equation:

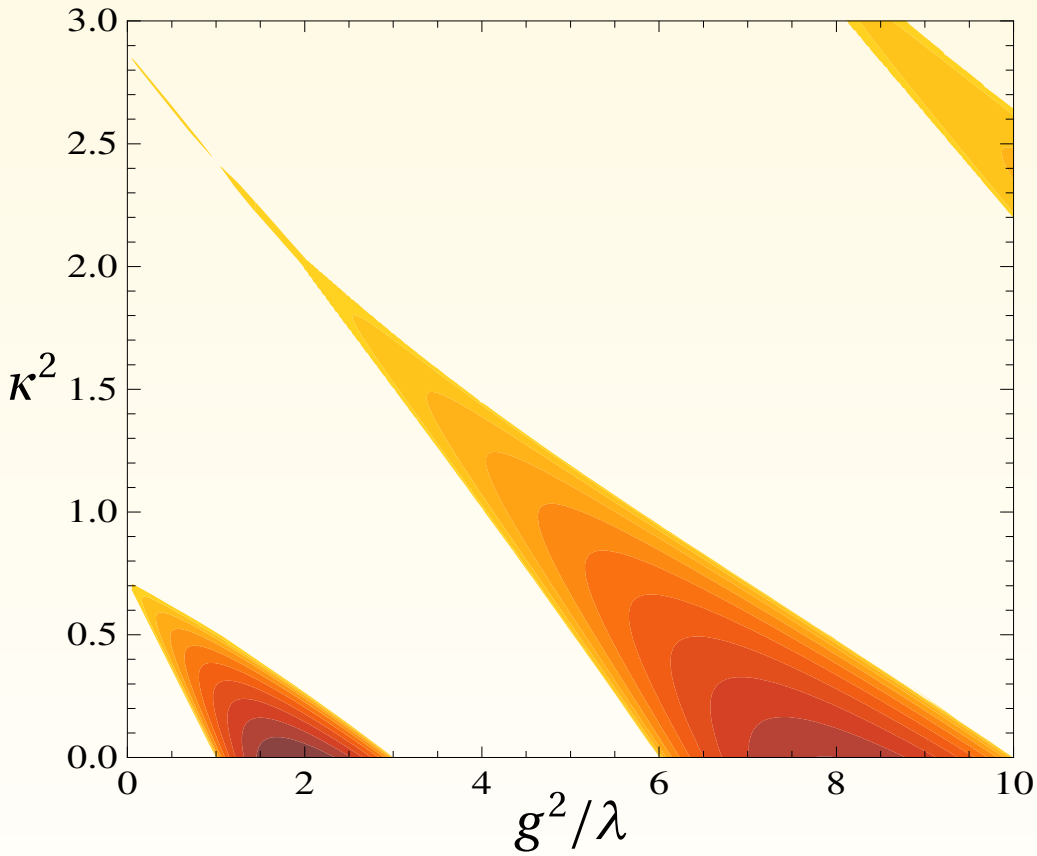

$$(a\chi_k)''+\left[\kappa^2+\frac{g^2}{\lambda}\mathrm{cn}^2\left(x,2^{-1/2}\right)\right](a\chi_k)=0$$

Development of Linear Instability

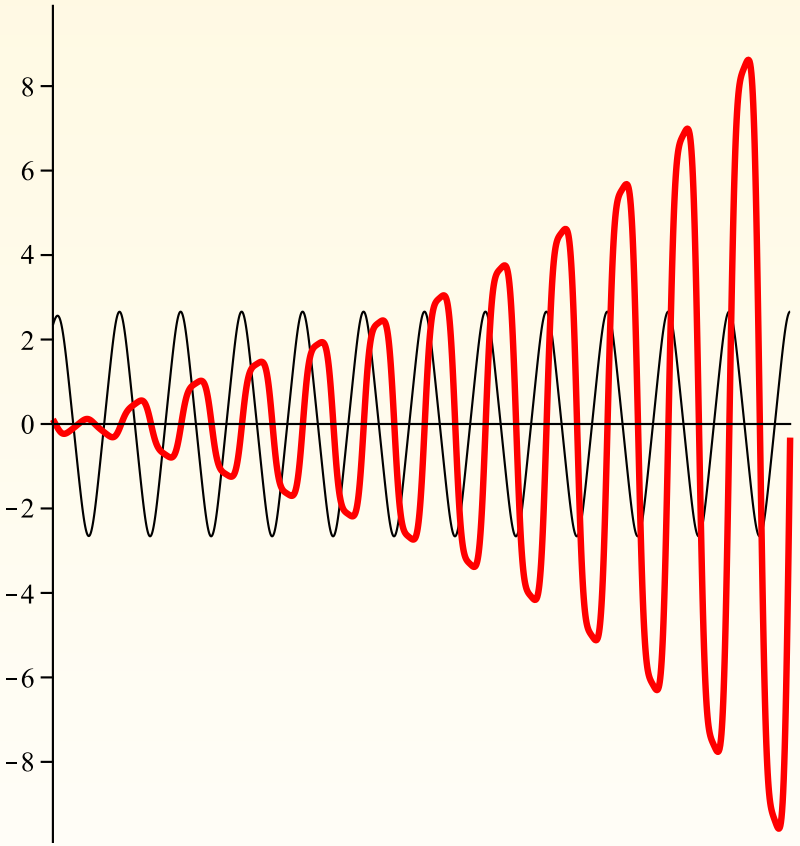

$g^2/\lambda = 2.99,\ \kappa^2 = 0$

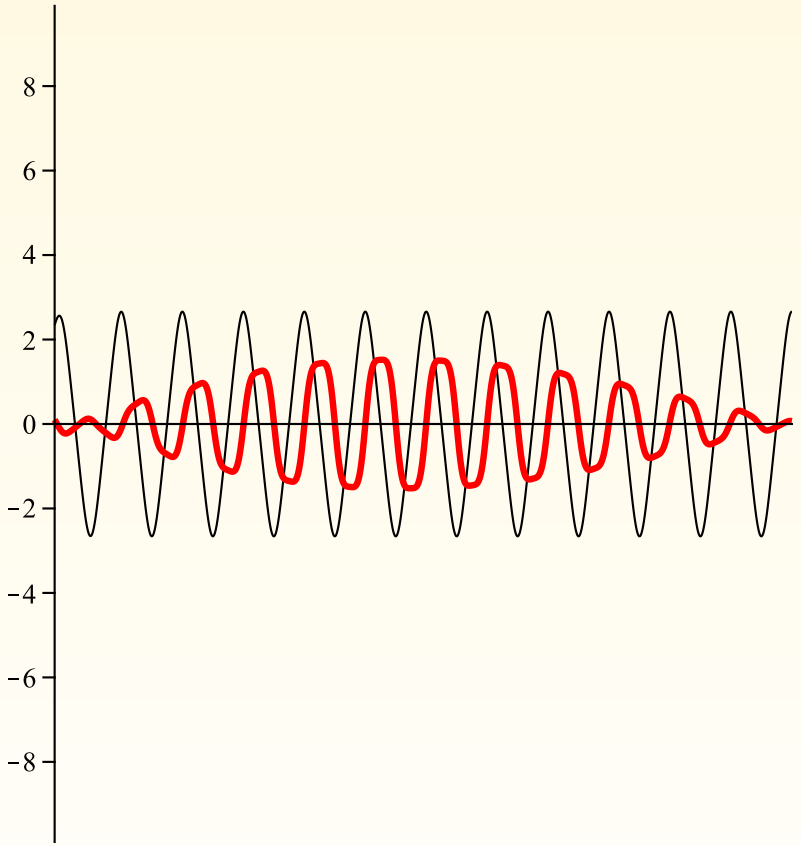

$g^2/\lambda = 3.01,\ \kappa^2 = 0$

Parametric Resonance is a Generic Feature

$$\chi_k'' + \left[\kappa^2 + q\cos^2(\tau)\right]\chi_k = 0$$

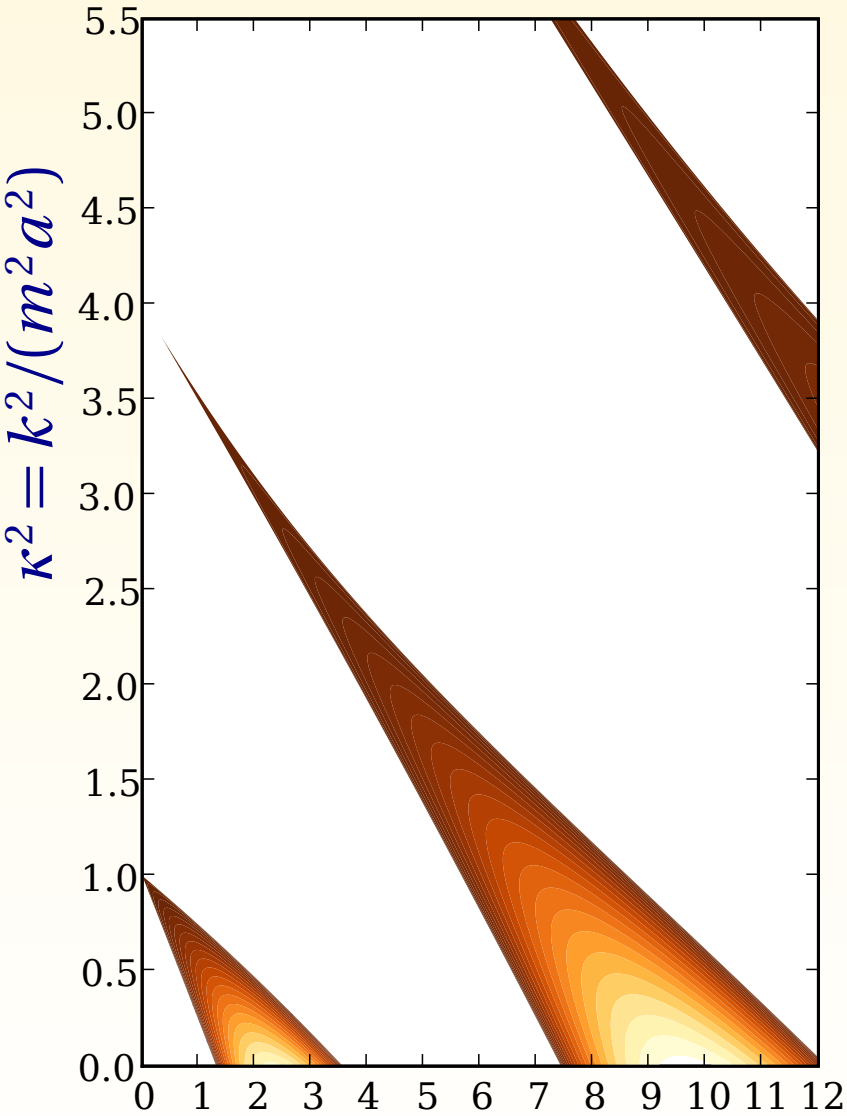

$$q = g^2\Phi_0^2/(m^2a^3)$$

$$\chi_k'' + \left[\kappa^2 + q\,\mathrm{cn}^2\left(\tau, 2^{-1/2}\right)\right]\chi_k = 0$$

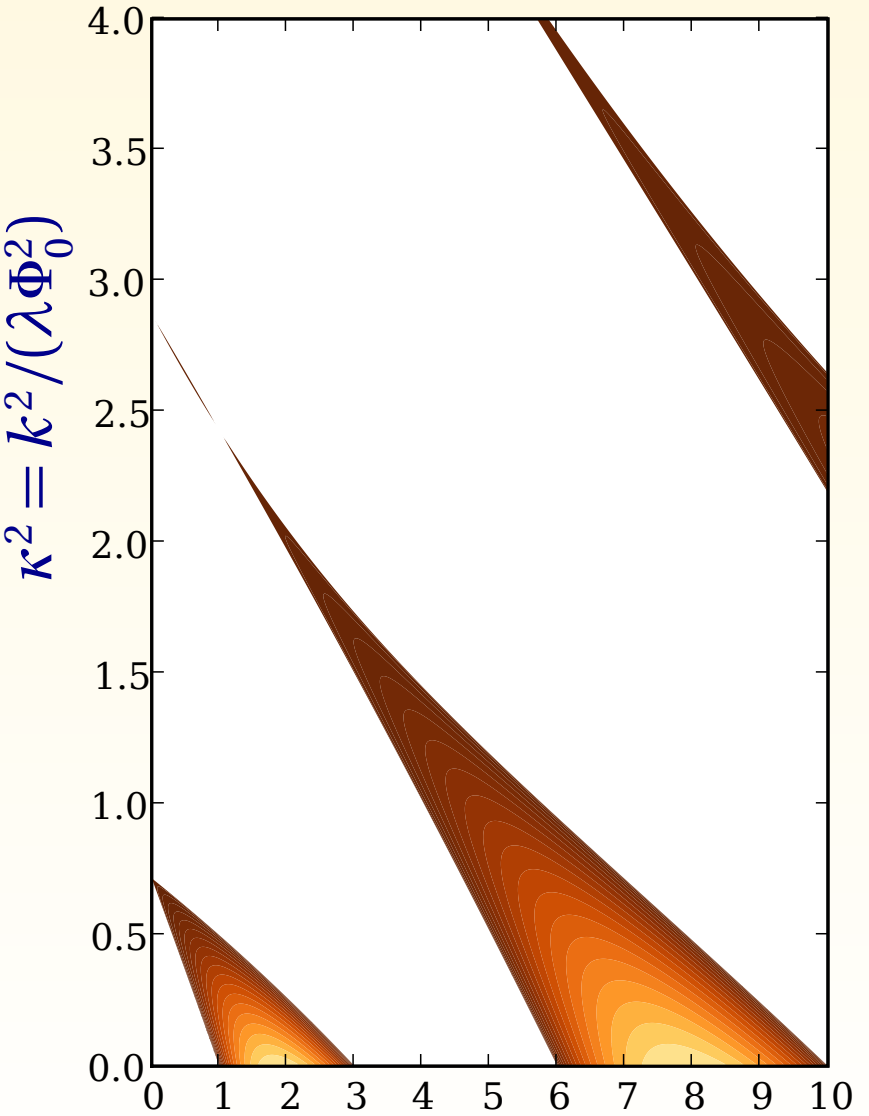

$$q = g^2/\lambda$$

DEFROST: A New 3D Numerical Solver

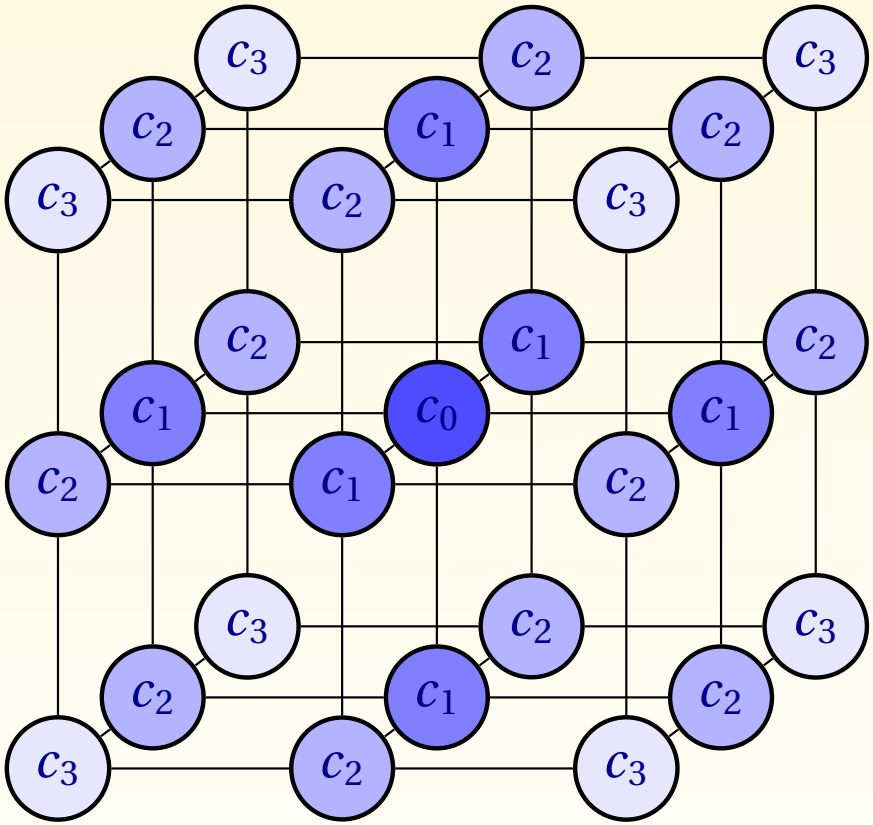

coefficient	c_3	c_2	c_1	$-c_0$
degeneracy	8	12	6	1
standard	0	0	1	6
isotropic A	0	$\frac{1}{6}$	$\frac{1}{3}$	4
isotropic B	$\frac{1}{12}$	0	$\frac{2}{3}$	$\frac{14}{3}$
isotropic C	$\frac{1}{30}$	$\frac{1}{10}$	$\frac{7}{15}$	$\frac{64}{15}$

http://www.sfu.ca/physics/cosmology/defrost

[Fortran-90, 600 lines, very fast, instrumented for 3D]

Field Evolution as a Chaotic Billiard

Density Evolution

$$\left[V(\phi,\chi)=\tfrac{1}{4}\lambda\phi^4+\tfrac{1}{2}g^2\phi^2\chi^2\right]$$

Density Evolution

$$\left[V(\phi,\chi)=\tfrac{1}{2}m^2\phi^2+\tfrac{1}{2}g^2\phi^2\chi^2\right]$$

Density Evolution

$$\left[V(\phi,\chi)=\frac{1}{2}m^2\phi^2+\frac{1}{2}\sigma\phi\chi^2+\frac{1}{4}\lambda\chi^4\right]$$

HERE IS HOW INSTABILITY DEVELOPS!

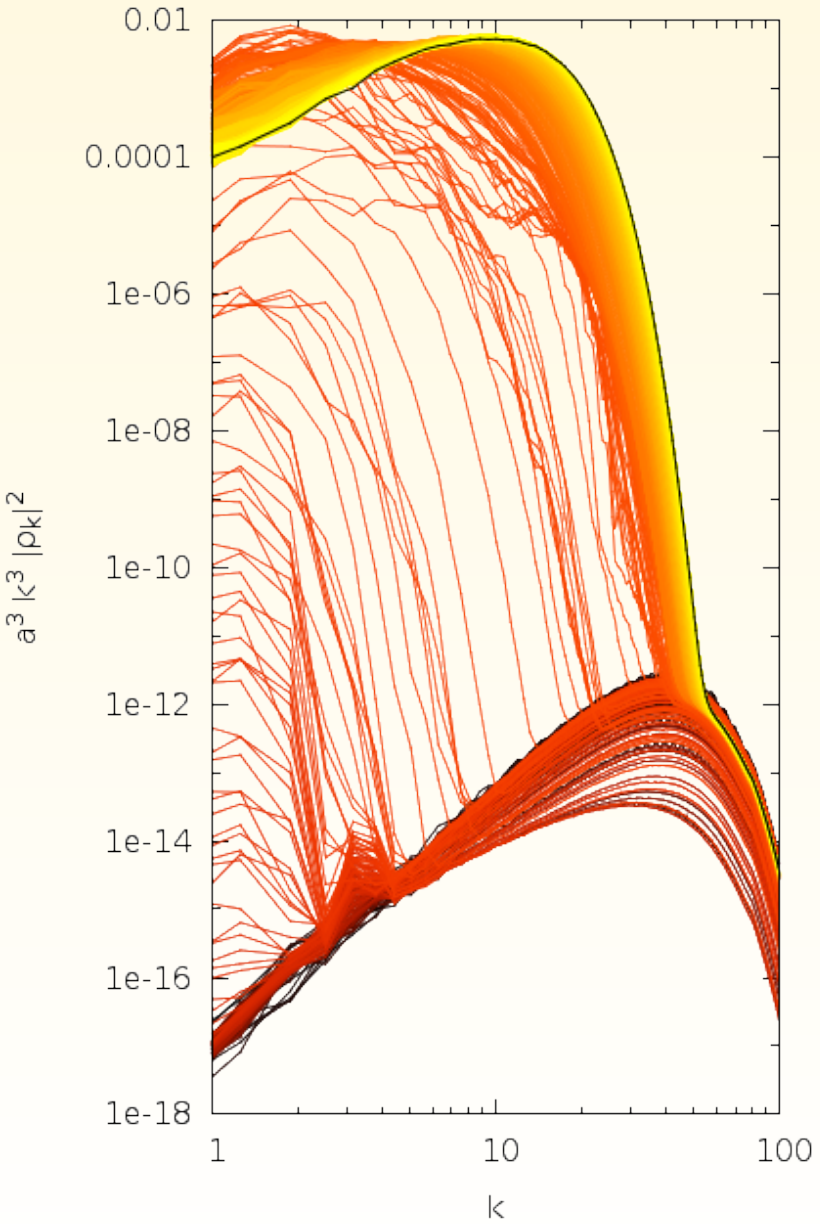

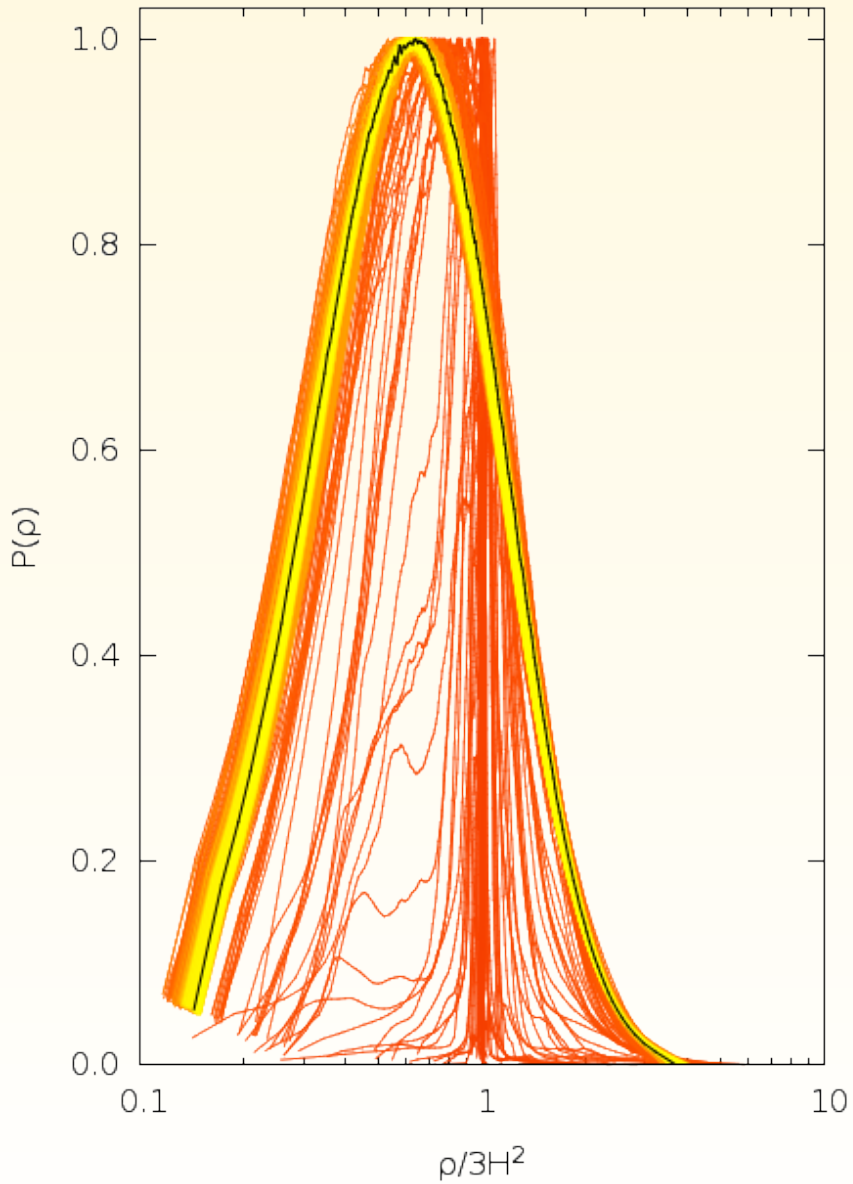

In Fact, It's Quite Log-Normal!

$$V(\phi,\chi)=\frac{1}{4}\lambda\phi^4+\frac{1}{2}g^2\phi^2\chi^2$$

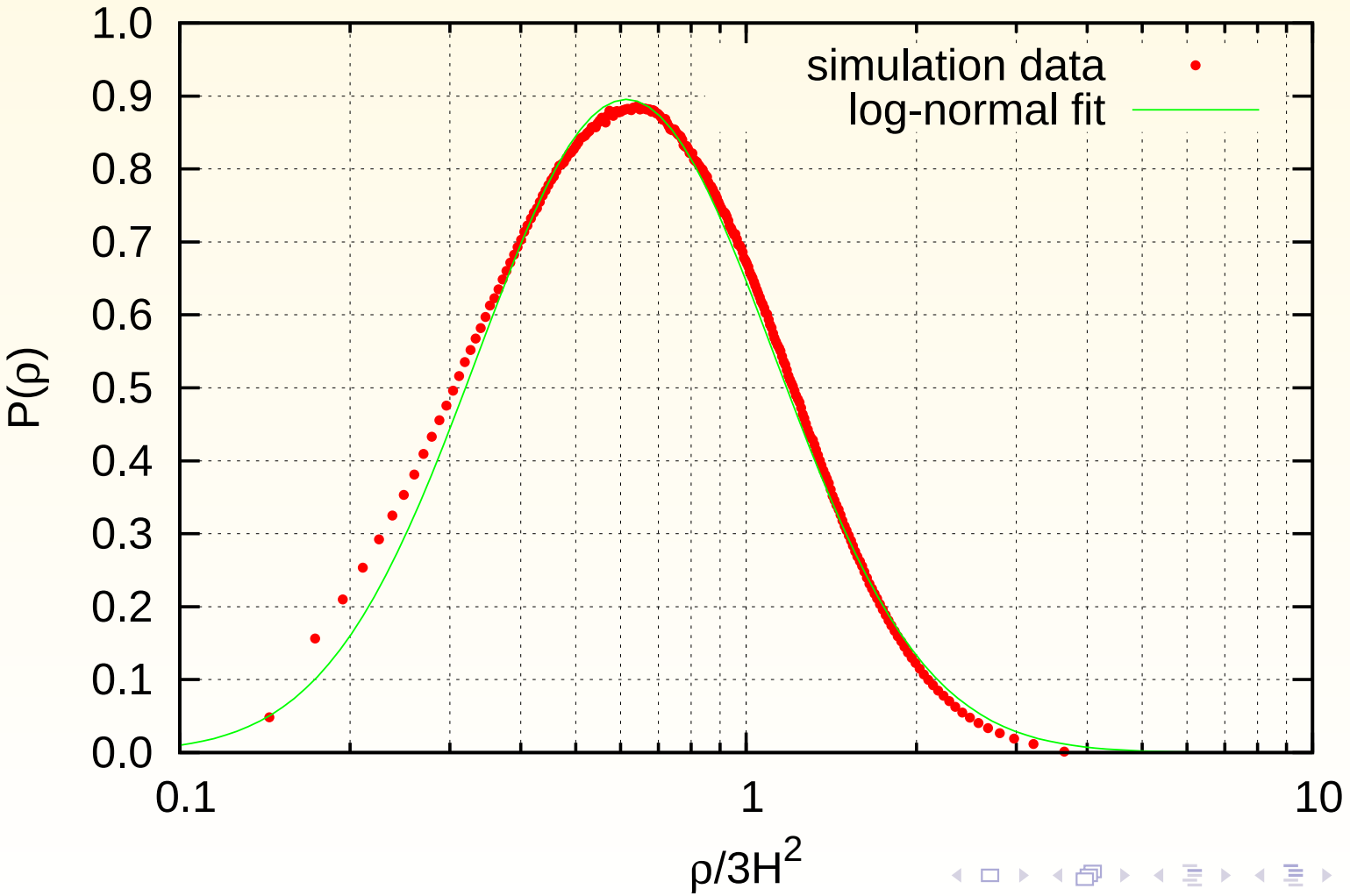

In Fact, It's Universally Log-Normal!

$$V(\phi,\chi)=\frac{1}{2}m^2\phi^2+\frac{1}{2}g^2\phi^2\chi^2$$

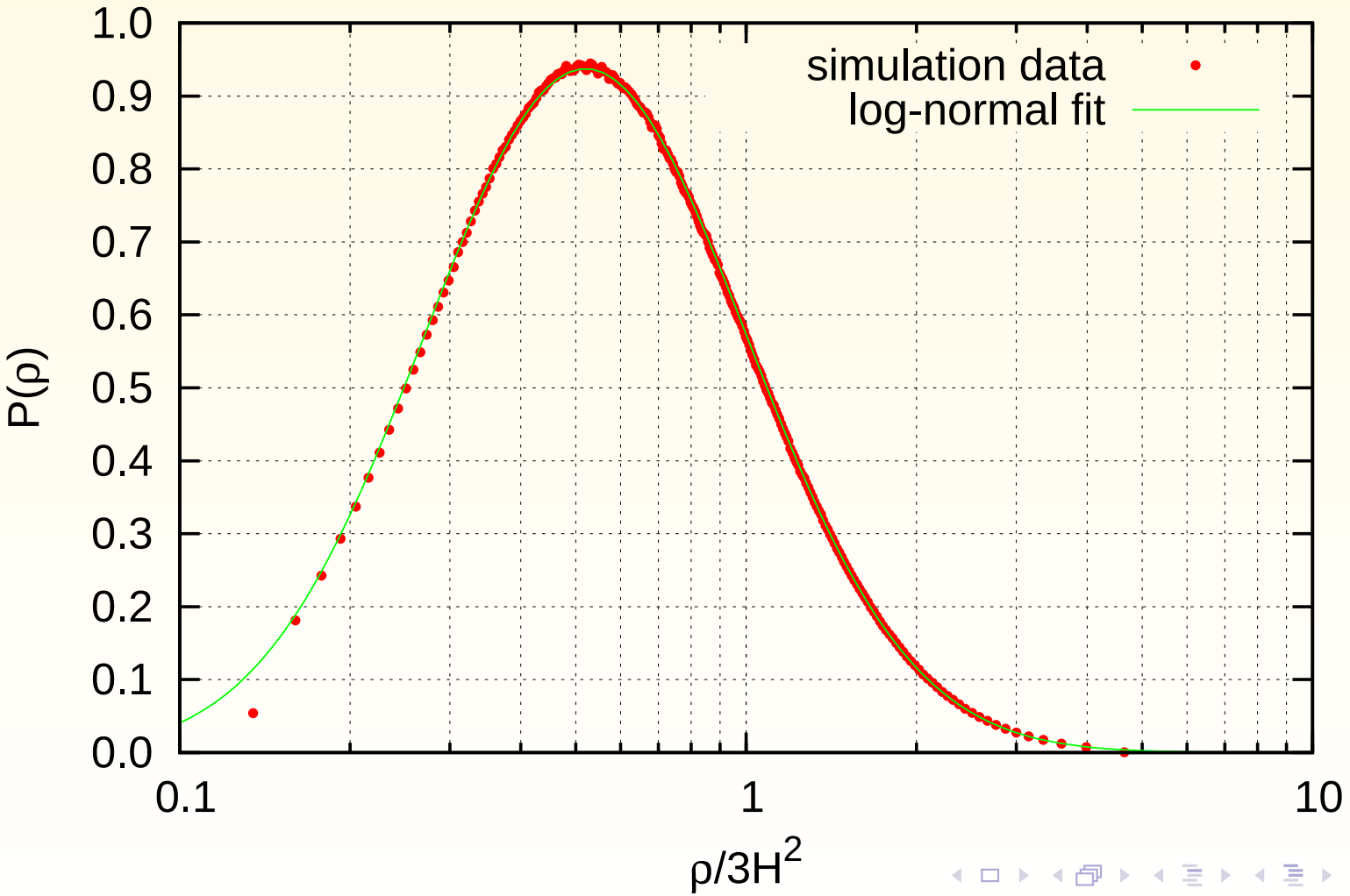

In Fact, It's Universally Log-Normal!

$$V(\phi,\psi)=\frac{1}{2}m^2\phi^2+\frac{1}{2}\sigma\phi\chi^2+\frac{1}{4}\lambda\chi^4$$

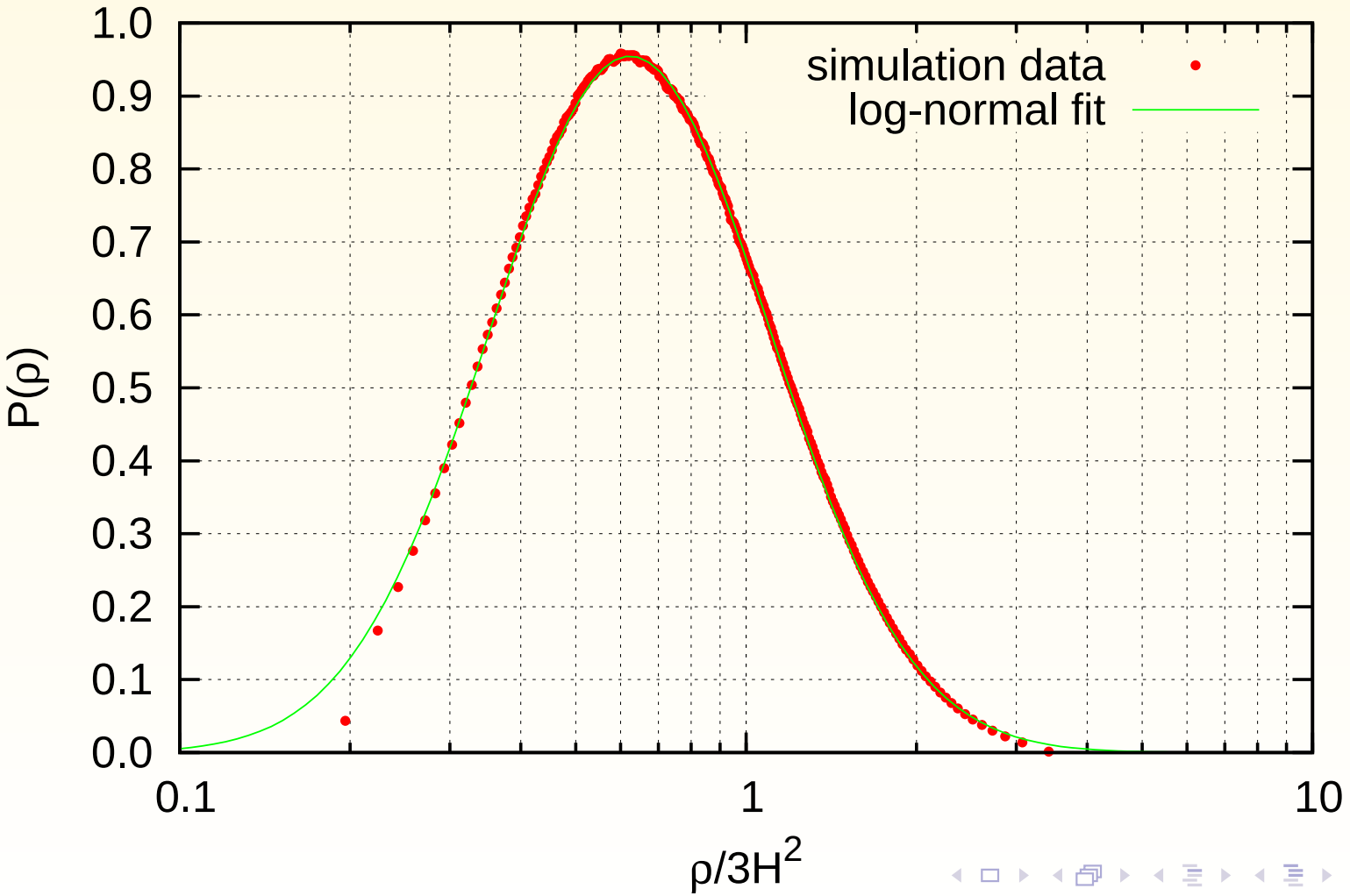

(Non-Thermal) Scalar Field Fixed Point?

$$V(\phi,\chi)=\frac{1}{4}\lambda\left(\phi^2+\chi^2-v^2\right)^2$$

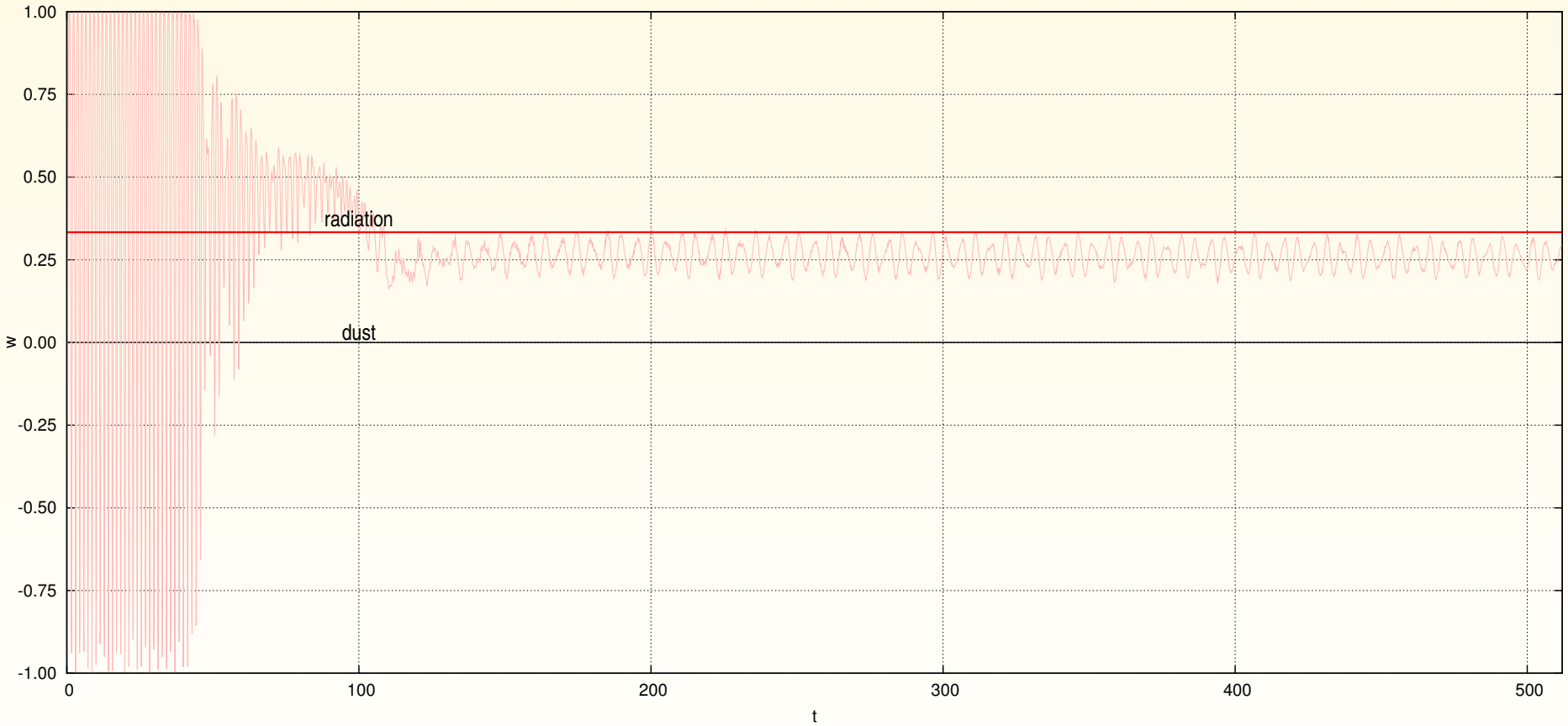

This Simply can't be Just a Coincidence...

A universal characteristic of random scalar field evolution?!

What's Going On Here?

Very tempting to blame scalar field turbulence!..

This Simply can't be Just a Coincidence...

A universal characteristic of random scalar field evolution?!

What's Going On Here?

Very tempting to blame scalar field turbulence!..

Are We Going to Ever See Any of This?

Thermal Bath Wipes Out Everything?!

Scales Too Small?!

We should look for things that can survive thermalization:

1. stable relics (primordial black holes)
2. decoupled fields (gravitational waves)
3. anomalies in expansion history (non-gaussianity)

Are We Going to Ever See Any of This?

Thermal Bath

Wipes Out Everything?!

Scales Too Small?!

We should look for things that can survive thermalization:

1. stable relics (primordial black holes)
2. decoupled fields (gravitational waves)
3. anomalies in expansion history (non-gaussianity)

Are We Going to Ever See Any of This?

Thermal Bath
Wipes Out Everything?!

Scales Too Small?!

We should look for things that can survive thermalization:

1. stable relics (primordial black holes)
2. decoupled fields (gravitational waves)
3. anomalies in expansion history (non-gaussianity)

Can Primoridal Black Holes Form? No...

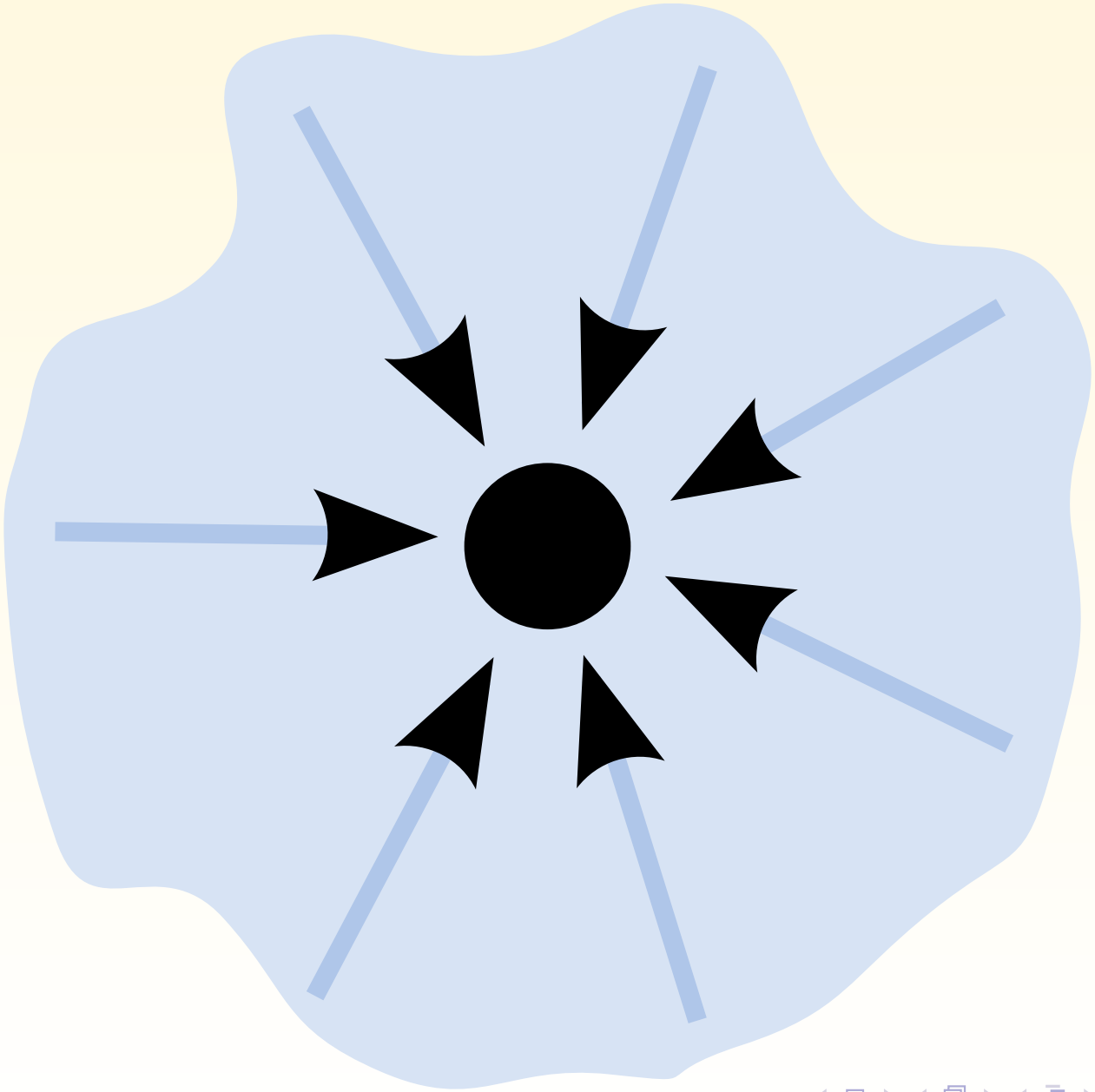

Can Primoridal Black Holes Form? No...

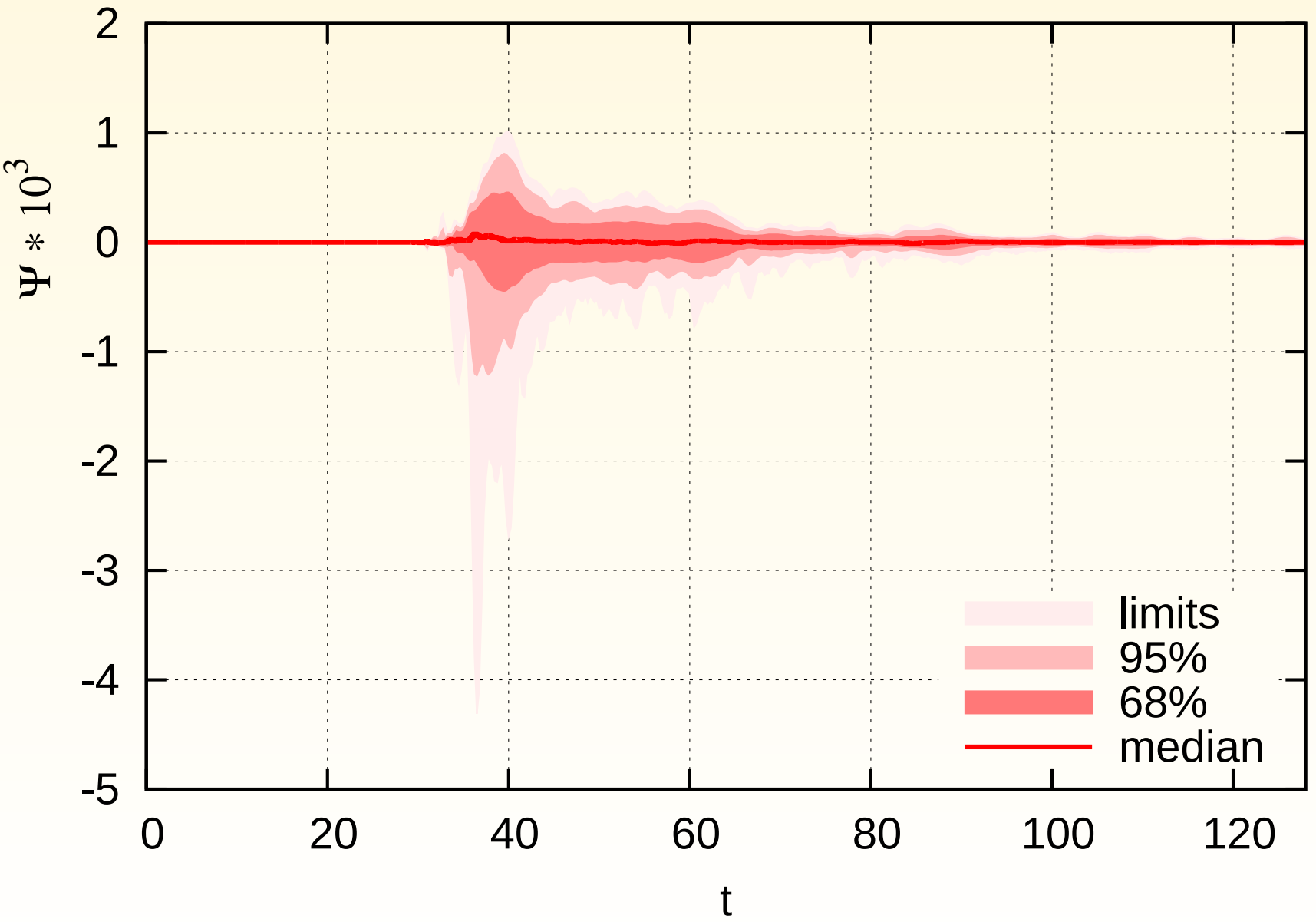

Gravitational Waves from Preheating?


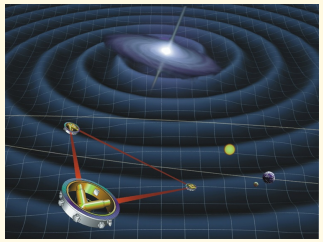
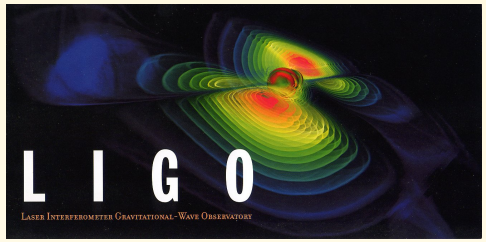



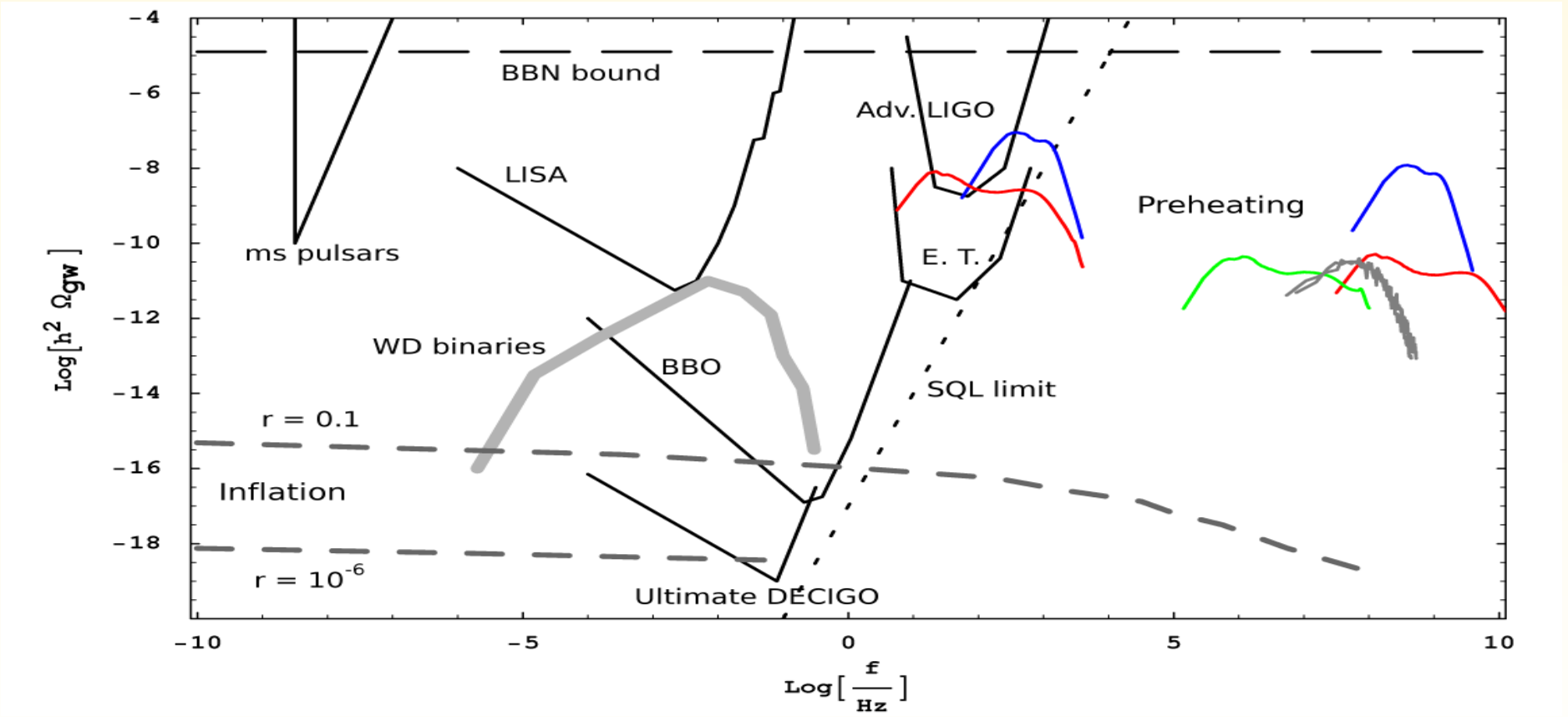

Dufaux, Felder, Kofman & Navros (2009)

Non-Gaussianity from Preheating?

CMB and Reheating scales different by 50+ e-folds!

Non-Gaussianity from Preheating?

CMB and Reheating scales different by 50+ e-folds!

Differences in Expansion can Modulate CMB

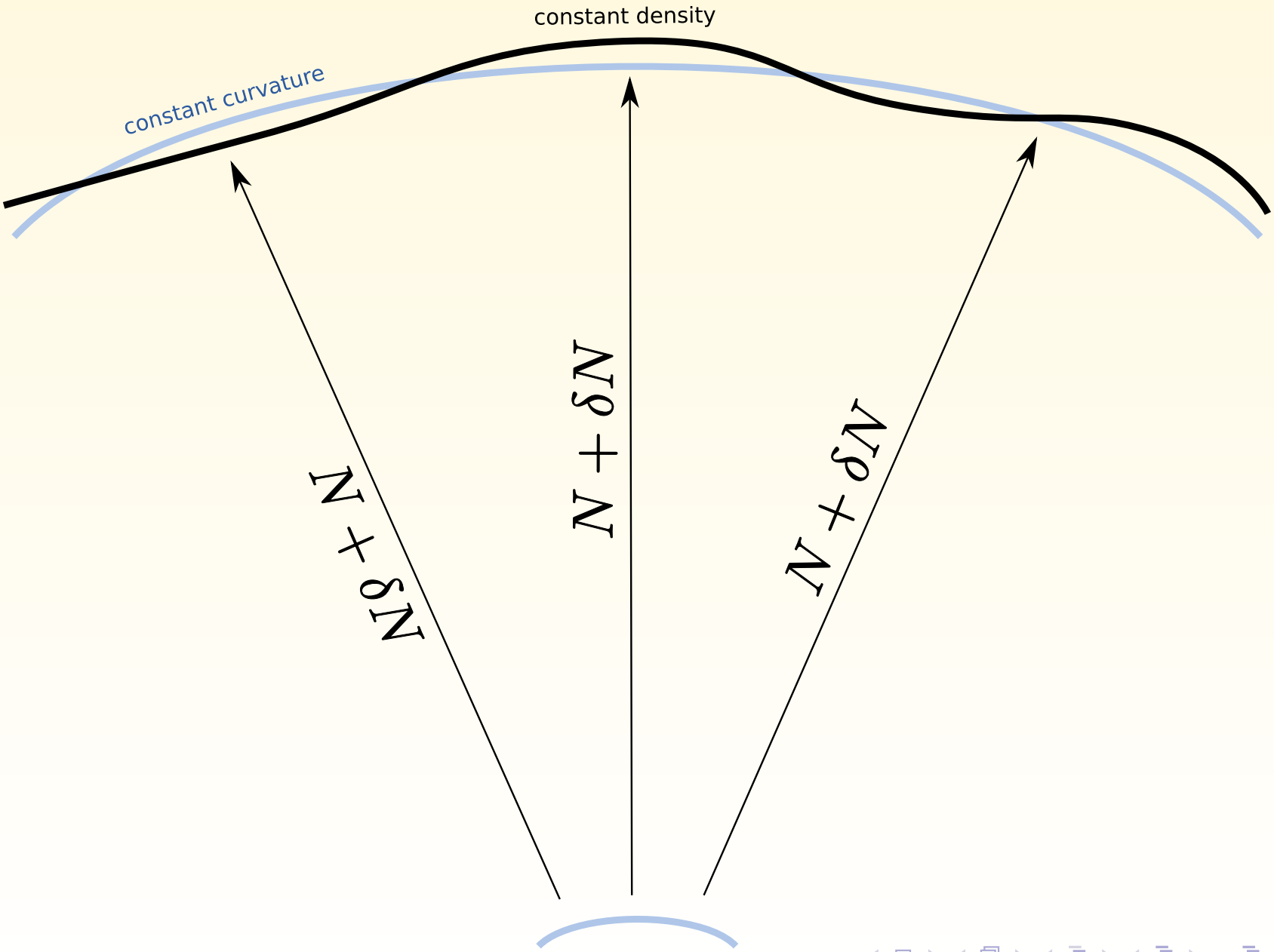

Modulation Comes from Isocurvature Mode

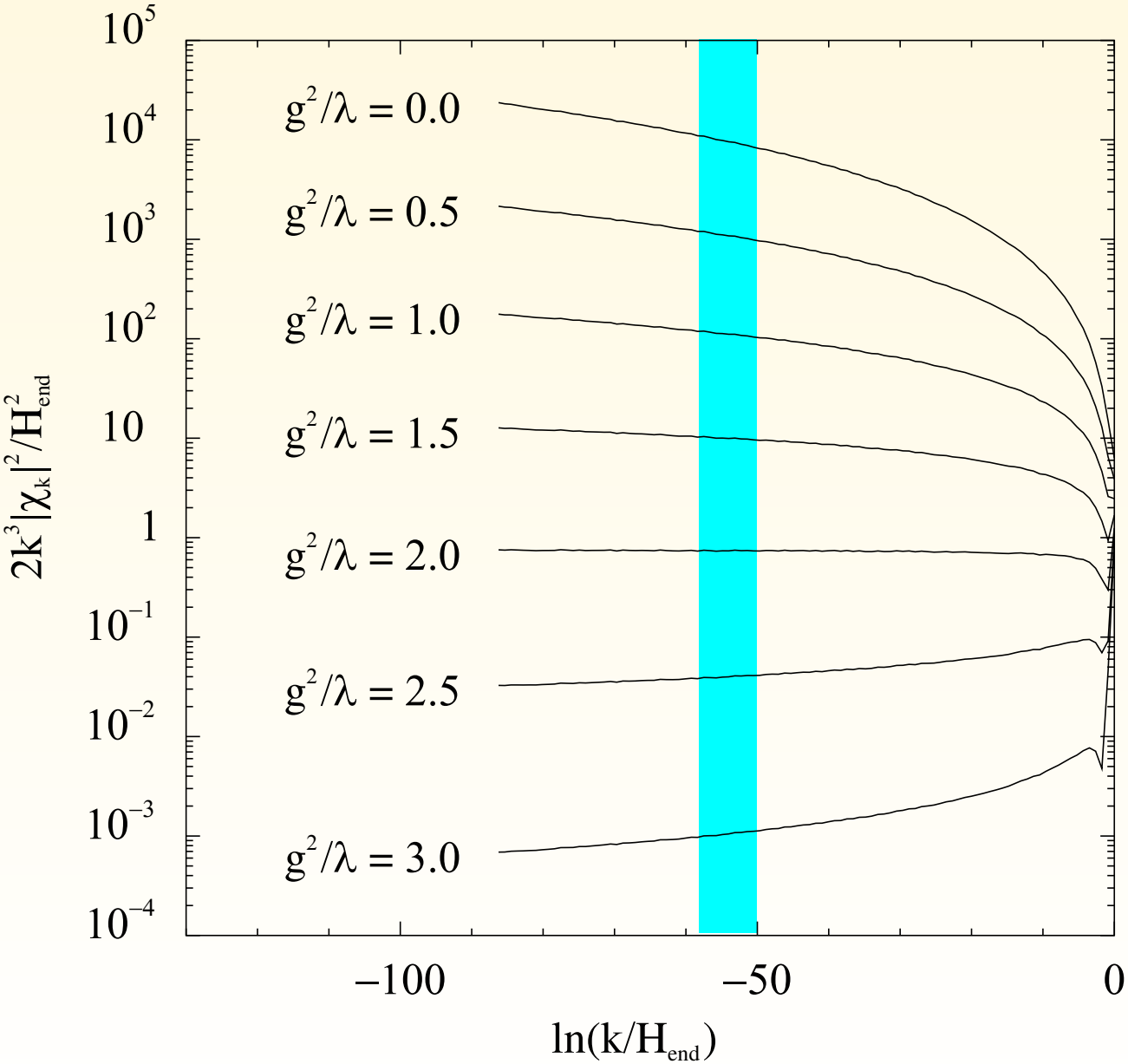

Evolution Depends on Initial Isocon Value

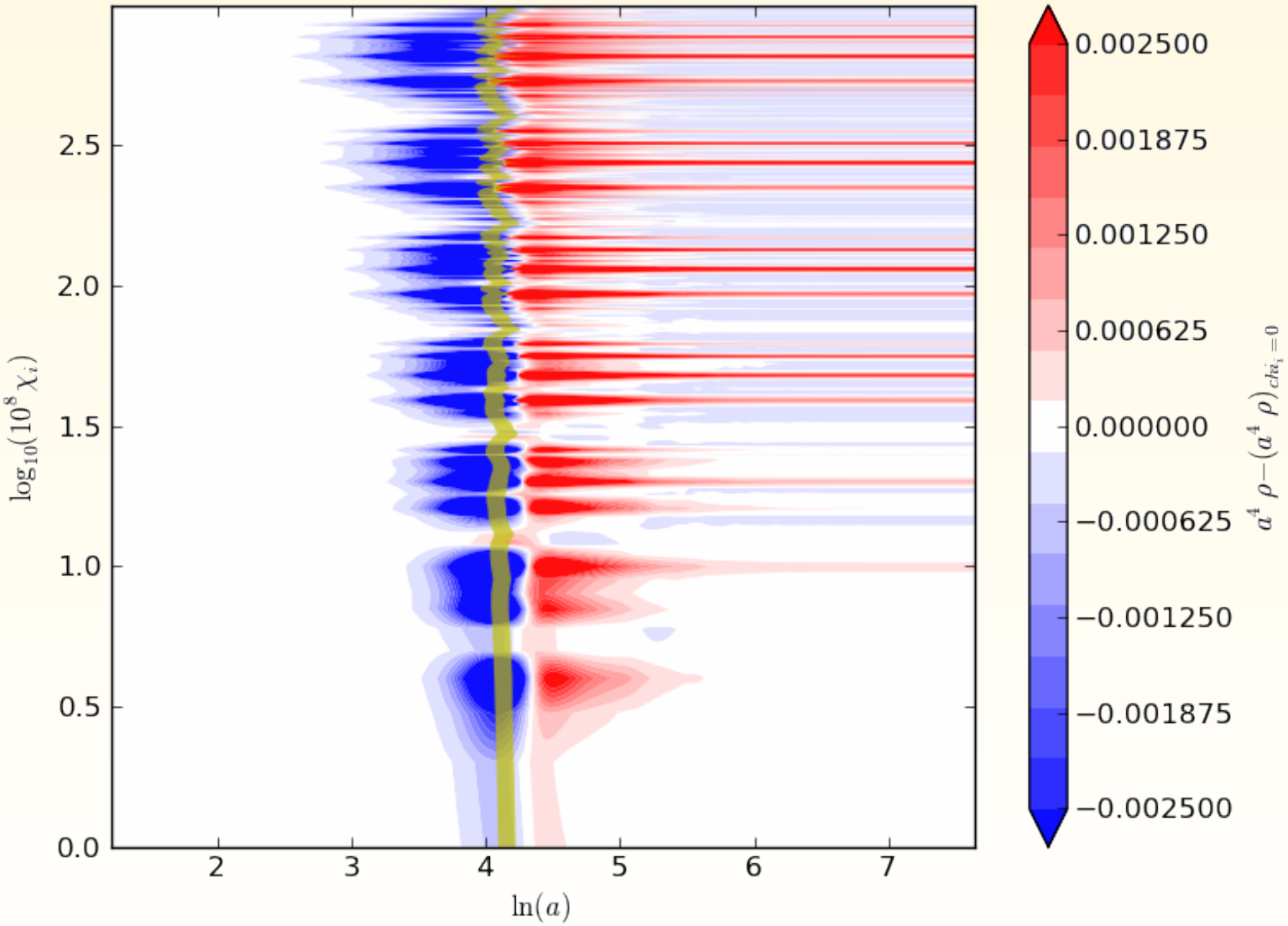

Symplectic Integrator to the Rescue!

Problem:

long-term oscillator evolution

$$H = \frac{p^2}{2} + \frac{q^4}{4}$$

4th order Runge-Kutta

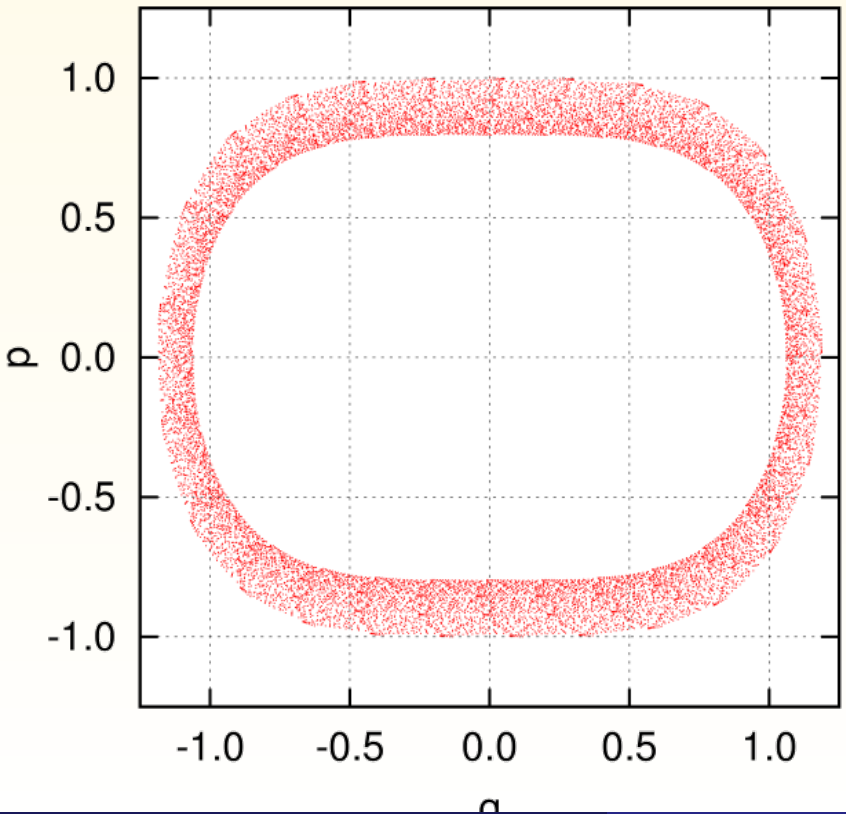

Symplectic Integrator to the Rescue!

Problem:

long-term oscillator evolution

$$H = \frac{p^2}{2} + \frac{q^4}{4}$$

4th order Runge-Kutta

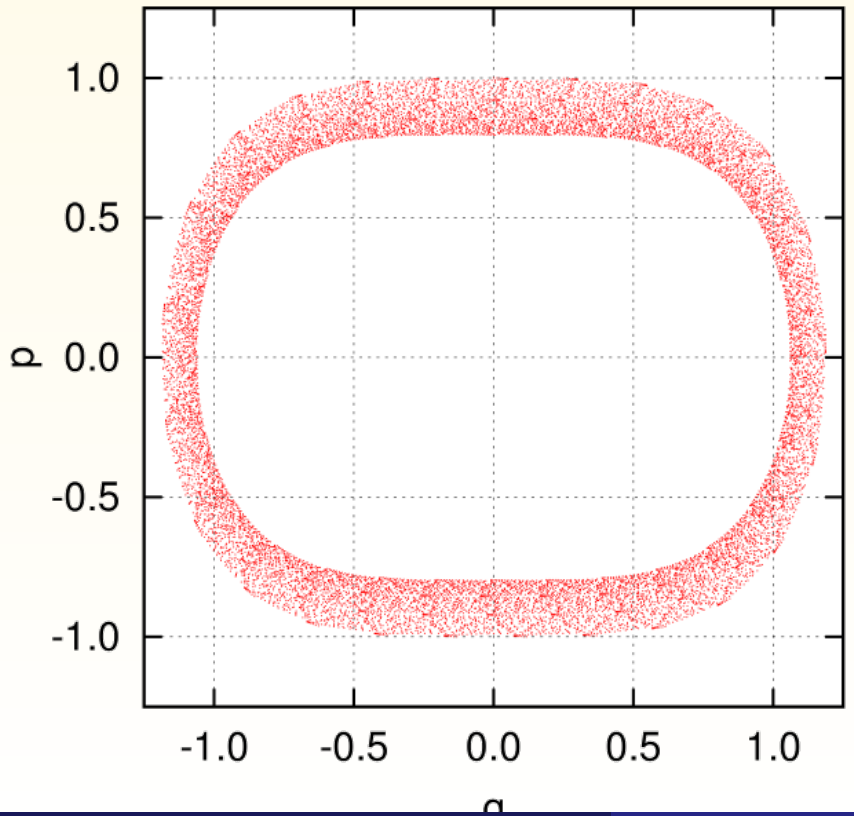

Solution:

enforce energy conservation

$$e^{A\,t/2}\,e^{B\,t}\,e^{A\,t/2} = e^{(A+B)t+O(t^3)}$$

4th order Symplectic

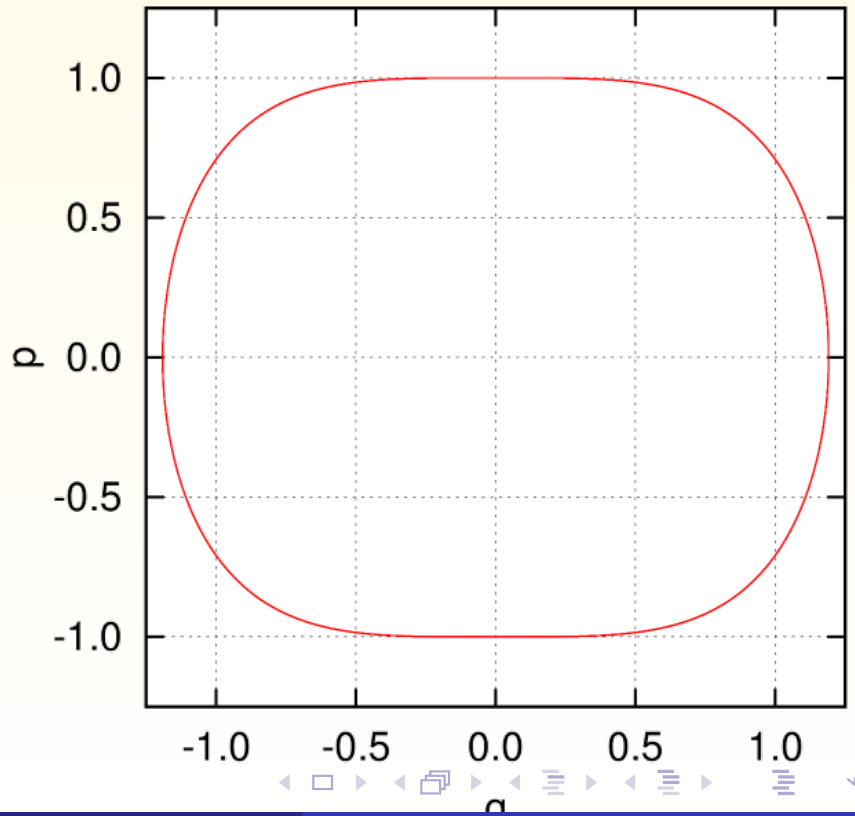

Isocurvature Mode Converts to Curvature

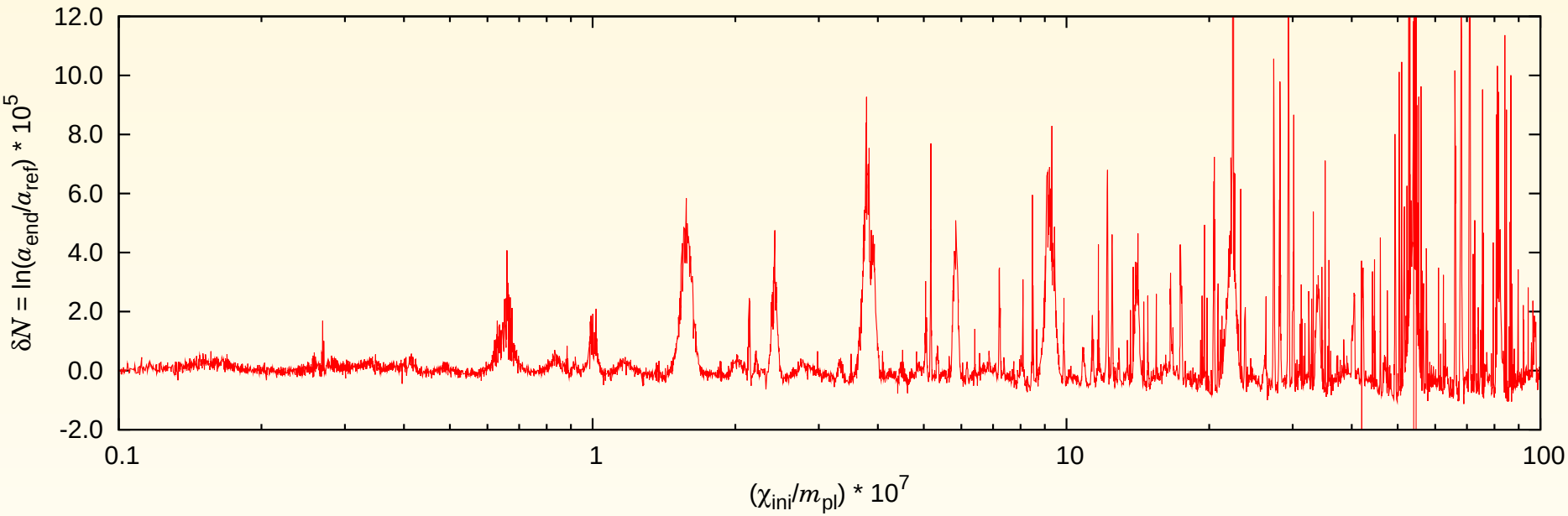

Are these peaks Real? Yes...

Isocurvature Mode Converts to Curvature

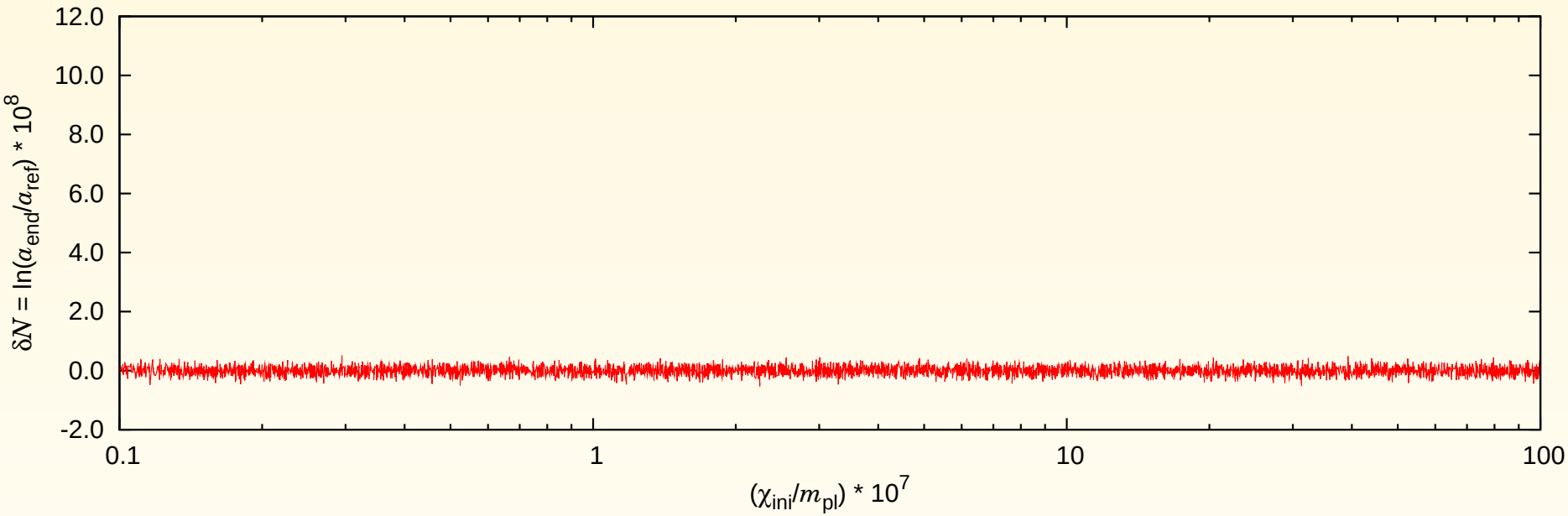

Are these peaks Real? Yes...

Primordial Non-Gaussianity is Produced!

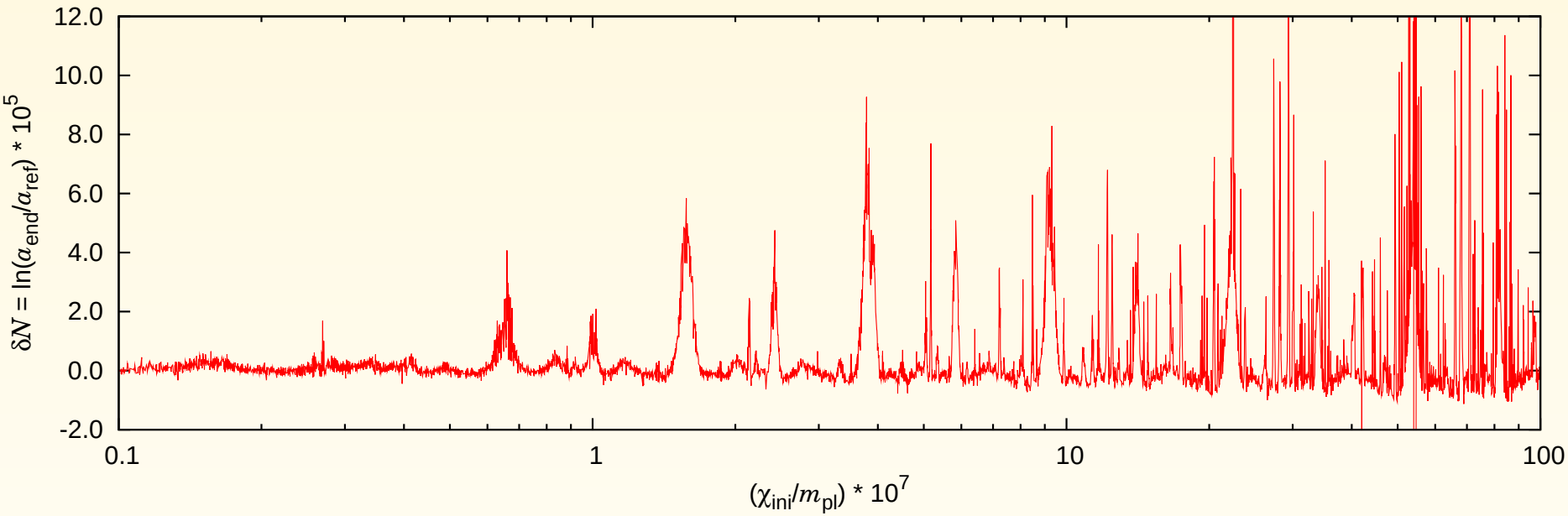

$$\Phi(\vec{x}) = \Phi_G(\vec{x}) + F_{NL}(\chi_G)$$

very different from f_{NL} parametrization!

Here is a Trajectory from the Peak

A Simple Analytical Model

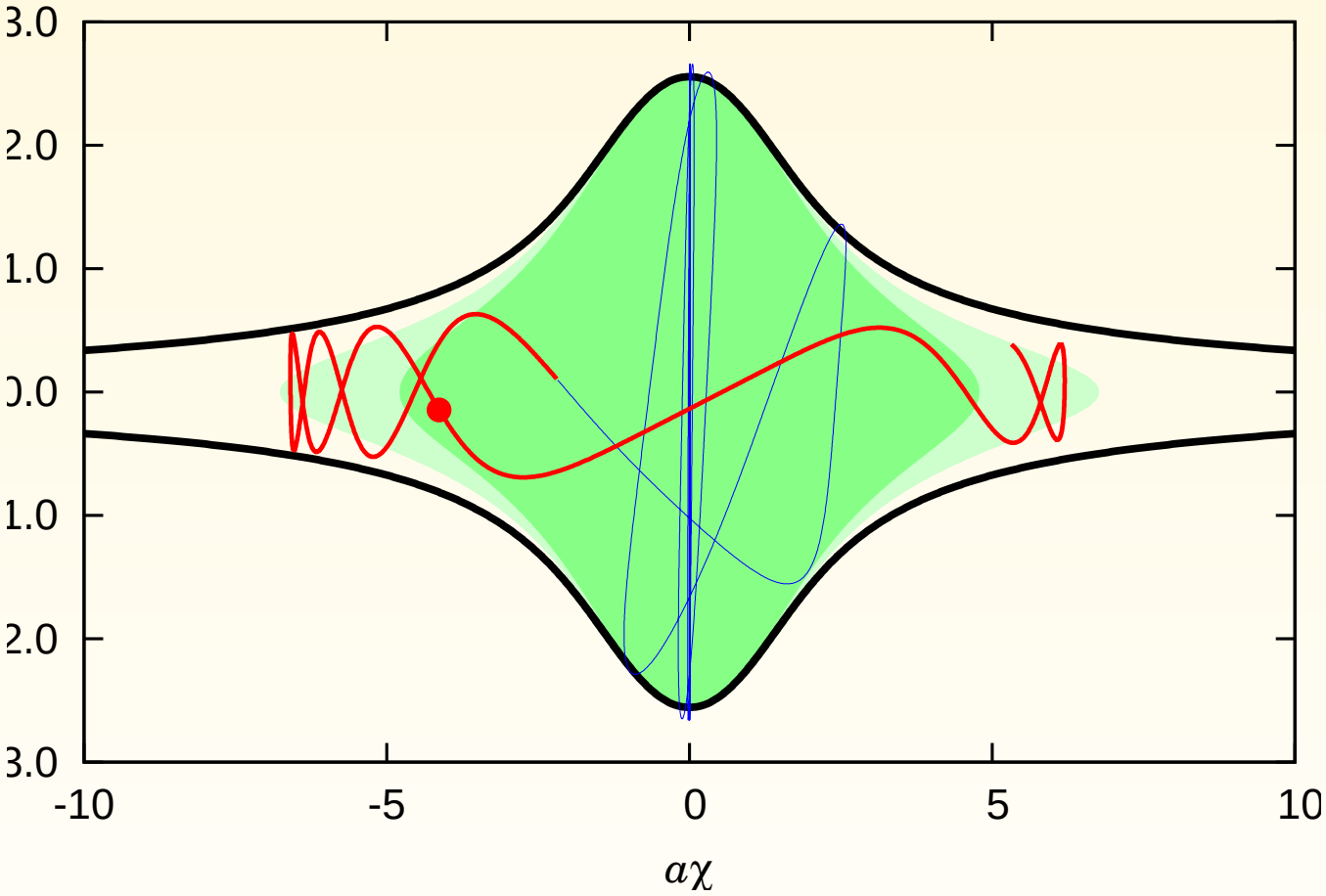

$$V_{\text{eff}}(\phi,\chi)=\frac{\lambda}{4}\phi^4+\frac{g^2}{2}\left(\phi^2+\langle\delta\phi^2\rangle\right)\chi^2$$

Time Evolution of Effective Potential

This Explains why Peaks are Log-Periodic!

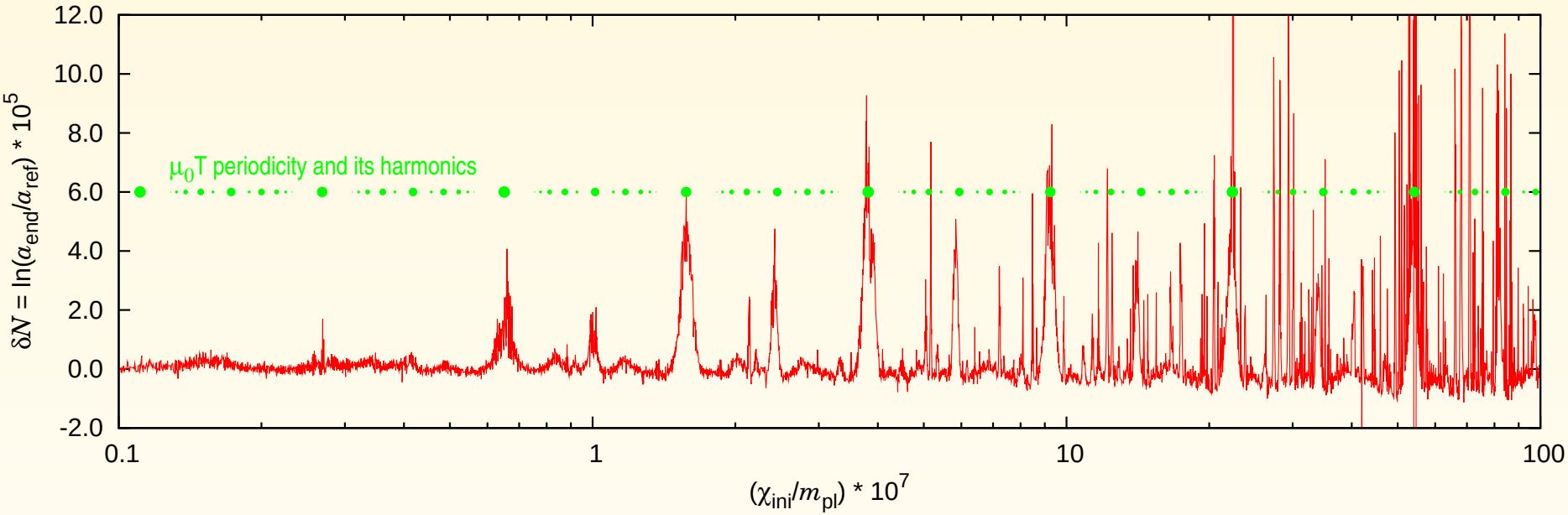

$$\phi(t+T) = \phi(t)$$
$$\chi(t+T) = \chi(t)e^{\mu_0 T}$$

Let's Explore the Parameter Space...

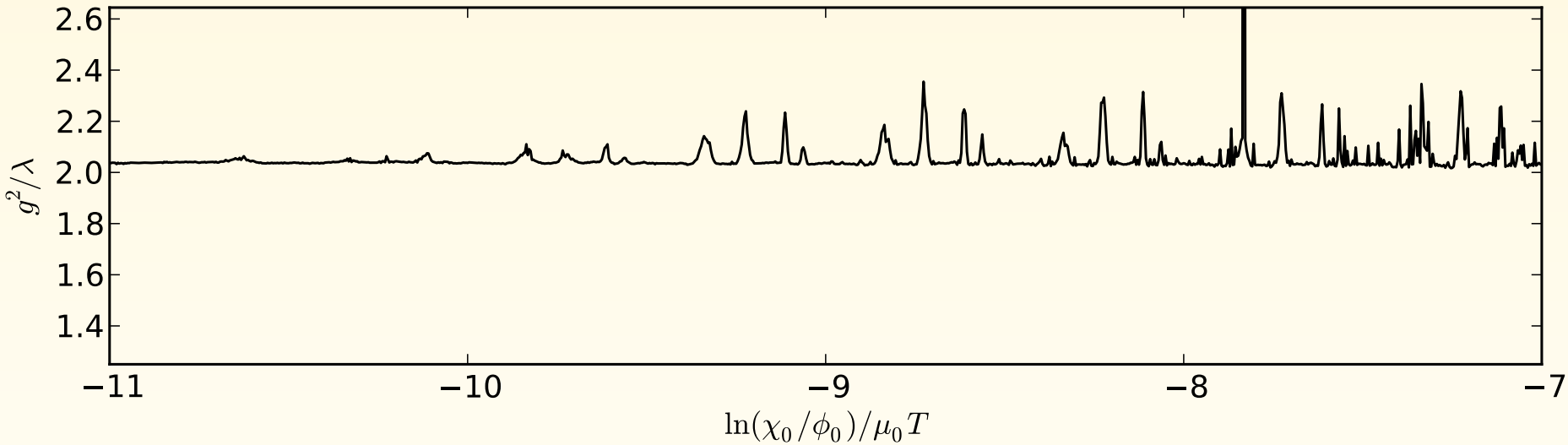

$$\phi(t+T) = \phi(t)$$
$$\chi(t+T) = \chi(t)e^{\mu_0 T}$$

Let's Explore the Parameter Space...

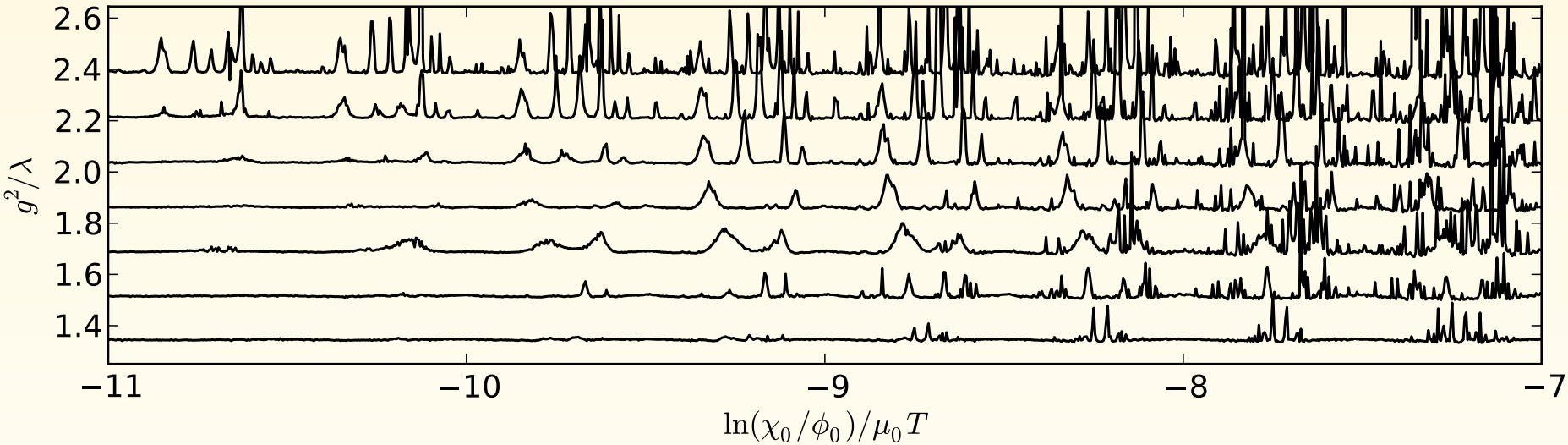

$$\phi(t+T) = \phi(t)$$
$$\chi(t+T) = \chi(t)e^{\mu_0 T}$$

Let's Explore the Parameter Space...

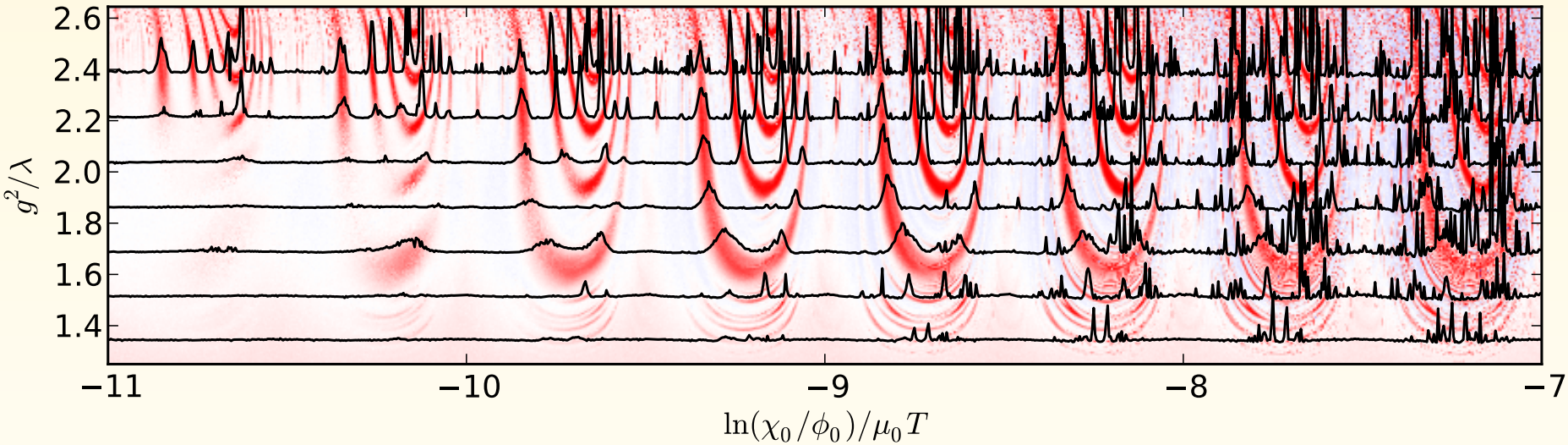

$$\phi(t+T) = \phi(t)$$
$$\chi(t+T) = \chi(t)e^{\mu_0 T}$$

Let's Explore the Parameter Space...

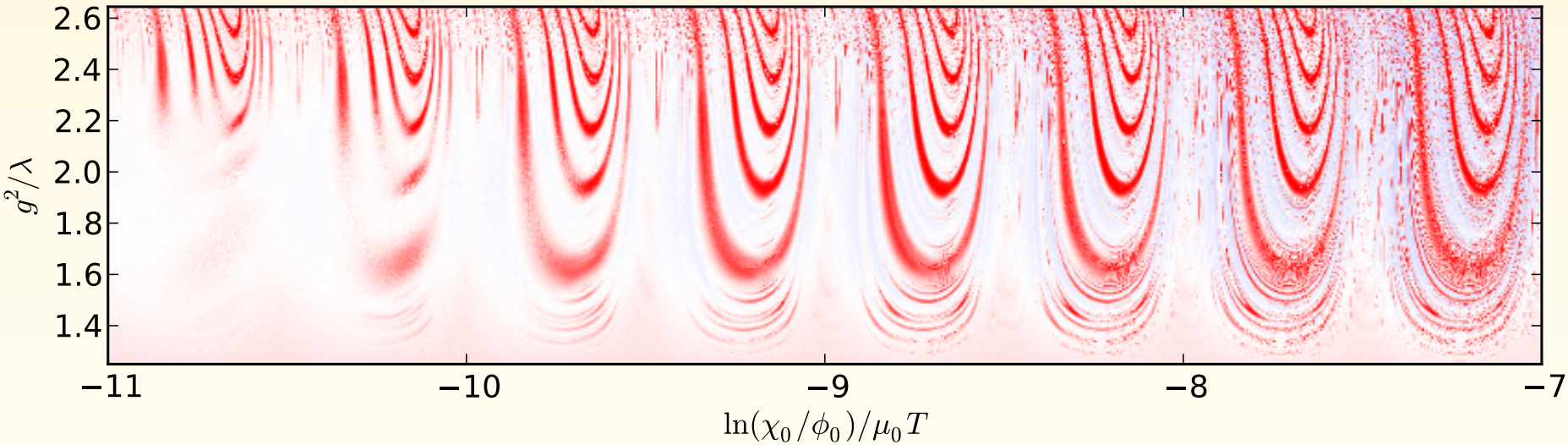

$$\phi(t+T) = \phi(t)$$
$$\chi(t+T) = \chi(t)e^{\mu_0 T}$$

... and Here's How Peaks Split & Multiply!

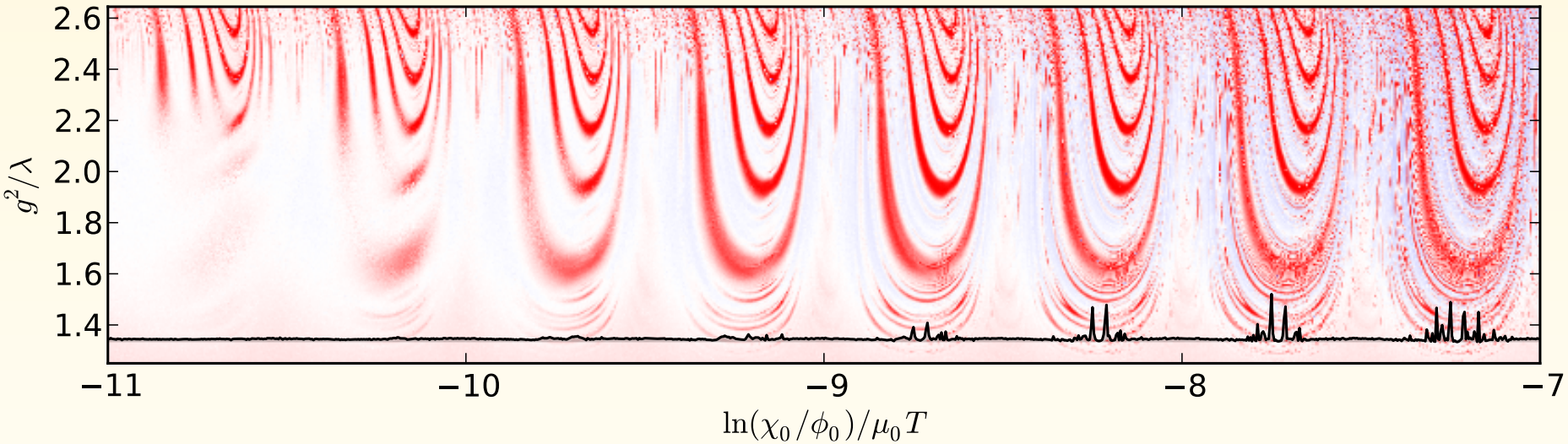

$$\phi(t+T) = \phi(t)$$
$$\chi(t+T) = \chi(t)e^{\mu_0 T}$$

... and Here's How Peaks Split & Multiply!

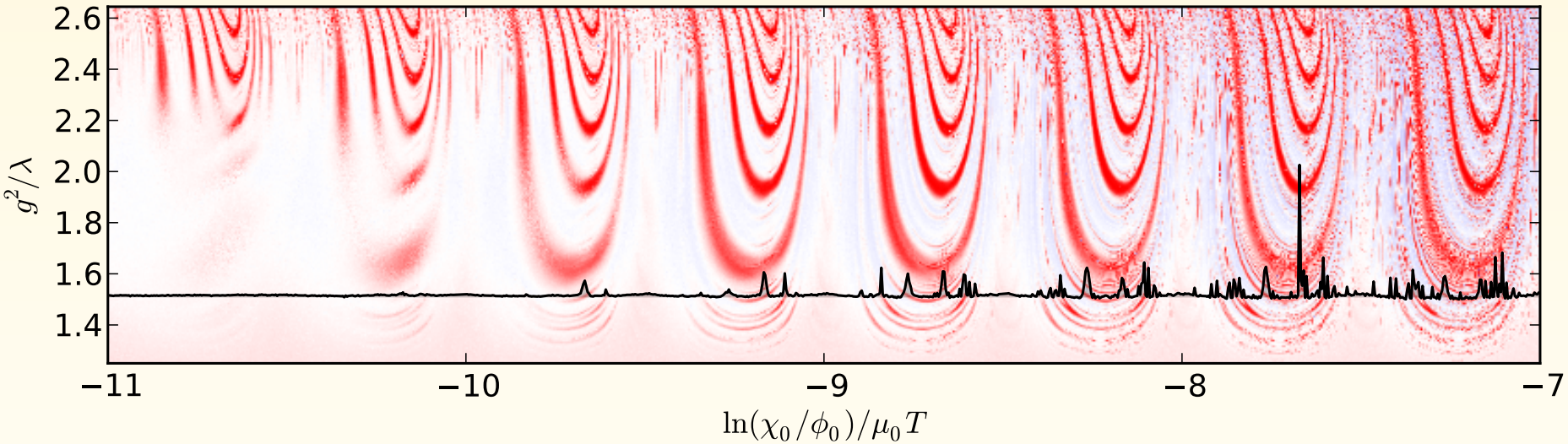

$$\phi(t+T) = \phi(t)$$
$$\chi(t+T) = \chi(t)e^{\mu_0 T}$$

... and Here's How Peaks Split & Multiply!

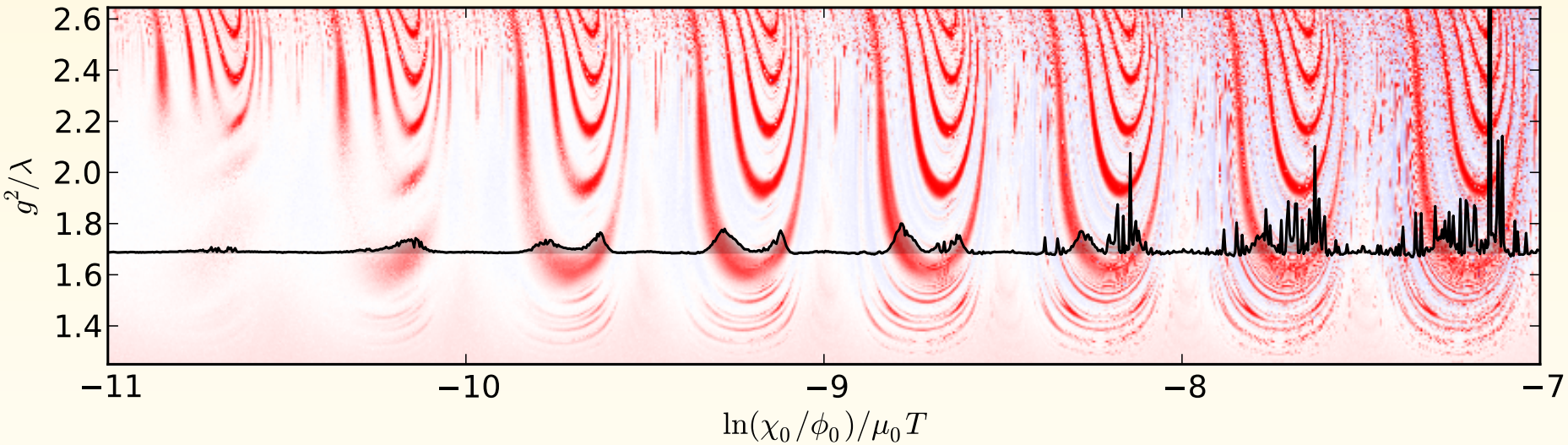

$$\phi(t+T) = \phi(t)$$
$$\chi(t+T) = \chi(t)e^{\mu_0 T}$$

... and Here's How Peaks Split & Multiply!

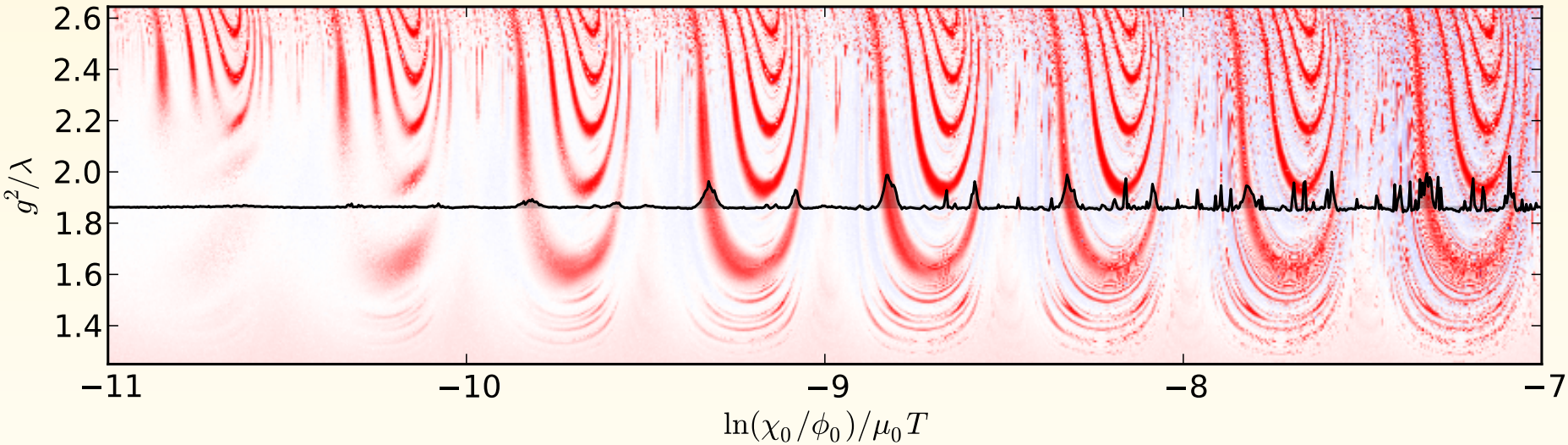

$$\phi(t+T) = \phi(t)$$
$$\chi(t+T) = \chi(t)e^{\mu_0 T}$$

... and Here's How Peaks Split & Multiply!

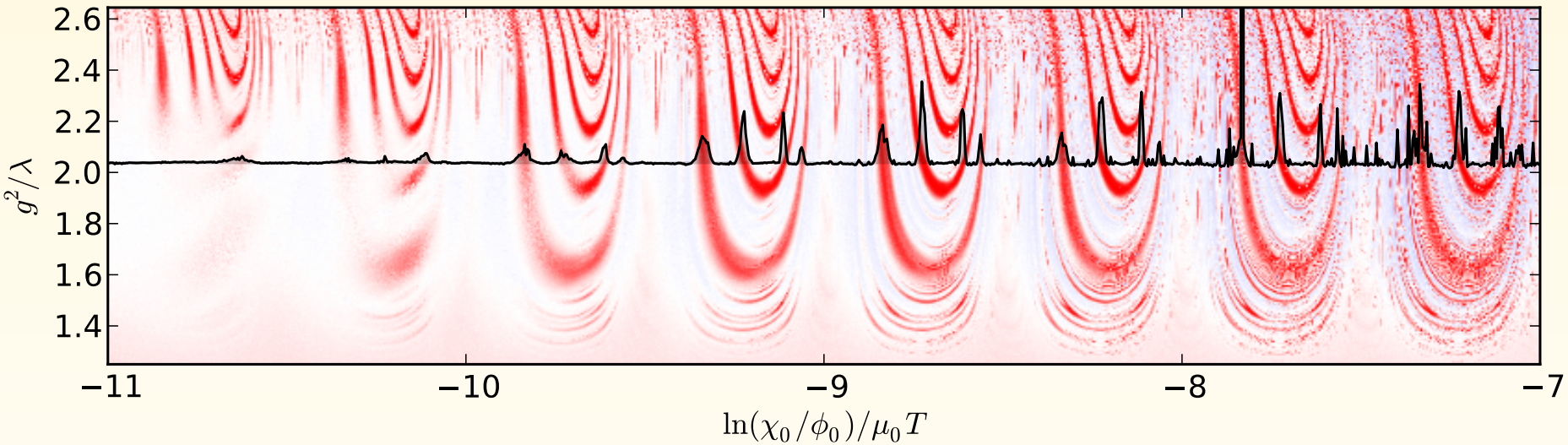

$$\phi(t+T) = \phi(t)$$
$$\chi(t+T) = \chi(t)e^{\mu_0 T}$$

... and Here's How Peaks Split & Multiply!

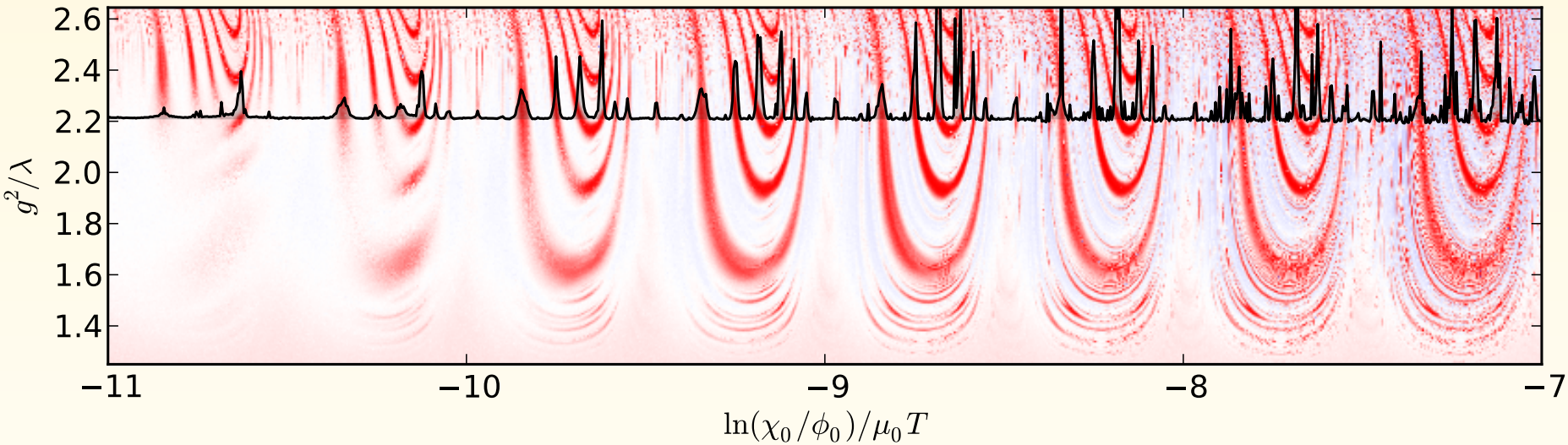

$$\phi(t+T) = \phi(t)$$
$$\chi(t+T) = \chi(t)e^{\mu_0 T}$$

... and Here's How Peaks Split & Multiply!

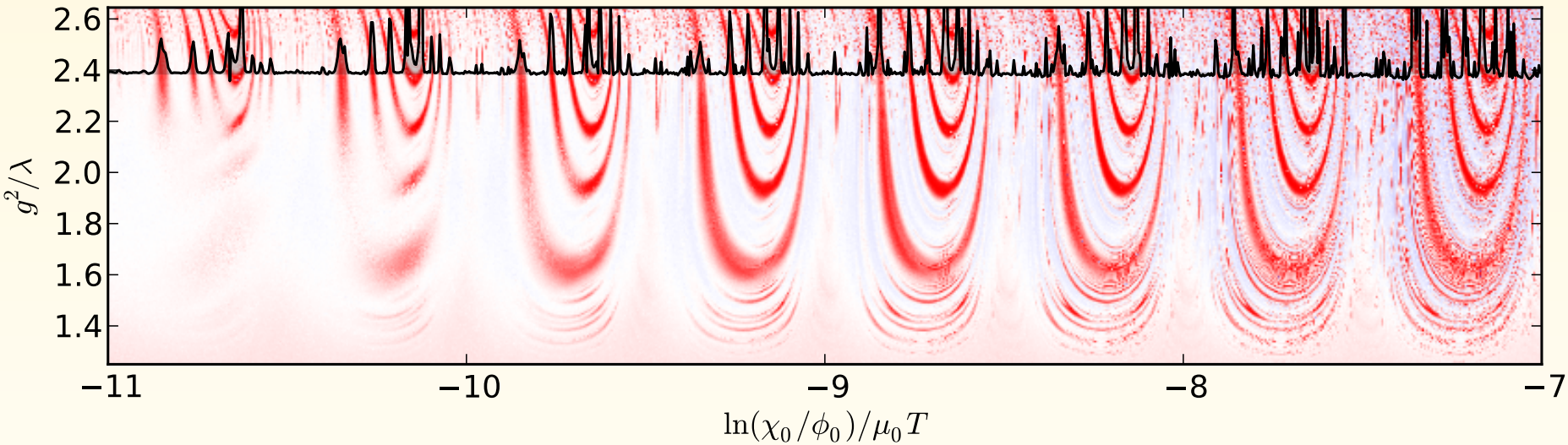

$$\phi(t+T) = \phi(t)$$
$$\chi(t+T) = \chi(t)e^{\mu_0 T}$$

PREHEATING CAN LEAVE A SIGNATURE IN CMB SKY!

the *way* inflation ends
can lead to a new signal:

usual non-Gaussianity:

$$\Phi(\vec{x}) = \Phi_G(\vec{x}) + f_{NL}\Phi_G^2(\vec{x})$$

new from preheating:

$$\Phi(\vec{x}) = \Phi_G(\vec{x}) + F_{NL}(\chi_G)$$

F_{NL} can be a *very*
non-trivial function:

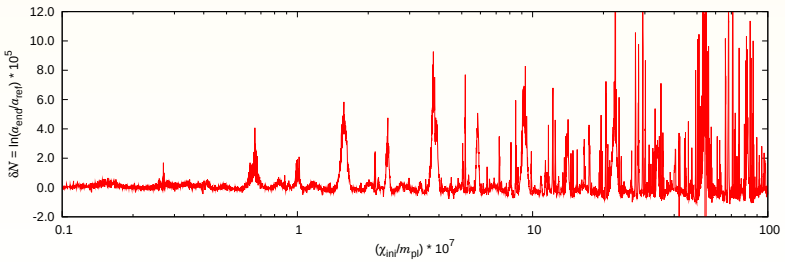

PREHEATING CAN LEAVE A SIGNATURE IN CMB SKY!

the *way* inflation ends can lead to a new signal:

usual non-Gaussianity:

$$\Phi(\vec{x}) = \Phi_G(\vec{x}) + f_{NL}\Phi_G^2(\vec{x})$$

new from preheating:

$$\Phi(\vec{x}) = \Phi_G(\vec{x}) + F_{NL}(\chi_G)$$

F_{NL} can be a *very* non-trivial function:

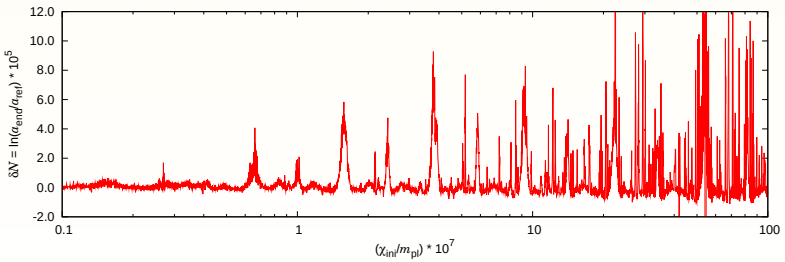

realization of *excursion set* can naturally give cold spots!

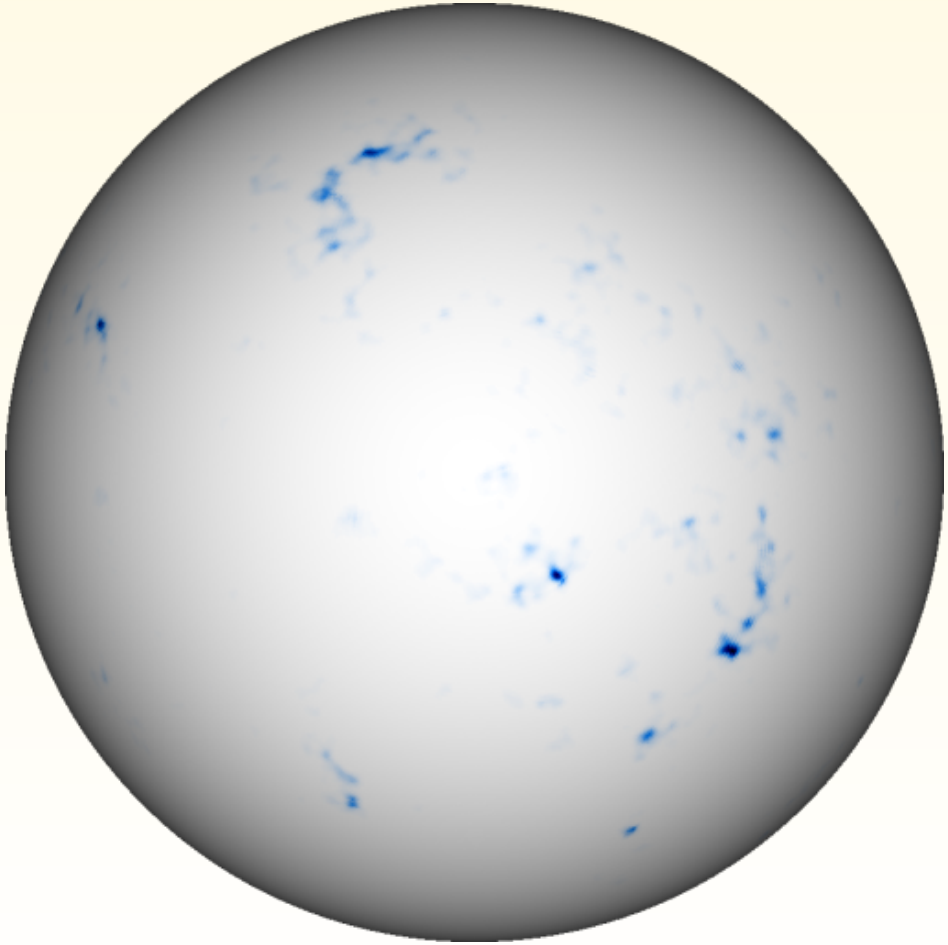

How Would It Look Like on the Sky?

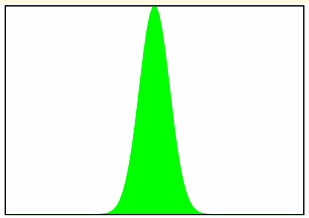

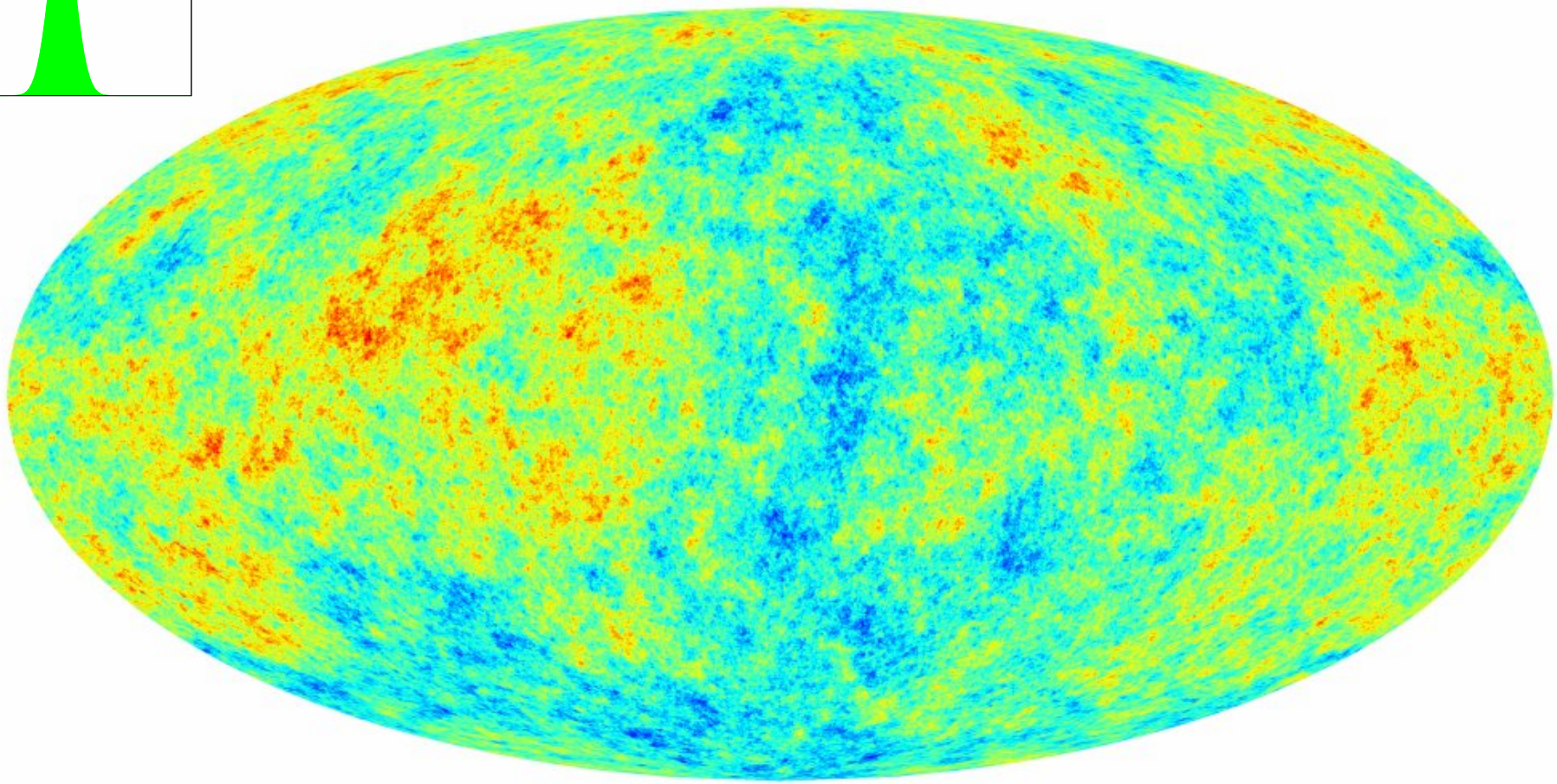

How Would It Look Like on the Sky?

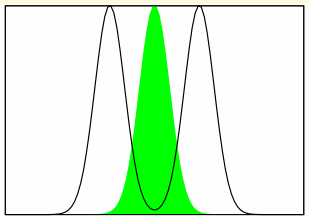

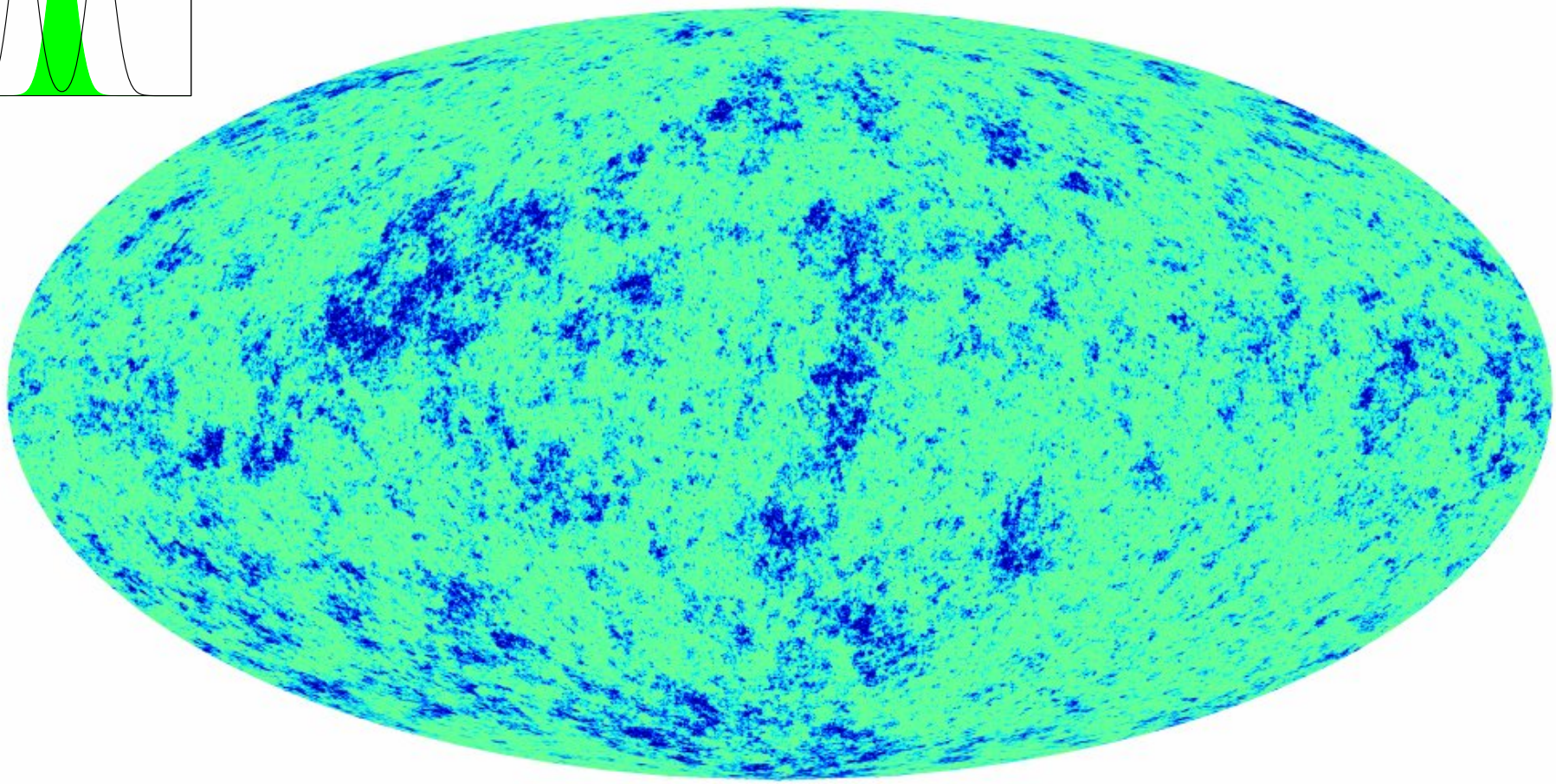

How Would It Look Like on the Sky?

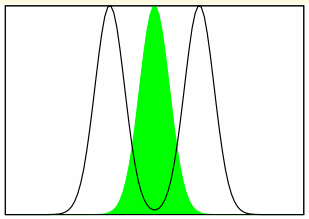

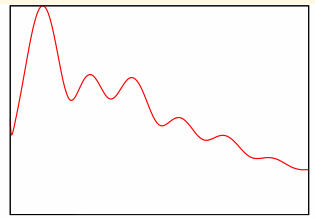

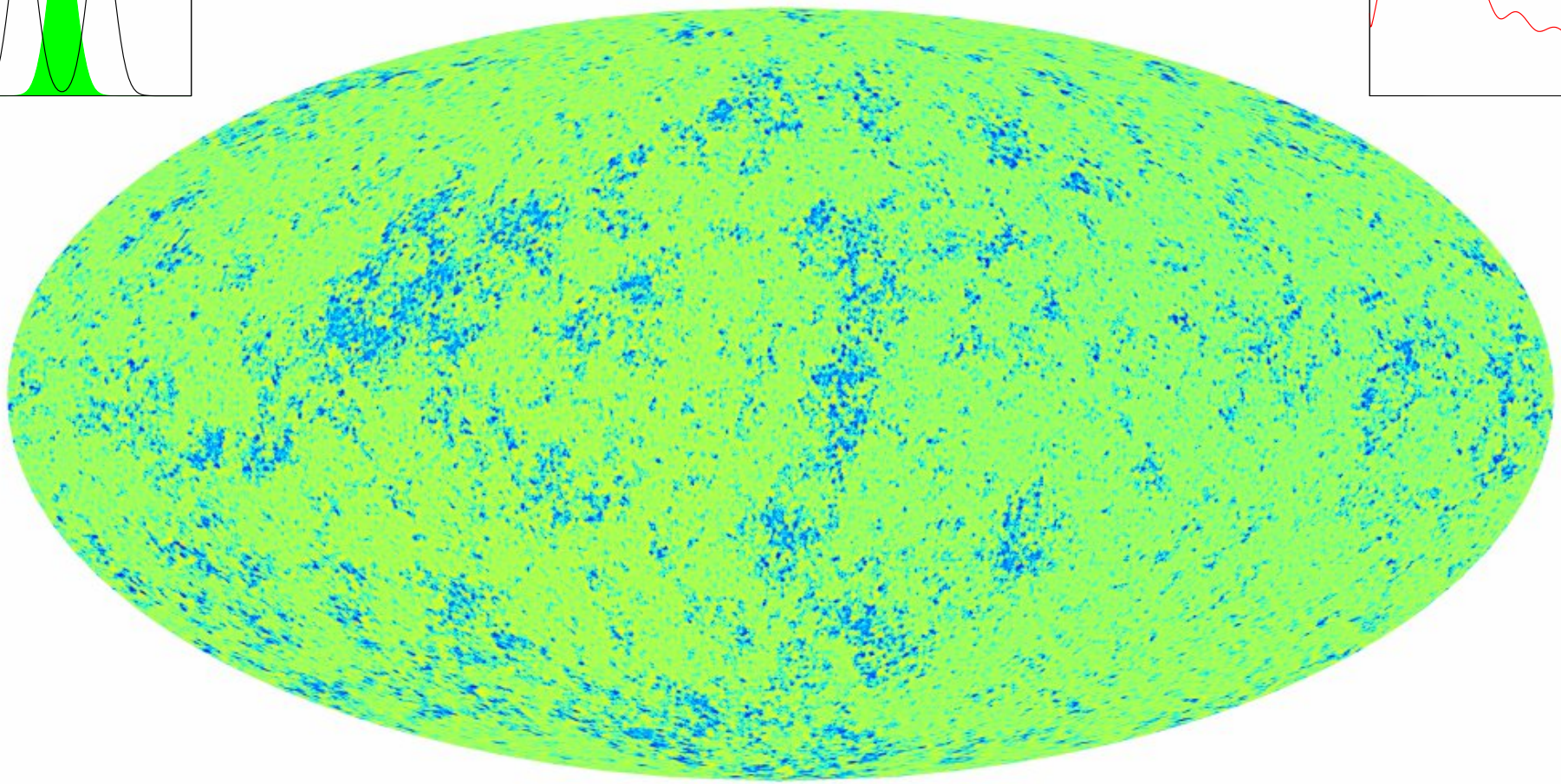

How Would It Look Like on the Sky?

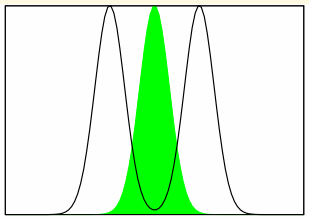

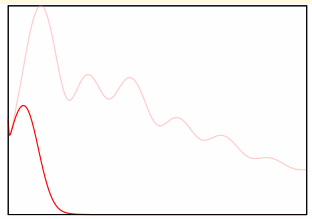

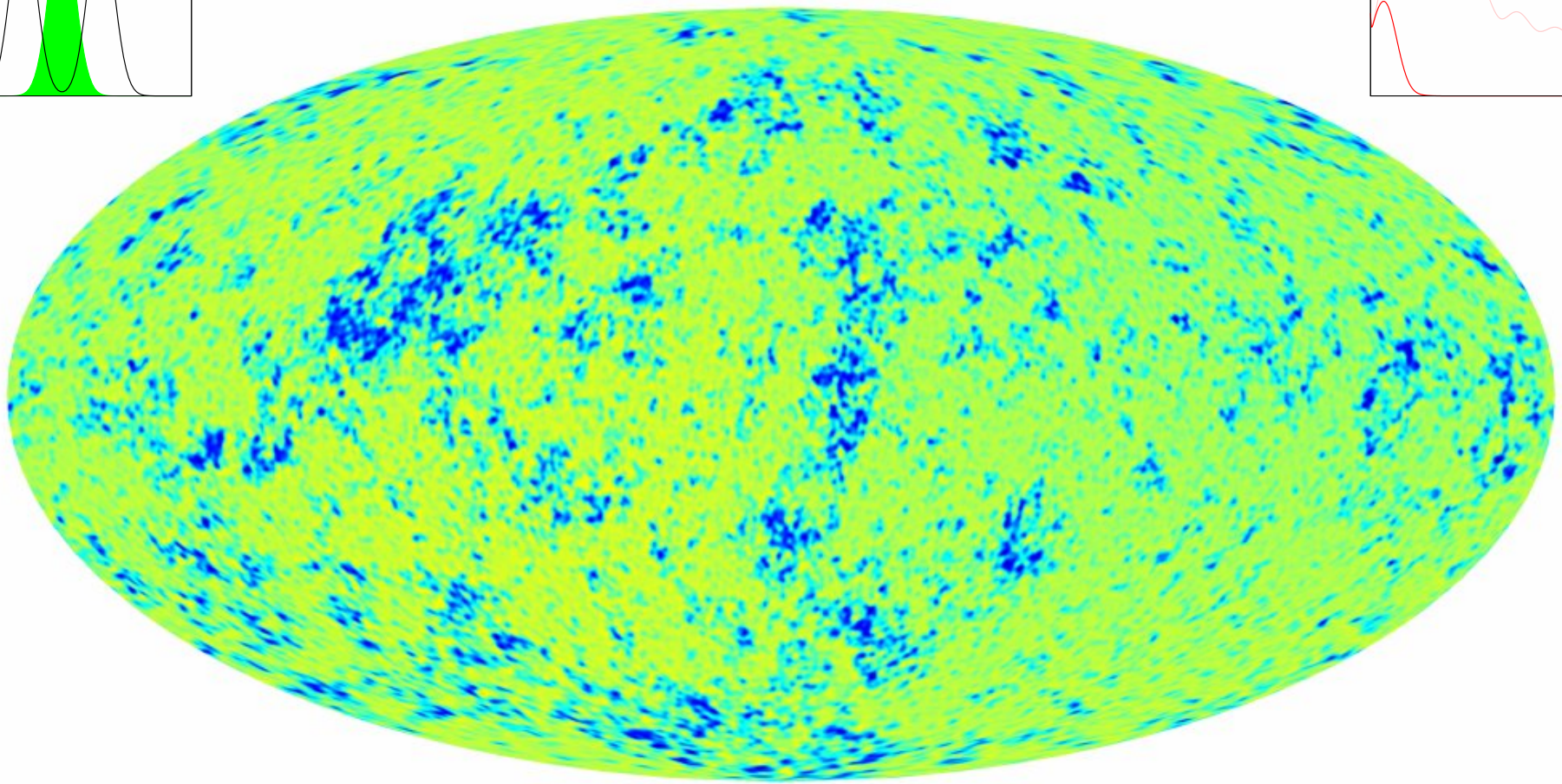

How Would It Look Like on the Sky?

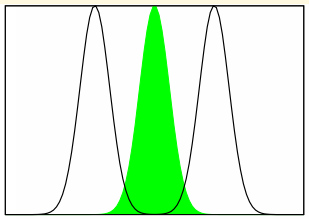

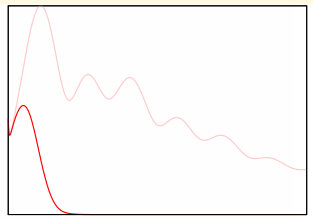

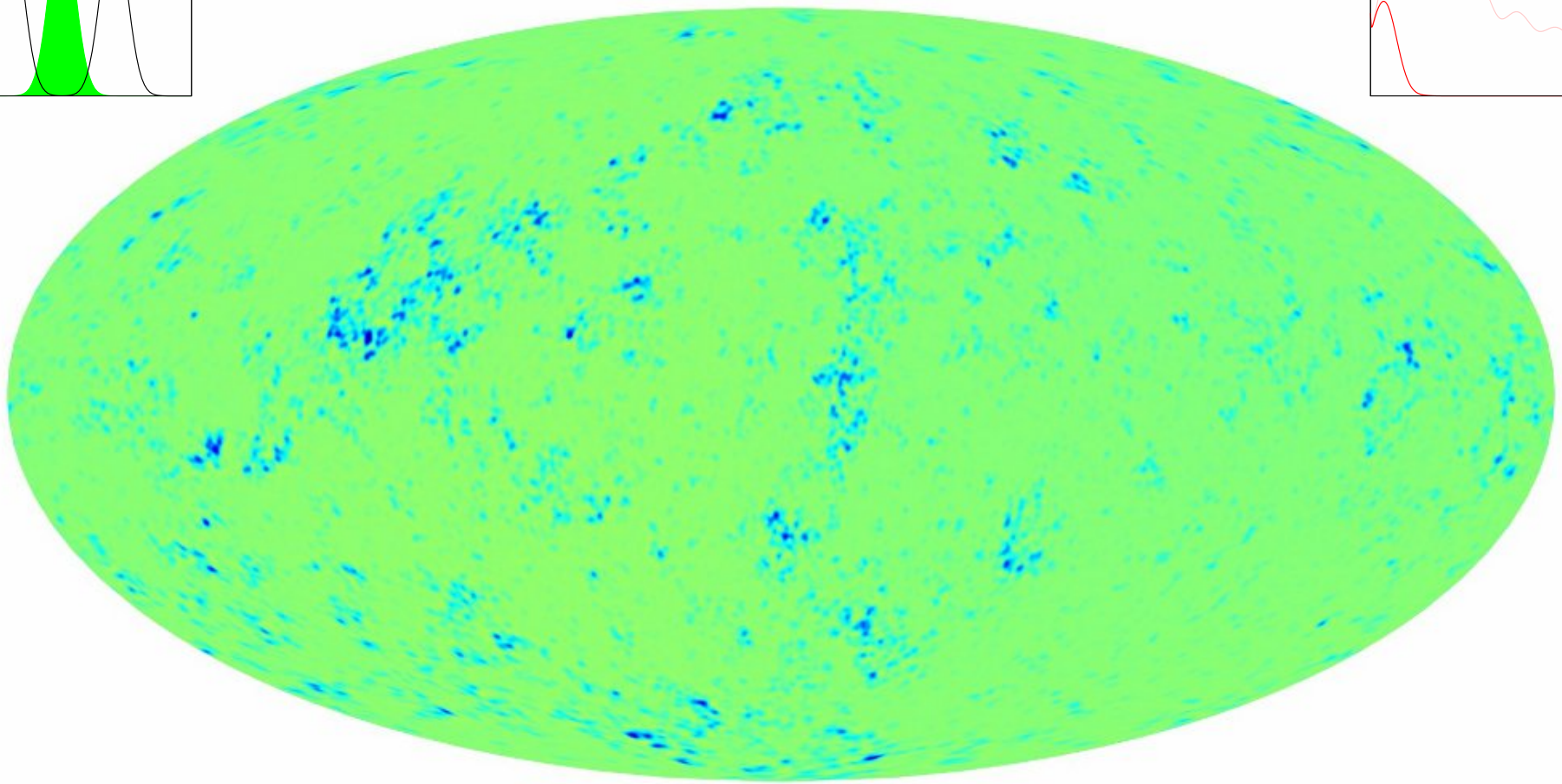

How Would It Look Like on the Sky?

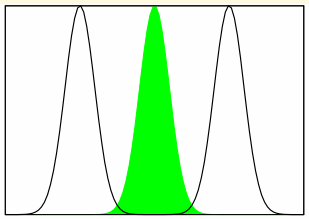

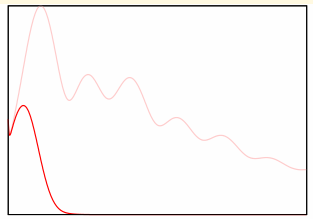

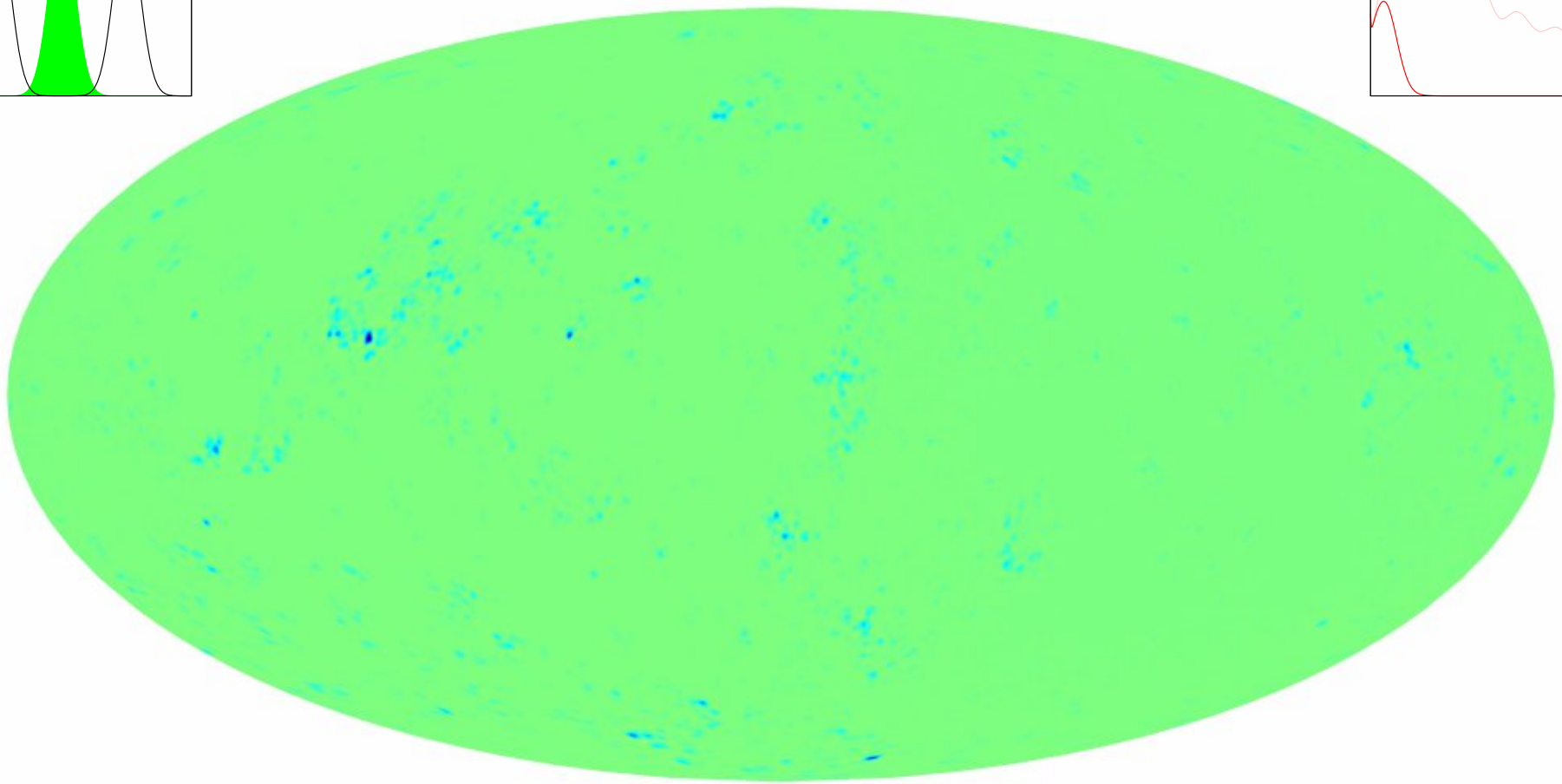

Err, There is a Cold Spot on CMB Sky!..

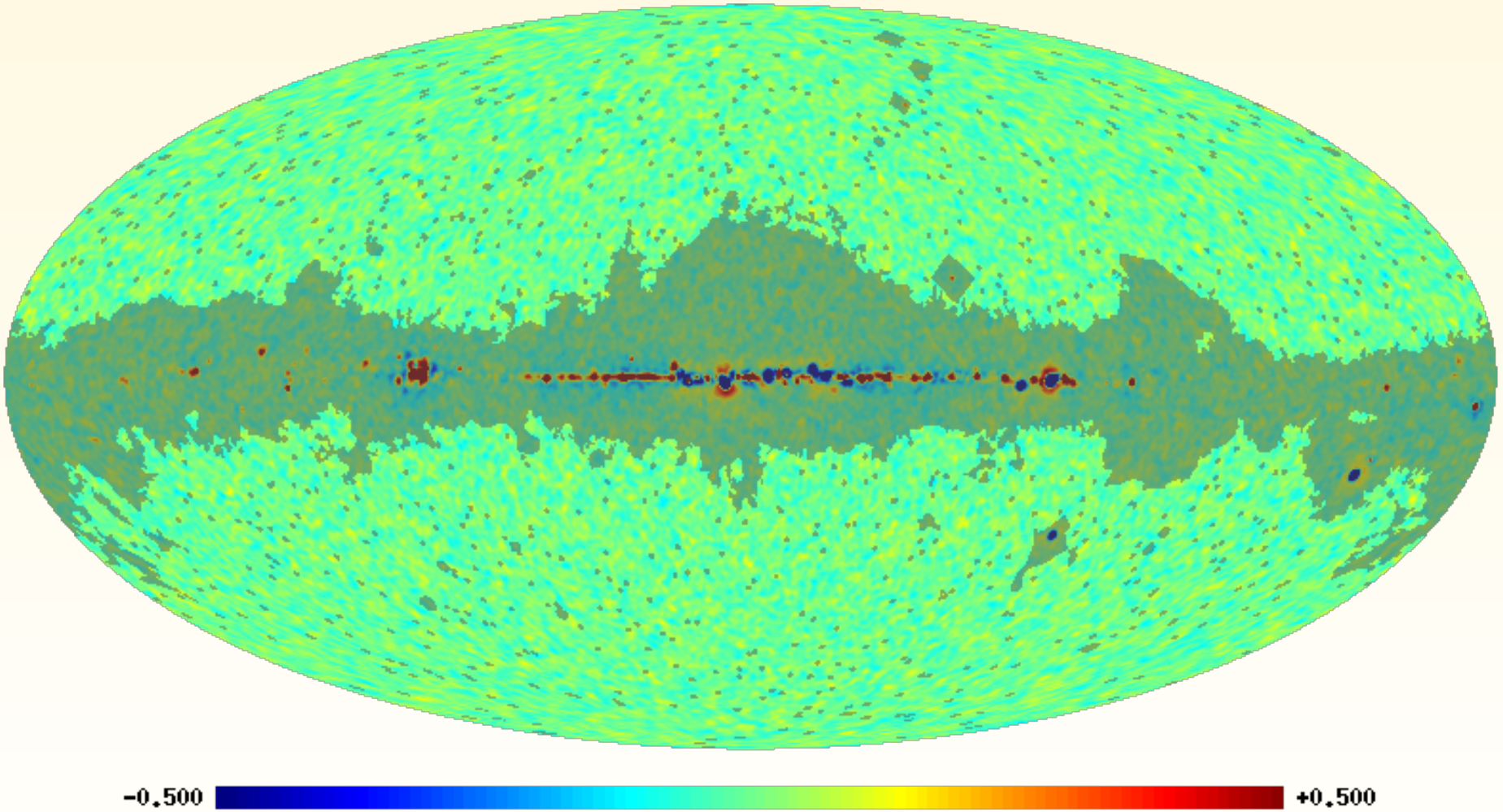

Err, There is a Cold Spot on CMB Sky!..

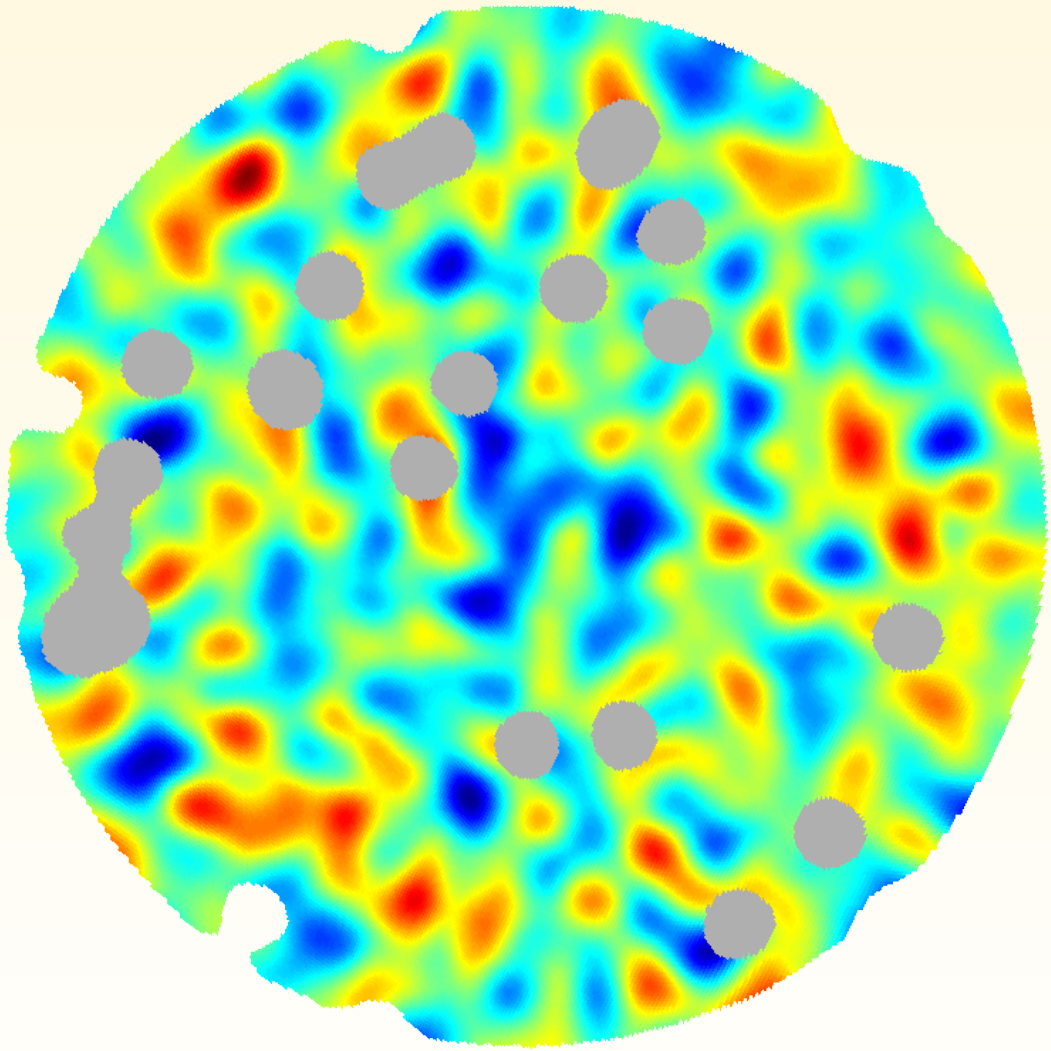

Err, There is a Cold Spot on CMB Sky!..

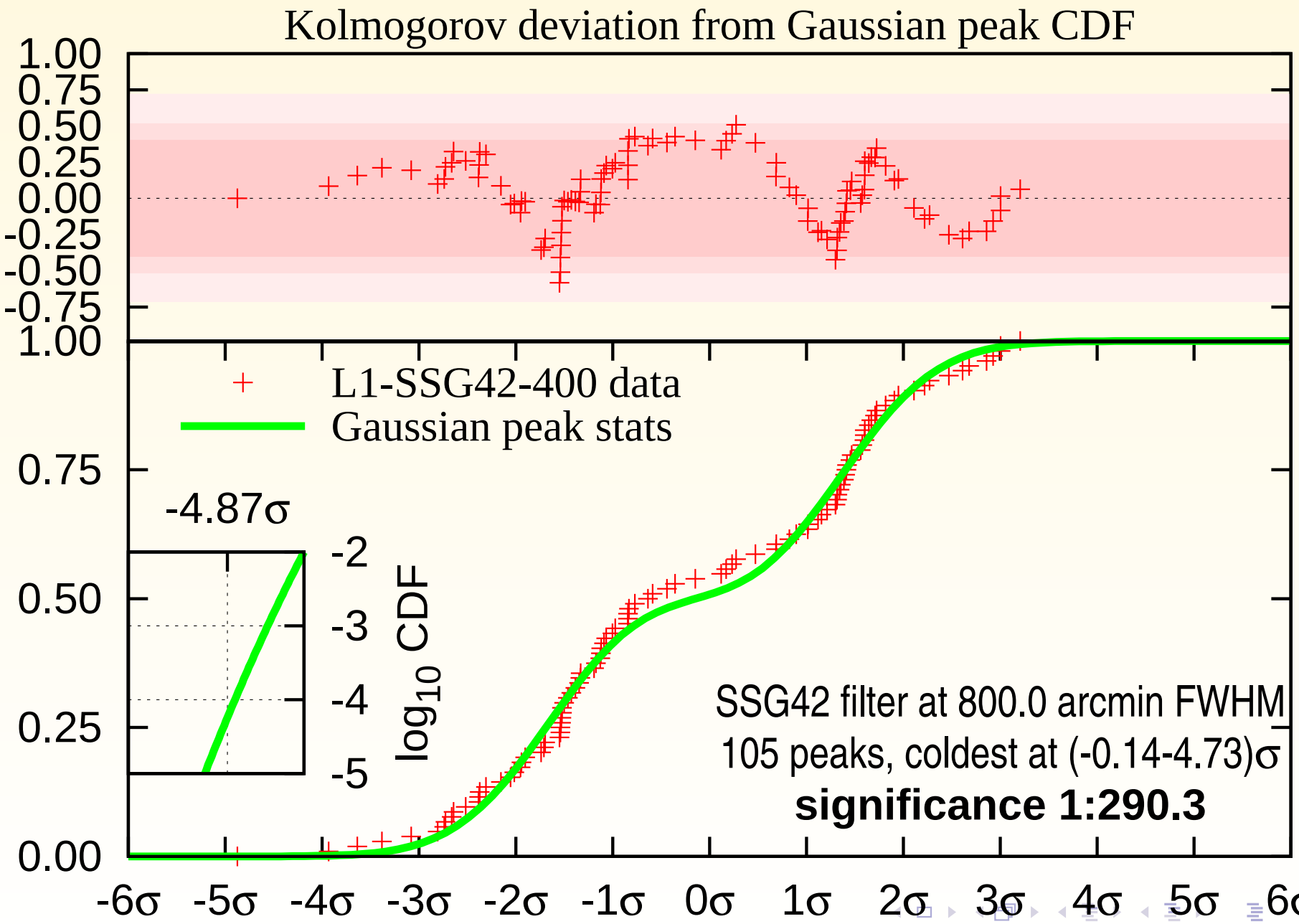

Polarization will Tell if it's Primordial!

Komatsu et. al. (2010)

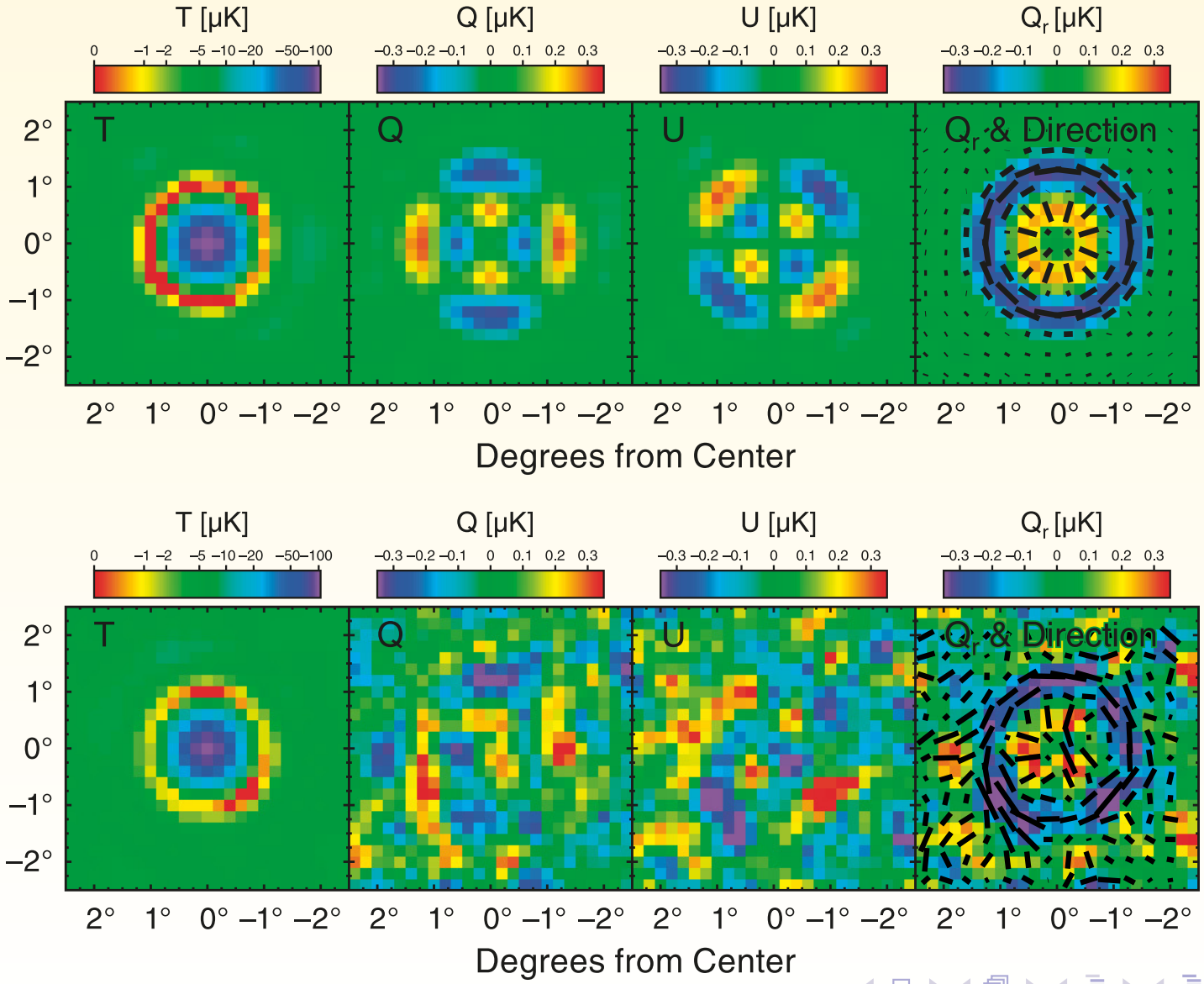

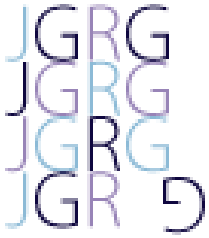

Jinn-Ouk Gong, JGRG 22(2012)111302

"Towards more precise estimates of the primordial bispectrum"

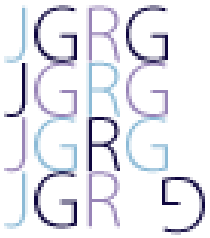

RESCEU SYMPOSIUM ON

GENERAL RELATIVITY AND GRAVITATION

JGRG 22



November 12-16 2012

Koshiba Hall, The University of Tokyo, Hongo, Tokyo, Japan



Towards more precise estimates of the primordial bispectrum

Jinn-Ouk Gong

APCTP, Pohang 790-784, Korea

RESCEU Symposium on General Relativity and Gravitation (JGRG22)
University of Tokyo, Tokyo, Japan
13th November, 2012

Celebrating 60th birthday of T. Futamase, H. Kodama and M. Sasaki

Based on

- C. T. Byrnes and JG, arXiv:1210.1851 [astro-ph.CO]
- A. Achucarro, JG, G. A. Palma and S. P. Patil, to appear
- JG, K. Schalm and G. Shiu, to appear

Outline

1. Introduction
2. Effects of non-trivial speed of sound
3. Bispectrum in general slow-roll
4. Running of $f_{\rm NL}$
5. Summary

General single field inflation

$$S=\int d^4x\sqrt{-g}\left[\frac{m_{\rm Pl}^2}{2}R+P(X,\phi)\right] \quad \text{with} \quad X\equiv-\frac{1}{2}g^{\mu\nu}\partial_\mu\phi\partial_\nu\phi$$

Originated from multi-field setup: light $\mathscr{R}$ and heavy $\mathscr{F}$

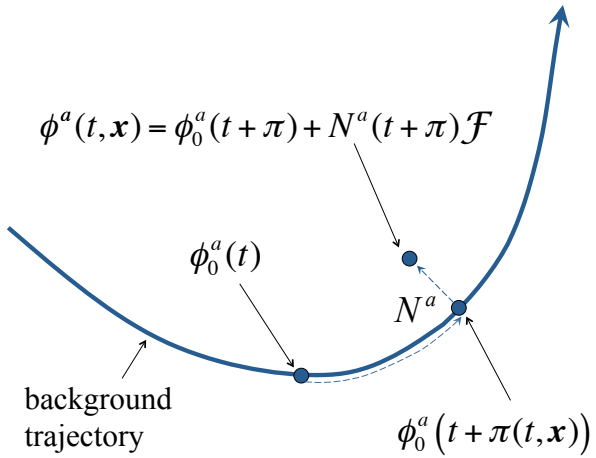

- Trajectory along the lightest direction
- Effects of heavy physics in curved traj
- Can we find universal features of "heavy" physics?

1. Write the action in terms of $\mathscr{R}$ (along traj) and $\mathscr{F}$ (off traj)
2. Integrate out $\mathscr{F}$: $e^{S_{\rm eff}[\mathscr{R}]}=\int[D\mathscr{F}]e^{S[\mathscr{R},\mathscr{F}]}$
   $\left[=\text{equiv to plugging linear sol: }\left(-\Box+M_{\rm eff}^2\right)\mathscr{F}=-2\dot{\theta}\left(\dot{\phi}_0/H\right)\dot{\mathscr{R}}\right]$
3. Effective single field action $S_{\rm eff}[\mathscr{R}]$

Effects of heavy physics as non-trivial c_s

Effects of heavy physics in "speed of sound"

$$c_s^{-2} \equiv 1 + \frac{4\dot{\theta}^2}{M_{\rm eff}^2} \quad (\dot{\theta}: \text{ angular velocity of traj})$$

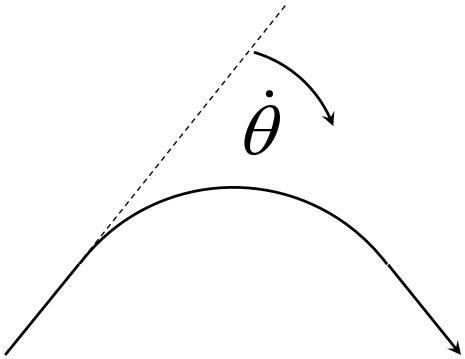

Single field theory with non-trivial c_s^2: Footprint of heavy physics

(Achucarro et al. 2012a)

$\mathscr{F}$ borrows kinetic energy of $\mathscr{R}$ → propagation speed c_s reduced

- EFT in $\Box/M_{\rm eff}^2$: universal footprint of heavy physics
- Many scalar fields in BSM, e.g. moduli
- New observables poorly constrained → to be tested in next decades

Splitting canonical action

EFT = canonical ($c_s = 1$) + (occasional) departure from $c_s = 1$

$$S = \underbrace{\int d^4x a^3 \epsilon m_{\rm Pl}^2 \left[\frac{\dot{\mathscr{R}}^2}{c_s^2} - \frac{(\nabla\mathscr{R})^2}{a^2} \right]}_{=S_2,\ \text{“free” part}} + S_3 + \cdots$$

$$= \underbrace{S_{2,\rm canonical}}_{c_s=1\ \text{part}} + \underbrace{\int d^4x a^3 \epsilon m_{\rm Pl}^2 \left(\frac{1}{c_s^2} - 1 \right) \dot{\mathscr{R}}^2}_{\equiv S_{2,\rm int}} + S_3 + \cdots$$

- Well known, accurate Green's function

  (For example, JG & Stewart 2001, Choe, JG & Stewart 2004)

- Interaction valid for a limited interval (c.f. Chen & Wang 2010)

c.f. Using $dy \equiv c_s d\tau = c_s dt/a$, $q^2 \equiv a^2\epsilon/c_s$ and $v = \sqrt{2} q \mathscr{R}$ (Baumann, Senatore & Zaldarriaga 2011)

$$S_2 = \int d^4x \frac{m_{\rm Pl}^2}{2} \left[(v')^2 - (\nabla v)^2 + \frac{q''}{q} v^2 \right]$$

But see later parts of this presentation

Features in the power spectrum

Interaction Hamiltonian at quadratic order

$$H^{(2)}_{\rm int}(t) = \int d^3x \left(\frac{\partial \mathscr{L}^{(2)}_{\rm int}}{\partial \dot{\mathscr{R}}} \dot{\mathscr{R}} - \mathscr{L}^{(2)}_{\rm int} \right) = \int d^3x a^3 \epsilon m_{\rm Pl}^2 \underbrace{\left(\frac{1}{c_s^2} - 1 \right)}_{\equiv -u(t)} \dot{\mathscr{R}}^2$$

Features in the power spectrum

$$\left\langle \hat{\mathscr{R}}_{\boldsymbol{k}}(\tau) \hat{\mathscr{R}}_{\boldsymbol{q}}(\tau) \right\rangle = -i \int_{\tau_{\rm in}}^{\tau} a(\tau') d\tau' \left\langle 0 \left| \left[\hat{\mathscr{R}}_{\boldsymbol{k}}(\tau) \hat{\mathscr{R}}_{\boldsymbol{q}}(\tau), H^{(2)}_{\rm int}(\tau') \right] \right| 0 \right\rangle = (2\pi)^3 \delta^{(3)}(\boldsymbol{k}+\boldsymbol{q}) \frac{2\pi^2}{k^3} \Delta\mathscr{P}_{\mathscr{R}}$$

$$\rightarrow \frac{\Delta\mathscr{P}_{\mathscr{R}}}{\mathscr{P}_{\mathscr{R}}} = \kappa \int_0^{\infty} dt u(t) \sin(2\kappa t) \quad \text{with} \quad \mathscr{P}_{\mathscr{R}} = \frac{H^2}{8\pi^2 m_{\rm Pl}^2 \epsilon}, t \equiv \frac{\tau}{\tau_\star}, \kappa \equiv \frac{k}{k_\star}$$

Inverting this relation to write u in terms of observable $\Delta\mathscr{P}_{\mathscr{R}}/\mathscr{P}_{\mathscr{R}}$

$$u(t) = \frac{2i}{\pi} \int_{-\infty}^{\infty} \frac{d\kappa}{\kappa} \frac{\Delta\mathscr{P}_{\mathscr{R}}}{\mathscr{P}_{\mathscr{R}}} \left(\frac{\kappa}{2} \right) e^{i\kappa\tau}$$

Correlated bispectrum and power spectrum: $B_{\mathscr{R}} = \int (\cdots \Delta\mathscr{P}_{\mathscr{R}}/\mathscr{P}_{\mathscr{R}})$

Leading bispectrum for varying c_s

Leading order action in terms of $u(t)$

$$S_3 \supset \int d^4x a^3 m_{\rm Pl}^2 \epsilon \left[3u\dot{\mathscr{R}}^2 \mathscr{R} - (u+2s)\mathscr{R}(\nabla\mathscr{R})^2 \right] \quad \left(s \equiv \frac{\dot{c}_s}{Hc_s} \right)$$

Assumption: H, ϵ and $\eta_{\|}$ approximately constant ($K \equiv k_1 + k_2 + k_3$)

$$B_{\mathscr{R}}(\boldsymbol{k}_1, \boldsymbol{k}_2, \boldsymbol{k}_3) = 2\Re \left\{ 2i\widehat{\mathscr{R}}_{k_1}(0)\widehat{\mathscr{R}}_{k_2}(0)\widehat{\mathscr{R}}_{k_3}(0) \left[3\epsilon \frac{m_{\rm Pl}^2}{H^2} \int_{-\infty}^{0} d\tau \frac{u}{\tau^2} \frac{d\widehat{\mathscr{R}}^*_{k_1}(\tau)}{d\tau} \frac{d\widehat{\mathscr{R}}^*_{k_2}(\tau)}{d\tau} \widehat{\mathscr{R}}^*_{k_3}(\tau) + 2 \text{ perm} \right.\right.$$

$$\left.\left. + \epsilon \frac{m_{\rm Pl}^2}{H^2} (\boldsymbol{k}_1 \cdot \boldsymbol{k}_2 + 2 \text{ perm}) \int_{-\infty}^{0} d\tau \frac{u+2s}{\tau^2} \widehat{\mathscr{R}}^*_{k_1}(\tau)\widehat{\mathscr{R}}^*_{k_2}(\tau)\widehat{\mathscr{R}}^*_{k_3}(\tau) \right] \right\}$$

$$= \frac{(2\pi)^4 \mathscr{P}_{\mathscr{R}}^2}{(k_1 k_2 k_3)^3} \left[\frac{3}{2}(k_1 k_2)^2 \left\{ \frac{1}{K} \frac{\Delta\mathscr{P}_{\mathscr{R}}}{\mathscr{P}_{\mathscr{R}}}\left(\frac{K}{2k_\star}\right) - k_3 \frac{d}{dk}\left[\frac{1}{k} \frac{\Delta\mathscr{P}_{\mathscr{R}}}{\mathscr{P}_{\mathscr{R}}}\left(\frac{k}{2k_\star}\right) \right] \right|_{k=K} \right\} + 2 \text{ perm} \right.$$

$$+ \frac{1}{2}(\boldsymbol{k}_1 \cdot \boldsymbol{k}_2 + 2 \text{ perm}) \left\{ \frac{K^2 - (k_1 k_2 + 2 \text{ perm})}{K} \frac{\Delta\mathscr{P}_{\mathscr{R}}}{\mathscr{P}_{\mathscr{R}}}\left(\frac{K}{2k_\star}\right) + k_1 k_2 k_3 \frac{d}{dk}\left[\frac{1}{k} \frac{\Delta\mathscr{P}_{\mathscr{R}}}{\mathscr{P}_{\mathscr{R}}}\left(\frac{k}{2k_\star}\right) \right] \right|_{k=K}$$

$$\left. - (k_1 k_2 + 2 \text{ perm}) \frac{d}{dk}\left[\frac{\Delta\mathscr{P}_{\mathscr{R}}}{\mathscr{P}_{\mathscr{R}}}\left(\frac{k}{2k_\star}\right) \right] \right|_{k=K} + k_1 k_2 k_3 \frac{d^2}{dk^2}\left[\frac{\Delta\mathscr{P}_{\mathscr{R}}}{\mathscr{P}_{\mathscr{R}}}\left(\frac{k}{2k_\star}\right) \right] \Bigg|_{k=K} \Bigg\} \Bigg]$$

(Achucarro, JG, Palma & Patil, to appear)

Correlation between spectra is manifest!

Modeling curvilinear trajectory

A cosh turn in otherwise straight trajectory in 2-field system

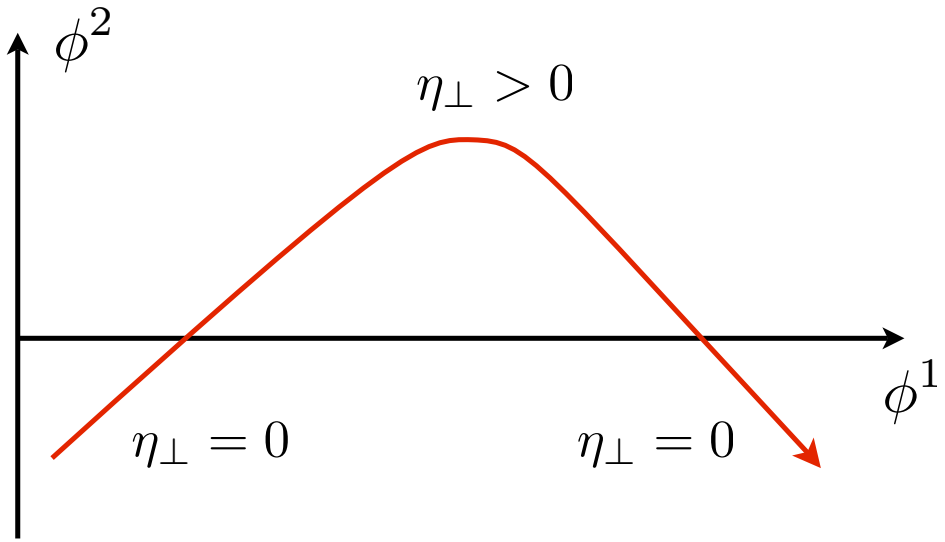

$$\eta_\perp = \frac{\dot{\theta}}{H} = \frac{\eta_{\perp,\max}}{\cosh^2\left[2(N-N_\star)/\Delta N\right]}$$

(Equations of motion: see Achucarro et al. 2011)

Features from smooth curvilinear trajectory

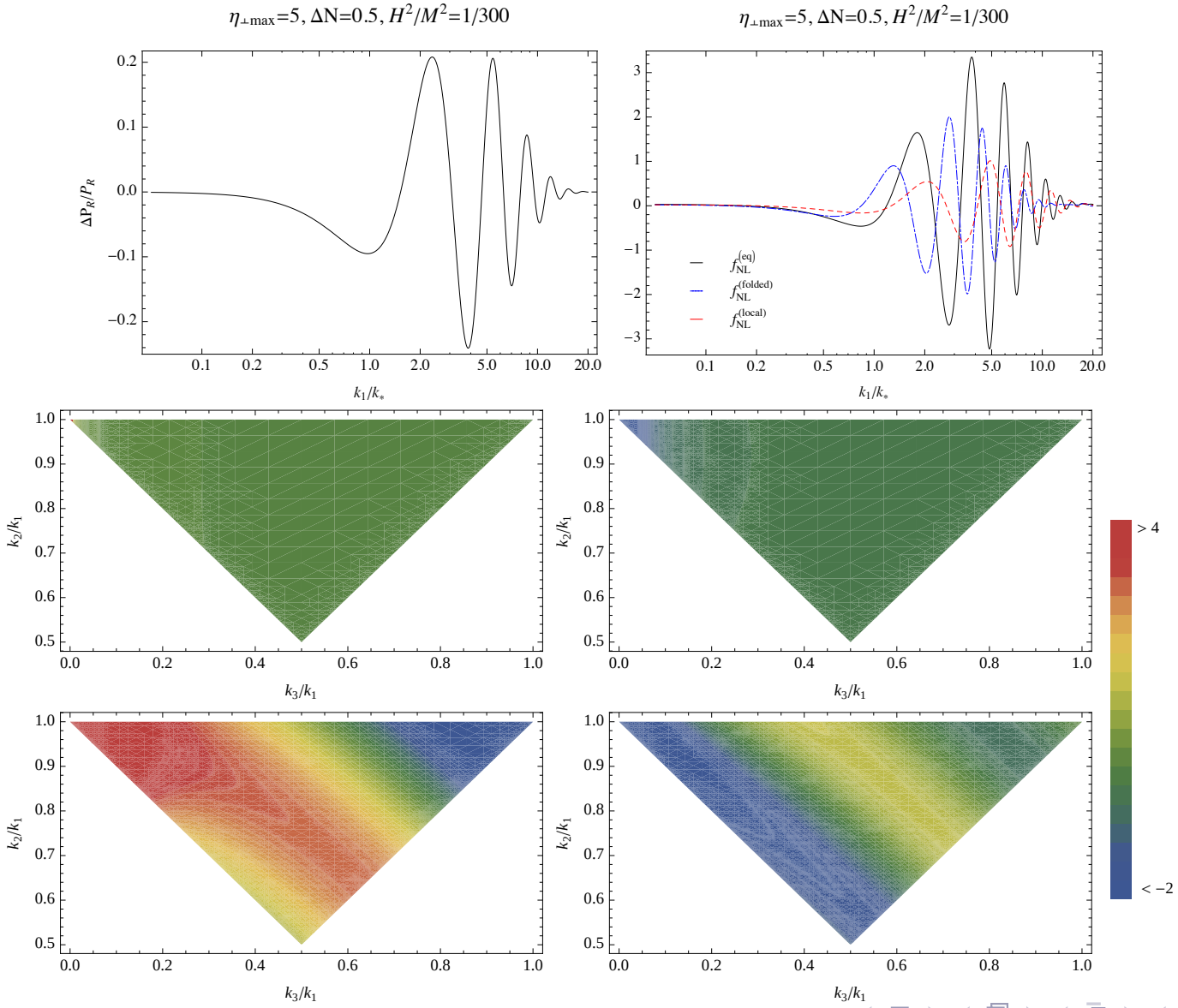

General slow-roll approximation

- $\widehat{\mathscr{R}}_k(\tau)$ = de Sitter piece + higher order corrections
- No guarantee for the hierarchy between slow-roll parameters
- Up to 1st order corrections in the standard SR known (Chen et al. 2007)
- Consistent account in more general contexts

Mode equation: $z^2 \equiv 2a^2 m_{\rm Pl}^2 \epsilon$, $y \equiv \sqrt{2k} z \widehat{\mathscr{R}}_k$, $dx = \equiv -k c_s dt/a$, $f \equiv 2\pi xz/k$

$$\underbrace{\frac{d^2y}{dx^2} + \left(1 - \frac{2}{x^2}\right) y}_{\text{de Sitter solution}} = \underbrace{\frac{1}{x^2} \underbrace{\frac{f'' - 3f'}{f}}_{\equiv g(\log x)} y}_{\text{departure from dS}} \qquad \left(f' \equiv \frac{df}{d\log x}\right) \quad \rightarrow \quad y_0(x) = \left(1 + \frac{i}{x}\right) e^{ix}$$

Green's function solution (JG & Stewart 2001)

$$\begin{aligned} y(x) =& y_0(x) + \frac{i}{2} \int_x^\infty \frac{du}{u^2} g(\log u) \left[y_0^*(u) y_0(x) - y_0^*(x) y_0(u) \right] y(u) \\ \equiv& y_0(x) + L(x,u) y(u) \\ =& y_0(x) + L(x,u) y_0(u) + L(x,u) L(u,v) y_0(v) + \cdots \end{aligned}$$

3rd order action reprocessed

$\dot{\mathscr{R}}^3$ and $\dot{\mathscr{R}}^2\mathscr{R}$: cumbersome to compute with many derivatives

$$\int \dot{\mathscr{R}}^3 \sim \int \left(\dot{y}_0 + \dot{L}y_0 + L\dot{y}_0 + \cdots\right)^3 \sim \text{☹}$$

Using partial int and linear eq to reduce the # of derivatives

$$\left.\frac{\delta L}{\delta \mathscr{R}}\right|_1 \equiv \frac{a^3\epsilon}{c_s^2}\left\{\ddot{\mathscr{R}} + \underbrace{\left[\frac{c_s^2}{a^2\epsilon}\frac{d}{dt}\left(\frac{a^2\epsilon}{c_s^2}\right) + H\right]}_{\equiv C = H(3+\eta-2s)}\dot{\mathscr{R}} - \frac{\Delta}{a^2}\mathscr{R}\right\}$$

$$\int A\dot{\mathscr{R}}^3 = \int \frac{\ddot{A} - 3\dot{A}C - 2A\dot{C} + 2AC^2}{2}\frac{d}{dt}\frac{\left(\mathscr{R}^3\right)}{3} + \cdots + \left.\frac{\delta L}{\delta \mathscr{R}}\right|_1 \frac{c_s^2}{a^3\epsilon}\left(\frac{\dot{A} - 2AC}{2}\mathscr{R}^2 + \cdots\right)$$

$$\int B\dot{\mathscr{R}}^2\mathscr{R} = \int \frac{-\dot{B} + BC}{2}\frac{d}{dt}\frac{\left(\mathscr{R}^3\right)}{3} + \cdots + \left.\frac{\delta L}{\delta \mathscr{R}}\right|_1 \frac{c_s^2}{a^3\epsilon}\frac{B}{2}\mathscr{R}^2$$

Field redefinition with more terms involved (JG, Schalm & Shiu, to appear)

$$S_3 = \int d\tau d^3x \underbrace{\frac{m_{\rm Pl}^2}{3}\frac{a^2\epsilon}{c_s}\left[-c_s aH\left(3s + \frac{\epsilon\eta}{2} + \epsilon s + 9us - 2s^2\right) - \frac{1}{2}\frac{d}{d\tau}\left(\frac{\eta}{c_s^2}\right)\right]}_{\equiv \mathfrak{C}}\frac{d}{d\tau}\left(\mathscr{R}^3\right) + (\text{higher SR terms})$$

1st order bispectrum in GSR

"Source" for the bispectrum

$$g_B(\log\tau) = \frac{c_s}{a^2 m_{\rm Pl}^2 \epsilon}\frac{-\tau}{f}\mathfrak{C} = \frac{1}{f}\left[c_s aH\left(3s + \frac{\epsilon\eta}{2} + \epsilon s + 9us - 2s^2\right) + \frac{1}{2}\frac{d}{d\log\tau}\left(\frac{\eta}{s}\right)\right]$$

Window functions constructed from homogeneous solution

$$y_0(k_1\tau)y_0(k_2\tau)y_0(k_3\tau) = W_B(k_1,k_2,k_3;\tau) + iX_B(k_1,k_2,k_3;\tau)$$
$$y_0(k_1\tau)y_0(k_2\tau)y_0^*(k_3\tau) = W_B(k_1,k_2,-k_3;\tau) + iX_B(k_1,k_2,-k_3;\tau) \equiv W_{B3} + iX_{B3}$$

Bispectrum up to 1st correction [i.e. $\mathcal{O}(g)$] (c.f. Adshead et al. 2011)

$$B_{\mathscr{R}}(\boldsymbol{k}_1,\boldsymbol{k}_2,\boldsymbol{k}_3) = \frac{(2\pi)^4}{4}\frac{\sqrt{\mathscr{P}_{\mathscr{R}}(k_1)}}{k_1^2}\frac{\sqrt{\mathscr{P}_{\mathscr{R}}(k_2)}}{k_2^2}\frac{\sqrt{\mathscr{P}_{\mathscr{R}}(k_3)}}{k_3^2}\int_0^\infty \frac{d\tau}{\tau} g_B(\log\tau)$$
$$\times\left\{\left(d_\tau - 3\frac{f'}{f}\right)W_B + \frac{1}{3}d_\tau(X_B + X_{B3})\int_0^\infty \frac{d\tilde\tau}{\tilde\tau} g(\log\tilde\tau)X(k_3\tilde\tau) + 2\text{ perm}\right.$$
$$-\frac{1}{3}d_\tau W_{B3}\int_\tau^\infty \frac{d\tilde\tau}{\tilde\tau} g(\log\tilde\tau)W(k_3\tilde\tau) - \frac{1}{3}d_\tau X_{B3}\int_0^\tau \frac{d\tilde\tau}{\tilde\tau} g(\log\tilde\tau)X(k_3\tilde\tau) + 2\text{ perm}$$
$$\left.-\frac{1}{2}d_\tau(X_B + X_{B3})\int_\tau^\infty \frac{d\tilde\tau}{\tilde\tau} g(\log\tilde\tau)\left(\frac{1}{k_3\tilde\tau} + \frac{1}{k_3^3\tilde\tau^3}\right) + 2\text{ perm}\right\} \quad \left(d_\tau \equiv \frac{d}{d\log\tau} + 3\right)$$

(JG, Schalm & Shiu, to appear)

Example: Starobinsky model

Starobinsky model: linear $V(\phi)$ + sudden slope change (Starobinsky 1992)

$$V(\phi) = V_0 \times \begin{cases} \left[1 - A(\phi - \phi_0)\right] & \text{for} \quad \phi < \phi_0 \\ \left[1 - (A + \Delta A)(\phi - \phi_0)\right] & \text{for} \quad \phi > \phi_0 \end{cases}$$

de Sitter approx: $\dfrac{f'}{f} = -\dfrac{\ddot{\phi}}{H\dot{\phi}}$, $g = -3\dfrac{V''}{V}$, $g_B = \dfrac{1}{f}\dfrac{d}{d\log\tau}\left(\dfrac{\ddot{\phi}}{H\dot{\phi}}\right)$ (Choe, JG & Stewart 2004)

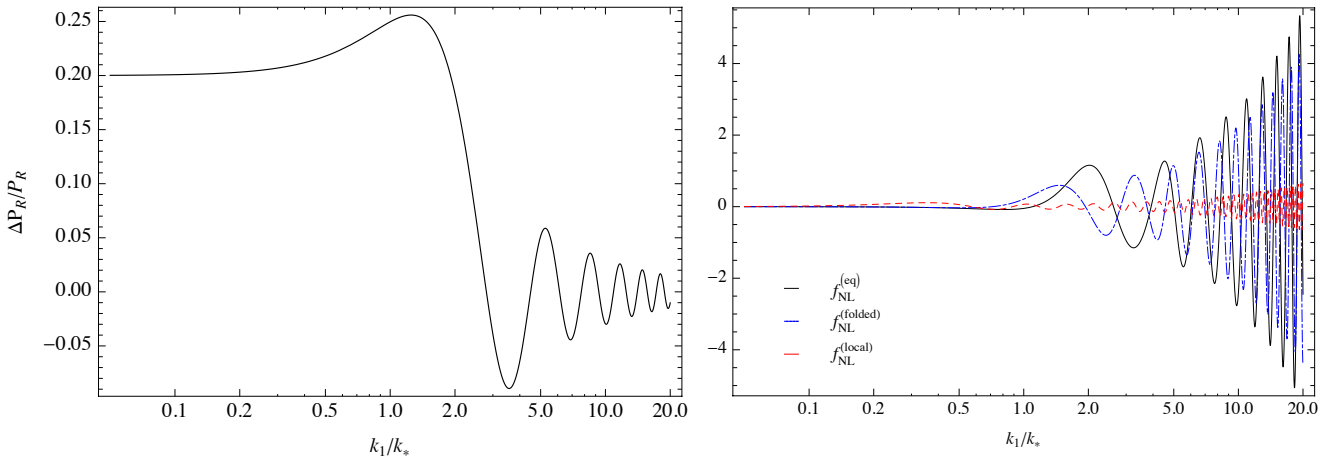

(cf. Arroja & Sasaki 2012)

Example: Starobinsky model

Starobinsky model: linear $V(\phi)$ + sudden slope change (Starobinsky 1992)

$$V(\phi) = V_0 \times \begin{cases} \left[1 - A(\phi - \phi_0)\right] & \text{for} \quad \phi < \phi_0 \\ \left[1 - (A + \Delta A)(\phi - \phi_0)\right] & \text{for} \quad \phi > \phi_0 \end{cases}$$

de Sitter approx: $\dfrac{f'}{f} = -\dfrac{\ddot{\phi}}{H\dot{\phi}}$, $g = -3\dfrac{V''}{V}$, $g_B = \dfrac{1}{f}\dfrac{d}{d\log\tau}\left(\dfrac{\ddot{\phi}}{H\dot{\phi}}\right)$ (Choe, JG & Stewart 2004)

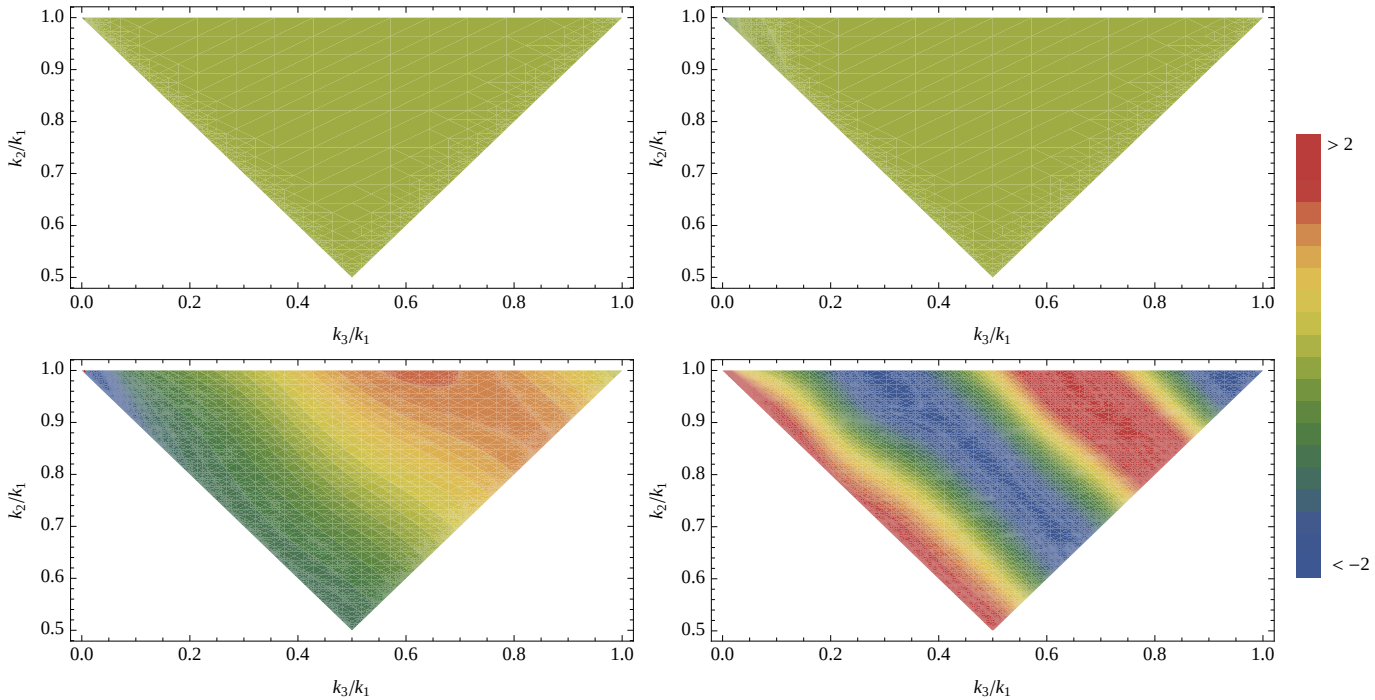

(cf. Arroja & Sasaki 2012)

Evolution of field fluctuations

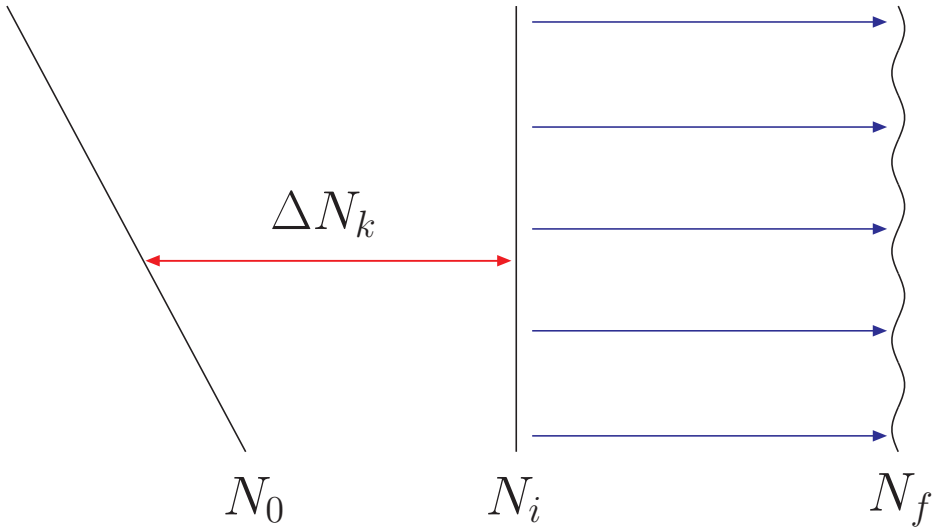

1. N_i: initial slice (flat) for the δN formalism, $\delta\phi^a_{\rm flat} \equiv Q^a$
2. N_f: final slice (comoving) for the δN formalism
3. N_0: horizon crossing of a mode k

$$Q^a(N_0) = \text{Gaussian} \rightarrow Q^a(N_i = N_0 + \Delta N_k) = \text{non-Gaussian}$$

$$\Delta N_k = \log\left(\frac{a_i}{a_0}\right) \approx \log\left[\frac{(aH)_i}{k}\right] \quad \rightarrow \quad k\text{-dependence}$$

Power spectrum and its running

Evolution equation of Q^a on large scales (Elliston, Seery & Tavakol 2012)

$$D_N Q^a = w^a{}_b Q^b + \frac{1}{2} w^a{}_{bc} Q^b Q^c + \cdots$$

$$w_{ab} = u_{(a;b)} + \frac{R_{c(ab)d}}{3} \frac{\dot\phi_0^c}{H} \frac{\dot\phi_0^d}{H} \qquad \left(u_a = -\frac{V_{;a}}{3H^2} \right)$$

$$w_{abc} = u_{(a;bc)} + \frac{1}{3} \left[R_{(a|de|b;c)} \frac{\dot\phi_0^d}{H} \frac{\dot\phi_0^e}{H} - 4 R_{a(bc)d} \frac{\dot\phi_0^d}{H} \right]$$

$$Q^a(N_i = N_0 + \Delta N_k) = Q^a(N_0) + \Delta N_k \left(w^a{}_b Q^b + \frac{1}{2} w^a{}_{bc} Q^b Q^c + \cdots \right) + \cdots$$

Power spectrum and the spectral index

$$\left\langle \mathcal{R}_{\boldsymbol{k}}(t_f) \mathcal{R}_{\boldsymbol{q}}(t_f) \right\rangle = (2\pi)^3 \delta^{(3)}(\boldsymbol{k}+\boldsymbol{q}) \frac{2\pi^2}{k^3} \mathcal{P}_{\mathcal{R}}(k) = N_a(t_i) N_b(t_i) \left\langle Q^a_{\boldsymbol{k}}(t_i) Q^b_{\boldsymbol{q}}(t_i) \right\rangle$$

$$\left\langle Q^a_{\boldsymbol{k}}(t_i) Q^b_{\boldsymbol{q}}(t_i) \right\rangle = \left\langle Q^a_{\boldsymbol{k}}(t_0) Q^b_{\boldsymbol{q}}(t_0) \right\rangle + 2\Delta N_k w^a{}_c \left\langle Q^b_{\boldsymbol{k}}(t_0) Q^c_{\boldsymbol{q}}(t_0) \right\rangle$$

$$\left\langle Q^a_{\boldsymbol{k}} Q^b_{\boldsymbol{q}} \right\rangle = \frac{H^2}{2k^3} \delta^{(3)}(\boldsymbol{k}+\boldsymbol{q}) \left(\gamma^{ab} + \epsilon^{ab} \right)$$

$$n_{\mathcal{R}} - 1 = \frac{D \log \mathcal{P}_{\mathcal{R}}}{d \log k} = -2\epsilon - 2 \frac{N_a N_b w^{ab}}{N_c N^c}$$ (Sasaki & Stewart 1996)

General formula for the running of $f_{\rm NL}$

$$\left\langle \mathcal{R}_{\boldsymbol{k}_1}(t_f)\mathcal{R}_{\boldsymbol{k}_2}(t_f)\mathcal{R}_{\boldsymbol{k}_3}(t_f)\right\rangle = (2\pi)^3\delta^{(3)}(\boldsymbol{k}_{123})B_{\mathcal{R}}(k_1,k_2,k_3)$$

$$= N_a N_b N_c \left\langle Q^a_{\boldsymbol{k}_1} Q^b_{\boldsymbol{k}_2} Q^c_{\boldsymbol{k}_3}\right\rangle + \frac{1}{2}\left\{N_{ab}N_cN_d\left\langle \left[Q^a \star Q^b\right]_{\boldsymbol{k}_1} Q^c_{\boldsymbol{k}_2} Q^d_{\boldsymbol{k}_3}\right\rangle + 2\ \text{perm}\right\}$$

1. 1st term: NL evolution between horizon crossing & initial slice

$$N_a(t_i)N_b(t_i)N_c(t_i)\left\langle Q^a_{\boldsymbol{k}_1}(t_i)Q^b_{\boldsymbol{k}_2}(t_i)Q^c_{\boldsymbol{k}_3}(t_i)\right\rangle$$

$$= (2\pi)^3\delta^{(3)}(\boldsymbol{k}_{123})N_a(t_i)N_b(t_i)N_c(t_i)\frac{H^4(t_0)}{4k_1^3k_2^3k_3^3}w^{abc}\left(k_1^3\Delta N_{k_1} + 2\ \text{perm}\right)$$

2. 2nd term: NL evolution between initial & final slices

$$\frac{1}{2}N_{ab}(t_i)N_c(t_i)N_d(t_i)\left\langle \left[Q^a(t_i)\star Q^b(t_i)\right]_{\boldsymbol{k}_1} Q^c_{\boldsymbol{k}_2}(t_i)Q^d_{\boldsymbol{k}_3}(t_i)\right\rangle$$

$$= (2\pi)^3\delta^{(3)}(\boldsymbol{k}_{123})N_{ab}(t_i)N_c(t_i)N_d(t_i)\frac{H^4(t_0)}{4k_1^3k_2^3}\left(\gamma^{ac}\gamma^{bd} + 2\Delta N_{k_1}w^{ac}\gamma^{bd} + 2\Delta N_{k_2}\gamma^{ac}w^{bd}\right)$$

$$\frac{6}{5}f_{\rm NL} = \frac{N_{ab}N^aN^b}{(N_cN^c)^2}\left\{1 - \Delta N_k\left[\underbrace{-\frac{N_aN_bN_cw^{abc}}{N_{de}N^dN^e} + 4w^{ab}\left(\frac{N_aN_b}{N_dN^d} - \frac{N_{ac}N_bN^c}{N_{de}N^dN^e}\right)}_{\equiv n_{f_{\rm NL}}}\right]\right\}$$

(Byrnes & JG 2012)

Summary

- General single field inflation
  1. From multi-field setup: by integrating out heavy field
  2. Non-trivial c_s: footprint of heavy physics
- Features in the power spectrum ($S_{2,\rm int}$) and bispectrum (S_3)
  1. Heavy quanta extract kinetic energy
  2. Non-trivial, oscillatory, correlated features
- General slow-roll scheme
  1. Terms with more derivatives → field redefinition
  2. More complete 1st order bispectrum
- Running of $f_{\rm NL}$
  1. Sensitive probe of early universe physics
  2. Non-trivial evolution after horizon crossing

WE WANT YOU!!!

APCTP cosmology groups (Ki Young Choi, JG and Arman Shafieloo) are looking for up to 5 post-doctoral fellows to start in 2013.

CV, list of publications, research statements + 3 reference letters to cosmopd2012@apctp.org

For further information, please consult APCTP homepage (http://www.apctp.org).

Teruaki Suyama, JGRG 22(2012)111303

“Testing the origin of primordial perturbation: Use of bi- and tri-spectrum”

RESCEU SYMPOSIUM ON

GENERAL RELATIVITY AND GRAVITATION

JGRG 22

November 12-16 2012

Koshiba Hall, The University of Tokyo, Hongo, Tokyo, Japan

Testing the origin of primordial perturbations
-Use of bi and tri-spectrum-

Teruaki Suyama (RESCEU, Univ. of Tokyo)

Collaborators: Kazuhide Ichikawa, Masahiro Kawasaki, Kazunori Nakayama, Toyokazu Sekiguchi, Fuminobu Takahashi, Tomo Takahashi, Takahiro Tanaka, Yuki Watanabe, Masahide Yamaguchi, Jun'ichi Yokoyama, Shuichiro Yokoyama

Primordial fluctuation

Primordial fluctuation

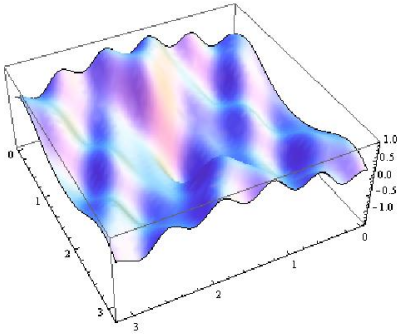

300,000yrs

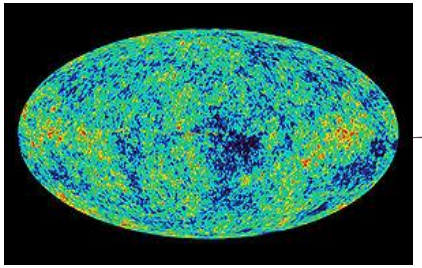

13 billion yrs



(WMAP data)

- matter fluctuation = fluctuation of spacetime (=curvature perturbation)
- It is a source of the current cosmic structure.
- From observations, we already know it does exist.
- But we don’t know its origin.

Generation of the primordial fluctuation

Basic paradigm

Inflation happened in the early Universe. During the inflationary stage, any light scalar field acquires fluctuations that are eventually stretched to cosmological scales.

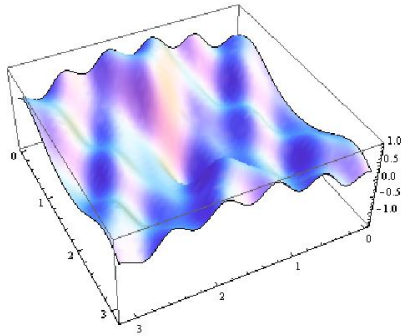

$$\delta\phi \simeq \frac{H}{2\pi}$$

When such a scalar field affects the expansion of the Universe, its fluctuating energy density creates the curvature perturbation through the Einstein equations.

$$R_{\mu\nu} - \frac{1}{2} g_{\mu\nu} R = 8\pi G \left(T^1_{\mu\nu} + T^2_{\mu\nu} + \cdots \right)$$

Generation of the primordial fluctuation

- **Minimal scenario**

  Inflaton fluctuations create the curvature perturbations.

$$\zeta \simeq \frac{H}{\dot{\phi}} \delta\phi$$

  - Almost scale invariant and almost Gaussian.
  - Good in the sense that it is simple, economical and consistent with all the observations so far. But this is just an assumption rather than a prediction.

Generation of the primordial fluctuations

- **Non-minimal scenario**

  Anything else

  Over the last decade, many non-minimal scenario have been proposed.

  Non-vacuum state, higher derivative interactions(DBI, Galileon, etc.), self-interactions, features in potential, conversion of isocurvature after inflation (multi-field models, curvaton, modulated reheating, multi-brid, inhomogeneous end of inflation, etc.), ….

Now, there are many models for the generation of the primordial fluctuation. We want to get useful information regarding its nature.

How can we reveal the origin of perturbations?

- Power spectrum

$$\langle \zeta_{\vec{k}_1} \zeta_{\vec{k}_2} \rangle = (2\pi)^3 P_\zeta(k_1) \delta(\vec{k}_1 + \vec{k}_2)$$

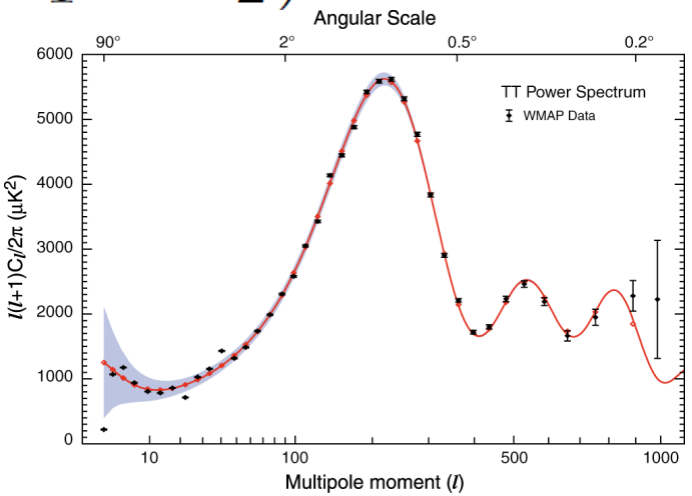

All the models predict nearly scale invariant spectrum.

$$n_S - 1 = \frac{d \log(k^3 P_\zeta)}{d \log k} = \mathcal{O}(0.01)$$

P is not enough to disentangle the degeneracy.

How can we reveal the origin of perturbations?

Is there another way other than the power spectrum?

3- and 4-point functions could be useful!!
(non-Gaussianity)

Bi-spectrum: 3-point function
Tri-spectrum: 4-point function

- Useful in the sense that they can provide us what cannot be probed by means of the power spectrum.
- Any deviation from the minimal scenario generically leads to the detectable level of non-Gaussianity.
- Potentially observable in the near future.

Various shapes of bi-spectrum

- Local type (Komatsu&Spergel 2001)

$$B(k_1, k_2, k_3) \propto \left(\frac{1}{k_1^3 k_2^3} + 2 \text{ perms.} \right)$$

- Equilateral type (Creminelli et al 2005)

$$B(k_1, k_2, k_3) \propto \left(\frac{3(k_1 + k_2 - k_3)(k_2 + k_3 - k_1)(k_3 + k_1 - k_2)}{k_1^3 k_2^3 k_3^3} \right)$$

- Orthogonal type (Senatore et al 2009)

$$B(k_1, k_2, k_3) \propto \left(-\frac{3}{k_1^3 k_2^3} - \frac{3}{k_2^3 k_3^3} - \frac{3}{k_3^3 k_1^3} - \frac{8}{k_1^2 k_2^2 k_3^2} + \frac{3}{k1 k_2^2 k_3^3} + 5 \text{ perms.} \right)$$

Detection of primordial non-gaussianity and distinction of the scale dependence allows to constrain the models.

How can we reveal the origin of perturbations?

From now on, I will focus on the so-called local type perturbation.

The curvature perturbation is generated from field perturbations on super-horizon scales. (curvaton, modulated reheating, inhomogeneous end of inflation, multi-brid, etc.)

How can we reveal the origin of perturbations?

Separate universe approach (Kodama&Hamazaki 1998, Nambu&Taruya 1998, Wands et al 2000)

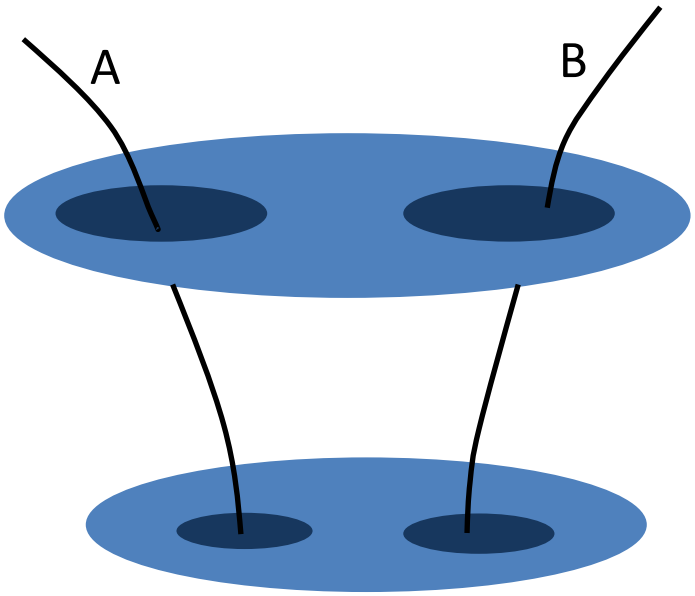





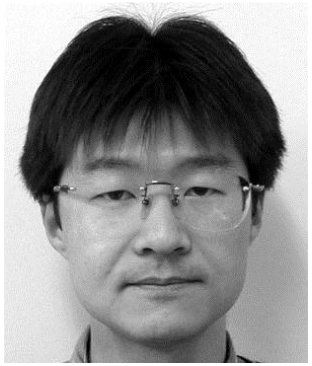

Perturbation is obtained by differentiating the background solutions.

Each Hubble region evolves like FLRW universe with different energy density and pressure.

δN formalism

(e.g. Starobinsky 1985, Salopek&Bond 1980, Sasaki&Stewart 1996, Sasaki&Tanaka 1998, Malik, Lyth&Sasaki 2004, Sugiyama,Komatsu&Futamase 2012)




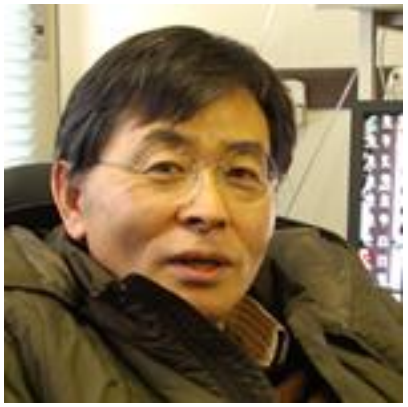

$$\zeta = \delta N$$

$$\zeta(t,\vec{x}) = \sum_a N_a(t)\delta\phi^a(\vec{x}) + \frac{1}{2}\sum_{ab} N_{ab}(t)\delta\phi^a(\vec{x})\delta\phi^b(\vec{x}) + \cdots$$

$$N_a(t) = \frac{\partial N(t)}{\partial \phi_a}, \quad N_{ab}(t) = \frac{\partial^2 N(t)}{\partial\phi_a\partial\phi_b}$$

Intuitive understanding of the δN formalism

Wisdom by T.Tanaka



Curvature = Expansion

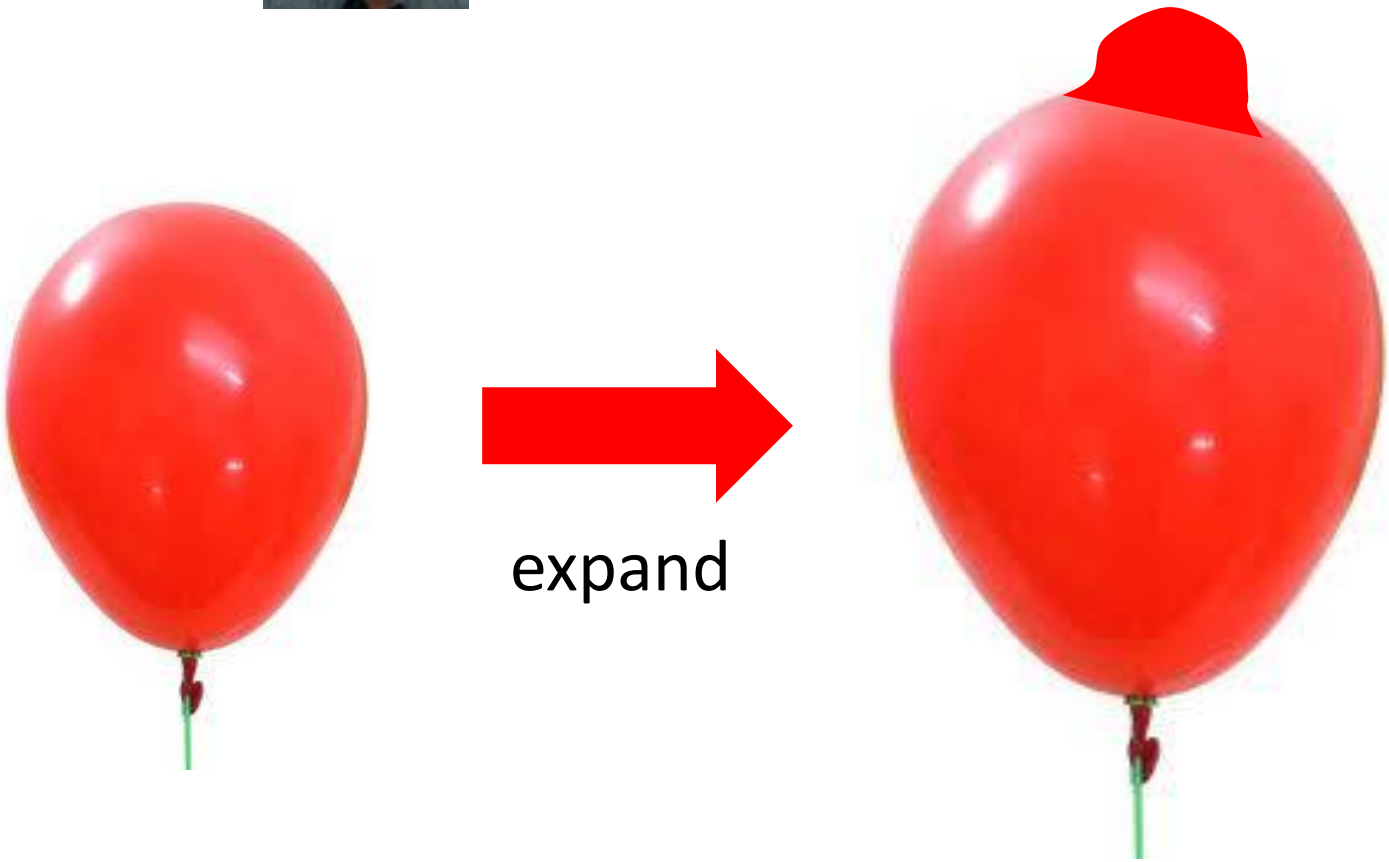

How can we reveal the origin of perturbations?

$$\zeta(t,\vec{x}) = \sum_a N_a(t)\delta\phi^a(\vec{x}) + \frac{1}{2}\sum_{ab} N_{ab}(t)\delta\phi^a(\vec{x})\delta\phi^b(\vec{x}) + \cdots$$

Same position

$\delta\phi^a(\vec{x})$: Gaussian(assumption)

This type of perturbation is realized if the focused scales are super-horizon at the time of its generation.

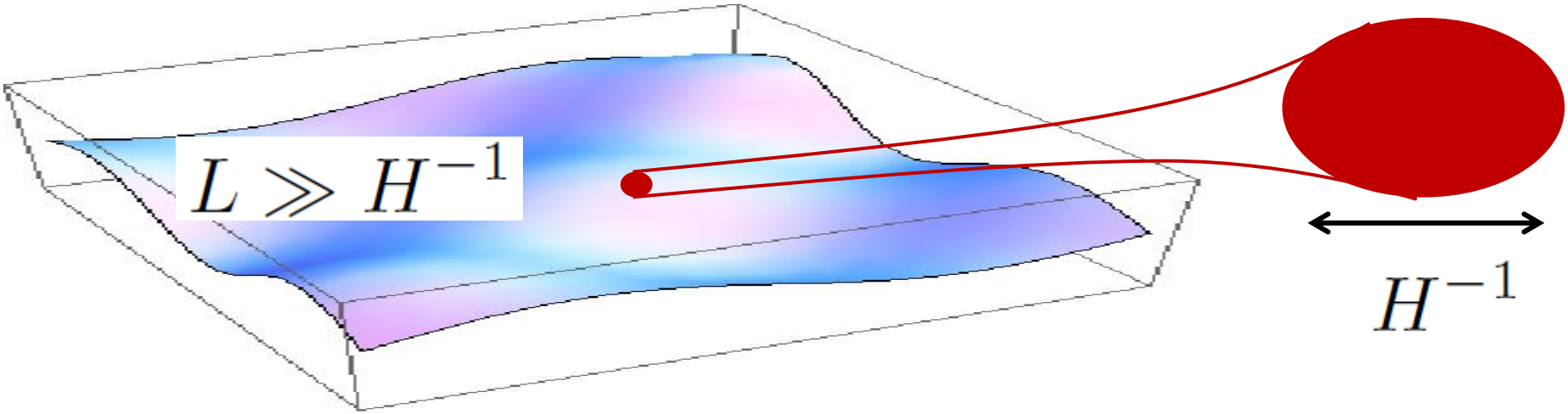

How can we reveal the origin of perturbations?

$$\zeta(t,\vec{x}) = \sum_a N_a(t)\delta\phi^a(\vec{x}) + \frac{1}{2}\sum_{ab} N_{ab}(t)\delta\phi^a(\vec{x})\delta\phi^b(\vec{x}) + \cdots$$

Two sources for non-Gaussianity of the curvature perturbation

- Non-gaussianity of field fluctuations

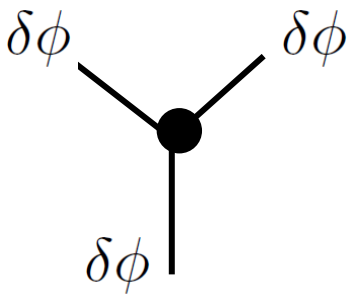

- Non-linear relation between field fluctuations and ζ

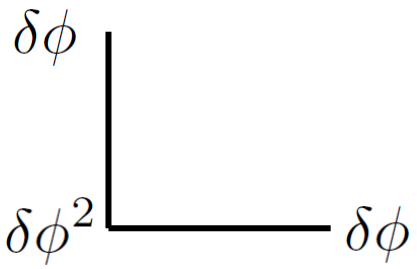

Non-Gaussianity(non-linearity) parameters

(Byrnes, Sasaki and Wands, 2006)

Bi-spectrum

$$\langle \zeta_{\vec{k}_1} \zeta_{\vec{k}_2} \zeta_{\vec{k}_3} \rangle = (2\pi)^3 B_\zeta(k_1, k_2, k_3) \delta(\vec{k}_1 + \vec{k}_2 + \vec{k}_3)$$

Tri-spectrum

$$\langle \zeta_{\vec{k}_1} \zeta_{\vec{k}_2} \zeta_{\vec{k}_3} \zeta_{\vec{k}_4} \rangle = (2\pi)^3 T_\zeta(\vec{k}_1, \vec{k}_2, \vec{k}_3, \vec{k}_4) \delta(\vec{k}_1 + \vec{k}_2 + \vec{k}_3 + \vec{k}_4)$$

$$B_\zeta(k_1, k_2, k_3) = \frac{6}{5} f_{\rm NL} \left(P_\zeta(k_1) P_\zeta(k_2) + P_\zeta(k_2) P_\zeta(k_3) + P_\zeta(k_3) P_\zeta(k_1) \right)$$

$$\begin{aligned} T_\zeta(\vec{k}_1, \vec{k}_2, \vec{k}_3, \vec{k}_4) \quad = \quad & \tau_{\rm NL} \left(P_\zeta(k_{13}) P_\zeta(k_3) P_\zeta(k_4) + 11 \text{ perms} \right) \\ & + \frac{54}{25} g_{\rm NL} \left(P_\zeta(k_2) P_\zeta(k_3) P_\zeta(k_4) + 3 \text{ perms} \right) \end{aligned}$$

Three non-linearity parameters that are observables.

Non-Gaussianity parameters

Current observational bounds on the non-linearity parameters

$$-10 < f_{\rm NL} < 70$$ (Komatsu et al., 2010)

$$-0.6 \times 10^4 < \tau_{\rm NL} < 3.3 \times 10^4$$

$$-7.4 \times 10^5 < g_{\rm NL} < 8.2 \times 10^5$$ (Smidt et al., 2010)

Planck is expected to give us $f_{\rm NL} < \mathcal{O}(1)$ and $\tau_{\rm NL} < 600$.

(Kogo and Komatsu, 2006)

More stringent bound may be obtained by using other cosmological probes. (e.g. Pajer&Zaldarriaga 2012)

Non-Gaussianity parameters

- Standard canonical inflaton fluctuation

$$f_{\rm NL} = \mathcal{O}(\epsilon)$$ (e.g. Maldacena 2002)

- Non-inflaton scenarios

$$f_{\rm NL} = \mathcal{O}(1) \text{ or } \gg \mathcal{O}(1)$$ depending on the model

Bispectrum can be useful to disentangle the degeneracy of models.

What can we say if we also include the trispectrum?

Local-type inequality

$$\frac{6}{5} f_{\rm NL} = \frac{N_a N_b N_{ab}}{(N_c N_c)^2} \qquad \tau_{\rm NL} = \frac{N_a N_b N_{ac} N_{bc}}{(N_d N_d)^3}$$

$$\tau_{\rm NL} \geq \left(\frac{6}{5} f_{\rm NL} \right)^2$$

(TS and M.Yamaguchi, 2008)

This is universal in the sense that it is independent of the underlying models.

Detection of fnl >20 means we surely detect $\tau_{\rm NL}$ as well.

This inequality also suggests a possibility that $f_{\rm NL}$ is small but $\tau_{\rm NL}$ can be very large.

Local-type inequality

More general statement (Smith, Lo Verde&Zaldarriaga 2011)

$$f_{NL} = \frac{5}{12} \lim_{k_1 \to 0} \frac{\langle \zeta_{\mathbf{k}_1} \zeta_{\mathbf{k}_2} \zeta_{\mathbf{k}_3} \rangle'}{P_\zeta(k_1) P_\zeta(k_2)},$$

$$\tau_{NL} = \frac{1}{4} \lim_{|\mathbf{k}_1 + \mathbf{k}_2| \to 0} \frac{\langle \zeta_{\mathbf{k}_1} \zeta_{\mathbf{k}_2} \zeta_{\mathbf{k}_3} \zeta_{\mathbf{k}_4} \rangle'_c}{P_\zeta(k_1) P_\zeta(k_3) P_\zeta(|\mathbf{k}_1 + \mathbf{k}_2|)}.$$



$$\tau_{\rm NL} \geq \left(\frac{6}{5} f_{\rm NL} \right)^2$$

Local-type inequality

More general statement (Sugiyama 2012)

$$\frac{6}{5} f_{NL} = \frac{1}{(\quad + \quad)^2} \left[\quad + \quad + 2 \quad \right]$$

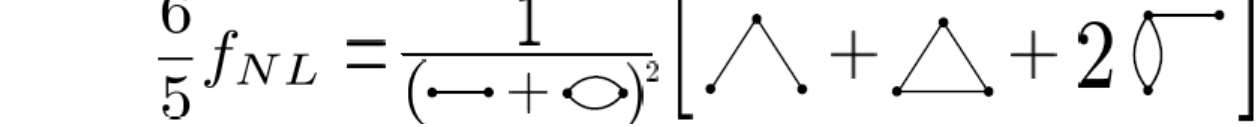

Inclusion of the loop corrections still leads to

$$\tau_{\rm NL} \geq \left(\frac{6}{5} f_{\rm NL} \right)^2$$

Local-type inequality

- Single source case (e.g. curvaton model)

$$\zeta = N_\phi \delta\phi + \frac{1}{2} N_{\phi\phi} \delta\phi^2 + \cdots$$

$$\frac{6}{5} f_{\rm NL} = \frac{N_a N_b N_{ab}}{(N_c N_c)^2} = \frac{N_{\phi\phi}}{N_\phi^2}$$

$$\tau_{\rm NL} = \frac{N_a N_b N_{ac} N_{bc}}{(N_d N_d)^3} = \frac{N_{\phi\phi}^2}{N_\phi^2}$$

$$\tau_{\rm NL} = \frac{36}{25} f_{\rm NL}^2$$

A consistency relation for the single source case

Local-type inequality

- Multi-source case (for example, inflaton and curvaton)

$$\zeta = N_\phi \delta\phi + N_\sigma \delta\sigma + \frac{1}{2} N_{\sigma\sigma} \delta\sigma^2 + \cdots$$ (Ichikawa et al. 2008)

Gaussian Non-Gaussian

$$\frac{25}{36} \frac{\tau_{\rm NL}}{f_{\rm NL}^2} = 1 + \frac{N_\phi^2}{N_\sigma^2} = 1 + \frac{\mathcal{P}_{\zeta\phi}}{\mathcal{P}_{\zeta\sigma}}$$

If the non-gaussian part is subdominant, the ratio becomes much larger than 1.

A ratio $\tau_{\rm NL}/f_{\rm NL}^2$ is a good indicator to get information of number of fields that contribute to the curvature perturbation.

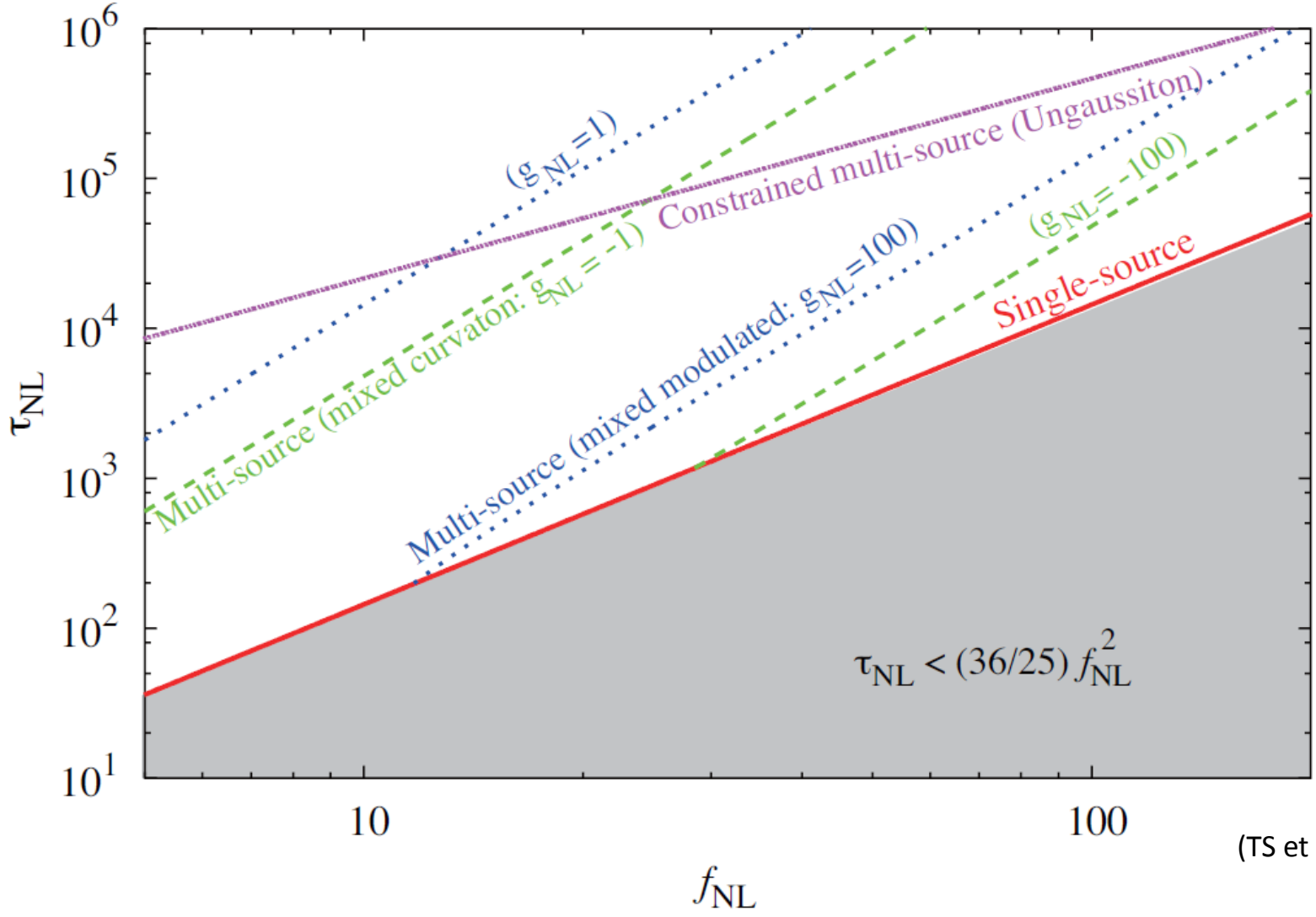
10^6
10^5
10^4
10^3
10^2
10^1
τ_{NL}
10
100
f_{NL}
$(g_{NL}=1)$
Constrained multi-source (Ungaussiton)
Multi-source (mixed curvaton: $g_{NL}=-1$)
$(g_{NL}=-100)$
Multi-source (mixed modulated: $g_{NL}=100$)
Single-source
$\tau_{NL} < (36/25) f_{NL}^2$

(TS et al. 2010)

Basic strategy to test the origin of perturbation

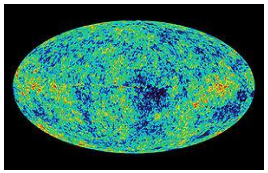

observation data

Detection of $f_{\rm NL}$

Non-detection of $f_{\rm NL}$

Non-detection of $\tau_{\rm NL}$

New idea needed

Detection of $\tau_{\rm NL}$

single source

$$\frac{25}{36}\frac{\tau_{\rm NL}}{f_{\rm NL}^2} = 1$$

$$\frac{25}{36}\frac{\tau_{\rm NL}}{f_{\rm NL}^2} > 1$$

multiple sources

Detection of $\tau_{\rm NL}$

Non-detection of $\tau_{\rm NL}$

Maybe, the minimal scenario

What about gnl?

$$\frac{54}{25} g_{\rm NL} = \frac{N_{abc} N_a N_b N_c}{(N_d N_d)^3}$$

This is not directly related to fnl and taunl. Thus, it brings another information specific to each model.

Example: self-interacting curvaton (e.g. Engvist&Nurmi 2005)

$$V(\sigma) = \frac{1}{2} m_\sigma^2 \sigma^2 + \lambda m_\sigma^4 \left(\frac{\sigma}{m_\sigma} \right)^n$$

$$g_{\rm NL} = -\frac{10}{3} f_{\rm NL} - \frac{575}{108}$$ without self-interaction

$$g_{\rm NL} \simeq A_{\rm NQ} f_{\rm NL}^2 + B_{\rm NQ} f_{\rm NL} + C_{\rm NQ}$$ with self-interaction

gnl is sesitive to the shape of the field potential.

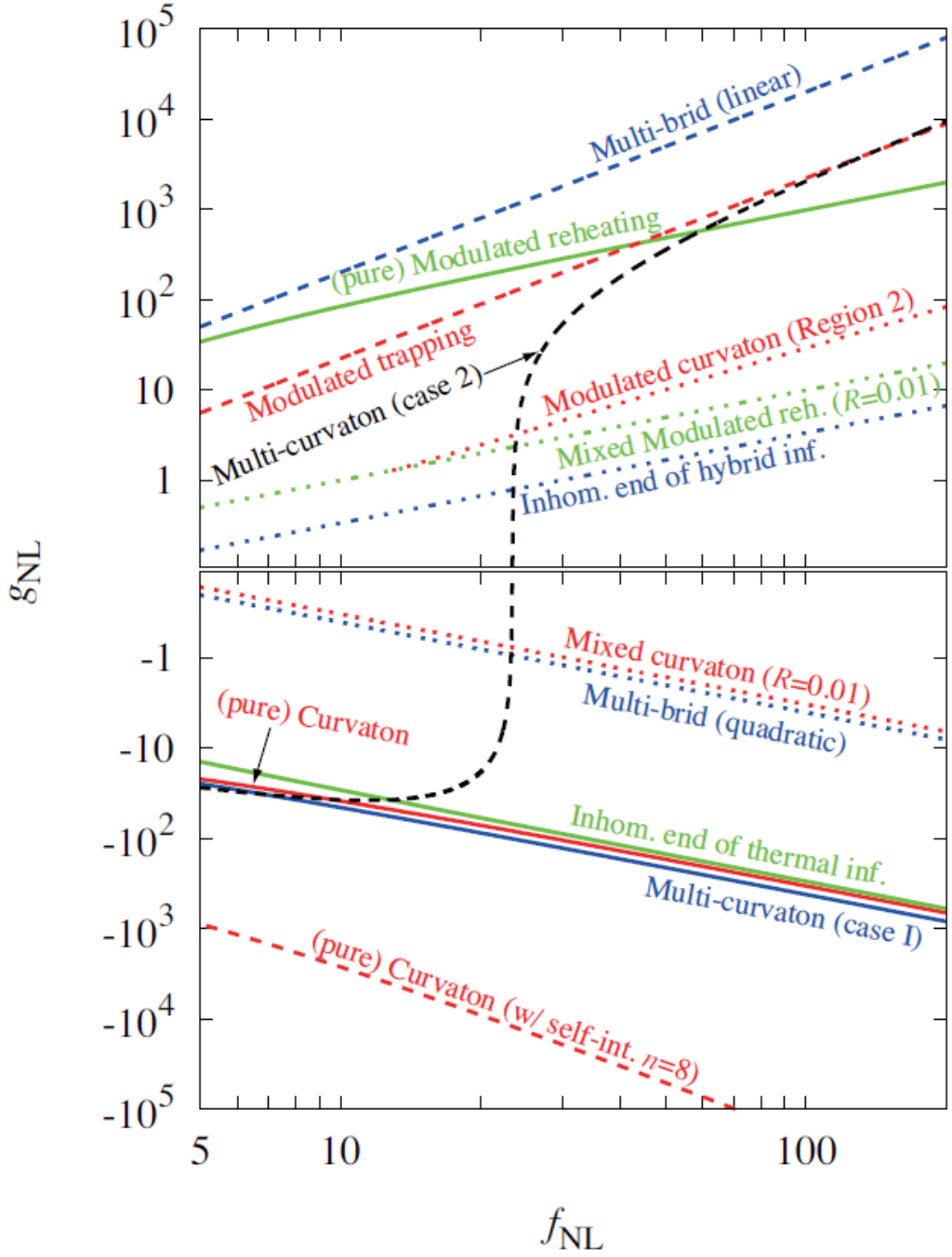
10^5
10^4
10^3
10^2
10
1
-1
-10
-10^2
-10^3
-10^4
-10^5
5
10
100
g_{NL}
f_{NL}
Multi-brid (linear)
(pure) Modulated reheating
Modulated trapping
Multi-curvaton (case 2)
Modulated curvaton (Region 2)
Mixed Modulated reh. (R=0.01)
Inhom. end of hybrid inf.
Mixed curvaton (R=0.01)
Multi-brid (quadratic)
(pure) Curvaton
Inhom. end of thermal inf.
Multi-curvaton (case I)
(pure) Curvaton (w/ self-int. n=8)

What about gnl?

We find gnl is model dependent. But, we can classify the models into three types:

- Suppressed $g_{\rm NL}$ type ($g_{\rm NL} \sim$ [suppression factor] $\times f_{\rm NL}$)
- Linear $g_{\rm NL}$ type ($g_{\rm NL} \sim f_{\rm NL}$)
- Enhanced $g_{\rm NL}$ type ($g_{\rm NL} \sim f_{\rm NL}^n$ with $n > 1$ or $n = 2$ for many models)

Consistency relations among non-linearity parameters

Category	$f_{\rm NL}$–$\tau_{\rm NL}$ relation	Examples and $f_{\rm NL}$–$g_{\rm NL}$ relation
Single-source	$\tau_{\rm NL} = (6f_{\rm NL}/5)^2$	(pure) curvaton (w/o self-interaction) $[g_{\rm NL} = -(10/3)f_{\rm NL} - (575/108)]^{(a)}$
		(pure) curvaton (w/ self-interaction) $[g_{\rm NL} = A_{\rm NQ}f_{\rm NL}^2 + B_{\rm NQ}f_{\rm NL} + C_{\rm NQ}]^{(b)}$
		(pure) modulated reheating $[g_{\rm NL} = 10f_{\rm NL} - (50/3)]^{(c)}$
		modulated-curvaton scenario $\left[g_{\rm NL} = 3r_{\rm dec}^{1/2}f_{\rm NL}^{3/2}\right]^{(d)}$
		Inhomogeneous end of hybrid inflation $[g_{\rm NL} = (10/3)\eta_{\rm cr}f_{\rm NL}]$
		Inhomogeneous end of thermal inflation $[g_{\rm NL} = -(10/3)f_{\rm NL} - (50/27)]^{(e)}$
		Modulated trapping $[g_{\rm NL} = (2/9)f_{\rm NL}^2]^{(f)}$
Multi-source	$\tau_{\rm NL} > (6f_{\rm NL}/5)^2$	mixed curvaton and inflaton $[g_{\rm NL} = -(10/3)(R/(1+R))f_{\rm NL} - (575/108)(R/(1+R))^3]^{(g)}$
		mixed modulated and inflaton $[g_{\rm NL} = 10(R/(1+R))f_{\rm NL} - (50/3)(R/(1+R))^3]^{(h)}$
		mixed modulated trapping and inflaton $[g_{\rm NL} = (2/9)((1+R)/R)f_{\rm NL}^2 = (25/162)\tau_{\rm NL}]^{(i)}$
		multi-curvaton $[g_{\rm NL} = C_{\rm mc}f_{\rm NL},\ \ g_{\rm NL} = (4/15)f_{\rm NL}^2]^{(j)}$
		Multi-brid inflation (quadratic potential) $[g_{\rm NL} = -(10/3)\eta f_{\rm NL},\ \ g_{\rm NL} = 2f_{\rm NL}^2]^{(k)}$
		Multi-brid inflation (linear potential) $[g_{\rm NL} = 2f_{\rm NL}^2]^{(l)}$
Constrained multi-source	$\tau_{\rm NL} = Cf_{\rm NL}^n$	ungaussiton ($C \simeq 10^3,\ n = 4/3$)

(TS et al. 2010)

Different consistency relations for different models.

Higher order correlators

3-point function

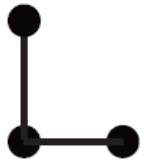

4-point function



5-point function

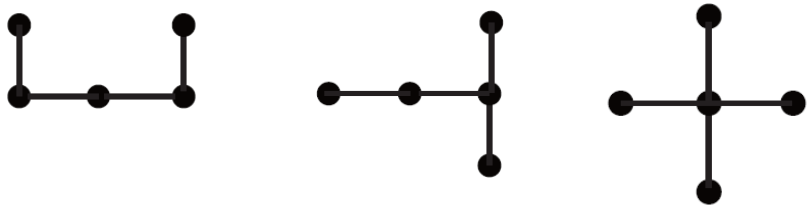

6-point function

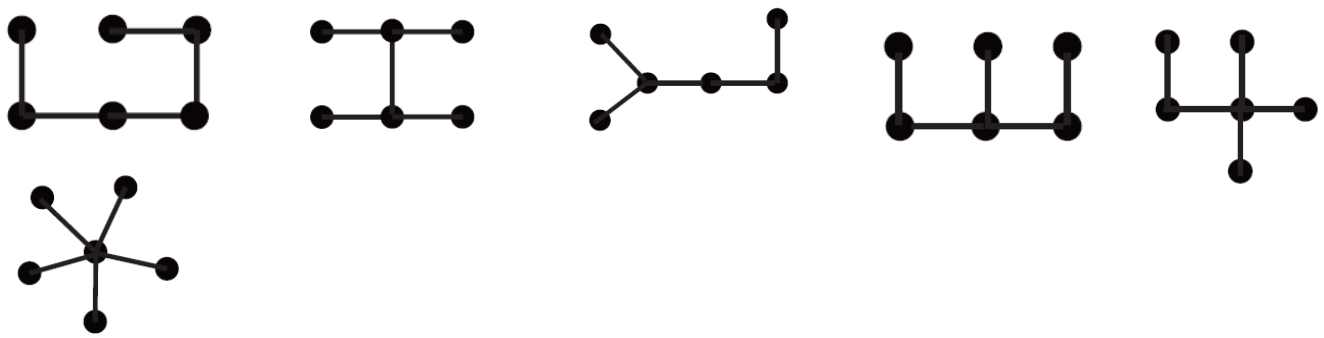

# of Non-linearity parameters=# of graphs with different topologies

General formula of # for arbitrary n is known. (Fry 1984)

The local type inequalities for n-point function (n:even)

General method to derive the local type inequalities

(TS and Yokoyama, 2011)

Example: 6-point function

$$\tau_6^{(1)}\tau_6^{(2)} \geq \left(g_6^{(1)}\right)^2$$

$$\tau_6^{(1)}\tau_4 \geq \left(f_5^{(1)}\right)^2, \qquad \tau_6^{(2)}\tau_4 \geq \left(f_5^{(2)}\right)^2$$

$$\tau_6^{(1)} \geq \tau_4^2, \qquad \tau_6^{(2)} \geq g_4^2$$

Five independent inequalities

$f_{\rm NL}$

suggests significant contribution of non-inflaton source.

$\tau_{\rm NL}$

clarifies if the perturbation is sourced by a single field or not.

$g_{\rm NL}$

probes interactions(parameters) of the candidate model.

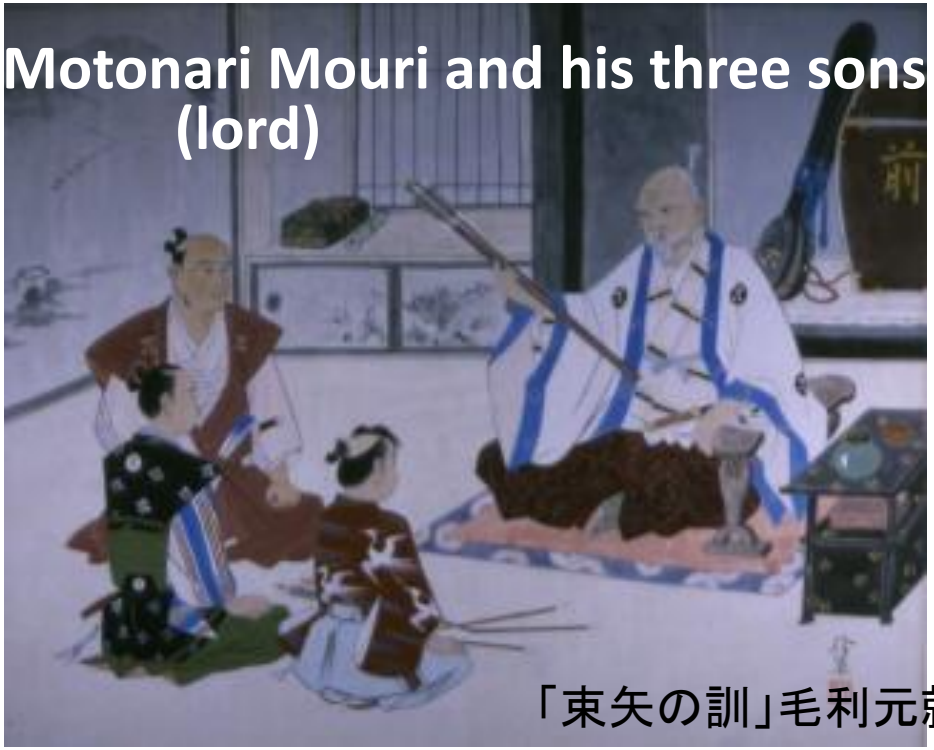

「束矢の訓」毛利元就一代絵（高増径草筆）

But, I do hope this is not the case for the following three persons. Individuals are already awesome for me.







Summary

Test of non-gaussianity can be useful to reveal the origin of primordial perturbations.

We can obtain information about number of fields contributing to the curvature perturbation by using fnl and taunl.

Detection of all the non-linearity parameters greatly helps us constrain the model of the early Universe.

Very soon, Planck results will tell us something.

Matthias Bartelmann, JGRG 22(2012)111304

"Recent developments in gravitational lensing"

RESCEU SYMPOSIUM ON

GENERAL RELATIVITY AND GRAVITATION

JGRG 22

November 12-16 2012

Koshiba Hall, The University of Tokyo, Hongo, Tokyo, Japan

RUPRECHT-KARLS-
UNIVERSITÄT
HEIDELBERG

Some recent developments in gravitational lensing

お誕生日おめでとうございます
to professors
Toshi Futamase, Hideo Kodama and Misao Sasaki

Matthias Bartelmann, Heidelberg University, Institute for Theoretical Astrophysics
JGRG22, Tokyo, Nov. 13, 2012

ZAH Zentrum für Astronomie Heidelberg
ARI+ITA+LSW

Lensing From Relativity

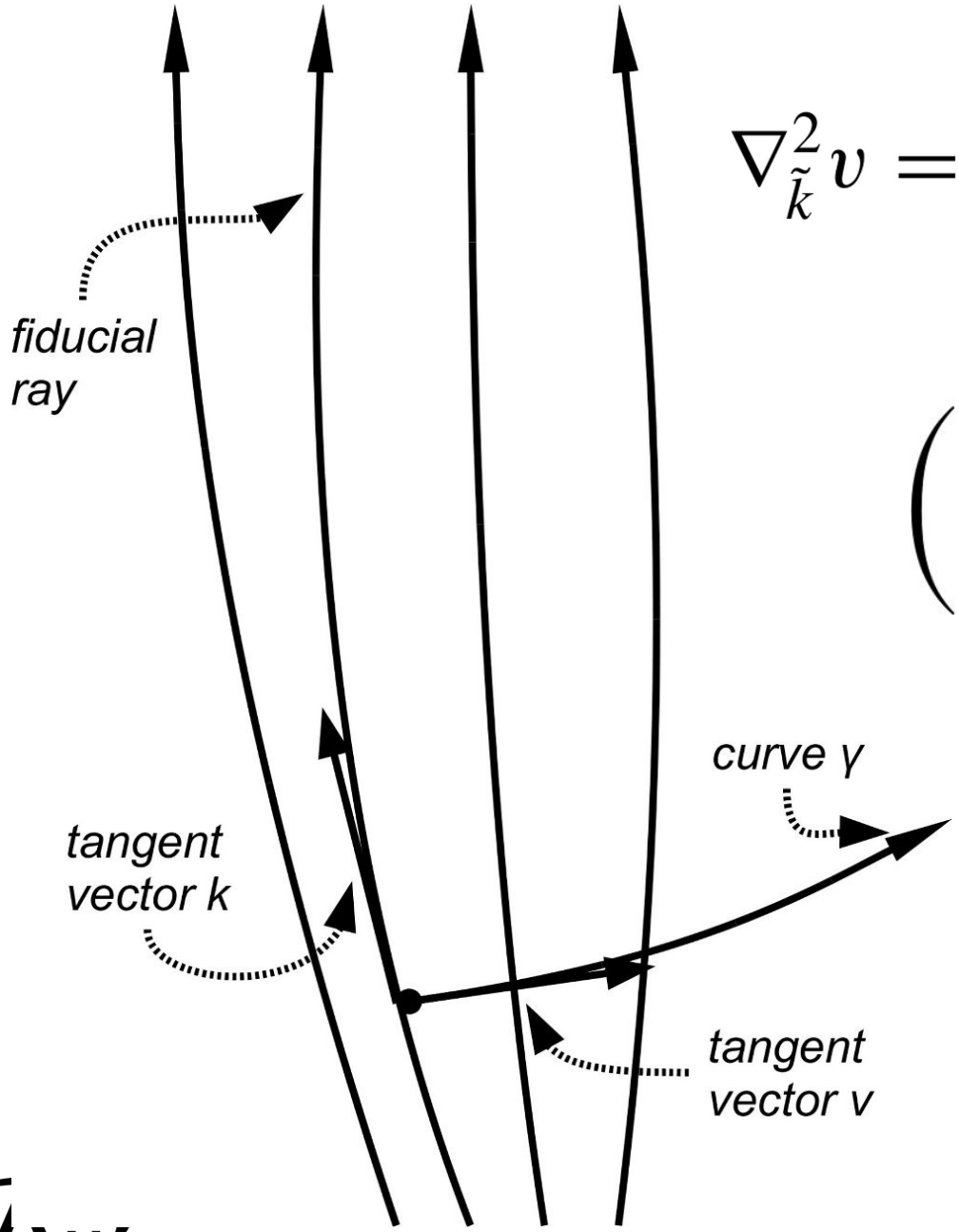

$$\nabla^2_{\tilde{k}} v = R(\tilde{k}, v)\tilde{k}$$

$$\left(\frac{\mathrm{d}^2}{\mathrm{d}w^2} + K\right) x^i = -2\partial^i \phi .$$

Ingredients:

1. Equation of geodesic deviation
2. Field equations: relations Between mass and curvature

[cf. MB, CQGr 27 (2010) w3001]

Lensing Quantities

effective lensing potential

$$\psi(\theta^j) = 2\int_0^{w_s} \mathrm{d}w' \frac{f_K(w_s - w')}{f_K(w')\, f_K(w_s)} \phi(f_K(w')\theta^j, w')$$

convergence $\kappa = \frac{1}{2}\partial^*\partial\psi$, $\gamma = \frac{1}{2}\partial^2\psi$ shear

$$\mathcal{F} = \partial\kappa = \frac{1}{2}\partial\partial^*\partial\psi \quad , \quad \mathcal{G} = \partial\gamma = \frac{1}{2}\partial^3\psi$$

spin-1 flexion spin-3 flexion

$$\left[\partial = \partial_1 + \mathrm{i}\partial_2\right]$$

edth operator (in flat space)

Cold Dark Matter Haloes

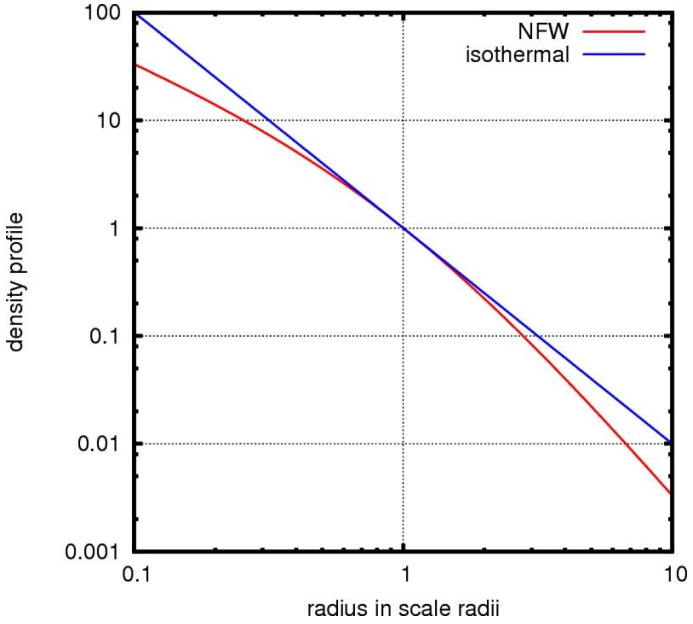

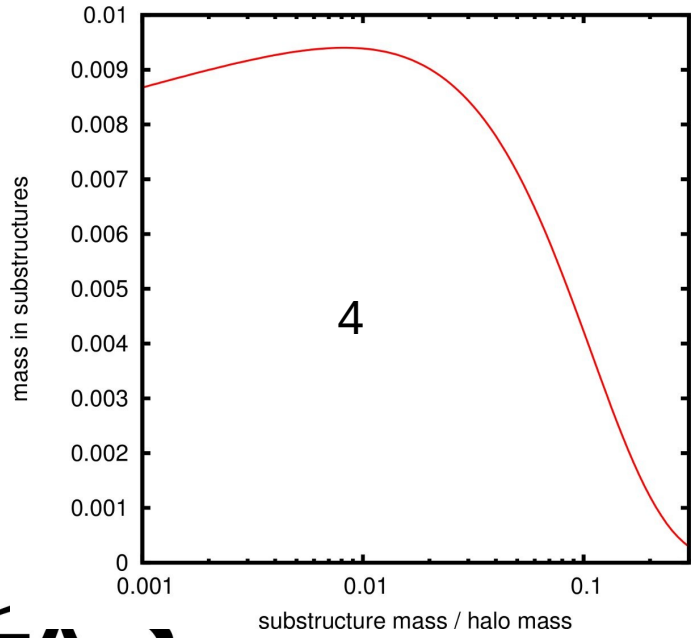

Simulation: Springel et al., profile: Navarro et al. 1997,
Substructure: Boylan-Kolchin et al. 2009



Concentration Parameter

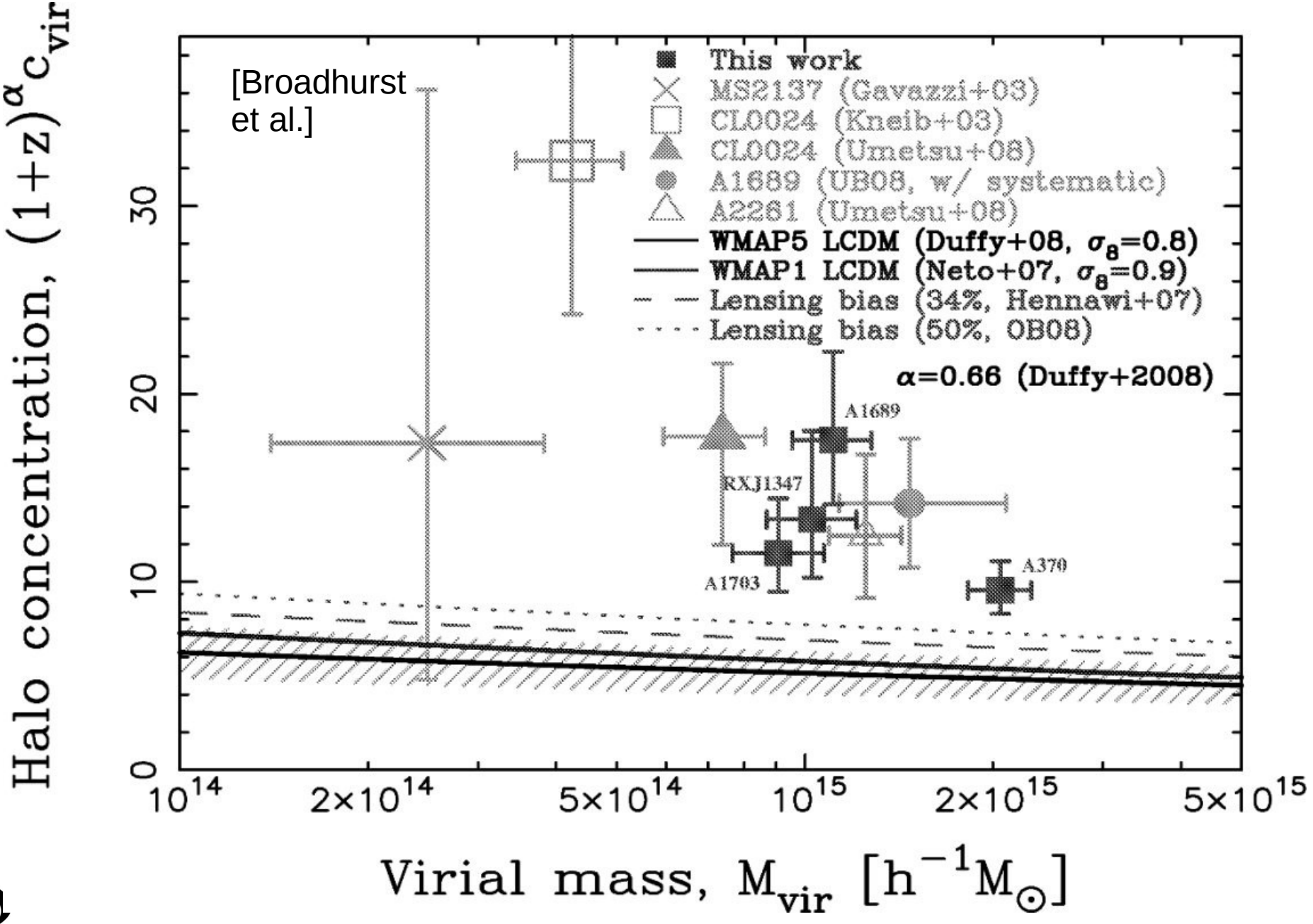

Cluster Lensing

MACS J 1206
[Umetsu et al. ApJ 755 (2012) 56]

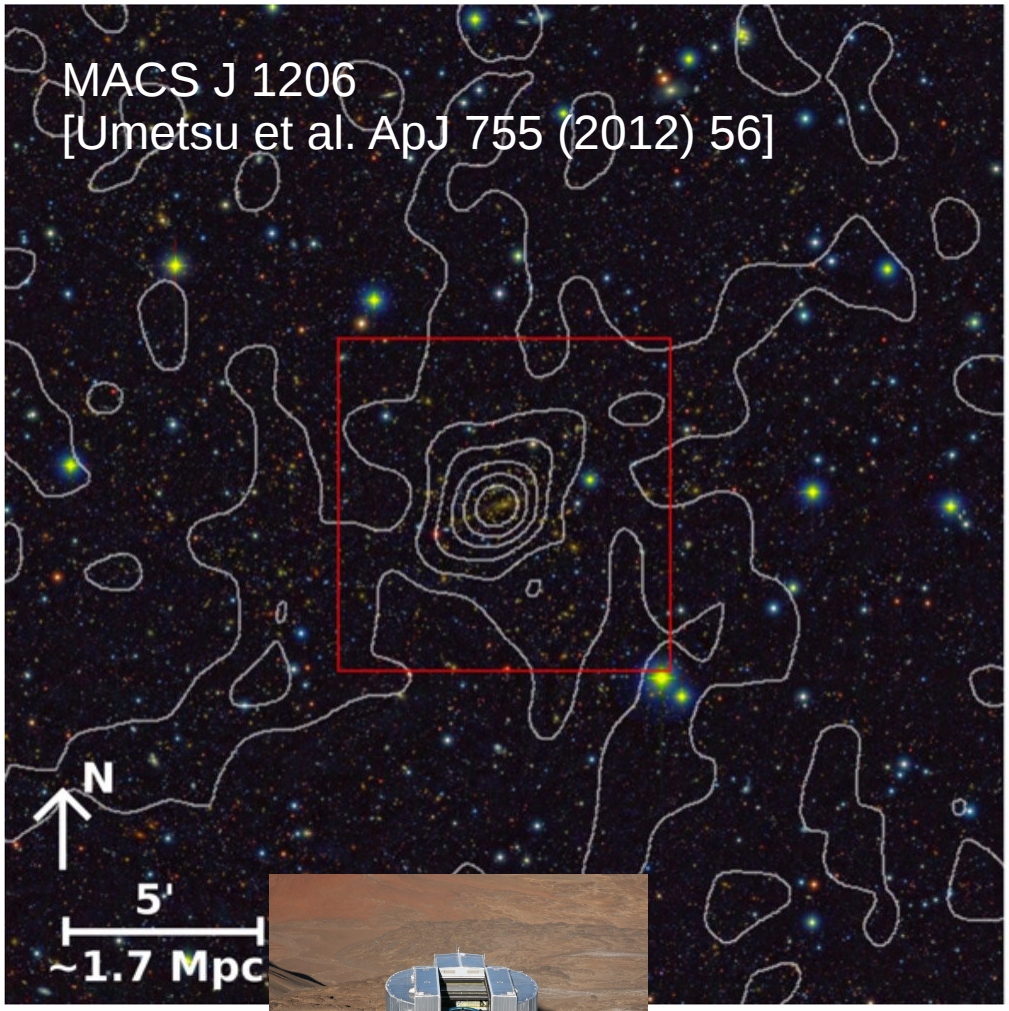

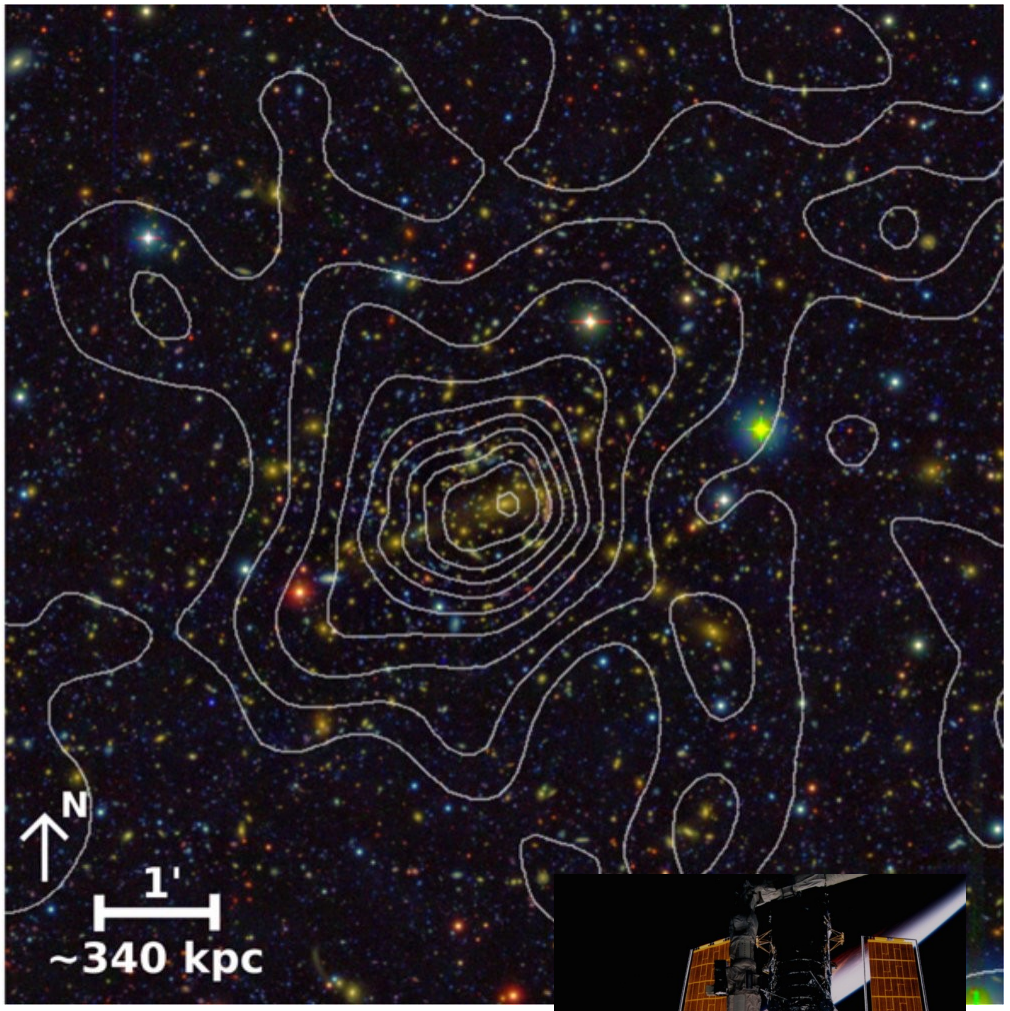

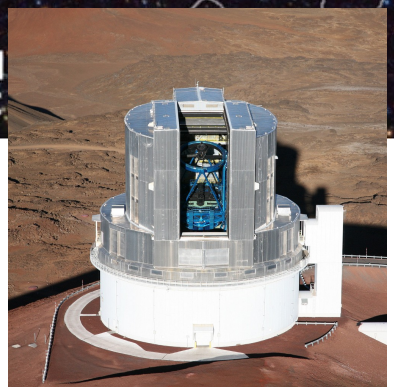

CLASH MCT Programme:
25 clusters in 16 bands
(HST and ground based)



Cluster Lensing: Example

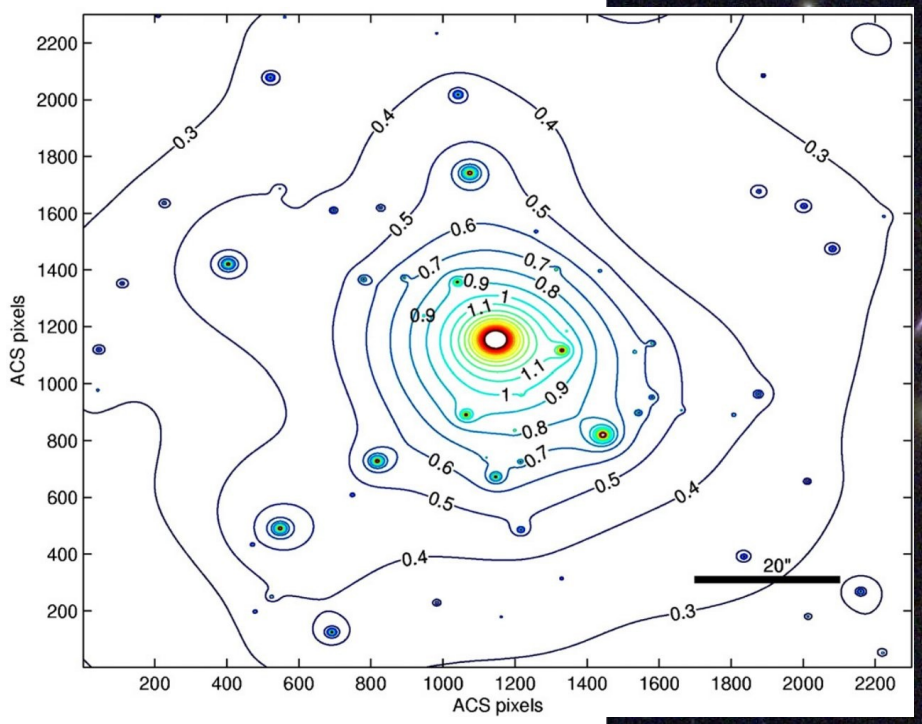

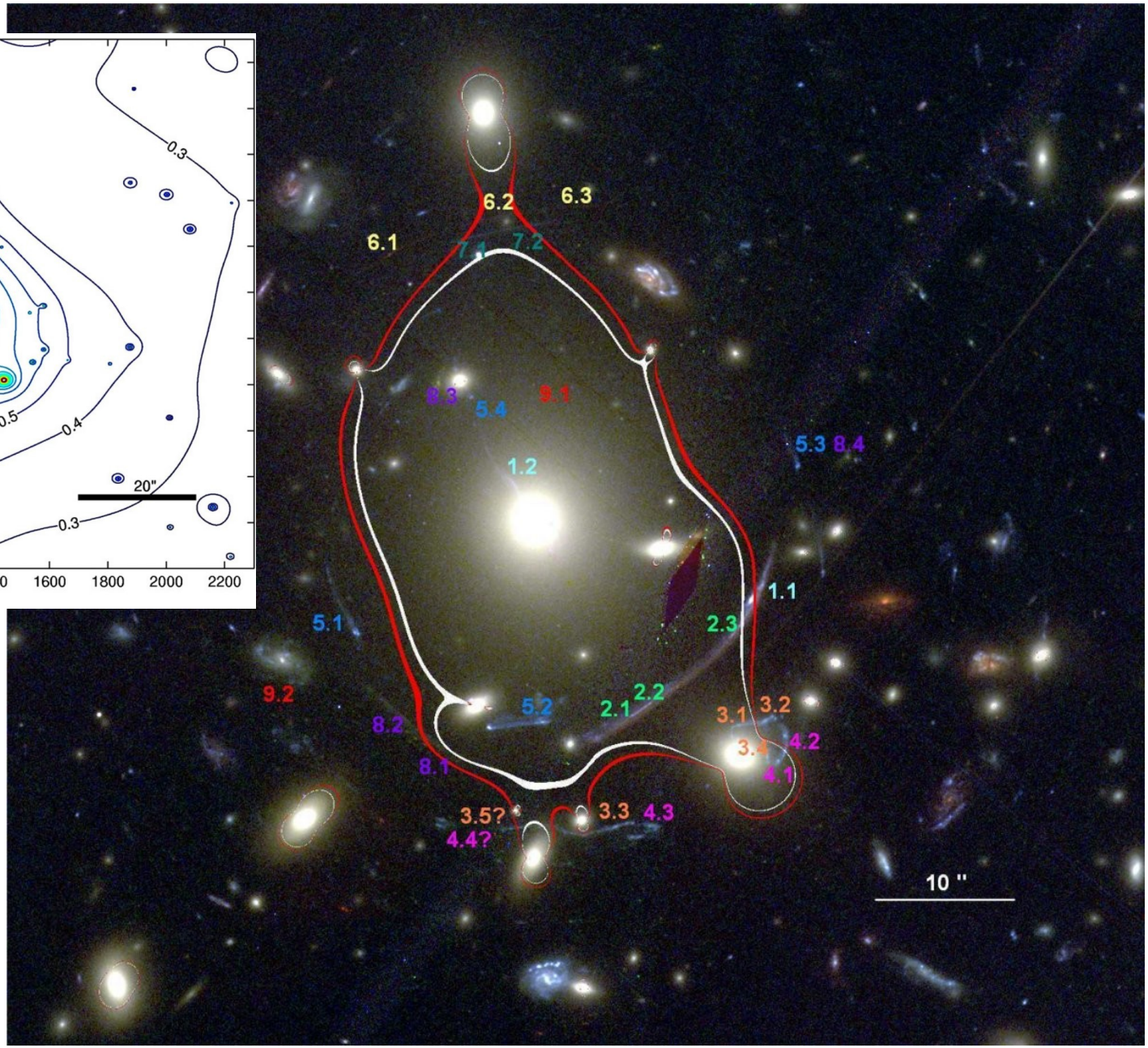

Abell 383
[Zitrin et al.
ApJ 742 (2011) 117]

Strong and Weak Lensing Combined

$$\chi^2 = \left(\varepsilon_i - \frac{Z_i\gamma_i}{1 - Z_i\kappa_i}\right) C_{ij}^{-1} \left(\varepsilon_j - \frac{Z_j\gamma_j}{1 - Z_j\kappa_j}\right)$$

[Bradač et al.
ApJ 706 (2009) 1201]

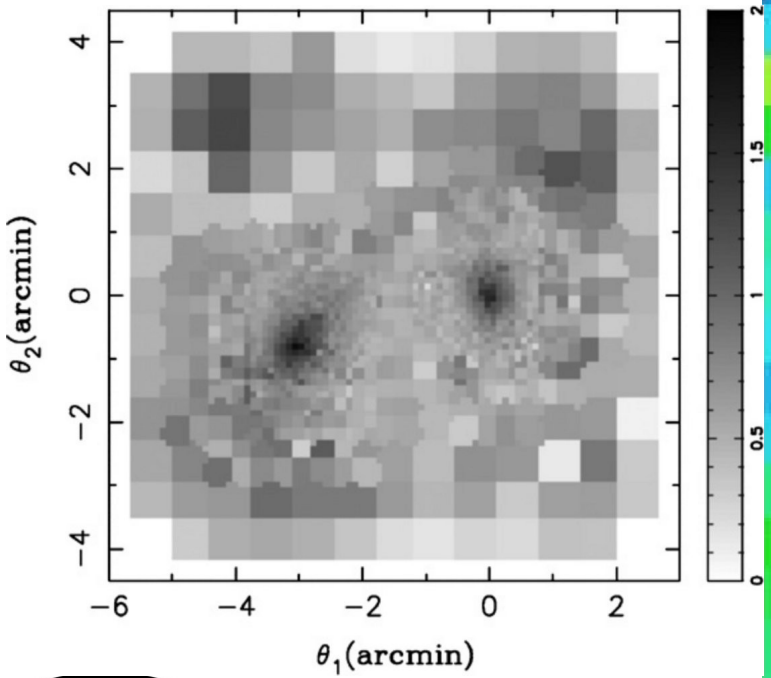

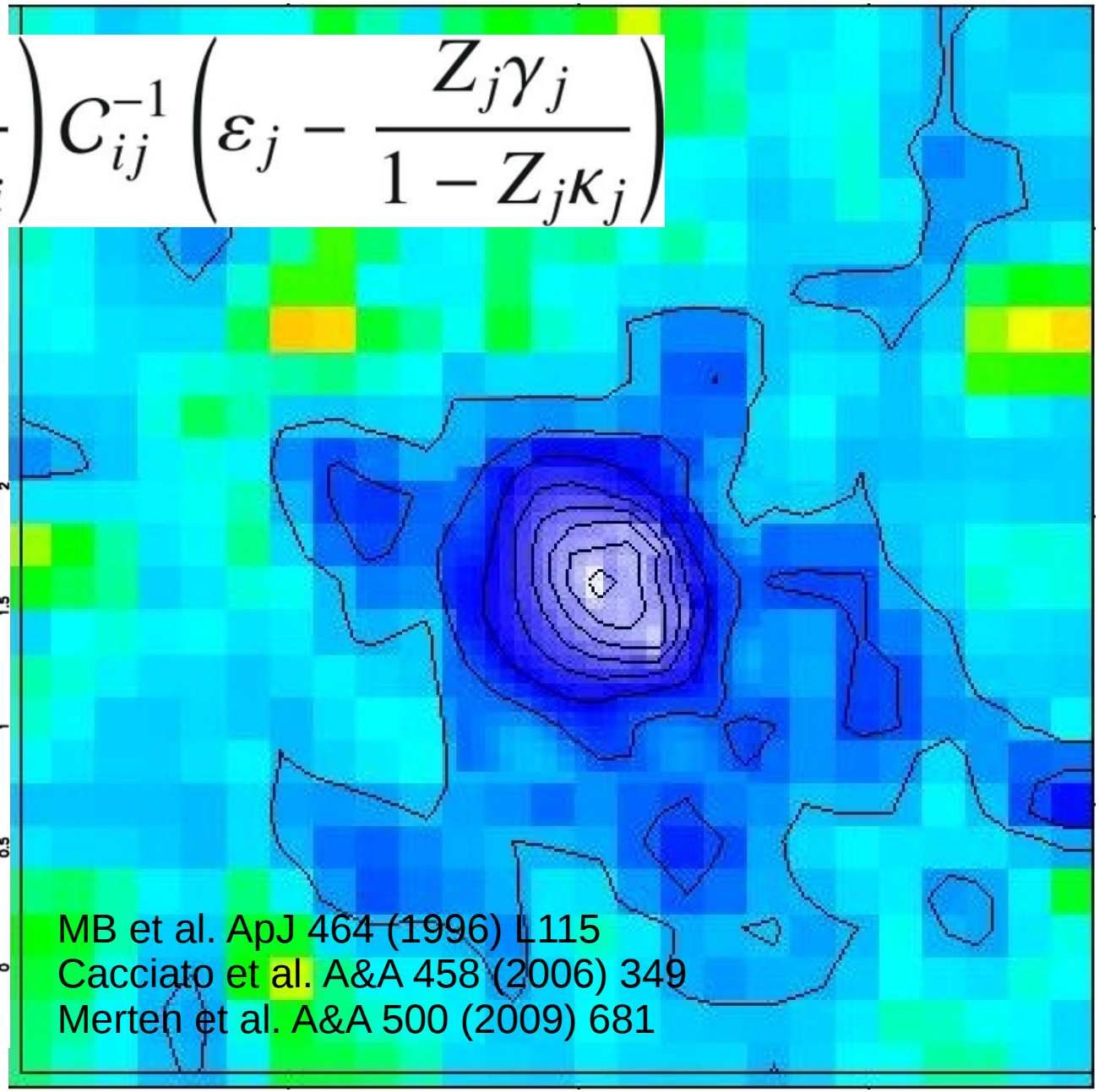

MB et al. ApJ 464 (1996) L115
Cacciato et al. A&A 458 (2006) 349
Merten et al. A&A 500 (2009) 681

Adaptive Reconstruction: Simulation

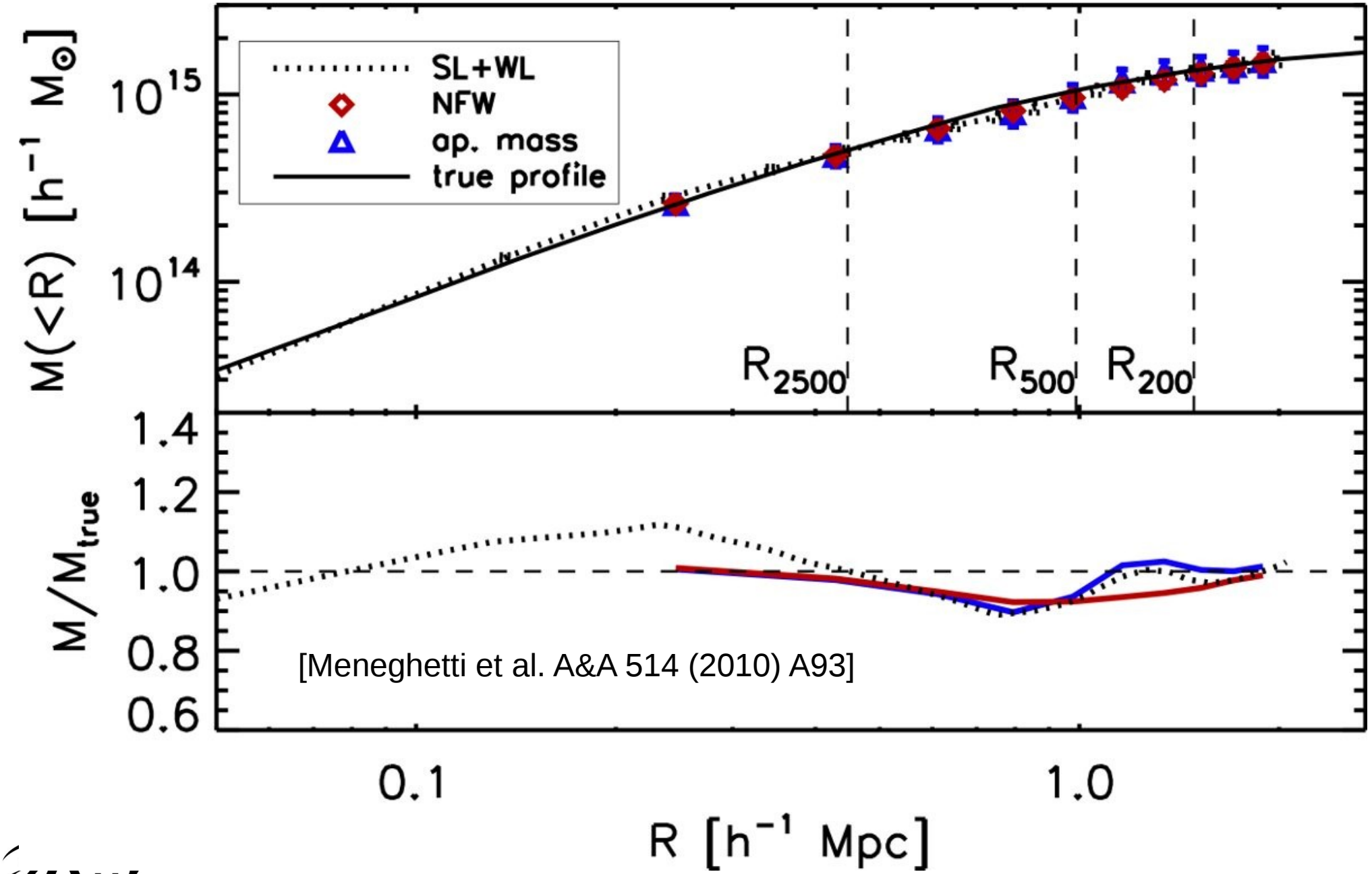

[Meneghetti et al. A&A 514 (2010) A93]

Strong and Weak Lensing Combined: Abell 2744

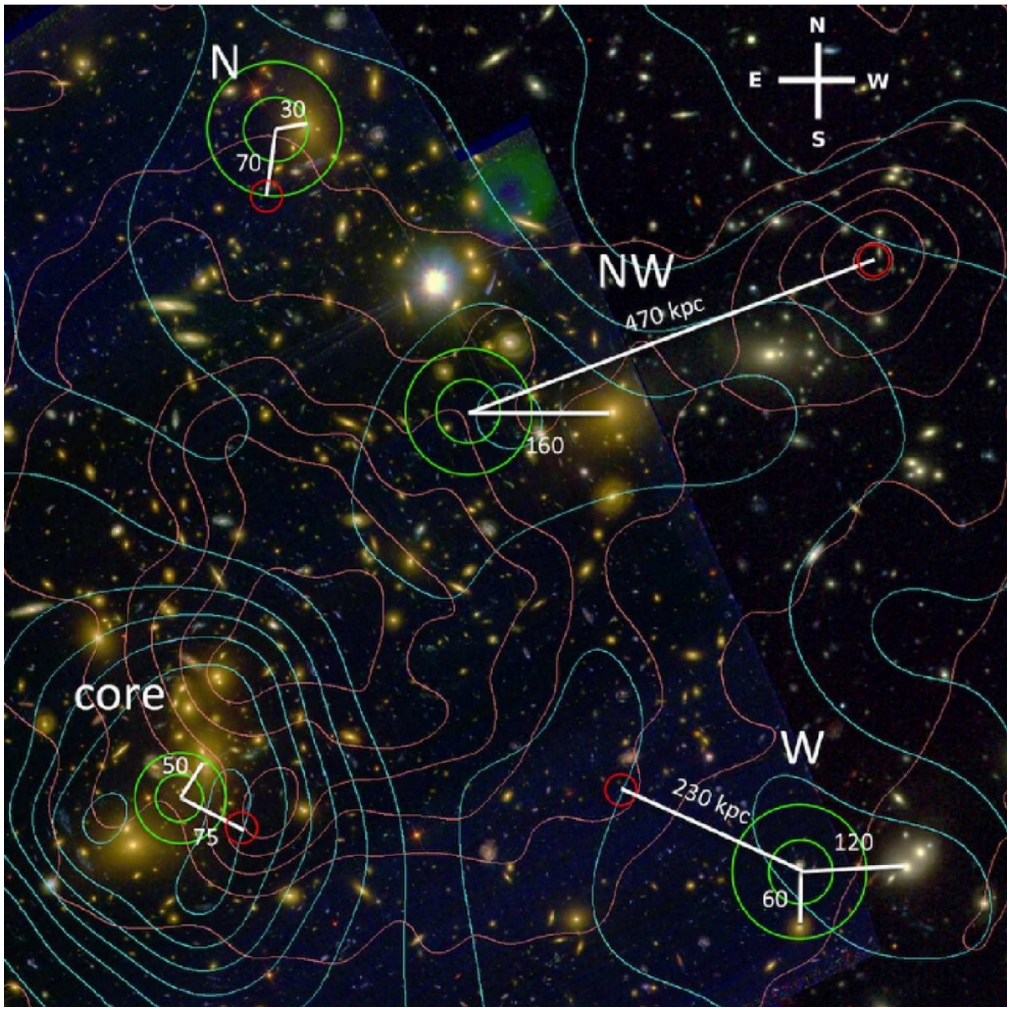

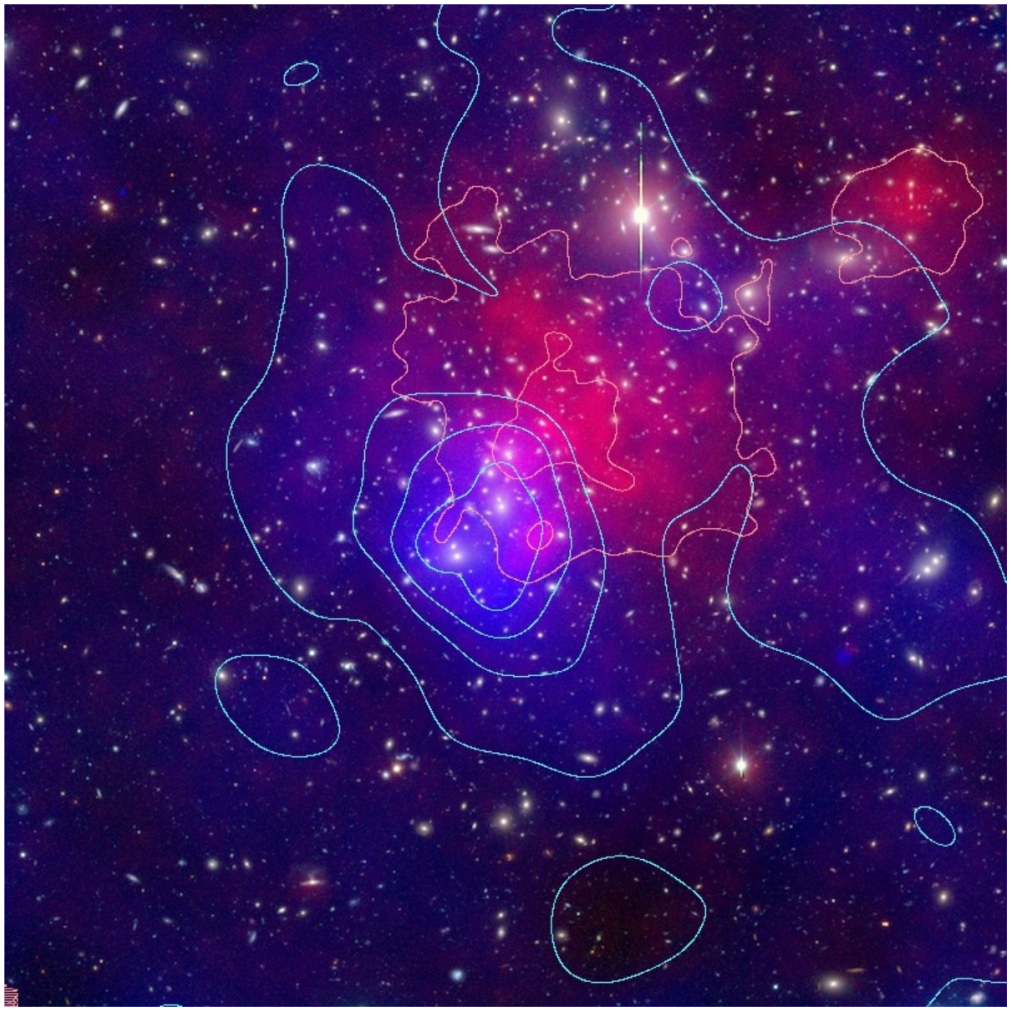

Abell 2744
[Merten et al. MNRAS 417 (2011), 333]

Recovered Density Profiles

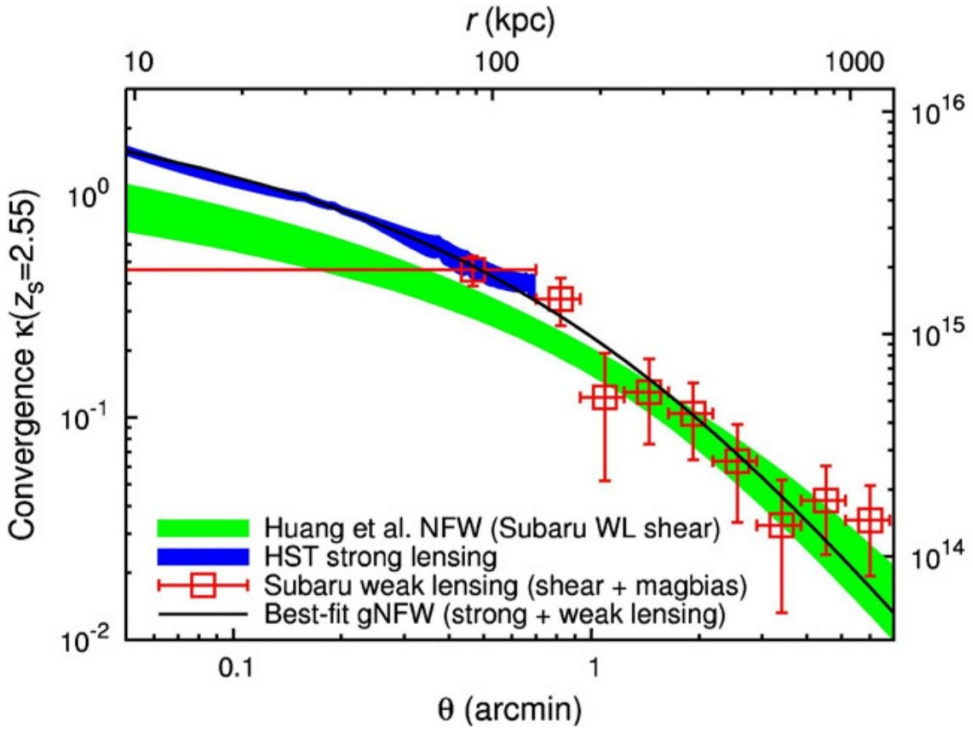

Abell 383
[Zitrin et al. ApJ 742 (2011) 117]

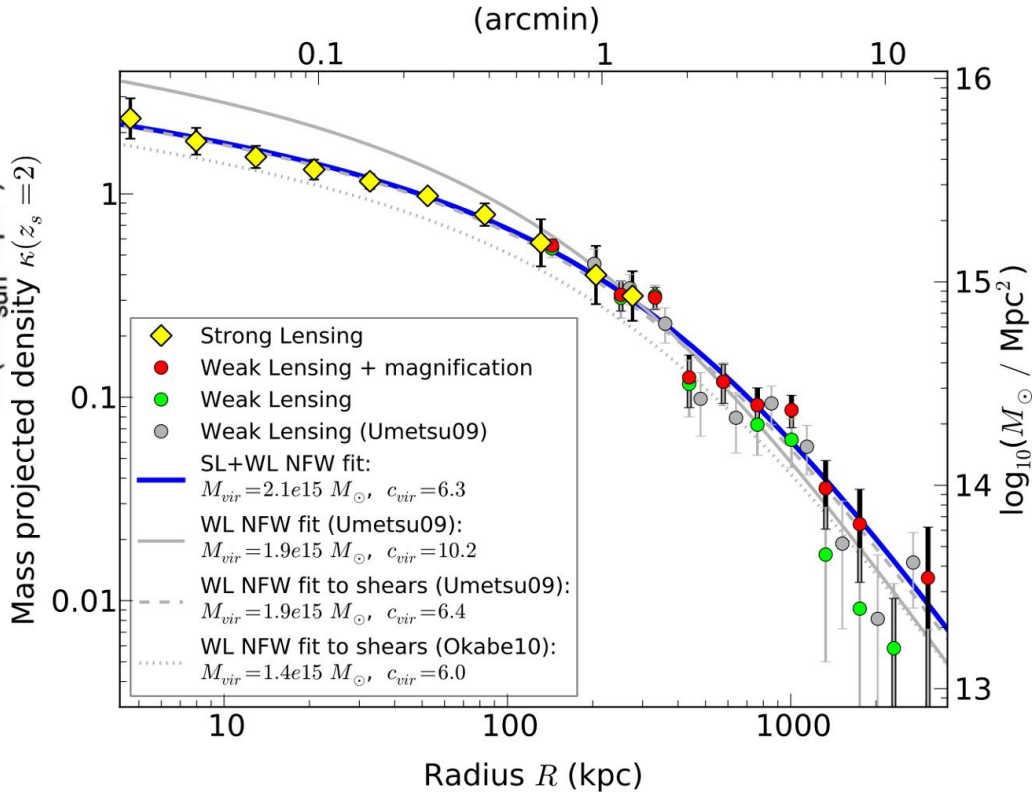

Abell 2261
[Coe et al. ApJ 757 (2012) 22]

Constraints on Concentration Parameter

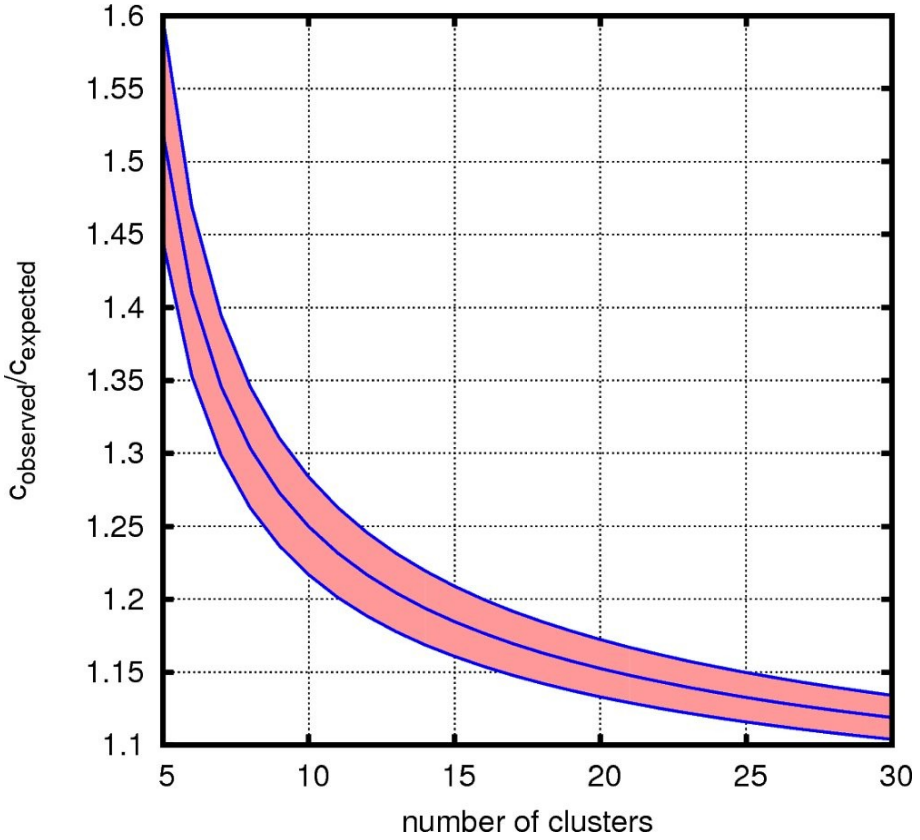

Expected significance with cluster sample
[from CLASH proposal]

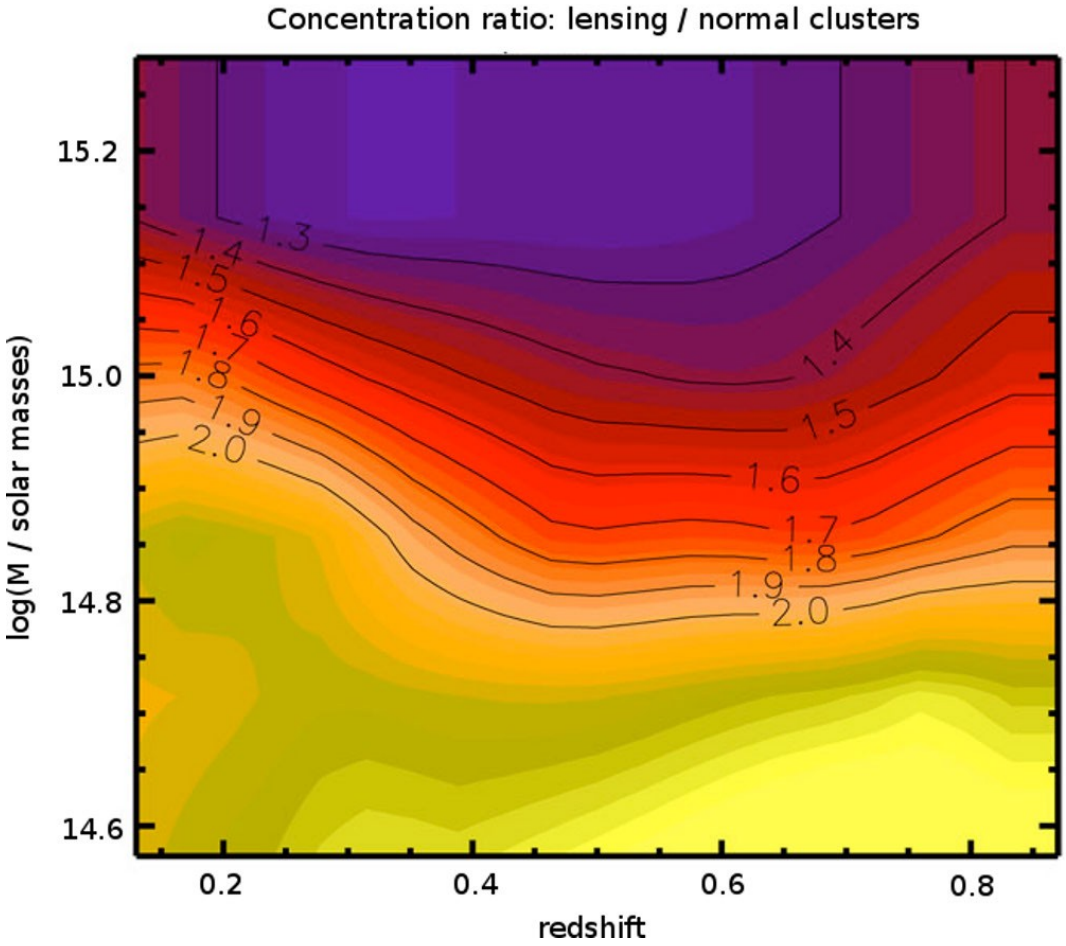

Concentration bias: 1.5 – 2 typically
[Meneghetti et al. A&A 519 (2010) 90]

Meaasured Concentration Parameters

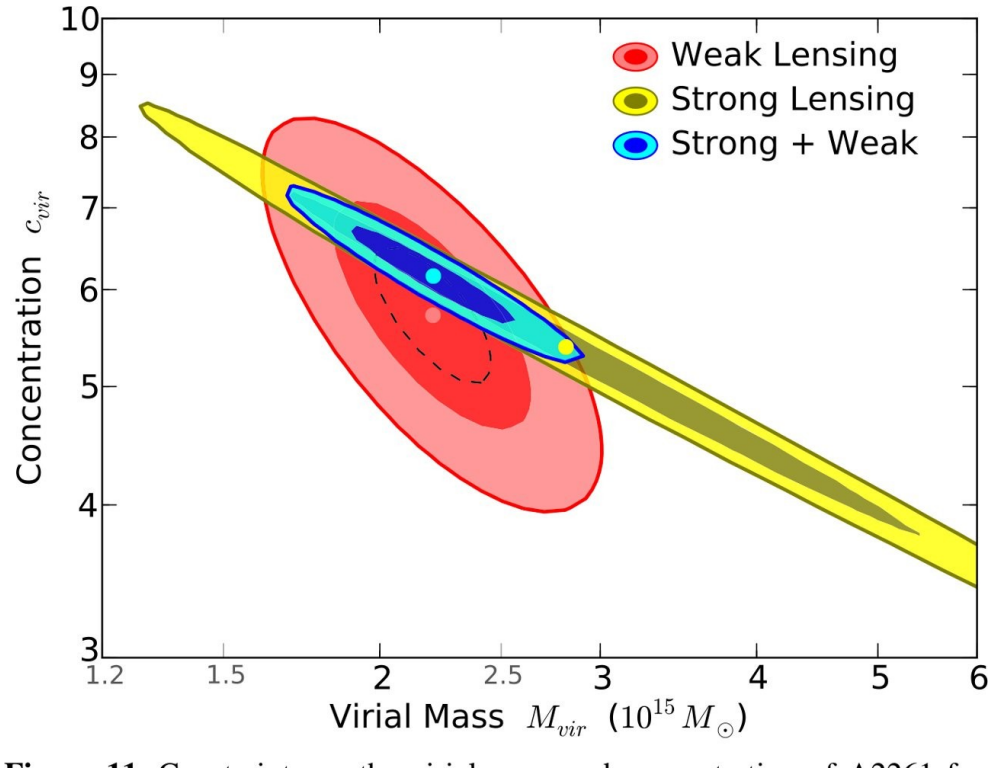

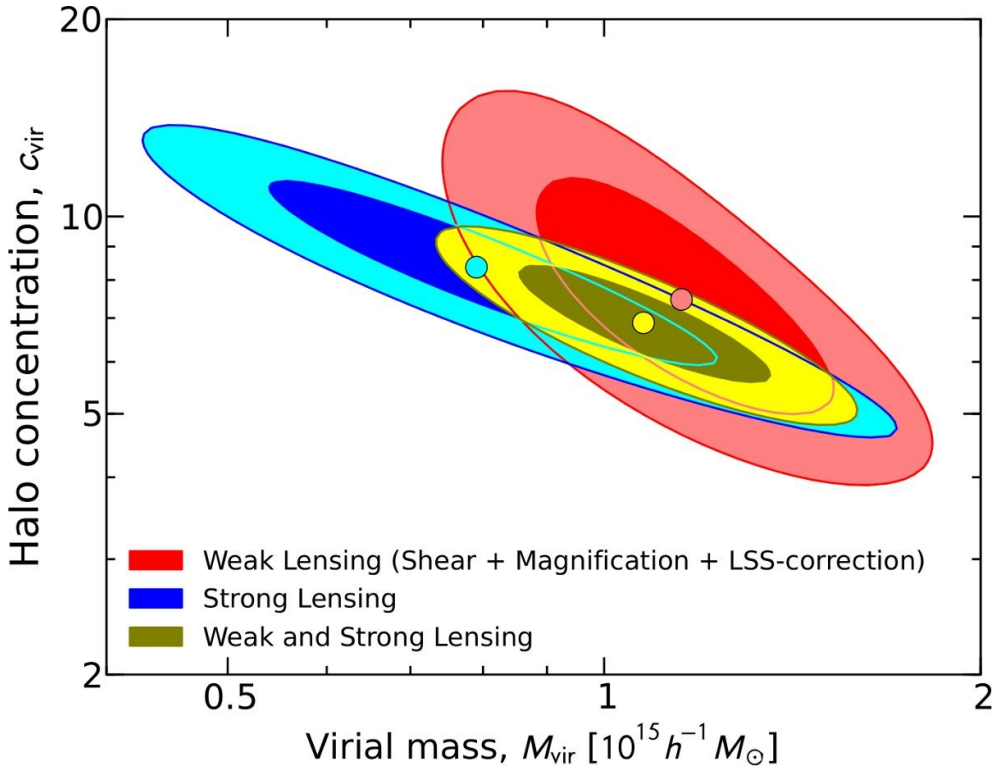

Abell 2261
[Coe et al. ApJ 757 (2012) 22]

MACS J 1206
[Umetsu et al. ApJ 755 (2012) 56]

Combined Results so Far

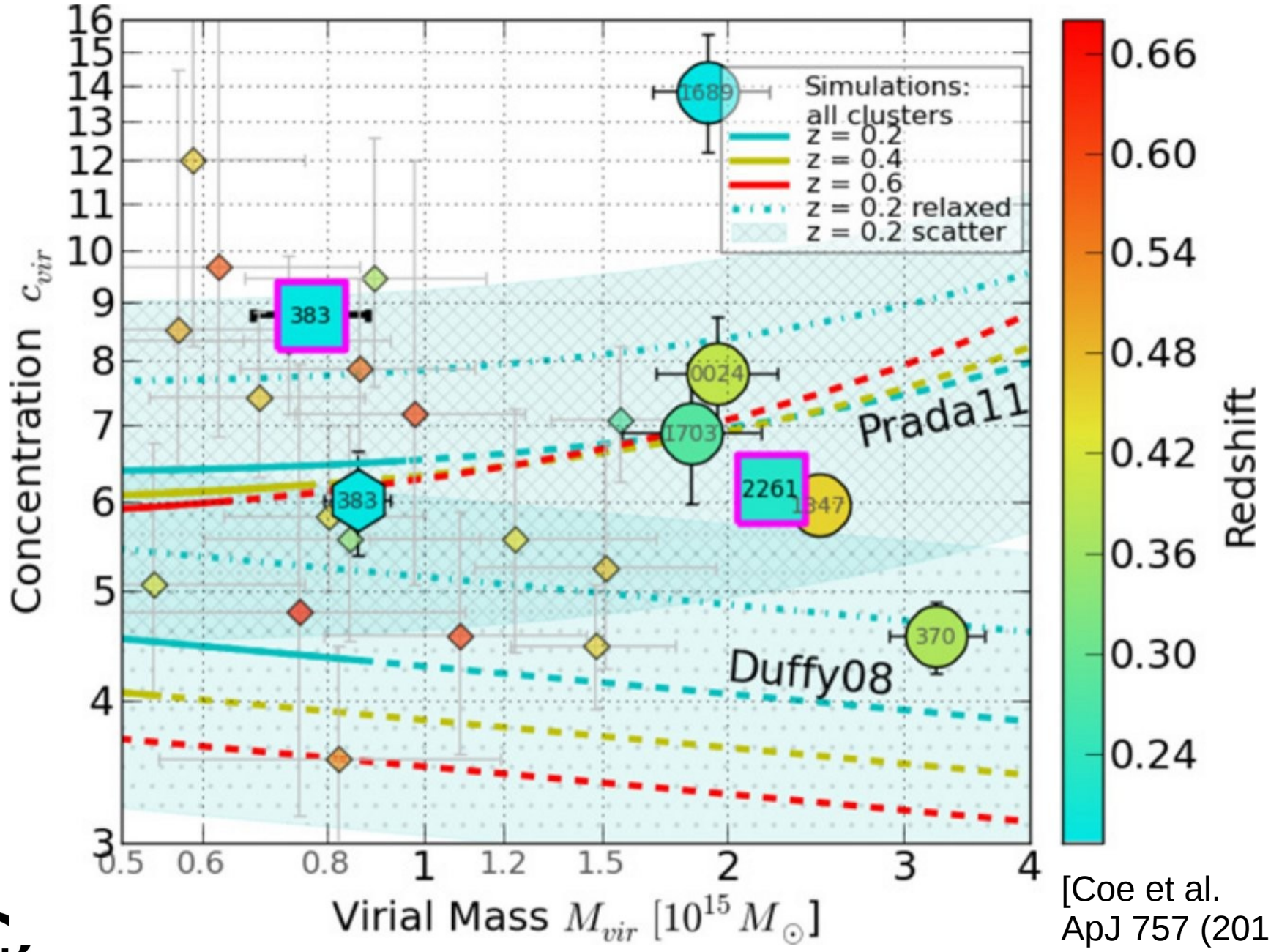

[Coe et al.
ApJ 757 (2012) 22]

Mass Reconstruction

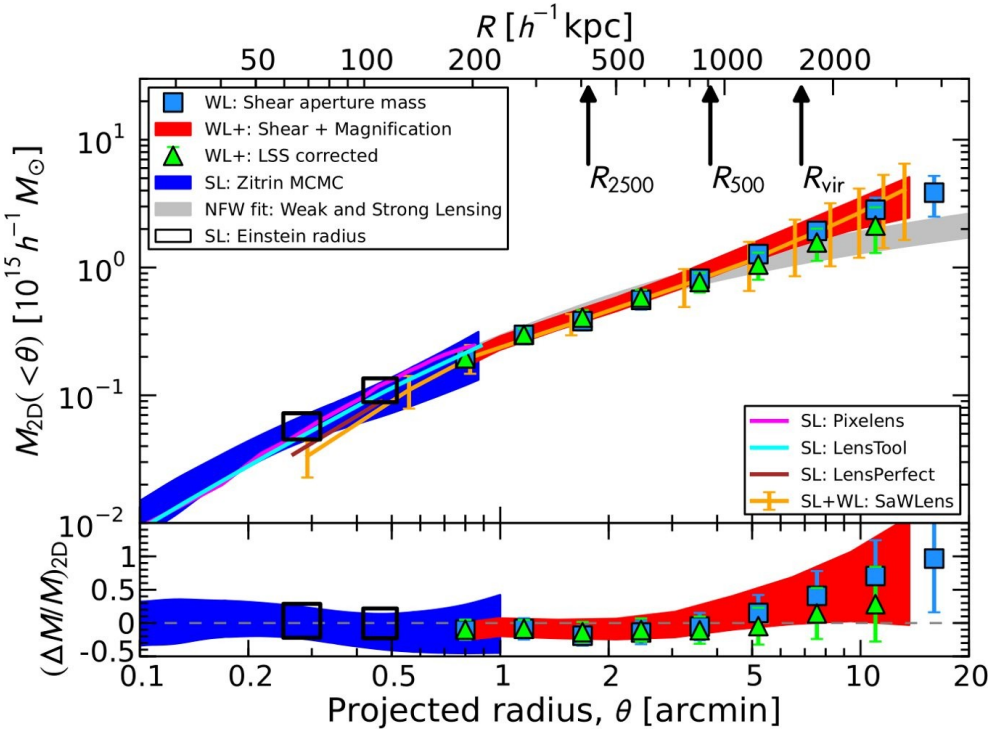

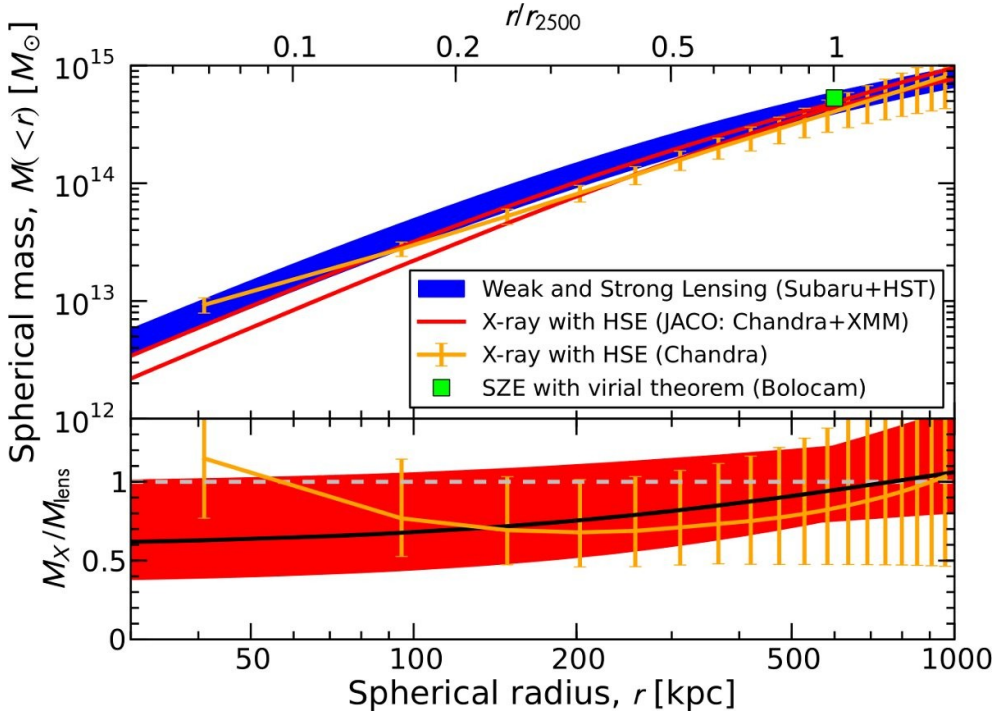

MACS J 1206
[Umetsu et al. ApJ 755 (2012) 56]

Lensing (left),
Lensing and X-ray emission (right)

Extreme Lenses?

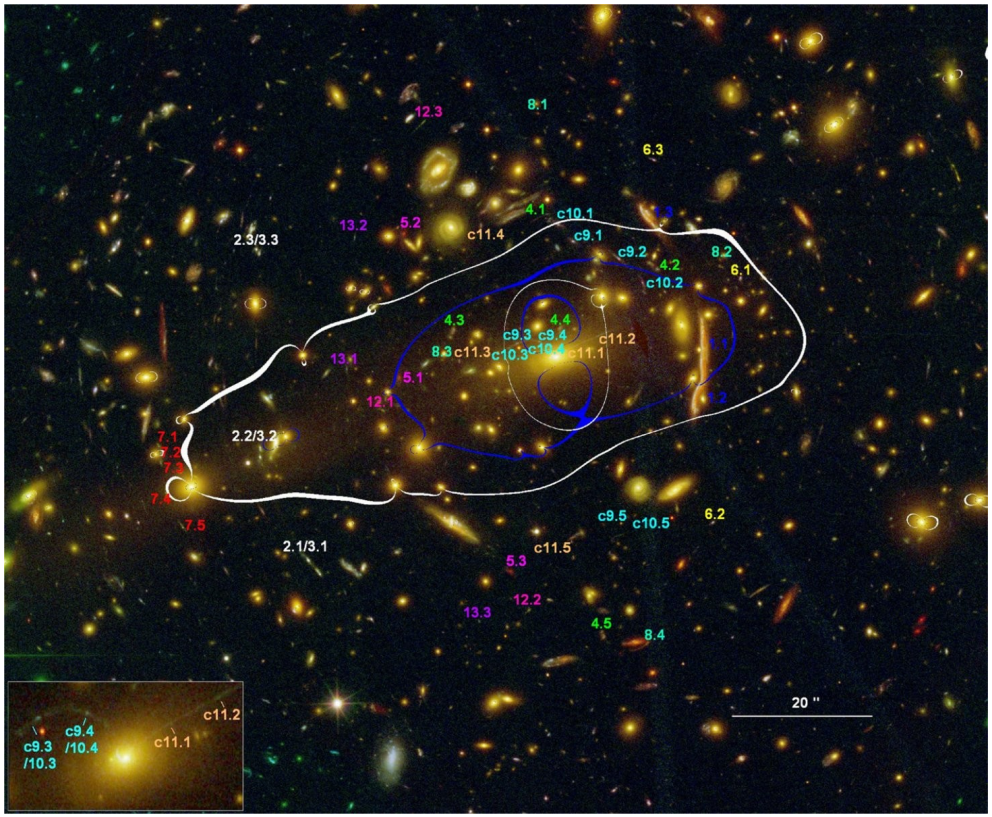

MACS J 1206
[Zitrin et al. ApJ 749 (2012) 97]

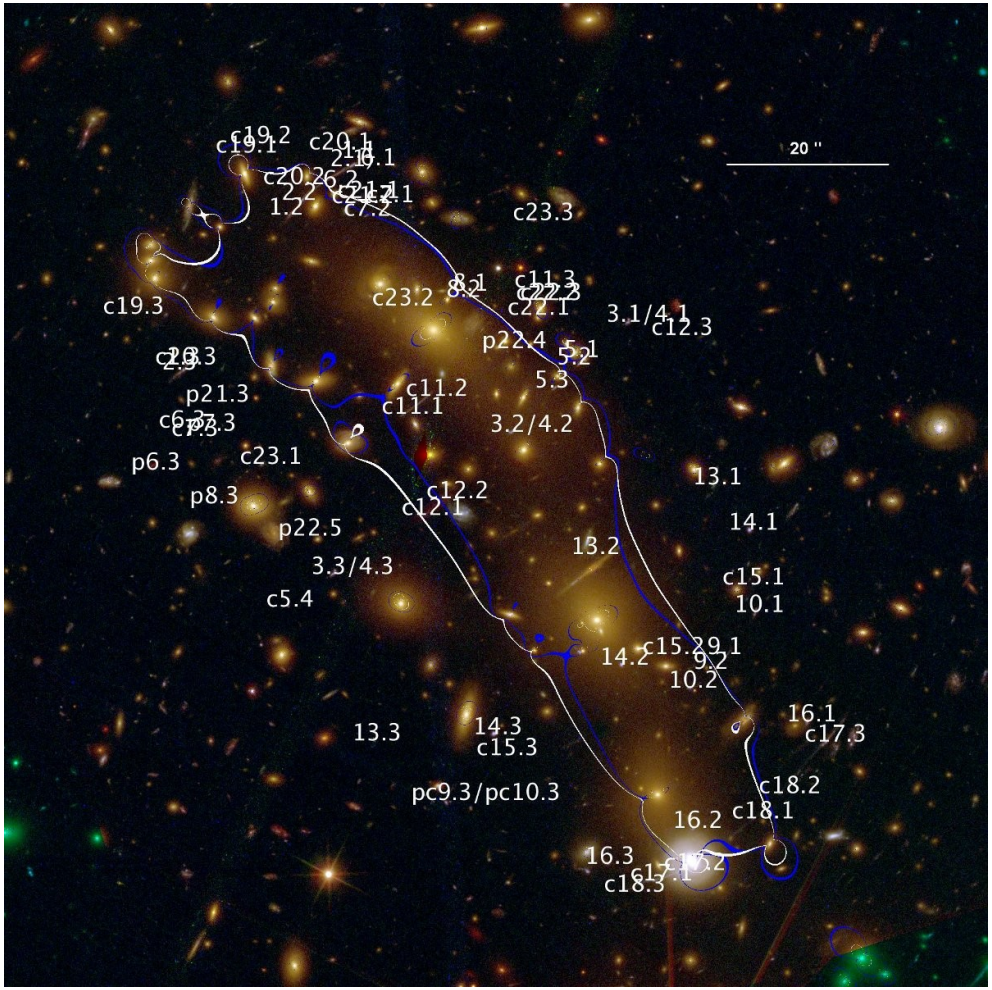

M 0416 [Zitrin et al. in prep.]

Extreme Lenses?

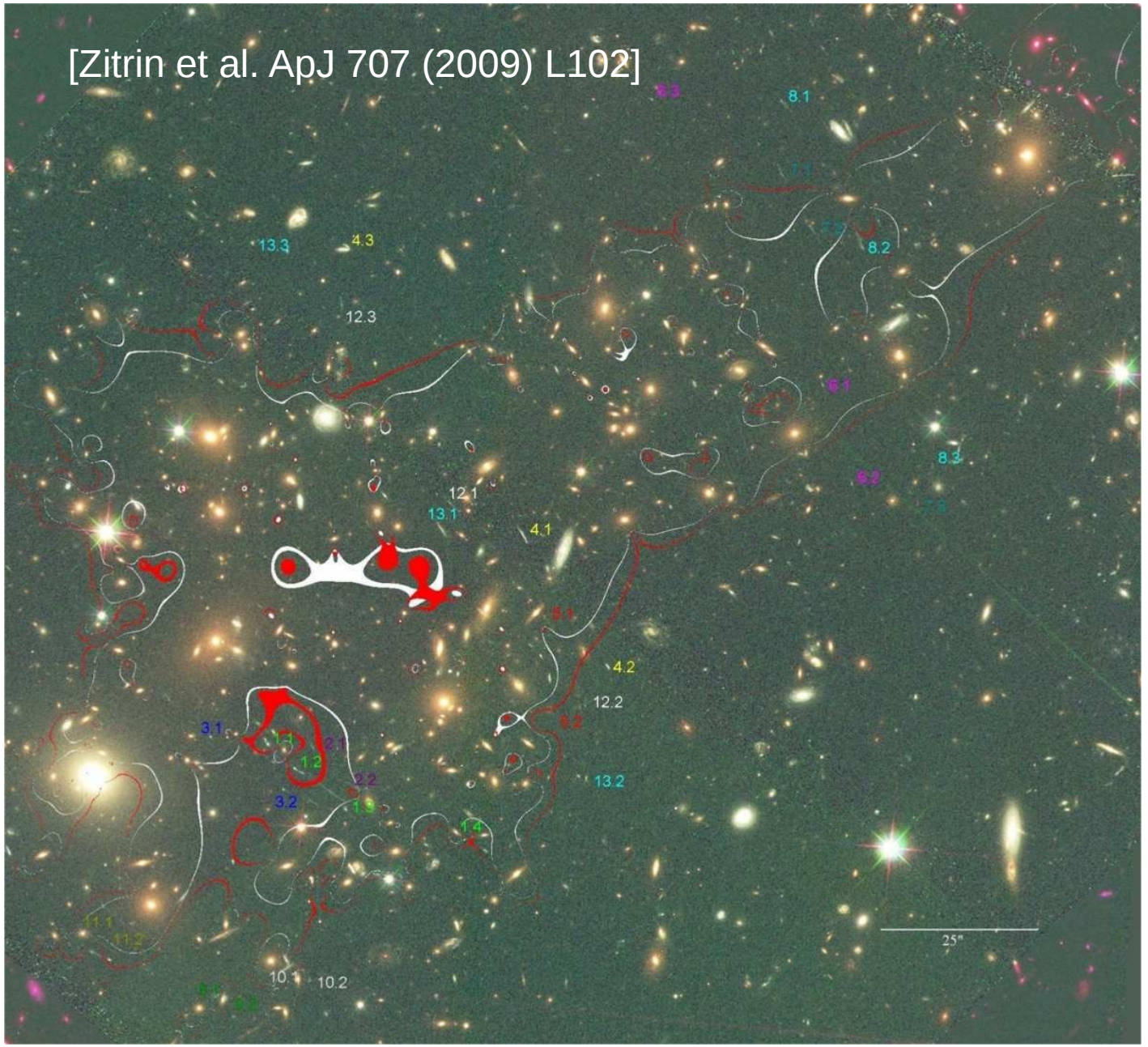

MACS
J 0717

Expectation of Large Critical Curves?

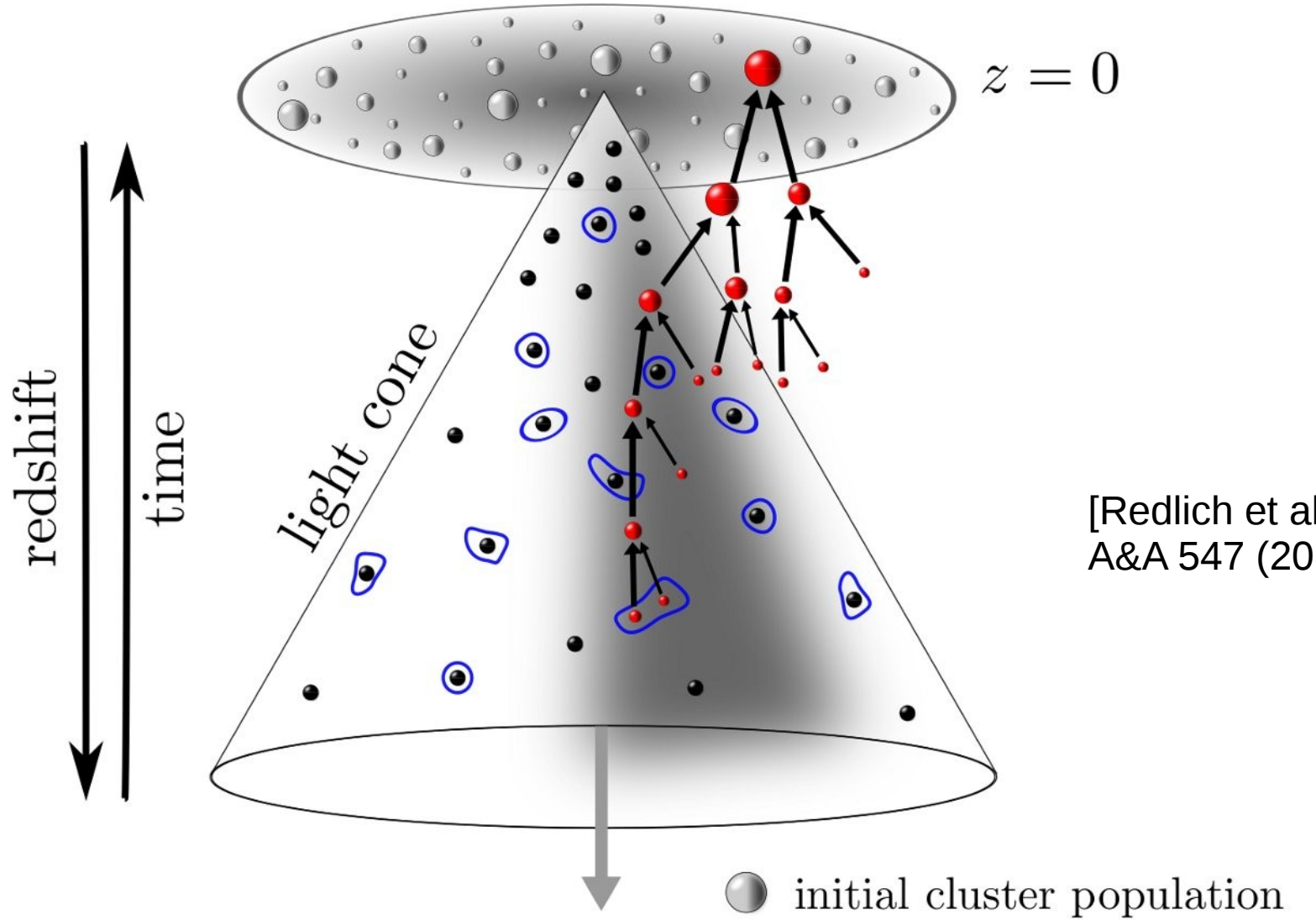

[Redlich et al.
A&A 547 (2012) A66]

Expectation of Large Critical Curves?

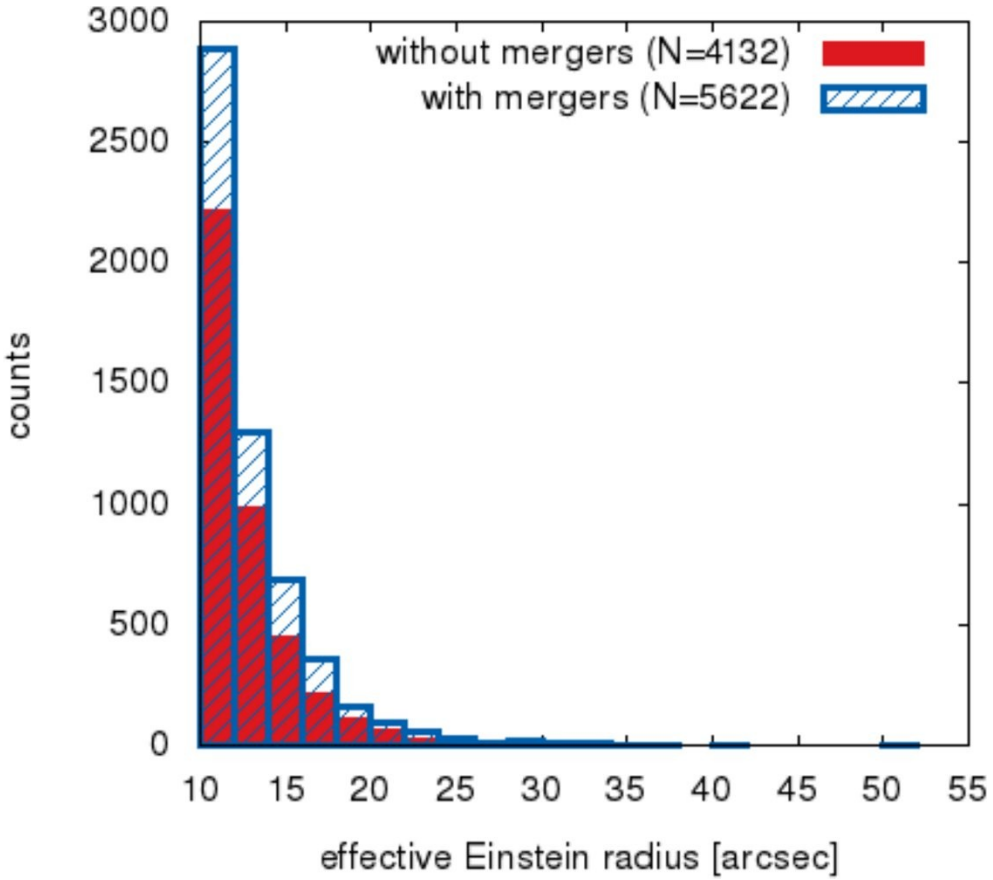

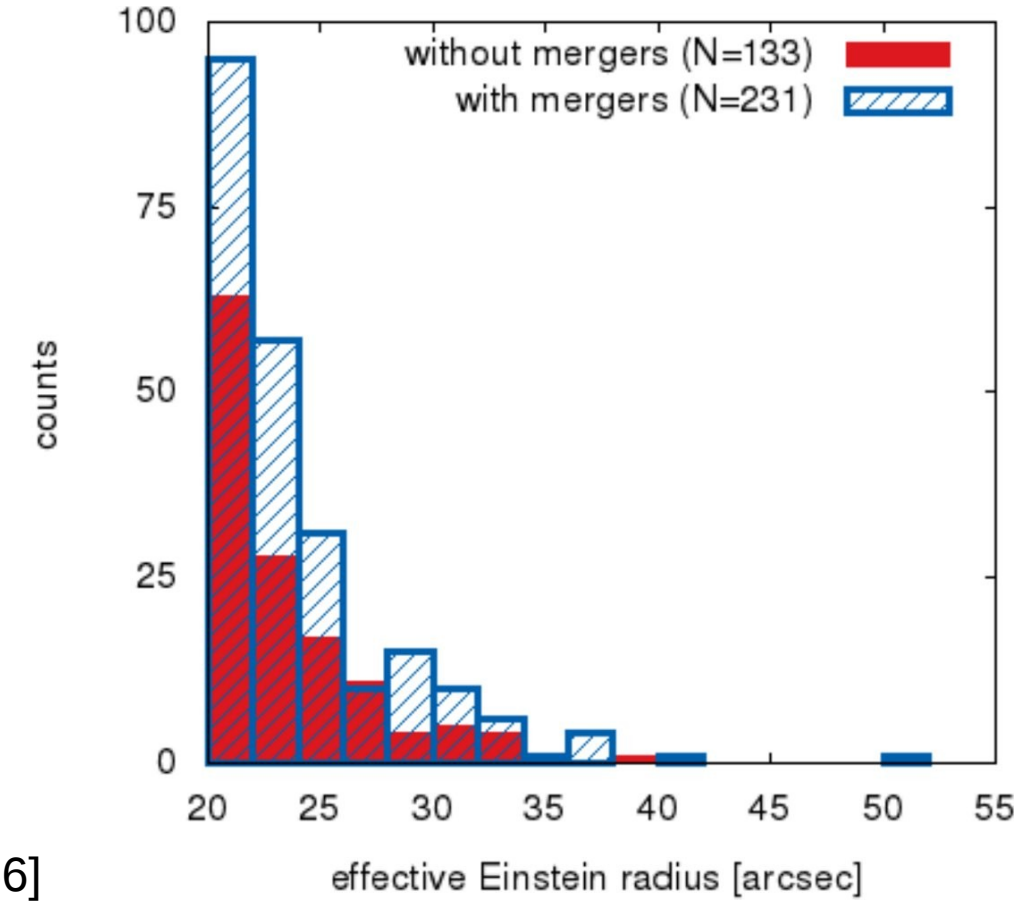

[Redlich et al. A&A 547 (2012) A66]

Extreme-Value Statistics

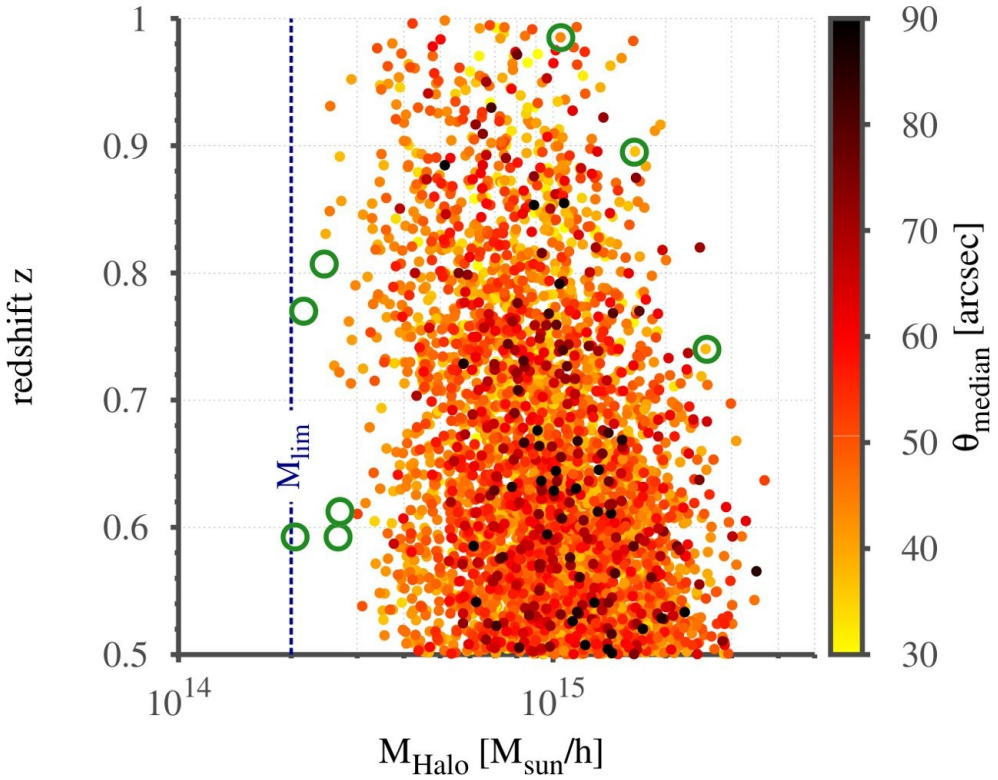

[Waizmann et al. A&A 547 (2012) A67]

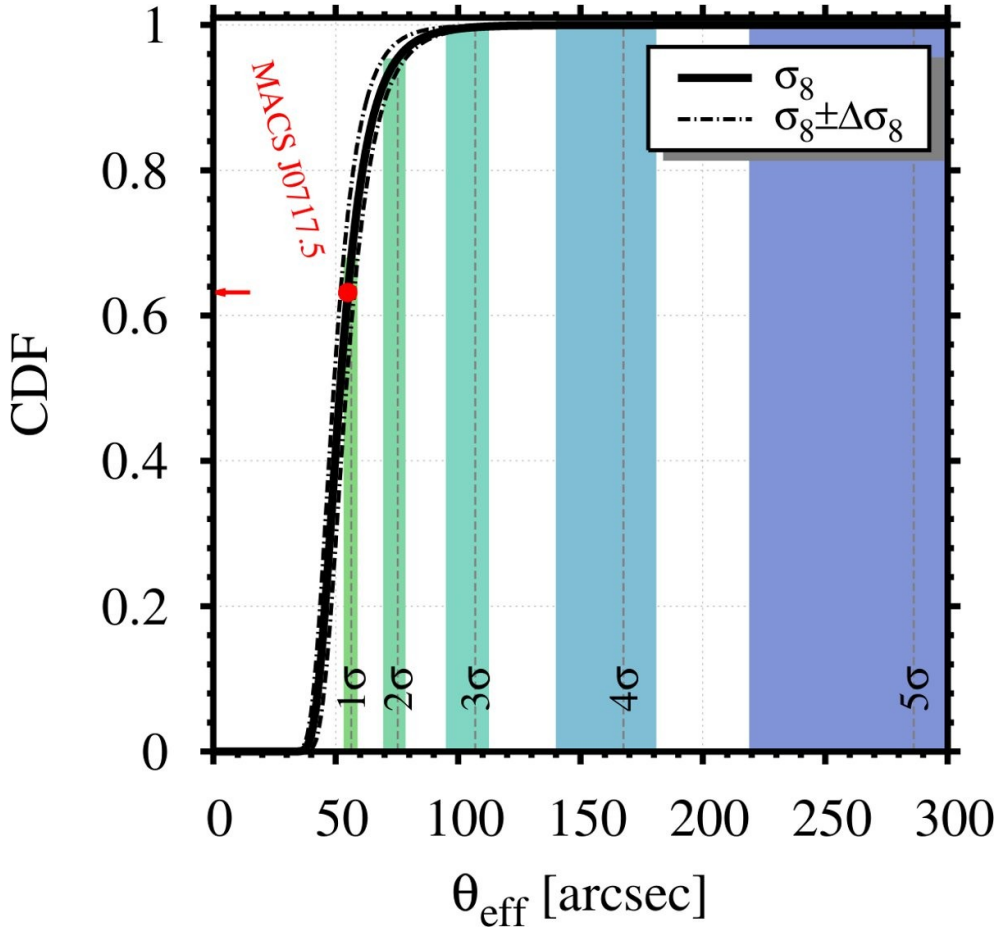

Extreme-Value Statistics

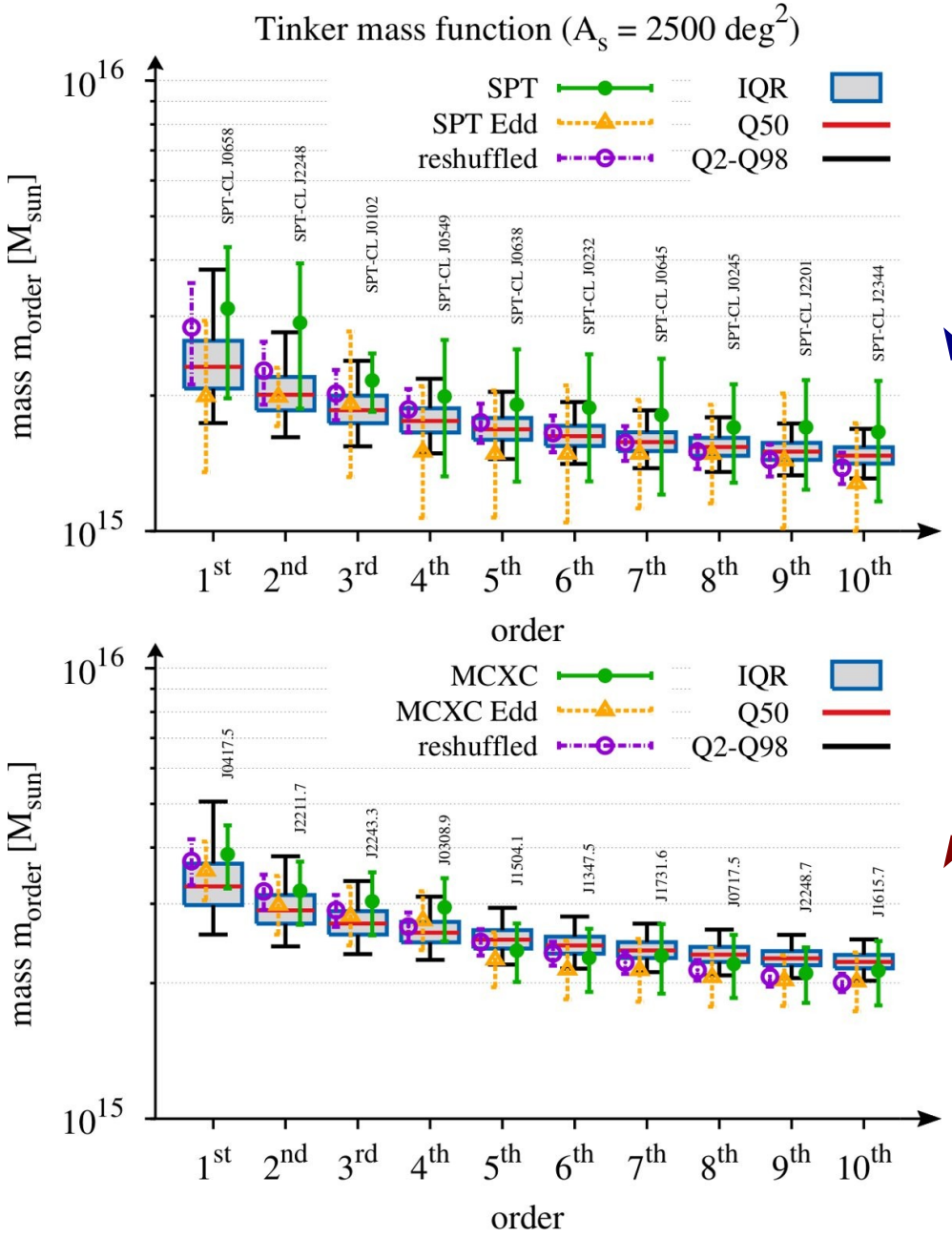

extreme SZ
and
X-ray clusters

[Waizmann et al. MNRAS (2012) submitted]

Gravitational Flexion

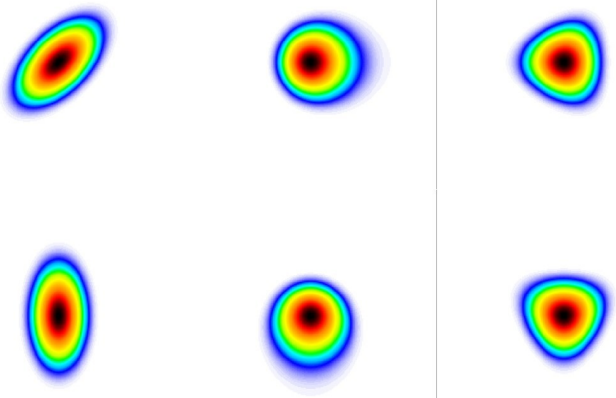

Gravitational flexion
Pioneering work by
T. Futamase, N. Okabe, Y. Okura, K. Umetsu

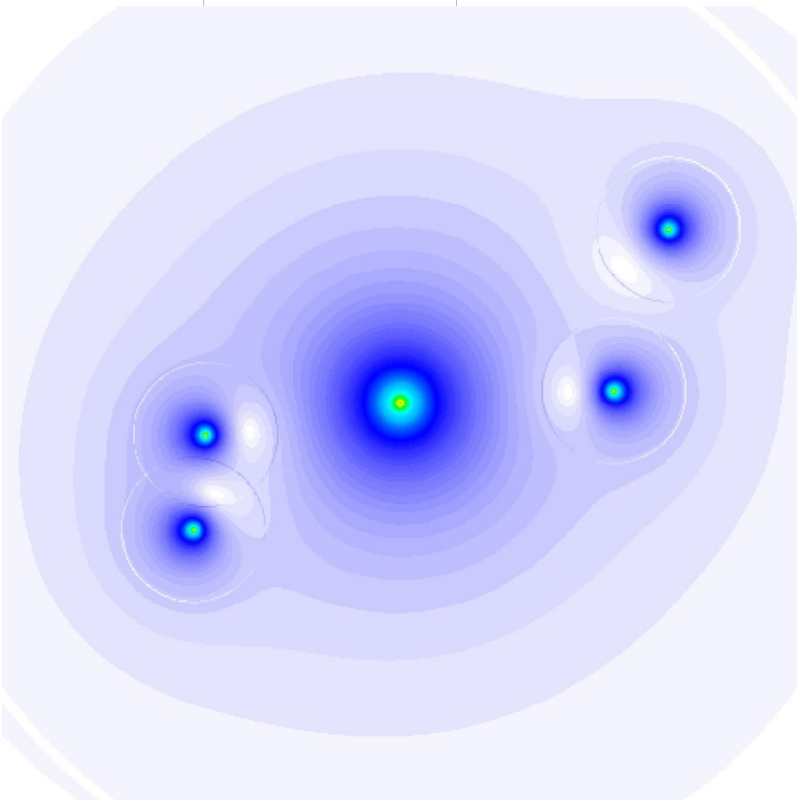

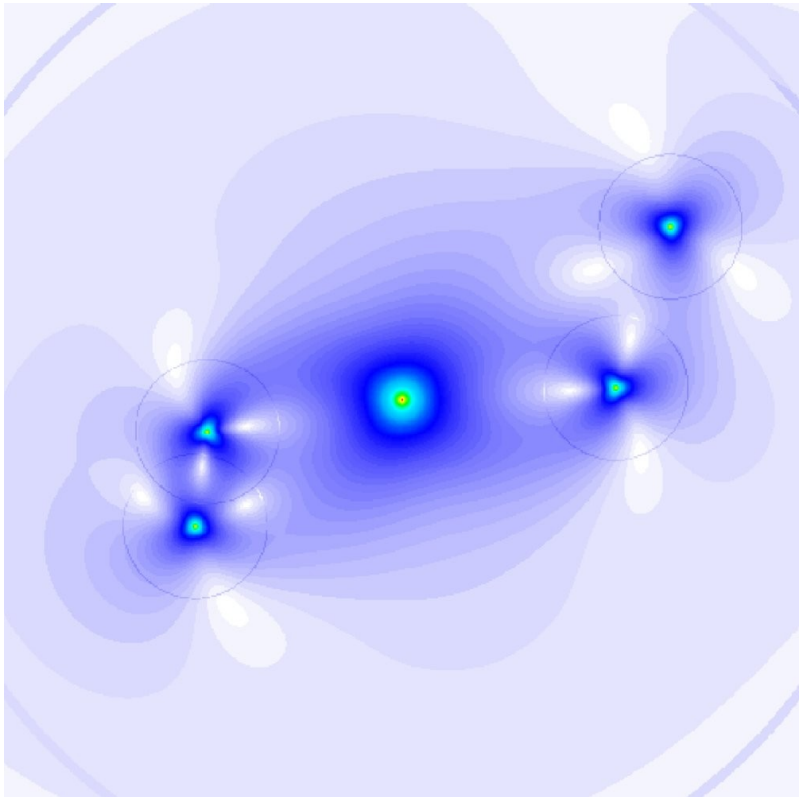

Flexion Measurement

$$\frac{4}{3}\langle\delta\rangle \simeq G + gF\left(19 - 24\frac{(TrQ)^2}{\xi}\right)$$

$$\langle\zeta\rangle - 2g\langle\zeta^\star\rangle \simeq F\left(\frac{9}{4} - 3\frac{(TrQ)^2}{\xi}\right) + g^\star G\left(\frac{9}{4} - \frac{(TrQ)^2}{\xi}\right) + 2F^\star g\left(3 - 4\frac{(TrQ)^2}{\xi}\right)$$

[Viola et al. MNRAS 419 (2012) 2215]

Table 1. Equations for deconvolving all moments up to order $n = 2$. The shown equations are specializations of equation (9).

$\{G\}_{0,0}\,\{P\}_{0,0} = \{G^\star\}_{0,0}$
$\{G\}_{0,1}\,\{P\}_{0,0} = \{G^\star\}_{0,1} - \{G\}_{0,0}\,\{P\}_{0,1}$
$\{G\}_{1,0}\,\{P\}_{0,0} = \{G^\star\}_{1,0} - \{G\}_{0,0}\,\{P\}_{1,0}$
$\{G\}_{0,2}\,\{P\}_{0,0} = \{G^\star\}_{0,2} - \{G\}_{0,0}\,\{P\}_{0,2} - 2\{G\}_{0,1}\,\{P\}_{0,1}$
$\{G\}_{1,1}\,\{P\}_{0,0} = \{G^\star\}_{1,1} - \{G\}_{0,0}\,\{P\}_{1,1} - \{G\}_{0,1}\,\{P\}_{1,0} - \{G\}_{1,0}\,\{P\}_{0,1}$
$\{G\}_{2,0}\,\{P\}_{0,0} = \{G^\star\}_{2,0} - \{G\}_{0,0}\,\{P\}_{2,0} - 2\{G\}_{1,0}\,\{P\}_{1,0}$

DEIMOS
[Melchior et al.
MNRAS 412 (2011) 1552]

Shear-Flexion Cross-Talk

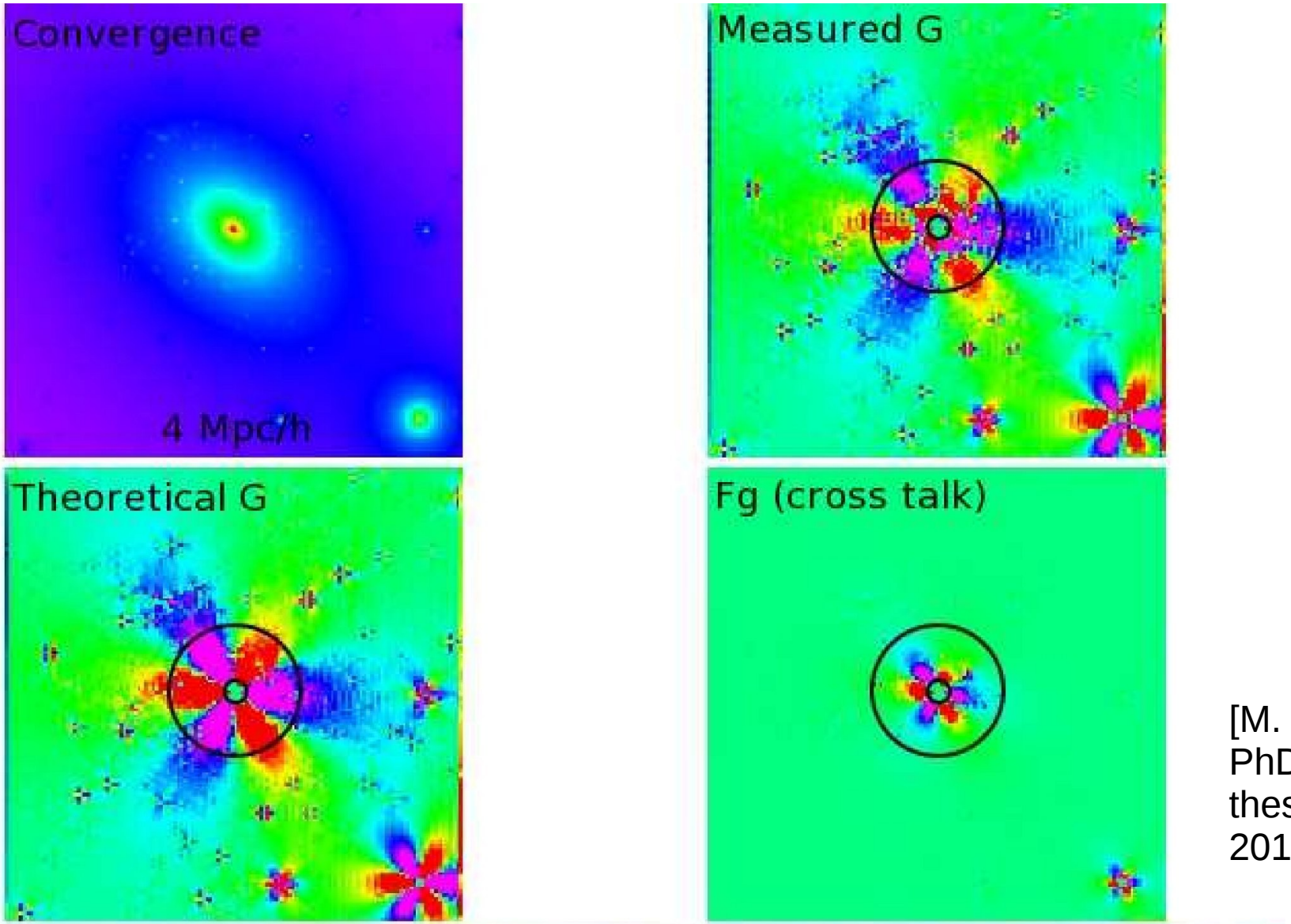

[M. Viola PhD thesis, 2010]

Combining Lensing and X-ray Data

[Konrad et al.
A&A (2012) submitted]

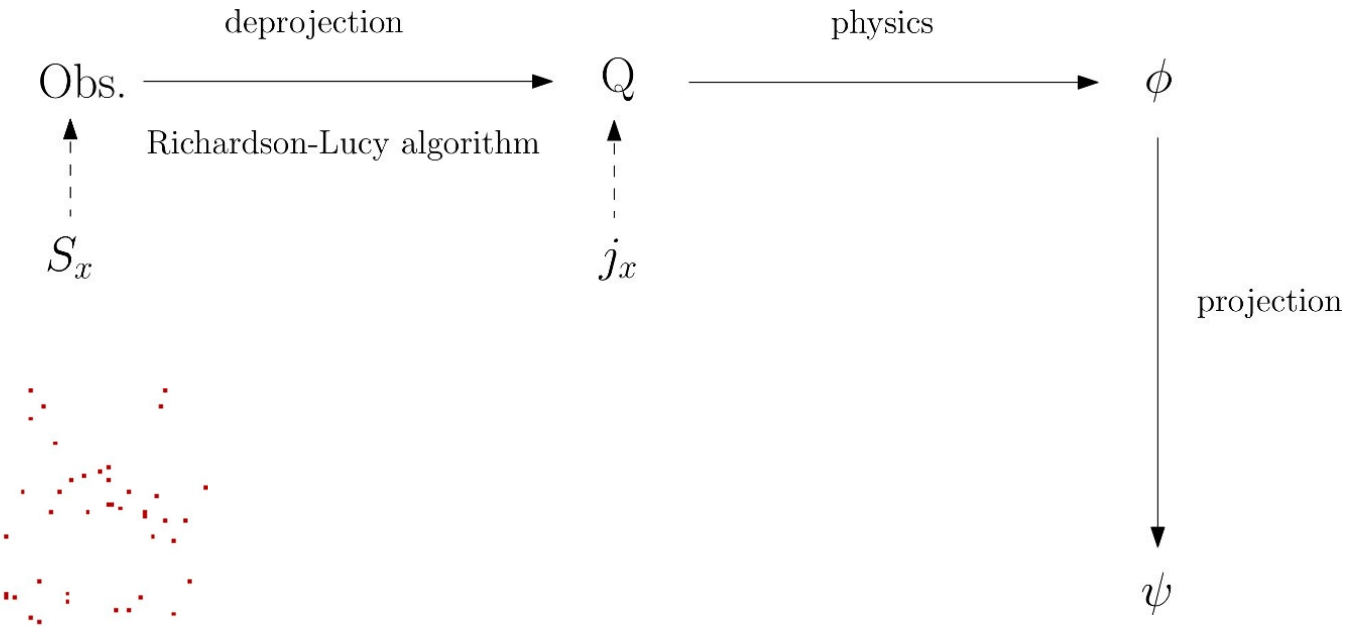

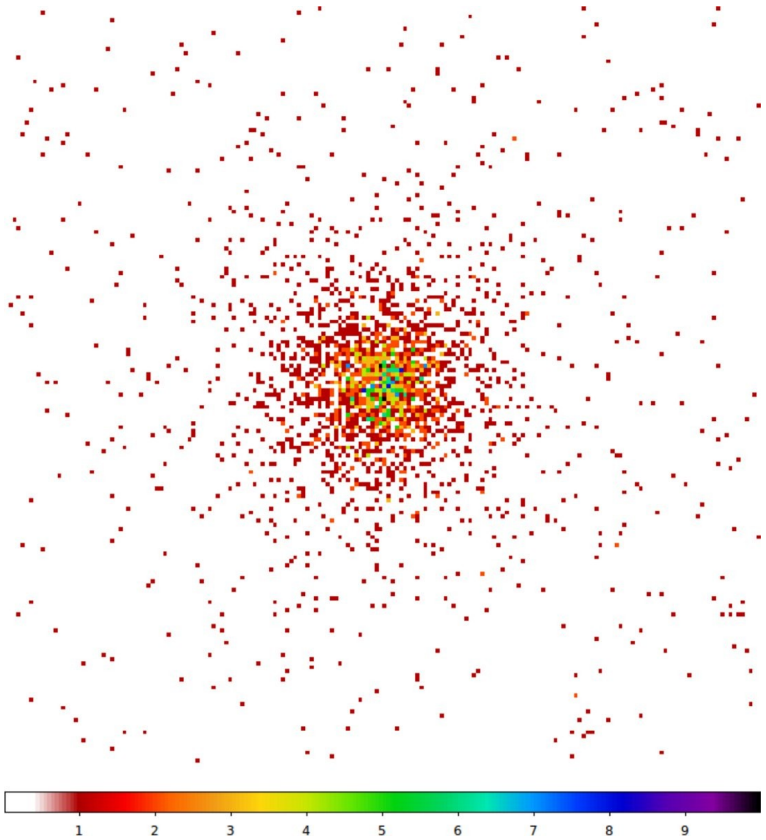

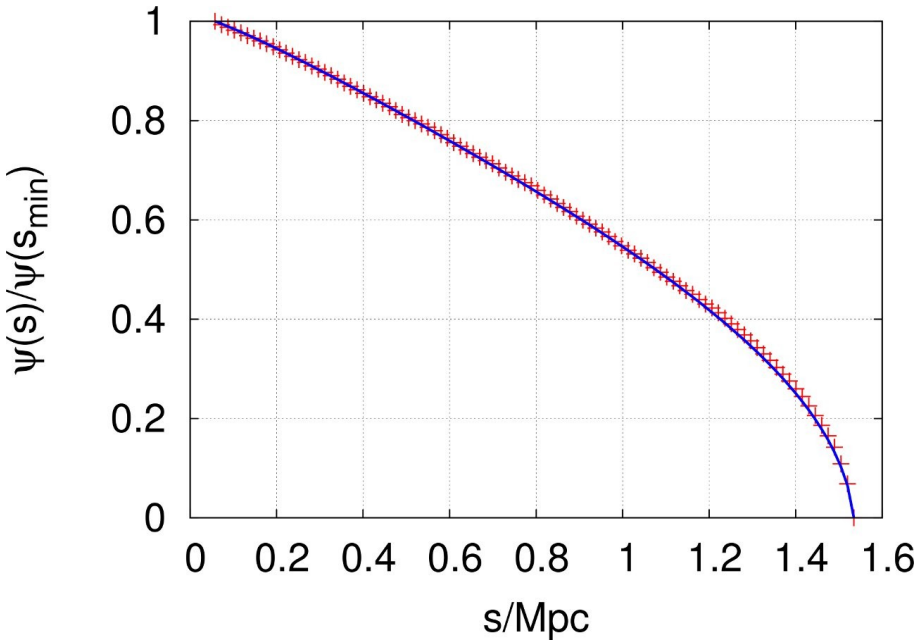

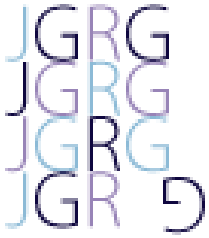

Ryo Tsutsui, JGRG 22(2012)111305

"Measuring distance with gamma-ray bursts"

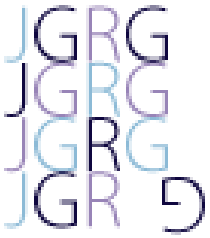

RESCEU SYMPOSIUM ON

GENERAL RELATIVITY AND GRAVITATION

JGRG 22



November 12-16 2012

Koshiba Hall, The University of Tokyo, Hongo, Tokyo, Japan



Distance measurement with (long) gamma-ray bursts

- Ryo Tsutsui (RESCEU)
  on behalf of GRB Cosmology Project
  and Hi-Z GUNDAM Project

JGRG22 2012/11/13

Table of Contents

- Brief introduction of gamma-ray bursts
- previous works and problems for distance measurements with gamma-ray bursts
- Their improvements and future prospects

Table of Contents

- Brief introduction of gamma-ray bursts
- previous works and problems for distance measurements with gamma-ray bursts
- Their improvements and future prospects

The simplest picture of long gamma-ray bursts

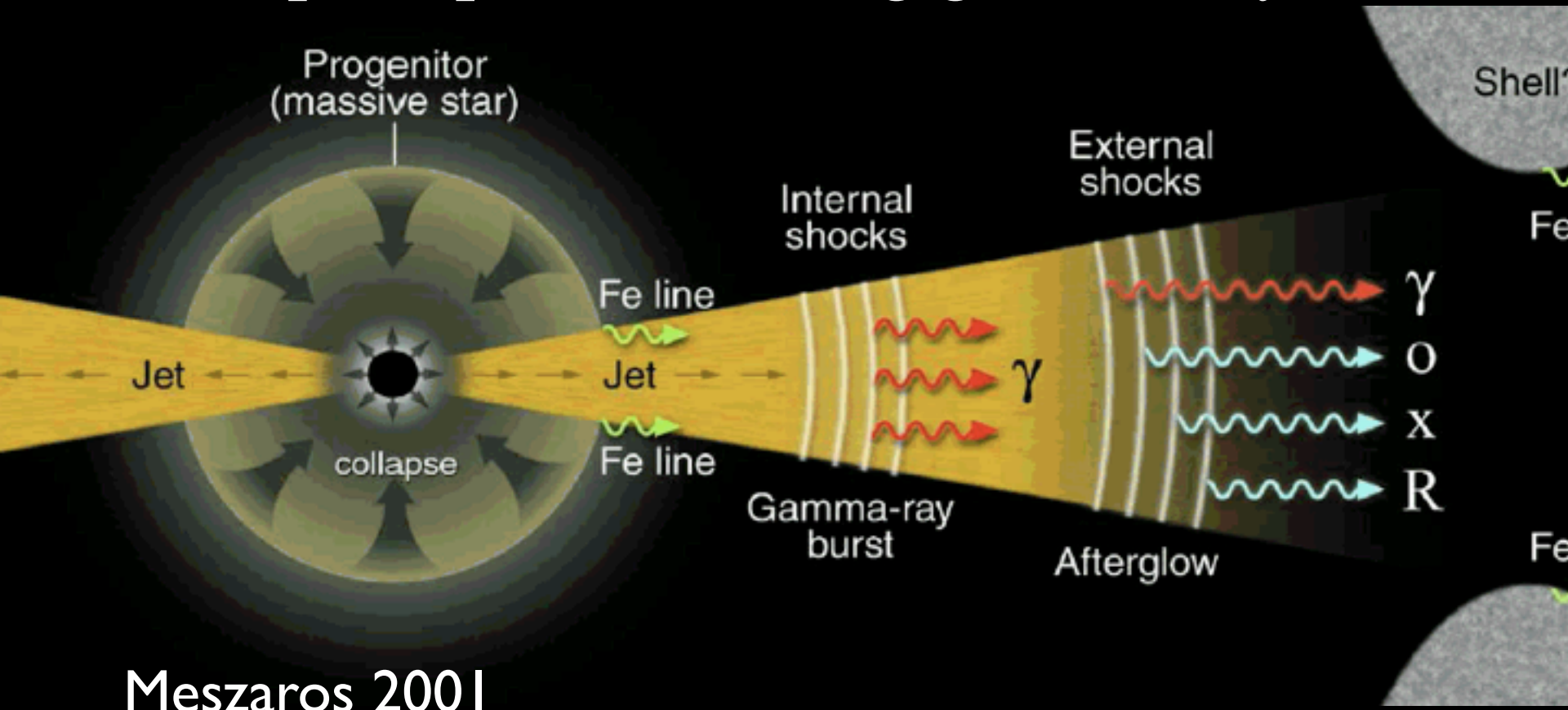

Meszaros 2001

- Energy release form central engine
- Radiation from relativistic jet Lorents factor ~ 100
- interaction between shell and interstellar medium

Time scale of GRBs

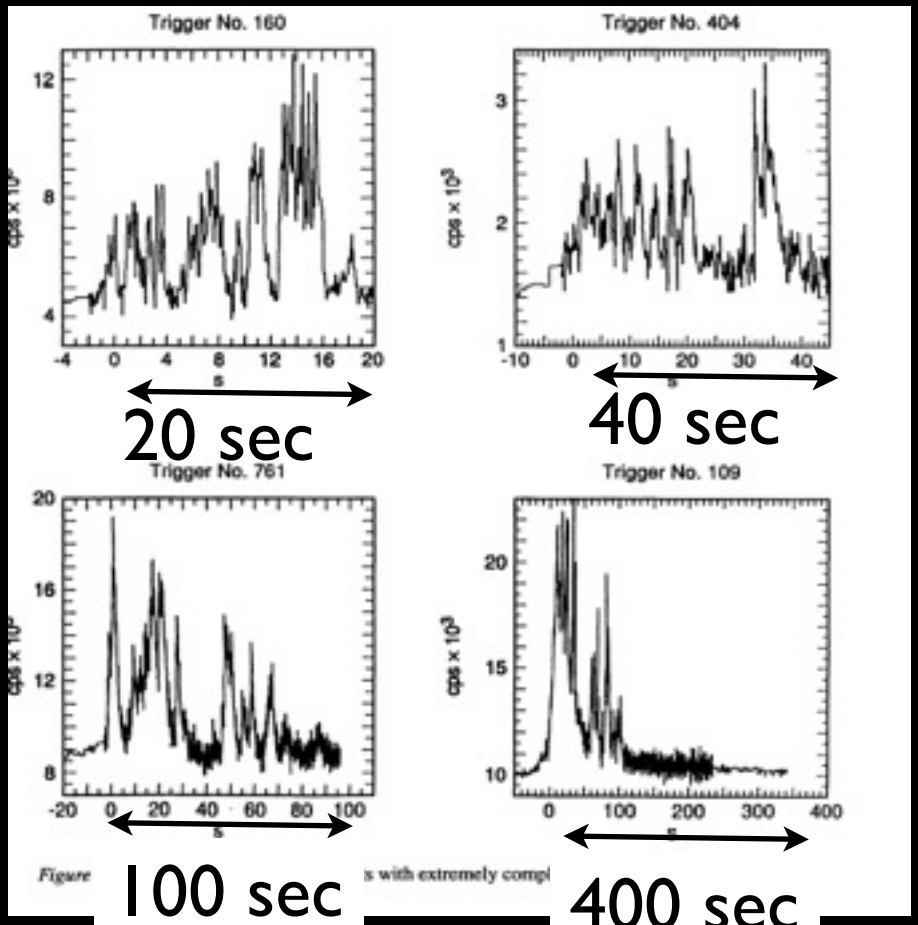

Complex time profile

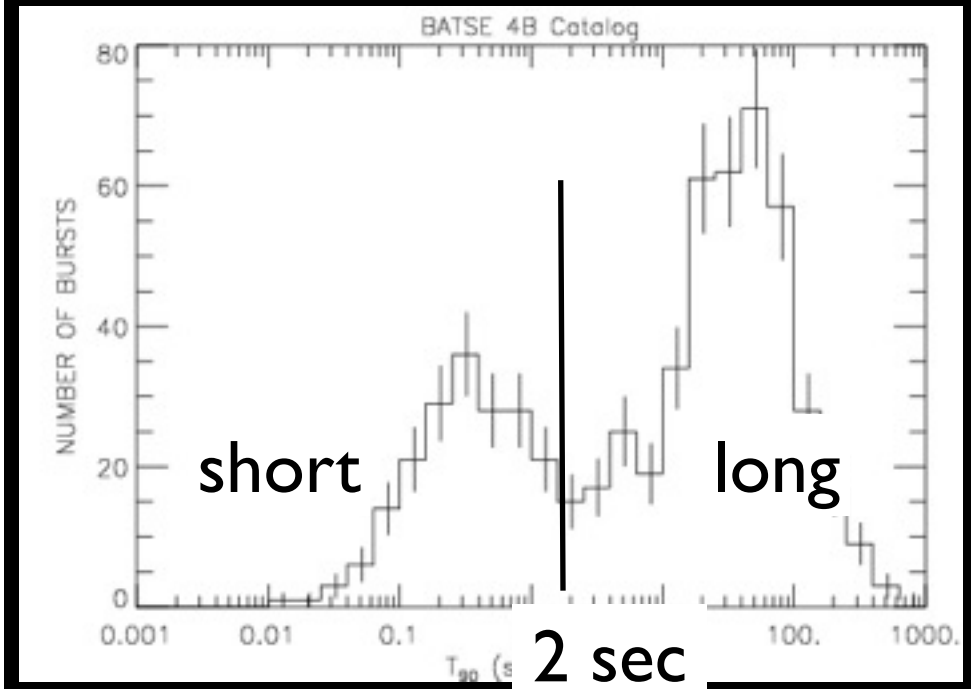

Two population
Long: core collapse
Short: merger?

Energy and distance of GRBs

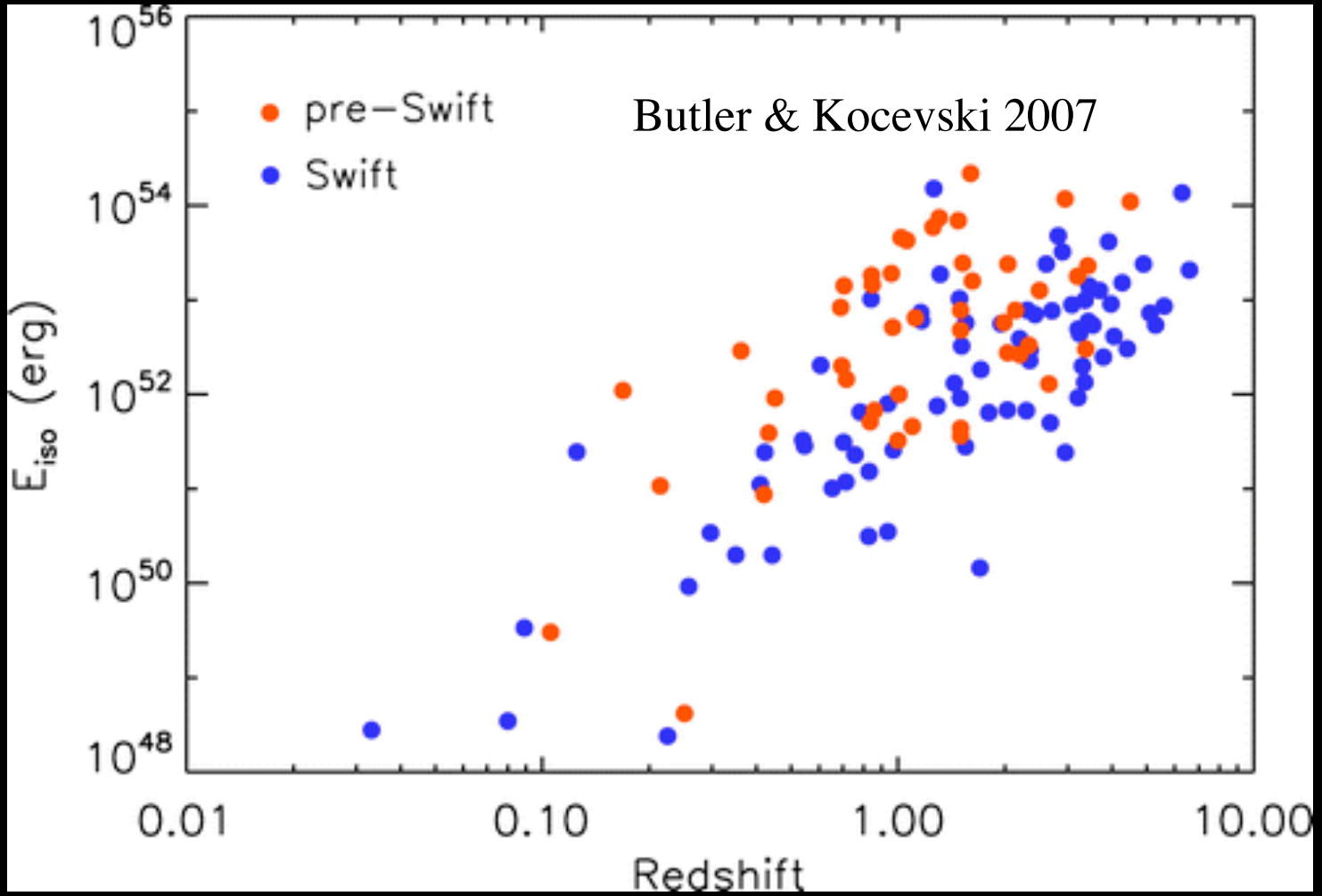

Spectra - Luminosity correlation

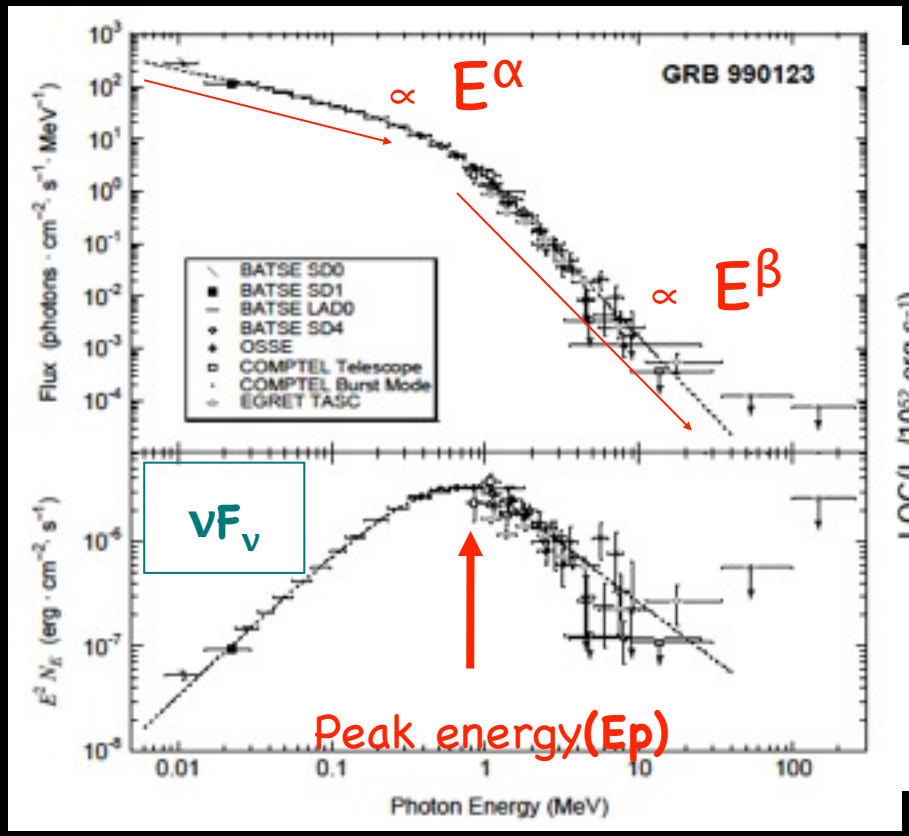

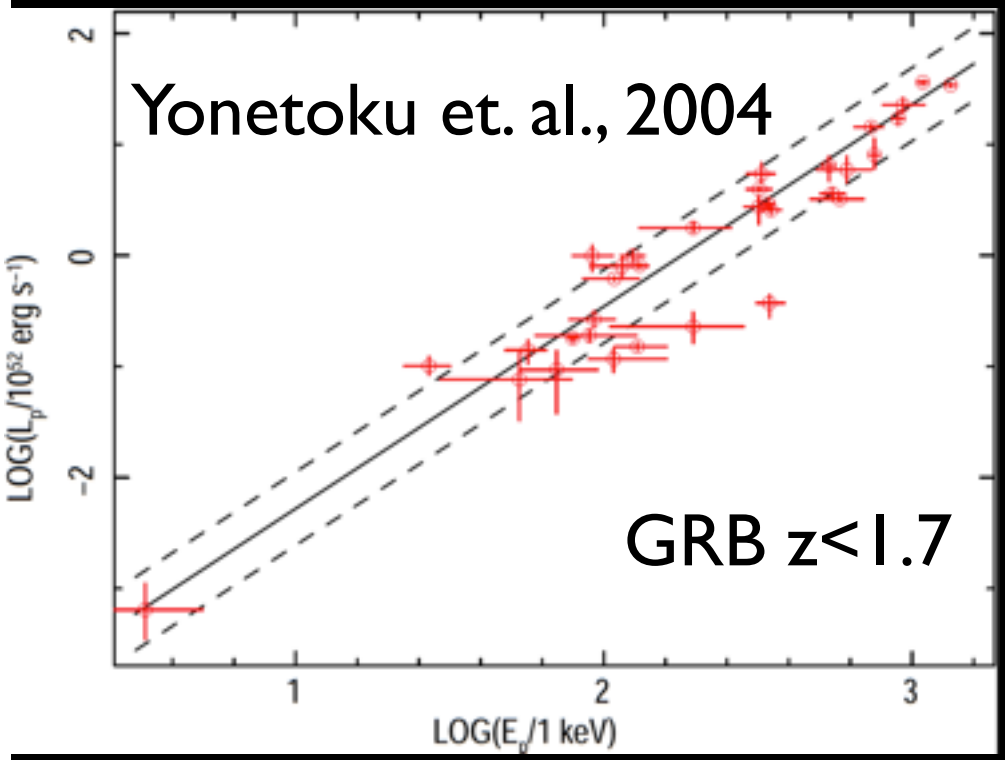

GRBs are "standardizable candles"

Luminosity of objects in the sky



Sun 10^{33} erg/s



Type Ia Supernovae 10^{43} erg/s



Gamma ray bursts 10^{53} erg/s

Table of Contents

- Brief introduction of gamma-ray bursts
- previous works and problems for distance measurements with gamma-ray bursts
- Their improvements and future prospects

Distance measurement with GRBs

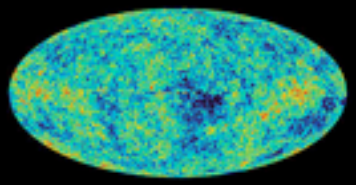

Kodama, RT + 2008

$(\Omega_m, \Omega_\Lambda) = (0, 1)$

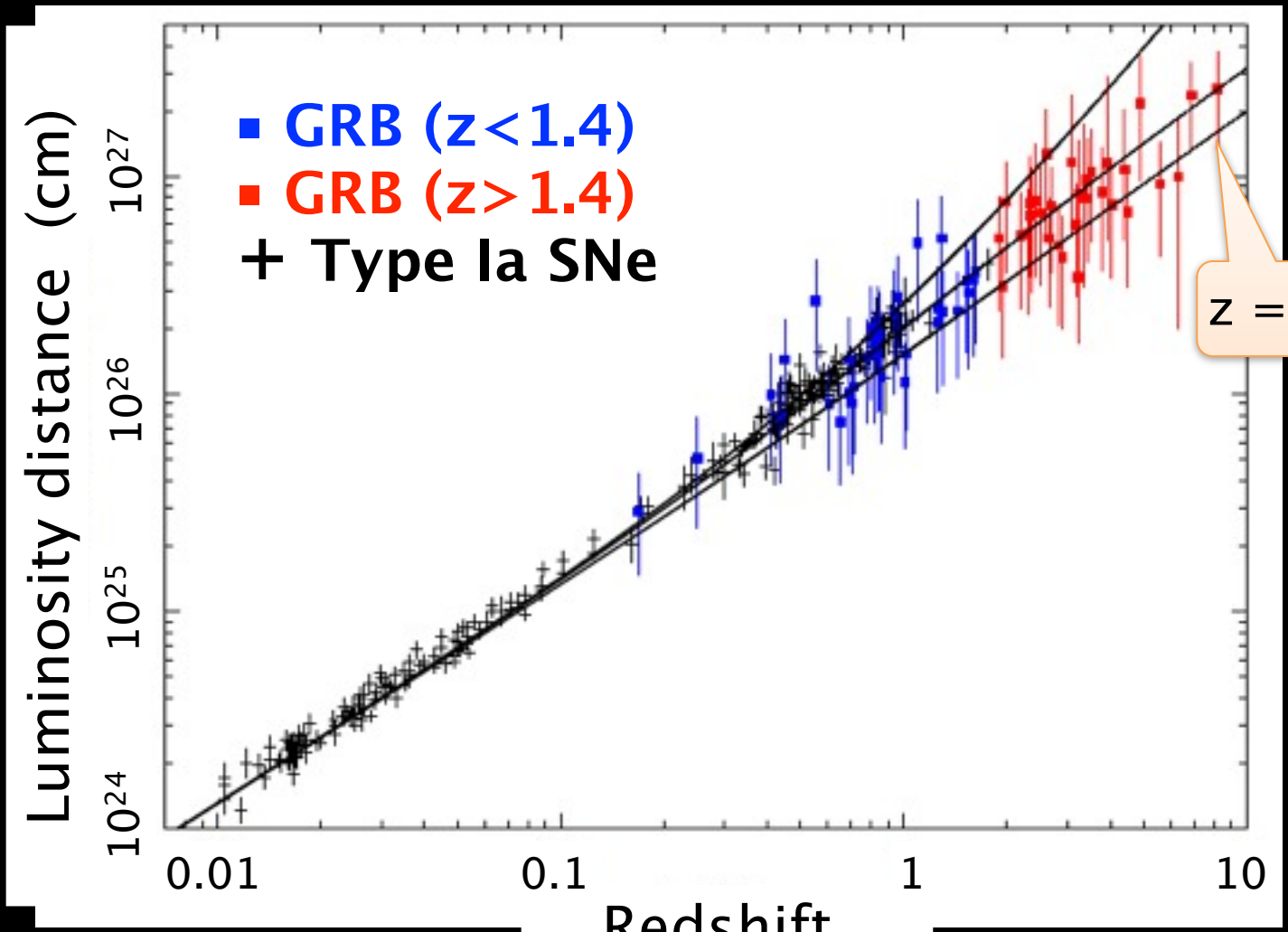

Kodama, RT + 2008

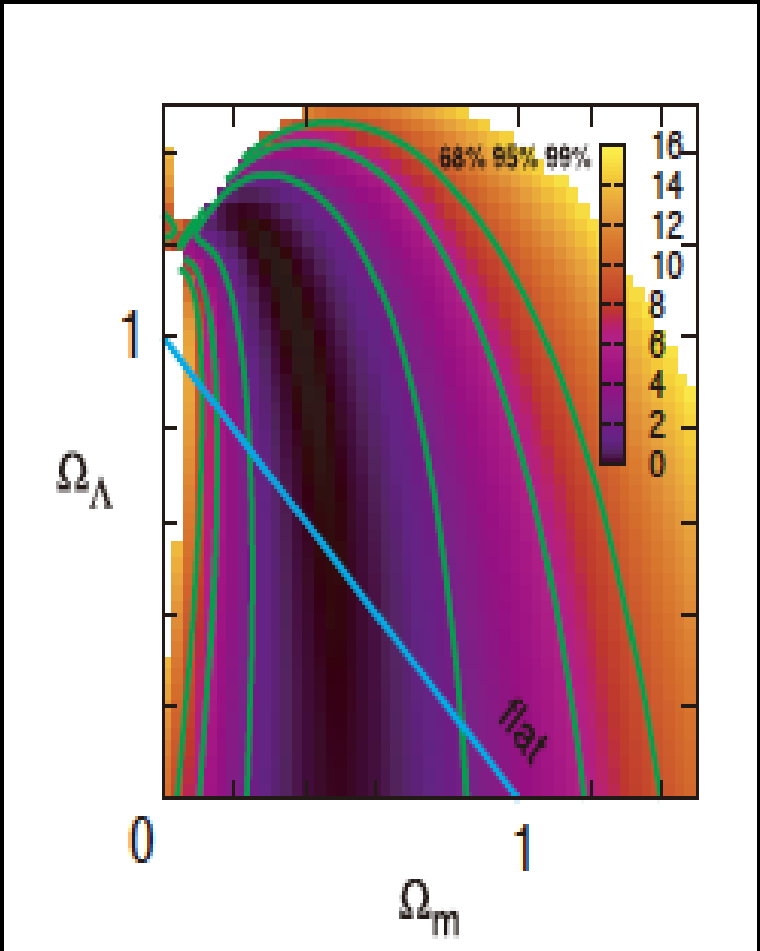

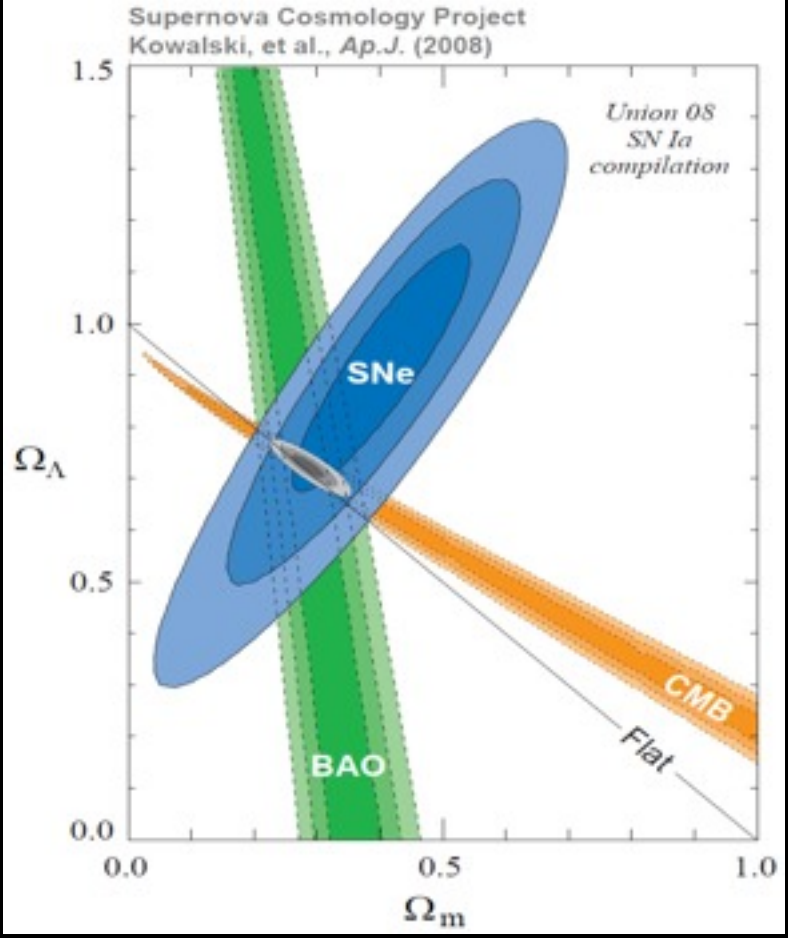

Major origin of error

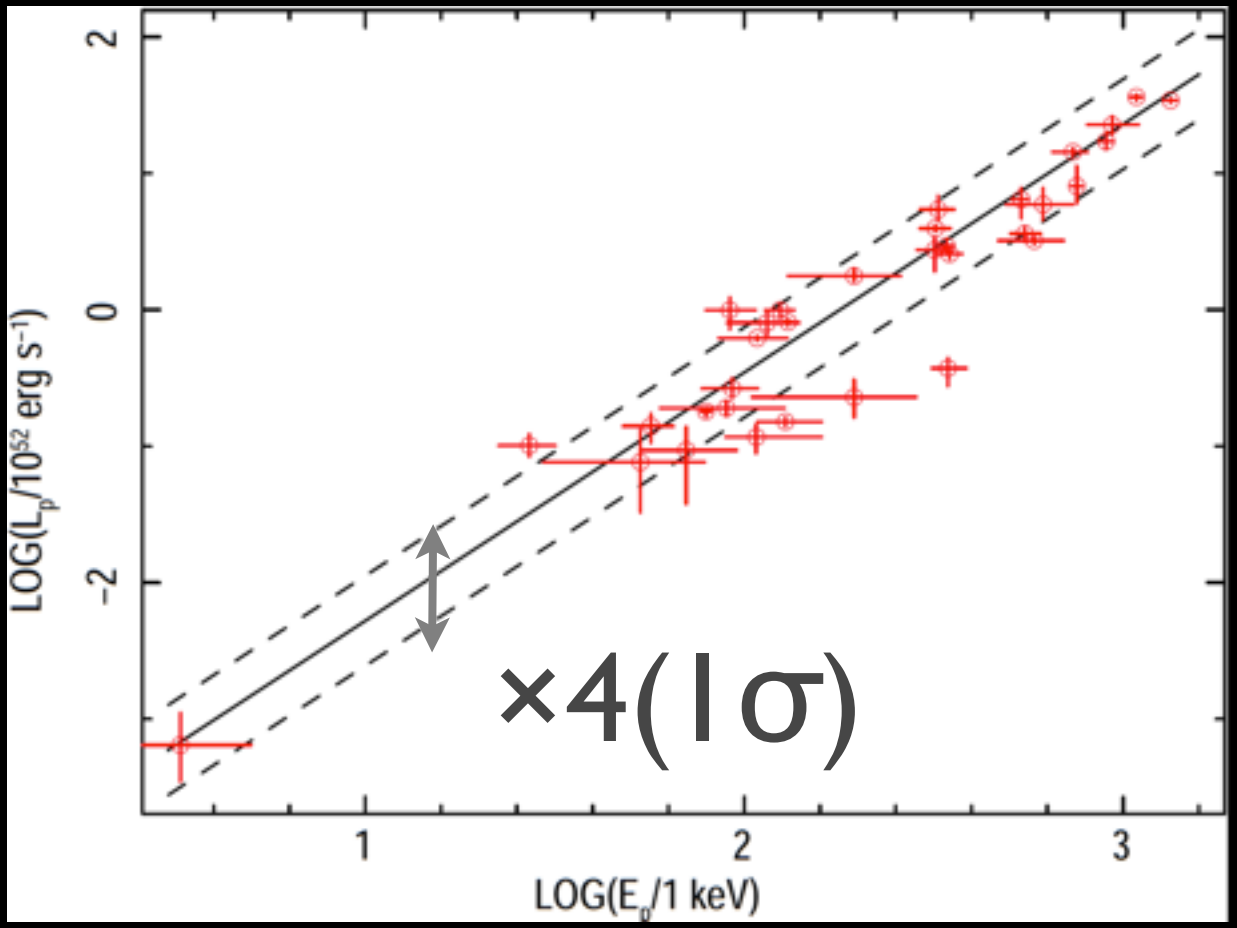

The upper dashed line is 4 times brighter than the lower one.
This means that we have two times uncertainty in distance measurement with Ep-Lp relation.

What means “Four times”

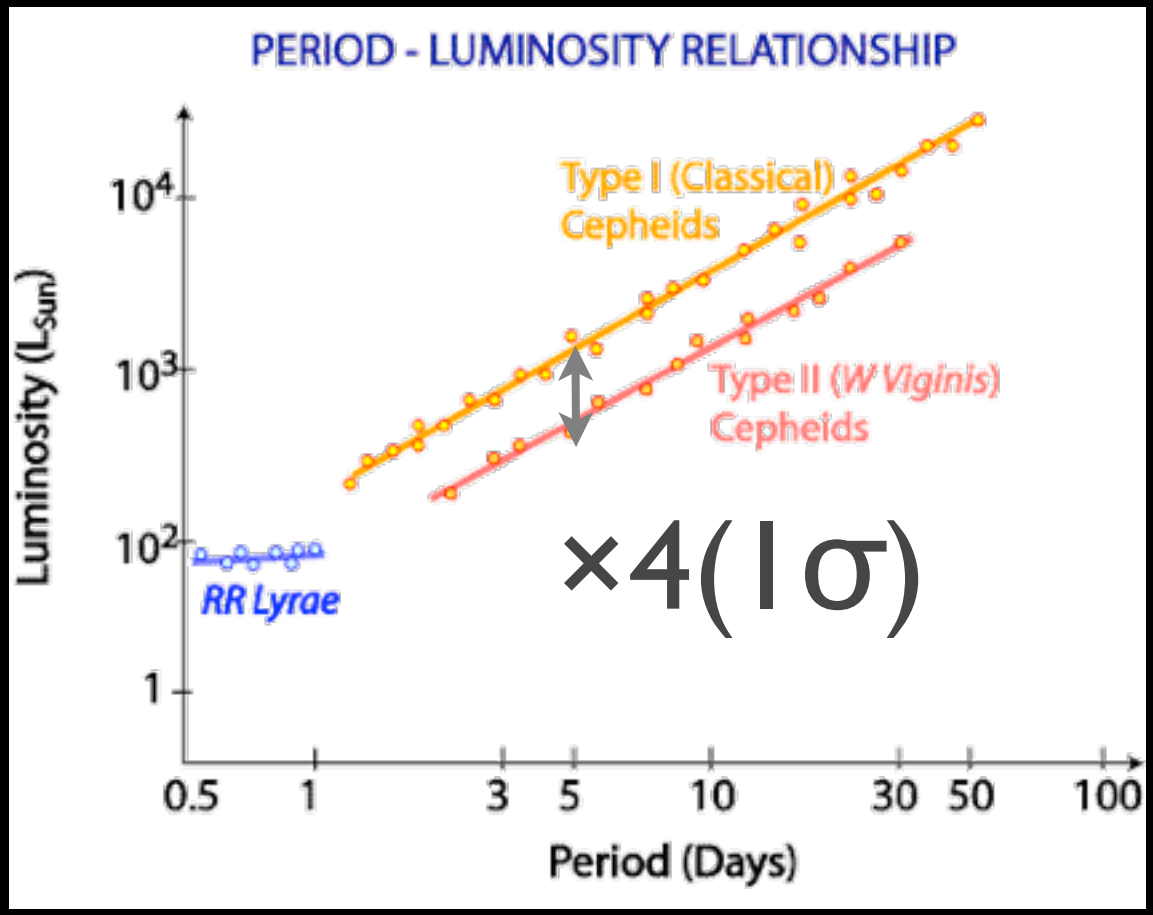

The difference between two P-L relations for Cepheid is comparable with dispersion of the Ep-Lp relation for long GRBs.

Result of the classification of Cepheid variable

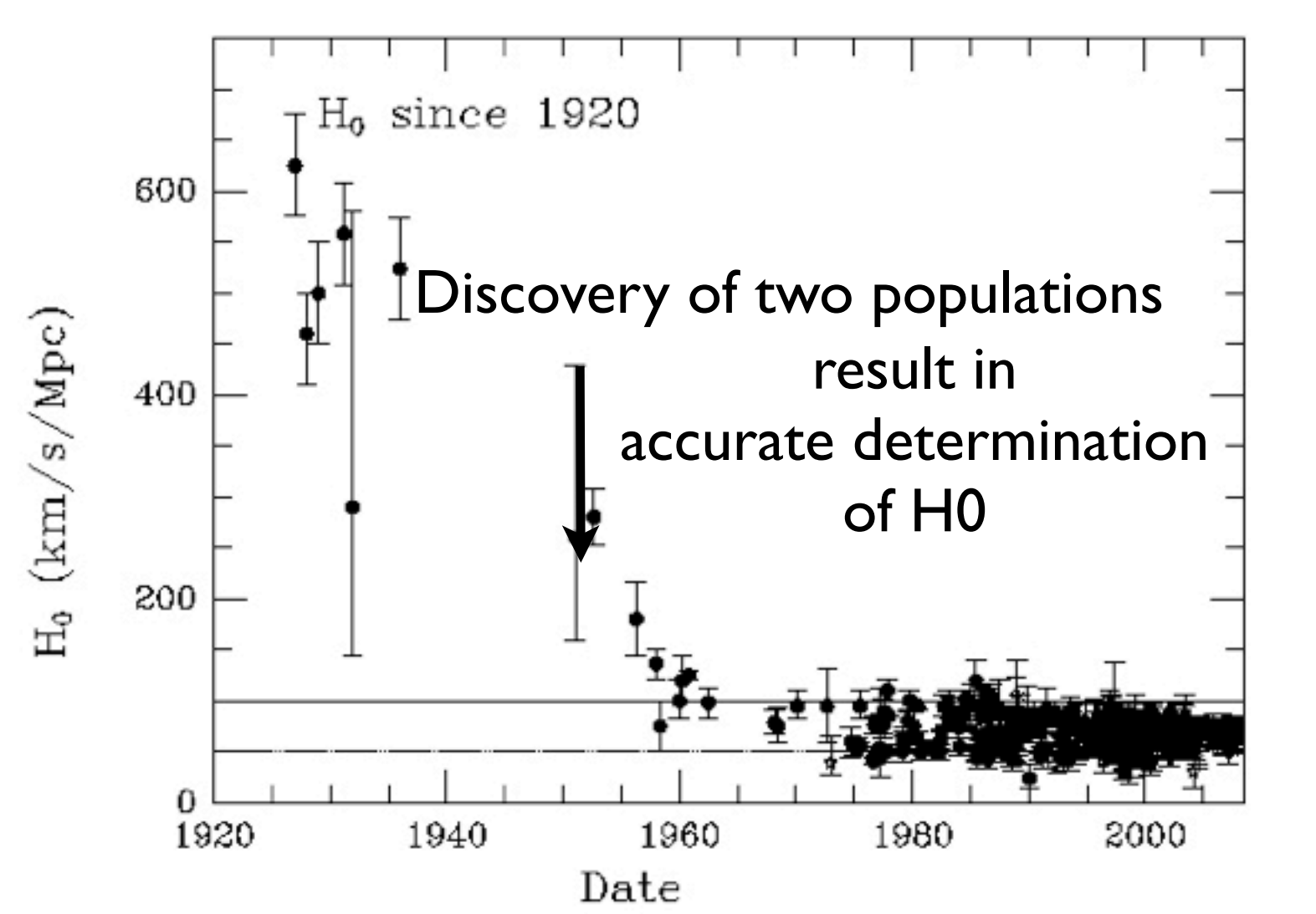

Clues for the existence of sub-classes of long GRBs I

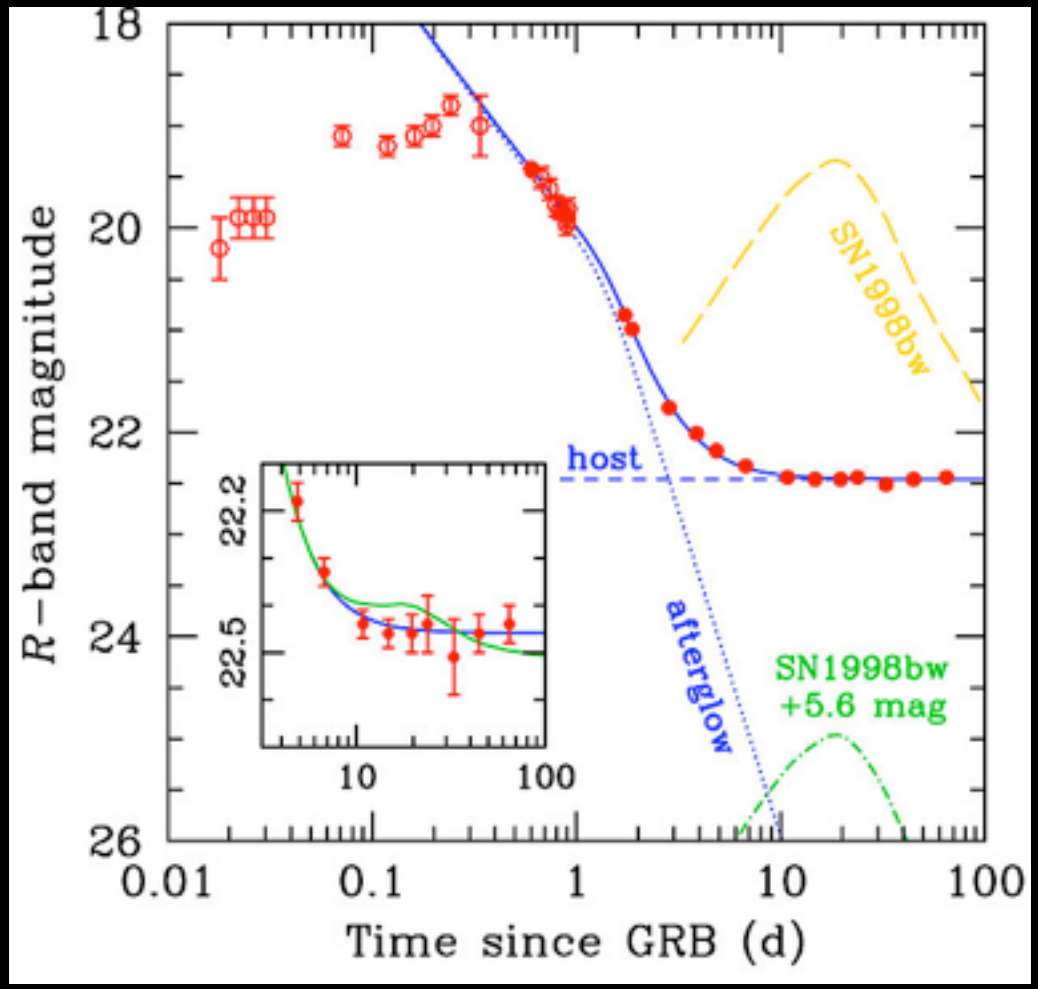

Some long GRB are associated with Type Ic SN, but some does not. These events may result in sub structure in the Ep-Lp relation.

Clues for the existence of sub-classes for long GRBs II

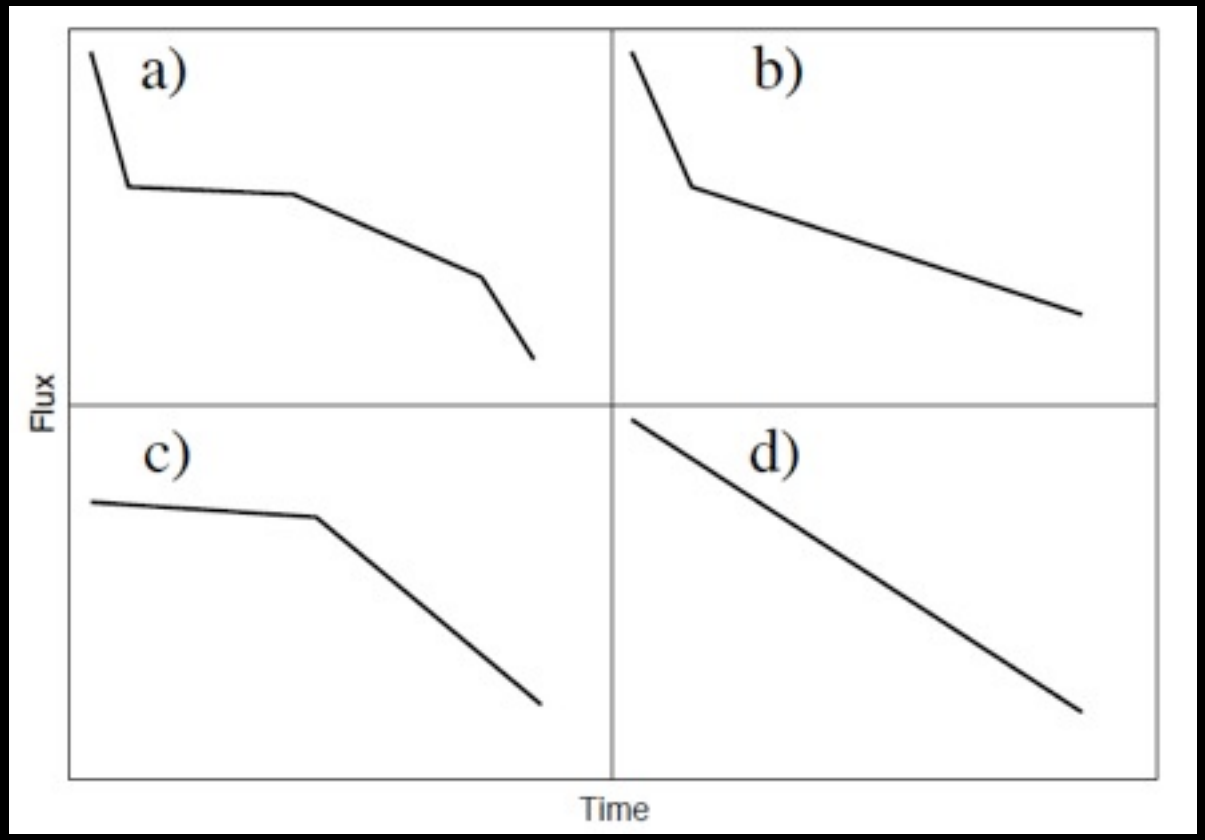

Diversity of X-ray AG light curve ($t \sim 100\text{-}10^6$ sec)

The most difficult problem which GRB study is facing. This suggests that there are some populations of long GRB.

Table of Contents

- Brief introduction of gamma-ray bursts
- previous works and problems for distance measurements with gamma-ray bursts
- Their improvements and future prospects

Toward accurate candles

- The use of accurate data.
- Redefinition of Lp in GRB rest frame time.
- The use of robust statistics and outlier rejection
- The second parameter : $T_L=E_{iso}/L_p$

Yonetoku, RT, + PASJ, 2010
RT, + PASJ, 2011

Two separate populations of long GRBs

RT. PASJ in press

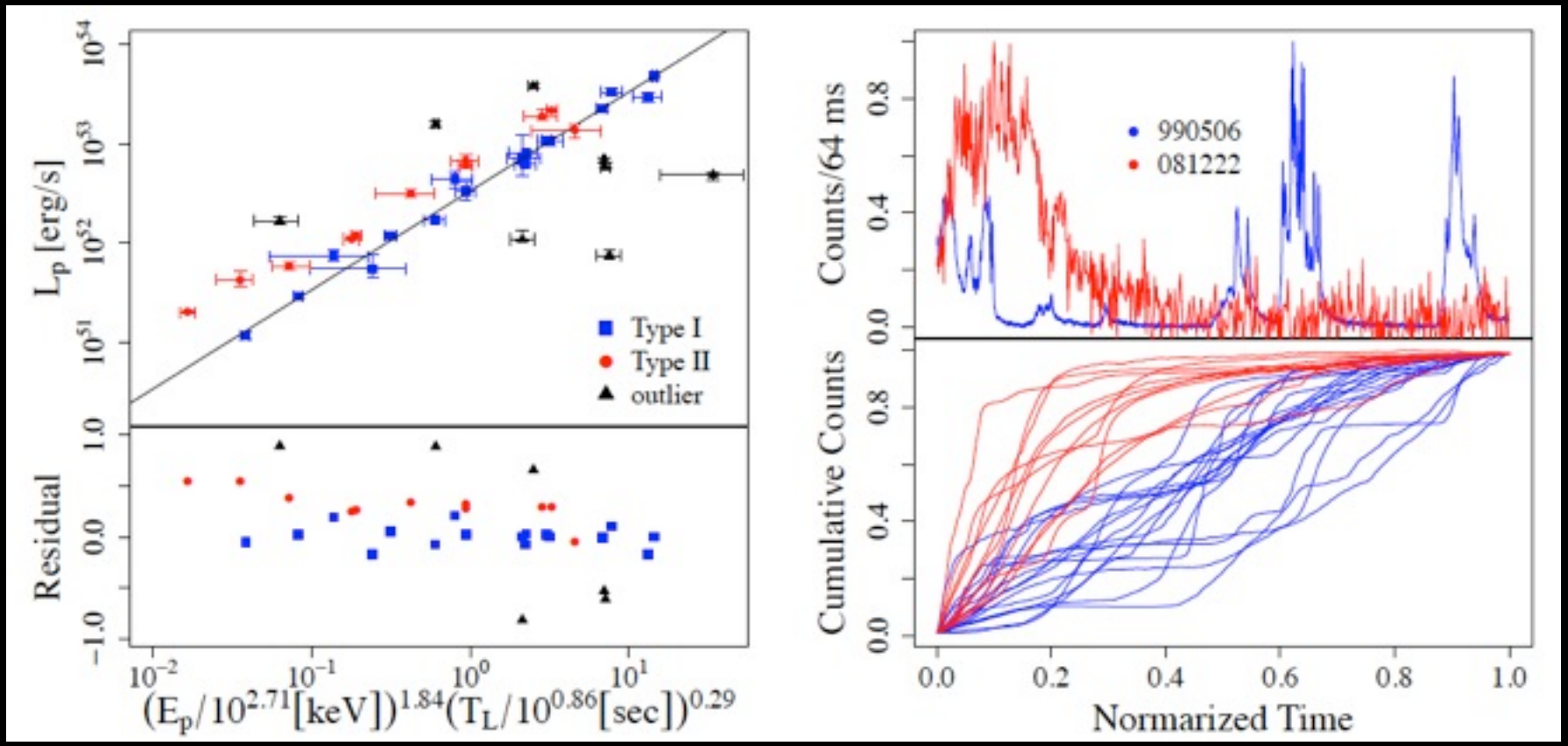

$T_L = E_{iso}/L_p$

Prompt-afterglow connection

Preliminary

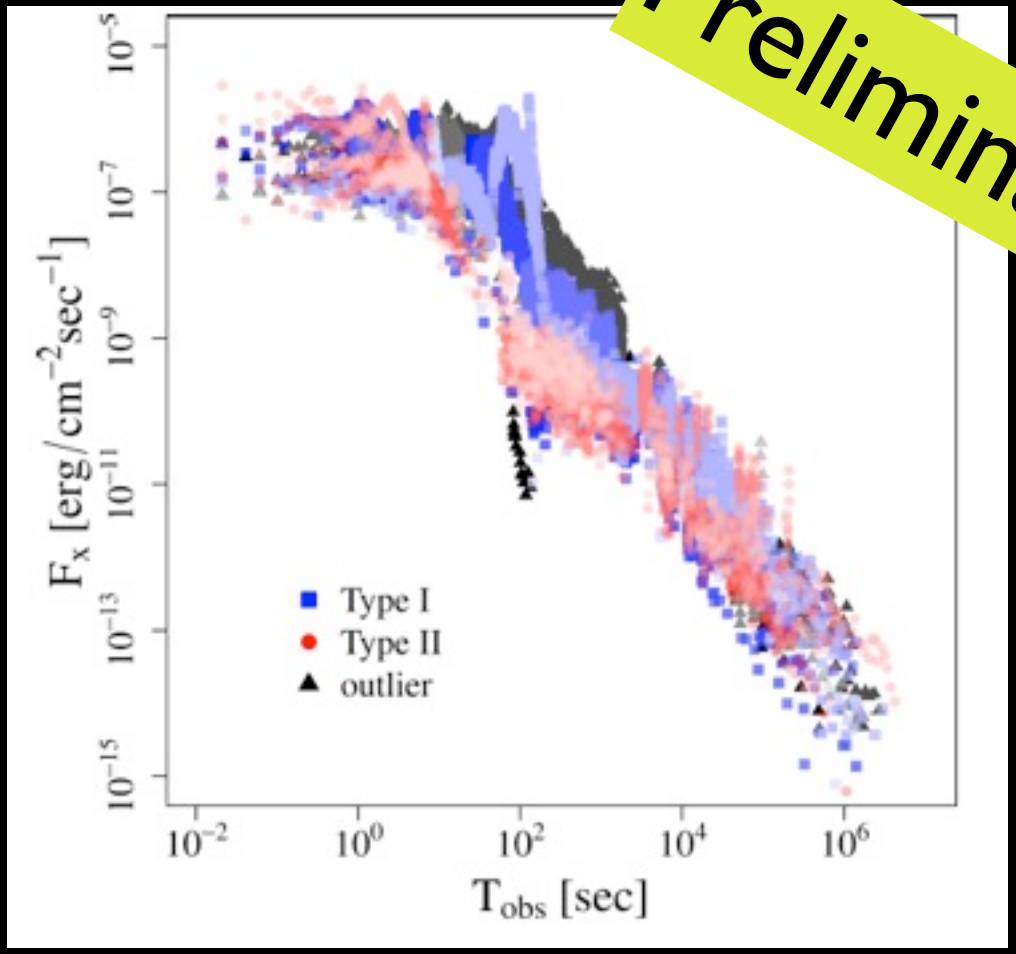

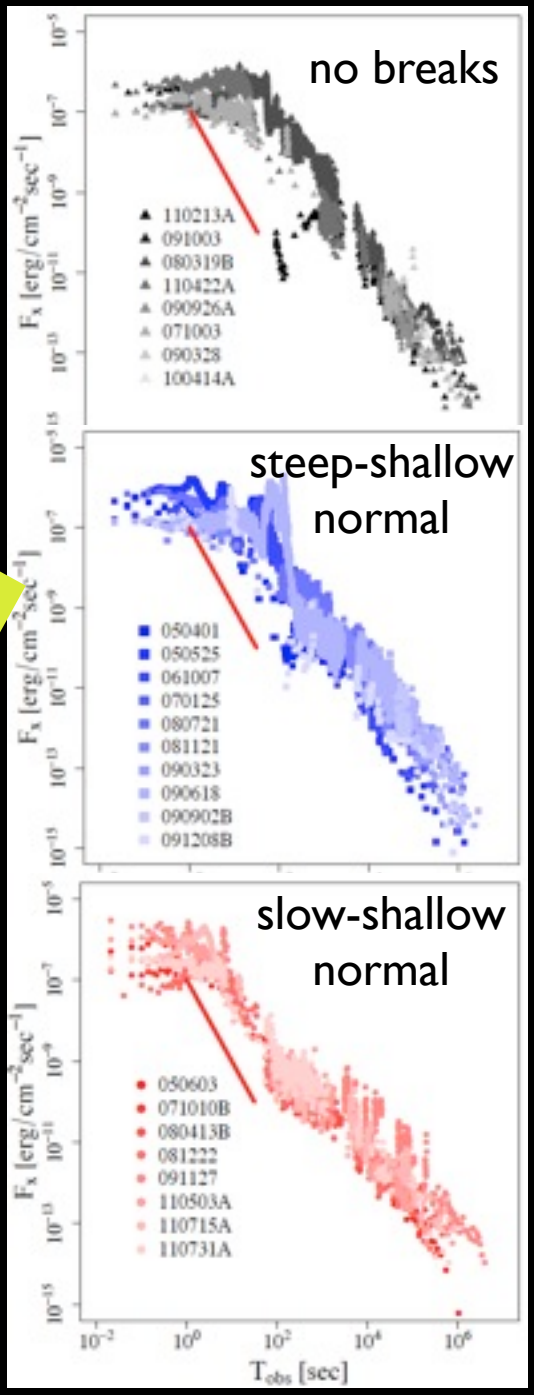

A new scaling law of Type II long GRBs

Preliminary

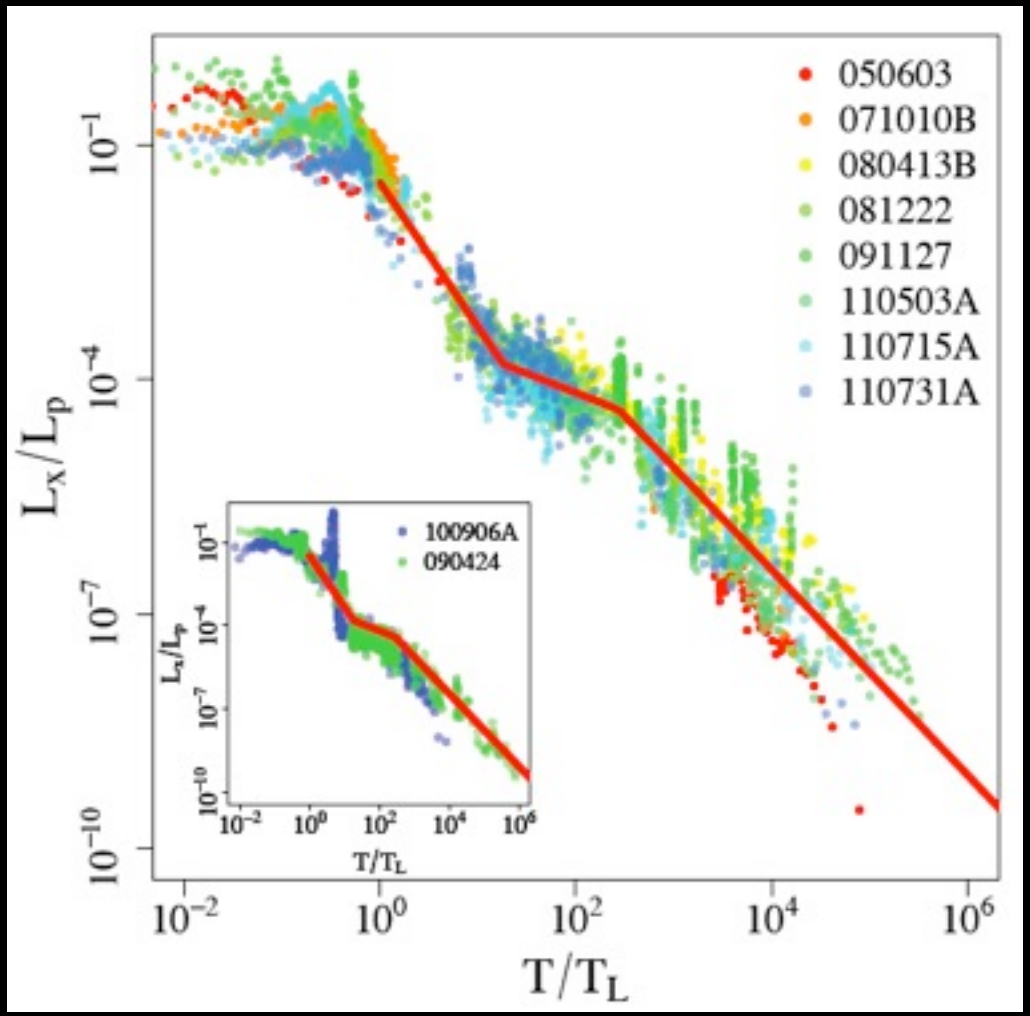

Division into sub classes reveals a beautiful scaling law of Type II long GRBs. This relation implies a universal mechanism which governing both of prompt and afterglow emissions.

Two separate populations of long GRBs

RT. PASJ in press

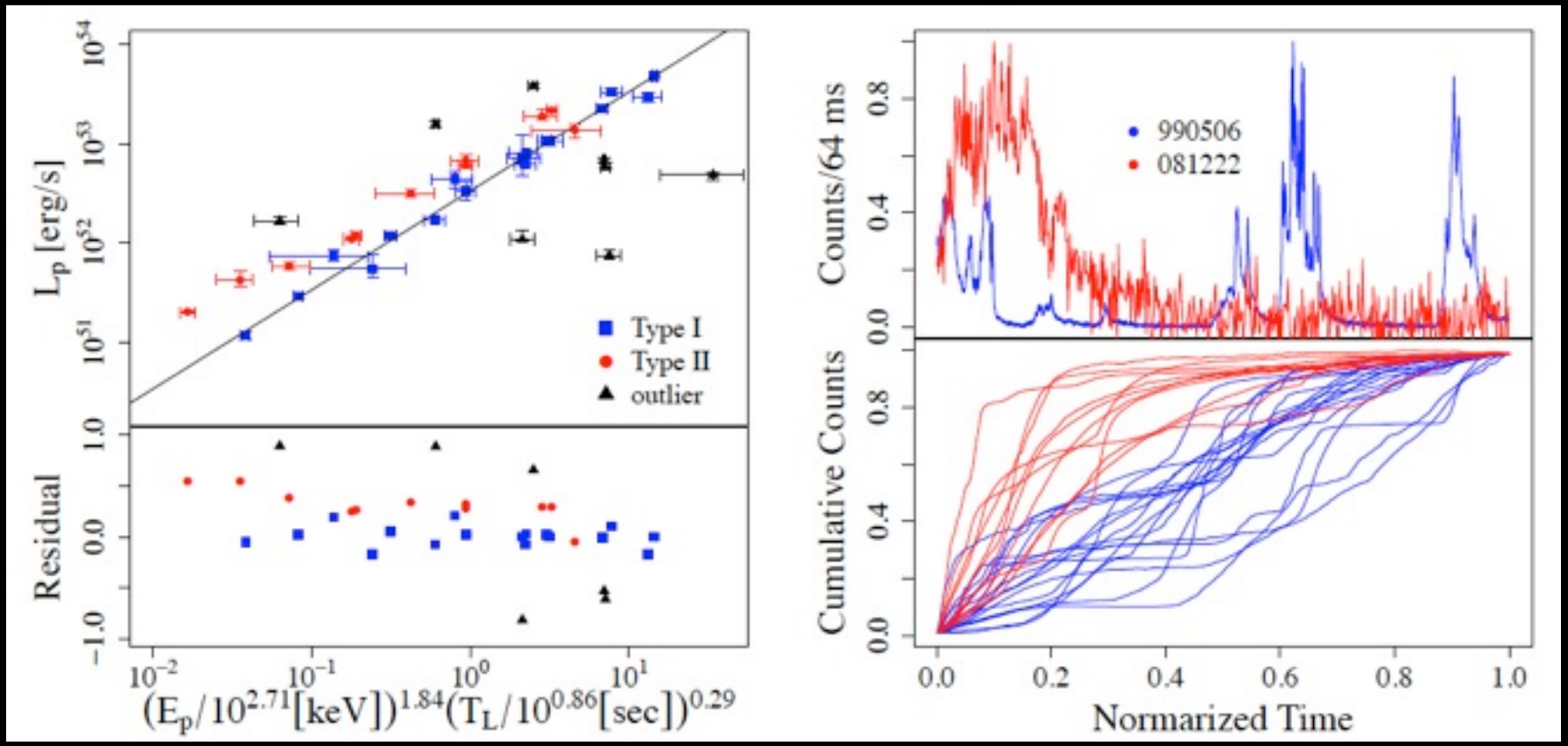

$T_L = E_{iso}/L_p$

Hubble diagram for Type I long GRBs

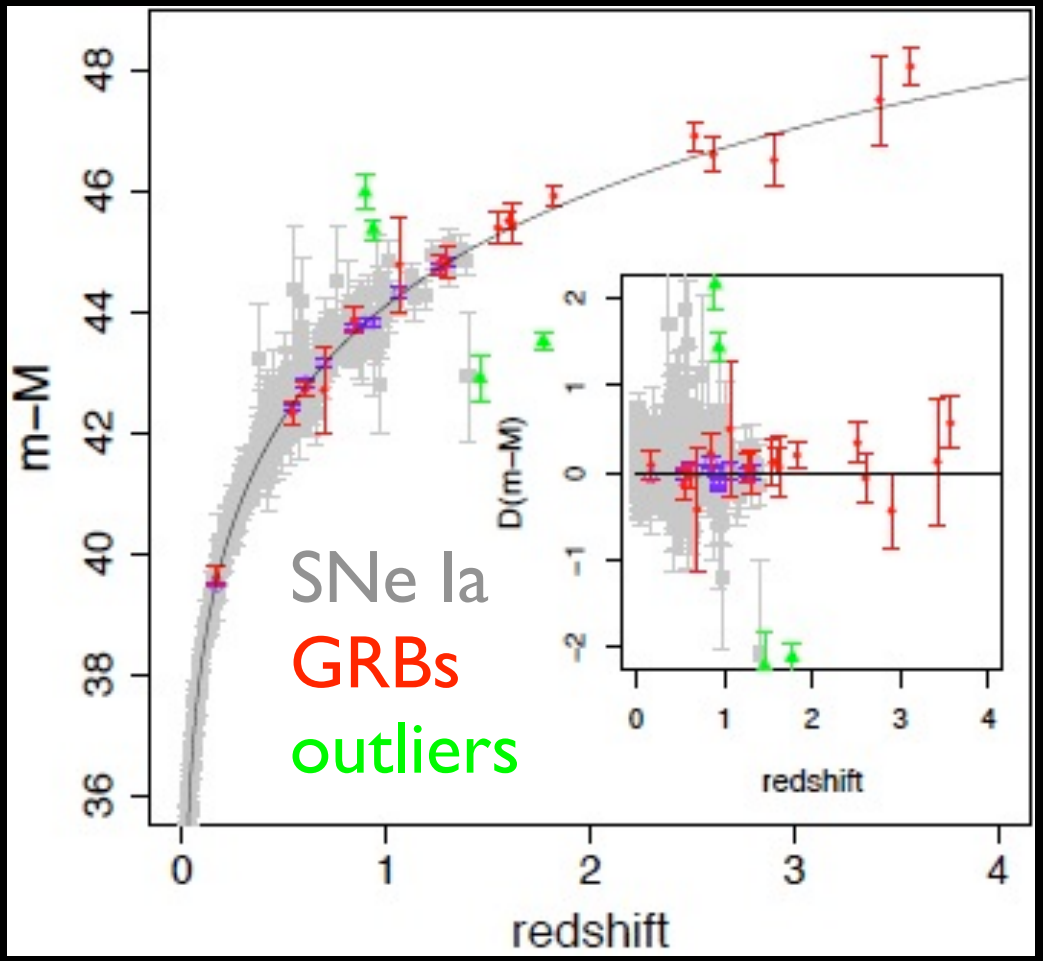

$(\Omega_m, \Omega_\Lambda) = (0, 1)$

$$\bar{\sigma}_{\mu,\mathrm{GRBs}} = 0.31$$

$$\bar{\sigma}_{\mu,\mathrm{SNeIa}} = 0.26$$

The error of LGRBs becomes as small as those of SNe Ia.

Constraint from Type I long GRBs

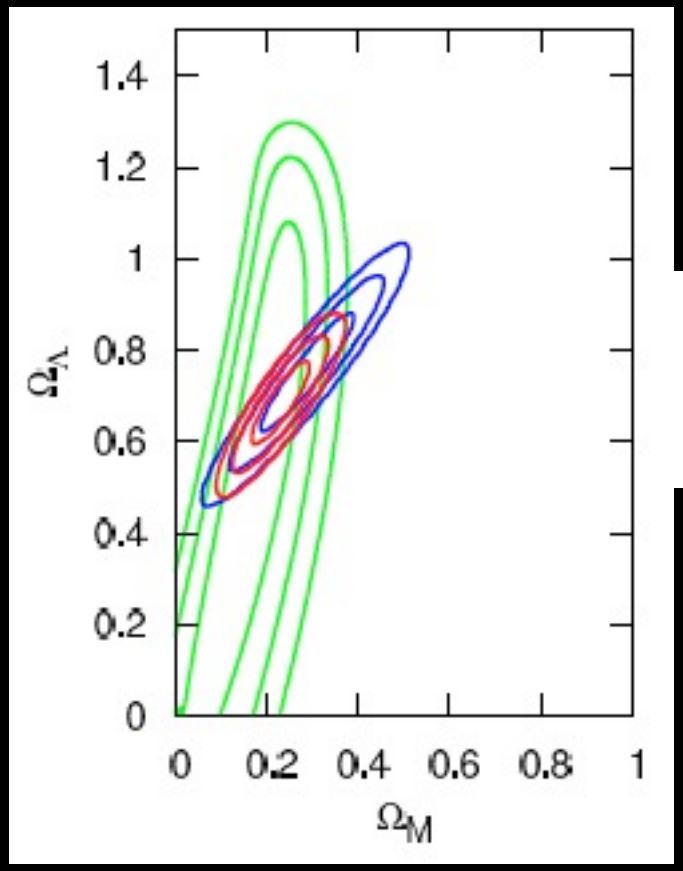

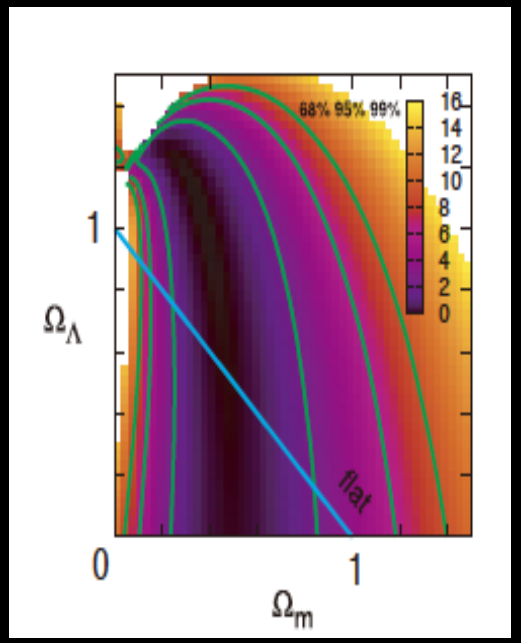

	Ω_M	Ω_Λ	χ^2/d.o.f
9 LGRBs (flat)	0.22 ± 0.04	-	5.09/7
557 SNe Ia (non-flat)	0.29 ± 0.10	0.76 ± 0.13	542.1/555
Combined (non-flat)	0.23 ± 0.06	0.68 ± 0.08	548.3/564

Future mission

HiZ-GUNDAM (High-z Gamma-ray bursts for Unraveling the Dark Ages Mission)

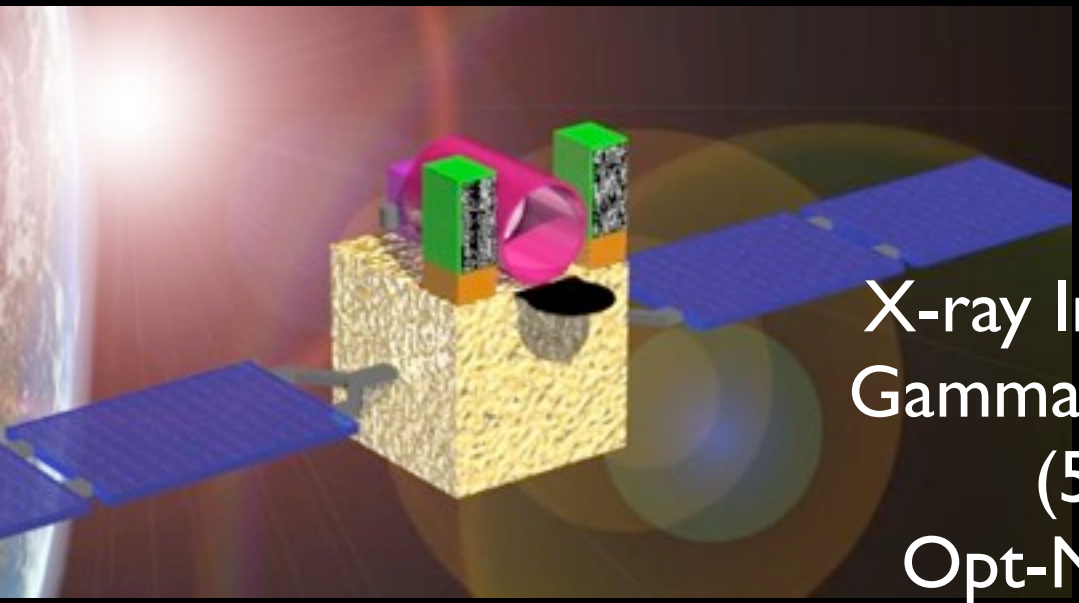

X-ray Imager (4-100keV)
Gamma-ray spectrometer
(50-1000keV)
Opt-NearIR Telescope
(0.3-1.7μm)

80 events/year (40 events for cosmology?)

Hubble diagram for Type I long GRBs

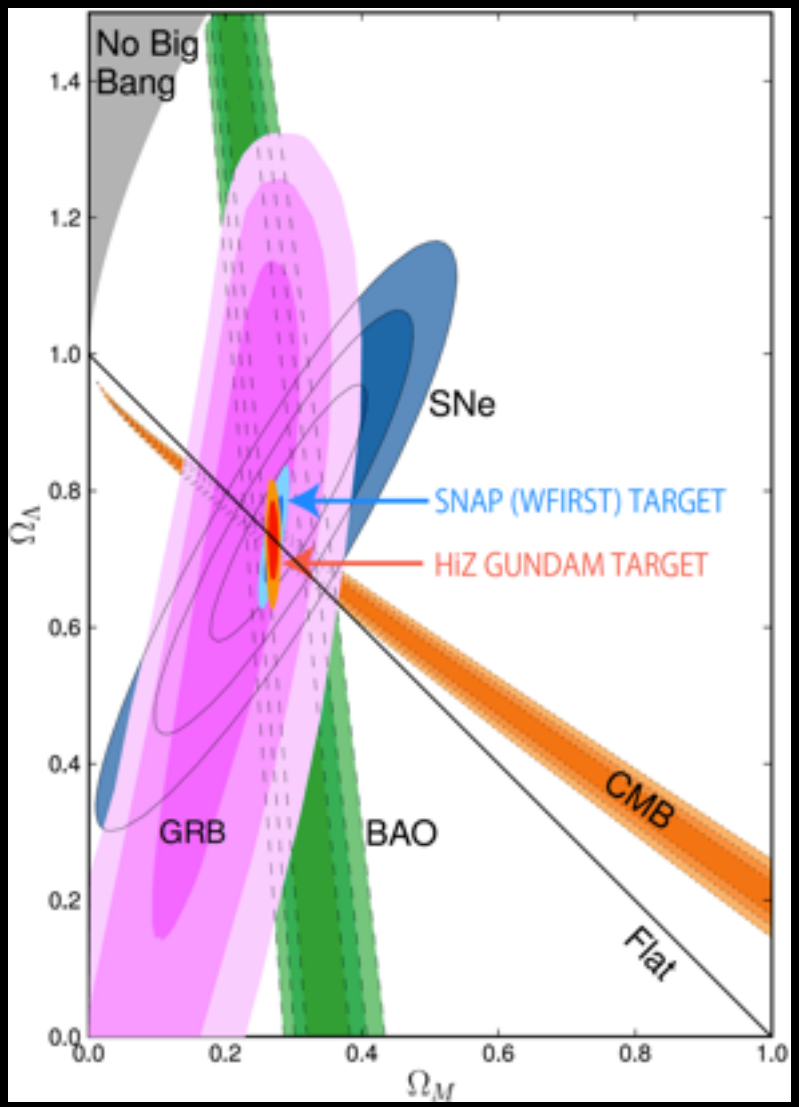

$\sigma_{\Omega m} \sim 0.01$ for 100 Type I long GRBs.

GUNDAM @ ODAIBA



Hi-Z GUNDAM Project has nothing to do with a famous japanese animation GUMDAM

If you go to Odedo-onsen by subway and monorail, you can find big gundam from monorail.

Summary

- We have found sub classes of long GRBs.
- Division into two classes drastically improve accuracy of distance measurement.

Two distinct spectral model

BAND model

$$f_{\rm BAND}(E) = \begin{cases} A\left(\frac{E}{100}\right)^{\alpha} \exp\left[-\frac{E(2+\alpha)}{E_{\rm peak}}\right], & E < E_c, \\ A\left[\frac{(\alpha-\beta)E_{\rm peak}}{100(2+\alpha)}\right]^{\alpha-\beta} \exp(\beta-\alpha)\left(\frac{E}{100}\right)^{\beta}, & E \geq E_c, \end{cases}$$

Cut off power law model

$$f_{\rm COMP}(E) = A\left(\frac{E}{E_{\rm piv}}\right)^{\alpha} \exp\left[-\frac{E(2+\alpha)}{E_{\rm peak}}\right].$$

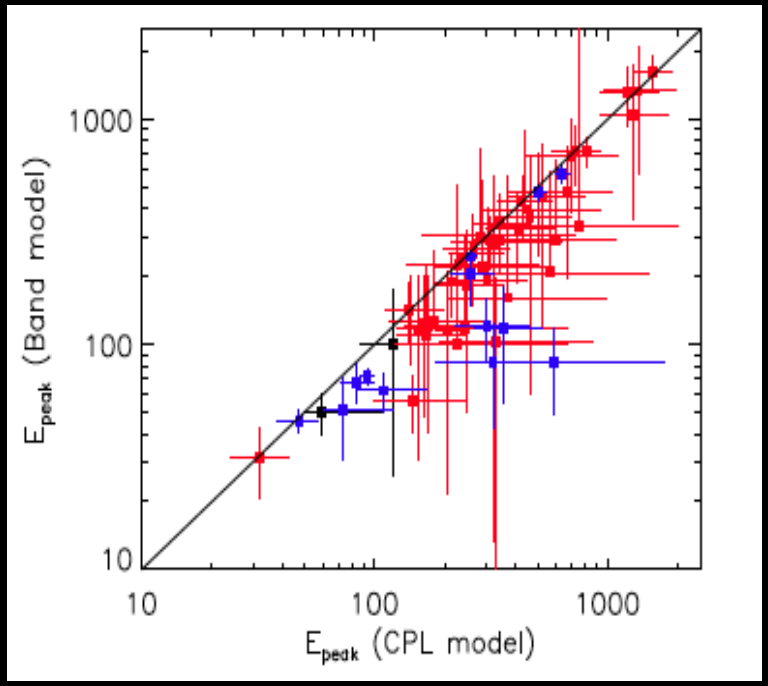

CPL Ep is alway higher than Band Ep

How to define Lp

1 sec in observer frame
→2.7 sec in GRB rest fram

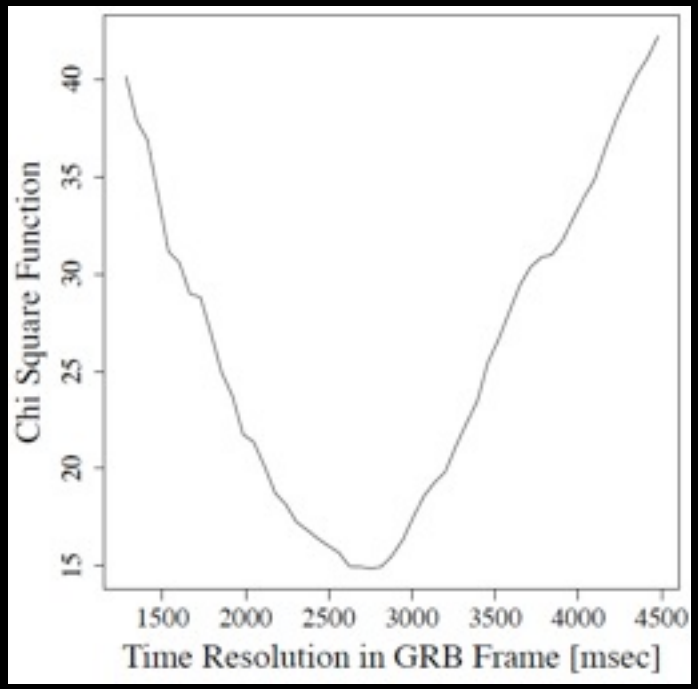

$\tau \approx 2.7$ sec is the best resolution for Lp

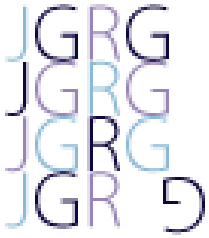

Yousuke Itoh, JGRG 22(2012)111306

"Stacking of cluster profiles"

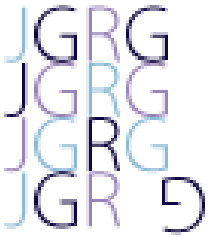

RESCEU SYMPOSIUM ON

GENERAL RELATIVITY AND GRAVITATION

JGRG 22



November 12-16 2012

Koshiba Hall, The University of Tokyo, Hongo, Tokyo, Japan





KAGRA

STACKING CLUSTERS

Yousuke Itoh

RESCEU, University of Tokyo

In Collaboration with T. Narikawa & Y. Suto

22nd workshop on General Relativity and Gravitation in Japan, RESCEU symposium, 2012 Sep. 12-16 @ University of Tokyo

In this talk…

1. Introduction
2. Universality of NFW?
3. Introduce the Hough transform as a semi-non-parametric method for the purpose 2.

Introduction

- One big mystery in astronomy: late time accelerated expansion of the universe.

$$\frac{1}{a}\frac{d^2a}{dt^2} > 0$$

- Possible solutions: Modified gravity or new form of matter (or …).

$$G = 8\pi\,(T_{ordinary} + T_{new})$$

or

$$G + \delta G = 8\pi\, T_{ordinary}$$

Introduction (cont'd)

- Assume modified gravity. It should coincide with the Newtonian grav. at smaller scale.

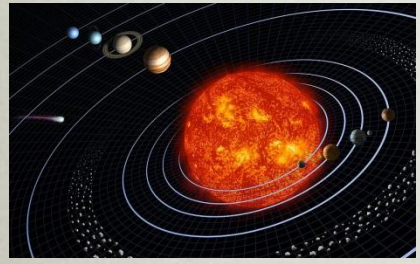

Small scale:
Solar system test.
Newtonian or GR.

Transition

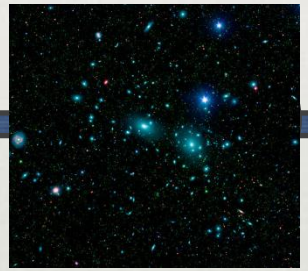

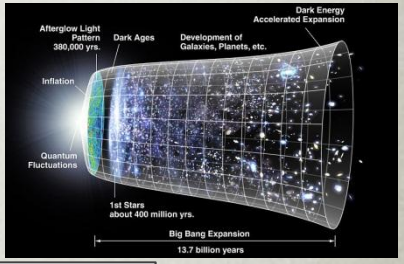

Large scale:
Acceleration.
Modified Gravity.

New test of modified gravity

Narikawa & Yamamoto (2012).
Narikawa's talk Wednesday afternoon for details.

- At the cluster of galaxies scale, scalar degrees of freedom may be apparent through, e.g., gravitational lensing.

$$\kappa \simeq \frac{f_K(\chi_S - \chi_L) f_K(\chi_L)}{f_K(\chi_S)} \int_0^{\chi_S} d\chi' \left[4\pi G \rho(r') - \frac{\alpha + 2\xi}{2} \frac{\triangle}{a_L^2} \varphi \right] a_L^2$$

Convergence = dimensionless surface mass density

Conventional part. Assuming NFW, gNFW, or Einasto.

Effect of Scalar dof

New test of modified gravity (cont'd)

Narikawa & Yamamoto (2012).
Narikawa's talk Wednesday afternoon for details.

- In principle, it seems work…, but.

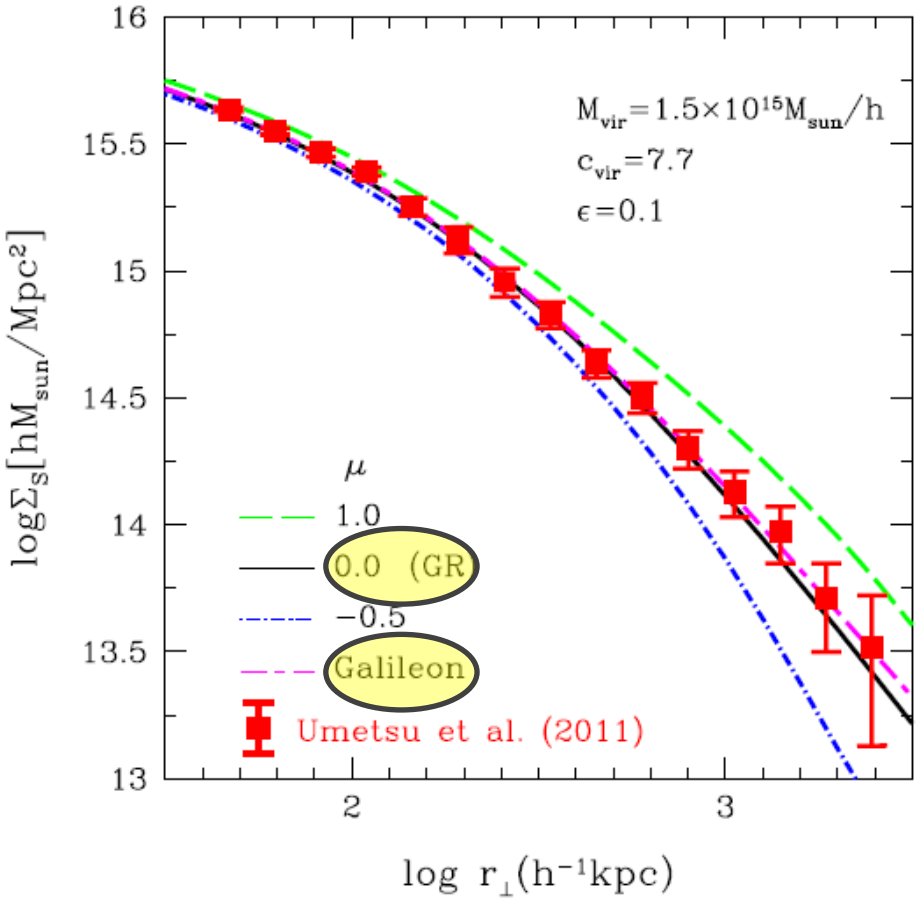

Difference between the galileon gravity and GR is very small.

Need a sufficiently accurate measurement of the cluster profile.

Stacking clusters of galaxies

- **Need a sufficiently accurate measurement of the cluster profile.**
- **Stacking many signals from clusters.**
  - **Averaging out "personalities" of clusters. (asymmetry, clumps, environment, …)**
- **Subtlity:**
  - **Even if the NFW (or other) is universal, it contains scaling radius/density.**

After all, is NFW really universal?

Reminder: NFW

- NFW: Navarro, Frenk & White ApJ (1996).
- ``Universal'' profile of a dark matter halo around a cluster of galaxies.

$$\rho(r) = \frac{\rho_s}{(r/r_s)(1+r/r_s)^2}$$

- Two parameters fimily: ρ_s and r_s
- In reality, each one may be deviated from NFW (environment, evolution history, asymmetry…).
- If stacking many $\rho(r)$'s, ...

Toy model for stacking experiment.

- NFW Cluster mass function (M_{ps} = 5x10^{14} solar masses)

$$p(>M) \propto \left(\frac{M}{M_{\rm PS}}\right)^{-1} \exp\left(-\frac{M}{M_{\rm PS}}\right)$$

- Cluster redshift distribution (z_0 = 0.45)

$$n(z)dz \propto z^2 \exp\left(-\frac{z}{z_0}\right) dz$$

- Concentration parameter (From Duffy 2011 Nbody simulation): $c = \bar{c} + \delta c$

$$\bar{c} = A(M/M_{\rm pivot})^B (1+z)^C$$

$$p(c_{200})dc_{200} = \frac{1}{\sqrt{2\pi\sigma^2_{\log_{10} c_{200}}}} \exp\left(-\frac{(\log_{10} c_{200} - \log_{10} \bar{c}_{200})^2}{2\sigma^2_{\log_{10} c_{200}}}\right) d\ln c_{200}$$

Toy model

Parameters of 100 toy NFW clusters.

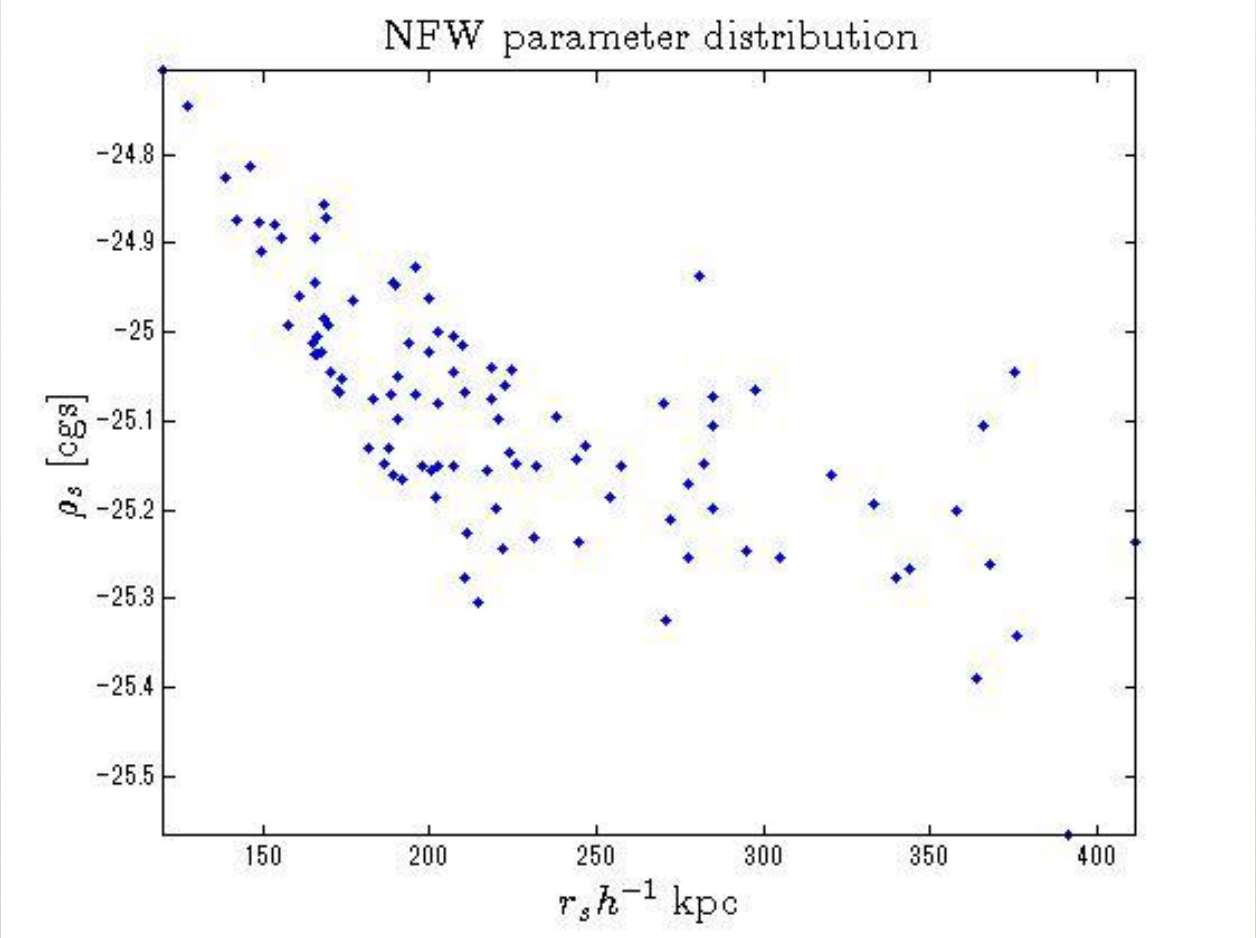

CMBCG catalogue contains over 55,000 clusters, though the number of known lensing clusters are much smaller than it at this moment….

With or Without scaling

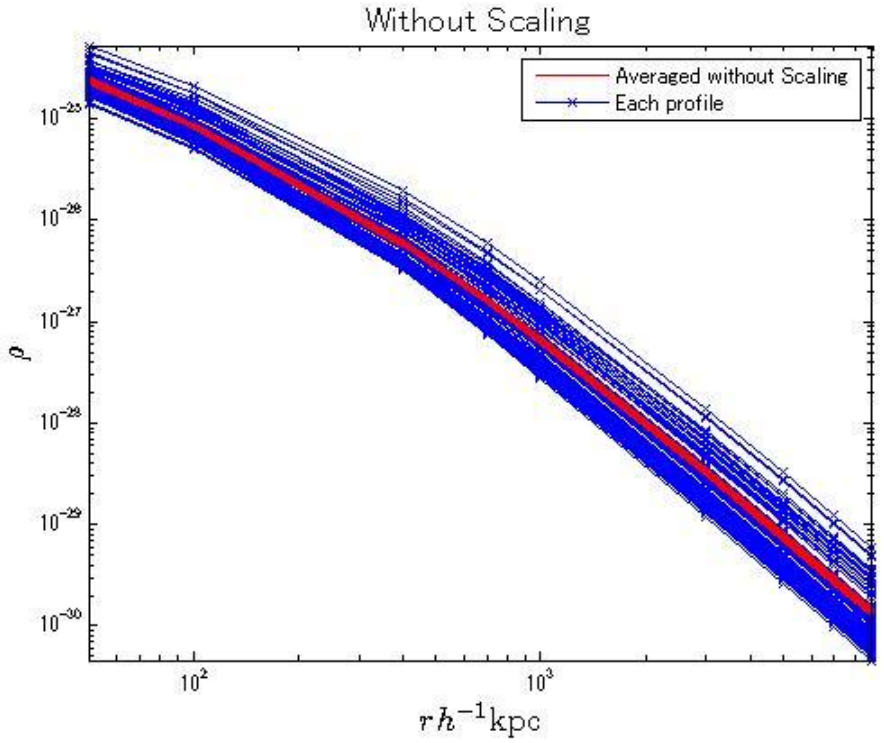

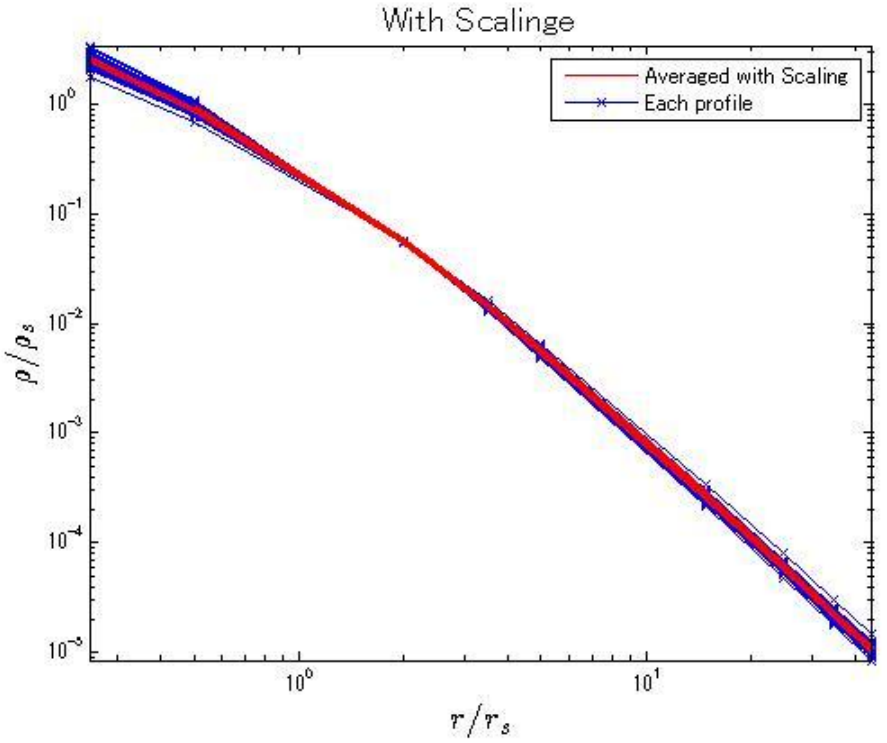

Blue: 100 cluster radial profiles (left: un-scaled, right: scaled)

Red: left: Averated, right: Scaled using true (M,$\bar{c}$) then Averaged.

$$\rho_{w.o\ scaling}(r;\ \{M_i, c_i\}_i) = \frac{1}{N}\sum_i^N \rho\ (r; M_i, c_i)$$

$$\bar{\rho}_{w\ scaling}(x; \{\delta c_i\}_i) = \frac{1}{N}\sum_i^N \frac{\rho(x\ r_{si}; M_i, \bar{c_i})}{\rho_{si}}$$

Estimating α : without noise.

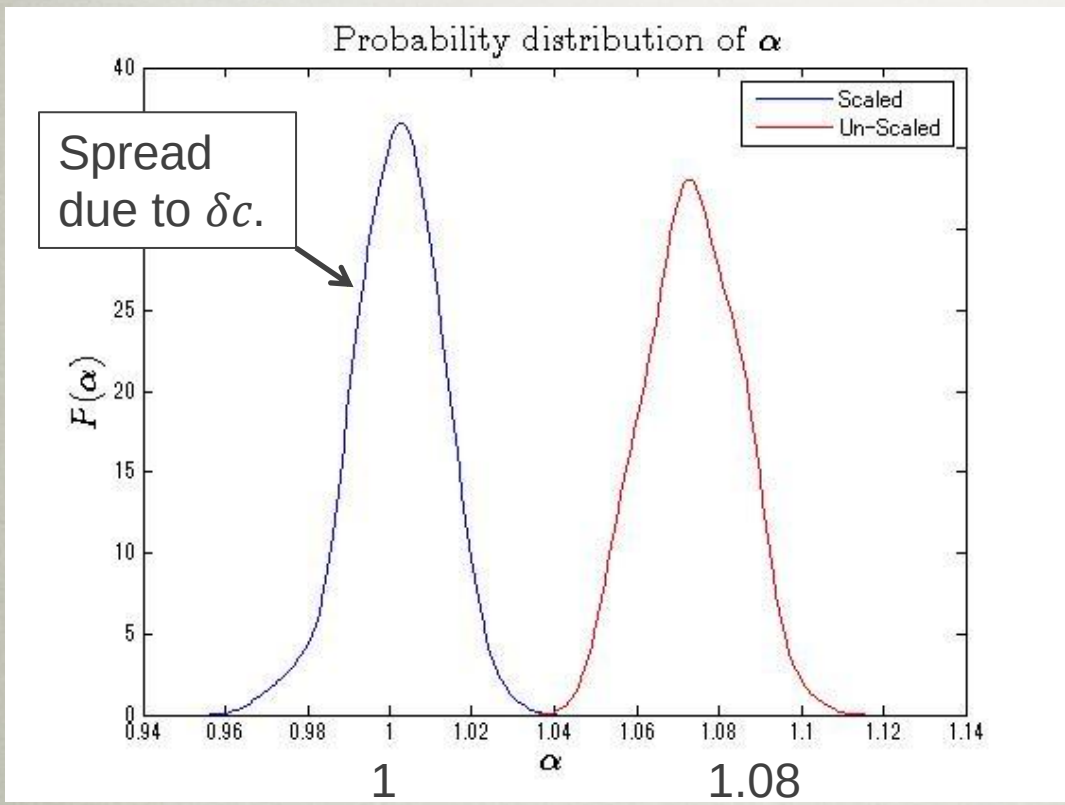

We estimate the inner power index α using 25 clusters and do it 100 times.

$$\rho(r) = \frac{\rho_s}{(r/r_s)^{\alpha}(1+r/r_s)^{3-\alpha}}$$

Ok, just small difference…

Toy model Including noise…

- Adding noise term to the NFW radial profile.

(r_i is the inner edge of the "observed" NFW profile.)

$$\begin{aligned} \rho(r) &= \rho_{\mathrm{NFW}}(r) + \delta\rho(r), \\ \delta\rho(r) &= 0.3\rho(r_i)\left(\frac{r_i}{r}\right)^2 \zeta(r), \\ \zeta &\sim N(0,1). \end{aligned}$$

At each radal bin, random noises ζ(r) follow Gaussian distribution with mean zero and variance 1.

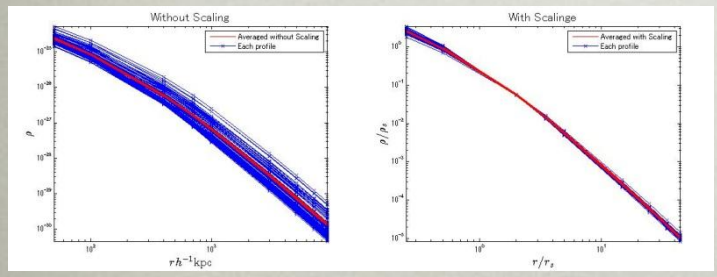

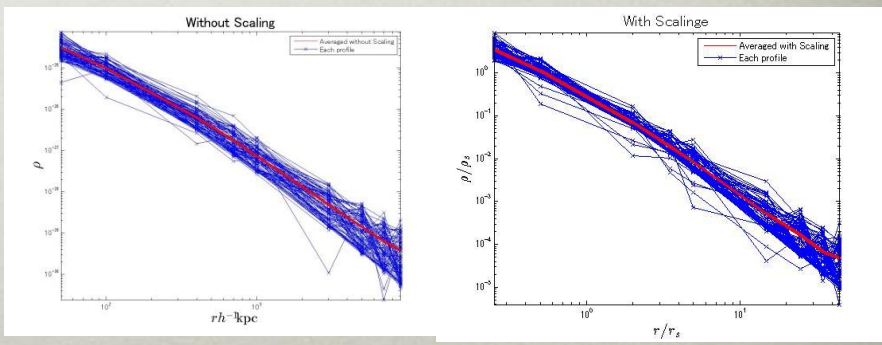

Toy model Including noise…

- Adding noise term to the NFW radial profile

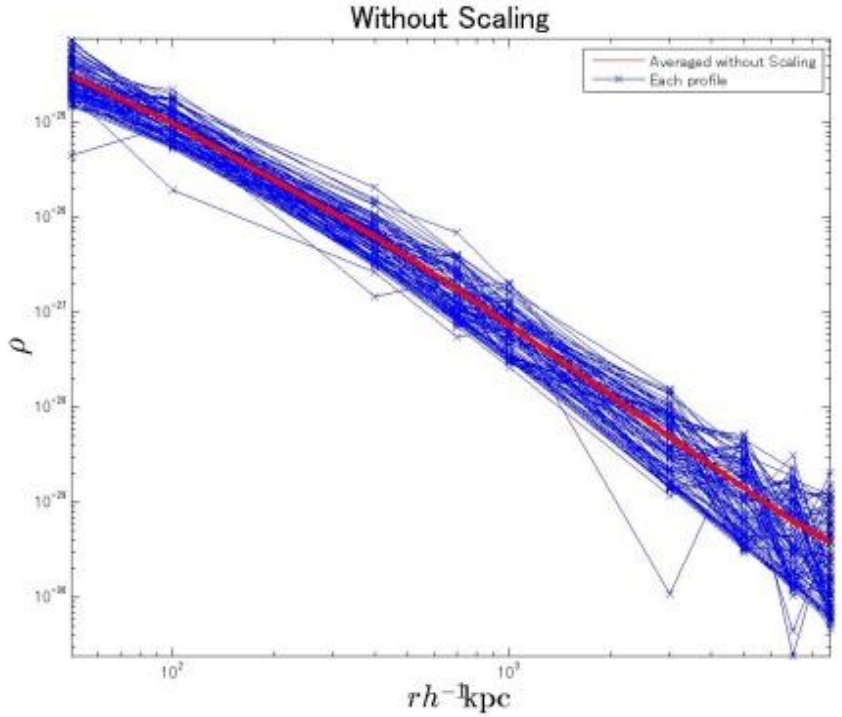

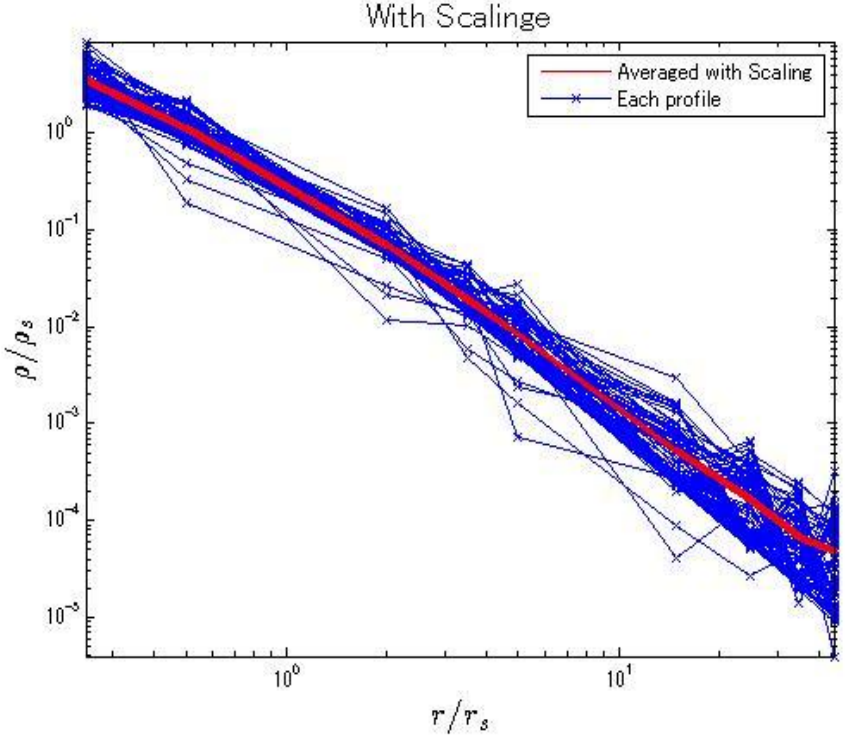

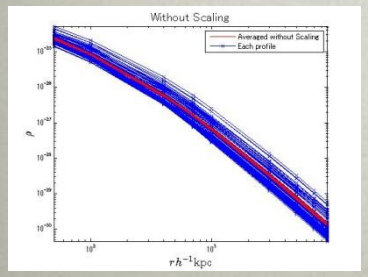

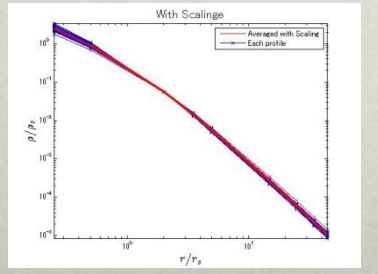



Estimating α : with noise.

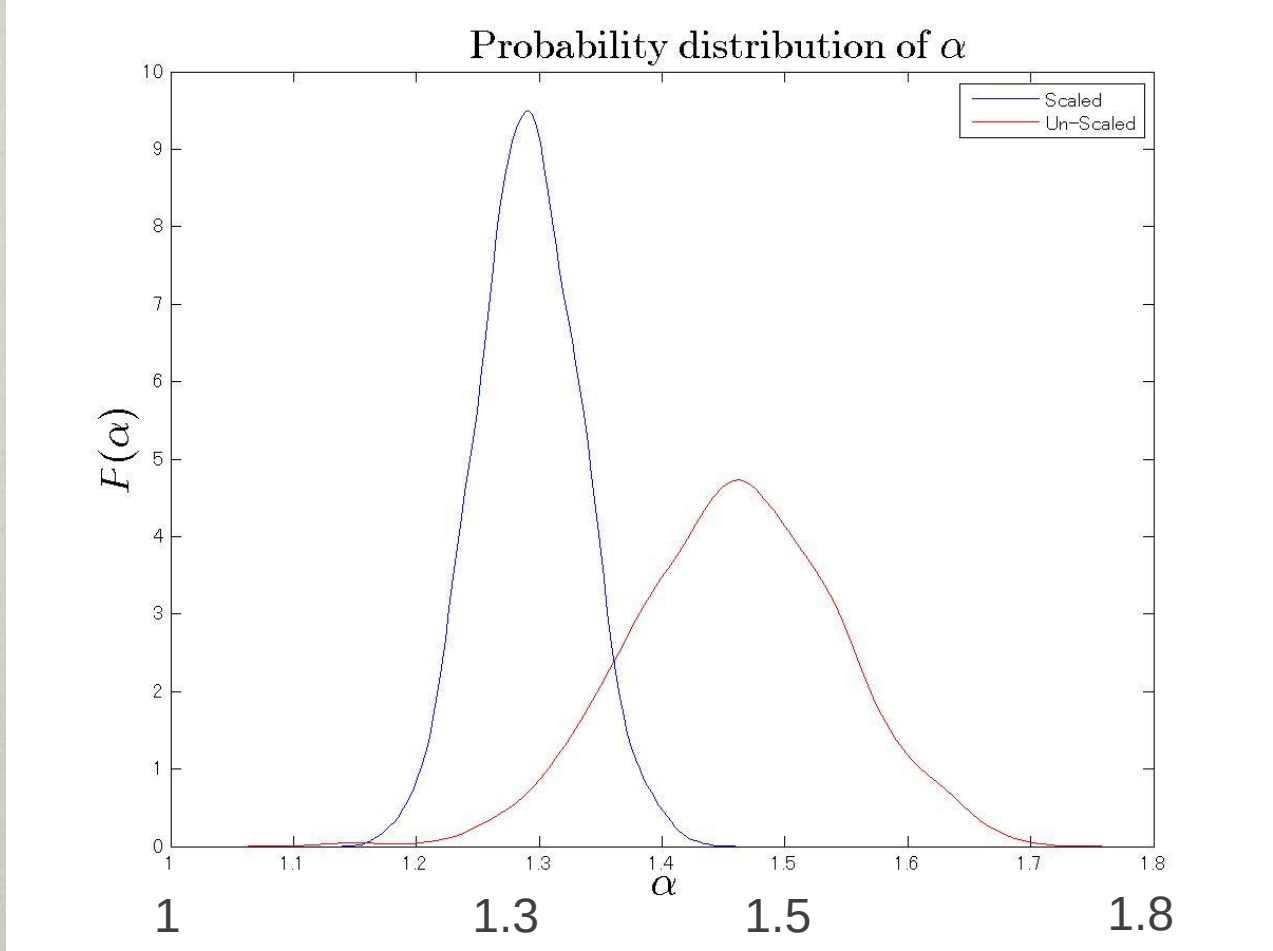

From 25 clusters estimate α, do it 1000 times.

Large bias for α from the constraint ρ(r)>0.
Noise is larger at smaller radius.

Concerns

- We do not know a priori the true NFW parameters ρ_s and r_s.
- How can we scale $\rho(r)$ if we do not know scaling parameters ρ_s and r_s?
- Estimating ρ_s and r_s for each cluster may bias results (e.g., test of modified gravity) if the NFW profile is not "the universal" profile in the first place.

Hough Transform (used in GW community as well)

- Assume a master equation $y = f(x; p_i)$ with M parameters p_i. (For explanation's sake, let's assume a curve for the master equation.)
- Given N>M pair of "data" (x_k, y_k), we obtain N curves in the M-dim param. space.
- If there is no noise, and if the master equation is correct, we get a solution as an intersection of the curves in the parameter space.
- When there is noise, there may be no solution. Yet, there may be a region where many intersections between two curves cluster.

Hough Transform (cont'd)

Straight line master eq.

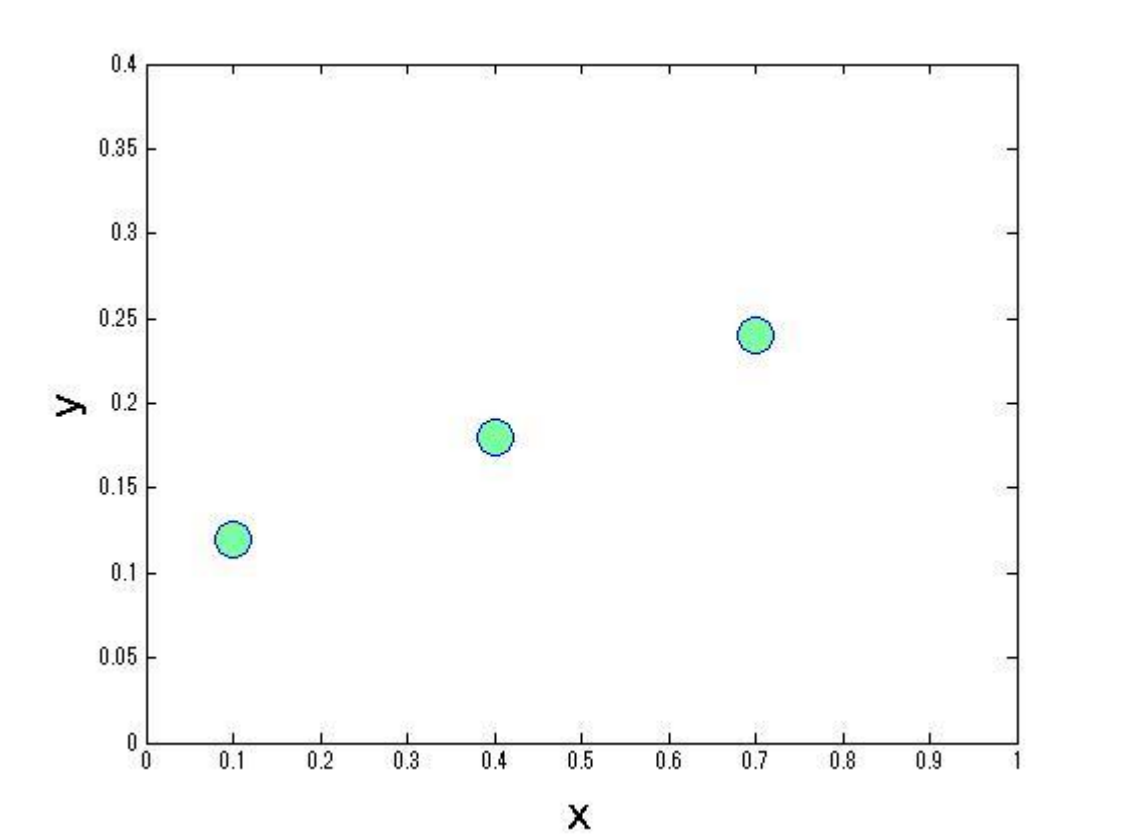

Given 3 "data".

Hough Transform (cont'd)

Straight line master eq.

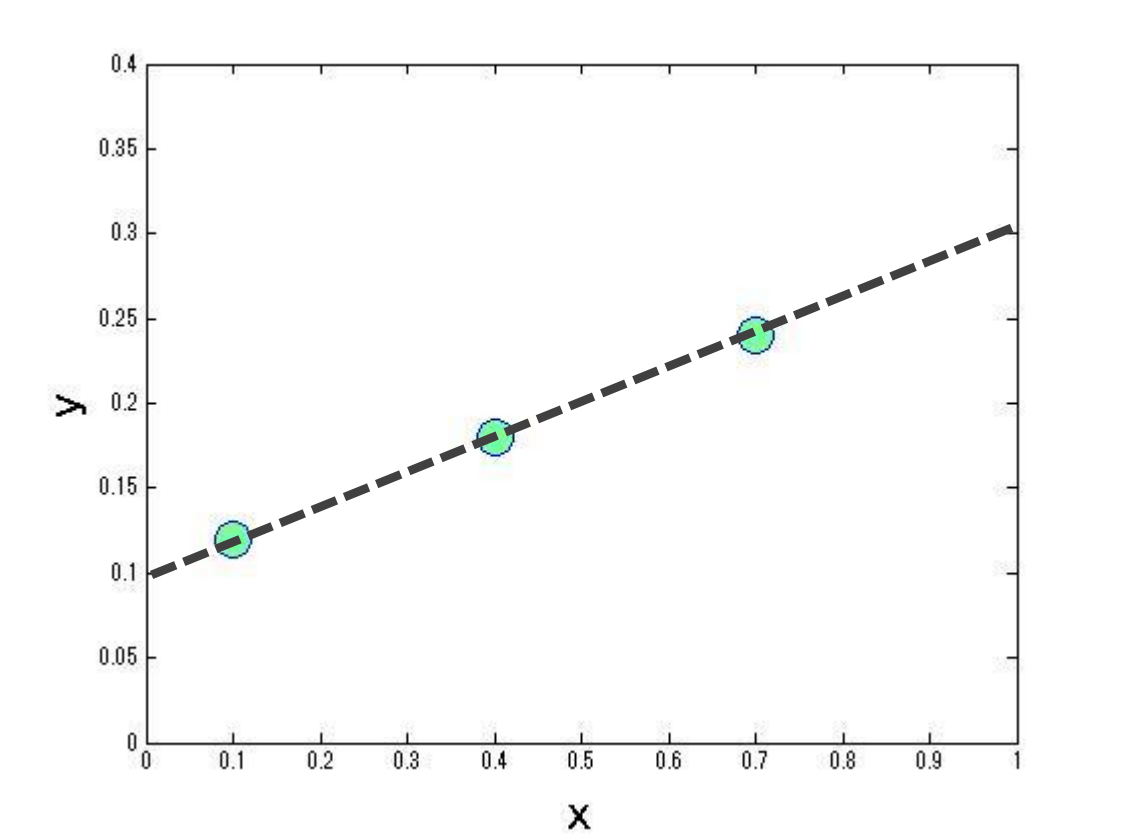

This "data" is actually on $y = 0.2\,x + 0.1$ line.

Hough Transform (cont'd)

Straight line master eq.

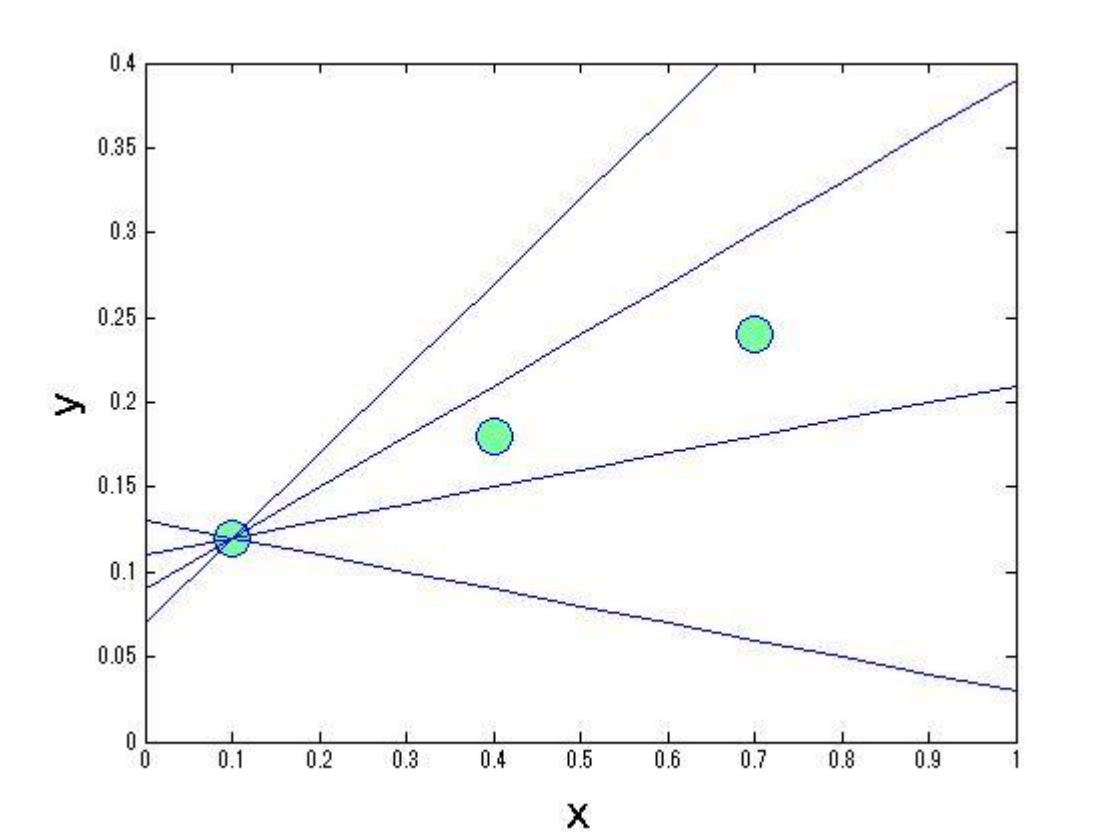

For the rightmost data, plot a master equation (straight line in this example) that pass through the data.

Hough Transform (cont'd)

Straight line master eq.

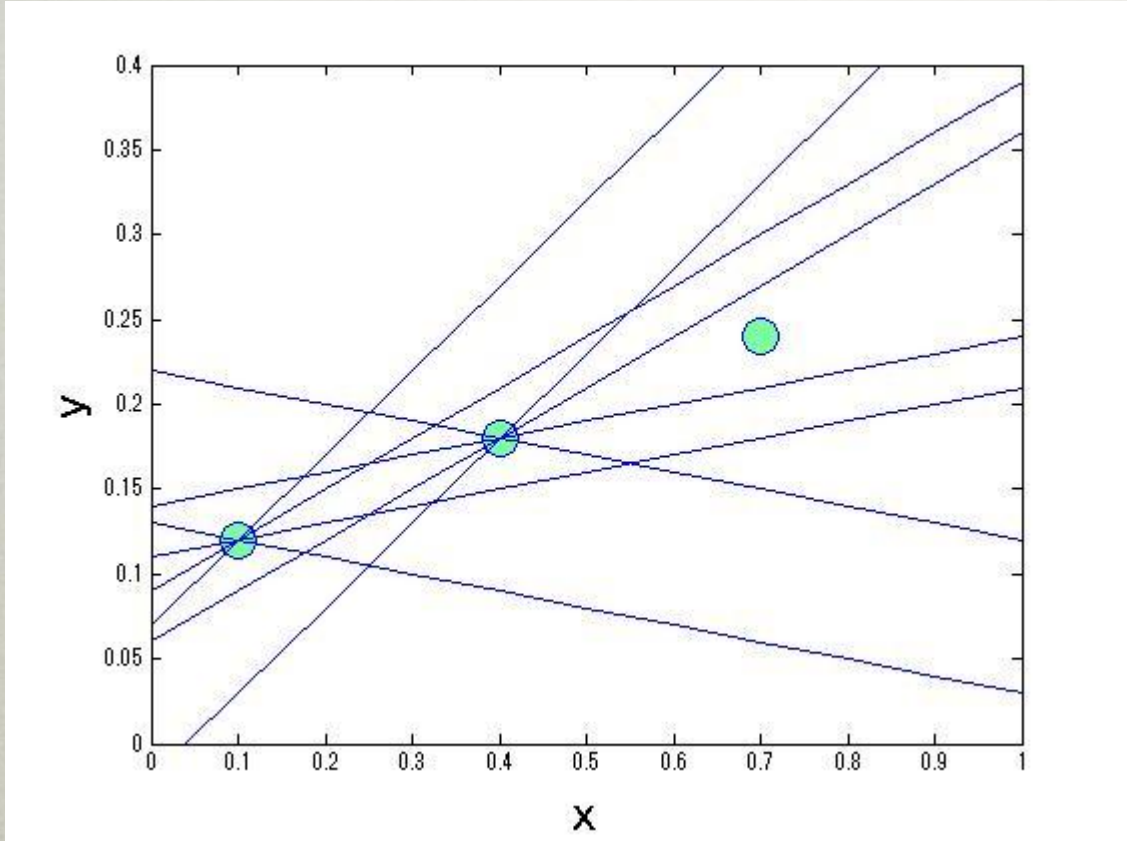

Do the same for the second data.

Hough Transform (cont'd)

Straight line master eq.

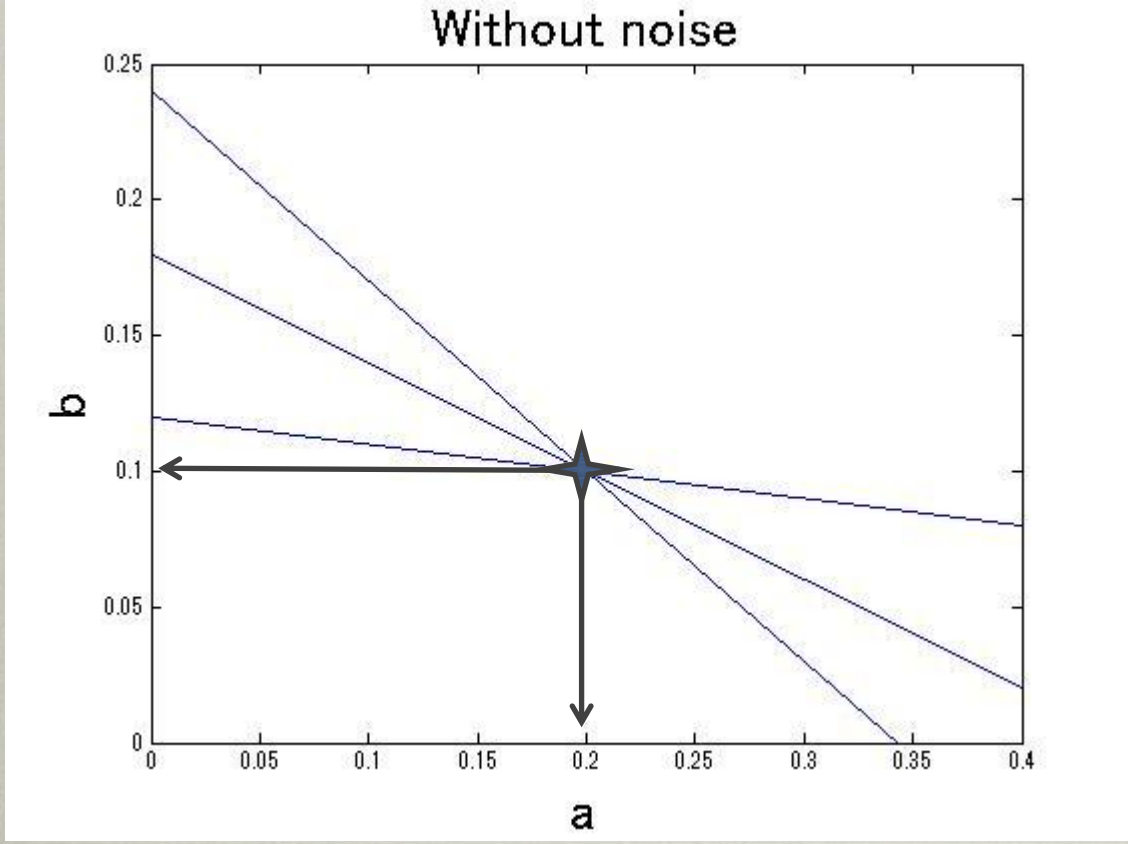

Move on to the parameter space.

If there is no noise, we have "the" solution.

NOTE:
Correct equation is
$y = 0.2\,x + 0.1$

Hough Transform (cont'd)

Straight line master eq.

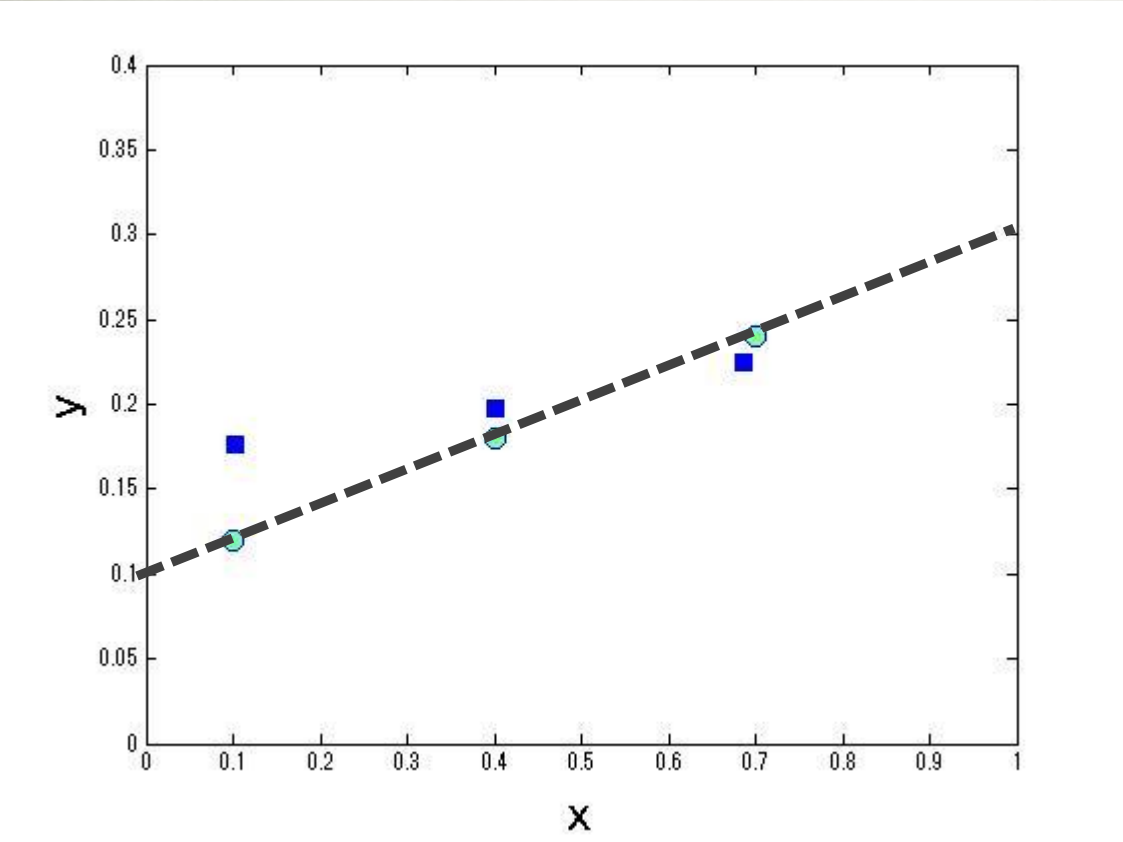

In reality,
there is noise.

Hough Transform (cont'd)

Straight line master eq.

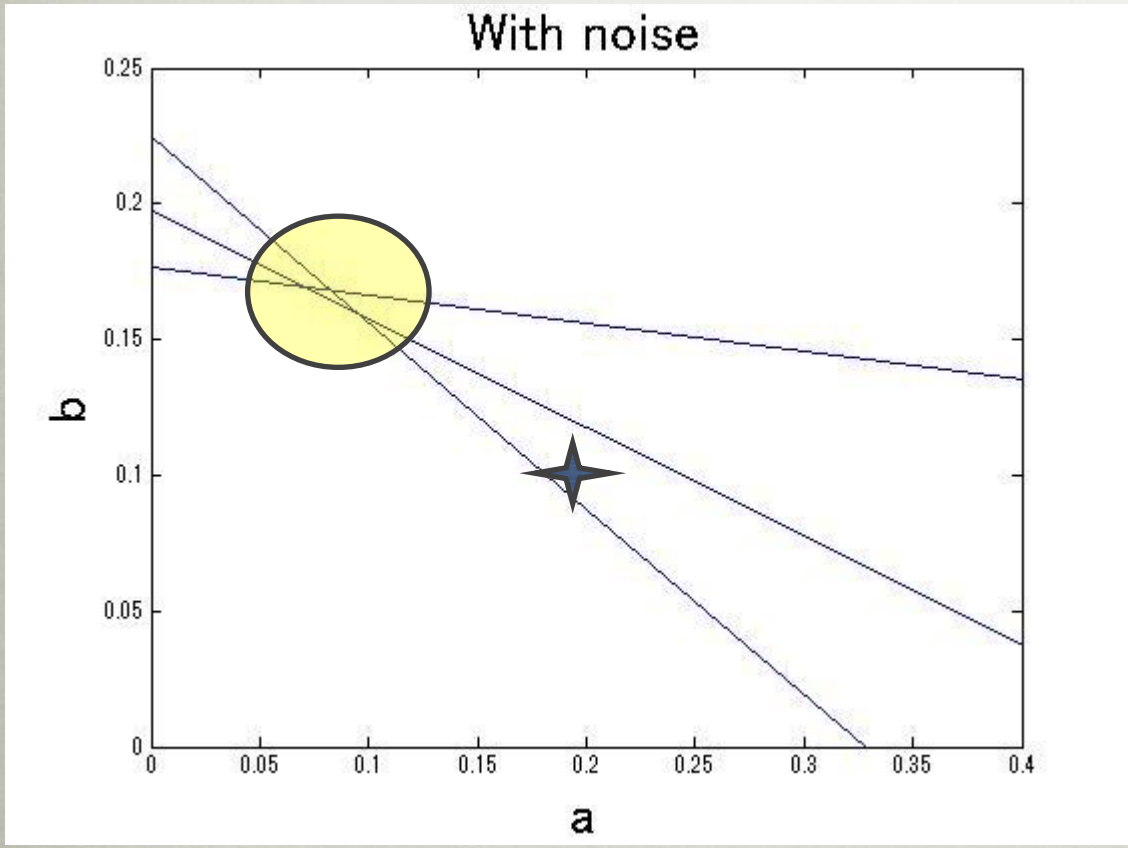

There is no "solution".
Yet the intersections cluster (hopefully) around the true value.

Do it many times….

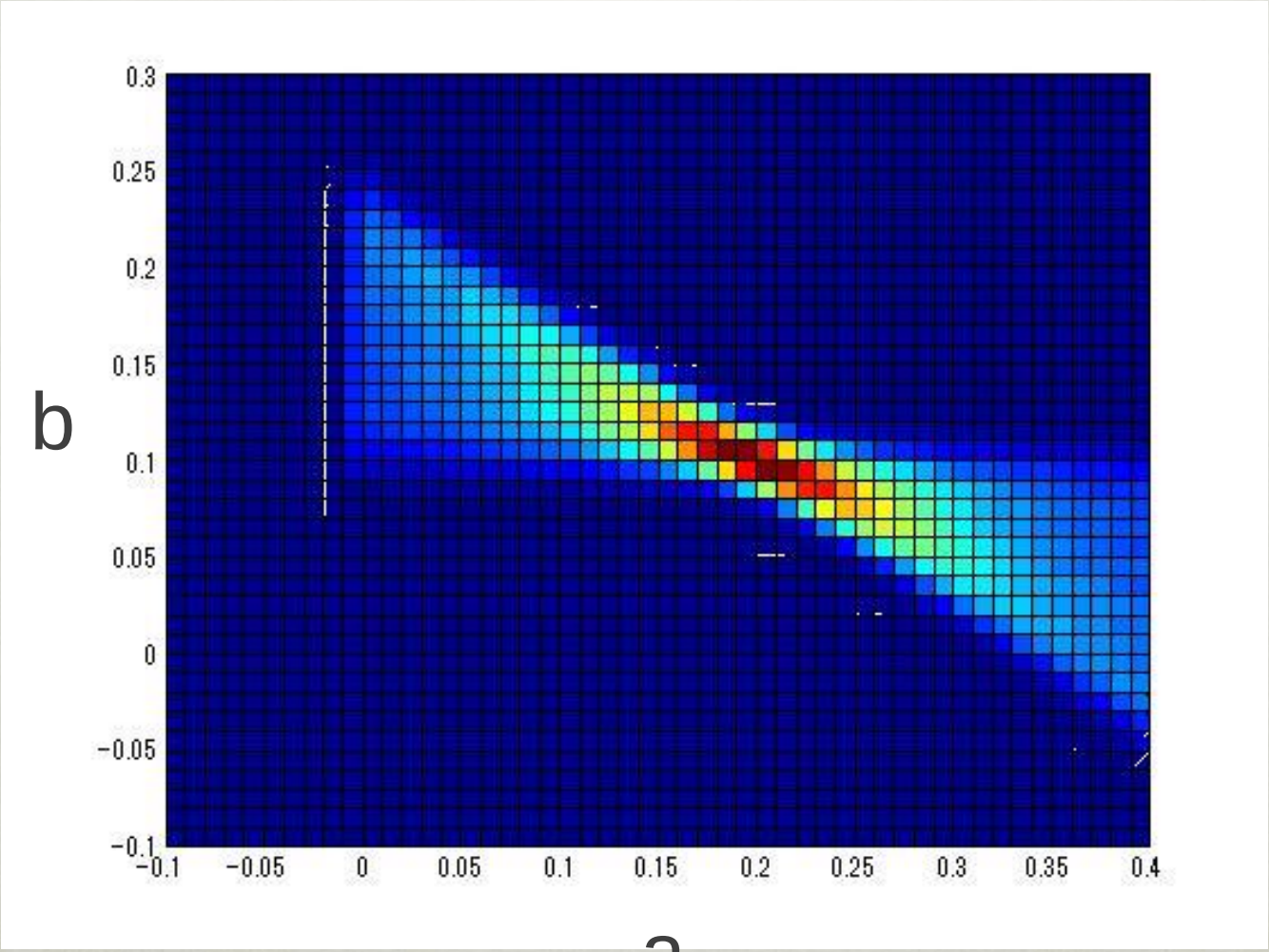

Even when b is random variable

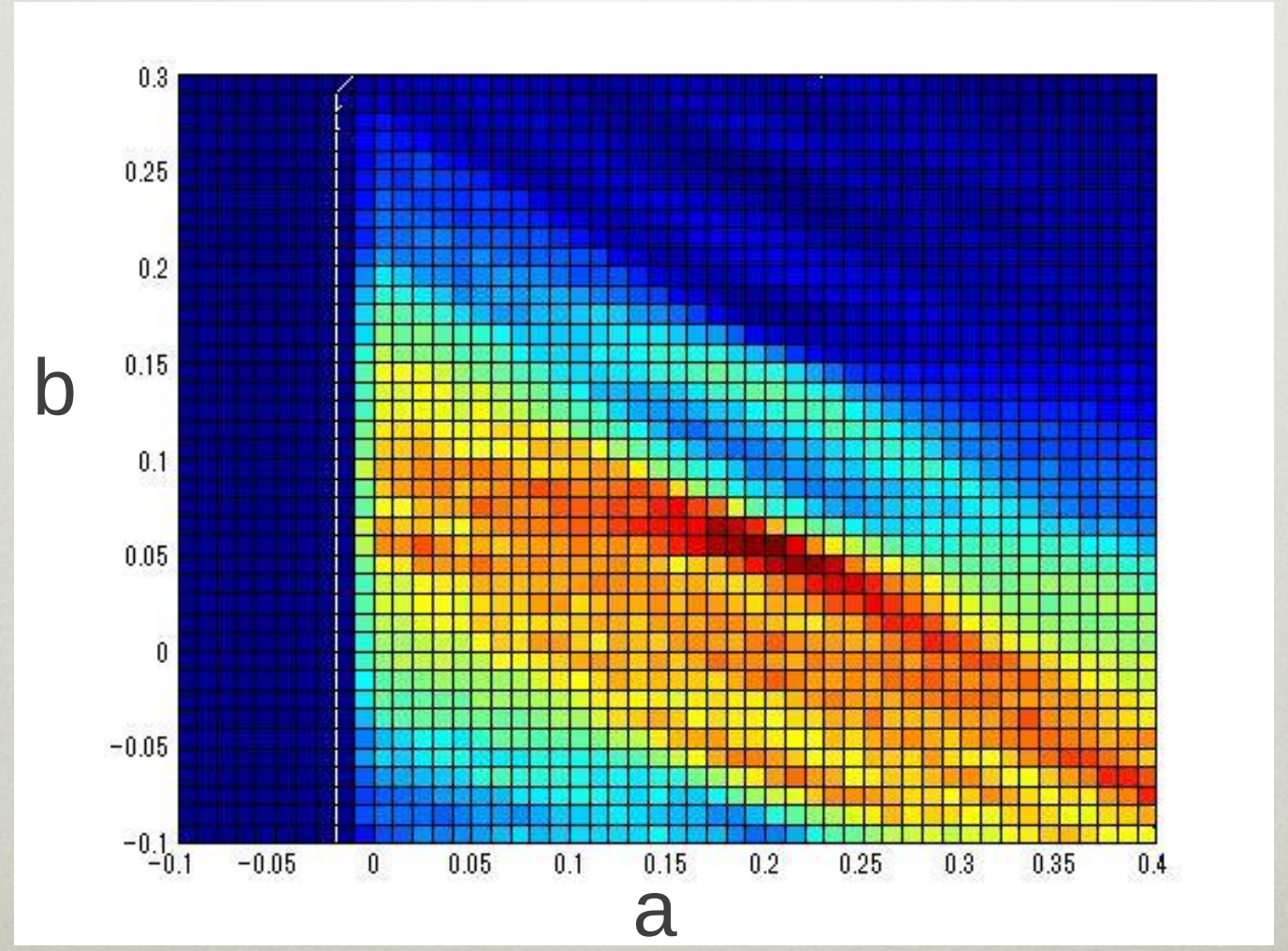

Semi-non-parametric HT on NFW profile.

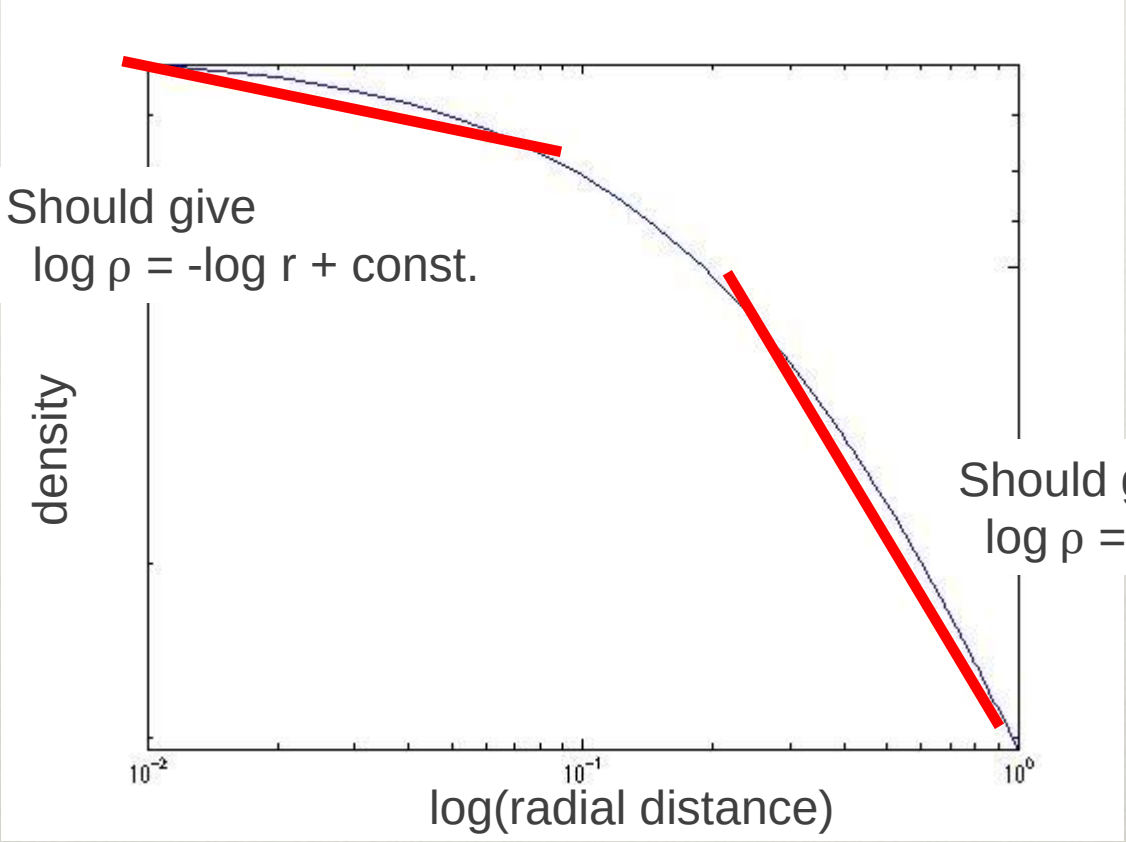

Master equation: $\log_{10} \rho(r) = a \log_{10} r + b$

Re-examining Toy model using Hough Transform

Fit 1000 $\log_{10}\rho(r)$ toy-data using a master equation $\log_{10}\rho(r) = a\log_{10} r + b$

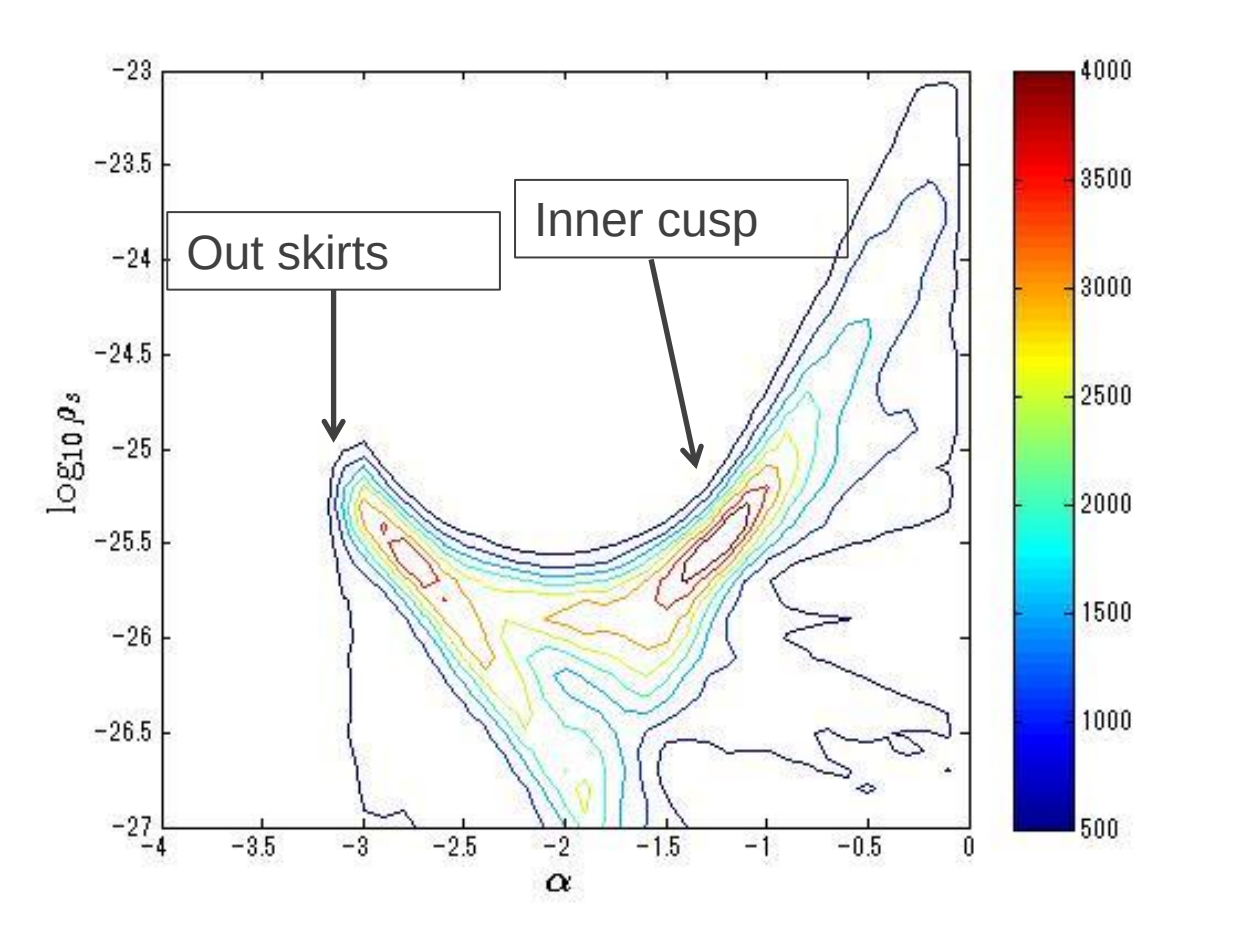

Conclusion: Stacking

- In the case of finding “the” cluster “universal” profile.
  - Without scaling, stacking gives biased results.
- Introduce Hough transform.
  - It seems useful in many fields including testing power-law indices of the averaged cluster radial profiles.

Appendix

Power of Stacking

Gravitational wave: Cutler & Schutz 2005.

“We show that gravitational waves from collection of the few brightest (in gravitational waves) neutron stars could perhaps be detected before the single brightest source, … ” (Cutler & Schutz PRD 2005).

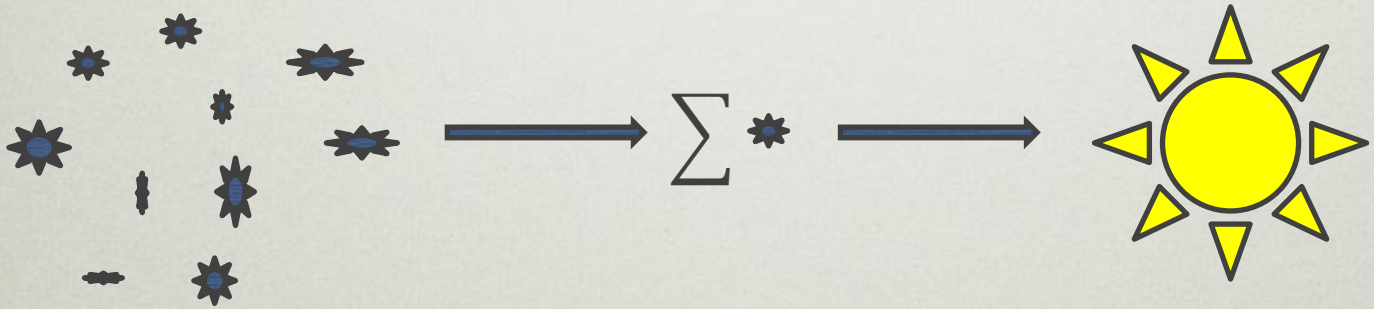

New test of modified gravity (cont'd)

Narikawa & Yamamoto (2012).
Narikawa's talk Wednesday afternoon for details.

- Assuming Navarro-Frenk-White (NFW), gNFW, or Einasto for the cluster density profile, the lensing potential becomes different from that of GR, due to the scalar DOF.
- At the outer-skirt of the lensing cluster observed, compare the observed tangential shear radial profile with the assumed one expected from the NFW density profile under GR.

New test of modified gravity (cont'd)

Narikawa & Yamamoto (2012).
Narikawa's talk Wednesday afternoon for details.

- Determine two parameters:
  - The strength of the modification to the Newtonian Gravity $G_{\rm eff} = G(1 + \mu)$
  - And the length scale smaller than which the Newtonian gravity is recovered.

$$r_V = 13.4\epsilon^{2/3}\left(\frac{M_{\rm vir}}{10^{15}{\rm M}_\odot}\right)^{1/3} h^{-1}{\rm Mpc}.$$

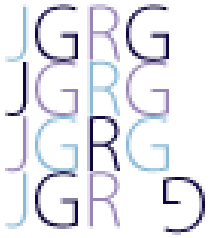

Kent Yagi, JGRG 22(2012)111307

"Black hole solution and binary gravitational waves in dynamical Chern-Simons gravity"

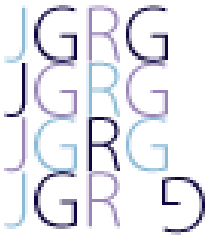

RESCEU SYMPOSIUM ON

GENERAL RELATIVITY AND GRAVITATION

JGRG 22



November 12-16 2012

Koshiba Hall, The University of Tokyo, Hongo, Tokyo, Japan



Black Hole Solution and Binary Gravitational Waves in Dynamical Chern-Simons Gravity

JGRG22 @ University of Tokyo

November 13th 2012

Kent Yagi

(Montana State University)

Collaborators:

Nicolas Yunes (Montana State Univ.)

Takahiro Tanaka (YITP)

Contents

§ 1 Introduction

§ 2 Black Hole Solutions

§ 3 Gravitational Waves from BH Binaries

§ 4 Summary & Future Work

Contents

§ 1 Introduction

§ 2 Black Hole Solutions

§ 3 Gravitational Waves from BH Binaries

§ 4 Summary & Future Work

Probing alternative theories of gravity using compact binaries

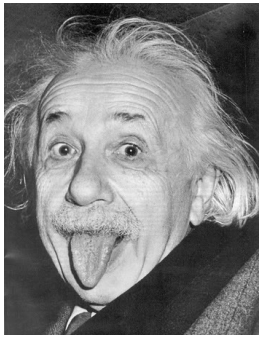

Why modifications of gravity ?

(I) Problems within GR can be naturally solved.

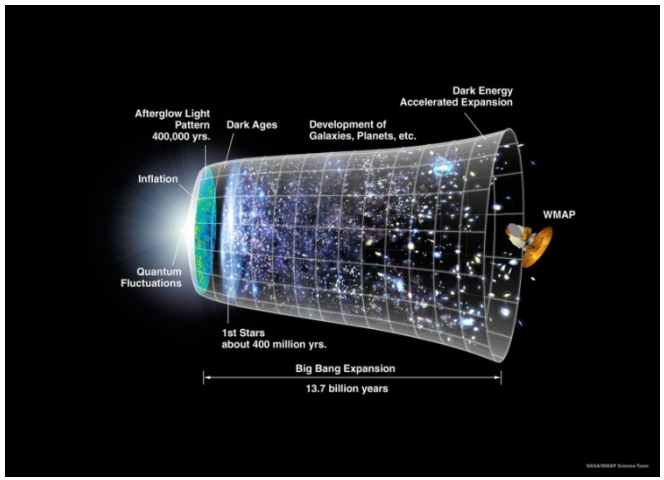

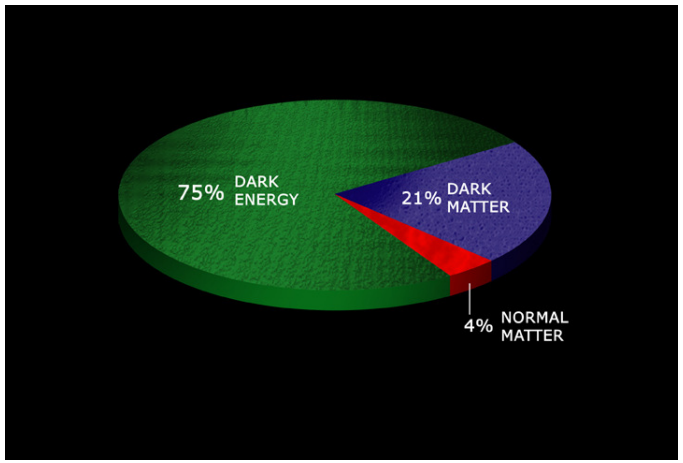

(II) Classical gravitational theory as a low-energy effective theory of a more fundamental theory

e.g. superstring theory ⇒ **Chern-Simons, Gauss-Bonnet, Scalar-tensor theories**

Testing GR

(I) Weak field, non-dynamical regime:

Solar System



Binary Pulsar

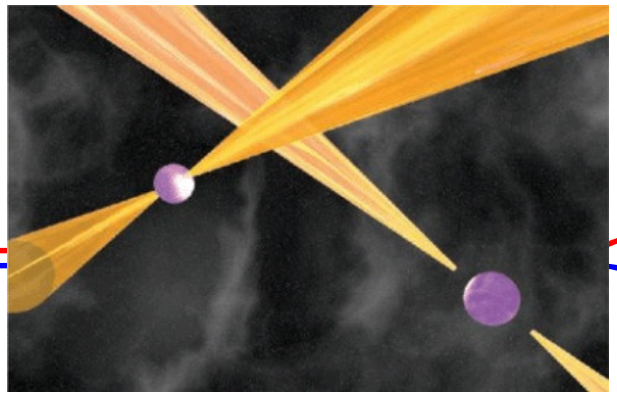

(II) Strong field, dynamical regime:

Gravitational Waves

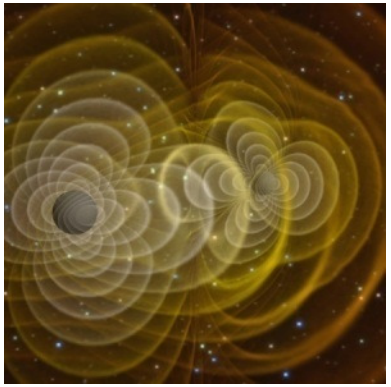

Dynamical Chern-Simons Gravity

- Standard Model
- Superstring Theory
- Loop Quantum Gravity
- Inflation

Dynamical Chern-Simons Gravity

-Standard Model
-Superstring Theory
-Loop Quantum Gravity
-Inflation

- Action:

$$S \equiv \int d^4x\sqrt{-g}\Big\{\kappa_g R + \frac{\alpha}{4}\vartheta R_{\nu\mu\rho\sigma}{}^*R^{\mu\nu\rho\sigma} - \frac{\beta}{2}[\nabla_\mu\vartheta\nabla^\mu\vartheta + 2V(\vartheta)] + \mathcal{L}_{\rm mat}\Big\}.$$

$c = G = 1$

$\kappa_g \equiv (16\pi)^{-1}$

Dynamical Chern-Simons Gravity

-Standard Model
-Superstring Theory
-Loop Quantum Gravity
-Inflation

- **Action:**

$$S \equiv \int d^4x\sqrt{-g}\Big\{\kappa_g R + \frac{\alpha}{4}\vartheta R_{\nu\mu\rho\sigma}{}^*R^{\mu\nu\rho\sigma} - \frac{\beta}{2}[\nabla_\mu\vartheta\nabla^\mu\vartheta + 2V(\vartheta)] + \mathcal{L}_{\rm mat}\Big\}.$$

$c = G = 1$

$\kappa_g \equiv (16\pi)^{-1}$

- **Field Eqs.:**

$$G_{\mu\nu}[g_{\mu\nu}] + \frac{\alpha}{\kappa_g}C_{\mu\nu}[\vartheta, g_{\mu\nu}] = \frac{1}{2\kappa_g}\left(T^{\rm mat}_{\mu\nu} + T^{\vartheta}_{\mu\nu}[\vartheta, g_{\mu\nu}]\right)$$

$$\Box\vartheta = -\frac{\alpha}{4\beta}{}^*RR + V'(\vartheta)$$

Dynamical Chern-Simons Gravity

-Standard Model
-Superstring Theory
-Loop Quantum Gravity
-Inflation

- **Action:**

$$S \equiv \int d^4x\sqrt{-g}\Big\{\kappa_g R + \frac{\alpha}{4}\vartheta R_{\nu\mu\rho\sigma}{}^*R^{\mu\nu\rho\sigma} - \frac{\beta}{2}[\nabla_\mu\vartheta\nabla^\mu\vartheta + 2V(\vartheta)] + \mathcal{L}_{\rm mat}\Big\}.$$

$c = G = 1$

$\kappa_g \equiv (16\pi)^{-1}$

- **Field Eqs.:**

$$G_{\mu\nu}[g_{\mu\nu}] + \frac{\alpha}{\kappa_g}C_{\mu\nu}[\vartheta, g_{\mu\nu}] = \frac{1}{2\kappa_g}\left(T^{\rm mat}_{\mu\nu} + T^{\vartheta}_{\mu\nu}[\vartheta, g_{\mu\nu}]\right)$$

$$\Box\vartheta = -\frac{\alpha}{4\beta}{}^*RR + V'(\vartheta)$$

- **Characteristic Length Scale:**

$$\xi^{1/4} \qquad \left(\xi \equiv \frac{\alpha^2}{\beta\kappa_g}\right)$$

Dynamical Chern-Simons Gravity

-Standard Model
-Superstring Theory
-Loop Quantum Gravity
-Inflation

- **Action:**

$$S \equiv \int d^4x\sqrt{-g}\Big\{\kappa_g R + \frac{\alpha}{4}\vartheta R_{\nu\mu\rho\sigma}{}^*R^{\mu\nu\rho\sigma} - \frac{\beta}{2}[\nabla_\mu\vartheta\nabla^\mu\vartheta + 2V(\vartheta)] + \mathcal{L}_{\rm mat}\Big\}.$$

$c = G = 1$

$\kappa_g \equiv (16\pi)^{-1}$

- **Field Eqs.:**

$$G_{\mu\nu}[g_{\mu\nu}] + \frac{\alpha}{\kappa_g}C_{\mu\nu}[\vartheta, g_{\mu\nu}] = \frac{1}{2\kappa_g}\left(T^{\rm mat}_{\mu\nu} + T^{\vartheta}_{\mu\nu}[\vartheta, g_{\mu\nu}]\right)$$

$$\Box\vartheta = -\frac{\alpha}{4\beta}{}^*RR + V'(\vartheta)$$

- **Characteristic Length Scale:**

$$\xi^{1/4} \qquad \left(\xi \equiv \frac{\alpha^2}{\beta\kappa_g}\right)$$

- **Small coupling approximation**

Dimensionless coupling constant: $\zeta \equiv \dfrac{\xi}{M^4} \ll 1$

For simplicity, we set $V(\vartheta) = 0$

Corrections to GWs from BH Binaries

(I) Dissipative

Scalar & Gravitational Radiation

→ Modifies the orbital evolution

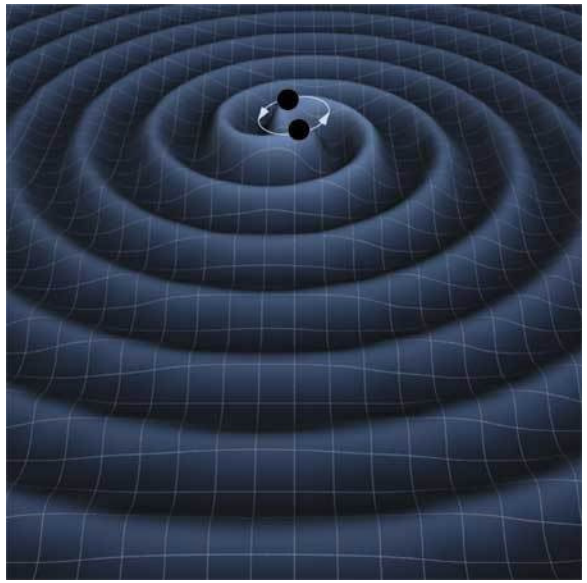

(II) Conservative

Modified BH Solution

→ Modifies the binding energy

→ Modifies the binary orbit

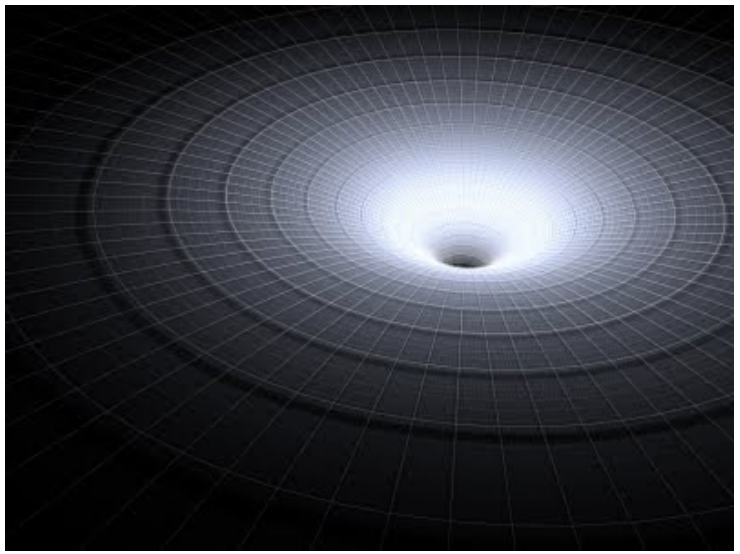

Dissipative Corrections in DCS Gravity

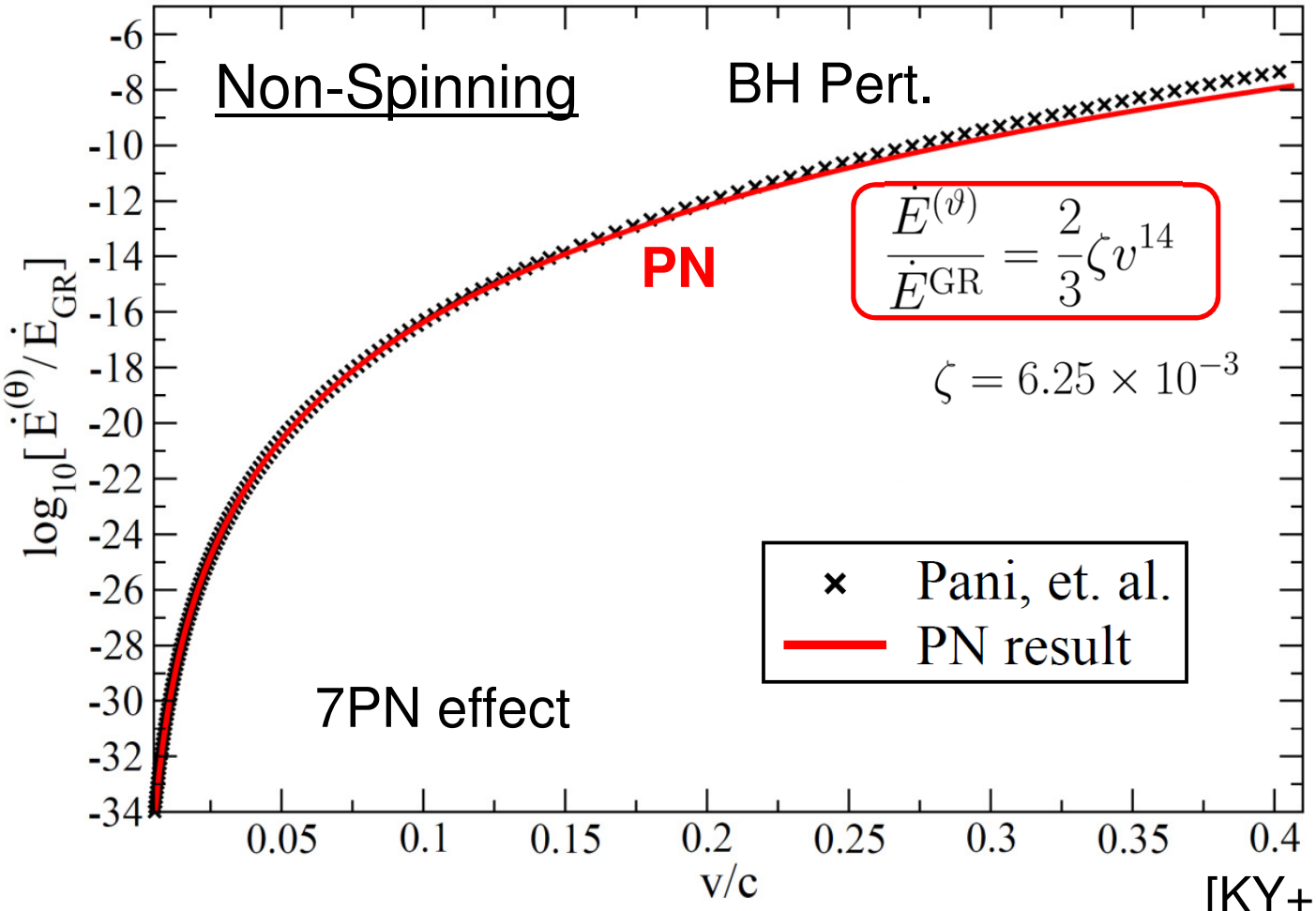

[KY+ (2012)]

For the spinning case, the correction is 2PN!

Now, we need to compute the conservative one.

Contents

§ 1 Introduction

§ 2 Black Hole Solutions

§ 3 Gravitational Waves from BH Binaries

§ 4 Summary & Future Work

(I) Non-Spinning

Spherical Symmetry

- $^*RR = 0$
- No CS correction
- Schwarzschild BH

(I) Non-Spinning

Spherical Symmetry

$\Rightarrow$ ${}^*RR = 0$

$\Rightarrow$ No CS correction

$\Rightarrow$ Schwarzschild BH

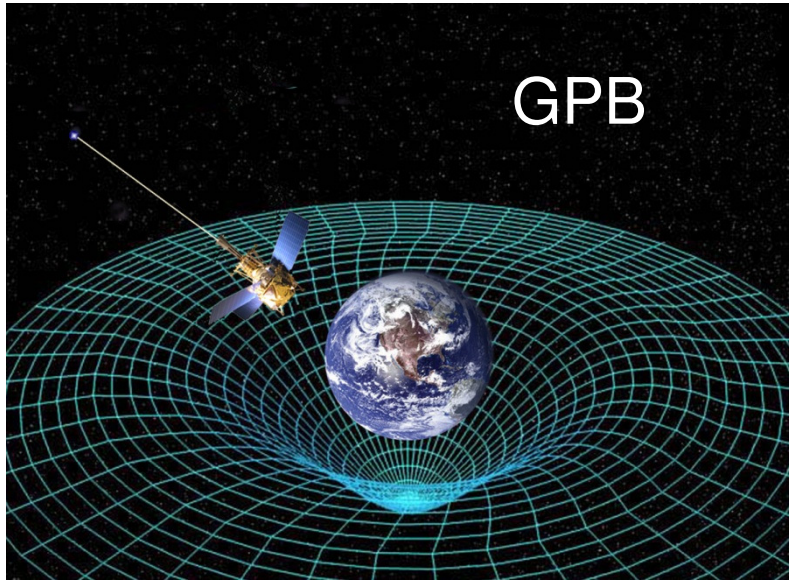

(II) Spinning

-Exact Solution unknown.

-Linear order in spin [Yunes & Pretorius (2009), Konno et al. (2009)]

$$ds^2 = ds^2_{\rm K} + \frac{5}{4}\frac{\alpha^2}{\beta\kappa}\frac{a}{r^4}\left(1+\frac{12}{7}\frac{M}{r}+\frac{27}{10}\frac{M^2}{r^2}\right)\sin^2\theta dt d\phi,$$

$\Rightarrow$ **frame-dragging effect**

Gravity Probe B $\Rightarrow$ $\xi^{1/4} < \mathcal{O}(10^8)\ {\rm km}$

[Ali-Haimoud & Chen (2011)]

BH Solution at Quadratic Order in Spin

Metric Perturbation: $g_{\mu\nu} = \boxed{g^{(0)}_{\mu\nu}} + \boxed{\alpha'^2 g^{(2)}_{\mu\nu}} + \mathcal{O}(\alpha'^4)$

GR CS

BH Solution at Quadratic Order in Spin

Metric Perturbation: $g_{\mu\nu} = \boxed{g^{(0)}_{\mu\nu}} + \boxed{\alpha'^2 g^{(2)}_{\mu\nu}} + \mathcal{O}(\alpha'^4)$

GR CS

Expansion in spin:

$$\boxed{g^{(0)}_{\mu\nu}} = g^{(0,0)}_{\mu\nu} + \chi' g^{(1,0)}_{\mu\nu} + \chi'^2 g^{(2,0)}_{\mu\nu} + \mathcal{O}(\chi'^3)$$

$$g^{(m,n)}_{\mu\nu} \propto \chi^m \alpha^n$$

BH Solution at Quadratic Order in Spin

Metric Perturbation: $g_{\mu\nu} = \boxed{g^{(0)}_{\mu\nu}} + \boxed{\alpha'^2 g^{(2)}_{\mu\nu}} + \mathcal{O}(\alpha'^4)$

GR CS

Expansion in spin:

$$\boxed{g^{(0)}_{\mu\nu}} = g^{(0,0)}_{\mu\nu} + \chi' g^{(1,0)}_{\mu\nu} + \chi'^2 g^{(2,0)}_{\mu\nu} + \mathcal{O}(\chi'^3)$$

$$\boxed{\alpha'^2 g^{(2)}_{\mu\nu}} = \alpha'^2 g^{(0,2)}_{\mu\nu} + \alpha'^2\chi' g^{(1,2)}_{\mu\nu} + \alpha'^2\chi'^2 g^{(2,2)}_{\mu\nu} + \mathcal{O}(\alpha'^2\chi'^3)\,,$$

$$g^{(m,n)}_{\mu\nu} \propto \chi^m \alpha^n$$

BH Solution at Quadratic Order in Spin

Metric Perturbation: $g_{\mu\nu} = g^{(0)}_{\mu\nu} + \alpha'^2 g^{(2)}_{\mu\nu} + \mathcal{O}(\alpha'^4)$

GR CS

Expansion in spin:

$$g^{(0)}_{\mu\nu} = g^{(0,0)}_{\mu\nu} + \chi' g^{(1,0)}_{\mu\nu} + \chi'^2 g^{(2,0)}_{\mu\nu} + \mathcal{O}(\chi'^3)$$

$$\alpha'^2 g^{(2)}_{\mu\nu} = \cancel{\alpha'^2 g^{(0,2)}_{\mu\nu}} + \alpha'^2 \chi' g^{(1,2)}_{\mu\nu} + \alpha'^2 \chi'^2 g^{(2,2)}_{\mu\nu} + \mathcal{O}(\alpha'^2 \chi'^3),$$

$$g^{(m,n)}_{\mu\nu} \propto \chi^m \alpha^n$$

BH Solution at Quadratic Order in Spin

Metric Perturbation: $g_{\mu\nu} = g^{(0)}_{\mu\nu} + \alpha'^2 g^{(2)}_{\mu\nu} + \mathcal{O}(\alpha'^4)$

GR CS

Expansion in spin:

$$g^{(0)}_{\mu\nu} = g^{(0,0)}_{\mu\nu} + \chi' g^{(1,0)}_{\mu\nu} + \chi'^2 g^{(2,0)}_{\mu\nu} + \mathcal{O}(\chi'^3)$$

$$\alpha'^2 g^{(2)}_{\mu\nu} = \alpha'^2 g^{(0,2)}_{\mu\nu} + \alpha'^2 \chi' g^{(1,2)}_{\mu\nu} + \alpha'^2 \chi'^2 g^{(2,2)}_{\mu\nu} + \mathcal{O}(\alpha'^2 \chi'^3),$$

Yunes & Pretorius, Konno et al.

$$g^{(m,n)}_{\mu\nu} \propto \chi^m \alpha^n$$

BH Solution at Quadratic Order in Spin

Metric Perturbation: $g_{\mu\nu} = g^{(0)}_{\mu\nu} + \alpha'^2 g^{(2)}_{\mu\nu} + \mathcal{O}(\alpha'^4)$

GR CS

Expansion in spin:

$$g^{(0)}_{\mu\nu} = g^{(0,0)}_{\mu\nu} + \chi' g^{(1,0)}_{\mu\nu} + \chi'^2 g^{(2,0)}_{\mu\nu} + \mathcal{O}(\chi'^3)$$

$$\alpha'^2 g^{(2)}_{\mu\nu} = \cancel{\alpha'^2 g^{(0,2)}_{\mu\nu}} + \alpha'^2 \chi' g^{(1,2)}_{\mu\nu} + \alpha'^2 \chi'^2 g^{(2,2)}_{\mu\nu} + \mathcal{O}(\alpha'^2 \chi'^3)\,,$$

Yunes & Pretorius, Konno et al.

New!!

$$g^{(m,n)}_{\mu\nu} \propto \chi^m \alpha^n$$

BH Solution at Quadratic Order in Spin

Metric Perturbation: $g_{\mu\nu} = g^{(0)}_{\mu\nu} + \alpha'^2 g^{(2)}_{\mu\nu} + \mathcal{O}(\alpha'^4)$

GR CS

Expansion in spin:

$$g^{(0)}_{\mu\nu} = g^{(0,0)}_{\mu\nu} + \chi' g^{(1,0)}_{\mu\nu} + \chi'^2 g^{(2,0)}_{\mu\nu} + \mathcal{O}(\chi'^3)$$

$$\alpha'^2 g^{(2)}_{\mu\nu} = \cancel{\alpha'^2 g^{(0,2)}_{\mu\nu}} + \alpha'^2\chi' g^{(1,2)}_{\mu\nu} + \alpha'^2\chi'^2 g^{(2,2)}_{\mu\nu} + \mathcal{O}(\alpha'^2\chi'^3)\,,$$

Yunes & Pretorius, Konno et al.

New!!

$$g^{(m,n)}_{\mu\nu} \propto \chi^m \alpha^n$$

Field Eqs.: $G^{(2,2)}_{\mu\nu}\left[g^{(0,0)}_{\mu\nu}, g^{(2,2)}_{\mu\nu}\right] = S^{(2,2)}_{\mu\nu}\left[g^{(0,0)}_{\mu\nu}, g^{(1,0)}_{\mu\nu}, g^{(1,2)}_{\mu\nu}, \vartheta^{(1,1)}\right]$

at order (2,2)

BH Solution at Quadratic Order in Spin

Metric Perturbation: $g_{\mu\nu} = g^{(0)}_{\mu\nu} + \alpha'^2 g^{(2)}_{\mu\nu} + \mathcal{O}(\alpha'^4)$

GR CS

Expansion in spin:

$$g^{(0)}_{\mu\nu} = g^{(0,0)}_{\mu\nu} + \chi' g^{(1,0)}_{\mu\nu} + \chi'^2 g^{(2,0)}_{\mu\nu} + \mathcal{O}(\chi'^3)$$

$$\alpha'^2 g^{(2)}_{\mu\nu} = \cancel{\alpha'^2 g^{(0,2)}_{\mu\nu}} + \alpha'^2\chi' g^{(1,2)}_{\mu\nu} + \alpha'^2\chi'^2 g^{(2,2)}_{\mu\nu} + \mathcal{O}(\alpha'^2\chi'^3)\,,$$

Yunes & Pretorius, Konno et al.

New!!

$$g^{(m,n)}_{\mu\nu} \propto \chi^m \alpha^n$$

Field Eqs.: $G^{(2,2)}_{\mu\nu}\left[g^{(0,0)}_{\mu\nu}, g^{(2,2)}_{\mu\nu}\right] = S^{(2,2)}_{\mu\nu}\left[g^{(0,0)}_{\mu\nu}, g^{(1,0)}_{\mu\nu}, g^{(1,2)}_{\mu\nu}, \vartheta^{(1,1)}\right]$

at order (2,2)

Known functions

BH Solution at Quadratic Order in Spin

Metric Perturbation: $g_{\mu\nu} = g^{(0)}_{\mu\nu} + \alpha'^2 g^{(2)}_{\mu\nu} + \mathcal{O}(\alpha'^4)$

GR CS

Expansion in spin:

$$g^{(0)}_{\mu\nu} = g^{(0,0)}_{\mu\nu} + \chi' g^{(1,0)}_{\mu\nu} + \chi'^2 g^{(2,0)}_{\mu\nu} + \mathcal{O}(\chi'^3)$$

$$\alpha'^2 g^{(2)}_{\mu\nu} = \cancel{\alpha'^2 g^{(0,2)}_{\mu\nu}} + \alpha'^2\chi' g^{(1,2)}_{\mu\nu} + \alpha'^2\chi'^2 g^{(2,2)}_{\mu\nu} + \mathcal{O}(\alpha'^2\chi'^3)\,,$$

Yunes & Pretorius, Konno et al.

New!!

$$g^{(m,n)}_{\mu\nu} \propto \chi^m \alpha^n$$

Field Eqs.: $G^{(2,2)}_{\mu\nu}\left[g^{(0,0)}_{\mu\nu}, g^{(2,2)}_{\mu\nu}\right] = S^{(2,2)}_{\mu\nu}\left[g^{(0,0)}_{\mu\nu}, g^{(1,0)}_{\mu\nu}, g^{(1,2)}_{\mu\nu}, \vartheta^{(1,1)}\right]$

at order (2,2)

Perturbation under Schw. BH

Known functions

BH Solution at Quadratic Order in Spin

Metric Perturbation: $g_{\mu\nu} = g^{(0)}_{\mu\nu} + \alpha'^2 g^{(2)}_{\mu\nu} + \mathcal{O}(\alpha'^4)$

GR CS

Expansion in spin:

$$g^{(0)}_{\mu\nu} = g^{(0,0)}_{\mu\nu} + \chi' g^{(1,0)}_{\mu\nu} + \chi'^2 g^{(2,0)}_{\mu\nu} + \mathcal{O}(\chi'^3)$$

$$\alpha'^2 g^{(2)}_{\mu\nu} = \cancel{\alpha'^2 g^{(0,2)}_{\mu\nu}} + \alpha'^2\chi' g^{(1,2)}_{\mu\nu} + \alpha'^2\chi'^2 g^{(2,2)}_{\mu\nu} + \mathcal{O}(\alpha'^2\chi'^3)\,,$$

Yunes & Pretorius, Konno et al.

New!!

$$g^{(m,n)}_{\mu\nu} \propto \chi^m \alpha^n$$

Field Eqs.: $G^{(2,2)}_{\mu\nu}\left[g^{(0,0)}_{\mu\nu}, g^{(2,2)}_{\mu\nu}\right] = S^{(2,2)}_{\mu\nu}\left[g^{(0,0)}_{\mu\nu}, g^{(1,0)}_{\mu\nu}, g^{(1,2)}_{\mu\nu}, \vartheta^{(1,1)}\right]$

at order (2,2)

Perturbation under Schw. BH

Known functions

Spherical harmonic decomposition

⇒ (r, θ) decouples

The New Metric [KY+ (2012)]

$$g_{tt}^{\rm CS} = \zeta\chi^2\frac{M^3}{r^3}\left[\frac{201}{1792}\left(1+\frac{M}{r}+\frac{4474}{4221}\frac{M^2}{r^2}-\frac{2060}{469}\frac{M^3}{r^3}+\frac{1500}{469}\frac{M^4}{r^4}-\frac{2140}{201}\frac{M^5}{r^5}+\frac{9256}{201}\frac{M^6}{r^6}-\frac{5376}{67}\frac{M^7}{r^7}\right)(3\cos^2\theta-1)\right.$$
$$\left.-\frac{5}{384}\frac{M^2}{r^2}\left(1+100\frac{M}{r}+194\frac{M^2}{r^2}+\frac{2220}{7}\frac{M^3}{r^3}-\frac{1512}{5}\frac{M^4}{r^4}\right)\right]+\mathcal{O}(\alpha'^2\chi'^4)\,, \tag{41}$$

$$g_{rr}^{\rm CS} = \zeta\chi^2\frac{M^3}{r^3f(r)^2}\left[\frac{201}{1792}f(r)\left(1+\frac{1459}{603}\frac{M}{r}+\frac{20000}{4221}\frac{M^2}{r^2}+\frac{51580}{1407}\frac{M^3}{r^3}-\frac{7580}{201}\frac{M^4}{r^4}\right.\right.$$
$$\left.-\frac{22492}{201}\frac{M^5}{r^5}-\frac{40320}{67}\frac{M^6}{r^6}\right)(3\cos^2\theta-1) \tag{42}$$
$$\left.-\frac{25}{384}\frac{M}{r}\left(1+3\frac{M}{r}+\frac{322}{5}\frac{M^2}{r^2}+\frac{198}{5}\frac{M^3}{r^3}+\frac{6276}{175}\frac{M^4}{r^4}-\frac{17496}{25}\frac{M^5}{r^5}\right)\right]+\mathcal{O}(\alpha'^2\chi'^4)\,,$$

$$g_{\theta\theta}^{\rm CS} = \frac{201}{1792}\zeta\chi^2M^2\frac{M}{r}\left(1+\frac{1420}{603}\frac{M}{r}+\frac{18908}{4221}\frac{M^2}{r^2}+\frac{1480}{603}\frac{M^3}{r^3}+\frac{22460}{1407}\frac{M^4}{r^4}+\frac{3848}{201}\frac{M^5}{r^5}+\frac{5376}{67}\frac{M^6}{r^6}\right)(3\cos^2\theta-1)$$
$$+\mathcal{O}(\alpha'^2\chi'^4)\,, \tag{43}$$

$$g_{\phi\phi}^{\rm CS} = \sin^2\theta g_{\theta\theta}^{\rm CS}+\mathcal{O}(\alpha'^2\chi'^4) \tag{44}$$

Contents

§ 1 Introduction

§ 2 Black Hole Solutions

§ 3 Gravitational Waves from BH Binaries

§ 4 Summary & Future Work

GWs from BH Binaries in CS Gravity

parameterized post-Einsteinian waveform: Yunes & Pretorius (2009)

$$\tilde{h}(f) = \tilde{h}_{\rm GR}(f)\,[1 + \alpha_{\rm ppE} u^{a_{\rm ppE}}]\,\exp\left(i\beta_{\rm ppE} u^{b_{\rm ppE}}\right)$$

$$u \equiv \pi \mathcal{M} f \propto v^3$$

GWs from BH Binaries in CS Gravity

parameterized post-Einsteinian waveform: Yunes & Pretorius (2009)

$$\tilde{h}(f) = \tilde{h}_{\rm GR}(f)\,[1 + \alpha_{\rm ppE} u^{a_{\rm ppE}}] \exp\left(i \beta_{\rm ppE} u^{b_{\rm ppE}}\right)$$

$$u \equiv \pi \mathcal{M} f \propto v^3$$

CS Gravity: $\alpha_{\rm ppE} = 0$ $\beta_{\rm ppE} = C(m_{1,2}, \hat{S}^i_{1,2})\zeta\chi^2$ $b_{\rm ppE} = -\frac{1}{3}$

2PN correction

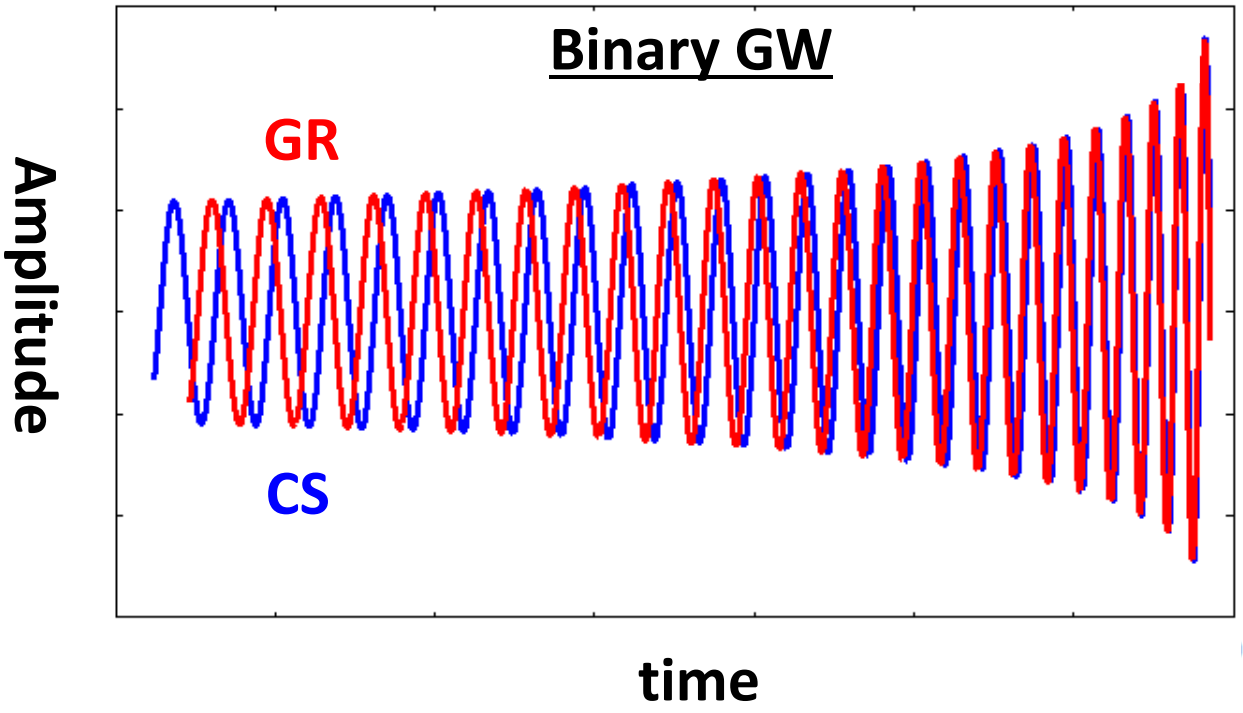

GW DETECTORS

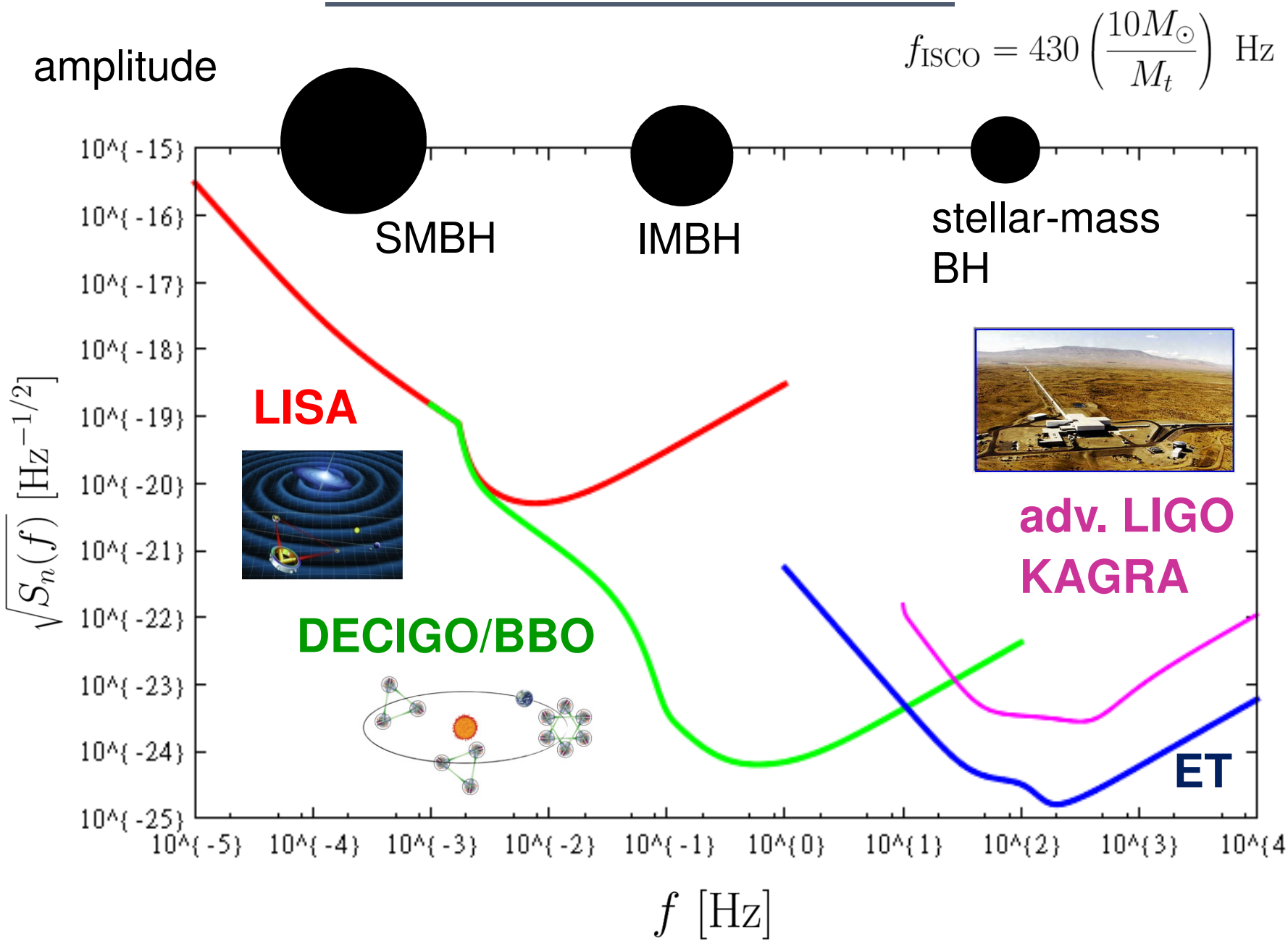

Results: Adv. LIGO, KAGRA

Constraints on $\xi^{1/4}(\mathrm{km})$

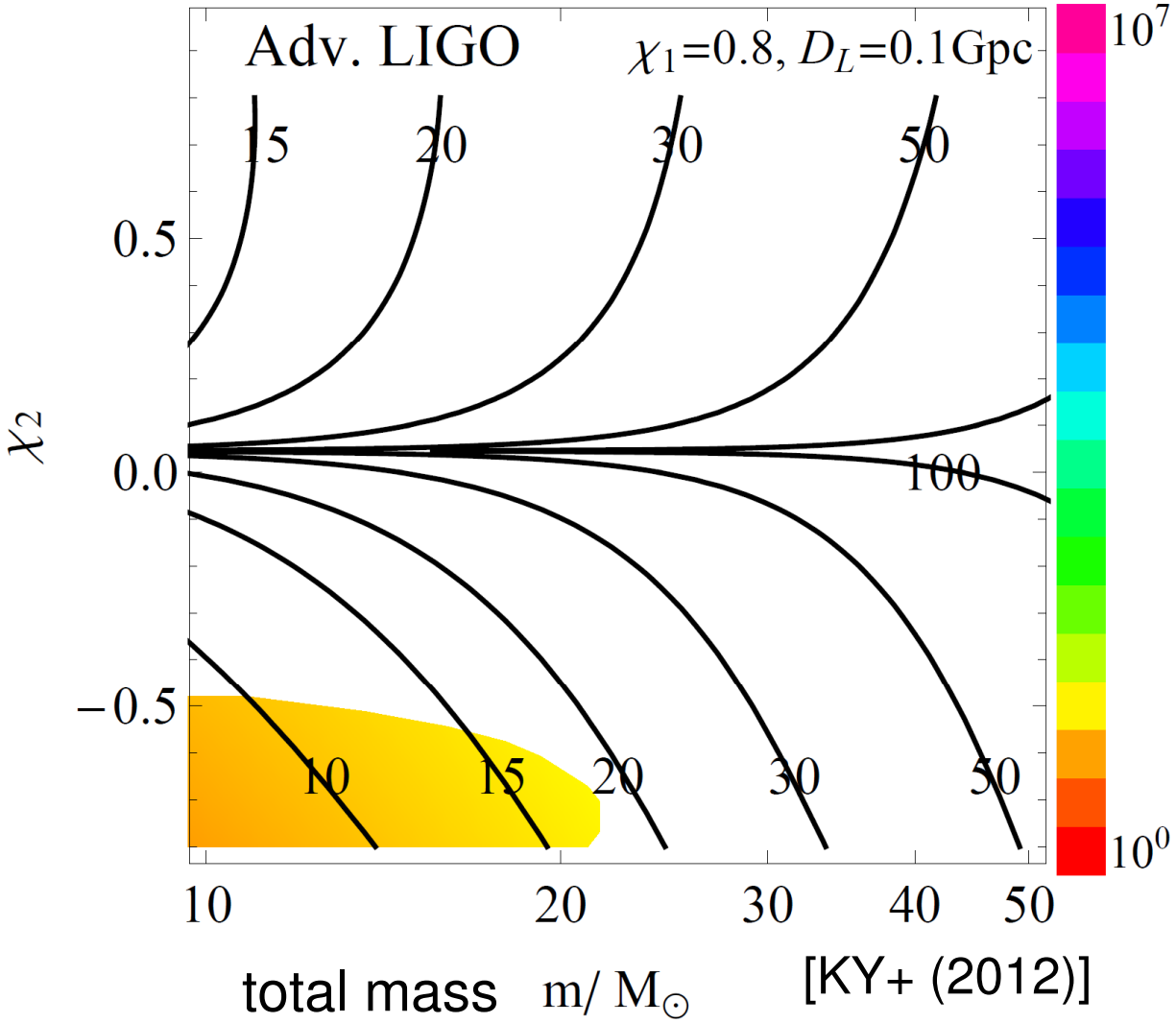

[KY+ (2012)]

$m_1/m_2 = 2$

Spins are known *a priori*

Colored Region:

$\Delta\zeta < 1$

Results: Adv. LIGO, KAGRA

Constraints on $\xi^{1/4}(\mathrm{km})$

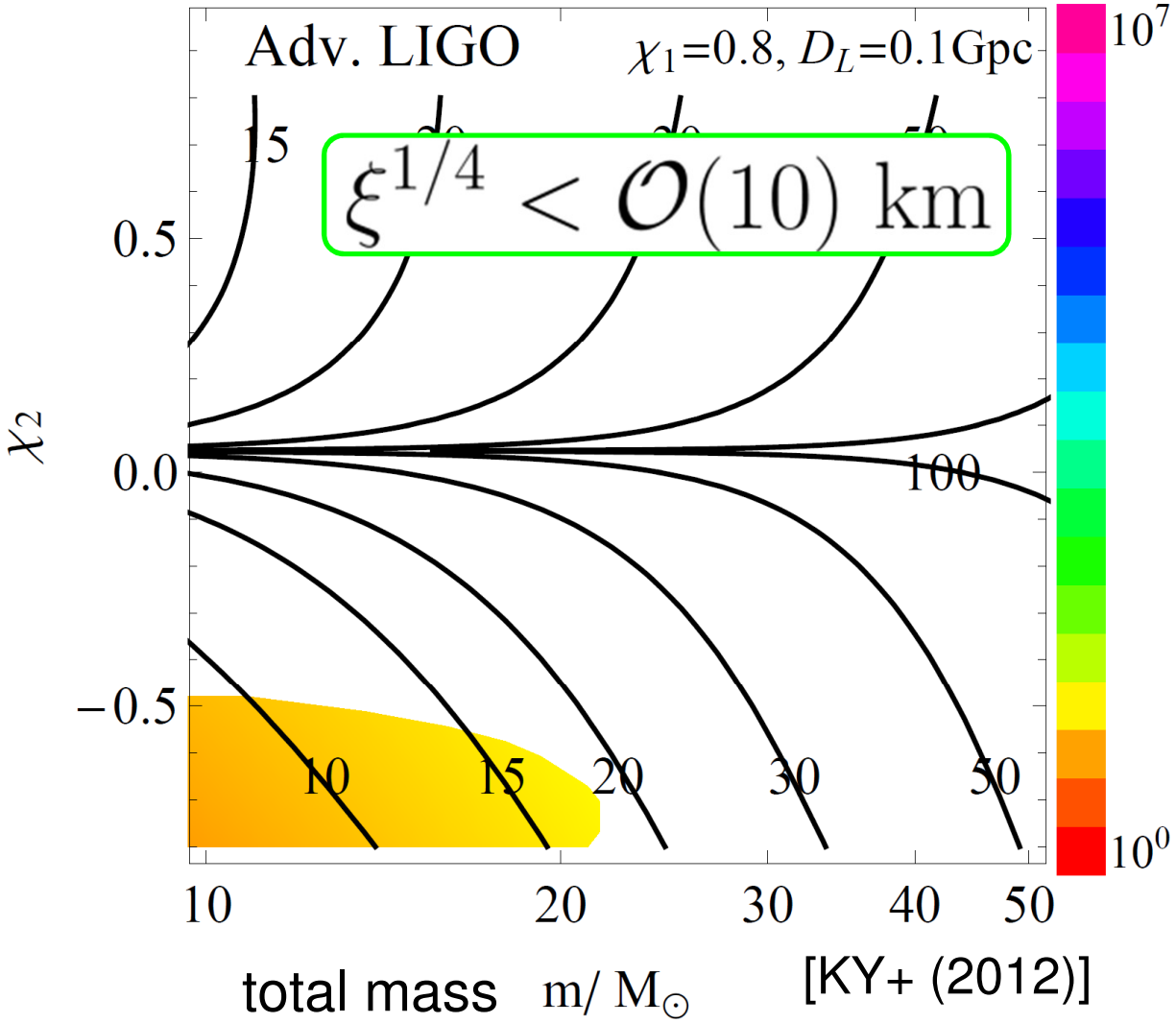

[KY+ (2012)]

$m_1/m_2 = 2$

Spins are known *a priori*

Colored Region:

$\Delta\zeta < 1$

Results: Adv. LIGO, KAGRA

Constraints on $\xi^{1/4}(\mathrm{km})$

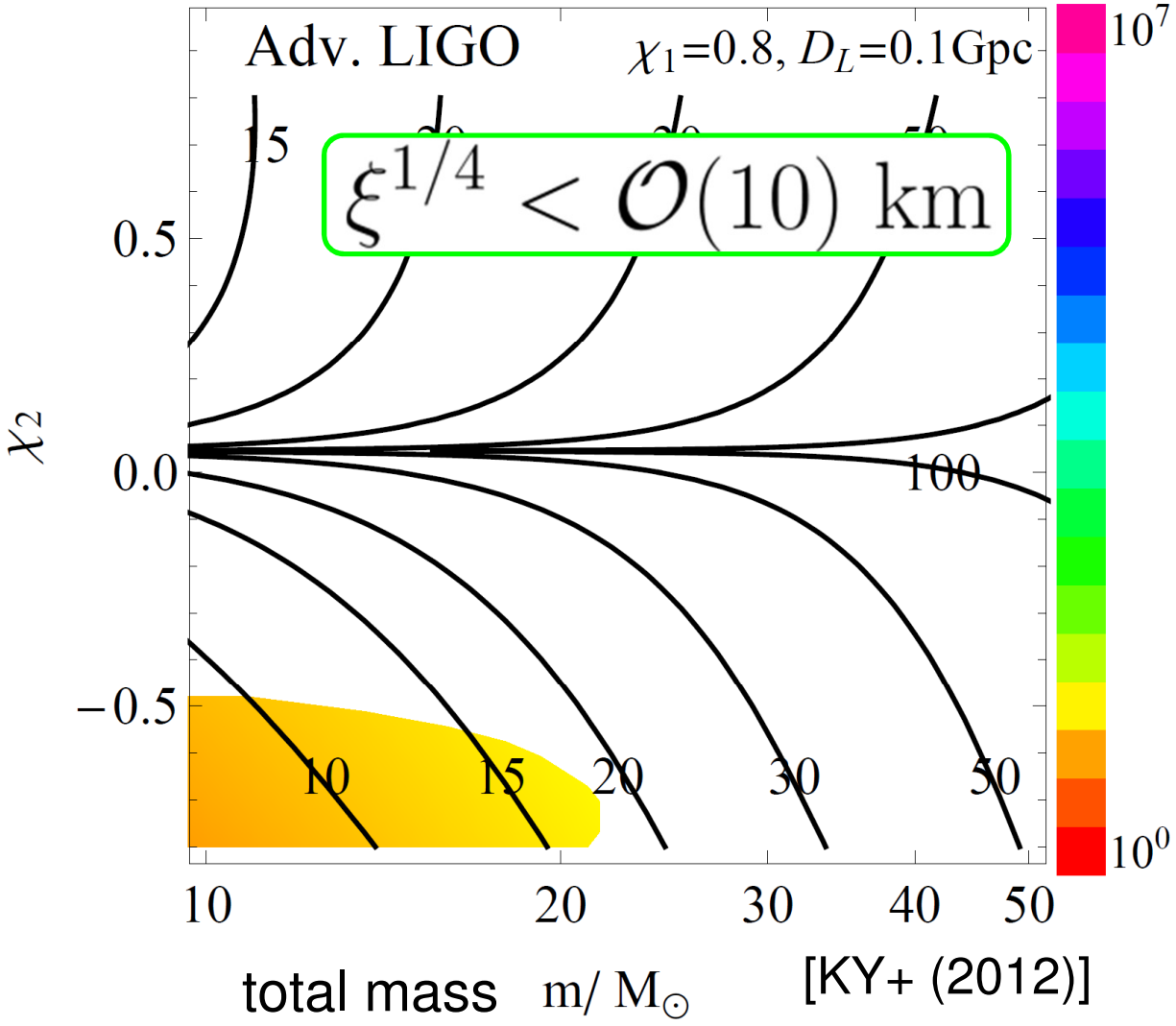

$m_1/m_2 = 2$

Spins are known *a priori*

Colored Region:

$$\Delta\zeta < 1$$

The bound roughly corresponds to the BH horizon size.

Results: Adv. LIGO, KAGRA

Constraints on $\xi^{1/4}(\mathrm{km})$

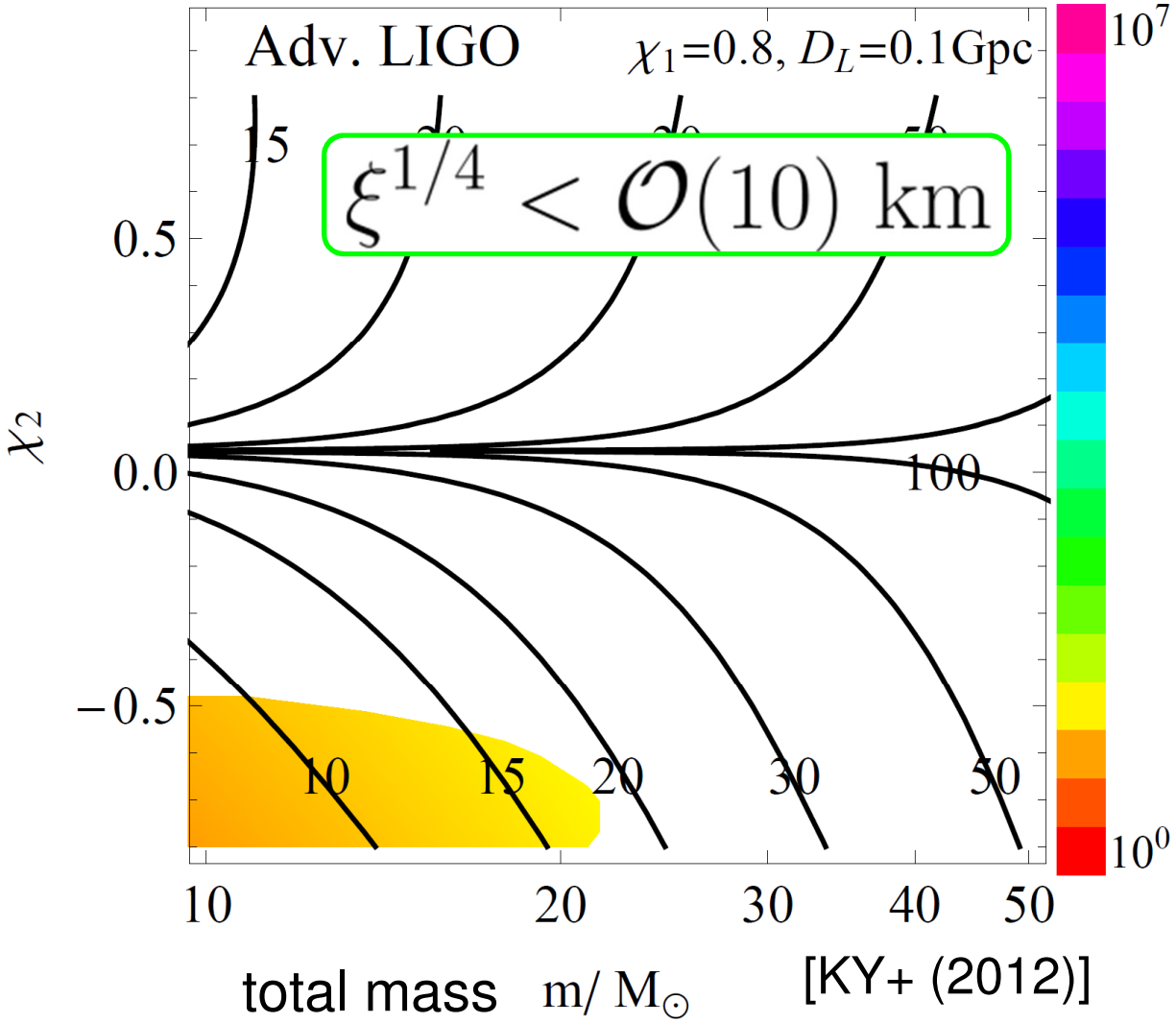

[KY+ (2012)]

$m_1/m_2 = 2$

Spins are known *a priori*

Colored Region:

$$\Delta\zeta < 1$$

The bound roughly corresponds to the BH horizon size.

Solar system:

$$\xi^{1/4} < \mathcal{O}(10^8)\ \mathrm{km}$$

Results: Adv. LIGO, KAGRA

Constraints on $\xi^{1/4}(\mathrm{km})$

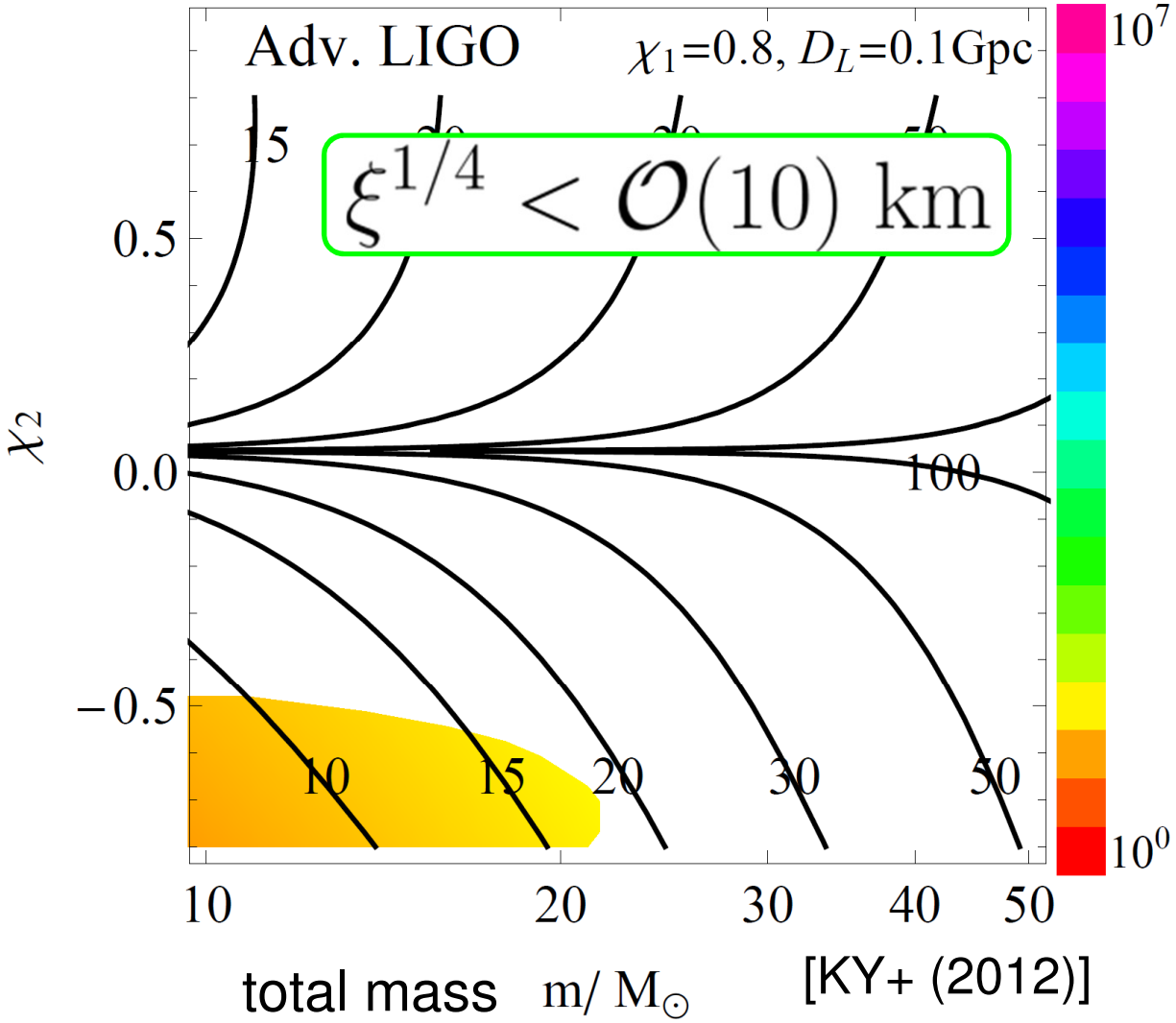

$m_1/m_2 = 2$

Spins are known *a priori*

Colored Region:

$$\Delta\zeta < 1$$

The bound roughly corresponds to the BH horizon size.

Solar system:

$$\xi^{1/4} < \mathcal{O}(10^8)\ \mathrm{km}$$

7 orders of magnitude stronger constraint than the solar system bound!!

Results: Other Detectors

spin (anti-)aligned binaries

(Spins are included into parameters.)

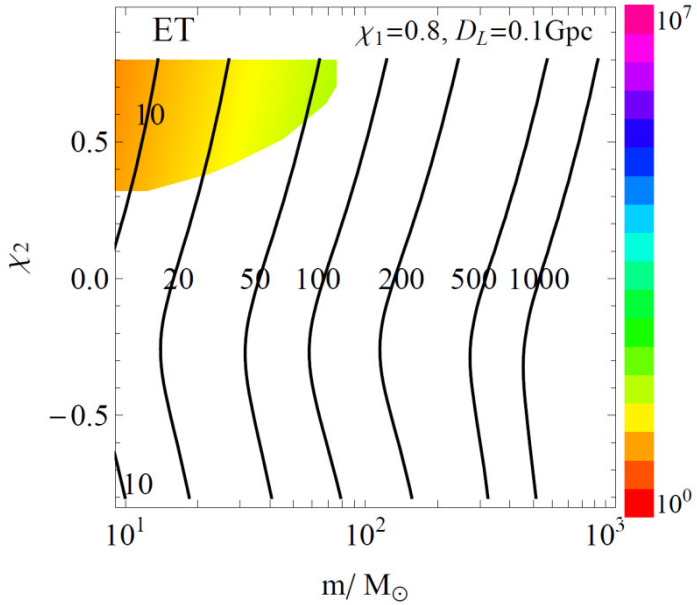

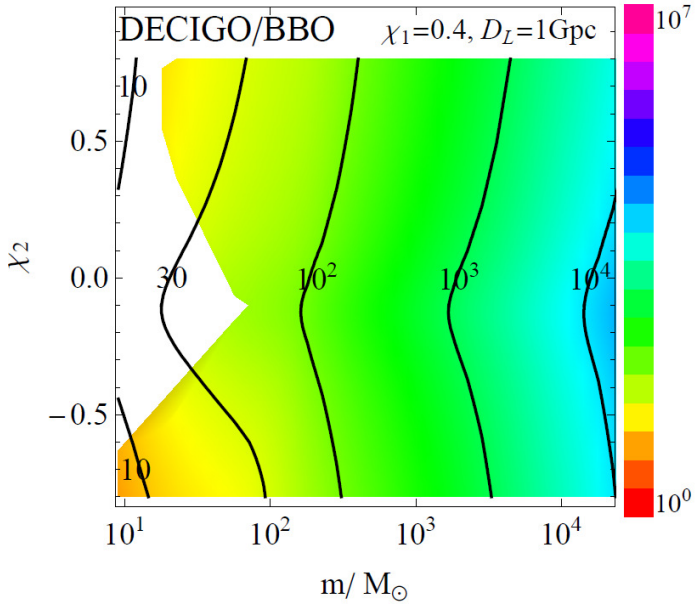

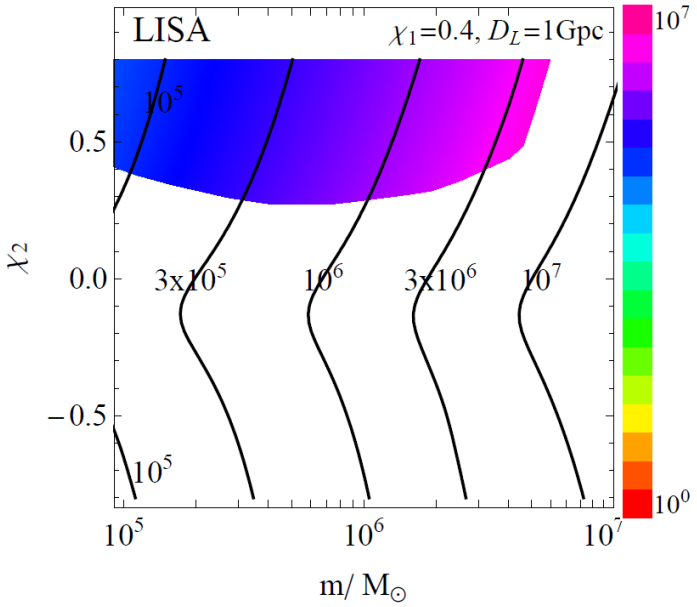

Contents

§ 1 Introduction

§ 2 Black Hole Solutions

§ 3 Gravitational Waves from BH Binaries

§ 4 Summary & Future Work

-New BH Solution to quadratic order in spin

⇨ 2PN Conservative Correction

-PN Scheme ⇨ 2PN Dissipative Correction

⇨ First self-consistent BH Binary gravitational waveforms

2nd generation ground-based interferometers

⇨ 7 orders of magnitude stronger constraint than the solar system bound!!

Future Work

- Precessing BH binaries
- Bayesian analysis, more realistic detector noises
- Modeling NSs in dynamical CS gravity
  - ⇨ Current constraints from double binary pulsar obs.

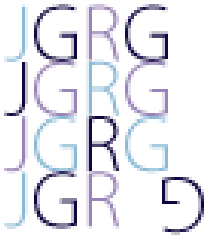

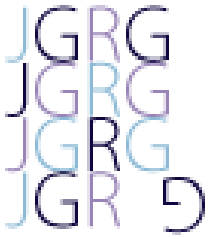

Hideki Maeda, JGRG 22(2012)111308

"Gauss-Bonnet braneworld redux: A novel scenario for the bouncing universe"

RESCEU SYMPOSIUM ON

GENERAL RELATIVITY AND GRAVITATION

JGRG 22

November 12-16 2012

Koshiba Hall, The University of Tokyo, Hongo, Tokyo, Japan





Gauss-Bonnet braneworld redux: A novel scenario for the bouncing universe

Hideki Maeda[1]

Centro de Estudios Científicos (CECs), Casilla 1469, Valdivia, Chile

Abstract

We propose a new scenario for the bouncing universe in a simple five-dimensional braneworld model in the framework of Einstein-Gauss-Bonnet gravity, which works even with ordinary matter on the brane. In this scenario, the so-called branch singularity located at a finite physical radius in the bulk spacetime plays an essential role. We show that a three-brane moving in the bulk may reach and pass through it in spite of the fact that it is a curvature singularity. The bulk spacetime is extended beyond the branch singularity in the C^0 sense and then the branch singularity is identified as a massive thin shell. From the bulk point of view, this process is the collision of the three-brane with the shell of branch singularity. From the point of view on the brane, this process is a sudden transition from the collapsing phase to the expanding phase of the universe. This manuscript is based on [1].

1 Preliminaries

We consider the following five-dimensional action for the bulk spacetime:

$$I = \frac{1}{2\kappa_5^2}\int d^5x\sqrt{-g}\Big(R - 2\Lambda + \alpha L_{\rm GB}\Big), \tag{1}$$

where the Gauss-Bonnet term $L_{\rm GB}$ is defined by

$$L_{\rm GB} := R^2 - 4R_{\mu\nu}R^{\mu\nu} + R_{\mu\nu\rho\sigma}R^{\mu\nu\rho\sigma}, \tag{2}$$

which does not give any higher-derivative term in the field equations. The constant α allows the GR limit $\alpha \to 0$. The gravitational equation given from the action (1) is

$$G^\mu{}_\nu + \alpha H^\mu{}_\nu + \Lambda\delta^\mu{}_\nu = 0, \tag{3}$$

where

$$H_{\mu\nu} := 2\Big(RR_{\mu\nu} - 2R_{\mu\alpha}R^\alpha{}_\nu - 2R^{\alpha\beta}R_{\mu\alpha\nu\beta} + R_\mu{}^{\alpha\beta\gamma}R_{\nu\alpha\beta\gamma}\Big) - \frac{1}{2}g_{\mu\nu}L_{\rm GB}. \tag{4}$$

The Gauss-Bonnet term in the action is obtained in the low-energy limit of heterotic superstring theory together with a dilaton in ten dimensions, in which case α is regarded as the inverse string tension and positive definite. We therefore assume $\alpha > 0$ throughout this paper. We also assume $\Lambda < 0$ and $1+4\alpha\Lambda/3 > 0$ in addition, the latter of which ensures the existence of nondegenerate maximally symmetric vacuum solutions.

1.1 Bulk solution

In this system, a vacuum solution is obtained as a warped product manifold $\mathcal{M}^5 \approx M^2 \times K^3$, where K^3 is a three-dimensional space of constant curvature. In the equations which follow, k denotes the curvature

[1]Email address: hideki@cecs.cl

of K^3 and takes the values 1 (positive curvature), 0 (zero curvature), and -1 (negative curvature). The metric of the vacuum solution is given by

$$ds_5^2 = g_{\mu\nu}dx^\mu dx^\nu = -h(r)dt^2 + \frac{dr^2}{h(r)} + r^2\left[d\chi^2 + f_k(\chi)^2(d\theta^2 + \sin^2\theta d\phi^2)\right], \tag{5}$$

$$h(r) := k + \frac{r^2}{4\alpha}\left(1 \mp \sqrt{1 + \frac{\alpha\mu}{r^4} + \frac{4}{3}\alpha\Lambda}\right), \tag{6}$$

where μ is constant, $f_0(\chi) := \chi$, $f_1(\chi) := \sin\chi$, and $f_{-1}(\chi) := \sinh\chi$ [2, 3].

It is seen that the solution has two branches corresponding to the sign in the metric function $h(r)$. We call the family with the minus (plus) sign the GR branch (non-GR branch). Only the GR branch solution has the general relativistic limit. The maximally symmetric vacuum in the non-GR branch was shown to be unstable [2] and so we only consider the solution in the GR branch in the present paper.

The global structures of this spacetime depending on the parameters have been clarified [4]. In this spacetime, there are two classes of curvature singularity for $\mu \neq 0$. One is the central singularity at $r = 0$ and the other is the branch singularity at $r = r_{\rm b} (> 0)$, where the term inside the square-root in the metric function (6) vanishes. $r_{\rm b}$ is explicitly given by

$$r_{\rm b} := \left(-\frac{3\alpha\mu}{3 + 4\alpha\Lambda}\right)^{1/4}. \tag{7}$$

The branch singularity exists if μ is negative. The metric and its inverse are finite at $r = r_{\rm b}$ (but their derivatives blow up) and the metric becomes complex and hence unphysical at $r < r_{\rm b}$.

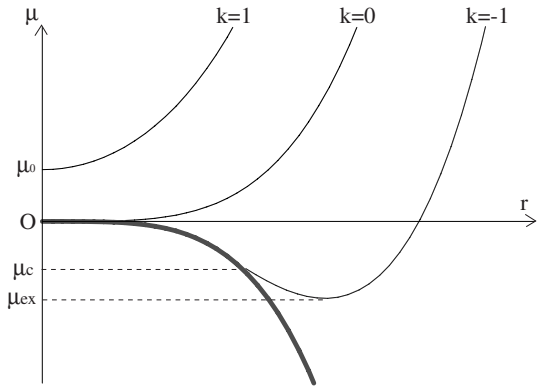

Figure 1: Thin curves show the relations between the mass parameter and the horizon radius for each k. A thick curve shows to the relation between the mass parameter and the branch-singularity radius. The metric becomes complex and unphysical below the thick curve.

Near the branch singularity, the metric function behaves as

$$h(r) \simeq \left(k + \frac{r_{\rm b}^2}{4\alpha}\right) - \frac{r_{\rm b}^{3/2}}{2\alpha}\sqrt{1 + \frac{4}{3}\alpha\Lambda}(r - r_{\rm b})^{1/2}. \tag{8}$$

Therefore, the branch singularity is timelike and spacelike for $k + r_{\rm b}^2/(4\alpha) > 0$ and $k + r_{\rm b}^2/(4\alpha) \leq 0$, respectively.

1.2 Friedmann equation on the brane

We consider a three-brane in the bulk spacetime (5), which is a timlike hypersurface described by $r = a(\tau)$ and $t = T(\tau)$, where the parameter τ is the proper time on the brane. The induced metric of the three-brane $\bar{g}_{ab}$ is given by

$$ds_4^2 = \bar{g}_{ab}dy^a dy^b = -d\tau^2 + a(\tau)^2\left[d\chi^2 + f_k(\chi)^2(d\theta^2 + \sin^2\theta d\phi^2)\right]. \tag{9}$$

This is the FRW metric with the spatial curvature k.

The dynamics of the three-brane, namely the behavior of the scale factor $a(\tau)$ on the brane, is determined by the junction condition. Here we simply assume the Z_2-symmetry of reflection with respect to the brane; we take two copies of the bulk spacetime with $r < a(\tau)$ and paste them at $r = a(\tau)$. Using the junction condition in Einstein-Gauss-Bonnet gravity [5, 6] with the following form of the energy-momentum tensor $S^a{}_b$ on the brane;

$$S^a{}_b = \mathrm{diag}(-\rho, p, p, p) + \mathrm{diag}(-\sigma, -\sigma, -\sigma, -\sigma,), \tag{10}$$

we obtain the modified Friedmann equation for the brane universe as

$$\frac{\kappa_5^4}{36}(\rho+\sigma)^2 = \left(\frac{h(a)}{a^2} + H^2\right)\left[1 + \frac{4\alpha}{3}\left(\frac{3k - h(a)}{a^2} + 2H^2\right)\right]^2, \tag{11}$$

where $H := \dot{a}/a$ and a dot denotes the differentiation with respect to τ [5, 7]. Here ρ and p are the energy density and pressure of a perfect fluid on the brane, and the constant σ is the brane tension.

We assume the following linear equation of state $p = (\gamma - 1)\rho$ and then the energy-conservation equation on the brane is integrated to give

$$\rho = \frac{\rho_0}{a^{3\gamma}}, \tag{12}$$

where a constant ρ_0 is assumed to be positive. Because $\gamma = 0$ is equivalent to the cosmological constant, we assume $0 < \gamma \leq 2$ which satisfies the dominant energy condition.

For $\alpha > 0$, Eq. (11) is solved to give the following modified Friedmann equation on the brane:

$$H^2 = V(a), \tag{13}$$

$$V(a) := \frac{1}{8\alpha}\left[-\frac{8k\alpha}{a^2} - 2 + \left\{A^{3/2} + 256\alpha^3P^2 + 16\sqrt{2\alpha^3P^2\left(128\alpha^3P^2 + A^{3/2}\right)}\right\}^{1/3} + A\left\{A^{3/2} + 256\alpha^3P^2 + 16\sqrt{2\alpha^3P^2\left(128\alpha^3P^2 + A^{3/2}\right)}\right\}^{-1/3}\right], \tag{14}$$

where

$$A := 1 + \frac{\alpha\mu}{a^4} + \frac{4}{3}\alpha\Lambda, \qquad P^2 := \frac{\kappa_5^4}{256\alpha^2}\left(\frac{\rho_0}{a^{3\gamma}} + \sigma\right)^2. \tag{15}$$

Here $V(a)$ denotes the effective potential and the region with $V(a) > 0$ is the allowed region for dynamics. Now we have a one-dimensional potential problem with one dynamical degree of freedom $a(\tau)$ and the qualitative behavior of a is completely understood by the form of the potential V.

2 Bouncing Gauss-Bonnet braneworld

The bouncing solution is characterized by the transition from the contracting phase ($\dot{a} < 0$) to the expanding one ($\dot{a} > 0$) of the universe. The bounce in a conventional sense occurs at the lower bound of this domain $a = a_\mathrm{B}$ satisfying $V(a_\mathrm{B}) = 0$. The evolution of the contracting universe in the domain $a > a_\mathrm{B}$ momentarily stops at $a = a_\mathrm{B}$ and then starts to expand in the domain $a > a_\mathrm{B}$. Therefore, the sufficient condition for this conventional bounce is $V(0) < 0$.

It is shown that the conventional bounce may occur in some cases in the Gauss-Bonnet braneworld with $\mu > 0$. In contrast, the situation in the Gauss-Bonnet braneworld with $\mu < 0$ is very different. The primary reason is that there is a branch singularity in the bulk and $a < r_\mathrm{b}$ is not in the physical domain of a. We will see what happens when the brane hits the branch singularity in the bulk.

2.1 Novel bounce for $\mu < 0$

For $\mu < 0$, $a < r_{\rm b}$ is not in the physical domain of a and so we focus on the behavior of the potential around $a = r_{\rm b}$. If the potential is non-negative, the brane reaches $a = r_{\rm b}$. If the potential is negative near $a = r_{\rm b}$, the bounce (in the conventional sense) occurs or a singularity appears at some $a > r_{\rm b}$.

First we present the condition that the brane hits the branch singularity in the bulk spacetime. The behavior of $V(a)$ around $a = r_{\rm b}$ is given by

$$V(a) \simeq V(r_{\rm b}) + O(a - r_{\rm b}), \tag{16}$$

where

$$V(r_{\rm b}) = -\frac{k}{r_{\rm b}^2} - \frac{1}{4\alpha} + P(r_{\rm b})^{2/3}. \tag{17}$$

Therefore, the brane reaches the branch singularity if $V(r_{\rm b}) \geq 0$. This condition is satisfied if

$$h(r_{\rm b}) = k + \frac{r_{\rm b}^2}{4\alpha} \leq 0. \tag{18}$$

Therefore, if the branch singularity is spacelike, which is realized only for $k = -1$, the brane reaches there. If the branch singularity is timelike, the condition $V(r_{\rm b}) \geq 0$ gives

$$\sigma \geq \frac{16\alpha}{\kappa_5^2}\left(\frac{k}{r_{\rm b}^2} + \frac{1}{4\alpha}\right)^{3/2} - \frac{\rho_0}{r_{\rm b}^{3\gamma}}. \tag{19}$$

It is noted that this condition is not so sensitive about γ and realized even with positive pressure ($\gamma > 1$). On the other hand, if

$$\sigma < \frac{16\alpha}{\kappa_5^2}\left(\frac{k}{r_{\rm b}^2} + \frac{1}{4\alpha}\right)^{3/2} - \frac{\rho_0}{r_{\rm b}^{3\gamma}} \tag{20}$$

is satisfied, $a = r_{\rm b}$ is not in the physical domains of a and hence the conventional bounce occurs or a singularity appears at some $a > r_{\rm b}$ instead.

We have seen the condition under which the brane hits the branch singularity in the bulk. Let us see what happens then. Now the important fact is that the curvature invariants on the brane do *not* blow up even when the brane approaches the branch singularity in the bulk. In fact, the behavior of the scale factor $a(\tau)$ near the branch singularity is obtained as

$$a(\tau) \simeq r_{\rm b} + a_1(\tau - \tau_{\rm b}) + O((\tau - \tau_{\rm b})^2), \tag{21}$$

$$a_1^2 := r_{\rm b}^2 V(r_{\rm b}), \tag{22}$$

where $\tau_{\rm b}$ is the cosmological time on the brane to reach the branch singularity. This is the Taylor series around $\tau = \tau_{\rm b}$ and hence the curvature invariants are all finite around there. However, because the allowed domain of a is $a \geq r_{\rm b}$, we must take the minus and plus signs of a_1 for $\tau < \tau_{\rm b}$ and $\tau > \tau_{\rm b}$, respectively. As a result, the evolution near $\tau = \tau_{\rm b}$ represents the transition from the collapsing phase ($\tau < \tau_{\rm b}$) to the expanding phase ($\tau > \tau_{\rm b}$). Thus, the bouncing universe is realized on the brane.

From the bulk point of view, this process is that the brane reaches the branch singularity and passes across it. It is emphasized that the spacetime on the brane is not free of singularities then, but there appears just a shell-type instantaneous singularity. In the generic case, the derivative of $a(\tau)$ (velocity) is not continuous and the metric on the brane is C^0 at $\tau = \tau_{\rm b}$. The junction condition on the brane then shows that there is a matter distribution on the spacelike hypersurface $\tau = \tau_{\rm b}$ on the brane. This means that a shell-type singularity appears instantaneously on the brane at $\tau = \tau_{\rm b}$ but it is rather harmless since it stems from the thin-shell approximation of the brane as well as the branch singularity. With a fine-tuning giving $a_1 \equiv 0$, in contrast, the metric on the brane becomes analytic around $\tau = \tau_{\rm b}$ and there is no shell-type singularity.

In summary, our claim is that the brane can reach the branch singularity and pass through it safely. In order to support this claim, we will show in the next subsections that the branch singularity is indeed harmless for a finite body moving radially and can be considered as a massive thin shell. From the bulk point of view, this novel bouncing process is the collision of the three-brane with the shell of branch singularity.

2.2 Branch singularity is weak

In this subsection, we show that the branch singularity is a weak singularity. The physical consequence of this property is that a finite body may reach there safely.

There are several definitions of the strength of a singularity. We first present the definition by Tipler [8]. Let $\bar{\gamma} : [\lambda_0, \lambda_s) \to M$ be an affinely parametrized causal geodesic which approaches a singularity as $\lambda \to \lambda_s^-$, where λ is an affine parameter. Define $J_{\lambda_1}(\bar{\gamma})$ for $\lambda_1 \in [\lambda_0, \lambda_s)$ to be a set of maps $Z_{(I)} : [\lambda_0, \lambda_s) \to TM$ (TM means the tangent bundle and $I = 1, 2, 3, 4$ ($I = 1, 2, 3$) for timelike (null) $\bar{\gamma}$) satisfying the following four:

$$Z^\mu_{(I)}(\lambda) \in T_{\bar{\gamma}(\lambda)}M, \tag{23}$$

$$Z^\mu_{(I)}(\lambda_1) = 0, \tag{24}$$

$$\ddot{Z}^\mu_{(I)} = -R^\mu{}_{\nu\rho\sigma} Z^\rho_{(I)} k^\nu k^\sigma, \tag{25}$$

$$Z^\mu_{(I)} k_\mu = 0. \tag{26}$$

where k^μ is the tangent of $\bar{\gamma}$. Equation (25) is called the Jacobi equation (or geodesic deviation equation). Along a timelike geodesic, four independent Jacobi fields define a volume element $V(\lambda)$ along $\bar{\gamma}$ by the exterior product. Along a null geodesic, three such fields define an area element which we also denote $V(\lambda)$. A singularity is called *Tipler strong* if

$$\lim_{\lambda \to \lambda_s^-} \inf V(\lambda) = 0 \tag{27}$$

is satisfied for all $\lambda_1 \in [\lambda_0, \lambda_s)$ and all four (three) linearly independent Jacobi fields $Z \in J_{\lambda_1}(\bar{\gamma})$ [8]. The singularity is called Tipler weak if it is not Tipler strong. This definition of the Tipler strong singularity intuitively says that any object that hits a strong singularity is crushed to zero volume (area).

The above definition ignores the case where $V(\lambda)$ blows up in the approach to the singularity. Also, $V(\lambda)$ may remain finite overall when some of the elements of $J_{\lambda_1}(\bar{\gamma})$ blow up but some others converge to zero. In order to include such situations, Ori defined deformationally strong singularity [9]. A singularity is called *deformationally strong* if it is either (i) Tipler strong, or (ii) if there exists an element of $J_{\lambda_1}(\bar{\gamma})$ that has infinite norm for $\lambda \to \lambda_s^-$ for all $\lambda_1 \in [\lambda_0, \lambda_s)$ [9]. A singularity is called deformationally weak if it is not deformationally strong. A singularity is Tipler weak if it is deformationally weak. Actually, it is shown by direct calculations that the branch singularity is deformationally weak along radial causal geodesics [1].

2.3 C^0 extension of the bulk beyond the branch singularity

In the previous subsection, we have seen that the branch singularity is harmless for radially moving finite bodies, which strongly supports our main claim. Then, the subsequent natural question is what the bulk spacetime on the other side of the branch singularity is. In order to answer to this question, we consider the extension of the bulk spacetime beyond $r = r_b$.

It is seen in (5) that the metric and its inverse are finite at the branch singularity. This implies that the spacetime can be extended beyond $r = r_b$ in the C^0 sense. The C^0 extension is not unique in general; however, thanks to the Birkhoff's theorem in the system [7], there are only two candidates for the extended spacetime, namely the GR and non-GR branches of the vacuum solution (5). Among these two, the GR branch should be chosen because of its dynamical stability. By attaching another the vacuum solution (5) in the GR-branch with the same mass parameter at the position of the branch singularity, we construct the C^0-extended bulk spacetime.

Now let us study the branch singularity in this extended spacetime in more detail. The induced metric on $r = r_b$ is given by

$$ds_4^2 = \bar{g}_{ab} dy^a dy^b = -h(r_b) dt^2 + r_b^2 \left[d\chi^2 + f_k(\chi)^2 (d\theta^2 + \sin^2\theta d\phi^2) \right]. \tag{28}$$

We know that the derivatives of h are not finite at $r = r_b$. The component of the extrinsic curvature K_{ab} of the hypersurface $r =$constant diverges in the limit $r \to r_b$. Nevertheless, the junction condition

provides a finite value of the energy-momentum tensor on $r = r_{\rm b}$. This implies that the branch singularity can be identified as a massive shell in the extended bulk spacetime. We consider the cases where $r = r_{\rm b}$ is timelike ($h(r_{\rm b}) > 0$) and spacelike ($h(r_{\rm b}) < 0$), separately. (A more careful treatment is required in the case of $h(r_{\rm b}) = 0$.)

First we consider the case where $r = r_{\rm b}$ is timelike. Then, we have

$$h(r_{\rm b}) = k + \frac{r_{\rm b}^2}{4\alpha} (> 0) \tag{29}$$

and the junction condition shows that $S^a{}_b$ on the hypersurface remains finite for $r \to r_{\rm b}$ as

$$\lim_{r \to r_{\rm b}} S^a{}_b = \mathrm{diag}(-\rho_{\rm b}, p_{\rm b}, p_{\rm b}, p_{\rm b}), \tag{30}$$

where

$$\rho_{\rm b} = -16\alpha \frac{h(r_{\rm b})^{3/2}}{r_{\rm b}^3}, \quad p_{\rm b} = \frac{8h(r_{\rm b})r_{\rm b}^4 - \mu}{2\sqrt{h(r_{\rm b})}r_{\rm b}^5}. \tag{31}$$

Thus, the branch singularity can be considered as a massive thin shell. Since $\rho_{\rm b} < 0$, the matter on $r = r_{\rm b}$ violates the weak energy condition.

Next we consider the case where $r = r_{\rm b}$ is spacelike. Then the junction condition gives the energy-momentum tensor $S^a{}_b$ on the spacelike hypersurface as

$$\lim_{r \to r_{\rm b}} S^a{}_b = \mathrm{diag}(P_{\rm b(r)}, P_{\rm b(t)}, P_{\rm b(t)}, P_{\rm b(t)}), \tag{32}$$

where

$$P_{\rm b(r)} = 16\alpha \frac{(-h(r_{\rm b}))^{3/2}}{r_{\rm b}^3}, \quad P_{\rm b(t)} = \frac{8h(r_{\rm b})r_{\rm b}^4 + \mu}{2\sqrt{-h(r_{\rm b})}r_{\rm b}^5}. \tag{33}$$

They are finite and hence the branch singularity may be considered as a massive spacelike thin shell. Since this is a spacelike shell, it is difficult to discuss the energy condition for the matter field there.

3 Summary and discussions

In this paper, we have presented a novel scenario for the bouncing universe in the five-dimensional braneworld in the framework of Einstein-Gauss-Bonnet gravity. In this scenario, the branch singularity located at the finite physical radius in the bulk, which appears for the negative mass parameter, plays an essential role. We have shown that the bulk spacetime is extended beyond the branch singularity in the C^0 sense and the branch singularity is identified as a massive thin shell. A three-brane may pass through the shell of branch singularity and then the bouncing universe is realized on the brane. This claim is strongly supported by the fact that the branch singularity is radially deformationally weak, which implies that the singularity is harmless for a finite body moving radially.

The present result opens a completely new possibility to achieve the bouncing brane universe as an effect of the higher-curvature terms. Our scenario is not sensitive about the equation of state for the matter on the brane and does work even with ordinary matter. Since the existence of the branch singularity stems from the quadratic nature of the theory, such a singularity is characteristic and must be quite generic in higher-curvature theories. In Lovelock higher-curvature gravity [10], which contains general relativity and Einstein-Gauss-Bonnet gravity as special cases, such a singularity appears in this class of vacuum solutions rather generically [11]. Interestingly, the central singularity is totally absent and the branch singularity is generic independent of the mass paraeter μ if there is a U(1) gauge field in the bulk spacetime in Einstein-Gauss-Bonnet gravity [12]. Undoubtedly, the effect of such singularities in cosmology is an interesting problem and should be investigated further.

References

[1] H. Maeda, Phys. Rev. D **85**, 124012 (2012).

[2] D. G. Boulware, and S. Deser, Phys. Rev. Lett. **55**, 2656 (1985).

[3] J. T. Wheeler, Nucl. Phys. **B268**, 737 (1986); D. Lorenz-Petzold, Mod. Phys. Lett. **A3**, 827 (1988); R.-G. Cai, Phys. Rev. D **65**, 084014 (2002); R.-G. Cai and Qi Guo, Phys. Rev. D **69**, 104025 (2004).

[4] T. Torii and H. Maeda, Phys. Rev. D**71**, 124002 (2005).

[5] S.C. Davis, Phys. Rev. D **67**, 024030 (2003).

[6] E. Gravanis and S. Willison, Phys. Lett. **B562**, 118 (2003); C. Garraffo, G. Giribet, E. Gravanis, and S. Willison, J. Math. Phys. **49**, 042502 (2008).

[7] C. Charmousis and J.-F. Dufaux, Class. Quant. Grav. **19**, 4671 (2002).

[8] F.J. Tipler, Phys. Lett. A **64**, 8 (1977).

[9] A. Ori, Phys. Rev. D **61**, 064016 (2000).

[10] D. Lovelock, J. Math. Phys. **12**, 498 (1971).

[11] H. Maeda, S. Willison, and S. Ray, Class. Quant. Grav. **28**, 165005 (2011).

[12] T. Torii and H. Maeda, Phys. Rev. D**72**, 064007 (2005).

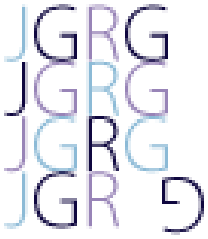

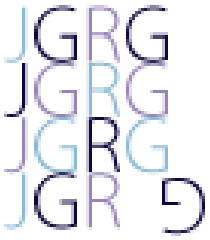

Tomohiro Takahashi, JGRG 22(2012)111311

"Instability of charged Lovelock black holes"

RESCEU SYMPOSIUM ON

GENERAL RELATIVITY AND GRAVITATION

JGRG 22

November 12-16 2012

Koshiba Hall, The University of Tokyo, Hongo, Tokyo, Japan





Instability of Charged Lovelock Black Holes

Tomohiro Takahashi[1(a)]

(a) *Department of Physics, Kyoto University, Kyoto 606-8502, Japan*

Abstract

We study stability of charged black hole solutions in Lovelock theory that is a natural higher dimensional extension of 4-dimensional Einstein theory. In the Lovelock-Maxwell system, there exist black hole solutions with two parameters, i.e., mass and charge. We examine the linear stability of this solution and construct master equations. We present the criterion for instability using these equations. By checking these criterion numerically, we show that nearly extreme black holes show instability in high frequency modes.

1 Introduction

In higher dimensional gravitational theory, when we adopt brane world scenarios, black holes might be created at colliders [1]. Thus it is important to examine the properties of higher dimensional black holes. There exist many properties, but linear stability is one of the most important property. This is because black holes with instability must not be created.

When we consider higher dimension, we must extend 4-dimensional Einstein theory into higher dimensional gravitational theory. In 4-dimensions, Einstein theory is constructed on the basis of two assumptions: the covariance and no higher derivative term. Thus, it is natural to extend the 4-dimensional gravitational theory keeping these assumptions. When we extend like this, the most general gravitational theory is not Einstein theory. It is Lovelock theory [2]. Therefore, it is important to examine stability of black hole solutions in Lovelock theory.

In Lovelock theory, there exist black hole solution with mass and stability of this solution has been already examined in [4]. However, it is supposed that black holes in colliders have charge because such objects result from proton-proton collisions. Thus we must regard Maxwell charge in examining stability. In the Lovelock-Maxwell system, there exist black holes with mass and charge, namely charged Lovelock black hole solutions. Here, we examine these solutions.

The organization is as follows. In section 2, we present charged Lovelock black hole solutions. In section 3, we examine the stability. The background solution has the spherical symmetry, so we can discuss tensor-type, vector-type and scalar-type perturbations separately. Thus we present the criteria for instability separately. Furthermore, we present a numerical result for 5-dimensional case. In section 4, we summarize the discussions.

2 Charged Lovelock Black Holes

In this section, we present charged Lovelock black hole as the solution of the Lovelock-Maxwell system. This system is governed by the action

$$\int d^D x\sqrt{\quad g}\quad \mathcal{L}_{\text{Lovelock}}\quad \frac{1}{4}F\quad F \tag{1}$$

where F is the eld strength of Maxwell eld A and $\mathcal{L}_{\text{Lovelock}}$ is

$$\mathcal{L}_{\text{Lovelock}}\quad =\quad \beta_1 R+\sum_{m=2}^{k}\frac{\beta_m(2m)!}{2^m m\prod_{p=1}^{2m}{}^{2}(n\quad p)}\ {}^{[}_{\kappa_1}{}^{1}_{}\ {}^{\sigma_1}_{1}\ {}^{2}_{\kappa_2}\quad\quad {}^{\sigma_m]}_{m}R\ {}_{1\sigma_1}{}^{\kappa_1\ 1}\quad\quad R\ {}_{m\sigma_m}{}^{\kappa_m\ m}\ . \tag{2}$$

[1]Email address: takahashi@tap.scphys.kyoto-u.ac.jp

Here n is related to the dimension D as $n = D \quad 2$ and β_ms are arbitrary constants which are called Lovelock coefficients. And k corresponds to the maximum order de ned as $k \quad [(D \quad 1)/2]$.

In this system, there exist spherically symmetric solutions. We here start from the ansatz

$$ds^2 = f(r)dt^2 + 1/f(r)dr^2 + r^2\gamma_{ij}dx^i dx^j, \tag{3}$$
$$F^{tr} = E(r), \quad \text{other components} = 0 \ . \tag{4}$$

Substituting these into the equations of motion derived from the above action, we obtain the following solution:

$$f(r) = 1 \quad r^2 \ (r) \ ,$$
$$\mathcal{P}[\ ] \quad \sum_{m=2}^{k} \frac{\beta_m}{m} \ ^m \ + \ = \frac{\mathcal{M}}{r^{n+1}} \quad \frac{\mathcal{Q}^2}{r^{2n}} \ , \tag{5}$$

and

$$E(r) = \sqrt{n(n \quad 1)}\mathcal{Q}/r^n \ . \tag{6}$$

Here $\mathcal{M}$ is a mass parameter of a black hole and $\mathcal{Q}$ corresponds to charge. In order to gain the explicit form, we must solve the k-th order polynomial equation (5). This equation has at most k roots, but there must only an asymptotically flat root. Here we call this asymptotic flat root charged Lovelock black hole.

3 Stability Analysis

In this section, we check the stability of this charged Lovelock black hole solution [3]. This solution has the spherical symmetry, so we can classify the rst order perturbations into tensor-type, vector-type and scalar-type and we can treat these separately.

3.1 Tensor-type Perturbations

Firstly, we discuss the tensor-type perturbations. The Maxwell eld A has no tensorial perturbations and then we only consider the gravitational perturbations

$$g_{tt} = \ g_{tr} = \ g_{ti} = \ g_{rr} = \ g_{ri} = 0, \quad g_{ij} = r^2\phi(r)e^{i\omega t}\mathcal{T}_{ij}. \tag{7}$$

Here, $\mathcal{T}_{ij}$ is tensor harmonics which is characterized by $\mathcal{T}_{ij}{}^{|k}{}_{|k} = \ (\ell(\ell+n \quad 1) \quad 2)\mathcal{T}_{ij}$. Using this metric perturbation, we can obtain

$$\partial_{r^*}^2 + V_g(r) \ \Psi = \omega^2\Psi \ , \tag{8}$$

where

$$\Psi = \phi(r)r\sqrt{T'(r)}, \ dr \ /dr = 1/f \ , \ T(r) = r^n \ ^1\partial_\psi\mathcal{P} \ ,$$
$$V_g(r) = \frac{\ell(\ell+n \quad 1)f}{(n \quad 2)r}\frac{T''}{T'} + \frac{1}{r\sqrt{T'}}\partial_{r^*}^2(r\sqrt{T'}) \ . \tag{9}$$

This is a Schrodinger-type equation and its eigenvalue is ω^2 and we decompose like $e^{i\omega t}$. Thus, if there exist negative eigenvalue states, charged Lovelock black holes are unstable. The effective potential for this equation is characterized by the function $T(r)$ and the constant ℓ. Then , for instance, negative eigenvalue states may exist if $T(r)$ behaves peculiar. Indeed, as is shown In [5], we can show that the Schrodinger equation for large ℓ modes has negative eigenvalue states if T' or T'' have negative regions. Thus what we have to do next is checking these criteria and we will do in subsection 3.4.

3.2 Vector-type Perturbations

For vector-type perturbations, we take the Regge-Wheeler gauge in which perturbative variables are expressed as

$$\begin{aligned} &A_t = \quad A_r = 0, \quad A_i = Ce^{i\omega t}\mathcal{V}_i \\ &g_{ti} = we^{i\omega t}\mathcal{V}_i, \quad g_{ri} = ve^{i\omega t}\mathcal{V}_i, \text{ otherwise} = 0 \ , \end{aligned} \tag{10}$$

where $\mathcal{V}_i$ is the vector harmonics which is characterized by ${\mathcal{V}_i}^{|l}{}_{|l} = \quad \kappa_v \mathcal{V}_i$. Substituting these into equation of motion and using suitable variables, we can gain the following master equation:

$$\partial_{r^*}^2 + \begin{matrix} V_g(r) & V_c(r) \\ V_c(r) & V_{em}(r) \end{matrix} \begin{matrix} \Psi \\ \zeta \end{matrix} = \omega^2 \begin{matrix} \Psi \\ \zeta \end{matrix} \ , \tag{11}$$

where

$$\begin{aligned} V_g(r) &= \frac{\kappa_v \quad (n \quad 1)}{n \quad 1}\frac{fT'}{rT} + r\sqrt{T'}\partial_{r^*}^2\frac{1}{r\sqrt{T'}} \ , \\ V_c(r) &= \quad 2(Er^n)\sqrt{\frac{\kappa_v \quad (n \quad 1)}{2(n \quad 1)}}\frac{f\sqrt{T'}}{r^{(n+2)/2}T} \ , \\ V_{em}(r) &= (\kappa_v + (n \quad 1))\frac{f}{r^2} + 2(Er^n)^2\frac{f}{r^{n+1}T} + r^{\ (n \ \ 2)/2}\partial_{r^*}^2 r^{(n \ \ 2)/2} \ . \end{aligned} \tag{12}$$

This is a Schrodinger equation with two components and ω^2 is its eigenvalue. In the same way as tensor-type, if the above Schrodinger equation has negative eigenstates, black holes are unstable. However, as is shown in [5], the Schrodinger operator is positive-de nite. Therefore, there is no negative eigenstate in the above system.

3.3 Scalar-type Perturbations

Finally, we consider the scalar-type perturbations. In the Zerilli gauge, perturbative variables are expressed as

$$\begin{aligned} &g_{tt} = fH_0\mathcal{Y}, \quad g_{tr} = H_1\mathcal{Y}, \quad g_{rr} = H\mathcal{Y}/f, \quad g_{ij} = r^2K\mathcal{Y}\gamma_{ij}, \\ &F_{tr} = X\mathcal{Y}, \quad F_{ti} = Y\mathcal{Y}_{|i}, \quad F_{ri} = Z\mathcal{Y}_{|i}, \text{ otherwise} = 0 \ , \end{aligned} \tag{13}$$

where $\mathcal{Y}$ is the scalar harmonics which is characterized by ${\mathcal{Y}_{|l}}^{|l} = \quad \kappa_s \mathcal{Y}$. Substituting these into equation of motion and using suitable variables which is discussed in [5], the perturbative equation can be summarized as

$$\partial_{r^*}^2 + \begin{matrix} V_g(r) & V_c(r) \\ V_c(r) & V_{em}(r) \end{matrix} \begin{matrix} \Psi \\ \zeta \end{matrix} = \omega^2 \begin{matrix} \Psi \\ \zeta \end{matrix} \ , \tag{14}$$

where

$$\begin{aligned} V_g(r) &= \kappa_s\frac{f}{nr} \quad 4(\kappa_s \quad n)\frac{T'}{\mathcal{A}T} \quad \frac{T''}{T'} \\ &\quad + \frac{2n(r^nE)^2f^2}{\mathcal{A}Tr^n} \quad \ln \quad \frac{fT'}{r^{n \ \ 2}(\mathcal{A}T)^2} \quad ' + \frac{\mathcal{A}T}{r\sqrt{T'}}f\partial_r\left(f\partial_r\frac{r\sqrt{T'}}{\mathcal{A}T}\right) \ , \\ V_c(r) &= \sqrt{\frac{\kappa_s \quad n}{n}}\frac{\sqrt{T'}}{r^{n/2}\mathcal{A}}\left[\ \kappa_s\frac{4(r^nE)f}{rT} + \frac{2n(r^nE)f^2}{T} \quad \ln \quad \frac{fT'}{r^{n \ \ 2}(\mathcal{A}T)^2} \quad '\right] \ , \\ V_{em}(r) &= fr^{(n \ \ 2)/2}\partial_r(f\partial_r\frac{1}{r^{(n \ \ 2)/2}}) \\ &\quad + \kappa_s\frac{f}{r^2} \quad 1 + \frac{4(Er^n)^2}{\mathcal{A}Tr^{n \ \ 1}} \quad + \frac{2n(r^nE)^2f^2}{r^n\mathcal{A}T} \quad \ln \quad \frac{r^{2n \ \ 2}(\mathcal{A}T)^2}{f} \quad ' \ , \\ \mathcal{A} &= 2\kappa_s + nrf' \quad 2nf \ . \end{aligned} \tag{15}$$

The above equation is Schrodinger equation. Thus, in the same way as tensor-type perturbations, whether negative energy states exist or not determines the stability of the background solutions. For this, as is shown in [5], we can prove that "if T' or $2T'^2 \quad TT''$ have negative regions, black holes show instability". Thus what we have to do next is checking the behaviors of the above functions and we examine these in the next subsection.

3.4 Numerical Result in 5-dimensions

Here, we check the behaviors of three function T', T'' and $2T'^2 \quad TT''$ numerically. For instance, we present the result for the 5-dimensional case. Fig.1 corresponds to this result.

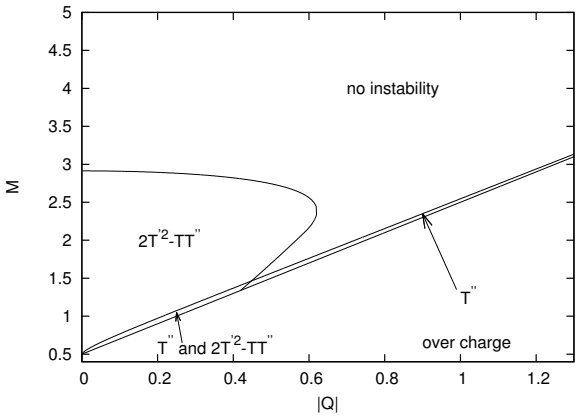

Figure 1: We show the unstable parameters in 5-dimensions. The horizontal axis correspond charge and the vertical one is mass. From this gure, there exist instability for nearly extreme black holes.

From this gure, we can easily see that nearly extreme black hole show instability. Note that this property is common to the other dimensions. Therefore, we can say that nearly extreme black holes are unstable in the Lovelock-Maxwell system.

4 Conclusion

We have studied the stability of charged black holes in Lovelock black holes. we have presented the master equation for each type of perturbations and shown the criteria for instability. We have also examined the criteria numerically and shown that nearly extreme black holes are unstable. These result indicates that black hole with nearly extreme mass are not created and very high energy is needed to produce black holes in colliders if Lovelock theory is true.

References

[1] S. B. Giddings and S. D. Thomas, Phys. Rev. D **65**, 056010 (2002) [arXiv:hep-ph/0106219];
S. B. Giddings and M. L. Mangano, Phys. Rev. D **78**, 035009 (2008) [arXiv:0806.3381 [hep-ph]].

[2] D. Lovelock, J. Math. Phys. **12** (1971) 498.

[3] R. Zegers, J. Math. Phys. **46**, 072502 (2005) [gr-qc/0505016].

[4] T. Takahashi and J. Soda, Prog. Theor. Phys. **124**, 911 (2010) [arXiv:1008.1385 [gr-qc]];
T. Takahashi and J. Soda, Prog. Theor. Phys. **124**, 711 (2010) [arXiv:1008.1618 [gr-qc]].

[5] T. Takahashi, PTEP **2013**, 013E02 (2013) [arXiv:1209.2867 [gr-qc]].

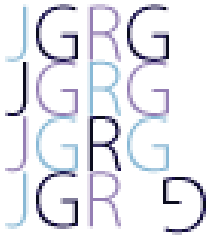

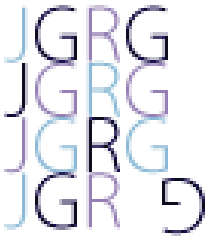

Naomasa Fushimi, JGRG 22(2012)111313

"Criterion for bound (or unbound) orbits in the Kottler spacetime"

RESCEU SYMPOSIUM ON

GENERAL RELATIVITY AND GRAVITATION

JGRG 22

November 12-16 2012

Koshiba Hall, The University of Tokyo, Hongo, Tokyo, Japan





Criterion for bound (or unbound) orbits in the Kottler spacetime

Naomasa Fushimi

Hirosaki University, Japan
with K.Yamada and H. Asada (Hirosaki)

JGRG22 in Tokyo November 12 - 16, 2012

Abstract: We discuss criteria for bound (or unbound) orbits of a test particle in the Kottler (Shcwarzschild-de Sitter) spacetime.

1 The equation of motion

The equation of motion for a test particle in Kottler spacetime:

$$\left(\frac{dr}{d\tau}\right)^2 = \frac{\Lambda}{3}r^2 + E + \frac{\Lambda}{3}j^2 + \frac{r_g}{r} - \frac{j^2}{r^2} + \frac{r_g j^2}{r^3} \tag{1}$$

where E , j^2 are constants defined by

$$E = \left(1 - \frac{r_g}{r} - \frac{\Lambda}{3}r^2\right)^2 \dot{t}^2 - 1$$
$$j^2 = r^2\dot{\phi}.$$

They are the energy per unit mass and angular momentum from correspondence with Newtonian mechanics, respectively.
And r_g is Schwarzschild radius, Λ is cosmological constant.

$$\frac{d^2r}{d\tau^2} = \frac{\Lambda}{3}r - \frac{r_g}{2r^2} + \frac{j^2}{4r^3} - \frac{r_g j^2}{6r^4} \tag{2}$$

2 Criterion for bound (or unbound) orbits

2.1 Sch

Well-known criterion for bound orbits near Schwarzschild blackhole.
$(k = \frac{3r_g^2}{j^2} < 1)$

$$j^2 < 3r_g^2$$
Unbound

$$3r_g^2 \le j^2 < 4r_g^2$$
$$\frac{-2(1-k)^{3/2} + 2 - 3k}{9k} < E < \frac{2(1-k)^{3/2} + 2 - 3k}{9k}$$

$$4r_g^2 \le j^2$$
$$\frac{-2(1-k)^{3/2} + 2 - 3k}{9k} < E < 0.$$

2.2 Kottler

Since we do not have a quintic formula, we cannot solve equation (1) nor equation (2), either. Then, Strum's theorem is applied.
equation (1) to six inequalities were obtained and equation (2) to three inequalities were obtained. Criterion for bound orbits in Kottler spacetime are found
$(\lambda = r_g^2\Lambda \ll 1)$

$$j^2 < 3r_g^2(1-18\lambda)$$
Unbound

$$3r_g^2(1-18\lambda) < j^2 < 4r_g^2[1-(10\lambda)^{1/3}]$$
$$\frac{-2(1-k)^{3/2} + 2 - 3k}{9k} - \lambda A_- < E < \frac{2(1-k)^{3/2} + 2 - 3k}{9k} + \lambda A_+$$
$$\left(A_\pm = 2\frac{16 - 60k + 69k^2 - 15k^3 - 12k^4 \pm \sqrt{1-k}(16 - 52k + 45k^2 + 2k^3 - 8k^4)}{k\{\pm 2(1-k)^{3/2} + 2 - 3k\}^3}\right)$$

$$4r_g^2[1-(10\lambda)^{1/3}] < j^2 < \frac{3}{16}r_g^2\left(\frac{3}{\lambda}\right)^{1/3}$$
$$\frac{-2(1-k)^{3/2} + 2 - 3k}{9k} - \lambda A_- < E < X^{1/3} - \frac{10\Lambda j^2}{27X^{1/3}} - \frac{\Lambda j^2}{8}$$
$$\left(X = \frac{5\Lambda\sqrt{6561r_g^4 + \frac{2560\Lambda j^6}{3}}}{648} - \frac{5r_g^2\Lambda}{8}\right)$$

$$\frac{3}{16}r_g^2\left(\frac{3}{\lambda}\right)^{1/3} < j^2$$
Unbound

The upper limit of angular momentum is new criterion.

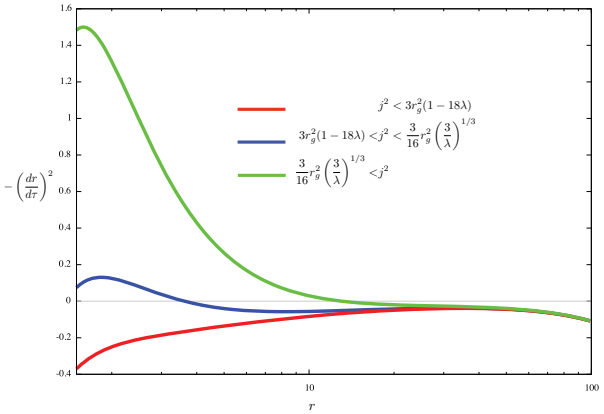

$(E = 0, \Lambda = 10^{-5}, r_g = 1)$

3 Outermost orbit

In equation (2), the fourth item loses its effect at the distant place. it changes into:

$$\frac{d^2r}{d\tau^2} \simeq \frac{\Lambda}{3}r - \frac{r_g}{2r^2} + \frac{j^2}{4r^3}. \tag{3}$$

On the boundary line at the distant place which changes from bound to unbound, it is required that the solution for r should become a multiple solution. Therefore, angular momentum is obtained as

$$j^2 = \frac{3}{16}r_g^2\left(\frac{3}{\lambda}\right)^{1/3}.$$

and r is obtained as

$$r = \frac{r_g}{2}\left(\frac{3}{\lambda}\right)^{1/3}. \tag{4}$$

This is outermost orbit.

4 Conclusion

We obtained criteria for bound (or unbound) orbits of a test particle.
Then substituting a suitable parameter value into obtained equation (4),

$$r \sim 10^{18}[\mathrm{m}]. \tag{5}$$

References

[1] F. Kottler, Ann. Phys. (Leipzig), 361, 401, (1918)

[2] J. M. A. Dandy, *Fundamentals of Celestial Mechanics,* 2nd ed. (William-Bell, VA, 1988).

[3] C. W. Misner, K. S. Thorne, J. A. Wheeler, *Gravitation*, (Freeman, New York, 1973).

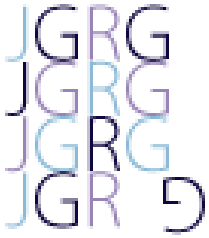

Kouji Nakamura, JGRG 22(2012)111315

"Problems in nth-order extension of the gauge-invariant perturbation theory"

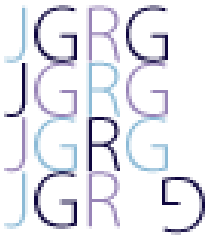

RESCEU SYMPOSIUM ON

GENERAL RELATIVITY AND GRAVITATION

JGRG 22



November 12-16 2012

Koshiba Hall, The University of Tokyo, Hongo, Tokyo, Japan



Problems in nth-order extension of the gauge-invariant perturbation theory

Kouji Nakamura (NAOJ)

References :

K.N. Prog. Theor. Phys., **110** (2003), 723. (arXiv : gr-qc/0303039).
K.N. Prog. Theor. Phys., **113** (2005), 413. (arXiv : gr-qc/0410024).
K.N. Adv. in Astron. **2010** (2010), 576273. (arXiv : 1001.2621[gr-qc]).
K.N. CQG **28** (2011), 122001. (arXiv : 1011.5272 [gr-qc]).
K.N. preprint (arXiv : 1105.4007 [gr-qc]).
K.N. Int. J. Mod. Phys. D **21** (2012), 1242004. (arXiv : 1203.6448 [gr-qc]).
K.N. in progress

I. Introduction

- The higher order perturbation theory in general relativity has very wide physical motivation.

  - **Cosmological perturbation theory**
    - Expansion law of inhomogeneous universe (ΛCDM v.s. inhomogeneous cosmology)
    - Non-Gaussianity in CMB (beyond WMAP)

  - **Black hole perturbations**
    - Radiation reaction effects due to the gravitational wave emission.

  - **Perturbation of a star (Neutron star)**
    - Rotation – pulsation coupling (Kojima 1997)

There are many physical situations to which higher order perturbation theory should be applied.

However, general relativistic perturbation theory requires very delicate treatments of “gauges”.

It is worthwhile to formulate the higher-order gauge-invariant perturbation theory from general point of view.

- According to this motivation, we have been formulating the general relativistic second-order perturbation theory in a gauge-invariant manner.
  - **General formulation :**
    - Framework of higher-order gauge-invariant perturbations :
      - K.N. PTP**110** (2003), 723; *ibid.* **113** (2005), 413.
    - Construction of gauge-invariant variables for the linear order metric perturbation :
      - K.N. CQG**28** (2011), 122001; 1105.4007[gr-qc]; IJMPD**21** (2012), 1242004.
    - **The nth-order extension of the definitions of gauge-invariant variables :**
      - K.N. in progress. (I am trying to resolve this issue.)
  - **Application to cosmological perturbation theory** :
    - Einstein equations : K.N. PRD**74** (2006), 101301R; PTP**117** (2007), 17.
    - Equations of motion for matter fields : K.N. PRD**80** (2009), 124021.
    - Consistency of the 2nd order Einstein equations : K.N. PTP**121** (2009), 1321.
    - Summary of current status of this formulation : K.N. Adv. in Astron. **2010** (2010), 576273.
    - Comparison with a different formulation : A.J. Christopherson, et al., CQG**28** (2011), 225024.

- In this poster presentation,
  - We propose an outline to define the gauge-invariant variables for nth-order general-relativistic perturbations.
  - Some problems to complete this outline are summarized.

II. “Gauge” in general relativity

(R.K. Sachs (1964).)

- There are two kinds of “gauge” in general relativity.
  - The concepts of these two “gauge” are closely related to the general covariance.
  - “General covariance” :

    There is no preferred coordinate system in nature.

- **The first kind “gauge”** is a coordinate system on a single spacetime manifold.

- **The second kind “gauge”** appears in the perturbation theory.

  This is a point identification between the physical spacetime and the background spacetime.
  - To explain this second kind “gauge”, we have to remind what we are doing in perturbation theory.

III. The second kind gauge in GR.

(Stewart and Walker, PRSL **A341** (1974), 49.)

Physical spacetime (PS)

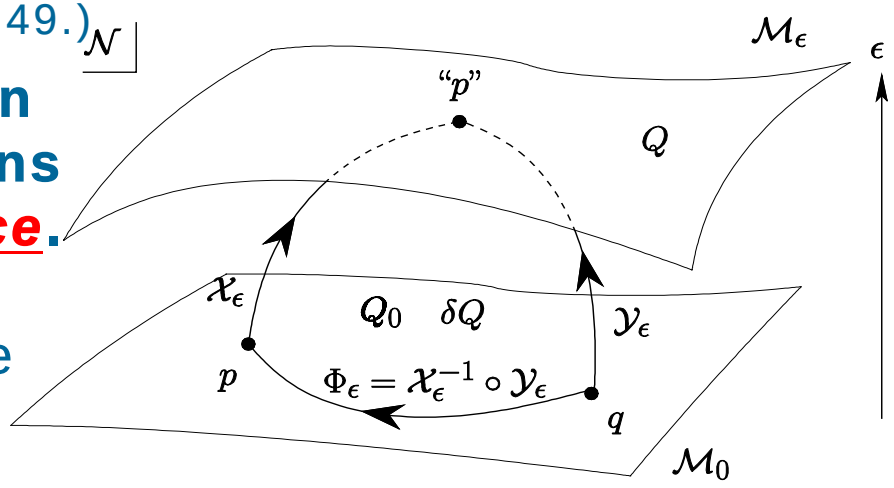

Background spacetime (BGS)

- **"*Gauge degree of freedom*" in general relativistic perturbations arises due to *general covariance*.**

- In any perturbation theories, we always treat two spacetimes :
  - *Physical Spacetime (PS);*
  - *Background Spacetime (BGS).*

- In perturbation theories, we always write equations like

$$Q(\text{“}p\text{”}) = Q_0(p) + \delta Q(p)$$

Through this equation, we always identify the points on these two spacetimes and this identification is called "gauge choice" in perturbation theory.

Gauge transformation rules to second order

Expansion of gauge choices :

We assume that each gauge choice is an exponential map.

$$Q_{\mathcal{X}} = \mathcal{X}_\epsilon^* Q = Q + \epsilon \pounds_u Q + \frac{1}{2}\epsilon^2 \pounds_u^2 Q + O(\epsilon^3)$$

$$Q_{\mathcal{Y}} = \mathcal{Y}_\epsilon^* Q = Q + \epsilon \pounds_v Q + \frac{1}{2}\epsilon^2 \pounds_v^2 Q + O(\epsilon^3)$$

$$\Phi_\epsilon^* Q = \left(\mathcal{X}_\epsilon^{-1} \circ \mathcal{Y}_\epsilon\right)^* Q = Q + \epsilon \pounds_{\xi_1} Q + \frac{1}{2}\epsilon^2 \left(\pounds_{\xi_2} + \pounds_{\xi_1}^2\right) Q + O(\epsilon^3)$$

(Sonego and Bruni, CMP, **193** (1998), 209.)

-------> $\xi_1 = u - v, \quad \xi_2 = [u, v]$

Expansion of the variable :

$$Q = Q_0 + \epsilon Q_1 + \frac{1}{2} Q_2 + O(\epsilon^3)$$

Order by order gauge transformation rules :

$$\mathcal{Y} Q_1 - \mathcal{X} Q_1 = \pounds_{\xi_1} Q_0$$

$$\mathcal{Y} Q_2 - \mathcal{X} Q_2 = 2 \pounds_{\xi_1} \mathcal{X} Q_1 + \left(\pounds_{\xi_2} + \pounds_{\xi_1}^2\right) Q_0$$

Gauge transformation rules for nth-order perturbations (Sonego and Bruni, CMP, **193** (1998), 209.)

- **Representation of general diffeomorphism :**

$$\Phi_\epsilon^* Q = \phi_{\frac{\epsilon^n}{(n)!}\xi_{(n)}} \circ \phi_{\frac{\epsilon^{n-1}}{(n-1)!}\xi_{(n-1)}} \circ \cdots \phi_{\frac{\epsilon^2}{(2)!}\xi_{(2)}} \circ \phi_{\frac{\epsilon}{(1)!}\xi_{(1)}} Q + O(\epsilon^{n+1})$$

$$= \sum_{l=0}^{n} \frac{\epsilon^l}{l!} \sum_{J_l} \frac{l!}{(1!)^{j_1}(2!)^{j_2}\cdots((l)!)^{j_l} j_1! j_2! \cdots j_l!} \pounds_{\xi_{(1)}}^{j_1} \pounds_{\xi_{(2)}}^{j_2} \cdots \pounds_{\xi_{(l)}}^{j_l} Q + O(\epsilon^{n+1})$$

where $J_l := \left\{ (j_1, \ldots, j_l) \in \mathbb{N}^l \,\middle|\, \sum_{i=1}^{l} i j_i = l \right\}$, $\phi_{\frac{\epsilon^l}{(l!)}\xi_{(l)}}$: the exponential map generated by $\frac{\epsilon^l}{(l!)}\xi_{(l)}^a$.

- **Expansion of the variable :** $Q = \sum_{l=0}^{n} \frac{\epsilon^l}{l!} Q_{(l)} + O(\epsilon^{n+1})$

- **Order by order gauge transformation rules :**

$$\mathcal{Y}Q_{(k)} = \sum_{l=0}^{k} \frac{k!}{(k-l)!} \sum_{J_l} \frac{1}{(1!)^{j_1}(2!)^{j_2}\cdots((l)!)^{j_l} j_1! j_2! \cdots j_l!} \pounds_{\xi_{(1)}}^{j_1} \pounds_{\xi_{(2)}}^{j_2} \cdots \pounds_{\xi_{(l)}}^{j_l} \mathcal{X}Q_{(k-l)}$$

To develop nth-order gauge-invariant perturbation theory, we have to construct gauge-invariant variables for each order perturbation through this gauge-transformation rule.

- **Problem 1 :**
  General diffeomorphism should form a group. How to prove?

III. Construction of gauge invariant variables in higher order perturbations

- metric perturbation : metric on PS : $\bar{g}_{ab}$, metric on BGS : g_{ab}

  metric expansion : $\bar{g}_{ab} = g_{ab} + \epsilon h_{ab} + \frac{1}{2}\epsilon^2 l_{ab} + O(\epsilon^3)$

  Our general framework of the second-order gauge invariant perturbation theory is based on a single assumption.

- **linear order (decomposition conjecture) :**

Suppose that the linear order perturbation h_{ab} is decomposed as

$$h_{ab} = \mathcal{H}_{ab} + \pounds_X g_{ab}$$

so that the variable $\mathcal{H}_{ab}$ and X^a are the gauge invariant and the gauge variant parts of h_{ab} , respectively.

These variables are transformed as

$$\mathcal{Y}\mathcal{H}_{ab} - \mathcal{X}\mathcal{H}_{ab} = 0 \qquad \mathcal{Y}X^a - \mathcal{X}X^a = \xi_1^a$$

under the gauge transformation $\Phi_\epsilon = \mathcal{X}_\epsilon^{-1} \circ \mathcal{Y}_\epsilon$.

This conjecture is almost proved but is still a conjecture due to the "zero-mode problem" !! (Problem 2)

[See K.N. CQG **28** (2011), 122001; arXiv:1105.4007[gr-qc]; IJMPD **21** (2012), 1242004.]

Second order :

Once we accept the above assumption for the linear order metric perturbation h_{ab} , we can always decompose the second order metric perturbations l_{ab} as follows :

$$l_{ab} =: \mathcal{L}_{ab} + 2\pounds_X h_{ab} + \left(\pounds_Z - \pounds_X^2\right) g_{ab}$$

where $\mathcal{L}_{ab}$ is gauge invariant part and Z_a is gauge variant part.

Under the gauge transformation $\Phi_\epsilon = \mathcal{X}_\epsilon^{-1} \circ \mathcal{Y}_\epsilon$, the vector field Z_a is transformed as $\quad {}_{\mathcal{Y}}Z^a - {}_{\mathcal{X}}Z^a = \xi_2^a + [\xi_1, X]^a$

Perturbations of an arbitrary matter field Q :

Using gauge variant part of the metric perturbation of each order, gauge invariant variables for an arbitrary tensor fields Q other than metric are defined by

- First order perturbation of Q : $\mathcal{Q}_1 := Q_1 - \pounds_X Q_0$
- Second order perturbation of Q :

$$\mathcal{Q}_2 := Q_2 - 2\pounds_X Q_1 - \left\{\pounds_Z - \pounds_X^2\right\} Q_0$$

The essence of the above construction of gauge-invariant variables is to find gauge-variant variables for each-order metric perturbations.

---> The definitions of gauge-invariant variables for an arbitrary matter field are automatically given through the gauge-variant variables for each-order metric perturbation.

We may concentrate on each-order metric perturbation.

The metric expansion : $$\bar{g}_{ab} = \sum_{l=0}^{n} \frac{\epsilon^l}{l!} {}^{(l)}g_{ab} + O(\epsilon^{n+1})$$

We denote the gauge-variant parts of the first- and the second-order metric perturbation as

$$ {}^{(1)}X^a := X^a, \quad {}^{(2)}X^a := Z^a. $$

Third-order metric perturbation [K.N. (2003)]

Gauge transformation rule :

$$
\begin{aligned}
{}^{(3)}_{\mathcal{Y}}g_{ab} \;=\; {}^{(3)}_{\mathcal{X}}g_{ab} + 3\pounds_{\xi_{(1)}}\,{}^{(2)}_{\mathcal{X}}g_{ab} + 3\left(\pounds^2_{\xi_{(1)}} + \pounds_{\xi_{(2)}}\right){}^{(1)}_{\mathcal{X}}g_{ab} \\
+ \left(\pounds^3_{\xi_{(1)}} + 3\pounds_{\xi_{(1)}}\pounds_{\xi_{(2)}} + \pounds_{\xi_{(3)}}\right) g_{ab}
\end{aligned}
$$

Inspecting this gauge-transformation rule, we define the variable ${}^{(3)}\hat{H}_{ab}$ by

$$
\begin{aligned}
{}^{(3)}\hat{H}_{ab} \;:=\; {}^{(3)}g_{ab} + 3\pounds_{-{}^{(1)}X}\,{}^{(2)}g_{ab} + 3\left(\pounds^2_{-{}^{(1)}X} + \pounds_{-{}^{(2)}X}\right){}^{(1)}g_{ab} \\
+ \left(\pounds^3_{-{}^{(1)}X} + 3\pounds_{-{}^{(1)}X}\pounds_{-{}^{(2)}X}\right) g_{ab}
\end{aligned}
$$

We can check that the gauge-transformation rule for ${}^{(3)}\hat{H}_{ab}$ is given by

$$
{}^{(3)}_{\mathcal{Y}}\hat{H}_{ab} - {}^{(3)}_{\mathcal{X}}\hat{H}_{ab} = \pounds_{\sigma_{(3)}}\,{}^{(0)}g_{ab}
$$

$$
\begin{aligned}
\sigma^a_{(3)} \;:=\; & \xi^a_{(3)} + 3[\xi_{(1)}, {}^{(2)}_{\mathcal{X}}X]^a + 3[\xi_{(1)}, \xi_{(2)}]^a + 3[{}^{(1)}_{\mathcal{X}}X, \xi_{(2)}]^a \\
& + 2[\xi_{(1)}, [\xi_{(1)}, {}^{(1)}_{\mathcal{X}}X]]^a + [{}^{(1)}_{\mathcal{X}}X, [\xi_{(1)}, {}^{(1)}_{\mathcal{X}}X]]^a
\end{aligned}
$$

Applying the above decomposition conjecture, we can decompose the variable ${}^{(3)}\hat{H}_{ab}$ into its gauge-invariant and gauge-variant parts as

$$
{}^{(3)}\hat{H}_{ab} =: {}^{(3)}\mathcal{H}_{ab} + \pounds_{{}^{(3)}X}\,{}^{(0)}g_{ab}, \quad {}^{(3)}_{\mathcal{Y}}\mathcal{H}_{ab} - {}^{(3)}_{\mathcal{X}}\mathcal{H}_{ab} = 0, \quad {}^{(3)}_{\mathcal{Y}}X^a - {}^{(3)}_{\mathcal{X}}X^a = \sigma^a_{(3)}.
$$

This implies that we have decomposed ${}^{(3)}g_{ab}$ as

$$
\begin{aligned}
{}^{(3)}g_{ab} \;=:\; & {}^{(3)}\mathcal{H}_{ab} + \pounds_{{}^{(3)}X} g_{ab} - 3\pounds_{-{}^{(1)}X}\,{}^{(2)}g_{ab} - 3\left(\pounds^2_{-{}^{(1)}X} + \pounds_{-{}^{(2)}X}\right){}^{(1)}g_{ab} \\
& - \left(\pounds^3_{-{}^{(1)}X} + 3\pounds_{-{}^{(1)}X}\pounds_{-{}^{(2)}X}\right) g_{ab}
\end{aligned}
$$

: gauge-invariant part, : gauge-variant part.

Fourth-order metric perturbation :

Gauge transformation rule :

$$
\begin{aligned}
{}^{(4)}_{\mathcal{Y}}g_{ab} \;=\; {}^{(4)}_{\mathcal{X}}g_{ab} &+ 4\pounds_{\xi_{(1)}}\,{}^{(3)}_{\mathcal{X}}g_{ab} + 6\left(\pounds_{\xi_{(2)}} + \pounds^2_{\xi_{(1)}}\right){}^{(2)}_{\mathcal{X}}g_{ab} + 4\left(\pounds_{\xi_{(3)}} + 3\pounds_{\xi_{(1)}}\pounds_{\xi_{(2)}} + \pounds^3_{\xi_{(1)}}\right){}^{(1)}_{\mathcal{X}}g_{ab} \\
&+ \left(\pounds_{\xi_{(4)}} + 3\pounds^2_{\xi_{(2)}} + 4\pounds_{\xi_{(1)}}\pounds_{\xi_{(3)}} + 6\pounds^2_{\xi_{(1)}}\pounds_{\xi_{(2)}} + \pounds^4_{\xi_{(1)}}\right) g_{ab}
\end{aligned}
$$

Inspecting this gauge-transformation rule, we define the variable ${}^{(4)}\hat{H}_{ab}$ by

$$
\begin{aligned}
{}^{(4)}\hat{H}_{ab} \;:=\; {}^{(4)}g_{ab} &+ 4\pounds_{-(1)X}\,{}^{(3)}g_{ab} + 6\left(\pounds_{-(2)X} + \pounds^2_{-(1)X}\right){}^{(2)}g_{ab} \\
&+ 4\left(\pounds_{-(3)X} + 3\pounds_{-(1)X}\pounds_{-(2)X} + \pounds^3_{-(1)X}\right){}^{(1)}g_{ab} \\
&+ \left(3\pounds^2_{-(2)X} + 4\pounds_{-(1)X}\pounds_{-(3)X} + 6\pounds^2_{-(1)X}\pounds_{-(2)X} + \pounds^4_{-(1)X}\right) g_{ab}
\end{aligned}
$$

We can check that the gauge-transformation rule for ${}^{(4)}\hat{H}_{ab}$ is given by

$$
{}^{(4)}_{\mathcal{Y}}\hat{H}_{ab} - {}^{(4)}_{\mathcal{X}}\hat{H}_{ab} = \pounds_{\sigma_{(4)}}\,{}^{(0)}g_{ab}
$$

$$
\begin{aligned}
\sigma^a_{(4)} \;:=\; &\xi^a_{(4)} + 4[\xi_{(1)},\xi_{(3)}]^a + 6[\xi_{(1)},[\xi_{(1)},\xi_{(2)}]]^a + 4[\xi_{(1)},{}^{(3)}X]^a + 3[\xi_{(2)},{}^{(2)}X]^a + 6[\xi_{(1)},[\xi_{(1)},{}^{(2)}X]]^a + 3[\xi_{(2)},[\xi_{(1)},{}^{(1)}X]]^a \\
&+3[{}^{(2)}X,[\xi_{(1)},{}^{(1)}X]]^a + 3[\xi_{(1)},[\xi_{(1)},[\xi_{(1)},{}^{(1)}X]]]^a + 3[\xi_{(1)},[{}^{(1)}X,[\xi_{(1)},{}^{(1)}X]]]^a + [{}^{(1)}X,[{}^{(1)}X,[\xi_{(1)},{}^{(1)}X]]]^a
\end{aligned}
$$

Applying the above decomposition conjecture, we can decompose the variable ${}^{(4)}\hat{H}_{ab}$ into its gauge-invariant and gauge-variant parts as

$$
{}^{(4)}\hat{H}_{ab} =: {}^{(4)}\mathcal{H}_{ab} + \pounds_{(4)X}\,{}^{(0)}g_{ab}, \qquad {}^{(4)}_{\mathcal{Y}}\mathcal{H}_{ab} - {}^{(4)}_{\mathcal{X}}\mathcal{H}_{ab} = 0, \qquad {}^{(4)}_{\mathcal{Y}}X^a - {}^{(4)}_{\mathcal{X}}X^a = \sigma^a_{(4)}.
$$

This implies that we have decomposed ${}^{(4)}g_{ab}$ as

$$
\begin{aligned}
{}^{(4)}g_{ab} \;=:\; {}^{(4)}\mathcal{H}_{ab} &+ \pounds_{(4)X}g_{ab} - 4\pounds_{-(1)X}\,{}^{(3)}g_{ab} - 6\left(\pounds_{-(2)X} + \pounds^2_{-(1)X}\right){}^{(2)}g_{ab} \\
&-4\left(\pounds_{-(3)X} + 3\pounds_{-(1)X}\pounds_{-(2)X} + \pounds^3_{-(1)X}\right){}^{(1)}g_{ab} \\
&- \left(3\pounds^2_{-(2)X} + 4\pounds_{-(1)X}\pounds_{-(3)X} + 6\pounds^2_{-(1)X}\pounds_{-(2)X} + \pounds^4_{-(1)X}\right) g_{ab}
\end{aligned}
$$

: gauge-invariant part, : gauge-variant part.

Problem 3 : nth-order metric perturbation :

Gauge transformation rule :

$$
\begin{aligned}
{}^{(n)}_{\mathcal{Y}}g_{ab} - {}^{(n)}_{\mathcal{X}}g_{ab} &= \sum_{l=1}^{n} \frac{n!}{(n-l)!} \sum_{J_l} \frac{1}{(1!)^{j_1}(2!)^{j_2}\cdots(l!)^{j_l} j_1! j_2! \cdots j_l!} \pounds^{j_1}_{\xi_{(1)}} \pounds^{j_2}_{\xi_{(2)}} \cdots \pounds^{j_l}_{\xi_{(l)}} {}^{(n-l)}_{\mathcal{X}}g_{ab} \\
&=: F\left[\xi^a_{(1)}, \cdots, \xi^a_{(n-1)}, \xi^a_{(n)}; {}^{(0)}_{\mathcal{X}}g_{ab}, {}^{(1)}_{\mathcal{X}}g_{ab}, \cdots, {}^{(n-1)}_{\mathcal{X}}g_{ab}\right]
\end{aligned}
$$

Inspecting this gauge-transformation rule, we define the variable ${}^{(n)}\hat{H}_{ab}$ by

$$
{}^{(n)}\hat{H}_{ab} := {}^{(n)}g_{ab} + F\left[-{}^{(1)}X^a, \cdots, -{}^{(n-1)}X^a, 0; {}^{(0)}g_{ab}, {}^{(1)}g_{ab}, \cdots, {}^{(n-1)}g_{ab}\right]
$$

We have to prove the following statement :
There exists a vector field $\sigma^a_{(n)}$ such that the gauge-transformation rule for the variable ${}^{(n)}\hat{H}_{ab}$ is given by ${}^{(n)}_{\mathcal{Y}}\hat{H}_{ab} - {}^{(n)}_{\mathcal{X}}\hat{H}_{ab} = \pounds_{\sigma_{(n)}} {}^{(0)}g_{ab}$

When the proof of the above statement is accomplished, we may apply the decomposition conjecture and we can decompose the variable ${}^{(n)}\hat{H}_{ab}$ into its gauge-invariant and gauge-variant parts as

$$
{}^{(n)}\hat{H}_{ab} =: {}^{(n)}\mathcal{H}_{ab} + \pounds_{{}^{(n)}X} {}^{(0)}g_{ab}, \quad {}^{(n)}_{\mathcal{Y}}\mathcal{H}_{ab} - {}^{(n)}_{\mathcal{X}}\mathcal{H}_{ab} = 0, \quad {}^{(n)}_{\mathcal{Y}}X^a - {}^{(n)}_{\mathcal{X}}X^a = \sigma^a_{(n)}.
$$

This implies that we have decomposed ${}^{(n)}g_{ab}$ as

$$
{}^{(n)}g_{ab} := {}^{(n)}\mathcal{H}_{ab} + \pounds_{{}^{(n)}X} g_{ab} - F\left[-{}^{(1)}X^a, \cdots, -{}^{(n-1)}X^a, 0; {}^{(0)}g_{ab}, {}^{(1)}g_{ab}, \cdots, {}^{(n-1)}g_{ab}\right]
$$

: gauge-invariant part, : gauge-variant part.

IV. Summary

We have summarized three problems in the nth-order extension of our general relativistic gauge-invariant perturbation theory.

Problems that we pointed out are as follows:

1. **Group properties of general diffeomorphisms;**
2. **Decomposition conjecture for linear metric perturbations;**
3. **Construction of nth-order gauge-invariant variables.**

Of course, the higher-order perturbation theory requires tough calculations to develop. However, we mainly focus on the essential problems in our formulation, i.e., the construction of gauge-invariant variables.

I am now trying to show the extendibility of our construction of gauge-invariant variables to nth-order perturbations by induction.

Kohkichi Konno, JGRG 22(2012)111316

"Non-inertial effects on Landau levels"

RESCEU SYMPOSIUM ON

GENERAL RELATIVITY AND GRAVITATION

JGRG 22

November 12-16 2012

Koshiba Hall, The University of Tokyo, Hongo, Tokyo, Japan

Non-Inertial Effects on Landau Levels

Kohkichi Konno

Collaborator : Rohta Takahashi

Tomakomai National College of Technology

K. Konno and R. Takahashi
"Space-time Rotation-Induced Landau Quantization"
Phys. Rev. D 85, 061502(R) (2012)
(arXiv:1201.5188)

Landau levels on a neutron star surface

e.g. G.F. Bignami et al., Nature 423, 725 (2003);
F. Haberl, Ap&SS 308, 181 (2007).

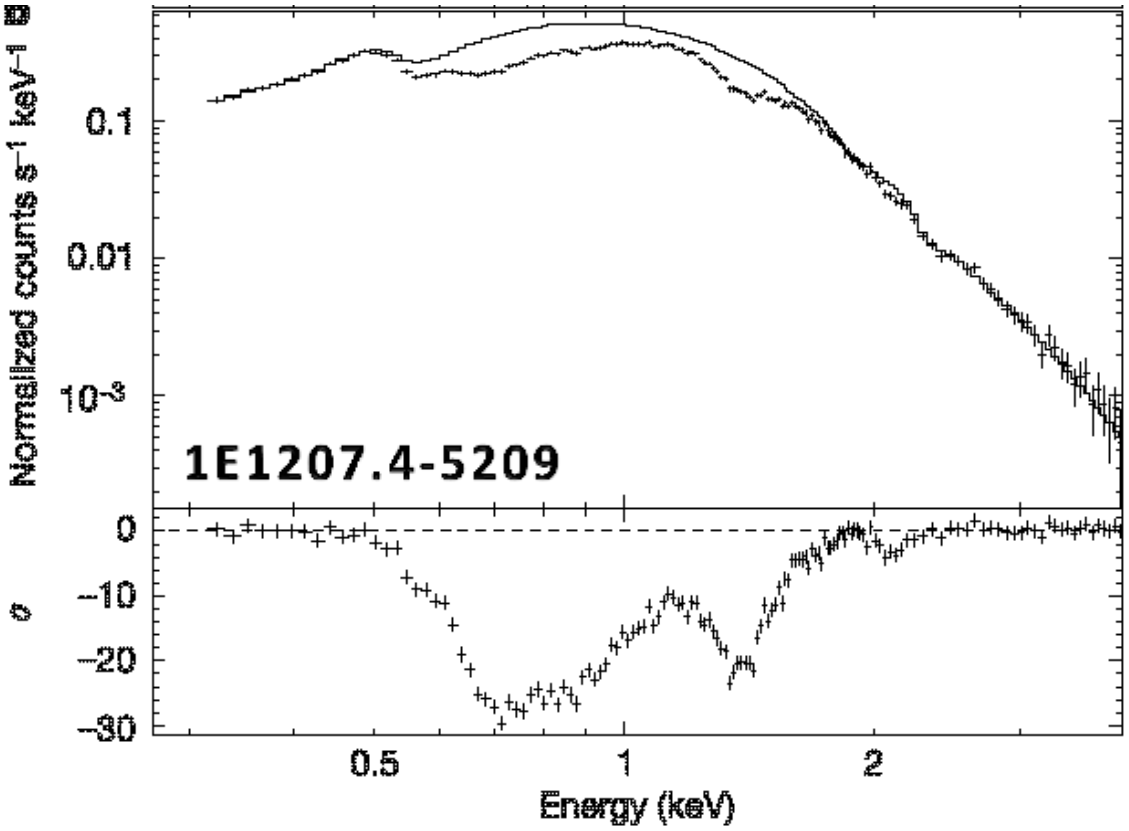

Other objects:

- RX J1605.3+3249
- RX J0720.4-3125
- RBS 1223
- RBS 1774
- etc

Quantum phenomena under strong gravity

Objective of our work

We consider quantum systems on the surface of a relativistic star to investigate quantum phenomena in the presence of both gravitational field and electromagnetic field.

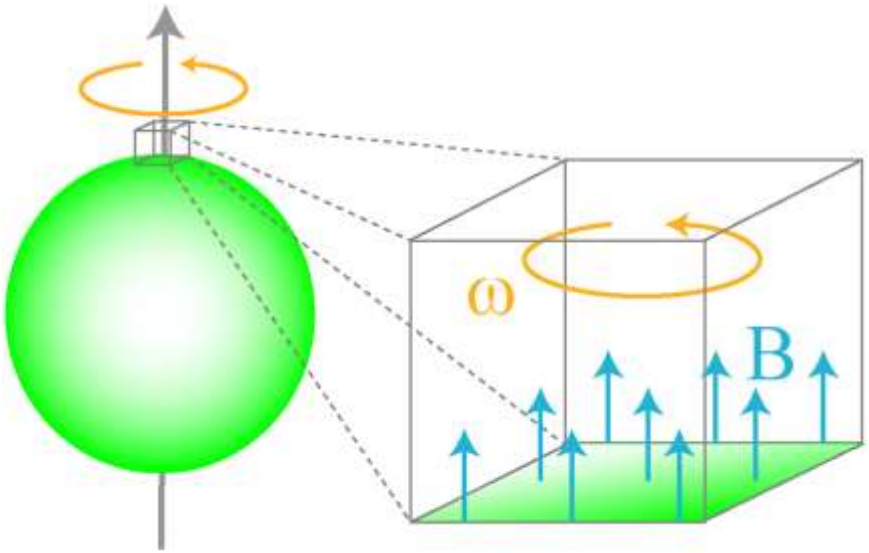

Assumptions:

- The star is rotating.
- The star has an axisymmetric magnetic field
- The rotational axis is aligned with the magnetic axis.
- Uniform magnetic field in the polar region

Our approach

Covariant Klein-Gordon equation

$$\left[g^{\mu\nu} \left(\nabla_\mu - \frac{ie}{\hbar} A_\mu \right) \left(\nabla_\nu - \frac{ie}{\hbar} A_\nu \right) + \frac{m^2 c^2}{\hbar^2} \right] \phi = 0$$

Neglecting intrinsic spin

Post-Newton expansion



$$\phi(x) = \Psi(x) \exp\left[-i \left(mc^2 / \hbar \right) t \right]$$

Schrodinger equation with relativistic corrections

Approximations

- **Slow rotation** ··· Kerr parameter: $\tilde{a} \ll 1$
- **Weak gravitational field** ··· $GM/\left(c^2 R\right) \ll 1$
- **Uniform magnetic field** ··· $\lambda_{\text{particle}} \ll L_B$

Deriving non-relativistic equation

$$\phi(x) = \Psi(x) \exp\left[-i \frac{mc^2}{\hbar} t \right]$$

Metric: $g_{\mu\nu}$,

4-Vector: $A_\mu = \left(0, \; -\frac{B}{2} y, \; \frac{B}{2} x, \; 0 \right)$



$$\left[g^{\mu\nu} \left(\nabla_\mu - \frac{ie}{\hbar} A_\mu \right) \left(\nabla_\nu - \frac{ie}{\hbar} A_\nu \right) + \frac{m^2 c^2}{\hbar^2} \right] \phi = 0$$

Spacetime metric

Slow rotation limit of the Kerr metric

$$
\begin{aligned}
ds^2 &= g_{\mu\nu} dx^\mu dx^\nu \\
&= \left(1 - \frac{2GM}{c^2 r}\right) dt^2 + \frac{4GMa}{cr} \sin^2\theta \, dt d\varphi \\
&\quad - \left(1 - \frac{2GM}{c^2 r}\right)^{-1} dr^2 - r^2 \left(d\theta^2 + \sin^2\theta d\varphi^2\right)
\end{aligned}
$$

Transformation to the surface of a rotating star

$$
\begin{cases}
x = x' \cos\Omega t - y' \sin\Omega t \\
y = x' \sin\Omega t + y' \cos\Omega t \\
z = z' + R
\end{cases}
$$

Schrodinger equation with relativistic corrections in the polar region

Neglecting the order of $O(1/c^2)$

$$i\hbar\frac{\partial}{\partial t}\Psi=\left[-\frac{\hbar^2}{2m}\nabla^2-\frac{GMm}{R}+mgz-\left(\frac{eB}{2m}+\varpi(R)\right)\hat{L}_z+\left(\frac{e^2B^2}{8m}+\frac{eB}{2}\varpi(R)\right)\left(x^2+y^2\right)\right]\Psi$$

where

$$\varpi(R)=\Omega-\frac{2GMa}{cR^3}$$

$$\hat{L}_z=-i\hbar\left(x\partial_y-y\partial_x\right)$$

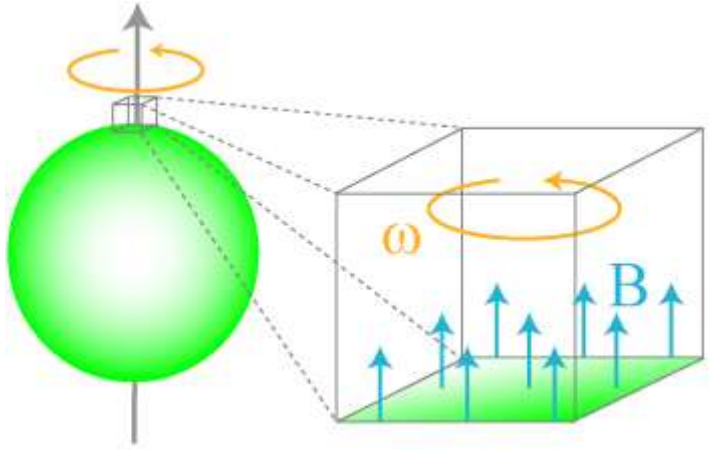

Separation of variables

Cylindrical coordinates: $\Psi(r,\theta,z)=\psi(r,\theta)\varphi(z)$

Vertical direction:

$$K\varphi=\left[-\frac{\hbar^2}{2m}\frac{\partial^2}{\partial z^2}+V(z)\right]\varphi$$

Horizontal direction :

$$(E-mU-K)\psi$$
$$=\left[-\frac{\hbar^2}{2m}\left(\partial_r{}^2+\frac{1}{r}\partial_r\right)+\frac{\hat{p}_\theta{}^2}{2mr^2}-\left(\frac{eB}{2m}+\varpi(R)\right)\hat{p}_\theta+\left(\frac{e^2B^2}{8m}+\frac{eB}{2}\varpi(R)\right)r^2\right]\psi$$

where

$$U=-GM/R,\quad \varpi(R)=\Omega-2GMa/(cR^3),$$
$$\hat{p}_\theta=-i\hbar\partial_\theta,\quad K=\text{constant}$$

Wave equation

$$\psi(r,\theta) = r^{\ell} \exp\left[i \frac{p_\theta}{\hbar} \theta \right] \exp\left[-\frac{\beta}{2} r^2 \right] F(r),$$

$$\ell = \pm \frac{p_\theta}{\hbar} \quad \text{for} \quad q = \pm e, \quad \beta = \left(\frac{q^2 B^2}{4\hbar^2} + \frac{mqB}{\hbar^2} \varpi(R) \right)^{1/2},$$

$$x = \beta r, \quad \varepsilon = \frac{2m}{\hbar^2}(E - mU - K_n) + \left(\frac{qB}{\hbar^2} + \frac{2m}{\hbar^2} \varpi(R) \right) p_\theta,$$

Transformation of variables

Confluent hypergeometric equation

$$\left[x \frac{d^2}{dx^2} + \{(\ell+1) - x\} \frac{d}{dx} - \left(\frac{\varepsilon}{4\beta} - \frac{\ell+1}{2} \right) \right] F(x) = 0$$

Integrability condition

$$\frac{\varepsilon}{4\beta} - \frac{\ell+1}{2} = n' \quad \text{(Integer)}$$

Energy eigenstates of the horizontal component

Wave function :

$$\psi = Ar^{\ell} \exp\left(-\frac{\beta}{2} r^2\right) L_n^{\ell}\left(\beta r^2\right)$$

$$\beta \equiv \sqrt{\frac{q^2 B^2}{4\hbar^2} + \frac{mqB}{\hbar^2}\varpi(R)}, \quad L_n^{\ell} : \text{ associated Laguerre function}$$

Eigen values :

$$E_{nn'} \simeq mU + \hbar\left(\frac{eB}{m} + 2\varpi(R)\right)\left(n + \frac{1}{2}\right) + K_{n'}$$

Non-inertial effects

Order estimates

As $B = 10^8 - 10^{15}[\mathrm{G}],\ M = M_\odot,\ R = 10[\mathrm{km}]$

$$\omega_B\left(m_e\right) = \frac{qB}{m_e} \simeq 10^{15} \sim 10^{22}[\mathrm{Hz}],$$

$$\omega_B\left(m_p\right) = \frac{qB}{m_p} \simeq 10^{12} \sim 10^{19}[\mathrm{Hz}],$$

$$\omega_\Omega = 2\Omega \simeq 10^3[\mathrm{Hz}], \quad \omega_a = \frac{4GMa}{cR^3} \simeq 10^2[\mathrm{Hz}],$$

Thermal effects : $\Delta\omega_T = k_\mathrm{B}T/\hbar \simeq 10^{17}[\mathrm{Hz}]$

Summary

We investigated quantum systems on a stellar surface. We seriously took account of non-inertial and gravitational effects for the quantum system through which magnetic field penetrates.

We obtained the analytic solution for the Schrodinger equation with relativistic corrections.



Landau levels are modified by the rotational and frame dragging effects.

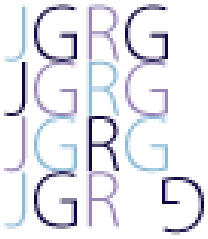

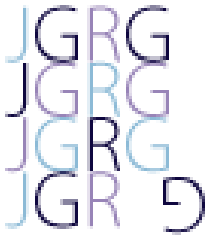

Hiroki Okawara, JGRG 22(2012)111317

"Quantum interferometer in Chern-Simons modified gravity"

RESCEU SYMPOSIUM ON

GENERAL RELATIVITY AND GRAVITATION

JGRG 22

November 12-16 2012

Koshiba Hall, The University of Tokyo, Hongo, Tokyo, Japan





Quantum Interferometry in Chern-Simons modified gravity

Hiroki Okawara
Hirosaki University, Japan
with K. Yamada, and H. Asada (Hirosaki)

JGRG22 in Tokyo Nov. 12 - 16, 2012

Accepted by Phys. Rev. Lett.

Abstract

Possible effects of Chern-Simons (CS) gravity on a quantum interferometer turn out to be dependent on the latitude and direction of the interferometer on the Earth in orbital motion around the Sun.

1 Chern-Simons (CS) gravity

CS gravity modifies GR via the addition of a correction

$$S_{CS} = \frac{1}{16\pi G}\int d^4x \frac{1}{4} f R^\star R, \tag{1}$$

Following [1], let us consider a system of nearly spherical bodies in the standard PPN point-particle approximation. The CS correction to the metric becomes

$$\delta_{CS} g_{0i} = \frac{2G}{c^3}\sum_A \frac{\dot{f}}{r_A}\left[\frac{m_A}{r_A}(\vec{v}_A\times\vec{n}_A)^i - \frac{J_A^i}{2r_A^2} + \frac{3}{2}\frac{(\vec{J}_A\cdot\vec{n}_A)}{r_A^2}n_A^i\right]. \tag{2}$$

2 Phase shifts in a quantum interferometer

We consider a quantum interferometer that consists of a closed path C (its area S) on the Earth, as shown by Fig 1. Δ is a phase difference induced by g_{0i} .
By using Stokes theorem, Δ is rewritten in the surface integral form over S

$$\Delta = \frac{mc}{\hbar}\oint_C \vec{g}\cdot d\vec{r} = \frac{mc}{\hbar}\int_S (\vec{\nabla}\times\vec{g}). \tag{3}$$

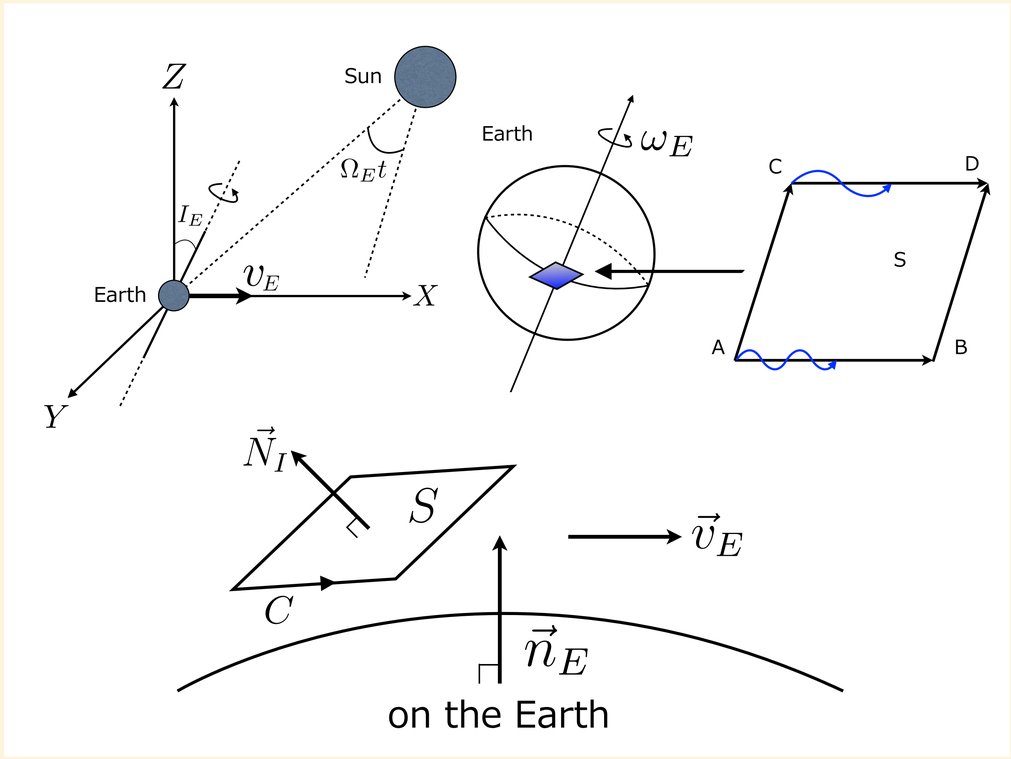

Figure 1: Quantum interferometer on the Earth orbiting around the Sun.

3 Phase shifts for Chern-Simons (CS) gravity

Let us substitute the CS term of Eq. (2) into Eq. (3) to obtain Δ for CS gravity. We focus on the Earth mass in CS gravity and use $r_E \gg \sqrt{S}$. Hence,

$$\Delta_{CS} = 2\dot{f}\frac{mGM_E S}{\hbar c^2 r_E^3}\tilde{\Delta}_{CS}, \tag{4}$$

$$\tilde{\Delta}_{CS} = [3(\vec{v}_E\cdot\vec{n}_E)\vec{n}_E - \vec{v}_E]\cdot\vec{N}_I. \tag{5}$$

Eq. (5) depends on the latitude and direction, and changes with the Earth's spin and orbital motion.

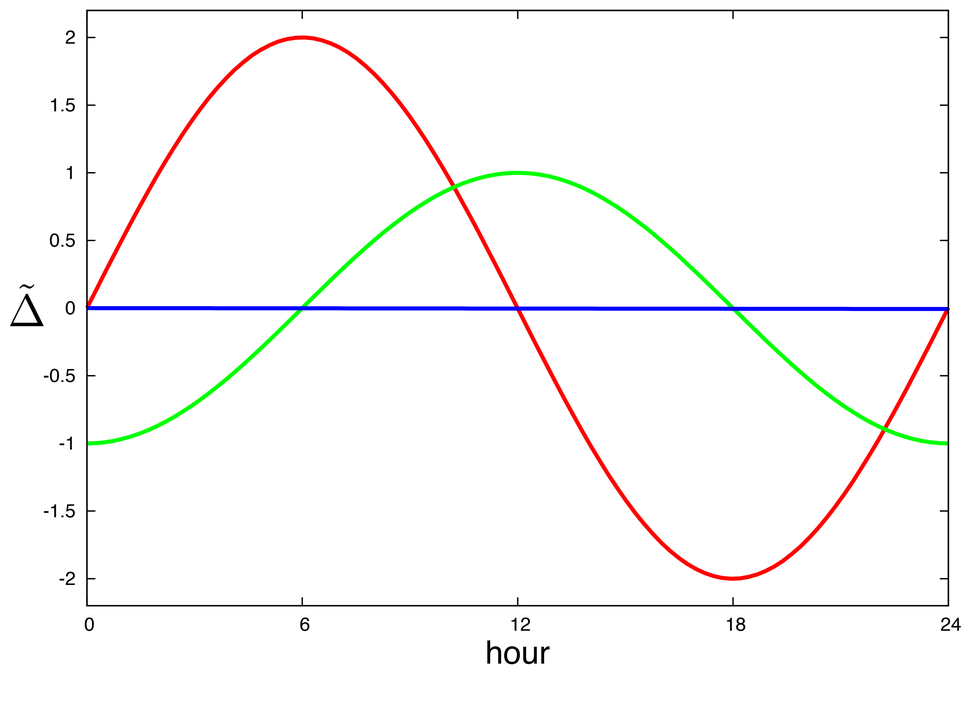

Figure 2: Daily variation in phase differences by CS effects. The red, green, and blue curves correspond to $\vec{N}_I$ for a horizontal plane and two vertical ones (one facing the East and the other facing the North), respectively.

4 Time variation and the latitude

By using the coordinate rotation $\vec{N}_I(t) = R(\omega_E t)\vec{N}_{I0}, \vec{n}_E(t) = R(\omega_E t)\vec{n}_{E0}$,
$\tilde{\Delta}_{CS}$ is rewritten in the rotating matrix $R(t)$

$$\tilde{\Delta}_{CS} = \left(R(t)^{-1}\vec{v}_E\right)^{\mathrm{T}}\left[3(\vec{n}_{E0}\cdot\vec{N}_{I0})\vec{n}_{E0} - \vec{N}_{I0}\right], \tag{6}$$

$$R(t)^{-1}\vec{v}_E = \{R(\phi)\}^{-1}\{R(\omega_E t)\}^{-1}\{R(\Omega_E t)\}^{-1}R(I_E)R(\Omega_E t)\begin{pmatrix} v_E \\ 0 \\ 0 \end{pmatrix}. \tag{7}$$

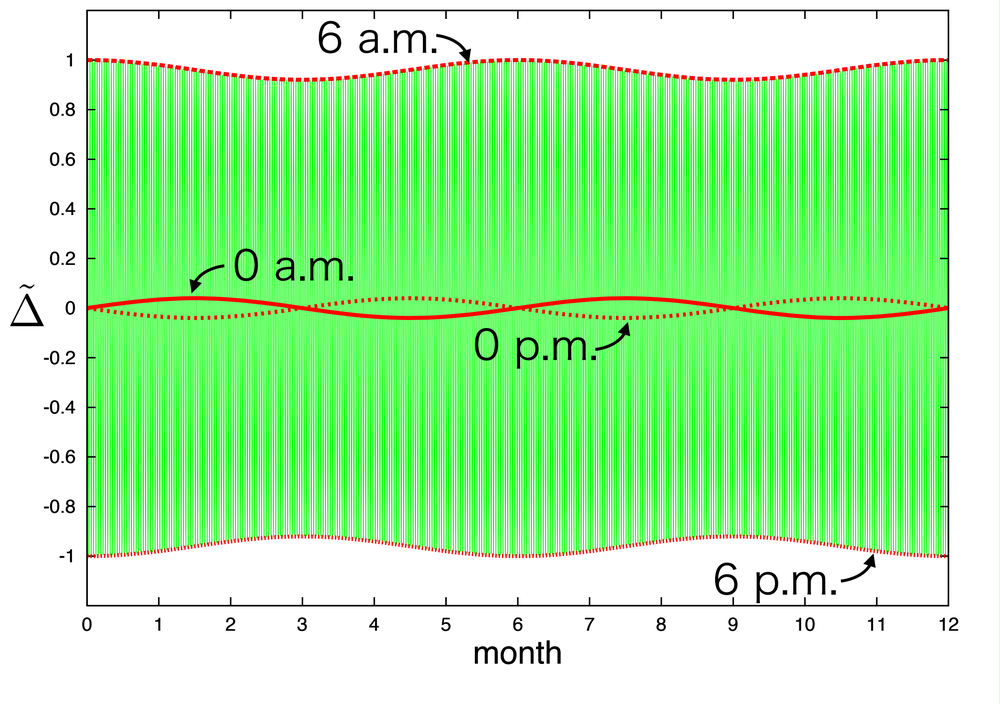

Figure 3: Seasonal variation in phase differences by CS effects. The green solid is full data points.

5 Possible constraint on $\dot{f}$

$\dot{f}$ induces the phase shift

$$|\Delta_{CS}| \sim 10^{-3}\mathrm{s}^{-1}\times\left(\frac{mc^2}{1\mathrm{GeV}}\right)\left(\frac{\dot{f}}{c}\right)\left(\frac{S}{0.4\mathrm{m}^2}\right). \tag{8}$$

Current phase mesurement accuracy at $O(10^{-3}) \rightarrow \dot{f}c^{-1} < 10^0$s bound.
GPB (Gravity Probe B), LAGEOS space mission $\rightarrow \dot{f}c^{-1} < 10^{-3}$s.

6 Conclusion

We considered effects of CS gravity on a quantum interferometer.

- Daily and seasonal variations in phase shifts are predicted with an estimate of the size of the effects.
- Neutron interferometry with ~ 5 meters arm length and $\sim 10^{-4}$ phase measurement accuracy would place a bound on a CS parameter comparable to Gravity Probe B satellite [2].

References

[1] S. Alexander and N. Yunes, Phys. Rev. Lett. **99**, 241101 (2007). [2] H. Okawara, K. Yamada, H. Asada, accepted Phys. Rev. Lett. (2012) (arXiv: **1210.4628**).

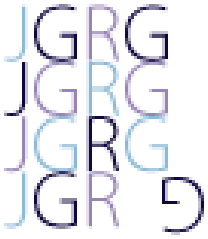

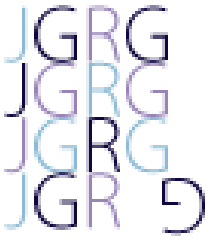

Masato Kaneyama, JGRG 22(2012)111318

"Excess power method with the Hilbert-Huang transform in search for gravitational wave signals"

RESCEU SYMPOSIUM ON

GENERAL RELATIVITY AND GRAVITATION

JGRG 22

November 12-16 2012

Koshiba Hall, The University of Tokyo, Hongo, Tokyo, Japan





Excess power method with the Hilbert-Huang transform in search for gravitational wave signals

Masato Kaneyama [1](a), Jordan B, Camp(b), Yuta Hiranuma(a)
Ken-ichi Oohara(a), Alexander Stroeer(c), and Hirotaka Takahashi(d)

(a) *raduate School of Science and Technology, Niigata University, Niigata 950-2181, Japan*
(b) *Laboratory for ravitational Physics, NASA oddard Space Flight Center, reenbelt, Maryland 20771, USA*
(c) *Center for ravitational Wave Astronomy, The University of Texas at Brownsville, Brownsville, Texas 78520, USA*
(d) *Department of Humanities, Yamanashi Eiwa College, Yamanashi 400-8555, Japan*

Abstract

We investigate the application of the Hilbert-Huang transform (HHT) to search for gravitational waves. The HHT is a novel and adaptive approach to time-series analysis. The HHT consists of an empirical mode decomposition and Hilbert spectral analysis. It can be applied to the analysis of gravitational-wave bursts, because this analysis does not assume the waveform. Thus, in this paper, we propose the excess power method with the HHT and estimate the detection efficiency of the proposed method.

1 Introduction

The Hilbert-Huang transform (HHT) [1, 2, 3] is a novel analysis of time series data which contain physical oscillatory modes. It is used to detect the signal in the noise and characterize physical oscillatory modes. The HHT consists of an empirical mode decomposition (EMD), followed by a Hilbert spectral analysis (HSA). It has a higher resolution of time-frequency than traditional analysis methods, because the EMD is an adaptive time-frequency decomposition. Thus, the HHT can be applied to non-linear and non-stationary time series data. On the other hand, traditional analysis methods such as the Fourier transform and wavelet transform also assume that the data is linear and stationary.

The HHT has been applied to various fields; biomedical engineering, financial engineering, image processing, seismic studies, ocean engineering, etc.

In this paper, we investigate the excess power method with the HHT to detect gravitational-wave bursts. This analysis does not require any knowledge of gravitational wave, for example, waveform etc. We also estimate the detection efficiency of the proposed method.

2 Hilbert spectral analysis and empirical mode decomposition

The Hilbert transform of function $u(t)$ is defined by

$$v(t) = \frac{1}{\pi} P \int_{-\infty}^{\infty} \frac{u(t')}{t - t'} dt', \tag{1}$$

where P indicates the Cauchy principal value. If the function $u(t) \in L^p(\mathbf{R})$ for $1 < p < \infty$, $v(t)$ is imaginary part of analytic function $F(t) = u(t) + iv(t) = a(t)e^{i\theta(t)}$. Then, an instantaneous amplitude (IA) $a(t)$ and instantaneous frequency (IF) $f(t)$ is defined by

$$a(t) = \sqrt{u^2(t) + v^2(t)}, \tag{2}$$

$$\theta(t) = \tan^{-1}\Big(\frac{v(t)}{u(t)}\Big), \tag{3}$$

$$f(t) = \frac{1}{2\pi}\frac{d\theta(t)}{dt}. \tag{4}$$

[1]Email address: kaneyama@astro.sc.niigata-u.ac.jp

Generally, it is not guaranteed that we obtain the physically meaningful IF. In order to obtain the meaningful IF, Huang et al. [2] showed that the data $u(t)$ should be satisfy the following two conditions: (I) A number of extrema and number of zero crossing equal or differ at most by one, (II) The mean value of the envelope defined using the local maxima and the envelope defined using the local minima is zero.

To satisfy the above conditions, we perform the EMD which is a series of high-pass filters in a sense. The EMD decomposes the data $u(t)$ to intrinsic mode functions (IMFs) and residual $r(t)$,

$$u(t) = \sum_i \mathrm{IMF}i + r(t). \tag{5}$$

Then, each IMF has a locally monochromatic frequency scale that is obtained empirically. The EMD algorithm is as follows:

- $h_1(t) = u(t)$
- for $i = 1$ to $i_{\max}$
  - ▷ $h_{i,1}(t) = h_i(t)$
  - ▷ for $k = 1$ to $k_{\max}$
    - ○ Identify the local maxima and minima of $h_{i,k}(t)$
    - ○ $U_{i,k}(t)$ = the upper envelope joining the local maxima using a cubic spline
    - ○ $L_{i,k}(t)$ = the lower envelope joining the local minima using a cubic spline
    - ○ $m_{i,k}(t) = (U_{i,k}(t) + L_{i,k}(t))/2$
    - ○ $h_{i,k+1}(t) = h_{i,k}(t) - m_{i,k}(t)$

    Exit from the loop k if a stoppage criterion $\dfrac{\sum_j |m_{i,k}(t_j)|}{\sum_j |h_{i,k}(t_j)|} < \epsilon$
  - ▷ $\mathrm{IMF}i = c_i(t) = h_{i,k}(t)$
  - ▷ $h_{i+1}(t) = h_i(t) - c_i(t)$
- residual: $r(t) = h_{i_{\max}+1}(t)$

The EMD frequently occurs mode mixing which is defined as a single IMF either consisting of signals of widely desperate scales or a signal of a similar scale residing in different IMF components. To suppress mode mixing, we perform the ensemble EMD (EEMD) [4],
(1) Add a white noise series to data,

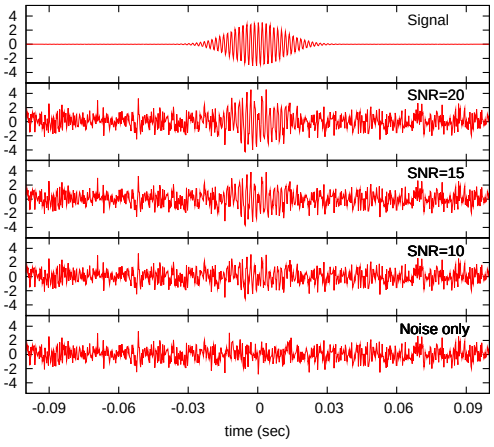

Figure 1: The sine-Gauss signal + the white-Gaussian noise

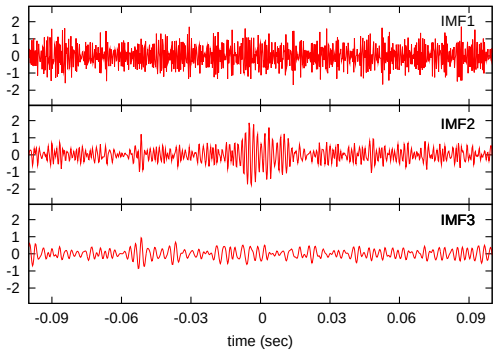

Figure 2: EEMD of the sine-Gauss signal in the white-Gaussian noise with SNR = 10

(2) Decompose the data with added white noise into IMFs,
(3) Repeat step (1) and (2) in many times with different white noise series each time,
(4) Obtain the ensemble means of corresponding IMFs of the decompositions as the final result.

To perform the EMD, we must be set the empirical EMD parameters which depend on the characteristic of the data [5]. End-of-loop-i condition is that residual becomes monotonic functions. We set the stoppage criterion $\epsilon = 10^{-4}$, consequently, k_{max} is almost equal to or lower than 100 in our simulations. The parameters for the EEMD are the size of ensemble N_e and standard deviation of white noise σ_e. We set $N_e = 200$ and $\sigma_e = 1.0$. We tried other values of σ_e but we found that this values is optimal. As for N_e, we verified that the results hardly change even with $N_e > 100$ but the value $N_e = 50$ is too small.

We apply the HHT to the sine-Gauss signal

$$h(t) = a\exp[-(t/\tau)^2]\sin(2\pi f t). \tag{6}$$

We set frequency of signal $f = 600$ Hz and $\tau = 0.1$ sec$/2\pi = 0.016$ sec. Moreover, we use a white-Gaussian noise with zero mean $\mu = 0$ and standard deviation $\sigma = 1.0$. Figure 1 plots the data used in our simulations. The signal-to-noise ratio (SNR) is defined by

$$\mathrm{SNR} = \sqrt{\sum_j h^2(t_j)}/\sigma. \tag{7}$$

The sampling frequency and data length is 4096 Hz and 1.0 sec, respectively. The results of EMD are showed in Fig. 2. The signal appears only in IMF2, because the sine-Gauss signal used in this case has a single frequency component.

3 Excess power methods

We propose an excess power method with the HHT to detect gravitational-wave bursts. If the IA $>$ IA$_c$ for a duration δt_c in some IMF, then we define the candidate of the detection for gravitational-wave bursts. Figure 3 plots the IAs for each IMF1, 2 and 3. The blue line represent the maxinum IA of noise only data. We evaluate the detection efficiency by using the receiver operating characteristics (ROC) curve, which shows the detection rate (DR) as a function of the false alarm rate (FAR). We perform the EEMD procedure for 1000 samples of each data which generated noise with a different seed.

Figure 4 plots the ROC curves for IMF1, 2 and 3 ($\delta t_c = 0$ msec). In IMF1 and IMF3, it does not detect gravtational-wave bursts for SNR $= 10$ and 15. We found that we obtatined the high detection efficiency in IMF2 : DR > 0.95 and FAR < 0.05 for SNR $= 10$.

Figure 5 plots the ROC curves of IMF2 for each SNR $= 10$, 15 and 20 and different δt_c. For SNR $=$ 15 and 20, we obtain better detection efficiency for any δt_c. When $\delta t_c = 4$ msec, we find DR > 0.97 and FAR < 0.05 for SNR $= 10$.

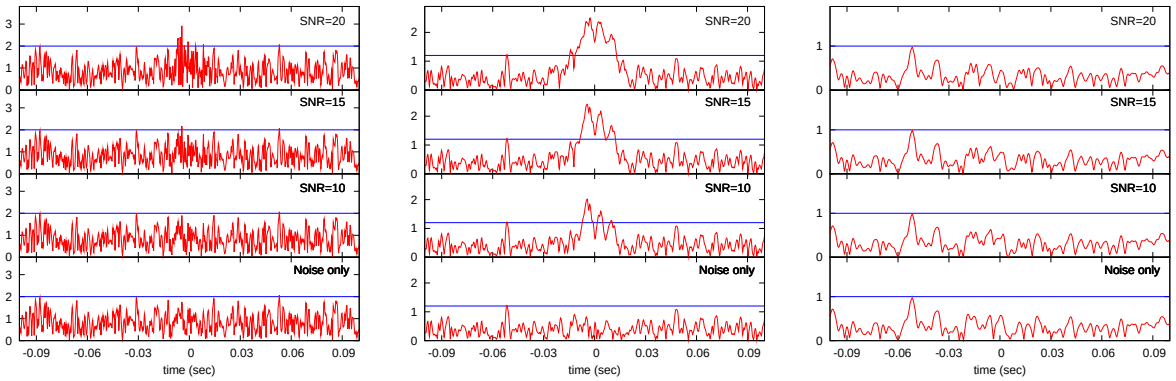

Figure 3: The IAs for each IMF1 (left), 2 (center), 3 (right)

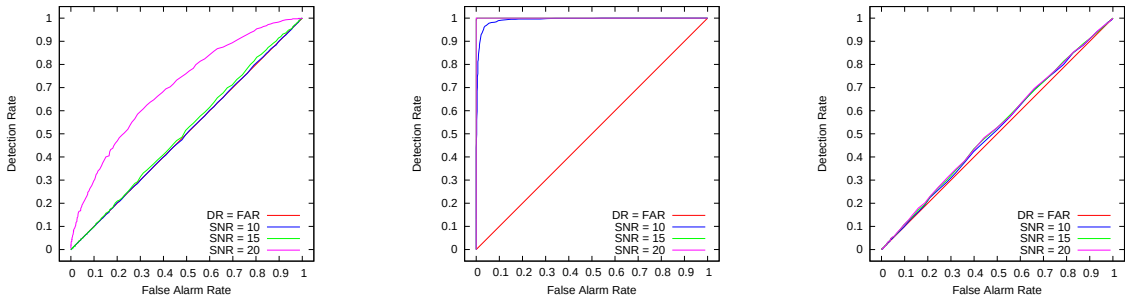

Figure 4: The ROC curves for each IMF1 (left), 2 (center), 3 (right)

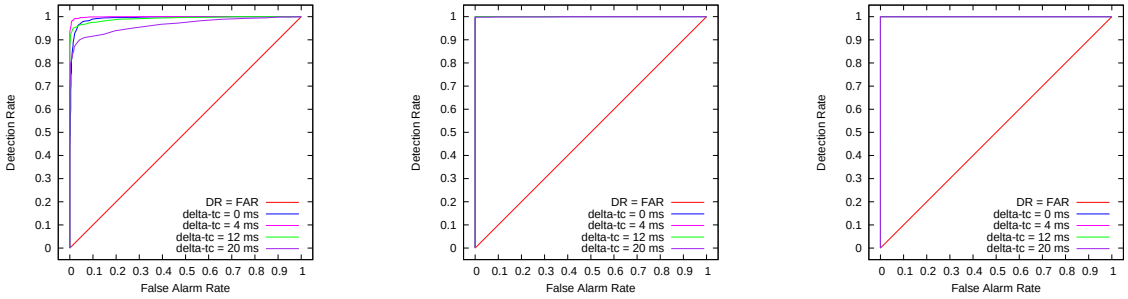

Figure 5: The ROC curves of IMF2 for each SNR = 10 (left), 15 (center), 20 (right)

4 Conclusion

We investigated the property of excess power method with the HHT for gravitational-wave bursts. We found the high detection efficiency only in IMF2. The signal almost appeared in IMF2, since the sine-Gauss signal used this paper had a single frequency component (f = 600 Hz).

Even if SNR = 10, we obtained DR > 0.95 and the FAR < 0.05. Moreover, when the duration time was $\delta t_c = 4$ msec, DR and FAR were better than that of $\delta t_c = 0$ msec.

We used the signal which had constant frequency. However, the real gravitational waves have complicate and large-scale frequency modulation. Since we expect to appear the signal in multiple IMFs, it is possible for us to obtain the better detection efficiency. We will report elsewhere.

Acknowledgments

This work was also supported in part by a Grant-in-Aid for Scientific Research on Innovative Areas (No. 24103005; K. Oohara and H. Takahashi) from the Ministry of Education, Culture, Sports, Science and Technology of Japan.

References

[1] N. E. Huang, S. R. Long and Z. Shen, Adv. Appl. Mech. **32**, 59 (1996).

[2] N. E. Huang, wt al. Proc. R. Soc. London, **454**, 903 (1998).

[3] N. E. Huang, Z. Shen, S. R. Long, Annu. Rev. Fluid Mech., **31**, 417 (1999).

[4] N. E. Huang and Z. Wu, Rev. Geophys. **46**, RG2006 (2006).

[5] H. Takahashi, K. Oohara, M. Kaneyama, Y. Hiranuma, and J. B. Camp, submitted to Advances in Adaptive Data Analysis (2013).

Junko Ohashi, JGRG 22(2012)111319

"Potential-driven Galileon inflation"

RESCEU SYMPOSIUM ON

GENERAL RELATIVITY AND GRAVITATION

JGRG 22

November 12-16 2012

Koshiba Hall, The University of Tokyo, Hongo, Tokyo, Japan

Potential-driven Galileon inflation

JCAP 1210, 035 (2012)

Junko Ohashi and Shinji Tsujikawa , Tokyo University of Science

Introduction

For the models of inflation driven by the potential energy of an inflaton field ϕ, the covariant Galileon Lagrangian $(\partial\phi)^2\Box\phi$ generally works to slow down the evolution of the field. On the other hand, if the Galileon self-interaction is dominant relative to the standard kinetic term, we show that there is no oscillatory regime of inflaton after the end of inflation. This is typically accompanied by the appearance of the negative propagation speed squared c_s^2 of a scalar mode, which leads to the instability of small-scale perturbations. For chaotic inflation and natural inflation we clarify the parameter space in which inflaton oscillates coherently during reheating. We also place observational constraints on the inflaton potentials from the information of the scalar spectral index n_s and the tensor-to-scalar ratio r.

Potential-driven inflation with Galileon term

We start with the following action

$$S=\int d^4x\sqrt{-g}\left[\frac{M_{\rm pl}^2}{2}R+X-V(\phi)-G_3(\phi,X)\Box\phi+\mathcal{L}_4+\mathcal{L}_5\right]$$

where

$$\mathcal{L}_4=G_4(\phi,X)R+G_{4,X}\left[(\Box\phi)^2-(\nabla_\mu\nabla_\nu\phi)(\nabla^\mu\nabla^\nu\phi)\right]$$

$$\mathcal{L}_5=G_5(\phi,X)G_{\mu\nu}(\nabla^\mu\nabla^\nu\phi)-\frac{1}{6}G_{5,X}\Big[(\Box\phi)^3-3(\Box\phi)(\nabla_\mu\nabla_\nu\phi)(\nabla^\mu\nabla^\nu\phi)+2(\nabla^\mu\nabla_\alpha\phi)(\nabla^\alpha\nabla_\beta\phi)(\nabla^\beta\nabla_\mu\phi)\Big]$$

For simplicity, we study the covariant Galileon theory in which only the G_3 term is present in the above action

$$G_3(\phi,X)=c_3\frac{X}{M^3},\ G_4(\phi,X)=0,\ G_5(\phi,X)=0$$

$c_3\dot\phi>0$ to avoid ghosts

Slow-roll equations

$$3M_{\rm pl}^2H^2\simeq V,\quad 3H\dot\phi(1+\mathcal{A})+V_{,\phi}\simeq 0,\qquad \mathcal{A}=\frac{3\delta_3}{\delta_X}$$

Slow-roll parameter

$$\epsilon=-\frac{\dot H}{H^2}\simeq\frac{\epsilon_\phi}{1+\mathcal{A}},\qquad \epsilon_\phi=\frac{M_{\rm pl}^2}{2}\left(\frac{V_{,\phi}}{V}\right)^2 \text{ (for standard inflation)}$$

- In the limit $|\mathcal{A}|\gg 1$ ($|\delta_3|\gg\delta_X$): $\epsilon\ll\epsilon_\phi$ (the evolution of ϕ slows down) ⇒ Galileon inflation
- In the limit $\mathcal{A}\to 0$ ($|\delta_3|\ll\delta_X$): $\epsilon\simeq\epsilon_\phi$ ⇒ Standard inflation

The transition from Galileon inflation to standard inflation can be quantified by the condition $\mathcal{A}(\phi_G)=1$.

slow-roll parameters

$$\delta_X=\frac{X}{M_{\rm pl}^2H^2},\quad \delta_3=\frac{c_3\dot\phi X}{M_{\rm pl}^2M^3H}$$

Results

Background analysis for $V(\phi)=(\lambda/n)\phi^n$ with Galileon term $X\Box\phi/M$

We have the critical mass $M_c=2^{-n/3}n^{(n-1)/3}M_{\rm pl}^{(n-1)/3}\lambda^{1/3}$

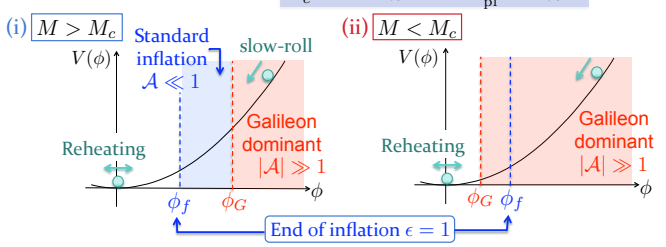

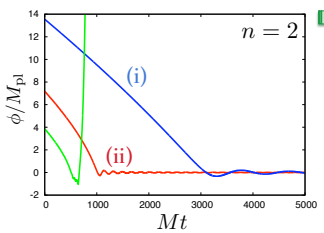

During the oscillating stage of inflaton

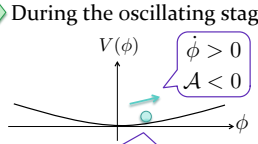

$\left(\mathcal{A}=-3\frac{H\dot\phi}{M^3}\right)$

$(1+2\mathcal{A})\ddot\phi\simeq -V_{,\phi}$

If $(1+2\mathcal{A})<0$, ϕ diverges. This can be happened for smaller M.

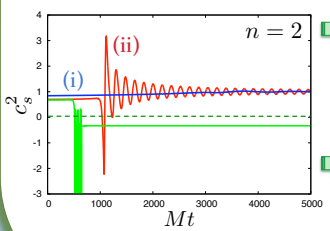

This is typically accompanied by the appearance of the negative propagation speed squared c_s^2 of a scalar mode, which leads to the instability of small-scale perturbations.

We find that the inflaton oscillations occur under the conditions

$M>2.5\times10^{-4}M_{\rm pl}$ (for $n=2$)

$M>9.5\times10^{-5}M_{\rm pl}$ (for $n=4$) (※1)

Observational constraints for $V(\phi)=(\lambda/n)\phi^n$

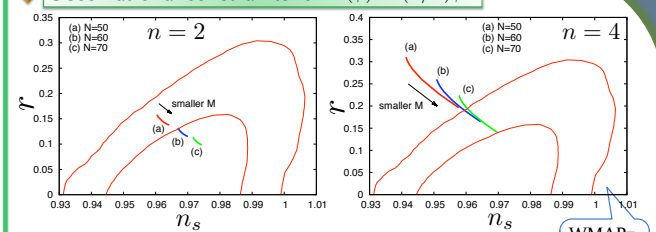

WMAP7, BAO, and HST

For smaller M, r gets smaller whereas n_s increases.

The quartic potential can be compatible with the current observations in the presence of the Galileon term. The model is within the 2σ contour for $M<7.7\times10^{-4}M_{\rm pl}$ (※2) with 60 e-foldings.

In terms of the parameter λ the conditions (※1) and (※2) translate into $3.4\times10^{-13}<\lambda<3.1\times10^{-10}$ (for $n=4$).

viable parameter space of λ

Natural inflation $V(\phi)=\Lambda^4[1+\cos(\phi/f)]$

In standard natural inflation

$f\gtrsim 3.5M_{\rm pl}$ for the consistency with the WMAP constraints. However, $f>M_{\rm pl}$ is not generally realized in particle physics.

In the presence of the Galileon term $X\Box\phi/M$

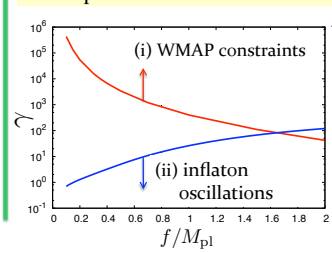

where $\gamma=\Lambda^4/(M^3M_{\rm pl})$

For the compatibility of two constraints we require that f is bounded to be $f>1.7M_{\rm pl}$. Hence the problem of the super-Planckian values of f in standard inflation is not improved significantly.

Conclusion

We have studied the viability of potential-driven Galileon inflation. The Galileon self-interactions generally lead to the slow down for the evolution of the field, which allows the possibility to accommodate steep inflaton potentials. The dominance of the Galileon self-interactions relative to the standard kinetic term X can modify the dynamics of reheating after inflation. In order to clarify this issue, we numerically solved the background equations for chaotic inflation and natural inflation. We found that, depending on the couplings G_i ($i=3,4,5$) and their associated mass scales M, there is no oscillatory regime of inflaton. Moreover the dominance of the Galileon terms generally gives rise to the negative scalar propagation speed squared c_s^2 during reheating, which leads to the instability of small-scale density perturbations.

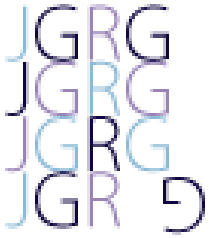

Ken'ichi Saikawa, JGRG 22(2012)111321

"Evolution and thermalization of axion dark matter in the condensed regime"

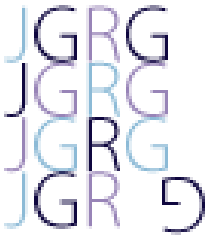

RESCEU SYMPOSIUM ON

GENERAL RELATIVITY AND GRAVITATION

JGRG 22



November 12-16 2012

Koshiba Hall, The University of Tokyo, Hongo, Tokyo, Japan



Evolution and thermalization of axion dark matter in the condensed regime

Ken'ichi Saikawa
ICRR, The University of Tokyo

Collaborate with M. Yamaguchi (Tokyo Institute of Technology)

Reference: KS and M. Yamaguchi, arXiv:1210.7080 [hep-ph]

Abstract

- Discuss the possibility that QCD axions form a Bose-Einstein condensate (BEC)
- Calculate time evolution of occupation number of axions in the condensed regime
  - Derive a formula for thermalization rate
  - Revisit axion cosmology

Peculiarities of axion dark matter

- Non-thermal production

$$H \lesssim m_a \quad (t = t_1)$$

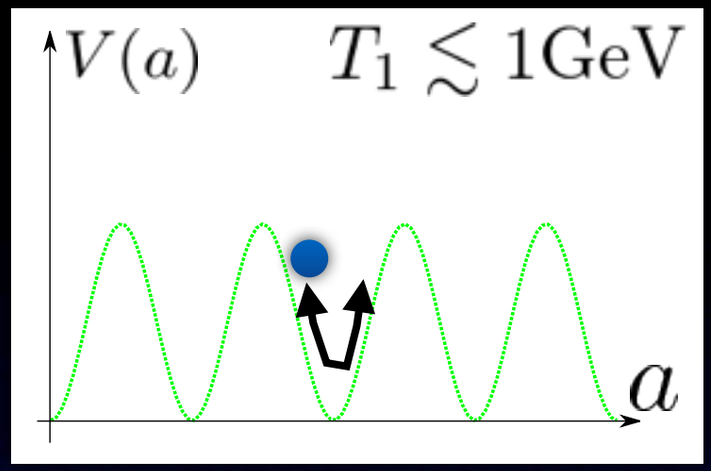

$$\Rightarrow \quad t_1 \sim 10^{-7}\mathrm{sec}$$

$$\delta v \sim \frac{\delta p}{m_a} \sim \frac{R(t_1)}{R(t_0)}\frac{1}{m_a t_1} \sim 3\times 10^{-17}\left(\frac{F_a}{10^{12}\mathrm{GeV}}\right)^{0.81}$$

"cold" dark matter ($\delta v < 10^{-8}$)

- Large occupation number

$$\mathcal{N} \sim n_a \frac{(2\pi)^3}{\frac{4\pi}{3}(m_a \delta v)^3} \sim 10^{61}\left(\frac{F_a}{10^{12}\mathrm{GeV}}\right)^{2.75}$$

($n_a \sim m_a F_a^2 (R(t_1)/R(t_0))^3$: number density of axions)

c.f. $\mathcal{N} \sim 10^{-18}\left(\frac{100\mathrm{GeV}}{m_{\mathrm{wimp}}}\right)^4$ for WIMPs

Do axions form a BEC ?

- Bose-Einstein condensate
  - Large fraction of bosons are in the lowest-energy state
  - Critical temperature

$$T_c = \left(\frac{\pi^2 n_a}{\zeta(3)}\right)^{1/3} \simeq 2\times 10^2 \mathrm{GeV}\left(\frac{F_a}{10^{12}\mathrm{GeV}}\right)^{0.54}\left(\frac{R(t_1)}{R(t)}\right)$$

$$\overset{!}{\gg} \delta\omega \sim \frac{1}{2} m_a (\delta v)^2 \sim 4\times 10^{-13}\mathrm{eV}\left(\frac{F_a}{10^{12}\mathrm{GeV}}\right)^{0.25}\left(\frac{R(t_1)}{R(t)}\right)^2$$

- Assumptions

	For axions
1. Particles are bosons	➡ satisfied
2. Number is conserved	➡ satisfied
3. Large occupation number	➡ satisfied
4. In thermal equilibrium	➡ ???

Axions vs WIMPs

- Thermalize if $\Gamma \sim \dot{\mathcal{N}}(p)/\mathcal{N}(p) > H$
- WIMPs : classical particle limit

$\hbar \longrightarrow 0$ while $E = \hbar\omega,\ \vec{p} = \hbar\vec{k}$ fixed

$\omega,\ \vec{k} \to \infty$ collection of classical "point particles"

evolution : use Boltzmann eq.

- axions : classical field limit

$\hbar \longrightarrow 0$ while $E = \mathcal{N}\hbar\omega,\ \vec{p} = \mathcal{N}\hbar\vec{k}$ fixed

$\mathcal{N} \to \infty \quad \delta\omega,\ \delta\vec{k} \sim \text{finite}$ "wavy field"

cannot use Boltzmann eq.

→ consider quantum mechanics

In quantum mechanics...

- We consider transitions between different quantum states.
- Two different regimes
- WIMPs $\omega \rightarrow \text{large}$

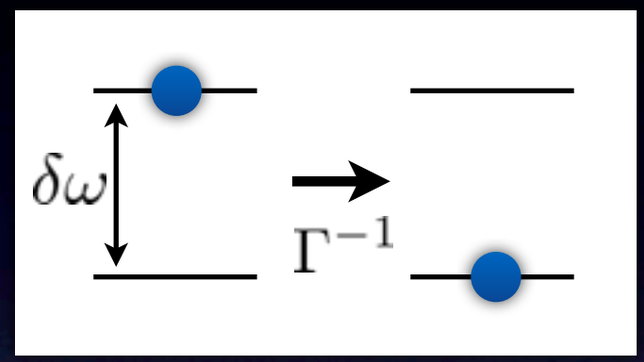

$$\delta\omega \gg \Gamma$$

energy exchanged in the transitions

transition rate

"particle kinetic regime"

- axions $\omega \rightarrow \text{small}$

$$\delta\omega \ll \Gamma$$

"condensed regime"

A transition makes sense if $\mathcal{N}\delta\omega \gg \Gamma$

Previous study

Erken, Sikivie, Tam, Yang, PRD85, 063520 (2012)

- Time evolution of quantum operators in the Heisenberg picture

l : label of the state (momentum)

$$H = \sum_i \omega_i a_i^\dagger a_i + \sum_{i,j,k,l} \frac{1}{4} \Lambda_{kl}^{ij} a_k^\dagger a_l^\dagger a_i a_j \qquad \mathcal{N}_l = a_l^\dagger a_l$$

$$\dot{\mathcal{N}}_l = i[H, \mathcal{N}_l]$$

$$= i \sum_{i,j,k} \frac{1}{2} (\Lambda_{ij}^{kl} a_i^\dagger a_j^\dagger a_k a_l e^{-i\Omega_{ij}^{kl} t} - \text{H.c.})$$

Leading contribution in the condensed regime

$$\Omega_{ij}^{kl} t \ll 1$$

$$\dot{\mathcal{N}}_l \sim \mathcal{O}(\Lambda_{ij}^{kl})$$

reduce to Boltzmann eq. in the particle kinetic regime

$$\Omega_{ij}^{kl} t \gg 1$$

$$\dot{\mathcal{N}}_l \sim \mathcal{O}(|\Lambda_{ij}^{kl}|^2)$$

$$+ \sum_{k,i,j} \frac{1}{2} |\Lambda_{ij}^{kl}|^2 [\mathcal{N}_i \mathcal{N}_j (\mathcal{N}_l + 1)(\mathcal{N}_k + 1)$$

$$- \mathcal{N}_l \mathcal{N}_k (\mathcal{N}_i + 1)(\mathcal{N}_j + 1)] \frac{2}{\Omega_{ij}^{kl}} \sin(\Omega_{ij}^{kl} t) + \dots$$

$$\Omega_{ij}^{kl} \equiv \omega_k + \omega_l - \omega_i - \omega_j$$

- What about the quantum-mechanical averages $\langle \dot{\mathcal{N}}_l(t) \rangle$?

Effects on cosmological parameters ?

- Thermalization rate is enhanced in the condensed regime → leads to axion BEC
- Thermalization rate with other species is also enhanced (?) Erken, Sikivie, Tam, Yang, PRD85, 063520 (2012); PRL108, 061304 (2012)
  - axions and photons have thermal contact

$$\rho_{\gamma i} = \frac{\pi^2}{15} T_{\gamma i}^4 = \rho_{\gamma f} + \rho_{af} = \frac{\pi^2}{30} T_{\gamma f}^4 (2+1)$$

$$\Rightarrow \quad T_{\gamma f} = (2/3)^{1/4} T_{\gamma i}$$

baryon-to-photon ratio at BBN $\eta_{\rm BBN} = (2/3)^{3/4} \eta_{\rm std.}$

effective # of neutrino d.o.f. $N_{\rm eff} = 6.77$ (obs. $N_{\rm eff} \simeq 3 - 4$)

- Is it true ? Does axion BEC conflict with standard cosmology?

In-in formalism

Weinberg, PRD72, 043514 (2005)

- Calculate expectation value of a quantum operator via perturbative expansion

$$\langle \mathcal{O}(t) \rangle = \langle \mathrm{in} | \mathcal{O}(t) | \mathrm{in} \rangle$$
$$= \langle \mathcal{O} \rangle + i \int_{t_0}^{t} dt_1 \langle [H_I(t_1), \mathcal{O}] \rangle$$
$$+ (i)^2 \int_{t_0}^{t} dt_2 \int_{t_0}^{t_2} dt_1 \langle [H_I(t_1), [H_I(t_2), \mathcal{O}]] \rangle + \dots$$

$\mathcal{O} = \mathcal{N}_n \equiv \dfrac{a_n^\dagger a_n}{V}$: number operator

$$\int \frac{d^3p}{(2\pi)^3} \to \frac{1}{V} \sum_{n_x, n_y, n_z}$$

(label becomes discrete)

$$H_I(t) = \frac{1}{V^4} \sum_{ijkl} \frac{1}{4} \Lambda_{kl}^{ij} e^{-i\Omega_{kl}^{ij} t} a_k^\dagger a_l^\dagger a_i a_j$$

(ignore axion # violating process)

(1) scalar self-coupling $\Lambda_{kl}^{ij} = -\dfrac{\lambda}{4m_a^2} V \delta_{i+j,k+l}$ ⬅ $H_I = -\int d^3x \dfrac{\lambda}{4!} \phi^4$

(2) gravity $\Lambda_{kl}^{ij} = -4\pi G m_a^2 \left(\dfrac{1}{|\mathbf{p}_k - \mathbf{p}_i|^2} + \dfrac{1}{|\mathbf{p}_k - \mathbf{p}_j|^2} \right) V \delta_{i+j,k+l}$ ⬅ $H_I = -\dfrac{G}{2} \int d^3x d^3x' \dfrac{\rho(\mathbf{x}, t) \rho(\mathbf{x}', t)}{|\mathbf{x} - \mathbf{x}'|}$

In state

- $|\mathrm{in}\rangle$ = a state which represents the coherent oscillation of axions
- Use a coherent state

$$|\alpha_i\rangle = e^{-\frac{1}{2}|\alpha_i|^2} \sum_{n=0}^{\infty} \frac{\alpha_i^n}{n!\sqrt{V^n}} (a_i^\dagger)^n |0\rangle \qquad \text{with} \quad a_i|0\rangle = 0$$

$$a_i|\alpha_i\rangle = V^{1/2}\alpha_i|\alpha_i\rangle$$

- Field amplitude

(assuming a mode with $|\mathbf{p}_n| \lesssim H \sim t^{-1}$)

$$\phi = \frac{1}{V}\sum_n \frac{1}{\sqrt{2E_{p_n}}}(e^{ip_n\cdot x}a_n + e^{-ip_n\cdot x}a_n^\dagger)$$

$$\langle\alpha_i|\phi|\alpha_i\rangle \simeq \frac{1}{\sqrt{2m_aV}}(e^{-im_at}\alpha_n + e^{im_at}\alpha_n^*) = \sqrt{\frac{2}{m_aV}}|\alpha_n|\cos(m_at-\beta)$$

(inside the horizon $\mathbf{p}_n \cdot \mathbf{x} \ll 1$)

classical field trajectory

- Mean square deviation

$$\Delta\phi = \sqrt{\langle\alpha_i|\phi^2|\alpha_i\rangle - \langle\alpha_i|\phi|\alpha_i\rangle^2} = \sqrt{\frac{1}{V}\sum_n \frac{1}{2E_n}}$$ vacuum fluctuation

“Zero modes”

- Assume plural (say K) oscillating modes

$$|\{\alpha\}\rangle = \prod_i^K e^{-\frac{1}{2}|\alpha_i|^2} \sum_{n=0}^{\infty} \frac{\alpha_i^n}{n!\sqrt{V^n}} (a_i^\dagger)^n |0\rangle$$

$$|\mathbf{p}_i| \lesssim H(t_1) \sim m_a(t_1)$$

for $i = 1, \ldots, K$

- number density

$$n_a = \frac{1}{V} \sum \langle \{\alpha\} | \mathcal{N}_n | \{\alpha\} \rangle = \frac{1}{V} \sum_i^K |\alpha_i|^2 \equiv \sum_i^K n_{c,i}$$

- Question : how these plural oscillating modes (“zero modes”) reach thermal equilibrium ?
  - decoupled axions
    = each of K modes oscillates independently
  - thermalized axions
    = transition between plural modes becomes significant

Evolution of occupation number

$$\langle \mathrm{in}|\mathcal{N}_p(t)|\mathrm{in}\rangle = \langle \mathcal{N}_p\rangle + i\int_{t_0}^{t} \langle [H_I(t_1),\mathcal{N}_p]\rangle + \mathcal{O}(H_I^2) + \dots$$

$$i\int_{t_0}^{t} dt_1 \langle [H_I(t_1),\mathcal{N}_p]\rangle \xrightarrow{t-t_0\to\infty} -\frac{1}{2V^2}\sum_j^K\sum_k^K\sum_l^K \left[\Lambda_{kl}^{pj}\frac{e^{-i\Omega_{kl}^{pj}t}}{\Omega_{kl}^{pj}}\alpha_k^*\alpha_l^*\alpha_j\alpha_p + \mathrm{c.c.}\right]$$

for $$|\mathrm{in}\rangle = \prod_i^K e^{-\frac{1}{2}|\alpha_i|^2}\sum_{n=0}^{\infty}\frac{\alpha_i^n}{n!\sqrt{V^n}}(a_i^\dagger)^n|0\rangle$$

coherent state

$$i\int_{t_0}^{t} dt_1 \langle [H_I(t_1),\mathcal{N}_p]\rangle = 0 \quad \text{for} \quad |\mathrm{in}\rangle = \prod_k \frac{1}{\sqrt{\mathcal{N}_k!V^{\mathcal{N}_k}}}(a_k^\dagger)^{\mathcal{N}_k}|0\rangle$$

number state

- First order term is relevant if

  (1) condensed regime $\Omega_{kl}^{pj}t \ll 1$

  (c.f. $e^{-i\Omega_{kl}^{pj}t} \approx 0$ for particle kinetic regime $\Omega_{kl}^{pj}t \gg 1$)

  (2) coherent state representation $|\mathrm{in}\rangle = |\{\alpha\}\rangle$

Thermalization rate

$$\Gamma \equiv \frac{1}{\mathcal{N}_p(t)} \frac{d\mathcal{N}_p(t)}{dt} \simeq \frac{1}{\mathcal{N}_p V^2} \sum_{j,k,l}^{K} \mathrm{Im}[\Lambda_{pj}^{kl} \alpha_k \alpha_l \alpha_j^* \alpha_p^*]$$

Using $\Lambda_{pj}^{kl} = \Lambda V \delta_{k+l,p+j}$ and $\mathcal{N}_p \simeq |\alpha_p|^2 \simeq \mathcal{N}/K$

we obtain

$$\Gamma_{\mathrm{condensed}} \simeq \Lambda \frac{\mathcal{N}}{V} = \Lambda n_a$$

n_a : number density of axions

- Recover the previous estimation Erken, Sikivie, Tam, Yang, PRD85, 063520 (2012)

scalar phi^4 $\quad \Gamma_{\mathrm{condensed},s} \simeq \dfrac{\lambda n_a}{4m_a^2} \quad \propto 1/R^3(t)$

gravity $\quad \Gamma_{\mathrm{condensed},g} \simeq \dfrac{4\pi G m_a^2 n_a}{(\delta p)^2} \quad \propto 1/R(t)$

$$\delta p \sim m_a \delta v \propto 1/R(t)$$

Formation of axion BEC

- Axions form a BEC when $\Gamma_{\mathrm{condensed},g} \gtrsim H$

  corresponding to the photon temperature

$$T_{\mathrm{BEC}} \simeq 2 \times 10^3 \mathrm{eV} \left(\frac{F_a}{10^{12} \mathrm{GeV}} \right)^{0.56}$$

- At this time, axions enter into thermal equilibrium with temperature

$$T_a(t_{\mathrm{BEC}}) \sim \frac{\delta p^2(t_{\mathrm{BEC}})}{3 m_a} \sim 2.5 \times 10^{-37} \mathrm{eV} \left(\frac{F_a}{10^{12} \mathrm{GeV}} \right)^{3.25}$$

  thermally excited modes

$$n_T(T_a(t_{\mathrm{BEC}})) \simeq \left(\frac{m_a T_a(t_{\mathrm{BEC}})}{2\pi} \right)^{3/2}$$

$$\frac{n_T(T_a(t_{\mathrm{BEC}}))}{n_a(t_{\mathrm{BEC}})} \simeq 7.5 \times 10^{-80} \left(\frac{F_a}{10^{12} \mathrm{GeV}} \right)^{-0.005}$$

- Almost all axions stay in the lowest energy state.

No photon cooling

- Interaction with other species b

$$H_{I,b}(t) = \frac{1}{V^4}\sum_{ijkl}\frac{1}{4}{\Lambda_b}^{ij}{}_{kl}e^{-i\Omega^{ij}_{kl}t}a^\dagger_k b^\dagger_l a_i b_j$$

- Assume b particles are represented as a number state

$$|\mathrm{in}\rangle = \prod_k \frac{1}{\sqrt{\mathcal{N}_k! V^{\mathcal{N}_k}}}(b^\dagger_k)^{\mathcal{N}_k}|\{\alpha\}\rangle$$

while $$|\{\alpha\}\rangle = \prod_i^K e^{-\frac{1}{2}|\alpha_i|^2}\sum_{n=0}^{\infty}\frac{\alpha_i^n}{n!\sqrt{V^n}}(a_i^\dagger)^n|0\rangle$$

- First order term exactly vanishes

$$\langle[H_{I,b}(t), \mathcal{N}_p]\rangle = 0$$

- Thermalization with other species is second order effect.
  - BEC axions do not have thermal contact with photons
    → does not affect cosmological parameters

Summary

- Derive the formula for thermalization rate in the condensed regime by using
  - in-in formalism
  - coherent state representation
- Formation of axion BEC occurs at $T_{\rm BEC} \sim \mathcal{O}(1)\mathrm{keV}$
- It does not conflict with standard cosmology
- Future directions
  - Extend the formalism including general relativistic corrections
  - Seek for other observable effects

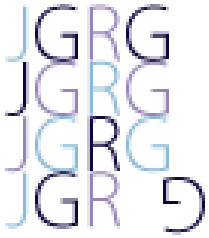

Kouichi Nomura, JGRG 22(2012)111322

"Ghost in multimetric gravity"

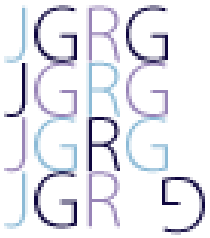

RESCEU SYMPOSIUM ON

GENERAL RELATIVITY AND GRAVITATION

JGRG 22



November 12-16 2012

Koshiba Hall, The University of Tokyo, Hongo, Tokyo, Japan



Ghost in Multimetric Gravity

Kyoto University

Kouichi Nomura, Jiro Soda

Phys. Rev. D86, 084052 (2012)

1. Introduction

Recently, the ghost problem in non-linear massive gravity has been solved.

Massive gravity : a challenge to give mass to graviton in general relativity

linear level : Pauli-Fiertz mass term ・・・ no problem

non linear level : a serious difficulty emerges

graviton has spin 2 ・・・ mssless : 2 degrees of freedom

massive : 5 degrees of freedom

In linear level, there are certainly 5 degrees of freedom.

However, in non-linear level, extra 6th degree of freedom emerges and turns out to be a ghost particle. → **BD ghost**

ghost particle : a particle having negative kinetic energy

For the consistency of the theory, ghost particles must be excluded.

Extension to bimetric gravity

In non-linear massive gravity, metric is always decomposed into backgroundand and fluctuation.

↓

The background metric can be promoted to a dynamical variable.

a theory of two dynamical metrics

It has been shown that no BD ghost is contained.

Question

Can we construct ghost-free theories with more than two metrics？

①：Trimetric case as a naïve extension of bimetric gravity is proposed. (2012, N. Khosravi et al)

→ The problem of BD ghost is unsolved.

②：Ghost-free multimetric gravity with vielbeins is proposed. (2012, K. Hinterbichler and R. A. Rosen)

→ ② dose not contain ①.

→ We solve the ghost problem in ①, and further develop our analysis to more general multimetric gravity.

2. Bimetric gravity g, f : metric

$$S_{bi} = M_g^2 \int d^4x \sqrt{-\det g} R[g] + M_f^2 \int d^4x \sqrt{-\det f} R[f]$$

Einstein Hilbert term

$$+ a \int d^4x \sqrt{-\det g} \Phi\left(\sqrt{g^{-1} f}\right)$$

Interaction term

M_g, M_f : Planck mass , $R[g], R[f]$: curvature , a : coupling constant

$\Phi(A)$: linear combination of $Tr(A)$, $(TrA)^2 - Tr(A^2)$,....

(up to fourth order in A)

No BD-ghost is contained,
and there exist one massless and one massive graviton.

→ degrees of freedom : $2 + 5 = 7$

3. Trimetric gravity g, f, h : metric

$$S_{tri} = M_g^2 \int d^4x \sqrt{-\det g} R[g] + M_f^2 \int d^4x \sqrt{-\det f} R[f] + M_h^2 \int d^4x \sqrt{-\det h} R[h]$$
$$+ a_1 \int \sqrt{-\det g} \Phi_1\left(\sqrt{g^{-1} f}\right) + a_2 \int \sqrt{-\det f} \Phi_2\left(\sqrt{f^{-1} h}\right) + a_3 \int \sqrt{-\det h} \Phi_3\left(\sqrt{h^{-1} g}\right)$$

a nive extension of bimetric case

In this case, we verified the exsistence of a BD-ghost.

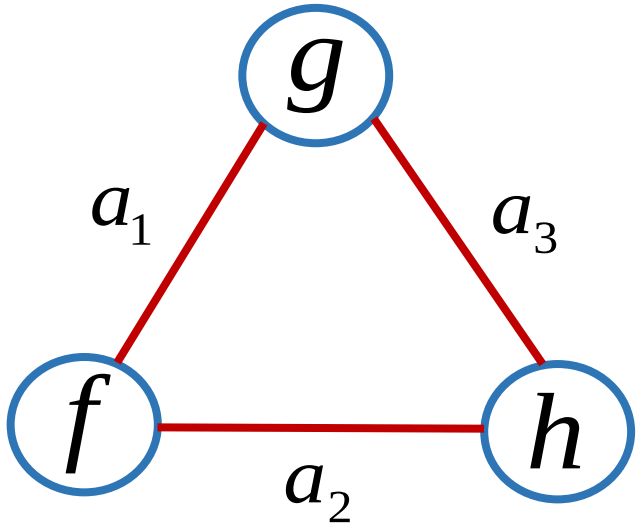

cutting one of interactions

Ghost-freedom is already shown in the vielbein formalism.

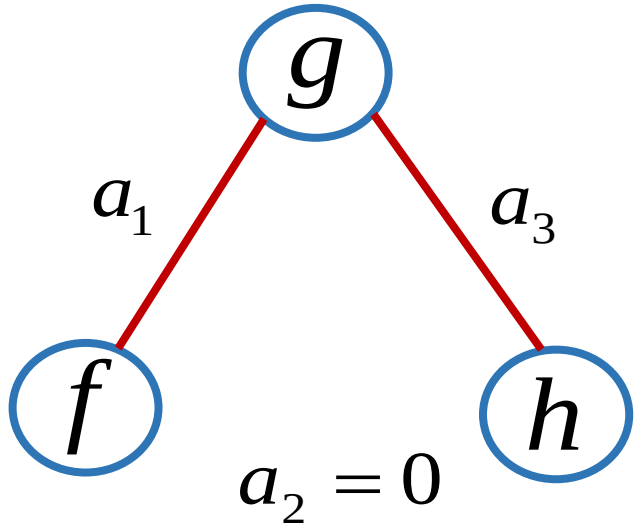

We perform the Hamiltonian analysis in homogeneous model.

$$g_{\mu\nu}dx^{\mu}dx^{\nu} = -N(t)^2 dt^2 + \gamma(t)_{ij}dx^i dx^j$$
$$f_{\mu\nu}dx^{\mu}dx^{\nu} = -L(t)^2 dt^2 + \omega(t)_{ij}dx^i dx^j$$
$$h_{\mu\nu}dx^{\mu}dx^{\nu} = -Q(t)^2 dt^2 + \rho(t)_{ij}dx^i dx^j$$

One of the metrics can be diagonalized through spacial rotations.

Hamiltonian : $H = NC_N + LC_L + QC_Q$

N, L, Q : Laglange multipliers

Constraints : $C_N = 0, C_L = 0, C_Q = 0$

Degrees of freedom : $3+6+6=15$

Constraints must be preserved in the time evolution.

$$\dot{C}_N = \{C_N, H\} = \{C_N, C_L\}L + \{C_N, C_Q\}Q \approx 0$$
$$\dot{C}_L = \{C_L, H\} = \{C_L, C_N\}N + \{C_L, C_Q\}Q \approx 0$$
$$\dot{C}_Q = \{C_Q, H\} = \{C_Q, C_N\}N + \{C_Q, C_L\}L \approx 0$$

$$\{C_N, C_L\} \propto a_1, \quad \{C_L, C_Q\} \propto a_2, \quad \{C_N, C_Q\} \propto a_3$$

$$\begin{pmatrix} 0 & a_1 & a_3 \\ -a_1 & 0 & a_2 \\ -a_3 & -a_2 & 0 \end{pmatrix} \begin{pmatrix} N \\ L \\ Q \end{pmatrix} = 0$$

We must determine the Lagrange multipliers to satisfy this condition.

Case 1:

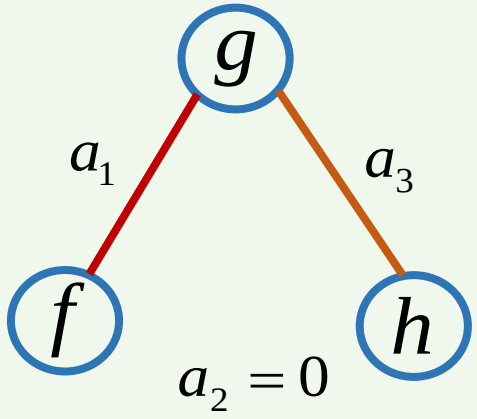

$$\begin{pmatrix} 0 & a_1 & a_3 \\ -a_1 & 0 & 0 \\ -a_3 & 0 & 0 \end{pmatrix} \begin{pmatrix} N \\ L \\ Q \end{pmatrix} = 0$$

Secondary Constraints $\quad a_1 \propto \{C_N, C_L\} \approx 0, \quad a_3 \propto \{C_N, C_Q\} \approx 0$

consistency in the time evolution

$$d\{C_N, C_L\}/dt = NC_{NL,N} + LC_{NL,L} + QC_{NL,Q} \approx 0$$
$$d\{C_N, C_Q\}/dt = NC_{NQ,N} + LC_{NQ,L} + QC_{NQ,Q} \approx 0$$

- One of the Lagrange multipliers is left undetermined. (one gauge freedom)
- The total number of constraints is five.

Total degrees of freedom : $(15 \times 2 - 5 - 1)/2 = 12$

- Masless graviton : 1
- Massive graviton : 2
- BD ghost : 0

Case 2:

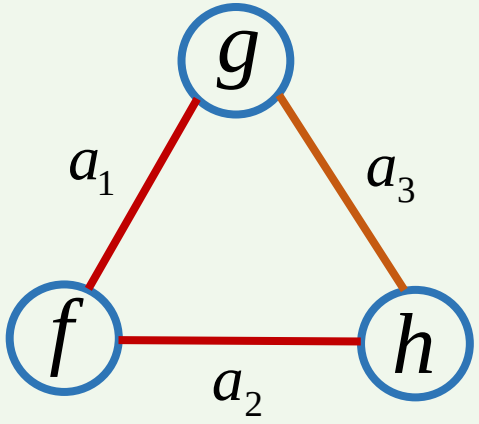

$$\begin{pmatrix} 0 & a_1 & a_3 \\ -a_1 & 0 & a_2 \\ -a_3 & -a_2 & 0 \end{pmatrix} \begin{pmatrix} N \\ L \\ Q \end{pmatrix} = 0$$

No seconday constraint

$$N = \frac{a_2}{a_1} Q, \quad L = -\frac{a_3}{a_1} Q, \quad Q : \text{arbitrary}$$

Constraints : 3
Gauge freedom : 1

Total degrees of freedom : $(15 \times 2 - 3 - 1)/2 = 13$

- Masless graviton : 1
- Massive graviton : 2
- BD ghost : 1

4. More general Multimetric gravity

$g_1, g_2, \ldots, g_n$: metrics

$$S_n = \sum_{k=1}^{n} M_k^2 \int d^4x \sqrt{-\det g_k}\, R[g_k] + \sum_{k=1}^{n} a_k \int d^4x \sqrt{-\det g_k}\, \Phi_k\left(\sqrt{g_k^{-1} g_{k+1}}\right)$$

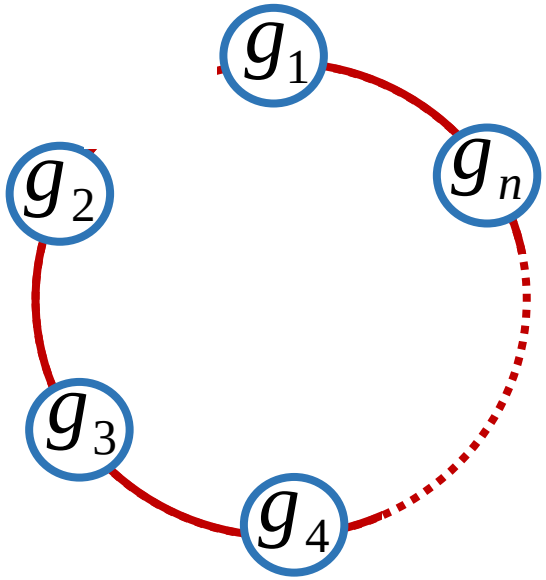

BD ghost : 0

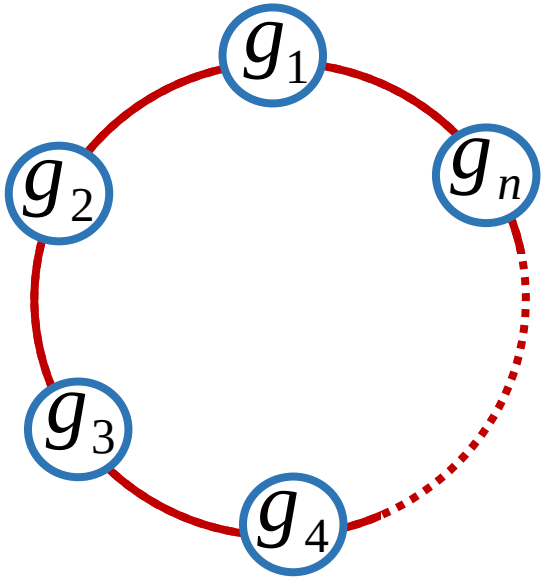

BD ghost : $(n-1)/2$ 個 (n:odd)

$(n-2)/2$ 個 (n:even)

5. summary

・We showed that there exists a BD-ghost in the trimetric gravity as a naive extension of the recently proposed ghost-free bimetric gravity.

・We also studied more general multi metric gravity, and showed there always exist BD-ghosts if loop type interactions are contained.

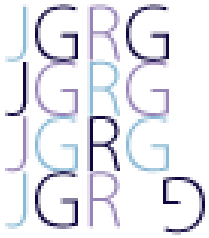

Shuichiro Yokoyama, JGRG 22(2012)111323

"Scale-dependent bias with the higher order primordial non-Gaussianity"

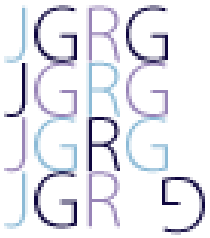

RESCEU SYMPOSIUM ON

GENERAL RELATIVITY AND GRAVITATION

JGRG 22



November 12-16 2012

Koshiba Hall, The University of Tokyo, Hongo, Tokyo, Japan



Scale-dependent bias with primordial higher order non-Gaussianity

~use of integrated Perturbation Theory~

Shuichiro Yokoyama (ICRR, the Univ. of Tokyo)
with Taka Matsubara (KMI, Nagoya Univ.)
arXiv:1210.2495, in prep.

Simplest parameterization

- **Focusing on Local type non-Gaussianity**

primordial curvature fluctuations (Komatsu & Spergel(2001), Byrnes, Sasaki & Wands(2006), …)

$$\Phi = \Phi_{\rm G} + f_{\rm NL}\left(\Phi_{\rm G}^2 - \langle\Phi^2\rangle\right) + g_{\rm NL}\Phi_{\rm G}^3 + \cdots$$

Gaussian fluc. $\sim 10^{-5}$ non-linearity parameters

→ **Non-zero higher order spectra**

(higher order correlation functions)

leadingly, …

- Bispectrum (3-point corr. func.) ⟺ $\langle\Phi(\mathbf{k}_1)\Phi(\mathbf{k}_2)\Phi(\mathbf{k}_3)\rangle$

$$B_\Phi(k_1,k_2,k_3) = 2f_{\rm NL}\left[P_\Phi(k_1)P_\Phi(k_2) + P_\Phi(k_2)P_\Phi(k_3) + P_\Phi(k_3)P_\Phi(k_1)\right]$$

- Trispectrum (4-point corr. func.) ⟺ $\langle\Phi(\mathbf{k}_1)\Phi(\mathbf{k}_2)\Phi(\mathbf{k}_3)\Phi(\mathbf{k}_4)\rangle_c$

Importance of trispcetrum

- **Trispectrum**

(Byrnes, Sasaki & Wands(2006), Boubekeur & Lyth(2006) …)

$$\langle \Phi_{\mathbf{k}_1} \Phi_{\mathbf{k}_2} \Phi_{\mathbf{k}_3} \Phi_{\mathbf{k}_4} \rangle_{\rm c} = (2\pi)^3 \delta^{(3)}(\mathbf{k}_1 + \mathbf{k}_2 + \mathbf{k}_3 + \mathbf{k}_4) T_\Phi(\mathbf{k}_1, \mathbf{k}_2, \mathbf{k}_3, \mathbf{k}_4)$$

$$T_\Phi(k_1, k_2, k_3, k_4) = 6 g_{\rm NL} \left[P_\Phi(k_1) P_\Phi(k_2) + 2 \text{ perms.} \right] + \frac{25}{9} \tau_{\rm NL} \{ P_\Phi(k_1) \left[P_\Phi(k_{13}) + P_\Phi(k_{23}) \right] + 10 \text{ perms.} \}$$

need two terms (different momentum-dependence)

Suyama and Yamaguchi (2008), …

We can generalize …

e.g.)

$$\Phi = \phi_{\rm G} + \psi_{\rm G} + f_{\rm NL} \left(\phi_{\rm G}^2 - \langle \phi_{\rm G}^2 \rangle \right)$$

$$\langle \phi_{\rm G} \psi_{\rm G} \rangle = 0$$

$$R \equiv P_\phi / P_\psi$$

$$\tau_{\rm NL} = \left(\frac{1+R}{R} \right) \left(\frac{6}{5} f_{\rm NL} \right)^2$$

$$\tau_{\rm NL} \geq \left(\frac{6}{5} f_{\rm NL} \right)^2$$

(Suyama, Takahashi, Yamguchi and SY (2010))

fNL vs tauNL

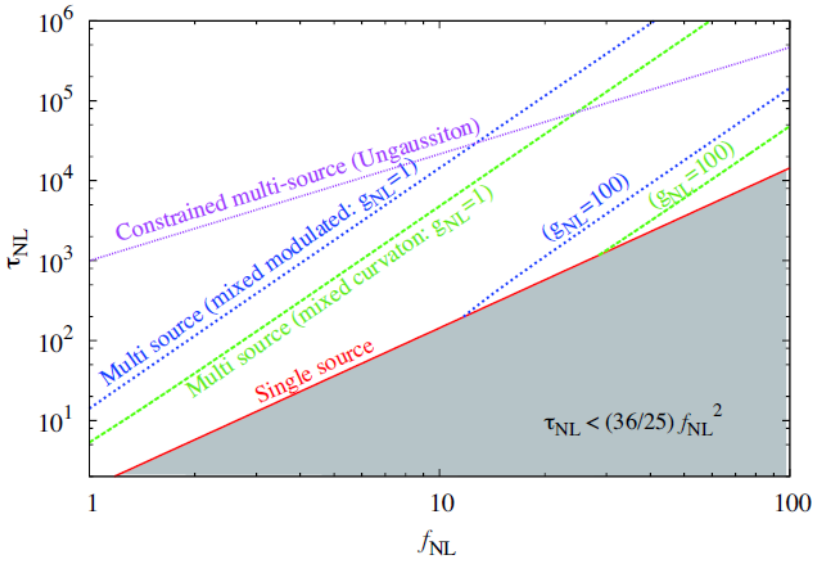

Different lines represent different models

distinguishing models !!!

fNL vs gNL

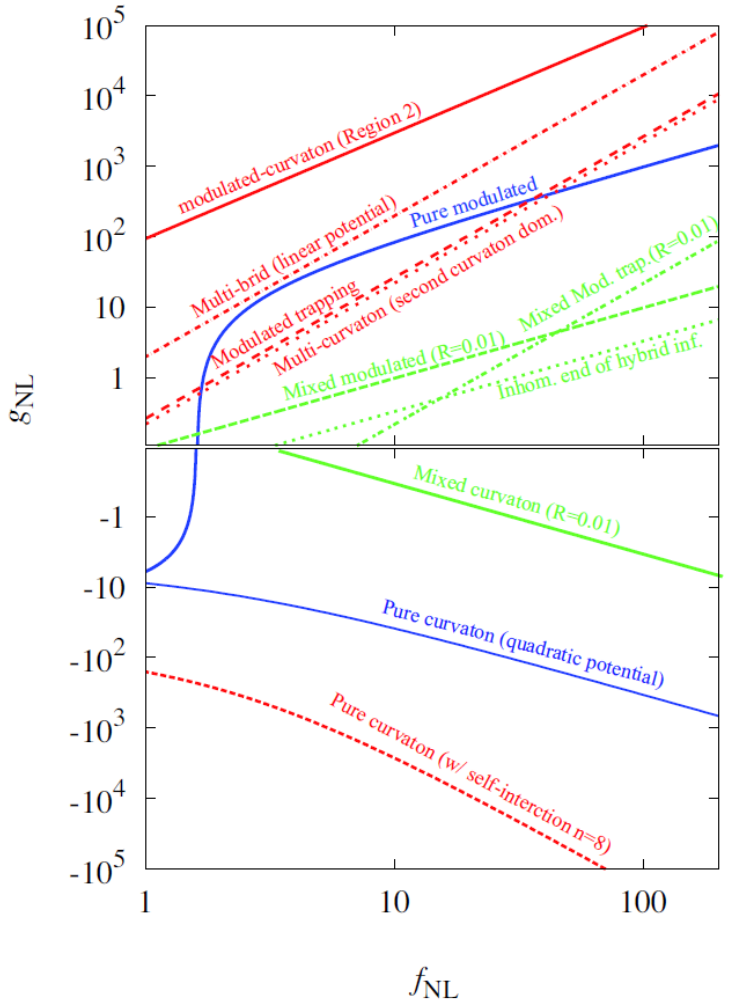

How accuracy can we measure these parameters with using cosmological observations?

Integrated Perturbation Theory (iPT)

Matsubara (2011), Matsubara (2012)

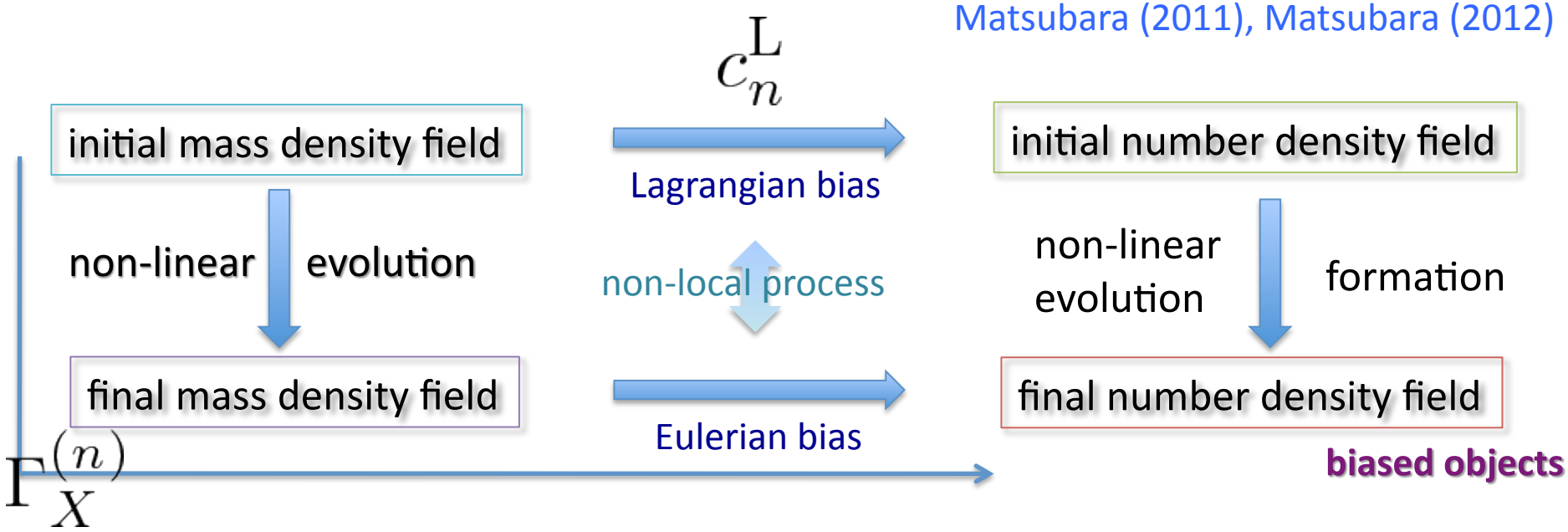

Non-linear perturbation theory integrated with non-local bias, redshift-distorsions, and primordial non-Gaussianity

initial mass density field; $\delta_{\rm L}$

final mass density field; δ_m

initial number density field; $\delta_X^{\rm L}$

final number density field; δ_X

Without high peak limit and peak-background split picture

- Introducing multi-point propagators

$$\left\langle \frac{\delta^n \delta_X(\mathbf{k})}{\delta\delta_{\rm L}(\mathbf{k}_1)\cdots\delta\delta_{\rm L}(\mathbf{k}_n)} \right\rangle = (2\pi)^{3-3n}\delta^{(3)}(\mathbf{k}_1+\cdots+\mathbf{k}_n-\mathbf{k})\Gamma_X^{(n)}(\mathbf{k}_1,\cdots,\mathbf{k}_n),$$



- Power spectrum of the biased objects with primordial non-Gaussianity

(without any high peak approximation, peak-backgroud picture, …)

Matsubara(2012)

$$\begin{aligned}
P_X(k) &= \left[\Gamma_X^{(1)}(\mathbf{k})\right]^2 P_{\rm L}(k) + \Gamma_X^{(1)}(\mathbf{k})\int\frac{d^3p}{(2\pi)^3}\Gamma_X^{(2)}(\mathbf{p},\mathbf{k}-\mathbf{p})B_{\rm L}(\mathbf{k},-\mathbf{p},\mathbf{k}+\mathbf{p}) \\
&+\frac{1}{3}\Gamma_X^{(1)}(\mathbf{k})\int\frac{d^3p_1d^3p_2}{(2\pi)^6}\Gamma_X^{(3)}(\mathbf{p}_1,\mathbf{p}_2,\mathbf{k}-\mathbf{p}_1-\mathbf{p}_2)T_{\rm L}(\mathbf{k},-\mathbf{p}_1,-\mathbf{p}_2,-\mathbf{k}+\mathbf{p}_1+\mathbf{p}_2) \\
&+\frac{1}{4}\int\frac{d^3p_1d^3p_2}{(2\pi)^6}\Gamma_X^{(2)}(\mathbf{p}_1,\mathbf{k}-\mathbf{p}_1)\Gamma_X^{(2)}(-\mathbf{p}_2,-\mathbf{k}+\mathbf{p}_2)T_{\rm L}(\mathbf{p}_1,\mathbf{k}-\mathbf{p}_1,-\mathbf{p}_2,-\mathbf{k}+\mathbf{p}_2)
\end{aligned}$$

$$\begin{cases}
P_{\rm L}(k) = \mathcal{M}(k)^2 P_\Phi(k) \\
B_{\rm L}(\mathbf{k}_1,\mathbf{k}_2,\mathbf{k}_3) = \mathcal{M}(k_1)\mathcal{M}(k_2)\mathcal{M}(k_3)B_\Phi(\mathbf{k}_1,\mathbf{k}_2,\mathbf{k}_3) \\
T_{\rm L}(\mathbf{k}_1,\mathbf{k}_2,\mathbf{k}_3,\mathbf{k}_4) = \mathcal{M}(k_1)\mathcal{M}(k_2)\mathcal{M}(k_3)\mathcal{M}(k_4)T_\Phi(\mathbf{k}_1,\mathbf{k}_2,\mathbf{k}_3,\mathbf{k}_4)
\end{cases}$$

$$\mathcal{M}(k) = \frac{2}{3}\frac{D(z)}{(1+z_*)D(z_*)}\frac{k^2T(k)}{{H_0}^2\Omega_{\rm m0}}$$

including growth factor, transfer function, Poisson equation, ..

- Diagrammatically, …

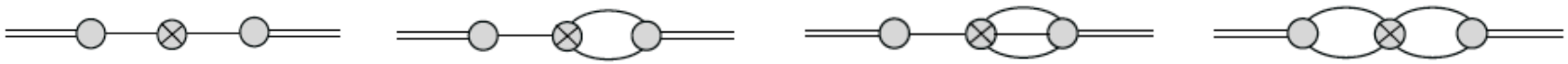

- Introducing renormalized bias functions

$$c_n^{\rm L}(\mathbf{k}_1,\mathbf{k}_2,\cdots,\mathbf{k}_n) = (2\pi)^{3n}\int \frac{d^3p}{(2\pi)^3}\left\langle \frac{\delta^n\delta_X^{\rm L}(\mathbf{p})}{\delta\delta_{\rm L}(\mathbf{k}_1)\cdots\delta\delta_{\rm L}(\mathbf{k}_n)}\right\rangle$$

← depend on the mass function of the biased objects

multiplicity function →

$$\Gamma_{\rm X}^{(1)}(\boldsymbol{k}) = 1 + c_1^{\rm L}(k)$$

$$\Gamma_{\rm X}^{(2)}(\boldsymbol{k}_1,\boldsymbol{k}_2) = F_2(\boldsymbol{k}_1,\boldsymbol{k}_2) + \left(1+\frac{\boldsymbol{k}_1\cdot\boldsymbol{k}_2}{{k_1}^2}\right)c_1^{\rm L}(k_2) + \left(1+\frac{\boldsymbol{k}_1\cdot\boldsymbol{k}_2}{{k_2}^2}\right)c_1^{\rm L}(k_1) + c_2^{\rm L}(\boldsymbol{k}_1,\boldsymbol{k}_2)$$

non-linear evolution
of the matter density field

$$F_n(\mathbf{k}_1,\mathbf{k}_2,\cdots,\mathbf{k}_n) \to 0$$

$$\mathbf{k}_1+\mathbf{k}_2+\cdots+\mathbf{k}_n = \mathbf{K} \to 0$$ (on large scales)

- Multiplicity function

$$n(M) = -\frac{2\bar{\rho}_0}{M}\frac{f_{\rm MF}(\nu)}{2}\frac{d\ln\sigma_M}{dM}$$

variance of $\delta_M(\boldsymbol{x}) = \int \frac{d^3k}{(2\pi)^3} e^{i\boldsymbol{k}\cdot\boldsymbol{x}} W(kR)\delta_{\rm L}(\boldsymbol{k})$

number density of the biased objects

multiplicity function

$\nu = \delta_c/\sigma_M$

critical density

Press-Schechter formalism,
Sheth-Tormen fitting formula, ..

Then,

$$c_n^{\rm L}(\boldsymbol{k}_1,\ldots,\boldsymbol{k}_n) = \frac{A_n(M)}{{\delta_{\rm c}}^n} W(k_1R)\cdots W(k_nR) + \frac{A_{n-1}(M)\,{\sigma_M}^n}{{\delta_{\rm c}}^n}\frac{d}{d\ln\sigma_M}\left[\frac{W(k_1R)\cdots W(k_nR)}{{\sigma_M}^n}\right]$$

$$A_n(M) \equiv \sum_{j=0}^{n}\frac{n!}{j!}{\delta_{\rm c}}^j\, b_j^{\rm L}(M)$$

$$b_n^{\rm L}(M) = (-1/\sigma_M)^n f_{\rm MF}^{(n)}/f_{\rm MF}$$

bias parameter can be evaluated!

Scale-dependent bias

- Bias parameter

$$P_X(k) \equiv b_X(k) P_{\rm L}(k)$$

on large scales $(k \to 0)$, $\boxed{b_X(k) \approx b_1(M)^2 + \Delta b(k)}$

Scale-dependent part;

$$\Delta b(k) \approx 4 f_{\rm NL} \frac{b_1(M)}{\mathcal{M}(k)} \left[b_2^{\rm L}(M) + 2 \frac{1 + \delta_c (b_1(M) - 1)}{\delta_c^2} \right] \sigma_M^2$$

→ k^-2-dependence

$$+ \left(g_{\rm NL} + \frac{25}{27} \tau_{\rm NL} \right) \frac{b_1(M)}{\mathcal{M}(k)}$$

→ k^-2-dependence

$$\times \left[b_3^{\rm L}(M) + \frac{2 + 2\delta_c (b_1(M) - 1) + \delta_c^2 b_2^{\rm L}(M)}{\delta_c^3} \left(4 + \frac{d \ln S_3(M)}{\ln \sigma_M} \right) \right] \sigma_M^4 S_3(M)$$

$$+ \frac{25}{9} \tau_{\rm NL} \frac{1}{\mathcal{M}(k)^2} \left[b_2^{\rm L}(M) + 2 \frac{1 + \delta_c (b_1(M) - 1)}{\delta_c^2} \right]^2 \sigma_M^4 ,$$

→ K^-4-dependence

$$S_3(M) = \frac{\langle \delta_M^3 \rangle}{\langle \delta_M^2 \rangle^2} \quad \delta_c = 1.68 \quad b_1(M) \equiv 1 + c_1^{\rm L}$$

Matsubara(2012), Yokoyama and Matsubara(2012)

- fNL vs gNL ; same k-dependence…

➔ Different redshift-dependence !

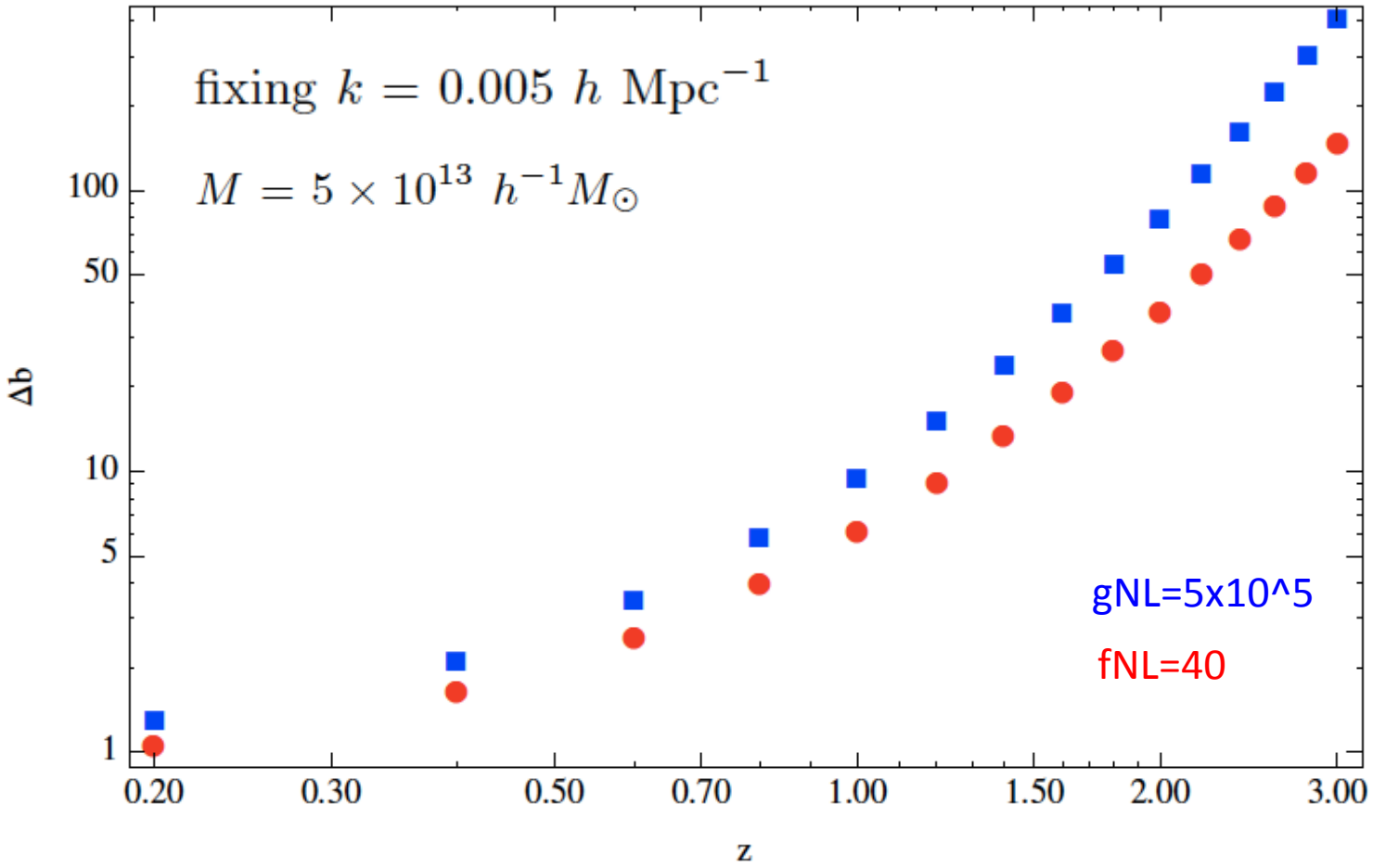

Higher redshift objects ➔ tighter constraints for gNL?

- fNL vs tauNL ; inequality $\tau_{\rm NL} \geq \left(\frac{6}{5} f_{\rm NL}\right)^2$

Introducing a stochasticity parameter;

$$r(k) \equiv \frac{P_{\rm m}(k) P_X(k)}{P_{{\rm m}X}(k)^2}.$$

$P_{{\rm m}X}(k)$; matter density field – biased objects cross power spectrum

$P_{\rm m}(k)$; matter density field power spectrum

On large scales,

$$r(k) \simeq 1 + \left(\frac{25}{9}\tau_{\rm NL} - 4 f_{\rm NL}^2\right) \frac{1}{b_1(k)^2 \mathcal{M}(k)^2} \left[\int \frac{d^3p}{(2\pi)^3} c_2^{\rm L}(\mathbf{p}, -\mathbf{p}) P_{\rm L}(p)\right]^2$$

Directly dependent on the inequality !

$$A_{\rm NL} = \tau_{\rm NL}/(6 f_{\rm NL}/5)^2$$

r(k) = 0, or < 0, or > 0 ??

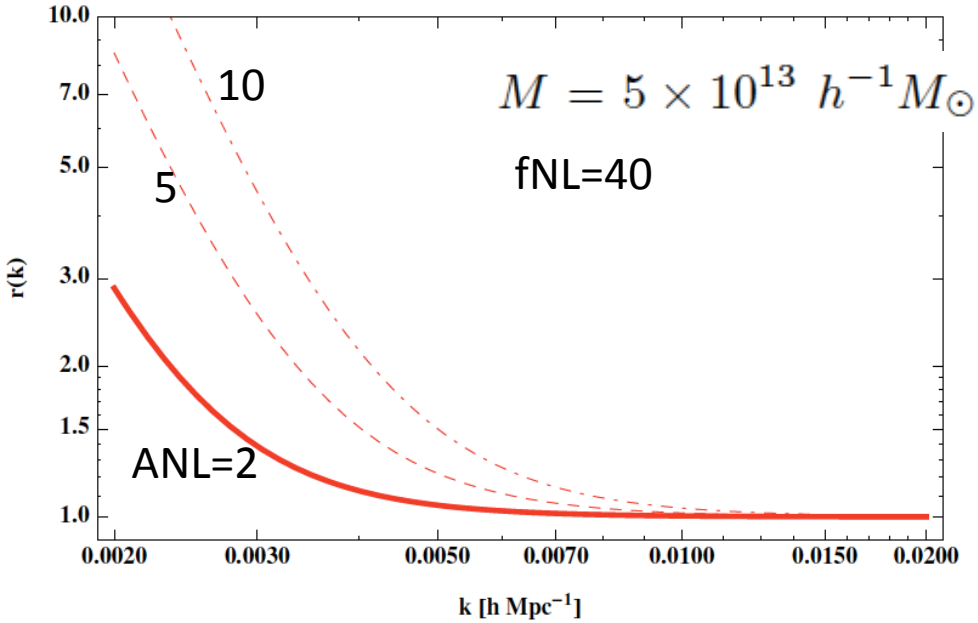

- Higher order from non-Gaussian mass function

$$f_{\rm MF} = f_{\rm PS(ST)} \times R^{\rm NG}$$ ⟹ b ?

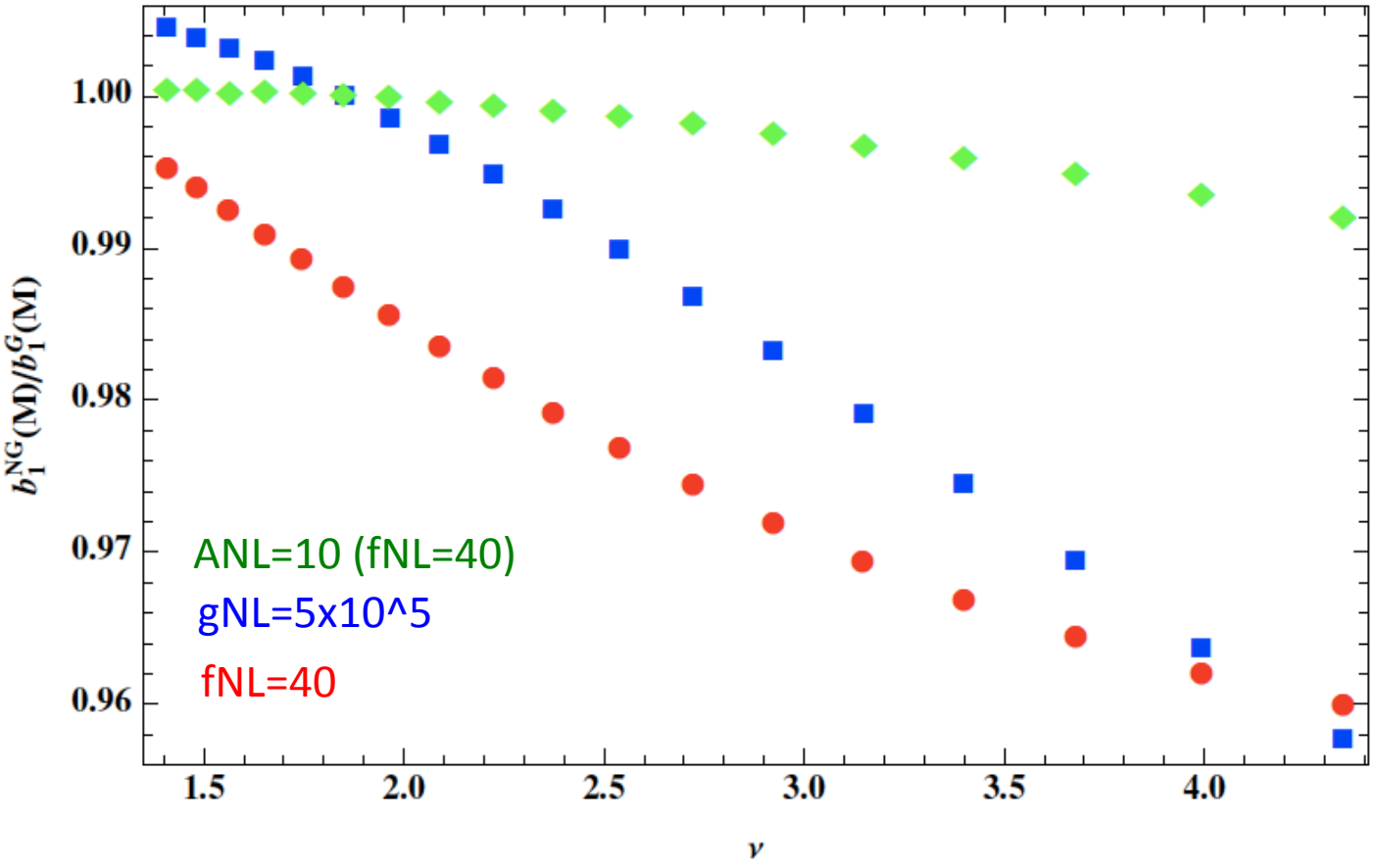

negligible for not so high peak objects..

- Higher order contribution (from b2, b3, …)

$$
\begin{aligned}
P_X(k) \;=\; & \sum_{n=1}^{\infty}\Bigg[\frac{1}{n!}\int\frac{d^3p_1\cdots d^3p_{n-1}}{(2\pi)^{3n}}\Gamma_X^{(n)}(\mathbf{p}_1,\mathbf{p}_2,\cdots,\mathbf{k}-\mathbf{P}_{n-1})^2 P_{\rm L}(p_1)P_{\rm L}(p_2)\cdots P_{\rm L}(|\mathbf{k}-\mathbf{P}_{n-1}|) \\
& +\frac{1}{(n-1)!}\int\frac{d^3p_1\cdots d^3p_n}{(2\pi)^{(3n)}}\Gamma_X^{(n)}(\mathbf{p}_1,\cdots,\mathbf{p}_{n-1},\mathbf{k}-\mathbf{P}_{n-1}) \\
& \quad\times\Gamma_X^{(n+1)}(-\mathbf{p}_1,\cdots,-\mathbf{p}_n,-\mathbf{k}+\mathbf{P}_n)P_{\rm L}(p_1)\cdots P_{\rm L}(p_{n-1})B_{\rm L}(\mathbf{k}-\mathbf{P}_{n-1},-\mathbf{p}_n,-\mathbf{k}+\mathbf{P}_n) \\
& +\frac{1}{3(n-1)!}\int\frac{d^3p_1\cdots d^3p_{n+1}}{(2\pi)^{3n+3}}\Gamma_X^{(n)}(\mathbf{p}_1,\cdots,\mathbf{p}_{n-1},\mathbf{k}-\mathbf{P}_{n-1}) \\
& \quad\times\Gamma_X^{(n+2)}(-\mathbf{p}_1,\cdots,-\mathbf{p}_{n+1},-\mathbf{k}+\mathbf{P}_{n+1})P_{\rm L}(p_1)\cdots P_{\rm L}(p_{n-1})T_{\rm L}(\mathbf{k}-\mathbf{P}_{n-1},-\mathbf{p}_n,-\mathbf{p}_{n+1},-\mathbf{k}+\mathbf{P}_{n+1})\Bigg] \\
& +\sum_{n=2}^{\infty}\frac{1}{4(n-2)!}\int\frac{d^3p_1\cdots d^3p_{n-1}d^3q}{(2\pi)^{3n}}\Gamma_X^{(n)}(\mathbf{p}_1,\cdots,\mathbf{p}_{n-1},\mathbf{k}-\mathbf{P}_{n-1}) \\
& \quad\times\Gamma_X^{(n)}(-\mathbf{p}_1,\cdots,-\mathbf{p}_{n-2},-\mathbf{q},-\mathbf{k}+\mathbf{P}_{n-2}+\mathbf{q}) \\
& \qquad\times P_{\rm L}(p_1)\cdots P_{\rm L}(p_{n-2})T_{\rm L}(\mathbf{p}_{n-1},\mathbf{k}-\mathbf{P}_{n-1},-\mathbf{q},-\mathbf{k}+\mathbf{P}_{n-2}+\mathbf{q}), \qquad (33)
\end{aligned}
$$

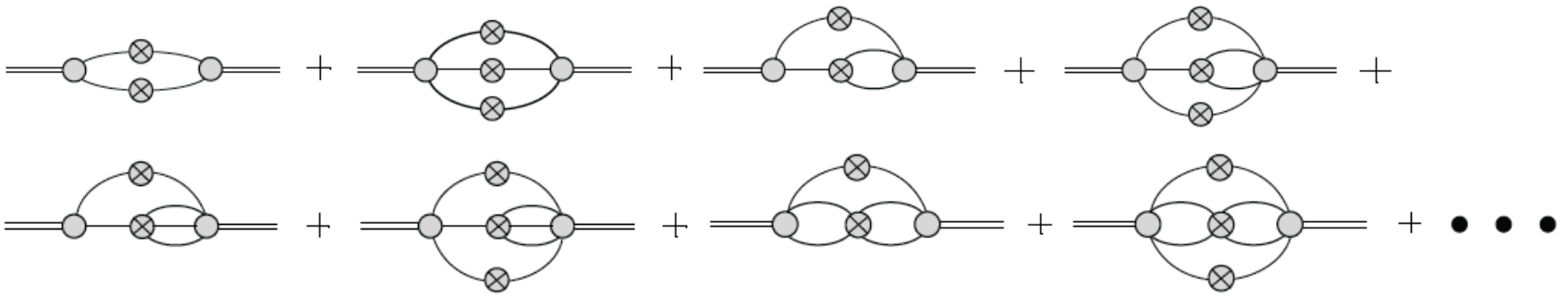

- Higher order in stochasticity parameter

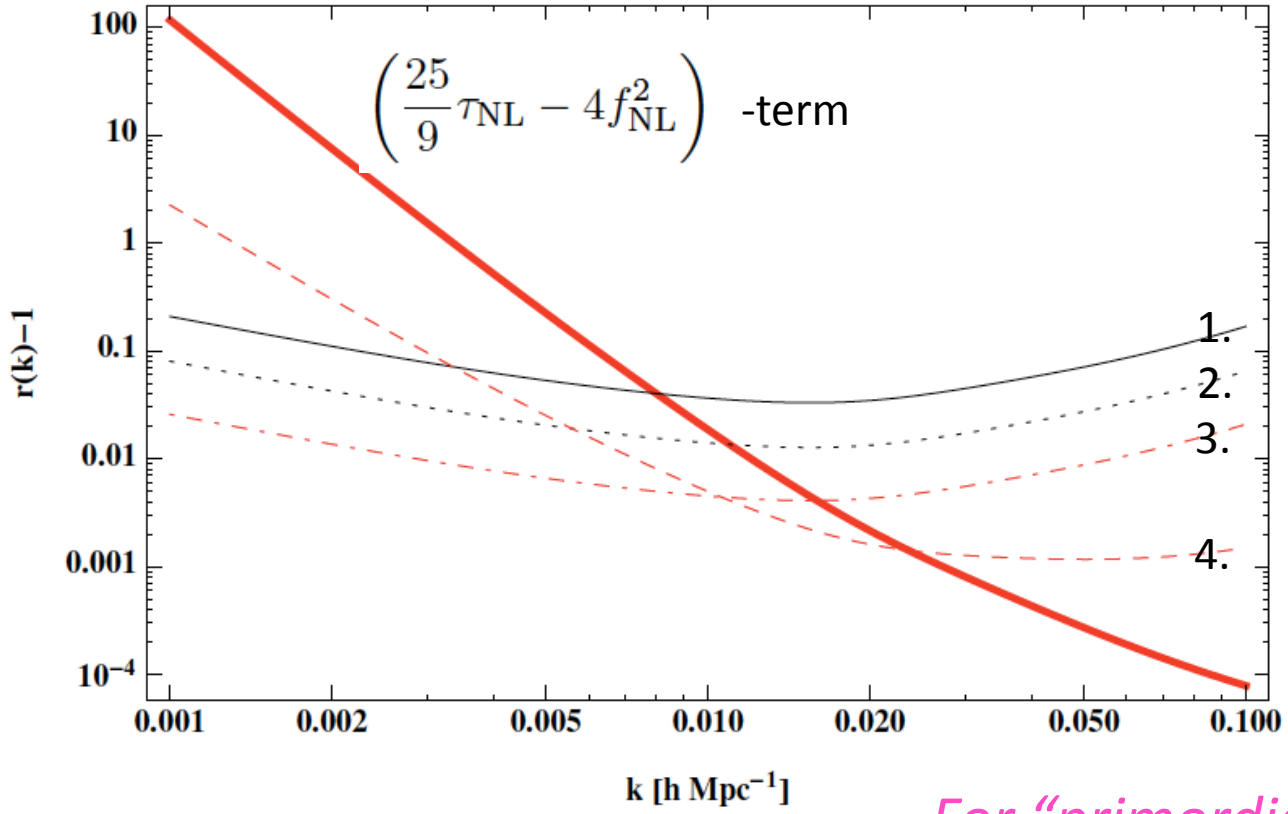

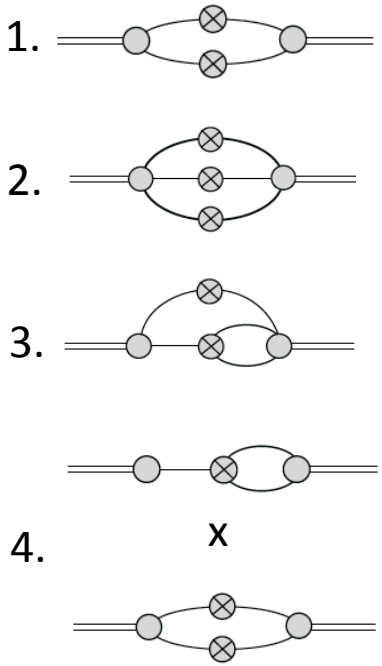

$f_{\rm NL} = 40$ and $\tau_{\rm NL} = 5 \times 36 f_{\rm NL}^2/25.$

fixing $z = 1$ and $M = 5 \times 10^{13}\ h^{-1} M_\odot$

For "primordial stochasticity",

$$k < O(10^{-2})\ h{\rm Mpc}^{-1}$$

is needed ??

- Equilateral ?

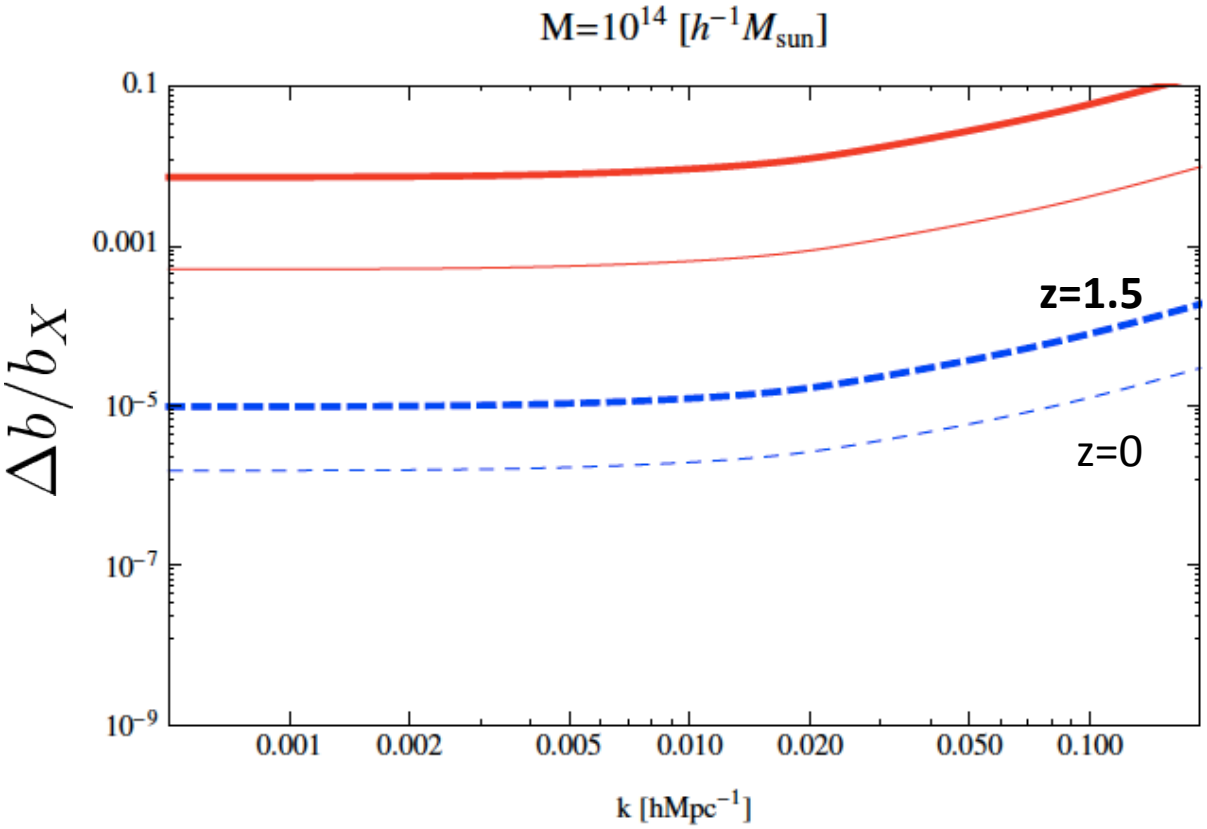

fNL^eq = 200

gNL^eq = 4x10^4
(= (fNL^eq)^2)

$$T_\Phi^{\rm eql}(-\mathbf{k},\mathbf{p}_1,\mathbf{p}_2,\mathbf{k}-\mathbf{p}_1-\mathbf{p}_2) \simeq \frac{25}{9}\frac{4^5 g_{\rm NL}^{\rm eql} k^2 P_\Phi(k)\mathcal{P}_\Phi^2}{p_1 p_2 |\mathbf{p}_1+\mathbf{p}_2| \left(p_1+p_2+|\mathbf{p}_1+\mathbf{p}_2|\right)^5}$$

See e.g., Mizuno and Koyama (2010)

Negligibly small contribution

Summary and Discussion

- Derive an accurate formula for the bias parameter with primordial non-Gaussianity by using integrated Perturbation Theory
- wide (large scales) and deep (redshift-dependence) surveys are needed.

- Galaxy bispectrum?
- Forecast for the constraints on fNL, gNL and tauNL? (HSC, …)

- preliminary

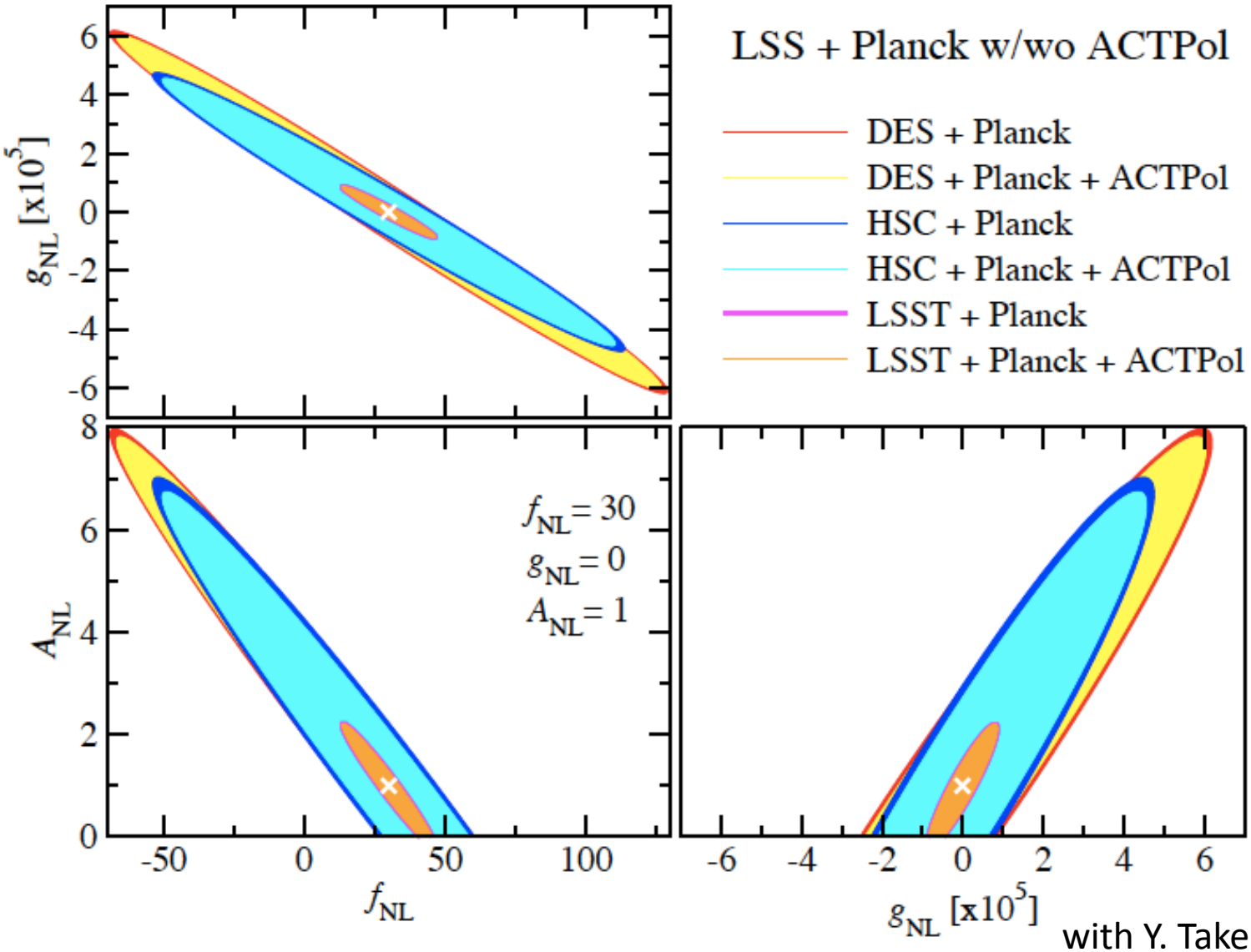

with Y. Takeuchi in prep.

- Bispectrum of the biased objects

Up to the one-loop order in the multi-point propagators, we have

$$
\begin{aligned}
B_X(\mathbf{k}_1,\mathbf{k}_2,\mathbf{k}_3) \;=\; & \left[\Gamma_X^{(1)}(\mathbf{k}_1)\Gamma_X^{(1)}(\mathbf{k}_2)\Gamma_X^{(2)}(-\mathbf{k}_1,-\mathbf{k}_2)P_{\rm L}(k_1)P_{\rm L}(k_2)+2\ \text{perms.}\right] \\
& +\Gamma_X^{(1)}(\mathbf{k}_1)\Gamma_X^{(1)}(\mathbf{k}_2)\Gamma_X^{(1)}(\mathbf{k}_3)B_{\rm L}(\mathbf{k}_1,\mathbf{k}_2,\mathbf{k}_3) \\
& +\frac{1}{2}\left[\Gamma_X^{(1)}(\mathbf{k}_1)\Gamma_X^{(1)}(\mathbf{k}_2)\int\frac{d^3p}{(2\pi)^3}T_{\rm L}(\mathbf{k}_1,\mathbf{k}_2,\mathbf{p},\mathbf{k}_3-\mathbf{p})+2\ \text{perms.}\right] \\
& +\left[\Gamma_X^{(1)}(\mathbf{k}_1)\Gamma_X^{(1)}(\mathbf{k}_2)\int\frac{d^3p}{(2\pi)^3}\Gamma_X^{(3)}(-\mathbf{k}_1,\mathbf{p},-\mathbf{k}_2-\mathbf{p})P_{\rm L}(k_1)B_{\rm L}(\mathbf{k}_2,\mathbf{p},-\mathbf{k}_2-\mathbf{p})+2\ \text{perms.}\right] \\
& +\cdots
\end{aligned}
$$

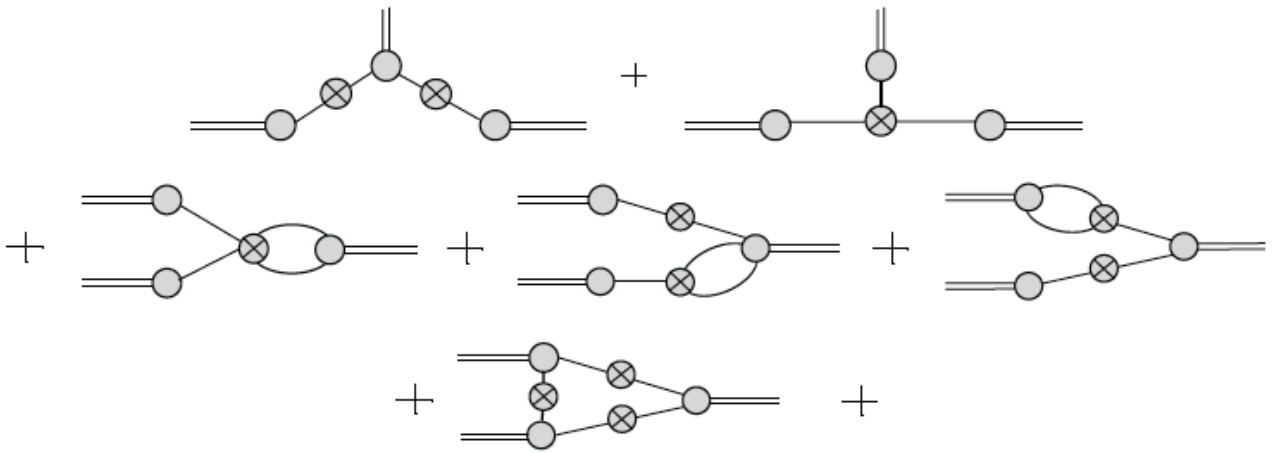

Takao Kitamura, JGRG 22(2012)111325

"Gravitational lensing by modified lens gravity"

RESCEU SYMPOSIUM ON

GENERAL RELATIVITY AND GRAVITATION

JGRG 22

November 12-16 2012

Koshiba Hall, The University of Tokyo, Hongo, Tokyo, Japan

Gravitational lensing by modified lens gravity

Takao Kitamura

Hirosaki University, Japan
with H. Asada (Hirosaki), K. Nakajima (Hirosaki)

JGRG22 in Tokyo Nov. 12 - 16, 2021
Abstract: IS DEMAGNIFICATION AN EVIDENCE FOR WORMHOLES ??

1 Deflection angle of light in the modified space-time metric (inverce power form)

In weak field limit, We consider a modified space-time metric as

$$ds^2 = -(1-\frac{\varepsilon_1}{r^n})dt^2 + (1+\frac{\varepsilon_2}{r^n})dr^2 + r^2(d\theta^2+\sin^2\theta d\phi). \tag{1}$$

This metric is rewritten up to O(ε) by comformal transformation as

$$ds^2 = (\frac{1}{1-\frac{\varepsilon_1}{r^n}})\tilde{ds}^2, \tag{2}$$

where

$$\tilde{ds}^2 \approx -dt^2 + (1+\frac{\varepsilon}{R^n})dR^2 + R^2(d\theta^2+\sin^2\theta d\phi^2) \tag{3}$$

with $R \equiv r^2/(1-\frac{\varepsilon_1}{r^n})$ and $\varepsilon \equiv n\varepsilon_1+\varepsilon_2$. We derivated deflection angle of light in this space-time as with method of schwartzchild case.

Derivated deflection angle is

$$\alpha = \frac{\varepsilon}{b^n}\cdot\int_0^{\frac{\pi}{2}}\cos^n\theta d\theta. \tag{4}$$

Especially, Equation (4) is rewritten as

$$\alpha = \frac{\varepsilon}{b^n}\cdot\frac{(n-1)!!}{n!!}\frac{\pi}{2} \quad \text{(n is even)}, \tag{5}$$

$$\alpha = \frac{\varepsilon}{b^n}\cdot\frac{(n-1)!!}{n!!} \quad \text{(n is odd)}. \tag{6}$$

b is impact parameter.

The Equation (4) coinside with schwarzschild case with $n=1$ and Ellis wormhole case with $n=2$.

2 Modified lens equation

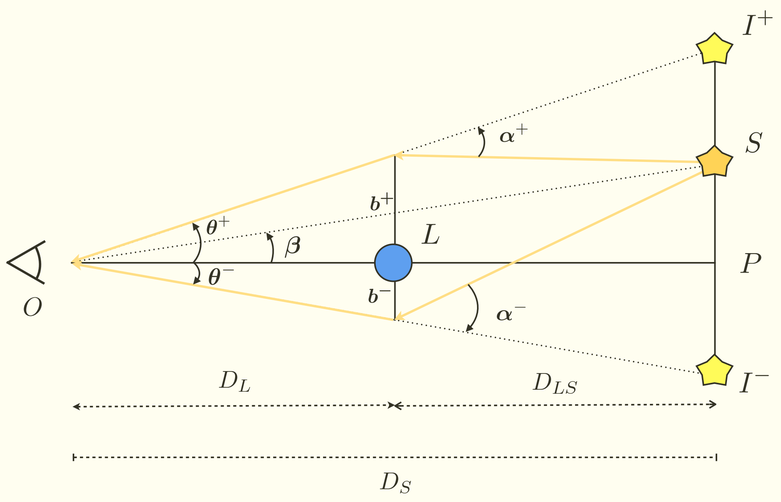

Lens equation for modified space-time is

$$\beta = \theta - \frac{1}{\theta^n} \quad (\theta>0), \tag{7}$$

$$\beta = \theta + \frac{1}{(-\theta)^n} \quad (\theta<0), \tag{8}$$

in the units of $\theta_E = \varepsilon^{\frac{1}{n+1}}$ that is Einstein ring radius with $\beta=0$. We call this equation as **Modified lens equation**.

We want to obtain analytical solution for modified lens equations. But no fomula of solution for fifth-order(or higher) equation. Therefore, we solve it using **asymptotic expansion**.

Then we consider source object pass through nearzone in proportion with Einstein ring radius ($\beta \ll |\theta_E|$).For $\beta<1$, Equation [7,8] are iteratively solved as

$$\theta_+ = 1+\frac{1}{n+1}\beta+\frac{1}{2}\frac{n}{(n+1)^2}\beta^2 \quad (\theta>0), \tag{9}$$

$$\theta_- = -1+\frac{1}{n+1}\beta-\frac{1}{2}\frac{n}{(n+1)^2}\beta^2 \quad (\theta<0). \tag{10}$$

3 Approximate prediction for amplification

Total amplification is

$$A \equiv \left|\frac{\theta_+}{\beta}\frac{d\theta_+}{d\beta}\right| + \left|\frac{\theta_-}{\beta}\frac{d\theta_-}{d\beta}\right|. \tag{11}$$

substitute Equations [9,10] in Equation (11):

$$A = \frac{1}{n+1}\frac{2}{\beta}. \tag{12}$$

Thus, magnifying condition ($A>1$) is rewritten as

$$\frac{2}{n+1} > \beta. \tag{13}$$

The meaning of Equation (13) is changing from magnification to demagnification with $\beta = 2/(n+1)$.

e.g. $n=10$, $\beta = 0.182$

4 Light curve by numerical calculations

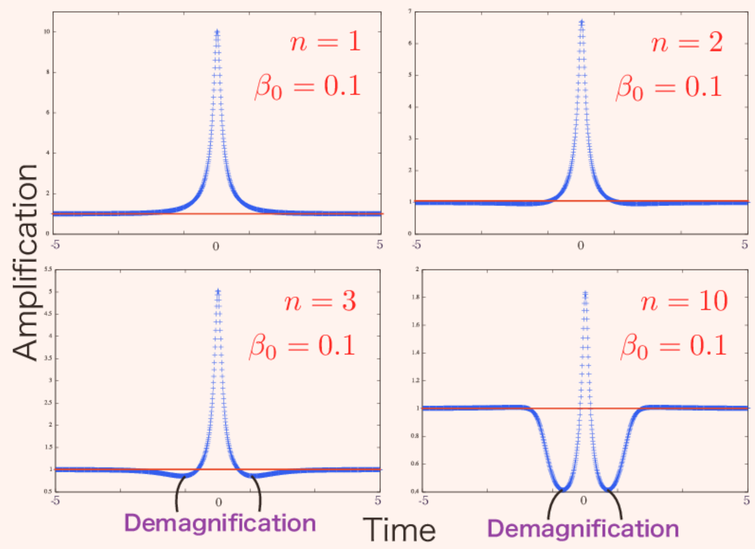

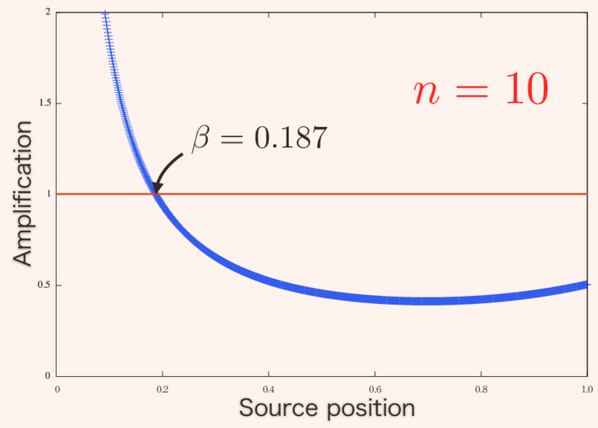

Blue line is light curve, and **Red line** is the brightness of source.
β_0 is the closest position from lens to source in units of θ_E.

Demagnified by **10 %, 60 %** from source brightness with $n=3$, $n=10$. The second figure shows β in the point which changes from magnification to demagnification is 0.187, this value is close to value of approximate prediction for foregoing section.

5 Conclusion

- **We obtained light curve for modified space-time metric**
- **Demagnification is an evidance EWH. But not always prove it !!**

Future work...

- Applying to modified gravity and exotic matter
- Mechanism of demagnification

References

[1] Fumio Abe 2010 ApJ 725 787.

[2] Y.Toki, T.Kitamura, H.Asada, F.Abe 2011 ApJ 740 121

[3] K. Nakajima, H. Asada 2011 Phys. Rev. D 85, 107501

[4] T.kitamura, K. Nakajima H. Asada arxiv

[5] Tsukamoto sann arxiv

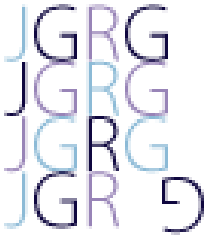

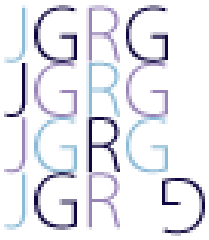

Yasumichi Sano, JGRG 22(2012)111327

"Gravitational field of a rotating ring around a Schwarzschild black hole"

RESCEU SYMPOSIUM ON

GENERAL RELATIVITY AND GRAVITATION

JGRG 22

November 12-16 2012

Koshiba Hall, The University of Tokyo, Hongo, Tokyo, Japan





P19

GRAVITATIONAL FIELD OF A ROTATING RING AROUND A SCHWARZSCHILD BLACK HOLE

～ Using Hertz Potential ～

Yasumichi SANO, Hideyuki TAGOSHI (Osaka University)

We calculated the perturbed space time metric of a Schwarzschild black hole (BH) and a rotating mass ring using Teukolsky equation and CCK (Chrzanowski, Cohen & Kegeles) formalism. We also visualized the result with tendex line and vortex line.

Introduction



- Black hole perturbation (1st order)
  - mass ratio (source/BH) as the small parameter

$$g_{\alpha\beta} = g^{(0)}_{\alpha\beta} + h_{\alpha\beta}$$

BH metric ⬆

- “Black hole ＋ moving point mass” perturbed metric
  → Self-force, gravitational wave
  - For Kerr BH, it is very difficult to calculate $h_{\alpha\beta}$
- Illuminating the method available with Kerr spacetime

Setting



- Schwarzschild black hole ＋ Rotating circular ring
  - Ring: a set of point particles in circular geodetic motion
  - Axisymmetric & steady problem
- Energy-momentum tensor of the ring ⬇
  - $2\pi m$: rest mass
  - u^α: four velocity
  - r_0: radius

$$T^{\alpha\beta} = \frac{m u^\alpha u^\beta}{u^t {r_0}^2}\delta(r-r_0)\delta(\cos\theta)$$

Method

- Finding $h_{\alpha\beta}$ via Hertz potential Ψ

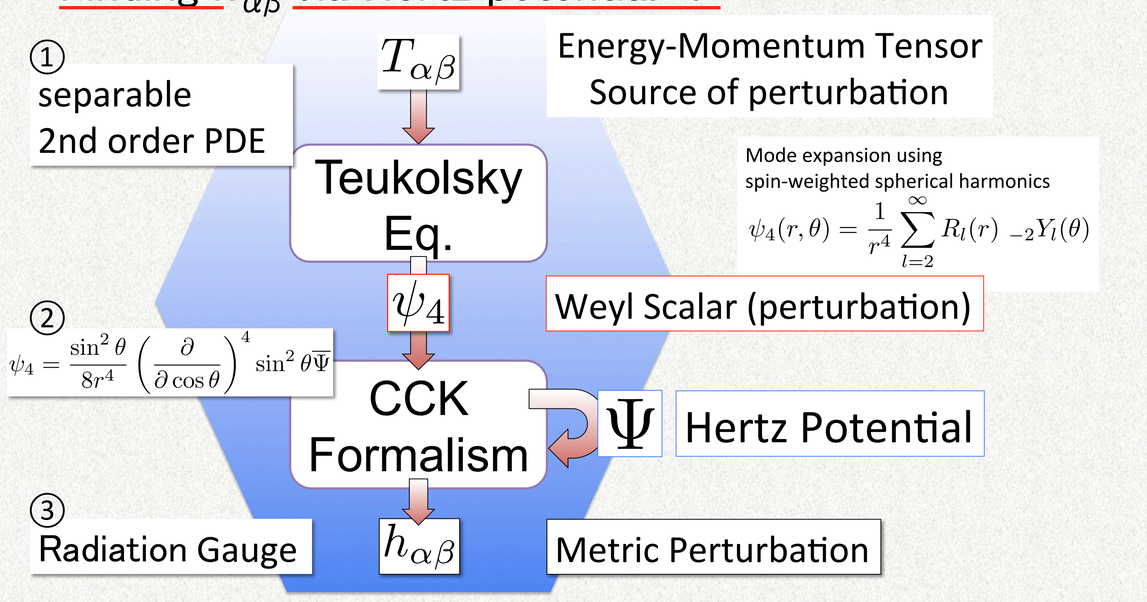

- Weyl scalar: Components of the Weyl tensor
  - 5 complex components (ψ_0, ψ_1, ψ_2, ψ_3, ψ_4)
- CCK: Chrzanowski (‘75), Cohen & Kegeles (‘79)
  In “Radiation gauge”, the perturbation $h_{\alpha\beta}$ is given by 2nd order partial derivative of Hertz potential
  - Hertz potential satisfies source free Teukolsky Eq.

Hertz potential

$$\Psi = \Psi_{\mathrm{P}} + \Psi_{\mathrm{H}}$$

- Assuming Hertz potential in the same mode expansion as Weyl scalar ($l \geq 2$), Eq.② reduces to algebraic Eq. ➡ The particular solution Ψ_{P} obtained easily
  - HOWEVER, Ψ_{P} gives singular Weyl tensor field, that is not continuous at the ring radius
- Determination of the Homogeneous solution Ψ_{H}
  - Some of degrees of freedom in Ψ_{H} are physical parameters (mass and angular momentum) ($l = 0,\ 1$ mode)
    ➡ By computing the mass and angular momentum, one can determine those parameters

$$M_{\mathrm{ring}} = -2\pi m u_\alpha \xi^\alpha \qquad J_{\mathrm{ring}} = 2\pi m u_\alpha \psi^\alpha$$

$\xi^\alpha = \left(\frac{\partial}{\partial t}\right)^\alpha$ $\psi^\alpha = \left(\frac{\partial}{\partial\phi}\right)^\alpha$: Killing vectors

  - J_{ring} completed the imaginary parts of all Weyl scalars, cancelling the discontinuities
  - M_{ring}, on the other hand, unexpectedly not cancelled the discontinuities of real parts of Weyl scalars

Visualizing (vortex line)

- A tensor representing frame-dragging effect
  - Weyl tensor $C_{\alpha\beta\gamma\delta}$ projected onto a 3 dimensional space

$$\mathcal{B}_{\hat{i}\hat{j}} = -\frac{1}{2}\epsilon_{\hat{i}\hat{p}\hat{q}} C_{\hat{0}\hat{j}}{}^{\hat{p}\hat{q}}$$

- Draw integral curves of the eigen vector field
- Ex. 1: Kerr BH
  - Outward curves in polar region

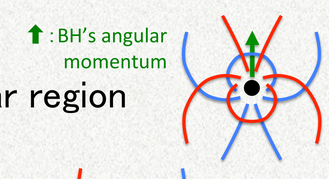

- Ex. 2: Line mass flow
  - Spiral around the (See only blue or red)



Result with only particular solution

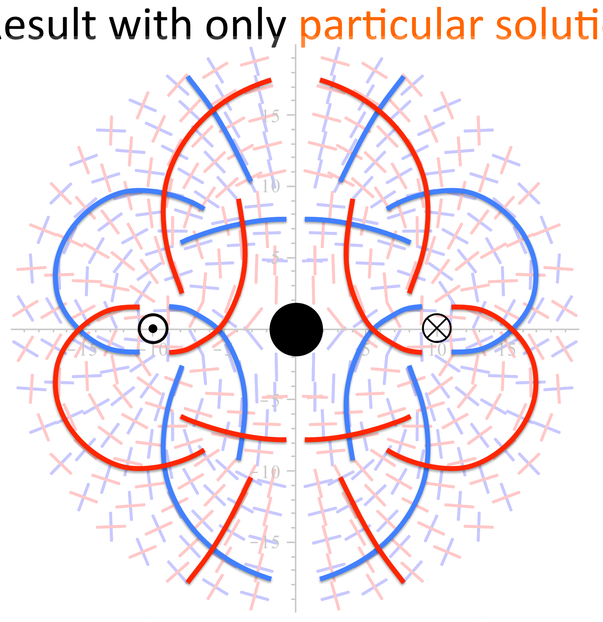

Not continuous at the ring radius
Outward curves upside down in color

With angular momentum

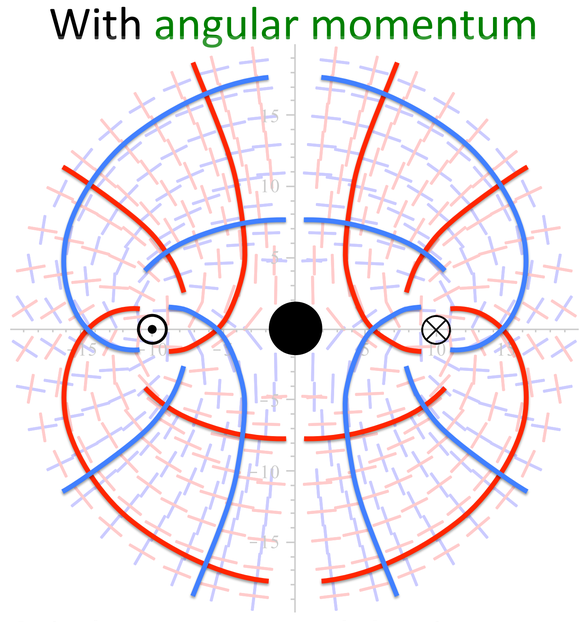

Spiral pattern around the ring
Continuous and interpretable

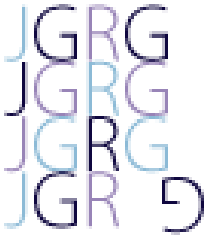

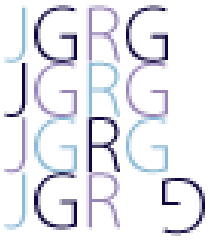

Hideyoshi Arakida, JGRG 22(2012)111328

"Effect of the cosmological constant on the bending of light and the cosmological lens equation"

RESCEU SYMPOSIUM ON

GENERAL RELATIVITY AND GRAVITATION

JGRG 22

November 12-16 2012

Koshiba Hall, The University of Tokyo, Hongo, Tokyo, Japan





Effect of the cosmological constant on the bending of light and the cosmological lens equation

Hideyoshi Arakida[1(a)], Masumi Kasai[(b)]

[(a)] *raduate School of Education, Iwate University*
[(b)] *raduate School of Science and Technology, Hirosaki University*

Abstract

We revisit the effect of cosmological constant Λ on the light deflection and its role in the cosmological lens equation. First, we re-examine the motion of photon in the Schwarzschild spacetime, and explicitly describe the trajectory of photon and deflection angle α up to the second-order in G. Then the discussion is extended to the contribution of the cosmological constant Λ in the Schwarzschild-de Sitter or Kottler spacetime. Contrary to the previous arguments, we emphasize the following points: (a) the cosmological constant Λ does appear in the orbital equation of light, (b) nevertheless the bending angle of light α does not change its form even if $\Lambda \neq 0$ since the contribution of Λ is thoroughly absorbed into the definition of the impact parameter, and (c) the effect of Λ is completely involved in the angular diameter distance D_A.

1 Introduction

Nowadays, it is widely regarded that the cosmological constant Λ or more generally dark energy is the most responsible candidate which explains accelerating expansion of Universe. Nonetheless the details of cosmological constant Λ or dark energy are still far from clear, then it is preferable and worthy to clarify the validity of this hypothesis by means of not only cosmological observations but also another astronomical/astrophysical ones.

Among such attempts, it would be the most natural idea to investigate the role of cosmological constant Λ in the classical tests of general relativity, e.g. the perihelion advance of planetary orbit and the bending of light path. So far, it was shown that the cosmological constant Λ causes the perihelion shift of planets at least in principle, even though its contribution is too small to detect in the current measurement technique (see [1, 2, 3] and the references therein).

While it has been believed for a long time that Λ does not contribute to the light deflection because there is no Λ in the second-order ordinary differential equation (ODE) of photon. However recently, Rindler and Ishak [4] pointed out that Λ does affect the bending angle by using the Schwarzschild-de Sitter or Kottler metric and the invariant formula of cosine. Subsequently many authors argued its appearance in diverse ways and generality assisted the fact that there appears Λ in the deflection angle α, see [5] for review and the references therein and also [6, 7, 8, 9, 10, 11, 12]. However, it seems that the conclusion has not converged yet; for instance whether the leading order effect of Λ is coupled with the mass of central body M or not and so on. In order to clear up the confusion, we will revisit the effect of the cosmological constant on the light deflection and its role in the cosmological lens equation.

2 Photon trajectory in Schwarzschild spacetime

Before discussing the influence of Λ on bending angle α, we shall begin with re-considering the solution of photon trajectory in the Schwarzschild spacetime. From the Schwarzschild metric in the Schwarzschild coordinates,

$$ds^2 = -\left(1-\frac{r_g}{r}\right)c^2dt^2 + \left(1-\frac{r_g}{r}\right)^{-1}dr^2 + r^2(d\theta^2+\sin^2\theta d\phi^2), \quad r_g = \frac{2GM}{c^2}, \tag{1}$$

[1]Email address: arakida@iwate-u.ac.jp

and the condition for null geodesic $ds^2 = 0$, we have the geodesic equation for equatorial plane ($\theta = \pi/2$),

$$\left(\frac{du}{d\phi}\right)^2 = \frac{1}{b^2} - u^2 + r_g u^3, \quad u \equiv \frac{1}{r}, \quad \frac{1}{b^2} \equiv \frac{E^2}{c^2 L^2}, \tag{2}$$

in which the two constants of motion, E and L are total energy and angular momentum, respectively. Alternatively, Eq. (2) can be expressed in the form of second-order ODE as,

$$\frac{d^2u}{d\phi^2} = -u + \frac{3}{2} r_g u^2, \tag{3}$$

nevertheless, hereinafter we use Eq. (2) instead of Eq. (3).

In order to obtain the photon trajectory up to the second-order in G, let us put the solution of Eq. (2) u as,

$$u = \frac{1}{b}\left(\sin\phi + r_g u_1 + r_g^2 u_2\right), \tag{4}$$

where u_1 and u_2 are, respectively, first $\mathcal{O}(G)$ and second $\mathcal{O}(G^2)$ order correction to zeroth-order solution $u_0 = \sin\phi/b$ (straight line). Hence u_1 and u_2 satisfy the following differential equations,

$$\frac{du_1}{d\phi} = -\frac{\sin\phi}{\cos\phi} u_1 + \frac{1}{2b}\frac{\sin^3\phi}{\cos\phi}, \tag{5}$$

$$\frac{du_2}{d\phi} = -\frac{\sin\phi}{\cos\phi} u_2 - \frac{1}{2\cos\phi}\left[\left(\frac{du_1}{d\phi}\right)^2 + u_1^2 - \frac{3}{b} u_1 \sin^2\phi\right]. \tag{6}$$

Noting that the integration constants of Eqs. (5) and (6) are chosen such that maximizing u (or minimizing r) for $\phi = \pi/2$, then we obtain the trajectory of photon up to the second-order in G as,

$$\frac{1}{r} = \frac{1}{b}\sin\phi + \frac{r_g}{4b^2}(3 + \cos 2\phi) + \frac{r_g^2}{64b^3}\big(37\sin\phi + 30(\pi - 2\phi)\cos\phi - 3\sin 3\phi\big), \tag{7}$$

where b is the impact parameter which represents the minimum value of r-coordinate for the undeflected light ray, i.e., $r_g = 0$. The bending angle α is shortly derived from Eq. (7) and it coincides with the famous formula by [13],

$$\alpha = 2\frac{r_g}{b} + \frac{15\pi}{16}\left(\frac{r_g}{b}\right)^2 = \frac{4GM}{c^2 b} + \frac{15\pi}{4}\frac{(GM)^2}{c^4 b^2} + \mathcal{O}(G^3). \tag{8}$$

It should be mentioned about the validity of the solution for light trajectory. The appropriateness of our solution, Eq. (7) can be verified readily by the direct substitution into Eq. (2) and it is found that the residual terms are order $\mathcal{O}(G^3)$, then it is perfectly valid up to the order of G^2. However, the photon trajectory given in previous works such as Eq. (18) of [14] and Eq. (16) of [5] are incorrect; in fact, there appears $\mathcal{O}(G^2)$ order residual term in the solution of photon trajectory in [5, 14].

3 Contribution of the cosmological constant

Now, let us investigate the contribution of Λ on light ray. For this purpose, we adopt the Schwarzschild-de Sitter or Kottler metric [15],

$$ds^2 = -\left(1 - \frac{r_g}{r} - \frac{\Lambda}{3}r^2\right)c^2 dt^2 + \left(1 - \frac{r_g}{r} - \frac{\Lambda}{3}r^2\right)^{-1} dr^2 + r^2(d\theta^2 + \sin^2\theta d\phi^2). \tag{9}$$

In the same way as the Schwarzschild case, the differential equation of light is given by

$$\left(\frac{du}{d\phi}\right)^2 = \frac{1}{b^2} - u^2 + r_g u^3 + \frac{\Lambda}{3}. \tag{10}$$

It should be emphasized here that the geodesic equation of light Eq. (10) does obviously include Λ. Therefore, previous arguments, such as "Λ does not appear in the geodesic equation of light", would be overstated. Actually, the second-order ODE derived from Eq. (10) reduces to Eq. (3), nevertheless its solution of light trajectory should be obtained in such a way that the integration constants satisfy Eq. (10).

Furthermore, the impact parameter is the minimum value of the coordinate r if the light ray were undeflected, i.e., $r_g = 0$. It is obvious from Eq. (10) that the impact parameter B in this case is defined by

$$\frac{1}{B^2} \equiv \frac{1}{b^2} + \frac{\Lambda}{3}. \tag{11}$$

Then, the form of Eq. (10) completely coincides with Eq. (2), except that the impact parameter b is replaced by B. Therefore, the solution of Eq. (10) becomes,

$$\frac{1}{r} = \frac{1}{B}\sin\phi + \frac{r_g}{4B^2}\left(3+\cos 2\phi\right) + \frac{r_g^2}{64B^3}\left(37\sin\phi + 30(\pi-2\phi)\cos\phi - 3\sin 3\phi\right), \tag{12}$$

and deflection angle is,

$$\alpha = 2\frac{r_g}{B} + \frac{15\pi}{16}\left(\frac{r_g}{B}\right)^2 = \frac{4GM}{c^2B} + \frac{15\pi}{4}\frac{(GM)^2}{c^4B^2} + \mathcal{O}(G^3). \tag{13}$$

It is worthy to note that the contribution of Λ is incorporated in Eqs. (12) and (13) through Eq. (11). As a consequence, it is found that the cosmological constant Λ does appears in both the geodesic equation and its solution, that is the trajectory of photon. However, the effect of Λ is completely absorbed into the definition of the the impact parameter (see Eq. (11)). Hence it is difficult to distinguish the influence of Λ from the observed deflection angle.

When we expand Eq. (13) by using $1/B = (1/b)\sqrt{1+\Lambda b^2/3} \simeq (1/b)(1+\Lambda b^2/6)$ and remain $\mathcal{O}(M, M\Lambda)$ terms, it follows that

$$\alpha \simeq \frac{4GM}{c^2 b} + \frac{2GMb\Lambda}{3c^2}, \tag{14}$$

in which second term coincides with the previous results, e.g. Eq. (5) and below in [16] and the third term of Eq. (15) in [10]. Hence it is found that these results are included in Eq. (13) as a limiting case.

It is clear that the trajectory of photon Eq. (12) strictly satisfies Eq. (10) up to the second-order in G based on the result in previous section.

4 Cosmological lens equation

Finally, we consider the contribution of Λ in the cosmological lens equation. Under the assumption that the thin lens approximation is valid, the lens equation relates the observed image position angle θ to the unlensed position angle β of the source as

$$\beta = \theta - \frac{D_A(z_L, z_S)}{D_A(0, z_S)}\alpha, \tag{15}$$

where $D_A(z_1, z_2)$ denotes the angular diameter distance from the redshift z_1 to z_2, and the arguments z_L and z_S are the redshift of the lens and the source, rwespectively. For the distance formula D_A in the unperturbed Friedmann-Lemaître-Robertson-Walker (FLRW) universe with Λ, see, e.g., [17].

Up to the first order in G, the bending angle α in the present case is

$$\alpha = \frac{4GM}{c^2 B}. \tag{16}$$

The impact parameter B is related to the image position angle θ by

$$B = D_A(0, z_L)\theta. \tag{17}$$

Then, from Eqs. (15), (16), and (17), the lens equation is finally

$$\beta = \theta - \frac{4GMD_A(z_L, z_S)}{c^2 D_A(0, z_L)\, D_A(0, z_S)} \frac{1}{\theta}. \tag{18}$$

Therefore, the contribution of Λ is completely involved in the form of the angular diameter distance D_A. No modifications due to Λ appear even if the term of $\mathcal{O}(G^2)$ in α is included. It should also be noted that Eq. (18) is exactly the same form appeared in [17, 18], where the authors have shown that the gravitational lensing effects are strongly dependent on the value of the cosmological constant and hence they provide us with useful means to test the cosmological constant.

Here, we mention that in paper [16], Sereno introduced the relation, $b_0 = D_d\vartheta$ (see Eq. (8) below of [16]) where b_0 is the impact factor of "Schwarzschild lens" (see Eq. (8) of [16]), D_d is the angular-diameter distance, and ϑ is the angular separation. Since in the case of cosmological lens, the cosmological distance, such as the angular diameter distance, is defined with Λ, then b_0 should be replaced by B, instead.

References

[1] A. W. Kerr, J. C. Hauck, B. Mashhoon, Class. Quant. Grav., **20**, 2727 (2003).

[2] W. Rindler, Relativity: Special, General, and Cosmological (2nd Ed.), Oxford Univ. Press, New York (2006).

[3] L. Iorio, Adv. Astron., id. 268647 (2008).

[4] W. Rindler, M. Ishak, Phys. Rev. D, **76**, id. 043006 (2007).

[5] M. Ishak, W. Rindler, Gen. Rel. Grav., **42**, 2247 (2010).

[6] K. Lake, Phys. Rev. D. **65**, id. 087301 (2002).

[7] M. Park, Phys. Rev. D, **78**, id. 023014 (2008).

[8] I. B. Khriplovich, A. A. Pomeransky, Int. J. Mod. Phys. D, **17**, 2255 (2008).

[9] F. Simpson, J. A. Peacock, A. F. Heavens, On lensing by a cosmological constant, MNRAS, **402**, 2009 (2010).

[10] A. Bhadra, S. Biswas, K. Sarkar, Phys. Rev. D, **82**, id. 063003 (2010).

[11] H. Miraghaei, M. Nouri-Zonoz, Gen. Rel. Grav. **42**, 2947 (2010)

[12] T. Biressa, J. A. de Freitas Pacheco, Gen. Rel. Grav., **43**, 2649 (2011).

[13] R. Epstein, I. I. Shapiro, Phys. Rev. D, **22**, 2947 (1980).

[14] J. Bodenner, C. M. Will, Am. J. Phys., **71**, 770 (2003).

[15] F. Kottler, Annalen. Phys., **361**, 401 (1918).

[16] M. Sereno, Phys. Rev. Lett., **102**, id. 021301 (2009).

[17] M. Fukugita, T. Futamase, M. Kasai, E. L. Turner, Astrophys. J., **393**, 3 (1992).

[18] M. Fukugita, T. Futamase, M. Kasai, Mon. Not. R. Astr. Soc., **246**, 24 (1990).

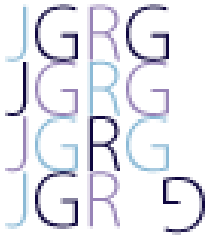

Takashi Torii, JGRG 22(2012)111329

"Graphical approach to the Lovelock black holes"

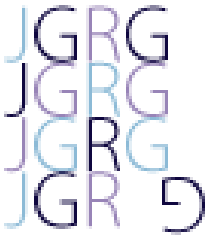

RESCEU SYMPOSIUM ON

GENERAL RELATIVITY AND GRAVITATION

JGRG 22



November 12-16 2012

Koshiba Hall, The University of Tokyo, Hongo, Tokyo, Japan



Graphical Approach to the Lovelock black holes

Takashi TORII

Osaka Institite of Technology
Osaka 535-8585, Japan

ABSTRACT

Recently a large number of studies have focused on the question of higher dimensions. One of the reasons for this is the fascinating new picture of our Universe called the braneworld universe. Because the fundamental scale could be about TeV in this senario, these models suggest that creation of tiny black holes in the upcoming large hadron collider will be possible. The braneworld model is an underlying fundamental theory, superstring/M-theory. Although superstring/M-theory has been highly elaborated, it is not enough to understand black hole physics in the string context. Hence at present to take string effects perturbatively into classical gravity is one approach to the study of quantum gravity effects.

With the restriction that the tension of a string be large as compared to the energy scale of other variables, i.e., in the α-expansion, the Gauss-Bonnet terms appear as the first curvature correction term to general relativity. Though many complicated combinations may appear for the higher order corrections, here we will adopt Lovelock gravitational theory expecting some aspects of higher curvature corrections are obtained. Lovelock gravitational theory is the most general theory which gives the e.o.m. with up to the second order derivative. In this theory we investigate the black hole solution and the spacetimes with product metric which are Nariai and Bertotti-Robinson types. The study of the black hole solution is the direct extension of the works by Whitt (1988) and Myers & Simon (1988). The study of the product metric will be applied to the spontaneous compactification mechanism without fluxes.

black hole solutions

In the first part of the poster we investigate black hole solutions in Lovelock gravity. Under the static ansatz the gravitational equation of motion becomes algebraic equation of the single metric function. Although it can not be solved analytically except for some simple cases, we show a technique to find the spacetime structure of the solution. We also consider the topological black hole solution whose submanifold has curvature k=0, -1. As some examples we study the solution in Gauss-Bonnet gravity and "M-theory" model.

Nariai and Bertotti-Robinson solutions

In the second part of the poster we investigate the solution with product metric in Lovelock gravity. Under the decomposition into 2-dim. Riemaninan manifold and (n-2)-dim. Euclidean submanifold with maximal symmetry, the gravitational equation of motion becomes algebraic equation of the single metric function. We will give the way to analyze such equation and to classify the solution into Nariai, anti-Nariai, Bertotti-Robindon, and Plebanski-Hachyan solutions. As some examples we study the solution in general relativity and Gauss-Bonnet gravity.

MODEL

Lagrangian

- We consider the Lovelock lagrangian up to Nth order, which gives a quasi-linear 2nd order gravitational equation

$$\mathcal{L} = \sum_{p=0}^{N} \frac{\alpha_p}{(n-2p)(n-2)!} \mathcal{L}_p$$

$$\mathcal{L}_p = 2^{-p} \delta^{\mu_1\nu_1\cdots\mu_p\nu_p}_{\rho_1\sigma_1\cdots\rho_p\sigma_p} R^{\rho_1\sigma_1}{}_{\mu_1\nu_1} \cdots R^{\rho_p\sigma_p}{}_{\mu_p\nu_p}.$$

$$N \leq \frac{n-1}{2}$$

α : coefficients

$\mathcal{L}_0$: cosmological constant

$\mathcal{L}_1$: Einstein-Hilbelt action

$\mathcal{L}_2$: Gauss-Bonnet term

Metric

- We assume the n-dimensional static spacetime whose metric is descrived by

$$ds^2 = -f(r)e^{-2\delta(r)}dt^2 + f^{-1}(r)dr^2 + R(r)^2 d\Omega^2_{n-2},$$

(n-2)-dim maximally sym. space

$$k = 1, 0, -1$$

BLACK HOLE SOLUTION

- gravitational equation

$$R \neq \text{const.} \xrightarrow[\text{gauge}]{} R = r$$

$$f(r) = k - r^2 F(r)$$

mass

$$U(F) := \sum_{p=0}^{N} \alpha_p F^p = \frac{\mu}{r^{n-1}} \qquad \delta \equiv 0$$

- vacuum: $U(F) = 0$
- infnity: $U(F_\infty) = 0$

$F_\infty = 0$: asymptotically flat

$F_\infty > 0$: asymptotically de Sitter

$F_\infty < 0$: asymptotically anti-de Sitter

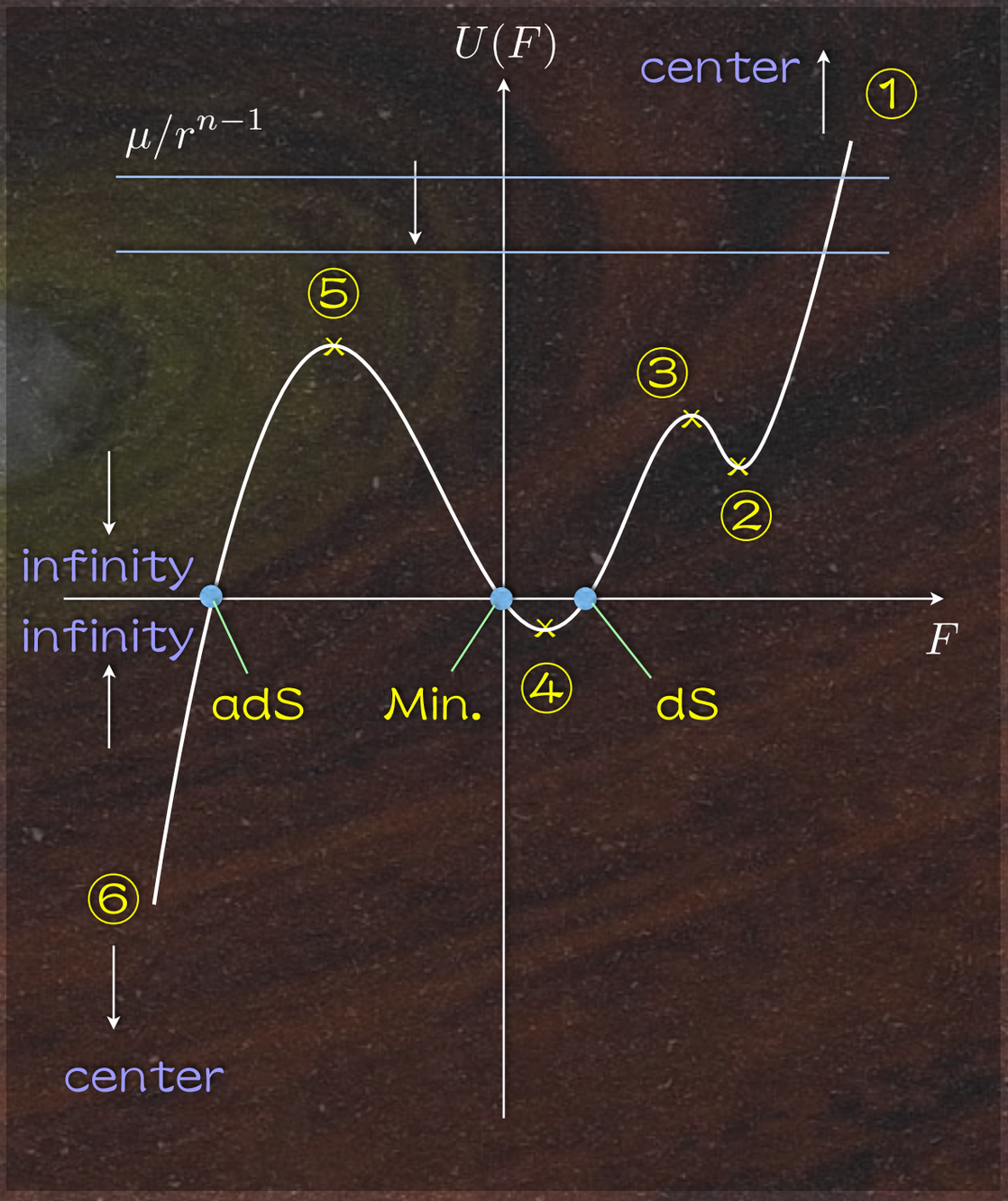

❖ singularity:

◆ central singularity: $r \to 0$

- n-1 > 2N
  - ① $F_0 > 0$: spacelike
  - ⑥ $F_0 < 0$: timelike
- n-1 = 2N
  - $\bar{k} > 0$: timelike
  - $\bar{k} = 0$: null
  - $\bar{k} < 0$: spacelike

$$\bar{k} := k \pm \left(\frac{\mu}{\alpha_p}\right)^{\frac{1}{p}} \qquad \bar{k} := k - \left(\frac{\mu}{\alpha_p}\right)^{\frac{1}{p}}$$

even N　　odd N

◆ branch singularity: $r \to r_b > 0$

② $|r| \to |r_b|_{+0}$: outer branch sing.

③-⑤ $|r| \to |r_b|_{-0}$: inner branch sing.

$$k + r_b^2 F_b \begin{cases} > 0 & \text{: timelike} \\ < 0 & \text{: spacelike} \\ = 0 & \begin{cases} \text{: timelike} \\ \text{: spacelike} \end{cases} \end{cases}$$

F-U diagram

event horizon

$$f(r_h) = k - r_h^2 F_h = 0 \quad \Rightarrow \quad \begin{cases} k = 0: & F_h = 0 \\ k \neq 0: & \mu \left(\dfrac{F_h}{k} \right)^{\frac{n-1}{2}} = 0 \end{cases}$$

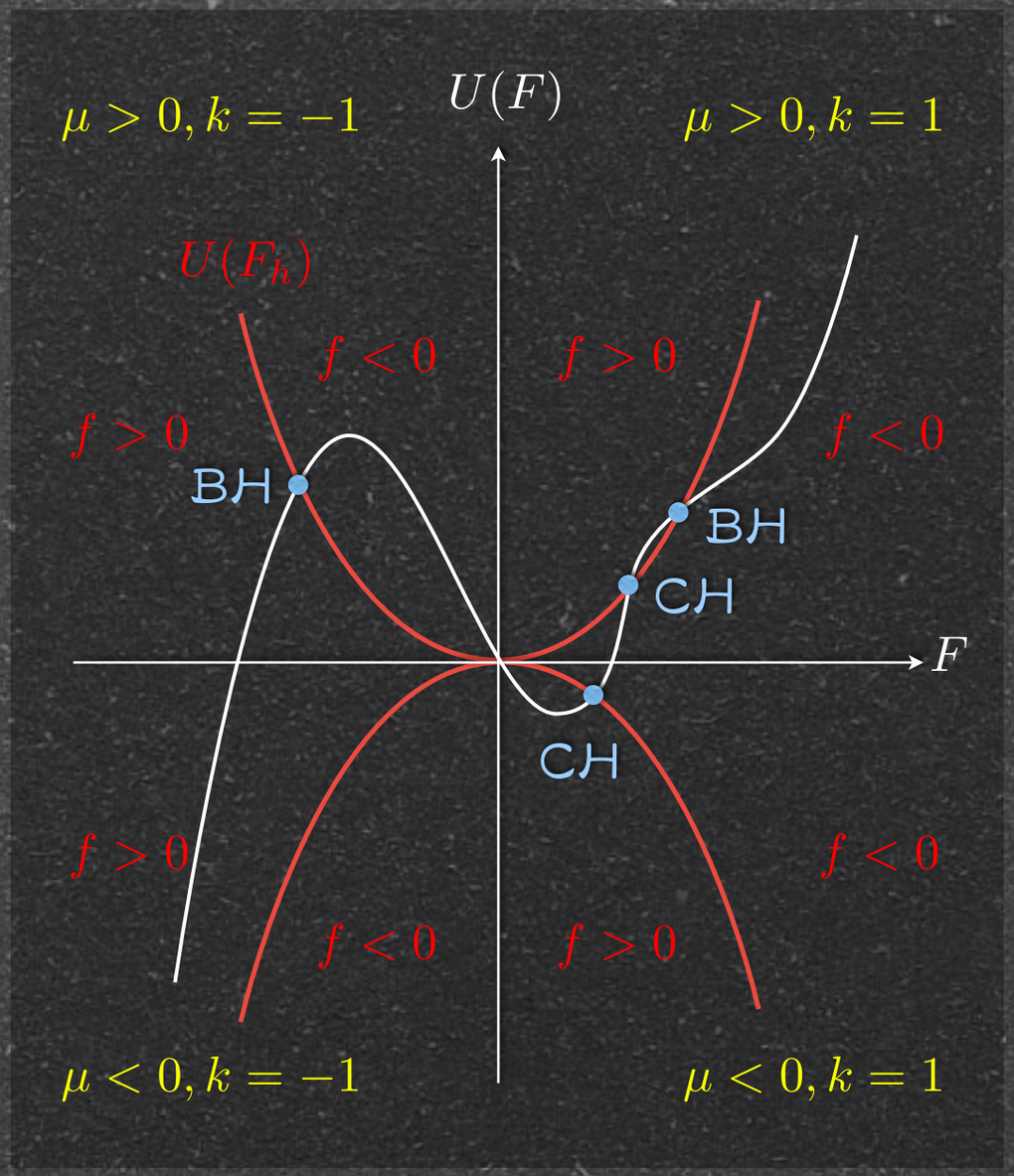

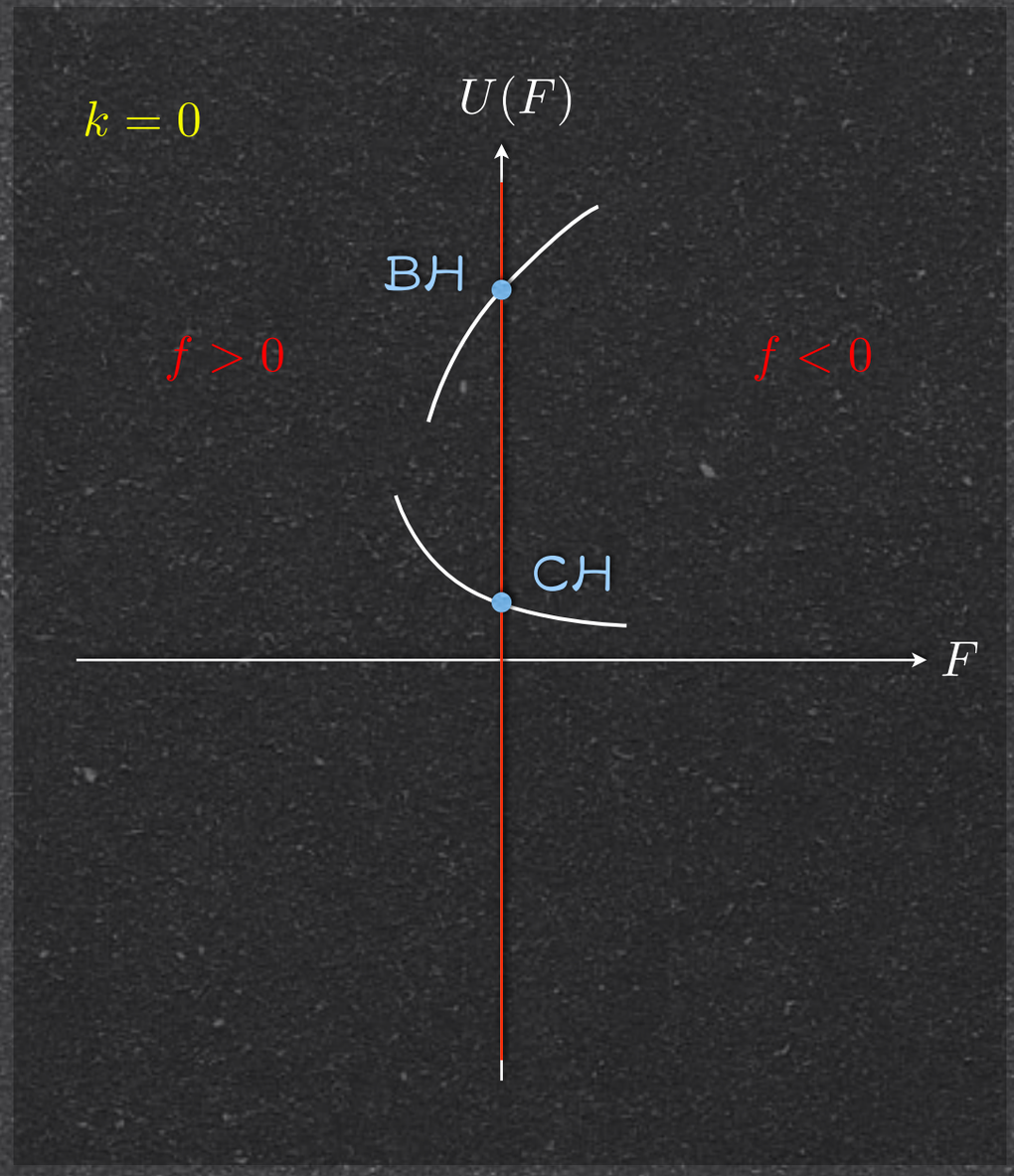

- Only the adS-branch solution has BH for k=0, -1.

Example 1: Gauss-Bonnet gravity

$\alpha_0 \neq 0,\ \alpha_1, \alpha_2 > 0$

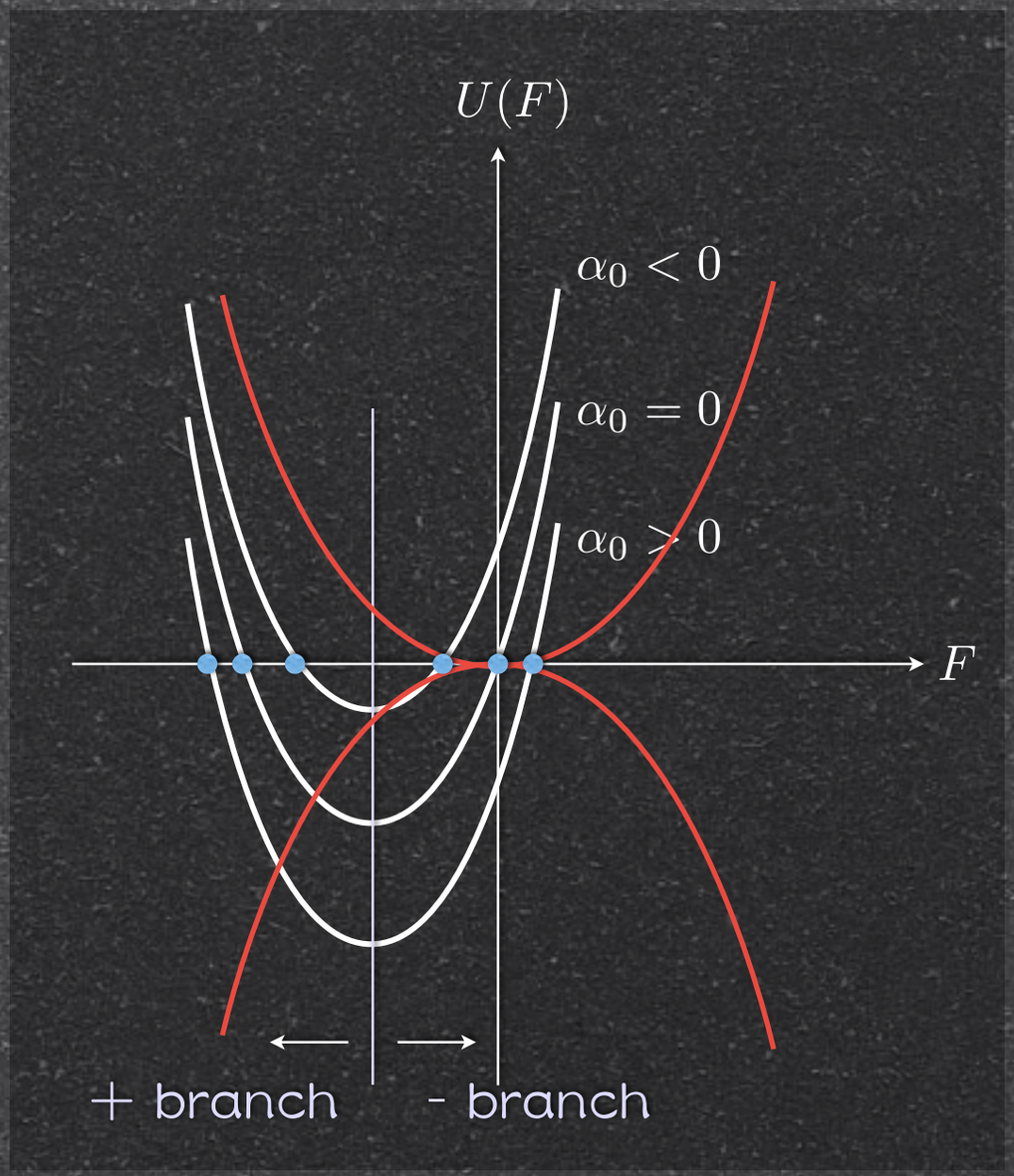

- $\alpha_1^2 - 4\alpha_0\alpha_2 > 0$ for the existence of relevant vacuum.
- Solutions in minus branch are asymptotically Mincowski/dS/adS for zero/negative/positive α_0, respectively.
- Solutions in plus branch are asymptotically adS.
- Negative mass solutions have branch singularity.
- Solutions in plus branch have BH horizons for k=-1.

- For details see
  TT & Maeda, PRD71, 124002 (2005)

Example 2: "M-theory" model

$$\alpha_1 > 0, \alpha_4 \neq 0, \ n = 10$$

Curvature corrections to M-theory consist of Lovelock part and other terms which gives higher derivative equation of motion. Here we consider only the Lovelock part.

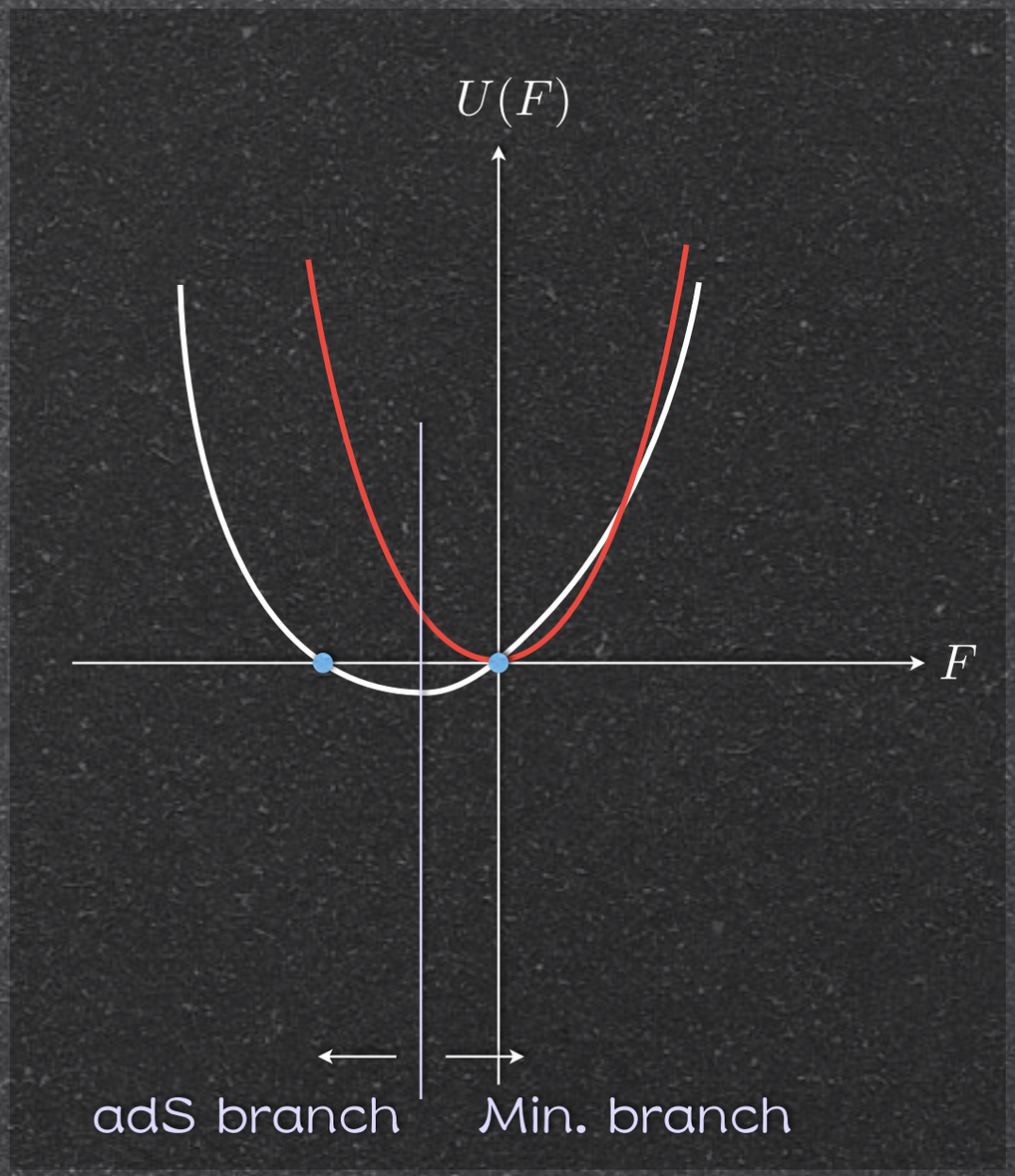

- Minkowski and adS branch exist.
- For positive mass, Minkowski-branch solution has spacetime central singularity, while adS-branch solution has timelike one.
- For positive mass, properties of the branch singularity depends on $\tilde{k}$.
- Horizon
  - Minkowski branch, positive mass:
    There is one BEH for k=1.
  - Minkowski branch, negative mass:
    There is one CEH for k=-1.
  - adS branch, positive mass:
    There are at least 2 horizons for k=-1.
  - adS branch, positive mass:
    There is at least 1 horizon for k=-1.

NARIAI & BERTOTTI-ROBINSON SOLUTION

- gravitational equation

$$R(r) \equiv B^2 = const.$$

$$\delta \equiv 0 \quad \text{(gauge)}$$

$$V(\tilde{B}^2) := \sum_{p=1}^{N} \alpha_p (k\tilde{B}^2)^p = -\alpha_0$$

$$f = 1 - \zeta_i r^2$$

$$\zeta_i := -\frac{\sum_{p=0}^{N} \alpha_p (n-2)_{2p+2} (k\tilde{B}_i^{-2})^p}{\sum_{p=0}^{N} \alpha_p (n-2)_{2p} (k\tilde{B}_i^{-2})^{p-1}}$$

$$\tilde{B} := B^{-1}$$

$$(n-p)_q = (n-p)(n-p-1)\cdots(n-q)$$

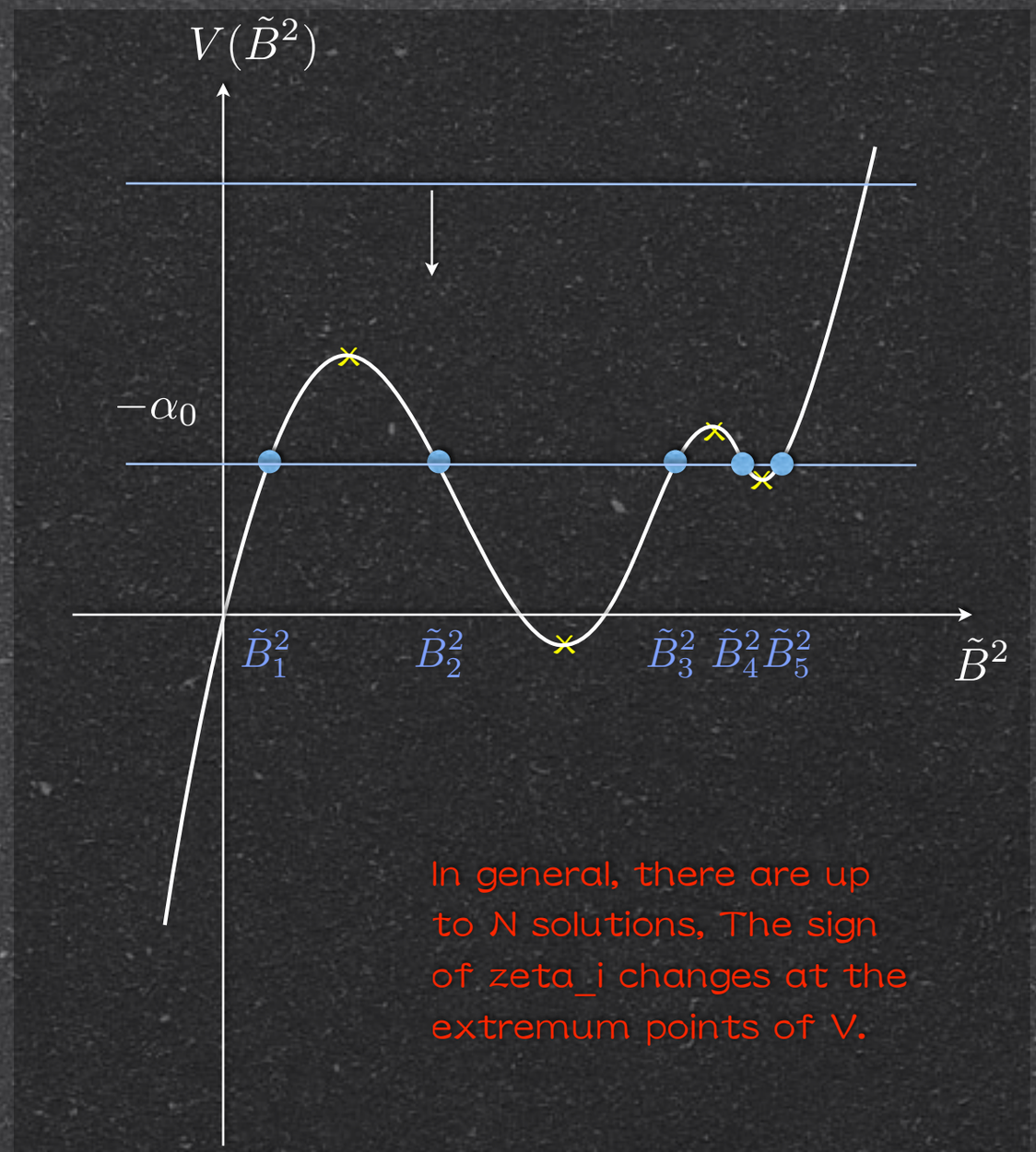

In general, there are up to N solutions, The sign of zeta_i changes at the extremum points of V.

Example 1: general relativity

$\alpha_o \neq 0, \ \alpha_1 > 0$

$$f = 1 + \frac{2\alpha_o}{(n-2)\alpha_1} r^2$$

$$B^2 = -\frac{\alpha_1}{\alpha_0} k \quad \longrightarrow \quad \alpha_0 k < 0$$

- k=1 and positive c.c. :
  - Nariai $(dS_2 \times S^{n-2})$
- k=-1 and negative c.c. :
  - anti-Nariai $(adS_2 \times H^{n-2})$

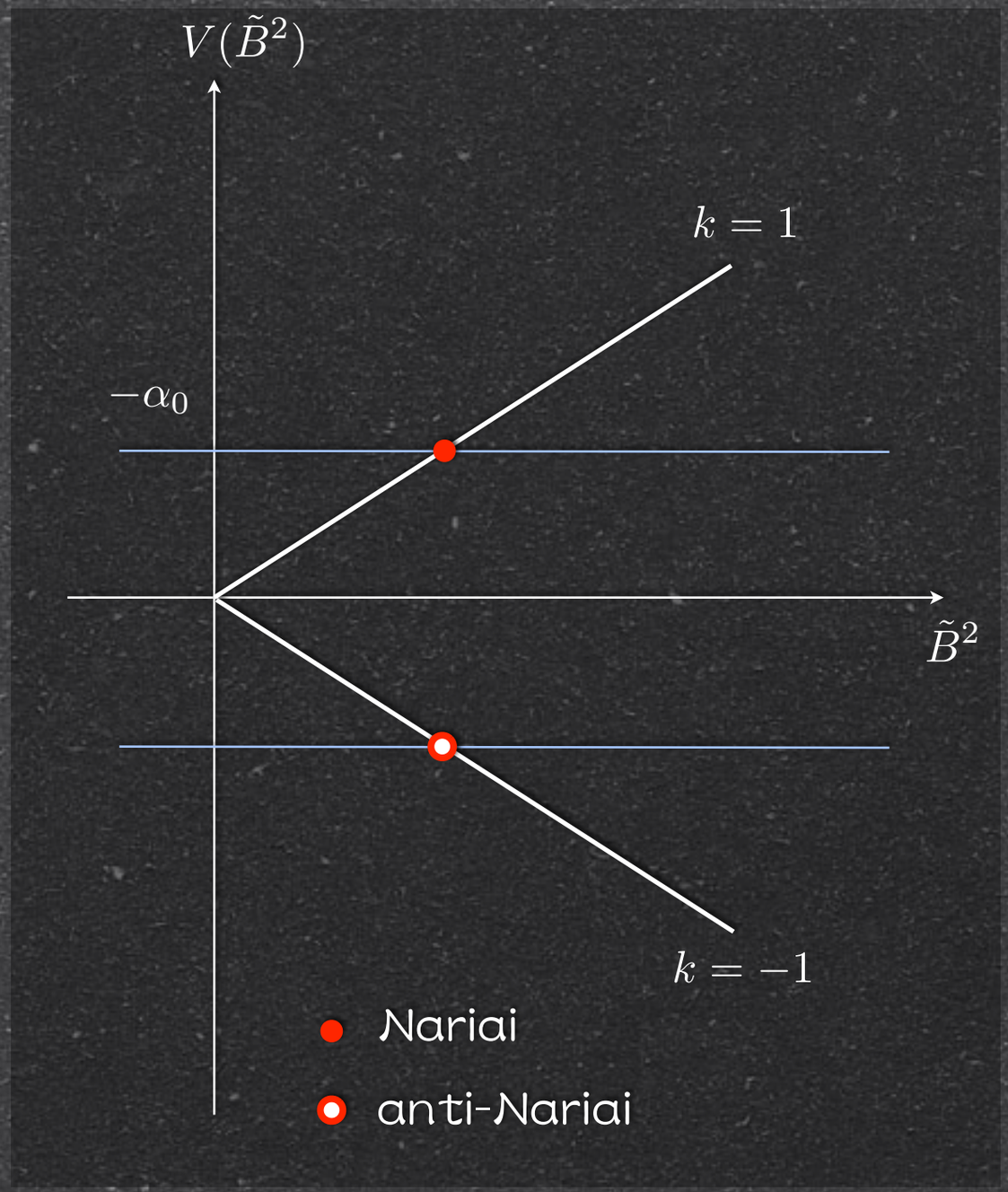

Example 2: Gauss-Bonnet gravity

$\alpha_o \neq 0,\ \alpha_1, \alpha_2 > 0$

$$V(\tilde{B}^2) = \alpha_1 k \tilde{B}^2 + \alpha_2 \tilde{B}^4$$

- Bertotti-Robinson solution exist for k=-1 case.
- These solution corresponds to extreme black hole solutions in the same system. There are certain coordinate transformation from them.

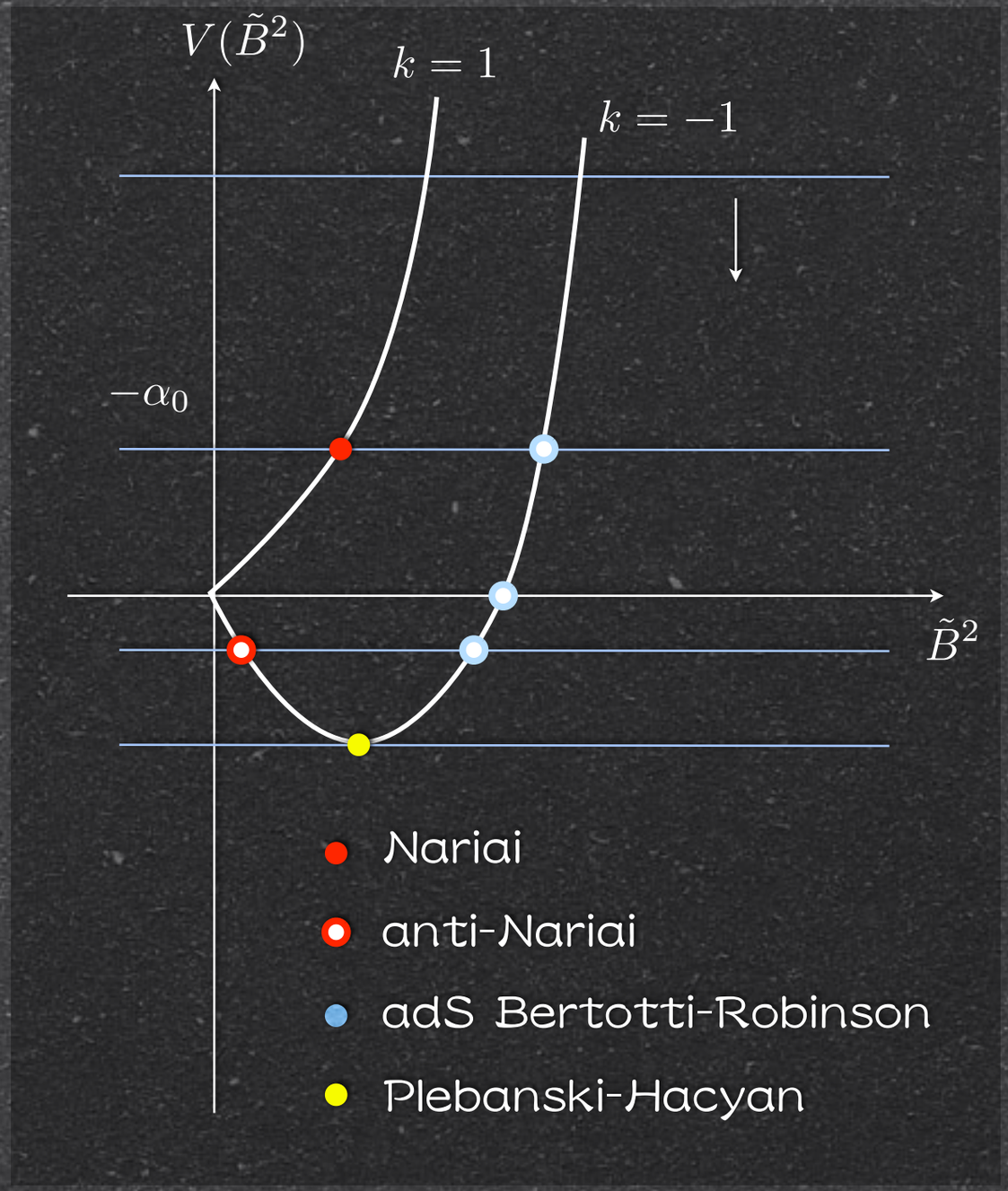

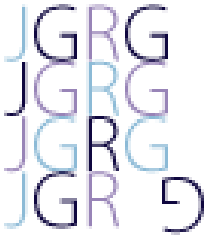

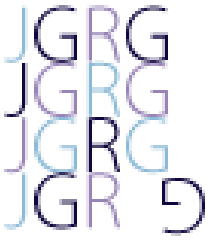

Haruna Murakami, JGRG 22(2012)111330

"Short-range gravity experiment searching for a large extra dimension"

RESCEU SYMPOSIUM ON

GENERAL RELATIVITY AND GRAVITATION

JGRG 22

November 12-16 2012

Koshiba Hall, The University of Tokyo, Hongo, Tokyo, Japan





Short-range gravity experiment searching for a large extra dimension

Haruna Murakami[1 a], Kazufumi Ninomiya[a,b], Hironori Nishio[a], Naruya Ogawa[a], Tomomi Sakuta[a], Saki Tanaka[a], Yumi Totsuka[a] and Jiro Murata[a]

[(a)] *Department of Physics, Rikkyo University, Nishi-Ikebukuro, Tokyo 171-8501, JAPAN*
[(b)] *RIKEN Nishina Center, 2-1 Hirosawa, Wako, Saitama 351-0198, JAPAN*

Abstract

According to the large extra dimension model, a deviation from Newtonian inverse square law is expected at sub millimeter scale. We have developed an experimental method using a torsion balance pendulum with an online digital image analysis system, aiming to test the Newton's gravitational law in a laboratory experiment.

1 Physics motivation

A question why gravity is extraordinary weak comparing to other three gauge interactions, is known as hierarchy problem, which prevent us to build a unified theory. A large extra dimension scenario was proposed to solve the hierarchy problem in a geometrical understandings, by assuming an existence of additional spacial dimensional world outside of our four dimensional space-time, where only gravitational field can propagate into the bulk space. In the ADD (N. Arkani-Hamed, S. Dimopoulos, G. Dvali) model [1], the extra dimensions are predicted to exist at below millimeter scale. As a result, modification of the Newtonian inverse square law is expected at the size of the extra dimensional space of below mm. In this scenario, form of gravitational force should be modified as;

$$\begin{cases} F_{r\geq\lambda} = G\frac{Mm}{r^2}, \\ F_{r\leq\lambda} = G_{4+d}\frac{Mm}{r^{2+d}}, \end{cases} \tag{1}$$

, where λ is interaction length corresponding to the size of the extra dimension, and d is the number of the large extra dimension. According to the ADD model, $\lambda = 0.1$mm at $d = 2$ is predicted, if modified Planck scale in the higher dimensional world is $E_{pl}^{ed} = 1$ TeV. Modified form of the gravitational potential is often expressed in a Yukawa interaction form as;

$$V = -G\frac{Mm}{r}\left(1 + \alpha e^{-\frac{r}{\lambda}}\right) \tag{2}$$

, where α is a coupling constant for the additional non-Newtonian potential. Newton's inverse square law has been experimentally tested in numbers of experiments, however, high precision tests of the inverse square law are limited only at astronomical scales [2]. Present study is aiming to perform a precision test of the inverse square law at below mm scale, where only poor experimental data exist.

2 Experimental principle

In our experiment, gravitational force is measured using a torsion pendulum and an online digital image analyzing system [3, 4]. The torsion pendulum is composed of two columns (targets) which attached to the ends of an aluminum bar. It is hanged by a $40\mu m$ thick tungsten wire. Motion of the torsion pendulum can be described with Hooke's law;

$$\tau = -\kappa\Delta\theta \tag{3}$$

[1]Email address: hrn@rikkyo.ac.jp

, where τ is torque, κ is the torsional spring constant and $\Delta\theta$ is angular displacement. The torsion spring constant κ can be estimated using relationship between measured oscillation period T and *kappa* with inertia moment I as;

$$\kappa = 4\pi \frac{I}{T^2} \tag{4}$$

Figure 1 shows the experimental principle of the measurement.

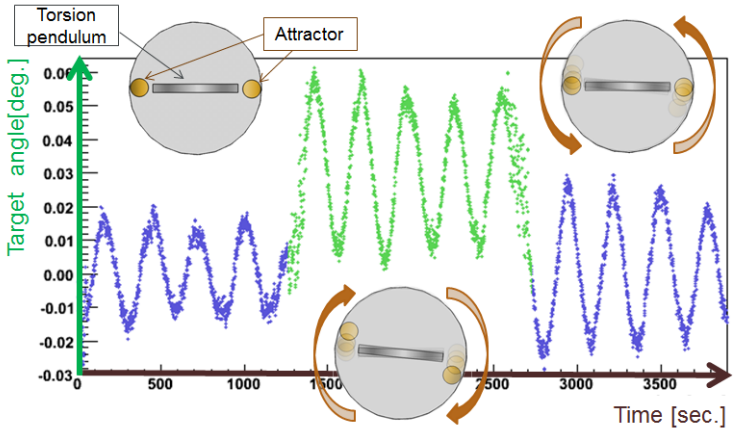

Figure 1: Principle of the measurement using torsion pendulum.

By changing the setting position of the gravity source (attractor) at around the torsion pendulum in a short time, a jumping gravitational signal is obtained as an twisting angular displacement of the torsion pendulum. Two copper attractors are set on a rotating table which rotation is driven by a stepping motor. The attractors are covered by an electrostatic shield made by copper. The entire system is set in a vacuum chamber, which vacuum level is maintained at below 1 Pa without keeping vacuum pump operation.

In addition to the jumping balanced position measurement using the torsion balance bar, we also tried an another method named "following measurement". In this measurement, the attractor continuously rotates very slowly comparing to the harmonic oscillation period, around the torsion pendulum. The balanced position dose not jumped, but continuously moved in this method. As a result, the torsion balance bar moves in the moving gravitational potential, which typical movements are shown in figure 2 .

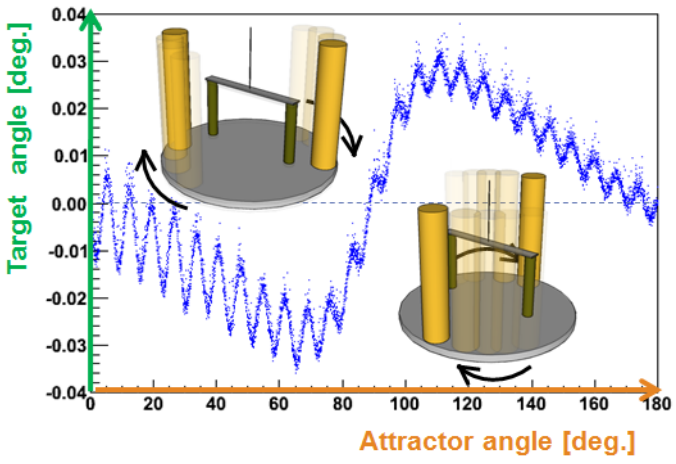

Figure 2: A typical result from the following measurement.

The motion of the torsion balance bar is monitored by a conventional digital video camera set on the top of the vacuum chamber, which captures movie information. The position and angular information of the torsion balance bar is extracted via a digital image analysis. The digital image analysis system used in this experiment is based on an optical alignment system (OASys) [3] developed for the PHENIX experiment at RHIC (Relativistic Heavy Ion Collider) which position resolution is about 10 nanometer. The present experiment utilized an dedicated position monitoring system developed using the OASys technique for the short range gravity experiment, achieving angular resolution of about 10^{-6} degrees [4].

3 Results

The experimental device, which consists of the torsion balance bar together with the digital image analysis system, are set on the forth basement of KEK-B Fuji experimental hall at KEK. It is because experimental environment considering mechanical vibration and temperature changing are relatively small at the basement hall. The data taking was performed with the following measurement method. Because of the 180 degrees symmetry of the device, two identical pattern is observed during a full 360 degrees rotation of the attractor. Ten cycles of this pattern were measured, and averaged. The obtained result is shown in figure 3, which is almost consistent with the Newtonian prediction, however, some points around 50 and 140 degree do not agree with the prediction. This systematic deviation can be understood as a misalignment effect.

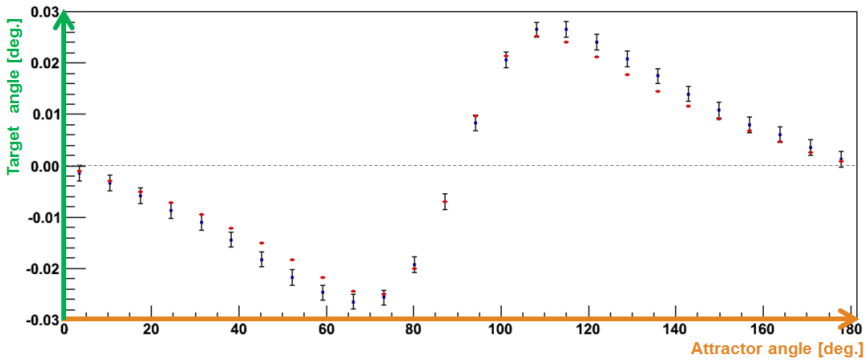

Figure 3: Observed gravity signal. Blue line is experiment data and red line is Newtonian prediction.

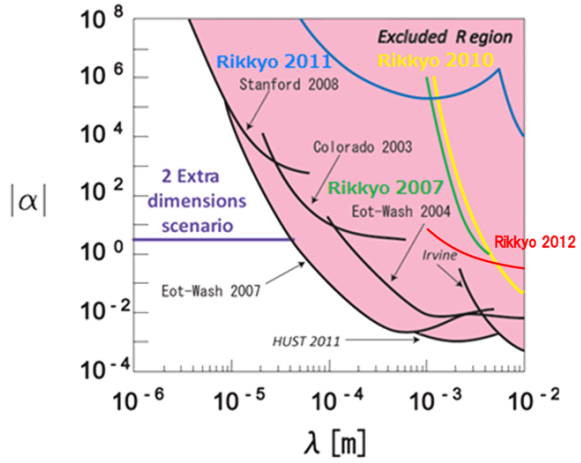

Figure 4: α-λ plot.

The obtained results are interpreted in the Yukawa potential expression (equation(2)). In this exper-

iment, distance between centers of objects ranges from 4.5mm to 74.5mm. Corresponding upper limit on the α-λ plot is shown in figure 4.

In conclusion, we have performed a short range gravity experiment motivated to test the Newtonian inverse square law at around mm scale, using a torsion balance bar device combined with our digital image analysis technique. A clear gravitational signal was observed, which are consistent with the Newtonian prediction. We are now developing the next generation device with higher symmetries which can reduce the systematic effects. The data taking has already been started in 2012, and will be reported in near future.

References

[1] Nima Arkani-Hamed, Savas Dimopoulos, Gia Dvali, Physics Letters B 429 (1998) 263-272.

[2] Ephraim Fishbach, Carrick Talmadge, Nature 356 (1992) 207-215; The Search for Non-Newtonian Gravity, Springer (1998) ISBN 0387984909.

[3] J. Murata et. al., Nucl. Instrum. Meth. A 500(2003) 309-317.

[4] Jiro Murata, Pico-Precision Displacement Sensor using Digital Image Analysish, IEEE Nuclear Science Symposium Conference Record 675 (2005).

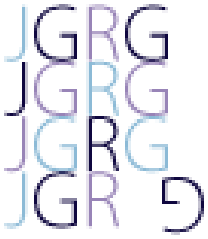

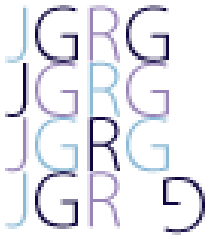

Jonathan White, JGRG 22(2012)111332

"Curvature perturbation in conformally related frames"

RESCEU SYMPOSIUM ON

GENERAL RELATIVITY AND GRAVITATION

JGRG 22

November 12-16 2012

Koshiba Hall, The University of Tokyo, Hongo, Tokyo, Japan





Curvature perturbation in conformally related frames

Jonathan White,[1] Masato Minamitsuji[2] and Misao Sasaki[3]

Yukawa Institute for Theoretical Physics,
Kyoto University, Kitashirakawa Oiwakecho, Sakyo-ku, Kyoto 606-8502, Japan

Abstract

We consider the curvature perturbation resulting from multi-field inflation models in which potentially all fields are non-minimally coupled to the Ricci scalar. We confirm that, unlike in the single field case, the curvature perturbations associated with the Jordan and Einstein frames are not the same, and that the difference is a direct consequence of the isocurvature perturbations inherent to multi-field models. Using the δN formalism, and focusing on analytically soluble examples, we see how the statistical properties of the two curvature perturbations are also not necessarily the same.

1 Introduction

Despite the agreement of predictions from single-field inflation models with current observational data, in the context of unifying and higher-dimensional theories it is natural to consider the presence of multiple fields during inflation. Moreover, as a consequence of the compactification of higher dimensions, or following renormalisation arguments, it is expected that these multiple fields be non-minimally coupled to the Ricci scalar [1]. It is therefore very important to determine any possible observational signatures that such multi-field models with non-minimal coupling might give rise to. The type of model that we are considering takes an action of the form

$$S = \int d^4x\sqrt{-g}\left\{f(\boldsymbol{\phi})R - \frac{1}{2}h_{ab}(\boldsymbol{\phi})g^{\mu\nu}\partial_\mu\phi^a\partial_\nu\phi^b - V(\boldsymbol{\phi})\right\}, \tag{1}$$

In determining the observational predictions of different inflation models, we are largely interested in the statistical properties of the primordial fluctuations they produce. In particular, we are interested in determining the curvature perturbation on constant density hypersurfaces, ζ, and its statistical properties. In order to make calculations more tractable for an action of the form (1) it is common practise to make the conformal transformation $g_{\mu\nu} = \Omega\tilde{g}_{\mu\nu}$ in order to bring the gravity part of the action into the canonical Einstein-Hilbert form, namely

$$S = \int d^4x\sqrt{-\tilde{g}}\left\{\frac{\tilde{R}}{2} - \frac{1}{2}S_{ab}(\boldsymbol{\phi})\tilde{g}^{\mu\nu}\partial_\mu\phi^a\partial_\nu\phi^b - \tilde{V}(\boldsymbol{\phi})\right\}, \tag{2}$$

with

$$S_{ab} = \frac{1}{2f}\left(h_{ab} + \frac{3f_af_b}{f}\right) \qquad \text{and} \qquad \tilde{V}(\boldsymbol{\phi}) = \frac{V}{4f^2}. \tag{3}$$

The action in its original form is referred to as being in the Jordan frame, and the transformed form as being in the Einstein frame. However, we see that we need to be careful to consider which metric matter is minimally coupled to, and if it is minimally to the original metric then we must be careful to relate $\tilde{\zeta}$ calculated in the Einstein frame back to the original ζ of the Jordan frame. In the case of a single non-minimally coupled field it is known that the two curvature perturbations are the same to all orders, and thus their statistical properties too, but this is no longer the case when multiple fields are considered [2]. The difference is a consequence of the isocurvature modes inherent to multi-field models

[1]Email address: jwhite@yukawa.kyoto-u.ac.jp
[2]Email address: masato@yukawa.kyoto-u.ac.jp
[3]Email address: misao@yukawa.kyoto-u.ac.jp

that are absent in the single-field case. Despite the difference in the curvature perturbations, however, it is important to note that any *observable* quantities will be independent of the frame in which they are calculated [3].

In this work we try to clarify the relation between the two curvature perturbations in the case of multiple non-minimally coupled fields. Using linear perturbation theory we first find that the notion of adiabaticity is not common to both frames. Namely, even if the curvature perturbation is conserved in one frame, it is not necessarily conserved in the other. We also find that the two curvature perturbations are of different magnitude. We then use the δN formalism, applied to analytically soluble examples, to confirm that predictions for the power spectrum, its tilt and non-gaussianity are in general different for ζ and $\tilde{\zeta}$ if one does not assume the vanishing of isocurvature modes before the end of inflation. If we expect that the isocurvature modes do eventually decay before the radiation domination era, where $\zeta = \tilde{\zeta}$, then this begs the question how is the $\zeta = \tilde{\zeta}$ limit reached, and how is the final curvature perturbation related to that at the end of inflation. The details of reheating therefore have to be considered more carefully.

2 Linear perturbations

In each frame we consider perturbations around a FLRW background of the form

$$ds^2 = -(1+2AY)dt^2 - 2aBY_i dt dx^i + a^2\left[(1+2\mathcal{R})\,\delta_{ij} + 2H_T\frac{1}{k^2}Y_{,ij}\right]dx^i dx^j, \tag{4}$$

The curvature perturbation on constant density hypersurfaces in the Jordan frame is given as

$$\zeta = \mathcal{R} - \frac{H}{\dot{\rho}}\delta\rho \tag{5}$$

and similarly in the Einstein frame.

The non-conservtion of ζ on super horizon scales is given as

$$\dot{\zeta} \simeq -\frac{H}{\rho + p}\delta p_{\rm nad} \tag{6}$$

where $\delta p_{\rm nad} = \delta p - \frac{\dot{p}}{\dot{\rho}}\delta\rho$. The explicit expressions for δp, $\delta\rho$ etc are given in terms of perturbations of the fields. It is useful to decompose these field perturbations into components along and perpendicular to the background trajectory - adiabatic and isocurvature modes respectively. On making this decomposition in the canonical two-field case, one finds that the isocurvature perturbations source the curvature perturbation when there is a turn in the background trajectory, thus leading to its non-conservation [4]. In the single-field case there is no such isocurvature component (on super-horizon scales) and thus the curvature perturbation is conserved. In our case we have N fields, meaning that there are $N-1$ isocurvature modes. These can be expressed in terms of the combination

$$\mathcal{K}^{ab} = \delta\phi^a\dot{\phi}^b - \delta\phi^b\dot{\phi}^a, \tag{7}$$

which we see will vanish for an adiabatic mode where $\delta\phi^a \propto \dot{\phi}^a$.

Making the metric decomposition (4) in the Jordan and Einstein frames we find the relation

$$\tilde{\mathcal{R}} = \mathcal{R} - \frac{\delta\Omega}{2\Omega}. \tag{8}$$

We thus see that the two curvature perturbations would be the same in a gauge corresponding to $\delta\Omega = 0$. In the single field case, as $\Omega = \Omega(\phi)$, $\delta\Omega = 0 \Rightarrow \delta\phi = 0$, which coincides with the constant energy and comoving gauge conditions in both frames. As such, one finds that the curvature perturbation on constant density hypersurfaces is the same in the two frames. More generally, however, the gauge $\delta\Omega = 0$ does not coincide with the comoving or constant energy density gauges of either frame. Moreover, if Ω is only a function of isocurvature modes, then there is no gauge for which $\delta\Omega = 0$, as isocurvature perturbations are gauge invariant.

Explicitly, on super horizon scales we find that the difference in the curvature perturbations on constant density hypersurfaces as defined in the two frames is of the form [5]

$$\zeta - \tilde{\zeta} \approx \mathcal{A}_{ab}\mathcal{K}^{ab} + \mathcal{B}_{ab}\dot{\mathcal{K}}^{ab}, \tag{9}$$

where $\mathcal{A}_{ab}$ and $\mathcal{B}_{ab}$ take some complex form in terms of background quantities. The important thing to note is that the difference is given in terms of the isocurvature modes $\mathcal{K}^{ab}$ and their derivatives. As such, in the absence of isocurvature modes, i.e. $\delta\phi^a \propto \dot{\phi}^a$, the two curvature perturbations do coincide.

With a non-zero difference between the two curvature perturbations we might also expect that their evolutions be different. In particular, it may be possible that despite being conserved in one frame, the curvature perturbation continues to evolve in the other.

In the Einstein frame we find that

$$\delta\tilde{p}_{nad} = -\frac{2S_{ab}\phi'^a}{(2\kappa^2 f)^2(\tilde{\rho}+\tilde{p})}S_{cd}\frac{D^{(S)}\phi'^d}{d\tilde{t}}\tilde{\mathcal{K}}^{bc}, \tag{10}$$

where a prime denotes a derivative with respect to $\tilde{t}$ ($d\tilde{t} = \sqrt{2f}dt$), $\tilde{\mathcal{K}}^{ab}$ is defined as in (7) but with dots replaced by primes and $D^{(S)}/d\tilde{t}$ is the covariant derivative with respect to the field-space metric S_{ab}. The curvature perturbation is thus sourced by the isocurvature modes when the background trajectory deviates from a geodesic of the field-space. This is the intuitive generalisation of the canonical two-field example given above.

Unfortunately, in the Jordan frame there seems to be no such intuitive interpretation as to when the curvature perturbations is conserved. However, with the difference between the two frames (9) given in terms of $\mathcal{K}^{ab}$, it is clear that the non-conservation in the Jordan frame will also be a result of sourcing from the isocurvature modes.

One interesting scenario would arise if the curvature perturbations in both frames were conserved but with a non-zero difference in their magnitudes. The first property might naively lead us to believe the evolution to be effectively single-field, but this would then be in disagreement with the second property. Using a two-field example we show that such a scenario is indeed possible [5].

We consider two fields ϕ and χ and require that $\dot{\chi} = 0$ and $f = f(\chi)$. This means that the χ field corresponds to the isocurvature mode and that the non-minimal coupling function only depends on this component. On imposing conservation of the curvature perturbation in the Einstein frame we find that the curvature perturbation in the Jordan frame is not necessarily conserved. However, if we further impose that the effective mass of the χ field be $\mathcal{O}(\epsilon)$ then we find

$$\frac{1}{H}\frac{\mathrm{d}}{\mathrm{d}t}\ln(\zeta - \tilde{\zeta}) \sim \mathcal{O}(\epsilon) \qquad \text{and} \qquad \zeta - \tilde{\zeta} = \frac{f_\chi}{2f\epsilon}\frac{H}{\sqrt{2k^3}}(1 + 3f_\chi^2/f)^{-1/2}, \tag{11}$$

so that to zeroth order in slow roll we also have conservation of ζ whilst maintaining a non-zero $\zeta - \tilde{\zeta}$. Comparing this expression with standard slow-roll expressions, we see that in order for ζ and $\tilde{\zeta}$ to be of the correct order of magnitude we require $f_\chi/\sqrt{f} \sim \mathcal{O}(\epsilon^{1/2})$.

The above two-field example indicates that we have a scenario such as that sketched in Figure 1. During inflation the two curvature perturbations are not equivalent, but both are conserved. The fact that we eventually require them to agree (under the assumption that an adiabatic limit is reached) then means that there must be an intermediate phase where the evolution of the curvature perturbation in the two frames is very different.

3 δN formalism

In applying the δN formalism we expand the total number of e-foldings between an initial flat hypersurface shortly after horizon crossing and a final constant energy hypersurface as a function of the initial field values on the flat hypersurface [6]. In the Jordan and Einstein frames we have

$$\zeta = \delta N = N_{,a}\delta\phi_f^a + \frac{1}{2}N_{,ab}\delta\phi_f^a\delta\phi_f^b + ... \qquad \text{and} \qquad \tilde{\zeta} = \delta\tilde{N} = \tilde{N}_a\delta\phi_{\tilde{f}}^a + \frac{1}{2}\tilde{N}_{ab}\delta\phi_{\tilde{f}}^a\delta\phi_{\tilde{f}}^b + ... \tag{12}$$

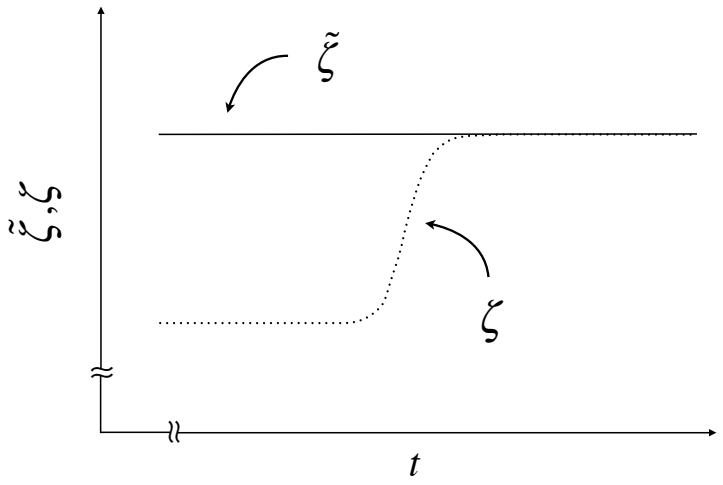

Figure 1:

respectively. Comparing these expansions we see that any difference between the curvature perturbations in the two frames comes from differences in the derivatives of N and $\tilde{N}$ with respect to the initial conditions and differences in the definition of the flat-gauge field perturbations $\delta\phi^a_f$ and $\delta\phi^a_{\tilde{f}}$.

By considering the definition of $\delta\phi^a_f$ and $\delta\phi^a_{\tilde{f}}$ at first order we see that

$$\delta\phi^a_f \equiv \delta\phi^a - \frac{\phi'^a}{\mathcal{H}}\mathcal{R} = (\delta^a_b + \frac{\phi'^a f_{,b}}{2f\mathcal{H}})\delta\phi^b_{\tilde{f}}, \tag{13}$$

where we have used $\tilde{\mathcal{R}} = \mathcal{R} + \frac{f_{,a}\delta\phi^a}{2f}$, $\tilde{\mathcal{H}} = \mathcal{H} + \frac{f'}{2f}$ and here a prime denotes a derivative with respect to conformal time. A similar relation can be found at second order [7][8].

Turning to the derivatives of N and $\tilde{N}$, the integral expressions for N and $\tilde{N}$ are given as

$$N = \int_E^* \mathcal{H}d\eta \qquad \text{and} \qquad \tilde{N} = \int_{\tilde{E}}^* \tilde{\mathcal{H}}d\eta = \int_{\tilde{E}}^* \mathcal{H}d\eta + \frac{1}{2}\ln\left(\frac{f_*}{f_{\tilde{E}}}\right) \tag{14}$$

respectively, where $*$ denotes the initial conditions, $E = $ const. specifies the final constant energy surface in the Jordan frame and $\tilde{E} = $ const. the final constant energy surface in the Einstein frame. We see that the differences thus come from the additional log term in the Einstein frame and the difference in the definition of the final constant energy surface.

Combining the results up to second order we find [8]

$$\begin{aligned}\zeta - \tilde{\zeta} = (N_a - N^{\tilde{E}}_a)\delta\phi^a_{\tilde{f}} + \frac{1}{2}(N_{ab} - N^{\tilde{E}}_{ab})\delta\phi^a_{\tilde{f}(1)}\delta\phi^b_{\tilde{f}(1)} \\ + \frac{f_b}{2f}\bigg|_{\tilde{E}}\frac{\partial\phi^b_{\tilde{E}}}{\partial\phi^a_*}\delta\phi^a_{\tilde{f}} + \left(\frac{f_{cd}}{2f}\bigg|_{\tilde{E}}\frac{\partial\phi^c_{\tilde{E}}}{\partial\phi^a_*}\frac{\partial\phi^d_{\tilde{E}}}{\partial\phi^b_*} - \frac{f_c f_d}{2f^2}\bigg|_{\tilde{E}}\frac{\partial\phi^c_{\tilde{E}}}{\partial\phi^a_*}\frac{\partial\phi^d_{\tilde{E}}}{\partial\phi^b_*} + \frac{f_c}{2f}\bigg|_{\tilde{E}}\frac{\partial^2\phi^c_{\tilde{E}}}{\partial\phi^a_*\partial\phi^b_*}\right)\delta\phi^a_{\tilde{f}(1)}\delta\phi^b_{\tilde{f}(1)},\end{aligned} \tag{15}$$

where

$$N^{\tilde{E}}_a = \frac{\partial}{\partial\phi^a_*}\left(\int_{\tilde{E}}^* \mathcal{H}d\eta\right). \tag{16}$$

It turns out that contributions to this difference coming from the relation between $\delta\phi^a_f$ and $\delta\phi^a_{\tilde{f}}$ cancel with those from the $\ln(f_*)$ term in (14), meaning that it is the difference in definition of the final constant energy surface that is important. If we consider an adiabatic limit, where final field values are independent of the initial conditions ($\partial\phi^a_{\tilde{E}}/\partial\phi^b_* = 0$) and the surfaces $E = $ const. and $\tilde{E} = $ const. coincide, then we see that $\zeta = \tilde{\zeta}$ is recovered.

To determine the power-spectrum, its tilt and non-gaussianity in the Jordan frame we can exploit relation (13) between $\delta\phi^a_f$ and $\delta\phi^a_{\tilde{f}}$ and our knowledge of the correlation functions of $\delta\phi^a_{\tilde{f}}$

$$\langle \delta\phi^a_{\tilde{f}\boldsymbol{k}} \delta\phi^b_{\tilde{f}\boldsymbol{k}'} \rangle = (2\pi)^3 \delta^3(\boldsymbol{k}+\boldsymbol{k}') \frac{\tilde{H}^2}{2k^3} S^{ab}. \tag{17}$$

Defining

$$\mathcal{N}_a = N_a + \frac{f_a}{2f} \qquad \text{and} \qquad \mathcal{N}_{ab} = \nabla_a\nabla_b N + \frac{\nabla_a\nabla_b f}{2f} - \frac{f_a f_b}{2f^2}, \tag{18}$$

we find

$$\mathcal{P}_\zeta(k) = \mathcal{N}_a\mathcal{N}_b S^{ab} \left(\frac{\tilde{H}}{2\pi}\right)^2 \qquad \text{and} \qquad f_{NL} = \frac{\mathcal{N}_a\mathcal{N}_b\mathcal{N}_{cd}S^{ac}S^{bd}}{\left[\mathcal{N}_e\mathcal{N}_f S^{ef}\right]^2}. \tag{19}$$

These are to be compared to the Einstein frame results

$$\mathcal{P}_{\tilde{\zeta}}(k) = \tilde{N}_a\tilde{N}_b S^{ab} \left(\frac{\tilde{H}}{2\pi}\right)^2 \qquad \text{and} \qquad \tilde{f}_{NL} = \frac{\tilde{N}_a\tilde{N}_b\nabla_c\nabla_d\tilde{N}S^{ac}S^{bd}}{\left[\tilde{N}_e\tilde{N}_f S^{ef}\right]^2}. \tag{20}$$

In general the derivatives of the total number of e-foldings with respect to the initial conditions must be calculated numerically. However, even in the case of non-minimal coupling there are cases where it can be done analytically. In the slow-roll approximation the equations of motion in the Jordan frame are of the form

$$\frac{d\phi^a}{dN} = 2f h^{ab}\frac{W_b}{W}, \tag{21}$$

where $W = V/f^2$. These can be solved analytically if $h^{ab} = \delta^{ab}$ and W is either product or sum separable. Taking the product separable case, in the Jordan frame $E = fW/2$ and we find [8]

$$N_c = \frac{1}{2f}\bigg|_E \frac{g^c_E}{g^c_*} \frac{\left(\frac{f_c}{f}\Big|_E + g^c_E\right)}{\sum_a \left(\frac{f_a}{f}\Big|_E + g^a_E\right) g^a_E} - \int_{\phi^a_E}^{\phi^a_*} \frac{f_c}{2f^2}\frac{g^c}{g^c_*}\frac{d\phi^a}{g^a} \tag{22}$$

whilst in the Einstein frame we have $\tilde{E} = W/4$, which gives

$$\tilde{N}_c = \frac{1}{2f}\bigg|_{\tilde{E}} \frac{g^c_{\tilde{E}}}{g^c_*} \frac{g^c_{\tilde{E}}}{\sum_a g^a_{\tilde{E}} g^a_{\tilde{E}}} - \int_{\phi^a_{\tilde{E}}}^{\phi^a_*} \frac{f_c}{2f^2}\frac{g^c}{g^c_*}\frac{d\phi^a}{g^a}, \tag{23}$$

where $g^a = W_a/W$.

Returning to the two-field example considered at linear order, but no longer imposing the conservation of $\tilde{\zeta}$, at linear level we find

$$\delta N - \delta\tilde{N} \simeq \frac{f_\chi}{2f\epsilon_E}\delta\chi_{\tilde{f}}, \tag{24}$$

which is in agreement with the previous result. Making the same argument as before that $f_\chi/\sqrt{f}$ should be $\mathcal{O}(\sqrt{\epsilon})$, and making some order of magnitude estimates, we find that $\tilde{f}_{NL} \sim \mathcal{O}(1) \times f_{\chi\chi}$ and that $(f_{NL} - \tilde{f}_{NL})/\tilde{f}_{NL} \sim \mathcal{O}(1)$. As such, the difference in non-gaussianity of ζ and $\tilde{\zeta}$ is potentially significant.

On a more general note, we see that at second order $f_{\chi\chi}$ contributes to possible discrepancies between ζ and $\tilde{\zeta}$. This means that even if f_χ gives a negligible difference between the results at linear order, a large $f_{\chi\chi}$ could still potentially give a significant difference at the level of non-gaussianity. Indeed, a well motivated form for the non-minimal coupling would be $f = 1 + \xi\chi^2$. In such a case, if the background trajectory is along $\chi = 0$, we would have $f_\chi = 0$ but $f_{\chi\chi} = 2\xi$. The consideration of specific forms for f and V and the resulting spectrum parameters is currently under way.

4 Conclusions

We have explored the relation between the Jordan and Einstein frame curvature perturbations on constant energy density hypersurfaces in the presence of multiple fields and non-minimal coupling. At linear order we saw explicitly that they are not the same and that the difference is a direct consequence of the isocurvature perturbations inherent to multi-field models. We also saw that conservation of the curvature perturbation in one frame does not imply conservation in the other, but that it is also possible that both are conserved with a non-zero difference in their magnitudes. At non-linear order we were able to implement the δN formalism in the Jordan and Einstein frames and saw explicitly that the non-gaussianity of the two curvature perturbations may also differ in the case that an adiabatic limit has not been reached. It was clear that the source of the difference is the difference in definition of the final constant energy surface in the Jordan and Einstein frames. These results highlight the non-observable nature of ζ itself, and the importance of knowing how both curvature perturbations evolve through reheating and are related to the temperature anisotropies of the Cosmic Microwave Background. Work in this direction is currently under way.

References

[1] E. J. Copeland, R. Easther and D. Wands, *"Vacuum fluctuations in axion - dilaton cosmologies,"* Phys. Rev. D **56** (1997) 874 [hep-th/9701082].

[2] J. O. Gong, J. C. Hwang, W. I. Park, M. Sasaki and Y. S. Song, *"Conformal invariance of curvature perturbation,"* JCAP **1109** (2011) 023 [arXiv:1107.1840 [gr-qc]].

[3] N. Deruelle and M. Sasaki, *"Conformal equivalence in classical gravity: the example of 'veiled' General Relativity,"* [arXiv:1007.3563 [gr-qc]].

[4] C. Gordon, D. Wands, B. A. Bassett and R. Maartens, *"Adiabatic and entropy perturbations from inflation,"* Phys. Rev. D **63** (2001) 023506 [astro-ph/0009131].

[5] J. White, M. Minamitsuji and M. Sasaki, *"Curvature perturbation in multi-field inflation with non-minimal coupling,"* JCAP **1207** (2012) 039 [arXiv:1205.0656 [astro-ph.CO]].

[6] D. H. Lyth, K. A. Malik and M. Sasaki, *"A General proof of the conservation of the curvature perturbation,"* JCAP **0505** (2005) 004 [astro-ph/0411220].

[7] K. A. Malik, *"Gauge-invariant perturbations at second order: Multiple scalar fields on large scales,"* JCAP **0511** (2005) 005 [astro-ph/0506532].

[8] J. White, M. Minamitsuji and M. Sasaki in preparation.

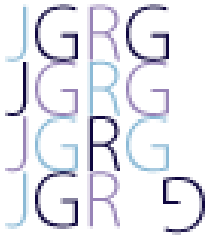

Ryo Saito, JGRG 22(2012)111333

"Features in the CMB spectrum as a probe of heavy physics during inflation"

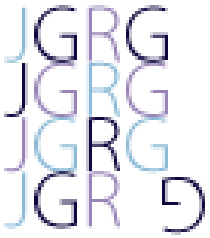

RESCEU SYMPOSIUM ON

GENERAL RELATIVITY AND GRAVITATION

JGRG 22



November 12-16 2012

Koshiba Hall, The University of Tokyo, Hongo, Tokyo, Japan





RESCEU SYMPOSIUM ON
GENERAL RELATIVITY AND GRAVITATION

JGRG22

November 12 - 16 2012
Koshiba Hall, The University of Tokyo, Hongo, Tokyo, Japan

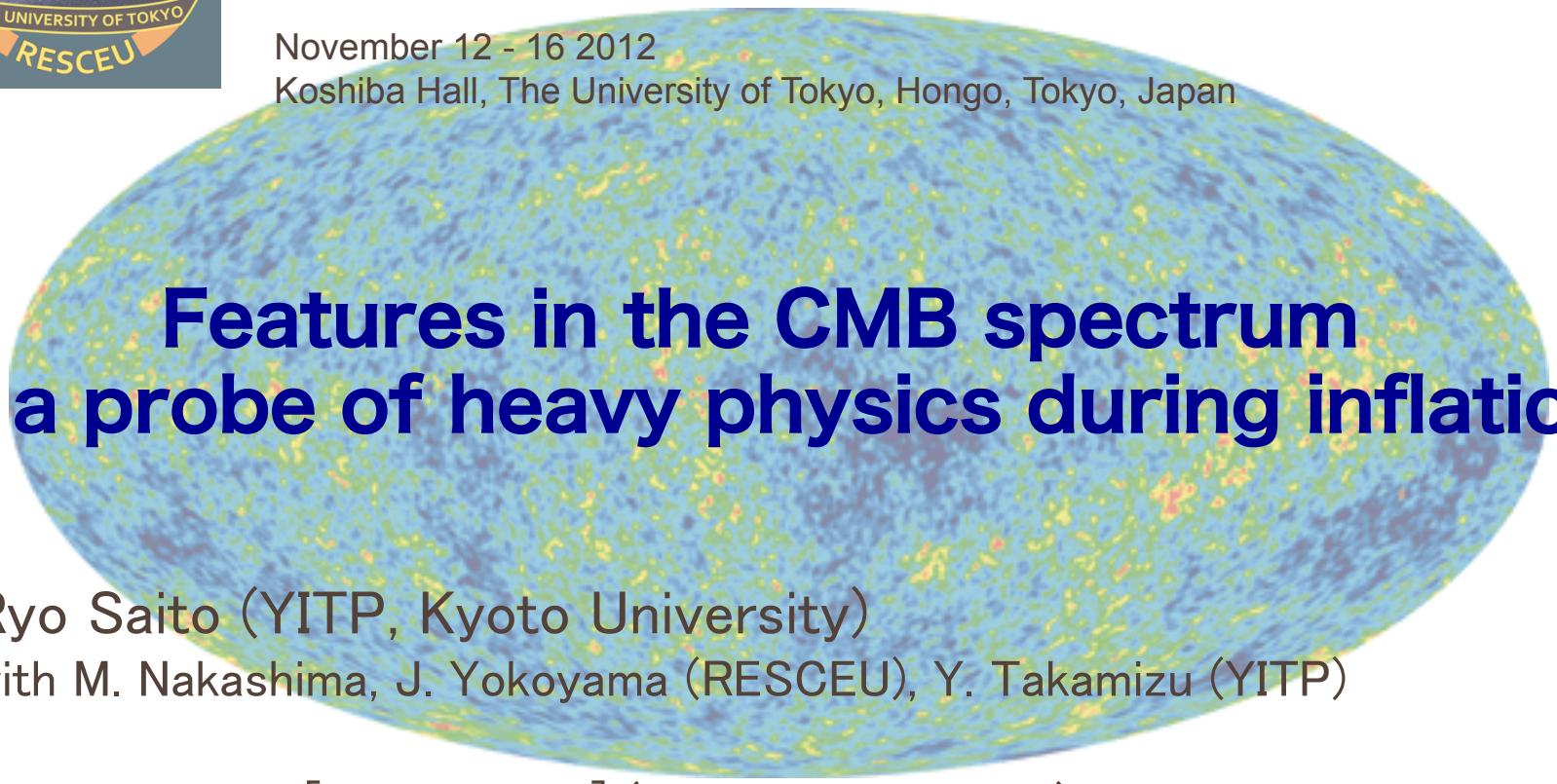

Features in the CMB spectrum as a probe of heavy physics during inflation

Ryo Saito (YITP, Kyoto University)
with M. Nakashima, J. Yokoyama (RESCEU), Y. Takamizu (YITP)

Ref: 1206.2164 [astro-ph.CO] (To appear in JCAP)
RS, J. Yokoyama, Y. Takamizu, in preparation

YITP
YUKAWA INSTITUTE FOR THEORETICAL PHYSICS

The simplest model of inflation:

Single-field slow-roll inflation

Predictions (with more technical assumptions)

The primordial fluctuations

- are adiabatic
- are nearly Gaussian-distributed
- have a nearly scale-invariant power spectrum

$$\Delta^2_{\mathcal{R}}(k) = \Delta^2_{\mathcal{R}}(k_0)(k/k_0)^{n_s-1}$$

No strong evidence to show that the Universe is described in a more complicated way.

"Single-field" does not mean that there is no field other than inflaton.

From a model-building point of view, in general, there are

many (scalar) degrees of freedom other than inflaton,

especially in models embedded in supergravity/string theory:
Moduli fields, Kaluza-Klein modes, Scalar SUSY-partner of inflaton,..

Usually, they are so heavy, $m \gg H$, that the models are treated *effectively* as single-field models.

The power spectrum is calculated by a single-field analysis with a reduced potential *assuming heavy fields are stuck to their potential minima*. [Yokoyama & Yamaguchi]

Is there any chance to probe heavy fields?

Heavy fields are *not necessarily* stuck to their potential minima and *can* affect the correlation functions.

They are displaced from their minima if they

- happen to be excited at the beginning of inflation.
  [Burgess, Cline, Lemieux, & Holman]

- are dynamically excited by e.g. turns of the inflaton trajectory.
  [Achucarro et al.], [Shiu & Xu], [Chen & Wang], [Sespedes et al.], [Pi & Sasaki],
  [Gao, Langlois, & Mizuno], [Burgess et al.],..

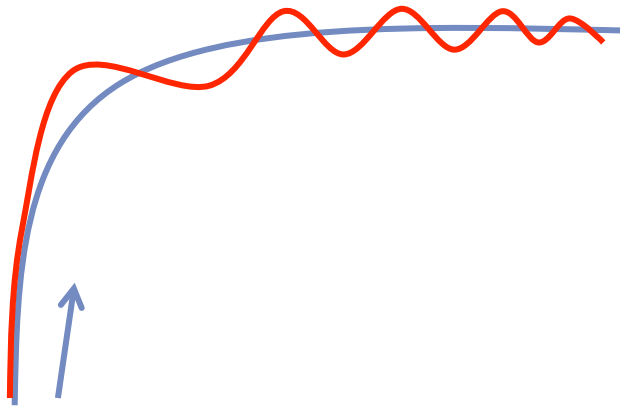

Heavy fields are displaced from their minima due to a centrifugal force.

When the turn is very sharp, the oscillation along the heavy direction can be excited after the turn.

What kind of effects are expected when heavy fields are excited from the potential minima?

- Large mixing between the light and heavy modes.
  [Achucarro et al.], [Shiu & Xu], [Chen & Wang], [Sespedes et al.], [Pi & Sasaki], [Gao, Langlois, & Mizuno],..

- Resonance between the excited oscillation and the fluctuations.
  [Chen] [RS, Nakashima, Takamizu, & Yokoyama]

The correction becomes larger for larger mass.

→ **It opens a possibility to probe heavy physics during inflation.**

Basic idea

[Chen] [RS, Nakashima, Takamizu, & Yokoyama]

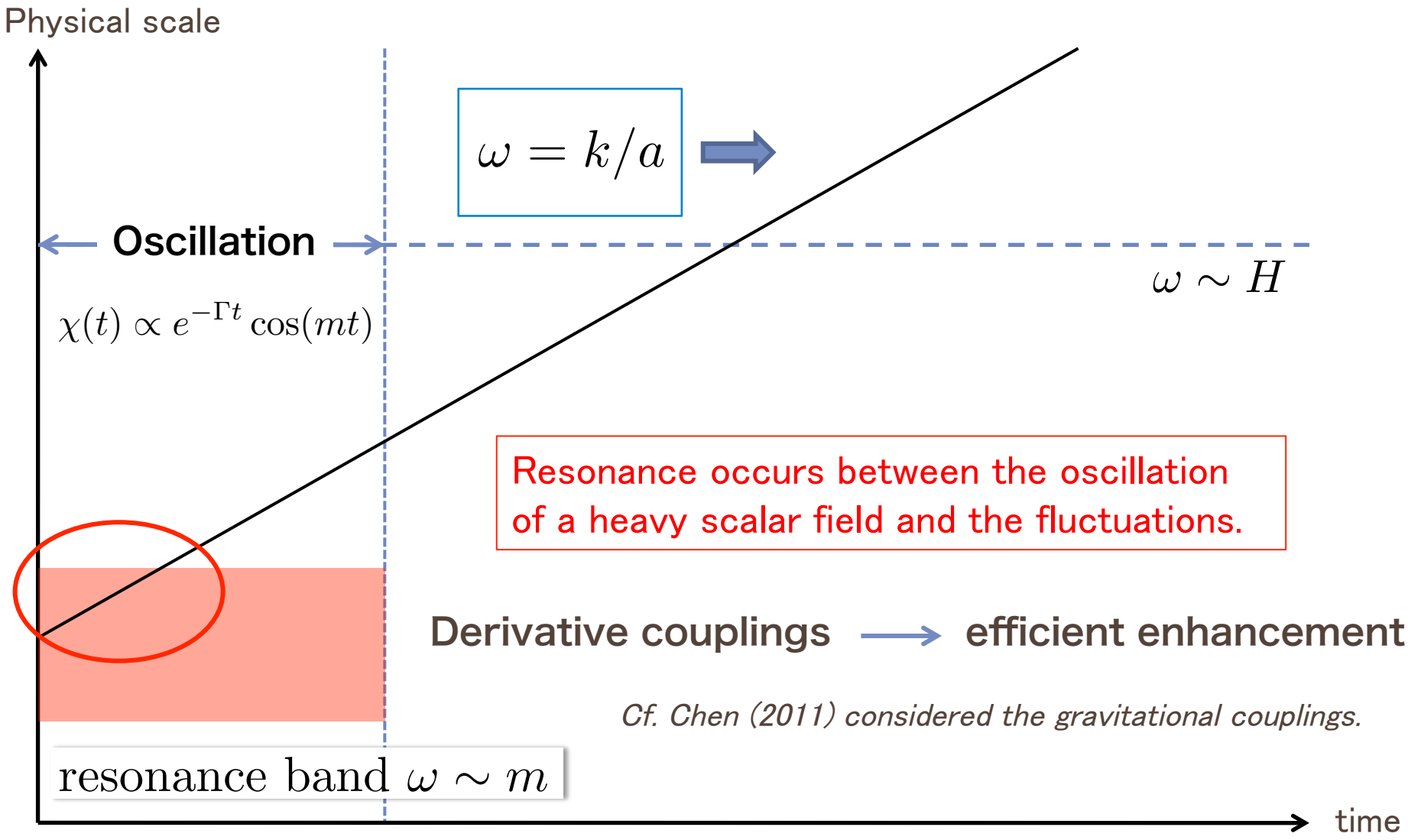

Model

Action: inflaton + a heavy scalar field with derivative couplings

$$S_m \equiv -\int \mathrm{d}x^4\sqrt{-g}\left[\frac{1}{2}(\partial\phi)^2 + V(\phi) + \frac{1}{2}(\partial\chi)^2 + \frac{m^2}{2}\chi^2 + K_n + K_d\right],$$

where

$$K_n \equiv \frac{\lambda_n}{2\Lambda_n}\chi(\partial\phi)^2$$

$$K_d \equiv \frac{\lambda_{d1}}{4\Lambda_d^4}(\partial\chi)^2(\partial\phi)^2 + \frac{\lambda_{d2}}{4\Lambda_d^4}(\partial\chi\cdot\partial\phi)^2$$

Decay rate of χ: Γ

Kn & Kd from the effective-field-theory point of view

[Weinberg]

$$\mathcal{L}_0 \equiv -\left[\frac{1}{2}(\partial\phi)^2 + V(\phi) + \frac{1}{2}(\partial\chi)^2 + \frac{m^2}{2}\chi^2\right],$$

is just the first term of the derivative expansion in a generic effective field theory.

Kn & Kd are next corrections to $\mathcal{L}_0$: most general ones if we assume parity & shift symmetry for the inflaton field.

They are usually unimportant, but could play an important role in the resonance region, which is deep inside the horizon and the heavy scalar field rapidly oscillates and then the derivatives are large.

Kn in specific models

– A heavy scalar field with a non-minimal coupling
(incl. a model with higher curvature terms),

- A pseudo-NG boson + a symmetry breaking field,
- Supergravity + higher order terms in the Kahler potential,..

Kd in specific models

– DBI action (Dp-brane):

$$S_{\rm DBI} = -T \int {\rm d}^4 x \int {\rm d}^{p-3} \lambda \sqrt{-\det \left(G_{MN} \partial_m \phi^M \partial_n \phi^N \right)} \quad (M, N = 0, \ldots, D-1)$$

Kd couplings appear expanding the square root in the action.

heavy scalar field = brane coordinates other than inflaton, KK modes

Setup

- Hierarchy of the energy scales

$$H < \Gamma < m < \Lambda_n, \Lambda_d$$

- Higher order terms are negligible

$$\chi < \Lambda_n, \ \dot{\phi}, \dot{\chi} < \Lambda_d^2$$

- The heavy scalar field is subdominant

$$f_\chi \equiv \frac{\rho_\chi}{\rho} \simeq \frac{\dot{\chi}^2 + m^2\chi^2}{6M_p^2H^2} \ll 1$$

- Flat potential

$$\epsilon_V \equiv \frac{M_p^2}{2}\left(\frac{V'}{V}\right)^2 \ll 1, \quad \eta_V \equiv M_p^2\frac{V''}{V} \ll 1$$

Power spectrum

We can make some simplifications (in the flat gauge):

The resonance takes place deep inside the horizon.

⟺ The gravitational effects are not important.

(The metric perturbations can be neglected.)

Small couplings & Large mass.

⟺ The fluctuations for the heavy field are smaller than those in the inflaton field and also do not satisfy the resonance condition ($\omega = \sqrt{m^2 + (k/a)^2} > m$).

(The perturbations in the heavy field can be neglected.)

Only the inflaton perturbations are relevant: $\phi = \phi_0 + \varphi$

Second-order action (flat gauge):

$$S_2 \simeq \int \mathrm{d}t\mathrm{d}^3x \, \frac{z_\phi^2}{2}\left[\dot{\varphi}^2 - c_s^2(\nabla\varphi)^2/a^2\right]$$

where

$$z_\phi^2 = a^3\left[1 + \lambda_n\frac{\chi}{\Lambda_n} + (\lambda_{d1}+\lambda_{d2})\,\frac{\dot{\chi}^2}{2\Lambda_d^4}\right]$$

$$c_s^2 \simeq 1 - \frac{\lambda_{d2}\dot{\chi}^2}{2\Lambda_d^4} + O\left(\frac{\dot{\chi}^4}{\Lambda_d^8}\right)$$

(the speed of sound)

Equation of motion (on subhorizon scales):

$$\frac{\mathrm{d}^2 v_k}{\mathrm{d}z^2} + \left[A_k - 2q\cos(2z)\right] v_k = 0$$

where

$$z \equiv mt,$$

$$v_k \equiv z_\phi \varphi,$$

$$A_k \equiv \left(\frac{k}{am}\right)^2,$$

$$q \equiv e^{-2\Gamma t}\left[\lambda_{d2}\frac{m^2\chi_0^2}{8\Lambda_d^4}\left(\frac{k}{am}\right)^2 + (\lambda_{d1}+\lambda_{d2})\frac{m^2\chi_0^2}{\Lambda_d^4}\right]$$

q_d

Form of the Mathieu equation ➡ **Parametric resonance**

A similar equation for the Kn-coupling case:

$$m \to m/2, \Gamma \to \Gamma/2, q \to \lambda_n q_n e^{-\Gamma t} \equiv \lambda_n \frac{\chi_0}{\Lambda_n} e^{-\Gamma t}$$

Condition for the parametric resonance

$$q \equiv e^{-2\Gamma t}\left[\lambda_{d2}\frac{m^2\chi_0^2}{8\Lambda_d^4}\left(\frac{k}{am}\right)^2+(\lambda_{d1}+\lambda_{d2})\frac{m^2\chi_0^2}{\Lambda_d^4}\right]<1$$

➡ **Narrow resonance**

$$|A_k-1|<q \quad \Rightarrow \quad (1-\tilde{q}/2)m<k/a<(1+\tilde{q}/2)m$$

where

$$\tilde{q}\equiv(2\lambda_{d1}+3\lambda_{d2})\frac{q_d}{8}e^{-2\Gamma t}\sim\left(\frac{V^{1/4}}{\Lambda_d}\right)^4 f_\chi$$

Number of resonance periods:

$$\Delta z\sim\frac{m}{H}\min(\tilde{q},H/\Gamma)$$

The resonance is more efficient for larger mass.

Spectra for different values of the mass

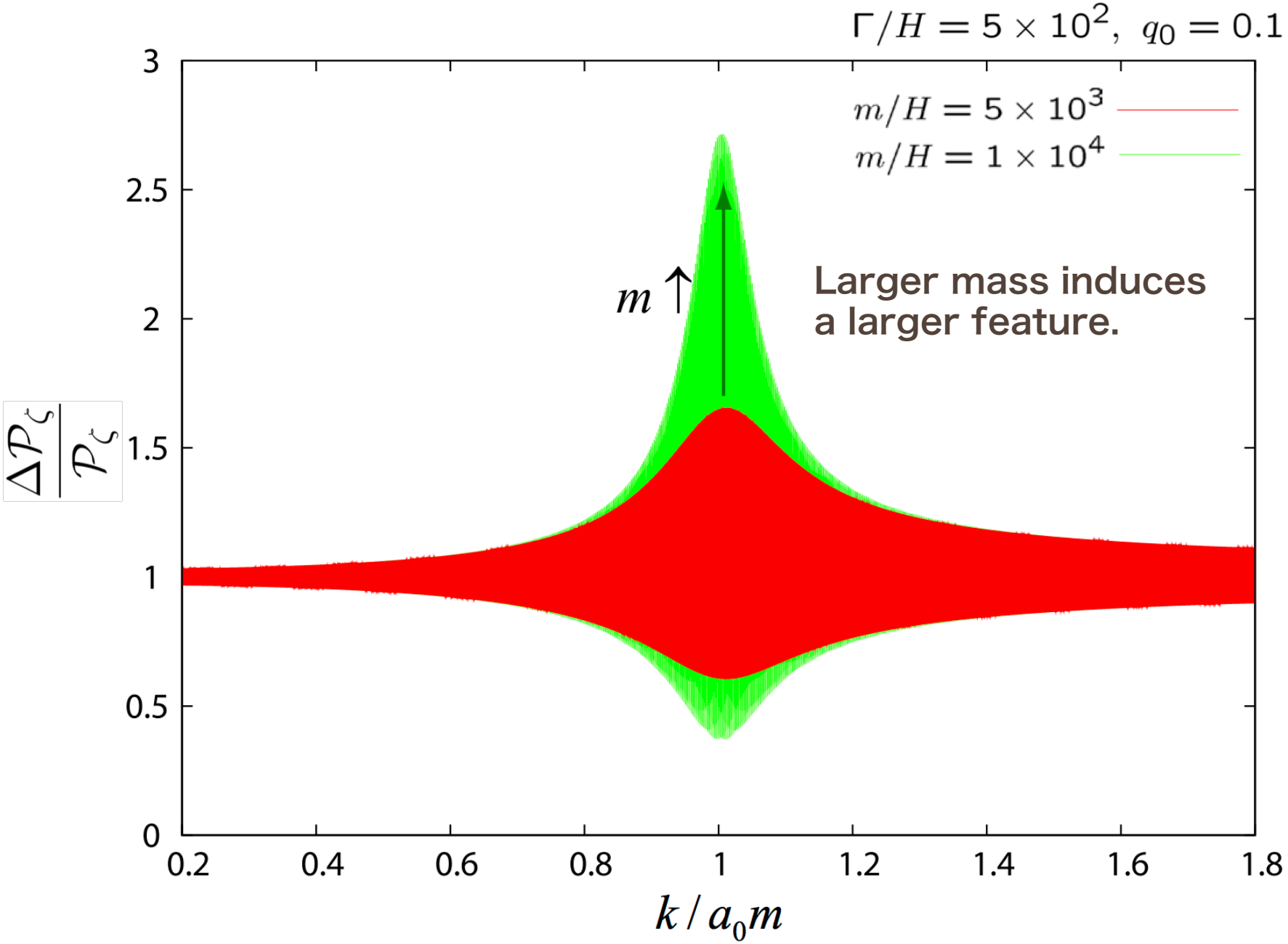

Bispectrum

The oscillation can also affect the higher-order correlation functions (non-Gaussianity, NG).

e.g., Bispectrum

$$\langle \zeta_{\mathbf{k}_1}(t)\zeta_{\mathbf{k}_2}(t)\zeta_{\mathbf{k}_3}(t)\rangle = (2\pi)^7\delta^3(\mathbf{k_1}+\mathbf{k_2}+\mathbf{k_3})F(\mathbf{k}_1,\mathbf{k}_2,\mathbf{k}_3)(\mathcal{P}_\zeta)^2$$

NG from the resonance

Resonant non-Gaussianity

[Chen, Easther, & Lim], [Flauger & Pajer], [Chen], [Behbahani et al.], [Gwyn Rummel, & Westphal],...

Relevant interactions

- contains an oscillatory component
- contains more derivatives

(The mixing with the fluctuations in the heavy field can be neglected.)

Kn couplings

$$\mathcal{L}_3 \supset -\frac{\lambda_n \chi}{\Lambda_n} \frac{\dot{\phi}}{2M_p^2 H} \left[\frac{1}{2}\varphi \left(\dot{\varphi}^2 + \frac{1}{a^2}(\partial\varphi)^2 \right) - \partial_i(\partial^{-2}\dot{\varphi})\dot{\varphi}\partial_i\varphi \right],$$

Kd couplings

$$\mathcal{L}_3 \supset -\frac{\lambda_{d1}\dot{\chi}^2}{2\Lambda_d^4} \frac{\dot{\phi}}{2M_p^2 H} \left[\frac{1}{2}\varphi \left(\dot{\varphi}^2 + \frac{1}{a^2}(\partial\varphi)^2 \right) - \partial_i(\partial^{-2}\dot{\varphi})\dot{\varphi}\partial_i\varphi \right]$$

$$-\frac{\lambda_{d2}\dot{\chi}^2}{2\Lambda_d^4} \frac{\dot{\phi}}{2M_p^2 H} \varphi\dot{\varphi}^2.$$

Interaction Hamiltonian

$$H^{\rm int} = \frac{\epsilon_\phi^{1/2}}{2\sqrt{2}a^2(2\pi)^6 M_p}\iiint {\rm d}^3k_1{\rm d}^3k_2{\rm d}^3k_3\ k_2k_3C_{\mathbf{k_1k_2k_3}}\varphi_{\mathbf{k}_1}\varphi_{\mathbf{k}_2}\varphi_{\mathbf{k}_3}\delta^3(\mathbf{k_1}+\mathbf{k_2}+\mathbf{k_3}),$$

where

$$C_{\mathbf{k_1k_2k_3}} \equiv C^n_{\mathbf{k_1k_2k_3}}e^{-\Gamma t}\cos(mt) + C^d_{\mathbf{k_1k_2k_3}}e^{-2\Gamma t}\sin^2(mt),$$

$$C^n_{\mathbf{k_1k_2k_3}} \equiv \lambda_n\left[1+\hat{\mathbf{k}}_2\cdot\hat{\mathbf{k}}_3\left(1-\frac{k_1}{k_2}\right)\right]q_n,$$

$$C^d_{\mathbf{k_1k_2k_3}} \equiv \left\{\frac{\lambda_{d1}}{2}\left[1+\hat{\mathbf{k}}_2\cdot\hat{\mathbf{k}}_3\left(1-\frac{k_1}{k_2}\right)\right]-\lambda_{d2}\right\}q_d,$$

The Bispectrum can be estimated by using the in-in formalism:

$$\langle \varphi_{\mathbf{k}_1}(t)\varphi_{\mathbf{k}_2}(t)\varphi_{\mathbf{k}_3}(t)\rangle = i\int \mathrm{d}t'\langle [H^{\mathrm{int}}(t'), \varphi_{\mathbf{k}_1}(t)\varphi_{\mathbf{k}_2}(t)\varphi_{\mathbf{k}_3}(t)]\rangle$$

$$= \mathrm{Re}\left(i\int \mathrm{d}t'\langle H^{\mathrm{int}}(t')\varphi_{\mathbf{k}_1}(t)\varphi_{\mathbf{k}_2}(t)\varphi_{\mathbf{k}_3}(t)\rangle \right)$$

Resonance at $K/a_* \simeq m$

$$H^{\mathrm{int}}(t') \sim \cos(mt')\varphi_{\mathbf{k}_1}(t')\varphi_{\mathbf{k}_2}(t')\varphi_{\mathbf{k}_3}(t') \sim \cos(mt')e^{-iK\eta'}$$

$$(K = k_1 + k_2 + k_3)$$

Resonance

➡ An additional contribution from the oscillatory region.

(There is no contribution from the subhorizon region in the usual case.)

Analytic estimation

Using the method of the steepest descent,

Dimensionless

$$F(\mathbf{k}_1,\mathbf{k}_2,\mathbf{k}_3)k_1^2k_2^2k_3^2$$
$$= -\frac{\epsilon_\phi}{16H}\int_0^\infty \mathrm{d}t'\ \frac{k_2k_3}{a^5}C_{\mathbf{k_1k_2k_3}}\cos(K\eta') + \text{cyclic}$$

The time of the excitation

$$\sim \frac{\sqrt{2\pi}\epsilon_\phi}{16}\left(\frac{2m}{H}\right)^{3/2}\left(\frac{k_2k_3}{K^2}\right)\left(\frac{K}{2m}\right)^{-3-2\Gamma/H}\cos\left\{\frac{2m}{H}\left[\ln\left(\frac{K}{2m}\right)+1\right]\right\}C^d_{\mathbf{k_1k_2k_3}} + \text{cyclic}$$

A similar equation for the Kn-coupling case:

$$m \to m/2, \Gamma \to \Gamma/2, C^d_{\mathbf{k_1k_2k_3}} \to C^n_{\mathbf{k_1k_2k_3}}$$

* We set the lower limit of integration as $-\infty$ instead of 0 to obtain the final expression. The function F is suppressed for K<m if we use 0 as the lower limit properly. (by a few factor for K=m)

A very large feature also appears in the Bispectrum.

$$\sim \epsilon_\phi q\left(\frac{m}{H}\right)^{3/2} \quad \text{at} \quad K \simeq m\ (\text{for } Kn), 2m\ (\text{for } Kd)$$

Summary

- We could obtain some hints on heavy physics during inflation by analyzing the local features of the CMB power spectrum.

- A heavy scalar field could leave non-negligible signatures in the CMB spectrum through parametric resonance between its background oscillations and the inflaton fluctuations.

- A large features could be induced in the higher-correlation functions, Non-Gaussianity, even when the feature in the power Spectrum is too small to be observed.

- If they are detected, they will improve our understanding of physics behind inflation.

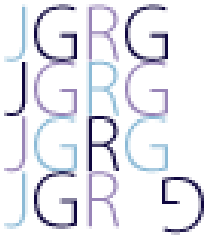

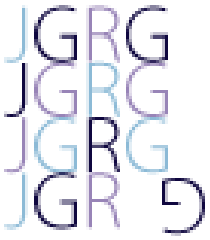

Keiki Saito, JGRG 22(2012)111334

"High frequency limit for gravitational perturbations of cosmological models in modified gravity theories"

RESCEU SYMPOSIUM ON

GENERAL RELATIVITY AND GRAVITATION

JGRG 22

November 12-16 2012

Koshiba Hall, The University of Tokyo, Hongo, Tokyo, Japan





High frequency limit for gravitational perturbations of cosmological models in modified gravity theories

Keiki Saito[1](a) and Akihiro Ishibashi(b)

(a) *Department of Particles and Nuclear Physics, The raduate University for Advanced Studies (SOKENDAI), 1-1 Oho, Tsukuba, Ibaraki 305-0801, Japan*
(b) *Department of Physics, Kinki University, Higashi-Osaka 577-8502, Japan*

Abstract

We study the effective gravitational stress-energy tensor for short-wavelength perturbations in modified gravity theories in the cosmological context. We consider $f(R)$ gravity theories on the assumptions that (i) the background has the Friedmann-Lemaître-Robertson-Walker symmetry and that (ii) when our $f(R)$ theory reduces to Einstein gravity. We show by explicit computation that the effective stress-energy tensor for a cosmological model in our $f(R)$ theories, as well as that obtained in the corresponding scalar-tensor theory, takes a similar form to that in general relativity and is in fact traceless, hence acting again like a radiation fluid. If the assumption (ii) above is dropped, then an undetermined integration constant appears and the resultant effective stress-energy tensor acquires a term that is in proportion to the background metric, hence being able to describe a cosmological constant. Whether this effective cosmological constant term is positive and whether it has the right magnitude as dark energy depends upon the value of the integration constant.

1 Introduction

Our observable universe appears to be homogeneous and isotropic on large scales, but highly inhomogeneous on small scales. It is therefore considerably interesting to consider whether the local inhomogeneities can have any effects on the global dynamics of our universe, in particular, any effect that corresponds to a positive cosmological constant or dark energy. A number of authors have explored this possibility of explaining the present cosmic accelerating expansion by some backreaction effects of the local inhomogeneities. Such a backreaction effect may be described in terms of an effective stress-energy tensor arising from metric as well as matter perturbations.

In general relativity, a consistent expansion scheme for short-wavelength perturbations and the corresponding effective stress-energy tensor were largely developed by Isaacson [1, 2], in which the small parameter, say ϵ, corresponds to the amplitude and at the same time the wavelength of perturbations. Isaacson's expansion scheme is called the high frequency limit or the short-wavelength approximation. It has been shown that this effective stress-energy tensor is traceless and satisfies the weak energy condition, i.e. acts like radiation [3, 4], and thus cannot provide any effects like dark energy in general relativity.

However, it is far from obvious if this traceless property of the effective stress-energy tensor is a nature specific only to the Einstein gravity or not. The purpose of this paper is to address this question in a simple, concrete model in the cosmological context. Among many, one of the simplest of modified theories so far proposed is the so called $f(R)$ theory. Since $f(R)$ gravity contains higher order derivative terms, we can anticipate the effective stress-energy tensor to be generally modified in the high frequency limit.

It is well-known that $f(R)$ gravity is equivalent to a scalar-tensor theory, which contains the coupling of the scalar curvature R to a scalar field ϕ in a certain way. The Brans-Dicke theory is one of the simplest examples. Therefore, our analysis can be performed, in principle, either (i) by first translating a given $f(R)$ theory into the corresponding scalar-tensor theory and then inspecting the stress-energy tensor for the scalar field ϕ, or (ii) by directly dealing with metric perturbations of the $f(R)$ theory. We may expect that the former approach is much easier than the latter metric approach, as one has to deal with metric perturbations of complicated combinations of the curvature tensors in the latter case. Nevertheless we

[1]Email address: saitok@post.kek.jp

will take the both approaches. In fact, in the metric approach, by directly taking up perturbations of the scalar curvature R, the Ricci tensor R_{ab} and the Riemann tensor $R^a{}_{bcd}$ involved in a given $f(R)$ theory, we can learn how to generalize our present analysis of a specific class of $f(R)$ gravity to analyses of other, different types of modified gravity theories that cannot even be translated into a scalar-tensor theory.

In the next section, we consider the high frequency limit in $f(R)$ gravity theory. Based on the Isaacson's scheme we expand the field equations for $f(R) = R + cR^2$ theory and first derive the general expression of the effective stress-energy tensor for gravitational perturbations in our $f(R)$ gravity. Then, assuming that our background metric has the FLRW symmetry and also that the resulting equations reduce to the corresponding equations for the Einstein gravity in the limit $c \to 0$, we see that the effective stress-energy tensor whose expression is significantly simplified, is in fact traceless as in the Einstein gravity case. As briefly mentioned above, when a given $f(R)$ gravity is translated into the corresponding scalar-tensor theory, the scalar field ϕ, which expresses an extra-degree of freedom in the $f(R)$ theory, possess a non-trivial potential term. In Sec. 3, we will make sure that the effective stress-energy tensor in Brans-Dicke theory is consistent with that in our $f(R)$ gravity. We will also see that in the Einstein frame, the traceless property of the effective stress-energy tensor is shown to hold in more generic circumstances. Section 4 is devoted to a summary and points to future research.

2 High frequency limit in $f\ R$ gravity

The field equations in the $f(R)$ gravity have terms consisting of higher order derivatives of R, and the order of those derivatives are higher than that of R: $\nabla_{a_1}\nabla_{a_2}\cdots\nabla_{a_m}R^{(n)}[h] \sim \mathrm{O}\left(\epsilon^{n-2-m}\right)$. Therefore it is expected that the effect of the short-wavelength approximation would be enhanced. In order to see whether this is the case, from now on we restrict our attention to the following concrete model $f(R) = R + cR^2$, where c is a constant. The field equations are

$$G^{f(R)}_{ab} \equiv G_{ab} + 2c\left(RR_{ab} - \frac{1}{4}g_{ab}R^2 - \nabla_a\nabla_b R + g_{ab}g^{cd}\nabla_c\nabla_d R\right) = \kappa^2 T^{(0)}_{ab}\,. \tag{1}$$

As in Isaacson's formula, we expand the above equations with respect to the small parameter ϵ. From now on, we consider the cosmological context. We assume that our background is spatially homogeneous and isotropic, that is, our background metric possesses the FLRW symmetry. Then, thanks to this background symmetry we can explicitly solve equations of the form $\nabla_a\nabla_b S(t,\vec{x}) = 0$. The equations of motion of $\mathrm{O}\left(\epsilon^{-3}\right)$ is solved to yield $R^{(1)}[h] = const.$ Taking the average, we find $R^{(1)}[h] = const. = \langle const.\rangle = \left\langle R^{(1)}[h]\right\rangle = 0$. Then, those of $\mathrm{O}\left(\epsilon^{-2}\right)$ become $\nabla_a\nabla_b R^{(2)}[h] = 0$. We find $R^{(2)}[h] \equiv S_1 =$ const. By using above equations, the equation of $\mathrm{O}\left(\epsilon^{-1}\right)$ immediately yields

$$\Box R^{(3)}[h] - R_{ab}[g^{(0)}]\Box h^{ab} = 0\,, \tag{2}$$

$$\left(1 + 2cR[g^{(0)}] + 2cS_1\right)R^{(1)}_{ab}[h] = 2c\left(\nabla_a\nabla_b R^{(3)}[h] - R_{cd}[g^{(0)}]\nabla_a\nabla_b h^{cd}\right)\,. \tag{3}$$

The effective stress-energy tensor is then expressed as

$$\begin{aligned}\kappa^2 T^{\mathrm{eff}}_{ab} = -\Big\langle &\left(1 + 2cR[g^{(0)}]\right)R^{(2)}_{ab}[h] - \frac{1}{2}g^{(0)}_{ab}S_1 \\ &+2c\left\{\left(R^{(3)}[h] - h^{cd}R_{cd}[g^{(0)}]\right)R^{(1)}_{ab}[h] + S_1\left(R_{ab}[g^{(0)}] + R^{(2)}_{ab}\right)\right\} \\ &-\frac{c}{2}g^{(0)}_{ab}\left(2R[g^{(0)}] + S_1\right)S_1 \\ &+2c\left(-g^{(0)}_{ab}h^{cd}\right)\left(\nabla_c\nabla_d R^{(3)}[h] - R_{ef}[g^{(0)}]\nabla_c\nabla_d h^{ef}\right)\Big\rangle\,.\end{aligned} \tag{4}$$

This is the most general expression of our effective stress-energy tensor.

We immediately notice that our expression (4) contains the integration constant S_1. There does not seem to be a definite way to determine S_1 within the framework of the present $f(R)$ theory itself. As a

sensible way to specify S_1, let us assume in the following that the effective stress-energy tensor (4) in the R^2 model should reduce to that in general relativity when $c = 0$, and accordingly choose S_1 $(= R^{(2)}[h])$ to be 0. Then, (4) becomes

$$\kappa^2 T^{\rm eff}_{ab} = -\left\langle \left(1 + 2cR[g^{(0)}]\right) R^{(2)}_{ab}[h] + 2c\left(R^{(3)}[h] - h^{cd}R_{cd}[g^{(0)}]\right) R^{(1)}_{ab}[h] \right\rangle , \tag{5}$$

where we have used (3) in the first equality above, and $\left\langle h^{cd}R^{(1)}_{cd}[h]\right\rangle = 0$ in the second equality so as to make the above expression compatible with that of general relativity in the $c = 0$ case. Then using this and $R^{(1)}[h] = 0$, we can find that $\kappa^2 T^{\rm eff}_{ab}$ is in fact traceless:

$$\kappa^2 T^{{\rm eff}a}{}_{a} = 0\,. \tag{6}$$

It should be stressed that as mentioned above, there is a prior no way to determine S_1 by the theory itself. If we choose S_1 to be, instead, a non-zero constant, then the effective stress-energy tensor, (4), has a term proportional to the background metric, that is, a cosmological-constant-looking term, even in the limit to the Einstein gravity.

3 The high frequency limit in scalar-tensor theory

In the previous section, the scalar curvature R and the Ricci tensor R_{ab} are taken up directly in the metric formalism of the $f(R)$ gravity. It is well-known that any $f(R)$ gravity theory is included in Brans-Dicke theory, which is one of the simplest examples of scalar-tensor theory. In this section, we will see that the results obtained in the previous section are indeed consistent with those obtained within the corresponding scalar-tensor theory.

In the Jordan frame, the $f(R)$ gravity of the metric formalism can be cast into the form of the above Brans-Dicke theory by setting $\phi = F(R) \equiv df(R)/dR$, $\omega_{\rm BD} = 0$ and $V = (FR - f)/2$. In this case, as one can find $R - 2\partial_\phi V = 0$, the equations of motion for ϕ and g_{ab} just given above become, respectively

$$\Box\phi - \frac{1}{2\phi}\nabla^a\phi\nabla_a\phi = \kappa^2 T^{(0)}_{\phi\ ab}\,, \tag{7}$$

$$G^{\rm ST}_{ab} \equiv \phi\left(R_{ab} - \frac{1}{2}g_{ab}R\right) - \nabla_a\nabla_b\phi + g_{ab}\left(g^{cd}\nabla_c\nabla_d\phi + V(\phi)\right) = \kappa^2 T^{(0)}_{ab}\,. \tag{8}$$

From now we consider short-wavelength perturbations for ϕ: $\phi = \phi_0 + \delta\phi$. We also assume that there is no coupling of matter fields with the second-order derivatives of ϕ, so that there are no non-vanishing terms of order $O(\epsilon^{-1})$ in the stress-energy tensor for matter fields. Then, the equation of motion for ϕ of O $\left(\epsilon^{-1}\right)$ is $\Box\delta\phi = 0$. and the equations of motion for g_{ab} of O $\left(\epsilon^{-1}\right)$ are

$$\phi_0\left(R^{(1)}_{ab}[h] - \frac{1}{2}g^{(0)}_{ab}R^{(1)}[h]\right) = \nabla_a\nabla_b\delta\phi - g^{(0)}_{ab}\Box\delta\phi\,. \tag{9}$$

Contracting with $g^{(0)ab}$, we have $R^{(1)}[h] = 3\Box\delta\phi/\phi_0 = 0$. From this, we can immediately find $R^{(1)}_{ab}[h] = 1\nabla_a\nabla_b\delta\phi/\phi_0$. The equations of motion in O (1) are given by $G^{\rm ST}_{ab}[g^{(0)}, \phi_0] = \kappa^2 T^{(0)}_{ab} + \kappa^2 T^{\rm eff}_{ab}$, where

$$\kappa^2 T^{\rm eff}_{ab} \equiv -\left\langle \phi_0 R^{(2)}_{ab}[h] + \delta\phi R^{(1)}_{ab}[h] - g^{(0)}_{ab}h^{cd}\nabla_c\nabla_d\delta\phi \right\rangle . \tag{10}$$

Here we would like to emphasise that so far we have made no assumptions concerning the form of $f(R)$ or the symmetry of our background metric $g^{(0)}_{ab}$; the above expression, (10), applies to the generic $f(R)$ theory with an arbitrary background metric.

If we restrict the form of $f(R)$ to be $f(R) = R + cR^2$, then by inspecting the expansions $\phi = \phi_0 + \delta\phi + \cdots$ and $F(R) = 1 + 2cR = \left(1 + 2cR[g^{(0)}]\right) + 2c\left(R^{(3)}[h] - h^{cd}R_{cd}[g^{(0)}]\right) + \cdots$, we find $\phi_0 = 1 + 2cR[g^{(0)}]$ and $\delta\phi = 2c\left(R^{(3)}[h] - h^{cd}R_{cd}[g^{(0)}]\right)$. Using these, we have

$$\begin{aligned}\kappa^2 T^{\rm eff}_{ab} = &-\Big\langle \left(1 + 2cR[g^{(0)}]\right) R^{(2)}_{ab}[h] \\ &+2c\left(R^{(3)}[h] - h^{cd}R_{cd}[g^{(0)}]\right) R^{(1)}_{ab}[h] - g^{(0)}_{ab}\phi_0 h^{cd}R^{(1)}_{cd}[h]\Big\rangle\,.\end{aligned} \tag{11}$$

Now we work on the cosmological situation so that the background metric has the FLRW symmetry. Provided that the limit $c \to 0$ should reproduce results in the case of the Einstein gravity, we finally obtain

$$\kappa^2 T^{\rm eff}_{ab} = -\left\langle \left(1 + 2cR[g^{(0)}]\right) R^{(2)}_{ab}[h] + 2c\left(R^{(3)}[h] - h^{cd}R_{cd}[g^{(0)}]\right) R^{(1)}_{ab}[h] \right\rangle . \tag{12}$$

We see that the expression (12) above is precisely the same as (5) derived within the metric formalism of the $f(R)$ gravity. This verifies our methods of Sec. 2 for dealing with short-wavelength perturbations of the $f(R)$ gravity within the metric formalism.

In the Einstein frame, the action becomes $S_{\rm E} = \int d^4x\sqrt{-\tilde{g}}\{\tilde{R} - (\tilde{\nabla}\tilde{\phi})^2 - \tilde{V}(\tilde{\phi})\}/(2\kappa^2)$, where $\tilde{g}_{ab} \equiv Fg_{ab}$, $\tilde{\phi} \propto \ln\phi$ and $\tilde{V} \equiv V/F^2$. From this action, one can find that the equation of motion of $\mathrm{O}\left(\epsilon^{-1}\right)$ is $\Box\delta\tilde{\phi} = 0$ and the effective stress-energy tensor is $\kappa^2 T^{\rm eff}_{ab} = \left\langle \tilde{\nabla}_a\delta\tilde{\phi}\tilde{\nabla}_b\delta\tilde{\phi} \right\rangle$. It then immediately follows that the effective stress-energy tensor must be traceless, i.e., $T^{{\rm eff}\,a}{}_a = 0$. This can be shown only on the assumption of the FLRW symmetry.

4 Summary

We have addressed the effective gravitational stress-energy tensor for short-wavelength perturbations in the simple class of $f(R)$ gravity of R^2 type in the cosmological context. By imposing that our background has the FLRW symmetry, we have derived our effective stress-energy tensor for short-wavelength metric perturbations in cosmological models. At this point, thanks to the background FLRW symmetry, the spacetime averaging over several wavelengths and our choice of the constant $S_1 = 0$, the expression of our effective stress-energy tensor has been significantly reduced to have the simple form, (5). We have also shown that the obtained effective stress-energy tensor is traceless, so that it acts like a radiation fluid as in the Einstein gravity case and thus, in particular, cannot mimic dark energy.

We would like to stress that in order to obtain the traceless feature of our effective stress-energy tensor, we have set $S_1 = 0$. However, the field equations for the Einstein gravity need not be, a prior, reproduced in the limit to the Einstein gravity: $c \to 0$. In that case S_1 could take a non-vanishing value and give rise to a cosmological-constant looking term in our effective stress-energy (4). It would be interesting to consider the question of whether there exists any sensible way to provide the right sign and magnitude for S_1 so that (4) can mimic dark energy within the framework of our modified gravity theory.

Our formulas derived in Sec. 2 deal directly with the scalar curvature R and the Ricci tensor R_{ab}, and therefore should be able to apply to similar analyses of other modified gravity theories which contain higher order curvature terms composed of R, R_{ab}, and $R^a{}_{bcd}$ and which cannot even be cast in the form of a scalar-tensor theory. It would be interesting to consider an extension of our present work to a wide class of modified gravity theories with high-rank curvatures.

Acknowledgements

We would like to thank Hideo Kodama, Hirotaka Yoshino, Robert M. Wald, and Stephen R. Green for useful discussions and comments. This work was supported in part by a Grant-in-Aid for JSPS Fellows under Grant No. 23-4465 (KS) and by the JSPS Grant-in-Aid for Scientific Research (C) No. 22540299 (AI) and by the Barcelona Supercomputing Center (BSC) under Grant No. AECT-2012-2-0005.

References

[1] R. A. Isaacson, Phys. Rev. **166**, 1263 (1968).

[2] R. A. Isaacson, Phys. Rev. **166**, 1272 (1968).

[3] G. A. Burnett, J. Math. Phys. **30**, 90 (1989).

[4] S. R. Green and R. M. Wald, Phys. Rev. D **83**, 084020 (2011).

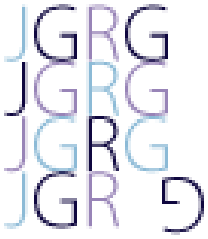

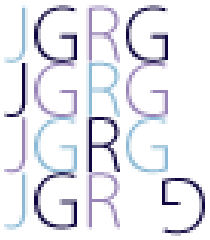

Hisaaki Shinkai, JGRG 22(2012)111336

"Wormhole dynamics in Gauss-Bonnet gravity"

RESCEU SYMPOSIUM ON

GENERAL RELATIVITY AND GRAVITATION

JGRG 22

November 12-16 2012

Koshiba Hall, The University of Tokyo, Hongo, Tokyo, Japan





Wormhole evolutions in higher-dimensional gravity

Hisa-aki Shinkai [1(a)] Takashi Torii [2(b)]

(a) *Dept. Information Science and Technology, Osaka Institute of Technology, Hirakata, Osaka 573-0196, Japan*
(b) *Dept. Engineering, Osaka Institute of Technology, Osaka, Osaka 535-8585, Japan*

Abstract

We know numerically the four-dimensional Ellis wormhole solution (the so-called Morris-Thorne's traversable wormhole) is unstable against an input of scalar-pulse from one side. We investigate this feature for higher-dimensional versions, both in n-dimensional general relativity and in 5-dimensional Gauss-Bonnet gravity. We derived Ellis wormhole solutions in n-dimensional general relativity, and evolved it numerically in dual-null coordinate with/without Gauss-Bonnet corrections. Preliminary results show that those are also unstable. We also find that the throat of wormhole in Gauss-Bonnet gravity tends to expand (or shrink) after an input of ghost-scalar pulse if the coupling constant α is positive (negative).

1 Introduction

Wormholes are popular tools in science ctions as a way for rapid interstellar travel, time machines and warp drives. However, wormholes are also a scienti c topic after the influential study of traversable wormholes by Morris & Thorne [1]. They considered "traversable conditions" for human travel through wormholes responding to Carl Sagan's idea for his novel (*Contact*), and concluded that such a wormhole solution is available if we allow "exotic matter" (negative-energy matter).

The introduction of exotic matter sounds to be unusual for the rst time, but such matter appears in quantum eld theory and in alternative gravitational theories such as scalar-tensor theories. The Morris-Thorne solution is constructed with a massless Klein-Gordon eld whose gravitational coupling takes the opposite sign to normal, which appears in Ellis's earlier work [2], who called it a drainhole.

Ellis (Morris-Thorne) wormhole solution was studied in many contexts. Among them, we focus its dynamical features. The rst numerical simulation on its stability behavior was reported by one of the authors [3]. They use a dual-null formulation for spherically symmetric space-time integration, and observed that the wormhole is unstable against Gaussian pulses in either exotic or normal massless Klein-Gordon elds. The wormhole throat suffers a bifurcation of horizons and either explodes to form an inflationary universe or collapses to a black hole, if the total input energy is negative or positive, respectively. These basic behaviors were repeatedly con rmed by other groups [4, 5]. [3]

The changes of wormhole either to a black hole or an expanding throat supports an uni ed understanding of black holes and traversable wormholes proposed by Hayward [8]. His proposal is that the two are dynamically interconvertible, and that traversable wormholes are understandable as black holes under negative energy density.

In this article, we introduce our extensional works of [3]; (a) constructing Ellis solutions in higher-dimensional general relativity, (b) dynamical effects of Gauss-Bonnet coupling constant in 5-dimensional wormhole solution.

[1]Email address: shinkai@is.oit.ac.jp
[2]Email address: torii@ge.oit.ac.jp
[3]Note that Armendariz-Picon[6] reports that the Ellis wormhole is stable using perturbation analysis. However, the conclusion is obtained with fixing the throat of wormhole and not the same situation with above numerical works[7].

2 Wormhole solutions in higher-dimensional general relativity

2.1 Field equations

We consider the following n-dimensional Einstein-Klein-Gordon system

$$S = \int d^n x\sqrt{\ g}\ \frac{1}{2\kappa_n^2}R \quad \frac{1}{2}\ (\partial\phi)^2 \quad V(\phi)\ , \tag{1}$$

where κ_n^2 is a n-dimensional gravitational constant, $= 1$ (or 1) for the normal (ghost) eld.

We consider the static and spherically symmetric space-time with the metric

$$ds_D^2 = f(r)dt^2 + f(r)\ ^1dr^2 + R(r)^2 h_{ij}dx^i dx^j \tag{2}$$

where $h_{ij}dx^i dx^j$ represents the line element of a $(n \quad 2)$-dimensional constant curvature space $S^{(n\ \ 2)}$ with curvature $k = \pm 1,\ 0$.

The Einstein tensor becomes

$$G_{tt} = \frac{n\quad 2}{2}f^2\ \frac{2R''}{R} + \frac{f'R'}{fR} + (n\quad 3)\frac{R'^2}{R^2}\ + \frac{f}{2R^2}{}^{(n\ \ 2)}\mathcal{R}, \tag{3}$$

$$G_{rr} = \frac{n\quad 2}{2}\frac{R'}{R}\ \frac{f'}{f} + (n\quad 3)\frac{R'}{R}\quad \frac{1}{2fR^2}{}^{(n\ \ 2)}\mathcal{R}, \tag{4}$$

$$G_{ij} = \left[\frac{f''}{2} + (n\quad 3)f\ \frac{R''}{R} + \frac{f'R'}{fR} + \frac{n\quad 4}{2}\frac{R'^2}{R^2}\ \right]g_{ij} + {}^{(n\ \ 2)}\mathcal{R}_{ij}\quad \frac{1}{2R^2}{}^{(n\ \ 2)}\mathcal{R}g_{ij}, \tag{5}$$

where ${}^{(n\ \ 2)}\mathcal{R}$ is the scalar curvature of $S^{(n\ \ 2)}$ and is obtained as

$${}^{(n\ \ 2)}\mathcal{R}_{ijkl} = k(h_{ik}h_{jl}\quad h_{il}h_{jk}), \tag{6}$$

$${}^{(n\ \ 2)}\mathcal{R}_{ij} = (n\quad 3)kh_{ij}, \tag{7}$$

$${}^{(n\ \ 2)}\mathcal{R} = (n\quad 2)(n\quad 3)k. \tag{8}$$

The non-zero components of the energy-momentum tensors

$$T\quad = \phi,\ \phi,\quad g\quad \Big[\frac{1}{2}\ (\nabla\phi)^2 + V(\phi)\Big], \tag{9}$$

are

$$T_{tt} = f\Big[\frac{1}{2}\ f\phi'^2 + V(\phi)\Big], \tag{10}$$

$$T_{rr} = f\ ^1\Big[\frac{1}{2}\ f\phi'^2\quad V(\phi)\Big], \tag{11}$$

$$T_{ij} = \Big[\frac{1}{2}\ f\phi'^2 + V(\phi)\Big]R^2 h_{ij}. \tag{12}$$

The Einstein equation, $G\quad = \kappa_n^2 T\quad$, becomes

$$(t,t): \qquad \frac{n\quad 2}{2}f^2\ \frac{2R''}{R} + \frac{f'R'}{fR} + (n\quad 3)\frac{R'^2}{R^2}\ + \frac{(n\quad 2)(n\quad 3)kf}{2R^2} = \kappa_n^2 f\Big[\frac{1}{2}\ f\phi'^2 + V(\phi)\Big], \tag{13}$$

$$(r,r): \qquad \frac{n\quad 2}{2}\frac{R'}{R}\ \frac{f'}{f} + (n\quad 3)\frac{R'}{R}\quad \frac{(n\quad 2)(n\quad 3)k}{2fR^2} = \frac{\kappa_n^2}{f}\Big[\frac{1}{2}\ f\phi'^2\quad V(\phi)\Big], \tag{14}$$

$$(i,j): \qquad \left[\frac{f''}{2} + (n\quad 3)f\ \frac{R''}{R} + \frac{f'R'}{fR} + \frac{n\quad 4}{2}\frac{R'^2}{R^2}\ \right]\quad \frac{(n\quad 3)(n\quad 4)k}{2R^2} = \kappa_n^2\Big[\frac{1}{2}\ f\phi'^2 + V(\phi)\Big] \tag{15}$$

The Klein-Gordon equation

$$\Box\phi = \frac{dV}{d\phi} \tag{16}$$

becomes

$$\frac{1}{R^{n-2}} R^{n-2} f\phi' \,' = \frac{dV}{d\phi}. \tag{17}$$

Hereafter, we assume that the scalar field is ghost, = 1.

2.2 Wormhole solution with massless scalar field in spacetime $k = 1$

We show the simplest solution, under the assumptions of the massless scalar field, $V(\phi) = 0$, in the closed universe, $k = 1$. Other cases are presented elsewhere [7]. The Klein-Gordon equation (17) is integrated as

$$\phi' = \frac{C}{fR^{n-2}}, \tag{18}$$

where C is an integration constant. The Einstein equations, then, are reduced to

$$\frac{(n-2)R'}{R}\left[\frac{(n-3)R'}{R} + \frac{f'}{f}\right] - \frac{(n-2)(n-3)}{fR^2} = \frac{\kappa_n^2 C^2}{f^2 R^{2(n-2)}} \tag{19}$$

$$\frac{(n-2)R''}{R} = \frac{\kappa_n^2 C^2}{f^2 R^{2(n-2)}} \tag{20}$$

We impose that the wormhole has a throat radius, a, at the coordinate $r = 0$. Then the regularity conditions are

$$R = a, \quad R' = 0, \quad f = f_0 \quad f' = 0, \tag{21}$$

where f_0 is a constant. We can assume $a = 1$ and $f_0 = 1$ without loss of generality, but we keep a in the equations for a while. Eq. (19) gives

$$\kappa_n^2 C^2 = (n-2)(n-3)a^{2(n-3)} \tag{22}$$

The solution of Eqs. (18)-(20) is

$$f = 1, \tag{23}$$

$$R' = \sqrt{1 - \left(\frac{a}{R}\right)^{2(n-3)}}, \tag{24}$$

$$\phi = \frac{\sqrt{(n-2)(n-3)}}{\kappa_n} a^{n-3} \int \frac{1}{R^{n-2}} dr. \tag{25}$$

The Eq. (24) is integrated to give

$$r(R) = mB_{R^m}\left(m, \frac{1}{2}\right) \frac{\sqrt{\Gamma[1-m]}}{\Gamma[m(n-4)]}, \tag{26}$$

where $m = \frac{1}{2(n-3)}$, and $B_z(p,q)$ is an incomplete beta function defined by

$$B_z(p,q) := \int_0^z t^{p-1}(1-t)^{q-1} dt \tag{27}$$

which can be expressed with the hypergeometric function $F(\ ,\beta,\gamma;z)$ as

$$B_z(p,q) = \frac{z^p}{p} F(p, 1-q, p+1; z). \tag{28}$$

Although Eq. (26) is implicit with respect to R, it is rewritten in the explicit form by using the inverse incomplete beta function.

For $n = 4$, this solution reduces to Ellis's wormhole solution. For $n \to \infty$, the function becomes $R = r + a$ and ϕ behaves like a step-function approaching $\phi \to /2$.

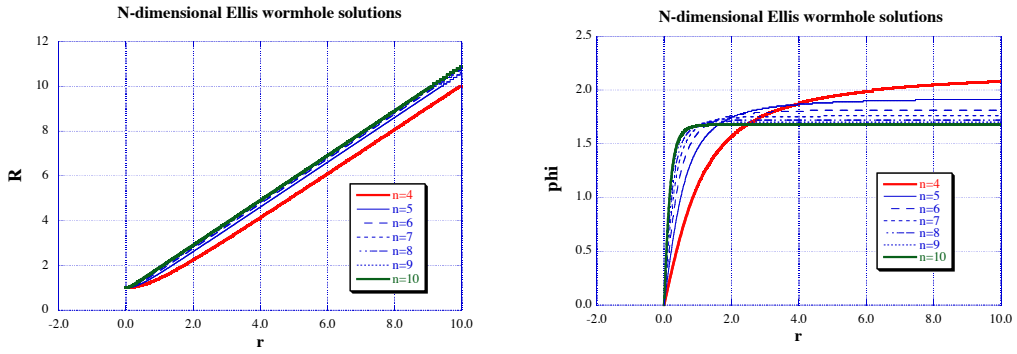

Figure 1: The n-dimensional wormhole solution. The circumference radius R (left panel) and the scalar eld ϕ (right panel) are plotted as a function of radial coordinate r. The cases of $n = 4$–10 are shown.

3 Effects of Gauss-Bonnet coupling constant in 5-dimensional wormhole evolution

3.1 Gauss-Bonnet gravity

Gauss-Bonnet gravity is derived from the superstring theory, with additional higher-order curvature correction terms to general relativity. Such higher-order corrections can be treated as an expansion of $\mathcal{R}$ in the action, but the Gauss-Bonnet term,

$$\mathcal{L}_{\rm GB} = \mathcal{R}^2 \quad 4\mathcal{R} \quad \mathcal{R} \quad + \mathcal{R} \quad {}_{\sigma}\mathcal{R} \quad {}^{\sigma}, \tag{29}$$

has nice properties such that it is ghost-free combinations[9] and does not give higher derivative equations but an ordinary set of equations with up to the second derivative in spite of the higher curvature combinations.

The Einstein-Gauss-Bonnet action in $(N+1)$-dimensional spacetime $(\mathcal{M}, g \quad)$ is described as

$$S = \int_{\mathcal{M}} d^{N+1}X\sqrt{\quad g} \ \frac{1}{2\kappa^2}\{ \ {}_{\rm GR}(\mathcal{R} \quad 2\Lambda) + \quad {}_{\rm GB}\mathcal{L}_{\rm GB}\} + \mathcal{L}_{\rm matter} \ , \tag{30}$$

where κ^2 is the $(N+1)$-dimensional gravitational constant, $\mathcal{R}$, $\mathcal{R} \quad$, $\mathcal{R} \quad {}_{\sigma}$ and $\mathcal{L}_{\rm matter}$ are the $(N+1)$-dimensional scalar curvature, Ricci tensor, Riemann curvature and the matter Lagrangian, respectively. This action reproduces the standard $(N+1)$-dimensional Einstein gravity, if we set the coupling constant ${}_{\rm GB}$ (≥ 0) equals to zero.

The action (30) gives the gravitational equation as

$${}_{\rm GR}\mathcal{G} \quad + \quad {}_{\rm GB}\mathcal{H} \quad = \kappa^2 \mathcal{T} \quad , \tag{31}$$

where

$$\mathcal{G} \quad = \quad \mathcal{R} \quad \frac{1}{2}g \quad \mathcal{R} + g \quad \Lambda, \tag{32}$$

$$\mathcal{H} \quad = \quad 2\Big[\mathcal{R}\mathcal{R} \quad 2\mathcal{R} \quad \mathcal{R} \quad 2\mathcal{R} \quad \mathcal{R} \quad + \mathcal{R} \quad {}^{\gamma}\mathcal{R} \quad {}_{\gamma}\Big] \quad \frac{1}{2}g \quad \mathcal{L}_{\rm GB}, \tag{33}$$

$$\mathcal{T} \quad = \quad 2\frac{\mathcal{L}_{\rm matter}}{g} + g \quad \mathcal{L}_{\rm matter}. \tag{34}$$

The higher-order curvature terms are considered as correction terms from string theory. These terms are known to produce two solution branches normally, only one of which has general-relativity limit. The theory is expected to have singularity-avoidance features in the context of gravitational collapses and/or

cosmology, but as far as we know there is no studies so far using fully numerical evolutions. (Numerical studies on critical phenomena are recently reported for small $_{\rm GB}$ [10, 11, 12]).

Studies on wormholes in Gauss-Bonnet gravity have long histories. Several solutions and their classifications are reported in [13, 14], while their energy conditions are considered in [15]. Similar researches are extended to the Lovelock gravity[16], and also to the Dilatonic Gauss-Bonnet system [17]. Our aim is to investigate their dynamical features.

3.2 Dual-null evolution system

In this article, we report our two initial numerical results. One is the evolution of 5D wormhole in general relativity. The other is its evolution in Gauss-Bonnet gravity.

We implemented our 4D dual-null evolution code [3] to 5D evolution code with Gauss-Bonnet terms. The system we consider is spherical symmetry, and expressed using dual-null coordinate

$$ds^2 = 2e^{f(x^+,x^-)}dx^+\,dx + r^2(x^+,x)d\Omega_3^2. \tag{35}$$

Wormhole is constructed with ghost scalar eld $\phi(x^+,x)$, but we also include normal scalar eld (x^+,x) contribution. The energy-momentum tensor is written as

$$\begin{aligned} T &= T^{\psi} + T^{\phi} \qquad (36)\\ &= , , g \frac{1}{2}(\nabla)^2 + V_1( ) + \phi, \phi, g \frac{1}{2}(\nabla\phi)^2 + V_2(\phi) , \end{aligned}$$

where = 1. This derives Klein-Gordon equations

$$\Box = \frac{dV_1}{d}, \qquad \Box\phi = \frac{dV_2}{d\phi}. \tag{37}$$

Following [3], we introduce the conformal factor Ω, expansion $\vartheta_\pm$, in-affinity $\nu_\pm$, and scalar momentum $_\pm, p_\pm$ as

$$\Omega = \frac{1}{r}, \tag{38}$$
$$\vartheta_\pm \quad 3\partial_\pm r, \tag{39}$$
$$\nu_\pm \quad \partial_\pm f, \tag{40}$$
$$_\pm \quad r\partial_\pm = \frac{1}{\Omega}\partial_\pm , \tag{41}$$
$$p_\pm \quad r\partial_\pm\phi = \frac{1}{\Omega}\partial_\pm\phi. \tag{42}$$

We also de ne

$$= \Omega^2 e^{f} + \frac{2}{9}\vartheta_+\vartheta , \tag{43}$$
$$\tilde{A} = {}_{\rm GR} + 4 {}_{\rm GB} e^f, \tag{44}$$
$$B = \kappa^2 T_+ + e^{f}\Lambda. \tag{45}$$

The set of evolution equations (x^+ and x -directions), then, are

$$\partial_\pm\Omega = \frac{1}{3}\vartheta_\pm\Omega^2 \tag{46}$$
$$\partial_\pm\vartheta_\pm = \nu_\pm\vartheta_\pm \frac{1}{\tilde{A}\Omega}\kappa^2 T_{\pm\pm} \tag{47}$$
$$\partial_\pm\vartheta_\mp = \frac{1}{\tilde{A}\Omega}(3 {}_{\rm GR} + B) \tag{48}$$
$$\partial_\pm f = \nu_\pm \tag{49}$$
$$\partial_\pm\nu_\mp = \frac{{}_{\rm GR}}{\tilde{A}}\left\{ \frac{4(3 {}_{\rm GR} B)}{3\tilde{A}} \right\} + \frac{(\kappa^2 T_{zz}\Omega^2 \Lambda)}{\tilde{A}e^f} + \frac{8 {}_{\rm GB}}{9\tilde{A}^3}\left\{ e^f(3 {}_{\rm GR} B)^2 \kappa^4 T_{++}T \right\} \tag{50}$$

together with Klein-Gordon equations

$$\partial_{\pm} = \Omega\ _{\pm}, \tag{51}$$
$$\partial_{\pm}\phi = \Omega p_{\pm}, \tag{52}$$
$$\partial_{+} = \frac{1}{6}\Omega\vartheta_{+} \quad \frac{1}{2}\Omega\vartheta \quad + \quad \frac{1}{2e^{f}\Omega}\frac{dV_1}{d}, \tag{53}$$
$$\partial_{+}p = \frac{1}{6}\Omega\vartheta_{+}p \quad \frac{1}{2}\Omega\vartheta \quad p_{+} \quad \frac{1}{2e^{f}\Omega}\frac{dV_2}{d\phi}, \tag{54}$$
$$\partial \quad _{+} = \frac{1}{2}\Omega\vartheta_{+} \quad \frac{1}{6}\Omega\vartheta \quad + \quad \frac{1}{2e^{f}\Omega}\frac{dV_1}{d}, \tag{55}$$
$$\partial \quad p_{+} = \frac{1}{2}\Omega\vartheta_{+}p \quad \frac{1}{6}\Omega\vartheta \quad p_{+} \quad \frac{1}{2e^{f}\Omega}\frac{dV_2}{d\phi}, \tag{56}$$

where the energy momentum tensor is written as

$$T_{++} = \Omega^2(\ ^2_{+} \quad p_{+}^2), \tag{57}$$
$$T \quad = \Omega^2(\ ^2 \quad p^2\ ), \tag{58}$$
$$T_{+} = e\ ^{f}\,(V_1(\ \ ) + V_2(\phi))\,, \tag{59}$$
$$T_{zz} = e^{f}(\ _{+} \quad p_{+}p\ ) \quad \frac{1}{\Omega^2}\,(V_1(\ \ ) + V_2(\phi))\,. \tag{60}$$

3.3 Preliminal results

We prepare the solution obtained in §2.2 as our initial data on $(x^+, x\ ) = (x^+, 0)$ hypersurface, and integrate along to x -direction using the set of equations above. Numerical integration techniques are the same with [3].

The preliminal results show that the wormhole throat is unstable, the expansion $\vartheta_{\pm}$ go splitting soon after the evolution begins. Fig. 2 shows their locations in $(x^+, x\ )$ plane. If the location of ϑ_{+} is outer (in x^+-direction) than that of $\vartheta\ $, then the region $\vartheta\ < x < \vartheta_{+}$ is judged as a black-hole. Otherwise the region $\vartheta_{+} < x < \vartheta\ $ can be judged as an expanding throat. Fig. 2 indicates the throat begins expanding, then turns to be a black hole. We also evolve the same initial data with Gauss-Bonnet terms $_{\rm GB} \neq 0$ and study their effects to the evolutions. We see if $_{\rm GB} > 0$ the throat expansion becomes slower. On the contrary, if $_{\rm GB} < 0$, then the throat expansion is accelerated in the initial stage.

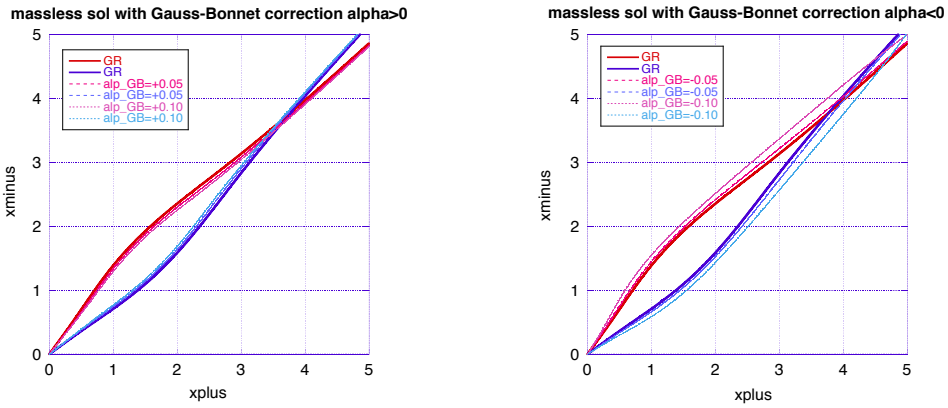

Figure 2: Location of the expansion ϑ_{+} (red lines) and $\vartheta\ $ (blue lines) for evolutions of a solution in §2.2 as a function of $(x_{+}, x\ )$. The throat begins expanding, then turns to be a black hole. When $_{\rm GB} > 0$ (left panel), expansions are slightly slowing down and $_{\rm GB} > 0$ affects to black hole formation earlier, while when $_{\rm GB} < 0$ (right panel) we see Gauss-Bonnet term accelerates expansion.

This work was supported partially by the Grant-in-Aid for Scienti c Research Fund of Japan Society of the Promotion of Science, No. 22540293 (HS). Numerical computations were carried out on SR16000 at YITP in Kyoto University, and on the RIKEN Integrated Cluster of Clusters (RICC).

References

[1] M. S. Morris & K. S. Thorne, Am. J. Phys. 56, 395 (1988).

[2] H. G. Ellis, J. Math. Phys. **14**, 395 (1973).

[3] H. Shinkai & S.A. Hayward, Phys. Rev. D 66, 044005 (2002).

[4] A. Doroshkevich, J. Hansen, I. Novikov, A. Shatskiy, IJMPD 18 (2009) 1665

[5] J. A. Gonzalez, F. S. Guzman & O. Sarbach, Class. Quantum Phys. 26 (2009) 015010, 015011; PRD80 (2009) 024023. O. Sarbach & T. Zannias, Phys. Rev. D 81, 047502 (2010).

[6] C. Armendariz-Picon, Phys. Rev. D 65, 104010 (2002) .

[7] T. Torii & H. Shinkai, in preparation.

[8] S A Hayward, Int. J. Mod. Phys. D8, 373 (1999).

[9] B. Zwiebach, Phys. Lett. B 156, 315 (1985).

[10] S. Golod & T. Piran, Phys. Rev. D 85, 104015 (2012).

[11] F. Izaurieta & E. Rodriguez, arXiv:1207.1496

[12] N. Deppe, C. D. Leonard, T. Taves, G. Kunstatter, R. B. Mann, arXiv:1208.5250

[13] B. Bhawal & S. Kar, Phys. Rev. D 46, 2464 (1992).

[14] G. Dotti, J. Oliva & R. Troncoso, Phys. Rev. D 76, 064038 (2007).

[15] H. Maeda & M. Nozawa, Phys. Rev. D 78, 024005 (2008).

[16] M H Dehghani & Z Dayyani, PRD 79, 064010 (2009).

[17] P Kanti, B Kleihaus & J Kunz, Phys. Rev. Lett. 107, 271101 (2011); Phys. Rev. D 85, 044007 (2012).

Yuta Yamada, JGRG 22(2012)111337

"Numerical study of 5-dimensional gravitational collapses"

RESCEU SYMPOSIUM ON

GENERAL RELATIVITY AND GRAVITATION

JGRG 22

November 12-16 2012

Koshiba Hall, The University of Tokyo, Hongo, Tokyo, Japan

Numerical Study of Five-dimensional Gravitational Collapses

[(a)]Yuta Yamada[1] and [(a),(b)]Hisa-aki Shinkai[2]

[(a)] *Faculty of Information Science and Technology, Osaka Institute of Technology, Hirakata, Osaka 573-0196, Japan*
[(b)] *Computational Astrophysics Laboratory, Institute of Physical & Chemical Research (RIKEN), Hirosawa, Wako, Saitama 351-0198, Japan*

Abstract

Five-dimensional black-hole and black-ring formation are investigated numerically. We model the initial matter distribution in homogeneous spheroidal and toroidal configurations under the momentarily static assumption and express the matter with collisionless particles. Evolutions of space-time and particles are followed by using ADM formalism ($4+1$ decomposition) and solving the geodesic equation. For spheroidal configurations, we repeat the simulation performed by Shapiro and Teukolsky (1991) that announced an appearance of a naked singularity, and also find similar results in the 5D version. For toroidal configurations in U(1)× U(1) symmetry, we consider the rotating collisionless particles which consist of equal numbers co-rotating and counter-rotating under a certain rotational law. We search both spherical(S^3) and ring-shaped($S^2 \times S^1$) horizons, and show topology change of apparent horizon from ring-shaped to spherical shape during its evolution. We also discuss whether an observer at the origin of the ring-horizon can escape out or not.

1 Introduction

For a decade, higher-dimensional black-holes are extensively studied linked with the so-called "large extra-dimensional models". The discovery of black-ring solution[1] with horizon of $S^2 \times S^1$ topology in U(1)× U(1) space, and its associated Saturn-type "black objects" reveal new features of higher-dimensional space-time. However, non-linear dynamical features, such as formation process, generality, and stability of black-objects, are not yet known. We plan to investigate these outstanding problems using numerical simulations. In this article, we report two models.

First topic is on the naked singularity formation. Shapiro and Teukolsky[2] (ST91) numerically showed that in four-dimensional(4D) space-time, collisionless matter particles in spheroidal distribution will collapse to singularity, without forming apparent horizon(AH) when the spheroids are highly prolate. We report their simulations and compare them with those in 5D(§3)[3].

Second topic is the formation of black-ring in 5D(§4). We distributed collisionless matter particles in toroidal configuration, and evolve them with/without their rotations. As the first step, we assume particles are counter-rotating and the system's net angular momentum is zero. We search both AH of spherical and ring-shaped during time evolution.

2 ur numerical code

For the simulation of spheroidal collapses, we evolve five-dimensional axisymmetric [symmetric on z-axis, SO(3)] or doubly-axisymmetric [symmetric both on x and z-axes, U(1)×U(1)], asymptotically flat space-time (see Figure 1). For the comparison, we also performed four-dimensional axisymmetric space-time evolutions.

We start our simulation from time symmetric and conformally flat initial data, which are obtained by solving the Hamiltonian constraint equations [4]. The asymptotical flatness is imposed throughout

[1]Email address: yamada@is.oit.ac.jp
[2]Email address: shinkai@is.oit.ac.jp

the evolution, which settles the fall-off condition to the metric as $\sim 1/r$ for 4D cases and $\sim 1/r^2$ for 5D cases.

The matter is described with 5000 collisionless particles, which move along the geodesic equations. We smooth out the matter by expressing each particle with Gaussian density distribution function with its typical width is twice as much as the numerical grid. The particles are homogeneously distributed in a spheroidal shape, parametrized with a and b (Figure 1), or eccentricity $e = \sqrt{1 - a^2/b^2}$.

By imposing axisymmetry or double-axisymmetry, our model becomes practically a (2+1)-dimensional problem. We construct our numerical grids with the Cartesian coordinate (x, z), and apply the so-called Cartoon method [5] to recover the symmetry of space-time.

The space-time is evolved using the Arnowitt-Deser-Misner (ADM) evolution equations. It is known that the ADM evolution equations excite an unstable mode (constraint-violation mode) in long-term simulations [6, 7]. However, we are free from this problem since gravitational collapse occurs within quite short time. By monitoring the violation of constraint equations during evolutions, we confirm that our numerical code has second-order convergence, and also that the simulation continues in stable manner. The results shown in this report are obtained with numerical grids, 129×129×2×2. We confirmed that higher resolution runs do not change the physical results.

We use the maximal slicing condition for the lapse function α, and the minimal strain condition for the shift vectors β^i. Both conditions are proposed for avoiding the singularity in numerical evolutions [8], and the behavior of α and β^i roughly indicates the strength of gravity, conversely. The iterative Crank-Nicholson method is used for integrating ADM evolution equations, and the Runge-Kutta method is used for matter evolution equations.

For discussing physics, we search the location of apparent horizon (AH), calculate the Kretschmann invariant ($\mathcal{I} = R_{abcd}R^{abcd}$) on the spacial hypersurface.

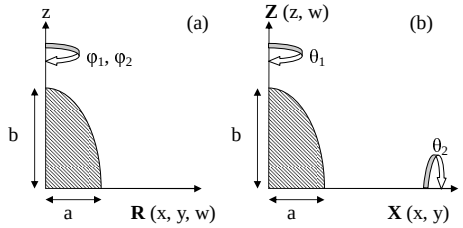

Figure 1: We evolve five-dimensional (a) axisymmetric [SO(3)] or (b) double-axisymmetric [U(1)× U(1)], asymptotically flat space-time using the Cartesian grid. The initial matter configuration is expressed with parameters a and b.

For the simulation of toroidal collapses, we evolve doubly-axisymmetric [symmetric both on x and z-axes, U(1)×U(1)], asymptotically flat space-time (see Figure 2). We use the maximal slicing condition for the lapse function α, and the zero shift condition for the shift vectors β^i.

In this paper, we consider the toroidal configuration which consist of equal number corotating and counter-rotating particles under the Kepler like law $V(r) \propto \xi/r$ where ξ is the arbitrary rotational parameter. Although each particles move on the x-z section, there are no net angular momentum. Hence we only solve the Hamiltonian constraint equation for preparing the initial data.

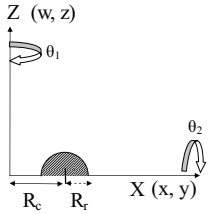

Figure 2: We evolve double-axisymmetric [U(1)× U(1)], asymptotically flat space-time using the Cartesian grid. The initial matter configuration is expressed with parameters R_c and R_r.

3 Results of spheroidal collapses

We prepare several initial data keeping the total ADM mass and the eccentricity of distribution, $e = 0.9$. By changing the initial matter distribution sizes, we observe the different final structures. Figure 3 shows snapshots of 5D axisymmetric evolutions of model $b/M = 4$ and 10 (model 5DSβ and 5DSδ, respectively; see Table 1); the former collapses to a black hole while the latter collapses without AH formation.

b/M $(t = 0)$	2.50	4.00	6.25	10.00
4D axisym.	4Dα	4Dβ	4Dγ	4Dδ
	AH-formed	no	no	no
	$e_{\rm AH} = 0.90$			
	$e_{\rm f} = 0.92$	$e_{\rm f} = 0.89$	$e_{\rm f} = 0.92$	$e_{\rm f} = 0.96$
5D axisym. SO(3)	5DSα	5DSβ	5DSγ	5DSδ
	AH-formed	AH-formed	no	no
	$e_{\rm AH} = 0.88$	$e_{\rm AH} = 0.88$		
	$e_{\rm f} = 0.82$	$e_{\rm f} = 0.84$	$e_{\rm f} = 0.88$	$e_{\rm f} = 0.96$
5D double axisym. U(1)×U(1)	5DUα	5DUβ	5DUγ	5DUδ
	AH-formed	AH-formed	AH-formed	no
	$e_{\rm AH} = 0.86$	$e_{\rm AH} = 0.87$	$e_{\rm AH} = 0.92$	
	$e_{\rm f} = 0.79$	$e_{\rm f} = 0.81$	$e_{\rm f} = 0.90$	$e_{\rm f} = 0.98$

Table 1: (above) Model-names and the results of their evolutions whether we observed AH or not. The eccentricity e the collapsed matter configurations is also shown; $e_{\rm AH}$ and $e_{\rm f}$ are at the time of AH formed (if formed), and on the numerically obtained final hypersurface, respectively.

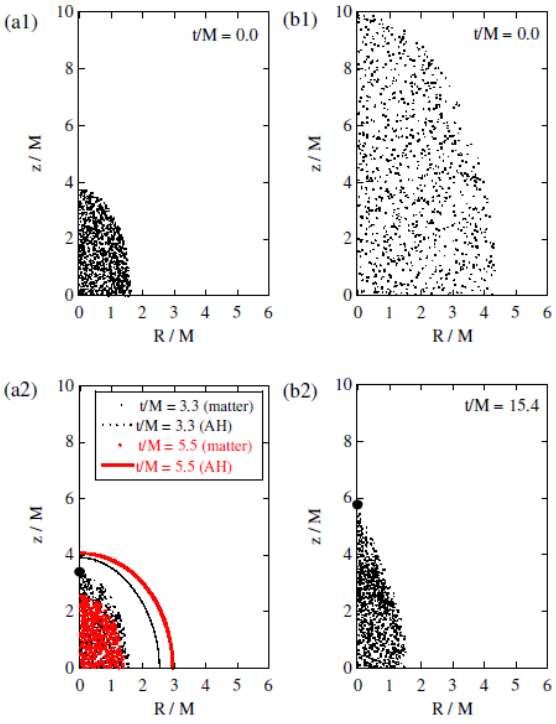

Figure 3: (right) Snapshots of 5D axisymmetric evolution with the initial matter distribution of $b/M = 4$ [Fig.(a1) and (a2); model 5DSβ in Table 1] and 10 [Fig.(b1) and (b2); model 5DSδ]. The big circle indicates the location of the maximum Kretschmann invariant $\mathcal{I}_{\rm max}$ at the final time at each evolution.

All the models we tried result in forming a singularity (i.e., diverging $\mathcal{I}$). We stop our numerical evolutions when the shift vector is not obtained with sufficient accuracy due to the large curvature. For model 5DSδ, we integrated up to the coordinate time $t/M = 15.4$ and the maximum of the Kretschmann invariant $\mathcal{I}_{\rm max}$ becomes $O(1000)$ on z-axis (see Figure 3), but AH is not formed.

When the initial matter is highly prolated, AH is not observed. This is consistent with 4D cases [2], and matches with the predictions from initial data analysis in 5D cases [4, 9]. The location of $\mathcal{I}_{\rm max}$ is on z-axis, and just outside of the matter. This is again the same with 4D cases [2]. The absence of AH with diverging $\mathcal{I}$ suggests a formation of naked singularity in 5D.

In order to compare the results with 4D and 5D, we reproduce the results of ST91. We then find that the $e = 0.9$ initial data with $b/M = 10$ (model 4Dδ) collapses without forming AH, and the code stops at the coordinate time $t = 20.91$ with $\mathcal{I}_{\rm max} = 84.3$ on the z-axis ($z/M = 6.1$); all the numbers match quite well with ST91. (Note that our slicing conditions and coordinate structure is not the same with ST91.)

We also performed 5D collapses with doubly-axisymmetric [U(1)×U(1)] space-time. The matter and space-time evolve quite similar to 5D and 4D axisymmetric cases, but we find that the critical configurations for forming AH is different. Table 1 summarizes the main results of 4D and two 5D cases. We find that AH in 5D is formed in larger b initial data than 4D cases. This result is consistent with our prediction from the sequence of initial data [4]. AH criteria with initial b is loosened for 5D doubly-axisymmetric cases. We show the eccentricity, $e_{\rm AH}$ and $e_{\rm f}$, which tell us that the doubly-axisymmetric assumption makes collapse less sharp when it forms AH, and makes collapse similar to 4D cases when it does not form AH. Table 1 indicates that the eccentricity itself is not a guiding measure for AH formation.

In Figure 4, we plotted $\mathcal{I}$ at the point which gives $\mathcal{I}_{\rm max}$ on the final hypersurface as a function of proper time. We see that 5D-collapse is proceeding rapidly than 4D collapses. We also see that collapses in doubly-axisymmetric space-time is proceeding slowly than single axisymmetric cases.

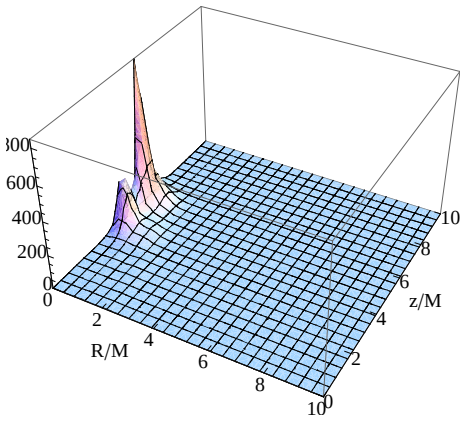

Figure 4: Kretschmann invariant $\mathcal{I}$ for model 5DSδ at $t/M = 15.4$. The maximum is $O(1000)$, and its location is on z-axis, just outside of the matter.

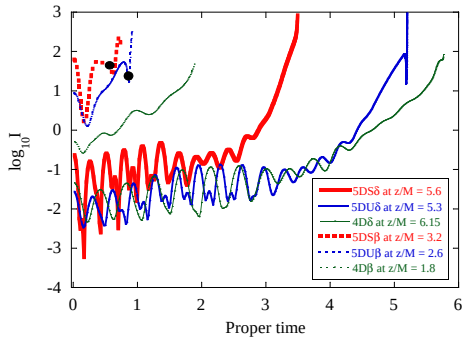

Figure 5: Kretschmann invariant $\mathcal{I}$ at the location of $\mathcal{I}_{\max}$ on the final hypersurface is plotted as a function of proper time at its location. labels indicate model-names in table 1. the time of ah formation (t=0.6 for model 5DSβ, t=0.9 for 5DUβ) is shown by a dot.

4 Results of toroidal matter collapses

Figure 6 shows that snapshots of evolutions of the non-rotating toroidal matter of which initial radius are (a) $R_c/r_s = 0.6$ and (b) 0.8, respectively. We observe a formation of spheroidal AH (common horizon) in upper panels, while we see a formation of toroidal AH (ring horizon) in a moment then it switches to common horizon in lower panels. Figure 7 shows the area of AHs as a function of coordinate time. Red and blue lines show the AH area during time evolutions of non-rotating and counter-rotating particles, respectively. We find that the area of horizon increases gradually during time evolution. We also find that for rotating-cases the appearance of AH delays and the area of horizon is smaller comparing to the non-rotating cases. These behavior are thought to be due to the delay of collapse by rotation effect. Furthermore, we show a numerical solution that the area of ring AH stays constant during time evolution (panel (b) in Fig.7). For the case of initial ring radius $R_c/r_s = 0.8$, AH is not formed during time evolution when parameter ξ is $\xi \geq 0.5$(the ratio of rotating energy to the total energy, $T/W = 0.19$). While for the case of initial ring radius $R_c/r_s = 1.5$, AH is not formed during time evolution when parameter ξ is greater than $0.2(T/W = 0.07)$.

For the case of $R_c(t = 0) = 0.8r_s$ and $\xi = 0$ (panel (a) in Fig.7), we check whether the observer at the origin who observed the appearance of the ring AH can escape outside or not. Fig.8 shows the snapshots of the hypersurfaces on x and z axis with the proper-time. In Fig.8, solid lines colored by red, blue and orange express a ring AH and common AH and light ray, respectively. For this case, the light ray which emitted from the inner ring AH reaches to the origin at proper-time $t = 0.75$ (left panel in Fig.8). Even if the observer tries to escape with the speed of light along to the Z-axis just after that time, he/she can not move outside of the common AH. We obtained the same result for the case of $R_c(t = 0) = 0.8r_s$ and $\xi = 0.3(T/W = 0.01)$. Our results indicate that when AH topology changes from ring-shaped to spherical, the observer cannot escape from these region. On the other hand, for the case of $R_c(t = 0) = 1.5r_s$ and $\xi = 0.1(T/W = 0.05)$ (panel (b) in Fig.7), as shown in Fig.9, the observer can escape from these region because of common AH is not formed.

5 Summary

In this article, we reported gravitational collapses of non-rotating spheroidal configurations, and non-rotating/counter-rotating toroidal configurations in 5D space-time. For time evolution of spheroidal configurations, we found the possibility of naked singularity formation. For time evolution of toroidal configurations, we see the formation of AH, and always we also found that topological transition of AH during the ring matter collapses where we observed monotonically increases of the area of AHs both

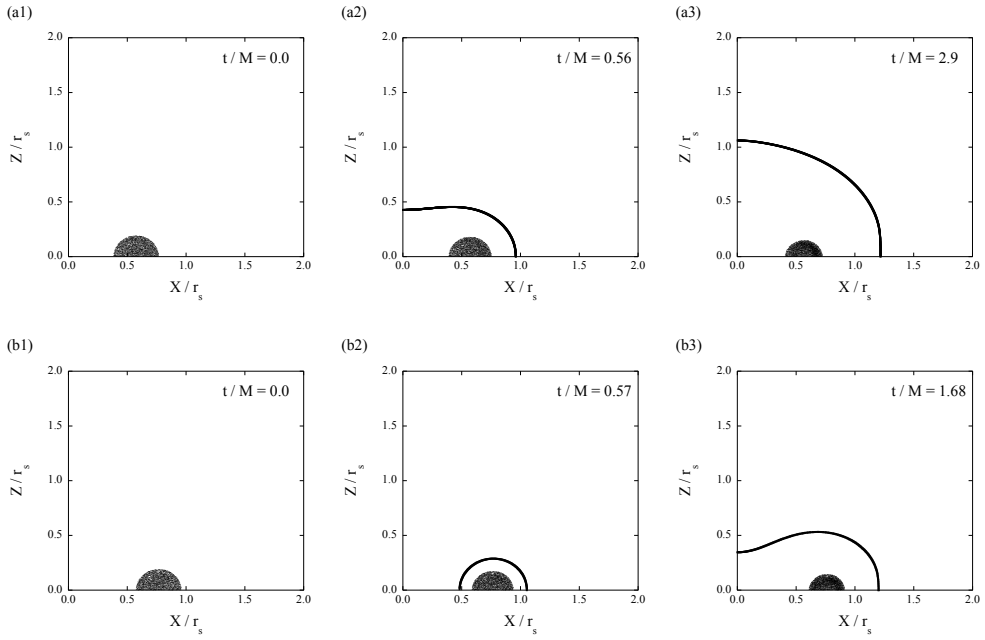

Figure 6: Snapshots of time evolutions, plotting particles and locations of AHs. We set initial ring radius $R_c/r_s = 0.6$ (upper panels), $R_c/r_s = 0.8$ (lower panels) and rotation parameter $\xi = 0$. We see that a common AH is directly formed at $t/M = 0.56$ in the panel (a2), while we see a topological transition of AHs from ring-shape to spherical at $t/M = 1.68$ in the panel (b3).

common and ring AHs.

Up to this moment, we only checked the existence of apparent horizons, and not the event horizons. The system does not include any net angular momentum. We are implementing our code to cover these studies.

This work was supported partially by the Grant-in-Aid for Scientific Research Fund of Japan Society of the Promotion of Science, No. 22540293. Numerical computations were carried out on SR16000 at YITP in Kyoto University, and on the RIKEN Integrated Cluster of Clusters (RICC).

References

[1] R. Emparan and H. S. Reall, Phys. Rev. Lett. **88**, 101101 (2002).

[2] S. L. Shapiro and S. A. Teukolsky, Phys. Rev. Lett. **66**, 994 (1991).

[3] Y. Yamada and H. Shinkai, Phys. Rev. D **83**, 064006 (2011).

[4] Y. Yamada and H. Shinkai, Class. Quant. Grav. **27**, 045012 (2010).

[5] M. Alcubierre, et al., Int. J. Mod. Phys. D**10**, 273 (2001).

[6] see e.g., H. Shinkai, J. Korean Phys. Soc. **54** 2513 (2009).

[7] H. Shinkai and G. Yoneda, Gen. Rel. Grav. **36** 1931 (2004).

[8] L. Smarr and J. W. York, Jr., Phys. Rev. D **17**, 2529 (1978).

[9] C-M. Yoo, K. Nakao and D. Ida, Phys. Rev. D **71**, 104014 (2005).

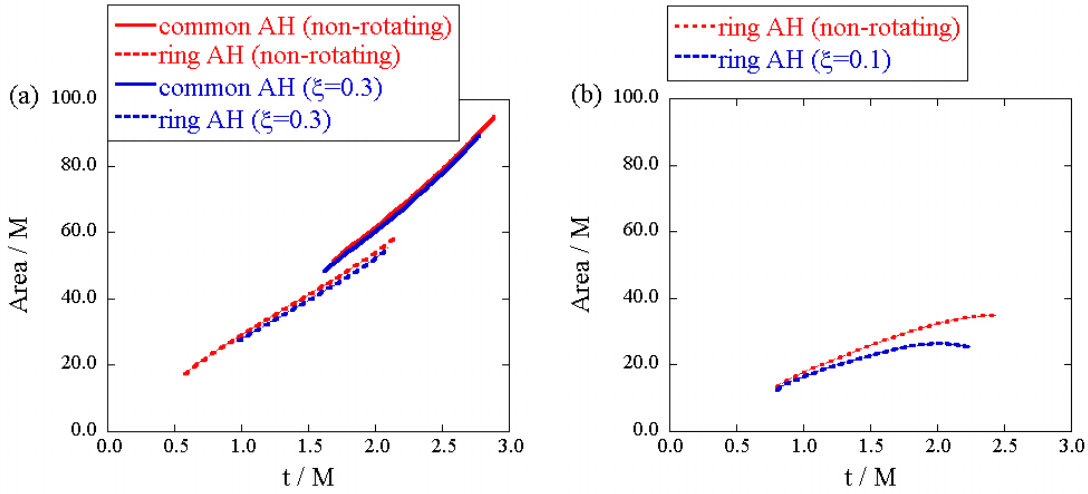

Figure 7: Area of AHs of both common and ring-shaped. The panels (a) and (b) show the results of time evolution for initial ring radius $R_c/r_s = 0.8$ and 1.5, respectively. Red and blue lines show AHs area during time evolution of non-rotating and counter-rotating particles, respectively. We see that the area of horizon increase gradually during time evolution. We also find that for rotating-cases the appearance of AH delays and the area of horizon is smaller comparing to the non-rotating cases.

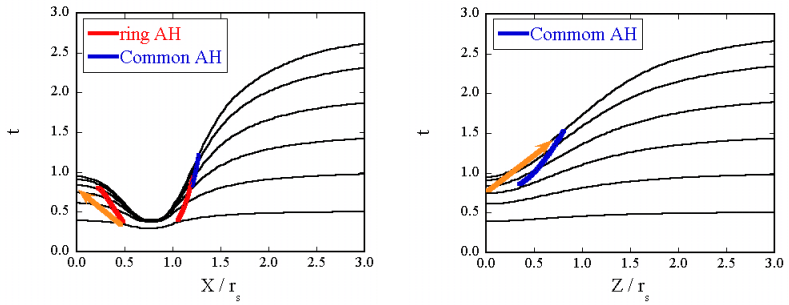

Figure 8: The snapshots of the hypersurfaces on x and z axis in the proper-time τ. The arrow indicates the path of light starting from the appearance of the ring horizon (left panel), and starting from the moment of such information arrives on the Z-axis. The arrow hits the common AH on Z-axis, which indicates the observer at the origin cannot escape if he/she observes the appearance of a ring-shaped horizon.

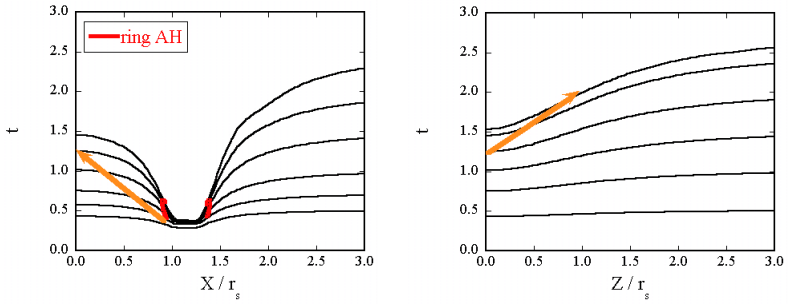

Figure 9: The same with Fig.8 for the case of $R_c(t=0) = 1.5r_s$ and $\xi = 0.1(T/W = 0.05)$. This case shows the observer at the origin can escape even if he/she observes the appearance of a ring-shaped horizon, since the common AH is not formed.

Takao Fukui, JGRG 22(2012)111338

"Effect of metric perturbations in vacuum 5D universe on material 4D universe"

RESCEU SYMPOSIUM ON

GENERAL RELATIVITY AND GRAVITATION

JGRG 22

November 12-16 2012

Koshiba Hall, The University of Tokyo, Hongo, Tokyo, Japan

Effect of Metric Perturbations in Vacuum 5D Universe on Material 4D Universe

Takao Fukui
Dokkyo University
1-1 Gakuencho, Soka, Saitama, 340-0042, Japan
tfukui@dokkyo.ac.jp

1.5D STM Universe [1)]

★ Field equations of the 5D Space（123）-Time（0）-Matter（4） Universe
(A bar over any quantity denotes its unperturbed value)

$${}^{5D}\overline{G}_{AB}=0 \qquad (A,B=0,123,4)$$

$${}^{5D}\overline{G}_{\alpha\beta}={}^{4D}\overline{G}_{\alpha\beta}+{}^{5thD}Extra\ \ terms=0 \quad (\alpha,\beta=0,123)$$

$${}^{5D}\overline{G}_{\alpha 5}=0, \quad {}^{5D}\overline{G}_{55}=0$$

★ Geometrical properties of the 5th coordinate
= Physical properties of the 4D Universe [2)]

$${}^{4D}\overline{G}_{\alpha\beta}=-{}^{5thD}Extra\ \ terms={}^{4D}Physical\ \ properties$$
$$=8\pi\overline{T}_{\alpha\beta}=8\pi\left[(\bar{\rho}+\bar{p})\bar{u}_{\alpha}\bar{u}_{\beta}-\bar{p}\bar{g}_{\alpha\beta}\right]$$

$c=G=1$ unit system is employed here.

★ Metric

$$ds^2=\sigma\left\{dt^2-a^2\left[\frac{dr^2}{1-kr^2}+r^2d\Omega^2\right]\right\}+\varepsilon b^2dl^2$$

★ Solutions [3)]

$$a^2=-\frac{(2Ft-g)^2+\kappa}{4F}$$

$$b=-\frac{4\varepsilon\sigma\hat{f}\hat{f}F^2t^2-2\hat{g}F^2t+g\hat{g}F-\varepsilon\sigma\hat{f}\hat{f}\left(g^2+\kappa\right)}{4afF^2}$$

★ The solutions determine the properties of matter of the 4D Universe through the unperturbed energy-momentum tensor for the perfect fluid

$${}^{4D}\overline{G}_{\alpha\beta}=8\pi\overline{T}_{\alpha\varphi}=8\pi\left[(\bar{\rho}+\bar{p})\bar{u}_{\alpha}\bar{u}_{\beta}-\bar{p}\bar{g}_{\alpha\beta}\right]$$

$$\frac{8\pi\bar{\rho}}{3}=-\frac{\varepsilon f^{2}}{a^{2}}-\frac{\kappa}{4\sigma a^{4}}$$

$$8\pi\bar{p}=\frac{\varepsilon f^{2}}{a^{2}}-\frac{\kappa}{4\sigma a^{4}}$$

$$F(l)\equiv\varepsilon\sigma f^{2}+k,\quad f=f(l),\quad g=g(l),\quad \hat{f}\equiv\frac{\partial f}{\partial l},\quad \hat{g}\equiv\frac{\partial g}{\partial l}$$

2.First-order perturbations [4]

$$g_{AB}=\bar{g}_{AB}+h_{AB}(t,r,l)$$

$$R_{AB}=\bar{R}_{AB}+H_{AB}+O(h^{2})$$

★ First order field equation of 5D STM theory

$${}^{5D}G_{AB}=\bar{R}_{AB}-\frac{1}{2}\bar{g}_{AB}\bar{R}+H_{AB}-\frac{1}{2}\bar{g}_{AB}H-\frac{1}{2}h_{AB}\bar{R}+\frac{1}{2}\bar{g}_{AB}\bar{g}^{CD}\bar{g}^{EF}h_{DF}\bar{R}_{CE}$$

★ Nonzero solutions of the off-diagonal components of ${}^{5D}G_{AB}=0$ for h_{AB}

$$h_{00}=\frac{\zeta_{0}^{1/2}r^{2}}{4\sqrt{\varepsilon\sigma}\,f^{3}q^{3/2}}$$

$$h_{55}=\frac{\zeta_{0}^{1/2}r^{2}\hat{f}^{2}q^{1/2}}{8(\varepsilon\sigma)^{5/2}f^{5}}$$

$$q\equiv 2\varepsilon\sigma t-f_{0}$$

★ The solutions determine the effects of the perturbations on ρ and p through

$$\begin{aligned}H_{\alpha\beta}&=8\pi\delta T_{\alpha\beta}\\&=8\pi\left[(\bar{\rho}+\bar{p})\bar{u}_{\alpha}\delta u_{\beta}+(\bar{\rho}+\bar{p})\bar{u}_{\beta}\delta u_{\alpha}+(\delta\rho+\delta p)\bar{u}_{\alpha}\bar{u}_{\beta}-\bar{p}h_{\alpha\beta}-\bar{g}_{\alpha\beta}\delta p\right]\end{aligned}$$

★ The dark side of the Universe [5] through $\delta\rho$ and δp

$$8\pi\delta\rho=\frac{3\zeta_{0}^{1/2}r^{2}}{2\sqrt{\varepsilon\sigma}\,f^{3}q^{7/2}}+\frac{6\zeta_{0}^{1/2}}{(\varepsilon\sigma)^{3/2}f^{5}q^{7/2}}$$

$$8\pi\delta p=-\frac{2\zeta_{0}^{1/2}}{(\varepsilon\sigma)^{3/2}f^{5}q^{7/2}}$$

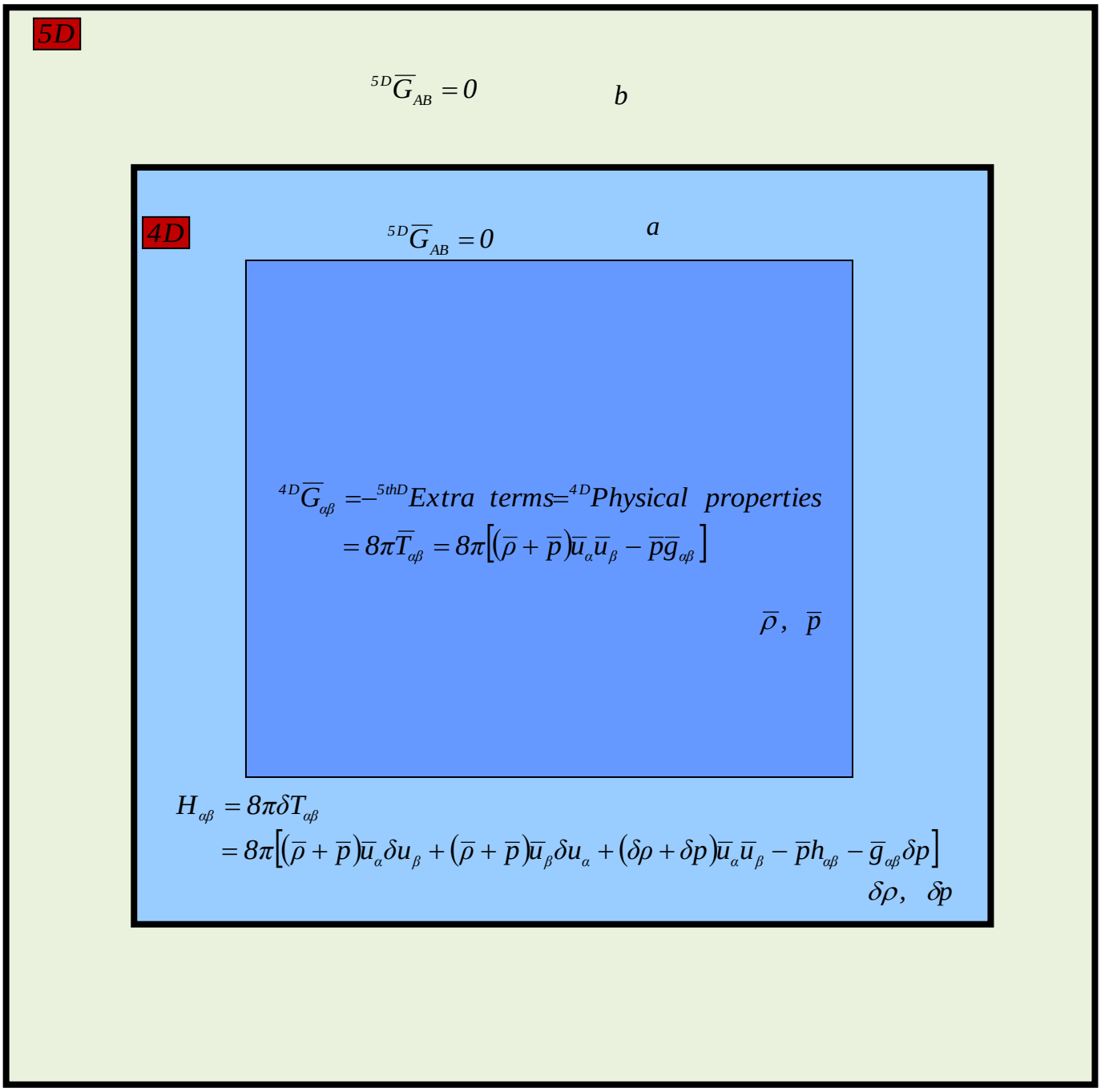

REFERENCES

1) P. S. Wesson, *Five-Dimensional Physics* (World Scientific, 2006).
2) T. Fukui, *Proceedings of the 11th Marcel Grossmann Meeting on General Relativity* (World Scientific, 2008)1287.
3) T. Fukui, S. S. Seahra, and P. S. Wesson, J. Math. Phys. **42**, 11, 5195, (2001).
4) S. Weinberg, *COSMOLOGY* (OXFORD, UNIVERSITY PRESS, 2008)219.
5) J. M. Overduin and P. S. Wesson, *DARKSKY, DARK MATTER* (IOP, 2003).

Saki Tanaka, JGRG 22(2012)111340

"Search of strong gravitational field around nuclei using electron-nuclear scattering experiment by geodesic precession"

RESCEU SYMPOSIUM ON

GENERAL RELATIVITY AND GRAVITATION

JGRG 22

November 12-16 2012

Koshiba Hall, The University of Tokyo, Hongo, Tokyo, Japan

Search of strong gravitational field around nuclei using electron-nuclear scattering experiment by geodetic precession

Saki Tanaka[1a], Yusuke Nakaya[a], Kazufumi Ninomiya[a,b],Hironori Nishio[a], Junichi Onishi[a], Robert Openshaw[c], Matthew Pearson[c], Yumi Totsuka[a] and Jiro Murata[a]

[(a)] *Department of Physics, Rikkyo University, Nishi-Ikebukuro, Tokyo 171-8501, JAPAN*
[(b)] *RIKEN Nishina Center, 2-1 Hirosawa, Wako, Saitama 351-0198, JAPAN*
[(c)] *TRIUMF, Vancouver, BC V6T 2A3, CANADA*

Abstract

The MTV-G experiment is a new unique experiment, aiming to search a large electron spin-precession in electron-nuclear scattering produced by a possible strong gravitational field around nuclei, which is predicted by the large extra-dimension model. This research is started at TRIUMF from 2011. The possible strong gravitational field can be detected as a large spin precession effect caused by the Geodetic precession predicted by the general relativity theory as a result of warped space-time around the nuclear mass. We utilize this phenomenon as a tool to explore the strong gravitational field using the MTV experimental setup.

1 Introduction

For particle and nuclear physicists, gravity has been regarded to be completely negligible in their observing phenomena. Needless to say, it is because the Newtonian gravity is about 10^{-38} weaker than other three gauge interactions. However, if we seriously consider about the possibility of strong gravitational field predicted by so called large extra dimension model which is known as ADD (N. Arkani-Hamed, S. Dimopoulos, G. Dvali) model [1], a small correction in nuclear phenomena coming from the enforced gravitational field should be carefully investigated. In fact, gravity is the most mysterious interaction among the four fundamental interactions. Its extreme weakness prevents particle theorists from building unified theories. Recently, a possible existence of very strong gravitational field at a microscopic scale is discussed based on the large extra dimension model. According to the ADD model, gravitational inverse square law can be modified due to existence of additional spatial dimensions. In order to naturally resolve the hierarchy problem unifying the Planck energy at around 1TeV in the higher dimensional world, at least two extra dimensions with its size of as large as a millimeter is requested, where no precision test of the inverse square law has been performed. Two possible ways to test the large extra dimension scenario were proposed. One way is to perform a direct laboratory test of gravitational law at below millimeter scale, using torsion balance pendulum or similar Cavendish-type devices [2]. Another way is based on a high energy collider experiment, trying to search quantum gravity related phenomena such as mono jet events and micro black hole creation [1, 3].

In the present study, we aim to investigate a possible strong gravitational field around nuclei as a new approach to search the large extra dimension. If there are two large extra dimension with 0.1 mm size, we can expect to see 10^{22} times stronger gravitational field comparing to the original Newtonian prediction. It can be shown in higher dimensional gravitational potential in $4+n$ dimension as;

$$V_{4+n}(r) = -\lambda^n G\frac{Mm}{r^{1+n}} = \left(\frac{\lambda}{r}\right)^n V_{Newton}(r). \quad (1)$$

If we assume that the size of the extra dimension is $\lambda = 0.1mm$ and the number of extra dimensions are $n = 2$, 3, and 4 cases, gravitational potential strength are modified as $V_{4+2,3,4}(r = 1fm) = 10^{22,33,44} \times V_{Newton}(r = 1fm)$

[1]Email address: saki_t@rikkyo.ac.jp

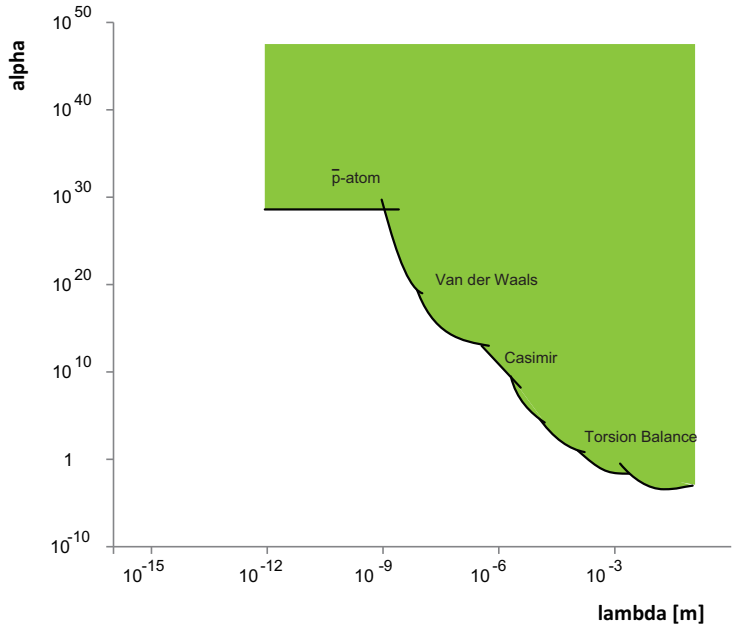

Figure 1: Summary of experimental search of the Yukawa term. Excluded region is illustrated as the green area. Region where present study aims to explore is indicated at around 100 fm.

Figure 1 shows summary of experimental tests of the Newtonian inverse square law at various length scales λ [4]. Vertical axis is coupling constant α of an additional Yukawa term defined in a modified gravitational potential with Yukawa term as;

$$V(r) = -G\frac{Mm}{r}\left(1 + \alpha e^{-r/\lambda}\right). \tag{2}$$

Shaded area of this figure indicates experimentally excluded region in the $\alpha - \lambda$ parameter space. It can be noticed that very little is known at below atomic scale. The length scale where $\alpha(\lambda) > 1$ indicates that even existence of the Newtonian gravity has not been confirmed in the current experimental precision. If we assume that the inverse square law is tested with 100% relative precision above 0.1 mm, i.e. $\alpha < 1$ at $\lambda > 0.1mm$, gravity can be as large as $10^{22}, 10^{33}, 10^{44}$ strength of the original Newtonian predictions for $n = 2, 3, 4$ cases, respectively. In the present study, we are aiming to test the inverse square law at a precision of around $\alpha \sim 10^{37}$ at around 100 fm scale.

2 Principle

An electron scattering experiment is performed in the present study as a tool to explore the possible strong gravitational field around nuclei. In a beta-decay process, emitted electrons are naturally polarized in its longitudinal direction because of parity violating nature of the weak interaction. Spin precession effects due to gravitational geodetic precession from the strong gravitational field around nuclei are examined in this experiment. The geodetic precession is a processioning effect of a spinning particle travelling in a warped spacetime produced as a gravitational field, which is predicted by the general relativity theory [5]. Existence of the geodetic precession phenomena itself is confirmed in 2011 by a NASA satellite Gravity Probe B as a precession of a gyroscope on the orbit around the Earth [6]. As shown in Figure 2, in our experiment, we regard the nuclei as the Earth, and the polarized electron as the gyroscope on the satellite.

We utilize an experimental device designed for the MTV experiment (Mott polarimetry for T-Violation experiment), which aims to search a large time reversal symmetry violation in nuclear beta decay [7], to measure a tiny transverse polarization of electrons using Mott scattering analyzing power. The MTV

experiment is measuring a transverse polarization of electrons emitted from spin-polarized ^{8}Li nuclei, which must be negligible in the standard model, in as well as 0.1% polarization precision. In this Mott-analyzer, backscattering left-right asymmetry from a Mott scattering at a thin lead foil is used as a measurement of the transverse polarization.

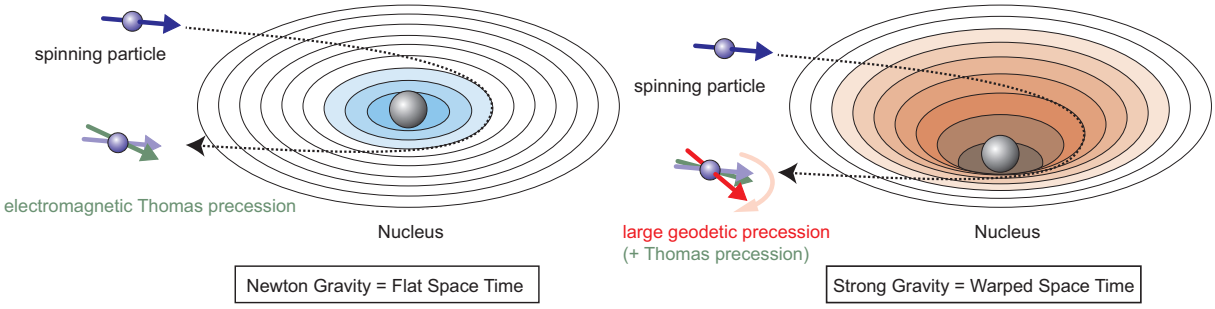

Figure 2: Probing principle using geodetic precession of spinning electron scattered by a nuclei.

For the present project aims to examine gravitational phenomena utilizing the MTV experimental device, it is named as MTV-G (MTV-Gravity) experiment. As shown in Figure 3, the MTV-G experiment consists of ^{90}Sr radiation source, primary scattering lead foil, and the MTV polarimeter with secondary scattering foil and electron tracking chamber. Existence of strong precession effects at the primary scattering foil is examined with the MTV polarimeter in the secondary scattering asymmetry.

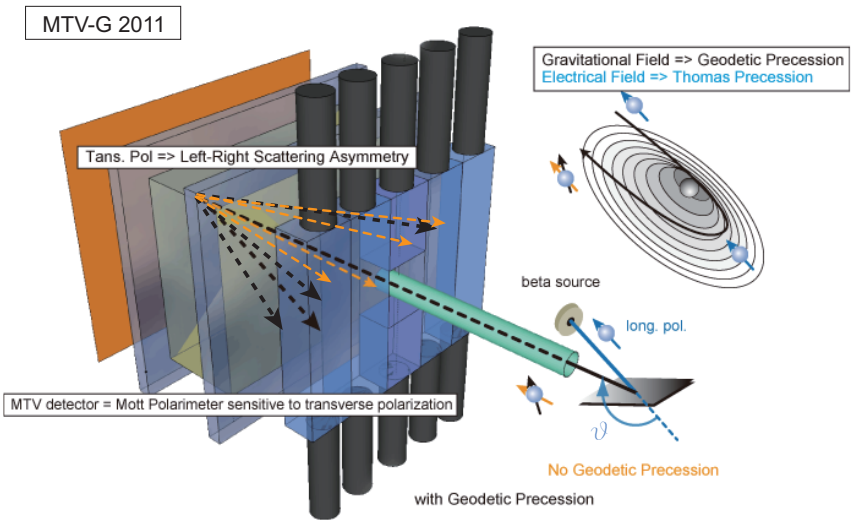

Figure 3: Setup of the MTV-G experiment.

3 Experiment and Results in 2011

The experiment was performed at TRIUMF in 2011 (Figure 3 and 4), at the MTV experimental beam line with 37MBq ^{90}Sr source for about two weeks of data taking. Relative setting angle of the radiation source and the primary scattering foil θ can be changed in order to see scattering angular dependence. By changing this scattering angle, we can measure the distance dependence from the nuclei. Secondary scattering left-right asymmetry defined as $Asymmetry = (N_{left} - N_{right})/(N_{left} + N_{right})$ are measured as functions of the primary scattering angle θ. In order to cancel out detector intrinsic efficiency deference, source configuration flipping between $UP/DOWN$ position settings are performed.

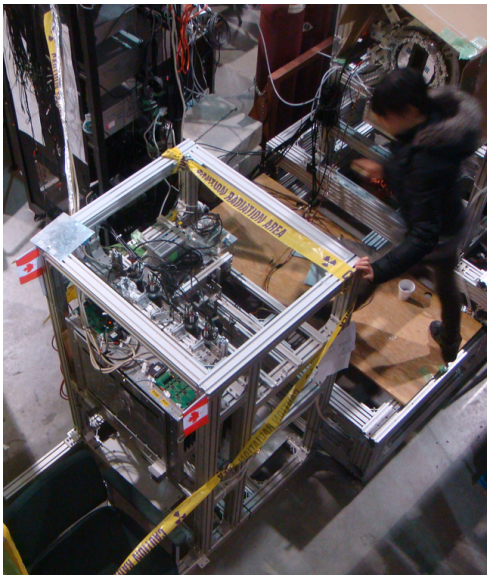

Figure 4: Experimental setup of the MTV-G experiment at TRIUMF in 2011.

In Figure 5, typical counting yield distributions are plotted as functions of secondary Mott scattering angle, for *UP* and *DOWN* configuration. The shape difference between *UP* and *DOWN* indicates the pure scattering asymmetry without suffering from detector efficiency difference. Here, we can see a clear evidence of transverse polarization as the non-zero asymmetry. The left-right asymmetry, which can be interpreted as the transverse polarization P, in $Asymmetry = P \times A$, using known analyzing power A of the Mott scattering. The analyzing power A includes de-polarization effects inside the scattering foils.

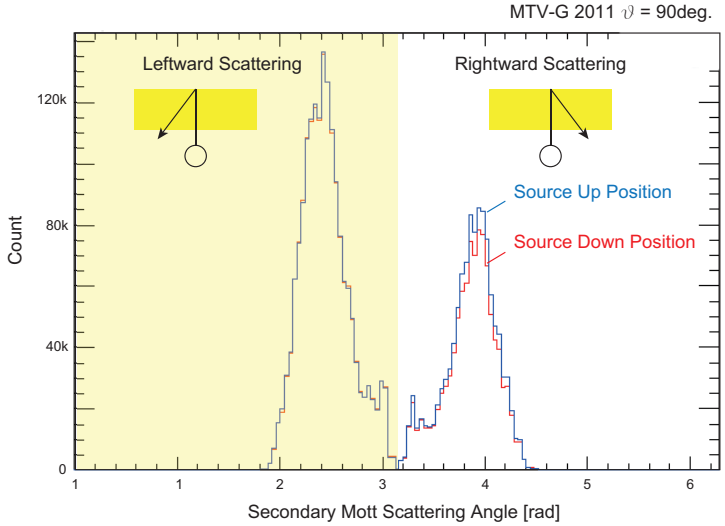

Figure 5: Example of backscattering angular distribution. A clear parity violating asymmetry can be noticed.

The obtained results are compared with possible Yukawa type interaction. In the Coulomb scattering, electron spin precession is dominated from electromagnetic Thomas precession, which exists even in zero magnetic fields. Contribution from the Thomas precession is estimated using a numerical simulation. After subtracting the Thomas precession contributions, maximum allowed strength α is estimated sup-

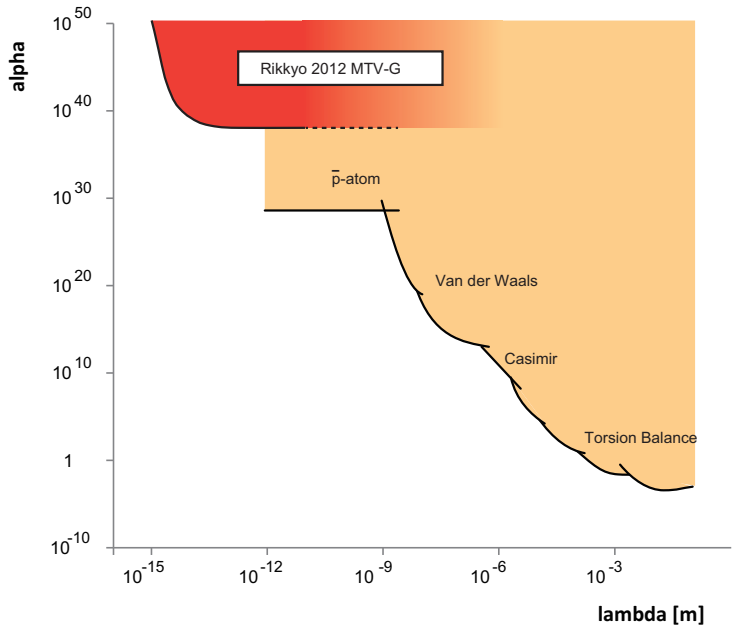

Figure 6: Constraint on the $\alpha - \lambda$ plot from the present result.

posing classical geodetic precession formula. We set a possible constraint on the $\alpha - \lambda$ parameter space using the obtained results, as shown in Figure 6. In the Figure 6, experimental limit at atomic scale is taken from an analysis of anti-protonic atom [**?**]. It can be seen that the present study set a new constraint at the shortest scale.

Present analysis supposes a classical geodetic precession expressed as

$$\vec{\Omega}_G = \frac{3}{2}\frac{GM}{r^3}\vec{r} \times \vec{v}, \tag{3}$$

which suppose the trajectory of the spinning particle obeying in a free fall motion in the gravitational field [5]. Here, M is mass of the nuclei, r is radius of electron orbit, $\vec{v}$ is electron velocity. The real situation is not a free fall, but dominated by the Coulomb potential. In addition, the phenomena is in a microscopic scale, therefore, classical treatment might not possible to be applied. Calculation of the present study based on quantum gravitational treatment with Coulomb field must be theoretically interesting and challenging subject for theorists.

The results shown in this paper is based on a first stage experiment with many parameter ambiguities, such as de-polarization factor, precision estimation of electromagnetic Thomas precession etc. We are now switching to a next generation experiment using cylindrical drift chamber (CDC) shown in Figure 7, which may provide a better results with increased precision.

4 Progress of 2012

Figure 7 and 8 show the experimental setup using the CDC. The radiation source is set at the center position of the CDC, together with the primary scattering foil. The secondary Mott analyzing foil is set outside of the CDC, followed by stopping scintillation counters. By measuring the azimuthal angular dependence around the symmetry axis of the CDC setup, experimental reliability is significantly improved from the previous setup with the planer drift chamber shown in Figure 3.

We have just performed the measurement using the CDC at TRIUMF in December 2012. Physics data taking was planned similar to the previous experiment using MWDC, by flipping the source direction in order to cancel the detector's intrinsic asymmetries. In addition to the statistical improvement because of the increased solid angle, we can expect to reduce systematic effects thanks to the detector's symmetric

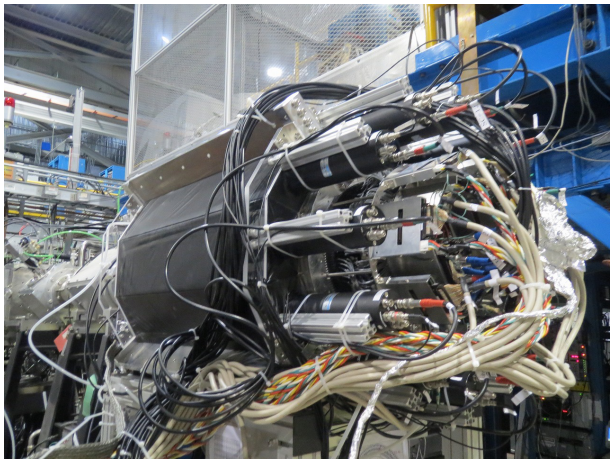

Figure 7: New MTV-G setup using CDC

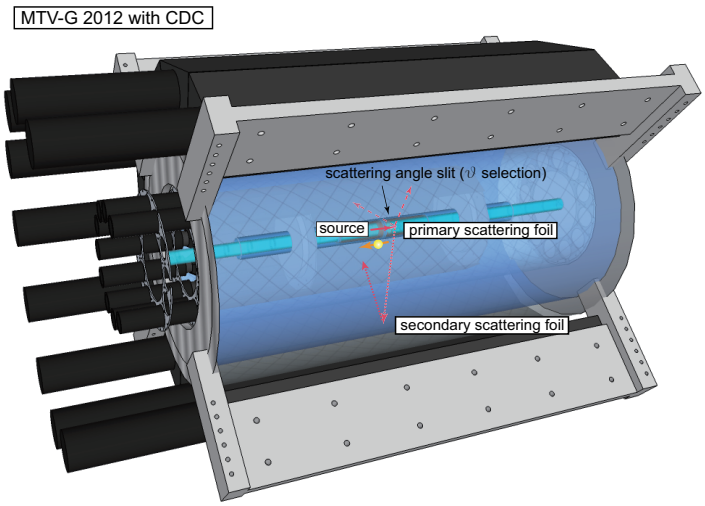

Figure 8: New setup and the image of electron scattering

geometry. Obtained data are now under analysis, which will be completed soon. Final data taking is schedule in 2013 summer, where our experience in this measurement in 2012 will be considered.

5 Conclusion and Future plan

In 2011, we have successfully performed the first gravity experiment, by applying an electron-nuclear scattering measurement. This is the first trial to search a strong gravitational field at an unexplored region of a nuclear scale. We succeeded to examine the existence of the strong gravity using electron spin direction changing which may include the Geodetic precession effect. As a result, we have succeeded to set a new constraint on the shortest length scale of around 100 fm on the $\alpha - \lambda$ plot, where no gravitational experimental test has been ever been performed.

In addition to the present study focusing on the 100 fm scale, we are interested to explore a wide field of physics in a scope of gravity. For an example, re-analysis of spectroscopic data of excited atoms is a good subject, which has not been analyzed as gravity data. If there are a strong gravitational force in addition to the Coulomb force, energy levels of the atomic states will be modified, which can be detected

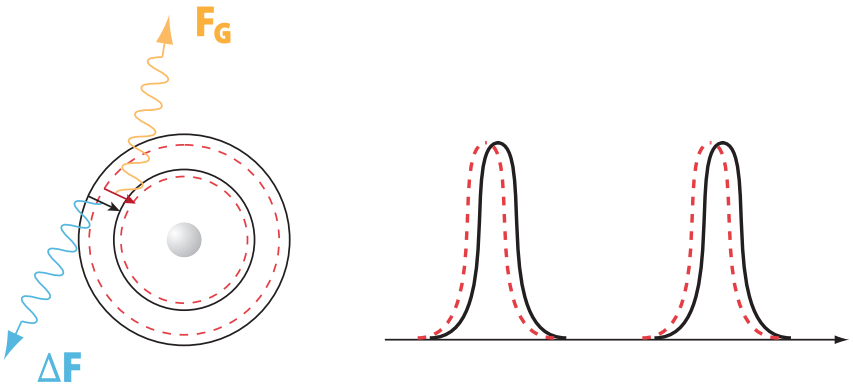

Figure 9: Measurement principle using exotic atom. Modification of the bounding potential can be detected as the frequency shifts.

as a wave length shift of the emitted photons. We will examine these atomic data and summarize them in the alpha-lambda plot, together with our original results obtained in the MTV-G experiment.

References

[1] N. Arkani-Hamed, S. Dimopoulos, G. Dvali, Phys. Lett. **B429**, 263 (1998).

[2] M. Hata *et al.*, J. Phys. **CS189**, 012019 (2009).

[3] ATLAS Collaboration, Phys. Lett. **B705**, 294 (2011).

[4] E. Fischbach and C.L. Talmadge, The search for non-Newtonian gravity, Springer Verlag, (1999).

[5] Hans Ohanian and Remo Ruffini, Gravitation and Spacetime, W.W. Norton & Co.

[6] C.W.F. Everitte *et al.*, Phys. Rev. Lett. **106** 221101 (2011).

[7] J. Murata *et al.*, J. Phys. **CS 312** (2011) 102011; J. Onishi *et al.*, J. Phys. **CS312** (2011) 102012

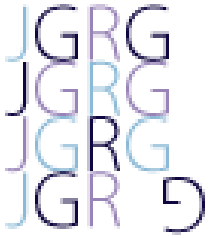

Hiromi Saida, JGRG 22(2012)111341

"Theory for observational verification of black hole existence"

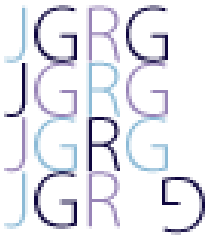

RESCEU SYMPOSIUM ON

GENERAL RELATIVITY AND GRAVITATION

JGRG 22



November 12-16 2012

Koshiba Hall, The University of Tokyo, Hongo, Tokyo, Japan



Theory for observational verification of black hole

Hiromi Saida (Daido Univ.) / saida@daido-it.ac.jp

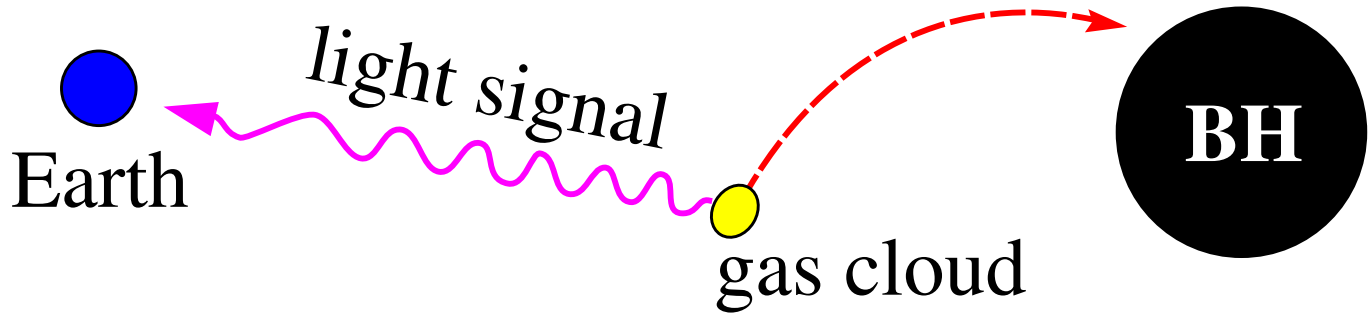

JGRG22, 2012.11.12–16 at Tokyo Univ.

1. Intro.

- I want to see black hole : **Directly observe the black hole horizon**

  → We suggest,

  - ◇ **The observable verifying the existence of BH horizon**
  - ◇ **The observable measuring the surface gravity of BH horizon**

- Note: **ur observable is realized in any wave propagating on BH spacetime GW, EM waves, and so on , and independent of details of BH environments.**

2. Set up a situation : a simple example

- Consider the radially alinged situation

$$\begin{cases} \text{Black hole} & : \text{Schwarzschild} \to \text{radius } R_{\rm BH} \\ \text{Source} & : \text{radial free fall (time like geodesic)} \\ \text{Wave} & : \text{propagate on a radial null geodesic} \\ \text{Observer} & : \text{rest at a distant point} \end{cases}$$

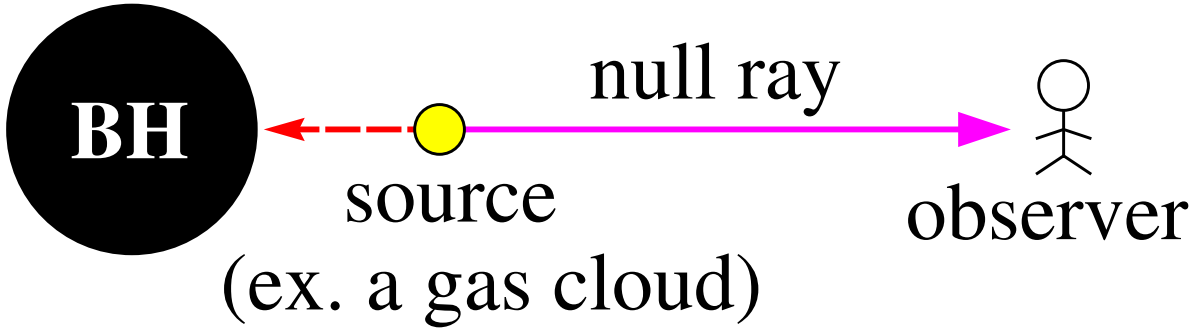

◇ Note: It is found observationally that, in next summer 2013, a gas cloud is going to fall into the BH candidate at the center of our galaxy.

3. The observable verifying the existence of BH horizon

• The source is falling into BH

→ The wave length of wave emitted by this source is
prolonged infinitely by the Grav. Doppler (redshift) due to BH horizon.

→ The infinite prolongation of wave length can
verify the existence of BH horizon.

⇓

The freezing of wave
should be observed.

(Numerical example is shown next)

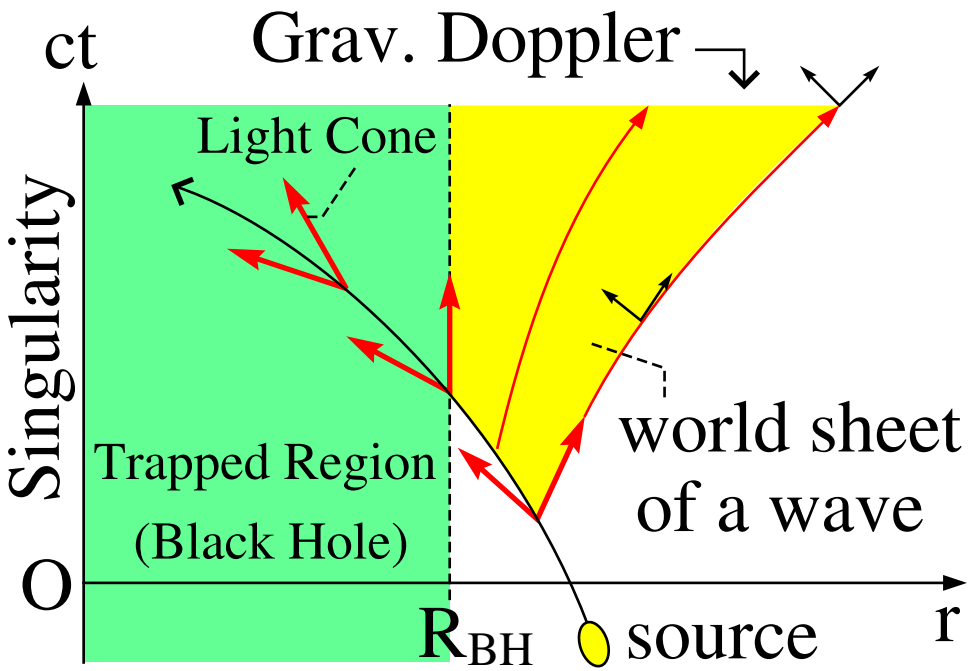

- Ex. Freezing oscillation of observed wave ($\downarrow$ "Gas's" $=$ "Source's" $\downarrow$)

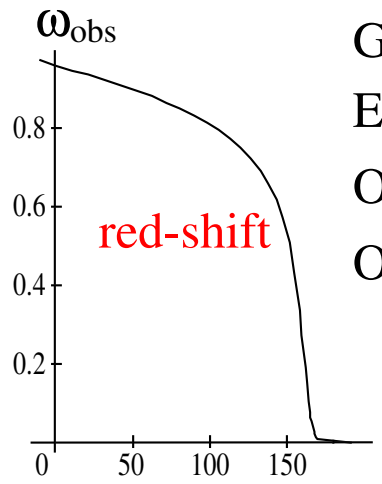

Gas's initial place $r_0 = 20\ R_{BH}$

Emission Freq. $\omega_{emit} = 1$

Observed red-shift ω_{obs}

Observed wave (model)

$$\Psi(t) = \mathrm{Sin}[\int \omega_{obs}\, d(t_{obs})]$$

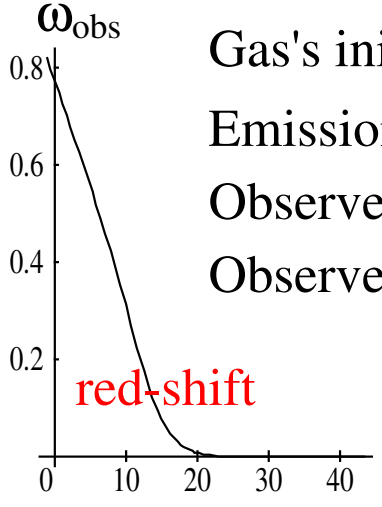

Gas's initial place $r_0 = 3\ R_{BH}$ (ISCO)

Emission Freq. $\omega_{emit} = 1$

Observed red-shift ω_{obs}

Observed wave (model)

$$\Psi(t) = \mathrm{Sin}[\int \omega_{obs}\, d(t_{obs})]$$

Near Horizon Behavior

$(r < (3/2)R_{BH})$

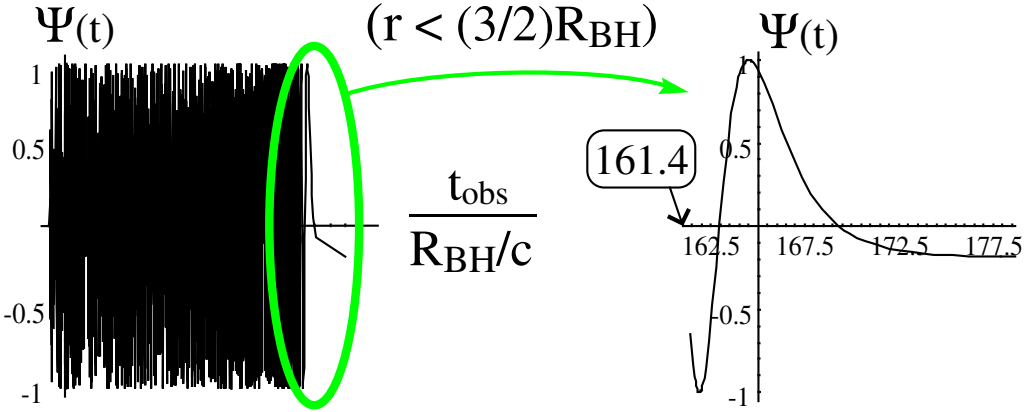

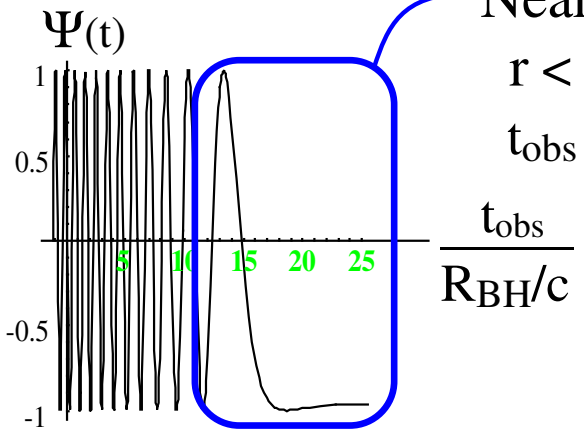

Near Horizon Behavior

$r < (3/2)R_{BH}$

$t_{obs} > 11.23\ R_{BH}/c$

$\rightarrow$ **The freezing oscillation appears in observation,**

when the source approaches BH horizon $r \sim 3M$ **.**

4. The observable measuring the mass and angular momentum of BH horizon

- Look precisely at the freezing ocsillation of observed wave:

  Time eovlution of the phase of observed oscillation (wave)

$$\Theta(t_{\rm obs}) = \int \omega_{\rm obs}\, {\rm d}t_{\rm obs} \sim \omega_0 \exp\left[-\frac{c\, t_{\rm obs}}{2R_{\rm BH}}\right] , \begin{cases} \omega_0 = \text{const.} \\ t_{\rm obs} = \text{observer's time} \end{cases}$$

$\rightarrow$ Power spectrum of this time evolution $\propto$ **Planckian distribution**

$$\begin{cases} \text{Typical oscillation} & : \Psi(t_{\rm obs}) = A(\omega_0) \exp[\, i\, \Theta(t_{\rm obs})\,] \\ \text{Fourier trans.} & : F(\Omega, \omega_0) = \displaystyle\int_{-\infty}^{\infty} e^{-i\,\Omega\, t_{\rm obs}}\, \Psi(t_{\rm obs})\ {\rm d}t_{\rm obs} \end{cases}$$

$$\therefore \quad P(\Omega) := \left|F(\Omega, \omega_0)\right|^2 \sim \frac{4\pi R_{\rm BH}|A|^2}{c}\, \frac{1}{\Omega}\, \frac{1}{e^{4\pi R_{\rm BH}\Omega/c} - 1}$$

→ [**"Temperature"** $\dfrac{\hbar c}{4\pi R_{\rm BH}}$ **shown in time evolution**]

$=$ [**Hawking temperature** $\dfrac{\kappa}{2\pi}$] (κ : surface gravity of BH)

for Kerr BH, $\kappa = \dfrac{\sqrt{M^2 - a^2}}{2\left(M^2 + M\sqrt{M^2 - a^2}\right)}$

→ **This gives a relation of M and a**

indepndent of details of BH environment.

→ Combining with the other observation,

M and a will be determined observationally.

• But there is a point of notice w.r.t. observation $\cdots$

Real observation detects the wave as an oscillation of "real number". ($\Psi(t_{\rm obs})$ should be a wave in real number.)

$\cdots$ continued to next page

$\rightarrow$ Wave in real number: $\Psi_{\rm R}(t_{\rm obs}) \;:=\; A(\omega_{\rm emit})\,\cos\Theta(t_{\rm obs})$

$\rightarrow$ Fourier trans.: $F_{\rm R}(\Omega,\omega_{\rm emit}) \;=\; \displaystyle\int_{-\infty}^{\infty} e^{-i\,\Omega\,t_{\rm obs}}\,\Psi_{\rm R}(t_{\rm obs})\;{\rm d}t_{\rm obs}$

$\rightarrow$ Power spectrum of time variation:

$$P_{\rm R}(\Omega) \;:=\; \left|F_{\rm R}(\Omega,\omega_{\rm emit})\right|^2 \;\sim\; \frac{\pi R_{\rm BH} A(\omega_{\rm emit})^2}{c}\,\frac{h(\Omega)}{\Omega}\,\frac{1}{e^{4\pi R_{\rm BH}\Omega/c}-1}$$

$$\text{where}\;\begin{cases} h(\Omega) \;=\; e^{4\pi R_{\rm BH}\Omega/c} + 2\,[\cos\Theta_\infty]\,e^{2\pi R_{\rm BH}\Omega/c} + 1 \\ \Theta_\infty \;=\; \Theta(t_{\rm obs}\to\infty) \;:\; \text{“Frozen” Phase} \end{cases}$$

Note 1: In real observation, the frozen phase Θ_∞ is required
in odrde to describe the curve fitting to observed data.

Note 2: $A(\omega_{\rm emit})$ is a constant depending only on the source,
not on the mass and angular momentum of BH.

5. Summary

- The observable verifying the existence of BH horizon

  → **The freezing oscillation found in time evolution of observed wave**

- The observable measuring the surface gravity of BH horizon

  → **The planckian distribution found in the power spectrum of time evolution of freezing oscillation**

  (Combining with the other observations, M and a will be determined.)

- Next issue (under consideration):
  - ◇ Application to gravitational collapse
  - ◇ Observation time required to obtain the Planckian distribution with good precision

Kotaro Fujisawa, JGRG 22(2012)111342

"Equilibrium states of magnetized disc-central compact object systems"

RESCEU SYMPOSIUM ON

GENERAL RELATIVITY AND GRAVITATION

JGRG 22

November 12-16 2012

Koshiba Hall, The University of Tokyo, Hongo, Tokyo, Japan

Equilibrium states of magnetized disc-central compact object systems

Kotaro Fujisawa[1](a), Rohta Takahashi(b),(c), Shijun Yoshida(d) and Yoshiharu Eriguchi(a)

(a) *Department of Earth Science and Astronomy, raduate School of Arts and Sciences, University of Tokyo, Komaba, Meguro-ku, Tokyo 153-8902, Japan*

(b) *Department of Natural and Physical Sciences, Tomakomai National College of Technology, Tomakomai 059-1275, Japan*

(c) *High Energy Astrophysics Laboratory, The Institute of Physical and Chemical Research (RIKEN), Saitama 351-0198, Japan*

(d) *Astronomical Institute, Tohoku University, Sendai 980-8578, Japan*

Abstract

We have obtained equilibrium states of magnetized disc-central compact object systems. Under the assumption of stationary and axisymmetry, we have derived generalized Grad-Shafranov equation (GS equation). We have succeed in solving GS equation and including not only poloidal but also toroidal magnetic fields under the ideal MHD approximation. We have obtained a toroid which sustains the extreme strong poloidal magnetic field near the central compact object.

1 Introduction

Recent GR simulations show that a few-solar-mass black hole and a highly dense toroid whose maximum density can reach $10^{10} - 10^{11}\mathrm{g/cm}^3$ around the black hole can be formed after the merging of binary neutron stars [1], the merging of a neutron and BH binary [2] and the collapsing of a massive star [3]. Therefore, dense toroids and central compact objects could be formed after collapsing or merging of compact objects. If the compact objects have strong magnetic fields such as a magneter, the toroid can also sustain the strong magnetic fields. Although, in order to understand the origin and dynamical formation processes of these systems, we must take into account many realistic physics and compute stationary configurations with magnetic fields in GR, nobody has yet succeeded in solving stationary states both with poloidal and toroidal magnetic fields in GR at present. Therefore, we explore such stationary states of axisymmetric magnetized barotropic systems in the framework of Newtonian gravity. Although there were many papers to obtain magnetized stationary states of discs/toroids only with poloidal magnetic fields (e.g. [4]) and discs/toroids only with toroidal magnetic fields inside the disks/toroids (e.g. [5]), no solutions both with poloidal and toroidal components of magnetic fields have been obtained yet. This is because it has been difficult to solve the Grad-Shafranov equation as well as the equations of motion consistently by some means.

Recently, Otani et al.[6] have obtained magnetized self-gravitating equilibrium states both with poloidal and toroidal magnetic fields self-consistently in the framework of Newtonian gravity. In this study we have extended the method employed in Otani's work. We calculate the equilibrium states of magnetized disc-central compact object systems with very strong magnetic field. We study what kind of magnetic configurations can sustain larger magnetic field energy.

2 Formulation and settings

Our formulation is essentially the same as that of Otani's work [6]. In order to obtain magnetized equilibrium states self-consistently, we solve the Euler equation,

$$\frac{1}{\rho}\nabla p = -\nabla\phi_g + \nabla\left(\frac{GM_c}{r}\right) + R\Omega^2\mathbf{e}_R + \frac{1}{\rho}\left(\frac{\boldsymbol{j}}{c}\times\boldsymbol{B}\right) \tag{1}$$

[1]Email address: fujisawa@ea.c.u-tokyo.ac.jp

and GS equation,

$$R\frac{\partial}{\partial R}\left(\frac{1}{R}\frac{\partial \Psi}{\partial R}\right)+\frac{\partial^2 \Psi}{\partial z^2}=-4\pi R\frac{j_\varphi(\Psi)}{c}, \tag{2}$$

self-consistently. Where, ρ, p, ϕ_g, M_c, Ω, $\boldsymbol{B}$, $\boldsymbol{j}$, G and c are mass density, pressure, gravitational potential of a toroid, mass of the central compact object, angular velocity of a toroid, magnetic field, current density, the gravitational constant and the speed of light. Ψ is a magnetic flux function defined as below:

$$\boldsymbol{B}_{\rm p}=\nabla\Psi\times\nabla\varphi. \tag{3}$$

$\boldsymbol{B}_p$ denotes a poloidal magnetic field. We solve GS equation by using Green function as below

$$\frac{\Psi(\boldsymbol{r})\sin\varphi}{R}=\frac{1}{c}\int_V\frac{j_\varphi(\boldsymbol{r'})}{|\boldsymbol{r}-\boldsymbol{r'}|}dV'. \tag{4}$$

The φ component of current density is expressed as an arbitrary function of flux function in our formulation as below:

$$\frac{j_\varphi}{c}=\frac{\kappa'(\Psi)\kappa(\Psi)}{4\pi R}+\rho R\mu(\Psi), \tag{5}$$

where $\kappa(\Psi)$ and $\mu(\Psi)$ are arbitrary functions of flux function Ψ. We can change the magnetic field structure by changing these arbitrary function forms [7]. We can integrate the Euler equation by using these arbitrary functions and obtain the first integral as below:

$$\int\frac{dp}{\rho}=-\phi_g+\frac{GM_c}{r}+\frac{1}{2}R^2\Omega^2(\Psi)+\int_\Psi\mu(\Psi)\,d\Psi+C. \tag{6}$$

C is a integral constant. In order to obtain the magnetized equilibrium state self-consistently, we fix one functional form and solve Eq.(4) and Eq.(6) iteratively until the system becomes convergence. Then, we obtain one magnetized equilibrium states after this iteration process.

In order to explore the magnetic field structure which sustains the large magnetic field energy, we calculate the critical equilibrium states of such systems beyond which no equilibrium states are allowed to exist when we fix one arbitrary functional forms set [6]. The critical model can sustain the largest magnetic filed energy with one functional form. A toroid can reach the central compact the most closely when the system is critical equilibrium state.

We assume that the mass of the central compact object, the toroid and the maximum density as below:

$$M_c=5.0M_\odot, \tag{7}$$

$$M_t=0.1M_\odot, \tag{8}$$

$$\rho_c=10^{11}{\rm g/cm^3}. \tag{9}$$

These values of physical quantities are typical ones obtained by the recent GR simulations [3].

3 Numerical Result

We show two critical configurations by changing the functional form of $\mu(\Psi)$ [7]. We set $\Omega(\Psi)=0$ in these calculations for simplicity. Therefore, these toroids are sustained by the magnetic pressure. mainly. Fig.1 shows the structures of the toroid (blue and red thick curves), the poloidal magnetic field lines (black curves) and the distributions of $\log_{10}|\boldsymbol{B}|$ (G) (color maps). The blue toroid (the left panel in Fig.1) has the largest magnetic fields among critical models in our parameter space, while the red has the smallest magnetic fields. Fig.2 shows the density distribution of each toroid in critical configuration. Both toroids have cusp structures at the inner edge. The blue toroid is stretched inward by the strong gravitational force of the central compact object.

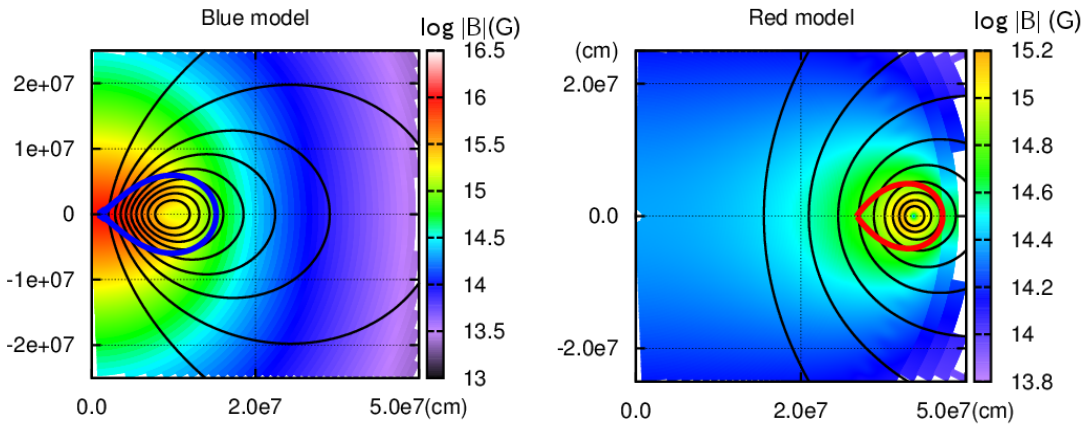

Figure 1: The magnetic field configuration and its magnitude ($\log_{10}|B|$ G). The curves denote magnetic field lines. The blue toroid (left) can approach near the central object because the magnetic pressure is larger than that of the red toroid (right).

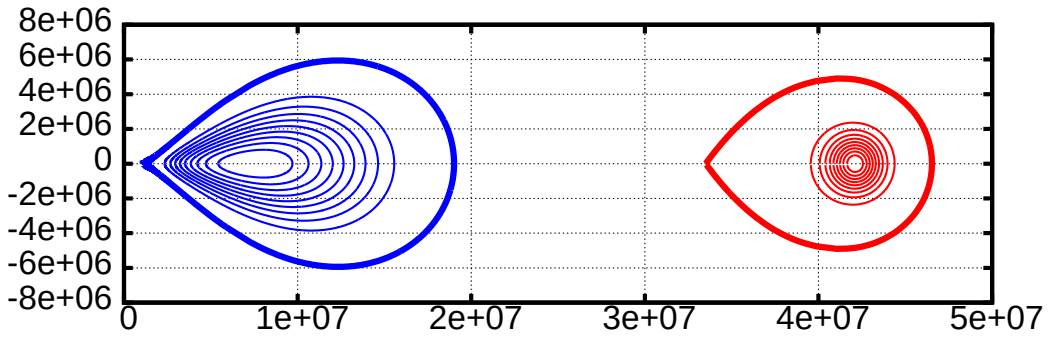

Figure 2: The density contours of toroids in the critical configuration. The blue toroid is stretched inward by the strong gravitational force of the central compact object.

4 Discussion and Conclusion

These toroids are sustained by the extreme strong magnetic pressure. As we have seen Fig.1 and Fig.2, the blue model can approach near the central compact object, because the strong magnetic fields pressure inside the toroid can balance the stronger gravity force of the central object. The distributions of magnetic fields of these models are different from each other. As seem from Fig.1, the magnetic field becomes maximum near the inner edge in the blue toroid model, while in the red toroid model, the magnetic fields become maximum near the center of the toroid. The magnitude of the magnetic fields of the blue model can reach about 10^{16} G near the inner edge of the toroid. The total magnetic field energy of the blue toroid is about three times as large as red toroid. Therefore, we conclude that the larger magnetic energy can be sustained in the toroid whose magnetic field is highly localized around the inner edge of the toroids and which locate closer to the central compact object.

Our model is, however, formulated in Newtonian gravity. The inner edge of the red toroid is located near the innermost stable circular orbit of the 5.0 $M_\odot$ central compact object. Since the Newtonian approximation near the region is invalid, we must treat this system by general relativistic formulation. We will extend our model to the general relativistic framework in the future.

References

[1] K. Hotokezaka, K. Kyutoku, H. Okawa, M. Shibata and K. Kiuchi, Phys. Rev. D **83**, 124008, (2011).

[2] K. Kyutoku, H. Okawa, M. Shibata and K. Taniguchi, Phys. Rev. D **84**, 064018, (2011).

[3] Y. Sekiguchi and M. Shibata, Astrophys. J. **737**, 6, (2011).

[4] Z.-Y. Li and F. H. Shu, Astrophys. J. **472**, 211, (1996).

[5] J. Ghanbari and S. Abbassi, Mon. Not. R. Astron. Soc. **350**, 1437, (2004).

[6] J. Otani, R. Takahashi and Y. Eriguchi, Mon. Not. R. Astron. Soc. **84**, 2152, (2009).

[7] K. Fujisawa, S. Yoshida and Y. Eriguchi, acMon. Not. R. Astron. Soc. **422**, 434, (2012).

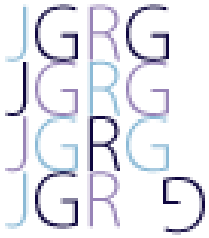

Seiju Ohashi, JGRG 22(2012)111343

"Gravitational collapse of the Einstein cluster in the Lovelock gravity"

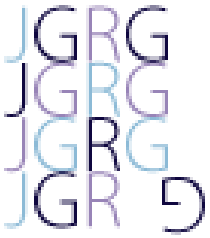

RESCEU SYMPOSIUM ON

GENERAL RELATIVITY AND GRAVITATION

JGRG 22



November 12-16 2012

Koshiba Hall, The University of Tokyo, Hongo, Tokyo, Japan



Gravitational Collapse of the Einstein Cluster in Lovelock gravity

Seiju Ohashi
Kyoto University

Contents

1.Introduction

2.Lovelock gravity

3.Collapse of Einstein cluster

4.Summary

1. 1 Introduction

Goal: Verify the Cosmic Censorship Conjecture

Cosmic Censorship Conjecture

No naked singularities form under physically reasonable condition.

- Which is the final state of gravitational collapse ?

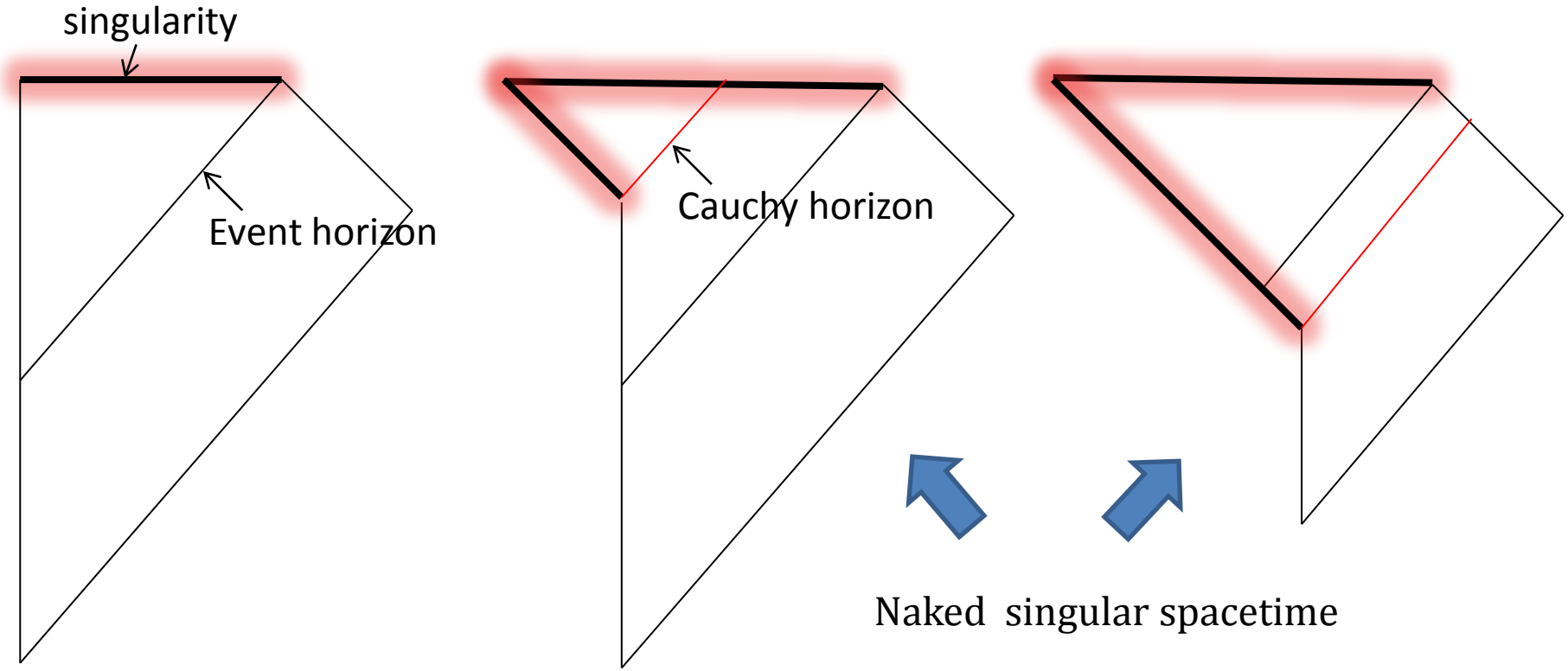

1. 2 Introduction

- Gravitational collapse and singularity formation are high energetic phenomena

- String theory is formulated in higher dimensional spacetime and predicts higher curvature correction to Einstein theory.



- It is important to study the gravitational collapse in higher dimensional spacetime in generalized Einstein gravity and verify whether the Cosmic Censorship Conjecture holds or not.

- Here we consider the Lovelock gravity as the generalized Einstein gravity theory

2.1 Lovelock gravity

Lovelock gravity is the natural extension of Einstein gravity to higher dimension and the most general theory which satisfies 3 conditions

- Field equation is second rank tensor

$$\mathcal{G}_{\mu\nu} = \mathcal{G}_{\nu\mu}$$

- Field equation is divergence free

$$\nabla_\mu \mathcal{G}^{\mu\nu} = 0$$

- Field equation contains the derivatives of metric tensor up to second order

$$\mathcal{G}(g, \partial g, \partial^2 g)$$

Einstein gravity is uniquely characterized by above conditions

2.2 Action for Lovelock gravity

- The most general action which satisfies abone 3 condition is

$$\mathcal{L} = \sum_{m=1}^{k} \frac{a_m}{m} \mathcal{L}_m$$

where

$$\mathcal{L}_m = \frac{1}{2^m} \delta^{\nu_1 \nu_2 \ldots \nu_{2m-1} \nu_{2m}}_{\mu_1 \mu_2 \ldots \mu_{2m-1} \mu_{2m}} R_{\nu_1 \nu_2}{}^{\mu_1 \mu_2} \ldots R_{\nu_{2m-1} \nu_{2m}}{}^{\mu_{2m-1} \mu_{2m}}$$

$$k = [(D-1)/2]$$

a_m : arbitrary constants

$\delta^{\nu_1 \nu_2 \ldots \nu_{2m-1} \nu_{2m}}_{\mu_1 \mu_2 \ldots \mu_{2m-1} \mu_{2m}}$: totally anti-symmetric tensor

3. 1 Collapse of Einstein Cluster

- We consider the gravitational collapse with **spherical symmetry.**
  In the previous paper , we study the spherical dust collapse in the Lovelock gravity .

Summary of dust case

Even dimensional case	Odd dimensional case
Only central singularity can be naked	Singularity at **finite radius** as well as central one can be naked

- Dust cloud, however, is not the realistic matter model. It is important to include the pressure.
  Here we consider the gravitational collapse of Einstein cluster.
  Einstein cluster is counter rotating dust cloud, which is equivalent to fluid which has **tangential pressure.**

3.2 Metrics and Field equation

- Metric for Einstein cluster

$$ds^2 = -A^2 dt^2 + \left(\left(\frac{R'}{R} \right)^2 \frac{J^2 + R^2}{W^2} \right) dr^2 + R^2 d\Omega^2$$

- Field equation for Einstein cluster

$$\sum_{m=1}^{k} c_m \left(\left(\frac{\dot{R}}{RA} \right)^2 + \frac{1}{R^2} - \frac{W^2}{J^2 + R^2} \right)^m = \frac{F(r)}{R^{n+1}}$$

$$c_l := \begin{cases} 1 & \text{if } \ l = 1 \\ \frac{a_l}{l} \prod_{p=1}^{2l-2} (n-p) & \text{if } \ 2 \leq l \leq k \end{cases}$$

$F(r)$: mass function

$J(r)$: specific angular momentum （J=0 corresponds to dust）

3.3 Singularity, apparent horizon and bounce point

Condition for Singularity formation $R = 0$

Odd dim

Apparent horizon $$H_{odd}(R) \equiv \sum_{m=1}^{k=(n+1)/2} c_m R^{n-2m+1} = F(r)$$

Bounce $$B_{odd}(R, J) \equiv \sum_{m=1}^{k=(n+1)/2} c_m R^{n+1-2m} \left(\frac{J^2}{J^2 + R^2} \right)^m = F(r)$$

Even dim

Apparent horizon $$H_{even}(R) \equiv \sum_{m=1}^{k=n/2} c_m R^{n-2m+1} = F(r)$$

Bounce $$B_{even}(R, J) \equiv \sum_{m=1}^{k=n/2} c_m R^{n+1-2m} \left(\frac{J^2}{J^2 + R^2} \right)^m = F(r)$$

3.4 Result : EVEN dimension

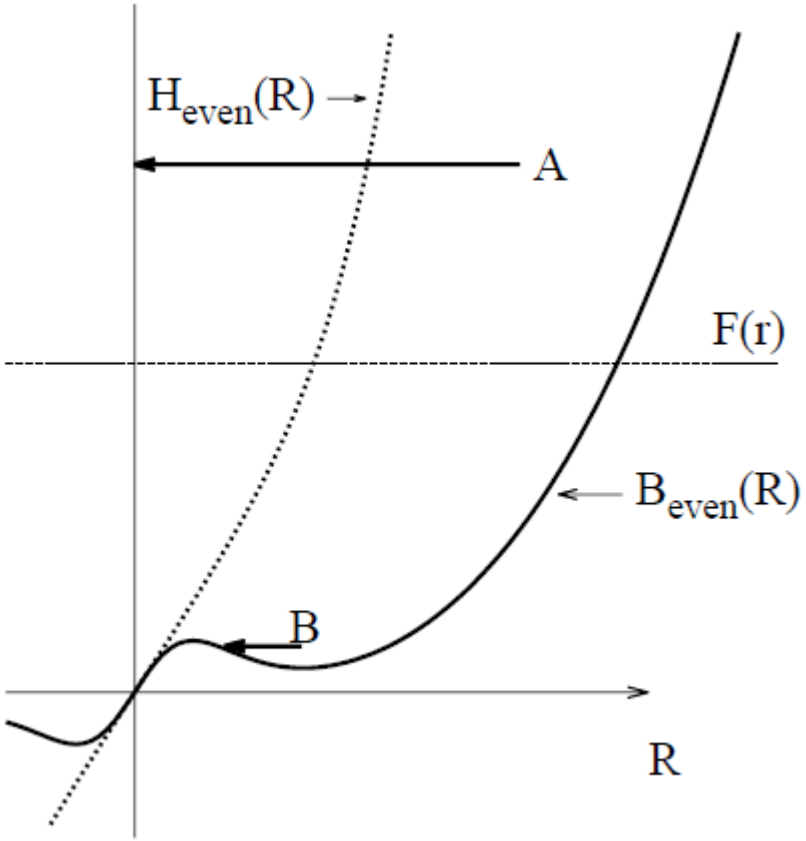

$r \neq 0$ case

- If J is sufficiently small, B_{even} has local maximum and shell can Bounce
- All the singularities are covered by apparent horizon and cannot be naked

$r = 0$ case

$$J^2(r) = j_4 r^4 + O(r^6)$$

$j_4 \neq 0$ ⇒ shell bounces

$j_4 = 0$ ⇒ shell does not bounce and singularity can be naked

3.5 Result : ODD dimension

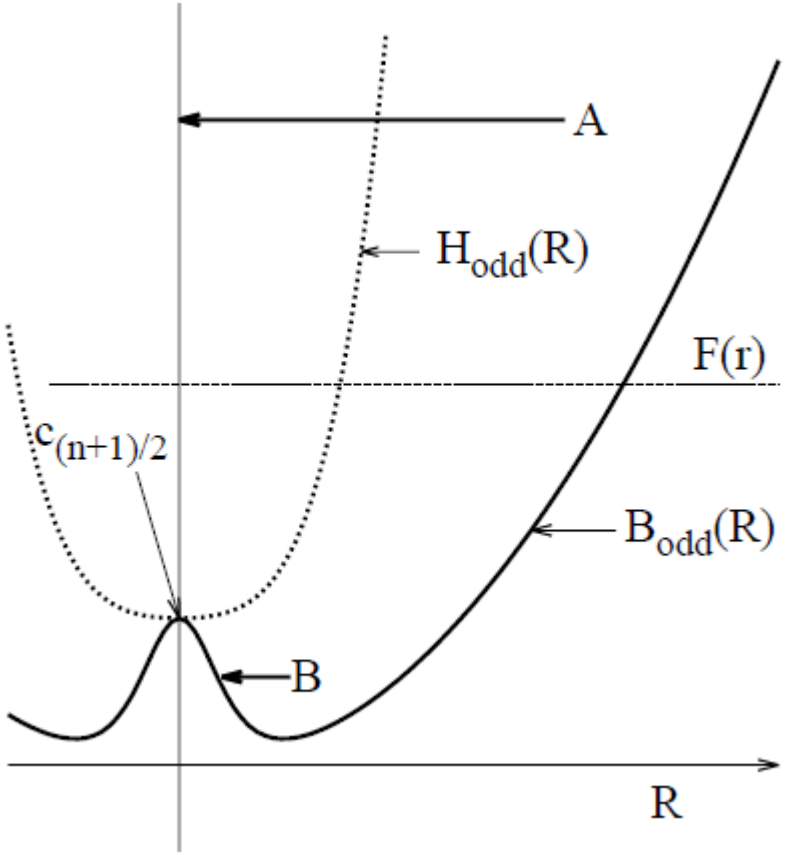

$r \neq 0$ case

- The shells which satisfy $F(r) < c_{(n+1)/2}$ inevitably bounce
- The other shells hit the singularity which cannot be naked

$r = 0$ case

$$J^2(r) = j_4 r^4 + O(r^6)$$

$j_4 \neq 0$ ⇒ shell bounces

$j_4 = 0$ ⇒ shell does not bounce and singularity can be naked

4. Summary

- We consider the gravitational collapse of Einstein cluster in Lovelock gravity, and investigate the effect of angular momentum (or pressure) on the Cosmic Censorship conjecture.

	Even dimension	Odd dimension
$r \neq 0$	J is sufficiently small ⇒ bounce No singularity can be naked.	$F(r) < c_{(n+1)/2}$ ⇒ bounce Other shell hit the singularity, but cannot be naked.
$r = 0$	$j_4 \neq 0$ ⇒ shell bounces $j_4 = 0$ ⇒ shell does not bounce and singularity can be naked	

Takuya Maki, JGRG 22(2012)111344

"Einstein equation of state and its cosmological applications"

RESCEU SYMPOSIUM ON

GENERAL RELATIVITY AND GRAVITATION

JGRG 22

November 12-16 2012

Koshiba Hall, The University of Tokyo, Hongo, Tokyo, Japan

Einstein equation of state and its cosmological applicationss

Takuya Maki[1](b) and Masaaki Morita [2](b)

(a)*Nikaido-gakuen, JWCPE, 8-19-1, Kita-karasuyama, Setagaya, Tokyo,157-8565, Japan*
(b)*Department of Integrated Arts and Science, Okinawa National College of Technology, 905 Henoko, Nago, Okinawa 905-2192, Japan*

Abstract

We investigate the applications of the Einstein equation of state to cosmological problems. In order to apply the cosmology, we expand the shear term in higher orders and find that the leading part of them are described in terms of the Weyl curvature . Consequently, the Penrose's Weyl curvature conjecture has been formulated from spacetime thermodynamical aspect.

1 Introduction

Recent cosmological observations suggest the cosmological scenario that the Universe has evolved from an almost homogeneous state to the present inhomogeneous state due to formation of the astronomical objects. If the Universe can be regarded as a system of the gravity theory, how can we describe evolution of the system? For this question, R.Penrose has proposed the following conjecture [1, 2], namely, 'The entropy of gravitational filed should be somehow related to the Weyl curvature' and 'The entropy, defined as a functional of the Weyl curvature, should be increasing in time.' The Wely curvature is traceless part of Riemann curvature tensor $R_{\alpha\beta\gamma\delta}$, which defined as

$$C_{\alpha\beta\gamma\delta} := R_{\alpha\beta\gamma\delta} - g_{\alpha[\gamma}R_{\delta]\beta} + g_{\beta[\gamma}R_{\delta]\alpha} + \frac{1}{3}Rg_{\alpha[\gamma}g_{\delta]\beta}, \tag{1}$$

Namly, this Penrose's Weyl curvature hypothesis means that gravitational field itself should carry an entropy, and it may be related to the Weyl tensor In this context, the Universe can be regard as a physical system with the following property, i.e. it has an almost homogeneous initial state that the gravitational entropy is nearly zero, After the formation of very inhomogeneous large scale structure, a final (present) state with large gravitational entropy. Then the gravitational entropy continues increasing globally from a initial equilibrium, Ricci dominant state to a final npn-equilibrium Weyl dominant state.
The entropy function mentioned above has been not clear to be defined by the fundamental gravity theory in spite of previous investigations, e.g. Grøn and Hervik(2001) by minisperspace model[3], Rudjord et. al(2012) introduce the gravitational entropy density $s(x)$ through examining the possibility to explain some kind of black hole entropy[4]. However these are just only phenomenological approach. Thus one of our aim of this report, we obtain more directly the conjecture from the fundamental gravitational theory. In this research, we study the cosmological applications of spacetime thermodynamics. This approach of gravity has recently been remarkably evolved and suggest the alternative of gravitational degree of freedom (detail in the next section). And we point out that the Penrose's Weyl curvature conjecture can be formulated naturally by expanding the shear term.

2 What is the Gravity?

The gravitational theory given by A. Einstein deduced by the principle of 'general relativity' and 'equivalent principle., in which the gravitational interaction is expressed by the Riemannian Manifold. Though

[1]Email address: maki@jwcpe.ac.jp
[2]Email address: morita@

the cosmological application has been successful, the quantization has difficulties due to the divergence of quantum renormalizations. However, it is widely known that the black hole thermodynamics seems to be related the quantum gravity. One of them so-called, 'Area theorem' has been studied from the quantum gravity aspects, e.g.D-brane, which states that the black hole entropy $S$is propotional to the stational black hole area A

$$S = \frac{1}{4G}A \tag{2}$$

Recently T. Jacobson (1995) give the alternative description to the gravity, namely, he has derive the Einstein equation from the Clausius's low and the area theorem applying to the local Rindler horizon at any point of any spacetime[5]. This gravity of approach seems to reviel the problem what the physical degree of freedom of gravity. Although the approach seems to be successful to the black hole thermodynamics, the cosmological applications have some problems due to just the construction.

3 Einstein equation of state

First we briefly review the Jacobson's derivation of the Einstein equation of state.
#1 **Equivalence Principe**
We can take a local inertial frame near any point in a spacetime manifold.

$$g_{\mu\nu}(X)\mathrm{d}X^\mu \mathrm{d}X^\nu = \left[\eta_{\mu\nu} + O(\ell^2)\right]\mathrm{d}X^\mu \mathrm{d}X^\nu, \tag{3}$$

We take a pacetime area $\Delta A(P)$ including P that is tangent to the light (here X_1 at P.
#2 **Local Rindler frame**
We consider the local Rindler flame (χ, η, X_2, X_3) from the local inertial flame $X_i (i = 0, 1, 2, 3)$ by the following transformation as

$$X^0 = \chi \sinh(\kappa\eta), \tag{4}$$
$$X^1 = -\chi \cosh(\kappa\eta), \tag{5}$$

where κ is a constant. Then the line element is given by

$$\mathrm{d}s^2 = -\kappa^2\chi^2\mathrm{d}\eta^2 + \mathrm{d}\chi^2 + \mathrm{d}\ell_\perp^2, \tag{6}$$

#3 **The observer and thermal system**
Consider an uniformally accelerating observer running away from the point near P in spatial direction of the light wavefront (X_1), whose trajectory is $\chi = const.$. Define χ^μ as a unit vector of this trajectory.
#4 **The local Rindler horizon** Then, for this observer, the null-geodesics $X^0 - X^1 = 0$ is a causal horizon which is parametrized by a affine parameter λ, X^2 and X^3.
When a unit vector k^μ of the null-geodesics with $X^2 = const.$ and $X^3 = const.$, then χ^μ i always approximate near the causal horizon as

$$\chi^\mu \approx -\kappa\lambda k^\mu \tag{7}$$

Thus we can regard the inside of the causal horizon as the thermal system for the observers.
#5 **The Clausius's low and construction of Einstein equation of state**
The Clausius's low is expressed in terms of the temperature T, entropy change δS and heat flow δQ of the thermodynamical system by

$$T\delta S \geq \delta Q \tag{8}$$

We can obtain the Einstein equation using the Area theorem $\delta S = \alpha\delta A$ for the entropy change, the Unruh temperature $T_u\sqrt{-g} = \frac{\hbar\kappa}{2\pi}$ [7] from the local Rindler horizon as the temperature$T$ and the energy flow through the horizon into the system as δQ.The energy flow is

$$\delta Q = \int_0^{\Delta\eta}\int_{\Delta A(\eta)} \lambda T_{\mu\nu}\chi^\mu k^\nu d\lambda dA = -\kappa\int_{\Delta\lambda} \lambda T_{\mu\nu}k^\mu k^\nu d\lambda dA \tag{9}$$

In the last step, we need to the change of the horizon area, i.e.

$$\delta A = \int_{\mathcal{S}} \theta \, \mathrm{d}\lambda \, \mathrm{d}\ell_{\perp}^2, \tag{10}$$

where the expansion θ of null congruence defined as $\theta = -\frac{1}{\Delta A}\frac{d\Delta A}{d\lambda}$ and ΔA is infinitesimal cross section to the null congruence at P. The change of expansion θ obeys at P with respect to λ with the Rauchaudhri's equation given by

$$\frac{d\theta}{d\lambda} = -\frac{1}{2}\theta^2 - \sigma^2 - R_{\mu\nu}k^\mu k^\nu \tag{11}$$

and of shear σ[8]:

$$\frac{d\sigma_{\mu\nu}}{d\lambda} = -\theta\sigma_{\mu\nu} - C_{\alpha\nu\mu\beta}k^\alpha k^\beta. \tag{12}$$

Now, under the preparation above, if we make a assumption $\theta\big|_P = 0, \sigma_{\mu\nu}\big|_P = 0$,, then

$$\begin{aligned} &T\delta S - \delta Q = 0 \\ &= -\kappa \int \lambda \, \mathrm{d}\lambda \int_{\mathcal{S}(\lambda)} \mathrm{d}\ell_{\perp}^2 \Big\{ \alpha \frac{\hbar}{2\pi} \Big[\theta/\lambda - \Big(\frac{1}{2}\theta^2 + \sigma_{\mu\nu}\sigma^{\mu\nu} + R_{\mu\nu}k^\mu k^\nu \Big) \Big]_P - T_{\mu\nu}k^\mu k^\nu \Big\}. \end{aligned} \tag{13}$$

up to $O(\lambda^2)$. Since this derivation is not depend on the point P, Eq.(**??**) yields the Einstein equation with cosmological constant by using the Bianchi identity and setting $\alpha = \frac{1}{4G\hbar}$. This result means that thermal equilibrium condition of the system, i.e. $T\delta S = \delta Q$ with $\theta\big|_P = 0, \sigma_{\mu\nu}\big|_P = 0$,,is equivalent to the Einstein equation.

4 Expansions of the shear term and the cosmological applications

Can the spacetime thermodynamics be applied to cosmological problems? How can we do it? The derivation of the Einstein equation of state is supposed that the evolution of the expansion θ and the shear $\sigma_{\mu\nu}$ depend on the point P in the spite of the independence of choice of P in the manifold. In order to apply the discussion above to any point on any geodesics parametrized by λ, we expand the θ and $\sigma_{\mu\nu}$ as

$$\theta = \theta\big|_P + \lambda\frac{d\theta}{d\lambda}\big|_P + \frac{1}{2!}\lambda^2\frac{d^2\theta}{d\lambda^2}\big|_P + \frac{1}{3!}\lambda^3\frac{d^3\theta}{d\lambda^3}\big|_P + \cdots \tag{14}$$

$$\sigma_{\mu\nu} = \sigma_{\mu\nu}\big|_P + \lambda\frac{d\sigma_{\mu\nu}}{d\lambda}\big|_P + \frac{1}{2!}\lambda^2\frac{d^2\sigma_{\mu\nu}}{d\lambda^2}\big|_P + \frac{1}{3!}\lambda^3\frac{d^3\sigma_{\mu\nu}}{d\lambda^3}\big|_P + \cdots \tag{15}$$

With conditions.(ref), the expansion θ at P ($\lambda = 0$) is expressed as

$$\theta = \theta\big|_P + \lambda\frac{d\theta}{d\lambda}\big|_P + \lambda^2\frac{d^2\theta}{d\lambda^2}\big|_P + \cdots + \lambda^n\frac{d^n\theta}{d\lambda^n}\big|_P + \cdots \tag{16}$$

$$\begin{aligned} &= 0 && 0th\ order \\ &+\Big(-\lambda R_{\mu\nu}k^\mu k^\nu\Big)\big|_P && 1st\ order \\ &+\lambda^2\frac{1}{2!}\Big(-\frac{d}{d\lambda}R_{\mu\nu}k^\mu k^\nu\Big)\big|_P && 2nd\ order \\ &+\lambda^3\frac{1}{3!}\Big(-\frac{d^2}{d\lambda^2}R_{\mu\nu}k^\mu k^\nu\Big)\big|_P + \lambda^3\frac{1}{3!}\Big(-E_{\alpha\gamma\delta\beta}k^\gamma k^\delta k^\alpha k^\beta\Big)\big|_P && 3rd\ order \\ &+\cdots \\ &+\lambda^n\frac{1}{n!}\Big(-\frac{d^{n-1}}{d\lambda^{n-1}}R_{\mu\nu}k^\mu k^\nu\Big)\big|_P + \lambda^n\frac{1}{n!}\Big(\frac{d^{n-3}}{d\lambda^{n-3}}(-E_{\alpha\gamma\delta\beta}k^\gamma k^\delta k^\alpha k^\beta\Big)\big|_P + Q_n(R_{\mu\nu}, C_{\alpha\nu\mu\beta}) && \mathrm{n}-th\ order \\ &+\cdots \end{aligned} \tag{17}$$

where

$$E_{\alpha\mu\nu\beta} := R_{\mu\nu}R_{\alpha\beta} + 2C_{\alpha\gamma\delta\beta}C_{\mu}{}^{\gamma\delta}{}_{\nu}. \tag{18}$$

In Eq.(17), we focus on the 1st and 2nd terms of each order $O(\lambda^n)$ and sum up these 1st terms and similarly the 2nd terms, The remaining terms $Q_n(R_{\mu\nu}, C_{\alpha\nu\mu\beta})$ have the leading term of higher order than those two terms. The summation of the two terms can be considered as the Taylor expansions of a functional given by integrating $-R_{\mu\nu}k^\mu k^\nu$ and $E_{\alpha\mu\nu\beta}k^\gamma k^\delta k^\alpha k^\beta$ with respect to λ.Then it is available at any point $\lambda = \lambda_1 \neq 0$ on the null geodesics by the analytical continuation. Therefore it is expected that spacetime thermodynamics can apply the discussions on a certain cosmological area. Thus we obtain the following inequality:

$$\begin{aligned} &T\delta S - \delta Q \\ &= \kappa \int \lambda \, \mathrm{d}\lambda \int_{\mathcal{S}(\lambda)} \mathrm{d}\ell_\perp^2 \Big[\alpha \frac{\hbar}{2\pi}(R_{\mu\nu}k^\mu k^\nu + E_{\alpha\gamma\delta\beta}k^\gamma k^\delta k^\alpha k^\beta) - T_{\mu\nu}k^\mu k^\nu)\Big]_p + O(\lambda^5)\Big\} \geq 0. \end{aligned} \tag{19}$$

The The 2nd term in the integrands is contributed from the shear term. We should note that this leading term is $O(\lambda^4)$. Comparing the derivation of the Einstein equation of state, this result can be interpreted as the case with non-equilibrium condition $T(\delta S + \delta S_i) = \delta Q$ instead of the Clausius's low [6]and then S_i is regarded as the internal entropy production term:

$$\delta S_i = \int \lambda \, \mathrm{d}\lambda \int_{\mathcal{S}(\lambda)} \mathrm{d}\ell_\perp^2 \Big\{(E_{\alpha\gamma\delta\beta})k^\gamma k^\delta k^\alpha k^\beta\Big\} \geq 0 \tag{20}$$

Consequently, we formulate the Penrose's Weyl curvature conjecture from spacetime thermodynamical point of view.

5 Summary and Outlook

·An attempt to define a gravitational entropy has been made elaborating Jacobson ' s spacetime thermodynamics.
· We have taken into account the higher orders of θ and $\sigma_{\mu\nu}$ with respect to an affine parameter λ, and then we obtained the non-equilibrium thermodynamical inequality which is satisfied at any λ on a light curve by the analytic continuation.
·The Weyl curvature naturally arises in the inequality of entropy variation associated with matter, and the intrinsic one. Consequently, we formulate the Penrose Conjecture from spacetime thermodynamical aspect.
·Now trying to extend the formula, defined only locally, to global one in order to apply to cosmological situations.

References

[1] R. Penrose, in *Proceedings of the First Marcel Grossmann Meeting on General Relativity*, ed R. Ruffini (North-Holland, 1977).

[2] R. Penrose, *J. Stat. Phys* **77**, 217 (1994).

[3] Ø. Grøn and S. Hervik, arXiv:gr-qc/0205026v1.

[4] Ø. Rudjord, Ø. Grøn and S. Hervik, *Phys. Scr.* **77**, 055901 (2008).

[5] T. Jacobson, *Phys. Rev. Lett.* **75**, 1260 (1995).

[6] G. Chirco and S. Liberati, *Phys. Rev. D* **81**, 024016 (2010).

[7] W. G. Unruh, *Phys. Rev. D* **14**, 870 (1976).

[8] R. M. Wald, *General Relativity* (The University of Chicago Press, 1984), p. 222.

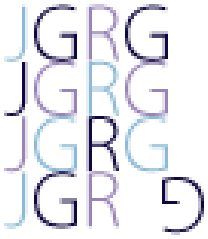

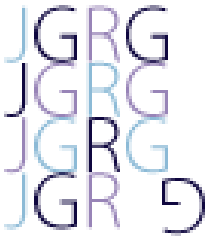

Hiromi Suzuki, JGRG 22(2012)111346

"Cosmic wiggly string in black hole spacetime"

RESCEU SYMPOSIUM ON

GENERAL RELATIVITY AND GRAVITATION

JGRG 22

November 12-16 2012

Koshiba Hall, The University of Tokyo, Hongo, Tokyo, Japan





Cosmic wiggly string in black hole spacetime

Hiromi Suzuki[1]

Department of Information and Science,
The Tokyo Woman's Christian University,
Zempukuji 2-6-1, Suginami-ku, Tokyo 167-8585, Japan

Abstract

We obtain two kinds of special solutions of test strings in the black hole spacetime because it is too difficult to obtain the general solutions of test string. One is the cosmic wiggly string of arc configuration which exhibits open string lying along the circular orbit in the equatorial plane outside the horizon. The other is the cosmic wiggly string of radial configuration which exhibits open string pointing toward the origin in the equatorial plane outside the horizon.

1 Introduction

A phase transition in the early Universe produced topological defects such as domain walls, strings and monopoles when the $U(1)$ symmetry breaks down in the unified theories. Topological defects are necessarily created due to the spontaneous symmetry breaking of vacuum state[see 1-4]. If the existence of the cosmic strings which are one of topological defects is confirmed, it is a strong evidence of vacuum phase transition in the universe. Besides the interests from the unified theories, it was proposed that cosmic strings can generate cosmological density fluctuations as seeds of the structure formation which can subsequently evolve into galaxies and large-scale structure[5,6]. However, this scenario was rejected due to the confliction with the precise observational data of cosmic microwave backgrounds[7,8].

Recently cosmic strings have been studied in the context of the superstring theories because fundamental strings and other string-like solitons such as D-strings could exist in the Universe as cosmic strings[9]. If such cosmic strings existin the Universe, it is an interesting subject how cosmic strings behave in the curved spacetime in general relativety. They have been investigatedby H. J. de Vega, N. G. Sánchez, V. P. Frolov and B. Carter[10-20]. The configuration of cosmic string in black hole spacetime is an interesting problem. It is well known how a test particle behaves in black hole spacetime. However, the motion of a test string in black hole spacetime is not known because the test string problem is significantly non-trivial due to the constraints. So we study the test string in detail. For the simplicity, we neglect the gravitational effects of string and assume that its thickness is zero.

We obtain two kinds of special solutions of test strings in the black hole spacetime because it is too difficult to obtain the general solutions of test string. One is the cosmic wiggly string of arc configuration which exhibits open string lying along the circular orbit in the equatorial plane outside the horizon. The other is the cosmic wiggly string of radial configuration which exhibits open string pointing toward the origin in the equatorial plane outside the horizon. We obtain interesting solutions though they are not the general solutions of test string.

Traditionally cosmic strings have been treated as fundamental strings and described by Nambu-Goto action$S_{N-G} = \int d\tau d\sigma \frac{1}{2\pi\alpha'} \sqrt{g^{ab} G_{\mu\nu} \partial_a X^\mu \partial_b X^\nu}$. However, some literatures claim that the so-called cosmic wiggly string is more favorable than the standard Nambu-Goto string to explain the possible role of extended cosmic string in cosmology or astronomy[21-27]. For the Nambu-Goto string the energy density and the tension are equal, while their relation in the wiggly string model is more relaxed to the extent that the energy density and the tension are not equal. In particular, it is known that the wiggly string of which the product of the energy density and the tension is constant behaves well. If the energy density is much larger than the string tension, its shape tends to wiggle. We mainly treat cosmic wiggly strings as cosmic strings.

[1]Email address: suzukihi@lab.twcu.ac.jp

2 Basic Equation of Cosmic Wiggly String

The induced metric on cosmic string is

$$h_{ab}(\tau,\sigma) = \partial_a X^\mu \partial_b X^\nu G_{\mu\nu}, \qquad (a,b=\tau,\sigma), \tag{1}$$

where τ and σ are the string coordinates, X^ν is the background coordinate and $G_{\mu\nu}$ is the background metric.

The two-dimensional energy-momentum tensor is given by

$$t^{ab} = (\mu - \tilde{T})u^a u^b + \tilde{T}h^{ab}, \tag{2}$$

where $\mu(\tau,\sigma)$ is the energy per unit length of string, $\tilde{T}(\tau,\sigma)$ is its tension, and $u^a(\tau,\sigma)$ is the fluid velocity parallel to the string with the normalization:$u^a u_a = -1$. The string has the energy density and the tension. This can be covariantly described by the energy-momentum tensor localized at the string as Eq. (2) introducing the velocity field. The physical reason for the energy-momentum tensor t^{ab} is not the issue of the present paper. It may come from the configurations of Higgs and gauge fields or just particles depending on the model.

The four-dimensional energy-momentum tensor by a cosmic string configuration is given by

$$T^{\mu\nu}(x) = \int d\tau d\sigma \sqrt{-h} t^{ab}(\tau,\sigma)\partial_a X^\mu(\tau,\sigma)\partial_b X^\nu(\tau,\sigma)\frac{\delta^4(x - X(\tau,\sigma))}{\sqrt{-G(X)}}, \tag{3}$$

where $h = det(h_{ab})$ and $G = det(G_{\mu\nu})$.

We derive the basic equation of motion of the cosmic wiggly string. The motion of the string is dictated by $D_\mu T^{\mu\nu}(x) = 0$ i.e., the conservation of energy and momentum.

We differentiate Eq. (3) by x^μ and sum over μ :

$$\begin{aligned}
\frac{\partial T^{\mu\nu}}{\partial x^\mu} &= \int d\tau d\sigma \sqrt{-h} t^{ab}(\tau,\sigma)\partial_a X^\mu(\tau,\sigma)\partial_b X^\nu(\tau,\sigma)\frac{\partial \delta^4(x - X(\tau,\sigma))}{\partial x^\mu}\frac{1}{\sqrt{-G(X)}}, \\
&= \int d\tau d\sigma \frac{\partial}{\partial \xi^a} \quad \sqrt{-h} t^{ab}(\tau,\sigma)\partial_b X^\nu(\tau,\sigma)\frac{1}{\sqrt{-G(X)}}\Bigg)\delta^4(x - X(\tau,\sigma)), \\
&= \int d\tau d\sigma \quad \frac{\partial(\sqrt{-h} t^{ab}\partial_b X^\nu)}{\partial \xi^a}\frac{1}{\sqrt{-G(X)}} + \sqrt{-h} t^{ab}\partial_b X^\nu \frac{\partial}{\partial \xi^a}\left(\frac{1}{\sqrt{-G(x)}}\right)\Bigg)\delta^4(x - X), \\
&= \int d\tau d\sigma \quad \frac{\partial(\sqrt{-h} t^{ab}\partial_b X^\nu)}{\partial \xi^a} + \sqrt{-h} t^{ab}\partial_b X^\nu \sqrt{-G(x)}\frac{\partial}{\partial \xi^a}\left(\frac{1}{\sqrt{-G(x)}}\right)\Bigg)\frac{\delta^4(x - X)}{\sqrt{-G(x)}}, \\
&= \int d\tau d\sigma \quad \partial_a(\sqrt{-h} t^{ab}\partial_b X^\nu) - \Gamma^\rho_{\mu\rho}\frac{\partial X^\mu}{\partial \xi^a}\sqrt{-h} t^{ab}\partial_b X^\nu\Bigg)\frac{\delta^4(x - X)}{\sqrt{-G(x)}}, \\
&= \int d\tau d\sigma \partial_a(\sqrt{-h} t^{ab}\partial_b X^\nu)\frac{\delta^4(x - X)}{\sqrt{-G(x)}} - \Gamma^\rho_{\mu\rho}\int d\tau d\sigma \sqrt{-h} t^{ab}\partial_a X^\mu \partial_b X^\nu \frac{\delta^4(x - X)}{\sqrt{-G(x)}}, \\
&= \int d\tau d\sigma \partial_a(\sqrt{-h} t^{ab}\partial_b X^\nu)\frac{\delta^4(x - X)}{\sqrt{-G(x)}} - \Gamma^\rho_{\mu\rho} T^{\mu\nu}.
\end{aligned} \tag{4}$$

The covariant derivative of tensor $T^{\mu\nu}$ is defined by

$$D_\mu T^{\mu\nu} = \frac{\partial T^{\mu\nu}}{\partial x^\mu} + \Gamma^\mu_{m\mu} T^{m\nu} + \Gamma^\nu_{m\mu} T^{m\mu}. \tag{5}$$

From Eqs.(3),(4), Eq.(5) becomes

$$\begin{aligned}
D_\mu T^{\mu\nu} &= \int d\tau d\sigma \partial_a(\sqrt{-h} t^{ab}\partial_b X^\nu)\frac{\delta^4(x - X)}{\sqrt{-G(x)}} + \Gamma^\mu_{\nu\lambda} T^{\nu\lambda} \\
&= \int d\tau d\sigma \quad \partial_a(\sqrt{-h} t^{ab}\partial_b X^\nu) + \sqrt{-h}\Gamma^\mu_{\nu\lambda} t^{ab}\partial_a X^\nu \partial_b X^\lambda\Bigg)\frac{\delta^4(x - X)}{\sqrt{-G(x)}}.
\end{aligned} \tag{6}$$

The conservation of energy and momentum is equivalent to

$$\frac{1}{\sqrt{-h}}\partial_a \quad \sqrt{-h}t^{ab}(\tau,\sigma)\partial_b X^\mu \quad + \Gamma^\mu_{\nu\lambda}\partial_a X^\nu \partial_b X^\lambda t^{ab} = 0, \qquad (\mu = 0,1,2,3). \tag{7}$$

Here $\Gamma^\mu_{\nu\lambda}$ is the affine connection computed from the background metric. This has to be solved for X^μ and u^a.

The covariant derivative of Einstein Eq. is given by

$$D^\mu(R_{\mu\nu} - \frac{1}{2}g_{\mu\nu}R) = 8\pi G D^\mu T_{\mu\nu}, \tag{8}$$

where the conservation of energy and momentum $D^\mu T_{\mu\nu} = 0$ is derived because the left hand of Eq. (8) is zero by the Bianchi identity. The conservation law gives the equation of motion for topological defects which are either a particle or a string. If we consider a particle and a string as a small defect of spacetime, its motion is given by the motion of background spacetime. This concept is the characteristic of general relativity and was discussed in detail by Einstein, Infeld and Hoffmann[28].

3 Cosmic wiggly strings of arc configuration in black hole spacetime

It is well known that the minimal radius of stable circular orbit for a test particle around the Schwarzschild black hole is three times the Schwarzschild radius. We concerns with the minimal radius of stable circular orbit for a test string around the black holes. We study the classical motion of cosmic wiggly strings of arc configuration in the various black holes and obtain the new special solutions of them. The cosmic wiggly strings exhibit open strings lying along the circular orbit in the equatorial plane outside horizon in the various black holes. The solutions in the various black holes are compared with them in the Schwarzschild black hole.

At first, because of the simplicity of the equations, we study the cosmic wiggly string in the Schwarzschild black hole. In the presence of small scale wiggles the macroscopically average value of the energy density μ would exceed its Nambu-Goto value, while the tension $\tilde{T}$ decreases. The particular case of equation of state for a wiggly cosmic string

$$\mu\tilde{T} = {\mu_0}^2, \qquad (\mu_0 : const.) \tag{9}$$

is simple in the analysis.

We make the ansatz

$$\theta = \frac{\pi}{2}, \tag{10}$$

$$r = const., \tag{11}$$

$$ct = d\tau + e\sigma, \tag{12}$$

$$\varphi = m\tau + n\sigma, \tag{13}$$

where d, e, m and n are constants to be determined in what follows.

The conservation of energy and momentum (7) becomes

$$\frac{1}{\sqrt{-h}}\partial_\tau \quad \sqrt{\frac{-\left(1-\frac{2MG}{r}\right)e^2 + n^2r^2}{-\left(1-\frac{2MG}{r}\right)d^2 - m^2r^2}}\left(-\mu(\tau) + 2\frac{{\mu_0}^2}{\mu(\tau)}\right)\dot{X}^\mu\Bigg)$$
$$+\Gamma^r_{tt}\partial_a t\partial_b t t^{ab} + \Gamma^r_{\varphi\varphi}\partial_a\varphi\partial_b\varphi t^{ab} = 0. \tag{14}$$

As we can choose the off-diagonal element of the induced metric $h_{\tau,}$ in Eq. (1) to be zero, the solution of Eq. (14) for an open string must satisfy the following condition:

$$-\left(1 - \frac{2MG}{r}\right)de + mnr^2 = 0. \tag{15}$$

The condition for the solution of Eq. (15) to be outside the horizon $r > 2MG$ reads

$$\frac{de}{mn} \quad 27(MG)^2. \tag{16}$$

From Eqs.(12)-(15), we obtain a particular solution[29]

$$r = \frac{\mu(dn + 2em) - 3\frac{{\mu_0}^2}{\mu}em}{\mu em + \frac{{\mu_0}^2}{\mu}(dn - 2em)}MG, \tag{17}$$

where the solution is outside the horizon if the tension $\frac{{\mu_0}^2}{\mu}$ of string is zero or the average value of energy density μ of string is zero and $2 > \frac{em}{dn} > 1/2$ (Fig.1). The angular velocity ω, the angular momentum M^{xy} and the energy P^0 are generally defined by

$$\omega := \frac{d\varphi}{dt} = \frac{m}{d}, \tag{18}$$

$$M^{xy} := \int (xT^{y0} - yT^{x0})dxdydz = \pi\sqrt{\omega en}(\mu - 3\frac{{\mu_0}^2}{\mu})r^2, \tag{19}$$

$$P^0 := \int T^{00}dxdydz = \pi(\sqrt{\frac{en}{\omega}}(\mu - 2\frac{{\mu_0}^2}{\mu}) - e\sqrt{\frac{e\omega}{n}}\frac{{\mu_0}^2}{\mu}). \tag{20}$$

In the strongly wiggly case($\mu \gg \mu_0$), we have a simple expression for the radius r in terms of the angular velocity ω from Eqs. (15), (17) and (18),

$$r = \frac{1}{\omega^{2/3}}(MG)^{1/3}. \tag{21}$$

We can determine the parameters d, e, m, n if the angular velocity ω, the energy P^0 and the angular momentum M^{xy} are given, except for the overall magnitude of d and m, which comes from the arbitrariness of the scale of τ.

We have obtained the solutions for open cosmic wiggly strings of circular configuration in the Schwarzschild black hole. For a closed cosmic string we can obtain a circular solution by restricting the parameter $n = 2$. The extended solutions for open cosmic wiggly strings of circular configuration outside the horizon have been found. The Nambu-Goto limit of the cosmic string has only a point-like solution, while the fundamental generic string has only a null particle solution. This is because the freedom of Nambu-Goto cosmic string is more than the one of the fundamental string. In contrast to our present work, Frolov and the co-authors got open string solutions lying in the radial direction and Ishihara and co-authors classified closed string solutions in Minkowski spacetime. We have obtained the solutions around the Schwarzschild black holes under the gauge condition $ct \propto (\tau \quad \alpha\sigma)$ while usually people choose the gauge condition $ct = \tau$. It remains to be clarified why only this particular class of gauge fixing condition works.

In the case of the Reisner-Nordström black hole, the open cosmic wiggly string lies in the equatorial plane and rotates along a circular orbit of a shorter radius outside the horizon comparing with the circular orbit in the Schwarzschild spacetime because of the existence of charge[30]. One might be interested in the string configuration in the extreme case (Q=M). However, no qualitatively distinctive feature arises in the extreme limit. On the other hand, there are only point-like solutions for the Nambu-Goto cosmic string because of its high symmetry, i.e. more constraints than the cosmic wiggly string.

In the case of the Kerr black hole, the open cosmic wiggly string lies in the equatorial plane and rotates in the same direction as the Kerr spacetime along a circular orbit of a smaller radius outside the horizon comparing with the circular orbit in the Schwarzschild spacetime because of the existence of the angular momentum[31]. We have compared the strongly wiggly string solution in the case of small Kerr parameter with the one in the Schwarzschild spacetime. In the case of positive Kerr parameter, the obtained radius is smaller than that of the solution for the Schwarzschild spacetime, while it is larger in the case of the negative Kerr parameter. This feature of stable circular orbit of a test string conforms with that of a test particle in the Kerr spacetime. The parameter regions for the wiggly string solution to be outside of the horizon have been indicated(Fig.2).

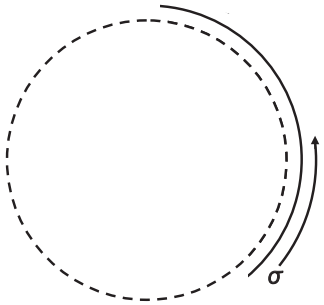

Figure 1: The string solution of arc configuration is shown. The dotted circle shows the horizon of spherically symmetric black hole, while the solid curve shows the string of arc configuration parametrized by the world sheet coordinate σ.

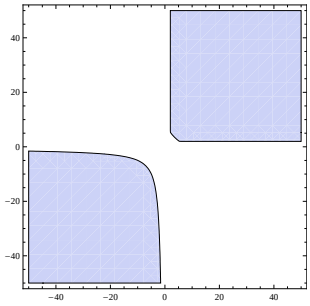

Figure 2: The shaded are parameter regions allowed in the case of $a = 1$, where the horizontal and vertical coordinate axes indicate d/m and e/n, respectively.

We have studied the relation of the string radius and the angular momentum in the case of a constant energy. The radius is larger with the decrease of the angular momentum for the positive Kerr parameter, while for the negative Kerr parameter the radius is smaller with the decrease of the angular momentum. The mechanism behind this phenomenon seems complicated and has not been fully understood. One might be interested in the string configuration in the expreme case($a = M$). However, no qualitatively distinctive feature arises in the extreme limit. On the other hand there are only point-like solutions for the Nambu-Goto cosmic string because of its high symmetry, i.e., more constraints. But we do not have any intuitive explanation for the existence of the extended solution in the case of the wiggly string. For example, we have found a curious but not fully understood phenomenon that the radius of the strongly wiggly string approaches the horizon as the angular velocity becomes larger.

We have obtained the solutions for open cosmic wiggly string in the Kerr-Newman black hole[32]. It is theoretically important to study the wiggly string solutions in the Kerr-Newman spacetime because the Kerr-Newman black hole is the most general stationary black hole. However, most of the black holes in the universe are generically rotating but there are no observational evidence that a black hole has a charge. We have showed that the solutions for the cosmic wiggly string reduced to a string-like extended

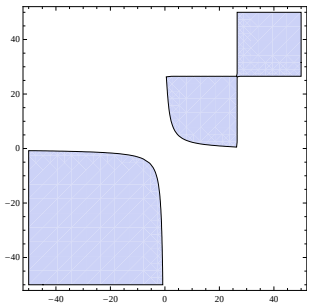

Figure 3: In the case of $a = 0.15$.

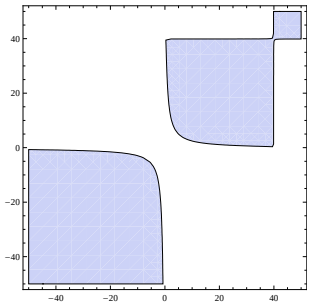

Figure 4: In the case of $a = 0.1$.

configuration in the Kerr-Newman spacetime and compared the solution with the cases of the Reisner-Nordström spacetime and the Kerr spacetime. We have found a new special solution of open wiggly strings in the (3+1)-dimensional stationally axially symmetric charged rotating black hole, though we cannot find any extended solution for the Nambu-Goto open string.

4 Cosmic wiggly strings of radial configuration in black hole spacetime

We have obtained the classical new special solutions of cosmic wiggly string of arc configuration in Sec. 3. Here we study classical motion of cosmic wiggly strings of radial configuration in the black holes as the extension of cosmic wiggly strings of arc configuration. The cosmic wiggly strings exhibit open strings pointing toward the origin in the equatorial plane outside the horizon in the various black holes. We show that there are two kinds of solutions : static and stationary solutions.

At first, because of the simplicity of the equations, we study classical motion of a string in (3+1)-dimensional spherically symmetric neutral black holes. We make the ansatz

$$\theta = \frac{\pi}{2}, \tag{22}$$

$$= const., \tag{23}$$

$$ct = \tau, \tag{24}$$

where we first study the static cosmic wiggly string by Eq. (23) for simplicity. Our string can be considered as an open string because our string solutions satisfy the free boundary condition at the end points $\sigma = 0$ and π,

$$\frac{\partial X_{\perp}{}^{\mu}}{\partial \sigma}|_{0,\pi} = 0, \tag{25}$$

where $X_{\perp}{}^{\mu}$ is the radial coordinate of the string, because $= const.$ in our case.

As we can choose the off-diagonal element of the induced metric h_{τ} in Eq. (2) to be zero while the two-dimensional energy-momentum tensor t has a finite value, the solution for a static string is given

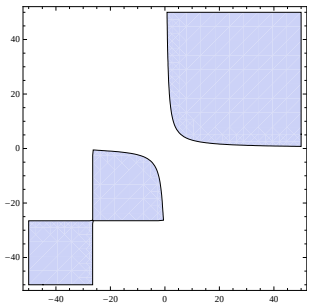

Figure 5: In the case of $a = -0.15$.

by the following equation:

$$\dot{r} = 0. \tag{26}$$

The essence of the dynamics of cosmic string can be described as the conservation of energy and stress. The conservation of energy and momentum (7) becomes

$$\mu M r'^2 + \frac{{\mu_0}^2}{\mu} \quad -5Mr'^2 + r(r-2M)r'' \quad = 0, \tag{27}$$

where $'$ is the derivative with respect to σ.

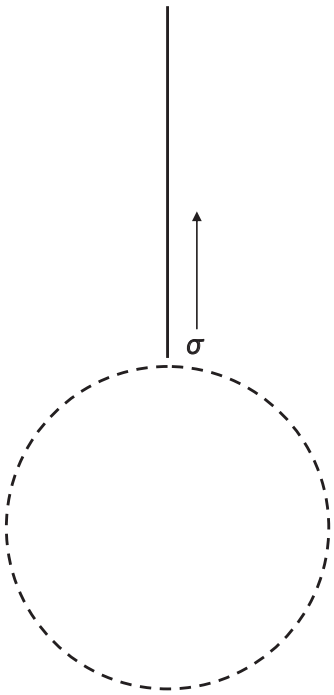

Figure 6: The string solution of radial configuration is shown. As the same as Fig. 1, the dotted circle shows the horizon of spherically symmetric black hole, while the solid line shows the string of radial configuration parametrized by the world sheet coordinate σ.

From Eq. (27), we obtain the solution of equation[33] (Fig. 6) as

$$\sigma = \frac{1}{b}\int_{r_0}^{r} dr \quad \frac{r}{r-2M} \quad ^{\frac{1}{2}(5-\frac{\mu^2}{{\mu_0}^2})}, (0 < \sigma < \pi) \tag{28}$$

where b is a constant that is defined by the following equation

$$b = r' \ \frac{r}{r-2M} \ ^{\frac{1}{2}(5-\frac{{\mu_0}^2}{\mu^2})}. \tag{29}$$

In the special case of the ratio $\frac{\mu^2}{{\mu_0}^2} = 4$ of the energy density to the tension we obtain the solution of equation as

$$\sigma(r=2) = 0, \tag{30}$$

$$\sigma = 2 \ \sqrt{\frac{r}{2}-1} \ \frac{r}{2} + \log \ \sqrt{\frac{r}{2}} + \sqrt{\frac{r}{2}-1} \quad . \tag{31}$$

The obtained cosmic wiggly string lies in the radial direction in the equatorial plane outside horizon and the string gets longer as the ratio $\frac{\mu^2}{{\mu_0}^2}$ of the energy density to the tension increases.

The energy P^0 is explicitly evaluated as

$$\begin{aligned} P^0 : &= \int T^{00} dxdydz \\ &= \frac{1}{c} \ \mu - 2\frac{{\mu_0}^2}{\mu} \quad r + 2M\log(r-2M) + A \ , \end{aligned} \tag{32}$$

where $T^{\mu\nu}$ is the four-dimensional energy-momentum tensor given by Eq. (3) and A is an integral constant.

we study a slowly stationary rotating cosmic wiggly string solution in the radial direction in the equatorial plane outside horizon in the Schwarzschild black hole.

We make the ansatz

$$\theta = \frac{\pi}{2}, \tag{33}$$

$$= \quad \tau, \tag{34}$$

$$ct = \tau, \tag{35}$$

where is a constant. Note that Eq. (34) implies a stationary rotation in contrast to Eq. (23).

The conservation of energy and momentum (7) becomes

$$\begin{aligned} &\mu(- \ ^2r^4 + 2M \ ^2r^3 + Mr - 2M^2){r'}^2 \\ &+\frac{{\mu_0}^2}{\mu} \ (3 \ ^2r^4 - 4M \ ^2r^3 - 5Mr + 10M^2){r'}^2 + r(- \ ^2r^3 + r - 2M)(r-2M)r'' \\ &= 0, \end{aligned} \tag{36}$$

where $'$ is the derivative with respect to σ and which corresponds to Eq. (27) in the case of $= 0$.

The obtained cosmic wiggly string is rotating very slowly outside horizon[33]. The maximum angular velocity of the cosmic wiggly string which starts from $r(\sigma = 0) = 2.01$ is about $= 0.03509$ where the cosmic wiggly string shrinks to a point. In the case of the ratio $\frac{\mu^2}{{\mu_0}^2} \leq 11$ of the energy density to the tension the maximum angular velocity of the cosmic wiggly string which starts from $r(\sigma = 0) = 2.1$ is about $= 0.10391$ where the cosmic wiggly string shrinks to a point. In the case of the ratio $\frac{\mu^2}{{\mu_0}^2}$ 11.9 of the energy density to the tension the cosmic wiggly string which starts from $r(\sigma = 0) = 2.1$ gets longer as the angular velocity increases and the wiggly string solution suddenly disappears. In the case of the intermediate ratio $\frac{\mu^2}{{\mu_0}^2} = 11.5$ of the energy density to the tension for example the cosmic wiggly string which starts from $r(\sigma = 0) = 2.1$ gets longer until the angular velocity reaches 0.045. and gets shorter and shrinks to a point at about $= 0.10391$.

The energy P^0 is generally defined by Eq. (32). The angular momentum M^{xy} is given by

$$\begin{aligned} M^{xy} &:= \int dxdydz(xT^{y0} - yT^{x0}) \\ &= (\mu - 2\frac{{\mu_0}^2}{\mu}) \ \int dr \frac{r^3}{\sqrt{(r-2M)(- \ ^2r^3 + r - 2M)}}. \end{aligned} \tag{37}$$

The solutions for open cosmic wiggly strings of radial configuration in the Reisner-Nordström black hole have been obtained in [33]. We have obtained the special solution of open cosmic wiggly string in the radial direction in a black hole spacetime which gets shorter with the increase of the charge. With the increase of the angular velocity the cosmic string gets longer or shorter depending on the strong or weak wiggliness. We can observe a curious behavior for the marginally wiggly case that is a little smaller than a certain value. The cosmic wiggly string gets shorter with the increase of the angular velocity and becomes a point when the ratio of the energy density to the tension is very smaller than the certain value (Fig. 7). In Figure 7, the flat regions indicate the regions where the cosmic wiggly string becomes a point. With the increase of charge the flat region shrinks and the maximum value of angular velocity $_{max}$ becomes larger.

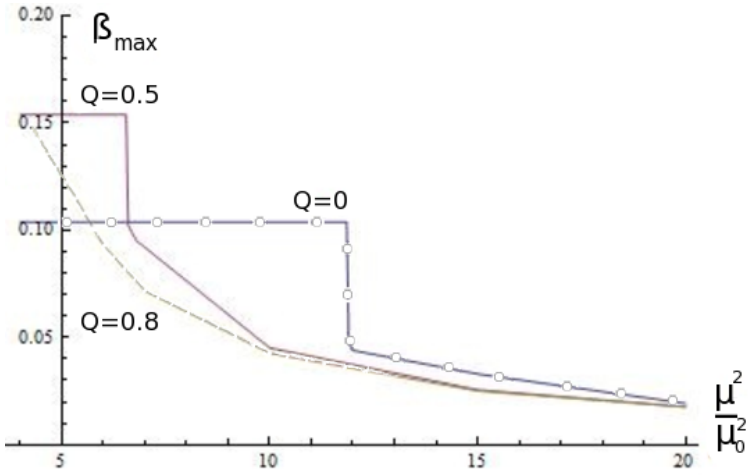

Figure 7: The relations between the ratio of the enaergy density to the tension $\frac{\mu^2}{{\mu_0}^2}$ and the maximum value of angular velocity $_{max}$ are shown in the cases of the charge $Q = 0, 0.5, 0.8$, where the horizontal and vertical coordinate axes indicate $\frac{\mu^2}{{\mu_0}^2}$, $_{max}$, respectively.

The solutions for open cosmic wiggly strings of radial configuration in the Kerr spacetime have been obtained[34]. We have obtained the special solution of open cosmic wiggly string in the radial direction in the Kerr spacetime which gets longer with the increase of the ratio of the energy density to the tension and shorter with the increase of the absolute of the Kerr parameter. With the increase of the angular velocity the cosmic string gets longer or shorter depending on the strong or weak wiggliness. We can observe a curious behavior for the marginally wiggly case that is slightly smaller than a certain value. The cosmic wiggly string gets shorter with the increase of the angular velocity and becomes a point when the ratio of the energy density to the tension is very smaller than the certain value (Fig. 8). Especially in the case of $a < 0$ the behavior is more complicated comparing the case of the Schwarzschild spacetime. In Figure 8, the flat regions indicate the regions where the cosmic wiggly string becomes a point. With the increase of Kerr parameter a the flat region is enlarged and the maximum value of angular velocity $_{max}$ becomes smaller. In the case of negative Kerr parameter, the flat region is larger than that of the case of positive Kerr parameter and the maximum value of angular velocity $_{max}$ takes the same value. One might be interested in the wiggly string configuration in the extreme case($a = 1$). However, nothing qualitatively distinctive feature arises in the extreme limit.

The solutions for open cosmic wiggly strings of radial configuration in the Kerr-Newman spacetime have been obtained[35]. The difference is the critical values of $\frac{\mu^2}{{\mu_0}^2}$ where the behavior of the string configuration drastically changes;shrinking to a point or the total disappearance after reaching the maximum radius. We have obtained the special solution of open cosmic wiggly string in the radial direction in the Kerr-Newman spacetime which gets longer with the increase of the ratio of the energy density to the tension, slightly shorter with the increase of the charge and shorter with the increase of the absolute of the Kerr parameter. This conclusion corresponds to the one in the Reisner-Nordström black hole and the Kerr black hole. With the increase of the angular velocity the cosmic wiggly string gets longer or shorter

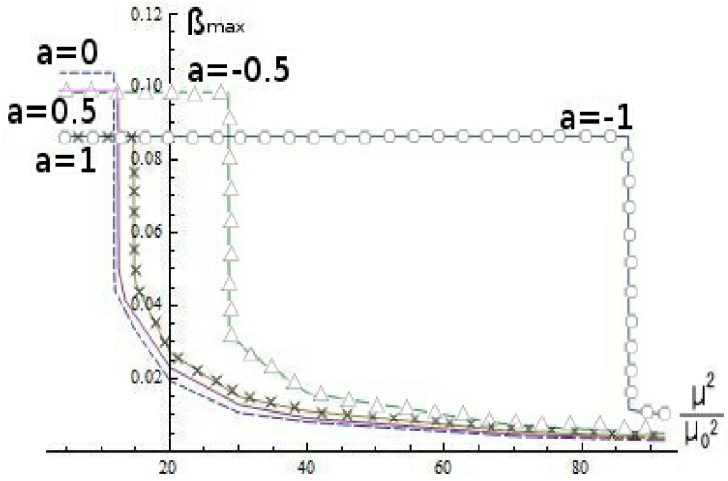

Figure 8: The relations between the ratio of the energy density to the tension $\frac{\mu^2}{{\mu_0}^2}$ and the maximum value of angular velocity $_{max}$ in the cases of the Kerr parameter $a = 0, 0.5, 1, -0.5, -1$

depending on the strong or weak wiggliness. We can observe a curious behavior for the marginally wiggly case that is a little smaller than a certain value. The cosmic wiggly string gets shorter with the increase of the angular velocity and becomes a point when the ratio of the energy density to the tension is very smaller than the certain value. Especially in the case of $a < 0$ the behavior is more complicated comparing the case of the Schwarzschild spacetime. One might be interested in the wiggly string configuration in the extreme case($a = 1$). However, nothing qualitatively distinctive feature arises in the extreme limit.

In contrast to our present work, V. Frolov *et al.* got rigidly rotating open string solutions lying in the radial direction which are the curved strings and not straight[19]. H. J. de Vega *et al.* got a straight nonoscillating string, radially disposed which rotates uniformly around the symmetry axis of the spacetime and which becomes an infinite static fundamental string from the horizon to infinity as the angular velocity approaches to zero[15]. H. Ishihara and H. Kozaki classified string solutions with geometrical symmetries in Minkowski spacetime[21].

In view of other solutions found by Frolov, de Vega and Ishihara et al. we suspect there will be rich variety of wiggly string solutions in a black hole background. The evolution of wiggly cosmic strings will be more interesting if they are trapped by black holes. However, its cosmological significance remains to be studied.

5 Conclusion

The cosmic wiggly string solutions have been obtained outside the horizon in all stationary black hole spacetimes. One is the cosmic wiggly string solutions of arc configuration. The other is the cosmic wiggly string solution of radial configuration in black hole spacetime, which exhibits finite open strings pointing toward the origin in the equatorial plane outside the horizon. The test string can exist near the horizon of black hole though the test particle cannot exist near the horizon of black hole. We hope that this investigation of test string as a probe further enchances the understanding of black holes.

References

[1] T. W. B. Kibble, *J. Phys.* **A9**, 1387 (1976).

[2] M. B. Hindmarsh and T. W. B. Kibble, *Rept. Prog. Phys.* **58**, 477 (1995). [arXiv:hep-ph/9411342].

[3] A. Vilenkin and E. P. S. Shellard,*Cosmic Strings and Other Topological Defects*(Cambridge University Press, 1994).

[4] M. R. Anderson, *The Mathematical Theory of Cosmic Strings* (Institute of Physics, Bristol 2003).

[5] Y. B. Zeldovich, *Mon. Not. Roy. Astron. Soc.* **192**, 663 (1980).

[6] A. Vilenkin, *Phys. Rev. Lett.* **46**, 1169 (1981).

[7] A. Albrecht, R. A. Battye and J. Robinson, *Phys. Rev. Lett.* **79**, 4736 (1997).

[8] A. Albrecht, R. A. Battye and J. Robinson, *Phys. Rev.* **D59**, 023508 (1998).

[9] E. J. Copeland, R. C. Myers and J. Polchinski, *High Energy Phys.* JHEP06, 013 (2004).

[10] H. J. de Vega and N. G. Sánchez, *Phys. Lett.* **B197**, 320 (1987).

[11] H. J. de Vega and N. G. Sánchez, *Phys. Rev.* **D47**, 3394 (1993) .

[12] H. J. de Vega, A. L. Larsen and N. G. Sánchez, *Nucl. Phys.* **B427**, 643 (1994).

[13] A. L. Larsen and N. G. Sánchez, *Phys. Rev.* **D50**, 7493 (1994).

[14] A. L. Larsen and N. G. Sánchez, *Phys. Rev.* **D51**, 6929 (1995).

[15] H. J. de Vega and I. L. Egusquiza, *Phys. Rev.* **D54**, 7513 (1996).

[16] *Phys. Rev.* **D60**, 125014 (1999).

[17] V. P. Frolov, V. D. Skarzhinsky, A. I. Zelnikov and O. Heinrich, *Phys. Lett.* **B224**, 255 (1989).

[18] B. Carter and V.P. Frolov, *Class. Quantum Grav.* **6**, 569 (1989).

[19] V. P. Frolov, S. Hendy and J. P. de Villiers, *Class. Quantum Grav.* **18**, 1535(2001)

[20] V. P. Frolov and D. Fursaev, *Class. Quantum Grav.* **14**, 1099(1997).

[21] H. Ishihara and H. Kozaki, *Phys. Rev.* **D72**, 061701 (2005).

[22] J. Hong, J. Kim and P. Sikivie, *Phys. Rev. Lett.* **69**, 2611 (1992).

[23] J. Kim and P. Sikivie, *Phys. Rev.* **D50**, 7410 (1994).

[24] B. Carter, *Phys. Rev.* **D41**, 3869 (1990).

[25] B. Carter, *Phys. Rev. Lett.* **74**, 3098 (1995).

[26] B. Carter, *Phys. Rev.* **D60**, 083502(1999).

[27] A. Arazi and C. Simeone, *Mod. Phys. Lett.* **A15**, 1369 (2000).

[28] A. Einstein, L. Infeld, and B. Hoffmann, *Ann. Math.* **39**, 65(1938).

[29] H. Suzuki, *Prog. Theor. Phys.* **120**, 865(2008).

[30] H. Suzuki, *Mod. Phys. Lett.* **A25**, 1233(2010).

[31] H. Suzuki, *Prog. Theor. Phys.* **124**, 181(2010).

[32] H. Suzuki, *Mod. Phys. Lett.* **A26**, 1221(2010).

[33] H. Suzuki, *Int. J. Mod. Phys.* **A26**, 3275(2011).

[34] H. Suzuki, *Mod. Phys. Lett.* **A26**, 1933(2011).

[35] H. Suzuki, *Gen. Relativ. Gravit.* **44**, 1937(2012).

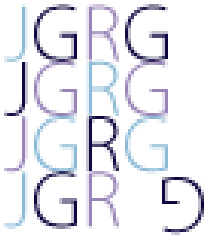

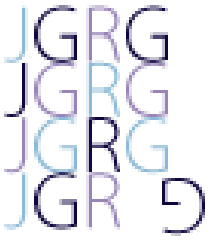

Kazunari Eda, JGRG 22(2012)111347

"Effect of dark matter halos around IMBHs on gravitational waves"

RESCEU SYMPOSIUM ON

GENERAL RELATIVITY AND GRAVITATION

JGRG 22

November 12-16 2012

Koshiba Hall, The University of Tokyo, Hongo, Tokyo, Japan





Effect of dark matter halos around IMBHs on the gravitational waves

Kazunari Eda

in collaboration with Y. Itoh, S. Kuroyanagi and J.Silk

RESCEU University of Tokyo

Introduction

IMBHs formation and their property

The purpose of this work is to estimate the effect of a dark matter (DM) halo around an intermediate mass black hole (IMBH) on GW. According to Ref.[3], there are two different IMBH formation scenarios. The first scenario is that IMBH is a remnant of collapse of a Pop III star. The second scenario is that IMBH is formed by cold gas within the early forming halos. Both scenarios predict that IMBH in the present is surrounded by dark matter mini-halo. (See Fig.1).

Dark matter mini-halo distribution

The DM profile of a mini-halo can be well approximated by Navarro, Frenk, and White (NFW) profile. But for simplicity, we assume that the DM density is distributed in a spherically symmetric manner around the IMBH and that the radial distribution is described by a power law between r_{min} and r_{max},

$$\rho(\boldsymbol{x}) = \rho_0 \left(\frac{r_0}{r}\right)^{\alpha} \quad (r_{\min} \le r \le r_{\max})$$

where ρ_0 500 $M_\odot$ /pc^3 and r_0 is 1.6 pc according to Ref[2]. r_{min} is a minimum value of the radial distance beyond which stable circular orbits are no longer allowed, that is, an Innermost Stable Circular Orbit (ISCO). So $r_{min} = r_{ISCO} = 6GM_{BH}/c^2$. r_{max} is the size of the DM mini-halo.

Formulation

Dark matter mini-halo distribution

We consider the binary systems which consist of a IMBH which has M_{BH}~10^3 $M_\odot$ and a star which has μ~1 $M_\odot$. The IMBH is surrounded by a DM halo which has a spherical density distribution and exists between r_{max} and r_{min}. We suppose that the DM density is still unperturbed even when the star orbits in the DM halo, which is justified by the fact that the DM total mass~10^6 $M_\odot$ is much larger than the star mass. In other words, we treat the star as a test-particle and we call it a "particle" in the following. The system that we examine here is idealized in comparison with the real astrophysical sources. However this idealization allows us to estimate the order of magnitude of DM effects on GW. In this situation, the equation of motion for the particle can be written as

$$\frac{d^2r}{dt^2} = -\frac{GM_{\rm eff}}{r^2} - \frac{F}{r^{\alpha-1}} + \frac{l^2}{r^3}$$

where l is the angular momentum of the particle per its mass, and M_{eff} and F is

$$M_{\rm eff} = \begin{cases} M_{\rm BH} + \dfrac{4\pi r_0^\alpha \rho_0}{3-\alpha}\left(r_{\max}^{3-\alpha} - r_{\min}^{3-\alpha}\right) \\ M_{\rm BH} - \dfrac{4\pi r_0^\alpha \rho_0}{3-\alpha} r_{\min}^{3-\alpha} \\ M_{\rm BH} \end{cases}, \quad F = \begin{cases} 0 & (r \ge r_{\max}) \\ \dfrac{4\pi G r_0^\alpha \rho_0}{3-\alpha} & (r_{\min} \le r \le r_{\max}) \\ 0 & (r \le r_{\min}) \end{cases}.$$

In the first term of the right hand side of this equation of motion, the dark matter mini-halo modifies the effective mass of the central BH. The second term contains interesting information of the DM halo radial distribution. The third term is regarded as a centrifugal force. We assume that the second term is much smaller than the first term,

$$\varepsilon r^{3-\alpha} \ll 1 \quad \left(\varepsilon \equiv \frac{F}{GM_{\rm eff}}\right),$$

that is, we can treat the term which involves DM halo as a perturbation. When the particle orbits circularly around the IMBH, the left hand side of the equation of motion vanishes, and we get the circular orbit radius F. Computing the GW waveforms, we obtain the amplitudes for $h+$ and $h\times$,

$$h_+ = \frac{1}{r}\frac{4G\mu\omega_s^2 R^2}{c^4}\frac{1+\cos^2\iota}{2}\cos(2\omega_s t)$$
$$h_\times = \frac{1}{r}\frac{4G\mu\omega_s^2 R^2}{c^4}\cos\iota\sin(2\omega_s t)$$

where ι is the inclination which is the angle between the normal to the orbit and the line-of-sight, and $2\omega_s$ is the GW frequency.

Waveforms including GW back-reaction

Then we include the effect of the GW back-reaction within linearized theory. The orbital radius and frequency is not constant any longer, because GW radiation energy E_{GW} is taken from the rotational energy E_{orbit} of the particle.

$$\frac{dE_{\rm orbit}}{dt} = -\frac{dE_{\rm GW}}{dt}.$$

This differential equation of time gives the relation between the orbital radius R and the time. Using this relation, we can compute the orbital frequency ω_s depending on time. So we replace ω_s and R in time-independent waveforms with time-dependent ω_s and R to get the waveform including the GW back-reaction.

In order to compare the theoretical waveforms with the experimental sensitivities, we must perform the Fourier transform of the waveforms. Using the stationary phase method with which only the slowly varying term in the Fourier integral can survive , we express the amplitude in Fourier space as expansions in ε,

$$\tilde{h}_+(f) = \left(\frac{5}{24}\right)^{\frac{1}{2}} \frac{e^{i\Psi_+(f)}}{\pi^{\frac{2}{3}} f^{\frac{7}{6}}} \frac{c}{r}\left(\frac{GM_c}{c^3}\right)^{\frac{5}{6}} \frac{1+\cos^2\iota}{2}\left[1 + \frac{7-2\alpha}{3}\left(\frac{GM_{\rm eff}}{\pi^2 f^2}\right)^{\frac{3-\alpha}{3}}\varepsilon + \cdots\right]$$

$$\tilde{h}_\times(f) = \left(\frac{5}{24}\right)^{\frac{1}{2}} \frac{e^{i\Psi_\times(f)}}{\pi^{\frac{2}{3}} f^{\frac{7}{6}}} \frac{c}{r}\left(\frac{GM_c}{c^3}\right)^{\frac{5}{6}} \cos\iota\left[1 + \frac{7-2\alpha}{3}\left(\frac{GM_{\rm eff}}{\pi^2 f^2}\right)^{\frac{3-\alpha}{3}}\varepsilon + \cdots\right]$$

$$\Psi_+ = 2\pi f\left(t_c + \frac{r}{c}\right) - \Phi_0 - \frac{\pi}{4} + 2\left(\frac{GM_c}{c^3}8\pi f\right)^{-\frac{5}{3}} \times \left[1 + \frac{10}{3}\frac{2\alpha-5}{2\alpha-11}\left(\frac{GM_{\rm eff}}{\pi^2 f^2}\right)^{\frac{3-\alpha}{3}}\varepsilon - \frac{5}{9}\frac{(2\alpha-1)(4\alpha-11)}{4\alpha-17}\left(\frac{GM_{\rm eff}}{\pi^2 f^2}\right)^{\frac{2(3-\alpha)}{3}}\varepsilon^2 + \cdots\right]$$

$$\Psi_\times = \Psi_+ + \frac{\pi}{2}$$

where t_c is the retarded time at coalescence, Φ_0 is the value of the phase at coalescence, M_c is the chirp mass, and $\Psi_\pm$ is the phase of the waveform $h_\pm$. These expansions are valid for the frequency f in which the higher order terms are negligible.

Definition of signal-to-noise ratio

To estimate the detectability, we must compute the signal-to-noise ratio, which is defined as S/N,

$$\left(\frac{S}{N}\right)^2 = 4\frac{\left[\int_{f_{\rm ini}}^{\infty} df\, \dfrac{\tilde{h}(f)\tilde{h}_t^*(f)}{S(f)}\right]^2}{\int_{f_{\rm ini}}^{\infty} df\, \dfrac{\left|\tilde{h}_t(f)\right|^2}{S(f)}}$$

where h(f) is the GW signal that is coming in the detector, h_t(f) is the template which is the GW signal we infer in advance, and S(f) is the spectral density that depends on the detector. We consider that the GW is detected by the evolved Laser Interferometer Space Antenna (eLISA). According to Ref [4], the sensitivity of eLISA is shown in Fig.2, which is the square root of the spectral density S(f).

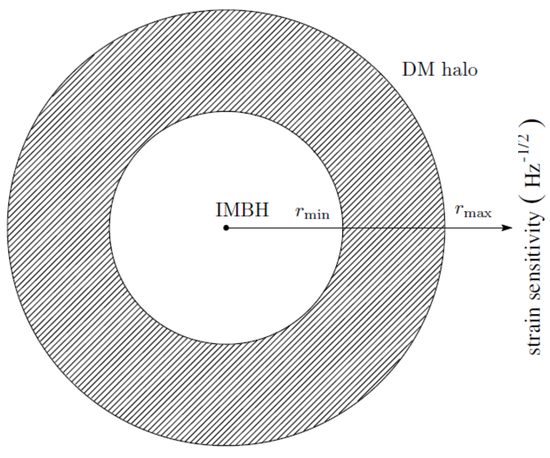

Fig.1: IMBH surrounded by DM mini-halo

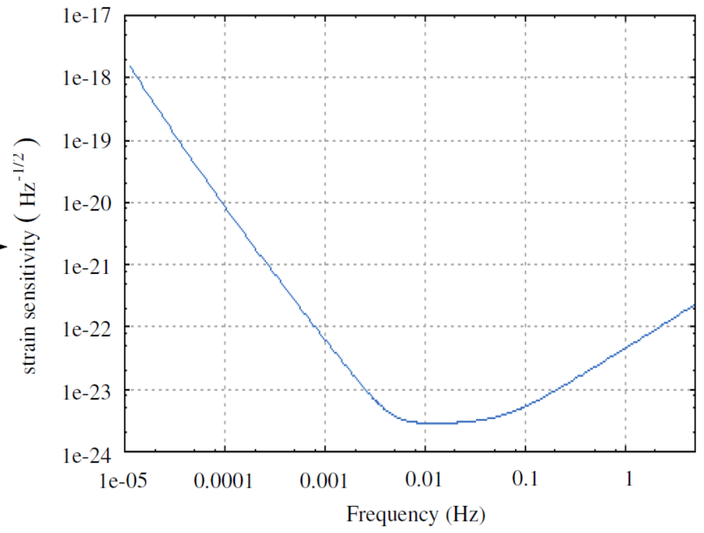

Fig.2: Sensitivity of eLISA

Conclusions

We assume that eLISA observes the GW for 5.0 years until the coalescence, then the interval of the frequency integration is from 22.7 mHz to infinity. P is defined as S/N in which a template is calculated including both the IMBH and the DM mini-halo gravitational potential and Q is defined as S/N in which a template is calculated including only IMBH. According to Ref [3], the power law index is α=7/3. So,

P/Q = 1.6×10^-3

This result means that in order to detect the GW from a binary where a star orbits around an intermediate mass black hole surrounded by a mini-halo in practice we must calculate the template including the effect of the DM halo. P/Q strongly depends on the power law index α. So if the GW is detected, the power law index would be determined very accurately.

Bibliography

[1] Maggiore, M "Gravitational Waves: Volume 1: Theory and Experiments" Oxford Unversity Press(2007)

[2] Zhao, H., Silk, J. "Dark minihalos with intermediate Mass Black Holes" Phys.Rev. Lett. 95, 011301(2005)

[3] Bertone, G., Zentner, A., Silk, J. "New signature of dark matter annihilations: Gamma rays from intermediate-mass black holes" Phys.Rev Lett. D 72, 103517(2005)

[4] "eLISA: Astrophysics and cosmology in the millihertz regime " arXive:1201.3621 (2012)

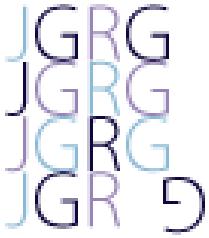

Yuhei Miyamoto, JGRG 22(2012)111348

"The effect of gauge fields on oscillating scalar fields at finite temperature"

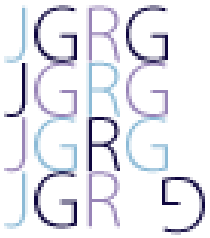

RESCEU SYMPOSIUM ON

GENERAL RELATIVITY AND GRAVITATION

JGRG 22



November 12-16 2012

Koshiba Hall, The University of Tokyo, Hongo, Tokyo, Japan



P37

The effect of gauge fields on oscillating scalar fields at finite temperature

Yuhei Miyamoto

RESCEU D1



Motivation

Our ultimate aim:
observational exploration of the early Universe
(mainly by using Gravitational Waves)

→We must consider all the sources of GWs.

→How about GWs from phase transition?

GW property depends on the types of phase transition.

(1st/2nd order? strong /weak 1st order?)

Question:
"How the fields affect the dynamics of
the scalar field?"

Previous study

- Effects from scalar bosons and a fermion have already studied.

  [Yamaguchi and Yokoyama, 97; Yokoyama, 04]

  → their contribution is interpreted as

  non-local memory terms and noise terms in the EoM of the scalar field.

$$\mathcal{L} = \frac{1}{2}(\partial_\mu\phi)^2 - \frac{1}{2}m_\phi\phi^2 - \frac{1}{4}\lambda\phi^4 + \frac{1}{2}(\partial_\mu\chi)^2 - \frac{1}{2}m_\chi\chi^2 - \mathcal{M}\phi\chi^2 - \frac{1}{4}h^2\chi^2\phi^2 + i\bar{\psi}\gamma^\mu\partial_\mu\psi - m_\psi\bar{\psi}\psi - f\phi\bar{\psi}\psi$$

$$(\Box + M^2)\phi(x) + \frac{\lambda}{3!}\phi^3(x) + \int_{-\infty}^{t} dt' \int d^3x' C_a(x-x')\phi(x') + \phi(x)\int_{-\infty}^{t} dt' \int d^3x' C_m(x-x')\phi^2(x')$$

non-local terms

$$= \xi_a(x) + \phi(x)\xi_m(x)$$

additive/multiplicative noise

Question:
How about gauge fields?
Is their effect similar to that of scalar boson?

settings

As a first step, we consider U(1) gauge field A_μ and complex scalar field Φ, whose interaction is determined by gauge principle.

Lagrangian density is as follows.

$$\begin{aligned}\mathcal{L} =& D_\mu\phi \cdot D^\mu\phi^* - m^2\phi\phi^* \\ =& (\partial_\mu - ieA_\mu)\phi \cdot (\partial^\mu + ieA^\mu)\phi^* - m^2\phi\phi^* \\ =& \partial_\mu\phi\partial^\mu\phi^* - m^2\phi\phi^* + ieA^\mu(\phi^*\partial_\mu\phi - \phi\partial_\mu\phi^*) + e^2A_\mu A^\mu\phi\phi^*\end{aligned}$$

Finite Temperature Field Theory

- Path integral expression for the generating functional $Z[J]$

$$Z[J;\beta] = \int \mathcal{D}\phi \, \exp\left[i \int_c d^4x \, (\mathcal{L}[\phi] + J(x)\phi(x)) \right]$$

J and Φ are defined on path c.
on "plus contour" and "minus contour",
we use J^+, J^-, ϕ^+, ϕ^- .

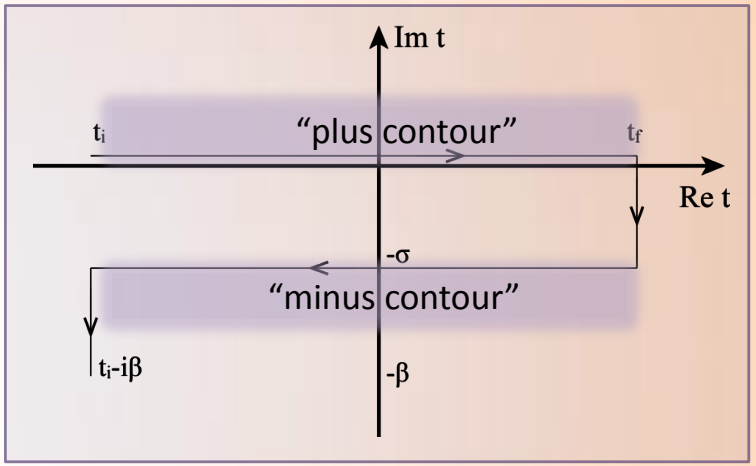

- We have 4 propagators with additional term representing finite temperature effect.
ex) scalar propagator in momentum space
(σ=0)

$$\tilde{G}^{++}(k) = \frac{i}{k^2 - m^2 + i\epsilon} + n(|k_0|)2\pi\delta(k^2 - m^2)$$
$$= \left(\tilde{G}^{--}(k)\right)^*$$
$$\tilde{G}^{+-}(k) = [n(|k_0|) + \theta(-k_0)]2\pi\delta(k^2 - m^2)$$
$$\tilde{G}^{-+}(k) = [n(|k_0|) + \theta(+k_0)]2\pi\delta(k^2 - m^2)$$

Effective Action

To describe the evolution of the expectation value of the scalar field, we use effective action.

Related quantyties:

$Z[J]$: Generating functional of correlation functions

$W[J]$: Generating functional of connected correlation functions

$$\exp\left[W[J]\right] = Z[J]$$

$\Gamma[\phi]$: Legendre transformation of $W[J]$ (variable: J→Φ)

$$\Gamma[\phi] = W[J] - \int J(x)\phi(x)\,dx$$

Only 1PI(one particle irreducible) diagrams contribute to $\Gamma[\phi]$.

Perturbative expansion

- It seems impossible to obtain full effective action.

  →Loop expansion also seems impossible.

  →perturbative expansion w.r.t. coupling constant
- The lowest order (order e^2)1PI diagrams are…

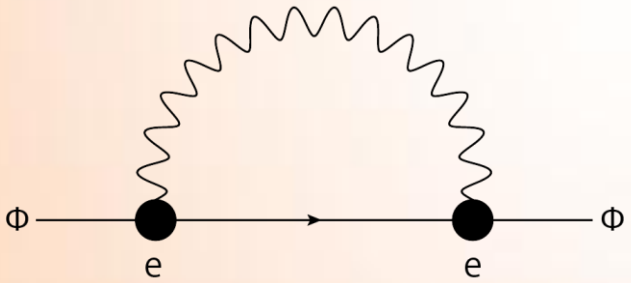

diagram 1

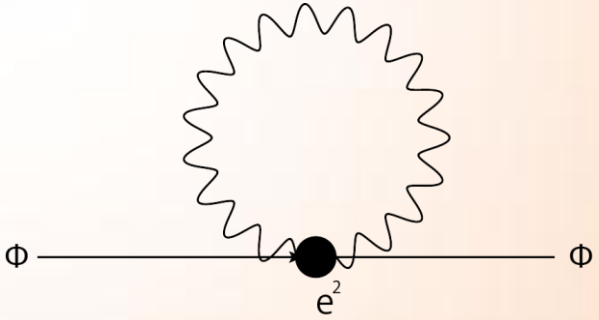

diagram 2

Finite temperature effective action

- The diagram 1 corresponds to the following effective action.

$$
\begin{aligned}
i\Gamma \supset & -e^2 \int d^4z_1 d^4z \phi^+(z_1)\phi^{+*}(z_2) \\
& \times \left[2\frac{\partial}{\partial z_1^\nu} D^{\mu\nu}_{++}(z_1-z_2)\cdot \frac{\partial}{\partial z_2^\mu} G^{++}(z_1-z_2) + 2\frac{\partial}{\partial z_2^\nu} D^{\mu\nu}_{++}(z_1-z_2)\cdot \frac{\partial}{\partial z_1^\mu} G^{++}(z_1-z_2) \right. \\
& \left. + 4D^{\mu\nu}_{++}(z_1-z_2)\frac{\partial}{\partial z_1^\mu}\frac{\partial}{\partial z_2^\nu} G^{++}(z_1-z_2) + \frac{\partial}{\partial z_1^\mu}\frac{\partial}{\partial z_2^\nu} D^{\mu\nu}_{++}(z_1-z_2) \times G^{++}(z_1-z_2) \right] \\
& -e^2 \int d^4z_1 d^4z \phi^-(z_1)\phi^{-*}(z_2) \\
& \times \left[2\frac{\partial}{\partial z_1^\nu} D^{\mu\nu}_{--}(z_1-z_2)\cdot \frac{\partial}{\partial z_2^\mu} G^{--}(z_1-z_2) + 2\frac{\partial}{\partial z_2^\nu} D^{\mu\nu}_{--}(z_1-z_2)\cdot \frac{\partial}{\partial z_1^\mu} G^{--}(z_1-z_2) \right. \\
& \left. + 4D^{\mu\nu}_{--}(z_1-z_2)\frac{\partial}{\partial z_1^\mu}\frac{\partial}{\partial z_2^\nu} G^{--}(z_1-z_2) + \frac{\partial}{\partial z_1^\mu}\frac{\partial}{\partial z_2^\nu} D^{\mu\nu}_{--}(z_1-z_2) \times G^{--}(z_1-z_2) \right] \\
& +e^2 \int d^4z_1 d^4z \left[\phi^+(z_1)\phi^{-*}(z_2) + \phi^{+*}(z_1)\phi^-(z_2) \right] \\
& \times \left[+2\frac{\partial}{\partial z_1^\nu} D^{\mu\nu}_{+-}(z_1-z_2)\cdot \frac{\partial}{\partial z_2^\mu} G^{+-}(z_1-z_2) + 2\frac{\partial}{\partial z_2^\nu} D^{\mu\nu}_{+-}(z_1-z_2)\cdot \frac{\partial}{\partial z_1^\mu} G^{+-}(z_1-z_2) \right. \\
& \left. + 4D^{\mu\nu}_{+-}(z_1-z_2)\frac{\partial}{\partial z_1^\mu}\frac{\partial}{\partial z_2^\nu} G^{+-}(z_1-z_2) + \frac{\partial}{\partial z_1^\mu}\frac{\partial}{\partial z_2^\nu} D^{\mu\nu}_{+-}(z_1-z_2)\cdot G^{+-}(z_1-z_2) \right]
\end{aligned}
$$

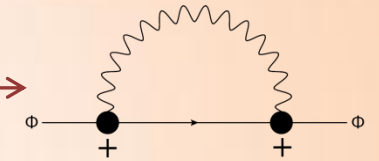

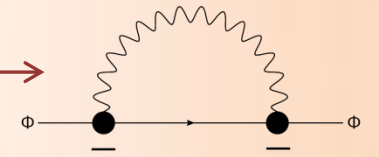

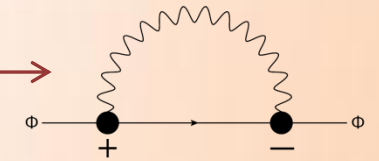

- The diagram 2 corresponds to the following effective action.

$$
\begin{aligned}
i\Gamma \supset \quad & ie^2 \int d^4z \left(\phi_\Delta \phi^*_\Delta + \frac{1}{2}\phi_c \frac{1}{2}\phi^*_c \right) \left(D^{\mu\,++}_\mu(0) - D^{\mu\,--}_\mu(0) \right) \\
& + ie^2 \int d^4z \frac{1}{2} \left(\phi_\Delta \phi^*_c + \frac{1}{2}\phi_c \frac{1}{2}\phi^*_\Delta \right) \left(D^{\mu\,++}_\mu(0) + D^{\mu\,--}_\mu(0) \right)
\end{aligned}
$$

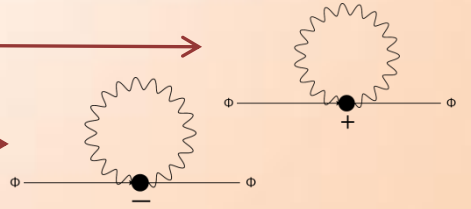

calculation of the effective action

- After some calculation, we can see there is an **IMAGINARY PART** in the effective action.
- imaginary part contains the following term.

$$i\Gamma \supset e^2 \int d^4z_1 d^4z_2 \left[\frac{1}{2}\phi_{\Delta \mathrm{R}}(z_1)\frac{1}{2}\phi_{\Delta \mathrm{R}}(z_2) + \frac{1}{2}\phi_{\Delta \mathrm{I}}(z_1)\frac{1}{2}\phi_{\Delta \mathrm{I}}(z_2)\right] \times 2\mathrm{Re}\gamma(z_1, z_2)$$

$$\begin{cases} \phi^+ = \phi_c + \frac{1}{2}\phi_\Delta \\ \phi^- = \phi_c - \frac{1}{2}\phi_\Delta \end{cases} \qquad \begin{cases} \phi_c = \frac{1}{\sqrt{2}}\left(\phi_{\mathrm{cR}} + i\phi_{\mathrm{cI}}\right) \\ \phi_\Delta = \frac{1}{\sqrt{2}}\left(\phi_{\Delta \mathrm{R}} + i\phi_{\Delta \mathrm{I}}\right) \end{cases}$$

$$\begin{aligned} &\gamma(z_1, z_2) \\ &\equiv -\left[2\frac{\partial}{\partial z_1^\nu}D^{\mu\nu}_{++}(z_1 - z_2)\cdot\frac{\partial}{\partial z_2^\mu}G^{++}(z_1 - z_2) + 2\frac{\partial}{\partial z_2^\nu}D^{\mu\nu}_{++}(z_1 - z_2)\cdot\frac{\partial}{\partial z_1^\mu}G^{++}(z_1 - z_2)\right. \\ &\quad \left. + 4D^{\mu\nu}_{++}(z_1 - z_2)\frac{\partial}{\partial z_1^\mu}\frac{\partial}{\partial z_2^\nu}G^{++}(z_1 - z_2) + \frac{\partial}{\partial z_1^\mu}\frac{\partial}{\partial z_2^\nu}D^{\mu\nu}_{++}(z_1 - z_2)\cdot G^{++}(z_1 - z_2)\right] \end{aligned}$$

Interpretation of imaginary part

- We would like to rewrite the imaginary part.
- According to previous studies, we hope to rewrite it as follows.

$$
\begin{aligned}
&\exp\left[i\Gamma\right] \\
&= \exp\left[i(\text{real function})\right] \times \exp\left[-\frac{1}{2}\int d^4x d^4y\, \phi(x) M(x,y)^{-1} \phi(y)\right] \\
&= \exp\left[i(\text{real function})\right] \times \int \mathcal{D}\xi \exp\left[-\frac{1}{2}\int d^4x d^4y\, \xi(x) M(x,y) \xi(y) + i\int d^4x\, \phi(x)\xi(x)\right] \\
&= \int \mathcal{D}\xi\, (\text{PDF}) \times \exp\left[i\left(\text{real function} + \int d^4x\, \phi(x)\xi(x)\right)\right] \\
&= \int \mathcal{D}\xi\, (\text{PDF}) \times \exp\left[iS_{\text{eff}}\right]
\end{aligned}
$$

formula of Gaussian integral:

$$
\begin{aligned}
&\int \mathcal{D}\xi \exp\left[-\frac{1}{2}\int d^4x d^4y\, \xi(x) M(x,y) \xi(y) + i\int d^4x\, \phi(x)\xi(x)\right] \\
&= \left(\det \frac{M}{2\pi}\right)^{-\frac{1}{2}} \cdot \exp\left[-\frac{1}{2}\int d^4x d^4y\, \phi(x) M(x,y)^{-1} \phi(y)\right]
\end{aligned}
$$

Difficulties in interpretation

- There seems to be a mathematical problem…
- The real part of eigenvalues of M should be POSITIVE to perform the Gaussian integral.

  → Re[γ(k)] should be always negative!

- But we find Re[γ](k) takes both positive and negative value.
- We can not rewrite the imaginary part of effective action!?

Remaining issue and work in progress

- Is it possible to rewrite the imaginary part of the effective action and interpret it as noise?

- One possibility: partial integral

ex.) $$i\Gamma \to \int d^4z_1 d^4z_2\, \dot{\phi}(z_1)\dot{\phi}(z_2) \times (\cdots)$$

→ EoM for ϕ contains not only ξ but also ∂ξ term?

- If we could obtain noise term, what property does it have? How much effect does it give to the scalar field? Does it behave like scalar boson?

$$\langle \xi(x)\, \xi(x') \rangle = ?$$

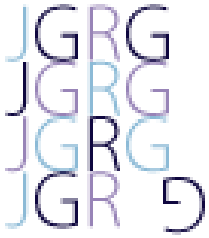

Hideyuki Tagoshi, JGRG 22(2012)111401

"Search for gravitational wave events with KAGRA and the world-wide network of laser interferometers in the advanced detector era"

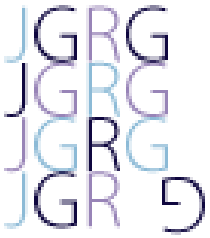

RESCEU SYMPOSIUM ON

GENERAL RELATIVITY AND GRAVITATION

JGRG 22



November 12-16 2012

Koshiba Hall, The University of Tokyo, Hongo, Tokyo, Japan



Search for gravitational wave events with KAGRA and the world-wide network of laser interferometers in the advanced era

Hideyuki Tagoshi

(Osaka University)

Contents

- Brief summary of sources
  - Compact binary Coalescence (CBC)
  - Supernova (Gravitational Collapse)
  - Pulsar
- Data analysis method
- Multi messenger astronomy and low latency search
- Parameter estimation
- KAGRA data analysis

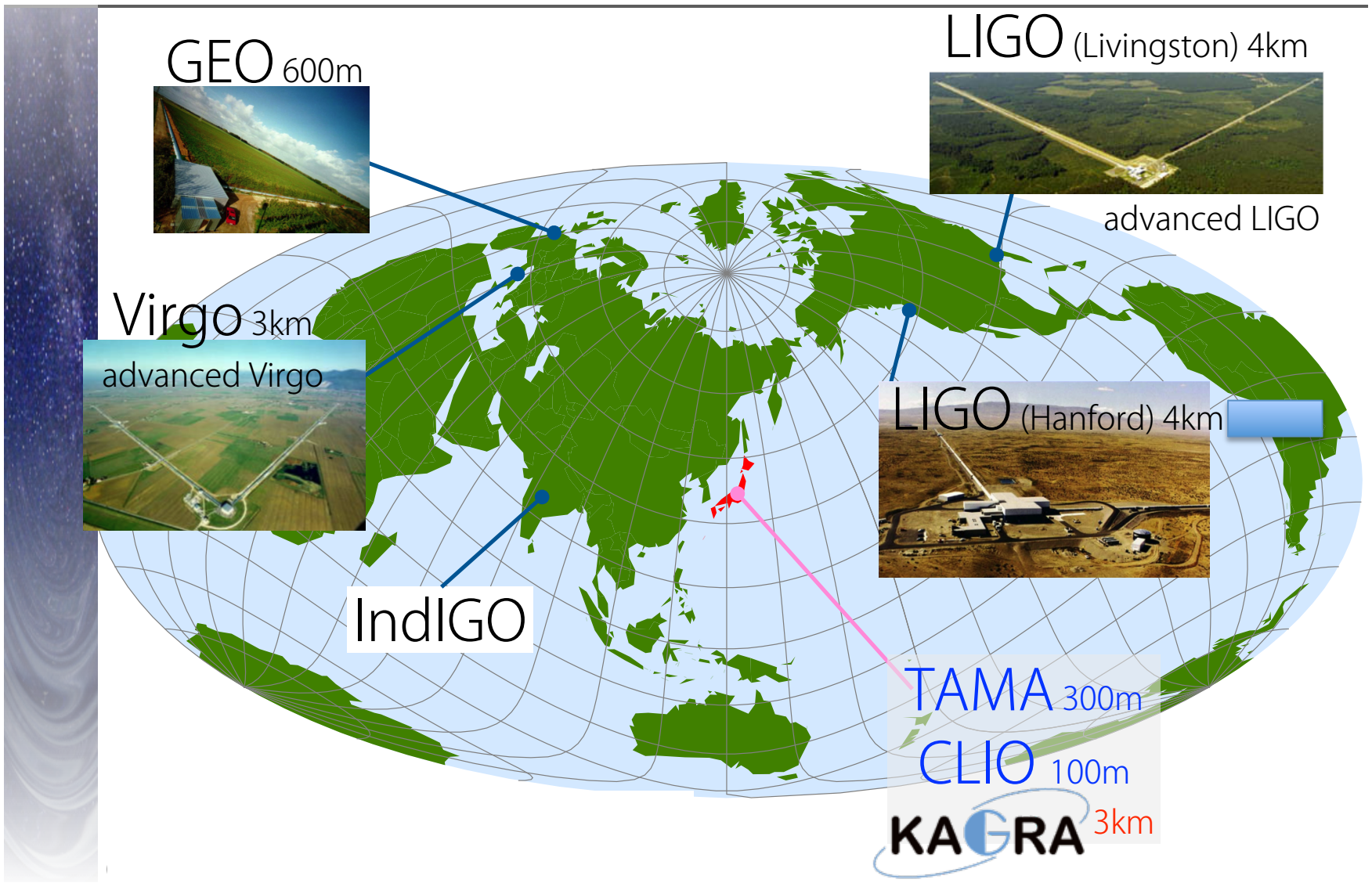
GEO 600m
LIGO (Livingston) 4km
advanced LIGO
Virgo 3km
advanced Virgo
LIGO (Hanford) 4km
IndIGO
TAMA 300m
CLIO 100m
KAGRA 3km

Generation of gravitational waves

In order to produce strong gravitational waves, we need

- Time variation of mass distribution

$$\frac{v}{c} \sim 1$$ and/or $$\left(\frac{v^2}{c^2} \sim\right) \frac{GM}{rc^2} \sim 1$$

high speed **strong gravity field**

- Non-spherically symmetric variation（time variation of quadrupole moment）

These factors restrict the source of strong gravitational waves

Sources of LIGO, Virgo, KAGRA

- Compact binary coalescence (CBC)
  neutron star (NS) and/or black hole(BH)
  inspiral, merger, ringdown

- Burst waves
  stellar core collapse
  pulsar glitches

- Continuous waves
  rotating neutron stars

- Stochastic background
  early universe origin, astrophysical origin

NS-NS merger rate

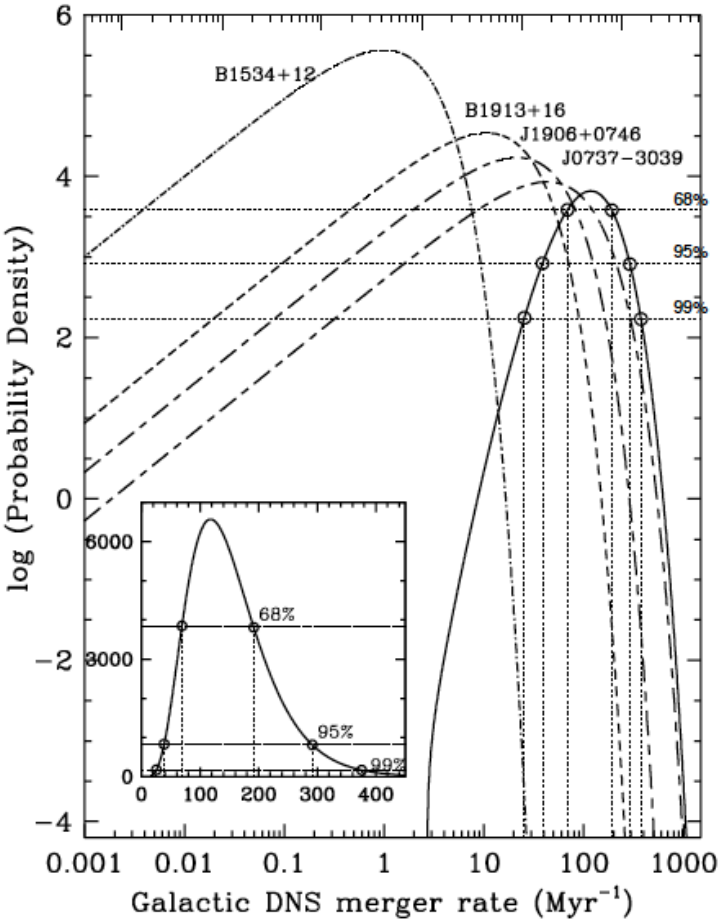

(Kim ('08), Lorimer ('08))

Galactic merger rate $118^{+174}_{-79}\,\mathrm{Myr}^{-1}$

A current official LCGT design (VRSE-D) gives horizon distance (@S/N=8) = 280Mpc (z=0.065)

Event rate for LCGT : $9.8^{+14}_{-6.6}\,\mathrm{yr}^{-1}$

However, systematic errors which are not included in this evaluation may be large.

See also: Abadie et al. CQG27, 173001(2010)

Physics in Compact Binary Coalescence

Inspiral → Merger → Ringdown (BH oscilation)

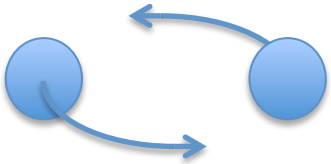

Numerical Relativity

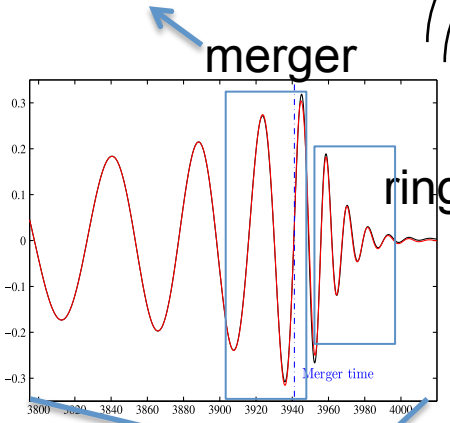

(BH perturbation)

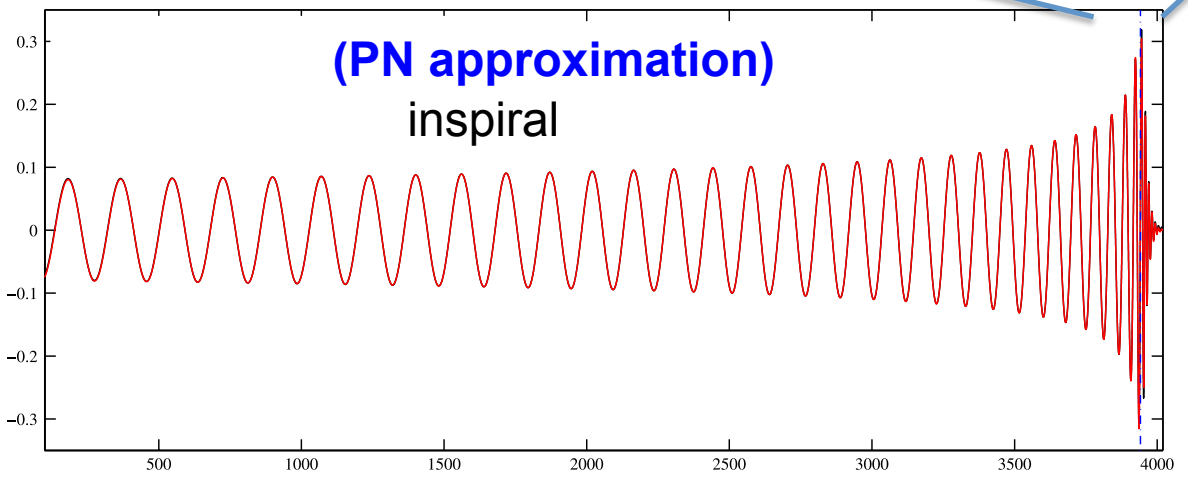

Basic value for the inspiral waveform

(m_1,m_2) [Msolar]	(1.4, 1.4)	(10, 1.4)	(10, 10)	(100, 1.4)
frequency@ISCO[Hz]	1570 Hz	386 Hz	220 Hz	43 Hz
duration(10Hz-ISCO)[sec]	1002 sec	224 sec	38 sec	46 sec
cycle(10Hz-ISCO)	16038	3585	605	743
orb. radius@10Hz[Mt]	174 Mt	68 Mt	47 Mt	16 Mt

$Mt=m_1+m_2$

ISCO: Inner most stable circular orbit.

NS-NS coalescence & HMNS

Hotokezaka, Kyutoku, Okawa, Shibata, Kiuchi, PRD83, 124008 (2011)

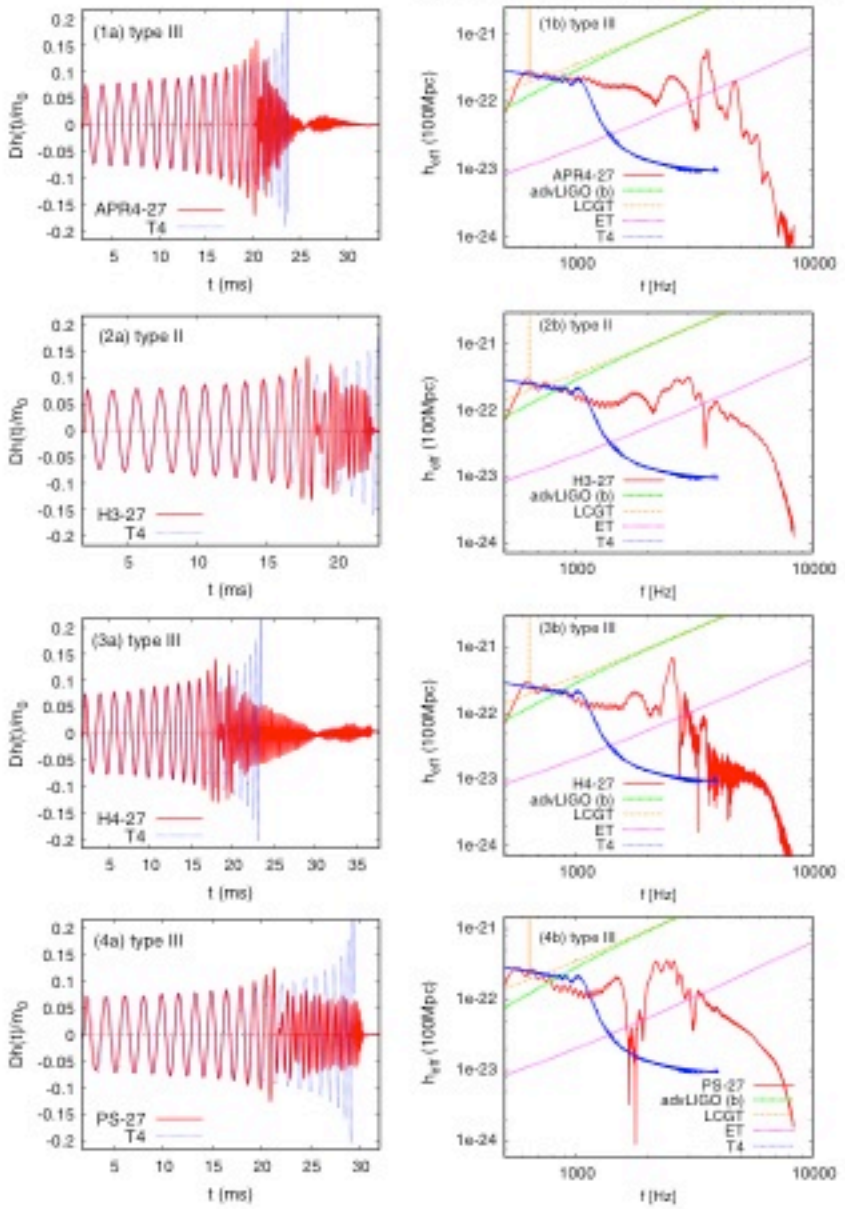

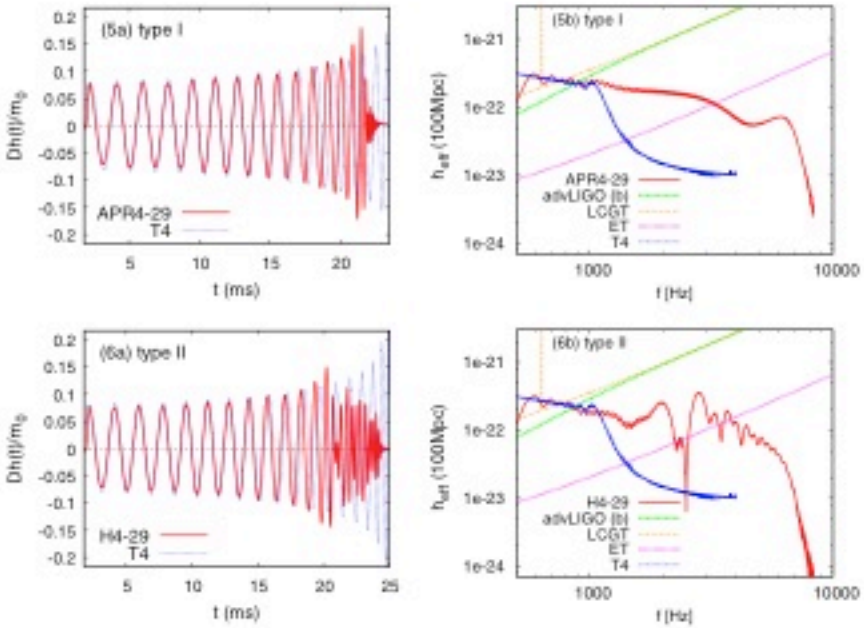

NS-NS for KAGRA

NS-NS binary coalescence
Horizon distance (S/N=8, optimal direction, face-on)

iKAGRA 29Mpc ➡ bKAGRA 280Mpc

(In LIGO's definition, 18Mpc) (173Mpc)

(LIGO's definition)=(KAGRA's definition)x($\sqrt{2}$)x(0.44)
(Assuming phase is measured. Averaged over the sky and inclination angle.)

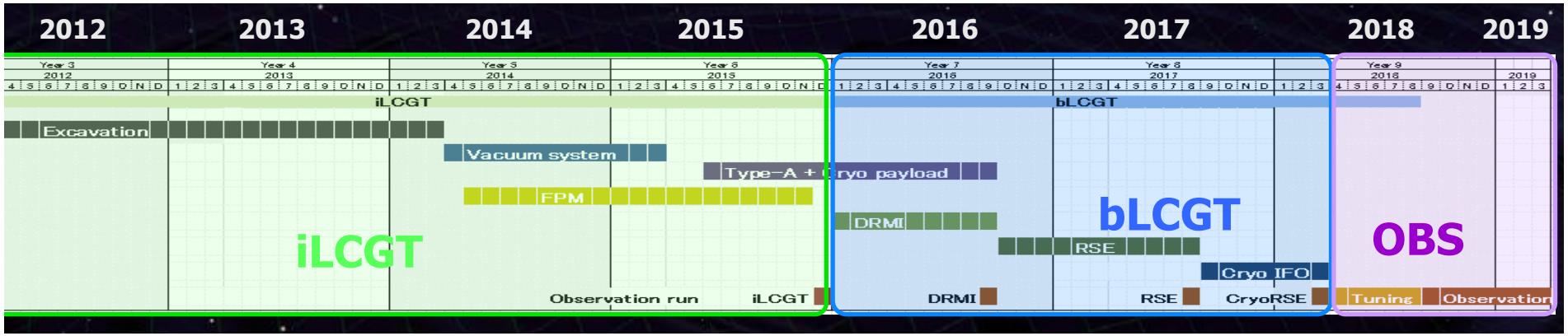

Event rate for bKAGRA : $9.8^{+14}_{-6.6}\,\mathrm{yr}^{-1}$

(based on Kim ('08), Lorimer ('08))

Supernova (Gravitational Collapse)

Review articles: Ott, CQG, 26, 063001 (2009), Fryer and New, LRR, 14, 1 (2011)

Various possible gravitational wave emission mechanism.

- Core collapse and bounce
- Rotational non-axisymmetric instabilities of proto-neutron star
- Post-bounce convection
- Non-radial pulsations of proto-neutron star

} Related to the explosion mechanism

- Anisotropic neutrino emission

etc.

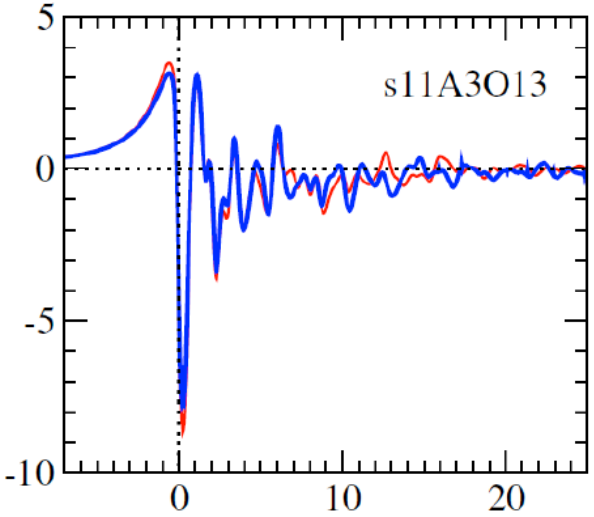

Collapse and bounce wave form from Dimmelmeier et al. 2008 [PRD 78, 064056]

Gravitational Collapse

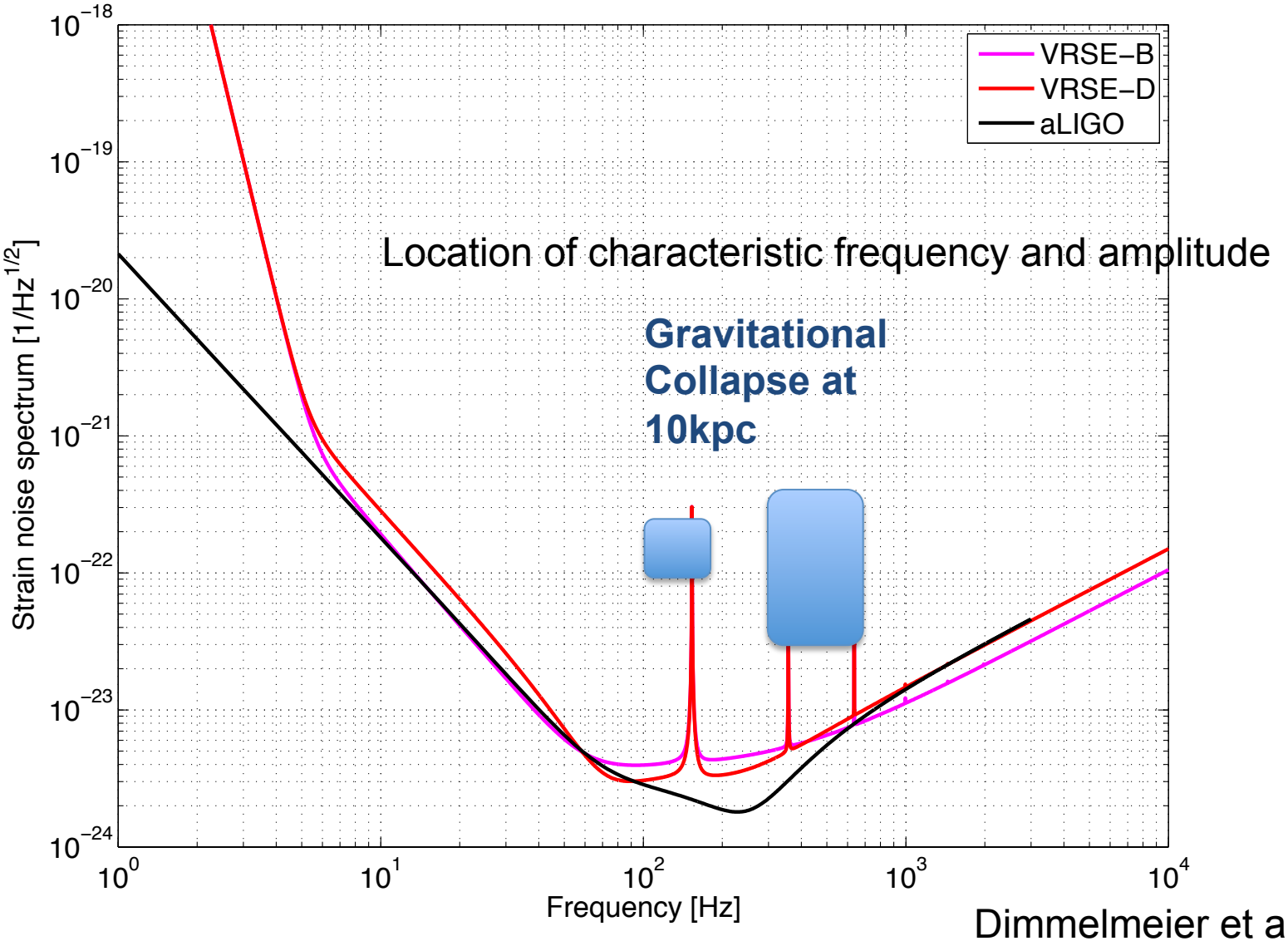

Dimmelmeier et al. ('08)
PRD 78, 064056

~several 100kpc can be seen by KAGRA

GW from core collapse

Dimmelmeier et al. PRD 78, 064056 ('08)

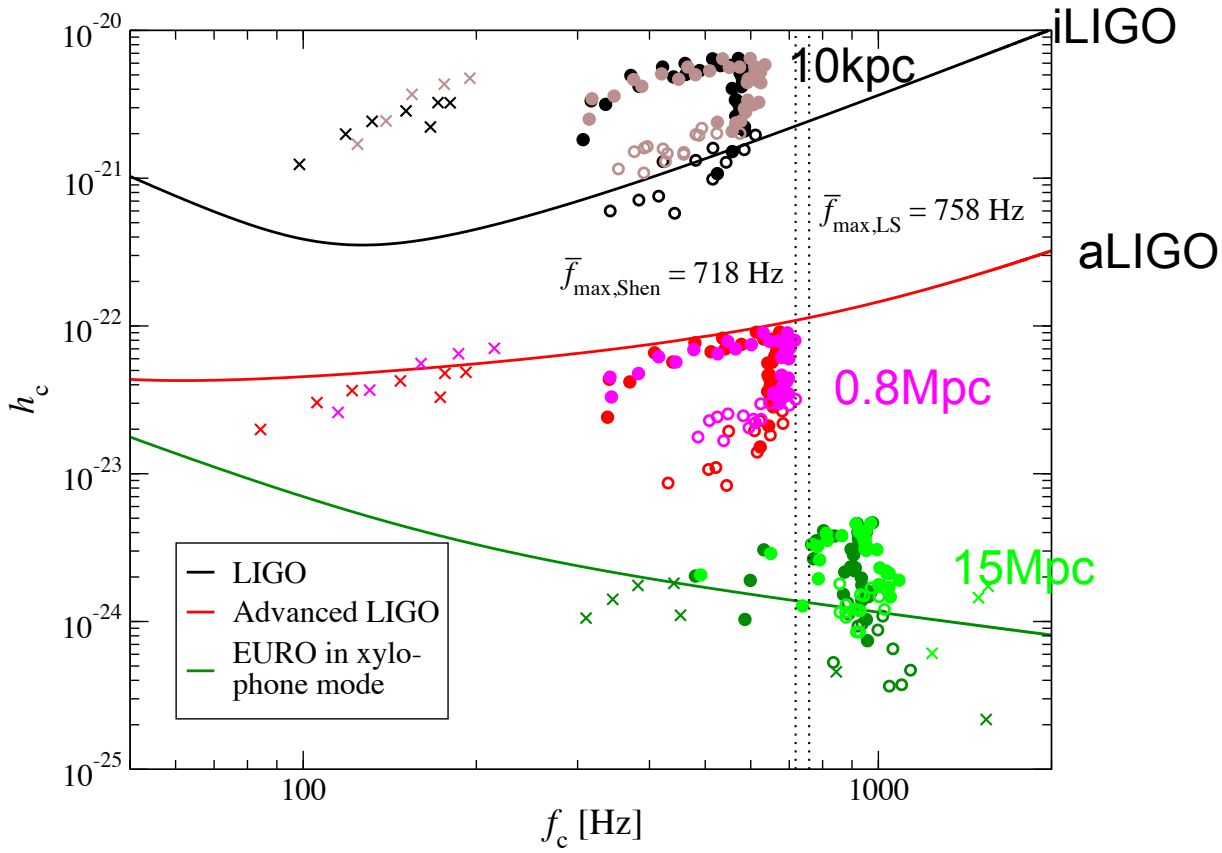

$$f_c = \left(\int_0^\infty \frac{\langle \hat{h}^2 \rangle}{S_h} f\, df\right)\left(\int_0^\infty \frac{\langle \hat{h}^2 \rangle}{S_h} df\right)^{-1} \qquad h_c = \left(3\int_0^\infty \frac{S_h c}{S_h}\langle \hat{h}^2 \rangle f\, df\right)^{1/2},$$

Continuous wave (rotating NS)

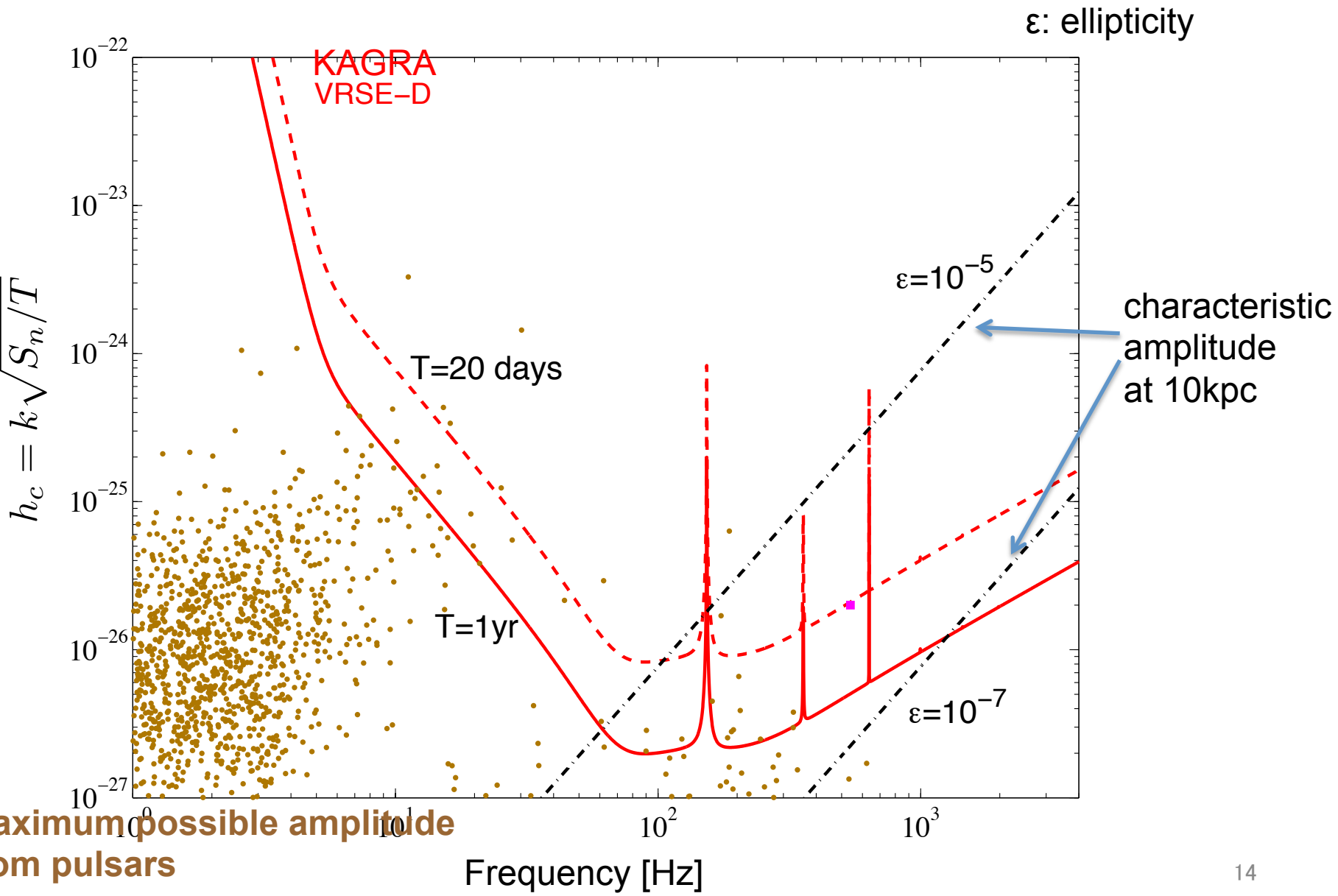

Maximum possible amplitude from pulsars

Data analysis method

Gravitational wave data analysis methods are categorized in various ways.

Characteristic of the sources

- Well-known waveform (expressed by a small number of parameters)
  CBC(inspiral, ringdown), Continuous wave (rotation neutron stars), …
- Unknown waveform (need complicated numerical simulations)
  Burst（Core collapse supernovae, merger phase of CBC, …)
- Random waveform (characterized only statistically)
  Stochastic background

Other factors:

- Short duration time（a few 10 minutes） rotation of the earth can be ignored
  CBC, Burst
- Long duration time（more than a few 10 minutes) rotation of the earth affects
  Continuous waves

How to detect the signal

- **Know waveform**

  "Matched filter"

  Cross-correlate data and templates with weight of inverse of noise power spectrum density

  Look for the parameter which realize the maximum of cross correlation.

- **Unknown waveform**

  "Excess power"

  Judge the presence of signal from the power excess of data.

How to detect the signal

- **Know waveform** Multiple detectors' case

  "Matched filter"

  Cross-correlate data and templates with weight of inverse of noise power spectrum density

  Look for the parameter which realize the maximum of cross correlation.

  ⇩ multiple detectors' case

  "Coherent matched filter" (Maximum likelihood method)

- **Unknown waveform**

  "Excess power"

  Judge the presence of signal from the power excess of data.

  ⇩ multiple detectors' case

  e.g., "Coherent WaveBurst" of LSC.

  "Coherent excess power" (Maximum likelihood method)

- **Random waveform**

  "Cross correlation"

  Cross correlation of data from different detectors.

Noise veto

In any laser interferometer detectors, the presence of non-stationary, non-Gaussian noise can not be ignored (at least so far, and probably in the future too).

In order to veto the fake events produced by such noise, noise veto scheme are introduced (case by case).

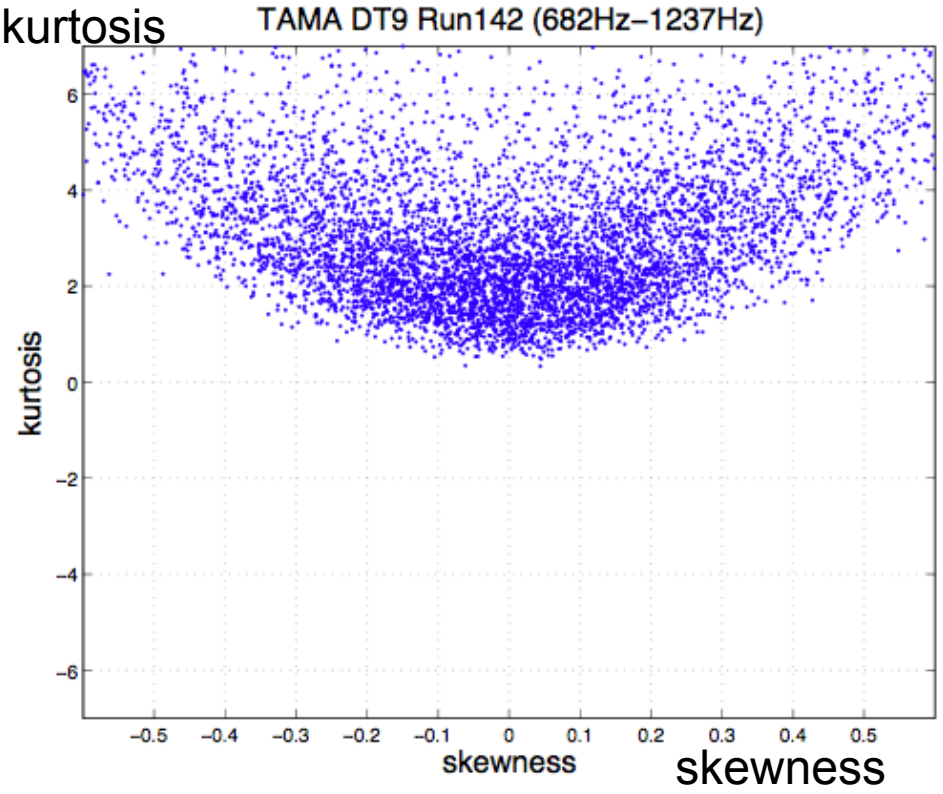

Non Gaussianity of TAMA data

Importance of network

For the gravitational wave astronomy, multiple detector network is important.

Why network?

needless to say but

- Improvement of S/N
- Improvement of reliability of detection

at the same time

- To determine the direction of the source,
- To determine two polarization mode of GW,
- To cover whole sky,

we need global network of (3 or more) detectors.

Accuracy of direction

NS-NS coalescence @180Mpc

L:LIGO-Livingston
H:LIGO-Hanford
V: Virgo
K: KAGRA
I:LIGO-India

median of δΩ [Deg^2]	LHV	LHVK	LHVI
(1.4, 1.4) Msolar	30.25	9.5	9.0

(95%CI)

e.g., J.Veitch et al., PRD85, 104045 (2012)
(Fisher matrix & simulation)

direction, inclination, polarization angle are given randomly

Source localization accuracy is 10 - 30 Deg^2 (@180Mpc, 95%CI).

see also Wen and Chen (2010)
Fairhurst (2011)

Importance of astronomical observation

- Triggered search

If we know the time and direction from other astronomical observation (EM, neutrino), it is a great benefit to the detection of the gravitational wave signal, since we can reduce the threshold.

(e.g., Kochanek,Piran (1993))

e.g, : GRB: Core collapse or CBC

Neutrino from Supernovae in nearby galaxies

Wide field optical/IR telescope monitoring SNe and GRB

- In fact, in the LIGO-Virgo analysis of 2009-2010 data, the triggered search using 154 GRBs information (time and direction), the threshold becomes 2 times lower than that which does not use such information.

This means 2 times longer distance of detection range.

(arXiv:1205.2216)

Importance of astronomical observation

- Follow up observation by astronomical telescopes

This is more challenging.
First, we detect GW signal.
Next, with the informaiton of time and direction,
astronomical observation are done.

- This useful for the improvement of the significance of detection, and for the detailed investigation of the physical process of the source.

- Since gravitational wave detectors are extremely wide fieldtelescope, this approach should also be a standard tool as a multi-messenger astronomy.

Low latency

For the follow-up search by the EM observatories,
low latency analysis is important.

For inspiral analysis, if we have 1Tflops computing power,
we can finish the analysis within 10 minutes (=length of template).

But 10 minutes are not very short if we consider, e.g., short gamma ray burst (the earlier, the better!).

In such case, we can reduce the mass range for the search.

If mass range between 1-2M_{solar}, the number of template is around 5000.
Then, if computing power is 1Tflops,
the computation time is less than1 second.
This is only for matched filtering computation.
Data transfer, calibration etc. must be tuned for this special purpose.

(See Kanda-san's talk)

Example of LIGO – Virgo

Ref. A&A 539, 124 (2012), A&A 541, 155 (2012

LIGO S6, Virgo VSR2 (12/17/2009-1/8/2010, 9/2-10/20/2010)

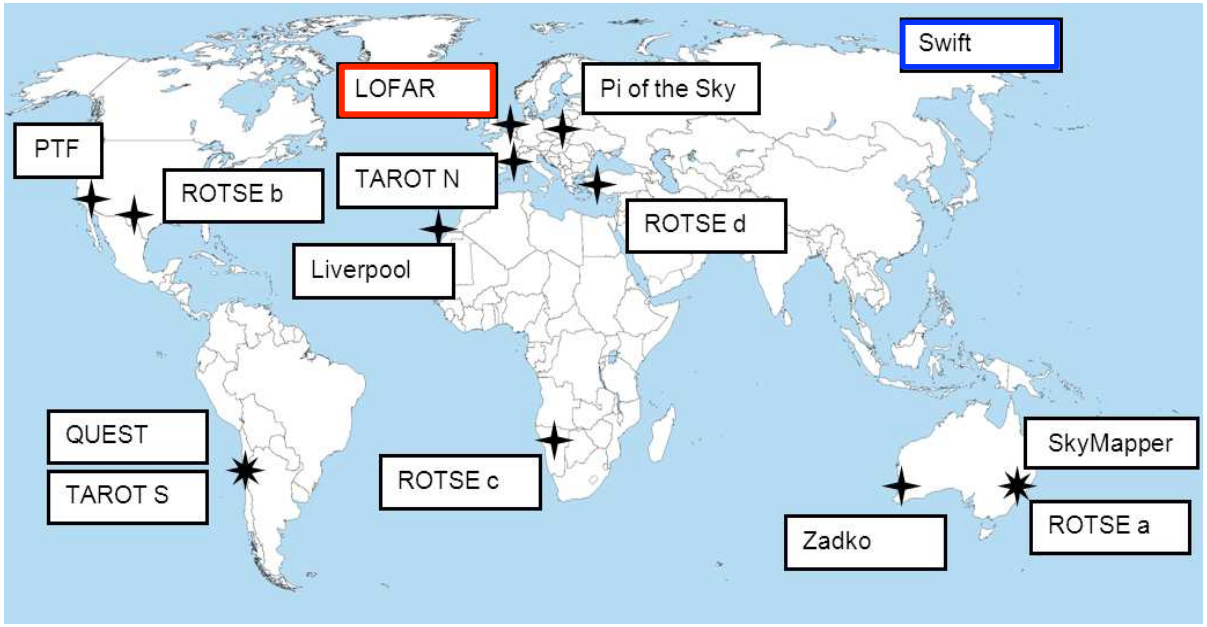

Participated observatories

Example of LIGO – Virgo

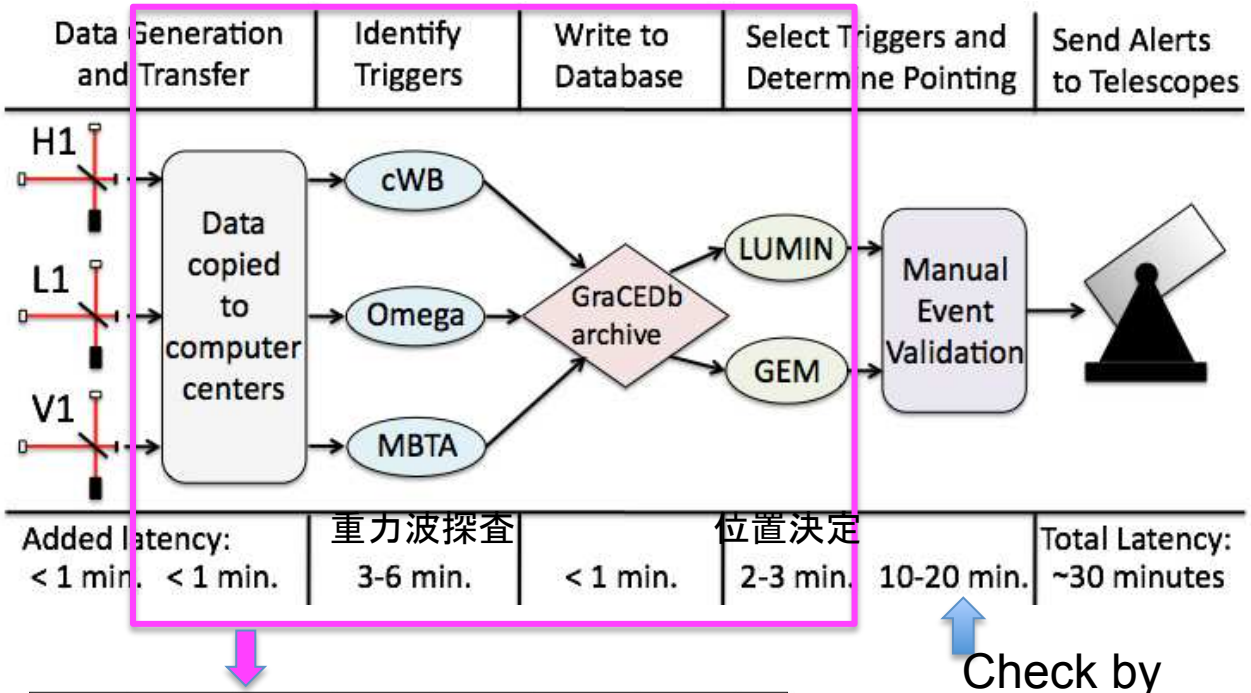

Check by human

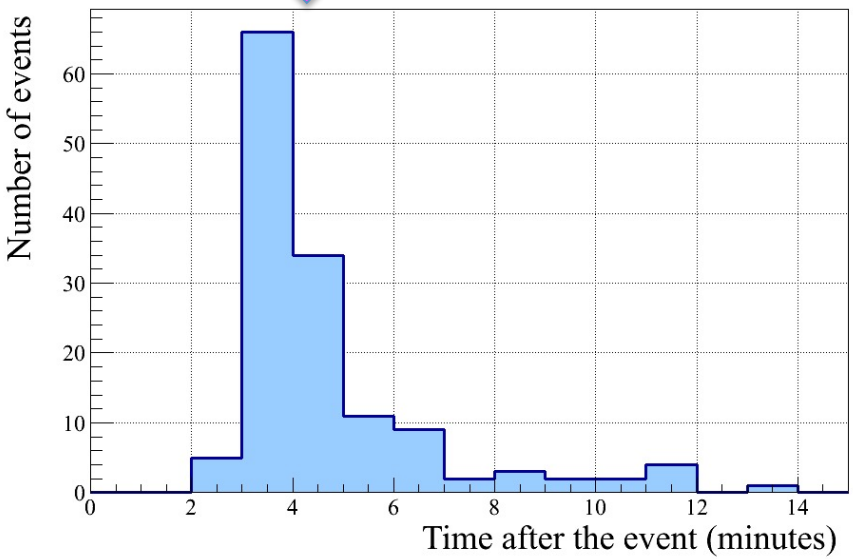

Automated part of MBTA(CBC) analysis was finished in 4 minutes typically.

A&A 541, 155 (2012)

Example of LIGO – Virgo

- Source localization accuracy is several 10～100sq. deg. (since these are by initial LIGO,Virgo).
Bigger than FOV of astronomical instruments.



- Use galactic catelog (GWGC)
and restrict the search region (up to 3-4deg^2).

GWGC: The Gravitational Wave Galaxy Catalog

Low latency search in KAGRA

- In KAGRA, we also plan to develop the high speed data analysis system and to establish the alert system to the astronomical observatories.
- Possible source direction must be restricted by using galactic catalog?
- In order to do this, we need to collaborate LIGO and Virgo.

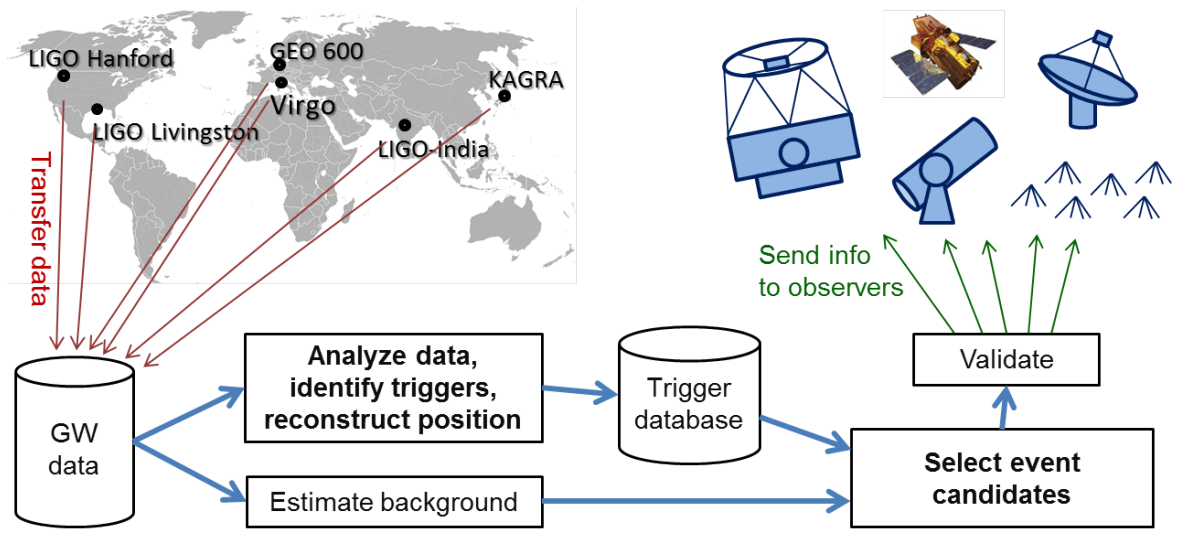

taken from arxiv:1206.6163

GW data analysis in advanced detector era

"Real detection"

Global network analysis
Collaboration of astronomers

} all of these are good for the detection

"GW astronomy and astrophysics" will begin as soon as GW is detected.

For astronomy and astrophysics, extraction of physical parameters are necessary.

Parameter estimation

- Known waveform (matched filter):
  Since theoretical waveform is done for the detection, parameter estimation is basically done at the same time of detection.

- Unknown waveform
  Theoretical waveform is not used. Reconstruction of buried signals, and extraction of physical parameters are necessary. This requires multiple detectors' data.

GW signal reconstruction・・・Gursel, Tinto (1989), Klimenko+ ('05,'08)
Supernova waveform model selection
・・・Summerscales+ (2008), Rover+ (2009), Logue+ (2012).

Time frequency analysis

For unmodeled burst signals, because of the lack of the accurate theoretical waveform, it also seems to be useful to employ some time-frequency representation of the data itself.

"plot of the energy distribution on the time-frequency plane"

- Spectrogram with STFT
- Wigner-Ville distribution
- Wavelet transform
- etc.

Other new methods

"Hilbert-Huang transform" (Huang+ ('98))
Empirical mode decomposition
+ instantaneous frequency by Hilbert transform

J.B.Camp et al.
H.Takahashi, K.Oohara et al.

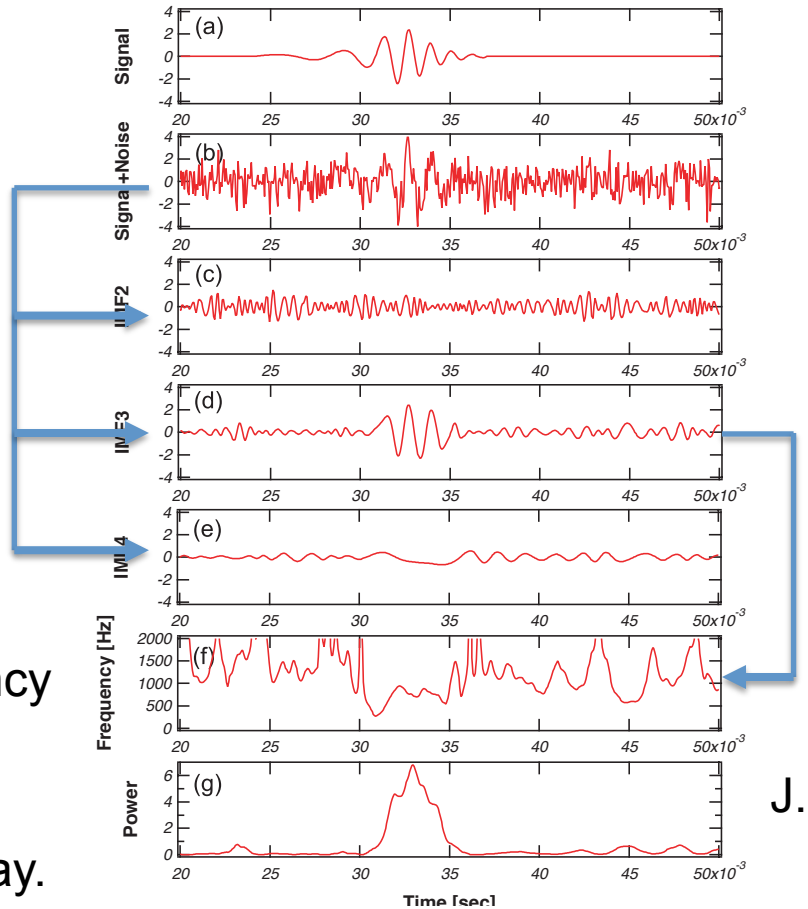

Instantaneous frequency

J.B.Camp+ ('07)

Analysis of HMNS is now underway.

KAGRA data analysis

- We need to have our own data analysis software in order to perform data analysis smoothly.
- We just started the development of the data analysis package for KAGRA.
- This should be compatible with existing software package of LIGO and Virgo.
- At the same time, we have to develop the package better than those of LIGO and Virgo's package at, at least, some points, since we develop new one from now.

incorporate new technology,
faster computation speed,
better accuracy, …

e.g., Fast computation with GPGPU
(K.Tanaka, N.Kanda,…)

KAGRA data analysis subsystem

- Core members: H.Tagoshi, Y.Itoh, H. Takahashi,
  N.Kanda (DMG), K.Hayama(DetChar), K.Oohara

+ graduate students

Clearly, we need more man power.

There are 4 postdoc positions at Osaka U. (2) and Osaka City U. (2).
If you are interested in, please contact us.

End

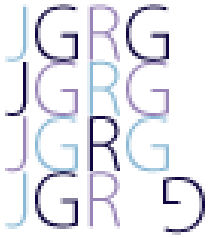

Takaaki Kajita, JGRG 22(2012)111402

"Status of KAGRA"

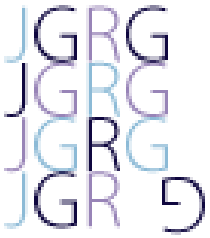

RESCEU SYMPOSIUM ON

GENERAL RELATIVITY AND GRAVITATION

JGRG 22



November 12-16 2012

Koshiba Hall, The University of Tokyo, Hongo, Tokyo, Japan



ICRR
Institute for Cosmic Ray Research
University of Tokyo

KAGRA

RESCEU Symposium on General Relativity and Gravitation
Nov. 12-16, 2012, Tokyo

Status of KAGRA

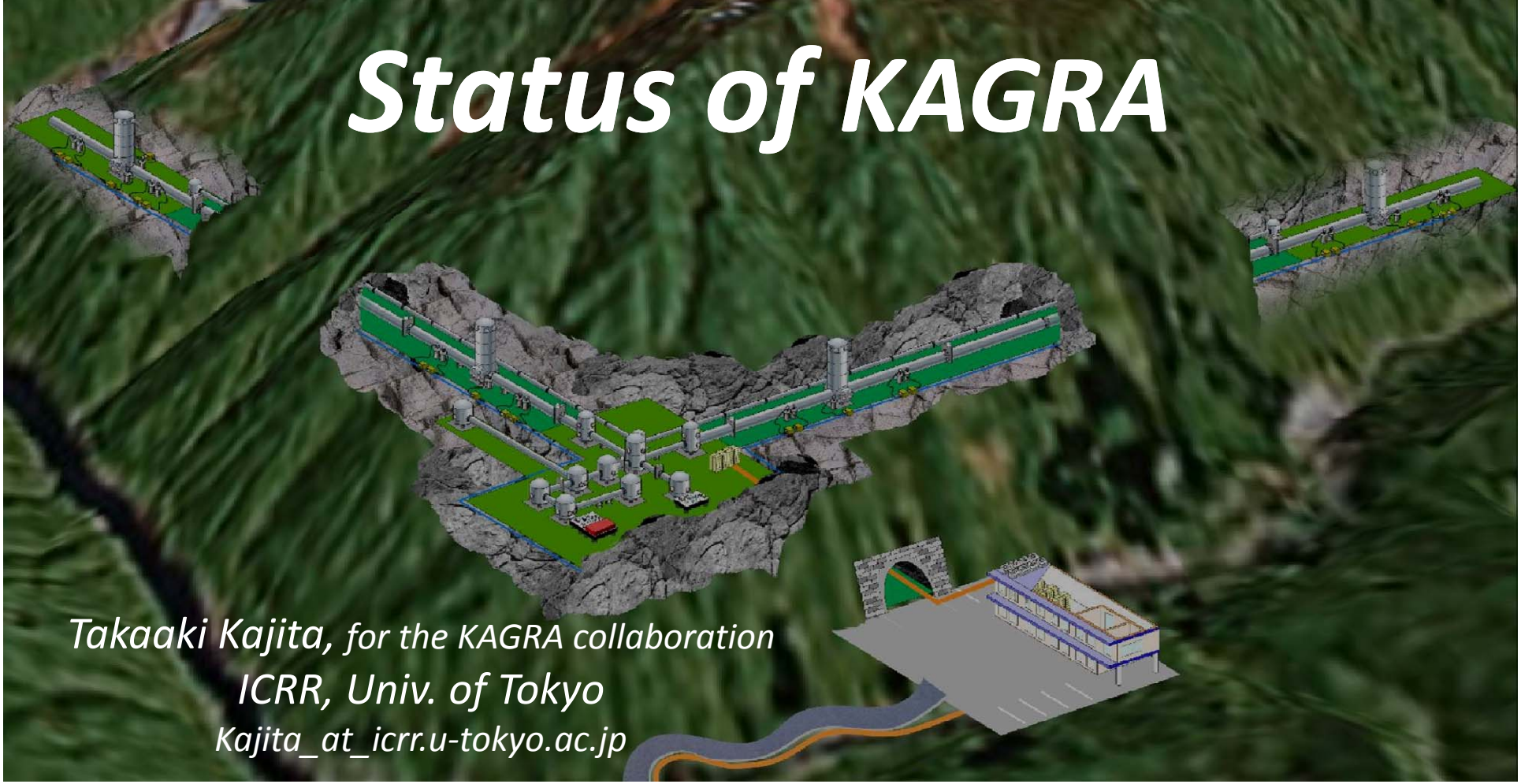

Takaaki Kajita, for the KAGRA collaboration
ICRR, Univ. of Tokyo
Kajita_at_icrr.u-tokyo.ac.jp

Outline

- General Introduction
- Overview of KAGRA
  - Key features
  - Science examples
- Status of construction
- Global GW network
- Summary

General Introduction: Why do we want to observe Gravitational Waves?

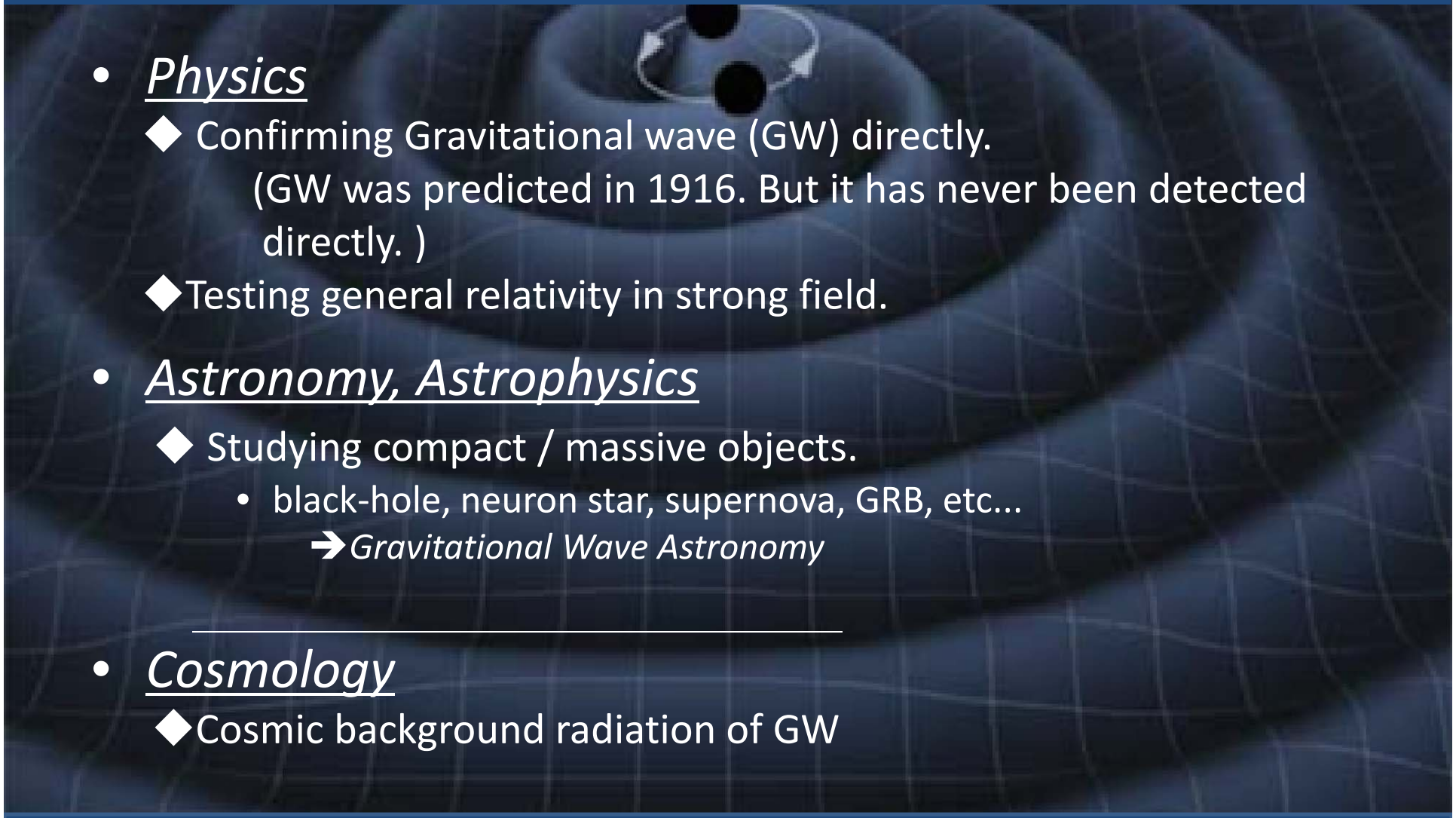

- *Physics*
  - ◆ Confirming Gravitational wave (GW) directly.
    (GW was predicted in 1916. But it has never been detected directly.)
  - ◆Testing general relativity in strong field.
- *Astronomy, Astrophysics*
  - ◆ Studying compact / massive objects.
    - black-hole, neuron star, supernova, GRB, etc...
      - ➔*Gravitational Wave Astronomy*

- *Cosmology*
  - ◆Cosmic background radiation of GW

Key requirements for high sensitivity ($\Delta L/L < 10^{-22}$)

Reduced ground motion

→*The interferometer should be build on a stable place*

→*Advanced seismic attenuation system*

Reduced thermal noise

→*Cryogenic mirrors*

Reduced photon fluctuation

→*High power, stable laser*

Longer baseline

→ *3km baseline*

→ *optical cavity to increase the effective baseline length*

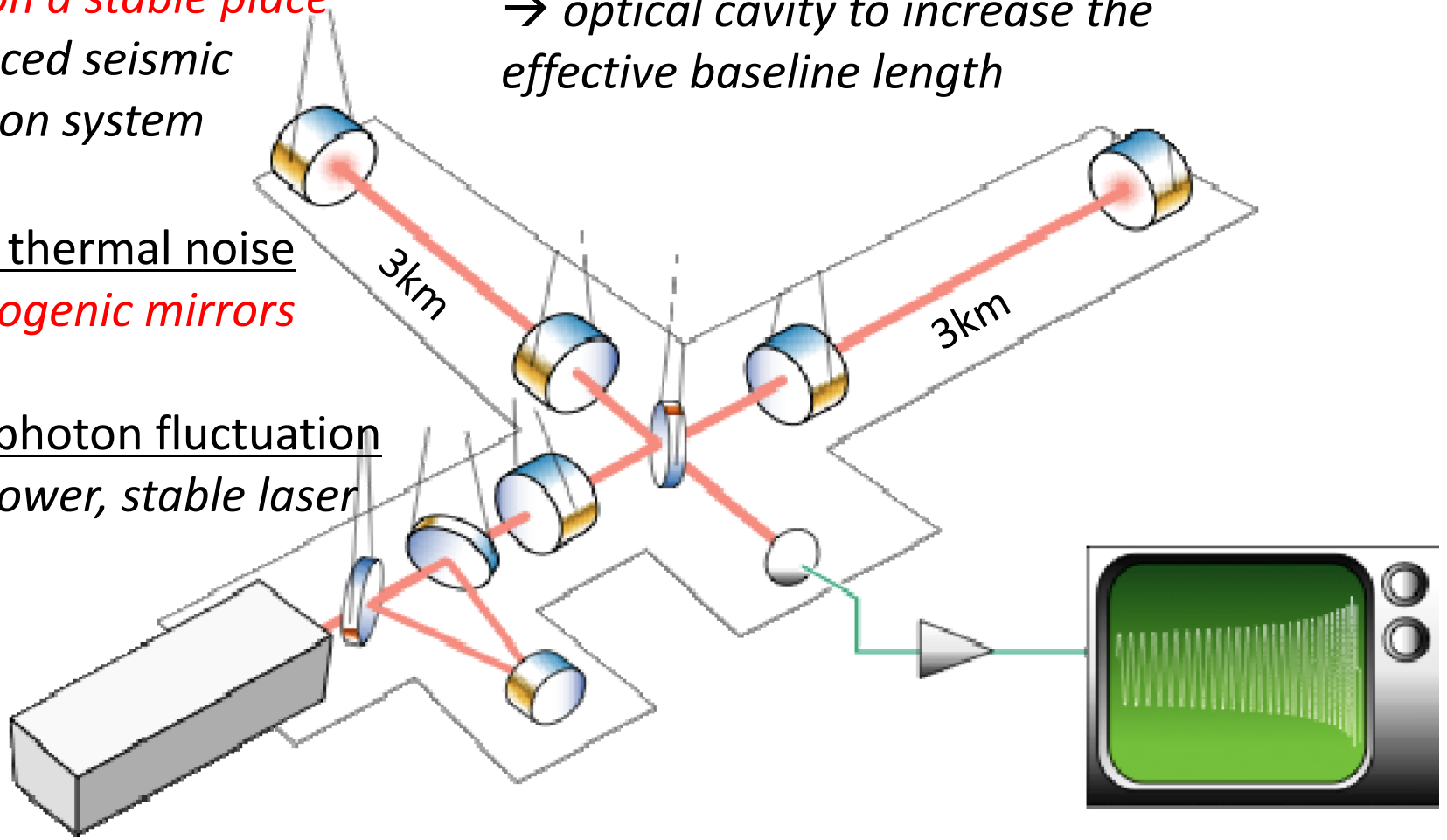

Key features of KAGRA

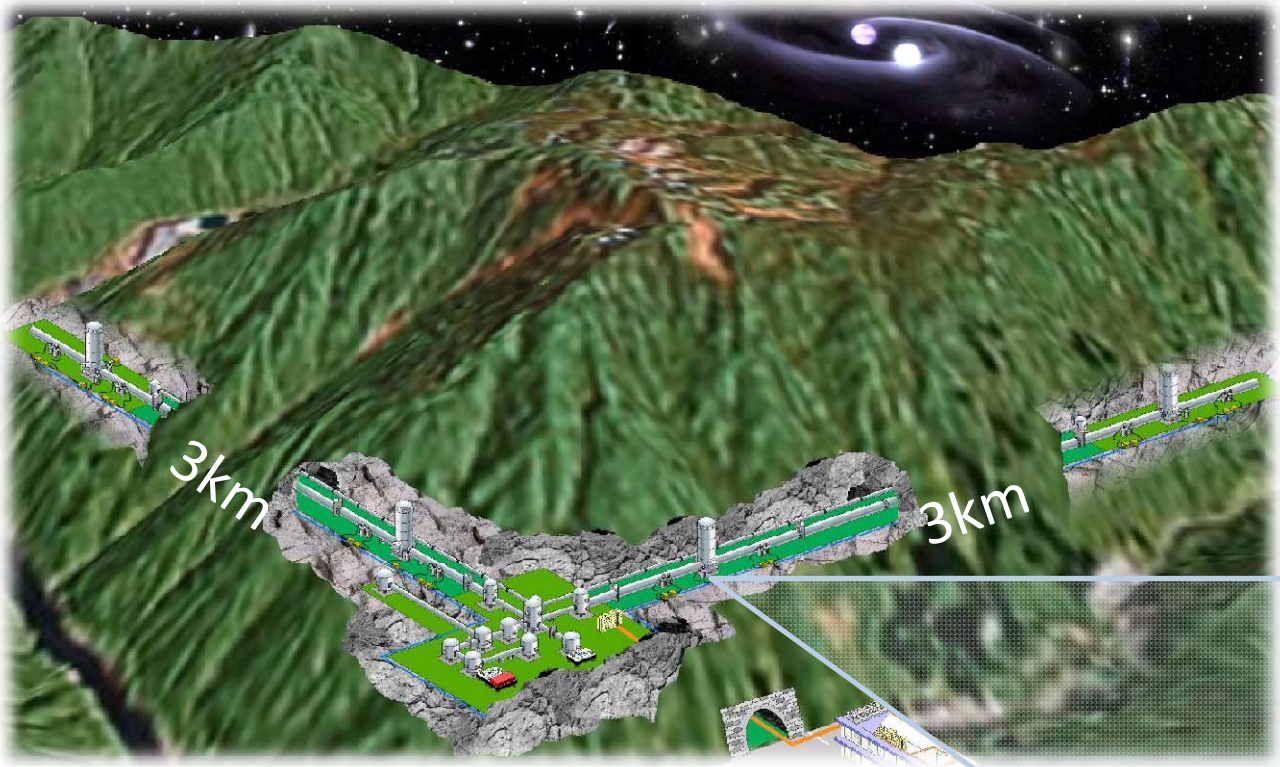



The detector will be constructed underground Kamioka.
➔ Reduction of seismic noise (to approximately 1/100).

Cryogenic mirrors will be used to reduce the thermal noise (in the 2nd phase).

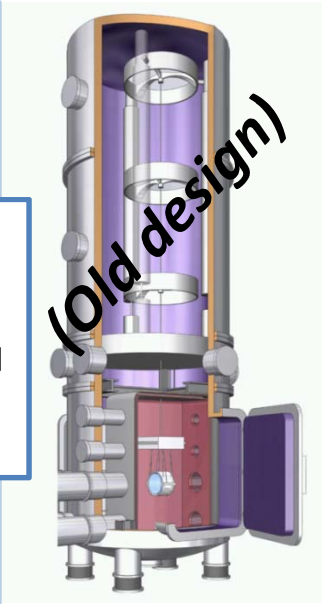

➔ Very high sensitivity.

Location


Mozumi
Kamioka
Observatory, ICRR
Super-
Kamiokande
3km
3km
K A G R A
New
Atotsu
Present mine entrance
Toyama airport
40min.
by car
Japan
Tokyo
Yokohama
Nagoya
Mt.Fuji

Sources of Gravitational Waves

1. Coalescence of neutron star binaries
2. Coalescence of black hole binaries
3. Core collapse of massive stars (Supernova)
   (good location; Super-Kamiokande at the same site)
4. Rotation of pulsars

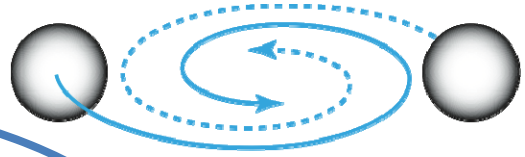

(H. Tagoshi)

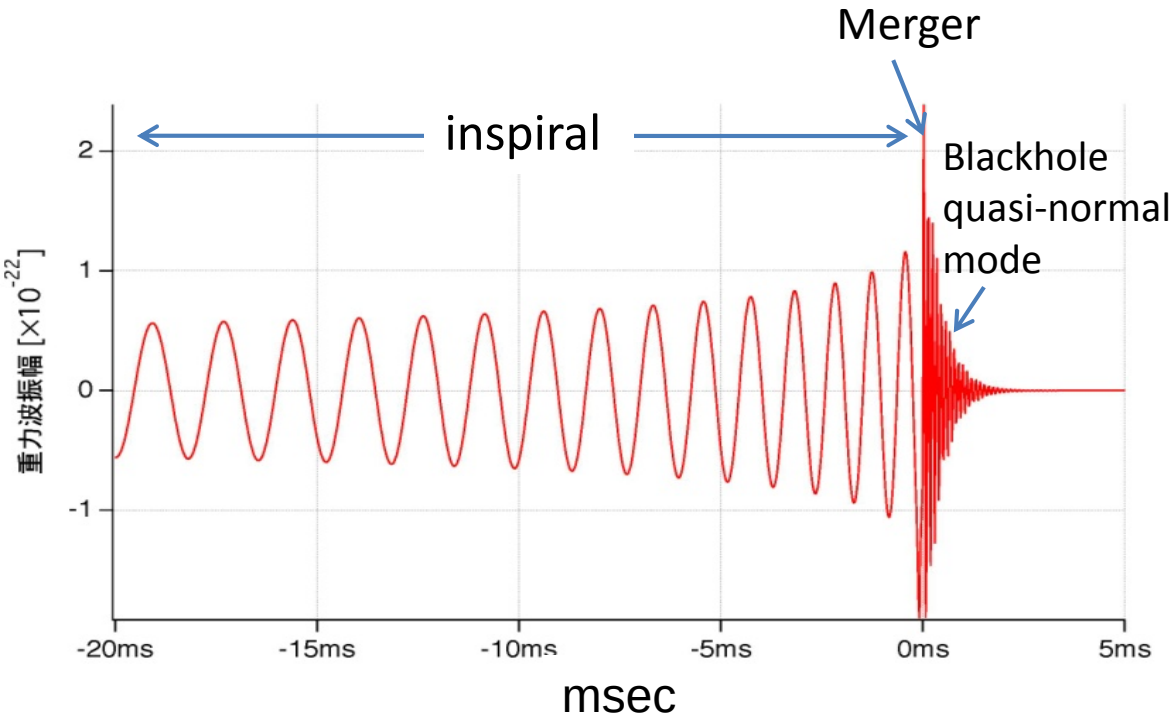

Sensitivities

GWIC report (2010)

Ad.-LIGO (USA), Ad-Virgo (Europe), KAGRA similar design sensitivities

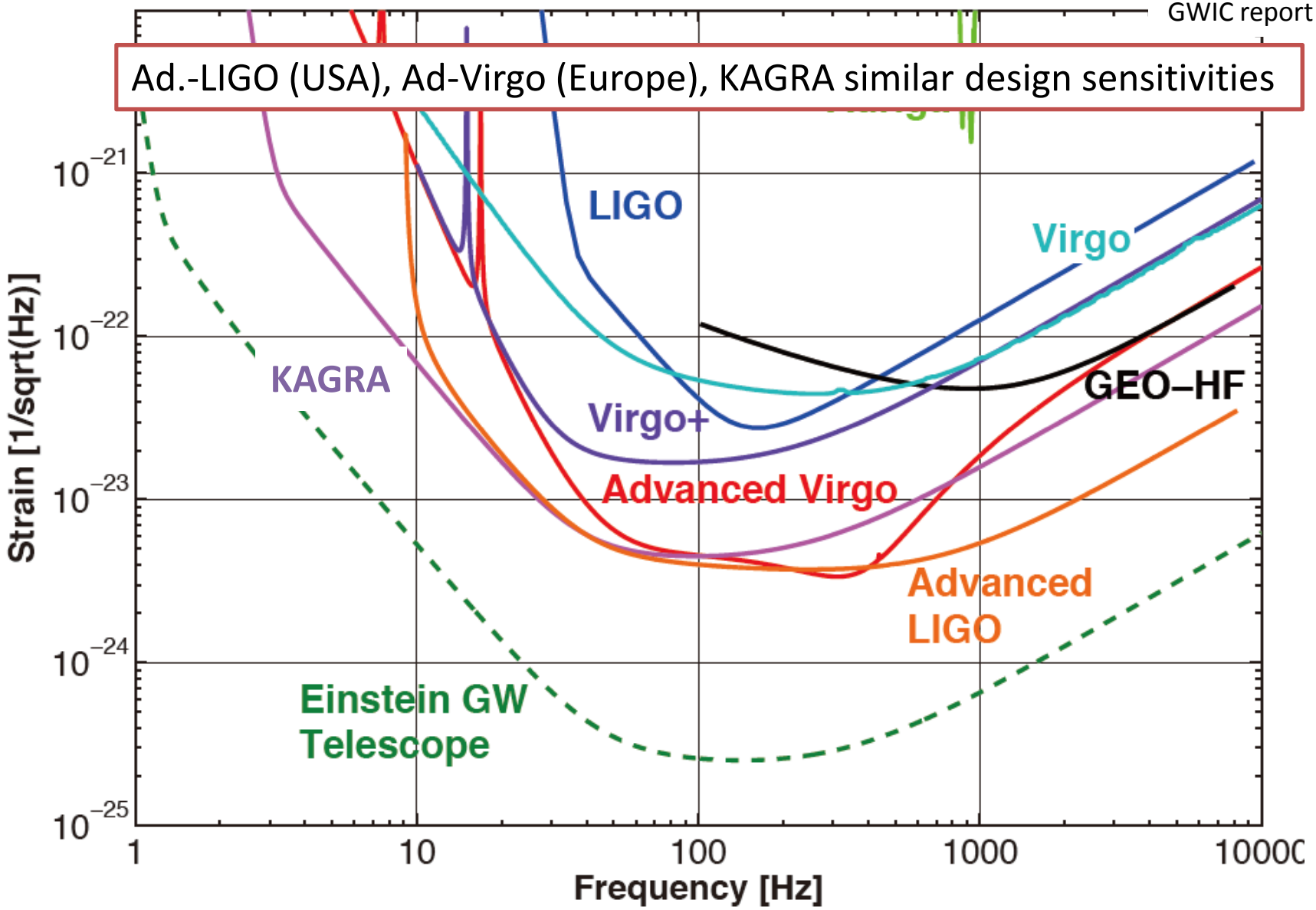

Expected NS-NS Coalescence signal

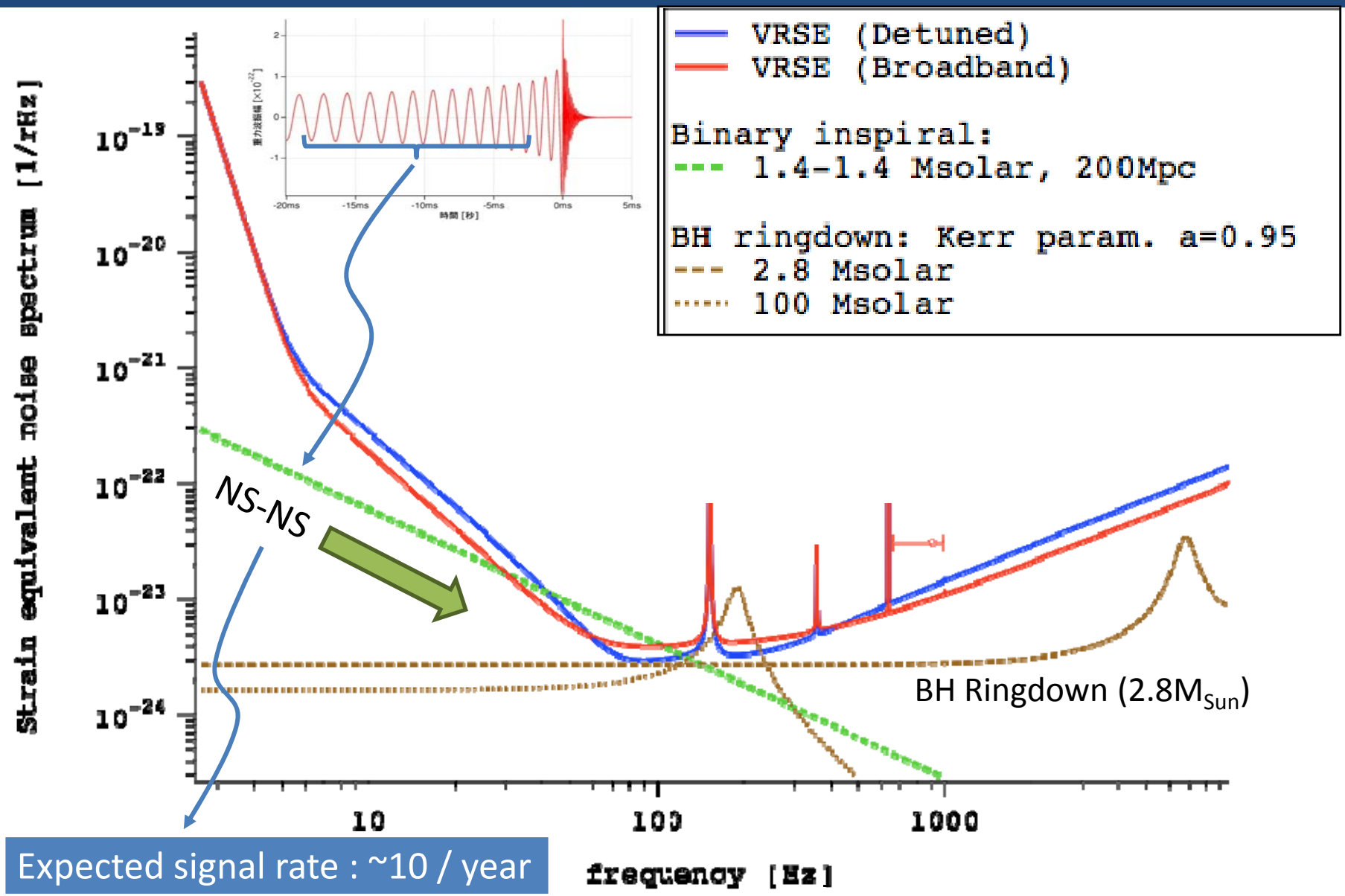

Expected signal rate : ~10 / year

Supernova

Various possible gravitational wave emission mechanism:

- Core collapse and bounce
- Rotational non-axisymmetric instabilities of proto-neutron star
- Post-bounce convection
- Anisotropic neutrino emission
- …

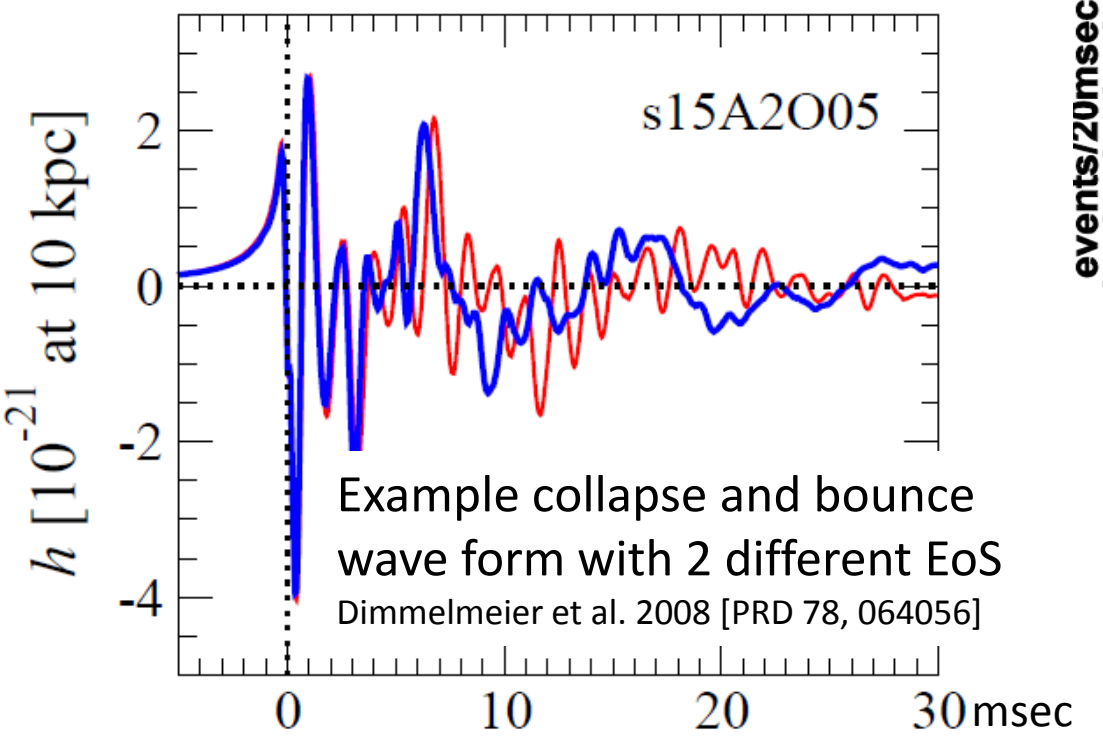

Example collapse and bounce wave form with 2 different EoS

Dimmelmeier et al. 2008 [PRD 78, 064056]

Neutrino (Super-K)

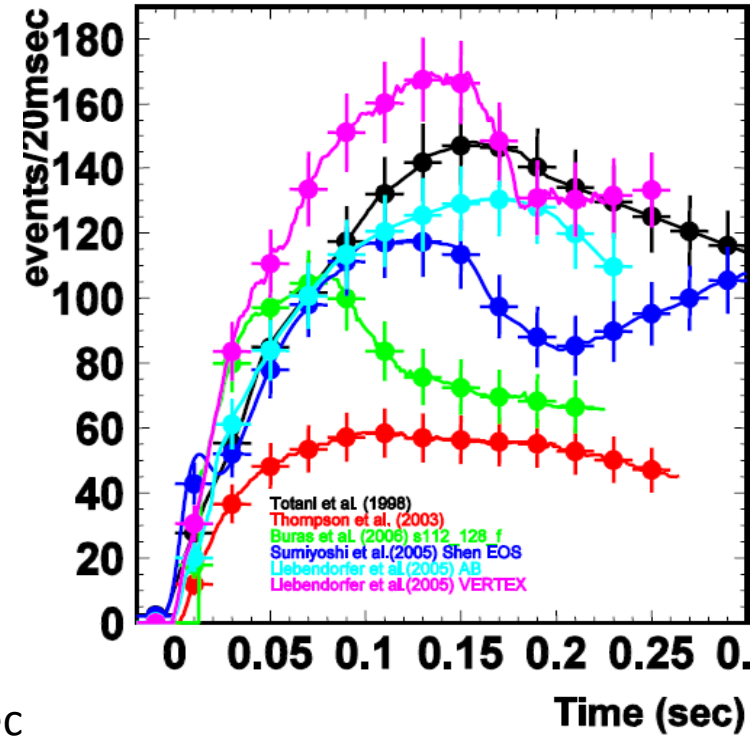

Expected SN signal

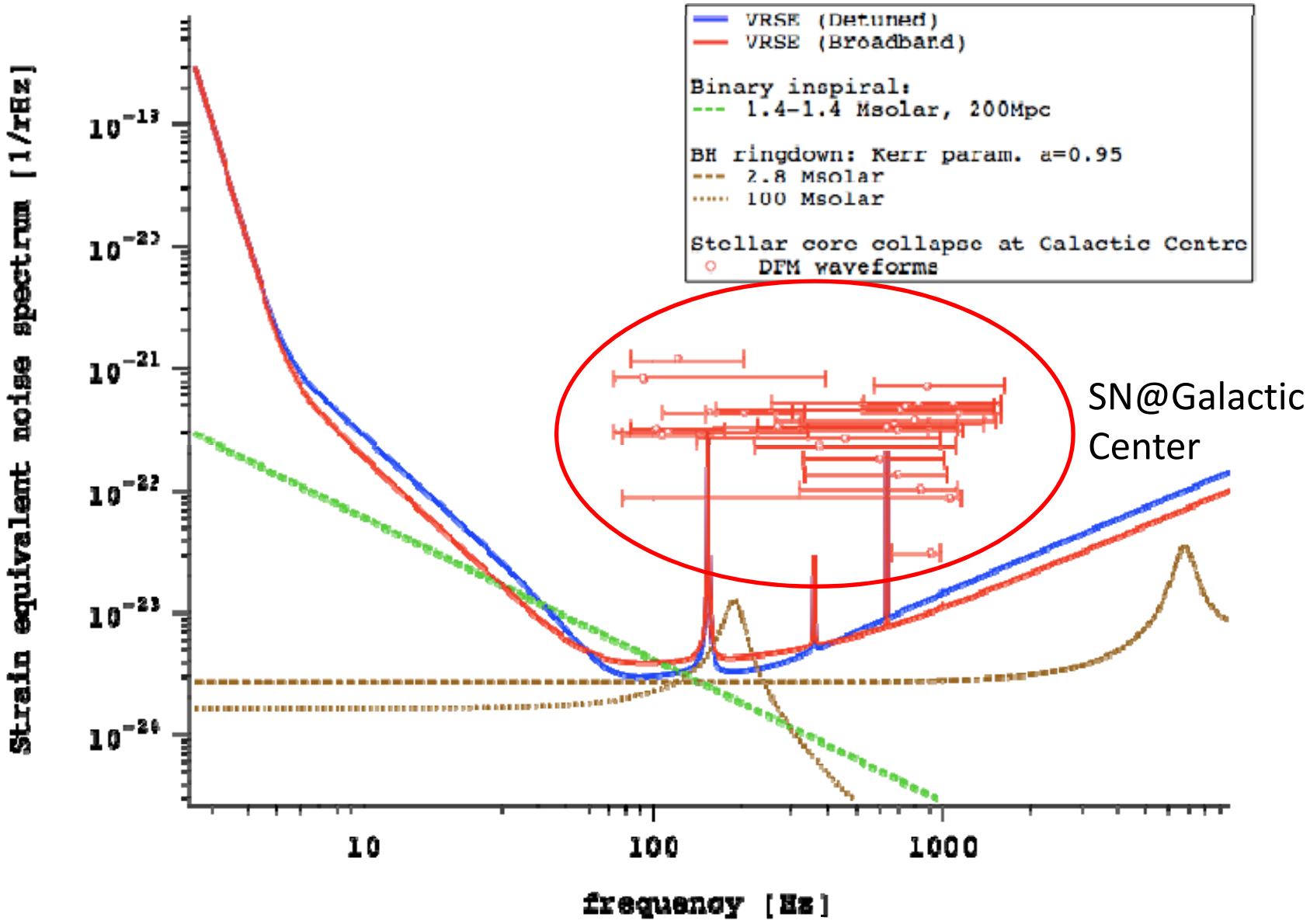

SN@Galactic Center

Time line (Construction and Observation)

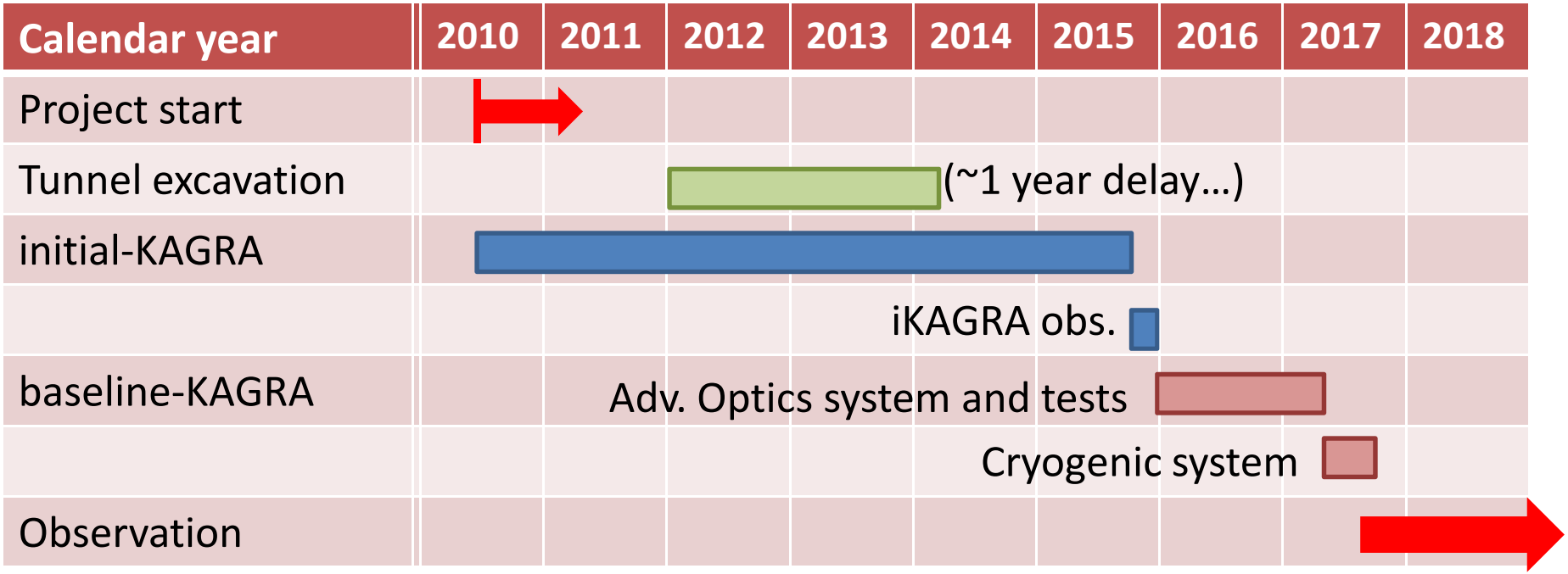

The construction/observation plan is in 2 stages:

- ✓In 2015, non-cryogenic observation (iKAGRA).
- ✓Operation with cryogenic system in 2017 (bKAGRA).
- ✓(High sensitivity operation in 2018?)

iKAGRA and bKAGRA

iKAGRA (~ 2015) → *bKAGRA (2016 ~)*

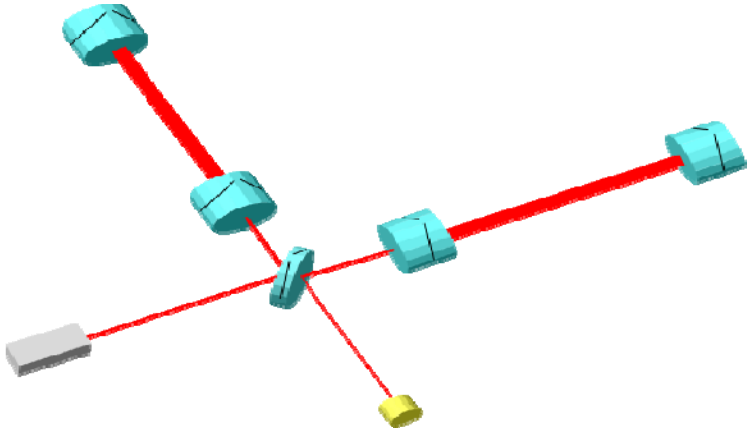

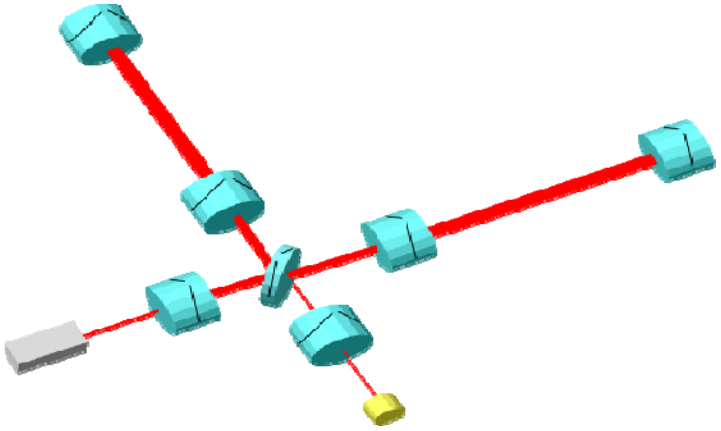

◆Simple interferometer with:
room temperature operation,
10W class laser, and
no power and signal recycling

◆ However, full end-to-end (relatively short) observation, in order to experience the operation and to understand the potential problems as soon as possible.

◆Advanced interferometer with:
power and signal recycling, but still room temperature operation.

↓

◆ Full bKAGRA with;
power and signal recycling,
cryogenic sapphire mirrors,
and >150W laser.

Status of the KAGRA Project

Tunnel excavation

- The blasting started on May 22, 2012.
- Excavation is carried out from the Mozumi and New-Atotsu entrances.
  - ➢ The excavated area are shown by red.

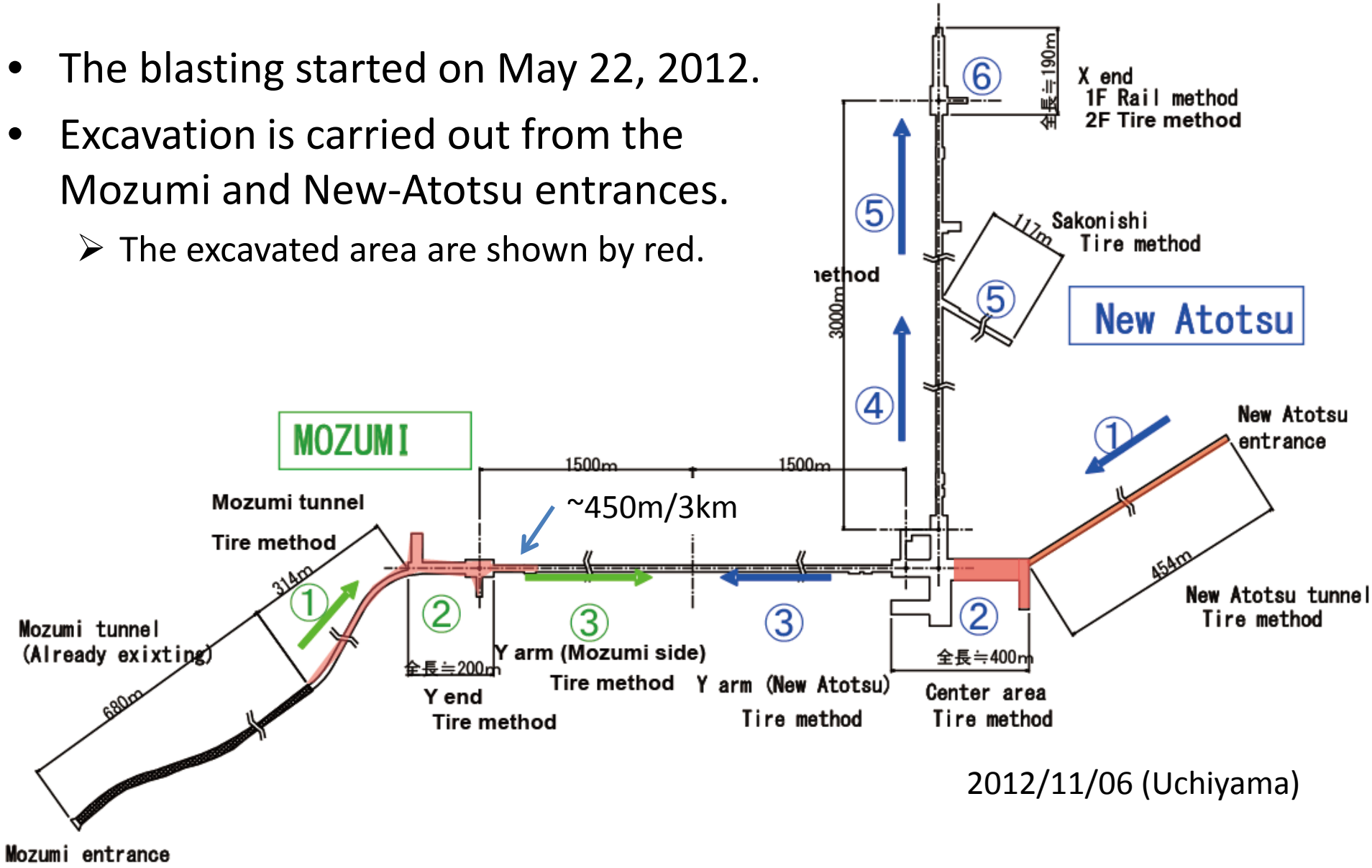

2012/11/06 (Uchiyama)

Tunnel excavation

New Atotsu entrance

End of April, 2012



Mid June, 2012



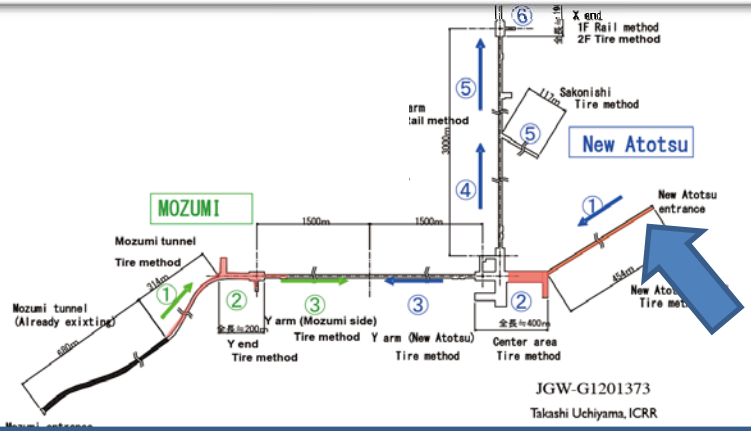

Excavation status (Y-end)



Y-end & Y-arm

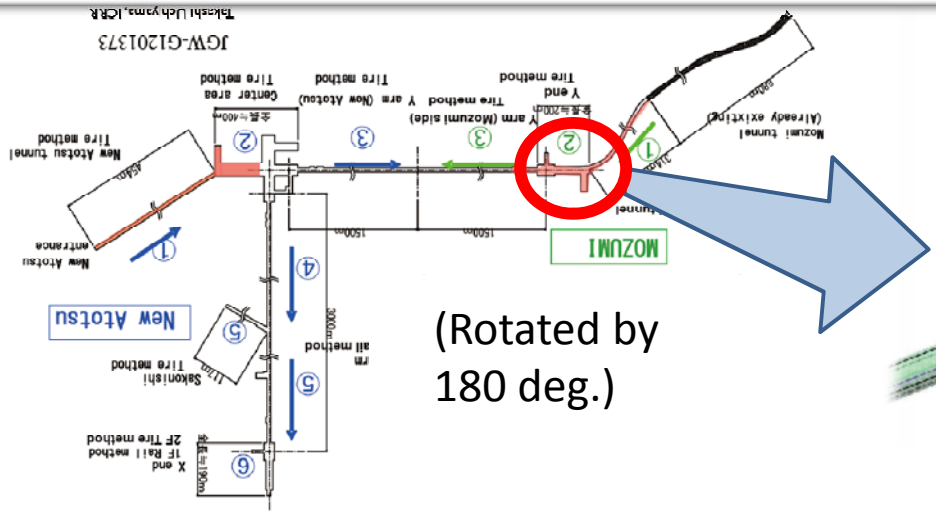

(Rotated by 180 deg.)

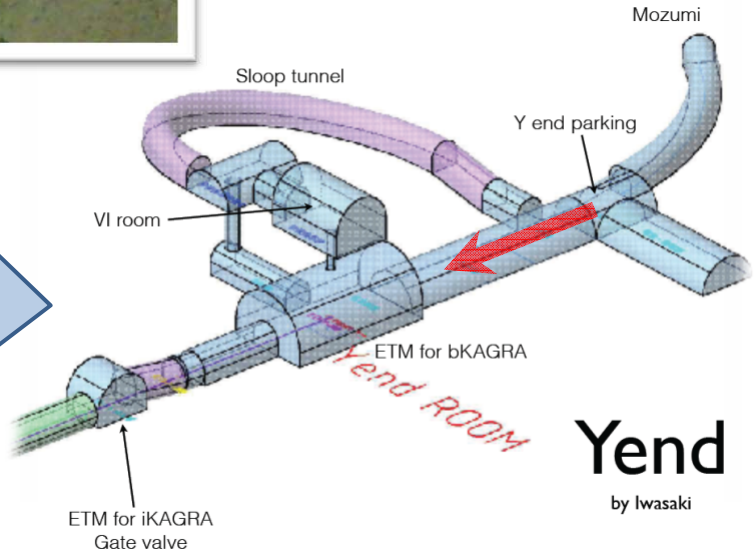

Excavation status (Center room)

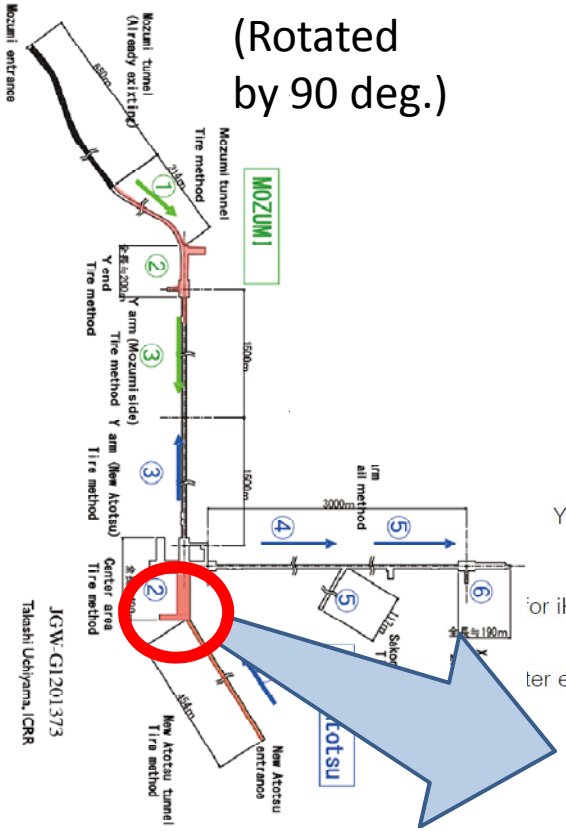

(Rotated by 90 deg.)



Center room

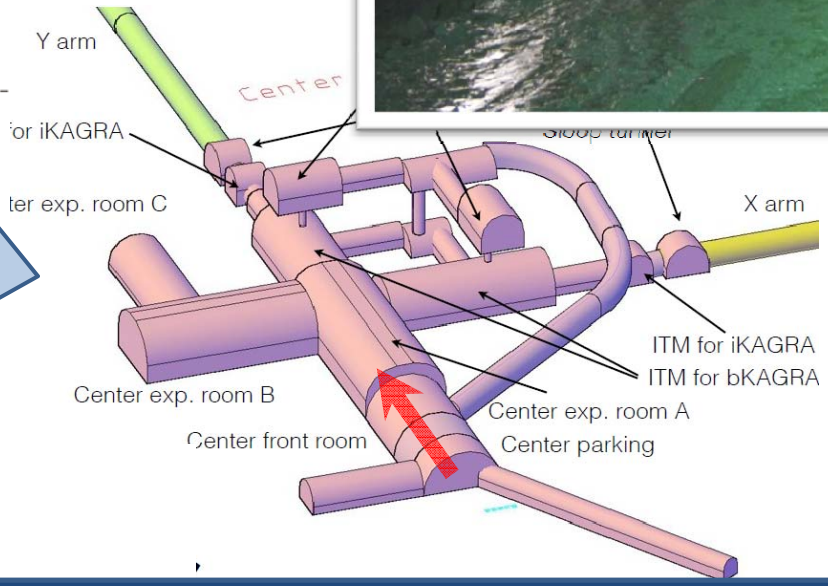

Status of construction: Surface building

- The refurbishment was finished in early Aug. We have just moved to this office.



Early June 2012



Aug.6, 2012



(Miyakawa, Uchiyama)

Status of preparation: Vacuum

- More than 70% of the pipes (total 6km) are produced and delivered to Kamioka.
- A mockup tunnel has been prepared at a factory near Kashiwa.



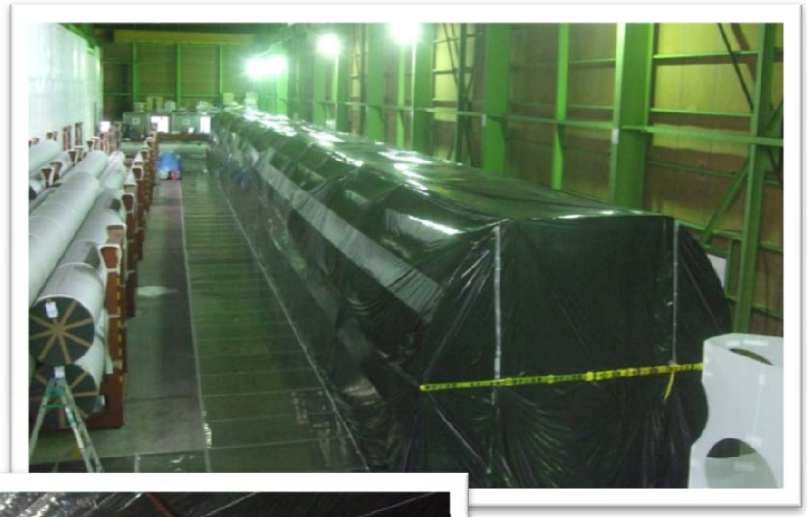

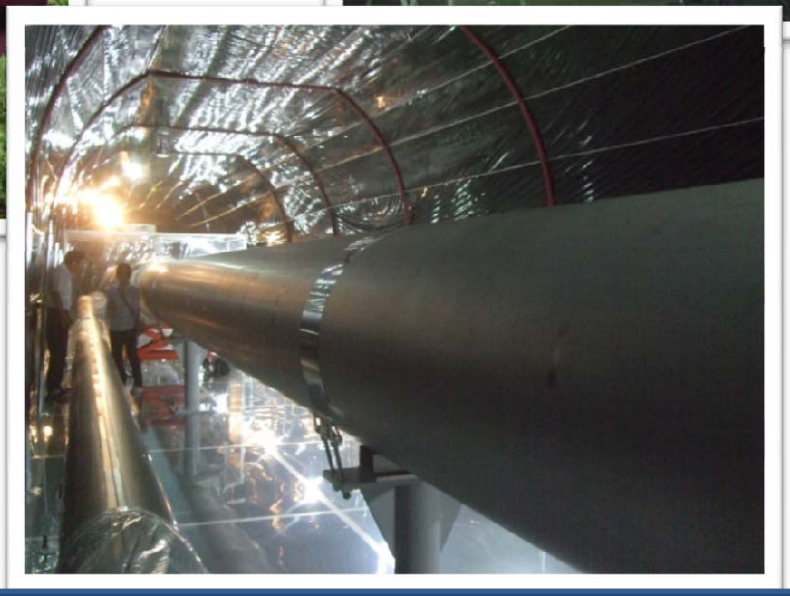

(Saito)

Status of construction: Seismic Attenuation

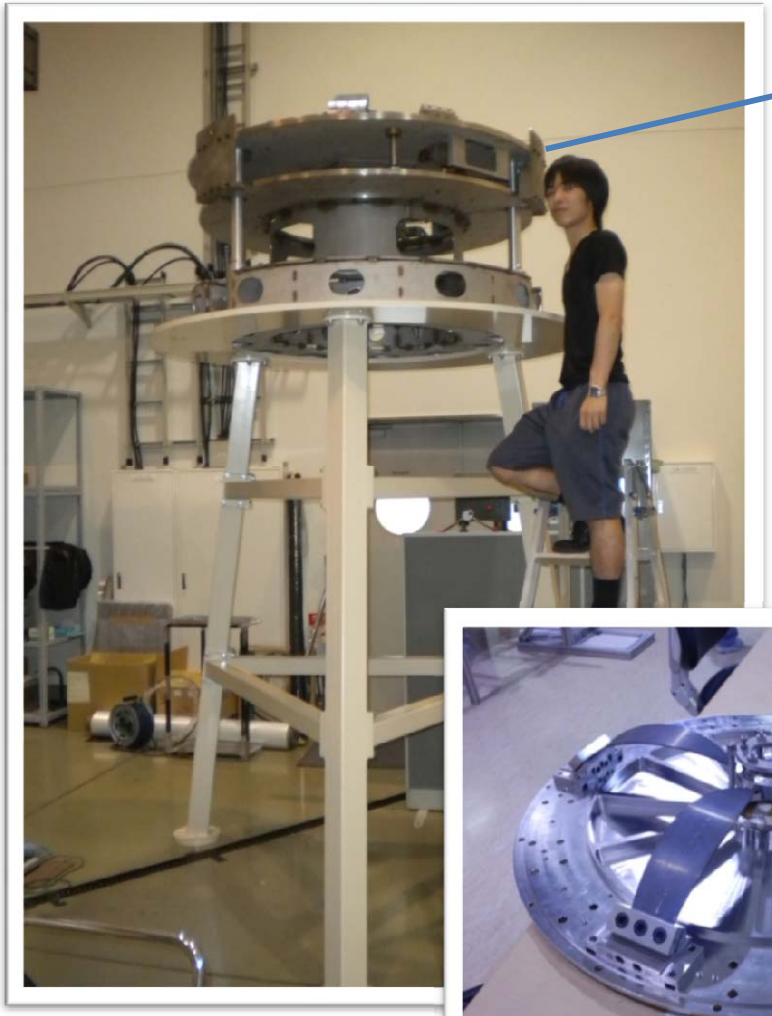

Top filter

Prototypes

Standard filter



(Takahashi et al)

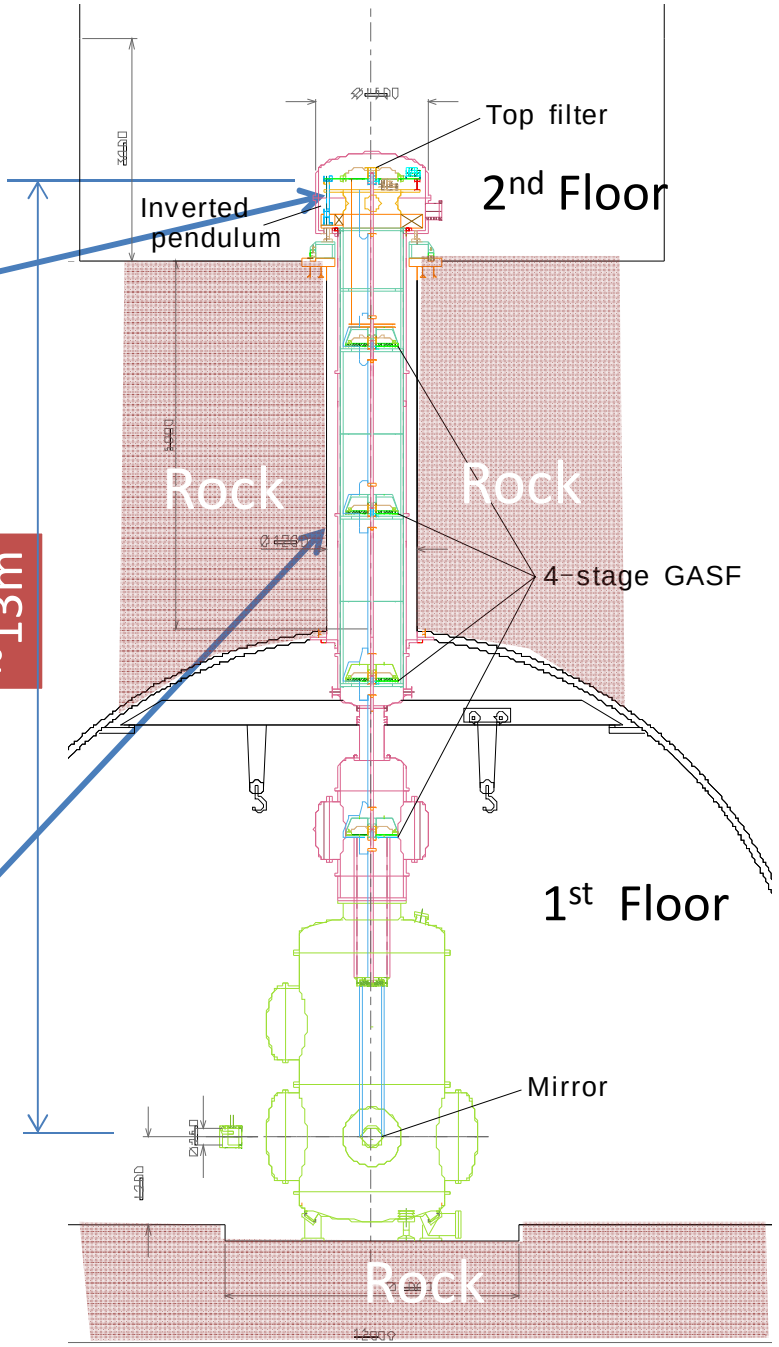

Status of preparation: Seismic Attenuation

Storage & Assembling in Akeno Observatory (ICRR)





Test of Pre-isolator (with the digital control system) at ICRR

Clean booth @Akeno



GAS filters delivered



Status of construction: Cryogenic system

Cryostat
Stainless steel t20mm
Diameter 2.4m
Height ~3.8m
M ~ 10 ton

to Seismic Attenuation system

Double radiation shield

Low vibration cryo-cooler units (4 units)

Main LASER beam

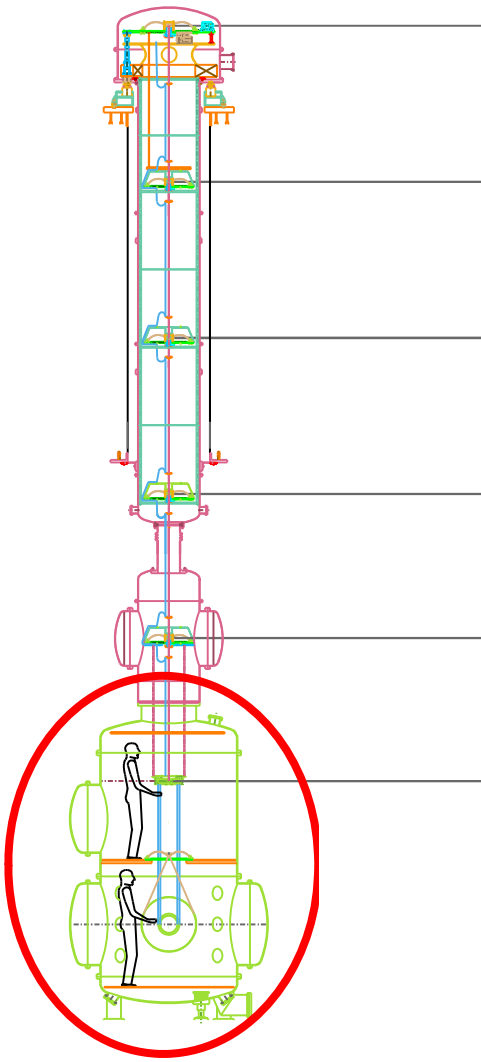

Status of construction: Cryogenic system



Cryostat construction
@Toshiba



Diameter 2.4m
Height ~3.8m
M ~ 10 ton

Status of construction: Cryogenic system



Cryostat (Vacuum chamber)
@Toshiba



Shield structure

Status of construction: Cryogenic system

Cryo-cooler unit

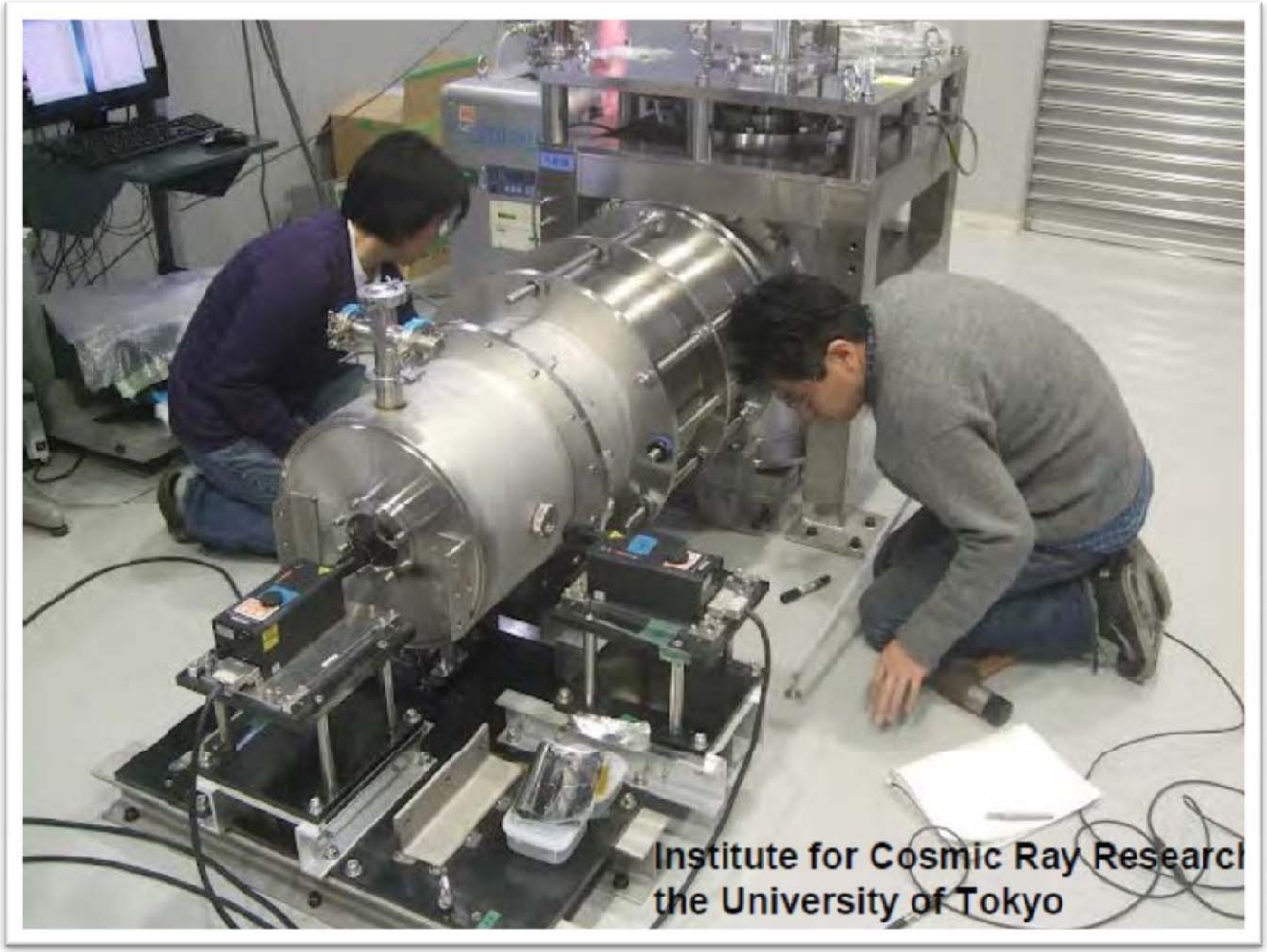

Vibration measurement is in progress

Status of preparation: Sapphire mirror

- First and second Sapphire crystal (C-axis, 22cmϕ, 15cm t) were delivered to Kashiwa in Aug. and Sep. 2012. (We do not know the quality yet…)

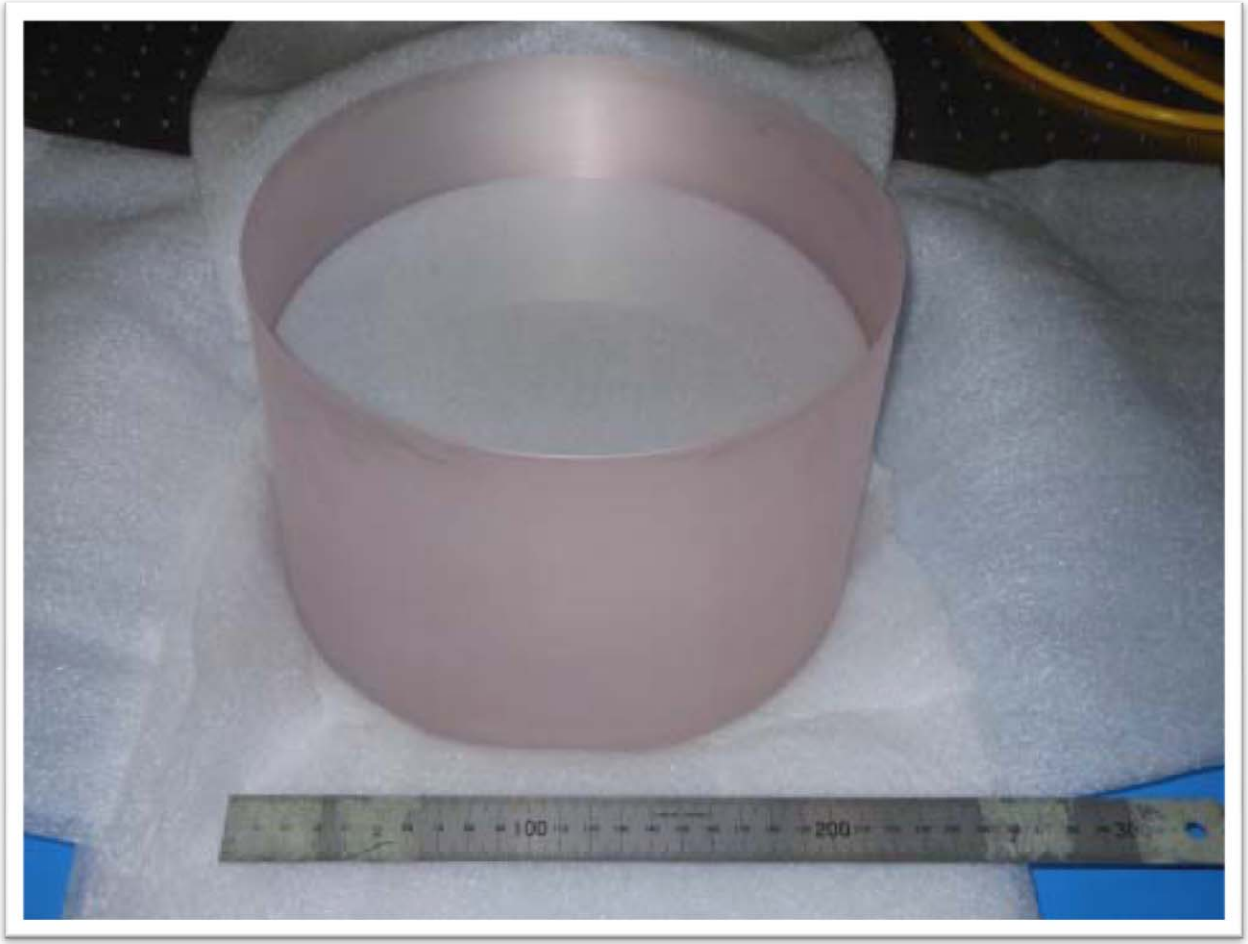

(Mio, Hirose)

Joining the global GW network

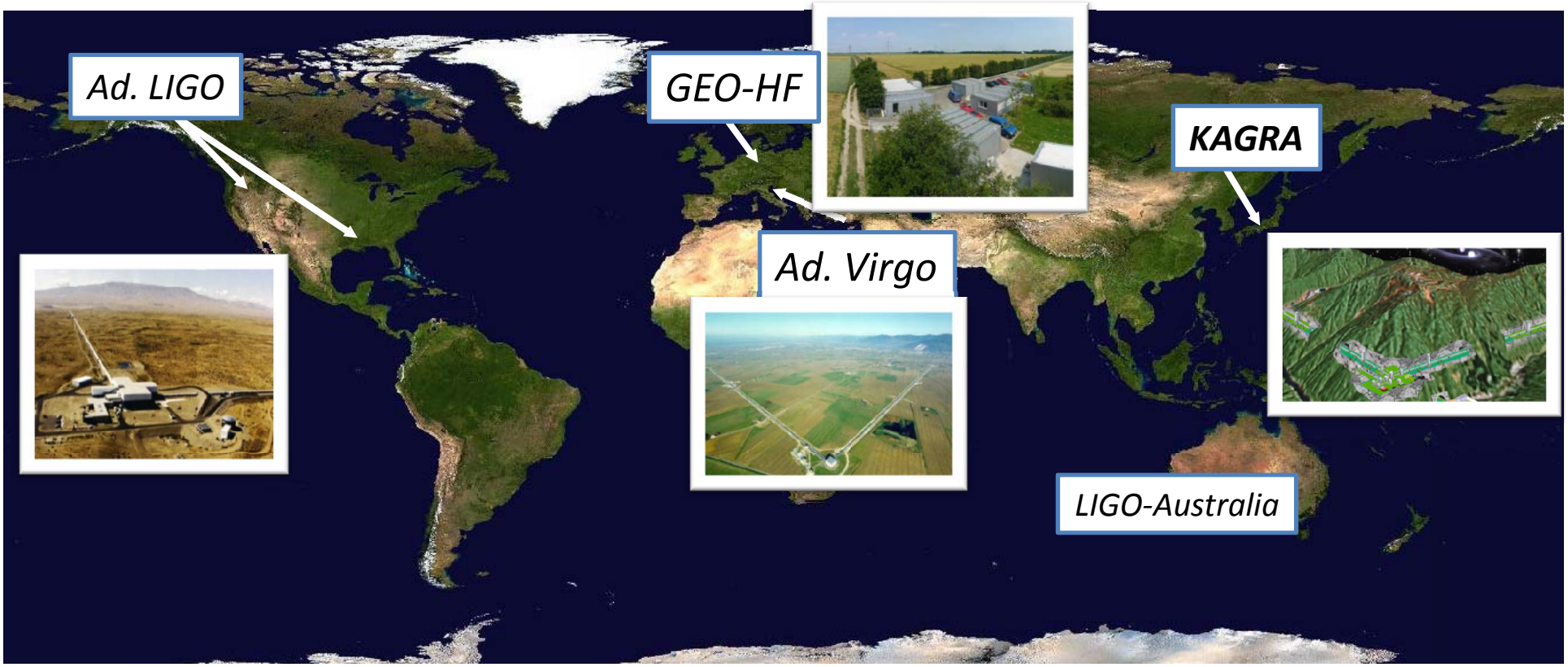

◆The scientific output will be maximized by the global network.

◆KAGRA has to learn various experiences / technologies from the existing interferometers.

◆KAGRA will join the worldwide network of gravitational wave detection / astronomy.

➔ MOU between LSC/Virgo/KAGRA (3 parties agreed.)

Importance of Global GW Network: Sky coverage

B. Schutz (Fijuwara Seminar, May 2009)

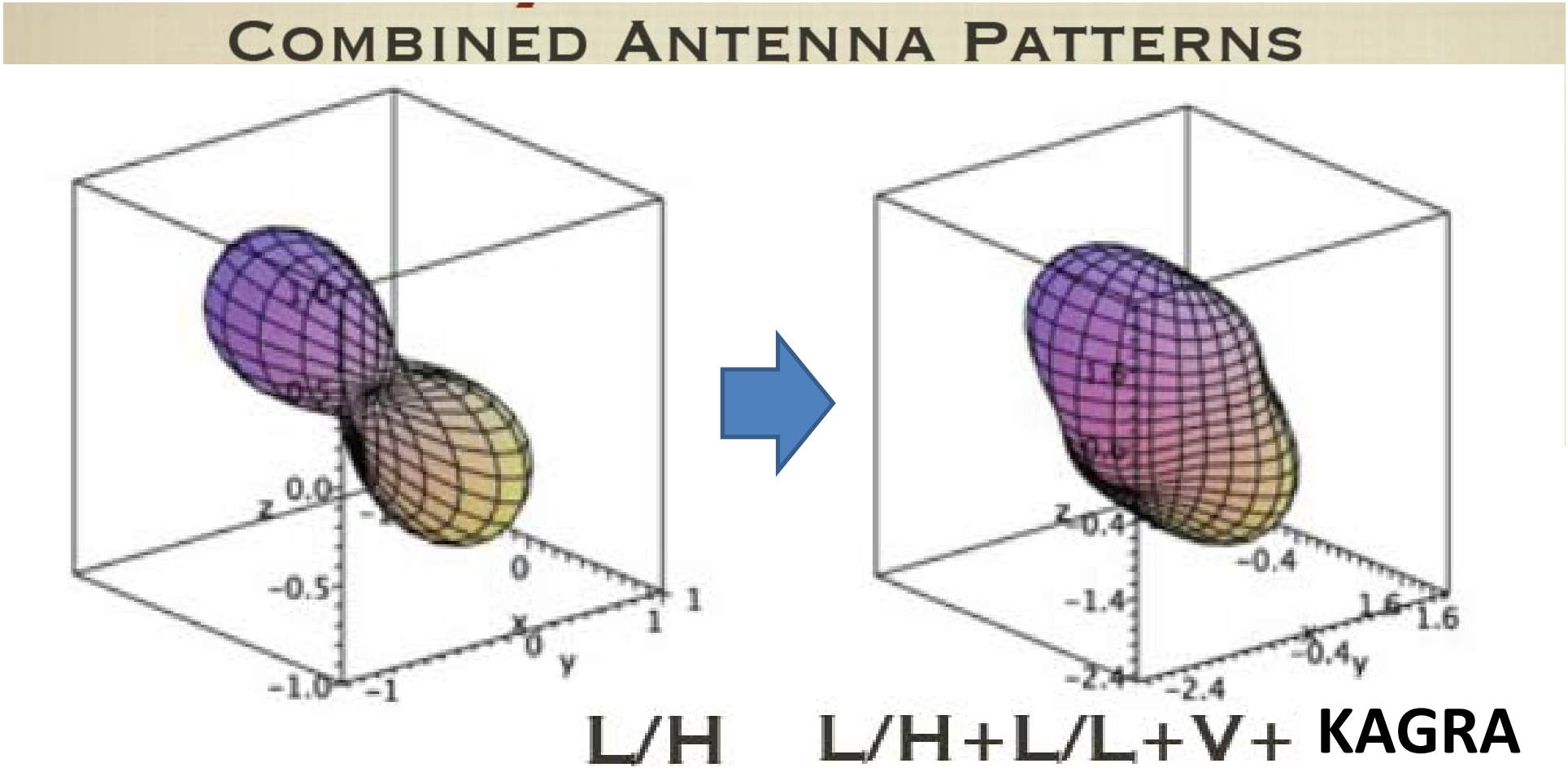

Much wider angular coverage !

Importance of Global GW Network: Angular res.

Wen and Chen, arXiv: 1003:2504

Determination of source sky position: 95%CL, supernova, S/N =10

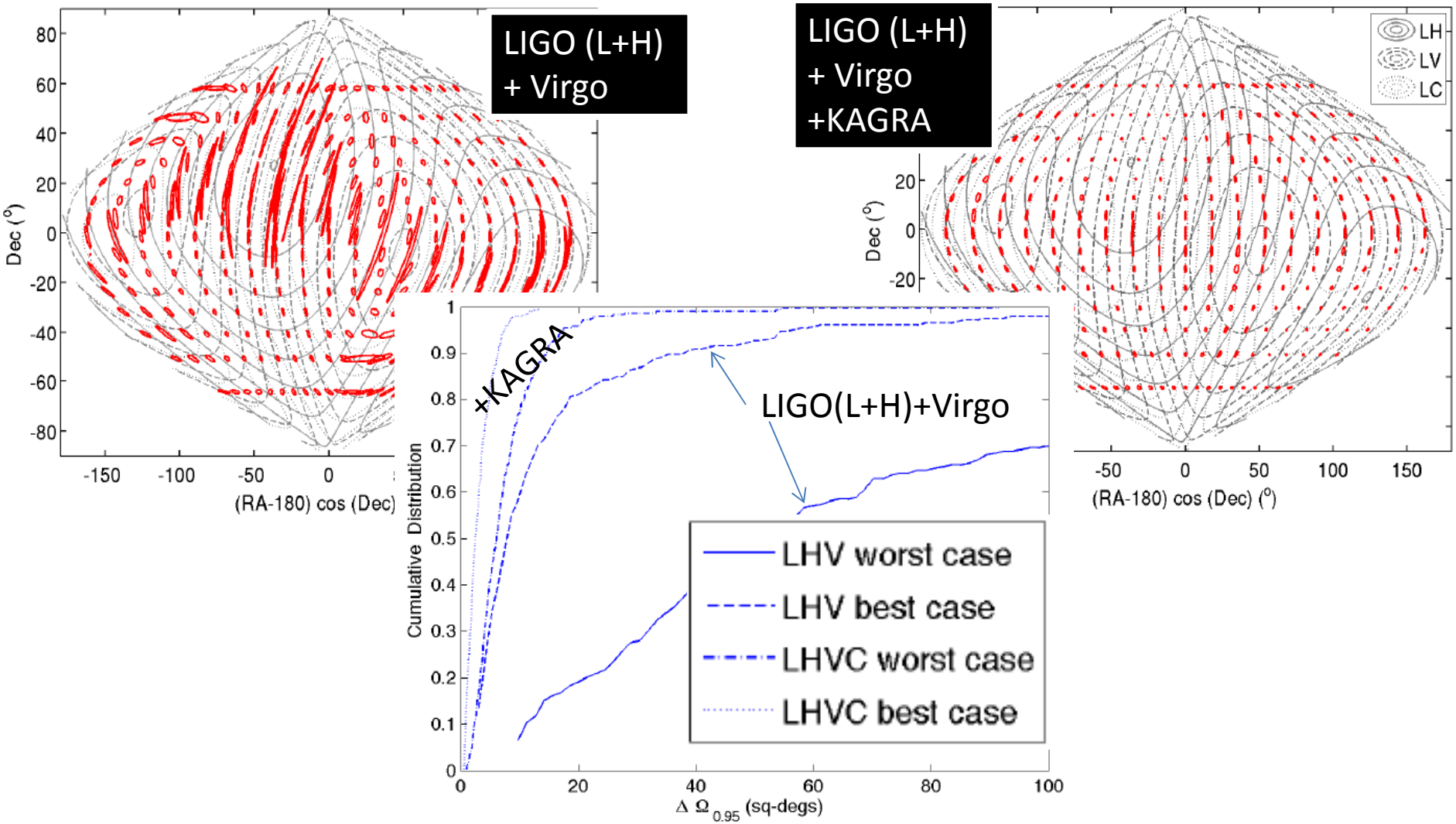

Multi-messenger astronomy: Example: Short Gamma Ray Burst

✓ NS-NS binary might be a progenitor of Short-GRB ?

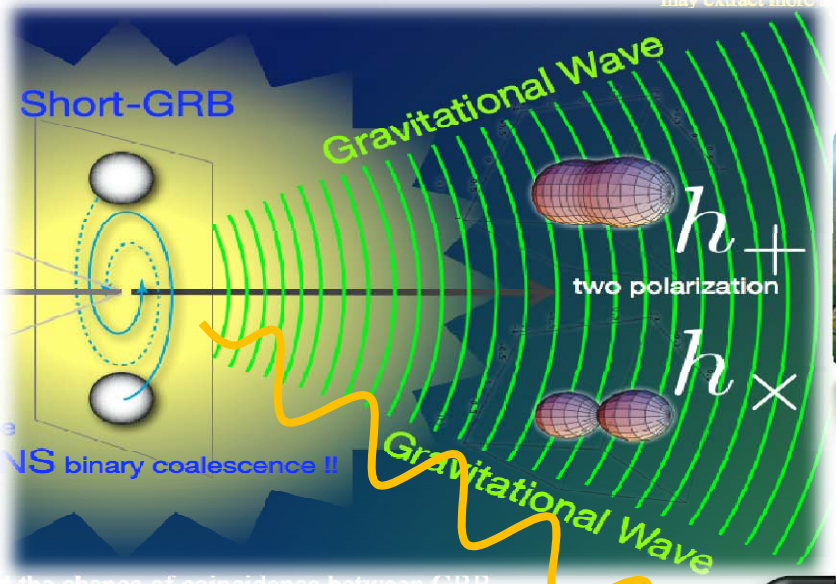



Gravitational wave (KAGRA, Adv.LIGO, Adv.Vergo, …)

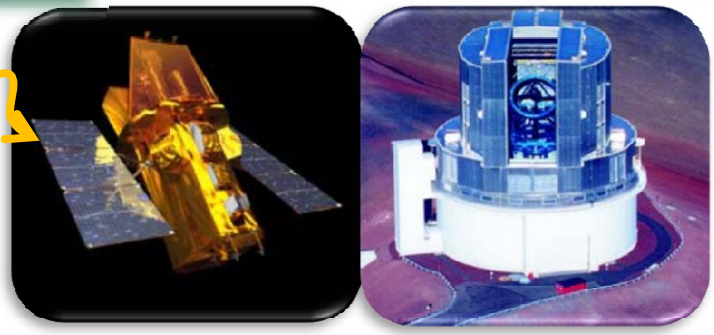

Gamma ray and optical observations

(H. Tagoshi)

Summary

- KAGRA is a unique GW interferometer with the underground site and the cryogenic technology.
- The KAGRA detector construction is in progress.
- Initial operation (iKAGRA) in late 2015.
- Preparation for the cryogenic system is also in progress.
- We plan to start the full cryogenic observation in 2017.
- KAGRA will join the global network of gravitational wave detection/astronomy.

Francesco Fidecaro, JGRG 22(2012)111403

"Virgo: design, results and perspectives"

RESCEU SYMPOSIUM ON

GENERAL RELATIVITY AND GRAVITATION

JGRG 22

November 12-16 2012

Koshiba Hall, The University of Tokyo, Hongo, Tokyo, Japan

Virgo: design, results and perspective

Francesco Fidecaro
For the Virgo Collaboration, the LSC and ET
Tokyo, November 14, 2012

Credit: Koppitz (AEI / ZIB), Rezzolla (AEI)

Outline

- GW detection peculiarities
- Gravitational wave spectrum
- The Virgo interferometer
- Some LSC-Virgo results (LSC and Virgo collaborations)
- Advanced Virgo
- The ET perspective (ET study group and science team)

GW detection

GW detection

- Need to measure changes in space time metric due to $T^{\mu\nu}$ variations
- The shape of the signal is given by the 2nd time derivative of Q^{ij}
- By measuring fields, and not energy, the signal amplitude varies as 1/R , distance from the source
- The amplitude of the detected signal depends smoothly on the incoming direction, due to the quadrupolar nature of the wave
- It scales as L, the size of the detector

Consequences

- Type of astrophysical / cosmological process identified by the signal shape (frequency components, phase)
- The number of observed sources, or recorded events, will raise as the distance (horizon) the detector is able to reach, to the 3rd power.
- Fixing the position of the source in the sky requires to measure the phase of the signal in more than one detector
- For long deterministic signals a single detector can be used (it moves !)
- The size of the detector determines the detectable GW wavelength

The reality

- Different detectors operate in different frequency bands, making their best to reduce noise
- Looking for amplitude one prefers massive compact astrophysical objects. The heavier the slower, but also the louder
- Studying the details of the process require higher spatial resolution, this translates into high frequency
- Options (remember that effects on single masses scale as 1/L)
  - Ground based, km size
  - Space based detectors
  - Galaxy based detectors
  - Universe based
  - No scale (stochastic background)
- Correspond to different sources
  - Compact binary systems
  - Binaries, massive black holes
  - Supermassive black holes
  - Stochastic background

The GW spectrum

Gravitational wave spectrum

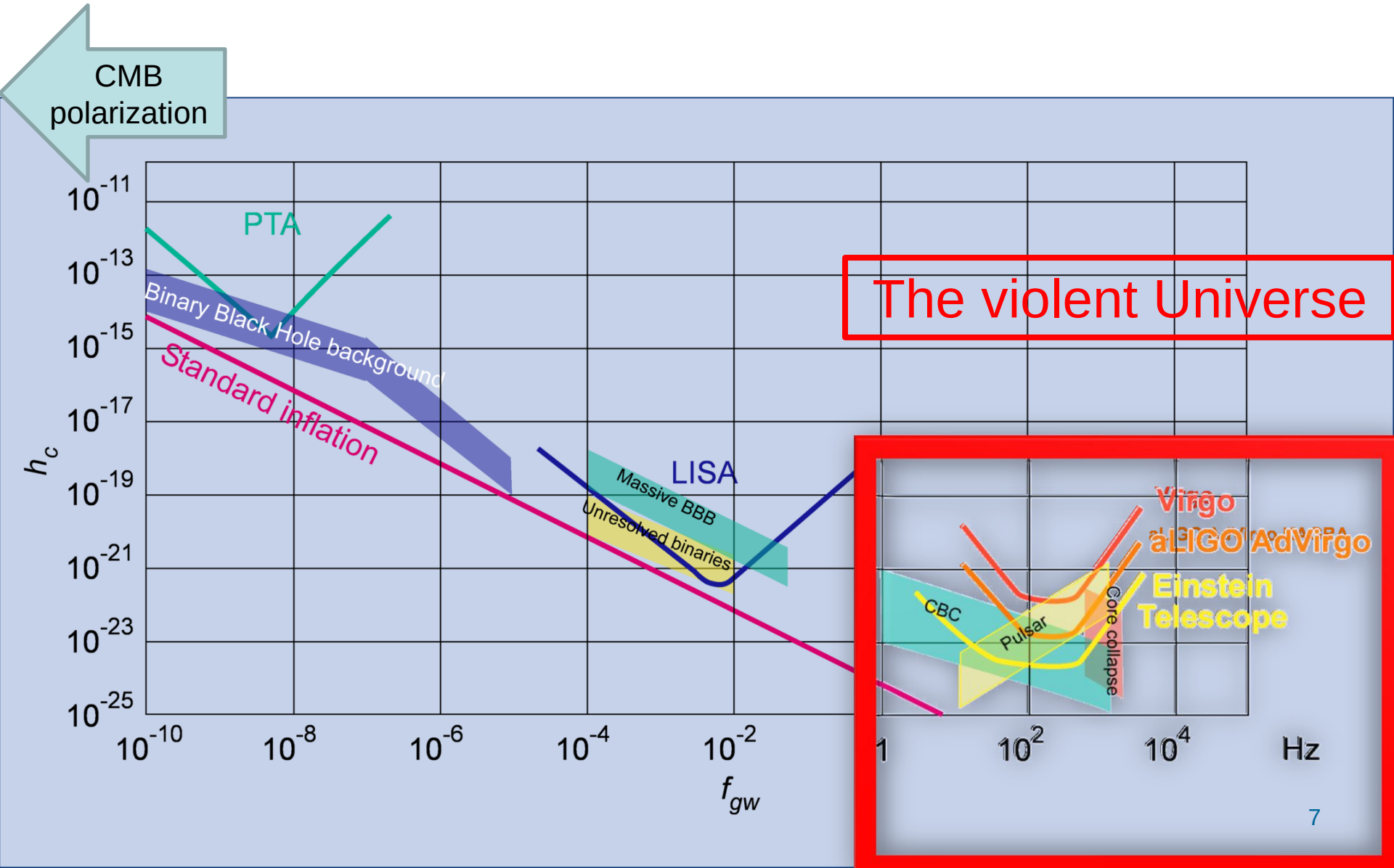

The violent Universe

- Ground based km scale interferometers will listen to the violent Universe, where gravity is strong over short distances

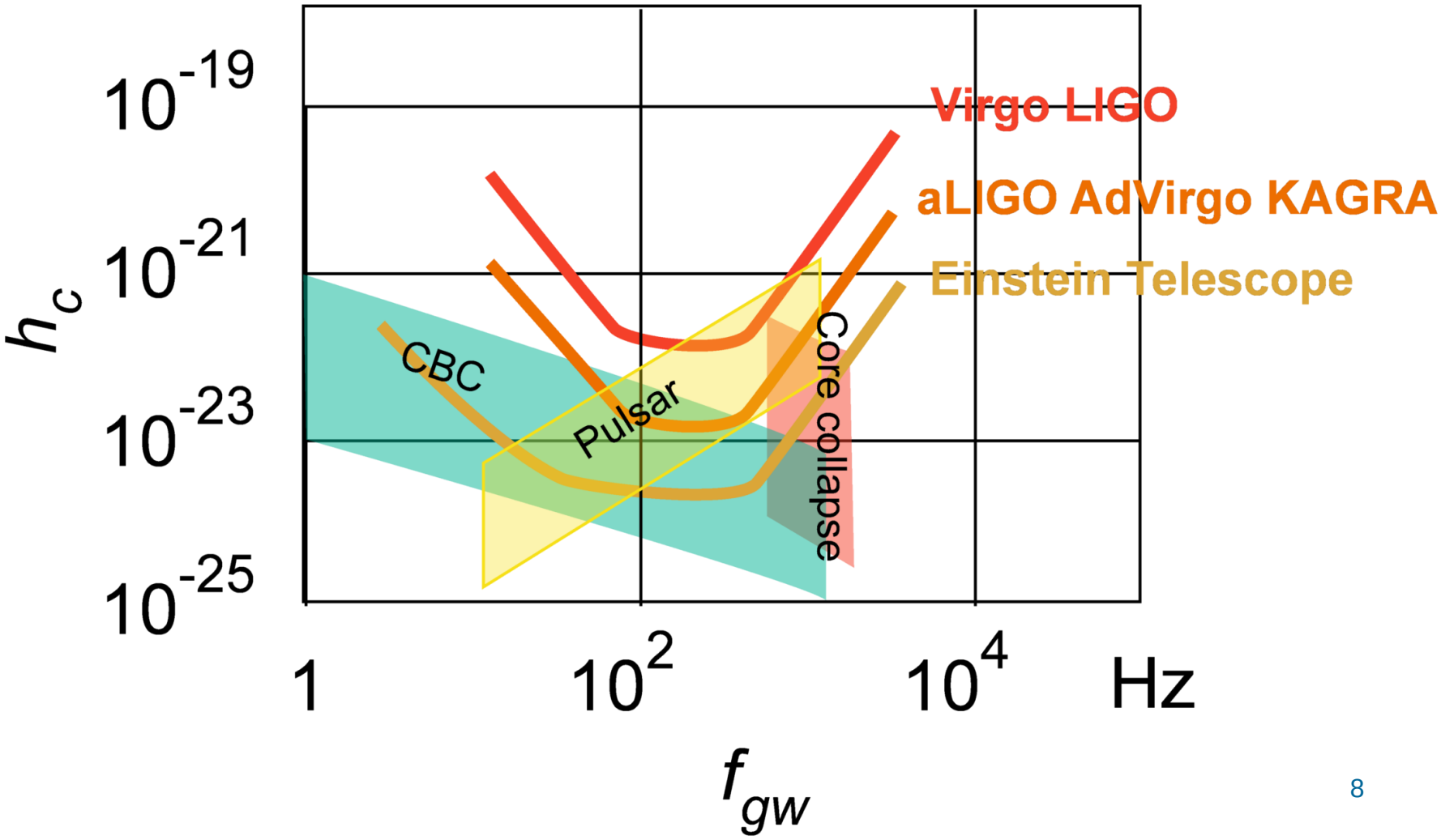

The Virgo detector

The Virgo Collaboration

T. Accadia[11], F. Acernese[5ac], F. Antonucci[8a], P. Astone[8a], G. Ballardin[2], F. Barone[5ac], M. Barsuglia[1], Th. S. Bauer[13a], M.G. Beker[13a], A. Belletoile[11], S. Birindelli[14a], M. Bitossi[7a], M. A. Bizouard[10a], M. Blom[13a], C. Boccara[10b], F. Bondu[14b], L. Bonelli[7ab], R. Bonnand[12], V. Boschi[7a], L. Bosi[6a], B. Bouhou[1], S. Braccini[7a], C. Bradaschia[7a], A. Brillet[14a], V. Brisson[10a], R. Budzyński[16b], T. Bulik[16cd], H. J. Bulten[13ab], D. Buskulic[11], C. Buy[1], G. Cagnoli[3a], E. Calloni[5ab], E. Campagna[3ab], B. Canuel[2], F. Carbognani[2], F. Cavalier[10a], R. Cavalieri[2], G. Cella[7a], E. Cesarini[3b], E. Chassande-Mottin[1], A. Chincarini[4], F. Cleva[14a], E. Coccia[9ab], C. N. Colacino[7a], J. Colas[2], A. Colla[8ab], M. Colombini[8b], A. Corsi[8a], J.-P. Coulon[14a], E. Cuoco[2], S. D'Antonio[9a], V. Dattilo[2], M. Davier[10a], R. Day[2], R. De Rosa[5ab], G. Debreczeni[17], M. del Prete[7ac], L. Di Fiore[5a], A. Di Lieto[7ab], M. Di Paolo Emilio[9ac], A. Di Virgilio[7a], A. Dietz[11], A. Dietz[11], M. Drago[15cd], V. Fafone[9ab], I. Ferrante[7ab], F. Fidecaro[7ab], I. Fiori[2], R. Flaminio[12], J.-D. Fournier[14a], J. Franc[12], S. Frasca[8ab], F. Frasconi[7a], A. Freise*, M. Galimberti[12], L. Gammaitoni[6ab], F. Garufi[5ab], M. E. Gáspár[17], G. Gemme[4], E. Genin[2], A. Gennai[7a], A. Giazotto[7a], R. Gouaty[11], M. Granata[1], C. Greverie[14a], G. M. Guidi[3ab], J.-F. Hayau[14b], H. Heitmann[14], P. Hello[10a], S. Hild**, D. Huet[2], P. Jaranowski[16e], I. Kowalska[16c], A. Królak[16af], N. Leroy[10a], N. Letendre[11], T. G. F. Li[13a], M. Lorenzini[3a], V. Loriette[10b], G. Losurdo[3a], E. Majorana[8a], I. Maksimovic[10b], N. Man[14a], M. Mantovani[7ac], F. Marchesoni[6a], F. Marion[11], J. Marque[2], F. Martelli[3ab], A. Masserot[11], C. Michel[12], L. Milano[5ab], Y. Minenkov[9a], M. Mohan[2], J. Moreau[10b], N. Morgado[12], A. Morgia[9ab], S. Mosca[5ab], V. Moscatelli[8a], B. Mours[11], I. Neri[6ab], F. Nocera[2], G. Pagliaroli[9ac], L. Palladino[9ac], C. Palomba[8a], F. Paoletti[7a,2], S. Pardi[5ab], M. Parisi[5b], A. Pasqualetti[2], R. Passaquieti[7ab], D. Passuello[7a], G. Persichetti[5ab], M. Pichot[14a], F. Piergiovanni[3ab], M. Pietka[16e], L. Pinard[12], R. Poggiani[7ab], M. Prato[4], G. A. Prodi[15ab], M. Punturo[6a], P. Puppo[8a], D. S. Rabeling[13ab], I. Rácz[17], P. Rapagnani[8ab], V. Re[15ab], T. Regimbau[14a], F. Ricci[8ab], F. Robinet[10a], A. Rocchi[9a], L. Rolland[11], R. Romano[5ac], D. Rosińska[16g], P. Ruggi[2], B. Sassolas[12], D. Sentenac[2], L. Sperandio[9ab], R. Sturani[3ab], B. Swinkels[2], A. Toncelli[7ab], M. Tonelli[7ab], O. Torre[7ac], E. Tournefier[11], F. Travasso[6ab], G. Vajente[7ab], J. F. J. van den Brand[13ab], S. van der Putten[13a], M. Vasuth[17], M. Vavoulidis[10a], G. Vedovato[15c], D. Verkindt[11], F. Vetrano[3ab], A. Viceré[3ab], J.-Y. Vinet[14a], H. Vocca[6a], M. Was[10a], M. Yvert[11]

- Early efforts
  - Brillet (optics)
  - Giazotto (suspensions)
- Collaboration started in 1992
- LAPP Annecy
- EGO Cascina
- Firenze-Urbino
- Genova
- Napoli
- OCA Nice
- NIKHEF Amsterdam
- LAL Orsay
- LMA Lyon
- APC Paris – ESPCI Paris
- Perugia
- Pisa
- Roma La Sapienza
- Roma Tor Vergata
- Trento-Padova
- IM PAN Warsaw
- RMKI Budapest
- LKB Paris
- 18 groups
- About 200 authors

Noise in mass position

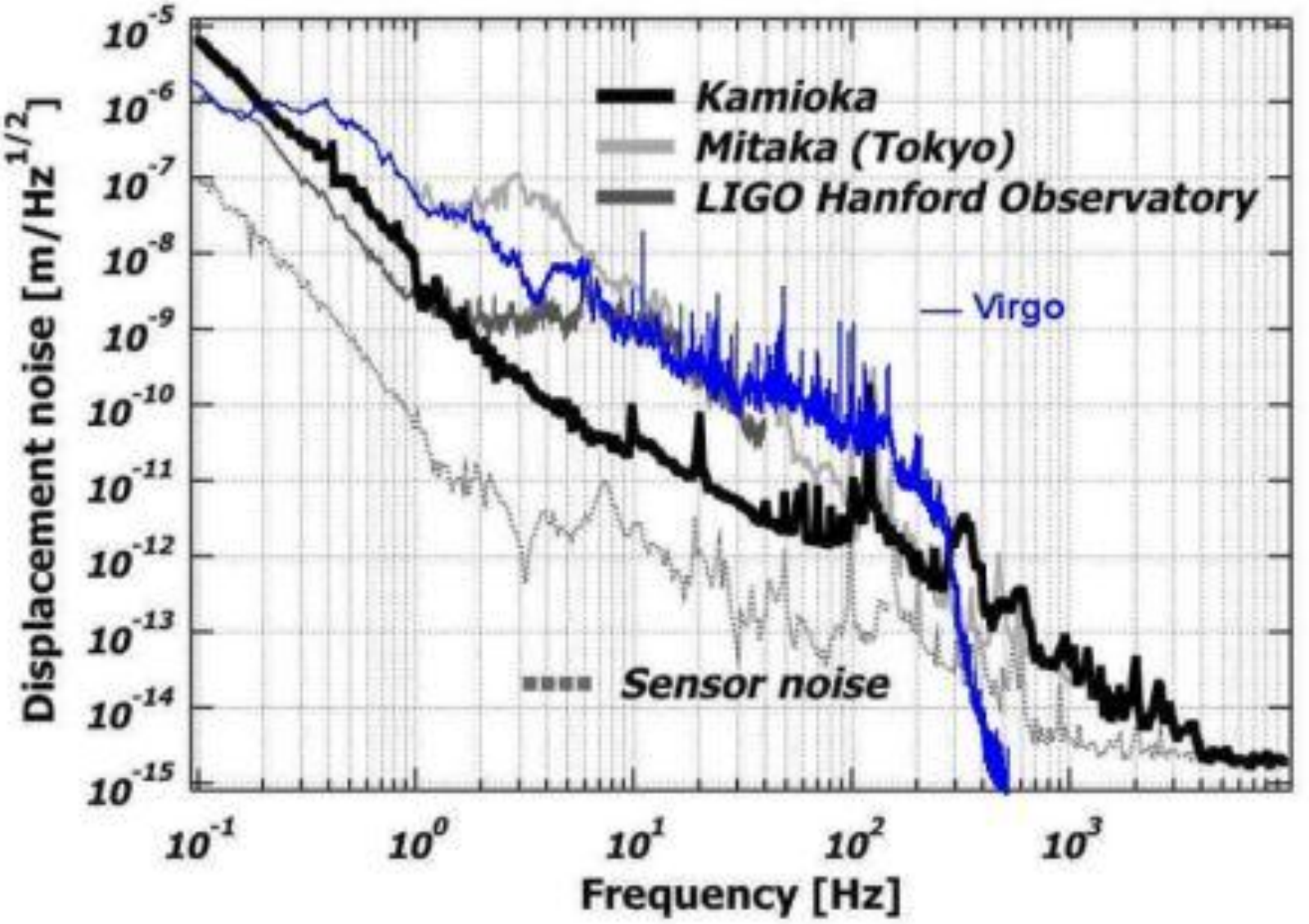

Superattenuator performance

- Excitation at top
- Use Virgo sensitivity and stability
- Integrate for several hours
- Upper limit for TF at 32 Hz:1,7 10^{-12}
- In some configurations a signal was found, but also along a direction perpendicular to excitation: compatible with magnetic cross talk

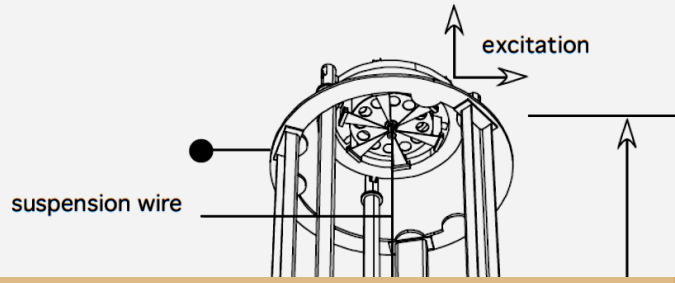

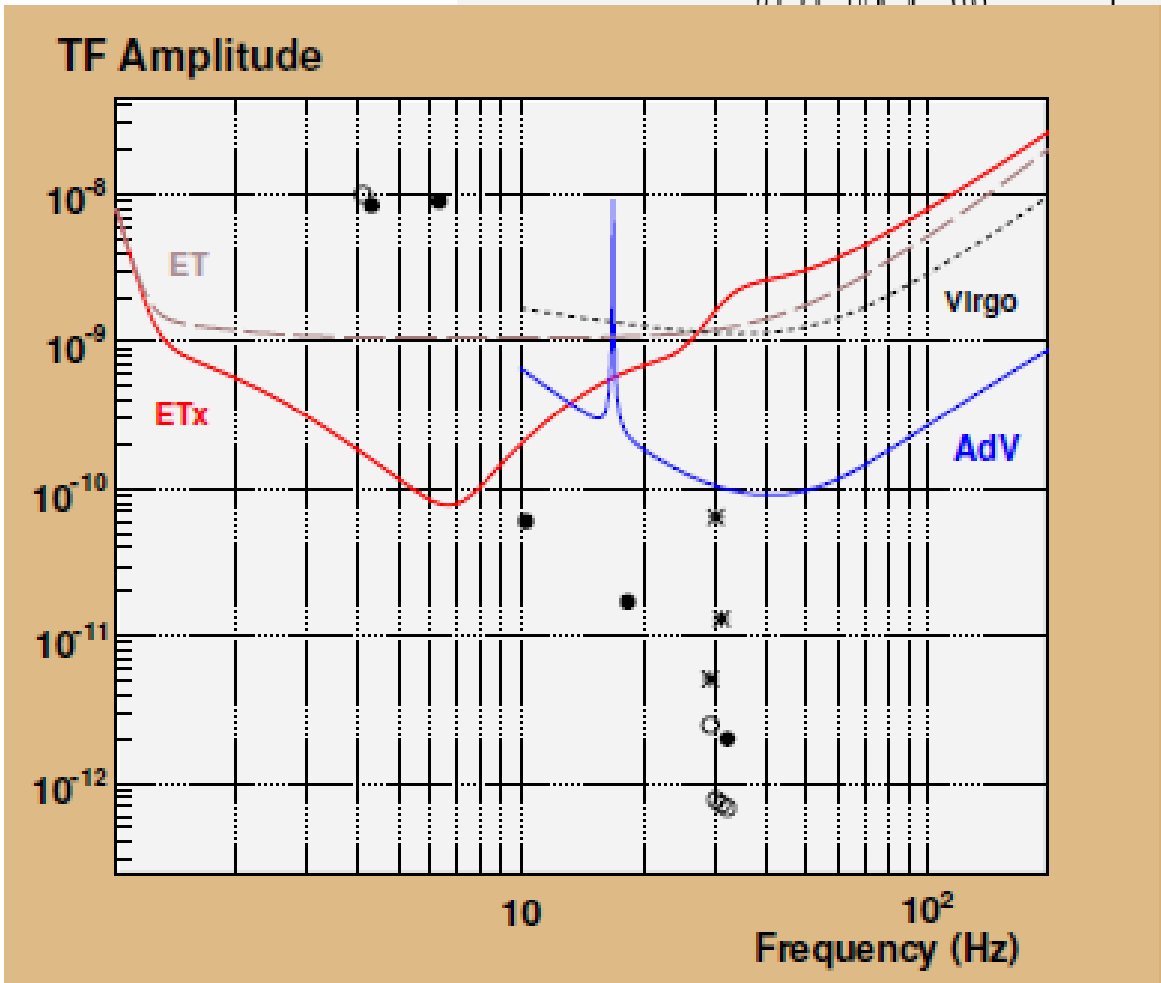

Issues in ser

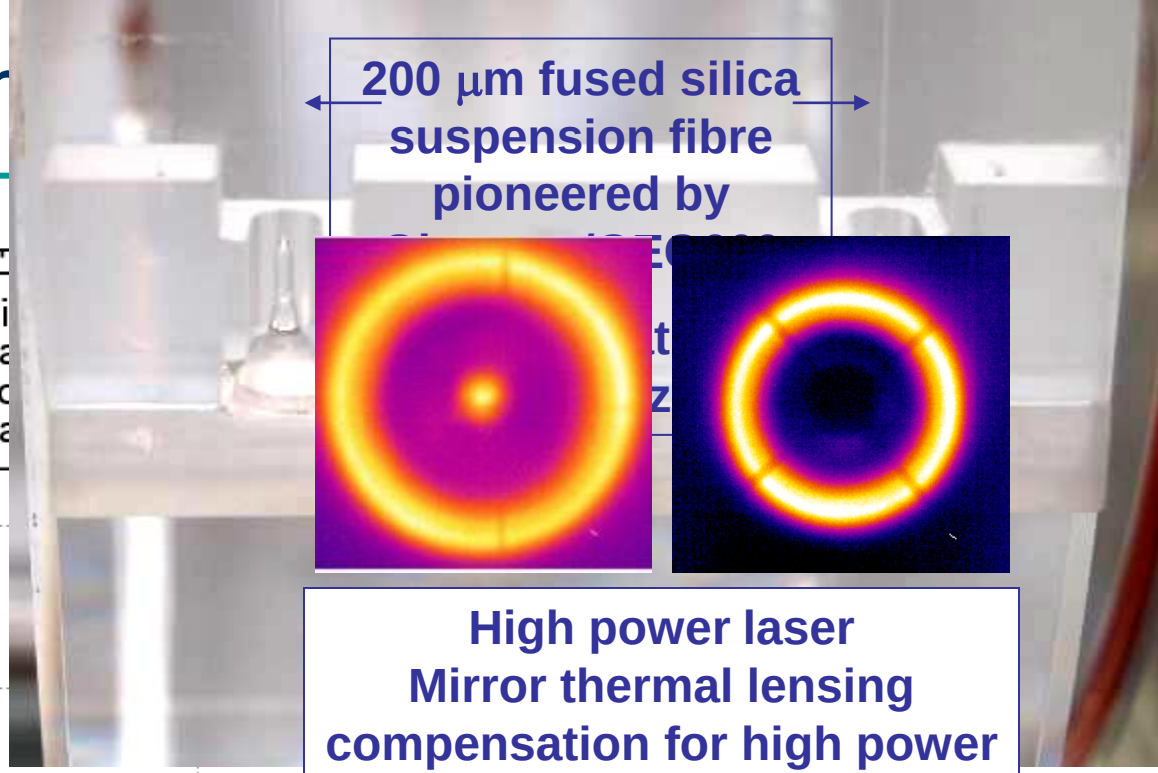

High power laser
Mirror thermal lensing compensation for high power
Signal recycling
Use of non standard light

Seismic attenuation

Local gravity fluctuations

Virgo site in Cascina



Noise understanding

- Noise sources and coupling are well understood
- Low frequency shows more structures
- Noise reduction in advanced detectors achieved with proper design

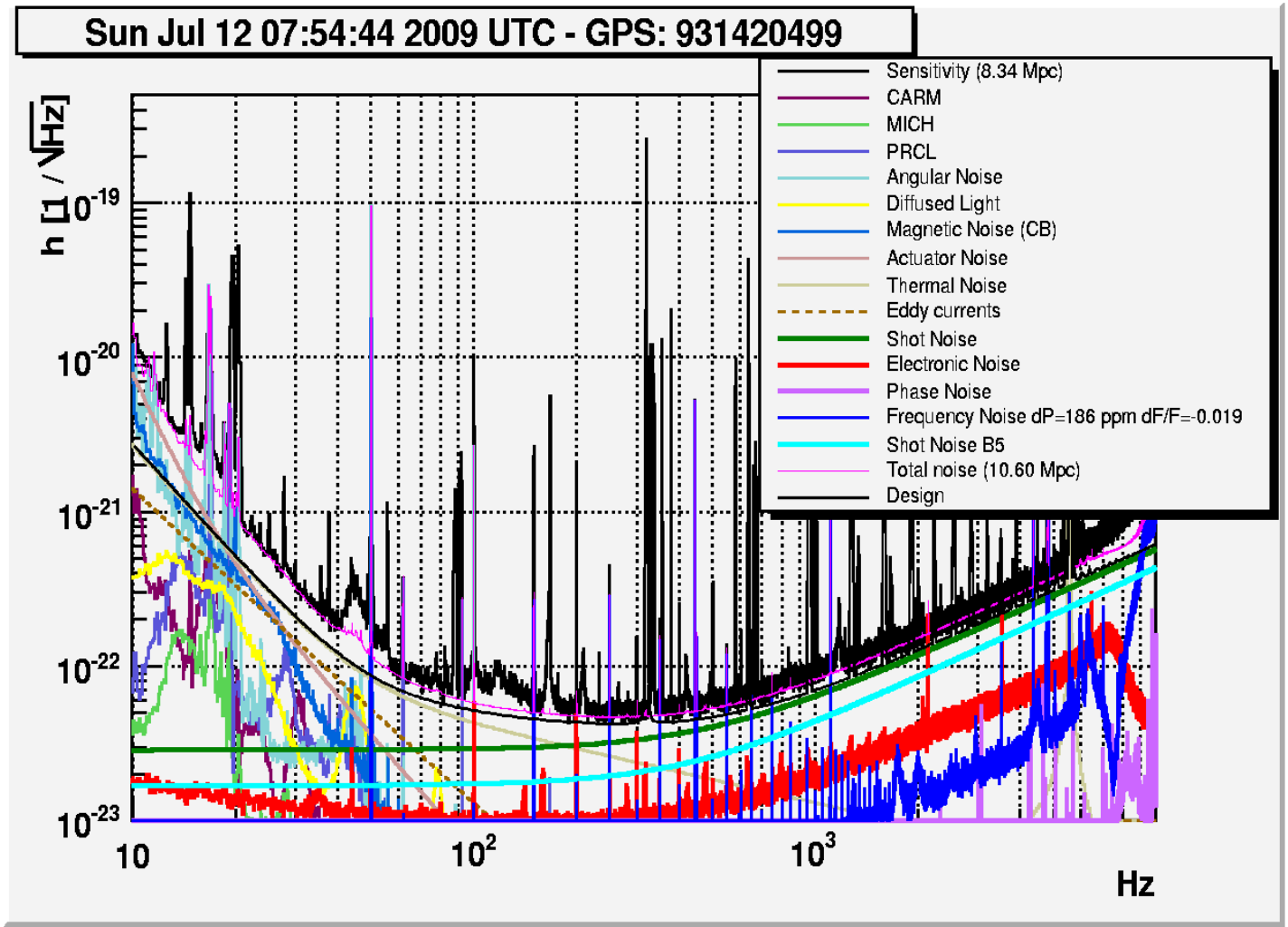

The noise budget

Lines
10.28 & arm (NI)
13-14 Cal
14.8 vert_rm
17 Mich
18.6 Env_Inj
20.1 Tz_rm
37 DET
78-82 Dihedron
130 (?)
166 Bs_violin
166 M1
210 M2

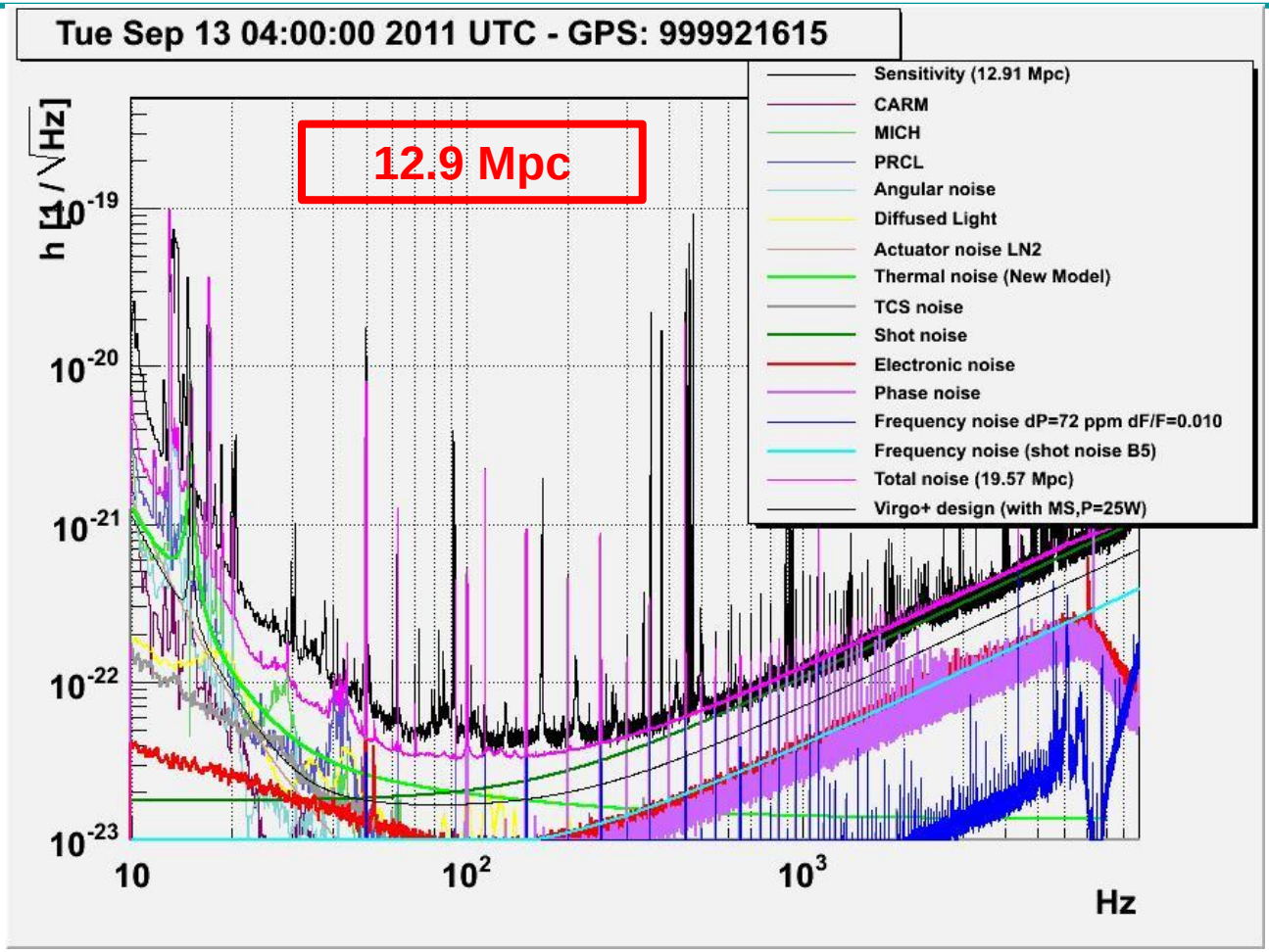

The noise budget. For frequency lower than about 300 Hz the sensitivity calculated as the quadratic sum of all noises - violet curve - does not explain the actual sensitivity - black curve.

Environmental noises studies

Investigations to understand the sources and the path to dark fringe

⇒ Coupling (paths) to dark fringe

- diffused light from in air optical benches
- diffused light related to Brewster window
- beam jitter on injection bench

⇒ Sources of environmental noise:

- air conditioning
- electronic racks

Need to work both on:

- reduction of coupling
- reduction of environmental noise

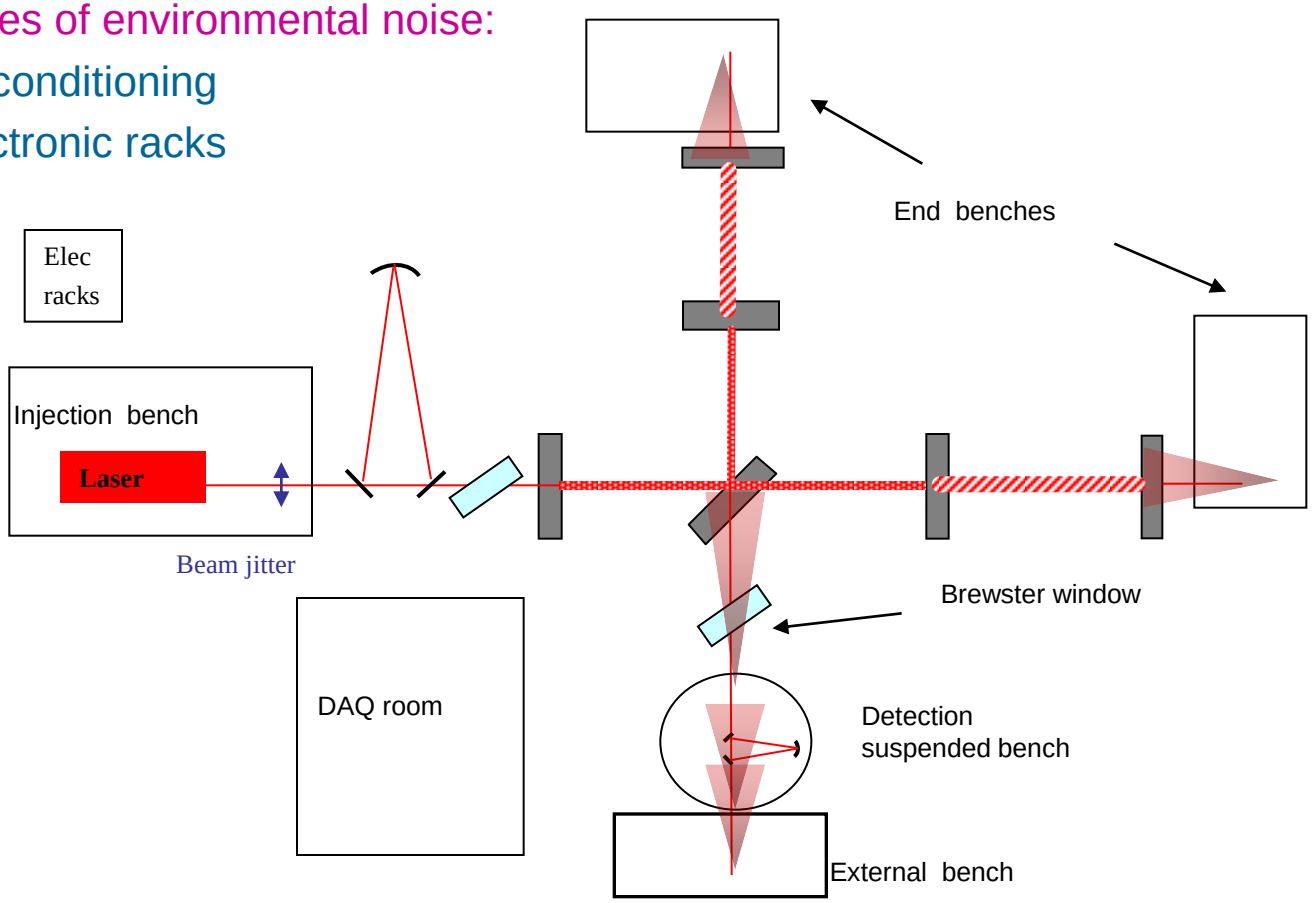

Virgo sensitivity progress

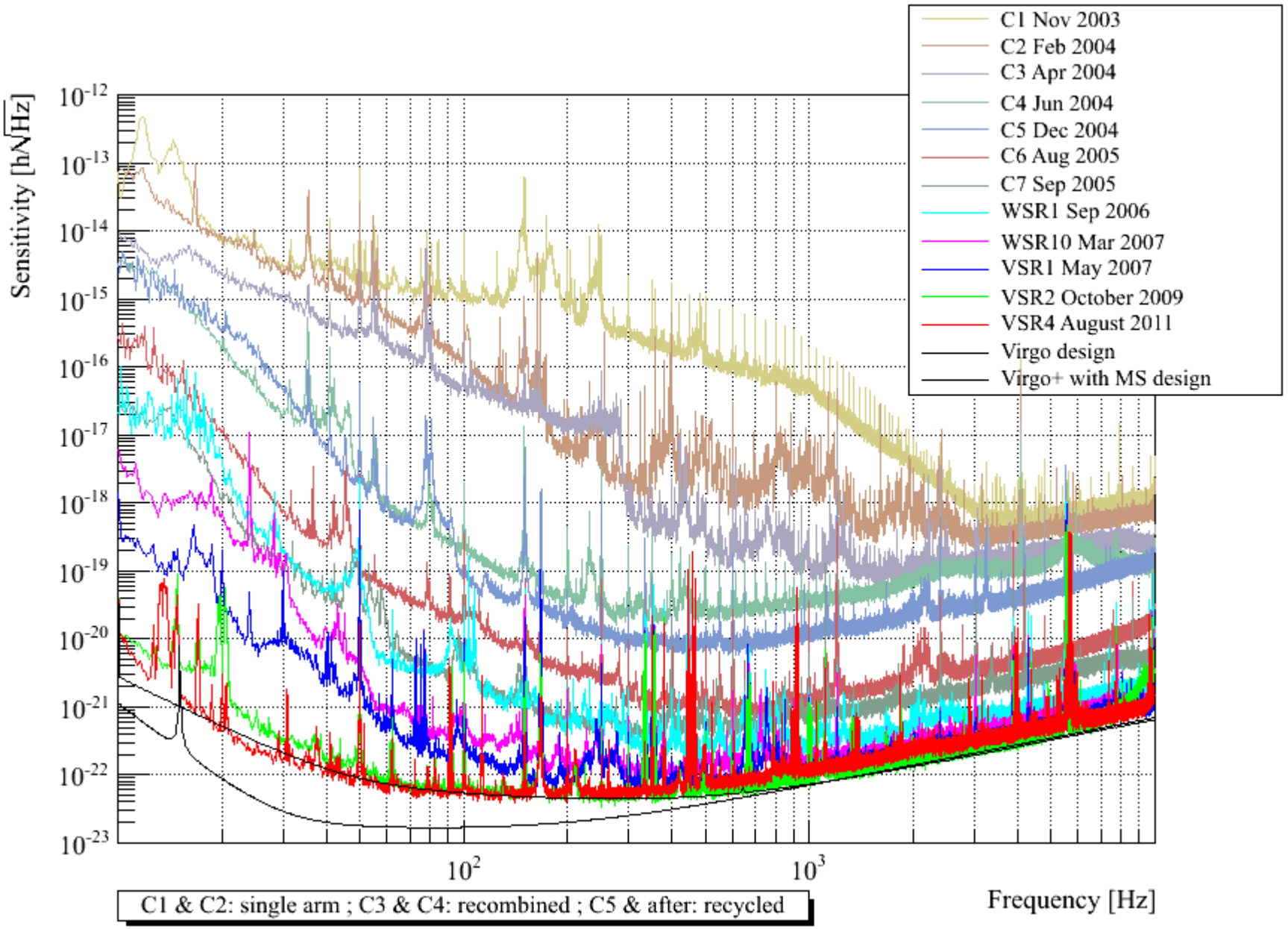

ROBUSTNESS

- Excellent robustness (and very good duty cycles) obtained by 1st generation detectors
- Not just sensitive instruments, but reliable ones!

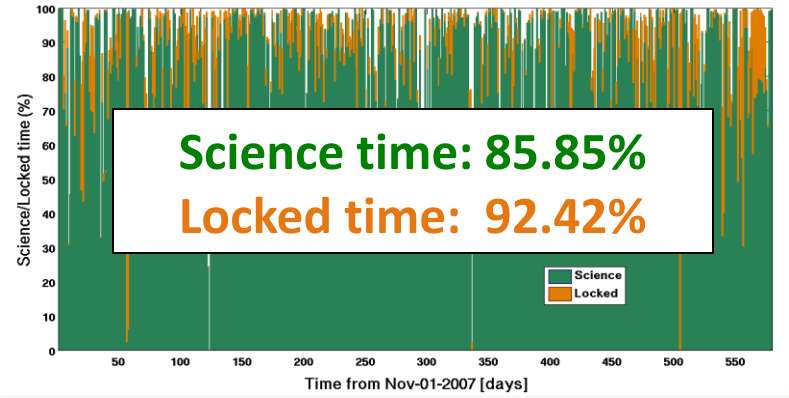

GEO: Nov 07 – Jun 09

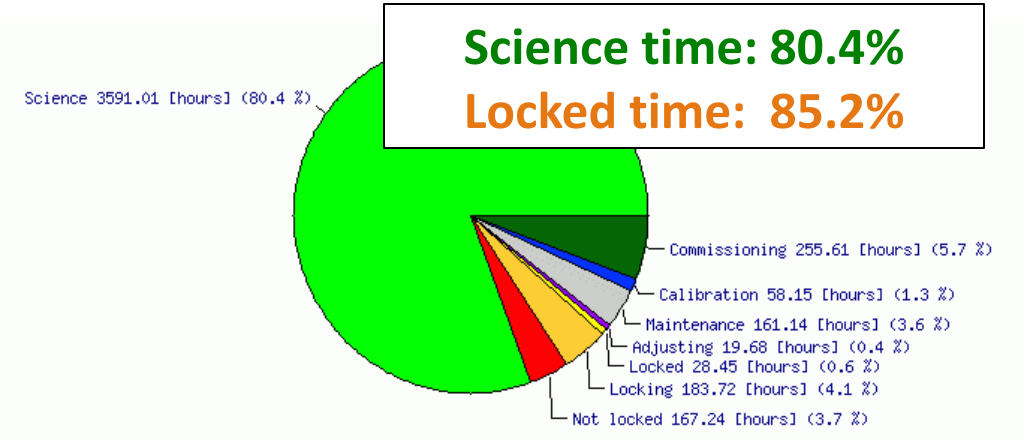

Virgo: Jul 09 – Jan 10

The global network

Motivation for a Global GW Detector Network

- *Source location*:
  - Ability to triangulate (or 'N-angulate') and more accurately pinpoint source locations in the sky
  - More detectors provides better source localization → *Multi-messenger astronomy*

- *Network Sky Coverage:*
  - GW interferometers have a limited antenna pat maximal sky coverage

- *Detection confidence*:
  - Redundancy – signals in multiple detectors

- *Maximum Time Coverage - 'Always listening'*:
  - Ability to be 'on the air' with one or more detect

- *Source parameter estimation:*
  - More accurate estimates of amplitude and phas
  - Polarization - array of oriented detectors is sen

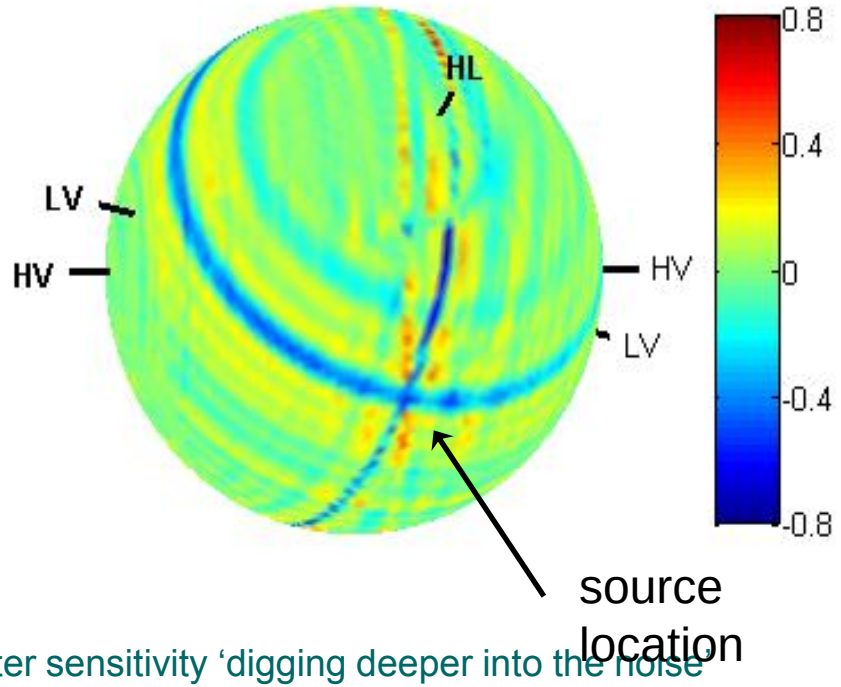

- *Coherent analysis*:
  - Combining data streams coherently leads to better sensitivity 'digging deeper into the noise'
  - Also, optimal waveform and coordinate reconstruction

World wide GW network: LV agreement

- "Among the **scientific benefits** we hope to achieve from the collaborative search are:
  - better confidence in detection of signals, better duty cycle and sky coverage for searches, and better source position localization and waveform reconstruction. In addition, we believe that the intensified sharing of ideas will also offer additional benefits."
- Collaborations keep their identities and independent governance

LV Agreement (I)

- “All data analysis activities will be open to all members of the LSC and Virgo Collaborations, in a spirit of cooperation, open access, full disclosure and full transparency with the goal of best exploiting the full scientific potential of the data.”

- Joint committees set up to coordinate data analysis, review results, run planning, and computing. The makeup of these committees decided by mutual agreement between the projects.

- Joint publication of observational data whether data from Virgo, or LIGO (GEO) or both

Some results from L-V

Horizon and event rate

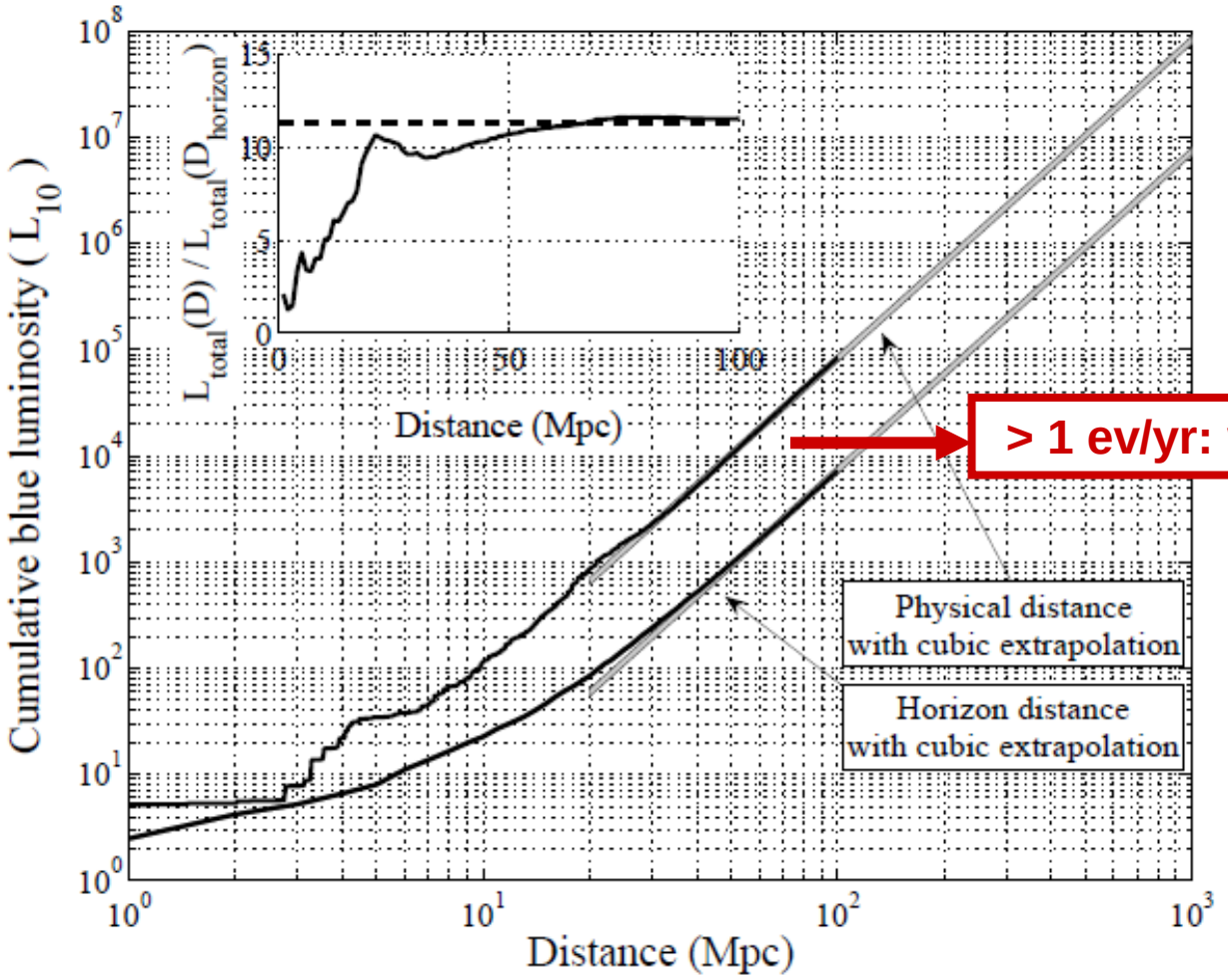

> 1 ev/yr: we did our best

FIG. 1: The total blue-light luminosity within a sphere of a given radius (top curve) and the accessible blue-light luminosity for a given horizon distance $D_{\rm horizon}$, taking location and orientation averaging into account (bottom curve). Gray shaded lines are cubic extrapolations. The inset shows the ratio between the top and bottom curves, which asymptotes to 2.26^3, as discussed in the text. Reproduced from [15] by permission of the AAS.

Predictions for the rates of compact binary coalescences observable … CQG, 10.1088/0264-9381/27/17/173001

VSR2 sensitivity for CW searches

Targeted searches.

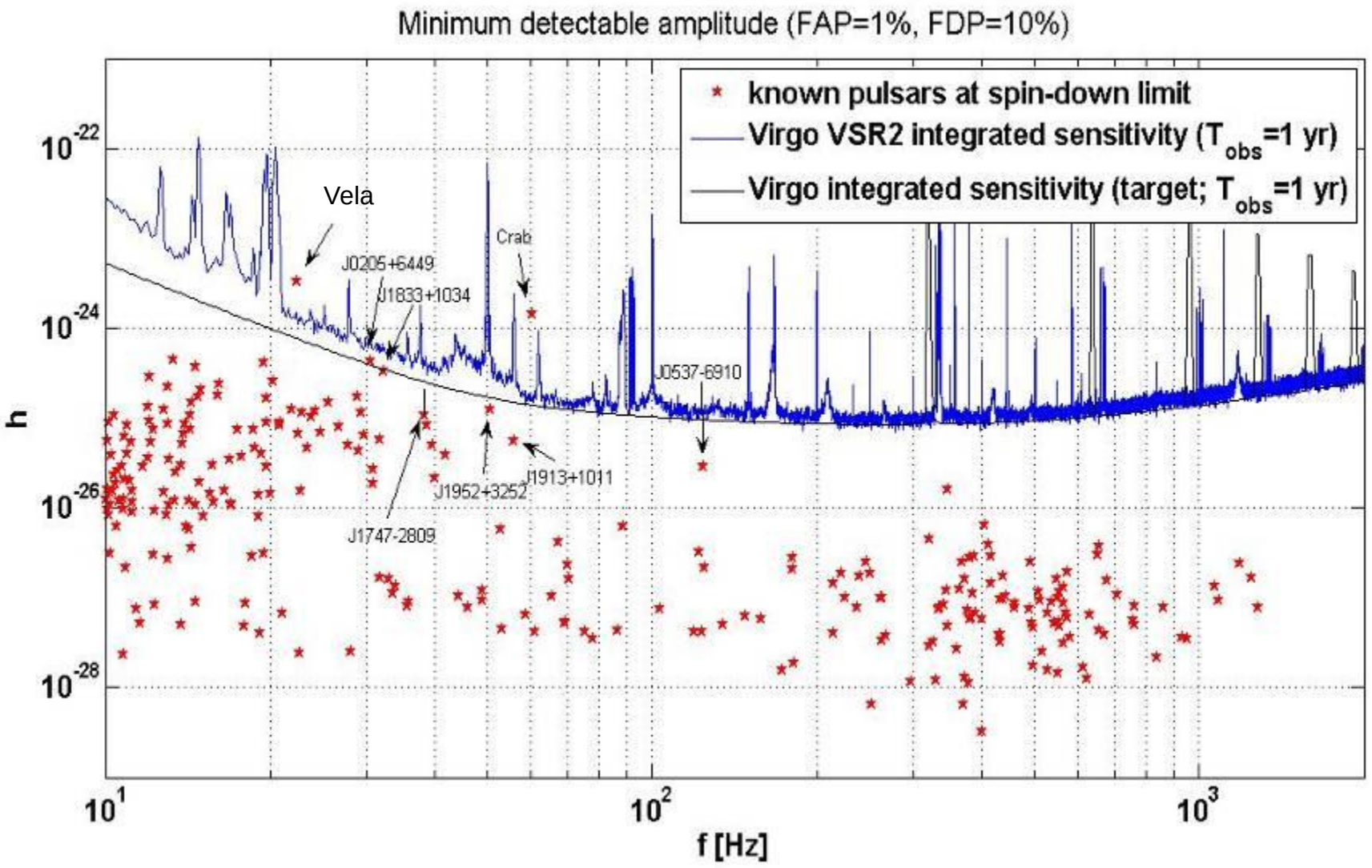

Vela pulsar spin down limit

THE ASTROPHYSICAL JOURNAL, 737:93 (16pp), 2011 August 20 doi:10.1088/0004-637X/737/2/93
© 2011. The American Astronomical Society. All rights reserved. Printed in the U.S.A.

BEATING THE SPIN-DOWN LIMIT ON GRAVITATIONAL WAVE EMISSION FROM THE VELA PULSAR

J. ABADIE[1], B. P. ABBOTT[1], R. ABBOTT[1], M. ABERNATHY[2], T. ACCADIA[3], F. ACERNESE[4,5], C. ADAMS[6], R. ADHIKARI[1],

- Spin down limit amplitude: 3.3 10^{-24} for VSR2
- Upper limit (known period, phase, orientation) < 2.2 10^{-24} 95% CL
- Local vibration disturbance (laser cooling pump)
- Improvements expected with VSR3 and VSR4

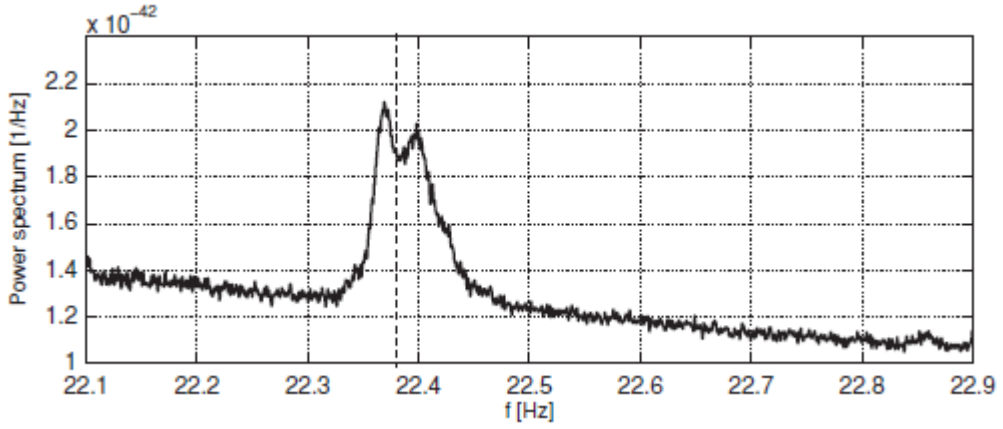

The Crab Pulsar: *Beating the Spin Down Limit!*

- Remnant from supernova in year 1054
- Spin frequency ν_{EM} = 29.8 Hz

  → $\nu_{gw} = 2\ \nu_{EM}$ = 59.6 Hz
- observed luminosity of the Crab nebula

accounts for < 1/2 spin down power

•spin down due to:

  - electromagnetic braking
  - particle acceleration
  - *GW emission?*

- early S5 result: $h < 3.9 \times 10^{-25}$ → ~ 4X *below*

  the spin down limit (assuming restricted priors)
- ellipticity upper limit: $\varepsilon < 2.1 \times 10^{-4}$
- GW energy upper limit < 6% of radiated energy is in GWs

Abbott, et al., *"Beating the spin-down limit on gravitational wave emission from the Crab pulsar,"* Ap. J. Lett. **683**, L45-L49, (2008).

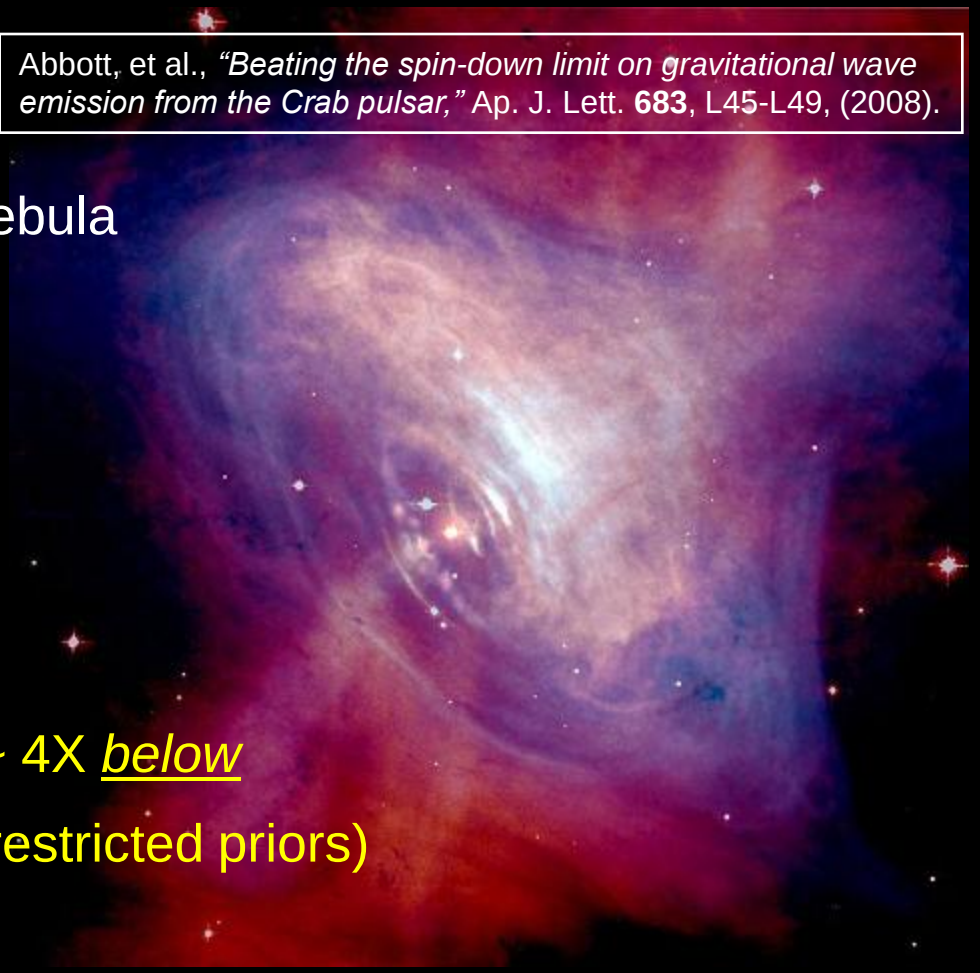

Searches for GWs from known pulsars

- Continuous gravitational-wave emission due to asymmetry rotation axis
  - elastic deformations of the solid crust or core
  - Distortion an extremely strong misaligned magnetic field
  - Weak emitters
- Spin-down limit:
- Crab pulsar (using LIGO data):
  - $h_0 < h_{sd}/7$, $E_{GW} < 0.02$ $h_{\mathrm{sd}} = \left(\frac{5}{2}\frac{GI_{zz}|\dot{\nu}|}{c^3 r^2 \nu}\right)^{1/2}$
- Vela pulsar (using Virgo data):
  - $h_0 < 0.66 h_{sd}$, $E_{GW} < 0.45 E_{total}$
- S5 search of 116 pulsars
  - Lowest upper-limit h_0: 2.3 x 10^{-26} (PSR J1603-7202)
  - Lowest upper-limit ellipticity: 7 x 10^{-8} (PSR J212

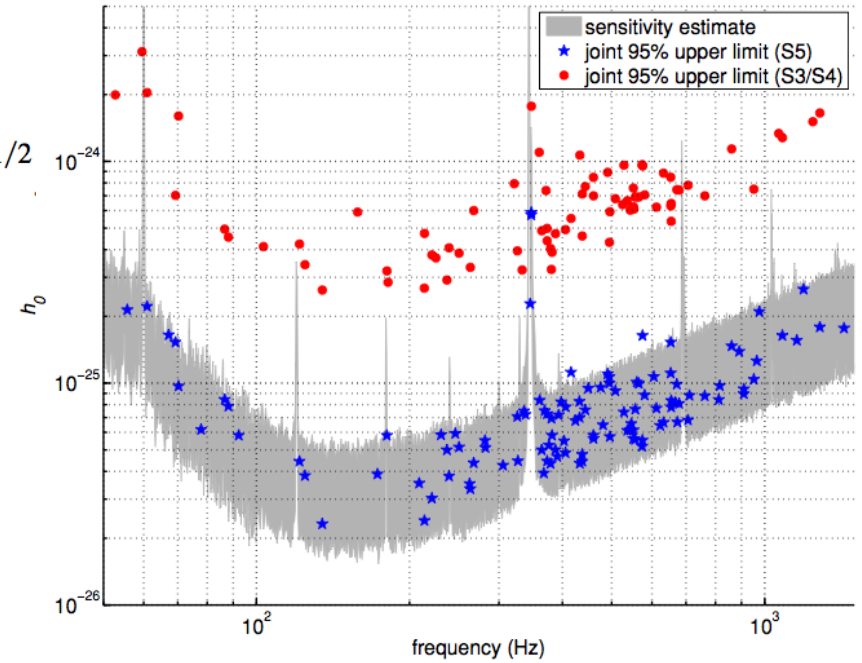

LIGO Scientific and Virgo Collaborations, "*Beating the spin-down limit on gravitational wave emission from the Crab pulsar",* Astrophys. J. Lett. 683 (2008) 45

LIGO Scientific and Virgo Collaborations, "*First search for gravitational waves from the youngest known neutron star",* Astrophys. J. 722 (2010) 1504

LIGO Scientific and Virgo Collaborations, "*Beating the spin-down limit on gravitational wave emission from the Vela pulsar,"* Astrophys. J. 737 (2011) 93

LIGO Scientific and Virgo Collaborations, "*Searches For Gravitational Waves From Known Pulsars With Science Run 5 LIGO Data*", Astrophys. J. 713 (2010) 671

3278-1.pdf - Adobe Reader
Vista Documento Strumenti Finestra ?
1 / 5 115% Trova

nature Vol 460|20 August 2009|doi:10.1038/nature08278

LETTERS

An upper limit on the stochastic gravitational-wave background of cosmological origin

The LIGO Scientific Collaboration* & The Virgo Collaboration*

A stochastic background of gravitational waves is expected to arise from a superposition of a large number of unresolved gravitational-wave sources of astrophysical and cosmological origin. It should carry unique signatures from the earliest epochs in the evolution of the Universe, inaccessible to standard astrophysical observations[1]. Direct measurements of the amplitude of this background are therefore of fundamental importance for understanding the evolution of the Universe when it was younger than one minute. Here we report limits on the amplitude of the stochastic gravitational-wave background using the data from a two-year science run of the Laser Interferometer Gravitational-wave Observatory[2] (LIGO). Our result constrains the energy density of the stochastic gravitational-wave background normalized by the critical energy density of the Universe, in the frequency band around

mirrors[2] is well suited to measure this differential strain signal due to gravitational waves. Over the past decade, LIGO has built three such multi-kilometre interferometers, at two locations[2]: H1 (4 km) and H2 (2 km) share the same facility at Hanford, Washington, USA, and L1 (4 km) is located in Livingston Parish, Louisiana, USA. LIGO, together with the 3 km interferometer Virgo[19] in Italy and GEO[20] in Germany, forms a network of gravitational-wave observatories. LIGO has completed science run S5 (between 5 November 2005 and 30 September 2007), acquiring one year of data coincident among H1, H2 and L1, at the interferometer design sensitivities (Fig. 1).

The search for the SGWB using LIGO data is performed by cross-correlating strain data from pairs of interferometers[8]. In the frequency (f) domain, the cross-correlation between two interferom-

Isotropic search: results

- Now we are beyond indirect BBN and CMB bounds
- We are beginning to probe models

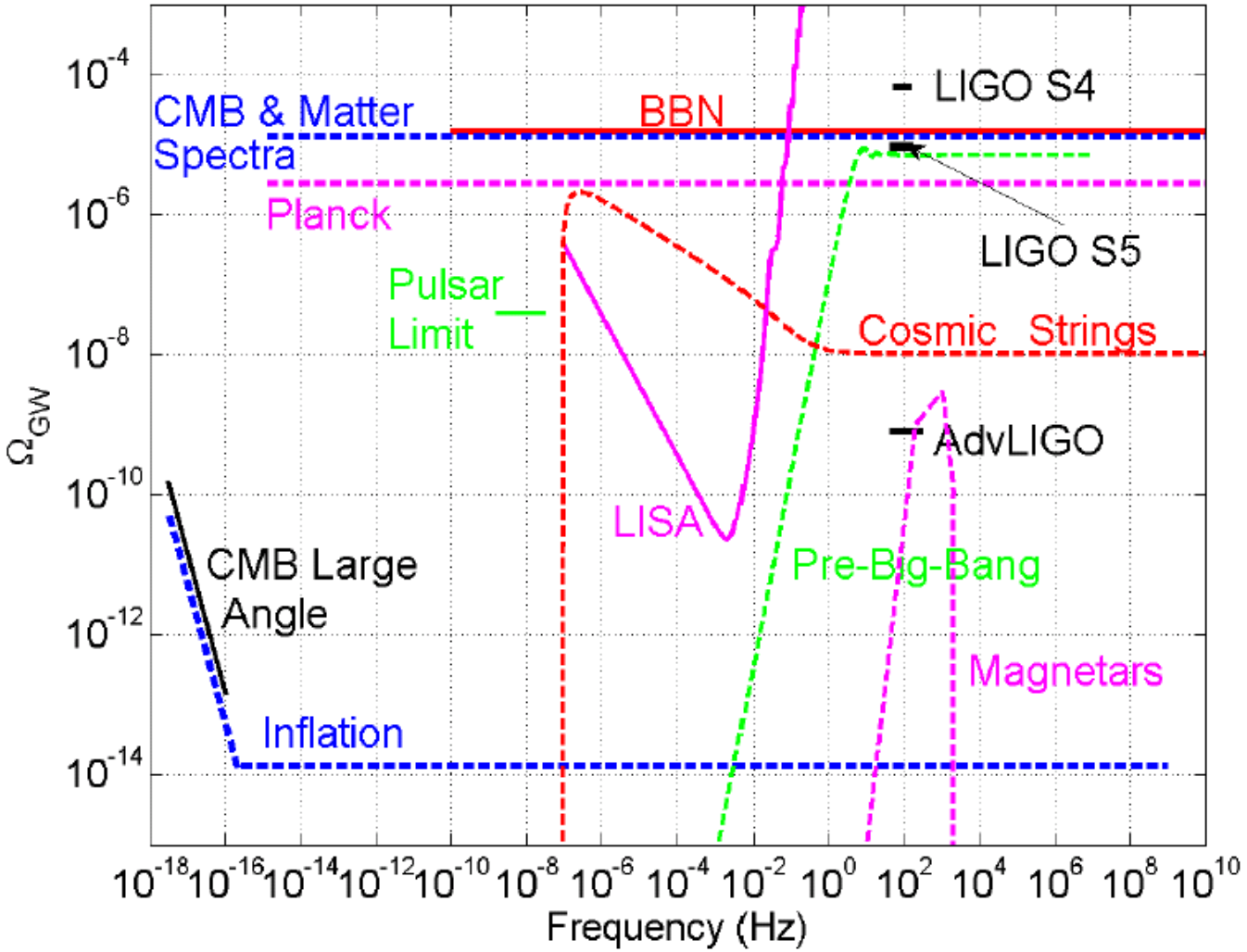

Pulsar Timing Array

Placing limits on the stochastic gravitational - wave background using European Pulsar Timing Array data (2011 GWIC prize thesis)

$$h_c(f) = A\left(\frac{f}{1yr^{-1}}\right)^{\alpha}$$

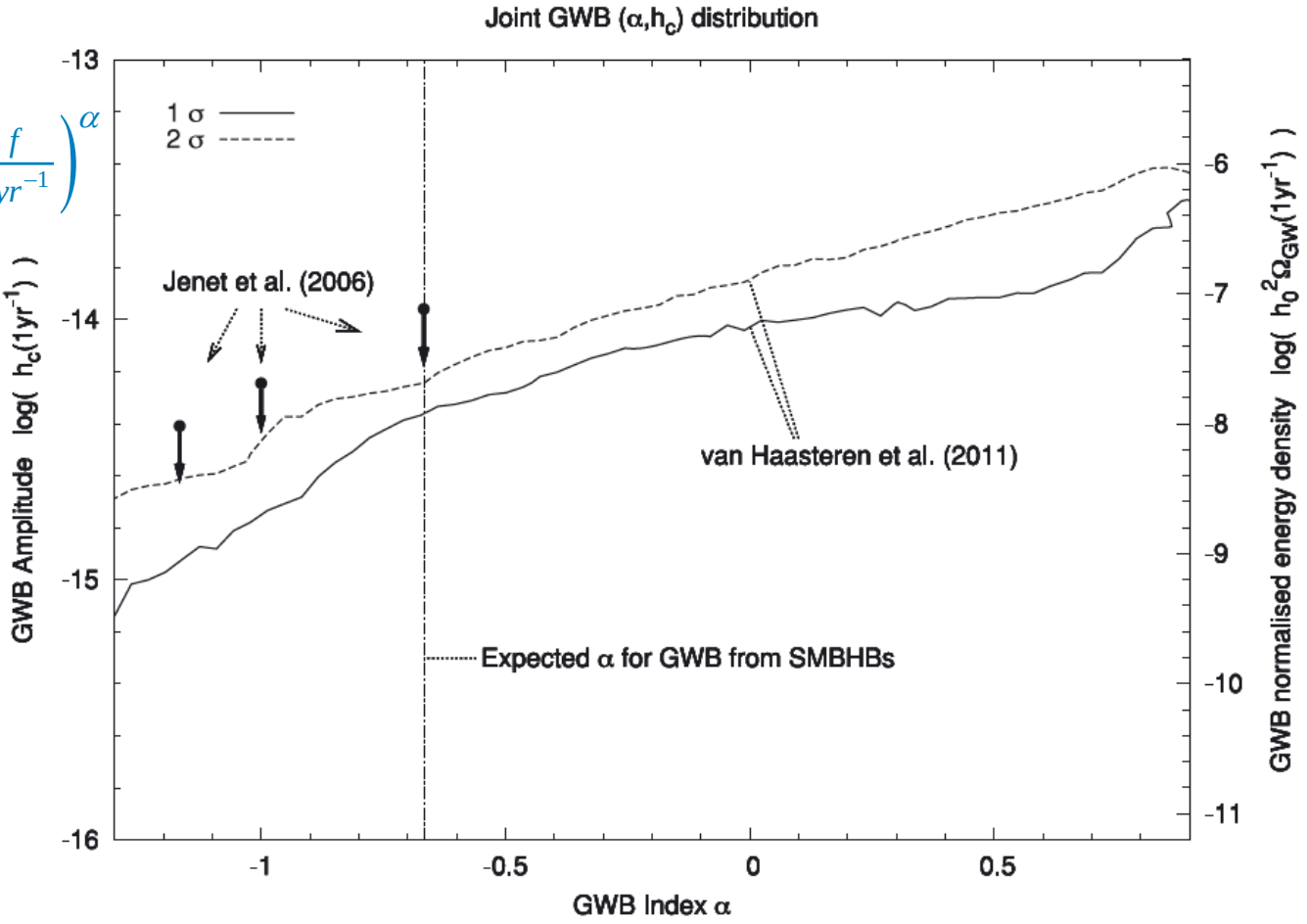

Monthly Notices of the Royal Astronomical Society
Volume 414, Issue 4, pages 3117-3128, 20 APR 2011 DOI: 10.1111/j.1365-2966.2011.18613.x
http://onlinelibrary.wiley.com/doi/10.1111/j.1365-2966.2011.18613.x/full#f5

Advanced Virgo

Slides by PL Giovanni Losurdo

ADVANCED VIRGO – ID CARD

- Advanced Virgo: upgrade of the Virgo interferometric detector of gravitational waves
- Goals:
  - improve the detection rate by ~1000
  - Participate to the early detections
  - Start the GW astronomy
- Funded by INFN, CNRS, EGO, Nikhef in Dec 2009: 23.8 ME
  - With some contributions from Poland and Hungary
- First light expected: fall 2015

Advanced detectors

- 2nd generation detectors
  - BNS inspiral range >10x better than Virgo
  - Detection rate: ~1000x better
  - 1 day of Adv data ≈ 3 yrs of data

Measured spectrum from
http://www.ligo.caltech.edu/~jzweizig/distribution/LSC_Data/

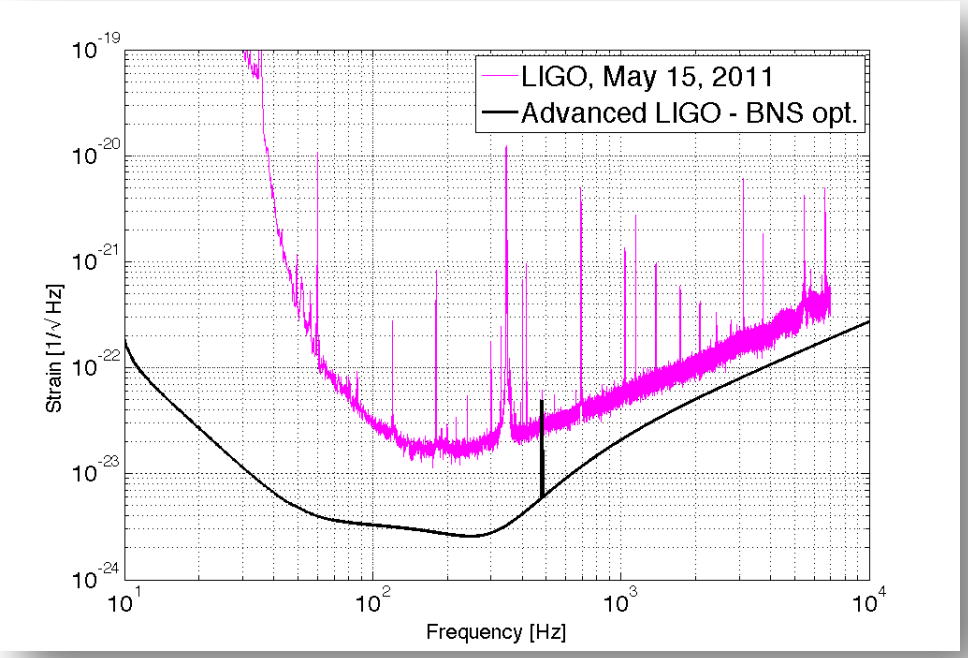

Measured spectrum courtesy of the Virgo Coll.

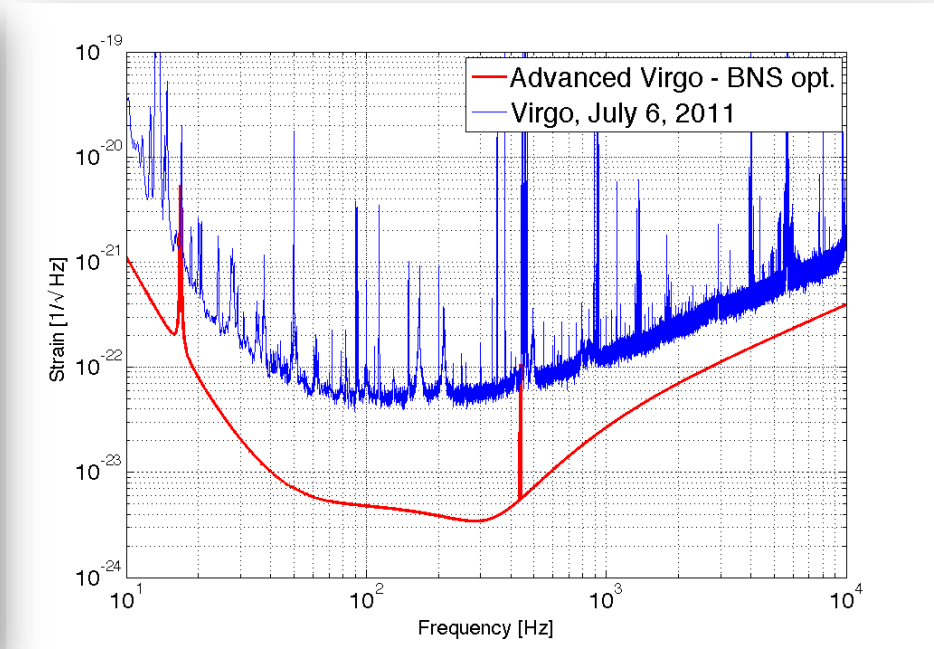

35

Advanced Virgo baseline design

- Plan to be back in 2015 with LIGO

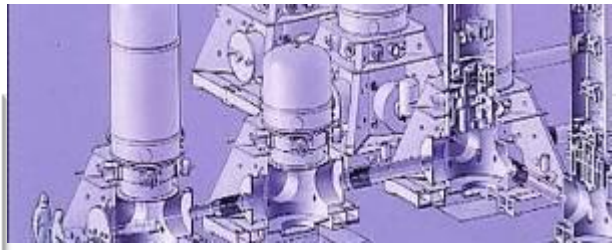

Larger central links
Cryotraps

Heavier mirrors

High finesse
3km FP cavities

Large spot size on TM

Non degenerate rec. cavities

High power laser

Signal Recycling (SR)

DC readout



Monolithic suspensions

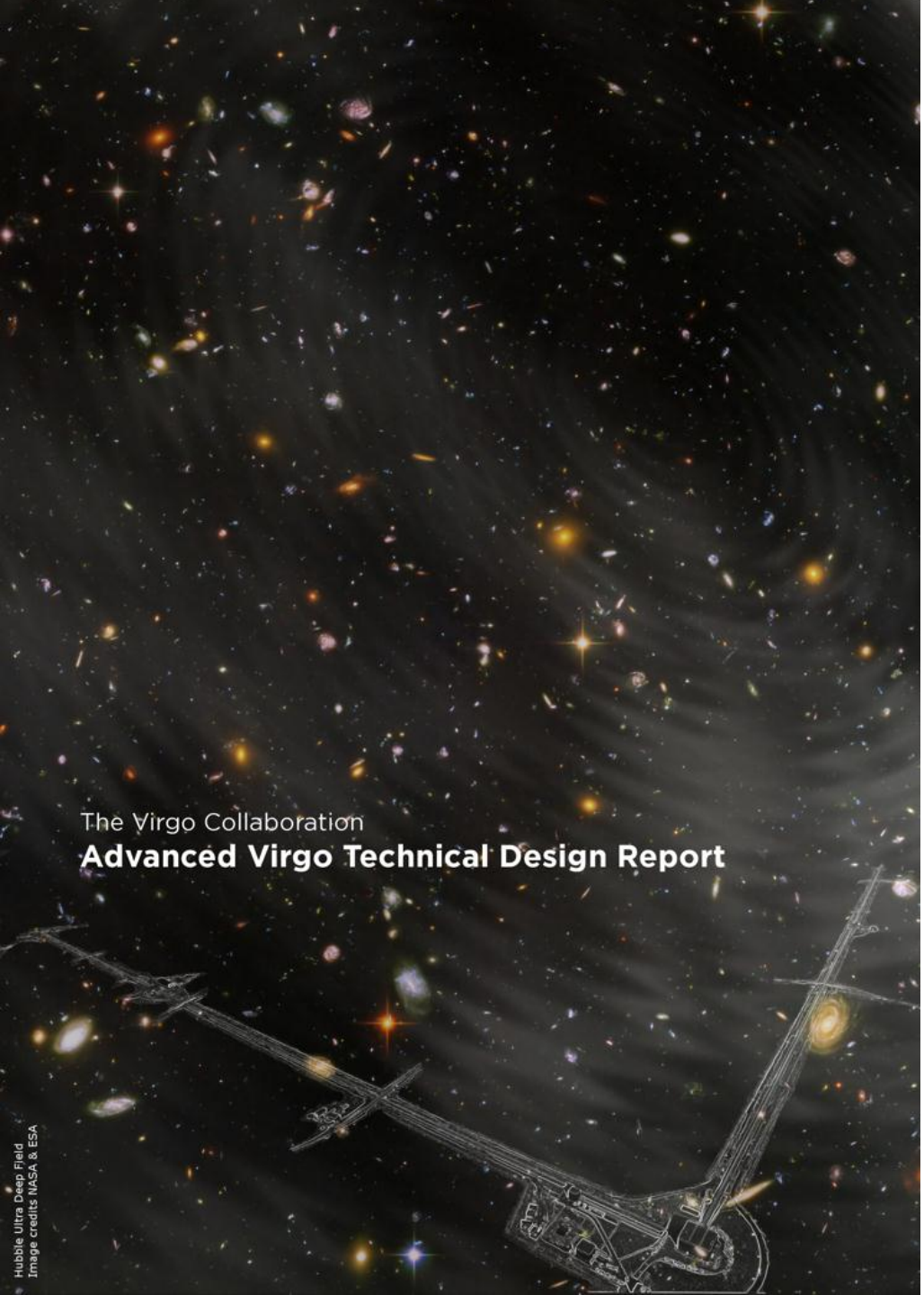

Advanced Virgo Technical Design Report

The Virgo Collaboration

VIR–0128A–12

April 13, 2012

OPTICAL LAYOUT

- MAIN CHANGES
  - Signal recycling
  - Larger beam
  - 200W rod laser
  - heavier mirrors

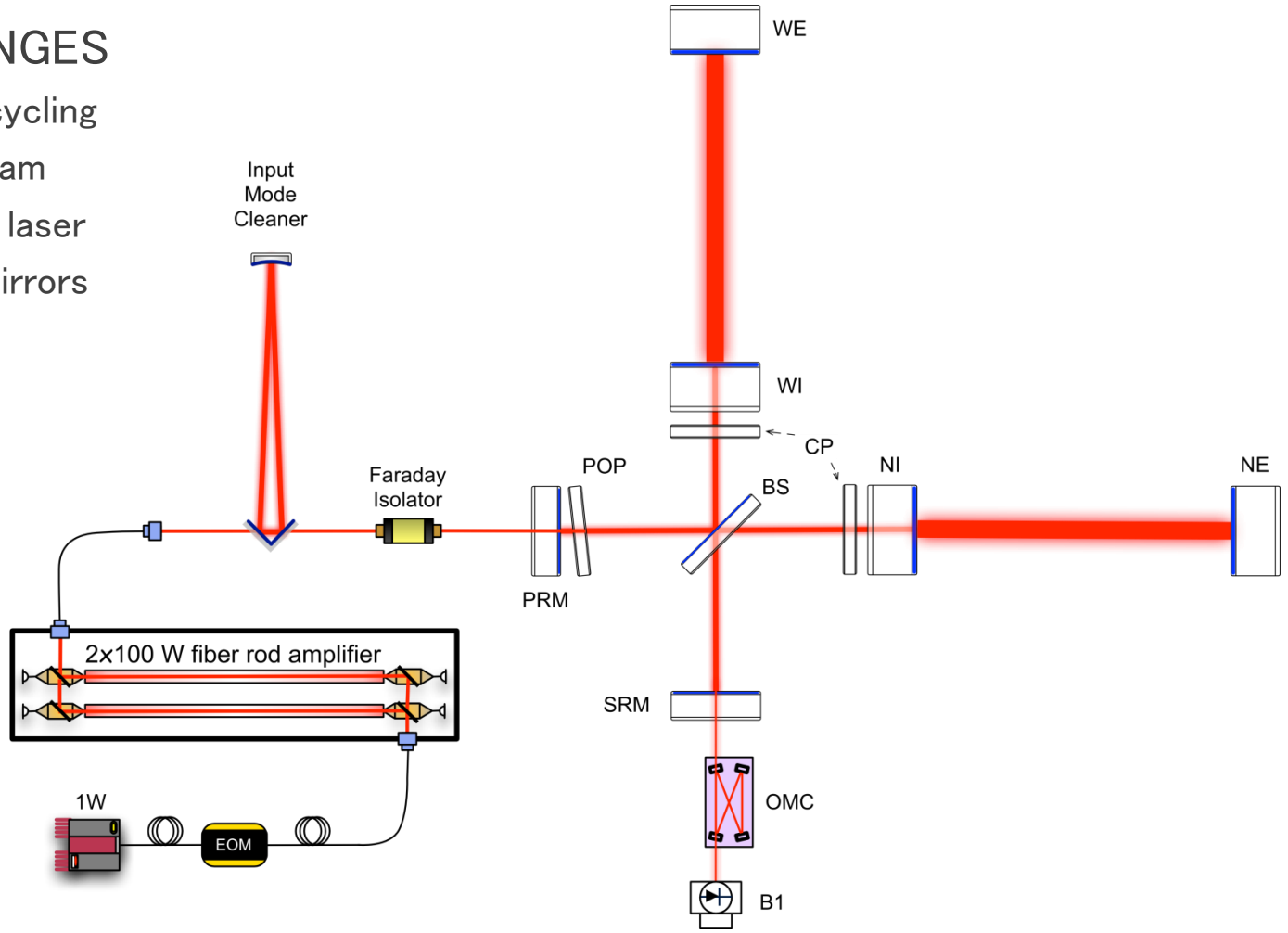

MIRRORS – SUBSTRATES

- Large high quality mirrors: 35cm diameter, 20cm thick, 42 kg
- Large beam splitter: 55cm diameter
- Manufacturer = **HERAEUS** (like in VIRGO), leader in low absorption silica
- New fused silica grade (Suprasil 3002):
  - **Better bulk absorption** (0.2 ppm/cm measured at LMA): better for thermal lensing
  - Good mechanical properties (High quality factor, > 10^7)





POLISHING

- Optical losses must be minimized to
  - Maximize the circulating power (and thus the sensitivity)
  - Minimize the scattered light (and the associated noise…)

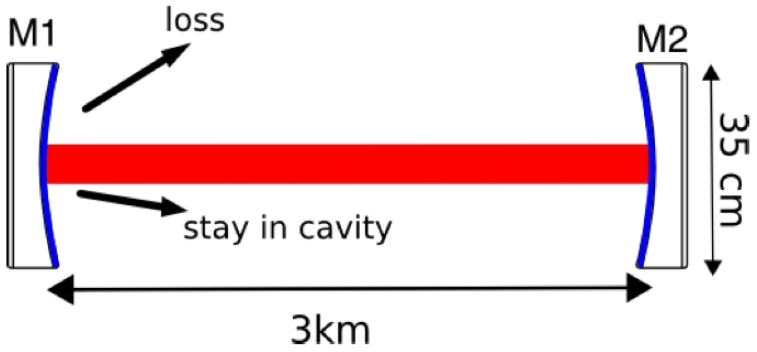

- AdV requirement: round-trip losses <50ppm →

  → mirror flatness < 0.5 nm rms
- Standard polishing may achieve flatness ~2 nm rms
- To reach specifications we apply "corrective coating" to polished mirrors

CORRECTIVE COATING

- Interferometric sensing of surface imperfections and correction by sputtering of silica molecules
- Mirror moved with respect to the silica beam by a robot (42kg mirror positioned with accuracy ~200 um)

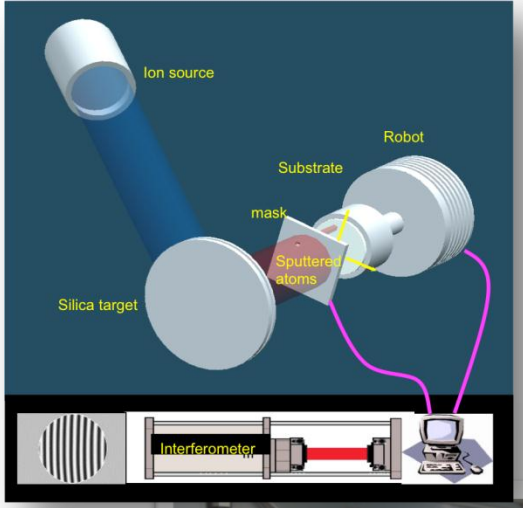

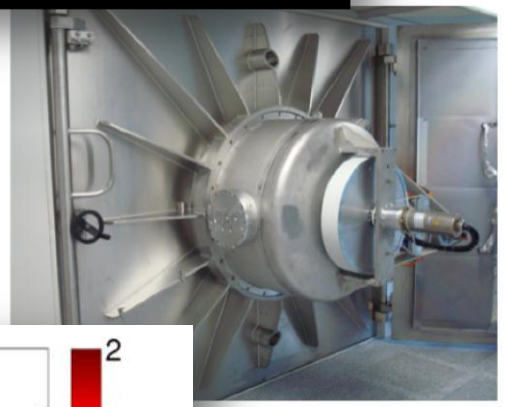

Exp. result:
RMS = 0.36 nm

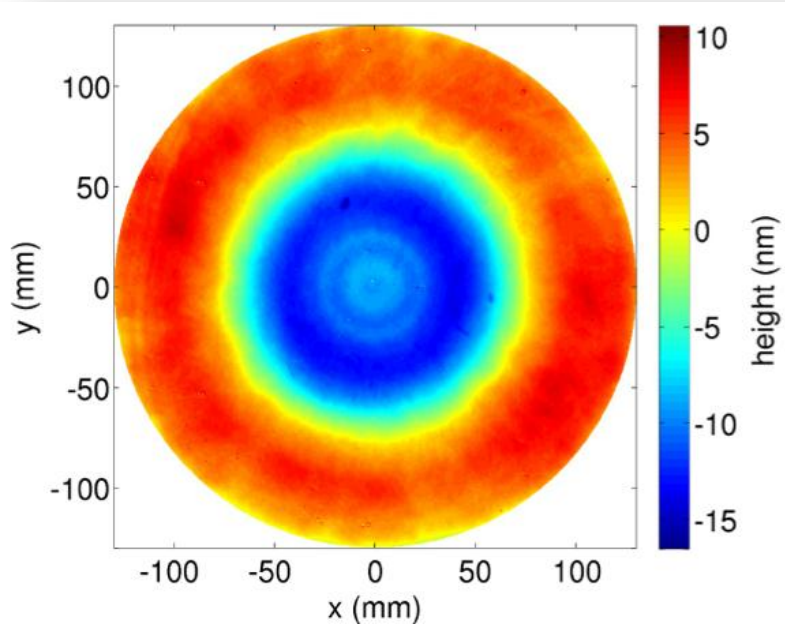

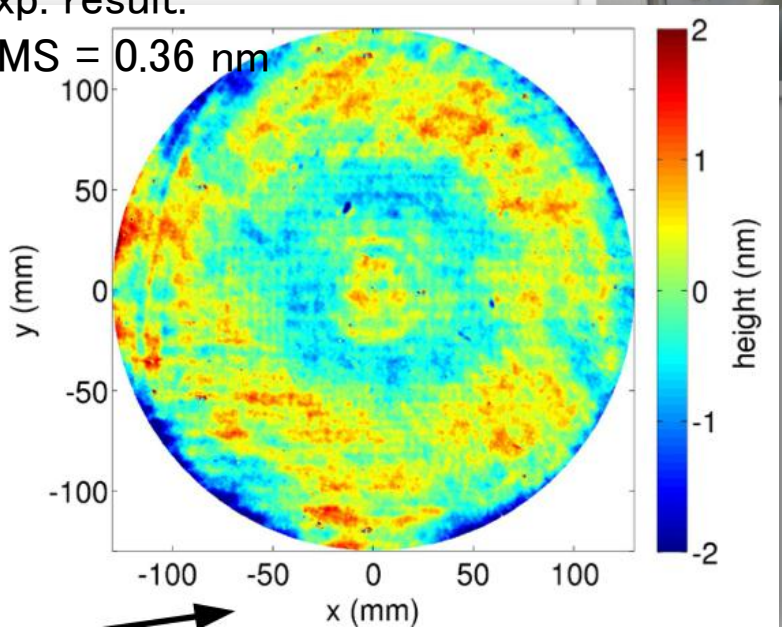

COATINGS

- Coating thermal noise is THE noise limiting sensitivity in the mid-range (dissipation dominated by the high refractive index layer)
- Doping Ta_2O_5 with Ti has improved it, but losses are still $O(10^{-4})$
- Advanced LIGO/Virgo use large spot size (~5cm) on the test masses

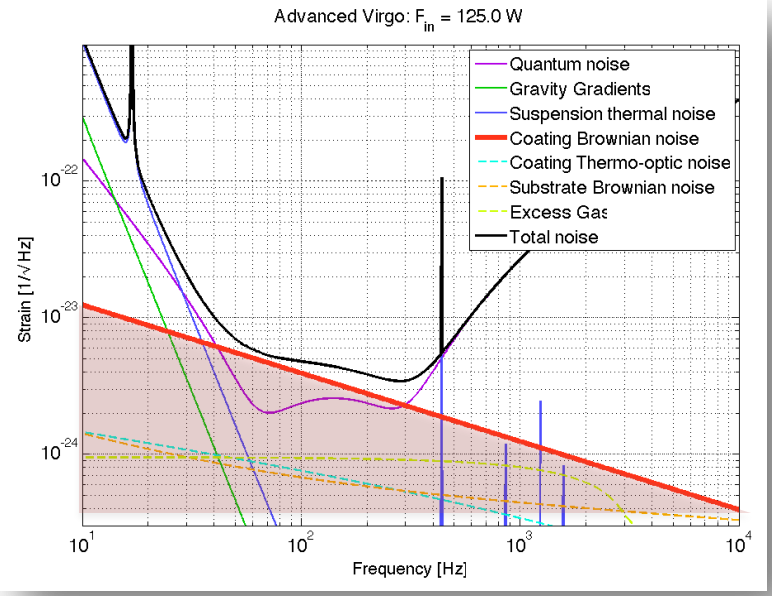

THERMAL COMPENSATION

- Aberrations (intrinsic mirror defects or thermal deformations of the mirrors) spoil the beam quality
- A set of sensors and thermal actuators has been conceived to get an "aberration free" interferometer

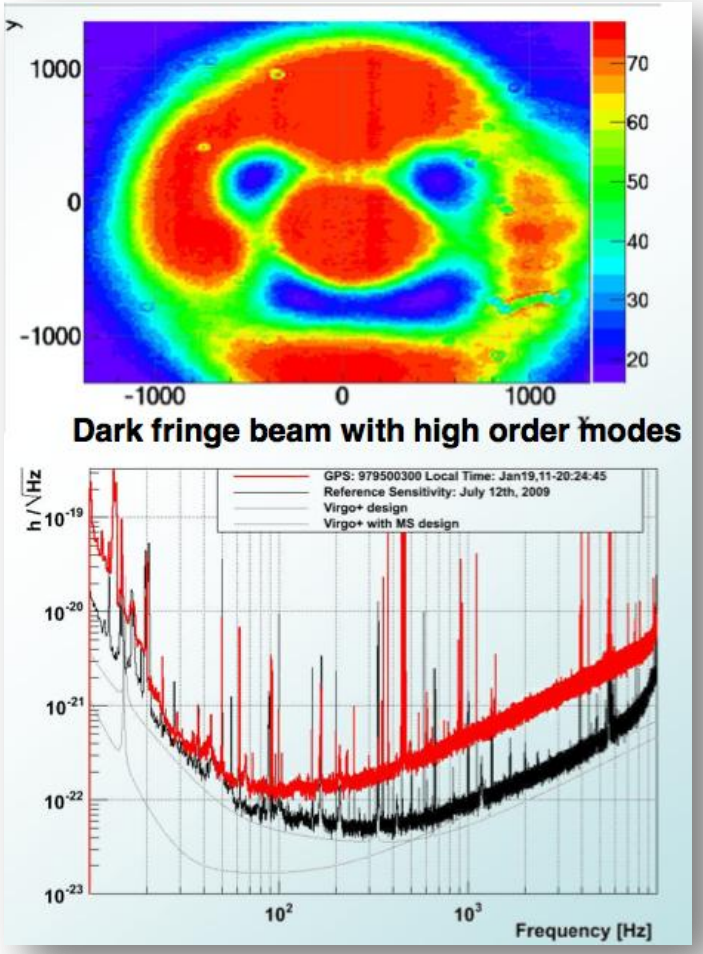

Effect of RoC asymmetry in Virgo+

CO2 laser

CO2 laser shined on the mirror: heat deposition where needed to compensate for aberrations

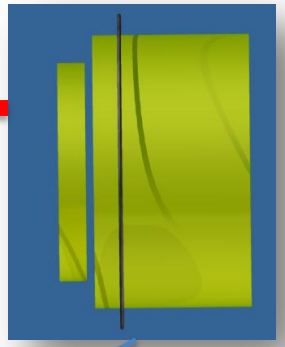

Heating rings around mirrors to tune RoC (accuracy: ~1m over 1500m)



STRAY LIGHT



- Scattered light has been one of the main issues of Virgo+
  - limiting the sensitivity in a wide frequency range
  - a lot of commissioning time used to mitigate it
- Thorough risk mitigation approach in AdV (large investment)



stray light on the output bench

SiC baffles added (+ other changes)

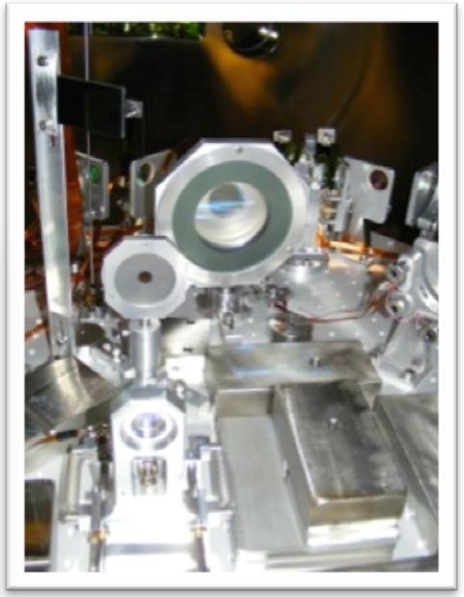

horizon more stable and higher

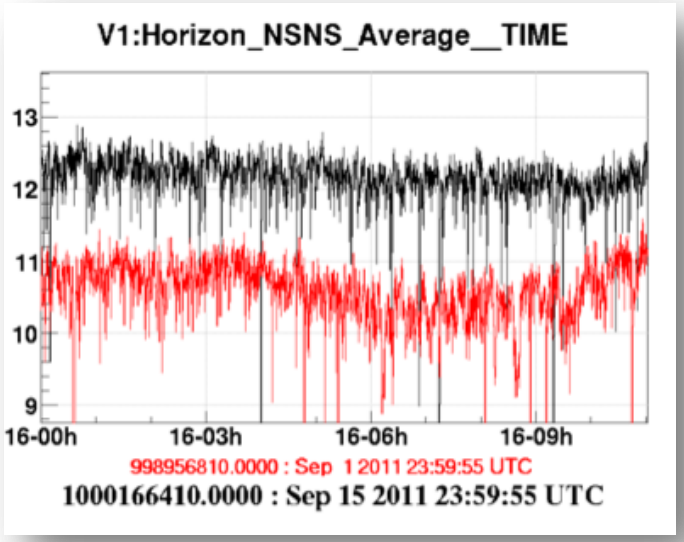

STRAY LIGHT MITIGATION

- Baffles to shield mirrors, pipes, vacuum chambers exposed to scattered light

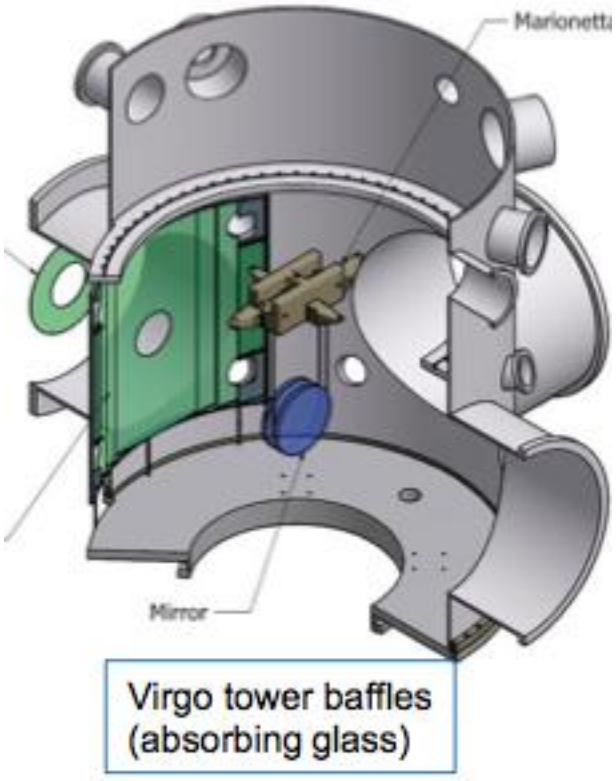

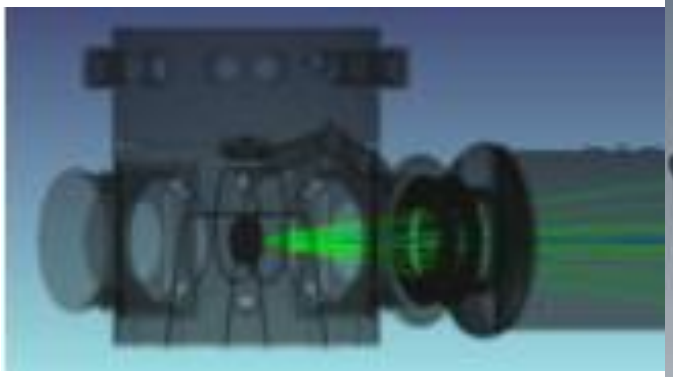

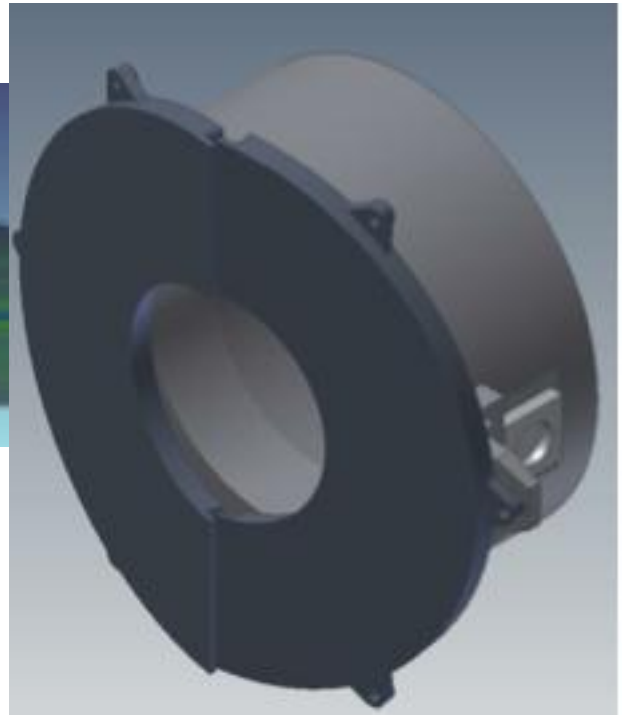

STRAY LIGHT MITIGATION



HVAC relocation
large suspended baffles

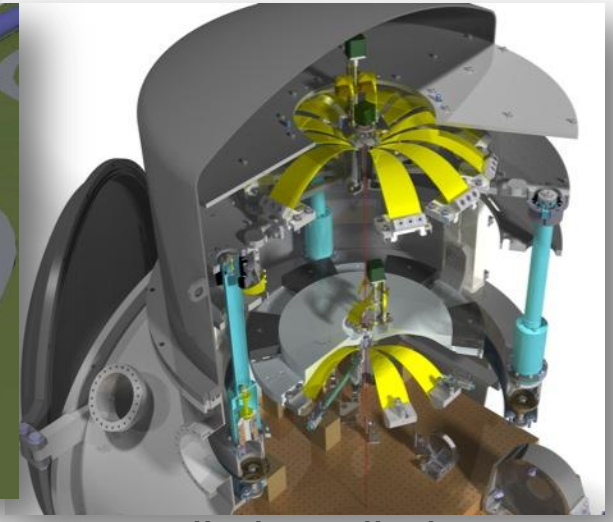

All photodiodes
seismically isolated
and In vacuum

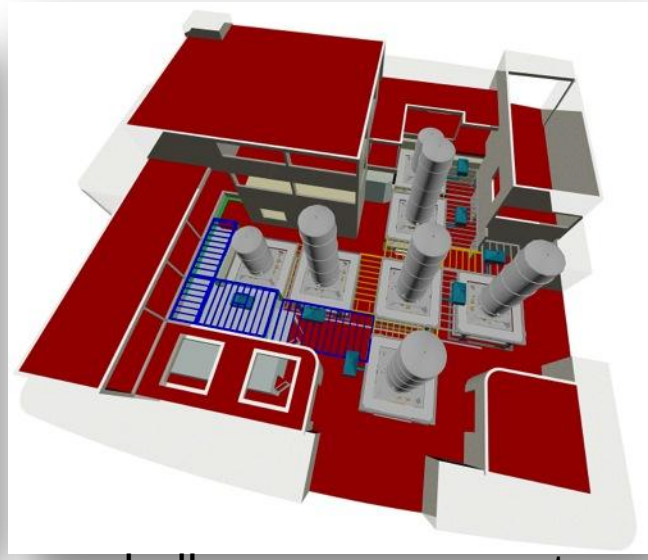

halls re-arrangements
for hosting minitowers

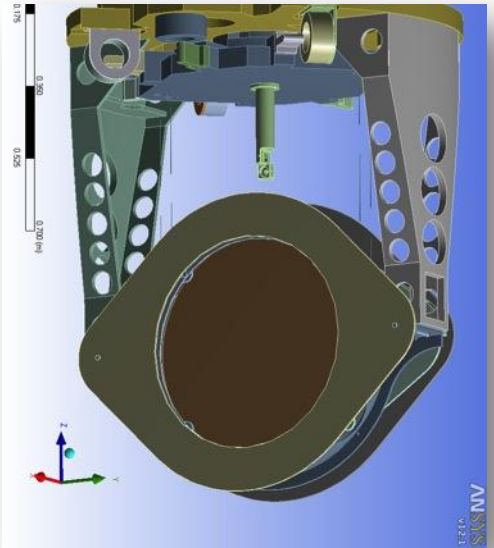

+
payloads/superattenuators/vacuum modifications
for the large baffles suspension
+ superpolished optics on suspended benches
+ …

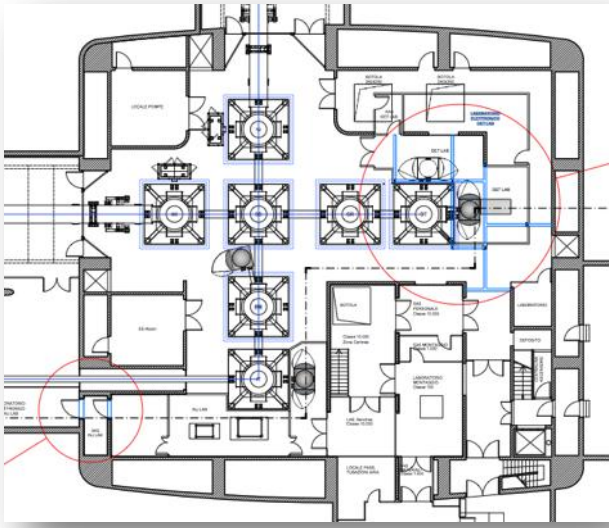

CRUCIAL DATES

- About 1 year of commissioning on parts of the interferometer before the end of installation
  - Allows speeding up the time needed for the first full lock
  - Requires early organization of the commissioning activities

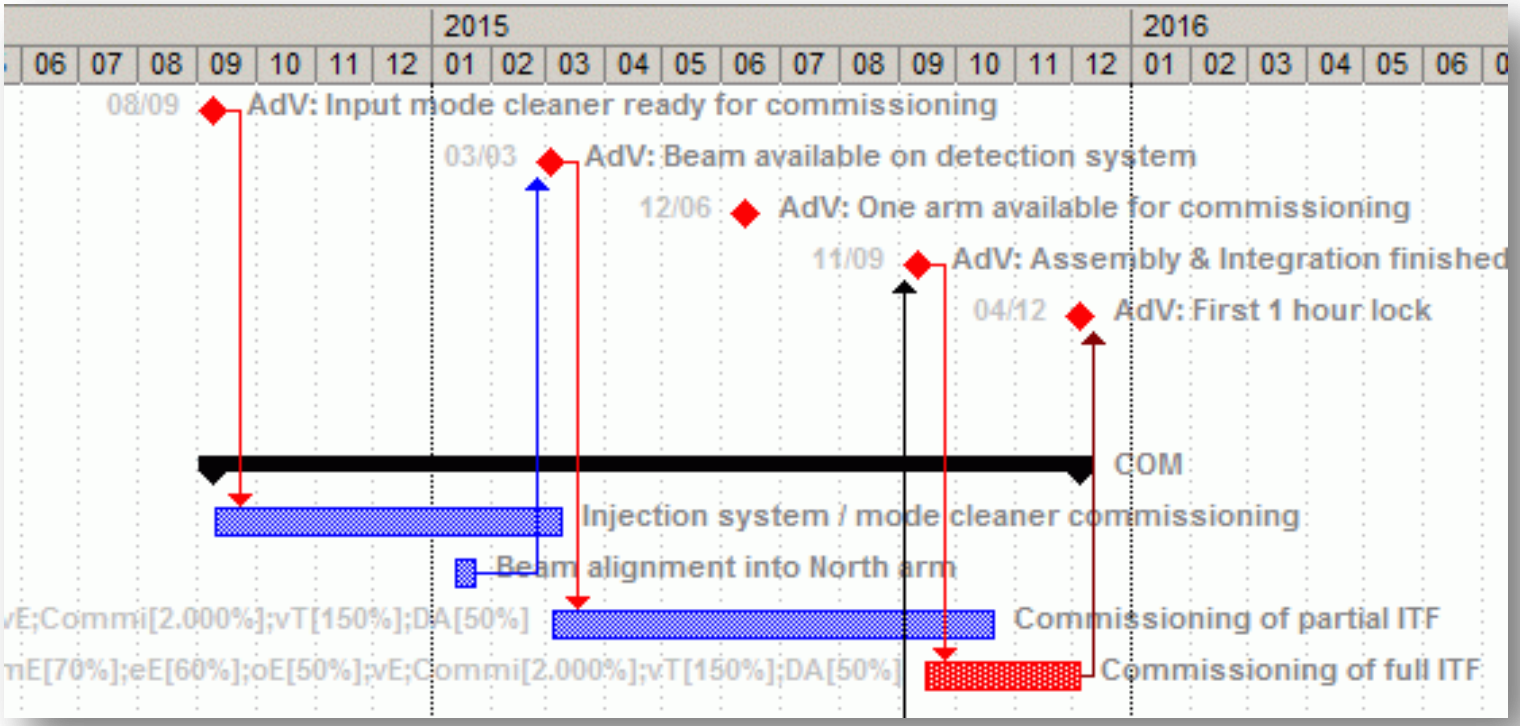

Perspective

Sensitivity future evolution

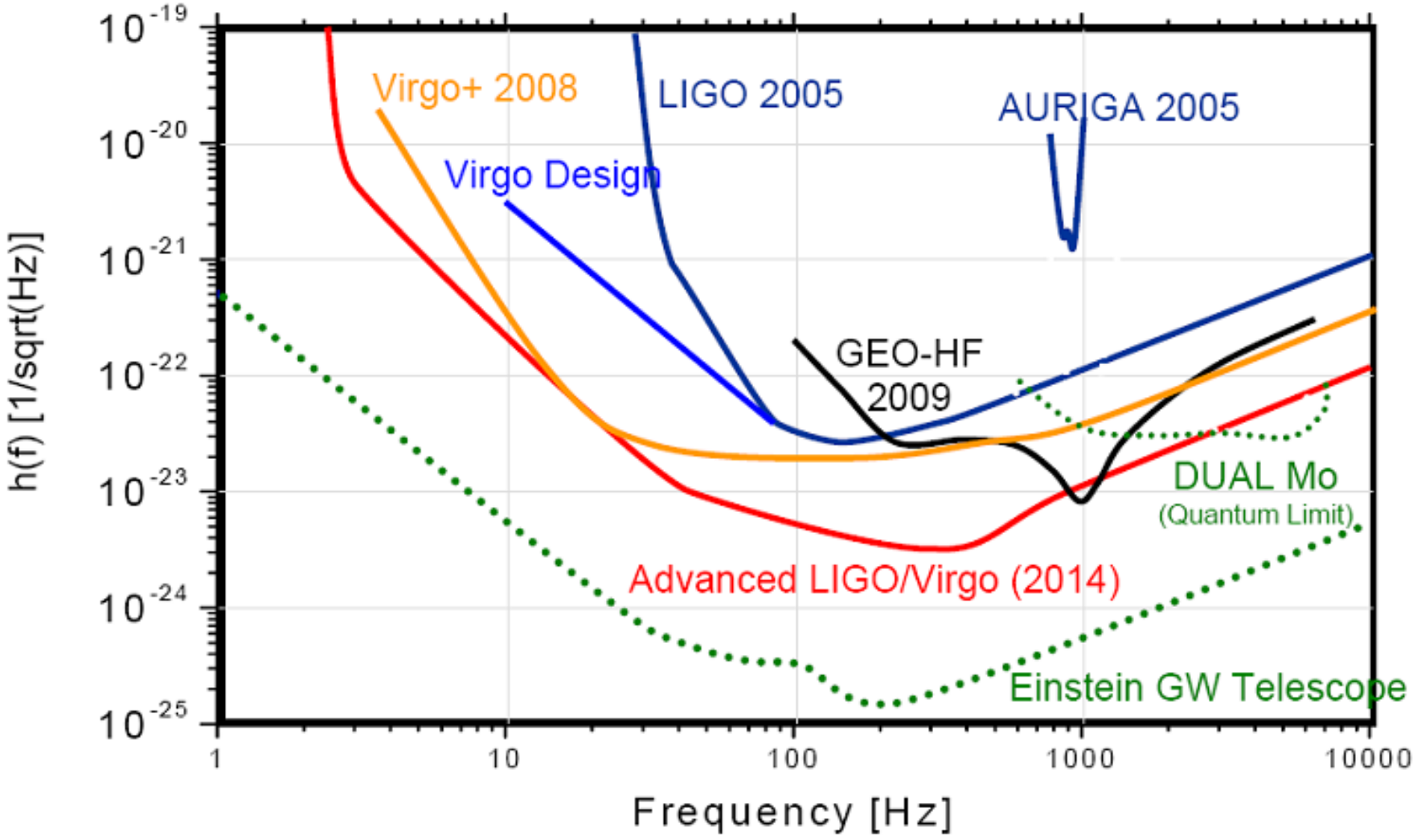

Conceptual Design Document

- ET conceptual design document released:
  - https://tds.ego-gw.it/ql/?c=7954
- ~400 pages describing the main characteristics of the observatory
- To be sent to the European Commission at the end of September
- To be published on CQG

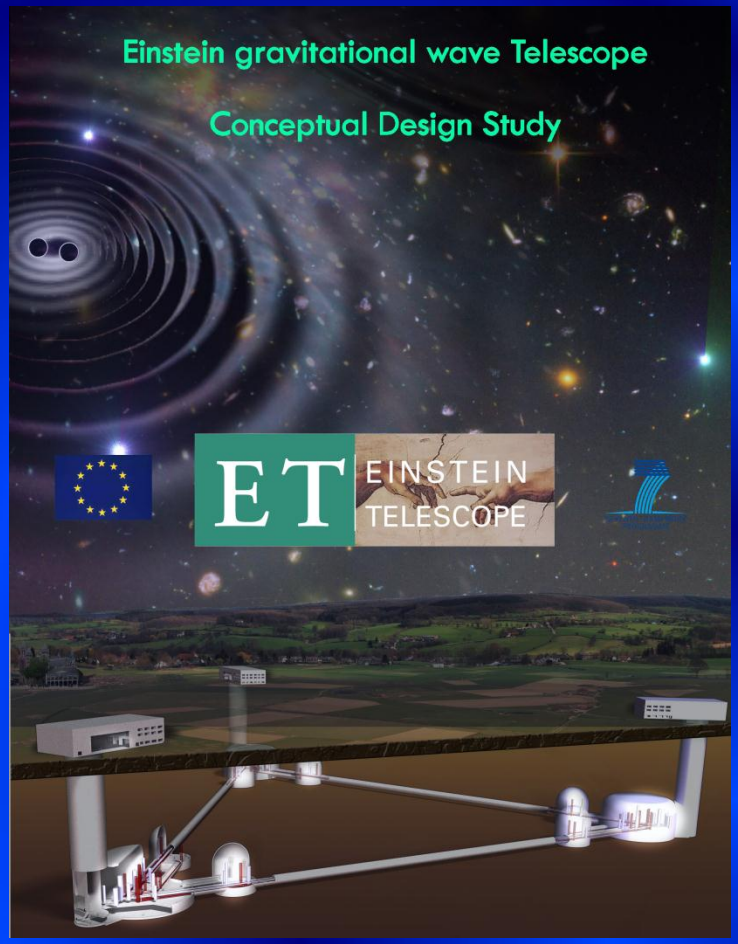

Artistic/Schematic views

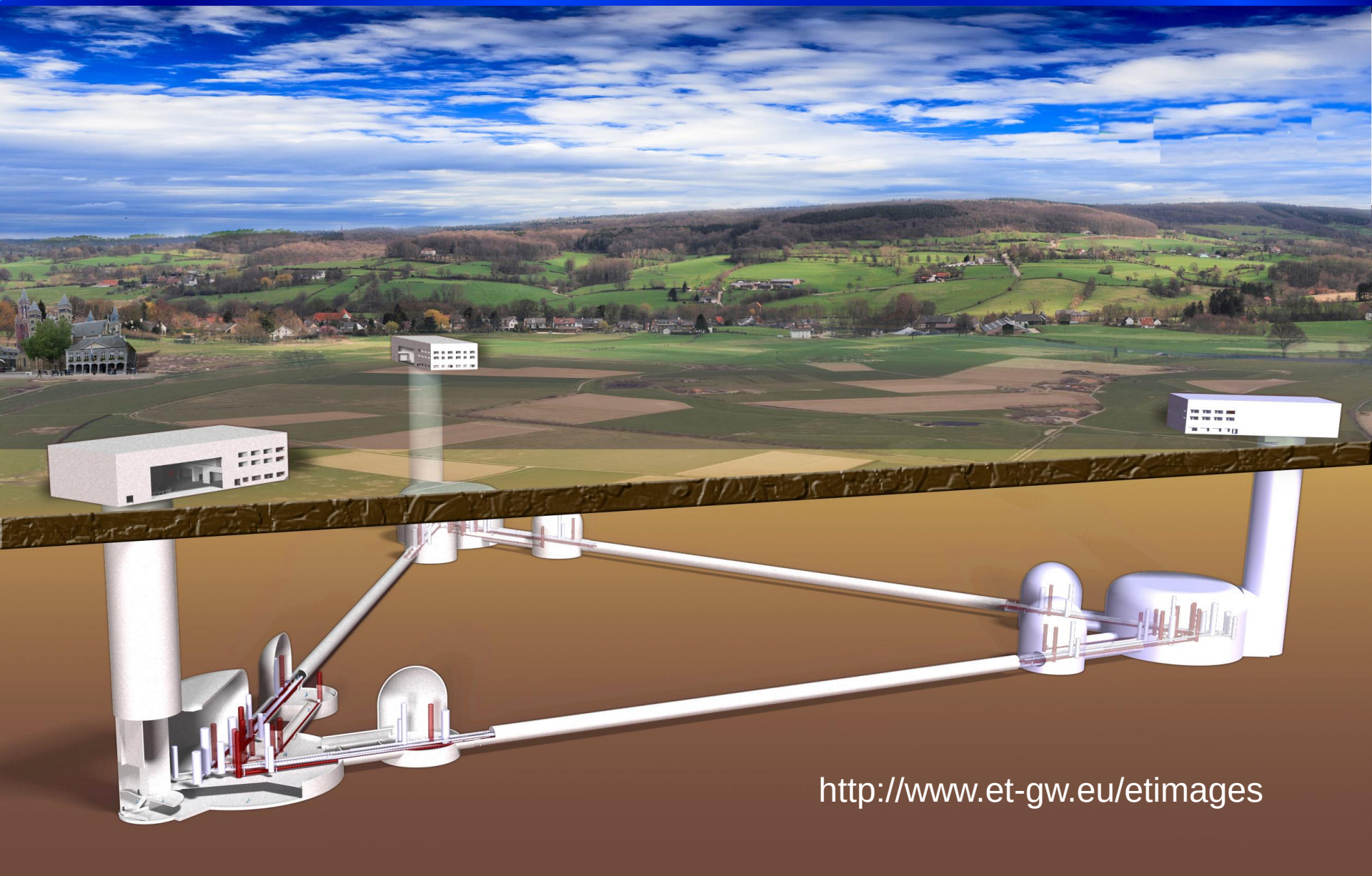

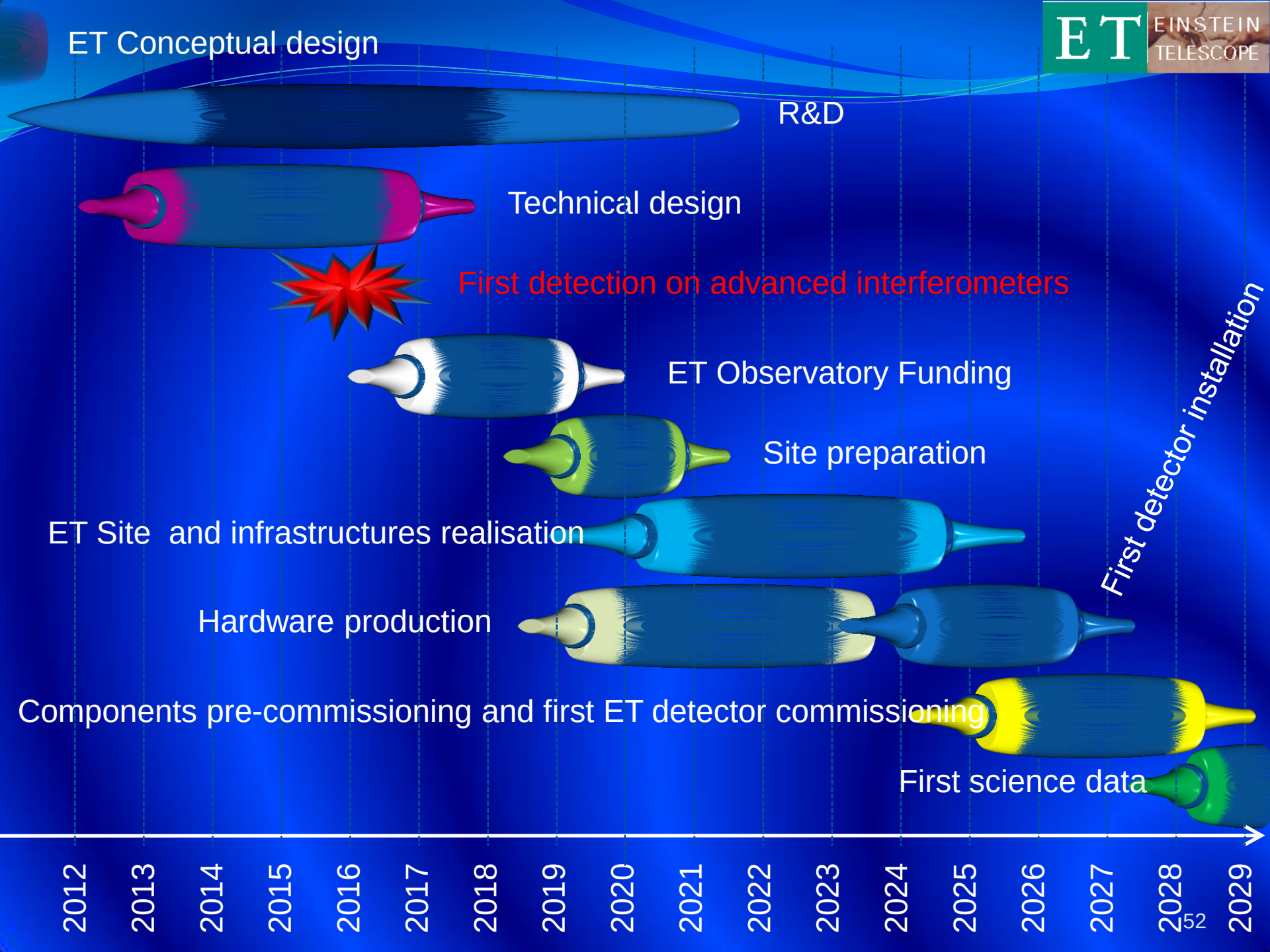
ET Conceptual design
R&D
Technical design
First detection on advanced interferometers
ET Observatory Funding
Site preparation
ET Site and infrastructures realisation
Hardware production
Components pre-commissioning and first ET detector commissioning
First science data
First detector installation
2012
2013
2014
2015
2016
2017
2018
2019
2020
2021
2022
2023
2024
2025
2026
2027
2028
2029

The ET Science

- Summary by B. Sathyaprakash, chair of ET WG 4 Astrophysics issues

Fundamental Physics

- Properties of gravitational waves
  - Testing GR beyond the quadrupole formula
    - Binary pulsars consistent with quadrupole formula; they don't measure properties of GW
  - How many polarizations are there?
    - In Einstein's theory only two polarizations; a scalar-tensor theory could have six
  - Do gravitational waves travel at the speed of light?
    - There are strong motivations from string theory to consider massive gravitons
    - Binary pulsars constrain the speed to few parts in a thousand
    - GW observations can constrain to 1 part in 10^{18}
- EoS of dark energy
  - Black hole binaries are standard candles/sirens
- EoS of supra-nuclear matter
  - Signature of EoS in GW emitted when neutron stars merge
- Black hole no-hair theorem and cosmic censorship
  - Are BH (candidates) of nature BH of general relativity?
- An independent constraint/measurement of neutrino mass
  - Delay in the arrival times of neutrinos and gravitational waves

Cosmology

- Cosmography
  - Build the cosmic distance ladder, strengthen existing calibrations at high z
  - Measure the Hubble parameter, dark matter and dark energy densities, dark energy EoS w, variation of w with z
- Black hole seeds
  - Black hole seeds could be intermediate mass black holes
  - Might explore hierarchical growth of central engines of black holes
- Dipole anisotropy in the Hubble parameter
  - The Hubble parameter will be "slightly" different in different directions due to the local flow of our galaxy
- Anisotropic cosmologies
  - In an anisotropic Universe the distribution of H on the sky should show residual quadrupole and higher-order anisotropies
- Primordial gravitational waves
  - Quantum fluctuations in the early Universe could produce a stochastic b/g
- Production of GW during early Universe phase transitions
  - Phase transitions, pre-heating, re-heating, etc., could produce detectable stochastic GW

Astrophysics

- Unveiling progenitors of short-hard GRBs
  - Understand the demographics and different classes of short-hard GRBs
- Understanding Supernovae
  - Astrophysics of gravitational collapse and accompanying supernova?
- Evolutionary paths of compact binaries
  - Evolution of compact binaries involves complex astrophysics
    - Initial mass function, stellar winds, kicks from supernova, common envelope phase
- Finding why pulsars glitch and magnetars flare
  - What causes sudden excursions in pulsar spin frequencies and what is behind ultra high-energy transients of EM radiation in magnetars
    - Could reveal the composition and structure of neutron star cores
- Ellipticity of neutron stars as small as 1 part in a billion (10μm)
  - Mountains of what size can be supported on neutron stars?
- NS spin frequencies in LMXBs
  - Why are spin frequencies of neutron stars in low-mass X-ray binaries bounded?
- Onset/evolution of relativistic instabilities
  - CFS instability and r-modes

Summary of Science with ET

- Fundamental Physics
  - Is the nature of gravitational radiation as predicted by Einstein?
  - Is Einstein theory the correct theory of gravity?
  - Are black holes in nature black holes of GR?
  - Are there naked singularities?
- Astrophysics
  - What is the nature of gravitational collapse?
  - What is the origin of gamma ray bursts?
  - What is the structure of neutron stars and other compact objects?
- Cosmology
  - How did massive black holes at galactic nuclei form and evolve?
  - What is dark energy?
  - What phase transitions took place in the early Universe?
  - What were the physical conditions at the big bang?

Conclusions

- We are at the edge of starting a new, fascinating field of science
- After “first words”, there is room for a large expansion in observations
- Room for unexpected
- In spite of the size, the instrument can be run by a single (clever) person
- New developments will be first by table top experiments
- High interdisciplinary views required
- Will reward junior and senior scientists

Thank you !

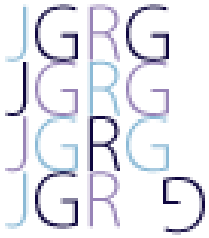

David Reitze, JGRG 22(2012)111404

"LIGO: Recent results, plans and prospects"

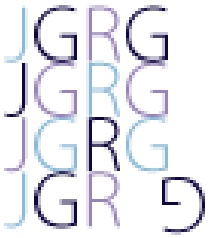

RESCEU SYMPOSIUM ON

GENERAL RELATIVITY AND GRAVITATION

JGRG 22



November 12-16 2012

Koshiba Hall, The University of Tokyo, Hongo, Tokyo, Japan



LIGO: Recent Results, Plans, and Prospects

David Reitze
LIGO Laboratory
California Institute of Technology

For the LSC and Virgo Collaboration

RESCEU SYMPOSIUM ON GENERAL RELATIVITY AND GRAVITATION

LIGO-G1201178-v1

Image: "Gravitational Waves", http://www.chaoscope.org/gallery.htm

LIGO

Topics

- Initial LIGO
- Selected Science Results from LIGO's S5 and S6 Science Runs
- Advanced LIGO – Status and Progress
- The Global Gravitational Wave Network
- LIGO-India: Status and Prospects

LIGO

LIGO Laboratory

LIGO Observatories are operated by Caltech and MIT





MIT

Caltech

Initial LIGO Concept

- Power-recycled Michelson interferometer
- 4 km long Fabry-Perot arm cavites
- Passive seismic isolation
- 10 kg mirrors figured to $\lambda/1000$
- 10 W → 30 W pre-stabilized laser operating at 1064 nm

- Passing GWs modulate the time-of-flight of light between the end test mass and the beam splitter
- The interferometer acts as a transducer, turning GWs into photocurrent
  - A coherent detector

$$h = \frac{2\mathrm{D}L}{L}$$

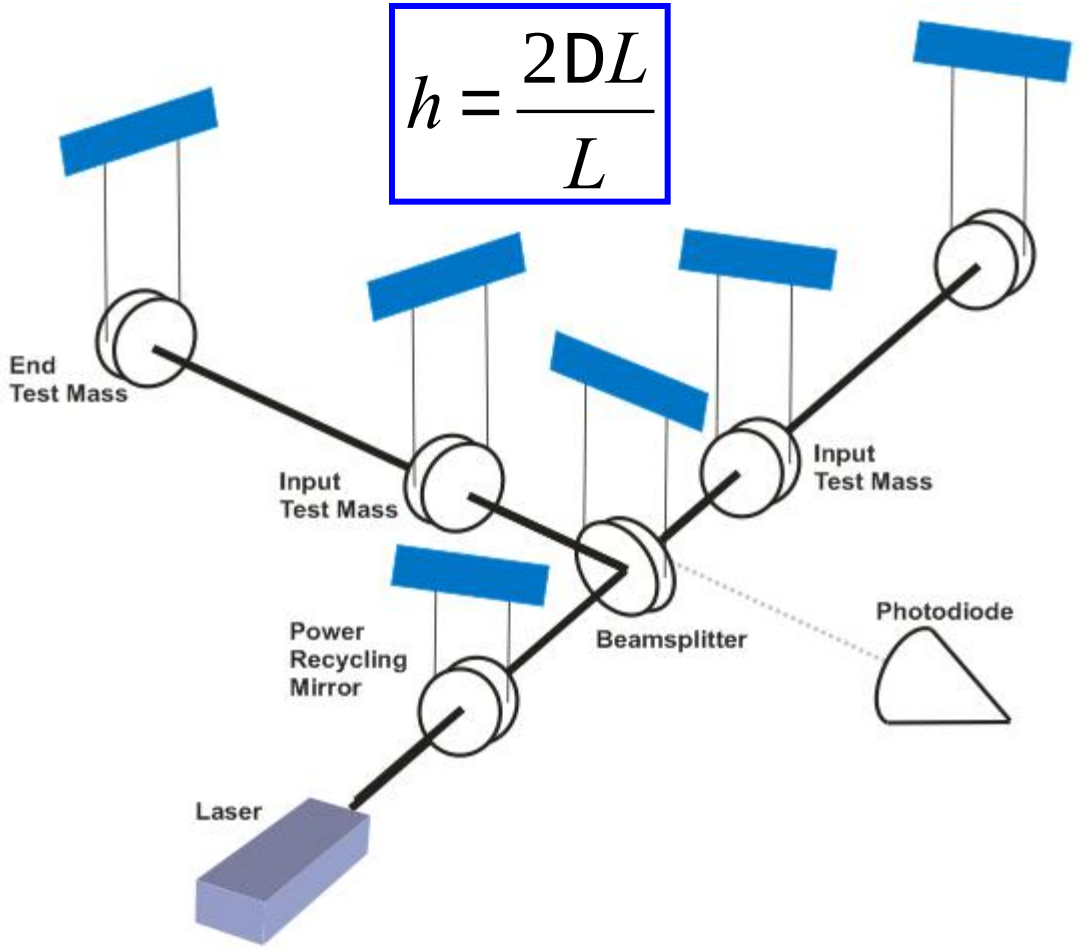

Initial LIGO Concept

$$h \sim \frac{\lambda}{L}$$

$$\times \frac{1}{N_{roundtrip}}$$

$$\times \sqrt{\frac{1}{\dot{N}_{photon}\tau_{storage}}}$$

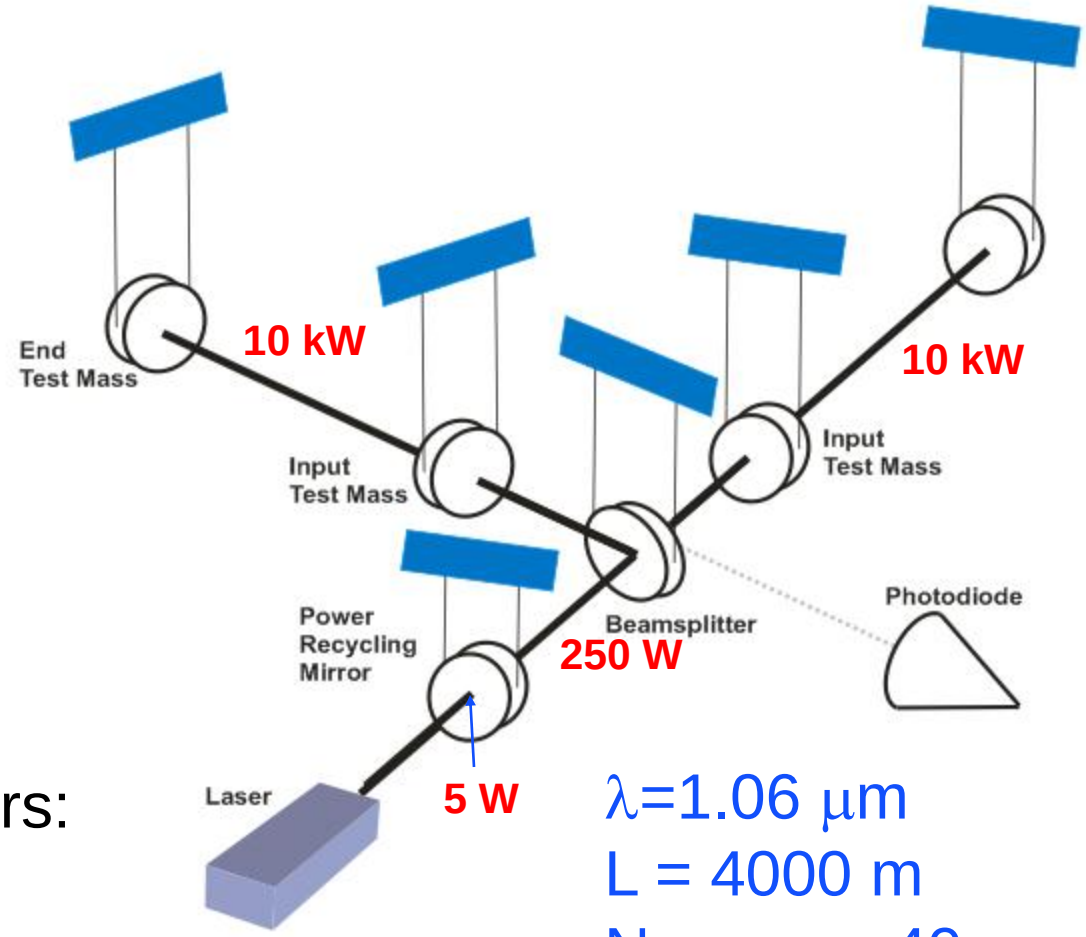

Putting in numbers:

$h \sim 10^{-21}$

λ=1.06 μm

L = 4000 m

$N_{roundtrip}$ = 40

LIGO

LIGO History

- **1989: LIGO Project proposed to NSF**
- 1992: LIGO Project funded by NSF
- 1995 – 1999: LIGO facilities construction at Hanford and Livingston
- 1998 – 2002: Installation/integration of initial LIGO interferometers
- 2002 - 2005: Interferometer commissioning interleaved with science runs (S1-S4)
- **Nov 4, 2005 – Sept 31, 2007: S5 science run**
  - » Design sensitivity reached; 15 Mpc range; > 1 year of triple coincidence data
- 2007 – 2009: Enhanced LIGO instrument upgrade
  - » Low cost upgrade, tests key Advanced LIGO technologies
- **April 2008: Advanced LIGO Construction begins**
- **July 7, 2009 – Oct 20, 2010: S6 science run**
  - » 18 Mpc range to merging binary neutron stars

Best Strain Sensitivities for the LIGO Interferometers

Comparisons among S1 - S5 Runs LIGO-G060009-03-Z

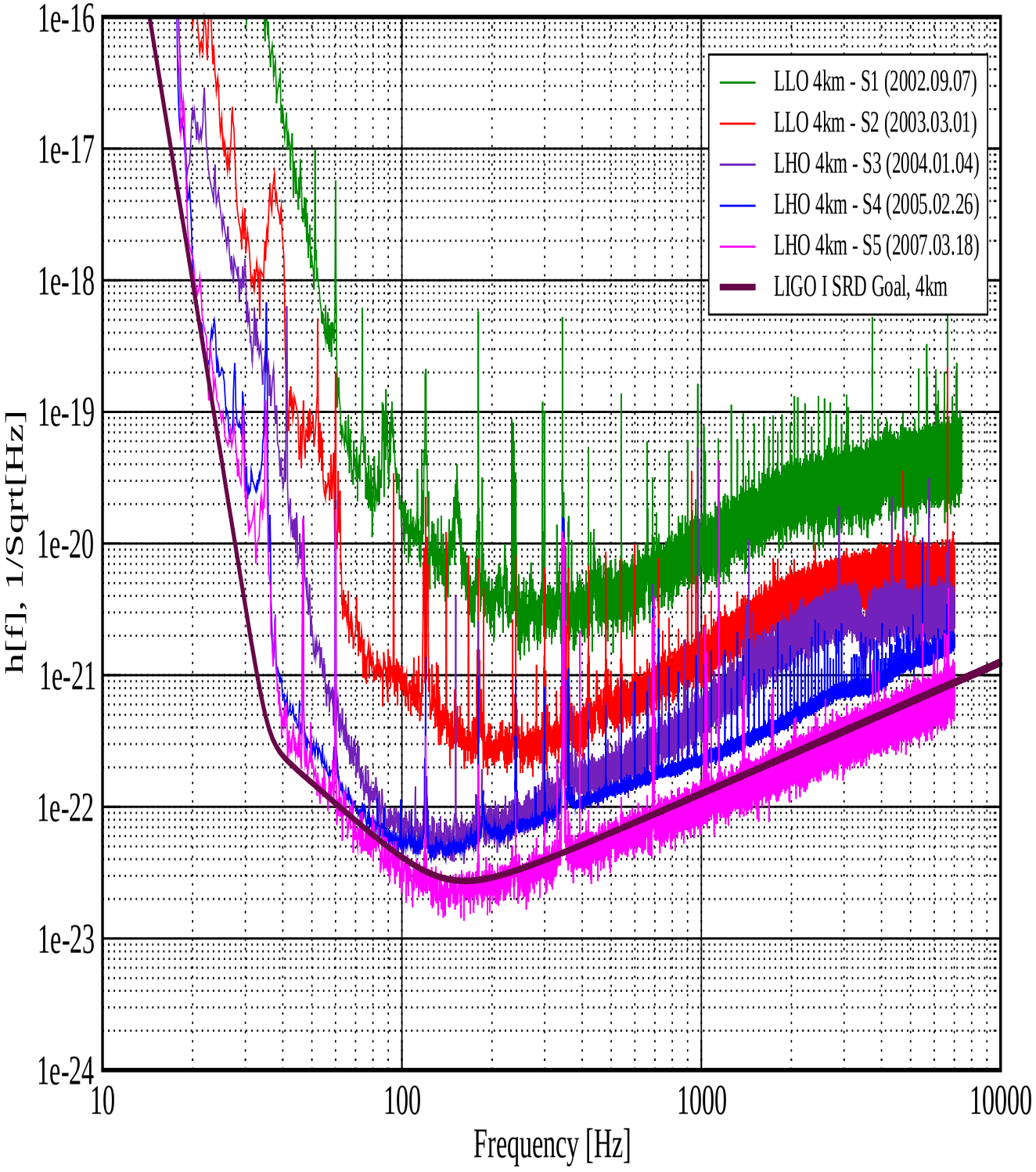

Best Strain Sensitivity: S6 Science Run

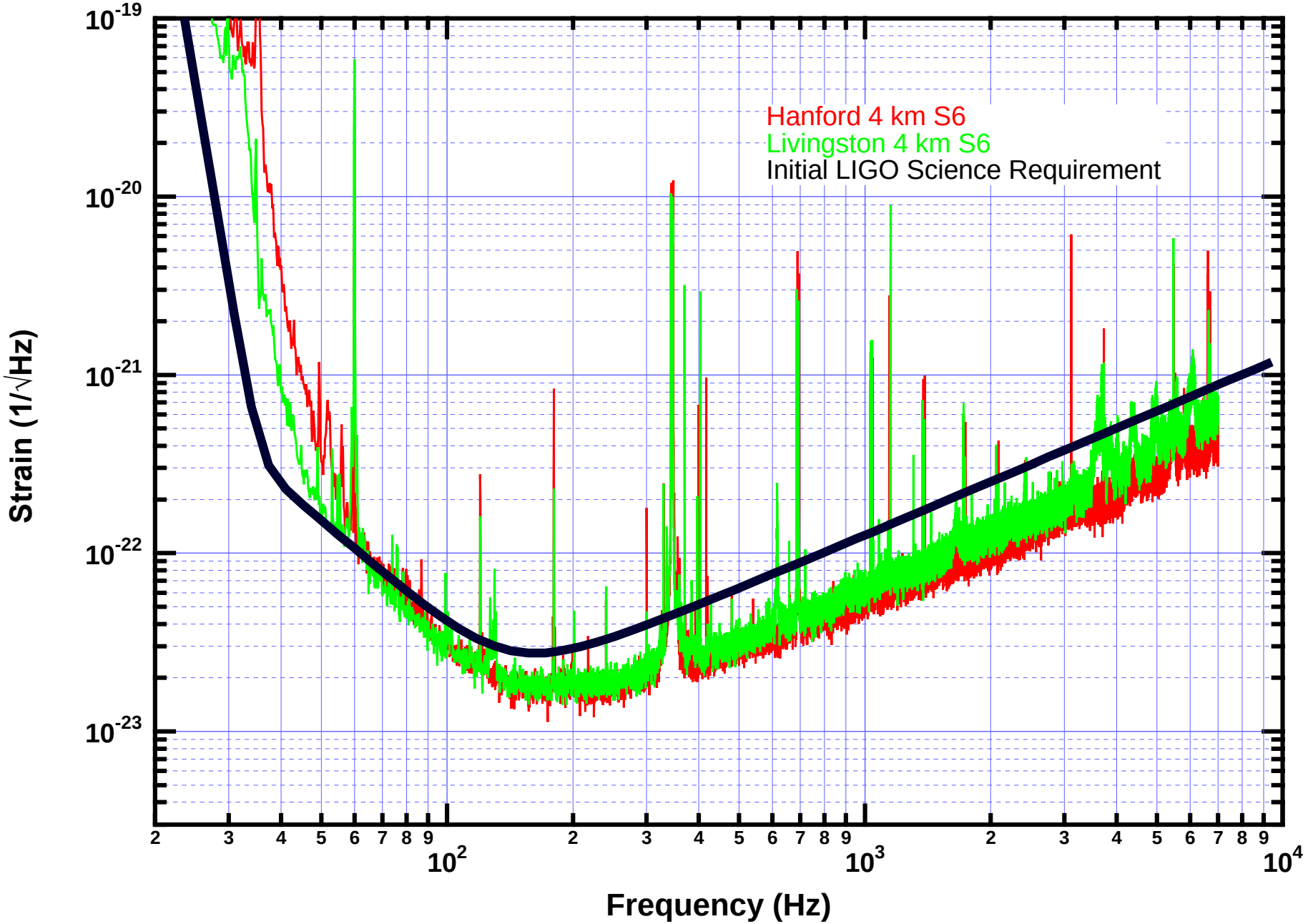

LIGO

Recent LIGO/Virgo/GEO science results

All LSC/Virgo Observational Papers: https://www.lsc-group.phys.uwm.edu/ppcomm/Papers.html

Astrophysical Sources of Gravitational Waves

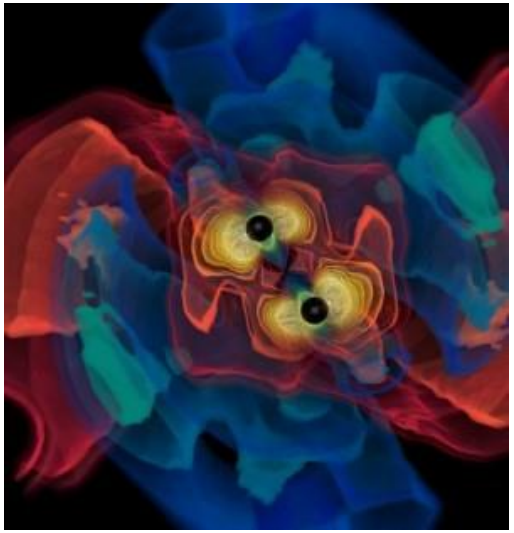

Credit: AEI, CCT, LSU

Coalescing Compact Binary Systems: Neutron Star-NS, Black Hole-NS, BH-BH

- Strong emitters, well-modeled,
- (effectively) transient

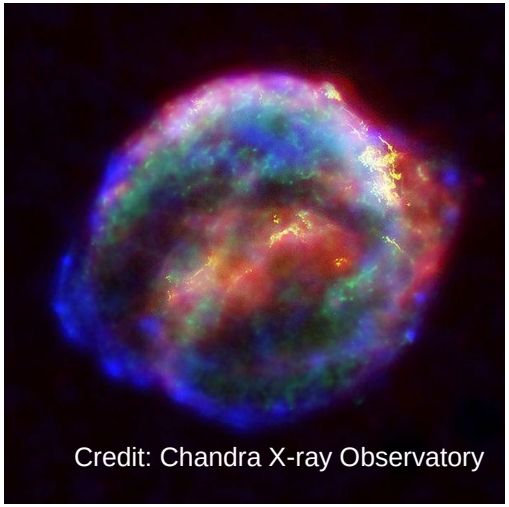

Credit: Chandra X-ray Observatory

Asymmetric Core Collapse Supernovae

- Weak emitters, not well-modeled ('bursts'), transient
- Cosmic strings, soft gamma repeaters, pulsar glitches also in 'burst' class

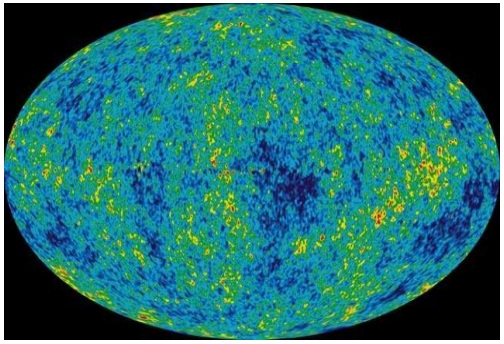

NASA/WMAP Science Team

Cosmic Gravitational-wave Background

- Residue of the Big Bang, long duration
- Long duration, stochastic background

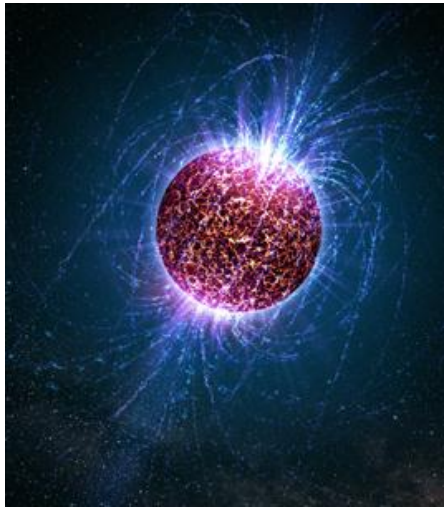

Casey Reed, Penn State

Spinning neutron stars

- (effectively) monotonic waveform
- Long duration

Astrophysical Sources of Gravitational Waves

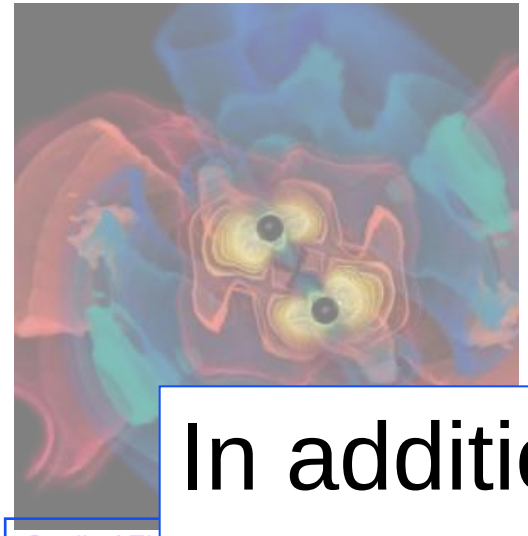

Credit: AEI,

Coalescing Compact Binary Systems: Neutron Star-NS, Black Hole- BH BH-BH

- Strong emitters,

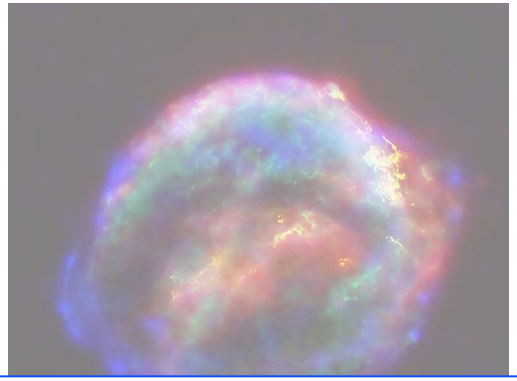

Asymmetric Core Collapse Supernovae

- Weak emitters, not well-modeled ('bursts'), transient

strings also
class

In addition to these known sources, there may be surprising sources of gravitational waves.

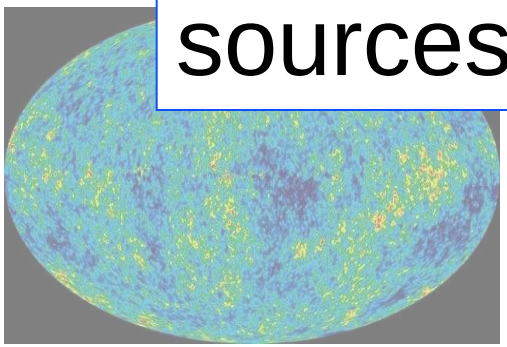

NASA/WMAP Science Team

- Residue of the Big Bang, long duration

- Stochastic, incoherent background

g neutron

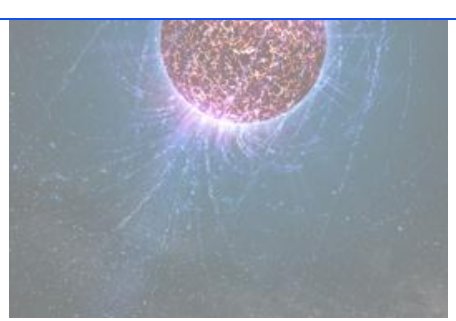

Casey Reed, Penn State

- (effectively) monotonic waveform

- Long duration

Compact binary inspiral, merger, ringdown

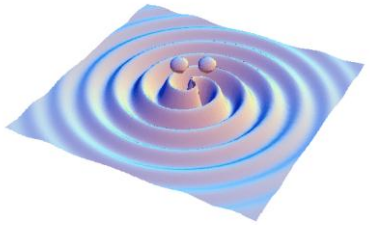

- There's a lot of physics and astrophysics in the waveforms!
- Waveform reconstruction (often buried in detector noise).

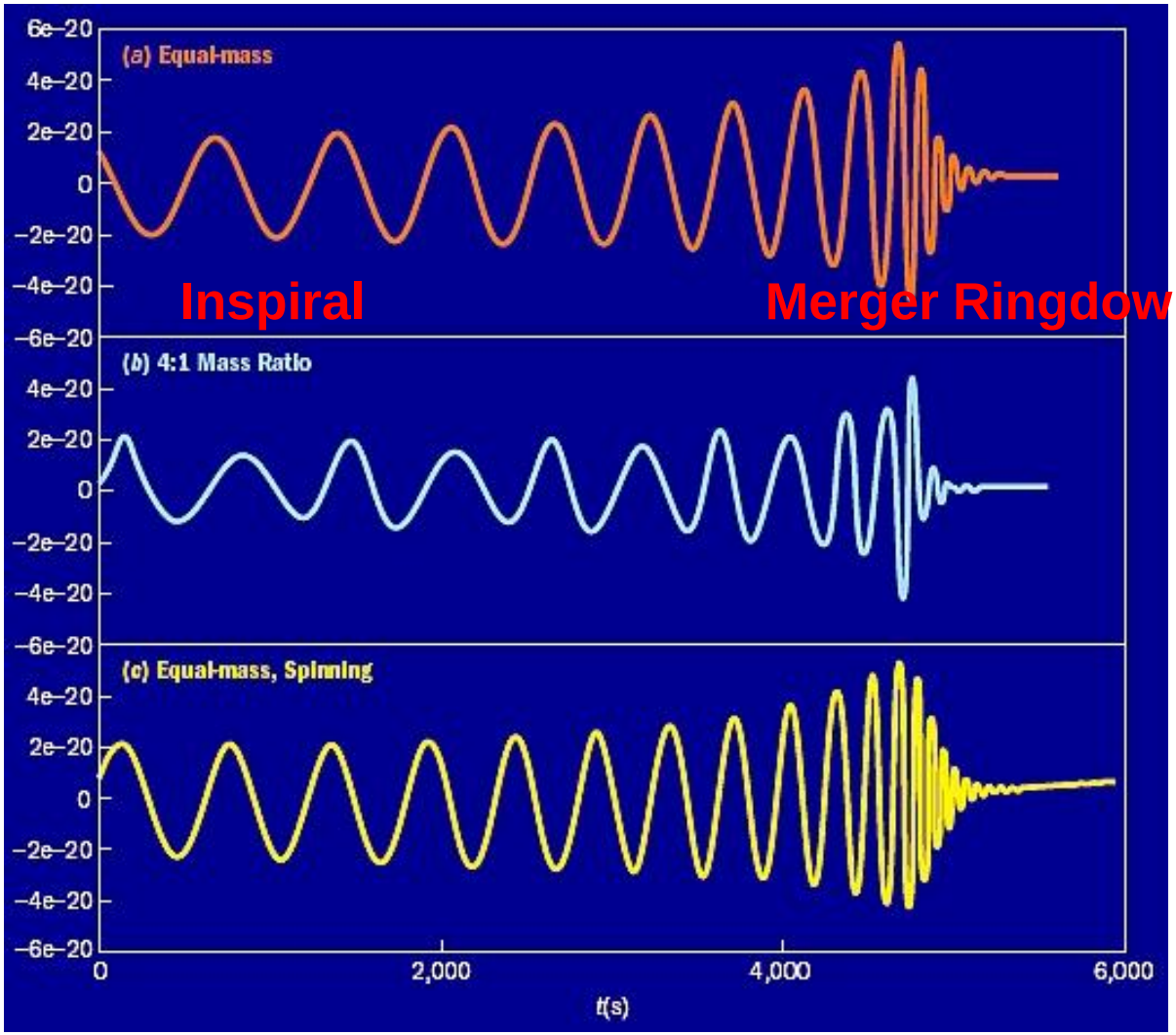

Searches for Binary Mergers

This source:



Produces this waveform:

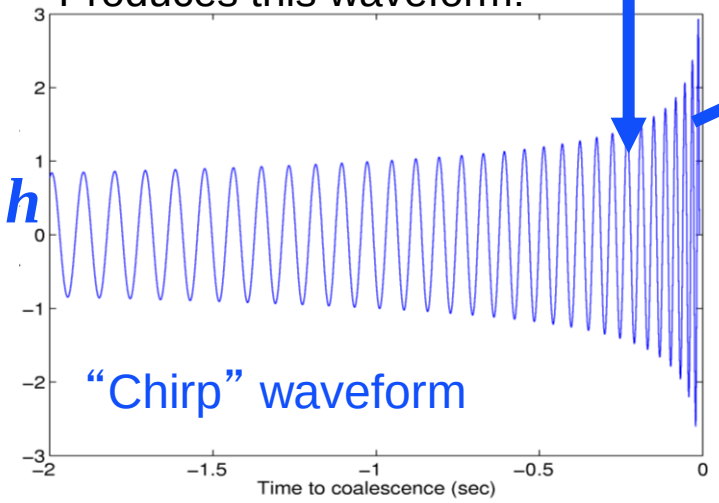

Buried in this noise stream:

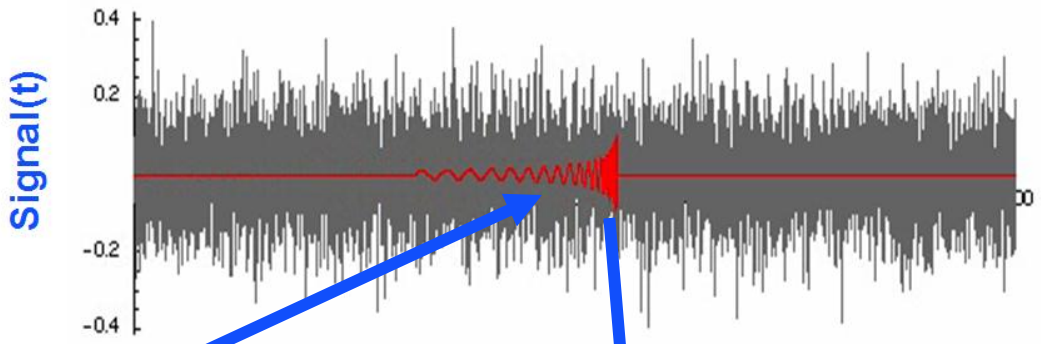

We use different methods (in this case optimal Wiener filtering using matched templates) to pull these signals from the noise:

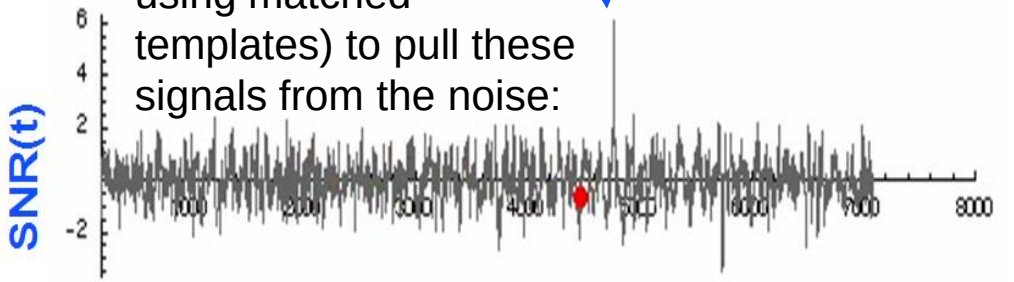

The problem is that non-astrophysical sources also produces signals (false positives)

The Current GW Detector Network

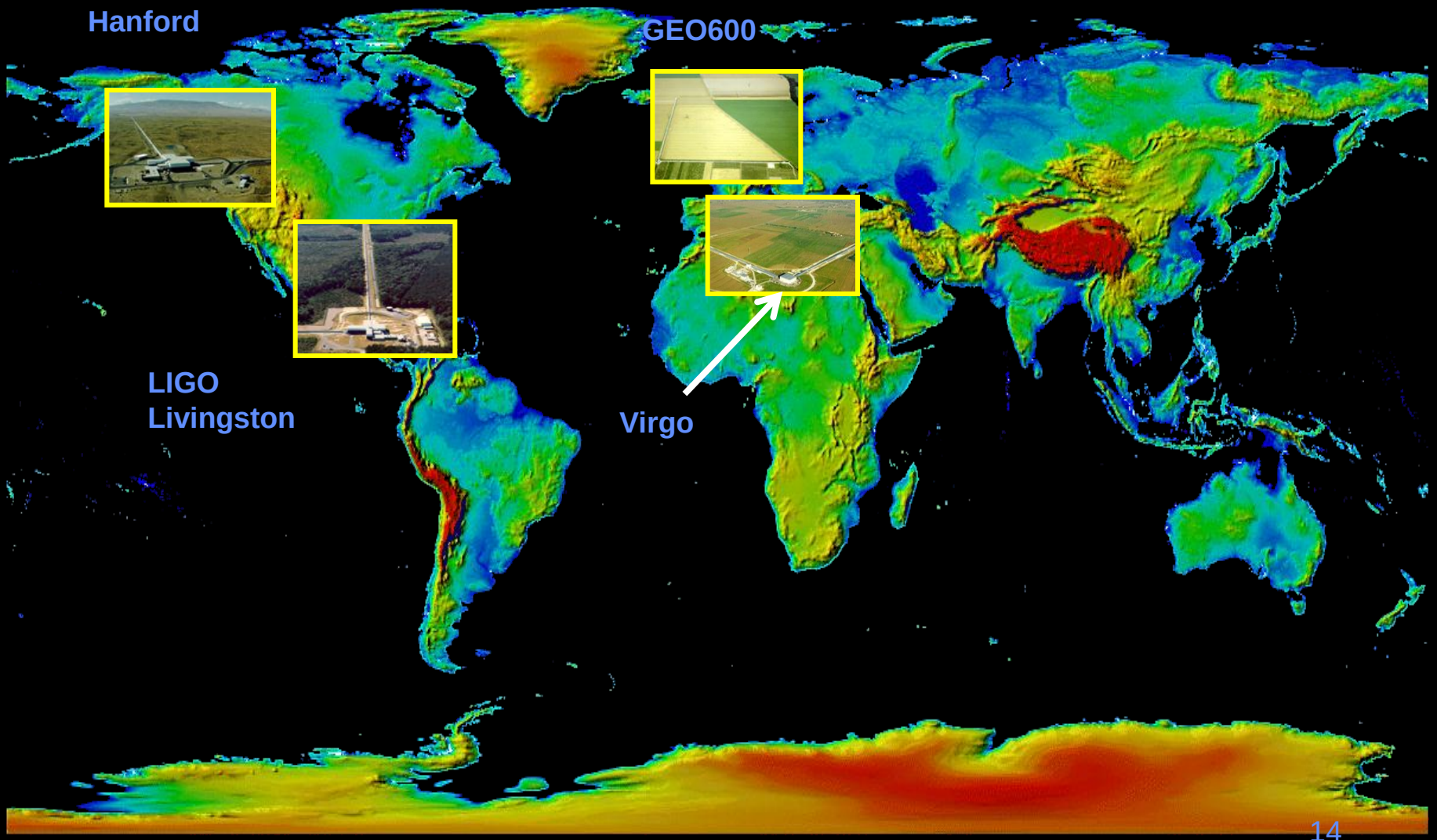

Global gravitational-wave detector network

- GW science is *greatly* enhanced by having distribution of global interferometers. Advantages include:
  - » Source localization
  - » Enhanced Network Sky Coverage
  - » Maximum Time Coverage - ‘Always listening’
  - » Detection confidence
- Since May 2007, LIGO, Virgo, and GEO600 has operated jointly as a global network

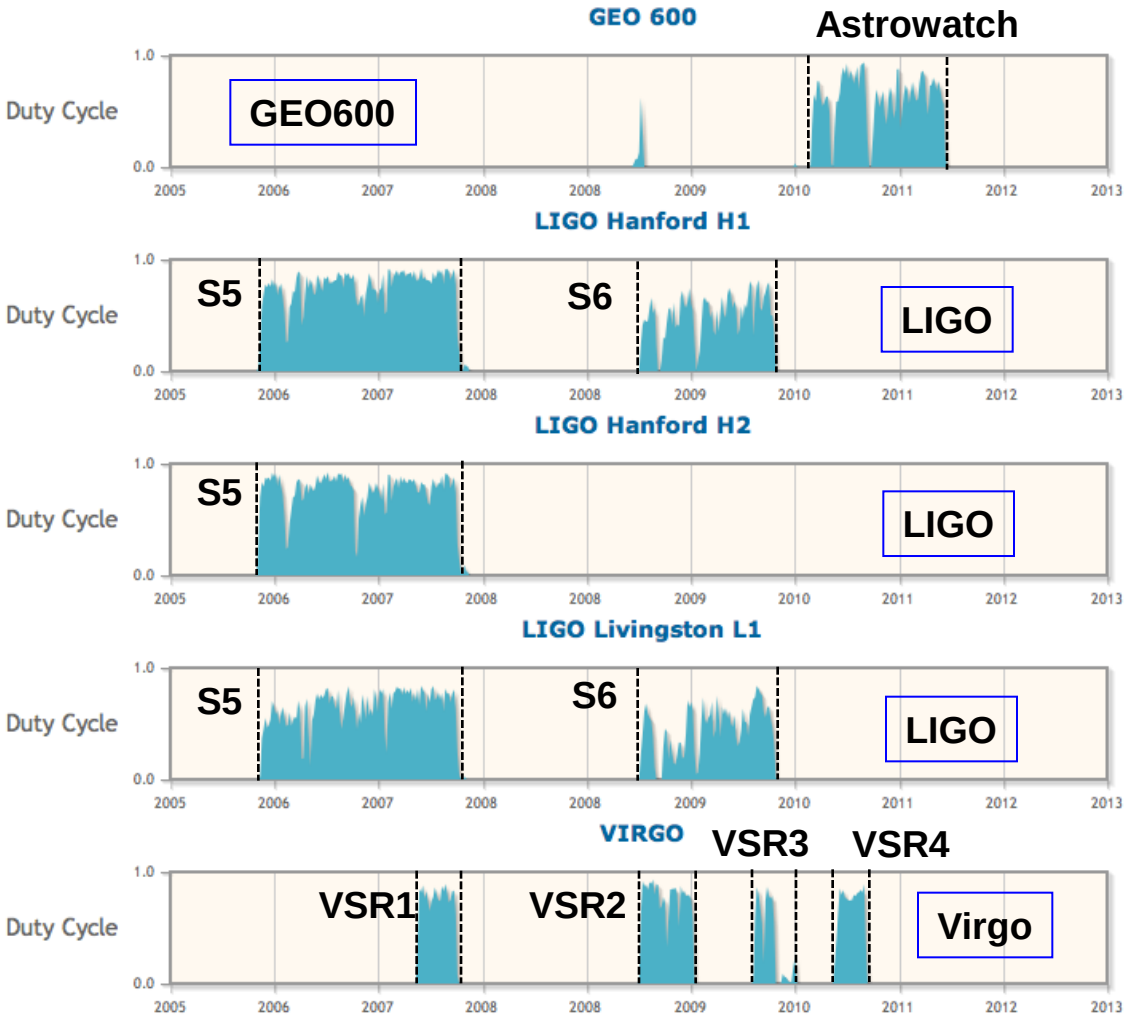

Expected detection rates for compact binary mergers

LIGO Scientific and Virgo Collaborations, "Predictions for the Rates of Compact Binary Coalescences Observable by Ground-based Gravitational-wave Detectors" Class. Quantum Grav. **27** (2010) 173001

- Binary coalescences rates
  - » neutron star (NS) = 1.4 $M_\odot$, Black Hole (BH) = 10 $M_\odot$

TABLE V: Detection rates for compact binary coalescence sources.

IFO	Source	$\dot{N}_{\rm low}$ $\rm yr^{-1}$	$\dot{N}_{\rm re}$ $\rm yr^{-1}$	$\dot{N}_{\rm pl}$ $\rm yr^{-1}$	$\dot{N}_{\rm up}$ $\rm yr^{-1}$
Initial LIGO	NS-NS	2×10^{-4}	0.02	0.2	0.6
	NS-BH	7×10^{-5}	0.004	0.1	
	BH-BH	2×10^{-4}	0.007	0.5	
	IMRI into IMBH			$< 0.001^b$	0.01^c
	IMBH-IMBH			$10^{-4\,d}$	$10^{-3\,e}$
Advanced LIGO	NS-NS	0.4	40	400	1000
	NS-BH	0.2	10	300	
	BH-BH	0.4	20	1000	
	IMRI into IMBH			10^b	300^c
	IMBH-IMBH			0.1^d	1^e

- **The error bar is large and important!**

Searching for Low Mass Compact Binary Coalescences

LIGO Scientific and Virgo Collaborations, “Search for Gravitational Waves from Low Mass Compact Binary Coalescence in LIGO's Sixth Science Run and Virgo's Science Runs 2 and 3”, Phys. Rev D**85** (2012) 082002

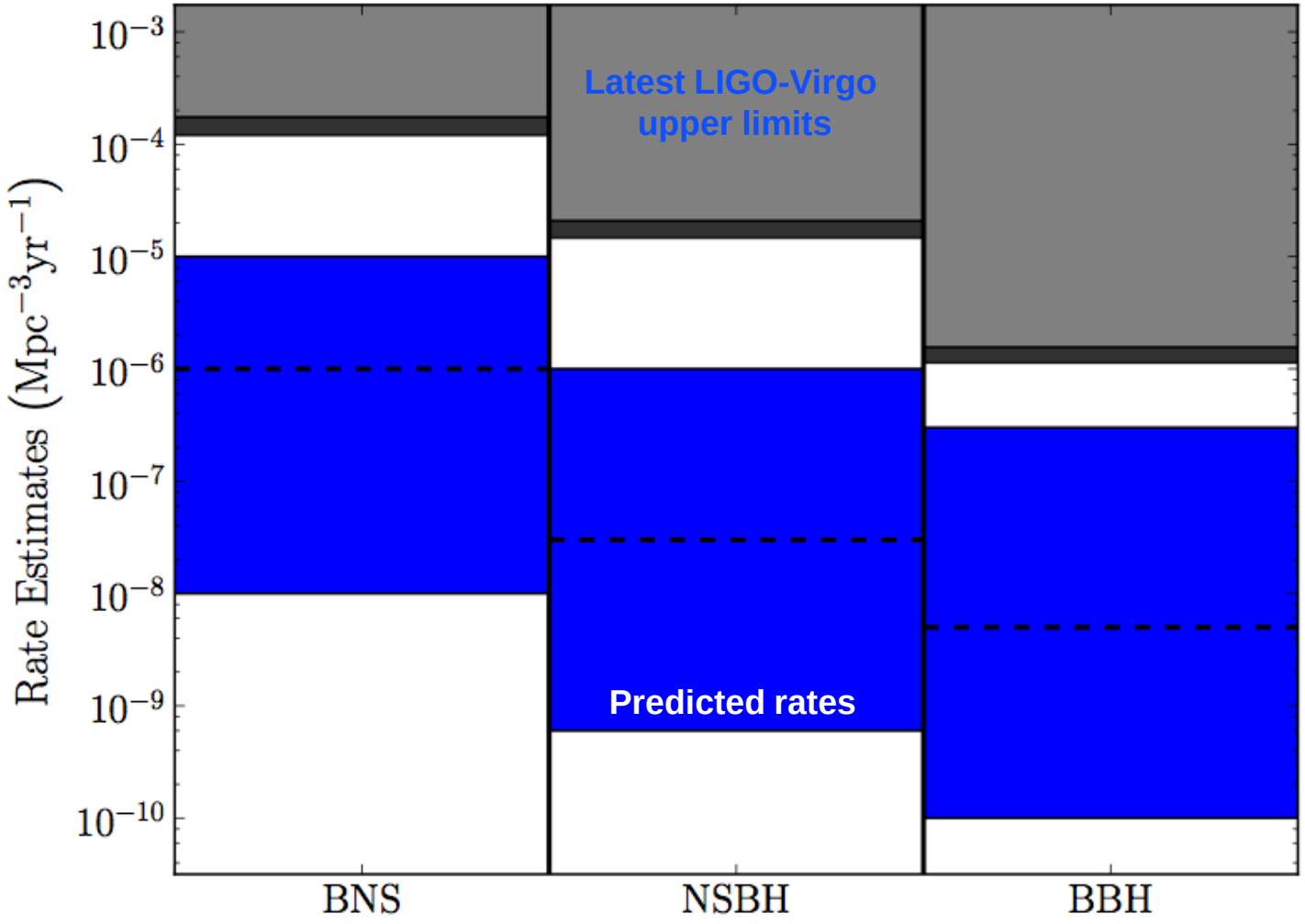

‘Event’ GW100916 – A Blind Injection

http://www.ligo.org/science/GW100916/

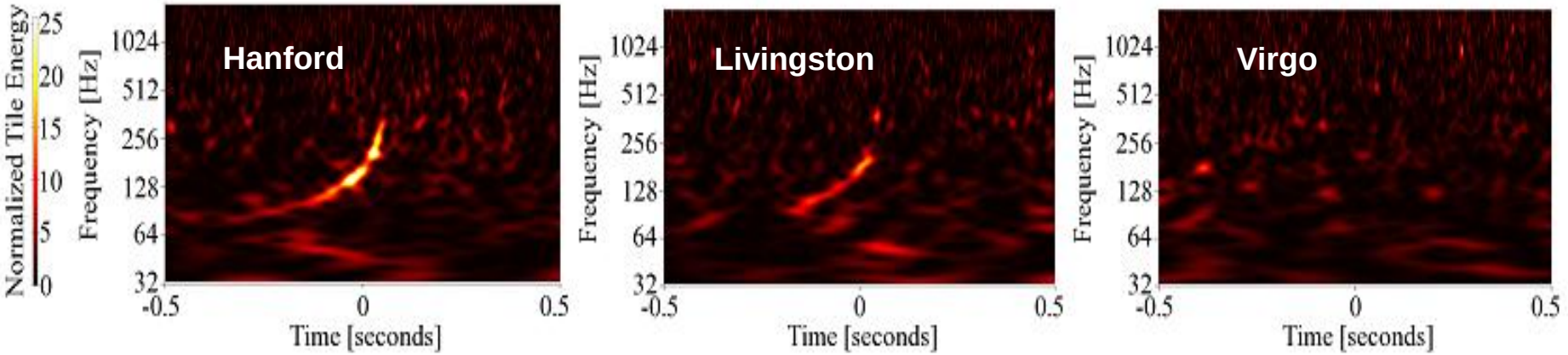

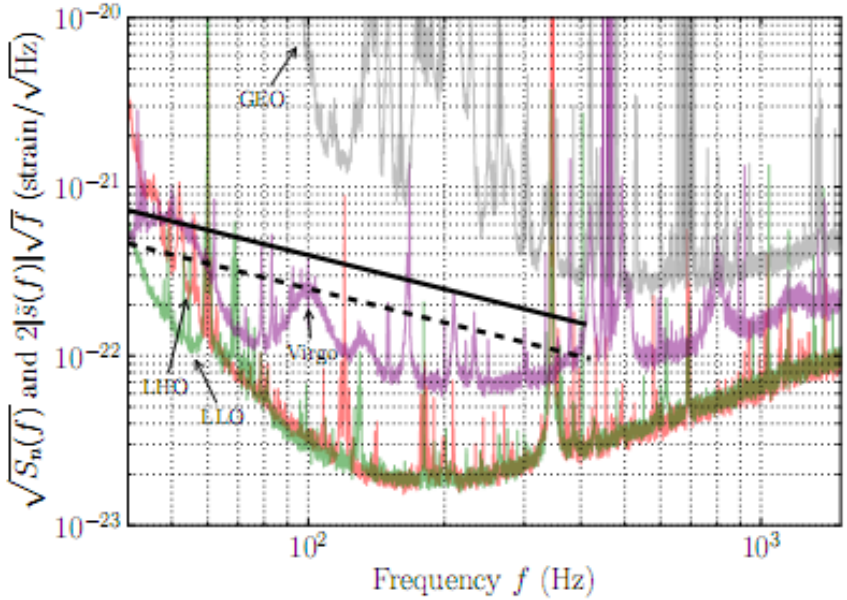

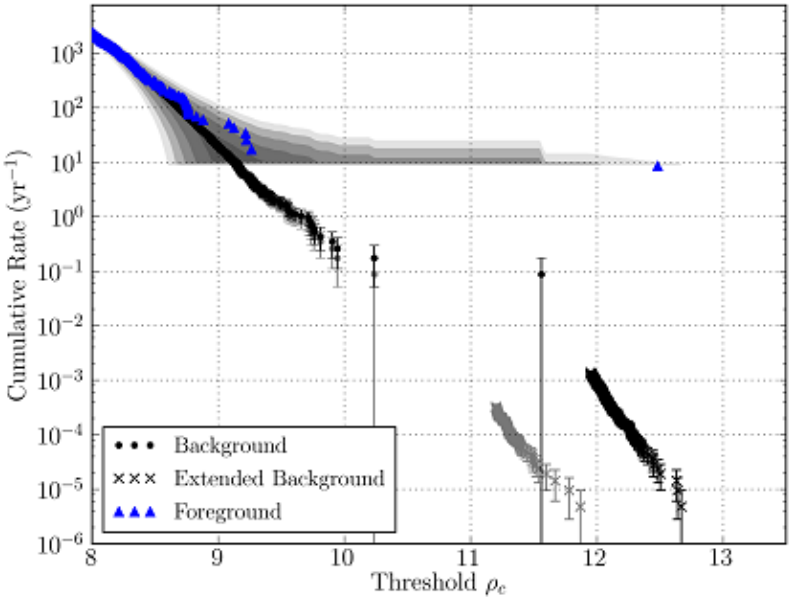

Triggered searches for gamma-ray bursts

- GRBs are good candidates for GW emission
- GRB progenitor models
  - Long GRB → Core collapse SN of a massively spinning star
  - Short GRB → coalescence of a neutron star and a compact object
    - ≤ 15% from neutron star quakes
- Compact, relativistic, asymmetric!
  - But measured red shifts → 10 Gpc

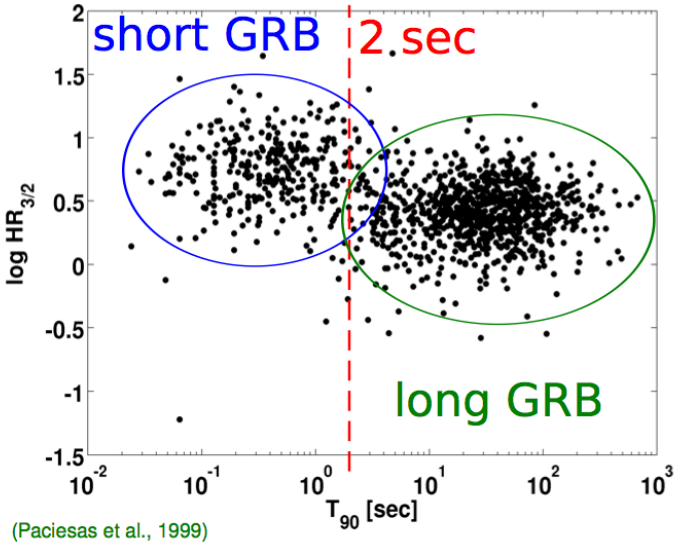

(Paciesas et al., 1999)

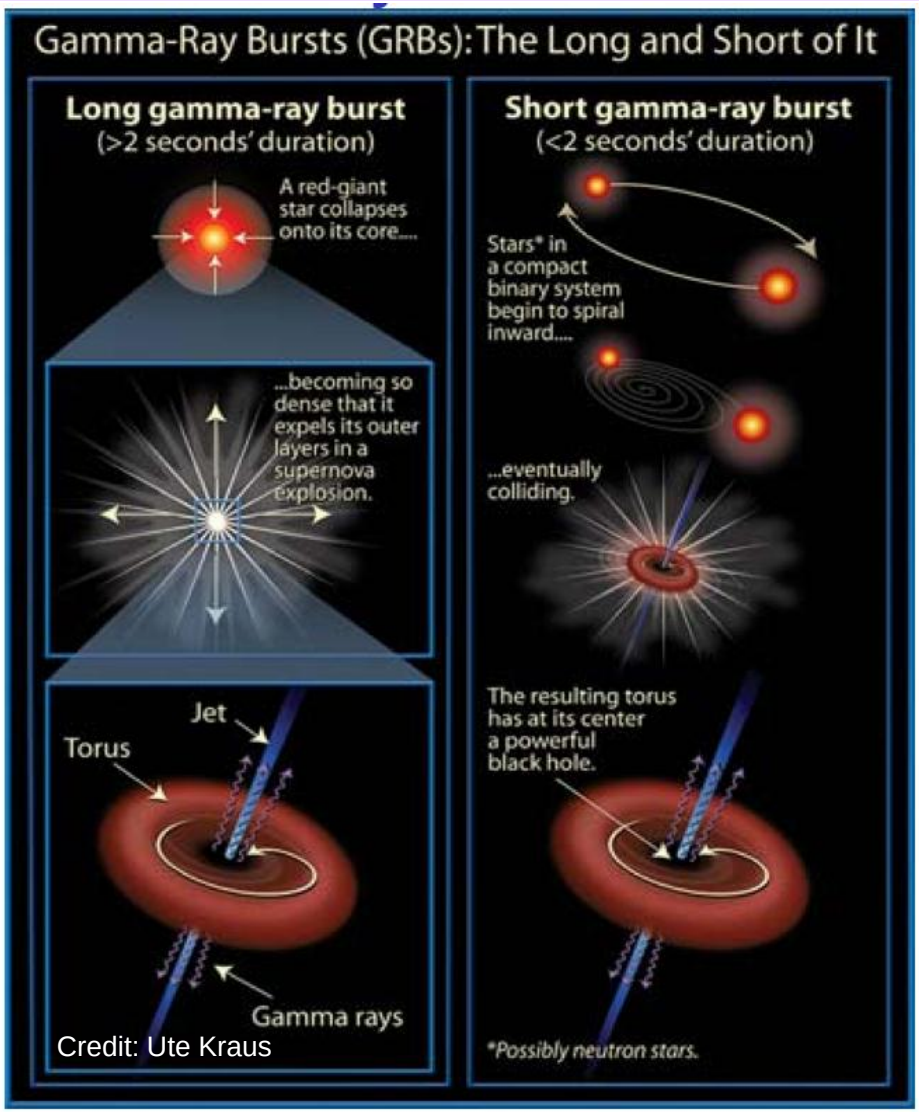

Searches for GWs from nearby GRB sources

- GRB050311, GRB070201: short GRBs with sky localizations that overlap nearby galaxies
  - » GRB050311 overlap with M81 (3.6 Mpc)
  - » GRB070201 overlap with M31 (770 kpc)
- Binary coalescence in M31 excluded at >99% confidence level
- BNS coalescence in M81 excluded at 98% confidence level

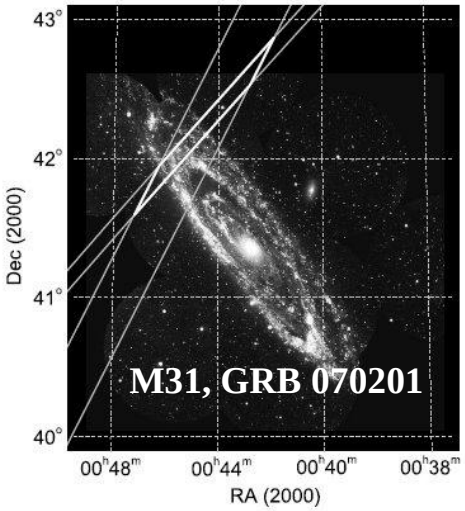

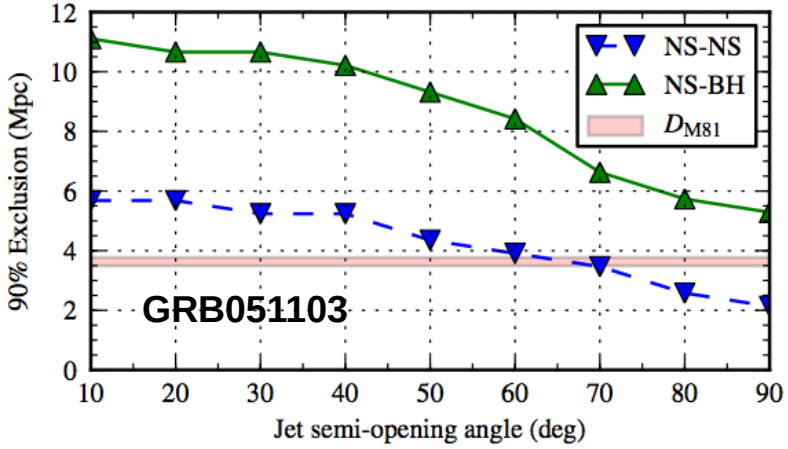

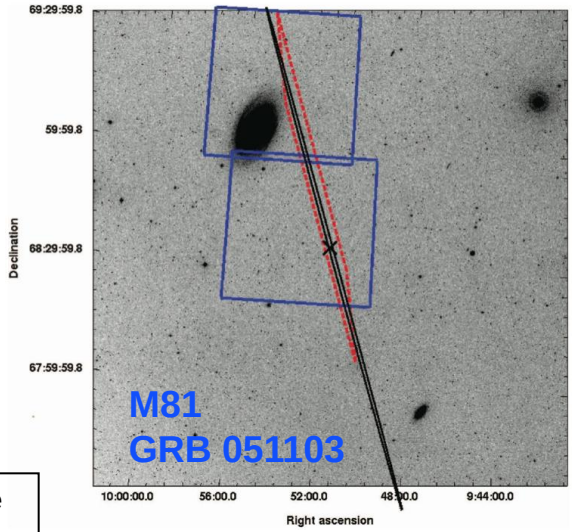

LIGO Scientific Collaboration, K. Hurley, "Implications for the Origin of GRB 070201 from LIGO Observations", Astrophys. J. **681** (2008) 1419

LIGO Scientific Collaboration, "Implications for the Origin of GRB 051103 from LIGO Observations", arXiv:1201.4413

Enabling multi-messenger astronomy with gravitational waves

- Many GWs sources are likely to radiate in the electromagnetic spectrum
- We want to see them via different observational methods simultaneously
- GW 'Aperture synthesis'
  - » Crude estimate of angular resolution

$$q_{GW} \sim l_{GW} / d \sim \text{few degrees}$$

→ wide field telescopes
  + Image tiling
  + Galaxy weighting

→ Neutrino observatories

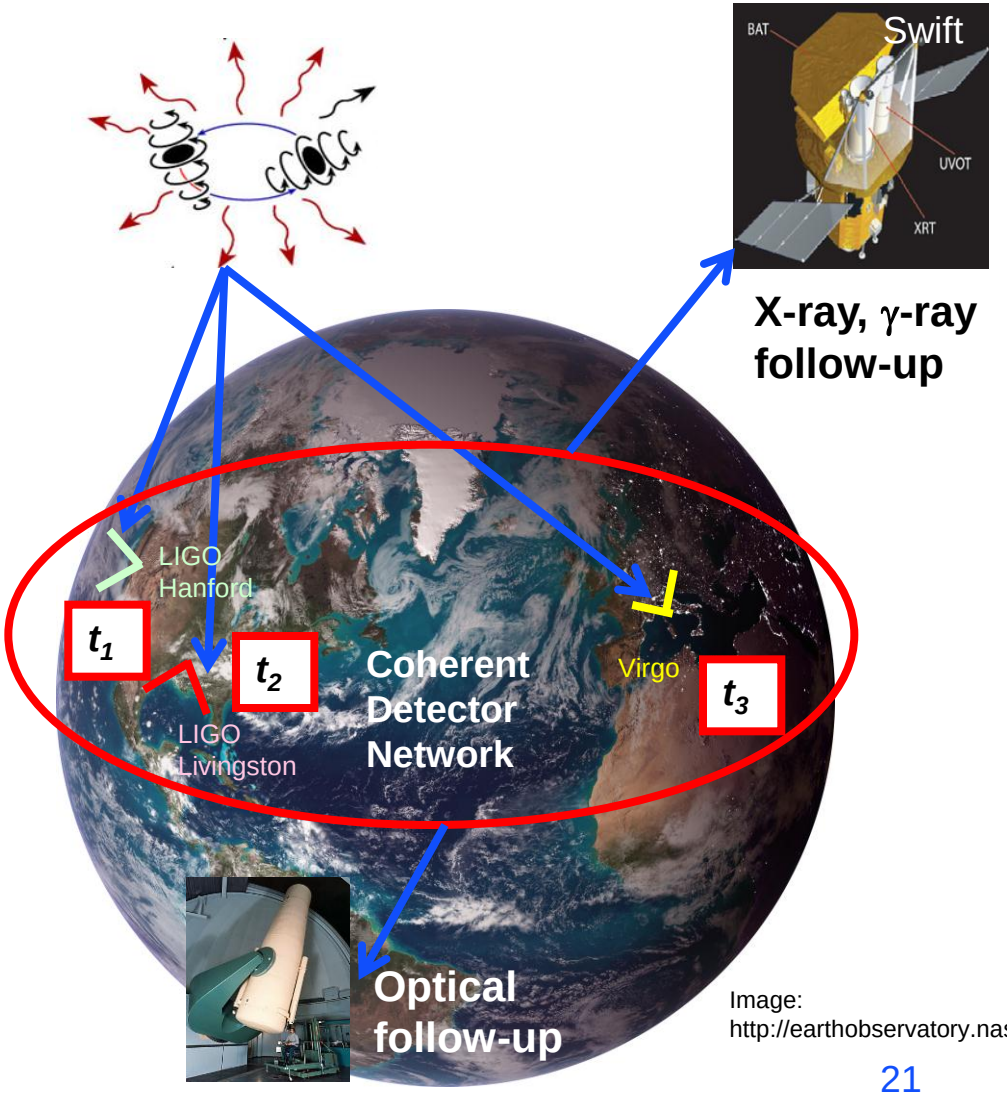

Image: http://earthobservatory.nasa.gov/

EM follow up of gravitational-wave triggers from S5, VSR1

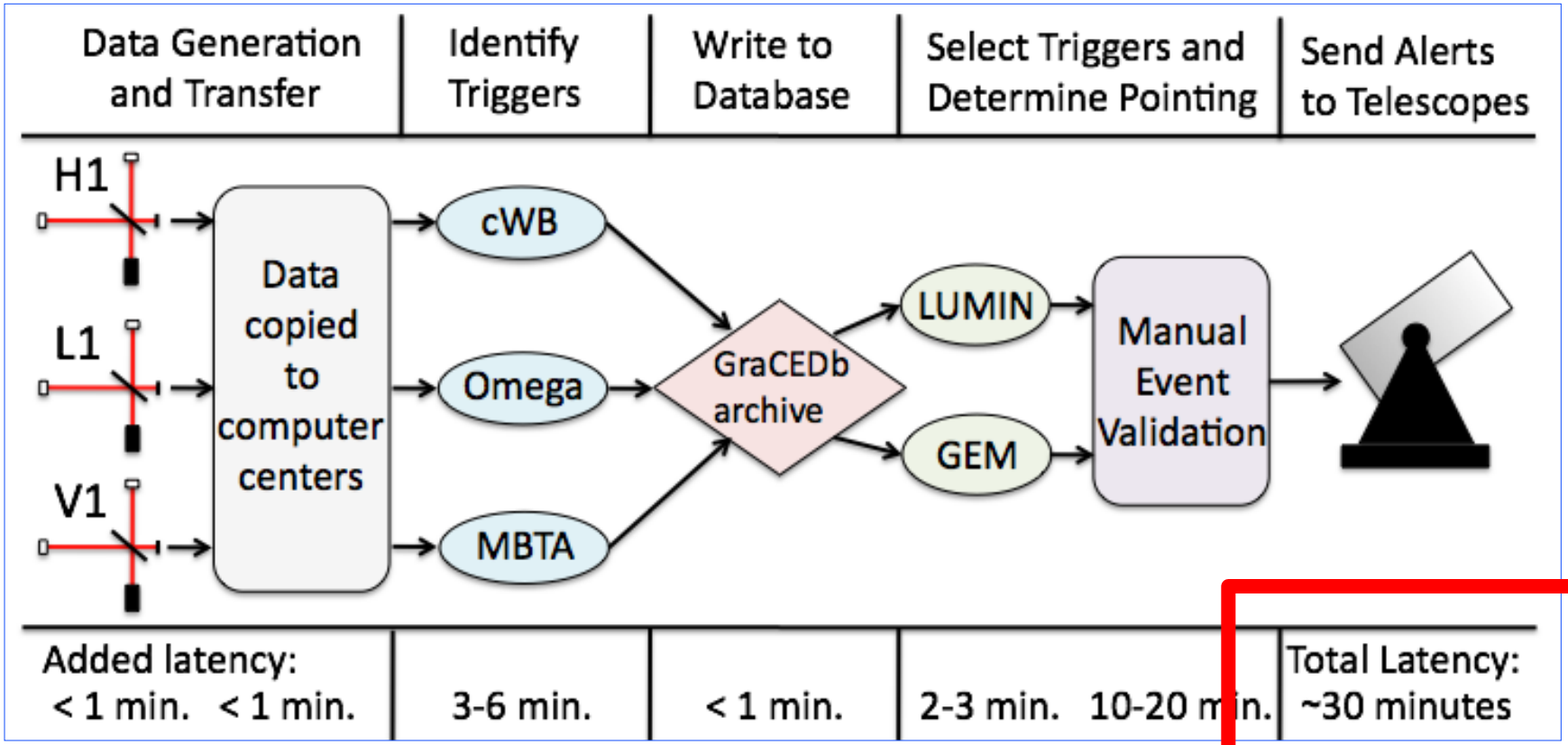

Observing Partners During 2009–2010

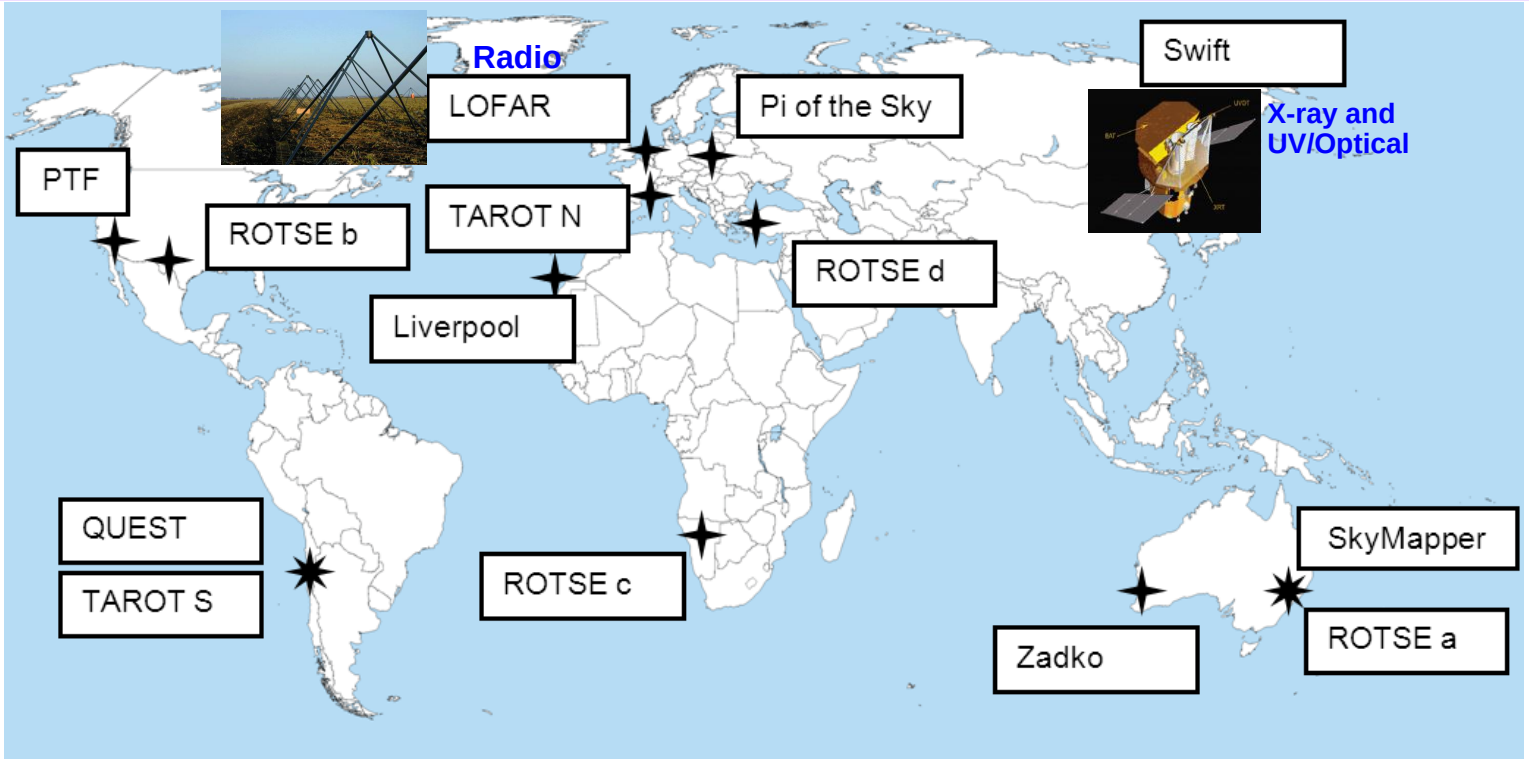

- Mostly (but not all) robotic wide-field optical telescopes
  - » Many of them used for following up GRBs and/or hunting for supernovae
- Nine event candidates in S6/VSR2,3 followed up by at least one scope

LIGO Scientific and Virgo Collaborations, "*Implementation and testing of the first prompt search for gravitational wave transients with electromagnetic counterparts*", A&A **539**, A124 (2012)

LIGO Scientific and Virgo Collaborations, "*First Low-Latency LIGO+Virgo Search for Binary Inspirals and their Electromagnetic Counterparts*", arXiv:1112.6005

Example: GW100916 Skymap

- LIGO-Virgo source localization ~ O(100 deg^2)
  - » Disconnected regions
- Top probability pixels imaged by Swift and other ground-based optical telescopes
- Swift pixels maximized probability on NGC2380 and ESO492-010

NGC2380
(Credit: Las Cumbras Observatory www.lcogt.net)



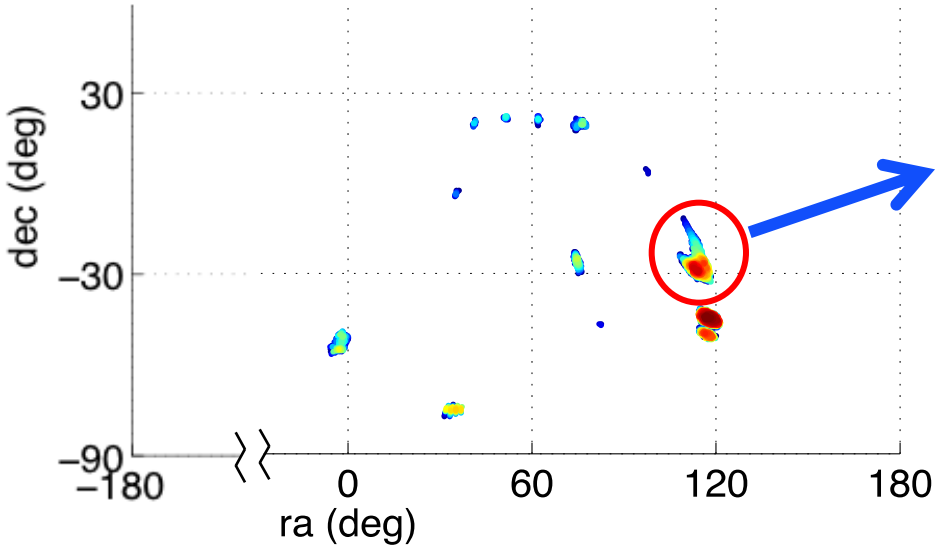

LIGO Scientific and Virgo Collaborations, "*Swift Follow-Up Observations Of Candidate Gravitational-Wave Transient Events*" arXiv:1205.1124

LIGO

Advanced LIGO

LIGO

CALTECH/MIT PROJECT

FOR A

LASER INTERFEROMETER

GRAVITATIONAL WAVE OBSERVATORY

December 1987

LIGO-M870001-00-M

By comparing the source strengths and benchmark sensitivities in Figure II-2 and in the periodic and stochastic figures A-4b,c (Appendix A), one sees that *(i) There are nonnegligible possibilities for wave detection with the first detector in the LIGO. (ii) Detection is probable at the sensitivity level of the advanced detector. (iii) The first detection is most likely to occur, not in the initial detector in the LIGO but rather in a subsequent one, as the sensitivity and frequency are being pushed downward from the middle curve toward the bottom curve of Figure II-2.*

Rochus Vogt, Ron Drever, Kip Thorne, Rai Weiss 1987

LIGO

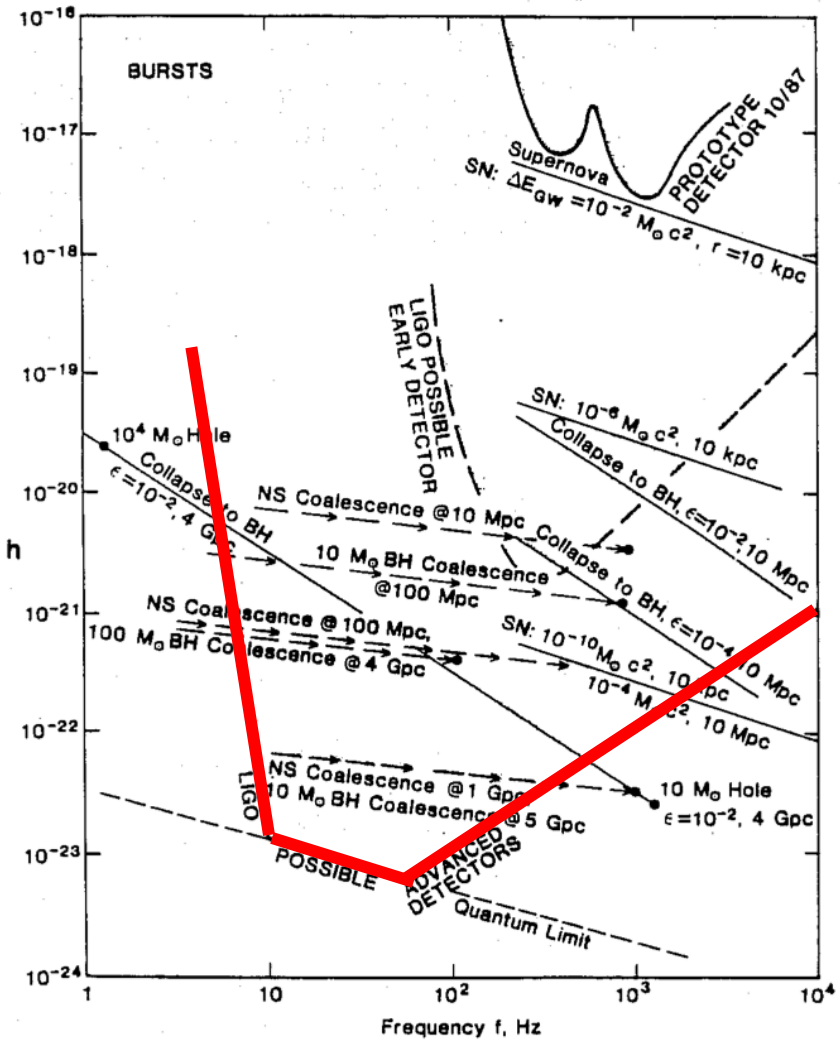

Rochus Vogt, Ron Drever, Kip Thorne, Rai Weiss 1987

Advanced LIGO

- Advanced LIGO – a complete upgrade of the LIGO interferometers
- Advanced LIGO is designed to increase the distance probed ('reach') by ~ 10X
  - » Leads to 1000X increase in volume → 1000X increase in event rate
- *Expect 10s of detections per year at design sensitivity*
  - » 1 aLIGO observational day = a few years of iLIGO

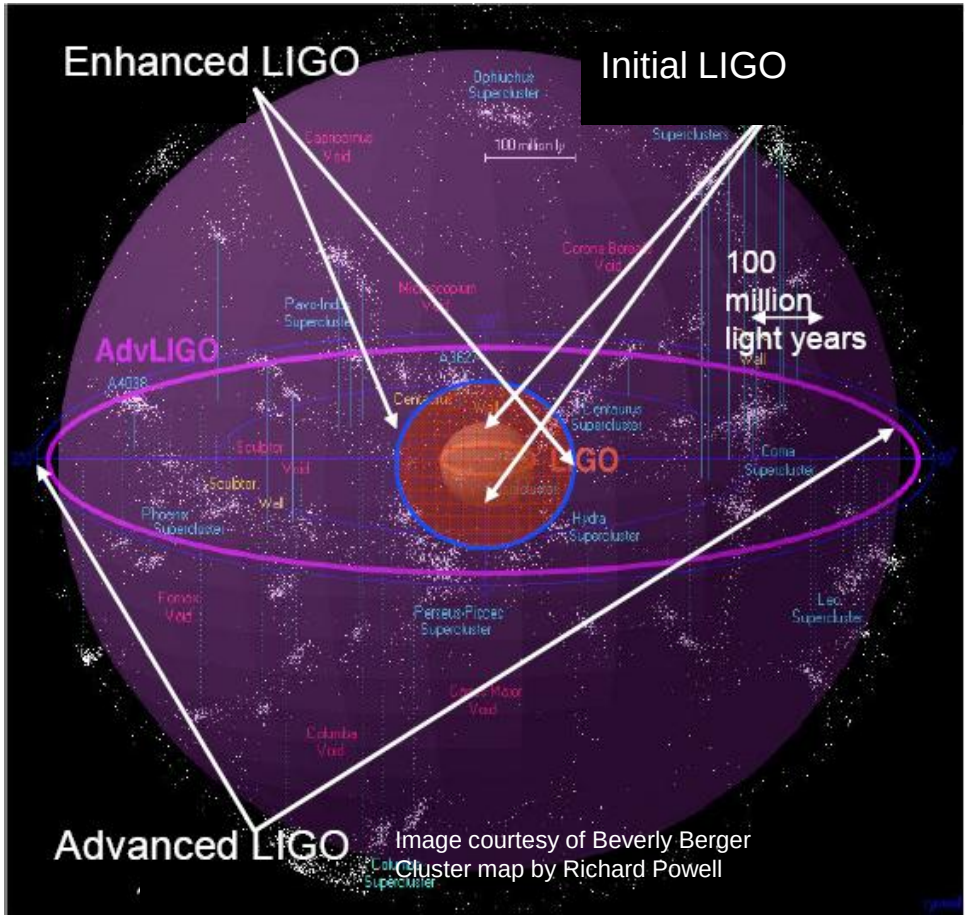

Expected detection rates for compact binary mergers

LIGO Scientific and Virgo Collaborations, "Predictions for the Rates of Compact Binary Coalescences Observable by Ground-based Gravitational-wave Detectors" Class. Quantum Grav. **27** (2010) 173001

- Binary coalescences rates
  - » neutron star (NS) = 1.4 $M_\odot$, Black Hole (BH) = 10 $M_\odot$

TABLE V: Detection rates for compact binary coalescence sources.

IFO	Source	$\dot{N}_{\rm low}$ $\rm yr^{-1}$	$\dot{N}_{\rm re}$ $\rm yr^{-1}$	$\dot{N}_{\rm pl}$ $\rm yr^{-1}$	$\dot{N}_{\rm up}$ $\rm yr^{-1}$
Initial LIGO	NS-NS	2×10^{-4}	0.02	0.2	0.6
	NS-BH	7×10^{-5}	0.004	0.1	
	BH-BH	2×10^{-4}	0.007	0.5	
	IMRI into IMBH			$< 0.001^b$	0.01^c
	IMBH-IMBH			$10^{-4\,d}$	$10^{-3\,e}$
Advanced LIGO	NS-NS	0.4	40	400	1000
	NS-BH	0.2	10	300	
	BH-BH	0.4	20	1000	
	IMRI into IMBH			10^b	300^c
	IMBH-IMBH			0.1^d	1^e

- **The error bar is large and important!**

Latest low mass CBC search results

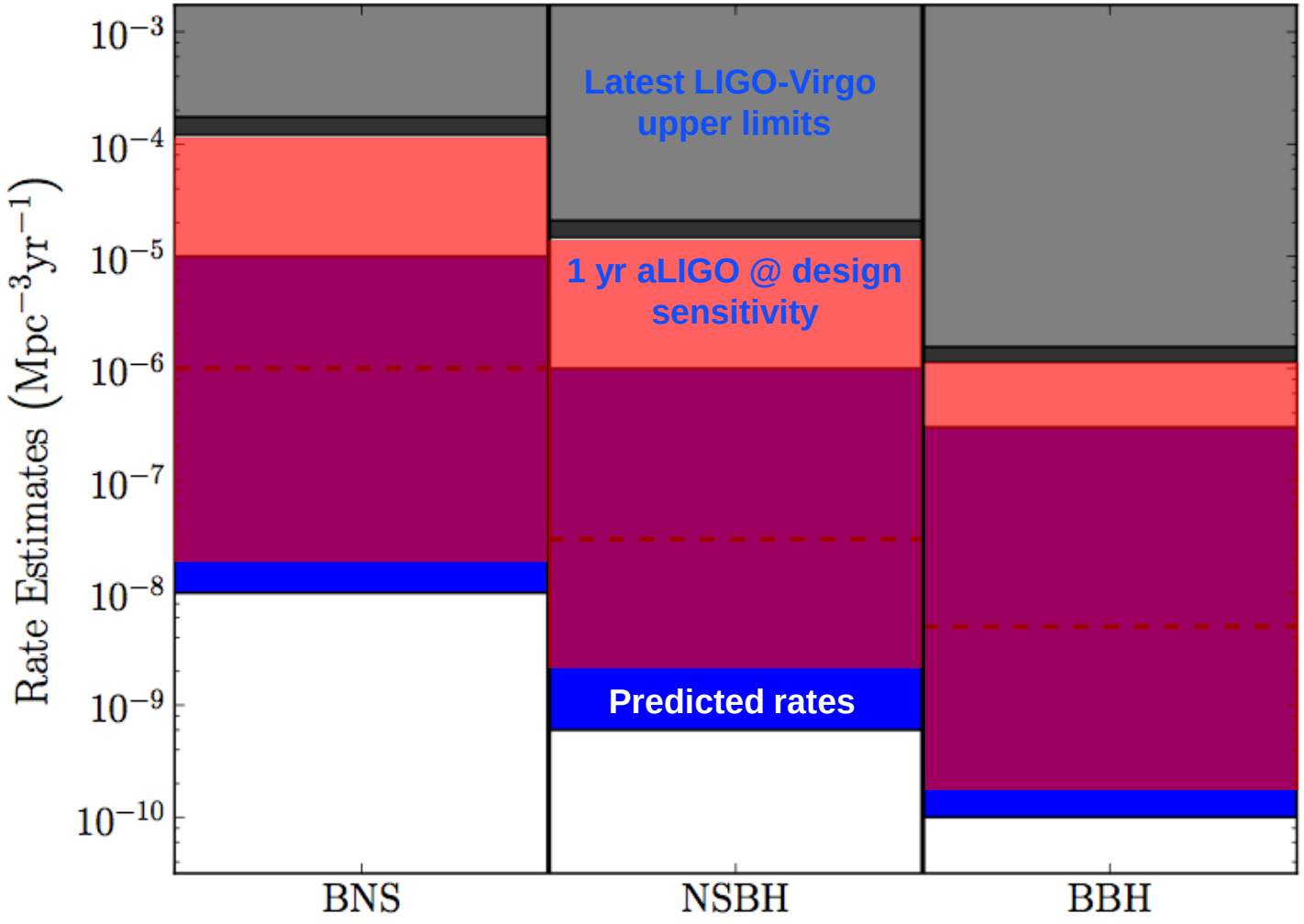

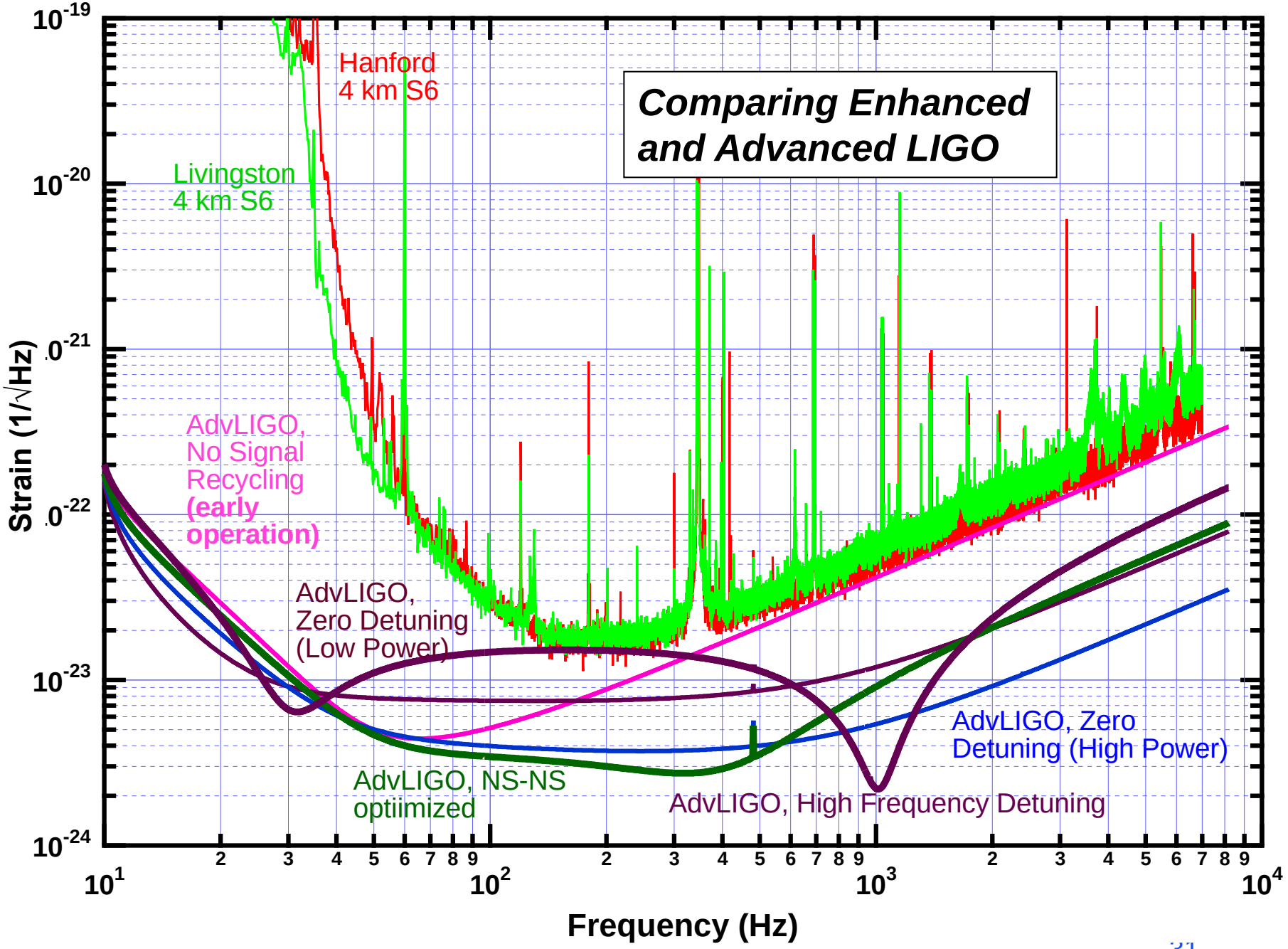
Comparing Enhanced and Advanced LIGO
Hanford 4 km S6
Livingston 4 km S6
AdvLIGO, No Signal Recycling (early operation)
AdvLIGO, Zero Detuning (Low Power)
AdvLIGO, NS-NS optiimized
AdvLIGO, High Frequency Detuning
AdvLIGO, Zero Detuning (High Power)
Strain (1/√Hz)
Frequency (Hz)
10^-19
10^-20
10^-21
10^-22
10^-23
10^-24
10^1
10^2
10^3
10^4

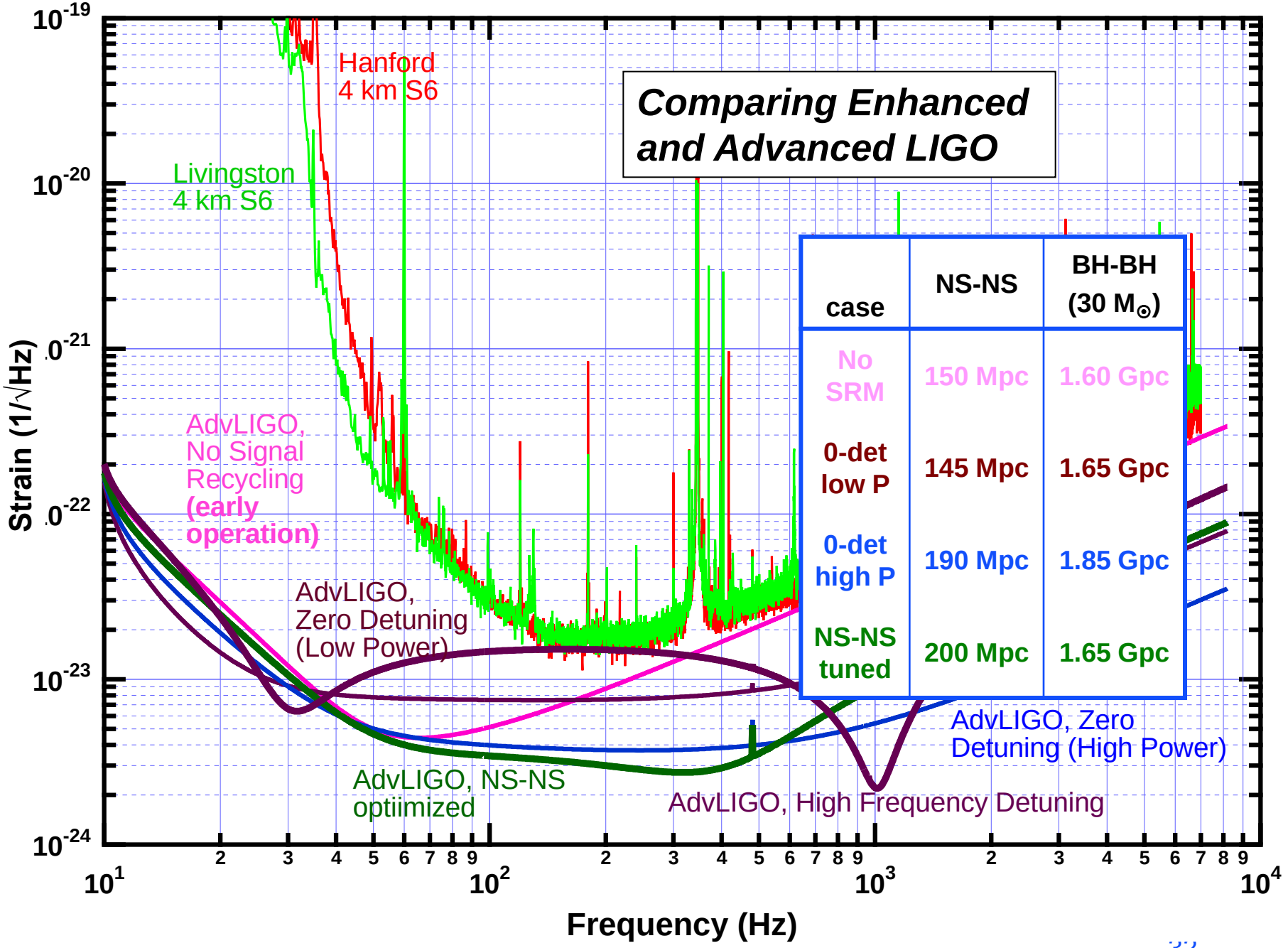
Comparing Enhanced and Advanced LIGO
Hanford 4 km S6
Livingston 4 km S6
AdvLIGO, No Signal Recycling (early operation)
AdvLIGO, Zero Detuning (Low Power)
AdvLIGO, NS-NS optiimized
AdvLIGO, High Frequency Detuning
AdvLIGO, Zero Detuning (High Power)
case | NS-NS | BH-BH (30 M⊙)
No SRM | 150 Mpc | 1.60 Gpc
0-det low P | 145 Mpc | 1.65 Gpc
0-det high P | 190 Mpc | 1.85 Gpc
NS-NS tuned | 200 Mpc | 1.65 Gpc
Strain (1/√Hz)
Frequency (Hz)

Advanced LIGO overview

What is Advanced?

Parameter	*Initial LIGO*	*Advanced LIGO*
Input Laser Power	10 W (10 kW arm)	180 W (>700 kW arm)
Mirror Mass	10 kg	40 kg
Interferometer Topology	Power-recycled Fabry-Perot arm cavity Michelson	Dual-recycled Fabry-Perot arm cavity Michelson (stable recycling cavities)
GW Readout Method	RF heterodyne	DC homodyne
Optimal Strain Sensitivity	3 x 10^{-23} / rHz	Tunable, better than 5 x 10^{-24} / rHz in broadband
Seismic Isolation Performance	f_{low} ~ 50 Hz	f_{low} ~ 13 Hz
Mirror Suspensions	Single Pendulum	Quadruple pendulum

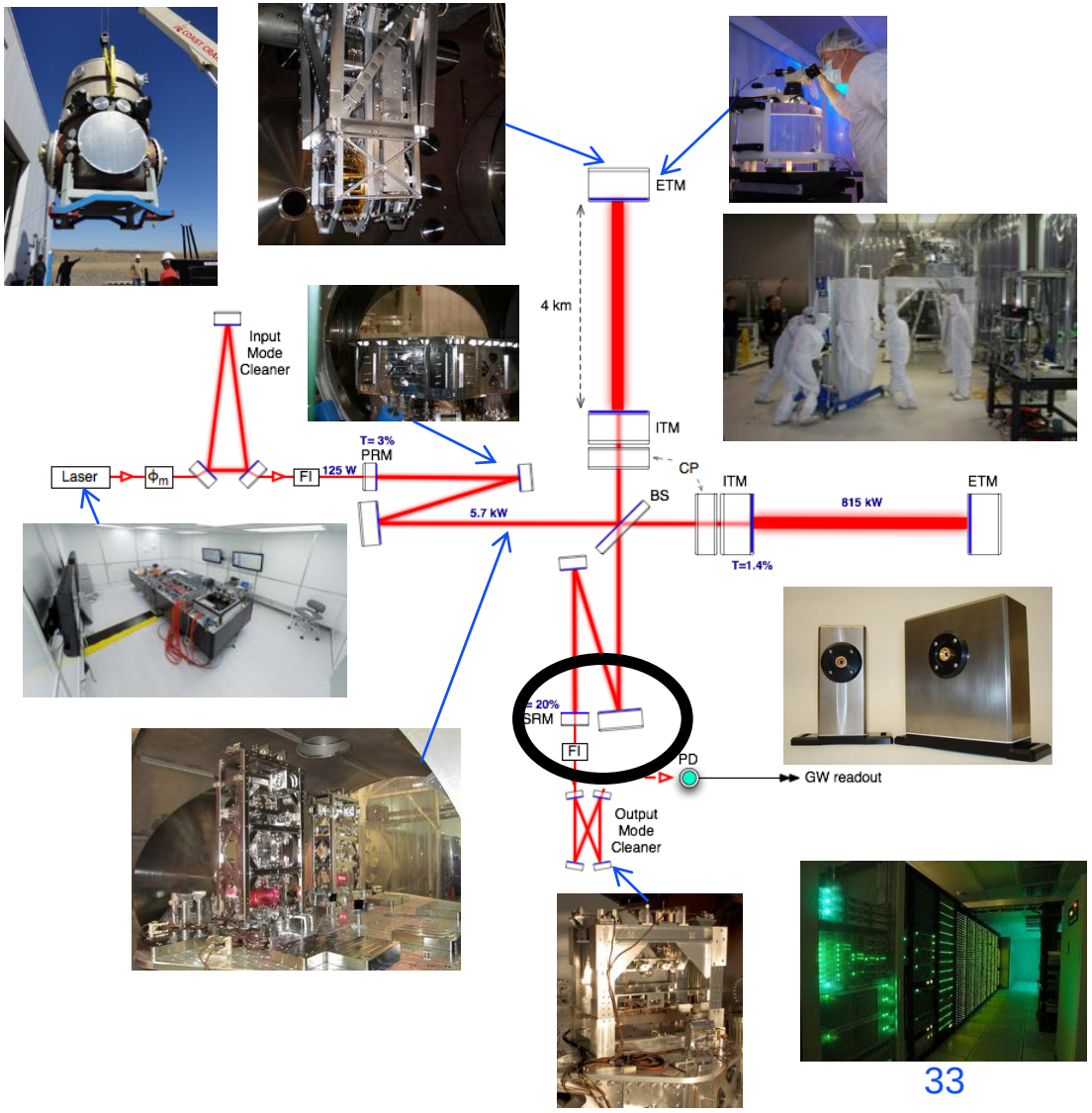



Advanced LIGO schedule

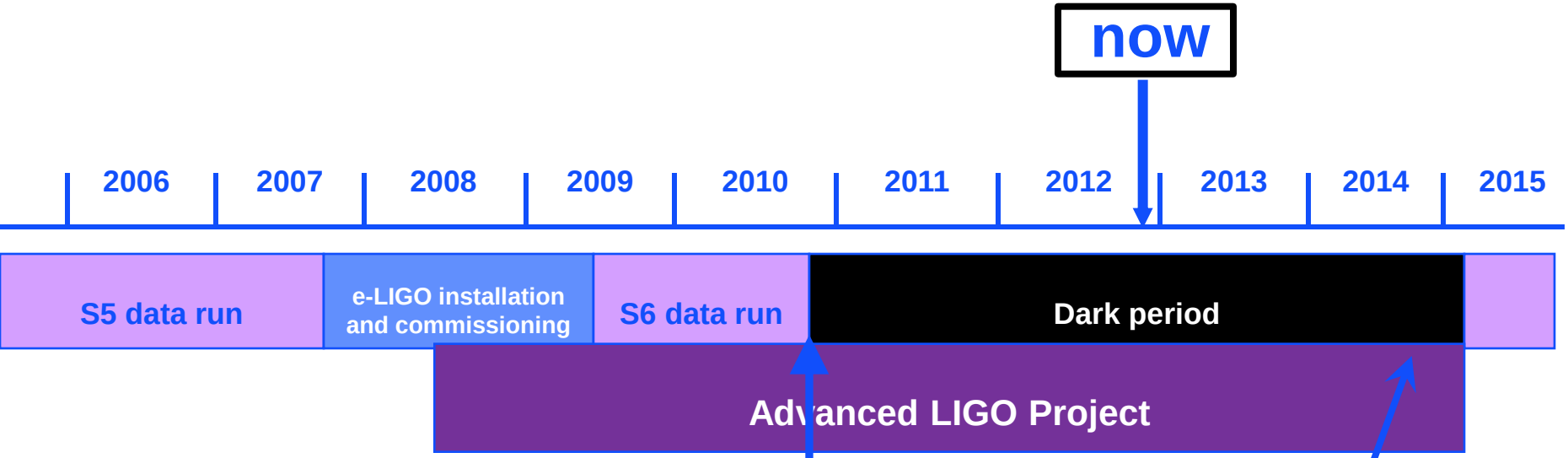

- ★ Fabrication, subsystem assembly, and installation ~ 80% complete
- ★ ***Interferometers operational in 2014***
- ★ ***First science data expected in 2015***

Adv LIGO Installation begins

Commissioning & initial data With Advanced LIGO

A Possible Upgrade: Squeezed Interferometry

Quantum Optics in service of Astrophysics!

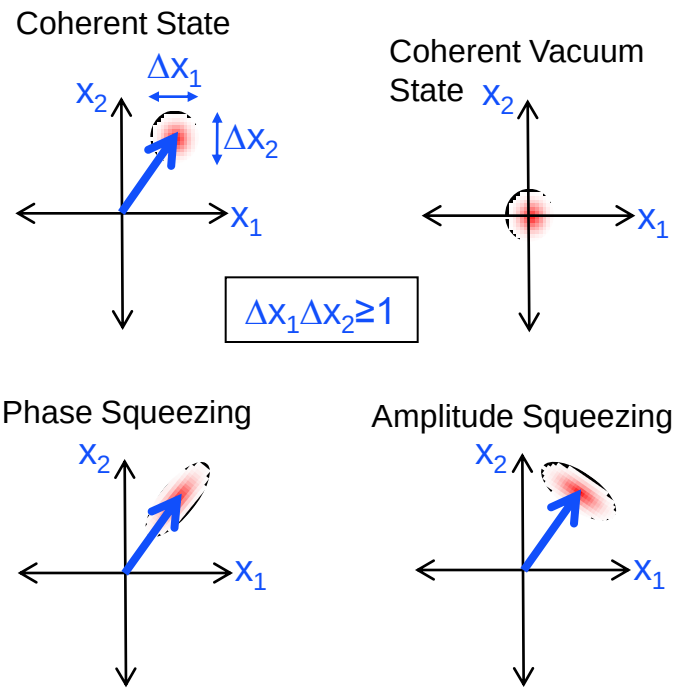

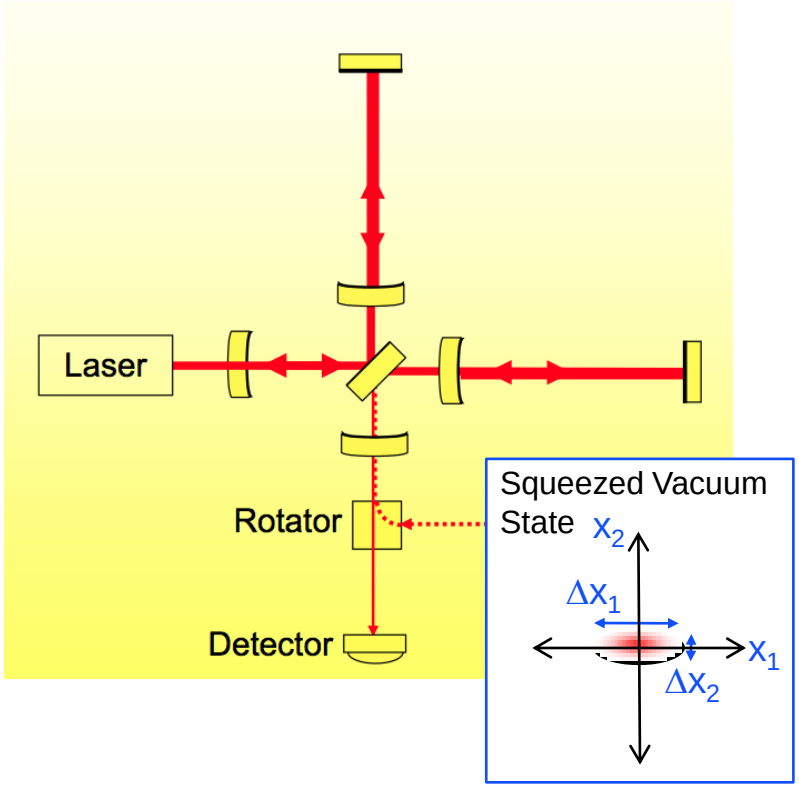

First Demonstration of Squeezed Interferometry in a Gravitational-wave Detector

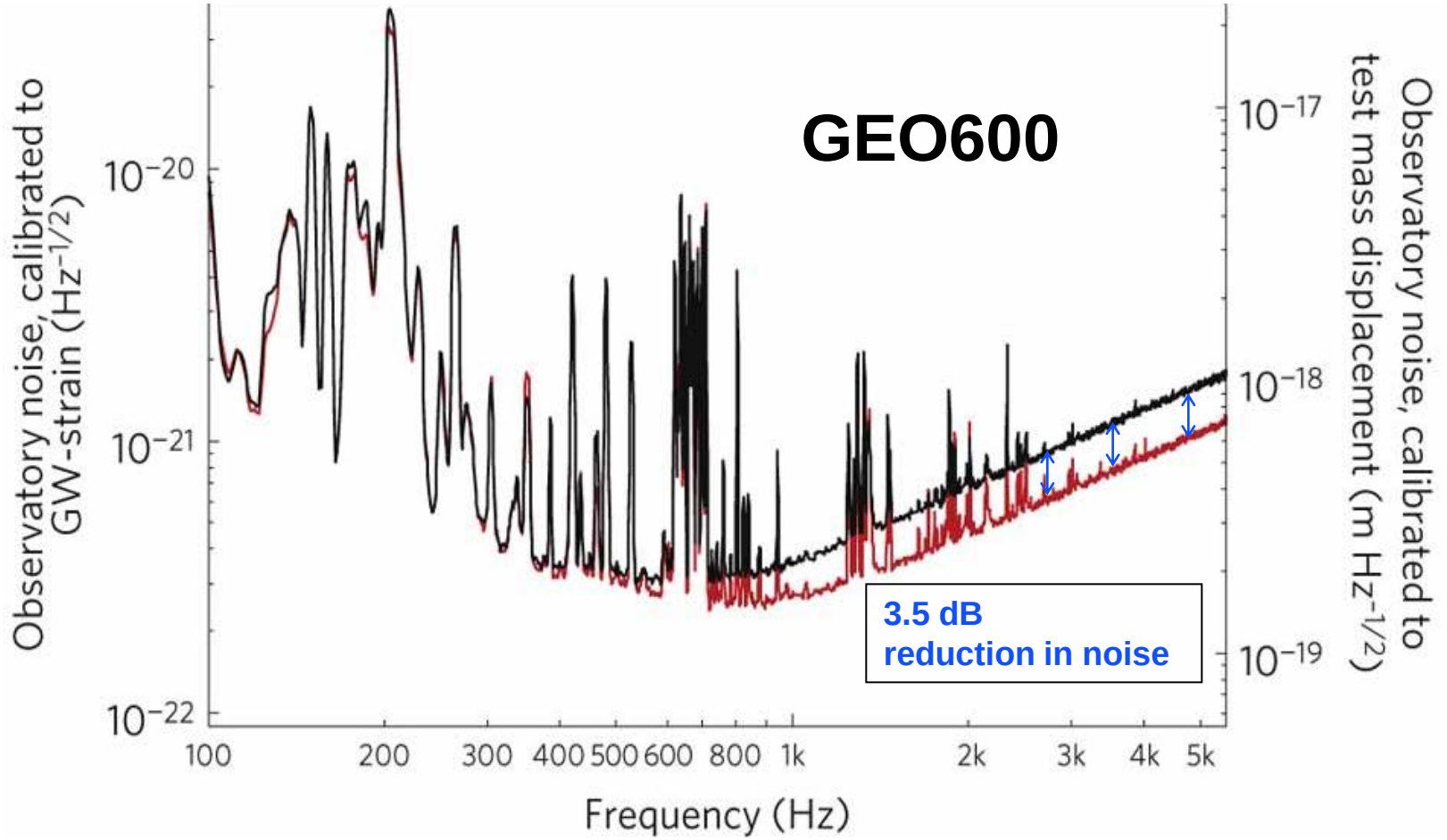

LIGO Scientific Collaboration, "*A gravitational wave observatory operating beyond the quantum shot-noise* limit", Nature Physics **7**, 962–965 (2011)

Using Squeezed Light to Improve LIGO Sensitivity

LSC, "Enhancing the astrophysical reach of the LIGO gravitational wave detector by using squeezed states of light", in preparation

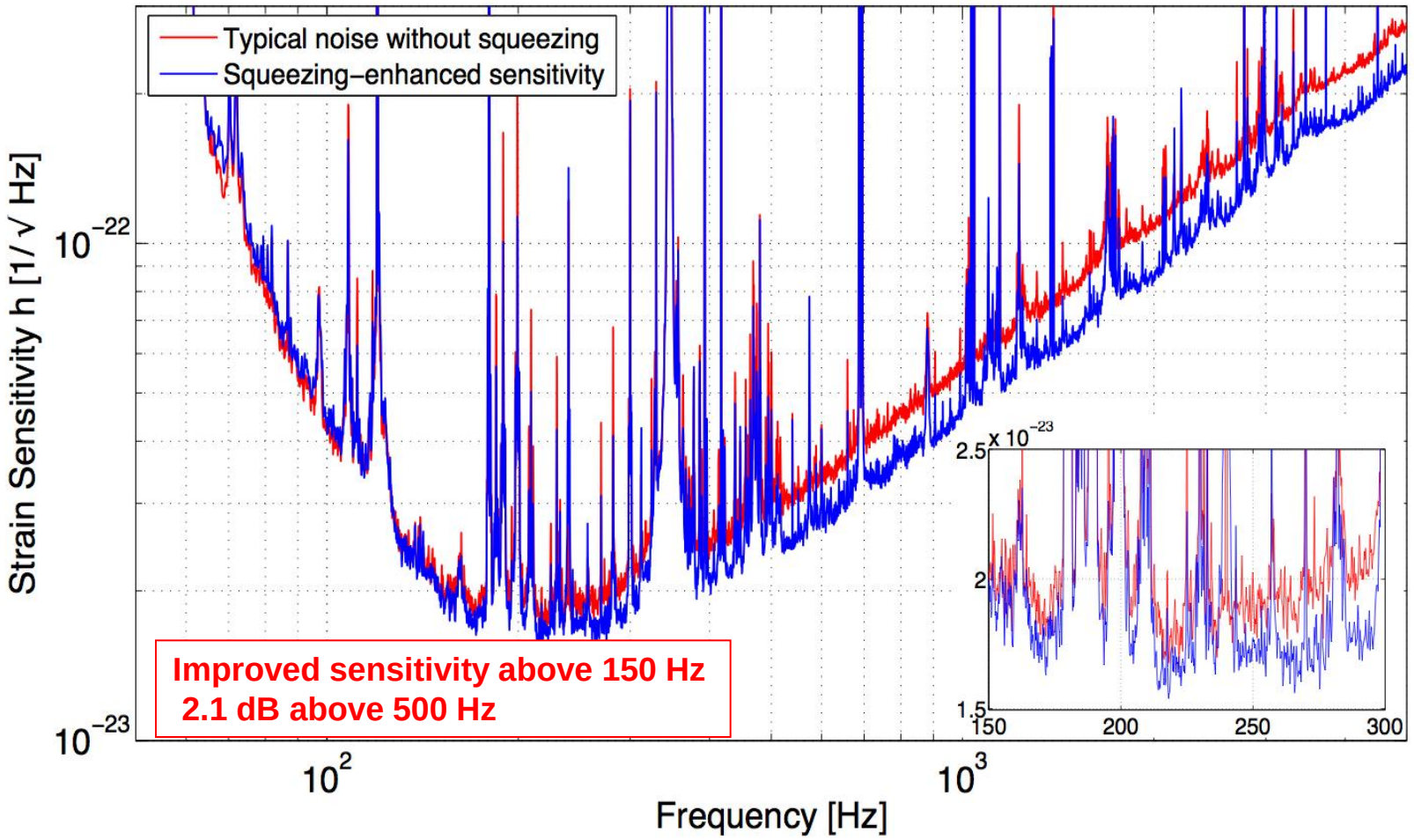

LIGO-India

- The idea in a nutshell–
- A direct partnership between LIGO Laboratory and India to build a LIGO interferometer on Indian soil
- Follows from earlier attempt to locate a LIGO detector in Australia



LIGO-India

- LIGO Lab (with its UK, German and Australian partners) provides components for one Advanced LIGO interferometer (H2) from the Advanced LIGO project
- India provides the infrastructure (site, roads, building, vacuum system), "shipping & handling," staff for installation & commissioning, operating costs

- Indian Institutional Participants:
  - Inter-University Centre for Astronomy and Astrophysics (Astrophysics, Site Selection, Computing)
  - Raja Ramanna Centre for Advanced Technology (Detector Development)
  - Institute for Plasma Research (Facility and Vacuum construction, control systems)
  - + IndIGO Consortium (broader scientific community in India)

- Indian funding – LIGO-India is a Mega-science Project
  - Total request of ~ $230M to fund construction and operations
  - Funding status: approved by DAE/DST, referred to Cabinet of the Prime Minister of India for approval
- US funding – funding for aLIGO components through MREFC (no new costs)
  - Total contribution $140M (includes aLIGO components, designs, documentation)

Binary Neutron Star Merger Localization: Hanford-Livingston-Virgo

3 site network
x denotes blind spots

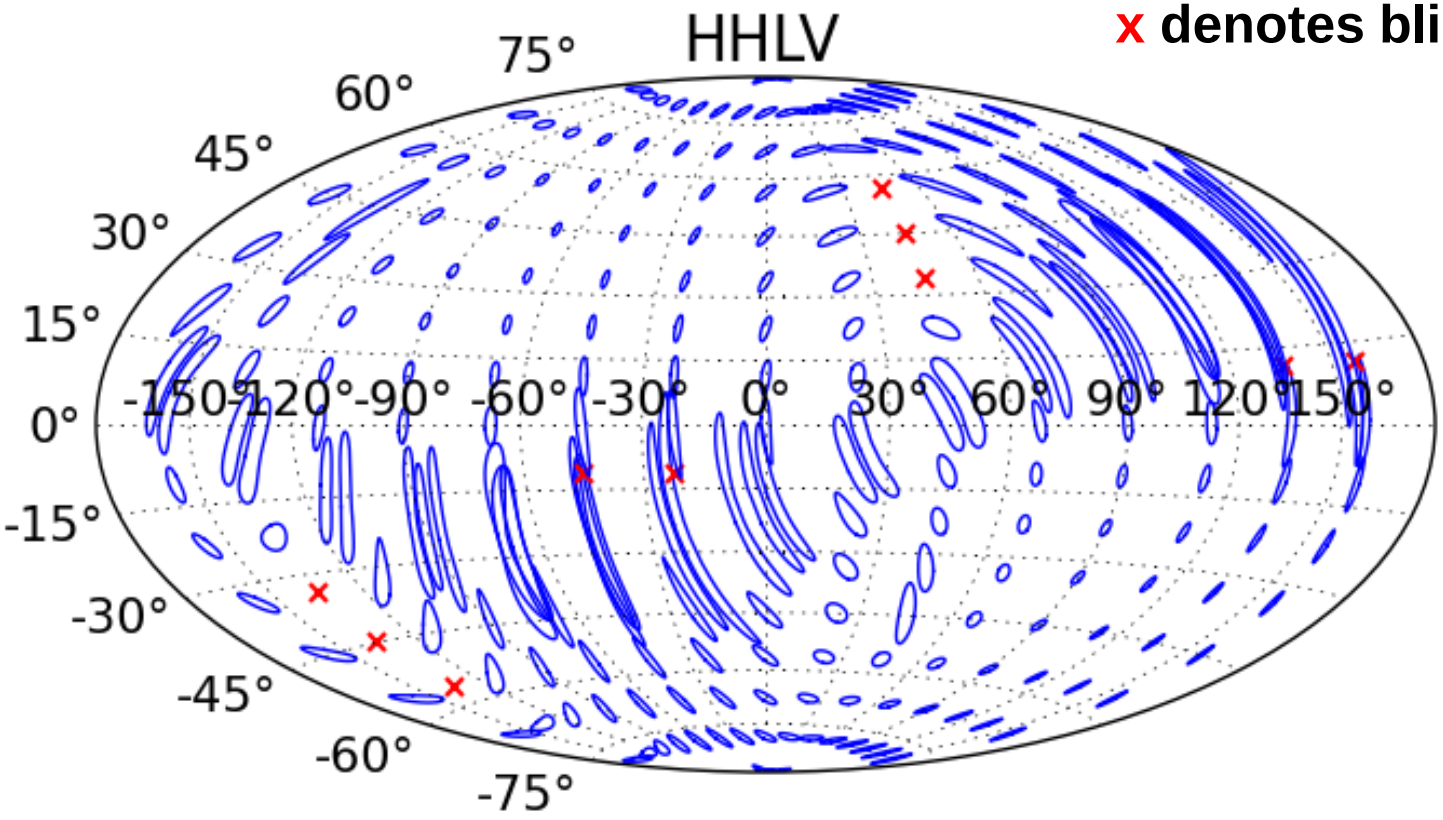

S. Fairhurst, "*Improved source localization with LIGO India*", arXiv:1205.6611v1

Binary Neutron Star Merger Localization: Hanford-Livingston-Virgo-India

4 site network

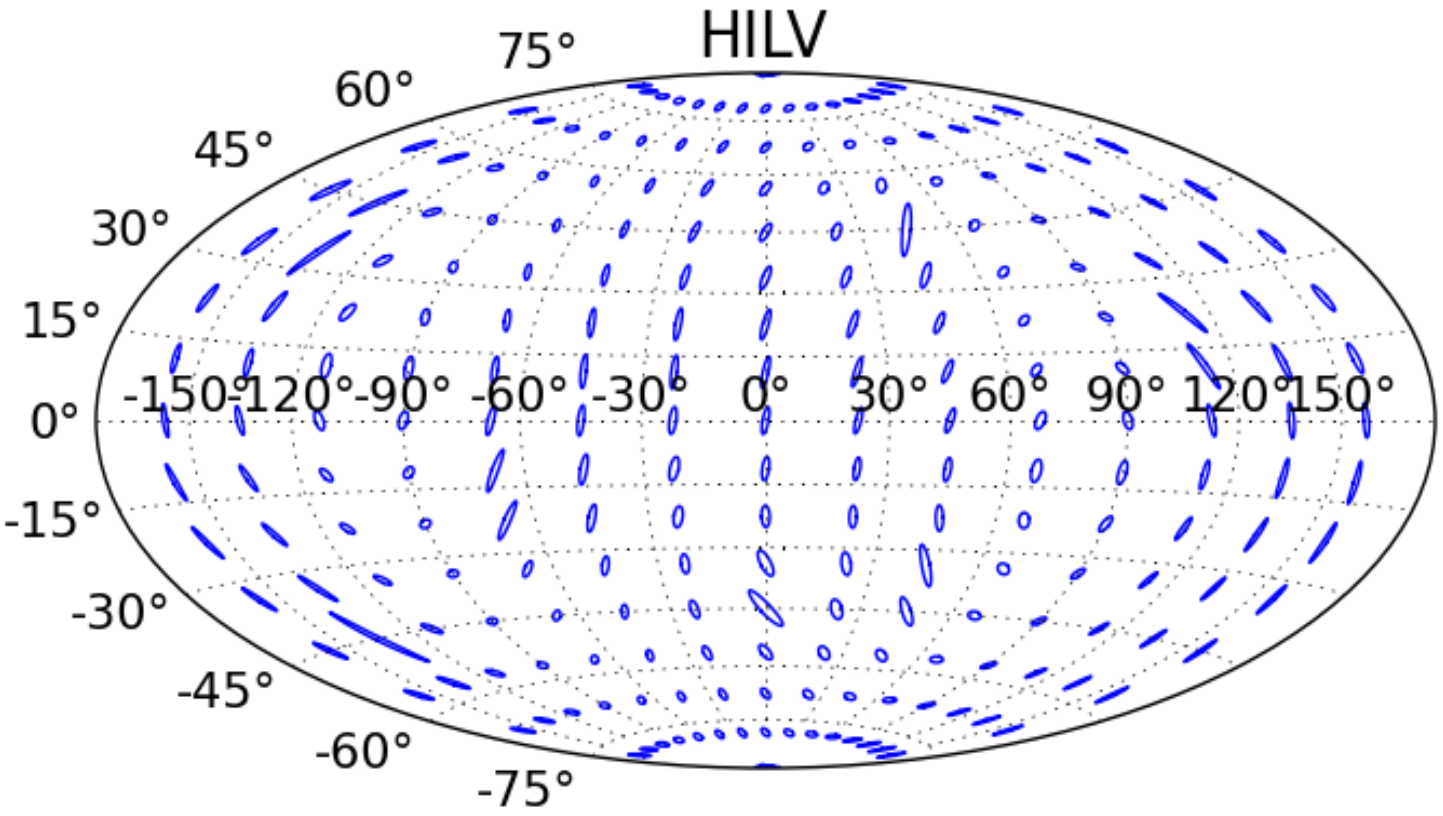

S. Fairhurst, "*Improved source localization with LIGO India*", arXiv:1205.6611v1

Binary Neutron Star Merger Localization: Hanford-Livingston-Virgo-KAGRA

4 site network

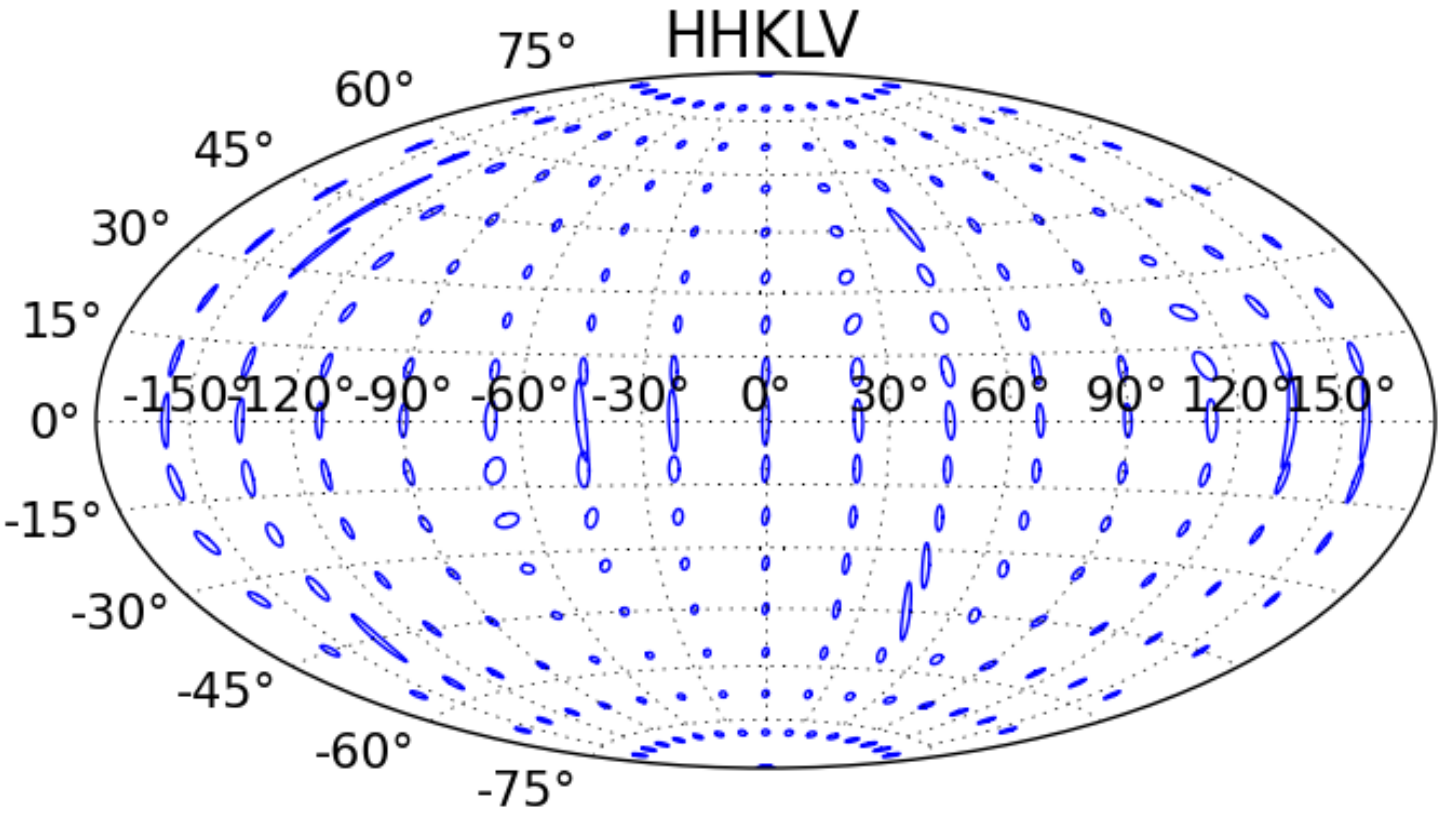

S. Fairhurst, "*Improved source localization with LIGO India*", arXiv:1205.6611v1

Binary Neutron Star Merger Localization: Hanford-Livingston-Virgo-India-KAGRA

5 site network

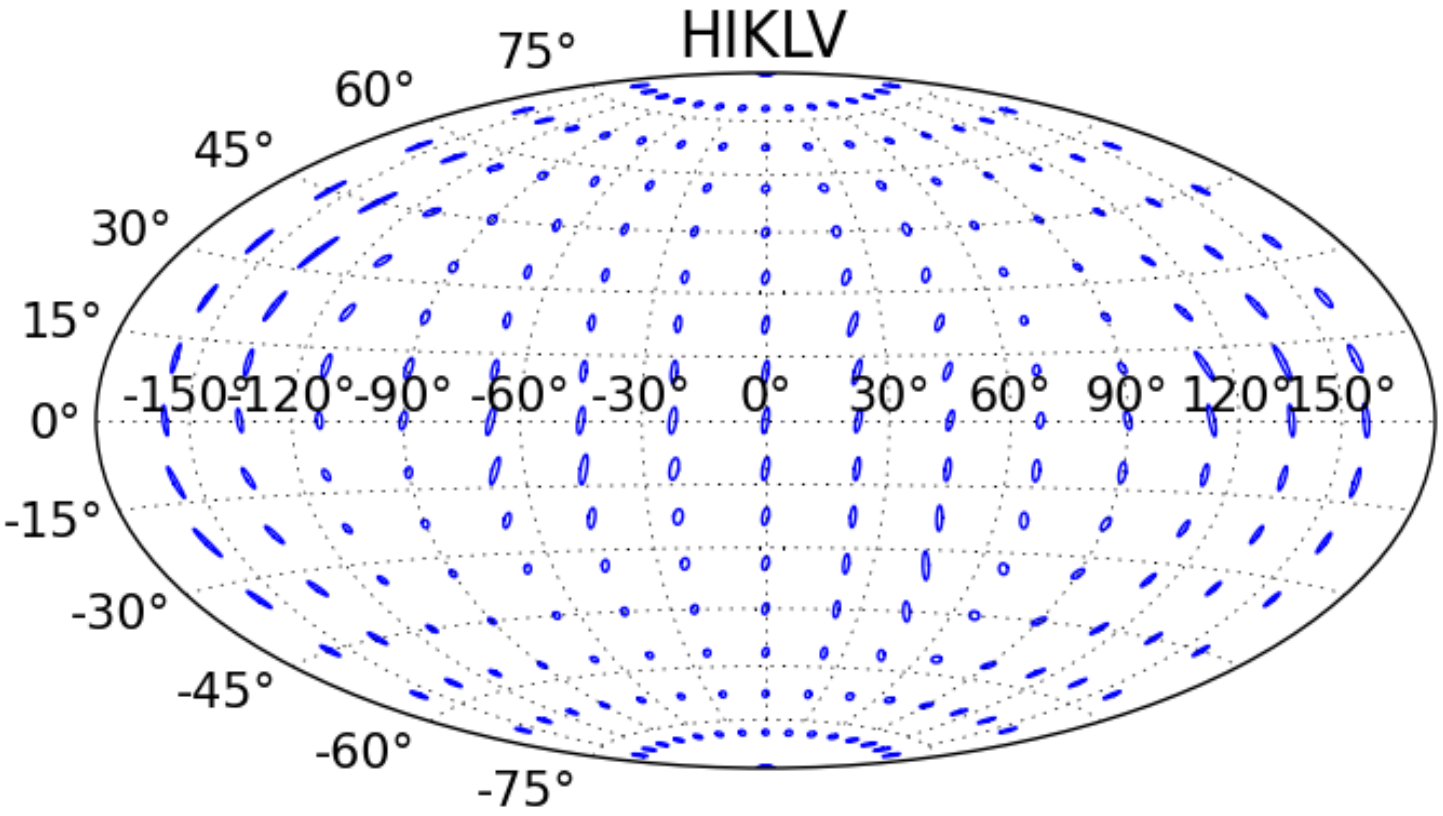

S. Fairhurst, "*Improved source localization with LIGO India*", arXiv:1205.6611v1

Sky Localization

For Binary Neutron Star Coalesence

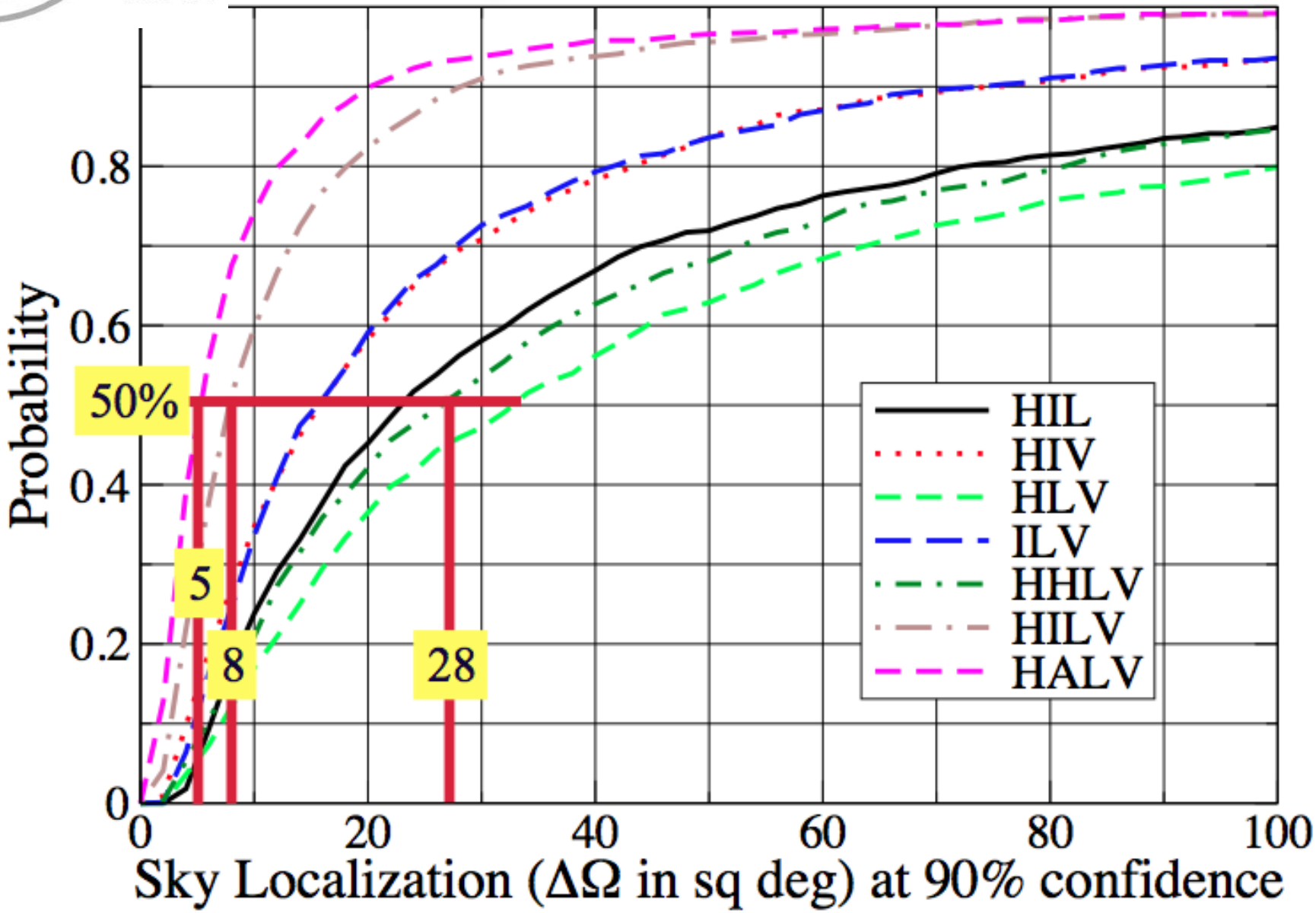

LIGO

LIGO-India Status

- Status in the US: -- the National Science Board has given permission to NSF, at its discretion, “to approve the proposed aLIGO Project in scope, enabling plans for the relocation of an advanced detector to India”
- Status in India – awaiting Cabinet approval and beginning of seed funding for facility design work
- Major activities in India are now focused on site evaluation/selection as well as development of a Tier 2 computing center @ IUCAA

- ***Expect LIGO-India to begin operations in 2020 or 2021***

Summary: The advanced GW detector network

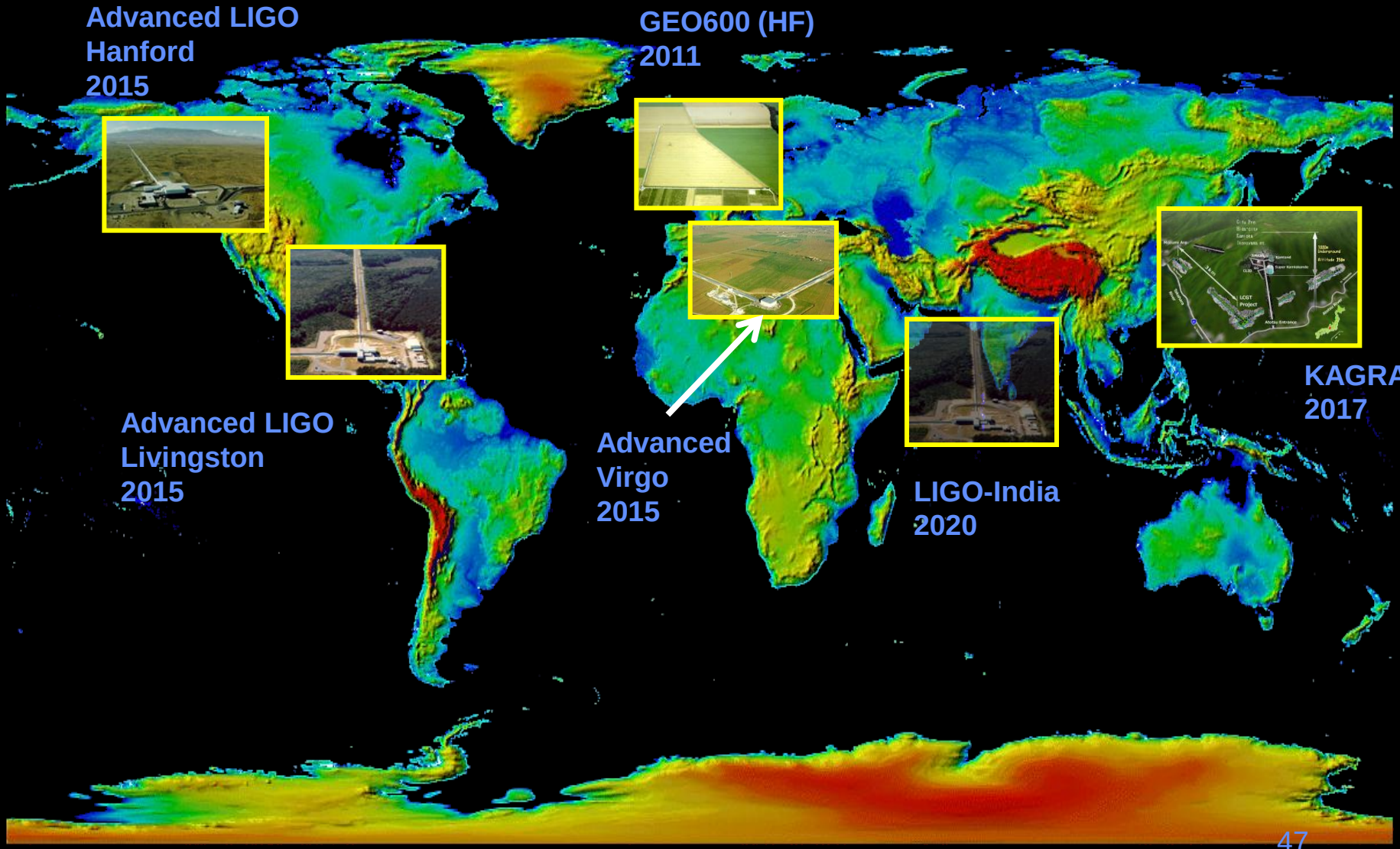

Summary: The advanced GW detector network

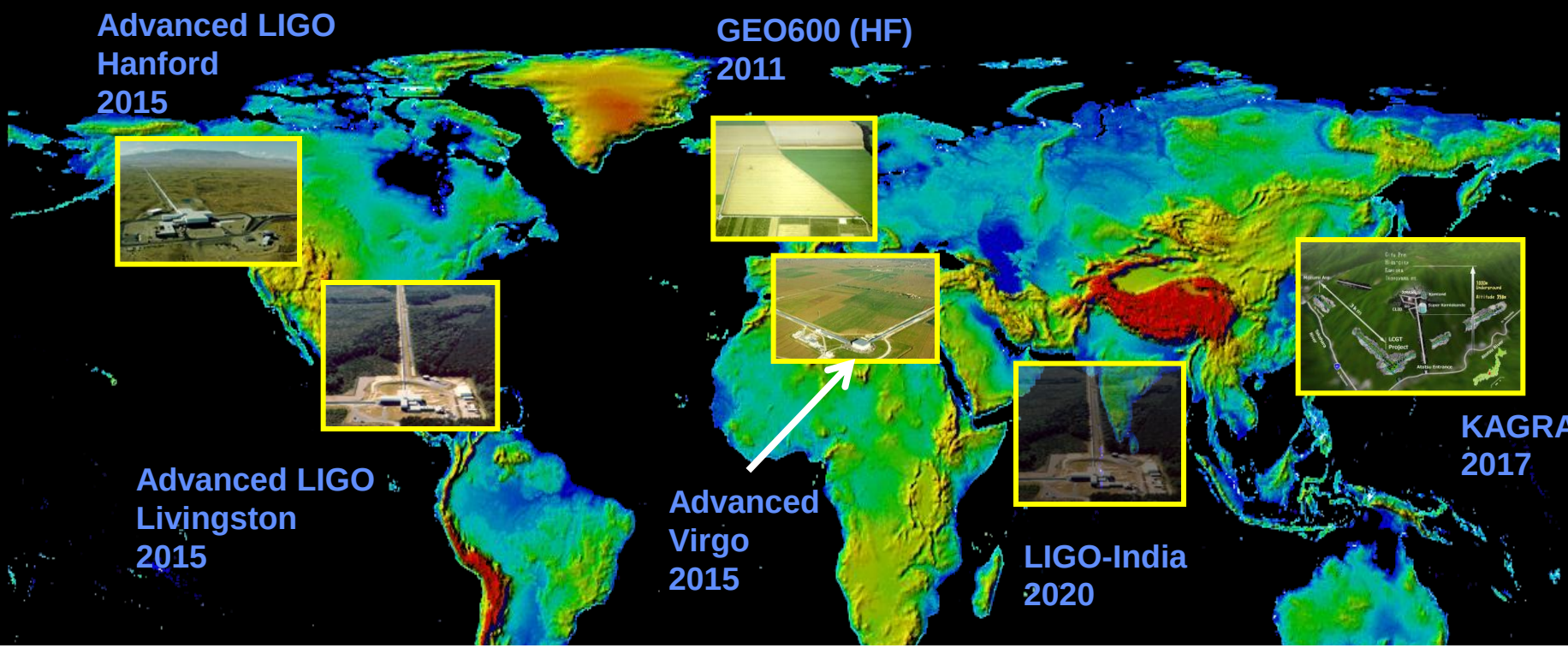

Memorandum of Understanding

between

KAGRA, LIGO and Virgo Scientific Collaborations

LIGO

Conclusion

These are exciting times for gravitational wave physicists and astronomers!

LIGO

Reducing the interferometer noises

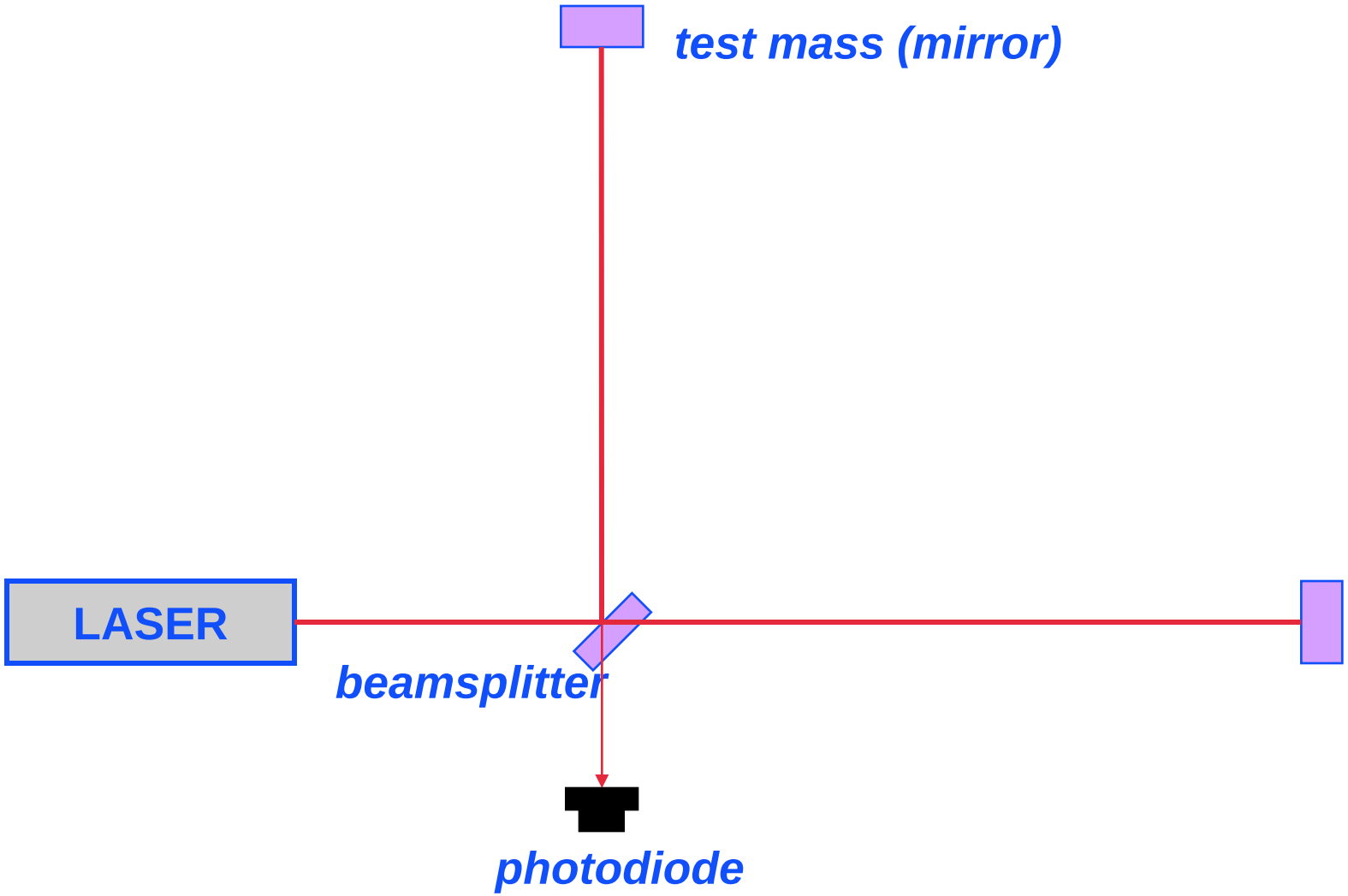

LIGO

Reducing the interferometer noises

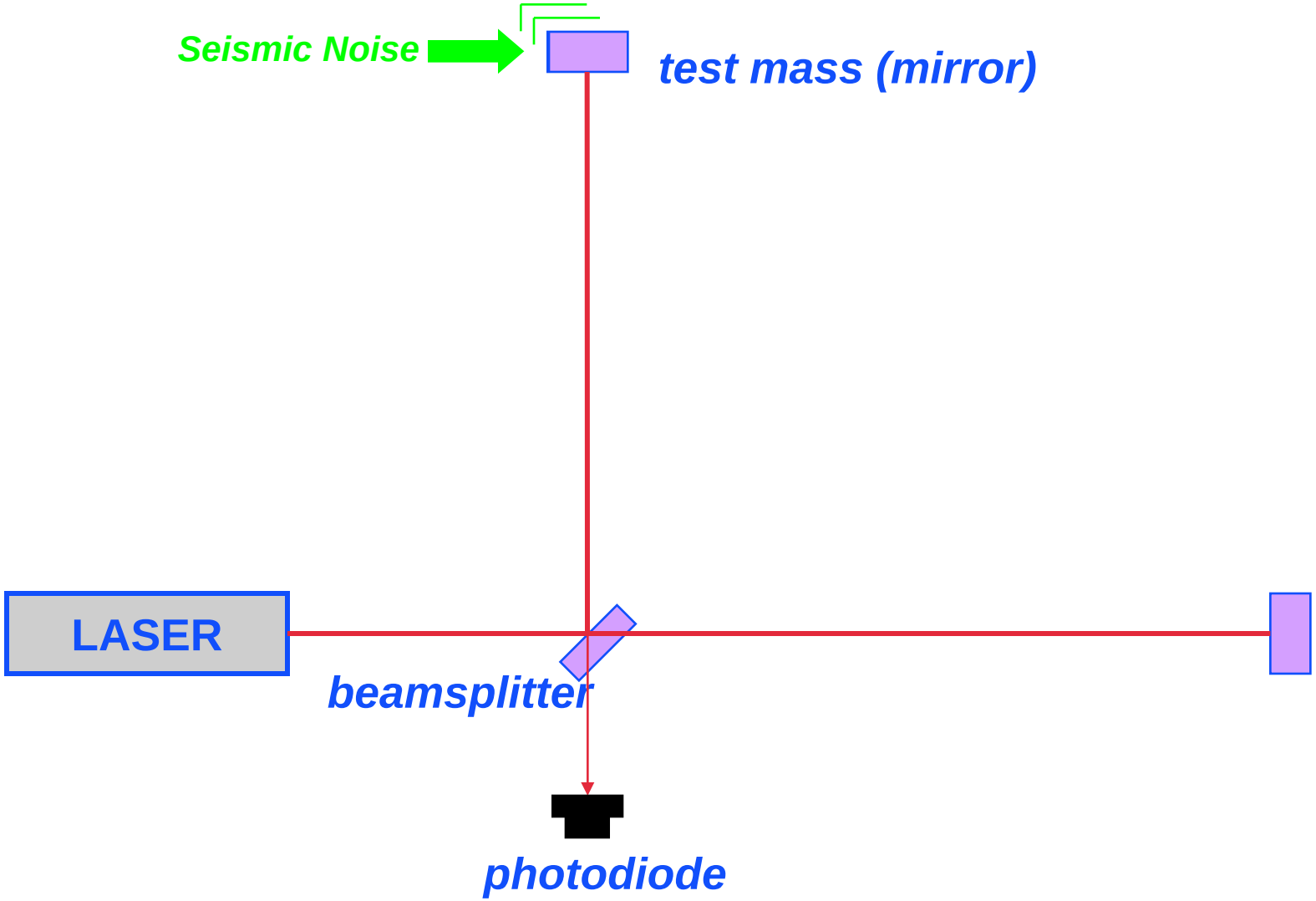

LIGO

Reducing the interferometer noises

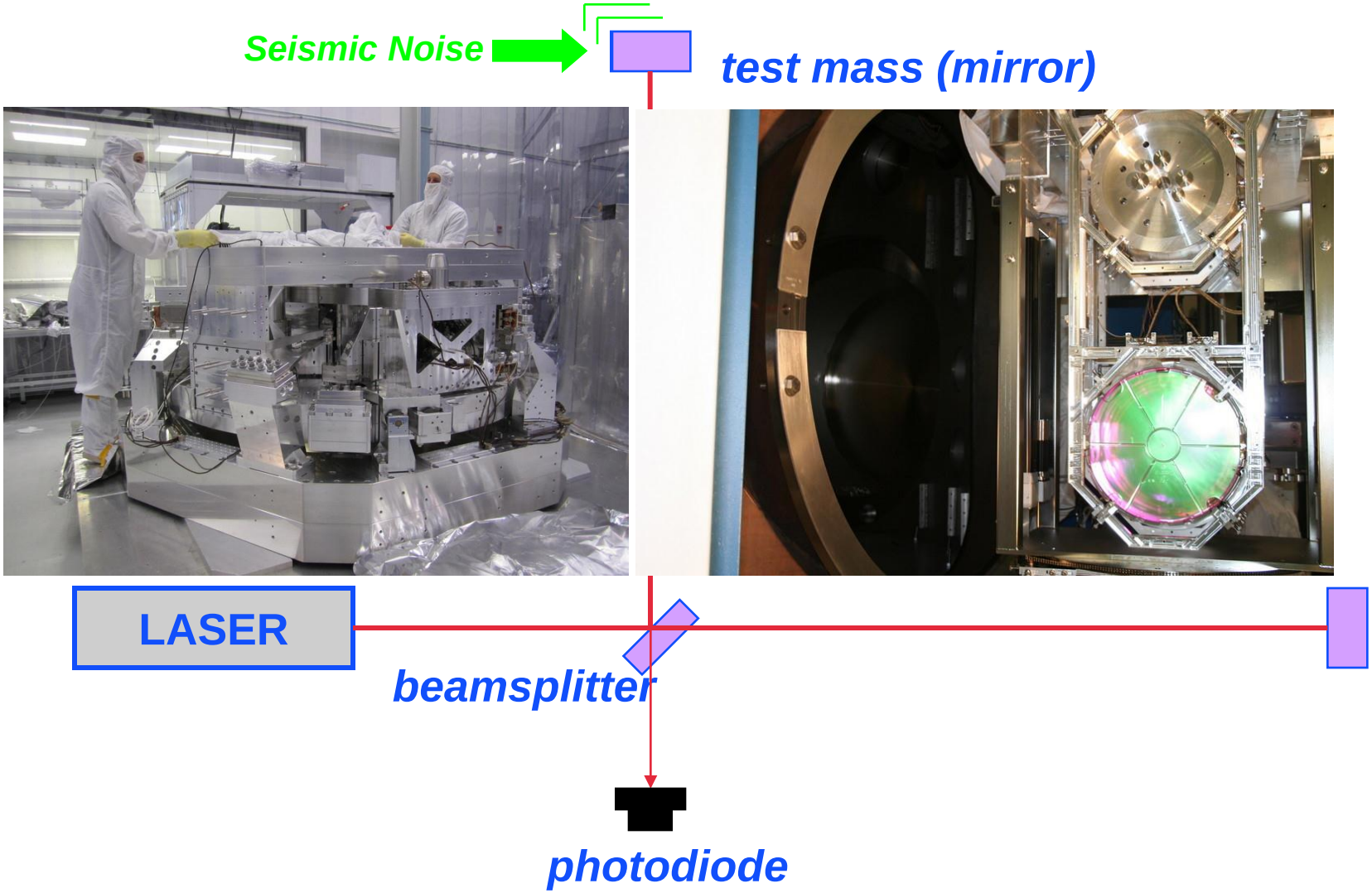

LIGO

Reducing the interferometer noises

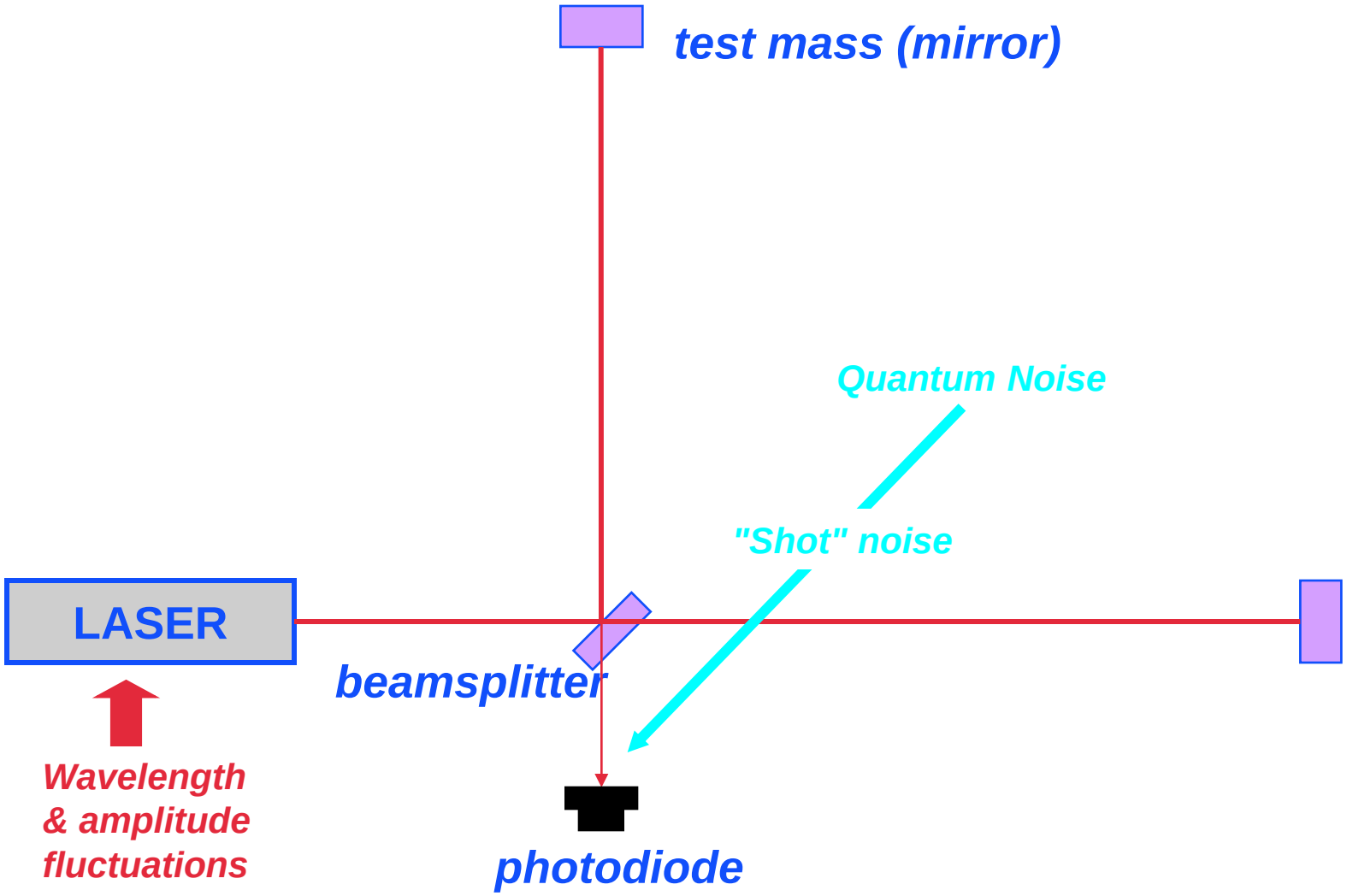

LIGO

Reducing the interferometer noises



est mass (mirror)

Quantum Noise

"Shot" noise

LASER

beamsplitter

Wavelength & amplitude fluctuations

photodiode

LIGO

Reducing the interferometer noises

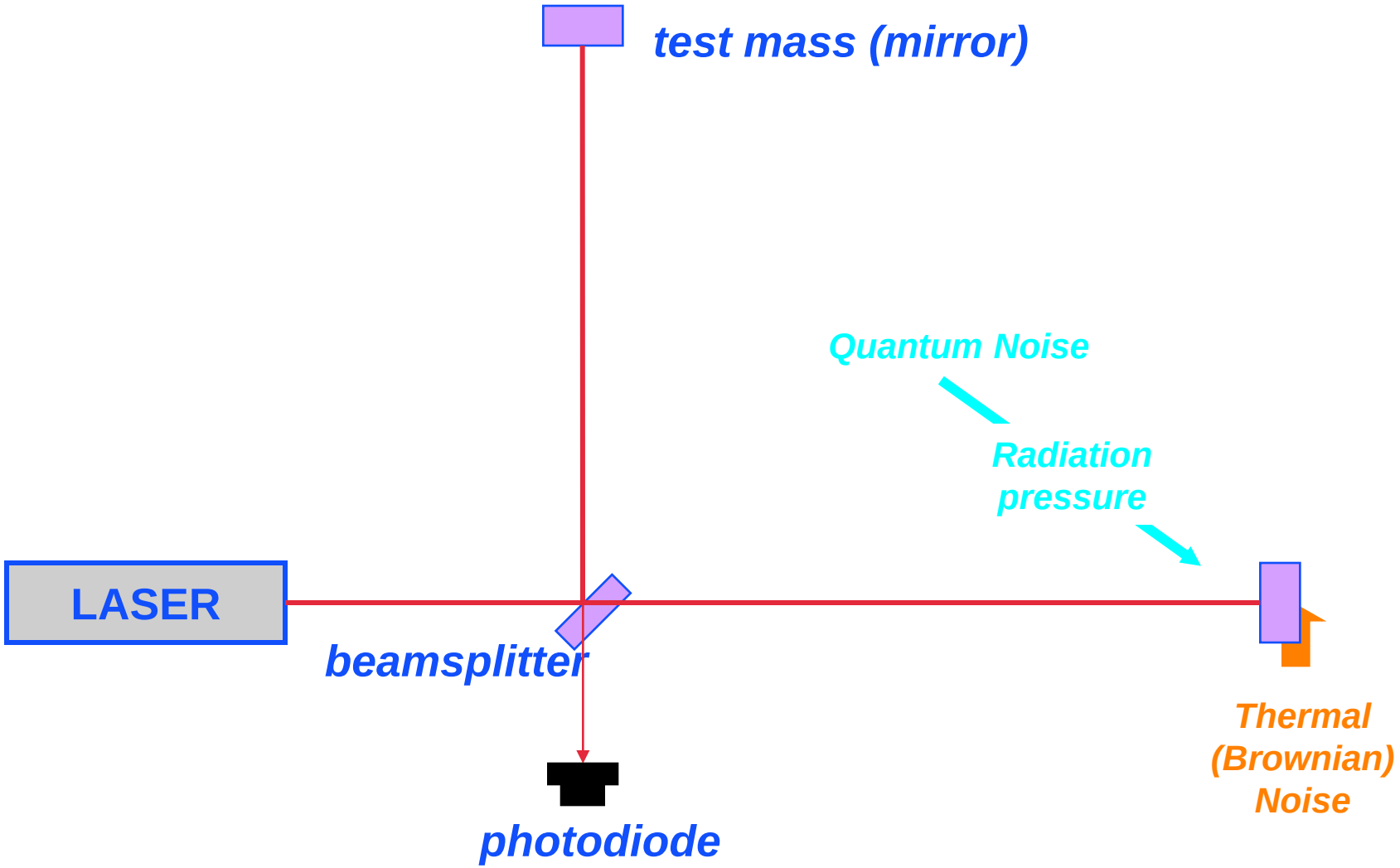

LIGO

Reducing the interferometer noises



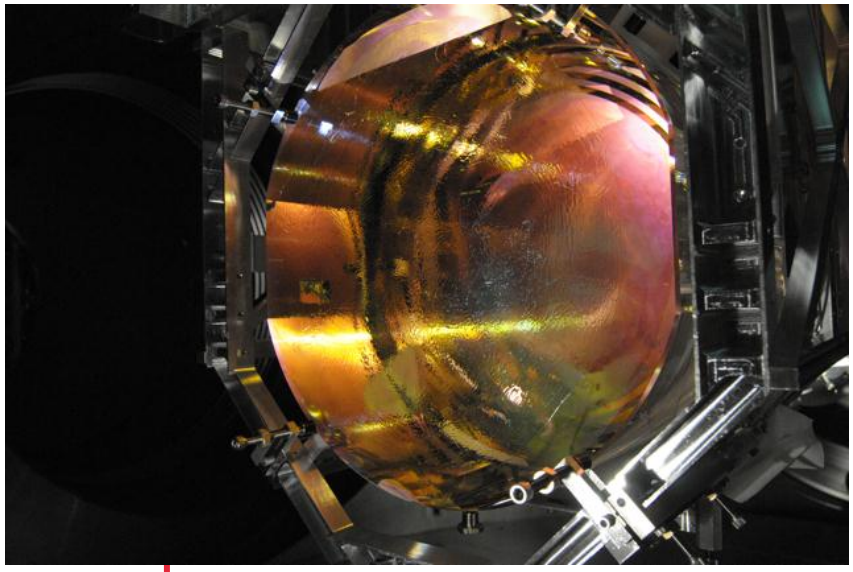

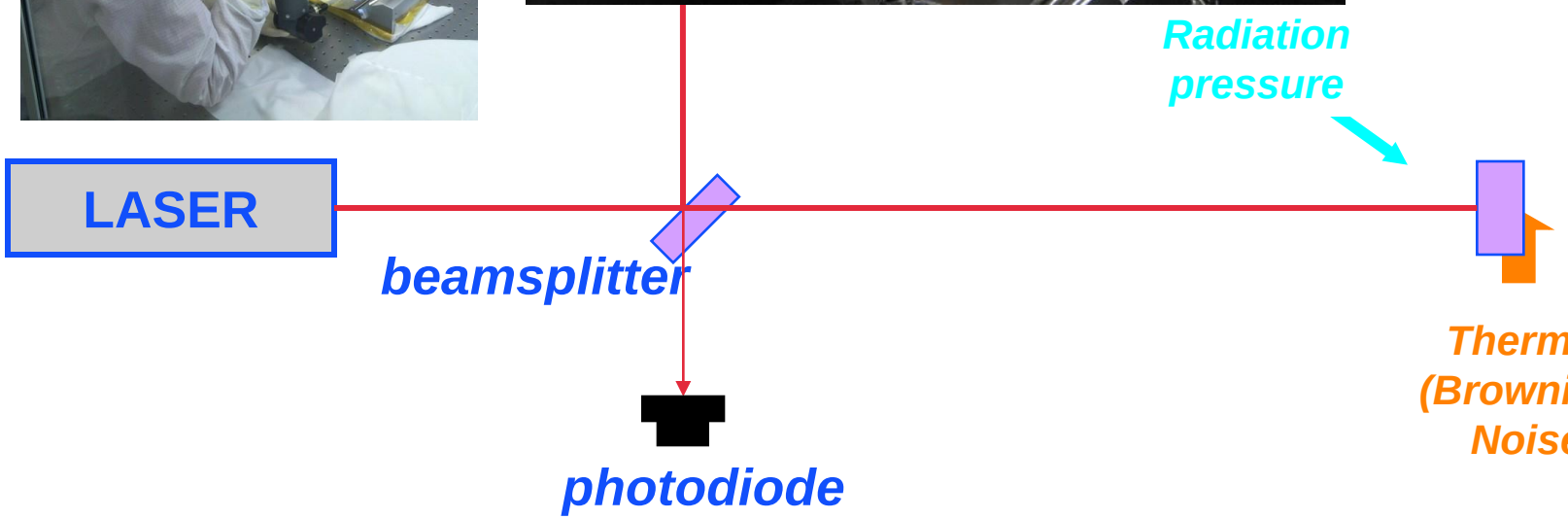

LIGO

Reducing the interferometer noises

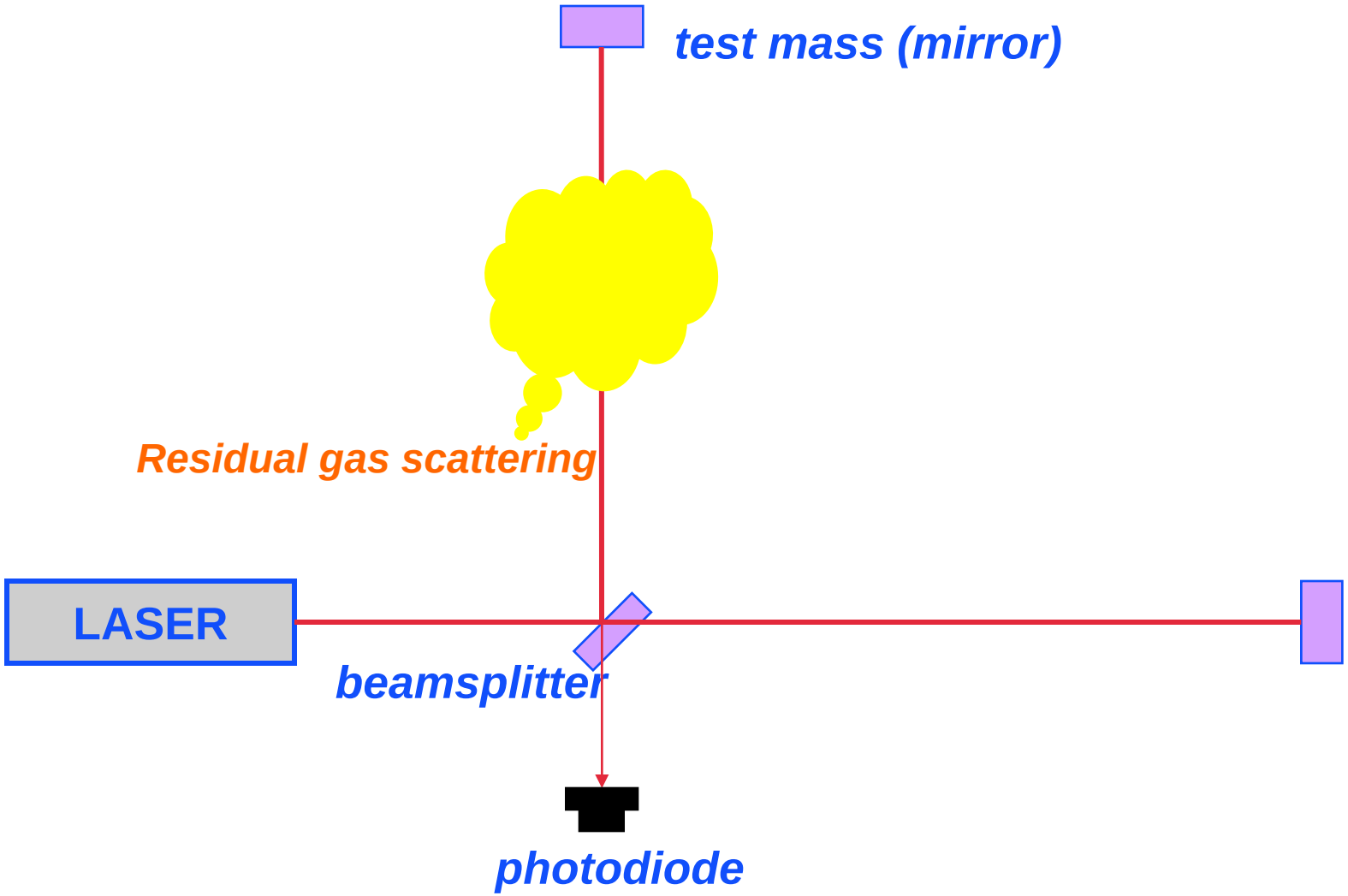

LIGO

Reducing the interferometer noises





LIGO

LIGO



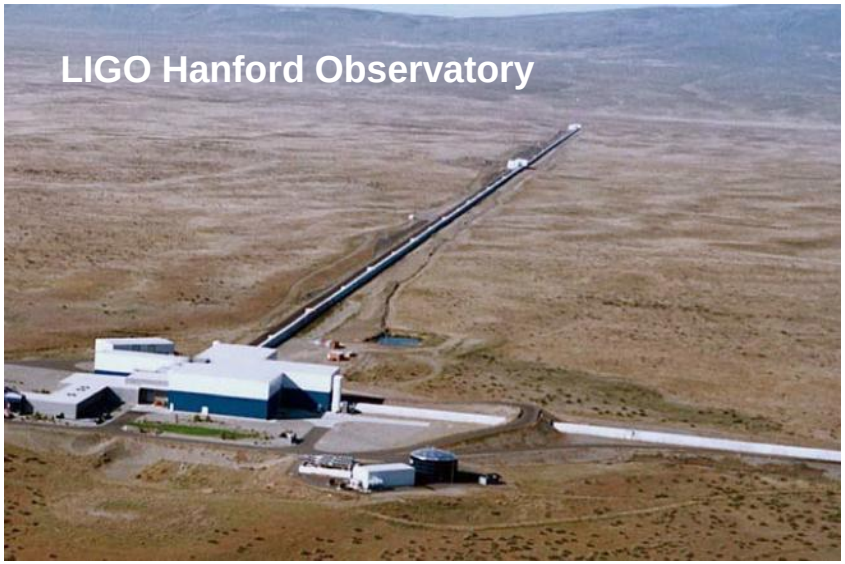

First Generation Interferometers



Initial LIGO
4 km long
Louisiana,
USA
2002-2010



Initial VIRGO
3 km long
Italy
2007 - 2011



Initial LIGO
4 km, 2 km long
Washington,
USA
2002-2010



Initial GEO600
600 m long
Germany
2002 - 2010

Gravitational-wave interferometers

- Enhanced Michelson interferometers
  - » LIGO, Virgo, and GEO600 use variations
- Passing GWs modulate the distance between the end test mass and the beam splitter
- The interferometer acts as a transducer, turning GWs into photocurrent
  - » A coherent detector

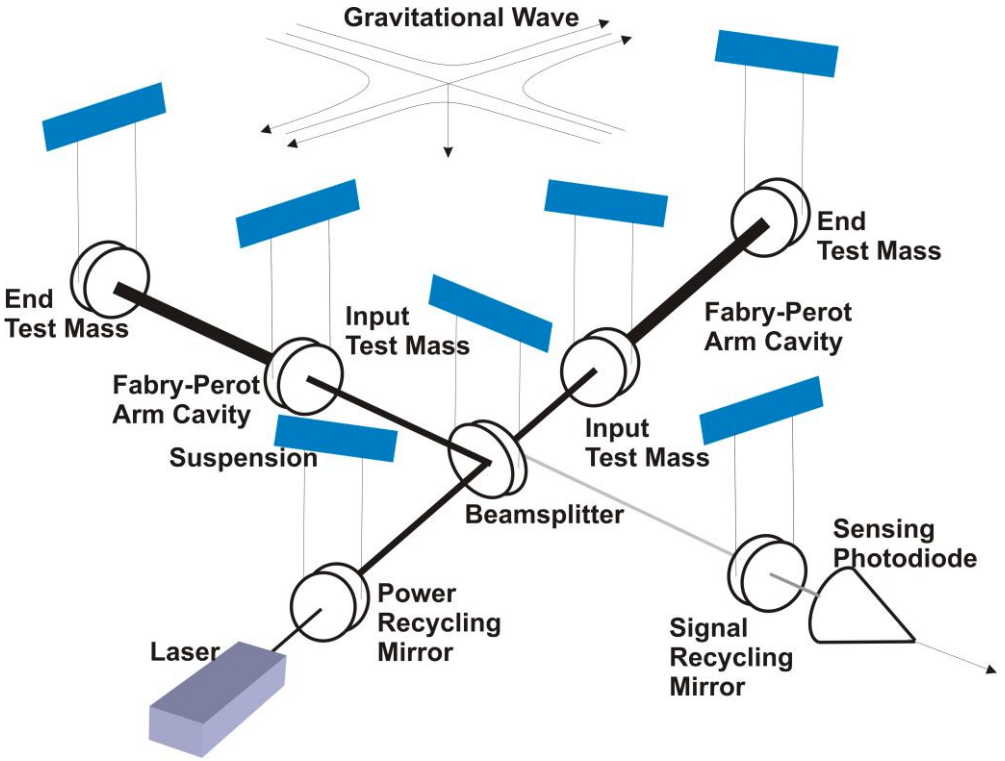

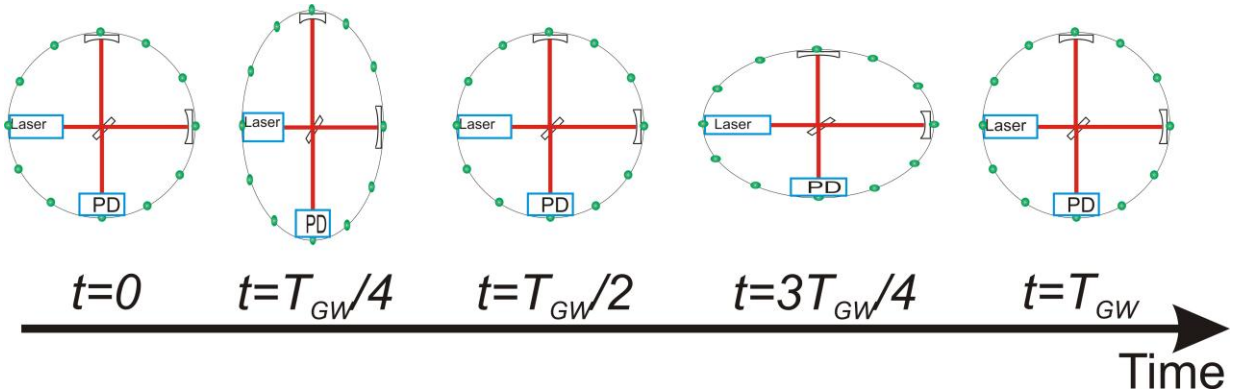

Searches for GWs from known pulsars

- Continuous gravitational-wave emission due to asymmetry rotation axis
  - » elastic deformations of the solid crust or core
  - » Distortion an extremely strong misaligned magnetic field
  - » Weak emitters
- Spin-down limit: $h_{sd} = \left(\frac{5}{2}\frac{GI_{zz}|\dot{\nu}|}{c^3 r^2 \nu}\right)^{1/2}$
- Crab pulsar (using LIGO data):
  - » $h_0 < h_{sd}/7$, $E_{GW} < 0.02E_{total}$
- Vela pulsar (using Virgo data):
  - » $h_0 < 0.66h_{sd}$, $E_{GW} < 0.45E_{total}$
- S5 search of 116 pulsars
  - Lowest upper-limit h_0: 2.3 x 10^{-26} (PSR J1603-7202)
  - Lowest upper-limit ellipticity: 7 x 10^{-8} (PSR J212[illegible] 3358)

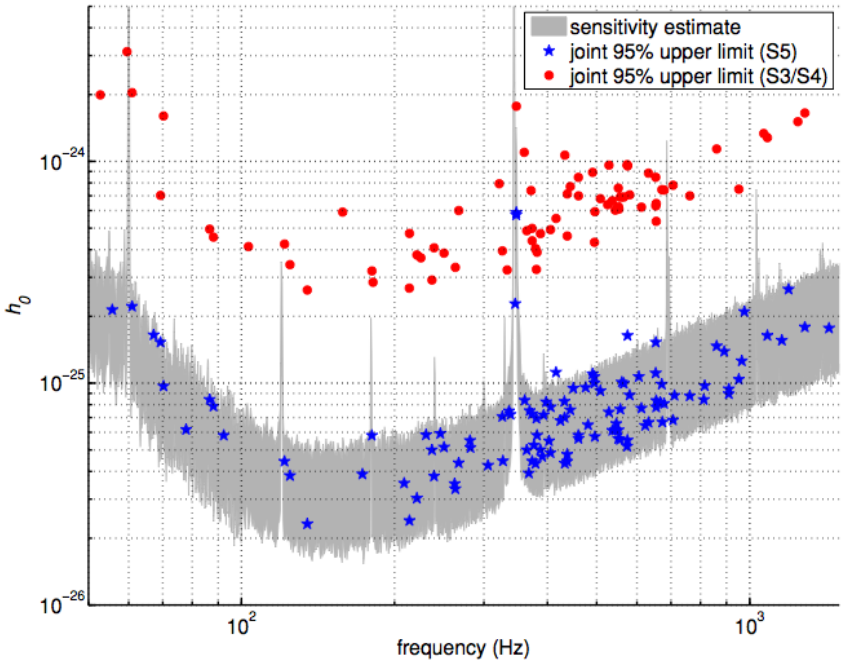

LIGO Scientific and Virgo Collaborations, "*Beating the spin-down limit on gravitational wave emission from the Crab pulsar",* Astrophys. J. Lett. **683** (2008) 45

LIGO Scientific and Virgo Collaborations, "*First search for gravitational waves from the youngest known neutron star",* Astrophys. J. **722** (2010) 1504

LIGO Scientific and Virgo Collaborations, "*Beating the spin-down limit on gravitational wave emission from the Vela pulsar,"* Astrophys. J. **737** (2011) 93

LIGO Scientific and Virgo Collaborations, "*Searches For Gravitational Waves From Known Pulsars With Science Run 5 LIGO Data*", Astrophys. J. **713** (2010) 671

Searches for stochastic gravitational waves

- Stochastic sources - primordial GWs or ensemble of incoherent point-like or extended emitters
- LIGO/Virgo S5 isotropic stochastic GW upper limit: $\Omega_0 < 6.9 \times 10^{-6}$
  - » Beats inferred upper limit from BBN: $\Omega_0^{BBN} < 1.1 \times 10^{-5}$
- LIGO/Virgo S5 directional search for point-like/extended emitters
  - » New: spherical harmonic decomposition for arbitrary angular distributions

LIGO Scientific and Virgo Collaborations, "*An upper limit on the stochastic gravitational-wave background of cosmological origin*", Nature, **460**: 990 (2009).

LIGO Scientific and Virgo Collaborations, "*Directional Limits on Persistent Gravitational Waves Using LIGO S5 Science Data*", Phys. Rev. Lett. **107** (2011) 271102

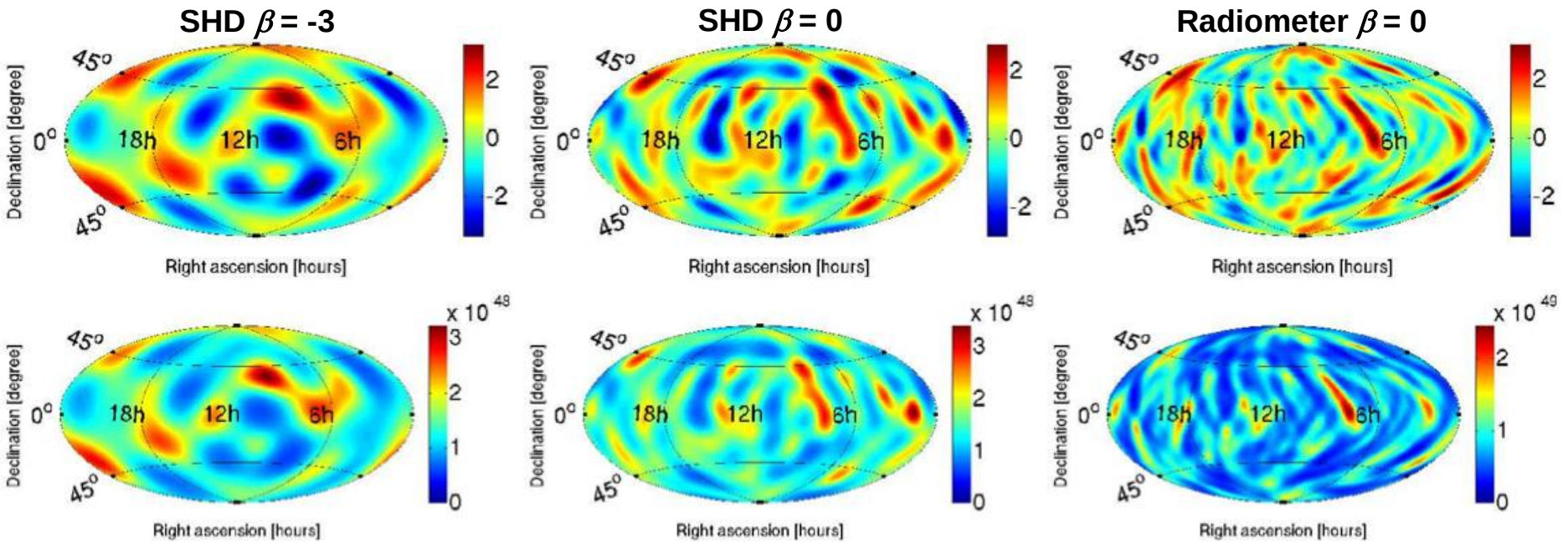

Joint GW-high energy neutrino searches with ANTARES

- Several plausible astrophysical joint GW-HEν emission sources
  - » Conventional: soft gamma repeaters, GRBs, choked GRBs
  - » More exotic: cosmic strings
- Both GWs and HEνs are very weakly interacting → information preserving, traveling unimpeded for cosmological distances
- Co-analysis with ANTARES Neutrino Telescope
  - » undersea, 40 km off southern coast of France
  - » 3D array of PMTs → ν position reconstruction
- 154 HEν triggers followed up with X-pipeline
  - » No candidates → exclusion distance

HEν candidates

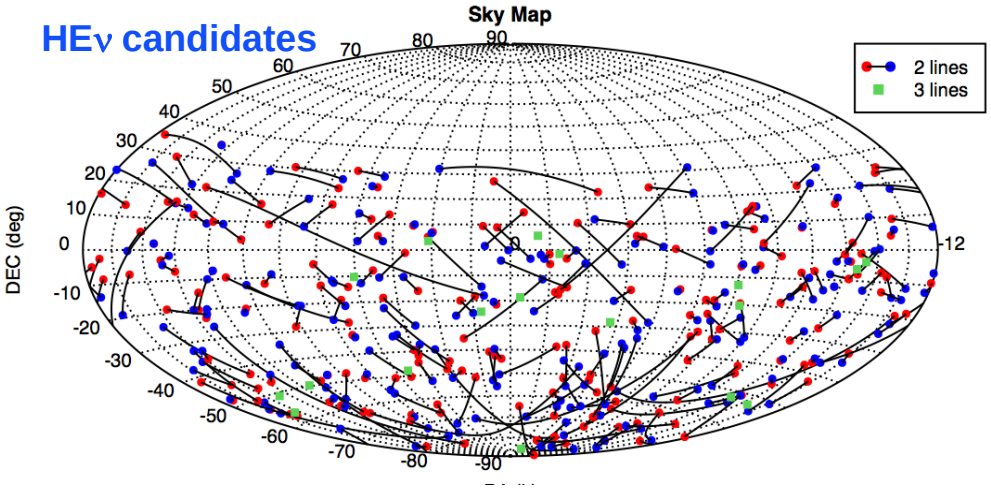

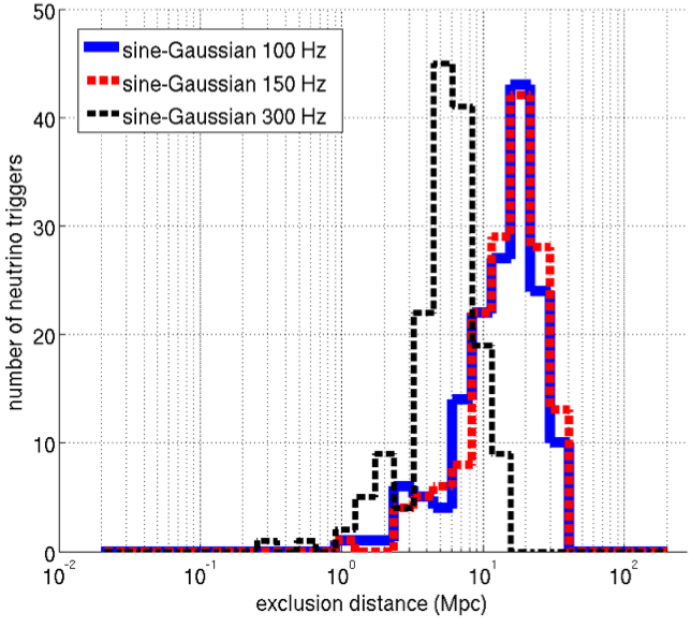

ANTARES, LIGO, AND Virgo Collaborations, "A first search for coincident gravitational waves and high energy neutrinos using LIGO, Virgo and ANTARES data from 2007", arXiv:1205.3018

The Current GW Detector Network

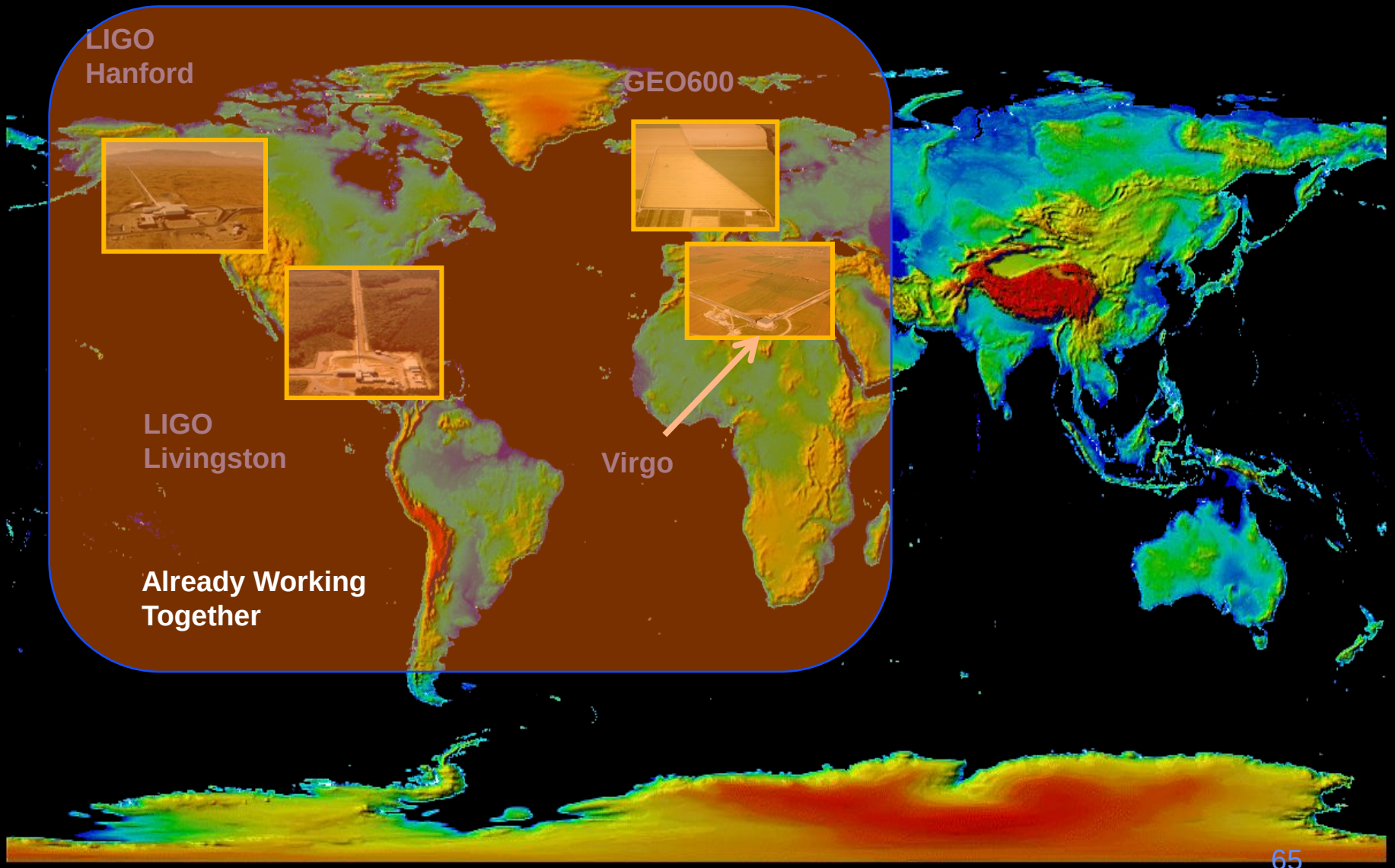

The Advanced GW Detector Network

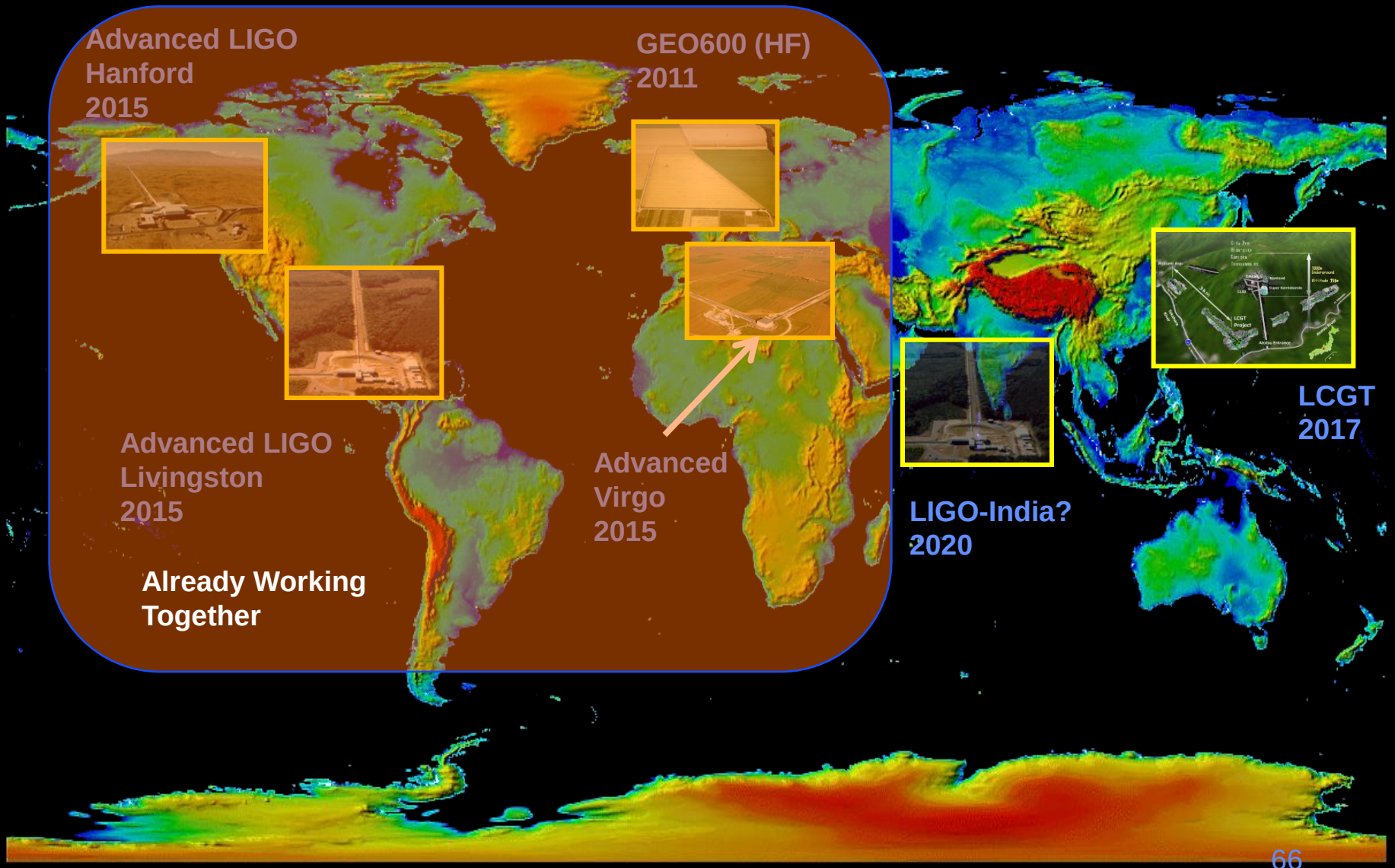

LIGO

LIGO Scientific Collaboration, "*LIGO: The Laser Interferometer Gravitational-Wave Observatory*", Rep. Prog. Phys. **72** (2009) 076901
H. Grote (for the LSC), "*The Upgrade of GEO600*", Class. Quantum Grav. **27**, 084003 (2010)
T. Accadia, et al., "*Virgo: a laser interferometer to detect gravitational waves*", J. Instrumentation **7**, P03012 (2012)

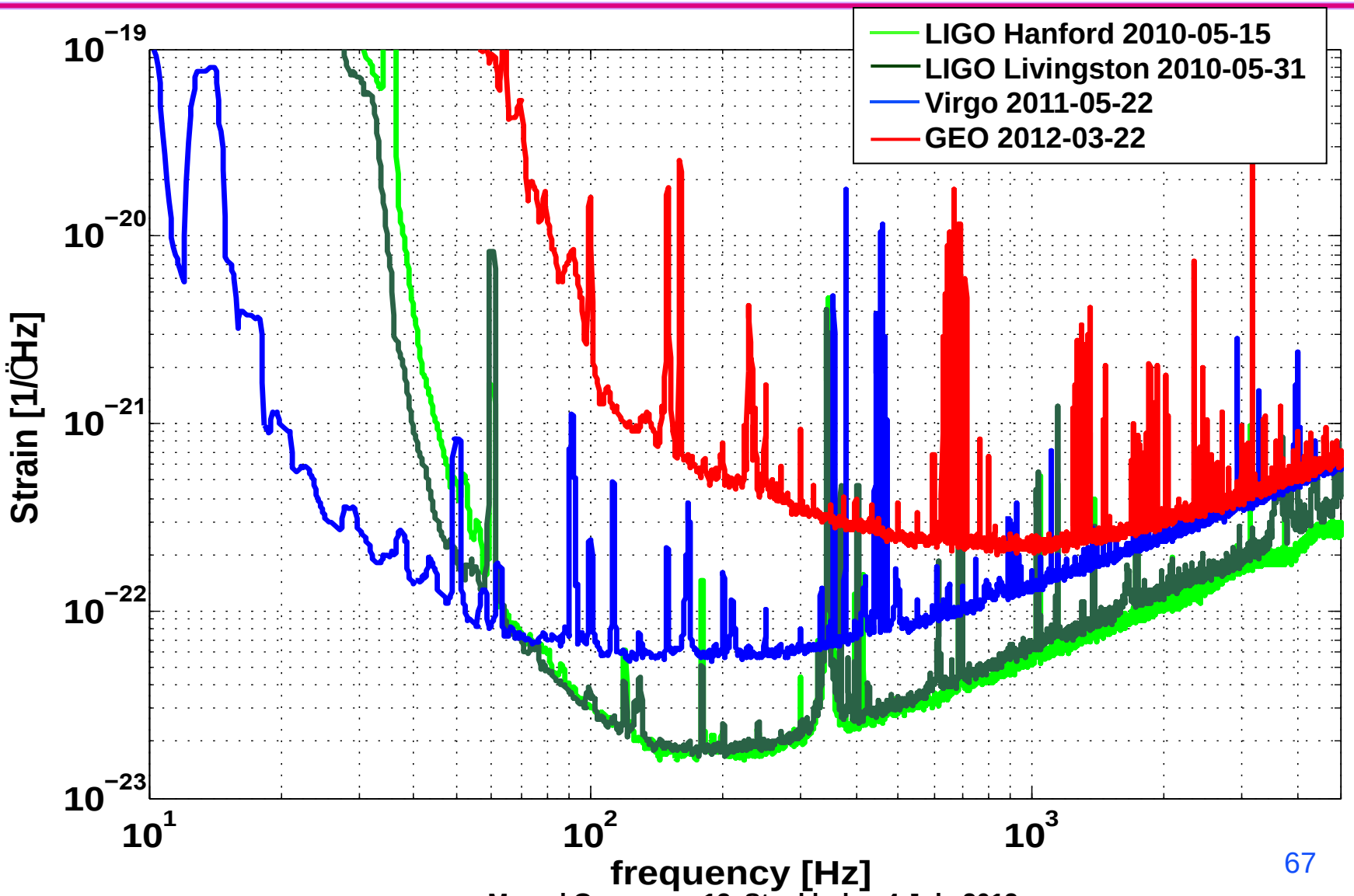

LIGO

LIGO Scientific Collaboration, "*LIGO: The Laser Interferometer Gravitational-Wave Observatory*", Rep. Prog. Phys. **72** (2009) 076901
H. Grote (for the LSC), "*The Upgrade of GEO600*", Class. Quantum Grav. **27**, 084003 (2010)
T. Accadia, et al., "*Virgo: a laser interferometer to detect gravitational waves*", J. Instrumentation **7**, P03012 (2012)

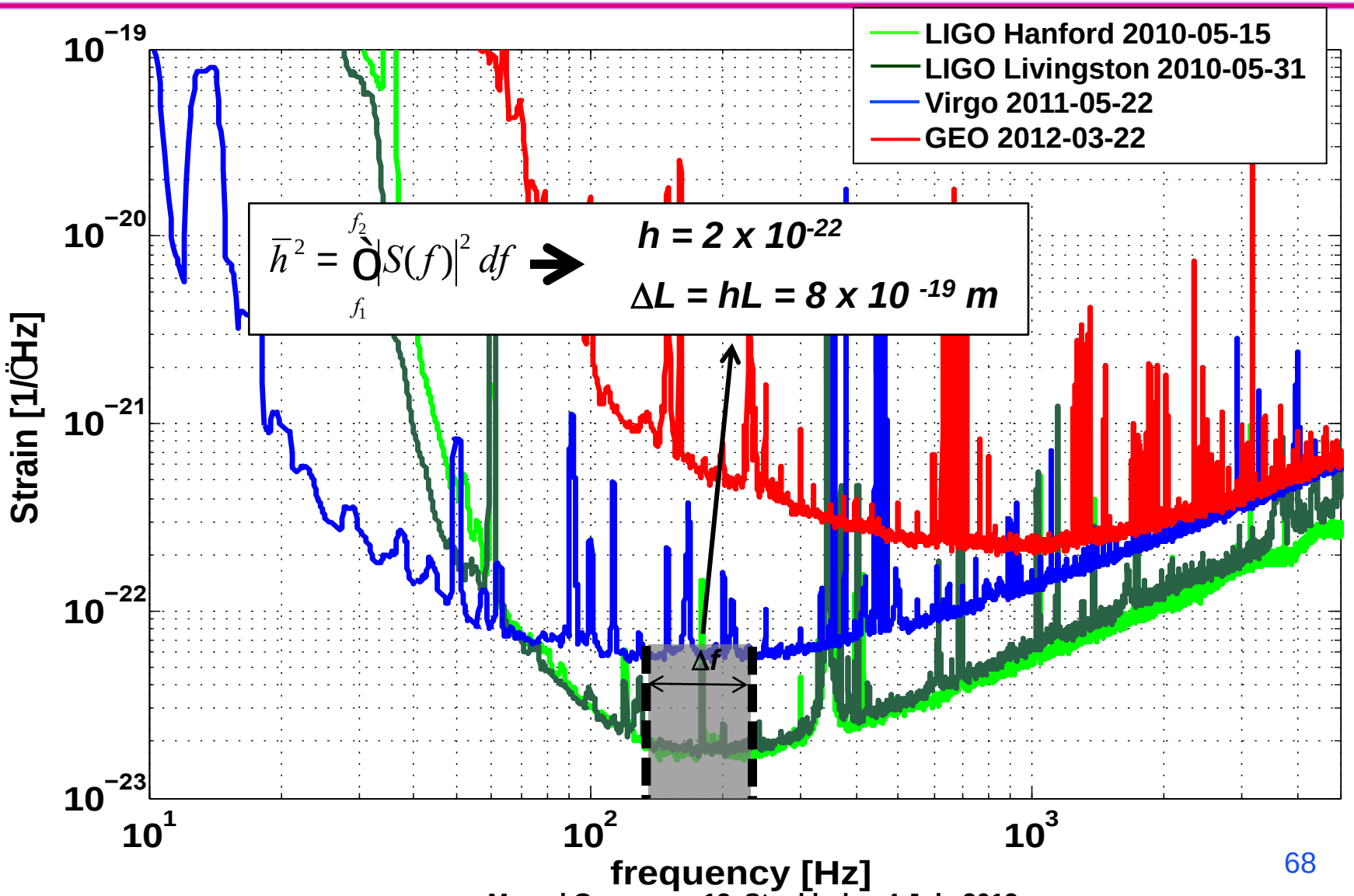

Triggered searches for gamma-ray bursts

- Data from LIGO S6 and Virgo VSR 2,3
- Modeled search for NS-NS, NS-BH coalescences
  - » TaylorF2 3.5 PN order templates, [2, 40) $M_\odot$ total mass range
- Unmodeled search for GW bursts
  - » Coherent network analysis ('X-pipeline'); time-frequency clustering
- 404 GRBs from Swift, Fermi, MAXI, SuperAGILE, INTEGRAL
- Require 2 detectors in science mode → 154 GRB triggers analyzed
  - » 10% with redshift; well beyond LIGO/Virgo range

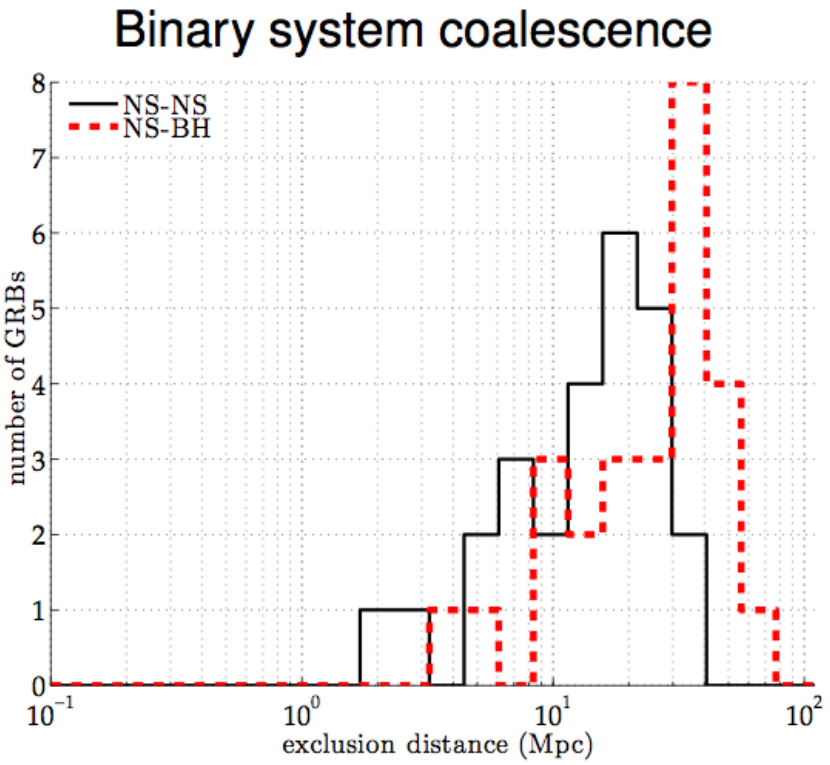

LIGO Scientific and Virgo Collaborations, Briggs, et al., "Search For Gravitational Waves Associated With Gamma-Ray Bursts During Ligo Science Run 6 And Virgo Science Runs 2 And 3", arXiv:1205.2216

Exclusion distance

Exclusion Distance vs. Jet Angle

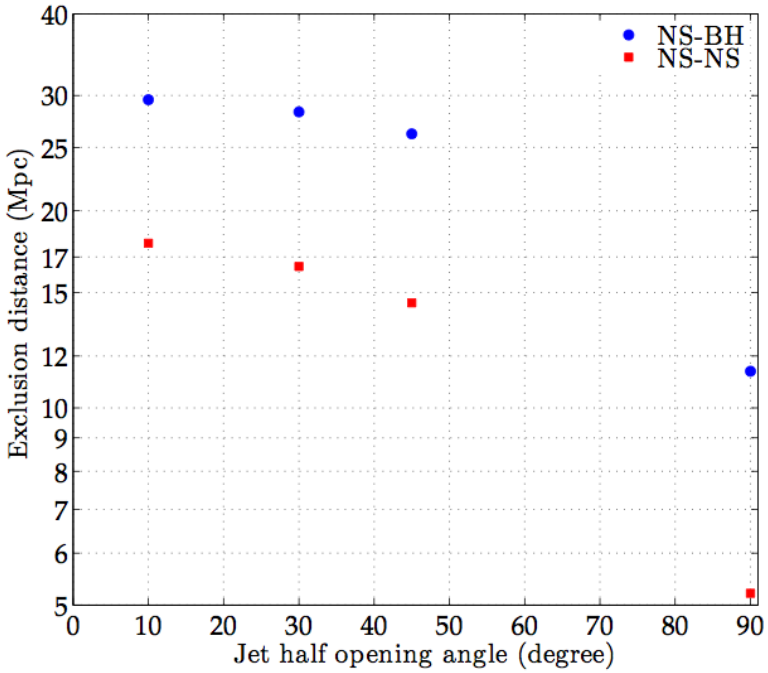

Cumulative Redshift Distribution

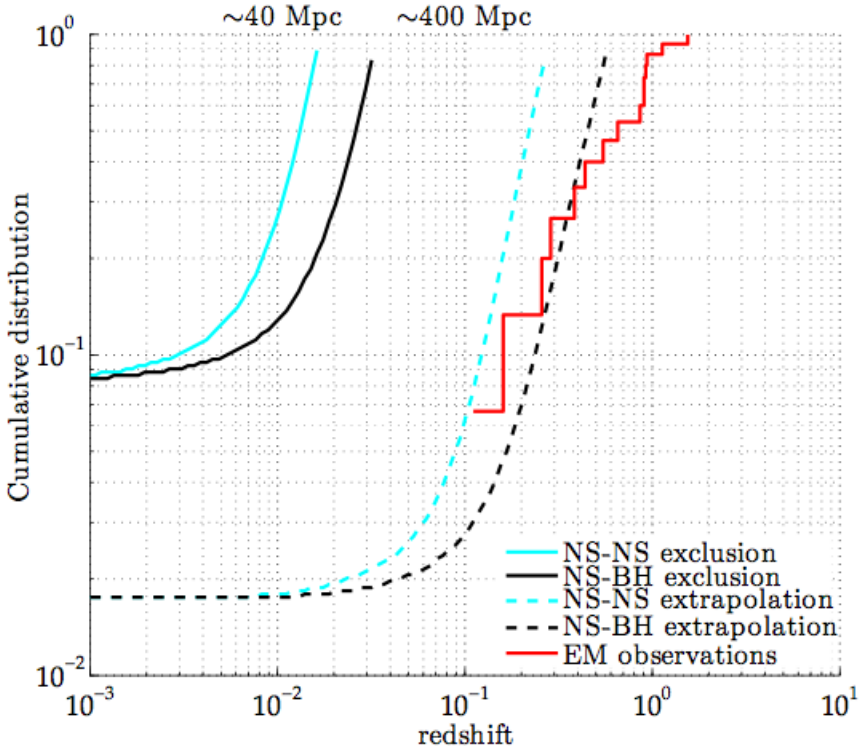

LIGO Scientific and Virgo Collaborations, Briggs, et al., "Search For Gravitational Waves Associated With Gamma-Ray Bursts During Ligo Science Run 6 And Virgo Science Runs 2 And 3", arXiv:1205.2216

Gravitational waves

- Gravitational waves are propagating solutions to the Einstein Field Equations in GR ('ripples' in space-time)
  - » Emissions from rapidly accelerating mass distributions
- Practically, need astrophysical objects moving near the speed of light

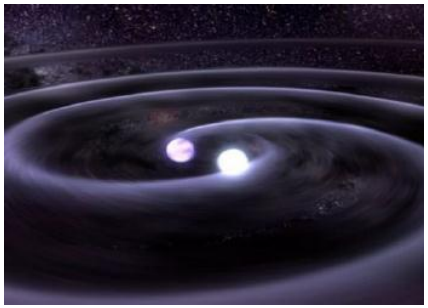

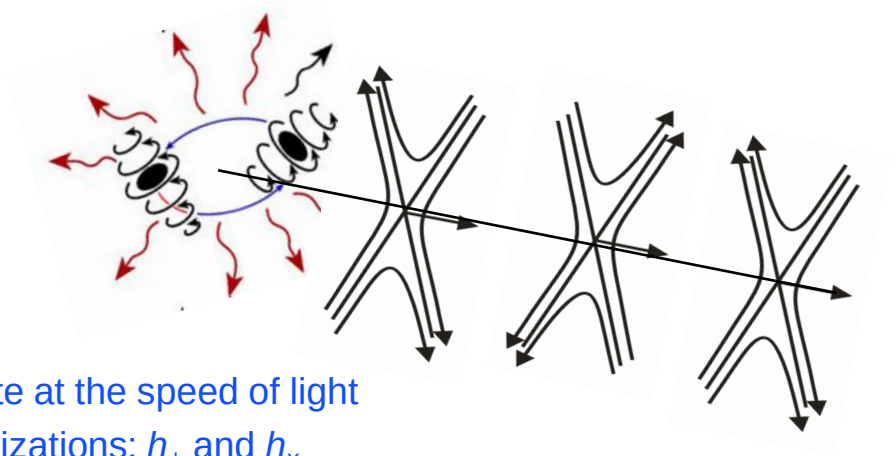

  - » According to GR, GWs propagate at the speed of light
  - » Quadrapolar radiation; two polarizations: h_+ and h_x
- Physically, gravitational waves are *strains*:

$$h = \frac{\Delta L(f)}{L}$$

- Sense of scale: strain from a binary neutron star pair
  - » M = 1.4 M⊙, r = 10^{23} m (15 Mpc, Virgo), R = 20 km, f_{orb} = 400 Hz

$$h \sim \frac{4\pi^2 G M R^2 f_{orb}^2}{c^4 r} \quad \Rightarrow \quad h \sim 10^{-21}$$

LIGO

Initial LIGO

Searching for High Mass Compact Binary Coalescences

- IMBH formation proposed to complete BH mass hierarchy…
  - » Via stellar collision in globular clusters, stalled supernovae of early pop III stars, progressive accumulation into higher mass
- …but their existence is uncertain
  - » Stellar winds suppression of runaway accumulation, merger recoil ejection of BH from GC
- Candidates exist: ultraluminous x-ray sources M82 X-1, NGC 1313 X-2
- S5/VSR1 search using constrained unmodelled waveform (Coherent WaveBurst algorithm)

Effective Range (Mpc) for H1H2L1V1

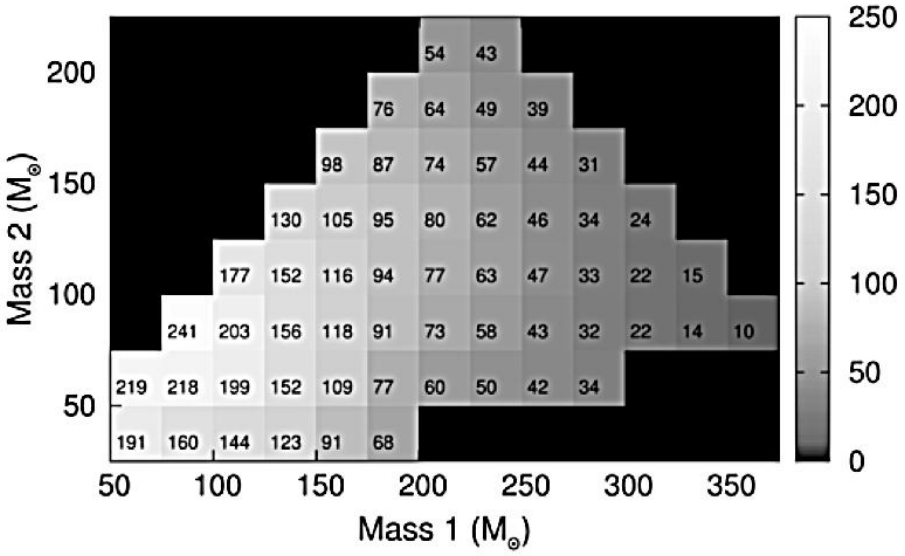

Rate Density Upper Limit (Mpc^{-3} Myr^{-1})

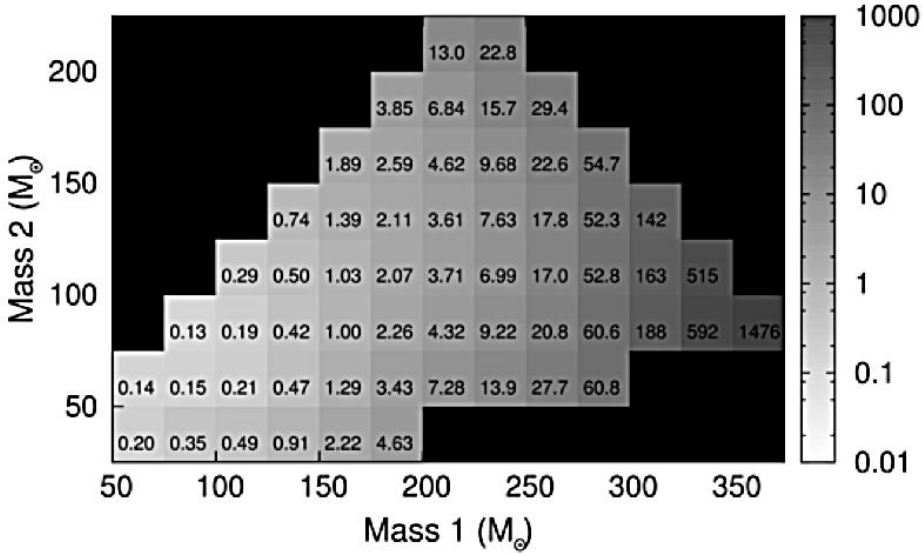

LIGO Scientific and Virgo Collaborations, "*Search for gravitational waves from intermediate mass binary black holes*", Phys. Rev. D**85**, 102004 (2012)

Squeezed Interferometry

- Shot noise and radiation pressure come from statistical fluctuations ultimately arising from the Heisenberg uncertainty principle
  - » These fluctuations exist in the vacuum state. They enter the interferometer at the output port.
- A noise reduction in one quadrature can be achieved at the expense of the other quadrature → 'squeezed light'
  - » 3 dB injected squeezed vacuum reduces noise by √ 2
  - » Possible to achieve 10 dB

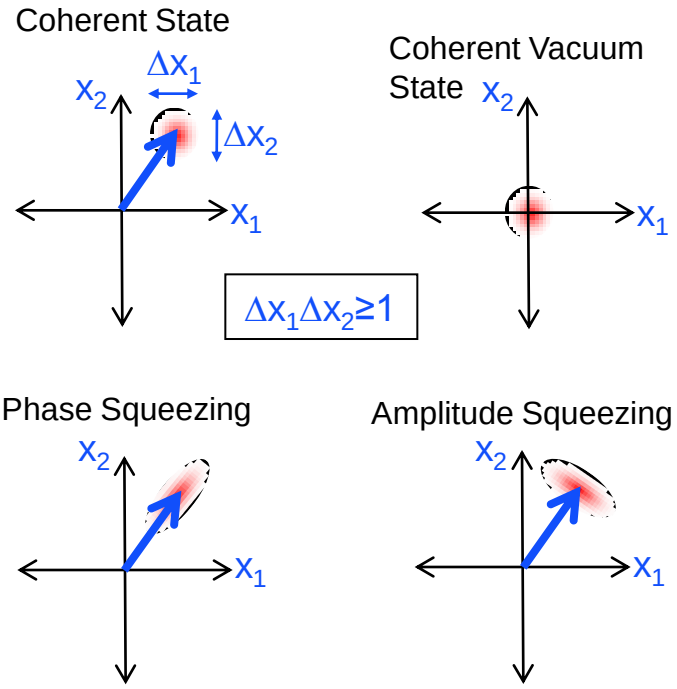

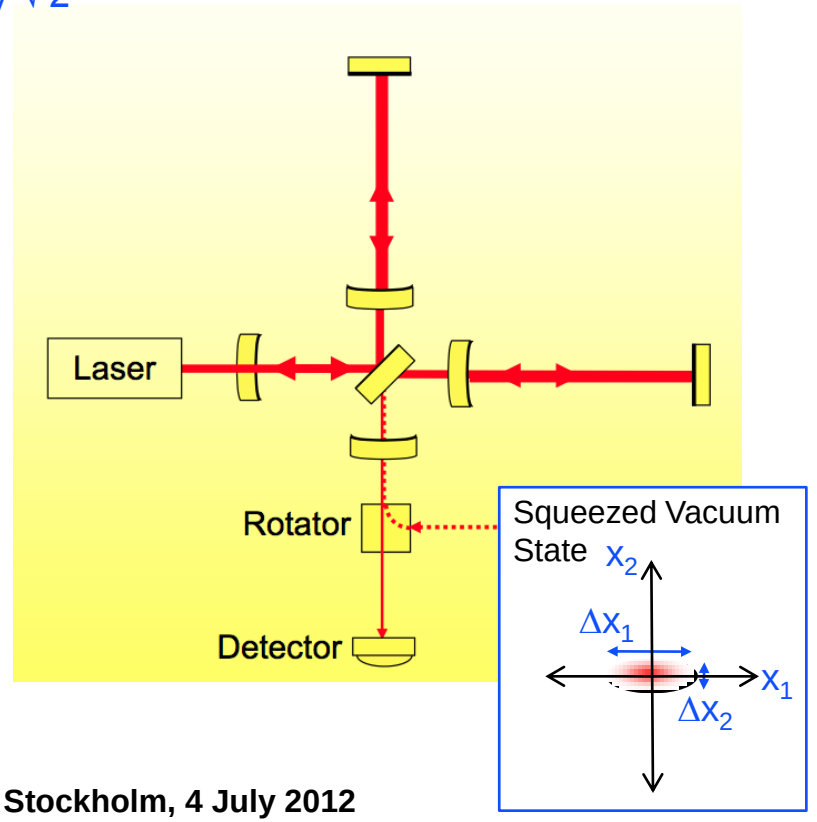

Advanced LIGO schedule

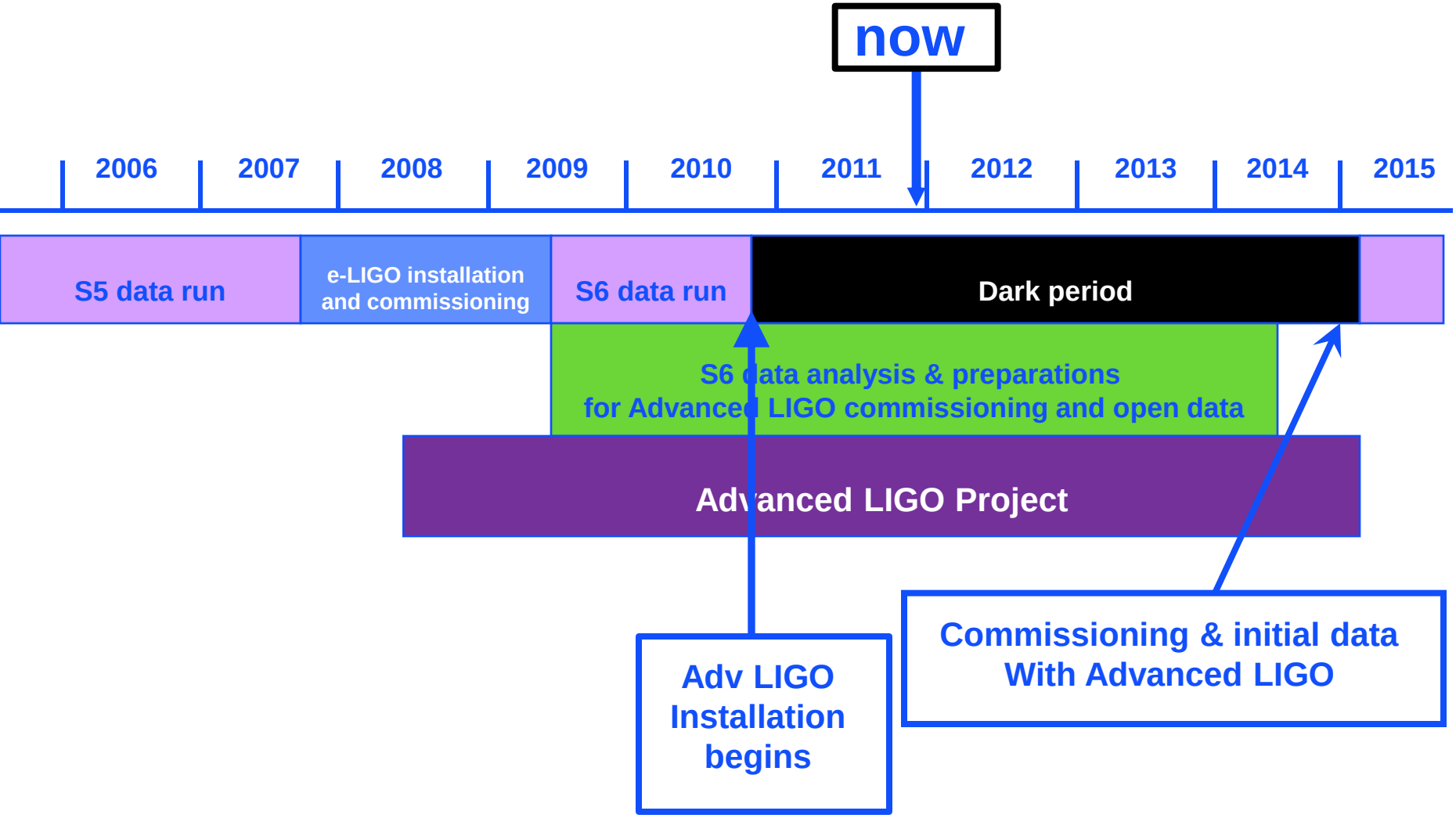

Koutarou Kyutoku, JGRG 22(2012)111405

"Electromagnetic counterparts to binary neutron star mergers"

RESCEU SYMPOSIUM ON

GENERAL RELATIVITY AND GRAVITATION

JGRG 22

November 12-16 2012

Koshiba Hall, The University of Tokyo, Hongo, Tokyo, Japan

Electromagnetic counterparts to binary neutron star mergers

Koutarou Kyutoku (KEK)

Collaborators:

Kunihito Ioka (KEK), Masaru Shibata (YITP)

Summary

Electromagnetic counterparts to gravitational waves from binary neutron star mergers will be important, and we still have no “perfect” counterpart model

We propose a possibility of ultra-relativistic outflows and associated X-ray-to-radio bands, second-to-day timescale emission from the shock breakout at the binary merger, ejecta-ISM shock, and synchrotron

This model is bright enough and has tight association with GWs, but it will be challenging to observe

Binary neutron star mergers

The most promising sources of gravitational waves

- neutron star masses, spins (if any), and radii
- supranuclear-density matter equations of state
- a way to (purely) gravitational-wave cosmology

Many electromagnetic signals are also expected

- short-hard gamma-ray bursts and afterglows
- radioactive decays of rapid-process elements
- interaction with surrounding interstellar media

Electromagnetic counterparts

The neutron star merger must be highly energetic

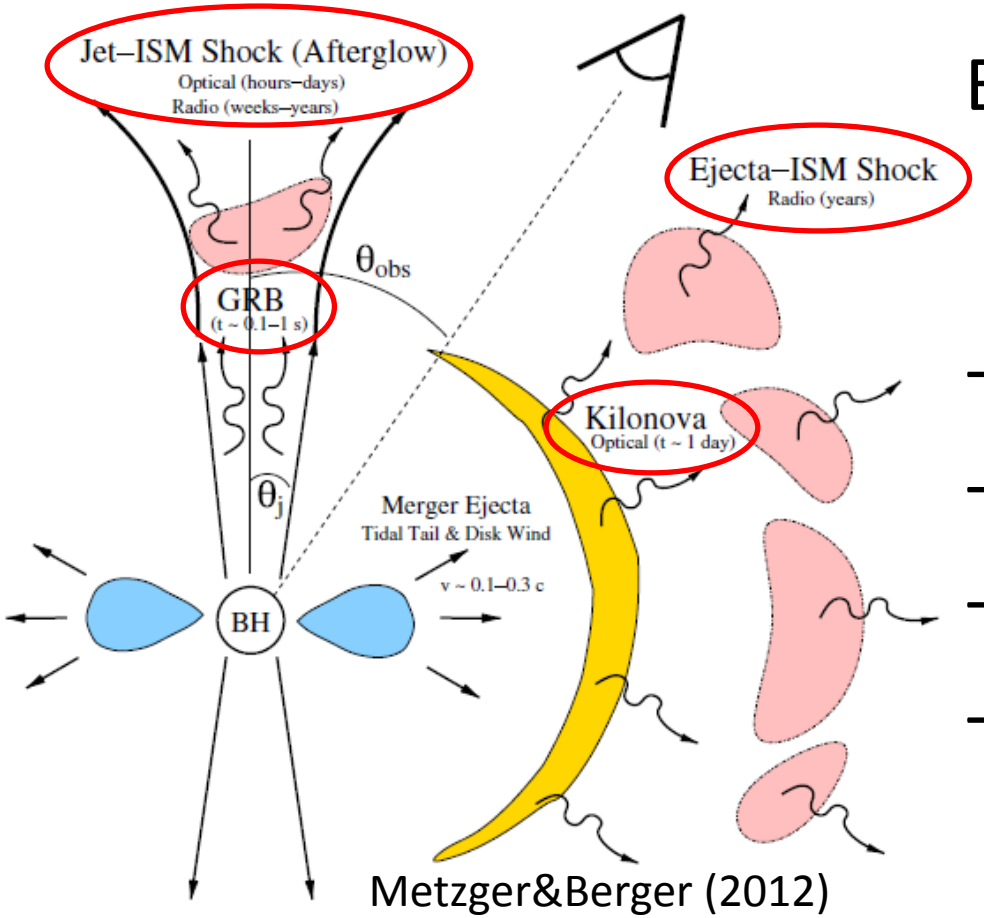

Metzger&Berger (2012)

EM emission with GWs are naturally expected

- detectable strength
- frequent association
- unique feature
- accurate localization

and so on are desired

Short-hard gamma-ray burst

The most energetic explosion

"Binary merger hypothesis"

should be tested by

simultaneous detection

(or its absence) of GWs and

short-hard gamma-ray bursts

Afterglows will localize events

with sufficient accuracy

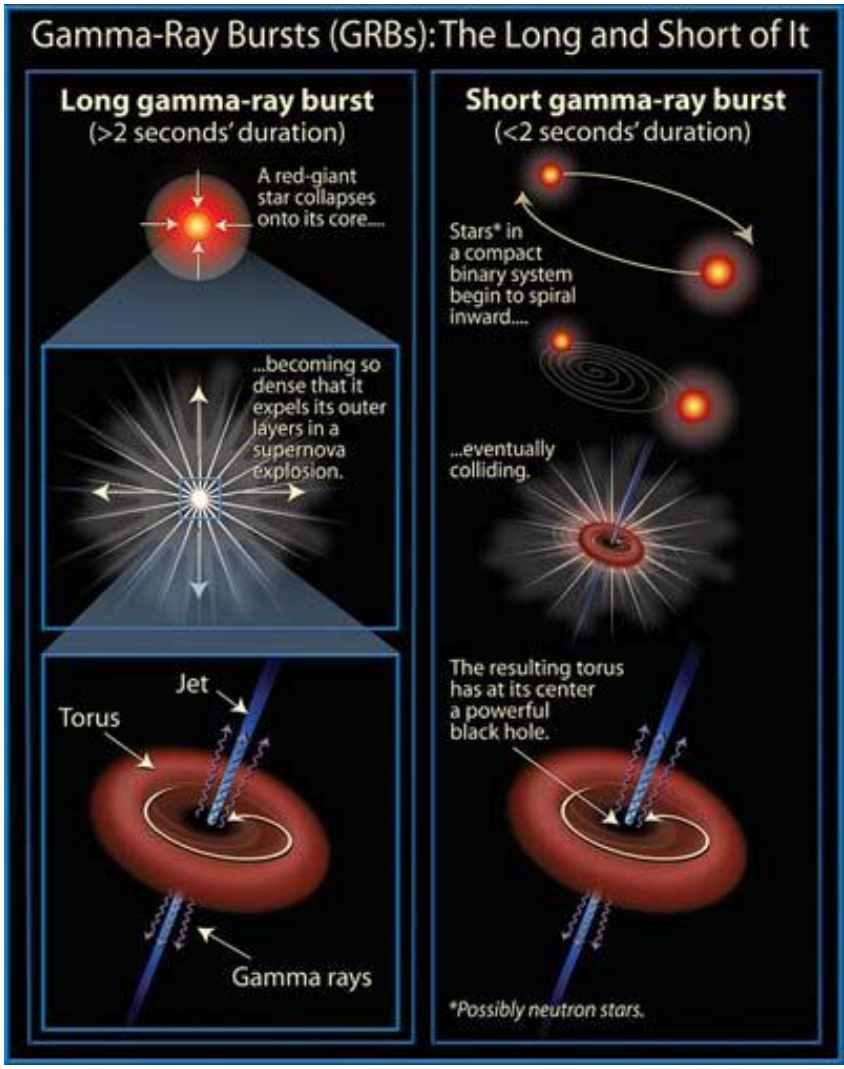

From encyclopedia of science

Problem: jet opening angle

Not necessarily accompany GWs due to the beaming

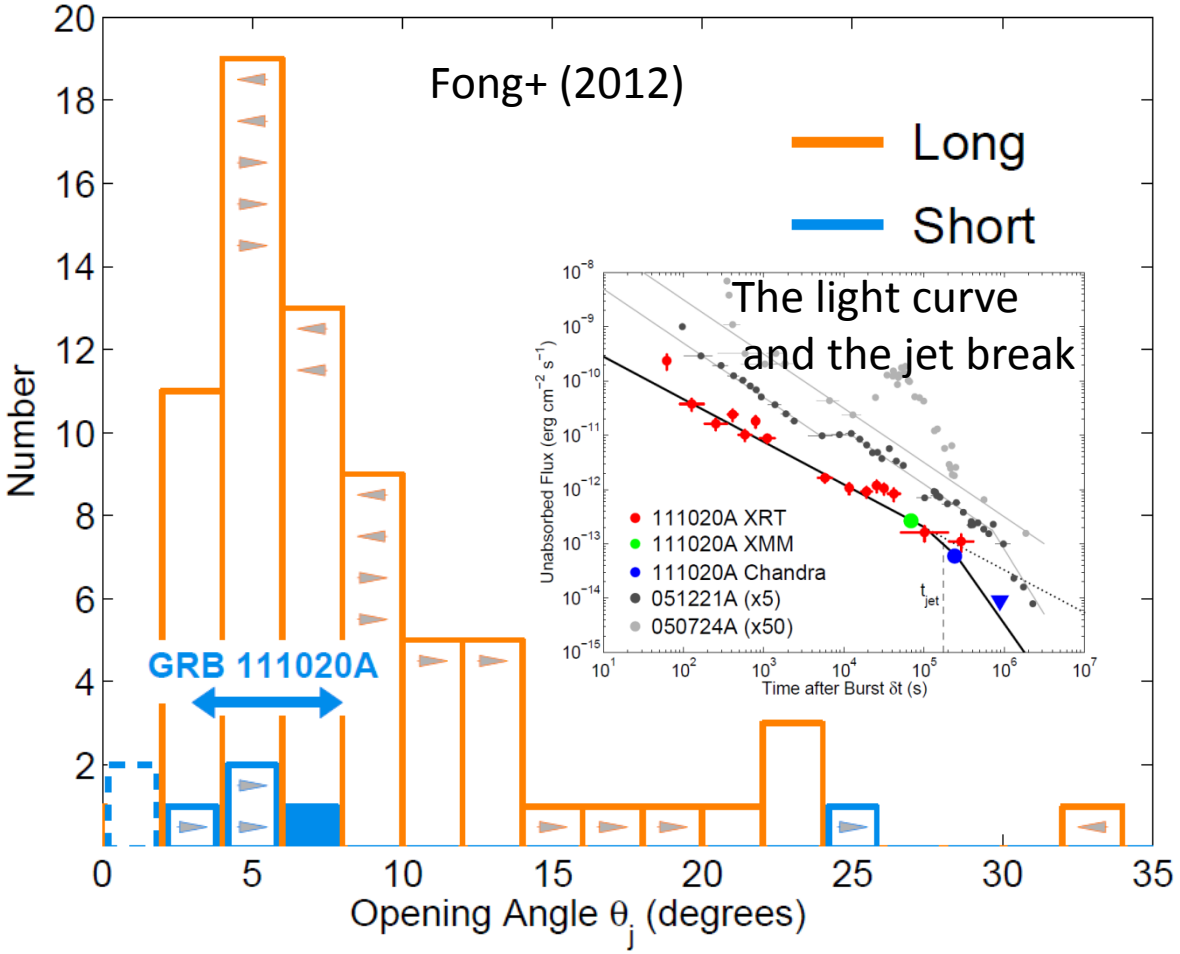

Two events suggest jet angle < 10 deg.

A few % of mergers accompany GRBs even if all mergers leads to the bursts

Mass ejection from the merger

- tidal torques by the rapidly (differentially) rotating, non-axisymmetric hypermassive neutron star

- heating by shocks generated at/after the merger

Nearly spherical:

"4π-counterpart"

mass: $10^{-2} - 10^{-3} M_\odot$

velocity: $0.15 - 0.25c$

kinetic E: $\sim 10^{50}$ erg

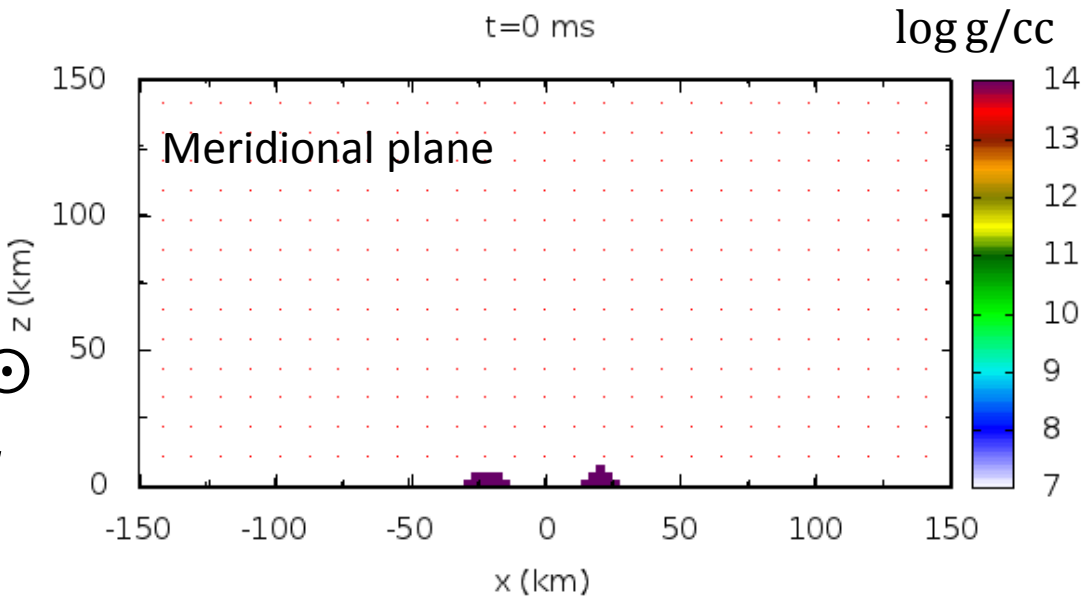

Hotokezaka, KK+ (submitted)

Movies made by Kenta Hotokezaka

Emission mechanisms

1. ejecta-ISM shock radio flare (Nakar&Piran 2011)
   synchrotron radiation like GRB afterglow and SNR
   O(year) to the peak: loose association with GWs

2. kilonova/macronova (Li&Paczynski 1992, Metger+ 2010)
   radioactive decay of r-process elements
   O(day) optical transients: many contaminations

No emission mechanism is perfect as counterparts

We need yet another electromagnetic counterpart!

Shock breakouts just at the merger

A contact surface is heated up to ~50MeV, so that hot material escape into the cold, low-density crust

The shock breakout should result unavoidably

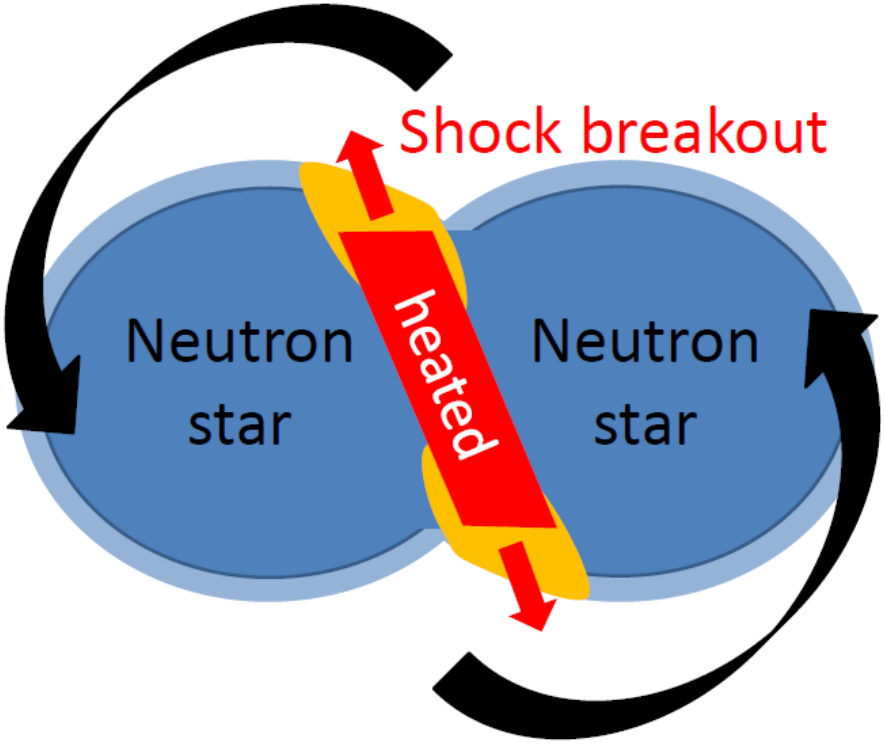

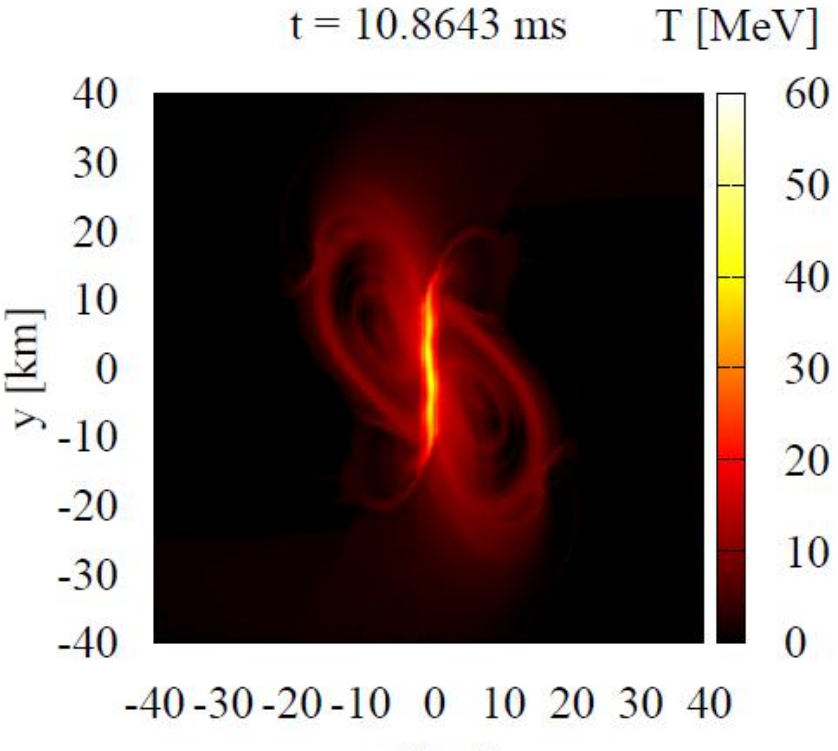

Shock and post-shock acceleration

A smaller mass is accelerated to a higher velocity

(Whitham 1958, Sakurai 1960, Johnson&Mckee 1971)

Shock acceleration

the acceleration of shock waves as they descend the density gradient = the neutron star crust

Post-shock acceleration

the acceleration of ejected material by converting thermal E. to kinetic. E and by the pressure gradient inside them

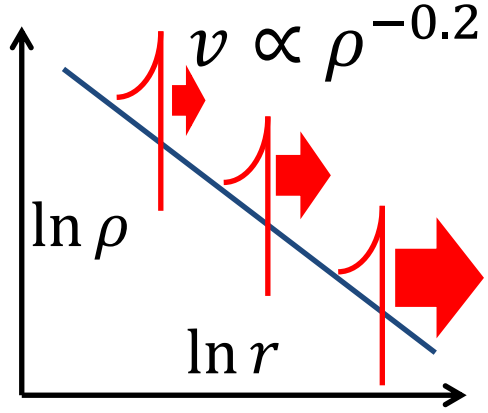

Ultra-relativistic outflows

Based on a spherical SNe model (Tan, Matzner, Mckee 2001)

Ejecta mass is $\sim 10^{-4} - 10^{-5} M_{\odot}$

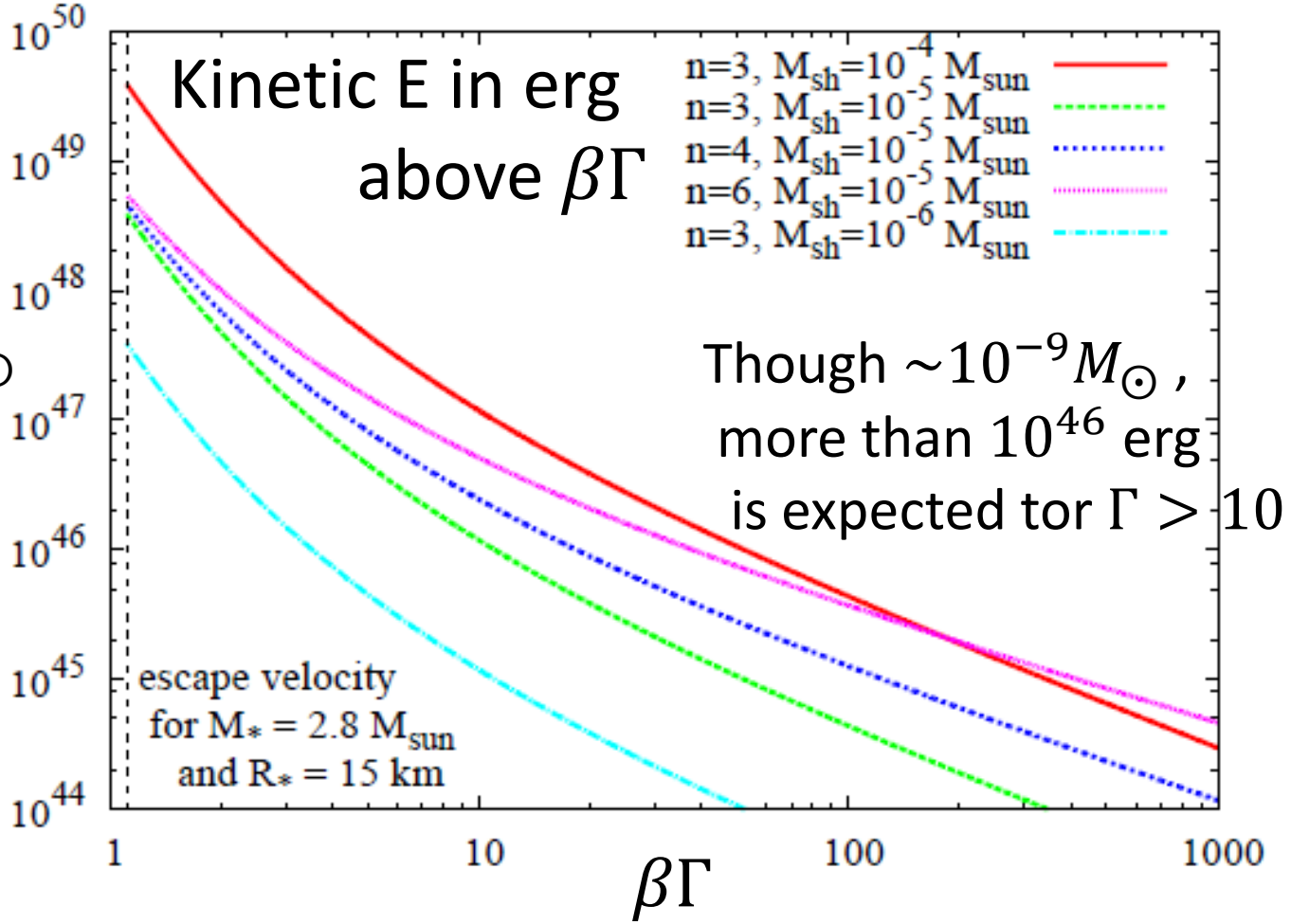

Though $\sim 10^{-9} M_{\odot}$, more than 10^{46} erg is expected tor $\Gamma > 10$

Blast waves and synchrotron emission

Ultra-relativistic -> fast and high-energy emission

How to observe in practice?

- GW alert
- galaxy monitor

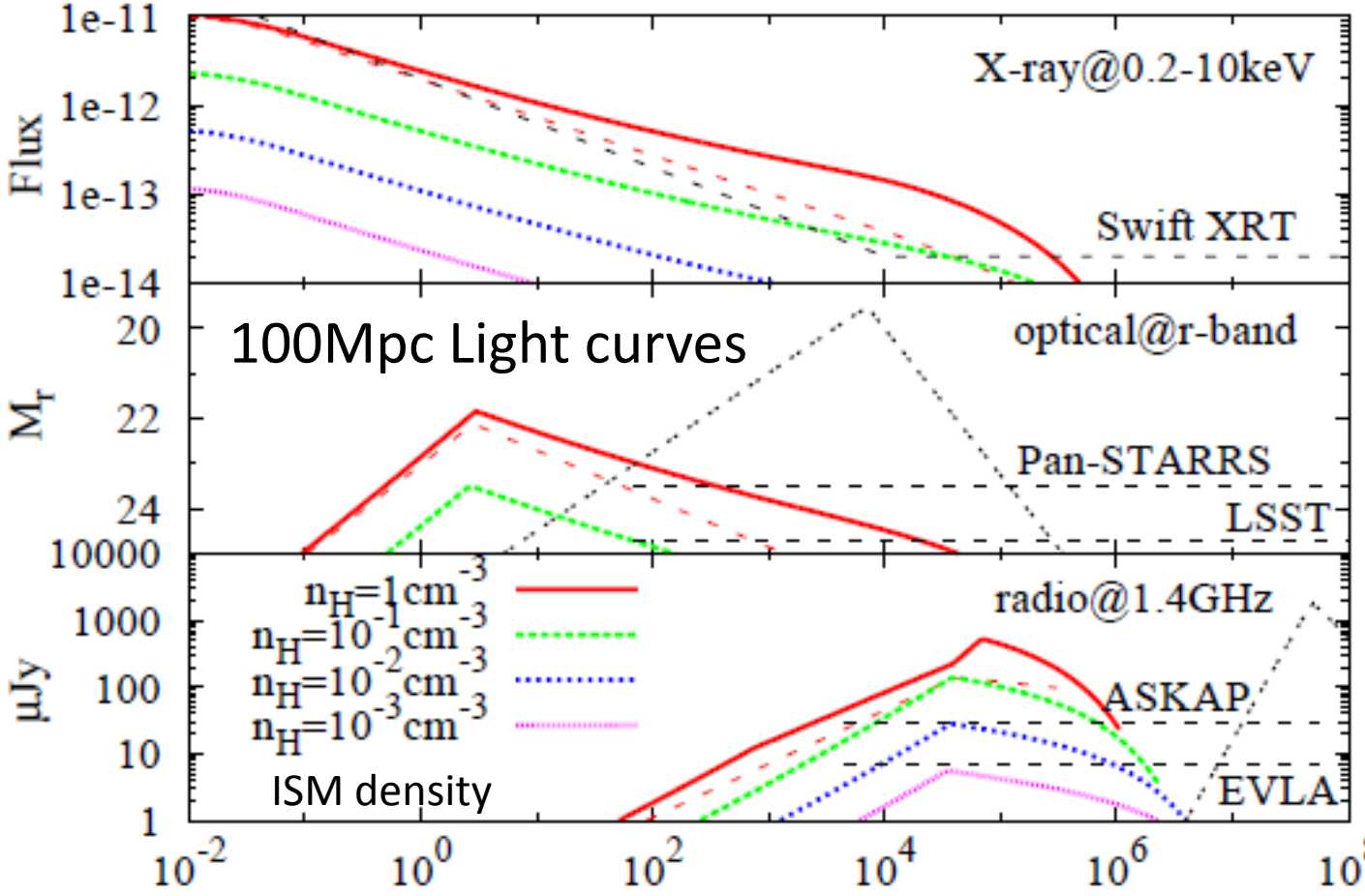

Summary

Electromagnetic counterparts to gravitational waves from binary neutron star mergers will be important, and we still have no “perfect” counterpart model

We propose a possibility of ultra-relativistic outflows and associated X-ray-to-radio bands, second-to-day timescale emission from the shock breakout at the binary merger, ejecta-ISM shock, and synchrotron

This model is bright enough and has tight association with GWs, but it will be challenging to observe

appendix

Horizon distance/detection rate

The signal-to-noise ratio threshold is taken to be ~8

For a best-oriented binaries (face-on to the detector), 445/927/2187Mpc for NSNS/BHNS/BHBH binaries

[a]To convert the rates per MWEG in Table II into detection rates, optimal horizon distances of 33 Mpc / 445 Mpc are assumed for NS-NS inspirals in the Initial / Advanced LIGO-Virgo networks. For NS-BH inspirals, horizon distances of 70 Mpc / 927 Mpc are assumed. For BH-BH inspirals, horizon distances of 161 Mpc / 2187 Mpc are assumed. These distances correspond to a choice of 1.4 $M_\odot$ for NS mass and 10 $M_\odot$ for BH mass. Rates for IMRIs into IMBHs and IMBH-IMBH coalescences are quoted directly from the relevant papers without conversion. See Section III for more details.

Detection rates are estimated with models

IFO	Source[a]	$N_{\rm low}$ $\rm yr^{-1}$	$N_{\rm re}$ $\rm yr^{-1}$	$N_{\rm high}$ $\rm yr^{-1}$	$N_{\rm max}$ $\rm yr^{-1}$
Initial	NS-NS	2×10^{-4}	0.02	0.2	0.6
	NS-BH	7×10^{-5}	0.004	0.1	
	BH-BH	2×10^{-4}	0.007	0.5	
	IMRI into IMBH			$< 0.001^b$	0.01^c
	IMBH-IMBH			$10^{-4\,d}$	$10^{-3\,e}$
Advanced	NS-NS	0.4	40	400	1000
	NS-BH	0.2	10	300	
	BH-BH	0.4	20	1000	
	IMRI into IMBH			10^b	300^c
	IMBH-IMBH			0.1^d	1^e

Abadie+ (2010)

Why we need counterparts?

One/two GW detectors cannot localize GW sources

O(10 degrees^2) for future GW detector networks

EM detection helps

- param. estimation
- host galaxy search

+ EM mechanisms

+ (psychologically)
  add GW evidences

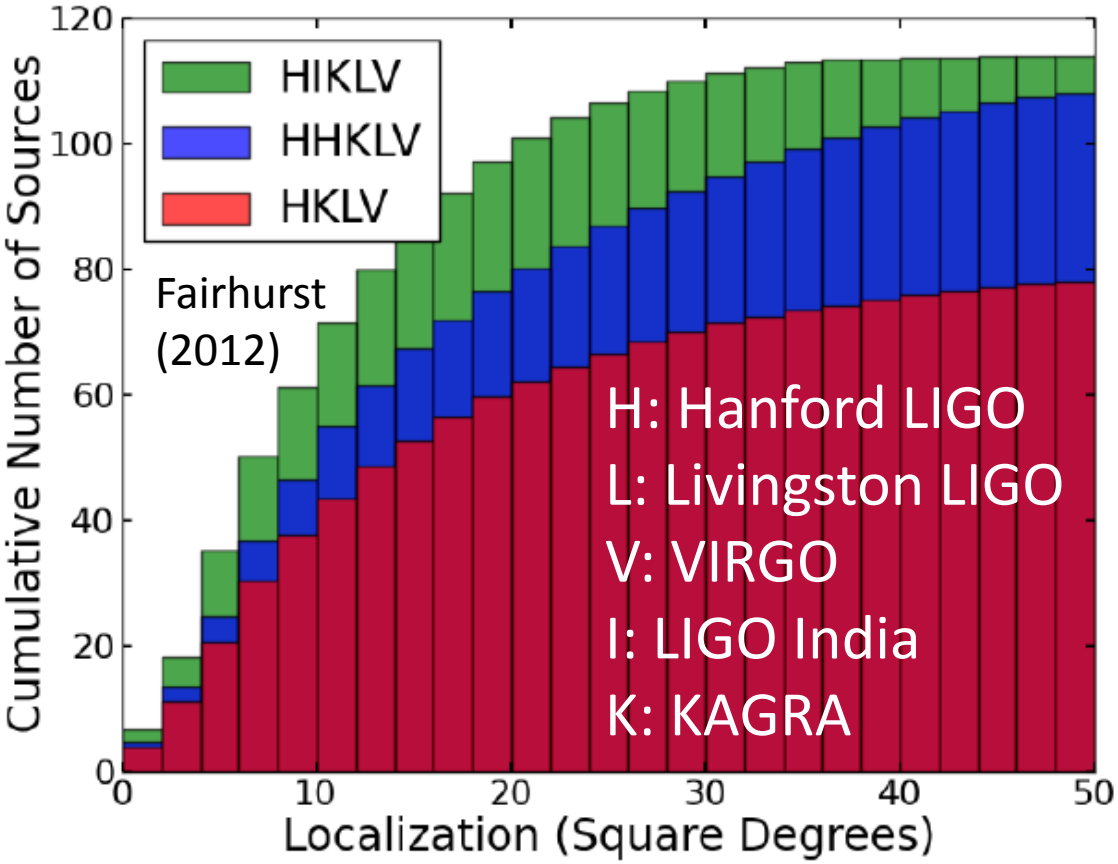

How to localize by GWs?

Triangulation by time delays between GW detectors

For three detectors, we obtain two crosses of circles

The fourth detector=KAGRA improves the situation

$$t_{\mathrm{delay}} = \frac{d\cos\theta}{c}$$

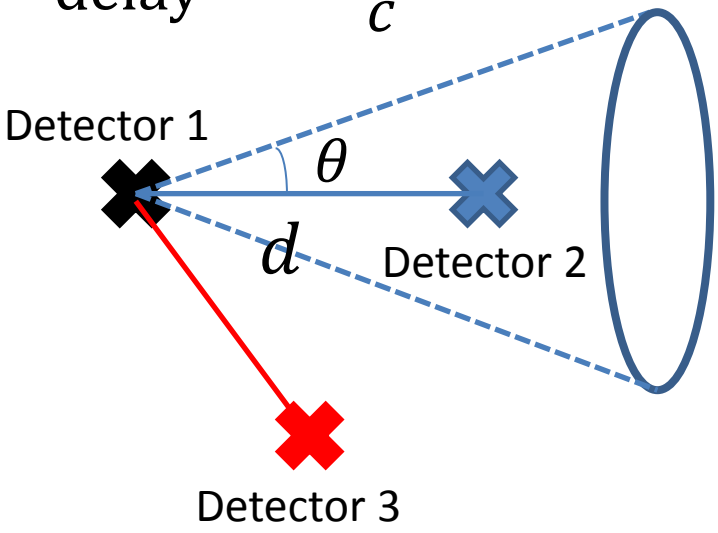

Source position
candidate circle

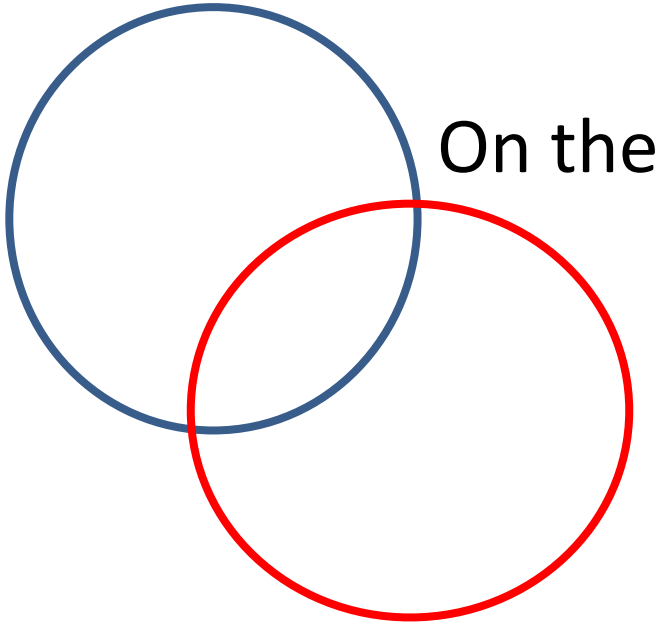

Radio flare

Ejecta forms blast waves colliding the ISM, and magnetic fields amplified & electrons accelerated

Radio synchrotron

O(year) to the peak…

Can we really declare association with GWs?

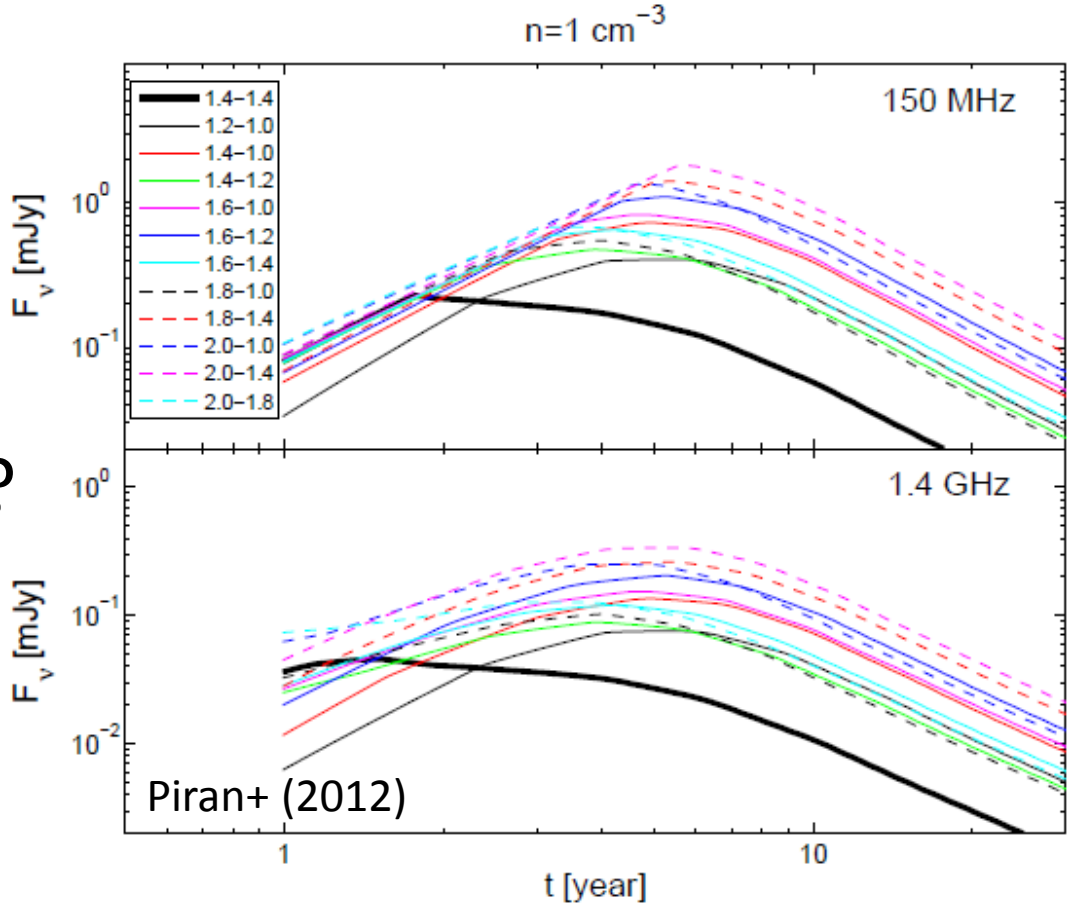

macronova/kilonova

Neutron-rich ejecta may accompany the r-process nucleosynthesis and radioactive nuclei formation

similar to SNe, only 1000 times brighter than novae

Shine in optical/UV

O(<day) to the peak

Uncertainty in r-process reaction, opacity…

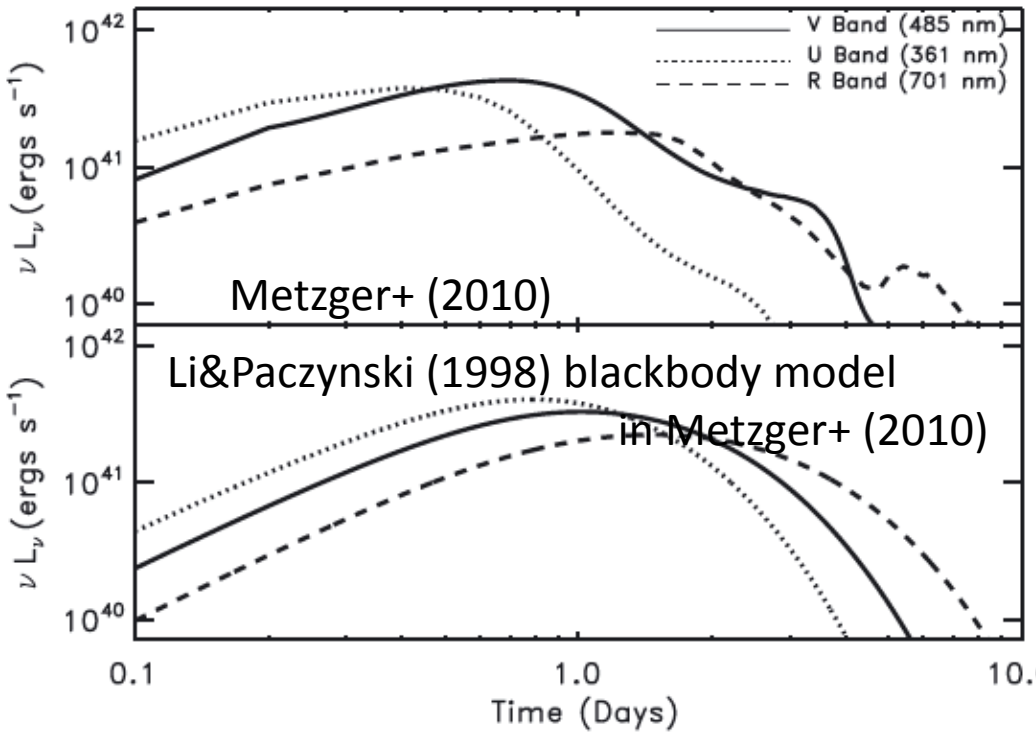

Shock acceleration in the envelope

Newtonian

$$\beta_s = A \left(\frac{\tilde{E}_{\rm in}}{\tilde{m}} \right)^{1/2} \left(\frac{\tilde{m} M_{\rm ej}}{\rho r^3} \right)^{\alpha_{\rm nr}}$$

$$\alpha_{\rm nr} \simeq 0.19$$

Semi-analytic

$$\Gamma_s \beta_s = p(1+p^2)^{0.12},$$

$$p \equiv A \left(\frac{\tilde{E}_{\rm in}}{\tilde{m}} \right)^{1/2} \left(\frac{\tilde{m} M_{\rm ej}}{\rho r^3} \right)^{\alpha_{\rm nr}}$$

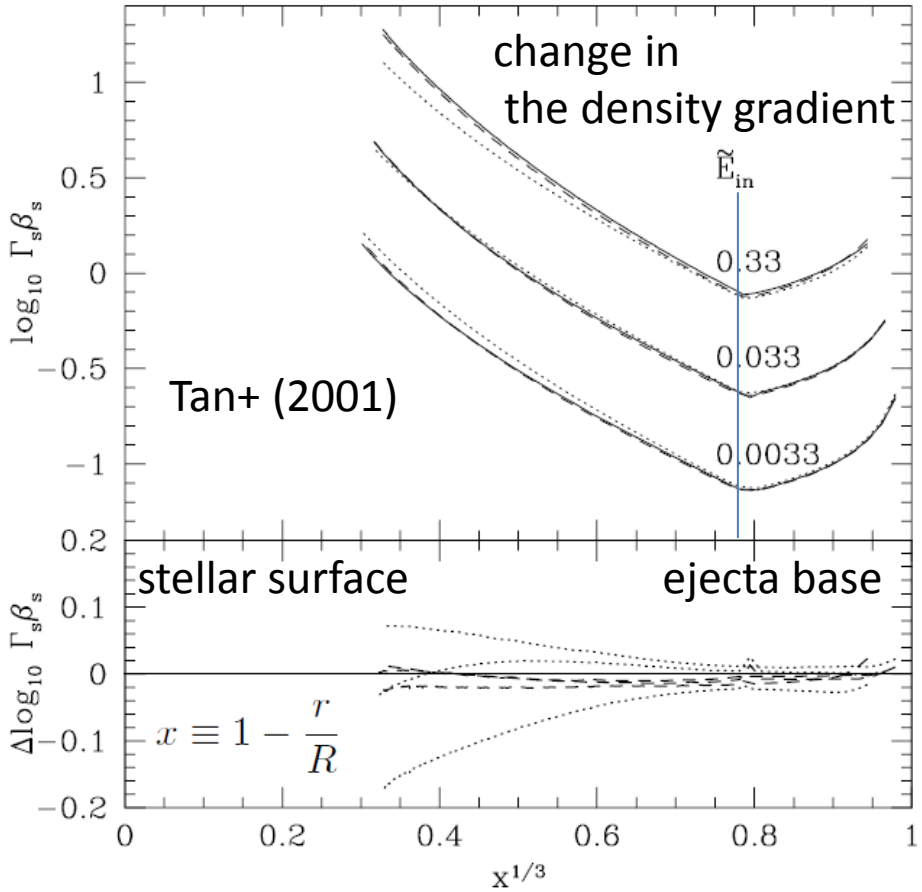

$$\rho = \rho_h \times \begin{cases} \left(\frac{R}{r_c} - 1\right)^n \left(\frac{r}{r_c}\right)^{-k_\rho}, & r < r_c \\ \left(\frac{R}{r} - 1\right)^n, & r_c < r < R. \end{cases}$$

Post-shock acceleration

Rankine-Hugonoit relation at the strong shock

$\beta_s/\beta_2 = 7/6$ for non-rela, $\Gamma_s/\Gamma_2 = \sqrt{2}$ for ultra-rela

After converting internal energy to thermal energy

$\beta_f/\beta_s = 6\sqrt{2}/7 = 1.21$ for non-rela

$\Gamma_f = 2{\Gamma_s}^2/3$ for ultra-rela (Blandford&Mckee(1976))

But post-shock acceleration is more efficient

$\beta_f/\beta_s = 2.04$ (Sakurai 1960)

$\Gamma_f \simeq \left(\Gamma_s/\sqrt{2}\right)^{1+\sqrt{3}}$ (Johnson&Mckee 1971)

Post-shock acceleration

Semi-analytic

$$\frac{\Gamma_f \beta_f}{\Gamma_s \beta_s} \simeq C_{\rm nr} + (\Gamma_s \beta_s)^{\sqrt{3}}$$

$$C_{\rm nr} = 2.03$$

Reproduce simulations

The distribution of velocity-kinetic E. is given taking the mass into account

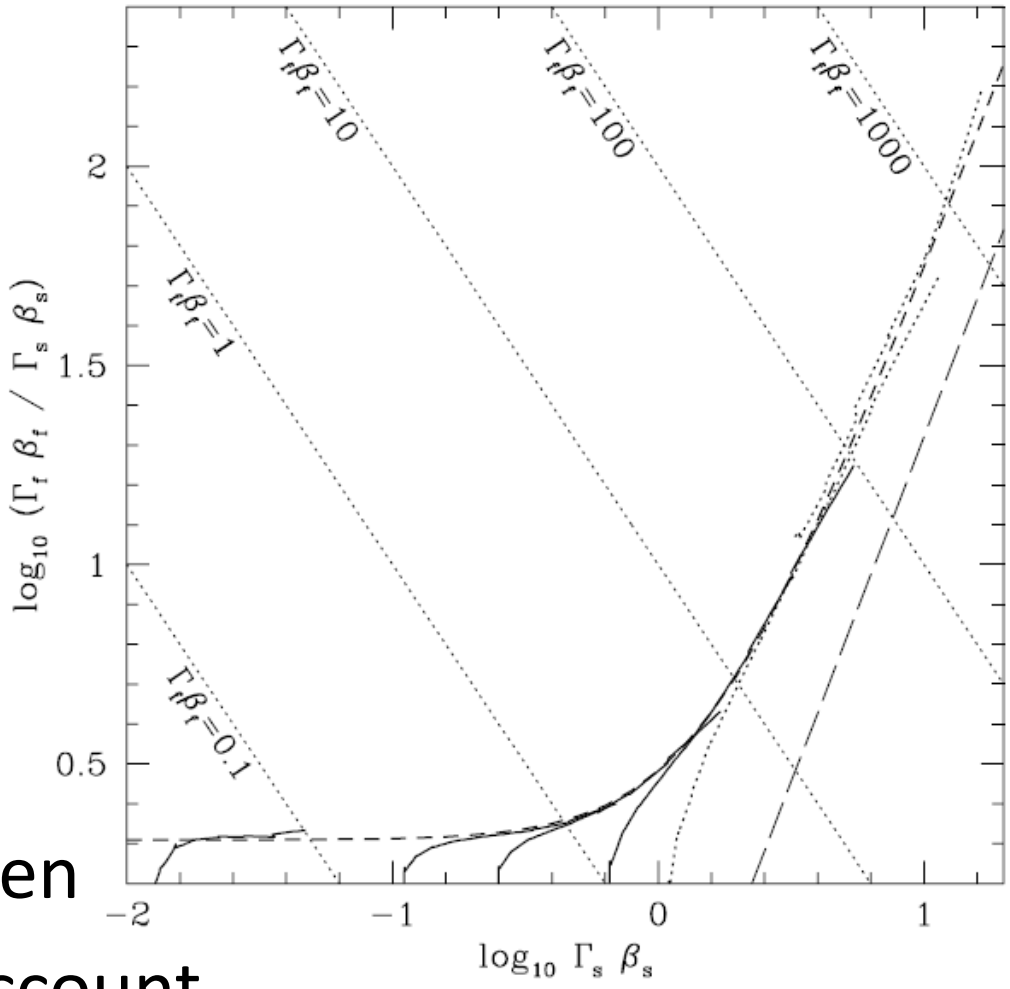

Neutron star crust

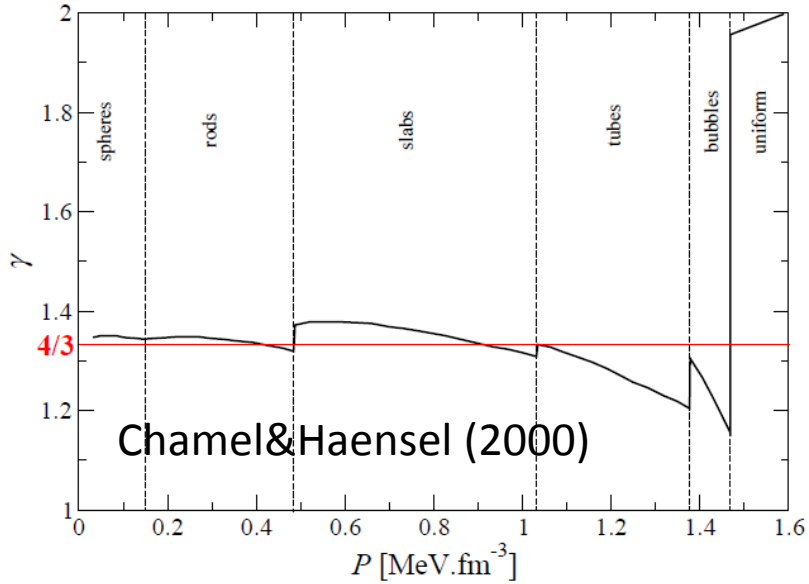

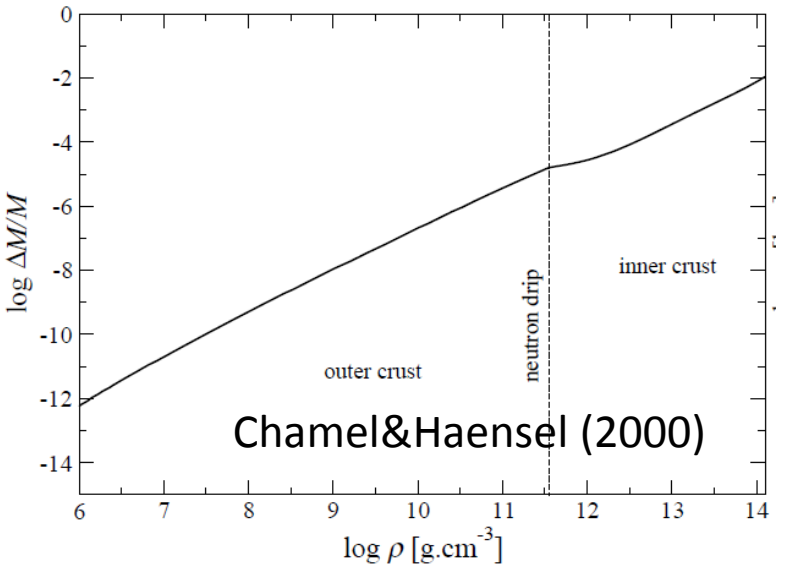

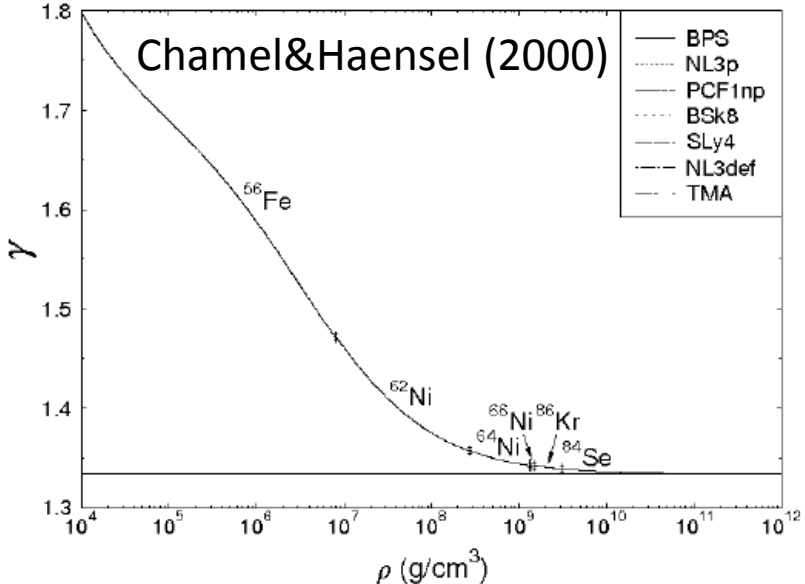

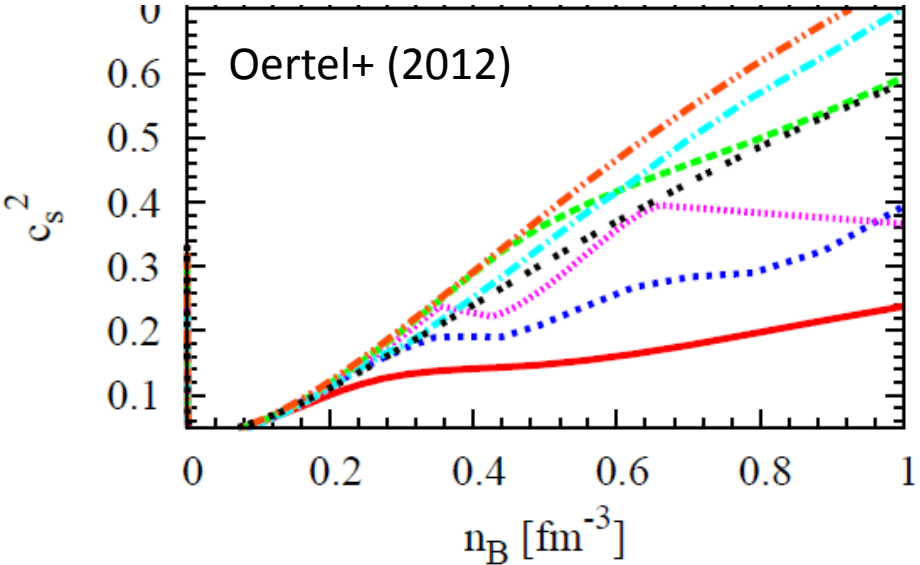

Estimation of the ejecta mass

Crust density profile: $\rho \propto (R-r)^n$, here $n \approx 3$

assume a core-crust interface is at some density ρ_0

Shock velocity: $v \propto \rho^{-0.2}$ for polytropic index $n = 3$

assume $v_{\rm ini}$ is the core sound velocity $\sim 0.25c$

$v_{\rm esc} = \sqrt{2GM/R} \sim 0.7c$ for a typical HMNS

Acceleration from initial to escape velocity gives the ratio between the density $\rho_{\rm esc}/\rho_0$

Integrate this with geometrical reduction gives the ejecta mass to be $10^{-2} \sim 10^{-3} M_{\rm crust} (\sim 0.01 M_\odot)$

Blast wave evolution

Blandford-Mckee's solution (Blandford&Mckee 1973): the evolution of relativistic self-similar blast waves

An initial shell has energy E and Lorentz factor Γ

BM begins when the shell obtains $\sim E$ from the ISM

$$R(t) \propto t^{1/4}, \Gamma(t) \propto t^{-3/8}$$

For a refreshed shock $E(>\Gamma) \propto \Gamma^{1-s}$

$$R(t) \propto t^{(s+1)/(s+7)}$$

$$\Gamma(t) \propto t^{-3/(s+7)}$$ (Rees&Meszaros 1998)

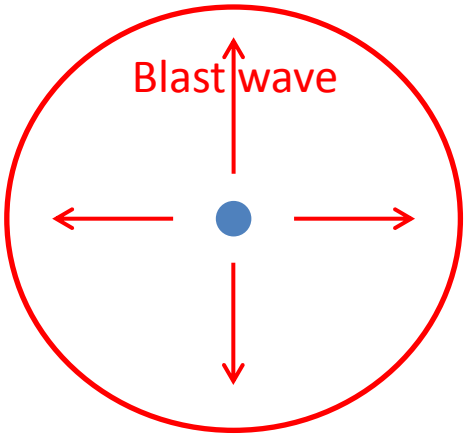

InterStellar Medium

Assumption for refreshed shocks

Fully adiabatic evolution (no radiation energy loss)

A radius-Lorentz factor closure relation: $R = 4\Gamma^2 ct$

this exact factor depends on situations

When the slower shell rear-ends, it is decelerated by the material accumulated by all the faster shells

$$E_0 \left(\frac{\Gamma}{\Gamma_0}\right)^{1-s} \sim \Gamma^2 R^3 n_{\rm H} m_p c$$

These relations determine the time evolution

Synchrotron radiation

Emission by relativistic electrons in a mangetic field

- electron acceleration behind a shock
- magnetic field amplification behind the shock

Fit the GRB afterglow and SNR well

Assume that the same model holds also in our case

- a smaller mass leads earlier deceleration
- more energetic electrons contribute to radiation

Synchrotron radiation

The electron number density in the Lorentz factor is assumed to have a power-law distribution

high frequency: cooling, low frequency: absorption

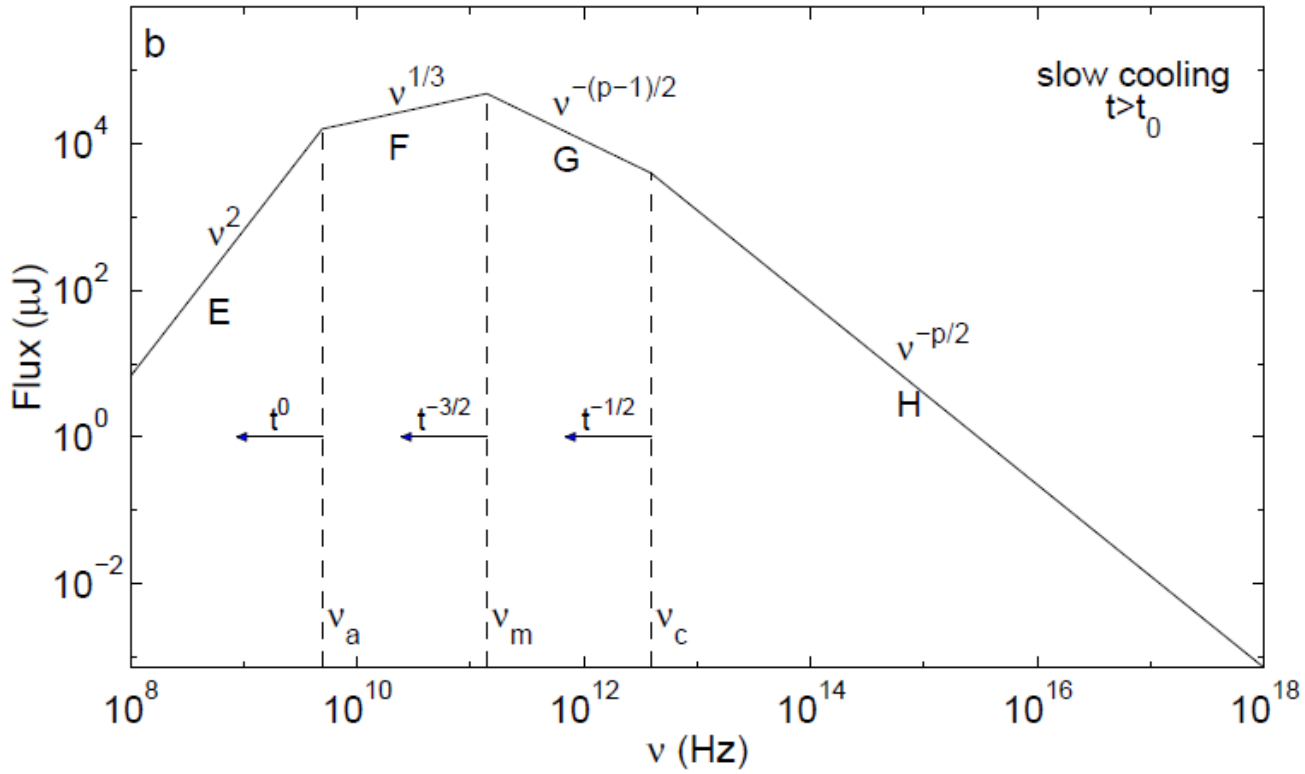

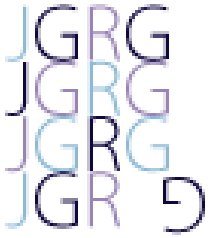

Kenta Kiuchi, JGRG 22(2012)111406

"General relativistic simulations of magnetized binary neutron star merger"

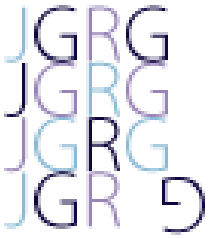

RESCEU SYMPOSIUM ON

GENERAL RELATIVITY AND GRAVITATION

JGRG 22



November 12-16 2012

Koshiba Hall, The University of Tokyo, Hongo, Tokyo, Japan



General relativistic simulation of magnetized binary neutron star mergers

Kenta Kiuchi

Collaborators : Masaru Shibata, Koutarou Kyutoku, Yuichiro Sekiguchi, Kenta Hotokezaka

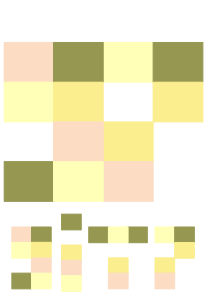

YITP

YUKAWA INSTITUTE FOR THEORETICAL PHYSICS





Magnetized Binary Neutron Star Mergers

Neutron stars have a magnetic field in general.

Magnetic Fields of NS (Manchester 04)

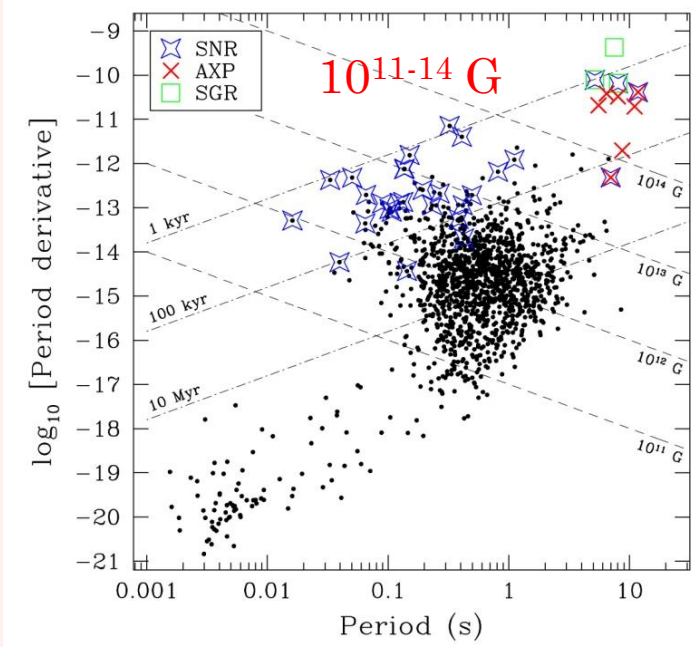

Period derivative

Spin period

What about in binary neutron star mergers ?

Possible amplification processes

- Kelvin-Helmholtz instability (Price-Rosswog 06, Gaicomazzo+ 11) @merger
- Magnetorotational instability (Balbus-Hawley 98, Rezzolla+ 11) in HMNS / disk
- Compression
- Magnetic winding

Outcome of binary neutron star mergers

Mass of observed NSs
(Lattimer & Paraksh 06)

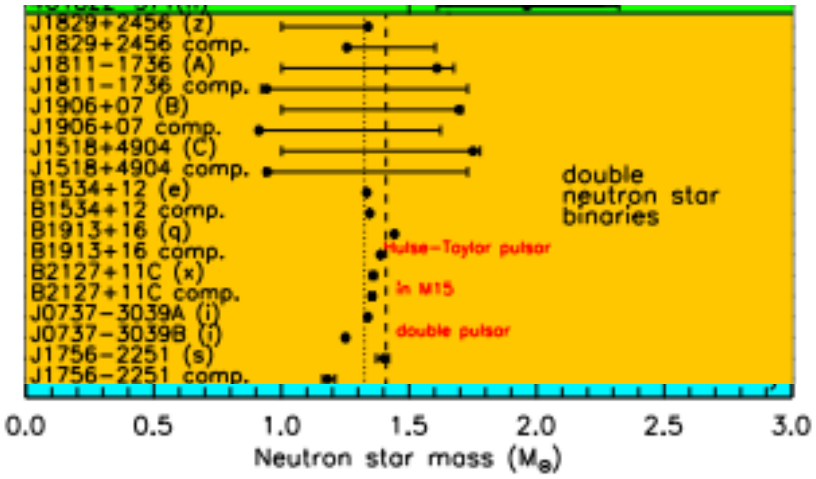

Shapiro-Time delay of PSRJ1614-2230
(Demorest+ 10)

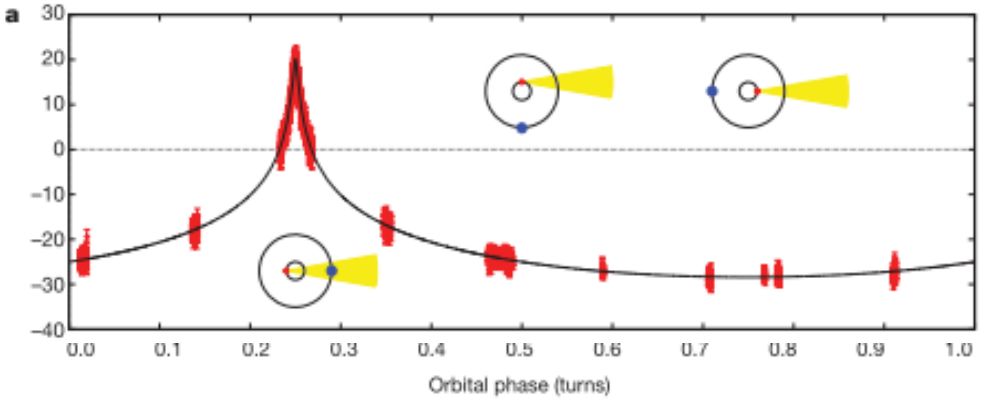

- Canonical mass of BNS = 2.7-2.8 $M_\odot$
- Maximum mass of spherical NS = 1.97 $\pm$0.04 $M_\odot$

Long-lived Hyper Massive Neutron Star (HMNS) would be formed after the merger

$\Rightarrow$ Magnetic fields would be an important player in binary neutron star mergers, e.g., angular momentum transport etc.

NR simulations for magnetized BNS mergers

✓Albert Einstein Institute (Giacomazzo+ 09, 11, Rezzolla+ 11)
- Γ-law EOS

✓Illinois University (Liu+ 08)
- Γ-law EOS

✓ Louisiana University+ (Anderson+ 08)
- Γ-law EOS

<u>All the simulations have been done so far</u>
- Relatively short duration $\lesssim$ 20 ms after merger or BH formation
- Applied only Γ-law EOS

<u>Our motivation</u>
- Long term simulation for exploring the magnetic amplification process
- Adopt the nuclear theory based EOS



GRMHD simulation of magnetized BNS mergers

Set up

- Equation of State : H4 based on RMF (Gledenning & Moszkowski 91)
  $M_{max} \gtrsim 2.03\ M_\odot$ and Γ-law for thermal part (Γ_{th}=1.8)
  $P = P_{cold} + P_{th}$
- BNS mass : 2.7 $M_\odot$, 2.8 $M_\odot$ (Equal mass system)
- Magnetic fields configuration : Confined

Confined field line (Liu+08)

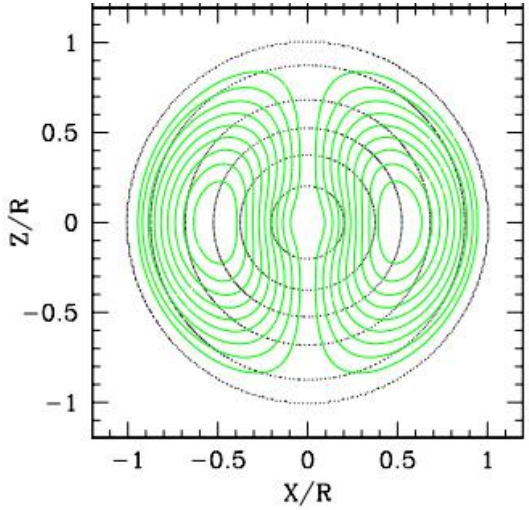

GRMHD simulation of magnetized BNS mergers

- Code description : FMR – GRMHD code based on Balsara's method preserving $\mathrm{Div} \cdot B = 0$ as well as the magnetic flux conservation (KK+ 12)

Formulation and Numerical scheme

- Baumgarte-Shapiro-Shibata-Nakamura formulation (Shibata-Nakamura 95, Baumgarte-Shapiro 99)
- 4th-order FD in space and time for the Einstein eqs.
- LLF flux and 3rd-order reconstruction for MHD
- Weno5 for reconstruction in the refinement boundary

Resolution Study

- High resolution $\Delta x = 230$ m (NS covered by 100 grid points)
- Medium resolution $\Delta x = 288$ m (NS covered by 80 grid points)
- Low resolution $\Delta x = 384$ m (NS covered by 60 grid points)

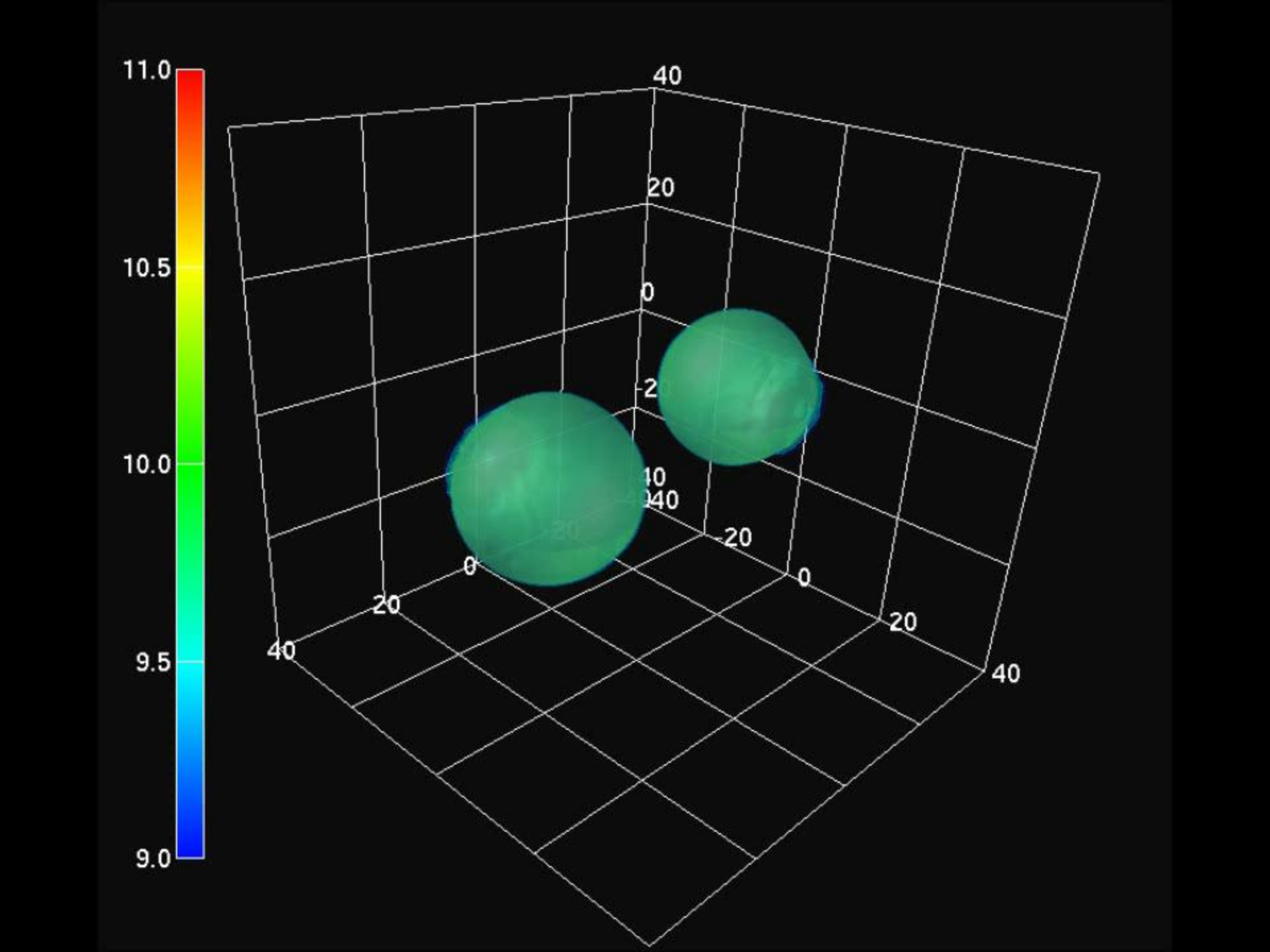
11.0
10.5
10.0
9.5
9.0
40
20
0
-2
10
40
-20
0
20
40
0
20
40

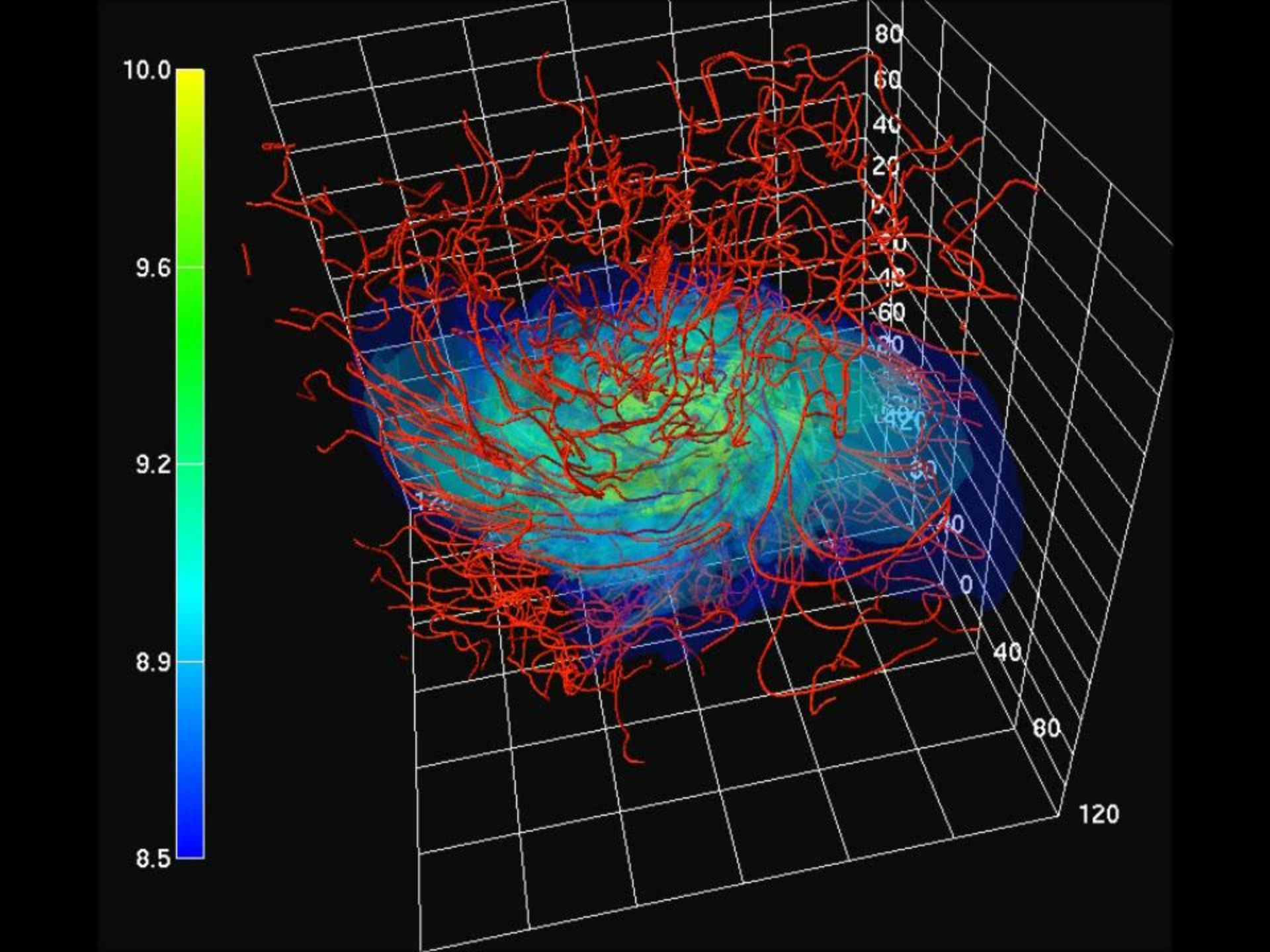
10.0
9.6
9.2
8.9
8.5
80
60
40
-60
0
40
80
120

Property of BH and torus

Density and angular velocity profile along x-axis

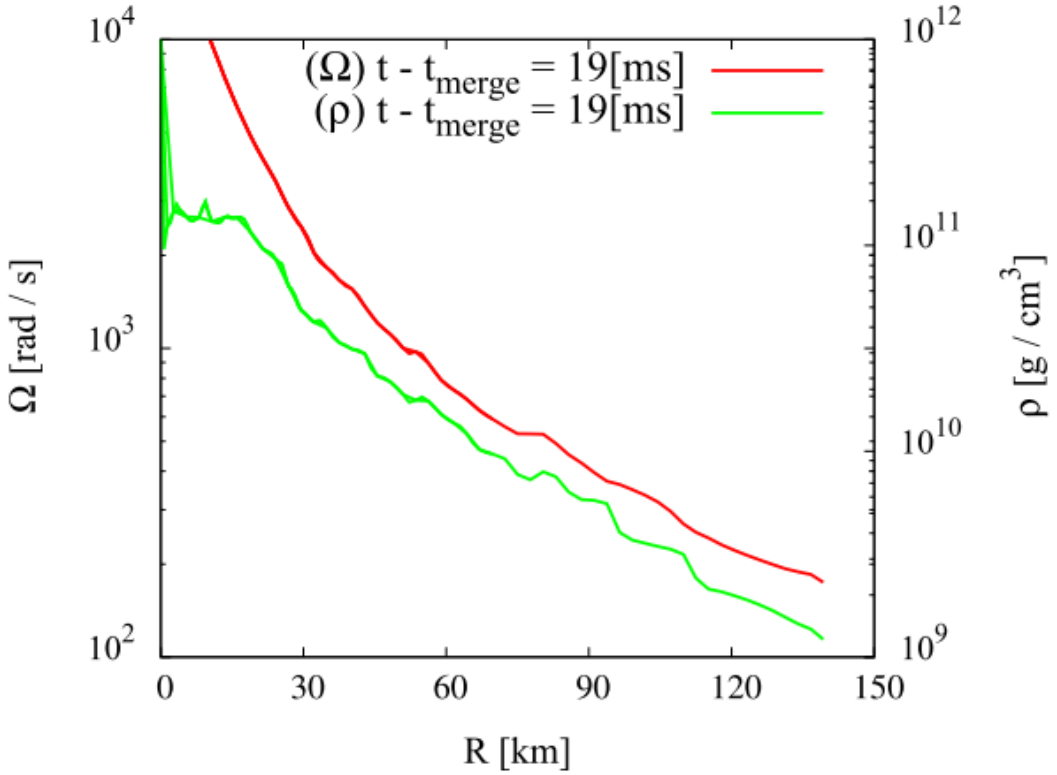

- Mass of BH is 2.6-2.7 $M_\odot$ and spin of BH is ≈ 0.7
- Almost Keplerian profile ($\propto R^{-3/2}$)
- Torus mass $\approx$ 0.03-0.04 $M_\odot$ @ 30 ms after BH formation
- MRI wavelength would be larger compared to HMNS, e.g., $\rho \approx 10^{15}$ g / cm^3

Magnetic field amplification (2.8 $M_\odot$ - confined model)

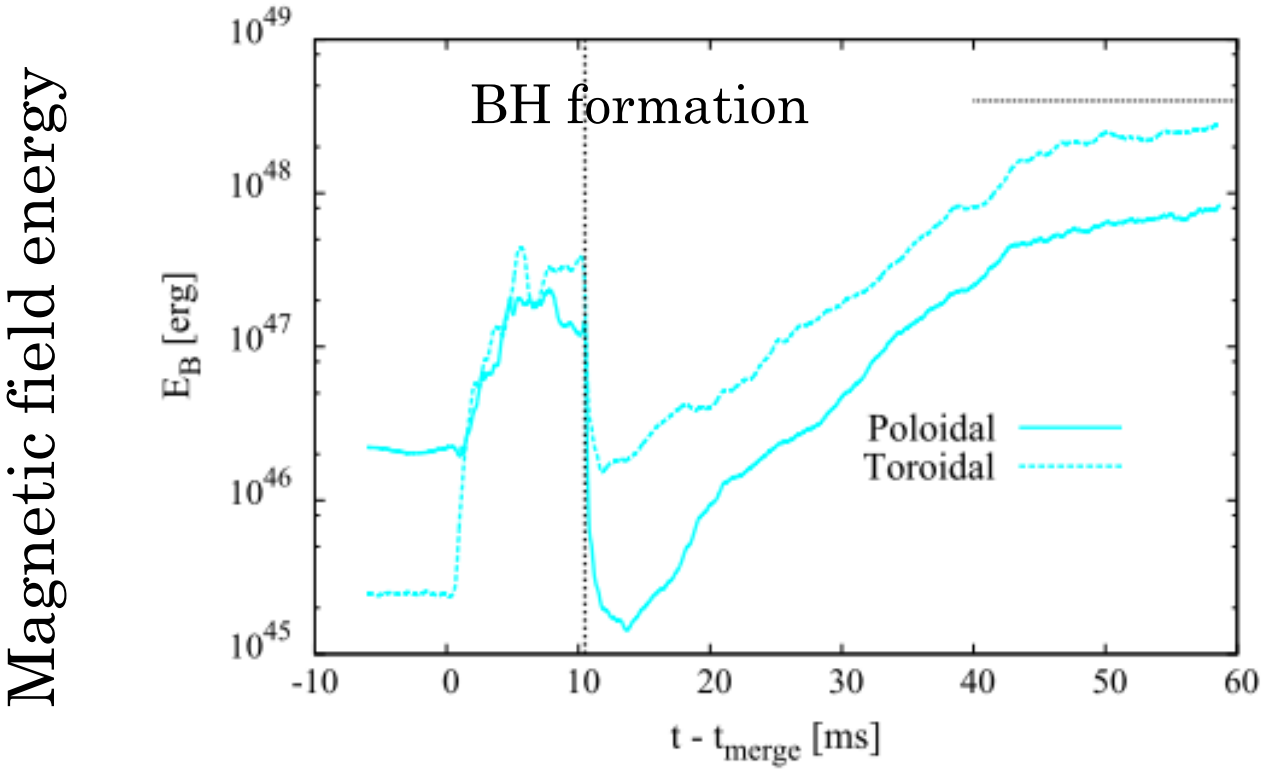

- Rapid increase at $t - t_{merge} \approx 0$ ms
- Slow increase in the HMNS phase
- Exponential growth after the BH formation (inside the torus)

Rapid increase at $t - t_{merge} \approx 0$ ms

Magnetic field strength

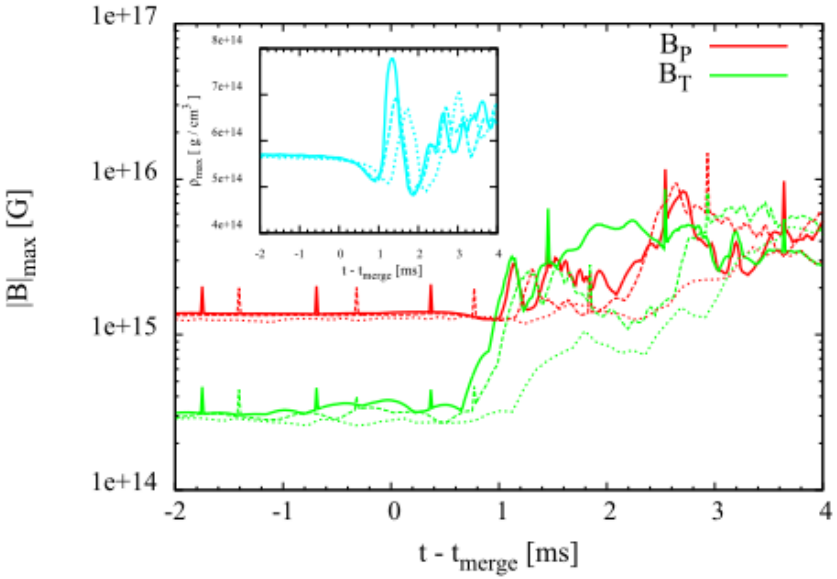

Vorticity @ $t - t_{merge} \approx 0$ ms

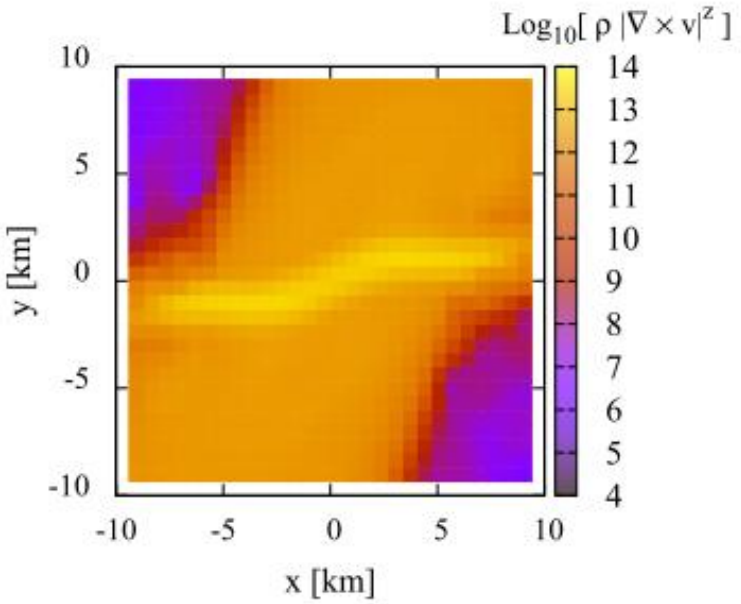

- Poloidal field increases by compression ~ $\rho^{2/3}$
- Toroidal field increases by the Kelvin-Helmholtz instability (Price-Rosswog 06, Anderson + 08, Gaicomazzo+ 11)
- Vortexes appear in the shear layer forming the two stars come into contact.

Slow increase in the HMNS phase

Magnetic field strength

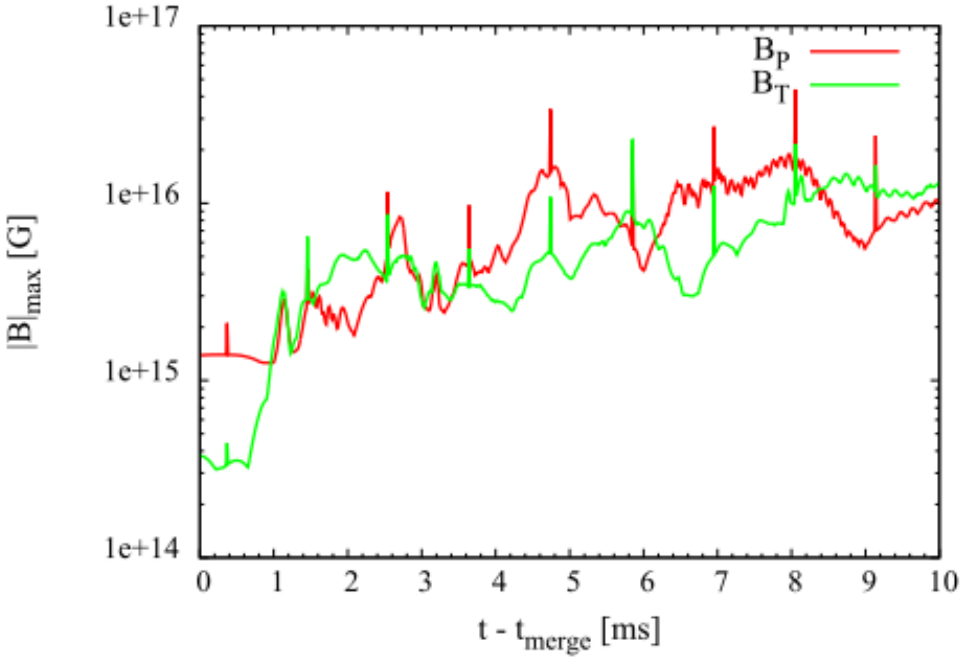

- Poloidal field increases due to the compression
- Toroidal field increases by the magnetic winding
- Very short MRI wavelength, i.e., $\rho \sim 10^{15}$ g / cm^3

Exponential growth after the BH formation

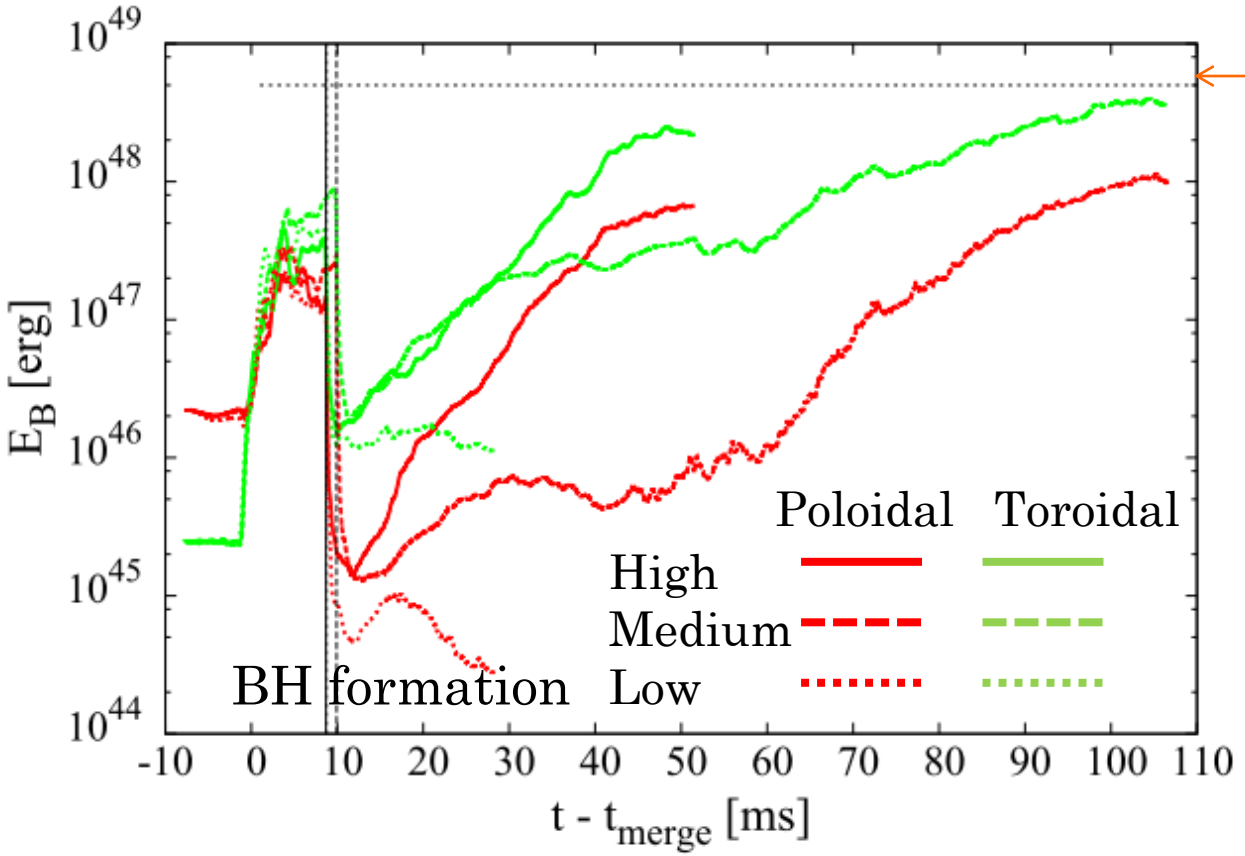

- Exponential growth in the high resolution, not in the low resolution, after the BH formation
- e-folding time ≈ 6 ms (high resolution model)
- Saturation level ≈ 3-5 × 10^{48} erg (1-2 % of kinetic energy)

Grid resolution vs MRI wavelength

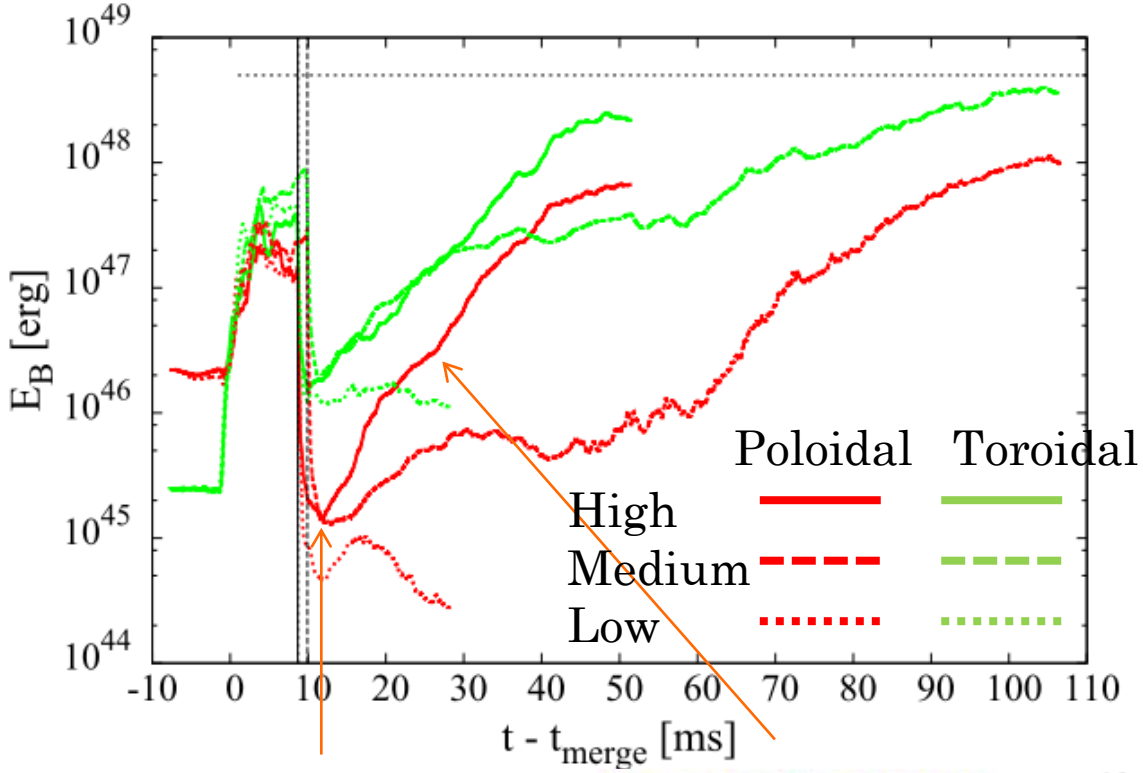

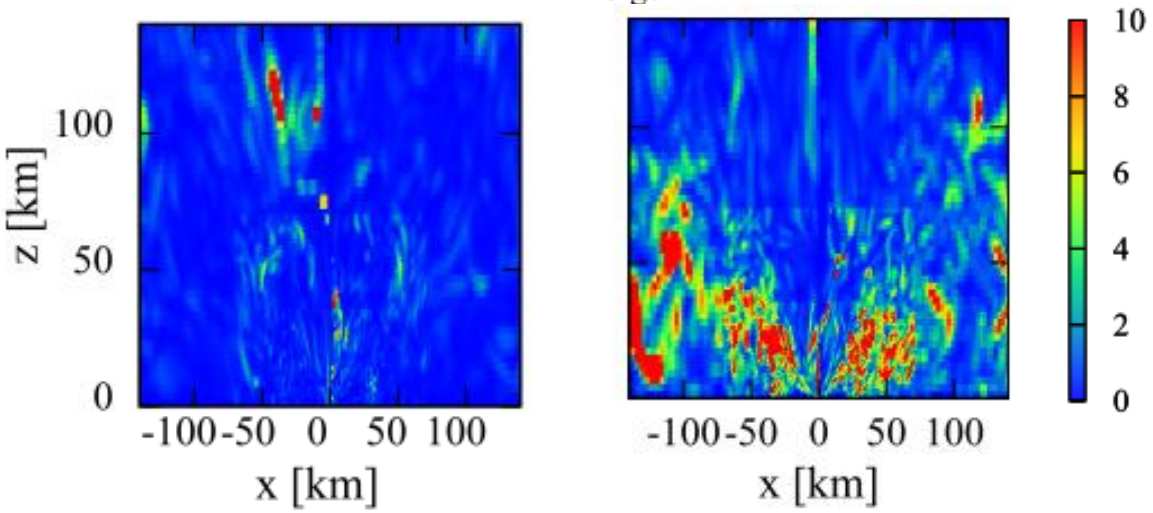

- Red region = MRI wavelength is covered by more than 10 grid points

2.7 $M_\odot$ model

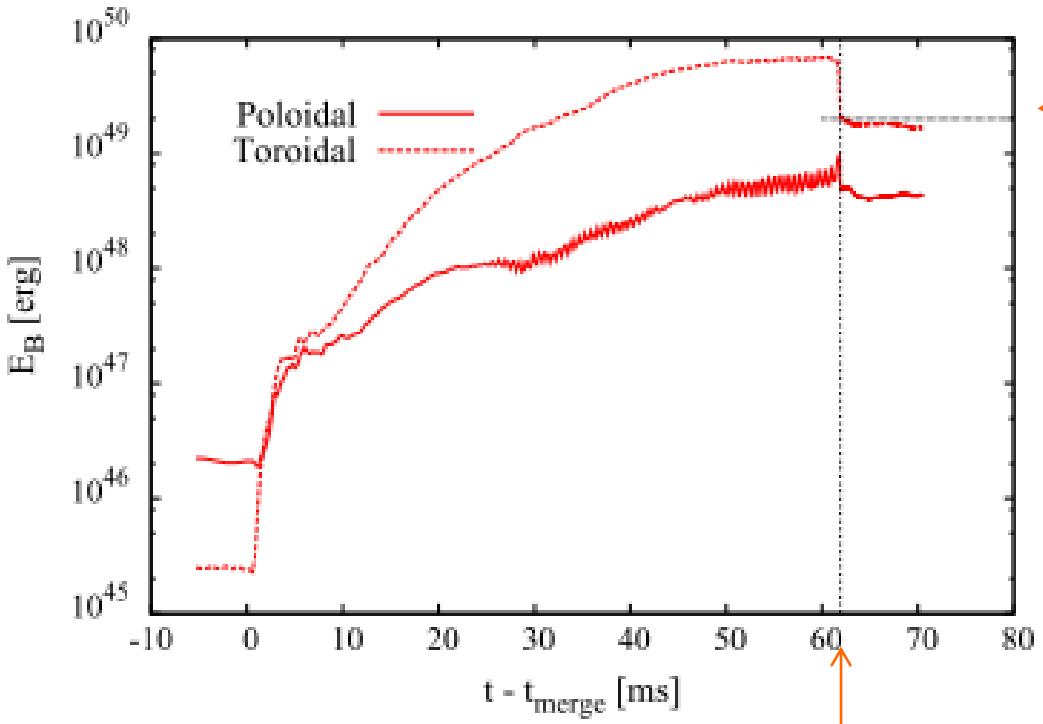

← Saturation

BH formation

- Strong magnetic pressure for the confined model
- 2.7 $M_\odot$ model is marginally stable
- Already reaches to a saturation level $\approx 2 \times 10^{49}$ erg (3-5 % of kinetic energy)

Mass ejection

Mass ejection is important for the electromagnetic counter part of BNS mergers

- synchrotron radiation (radio) (Nakar & Piran 11)

~ 2.5 mJy $(E_0/10^{49}\mathrm{erg})(n_0/1\mathrm{cm}^{-3})^{1/2}(\beta/0.2)^{-1}(D/300\mathrm{Mpc})^{-2}$

- r-process elements (optical) (Li-Paczynski 98, Metzger+10, 12)

t_{peak} ~ 0.1 day $(\beta/0.2)^{-1/2}(M_{eje}/10^{-3}\,M_\odot)^{1/2}$

L_{peak} ~ 7×10^{41} erg/s $(f/3\times10^{-6})(\beta/0.2)^{1/2}(M_{eje}/10^{-3}\,M_\odot)^{1/2}$

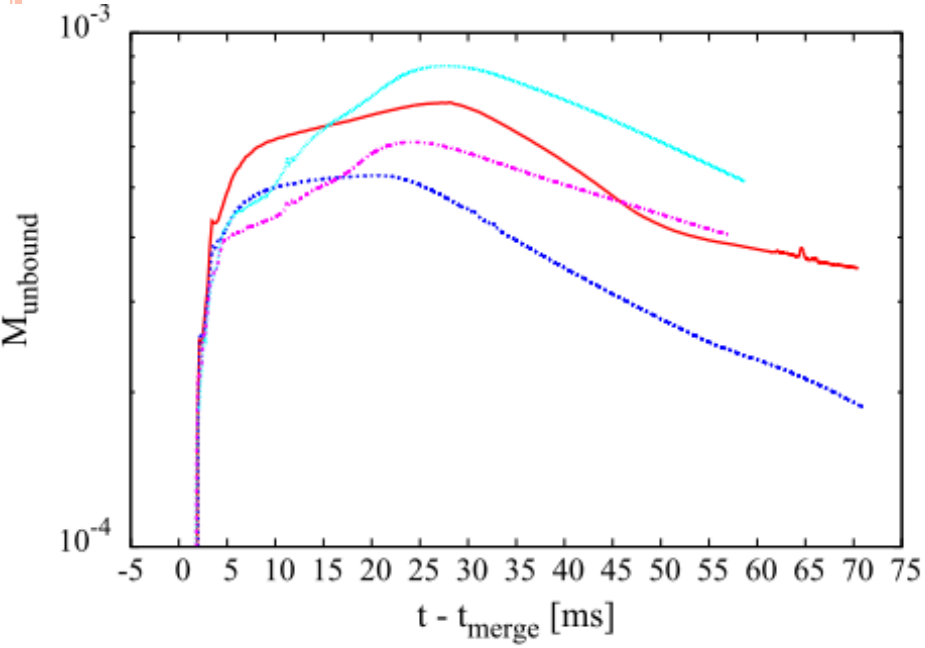

2.7 $M_\odot$– confined B

2.8 $M_\odot$– confined B

- Rapid rise due to the gravitational torque @ the merger
- M_{eje} ≈ several $\times10^{-4}\,M_\odot$
- Kinetic energy E_0 ≈$10^{49\text{-}50}$ erg

Summary for magnetized BNS mergers

- Torus around the BH is subject to the MRI

Long term and high-resolution simulation is essential

- Turbulent magnetic field develops inside the torus
- Saturation of MRI : magnetic energy ≈ 1-5 % of kinetic energy

<u>Future work</u>

- Higher resolution simulation, ultimately $\Delta x \approx 100$ m on K computer
- Weak magnetic field, e.g., $10^{11\text{-}13}$ G for observed NSs
- Systematic study for EOS
- Equilibrium configuration of magnetized binary neutron stars as initial conditions



Luminosity

2.7 $M_\odot$ model

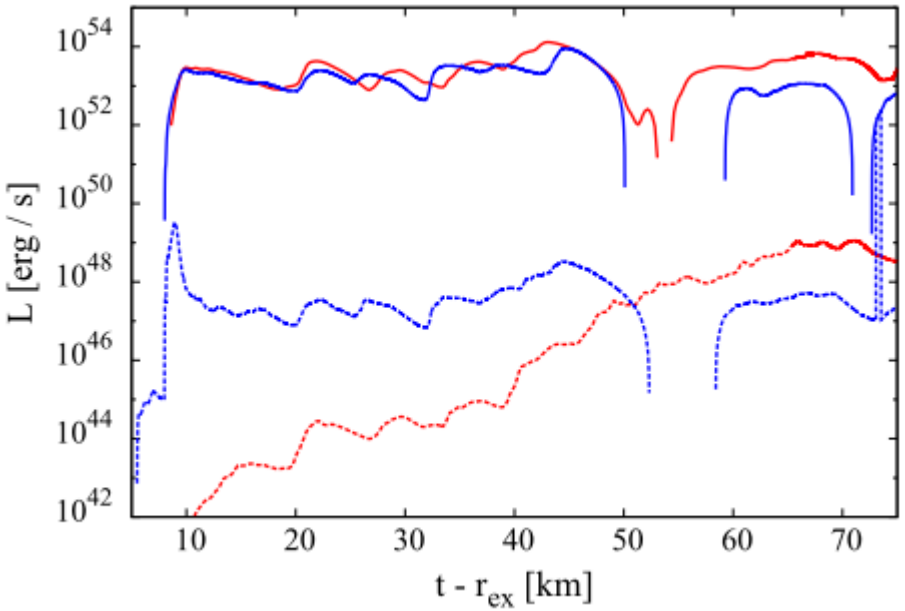

2.8 $M_\odot$ model

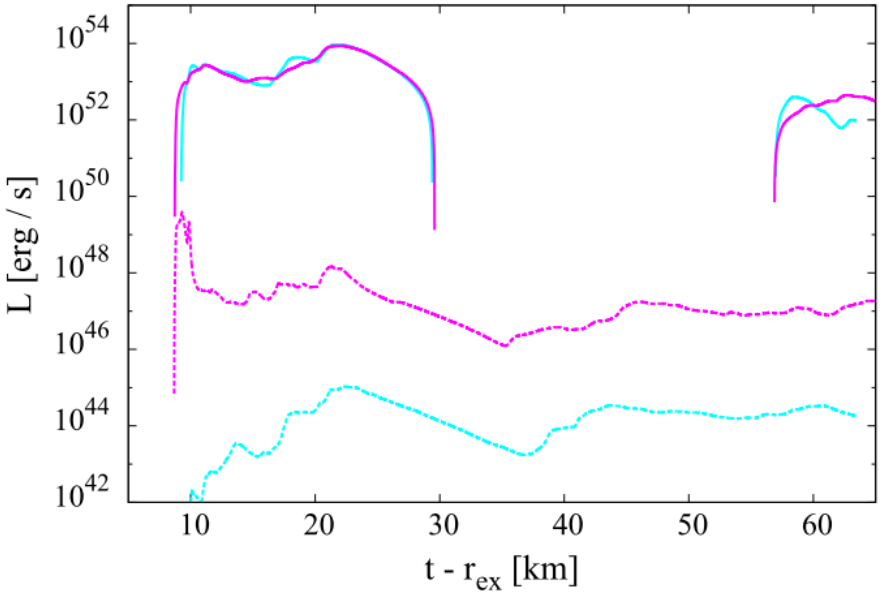

Gravitational wave astronomy and binary neutron star mergers

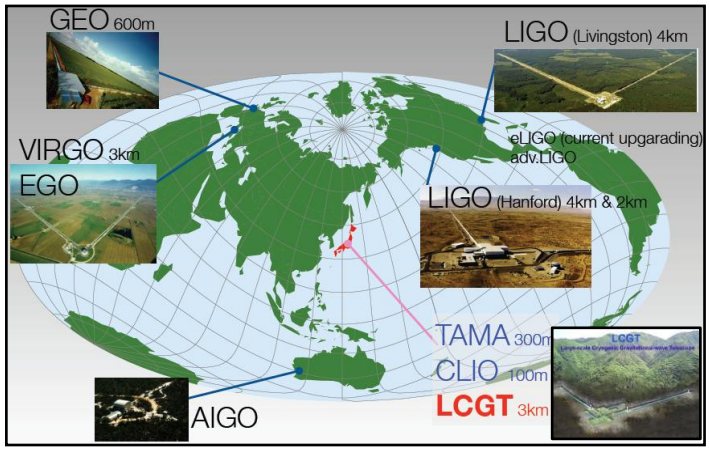

Gravitational waves

- Imprinting "raw" information of sources
- Extremely weak signal, $h_c \sim 10^{-22}$

Binary neutron star (BNS) mergers

- Promising source of GWs : 10 events / yr for KAGRA
- High-end laboratory for the nuclear theory :

Reconstruction of Mass-Radius relation

- Theoretical candidate of Short-Gamma-Ray Burst

(Narayan+ 92)

Numerical Relativity

BNS mergers

- Density ~10^{15} g / cm^3 (Strong interaction)
- Temperature ~10^{11} K (Weak interaction)
- Strong gravity (Gravity)
- Magnetic field ~$10^{11\text{-}14}$ Gauss (Electromagnetic force)

Numerical Relativity : Simultaneously solving

- the Einstein equations
- Relativistic (magneto) hydrodynamics
- Radiation field for neutrino

Unique approach to explore phenomena in strong gravity



Dipole model

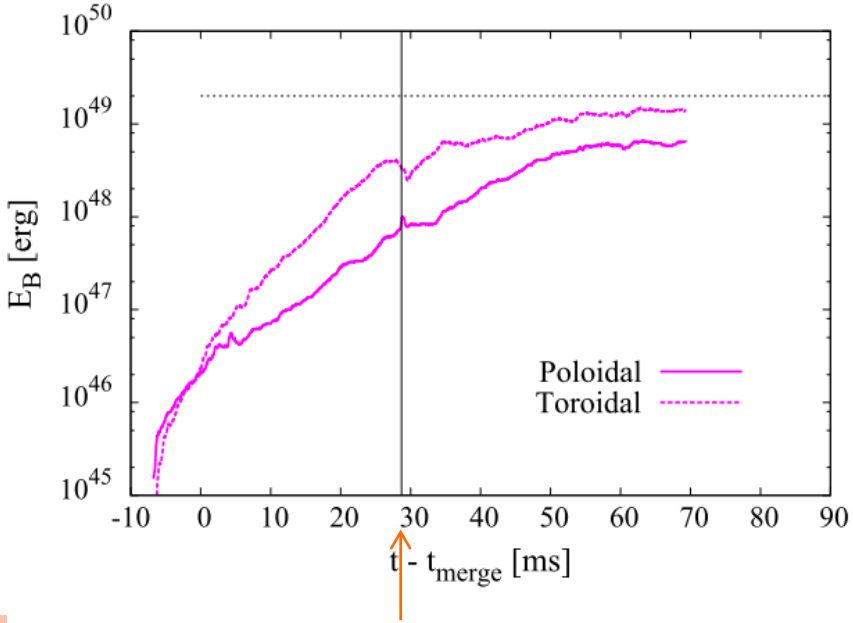

BH formation

Dipole field line

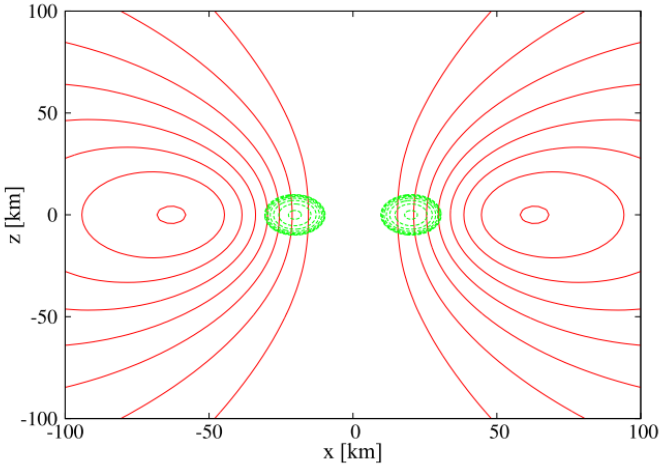

2.8 $M_\odot$ - Dipole model

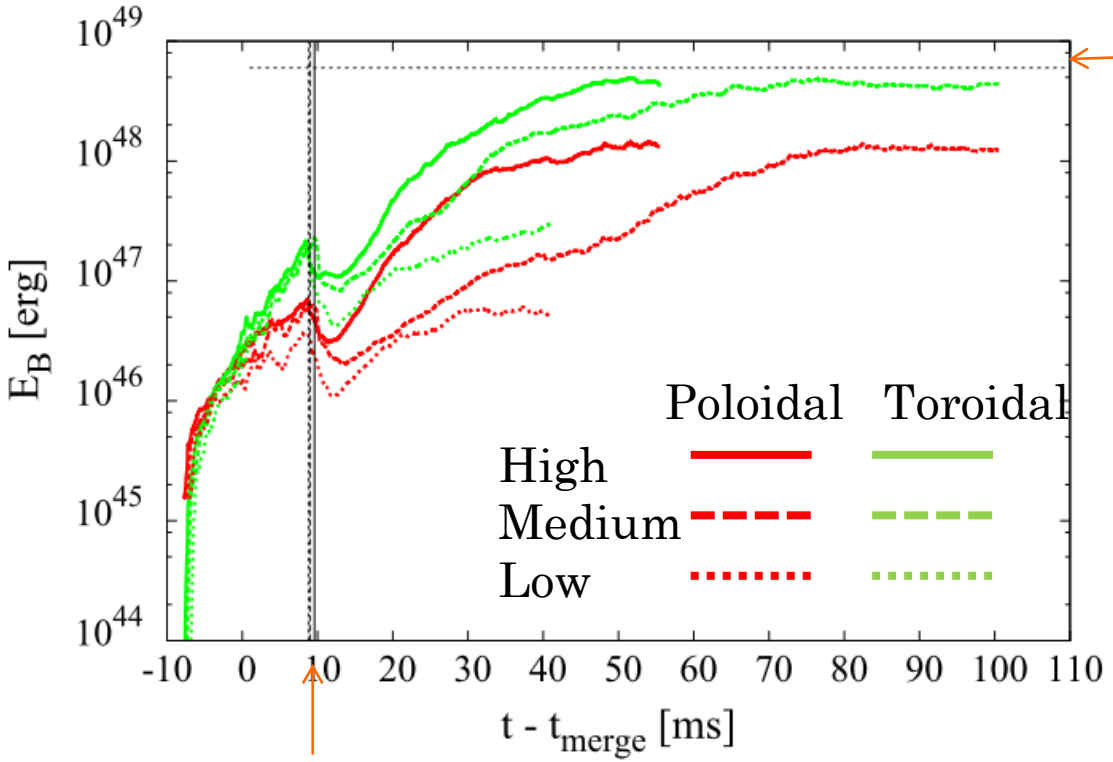

- Exponential growth in the high and middle resolution, not in the low resolution after the BH formation
- e-folding time ≈ 6 ms (high resolution model)
- Saturation level ≈ 6-7 $\times 10^{48}$ erg (2-3 % of the kinetic energy)

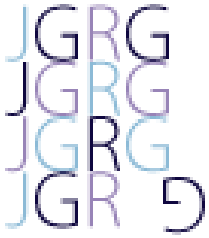

Hajime Sotani, JGRG 22(2012)111407

"Shear oscillations in hadron-quark mixed phase"

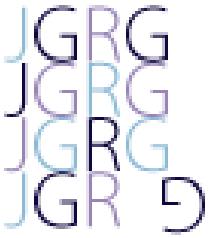

RESCEU SYMPOSIUM ON

GENERAL RELATIVITY AND GRAVITATION

JGRG 22



November 12-16 2012

Koshiba Hall, The University of Tokyo, Hongo, Tokyo, Japan



Shear Oscillations in Hadron-Quark Mixed Phase

Hajime Sotani (YITP)

T. Maruyama (JAEA)
T. Tatsumi (Kyoto Univ.)

Hadron-Quark Mixed Phase

- Nonuniform structure between the crust and core (pasta).
- As increasing the density, hadronic matter could change to quark matter with the *phase transition*.
- Similar to the pasta in crust region, the hadron-quark mixed phase may become nonuniform structure, whose properties depend strongly on the surface tension.
  - 10 MeV fm^{-2} < σ < 70 MeV fm^{-2}
- *How can we see such properties ??*

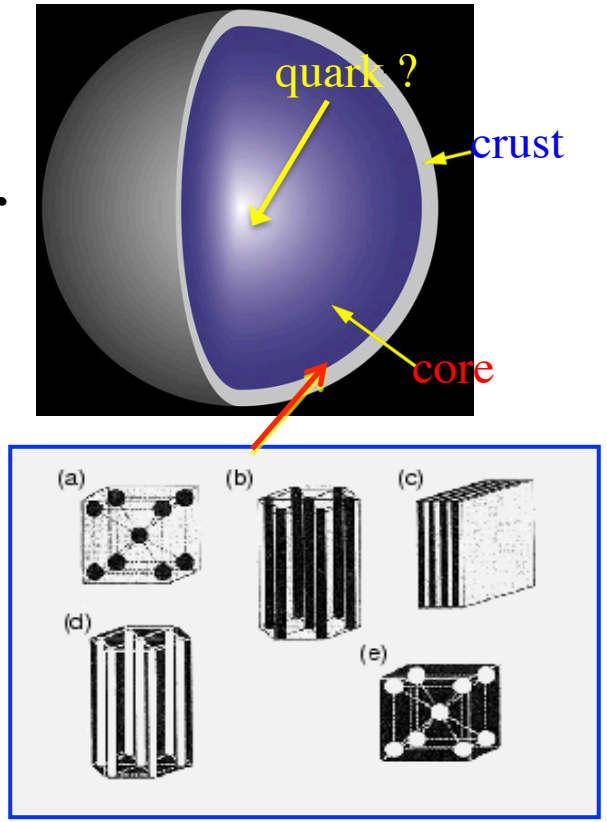

Asteroseismology

- Via the observations of stellar oscillations

  → One can get the interior information (**asteroseismology**)

  e.g., helioseismology for Sun

- With this technique, the possibilities to get the information of NSs have been suggested.

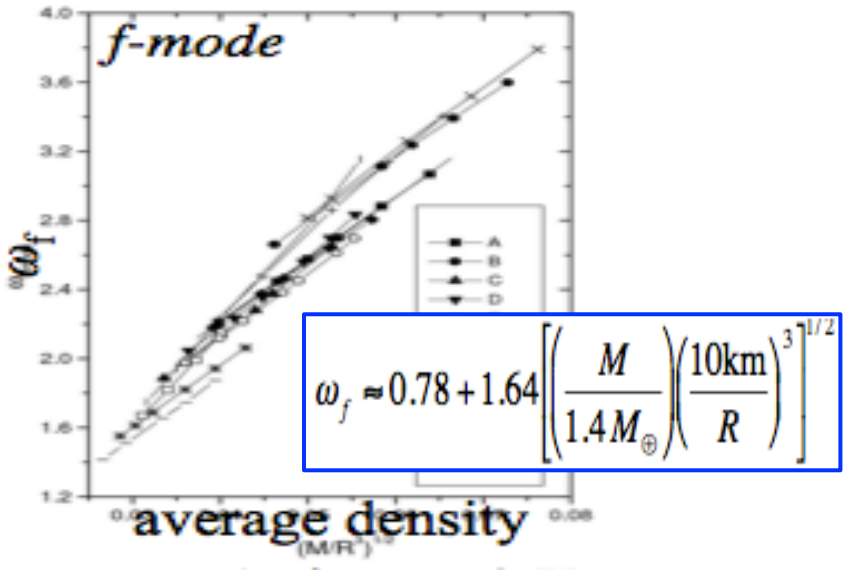

Andersson & Kokkotas (1998)

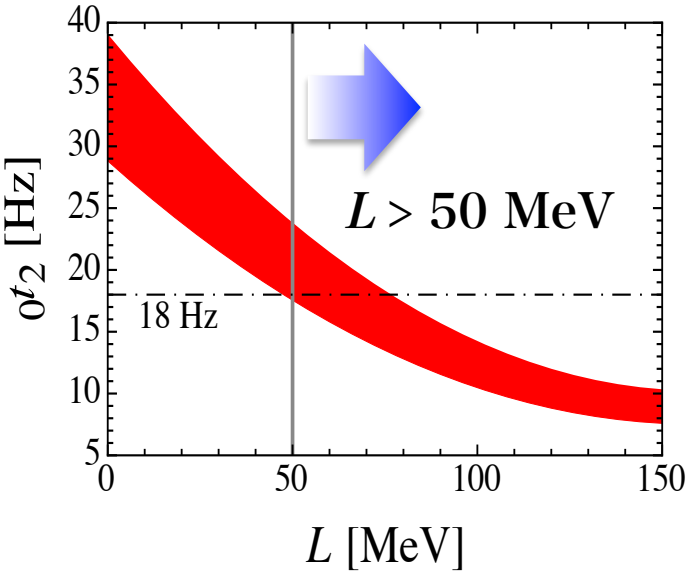

HS+2012

Shear Oscillations

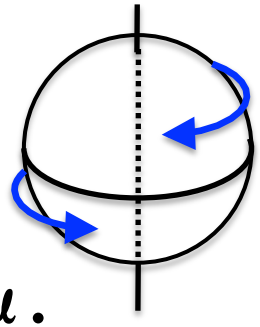

- Shear oscillations can be characterized by μ.
- We know the formula of μ only in bcc lattice.
  - considering the shear only in quark spherical droplet.
  - frequency of fundamental oscillation $\propto v_s$ ($v_s^2 \sim \mu/\rho$)
  - calculated frequencies could be lower limit

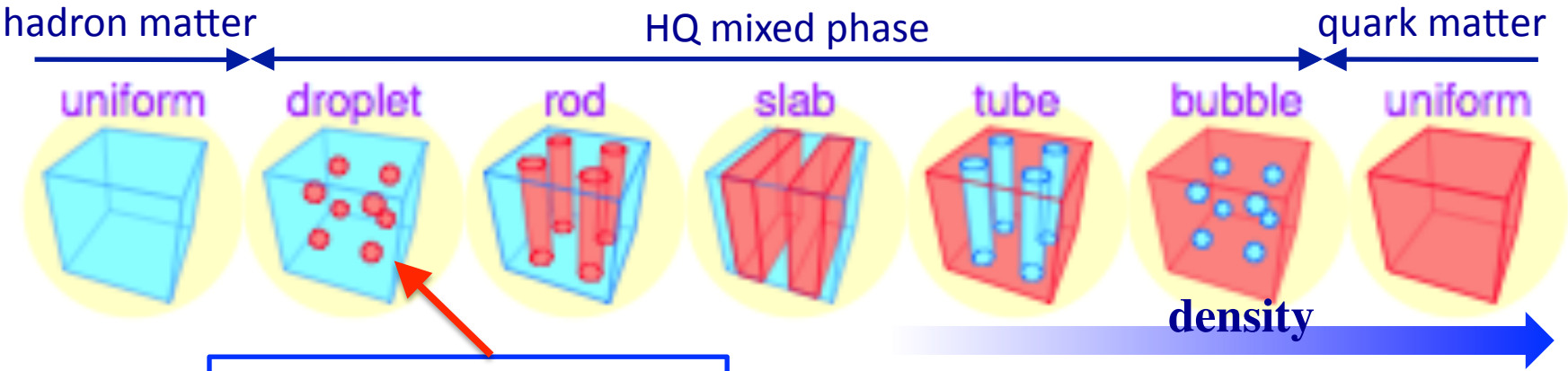

$$\mu = 0.1194 \frac{n_i (Ze)^2}{a}$$

strohmayer et al., 1991

n_i : number density of quark droplet
Z : charge of quark droplet
a : spacing of quark droplet

Shear Modulus

- $\mu \sim 10^{-10}$-10^{-9} in crust
- $\mu \sim 10^{-7}$-10^{-6} in HQ mixed phase
  - number of "charge" is quite different

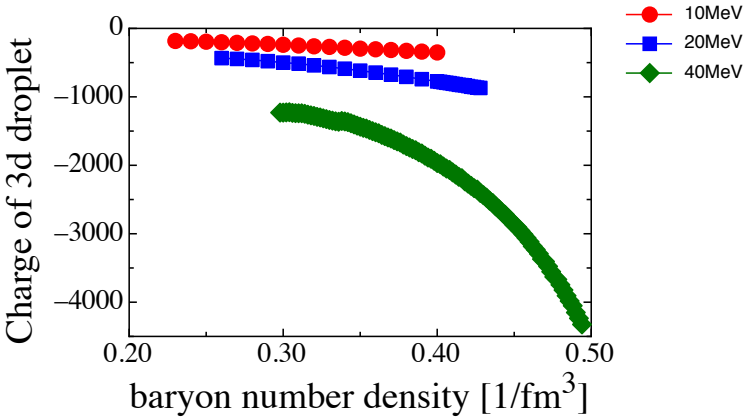

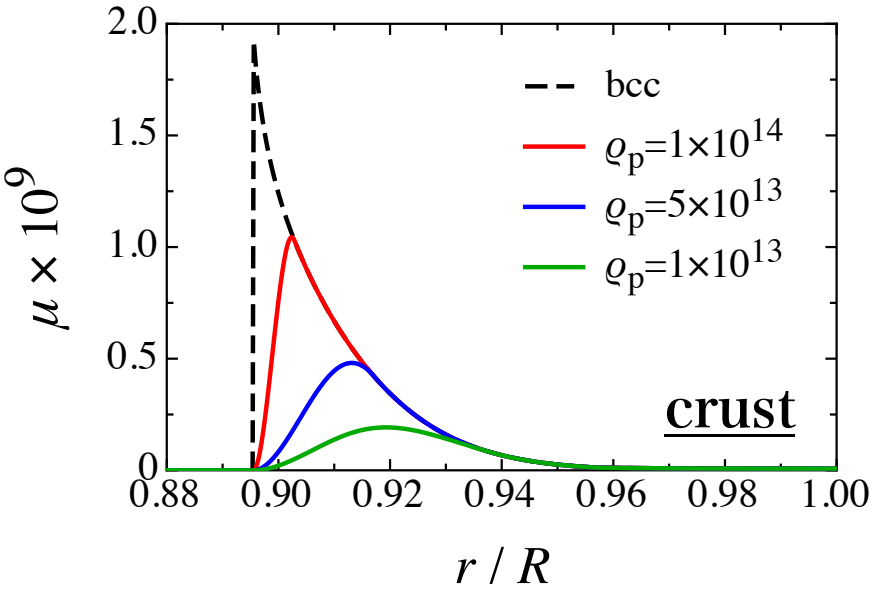

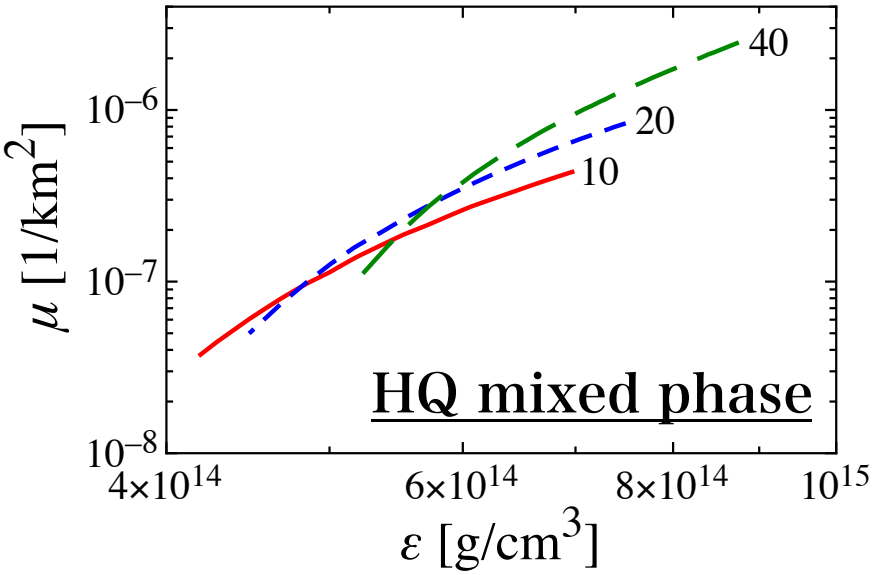

Estimations

- Compared with crust properties,
  - μ becomes ~10^3 times larger
  - ρ becomes ~10 times larger
  - $v_s = (\mu/\rho)^{1/2}$ could be ~10 times larger
- Frequencies of shear oscillations $\propto v_s$
  - In HQ mixed phase, the frequencies of shear oscillations could become ~10 times larger than that in crust.

Fundamental Oscillations 1

- Frequencies of fundamental shear oscillations as a function of stellar mass
  - those depend strongly on the surface tension

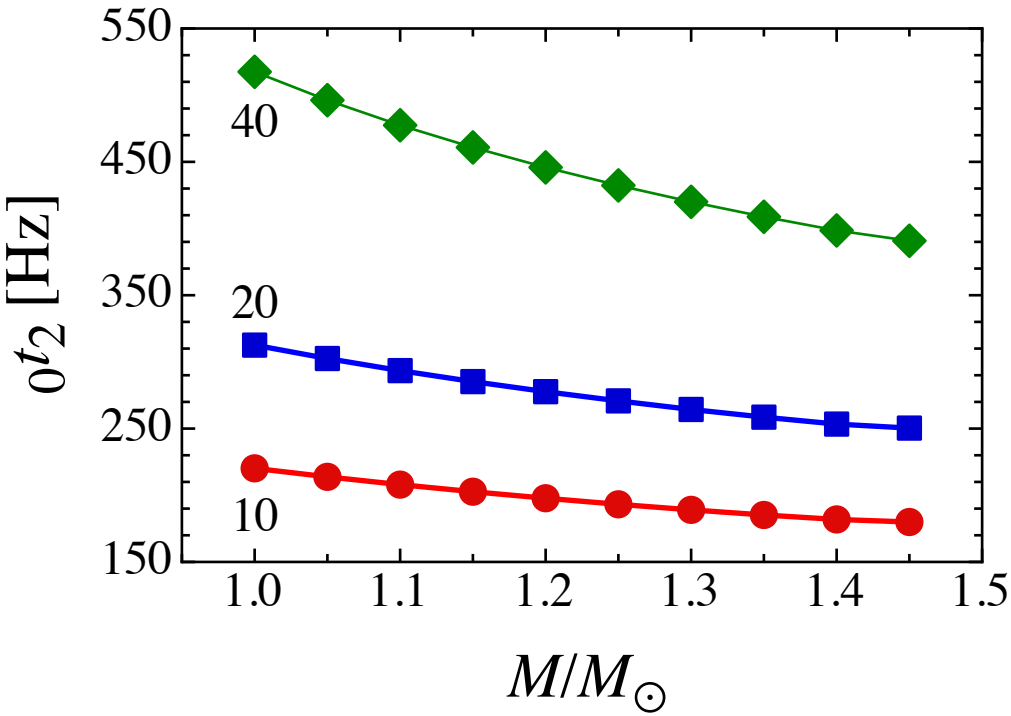

c.f.) $_0t_2$ in crust ~ 20 - 30 Hz

Fundamental Oscillations 2

- We find that the frequencies of fundamental shear oscillations are almost proportional to σ.
- With the help of the observation of stellar mass, it might be possible to obtain the value of σ.

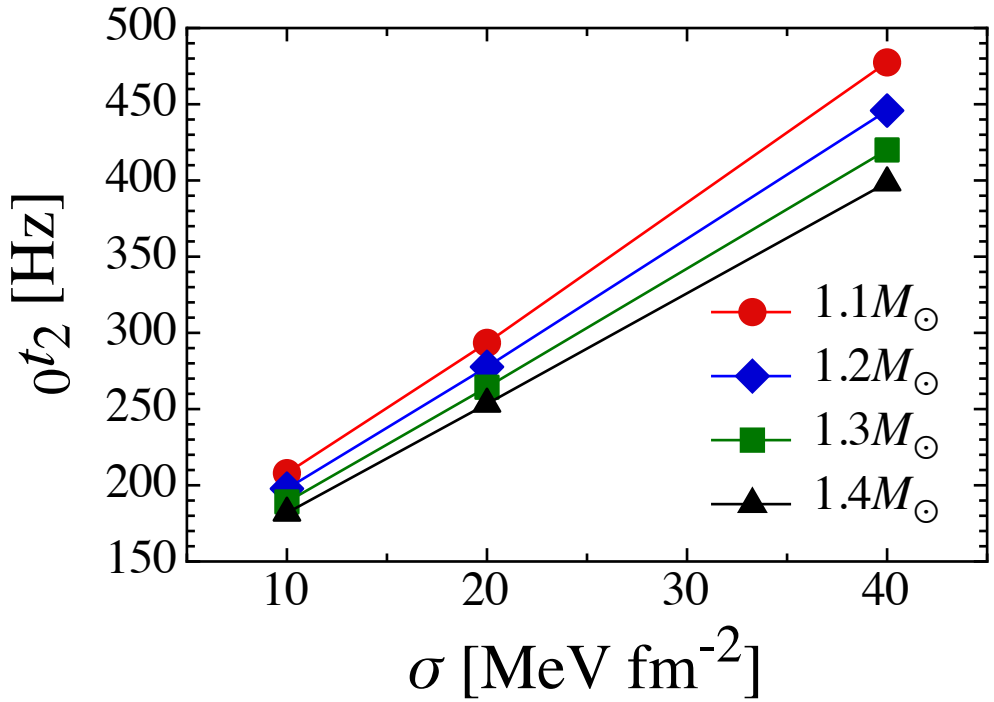

Fundamental Oscillations 2

- We find that the frequencies of fundamental shear oscillations are almost proportional to σ.
- With the help of the observation of stellar mass, it might be possible to obtain the value of σ.

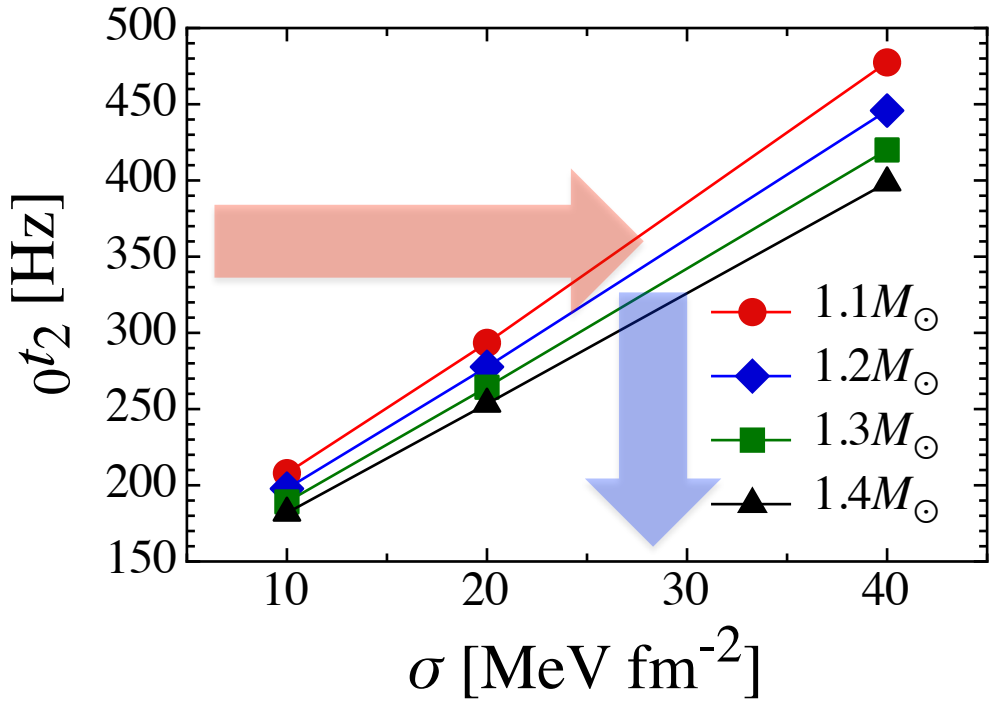

Conclusion

- We consider the shear oscillations in hadron-quark mixed phase, whose properties depends strongly on the surface tension.
- Frequencies of shear oscillations in HQ phase becomes ~10 times larger than those in crust.
- Frequencies of fundamental oscillations are proportional to surface tension.
- We show the possibility to determine the value of σ.
  - With the help of the observation of stellar mass, one might be possible to obtain the value of σ via the observation of shear oscillations.

1st Overtones

- Frequencies of 1st overtone shear oscillation as a function of stellar mass
- We can not see the linearity with respect to σ.

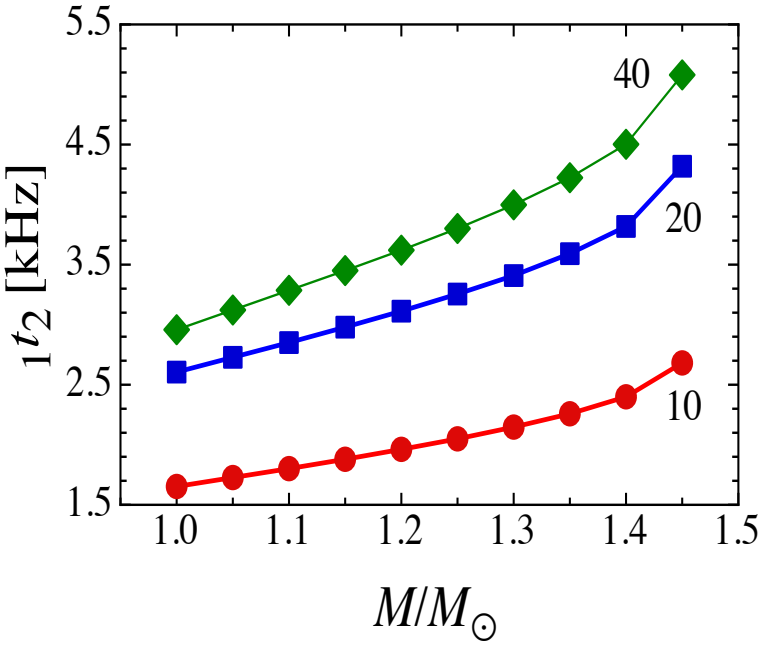

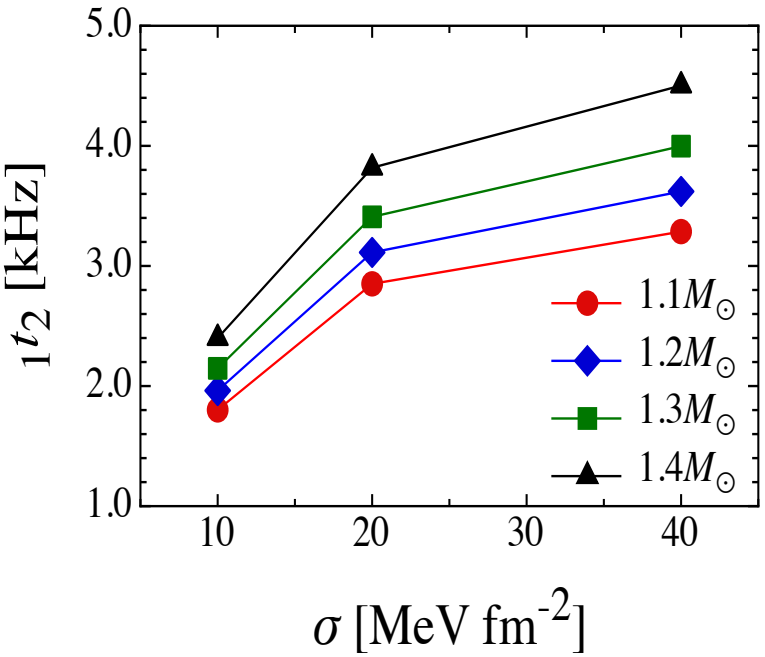

Comparison with QPO frequencies

HS+(2012b)

- Comparison of frequencies of torsional oscillations with the QPO frequencies observed in SGR 1806-20

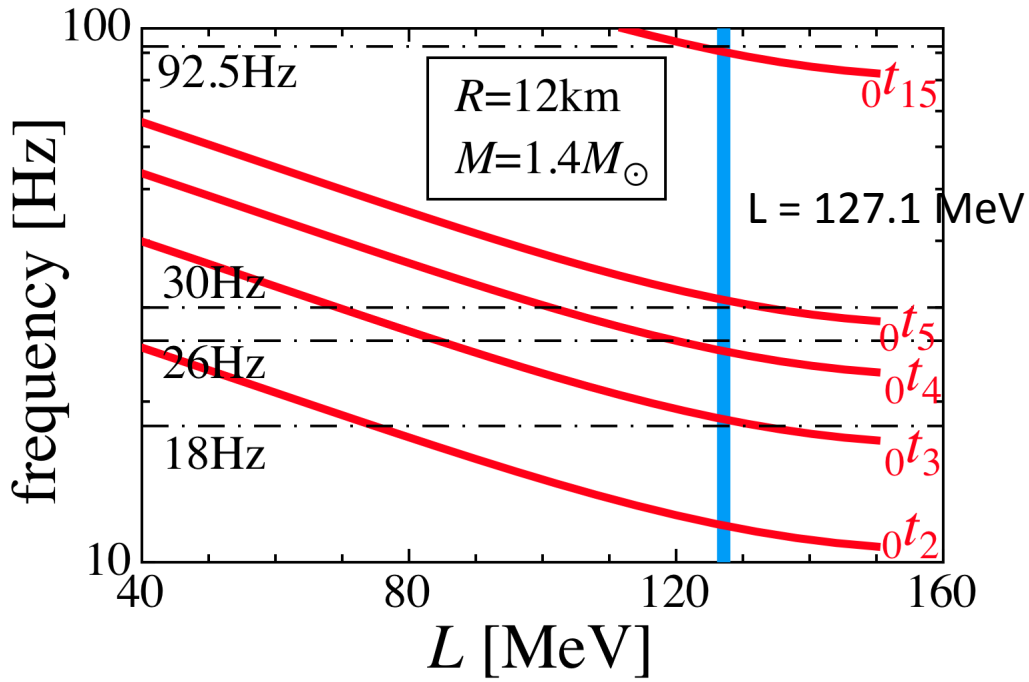

- less than 5% accuracy

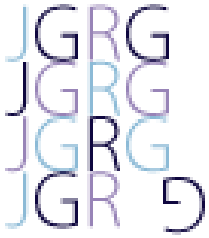

Shin'ichirou Yoshida, JGRG 22(2012)111408

"Non-axisymmetric oscillations of rotating relativistic stars by conformally flat approximation"

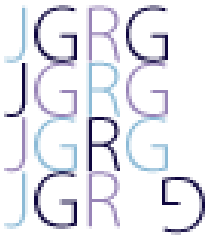

RESCEU SYMPOSIUM ON

GENERAL RELATIVITY AND GRAVITATION

JGRG 22



November 12-16 2012

Koshiba Hall, The University of Tokyo, Hongo, Tokyo, Japan



Non-axisymmetric oscillations of rotating relativistic stars by conformally flat approximation

Shin'ichirou Yoshida (The University of Tokyo)

Studies of oscillations of rapidly rotating relativistic stars

<u>astrophysical interests</u>

as sources of gravitational wave $\nu \sim \mathrm{several} \cdot (10^2 - 10^3)\mathrm{Hz}$

ground-based laser-interferometers
resonant detectors

stability of stars

determining maximum masses/rotational period of NS

Aim of the studies:

Compute characteristic(eigen-) frequencies of "realistic" NS models.

Determine the stability boundaries of a parameter space of rotating stars.

Preceding studies of oscillations of rotating stars in GR

via traditional eigenvalue problem

Kojima (1992,1997) slow-rotation
Yoshida & Kojima (1997) slow-rotation

Cutler & Lindblom (1992) post-Newtonian

Yoshida & Eriguchi (1997,1999) Cowling; f-modes
Yoshida & Eriguchi (2001) Cowling; axisymmetric modes
Yoshida et al. (2002,2005) Cowling; f-modes

Lockitch et al. (2001) slow-rotation, relativistic inertial modes

Ruoff & Kokkotas (2001,2002) slow-rotation, relativistic r-modes

Ferrari et al. (2004) Cowling; rotating proto-NS
Passamonti et al. (2006) slow-rotation
Ferrari et al. (2007)

via direct hydrodynamical simulations

Font et al. (2001) Cowling; axisymmetric oscillations
Dimmelmeier et al. (2006) spatially conformal-flat; axisymmetric oscillations

Saijo et al. (2001) post-Newtonian
Saijo (2005) spatially conformal-flat

Shibata & Sekiguchi (2003) full GR; axisymmetric oscillations
Shibata & Karino (2004) post-Newtonian; bar-mode instability
Shibata & Sekiguchi (2005) full GR; dynamical instability

Stavridis et al. (2007) slow-rotation(differential)
Kastaun et al. (2010) Cowling
Krueger et al. (2010) Cowling
Gaertig & Kokkotas (2009,2011) Cowling (also g-modes)

Baiotti et al. (2007) full GR; bar-mode instability
Manca et al. (2007) full GR; dynamical instability
Takami et al. (2011) full GR; axisymmetric instability

"Cowling"=*Cowling approximation* where metric perturbation is neglected

* *non-linear hydrodynamic simulation*

* *linear hydrodynamic simulation*

Full GR treatment is rather expensive!

* eigenvalue problem - no formulation exists except for slowly rotating cases!
(messy equations; how do we impose boundary conditions?)

* direct numerical simulations - numerically expensive
identification & extraction of eigenmodes?

For a "fluid mode", its gravitational damping time is several orders of magnitude longer than the period ⟶ We may neglect the gravitational radiation effect.

But, neglecting all the gravitational perturbation (Cowling approximation) is not satisfactory, especially for the low-order modes.

We want something better than Cowling, but easier to handle than "full GR".

↓

Conformally flat approximation!!

General relativistic hydrodynamics with spatially conformally-flat approximation

Isenberg (1978) ;Wilson et al. (1996) : Solving system of elliptic eqs. for metrics
"Isenberg-Wilson-Mathews theory"

Applications

Wilson et al.(1996) - binary NS quasi-equilibrium

Glanclement et al. (2002) - binary BH quasi-equilibrium

Oechslin et al. (2002;2004) - NS merger

Faber et al. (2004) - NS merger

Dimmelmeier et al.(2002) - Core-collapse SN

Saijo (2005) - bar-instability in core collapse

Dimmelmeier et al.(2006) - Non-linear oscillations of NS

Formulation

assumptions
+ a background star - stationary, axisymmetric, isentropic
+ barotropic EOS - no buoyancy (no g-modes)
+ linear perturbation
+ spatially conformally flat approximation (CFA) of gravity
  - both equilibrium & perturbed state

[CFA]

$$ds^2 = -\alpha^2 dt^2 + \psi^4 f_{ij}(dx^i + \beta^i dt)(dx^j + \beta^j dt); \quad f_{ij}: \text{ flat metric}$$

"(3+1)-" form of Einstein's equation in CFA:
Hamiltonian & Momentum constraint, "evolution" of Kij (K=0)

$$\hat{\nabla}^i \hat{\nabla}_i \psi = -2\pi\psi^5 \left(\rho_H + \frac{1}{64\pi\alpha^2} \hat{\Lambda}_{ij} \hat{\Lambda}^{ij} \right)$$

$$\hat{\nabla}^i \hat{\nabla}_i (\alpha\psi) = 2\pi\alpha\psi^5 \left(\rho h(3(\alpha u^t)^2 - 2) + 5p + \frac{7}{64\pi\alpha^2} \hat{\Lambda}_{ij} \hat{\Lambda}^{ij} \right)$$

$$\hat{\nabla}^i \hat{\nabla}_i \beta^j = 16\pi\alpha\psi^4 S^j - \frac{1}{3} \hat{\nabla}^j (\hat{\nabla}_k \beta^k) + \hat{\Lambda}^{jk} \hat{\nabla}_k \ln \left(\frac{\alpha}{\psi^6} \right)$$

$$\rho_H := n_a n_b T^{ab} \quad S^j := -\delta^j_a n_c T^a_c \quad \hat{\Lambda}^{ij} := \hat{\nabla}^i \beta^j + \hat{\nabla}^j \beta^i - \frac{2}{3} f^{ij} \hat{\nabla}_k \beta^k$$

$$T^{ap} := \rho h u^a u^b + p g^{ab}$$

Formulation - contd.

[equations of hydrodynamics]

rest mass conservation

$$\partial_a \pi^a + \pi^a \partial_a \ln\left(\frac{\rho}{h}\right) + \pi^a \left(\frac{\partial_a \alpha}{\alpha} + \frac{6\partial_a \psi}{\psi} + \frac{2}{r}\delta^r_a + \cot\theta \delta^\theta_a\right) = 0$$

momentum equation

$$\pi^b \partial_b \pi_j - \pi^b \partial_j \pi_b = 0$$

$$\pi_a := h u_a$$

Linearizing equations above and supplementing with boundary conditions, we set up an eigenvalue problem.

% boundary conditions

+ metric components $\psi,\ \alpha,\ \beta^j$ --- regularity at the origin & at the infinity
+ fluid variables $h,\ \pi_j$ --- regularity at the origin
  stress free surface :
  $\Delta p = 0$ (Lagrangian perturbation of pressure vanishes).

Numerical treatment

(A) metric part: given sources (S), formal solutions are obtained by Green's functions

$$\hat{\nabla}_i \hat{\nabla}^i q = S \quad \rightarrow \quad q = \int S(\vec{y}) G(\vec{x}|\vec{y}) dV_y$$

(B) fluid part: equations are descretized

$$\mathbf{U}(\mathbf{f}) = \mathfrak{g}(q)$$

$\mathbf{f}$: array vector of fluid variables

$\mathbf{U}$: array of operators describing hydro-equations

regarded as source terms when q is given

Equations of fluid part are solved by Newton-Raphson method.

(A) and (B) are iteratively solved. => eigenmode!

Numerical treatment - contd.

* background star is stationary and axisymmetric
  => perturbation is decomposed into harmonic components

$$\delta f \sim \exp[-i\sigma t + im\varphi] \cdot F(r,\theta)$$

The problem is reduced to 2D eigenvalue problem.

* Surface-fitted coordinate: $r = R_s(\theta^*)\ r^*$ $\quad p(R_s,\theta) = 0$ (equilibrium surface)

$$\theta = \theta^*$$

Equilibrium stellar surface is always mapped to r*=1.
==> Boundary condition is easy to impose.

computational grids

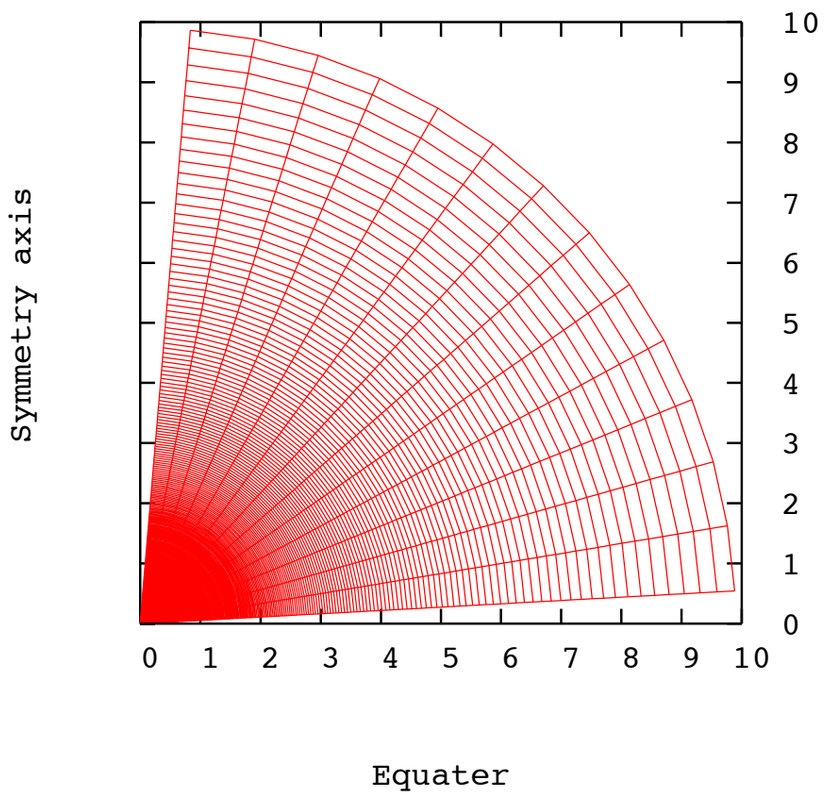

* radial grid points: non-uniform distribution (r*=1 on the equatorial surface)
* angular grid points: zeroes of Legendre function

-- For stellar interior, "fluid" and "metric" grids are staggered.

Results - quadrupole modes of slowly rotating star

$$\delta f \sim \exp(-i\sigma t + im\varphi)$$

$$\sigma = \sigma^0 + m\ \sigma'\ \Omega$$

non-rotating　　rotational correction

Mode	M / R	$\sigma^0_{CFA}/\sigma^0_R$	σ^0_{Cw}/σ^0_R	σ'_{CFA}/σ'_R	σ'_{Cw}/σ'_R
f	0.100	0.998	1.26	0.998	1.02
	0.200	0.997	1.15	1.00	1.01
P_1	0.100	1.00	1.10	0.994	1.00
	0.200	0.997	1.11	0.991	1.01
P_2	0.100	1.00	1.05	0.997	1.00
	0.200	0.999	1.06	1.00	1.00

EOS --- $p = K\epsilon^2$

Cw: Cowling approximation (Yoshida & Kojima 1997)

Results - quadrupole modes of slowly rotating star

eigenfunctions of P_l mode

δh

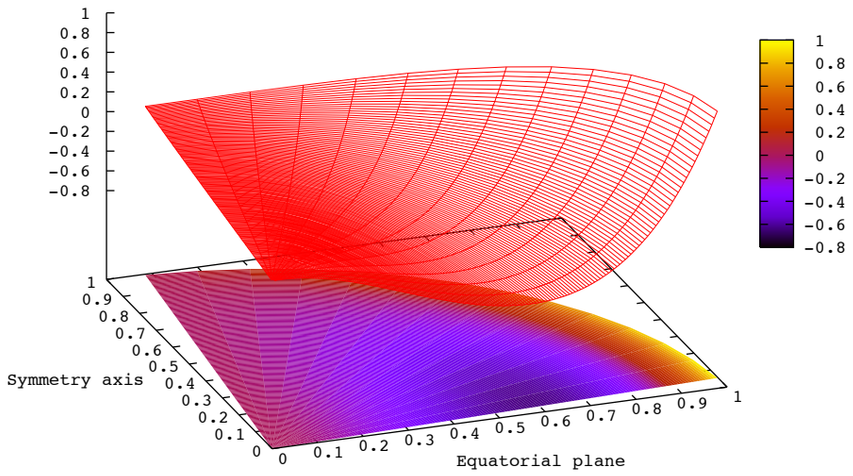

$\delta \pi_r$

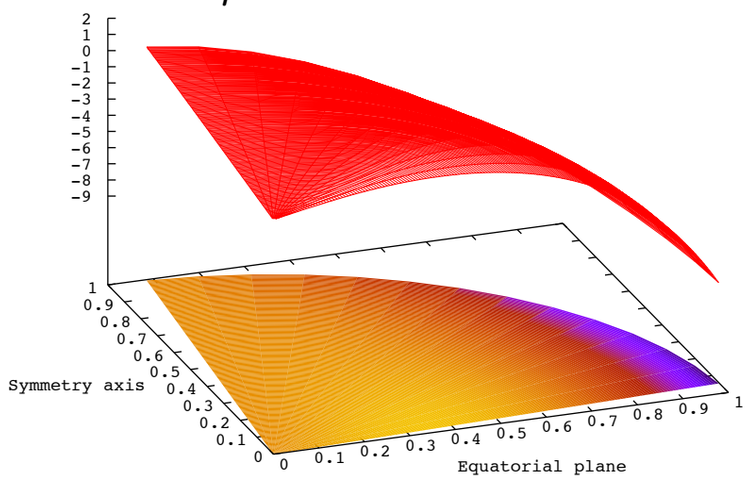

$\delta \pi_\theta$

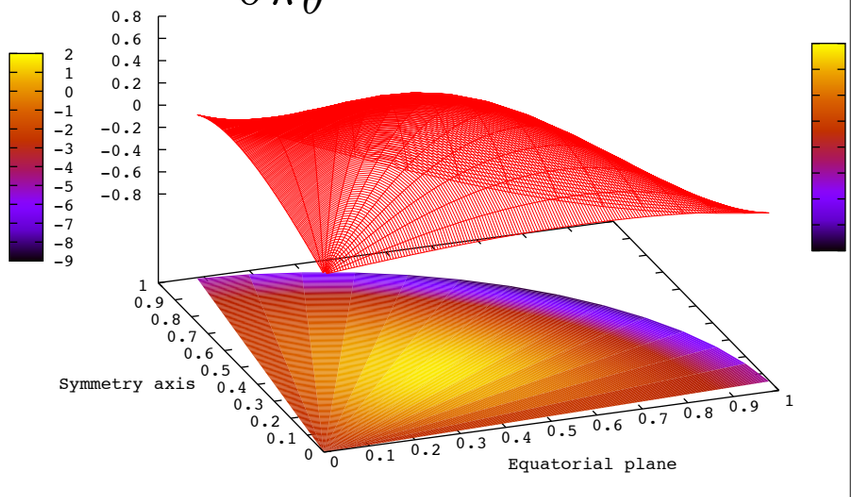

$\delta \alpha$

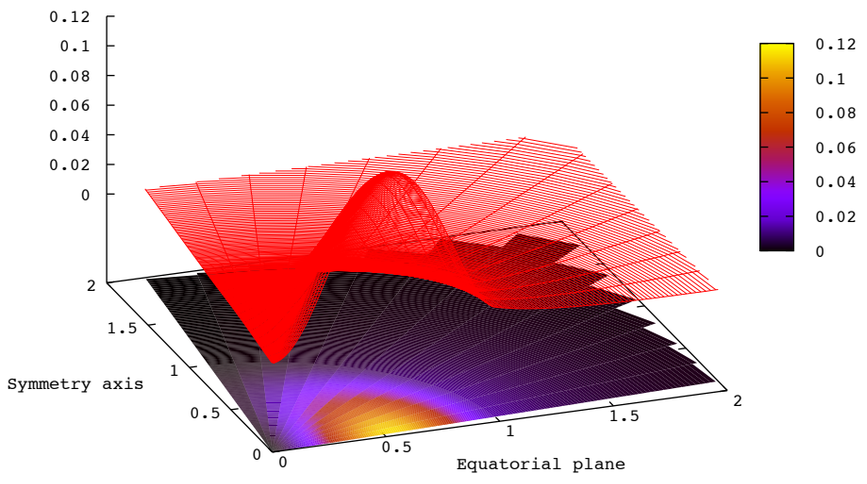

$\delta \psi$

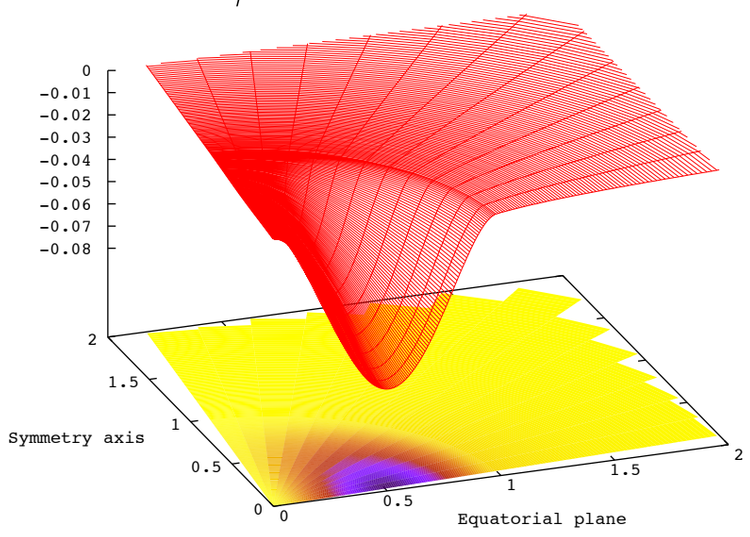

$\delta \beta^\theta$

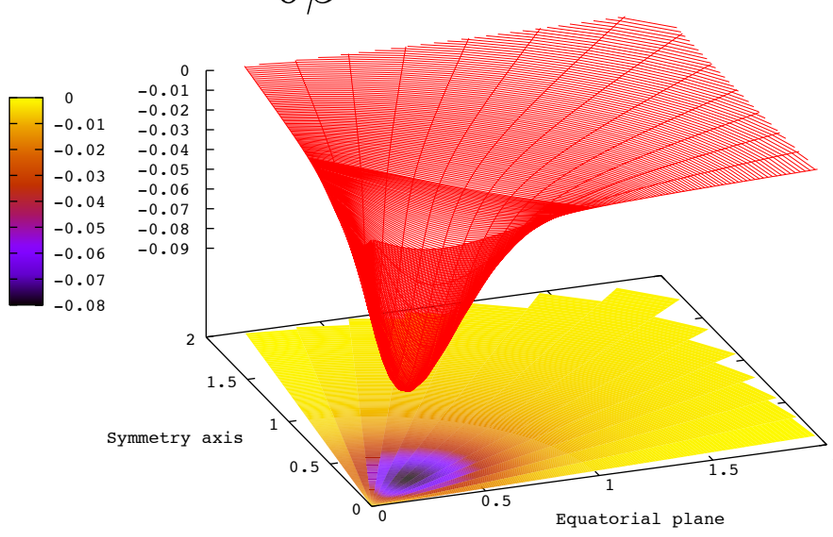

CFS instability Chandrasekhar (1970), Friedman & Schutz (1985)

instability in pulsations of rotating stars that couple to (gravitational) radiation field --- f-mode, r-mode instability

From the inertial frame, the star (with a marker dot) and the mode pattern is rotating in clockwise direction.

Angular momentum carried away by gravitational wave has the same sign as that of the star.

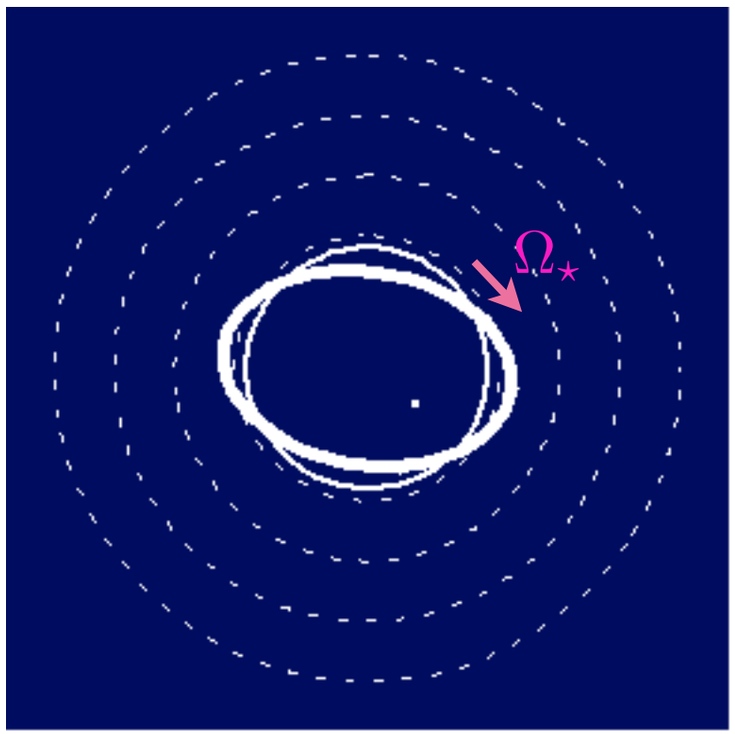

inertial frame view

From the corotating frame of star (in which the star is at rest), the mode pattern is rotating in counter-clockwise direction. This mode has an opposite sign of canonical angular momentum to that of star (and that of gravitational wave).

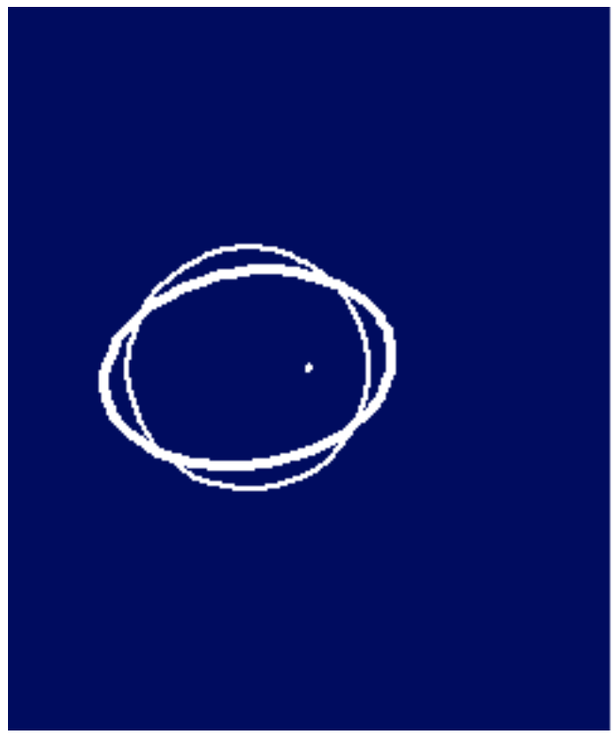

corotating frame view

zeroes of frequency (seen from the inertial frame) marks the onsets of the instability.

Results - sequences of counter-rotating f-modes

Equilibria: computed by COCAL code (Uryu & Tsokaros 2012)

EOS: $p = K\rho^2$

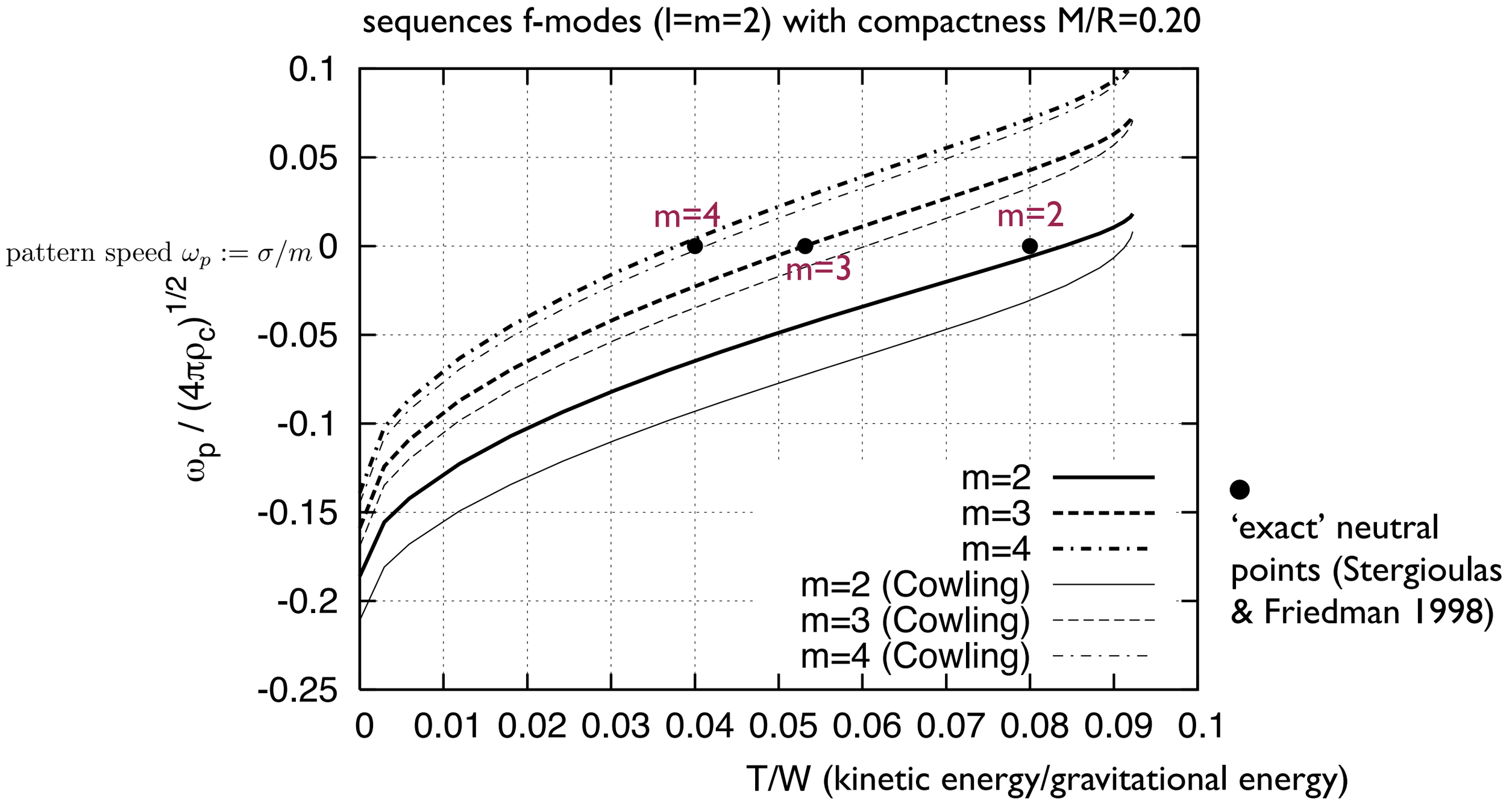

Summary

We developed a new code to solve eigenmode problem of rotating star with arbitrary rotation.

spatially conformal flatness approximation
=> suppressing gravitational radiation

Compared to conventional Cowling approximation, the eigenmodes obtained are highly improved.

What' s coming next?

* differential rotation --- proto-NS ; dynamical instability of rotating stars
* nuclear EOS --- asteroseismology of NS
* stably stratified star --- g-modes of rotating stars in GR

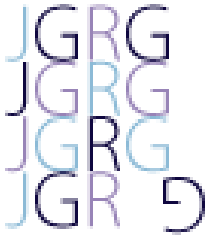

Motoyuki Saijo, JGRG 22(2012)111409

"Nonlinear effect of r-mode instability in uniformly rotating stars"

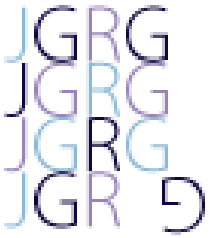

RESCEU SYMPOSIUM ON

GENERAL RELATIVITY AND GRAVITATION

JGRG 22



November 12-16 2012

Koshiba Hall, The University of Tokyo, Hongo, Tokyo, Japan



Nonlinear Effect of R-mode Instability in Uniformly Rotating Stars

Motoyuki Saijo (Rikkyo University)

CONTENTS

1. Introduction

2. Dynamical approach beyond acoustic timescale

3. Nonlinear r-mode instability

4. Summary

22nd General Relativity and Gravitation in Japan
14 November 2012 @RESCEU, The University of Tokyo, Japan

1. Introduction

Various Instabilities in Secular Timescale

CFS instability

(Chandrasekhar 70, Friedman & Schutz 78)

- Fluid modes (f, p, g-modes) may become unstable due to gravitational radiation
- Instability occurs in dissipative timescale

r-mode instability

(Andersson 98, Friedman & Morsink 98)

- Fluid elements oscillate due to Coriolis force
- Instability occurs due to gravitational radiation

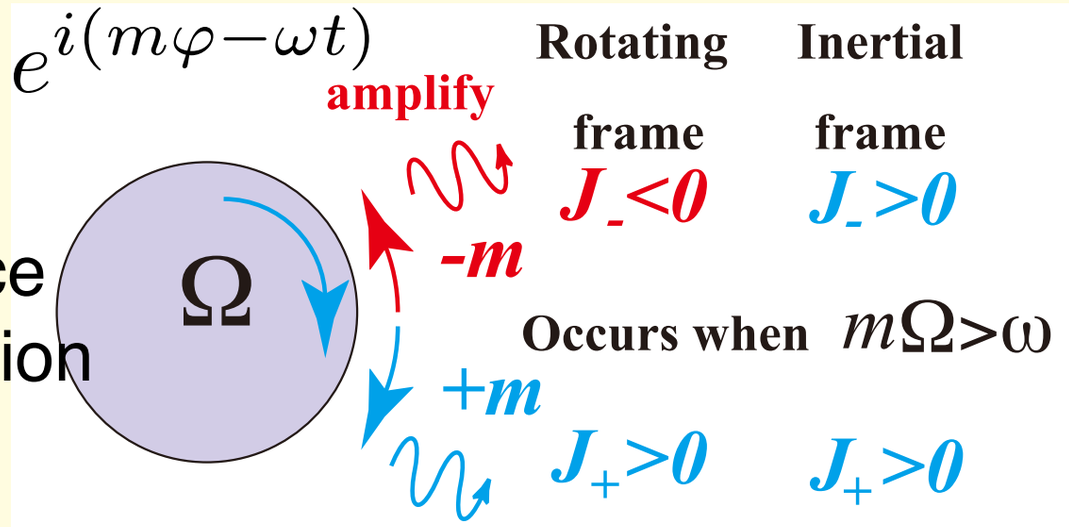

g-mode instability

- Fluid elements oscillate due to restoring force of buoyancy
- Instability occurs in nonadiabatic evolution or in convective unstable cases

Kelvin-Helmholtz instability

- Instability occurs when the deviation of the velocity between the different fluid layers exceeds some critical value

Dynamics of r-mode instabilities

Saturation amplitude of r-mode instability

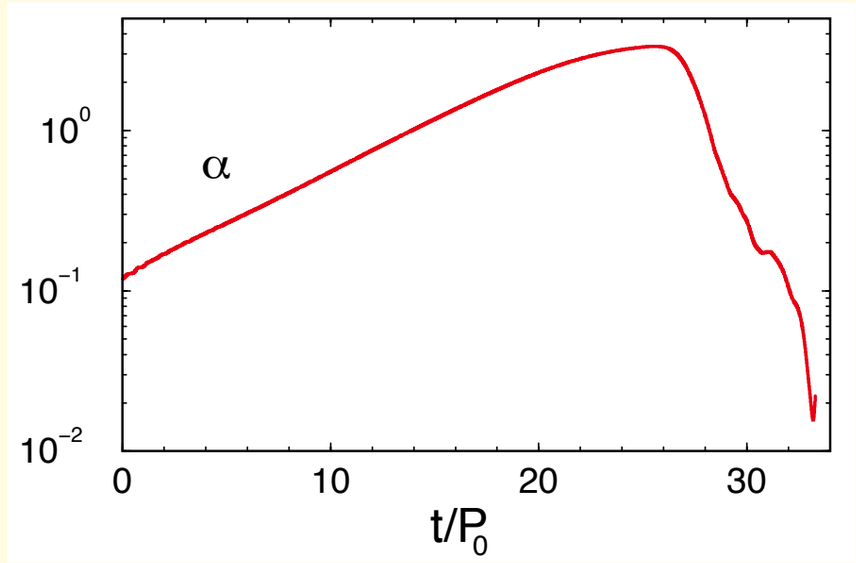

3D simulation

- Saturation amplitude of o(1)
- Imposing large amplitude of radiation reaction potential in the system to control secular timescale with dynamics (Lindblom et al. 00)

1D evolution with partially included 3 wave interaction

- Saturation amplitude of ~ o(0.001), which depends on interaction term

Final fate of r-mode instability

(Schenk et al. 2001)

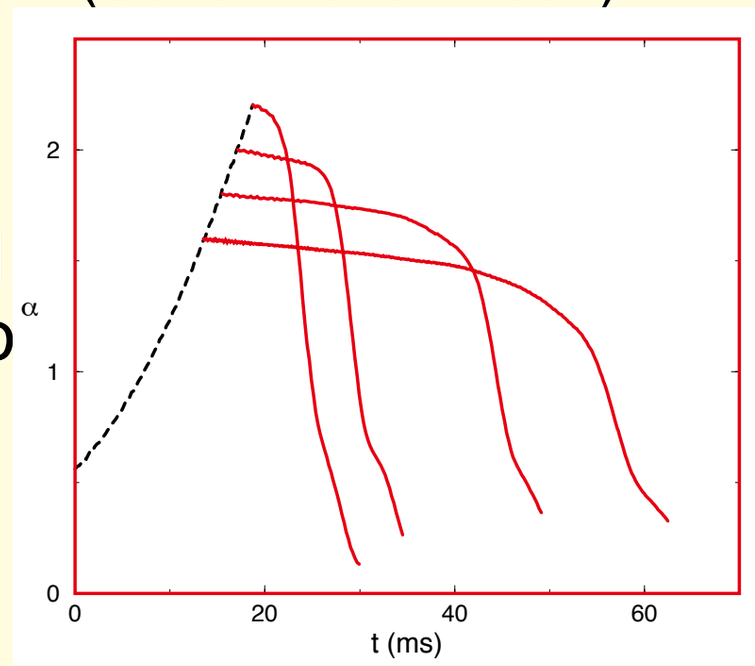

3D simulation

- Evolution starting from the amplitude o(1)
- Imposing large amplitude of radiation reaction potential
- Energy dissipation of r-mode catastrophically decays to differentially rotating configuration in dynamical timescale

1D evolution including mode couplings network

- After reaching the saturation amplitude ~o(0.001), Kolmogorov-type cascade occurs
- Destruction timescale is secular

(Gressman et al. 02, Lin & Suen 06)

Dynamics of r-mode instabilities

Saturation amplitude of r-mode instability

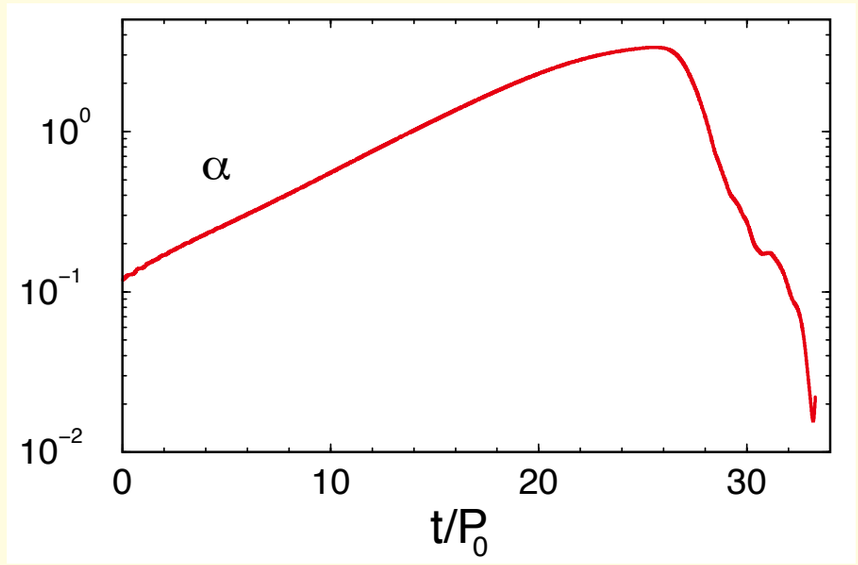

3D simulation

- Saturation amplitude of o(1)
- Imposing large amplitude of radiation reaction potential in the system to control secular timescale with dynamics (Lindblom et al. 00)

1D evol

- Satur n

Final fa 2001)

3D si

- Evolut
- Imposing large amplitude of radiation reaction potential
- Energy dissipation of r-mode catastrophically decays to differentially rotating configuration in dynamical timescale

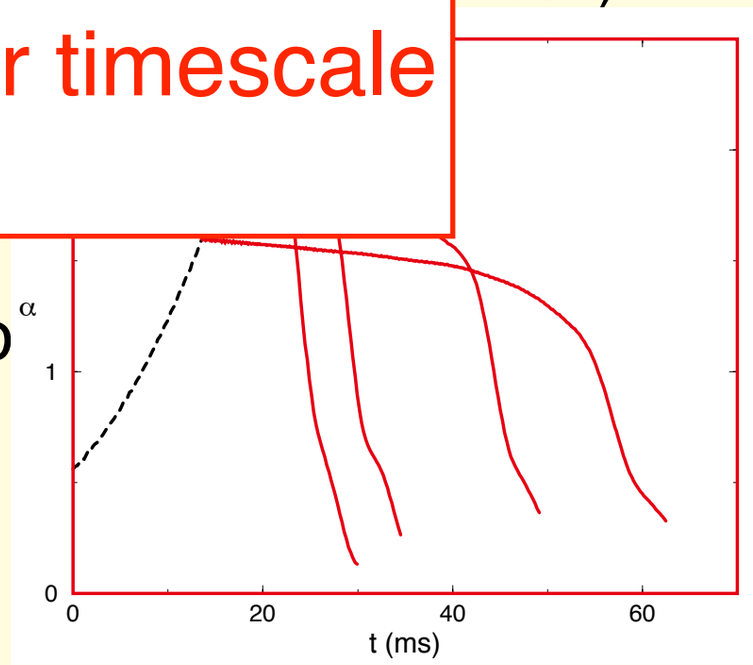

1D evolution including mode couplings network

- After reaching the saturation amplitude ~o(0.001), Kolmogorov-type cascade occurs
- Destruction timescale is secular

(Gressman et al. 02, Lin & Suen 06)

Alternative approaches

- From linear regime to nonlinear regime
- From dynamical timescale to secular timescale

are necessary!

Amplitude of r-mode instability (LIGO 10)

- Isolated compact object in the supernova remnant Cassiopeia A
- Compelling evident that the central compact object is neutron star
- Restriction to the amplitude of the r-mode instability by not detecting gravitational waves

$$\alpha \approx 0.14 - 0.005$$



Possibility of gravitational wave source (Bondarescu et al. 09)

- Possibility of parametric resonance by nonlinear mode-mode interaction
- Amplification to $\alpha \sim 1$

Necessary to obtain a common knowledge for the basic properties of r-mode instability !

2. Dynamics beyond acoustic timescale

- Timescale which cannot be reached by GR hydrodynamics
  - ▶ Need to separate the hydrodynamics and the radiation term
- Instability driven by gravitational radiation
  - ▶ Need to impose gravitational waves

"Newton gravity + gravitaional radiation reaction" are at least necessary

Gravitational radiation reaction

(Blanchet, Damour, Schafer 90)

Quadrupole radiation metric

(includes 2.5PN term)

$$h_{ij} = -\frac{4G}{5c^5}\epsilon\frac{d^3 I_{ij}^{TT}}{dt^3}$$

amplification factor to control the radiation reaction timescale

Gravitational radiation reaction potential

$$\Phi^{(\mathrm{RR})} = \frac{1}{2}(-\psi + h_{ij}x^j\nabla_i\Phi)$$

$$\triangle\psi = 4\pi h_{ij}x^j\nabla^i\rho$$

Dynamics beyond the acoustic timescale

- Shortest timescale in the system restricts the maximum timestep for evolution
  ▶ Acoustic timescale in Newtonian gravity (control acoustic timescale)
- Relax the restriction from the rotation of the background star
  ▶ Introduce rotating reference frame

Anelastic approximation

Kill the degree of freedom of the sound wave propagation

$$v^j \nabla_j h + (\Gamma - 1) h \nabla_j v^j = 0$$

▼ No shocks

$$\nabla_j (\rho v^j) = 0$$

Linear regime (Villain & Bonazzolla 02)

$$\nabla_j (\rho_{\rm eq} v^j) = 0$$

Propagation of the sound wave

$$\frac{\partial \rho}{\partial t} = \frac{1}{c_s^2}\frac{\partial P}{\partial t} = -\nabla_j (\rho v^j)$$

$$\frac{\partial}{\partial t}\nabla_j (\rho v^j) + \triangle P = S$$

▶ $$\left(\triangle - \frac{1}{c_s^2}\frac{\partial}{\partial t}\right) P = S$$

Imposing the anelastic approximation changes the structure of the pressure equation

Basic equations in rotating reference frame (Lie derivative)

Time evolution

$$\frac{\partial \rho}{\partial t} = 0$$

$$\frac{\partial}{\partial t}(\rho u_i) + \nabla_j(\rho u_i v^j) = -\nabla_i p - \rho \nabla_i(\Phi + \Phi^{(\mathrm{RR})}) - \rho(v^j_{(\mathrm{eq})} + v^j)\nabla_j u_{i\ (\mathrm{eq})} + \rho u_j \nabla_i v^j_{(\mathrm{eq})}$$

up to 1st order of ϵ

Spatial component of the momentum velocity

$$u_{i(\mathrm{eq})} + u_i = \tilde{\gamma}_{ij}(v^j_{(\mathrm{eq})} + v^j)$$

spatial metric $\tilde{\gamma}_{ij} = \delta_{ij} + h_{ij}$

Pressure poisson equation

$$\triangle p = S_p$$

Boundary condition:
P=0 at the stellar surface

Anelastic approximation (constraint)

$$\nabla_j(\rho v^j) = 0$$

Need a special technique to satisfy constraints throughout the evolution

Procedure

Similar procedure to SMAC method, which is used to solve Navie-Stokes incompressible fluid (McKee et al. 08)

1. Time update the linear momentum

$$(\rho\Delta u_i)^{(*)} = (\rho\Delta u_i)^{(n)} - \Delta t[\nabla_i p + \cdots]$$

Note that the velocity does not automatically satisfy anelastic condition

2. Introduce an auxiliary function ϕ and solve the following Poisson's equation

$$(\triangle\phi)^{(*)} = \partial_j(\rho\Delta v^j)^{(*)}$$

Boundary Condition: $\phi = 0$ at the stellar surface

3. Adjust the 3-velocity in order to satisfy the anelastic condition

$$(\rho\Delta v^i)^{(n+1)} = (\rho\Delta v^i)^{(*)} - (\partial^i\phi^{(*)})$$

4. Introduce another auxiliary function ψ and solve the following Poisson's equation

$$\triangle\psi = \delta^{ij}[\partial_j(\rho\Delta u_i)^{(*)} - \partial_j(\rho\Delta u_i)^{(n+1)}]$$

Boundary Condition: $\psi = 0$ at the stellar surface

5. Time update the pressure

$$p^{(n+1)} = p^{(n)} + \frac{\psi^{(*)}}{\Delta t}$$

3. Nonlinear r-mode instability

Equilibrium configuration of the star

- Rapidly rotating neutron star
- Uniformly rotating, n=1 polytropic equation of state

r_p/r_e	T/W
0.55	0.102
0.65	0.088
0.70	0.076
0.75	0.062

Eigenfunction and eigenvector of r-mode in incompressible star

Eigenfunction of the velocity

$$\delta v = \alpha \Omega R \left(\frac{r}{R}\right)^l Y_{ll}^{(B)} \qquad \alpha = 1 \times 10^{-4}$$

Impose eigenfunction type perturbation on the equilibrium velocity to trigger r-mode instability

Eigenfrequency (rotating reference frame)

$$\omega = \frac{2m}{l(l+1)}\Omega$$

Incompressible star case

Check the excitation of the eigenfrequency

Spectrum

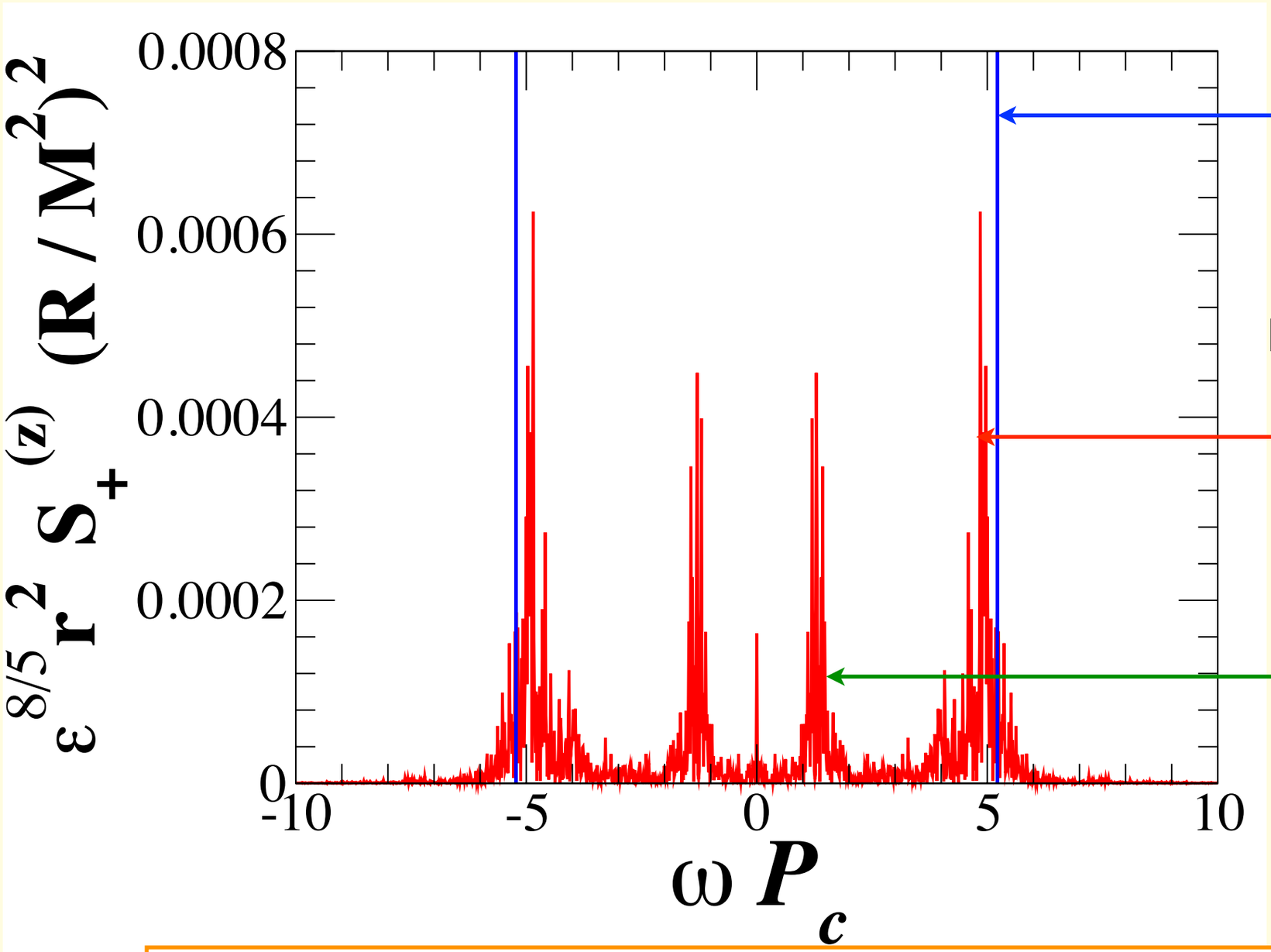

Eigenfrequency of the r-mode from slow rotation approximation

(Yoshida & Lee 01)

Our excitation frequency

g-mode ?

Due to

- slow rotation approximation
- anelastic approximation

the eigenfrequency does not perfectly agree

Gravitational Waveform

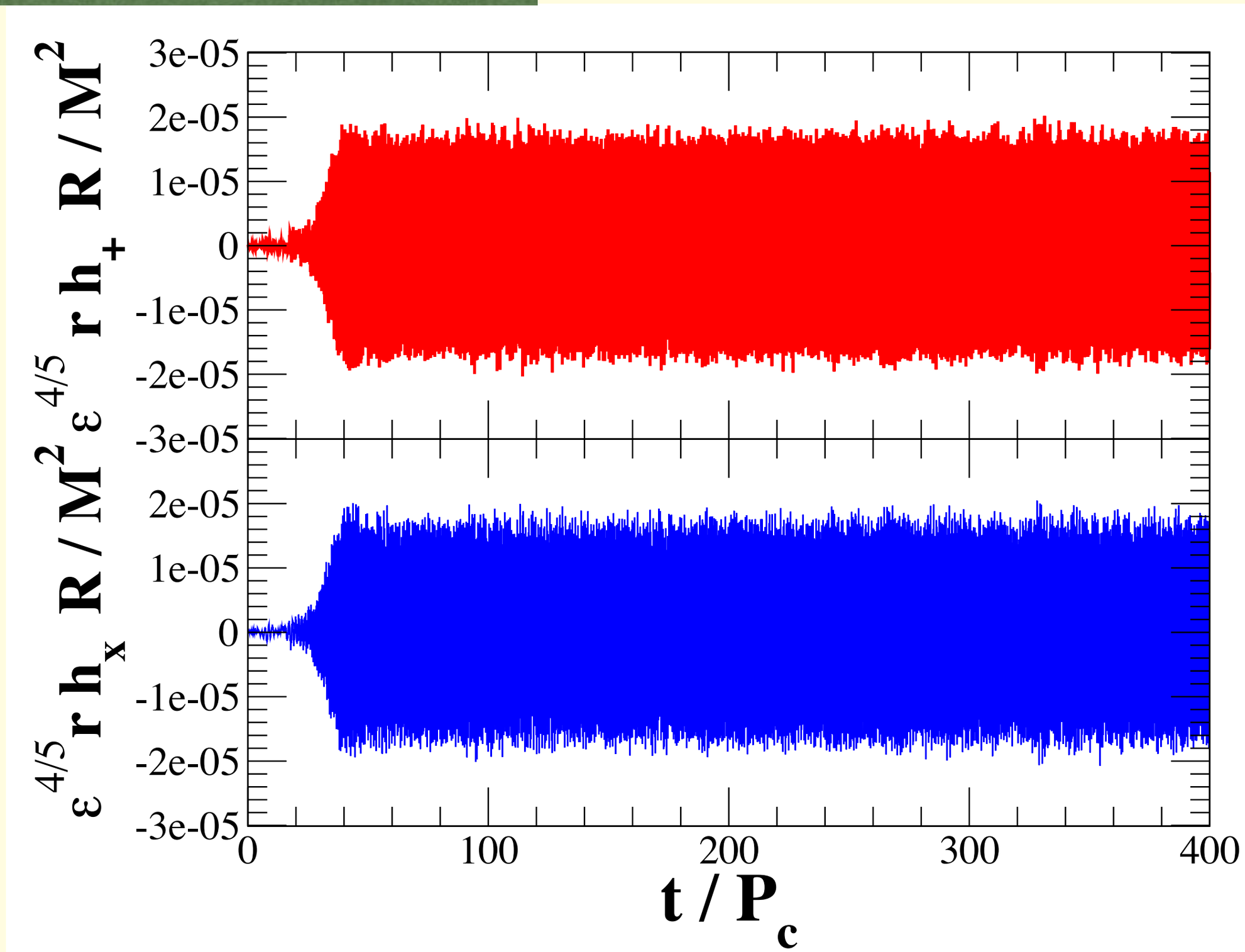

Saturation amplitude is around $\alpha \approx 10^{-3}$

Velocity profile

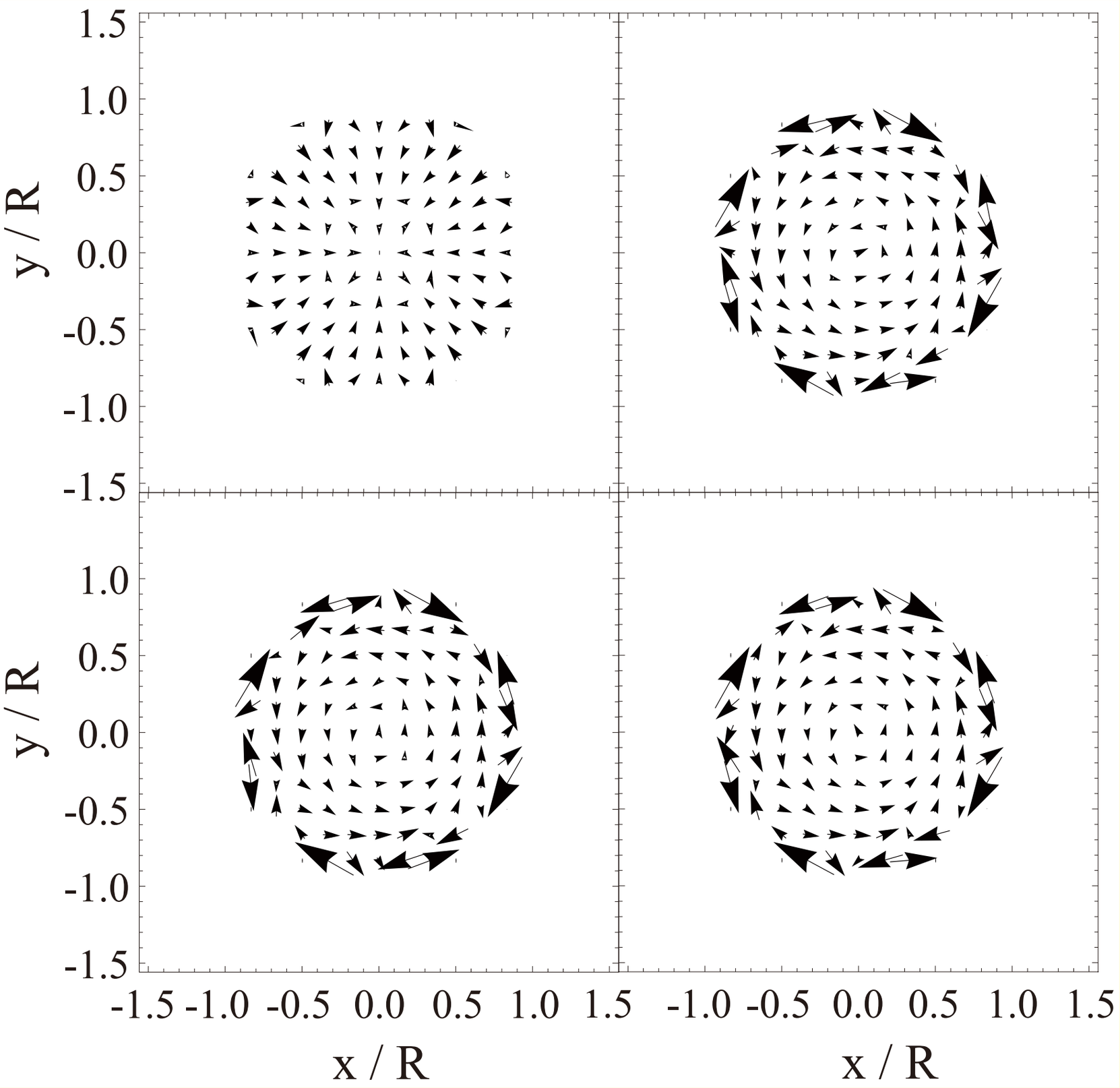

- No velocity profile appears in the equatorial plane in linear and slow rotation regime of r-mode instability

  ▶ Effect of rapid rotation and nonlinearity

- Shock wave seems to form at the surface as the times goes on

  ▶ “Destruction” of r-mode instability

Comment to the Catastrophic Decay?

- Lindblom et al. shows in their paper that the catastrophic decay is due to the shocks and the breaking waves at the surface

- Anelastic approximation kills the dominant contribution of the density fluctuation

- Computation with small amplitude of velocity perturbation with Newtonian hydrodynamics may answer the question

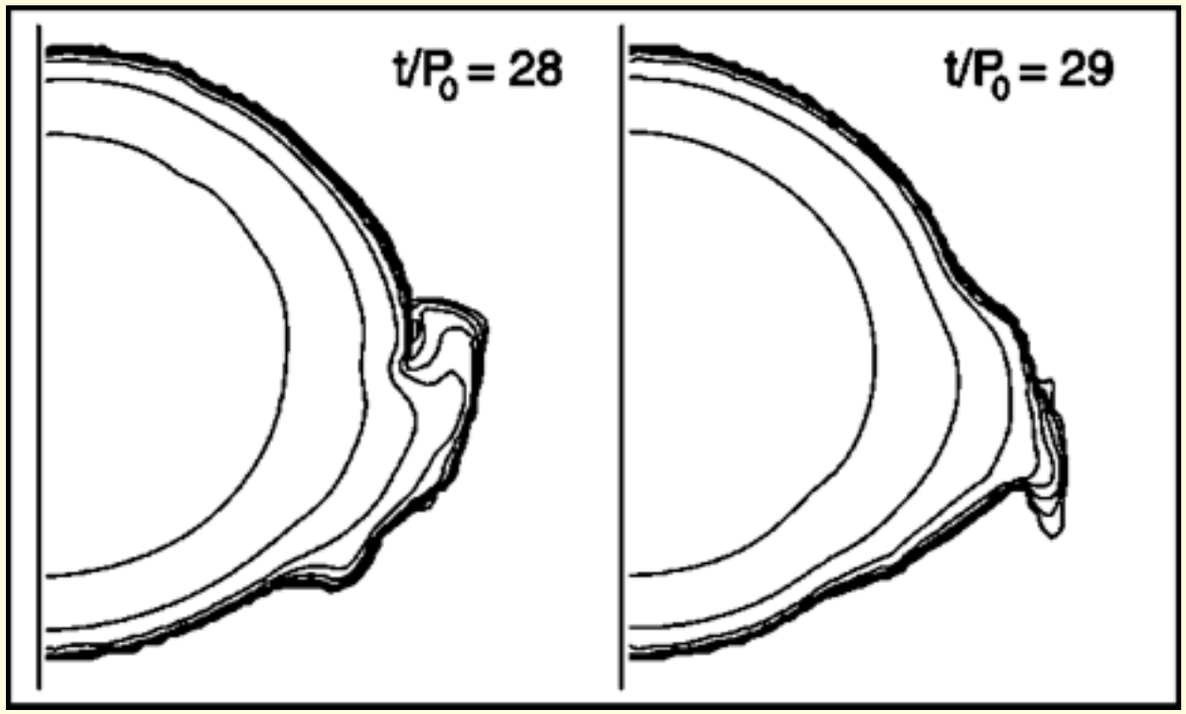

(Lindblom et al. 02)

Might be very difficult

4. Summary

We investigate the r-mode instability of uniformly rotating stars by means of three dimensional hydrodynamical simulations in Newtonian gravity with radiation reaction

- We have succeeded in constructing a nonlinear anelastic approximation in the rotating reference frame, which kills the propagation of sound speed, in order to evolve the system beyond the dynamical timescale.
- When the current multipole contribution is dominant to the r-mode instability (density fluctuation effect is negligible), the instability seems to last for at least hundreds of rotation periods
- Studies of no anelastic approximation with small amplitude of velocity perturbation may help us for a better understanding

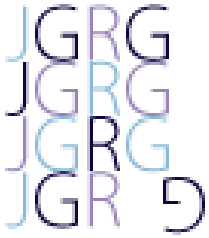

Tomohiro Harada, JGRG 22(2012)111410

"Upper limits of particle emission from high-energy collision and reaction near a maximally rotating Kerr black hole"

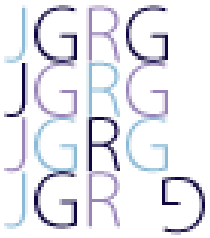

RESCEU SYMPOSIUM ON

GENERAL RELATIVITY AND GRAVITATION

JGRG 22



November 12-16 2012

Koshiba Hall, The University of Tokyo, Hongo, Tokyo, Japan



Upper limits of particle emission from high-energy collision and reaction near a maximally rotating Kerr black hole

Tomohiro Harada
in collaboration with H. Nemoto and U. Miyamoto

Department of Physics, Rikkyo University

12-16/11/2012 JGRG22@RESCEU, U Tokyo

Introduction

- “Kerr BHs as particle accelerators” (Bañados, Silk & West 2009): Collision with an arbitrarily high centre-of-mass (CM) energy near the horizon of a maximally rotating BH. Implication to DM particles pair annihilation.
- Critical comments: Berti et al. 2009, Jacobson & Sotirou 2010
- Astrophysical relevance: Harada & Kimura 2011abc

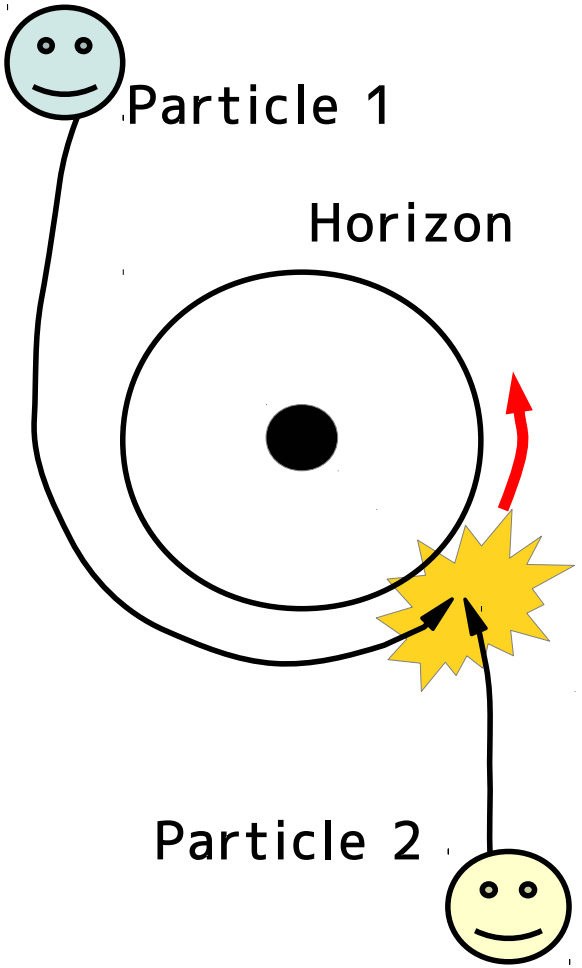

Can we observe new physics?

- Particle collision with extremely high CM energy might produce an exotic particle. Can we observe it?
- If a high-energy and/or super-heavy particle is to be emitted from the collision of ordinary particles, we need energy extraction from the BH.
- This is possible in general for a rotating BH, as is well known.

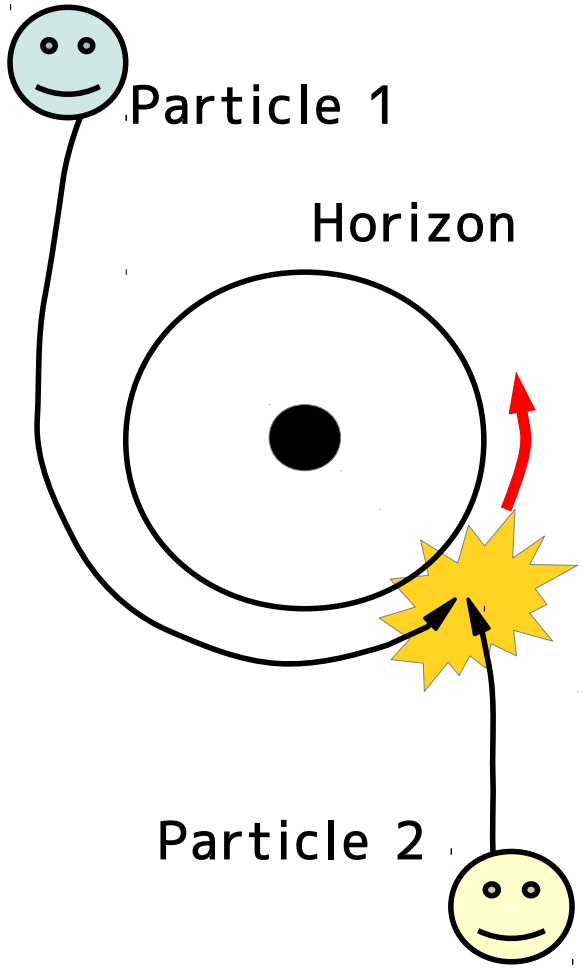

Collisional Penrose Process

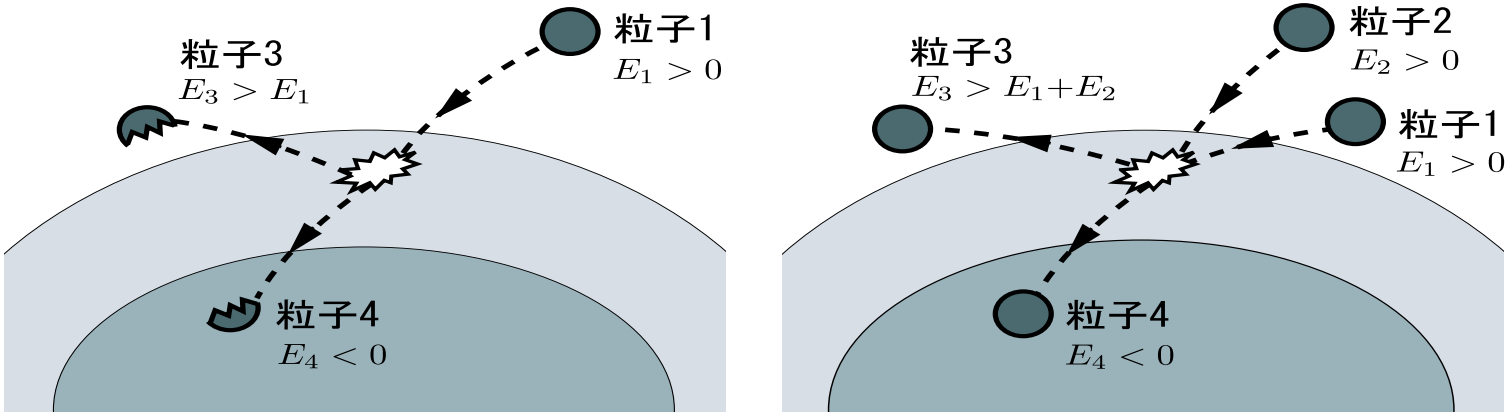

Figure: Left: Penrose process, right: Collisional Penrose process. The light and deep shaded regions denote the ergoregions and BHs, respectively.

- Energy can be extracted from a rotating BH due to the negative energy orbit in the ergoregion.
- Collisional Penrose process (Piran, Shaham & Katz 1975)
- Jacobson & Sotiriou (2010) argue that no energy extraction occurs through the BSW collision.

Maximally rotating BH

- Maximally rotating Kerr BH
  - Boyer-Lindquist coordinates: (t, r, θ, ϕ)
  - $a = M$: $r_H = M$, $\Omega_H = 1/(2M)$, $\kappa_H = 0$
  - Ergoregion: $M < r < M(1 + \sin\theta)$
- Geodesic motion in the equatorial plane
  - 1D potential problem

$$\frac{1}{2}(p^r)^2 + V(r) = 0, \quad \text{or} \quad p^r = \sigma\sqrt{-2V(r)}, \quad \text{where} \quad p^r = \frac{dr}{d\lambda},$$

where λ is the affine parameter,

$$V(r) = -\frac{Mm^2}{r} + \frac{L^2 - a^2(E^2 - m^2)}{2r^2} - \frac{M(L - aE)^2}{r^3} - \frac{E^2 - m^2}{2},$$

and E and L are conserved.

  - Forward-in-time condition: $p^t = dt/d\lambda > 0$
  - This implies $2E - \tilde{L} \geq 0$ in the limit $r \to r_H$, where $\tilde{L} = L/M$. We define a critical particle as a particle satisfying $2E - \tilde{L} = 0$.

Collision and reaction

- Collision and reaction: $1 + 2 \to 3 + 4$
  - CM energy: $E_{\rm cm}^2 = -(p_1^a + p_2^a)(p_{1a} + p_{2a}) = -(p_3^a + p_4^a)(p_{3a} + p_{4a})$
  - Conservation: $E_1 + E_2 = E_3 + E_4$ and $\tilde{L}_1 + \tilde{L}_2 = \tilde{L}_3 + \tilde{L}_4$
  - Radial momentum conservation : $p_1^r + p_2^r = p_3^r + p_4^r$
- BSW collision: particle 1 is critical ($2E_1 - \tilde{L}_1 = 0$), while particle 2 is subcritical ($2E_2 - \tilde{L}_2 > 0$). If the two particles collide at $r = M/(1-\epsilon)$ $(0 < \epsilon \ll 1)$ with $p^r < 0$,

$$E_{\rm cm} \approx \sqrt{\frac{2(2E_1 - \sqrt{3E_1^2 - m_1^2})(2E_2 - \tilde{L}_2)}{\epsilon}}.$$

$E_{\rm cm} \to \infty$ as $\epsilon \to 0$.

Particle motion near the horizon

- Let $\tilde{L} = 2E(1+\delta)$, $\delta = \delta_{(1)}\epsilon + \delta_{(2)}\epsilon^2 + O(\epsilon^3)$.
- The forward-in-time condition at $r = M/(1-\epsilon)$ yields $\delta < \epsilon + O(\epsilon^2)$.
- Turning points of the potential

$$r_{t,\pm}(e) = M\left(1 + \frac{2e}{2e \mp \sqrt{e^2+1}}\delta_{(1)}\epsilon\right) + O(\epsilon^2), \quad \text{where } e = E/m.$$

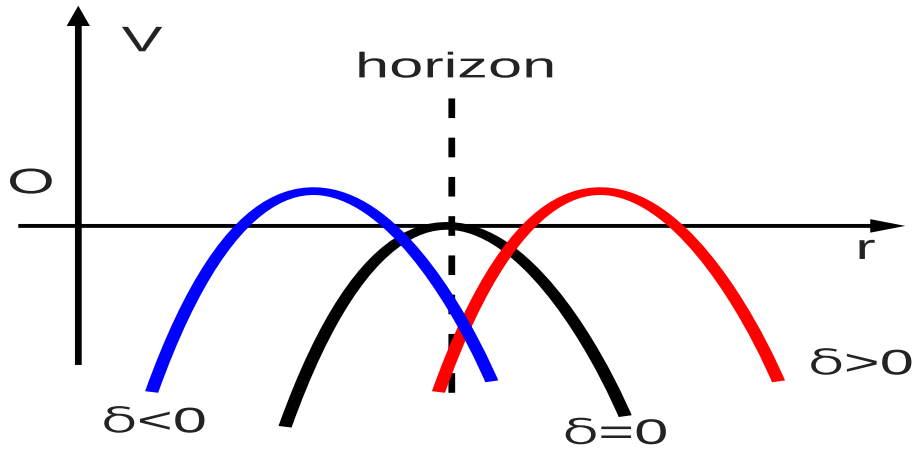

- To escape to infinity from $r = M/(1-\epsilon)$, we need $e \geq 1$ and
  - (a) $\delta_{(1)} < 0$ and $\sigma = 1$
  - (b) $\delta_{(1)} > 0$ and $r \geq r_{t,+}(e)$ or $0 < \delta_{(1)} \leq \delta_{(1),\max} = (2e - \sqrt{e^2+1})/(2e)$.

Collision and reaction near the horizon

- Let us consider a collision at $r = M/(1-\epsilon)$.
- Let $\tilde{L}_3 = 2E_3(1+\delta)$, $\sigma_3 = \pm 1$ and $\sigma_4 = -1$.
- The forward-in-time condition is taken into account.
- The radial momentum conservation: $p^r_1 + p^r_2 = p^r_3 + p^r_4$.
  - Expand p^r_i $(i = 1,2,3,4)$ in terms of ϵ.
  - The radial momentum conservation implies at $O(\epsilon)$

$$(2E_1 - \sqrt{3E_1^2 - m_1^2}) + 2E_3(\delta_{(1)} - 1) = \sigma_3 \sqrt{E_3^2(3 - 8\delta_{(1)} + 4\delta_{(1)}^2) - m_3^2}.$$

  - It implies at $O(\epsilon^2)$ an equation including m_4. With this equation, we can check whether $m_4^2 \geq 0$ is satisfied or not.

The energy of the escaping particle

- The radial momentum conservation implies at $O(\epsilon)$

$$(2E_1 - \sqrt{3E_1^2 - m_1^2}) + 2E_3(\delta_{(1)} - 1) = \sigma_3 \sqrt{E_3^2(3 - 8\delta_{(1)} + 4\delta_{(1)}^2) - m_3^2}. \tag{1}$$

- Squaring the both sides of Eq. (1) yields the following quadratic equation for E_3.

$$4A_1E_3(1 - \delta_{(1)}) = A_1^2 + (E_3^2 + m_3^2), \tag{2}$$

where $A_1 = 2E_1 - \sqrt{3E_1^2 - m_1^2} > 0$.

- Solving Eq. (2) for $\delta_{(1)}$ and substituting it into Eq. (1) yields

$$A_1^2 - (E_3^2 + m_3^2) = 2\sigma_3 A_1 \sqrt{E_3^2(3 - 8\delta_{(1)} + 4\delta_{(1)}^2) - m_3^2}. \tag{3}$$

Upper limits of the emitted particle's energy

- We assume $E_1 \geq m_1$ so that particle 1 is initially at infinity.

(i) $\sigma_3 = 1$: Eq. (3) immediately implies $E_3 \leq \sqrt{A_1^2 - m_3^2} < E_1$, i.e., no energy extraction.

(ii) $\sigma_3 = -1$ and $0 < \delta_{(1)} \leq \delta_{(1),\mathrm{max}}$: $E_3 = 2.186 E_1$ is possible.

- Eq. (2) immediately implies $\lambda_- \leq E_3 \leq \lambda_+$, where $\lambda_\pm = 2A_1 \pm \sqrt{3A_1^2 - m_3^2}$ and the equality holds for $\delta_{(1)} = 0$.
- This implies that E_3/E_1 takes a maximum $(2 - \sqrt{2})/(2 - \sqrt{3}) \simeq 2.186$ for $E_1 = m_1$, $m_3 = 0$ and $\delta_{(1)} = +0$.

Escape without and with bounce

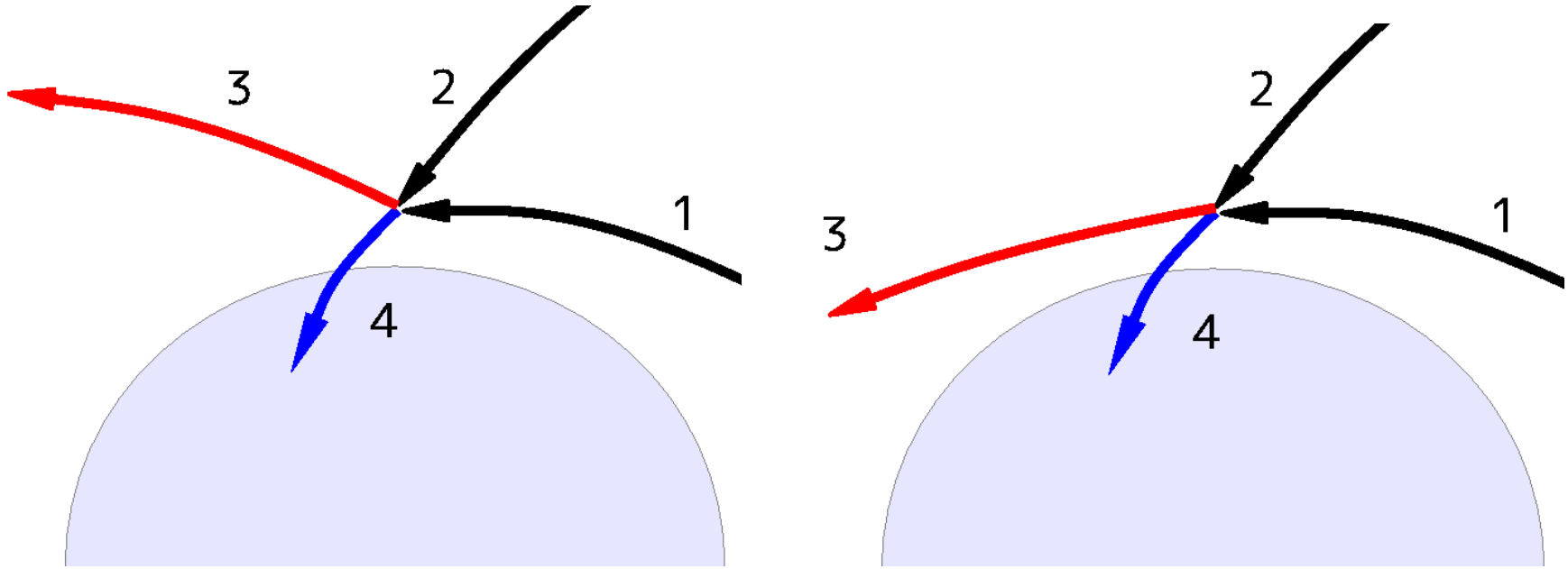

Figure: Left: escape without bounce ($\sigma = 1$), right: escape with bounce ($\sigma = -1$).

- Energy extraction is possible only with bounce ($\sigma_3 = -1$).

Energy gain efficiency

- The upper limit of the energy gain efficiency $\eta = E_3/(E_1 + E_2)$ can be further studied based on $O(\epsilon^2)$ equation.
- The upper limit of the efficiency for $E_3 = E_B$ is given by 146.6 % for any BSW collision.
- The upper limits are 117.6 % for perfectly elastic collision, 137.2 % for inverse Compton scattering and 109.3 % for pair annihilation.
- Our result agrees with a numerical work by Bejger, Piran, Abramowicz & Hakanson (2012) and contradicts a simplistic argument by Jacobson & Sotiriou (2010).
- On the other hand, the efficiency is not very high but modest at most.

Summary

- The rotational energy of a maximally rotating BH can be extracted through a BSW collision, whereas the emitted particle cannot be highly energetic.
- Note, however, that the BSW collision may open a new reaction channel because of high CM energy, which can leave its features on the gamma-ray spectrum (cf. Cannoni, Gomez, Perez-Garcia & Vergados 2012).

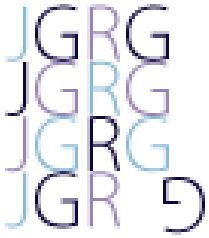

Hideki Ishihara, JGRG 22(2012)111411

"Stable null bound orbits around a black ring"

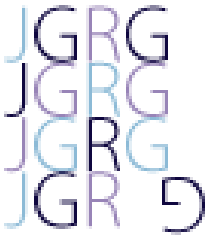

RESCEU SYMPOSIUM ON

GENERAL RELATIVITY AND GRAVITATION

JGRG 22



November 12-16 2012

Koshiba Hall, The University of Tokyo, Hongo, Tokyo, Japan



Stable Bound Null Orbit around a Black Ring

Hideki Ishihara



T.Igata, H.Ishihara, and Y.Takamori
(Osaka City University)

Introduction

Higher-dim. Black Hole is a key
for a verification of extra dimensions?

$D = 4$

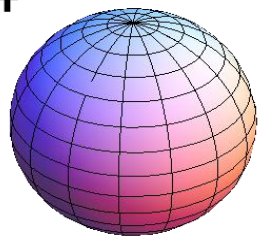

S^2

Kerr Black Hole

$D = 5$

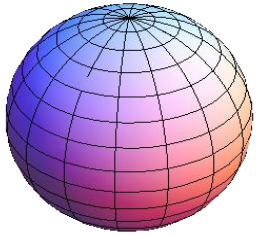

S^3

Black Hole
Myers & Perry (1986)

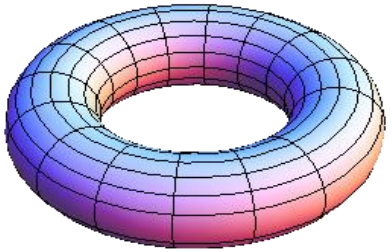

$S^2 \times S^1$

Black Ring
Emparan & Reall (2002)

Geodesics around a Black Hole

Geodesic particles are important probes of gravitational field around a black hole.

$D = 4$

- ISCO appears for timelike particles
- Unstable circular orbits exist for null particles
- Geodesic equations in Kerr geometry are separable

$D = 5$

For spherical black holes (the Myers-Perry metric)

- No stable circular orbit exists for timelike particles
- Unstable circular orbits exist for null and timelike particles
- Geodesic equations are separable

V.P.Frolov and D.Stojkovic(2003)

For black rings (the Emparan-Real metric)

- Stable stationary orbits exist for timelike particles
- Geodesic equations would not be separable

J.Hoskisson(2008), M.Durkee(2009),
T.Igata, H.Ishihara, and Y.Takamori(2010),(2011)
S.Grunau, V.Kagramanova, J.Kunz, C.Lammerzahl(2012)

Stable Bound Orbits

Orbits stable against small perturbations, and bounded in a finite domain outside the black hole horizon.

	Stable Bound Orbit	
	Timelike	Null
4-D Black Holes	Yes	No
5-D Black Holes	No	No
5-D Black Rings	Yes	?

T.Igata, H.Ishihara, and Y.Takamori,
Phys. Rev. D82, 101501 (2010)

Particle Motion around a Black Hole

4−dim. Schwarzschild BH case

Effective potential : $V_4(r;L) = \dfrac{L^2}{r^2} - \dfrac{M}{r} - \dfrac{ML^2}{r^3}$

$V_4(r;L)$

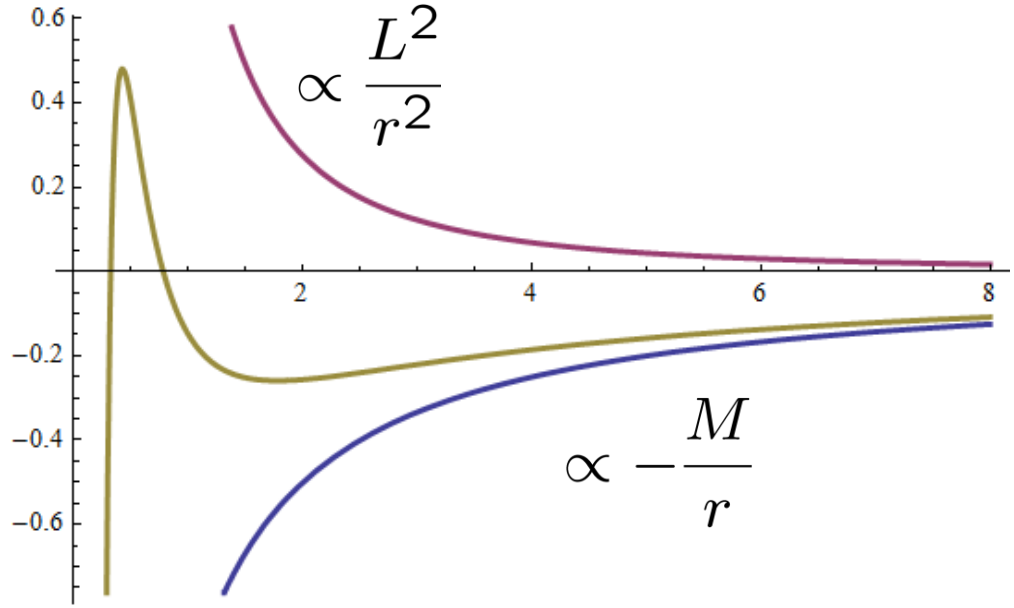

Particle Motion around a Black Hole

D−dim. Schwarzschild BH case

Effective potential : $V_D(r;L) = \dfrac{L^2}{r^2} - \dfrac{M}{r^{D-3}} - \dfrac{ML^2}{r^{D-1}}$

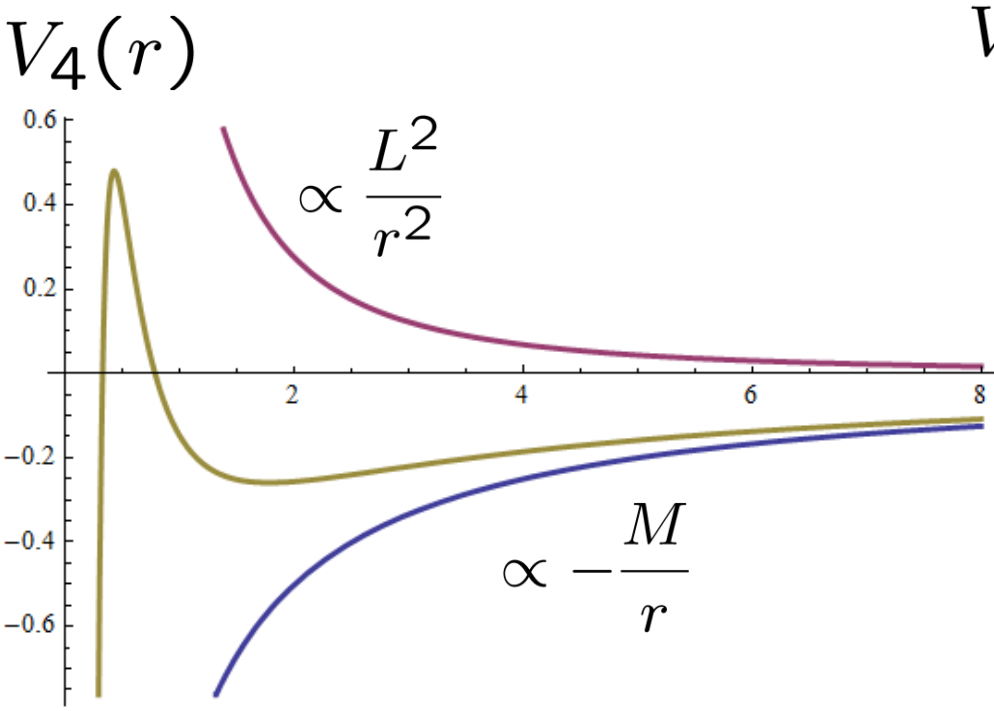

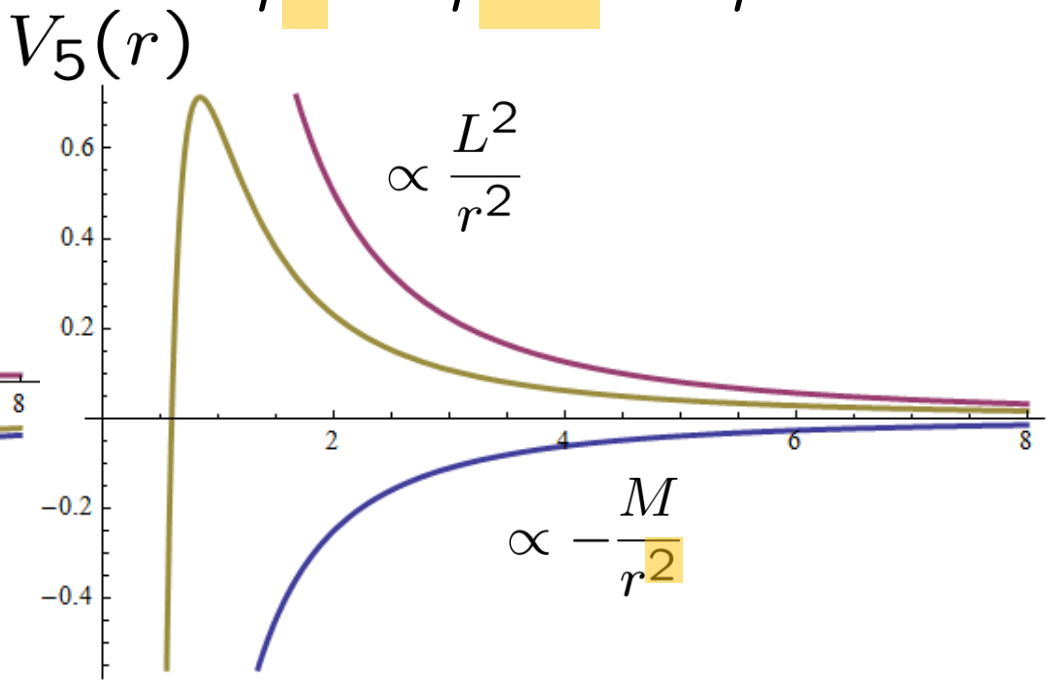

No stable bound orbits for $D \geq 5$

Stationary Points Set for Effective Potential

Effective potential for D−dim. Schwarzschild BH

$$V_D(r;L) = \frac{L^2}{2r^2} - \frac{M}{r^{D-3}} - \frac{ML^2}{r^{D-1}}$$

Stationary condition

$$\partial_r V_D(r;L) = -\frac{L^2}{r^3} + (D-3)\frac{M}{r^{D-2}} + (D-1)\frac{ML^2}{r^D} = 0$$

Stationary Points Set

$$L(r) = \sqrt{\frac{(D-3)Mr^2}{r^{D-3} - (D-1)M}}$$

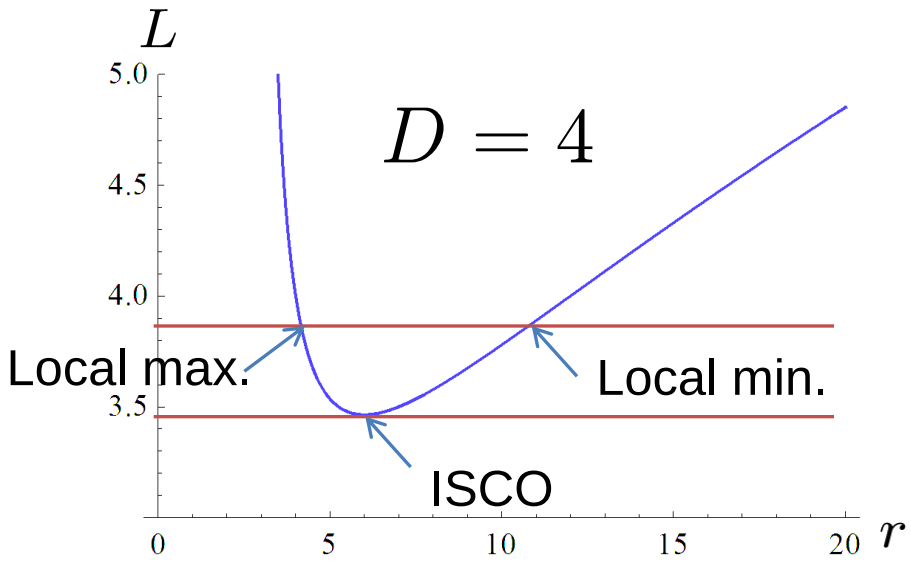

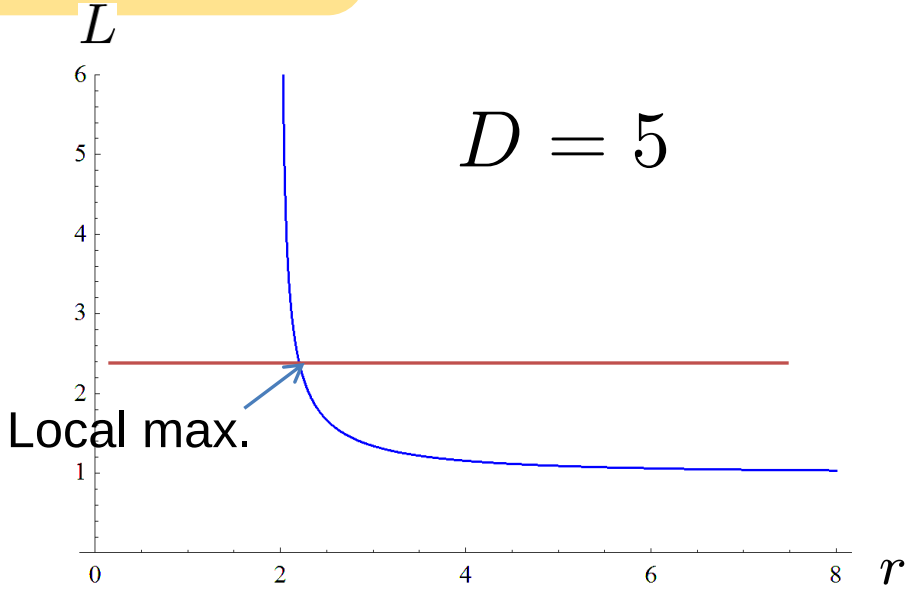

no stable bound orbits

How about

Black Ring ?

5D Singly Rotating Black Ring

Metric

Emparan & Reall (2002)

$$ds^2 = -\frac{F(y)}{F(x)}\left(dt - CR\frac{1+y}{F(y)}d\psi\right)^2 + \frac{R^2}{(x-y)^2}F(x)\left(-\frac{G(y)}{F(y)}d\psi^2 - \frac{dy^2}{G(y)} + \frac{dx^2}{G(x)} + \frac{G(x)}{F(x)}d\phi^2\right),$$

$$F(\xi) = 1+\lambda\xi, \quad G(\xi) = (1-\xi^2)(1+\nu\xi), \quad C = \sqrt{\lambda(\lambda-\nu)\frac{1+\lambda}{1-\lambda}}, \quad \lambda = \frac{2\nu}{1+\nu^2}$$

Free parameters

R : ring radius

ν : thickness (thin $0 < \nu < 1$ fat)

Killing vectors

$$\partial_t, \quad \partial_\phi, \quad \partial_\psi$$

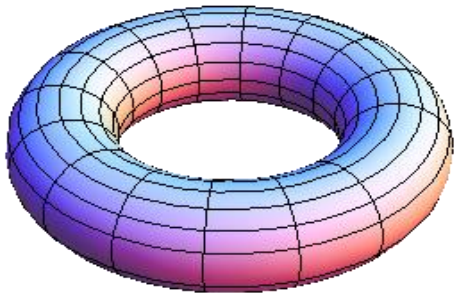

Horizon topology

$$S^2 \times S^1$$

Coordinates for the Black Ring

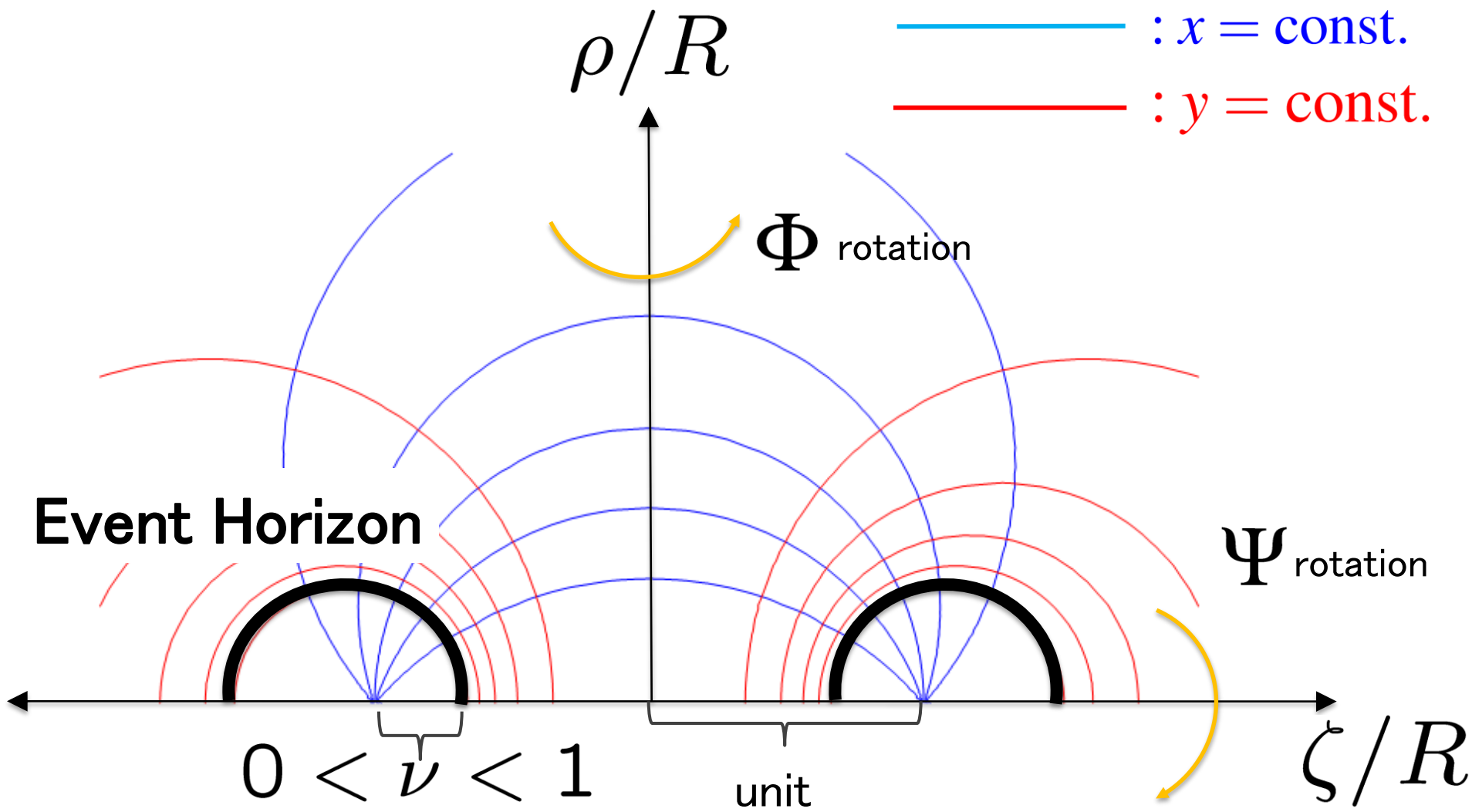

(t, Φ, Ψ) are suppressed.

(ρ, Φ), (ζ, Ψ): polar coordinates on the independent two planes, respectively.

Hamiltonian formalism for a Null particle

Constants of motion

$$E = -k_t, L_\phi = k_\phi, L_\psi = k_\psi$$

Hamiltonian

$$H = \frac{1}{2} g^{\alpha\beta} k_\alpha k_\beta$$

$$= \frac{1}{2} \left(g^{\zeta\zeta} k_\zeta^2 + g^{\rho\rho} k_\rho^2 + E^2 \, U \right) = 0,$$

Effective Potential

$$U(\zeta, \rho; l_\psi, l_\phi) = g^{tt} + g^{\phi\phi} l_\phi^2 + g^{\psi\psi} l_\psi^2 - 2 g^{t\psi} l_\psi$$

$$(l_\phi := L_\phi / E, \quad l_\psi := L_\psi / E)$$

Stationary Orbits

Stationary Solutions

$$\dot{\rho} = \dot{\zeta} = 0 \longrightarrow k_\rho = k_\zeta = 0$$

$$\longrightarrow \partial_\zeta U(\zeta, \rho; l_\psi, l_\phi) = \partial_\rho U(\zeta, \rho; l_\psi, l_\phi) = 0$$

$$\longrightarrow \quad l_\psi = l_\psi(\zeta, \rho), \qquad l_\phi = l_\phi(\zeta, \rho)$$

Stationary Points Set

$$\Sigma = \{(\zeta, \rho, l_\psi(\zeta, \rho), l_\phi(\zeta, \rho))\}$$

defines 2-dimensional surface embedded
in the 4-dimensional space

$$\mathcal{N} = \{(\zeta, \rho, l_\psi, l_\phi)\}$$

Null condition for the stationary orbits is $U|_\Sigma = 0$

Stability conditions

Local minimum of $U(\zeta, \rho; l_\psi, l_\phi)$ ⟷ Stable Stationary orbit

↕

Two eigenvalues of Hessian matrix

$$\mathcal{H}(U) = \begin{pmatrix} \partial_\zeta^2 U & \partial_\zeta \partial_\rho U \\ \partial_\rho \partial_\zeta U & \partial_\rho^2 U \end{pmatrix}$$

are positive at the stationary point.

↕

$$\det \mathcal{H}(U)|_\Sigma > 0 \quad \text{and} \quad \mathrm{tr}\, \mathcal{H}(U)|_\Sigma > 0$$

Existence of Stable Stationary Orbits

Projection of Σ into the ζ - ρ plane for $\nu = 0.1$

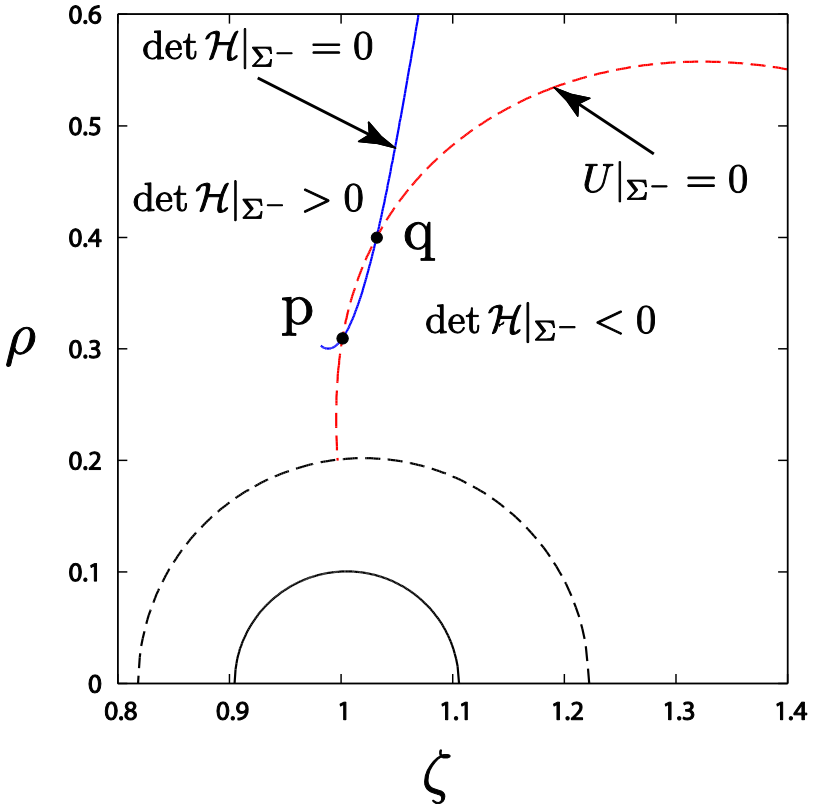

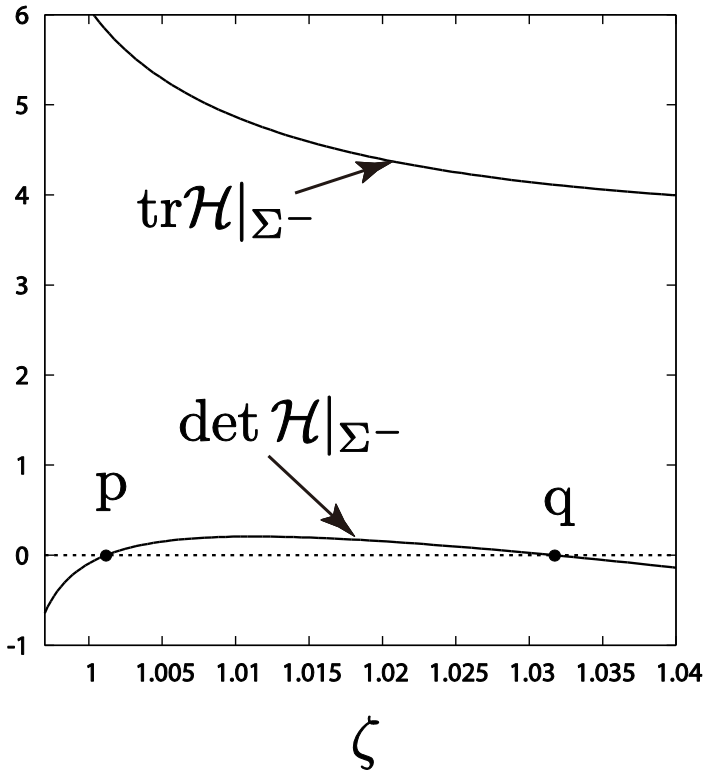

Stable Toroidal Spiral Orbits

The stable stationary orbit is tangent to a null Killing vector

$$\partial_t + \alpha(l_\psi, l_\phi)\partial_\psi + \beta(l_\psi, l_\phi)\partial_\phi \,.$$

The projection of a orbit on a $t = const$ surface is a toroidal spiral on $\mathrm{S}^1 \times \mathrm{S}^1$.

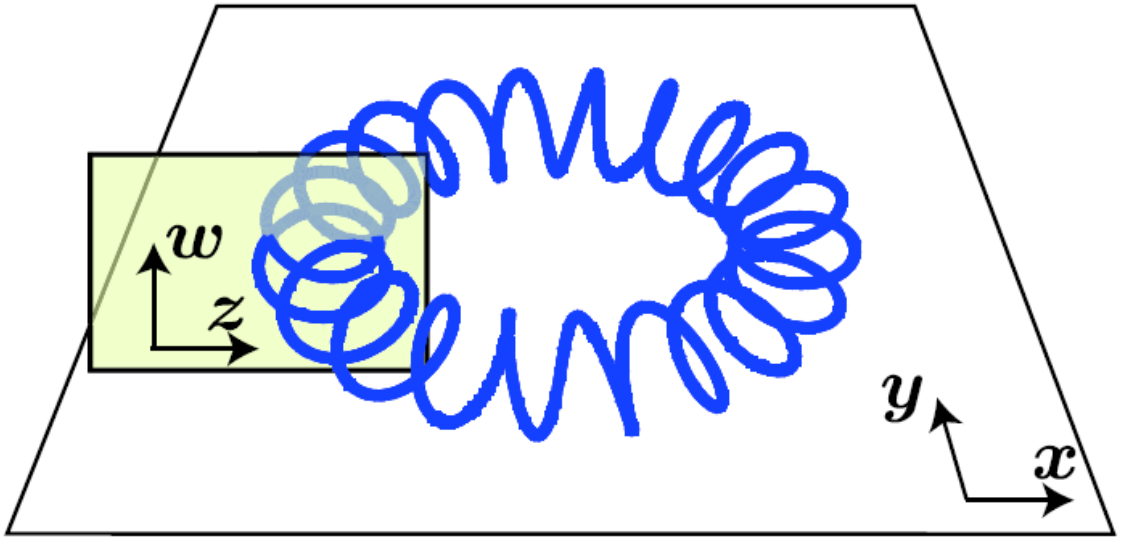

Critical Thickness

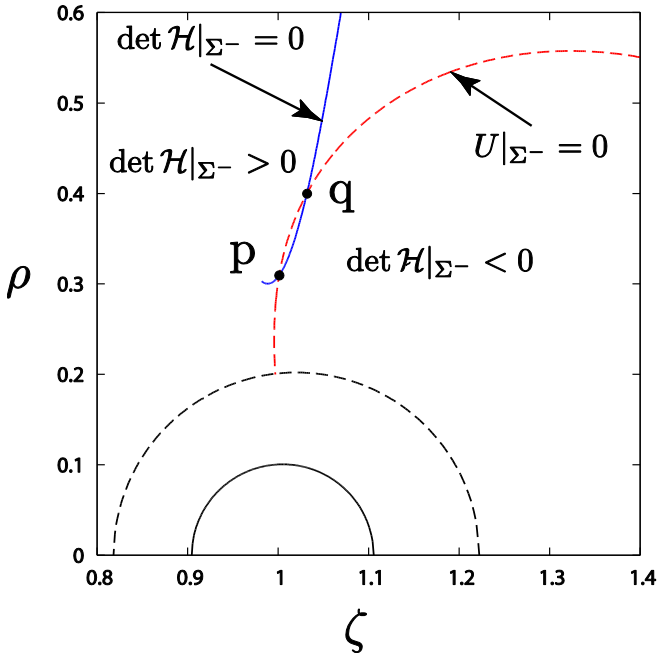

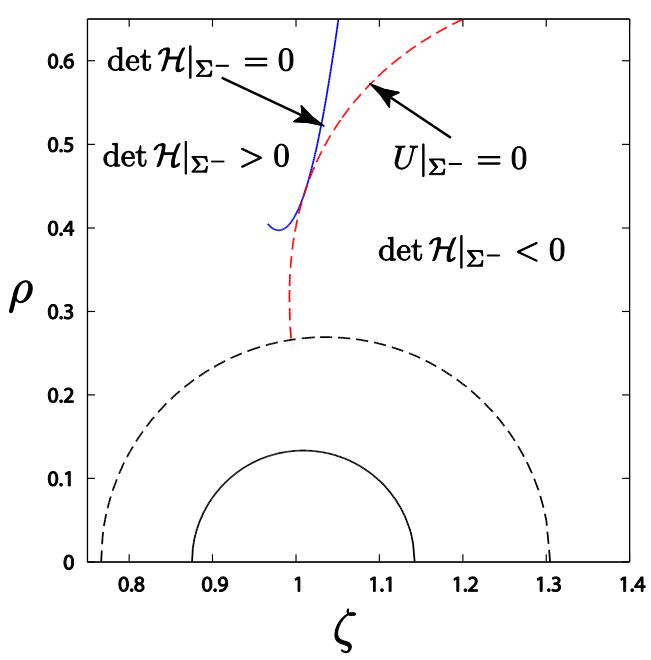

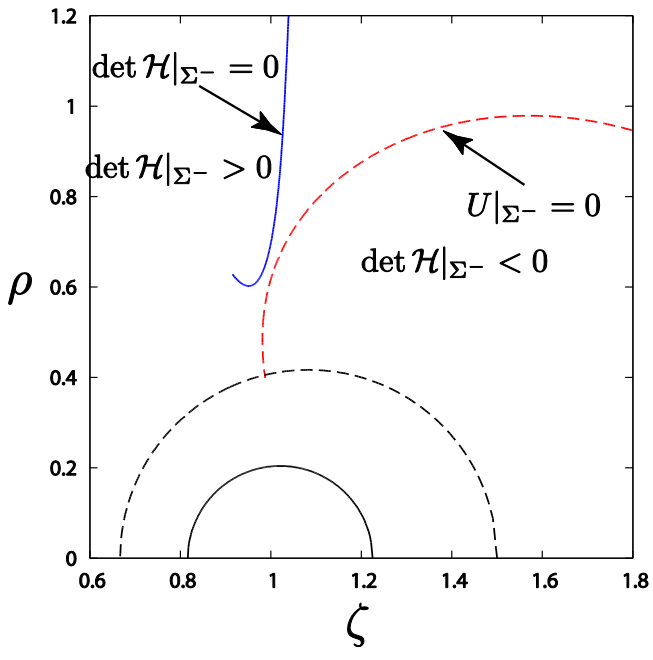

$\nu = 0.1$ $\nu = 0.13224 \simeq \nu_c$ $\nu = 0.2$

p : Innermost Stable Toroidal Spiral Orbit (ISTSO)

q : Outermost Stable Toroidal Spiral Orbit (OSTSO)

Cusps

Projection of Σ into the l_ψ - l_ϕ plane for $\nu = 0.1$

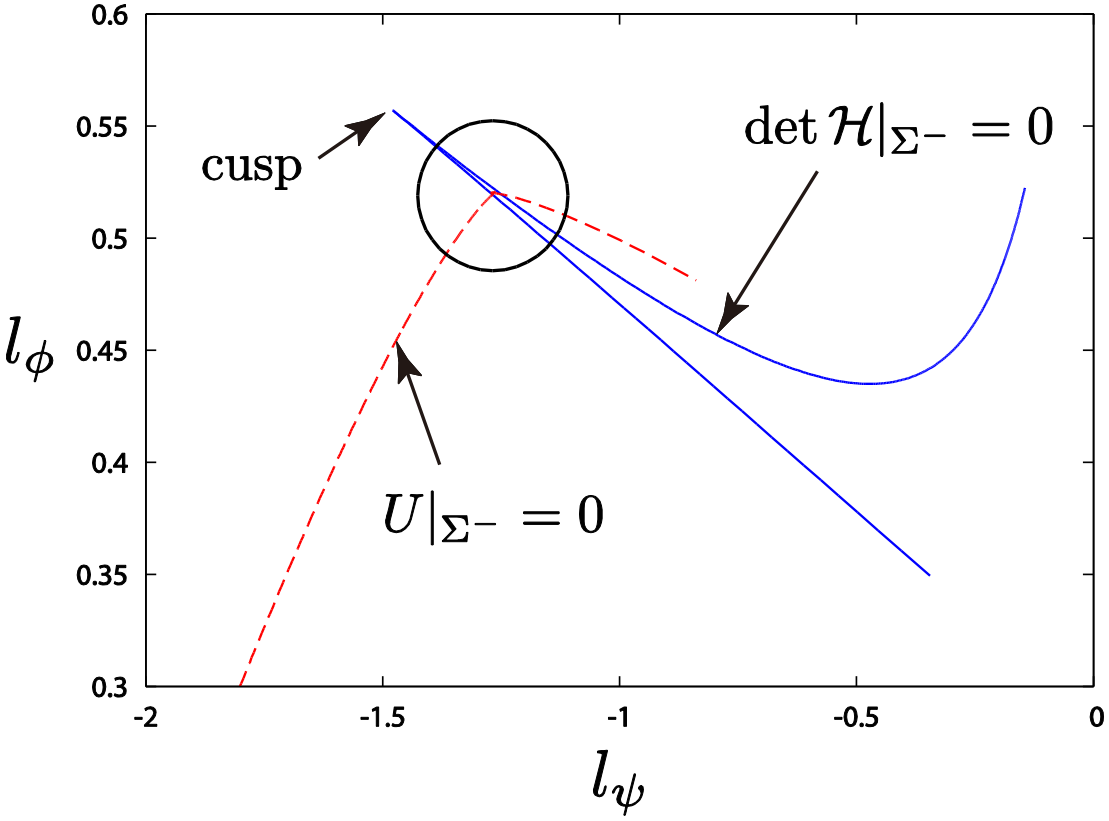

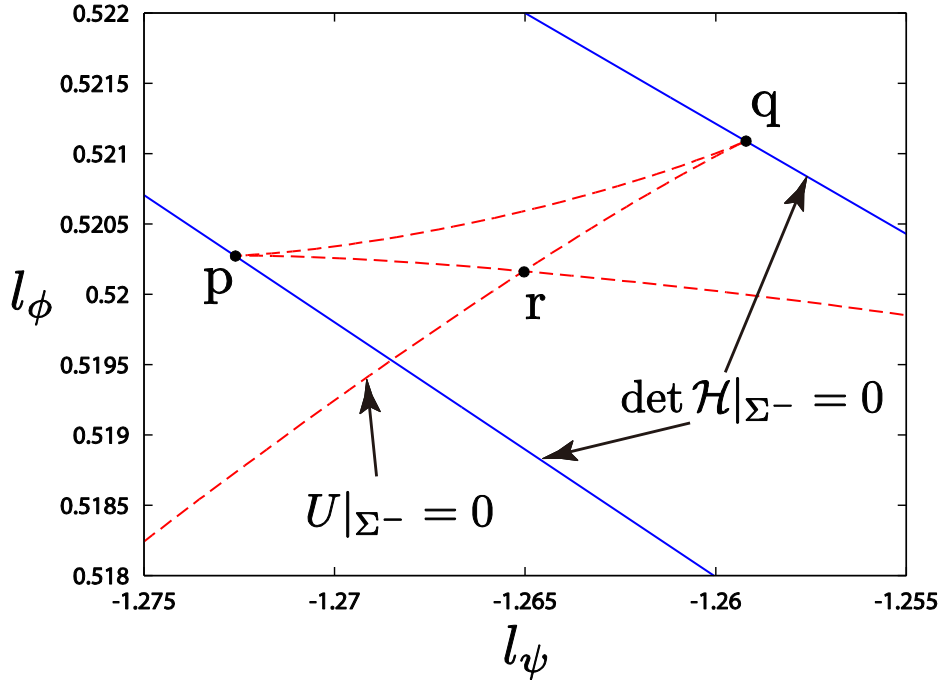

Stationary Points Set

2-dim. surface embedded
in 4-dimensional space

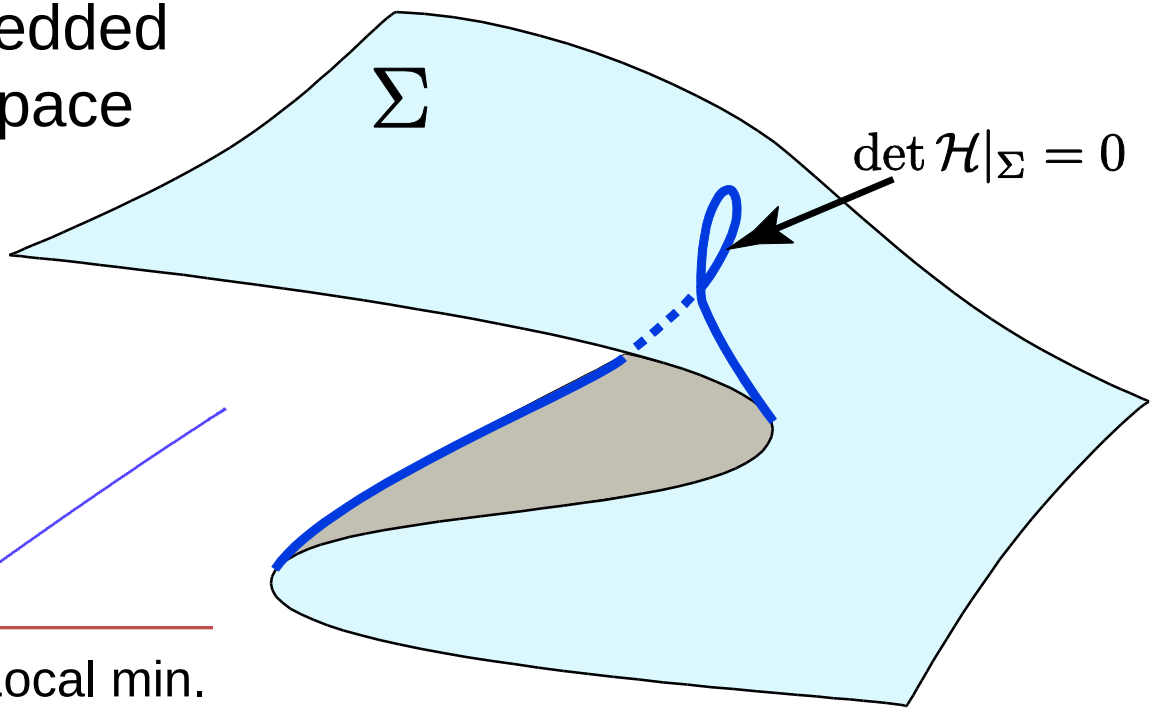

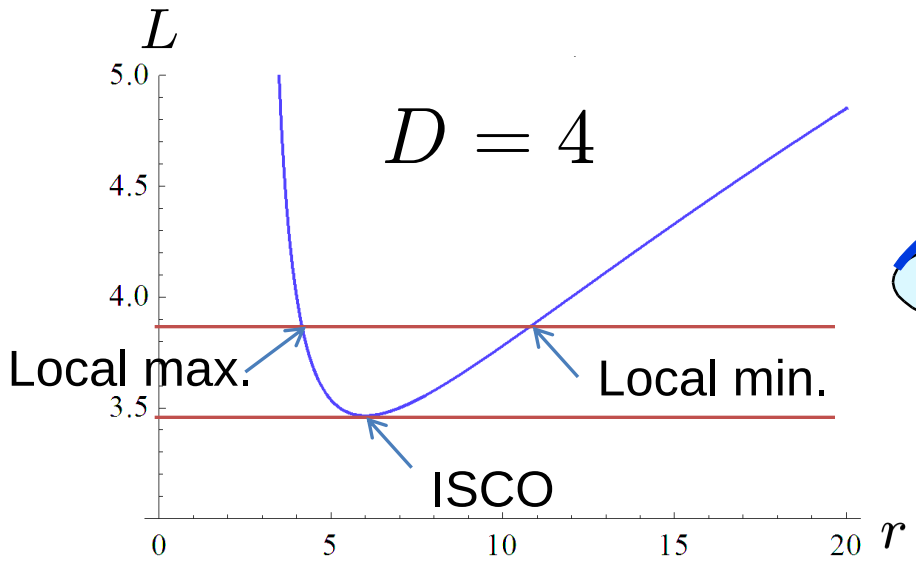

Stationary Points

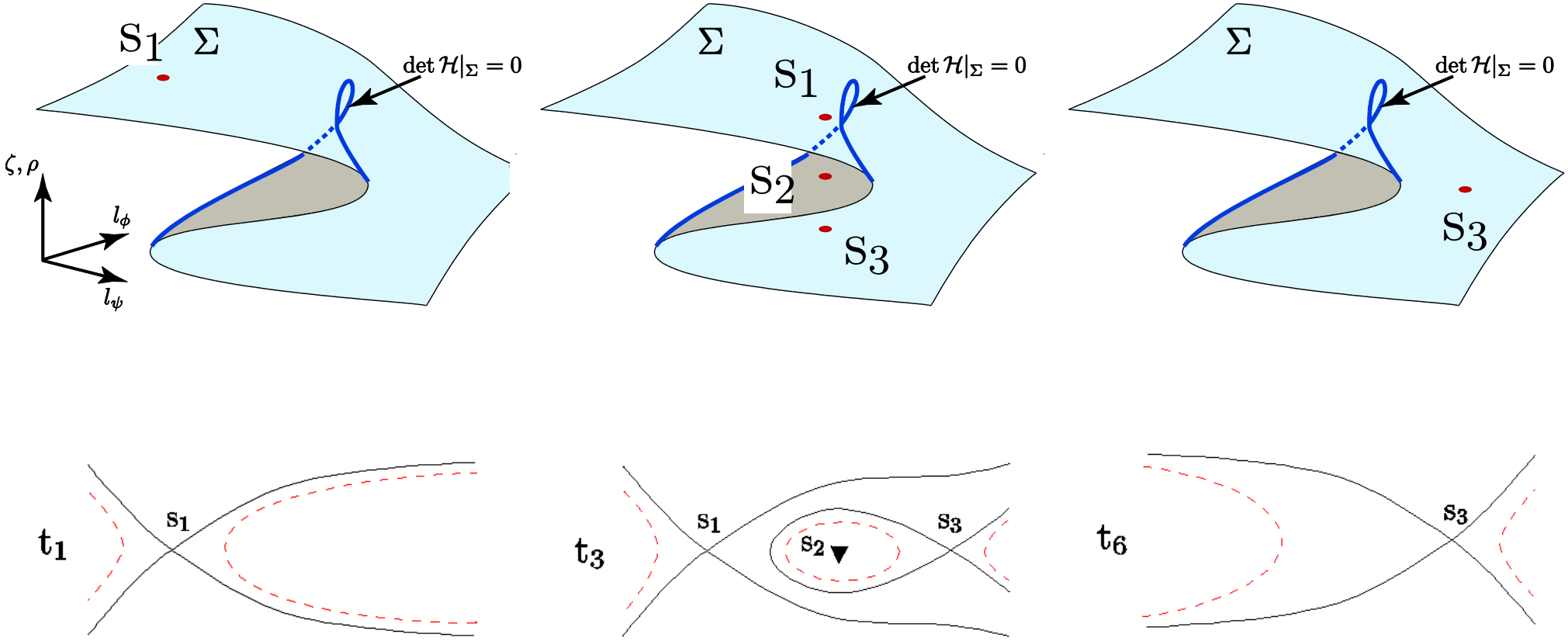

Stationary Points

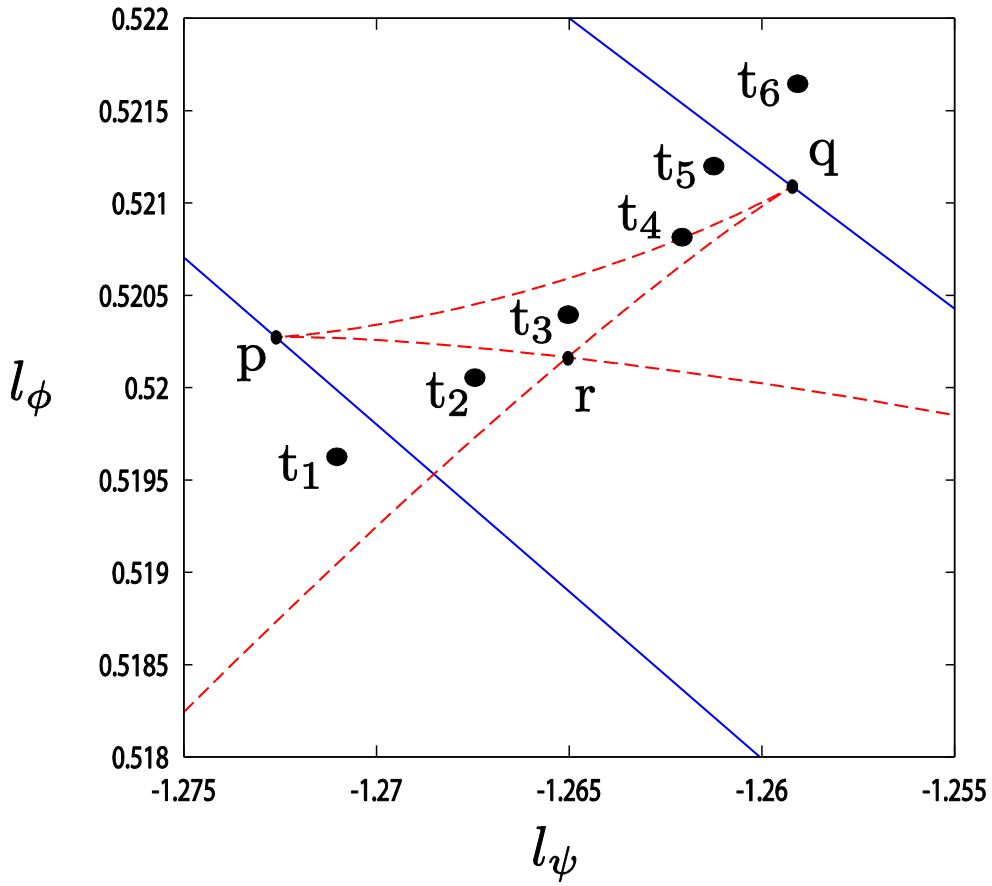

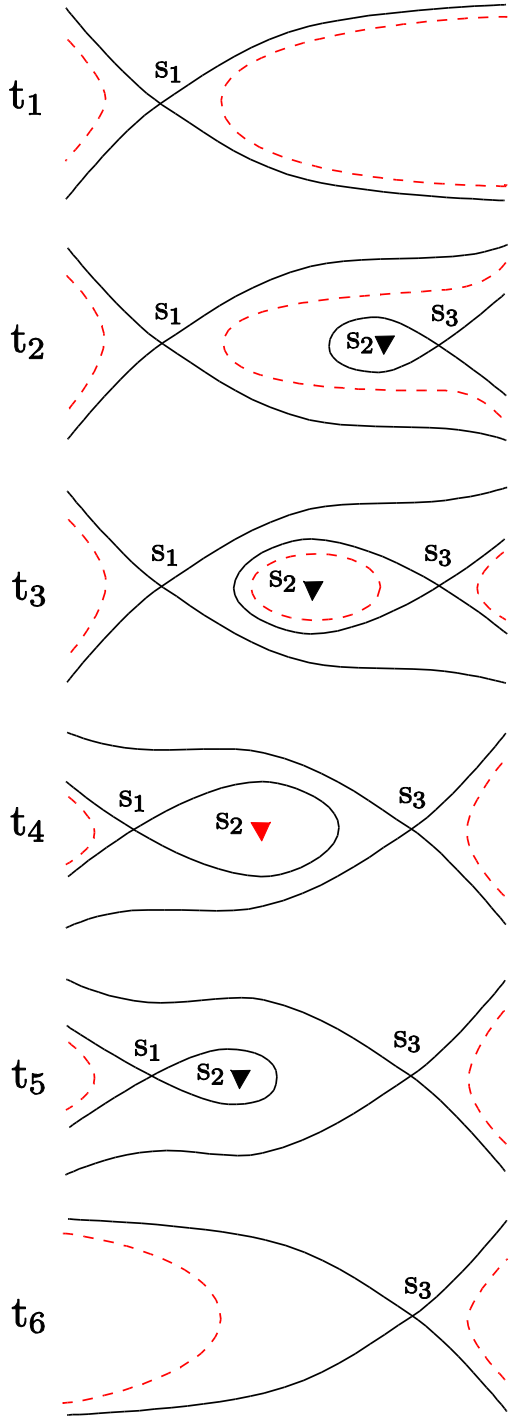

Bounded Null Orbits

Non stationary bounded orbits appear

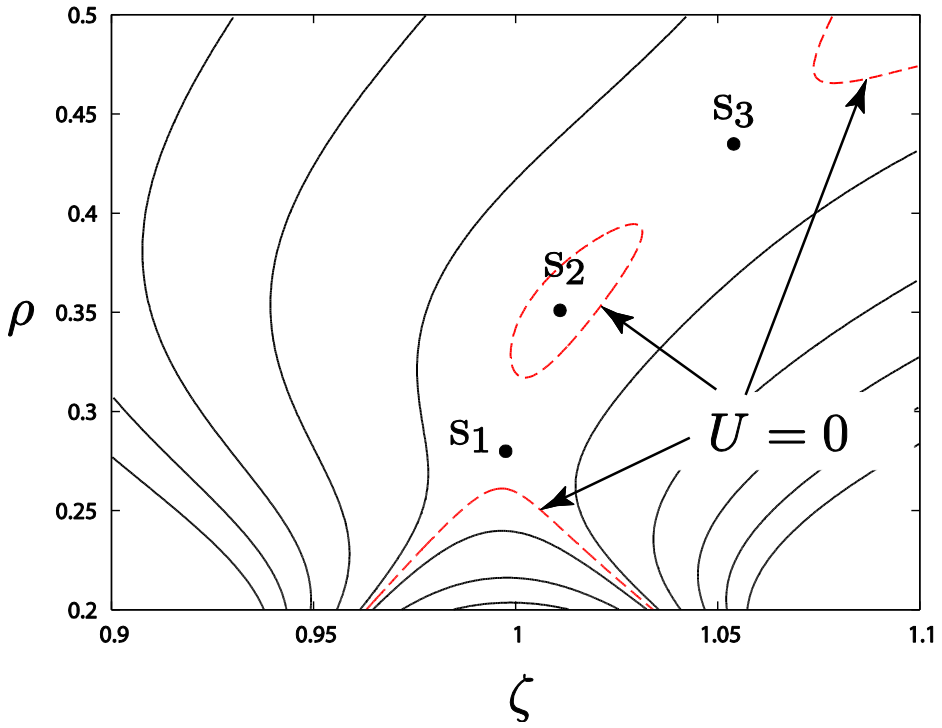

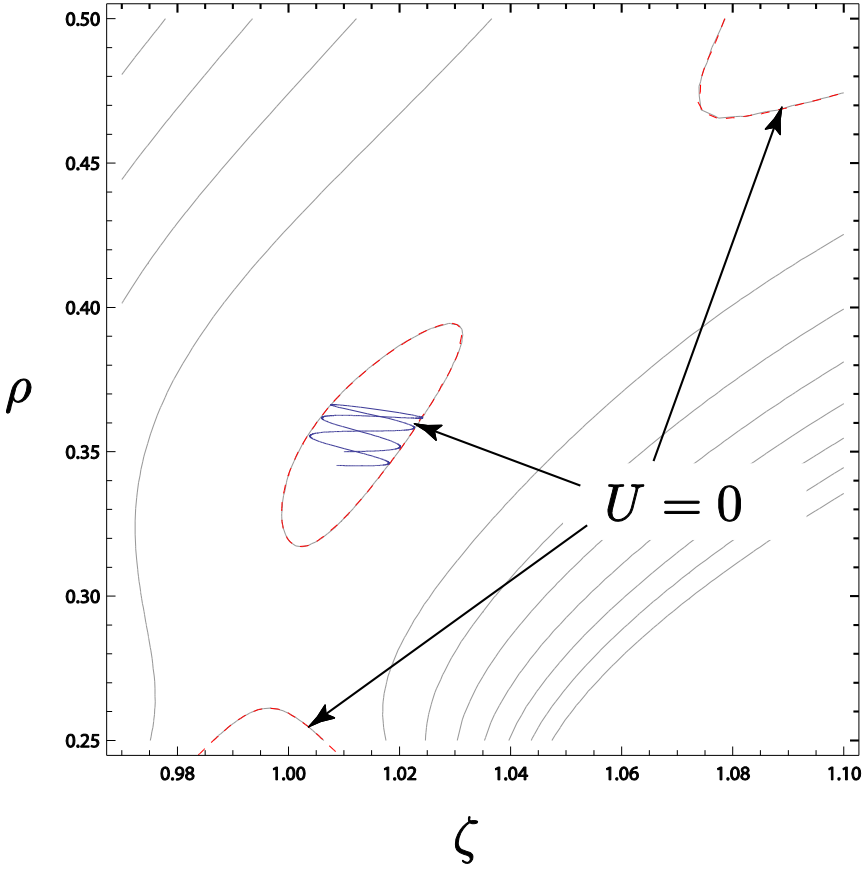

Summary

Stable bound null orbits exist around a Black Ring.

for $\nu \leq \nu_c = 0.13224\cdots$

	Stable Bound Orbit	
	Timelike	Null
4-D Black Holes	Yes	No
5-D Black Holes	No	No
5-D Black Rings	Yes	Yes

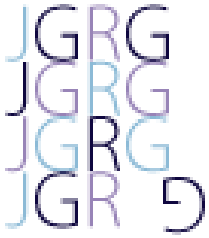

Hirotaka Yoshino, JGRG 22(2012)111412

"Axion bosenova"

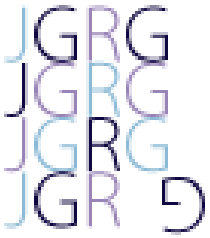

RESCEU SYMPOSIUM ON

GENERAL RELATIVITY AND GRAVITATION

JGRG 22



November 12-16 2012

Koshiba Hall, The University of Tokyo, Hongo, Tokyo, Japan



Axion Bosenova

Hirotaka Yoshino
Hideo Kodama *(KEK)*

Prog. Thoer. Phys. 128, 153-190 (2012),
arXiv:1203.5070[gr-qc]

JGRG22 @ RESCEU University of Tokyo
(November 14, 2012)

Contents

- Introduction
- Simulation
- Discussion
- Summary

Introduction

Axiverse

- QCD axion
  - QCD axion was introduced to solve the Strong CP problem.
  - It is one of the candidates of dark matter.

- String axions

Arvanitaki, Dimopoulos, Dubvosky, Kaloper, March-Russel, PRD81 (2010), 123530.

  - String theory predicts the existence of 10-100 axion-like massive scalar fields.
  - There are various expected phenomena of string axions.

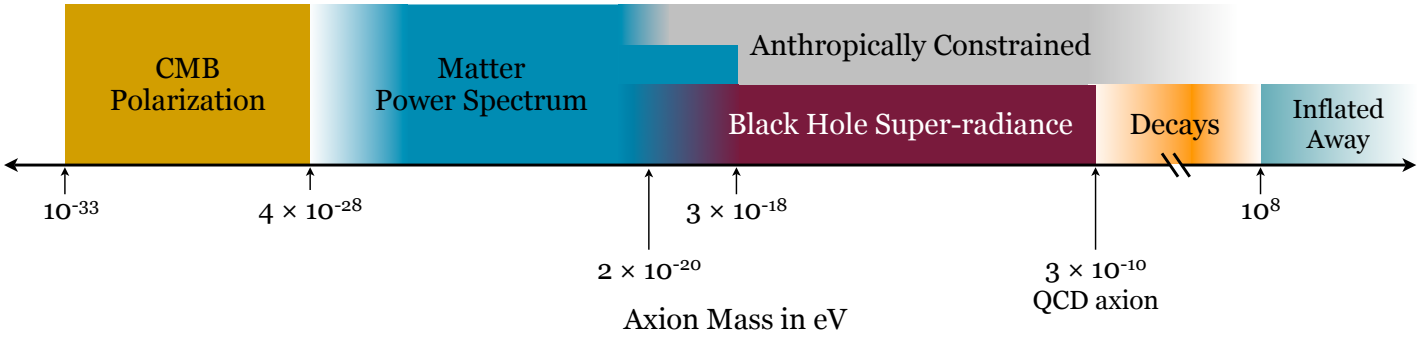

Axion field around a rotating black hole

- Axion field forms a cloud around a rotating BH and extract energy of the BH by “superradiant instability”.

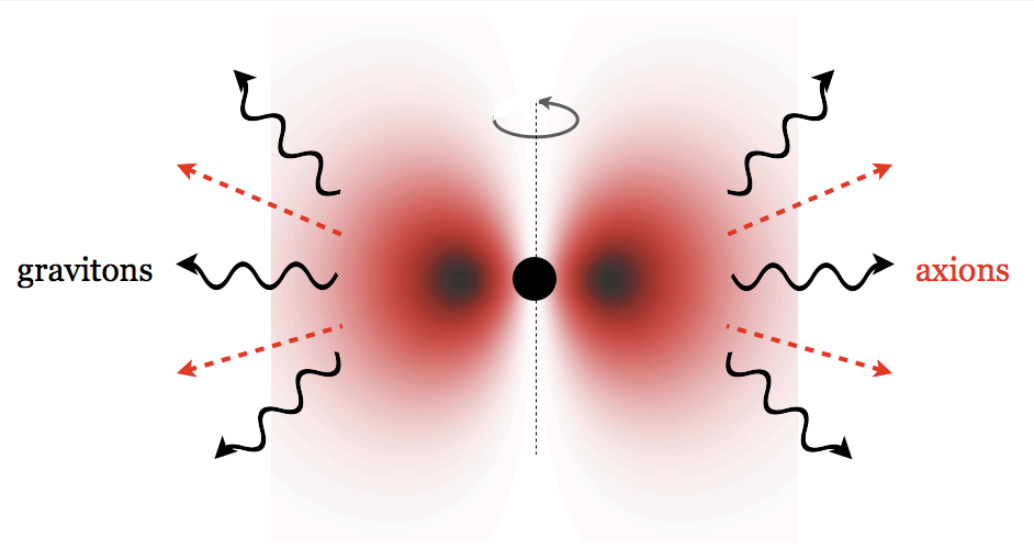

Arvanitaki, Dimopoulos, Dubvosky, Kaloper, March-Russel, PRD81 (2010), 123530.

Arvanitaki and Dubovsky, PRD83 (2011), 044026.

Superradiance

Zel'dovich (1971)

- Massless Klein-Gordon field $\nabla^2 \Phi = 0$

$$\Phi = \mathrm{Re}[e^{-i\omega t} R(r) S(\theta) e^{im\phi}]$$

$$R = \frac{u}{\sqrt{r^2 + a^2}} \quad \Rightarrow \quad \frac{d^2 u}{dr_*^2} + \left[\omega^2 - V(\omega)\right] u = 0$$

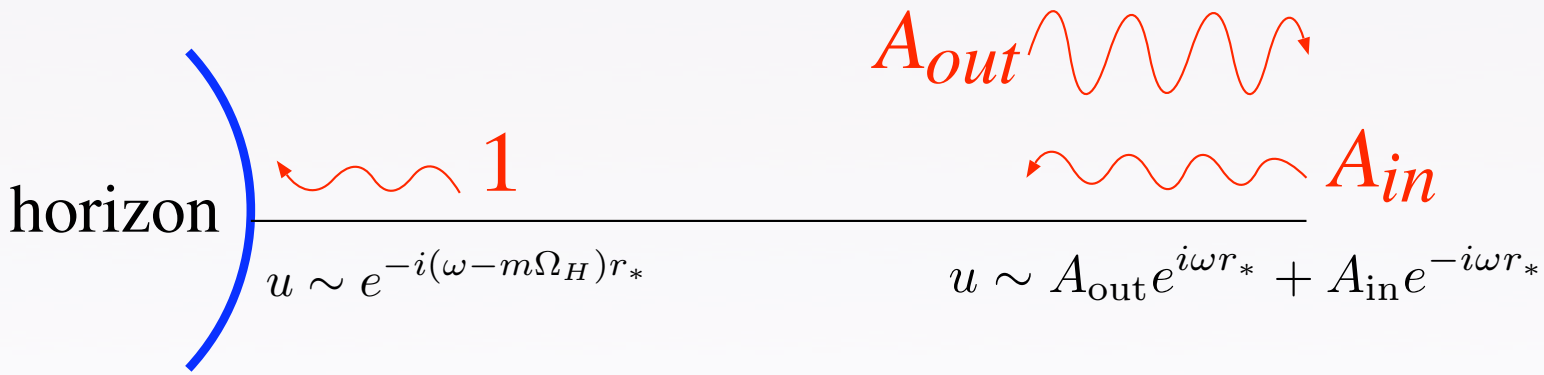

$$\left(1 - \frac{m\Omega_H}{\omega}\right) |T|^2 = 1 - |R|^2$$

Superradiant condition:

$$\omega < \Omega_H m$$

Bound state

Zouros and Eardley, Ann. Phys. 118 (1979), 139.
Detweiler, PRD22 (1980), 2323.

- Massive Klein-Gordon field $\nabla^2\Phi - \mu^2\Phi = 0$

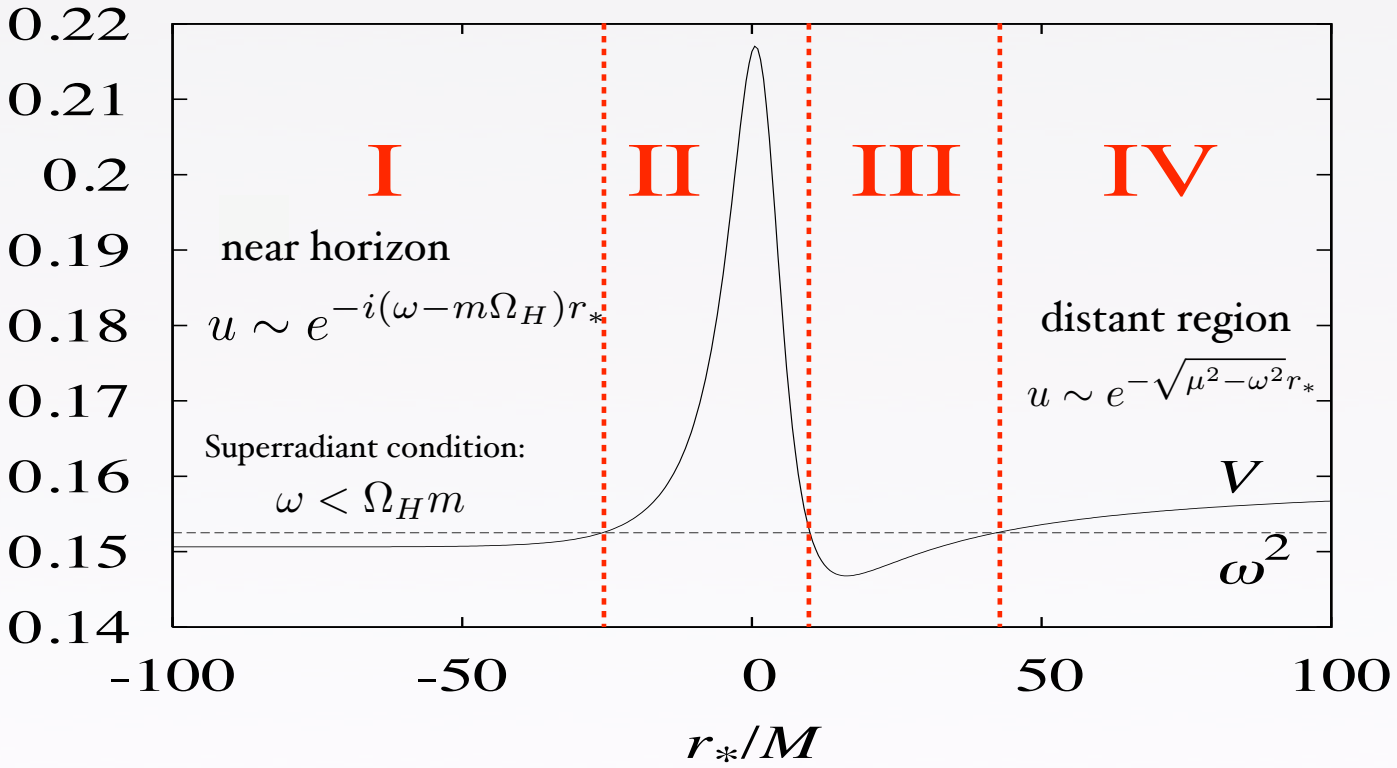

Typical time scale $\sim 10^7 M \sim \begin{cases} 50\ \text{s} & (M = 10 M_\odot) \\ 1.6\ \text{year} & (M = 10^6 M_\odot) \end{cases}$

BH-axion system

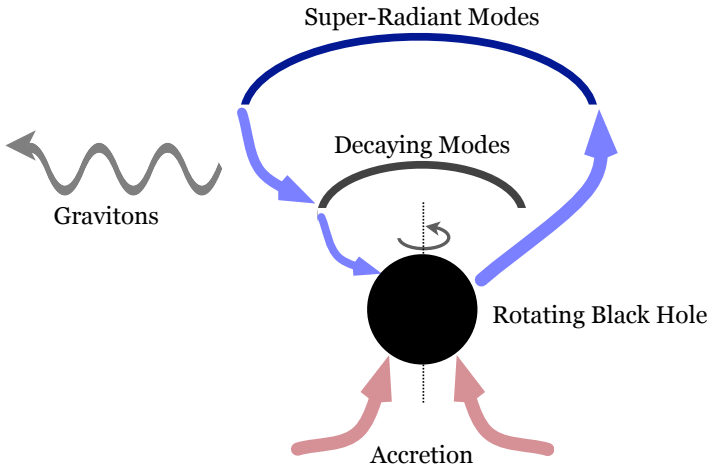

Arvanitaki and Dubovsky, PRD83 (2011), 044026.

- Superradiant instability
  - Emission of gravitational waves
    (Level transition, Pair annihilation of axions)
- Effects of nonlinear self-interaction
  - Bosenova
  - Mode mixing

Nonlinear effect

- Typically, the potential of axion field becomes periodic

$$V = f_a^2 \mu^2 [1 - \cos(\Phi / f_a)]$$

$$\Rightarrow \quad \boxed{\nabla^2 \varphi - \mu^2 \sin \varphi = 0} \qquad \varphi \equiv \frac{\Phi}{f_a}$$

- c.f., QCD axion

PQ phase transition

U(1)PQ symmetry $\Rightarrow$ Potential becomes like a wine bottle

QCD phase transition

$\Rightarrow$ Z(N) symmetry

BH-axion system

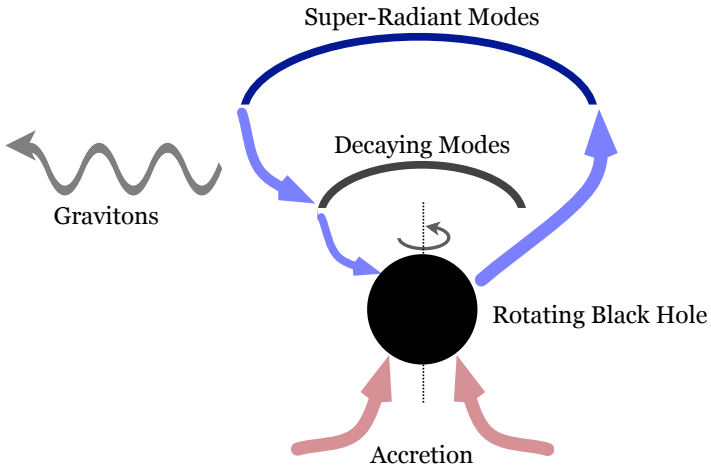

Arvanitaki and Dubovsky, PRD83 (2011), 044026.

- Superradiant instability
  - Emission of gravitational waves
    (Level transition, Pair annihilation of axions)
- Effects of nonlinear self-interaction
  - Bosenova
  - Mode mixing

Bosenova in condensed matter physics

http://spot.colorado.edu/~cwieman/Bosenova.html

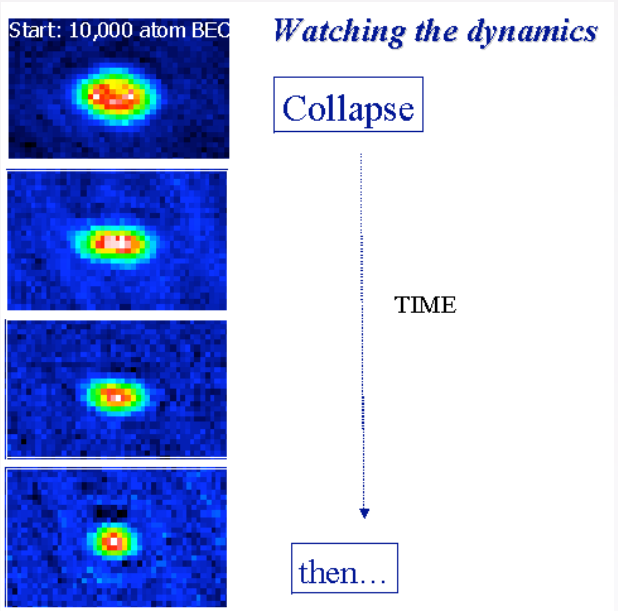

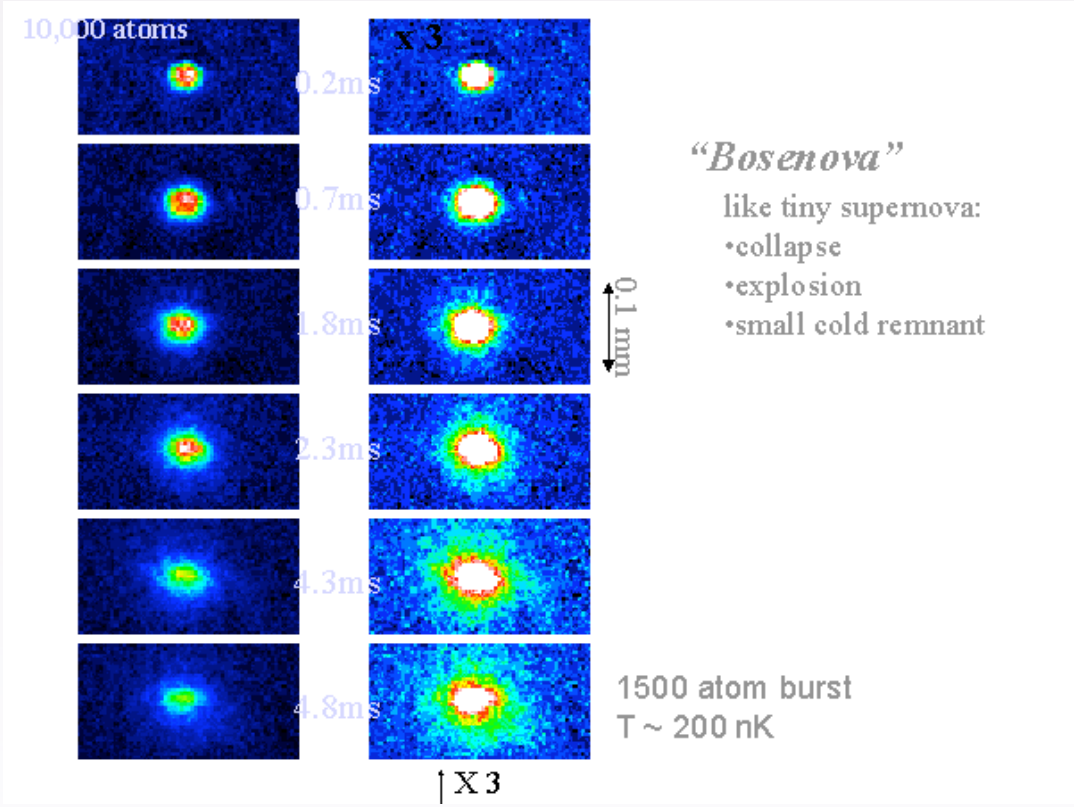

BEC state of Rb85 (interaction can be controlled)

Switch from repulsive interaction to attractive interaction

Wieman et al., Nature 412 (2001), 295

What we would like to do

- We would like to study the phenomena caused by axion cloud generated by the superradiant instability around a rotating black hole.

- In particular, we study numerically whether “Bosenova” happens when the nonlinear interaction becomes important.

- We adopt the background spacetime as the Kerr spacetime, and solve the axion field as a test field.

Simulations

- Typical two simulations
- Does the bosenova really happen?

Numerical simulation

- Sine-Gordon equation

$$\nabla^2\varphi - \mu^2 \sin\varphi = 0$$

- Setup $\quad a/M = 0.99, \quad M\mu = 0.4$

As the initial condition, we choose the bound state of the Klein-Gordon field of the $l = m = 1$ mode.

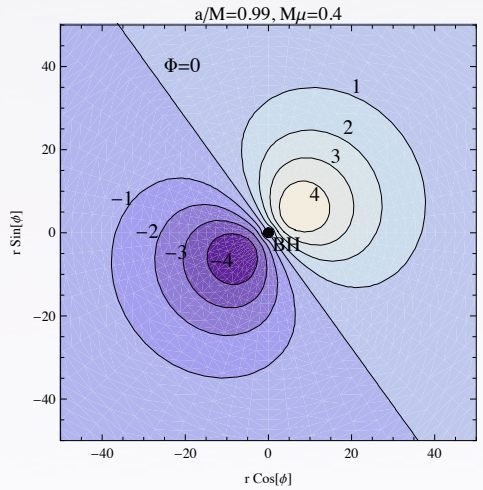

	Initial peak value	$E/[(f_a/M_p)^2 M]$
(A)	0.6	1370
(B)	0.7	1862

Simulation (A)

$\varphi_{\rm peak}(0) = 0.6$

- Axion field on the equatorial plane $(\theta = \pi/2)$

$(\phi = 0)$

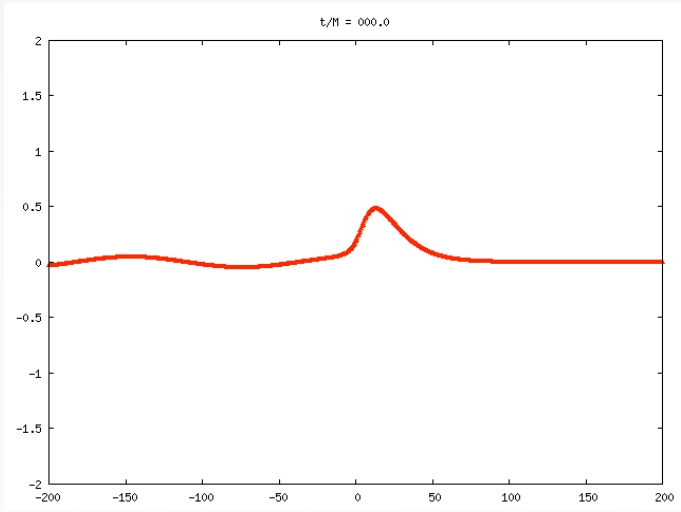

Φ

$-200 \leq r_*/M \leq 200$

(Equatorial plane)

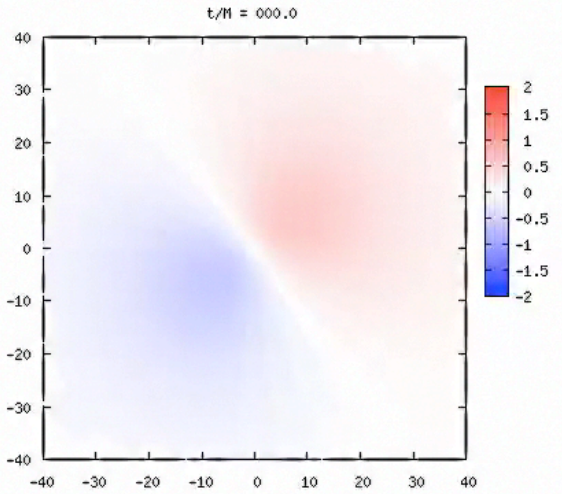

$r \sin\phi$

$r \cos\phi$

Simulation (A)

- Peak value and peak location

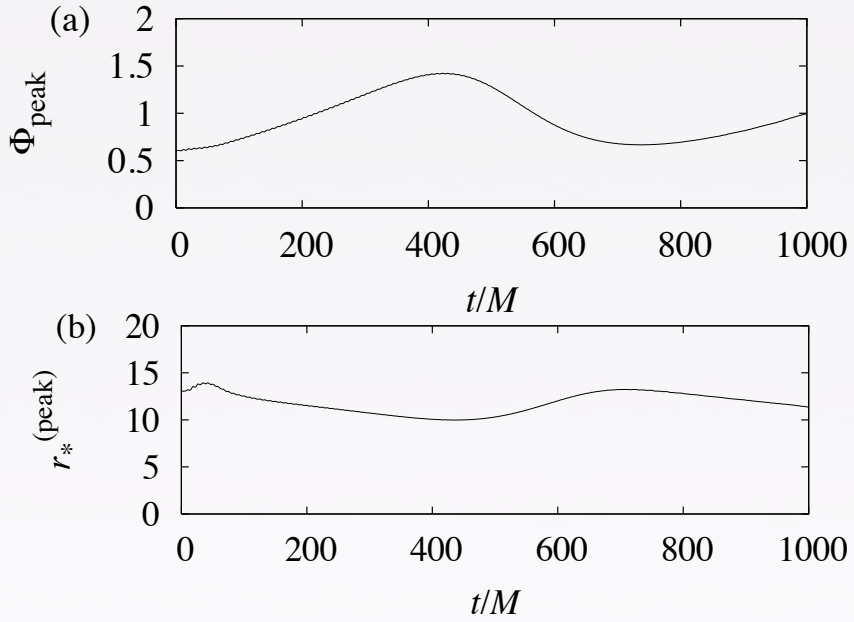

- Fluxes toward the horizon

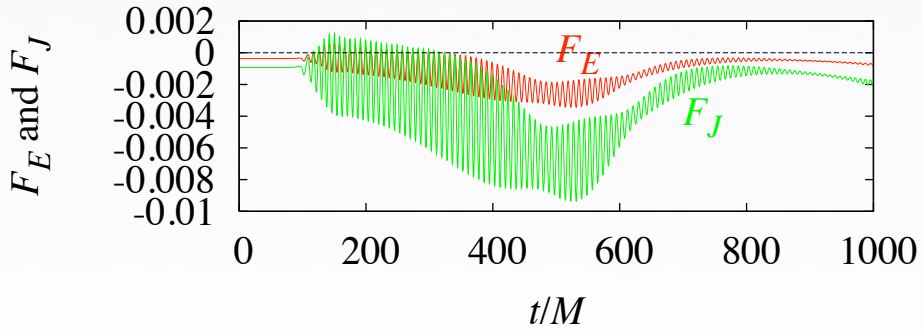

- Energy and angular momentum distribution

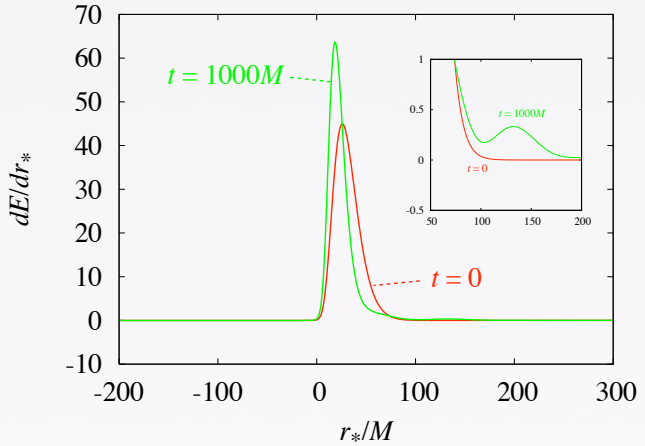

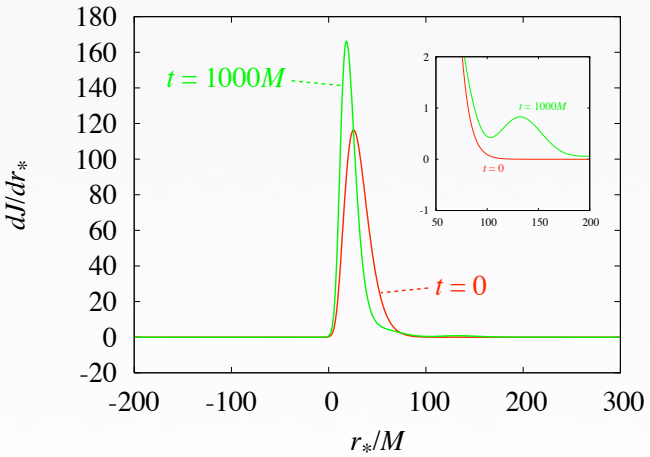

Simulation (B)

$\varphi_{\rm peak}(0) = 0.7$

- Axion field on the equatorial plane $(\theta = \pi/2)$

$(\phi = 0)$

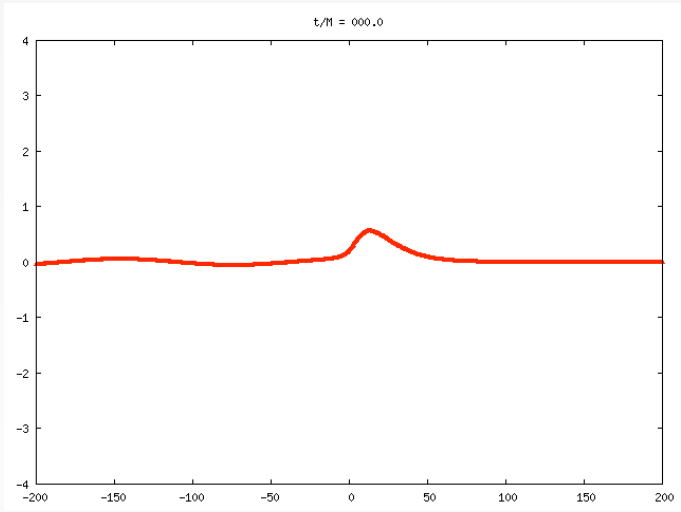

Φ

$-200 \leq r_*/M \leq 200$

(Equatorial plane)

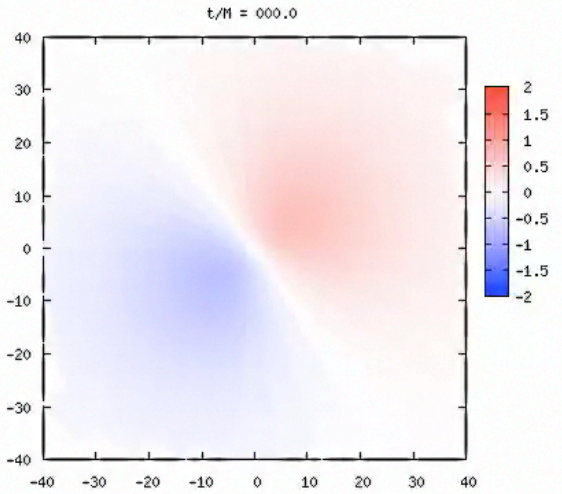

$r \sin\phi$

$r \cos\phi$

Simulation (B)

- Peak value and peak location

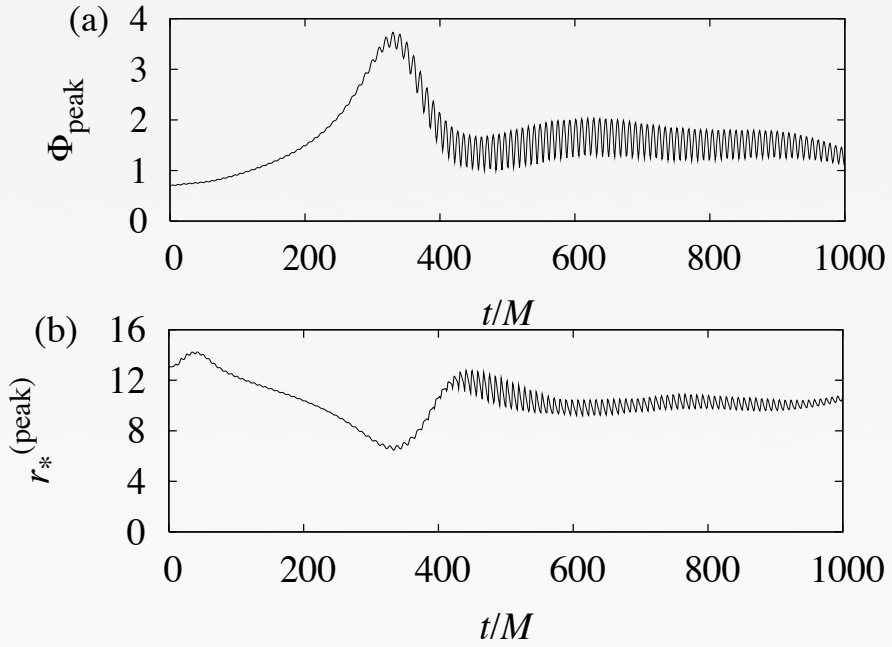

- Fluxes toward the horizon

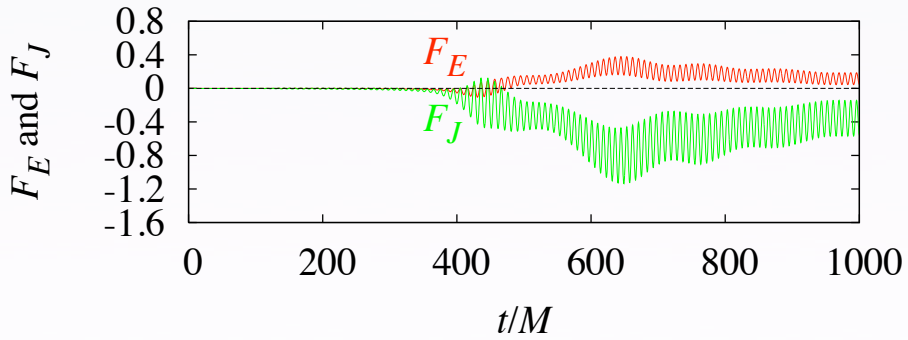

- Energy and angular momentum distribution

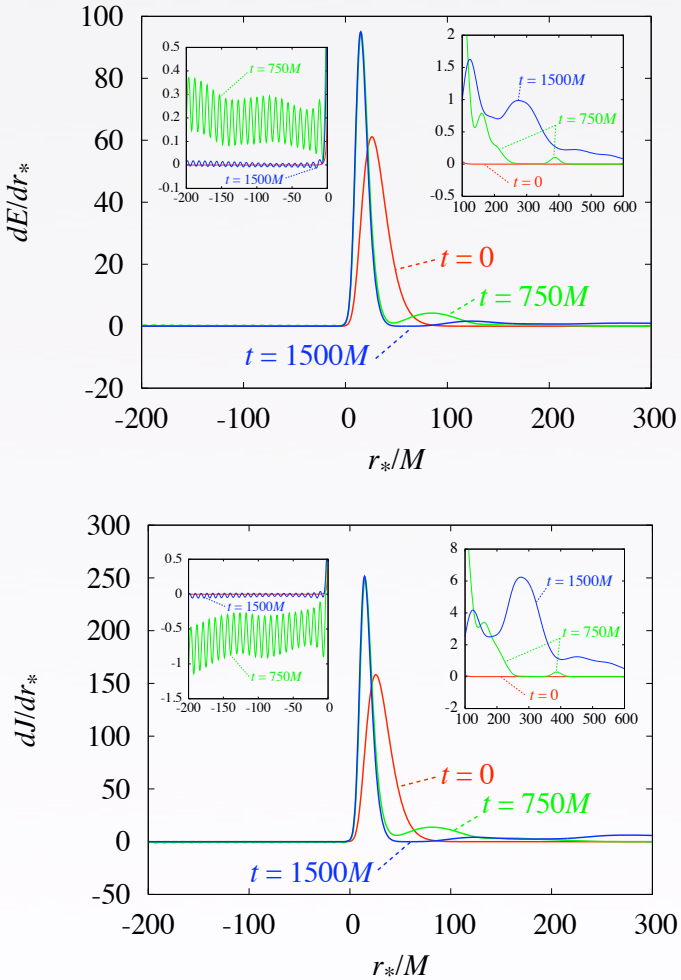

Simulation (B)

- Energy distribution

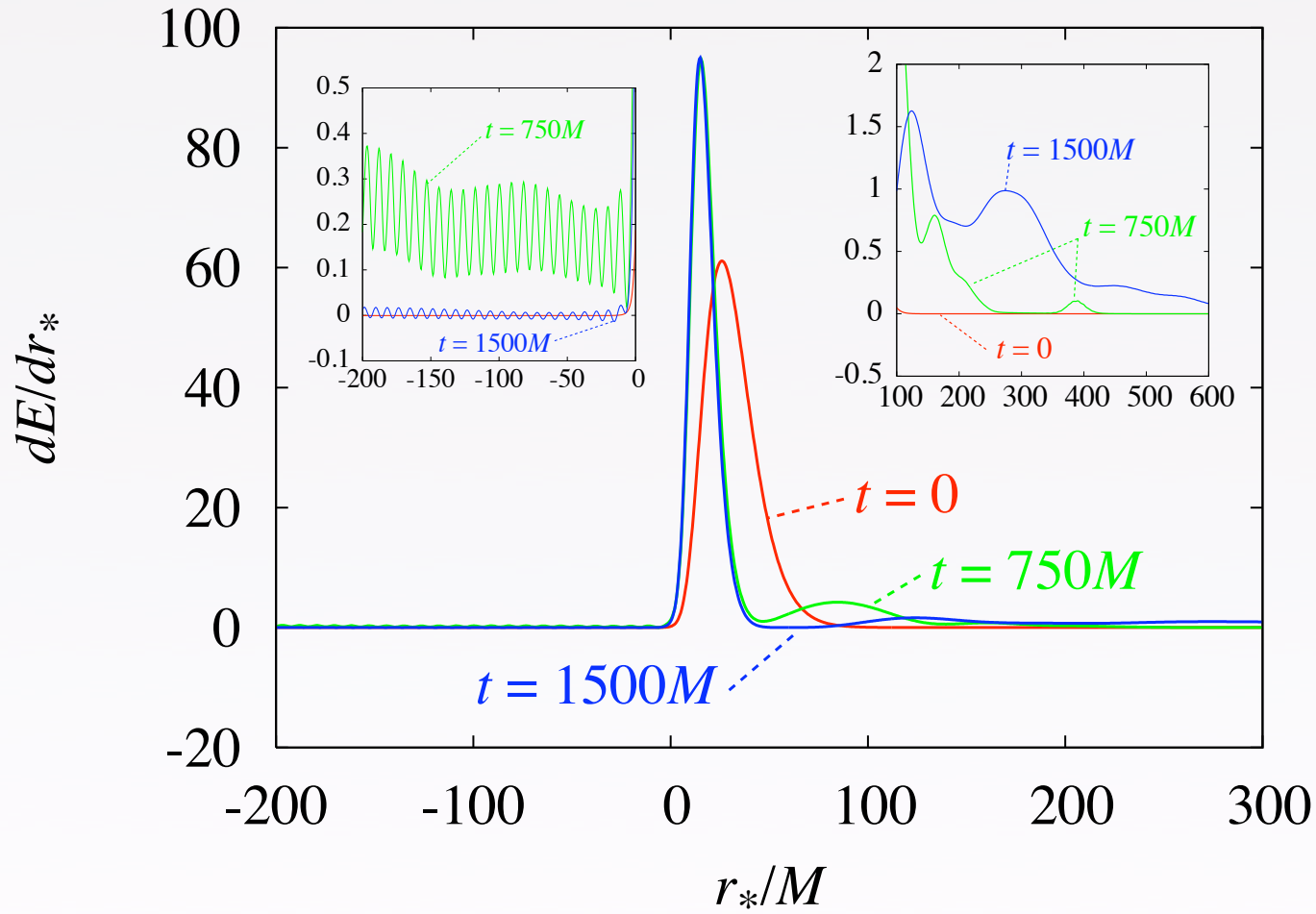

Simulations

- Typical two simulations
- Does the bosenova really happen?

Does bosenova really happen?

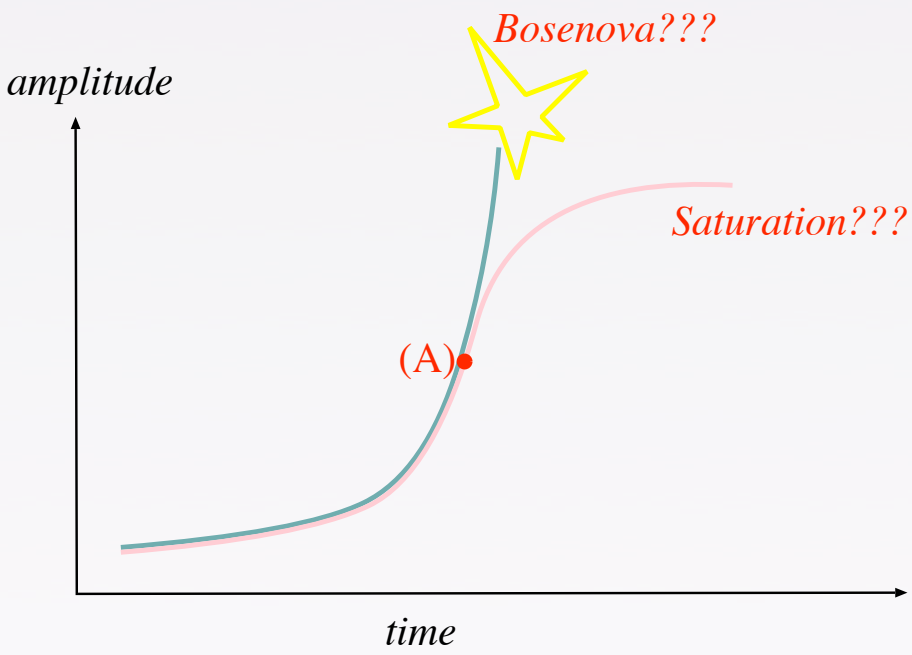

- Additional simulation:

$$\varphi(0) = C\varphi^{(\mathrm{A})}(1000M)$$
$$\dot{\varphi}(0) = C\dot{\varphi}^{(\mathrm{A})}(1000M)$$

$$C = \begin{cases} 1.05 \\ 1.08 \\ 1.09 \end{cases}$$

Supplementary simulation

$$\varphi(0) = C\varphi^{(\mathrm{A})}(1000M)$$
$$\dot{\varphi}(0) = C\dot{\varphi}^{(\mathrm{A})}(1000M)$$

- Energy absorbed by the black hole $\Delta E := \int_0^t F_E dt$ $\quad C = \begin{cases} 1.05 \\ 1.08 \\ 1.09 \end{cases}$

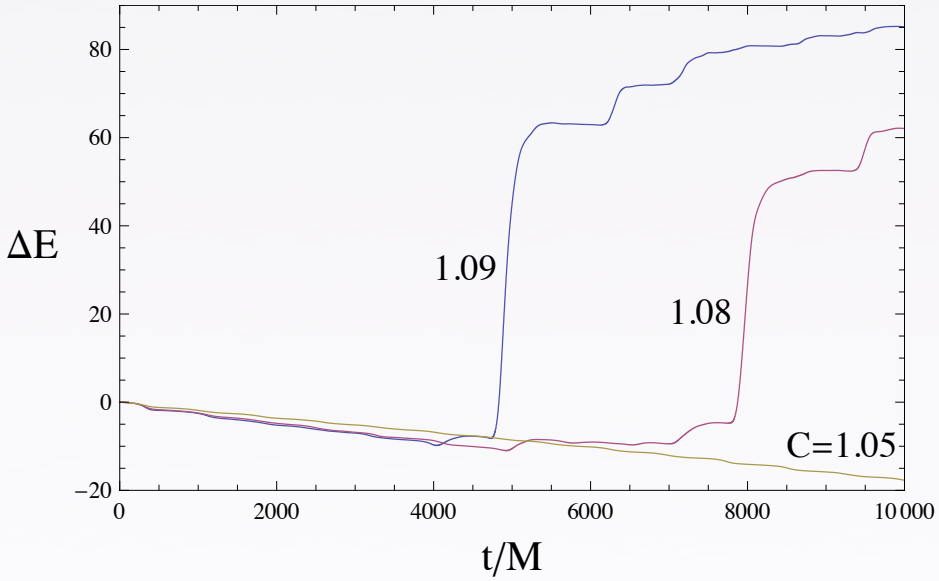

The bosenova happens when $E \simeq 1600 \times (f_a/M_p)^2 M$

Discussions

- Effective theory
- Gravitational waves

Effective theory (I)

- Action $\hat{S} = \int d^4x\sqrt{-g}\left[-\frac{1}{2}(\nabla\varphi)^2 - \mu^2\left(\frac{\varphi^2}{2} + \hat{U}_{\rm NL}(\varphi)\right)\right],$

- Non-relativistic approximation

$$\varphi = \frac{1}{\sqrt{2\mu}}\left(e^{-i\mu t}\psi + e^{i\mu t}\psi^*\right)$$

$$\Rightarrow \quad \hat{S}_{\rm NR} = \int d^4x\left[\frac{i}{2}\left(\psi^*\dot{\psi} - \psi\dot{\psi}^*\right) - \frac{1}{2\mu}\partial_i\psi\partial_i\psi^* + \frac{\alpha_g}{r}\psi^*\psi - \mu^2\tilde{U}_{\rm NL}(|\psi|^2/\mu)\right]$$

$$\tilde{U}_{\rm NL}(x) = -\sum_{n=2}^{\infty}\frac{(-1/2)^n}{(n!)^2}x^n.$$

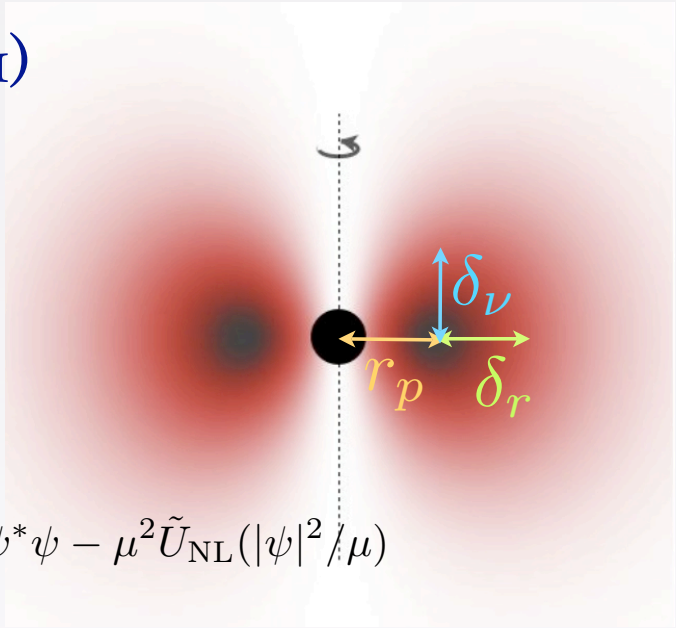

- Approximate the axion cloud as a Gaussian wavepacket

$$\psi = A(t,r,\nu)e^{iS(t,r,\nu)+im\phi} \qquad (\nu = \cos\theta)$$

$$A(t,r,\nu) \approx A_0\exp\left[-\frac{(r-r_p)^2}{4\delta_r r_p^2} - \frac{(\nu-\nu_p)^2}{4\delta_\nu}\right],$$

$$S(t,r,\nu) \approx S_0(t) + p(t)(r-r_p) + P(t)(r-r_p)^2 + \pi_\nu(t)(\nu-\nu_p)^2 + \cdots,$$

Effective theory (2)

- Effective Lagrangian: $L = T - V$

$$T = \frac{1}{2}A\dot{\delta}_r^2 + B\dot{\delta}_r\dot{r}_p + \frac{1}{2}C\dot{r}_p^2 + \frac{1}{2}D\dot{\delta}_\nu^2,$$

$$\frac{V}{\mu\alpha_g^2} = \frac{1}{2(\alpha_g\mu r_p)^2(1+\delta_r)}\left(1+\delta_\nu+\frac{1}{4\delta_r}+\frac{1}{4\delta_\nu}\right) - \frac{1}{(\alpha_g\mu r_p)(1+\delta_r)}$$
$$-\alpha_g^{-2}\sum_{n=2}^{\infty}\frac{(-1/2)^n}{(n!)^2 n}\left[\frac{N_*}{\sqrt{\delta_r\delta_\nu}(\alpha_g\mu r_p)^3(1+\delta_r)}\right]^{n-1}.$$

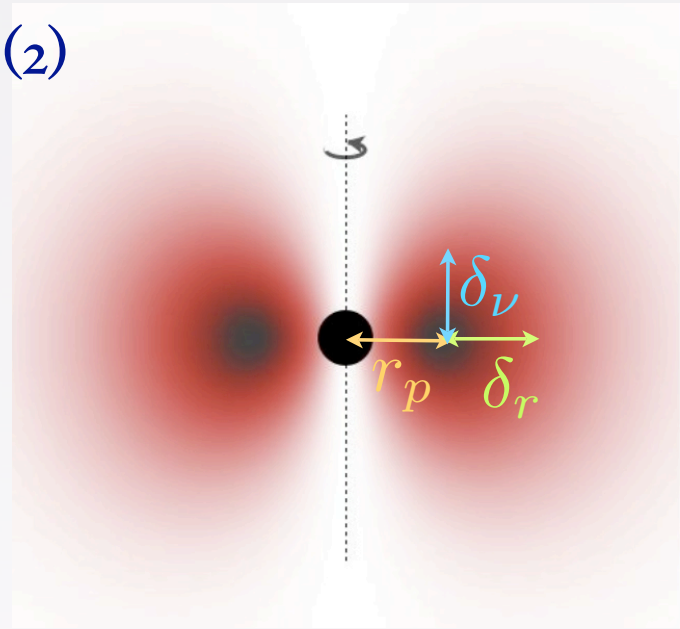

- Potential

$\alpha_g = 0.1$

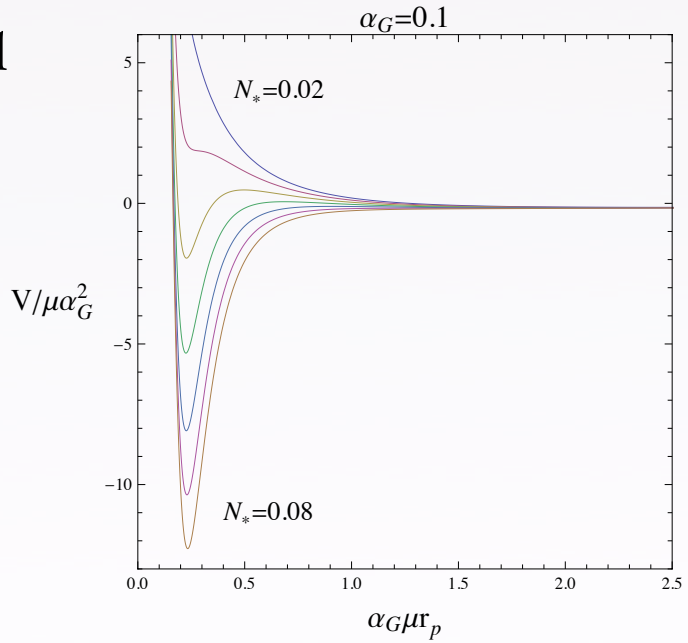

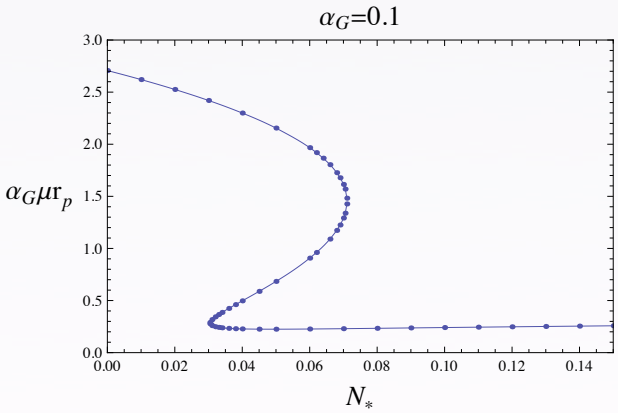

Small oscillations

- Oscillation around a equilibrium point $\quad \Delta q_i = (\Delta\delta_r, \Delta\delta_\nu, \alpha_g \mu \Delta r_p)$

$$\Rightarrow \quad \frac{d^2(\Delta q_i)}{dt^2} = -\sum_j \omega_{ij} \Delta q_j$$

- Oscillation frequencies
  - $\alpha_g = 0.4, N_* = 1.1$

$$\omega^2 = 1.141, \quad 0.249, \quad 0.0166, \qquad \boxed{\Delta t \approx 761M}$$

$$\Rightarrow \quad \delta q = \begin{pmatrix} 0.110 \\ -0.027 \\ 0.994 \end{pmatrix}, \quad \begin{pmatrix} 0.075 \\ 0.724 \\ 0.686 \end{pmatrix}, \quad \begin{pmatrix} -0.378 \\ -0.005 \\ 0.925 \end{pmatrix}.$$

  - $\alpha_g = 0.4, N_* = 1.3$

$$\omega^2 = 14.06, \quad 5.59, \quad 0.175, \qquad \boxed{\Delta t \approx 26M}$$

$$\Rightarrow \quad \Delta q = \begin{pmatrix} 0.218 \\ -0.030 \\ 0.975 \end{pmatrix}, \quad \begin{pmatrix} 0.070 \\ 0.927 \\ 0.367 \end{pmatrix}, \quad \begin{pmatrix} -0.640 \\ -0.085 \\ 0.763 \end{pmatrix}.$$

Discussions

- Axion cloud model
- Gravitational waves

GWs emitted in the bosenova (rough estimate)

- Assumption:
  - Quadrupole approximation
  - Change in the quadrupole moment by the infall of energy in the bosenova

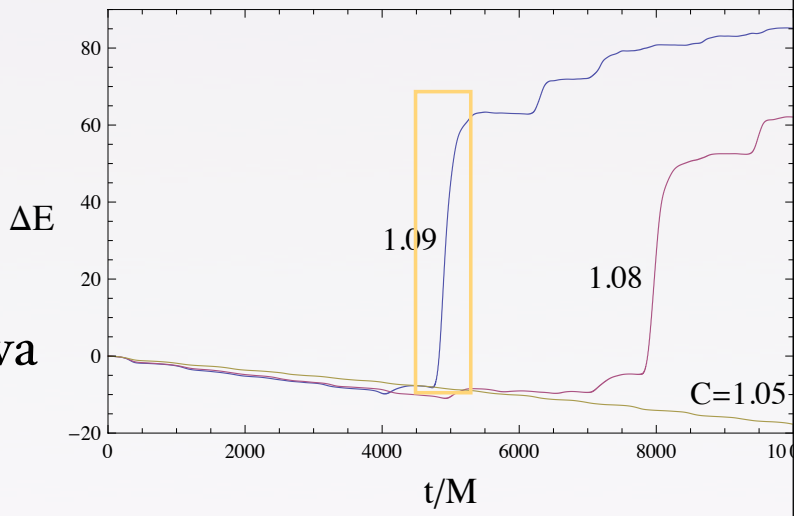

$$Q_{ij} \sim r_p^2 E$$

$10M$

$$E_0 + \frac{1}{2}(\Delta E)\left[\cos\left(\pi\frac{t}{\Delta t}\right) - 1\right]$$

$10^{-3}M$ $0.05E_0$ $500M$

- Amplitude of generated GWs

$$h \sim \frac{\ddot{Q}_{ij}}{r_{\rm obs}} \sim 10^{-7}\frac{M}{r_{\rm obs}}$$

Detectability

$$h \sim \frac{\ddot{Q}_{ij}}{r_{\rm obs}} \sim 10^{-7}\frac{M}{r_{\rm obs}}$$

- Supermassive BH of our galaxy (Sagittarius A*)

$$h_{\rm rss} := \left[\int |h|^2 dt\right]^{1/2} \sim 10^{-16}({\rm Hz})^{-1/2}$$

⇨ *Detectable by the eLISA*

- Solar-mass BH (e.g., Cygnus X-1)

$$h_{\rm rss} \sim 10^{-24}({\rm Hz})^{-1/2}$$

⇨ *below the sensitivity of the KAGRA, Advanced LIGO, Advanced Virgo, etc.*

$(10^{-4}$ Hz)

↑

Angular frequency of GW

↓

$(10^{2}$ Hz)

Summary

Summary

- We developed a reliable code and numerically studied the behaviour of axion field around a rotating black hole.
- The nonlinear effect enhances the rate of superradiant instability when the amplitude is not very large.
- The bosenova collapse would happen as a result of superradiant instability.

Ongoing studies

- Calculation of the gravitational waves emitted in bosenova.
- The case where axions couple to magnetic fields.

Appendix

Superradiant instability

Massive scalar fields around a Kerr BH

- Metric

$$ds^2 = -\left(\frac{\Delta - a^2\sin^2\theta}{\Sigma}\right)dt^2 - \frac{2a\sin^2\theta(r^2+a^2-\Delta)}{\Sigma}dtd\phi + \left[\frac{(r^2+a^2)^2 - \Delta a^2\sin^2\theta}{\Sigma}\right]\sin^2\theta d\phi^2 + \frac{\Sigma}{\Delta}dr^2 + \Sigma d\theta^2$$

$$\Sigma = r^2 + a^2\cos^2\theta,$$
$$\Delta = r^2 + a^2 - 2Mr.$$

- Massive scalar field
  - Lagrangian density

$$\mathcal{L} = -\sqrt{-g}\left[\frac{1}{2}g^{ab}\nabla_a\Phi\nabla_b\Phi + U(\Phi)\right], \quad U(\Phi) = \frac{1}{2}\mu^2 f_a^2\sin^2(\Phi/f_a) \simeq \frac{1}{2}\mu^2\Phi^2$$

  - Klein-Gordon equation $\nabla^2\Phi - U'(\Phi) = 0$

Massive scalar field around a Kerr BH

- Separation of variables $\Phi = e^{-i\omega t} R(r) S(\theta) e^{im\phi}$

$$\frac{1}{\sin\theta}\frac{d}{d\theta}\sin\theta\frac{dS}{d\theta} + \left[-k^2 a^2\cos^2\theta - \frac{m^2}{\sin^2\theta} + E_{lm}\right] S = 0$$

$$\frac{d}{dr}\Delta\frac{dR}{dr} + \left[\frac{K^2}{\Delta} - \lambda_{lm} - \mu^2 r^2\right] R = 0$$

$$K = (r^2 + a^2)\omega - am$$

$$k^2 = \mu^2 - \omega^2$$

$$\lambda_{lm} = E_{lm} + a^2\omega^2 - 2am\omega$$

Massive scalar field around a Kerr BH

$$\frac{d}{dr}\Delta\frac{dR}{dr}+\left[\frac{K^2}{\Delta}-\lambda_{lm}-\mu^2 r^2\right]R=0$$

- distant region $R\sim r^{-1\pm\frac{\mu^2-2\omega^2}{k}}\exp(\pm kr)$ $\qquad k=\sqrt{\mu^2-\omega^2}$

- near horizon $R\sim e^{\pm i\omega_* r_*}$ (outgoing / ingoing) $\qquad \boxed{\omega_*=\omega-\Omega_H m}$

(tortoise coordinate) r_* $\qquad dr_*=\dfrac{r^2+a^2}{\Delta}dr$

- Energy flux $\qquad P^\mu=-T^\mu_{\ \nu}\xi^\nu$

$$-P_{r_*}=\nabla_{r_*}\Phi\nabla_t\Phi\propto(\omega-\Omega_H m)\omega$$

If $\omega<\Omega_H m$, negative energy falls into the black hole ⇨ superradiance

Bound state

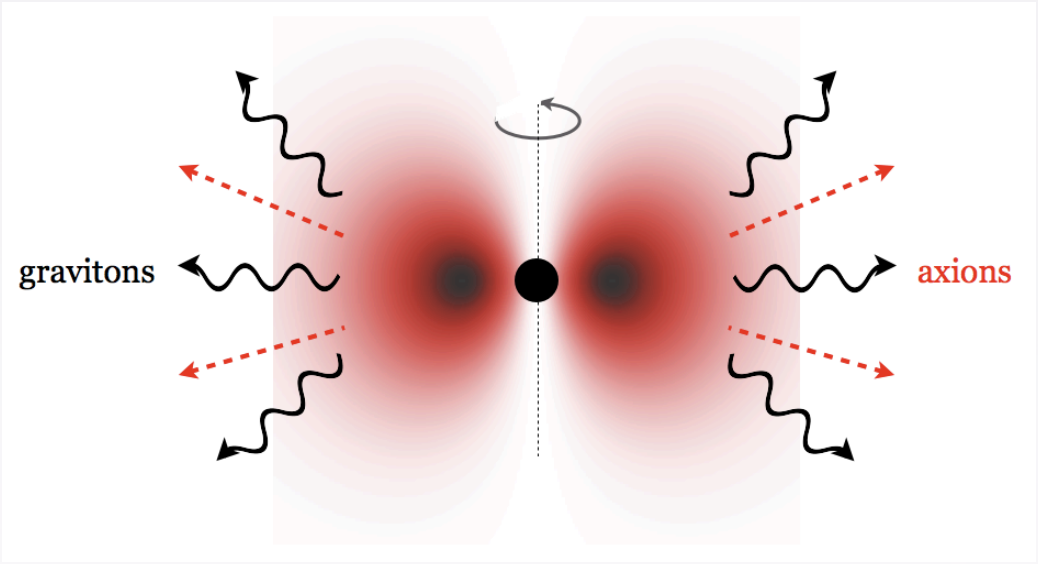

- Matching method — Detweiler, PRD22 (1980), 2323. $M\mu \simeq M\omega \ll 1$
- WKB method — Zouros and Eardley, Ann. Phys. 118 (1979), 139. $M\mu \gg 1$
- Numerical analysis — Dolan, PRD76 (2007), 084001.

Bound state

Zouros and Eardley, Ann. Phys. 118 (1979), 139.

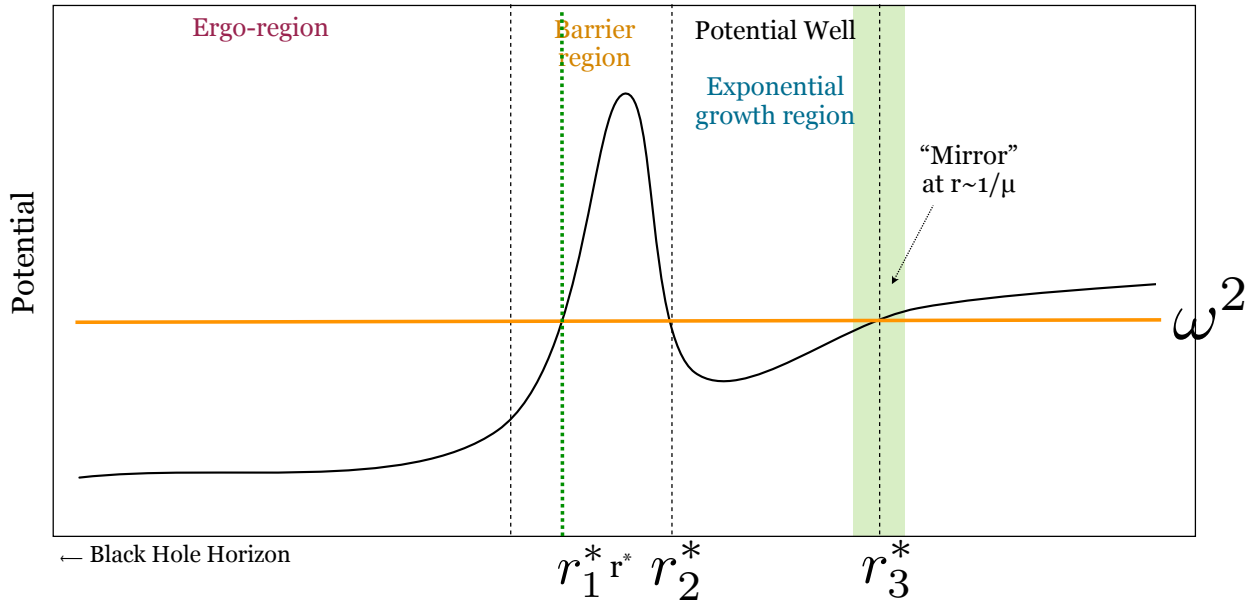

$$R = \frac{u}{\sqrt{r^2 + a^2}} \quad \Rightarrow \quad \frac{d^2u}{dr_*^2} + \left[\omega^2 - V(\omega)\right] u = 0$$

$$V(\omega) = \frac{\Delta\mu^2}{r^2 + a^2} + \frac{4Mam\omega r - a^2m^2 + \Delta\left[E_{lm} + (\omega^2 - \mu^2)a^2\right]}{(r^2 + a^2)^2} + \frac{\Delta}{(r^2 + a^2)^3}\left(3r^2 - 4Mr + a^2 - \frac{3\Delta r^2}{r^2 + a^2}\right)$$

Qualitative discussion on "Bosenova"

Arvanitaki and Dubovsky, PRD83 (2011), 044026.

- action

$$S = \int d^4x\sqrt{-g}\left[\frac{1}{2}g^{ab}\nabla_a\Phi\nabla_b\Phi + U(\Phi)\right]$$

$$U(\Phi) = \frac{1}{2}\mu^2 f_a^2 \sin^2(\Phi/f_a)$$

- Nonrelativistic approximation

$$\Phi = \frac{1}{\sqrt{2\mu}}\left(e^{-i\mu t}\psi + e^{i\mu t}\psi^*\right)$$

$$S = \int d^4x\left[i\Psi^*\partial_t\psi - \frac{1}{2\mu}\partial_i\psi\partial_i\psi - \mu V_N\psi^*\psi + \frac{1}{16 f_a^2}(\psi^*\psi)^2\right]$$

- Effective potential

$$V(r) \approx N\frac{l(l+1)+1}{2\mu r^2} - \frac{NM\mu}{r} - \frac{N^2}{32\pi f_a^2 r^3}$$

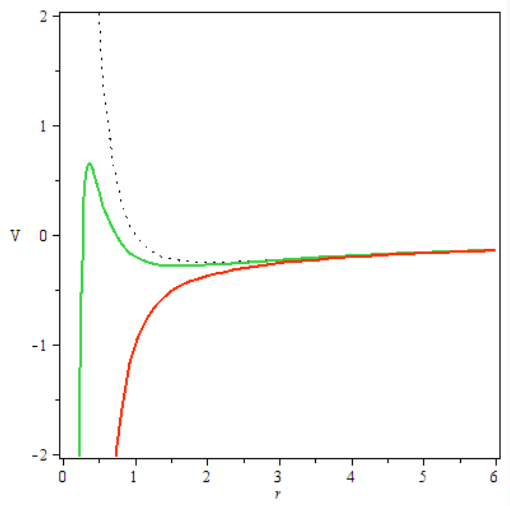

Code

First difficulty

- Stable simulation cannot be realized in Boyer-Lindquist coordinates.

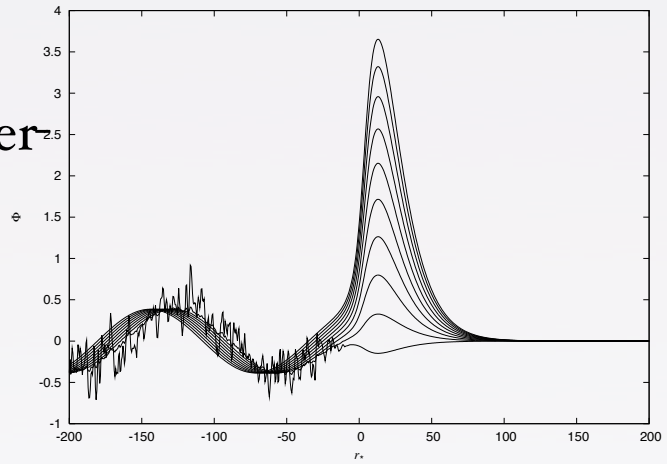

First difficulty

- Stable simulation cannot be realized in Boyer-Lindquist coordinates.

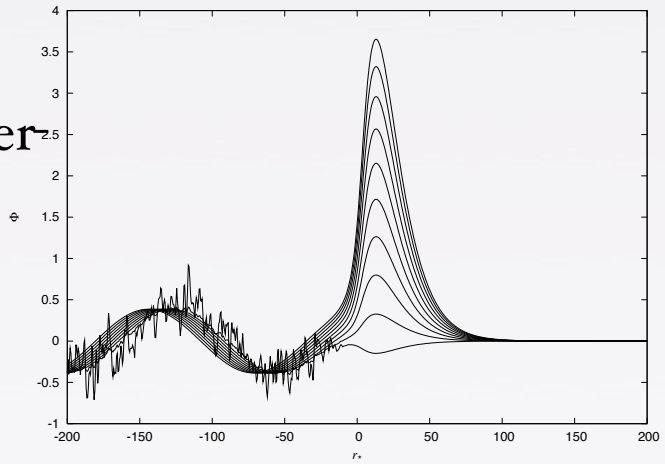

⇨ We use ZAMO coordinates.

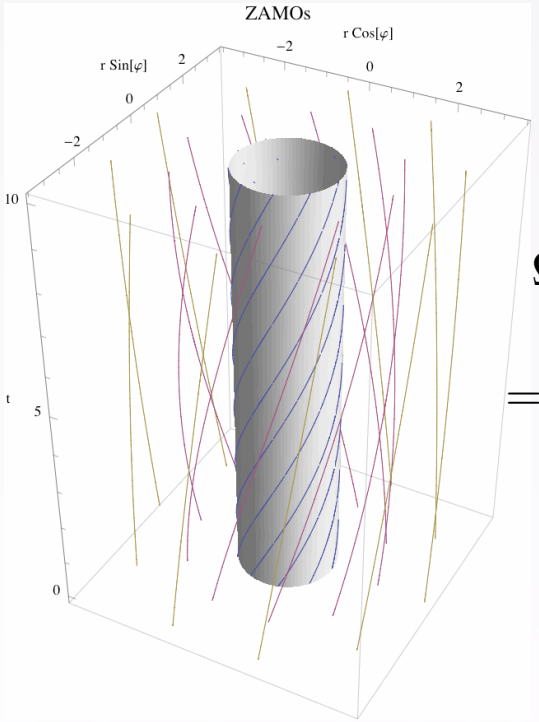

$$\Omega = \frac{d\phi}{dt} = \frac{u^\phi}{u^t} = -\frac{g_{t\phi}}{g_{\phi\phi}} = \frac{2Mar}{(r^2+a^2)^2 - \Delta a^2 \sin^2\theta}$$

$$\begin{aligned}
\tilde{t} &= t, \\
\tilde{\phi} &= \phi - \Omega(r,\theta)t, \\
\tilde{r} &= r, \\
\tilde{\theta} &= \theta,
\end{aligned}$$

Numerical solution in the ZAMO coordinates

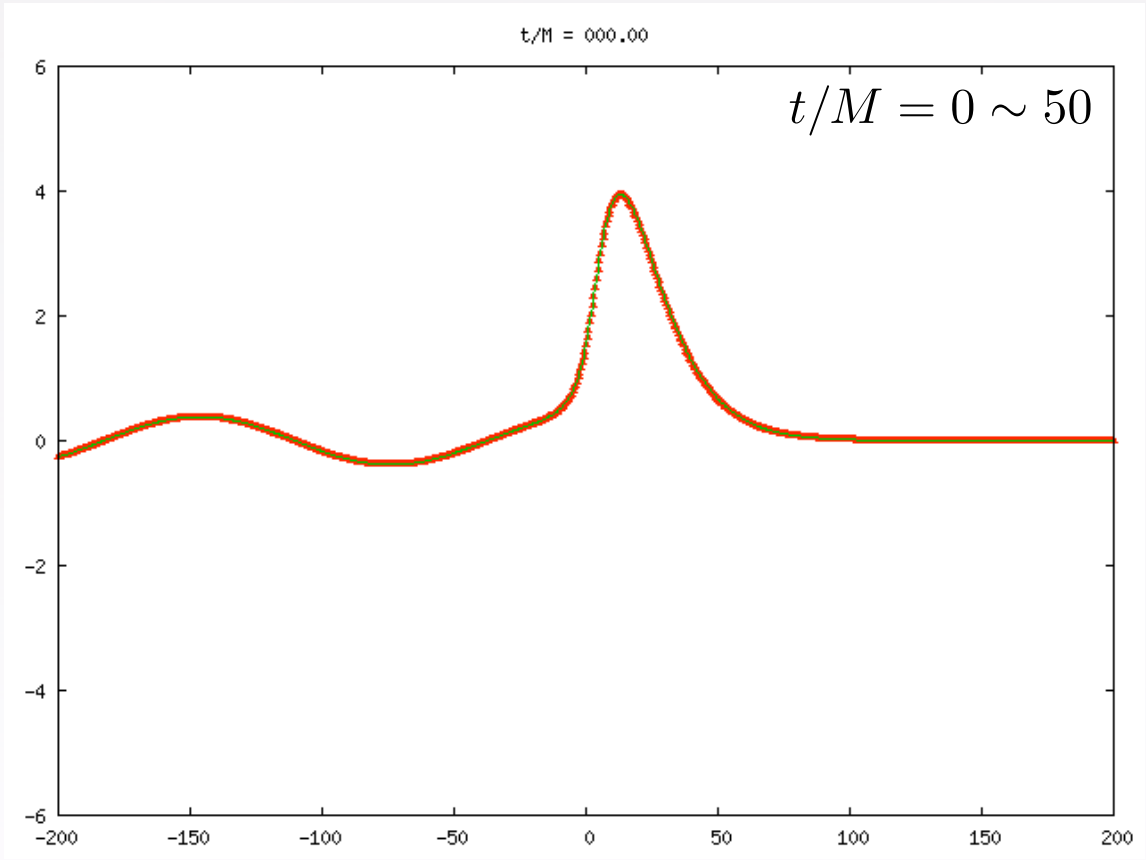

Second difficulty

- ZAMO coordinates become more and more distorted in the time evolution

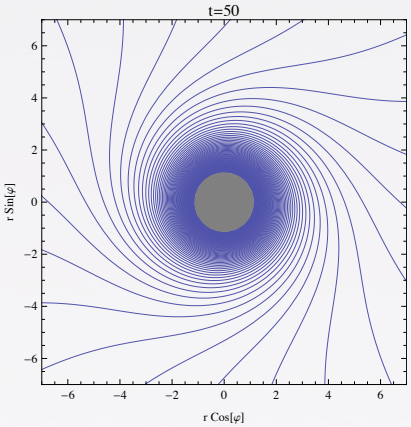

Second difficulty

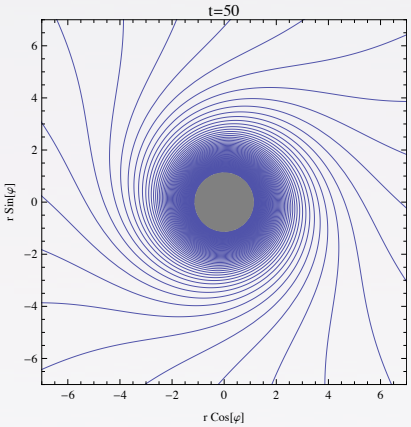

- ZAMO coordinates become more and more distorted in the time evolution

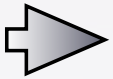

We “pull back” the coordinates

$$nT_P \leq t \leq (n+1)T_P :$$

$$\begin{aligned} t^{(n)} &= t, \\ \phi^{(n)} &= \phi - \Omega(r,\theta)(t - nT_P), \\ r^{(n)} &= r, \\ \theta^{(n)} &= \theta. \end{aligned}$$

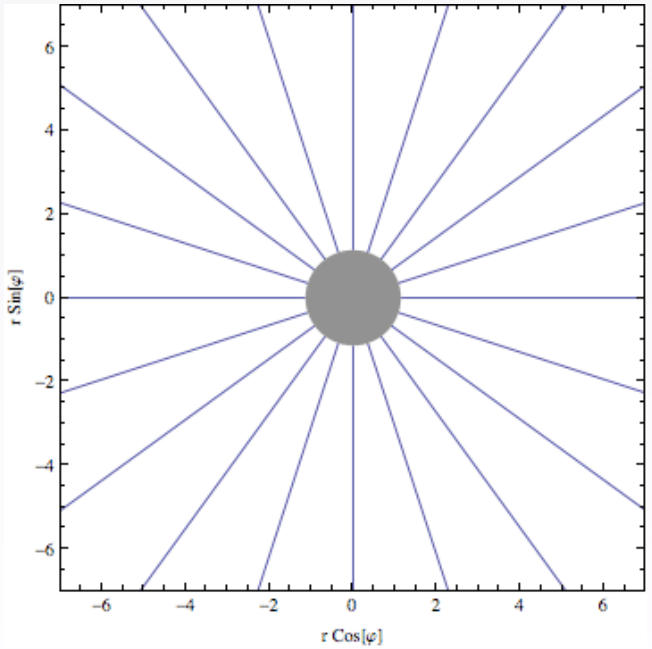

Our 3D code

- Space direction：6th-order finite discretization
- Time direction：4th-order Runge-Kutta
- Grid size: $\Delta r_* = 0.5 \quad (M = 1)$
  $\Delta\theta = \Delta\phi = \pi/30$
- Courant number: $C = \dfrac{\Delta t}{\Delta r_*} = \dfrac{1}{20}$
- Pure ingoing BC at the inner boundary,
  Fixed BC at the outer boundary
- Pullback: 7th-order Lagrange interpolation

Code check (I)

- Comparison with semianalytic solution of the Klein-Gordon case

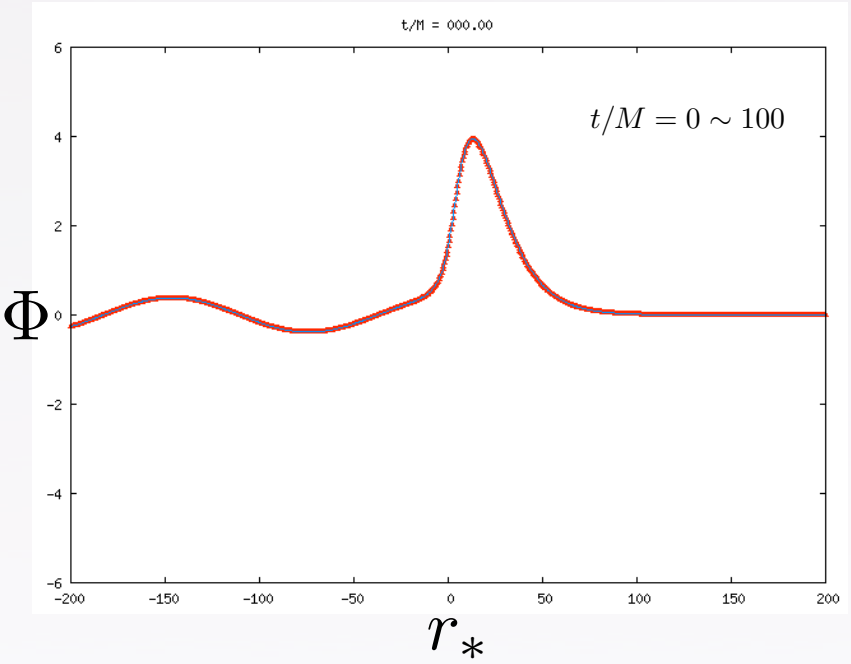

- Growth rate

$$\omega_I = \frac{\dot{E}}{2E} \simeq \frac{E(100M) - E(0)}{200ME(0)}$$

$$\omega_I^{(\mathrm{CF})}/\mu = 3.31 \times 10^{-7}$$

$$\omega_I^{(\mathrm{Numerical})}/\mu = 3.26 \times 10^{-7}$$

Code check (2)

- Convergence

$(t = 12.5M)$

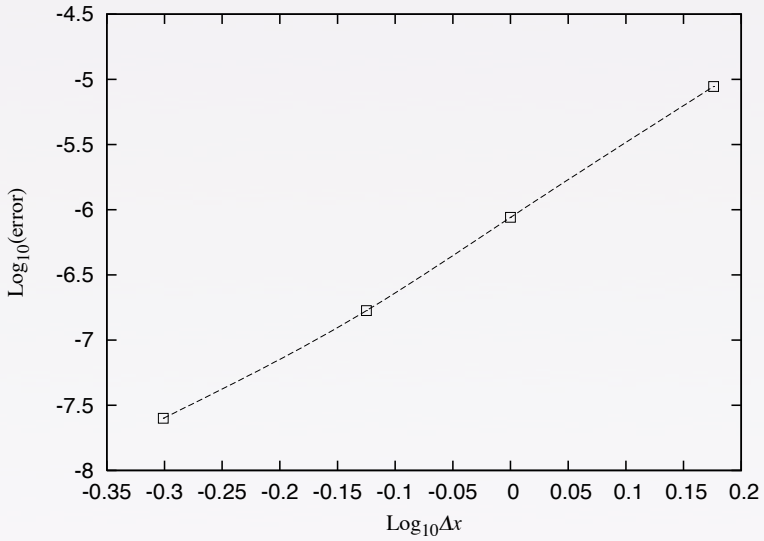

- Conserved quantities

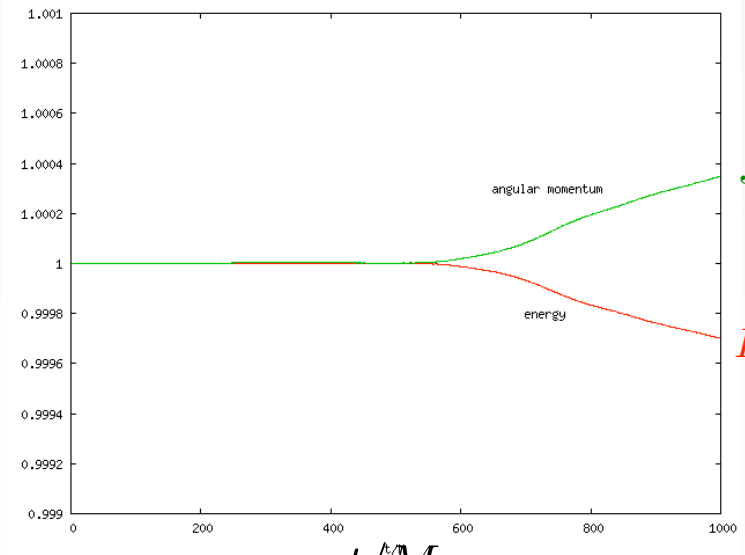

J/J_0

E/E_0

Comparison with BEC

Action

Saito and Ueda, PRA63 (2001), 043601

BEC

- Action

$$S = N\hbar \int d^3x dt \left[i\psi^* \dot{\psi} + \frac{1}{2}\psi^* \nabla^2 \psi - \frac{r^2}{2}\psi^* \psi - \frac{g}{2}(\psi^* \psi)^2 \right]$$



$$i\dot{\psi} = -\frac{1}{2}\nabla^2 \psi + \frac{r^2}{2}\psi + g|\psi|^2 \psi$$

Gross-Pitaevskii equation

BH-axion

- Action

$$\hat{S} = \int d^4x \sqrt{-g} \left[-\frac{1}{2}(\nabla\varphi)^2 - \mu^2 \left(\frac{\varphi^2}{2} + \hat{U}_{\rm NL}(\varphi) \right) \right],$$

- Non-relativistic approximation

$$\varphi = \frac{1}{\sqrt{2\mu}} \left(e^{-i\mu t}\psi + e^{i\mu t}\psi^* \right)$$

$$\hat{S}_{\rm NR} = \int d^4x \left[\frac{i}{2}\left(\psi^* \dot{\psi} - \psi \dot{\psi}^* \right) - \frac{1}{2\mu}\partial_i \psi \partial_i \psi^* + \frac{\alpha_g}{r}\psi^* \psi - \mu^2 \tilde{U}_{\rm NL}(|\psi|^2/\mu) \right]$$

$$\tilde{U}_{\rm NL}(x) = -\sum_{n=2}^{\infty} \frac{(-1/2)^n}{(n!)^2} x^n.$$

Effective theory

Saito and Ueda, PRA63 (2001), 043601

$(\nu = \cos\theta)$

- BEC $\psi = A(x,y,z,t)e^{i\phi(x,y,z,t)}$

$$A = \frac{\exp\left[-\left(\frac{x^2}{2d_x^2(t)} + \frac{y^2}{2d_y^2(t)} + \frac{z^2}{2d_z^2(t)}\right)\right]}{\sqrt{\pi^{3/2} d_x(t) d_y(t) d_z(t)}}$$

$$\phi = \frac{\dot{d}_x(t)}{2d_x(t)}x^2 + \frac{\dot{d}_y(t)}{2d_y(t)}y^2 + \frac{\dot{d}_z(t)}{2d_z(t)}z^2$$

- Spherical case $d_x = d_y = d_z = r(t)$

$$S = \frac{N\hbar}{4}\int dt\left[3\dot{r}^2 + 3\dot{r} - f(r)\right]$$

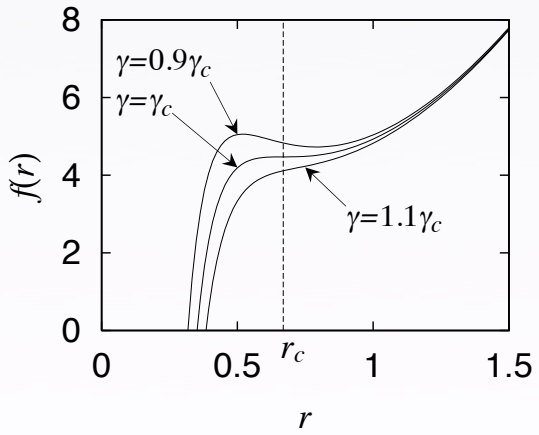

- BH-axion $\psi = A(t,r,\nu)e^{iS(t,r,\nu)+im\phi}$

$$A(t,r,\nu) \approx A_0 \exp\left[-\frac{(r-r_p)^2}{4\delta_r r_p^2} - \frac{(\nu-\nu_p)^2}{4\delta_\nu}\right],$$

$$S(t,r,\nu) \approx S_0(t) + p(t)(r-r_p) + P(t)(r-r_p)^2 + \pi_\nu(t)(\nu-\nu_p)^2 + \cdots,$$

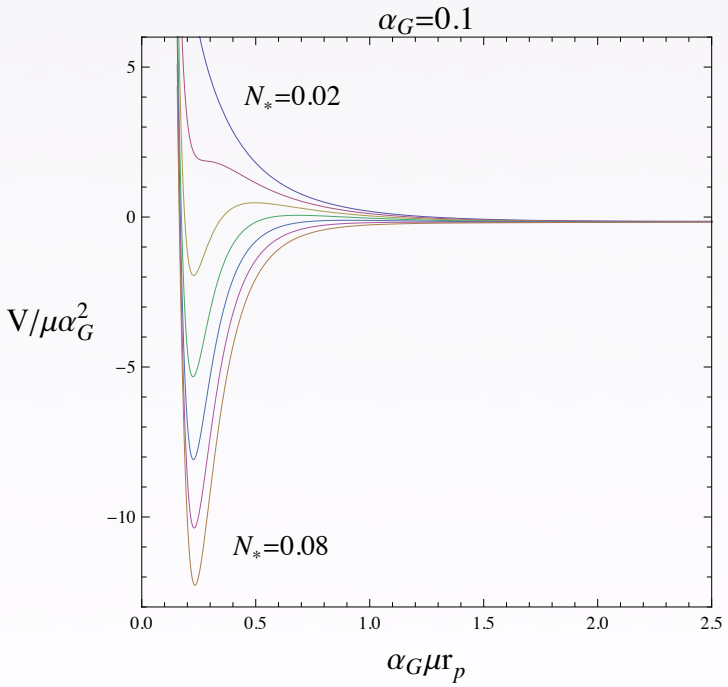

Simulation results

Saito and Ueda, PRA63 (2001), 043601

- BEC

$$i\dot{\psi} = -\frac{1}{2}\nabla^2\psi + \frac{r^2}{2}\psi + g|\psi|^2\psi - \frac{i}{2}\left(\frac{L_2}{2}|\psi|^2 + \frac{L_3}{6}|\psi|^4\right)\psi$$

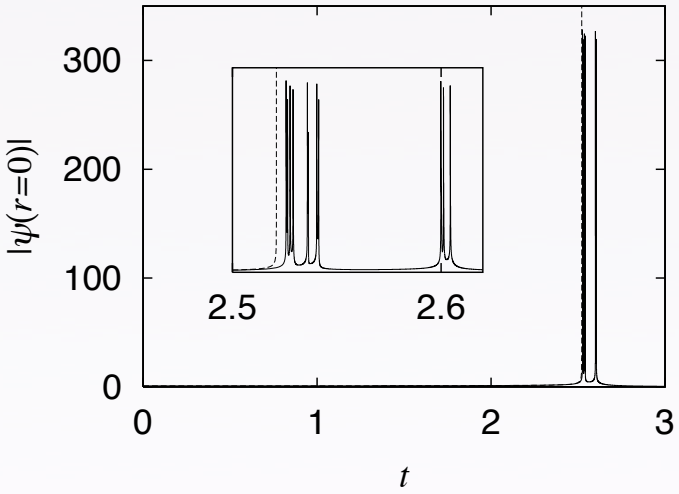

- BH-axion
  - Our simulation results

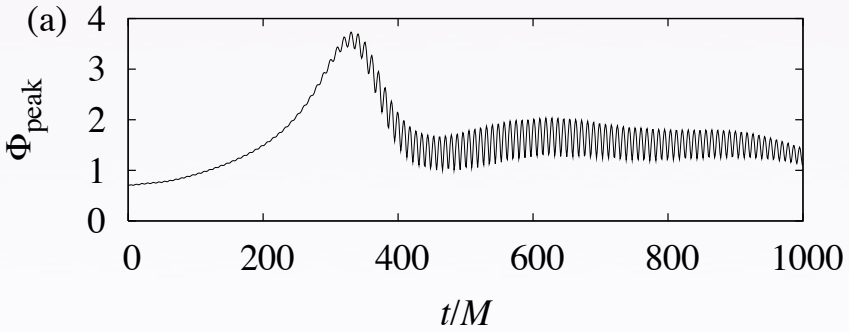

Green's function analysis

Simulation (B)

- Snapshots

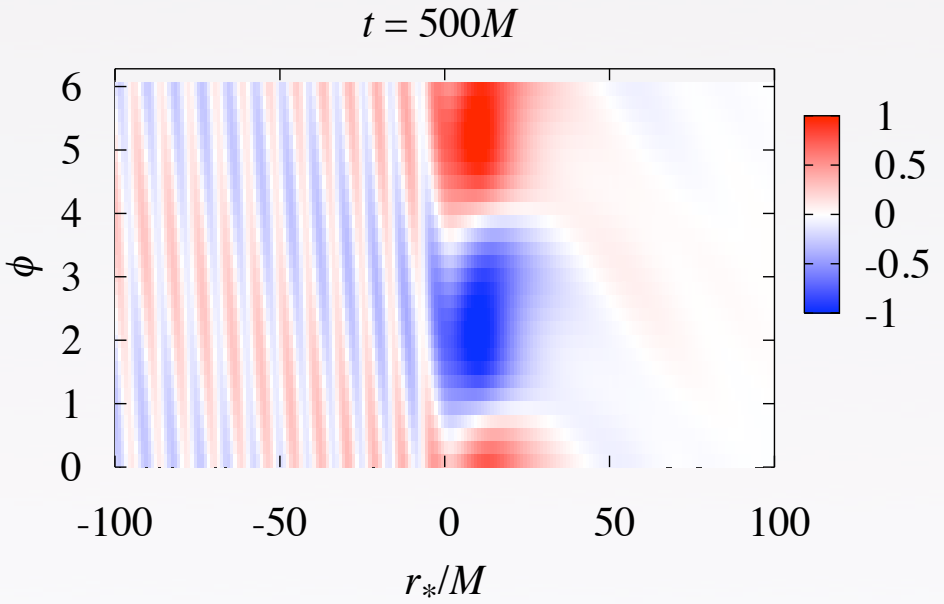

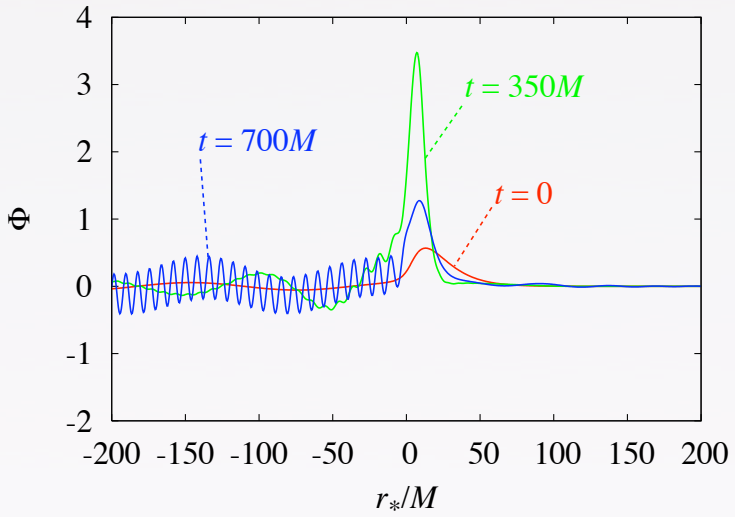

m=-1 mode is generated!

(Near the horizon)

$$\Phi \sim e^{-i\omega t} e^{-i\tilde{\omega} r_*}$$

$$\tilde{\omega} = \omega - m\Omega_H$$

$$M\omega_{\rm KG} = 0.39 \qquad M\omega_{\rm NL} = 0.35$$

$$M\tilde{\omega}_{\rm KG} = -0.04 \qquad M\tilde{\omega}_{\rm NL} = 0.87$$

Green's function approach (1)

- Approximation

$$\varphi(x) = \varphi_0(x) + \Delta\varphi, \qquad \varphi_0 = 2\mathrm{Re}\left[e^{(\gamma - i\omega_0)t} P(r) S_1^1(\cos\theta) e^{i\phi}\right],$$

$O(\varphi_0^4)$ is ignored

- Equation

$$(\nabla^2 - \mu^2)\Delta\varphi = J(\varphi_0) := -\frac{\mu^2}{6}\varphi_0^3$$

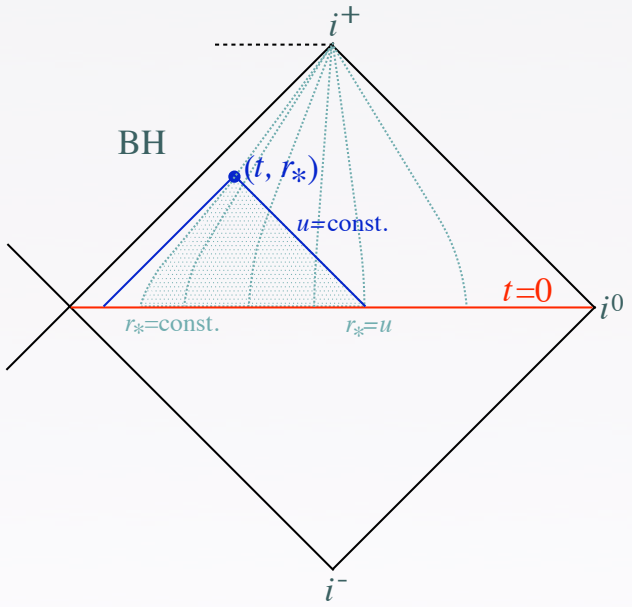

- Green's function

$$(\nabla^2 - \mu^2)_{x'} G(x, x') = \delta^4(x, x')$$

- Formal solution

$$\Delta\varphi(x) = \int_{D'} d^4x' \sqrt{-g(x')} G(x, x') J(\varphi_0(x'))$$

Green's function approach (2)

- Constructing the Green's function

$$G(x,x') = \frac{1}{(2\pi)^2}\sum_{\ell,m}\int_{-\infty}^{\infty} d\omega G^{\omega}_{\ell m}(r,r') e^{-i\omega(t-t')+im(\phi-\phi')} S^m_\ell(\cos\theta)\bar{S}^m_\ell(\cos\theta'),$$

$$G^{\omega}_{\ell m}(r,r') = \frac{1}{W_{\ell m\omega}}\left[\theta(r-r')R^+_{\ell m\omega}(r)R^-_{\ell m\omega}(r') + \theta(r'-r)R^-_{\ell m\omega}(r)R^+_{\ell m\omega}(r')\right],$$

- Radial function $\quad k = \sqrt{\omega^2-\mu^2}, \mathrm{Im}[k] \geq 0$

$$R^+_{\ell m\omega} \simeq \begin{cases} C^+_{\ell m\omega} e^{ikr}/r, & r\to\infty; \\ A^+_{\ell m\omega} e^{i\tilde{\omega}r_*} + B^+_{\ell m\omega} e^{-i\tilde{\omega}r_*}, & r\simeq r_+, \end{cases}$$

$$R^-_{\ell m\omega} \simeq \begin{cases} A^-_{\ell m\omega} e^{-ikr}/r + B^-_{\ell m\omega} e^{ikr}/r, & r\to\infty; \\ C^-_{\ell m\omega} e^{-i\tilde{\omega}r_*}, & r\simeq r_+, \end{cases}$$

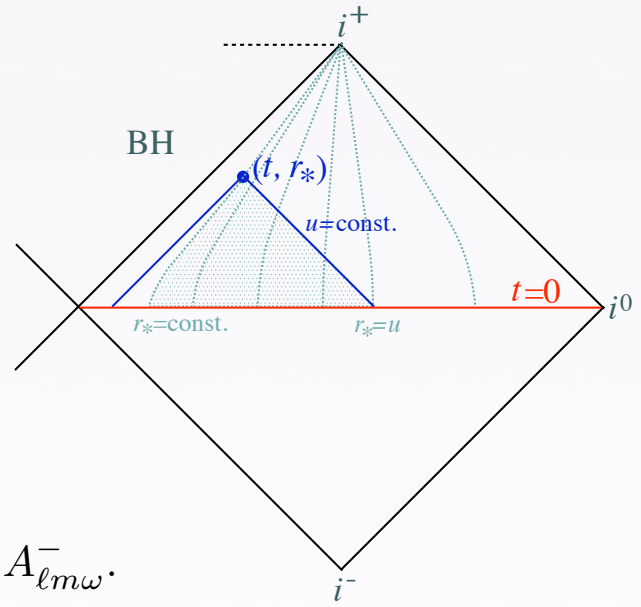

$$W(R^-,R^+) = 2i\tilde{\omega}(r_+^2+a^2)C^-_{\ell m\omega}A^+_{\ell m\omega} = 2ikC^+_{\ell m\omega}A^-_{\ell m\omega}.$$

Green's function approach (3)

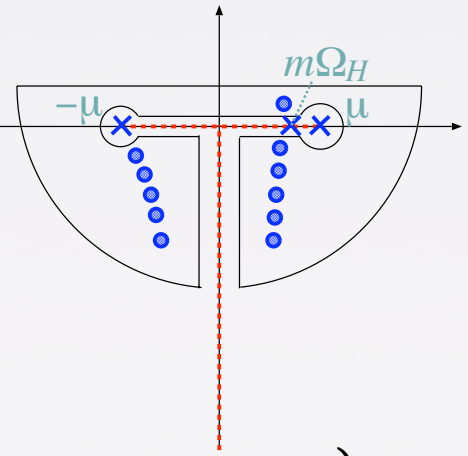

- Near-horizon solution

$$\Delta\varphi = \sum_{\ell,m} e^{im\phi} S_\ell^m(\cos\theta) \frac{e^{im\Omega_H r_*}}{2i(r_+^2 + a^2)}$$
$$\times \left\{ e^{(3\gamma - im\omega_0)u} D_{\ell m}(u, r_*) - \int_{-\infty}^{\infty} d\omega \frac{e^{-i\omega u}}{\tilde{\omega} A_{\ell m}^{+(\omega)} [3\gamma + i(\omega - m\omega_0)]} E_{\ell m}^{(\omega)}(u, r_*) \right\},$$

  - First term $\sim e^{-i(m\omega_0 + 3i\gamma)t}$
  - Second term
    - Pole $\omega = m\omega_0 + 3i\gamma$ ⇨ $\sim e^{-i(m\omega_0 + 3i\gamma)t}$
    - Pole $A_{\ell m}^{+(\omega_{\rm BS}^{(\ell mn)})} = 0$ ⇨ $\sim \sum_n (\cdots) e^{-i\omega_{\rm BS}^{(\ell mn)} t}$

$$\omega_{\rm BS}^{(n)} \simeq \pm\mu \simeq \pm\omega_0$$

Nonlinear term makes transfer from growing bound state to decaying bound state with negative frequency.

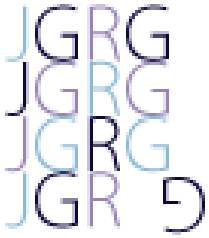

Osamu Seto, JGRG 22(2012)111413

"Curvaton induced modulated reheating"

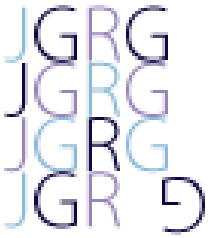

RESCEU SYMPOSIUM ON

GENERAL RELATIVITY AND GRAVITATION

JGRG 22



November 12-16 2012

Koshiba Hall, The University of Tokyo, Hongo, Tokyo, Japan



Curvaton induced modulated reheating

Osamu Seto (Hokkai-Gakuen Univ.)

With Ki-Young Choi (APCTP and POSTECH)

Based on: corrected* **Phys. Rev. D 85, 123528 (2012)**

*Thanks to S.Yokoyama, T.Suyama and D.Wands

Are you ready for this?

First year Planck observations:
Full sky maps and cosmological implications.

Authors.....

Abstract We present full sky microwave from the Planck first year sky survey. …. The age of the Universe…….Nonlinearity of local type f_NL^local(k_0=0.002 Mpc^-1)=15 +/- 9 (95% CL) is detected. …. index n_s = 0.97 +/- 0.02... The B-mode polarization is also detected. The corresponding tensor-to-scalar ratio is estimated as rT(k_0=0.002 Mpc^-1)=0.10 +/- 0.03 (95% CL).

§ Introduction

- Inflation

  is an elegant solution to

  horizon, flatness, monopole problem

  and

  provides the seed of density fluctuation of

  adiabatic,

  almost scale invariant, and Gaussian

  as well as tensor modes.

Non-Gaussianity in perturbation generation

- Inflaton ϕ [Hawking, Guth and Pi,… 1982]

  $f_{NL} = O(\epsilon,\eta)$ [Maldacena 2003]

- Curvaton σ [Lyth and Wands, Moroi and Takahashi, Enqvist and Sloth 2001~2]

  $f_{NL} = O(1/R)$ [Lyth et al 2003,…]

- Modulated reheating by a light scalar σ [Kofman 2003, Dvali et al 2004]

  $$\delta\Gamma_{\phi[\sigma]} \neq 0 \quad \Longrightarrow \quad \delta T/T \neq 0$$

  $f_{NL} = f_{NL}(\Gamma, \partial\Gamma, \ldots)$ [Zaldarriaga 2004,…]

System in perturbation generation

- Inflaton ϕ [Hawking, Guth and Pi,… 1982]

  Inflaton ϕ

- Curvaton σ [Lyth and Wands, Moroi and Takahashi, Enqvist and Sloth 2001~2]

  Inflaton ϕ + Curvaton σ

- Modulated reheating by a light scalar σ [Kofman 2003, Dvali et al 2004]

  Inflaton ϕ + Light scalar σ

System in perturbation generation

- Inflaton ϕ [Hawking, Guth and Pi,… 1982]

  Inflaton ϕ

- Curvaton σ [Lyth and Wands, Moroi and Takahashi, Enqvist and Sloth 2001~2]

  "massive" + "decaying" + "non ϕ interacting"

  Inflaton ϕ + Curvaton σ

- Modulated reheating by a light scalar σ [Kofman 2003, Dvali et al 2004]

  What's difference?

  Inflaton ϕ + Light scalar σ

  "massless" + "ϕ interacting"

§ ϕ-σ interaction

- Inflaton ϕ - Curvaton/light scalar σ interactions may exist.

- If ϕ and σ are singlet, there might be

$$\mathcal{L}_{\rm int} = \phi\, \sigma\, \mathcal{O}_{\rm SM} + \text{tiny } \phi^2\, \sigma^2 + \ldots, .$$

- ex.)

$$\mathcal{L}_{\rm int} = \phi\, \sigma\, |\Phi|^2 \qquad \text{then} \qquad \Gamma_\phi \propto \sigma^2$$

- Modulated reheating by curvaton [Suyama et al 2010]

§ General analysis

- Inflaton ϕ and another scalar σ
- Thermal history after inflation

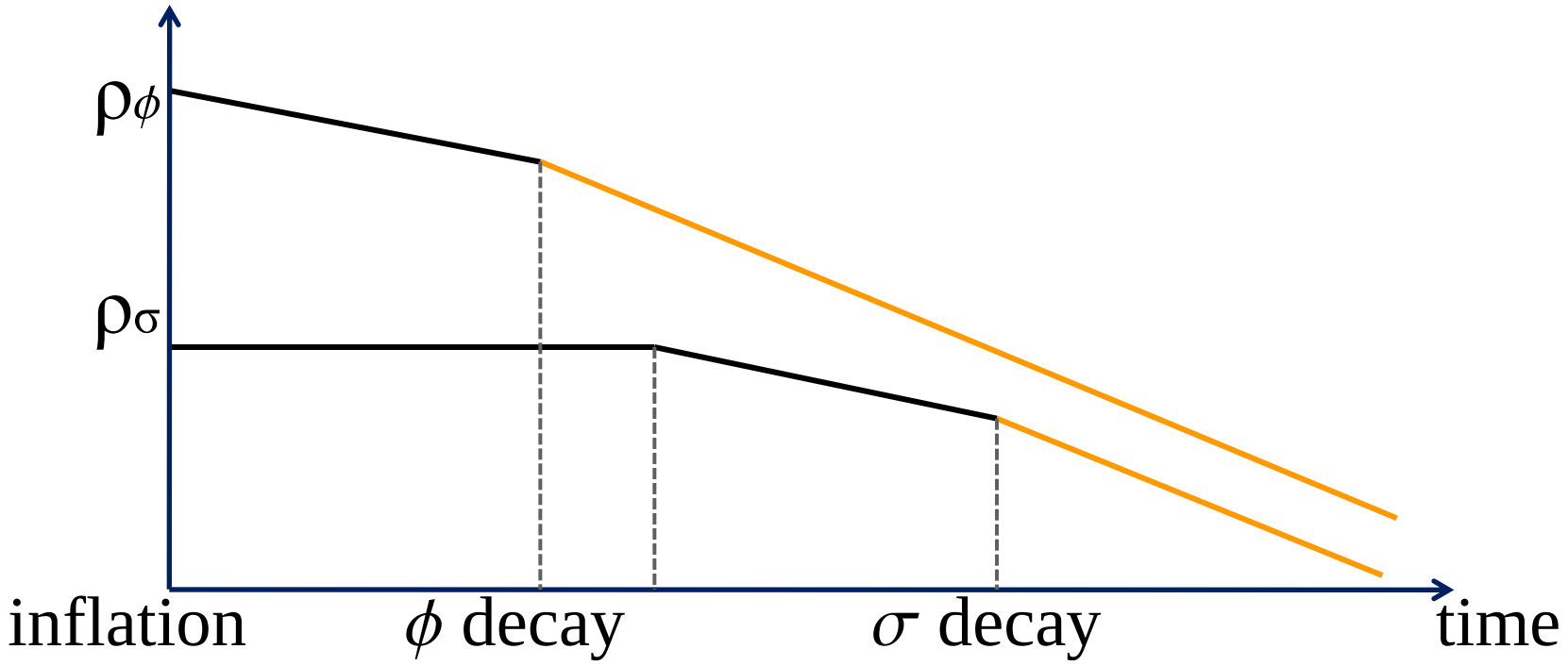

§ General analysis

- Inflaton ϕ and another scalar σ
- Thermal history after inflation

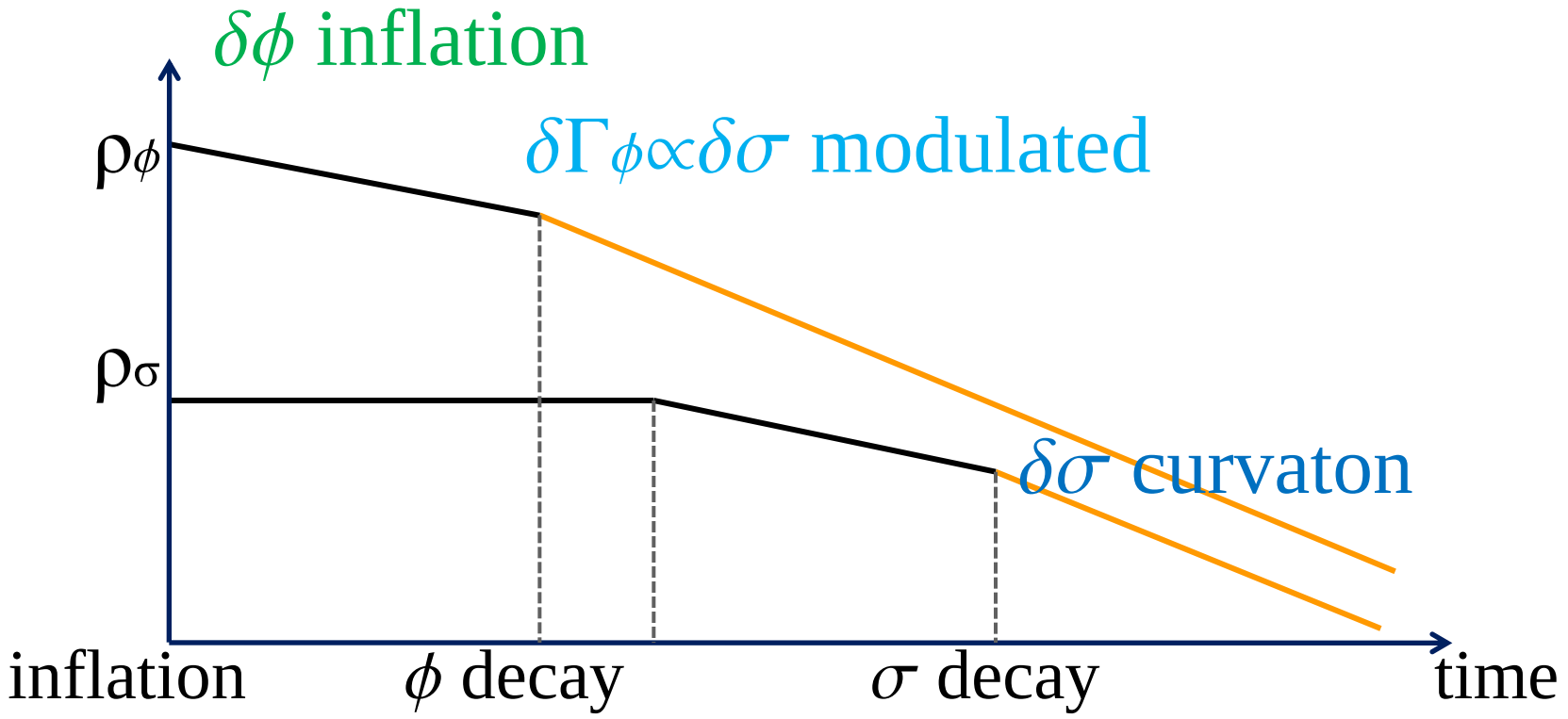

§ § Formula of perturbation

- After σ decay:

  inflaton-modulated mixed [Zaldarriaga 2004, Ichikawa et al 2008] + curvaton

- On uniform σ density hypersurface

$$\zeta = (1-R)\zeta_r + R\zeta_\sigma = \zeta_r + \frac{R}{3}S_\sigma$$

$$R \equiv \left.\frac{3\rho_\sigma}{4\rho_r + 3\rho_\sigma}\right|_{H=\Gamma_\sigma} \qquad S_\sigma \equiv 3(\zeta_\sigma - \zeta_r)$$

- Power spectrum

Q is a function of $\Gamma_\phi(\sigma)/H_c$

$$\mathcal{P}_\zeta = \frac{1}{2M_P^2\epsilon_*}\mathcal{P}_{\delta\phi_*} + \left(Q_\sigma + \frac{2R}{3\sigma_*}\right)^2 \mathcal{P}_{\delta\sigma_*}$$

§ § Resultant perturbation

- Important parameters: σ_*, R, $\{\sigma_* Q_\sigma, \sigma_*^2 Q_{\sigma\sigma}, \ldots\}$

ϕ-σ ratio Modulated

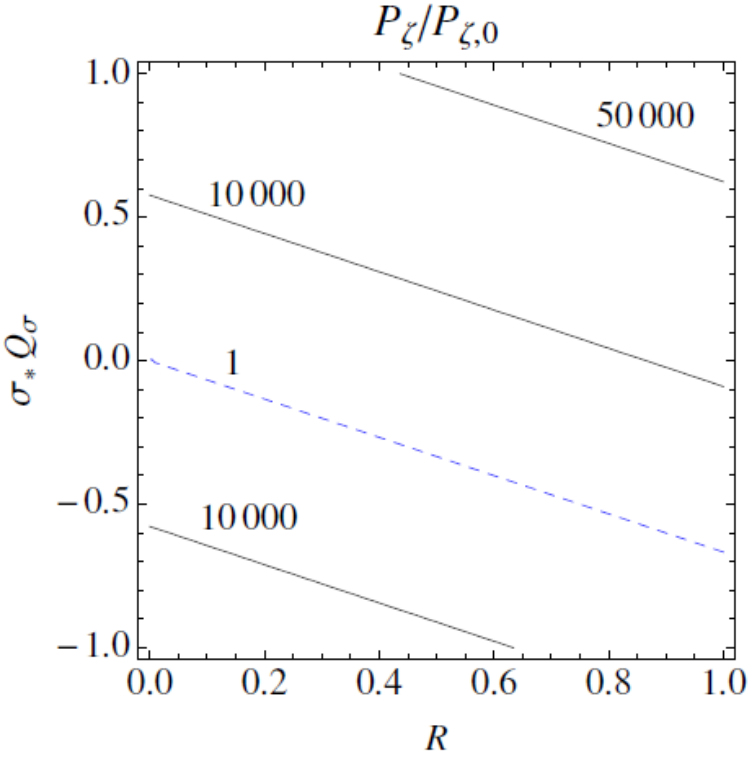

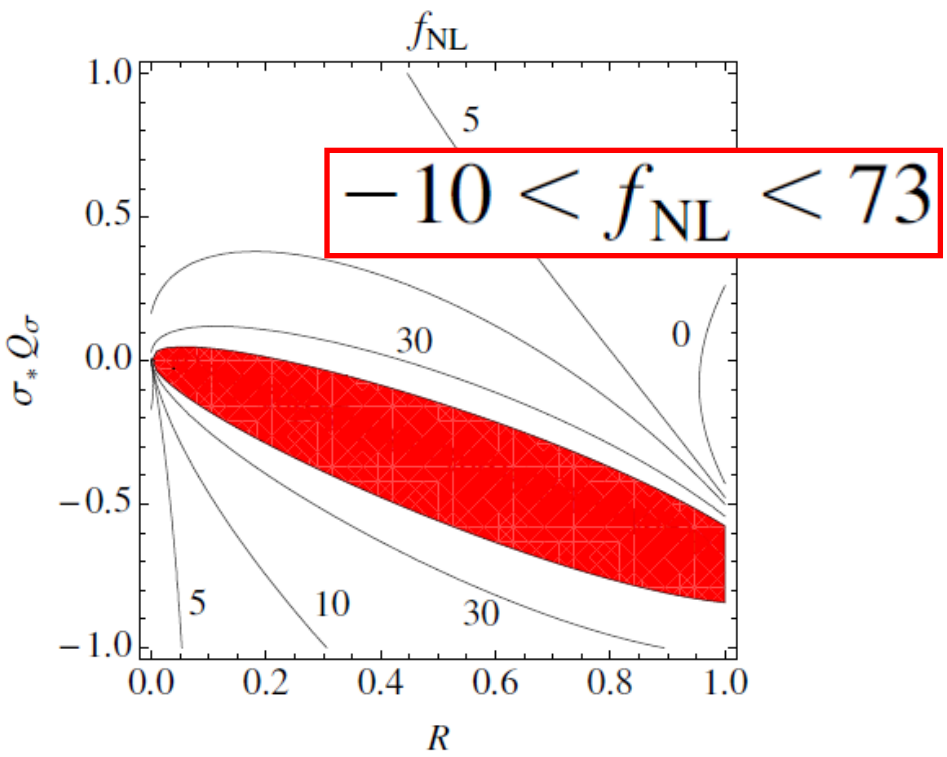

- Small σ_* case : mainly σ originated

§ Simplest case

- Potential

$$V[\phi, \sigma] = \frac{1}{2} m_\phi^2 \phi^2 + \frac{1}{2} m_\sigma^2 \sigma^2$$

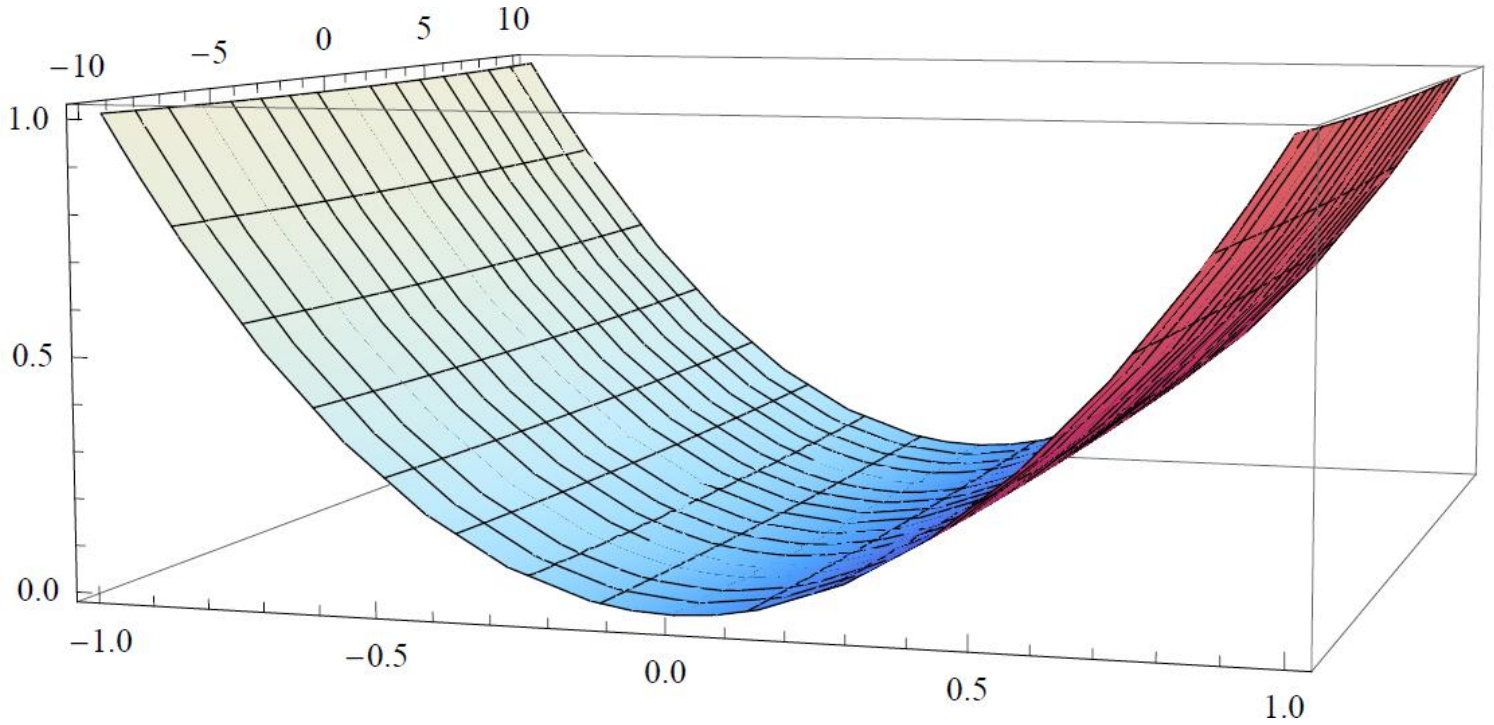

§ § Power spectrum

- Power spectrum

$$\mathcal{P}_\zeta \simeq \frac{1}{6(2\pi)^2}\frac{m_\phi^2}{M_P^2}(2N_{\rm inf}+1)^2 + \left\{Q_\sigma \sigma_* + \frac{2R}{3}\right\}^2 \frac{m_\phi^2}{3(2\pi\sigma_*)^2}(2N_{\rm inf}+1)$$

§ § Power spectrum

- Power spectrui

$$\mathcal{P}_\zeta \simeq \frac{1}{6(2\pi)^2}\frac{m_\phi^2}{M_P^2}(2N_{\rm inf}$$

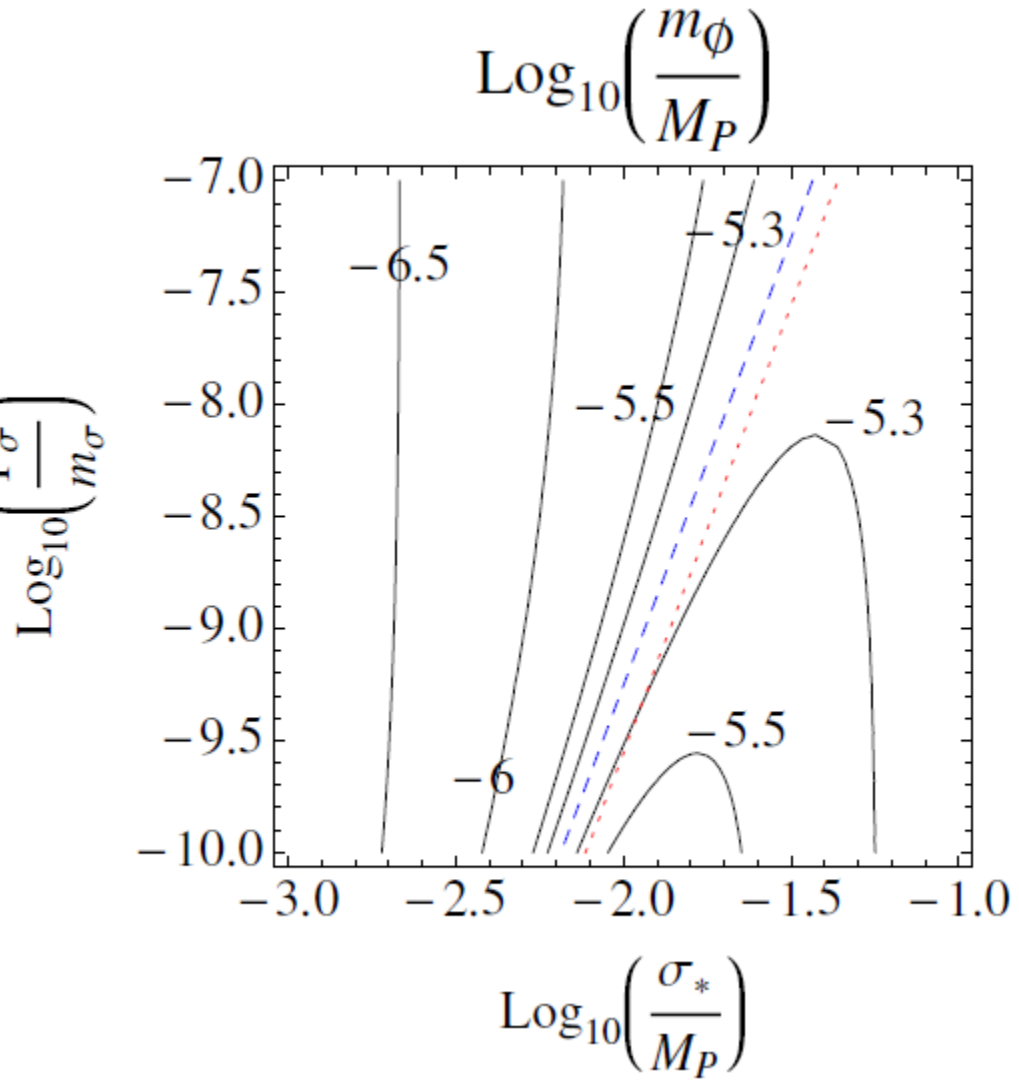

§ § Tensor and nonlinearity

- Model I
- Interaction

$$\mathcal{L}_{\rm int} = \lambda |\Phi|^2 \phi \sigma$$

- Decay rate

$$\Gamma_{\phi}^{\rm CD}(\sigma) = \frac{1}{8\pi m_{\phi}} \lambda^2 \sigma^2$$

$$(Q_{\sigma}\sigma_{*}, Q_{\sigma\sigma}\sigma_{*}^2, Q_{\sigma\sigma\sigma}\sigma_{*}^3) = \left(-\tfrac{1}{3}, \quad \tfrac{1}{3}, \quad -\tfrac{2}{3} \right)$$

§ § Tensor and nonlinearity

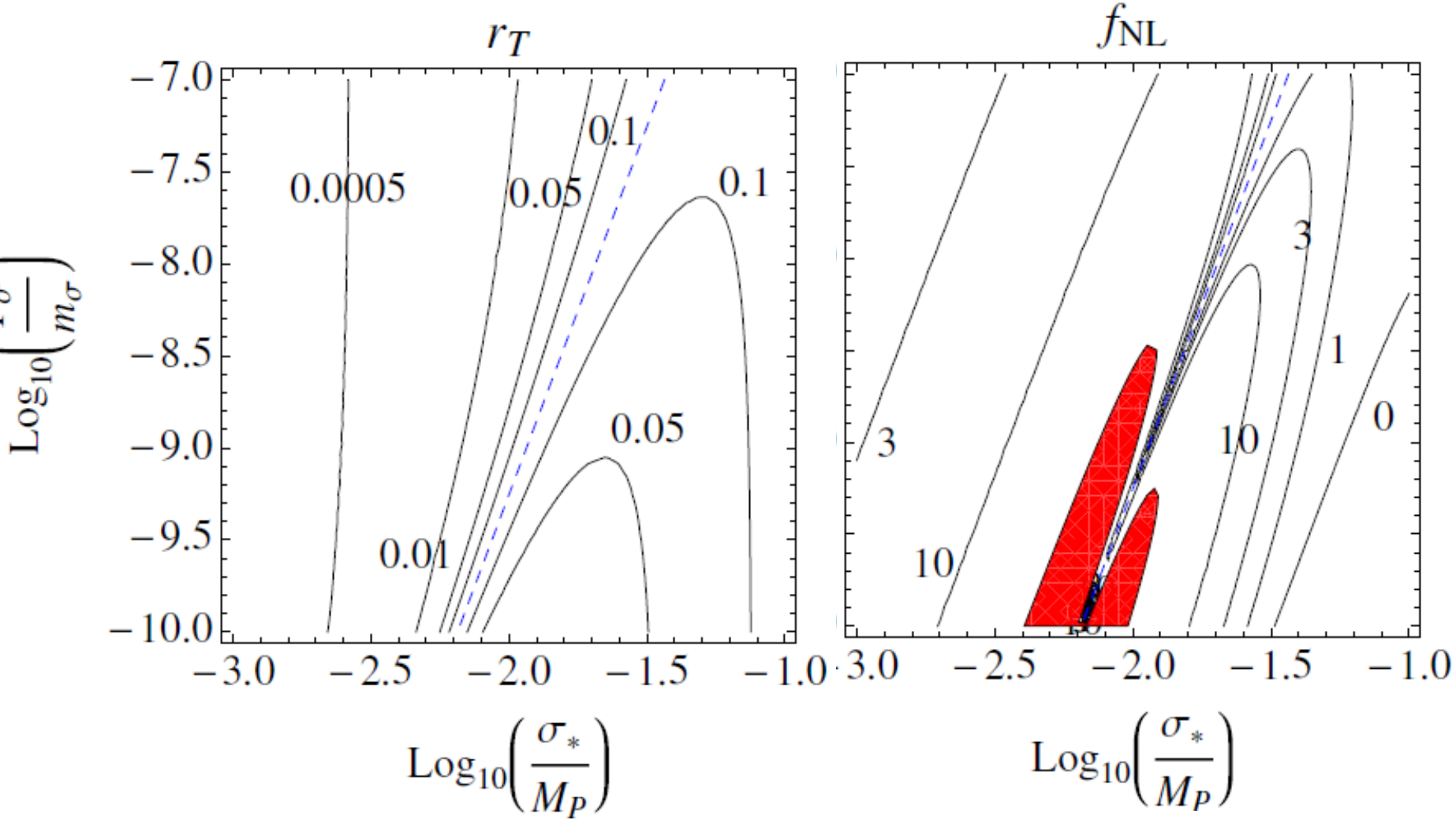

§ § Tensor and nonlinearity

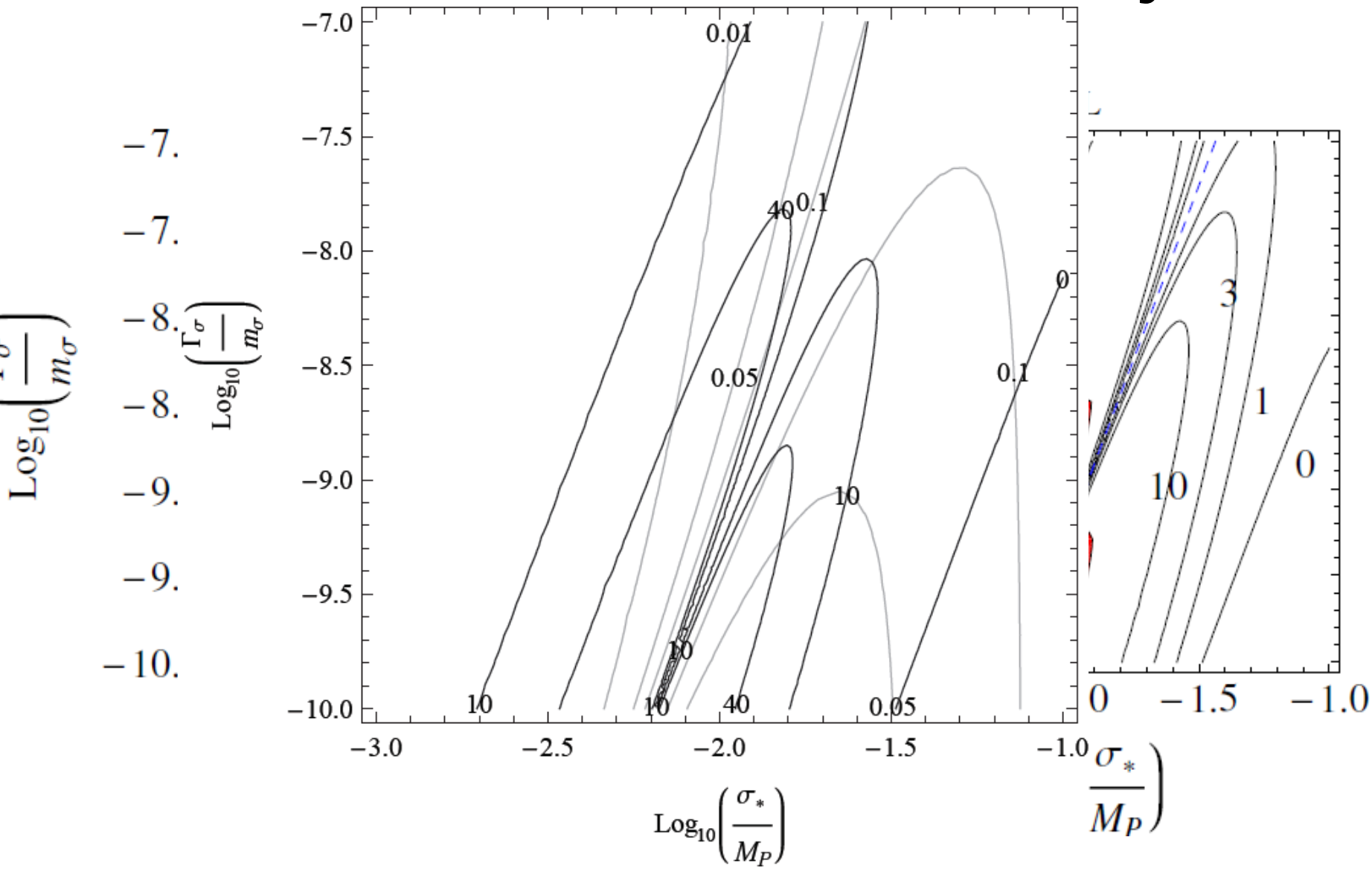

§ Summary

- ***"Inflaton-modulated-curvaton mixed"***
- Interaction between ϕ and σ is a subject to be studied.
- An interesting possibility: simultaneous large f_{NL} and r_T

Kazuharu Bamba, JGRG 22(2012)111414

"Finite-time future singularities and rip cosmology in f(T) gravity"

RESCEU SYMPOSIUM ON

GENERAL RELATIVITY AND GRAVITATION

JGRG 22

November 12-16 2012

Koshiba Hall, The University of Tokyo, Hongo, Tokyo, Japan

Finite-time future singularities and Rip cosmology in $f(T)$ gravity

Kazuharu Bamba[1(a)], Ratbay Myrzakulov[2(b)], Shin'ichi Nojiri[3(a),(c)] and Sergei D. Odintsov[4(b),(c),(d),(e),(f)]

(a) *Kobayashi-Maskawa Institute for the Origin of Particles and the Universe, Nagoya University, Nagoya 464-8602, Japan*
(b) *Eurasian International Center for Theoretical Physics, Eurasian National University, Astana 010008, Kazakhstan*
(c) *Department of Physics, Nagoya University, Nagoya 464-8602, Japan*
(d) *Institució Catalana de Recerca i Estudis Avançats (ICREA), Barcelona, Spain*
(e) *Institut de Ciencies de l'Espai (CSIC-IEEC), Campus UAB, Facultat de Ciencies, Torre C5-Par-2a pl, E-08193 Bellaterra (Barcelona), Spain*
(f) *Tomsk State Pedagogical University, Tomsk, Russia*

Abstract

We show that the nite-time future singularities appear in $f(T)$ gravity with T being the torsion scalar. We reconstruct $f(T)$ gravity models with realizing the nite-time future singularities. It is explicitly demonstrated that a power-law type correction term T^{β} ($\beta > 1$) such as a T^2 term can remove the nite-time future singularities in $f(T)$ gravity. We also investigate $f(T)$ models with realizing inflation in the early universe, the ΛCDM model, Little Rip cosmology and Pseudo-Rip cosmology.

1 Introduction

Cosmological observations such as Type Ia Supernovae (SNe Ia), cosmic microwave background (CMB) radiation, large scale structure (LSS), baryon acoustic oscillations (BAO), and weak lensing have suggested the current accelerated expansion of the universe. There is two representative approaches to understand this phenomenon. The first is to introduce the so-called "dark energy" (for a very recent review, see, e.g., [1]). The second is to extend the gravitational theory, for example, $F(R)$ gravity (for reviews, see, e.g., [2]). There also exists "teleparallelism" constructed by using the Weitzenböck connection. This is an alternative gravity theory to general relativity and it is described by the torsion scalar T and not the scalar curvature R defined with the Levi-Civita connection [3]. It has recently been revealed that the late time cosmic acceleration [4, 5, 6] as well as in ation [7] can be realized by extending this theory to $f(T)$ gravity, similarly to that in $F(R)$ gravity. In this paper, we review our results in Ref. [8]. In particular, we demonstrate the existence of finite-time future singularities in $f(T)$ gravity. We note that the procedure used here has also been extended to Loop quantum cosmology [9]. In addition, we explain the relevant cosmologies to future singularities. We use units of $k_{\rm B} = c = \hbar = 1$ and denote the gravitational constant $8\pi G$ by $^2 \equiv 8\pi/{M_{\rm Pl}}^2$ with the Planck mass of $M_{\rm Pl} = G^{-1/2} = 1.2 \times 10^{19}$GeV.

2 Finite-time future singularities in $f(T)$ gravity

In the teleparallelism, the metric $g^{\mu\nu}$ is written $g_{\mu\nu} = \eta_{AB} e^A_\mu e^B_\nu$ with $e_A(x^\mu)$ orthonormal tetrad components, where $A = 0, 1, 2, 3$ for the tangent space at each point x^μ of the manifold, $\mu, \quad = 0, 1, 2, 3$ are coordinate indices on the manifold, and e^μ_A is the tangent vector of the manifold. The teleparallel Lagrangian density is expressed by using the torsion scalar T, although in general relativity the Lagrangian density is described by the Ricci scalar R. The torsion scalar T is given by $T \equiv S_\rho{}^{\mu\nu} T^\rho{}_{\mu\nu}$

[1]Email address: bamba@kmi.nagoya-u.ac.jp
[2]Email address: rmyrzakulov@gmail.com
[3]Email address: nojiri@phys.nagoya-u.ac.jp
[4]Email address: odintsov@ieec.uab.es

Table 1: Conditions for the finite-time future singularities to occur on q in the expressions of H in Eq. (1), $\rho_{\rm DE}$, $P_{\rm DE}$, and the behaviors of H and $\dot{H}$ in the limit $t \to t_{\rm s}$.

$q(\neq 0, -1)$	H $(t \to t_{\rm s})$	$\dot{H}$ $(t \to t_{\rm s})$	$\rho_{\rm DE}$	$P_{\rm DE}$
q 1 [Type I ("Big Rip") singularity]	$H \to \infty$	$\dot{H} \to \infty$	$J_1 \neq 0$	$J_1 \neq 0$ or $J_2 \neq 0$
$0 < q < 1$ [Type III singularity]	$H \to \infty$	$\dot{H} \to \infty$	$J_1 \neq 0$	$J_1 \neq 0$
$-1 < q < 0$ [Type II ("sudden") singularity]	$H \to H_{\rm s}$	$\dot{H} \to \infty$		$J_2 \neq 0$
$q < -1$, but q is not any integer [Type IV singularity]	$H \to H_{\rm s}$	$\dot{H} \to 0$ (Higher derivatives of H diverge.)		

with $T^{\rho}{}_{\mu\nu} \equiv e^{\rho}_{A}\left(\partial_{\mu}e^{A}_{\nu} - \partial_{\nu}e^{A}_{\mu}\right)$ the torsion tensor and $S_{\rho}{}^{\mu\nu} \equiv (1/2)\left(K^{\mu\nu}{}_{\rho} + \delta^{\mu}_{\rho}\, T^{\alpha\nu}{}_{\alpha} - \delta^{\nu}_{\rho}\, T^{\alpha\mu}{}_{\alpha}\right)$, where $K^{\mu\nu}{}_{\rho} \equiv -(1/2)\left(T^{\mu\nu}{}_{\rho} - T^{\nu\mu}{}_{\rho} - T_{\rho}{}^{\mu\nu}\right)$ is the contorsion tensor. The modified teleparallel action is given by [5] $I = \int d^4x|e|\left[f(T)/\left(2\ \ ^2\right) + \mathcal{L}_{\rm M}\right]$, where $|e| = \det\left(e^{A}_{\mu}\right) = \sqrt{-g}$ and $\mathcal{L}_{\rm M}$ is the Lagrangian of matter.

We take the four-dimensional at Friedmann-Lemaître-Robertson-Walker (FLRW) space-time with the metric $ds^2 = dt^2 - a^2(t)\sum_{i=1,2,3}\left(dx^i\right)^2$, where $a(t)$ is the scale factor. In this background, we have $g_{\mu\nu} = {\rm diag}(1, -a^2, -a^2, -a^2)$ and the tetrad components $e^{A}_{\mu} = (1, a, a, a)$. The torsion scalar $T = -6H^2$ with $H = \dot{a}/a$ the Hubble parameter, where the dot denotes the time derivative, $\partial/\partial t$. In the at FLRW background, the gravitational field equations read $H^2 = \left(\ ^2/3\right)(\rho_{\rm M} + \rho_{\rm DE})$ and $\dot{H} = -\left(\ ^2/2\right)(\rho_{\rm M} + P_{\rm M} + \rho_{\rm DE} + P_{\rm DE})$ with where $\rho_{\rm M}$ and $P_{\rm M}$ the energy density and pressure of all perfect uids of generic matter, respectively. The perfect uid satisfies the continuity equation $\dot{\rho}_{\rm M} + 3H(\rho_{\rm M} + P_{\rm M}) = 0$. In addition, the energy density and pressure of dark components become $\rho_{\rm DE} = \left[1/\left(2\ ^2\right)\right]J_1$ and $P_{\rm DE} = -\left[1/\left(2\ ^2\right)\right](4J_2 + J_1)$, respectively, where $J_1 \equiv -T - f + 2TF$ and $J_2 \equiv (1 - F - 2TF')\dot{H}$ with $F \equiv df/dT$ and $F' = dF/dT$. The standard continuity equation is also satisfied as $\dot{\rho}_{\rm DE} + 3H(\rho_{\rm DE} + P_{\rm DE}) = 0$.

3 $f(T)$ models with realizing cosmologies

In the FLRW background, the e ective equation of state (EoS) for the universe is written as [2] $w_{\rm eff} \equiv P_{\rm eff}/\rho_{\rm eff} = -1 - 2\dot{H}/\left(3H^2\right)$ with $\rho_{\rm eff} \equiv 3H^2/\ ^2$ and $P_{\rm eff} \equiv -\ 2\dot{H} + 3H^2\ \ /\ ^2$ the total energy density and pressure of the universe, respectively. At the dark energy dominated stage, we have $w_{\rm DE} \approx w_{\rm eff}$. In the following, we consider this case that dark energy is completely dominant over matter because we explore the evolution of the universe around the time when the finite-time future singularities appear. For $\dot{H} < 0$ (> 0), we find $w_{\rm eff} > -1$ (< -1), which describes the non-phantom [namely, quintessence] (phantom) phase. The case that $w_{\rm eff} = -1$ for $\dot{H} = 0$ corresponds to the cosmological constant.

It is known that there exist four types of the finite-time future singularities [10]. Type I ("Big Rip" [11]): For the limit $t \to t_{\rm s}$, $a \to \infty$, $\rho_{\rm eff} \to \infty$ and $|P_{\rm eff}| \to \infty$. The case that $\rho_{\rm eff}$ and $P_{\rm eff}$ are finite values at $t = t_{\rm s}$ [12] is included. (ii) Type II ("sudden" [13]): For the limit $t \to t_{\rm s}$, $a \to a_{\rm s}$, $\rho_{\rm eff} \to \rho_{\rm s}$ and $|P_{\rm eff}| \to \infty$. (iii) Type III: For the limit $t \to t_{\rm s}$, $a \to a_{\rm s}$, $\rho_{\rm eff} \to \infty$ and $|P_{\rm eff}| \to \infty$. (iv) Type IV: For the limit $t \to t_{\rm s}$, $a \to a_{\rm s}$, $\rho_{\rm eff} \to 0$, $|P_{\rm eff}| \to 0$, and higher derivatives of H diverge. Also, the case that $\rho_{\rm eff}$ and/or $|P_{\rm eff}|$ become finite values at $t = t_{\rm s}$ is included. Here, $t_{\rm s}$ is the time when the finite-time future singularities occur, and $a_{\rm s}(\neq 0)$ and $\rho_{\rm s}$ are constants. We examine the case that H is expressed as [14]

$$H \sim h_{\rm s}\left(t_{\rm s} - t\right)^{-q} \ \text{ for } \ q > 0\,, \quad H \sim H_{\rm s} + h_{\rm s}\left(t_{\rm s} - t\right)^{-q} \ \text{ for } \ q < -1,\ \ -1 < q < 0\,, \tag{1}$$

where $h_{\rm s}(> 0)$ and $H_{\rm s}(> 0)$ are positive constants, and $q(\neq 0, -1)$ is a non-zero constant. Only the period $0 < t < t_{\rm s}$ is studied because H should be a real number. In Table 1, we show the conditions for the finite-time future singularities to exist on q in the expression of H in Eq. (1), $\rho_{\rm DE}$, $P_{\rm DE}$, and the behaviors of H and $\dot{H}$ in the limit $t \to t_{\rm s}$.

Table 2: Necessary conditions on the model parameters of a power-law model of $f(T)$ in order to realize the finite-time future singularities, what types of the finite-time future singularities finally emerge, and those of the correction term $f_{\rm c}(T) = BT^{\beta}$ with removing the finite-time future singularities.

$q(\neq 0, -1)$	Final behavior	$f(T) = AT^{\alpha}$ $(A \neq 0, \alpha \neq 0)$	$f_{\rm c}(T) = BT^{\beta}$ $(B \neq 0, \quad \neq 0)$
$q \quad 1$ [Type I ("Big Rip") singularity]	emerges	$\alpha < 0$	> 1
$0 < q < 1$ [Type III singularity]	—	$\alpha < 0$	> 1
$-1 < q < 0$ [Type II ("sudden") singularity]	—	$\alpha = 1/2$	$\neq 1/2$
$q < -1$, but q is not any integer [Type IV singularity]	emerges	$\alpha = 1/2$	$\neq 1/2$

For H in Eq. (1), we reconstruct models of $f(T)$ gravity where the finite-time future singularities occur. We note that there have been proposed reconstruction method for modified gravity such as an $F(R)$ gravity in Ref. [15]. As a result, we find that for a power-law form of $f(T)$ as $f(T) = AT^{\alpha}$ with $A(\neq 0)$ and $\alpha(\neq 0)$ non-zero constants, in the at FLRW background both the two gravitational filed equations can be satisfied. In addition, we investigate a correction term to remove the finite-time future singularities. As an example of a correction term $f_{\rm c}(T)$, we take $f_{\rm c}(T) = BT^{\beta}$ where $B(\neq 0)$ and $(\neq 0)$ are non-zero constants. In $F(R)$ gravity, the correction term with $= 2$, namely, a T^2 term can cure the finite-time future singularities [2]. Consequently, we see that for the combined form as $f(T) = AT^{\alpha} + BT^{\beta}$, the two gravitational filed equations cannot be met simultaneously. This implies that such a power-low correction term can remove the finite-time future singularities. In Table 2, we depict necessary conditions for the model parameters of a power-law form of $f(T)$ where the finite-time future singularities appear, those of a power-low the correction term which can remove the finite-time future singularities. We also describe what types of the finite-time future singularities eventually appear. The finite-time future singularities with the large absolute value of q can emerge. In addition, we explicitly derive $f(T)$ models in which (a) in ation in the early universe, (b) the CDM model, (c) Little Rip cosmology [16], and (d) Pseudo-Rip cosmology [17, 18] can be realized. In Table 3, we represent forms of H and $f(T)$ with realizing these cosmological scenarios.

Furthermore, we study Little Rip cosmology which corresponds to a mild phantom scenario. The Little Rip scenario has been proposed to avoid the finite-time future singularities, in particular a Big Rip singularity. In this scenario, the energy density of dark energy increases in time with $w_{\rm DE}$ being less than -1 and then $w_{\rm DE}$ asymptotically approaches $w_{\rm DE} = -1$. However, such a scenario eventually leads to the dissolution of bound structures at some time in the future via the increase of an inertial force between objects. This process is called the "Little Rip". We also investigate Pseudo-Rip cosmology. The above four cosmological models can be classified by using the behavior of the Hubble parameter as follows [17]. (a) power-law in ation: $H(t) \to \infty, \quad t \to 0$. (b) the CDM model or exponential in ation: $H(t) = H(t_0) =$ constant with t_0 the present time. (c) Little Rip cosmology: $H(t) \to \infty, \quad t \to \infty$. (d) Pseudo-Rip cosmology, which is also phantom asymptotically de Sitter universe: $H(t) \to H_{\infty} < \infty$, $t \to \infty$. Here, $t \quad t_0$, and $H_{\infty}(> 0)$ is a positive constant. We also note that for a Big Rip singularity, $H(t) \to \infty, \quad t \to t_{\rm s}$, as shown in Table 1.

4 Summary

We have illustrated that there appear finite-time future singularities (Type I and IV) in $f(T)$ gravity and reconstructed an $f(T)$ gravity model with realizing the finite-time future singularities. Furthermore, it has been verified that a power-law type correction term T^{β} (> 1) such as a T^2 term can remove the finite-time future singularities in $f(T)$ gravity. This is the same feature as in $F(R)$ gravity. In addition, we have derived the expressions of $f(T)$ gravity models in which (a) Power-law in ation, (b) CDM model, (c) Little Rip cosmology, and (d) Pseudo Rip Cosmology can be realized.

Table 3: Forms of H and $f(T)$ which can realize (a) in ation in the early universe, (b) the CDM model, (c) Little Rip cosmology and (d) Pseudo-Rip cosmology.

Cosmology	H	$f(T)$
(a) Power-law in ation	$H = h_{\rm inf}/t\,,$	$f(T) = AT^{\alpha}\,,$
(In the limit $t \to 0$)	$h_{\rm inf}(> 1)$	$\alpha < 0$ or $\alpha = 1/2$
(b) CDM model	$H = \sqrt{\ /3} = \text{constant}\,,$	$f(T) = T - 2\ \ ,$
or exponential in ation	> 0	> 0
(c) Little Rip cosmology	$H = H_{\rm LR}\exp(\xi t)\,,$	$f(T) = AT^{\alpha}\,,$
(In the limit $t \to \infty$)	$H_{\rm LR} > 0$ and $\xi > 0$	$\alpha < 0$ or $\alpha = 1/2$
(d) Pseudo-Rip cosmology	$H = H_{\rm PR}\tanh(t/t_0)\,, \quad H_{\rm PR} > 0$	$f(T) = A\sqrt{T}$

References

[1] K. Bamba, S. Capozziello, S. Nojiri and S. D. Odintsov, Astrophys. Space Sci. **342**, 155 (2012).

[2] S. Nojiri and S. D. Odintsov, Phys. Rept. **505**, 59 (2011); eConf **C0602061**, 06 (2006) [Int. J. Geom. Meth. Mod. Phys. **4**, 115 (2007)] [arXiv:hep-th/0601213].

[3] F. W. Hehl, P. Von Der Heyde, G. D. Kerlick and J. M. Nester, Rev. Mod. Phys. **48**, 393 (1976); K. Hayashi and T. Shirafuji, Phys. Rev. D **19**, 3524 (1979) [Addendum-ibid. D **24**, 3312 (1981)]; E. E. Flanagan and E. Rosenthal, *ibid.* **75**, 124016 (2007).

[4] G. R. Bengochea and R. Ferraro, Phys. Rev. D **79**, 124019 (2009).

[5] E. V. Linder, Phys. Rev. D **81**, 127301 (2010) [Erratum-ibid. D **82**, 109902 (2010)].

[6] K. Bamba, C. Q. Geng and C. C. Lee, arXiv:1008.4036 [astro-ph.CO]; K. Bamba, C. Q. Geng, C. C. Lee and L. W. Luo, JCAP **1101**, 021 (2011).

[7] R. Ferraro and F. Fiorini, Phys. Rev. D **75**, 084031 (2007); *ibid.* **78**, 124019 (2008).

[8] K. Bamba, R. Myrzakulov, S. Nojiri and S. D. Odintsov, Phys. Rev. D **85**, 104036 (2012).

[9] K. Bamba, J. de Haro and S. D. Odintsov, arXiv:1211.2968 [gr-qc], to appear in JCAP.

[10] S. Nojiri, S. D. Odintsov and S. Tsujikawa, Phys. Rev. D **71**, 063004 (2005).

[11] R. R. Caldwell, M. Kamionkowski and N. N. Weinberg, Phys. Rev. Lett. **91**, 071301 (2003); B. McInnes, JHEP **0208** (2002) 029.

[12] Y. Shtanov and V. Sahni, Class. Quant. Grav. **19**, L101 (2002).

[13] J. D. Barrow, Class. Quant. Grav. **21**, L79 (2004); S. Nojiri and S. D. Odintsov, Phys. Lett. B **595**, 1 (2004).

[14] S. Nojiri and S. D. Odintsov, Phys. Rev. D **78**, 046006 (2008).

[15] S. Nojiri and S. D. Odintsov, Phys. Rev. D **74**, 086005 (2006); J. Phys. Conf. Ser. **66**, 012005 (2007) [arXiv:hep-th/0611071].

[16] P. H. Frampton, K. J. Ludwick and R. J. Scherrer, Phys. Rev. D **84**, 063003 (2011); I. Brevik, E. Elizalde, S. Nojiri and S. D. Odintsov, *ibid.* **84**, 103508 (2011); P. H. Frampton, K. J. Ludwick, S. Nojiri, S. D. Odintsov and R. J. Scherrer, Phys. Lett. B **708**, 204 (2012);

[17] P. H. Frampton, K. J. Ludwick and R. J. Scherrer, Phys. Rev. D **85**, 083001 (2012).

[18] A. V. Astashenok, S. Nojiri, S. D. Odintsov and A. V. Yurov, Phys. Lett. B **709**, 396 (2012).

Soichiro Isoyama, JGRG 22(2012)111415

"Adiabatic evolution of resonant orbits in Kerr space time"

RESCEU SYMPOSIUM ON

GENERAL RELATIVITY AND GRAVITATION

JGRG 22

November 12-16 2012

Koshiba Hall, The University of Tokyo, Hongo, Tokyo, Japan

Adiabatic evolution of resonant orbits on err spacetime

Soichiro Isoyama [1(a)]

[(a)] *Yukawa Institute for Theoretical Physics, Kyoto university, Kyoto, 606-8502, Japan*

Abstract

We discuss the inspiral of a small body in a background Kerr spacetime. In the adiabatic regime, the radiation reaction is solely characterized by the averaged rate of the change of the constants of motion, the energy E, the azimuthal angular momentum L and the Carter constant Q. Despite the lack of the global conservation law for the Carter constant, it has been shown that its long time averaged rate of change can be simply computed via "global conservation law like" formula when there exists a simultaneous turning point of the radial and polar oscillations. However, an inspiralling orbit may cross a *resonance* point, where the frequencies of the radial and polar orbital oscillations are in a rational ratio. At the resonant point, one cannot find a simultaneous turning point in general, thus a direct computation of the self-forces, quite challenging especially in the Kerr background, seems to be necessary. Contrary to this expectation, we here show that we can still compute the averaged rate of change of the Carter constant in a relatively simple manner even at the resonance point.

1 Introduction

A supermassive black hole accompanied by a compact object is one of the potential sources of the low frequency gravitational waves. This system can be considered as a particle with mass μ moving along a bound orbit on a much larger Kerr black hole with the mass $M(\gg \mu)$ and the spin parameter a. Then, the dominant part of the long time orbital evolution due to the radiation reaction of the gravitational wave emission is dictated by the long time averaged rates of the change of three constants of motion: the energy E, the azimuthal angular momentum L and the Carter constant Q as long as the characteristic time scale of the secular orbital evolution due to the radiation reaction is sufficiently longer than the orbital period. This method is called the adiabatic approximation [1, 2].

The averaged rates of change of the energy and the azimuthal angular momentum of the particle can be balanced with the ones carried by the gravitational waves due to their global conservation laws. Although we do not have any balance argument for the Carter constant, based on Mino's work [1], it has shown that the averaged rate of change of the Carter constant can be also computed by a practically simple formula [2, 3]. However, the derivation of above mentioned formula implicitly assumes that there exists a simultaneous turning point of the radial and polar oscillations. The problem is that we cannot find such a turning point for a inspiral that crosses a resonant point, where the inspiral's radial and polar orbital frequencies, Ω_r and Ω_θ, takes $\Omega_r/\Omega_\theta = j_r/j_\theta$ with coprime integers, j_r and j_θ.

The purpose of this article is overviewing our claim that we can still easily compute the adiabatic evolution of the Carter constant in the resonance case, together with the scalar toy model: a point scalar particle with mass μ_0 and charge q coupled to its own scalar field, and moving on the resonant bounded geodesic around the Kerr black hole. Further details are presented in our preparing manuscript [5]. In this paper, we use geometrical units $G = c = 1$ and take the sign convention of the metric is $(-,+,+,+)$. For saving the space of the article, the basic tools required for the adiabatic evolution of the scalar toy model, such as the solution of geodesic equation and the mode-decomposed retarded solution of the scalar field, are borrowed from Drasco *et al.*[6] without derivation.

[1]Email address: isoyama@yukawa.kyoto-u.ac.jp

2 A bounded resonant geodesic in err spacetime

We label the geodesic motion of a scalar particle with the bare rest mass $\mu = 1$ and a scalar charge q as $z(\lambda) := (t(\lambda),\ r(\lambda),\ \theta(\lambda),\ \phi(\lambda))$ with the "Mino time" λ, which is related to the proper time τ as $d\lambda := d\tau/\Sigma$ with $\Sigma := r^2 + a^2\cos^2\theta$. In terms of the Mino time, the r and θ oscillations are independently periodic for bound orbits:

$$r(\lambda) = r(\lambda + n\Lambda_r), \qquad \theta(\lambda) = \theta(\lambda + k\Lambda_\theta), \tag{1}$$

where n and k are integers, and Λ_r and Λ_θ are the periods with respect to the Mino time λ. The precise meaning of the resonance is that the orbital frequencies $\Upsilon_{r,\theta} := 2\pi/\Lambda_{r,\theta}$ with respect to the Mino time λ, or the frequency $\Omega_{r,\theta} = \Upsilon_{r,\theta}/\Upsilon_t$ with respect to t are related to each other as

$$\frac{\Upsilon_r}{j_r} = \frac{\Upsilon_\theta}{j_\theta} =: \Upsilon\ , \tag{2}$$

where j_r and j_θ are coprime integers. In the resonance case, there is always a difference between the times reaching the minima of r and θ oscillations. We call this difference "offset phase" and denote it as $\Delta\lambda$,and choose $\Delta\lambda$ such that $|\Delta\lambda| \le \Lambda'/2$, where $\Lambda' = (2\pi/\Upsilon)/(j_r + j_\theta)$.

The motion in the t and ϕ directions is also decoupled into r- and θ-dependent parts. Indeed, we have

$$t(\lambda) = \Upsilon_t\lambda + \Delta t_r(\lambda - \Delta\lambda) + \Delta t_\theta(\lambda), \qquad \phi(\lambda) = \Upsilon_\phi\lambda + \Delta\phi_r(\lambda - \Delta\lambda) + \Delta\phi_\theta(\lambda), \tag{3}$$

where Υ_t and Υ_ϕ are the averaged orbital frequency, and Δt_r and $\Delta\phi_r$ are the oscillating function with the period Λ_r. The meaning of the functions Δt_θ and $\Delta\phi_\theta$ can be understood in the same manner.

For detailed derivations, see Draso *et al.*[6].

3 Adiabatic evolution of the Carter constant with resonance

Due to the lack of the global conservation law for the Carter constant, we go back to the definition of the Carter constant, and start from the bare formula of its long time averaged rate of the change, which is written in terms of the scalar self-force acting on the particle. The Carter constant in the Kerr spacetime is defined as (*e.g.*. see Ref. [3])

$$Q := \left(\frac{L}{\sin\theta} - a\sin\theta E\right)^2 + a^2\cos^2\theta + \Sigma^2(u^\theta)^2, \tag{4}$$

where $u^\alpha := dz^\alpha/d\tau$, and E and L are the conserved energy and the azimuthal angular momentum of the particle, respectively. With the aid of the geodesic equations, the expression of the long time averaged value of the Mino-time derivative of the Carter constants takes

$$\left\langle \frac{dQ}{d\lambda} \right\rangle_\lambda = -2q \left\langle \left\{ \left(V_{tr}(r)\partial_t + V_{\phi r}(r)\partial_\phi + \frac{dr(\lambda)}{d\lambda}\partial_r \right) \left[\Sigma(x)\Phi^{(R)}(x) \right] \right\}_{x=z(\lambda)} \right\rangle_\lambda , \tag{5}$$

where $V_{tr}(r)$ and $V_{\phi r}(r)$ are the r-dependent potentials of the t and ϕ components of the geodesic equations [6]. In Eq. (5), the symbol $\langle \dots \rangle$ denotes the λ average: $\langle F(\lambda)\rangle_\lambda := \lim_{T\to+\infty}(1/(2T))\int_{-T}^{+T} d\lambda' F(\lambda')$ for a function $F(\lambda)$. The field $\Phi^{(R)}(x)$ is the R-part of the retarded scalar field, which is regular even at the particle's location [7]. With the aid of the "radiative (anti-symmetric)" field defined by the half-retarded *minus* half-advanced fields, and the "symmetric" field also defined by the half-retarded *plus* half-advanced field, we have $\Phi^{(R)}(x) := \Phi^{(\mathrm{rad})}(x) + \left\{\Phi^{(\mathrm{sym})}(x) - \Phi^{(S)}(x)\right\}$, where $\Phi^{(S)}(x)$ is the S-part of the retarded field, which is the symmetric for the argument of the Green function, satisfies the same inhomogeneous Klein-Gordon equation as retarded solution, and shares the same singular structure as the one of retarded/advanced field. To ensure the regularity of $\Phi^{(R)}(x)$, the subtraction of $\Phi^{(S)}(x)$ is essential.

Noting that either radiative, symmetric and S-part field, which we put the symbol $\Phi^{(\sharp)}$ to schematically denote them, is defined through the Green function as $\Phi^{(\sharp)} := -q\int d\lambda\Sigma[z(\lambda)]G^{(\sharp)}[x, z(\lambda)]$, Eq. (5) can

be rewritten with these Green functions. After integral by parts of Eq. (5) and rather involved algebra, we arrive at expression for the radiative part:

$$\left\langle \frac{dQ}{d\lambda} \right\rangle_\lambda^{(\mathrm{rad})} = 2q^2 \int_{-\infty}^{+\infty} d\lambda' \, \Sigma[z(\lambda')] \left\langle \left[\Sigma(x) \left(\langle V_{tr} \rangle \partial_t - \langle V_{\phi r} \rangle \partial_\phi \right) G^{(\mathrm{rad})}(x, z(\lambda')) \right]_{x=z(\lambda)} \right\rangle_\lambda - 2q^2 \int_{-\infty}^{+\infty} d\lambda' \left[\Sigma(x') \frac{d}{d(\Delta\lambda)} \left\langle \Sigma[z(\lambda)] G^{(\mathrm{rad})}(z(\lambda), x') \right\rangle_\lambda \right]_{x'=z(\lambda')} . \tag{6}$$

Note that $z(\lambda)$ implicitly depends on the offset phase $\Delta\lambda$.

The symmetric and S-part contribution to $\langle dQ/dt \rangle^{(\sharp)}$ is more tricky since the each of $G^{(\mathrm{sym})}[z(\lambda), z(\lambda')]$ and $G^S[z(\lambda), z(\lambda')]$ diverges in the coincidence limit $z(\lambda) \to z(\lambda')$, while their difference is regular in this limit. The problem here is that we can just compute symmetric and S-part field separately since the S-part Green function is only defined near the particle location[7]. To remedy this situation, we here introduce the point splitting regularization by displacing the orbits $z(\lambda)$ and $z(\lambda')$ as $z(\lambda) \to z_+(\lambda) := z(\lambda) + (\epsilon/2)\xi$, and $z(\lambda') \to z_-(\lambda') := z(\lambda') - (\epsilon/2)\xi$ with a small parameter $\epsilon \ll 1$, and the Killing field $\xi := \cos\zeta \, \xi^{(t)\mu} + (\Omega_\phi \cos\zeta - \Omega \sin\zeta) \, \xi^{(\phi)\mu}$ as well as the Killing vectors associated with the stationarity and axisymmetry of the Kerr spacetime: $\xi^{(t)\mu}$ and $\xi^{(\phi)\mu}$. Here Ω_ϕ and Ω are the orbital frequency with respect to t, not to the Mino-time, and we introduce the parameter ξ to specify the Killing field.

Taking care of this point splitting regularization, the symmetric contribution to $\langle dQ/dt \rangle$, after subtracting the S-part contribution and making it regularized, can be written as

$$\left\langle \frac{dQ}{d\lambda} \right\rangle_\lambda^{(\mathrm{sym}-S)} = -\lim_{\epsilon \to 0} q^2 \frac{d}{d(\Delta\lambda)} \left[\Psi^{(\mathrm{sym})}(\Delta\lambda, \epsilon) - \Psi^{(S)}(\Delta\lambda, \epsilon) \right] . \tag{7}$$

where we introduce the symmetric and S-part potential $\Psi^{(\mathrm{sym})/(S)}(\Delta\lambda, \epsilon)$ defined by

$$\Psi^{(\mathrm{sym})/(S)}(\Delta\lambda, \epsilon) := \int_{-\infty}^{+\infty} d\lambda' \Sigma[z_-(\lambda')] \left\langle \Sigma[z_+(\lambda)] G^{(\mathrm{sym})/\mathrm{S}}[z_+(\lambda), z_-(\lambda')] \right\rangle_\lambda . \tag{8}$$

4 Simplified formula for the regularized symmetric part

The expressions Eqs. (6) and (7) are rewritten as more practical expressions if we take care of that the variables of the scalar Klein-Gordon equation is separable in the Kerr spacetime. In fact, its homogeneous solution, namely mode functions is written by $\pi^\flat_{\omega\ell m}(t, r, \theta, \phi) := (2/\sqrt{r^2 + a^2}) e^{-i\omega t} e^{im\phi} \theta_{\omega\ell m}(\theta) u^\flat_{\omega\ell m}(r^*)$ where m is the integer, r^* is the tortoise coordinate defined by $dr^* := ((r^2 + a^2)/(r^2 - 2Mr + a^2))dr$, and $\theta_{\omega\ell m}(\theta) e^{im\phi} := S_{\omega\ell m}(\theta, \phi)$ is the spheroidal harmonics normalized as $\int d\theta d\phi \sin\theta S_{\omega\ell m}(\theta, \phi)^* S_{\omega\ell' m'}(\theta, \phi) = \delta_{\ell\ell'}\delta_{mm'}$.. The symbol $\flat$ represents one of the four distinct boundary conditions: "up", "down", "in" and "out". The corresponding radial functions $u^\flat_{\omega\ell m}(r^*)$ are respectively defined in *e.g.* Ref.[6]. The mode functions enable us to write down the retarded Green function as the factorized form:

$$G^{(\mathrm{ret})}(x, x') = \frac{1}{16\pi i} \int_{-\infty}^{+\infty} d\omega \sum_{\ell=0}^{+\infty} \sum_{m=-\ell}^{\ell} \frac{\omega}{|\omega|} \frac{1}{\alpha_{\omega\ell m} \beta_{\omega\ell m}} \times \left[\pi^{\mathrm{up}}_{\omega\ell m}(x) \pi^{\mathrm{out}\,*}_{\omega\ell m}(x') H(r - r') + \pi^{\mathrm{in}}_{\omega\ell m}(x) \pi^{\mathrm{down}\,*}_{\omega\ell m}(x') H(r' - r) \right] \tag{9}$$

with the Heaviside step function $H(x) := \int_{-\infty}^{x} \delta(y) dy$. Thinking of the definition of the radiative and the symmetric field, at least, the Green functions associated with these two field are also written in the factorized form with the relation given by $G^{(\mathrm{rad})}(x, x') := (1/2)[G^{(\mathrm{ret})}(x, x') - G^{(\mathrm{ret})}(x', x)]$ and $G^{(\mathrm{sym})}(x, x') := (1/2)[G^{(\mathrm{ret})}(x, x') + G^{(\mathrm{ret})}(x', x)]$ with $G^{(\mathrm{ret})}(x, x') = G^{(\mathrm{adv})}(x', x)$. Their explicit forms will be shown our manuscript [5].

The simplified formula is essentially derived by substituting the radiative and the symmetric Green function in the factorized form into Eqs. (6) and (7). Considering $\langle dQ/d\lambda \rangle_\lambda^{(\mathrm{rad})}$ has already computed by both Flanagan *et.al.* [8] and us [5], we bravely skip to show its explicit form here. See above two references for technical issues and its final form.

Compared to $\langle dQ/d\lambda\rangle_\lambda^{(\rm rad)}$, the simplification of $\langle dQ/d\lambda\rangle_\lambda^{(\rm sym)}$ and $\langle dQ/d\lambda\rangle_\lambda^{(S)}$ is much involved. The main obstacle is that the S-part Green function does not admit the mode decomposition in terms of the spheroidal harmonics, while we can easily decompose the symmetric Green function with the aid of Eq. (9). Here, the key observation here is what we need is the mode decomposition of the potentials defined in Eq. (8), rater than that of the Green functions themselves. We note that the bound geodesic allows to discretized the frequency ω as $\omega_{mN} := m\Omega_\phi + N\Omega$ with the integer N. With the aid of this information and the retarded Green fucntion in mode decomposed form given in Eq. (9), it is straightforward to obtain the regularized symmetric potential in the (N, m)-decomposed form:

$$\Psi^{(\rm sym)}(\Delta\lambda;\epsilon) = \sum_{Nm} e^{i(\epsilon_1 N+\epsilon_2 m)\Omega}\Psi^{(\rm sym)}_{Nm}(\Delta\lambda), \tag{10}$$

where $\epsilon_1 = \epsilon\cos\zeta$ and $\epsilon_2 = \epsilon\sin\zeta$. remarkably, Eq. (10) is nothing but a two-dimensional Fourier series expansion of $\Psi^{(\rm sym)}(\Delta\lambda;\epsilon)$. In other words, the (N, m)-mode decomposition is simply achieved via its inverse Fourier transformation. This is clearly good news for the S-part potential since its local expansion near the particle can be computed as

$$\Psi^{(S)}(\Delta\lambda;\epsilon) = -\frac{\psi(\zeta)}{\epsilon} + O(\epsilon), \tag{11}$$

with a ζ-dependent function. Thus, the (N, m)-mode decomposition of Eq. (11) is just derived as

$$\Psi^{(S)}_{Nm}(\Delta\lambda) = \frac{\Omega^2}{4\pi^2}\int_{-\frac{\pi}{\Omega}}^{\frac{\pi}{\Omega}} d\epsilon_1 \int_{-\frac{\pi}{\Omega}}^{\frac{\pi}{\Omega}} d\epsilon_2 e^{-i(\epsilon_1 N+\epsilon_2 m)\Omega}\Psi^{(S)}(\Delta\lambda;\epsilon) \tag{12}$$

All in all, the expression given in Eq. (7) can be computed as by mode-by-mode subtraction:

$$\left\langle \frac{dQ}{dt}\right\rangle_t^{(\rm sym)} = -\frac{q^2}{\Upsilon_t}\sum_{Nm} e^{i(\epsilon_1 N+\epsilon_2 m)\Omega}\left[\frac{d}{d(\Delta\lambda)}\left\{\Psi^{(\rm sym)}_{Nm}(\Delta\lambda) - \Psi^{(S)}_{Nm}(\Delta\lambda)\right\}\right]. \tag{13}$$

The merit of Eq. (13) is that both (N, m)-modes of the symmetric and S-part potentials are easily handled in the numerical implementation without bothering the divergence. In addition, the S-part has already subtracted at the level of mode decomposed form, we do not see any divergence even after summing up with respect to the N and m modes of the right hand side of Eq. (13). Again, further technical details will be explained our manuscript [5].

References

[1] Y. Mino, Phys. Rev. D **67**, 084027 (2003).

[2] T. Hinderer and E. E. Flanagan, Phys. Rev. D **78**, 064028 (2008).

[3] N. Sago, T. Tanaka, W. Hikida, K. Ganz and H. Nakano, Prog. Theor. Phys. **115**, 873 (2006).

[4] E. E. Flanagan and T. Hinderer, Phys. Rev. Lett. **109**, 071102 (2012).

[5] S. Isoyama, N. Sago, H. Nakano, R. Fujita and T. Tanaka, *in preparation.*

[6] S. Drasco, E. E. Flanagan and S. A. Hughes, Class. Quant. Grav. **22**, S801 (2005).

[7] S. L. Detweiler and B. F. Whiting, Phys. Rev. D **67**, 024025 (2003).

[8] E. E. Flanagan, S. A. Hughes and U. Ruangsri, arXiv:1208.3906 [gr-qc].

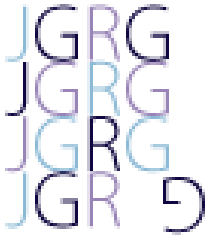

Toshiya Namikawa, JGRG 22(2012)111416

"An improved method for CMB lensing reconstruction and its cosmological applications"

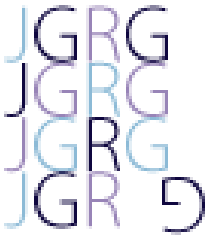

RESCEU SYMPOSIUM ON

GENERAL RELATIVITY AND GRAVITATION

JGRG 22



November 12-16 2012

Koshiba Hall, The University of Tokyo, Hongo, Tokyo, Japan



An Improved Method for CMB Lensing Reconstruction and Its Cosmological Applications

Toshiya Namikawa (The University of Tokyo)

Nov.12-16, 2012, JGRG @ Tokyo

Introduction

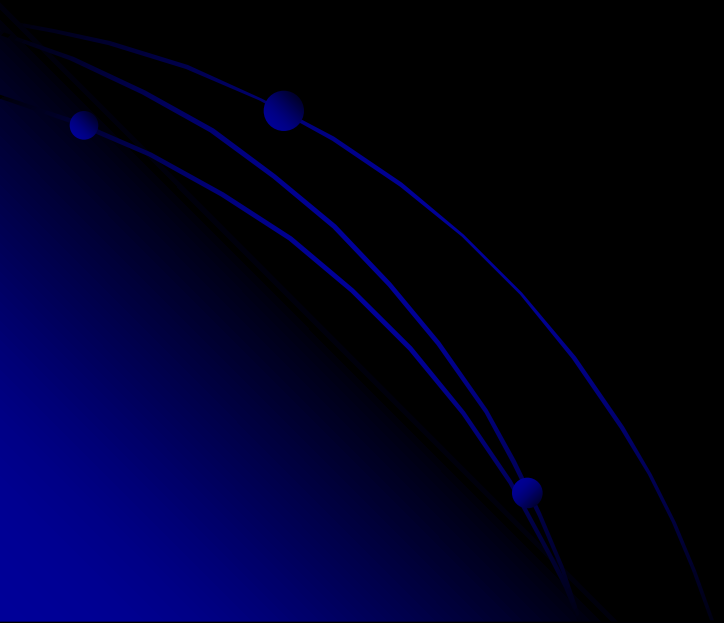

Cosmic Microwave Background (CMB)

- **Precise measurements of CMB fluctuations**

COBE

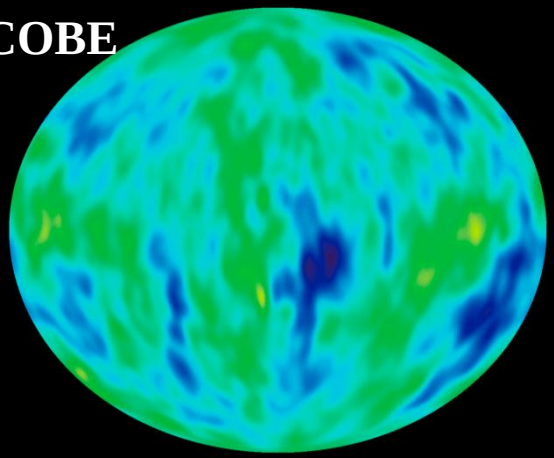

WMAP

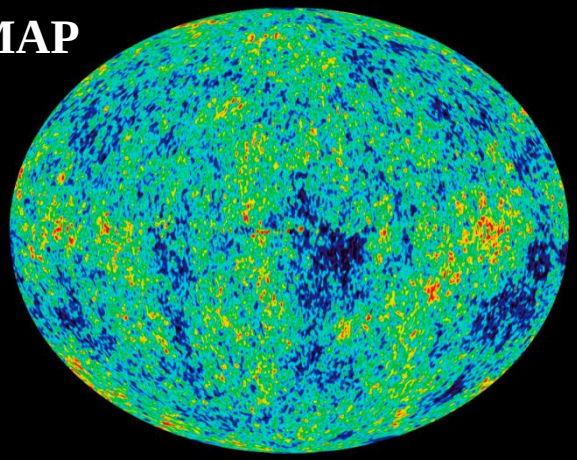

from LAMBDA web site (http://lambda.gsfc.nasa.gov/)

- **The energy components of Universe is well described by ΛCDM model**

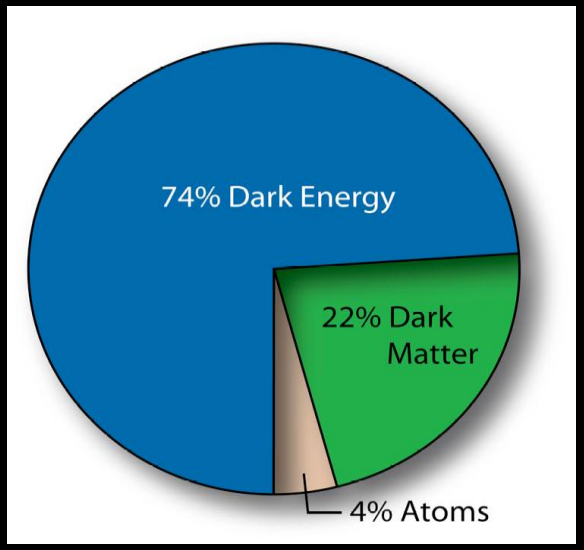

- ✓ **dark energy, dark matter**
- ✓ **mass of neutrinos**

⋮

Cosmological observations

➢ Observations

- CMB temperature/ polarizations
- Type-Ia Super Novae
- Baryon Acoustic Oscillations
- Cluster abundance
- Weak Lensing
- 21cm brightness temperature

➢ CMB lensing

- ✓ Sensitive to both geometry and density fluctuations at z=1~5
- ✓ The most high-z source for weak lensing
- ✓ The physical properties of source (CMB) is well known

dark energy, neutrino mass, …

primordial gravitational waves, primordial non-Gaussianity

Lensing effect on CMB

- **CMB Lensing**
  = Distortion of the pattern of the temperature/polarizations anisotropies

(Reviews : Lewis&Challinor'06, Hanson+'10)

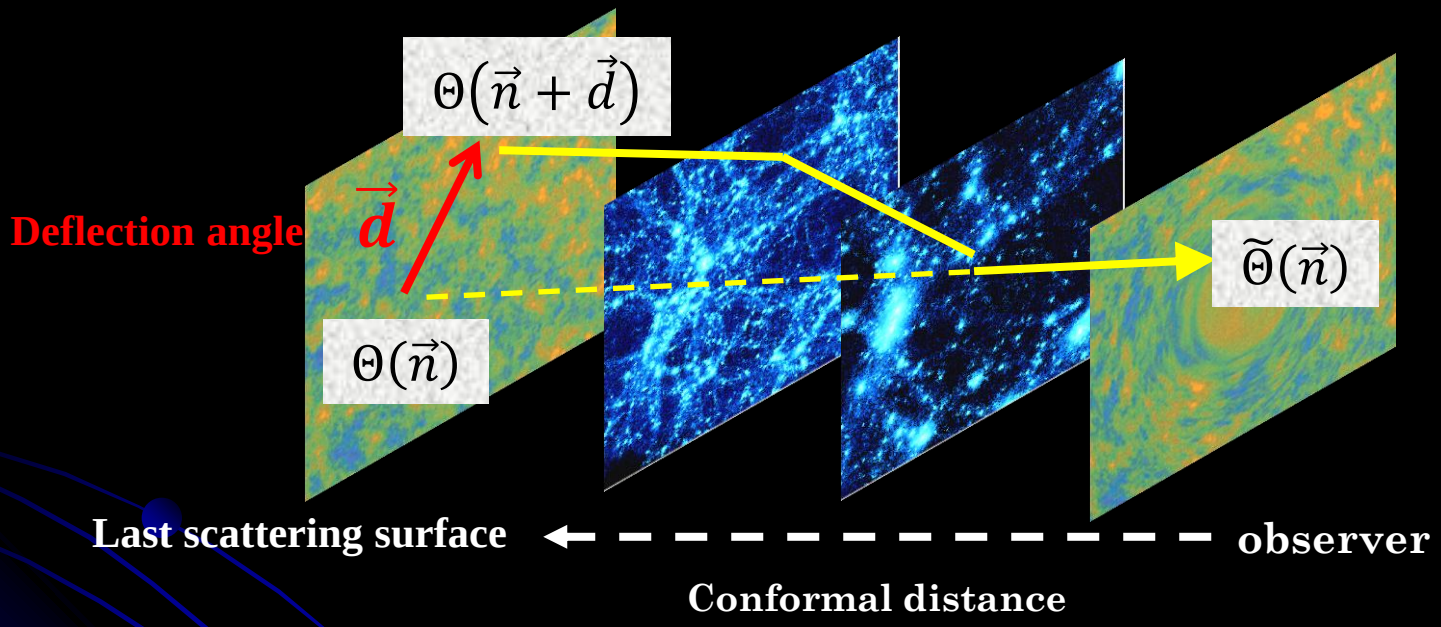

- **Lensed anisotropies**

$$\tilde{\Theta}(\vec{n}) = \Theta\left(\vec{n} + \vec{d}(\vec{n})\right)$$

Lensing potential

Gravitational potential

$$\nabla\left(-2\int_0^{\chi_s} d\chi \frac{\chi_s - \chi}{\chi\chi_s}\overline{\psi(\eta_0 - \chi, \chi\vec{n})}\right)$$

Lensed temperature anisotropies

- **Angular power spectrum**

$$\widetilde{\Theta}(\vec{n}) \Rightarrow \widetilde{\Theta}_{\ell m} = \int d\vec{n}\, Y^*_{\ell m}(\vec{n})\widetilde{\Theta}\,(\vec{n}) \Rightarrow \langle \widetilde{\Theta}_{\ell m}\widetilde{\Theta}^*_{\ell' m'}\rangle = \delta_{\ell\ell'}\delta_{mm'}\tilde{C}_\ell^{\Theta\Theta}$$

Harmonics space — Angular power spectrum

- **Lensed angular power spectrum**

(Lewis&Challinor'06)

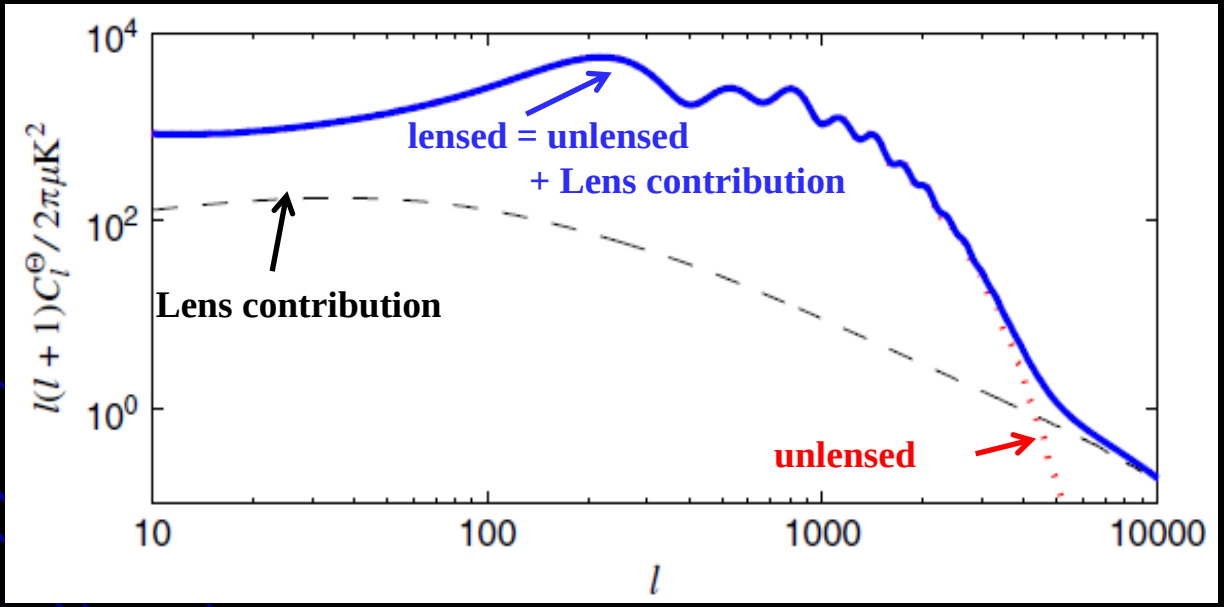

Lensing effect becomes dominate at Silk damping scale: $\ell > 2000$ (~ few arcmin)

→ **A few arcmin angular resolution is required**

Lensed polarizations anisotropies

- **CMB polarizations**
  - **Decomposition with parity** (patterns of E/B-modes)

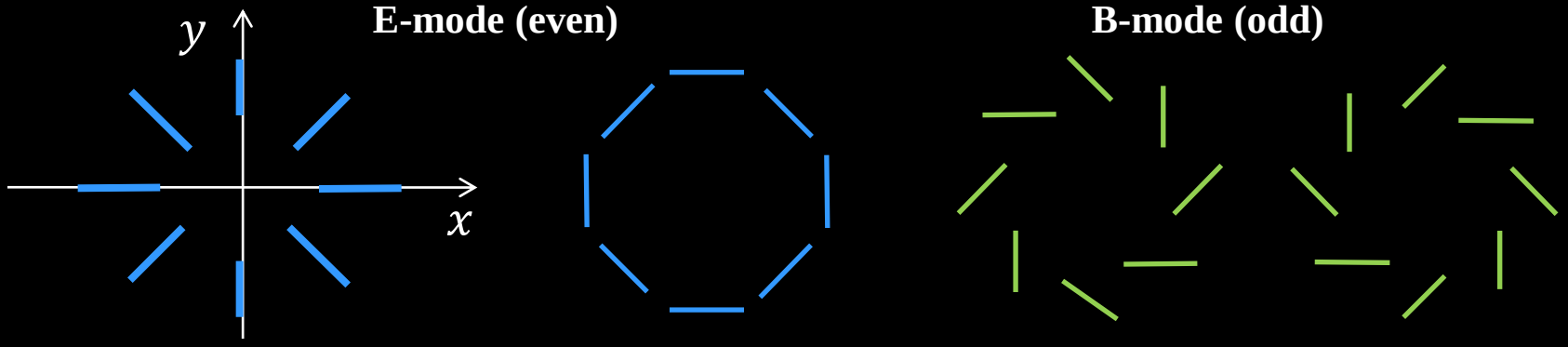

- **Lensed E/B-modes angular power spectra** (Lewis&Challinor'06)
  - **B-mode from lensing**

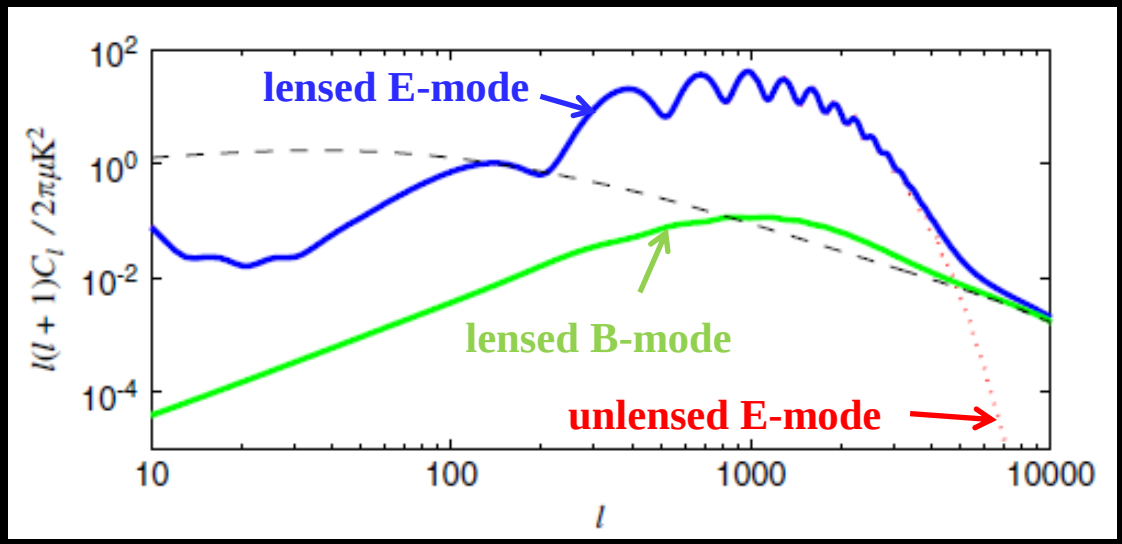

Lensed polarizations anisotropies

- **CMB polarizations**
  - **Decomposition with parity** (patterns of E/B-modes)

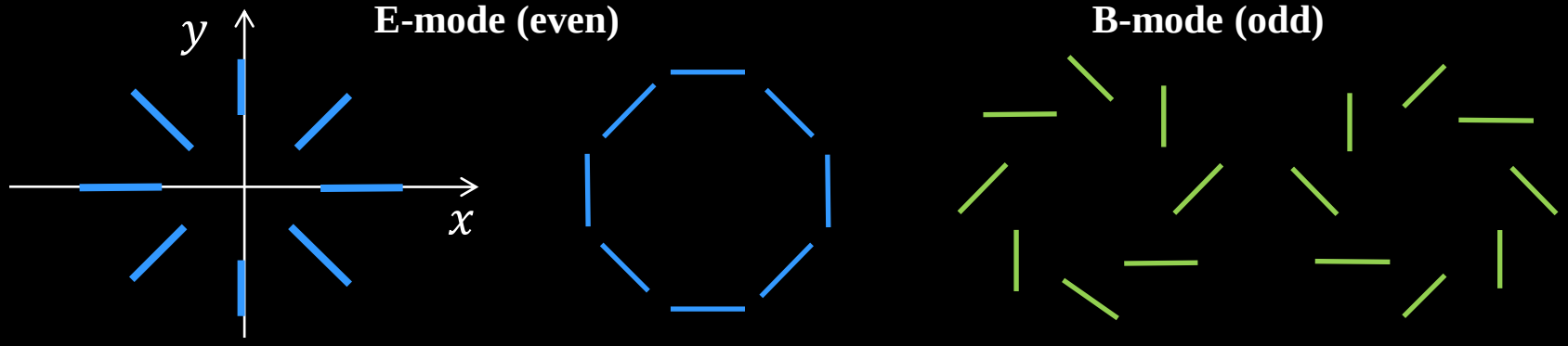

- **Lensed E/B-modes angular power spectra** (Lewis&Challinor'06)
  - **B-mode from lensing**

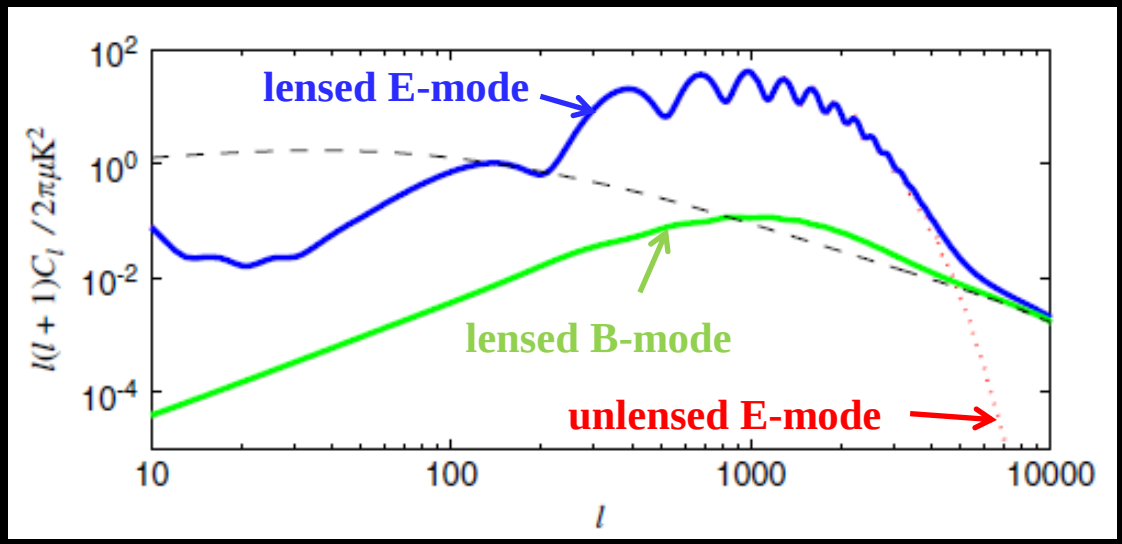

How to measure lensing effect from CMB

- **Lensed CMB power spectrum, e.g., C_ℓ^{BB}**
  - ✓ **easy to mitigate biases from, e.g., masking compared to reconstruction**
  - ✓ **estimation of power spectrum of lensing potentials, $C_\ell^{\phi\phi}$, is difficult**

- **CMB lensing reconstruction = estimate lensing potentials itself**
  - ✓ **useful for cross-correlation studies with, e.g., cosmic shear, galaxy clustering, etc**
  - ✓ **also useful to study, e.g., three-point correlation of lensing potentials, etc**

CMB lensing reconstruction

- **Essence of lensing reconstruction** (Review: Hanson+'10)

  Lensing induces mode coupling in the temperature anisotropies

$$\widetilde{\Theta}_{\vec{\ell}} = \Theta_{\vec{\ell}} - \int d^2L \, (\vec{\ell} \cdot \vec{L}) \phi_{\vec{L}-\vec{\ell}} \Theta_{\vec{L}}$$

  Lensing potentials would be estimated from mode coupling $\widetilde{\Theta}_{\ell} \widetilde{\Theta}_{\vec{L}}$ $(\ell \neq L)$

- **Estimator** (e.g., Hu&Okamoto'02; Hanson+'09)

$$\hat{\phi}_L^{(C)} = \hat{\phi}_L^{(S)} - \langle \hat{\phi}_L^{(S)} \rangle$$

Mean-field bias: induced by non-lensing effect (mask, inhomogeneous noise, beam asymmetry, …)

$$\hat{\phi}_L^{(S)} = \int d^2\ell \; F_{\ell,L}^{\phi} \, \overline{\Theta}_{\ell} \overline{\Theta}_{\vec{L}-\vec{\ell}} \qquad \left(\overline{\Theta}_{\ell} = \frac{\widetilde{\Theta}_L}{C_L^{\Theta\Theta}} \right)$$

$(L \neq 0)$

includes "observed lensed" Cl's

Lensing reconstruction from current data

- **Smith+ '07** **(3.4σ)**

  WMAP
  + NVSS (NARO VLA Sky Survey)

- **Hirata+ '08** **(2.5σ)**

  WMAP
  + NVSS + SDSS (Sloan Digital Sky Survey)

- **Das+ '11**

  WMAP
  + Atacama Cosmology Telescope (ACT)

- **van Engelen+ '12**

  WMAP + South Pole Telescope (SPT)

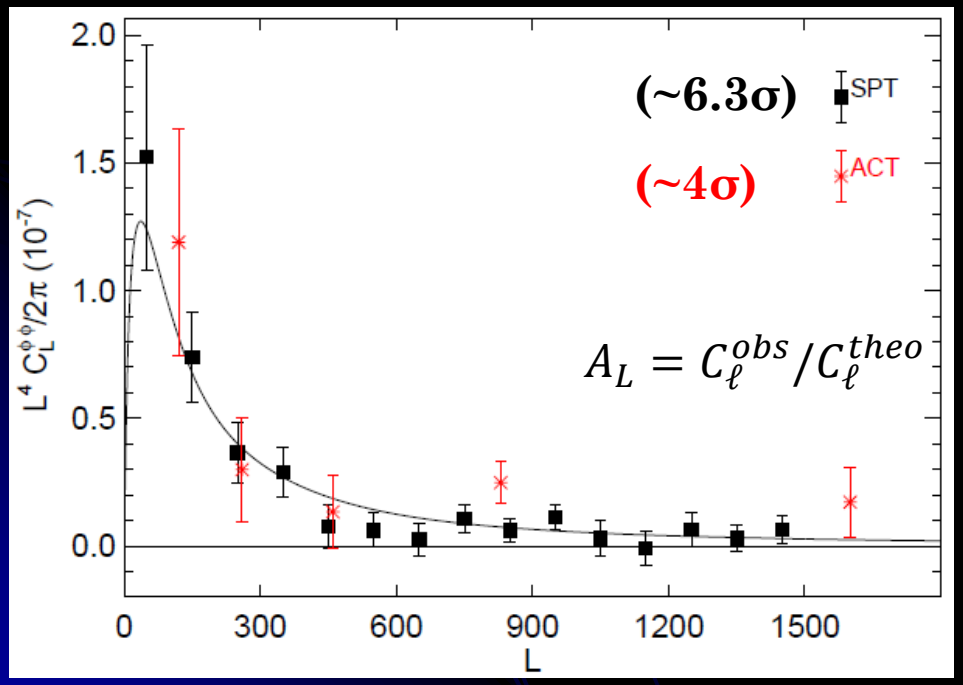

Angular power spectrum of lensing potentials

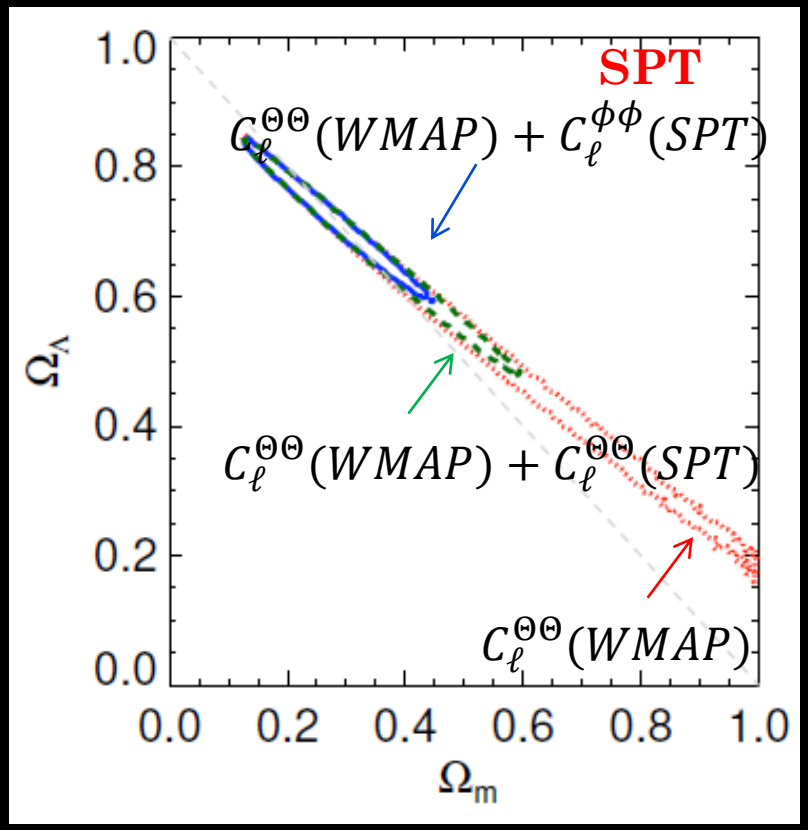

Future prospects

- **Ongoing/upcoming and next generation CMB experiments**
  - ✓ **Space** PLANCK, CMBPol, LiteBIRD, …
  - ✓ **Ground** PolarBear, ACTPol, SPTpol, Polar…

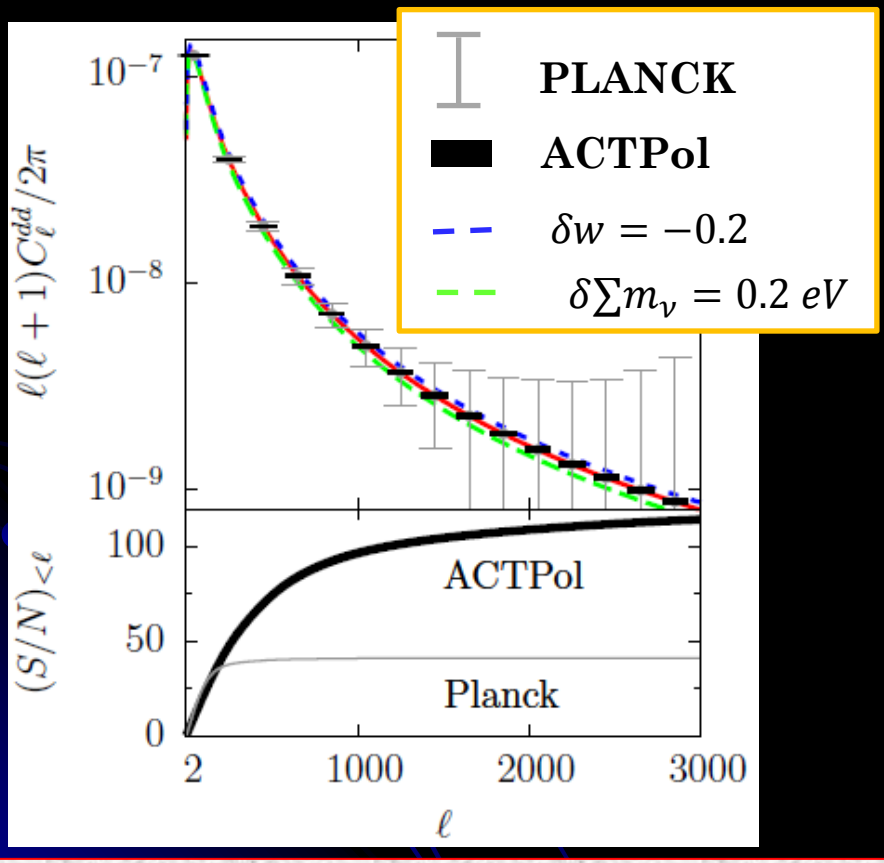

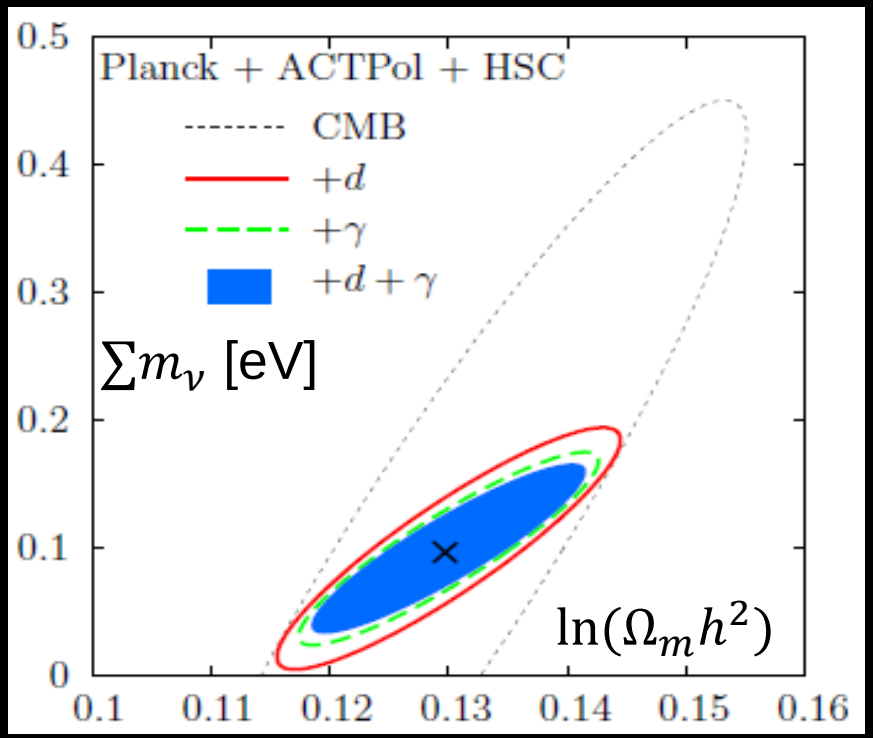

TN, Saito & Taruya '10

Lensing signals would be detected with enough precision to probe, e.g., dark energy and massive neutrinos

Lensing reconstruction from CMB map and Its Cosmological Applications

Gradient/Curl modes

- **Deflection angle**

  2 components
  - Gradient --- linear density fluctuations…
  - Curl --- any vector and tensor sources (gravitational waves (GWs), cosmic strings, magnetic field…)

2D Levi-Chivita tensor

$$d_i(\vec{n}) = \underbrace{\partial_i \phi(\vec{n})}_{\text{gradient}} + \underbrace{\epsilon_{ij}\partial_j \omega(\vec{n})}_{\text{curl}}$$

- **Application of curl-mode reconstruction**
  - Probing, e.g., cosmic strings, GWs, magnetic field …
  - Check systematics

- **Outline**

  1. derive estimator for gradient and curl modes
  2. reconstruct from current CMB data
  3. discuss future prospects

Estimator

- **Estimator** TN, Yamauchi & Taruya '12

$$\hat{\phi}^{(XY)}_{\ell m} = (-1)^m \sum_{L_1 M_1} \sum_{L_2 M_2} F^{XY}_{\ell L_1 L_2} \begin{pmatrix} \ell & L_1 & L_2 \\ -m & M_1 & M_2 \end{pmatrix} \tilde{\mathrm{X}}_{L_1 M_1} \tilde{Y}_{L_2 M_2}$$

$$\hat{\omega}^{(XY)}_{\ell m} = (-1)^m \sum_{L_1 M_1} \sum_{L_2 M_2} G^{XY}_{\ell L_1 L_2} \begin{pmatrix} \ell & L_1 & L_2 \\ -m & M_1 & M_2 \end{pmatrix} \tilde{\mathrm{X}}_{L_1 M_1} \tilde{Y}_{L_2 M_2}$$

mode coupling

$\tilde{X}_{\ell m}$, $\tilde{Y}_{\ell m}$: **Lensed quantities** ($\tilde{\Theta}_{\ell m}, \tilde{E}_{\ell m}$, **or** $\tilde{B}_{\ell m}$)

- **Weight functions are determined so that**

1. **Gradient / curl mode estimators do not include curl / gradient mode, respectively**
2. **The variance of estimator is minimized**

Thanks to the distinctive property of parity (∇ and $\star\nabla$), we can estimate gradient and curl mode separately

Lensing reconstruction from current data

- Data **ACT**

(Dunner+'12)

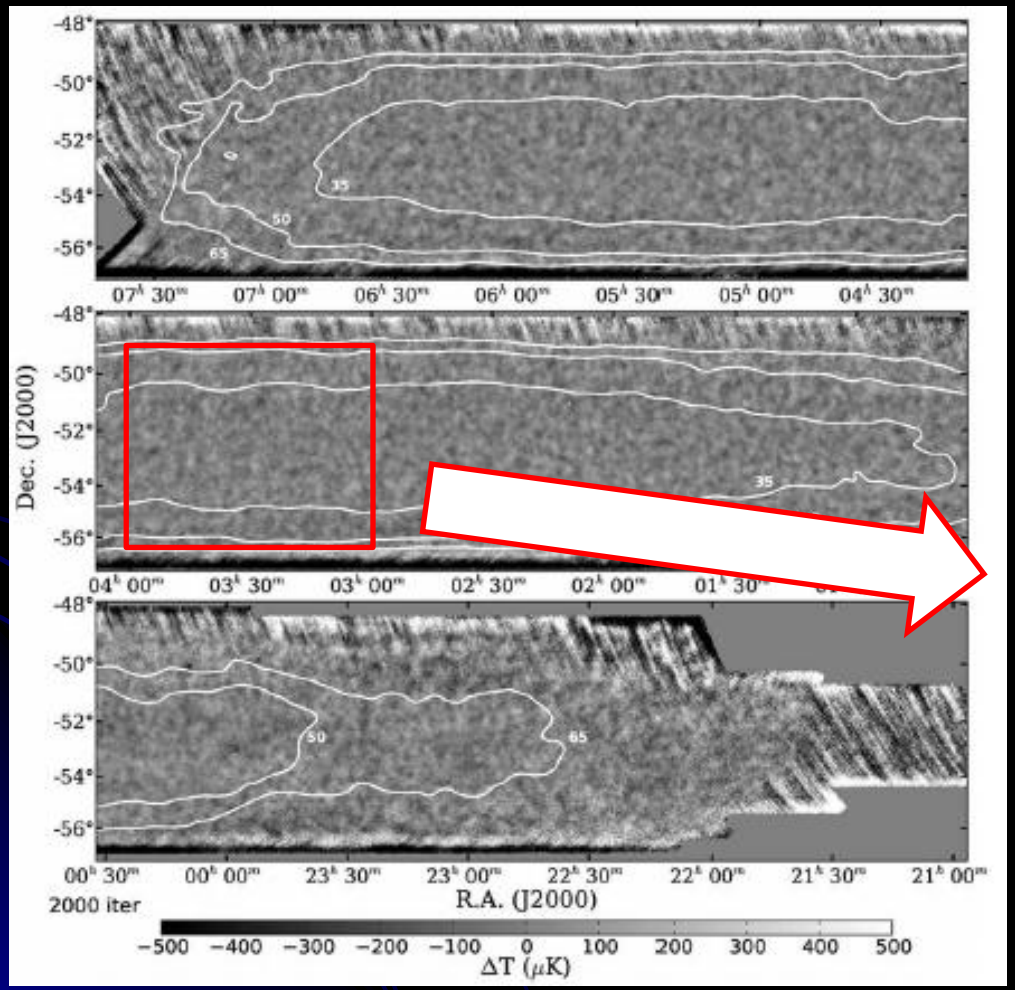

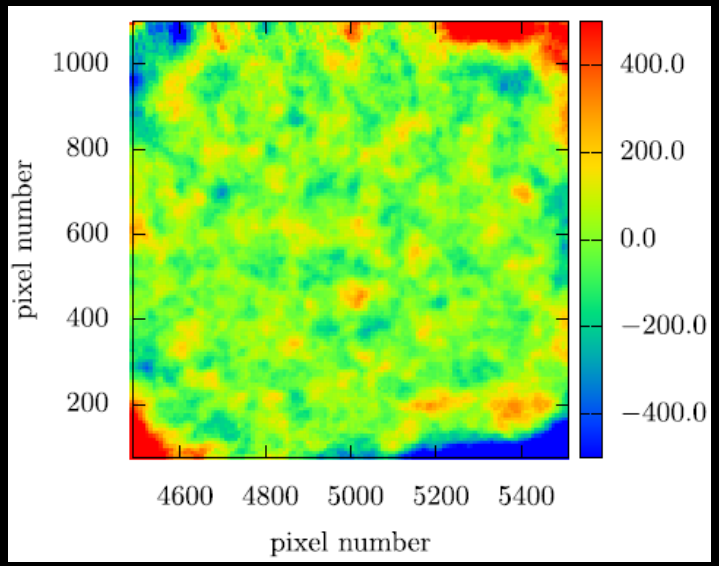

Data is taken from http://lambda.gsfc.nasa.gov/product/act/act_prod_table.cfm (LAMBDA)

Estimating lensing power spectrum

- **Power spectrum of lensing estimator** **(e.g., Hanson+'11)**

$$\hat{x}_L = \int d\vec{\ell}\ F^x_{\ell,L}\ \widetilde{\Theta}_\ell \widetilde{\Theta}_{\vec{L}-\vec{\ell}}$$

$$\rightarrow \quad \langle|\hat{x}_L|^2\rangle = \int d\vec{\ell}_1 \int d\vec{\ell}_2\, F^x_{L,\ell_1} F^x_{L,\ell_2} \langle \widetilde{\Theta}^*_{\ell_1} \widetilde{\Theta}^*_{\vec{L}-\vec{\ell}_1} \widetilde{\Theta}_{\ell_2} \widetilde{\Theta}_{\vec{L}-\vec{\ell}_2} \rangle$$

decomposed into disconnected/connected part

$$\rightarrow \quad \langle|\hat{x}_L|^2\rangle \simeq N^{x,(0)}_\ell + C^{xx}_\ell + \sum_x N^{x,(1)}_\ell + O[(C^{xy}_\ell)^2]$$

disconnected part (Gaussian bias)

connected part

[Note] several techniques for power spectrum estimation can reduce uncertainties in Gaussian bias

(Hu'02, Sherwin&Das'11, *TN*,Hanson&Takahashi'12)

Cosmological implications

- **An example of cosmological implications from curl mode**

$\ell^4|\hat{\varpi}_L|^2/2\pi$

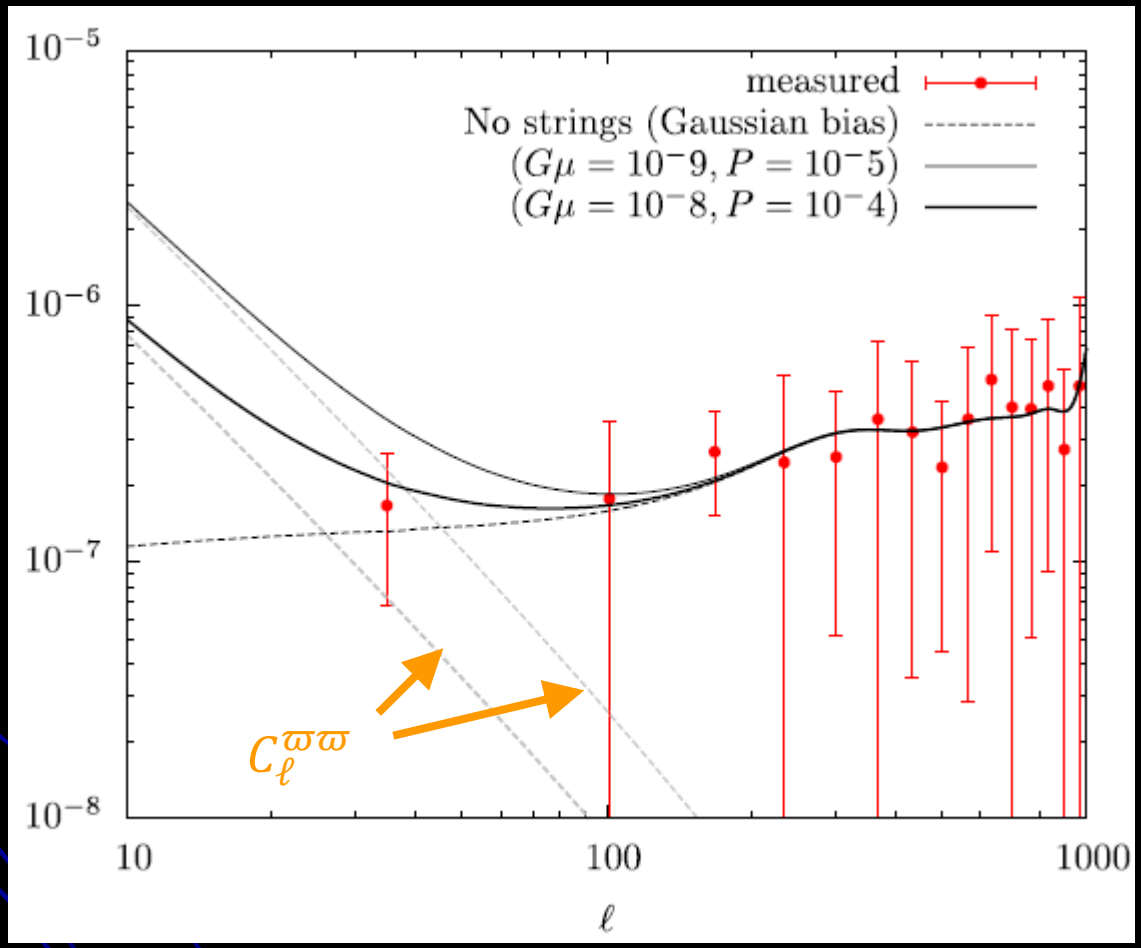

From ACT data, parameter region which is not ruled out from CMB temperature power spectrum, e.g., $G\mu \sim 10^{-9}$ with P $\sim 10^{-5}$ seems to be ruled out

Cosmological implications (Future Prospects)

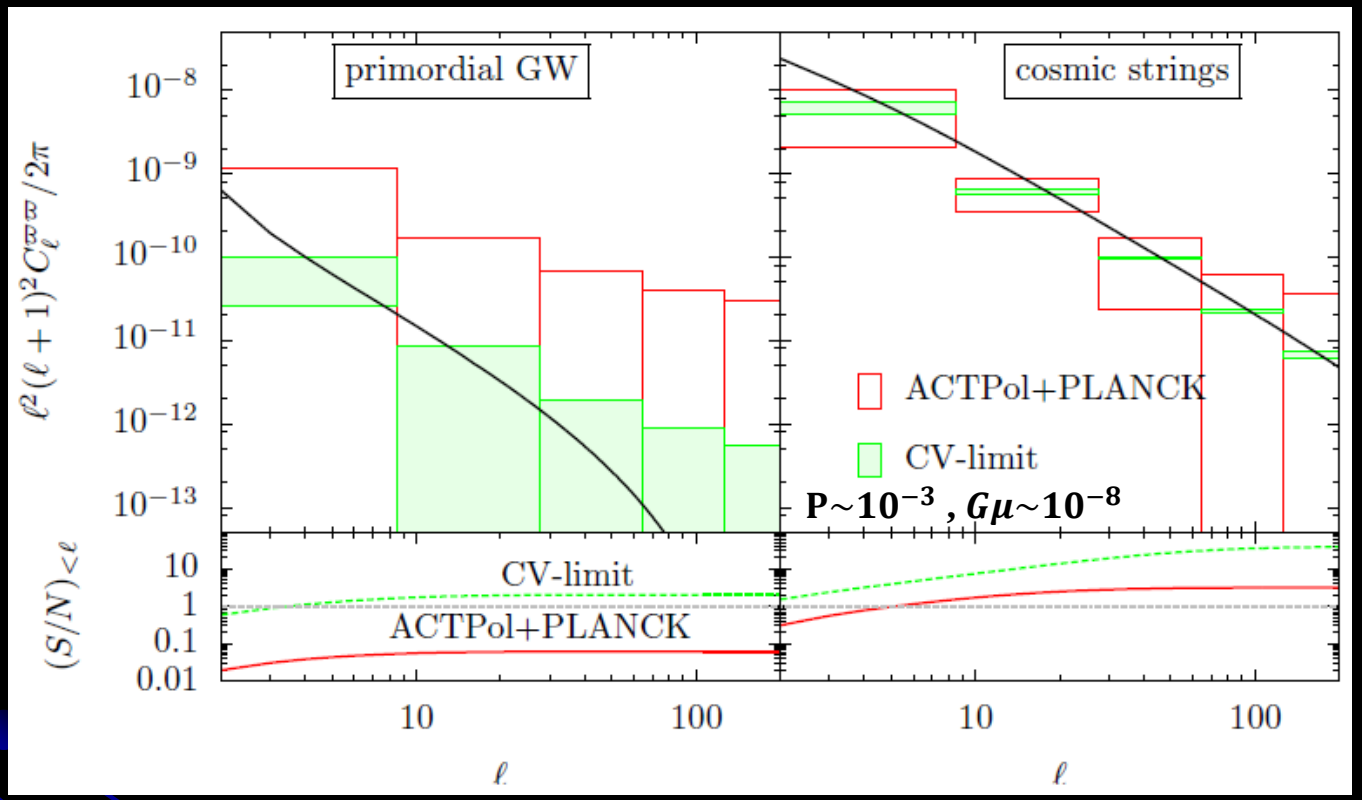

TN, Yamauchi & Taruya '12

- ✓ **Primordial GWs --- even r=0.1 would be difficult to detect.**
- ✓ **Cosmic strings --- can be explored with upcoming experiments**

(This would be a new probe of cosmic strings from CMB)

Summary

- **Formulation of CMB lensing reconstruction in the presence of both gradient and curl modes**
  - ✓ **Gradient and curl modes are estimated separately thanks to the distinctive property of parity**
- **Lensing reconstruction from current CMB map**
  - ✓ **Show an example of cosmological implications from curl mode**
- **Future prospects of CMB lensing reconstruction**
  - ✓ **Lensing signals from upcoming and future CMB experiments and galaxy imaging surveys would constrain not only mass of neutrinos, property of dark energy, but also e.g., cosmic strings and other non-scalar components**
  - ✓ **If $r<0.01$, lensing reconstruction is important to probe primordial gravitational waves from B-polarization**

- **Gradient mode**

$\ell^4 \left|\hat{\phi}_L\right|^2 / 2\pi$

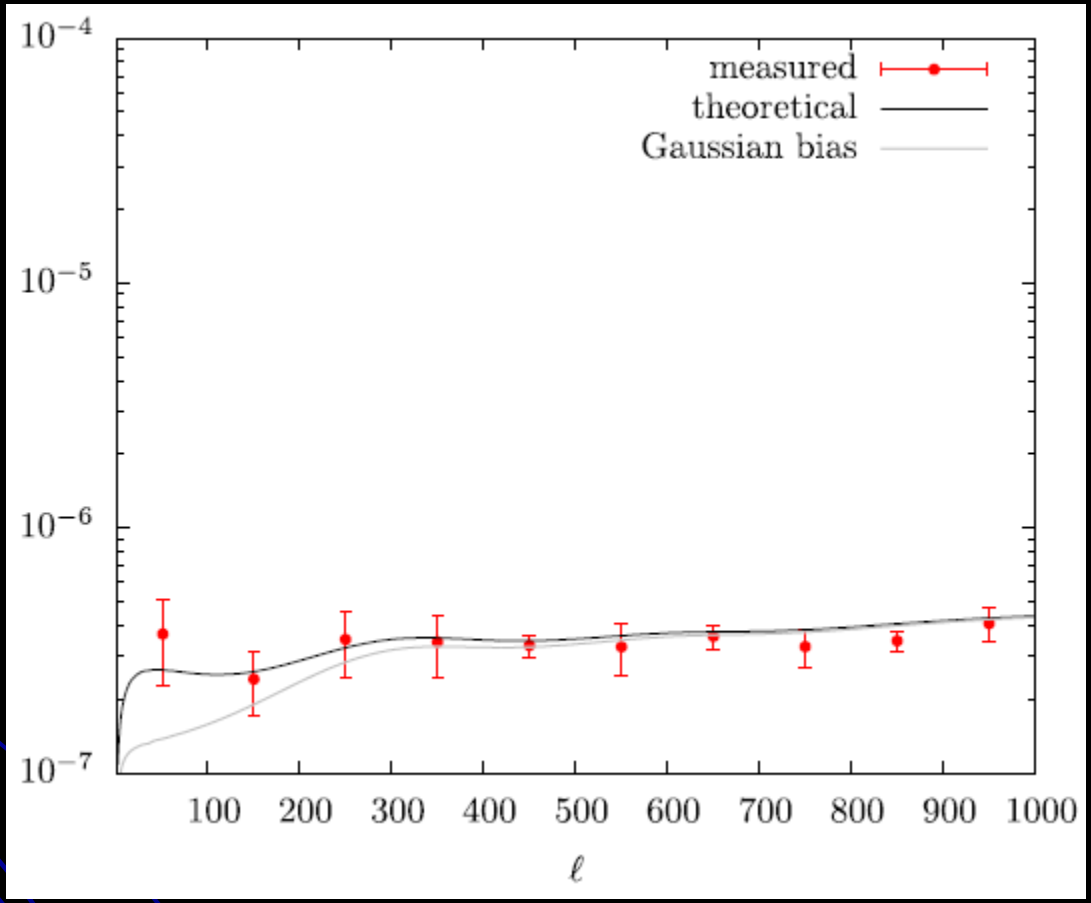

Estimating lensing power spectrum

- **Bias contributions** **(e.g., Hanson+'11)**

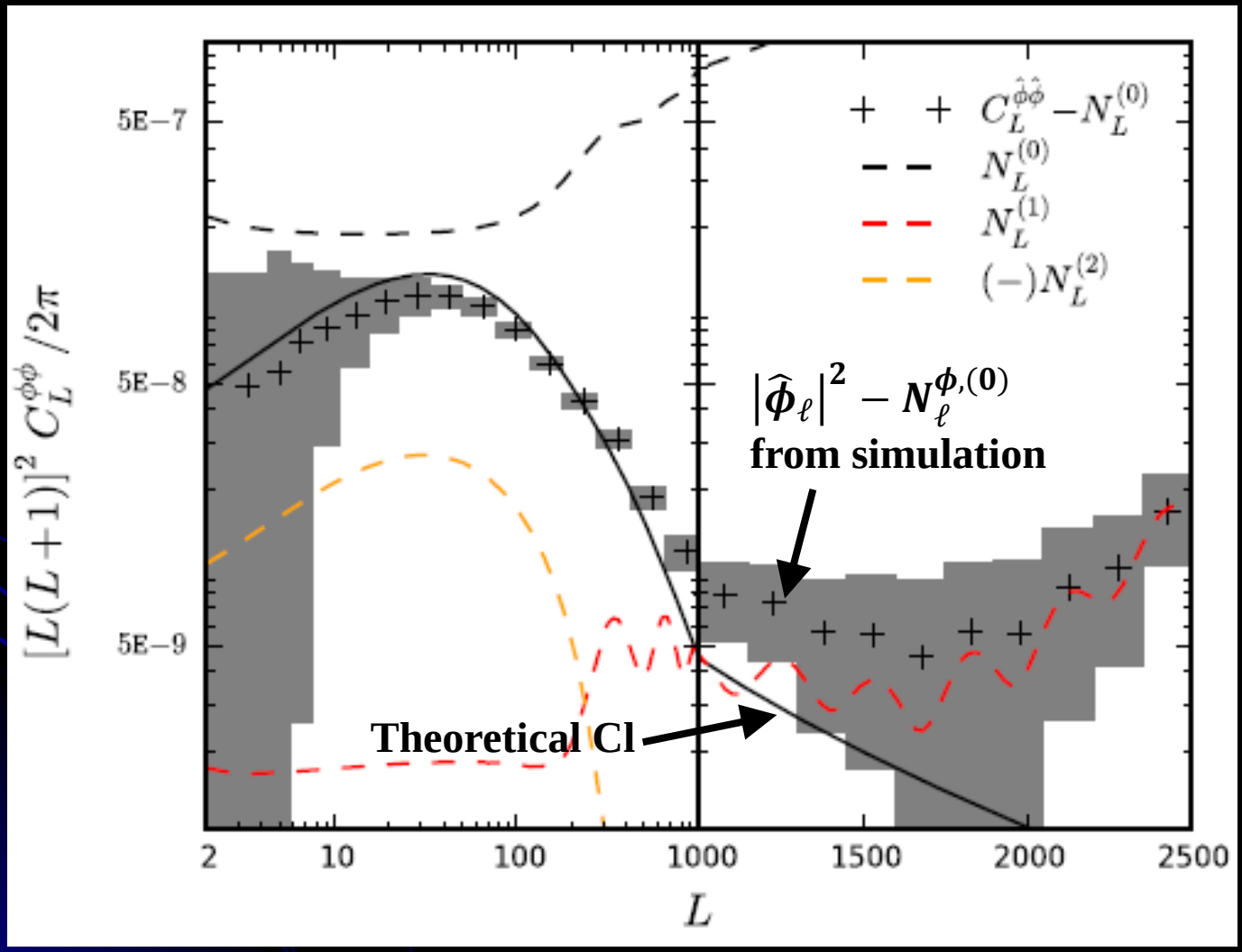

Reduced-bias estimator

(2) improve "standard" estimator to remove "mean field"

$$\langle \hat{\phi}_{\vec{\ell}} \rangle = R_\ell^{\phi M} M_\ell \quad \longrightarrow \quad \langle \hat{\phi}_{\vec{\ell}}^{BR} \rangle = 0$$

We consider "lensing" and "mask" estimators:

$$\widehat{M}_\ell = N_\ell^{MM} \int d\vec{L} \frac{f_{\ell,L}^{\phi} f_{\ell,L}^{M}}{2\tilde{C}_\ell^{\Theta\Theta} \tilde{C}_L^{\Theta\Theta}}$$

$$f_{\ell,L}^{\phi} = \vec{\ell} \cdot \vec{L} \tilde{C}_L^{\Theta\Theta} + \vec{\ell} \cdot (\vec{\ell} - \vec{L}) \tilde{C}_{|\vec{\ell}-\vec{L}|}^{\Theta\Theta}$$

$$f_{\ell,L}^{M} = [\tilde{C}_L^{\Theta\Theta} + \tilde{C}_{|\vec{\ell}-\vec{L}|}^{\Theta\Theta}]$$

$$R_\ell^{ab} = N_\ell^{aa} \int d\vec{L} \frac{f_{\ell,L}^{a} f_{\ell,L}^{b}}{2\tilde{C}_\ell^{\Theta\Theta} \tilde{C}_L^{\Theta\Theta}}$$

$$[N_\ell^{aa}]^{-1} = \int d\vec{L} \frac{f_{\ell,L}^{a} f_{\ell,L}^{a}}{2\tilde{C}_\ell^{\Theta\Theta} \tilde{C}_L^{\Theta\Theta}}$$

Since

$$\langle \hat{\phi}_\ell \rangle_{CMB} = \phi_\ell + R_\ell^{\phi M} M_\ell$$

$$\langle \widehat{M}_\ell \rangle_{CMB} = R_\ell^{M\phi} \phi_\ell + M_\ell$$

we define a new estimator

$$\hat{\phi}_\ell^{BR} = \frac{\hat{\phi}_\ell - R_\ell^{\phi M} \widehat{M}_\ell}{1 - R_\ell^{\phi M} R_\ell^{M\phi}}$$

Appendix: Filter functions

- **"standard" quadratic estimator**

$$F^{a}_{\vec{\ell},\vec{L}} = -N^{aa}_{\ell} f^{a}_{\ell,L}$$

$$[N^{aa}_{\ell}]^{-1} = \int d\vec{L} \frac{f^{a}_{\ell,L} f^{a}_{\ell,L}}{2\tilde{C}^{\Theta\Theta}_{\ell}\tilde{C}^{\Theta\Theta}_{L}}$$

$$f^{\phi}_{\ell,L} = \vec{\ell}\cdot\vec{L}C^{\Theta\Theta}_{L} + \vec{\ell}\cdot(\vec{\ell}-\vec{L})C^{\Theta\Theta}_{|\vec{\ell}-\vec{L}|}$$

$$f^{\varpi}_{\ell,L} = (\star\vec{\ell})\cdot\vec{L}C^{\Theta\Theta}_{L} + (\star\vec{\ell})\cdot(\vec{\ell}-\vec{L})C^{\Theta\Theta}_{|\vec{\ell}-\vec{L}|}$$

- **Our "bias-reduced" estimator**

$$F'^{\phi}_{\vec{\ell},\vec{L}} = \frac{F^{\phi}_{\ell,L} - R^{\phi M}F^{M}_{\ell,L}}{1 - R^{\phi M}R^{M\phi}}$$

$$R^{ab}_{\ell} = N^{aa}_{\ell}\int d\vec{L} \frac{f^{a}_{\ell,L} f^{b}_{\ell,L}}{2\tilde{C}^{\Theta\Theta}_{\ell}\tilde{C}^{\Theta\Theta}_{L}}$$

$$f^{\phi}_{\ell,L} = \vec{\ell}\cdot\vec{L}\tilde{C}^{\Theta\Theta}_{L} + \vec{\ell}\cdot(\vec{\ell}-\vec{L})\tilde{C}^{\Theta\Theta}_{|\vec{\ell}-\vec{L}|}$$

$$f^{\varpi}_{\ell,L} = (\star\vec{\ell})\cdot\vec{L}\tilde{C}^{\Theta\Theta}_{L} + (\star\vec{\ell})\cdot(\vec{\ell}-\vec{L})\tilde{C}^{\Theta\Theta}_{|\vec{\ell}-\vec{L}|}$$

$$f^{M}_{\ell,L} = [\tilde{C}^{\Theta\Theta}_{L} + \tilde{C}^{\Theta\Theta}_{|\vec{\ell}-\vec{L}|}]$$

Lensing Reconstruction

Information on the deflection angle is included in the observed lensed anisotropies

$$\widetilde{\Theta}(\vec{n}) = \Theta\left(\vec{n} + \vec{d}\right) \simeq \Theta(\vec{n}) + d(\vec{n}) \cdot \nabla\Theta(\vec{n})$$

We need to reconstruct the deflection angle only from the statistical properties of lensed and unlensed CMB

Result 2. Cosmological applications

We consider two sources of curl mode: primordial GWs and cosmic strings

Model of cosmic strings

See Yamauchi, *TN* & Taruya '12 for details of cosmic strings

- **We consider straight string, randomly oriented**
- **Motion of strings is determined by velocity-dependent one scale model which depends on string tension, $G\mu$ and intercommuting probability, P**



- **Lensing is induced by metric perturbations from strings in our line-of-site**

Noise spectrum

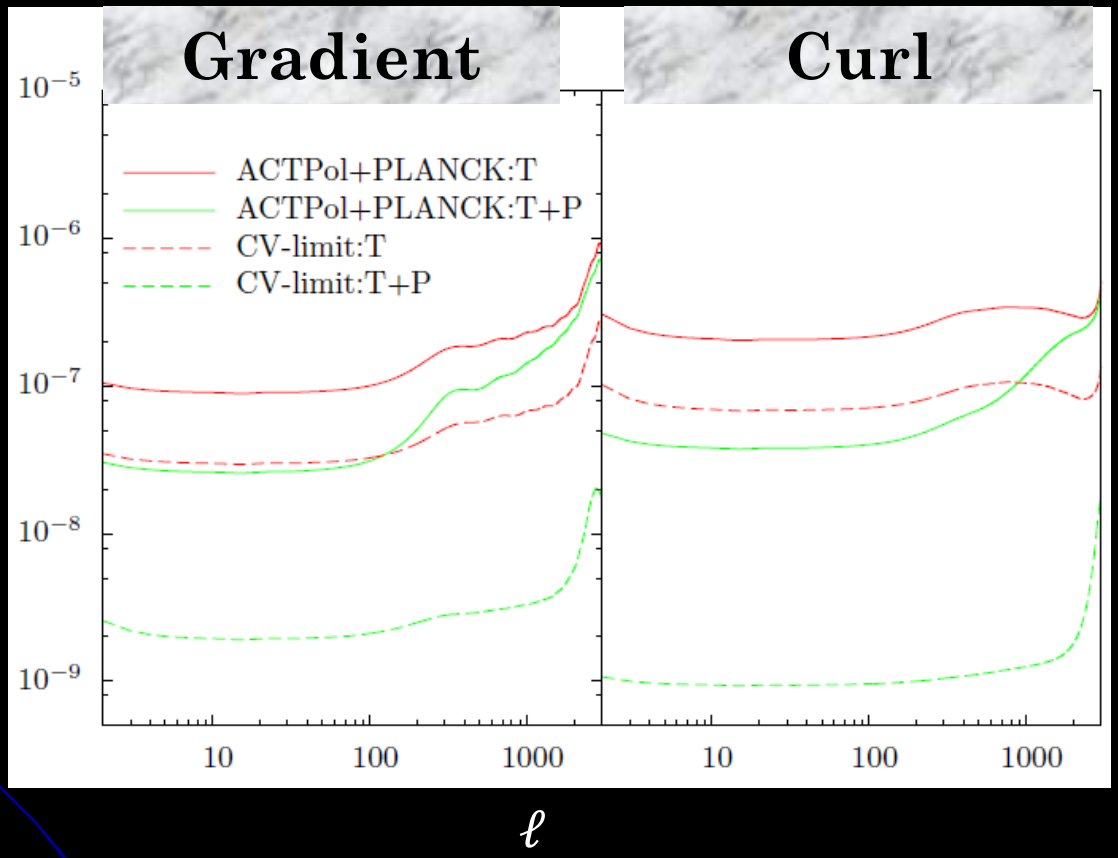

- **The variance of curl-mode estimator is similar to that of gradient-mode**
- **If we include polarization, the variance of curl-mode estimator is improved efficiently compared to that of gradient mode**

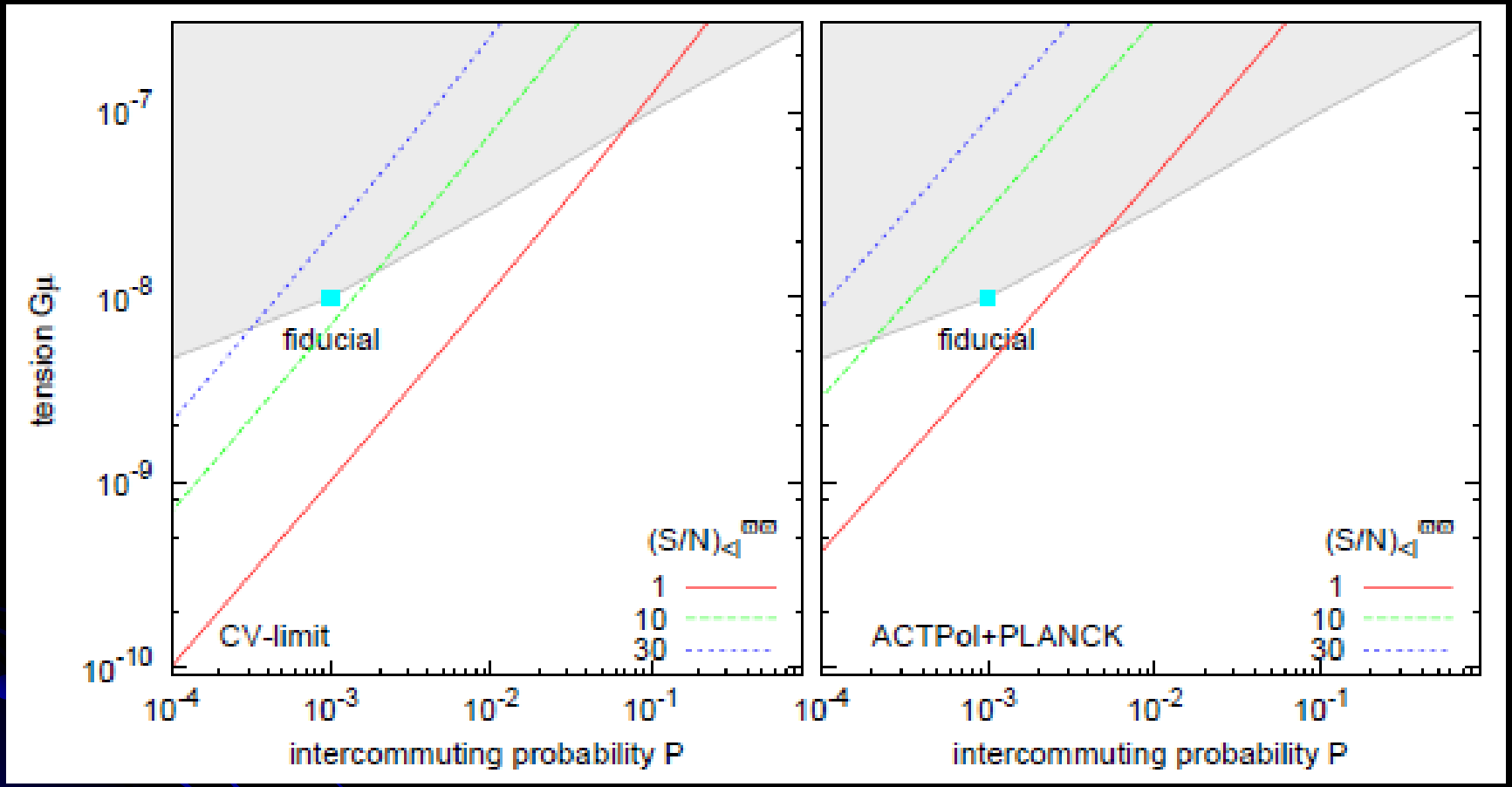

$$\omega(\theta,\varphi) = \int_0^{\chi_s} d\chi \frac{\chi_s - \chi}{\chi_s \chi} \frac{1}{\sin\theta} \frac{d}{d\chi} \left(\frac{\partial \Omega_\theta}{\partial \varphi} - \frac{\partial \Omega_\varphi}{\partial \theta} \right)$$

Vector and tensors contributions

Purposes

➢ Previous work including curl-mode reconstruction

✓ Cooray+'05

- empirically defined a quadratic estimator in flat-sky
- claimed that the gradient-mode estimator given in previous studies are biases in the presence of curl mode

➢ Our purposes

1. Derive estimator including curl mode

2. Lensing reconstruction from current CMB data and show cosmological implications

3. Compute the detectability of curl mode from primordial GWs and cosmic strings with full-sky estimator., and also compare with that of B-mode shear generated from cosmic strings.

Comparison with B-mode shear

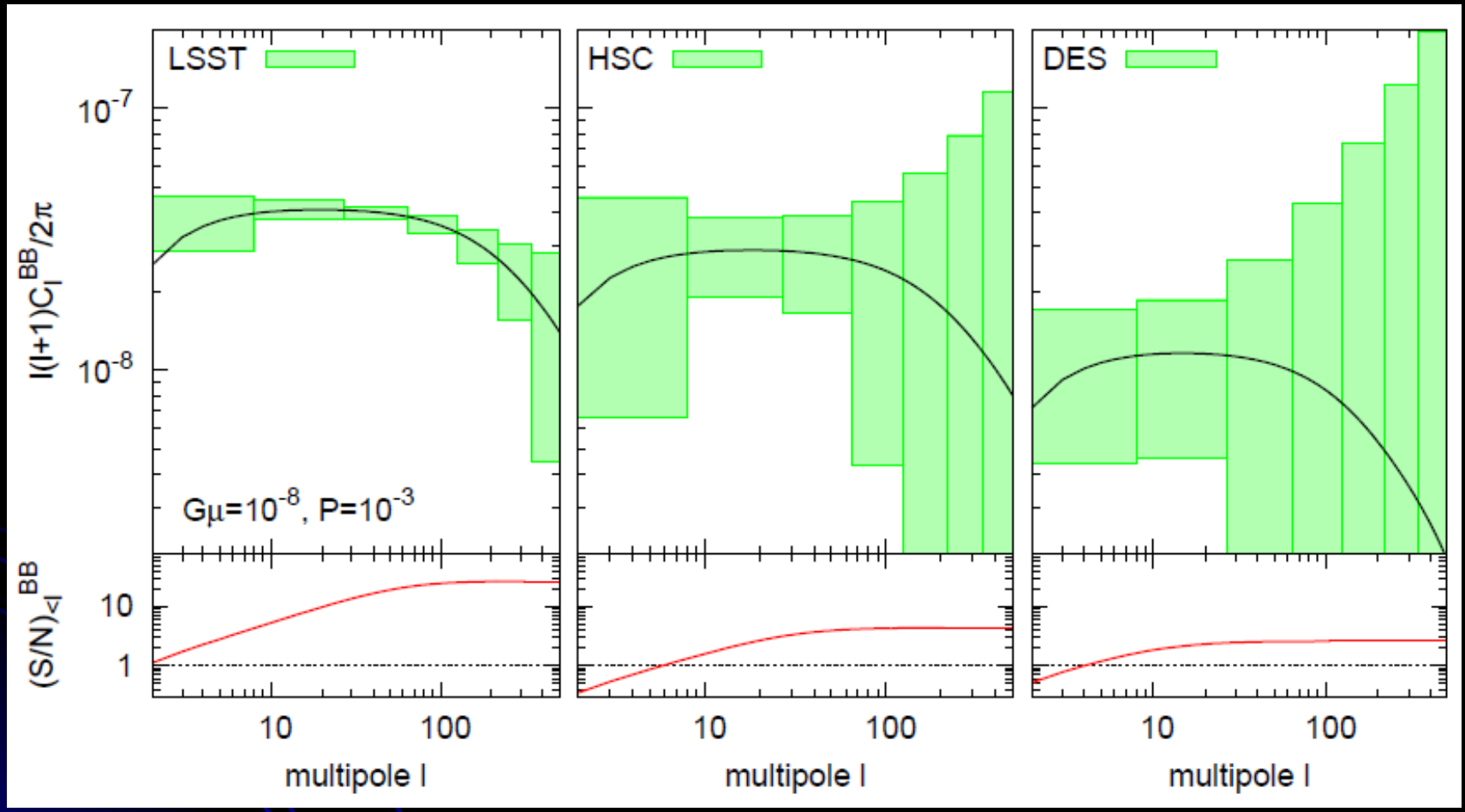

Yamauchi, TN & Taruya '12

Comparison with power spectrum

- S/N on $P - G\mu$ plane

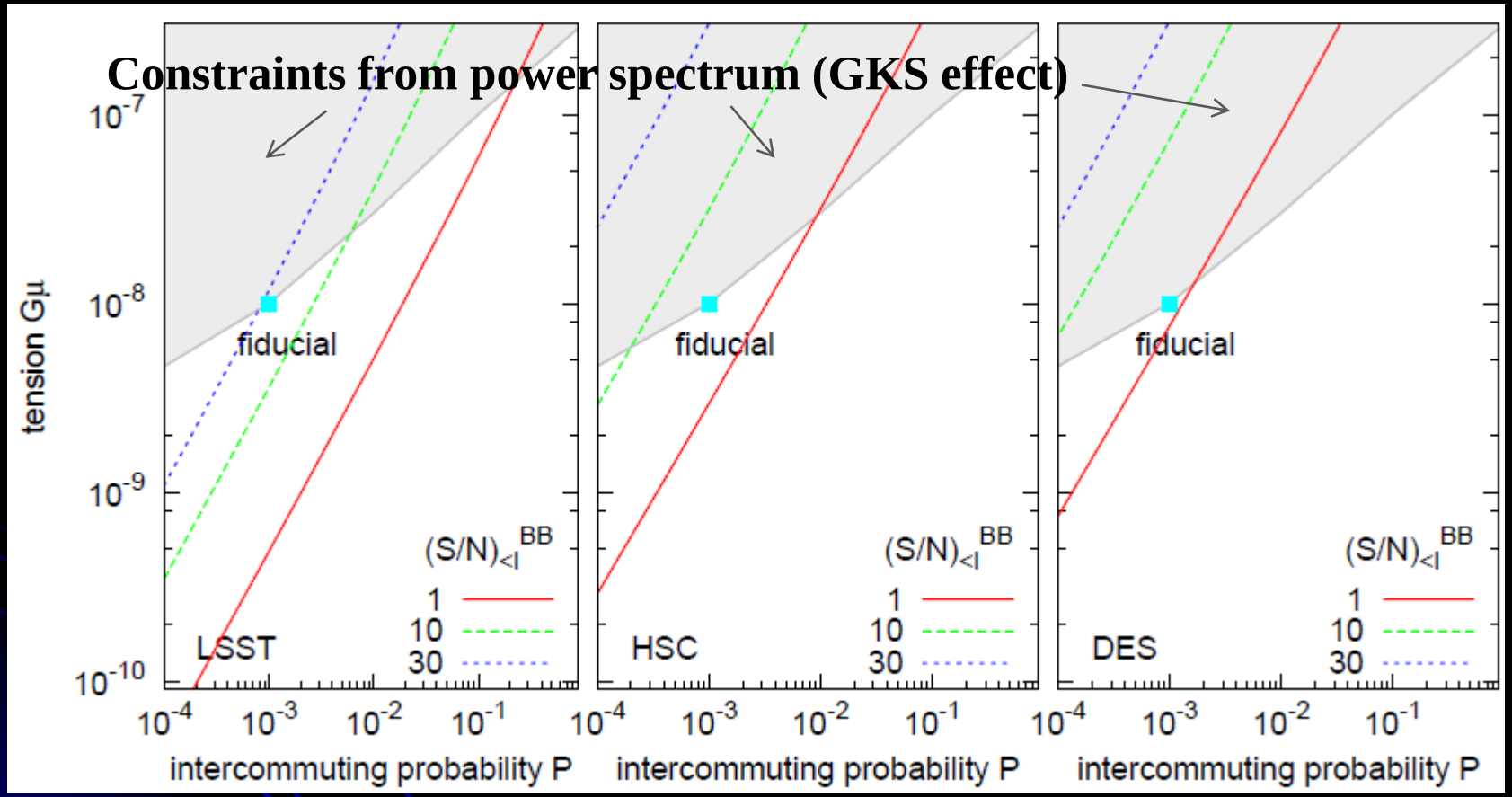

Yamauchi, TN & Taruya '12

LSST has sensitivity to cosmic strings with P~0.1 and $G\mu \sim 10^{-7}$

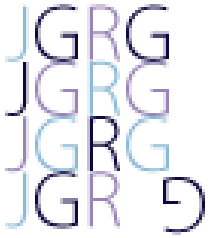

Hayato Motohashi, JGRG 22(2012)111417

"Cosmological constraints on sterile neutrino mass in f(R) gravity"

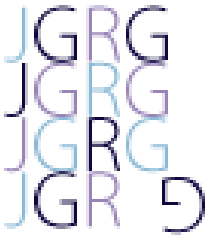

RESCEU SYMPOSIUM ON

GENERAL RELATIVITY AND GRAVITATION

JGRG 22



November 12-16 2012

Koshiba Hall, The University of Tokyo, Hongo, Tokyo, Japan



Cosmological constraints on sterile neutrino mass in $f(R)$ gravity

Hayato Motohashi
本橋 隼人
(RESCEU, The University of Tokyo)

in collaboration with
Alexei A. Starobinsky (Landau Inst.)
Jun'ichi Yokoyama (RESCEU)

2012.11.12-16 RESCEU symposium and JGRG22, Univ. of Tokyo

Two regimes of accelerated expansion

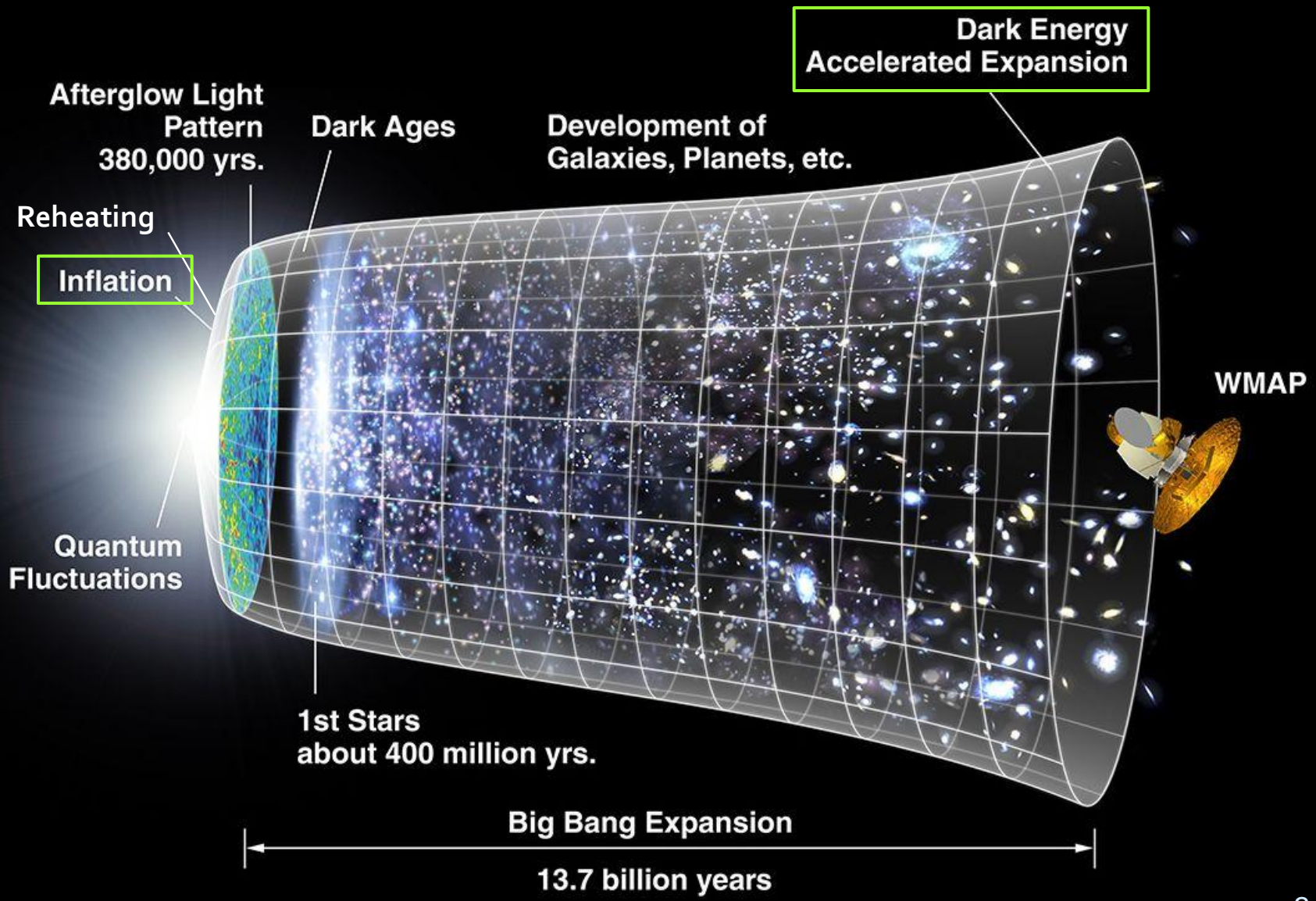

$f(R)$ gravity

can describe the accelerated expansion.

$$S = \frac{1}{16\pi G}\int d^4x\sqrt{-g}f(R) + S_m$$

Primordial inflation

Starobinsky, Phys.Lett. B91 (1980) 99

$$f(R) = R + \frac{R^2}{6M^2}$$

Late-time acceleration

Starobinsky, JETP Lett. 86, 157 (2007) [arXiv:0706.2041]

$$f(R) = R + \lambda R_s\left[\left(\frac{R^2}{R_s^2}+1\right)^{-n} - 1\right]$$

cf. $f(R)$ model for both accelerated expansion

Appleby, Battye, Starobinsky, JCAP 1006, 005 (2010) [arXiv:0909.1737]
H.M., Nishizawa, PRD 86 (2012) 093514 [arXiv:1204.1472]

Testing modified gravity



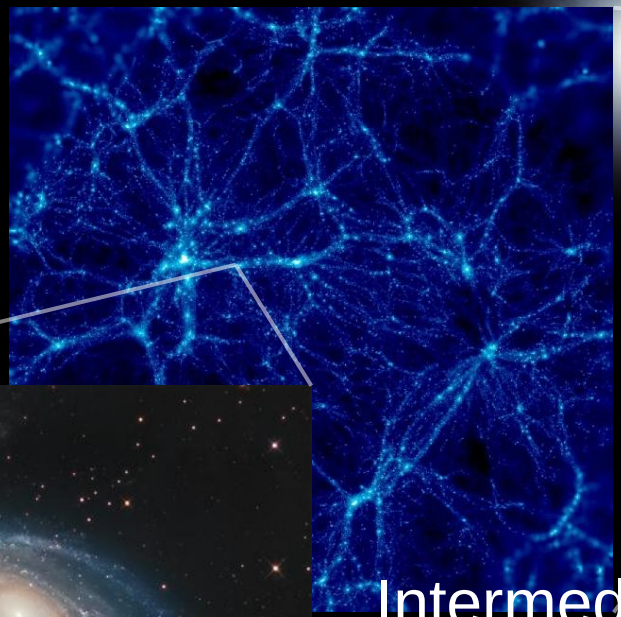





Horizon scale

$\sim 1\mathrm{Gpc}\ (10^{25}\mathrm{m})$

Expansion history

Intermediate scale

$\sim 100\mathrm{Mpc}\ (10^{24}\mathrm{m})$

Large scale structure

Local scale $\sim 1\mathrm{AU}\ (10^{11}\mathrm{m})$

Solar system test

Time variation of EoS parameter $w \equiv P/\rho$

$$w_{\rm DE} = w_0 + \frac{w_a z}{1+z}$$

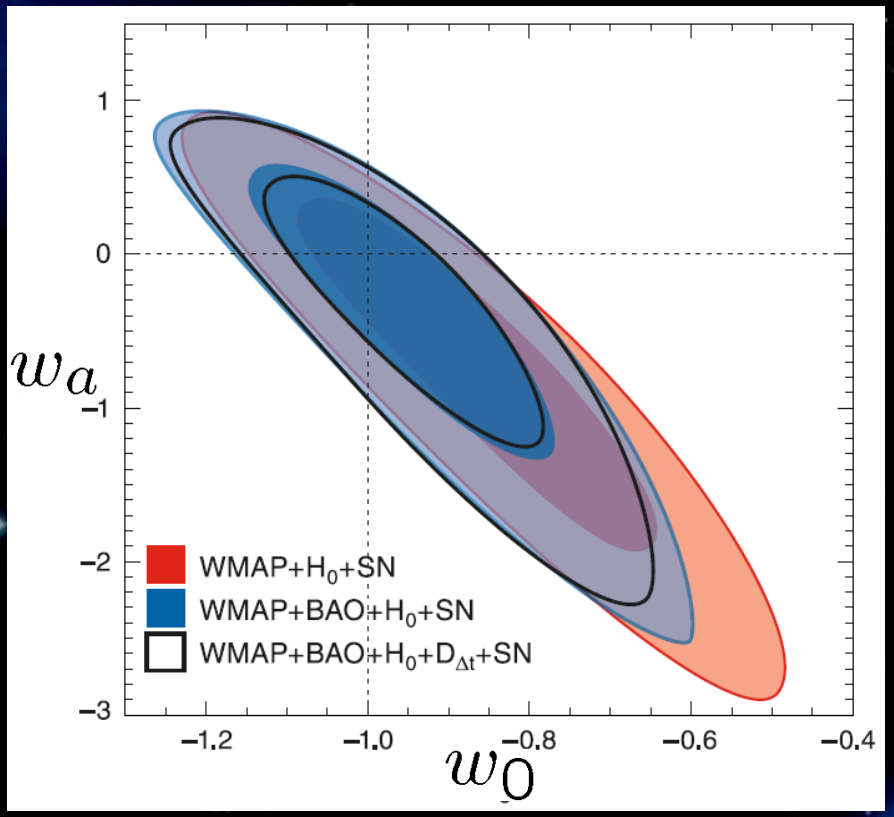

Komatsu et al.,
APJ Suppl. 192, 18 (2011)
[arXiv:1001.4538]

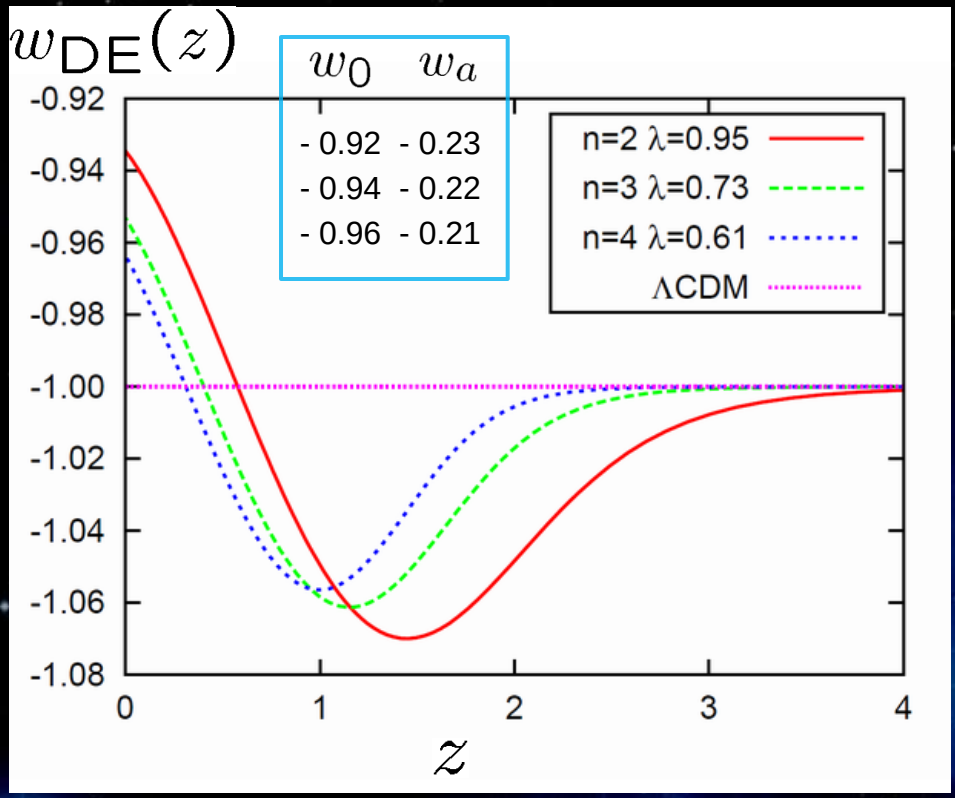

H.M., Starobinsky, Yokoyama
PTP 123 (2010) 887 [arXiv:1002.1141]

Growth index $\gamma(z)$

$$\frac{d\log\delta}{d\log a} = \Omega_m(z)^{\gamma(z)}$$

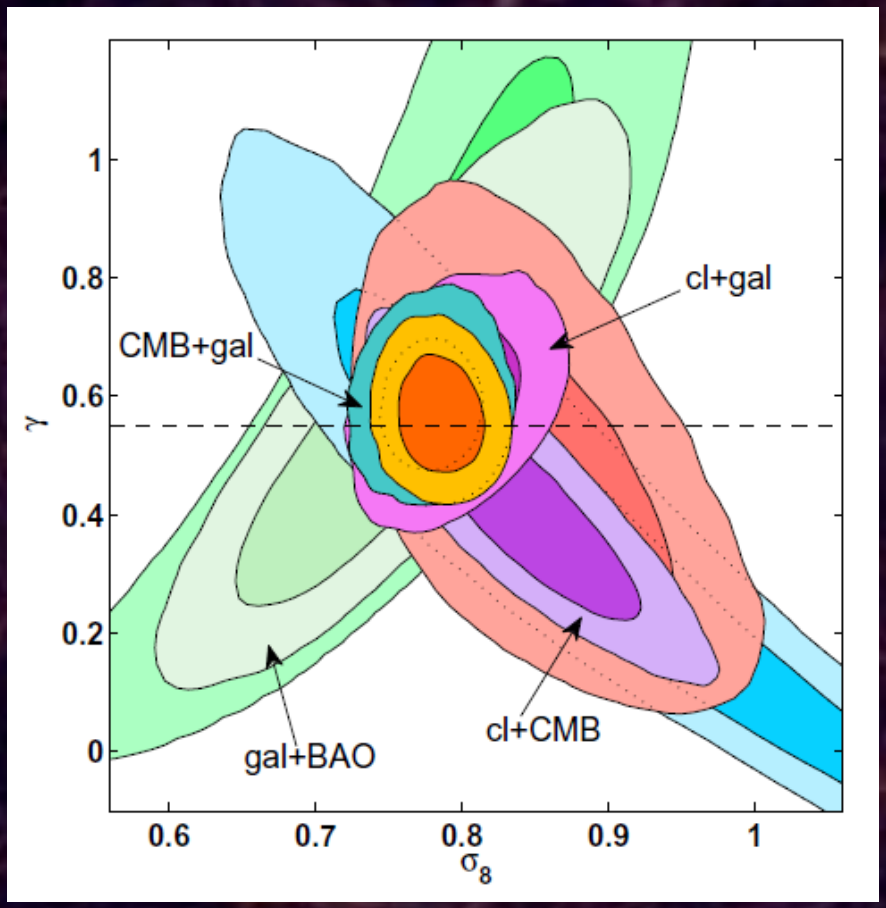

Rapetti et al., arXiv: 1205.4679

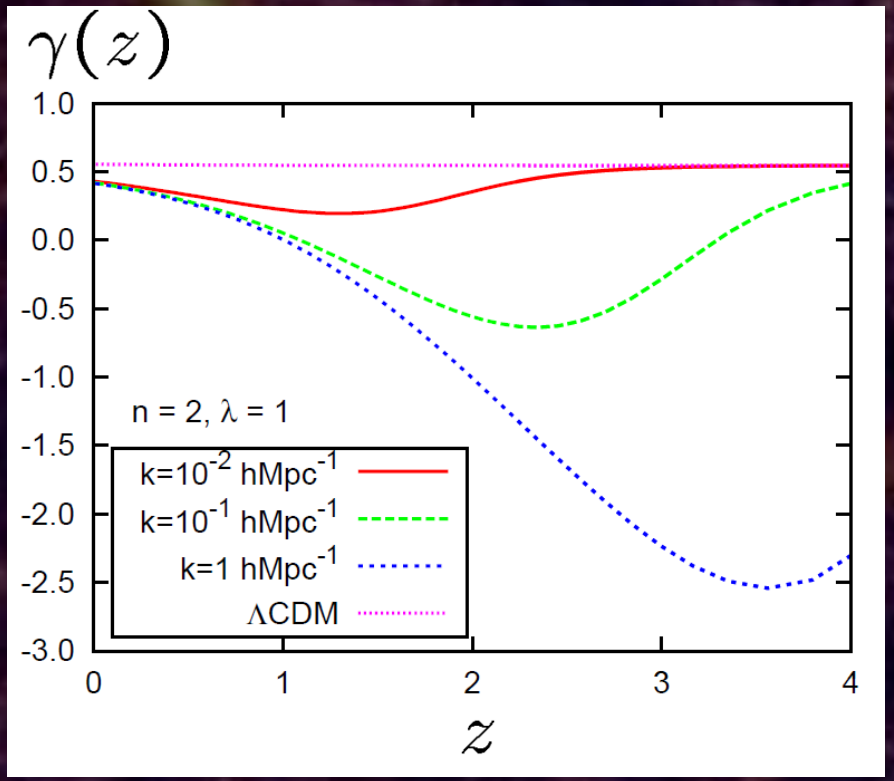

H.M., Starobinsky, Yokoyama
PTP 123 (2010) 887 [arXiv:1002.1141]

Additional transfer function in $f(R)$ gravity

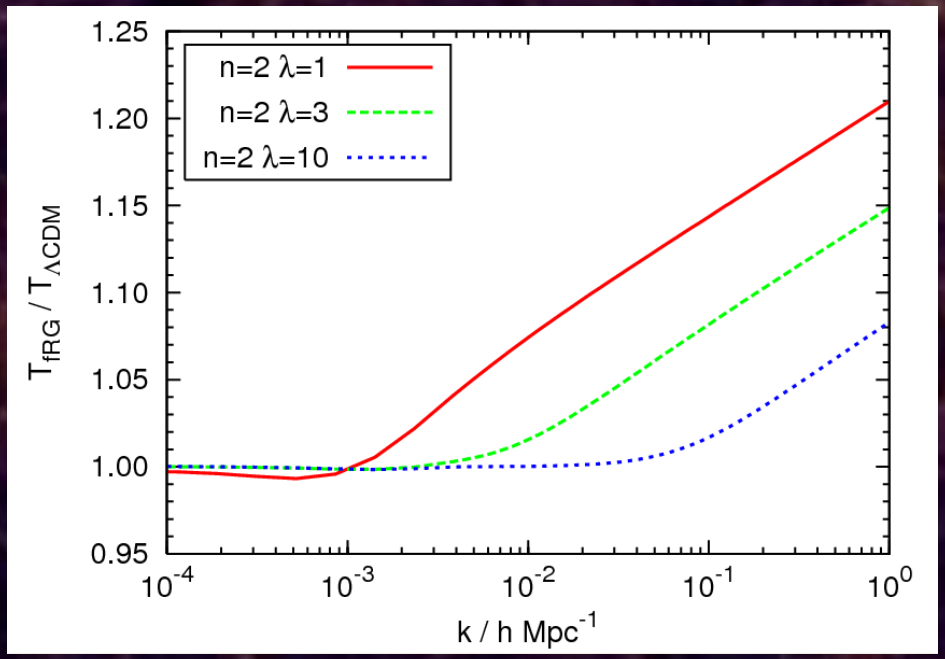

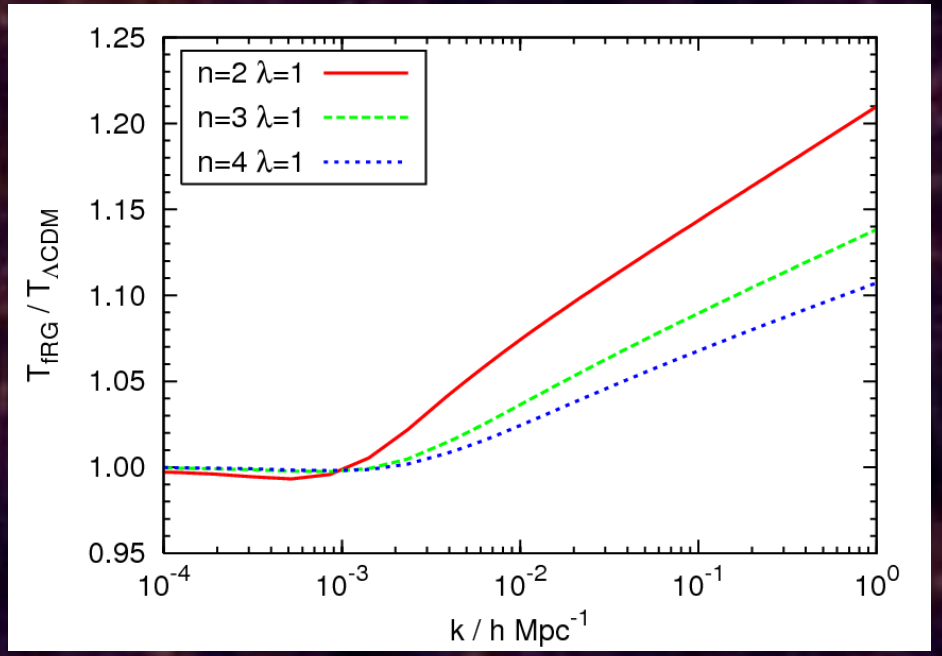

$f(R)$ gravity enhances matter power spectrum.

↕ cancel

Massive neutrino suppresses matter power spectrum.

Constraint on $N_{\rm eff}$ from BBN

Abazajian et al [arXiv:1204.5379]

Model	Data	68% (95%) N_{eff}	Ref.
η+N_{eff}	η_{CMB}+Y_p+D/H	$3.8^{(+0.8)}_{(-0.7)}$	[331]
	η_{CMB}+Y_p+D/H	$< (4.05)$	[332]
	Y_p+D/H	3.85 ± 0.26	[333]
	Y_p+D/H	3.82 ± 0.35	[333]
	Y_p+D/H	3.13 ± 0.21	[333]
η+N_{eff}, ($\Delta N_{eff} \equiv N_{eff} - 3.046 \geq 0$)	η_{CMB}+D/H	3.8 ± 0.6	[122]
	η_{CMB}+Y_p	$3.90^{+0.21}_{-0.58}$	[122]
	Y_p+D/H	$3.91^{+0.22}_{-0.55}$	[122]

[331] Izotov, Thuan, Astrophys.J. 710, L67 (2010) [arXiv:1001.4440]
[332] Mangano,Serpico, Phys.Lett. B701, 296 (2011) [arXiv:1103.1261]
[333] Nollett, Holder [arXiv:1112.2683]
[122] Hamann et al, JCAP 1109, 034 (2011) [arXiv:1108.4136]

Constraints on $N_{\rm eff}$ and $\sum m_\nu$ in ΛCDM

CMB

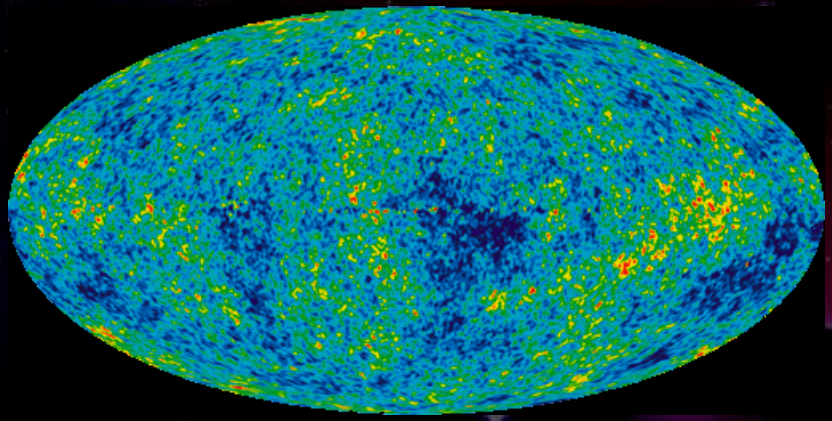

Komatsu et al.,
APJ Suppl. 192, 18 (2011)
[arXiv:1001.4538]

+

ΛCDM

⇩

LSS

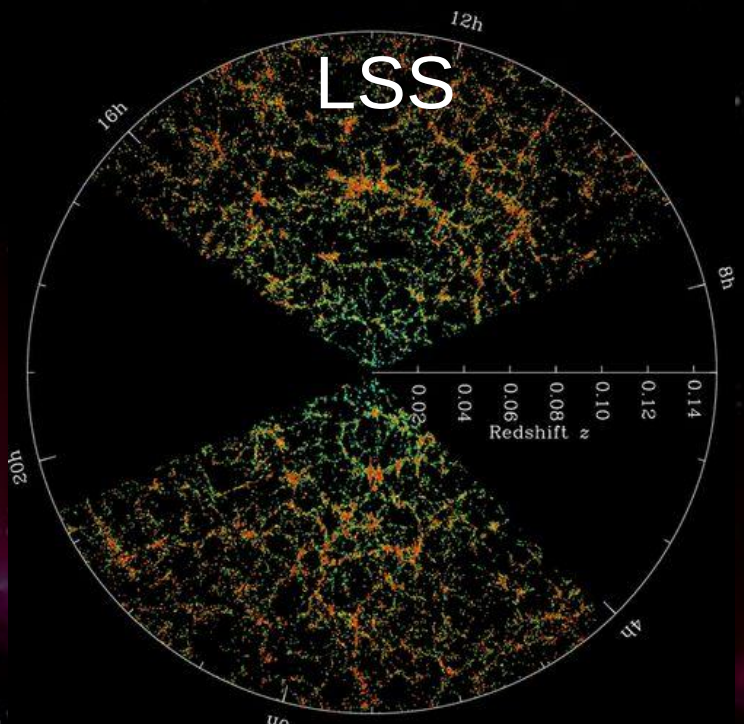

Reid et al,
Mon.Not.Roy.Astron.Soc. 404
(2010) 60 [arXiv:0907.1659]

$$\sum m_\nu < 0.44\text{eV} \quad (95\%\ \text{CL})$$

$$N_{\rm eff} = 4.34^{+0.86}_{-0.88} \quad (68\%\ \text{CL})$$

Constraints on $N_{\rm eff}$ and $\sum m_\nu$ in ΛCDM

ABSTRACT

Recent indications from both particle physics and cosmology suggest the existence of more than three neutrino species. In cosmological analyses the effects of neutrino mass and number of species can in principle be disentangled for fixed cosmological parameters. However, since we do not have perfect measurements of the standard Λ Cold Dark Matter model parameters some correlation remains between the neutrino mass and number of species, and both parameters should be included in the analysis. Combining the newest observations of several cosmological probes (cosmic microwave background, large scale structure, expansion rate) we obtain $N_{\rm eff} = 3.58^{+0.15}_{-0.16}(68\%\,{\rm CL})^{+0.55}_{-0.53}(95\%\,{\rm CL})$ and $\sum m_\nu < 0.60\,{\rm eV}(95\%\,{\rm CL})$, which are currently the strongest constraints on $N_{\rm eff}$ and $\sum m_\nu$ from an analysis including both parameters. The preference for $N_{\rm eff} > 3$ is now at a 2σ level.

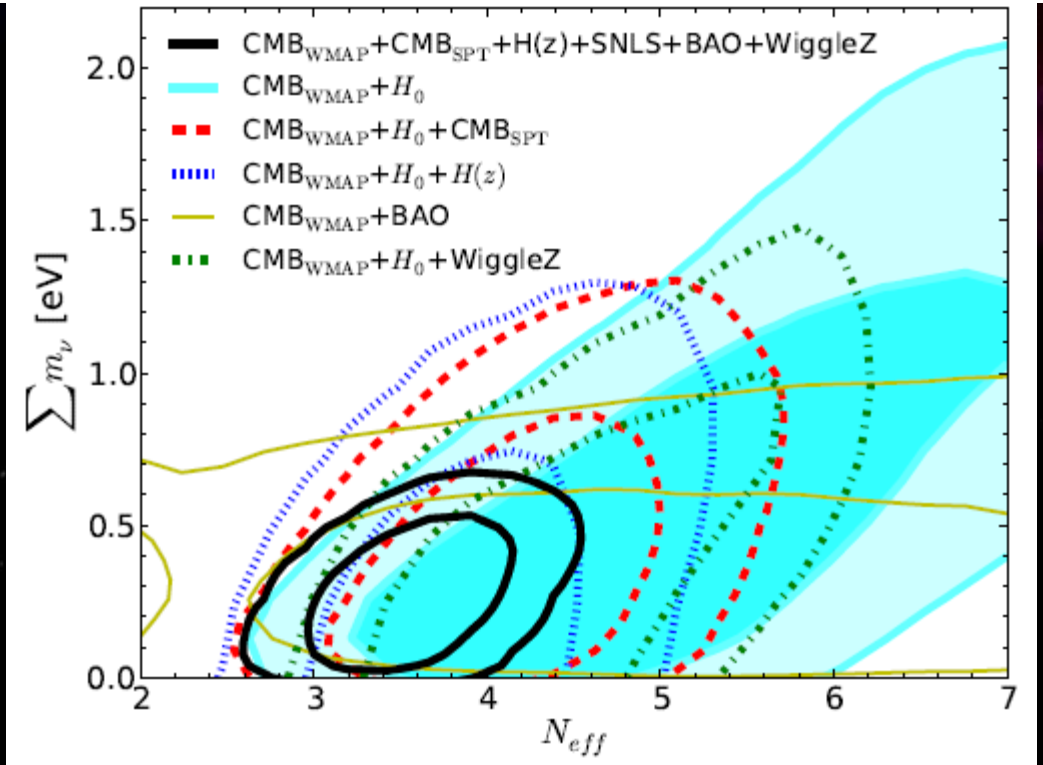

Riemer-Sorensen et al [arXiv:1210.2131]

ΛCDM cosmology

⇩

sub-eV

sterile neutrino

Neutrino oscillation

Sterile neutrino mass $\gtrsim$ 1 eV

⇔ ΛCDM model

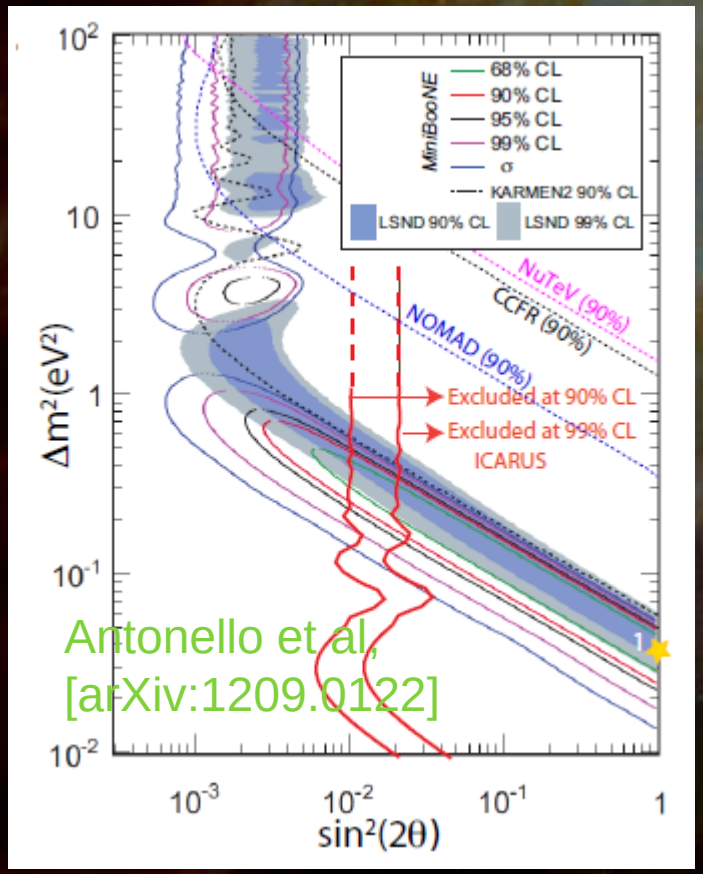

Antonello et al,
[arXiv:1209.0122]

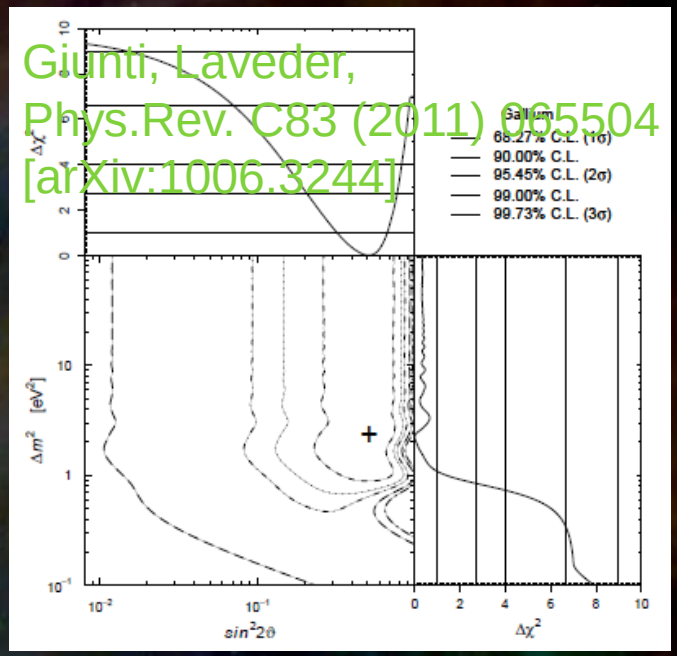

Giunti, Laveder,
Phys.Rev. C83 (2011) 065504
[arXiv:1006.3244]

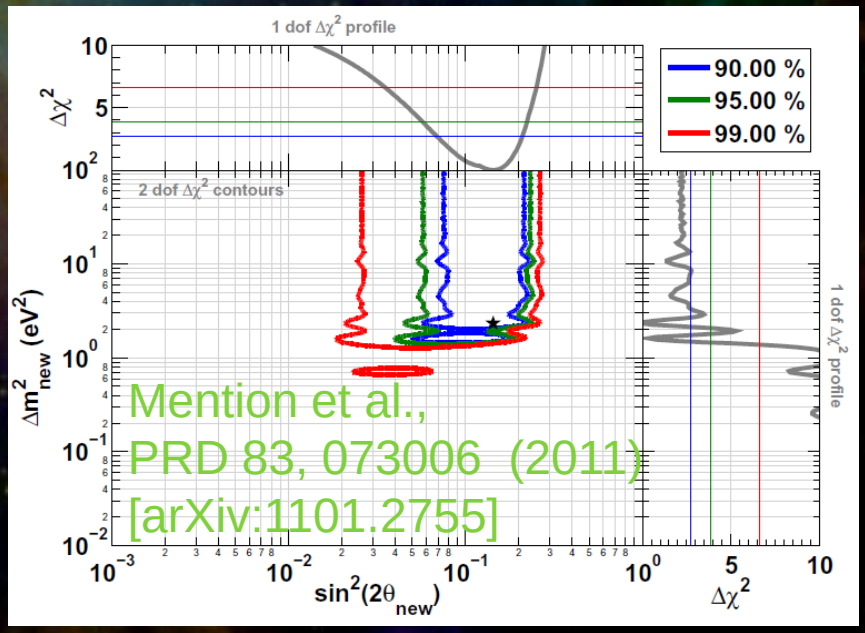

Mention et al.,
PRD 83, 073006 (2011)
[arXiv:1101.2755]

MCMC analysis: ΛCDM vs $f(R)$ gravity

H.M., Starobinsky and Yokoyama, arXiv:1203.6828

- 3 massless and 1 massive neutrino with mass = 1 eV
- WMAP7, SDSS DR 7 $(0.02h\mathrm{Mpc}^{-1} \leq k \leq 0.08h\mathrm{Mpc}^{-1})$
- Better fit : $\Delta\chi^2 = 10.7$ $(\Delta\mathrm{AIC} = 8.7)$
- GR : $\sigma_8 = 0.661^{+0.023}_{-0.027}$, $f(R) : \sigma_8 = 0.815^{+0.105}_{-0.066}$

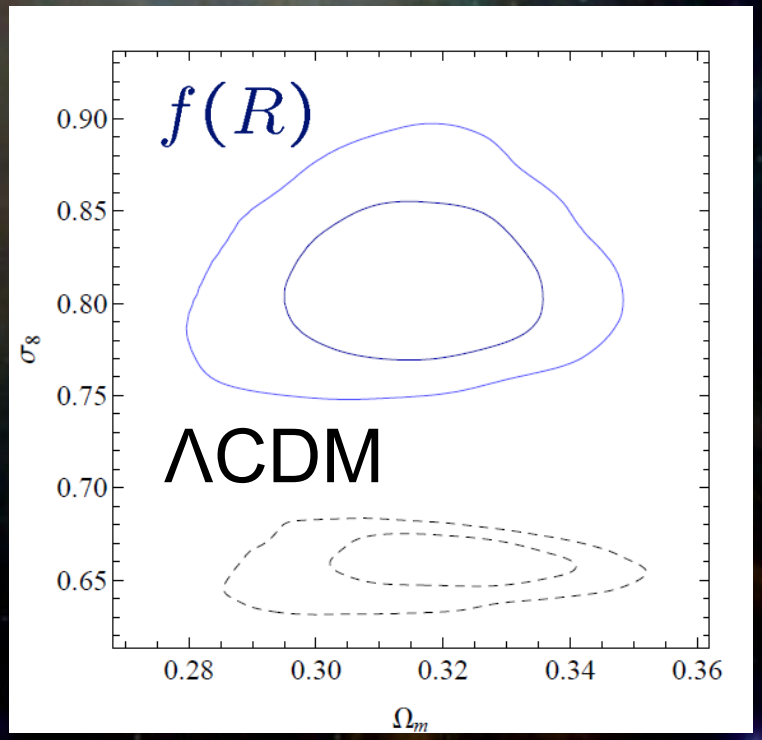

MCMC analysis: ΛCDM vs $f(R)$ gravity

H.M., Starobinsky and Yokoyama, arXiv:1203.6828

- 3 massless and 1 massive neutrino with mass = 1 eV
- WMAP7, SDSS DR 7 $(0.02h\mathrm{Mpc}^{-1} \leq k \leq 0.08h\mathrm{Mpc}^{-1})$
- Better fit : $\Delta\chi^2 = 10.7$ $(\Delta\mathrm{AIC} = 8.7)$
- GR : $\sigma_8 = 0.661^{+0.023}_{-0.027}$, $f(R)$: $\sigma_8 = 0.815^{+0.105}_{-0.066}$

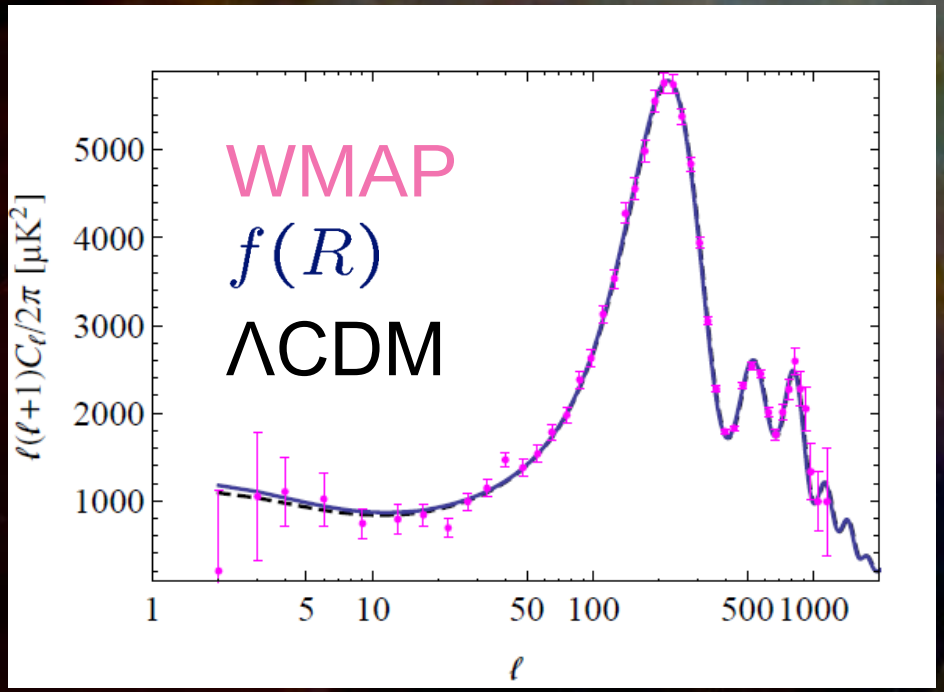

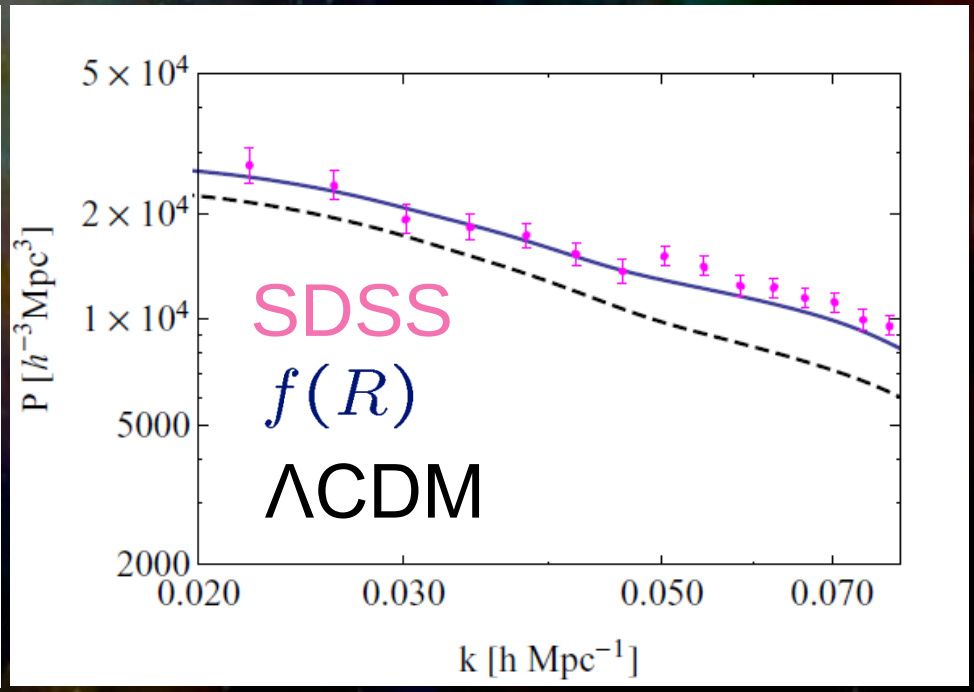

Summary

- Cosmology based on ΛCDM model

  Sterile neutrino mass $<$ 1 eV

- Neutrino oscillation experiments

  Sterile neutrino mass $\gtrsim$ 1 eV

- $f(R)$ gravity can resolve the tension.

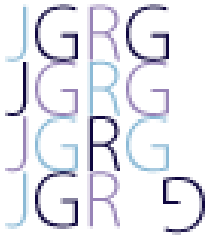

Tatsuya Narikawa, JGRG 22(2012)111418

"Testing gravity with galaxy cluster"

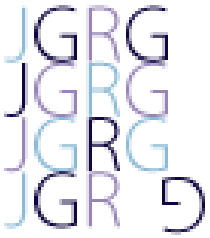

RESCEU SYMPOSIUM ON

GENERAL RELATIVITY AND GRAVITATION

JGRG 22



November 12-16 2012

Koshiba Hall, The University of Tokyo, Hongo, Tokyo, Japan



JGRG22 RESCEU November 14th, 2012

Testing gravity with galaxy cluster

Tatsuya Narikawa

(RESCEU,U-Tokyo)



Outline

- Modified gravity
- Screening mechanism
- Cluster lensing
- Summary

Based on
TN, Yamamoto, JCAP (2012)
TN, Kobayashi, Yamauchi, Saito, work in progress

Modified Gravity

- Motivation: Discovery of current cosmic acceleration

  [Riess, Schmidt et al. '98, Perlmutter et al. '99]

$\ddot{a} > 0$

→Breakdown of GR at large-scales ?

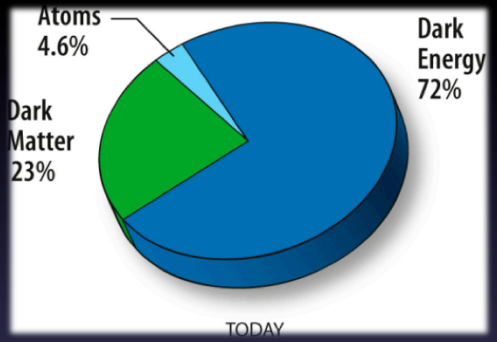

[WMAP]

- As an alternative to dark energy

- Modified gravity with extra fields ϕ

Scalar-tensor gravity, f(R) gravity, DGP model,

Galileon model, Decoupling-limit of Ghost-free massive gravity, etc.

[Mukohyama-san's talk]

Local Gravity Constraints

- In MG, new d.o.f. ϕ mediates fifth-force.

$\rightarrow$deviation from GR on large-scales.

- However, local gravity constraints are strong:
  - e.g. $\gamma_{PPN}-1=(2.1\pm2.3)\times10^{-5}$ by time-delay [Bertotti et al. '03]
- MG need to evade local gravity tests with screening mechanisms!

[Cassini spacecraft]

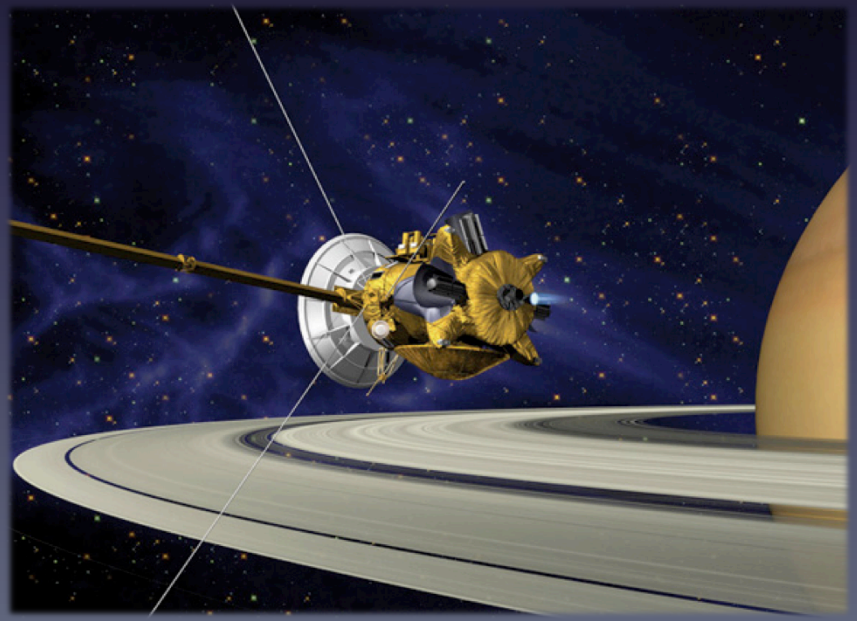

Screening Mechanisms of ϕ in Local Region

- Kinetic type: Vainshtein mechanism [Vainshtein '72]
  - Large kinetic term⇔weak coupling: Galileon-type
- Potential type: Chameleon mechanism, Symmetron
  [Khoury & Weltman '04, Hinterbichler & Khoury '10]
  - Large curvature of potential⇔massive scalar field m_ϕ

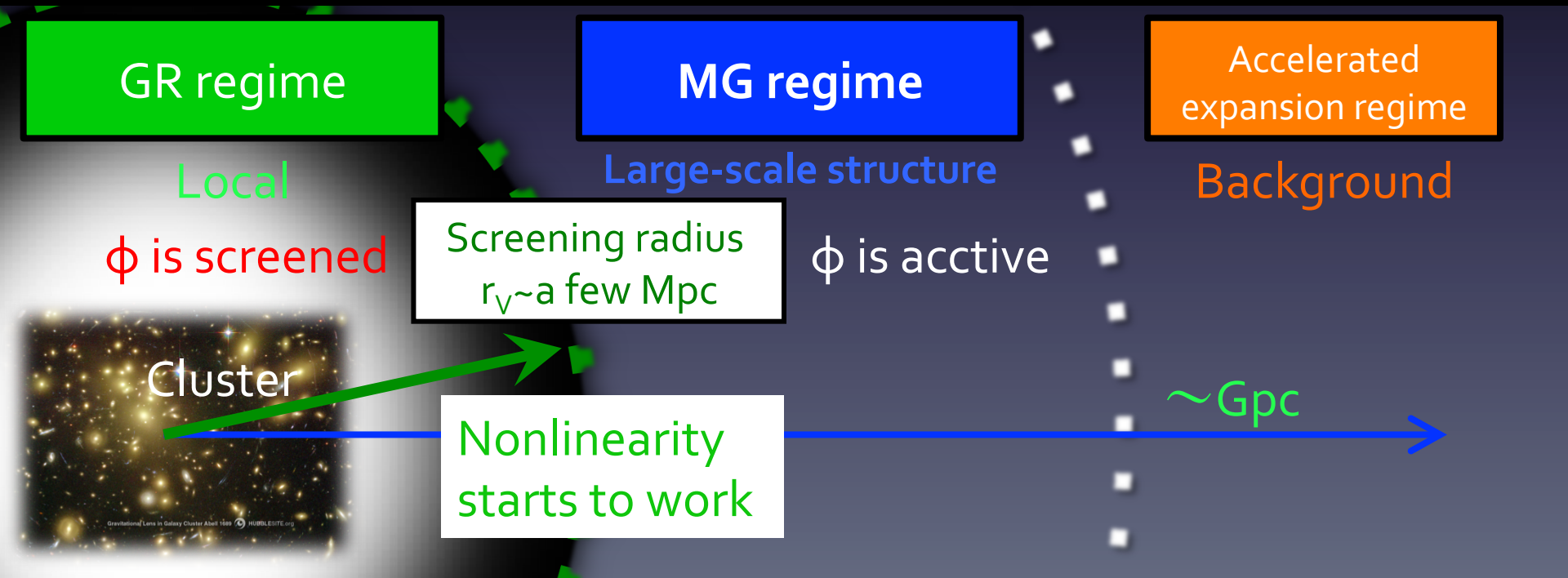

Observational Test of Modified Gravity

- Whether the screening mechanism works completely or not around high-density regions ?
- Gravitational lensing of galaxy clusters may be useful to test modified gravity
- Key: lensing potential $\triangle\Phi_+ \equiv \triangle(\Phi+\Psi)/2$

[TN, Yamamoto, '12]

- Large amount of data of cluster lensing will be provided by Hyper Suprime-Camera (HSC) [Takada-san's talk]

Stacked Cluster Lensing Analysis

The average distortion profile [Itoh-san's talk]

- is less sensitive to individual substructures/asphericity
- helps to improve the S/N

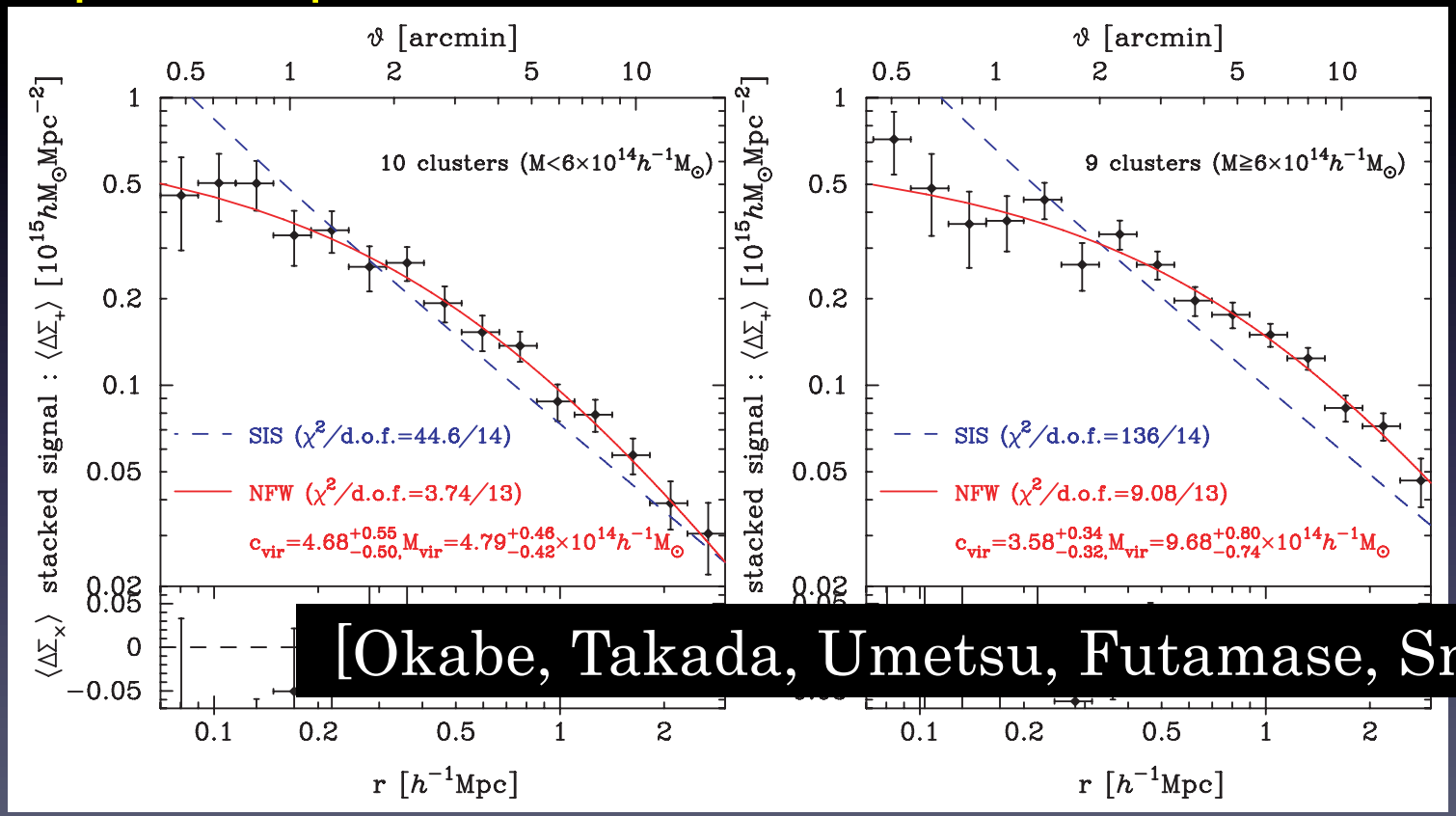

[Okabe, Takada, Umetsu, Futamase, Smith '10]

- may be also useful to test modified gravity

Galileon-type Modified Gravity

- Motivation: decoupling limit of DGP model

$\mathcal{L}_{\rm int} \sim X\Box\phi$: higher-derivative term

where ϕ : scalar field, $X \equiv -\frac{1}{2}(\partial\phi)^2$

enjoy Galileon shift symmetry: $\partial_\mu\phi \to \partial_\mu\phi + c_\mu$

$\to$ 「
- Cosmic acceleration
- 2nd order EOM
- Vainshtein mechanism 」

[DLofDGP] Luty, Porrati & Rattazzi '03, Nicolis & Rattazzi '04

Vainshtein Mechanism in Simple Model

$$\mathcal{L}_\phi = 3\phi\Box\phi - \frac{2}{\Lambda^3}(\partial\phi)^2\Box\phi + \frac{2}{M_{\rm Pl}}\phi T$$



ϕEOM

$$3\Box\phi + \frac{1}{\Lambda^3}\left((\Box\phi)^2 - (\partial_\mu\partial_\nu\phi)^2\right) = -\frac{1}{M_{\rm Pl}}T$$

At $r \ll r_V$: Large kinetic term ⇔ Weak coupling to matter

$$\phi'(r) \sim \left(\frac{M}{2M_{\rm Pl}}\frac{\Lambda^3}{r}\right)^{1/2} \ll \partial_r\Phi_{\rm N} \quad \leftarrow \text{screened !}$$

where Vainshtein radius: $r_V \equiv (M/M_{\rm Pl})\Lambda^{-1}$

[Luty, Porrati & Rattazzi '03, Nicolis & Rattazzi '04]

The Most General Second-Order Scalar-Tensor Theory [Horndesky '74]

$$S = \int d^4x\sqrt{-g}[\mathcal{L} + \mathcal{L}_m]$$

assume matter do not directly couple to ϕ

$$\mathcal{L} = K(\phi, X) - G_3(\phi, X)\Box\phi$$
$$+ G_4(\phi, X)R + G_{4X} \times (\text{field derivatives})$$
$$+ G_5(\phi, X)G_{\mu\nu}\nabla^\mu\nabla^\nu\phi$$
$$- \frac{1}{6}G_{5X} \times (\text{field derivatives})$$

where $G_{iX} \equiv \partial G_i/\partial X$

4 arbitrary functions of ϕ, X

is equivalent to the generalized galileon

[Deffayet et al. '11, Kobayashi, Yamaguchi , Yokoyama '11]

Background solution

$$ds^2 = \eta_{\mu\nu} dx^\mu dx^\nu$$

$$\phi = \phi_0 = \text{const}, \;\; X = 0$$

Inorder to admit this solution, we require that

$$K(\phi_0, 0) = 0, \;\; K_\phi(\phi_0, 0) = 0$$

Spherical symmetric perturbations produced by a nonrelativistic matter

$$ds^2 = -[1 + 2\Phi(r)]dt^2 + [1 - 2\Psi(r)]\delta_{ij} dx^i dx^j$$

$$\phi = \phi_0 + \varphi(r)$$

All the coefficients are evaluated at the background.

We will ignore the mass term $K_{\phi\phi}$.

Static-Spherically Symmetric Configurations

Metric EOM:

$$\frac{M_{\rm Pl}^2}{2}\frac{(r^2\Psi')'}{r^2} - M_{\rm Pl}\xi\frac{(r^2\varphi')'}{2r^2} - \frac{M_{\rm Pl}}{\Lambda^3}\alpha\frac{[r(\varphi')^2]'}{2r^2} - \frac{3M_{\rm Pl}}{\Lambda^6}\beta\frac{[(\varphi')^3]'}{6r^2} = -\frac{1}{4}T_t{}^t$$

$$M_{\rm Pl}^2(\Psi'-\Phi') - 2M_{\rm Pl}\xi\varphi' - \frac{M_{\rm Pl}}{\Lambda^3}\alpha\frac{(\varphi')^2}{r} = 0$$

ϕEOM:

$$\eta\frac{(r^2\varphi')'}{r^2} - 2\frac{\mu}{\Lambda^3}\frac{[r(\varphi')^2]'}{r^2} + 2M_{\rm Pl}\xi\frac{[r^2(2\Psi-\Phi)']'}{r^2} + 4\frac{M_{\rm Pl}}{\Lambda^3}\alpha\frac{[r\varphi'(\Psi'-\Phi')]'}{r^2} + 2\frac{\nu}{\Lambda^6}\frac{[(\varphi')^3]'}{r^2} - \frac{6M_{\rm Pl}}{\Lambda^6}\beta\frac{[(\varphi')^2\Phi']'}{r^2} = 0$$

where six dimensionless parameters:

ξ, η, μ, α, ν, β are functions of K_X, $G_{3\phi}$, G_{3X}, G_{4X}, $G_{5\phi}$,.....

(cf. Vainshtein mechanism under considering background evolution [Kimura, Kobayashi, Yamamoto '12])

Quintic Scalar-Field Equation

We arrive at

$$P(x,A) := \xi A(r) + \left(\frac{\eta}{2} + 3\xi^2\right) x + \left[\mu + 6\alpha\xi - 3\beta A(r)\right] x^2$$
$$+ \left(\nu + 2\alpha^2 + 4\beta\xi\right) x^3 - 3\beta^2 x^5 = 0$$

where we define

$$x = \frac{1}{\Lambda^3}\frac{\varphi'}{r}, \quad A(r) = \frac{1}{M_{\rm Pl}\Lambda^3}\frac{M(r)}{8\pi r^3}$$

which are dimensionless.

M(r) is the enclosed mass.

Scalar-Field Equation [cf. Sbisa, Niz, Koyama, Tasinato '12]

We solve

$$x = \frac{1}{\Lambda^3}\frac{\varphi'}{r}, \quad A(r) = \frac{1}{M_{\rm Pl}\Lambda^3}\frac{M(r)}{8\pi r^3}$$

$$P(x,A) := \xi A(r) + \left(\frac{\eta}{2} + 3\xi^2\right)x + \left[\mu + 6\alpha\xi - 3\beta A(r)\right]x^2$$

$$+ \left(\nu + 2\alpha^2 + 4\beta\xi\right)x^3 - 3\beta^2 x^5 = 0$$

for the inner region (A>>1) and the outer region (A<<1).

We then derive the conditions under which the two solutions are matched smoothly in an intermediate region.

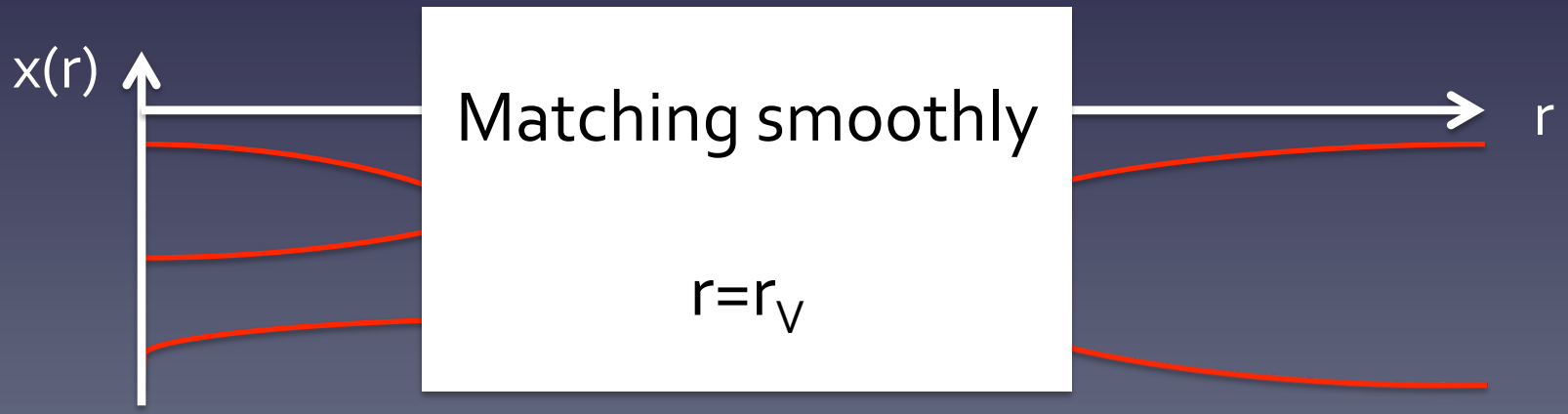

Outer Solution: Asymptotically Flat

- In the outer region (A<<1), there is always a decaying solution,

$$x \approx x_{\rm f} := -\frac{2\xi A(r)}{\eta + 6\xi^2}$$

which is obtained by neglecting the nonlinear terms in P(x,A)=0.

The other solutions do not correspond to an asymptotically flat spacetime.

Inner Solution: Vainshtein

- In the inner region (A>>1), P=0 reduces to

$$P(x, A) \approx \xi A - 3\beta A x^2 - 3\beta^2 x^5 \approx 0$$

We have a solution (ξβ>0):

$$x \approx x_\pm := \pm\sqrt{\frac{\xi}{3\beta}} = \text{const}$$

(P(x-,A) does not depend on A.)

For this solution, we have Newtonian behavior:

$$\Psi'/r \simeq \Phi'/r \propto A$$

This is therefore the Vainshtein solution.

For simplicity we focus on the case of ξ>0.

Matching of Two Solutions

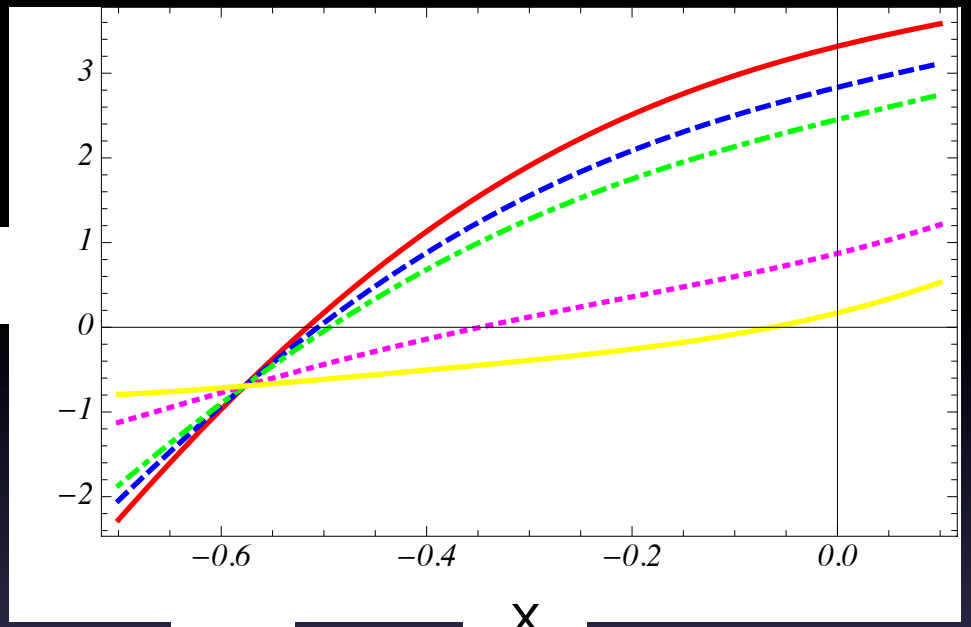

↑
A
↓

In this case, P(x)=o has a single real root in (x-,o) for any A>o.

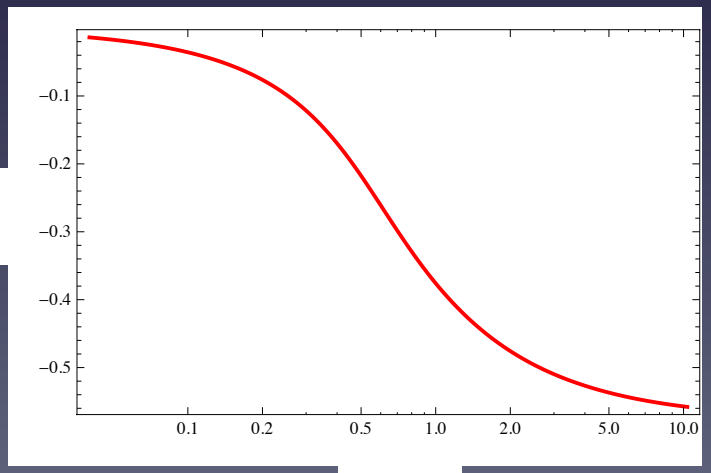

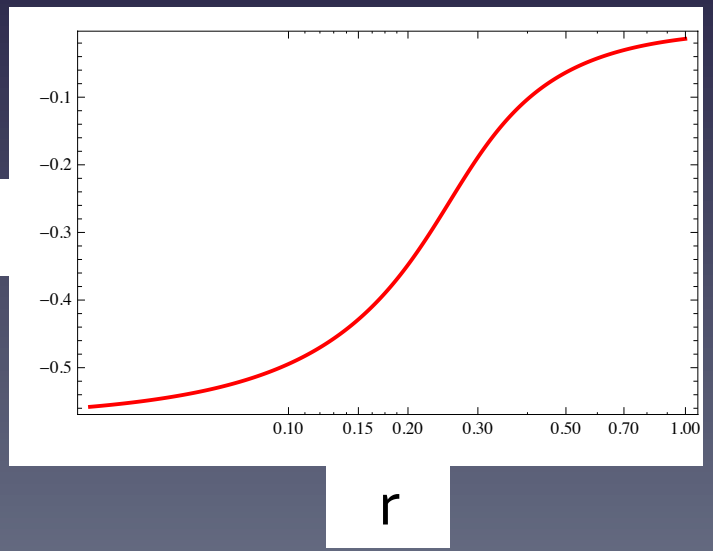

Decoupling Limit of Massive Gravity

[de Rham, Heisenberg '11]

Decoupling limit: $M_{pl}\to\infty$, $m_g\to 0$, $\Lambda^3=M_{pl}m_g^2$ =fixed.

The corresponds to

$$\mathcal{E}^{\alpha\beta}_{\mu\nu}H_{\alpha\beta}$$

$$K=0=G_3,\ G_4=\frac{M_{\rm pl}^2}{2}+M_{\rm Pl}\phi+\frac{M_{\rm Pl}}{\Lambda^3}\alpha X,\ G_5=-3\frac{M_{\rm Pl}}{\Lambda^6}\beta X$$

One finds

$$\eta=\mu=\nu=0,\ \xi=1,\ \alpha\neq 0,\ \beta\neq 0$$

The condition of smooth matching of the two solutions:

$$\alpha < 0 \text{ or } \frac{\sqrt{\beta}}{\alpha} \geq \sqrt{\frac{5+\sqrt{13}}{24}} \sim 0.6$$

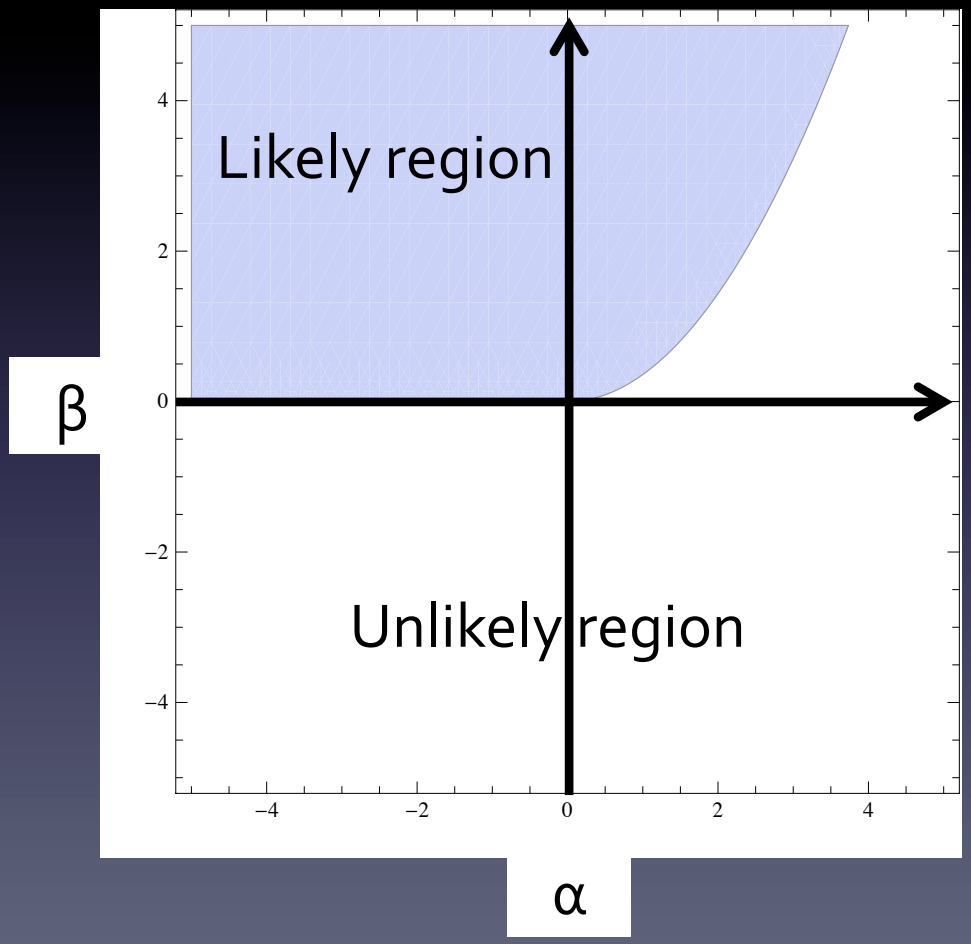

Explore the observationally allowed region with cluster lensing.

Cluster Lensing

Mass map (shear)

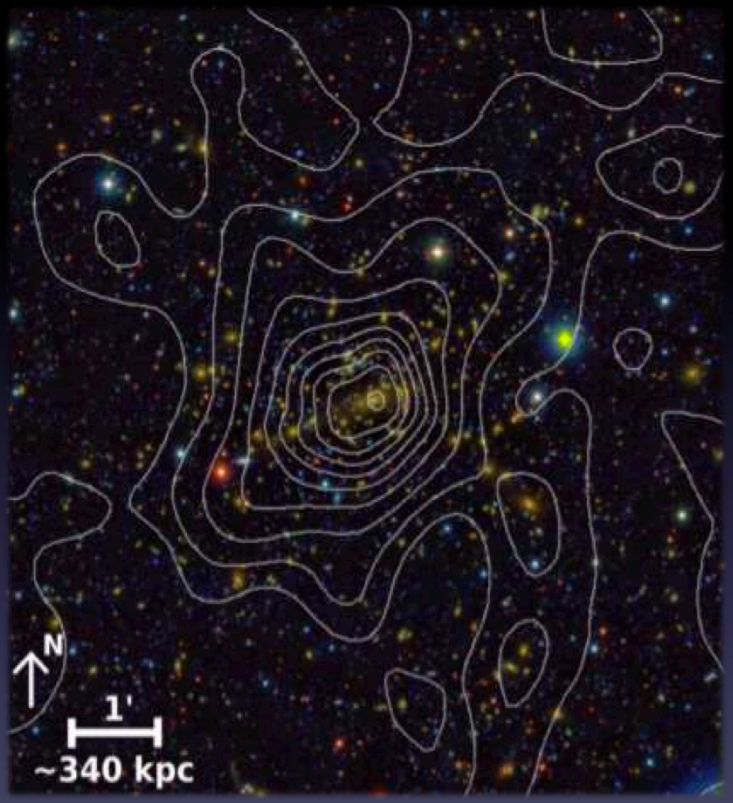

[Bartelmann's talk]

Surface mass density $\Sigma_S(r_{perp})$

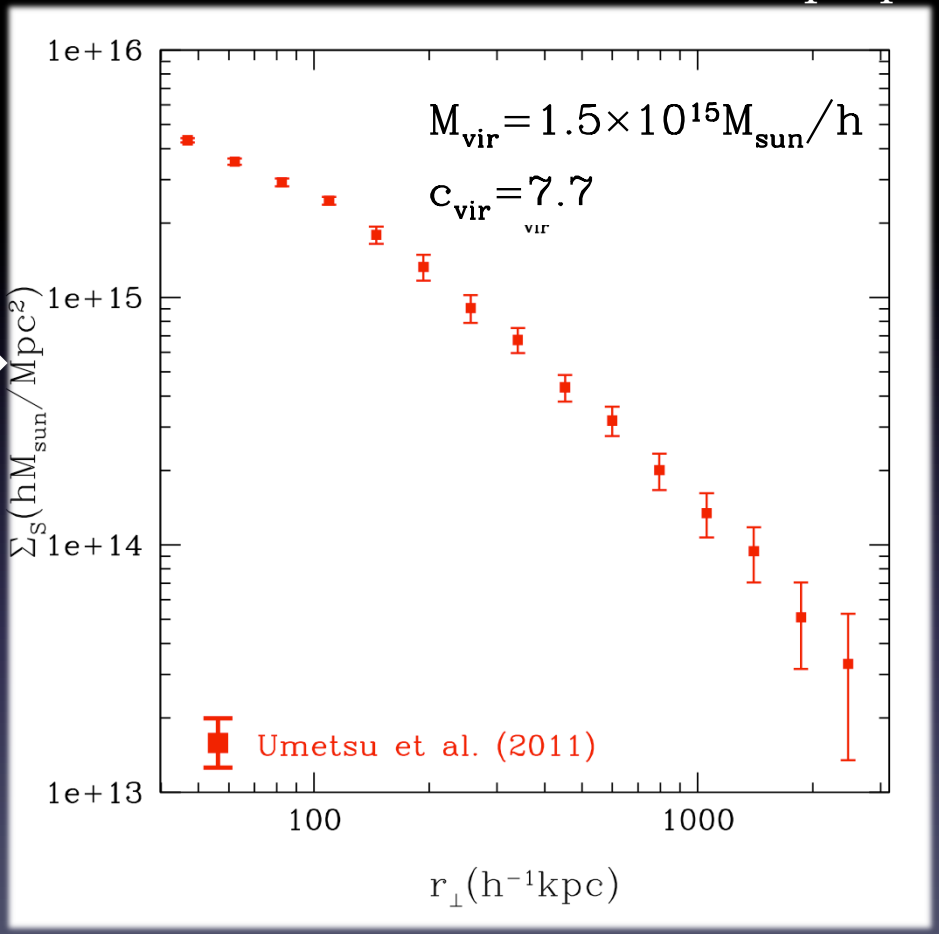

[Umetsu et al. '11,
cf. Oguri et al. '12]

Gravitational Lensing in Massive Gravity

- Geodesic equation

$$\frac{d^2}{d\chi^2}(\chi\theta^i) = 2\Phi_{+,i}, \quad i = 1,2 \qquad \Phi_+ \equiv (\Phi + \Psi)/2$$

- Surface mass density $\Sigma_S(r_{perp}) \propto \kappa(r_{perp})$

$$\Sigma_S \propto \int_0^\infty dZ \triangle^{(2D)} \Phi_+$$

$$r = \sqrt{r_\perp^2 + Z^2}$$

where lensing potential in massive gravity:

$$\triangle\Phi_+ = \frac{\Lambda^3}{M_{\rm Pl}} \frac{\left[\left(\alpha x^2 + 2\beta x^3 + 2A\right) r^3\right]'}{2r^2}$$

Assume $\delta\rho(r)$ as NFW profile: $\rho(r) = \dfrac{\rho_s}{(r/r_s)(1 + r/r_s)^2}$

Surface Mass Density in Massive Gravity

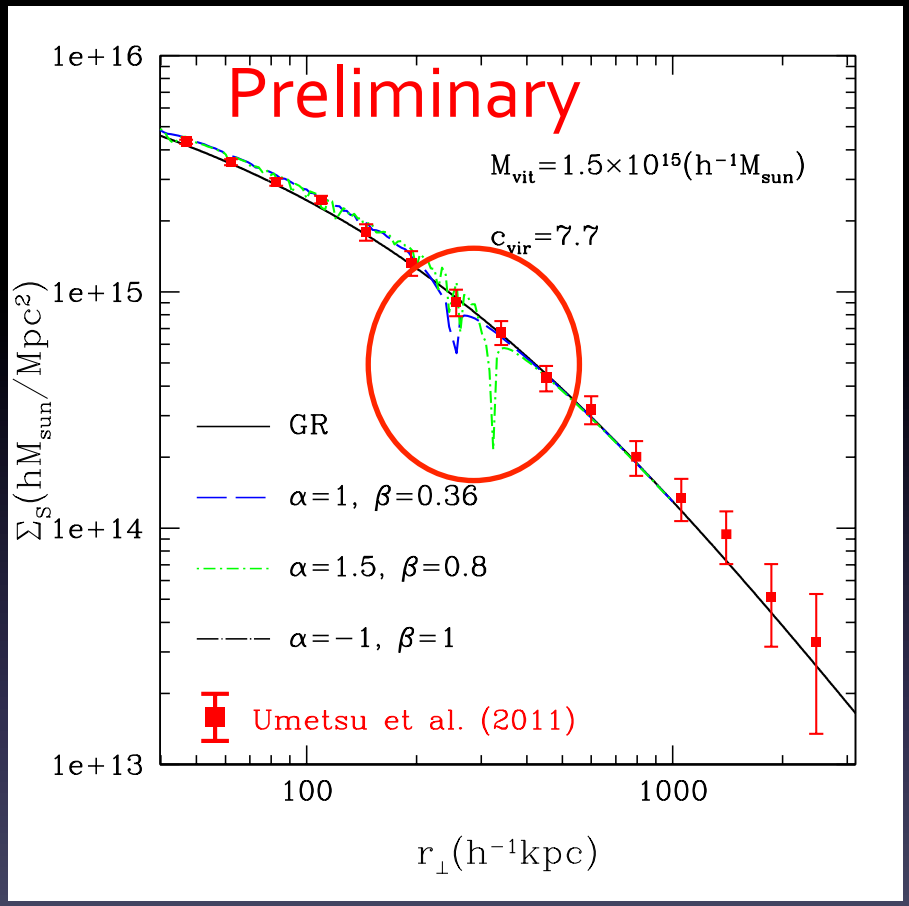

Parameters:{α,β,Λ;ρ_s,r_s}

(Λ=0.01/H_0, ρ_s, r_s fixed)

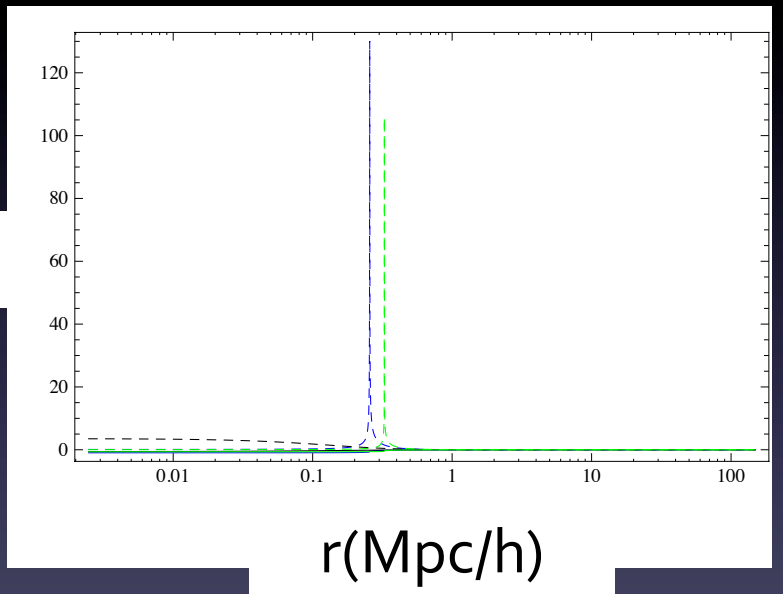

Origin of dip: x′(<=>ϕ″)

Dip appears at $r\sim r_V:=(r_sM_{Pl}/\Lambda^3)^{1/3}$

→allows us to put constraint

Summary

- Static-spherically symmetric solutions of ϕEOM in the context of Horndeski's theory.
- We explore the possibility of testing modified gravity exhibiting the Vainshtein mechanism against observation of cluster lensing.

- Key effects on cluster lensing Σ_S is that x'(<=>ϕ'') can substantially be large at the transition from screened to unscreened regions.

→This allows us to put observational constraints on modified gravity.

Thank you for your attention

Rampei Kimura, JGRG 22(2012)111419

"Constraints on general second-order scalar-tensor models from gravitational Cherenkov radiation"

RESCEU SYMPOSIUM ON

GENERAL RELATIVITY AND GRAVITATION

JGRG 22

November 12-16 2012

Koshiba Hall, The University of Tokyo, Hongo, Tokyo, Japan

Constraints on general second-order scalar-tensor models from gravitational Cherenkov radiation

Rampei Kimura
Hiroshima University

JGRG @Tokyo University 11/14/2012

Based on
RK and Kazuhiro Yamamoto, JCAP 07 (2012) 050

Introduction

- Accelerating universe
  - Implication of cosmological constant?

$$G_{\mu\nu}+\Lambda g_{\mu\nu} = 8\pi G T_{\mu\nu}$$

  - Observationally, fine !!
  - **Cosmological constant problem**

    121 orders of magnitude differences

Can **modification of gravity** solve this puzzle ???

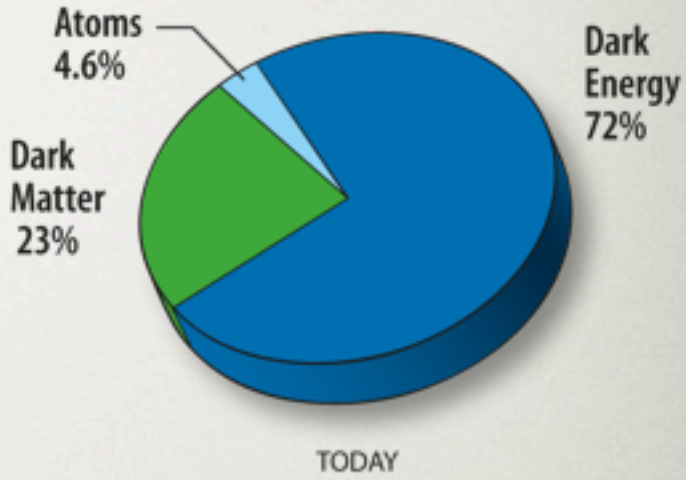

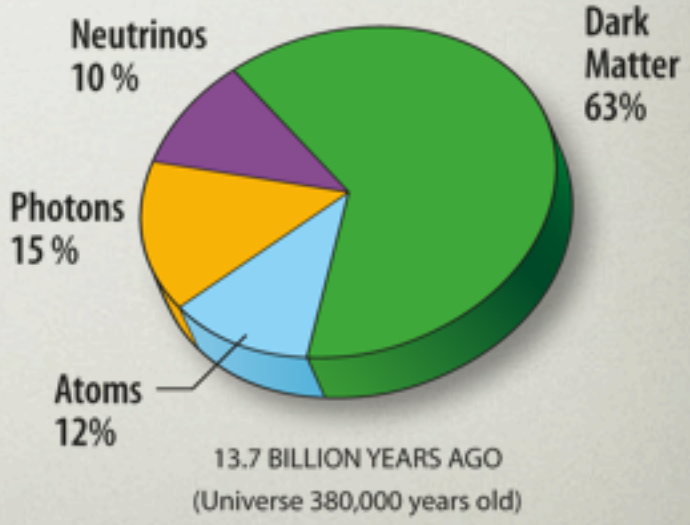

(from WMAP website)

Galileon theory

✓ Galileon (Nicolis et al. '09)

$$\Box = \nabla_\mu \nabla^\mu$$

$$\mathcal{L} \supset (\partial\varphi)^2 \Box\varphi$$

second derivative with respect to space-time

✓ Galileon term contains the second derivative term, but ...

coupling between scalar and curvature

$$\text{EOM} \supset (\Box\varphi)^2 - (\nabla_\mu \nabla_\nu \varphi)^2 - R_{\mu\nu}\nabla^\mu\varphi\nabla^\nu\varphi$$

No higher-order derivative terms in EOM !!

Most general second-order scalar-tensor theory (MGST)

✓ Horndeski found the most general Lagrangian whose EOM is second-order differential equation for ϕ and $g_{\mu\nu}$ (also known as **Generalized galileon**)

Horndeski, Int. J. Theor. Phys. 10,363 (1974) , Deffayet, Gao, Steer (2011)

$$\mathcal{L}_2 = K(\phi, X)$$

K-essence term $\mathcal{L}_2 \supset (\partial\phi)^2,\ V(\phi)$

$$\mathcal{L}_3 = -G_3(\phi, X)\Box\phi$$

Cubic galileon term

$\mathcal{L}_3 \supset (\partial\phi)^2\Box\phi$

$$\mathcal{L}_4 = G_4(\phi, X)R + G_{4,X}[(\Box\phi)^2 - (\nabla_\mu\nabla_\nu\phi)(\nabla^\mu\nabla^\nu\phi)]$$

Einstein-Hilbert term

$\mathcal{L}_4 \supset (M_{\rm Pl}^2/2)R$

$$\mathcal{L}_5 = G_5(\phi, X)G_{\mu\nu}(\nabla^\mu\nabla^\nu\phi) - \frac{1}{6}G_{5,X}\Big[(\Box\phi)^3 - 3(\Box\phi)(\nabla_\mu\nabla_\nu\phi)\,(\nabla^\mu\nabla^\nu\phi) + 2(\nabla^\mu\nabla_\alpha\phi)(\nabla^\alpha\nabla_\beta\phi)(\nabla^\beta\nabla_\mu\phi)\Big]$$

Non-minimal derivative coupling

$\mathcal{L}_5 \supset G^{\mu\nu}\nabla_\mu\phi\nabla_\nu\phi$

(Germani et al. 2011; Gubitosi, Linder 2011)

$X = -(\partial\phi)^2/2, \quad G_{iX} = \partial G_i/\partial X$

Why galileon??

- **Self-accelerating solution**
- **Free of ghost-instabilities**
- **Vainshtein mechanism** (Vainshtein 1972)
  - Scalar field is effectively weakly coupled to matter in a high density region
  - Reduce general relativity at small scales
- Relation with decoupling limit in **massive gravity**

(de Rham, Gabadadze, Tolley, 2010)

Cosmological observations

RK, Kazuhiro Yamamoto, JCAP 04 (2011) 025
RK, Tsutomu Kobayashi, Kazuhiro Yamamoto, Physical Review D 85 (2012) 123503

- Standard rulers (supernovae + CMB shift parameter)
  - **Not powerful tools** to constrain model parameters in modified gravity theories, but **useful tools** to determine cosmological parameters
- Galaxy distribution (SDSS LRG sample)
  - **The error bar is still large** to constrain model parameters
- Cross correlation between LSS and ISW
  - **Excellent tool** to constrain modified gravity
  - Indicates that the effective gravitational coupling **G_{eff} has to be smaller than ~1.2 G_N**, otherwise CCF becomes **negative** which contradicts with observations

Other signatures ??

Sound speed of graviton in MGST

- Quadratic action for **a tensor mode** in the most general scalar-tensor theory

  Kobayashi, Yamaguchi, Yokoyama, Prog. Theor. Phys. 126, 511 (2011),

$$S_T^{(2)} = \frac{1}{8}\int dtd^3xa^3\left[\mathcal{G}_T\dot{h}_{ij}^2 - \frac{\mathcal{F}_T}{a^2}(\vec{\nabla}h_{ij})^2\right]$$

- Sound speed of graviton

$$c_T^2 \equiv \frac{\mathcal{F}_T}{\mathcal{G}_T}$$

$$\mathcal{F}_T \equiv 2\left[G_4 - X\left(\ddot{\phi}G_{5X} + G_{5\phi}\right)\right]$$

$$\mathcal{G}_T \equiv 2\left[G_4 - 2XG_{4X} - X\left(H\dot{\phi}G_{5X} - G_{5\phi}\right)\right]$$

Sound speed of graviton could be **different from speed of light** !!!

Gravitational Cherenkov Radiation

- If the sound speed of graviton is smaller than the speed of light, **particle should emit graviton** through the similar process to Cherenkov radiation

Moore and Nelson (2001)

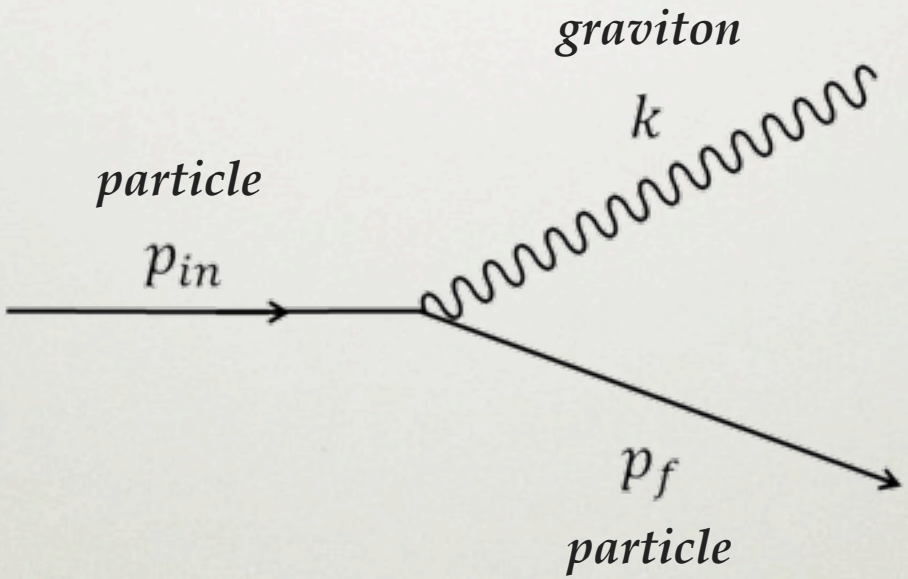

- Highest energy cosmic ray (p ~ 3×10^{11} GeV) can provide us **the lower bound on the sound speed of graviton**

Gravitational Cherenkov Radiation

- Consider the complex scalar in **a FRW background**

$$S_m = \int d^4x\sqrt{-g}\left[-g^{\mu\nu}\partial_\mu\Psi^*\partial_\nu\Psi - m^2\Psi^*\Psi - \xi R\Psi^*\Psi\right]$$

- Quantize the complex scalar and tensor field as

$$\hat{\Psi}(\eta,\mathbf{x}) = \frac{1}{a}\int\frac{d^3p}{(2\pi)^{3/2}}\left[\hat{b}_{\mathbf{p}}\psi_p(\eta)e^{i\mathbf{p}\cdot\mathbf{x}} + \hat{c}^\dagger_{\mathbf{p}}\psi^*_p(\eta)e^{-i\mathbf{p}\cdot\mathbf{x}}\right]$$

$$\hat{h}_{\mu\nu} = \frac{1}{a}\sqrt{\frac{2}{\mathcal{G}_T}}\sum_\lambda\int\frac{d^3k}{(2\pi)^{3/2}}\left[\varepsilon^{(\lambda)}_{\mu\nu}\hat{a}_{\mathbf{k}}h_k(\eta)e^{i\mathbf{k}\cdot\mathbf{x}} + \varepsilon^{(\lambda)}_{\mu\nu}\hat{a}^\dagger_{\mathbf{k}}h^*_k(\eta)e^{-i\mathbf{k}\cdot\mathbf{x}}\right]$$

$$[\hat{b}_{\mathbf{p}},\hat{b}^\dagger_{\mathbf{p}'}] = \delta(\mathbf{p}-\mathbf{p}')$$

$$[\hat{c}_{\mathbf{p}},\hat{c}^\dagger_{\mathbf{p}'}] = \delta(\mathbf{p}-\mathbf{p}')$$

- Mode functions satisfy

$$\left(\frac{d^2}{d\eta^2} + p^2 + m^2a^2\right)\psi_p(\eta) = 0$$

$$\left(\frac{d^2}{d\eta^2} + c_T^2k^2 - \frac{a''}{a}\right)h_k(\eta) = 0$$

Gravitational Cherenkov Radiation

- The total radiation energy from the complex scalar field

$$E = \sum_{\lambda} \sum_{\mathbf{k}} (\omega_k / a) \left\langle \hat{a}_{\mathbf{k}}^{\dagger(\lambda)} \hat{a}_{\mathbf{k}}^{(\lambda)} \right\rangle$$

where

$$\left\langle \hat{a}_{\mathbf{k}}^{\dagger(\lambda)} \hat{a}_{\mathbf{k}}^{(\lambda)} \right\rangle = 2\Re \int_{t_{\rm in}}^{t} dt_2 \int_{t_{\rm in}}^{t_2} dt_1 \left\langle H_I(t_1) \hat{a}_{\mathbf{k}}^{\dagger(\lambda)} \hat{a}_{\mathbf{k}}^{(\lambda)} H_I(t_2) \right\rangle$$

$$H_I = a \int d^3x h_{ij} \partial_i \Psi \partial_j \Psi^*$$

- Graviton emission rate (using sub-horizon approximation)

$$\frac{dE}{dt} \simeq \frac{G_N \, p_{\rm in}^4}{a^4} \frac{4(1-c_T)^2}{3(1+c_T)^2}$$

- A particle with momentum p **cannot** possibly have been traveling for **longer than**

$$t \sim \frac{a^4}{G_N} \frac{(1+c_T)^2}{4(1-c_T)^2} \frac{1}{p^3}$$

Gravitational Cherenkov Radiation

- Observations from cosmic rays tells

Time scale that cosmic ray turn into radiation energy of graviton $>$ **Time scale that cosmic ray travels from origin to us**

- The highest energy cosmic ray
  - Energy
  - Distance

$$E_{\rm highest} \sim 10^{11}{\rm GeV}$$

$$c\,t \sim 10\,{\rm kpc}$$

- **Constraint on the sound speed of graviton**

$$1 - c_T \lesssim 2 \times 10^{-15}$$

Toy Model 1

- Gubitosi and Linder model (Gubitosi and Linder 2011)

$$S = \int d^4x\sqrt{-g}\left[\frac{M_{\rm Pl}^2}{2}R + X + \frac{\lambda}{M_{\rm Pl}^2}G^{\mu\nu}\nabla_\mu\phi\nabla_\mu\phi + \mathcal{L}_m[g_{\mu\nu},\psi]\right]$$

$$K = X$$
$$G_3 = 0$$
$$G_4 = M_{\rm Pl}^2/2$$
$$G_5 = -\lambda\phi/M_{\rm Pl}^2$$

- Condition for existence of self-accelerating solution and avoiding the ghost-instability

$$-\frac{1}{18}\frac{M_{\rm Pl}^2}{H_0^2} < \lambda < -\frac{1}{30}\frac{M_{\rm Pl}^2}{H_0^2}$$

λ is always negative

- Sound speed of graviton

$$c_T^2 = \frac{M_{\rm Pl}^2 + 2\lambda\dot{\phi}^2/M_{\rm Pl}^2}{M_{\rm Pl}^2 - 2\lambda\dot{\phi}^2/M_{\rm Pl}^2} < 1$$

Inconsistent with the constraint from the gravitational Cherenkov radiation...

Toy Model 2

$c_T > 1 - \epsilon$

$\epsilon = 2 \times 10^{-15}$

Extended galileon model (De Felice and Tsujikawa 2011)

$$K = -c_2 M_2^{4(1-p_2)} X^{p_2},$$
$$G_3 = c_3 M_3^{1-4p_3} X^{p_3},$$
$$G_4 = \frac{1}{2} M_{\rm pl}^2 - c_4 M_4^{2-4p_4} X^{p_4},$$
$$G_5 = 3 c_5 M_5^{-(1+4p_5)} X^{p_5},$$

$$p_2 = p$$
$$p_3 = p + (2q - 1/2)$$
$$p_4 = p + 2q$$
$$p_5 = p + (6q - 1)/2$$

4 model parameters p, q, $\alpha(c_3)$, β (c_4)

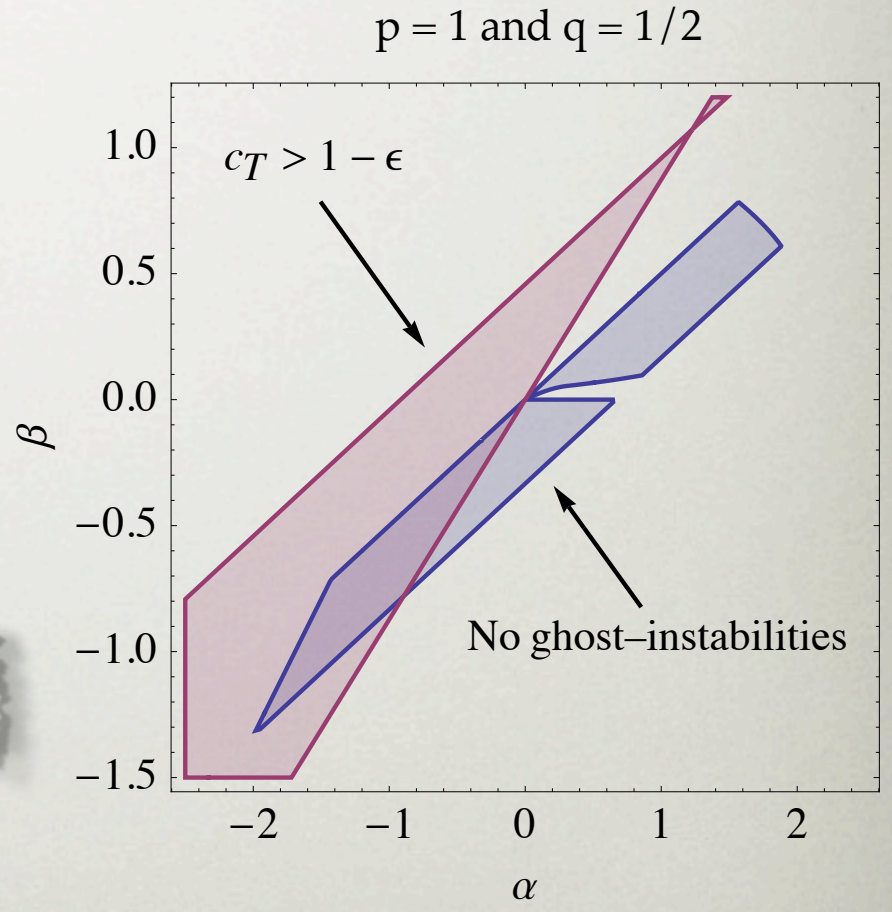

Strong constraints for the model parameters α and β

Summary

- In the most general scalar-tensor theory, sound speed of graviton could be different from speed of light
- The constraints from **gravitational Cherenkov radiation** would be a powerful probe.
- **Gravitational Cherenkov radiation** could be a criteria for the construction of modification of gravity

Gravitational Cherenkov radiation for massive graviton

- Quadratic action for **a tensor mode** for massive graviton

Gumrukcuoglu, Kuroyanagi, Lin, Mukohyama, Tanahashi (2012)

$$I^{(2)}_{tensor} = \frac{M^2_{Pl}}{8}\int dtd^3x\, N a^3\sqrt{\Omega}\left[\frac{1}{N^2}\dot{\gamma}^{ij}\dot{\gamma}_{ij} + \frac{c_g^2(t)}{a^2}\gamma^{ij}\left(\triangle - 2K\right)\gamma_{ij} - M^2_{GW}(t)\gamma^{ij}\gamma_{ij}\right]$$

- Dispersion relation

$$\omega_k^2 = c_g^2 k^2 + a^2 M^2_{GW}$$

For c_g=c, there is **no gravitational Cherenkov radiation** even if m≠0

Currently, checking the case c_g≠c and m≠0...

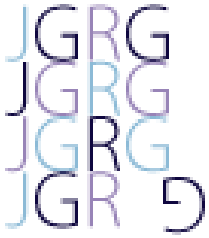

Daisuke Yamauchi, JGRG 22(2012)111420

"Weak lensing generated by vector perturbations and detectability of cosmic strings"

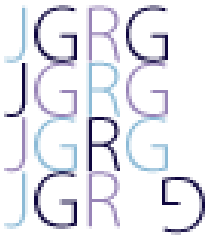

RESCEU SYMPOSIUM ON

GENERAL RELATIVITY AND GRAVITATION

JGRG 22



November 12-16 2012

Koshiba Hall, The University of Tokyo, Hongo, Tokyo, Japan



Weak lensing generated by vector perturbations and detectability of cosmic strings

Daisuke Yamauchi

ICRR, U. Tokyo

DY, A. Taruya (U Tokyo, RESCEU), T. Namikawa (U Tokyo)

- JCAP 1201 (2012) 007, arXiv:1110.1718 [astro-ph.CO]
- JCAP 1210 (2012) 030, arXiv:1205.2139 [astro-ph.CO]
- arXiv:12??.????

Vector mode in cosmology

Scalar mode

- dominant component, gravitational clustering,…

Vector mode

- very minor component and does not serve as a seed of structure formation
- In absence of sources, it decays away, and rapidly becomes negligible …

✓ BUT! It can be generated via a variety of mechanisms :
cosmic strings, magnetic fields, massive neutrinos,
2nd-order density perturbations, modification of gravity,…

…The detection/measurement of them offers an important clue to probe the unknown physics and history of the very early universe!

Gravitational Lensing
= method to ``see'' invisibles

NASA/ESA

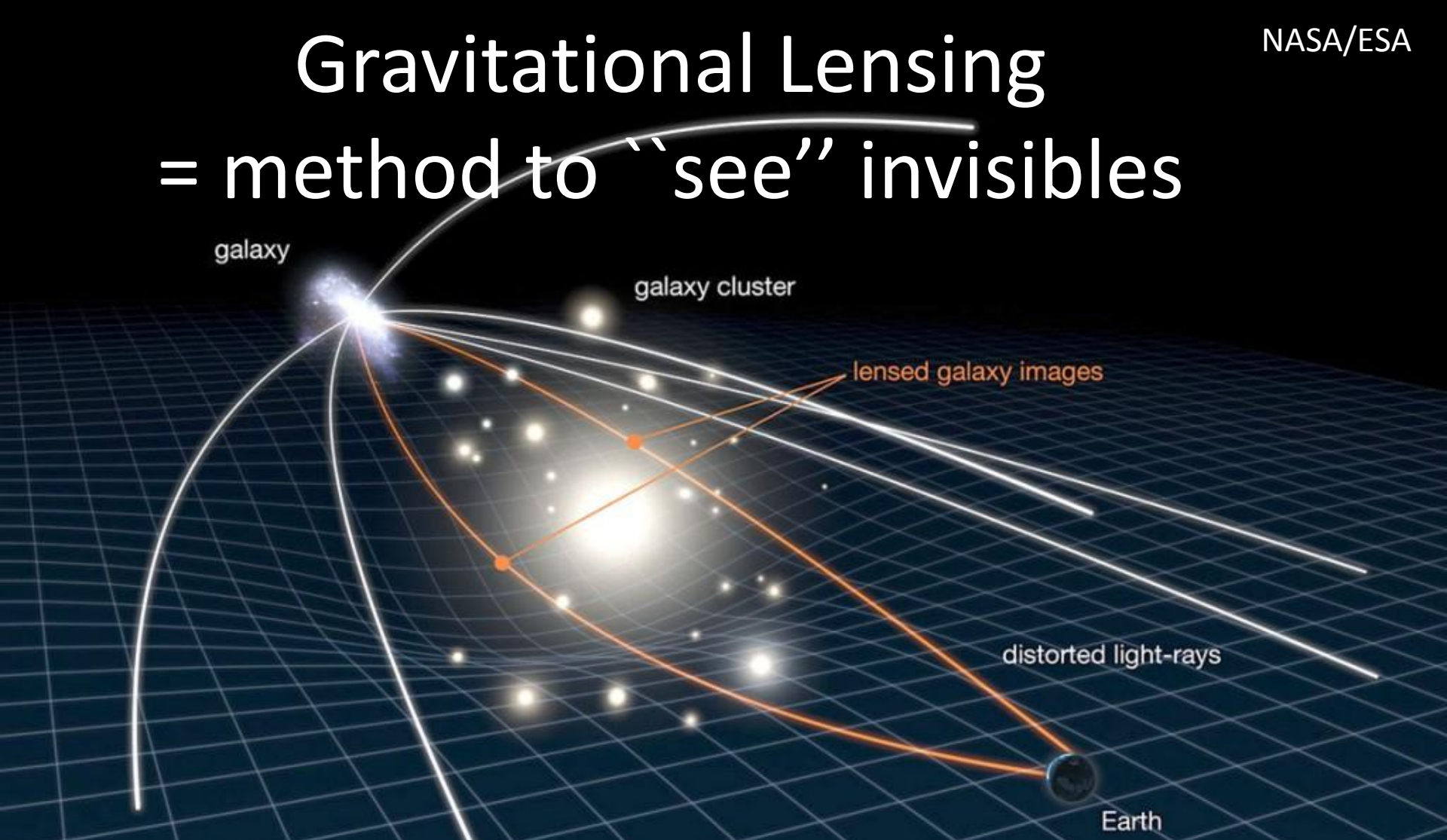

WEAK LENSING observations can provide a direct evidence for the intervening ``VECTOR MODES'' along a line of sight by measuring the spatial patterns of the deformation of the photon path.

Main Goal

1. We derive the full-sky formulas for

   - vector-induced cosmic shear for galaxy survey
   - vector-induced deflection angle for CMB-lensing

2. As a prospect for detecting shear/deflection,
   we consider a cosmic string network as
   a possible source for seeding vector perturbations.

Cosmic shear

Galaxies randomly distributed

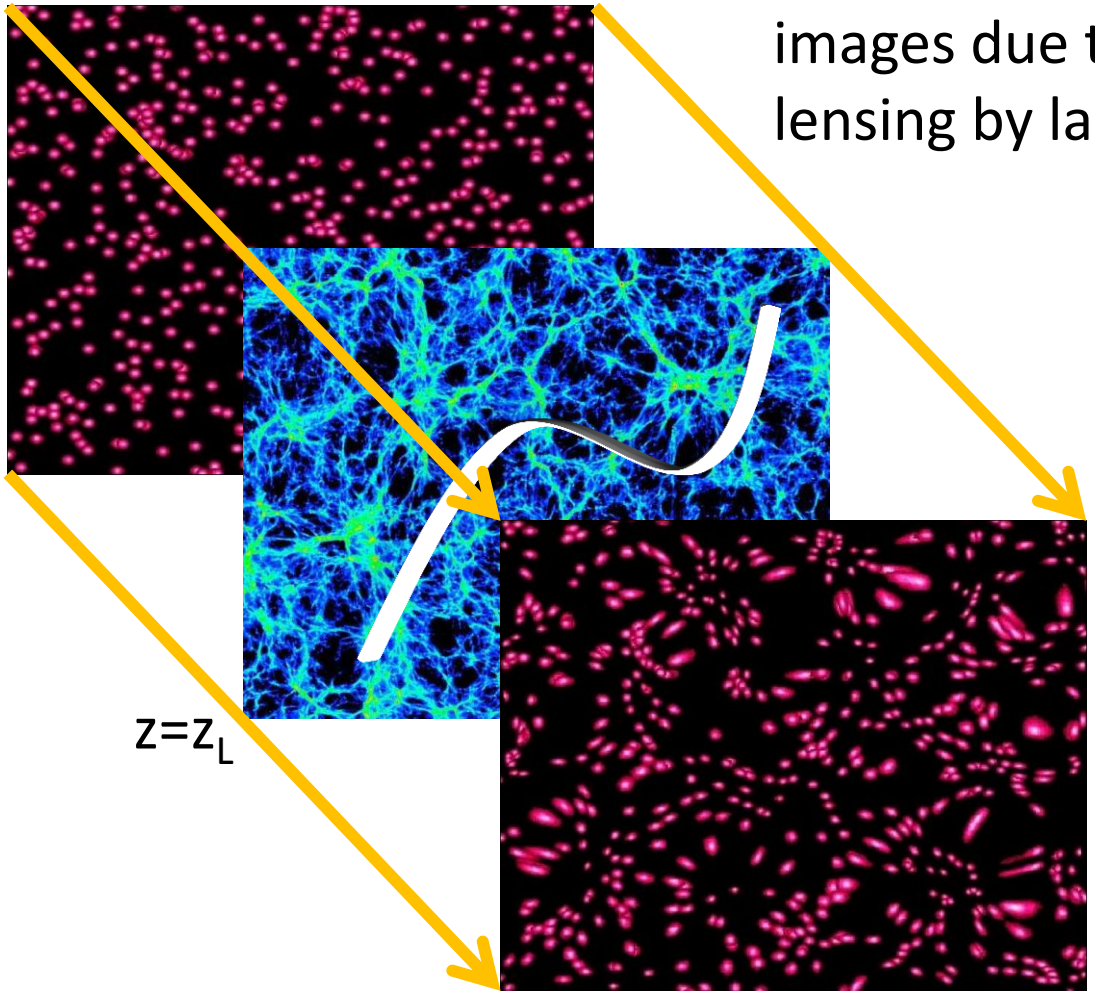

:the deformation of distant-galaxy images due to weak gravitational lensing by large-scale structure

…+ exotic objects

Intrinsic shape of a background galaxy

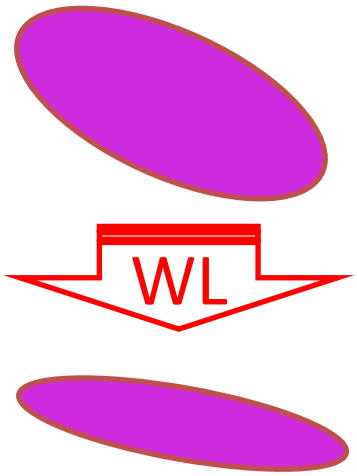

Galaxy shape actually seen after WL

E-/B-mode decomposition in WL

The spatial pattern of lensing shear fields can be decomposed into even-parity part (E-mode) and odd-parity part (B-mode).

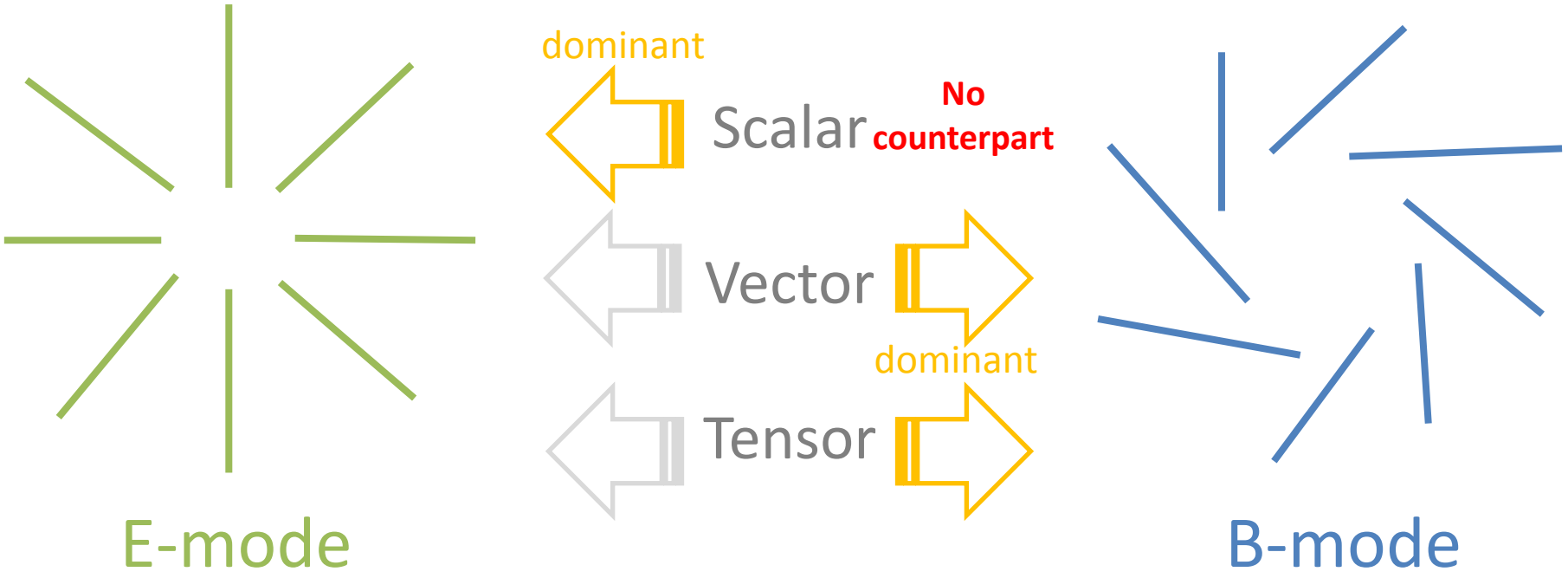

The non-vanishing B-mode shear signal would be a direct evidence for non-scalar metric perturbations .

(See [Dodelson+('03), Schmidt+('12),…] for primordial GW)

Formula for vector-induced B-mode shear

[**DY**+Namikawa+Taruya, 1205.2139]

- vector perturbations

$$\mathrm{d}s^2 = a^2(\eta)\left[-\mathrm{d}\eta^2 + 2B_i \mathrm{d}\eta \mathrm{d}x^i + \left(\delta_{ij} + 2H_{(i|j)}\right)\mathrm{d}x^i \mathrm{d}x^j\right]$$

$\sigma_{\mathrm{g},i} \equiv \dot{H}_i - B_i$: gauge-invariant vector perturbations

Solving the geodesic deviation equation,…

comoving distance

$$C_\ell^{\mathrm{BB}} = \frac{1}{2\pi}\frac{(\ell-1)!(\ell+2)!}{(\ell+1)!(\ell-2)!}\int_0^\infty k^2 \mathrm{d}k \int_0^{\chi_\mathrm{S}} \mathrm{d}\chi \int_0^{\chi_\mathrm{S}} \mathrm{d}\chi' \times \frac{j_\ell(k\chi)}{\chi}\frac{j_\ell(k\chi')}{\chi'} P_{\sigma_\mathrm{g}\sigma_\mathrm{g}}(k; \eta_0-\chi, \eta_0-\chi')$$

CMB lensing

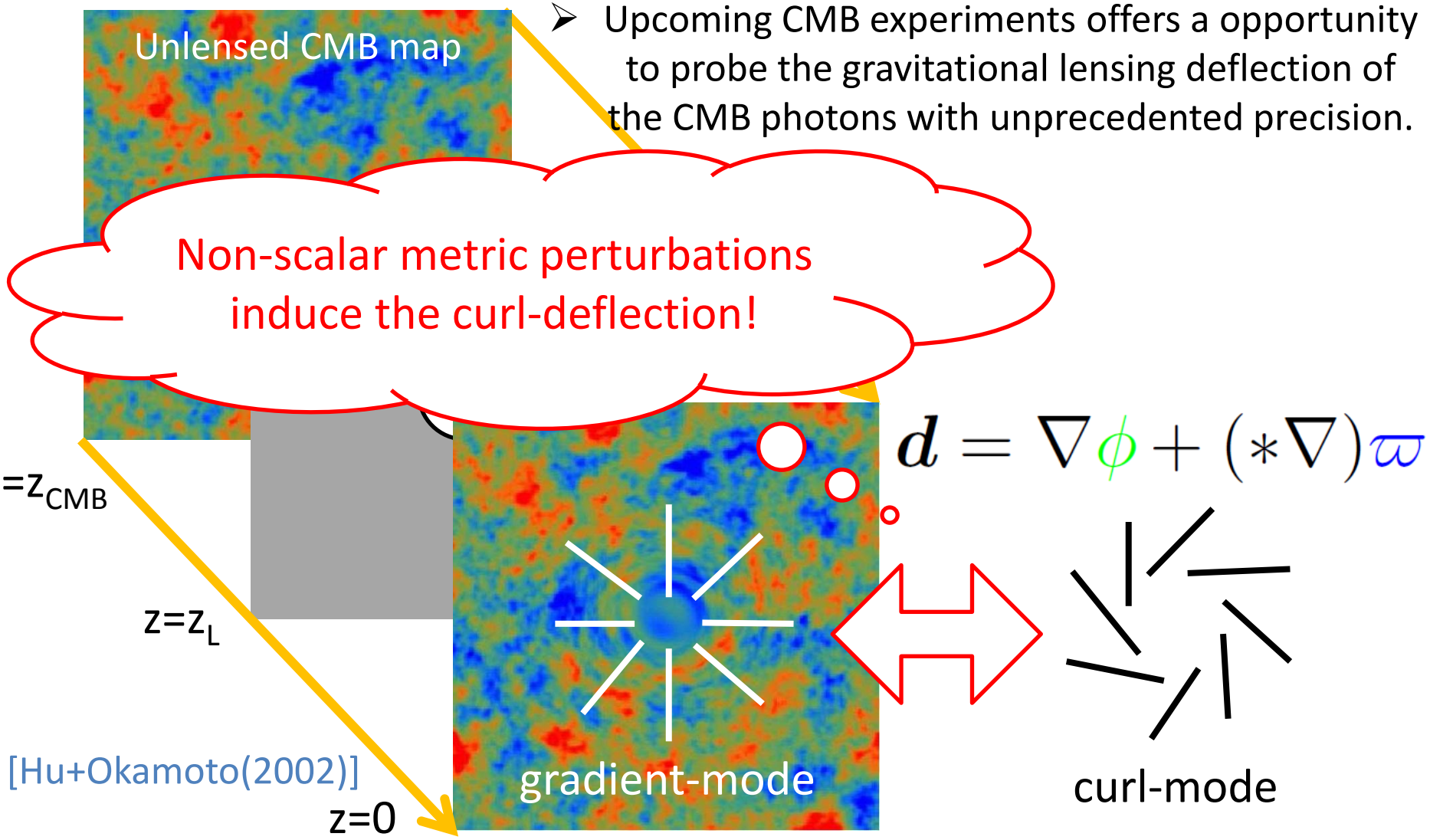

- Upcoming CMB experiments offers a opportunity to probe the gravitational lensing deflection of the CMB photons with unprecedented precision.

Formula for vector-induced curl-mode

[**DY**+Namikawa+Taruya, 1205.2139]

$$\mathrm{d}s^2 = a^2(\eta)\left[-\mathrm{d}\eta^2 + 2B_i \mathrm{d}\eta \mathrm{d}x^i + \left(\delta_{ij} + 2H_{(i|j)}\right)\mathrm{d}x^i \mathrm{d}x^j\right]$$

$\sigma_{\mathrm{g},i} \equiv \dot{H}_i - B_i$: vector perturbations

$$C_\ell^{\varpi\varpi} = \frac{1}{2\pi}\frac{(\ell-1)!}{(\ell+1)!}\int_0^\infty k^2 \mathrm{d}k \int_0^{\chi_{\mathrm{CMB}}} \mathrm{d}\chi \int_0^{\chi_{\mathrm{CMB}}} \mathrm{d}\chi' \times \frac{j_\ell(k\chi)}{\chi}\frac{j_\ell(k\chi')}{\chi'} P_{\sigma_\mathrm{g}\sigma_\mathrm{g}}(k; \eta_0 - \chi, \eta_0 - \chi')$$

Note : Considering a single light source, we can extract the vector-induced gradient-/curl-modes from the vector-induced shear fields.

$$C_\ell^{\phi\phi} = 4\frac{(\ell-2)!}{(\ell+2)!}C_\ell^{\mathrm{EE}}, \quad C_\ell^{\varpi\varpi} = 4\frac{(\ell-2)!}{(\ell+2)!}C_\ell^{\mathrm{BB}}$$

CMB-lensing reconstruction

Lensing induces higher-order term, i.e., **non-Gaussianity**, in measured CMB anisotropies.

➢ NG can be used to reconstruct the lensing angular power spectrum.

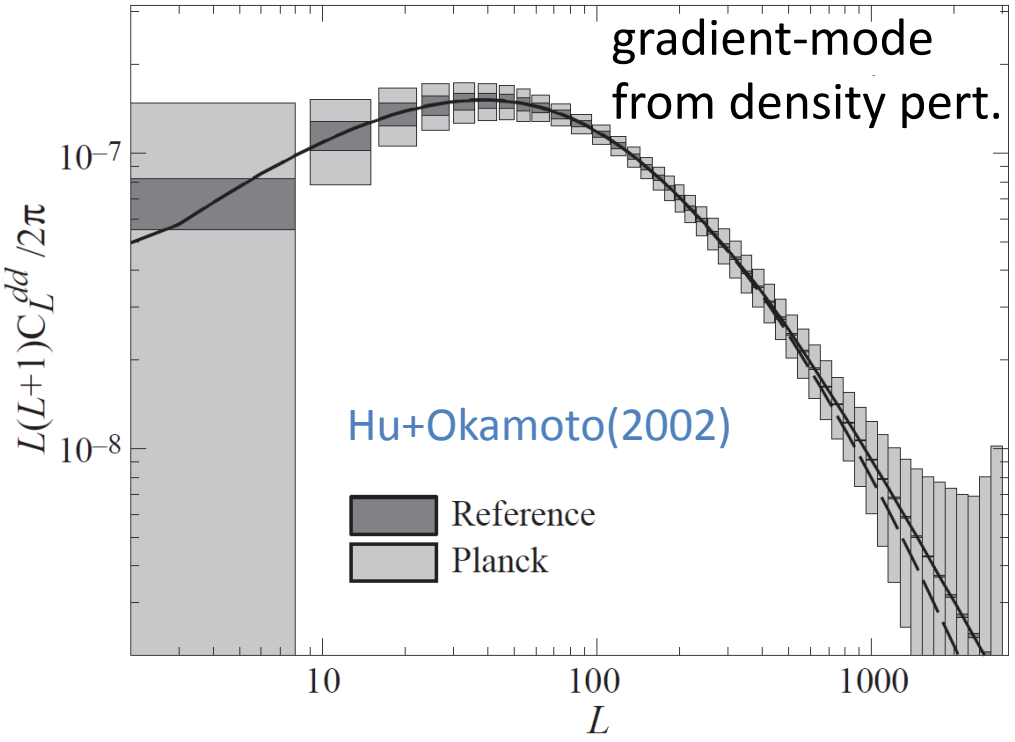

$$\boldsymbol{d} = \nabla\phi + (*\nabla)\varpi$$

✓ Gradient-mode ϕ
[Hu+Okamoto (2002),…]

✓ Curl-mode ω
[Cooray+ (2005),
Namikawa+**DY**+Taruya (2011)]

A cosmic string network as a source of vector perturbations

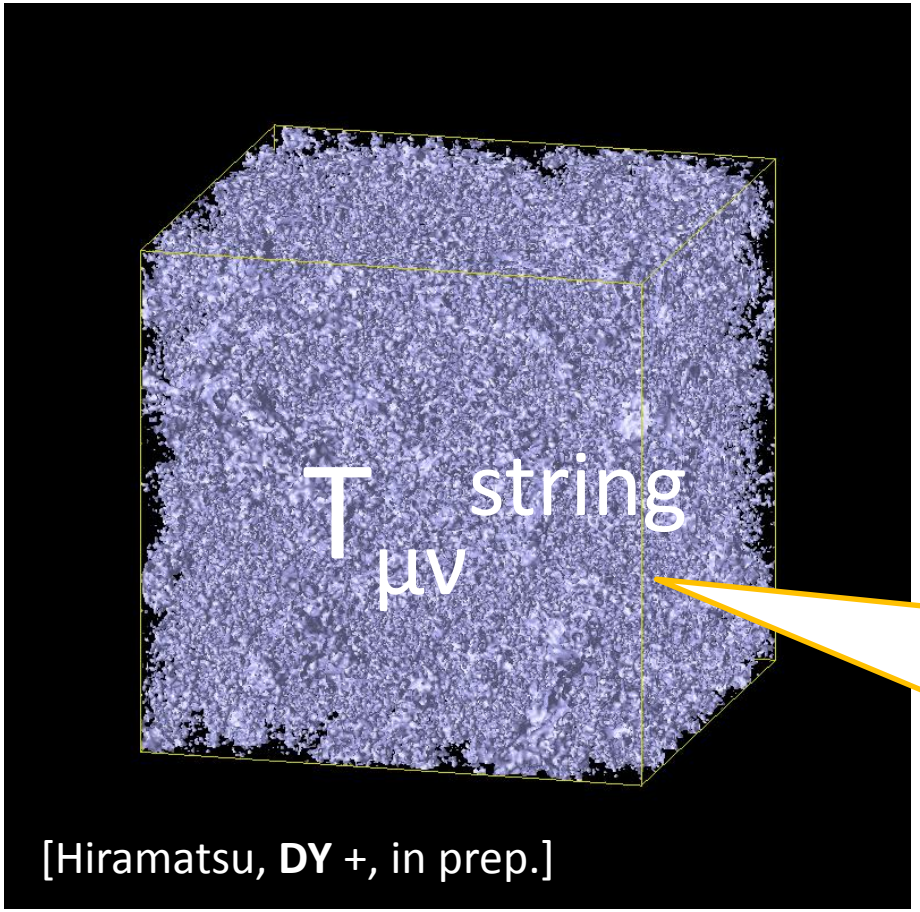

[Hiramatsu, **DY** +, in prep.]

``COSMIC STRINGS'' : relics from the early universe and exist in a wide variety of particle-physics models.

The vector metric perturbations, ``$\sigma_{g,i}$'', are sourced by the non-vanishing vector mode of string stress-energy tensor.

(For convenience, we use the simple analytic model for the network evolution and the correlations.)

B-mode shear from cosmic strings

[**DY**+Namikawa+Taruya, 1205.2139]

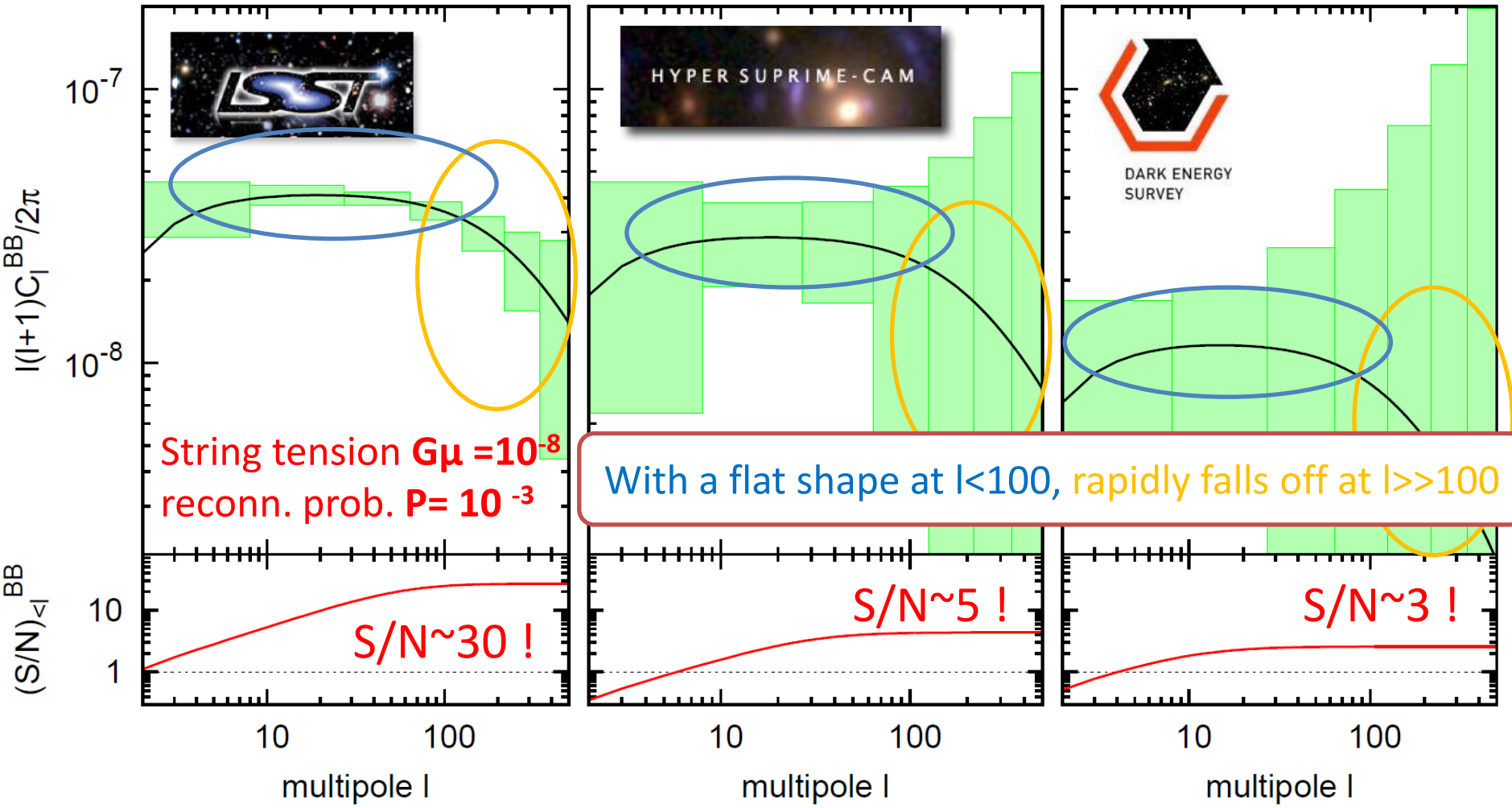

[DY+Namikawa+Taruya, 1205.2139]

S/N for string-induced B-mode shear

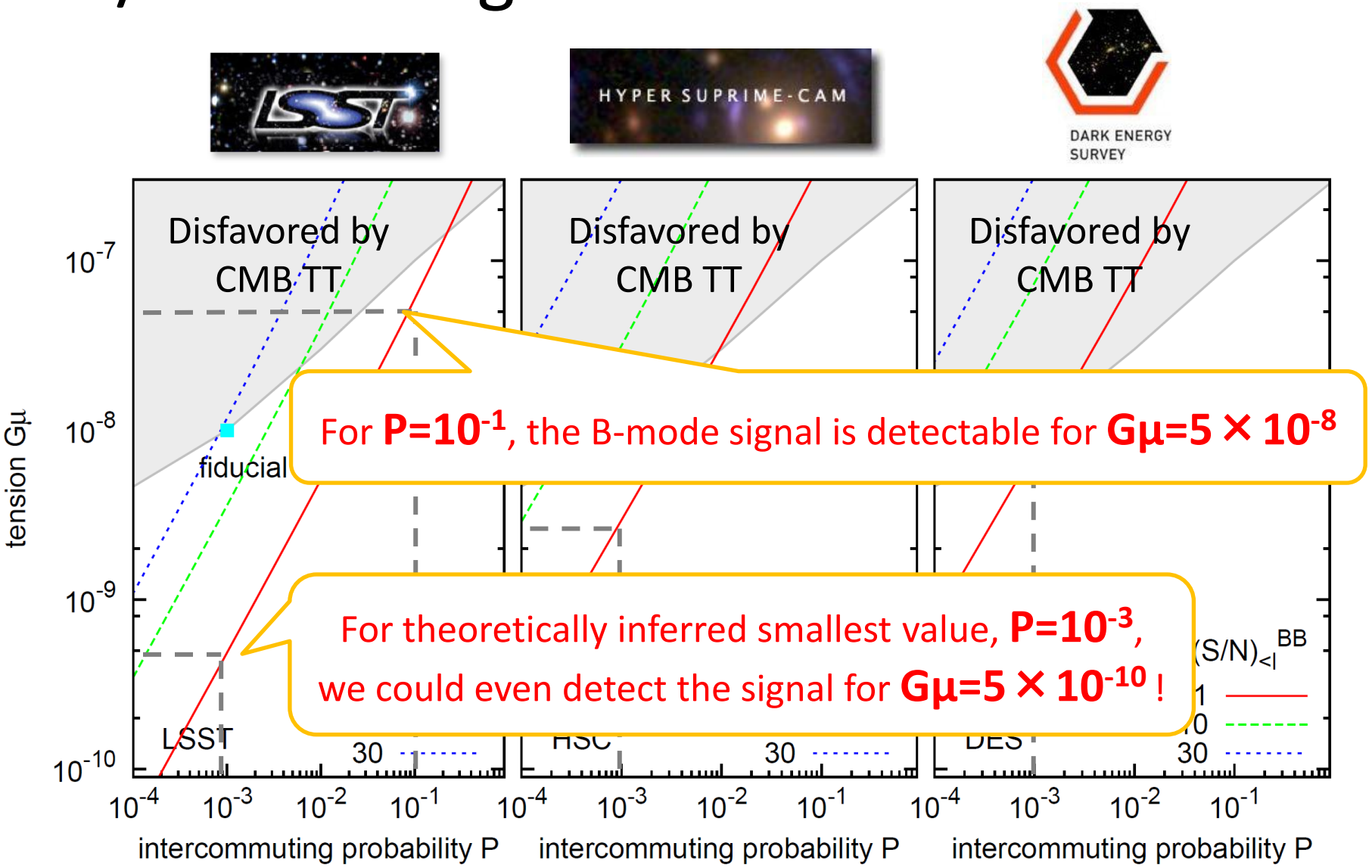

Curl-deflection from cosmic strings

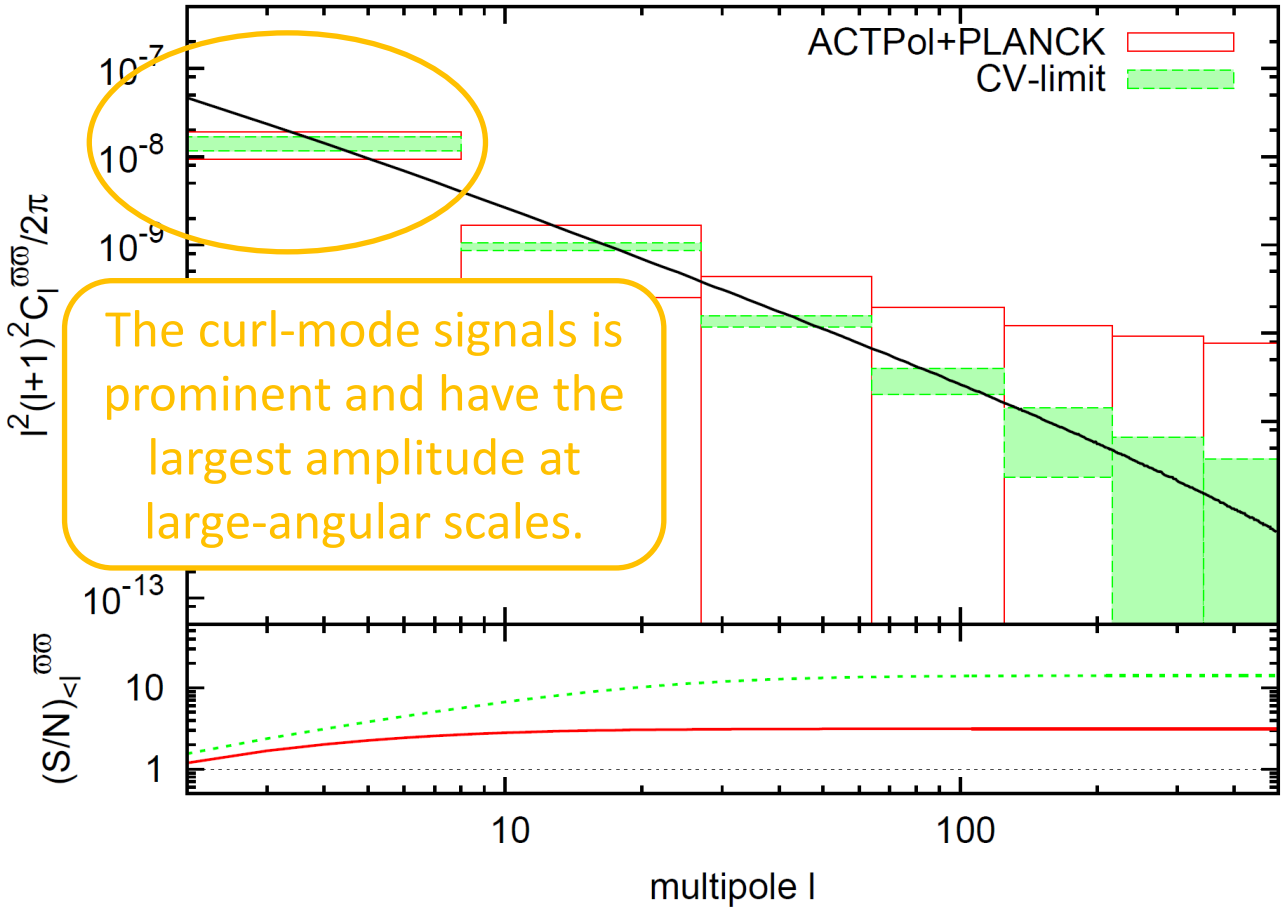

The curl-mode signals is prominent and have the largest amplitude at large-angular scales.

[**DY**+Namikawa+Taruya, 1205.2139]

String tension **Gμ =10^{-8}**
reconn. prob. **P= 10^{-3}**

S/N ~ 10 !
S/N ~ 3 !

The CURL-MODE measurement would provide not only a direct probe of cosmic strings, but also a diagnosis helpful to check the systematics in the derived constraints from the CMB TT.

S/N for string-induced curl-deflection

[**DY**+Namikawa+Taruya, 1205.2139]

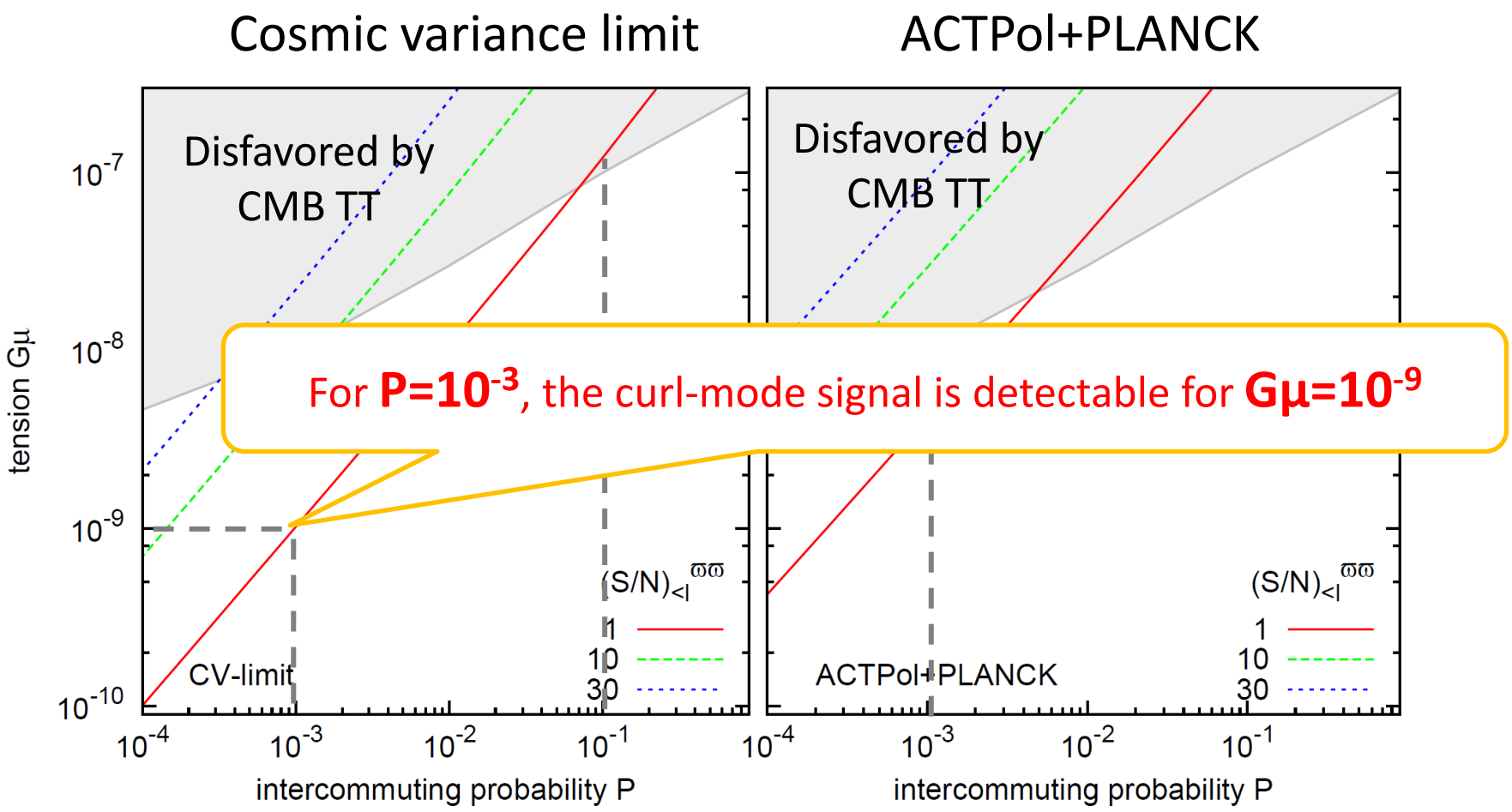

Summary

- We study how vector metric perturbations affect weak gravitational lensing and possible signatures.

- As an application, we consider a cosmic string network as a possible source for seeding vector perturbations.

  ✓ B-mode of shear fields

  - $P<10^{-1} \rightarrow G\mu > 5 \times 10^{-8}$, $P=10^{-3} \rightarrow G\mu > 5 \times 10^{-10}$

  ✓ Curl-mode of deflection angle

  - $P<10^{-1} \rightarrow G\mu > 4 \times 10^{-9}$, $P=10^{-3} \rightarrow G\mu > 10^{-9}$

- There are several missing pieces including

  the contribution of tensor perturbations,
  the additional correlations, and the other sources

[**DY**, Namikawa, Taruya, in prep.]

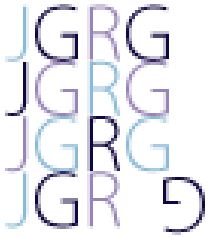

Dmitry Gorbunov, JGRG 22(2012)111421

"Higgs-inflation and the latest LHC results"

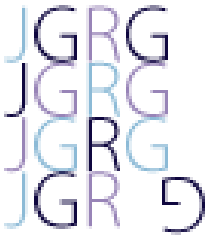

RESCEU SYMPOSIUM ON

GENERAL RELATIVITY AND GRAVITATION

JGRG 22



November 12-16 2012

Koshiba Hall, The University of Tokyo, Hongo, Tokyo, Japan



Higgs-inflation and the latest LHC results

Dmitry Gorbunov

Institute for Nuclear Research of RAS, Moscow

RESCEU Symposium on General Relativity and Gravitation

JGRG22, Tokyo

Outline

1. Inflation: general ideas
2. Higgs-inflation
   - Mechanism, Reheating, Predictions for perturbation spectra
   - Extensions: to solve neutrino, DM, BAU
3. LHC: the Higgs boson mass
4. Higgs-inflation and QFT
   - Nonremormalizability and strong coupling
   - BAU, neutrino oscillations due to nonrenormalizable operators?
5. Summary

Outline

1. Inflation: general ideas
2. Higgs-inflation
   - Mechanism, Reheating, Predictions for perturbation spectra
   - Extensions: to solve neutrino, DM, BAU
3. LHC: the Higgs boson mass
4. Higgs-inflation and QFT
   - Nonremormalizability and strong coupling
   - BAU, neutrino oscillations due to nonrenormalizable operators?
5. Summary

Inflationary solution of Hot Big Bang problems

Temperature fluctuations

$\delta T/T \sim 10^{-5}$

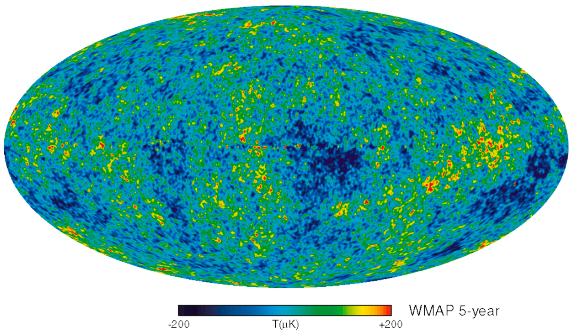

Universe is uniform!

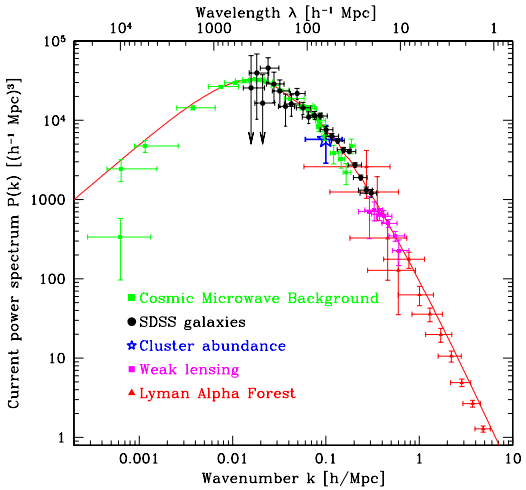

$\delta\rho/\rho \sim 10^{-5}$

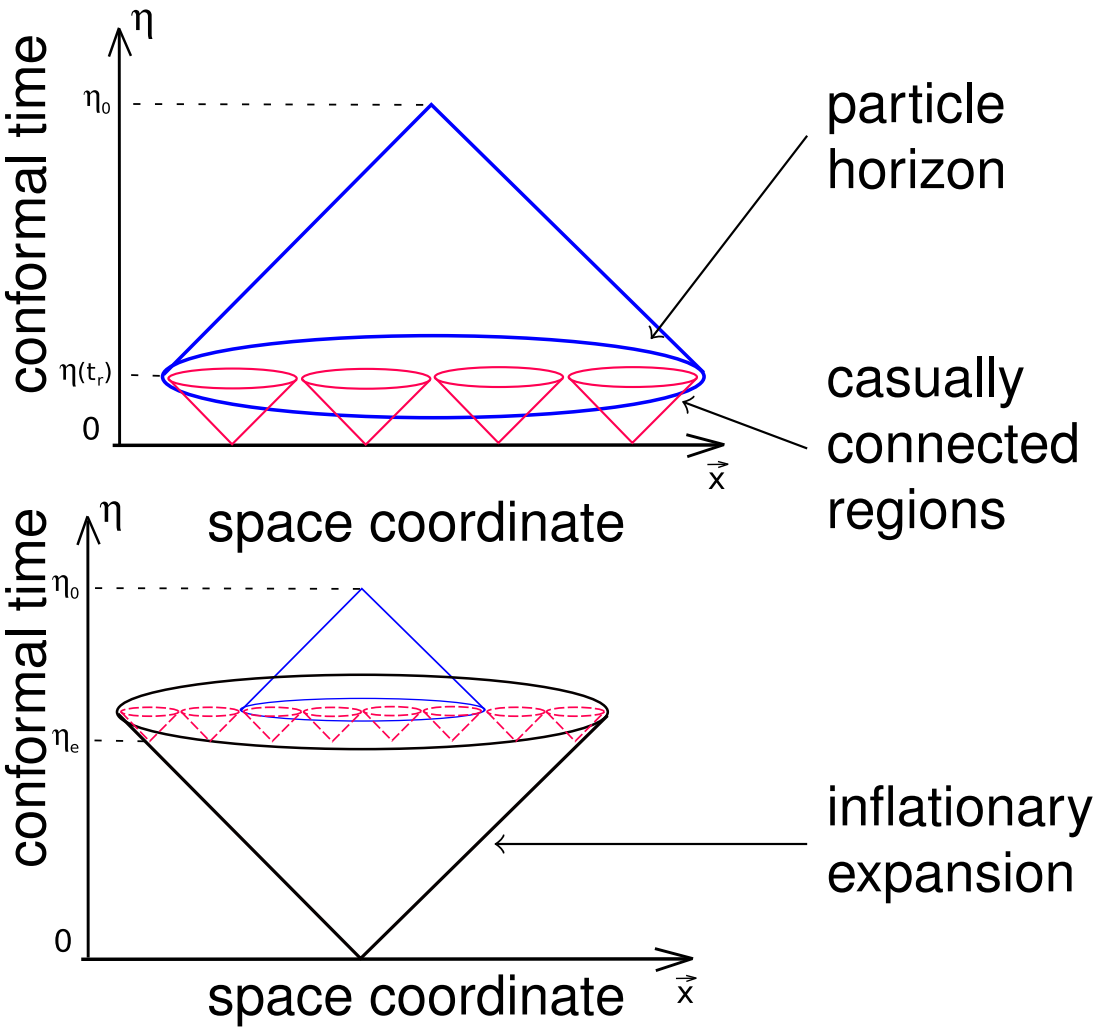

Chaotic inflation: simple realization

$$S=\int d^4x\sqrt{-g}\left(-\frac{M_P^2}{2}R+\frac{(\partial_\mu X)^2}{2}-\beta X^4\right)$$

$$\ddot{X}+3H\dot{X}+V'(X)=0$$

$$\frac{\dot{a}^2}{a^2}=H^2=\frac{1}{M_P^2}V(X)\,,\qquad a(t)\propto e^{Ht}$$

Chaotic inflation, A.Linde (1983)

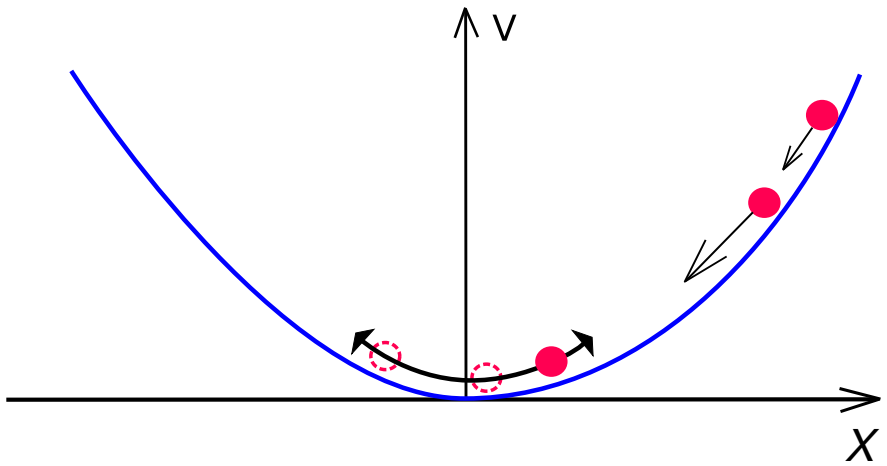

slow roll conditions get satisfied at
$X_e > M_{Pl}$ $\qquad M_P^2 = M_{Pl}^2/(8\pi)$

generation of scale-invariant scalar (and tensor) perturbations from exponentially stretched quantum fluctuations of X

$\Longrightarrow$

$\delta\rho/\rho \sim 10^{-5}$ requires
$V=\beta X^4 : \beta \sim 10^{-13}$

We have scalar in the SM! The Higgs field!

In a unitary gauge $H^T=\left(0\,,(h+v)/\sqrt{2}\right)$ (and neglecting $v=246$ GeV) $\lambda \sim 0.1-1$

$$S=\int d^4x\sqrt{-g}\left(-\frac{M_P^2}{2}R+\frac{(\partial_\mu h)^2}{2}-\frac{\lambda h^4}{4}\right)$$

Chaotic inflation: simple realization

$$S=\int d^4x\sqrt{-g}\left(-\frac{M_P^2}{2}R+\frac{(\partial_\mu X)^2}{2}-\beta X^4\right)$$

$$\ddot{X}+3H\dot{X}+V'(X)=0$$

$$\frac{\dot{a}^2}{a^2}=H^2=\frac{1}{M_P^2}V(X)\,,\qquad a(t)\propto e^{Ht}$$

Chaotic inflation, A.Linde (1983)

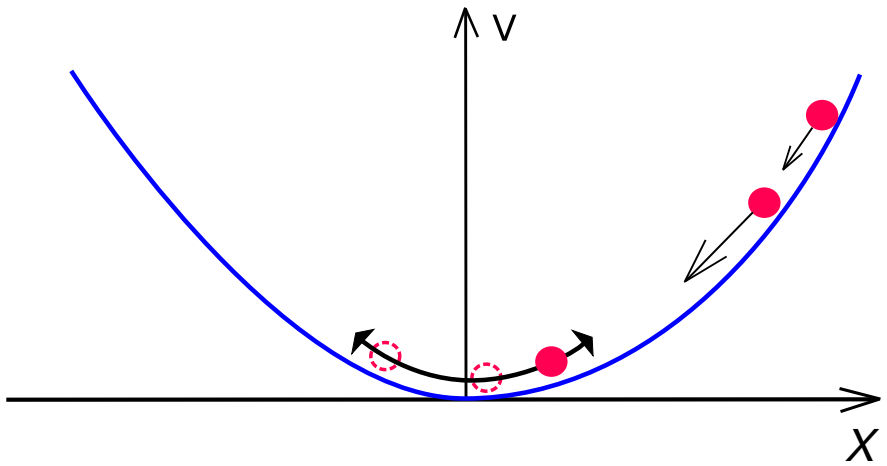

slow roll conditions get satisfied at
$X_e > M_{Pl}$ $\qquad M_P^2=M_{Pl}^2/(8\pi)$

generation of scale-invariant scalar (and tensor) perturbations from exponentially stretched quantum fluctuations of X $\Longrightarrow$

$\delta\rho/\rho\sim 10^{-5}$ requires
$V=\beta X^4$: $\beta\sim 10^{-13}$

We have scalar in the SM! The Higgs field!

In a unitary gauge $H^T=\left(0\,,(h+v)/\sqrt{2}\right)$ (and neglecting $v=246\,\text{GeV}$) $\qquad \lambda\sim 0.1-1$

$$S=\int d^4x\sqrt{-g}\left(-\frac{M_P^2}{2}R+\frac{(\partial_\mu h)^2}{2}-\frac{\lambda h^4}{4}\right)$$

Outline

1. Inflation: general ideas
2. Higgs-inflation
   - Mechanism, Reheating, Predictions for perturbation spectra
   - Extensions: to solve neutrino, DM, BAU
3. LHC: the Higgs boson mass
4. Higgs-inflation and QFT
   - Nonremormalizability and strong coupling
   - BAU, neutrino oscillations due to nonrenormalizable operators?
5. Summary

Higgs-inflation

F.Bezrukov, M.Shaposhnikov (2007)

$$S=\int d^4x\sqrt{-g}\left(-\frac{M_P^2}{2}R-\xi H^\dagger HR+\mathscr{L}_{SM}\right)$$

In a unitary gauge $H^T=\left(0,(h+v)/\sqrt{2}\right)$ (and neglecting $v=246\,\text{GeV}$)

$$S=\int d^4x\sqrt{-g}\left(-\frac{M_P^2+\xi h^2}{2}R+\frac{(\partial_\mu h)^2}{2}-\frac{\lambda h^4}{4}\right)$$

slow roll behavior due to modified kinetic term even for $\lambda\sim 1$

Go to the Einstein frame: $(M_P^2+\xi h^2)R\to M_P^2\tilde{R}$

$$g_{\mu\nu}=\Omega^{-2}\tilde{g}_{\mu\nu}\,,\qquad \Omega^2=1+\frac{\xi h^2}{M_P^2}$$

with canonically normalized χ:

$$\frac{d\chi}{dh}=\frac{M_P\sqrt{M_P^2+(6\xi+1)\xi h^2}}{M_P^2+\xi h^2}\,,\quad U(\chi)=\frac{\lambda M_P^4 h^4(\chi)}{4(M_P^2+\xi h^2(\chi))^2}\,.$$

we have a flat potential at large fields: $U(\chi)\to\text{const}$ @ $h\gg M_P/\sqrt{\xi}$

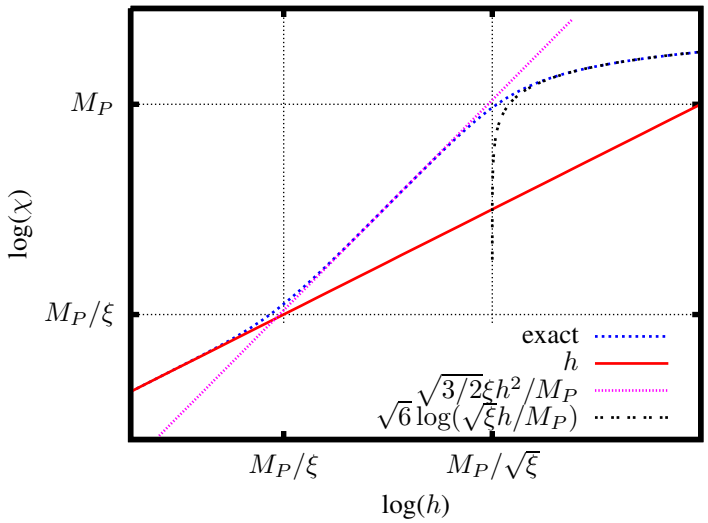

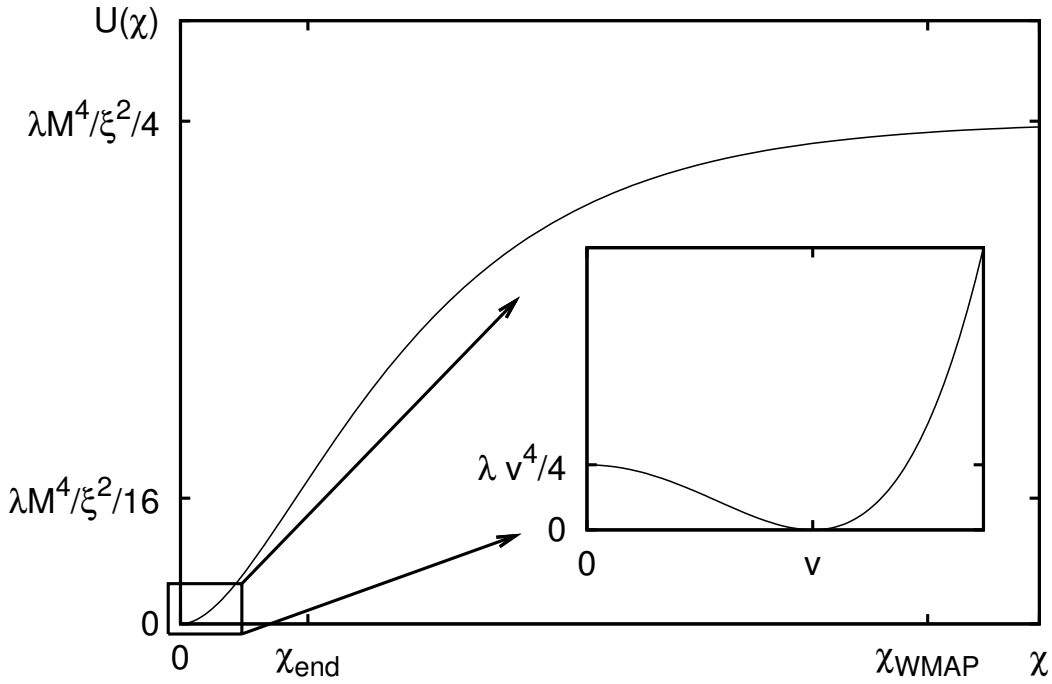

Reheating by Higgs field

after inflation: $M_P/\xi < h < M_P/\sqrt{\xi}$

effective dynamics : $h^2 \to \chi$

$$\mathscr{L} = \frac{1}{2}\partial_\mu\chi\partial^\mu\chi - \frac{\lambda}{6}\frac{M_P^2}{\xi^2}\chi^2$$

Advantage: NO NEW interactions
to reheat the Universe
inflaton couples to all SM fields!

exponentially flat potential! @ $h \gg M_P/\sqrt{\xi}$:

$$U(\chi) = \frac{\lambda M_P^4}{4\xi^2}\left(1 - \exp\left(-\frac{\sqrt{2}\chi}{\sqrt{3}M_P}\right)\right)^2$$

coincides with R^2-model!

But NO NEW d.o.f. 0812.3622, 1111.4397
Different reheating temperature...

from WMAP-normalization: $\xi \approx 47000 \times \sqrt{\lambda}$

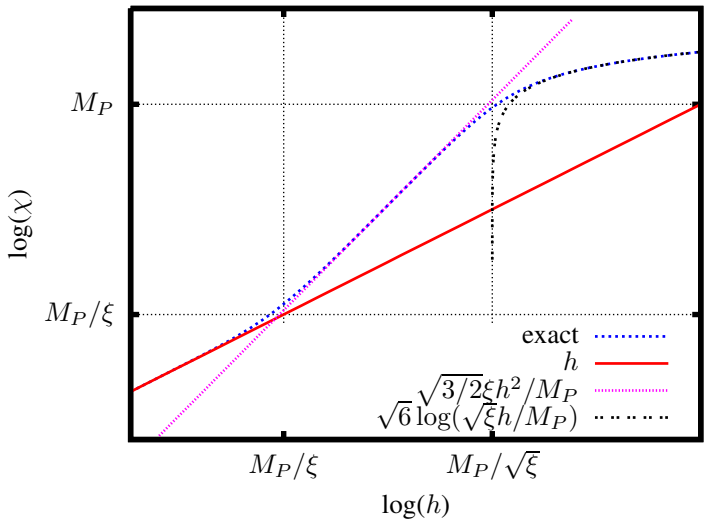

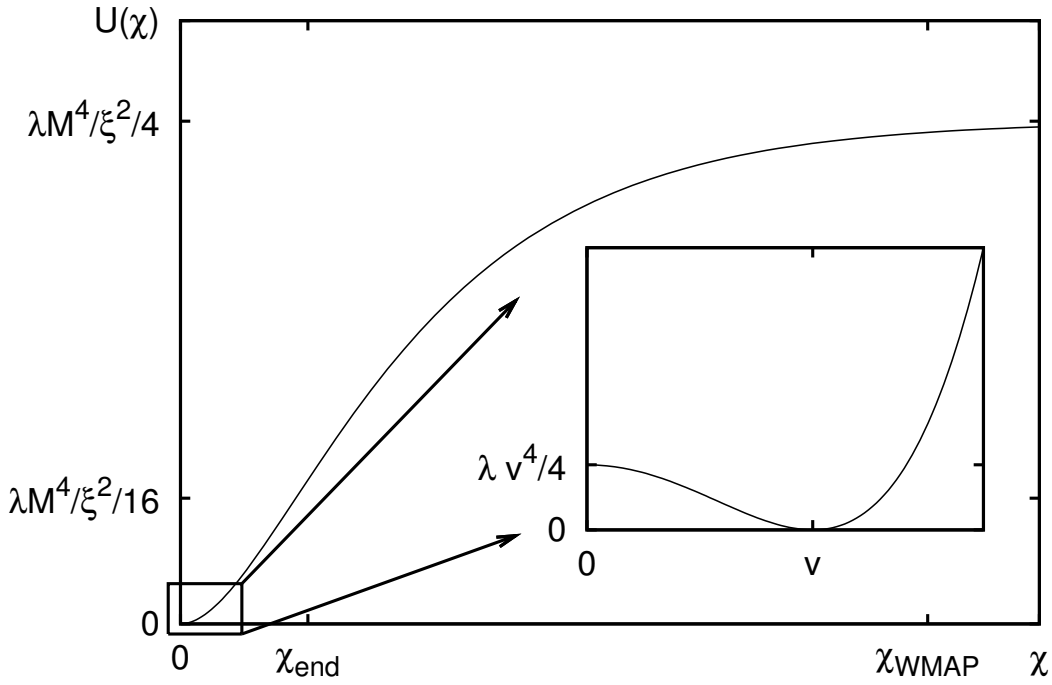

Reheating by Higgs field

after inflation: $M_P/\xi < h < M_P/\sqrt{\xi}$

exponentially flat potential! @ $h \gg M_P/\sqrt{\xi}$:

effective dynamics : $h^2 \to \chi$

$$U(\chi) = \frac{\lambda M_P^4}{4\xi^2}\left(1-\exp\left(-\frac{\sqrt{2}\chi}{\sqrt{3}M_P}\right)\right)^2$$

$$\mathscr{L} = \frac{1}{2}\partial_\mu\chi\partial^\mu\chi - \frac{\lambda}{6}\frac{M_P^2}{\xi^2}\chi^2$$

coincides with R^2-model!

But NO NEW d.o.f. 0812.3622, 1111.4397
Different reheating temperature. . .

Advantage: NO NEW interactions
to reheat the Universe
inflaton couples to all SM fields!

from WMAP-normalization: $\xi \approx 47000 \times \sqrt{\lambda}$

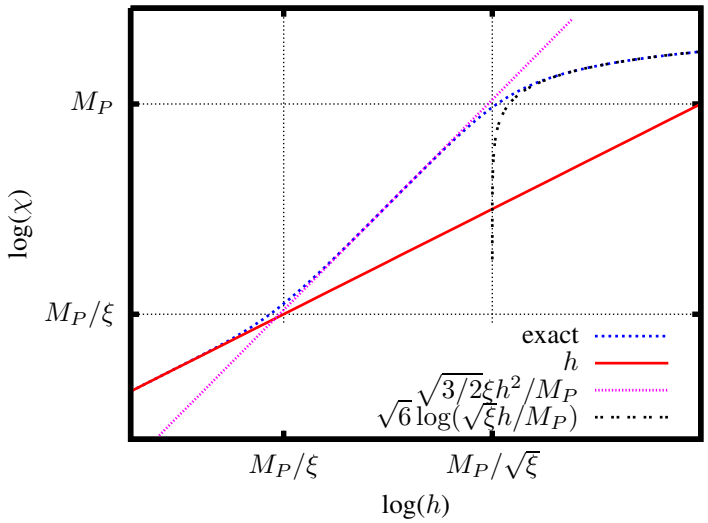

F.Bezrukov, D.G., M.Shaposhnikov, 0812.3622

$$m_W^2(\chi) = \frac{g^2}{2\sqrt{6}} \frac{M_P |\chi(t)|}{\xi}$$

$$m_t(\chi) = y_t \sqrt{\frac{M_P |\chi(t)|}{\sqrt{6}\,\xi}}\, \mathrm{sign}\,\chi(t)$$

Reheating by Higgs field

after inflation: $M_P/\xi < h < M_P/\sqrt{\xi}$

reheating via W^+W^-, ZZ production at zero crossings

then nonrelativistic gauge bosons scatter to light fermions

$$\chi \to W^+W^- \to f\bar{f}$$

effective dynamics : $h^2 \to \chi$

$$\mathscr{L} = \frac{1}{2}\partial_\mu\chi\partial^\mu\chi - \frac{\lambda}{6}\frac{M_P^2}{\xi^2}\chi^2$$

Hot stage starts almost from $T = M_P/\xi \sim 10^{14}$ GeV:

$$3.4\times10^{13}\,\mathrm{GeV} < T_r < 9.2\times10^{13}\left(\frac{\lambda}{0.125}\right)^{1/4}\mathrm{GeV}$$

Advantage: NO NEW interactions
to reheat the Universe
inflaton couples to all SM fields!

$n_s = 0.967$, $r = 0.0032$ F.Bezrukov, D.G.,

WMAP-normalization: $\xi \approx 47000\times\sqrt{\lambda}$ 1111.4397

True Extension of the Standard Model should

- Reproduce the correct neutrino oscillations
- Contain the viable DM candidate
- Be capable of explaining the baryon asymmetry of the Universe
- Have the inflationary mechanism operating at early times

Guiding principle:

use as little “new particle physics” as possible

Why?

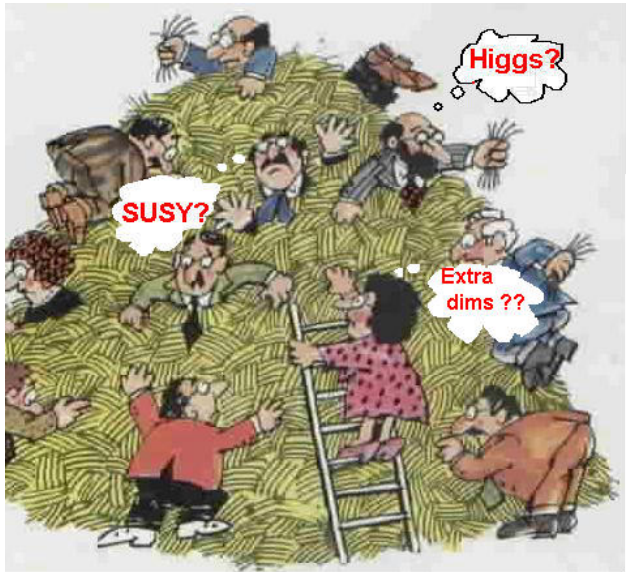

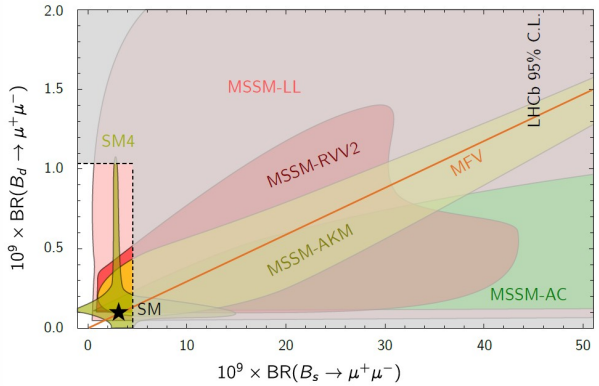

No any hints observed so far!

No FCNC

No WIMPs

No . . .

Nothing new at all

(apart of QCD. . .)

Straightforward renormalizable completion: νMSM

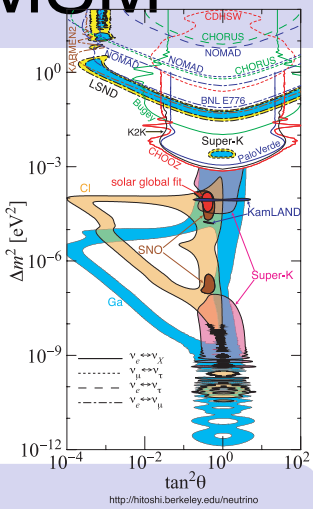

- Use as little "new physics" as possible
- Require to get the correct neutrino oscillations
- Explain DM and baryon asymmetry of the Universe

Lagrangian

Most general renormalizable with 3 right-handed neutrinos N_I

$$\mathscr{L}_{\nu MSM} = \mathscr{L}_{MSM} + \overline{N}_I i\partial\!\!\!/ N_I - f_{I\alpha} H \overline{N}_I L_\alpha - \frac{M_I}{2}\overline{N}_I^c N_I + \text{h.c.}$$

Extra coupling constants:

3 Majorana masses M_i — T.Asaka, S.Blanchet, M.Shaposhnikov (2005)

15 new Yukawa couplings — T.Asaka, M.Shaposhnikov (2005)
(Dirac mass matrix $M^D = f_{I\alpha}\langle H\rangle$ has 3 Dirac masses,
6 mixing angles and 6 CP-violating phases)

The model is remarkably simple:

It explains

- inflation without introducing a new scalars
- post-inflationary reheating without new interactions with SM fields

It may be further modified (e.g. by νMSM) to resolve other phenomenological problems of the SM:

- neutrino oscillations
- dark matter
- baryon asymmetry of the Universe

Outline

1. Inflation: general ideas
2. Higgs-inflation
   - Mechanism, Reheating, Predictions for perturbation spectra
   - Extensions: to solve neutrino, DM, BAU
3. LHC: the Higgs boson mass
4. Higgs-inflation and QFT
   - Nonremormalizability and strong coupling
   - BAU, neutrino oscillations due to nonrenormalizable operators?
5. Summary

Naively all we need is $V \sim \lambda\,\phi^4 > 0$...

(here in the Einstein frame)

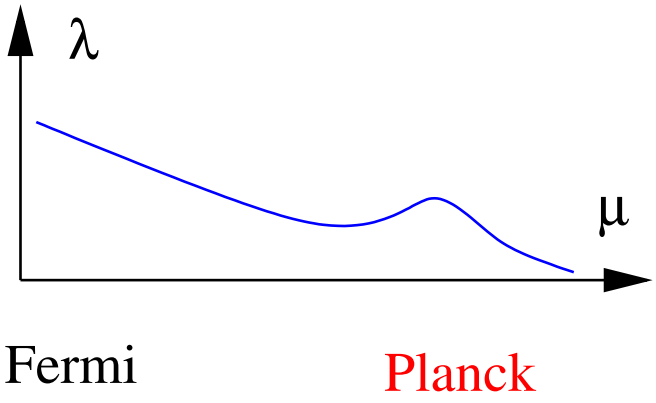

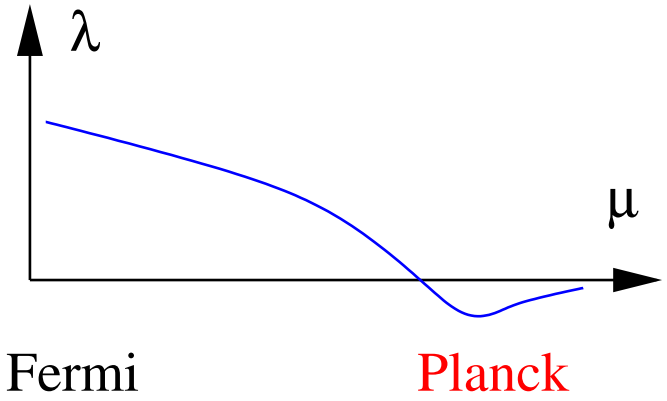

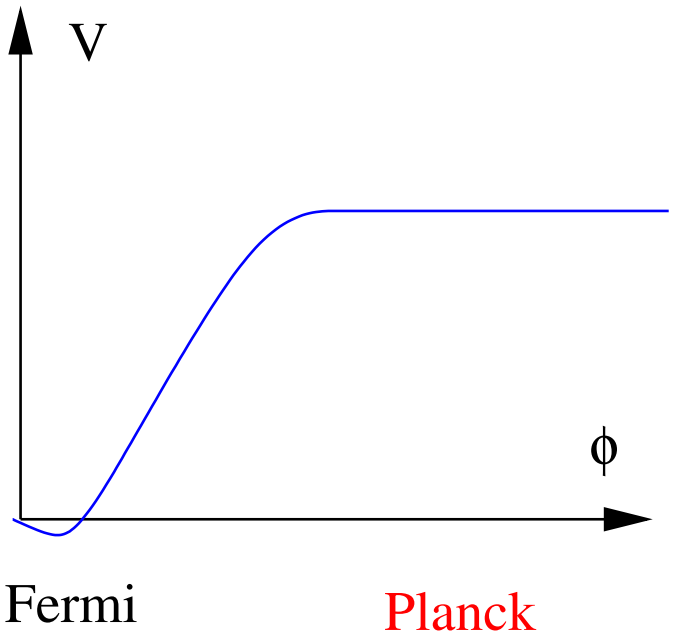

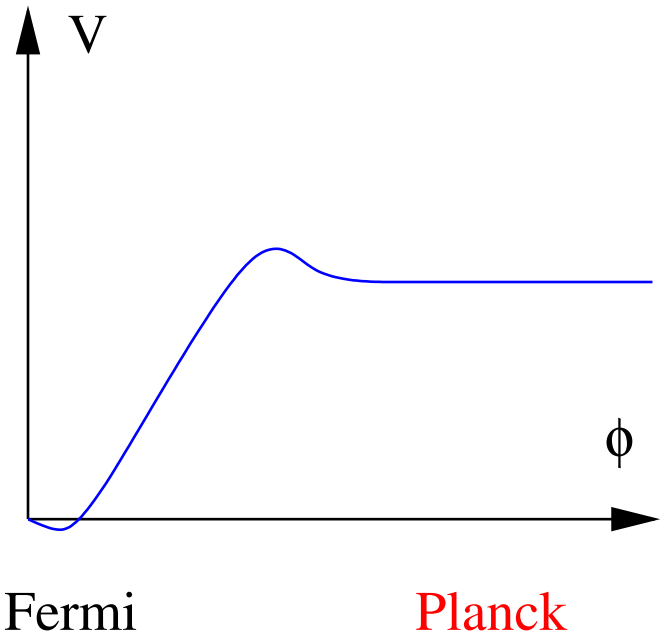

Critical point: where EW-vacuum becomes unstable

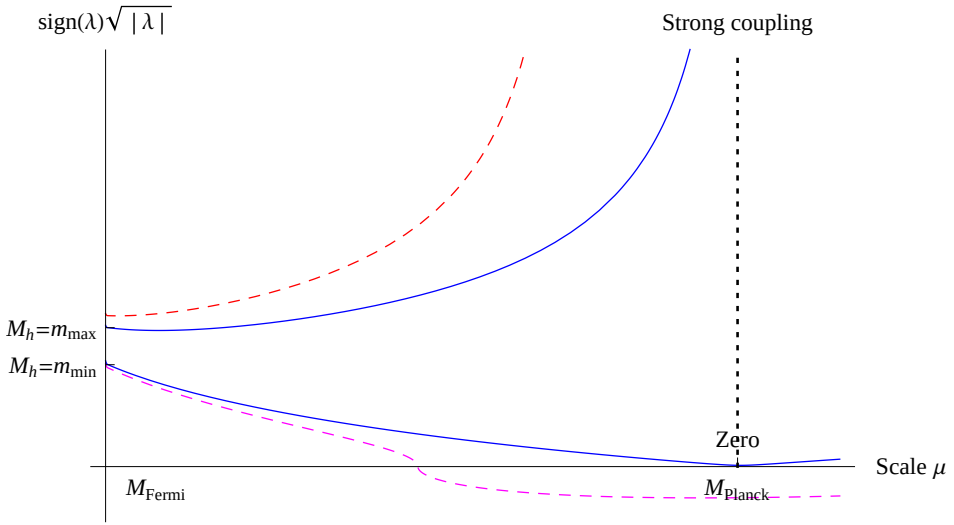

Higgs mass M_h=124 GeV

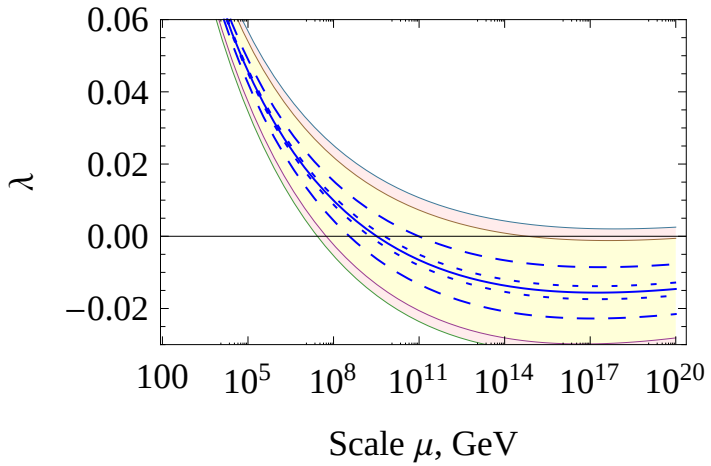

F.Bezrukov, M.Shaposhnikov (2009)
F.Bezrukov, D.G. (2011)
F.Bezrukov, M.Kalmykov, B.Kniehl, M.Shaposhnikov (2012)
G. Degrassi et al (2012)

$$m_h^{\mathrm{H}} > \left[129.0 + \frac{m_t - 172.9\,\mathrm{GeV}}{1.1\,\mathrm{GeV}} \times 2.2 - \frac{\alpha_s(M_Z) - 0.1181}{0.0007} \times 0.56\right] \mathrm{GeV}$$

present measurements at CMS and ATLAS:

$$m_h \simeq 125.5 \pm 1\ \mathrm{GeV}$$

Update at HCP2012, Nov.12-16

Higgs mass M_h=127 GeV

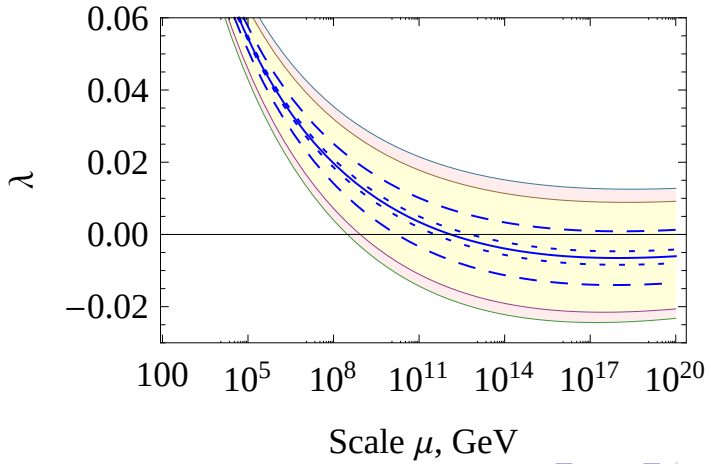

Multiple point principle: D.Bennett, H.Nielsen (1993), C.Froggatt, H.Nielsen (1995)

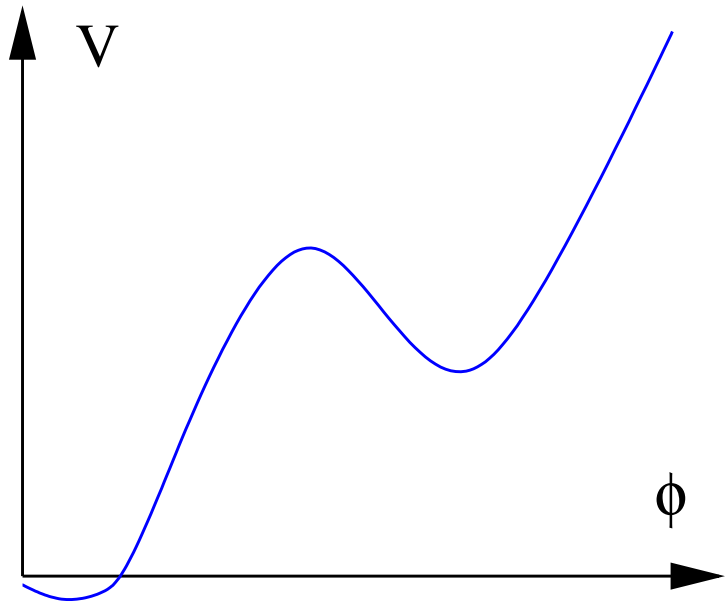

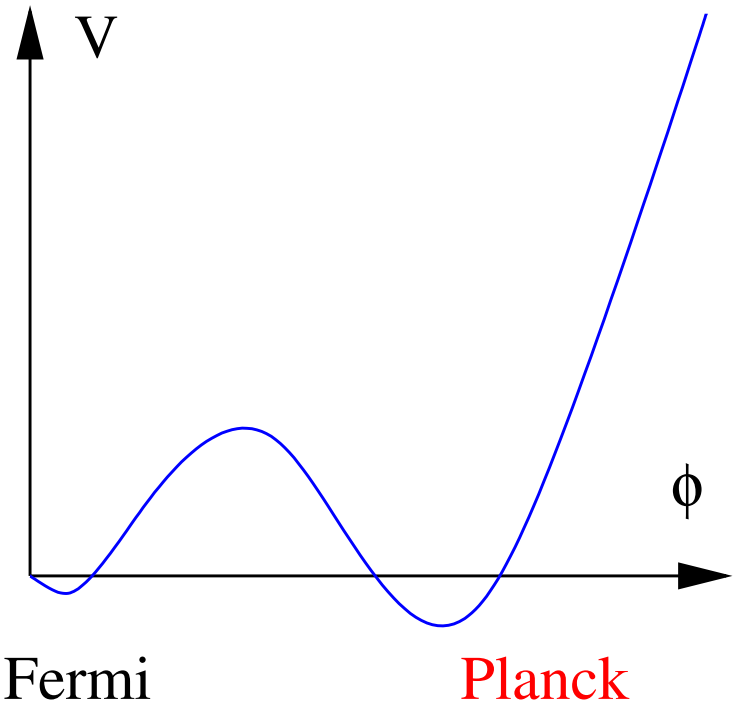

$$\Lambda \simeq 0 \Rightarrow V(\phi_{EW}) = V(\phi_{Planck}) = 0 \Rightarrow \lambda(\mu_{Planck}) = 0$$

Planck scale enters $\Rightarrow V'(\phi_{EW}) = V'(\phi_{Planck}) = 0 \Rightarrow \dfrac{d\lambda(\mu)}{d\log\mu}(\mu_{Planck}) = 0$

It gives $m_t \simeq 173$ GeV and $m_h \simeq 129$ GeV

Upper limit on the Higgs boson mass

Higgs-inflation: selfconsistency, $h \sim M_{Pl}$

F.Bezrukov, M.Shaposhnikov (2009)
F.Bezrukov, D.G. (2011)
F.Bezrukov, M.Kalmykov, B.Kniehl, M.Shaposhnikov (2012)
G. Degrassi et al (2012)

$$m_h^{\mathrm{H}} > \left[129.0 + \frac{m_t - 172.9\,\mathrm{GeV}}{1.1\,\mathrm{GeV}} \times 2.2 - \frac{\alpha_s(M_Z) - 0.1181}{0.0007} \times 0.56\right] \mathrm{GeV}$$

critical value refers to $\lambda(h \to M_P) \to 0$

WMAP-normalization: $\xi \approx 47000 \times \sqrt{\lambda} \cdots \to 0$?

$\xi \sim 1$ would imply $\lambda \sim 10^{-13}$ at finit interval $\Delta h \sim M_{Pl}$

$$\frac{d\lambda}{d\log\mu} = +\#\lambda^2 - Y_t^4 + \alpha_W + \ldots$$

Can not be arranged...

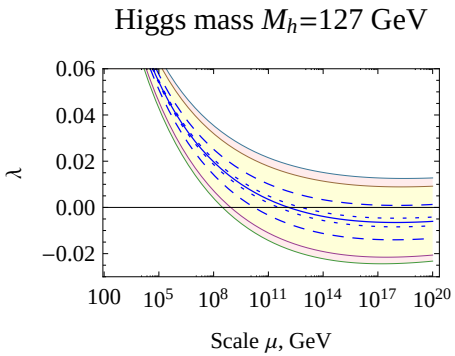

errors in M_W give uncertainties < 0.2 GeV

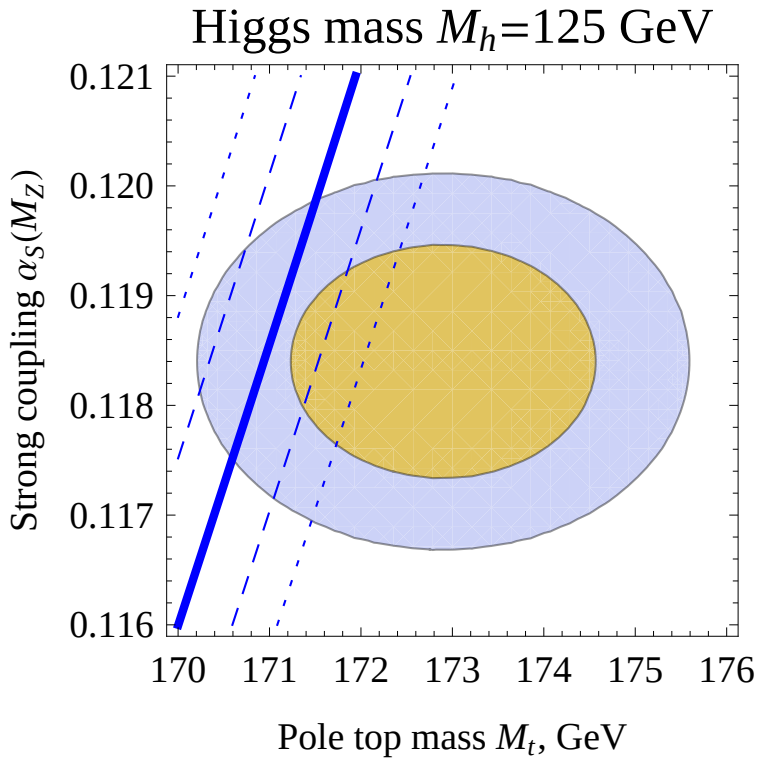

Experimental uncertainties: 2-3 GeV
Theoretical uncertainties: 1-2 GeV

Important for further improvement:

- 3-loop matching and QCD for t
- measurement of α_s, m_t and m_h at LHC(?)

The SM Higgs boson (?) found @ 125 GeV

- When the digit matters. . . !!
- Smooth incorporation of gravity @ M_{Pl}?

  – Great desert up to Gravity scale (asymptotic safety?)

  (no gauge hierarchy problem: all NP we need is either @ EW-scale or in gravity sector)

  – viable (ν, DM, BAU) SM extensions: R^2-inflation with νMSM, Higgs-inflation (can $S^2 H^\dagger H$ help?), . . .
- It's another scale: e.g. PQ-scale, or Leptogenesis, etc
- Just a coincidence, e.g. as GUT

  – gauge coupling unification $\rightarrow$ (gauge hierarchy problem, then not at a single point) $\rightarrow$ SUSY

  – there are other "hints":

  $m_h^2 \approx m_Z m_t$, $m_h \approx v/2 \approx 3m_Z/2$, $\lambda\,(m_h = 125\ \text{GeV}) \approx 0.125$

  Is Nature aware of GeV and decimal system?

Outline

1. Inflation: general ideas
2. Higgs-inflation
   - Mechanism, Reheating, Predictions for perturbation spectra
   - Extensions: to solve neutrino, DM, BAU
3. LHC: the Higgs boson mass
4. Higgs-inflation and QFT
   - Nonremormalizability and strong coupling
   - BAU, neutrino oscillations due to nonrenormalizable operators?
5. Summary

Fine theoretical descriptions both in

$$\text{UV:}\ \ \chi \gg M_P\ ,\ \ U = \text{const} + \mathcal{O}\left(\exp\left(-\sqrt{2}\,\chi/\sqrt{3}M_P\right)\right)$$

and in

$$\text{IR:}\ \ h \ll M_P/\xi\ ,\ \ U = \frac{\lambda}{4}h^4$$

no gravity corrections at inflation!
(Unlike βX^4) All inflationary predictions are robust

Obvious problem with QFT-description of IR/UV matching at intermediate $\chi < \chi_{\rm end}$ and $h < M_P/\sqrt{\xi}$

Hence no reliable prediction for the SM Higgs boson mass $m_h = \sqrt{2\lambda}\,v$ except the absence of Landau pole and wrong minimum of Higgs potential (well) below M_P/ξ

$$130\,\text{GeV} \lesssim m_h \lesssim 190\,\text{GeV}$$

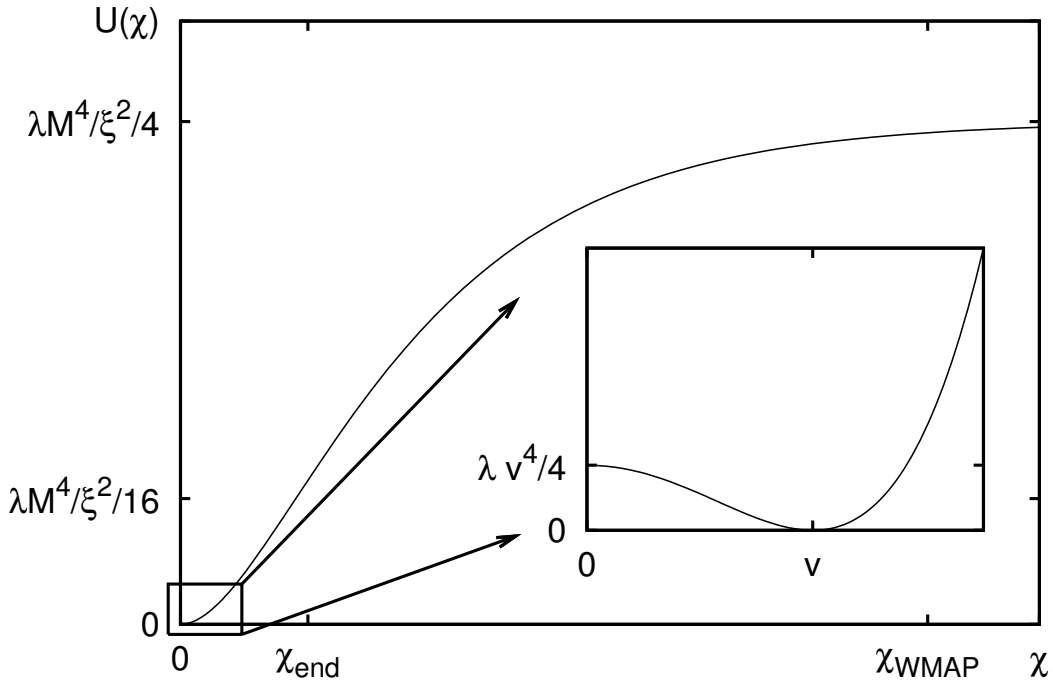

exponentially flat potential! @ $h \gg M_P/\sqrt{\xi}$:

$$U(\chi) = \frac{\lambda M_P^4}{4\xi^2}\left(1 - \exp\left(-\frac{\sqrt{2}\,\chi}{\sqrt{3}M_P}\right)\right)^2$$

coincides (apart of $T_{reh} \simeq 10^{14}$ GeV) with R^2-model!
But NO NEW d.o.f. 0812.3622

$$n_s = 0.967\ ,\ \ r = 0.0032\ ,\ \ N = 57.7$$

from WMAP-normalization: $\xi \approx 47000 \times \sqrt{\lambda}$

Fine theoretical descriptions both in

$$\text{UV:}\ \ \chi \gg M_P\ ,\ \ U = \text{const} + \mathcal{O}\left(\exp\left(-\sqrt{2}\chi/\sqrt{3}M_P\right)\right)$$

and in

$$\text{IR:}\ \ h \ll M_P/\xi\ ,\ \ U = \frac{\lambda}{4}h^4$$

no gravity corrections at inflation!
(Unlike βX^4) All inflationary predictions are robust

Obvious problem with QFT-description of IR/UV matching at intermediate $\chi < \chi_{\rm end}$ and $h < M_P/\sqrt{\xi}$

Hence no reliable prediction for the SM Higgs boson mass $m_h = \sqrt{2\lambda}\, v$ except the absence of Landau pole and wrong minimum of Higgs potential (well) below M_P/ξ

$$130\,\text{GeV} \lesssim m_h \lesssim 190\,\text{GeV}$$

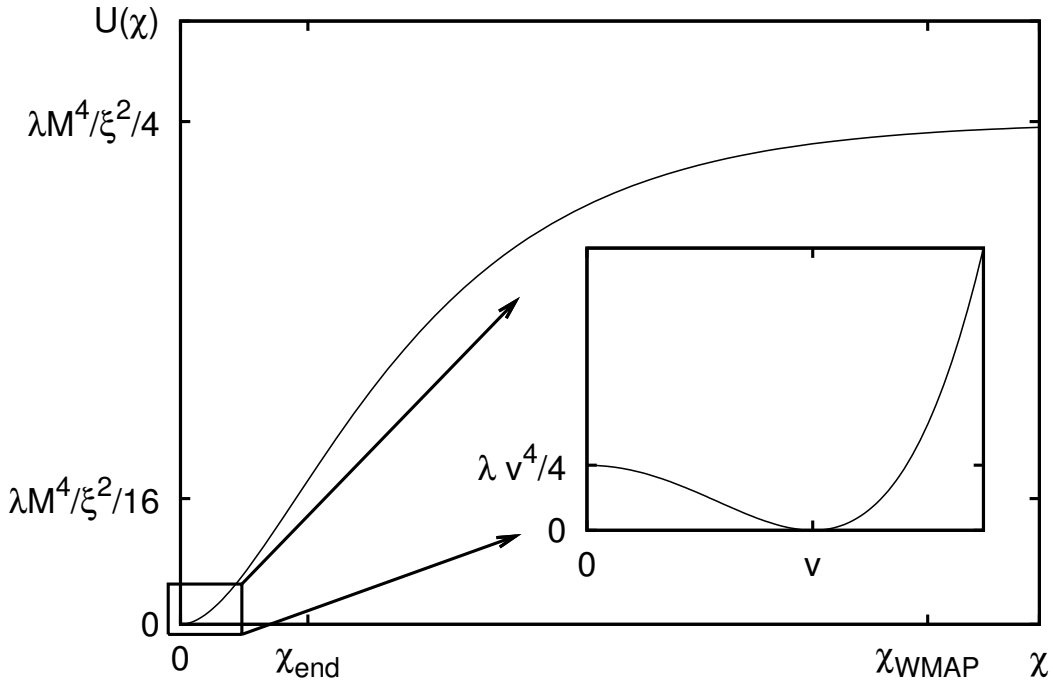

exponentially flat potential! @ $h \gg M_P/\sqrt{\xi}$:

$$U(\chi) = \frac{\lambda M_P^4}{4\xi^2}\left(1 - \exp\left(-\frac{\sqrt{2}\chi}{\sqrt{3}M_P}\right)\right)^2$$

coincides (apart of $T_{reh} \simeq 10^{14}$ GeV) with R^2-model!
But NO NEW d.o.f. 0812.3622

$$n_s = 0.967\ ,\ \ r = 0.0032\ ,\ \ N = 57.7$$

from WMAP-normalization: $\xi \approx 47000 \times \sqrt{\lambda}$

Strong coupling in Higgs-inflation: scatterings

Jordan frame

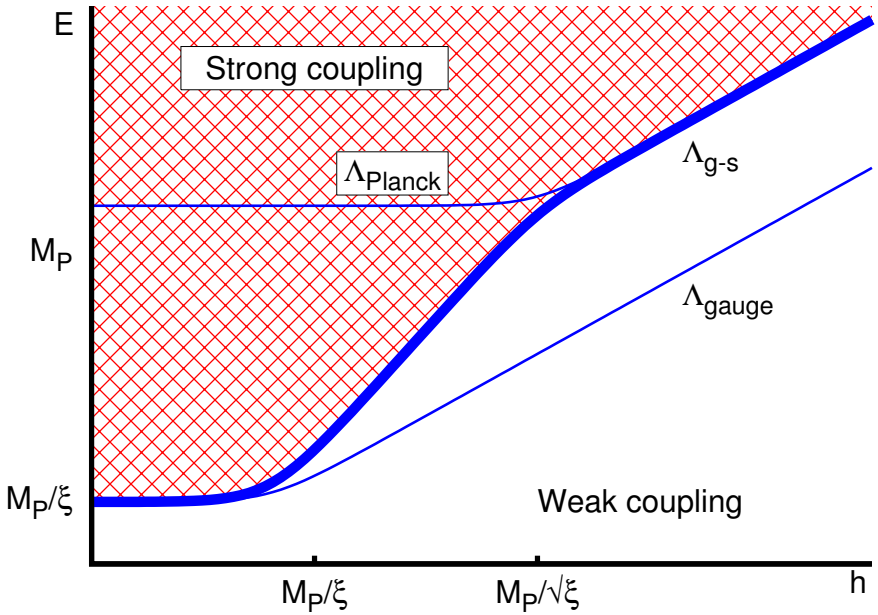

Einstein frame

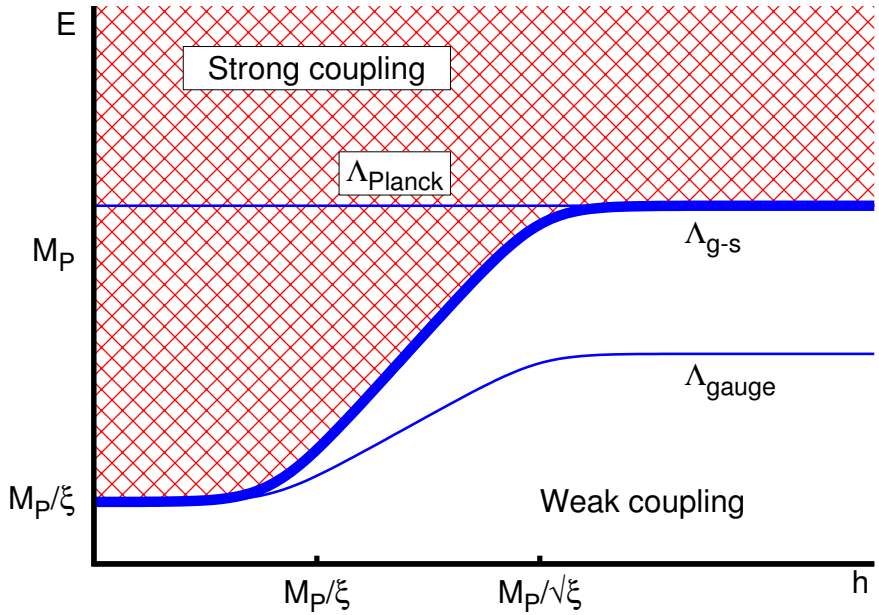

gravity-scalar sector:

$$\Lambda_{g-s}(h) \simeq \begin{cases} \frac{M_P}{\xi}, & \text{for } h \lesssim \frac{M_P}{\xi}, \\ \frac{\xi h^2}{M_P}, & \text{for } \frac{M_P}{\xi} \lesssim h \lesssim \frac{M_P}{\sqrt{\xi}}, \\ \sqrt{\xi} h, & \text{for } h \gtrsim \frac{M_P}{\sqrt{\xi}}. \end{cases}$$

gravitons: $\Lambda^2_{\text{Planck}} \simeq M_P^2 + \xi h^2$

gauge interactions:

$$\Lambda_{\text{gauge}}(h) \simeq \begin{cases} \frac{M_P}{\xi}, & \text{for } h \lesssim \frac{M_P}{\xi}, \\ h, & \text{for } \frac{M_P}{\xi} \lesssim h, \end{cases}$$

1008.5157

Strong coupling at M_P/ξ ...

Introducing new fields to push the scale up: out of the logic

Can it change the initial conditions of the Hot Big Bang?

1. reheating temperature
2. baryon (lepton) asymmetry of the Universe
3. dark matter abundance

Let's test these options adding all possible nonrenormalizable operators to the model

What can nonrenormalizable operators do?

F.Bezrukov, D.G., Shaposhnikov (2011)

$$\delta\mathscr{L}_{\rm NR} = -\frac{a_6}{\Lambda^2}(H^\dagger H)^3 + \cdots$$
$$+\frac{\beta_L}{4\Lambda}F_{\alpha\beta}\bar{L}_\alpha\tilde{H}H^\dagger L^c_\beta + \frac{\beta_B}{\Lambda^2}O_{\text{baryon violating}} + \cdots + \text{h.c.}$$
$$+\frac{\beta_N}{2\Lambda}H^\dagger H\bar{N}^c N + \frac{b_{L_\alpha}}{\Lambda}\bar{L}_\alpha(\not{\partial}N)^c\tilde{H} + \cdots\,,$$

L_α are SM leptonic doublets, $\alpha = 1,2,3$, N stands for right handed sterile neutrinos potentially present in the model, $\tilde{H}_a = \varepsilon_{ab}H^*_b$, $a,b = 1,2$;

and

$$\Lambda = \Lambda(h) = \left\{\Lambda_{g-s}(h)\,,\ \Lambda_{\text{gauge}}(h)\,,\ \Lambda_{\text{Planck}}(h)\right\}$$

couplings can differ significantly in different regions of h:
today $h < M_P/\xi$, at preheating $M_P/\xi < h < M_P/\sqrt{\xi}$

LFV, BV nonrenormalizable operators today

Neutrino masses: easily

$$\mathscr{L}^{(5)}_{\nu\nu} = \frac{\beta_L v^2}{4\Lambda}\frac{F_{\alpha\beta}}{2}\bar{\nu}_\alpha \nu^c_\beta + \text{h.c.}$$

hence

$$\Lambda \sim 3\times 10^{14}\,\text{GeV}\times\beta_L\times\left(\frac{3\times 10^{-3}\,\text{eV}^2}{\Delta m^2_{\text{atm}}}\right)^{1/2}$$

when

$$\Lambda = \frac{M_P}{\xi} \sim 0.6\times 10^{14}\,\text{GeV}$$

can explain with

$$\beta_L \sim 0.2$$

Proton decay: probably

$$\mathscr{L}^{(6)} \propto \frac{\beta_B}{\Lambda^2} QQQL$$

then from experiments

$$\Lambda \gtrsim \sqrt{\beta_B}\times 10^{16}\,\text{GeV}\times\left(\frac{\tau_{p\to\pi^0 e^+}}{1.6\times 10^{33}\,\text{years}}\right)^{1/4}$$

with the same

$$\Lambda = \frac{M_P}{\xi} \sim 0.6\times 10^{14}\,\text{GeV}$$

one needs

$$\beta_B < 0.4\times 10^{-4}$$

Either B and L_α are significantly different
or we will observe proton decay in the next generation experiment

LFV, BV nonrenormalizable operators today

Neutrino masses: easily

$$\mathscr{L}^{(5)}_{\nu\nu} = \frac{\beta_L v^2}{4\Lambda}\frac{F_{\alpha\beta}}{2}\bar{\nu}_\alpha \nu^c_\beta + \text{h.c.}$$

hence

$$\Lambda \sim 3\times 10^{14}\,\text{GeV}\times\beta_L\times\left(\frac{3\times 10^{-3}\,\text{eV}^2}{\Delta m^2_{\text{atm}}}\right)^{1/2}$$

when

$$\Lambda = \frac{M_P}{\xi} \sim 0.6\times 10^{14}\,\text{GeV}$$

can explain with

$$\beta_L \sim 0.2$$

Proton decay: probably

$$\mathscr{L}^{(6)} \propto \frac{\beta_B}{\Lambda^2} QQQL$$

then from experiments

$$\Lambda \gtrsim \sqrt{\beta_B}\times 10^{16}\,\text{GeV}\times\left(\frac{\tau_{p\to\pi^0 e^+}}{1.6\times 10^{33}\,\text{years}}\right)^{1/4}$$

with the same

$$\Lambda = \frac{M_P}{\xi} \sim 0.6\times 10^{14}\,\text{GeV}$$

one needs

$$\beta_B < 0.4\times 10^{-4}$$

Either B and L_α are significantly different
or we will observe proton decay in the next generation experiment

LFV, BV nonrenormalizable operators today

Neutrino masses: easily

$$\mathscr{L}^{(5)}_{\nu\nu} = \frac{\beta_L v^2}{4\Lambda}\frac{F_{\alpha\beta}}{2}\bar{\nu}_\alpha \nu^c_\beta + \text{h.c.}$$

hence

$$\Lambda \sim 3\times 10^{14}\,\text{GeV}\times\beta_L\times\left(\frac{3\times 10^{-3}\,\text{eV}^2}{\Delta m^2_{\text{atm}}}\right)^{1/2}$$

when

$$\Lambda = \frac{M_P}{\xi} \sim 0.6\times 10^{14}\,\text{GeV}$$

can explain with

$$\beta_L \sim 0.2$$

Proton decay: probably

$$\mathscr{L}^{(6)} \propto \frac{\beta_B}{\Lambda^2} QQQL$$

then from experiments

$$\Lambda \gtrsim \sqrt{\beta_B}\times 10^{16}\,\text{GeV}\times\left(\frac{\tau_{p\to\pi^0 e^+}}{1.6\times 10^{33}\,\text{years}}\right)^{1/4}$$

with the same

$$\Lambda = \frac{M_P}{\xi} \sim 0.6\times 10^{14}\,\text{GeV}$$

one needs

$$\beta_B < 0.4\times 10^{-4}$$

Either B and L_α are significantly different
or we will observe proton decay in the next generation experiment

Leptogenesis, $\Delta_B \approx \Delta_L/3$: can be successful

$$i\frac{d}{dt}\hat{Q}_L = \left[\hat{H}_{\rm int}, \hat{Q}_L\right] , \quad \Delta n_L \equiv n_L - n_{\bar{L}} = \langle Q_L \rangle$$

$$\mathscr{L}_Y = -Y_\alpha \bar{L}_\alpha H E_\alpha + \text{h.c.} , \qquad \mathscr{L}^{(5)}_{\nu\nu} = \frac{\beta_L}{4\Lambda} F_{\alpha\beta} \bar{L}_\alpha \tilde{H} H^\dagger L^c_\beta + \text{h.c.}$$

$$d\Delta n_L/dt \propto \text{Im}\left(\beta_L^4 \,\text{Tr}\left(FF^\dagger FYYF^\dagger YY\right)\right) \propto \beta_L^4 y_\tau^4 \cdot \text{Im}\left(F_{3\beta} F^*_{\alpha\beta} F_{\alpha 3} F^*_{33}\right)$$

for the gauge cutoff $\Lambda = h$ one has

$$\beta_L^4 \left(\frac{y_\tau}{0.01}\right)^4 \left(\frac{0.25}{\lambda}\right)^{5/4} \times 10^{-10} < \Delta_L < \beta_L^4 \left(\frac{y_\tau}{0.01}\right)^4 \left(\frac{0.25}{\lambda}\right) \times 10^{-9} ,$$

for gravity-scalar cutoff $\Lambda = \xi\, h^2/M_P$

$$\beta_L^4 \left(\frac{y_\tau}{0.01}\right)^4 \left(\frac{0.25}{\lambda}\right)^{13/4} \times 6.3 \times 10^{-13} < \Delta_L < \beta_L^4 \left(\frac{y_\tau}{0.01}\right)^4 \left(\frac{0.25}{\lambda}\right)^2 \times 2.4 \times 10^{-10}$$

In both cases the asymmetry can be (significantly) increased with operator

$$\delta\mathscr{L}^\tau = y_\tau L_\tau H E_\tau + \beta_y L_\tau H E_\tau \frac{H^\dagger H}{\Lambda^2} + \cdots$$

one can fancy the hierarchy

$$1 \sim \beta_y \gg y_\tau \sim 10^{-2} .$$

gives a factor up to 10^8 !

Leptogenesis, $\Delta_B \approx \Delta_L/3$: can be successful

$$i\frac{d}{dt}\hat{Q}_L = \left[\hat{H}_{\rm int}, \hat{Q}_L\right], \quad \Delta n_L \equiv n_L - n_{\bar{L}} = \langle Q_L \rangle$$

$$\mathscr{L}_Y = -Y_\alpha \bar{L}_\alpha H E_\alpha + \text{h.c.}, \qquad \mathscr{L}^{(5)}_{\nu\nu} = \frac{\beta_L}{4\Lambda} F_{\alpha\beta} \bar{L}_\alpha \tilde{H} H^\dagger L^c_\beta + \text{h.c.}$$

$$d\Delta n_L/dt \propto \text{Im}\left(\beta_L^4 \,\text{Tr}\left(FF^\dagger FYYF^\dagger YY\right)\right) \propto \beta_L^4 y_\tau^4 \cdot \text{Im}\left(F_{3\beta} F^*_{\alpha\beta} F_{\alpha 3} F^*_{33}\right)$$

for the gauge cutoff $\Lambda = h$ one has

$$\beta_L^4 \left(\frac{y_\tau}{0.01}\right)^4 \left(\frac{0.25}{\lambda}\right)^{5/4} \times 10^{-10} < \Delta_L < \beta_L^4 \left(\frac{y_\tau}{0.01}\right)^4 \left(\frac{0.25}{\lambda}\right) \times 10^{-9},$$

for gravity-scalar cutoff $\Lambda = \xi\, h^2/M_P$

$$\beta_L^4 \left(\frac{y_\tau}{0.01}\right)^4 \left(\frac{0.25}{\lambda}\right)^{13/4} \times 6.3 \times 10^{-13} < \Delta_L < \beta_L^4 \left(\frac{y_\tau}{0.01}\right)^4 \left(\frac{0.25}{\lambda}\right)^{2} \times 2.4 \times 10^{-10}$$

In both cases the asymmetry can be (significantly) increased with operator

$$\delta\mathscr{L}^\tau = y_\tau L_\tau H E_\tau + \beta_y L_\tau H E_\tau \frac{H^\dagger H}{\Lambda^2} + \cdots$$

one can fancy the hierarchy

$$1 \sim \beta_y \gg y_\tau \sim 10^{-2}.$$

gives a factor up to 10^8 !

Dark matter: an example of sterile fermion

$$\mathscr{L}_{\rm int} = \beta_N \frac{H^\dagger H}{2\Lambda} \bar{N}^c N = \frac{\beta_N}{4} \frac{h^2}{\Lambda(h)} \bar{N}^c N$$

can be produced at preheating or at the hot stage

DM fermion has to be light! (WDM?)

Indeed, today

$\frac{b_{L_\alpha}}{\Lambda} \bar{L}_\alpha (\not{D} N)^c \tilde{H}$

$$f_\alpha \sim b_{L_\alpha} \frac{M_N}{\Lambda} \,.$$

So, N is unstable with the $\gamma\nu$ partial width of the order

$$\Gamma_{N\to\gamma\nu} \sim \frac{9\, b_{L_\alpha}^2\, \alpha\, G_F^2}{512\pi^4} \frac{v^2 M_N^5}{\Lambda^2} \,.$$

EGRET gives $\tau_{\gamma\nu} \gtrsim 10^{27}$ s, hence 0709.2299

$$\text{for } \Lambda = M_P: \quad M_N \lesssim 200\,\text{MeV}, \qquad \text{for } \Lambda = M_P/\xi: \quad M_N \lesssim 4\,\text{MeV}$$

Outline

1. Inflation: general ideas
2. Higgs-inflation
   - Mechanism, Reheating, Predictions for perturbation spectra
   - Extensions: to solve neutrino, DM, BAU
3. LHC: the Higgs boson mass
4. Higgs-inflation and QFT
   - Nonremormalizability and strong coupling
   - BAU, neutrino oscillations due to nonrenormalizable operators?
5. Summary

Summary

LHC hints at 125 GeV may point at:

- Multiple point principle ...?
- No new particle physics upto gravity scale
- Higgs-inflation: $129\ \text{GeV} \lesssim m_h \lesssim 195\ \text{GeV}$

  needs better precision in measurement of m_h, m_t, y_t, α_s

  may ask for UV-completion... asymptotic safety?

  Some other inflationary models also point at $m_h \sim 125\,\text{GeV}$ (e.g. hill-top potential in simple tensor-scalar gravity I.Masina, A.Notari (2012))
- Higgs-inflation may be easily completed to account for
  - neutrino oscillations
  - dark matter
  - baryon asymmetry of the Universe

  Examples: νMSM, nonrenormalizable operators at strong coupling UV-scale

Backup slides

Absence of the Landau pole upto inflationary scale $\sim 10^{13}$ GeV and stability of the Higgs potential at large post-inflationary values of the Higgs boson field $h \sim M_{Pl}$

$$129\,\text{GeV} \lesssim m_h \lesssim 195\,\text{GeV}$$

F.Bezrukov, D.G. (2010)

Lower bound refer to the case of $\lambda(M_{Pl}) = 0$

Message: Zero Planck-scale corrections from gravity?

PAST: gauge coupling unification...
Message: $\lambda(125\ \text{GeV}) = 0.125$
Nature knows

GeV and decimal system !!

THIS MODEL HAS ALREADY BEEN CORNERED BY LHC !!

RG-evolution with energy scale μ:

$$\frac{d\lambda}{d\log\mu^2} \propto +\#\cdot\lambda^2 - \#\cdot Y_t^4$$

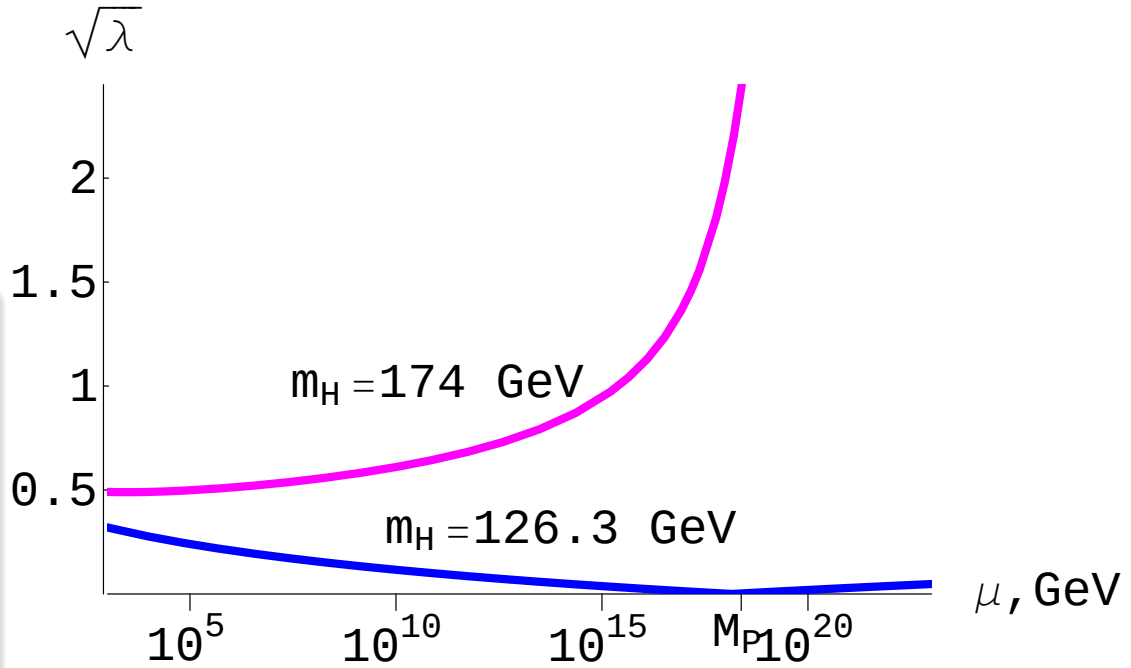

$h \to W^+W^-, ZZ$

$T_{reh} \simeq 3 \times 10^{13}$ GeV

F.Bezrukov, D.G., M.Shaposhnikov (2009)

Models without NEW scalar(s) in PARTICLE PHYSICS SECTOR

A.Starobinsky (1980) R^2-inflation

$$S^{JF}=-\frac{M_P^2}{2}\int\sqrt{-g}\,d^4x\left(R-\frac{R^2}{6\mu^2}\right)+S^{JF}_{matter}\,,$$

Higgs-inflation F.Bezrukov, M.Shaposhnikov (2007)

$$S^{JF}=\int\sqrt{-g}\,d^4x\left(-\frac{M_P^2}{2}R-\xi H^\dagger HR\right)+S^{JF}_{matter}$$

In this two models "inflatons" couple to the SM fields in different ways

R^2-inflation: gravity, $\mathscr{L}\propto\phi/M_P$

D.G., A.Panin (2010)

$$T_{reh}\approx 3\times 10^9\ \text{GeV}$$

Higgs-inflation: finally, at $\phi\lesssim M_P/\xi$ like in SM

F.Bezrukov, D.G., M.Shaposhnikov (2008)

$$T_{reh}\approx 6\times 10^{13}\ \text{GeV}$$

with different length of the post inflationary matter domination stage: F.Bezrukov, D.G. (2011)

- somewhat different perturbation spectra

  $n_s=0.965\,,\ r=0.0032$ $\qquad$ $n_s=0.967\,,\ r=0.0036$

  break in primordial gravity wave spectra at different frequencies
- in R^2 perturbations 10^{-5} enter nonlinear regime:

  gravity waves from inflaton clumps
- SM Higgs potenial is OK up to the reheating scale:

  $m_h\gtrsim 116\ \text{GeV}$ $\qquad$ $m_h\gtrsim 120-129\ \text{GeV}$

The power spectra of primordial perturbations

The same potential, the same ϕ at the end of inflation

e.g. F.Bezrukov, D.G., M.Shaposhnikov (2008)

$$n_s \simeq 1 - \frac{8(4N+9)}{(4N+3)^2}\,, \qquad r \simeq \frac{192}{(4N+3)^2}$$

But WMAP observes different N in the two models:
$k/a_0 = 0.002/\mathrm{Mpc}$ exits horizon at different moments

$$N = \frac{1}{3}\log\left(\frac{\pi^2}{30\sqrt{27}}\right) - \log\frac{(k/a_0)}{T_0 g_0^{1/3}} + \log\frac{V_*^{1/2}}{V_e^{1/4} M_P} - \frac{1}{3}\log\frac{V_e^{1/4}}{10^{13}\,\mathrm{GeV}} - \frac{1}{3}\log\frac{10^{13}\,\mathrm{GeV}}{T_{reh}}$$

The difference is

F.Bezrukov, D.G. (2011)

$$N_* \approx 57 - \frac{1}{3}\log\frac{10^{13}\,\mathrm{GeV}}{T_{reh}}\,, N_{R^2} = 54.37,\ N_H = 57.66.$$

R^2-inflation: $n_s = 0.965,\quad r = 0.0036,$

Higgs-inflation: $n_s = 0.967,\quad r = 0.0032.$

Planck(?), CMBPol(1-2σ)

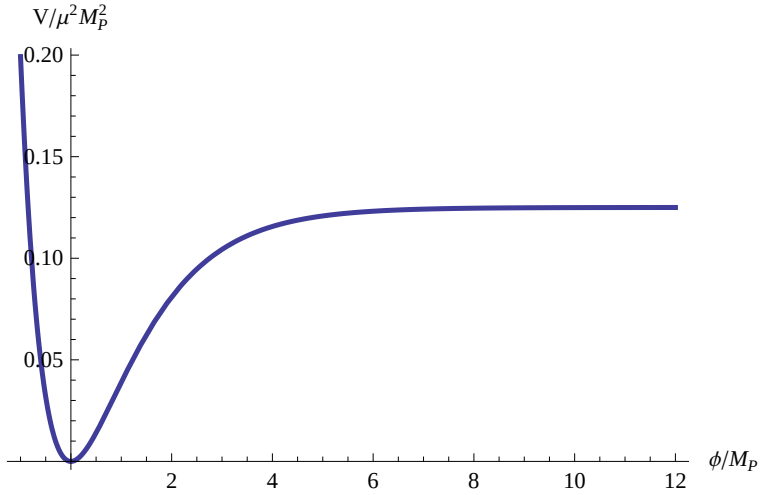

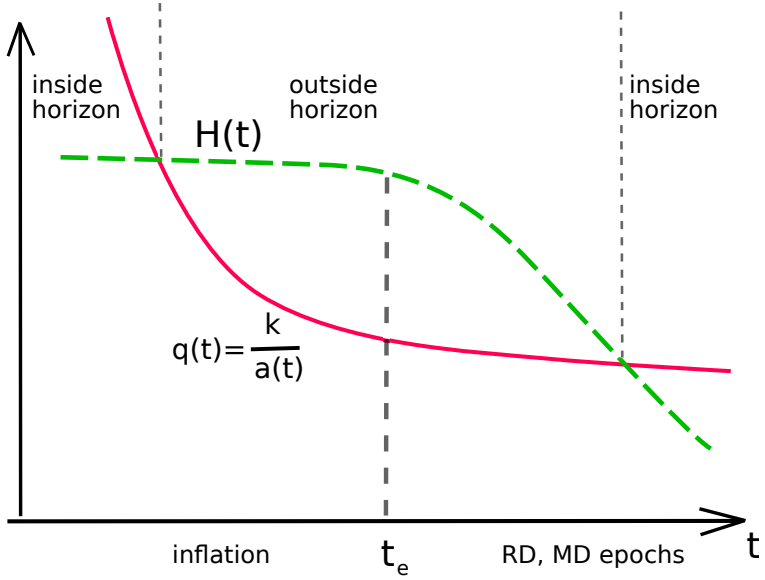

Upper limit on the Higgs boson mass

R^2-inflation: stability while the Universe evolves from $Q = T_{reh} \approx 3 \times 10^9$ GeV

J.Espinosa, G.Giudice, A.Riotto (2007) F.Bezrukov, D.G. (2011)

$$m_h^{R^2} > \left[116.5 + \frac{m_t - 172.9\,\text{GeV}}{1.1\,\text{GeV}} \times 2.6 - \frac{\alpha_s(M_Z) - 0.1181}{0.0007} \times 0.5\right] \text{GeV}$$

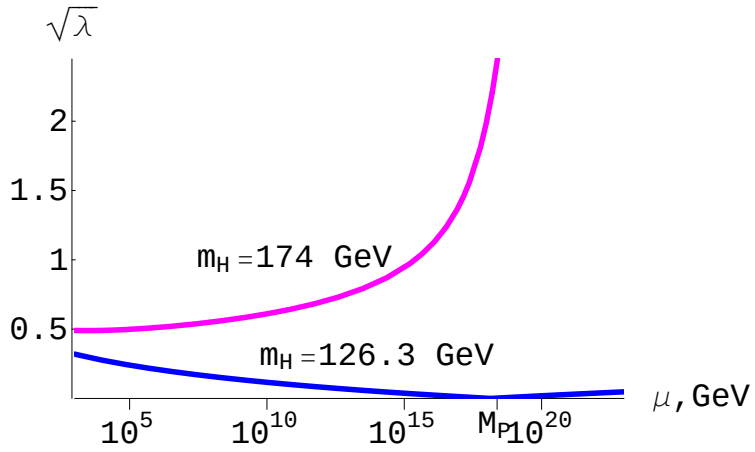

Higgs-inflation: stability while the Universe evolves from $Q = T_{reh} \approx 6 \times 10^{13}$ GeV

F.Bezrukov, M.Shaposhnikov (2009) F.Bezrukov, D.G. (2011)

$$m_h^{\text{H}} > \left[120.0 + \frac{m_t - 172.9\,\text{GeV}}{1.1\,\text{GeV}} \times 2.1 - \frac{\alpha_s(M_Z) - 0.1181}{0.0007} \times 0.5\right] \text{GeV}$$

stability while the Universe evolves right after inflation $h \approx 10^{13}$ GeV

$$m_h^{\text{H}} > [129.0 + \ldots]\ \text{GeV}$$

present limit from CMS: $m_h < 127$ GeV @ 95%CL

Uncertainties: about $2-3$ GeV due to unknown QCD-corrections

Important for further improvement:

- (N)NLO corrections in QCD coupling
- measurement of m_t and m_h at LHC

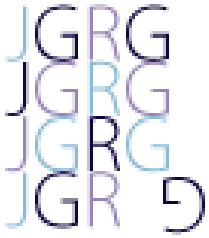

Yingli Zhang, JGRG 22(2012)111422

"Tunneling fields in non-linear massive gravity"

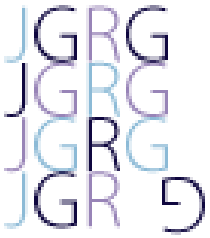

RESCEU SYMPOSIUM ON

GENERAL RELATIVITY AND GRAVITATION

JGRG 22



November 12-16 2012

Koshiba Hall, The University of Tokyo, Hongo, Tokyo, Japan



YUKAWA INSTITUTE FOR THEORETICAL PHYSICS

RESCEU SYMPOSIUM ON GENERAL RELATIVITY AND GRAVITATION

JGRG22

November 12 - 16 2012

Hawking-Moss instantons in non-linear Massive Gravity

Ying-li Zhang

YITP , Kyoto University

Cooperator: Ryo Saito, Misao Sasaki

arxiv: 1210.6224

In Massive Gravity (MG), the mass of graviton is non-vanishing, which breaks the gauge invariance

Generally speaking, the dof is

$$10 - 4 = 6$$

Constraint equations

Helicity $\pm 2, \ \pm 1, \ 0,$



Recently, a non-linear construction of massive gravity theory (dRGT) is proposed, where the BD ghost is removed by specially designed non-linear terms, so that the lapse function N becomes a Lagrangian Multiplier, which removes the ghost degree of freedom.

Non-linear Massive Gravity (dRGT)

C. de Rham, G. Gabadadze, Phys. Rev. D 82, 044020 (2010);
C. de Rham, G. Gabadadze and A. J. Tolley, Phys. Rev. Lett 106, 231101 (2011);
S. F. Hassan and R. A. Rosen, JHEP 1107, 009 (2011)

$$S_{MG} = \int d^4x \, \sqrt{-g} \left[\frac{R}{2} + m_g^2 (\mathcal{L}_2 + \alpha_3 \mathcal{L}_3 + \alpha_4 \mathcal{L}_4) \right],$$

where $[\mathcal{K}] = tr\left(K_\mu^\nu\right)$

$$\mathcal{L}_2 = \frac{1}{2}\left([\mathcal{K}]^2 - \left[\mathcal{K}^2\right] \right),$$

$$\mathcal{L}_3 = \frac{1}{6}\left([\mathcal{K}]^3 - 3\,[\mathcal{K}]\left[\mathcal{K}^2\right] + 2\left[\mathcal{K}^3\right] \right),$$

$$\mathcal{L}_4 = \frac{1}{24}\left([\mathcal{K}]^4 - 6\,[\mathcal{K}]^2\left[\mathcal{K}^2\right] + 3\left[\mathcal{K}^2\right]^2 + 8\,[\mathcal{K}]\left[\mathcal{K}^3\right] - 6\left[\mathcal{K}^4\right] \right),$$

$$\mathcal{K}_\nu^\mu \equiv \delta_\nu^\mu - \sqrt{g^{\mu\sigma} G_{ab}(\phi) \partial_\nu \phi^a \partial_\sigma \phi^b}.$$

fiducial metric

Stuckelberg field

Self-accelerating solution is found in context of non-linear massive gravity, where two branches exist with effective cosmological constant consists of a contribution from mass of graviton. A. E. Gumrukcuoglu et. al. JCAP 106, 231101(2011);

$$\Lambda_{\pm} = -\frac{m_g^2}{(\alpha_3+\alpha_4)^2}\left[(1+\alpha_3)\left(2+\alpha_3+2\,\alpha_3^2-3\,\alpha_4\right) \pm 2\,\left(1+\alpha_3+\alpha_3^2-\alpha_4\right)^{3/2}\right],$$

There seems to be some hope to explain the current acceleration, but…

still there exists the Cosmological Constant Problem

A possible resolution: Anthropic Landscape of Vacua

S. Weinberg, Rev. Mod. Phys. 61, 1 (1989)

• The Landscape has several local minima;

• the fields can (and will) tunnel from a metastable minimum to a lower one;

• this process is driven by instanton.

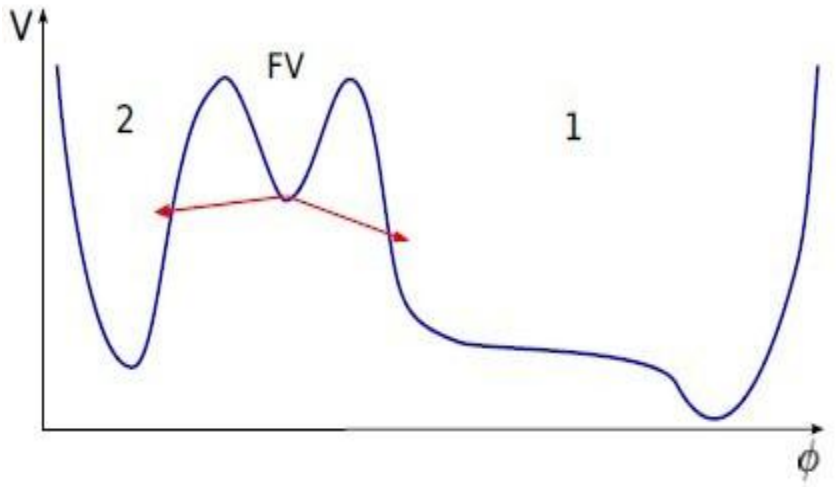

S. Coleman and F. de Luccia, Phys.Rev. D21, 3305, (1980)

→ it is interesting to investigate how the stability of a vacuum is determined in the context of non-linear Massive Gravity

Setup of model

$$S = S_{MG} + S_m,$$

$$S_m \equiv -\int d^4x\, \sqrt{-g}\left[\frac{1}{2}(\partial\sigma)^2 + V(\sigma)\right],$$

- potential $V(\sigma)$

  local minima: σ_F

  global minima: σ_T

  local max: $\sigma_{\rm top}$

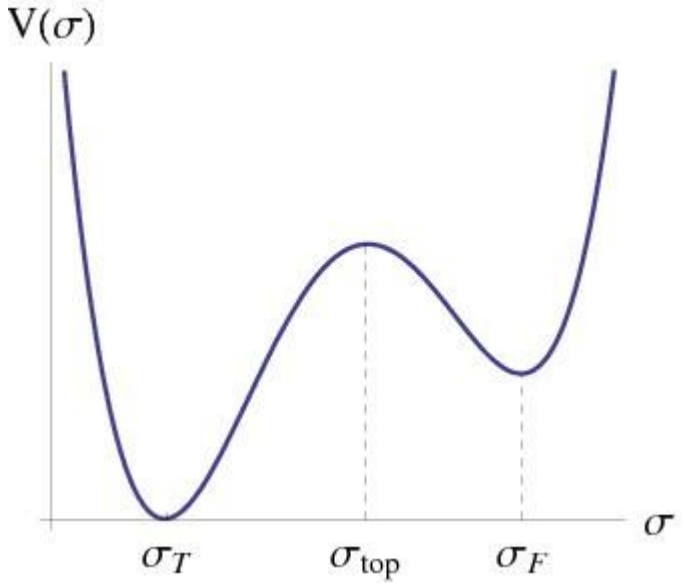

- tunneling probability per unit time per unit volume

$$\Gamma/V = Ae^{-B},$$

$$B = S_E[g_{\mu\nu,B}, \phi_B] - S_E[g_{\mu\nu,F}, \phi_F],$$

bounce solution

'false vacuum'

Lowest action

usually, bounce solutions are explored by assuming an O(4) symmetry

➢ spacetime metric: Euclidean

$$g_{\mu\nu}dx^\mu dx^\nu = N(\xi)^2 d\xi^2 + a(\xi)^2 \Omega_{ij} dx^i dx^j,$$

$$\Omega_{ij} \equiv \delta_{ij} + \frac{K\delta_{il}\delta_{jm}x^l x^m}{1 - K\delta_{lm}x^l x^m}, \quad K > 0$$

Note: the fiducial metric may not respect the symmetry

- fiducial metric: deSitter

$$G_{ab}(\phi)d\phi^a d\phi^b \equiv -(d\phi^0)^2 + b(\phi^0)^2\Omega_{ij}d\phi^i d\phi^j,$$

$$b(\phi^0) \equiv F^{-1}\sqrt{K}\cosh(F\phi^0).$$

fiducial Hubble parameter

→ the O(4)-symmetric solutions are obtained by setting

$$\phi^0 = f(\xi), \quad \phi^i = x^i.$$

Inserting these ansatz into the action, we obtain the constraint equation by varying with respect with f

$$(i\dot{a} + Nb_{,f}) \left[\left(3 - \frac{2b}{a}\right) + \alpha_3 \left(1 - \frac{b}{a}\right)\left(3 - \frac{b}{a}\right) + \alpha_4 \left(1 - \frac{b}{a}\right)^2 \right] = 0,$$

$$\dot{a} \equiv \frac{da}{d\xi} \qquad b_{,f} \equiv \frac{db}{df} = \sqrt{K}\sinh(Ff)$$

→

Branch I $\quad Nb_{,f} = -i\dot{a},$ (equivalent to branch II)

Branch II $\quad \left(3 - \frac{2b}{a}\right) + \alpha_3 \left(1 - \frac{b}{a}\right)\left(3 - \frac{b}{a}\right) + \alpha_4 \left(1 - \frac{b}{a}\right)^2 = 0.$

→

$$b = X_{\pm} a, \qquad X_{\pm} \equiv \frac{1 + 2\,\alpha_3 + \alpha_4 \pm \sqrt{1 + \alpha_3 + \alpha_3^2 - \alpha_4}}{\alpha_3 + \alpha_4}.$$

Friedmann equation & EOM for tunneling field

$$\begin{cases} \dfrac{3}{a^2}\left(\dfrac{da}{d\tau}\right)^2 - \dfrac{3K}{a^2} = \dfrac{1}{2}\left(\dfrac{d\sigma}{d\tau}\right)^2 - V(\sigma) - \Lambda_{\pm}, \\ \dfrac{d^2\sigma}{d\tau^2} + 3\left(\dfrac{da}{d\tau}\right)\dfrac{d\sigma}{d\tau} - V_{,\sigma}(\sigma) = 0 \end{cases}$$

where $\mathrm{d}\tau \equiv N\mathrm{d}t,$

$$\Lambda_{\pm} \equiv -\frac{m_g^2}{(\alpha_3+\alpha_4)^2}\left[(1+\alpha_3)\left(2+\alpha_3+2\,\alpha_3^2-3\,\alpha_4\right) \pm 2\,\left(1+\alpha_3+\alpha_3^2-\alpha_4\right)^{3/2}\right],$$

Hawking-Moss(HM) solution

- HM solution can be found at the local maximum of the potential $\sigma = \sigma_{\rm top}$ under boundary condition $a_{\rm HM}(H_{\rm HM}\tau = \pm\pi/2) = 0\,,$

$$a_{\rm HM}(\tau) = H_{\rm HM}^{-1}\sqrt{K}\cos\left(H_{\rm HM}\tau\right)\,,$$

$\mathrm{d}\tau \equiv N\mathrm{d}\xi$

$$H_{\rm HM} \equiv \sqrt{\frac{\Lambda_{\pm} + V(\sigma_{top})}{3}}$$

- inserting this result into the Euclidean action and evaluate by integrating in the range $H_{\rm HM}\tau = -\pi/2 \longrightarrow \pi/2$, we finally express the HM action

$$Y_\pm \equiv 3(1-X_\pm) + 3\alpha_3(1-X_\pm)^2 + \alpha_4(1-X_\pm)^3$$

$$S_E[a_{\rm HM}, \sigma_{\rm top}] = -\frac{8\pi^2}{H_{\rm HM}^2}\left[1 - \frac{Y_\pm X_\pm}{6\alpha^4}\left(\frac{m_g}{H_{\rm HM}}\right)^2\left(2 - \sqrt{1-\alpha^2}(2+\alpha^2)\right)\right]$$

standard HM solution

Correction due to the mass of graviton

$$\alpha \equiv X_\pm \frac{F}{H_{\rm HM}} \in [0,1]$$

Comparing with GR case, recalling the tunneling probability $\Gamma/V = Ae^{-B}$, we obtains:

$$\Delta B \equiv B^{(\rm MG)} - B^{(\rm GR)} = CY_\pm\,, \quad C<0$$

Tunneling rate is enhanced for $Y_\pm > 0$,
suppressed for $Y_\pm < 0$.

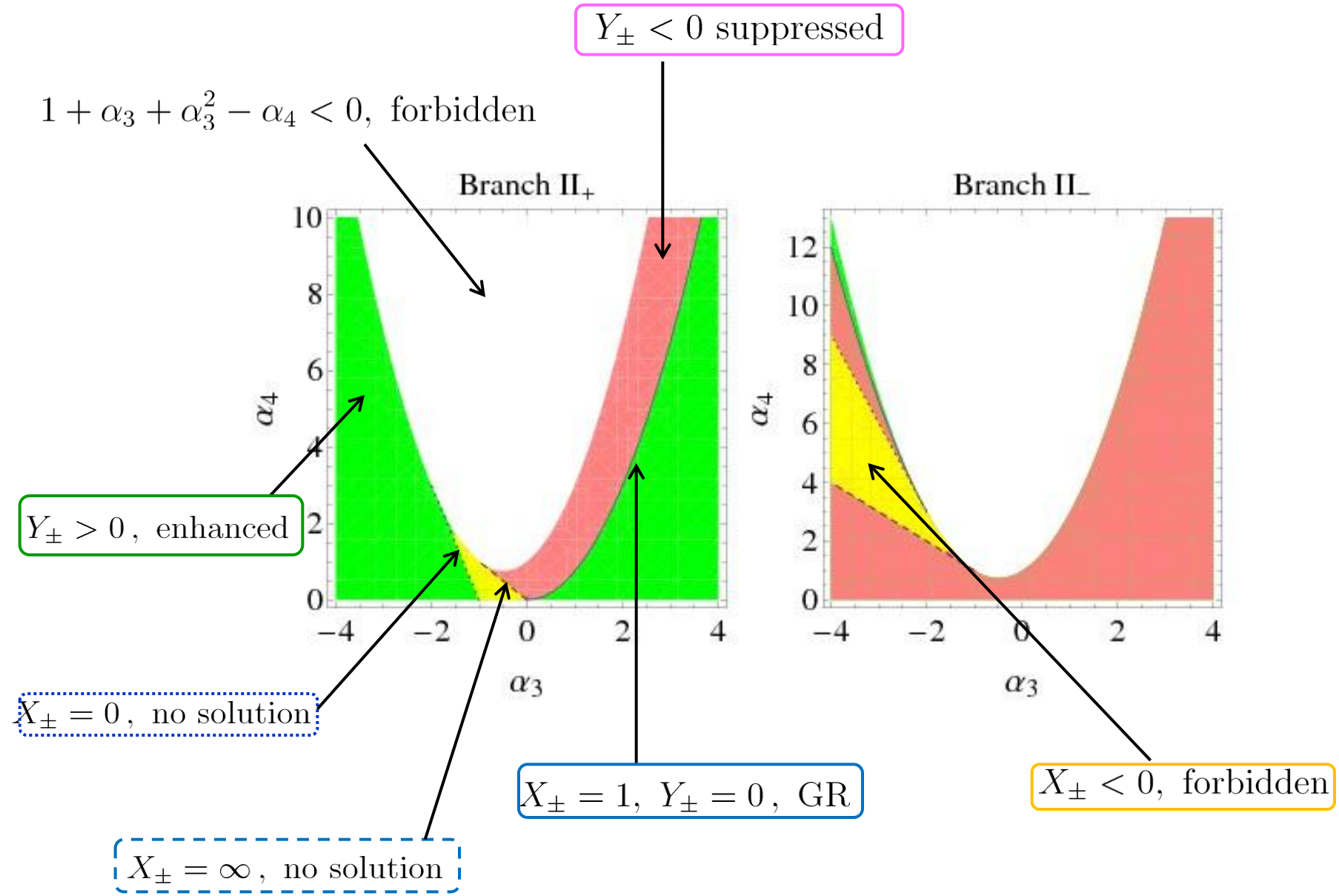
$Y_\pm < 0$ suppressed
$1 + \alpha_3 + \alpha_3^2 - \alpha_4 < 0$, forbidden
Branch II$_+$
Branch II$_-$
α_4
α_3
$Y_\pm > 0$, enhanced
$X_\pm = 0$, no solution
$X_\pm = 1$, $Y_\pm = 0$, GR
$X_\pm < 0$, forbidden
$X_\pm = \infty$, no solution

Summary and future work

- We constructed a model in which the tunneling field minimally couples to the non-linear massive gravity;
- corrections of HM solution from mass term is found, which implies suppression or enhancement of tunneling rate, depending on the choices of parameters;
- analysis of Colemann-DeLuccia solutions is under work;
- it would be interesting to investigate the case where the tunneling field couples to the non-linear massive gravity non-minimally.

- Appendix

$$Y_\pm \equiv 3(1-X_\pm) + 3\alpha_3(1-X_\pm)^2 + \alpha_4(1-X_\pm)^3$$

$$S_E[a_{\rm HM}, \sigma_{\rm top}] = \int \mathrm{d}^3x\sqrt{\Omega}\int_{-\pi/2H_{\rm HM}}^{\pi/2H_{\rm HM}} \mathrm{d}\tau\; a_{HM}^3 \left(2\Lambda_{\pm,\rm eff} - \frac{6K}{a_{\rm HM}^2} + m_g^2 Y_\pm \sqrt{-\left(\frac{df_{\rm HM}}{d\tau}\right)^2} \right)$$

$$\Lambda_{\pm,\rm eff} \equiv \Lambda_\pm + V(\sigma_{\rm top})$$

$$b_{\rm HM} = F^{-1}\sqrt{K}\cosh(F f_{\rm HM}) = X_\pm a_{\rm HM} \Longrightarrow \left(\frac{df_{\rm HM}}{d\tau}\right)^2 = \frac{X_\pm^2 \sin^2(H_{\rm HM}\tau)}{\alpha_{\rm HM}^2\cos^2(H_{\rm HM}\tau) - 1}$$

$$\alpha_{\rm HM} \equiv X_\pm \frac{F}{H_{\rm HM}} \in [0,1]$$

- Note: for the Minkowski fiducial metric, $b_{\rm HM} = \sqrt{K} f_E$, by setting $f_E = -if$

$$\frac{df_{E,\rm HM}}{d\tau} = -X_\pm \sin(H_{\rm HM}\tau)$$

so we recover the Minkowski one by setting $\alpha_{\rm HM} = 0$.

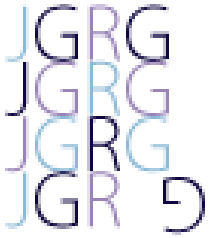

Atsushi Nishizawa, JGRG 22(2012)111423

"Probing for massive gravitational-wave background with a ground-based detector network"

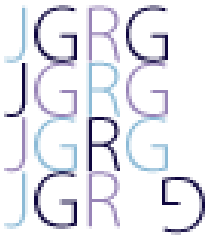

RESCEU SYMPOSIUM ON

GENERAL RELATIVITY AND GRAVITATION

JGRG 22



November 12-16 2012

Koshiba Hall, The University of Tokyo, Hongo, Tokyo, Japan



Probing for massive GW background with a ground-based detector network

Atsushi Nishizawa (YITP, Kyoto Univ.)

Collaborator: Kazuhiro Hayama (NAOJ)



Nov. 12-16, 2012, JGRG22 @ Tokyo Univ.

Introduction

So far, various modified gravity theories have been suggested.
(Scalar-tensor theory, f(R) gravity, higher derivative gravity, bimetric gravity, nonlinear massive gravity etc.)

Those theories could alter tensor perturbations and predict the properties of GWs different from GR:

- massive gravitons
- different phase evolution of GWs
- additional GW polarizations (scalar & vector pols.)



GW observation can be utilized for
- direct test of general relativity
- probing the extended theories beyond GR

Here we focus on massive graviton and its detectability with GW detectors.

Massive graviton & GW

Dispersion relation of graviton $\omega^2 = m_g^2 + k^2$

- minimum frequency of GW $\omega_{\rm min} = m_g$
- propagating speed of GW (group velocity)

$$v_g(\omega; m_g) \equiv \frac{d\omega}{dk} = \sqrt{1 - \frac{m_g^2}{\omega^2}}$$

Modification of GW waveform from a compact binary

[Will 1998, Berti et al. 2005, Yagi & Tanaka 2010]

aLIGO: $m_g \lesssim 10^{-22}\,{\rm eV}$ LISA: $m_g \lesssim 10^{-25}\,{\rm eV}$

- phase velocity of GW

$$v_p(\omega; m_g) \equiv \frac{\omega}{k} = \left(\sqrt{1 - \frac{m_g^2}{\omega^2}}\right)^{-1}$$

GW polarizations

In general metric theory of gravity, six polarizations are allowed.
[Eardley et al. 1973, Will 1993].

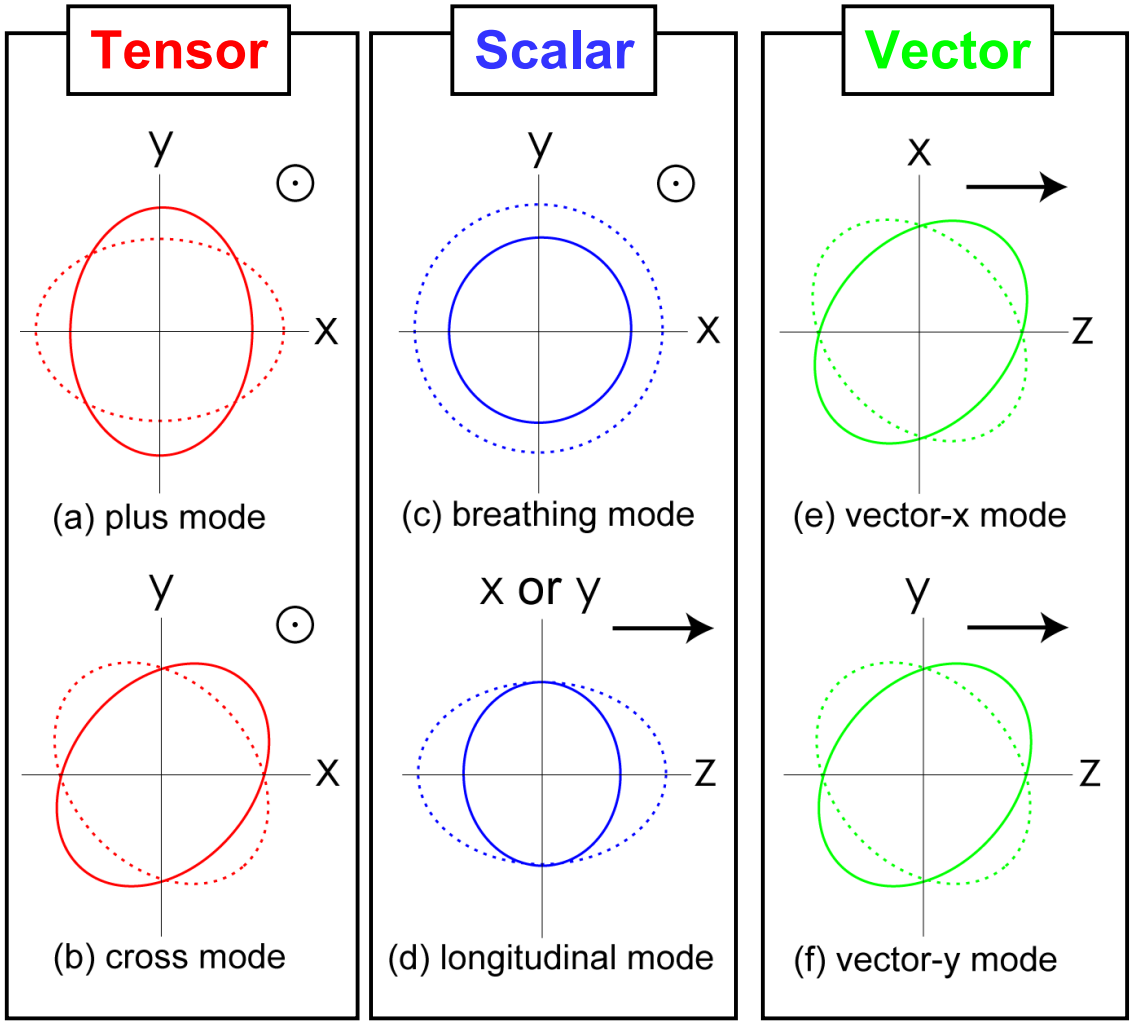

Current mass constraints

Solar system	$m_g \lesssim 10^{-21}\,\mathrm{eV}$	[Talmadge et al. 1988, Will 1998]
Galaxy cluster	$m_g \lesssim 10^{-29}\,\mathrm{eV}$	[Goldhaber & Nieto 1974]
Weak lensing	$m_g \lesssim 10^{-31}\,\mathrm{eV}$	[Choudhury et al. 2004]
CMB	$m_g \lesssim 10^{-30}\,\mathrm{eV}$	[Dubovsky et al. 2010]

The above is static bounds based on the modification of Newtonian potential (background level).

Binary pulsar	$m_g \lesssim 10^{-20}\,\mathrm{eV}$	[Finn & Sutton 2002]

This bound is applied to only tensor polarization mode.

Constraints on scalar and vector mode of GW is NOT so strong and they can be quite massive.

GW background

Here we consider massive GW background.

Detector output of GW background

$$h(t,\vec{X}) = \sum_A \int_{S^2} d\hat{\Omega} \int_{-\infty}^{\infty} df\, \tilde{h}_A(f,\hat{\Omega})\, e^{2\pi i f(t-\hat{\Omega}\cdot\vec{X}/v_p)} F_A(\hat{\Omega})$$

detector response func.

$$v_p(\omega; m_g) \equiv \frac{\omega}{k} = \left(\sqrt{1-\frac{m_g^2}{\omega^2}}\right)^{-1}$$

Energy density of GW background

$$\Omega_{\rm gw}(f) \equiv \frac{1}{\rho_c}\frac{d\rho_{\rm gw}}{d\ln f}$$

tensor $\quad \Omega^T_{\rm gw} \equiv \Omega^+_{\rm gw} + \Omega^\times_{\rm gw} \qquad (\Omega^+_{\rm gw} = \Omega^\times_{\rm gw})\ ,$

vector $\quad \Omega^V_{\rm gw} \equiv \Omega^x_{\rm gw} + \Omega^y_{\rm gw} \qquad (\Omega^x_{\rm gw} = \Omega^y_{\rm gw})\ ,$

scalar $\quad \Omega^S_{\rm gw} \equiv \frac{1}{3}\left(\frac{1+2\kappa}{1+\kappa}\right)(\Omega^b_{\rm gw} + \Omega^\ell_{\rm gw})\ , \qquad \kappa \equiv \Omega^\ell_{\rm gw}/\Omega^b_{\rm gw}$

Correlation analysis of GW background

Single detector cannot distinguish GWB and random detector noise.
Also in most cases GW signal is small compared to noise.

$$h(t) \ll n(t)$$

Signal of detector 1: $s_1(t) = h(t) + n_1(t)$

Signal of detector 2: $s_2(t) = h(t) + n_2(t)$



correlation

$$\int dt\, s_1(t)\, s_2(t) = \int dt\, \left[h^2(t) + h(t)n_1(t) + h(t)n_2(t) + n_1(t)n_2(t)\right]$$

$\propto T$ $\propto \sqrt{T}$

Signal to noise ratio

$$\mathrm{SNR} \approx \frac{\int dt\, h^2(t)}{\int dt\, n_1(t)n_2(t)} \propto \sqrt{T}$$

Correlation signal

Correlation signal in a frequency bin:

$$\mu_i(f) = \frac{3H_0^2}{10\pi^2} T\, f^{-3} \sum_A \gamma_i^A \Omega_{\rm gw}^A(f) \Delta f$$

Overlap reduction function

tensor $$\gamma_{IJ}^T(f; m_g^T) \equiv \frac{5}{2} \int_{S^2} \frac{d\hat{\Omega}}{4\pi} \left(F_I^+ F_J^+ + F_I^\times F_J^\times\right) \exp\left[i \frac{2\pi f\, \hat{\Omega} \cdot \Delta\vec{X}}{v_p(f; m_g^T)}\right] ,$$

vector $$\gamma_{IJ}^V(f; m_g^V) \equiv \frac{5}{2} \int_{S^2} \frac{d\hat{\Omega}}{4\pi} \left(F_I^x F_J^x + F_I^y F_J^y\right) \exp\left[i \frac{2\pi f\, \hat{\Omega} \cdot \Delta\vec{X}}{v_p(f; m_g^V)}\right] ,$$

scalar $$\gamma_{IJ}^S(f; m_g^S) \equiv \frac{15}{1+2\kappa} \int_{S^2} \frac{d\hat{\Omega}}{4\pi} \left(F_I^b F_J^b + \kappa F_I^\ell F_J^\ell\right) \exp\left[i \frac{2\pi f\, \hat{\Omega} \cdot \Delta\vec{X}}{v_p(f; m_g^S)}\right]$$

$$\kappa \equiv \Omega_{\rm gw}^\ell / \Omega_{\rm gw}^b$$

Overlap reduction function

$$\gamma_{IJ}^{T}(f;m_g^T) \equiv \frac{5}{2}\int_{S^2}\frac{d\hat{\Omega}}{4\pi}\left(F_I^{+}F_J^{+}+F_I^{\times}F_J^{\times}\right)\exp\left[i\,\frac{2\pi f\,\hat{\Omega}\cdot\Delta\vec{X}}{v_p(f;m_g^T)}\right]$$

@ low freq. ⟶ Const. @ high freq. ⟶ Damping oscillation

LIGO H1-L1 pair

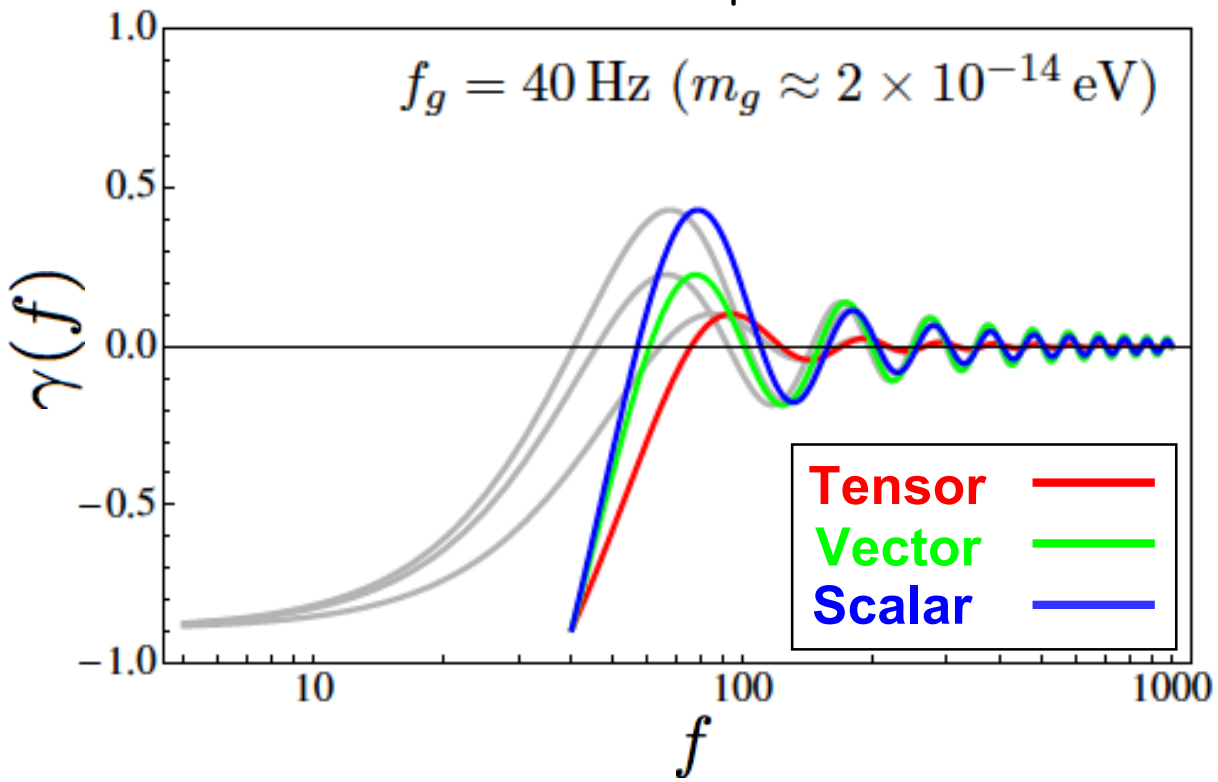

For massive graviton, effective distance between detectors is smaller than massless case.

$$\frac{\Delta\vec{X}}{c} \longrightarrow \frac{\Delta\vec{X}}{v_p}$$

- stronger correlation
- low freq. cutoff

Mass detection

Case (i): small mass

Case (ii): intermediate mass

Case (iii): large mass

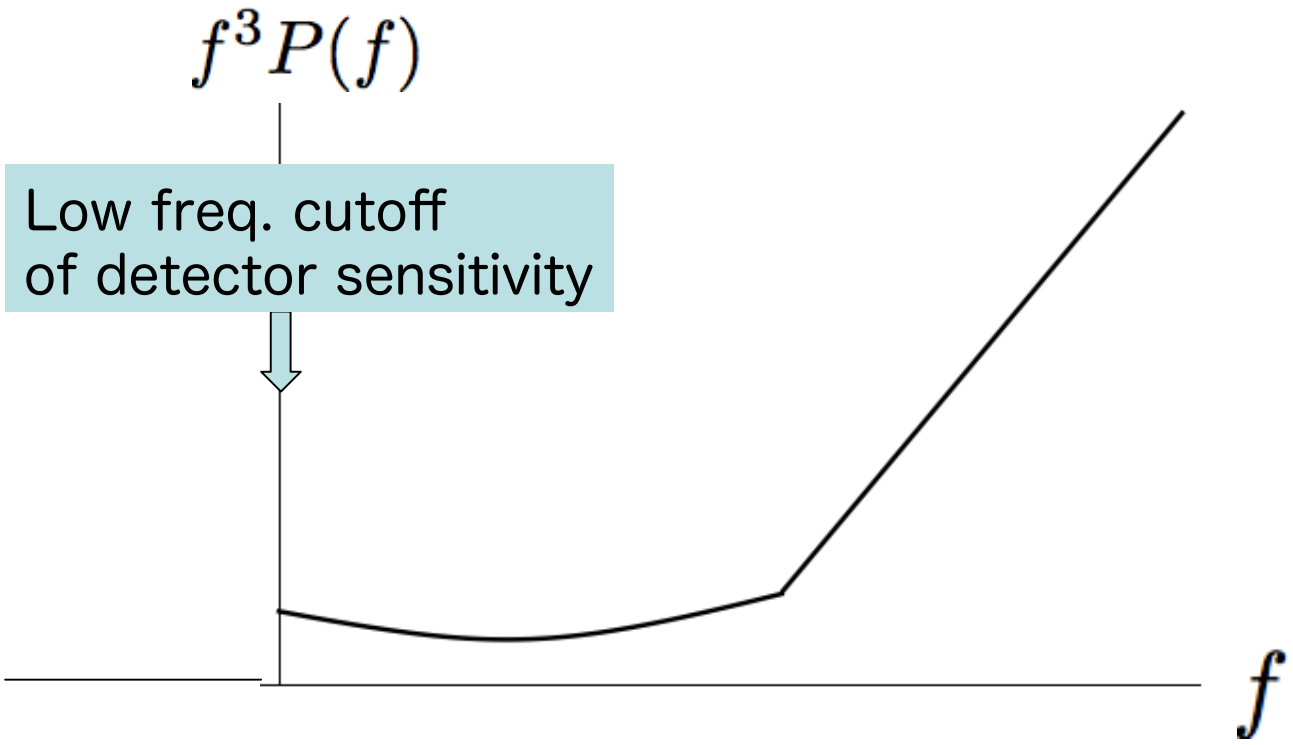

Mass detection

Case (i): small mass

Case (ii): intermediate mass

Case (iii): large mass

Indistinguishable
from massless case

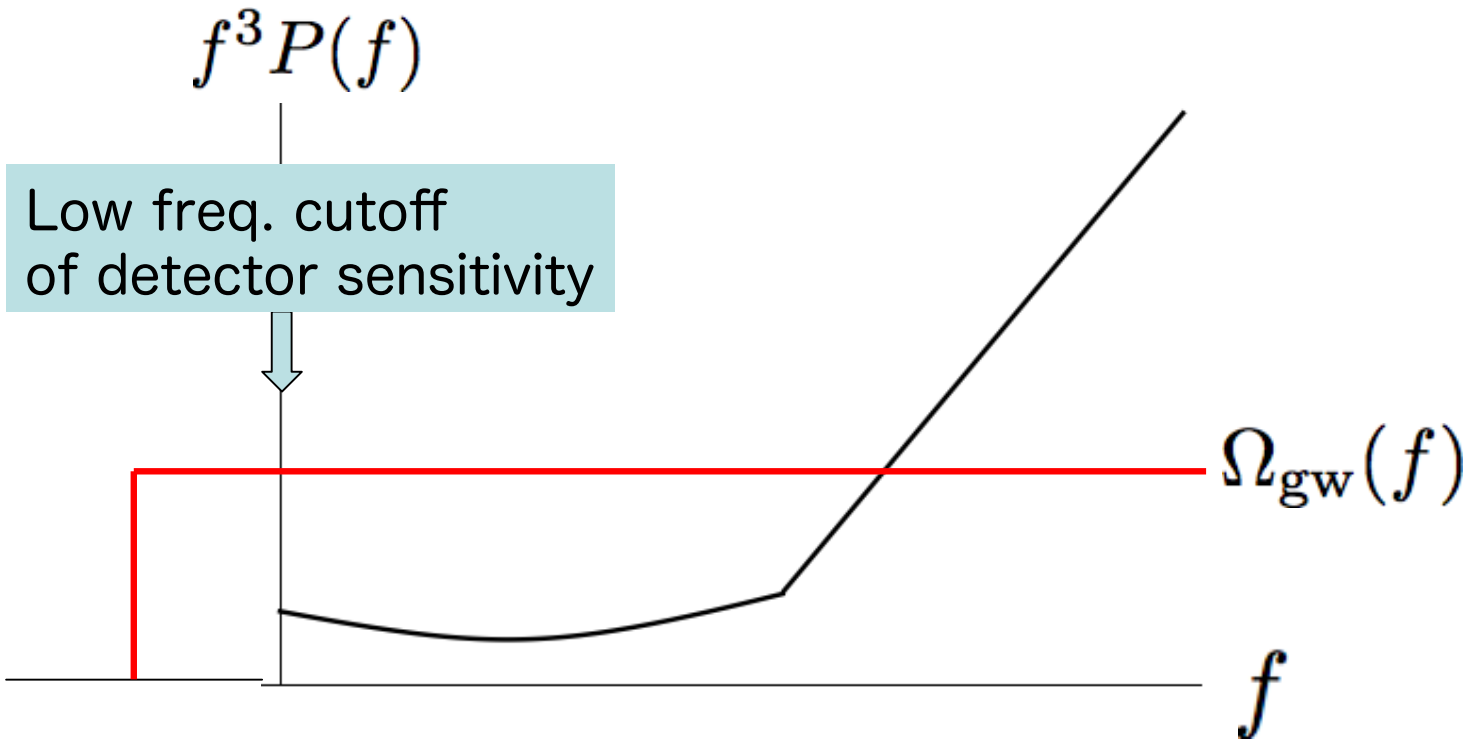

Mass detection

Case (i): small mass

Case (ii): intermediate mass

Case (iii): large mass

Characteristic jump of GWB spectrum is seen.

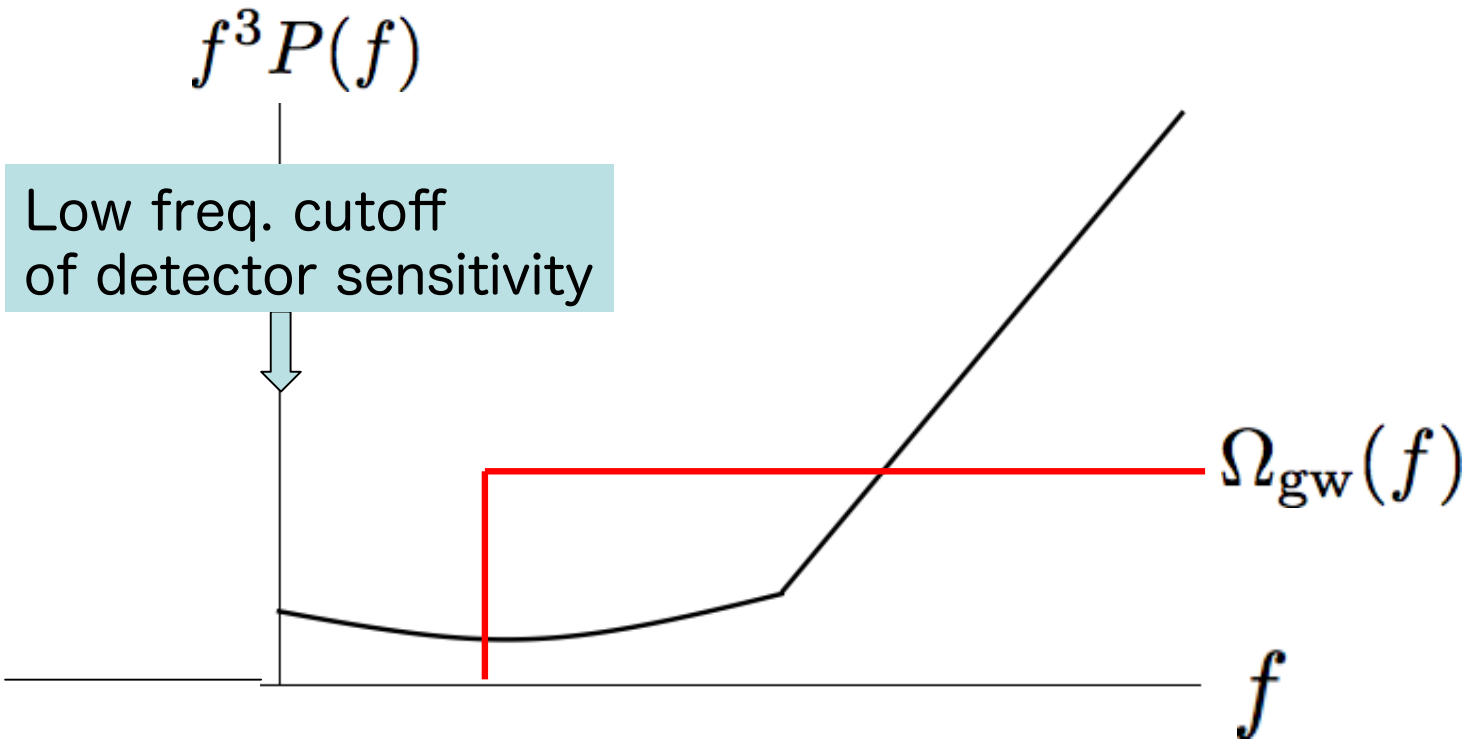

Mass detection

Case (i): small mass

Case (ii): intermediate mass

Case (iii): large mass

Even if large GWB exists, we see nothing.

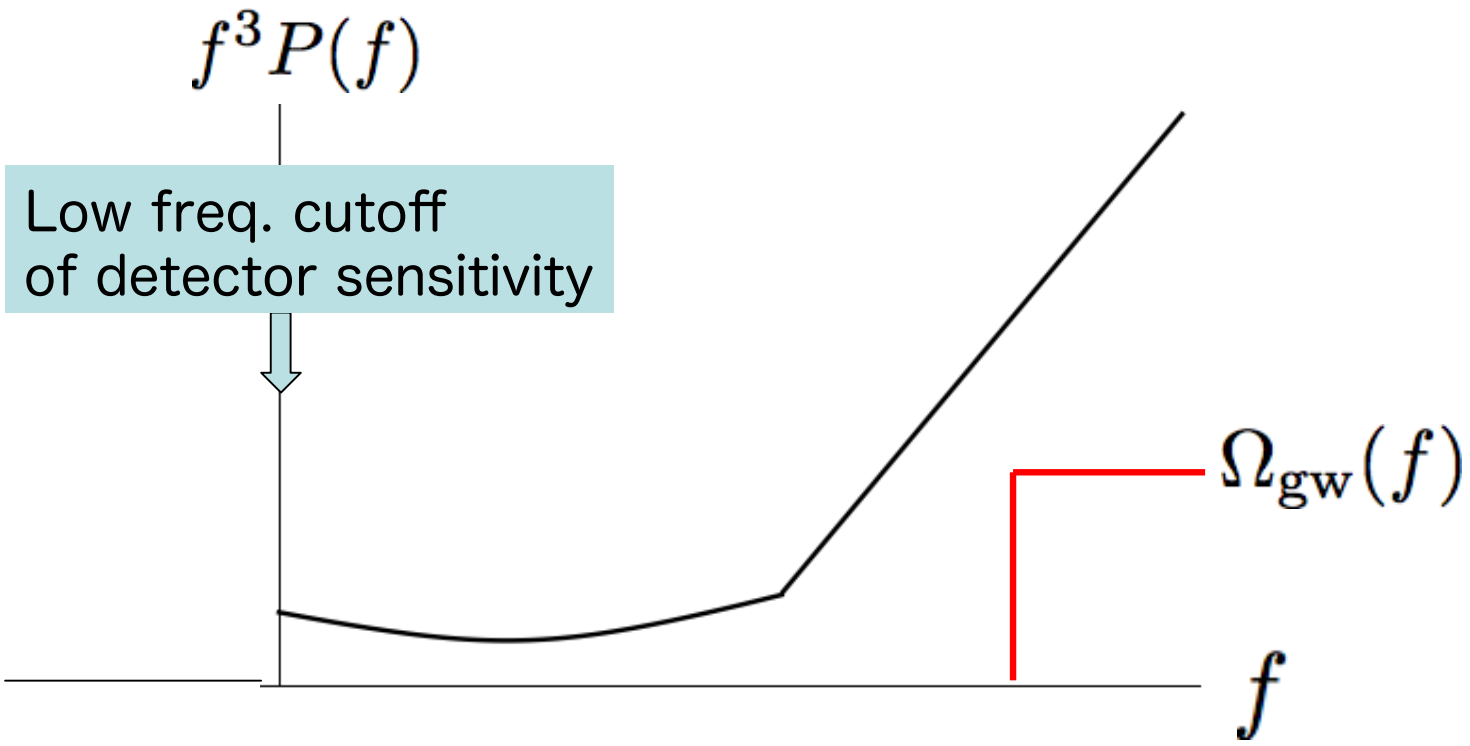

Fisher matrix & graviton mass determination

Typical mass scale detectable with a GW detector:

$$m_g \approx 6.58 \times 10^{-14} \left(\frac{f_g}{100\,\mathrm{Hz}} \right) \mathrm{eV}$$

Use Fisher matrix to estimate measurement accuracy of m_g

$$F_{ab} = \sum_{i=1}^{N_{\mathrm{pair}}} \sum_{A} \int_0^\infty df \left[\frac{C(f)\{\gamma_i^A(f)\}^2 \partial_a \Omega_{\mathrm{gw}}(f) \partial_b \Omega_{\mathrm{gw}}(f)}{\mathcal{N}_i(f)} + \frac{\partial_a \gamma_i^A(f) \partial_b \gamma_i^A(f) + \gamma_i^A(f) \partial_a \partial_b \gamma_i^A(f)}{3\{\gamma_i^A(f)\}^2} \right]$$

$$C(f) \equiv \frac{9 H_0^4 T}{50 \pi^4 f^6}\,, \qquad \mathcal{N}_i(f) \equiv P_I(f) P_J(f)$$

Fisher matrix & graviton mass determination

Typical mass scale detectable with a GW detector:

$$m_g \approx 6.58 \times 10^{-14} \left(\frac{f_g}{100\,\mathrm{Hz}} \right) \mathrm{eV}$$

Use Fisher matrix to estimate measurement accuracy of m_g

$$F_{ab} = \sum_{i=1}^{N_{\mathrm{pair}}} \sum_{A} \int_0^\infty df \left[\frac{C(f)\{\gamma_i^A(f)\}^2 \partial_a \Omega_{\mathrm{gw}}(f) \partial_b \Omega_{\mathrm{gw}}(f)}{\mathcal{N}_i(f)} + \frac{\partial_a \gamma_i^A(f) \partial_b \gamma_i^A(f) + \gamma_i^A(f) \partial_a \partial_b \gamma_i^A(f)}{3\{\gamma_i^A(f)\}^2} \right]$$

$$C(f) \equiv \frac{9 H_0^4 T}{50 \pi^4 f^6}\,, \qquad \mathcal{N}_i(f) \equiv P_I(f) P_J(f)$$

We ignore the contribution from the 2nd term for safety.
Then our estimate is conservative one.

Computation setup

Model of GW background:

$$\Omega_{\rm gw}(f) = \Omega_{\rm gw,0}\left(\frac{f}{f_0}\right)^{n_t}\Theta[f-f_g]$$

We assume only a single pol. mode exists.
(not mixture of 3 pols.)

Free parameters: $\Omega_{\rm gw,0},\ n_t,\ f_g$

Fiducial values: $\Omega_{\rm gw,0}=10^{-7},\ n_t=0.$ & all f_g

Detector network:

Consider 4 GW detectors: aLIGO (H1&L1), aVIRGO, KAGRA

Correlation pairs are HL, HV, LV, HK, KL, KV.

(all noise spectra are assumed to be that of aLIGO.)

SNR of a detector network

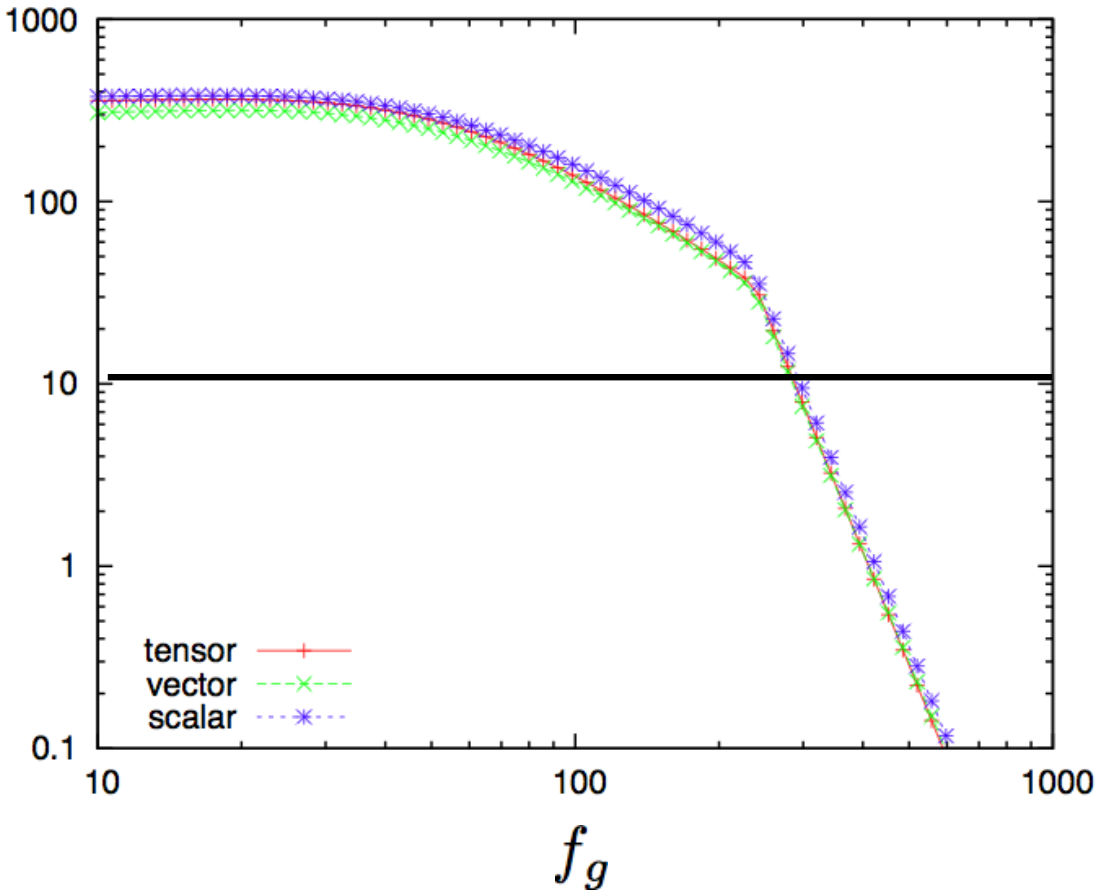

No significant difference between polarization modes. A detector network has almost the same sensivity to GWB.

Detector low freq. cutoff = 10 Hz.

SNR threshold = 10 ⟶ High freq. cutoff = 300 Hz

Mass measurement accuracy

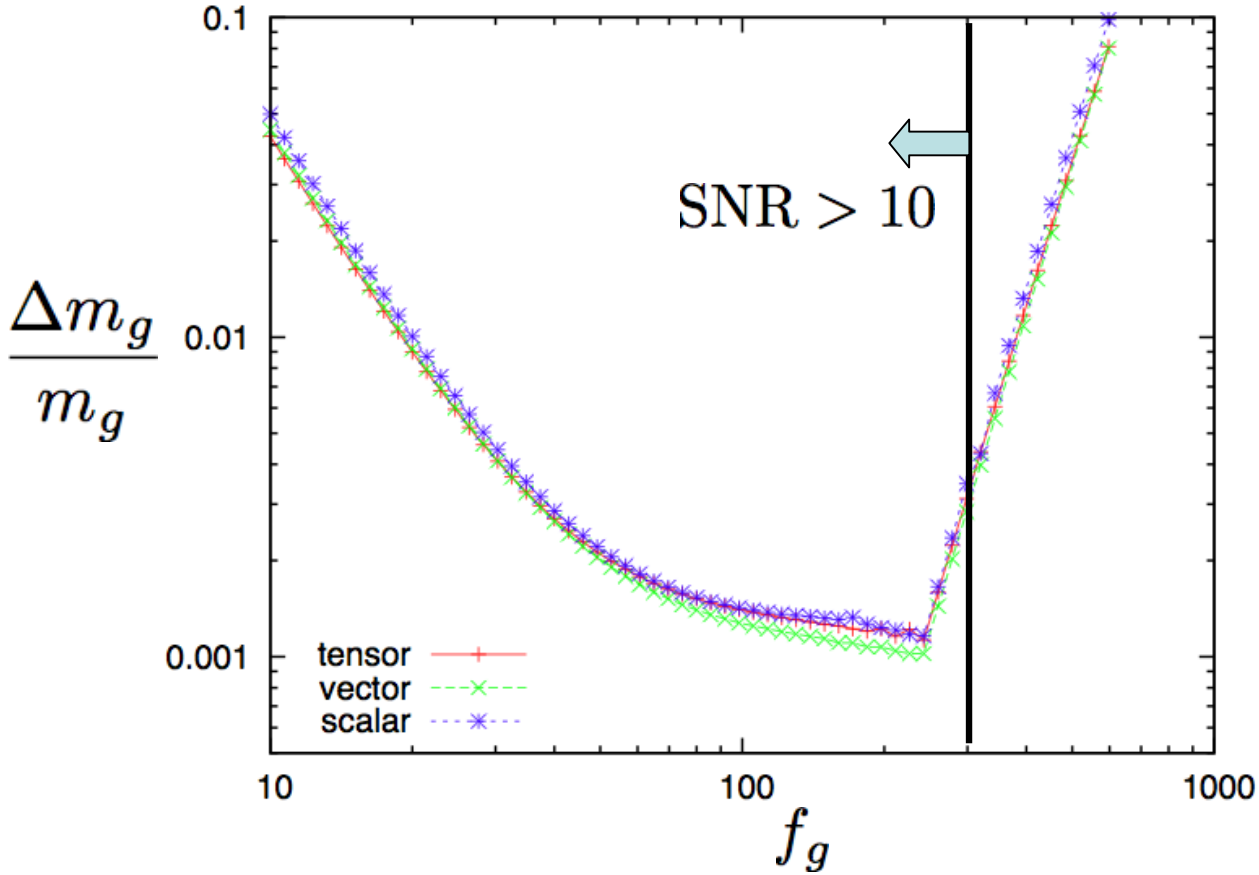

In the available frequency range, graviton mass is well determined.

$$10\,\mathrm{Hz} \leq f \leq 300\,\mathrm{Hz}$$

$$6.7 \times 10^{-15}\,\mathrm{eV} \leq m_g \leq 2.0 \times 10^{-13}\,\mathrm{eV}$$

for $\Omega_{\mathrm{gw},0} = 10^{-7}$, $n_t = 0$

Summary

- Search for graviton mass and polarization enable us to perform model-independent test of gravity and to constrain alternative theory of gravity.
- We considered massive GWB and showed that if GWB is detected, advanced-detector network can search for graviton mass in the range.

$$6.7 \times 10^{-15}\,\mathrm{eV} \leq m_g \leq 2.0 \times 10^{-13}\,\mathrm{eV}$$

Note1: If the correlation signal is a mixture of 3 pol. modes, we can robustly separate these mode with a detector network as shown in

[AN et al., PRD 79, 082002 (2009); PRD 81, 104043 (2010)]

Note2: If we take the Fisher matrix for $\gamma(f)$ into account, detectable mass range would broaden.

Note3: It'd be interesting to consider space-based detectors and pulsar timing, which can constrain different mass range.

Large peak on GWB spectrum?

[Gumrukcuoglu et al., arXiv:1208.5975]

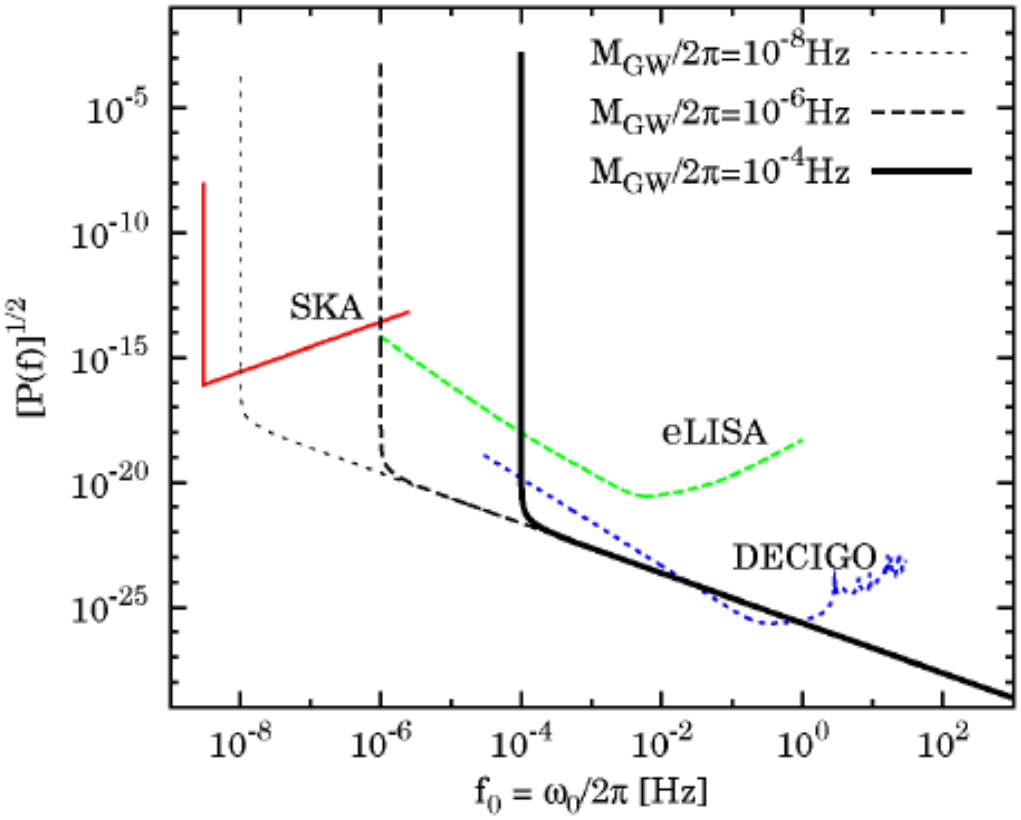

$$\mathcal{P}(\omega_0) \equiv \frac{d}{d\ln\omega_0}\langle\gamma_{ij}\gamma^{ij}\rangle\Big|_{t=t_0} = \frac{\omega_0^2}{\omega_0^2 - M_{GW,0}^2}\frac{2k^3}{\pi^2}\left|\gamma_k(t_0)\right|^2$$

Observational constraints on GWB

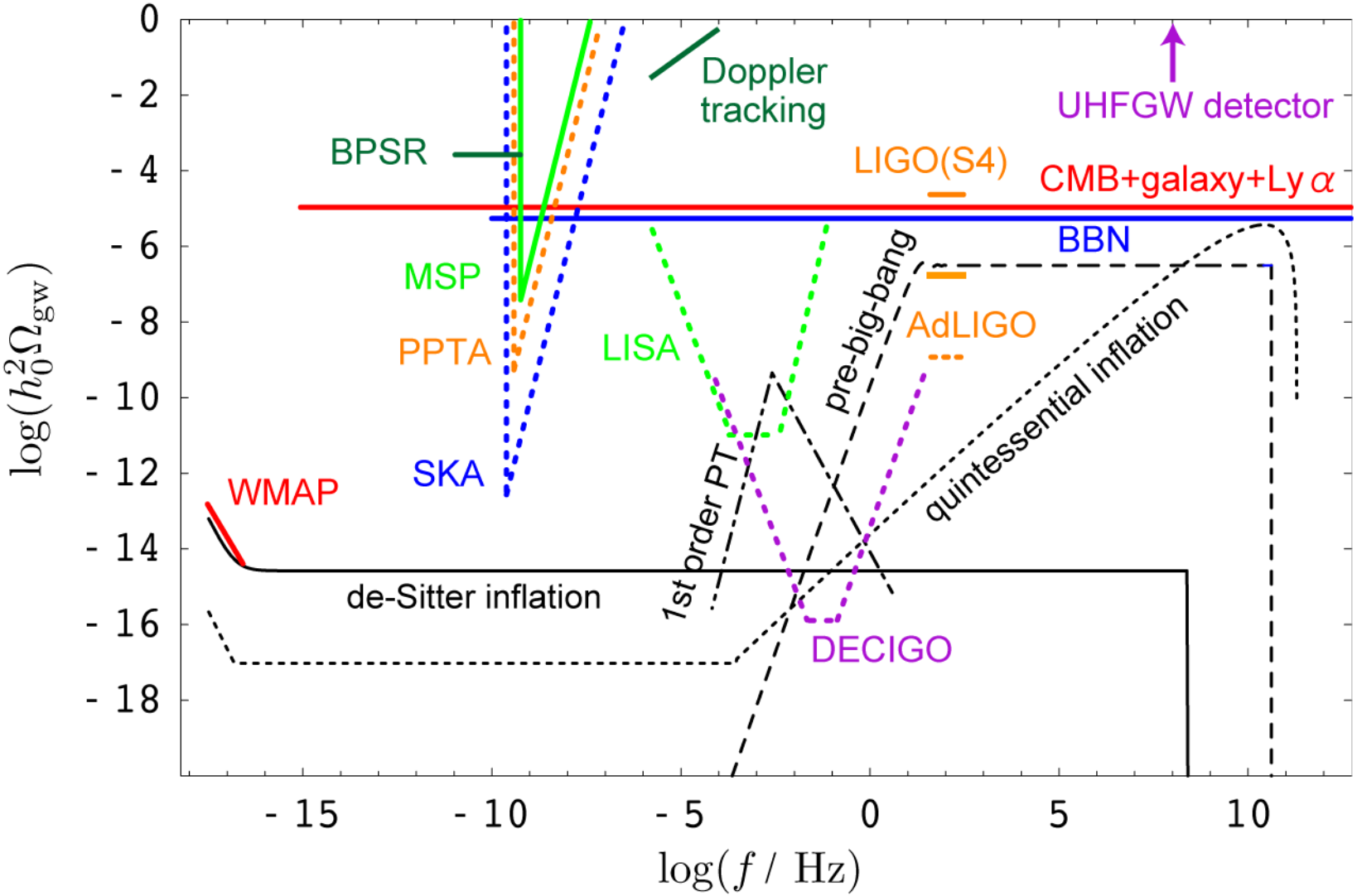

Angular response functions

[Tobar, Suzuki & Kuroda 1999]

$$\sqrt{F_+^2 + F_\times^2}$$

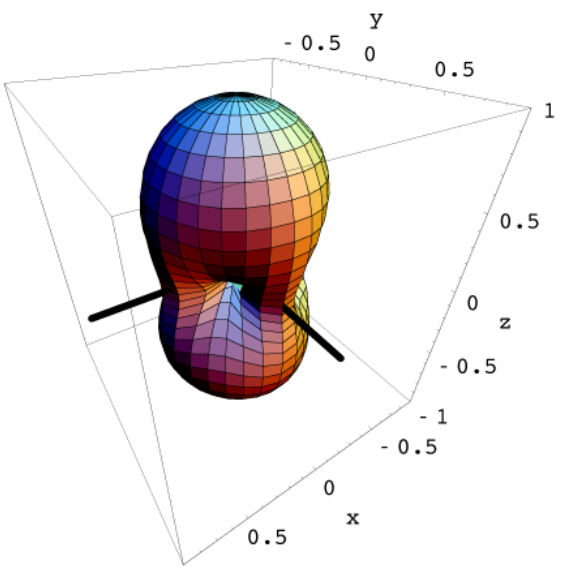

Tensor

$$\sqrt{F_x^2 + F_y^2}$$

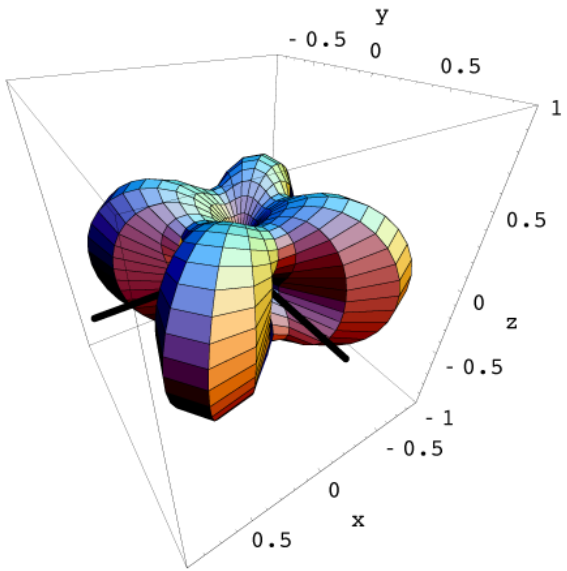

Vector

$$\sqrt{F_b^2 + F_\ell^2}$$

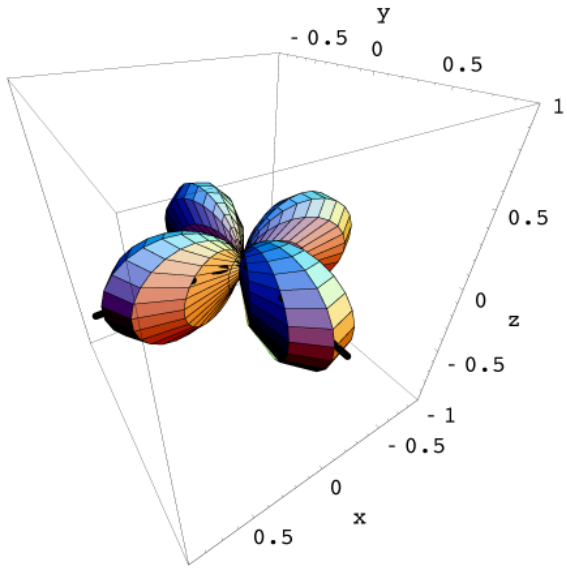

Scalar

Vector and scalar modes are also detectable with an interferometer.

Overlap reduction function (KV)

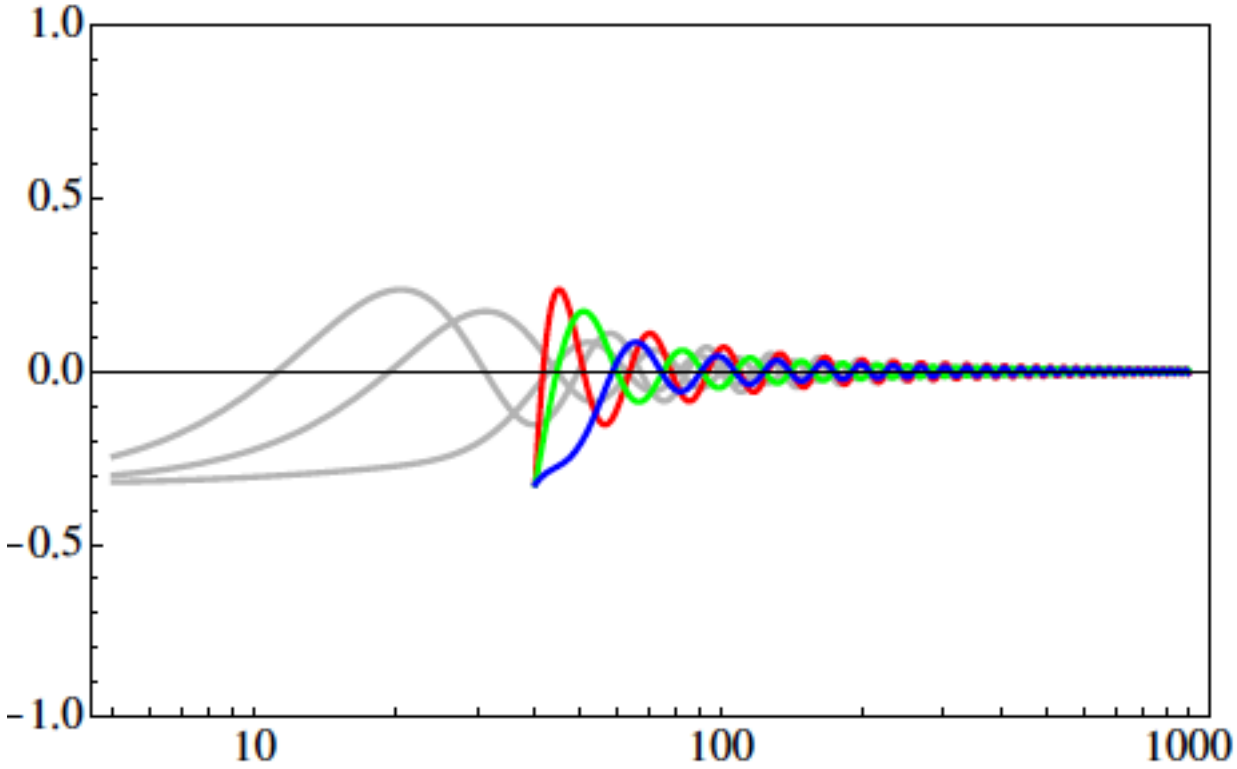

Overlap reduction function (LV)

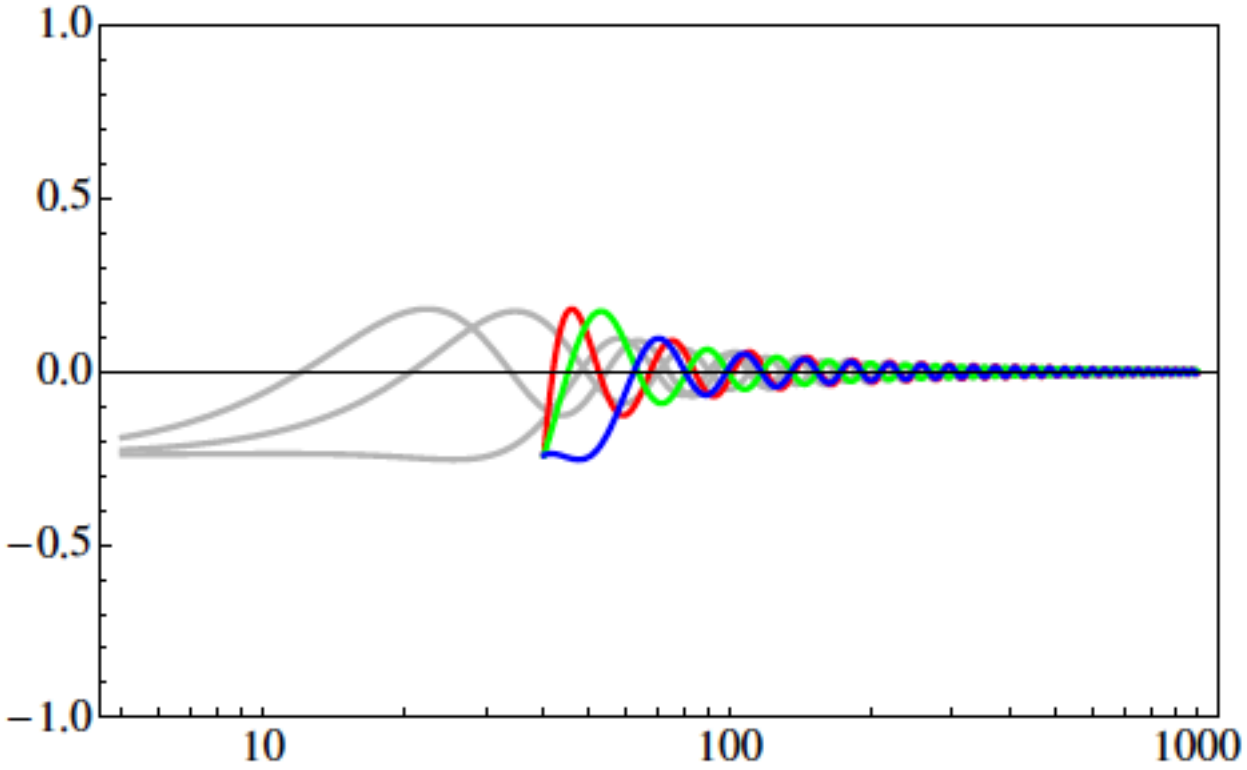

Overlap reduction function (HV)

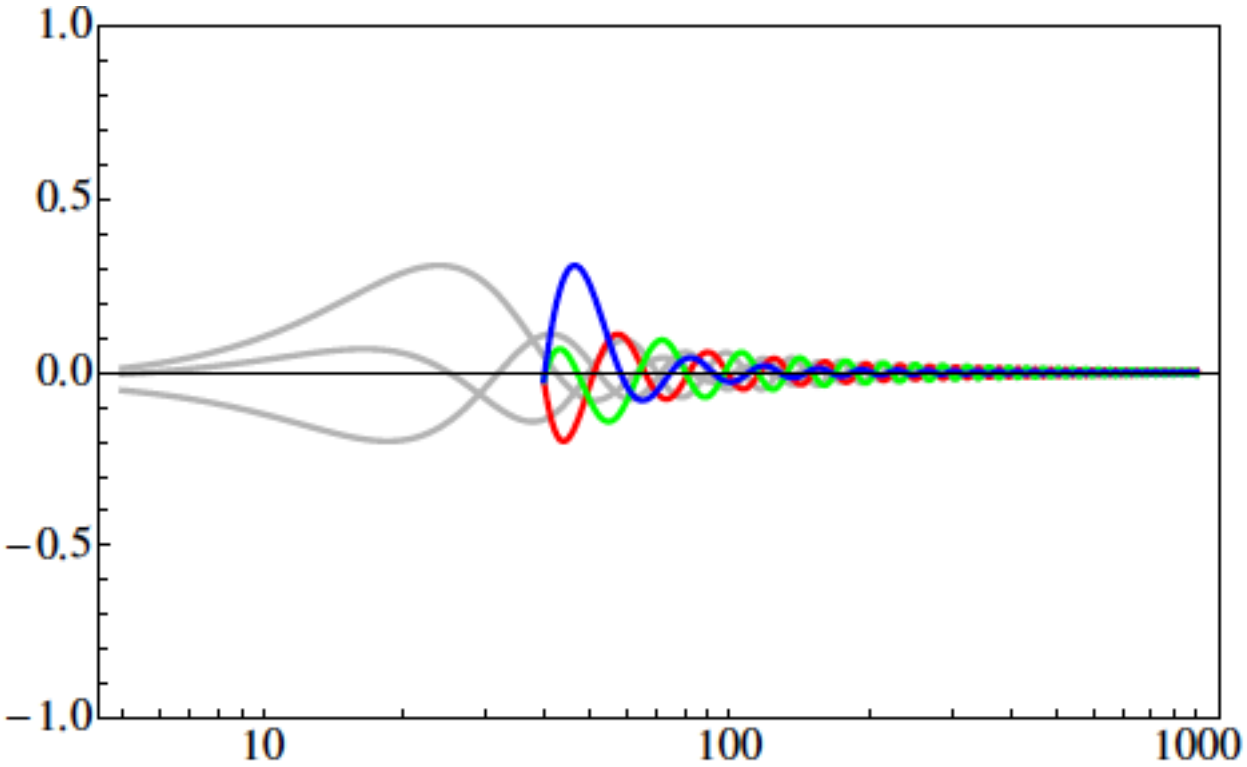

Overlap reduction function (KH)

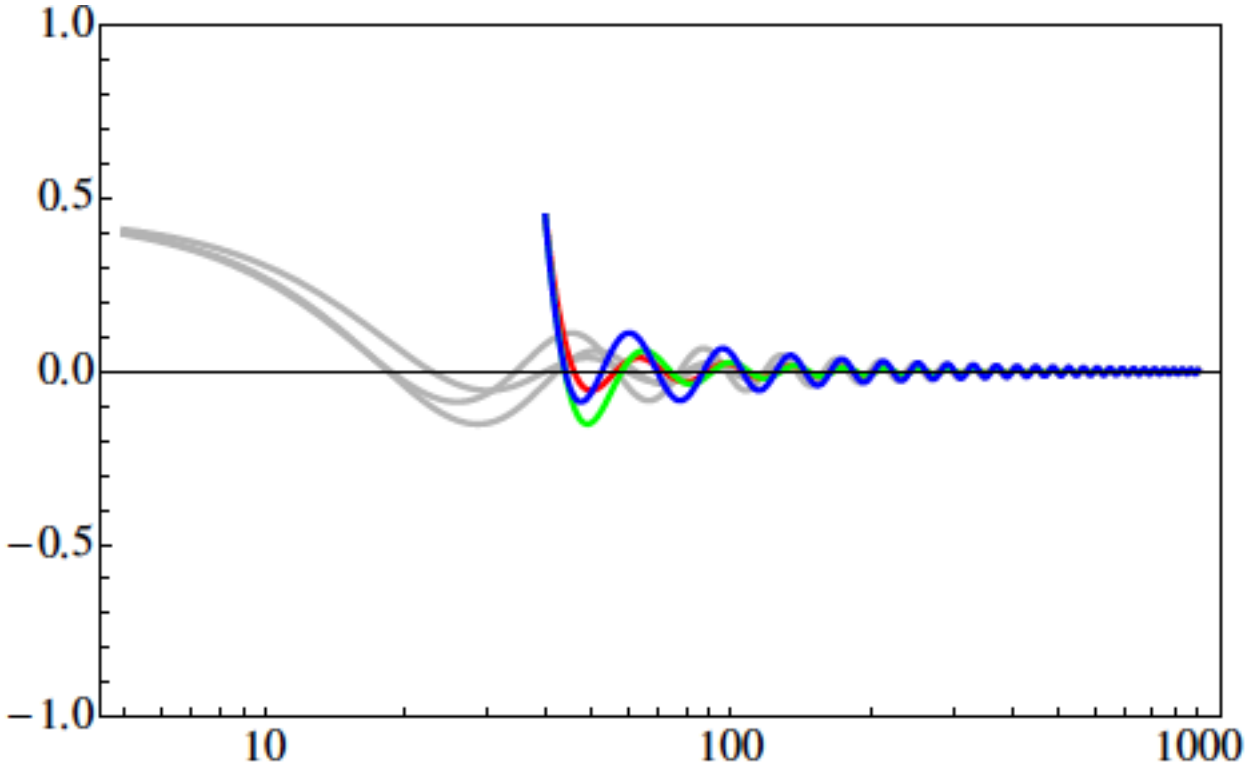

Overlap reduction function (KL)

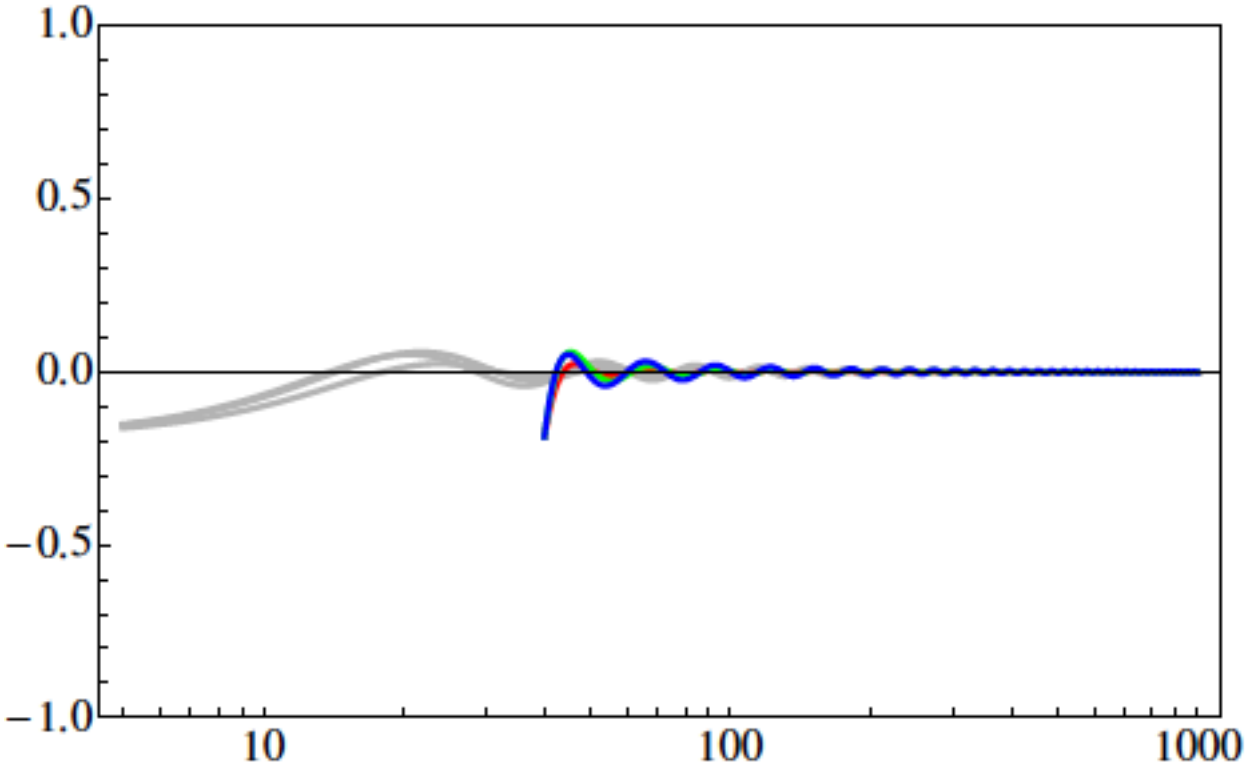

Mode separation

Correlation signal of GW at a frequency bin

$$Z_{IJ}(f) \equiv \Omega^T_{\rm gw}(f)\gamma^T_{IJ}(f) + \Omega^V_{\rm gw}(f)\gamma^V_{IJ}(f) + \xi\Omega^S_{\rm gw}(f)\gamma^S_{IJ}(f)$$

In principle, three detectors allow us to separate the modes.

$$\begin{pmatrix} Z_{12} \\ Z_{23} \\ Z_{31} \end{pmatrix} = \mathbf{\Pi} \begin{pmatrix} \Omega^T_{\rm gw} \\ \Omega^V_{\rm gw} \\ \xi\Omega^S_{\rm gw} \end{pmatrix} \qquad \mathbf{\Pi} \equiv \begin{pmatrix} \gamma^T_{12} & \gamma^V_{12} & \gamma^S_{12} \\ \gamma^T_{23} & \gamma^V_{23} & \gamma^S_{23} \\ \gamma^T_{31} & \gamma^V_{31} & \gamma^S_{31} \end{pmatrix}$$

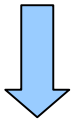

Mode separation

$$\begin{pmatrix} \Omega^T_{\rm gw} \\ \Omega^V_{\rm gw} \\ \xi\Omega^S_{\rm gw} \end{pmatrix} = \mathbf{\Pi}^{-1} \begin{pmatrix} Z_{12} \\ Z_{23} \\ Z_{31} \end{pmatrix}$$

Separability strongly depends on $\det \mathbf{\Pi}$. $\mathrm{SNR}(f) \propto \det \mathbf{\Pi}(f)$

If the modes are not separable ($\det \mathbf{\Pi} = 0$),
GWB signal does not contribute to the SNR at the frequencies.

Detectors & Earth coordinate

5 advanced detectors on the ground.
[A=AIGO, C=LCGT, H=AdvLIGO(H1), L=AdvLIGO(L1), V=AdvVIRGO.]

Detector pair is completely characterized by three parameters.

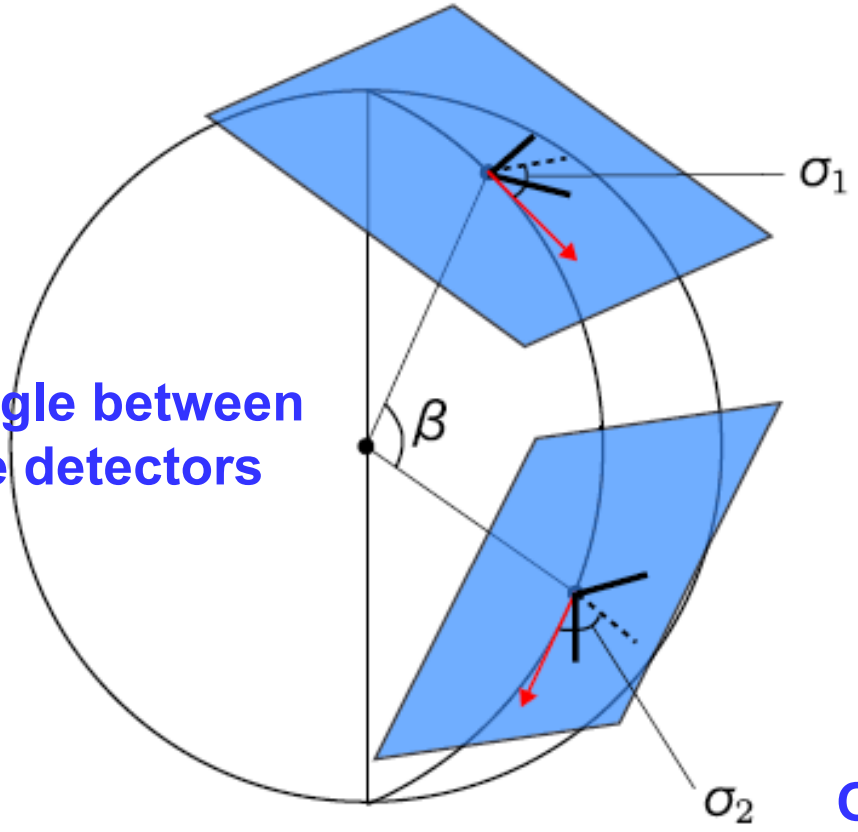

Orientation of det. 1

Angle between the detectors

Orientation of det. 2

SNR (single pol.)

Assume that GWB has only one polarization mode.

$$\text{normalized SNR} = \frac{\text{SNR}(\beta)}{\text{SNR}(\beta = 0)},$$

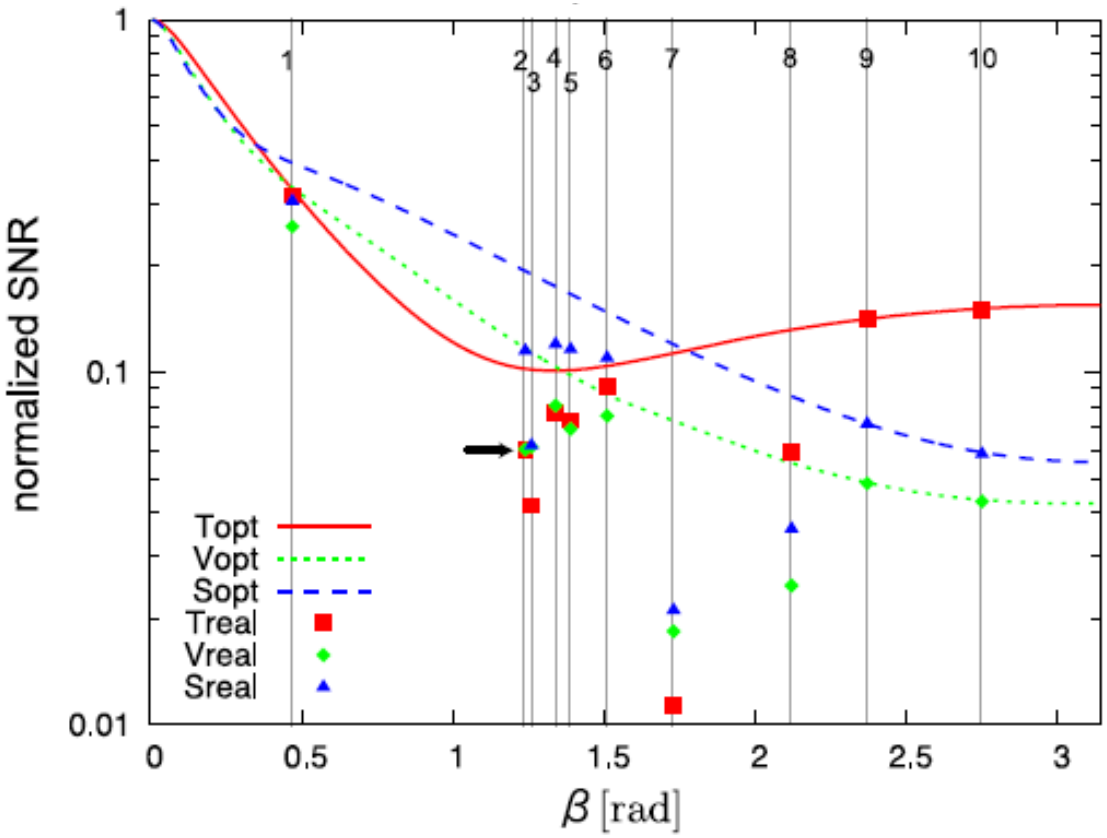

Detector pair
1=HL,
2=AC,
3=CH,
4=LV,
5=HV,
6=CV,
7=CL,
8=AV,
9=AH,
10=AL.

This is also true for current detectors.

Detectable GWB with single pol.

5 advanced detectors on the ground.
[A=AIGO, C=LCGT, H=AdvLIGO(H1), L=AdvLIGO(L1), V=AdvVIRGO.]

All detectors have the same noise spectrum as that of AdvLIGO.

Observation time $T = 3\mathrm{yr}.$ $\mathrm{SNR} = 5$

detector pair	$h_0^2\Omega_{\rm gw}^T$	$h_0^2\Omega_{\rm gw}^V$	$\xi h_0^2\Omega_{\rm gw}^S$
A - C	8.6×10^{-9}	8.6×10^{-9}	4.5×10^{-9}
A - H	3.6×10^{-9}	1.1×10^{-8}	7.3×10^{-9}
A - L	3.4×10^{-9}	1.2×10^{-8}	8.8×10^{-9}
A - V	8.7×10^{-9}	2.1×10^{-8}	1.4×10^{-8}
C - H	1.2×10^{-8}	8.4×10^{-9}	8.4×10^{-9}
C - L	4.5×10^{-8}	2.8×10^{-8}	2.5×10^{-8}
C - V	5.7×10^{-9}	6.9×10^{-9}	4.7×10^{-9}
H - L	1.6×10^{-9}	2.0×10^{-9}	1.7×10^{-9}
H - V	7.1×10^{-9}	7.5×10^{-9}	4.5×10^{-9}
L - V	6.7×10^{-9}	6.4×10^{-9}	4.3×10^{-9}

most sensitive

All modes are detectable with almost the same SNRs.

Detectable GWB after mode separation

- Advanced detectors on the ground

[A=AIGO, C=LCGT, H=AdvLIGO(H1), L=AdvLIGO(L1), V=AdvVIRGO.]

- Assume the same noise spectrum as that of AdvLIGO.

detector set	$h_0^2\Omega_{\rm gw}^T$	$h_0^2\Omega_{\rm gw}^V$	$\xi h_0^2\Omega_{\rm gw}^S$
A - C - H	5.2×10^{-9}	8.1×10^{-9}	5.5×10^{-9}
A - C - L	6.0×10^{-9}	1.5×10^{-8}	8.3×10^{-9}
A - C - V	1.3×10^{-8}	1.0×10^{-8}	6.8×10^{-9}
A - H - L	3.8×10^{-9}	1.2×10^{-8}	1.0×10^{-8}
A - H - V	8.5×10^{-9}	2.2×10^{-8}	2.1×10^{-8}
A - L - V	6.0×10^{-9}	2.4×10^{-8}	2.3×10^{-8}
C - H - L	1.4×10^{-8}	1.9×10^{-8}	1.9×10^{-8}
C - H - V	1.1×10^{-8}	1.0×10^{-8}	7.6×10^{-9}
C - L - V	1.2×10^{-8}	2.0×10^{-8}	1.7×10^{-8}
H - L - V	6.1×10^{-9}	1.3×10^{-8}	6.0×10^{-9}

$$T = 3\mathrm{yr}.$$

$$\mathrm{SNR} = 5$$

Mode separation hardly degrade the SNRs.
(Almost the same sensitivity to GWB in the presence of a single pol. mode)

Daisuke Yoshida, JGRG 22(2012)111424

"New cosmological solutions in massive gravity"

RESCEU SYMPOSIUM ON

GENERAL RELATIVITY AND GRAVITATION

JGRG 22

November 12-16 2012

Koshiba Hall, The University of Tokyo, Hongo, Tokyo, Japan

New Cosmological Solutions in Massive Gravity

Daisuke Yoshida[1(a)] ,Tsutomu Kobayashia[2(b)] ,Masaru Siinoa[3(a)] ,Masahide Yamaguchia[4(a)]

(a) *Department of Physics, Tokyo Institute of Technology, Tokyo 152-8551, Japan*

(b) *Department of Physics, Rikkyo University, Toshima, Tokyo 175-8501, Japan*

Abstract

In massive gravity,we find a series of the metrics for which the effective energy momentum tensor from the graviton mass behave as a cosmological constant. As a result,the metric that is exact solution in general relativity with cosmological constant is a exact solution also in massive gravity. Especially,these solutions include expanding cosmological solutions with flat,open and closed spacial curvature.

1 Introduction

It is very intriguing to explore whether or not the graviton can have a mass. The first attempt to add a mass term to the gravity action was made by Fierz and Pauli [1], who considered the quadratic action for the graviton $h_{\mu\nu}$ in flat space with the mass term

$$m^2 \left(h_{\mu\nu}h^{\mu\nu} - h^2\right). \tag{1}$$

The linear theory with the Fierz-Pauli mass term is ghost-free. However, the theory does not reproduce general relativity in the massless limit $m \to 0$. The extra three degrees of freedom in a massive spin 2 survive even in this limit, and therefore the prediction for light bending is away from that of general relativity, which clearly contradicts solar-system tests. This is called the vDVZ discontinuity [2].

As pointed out by Vainshtein [3], the discontinuity can in fact be cured by going beyond the linear theory. Massive gravity has a new length scale called the Vainshtein radius, below which the nonlinearities of the theory come in and the effect of the extra degrees of freedom is screened safely. The Vainshtein radius becomes larger as m gets smaller, and thereby a smooth massless limit is attained.

However, the very nonlinearities turned out to cause another trouble. Boulware and Deser argued that there appears the sixth scalar degree of freedom at nonlinear order, which has a wrong sign kinetic term, *i.e.,* the sixth mode is a ghost [4]. The presence of the Boulware-Deser (BD) ghost has hindered us from constructing a consistent theory of massive gravity.

Recently, a theoretical breakthrough in this field has been made. Adding higher-order self-interaction terms and tuning appropriately their coefficients, de Rham and collaborators successfully eliminated the dangerous scalar mode from the theory in the decoupling limit [5, 6]. Then, Hassan and Rosen established a complete proof that the theory does not suffer from the BD ghost instability to all orders in perturbations and away from the decoupling limit [7]. Thus, there certainly exists a nonlinear theory of massive gravity that is free of the BD ghost.

2 Action of Ghost Free Massive Gravity

The action of the ghost free massive gravity [6] is following:

$$S = S_{EH} + S_{mass} + S_{matter}, \tag{2}$$

[1]Email address: yoshida"at"th.phys.titech.ac.jp
[2]Email address: tsutomu"at"rikkyo.ac.jp
[3]Email address: msiino"at"th.phys.titech.ac.jp
[4]Email address: gucci"at"phys.titech.ac.jp

here,S_{EH} and S_{matter} is usual Einstein-Hilbert action and matter's action. The additional mass term S_{mass} is

$$S_{mass} = \frac{M_{PL}^2}{2}\int d^4x\sqrt{-g}m^2\left(\mathcal{U}_2 + \alpha_3\mathcal{U}_3 + \alpha_4\mathcal{U}_4\right). \tag{3}$$

with graviton mass m and free parameters α_3, α_4. Here,

$$\mathcal{U}_2 := [\mathcal{K}]^2 - [\mathcal{K}^2], \tag{4}$$
$$\mathcal{U}_3 := [\mathcal{K}]^3 - 3[\mathcal{K}][\mathcal{K}^2] + 2[\mathcal{K}^3], \tag{5}$$
$$\mathcal{U}_4 := [\mathcal{K}]^4 - 6[\mathcal{K}^2][\mathcal{K}]^2 + 8[\mathcal{K}^3][\mathcal{K}] + 3[\mathcal{K}^2]^2 - 6[\mathcal{K}^4]. \tag{6}$$

"[ ]" represents trace:

$$[\mathcal{K}] = \mathcal{K}^\mu_\mu, \quad [\mathcal{K}^2] = \mathcal{K}^\mu_\nu\mathcal{K}^\nu_\mu, \quad \cdots, \tag{7}$$

and $\mathcal{K}^\mu_\nu$ is

$$\mathcal{K}^\mu_\nu = \delta^\mu_\nu - \sqrt{g^{\mu\rho}\partial_\rho\phi^a\partial_\nu\phi^b\eta_{ab}}. \tag{8}$$

the Square root of a tensor is defind as follow:

$$\sqrt{A^\mu_\rho}\sqrt{A^\rho_\nu} = A^\mu_\nu. \tag{9}$$

ϕ^a $(a = 0, 1, 2, 3)$ are scalar fields called Stückelberg field.

In the action,Stückelberg fields appear throught the conbination $\partial_\mu\phi^a\partial_\nu\phi^b\eta_{ab} \equiv \Sigma_{\mu\nu}$, and , We call this tensor "fiducial metric". In the coordinate

$$x^0 = \phi^0, x^1 = \phi^1, x^2 = \phi^2, x^3 = \phi^3, \tag{10}$$

the fiducial metric becomes the diagonal Minkowski metric:

$$\Sigma_{\mu\nu} = \eta_{\mu\nu}, \tag{11}$$

and,this coordinate called "unitary gauge".

The equation of motion derived from this action is

$$G_{\mu\nu} + m^2X_{\mu\nu} = \frac{1}{M_{PL}^2}T_{\mu\nu}. \tag{12}$$

Here,$G_{\mu\nu}$is the Einstein tensor,$T_{\mu\nu}$is the energy momentum tensor of the matter,and $m^2X_{\mu\nu}$ is effective energy momentum tensor from graviton mass:

$$m^2X_{\mu\nu} = \frac{1}{\sqrt{-g}}\frac{\delta S_{mass}}{\delta g^{\mu\nu}} \tag{13}$$

Note that if $m^2X_{\mu\nu} \propto g_{\mu\nu}$, this term behave as a cosmological constant, therefore the equation of motion coincides with the Einstein equation with a cosmological constant.

3 Cosmological Solutions

In massive gravity, a change of coordinate transforms not only $g_{\mu\nu}$ but also $\Sigma_{\mu\nu}$. So, in the coordinate where $g_{\mu\nu}$ is the usual diagonal form:

$$g_{\mu\nu}dx^\mu dx^\nu = -dt^2 + a^2(t)\left[\frac{dr^2}{1-Kr^2} + r^2d\Omega^2\right], \tag{14}$$

the fiducial metric $\Sigma_{\mu\nu}$ is a generally complicated form.

The first attempt to find a cosmological solution was made by D'Amico et al [8]. In this analysis, the free parameterα_3, α_4 set to zero,the spacial curvature is flat , and in the familiar diagonal FLRW coordinate of teh physical metric,the fiducial metric is the diagonal Minkowski form ($\phi^\mu = x^\mu$):

$$g_{\mu\nu}dx^\mu dx^\nu = -dt^2 + a^2(t)\delta_{ij}dx^i dx^j \tag{15}$$
$$\Sigma_{\mu\nu}dx^\mu dx^\nu = \eta_{\mu\nu}dx^\mu dx^\nu, \tag{16}$$

or has same symmetry as the physical metric($\phi^0 = f(t), \phi^i = x^i$):

$$g_{\mu\nu}dx^\mu dx^\nu = -dt^2 + a^2(t)\delta_{ij}dx^i dx^j, \tag{17}$$
$$\Sigma_{\mu\nu}dx^\mu dx^\nu = -\dot{f}^2(t)dt^2 + \delta_{ij}dx^i dx^j. \tag{18}$$

In both cases, equation of motion implies $\dot{a} = 0$, as a result ,our univers can not expand.

To obtain the expanding FLRW solution,we must consider more complicated case. One way is to consider the open FLRW space time [9] ,or more general fiducial metric [8] [10]. But , we take another approach. We choose the coordinate where the fiducial metric is the diagonal Minkowski form(unitary gauge), and the physical metric is not usual diagonal form.

Before our work,the de Sitter solution was already found [11]. In this analysis,the de Sitter space time is described by the Painlevé-Gullstrand (PG) coordinate in the unitary gauge:

$$g_{\mu\nu}dx^\mu dx^\nu = -\kappa^2 dt^2 + \tilde{\alpha}^2\left(dr \pm \sqrt{\frac{\Lambda}{3}}\kappa r dt\right)^2 + \tilde{\alpha}^2 r^2 d\Omega^2 \tag{19}$$
$$\Sigma_{\mu\nu}dx^\mu dx^\nu = \eta_{\mu\nu}dx^\mu dx^\nu. \tag{20}$$

In addition, free parameter α_3, α_4 was choosed as following:

$$\alpha_3 = \frac{1}{3}(\alpha - 1), \alpha_4 = \frac{1}{12}(\alpha^2 - \alpha + 1), \alpha = \frac{\tilde{\alpha}}{1 - \tilde{\alpha}}. \tag{21}$$

In this case,the effective energy momentum tensor from the graviton mass is

$$m^2 X_{\mu\nu} = \frac{m^2}{\alpha}g_{\mu\nu}. \tag{22}$$

Therefore, the equation of motions are Einstein equation with the effective coupling constant m^2/α.So for $\Lambda = m^2/\alpha$,this de Sitter solution is an exact solution in massive gravity.

We extend this analysis to the FLRW space time. The key observation is that ,as the de Sitter space time, the FLRW space time can be described by the PG coordinate[13].So,we impose this form of the physical metric in the unitary gauge:

$$g_{\mu\nu}dx^\mu dx^\nu = -\kappa^2 dt^2 + \frac{\tilde{\alpha}^2}{1 - K\tilde{\alpha}^2 r^2/a^2(t)}\left(dr \pm \frac{\dot{a}}{a}\kappa r dt\right)^2 + \tilde{\alpha}^2 r^2 d\Omega^2 \tag{23}$$
$$\Sigma_{\mu\nu}dx^\mu dx^\nu = \eta_{\mu\nu}dx^\mu dx^\nu. \tag{24}$$

We use same parameters as (21). In the set up ,the effective energy momentum tensor from the graviton mass is same as eq.(22),and,as expected,the equation of motion is the Einstein equation with a cosmological constant. So, as in general relativity,these FLRW space times are solutions in massive gravity.

We can transform the coordinate to the familiar diagonal FLRW coordinate by $r \to R = \tilde{\alpha}r/a(t), t \to T = \kappa t$,

$$g_{\mu\nu}dx^\mu dx^\nu = -dT^2 + a^2(T)\left[\frac{dR^2}{1 - KR^2} + R^2 d\Omega^2\right] \tag{25}$$
$$\Sigma_{\mu\nu}dx^\mu dx^\nu = -\left(\frac{1}{\kappa^2} - \frac{\dot{a}^2 R^2}{\tilde{\alpha}^2}\right)dT^2 + \frac{2a\dot{a}R}{\tilde{\alpha}^2}dTdR + \frac{a^2}{\tilde{\alpha}^2}(dR^2 + R^2 d\Omega^2). \tag{26}$$

In this coordinate,the fiducial metric is inhomogenious form. Thus,the fiducial metric is the form out of ansatz eq.(16),eq.(18).

4 More General Solutions

We can generalize our cosmological solutions. Instead of the PG form FLRW metric (23) ,we use the following general PG form metric:

$$g_{\mu\nu}dx^{\mu}dx^{\nu} = -U^2(x^{\mu})dt^2 + V^2(x^{\mu})\left(dr + f(x^{\mu})dt\right)^2 + \tilde{\alpha}^2 r^2 d\Omega^2. \quad (27)$$

Here,U, V, f are arbitrary functions. Also,in this set up,the effective energy momentum tensor is same as (22). As a result,the metric that is an exact solution in general relativity with a cosmological constant ,is a exact solution also in massive gravity.

For example,the Lemaître-Tolman-Bondi (LTB) metric can be described by PG form[13]. Therefore the LTB solution is an exact solution in massive gravity. we can use this solution to study spherical collapse of a perfect fluid in massive gravity.

5 Concludion

We have found new cosmological solutions in massive gravity with flat,open,and closed spatial geometries. Our solutions can be extended to general spherical space time,including LTB space time. In both cases, the key was that general PG form metric (27)gives rise to an effective energy momentum tensor of a cosmological constant m^2/α for the special choice of the parameters (21). This is essential for being able to get analytic solutions in massive gravity easily from the seed solutions in general relativity.

References

[1] M. Fierz and W. Pauli, Proc. Roy. Soc. Lond. A **173**, 211 (1939).

[2] H. van Dam and M. J. G. Veltman, Nucl. Phys. B **22**, 397 (1970); Zakharov, JETP Letters (Sov. Phys.) **12**, 312 (1970).

[3] A. I. Vainshtein, Phys. Lett. B **39**, 393 (1972).

[4] D. G. Boulware and S. Deser, Phys. Rev. D **6**, 3368 (1972).

[5] C. de Rham and G. Gabadadze, Phys. Rev. D **82**, 044020 (2010) [arXiv:1007.0443 [hep-th]].

[6] C. de Rham, G. Gabadadze and A. J. Tolley, Phys. Rev. Lett. **106**, 231101 (2011) [arXiv:1011.1232 [hep-th]].

[7] S. F. Hassan and R. A. Rosen, Phys. Rev. Lett. **108**, 041101 (2012) [arXiv:1106.3344 [hep-th]].

[8] G. D'Amico, C. de Rham, S. Dubovsky, G. Gabadadze, D. Pirtskhalava and A. J. Tolley, Phys. Rev. D **84**, 124046 (2011) [arXiv:1108.5231 [hep-th]].

[9] A. E. Gumrukcuoglu, C. Lin and S. Mukohyama, JCAP **1111**, 030 (2011) [arXiv:1109.3845 [hep-th]].

[10] P. Gratia, W. Hu, M. Wyman, arXiv:1205.4241 [hep-th].

[11] L. Berezhiani, G. Chkareuli, C. de Rham, G. Gabadadze and A. J. Tolley, Phys. Rev. D **85**, 044024 (2012) [arXiv:1111.3613 [hep-th]].

[12] P. Painlevé C. R. Acad. Sci. (Paris) **173**, 677 (1921); A. Gullstrand, Arkiv. Mat. Astron. Fys. **16**, 1 (1922).

[13] Y. Kanai, M. Siino and A. Hosoya, Prog. Theor. Phys. **125**, 1053 (2011) [arXiv:1008.0470 [gr-qc]].

Yuki Sakakihara, JGRG 22(2012)111425

"Inflation in bimetric gravity"

RESCEU SYMPOSIUM ON

GENERAL RELATIVITY AND GRAVITATION

JGRG 22

November 12-16 2012

Koshiba Hall, The University of Tokyo, Hongo, Tokyo, Japan

2012/11/14 jgrg

Inflation in Bimetric Gravity

Yuki Sakakihara Kyoto University, M2

with Jiro Soda and Tomohiro Takahashi

What is bimetric gravity?

Introduce massive graviton
→ ”massive gravity theory”

When there is general covariance, graviton cannot have mass.

Introduce “reference metric”.

It breaks general covariance, then graviton can have mass.

* reference metric is non dynamical in massive gravity

Make the reference metric dynamical

bi(metric)gravity

Bigravity action

$$S = \frac{M_g^2}{2}\int d^4x\sqrt{-g}R[g_{\mu\nu}] + \frac{M_f^2}{2}\int d^4x\sqrt{-f}R[f_{\mu\nu}] + m^2M_e^2\int d^4x\sqrt{-g}\,F_2$$

EH action of $g_{\mu\nu}$ | EH action of $f_{\mu\nu}$ | Interaction term

$g_{\mu\nu}$: physical metric

$f_{\mu\nu}$: reference metric

$$F_2[L^\mu_\nu] = \frac{1}{2}([L]^2 - [L^2])$$

trace

$$L^\mu_\nu = \delta^\mu_\nu - (\sqrt{g^{-1}f})^\mu_\nu$$

m^2 : coupling constant

$$M_e^2 = (\frac{1}{M_g^2} + \frac{1}{M_f^2})^{-1}$$

: reduced Plank scale

The motivation of our study

We would like to investigate dynamics of spacetime with matter in bimetric gravity.

As the simple case,
we think of bimetric theory with cosmological constants.

$$S = \frac{M_g^2}{2}\int d^4x\sqrt{-g}(R[g_{\mu\nu}] - 2\Lambda_g) + \frac{M_f^2}{2}\int d^4x\sqrt{-f}(R[f_{\mu\nu}] - 2\Lambda_f)$$
$$+m^2 M_e^2 \int d^4x\sqrt{-g}F_2[L^\mu_\nu],$$

* We can think of cosmological constants as scalar fields in slow roll approximation.

We can also discuss inflation.

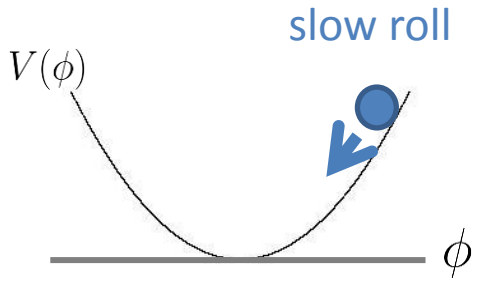

de Sitter solution

$$a_g = \frac{M_e^2}{M_g^2}, \quad \xi = \frac{m^2}{M_e^2}, \quad \lambda_g = \frac{\Lambda_g}{3M_e^2}, \quad \lambda_f = \frac{\Lambda_f}{3M_e^2}, \quad ' = \frac{1}{M_e}\frac{\mathrm{d}}{\mathrm{d}t}.$$

homogeneous metric ansatz

$$ds^2 = -N^2(t)dt^2 + e^{2\alpha}(t)[dx^2 + dy^2 + dz^2]$$
$$ds'^2 = -M^2(t)dt^2 + e^{2\beta}(t)[dx^2 + dy^2 + dz^2]$$

From variational principle of action

$$\left(\frac{\alpha'}{N}\right)' - \xi a_g(M - N\epsilon)\left(\frac{3}{2} - \epsilon\right) = 0, \quad \text{: EoM of } \alpha$$

$$\epsilon = e^{\beta-\alpha}$$

$$\left(\frac{\beta'}{M}\right)' + \xi(1 - a_g)\epsilon^{-3}(M - N\epsilon)\left(\frac{3}{2} - \epsilon\right) = 0, \quad \text{: EoM of } \beta$$

$$\left(\frac{\alpha'}{N}\right)^2 = \lambda_g + \xi a_g(2 - \epsilon)(\epsilon - 1), \quad \text{: constraint (from variation with respect to N)}$$

$$\left(\frac{\beta'}{M}\right)^2 = \lambda_f + \xi(1 - a_g)\epsilon^{-3}(1 - \epsilon). \quad \text{: constraint (from variation with respect to M)}$$

$$\xi\left(\frac{3}{2} - \epsilon\right)\left(\frac{\beta' e^{\beta}}{M} - \frac{\alpha' e^{\alpha}}{N}\right) = 0 \quad \text{: consistency relation (secondary constraint)}$$

de Sitter solution is represented as positive roots of $g(\epsilon)$: ϵ_0 = const. → $\alpha' = \beta' = H_0$

$$g(\epsilon) = (\lambda_f + \xi a_g)\epsilon^3 - 3\xi a_g \epsilon^2 + [-\lambda_g + 2\xi a_g - \xi(1 - a_g)]\epsilon + \xi(1 - a_g) = 0.$$

de Sitter solution

$$a_g = \frac{M_e^2}{M_g^2}, \quad \xi = \frac{m^2}{M_e^2}, \quad \lambda_g = \frac{\Lambda_g}{3M_e^2}, \quad \lambda_f = \frac{\Lambda_f}{3M_e^2}, \quad ' = \frac{1}{M_e}\frac{\mathrm{d}}{\mathrm{d}t}.$$

homogeneous metric ansatz

$$ds^2 = -N^2(t)dt^2 + e^{2\alpha}(t)[dx^2 + dy^2 + dz^2]$$
$$ds'^2 = -M^2(t)dt^2 + e^{2\beta}(t)[dx^2 + dy^2 + dz^2]$$

From variational principle of action

$$\left(\frac{\alpha'}{N}\right)' - \xi a_g(M - N\epsilon)\left(\frac{3}{2} - \epsilon\right) = 0, \quad \text{: EoM of } \alpha$$

$$\epsilon = e^{\beta-\alpha}$$

$$\left(\frac{\beta'}{M}\right)' + \xi(1 - a_g)\epsilon^{-3}(M - N\epsilon)\left(\frac{3}{2} - \epsilon\right) = 0, \quad \text{: EoM of } \beta$$

$$\left(\frac{\alpha'}{N}\right)^2 = \lambda_g + \xi a_g(2 - \epsilon)(\epsilon - 1), \quad \text{: constraint (from variation with respect to N)}$$

$$\left(\frac{\beta'}{M}\right)^2 = \lambda_f + \xi(1 - a_g)\epsilon^{-3}(1 - \epsilon). \quad \text{: constraint (from variation with respect to M)}$$

$$\xi\left(\frac{3}{2} - \epsilon\right)\left(\frac{\beta' e^{\beta}}{M} - \frac{\alpha' e^{\alpha}}{N}\right) = 0 \quad \text{: con}$$

Expansion rate (Hubble)

$$H_0^2 = \lambda_g + \xi a_g(2 - \epsilon_0)(\epsilon_0 - 1)$$

de Sitter solution is represented as positive roots of $g(\epsilon)$: ϵ_0 = const. → $\alpha' = \beta' = H_0$

$$g(\epsilon) = (\lambda_f + \xi a_g)\epsilon^3 - 3\xi a_g \epsilon^2 + [-\lambda_g + 2\xi a_g - \xi(1 - a_g)]\epsilon + \xi(1 - a_g) = 0.$$

The conditions for the existence of de Sitter solution

Condition① : There exist positive roots of $g(\epsilon)$

Condition② : The roots satisfy $H_0^2 > 0$

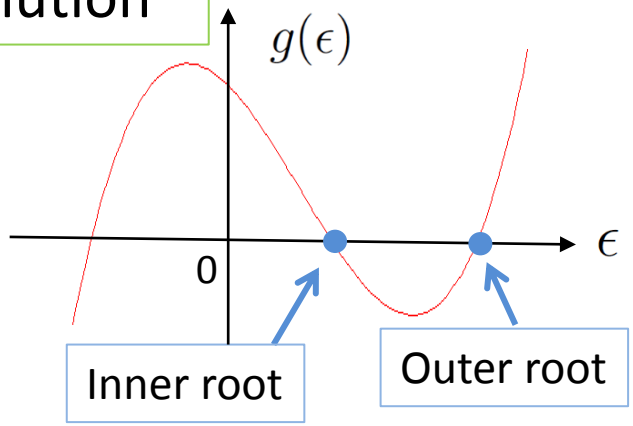

Inner root

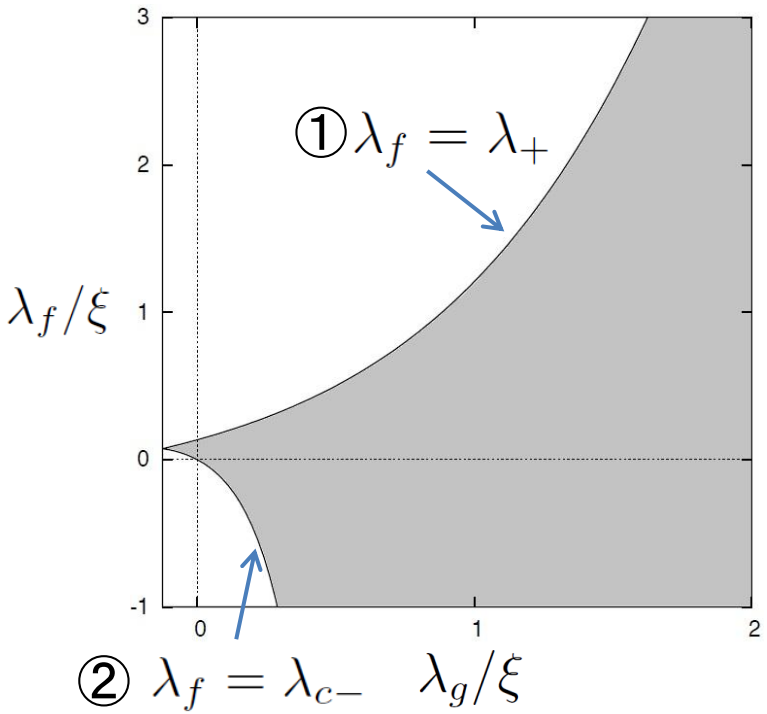

Outer root

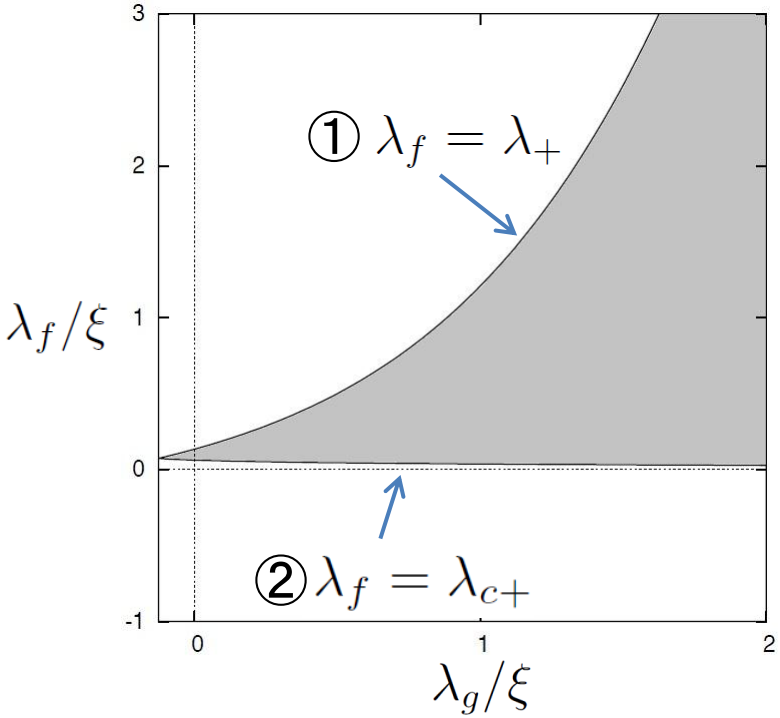

where $\lambda_+ = \lambda_+(\xi, a_g, \lambda_g)$, $\lambda_{c\pm} = \xi(1-a_g)\left(\frac{1}{2} \pm \sqrt{\frac{\lambda_g}{\xi a_g} + \frac{1}{4}}\right) \Big/ \left(\frac{3}{2} \pm \sqrt{\frac{\lambda_g}{\xi a_g} + \frac{1}{4}}\right)^3$

Anisotropic perturbation

anisotropic ansatz

$$ds^2 = -N^2(t)dt^2 + e^{2\alpha(t)}\left[e^{-4\sigma(t)}dx^2 + e^{2\sigma(t)}(dy^2+dz^2)\right],$$

$$ds'^2 = -M^2(t)dt^2 + e^{2\beta(t)}\left[e^{-4\lambda(t)}dx^2 + e^{2\lambda(t)}(dy^2+dz^2)\right],$$

From variational principle of action,

$$\sigma'' + 3H_0\sigma' - \xi a_g \epsilon_0 (3-2\epsilon_0) q = 0 \quad : \text{EoM of } \sigma$$

$$\lambda'' + 3H_0\lambda' + \xi(1-a_g)\frac{1}{\epsilon_0}(3-2\epsilon_0) q = 0 \quad : \text{EoM of } \lambda$$

$$q = \lambda - \sigma$$

From the difference of EoMs,

$$q'' + 3H_0 q' + \xi\left[a_g\epsilon_0 + (1-a_g)\frac{1}{\epsilon_0}\right](3-2\epsilon_0) q = 0$$

$$\omega_0^2 = \xi\left[a_g\epsilon_0 + (1-a_g)\frac{1}{\epsilon_0}\right](3-2\epsilon_0)$$

: Effective mass of massive graviton

The stability towards the anisotropic perturbation

$$\omega_0^2 = \xi\left[a_g\epsilon_0 + (1-a_g)\frac{1}{\epsilon_0}\right](3-2\epsilon_0)$$

positive definite

The stability is determined by the sign of oscillational term

whether ϵ_0 is larger/smaller than $\frac{3}{2}$

Inner root

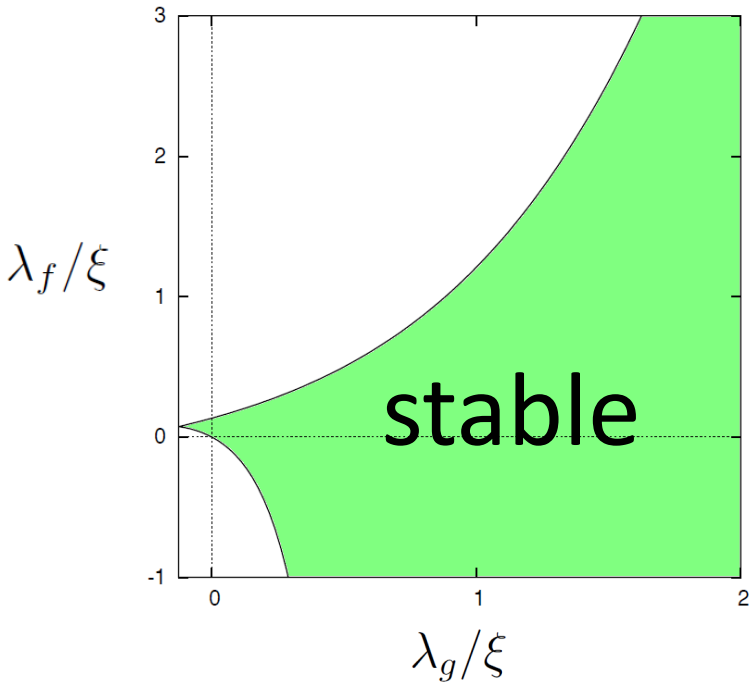

Outer root

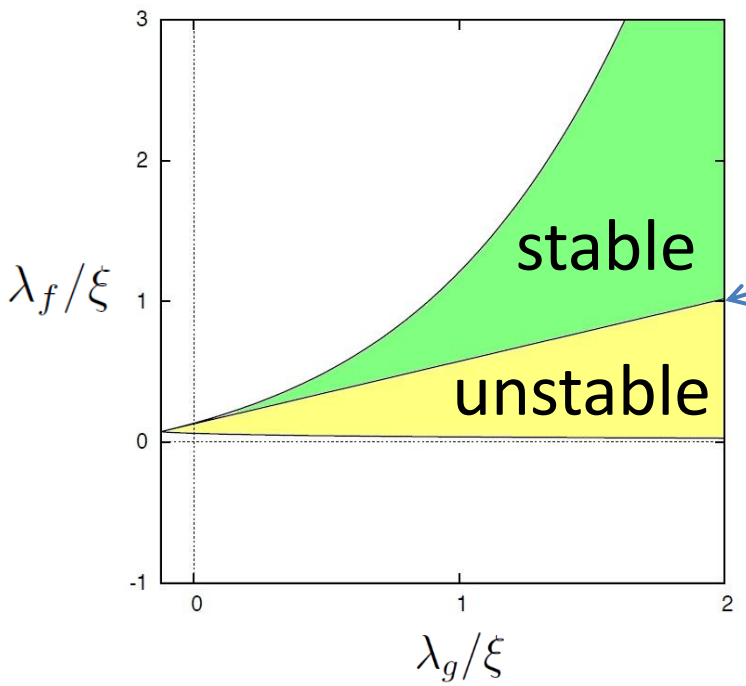

where $\lambda_{\frac{3}{2}} = \frac{4}{27}\left[3\left(\lambda_g + \frac{\xi a_g}{4}\right) + \xi(1-a_g)\right]$

Evaluation of effective mass ω_0^2

$$\beta = \frac{\omega_0^2}{H_0^2} = \frac{\xi[a_g\epsilon_0 + (1-a_g)\frac{1}{\epsilon_0}](3-2\epsilon_0)}{\lambda_g + \xi a_g(2-\epsilon_0)(\epsilon_0-1)}$$

: the ratio of effective mass to Hubble scale

Inner root ➡ $\beta > 2$

Outer root ➡ $\beta < 2$

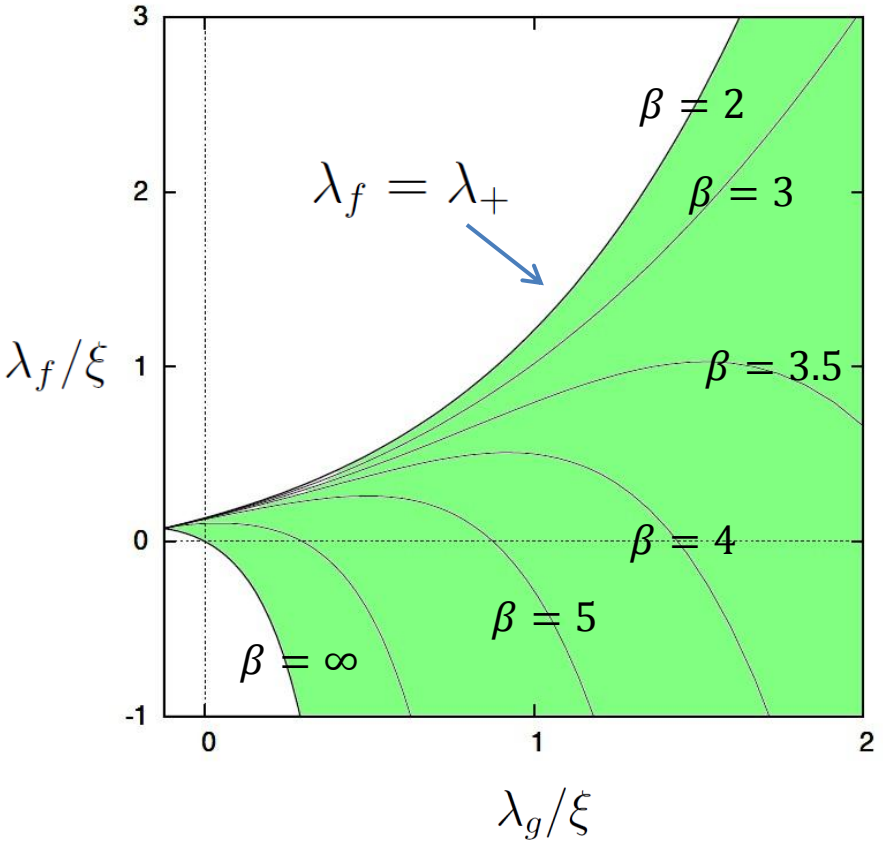

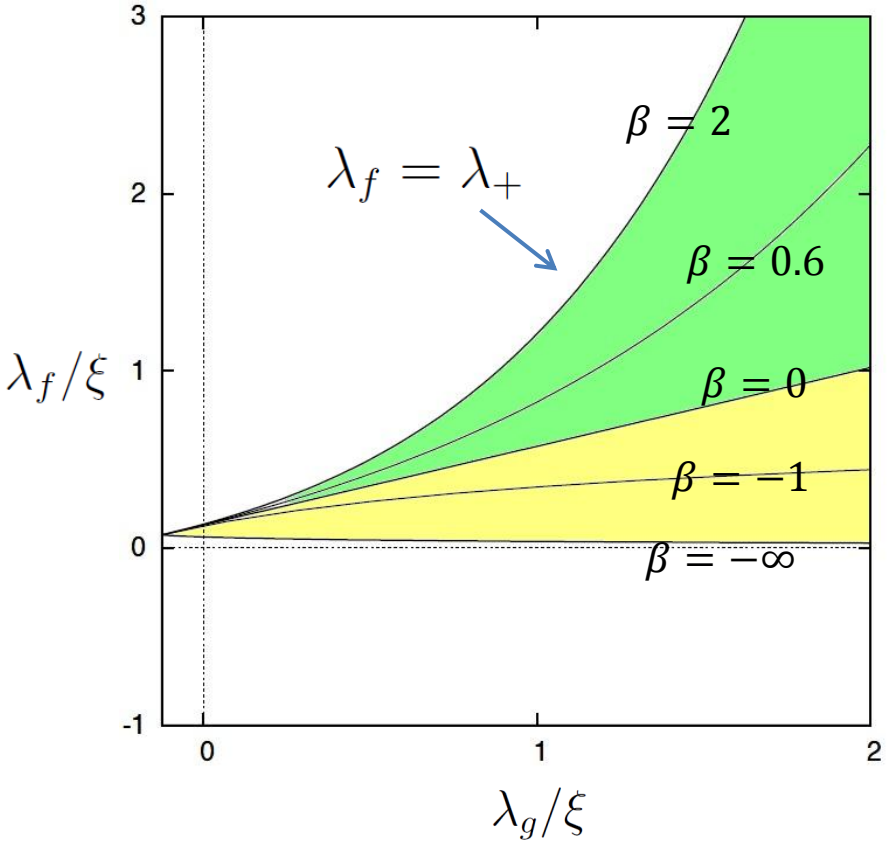

Effective mass exactly equals to $2H_0^2$ on $\lambda_f = \lambda_+$!

Summery

(1) homogeneous isotropic metric ansatz

➡ the condition that de Sitter solution exists

There are two series of solutions: inner root and outer root.

(2) anisotropic perturbation around de Sitter sol.

➡ the stability for the perturbation

- inner root → stable
- outer root → stable for $\lambda_f > \lambda_{\frac{3}{2}}$ and unstable for $\lambda_f < \lambda_{\frac{3}{2}}$

➡ effective mass of massive graviton corresponding to the anisotropy.

- inner root → $\omega_0^2 > 2H_0^2$
- outer root → $\omega_0^2 < 2H_0^2$

For inner root, effective mass is bounded above Hubble scale.
If we consider inflation then the anisotropy decays in inflation time scale.

Future work

When we consider perturbations on de Sitter background in massive gravity, the square of graviton mass should be larger than $2H_0^2$ (Higuchi bound)

ref. A.Higuchi, Nucl,Phys. B 282,397 (1987)

- In our analysis,

  Effective mass exactly equals to $2H_0^2$ on $\lambda_f = \lambda_+$!

  i.e. the critical condition for the existence of de Sitter solutions

  ⇔ coincide with Higuchi bound

- Is there really the relation between them ?
  - explicitly calculating the mass bound of massive graviton in bimetric gravity

$$S = \frac{M_g^2}{2}\int d^4x\sqrt{-g}R[g_{\mu\nu}] + \frac{M_f^2}{2}\int d^4x\sqrt{-f}R[f_{\mu\nu}]$$
$$+m^2M_e^2\int d^4x\sqrt{-g}\sum_{n=0}^{4}\beta_n e_n[(\sqrt{g^{-1}f})^\mu_\nu]$$

$$e_n[X^\mu_\nu] = \frac{(-1)^n}{n!}\sum_{\sigma\in S_n}\mathrm{sig}(\sigma)X^{\mu_{\sigma(1)}}_{\mu_1}X^{\mu_{\sigma(2)}}_{\mu_2}\cdots X^{\mu_{\sigma(n)}}_{\mu_n}$$

equivalent

$$\beta_0 = \alpha_0 - 4\alpha_1 + 6\alpha_2 - 4\alpha_3 + \alpha_4$$
$$\beta_1 = \alpha_1 - 3\alpha_2 + 3\alpha_3 - \alpha_4$$
$$\beta_2 = \alpha_2 - 2\alpha_3 + \alpha_4$$
$$\beta_3 = \alpha_3 - \alpha_4$$
$$\beta_4 = \alpha_4$$

← cosmological const of physical metric

← cosmological constant of reference metric

$$S = \frac{M_g^2}{2}\int d^4x\sqrt{-g}R[g_{\mu\nu}] + \frac{M_f^2}{2}\int d^4x\sqrt{-f}R[f_{\mu\nu}]$$
$$+m^2M_e^2\int d^4x\sqrt{-g}\sum_{n=0}^{4}\alpha_n e_n[(1-\sqrt{g^{-1}f})^\mu_\nu]$$

The condition for the existence of de Sitter solution

* We fix $\xi,\ a_g,\ \lambda_g$ and vary λ_f in the following. Then root of $g(\epsilon)$ is function of λ_f .

$$\epsilon_0 = \epsilon_0(\lambda_f)$$

Condition(1) : There exist positive roots of $g(\epsilon)$

$$\lambda_f \leq \lambda_+(\xi, a_g, \lambda_g)$$

Condition(2) : The roots satisfy $H_0^2 > 0$

Expansion rate is determined from constraint.

$$H_0^2 = \lambda_g + \xi a_g(2-\epsilon_0)(\epsilon_0 - 1)$$

$$\epsilon_{c-} < \epsilon_0(\lambda_f) < \epsilon_{c+}$$

where $\epsilon_{c\pm} = \frac{3}{2} \pm \sqrt{\frac{\lambda_g}{\xi a_g} + \frac{1}{4}}.$

The behavior of the roots of $g(\epsilon)$

- $\lambda_f = \lambda_+$

$\frac{\mathrm{d}\epsilon_{\mathrm{in}}}{\mathrm{d}\lambda_f} > 0.$ $\frac{\mathrm{d}\epsilon_{\mathrm{out}}}{\mathrm{d}\lambda_f} < 0.$

There exists a positive multiple root .

$$\epsilon_*$$

This root satisfies

$$\epsilon_{c-} < \epsilon_* < \epsilon_{c+}$$

- $\lambda_f < \lambda_+$

There ordinarily exist two positive roots.

ϵ_{in} and ϵ_{out} (inner root and outer root)

As we decrease λ_f, { ϵ_{in} decreases. / ϵ_{out} increases. }

➡ Sometime, { ϵ_{in} becomes smaller than ϵ_{c-} / ϵ_{out} becomes larger than ϵ_{c+} }

$$\epsilon_{\mathrm{in}} < \epsilon_*$$
$$\epsilon_{\mathrm{out}} > \epsilon_*$$

The critical λ_f is λ_{c-} , λ_{c+} , respectively.

we can rewrite the following value as

$$\omega_0^2(\epsilon_0) - 2H_0^2(\epsilon_0) = (\epsilon_* - \epsilon_0) \times (\text{positive definite})$$

$$\begin{aligned} \omega_0^2 > 2H_0^2 &\quad\Leftrightarrow\quad \epsilon_0 < \epsilon_* \\ \omega_0^2 = 2H_0^2 &\quad\Leftrightarrow\quad \epsilon_0 = \epsilon_* \\ \omega_0^2 < 2H_0^2 &\quad\Leftrightarrow\quad \epsilon_0 > \epsilon_* \end{aligned}$$

From $\begin{aligned} \epsilon_{\text{in}} &< \epsilon_* \\ \epsilon_{\text{out}} &> \epsilon_* \end{aligned}$, inner root satisfies $\omega_0^2 > 2H_0^2$

outer root satisfies $\omega_0^2 < 2H_0^2$

Bigravity action

$$S = \frac{M_g^2}{2}\int d^4x\sqrt{-g}R[g_{\mu\nu}] + \frac{M_f^2}{2}\int d^4x\sqrt{-f}R[f_{\mu\nu}] + m^2M_e^2\int d^4x\sqrt{-g}\,F_2$$

EH action of $g_{\mu\nu}$ | EH action of $f_{\mu\nu}$ | Interaction term

$g_{\mu\nu}$: physical metric

$f_{\mu\nu}$: reference metric

$$F_2[L^\mu_\nu] = \frac{1}{2}([L]^2 - [L^2])$$

trace

$$L^\mu_\nu = \delta^\mu_\nu - (\sqrt{g^{-1}f})^\mu_\nu$$

m^2 : coupling constant

$$M_e^2 = \left(\frac{1}{M_g^2} + \frac{1}{M_f^2}\right)^{-1}$$

: reduced Plank scale

* when we make the general coordinate transformation at the same time for both metrics, the action is unchanged. (there are only 4 DOF as general covariance.)

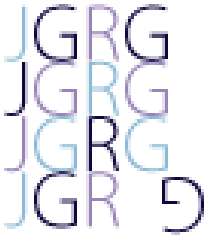

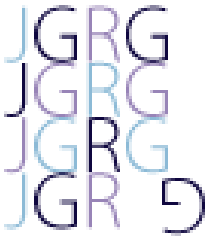

Maresuke Shiraishi, JGRG 22(2012)111426

"Parity violation in the CMB bispectrum"

RESCEU SYMPOSIUM ON

GENERAL RELATIVITY AND GRAVITATION

JGRG 22

November 12-16 2012

Koshiba Hall, The University of Tokyo, Hongo, Tokyo, Japan





Parity violation in the CMB bispectrum

Maresuke Shiraishi[1](a)

(a) *Department of Physics and Astrophysics, Nagoya University, Nagoya, Aichi, 464-8602, Japan*

Abstract

We analyze the response of the parity violation in the primordial non-Gaussianity to the CMB bispectrum. We find that the parity-violating non-Gaussianity creates III, IIE, IEE, IBB, EEE, EBB spectra obeying $\sum_{n=1}^{3}\ell_n =$ odd and IIB, IEB, EEB, BBB spectra satisfying $\sum_{n=1}^{3}\ell_n =$ even. We confirm these features through the case where the parity-violating Weyl cubic action or primordial helical magnetic field exists.

1 Introduction

Non-Gaussian features in the cosmological perturbations include detailed information on the nature of the early Universe, and there have been many works that attempt to extract them from the bispectrum (three-point function) of the cosmic microwave background (CMB) anisotropies (e.g., Ref. [1]). However, most of these discussions are limited in the cases that the scalar-mode contribution dominates in the non-Gaussianity and also are based on the assumption of rotational invariance and parity conservation.

In contrast, there are several studies on the non-Gaussianities of not only the scalar-mode perturbations but also the vector- and tensor-mode perturbations [2]. These sources produce the additional signals on the CMB bispectrum [3] and can give a dominant contribution by considering such highly non-Gaussian sources as the stochastic magnetic elds [4]. Furthermore, even in the CMB bispectrum induced from the scalar-mode non-Gaussianity, if the rotational invariance is violated in the non-Gaussianity, the characteristic signals appear [5]. Thus, it is very important to clarify these less-noted signals to understand the precise picture of the early Universe.

This paper discusses how the parity violation in the primordial non-Gaussianity affects in the CMB bispectrum. The effects on the cosmic microwave background (CMB) have been well-studied and the cosmological parity violation has been veri ed by analyzing the non-vanishing cross-correlated power spectra between the intensity (I) and B-mode polarization (B) anisotropies and those between E-mode (E) and B-mode polarization anisotropies. Furthermore, beyond the linear-order effects, the impacts of the parity violation on the graviton non-Gaussianities have recently been discussed [6, 7]. According to the concept of this literature, in Ref. [8], we have formulated the CMB bispectrum generated from the parity-violating graviton non-Gaussianities and nd special signatures of primordial parity violation. Moreover, Ref. [9] have evaluated the detectability of the parity-violating non-Gaussianity by using the CMB III bispectrum under an assumption of the existence of large-scale helical magnetic elds.

This paper corresponds to a review of our papers [8, 9]. Detailed organization is as follows. In the next section, we summarize the effects of the parity in the primordial non-Gaussianity on the CMB bispectrum. In Secs. 3 and 4, we present the CMB bispectra sourced from the non-Gaussianities due to the parity-violating Weyl gravity and primordial helical magnetic elds. The nal section is devoted to summary and discussion.

2 Response of parity in non-Gaussianity to CMB bispectrum

The CMB fluctuation on any direction, $\hat{\mathbf{n}}$, is quanti ed in multipole space as

$$\frac{\Delta X(\hat{\mathbf{n}})}{X} = \sum_{\ell m} a_{X,\ell m} Y_{\ell m}(\hat{\mathbf{n}}) \ , \tag{1}$$

[1]Email address: mare@nagoya-u.jp

where X denotes the intensity (I) and two polarization elds (E, B). If keeping the rotational invariance of the primordial non-Gaussianity, the CMB bispectrum is also de ned in multipole space as

$$B_{X_1X_2X_3,\ell_1\ell_2\ell_3} = \sum_{m_1m_2m_3} \begin{matrix}\ell_1 & \ell_2 & \ell_3\\ m_1 & m_2 & m_3\end{matrix} \left\langle \prod_{n=1}^{3} a_{X_n,\ell_m m_n} \right\rangle \tag{2}$$

The multipole con guration of the CMB bispectrum can be easily understood only if one consider the parity transformation of the CMB intensity and polarization elds in real space. III, IIE, IEE, IBB, EEE and EBB spectra from parity-conserving non-Gaussianity, and IIB, IEB, EEB, and BBB spectra from parity-violating non-Gaussianity have even parity, namely,

$$\left\langle \prod_{i=1}^{3} \frac{\Delta X_i(\hat{\mathbf{n}}_\mathbf{i})}{X_i} \right\rangle = \left\langle \prod_{i=1}^{3} \frac{\Delta X_i(\quad \hat{\mathbf{n}}_\mathbf{i})}{X_i} \right\rangle \ . \tag{3}$$

Then, from the multipole expansion (1) and its parity flip version as

$$\frac{\Delta X(\quad \hat{\mathbf{n}})}{X} = \sum_{\ell m} a_{X,\ell m} Y_{\ell m}(\quad \hat{\mathbf{n}}) = \sum_{\ell m} (\quad 1)^{\ell} a_{X,\ell m} Y_{\ell m}(\hat{\mathbf{n}}) \ , \tag{4}$$

one can notice that $\sum_{n=1}^{3} \ell_n =$ even must be satis ed. On the other hand, since IIB, IEB, EEB, and BBB spectra from parity-conserving non-Gaussianity, and III, IIE, IEE, IBB, EEE, and EBB spectra from parity-violating non-Gaussianity have odd parity, namely,

$$\left\langle \prod_{i=1}^{3} \frac{\Delta X_i(\hat{\mathbf{n}}_\mathbf{i})}{X_i} \right\rangle = \quad \left\langle \prod_{i=1}^{3} \frac{\Delta X_i(\quad \hat{\mathbf{n}}_\mathbf{i})}{X_i} \right\rangle \ , \tag{5}$$

one can obtain $\sum_{n=1}^{3} \ell_n =$ odd.

3 CMB signatures from parity-violating Weyl gravity

Primordial non-Gaussianity from parity-odd (parity-violating) Weyl cubic action has been rstly reported by Ref.[6] in the context of ultraviolet modi cation of gravity. After that, careful treatments by Ref. [7] have shown that resultant parity-violating non-Gaussianity of the primordial gravitational waves emerges not in the exact de Sitter space-time but in the quasi de Sitter space-time, and hence, its amplitude is proportional to a slow-roll parameter. In these studies, the authors have assumed that the coupling constant of the Weyl cubic terms is independent of time.

In this section, we focus on the graviton non-Gaussianity generated from the parity-violating Weyl gravity with the running coupling constant as a function of a conformal time, $f(\ )$, whose action is given by

$$S = \int d\ d^3x \frac{f(\ )}{\Lambda^2} \qquad W \quad _\gamma W^\gamma \ _\sigma W^\sigma \qquad . \tag{6}$$

Here, $W \quad _\gamma$ denotes the Weyl tensor, is a 4D Levi-Civita tensor normalized as $^{0123} = 1$, and Λ is a scale that sets the value of the higher derivative corrections [6]. The coupling constant is assumed as the power-law type: $f(\ ) = (\ /\ )^A$, where is a conformal time. Here, we have set $f(\quad) = 1$. Such a coupling can be readily realized by considering a dilaton-like coupling in the slow-roll inflation. In this case, depending on time dependence of coupling, we can realize nite non-Gaussianity of gravitational waves even in the exact de Sitter space time. Note that primordial tensor bispectrum from such non-Gaussianity is categorized as the equilateral type.

Figure. 1 shows an example of the CMB III and BBB bispectra from such primordial tensor bispectrum. Here, we plot the reduced bispectrum de ned by

$$b_{X_1X_2X_3,\ell_1\ell_2\ell_3} \quad (G_{\ell_1\ell_2\ell_3}) \ ^1B_{X_1X_2X_3,\ell_1\ell_2\ell_3} \tag{7}$$

with

$$G_{\ell_1\ell_2\ell_3} \quad \frac{2\sqrt{\ell_3(\ell_3+1)\ell_2(\ell_2+1)}}{\ell_1(\ell_1+1) \quad \ell_2(\ell_2+1) \quad \ell_3(\ell_3+1)}\sqrt{\frac{\prod_{n=1}^{3}(2\ell_n+1)}{4}} \quad \begin{matrix}\ell_1 & \ell_2 & \ell_3\\ 0 & 1 & 1\end{matrix} \quad . \tag{8}$$

It is observed that III and BBB spectra obey $\sum_{n=1}^{3}\ell_n = \text{odd}$ and $\sum_{n=1}^{3}\ell_n = \text{even}$, respectively. These are consistent with the discussion in the previous section and characteristic imprints of the parity-violating non-Gaussianity.

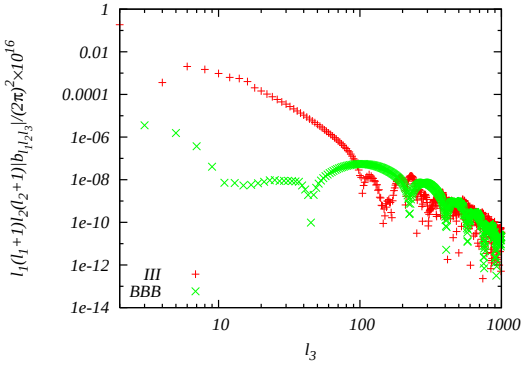

Figure 1: Absolute values of the CMB III and BBB spectra from parity-violating graviton non-Gaussianity. Here, three multipoles are xed as $\ell_1 \quad 2 = \ell_2 \quad 1 = \ell_3$. Here, we x the parameters as $\Lambda = 3 \quad 10^6$GeV, $A = 1$ and $= \quad k \ ^1 = \quad 14$Gpc, and other cosmological parameters are xed as the mean values limited from the WMAP 7-yr data [10].

4 CMB signatures from helical magnetic fields

If there exists the primordial magnetic eld (PMF), which is a favored candidate for the seed eld of microgauss-level magnetic elds in galaxies and cluster of galaxies, their power spectrum may involve the parity-violating component. Assuming Gaussianity of such PMF, bene cial signals are generated in the CMB bispectra due to the quadratic dependence of the CMB fluctuation on the PMF. In the case where only parity-conserving component exists, the contributions of PMFs to the primordial non-Gaussianities and the CMB bispectra have been deeply investigated in e.g., Ref. [4].

In this section, let us consider the effects of PMFs including the parity violation on the CMB bispectrum. We shall start from the convention of the parametrization for the PMF as

$$\langle B_a(\mathbf{k})B_b(\mathbf{k}')\rangle = \frac{(2\ )^3}{2}\left[P_B(k)P_{ab}(\hat{\mathbf{k}}) + i\ _{abc}\hat{k}_c P_{\mathcal{B}}(k)\right] \ (\mathbf{k}+\mathbf{k}') \ , \tag{9}$$

where $\hat{\mathbf{k}}$ is a unit vector, $_{abc}$ is the 3D Levi-Civita tensor normalized by $_{123} = 1$, and $P_{ab}(\hat{\mathbf{k}}) \quad _{ab} \quad \hat{k}_a\hat{k}_b$ is a projection tensor coming from the divergence free nature of PMFs. The rst and second terms in the bracket of r.h.s. represent non-helical and helical contributions, respectively. The magnetic anisotropic stress, which depends quadratically on the PMF, acts as a source of metric perturbations prior to neutrino decoupling. Then, due to Gaussianity of the PMF, resulting curvature perturbation and gravitational wave become highly non-Gaussian elds. Such non-Gaussianities result in nite CMB bispectra of scalar and tensor modes.

Figure 2 describes the signal-to-noise ratio from the parity-violating components of the CMB III bispectrum ($\sum_{n=1}^{3}\ell_n = \text{odd}$) in the cosmic variance limit. As shown in this gure, at large scales, tensor mode dominates over scalar one because of the ISW ampli cation. Note that the auto-correlated bispectrum of scalar modes is exactly zero because the scalar mode has no spin dependence and cannot hold the information on parity. The parity-odd III bispectrum depends on $P_B^2 P_{\mathcal{B}}$. Introducing the PMF strengths smoothed on 1Mpc, namely, $B_{1\mathrm{Mpc}}(\propto P_B^{1/2})$ and $\mathcal{B}_{1\mathrm{Mpc}}(\propto P_{\mathcal{B}}^{1/2})$, we can conclude that the signal-to-noise ratio from parity-odd III bispectrum exceeds unity if $B_{1\mathrm{Mpc}}^{2/3}\mathcal{B}_{1\mathrm{Mpc}}^{1/3} > 2.3$nG.

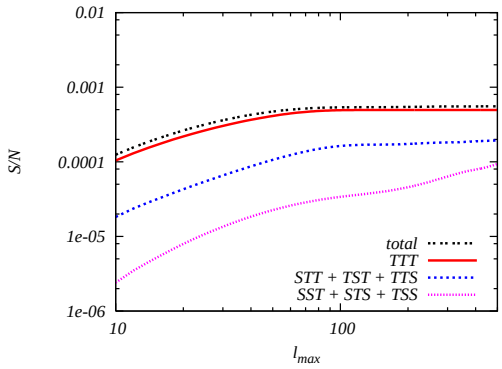

Figure 2: Signal-to-noise ratios from the parity-odd CMB III bispectra coming from $\sum_{n=1}^{3}\ell_n = \text{odd}$, respectively, in the cosmic variance limit. The "total" line denotes S/N obtained from the total spectrum of $TTT, STT, TST, TTS, SST, STS$ and TSS modes, and the others correspond to S/N's coming from each mode. Here, we x the PMF parameters as $B_{1\mathrm{Mpc}} = 1.0\mathrm{nG}, \mathcal{B}_{1\mathrm{Mpc}} = 0.287\mathrm{nG}$, and assume the PMF generation at the GUT scale and nearly scale invariance of P_B and $P_{\mathcal{B}}$. The other parameters are identical to the mean values obtained from the WMAP-7yr data [10].

5 Summary and discussion

In this paper, we have summarized the impacts of parity-violating non-Gaussianities on the CMB bispectra. Non-Gaussian level party violation limits the multipole con gurations of the CMB bispectra. That is, III, IIE, IEE, IBB, EEE, EBB spectra obey $\sum_{n=1}^{3}\ell_n = \text{odd}$, and IIB, IEB, EEB, BBB spectra arise if satisfying $\sum_{n=1}^{3}\ell_n = \text{even}$. Actually, these special properties associated with parity-violating non-Gaussianity can be predicted in the several early Universe models, such as the Weyl gravity and inflation with the electromagnetic eld [8, 9]. Constraining these models from the CMB observation remains as a future issue.

References

[1] N. Bartolo, E. Komatsu, S. Matarrese and A. Riotto, Phys. Rept. **402** (2004), 103 [arXiv:astro-ph/0406398].

[2] J. M. Maldacena, JHEP **0305** (2003), 013 [arXiv:astro-ph/0210603].

[3] M. Shiraishi, D. Nitta, S. Yokoyama, K. Ichiki and K. Takahashi, Prog. Theor. Phys. **125** (2011), 795 [arXiv:1012.1079 [astro-ph.CO]].

[4] M. Shiraishi, D. Nitta, S. Yokoyama and K. Ichiki, JCAP **1203**, 041 (2012) [arXiv:1201.0376 [astro-ph.CO]].

[5] M. Shiraishi and S. Yokoyama, arXiv:1107.0682 [astro-ph.CO].

[6] J. M. Maldacena, G. L. Pimentel, JHEP **1109** (2011), 045. [arXiv:1104.2846 [hep-th]].

[7] J. Soda, H. Kodama, M. Nozawa, JHEP **1108** (2011), 067. [arXiv:1106.3228 [hep-th]].

[8] M. Shiraishi, D. Nitta and S. Yokoyama, Prog. Theor. Phys. **126**, 937 (2011) [arXiv:1108.0175 [astro-ph.CO]].

[9] M. Shiraishi, JCAP **1206**, 015 (2012) [arXiv:1202.2847 [astro-ph.CO]].

[10] E. Komatsu *et al.* [WMAP Collaboration], Astrophys. J. Suppl. **192** (2011), 18 [arXiv:1001.4538 [astro-ph.CO]].

Jerome Martin, JGRG 22(2012)111501

"The cosmological constant problem"

RESCEU SYMPOSIUM ON

GENERAL RELATIVITY AND GRAVITATION

JGRG 22

November 12-16 2012

Koshiba Hall, The University of Tokyo, Hongo, Tokyo, Japan

The Cosmological Constant Problem



Jérôme Martin

Institut d'Astrophysique de Paris & Research Center for the Early Universe (Tokyo University)

"Joyeux anniversaire et meilleurs voeux aux professeurs Futamase, Kodama & Sasaki!"

RESCEU SYMPOSIUM ON GENERAL RELATIVITY AND GRAVITATION
JGRG22 November 12 - 16 2012

Outline

1- Introduction: the cosmological constant in the Einstein equations.

2- Observational constraints on the *CC*.

3- Regularization (or renormalization) of the vacuum energy density.

4- Possible loopholes in our approach to the *CC* problem.

5- General conclusions.

Based on

"Everything you always wanted to know about the Cosmological constant problem (but were afraid to ask)"

Comptes Rendus Physique 13 (2012) 566-665

arXiv:1205.3365

See also:

- S. Weinberg, Rev. Mod. Phys. 61, 1 (1989)
- V. Sahni & A. Starobinsky, astro-ph/9904398
- T. Padmanabhan, hep-th/0212290
- J. Yokoyama, gr-qc/0305068
- J. Polchinsky, hep-th/0603249
- M. Li, X. Li, S. Wang & Y. Wang, arXiv:1103.5870

Historically introduced by Einstein to find a static cosmological solution in General Relativity (GR) [see N. Straumann, gr-qc/0208027]

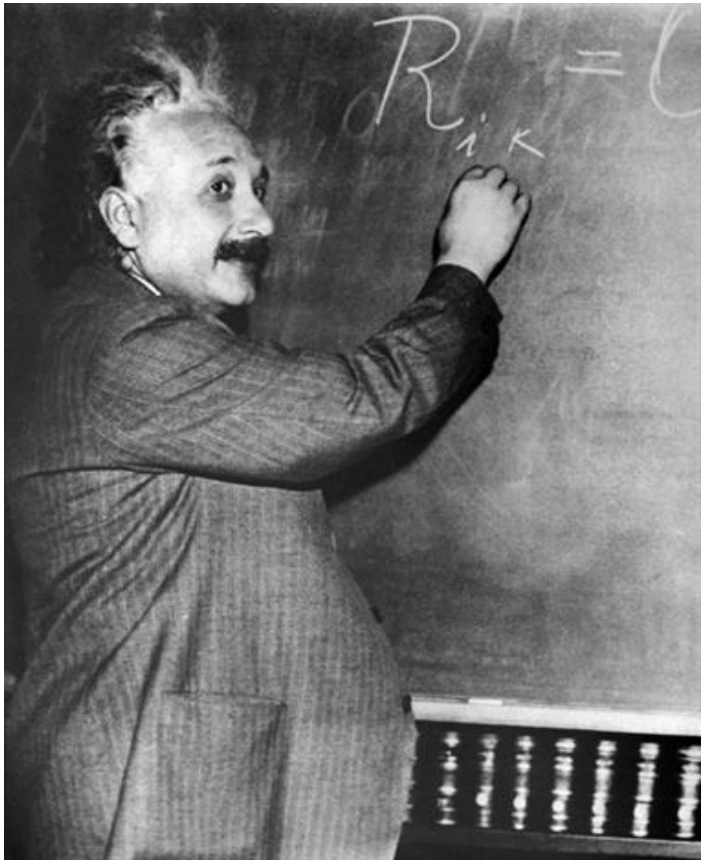

PROCEEDINGS
OF THE
NATIONAL ACADEMY OF SCIENCES
Volume 18 March 15, 1932 Number 3

ON THE RELATION BETWEEN THE EXPANSION AND THE MEAN DENSITY OF THE UNIVERSE

BY A. EINSTEIN AND W. DE SITTER

Communicated by the Mount Wilson Observatory, January 25, 1932

In a recent note in the *Göttinger Nachrichten*, Dr. O. Heckmann has pointed out that the non-static solutions of the field equations of the general theory of relativity with constant density do not necessarily imply a positive curvature of three-dimensional space, but that this curvature may also be negative or zero.

There is no direct observational evidence for the curvature, the only directly observed data being the mean density and the expansion, which latter proves that the actual universe corresponds to the non-statical case. It is therefore clear that from the direct data of observation we can derive neither the sign nor the value of the curvature, and the question arises whether it is possible to represent the observed facts without introducing a curvature at all.

Historically the term containing the "cosmological constant" λ was introduced into the field equations in order to enable us to account theoretically for the existence of a finite mean density in a static universe. It now appears that in the dynamical case this end can be reached without the introduction of λ.

If we suppose the curvature to be zero, the line-element is

$$ds^2 = -R^2(dx^2 + dy^2 + dz^2) + c^2dt^2, \qquad (1)$$

where R is a function of t only, and c is the velocity of light. If, for the sake of simplicity, we neglect the pressure p,[1] the field equations without λ lead to two differential equations, of which we need only one, which in the case of zero curvature reduces to:

$$\frac{1}{R^2}\left(\frac{dR}{cdt}\right)^2 = \frac{1}{3}\kappa\rho. \qquad (2)$$

The observations give the coefficient of expansion and the mean density:

$$\frac{1}{R}\frac{dR}{cdt} = h = \frac{1}{R_B}; \quad \rho = \frac{2}{\kappa R_A^2}.$$

In presence of a Cosmological Constant, the Einstein field equations read

$$\underbrace{R_{\mu\nu} - \frac{R}{2} g_{\mu\nu}}_{\text{geometry}} + \underbrace{\Lambda_{\mathrm{B}} g_{\mu\nu}}_{\text{CC}} = \underbrace{\kappa T_{\mu\nu}}_{\text{matter}}$$

- Preserves covariance
- Covariant derivative vanishes hence compatible with a conserved energy momentum tensor
- Dimension length^ (-2)
- The CC can always been seen as an extra source of matter: $T_{\mu\nu} = -\frac{\Lambda_{\mathrm{B}}}{\kappa} g_{\mu\nu}$
- The equation of state of the CC is: $w = \frac{p}{\rho} = -1$. The effective pressure is negative.

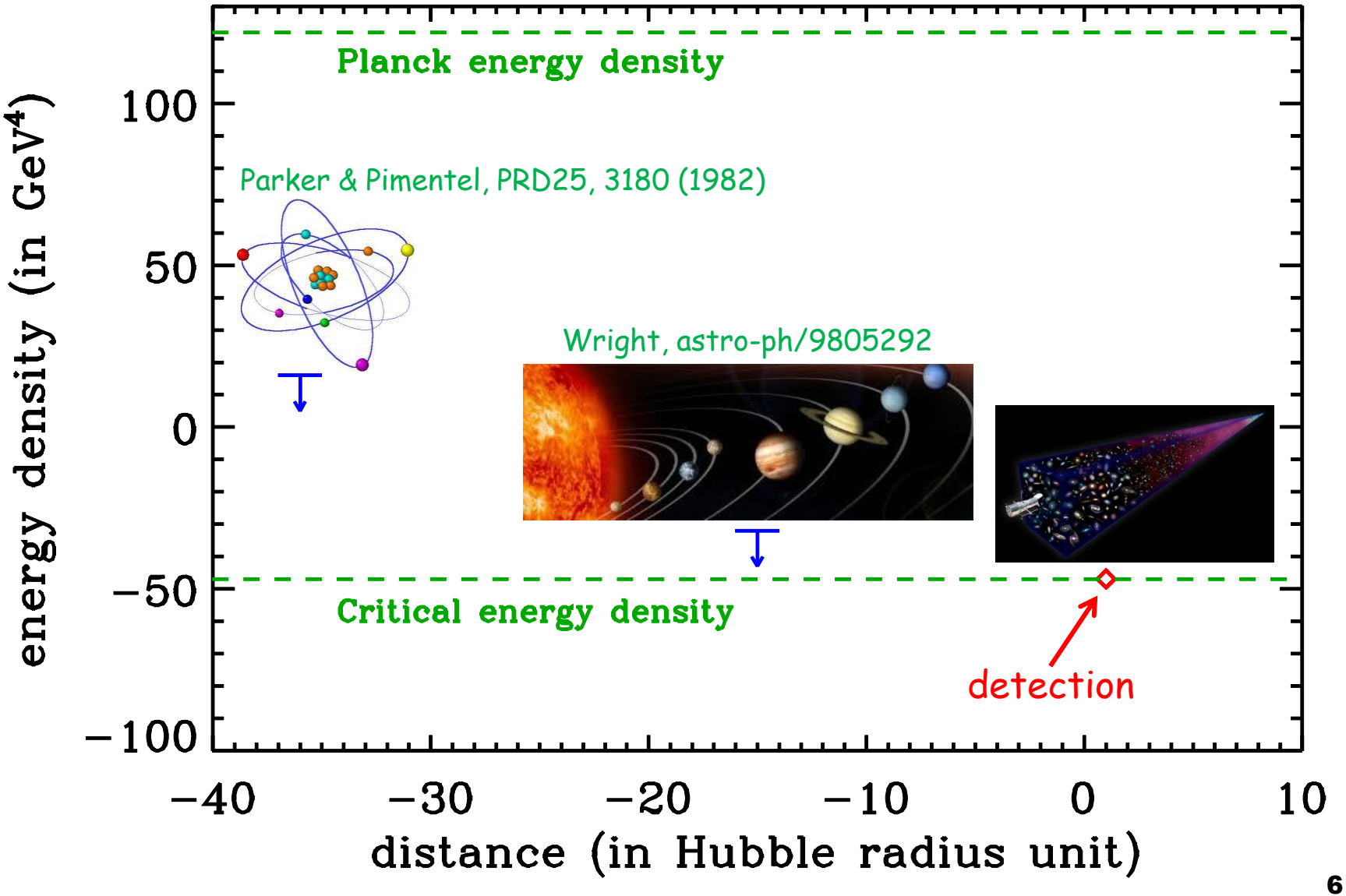
Planck energy density
Parker & Pimentel, PRD25, 3180 (1982)
Wright, astro-ph/9805292
Critical energy density
detection
energy density (in GeV⁴)
100
50
0
−50
−100
−40
−30
−20
−10
0
10
distance (in Hubble radius unit)

In 1998, two groups measure the expansion of the Universe and claim detection of a non-vanishing CC.

THE ASTRONOMICAL JOURNAL, 116:1009–1038, 1998 September
© 1998. The American Astronomical Society. All rights reserved. Printed in U.S.A.

OBSERVATIONAL EVIDENCE FROM SUPERNOVAE FOR AN ACCELERATING UNIVERSE AND A COSMOLOGICAL CONSTANT

ADAM G. RIESS,[1] ALEXEI V. FILIPPENKO,[1] PETER CHALLIS,[2] ALEJANDRO CLOCCHIATTI,[3] ALAN DIERCKS,[4] PETER M. GARNAVICH,[2] RON L. GILLILAND,[5] CRAIG J. HOGAN,[4] SAURABH JHA,[2] ROBERT P. KIRSHNER,[2] B. LEIBUNDGUT,[6] M. M. PHILLIPS,[7] DAVID REISS,[4] BRIAN P. SCHMIDT,[8,9] ROBERT A. SCHOMMER,[7] R. CHRIS SMITH,[7,10] J. SPYROMILIO,[6] CHRISTOPHER STUBBS,[4] NICHOLAS B. SUNTZEFF,[7] AND JOHN TONRY[11]

Received 1998 March 13; revised 1998 May 6

ABSTRACT

We present spectral and photometric observations of 10 Type Ia supernovae (S
range $0.16 \leq z \leq 0.62$. The luminosity distances of these objects are determined by
relations between SN Ia luminosity and light curve shape. Combined with pre
High-z Supernova Search Team and recent results by Riess et al., this expanded
supernovae and a set of 34 nearby supernovae are used to place constraints on
logical parameters: the Hubble constant (H_0), the mass density (Ω_M), the cosmolog
vacuum energy density, Ω_Λ), the deceleration parameter (q_0), and the dynamical ag
The distances of the high-redshift SNe Ia are, on average, 10%–15% farther than e
density ($\Omega_M = 0.2$) universe without a cosmological constant. Different light curve f
subsamples, and prior constraints unanimously favor eternally expanding models
logical constant (i.e., $\Omega_\Lambda > 0$) and a current acceleration of the expansion (i.e., $q_$
constraint on mass density other than $\Omega_M \geq 0$, the spectroscopically confirmed S
consistent with $q_0 < 0$ at the 2.8 σ and 3.9 σ confidence levels, and with $\Omega_\Lambda > 0$ a
confidence levels, for two different fitting methods, respectively. Fixing a "minimal
0.2, results in the weakest detection, $\Omega_\Lambda > 0$ at the 3.0 σ confidence level from on
For a flat universe prior ($\Omega_M + \Omega_\Lambda = 1$), the spectroscopically confirmed SNe Ia
and 9 σ formal statistical significance for the two different fitting methods. A univer
matter (i.e., $\Omega_M = 1$) is formally ruled out at the 7 σ to 8 σ confidence level for th
methods. We estimate the dynamical age of the universe to be 14.2 ± 1.7 Gyr inclu
tainties in the current Cepheid distance scale. We estimate the likely effect of several sources of system-
atic error, including progenitor and metallicity evolution, extinction, sample selection bias, local
perturbations in the expansion rate, gravitational lensing, and sample contamination. Presently, none of
these effects appear to reconcile the data with $\Omega_\Lambda = 0$ and $q_0 \geq 0$.

Key words: cosmology: observations — supernovae: general



From left, Adam Riess, Saul Perlmutter and Brian Schmidt shared the Nobel Prize in physics awarded Tuesday.

[1] Department of Astronomy, University of California at Berkeley, Berkeley, CA 94720-3411.
[2] Harvard-Smithsonian Center for Astrophysics, 60 Garden Street, Cambridge, MA 02138.
[3] Departamento de Astronomía y Astrofísica, Pontificia Universidad Católica, Casilla 104, Santiago 22, Chile.
[4] Department of Astronomy, University of Washington, Box 351580, Seattle, WA 98195.
[5] Space Telescope Science Institute, 3700 San Martin Drive, Baltimore, MD 21218.
[6] European Southern Observatory, Karl-Schwarzschild-Strasse 2, D-85748 Garching bei München, Germany.
[7] Cerro Tololo Inter-American Observatory, National Optical Astronomy Observatories, Casilla 603, La Serena, Chile. NOAO is operated by the Association of Universities for Research in Astronomy, Inc., under cooperative agreement with the National Science Foundation.
[8] Mount Stromlo and Siding Spring Observatories, Private Bag, Weston Creek, ACT 2611, Australia.
[9] Visiting Astronomer, Cerro Tololo Inter-American Observatory.
[10] Department of Astronomy, University of Michigan, 834 Dennison Building, Ann Arbor, MI 48109.
[11] Institute for Astronomy, University of Hawaii, 2680 Woodlawn Drive, Honolulu, HI 96822.

1. INTRODUCTION

This paper reports observations of 10 new high-redshift Type Ia supernovae (SNe Ia) and the values of the cosmological parameters derived from them. Together with the four high-redshift supernovae previously reported by our High-z Supernova Search Team (Schmidt et al. 1998; Garnavich et al. 1998a) and two others (Riess et al. 1998b), the sample of 16 is now large enough to yield interesting cosmological results of high statistical significance. Confidence in these results depends not on increasing the sample size but on improving our understanding of systematic uncertainties.

The time evolution of the cosmic scale factor depends on the composition of mass-energy in the universe. While the universe is known to contain a significant amount of ordinary matter, Ω_M, which decelerates the expansion, its dynamics may also be significantly affected by more exotic forms of energy. Preeminent among these is a possible energy of the vacuum (Ω_Λ), Einstein's "cosmological con-

THE ASTROPHYSICAL JOURNAL, 517:565–586, 1999 June 1
© 1999. The American Astronomical Society. All rights reserved. Printed in U.S.A.

MEASUREMENTS OF Ω AND Λ FROM 42 HIGH-REDSHIFT SUPERNOVAE

S. PERLMUTTER,[1] G. ALDERING, G. GOLDHABER,[1] R. A. KNOP, P. NUGENT, P. G. CASTRO,[2] S. DEUSTUA, S. FABBRO,[3] A. GOOBAR,[4] D. E. GROOM, I. M. HOOK,[5] A. G. KIM,[1,6] M. Y. KIM, J. C. LEE,[7] N. J. NUNES,[2] R. PAIN,[3] C. R. PENNYPACKER,[8] AND R. QUIMBY
Institute for Nuclear and Particle Astrophysics, E. O. Lawrence Berkeley National Laboratory, Berkeley, CA 94720
C. LIDMAN
European Southern Observatory, La Silla, Chile
R. S. ELLIS, M. IRWIN, AND R. G. MCMAHON
Institute of Astronomy, Cambridge, England, UK
P. RUIZ-LAPUENTE
Department of Astronomy, University of Barcelona, Barcelona, Spain
N. WALTON
Isaac Newton Group, La Palma, Spain
B. SCHAEFER
Department of Astronomy, Yale University, New Haven, CT
B. J. BOYLE
Anglo-Australian Observatory, Sydney, Australia
A. V FILIPPENKO AND T. MATHESON
Department of Astronomy, University of California, Berkeley, CA
A. S. FRUCHTER AND N. PANAGIA[9]
Space Telescope Science Institute, Baltimore, MD
H. J. M. NEWBERG
Fermi National Laboratory, Batavia, IL
AND
W. J. COUCH
University of New South Wales, Sydney, Australia
(THE SUPERNOVA COSMOLOGY PROJECT)

Received 1998 September 8; accepted 1998 December 17

ABSTRACT

We report measurements of the mass density, Ω_M, and cosmological-constant energy density, Ω_Λ, of the universe based on the analysis of 42 type Ia supernovae discovered by the Supernova Cosmology Project. The magnitude-redshift data for these supernovae, at redshifts between 0.18 and 0.83, are fitted jointly with a set of supernovae from the Calán/Tololo Supernova Survey, at redshifts below 0.1, to yield values for the cosmological parameters. All supernova peak magnitudes are standardized using a SN Ia light-curve width-luminosity relation. The measurement yields a joint probability distribution of the cosmological parameters that is approximated by the relation $0.8\Omega_M - 0.6\Omega_\Lambda \approx -0.2 \pm 0.1$ in the region of interest ($\Omega_M \lesssim 1.5$). For a flat ($\Omega_M + \Omega_\Lambda = 1$) cosmology we find $\Omega_M^{\rm flat} = 0.28^{+0.09}_{-0.08}$ (1 σ statistical) $^{+0.05}_{-0.04}$ (identified systematics). The data are strongly inconsistent with a $\Lambda = 0$ flat cosmology, the simplest inflationary universe model. An open, $\Lambda = 0$ cosmology also does not fit the data well: the data indicate that the cosmological constant is nonzero and positive, with a confidence of $P(\Lambda > 0) = 99\%$, including the identified systematic uncertainties. The best-fit age of the universe relative to the Hubble time is $t_0^{\rm flat} = 14.9^{+1.4}_{-1.1}(0.63/h)$ Gyr for a flat cosmology. The size of our sample allows us to perform a variety of statistical tests to check for possible systematic errors and biases. We find no significant differences in either the host reddening distribution or Malmquist bias between the low-redshift Calán/Tololo sample and our high-redshift sample. Excluding those few supernovae that are outliers in color excess or fit residual does not significantly change the results. The conclusions are also robust whether or not a width-luminosity relation is used to standardize the supernova peak magnitudes. We discuss and constrain, where possible, hypothetical alternatives to a cosmological constant.

Subject headings: cosmology: observations — distance scale — supernovae: general

[1] Center for Particle Astrophysics, University of California, Berkeley, California.
[2] Instituto Superior Técnico, Lisbon, Portugal.
[3] LPNHE, CNRS-IN2P3, and University of Paris VI and VII, Paris, France.
[4] Department of Physics, University of Stockholm, Stockholm, Sweden.
[5] European Southern Observatory, Munich, Germany.
[6] PCC, CNRS-IN2P3, and Collège de France, Paris, France.
[7] Institute of Astronomy, Cambridge, England, UK.
[8] Space Sciences Laboratory, University of California, Berkeley, California.
[9] Space Sciences Department, European Space Agency.

- The hard fact is that the following equation does not fit well the data

$$H^2 = \frac{1}{3M_{\rm Pl}^2}\rho_{\rm CDM}$$

- The hard fact is that the following equation does not fit well the data

$$H^2 = \frac{1}{3M_{\rm Pl}^2}\rho_{\rm CDM}$$

- If the Universe is homogeneous and isotropic and if gravity is described by GR and if there is no other exotic fluid then the CC is non-vanishing.

$$\begin{aligned} \rho_\Lambda &\sim 10^{-47}{\rm GeV}^4 \sim \rho_{\rm cri} \\ &\sim \left(10^{-3}{\rm eV}\right)^4 \end{aligned}$$

- The hard fact is that the following equation does not fit well the data

$$H^2 = \frac{1}{3M_{\rm Pl}^2}\rho_{\rm CDM}$$

- If the Universe is homogeneous and isotropic and if gravity is described by GR and if there is no other exotic fluid then the CC is non-vanishing.

- In this framework, the Universe is accelerating.

- The hard fact is that the following equation does not fit well the data

$$H^2 = \frac{1}{3M_{\rm Pl}^2}\rho_{\rm CDM}$$

- If the Universe is homogeneous and isotropic and if gravity is described by GR and if there is no other exotic fluid then the CC is non-vanishing.
- In this framework, the Universe is accelerating.
- 2012: there is now a bunch of different and independent measurements pointing towards this conclusion (age of the universe, SNIa, clusters abundance, lensing etc …)

Example: using the CMB only, a vanishing CC now seems to be ruled out at more than 5 sigma …

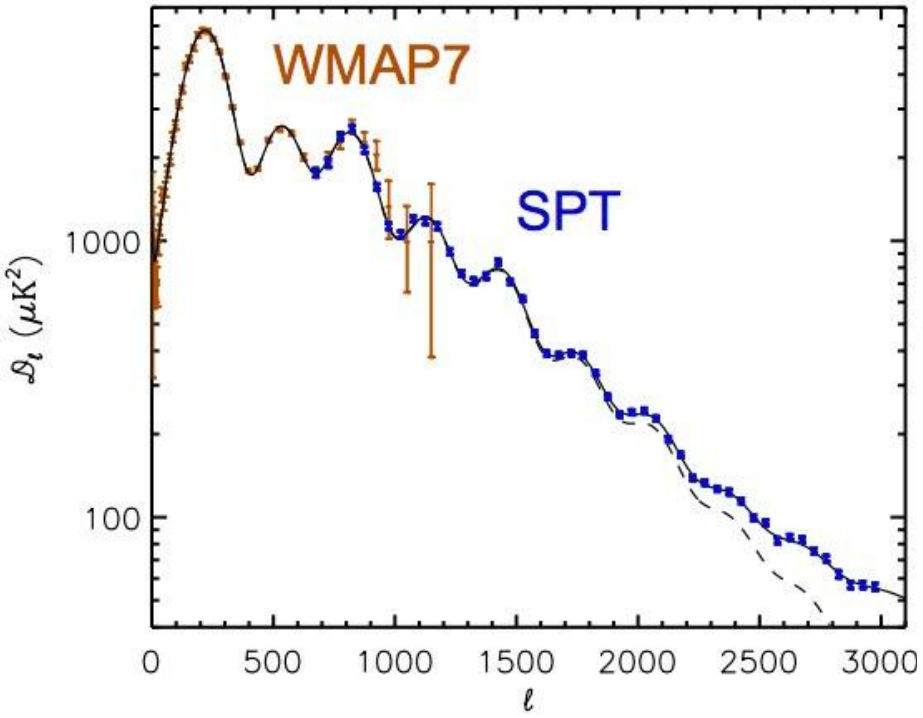

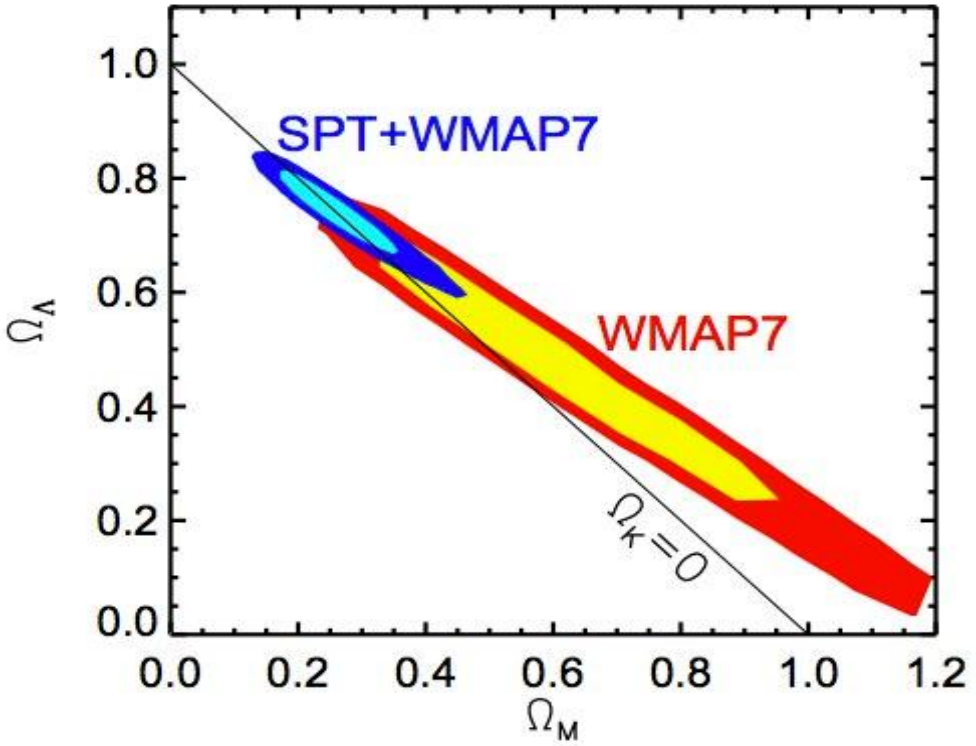

SPT data, arXiv:1210.7231

- The hard fact is that the following equation does not fit well the data

$$H^2 = \frac{1}{3M_{\rm Pl}^2}\rho_{\rm CDM}$$

- If the Universe is homogeneous and isotropic and if gravity is described by GR and if there is no other exotic fluid then the CC is non-vanishing.
- In this framework, the Universe is accelerating.
- 2012: there is now a bunch of different and independent measurements pointing towards this conclusion (age of the universe, SNIa, clusters abundance, lensing etc …)
- The other alternatives (in-homogeneous universe, modified gravity, quintessence etc …) have their own problems.

A possible alternative is that there is no CC but a scalar field ("quintessence") playing the role of a "dark energy".

$$H^2 = \frac{1}{3M_{\rm Pl}^2}\left(\rho_{\rm CDM} + \rho_{\rm DE}\right)$$

$$\frac{\ddot{a}}{a} = -\frac{1}{6M_{\rm Pl}^2}\left(\rho_{\rm CDM} + \underbrace{\rho_{\rm DE} + 3p_{\rm DE}}_{\text{must be <0}}\right)$$

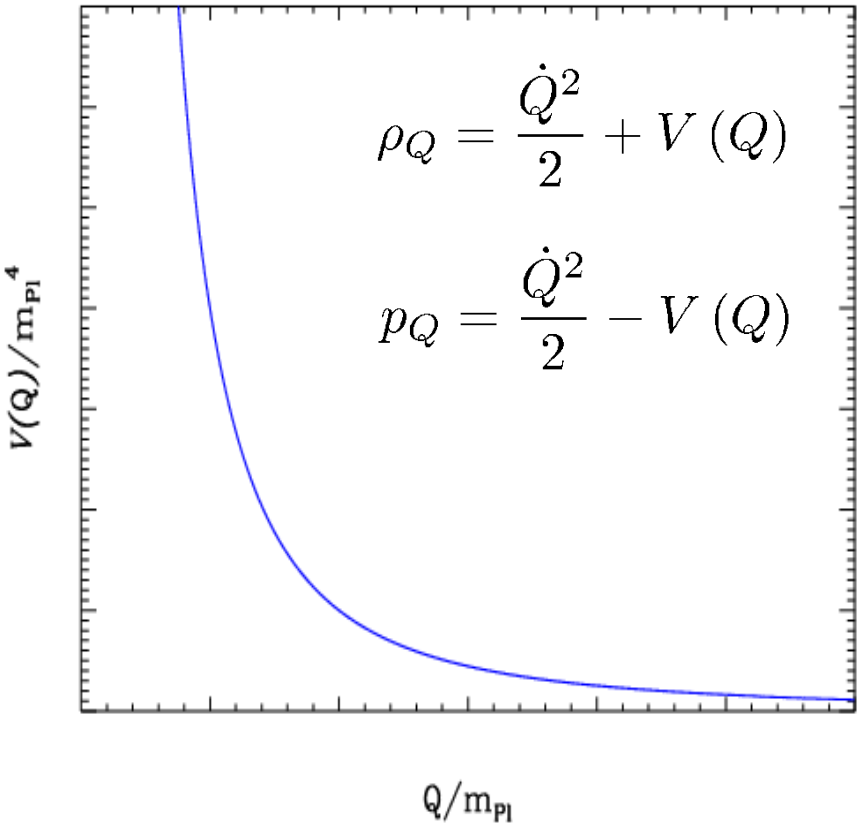

Ratra & Peebles, PRD37 3406 (1988)

In these models, dark energy is dynamical and the equation of state is a time-dependent quantity. Falsifiable since different from the CC

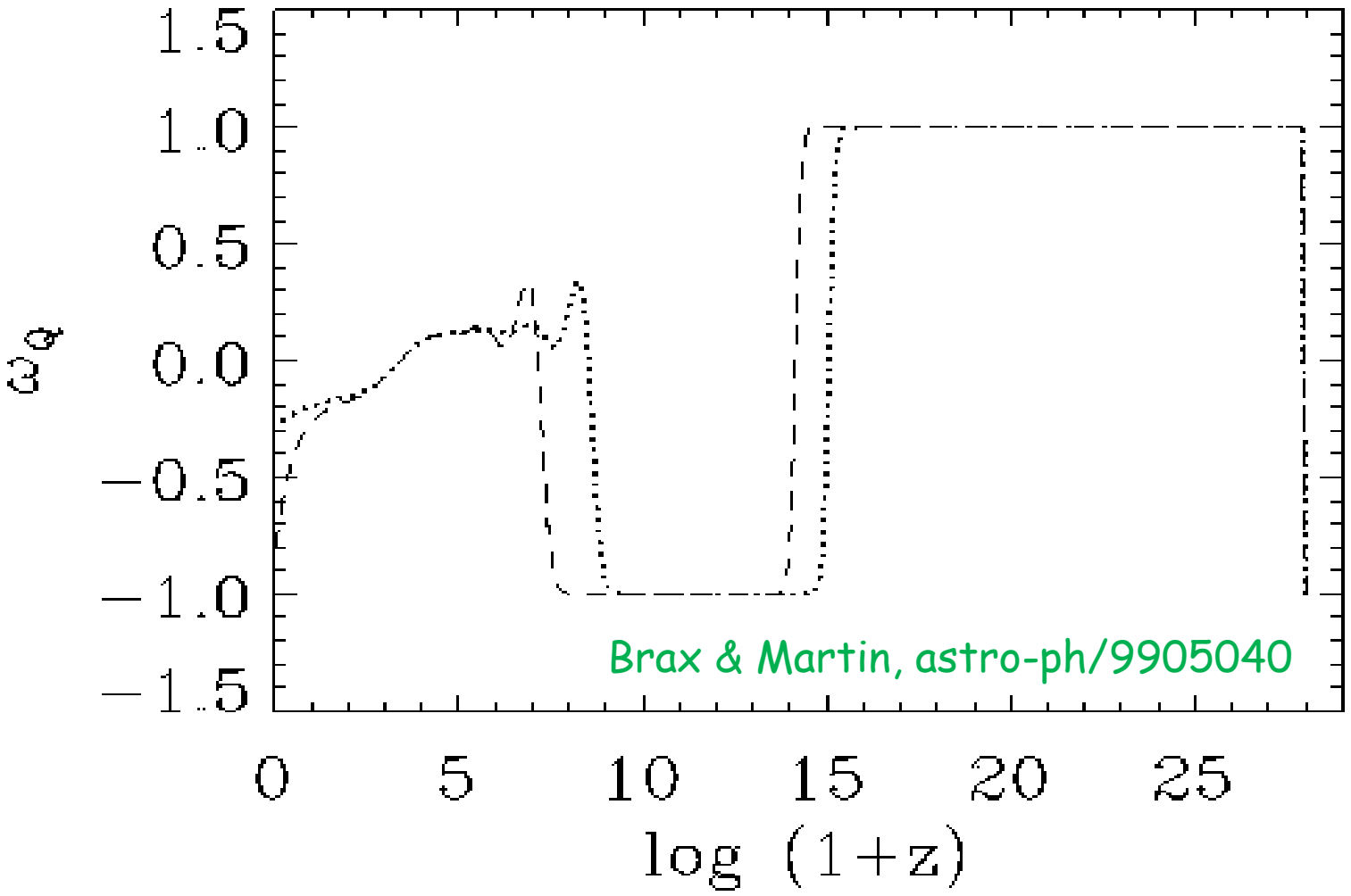

- Hard to find good models of particle physics which lead to the correct potentials
- Hard to control the interactions of quintessence with the other fields
- Hard not to destroy the flatness of the potential by quantum corrections
- Everything seems to indicate that w=-1 …

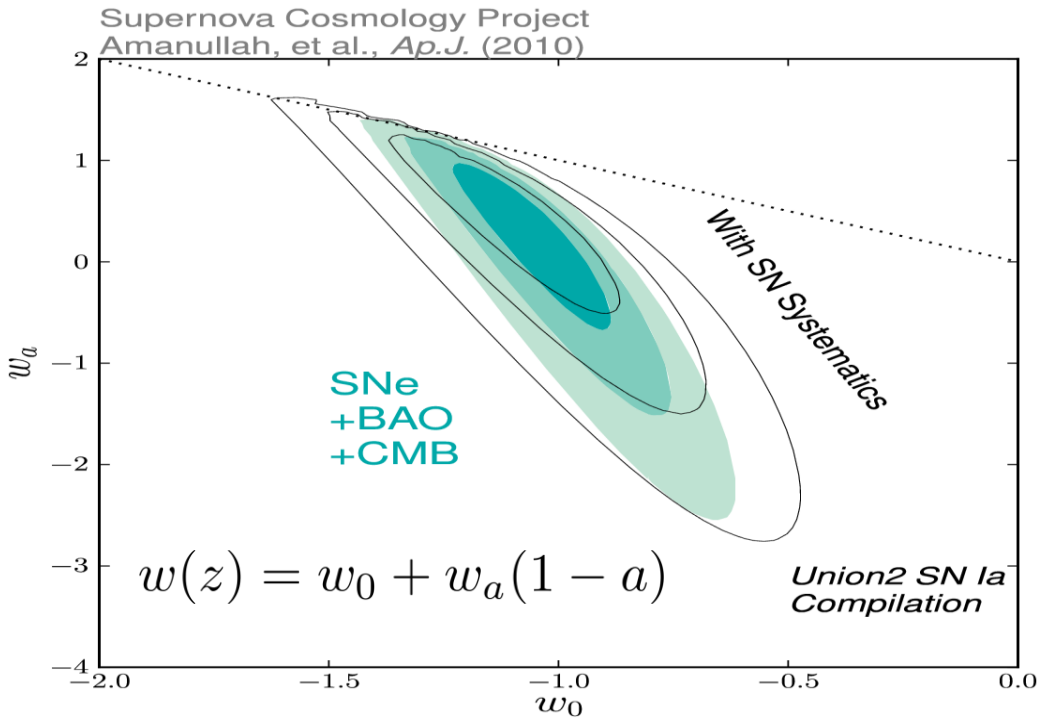

- The hard fact is that the following equation does not fit well the data

$$H^2 = \frac{1}{3M_{\rm Pl}^2}\rho_{\rm CDM}$$

- If the Universe is homogeneous and isotropic and if gravity is described by GR and if there is no other exotic fluid then the CC is non-vanishing.
- In this framework, the Universe is accelerating.
- 2012: there is now a bunch of different and independent measurements pointing towards this conclusion. (age of the universe, SNIa, clusters abundance, lensing etc …)
- The other alternatives (in-homogeneous universe, modified gravity, quintessence etc …) have their own problems.
- Even if what we see in cosmology is not the CC, this implies a new upper limit on the CC energy density

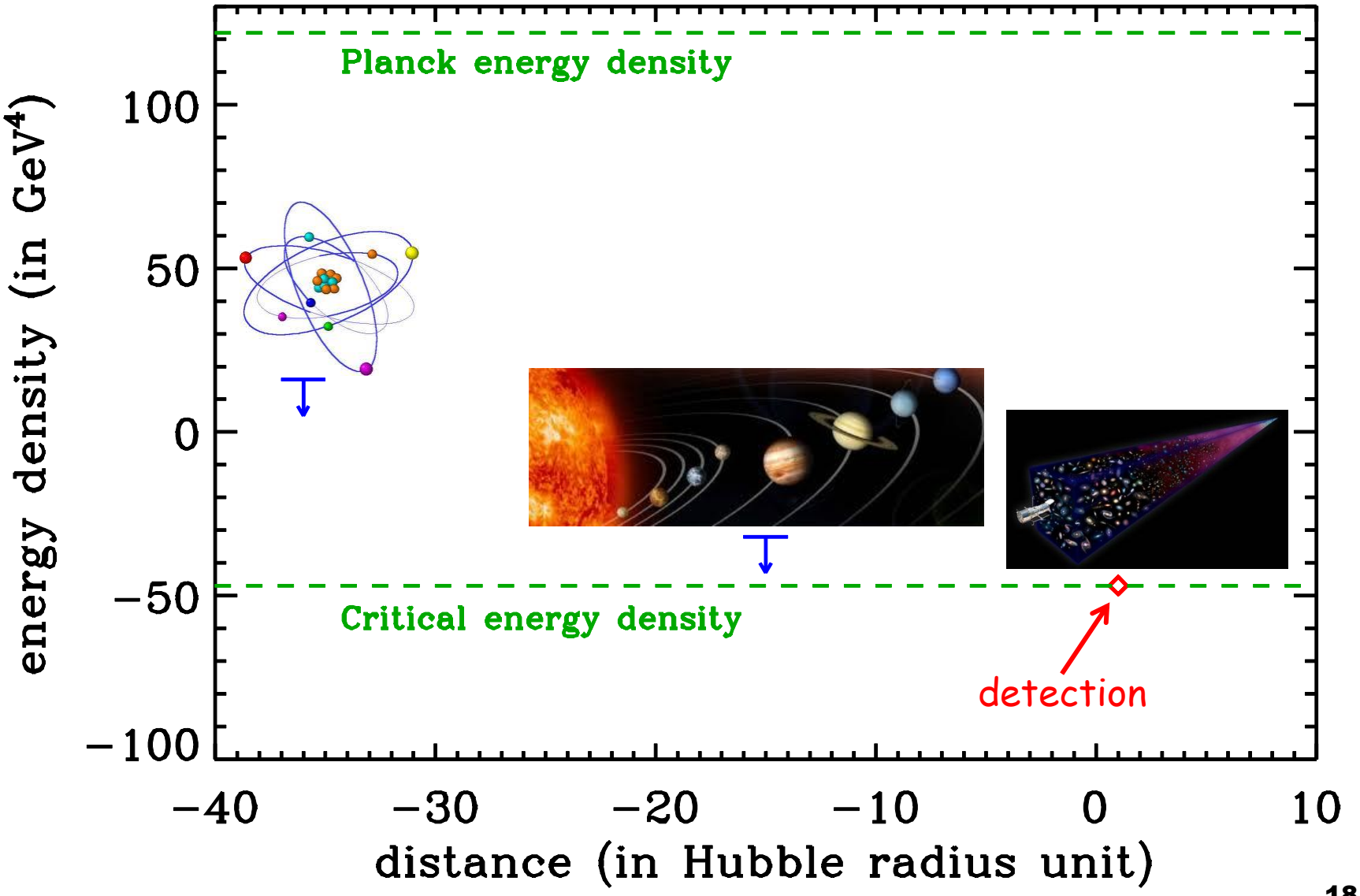
Planck energy density
Critical energy density
detection
energy density (in GeV⁴)
100
50
0
−50
−100
−40
−30
−20
−10
0
10
distance (in Hubble radius unit)

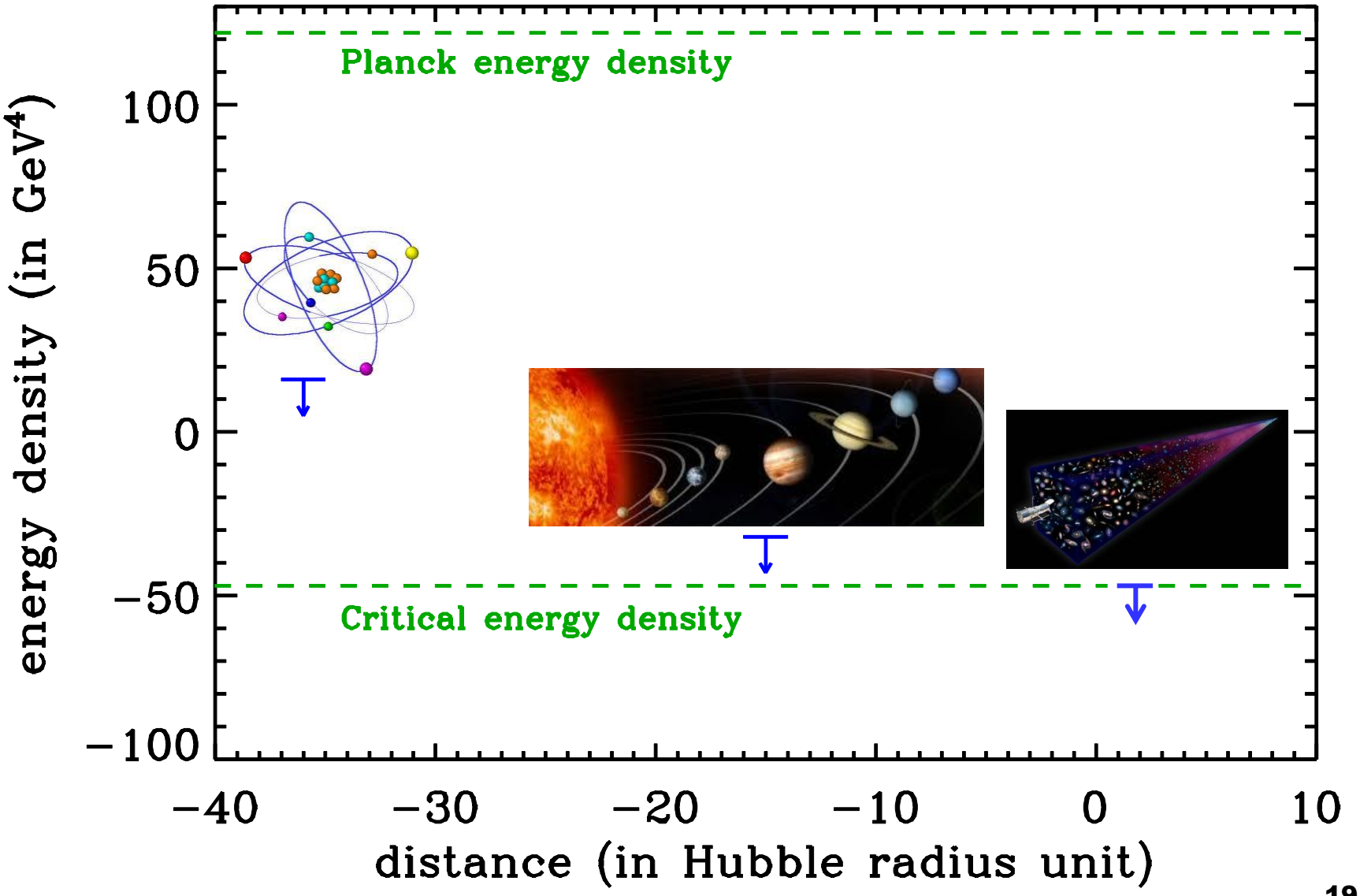
Planck energy density
Critical energy density
energy density (in GeV⁴)
100
50
0
−50
−100
−40
−30
−20
−10
0
10
distance (in Hubble radius unit)

- Therefore, the CC remains the simplest explanation of the different cosmological measurements

- There is no sign in the observations that we need a dark energy different from the CC

- At this (classical) level, we have a theory with a new fundamental constant and its value has been determined by the measurements to be

$$\Lambda_{\rm B} \simeq 10^{-52} m^{-2}$$

- The CC is such that it is very difficult to check this value elsewhere than in cosmology … always a negligible effect.

When QM and QFT are taken into account, the nature of the discussion is however drastically modified [A. Sakharov, Sov. Phys. Dokl. 12, 1040 (1968)]

- The vacuum state has the following stress-energy tensor

$$\langle T_{\mu\nu} \rangle = - \left[V\left(\phi_{\min}\right) + \rho_{\rm vac} \right] g_{\mu\nu}$$

$$\Lambda_{\rm eff} = \Lambda_{\rm B} + \frac{1}{M_{\rm Pl}^2} \left[V\left(\phi_{\min}\right) + \rho_{\rm vac} \right]$$

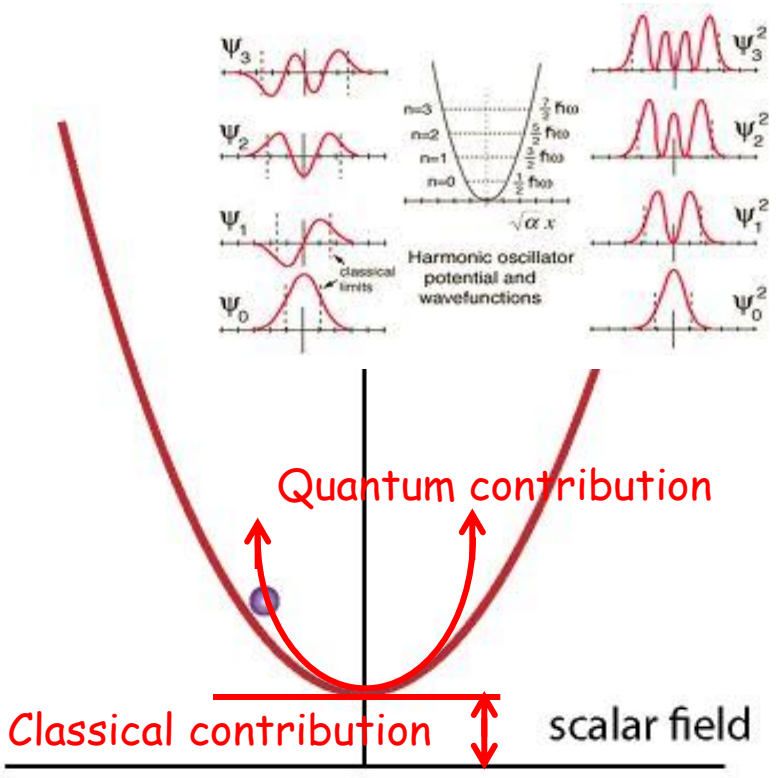

- In flat spacetime, only differences of energy are measurable so not important … In curved spacetime, the absolute value is important.

- A priori, the vacuum fluctuations gravitate as any other form of energy

An example is the Electro-Weak transition

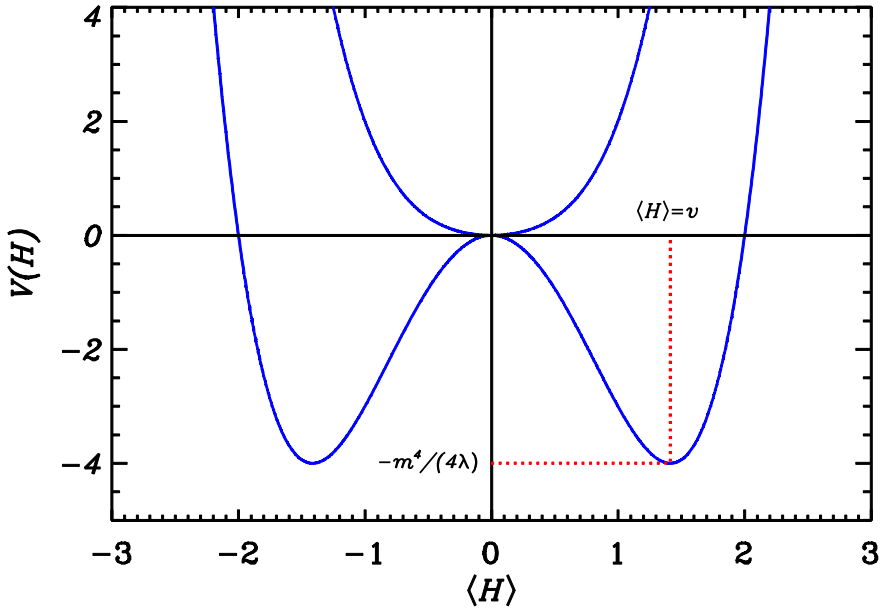

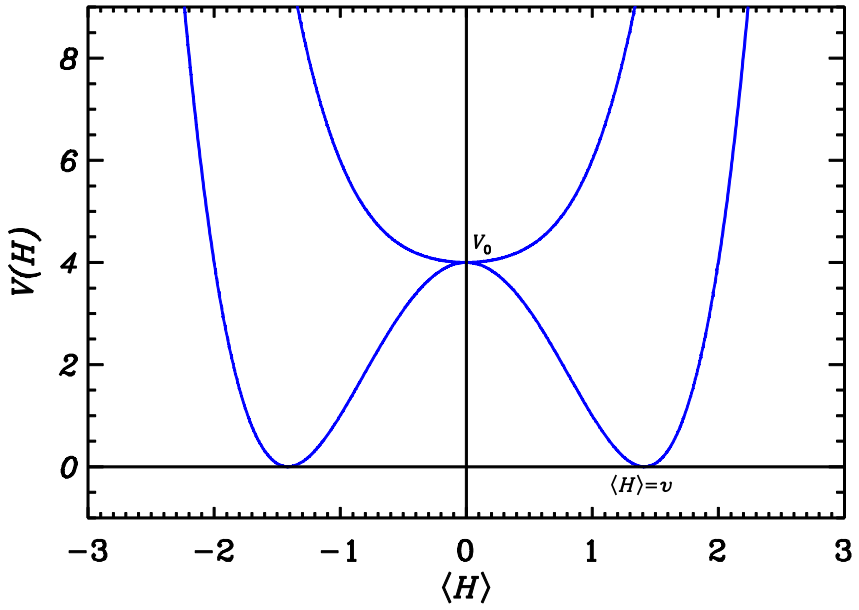

$$V\left(\phi_{\min}\right) = -\frac{1}{4} m_{\mathrm{H}}^2 v^2 = -\frac{\sqrt{2}}{16} \frac{m_{\mathrm{H}}^2}{G_{\mathrm{F}}^2} \simeq -1.2 \times 10^8 \,\mathrm{GeV}^4$$

- Because of Heisenberg principle the position and the velocity of a quantum harmonic oscillator cannot vanish at the same time

$$\langle H \rangle = \frac{\hbar\omega}{2}$$

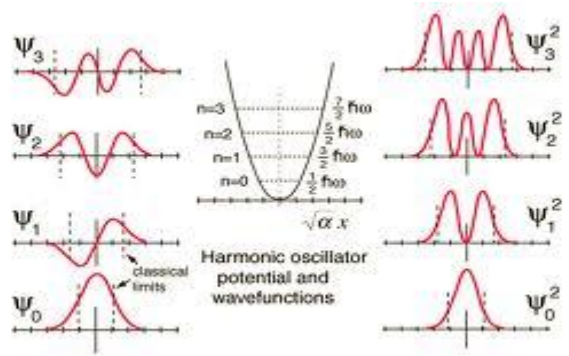

- A quantum field=infinite collections of quantum oscillators

$$\langle H \rangle = \sum \frac{\hbar\omega}{2} = \infty$$

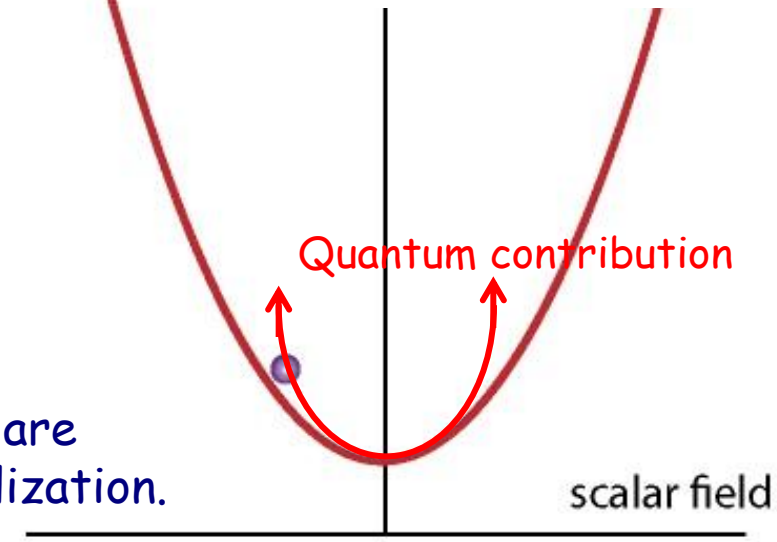

- This should not cause any panic since we are used to tame infinities in QFT: renormalization.

- However, this particular type of infinity is usually not renormalized but ignored on the basis that, in flat spacetime, only differences of energies are measurable.

The first attempt to estimate the gravitational impact of vacuum fluctuations was done by W. Pauli [see "Die allgemeinen Principein des Wellenmechanik"]

$$H^2 + \frac{k}{a^2} = \frac{1}{3M_{\rm Pl}^2}\rho + \frac{\Lambda}{3}$$

$$-\left(2\frac{\ddot{a}}{a} + H^2 + \frac{k}{a^2}\right) = \frac{1}{M_{\rm Pl}^2}p - \Lambda$$

Einstein static universe

$$a^2 = \frac{2M_{\rm Pl}^2}{\rho} \qquad a \simeq 31 \text{ kms}$$

$$\rho = \frac{1}{8\pi^2}\omega_{\rm max}^4$$

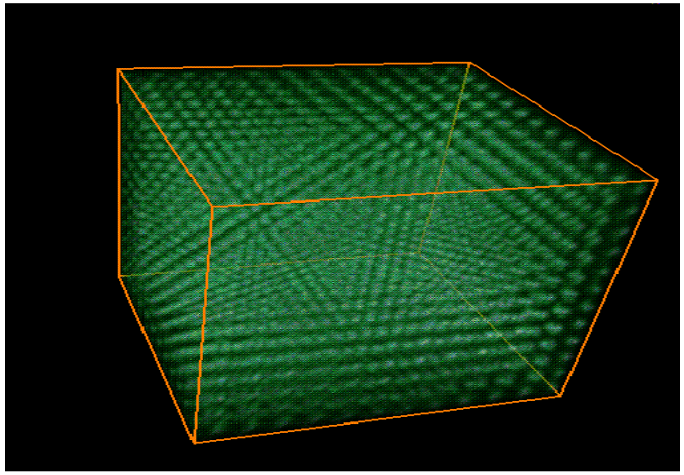

Radiation field in a box

"it could not even reach to the moon"



In a modern language, the main issue is how to renormalize the vacuum energy density

$$\Lambda_{\rm eff} = \Lambda_{\rm B} + \frac{1}{M_{\rm Pl}^2}\frac{1}{(2\pi)^3}\int {\rm d}^3\mathbf{k}\frac{1}{2}\omega(\mathbf{k}) = \Lambda_{\rm B} - \frac{m^2}{4M_{\rm Pl}^2}$$

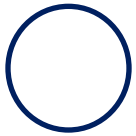

- The vacuum contribution is expressed in terms of Feynman bubble diagrams, ie diagrams with no external leg.
- These diagrams have bad convergence properties, worst than ordinary loop diagrams: they remain infinite even in the QM limit.
- In non-gravitational physics, these graphs always cancel out.
- When gravity is taken into account, one must regularize them.

Renormalization leads to the following expression for the CC

$$\rho_{\rm vac} = \rho_{\rm B} + \rho_{\rm vac}^{\rm EW} + \rho_{\rm vac}^{\rm QCD} + \sum_i n_i \frac{m_i^4}{64\pi^2} \ln\left(\frac{m_i^2}{\mu^2}\right)$$

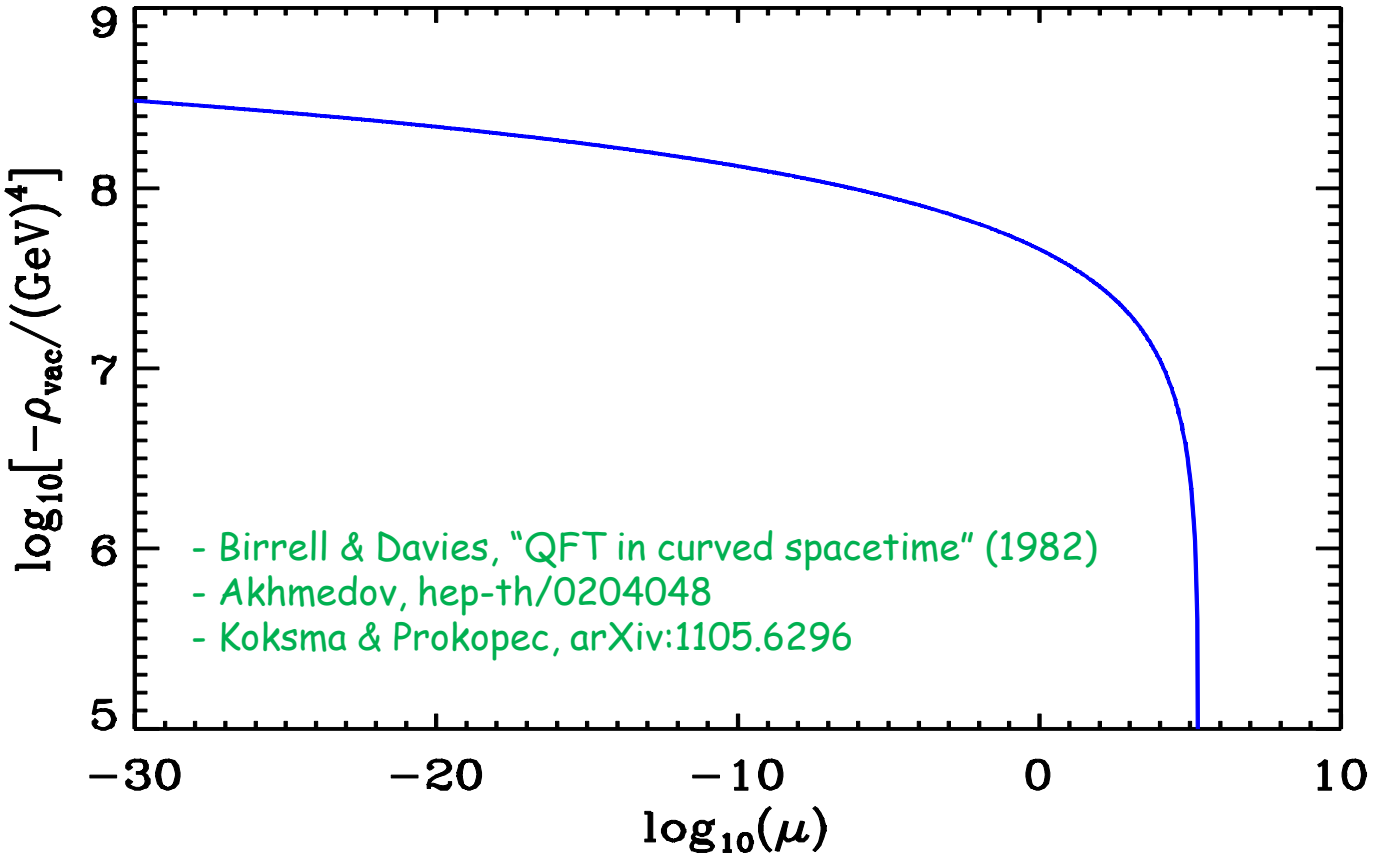

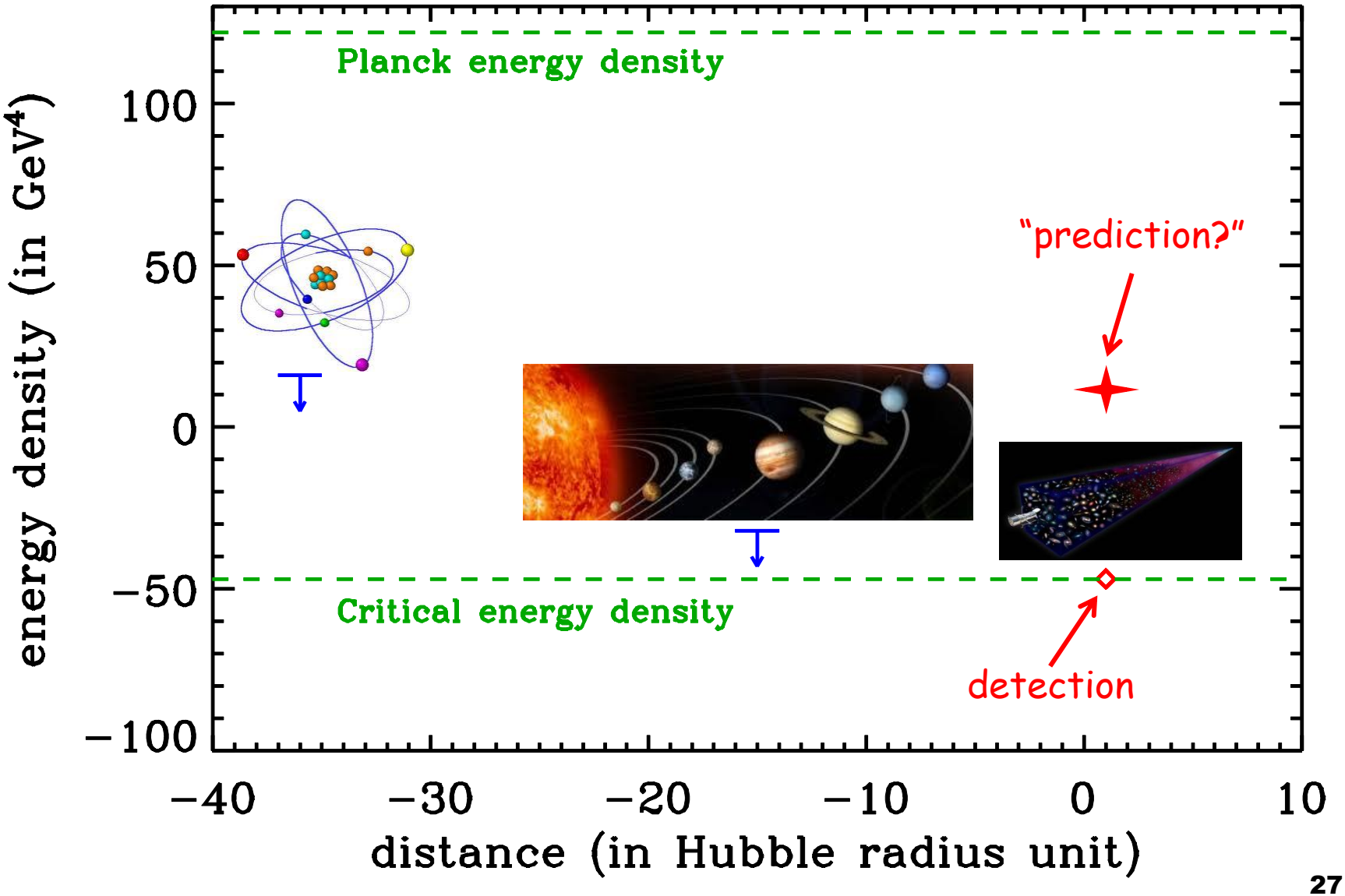
Planck energy density
Critical energy density
"prediction?"
detection
energy density (in GeV⁴)
100
50
0
−50
−100
−40
−30
−20
−10
0
10
distance (in Hubble radius unit)

- A possible loophole is that vacuum fluctuations are just an artifact of QFT. However, we observe their influence in the Casimir effect or in the Lamb shift effect.

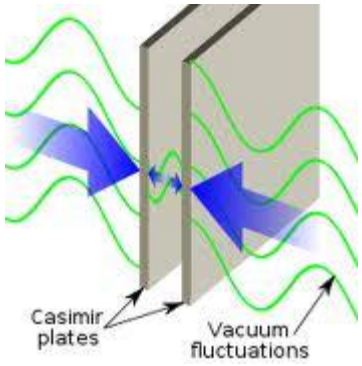

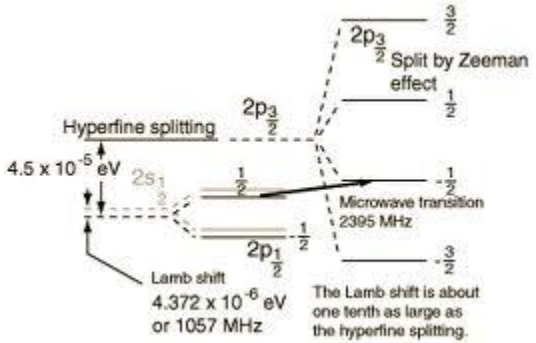

- Maybe vacuum fluctuations have abnormal gravitational properties?? But vacuum fluctuations participate for a non-negligible amount to the mass of nuclei … and they are observed to obey the UFF (WEP).

- What about the EP (UFF) in the quantum regime??

The UFF in QM is described by the following Schrodinger equation

$$i\hbar\frac{\partial\Psi(t,z)}{\partial t} = -\frac{\hbar^2}{2m_{\rm ini}}\frac{\partial^2\Psi(t,z)}{\partial z^2} + m_{\rm grav}gz\Psi(t,z)$$

- The validity of this equation has been experimentally checked by the Collela Overhausser Werner (COW) experiment and by atomic interferometry.
- UFF can be checked by measuring times of flight of quantum particles.
- The classical result is recovered if $|L - z_{\rm max}| \gg \ell_g$

$$\ell_g = \left(\frac{\hbar^2}{2m_{\rm ini}m_{\rm grav}g}\right)^{1/3} = \left(\frac{\hbar^2 r_\oplus^2}{2m_{\rm ini}m_{\rm grav}GM_\oplus}\right)^{1/3}$$

One gram particle: $\ell_g = 10^{-10}\,\mathrm{m}$

Neutron: $\ell_g = 1.5\,\mathrm{mm}$

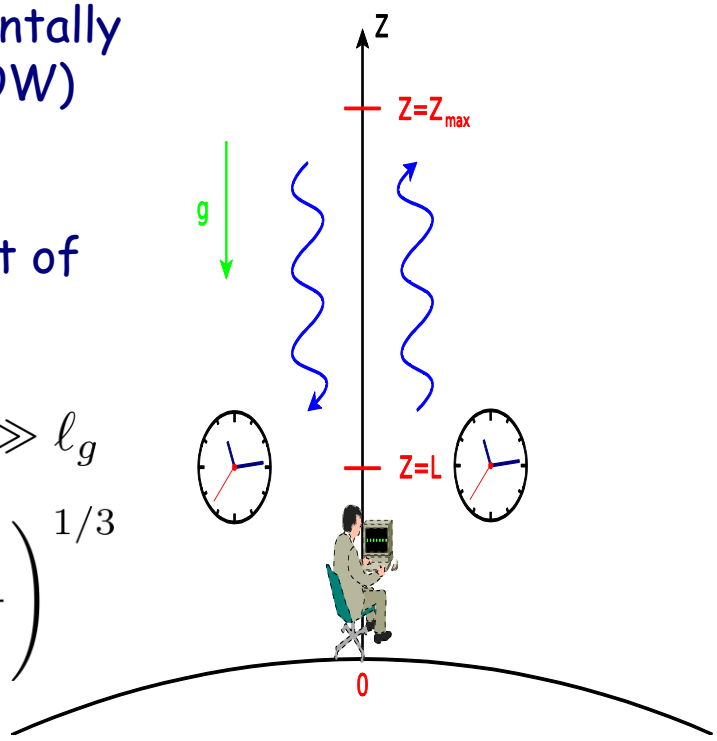

P. Davies, CQG 21 5677 (2004)

Conclusions:

- The cosmological constant problem is the impossibility to reconcile the renormalized value of vacuum energy with its observed value in cosmology and/or with the upper contraints obtained in others experimental situations.

- It is then natural to question the assumptions made to arrive at this result: failure of our renormalization technique, vacuum fluctuations=fake , abnormal gravitational properties of the vacuum etc …

- However, investigating these issues does not seem to reveal any inconsistencies (at the theoretical/observational level).

- It is frustrating that cosmology be the only situation where one can measure (and not only constrain) the *CC*!

- The *CC* problem is a deep problem since it lies at the crossroads between gravity and QM. In brief, the question is: what are the gravitational properties of the quantum vacuum?

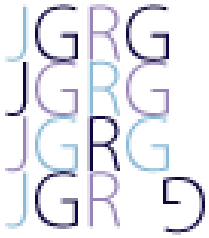

Masahiro Takada, JGRG 22(2012)111502

"SuMIRe project: Hyper Suprime-Cam (HSC) and Prime Focus Spectrograph (PFS)"

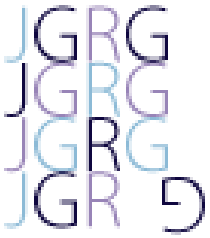

RESCEU SYMPOSIUM ON

GENERAL RELATIVITY AND GRAVITATION

JGRG 22



November 12-16 2012

Koshiba Hall, The University of Tokyo, Hongo, Tokyo, Japan



SuMIRe project:
Hyper Suprime-Cam (HSC)
and
Prime Focus Spectrograph (PFS)

Masahiro Takada
(Kavli IPMU, U. Tokyo)

KAVLI IPMU
INSTITUTE FOR THE PHYSICS AND MATHEMATICS OF THE UNIVERSE

@ JGRG, U Tokyo, Nov 15, 2012

Futamase-sensei

- Congratulations on your 60th birthday!
- Congratulations to Sasaki-san and Kodama-san, too
- I was a graduated student of Futamase-sensei at Tohoku University
- My master thesis project as “Post-Newtonian Lagrangian perturbation approach to the large-scale structure formation” (1998)
- My PhD thesis project was “Weak lensing effect on CMB” (2001)

The golden age of cosmology

- Various data sets are now available
- The measurement accuracies are increasing improved
- Can test cosmological models/scenarios very precisely: the expansion history and the growth of structure formation

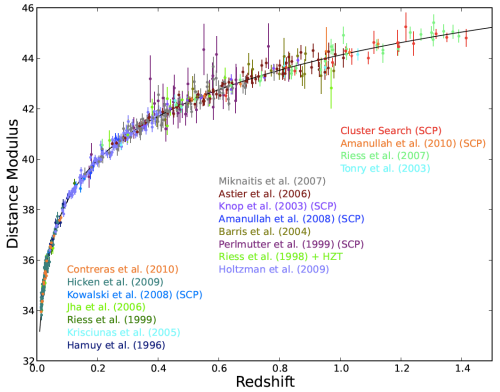

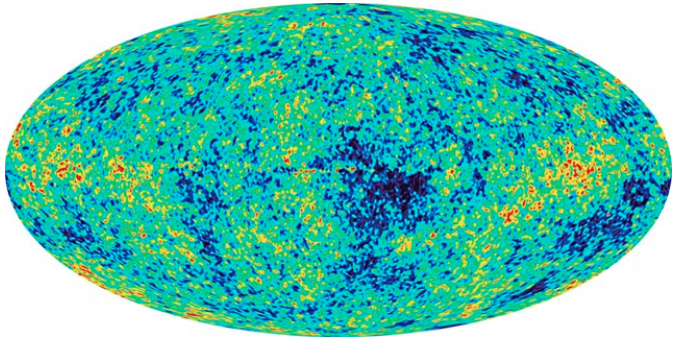

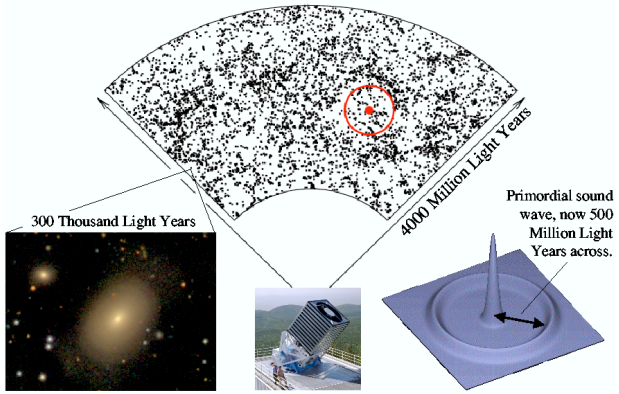

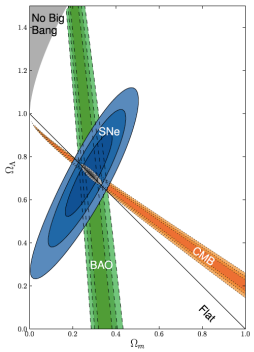

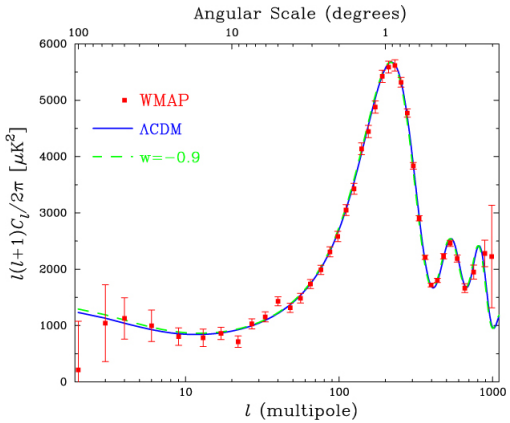

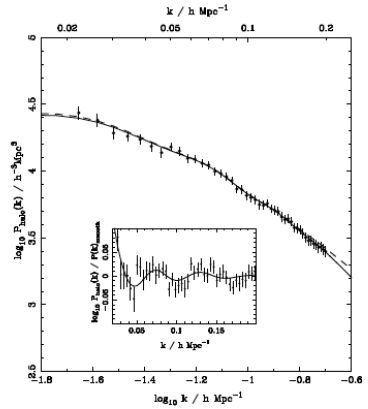

Big Questions in Cosmology

- What is the universe made of? – the nature of dark matter
- What is its fate? – the nature of dark energy
- How did the universe begin? – the nature of primordial fluctuations

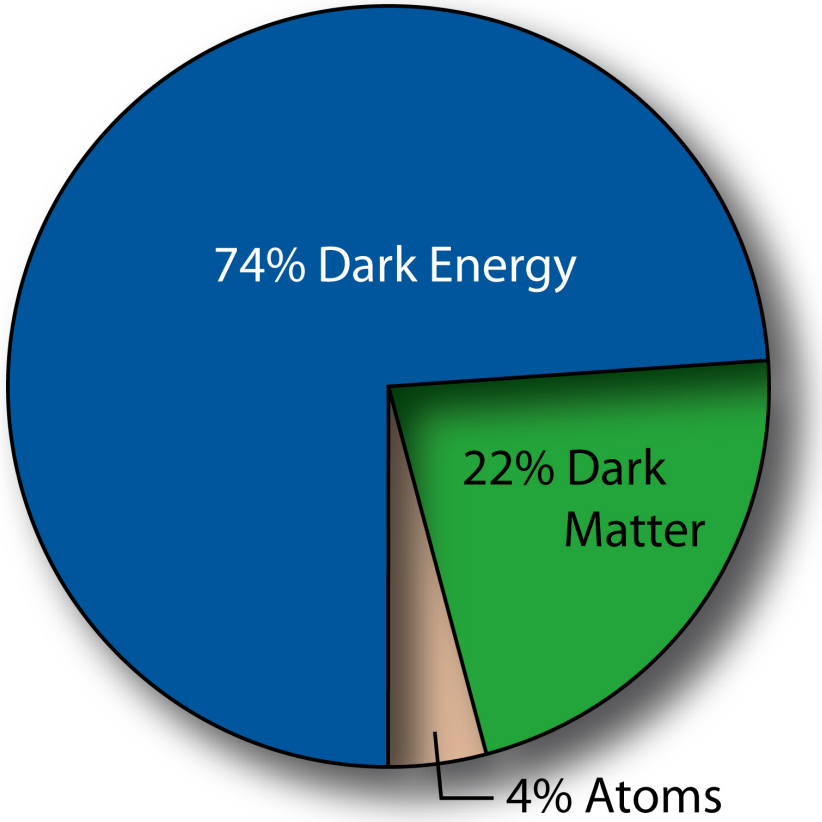

From WMAP

Test of cosmic acceleration

- Geometrical test

$$H^2(z) = H_0^2\left[\Omega_{m0}(1+z)^3 - \frac{K}{H_0^2}(1+z)^2 + \frac{\rho_{\rm de}(z)}{\rho_{\rm cr0}}\right]$$

Dark Energy

  - CMB, Type-Ia SNe, Baryonic Acoustic Oscillation (BAO)
- Growth of structure formation

$$\ddot{\delta}_m + 2H\dot{\delta}_m - 4\pi G\bar{\rho}_m\delta_m = 0$$

Cosmic Expansion *Gravity*

  - Weak Lensing, Galaxy clustering, Counts of galaxy clusters
- *Goal*: Combine the geometrical and structure formation probes to distinguish DE and modification of gravity for the origin of cosmic acceleration

Large-scale structure formation

- The initial conditions are now well constrained by CMB
- The ΛCDM model gives specific predictions of the subsequent structure formation, based on the analytic and simulation methods
- The growth of structures arises from the competing effects; *cosmic expansion vs. gravity*
- Dark energy affects the structure formation
- The models can be tested by precise data

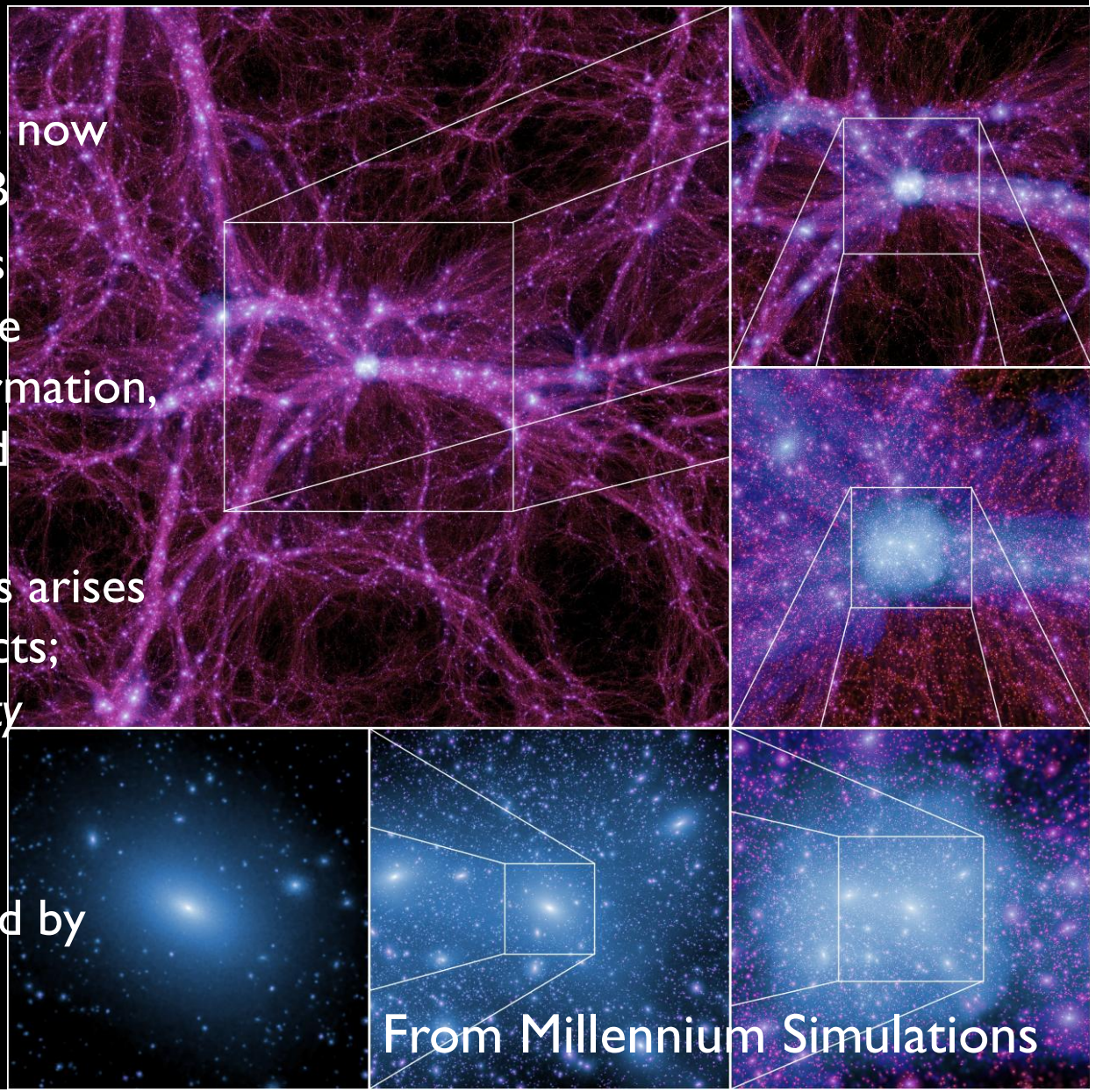

Galaxy survey; imaging vs. spectroscopy

Imaging

- Find objects
  - Stars, galaxies, galaxy clusters
- Measure the image shape of each object → *weak gravitational lensing*
- For cosmology purpose
  - *Pros*: many galaxies, a reconstruction of dark matter distribution
  - *Cons*: 2D information, limited redshift info. (photo-z at best)



Spectroscopy

- Measure the photon-energy spectrum of *target* object
- Distance to the object can be known → *3D clustering analysis*
- For cosmology
  - *Pros*: more fluctuation modes in 3D than in 2D
  - *Cons*: need the pre-imaging data for targeting; observationally more expensive (or less galaxies)

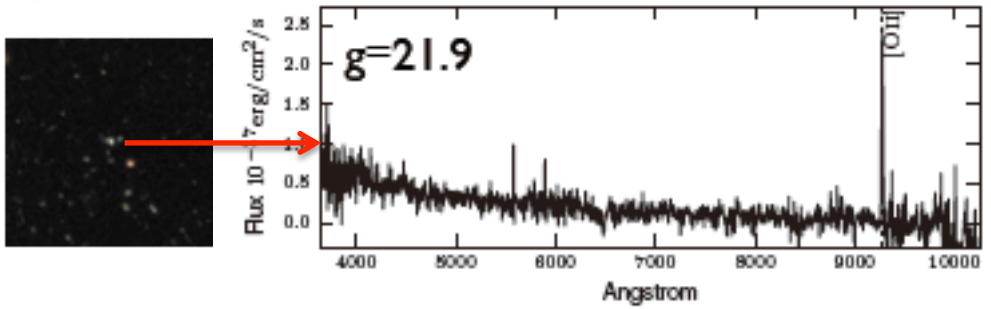

Impact of *unbiased* wide-area imaging/spectroscopic survey

- Examples; SDSS, COSMOS
- Legacy data set

The table shows scientific impacts of each optical telescope and survey, based on the stats of 2008-year papers published in journals

SDSS(2.5m) has brought more impacts than HST or 8m Tels

Trimble & Ceja (2010)

Table 6: Optical papers and citations by telescope/observatory.

Telescope	Papers[1]	Citat.[1]	C/P[1]	Papers[2]
HST	206.6	765	3.70	391.5
VLT	139.1	452	3.25	290.6
Keck	59.6	333	5.59	121.5
CFHT	38.0	152	4.00	69.6
Gemini	34.3	108	3.15	63.7
Subaru	33.0	138	4.18	70.0
AAT	23.0	83	3.61	42.4
WHT	19.5	55	2.82	34.7
IRTF	16.9	46	2.72	31.2
UKIRT	15.8	54	3.42	34.3
Okayama 1.88m	9.9	30	3.03	17.0
U.Hi. 2.2m	5.1	17	3.33	10.4
HET	5.0	35	7.00	8.9
LBT	4.8	18	3.75	8.2
MDM 2.4m	4.6	17	3.70	7.0
APO 3.5m	4.5	16	3.56	9.5
Lyot (PduM)	3.0	5	1.67	8.9
abridged …				
SDSS	133.0	863	6.49	336.1
2MASS	136.2	479	3.52	275.8
48” Schmidts	45.8	95	2.07	100.7
MACHO, ASAS, etc.	29.1	123	4.23	47.1
TOTAL OPTICAL	1233.8	4764	3.86	2530.4



SuMIRe = Subaru Measurement of Images and Redshifts



- IPMU director Hitoshi Murayama funded (~ $32M) by the Cabinet in Mar 2009, as one of the stimulus package programs
- Build *wide-field* camera (Hyper SuprimeCam) and *wide-field* multi-object spectrograph (Prime Focus Spectrograph) for the Subaru Telescope (8.2m)
- Explore the fate of our Universe: dark matter, dark energy
- Keep the Subaru Telescope a world-leading telescope in the TMT era
- Precise images of 1B galaxies
- Measure distances of 1M galaxies

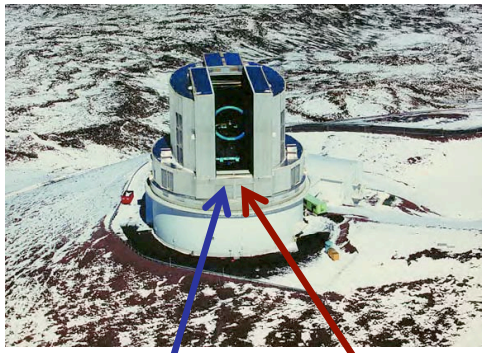

Subaru (NAOJ)



HSC

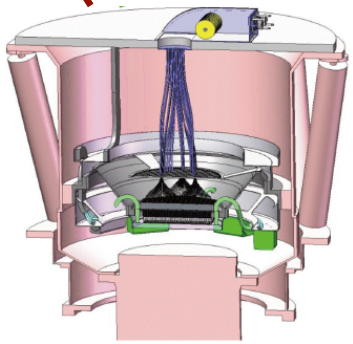

PFS



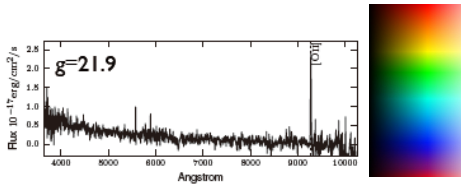

Subaru Telescope



Prime-Focus Instrument



Subaru Telescope

@ summit of Mt. Mauna Kea (4200m), Big Island, Hawaii

Dark Energy Competition



BOSS (2009-)



KIDS (2012-)

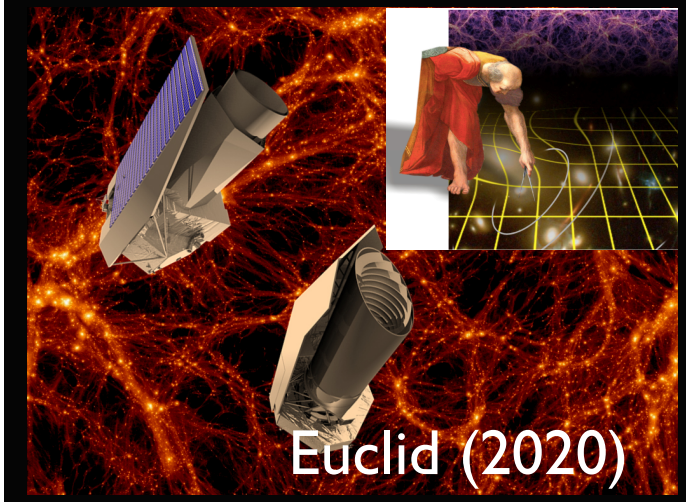

Euclid (2020)

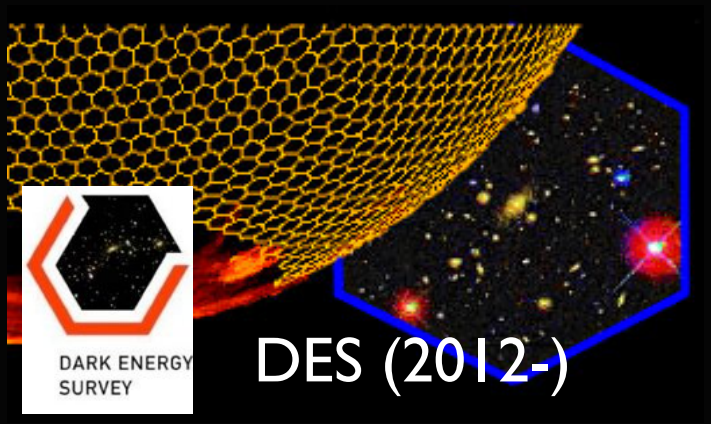

DES (2012-)

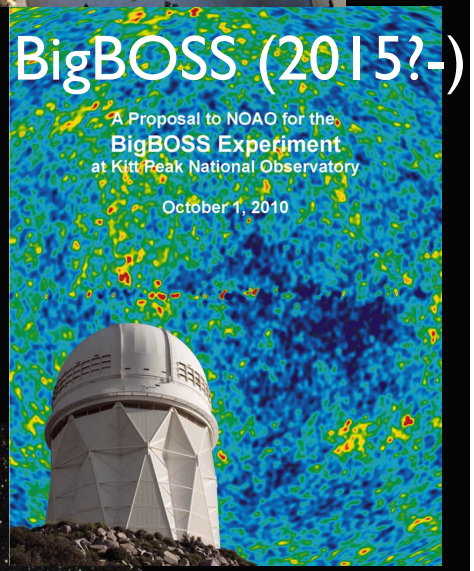

BigBOSS (2015?-)





LSST (2020?-)

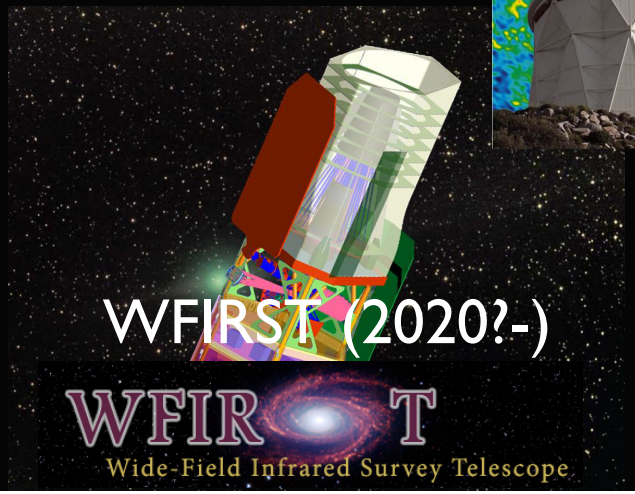

WFIRST (2020?-)

Time line (DE experiments)

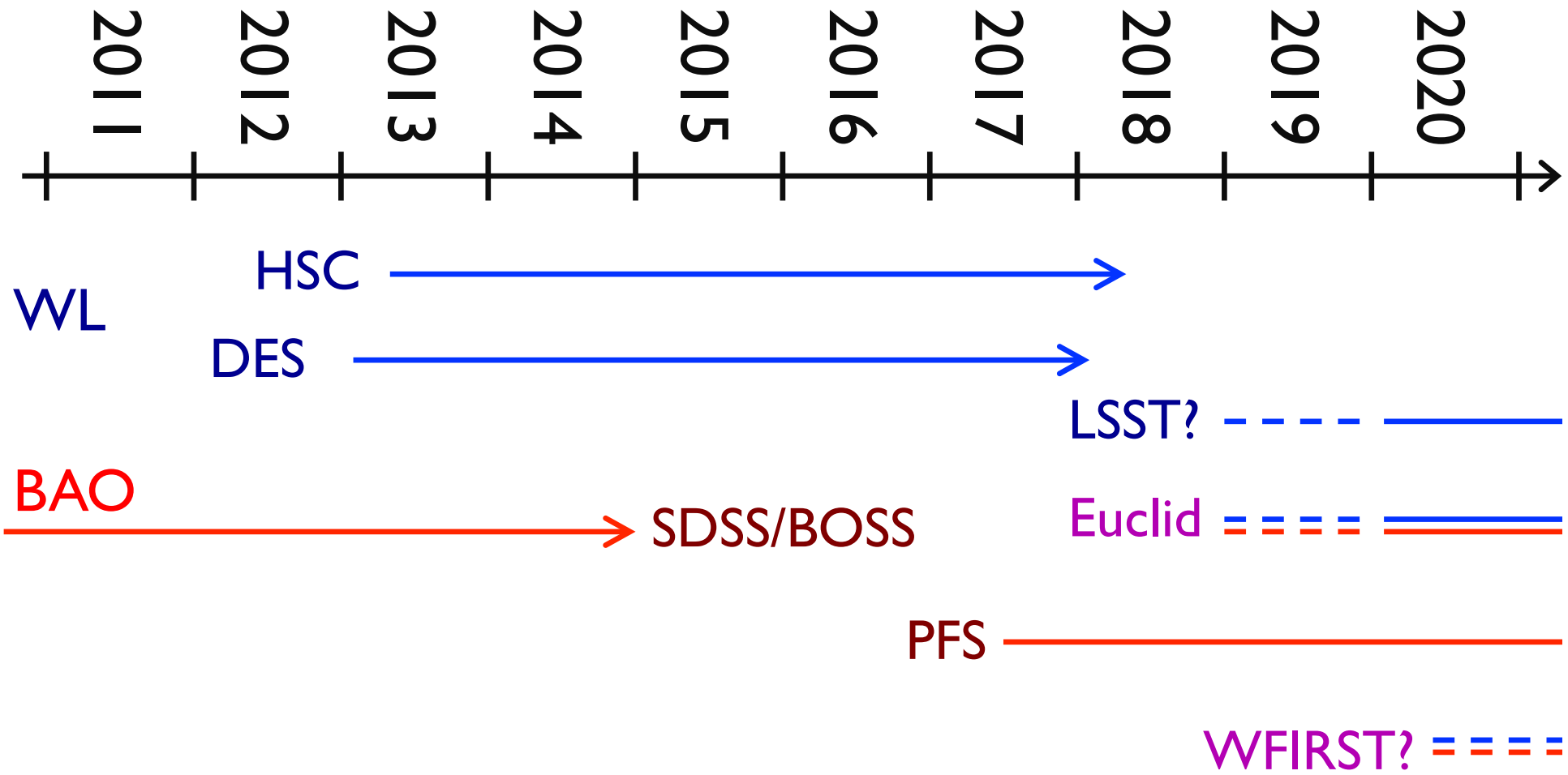

We are in a good position!



Hyper Suprime-Cam (HSC)

- Upgrade the prime focus camera
- Funded, started since 2006: total cost ~$50M
- International collaboration: Japan (NAOJ, IPMU, Tokyo, Tohoku, Nagoya, +), Princeton, Taiwan
- FoV (1.5° in diameter): ~10×Suprime-Cam
- Keep the excellent image quality
- Instrumentation well underway (being led by S. Miyazaki, NAOJ)
- HSC survey starting from 2012 - 2017
- Deep multi-band imaging (grizy; i~26, y~24) with 1400 square degrees

Hyper Suprime-Cam Project

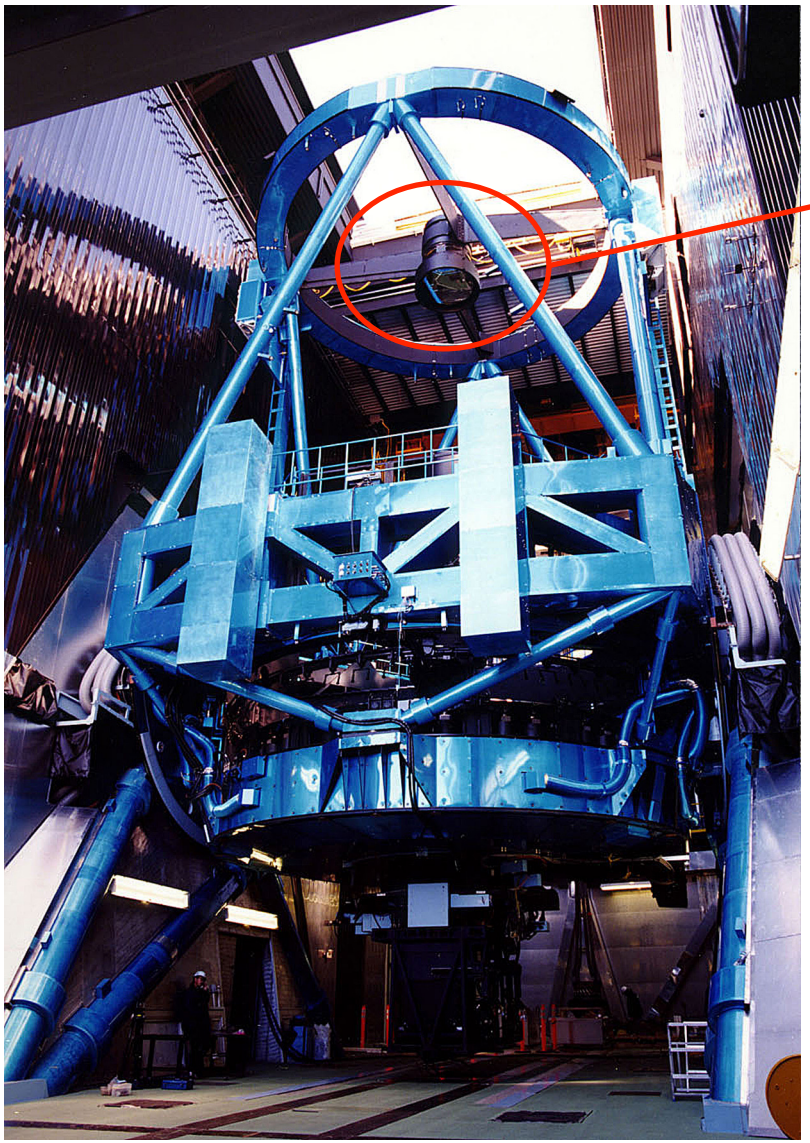



- All instruments at Mauna Kea
- The *largest* camera in the world
- 3m high
- 3 tons weighed
- 116 CCD chips (870 millions pixels)

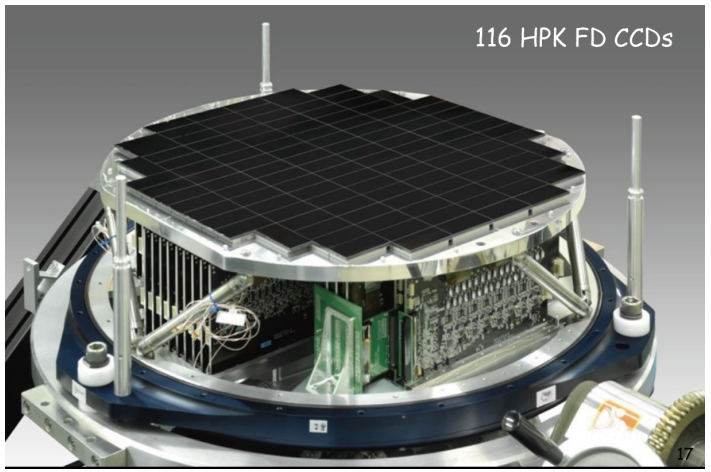

The Engineering first light!

From Satoshi Miyazaki (NAOJ, HSC PI)



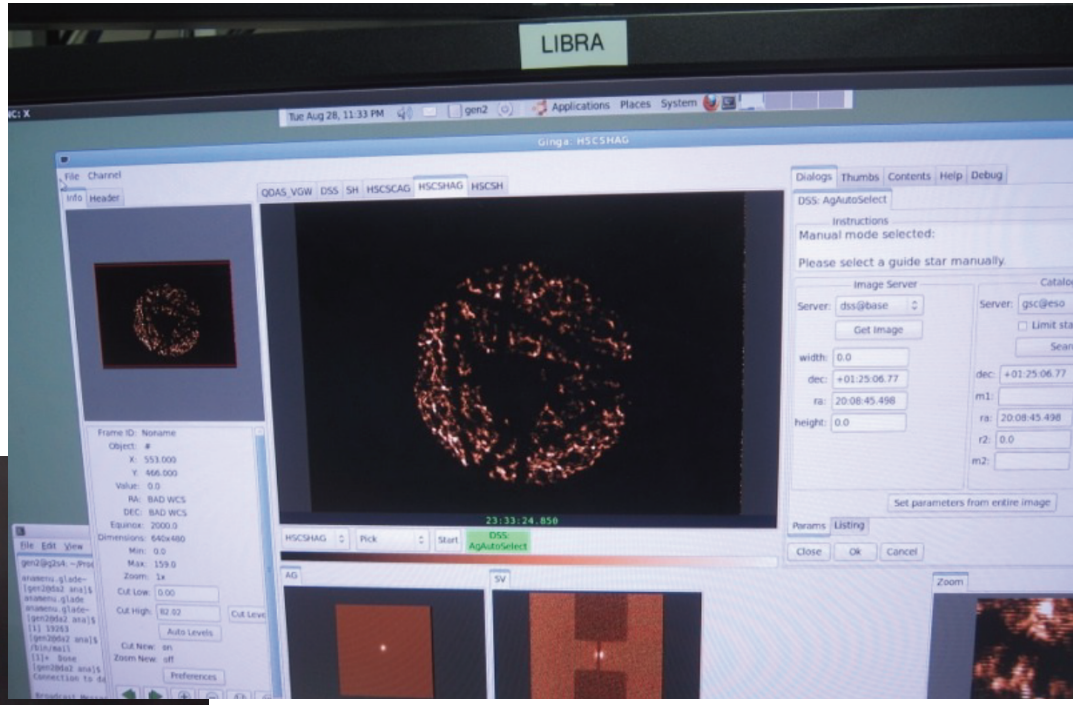

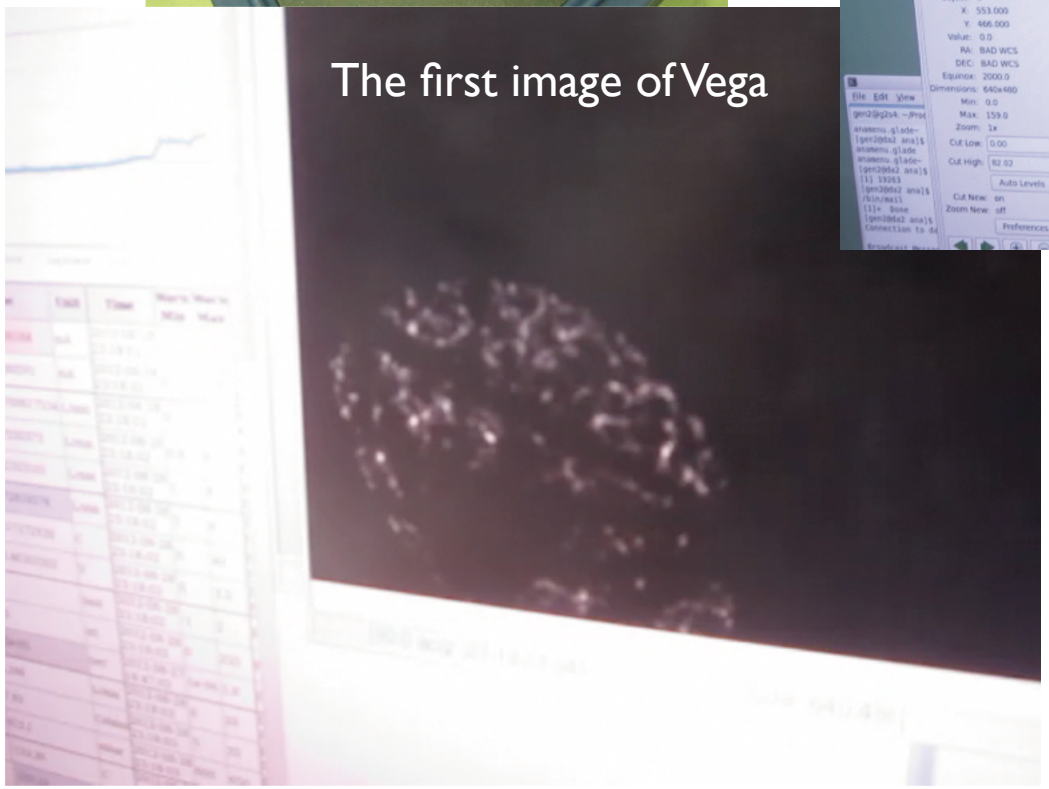

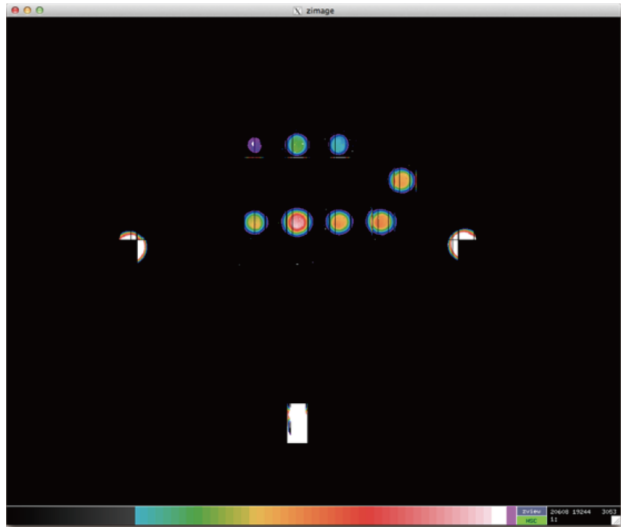

HSC Engineering First Light





- Press release (Sep 12)
- From homepages of IPMU and NAOJ
- Nature, the newspapers in Japan, YouTube
- YouTube: 3,998 hits (as of Nov 13)

Planned HSC Survey

- Wide Layer: 1400 sq. degs., *grizy* (i_{AB}=26, 5σ)
  - Weak gravitational lensing
  - Galaxy clustering, properties of z~1 L_* galaxy
  - *Dark Energy*, *Dark Matter*, neutrino mass, the early universe physics (primordial non-Gaussianity, spectral index)
- Deep Layer: 28 sq. degs, *grizy*+NBs (*i*=27)
  - For calibration of galaxy shapes for HSC-Wide WL
  - Lyman-alpha emitters, Lyman break galaxies, QSO
  - Galaxy evolution up to z~7
  - *The physics of cosmic reionization*
- Ultra-deep Layer: 2FoV, *grizy*+NBs (i~28)
  - Type-Ia SNe up to z~1.4
  - LAEs, LBGs
  - Galaxy evolution
  - *Dark Energy, the cosmic reionization*

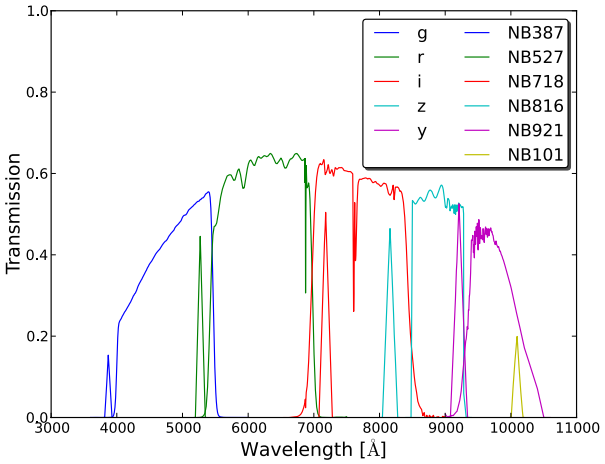

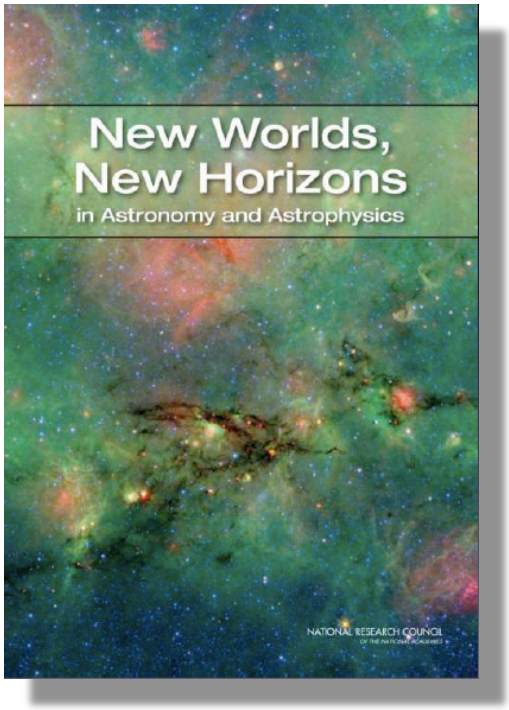

Planned HSC Survey

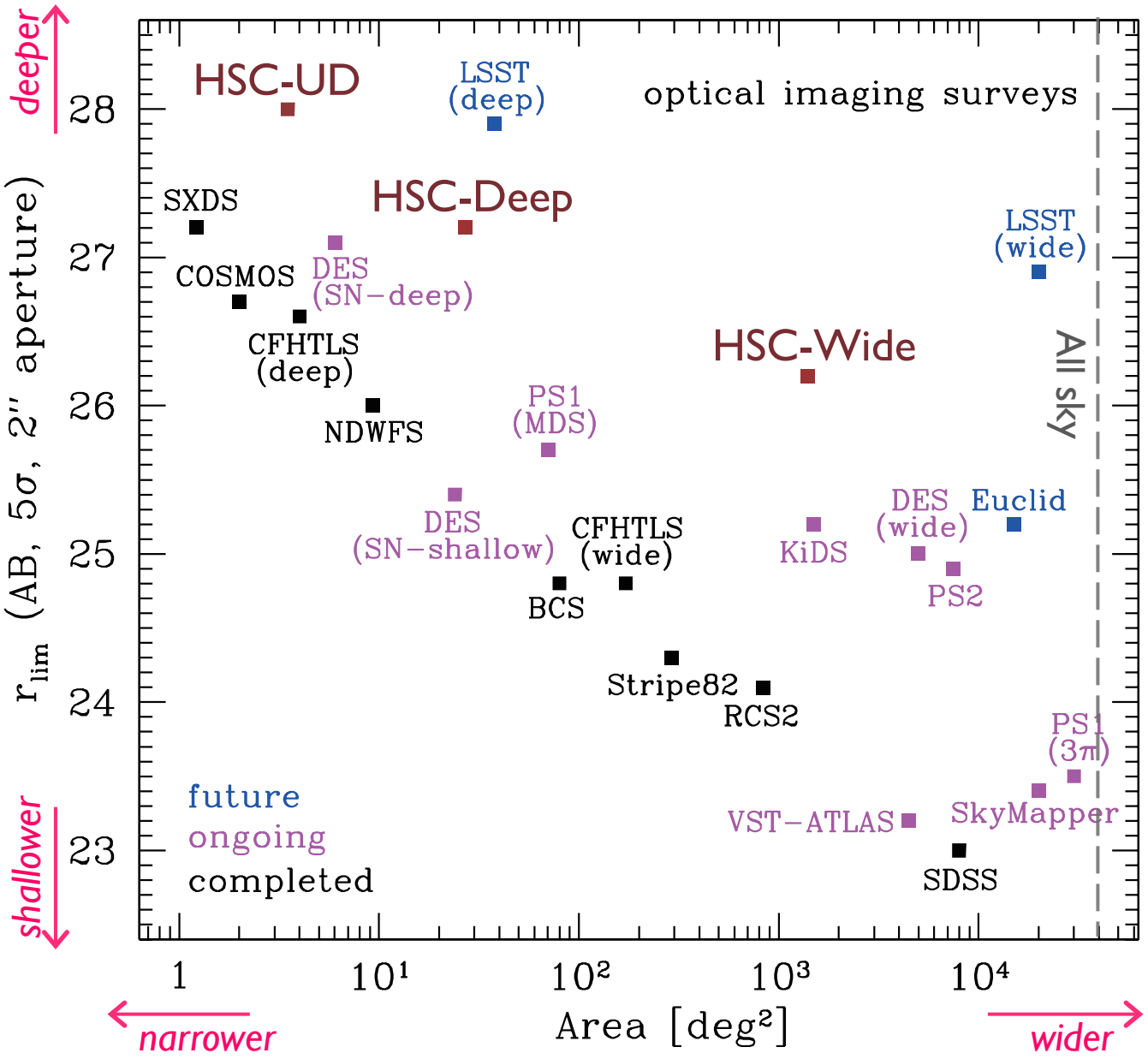

Black: existing

Magenta: upcoming

Blue: future

HSC Layers will explore new regions in survey parameter space

HSC Survey Fields

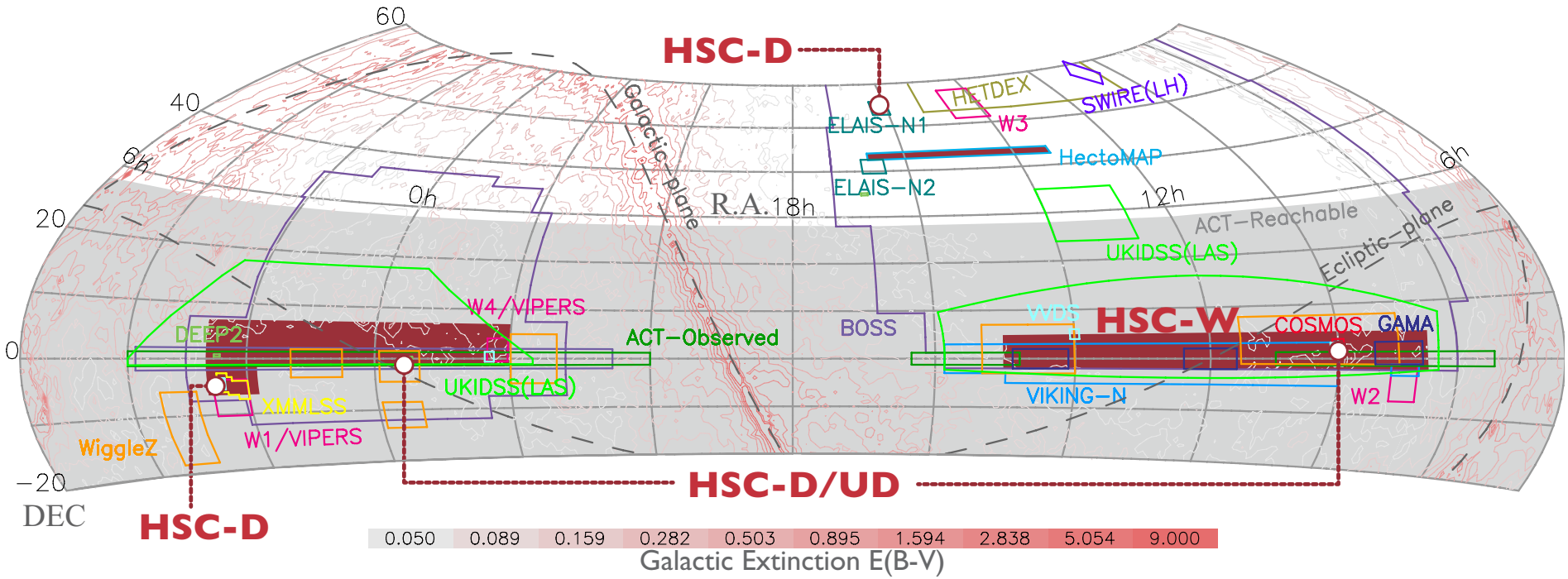

- The HSC fields are selected based on …
  - Synergy with other data sets: SDSS/BOSS, The Atacama Cosmology Telescope CMB survey (from Chile), X-ray (XMM-LSS), spectroscopic data sets
  - Spread in RA
  - Low dust extinction

Gravitational Lensing =Einstein's prediction

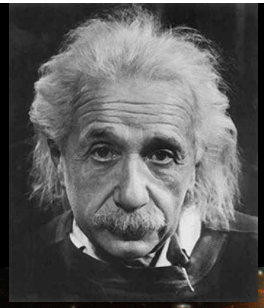

$$G_{\mu\nu} = \frac{8\pi G}{c^4} T_{\mu\nu}$$

$$\Rightarrow \text{ light path: } \boldsymbol{x} = \boldsymbol{x}[z; g_{\mu\nu}]$$

The *curved* space-time bends "light path"

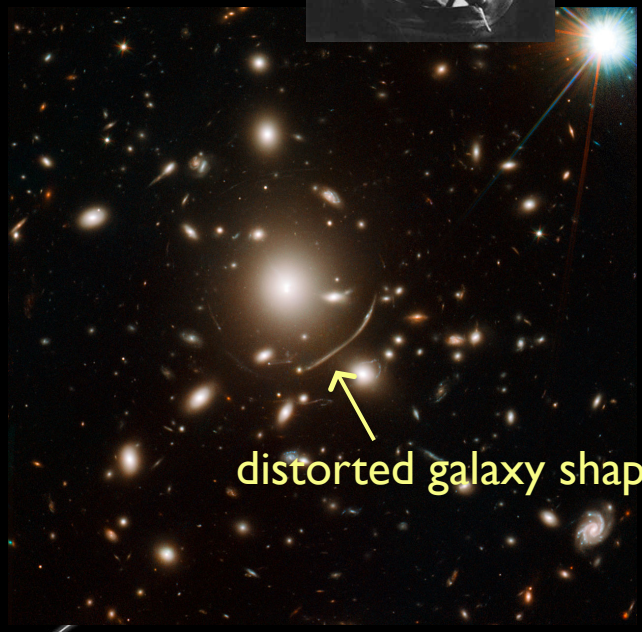

The curvature of space-time is measurable via galaxy shapes

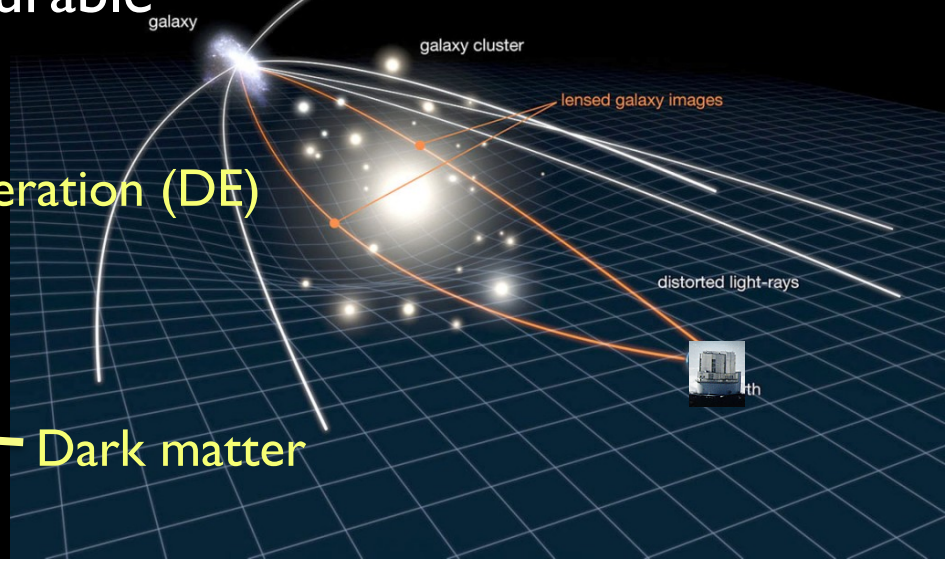

Lensing strength =

(geometry of the universe) ← Cosmic acceleration (DE)

× (total matter of lens(es)) ← Dark matter

Subaru Telescope: wide FoV & excellent image quality

- **Fast, Wide, Deep & Sharp**
- a cosmological survey needs these





HST

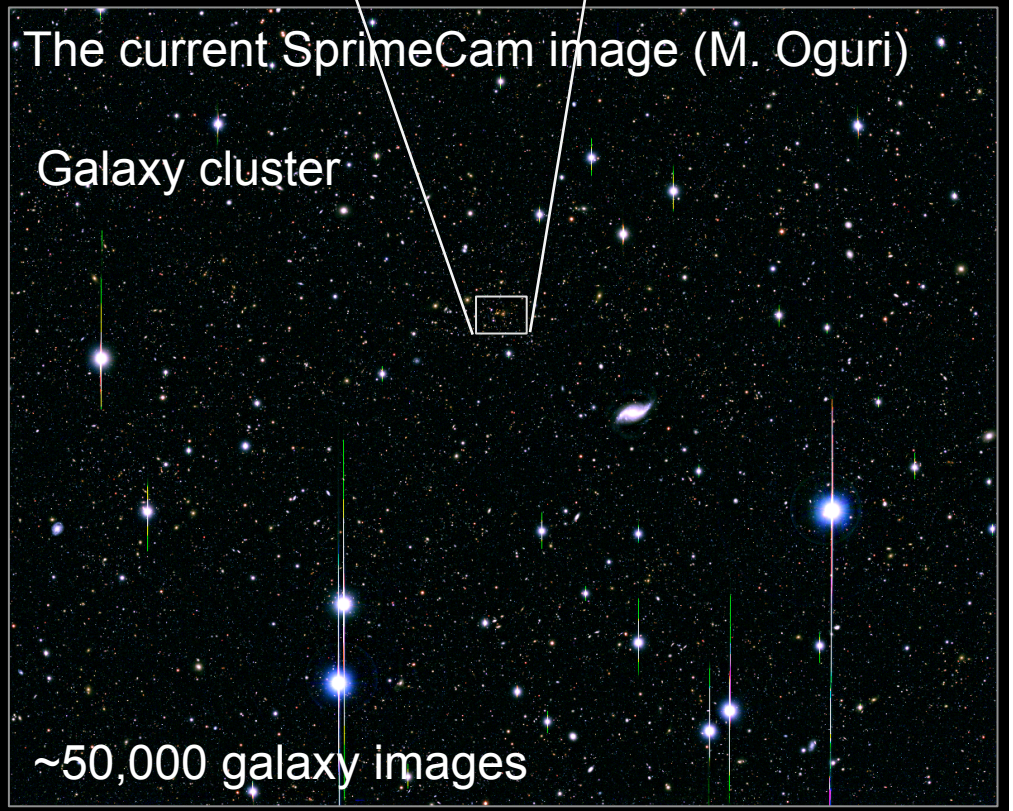

Hyper Suprime-Cam FoV

- **Fast**
- a cos



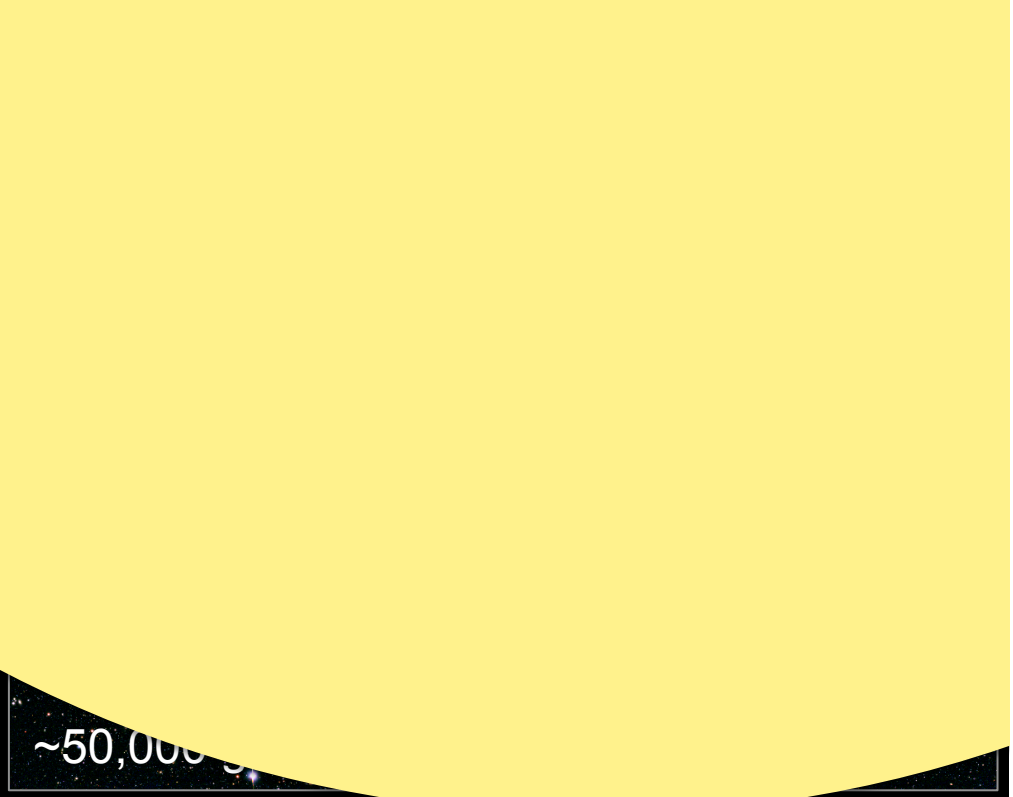

Statistical weak lensing

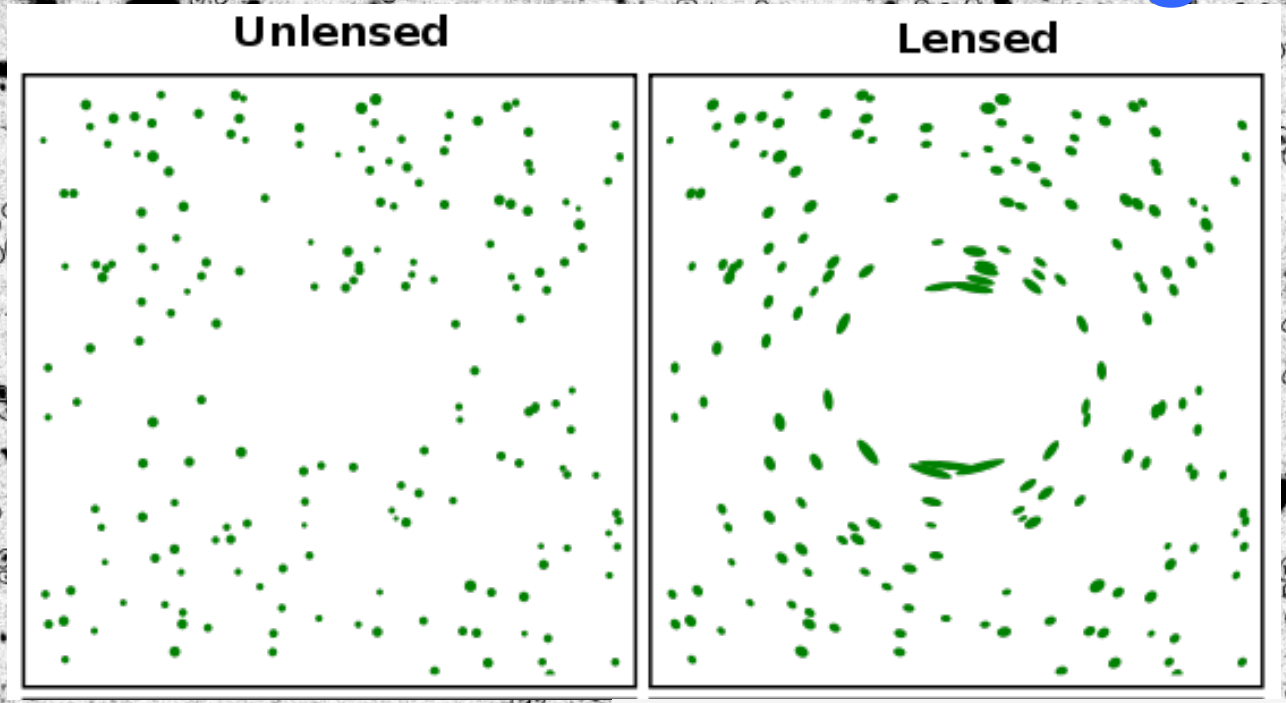

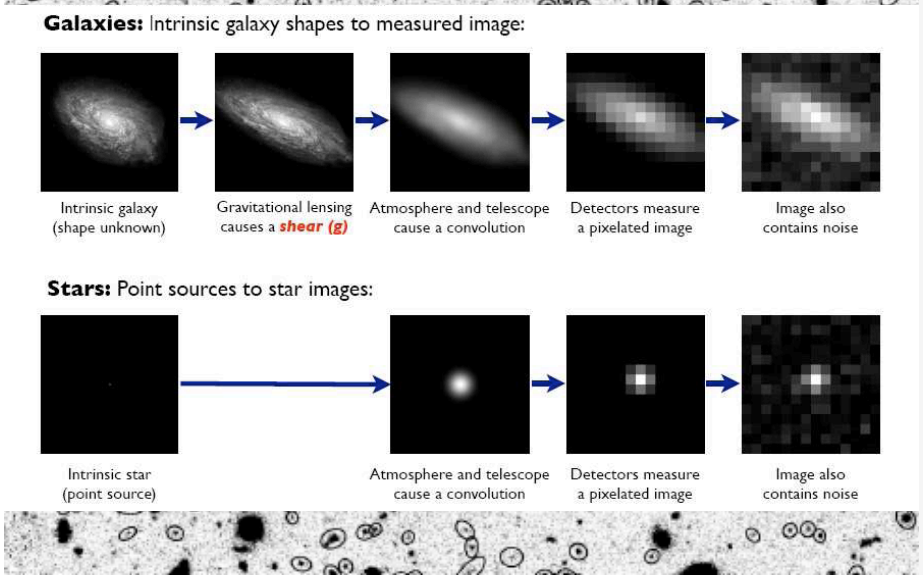

- Need statistics to reduce the intrinsic shape contamination
- Excellent image quality and deep image needed for an accurate WL measurement
- Issues; accurate shape measurements, PSF correction, pixelization effect

Stacked lensing: halo-shear correlation

$$\gamma_+^{\rm obs}(\theta_i) = \gamma_+^{\rm cluster}(\theta_i) + \gamma_+^{\rm LSS}(\theta_i) + \varepsilon_+(\theta_i)$$

Oguri & MT 11

projection effect

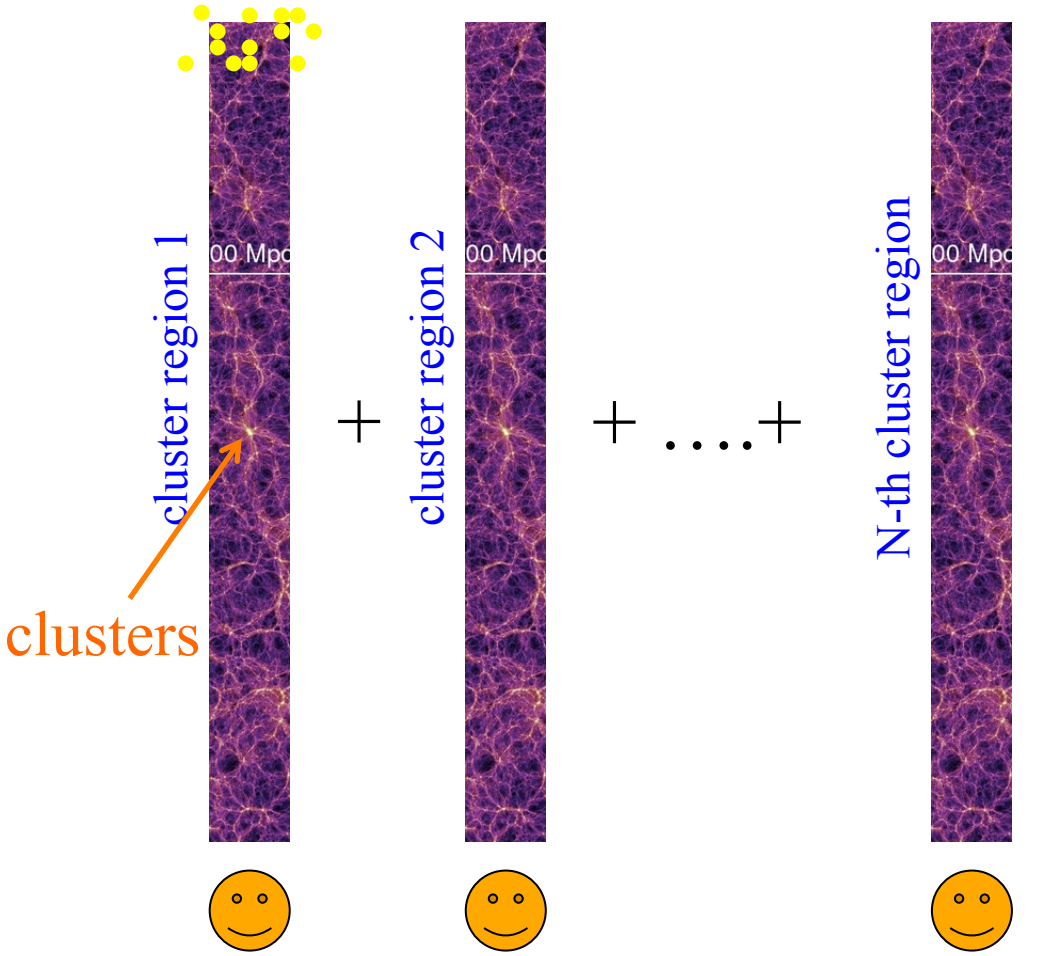

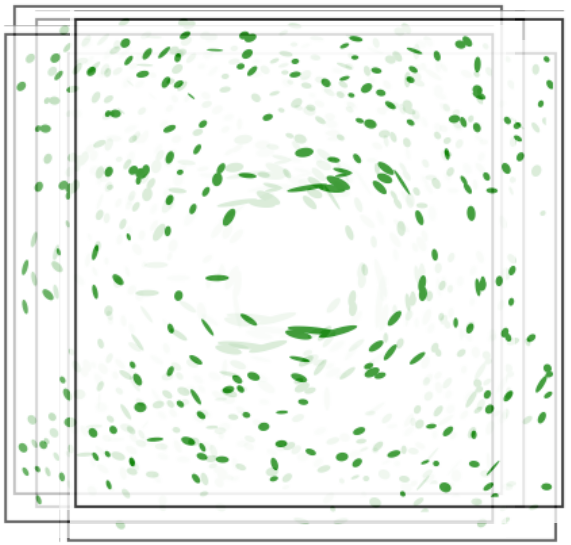

$$\langle\gamma_+\rangle(\theta) = \frac{1}{N_{cl}} \sum_{a=1}^{N_{cl}} \sum_{|\vec{\theta}'|\subset\theta} \gamma_{+(a\text{-th cluster})}(\vec{\theta}') \approx \left\langle \gamma_+^{\rm cluster} \right\rangle(\theta)$$

Less affected by projection effect, intrinsic alignment, sys. errors ….

Note: halo center

Average DM distribution of galaxy clusters

Okabe, MT, Umetsu, Graham, Futamase 10
Okabe, MT, Futamase et al. in prep.

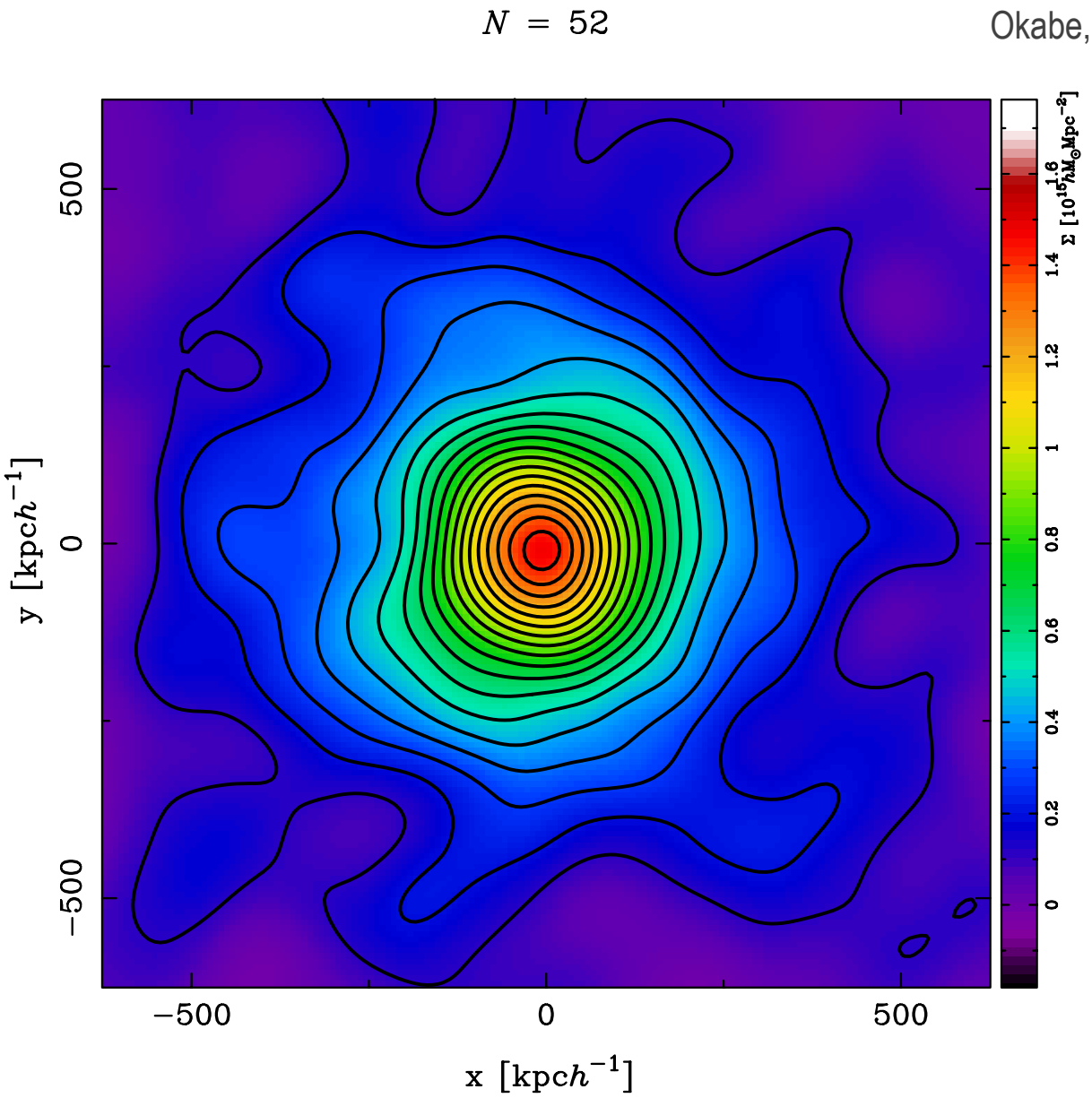

Stacked cluster lensing (all the ROSAT-selected clusters in z=0.15-0.3)

Have obtained Subaru data of all the 52 previously-known, X-ray luminous clusters in 0.15<z<0.3; S/N~50

Used ~*1M* galaxies in total for WL analysis

This projected started in 2005; it has taken 6 years so far (10 nights)

Stacked Lensing (contd.)

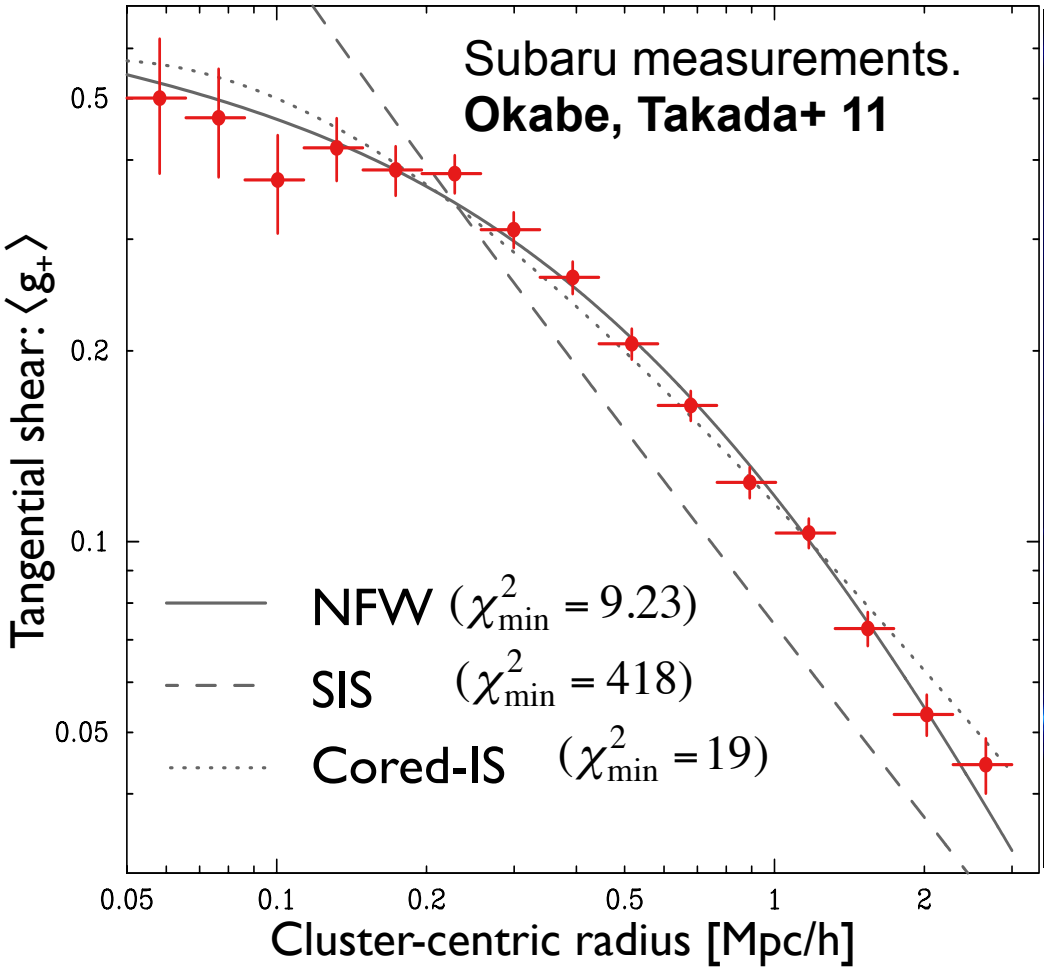

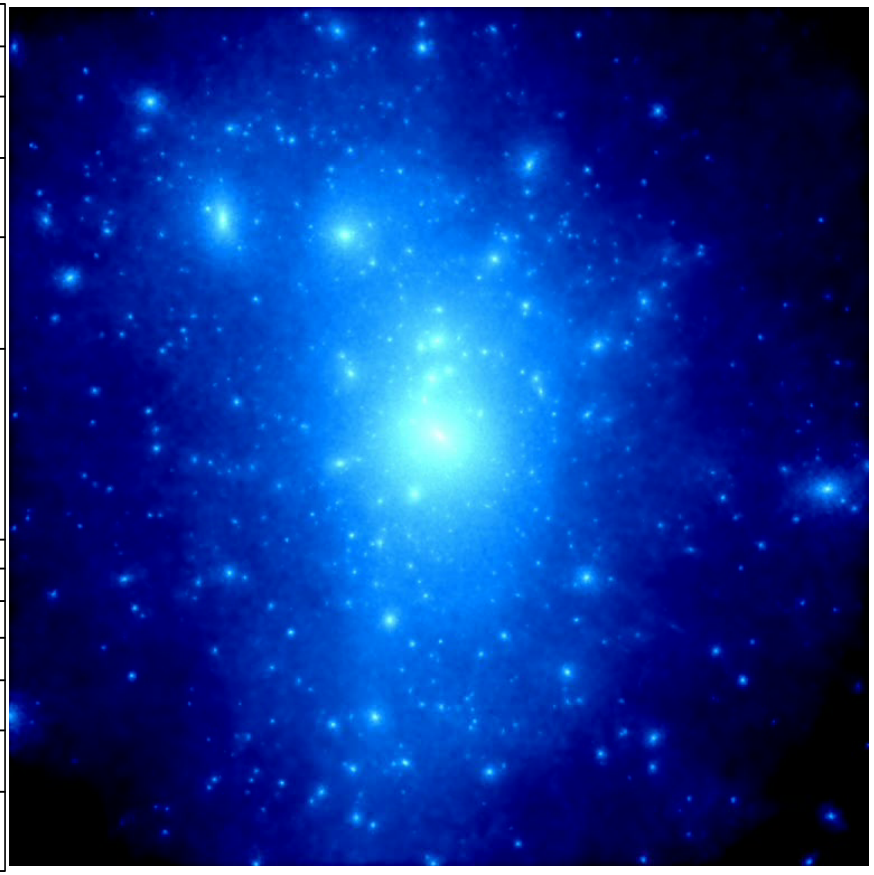

The precise meas. of mean mass: M_{vir}/10^14=$6.75^{+0.33}_{-0.32}$ (4%), c_{vir}=$4.10^{+0.21}_{-0.20}$(5%)
Excellent agreement with CDM simulation predictions

Forecast for stacked lensing with HSC

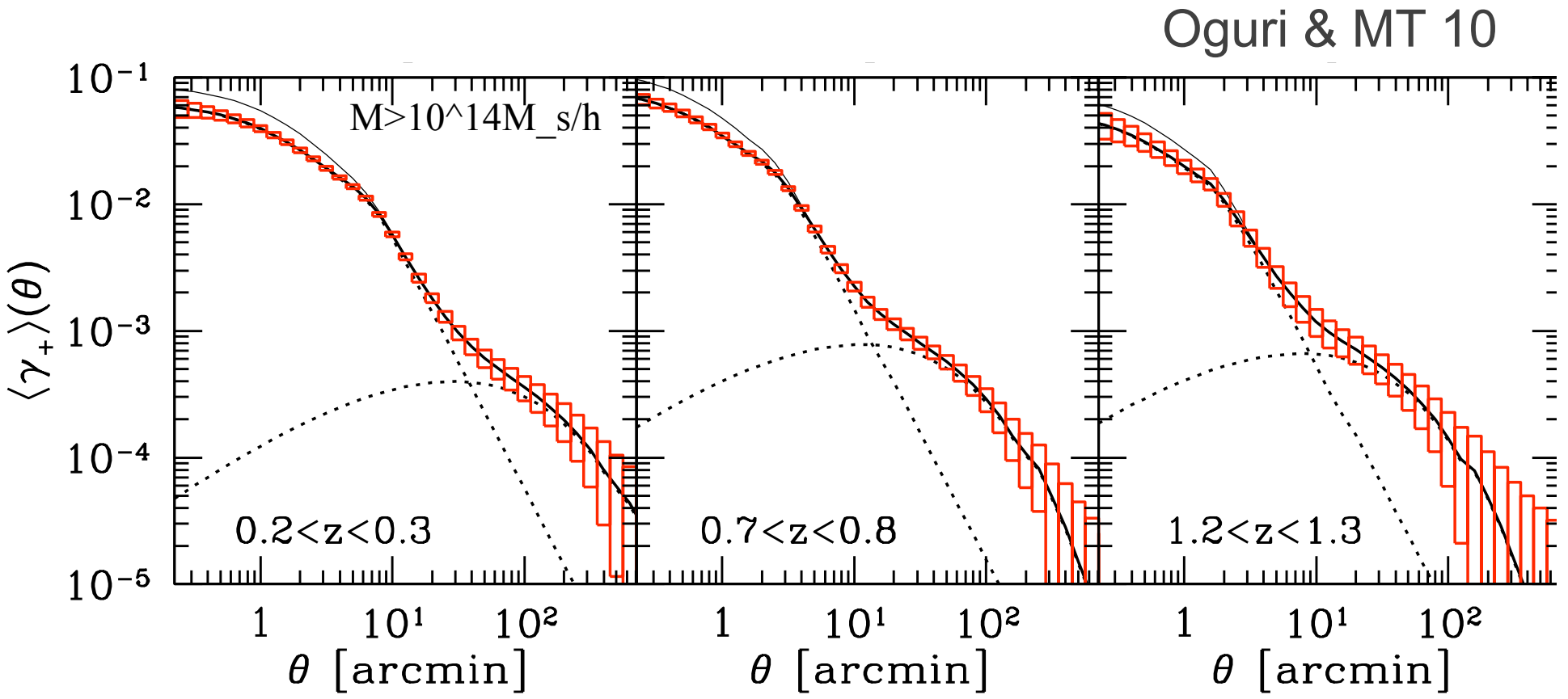

- HSC can achieve a high S/N detection of stacked WL signals out to z~1.3
- Small-angle signals are from one halo (the mean halo mass and the average shape of mass profile)
- Large-angle signals are from the mass distribution in large-scale structure

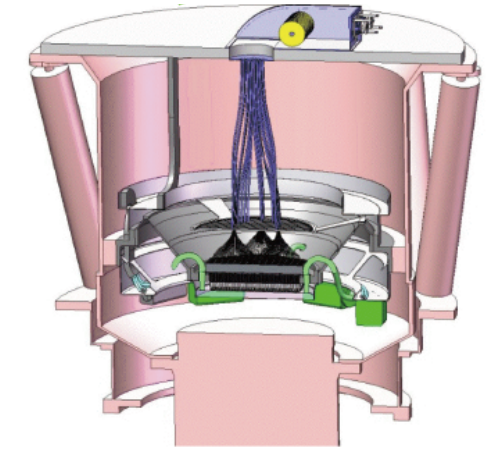

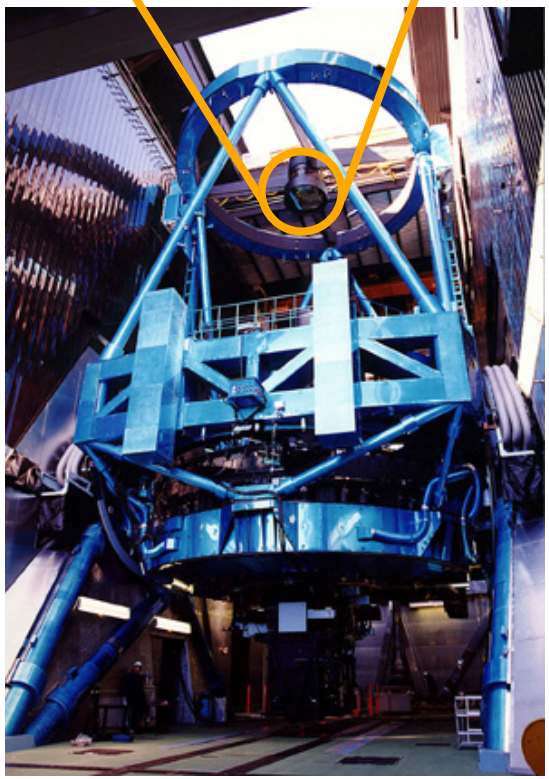

Prime Focus Spectrograph (PFS)

- Multi object fiber spectrograph for 8.2m Subaru
- International collaboration; Japan (IPMU+), Princeton, JHU, Caltech/JPL, LAM, Brazil, ASIAA
- Initiated by the stimulus funding (~$30M secure); $50M needed for the instrumentation
- The current baseline design
  - The same optics to HSC
  - 2400 fibers
  - 380-1300nm wavelength coverage
  - R~2000, 3000, 5000 (blue, red, NIR)
- The target first light; around 2017
- Capable of various science cases: cosmology, galaxy, galactic archeology

PFS Positioner

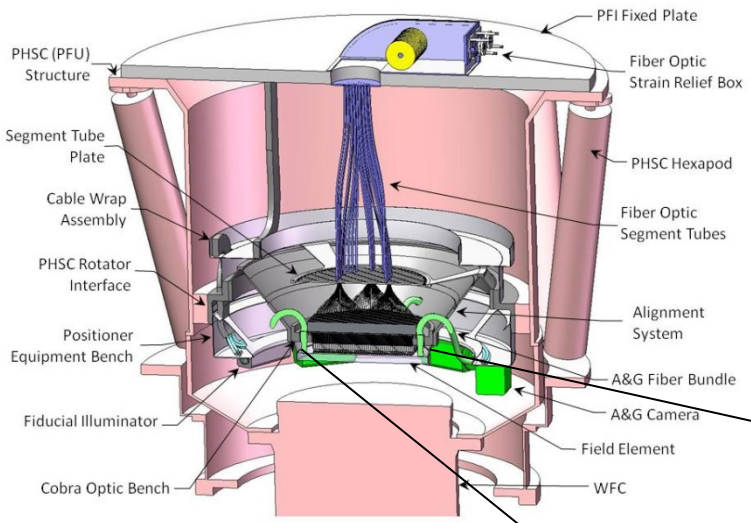

Positioner Unit - *Cobra*



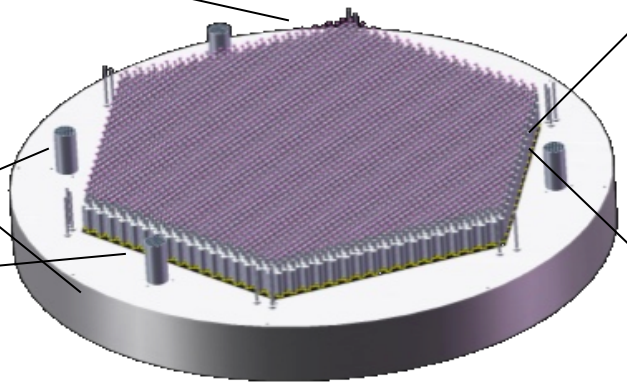

A&G Fiber Guides

Optical Bench with Positioner Units

Cobra system is the most essential part of PFS, and will be built at JPL
Designed to achieve 5 μ m accuracy in < 8 iterations (40 sec)

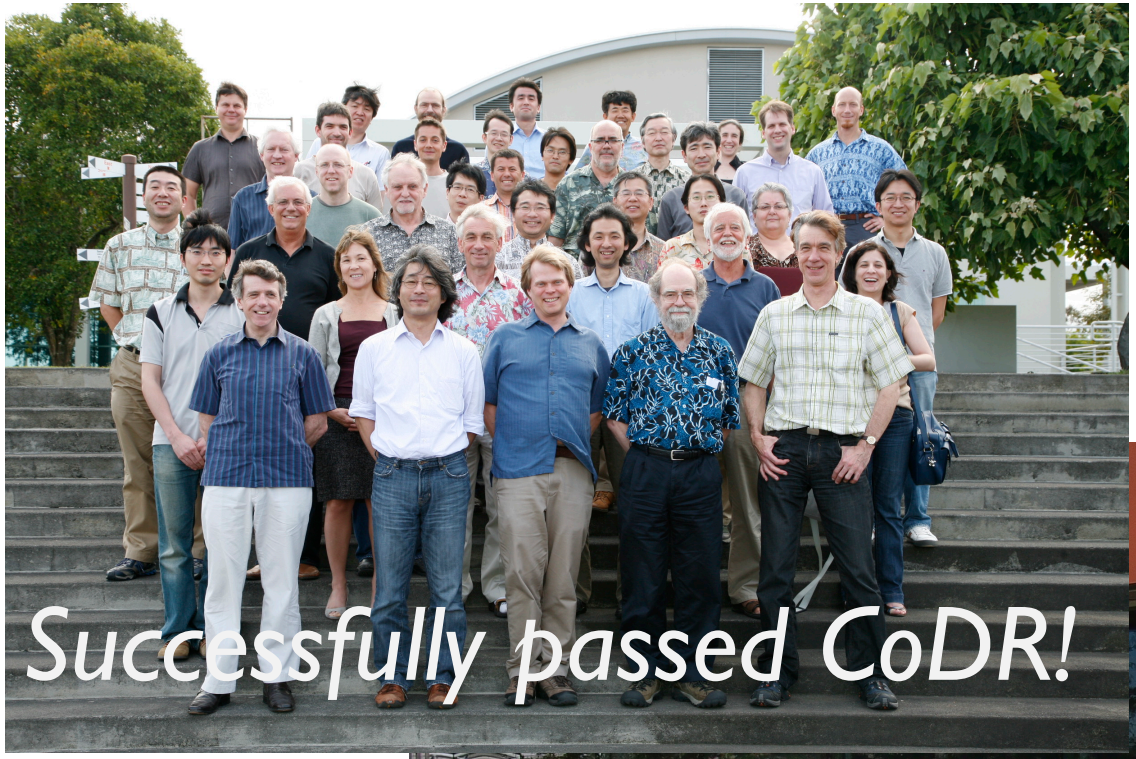

- *Concept Design Review* (Mar 2012)
- Next milestone: Preliminary Design Review (Feb or Mar 2013)



PFS Science Document in arXiv

DRAFT VERSION JUNE 21, 2012
Preprint typeset using LaTeX style emulateapj v. 5/2/11

arXiv:1206.0737v2 [astro-ph.CO] 19 Jun 2012

EXTRAGALACTIC SCIENCE AND COSMOLOGY WITH THE SUBARU PRIME FOCUS SPECTROGRAPH (PFS)

RICHARD ELLIS[1], MASAHIRO TAKADA[2], HIROAKI AIHARA[2,3], NOBUO ARIMOTO[4], KEVIN BUNDY[2], MASASHI CHIBA[5], JUDITH COHEN[1], OLIVIER DORE[6,1], JENNY E. GREENE[7], JAMES GUNN[7], TIMOTHY HECKMAN[8], CHRIS HIRATA[1], PAUL HO[9], JEAN-PAUL KNEIB[10], OLIVIER LE FEVRE[10], HITOSHI MURAYAMA[2,11], TOHRU NAGAO[12], MASAMI OUCHI[13], MICHAEL SEIFFERT[4,1], JOHN SILVERMAN[2], LAERTE SODRÉ JR[14], DAVID N. SPERGEL[7], MICHAEL A. STRAUSS[7], HAJIME SUGAI[2], YASUSHI SUTO[3], HIDEKI TAKAMI[4], ROSEMARY WYSE[8], & THE PFS TEAM

Draft version June 21, 2012

ABSTRACT

The Subaru Prime Focus Spectrograph (PFS) is a massively-multiplexed fiber-fed optical and near-infrared spectrograph ($N_{\rm fiber}$=2400, $380 \leq \lambda \leq 1300$nm), offering unique opportunities in survey astronomy. Following a successful external design review the instrument is now under construction with first light predicted in late 2017. Here we summarize the science case for this unique instrument in terms of provisional plans for a Subaru Strategic Program of $\simeq$300 nights. We describe plans to constrain the nature of dark energy via a survey of emission line galaxies spanning a comoving volume of $9.3h^{-3}$Gpc^3 in the redshift range $0.8 < z < 2.4$. In each of 6 independent redshift bins, the cosmological distances will be measured to 3% precision via the baryonic acoustic oscillation scale and redshift-space distortion measures will be used to constrain structure growth to 6% precision. As the near-field *cosmology* program, radial velocities and chemical abundances of stars in the Milky Way and M31 will be used to infer the past assembly histories of both spiral galaxies as well as the structure of their dark matter halos. Complementing the goals of the Gaia mission ($V < 17$), radial velocities and metallicities will be secured for 10^6 Galactic stars to $17 < V < 20$. Data for fainter stars to $V \simeq 21$ will be secured in areas containing Galactic tidal streams. The M31 campaign will target red giant branch stars with $21 < V < 22.5$ over an unprecedented area of 65 deg^2. For the extragalactic program, our simulations suggest the wide wavelength range of PFS will be particularly powerful in probing the galaxy population and its clustering over a wide redshift range and we propose to conduct a color-selected survey of $1 < z < 2$ galaxies and AGN over 16 deg^2 to $J \simeq 23.4$, yielding a fair sample of galaxies with stellar masses above $\sim 10^{10} M_\odot$ at $z \simeq 2$. A two-tiered survey of higher redshift Lyman break galaxies and Lyman alpha emitters will quantify the properties of early systems close to the reionization epoch. PFS will also provide unique spectroscopic opportunities beyond these currently-envisaged surveys, particularly in the era of Euclid, LSST and TMT.

Subject headings: PFS — cosmology — galactic archaeology — galaxy evolution

1. INTRODUCTION

There is currently a major expansion in survey imaging capability via the use of CCD and near-infrared detector mosaics on a wide range of ground-based telescopes. Such imaging surveys provide accurate photometric and other data to enable the study of gravitational lensing signals which trace the distribution of dark matter and to conduct census studies of Galactic structures and distant star-forming galaxies. For over a decade it has been recognized that a similar revolution

[1] California Institute of Technology, Pasadena, CA 91125, U.S.A
[2] Kavli Institute for the Physics and Mathematics of the Universe (Kavli

Baryon Acoustic Oscillation (BAO)

Sloan Digital Sky Survey (SDSS-I,II) (2000-2008)

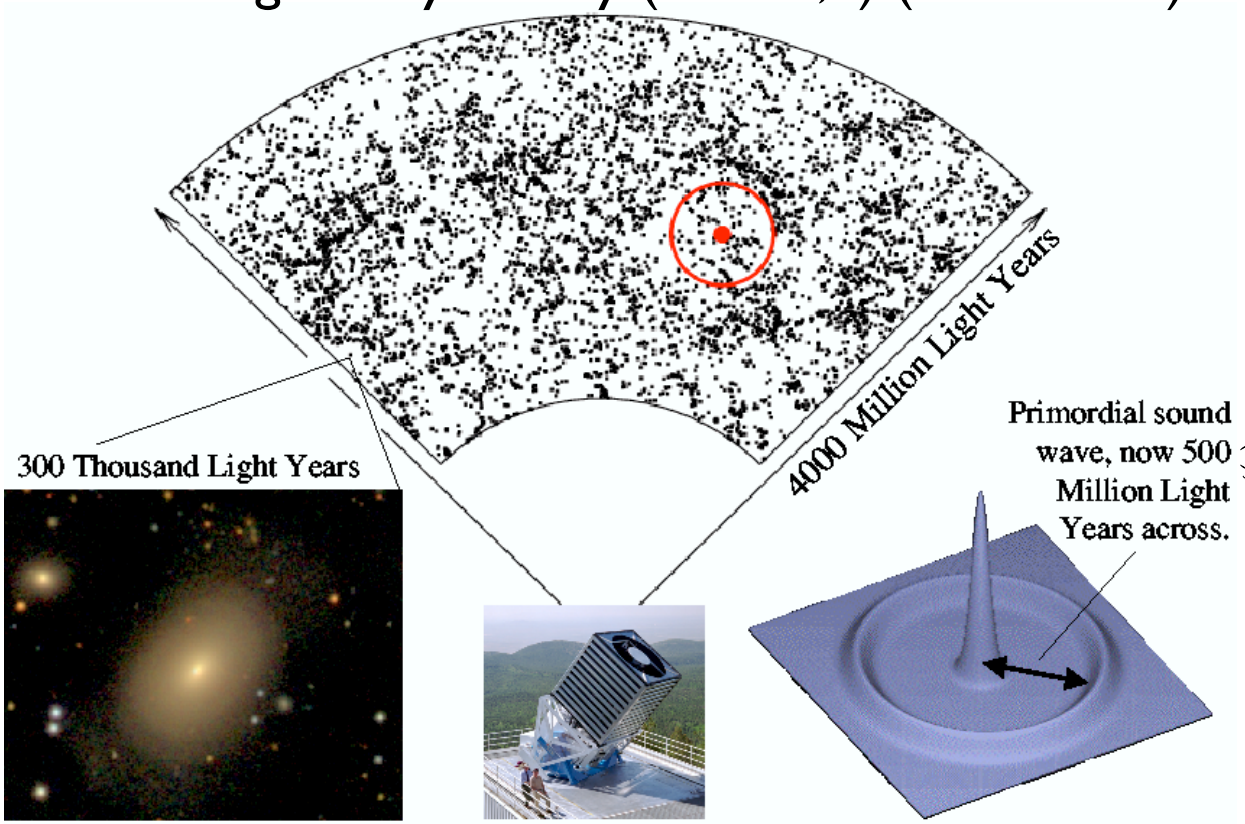

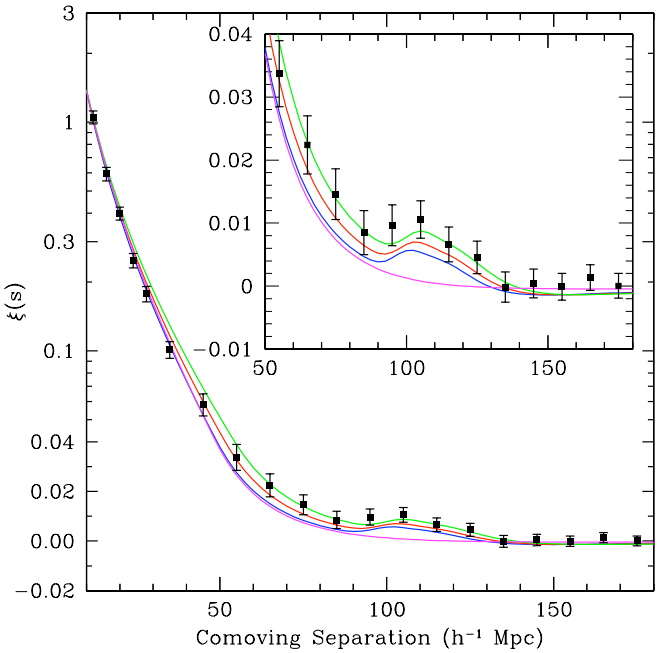

Eisenstein et al. (05)

$$r_{\mathrm{BAO}} = D_A(z)\Delta\theta_{\mathrm{obs}} \qquad r_{\mathrm{BAO}} = \frac{\Delta z_{\mathrm{obs}}}{H(z_{\mathrm{survey}})}$$

Dark Energy Task Force Report (DETF)

a. The **BAO** technique has only recently been established. It is less affected by astrophysical uncertainties than other techniques.

BAO geometrical test

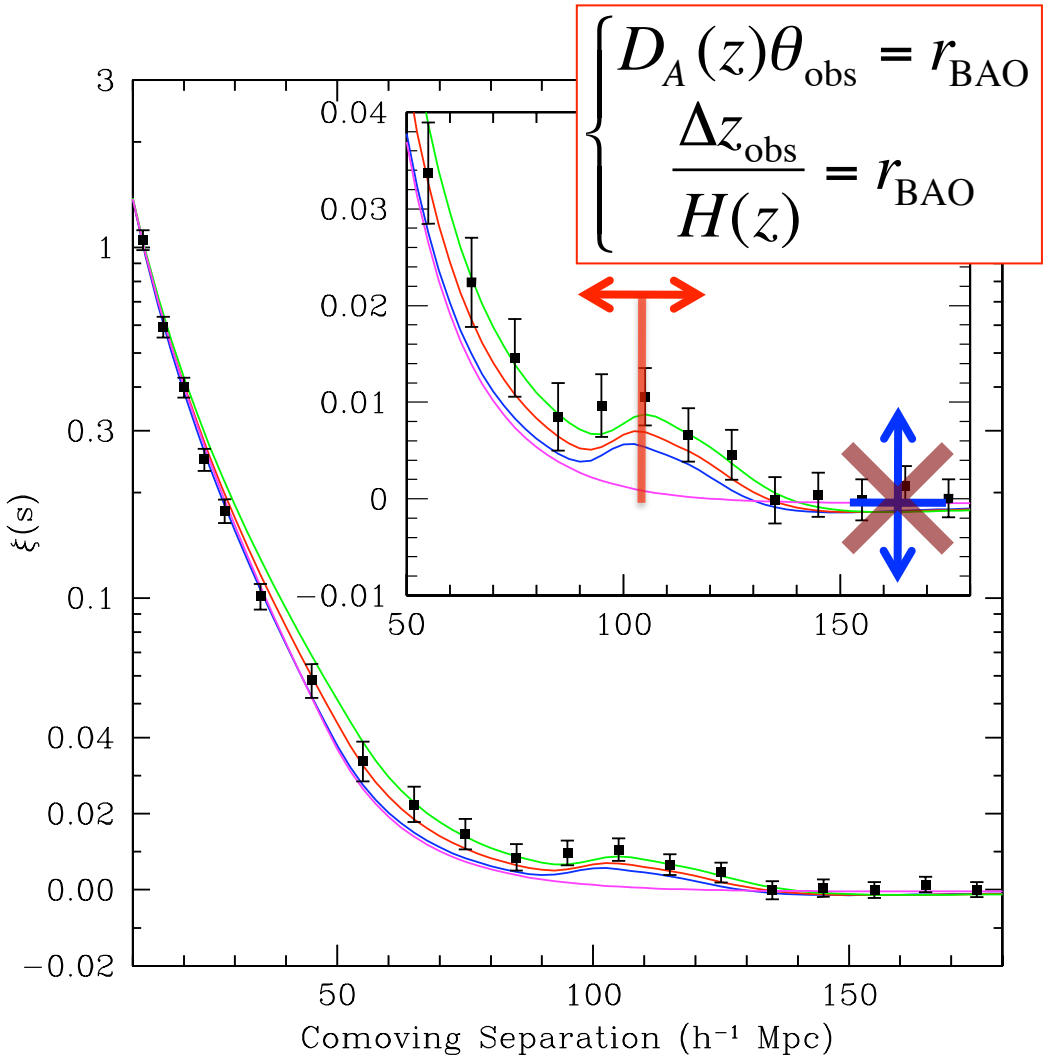

- Measure *the single length scale* (BAO) from the galaxy distribution
- *Not* use the clustering amplitude information to do cosmology due to galaxy bias uncertainties, even though much higher signal-to-noise ratios in the amplitude signals
- The amplitude uncertainty is marginalized over to obtain the distance constraints

Redshift range for PFS survey

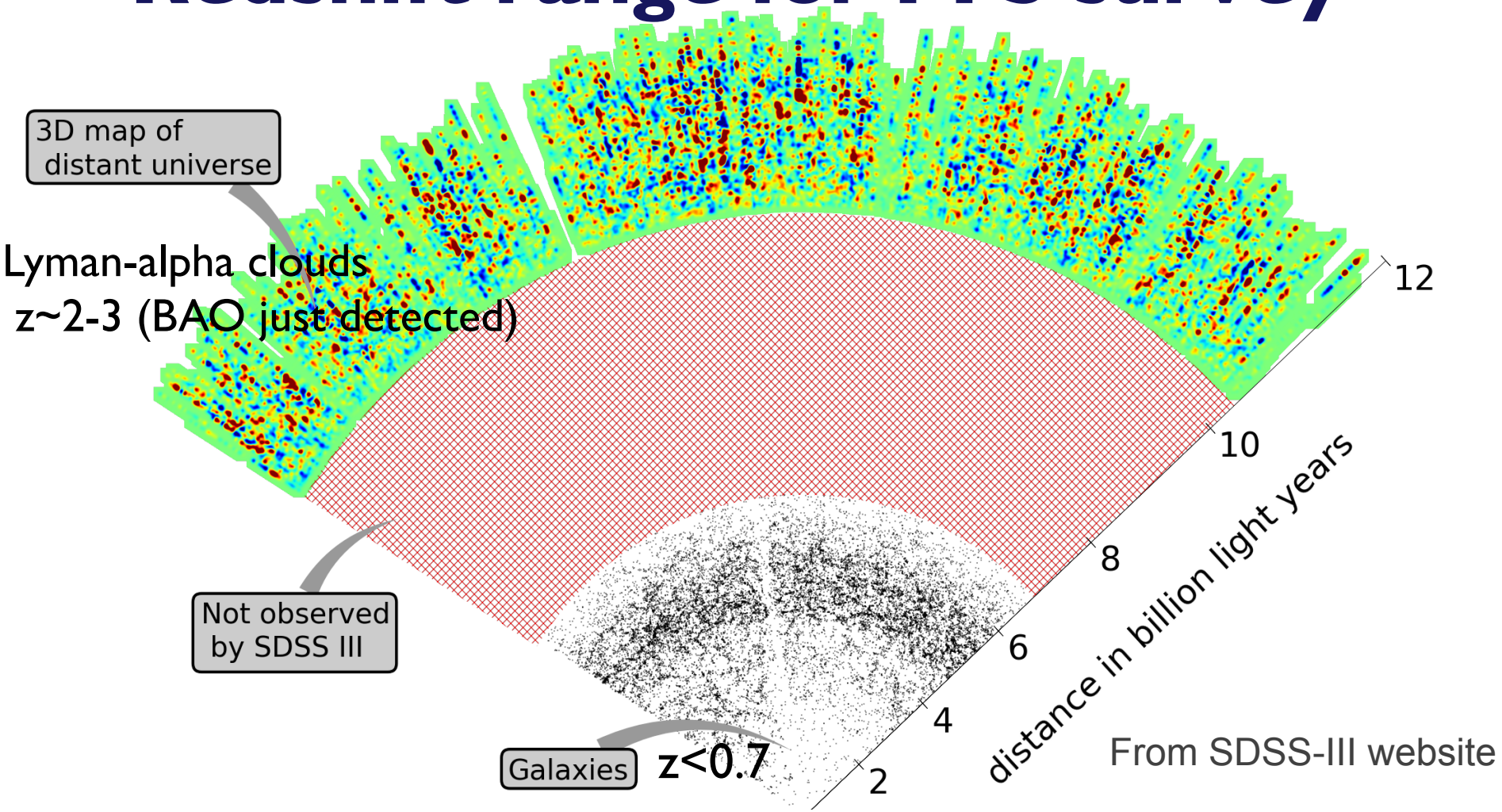

- 0.7<z<2 universe not yet observed
- SuMIRe = Imaging & spectroscopic surveys of the *same* region of the sky with the *same* telescope

PFS spectrograph design

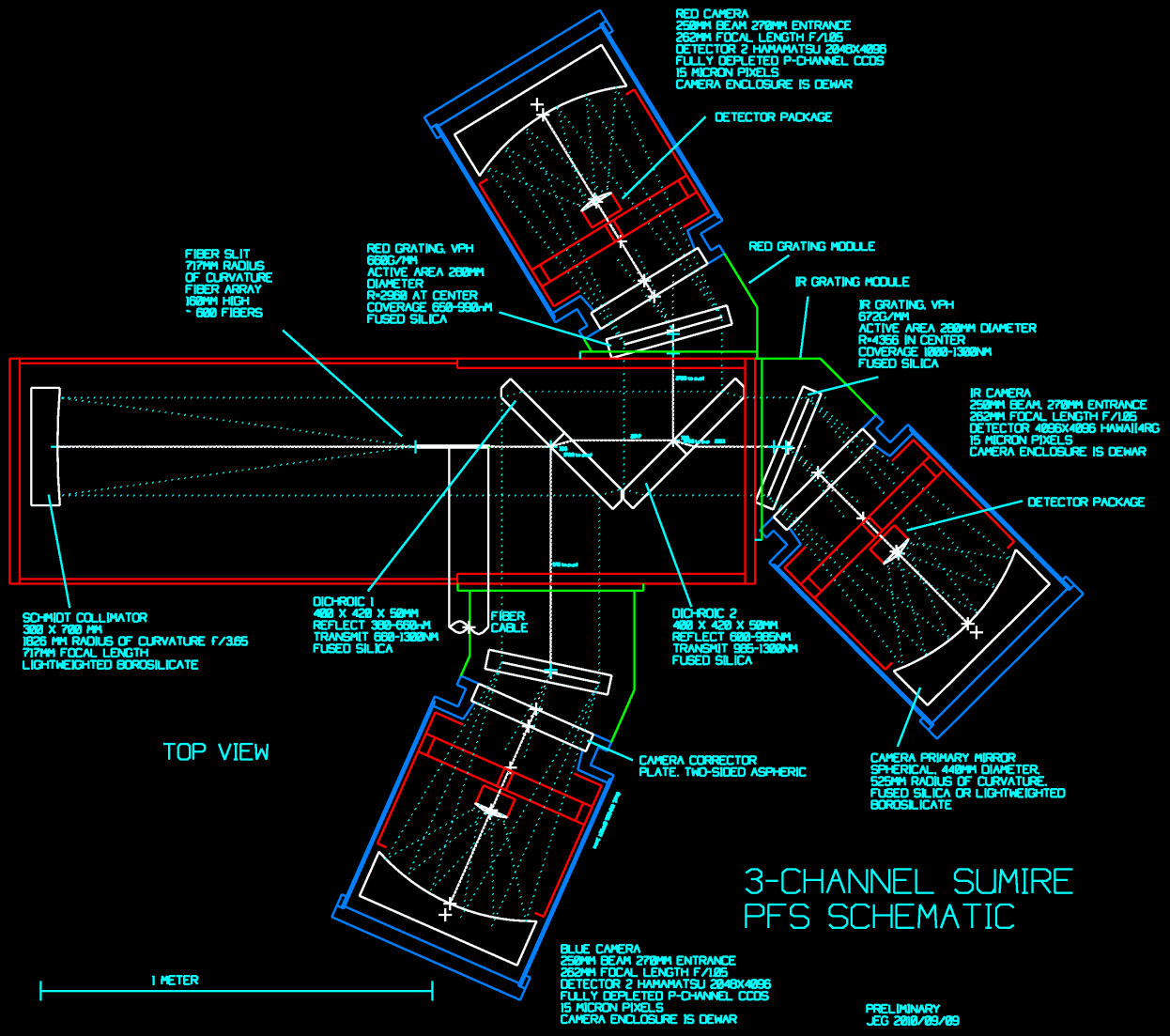

- Wide wavelength coverage: Blue (380-670), Red (650-1000) and NIR (970-1300) spectra at the same time

Unique capability of PFS: high performance

A working example:

$f_{[OII]}=5\times10^{-17}$erg/cm^2/s, σ_v=70 km/s, r_{eff}=0.3"

t_{exp}=2×450sec (15min in total)

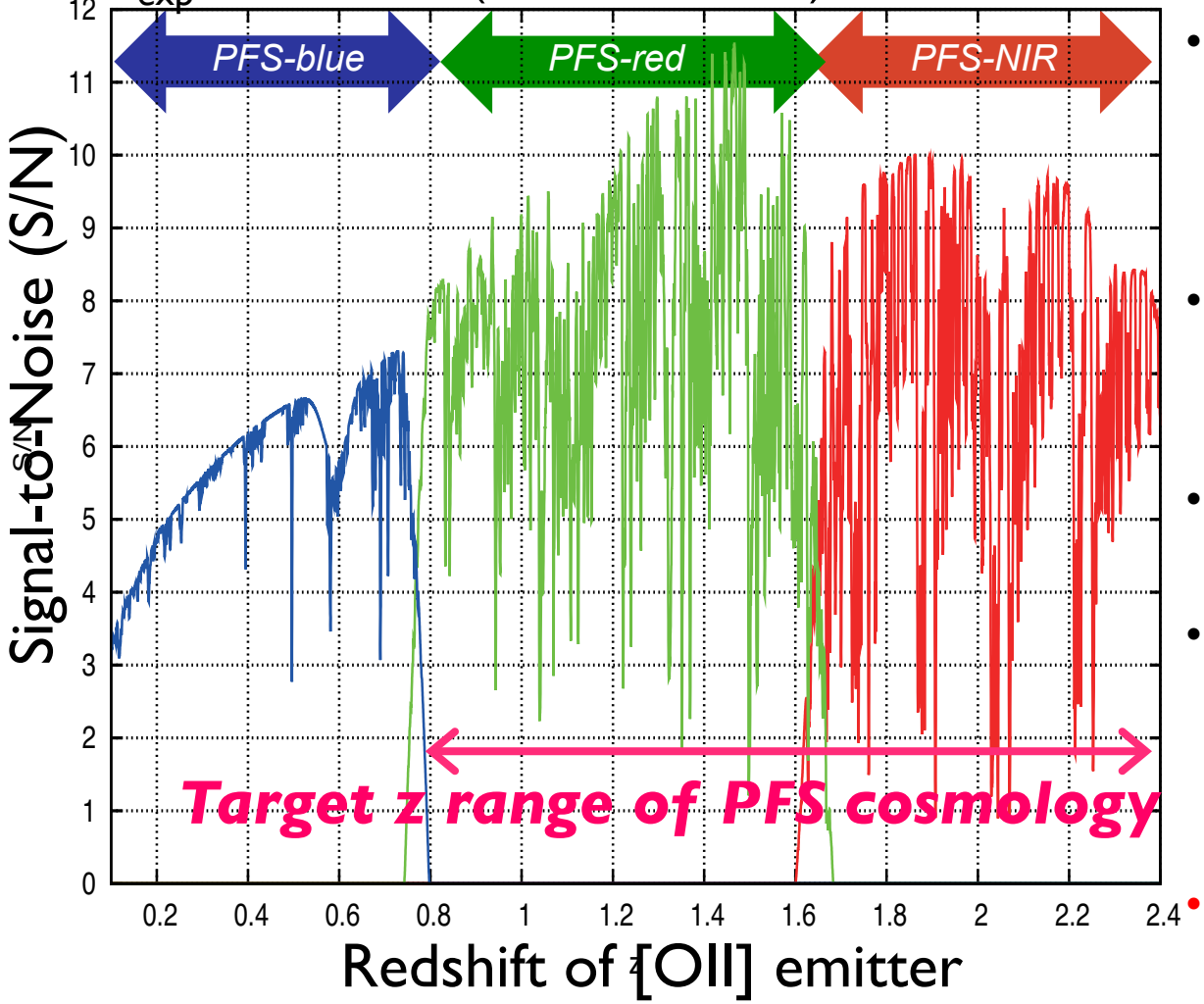

- [OII] line (3727Å) feature used for cosmology survey
- Assuming baseline instrument parameters (fiber size, throughput, readout noise, etc.)
- *Conservative assumption*: 0.8" seeing, at FoV edge, 26 deg. zenith angle
- *Included sky continuum & OH lines*
- The PFS design allows a matched S/N in Red and NIR arms → a wide redshift coverage, **0.8<z<2.4**
- LSS more linear at higher *z*

Target selection of [OII] emitters

- Mock Catalog, based on the COSMOS 30 bands, zCOSMOS and DEEP2 (Jouvel et al. 2009, + further updates)
- The wide z-range allows an efficient target selection based on the color cut:

$$22.8<g<24.2 \ \& \ -0.1<g-r<0.3$$

- 7847 targets per the PFS FoV (1.3 deg. diameter)~ 3×(# of PFS fibers)
- ~75% success rate for 2 visits of each field

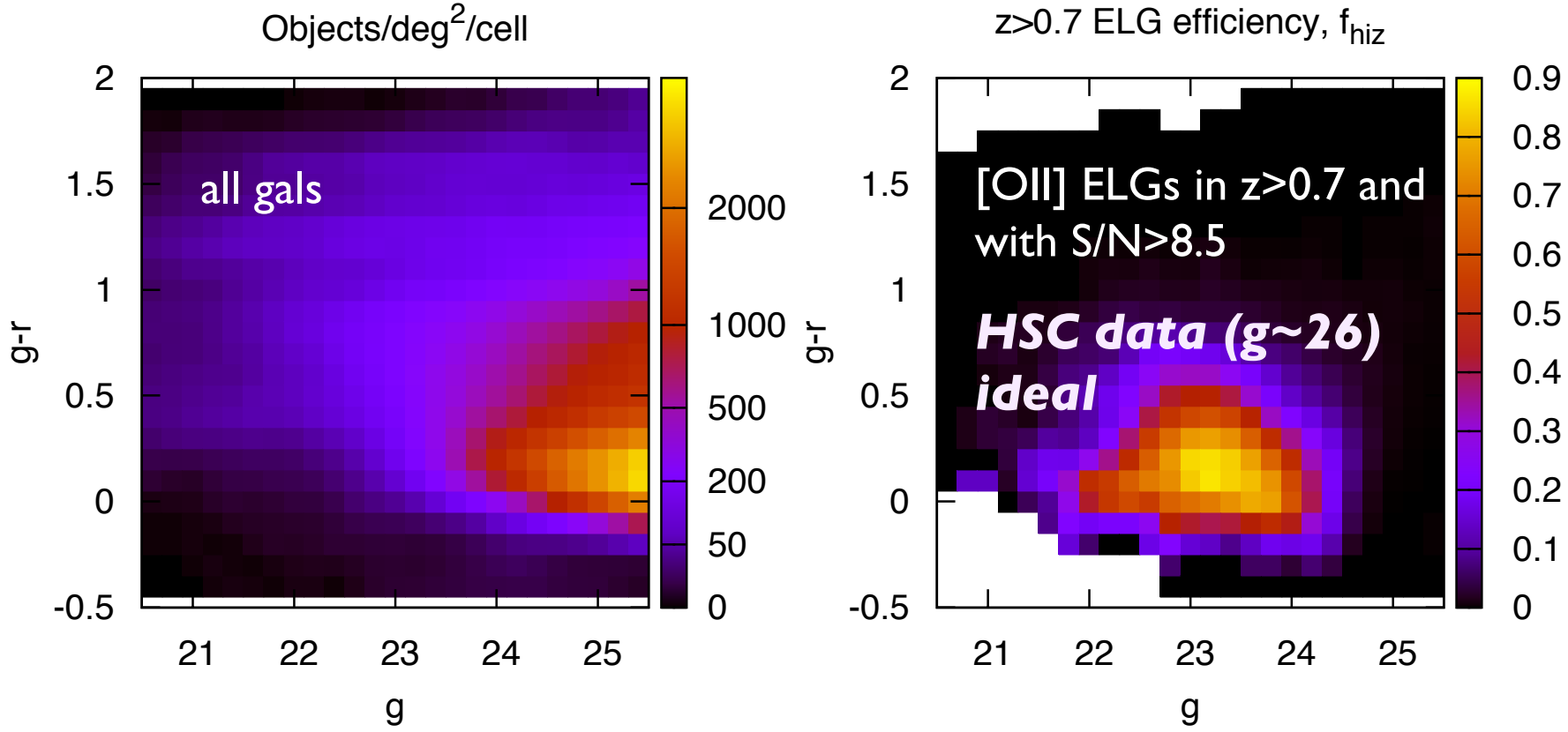

PFS Cosmology Survey

- Assume 100 clear nights to meet the scientific goals → the area of PFS survey

$$\frac{100[\text{nights}]\times 8[\text{hours}]\times 60[\text{min}]}{2[\text{visits}]\times(15[\text{min}]+3[\text{min}])}\times 1.098[\text{sq. deg. FoV}]=1464\ \text{sq. deg.}$$

Redshift	V_{survey} (h^{-3} Gpc^3)	# of galaxies (per FoV)	n_g ($10^{-4}\,h^3$ Mpc^{-3})	bias	$n_gP(k)$ @k=0.1hMpc^{-1}
0.8<z<1.0	0.79	358	6.0	1.26	2.23
1.0<z<1.2	0.96	420	5.8	1.34	2.10
1.2<z<1.4	1.09	640	7.8	1.42	2.64
1.4<z<1.6	1.19	491	5.5	1.5	1.78
1.6<z<2.0	2.58	598	3.1	1.62	0.95
2.0<z<2.4	2.71	539	2.7	1.78	0.76

- The total volume: ~9 (Gpc/h)3 ~ 2 × BOSS survey
- Assumed galaxy bias (poorly known): b=0.9+0.4z
- PFS survey will have $n_gP(k)$~a few@k=0.1Mpc/h in each of 6 redshift bins

Expected BAO constraints

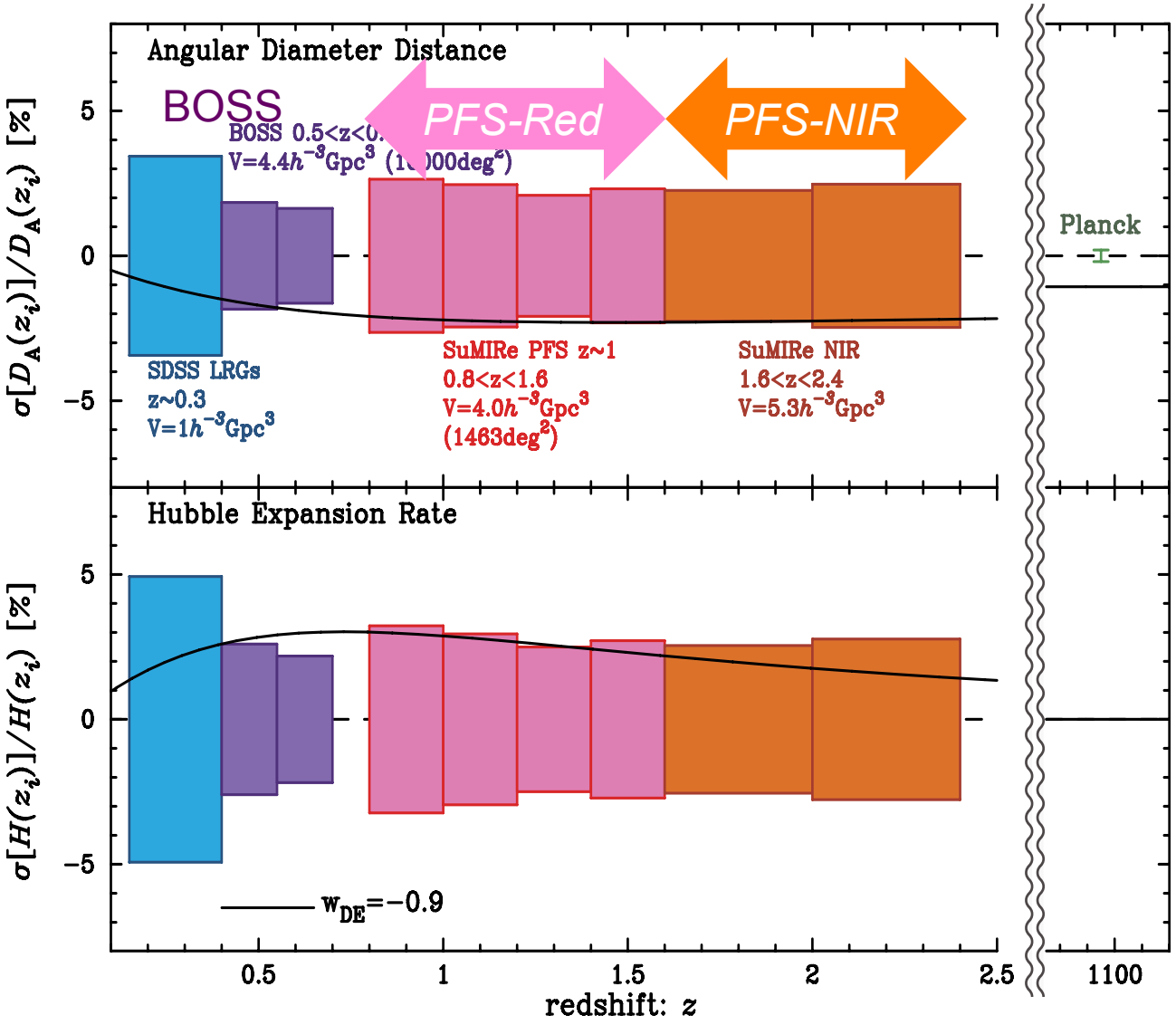

- The PFS cosmology survey enables a *3%* accuracy of measuring $D_A(z)$ and $H(z)$ in each of 6 redshift bins, over $0.8<z<2.4$
- This accuracy is *comparable* with BOSS, but extending to higher redshift range
- Also very efficient given competitive situation
  - BOSS (2.5m): 5 yrs
  - PFS (8.2m): 100 nights

Model-independent DE reconstruction

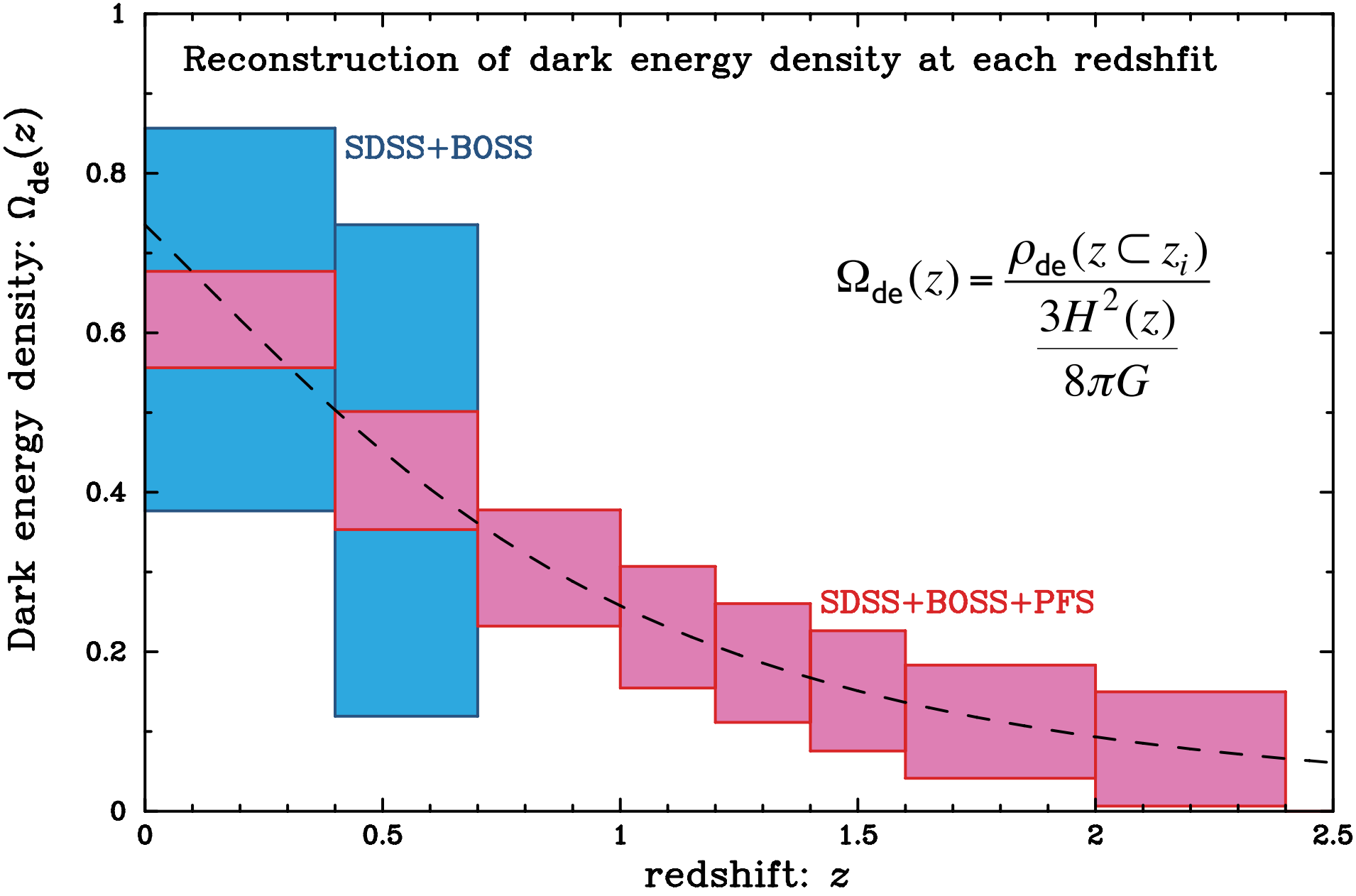

PFS vs. BigBOSS

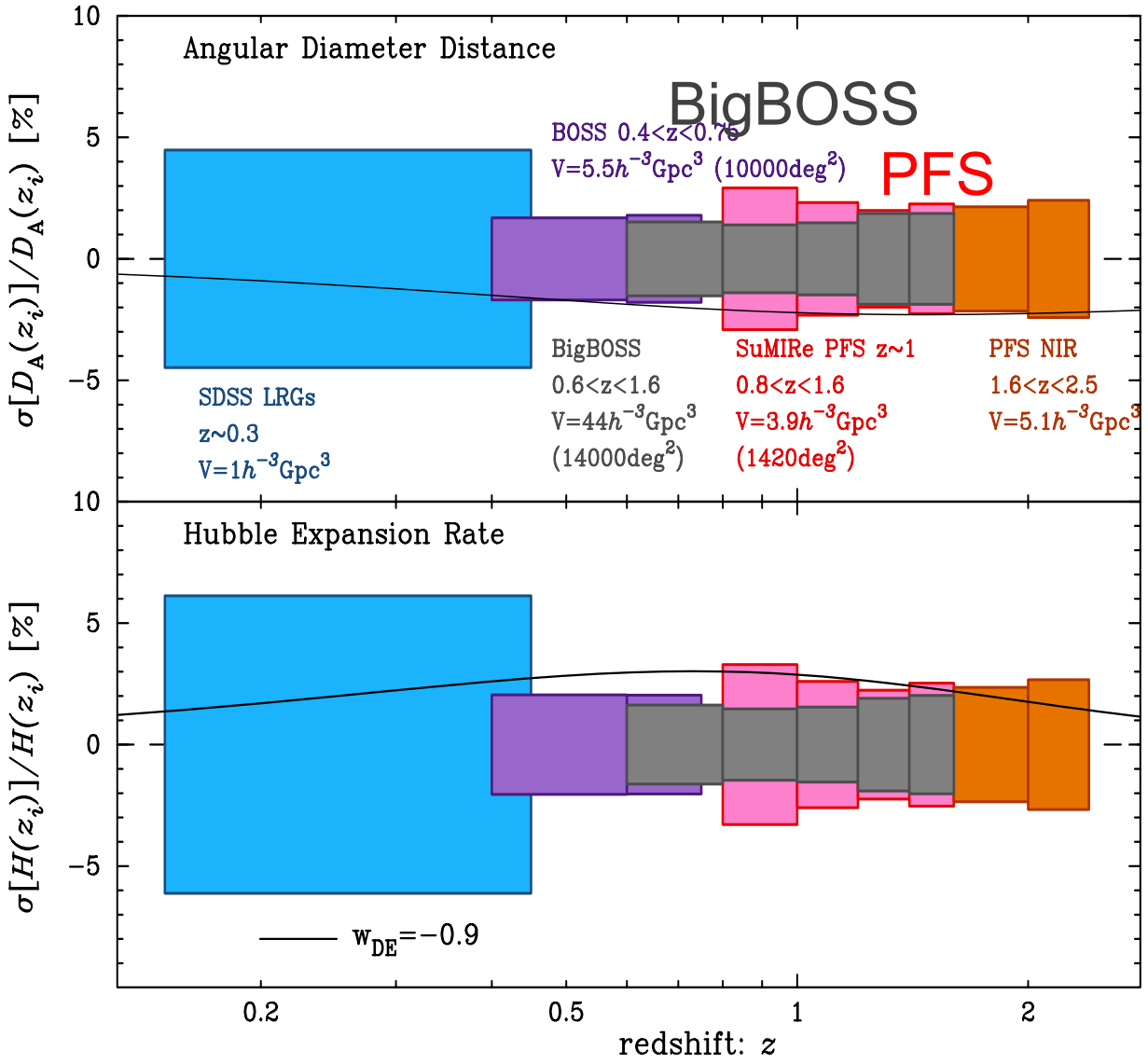

- 500 vs. 100 nights
- 14000 vs. 1420 sq. deg.
- BAO constraints; BigBOSS a factor 3 more powerful than PFS?

- *No! PFS has a comparable power with BigBOSS in z=1.2-1.6, also probes the new z-range*

Expected growth rate constraints

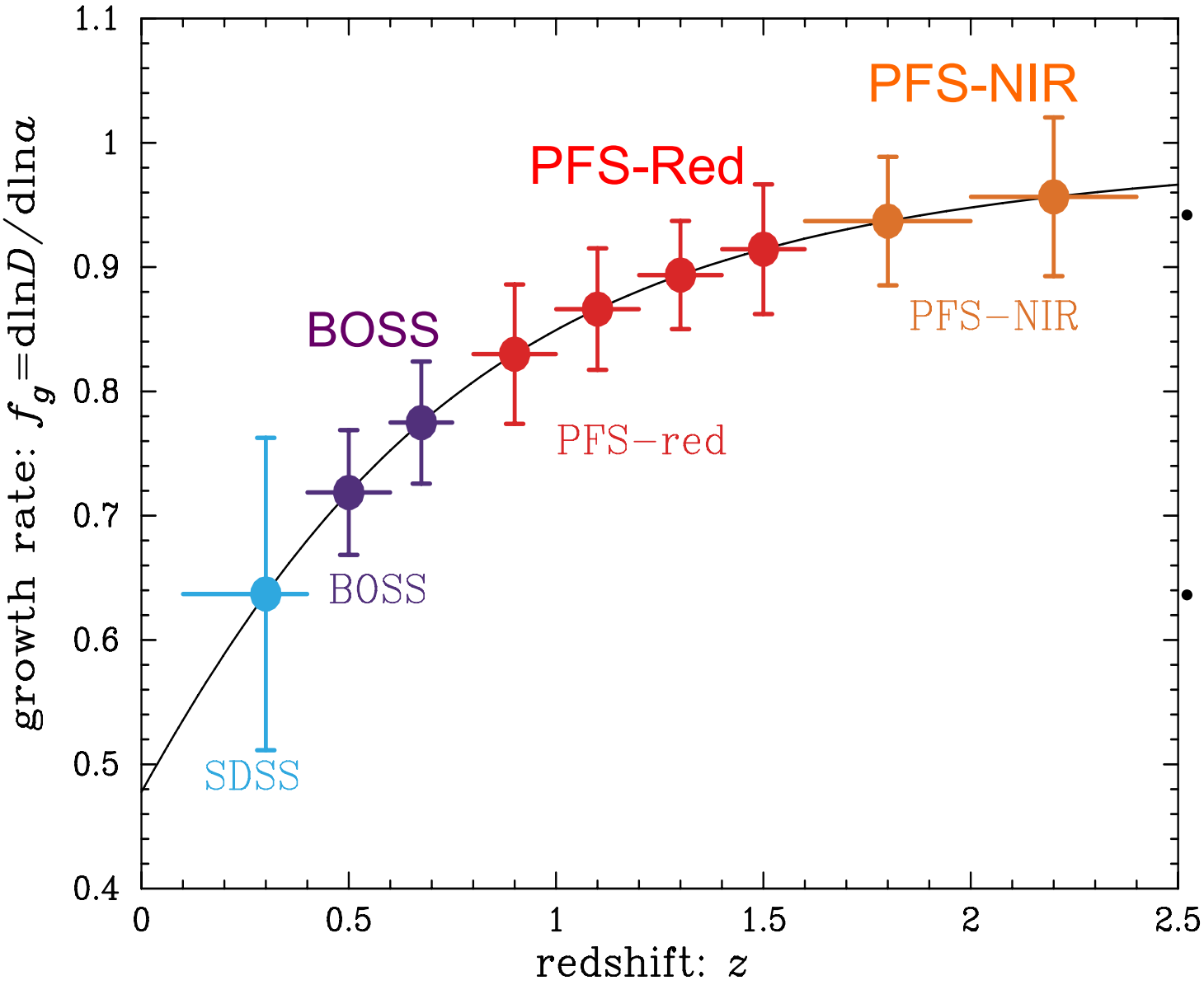

- The PFS survey design allows a 5% accuracy of constraining the growth rate in each redshift (each of 6 bins)
- Again complementary to BOSS

SuMIRe: HSC+PFS forecast

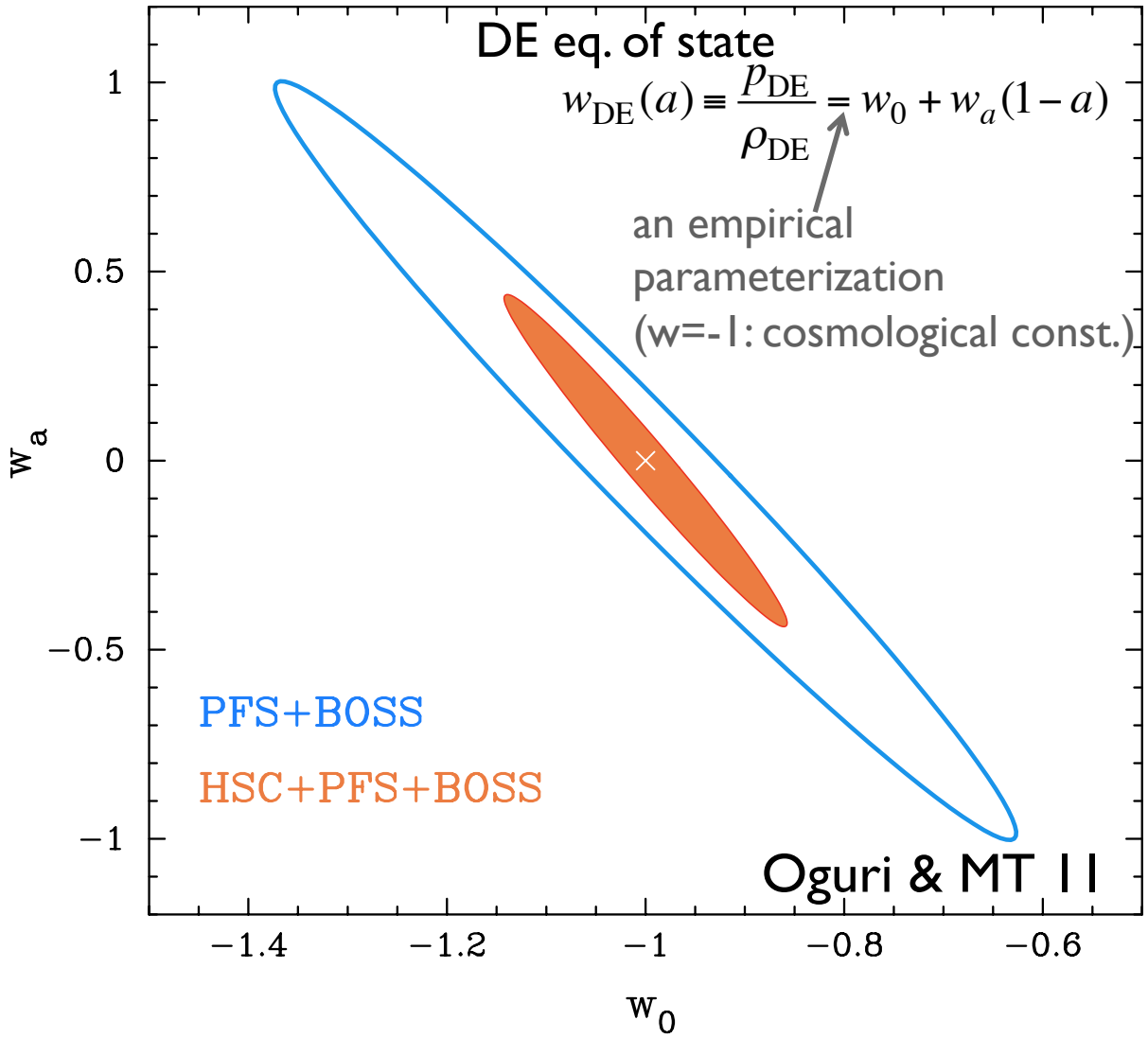

- Improves the dark energy FoM by a factor of 6 from either alone of the two
- σ(w_const)=0.02: equivalent to Stage-IV DE experiment
- There are more rooms to explore the synergy (not yet fully explored in the literature)
- Calibration issues of various systematics in each imaging and spectroscopic surveys

Cosmology frontier survey needs *help* from theory people!

- Need to resolve *many* issues in both theory and observation
- *New* ideas can be tested with upcoming data sets (SuMIRe in particular)
- Japan is *behind* observational cosmology (theory is stronger in Japan)
- *A big chance/opportunity* for Japanese community to *make a leap* to the *world frontier*
- *Discovery channels (hope serendipitous discoveries as in SK)*

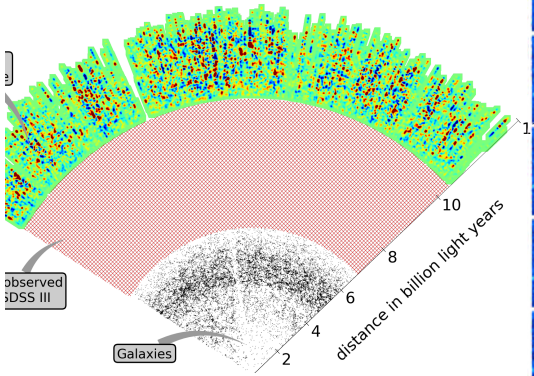

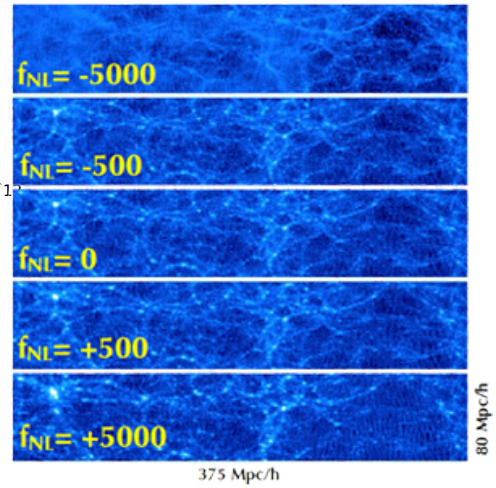

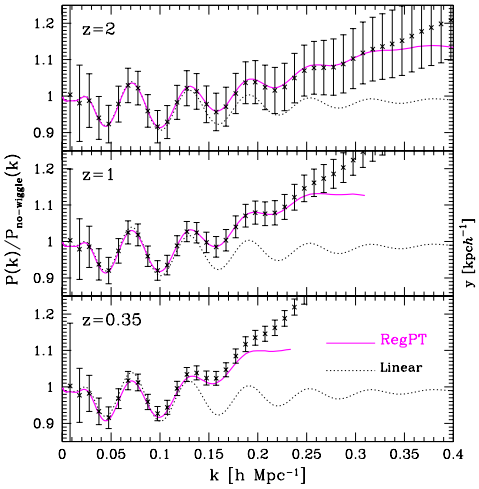

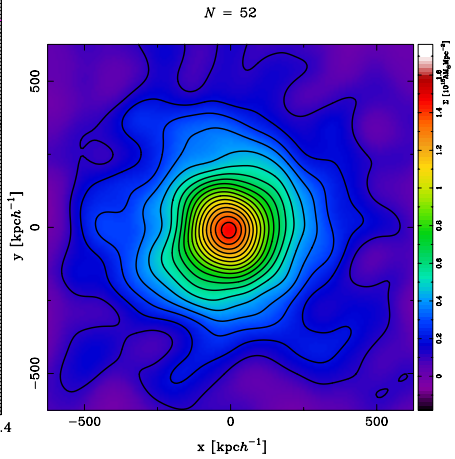

Current obs. cosmology driven by data

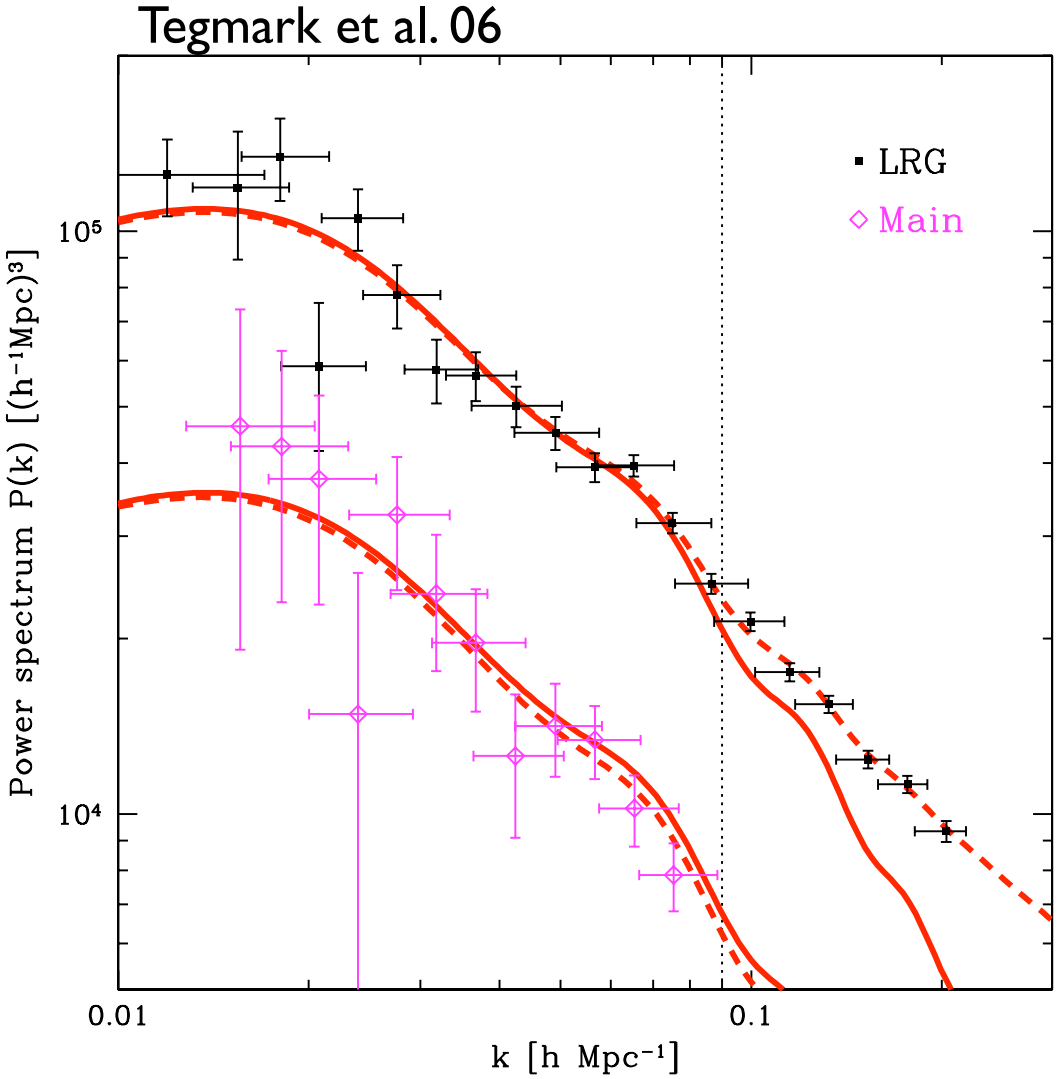

$$P_g(k) = b^2 P_m^L(k) \frac{1 + Q_{\rm nl} k^2}{1 + 1.4k}$$

- The high-precision measurements/data available
- Empirical models often used
- Data is more advanced than the accuracy of model

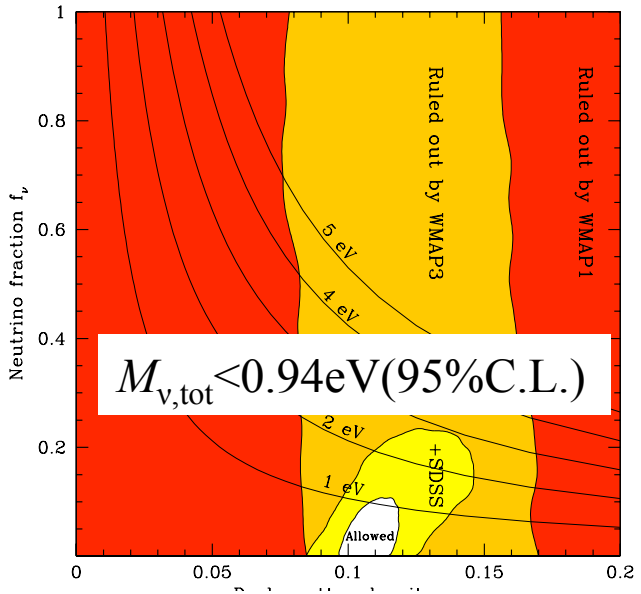

New development in modeling nonlinear power spectrum

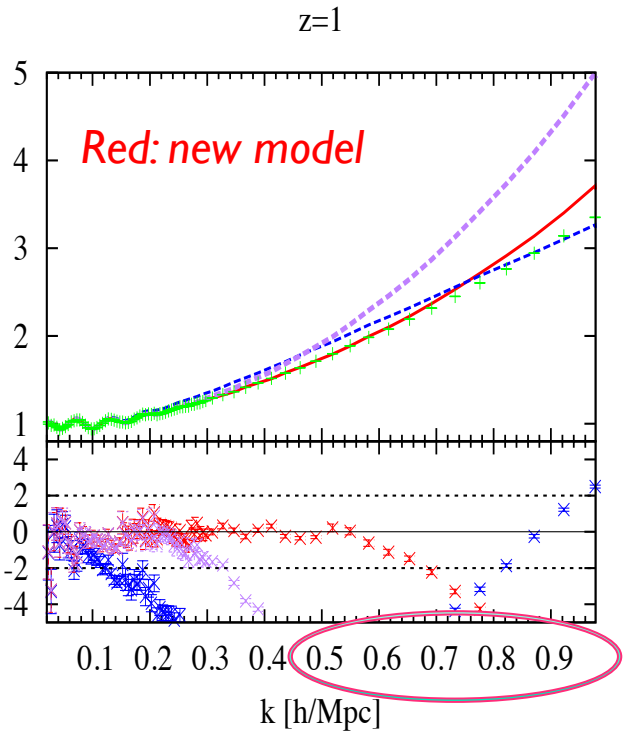

Sugiyama & Futamase 12

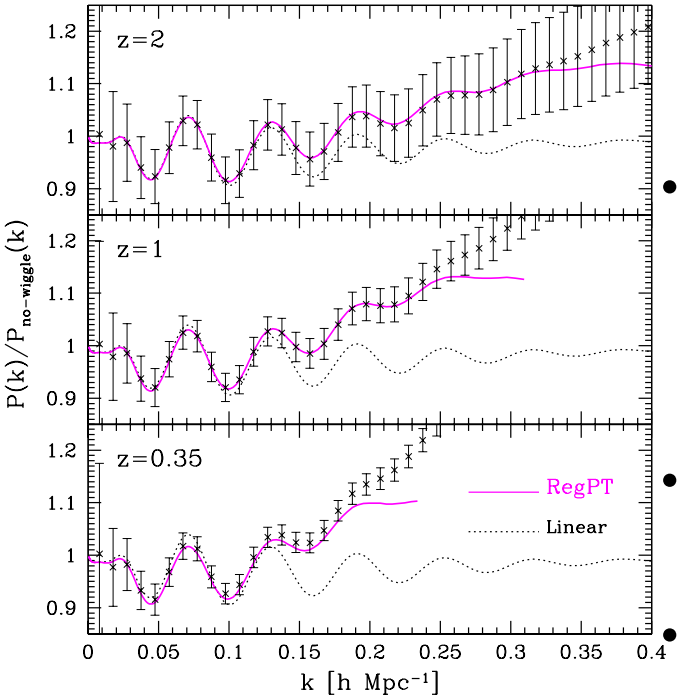

Taruya et al. 12
(also see Matsubara 08…)

- Various new methods to compute nonlinear power spectra have revisited
- Good examples; new ideas from theory people help! (for analysis/interpretation)
- The field led by many Japanese cosmologists
- Based on pioneer works; Kodama & Sasaki (84), Suto & Sasaki (91), Makino, Suto & Sasaki (92)

Summary

- SuMIRe = Subaru Measurement of Images and Redshifts
  - Unique capabilities of 8.2m Subaru Telescope (other projects all 4m-class telescopes besides LSST)
- Hyper Suprime-Cam Survey (HSC) = imaging of 1B gals
  - Start the wide-area survey from around Aug 2013 for 5 years
  - Use WL to recover the DM distribution up to z~1
- Prime Focus Spectrograph (PFS) = redshifts of 4M gals
  - Start the wide area survey from around 2018 for 5 years
  - Baryon Acoustic Oscillations to measure the cosmic expansion rate
- Imaging + spectroscopic survey is a very powerful combination
  - Cosmology: DE, DM, neutrino masses, curvature, inflation models (f_NL)
  - Not only for cosmology, also for galaxy evolution, the origin of Milky Way
- Great opportunities for young cosmologists to jump into, to "test" your models/ideas

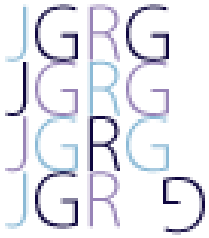

Luc Blanchet, JGRG 22(2012)111503

"The first law of binary black hole dynamics"

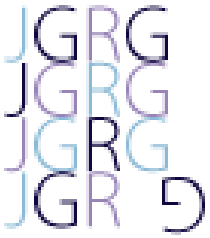

RESCEU SYMPOSIUM ON

GENERAL RELATIVITY AND GRAVITATION

JGRG 22



November 12-16 2012

Koshiba Hall, The University of Tokyo, Hongo, Tokyo, Japan



INSTITUT D'ASTROPHYSIQUE DE PARIS
Unité mixte de recherche 7095 CNRS - Université Pierre et Marie Curie

FIRST LAW OF BINARY BLACK HOLE DYNAMICS

dedicated to the 60th birthday of
Toshi Futamase, Hideo Kodama, Misao Sasaki

Luc Blanchet

Gravitation et Cosmologie ($\mathcal{GR}\varepsilon\mathbb{C}\mathcal{O}$)
Institut d'Astrophysique de Paris

15 novembre 2012

Four Laws of Black Hole Dynamics

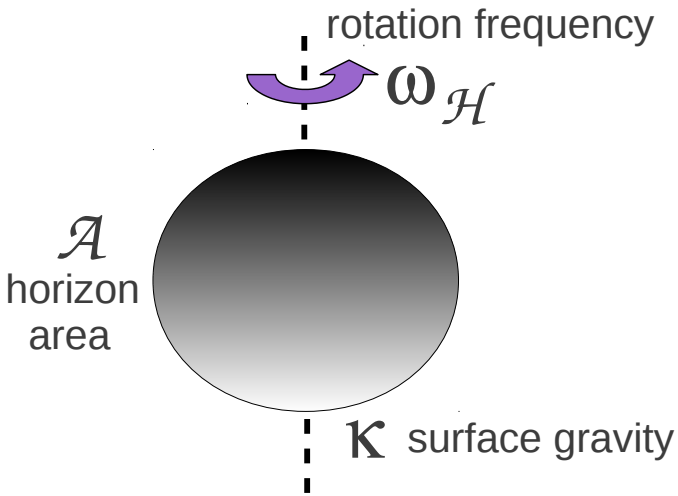

ZEROTH LAW

Surface gravity κ is constant over the horizon of a stationary black hole

FIRST LAW

Mass M and angular momentum J of BH change according to [Bardeen, Carter & Hawking 1973]

$$\delta M - \omega_{\mathcal{H}}\, \delta J = \frac{\kappa}{8\pi} \delta \mathcal{A}$$

SECOND LAW

In any physical process involving one or several BHs with or without an environment [Hawking 1971]

$$\delta A \geqslant 0$$

THIRD LAW

It is impossible to achieve $\kappa = 0$ in any process

Four Laws of Black Hole Dynamics

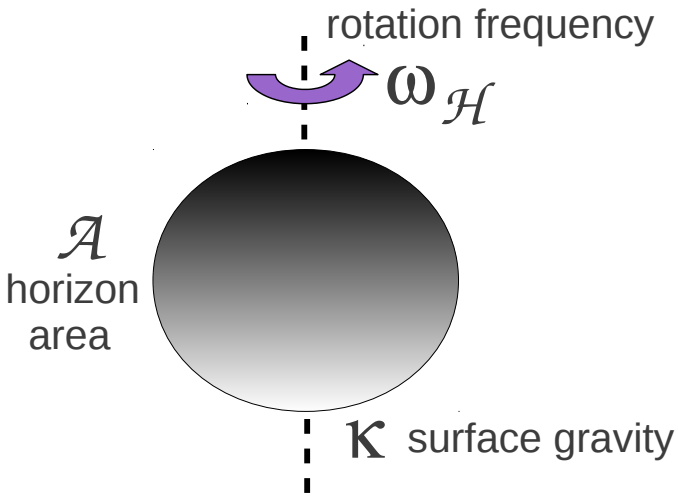

ZEROTH LAW

Surface gravity κ is constant over the horizon of a stationary black hole

FIRST LAW

Mass M and angular momentum J of BH change according to [Christodoulou 1970, Smarr 1973]

$$M - 2\omega_{\mathcal{H}} J = \frac{\kappa}{4\pi}\mathcal{A}$$

SECOND LAW

In any physical process involving one or several BHs with or without an environment [Hawking 1971]

$$\delta A \geqslant 0$$

THIRD LAW

It is impossible to achieve $\kappa = 0$ in any process

Fourty Years of BH Thermodynamics [Bekenstein 1972, Hawking 1976]

- Using arguments involving a piece of matter with entropy thrown into a BH, Bekenstein derived the BH entropy

$$S_{\rm BH} = \alpha \, \mathcal{A}$$

  This would require $T_{\rm BH} = \frac{\kappa}{8\pi\alpha}$ but the thermodynamic temperature of a *classical* BH is absolute zero since a BH is a perfect absorber
- However Hawking proved that *quantum* particle creation effects near a BH result in a black body temperature $T_{\rm BH} = \frac{\kappa}{2\pi}$. This leads to the famous

Bekenstein-Hawking entropy of a stationary black hole

$$S_{\rm BH} = \frac{c^3 k}{\hbar G} \frac{\mathcal{A}}{4}$$

The analogy between BH dynamics and the laws of thermodynamics is complete

Toward a Generalized First Law for a System of BHs

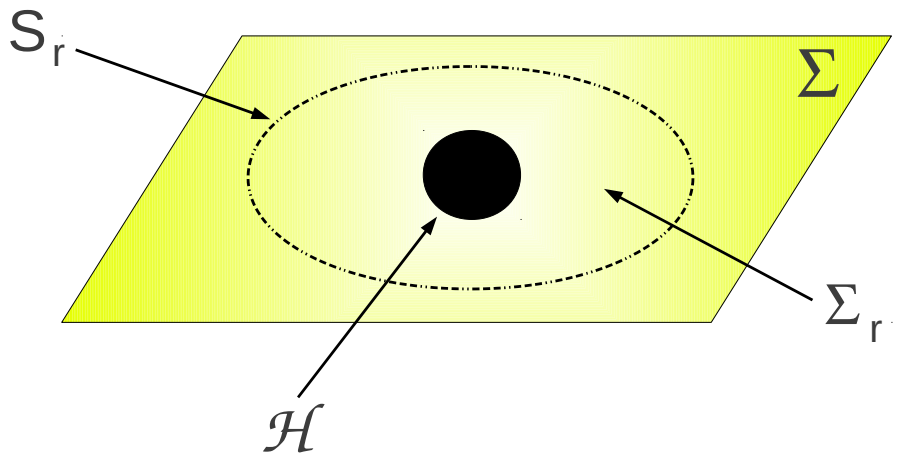

- The mass and the angular momentum of the BH are given by Komar surface integrals at spatial infinity

$$M = -\frac{1}{8\pi} \lim_{r\to\infty} \oint_{S_r} \nabla^\mu t^\nu \, \mathrm{d}S_{\mu\nu}$$

$$J = \frac{1}{16\pi} \lim_{r\to\infty} \oint_{S_r} \nabla^\mu \phi^\nu \, \mathrm{d}S_{\mu\nu}$$

where t^μ and ϕ^μ are the two stationary and axi-symmetric Killing vectors

Toward a Generalized First Law for a System of BHs

- The first law of BH dynamics expresses the change

$$\delta Q = \delta M - \omega_{\mathcal{H}}\, \delta J$$

in the Noether charge Q between two nearby BH configurations, where Q is associated with the Killing vector

$$K^\mu = t^\mu + \omega_{\mathcal{H}}\, \phi^\mu$$

which is the null generator of the BH horizon

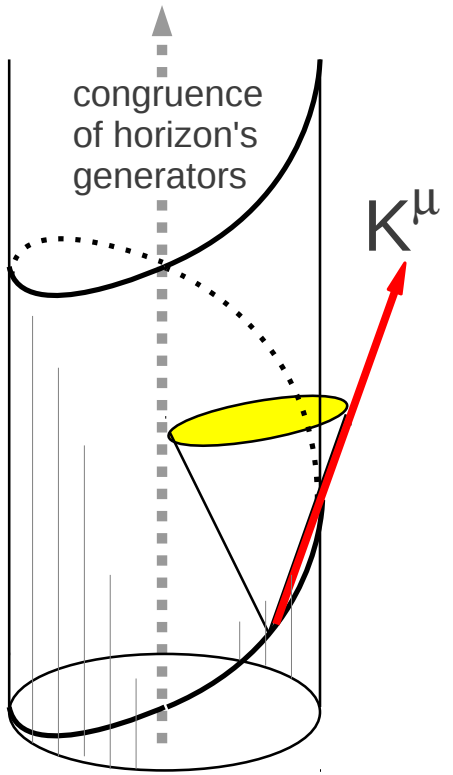

Toward a Generalized First Law for a System of BHs

- A generalized First Law valid for systems of BHs can be obtained when the geometry admits a Helical Killing Vector (HKV)

$$K^\mu \partial_\mu = \partial_t + \Omega\, \partial_\varphi$$

  where ∂_t is time-like and ∂_φ is space-like (with closed orbits), even when ∂_t and ∂_φ are not separately Killing vectors
- This applies to the case of two Kerr BHs moving on exactly circular orbits with orbital frequency Ω
- The two BHs should be in corotation, so that $\omega_{\mathcal{H}}$ should approximately be equal to Ω. In particular the spins should be aligned with the orbital angular momentum

Toward a Generalized First Law for a System of BHs

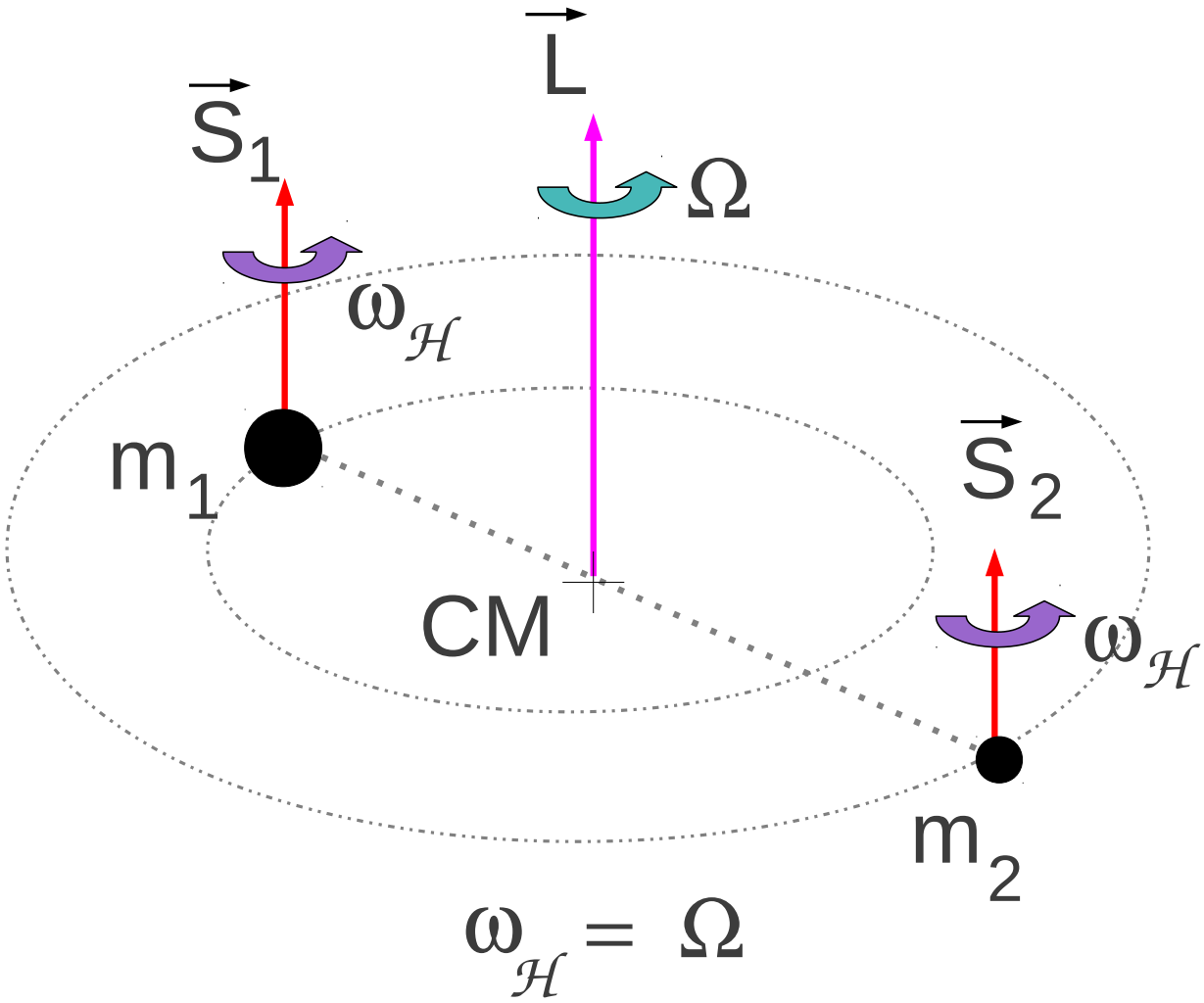

Toward a Generalized First Law for a System of BHs

1. With the Helical Killing Vector $K^\mu \partial_\mu = \partial_t + \Omega\, \partial_\varphi$ the change in the associated Noether charge is given by

$$\delta Q = \delta M - \Omega\, \delta J$$

   provided that the space-time is asymptotically flat [Friedman, Uryū & Shibata 2002]

2. However exact solutions of the Einstein field equations with Helical Killing symmetry cannot be asymptotically flat since they are periodic which contradicts the decrease of the Bondi mass at $\mathcal{J}^+$ [Gibbons & Stewart 1983]

Toward a Generalized First Law for a System of BHs

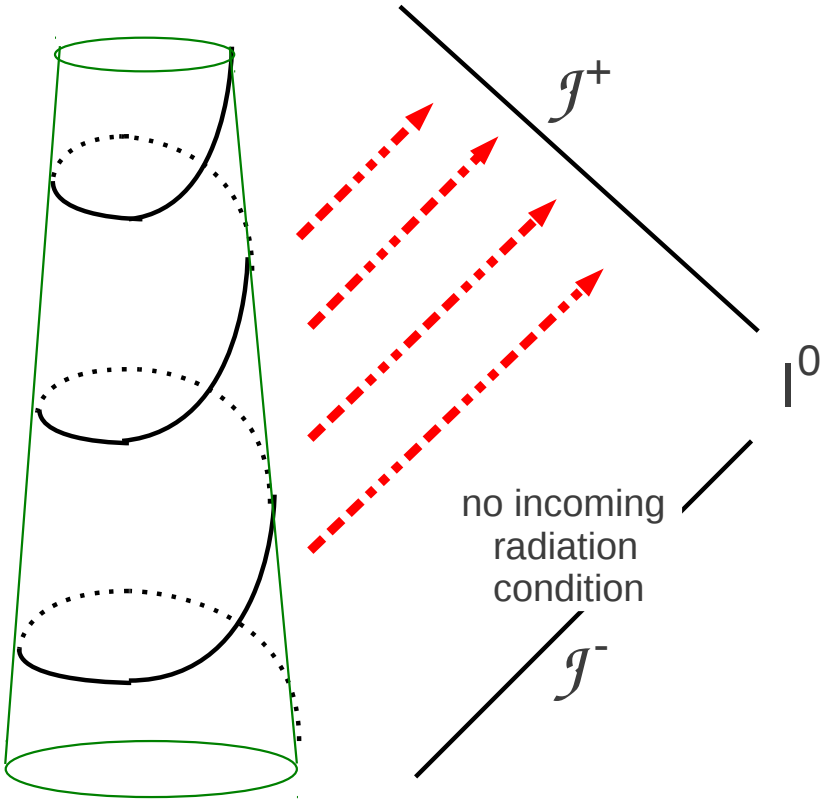

Physical situation

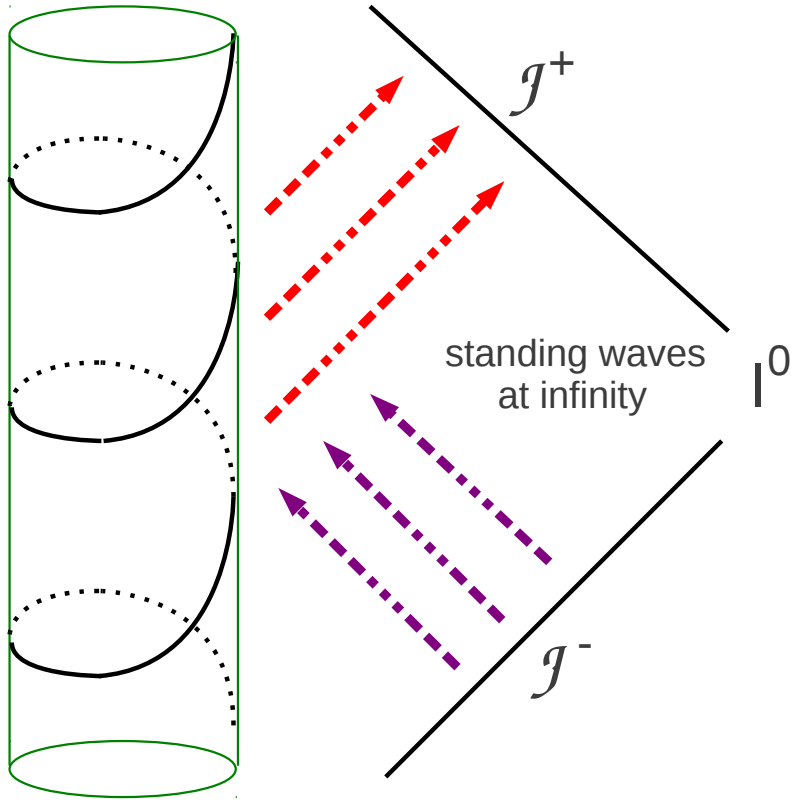

Situation with the HKV

Looking at the Conservative Part of the Dynamics

- One way to deal with the problem is to look at approximate solutions which are asymptotically flat. A possible solution is to suppress radiation degrees of freedom by imposing a condition of conformal flatness for the spatial metric
  [Isenberg & Nester 1980; Wilson & Mathews 1989]

- Here we follow a different route which is to consider only the conservative part of the dynamics in a post-Newtonian (PN) expansion, neglecting the dissipative effects due to the emission of gravitational radiation

- Thus we derive the First Law for a class of conservative PN space-times admitting a HKV and describing point particles (possibly with spins) moving on an exactly circular orbit

Two Point Particles on an Exactly Circular Orbit

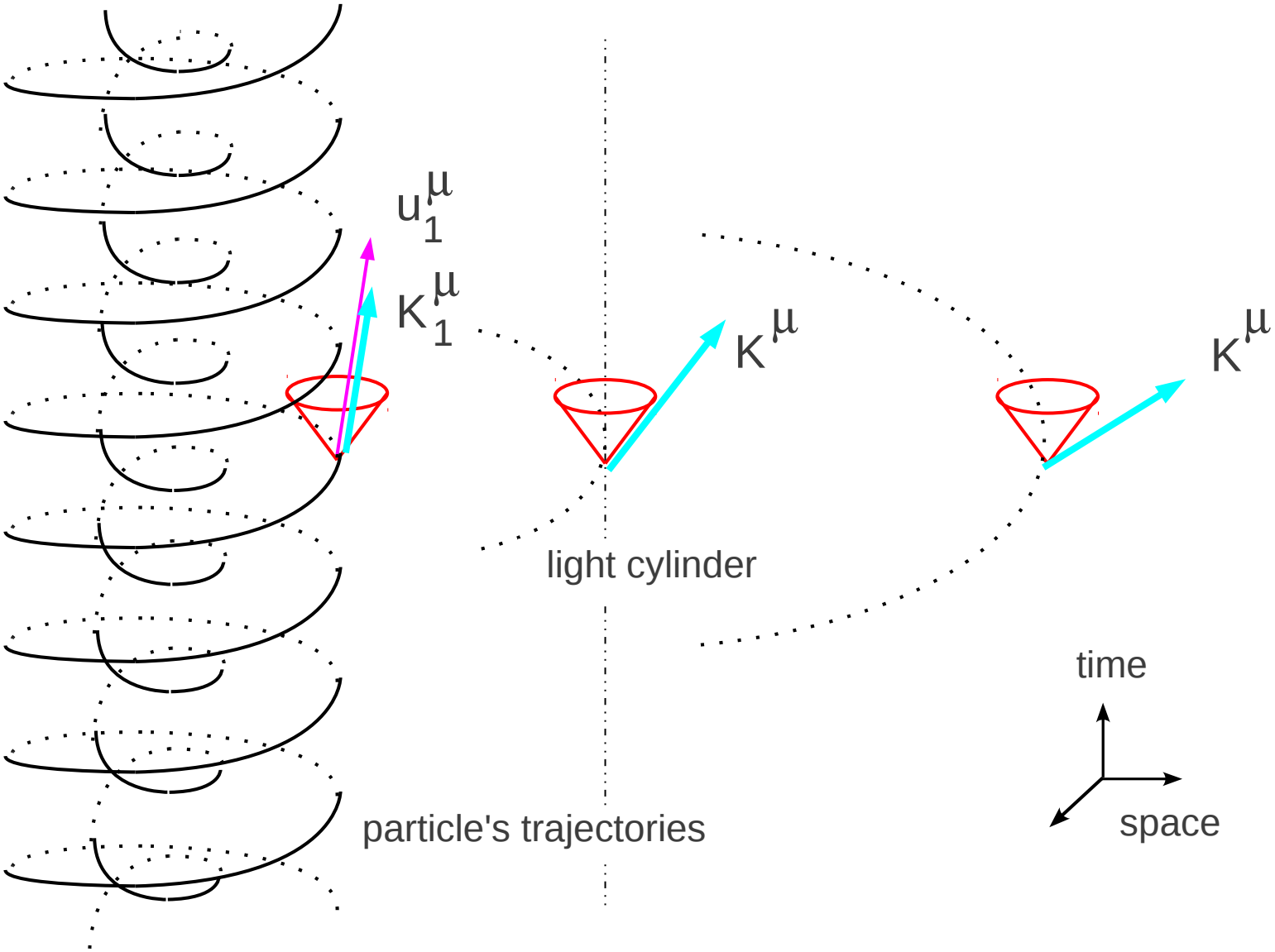

Conservative versus Dissipative Dynamics in PN theory

- Internal acceleration of a matter system is written as a formal PN expansion

$$\frac{\mathrm{d}\mathbf{v}}{\mathrm{d}t} = \mathbf{A}_{\mathrm{N}} + \frac{1}{c^2}\mathbf{A}_{\mathrm{1PN}} + \frac{1}{c^4}\mathbf{A}_{\mathrm{2PN}} + \frac{1}{c^5}\mathbf{A}_{\mathrm{2.5PN}} + \frac{1}{c^6}\mathbf{A}_{\mathrm{3PN}} + \frac{1}{c^7}\mathbf{A}_{\mathrm{3.5PN}} + \frac{1}{c^8}\mathbf{A}_{\mathrm{4PN}} + \mathcal{O}\left(\frac{1}{c^9}\right)$$

- Naive split would be to say that conservative effects are those which carry an even power of $1/c$, while dissipative effects, linked to gravitational radiation reaction, are those which carry an odd power of $1/c$

Conservative versus Dissipative Dynamics in PN theory

- This is correct at leading 2.5PN order where the force derives from a scalar in an appropriate gauge, $\mathbf{A}_{2.5\mathrm{PN}} = \boldsymbol{\nabla} V_{2.5\mathrm{PN}}$ with [Burke & Thorne]

$$V_{2.5\mathrm{PN}}(\boldsymbol{x},t) = -\frac{1}{5}\, x^i x^j I^{(5)}_{ij}(t)$$

  This term would change sign if we change the prescription of retarded potentials to the advanced potentials

- This is still correct at sub-leading order 3.5PN where the force involves both scalar and vector potentials given by [Blanchet 1997]

$$\begin{aligned} V_{3.5\mathrm{PN}} &= \frac{1}{189} x^i x^j x^k I^{(7)}_{ijk}(t) - \frac{1}{70} \boldsymbol{x}^2 x^i x^j I^{(7)}_{ij}(t) \\ V^i_{3.5\mathrm{PN}} &= \frac{1}{21} x^{\langle i} x^j x^{k\rangle} I^{(6)}_{jk}(t) - \frac{4}{45} \varepsilon_{ijk} x^j x^l J^{(5)}_{kl}(t) \end{aligned}$$

  which also change sign from retarded to advanced potentials

Dissipative Tail Effect in the PN Dynamics

However the naive split fails starting at 4PN order because of the appearance of tails in the radiation reaction force [Blanchet & Damour 1988]

$$V_{\rm 4PN} = -\frac{4M}{5}\, x^i x^j \int_{-\infty}^{t} \mathrm{d}t'\, I_{ij}^{(7)}(t') \ln\left(\frac{t-t'}{2r}\right)$$

This term is not invariant when we go from retarded to advanced potentials

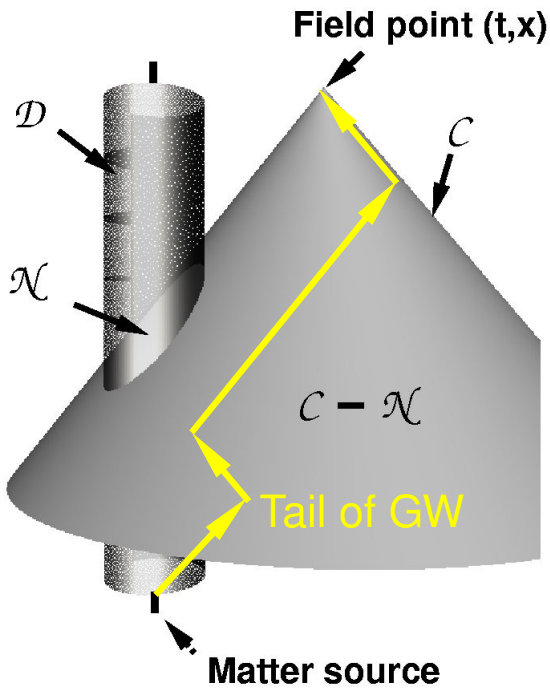

Logarithms at 4PN order in the Conservative Dynamics

With the HKV we have at our disposal the binary's orbital period $P = 2\pi/\Omega$. We split

$$\ln\left(\frac{t-t'}{2r}\right) = -\ln\left(\frac{r}{P}\right) + \ln\left(\frac{t-t'}{2P}\right)$$

Tails produce a conservative 4PN logarithmic term

$$V_{\rm 4PN} = -\frac{4M^2}{5}\, x^i x^j \Bigg[\underbrace{-I^{(6)}_{ij}(t) \ln\left(\frac{r}{P}\right)}_{\text{conservative 4PN log term}} + \underbrace{\int_{-\infty}^{t} \mathrm{d}t'\, I^{(7)}_{ij}(t') \ln\left(\frac{t-t'}{2P}\right)}_{\text{dissipative term (neglected)}} \Bigg]$$

We shall see appearing at 4PN and higher orders like 5PN some logarithmic contributions in the conservative part of the dynamics of binary black holes

Short History of the PN Approximation

Equations of motion

- 1PN equations of motion [Lorentz & Droste 1917; Einstein, Infeld & Hoffmann 1938]
- Radiation-reaction controvercy [Ehlers *et al* 1979; Walker & Will 1982]
- 2.5PN equations of motion and GR prediction for the binary pulsar [Damour & Deruelle 1982; Damour 1983]
- The "3mn" Caltech paper [Cutler, Flanagan, Poisson & Thorne 1993]
- 3.5PN equations of motion [Jaranowski & Schäfer 1999; BF 2001; ABF 2002; BI 2003; Itoh & Futamase 2003, Foffa & Sturani 2011]
- Ambiguity parameters resolved [DJS 2001; BDE 2003]

Radiation field

- 1918 Einstein quadrupole formula
- 1940 Landau-Lifchitz formula
- 1960 Peters-Mathews formula
- EW moments [Thorne 1980]
- BD moments and wave generation formalism [BD 1989; B 1995, 1998]
- 1PN phasing [Wagoner & Will 1976; BS 1989]
- Test-particle limit using BH perturbations [Tagoshi & Sasaki 1994]
- 2PN waveform [BDIWW 1995]
- 3.5PN phasing and 3PN waveform [BFIJ 2003, BFIS 2007]
- Ambiguity parameters resolved [BI 2004; BDEI 2004, 2005]

The Gravitational Chirp of Compact Binaries

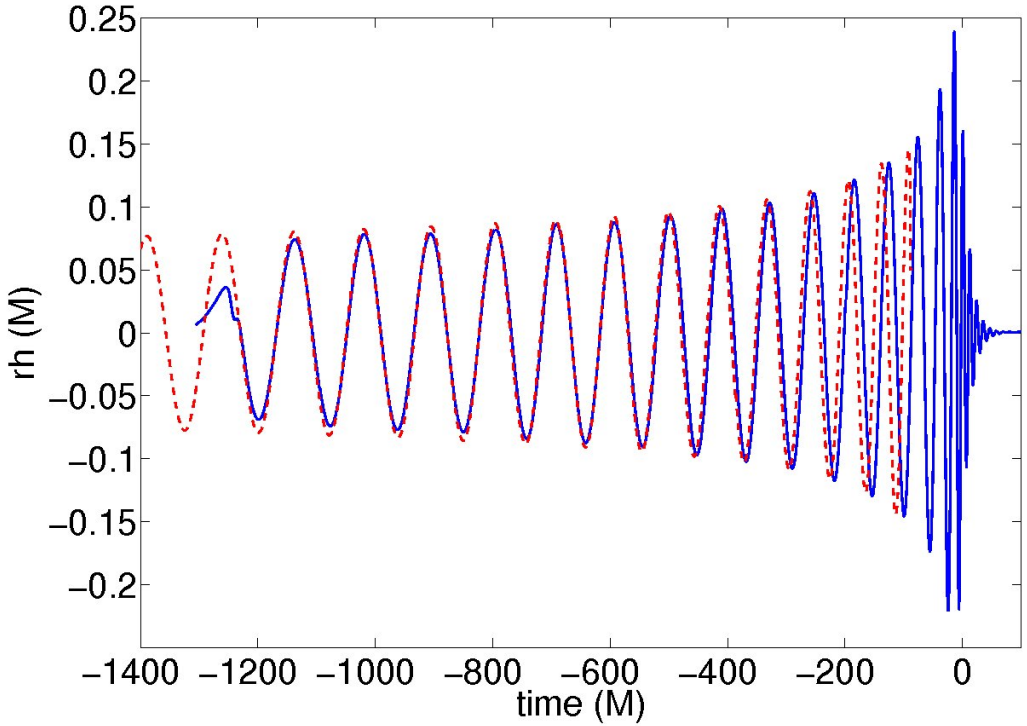

The waveform is obtained by matching a high-order post-Newtonian waveform describing the long inspiralling phase and a highly accurate numerical waveform describing the final merger and ringdown phases

3.5PN Equations of Motion of Compact Binary Systems

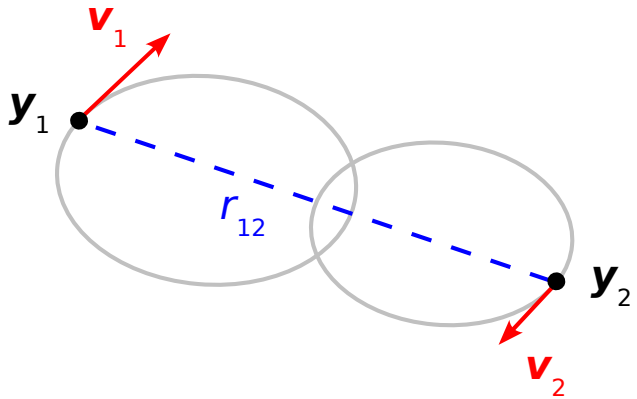

Explicit EOM for non-spinning compact binaries

$$\frac{\mathrm{d}v_1^i}{\mathrm{d}t} = -\frac{Gm_2}{r_{12}^2}n_{12}^i$$
$$+\overbrace{\frac{1}{c^2}\left\{\left[\frac{5G^2m_1m_2}{r_{12}^3}+\frac{4G^2m_2^2}{r_{12}^3}+\frac{Gm_2}{r_{12}^2}\left(\frac{3}{2}(n_{12}v_2)^2-v_1^2-2v_2^2\right)\right]n_{12}^i+\cdots\right\}}^{\text{1PN}}$$
$$+\underbrace{\frac{1}{c^4}[\cdots]}_{\text{2PN}}+\underbrace{\frac{1}{c^5}[\cdots]}_{\text{2.5PN}}+\underbrace{\frac{1}{c^6}[\cdots]}_{\text{3PN}}+\underbrace{\frac{1}{c^7}[\cdots]}_{\text{3.5PN}}+\mathcal{O}\left(\frac{1}{c^8}\right)$$

Spin effects arise at orders 1.5PN for the spin-orbit and 2PN for the spin-spin.

Mass and Angular Momentum of Compact Binaries

It is convenient tu use the gauge invariant PN parameter

$$x = \left(\frac{Gm\Omega}{c^3}\right)^{3/2}$$

with the mass parameters $m = m_1 + m_2$ and $\nu = m_1 m_2/m^2$.

Conservative PN energy for circular orbits

$$E = -\frac{1}{2}m\nu\left\{1 + \overbrace{\left(-\frac{3}{4} - \frac{\nu}{12}\right)x}^{\text{1PN}} + \overbrace{[\cdots]\,x^2}^{\text{2PN}} + \overbrace{[\cdots]\,x^3}^{\text{3PN}} + \overbrace{\left(\cdots + \frac{448}{15}\nu\ln x\right)x^4}^{\text{4PN}} + \overbrace{\left(\cdots + \left[-\frac{4988}{35} - 6565\nu\right]\nu\ln x\right)x^5}^{\text{5PN}} + \mathcal{O}\left(x^6\right)\right\}$$

The 4PN and 5PN conservative logarithmic terms have been computed recently

[Blanchet, Detweiler, Le Tiec & Whiting 2010]

Mass and Angular Momentum of Compact Binaries

The angular momentum J is checked to satisfy for all the terms up to 3PN order, and also for the 4PN and 5PN log terms, the

Thermodynamic relation valid for circular orbits

$$\frac{\partial M}{\partial \Omega} = \Omega \frac{\partial J}{\partial \Omega}$$

which constitutes the first ingredient in the First Law of binary black holes.

- The thermodynamic relation states that the flux of energy emitted in the form of gravitational waves is proportional to the flux of angular momentum
- It is used in numerical computations of the binary evolution based on a sequence of quasi-equilibrium configurations [Gourgoulhon *et al* 2002]

The Redshift Observable [Detweiler 2008]

- The geometry has a Helical Killing Vector (HKV) asymptotically given by

$$K^\mu \partial_\mu = \partial_t + \Omega\, \partial_\varphi$$

- The four-velocity u_1^μ of the particle must be proportional to the HKV at the location of the particle

$$K_1^\mu = z_1\, u_1^\mu$$

- In suitable coordinate systems z_1 reduces to the inverse of the zeroth component of the particle's velocity,

$$z_1 = \frac{1}{u_1^t} = \sqrt{-(g_{\mu\nu})_1\, v_1^\mu v_1^\nu}$$

- The relation $z_1(\Omega)$ is a well-defined observable which can be computed to high precision in PN theory

The Redshift Observable [Detweiler 2008]

- The redshift obervable was introduced in self-force computations of the motion of a particle around the black hole in the limit $m_1/m_2 \ll 1$
- It represents the redshift of light rays emitted by the particle and received at infinity along the symmetry axis

$$z_1 = \frac{(k_\mu u^\mu)_{\text{rec}}}{(k_\mu u^\mu)_{\text{em}}} = \frac{1}{u_1^t}$$

- This is also the Killing energy of the particle associated with the HKV

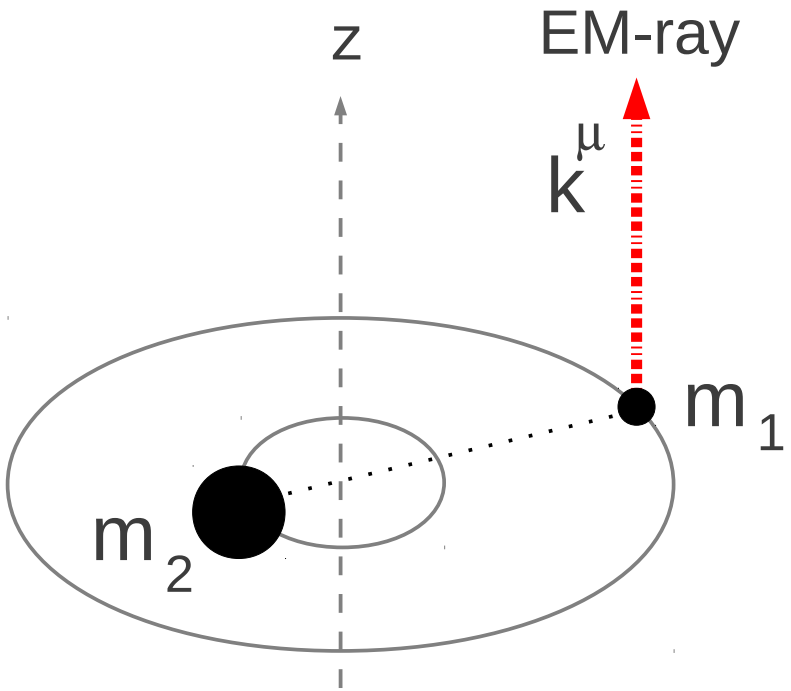

Post-Newtonian Computation of the Redshift Observable

The PN metric is to be evaluated at the location of one of the particles

$$z_1 = \left[- \underbrace{(g_{\mu\nu})_1}_{\text{regularized metric}} v_1^\mu v_1^\nu \right]^{1/2}$$

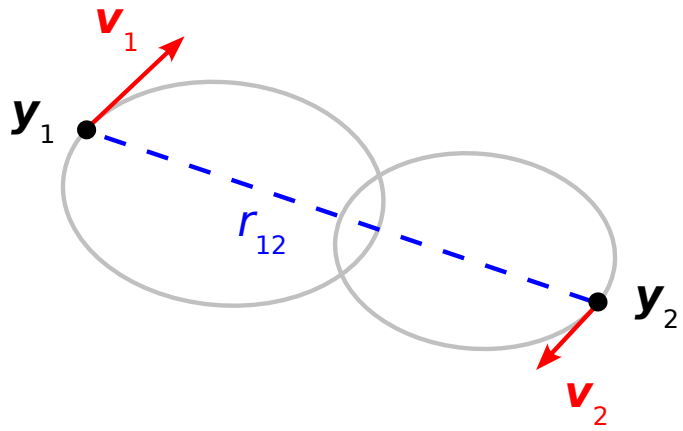

A self-field regularization is required

- Hadamard's regularization [Hadamard 1932; Schwartz 1978] is convenient but has been shown to yield ambiguities at the 3PN order
- Dimensional regularization ['t Hooft & Veltman 1972] is extremely powerful and is free of any ambiguity at 3PN order

High-order PN result for the Redshift Observable

[Blanchet, Detweiler, Le Tiec & Whiting 2010ab]

- Posing $X_1 = m_1/m$ and still $x = (Gm\Omega/c^3)^{3/2}$, the redshift observable of particle 1 through 3PN order and augmented by 4PN and 5PN logarithmic contributions is

$$z_1 = 1 + \left(-\frac{3}{2}X_1 + \frac{\nu}{2}\right)x + \overbrace{[\cdots]\,x^2}^{\text{1PN}} + \overbrace{[\cdots]\,x^3}^{\text{2PN}} + \overbrace{[\cdots]\,x^4}^{\text{3PN}} + \left(\cdots \underbrace{+\,[\cdots]\,\nu \ln x}_{\text{4PN log}}\right)x^5 + \left(\cdots \underbrace{+\,[\cdots]\,\nu \ln x}_{\text{5PN log}}\right)x^6 + \mathcal{O}\left(x^7\right)$$

- We can re-expand in the small mass-ratio limit $\nu = m_1 m_2/m^2 \ll 1$ so that

$$z_1 = z_{\rm Schw} + \underbrace{\nu\, z_{\rm SF}}_{\text{self-force}} + \underbrace{\nu^2\, z_{\rm PSF}}_{\text{post-self-force}} + \mathcal{O}(\nu^3)$$

High-order PN fit to the Numerical Self Force

- The 3PN prediction agrees with the SF value with 7 significant digits

3PN value	SF fit
$a_3 = -\frac{121}{3} + \frac{41}{32}\pi^2 = -27.6879026\cdots$	$-27.6879034 \pm 0.0000004$

- Post-Newtonian coefficients are fitted up to 7PN order

PN coefficient	SF value
a_4	$-114.34747(5)$
a_5	$-245.53(1)$
a_6	$-695(2)$
b_6	$+339.3(5)$
a_7	$-5837(16)$

Comparison with the Self-Force Prediction

[Blanchet, Detweiler, Le Tiec & Whiting 2010]

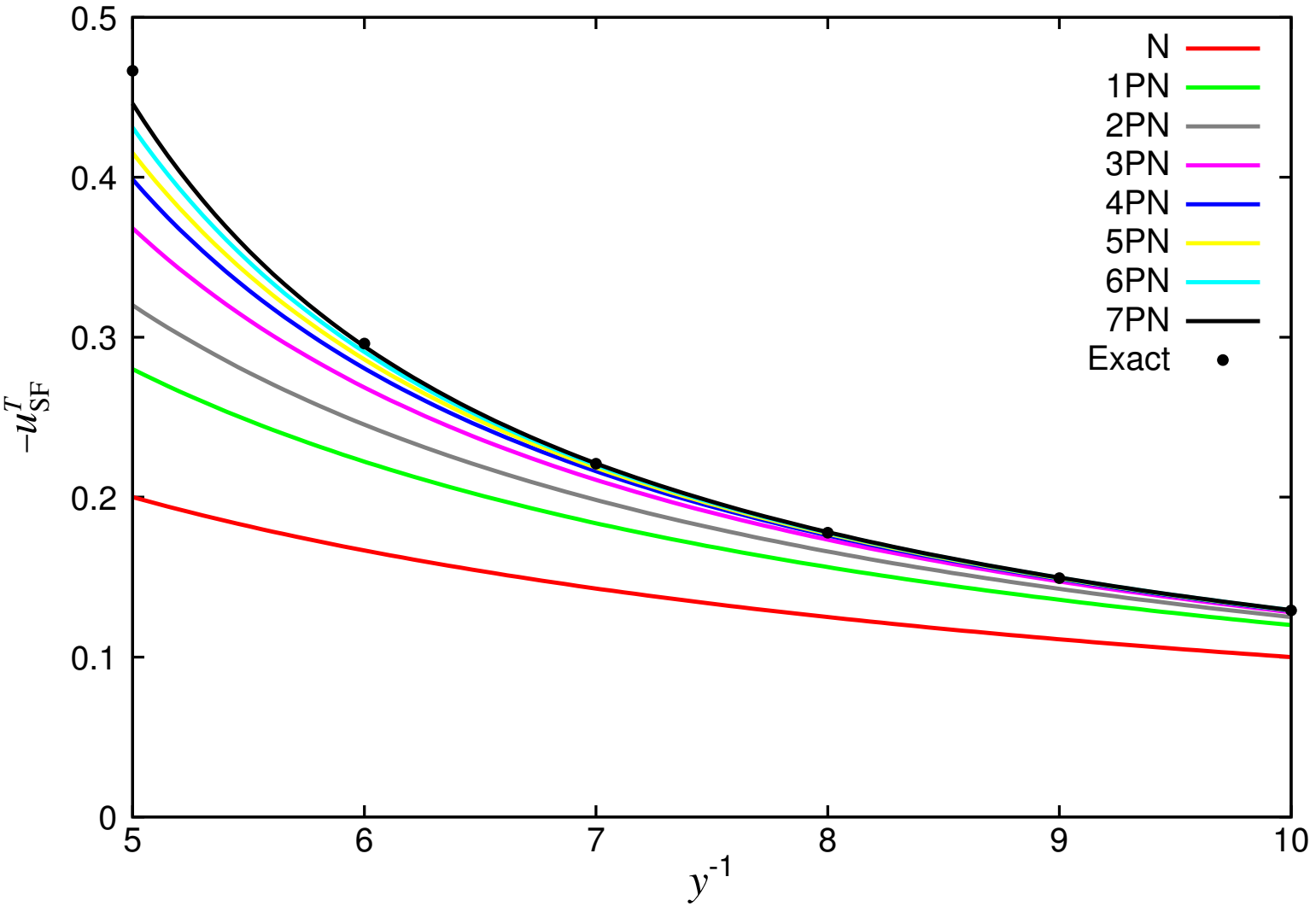

First Law of Binary Point Particle Mechanics

[Le Tiec, Blanchet & Whiting 2011]

1. We find by direct computation that the redshift observables z_1 and z_2 are related to the ADM mass and angular momentum by

$$\frac{\partial M}{\partial m_1} - \Omega \frac{\partial J}{\partial m_1} = z_1 \quad \text{and} \quad (1 \leftrightarrow 2)$$

2. Finally those relations can be summarized into the

First law of binary point-particles mechanics

$$\delta M - \Omega\, \delta J = z_1\, \delta m_1 + z_2\, \delta m_2$$

The first law tells how the ADM quantities change when the individual masses m_1 and m_2 of the particles vary (keeping the frequency Ω fixed)

3. An interesting consequence is the remarkably simple relation

First integral of the first law

$$M - 2\Omega J = z_1 m_1 + z_2 m_2$$

Agreement with the Generalized First Law of Mechanics

[Friedman, Uryū & Shibata 2002]

- Space-time generated by black holes and perfect fluid matter distributions
- Globally defined HKV field
- Asymptotic flatness

Generalized law of perfect fluid and black hole mechanics

$$\delta M - \Omega \delta J = \int_\Sigma \left[\bar{\mu}\, \Delta(\mathrm{d}m) + \bar{T}\, \Delta(\mathrm{d}S) + w^\mu \Delta(\mathrm{d}C_\mu) \right] + \sum_n \frac{\kappa_n}{8\pi}\, \delta A_n$$

where Δ denotes the Lagrangian variation of the matter fluid, where $\mathrm{d}m$ is the conserved baryonic mass element, and where $\overline{T} = zT$ and $\overline{\mu} = z(h - Ts)$ are the redshifted temperature and chemical potential

In the point-particle limit for the fluid bodies (without BHs) one recovers formally the PN result

First law of mechanics for binary point particles with spins

[Blanchet, Buonanno & Le Tiec 2012]

The spins must be aligned or anti-aligned with the orbital angular momentum.

First law of binary point particles with spins

$$\delta M - \Omega\, \delta J = \sum_{n=1}^{2} \Big[z_n\, \delta m_n + (\Omega_n - \Omega)\, \delta S_n \Big]$$

- The precession frequency Ω_n of the spins obeys

$$\frac{\mathrm{d}\boldsymbol{S}_n}{\mathrm{d}t} = \boldsymbol{\Omega}_n \times \boldsymbol{S}_n$$

- The total angular momentum is related to the orbital angular momentum by

$$J = L + S_1 + S_2$$

Analogies with single and binary black holes

1. Single black hole [Bardeen et al 1972]

$$\delta M - \omega_{\mathcal{H}}\, \delta J = \frac{\kappa}{8\pi} \delta \mathcal{A}$$

2. Two black holes [Friedman, Uryū & Shibata 2002]

$$\delta M - \Omega\, \delta J = \sum_{n=1}^{2} \frac{\kappa_n}{8\pi} \delta \mathcal{A}_n$$

3. Two point particles [Le Tiec, LB & Whiting 2012]

$$\delta M - \Omega\, \delta J = \sum_{n=1}^{2} z_n \delta m_n$$

4. Two spinning point particles [LB, Buonanno & Le Tiec 2012]

$$\delta M - \Omega\, \delta J = \sum_{n=1}^{2} \Big[z_n\, \delta m_n + (\Omega_n - \Omega)\, \delta S_n \Big]$$

Analogies with single and binary black holes

1. Single black hole [Smarr 1973]

$$M - 2\omega_{\mathcal{H}}\, J = \frac{\kappa}{4\pi}\mathcal{A}$$

2. Two black holes [Friedman, Uryū & Shibata 2002]

$$M - 2\Omega\, J = \sum_{n=1}^{2} \frac{\kappa_n}{4\pi}\mathcal{A}_n$$

3. Two point particles [Le Tiec, LB & Whiting 2012]

$$M - 2\Omega\, J = \sum_{n=1}^{2} z_n m_n$$

4. Two spinning point particles [LB, Buonanno & Le Tiec 2012]

$$M - 2\Omega\, J = \sum_{n=1}^{2} \Big[z_n\, m_n + 2\,(\Omega_n - \Omega)\, S_n \Big]$$

Analogies with single and binary black holes

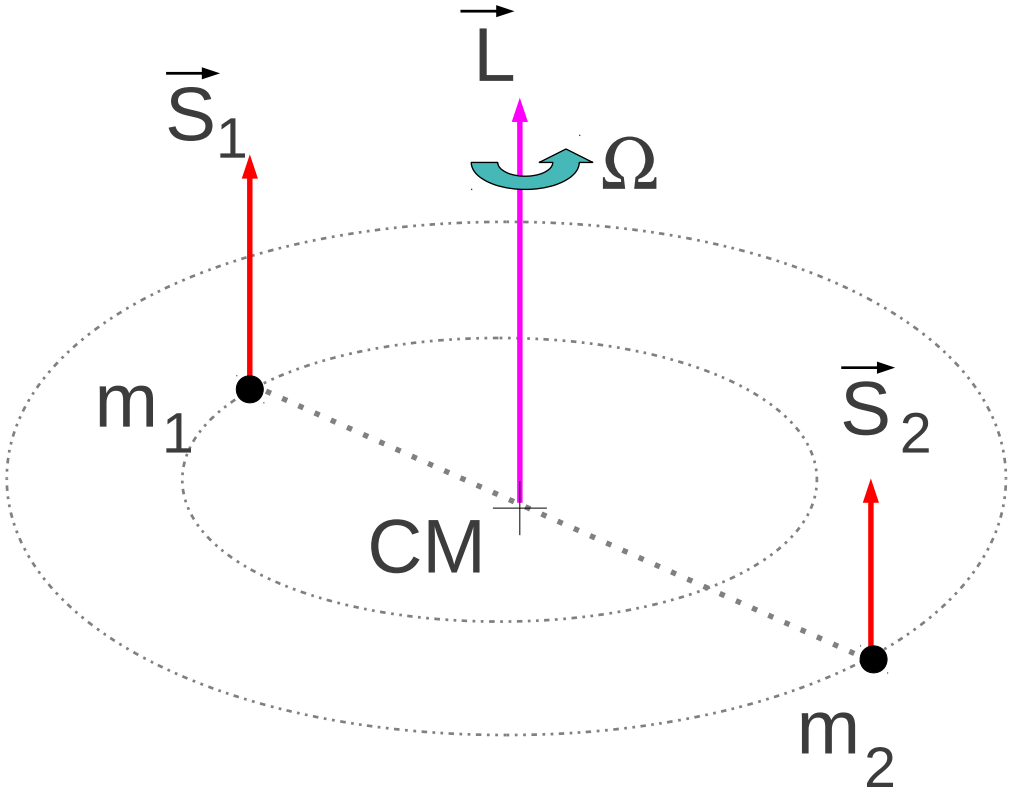

For point particles which have no finite extension the notion of rotation frequency of the body is meaningless. Thus the First Law is valid for arbitrary aligned or anti-aligned spins

The first law for Binary Corotating Black Holes

1. To describe extended bodies such as black holes one must suplement the point particles with some internal constitutive relation of the type

$$m_n = m_n\left(m_n^{\text{irr}}, S_n\right)$$

where S_n is the spin and m_n^{irr} is some "irreducible" constant mass

2. We define the response coefficients associated with the internal structure

$$c_n = \left(\frac{\partial m_n}{\partial m_n^{\text{irr}}}\right)_{S_n}, \qquad \omega_n = \left(\frac{\partial m_n}{\partial S_n}\right)_{m_n^{\text{irr}}}$$

where in particular ω_n is the rotation frequency of the body

3. The First Law becomes

$$\delta M - \Omega\,\delta J = \sum_{n=1}^{2}\left[z_n\, c_n\, \delta m_n^{\text{irr}} + (z_n\,\omega_n + \Omega_n - \Omega)\,\delta S_n\right]$$

The First Law for Binary Corotating Black Holes

Corotation condition for extended particles [LB, Buonanno & Le Tiec 2012]

$$z_n \, \omega_n = \Omega - \Omega_n$$

The First Law is then in agreement with the first law of two black holes [Friedman, Uryū & Shibata 2002]

$$\delta M - \Omega \, \delta J = \sum_{n=1}^{2} \frac{\kappa_n}{8\pi} \delta \mathcal{A}_n$$

provided that we make the identifications

$$\begin{aligned} m_n^{\text{irr}} &\longleftrightarrow \sqrt{\frac{\mathcal{A}_n}{16\pi}} \\ z_n \, c_n &\longleftrightarrow 4 m_n^{\text{irr}} \kappa_n \end{aligned}$$

Conclusions

1. Compact binary star systems are the most important source for gravitational wave detectors LIGO/VIRGO and LISA
2. Post-Newtonian theory has proved to be the appropriate tool for describing the inspiral phase of compact binaries up to the ISCO
3. For massive BH binaries the PN templates should be matched to the results of numerical relativity for the merger and ringdown phases
4. The PN approximation is now tested against different approaches such as the SF and performs extremely well
5. The conservative part of the dynamics of compact binaries exhibits a First Law which is the analogue of the First Law of black hole mechanics

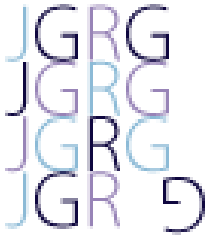

Hideo Kodama, JGRG 22(2012)111504

"Charmed by spacetime physics – from four to higher dimensions"

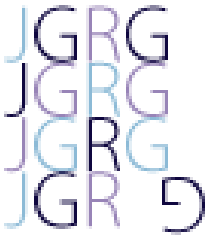

RESCEU SYMPOSIUM ON

GENERAL RELATIVITY AND GRAVITATION

JGRG 22



November 12-16 2012

Koshiba Hall, The University of Tokyo, Hongo, Tokyo, Japan



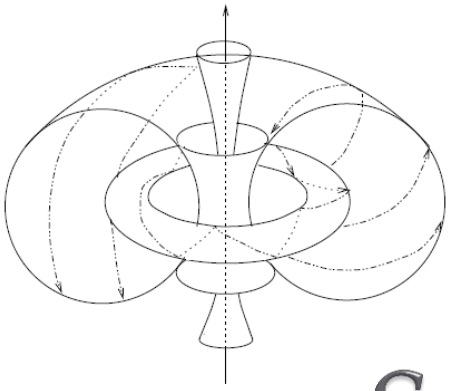

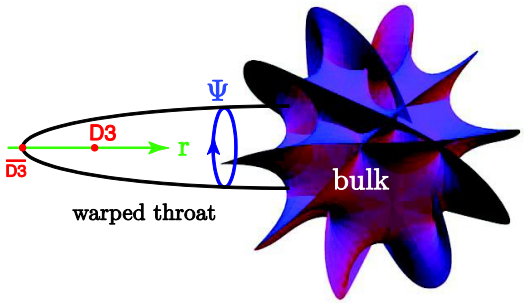

Charmed by Spacetime Physics

— From Four to Higher Dimensions —

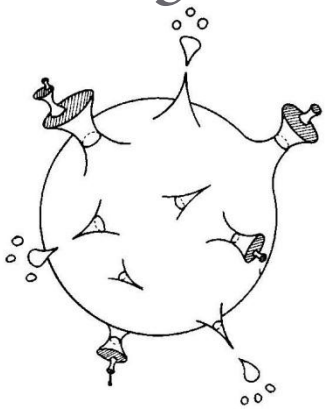

Hideo Kodama
Theory Center, KEK

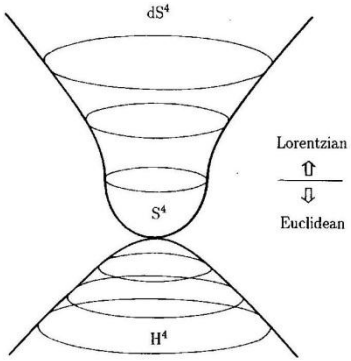

The 22th JGRG symposium
2012.11.15 Koshiba Hall, University of Tokyo

In Hayashi School

- 1975-1983

Bitter start

1975/4 Nuclear Astrophysics Group
led by late Prof. Chushiro Hayashi
in Kyoto University.

- 1969 Lagrangian quantum cosmology (Misner)

  Particle creation in an expanding universe (Parker)
- 1970 Singularity theorems (Hawking, Penrose)
- 1973 BH entropy (Bekenstein)

  Hawking –Ellis textbook
- 1974 BH evaporation (Hawking)



1975　研究室ハイキング、洛南鷲峰山の行者場、回想：鈴木博子君も非常に険しい道を降り下った



1999 佐藤文隆氏の紫綬褒章受賞祝賀会、於京都ロイヤルホテル、写真の左半分



同写真の右半分

Bitter start

1975/4 Nuclear Astrophysics Group
led by late Prof. Chushiro Hayashi
in Kyoto University.

1975/7 My daughter was born.

1977/1 My son was born.

1977/12 Two papers on quantum gravity.

- "Quantization of Gauge Fields by the Reduce
  Formalism. 1. The Case of the Yang-Mills Field
- "Quantization of Gauge Fields by the Reduce
  Formalism. 2. The Case of the Gravitational F

Both were rejected!!

Lesson 1

Do not be too self-confident !

First Papers

After struggles of two years,

- "Inevitability of a naked singularity associated with the black hole evaporation", *Kodama H: PTP 62, L1434-1435 (1979) .*

- "Conserved energy flux for the spherically symmetric system and the back reaction problem in the black hole evaporation", *Kodama H: PTP 63, 1217-1228 (1980).*

$$K := *(dr \wedge r^n \Omega_n), \quad S^\mu := G^\mu_\nu K^\nu \Rightarrow \quad \nabla_\mu S$$

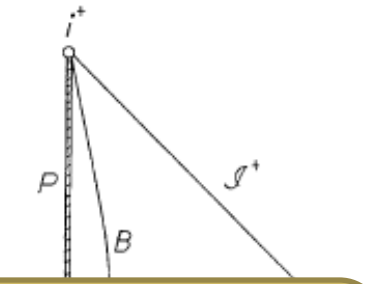

Lesson 2

The origial motivation of a paper will be soon forgotten !

Moving to Physical Cosmology

1981/3 Degree of DS

"On the particle-defining modes for a free neutral scalar field in spatially homogeneous and isotropic universes"

Kodama H: PTP65, 507-524 (1981).

But, I was still struggling …

1981-82 Invited to collaboration on the inflationary universe model by Katsuhiko Sato (with Maeda K, Sasaki M)

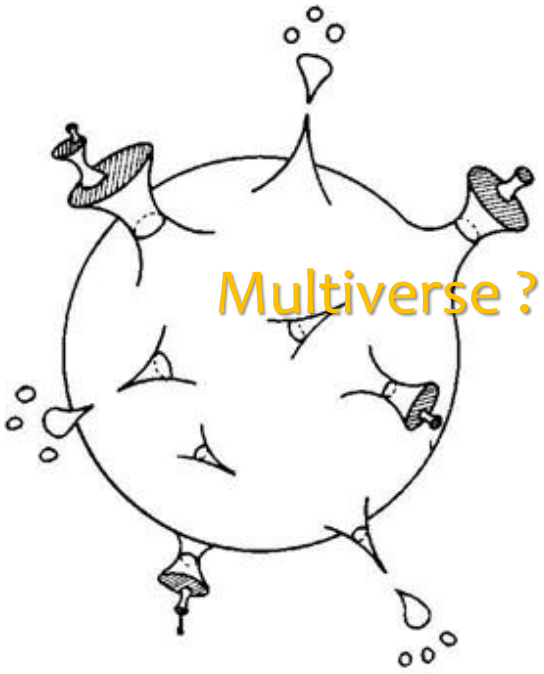

This collaboration opened up a new research avenue for me!!

K. Sato's New Group in U. Tokyo

- 1983-1987

The Early History of Inflation Theory

1974 SU(5) GUT (George H & Glashow SL)

1980 GUT inflation (Sato K, Kazanas D, Guth A)

1981 New inflation model (Linde A, Albrecht & Steinhardt)

1982 Cosmological perturbations from quantum fluctuations (Linde A, Hawking SW & Moss I, Starobinsky AA)

Creation of the Universe from Nothing (Vikenkin A)

1983 Wave function of the universe (Hartle J, Hawking SW)

Chaotic inflation (Linde A)

1984 Birth of superstring theories

From Inflation to Cosmological Perturbations

The old inflation model ➔ too inhomogeneous universe.

The new inflation model ➔ too "bold" universe.

How did the present inhomogeneous structures emerge?

Gauge-invariant formulation for perturbations

"Gauge Invariant Cosmological Perturbations", Bardeen J: PRD22, 1882 (1980)

Extension to multi-component systems

- "Cosmological perturbation theory"
  Kodama H, Sasaki M: PTP Suppl. 78, 1-166 (1984).
- "Constraint on the amplitude of isothermal perturbations imposed by an isotropy of the cosmic microwave background radiation"
  Suto Y, Sato K, Kodama H: APJ Lett 292, 1-4 (1985)

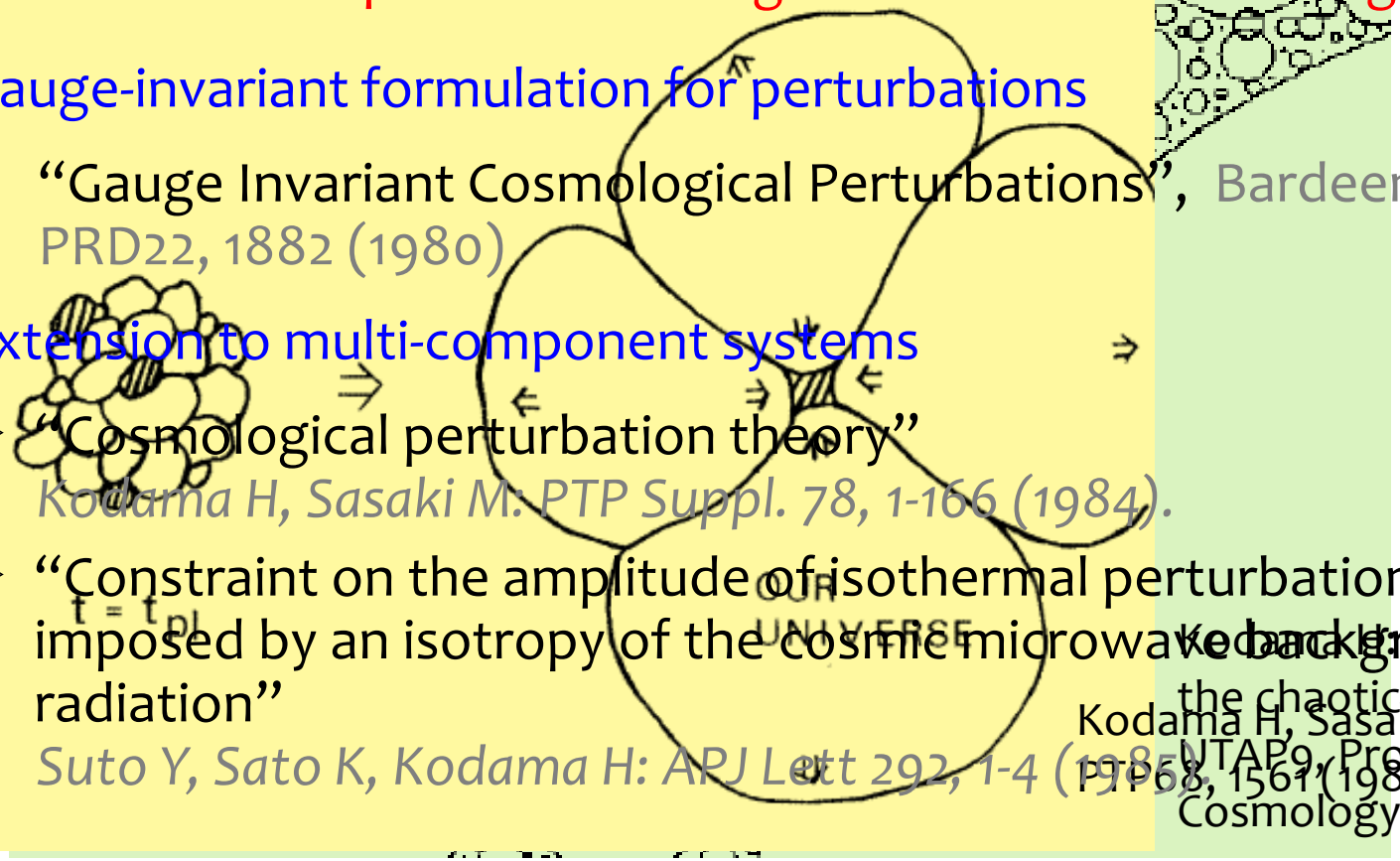

Kodama H, Sasaki M, Sato K: "Comments on the chaotic inflation", PTP68, 1561(1982)

Kodama H, Sasaki M, Sato K: IJTAP9, Proc. GUT & Cosmology, Tsukuba 1983.

More on Cosmology

We introduced the concept of "isocurvature perturbations" and studied their cosmological consequences.

- "Evolution of isocurvature perturbations I: Photon-baryon universe"
  Kodama H , Sasaki M: IJMP A 1, 265-301 (198
- "Evolution of isocurvature perturbations
  universe"
  Kodama H, Sasaki M: IJMP A 2, 491-560 (198

- Decaying CDM (with Suto & Sato)
- Baryogenesis after inflation (with Yokoya
- Dynamics of quark –hadron phase transit o)

Lesson 3

Do not insist on your preference wrt research subjects !

Back to Kyoto U.

- 1987-1993

Back to Quantum Gravity

Interpretation of quantum cosmology

- "Quantum Cosmology In Terms Of The Wigner Function." , Kodama H(1988), MG5 (Perth, Australia)

I was struggling again. ..

New canonical formulation by Ashtekar.

"New Variables for Classical and Quantum Gravity."
Ashtekar A: PRL 57, 2244-2247 (1986)

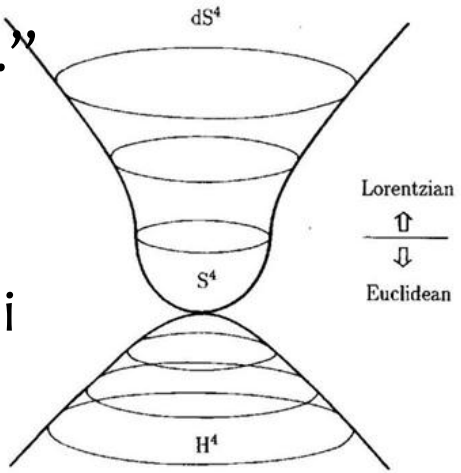

Application to cosmology.

- "Specialization of Ashtekar's Formalism to Bianchi Cosmology"
  Kodama H: PTP 80, 1024-1040 (1988).
- "Holomorphic Wavefunction of the Universe"
  Kodama H: PRD 42, 2548-2565 (1990).

$$\Psi = \exp\left(-\frac{i}{\Lambda} S_{\mathrm{CS}}[\mathscr{A}]\right)$$

New Research Group

Compact Bianchi models

- "Comments on closed Bianchi models"
  Fujiwara Y, Ishihara H, Kodama H: CQG 10, 859-868 (1993)

Domain wall dynamics

- "Does a domain wall emit gravitational w
  invariant perturbative treatment"
  Kodama H, Ishihara H, Fujiwara Y: PRD 50, 7

Maximum mass of dS BH

- "Can Large Black Holes Collide in de Sitte
  Inflationary Scenario of Inhomogeneous
  Shiromizu T, Nakano K, Kodama H, Maeda
  (1993).

Lesson 4

Do not do research alone!

In Yukawa Institute (Uji Branch)

- 1993-1995

New Formulation for Canonical QG

Dirac formalism for the canonical quantum gravity

$$\mathscr{C}_g \Psi = 0, \ \mathscr{H}_m \Psi = 0, \ \mathscr{H}_\perp \Psi = 0$$

$$H = \langle N^\alpha, \mathscr{H}_\alpha \rangle \approx 0$$

$$T \text{ is a time variable} \quad \Leftrightarrow \quad [H, T] \not\approx 0$$
$$X \text{ is a Dirac observable} \quad \Leftrightarrow \quad [\mathscr{H}_\alpha, X] \approx 0.$$

New quantum formulation for totally constrained systems.

- "Dynamics of Totally Constrained Systems I. Classical Theory"

  Kodama H : PTP 94, 475-501 (1995)
- "Dynamics of Totally Constrained Systems II. Quantum Theory"

  Kodama H : PTP 94, 937-987 (1995)

These are the the least cited papers among my papers, but I believe that these are the most original and deep work in my life.

Web Formalism for a Totally Constrained System

Totally Constrained System

$$H = n^\alpha h_\alpha : \quad [h_\alpha, h_\beta] = h_\gamma f^\gamma_{\alpha\beta}$$

The state vector is just a bookkeeper of measurement info:

$$\Phi \in \mathscr{H} \mapsto P(x_n) = |\langle x_n|\Phi\rangle|^2, \;\; X|x_n\rangle = x_n|x_n\rangle$$

The c… mposed on an unbounded linear funct… escribes dynamics:

$$\Psi(h \quad \Leftrightarrow \quad \Psi(\mathscr{N}) = 0, \;\; \mathscr{N} = \sum \text{range } h_\alpha$$

Time… n 'instantaneous state space' $\mathscr{L}$:

$$\mathscr{L} \cap \mathscr{N} = 0$$

On $\mathscr{L}$… e usual wavefunction:

$$\Phi \in \mathscr{L}$$

Lesson 5

Formulation must be timely and productive!

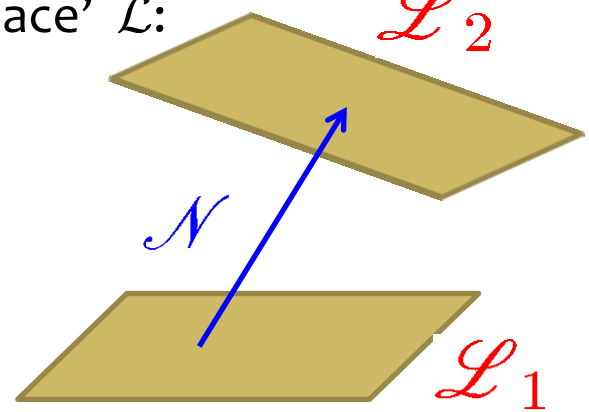


In Yukawa Institute
(Kitashirakawa)
1995-2007

Bianchi Cosmology

Hosoya Group in Titech

"Compact homogeneous universes."
Koike T, Tanimoto M, Hosoya A: JMP35 , 4855 (1994) [grcq/9405052]

Thurston conjecture (=> proved by G Perelman 2002-2003)

Locally homogeneous & compact 3D ➔ $M = \tilde{M}/\Gamma$

$\tilde{M} = E^3,\ S^3,\ H^3,\ S^2 \times E^1,\ H^2 \times E^1,$ Nil, Sol, $\widetilde{\mathbf{SL}_2\mathbb{R}}$

Hamiltonian str… …hi models

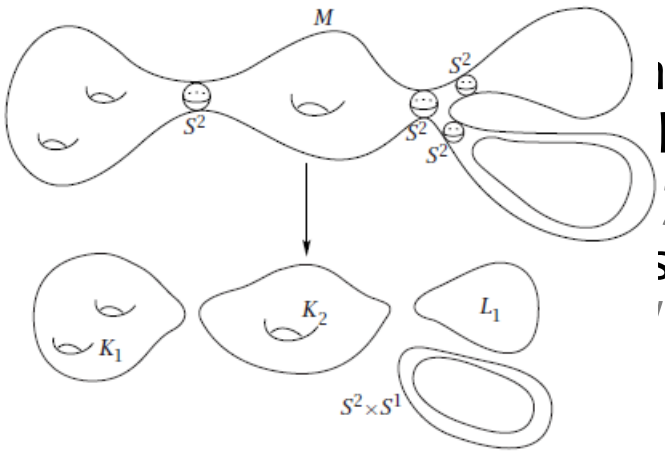

- "Canonical Str… …neous Systems on Compact Closed 3-Mani… …l"
  Kodama H : PT… …705066].
- "Phase Space … …s with Fluid"
  Kodama H : PT… …0109064].

Back to Inflationary Cosmology

Is the Bardeen parameter conserved during reheating?

- "Evolution of cosmological perturbations in a stage dominated by an oscillatory scalar field"
  Kodama H, Hamazaki T : PTP 96, 949 (1996)[gr-qc/9608022].
- "Evolution of cosmological perturbations during reheating"
  Hamazaki T, Kodama H: PTP96, 1123 (1996)[gr-qc/9609036].
- "Evolution of Cosmological Perturbations in the Long Wavelength Limit"
  Kodama H, Hamazaki T: PRD 57, 7177(1998) [gr-qc/9712045].

To Higher Dimensions

Braneworld model

"A Large mass hierarchy from a small extra dimension"
Randall L , Sundrum R: PRL83 , 3370-3373 (1999)
"An Alternative to compactification"
Randall L, Sundrum R: PRL83 , 4690-4693 (1999)

Perturbations with model generalisation

$$\tilde{M} = \mathcal{N} \times K : \quad ds^2 = g_{ab}(y)dy^a dy^b + r(y)^2 d\sigma_K^2$$

- Brane World Cosmology — Gauge-Invariant Formalism for Perturbation —
  Kodama H, Ishibashi A, Seto O: PRD62, 064022(2000)[hep-th/0004160].

Cf. "Gauge invariant gravitational perturbations of maximally symmetric space-times", Mukohyama S: PRD62, 084015 (2000)[hep-th/0004067]

Higher-Dimensional Black Holes

Static black holes in higher dimensions

$$ds^2 = -f(r)dt^2 + f(r)^{-1}dr^2 + r^2 d\sigma_n^2$$

Three types of perturbations

- tensor perturbations : trivial
- vector perturbations : easy
- scalar perturbations : difficult ➔ Original paper by Zerilli

Generalisation of the Regge-Wheeler & Zerilli equations

- "A master equation for gravitational perturbations of maximally symmetric black hole in higher dimensions"
  Kodama H, Ishibashi A.: PTP110, 701-722 (2003)
- "Stability of higher-dimensional Schwarzschild black holes"
  Ishibashi A, Kodama H : PTP110, 901-919 (2003)
- "Master equations for perturbations of generalized static black holes with charge in higher dimensions"
  Kodama H, Ishibashi A.: PTP111, 29-73 (2004)

Thanks to Maple!!

To HD Unified Theories

The first realistic string inflation model (KKLT):

"de Sitter Vacua in String Theory"

Kachru S, Kallosh R, Linde A, Trivedi S : PRD68, 046005 (2003).

Systematic classification of BPS solutions to sugra of D=5 – 11:

Gauntlett JP, Gutowski JB (2003), …

Dynamics of warped compactification

- "Moduli Instability in Warped Compactifications of the Type IIB Supergravity

  Kodama H. and Uzawa K.: JHEP 0507, 061:1-16 (2005) [hep-th/0504193].

- "Comments on the four-dimensional effective theory for warped compactification"

  Kodama H. and Uzawa K.: JEHP 0603, 053:1-18 (2006) [hep-th/0512104].

Bottom Up Analysis

Standard model ⇒ GUT: gauge-sector unification

- αunification, hypercharge structure, neutrino mass
- Baryon asymmetry, strong CP(Peccei-Quinn symmetry)

GUT ⇒ SGUT: boson-fermion correspondence

- Dark matter, Λ problem, hierarchy problem

SGUT ⇒ Sugra GUT: inclusion of gravity

- Flat inflaton potential

Sugra GUT ⇒ HD Sugra GUT: matter sector unification

- Generation repitition, Cabibo/neutrino mixing, CP violation
- Origin of the Higgs in the adjoint representation

HD Sugra GUT ⇒ Superstring/M theory

- Consistency as a quantum theory, finite control parameters
- No Λ freedom (M-theory)

Research History

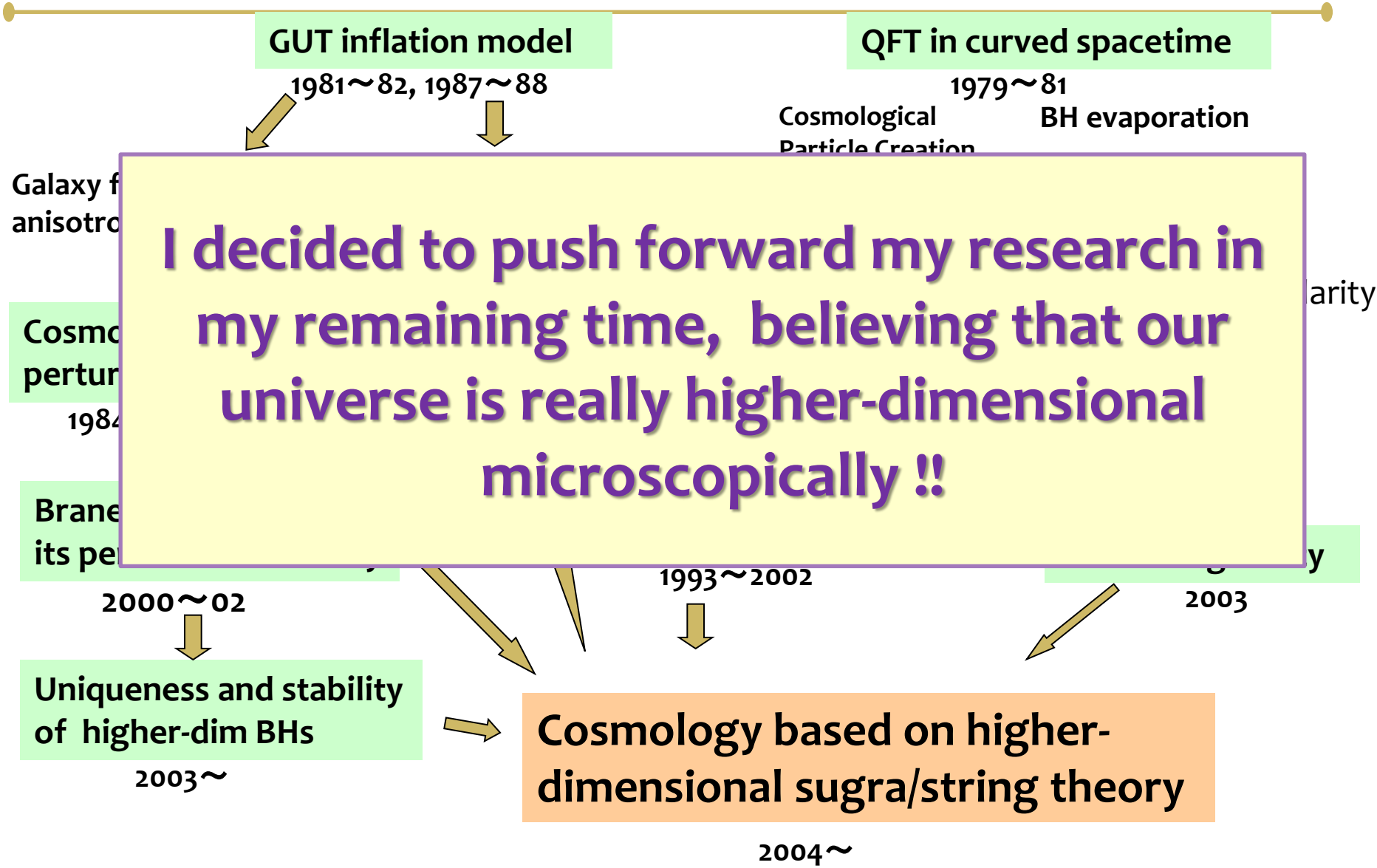

I decided to push forward my research in my remaining time, believing that our universe is really higher-dimensional microscopically !!

New Group in KEK

- 2007 -- 2016

Cosmophysics Group Key Projects

- Test unified theory of all interactions including gravity by the early evolution of the Universe
- High energy physics of cosmic jets and black holes

Problems to be solved in HUnT

- Dark Energy / Inflation Problems
  - Supersymmetry is necessary to control the vacuum energy but not sufficient to make it small.
    - ☞ New symmetry?
  - How to circumvent the No-Go theorem against inflation?
    - ☞ Higher-order corrections? Singularities? Open extra-dimensions?
- Compactification problem
  - No compactification with stabilised moduli consistent with the SM has been found.
    - ☞ Can we reproduce the SM ?
  - Landscape problem, breaking and restoration of SUSY
    - ☞ Dynamical comparison of compactification and ground states.

Messengers of Fundamental Physics in Cosmophysics

- Indirect

  CMB /LSS ➔ Inflation

- Direct

  DM: neutralinos $E \sim E_{SUSY} = 1\text{TeV} \sim 10^{10}$ GeV

  gravitinos $E \sim E_{SUSY}$, almost undetectable

  axions $E \sim f_a = 10^8$ GeV $\sim m_{pl}$

  GW: $E \lesssim m_{pl}$

  Dark radiations ???

Axiverse

Among these, axions are quite unique in the following points:

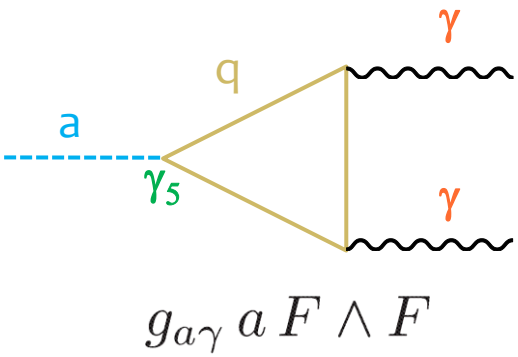

- The shift symmetry leads to Chern-Simons interactions producing interesting and rich cosmophysical phenomena.
- Non-perturbative effects produce vey tiny mass, which is consistent with experiments due to its pseudo-scalar nature. The Compton wavelength can be of cosmological scales.
- Axion is an indispensable ingredient in the anomaly cancelation and appears ubiquitously in string compactification.

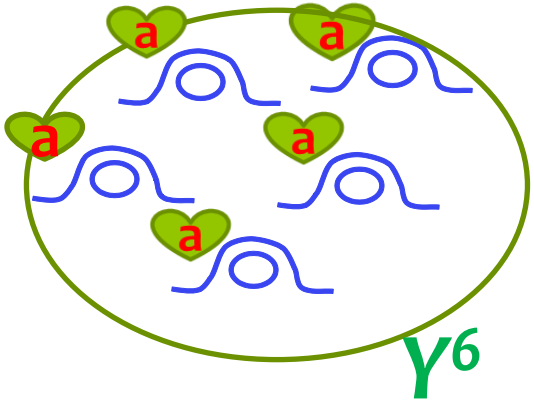

Thus, axions provide us the possibility to probe physics on the highest energy scales by low energy cosmophysical phenomena.

Back to Four Dimensions



I believe that axion is the most promising research subject in the future.

So, on the occasion of my becoming 60 years old, I propose the subject "axion cosmophysics" as the baton to the next generation.

	1	2	3	4	5	6	7	8	9	10
十干	甲	乙	丙	丁	戊	己	庚	辛	壬	癸
十二支	子	丑	寅	卯	辰	巳	午	未	申	酉
	11	12	13	14	15	16	17	18	19	20
十干	甲	乙	丙	丁	戊	己	庚	辛	壬	癸
十二支	戌	亥	子	丑	寅	卯	辰	巳	午	未
	21	22	23	24	25	26	27	28	29	30
十干	甲	乙	丙	丁	戊	己	庚	辛	壬	癸
十二支	申	酉	戌	亥	子	丑	寅	卯	辰	巳
	31	32	33	34	35	36	37	38	39	40
十干	甲	乙	丙	丁	戊	己	庚	辛	壬	癸
十二支	午	未	申	酉	戌	亥	子	丑	寅	卯
	41	42	43	44	45	46	47	48	49	50
十干	甲	乙	丙	丁	戊	己	庚	辛	壬	癸
十二支	辰	巳	午	未	申	酉	戌	亥	子	丑
	51	52	53	54	55	56	57	58	59	60
十干	甲	乙	丙	丁	戊	己	庚	辛	壬	癸
十二支	寅	卯	辰	巳	午	未	申	酉	戌	亥


www-conf.kek.jp
AIU 12
KEK, Tsukuba, Japan
6-9 Nov. 2012
http://www-conf.kek.jp/AIU12/
AXION
COSMOPHYSICS
SOC:
Hideo Kodama (KEK, Chair)
Masataka Fukugita (IPMU)
Masashi Hazumi (KEK)
Kunihito Ioka (KEK)
Akihiro Ishibashi (Kinki U)
Masahiro Kawasaki (ICRR)
Tatsuo Kobayashi (Kyoto U)
Kazunori Kohri (KEK)
Shun'ya Mizoguchi (KEK)
Shinji Mukohyama (IPMU)
Kazunori Nakayama (U Tokyo)
Nobuyoshi Ohta (Kinki U)
Jiro Soda (Kyoto U)
Fuminobu Takahashi (Tohoku U)
Takayuki Tomaru (KEK)
Masahide Yamaguchi (Titech)
Jun'ichi Yokoyama (RESCEU)
Invited Speakers:
Markus Ackermann (DESY)
Karl van Bibber (UCB)
Charles D. Dermer (USNRL)
Sergei Dubovsky (New York U)
Pedro G. Ferreira (U Oxford)
Yutaka Fujita (Osaka U)
Shuji Matsuura (JAXA)
Makoto Minowa (U Tokyo)
Shinji Mukohyama (IPMU)
Kazuyuki Omukai (Kyoto U)
Jonathan R. Pritchard (Harvard U)
Georg G. Raffelt (MPP)
Tetsuya Shiromizu (Kyoto U)
Osamu Seto (Hokkaigakuen U)

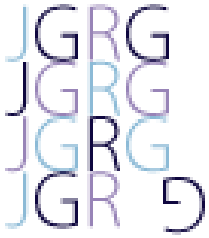

Misao Sasaki, JGRG 22(2012)111505

"A few thoughts on gravity and cosmology"

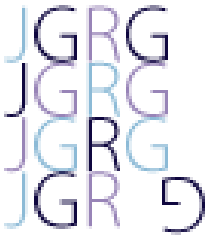

RESCEU SYMPOSIUM ON

GENERAL RELATIVITY AND GRAVITATION

JGRG 22



November 12-16 2012

Koshiba Hall, The University of Tokyo, Hongo, Tokyo, Japan



YUKAWA INSTITUTE FOR THEORETICAL PHYSICS

JGRG22
15 November, 2012

A Few Thoughts on Gravity and Cosmology

- geemunu, geemunu, geemunu...-

Misao Sasaki
YITP, Kyoto University

a bit of recollections

cosmological perturbation theory (CPT)

collaboration with
H Kodama

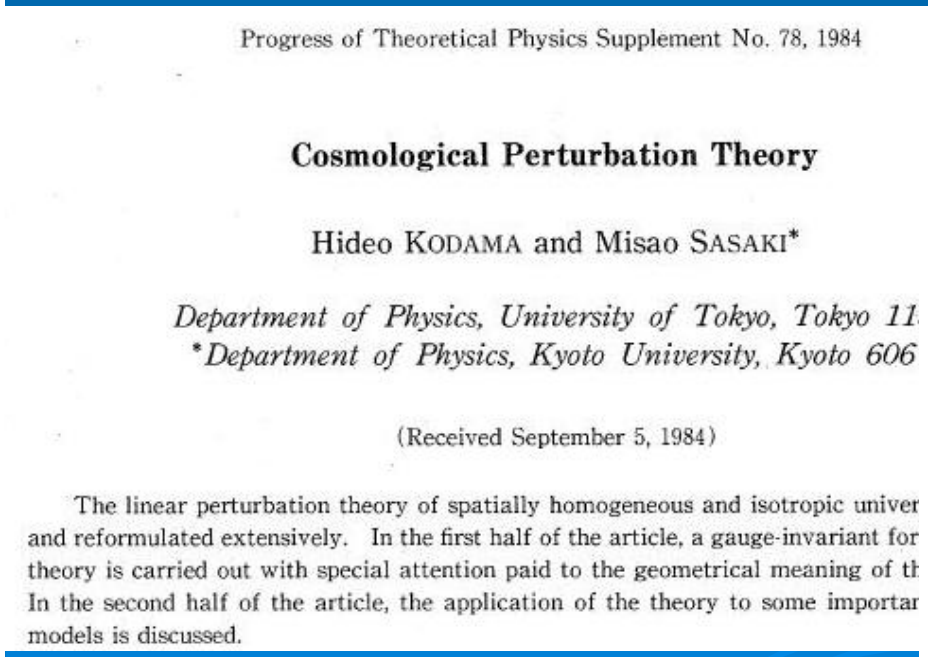

Progress of Theoretical Physics Supplement No. 78, 1984

Cosmological Perturbation Theory

Hideo KODAMA and Misao SASAKI*

Department of Physics, University of Tokyo, Tokyo 11
**Department of Physics, Kyoto University, Kyoto 606*

(Received September 5, 1984)

The linear perturbation theory of spatially homogeneous and isotropic univer
and reformulated extensively. In the first half of the article, a gauge-invariant for
theory is carried out with special attention paid to the geometrical meaning of th
In the second half of the article, the application of the theory to some importar
models is discussed.

gravitational waves (GW)

collaboration with
T Futamase through
TAMA300
(+ gravitational lensing)

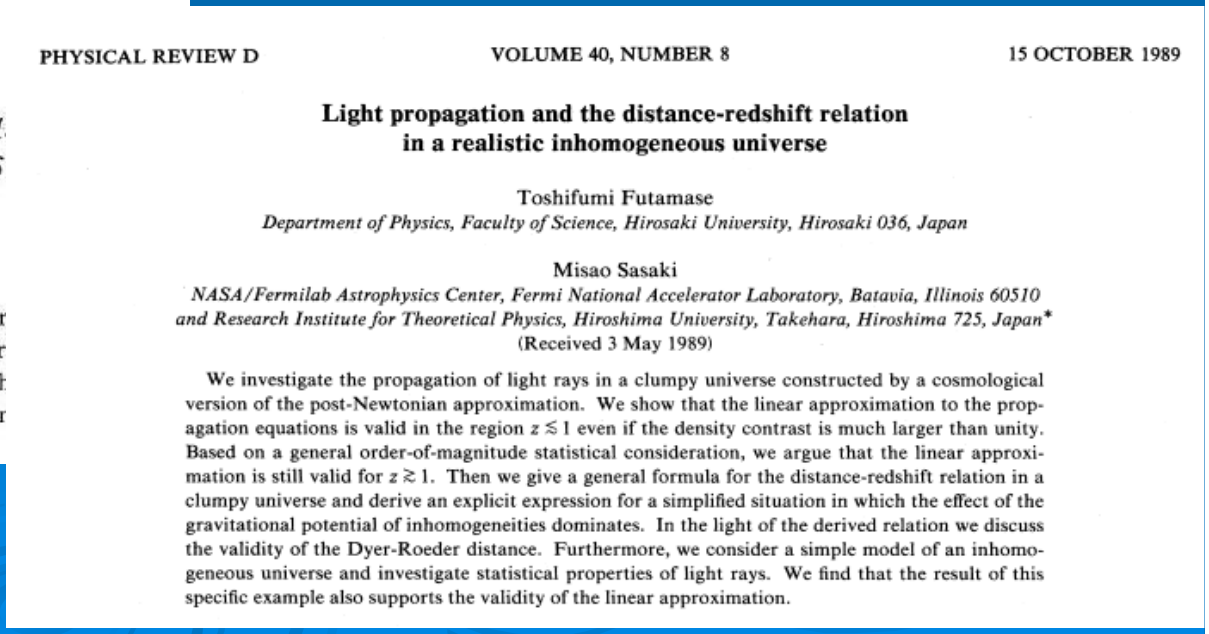

PHYSICAL REVIEW D VOLUME 40, NUMBER 8 15 OCTOBER 1989

Light propagation and the distance-redshift relation in a realistic inhomogeneous universe

Toshifumi Futamase
Department of Physics, Faculty of Science, Hirosaki University, Hirosaki 036, Japan

Misao Sasaki
*NASA/Fermilab Astrophysics Center, Fermi National Accelerator Laboratory, Batavia, Illinois 60510 and Research Institute for Theoretical Physics, Hiroshima University, Takehara, Hiroshima 725, Japan**
(Received 3 May 1989)

We investigate the propagation of light rays in a clumpy universe constructed by a cosmological version of the post-Newtonian approximation. We show that the linear approximation to the propagation equations is valid in the region $z \lesssim 1$ even if the density contrast is much larger than unity. Based on a general order-of-magnitude statistical consideration, we argue that the linear approximation is still valid for $z \gtrsim 1$. Then we give a general formula for the distance-redshift relation in a clumpy universe and derive an explicit expression for a simplified situation in which the effect of the gravitational potential of inhomogeneities dominates. In the light of the derived relation we discuss the validity of the Dyer-Roeder distance. Furthermore, we consider a simple model of an inhomogeneous universe and investigate statistical properties of light rays. We find that the result of this specific example also supports the validity of the linear approximation.

a bit of recollections

cosmological perturbation theory (CPT)

gravitational waves (GW)

- during 80's, GWs were regarded as more realistic, of firm GR foundation.
- during 90's, CPT became realistic, thanks to COBE/DMR measured anisotropy.
- during 00's, both became realistic. But...

fairy tales are necessary for healthy growth of children
(H Sato at a theory group workshop, 中間発表会, in '90s)

(chukan-happyo-kai)

so WE (at least I) need fairy tales...

Gravity Today

- No deviation from General Relativity

cf. Will's living review '06

- solar system tests – PPN parameters

$$g_{oo} = -1 + 2\psi - 2\beta\psi^2 + \cdots : \quad \beta_{GR} = 1$$
$$g_{ij} = \delta_{ij}\left(1 + 2\gamma\psi + \cdots\right) \quad : \quad \gamma_{GR} = 1$$

$|\gamma - 1| < 2.3 \times 10^{-5}$: Shapiro time delay (Bertotti et al. '03)

$|4\beta - \gamma - 3| < 4.4 \times 10^{-4}$: Strong EP (Baessler et al. '99)

- constancy of gravitational constant

$|d\log G/dt| < 10^{-12}$ yr^{-1}: Lunar laser ranging (Williams et al '04)

- binary pulsar – GW emission rate

Hulse-Taylor binary (B1913+16)

- orbital change due to GW emission

$$\frac{\dot{P}_{\mathrm{B1913+16}}}{\dot{P}_{GR}} = 1.0013 \pm 0.0021$$

perfect match with GR predictions

- periastron time shift

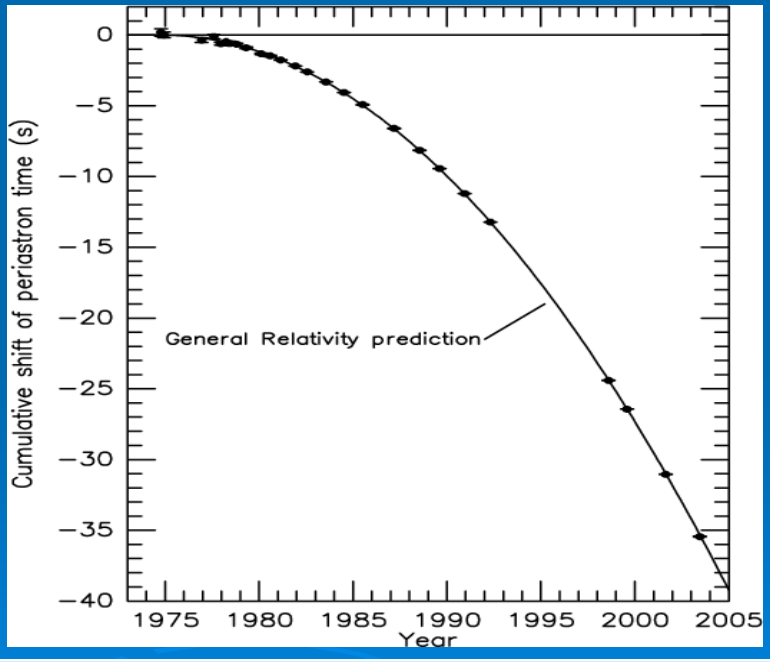

gravitational wave astronomy will further test GR

Cosmology Today

- Big Bang theory has been firmly established

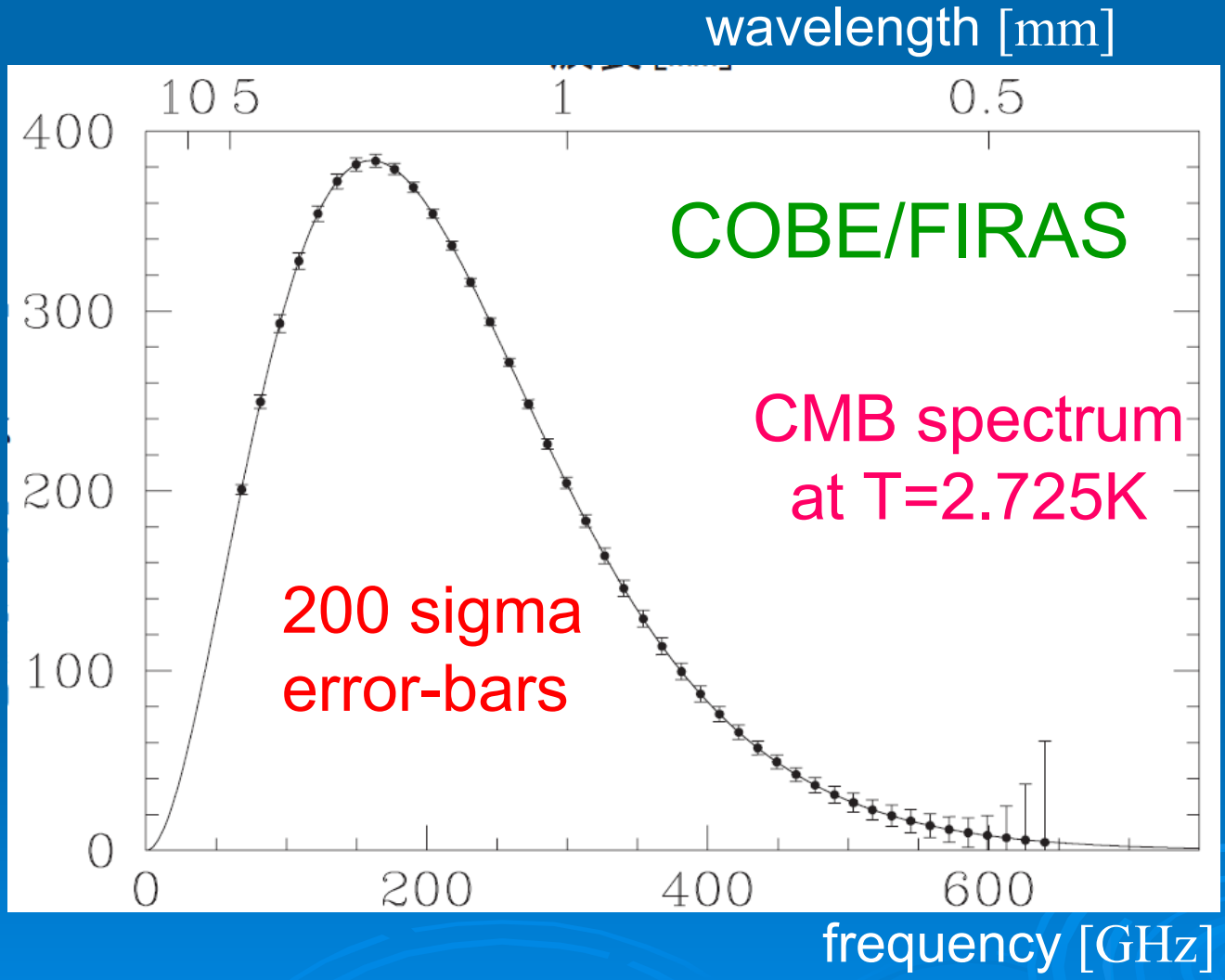

another strong evidence for GR

Strong evidence for Inflation

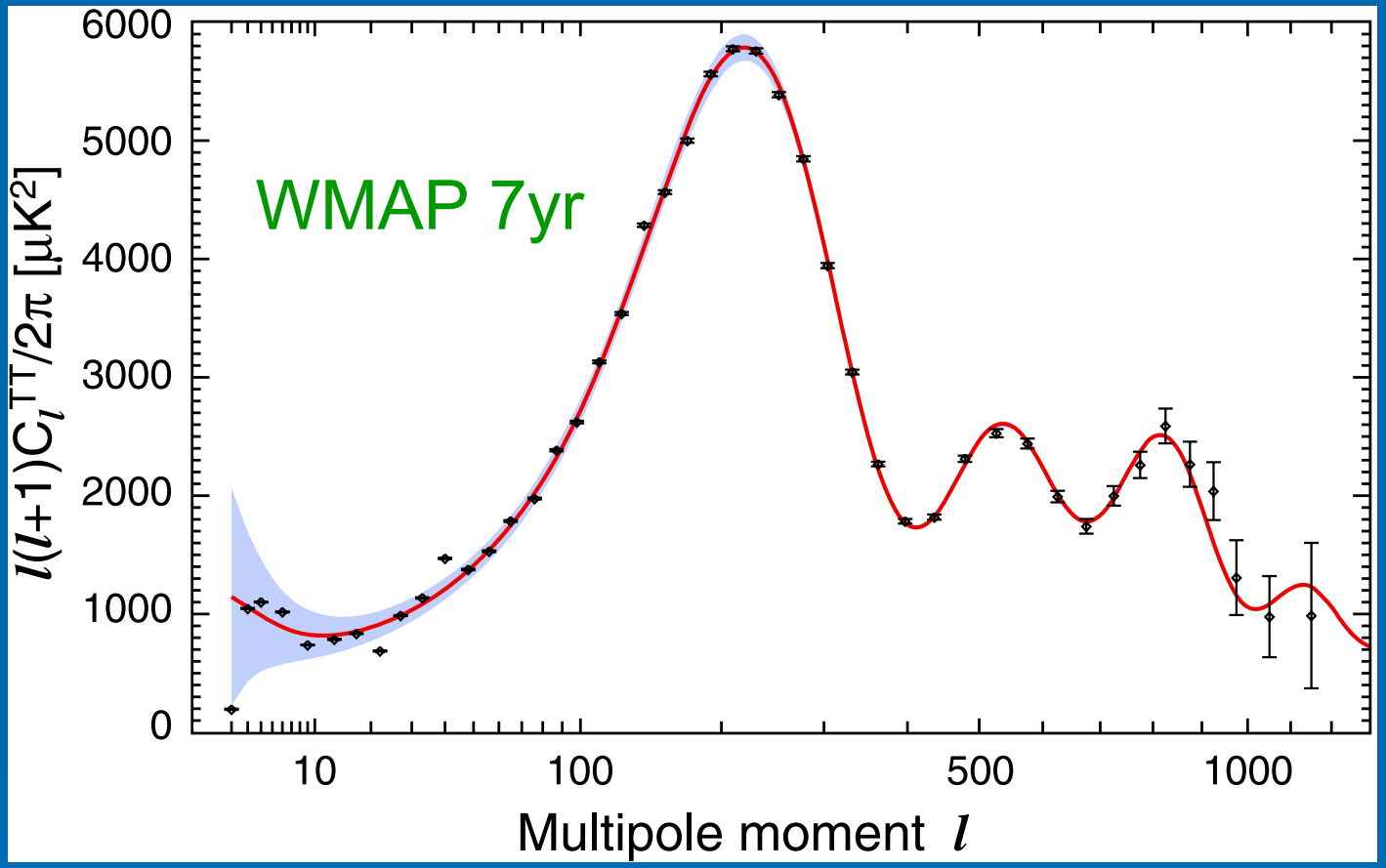

$$\left\langle \Delta T(\vec{n}_1)\Delta T(\vec{n}_2)\right\rangle = \sum_{\ell=0}^{\infty}\frac{2\ell+1}{4\pi}C_\ell P_\ell(\cos\theta).$$

- highly Gaussian fluctuations
- almost scale-invariant spectrum

only to be confirmed (by tensor modes?)

Fundamental(?) Issues

- Dark Matter

  Is it really `matter'?

  Perhaps yes, because it gravitates.

  fermion? boson? primordial BH?
  something else?

Is there a way to generically distinguish them?

- Dark Energy

  - apparent accelerated expansion of the universe

    Is the expansion really accelerating?
    e.g. inhomogeneous universe models

    How can we confirm acceleration?

  - modified gravity vs unknown matter field

    How to distinguish?

    large scale structure formation
    $w<-1$ implies modified gravity,etc...

    Can we falsify GR?

    any other effective discriminators?

comments on modified gravity

IR modification ⟵ GR ⟶ UV modification

↕ ?

long distance

↕ ?

short distance

- time is important in spacetime!
- any smooth function f(x) contains infinitely large Fourier modes...
- amplitude of Riemann? in which frame?

- Inflation

- How did inflation begin?

  what guarantees homogeneity and isotropy?

  quantum cosmology/gravity?

- What is 'inflaton'?

  what determines the end of inflation?

  flatness / open inflation?

  non-Gaussianity? tensor-scalar ratio?

  eternal inflation, anthropic principle, probability measure,...

new guiding principle / working hypothesis?

What's next?
Which direction?

With a bit of 我田引水 (ga den-in sui)

which means ‘self advocacy’, more or less...

String Theory Landscape!

Isn’t there a landscape in LQG?

(a question to Abhay)

String theory landscape

Bousso & Pochinski ('00), Susskind, Douglas, KKLT ('03), ...

- There are ~ 10^{500} vacua in string theory
  - vacuum energy ρ_V may be positive or negative
  - typical energy scale ~ M_P^4
  - some of them have $\rho_V << M_P^4$

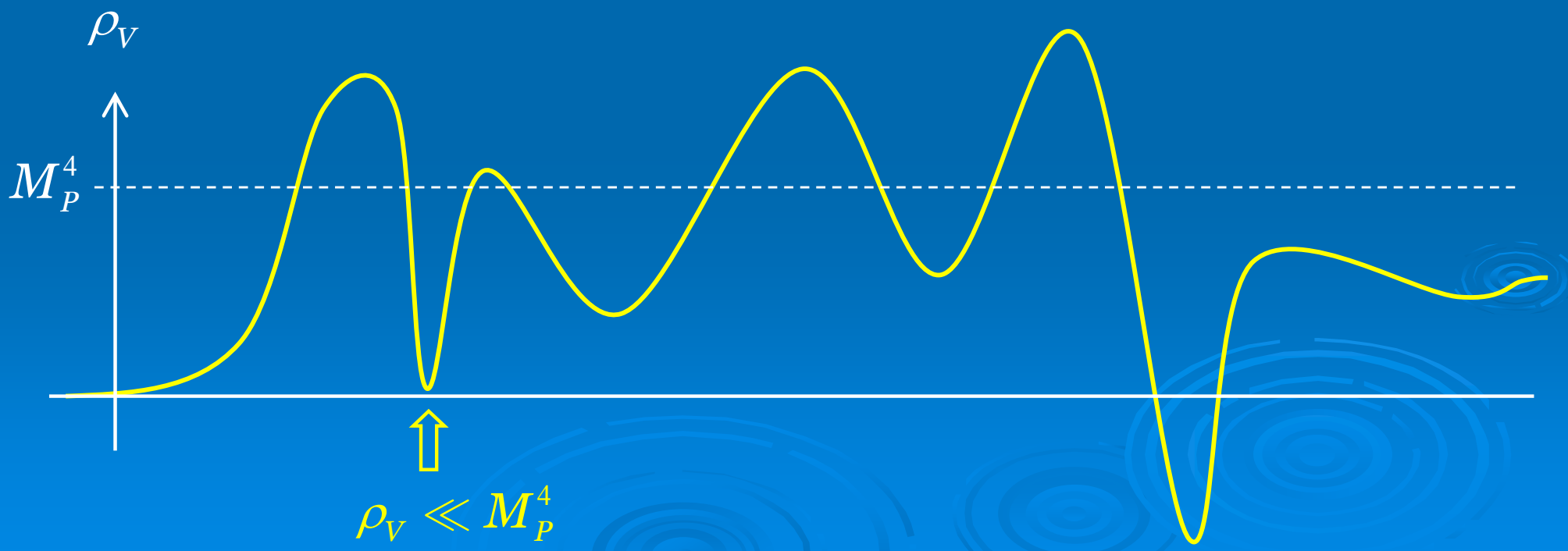

testing string theory landscape in cosmology?

Cosmic Landscape

various vacua realized in the early universe

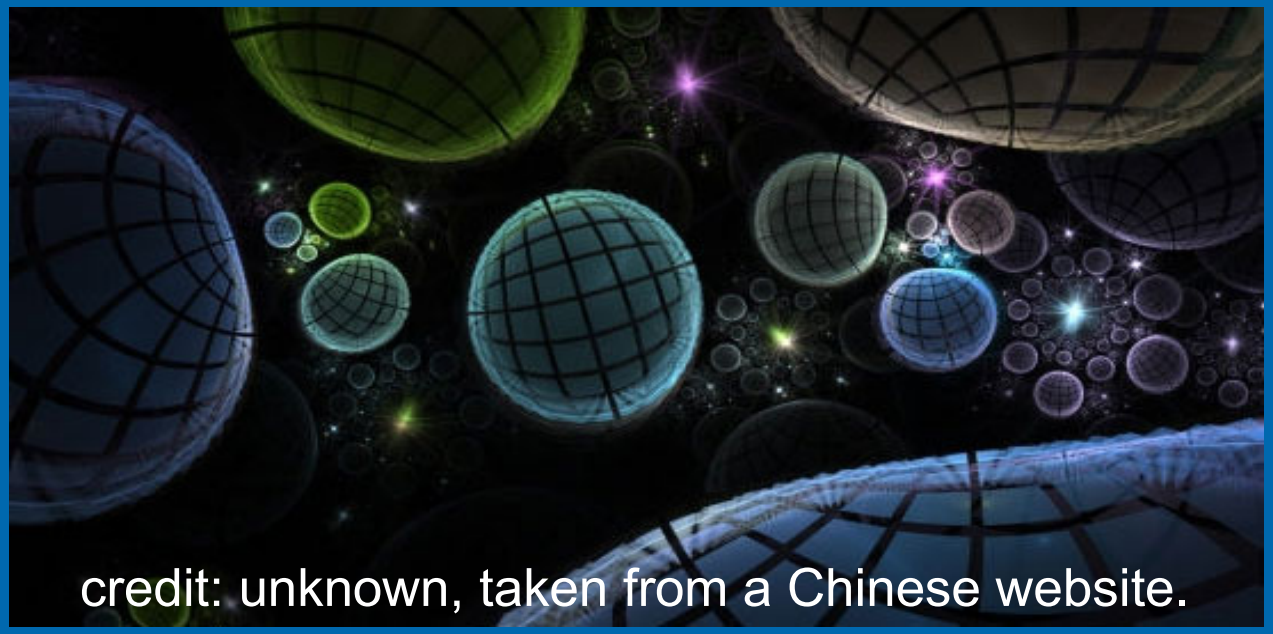

credit: unknown, taken from a Chinese website.

distribution determined by various factors

probability measure, density of states,
quantum equilibrium, ...

quantum transitions between various vacua

Creation of open universe

de Sitter (dS) vacuum: O(4,1)

⬇

Euclidean bubble: O(4)

⬇

nucleated bubble: O(3,1)
=open universe

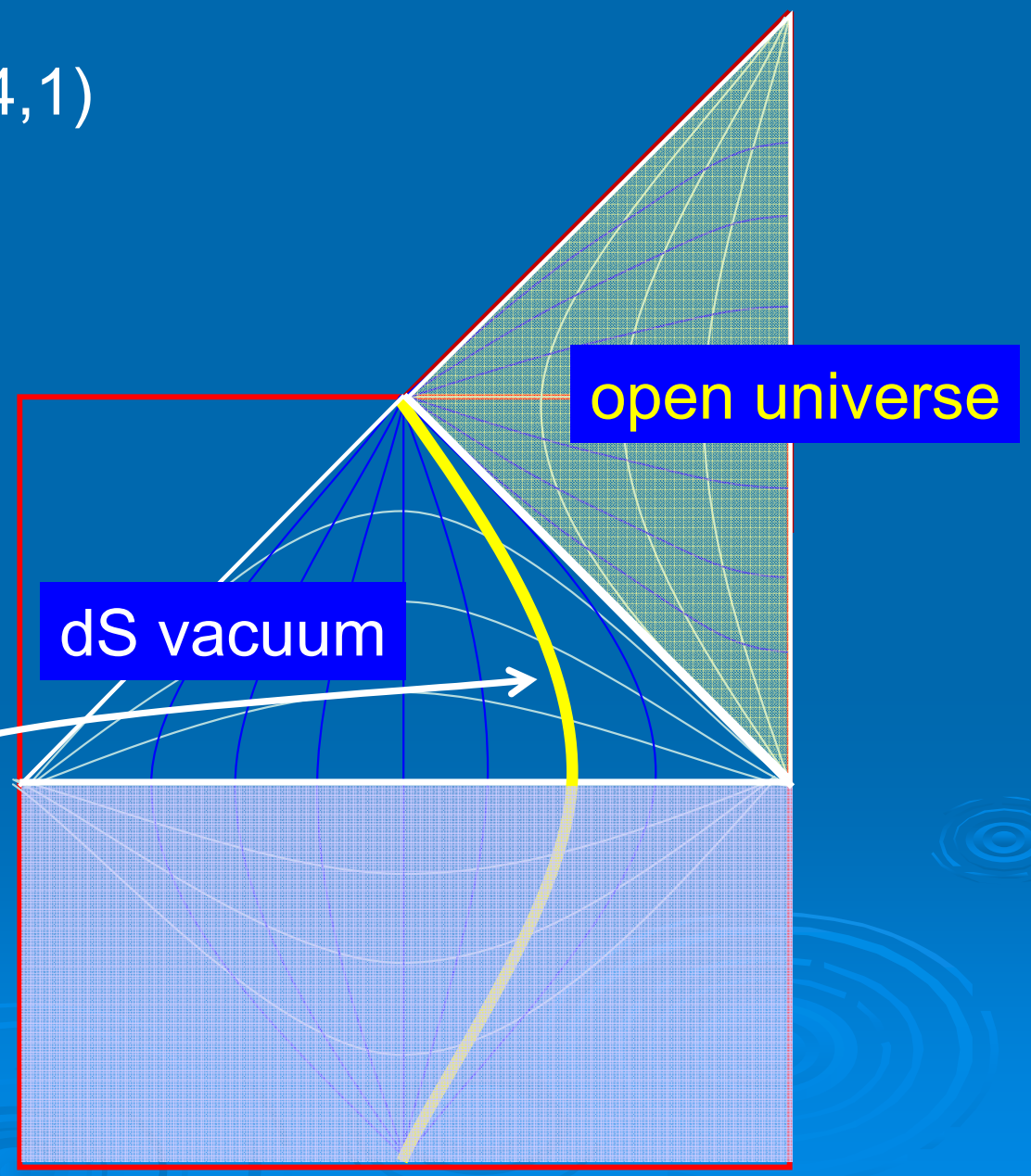

Our Universe was born out of quantum tunneling!

- two possibilities

1. inflation after tunneling was short enough (N~60)

$$1-\Omega_0 = 10^{-2} \sim 10^{-3}$$ "open universe"

➡ signatures in large angle CMB anisotropies

Yamauchi, Linde, Naruko, Tanaka & MS (2011)

2. inflation after tunneling was long enough (N>>60)

$$1-\Omega_0 \ll 1$$ "flat universe"

➡ signatures from bubble collisions

Sugimura, Yamauchi & MS (2012)

Sugimura's talk: parallel session on Monday

trace of bubble collisions

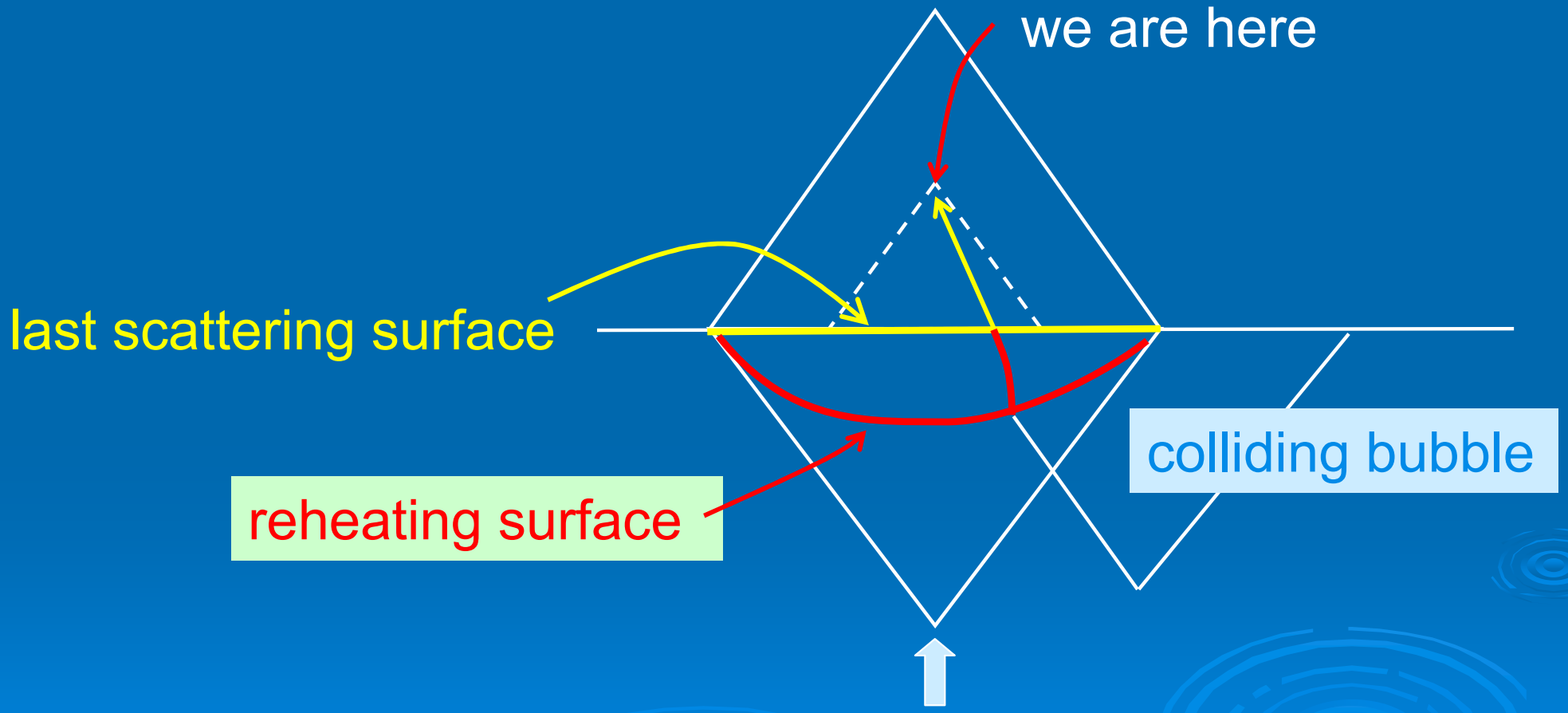

➢ simple model

- no (spherically symmetric) bubble seen in the CMB map

⇔ negligible effect on curvature perturbation (~Newton potential) at leading order

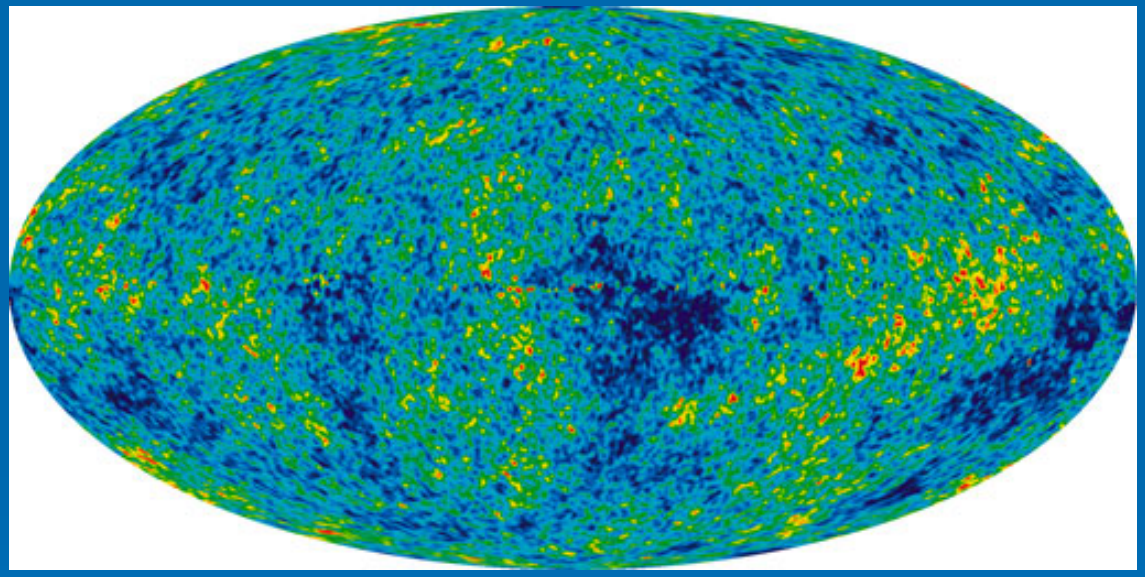

bubbles may be seen as “localized” non-Gaussianity

$$\Phi(x) = \Phi_{Gauss}(x) + f_{NL}(x)\Phi^2_{Gauss}(x) + \ldots$$

↳ space-dependent

Non-Gaussian bubbles in the CMB Sky

Sugimura, Yamauchi & MS (2012)

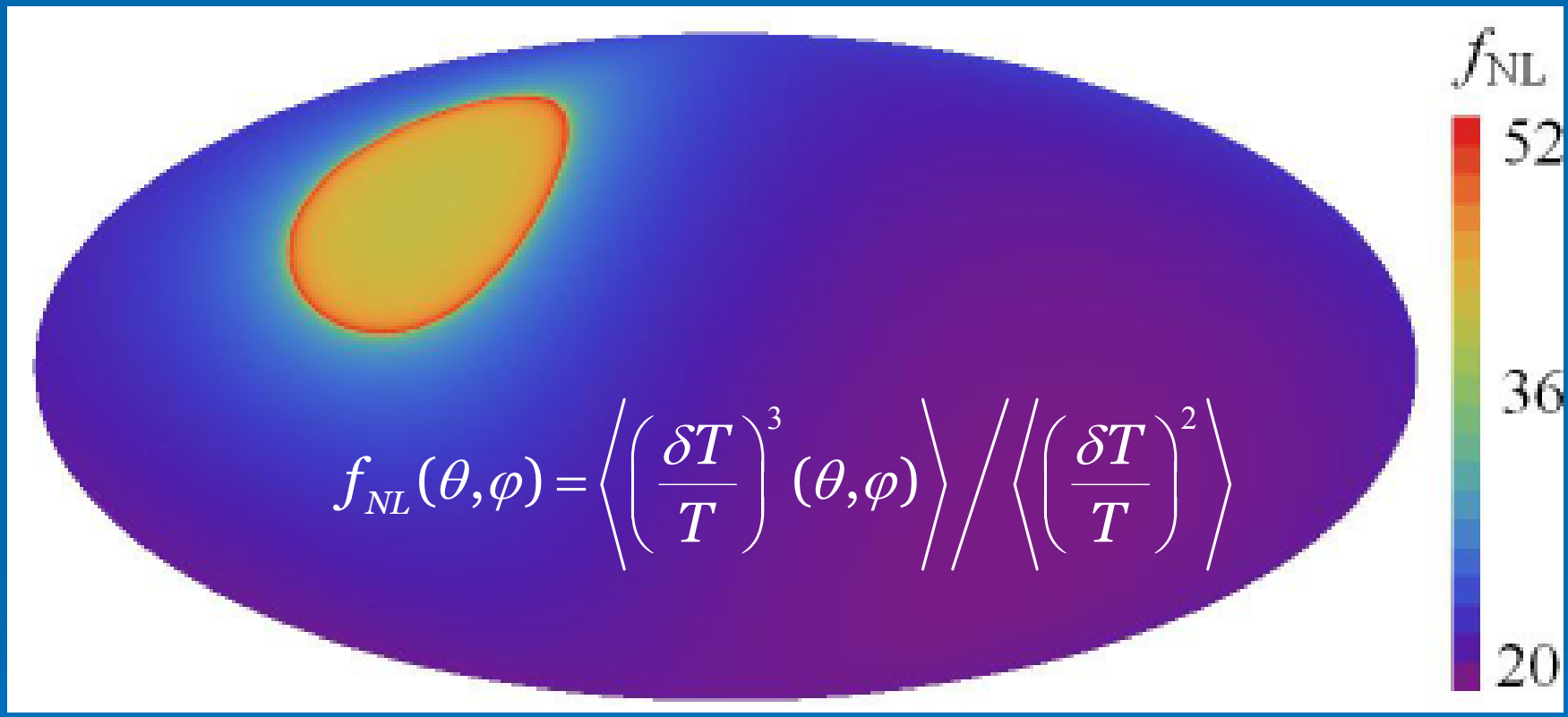

detection of a spherically symmetric "localized" non-Gaussianity will be the first observational signature of string theory!

Summary without summary...

We are entering an era of

precision cosmology

gravitational wave astronomy

any tiny deviation from GR would be revolutionary

develop ‘realistic’ GR cosmology

perturbative, non-perturbative, numerical, observational...

continued to T Futamase’s talk

Toshifumi Futamase, JGRG 22(2012)111506

"GR in the observational cosmology"

RESCEU SYMPOSIUM ON

GENERAL RELATIVITY AND GRAVITATION

JGRG 22

November 12-16 2012

Koshiba Hall, The University of Tokyo, Hongo, Tokyo, Japan

GR in the observational Cosmology

T. Futamase
Astronomical Institute, Tohoku University

- Ph. D 1981 “Radiation reaction in EOM in GR”
  Supervisor: Bernard Schutz
- Humboldt Fellow at MPA
  Jurgen Ehlers, Peter Schneider, Matthias Bartelmann,
  Thomas Buchert …..
- 1988 I got a position at Hirosaki University
  Kasai-san, Fukugida-san, Yoshida-san, Hamana-san, Asada san
  Sasaki san
- 1995 I moved to Astronomical Institute at Tohoku University
  Tosa sensei,
  Takada san, Umetsu san, Komatsu san, Itoh kun, Okura-kun,
  Okabe kun, …
- 1991 Subaru First light
- 2012 HSC

DM sub halos in Coma Cluster

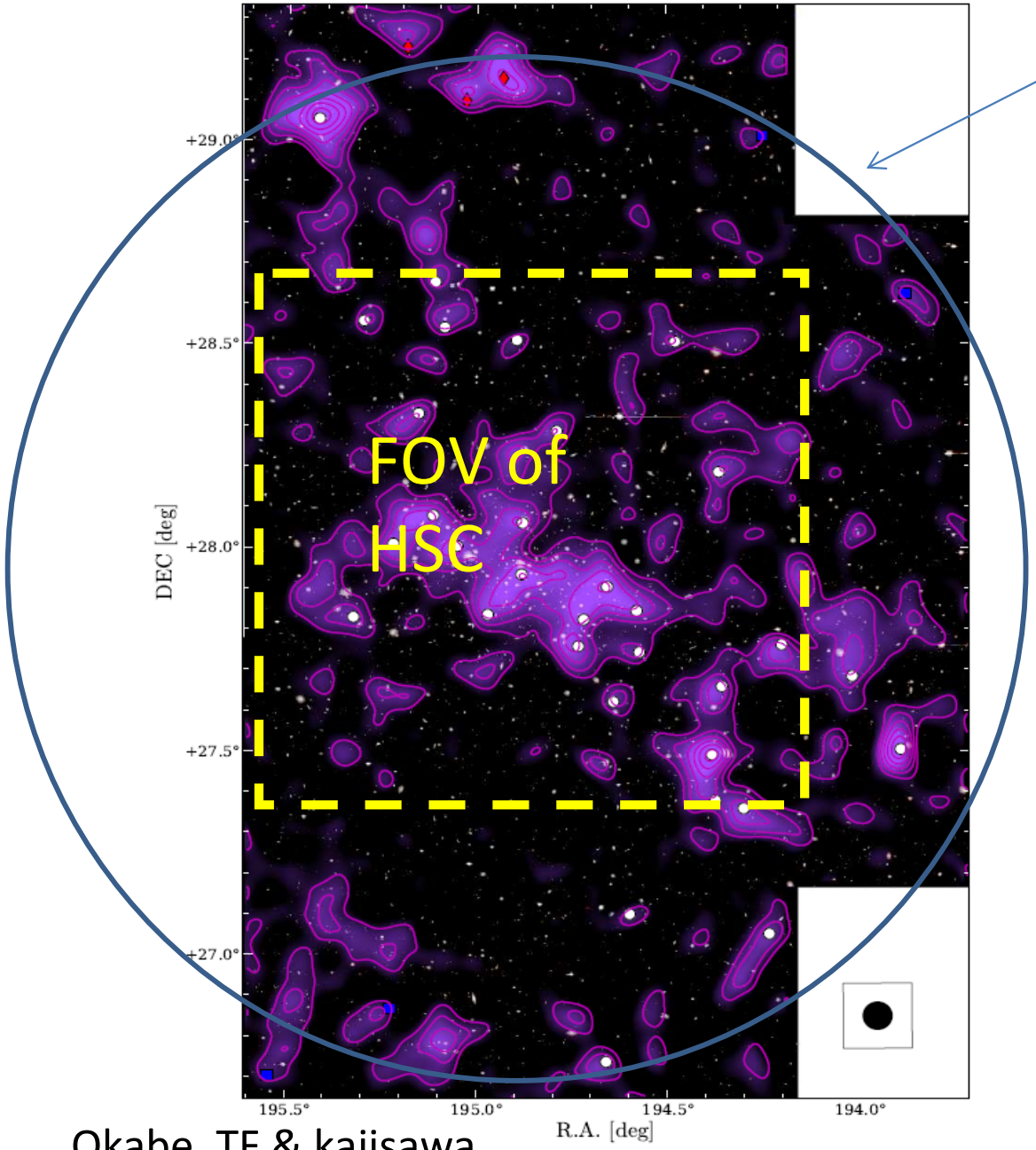

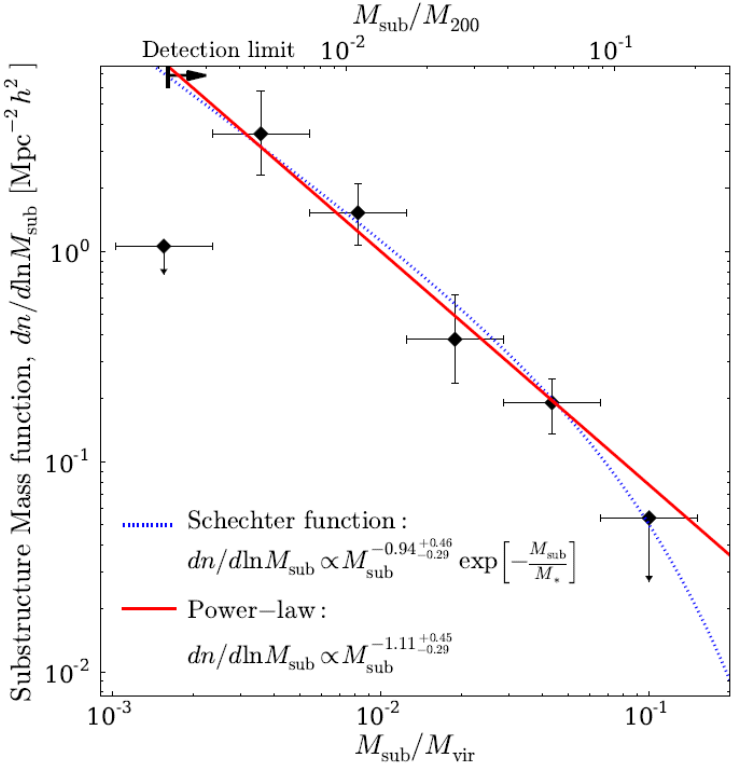

Okabe, TF & kajisawa

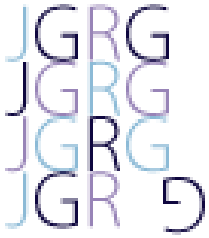

Yuichiro Sekiguchi, JGRG 22(2012)111601

"Gravitational-wave and neutrino emissions from black hole-neutron star binary merger"

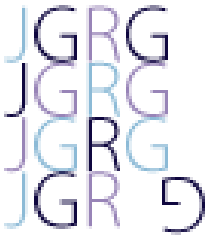

RESCEU SYMPOSIUM ON

GENERAL RELATIVITY AND GRAVITATION

JGRG 22



November 12-16 2012

Koshiba Hall, The University of Tokyo, Hongo, Tokyo, Japan



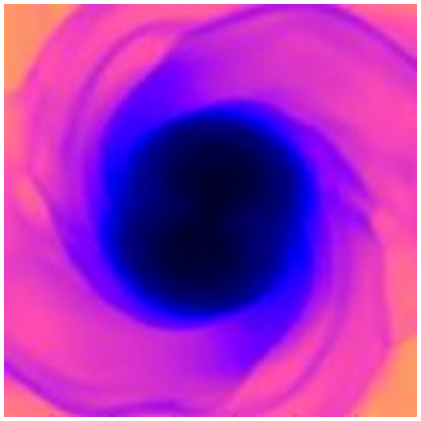

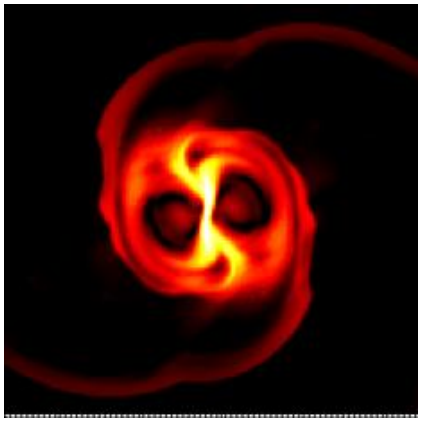

Current Status of Numerical Relativity Simulations

Yuichiro Sekiguchi (YITP)

K. Kiuchi, K. Kyutoku, M. Shibata, K. Hotokezaka

K computer

What is Numerical Relativity ?

- Solving Einstein eq. and source field eqs. to clarify dynamical phenomena in the universe where strong gravity plays a role

$$G_{ab} = \frac{8\pi G}{c^4} T_{ab}$$

$$\nabla_a T^{ab} = 0 \quad (T^{ab} = (T_{\rm Fluid} + T_{\rm EM} + T_\nu + ...)^{ab})$$

$$\nabla_a J^a = 0 \quad (J^a \sim (n_{\rm baryon},\ n_{\rm lepton}(n_e, n_\nu, ...),\ ...)u^a)$$

- All four known interactions play important roles
  - **Gravity** : GR, BH formation, ISCO, etc
  - **Strong** : EOS (equation of state) of dense nuclear/hadronic matter
  - **EM** : MHD phenomena, EOS of dense matter
  - **Weak** : Electron capture, Neutrino production
    - 99% gravitational binding energy released is carried away by neutrinos in SNe



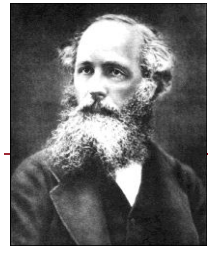
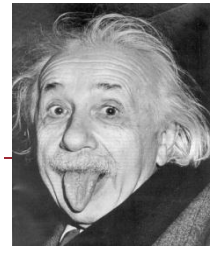

Targets of Numerical Relativity

- Dynamical phenomena with strong gravity
  - Black hole formation
  - Stellar core collapse
  - Merger of compact object binary

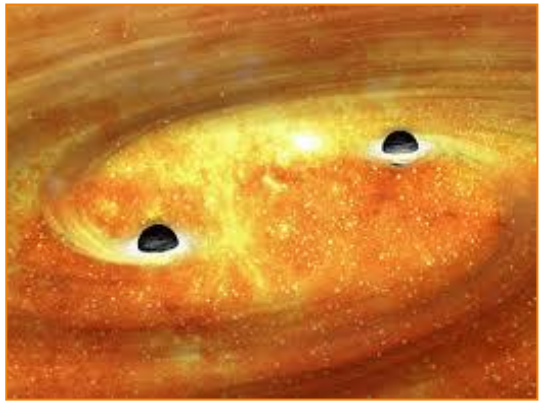

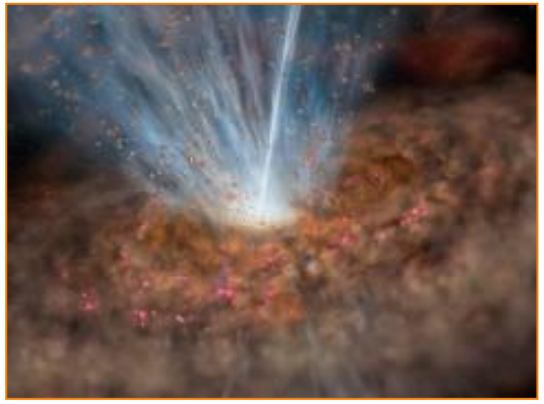

General relativistic gravity is important
Highly nonlinear and dynamical

→ **Numerical Relativity**

Targets of Numerical Relativity

- Dynamical phenomena with strong gravity
  - Black hole formation
  - Stellar core collapse
  - Merger of compact object binary
- **Gravitational waves from them**
  - **NR should provide GW templates**

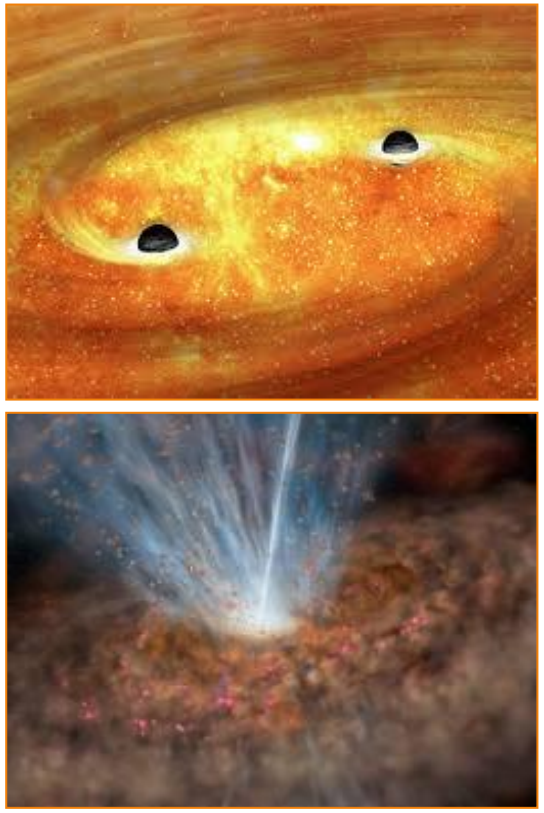

General relativistic gravity is important
Highly nonlinear and dynamical

→ **Numerical Relativity**

Current & up-coming GW detectors

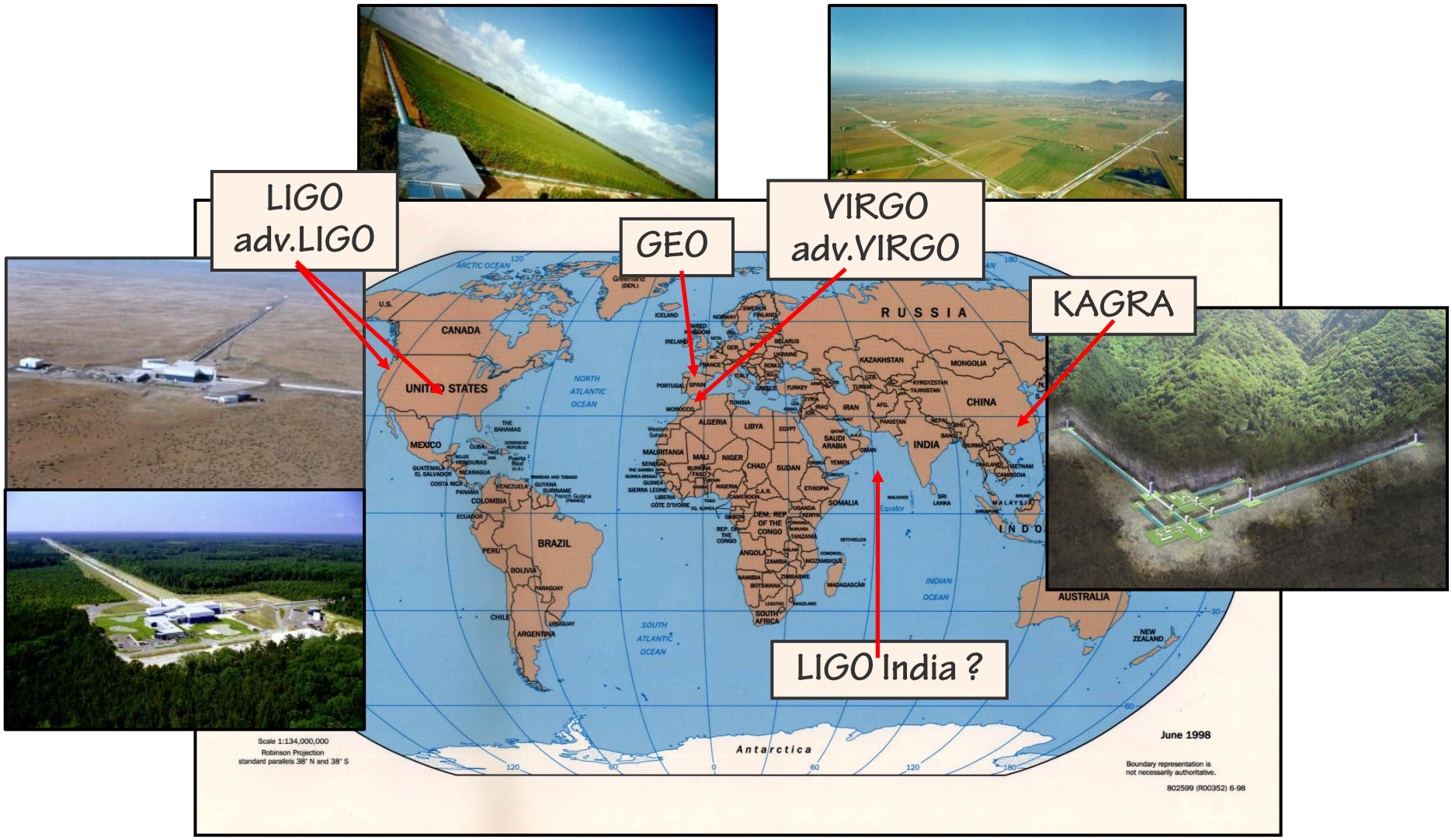

BNS 1.35-1.35Msolar optimal @ 100Mpc

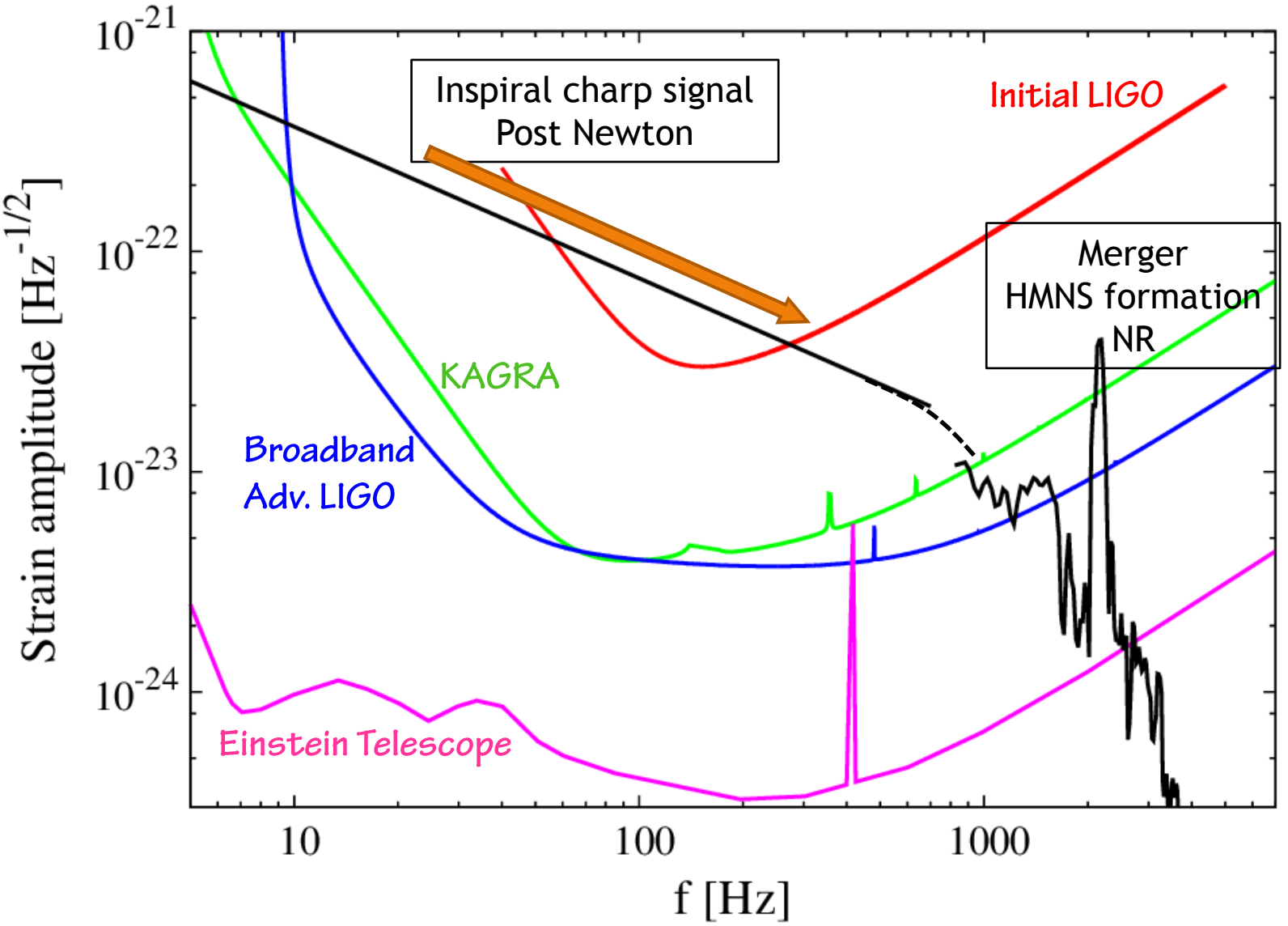

Targets of Numerical Relativity

- Dynamical phenomena with strong gravity
  - Black hole formation
  - Stellar core collapse
  - Merger of compact object binary
- Gravitational waves from them
  - NR should provide GW template
  - **Towards GW astronomy**
    - **Exploring physics and astrophysics by GW**

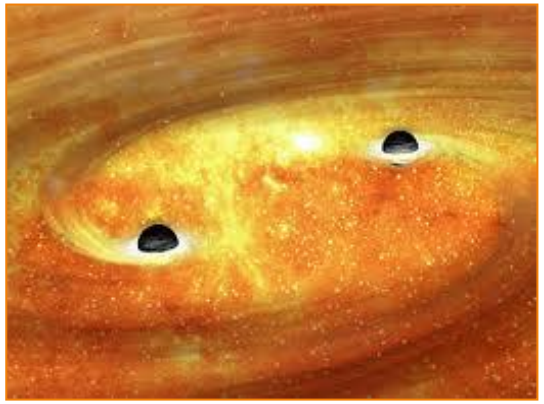

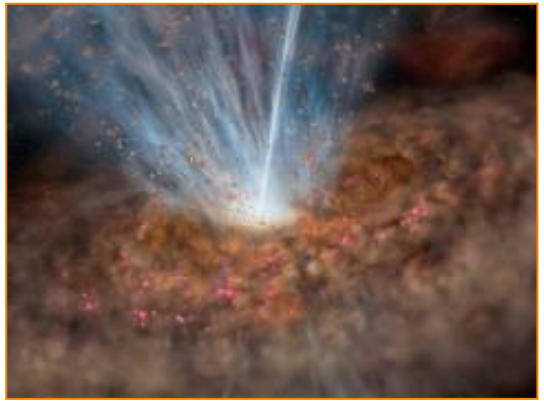

General relativistic gravity is important
Highly nonlinear and dynamical

→ **Numerical Relativity**

Neutron star & physics of dense matter

- Neutron star (NS) as a laboratory of dense matter physics
- There are a large number theoretical models
  - Equation of State (EOS)

$$P = P(\rho, T, X_i)$$

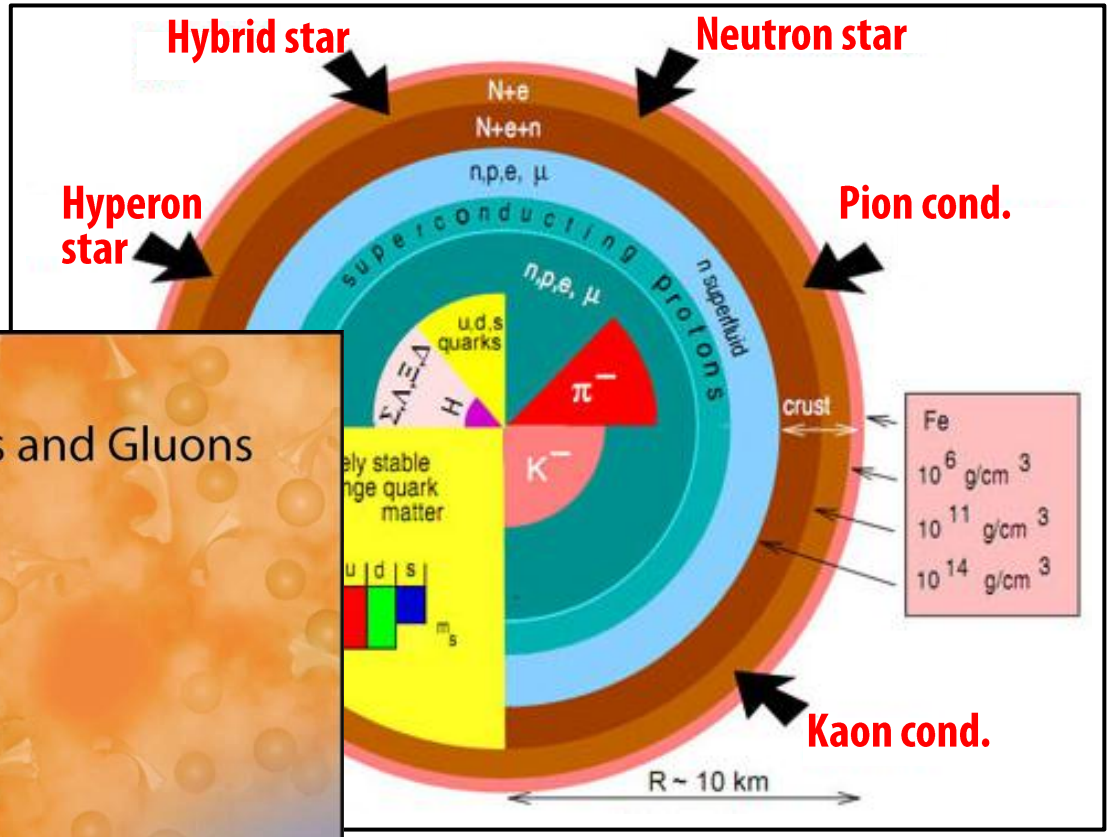

F. Weber (2005)

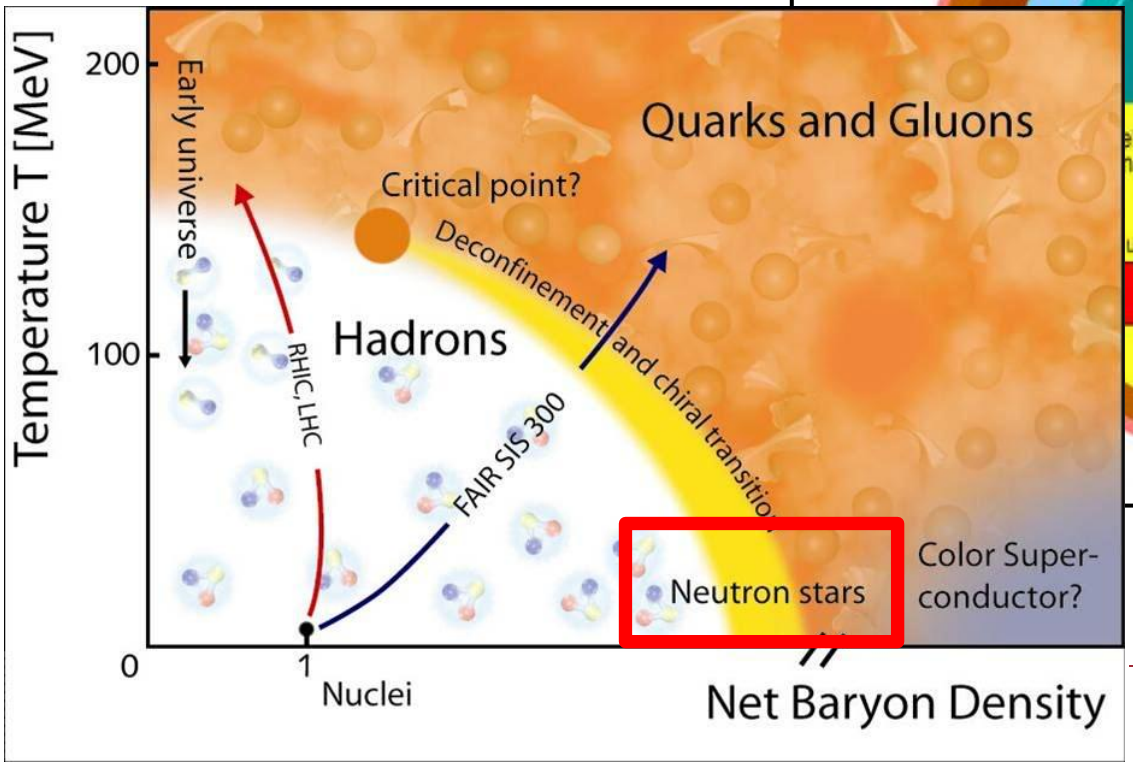

www.gsi.de

Open Question



- Given the theoretical uncertainty, which one
- Traditional method to constrain the models
  - **Mass-Radius relation** :
    - Estimation of mass and radius observation of X-ray binary
    - Large systematic error
  - **Maximum mass** :
    - Just find a massive NS
  - **PSR J1614-2230 (NS-WD)**
    - NS of 1.97Msolar
    - Mass measurement by Shapiro time delay
    - Too soft EOSs are excluded
  - Still we have a number of theoretical models

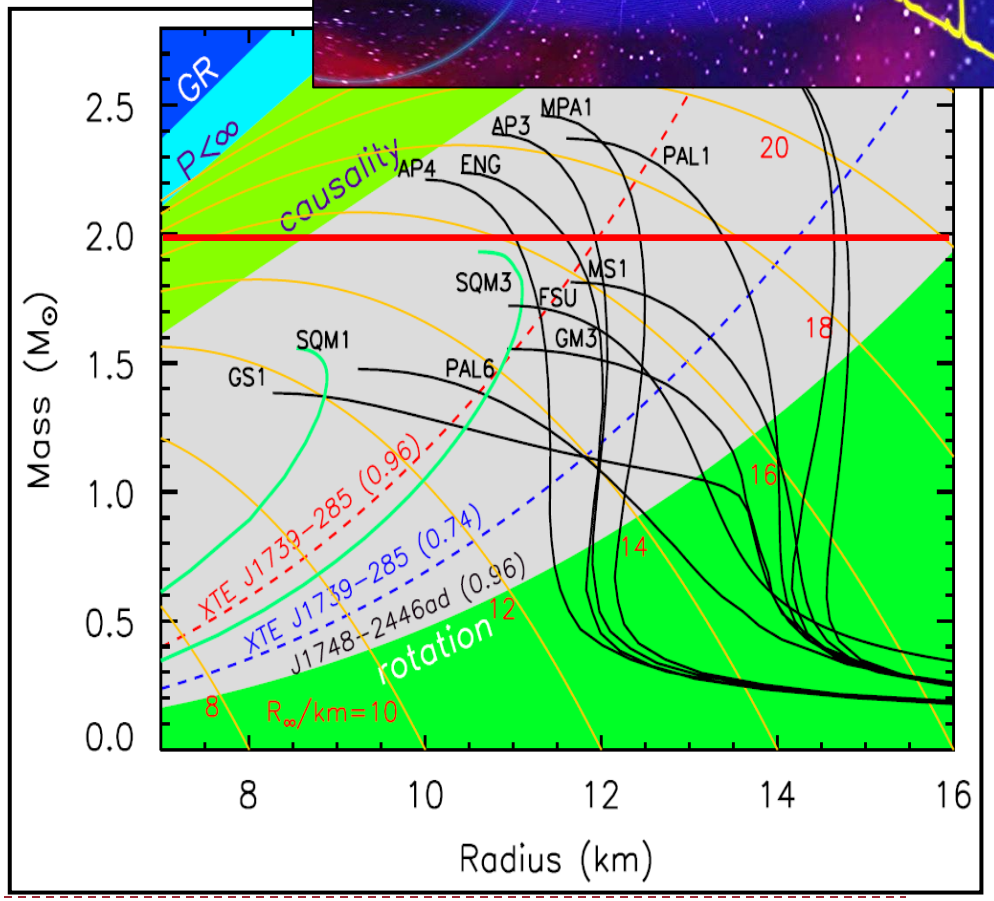

Lattimer & Prakash (2007)

Compact binary merger as cosmological collider

- NS-NS merger
  - Collision of giant nuclear matter objects
    - Tell BH or NS by GW ⇒ maximum mass
    - Both M and R are contained in GW
  - We may explore the physics of dense matter by ‘seeing’ NS interior by GW
- BH-BH merger
  - Collision of strongest gravity sources
  - Testing gravity in extremely strong regime
    - Beyond Einstein gravity ?
    - Higher dimension ?
- Comparison of observations with NR modeling

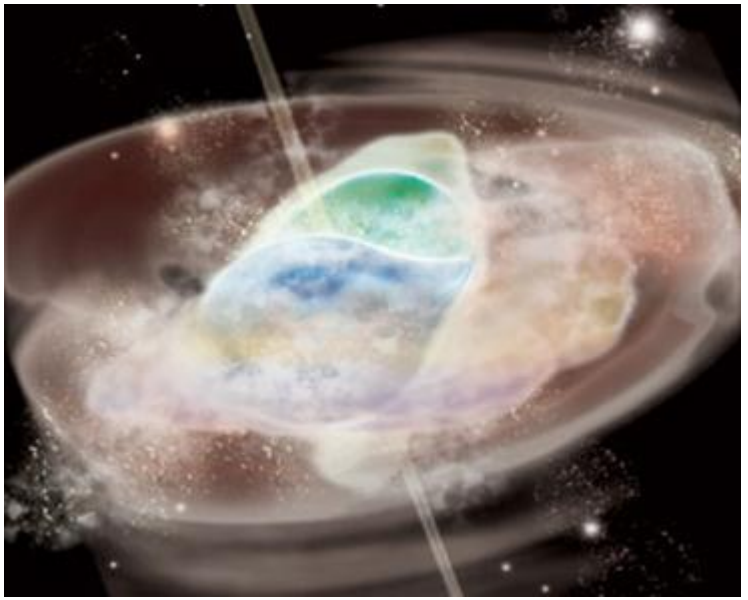

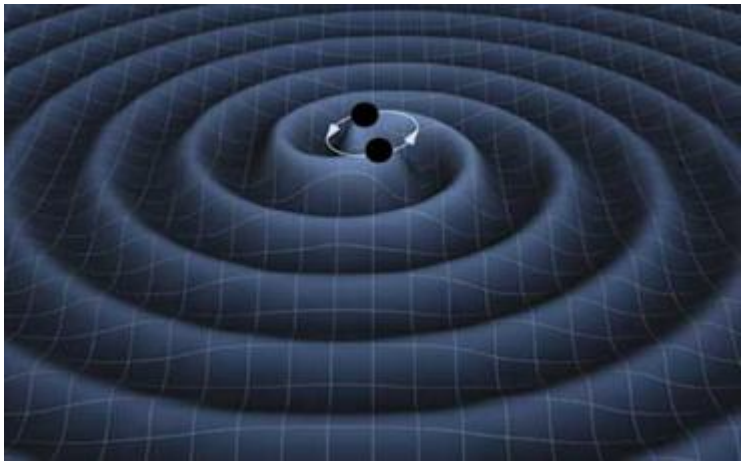

Targets of Numerical Relativity

- Dynamical phenomena with strong gravity
  - Black hole formation
  - Stellar core collapse
  - Merger of compact object binary
- Gravitational waves from them
  - NR should provide GW template
  - Towards GW astronomy
    - E.g. NS as a laboratory for dense matter physics
- **High energy phenomena in astrophysics**
  - **Gamma-ray bursts**
  - Supernova explosions

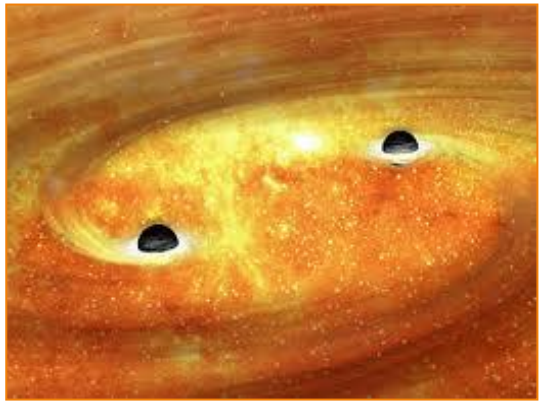

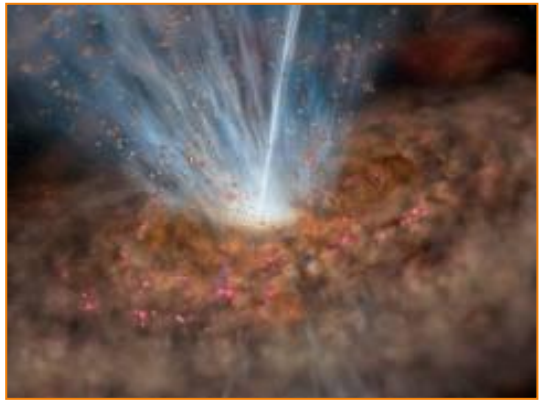

General relativistic gravity is important
Highly nonlinear and dynamical

→ **Numerical Relativity**

Central engine o

- Gamma-ray burst (GRB) : ba
  - Short and intense burst of gam
    - Discovered accidentally in the la
    - With rapid time variability : Δt ~
  - Duration : T ~ 0.01-1000 s.
    - Bimodal distribution :
    - T < 2 s : Short GRB (SGRB)
    - T > 2 s : Long GRB (LGRB)
  - Energy :
    - LGRB ~ 10^{51}erg (with beaming)
    - SGRB ~ 10^{49} erg
  - Central engine model
    - BH + accretion disk formed by
    - SGRB : NS-NS, BH-NS merger
    - LGRB : Stellar core collapse

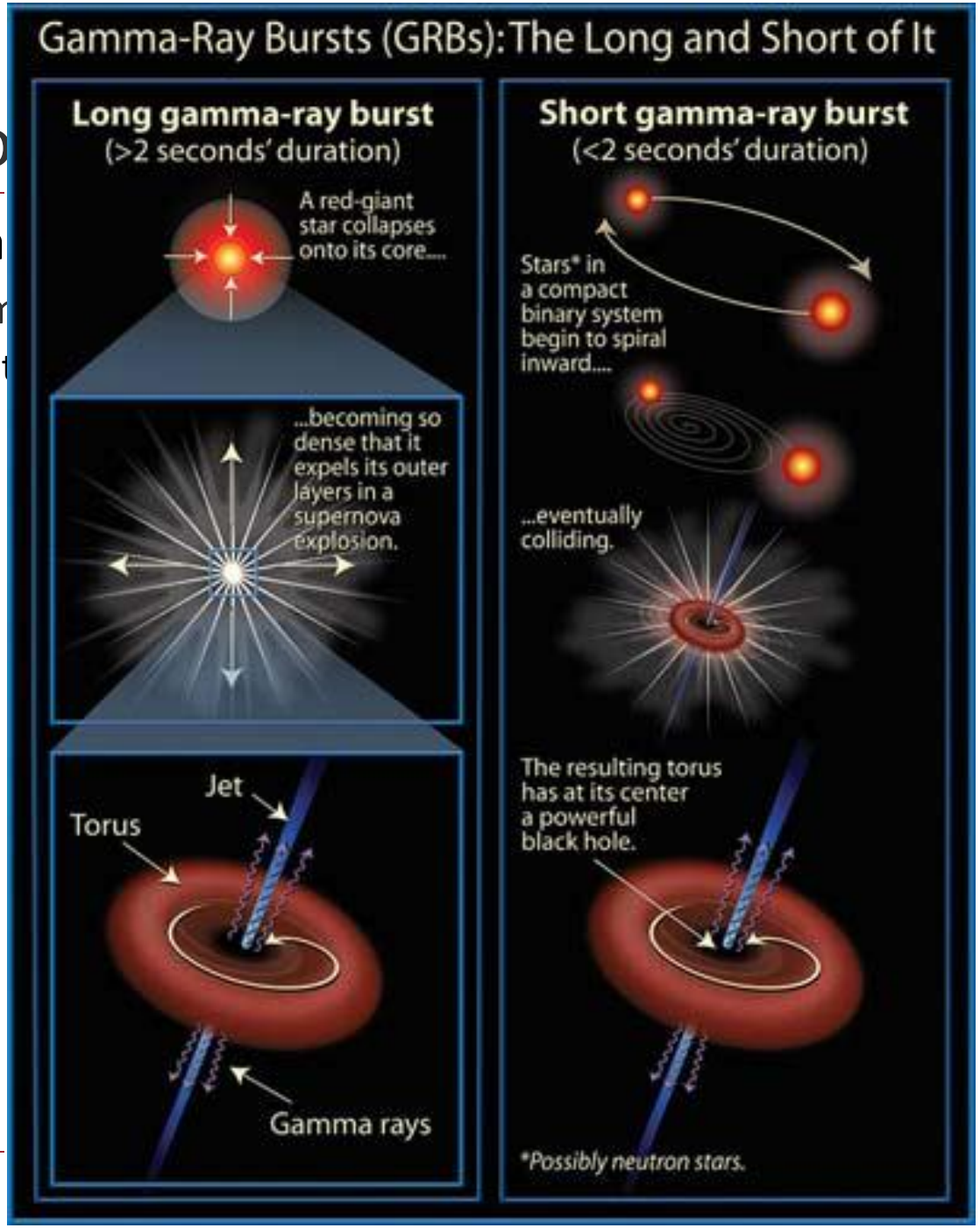

How does the GRB jet launch ?

- One possible scenario : **neutrino pair annihilation**
  - Emission of neutrinos in the hot accretion disk
  - Deposition of energy through neutrino annilihation in the baryon-poor funnel around the rotation axis driving a baryonic jet
    - Emission of gamma-ray photons in internal shocks
  - Energetics
    - Disk mass : 0.05Msolar
    - Gravitational energy at ISCO ~ 10^{53} erg
    - Neutrino Luminosity ~ Gravitational energy ?
    - Neutrino pair annihilation efficiency of 0.1--1% ?

      ⇒ jet energy of $10^{50\text{-}51}$ erg ?

      ⇒ GRB energy of 10^{49} erg ?

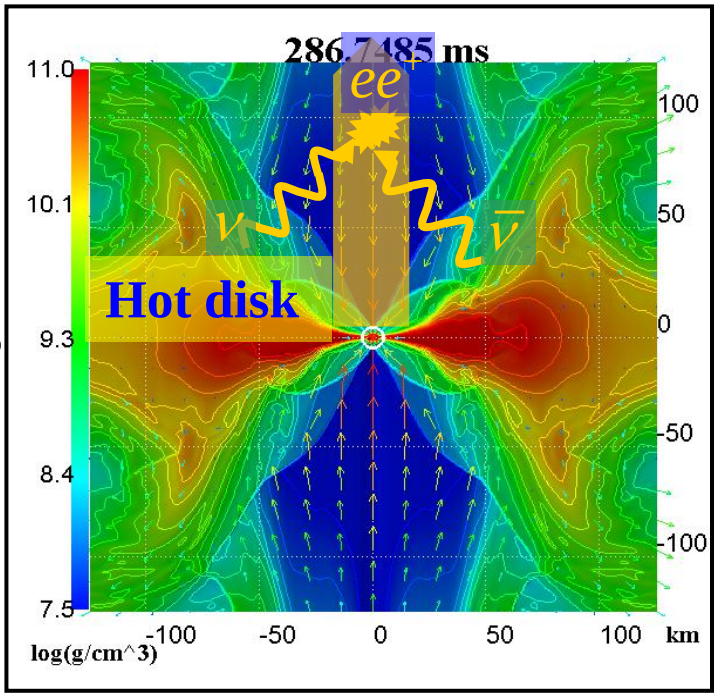

Sekiguchi & Shibata 2007

Current status of NR (1)

- **Solving Einstein equation ○**
  - ADM formulation (unstable) ⇒ BSSN formulation (stable)
    - Shibata & Nakamura (1995), Baumgarte & Shapiro (1999)
  - Stable and less time-consuming coordinate conditions (1990~)
- **Numerical scheme for GR hydrodynamics ○**
  - High resolution shock capturing scheme (Valencia, Munich 1990~)
  - GR Magnetohydrodynamics (GRMHD; 2000~) Kiuchi-kun's talk
- **Treatment of BH ○**
  - First successful binary BH simulation by Pretorius in 2005
  - BSSN-puncture : adopt nice coordinates and variables (Campanelli+ 2006)
- **Other issues ○**
  - Locating Apparent Horizon
  - GW extraction techniques from the metric
  - Mesh refinement techniques (E.g. Yamamoto+ 2008)
  - Powerful Supercomputers

Current status of NR (2)

- **Towards more 'realistic' or physical modeling …….**
  - **Trend in 2010~**
- **Equation of state (EOS) ○**
  - Nuclear-theory-based finite temperature EOS tables
    - Sekiguchi 2007,2010; O
- **Neutrino treatment ○**
  - Weak interactions (Sek
    - $e^{\pm}$ captures, $e^{\pm}$ annihila
  - Neutrino cooling (Sekig
  - Neutrino heating (Kurc
  - ***Neutrino transfer*** base
    - Solving Boltzmann equa
      ⇒ approximate solutio

Takahashi, Ohsuga, Sekiguchi, Inoue, & Tomida

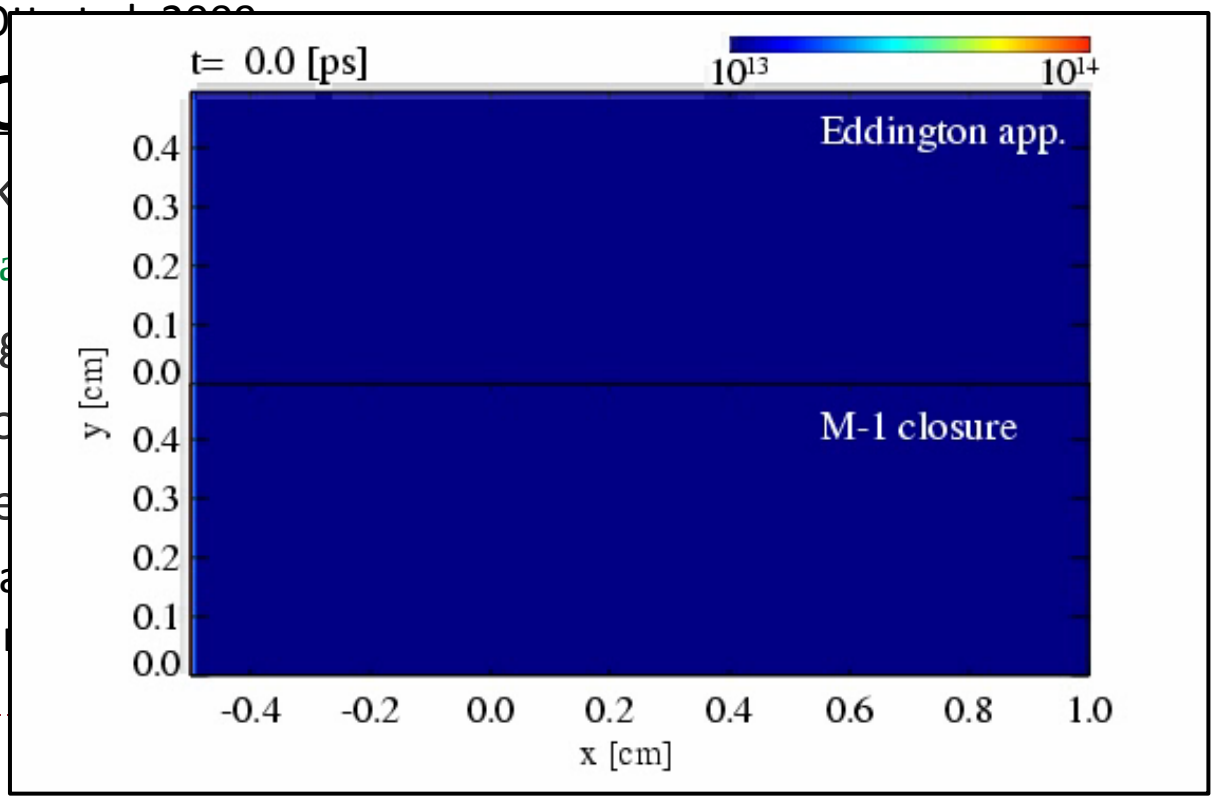

Neutrino transfer : last frontier in NR

- Solving Boltzmann equation (6+1 dims. !) is not feasible at current status
- Approximate solution by Moment scheme with a closure relation
  - Neutrino heating (absorption on proton/neutron) can be treated
  - Some approximate treatment is required for ν annihilation

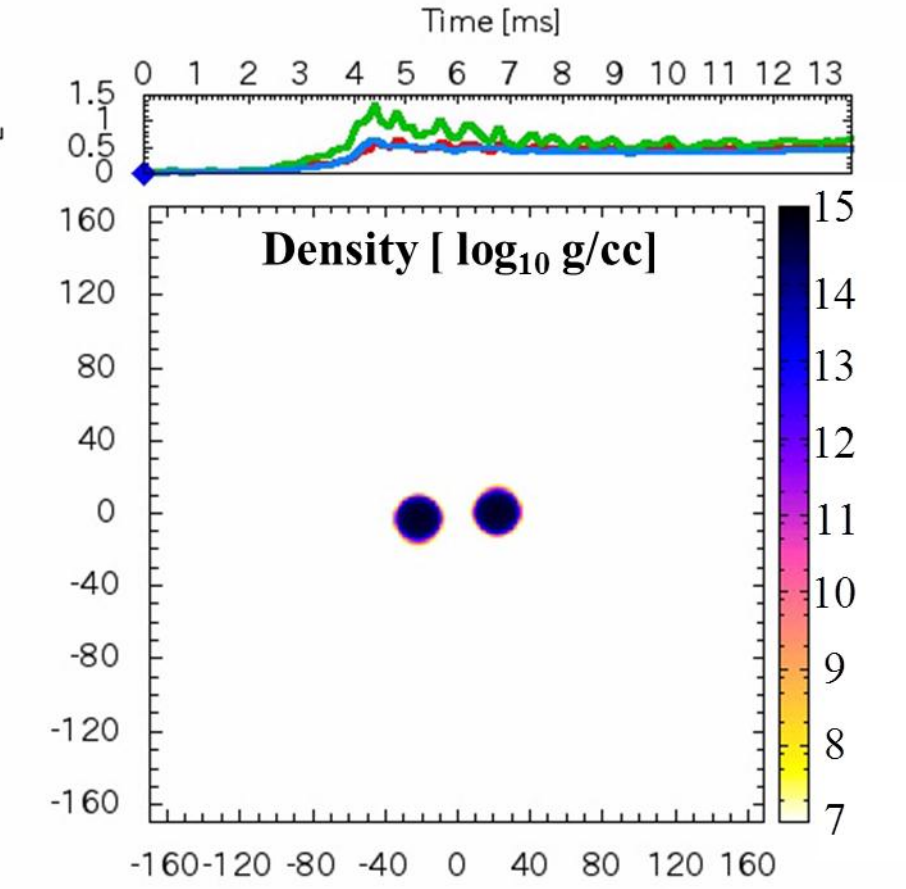

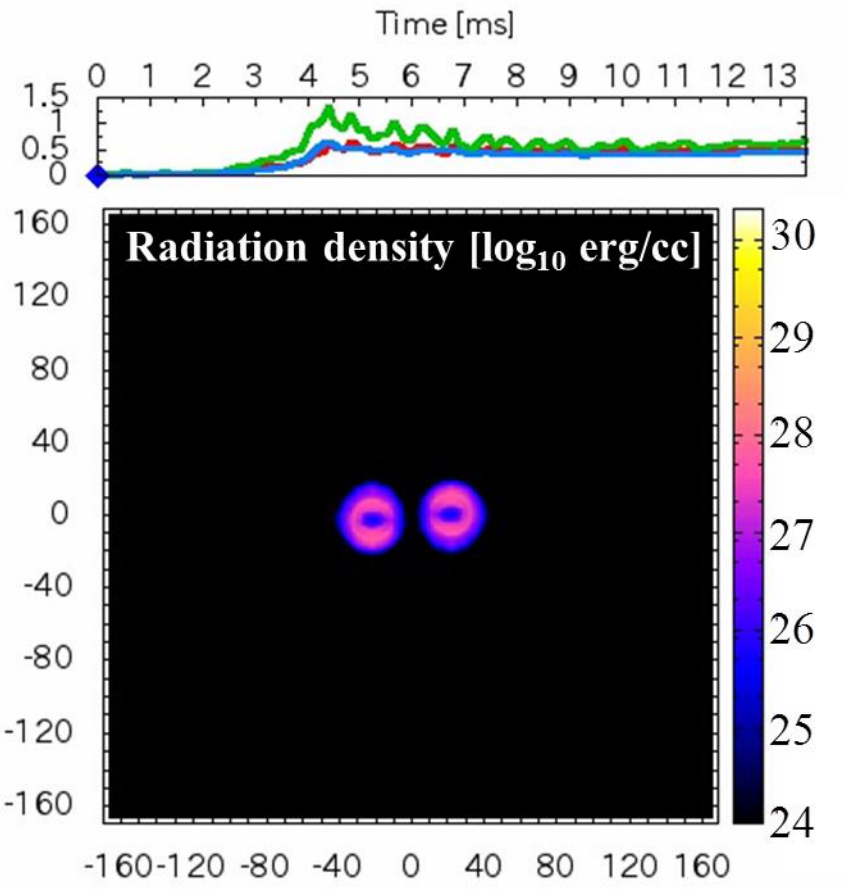

Neutrino transfer : last frontier in NR

- Solving Boltzmann equation (6+1 dims. !) is not feasible at current status
- Approximate solution by Moment scheme with a closure relation
  - Neutrino heating (absorption on proton/neutron) can be treated
  - Some approximate treatment is required for ν annihilation

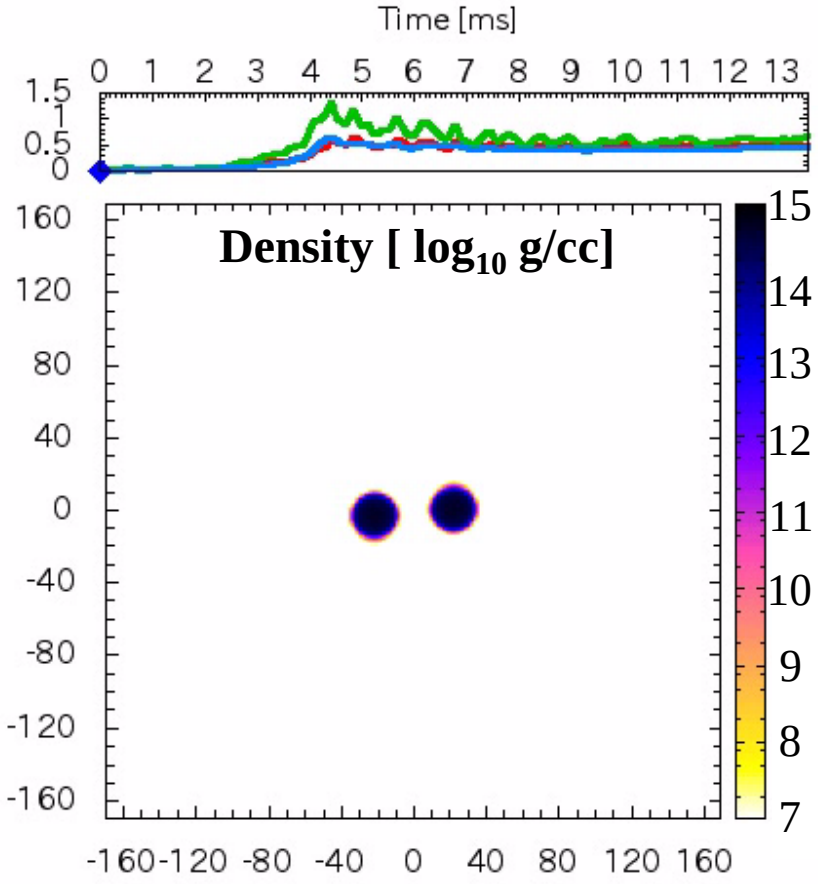

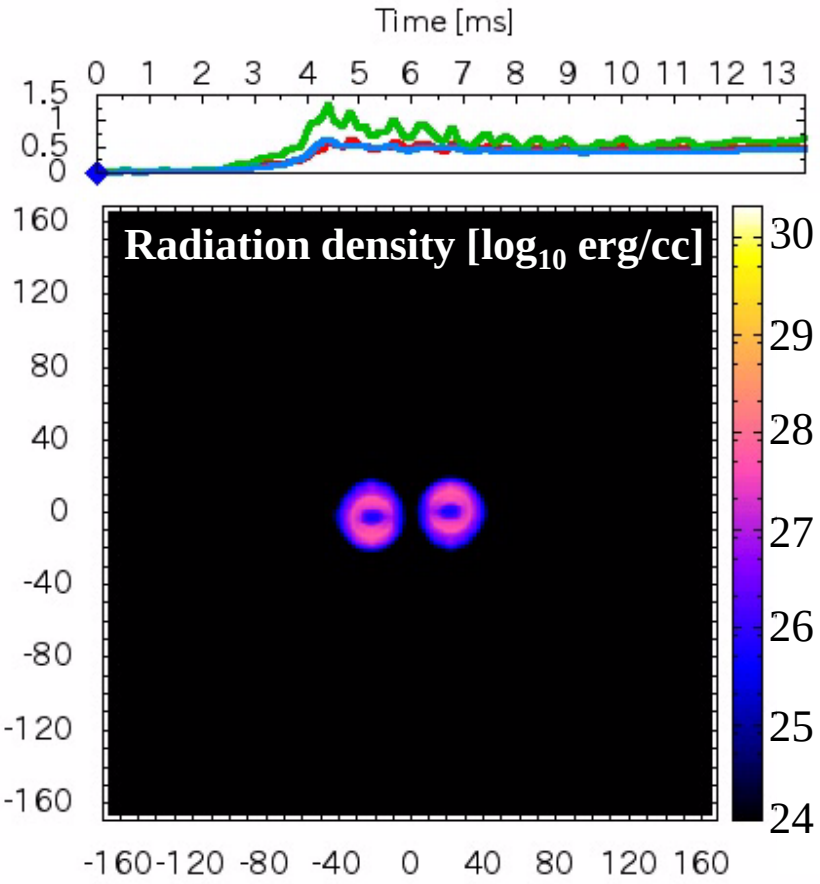

NR simulations with a physical modeling is now possible !

- Einstein's equations: Shibata-Nakamura (BSSN) formalism
  - 4th order finite difference in space, 4th order Runge-Kutta time evolution
  - Gauge conditions : 1+log slicing, dynamical shift
- GR Hydrodynamics ***with neutrinos*** (Sekiguchi 2010)
  - **Nuclear-theory-based finite temperature EOS**
  - **EOM of Neutrinos**
  - **Lepton Conservations**
  - **Weak Interactions**
    - $e^{\pm}$ captures, pair annihilation, plasmon decay, Bremsstrahlung
  - A detailed neutrino opacities
  - High-resolution-shock-capturing scheme
- **BH excision technique**
- **(Fixed) Mesh refinement technique**

$$\nabla_a T^a_b = -Q^{(\mathrm{leak})}_b$$
$$\nabla_a T^a_b{}^{(\nu,\mathrm{stream})} = Q^{(\mathrm{leak})}_b$$

$$\nabla_a(\rho Y_e u^a) = -\gamma_{\mathrm{e-cap}} + \gamma_{\mathrm{e+cap}}$$
$$\nabla_a(\rho Y_{\nu_e} u^a) = \gamma_{\mathrm{e-cap}} + \gamma_{\mathrm{pair}} + \gamma_{\mathrm{plasmon}} + \gamma_{\mathrm{Brems}} - \gamma_{\nu_e \mathrm{leak}}$$
$$\nabla_a(\rho Y_{\bar{\nu}_e} u^a) = \gamma_{\mathrm{e+cap}} + \gamma_{\mathrm{pair}} + \gamma_{\mathrm{plasmon}} + \gamma_{\mathrm{Brems}} - \gamma_{\bar{\nu}_e \mathrm{leak}}$$
$$\nabla_a(\rho Y_{\nu_{\mu,\tau}} u^a) = \gamma_{\mathrm{pair}} + \gamma_{\mathrm{plasmon}} + \gamma_{\mathrm{Brems}} - \gamma_{\nu_{\mu,\tau}\,\mathrm{leak}}$$

Sekiguchi (2010) Progress of Theoretical Physics **124**, 331

Compact object binary mergers

- NS–NS and BH–NS merger



Evolution of NS-NS

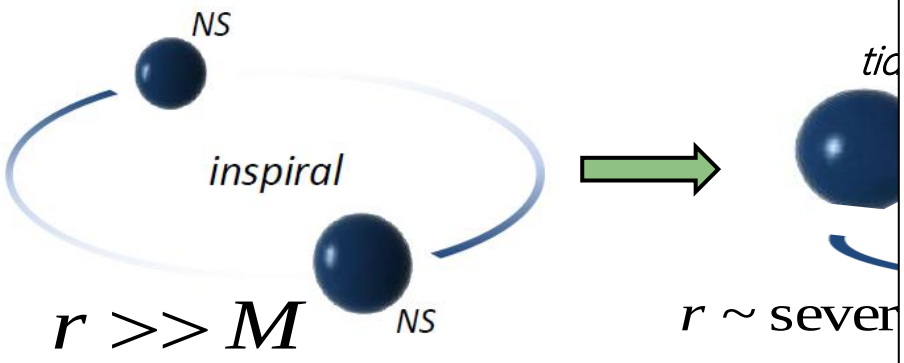

More Likely

M_{total}



Hyper Massive NS (HMNS)

$M_{\text{total}} < M_{\text{NS, max}}$

$M_{\text{total}} > M_{\text{NS,}}$



stable



accretion

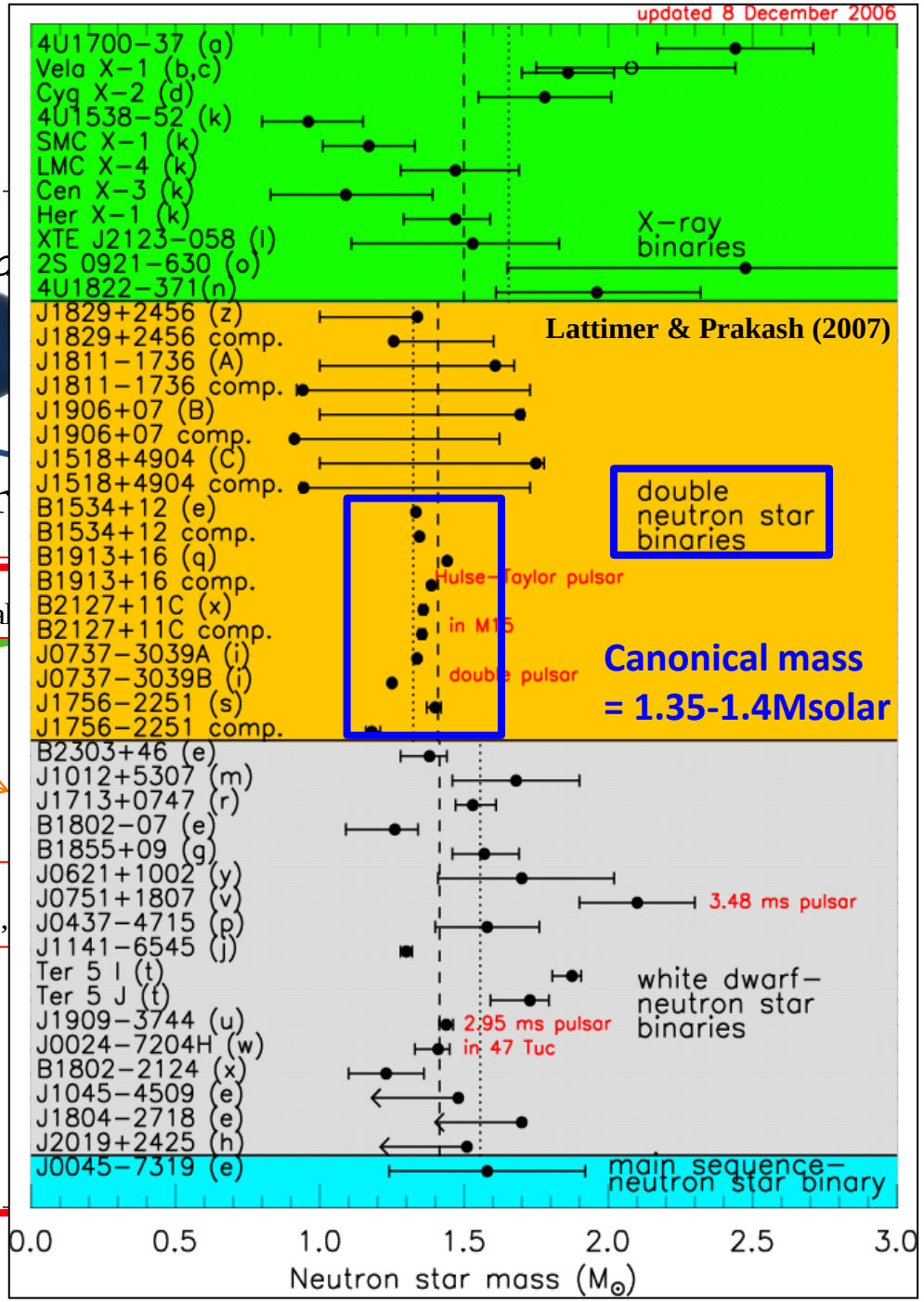

Hotokezaka et al. (2011); (2012)

GW from NS-NS (**long lived HMNS**)

NS(1.2Msolar)-NS(1.5Msolar) binary (APR EOS)

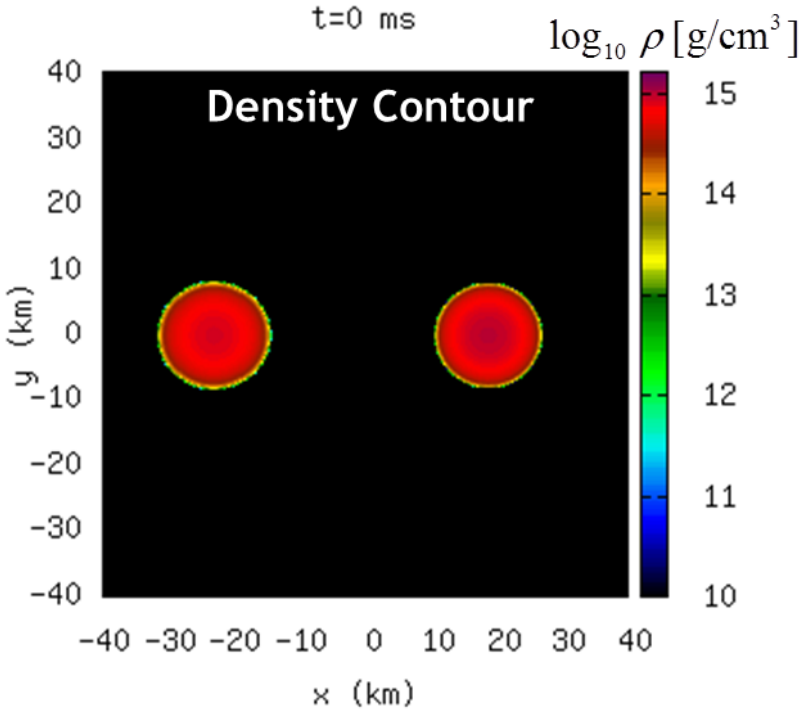

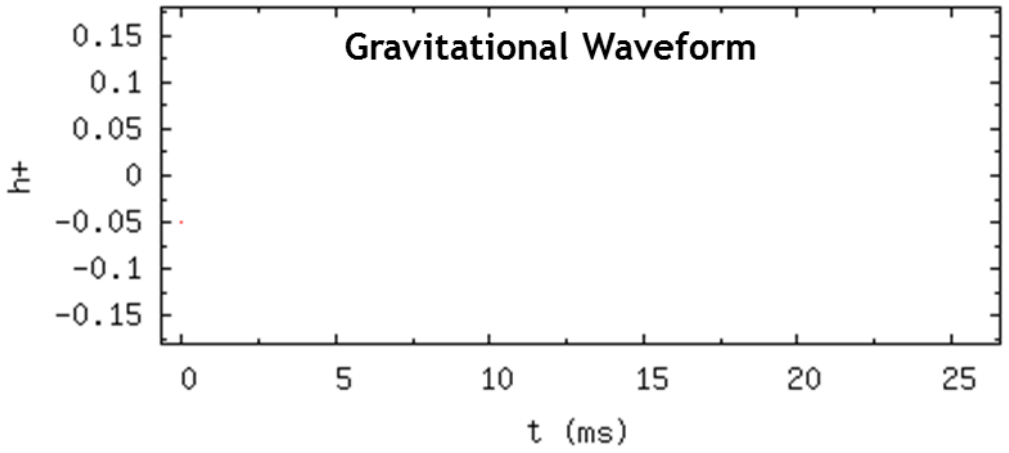

Animation by Hotokezaka

Hotokezaka et al. (2011); (2012)

GW from NS-NS (**long lived HMNS**)

NS(1.2Msolar)-NS(1.5Msolar) binary (APR EOS)

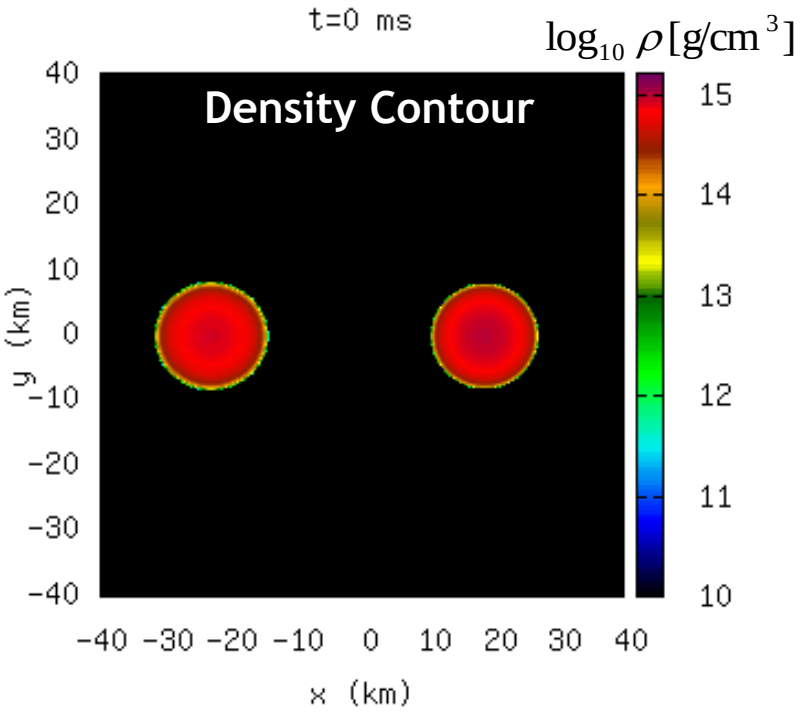

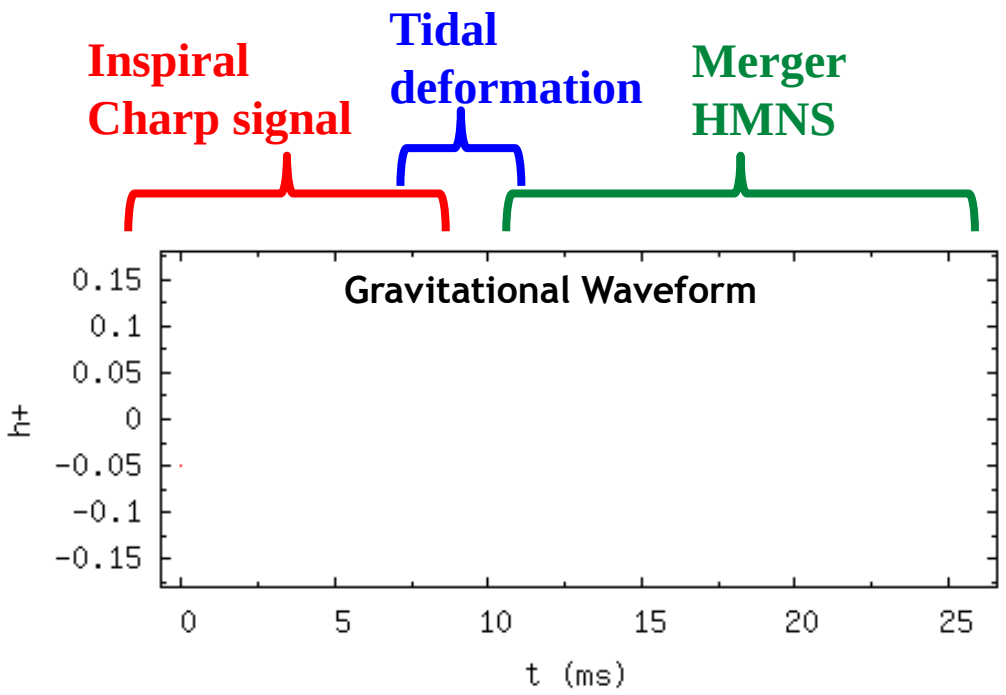

Animation by Hotokezaka

Hotokezaka et al. (2011); (2012)

GW from NS-NS (**Prompt BH formation**)

NS(1.3Msolar)-NS(1.6Msolar) binary (APR EOS)

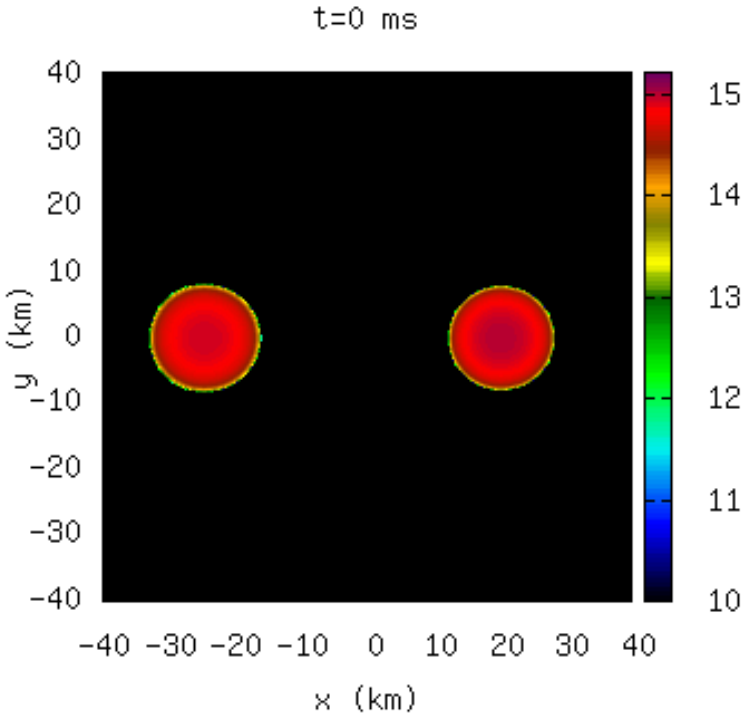

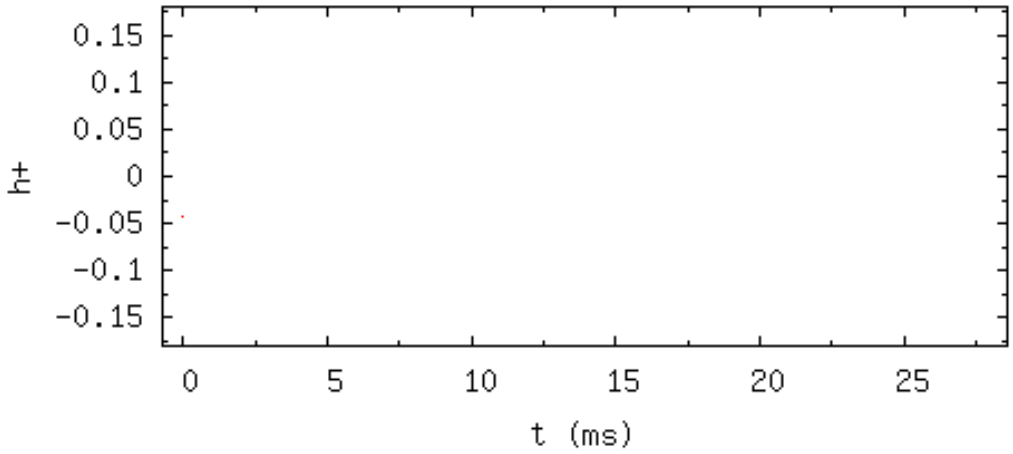

Animation by Hotokezaka

Exploring Dense matter physics by GW

Inspiral phase

- Point particle approximation
- Information of orbits, **neutron star mass** etc.

Tidal deformation

- Finite size effect
- Deviation from charp ⇒ **NS radius**

Merger and oscillation of HMNS

- BH or NS ⇒ **maximum mass**
- GW from rotating HMNS ⇒ **NS radius (and EOS)**

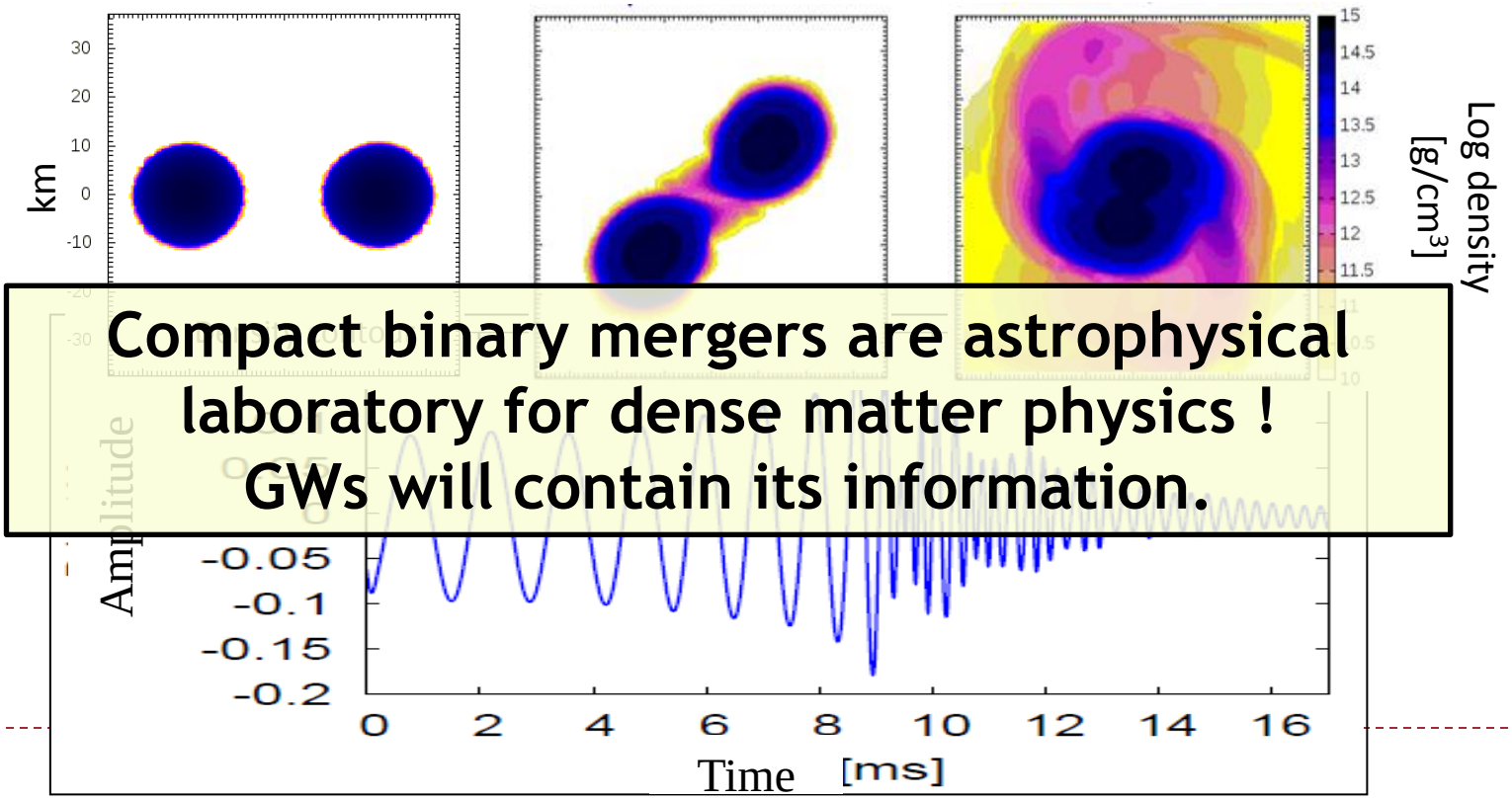

Compact binary mergers are astrophysical laboratory for dense matter physics ! GWs will contain its information.

Hotokezaka et al. (2011); (2012)

GWs from HMNS (1.3-1.4 Msolar Merger)

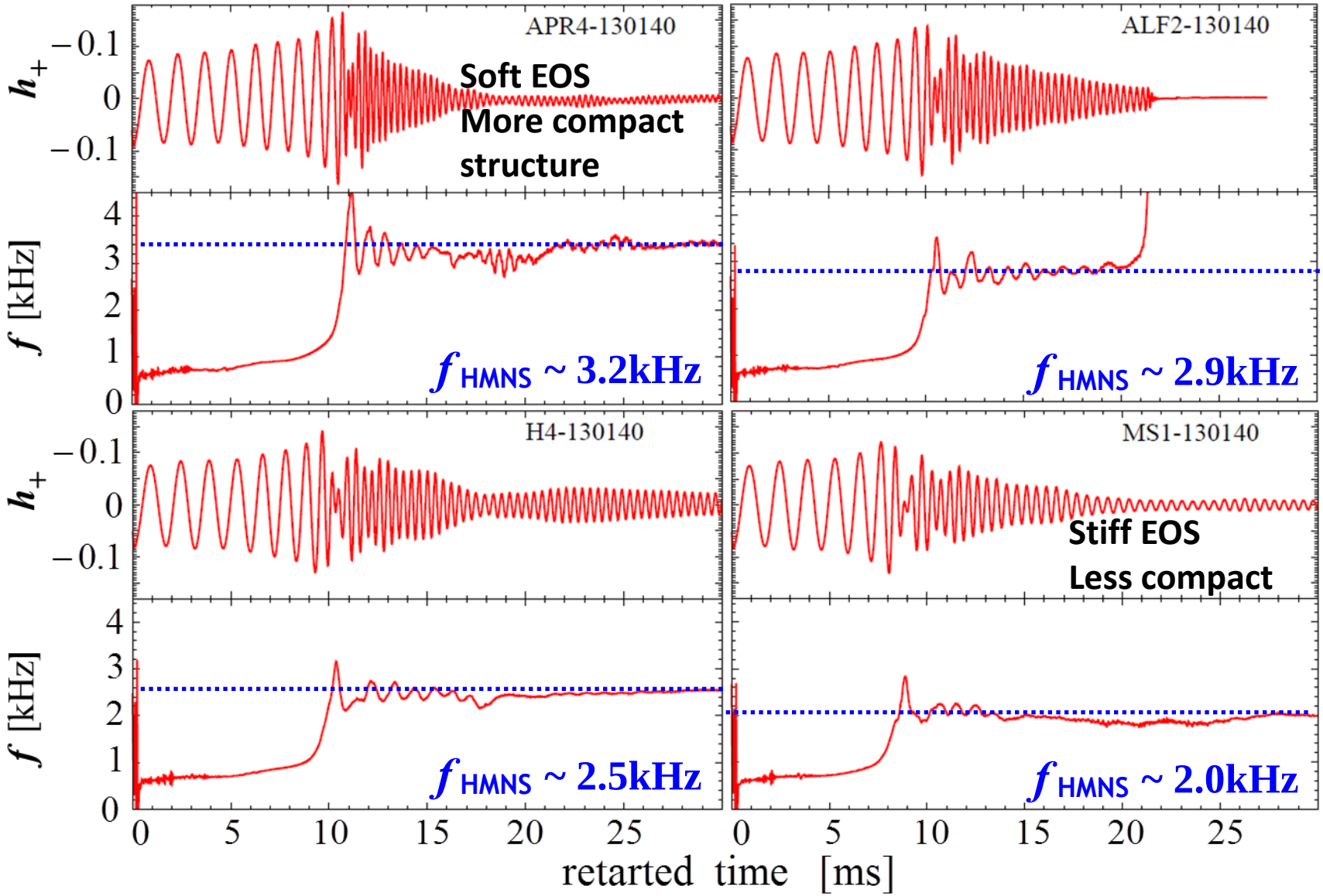

Hotokezaka et al. (2011); (2012)

GW spectra (1.35-1.35 Msolar)

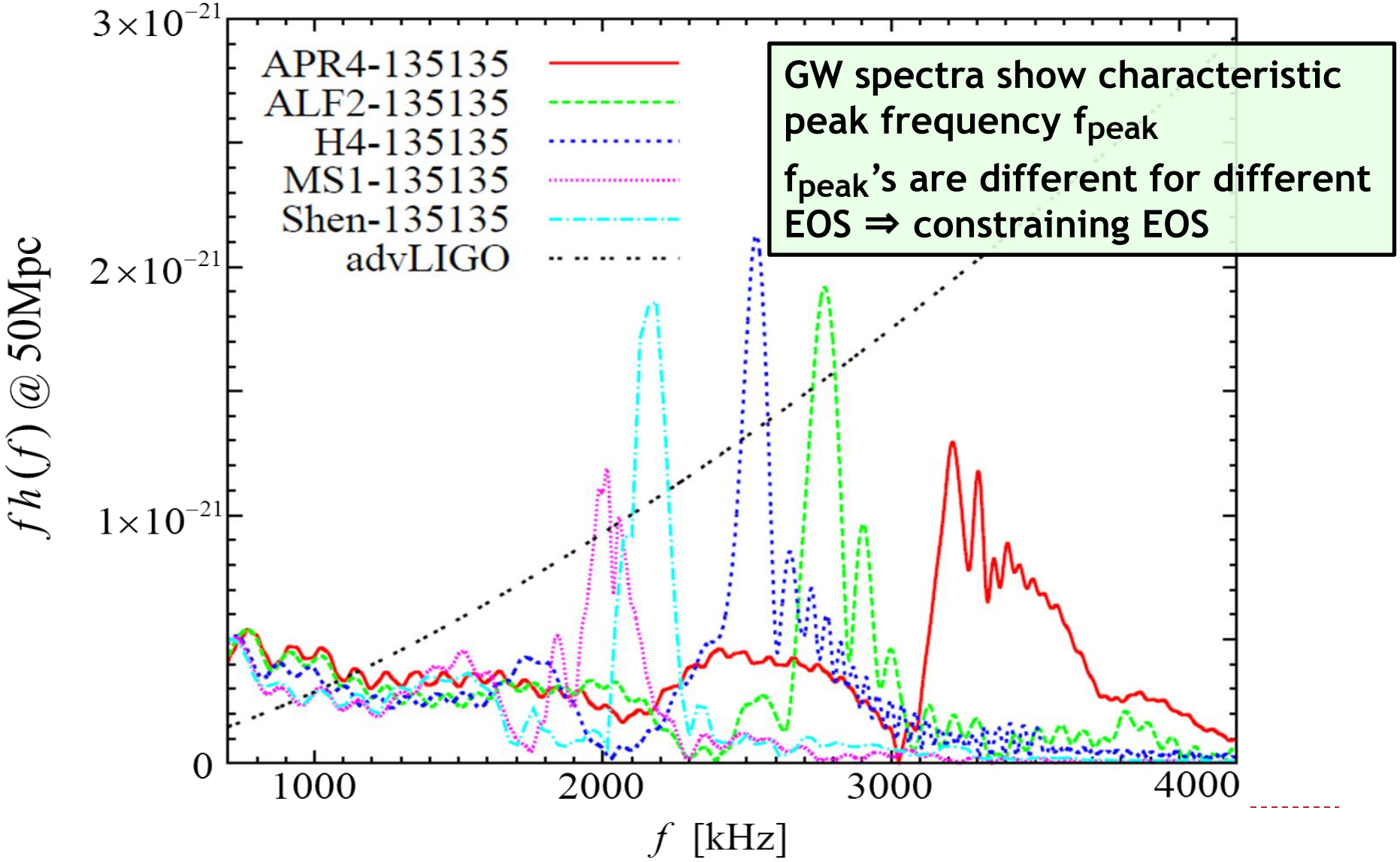

GW spectra show characteristic peak frequency f_{peak}

f_{peak}'s are different for different EOS ⇒ constraining EOS

Evolution of BH-NS

Shibata & Taniguchi (2008)
Kyutoku et al. (2010), (2011)

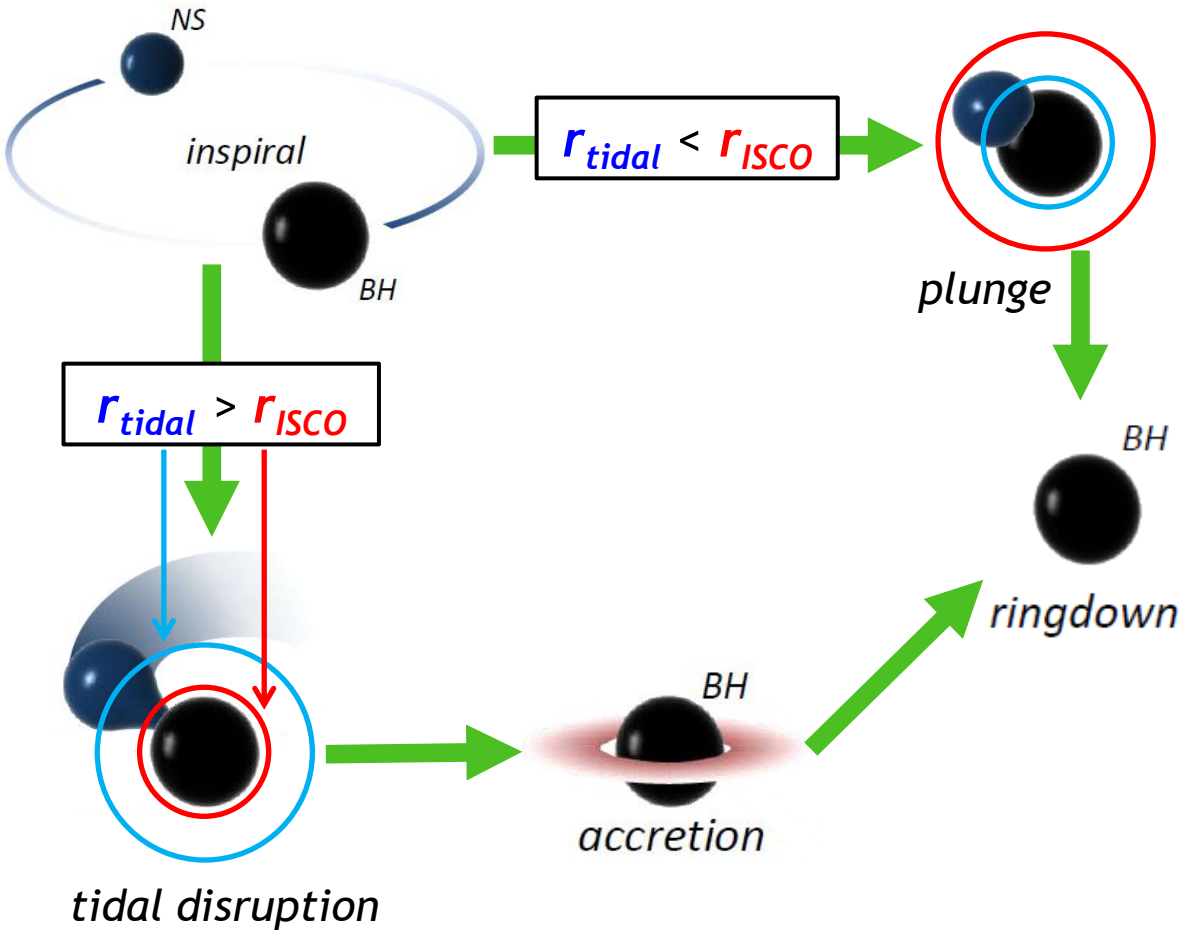

$$r_{\rm ISCO} = r_{\rm ISCO}(M_{\rm BH}, a_{\rm BH})$$

BH spin dependence
larger a_{BH} ⇒ smaller r_{ISCO}

tidal force = self gravity of NS

$$\frac{r_{\rm tidal}}{M_{\rm BH}} = \left(\frac{M_{\rm NS}}{M_{\rm BH}}\right)^{2/3} \left(\frac{M_{\rm NS}}{R_{\rm NS}}\right)^{-1}$$

Compactness of NS
⇒ NS structure (EOS)

Imre Bartos, GECo, Columbia University
(Bartos et al. 2013, in prep.)

GW from BH-NS merger

Kyutoku et al. (2010), (2011)

- **Tidal disruption**
  - GW amplitude shutdown suddenly
  - Widespread tidal arm and accretion disk form
- **Plunge/Weak disruption**
  - inspiral orbit sustains in more inner regions
  - NS hits BH and quasi-normal mode is excited

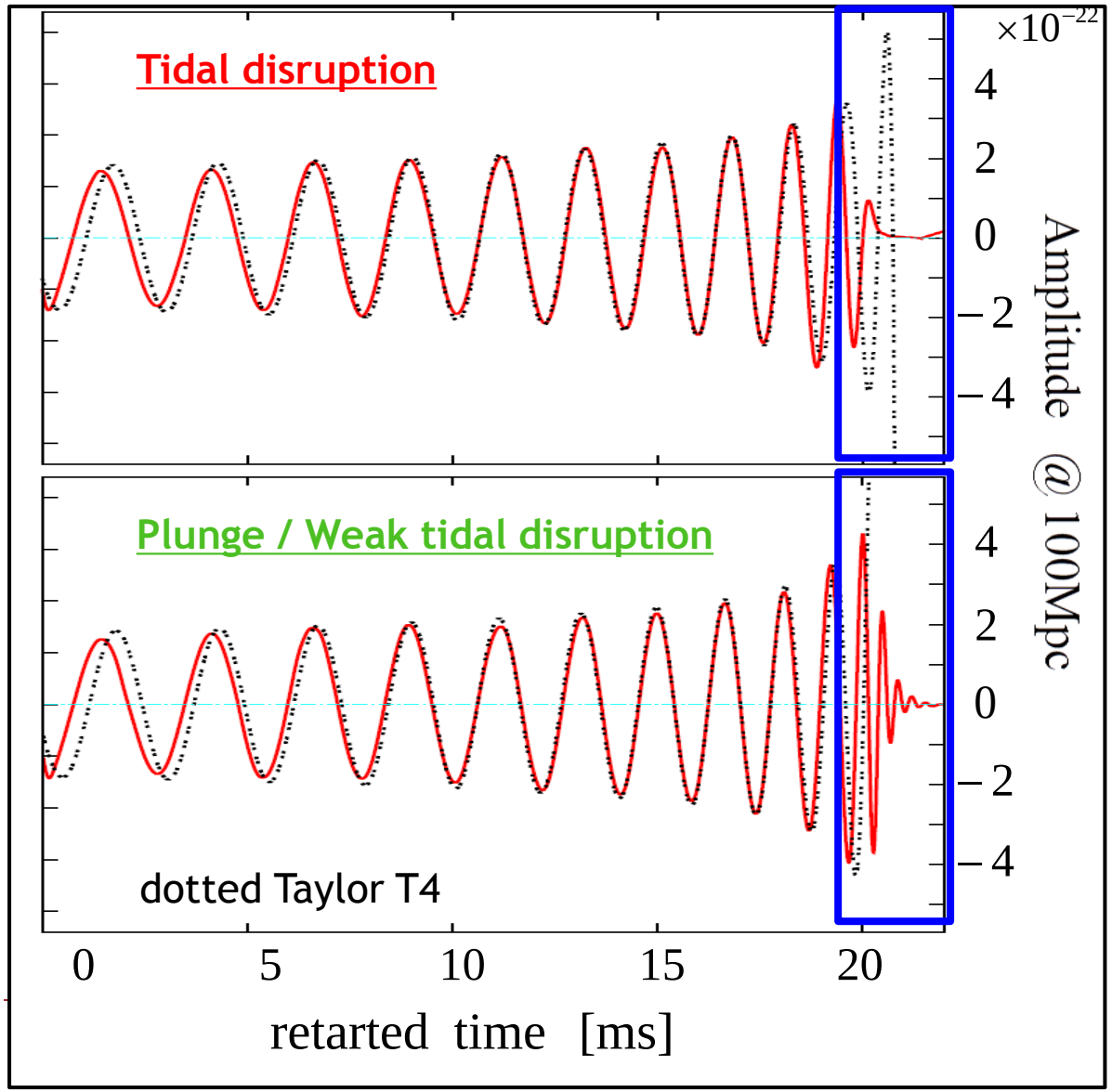

What GW spectra tell us

Kyutoku et al. (2010), (2011)

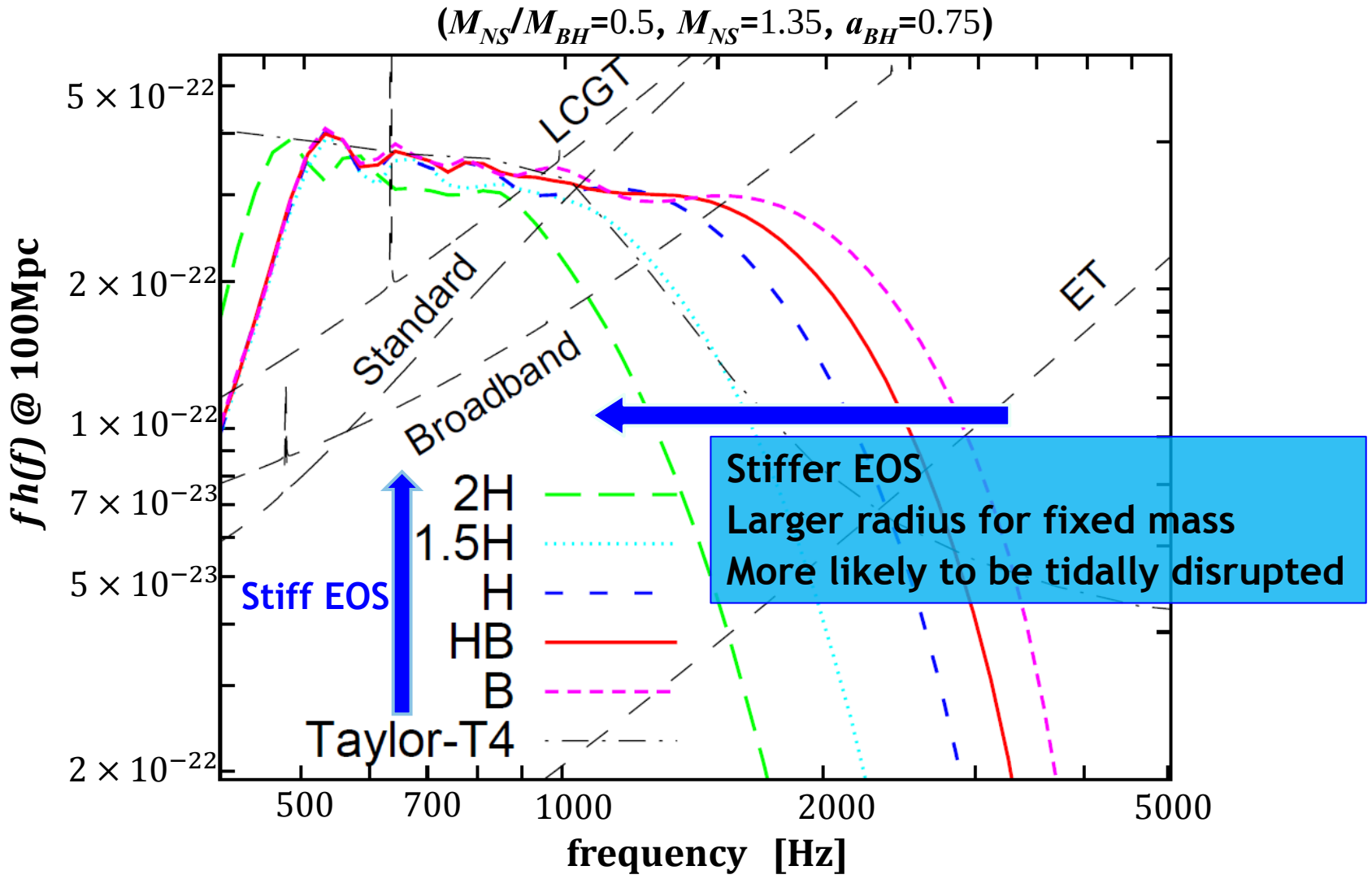

Kyutoku et al. (2011)

NR simulations with microphysics

- Towards central engine of GRB



Sekiguchi et al. PRL (2011) **107**, 051102; **107**, 211101

NS-NS merger (1.6-1.6Msolar)

- Hyper massive NS (HMNS) is first formed
  - Temperature increases significantly by compression and shock heating
  - Shocks occur in spiral arms
- HMNS eventually collapse to a BH due to emission of GW and neutrinos
  - accretion disk (with Mdisk < 0.1Msolar) forms around the BH

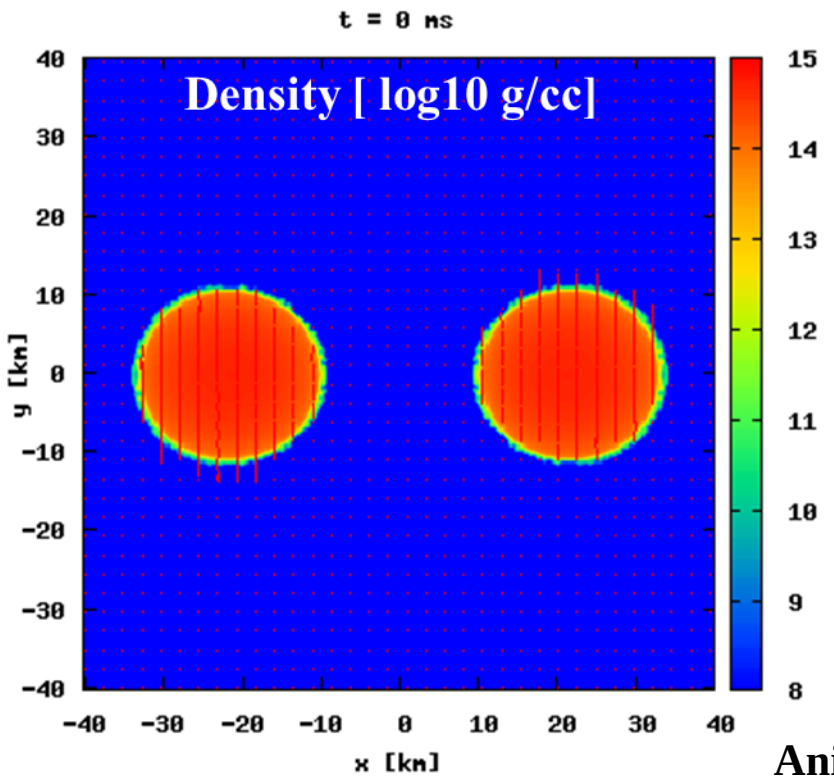

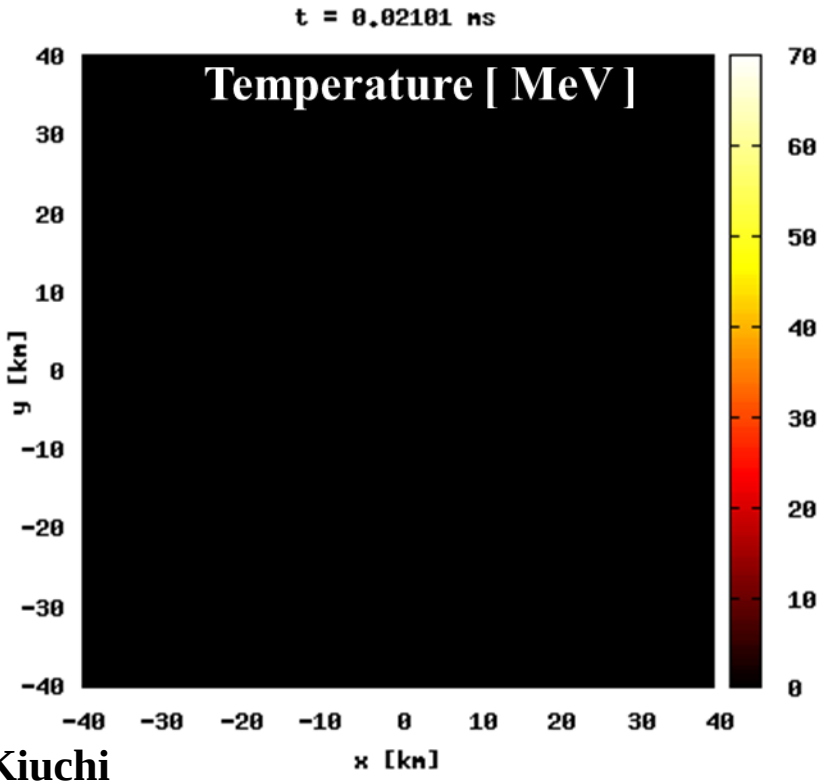

Animation by Kiuchi

Sekiguchi et al. PRL (2011) **107**, 051102; **107**, 211101

NS-NS merger (1.6-1.6Msolar)

- Hyper massive NS (HMNS) is first formed
  - Temperature increases significantly by compression and shock heating
  - Shocks occur in spiral arms
- HMNS eventually collapses to a BH due to emission of GW and neutrinos
  - accretion disk (with Mdisk < 0.1Msolar) forms around the BH

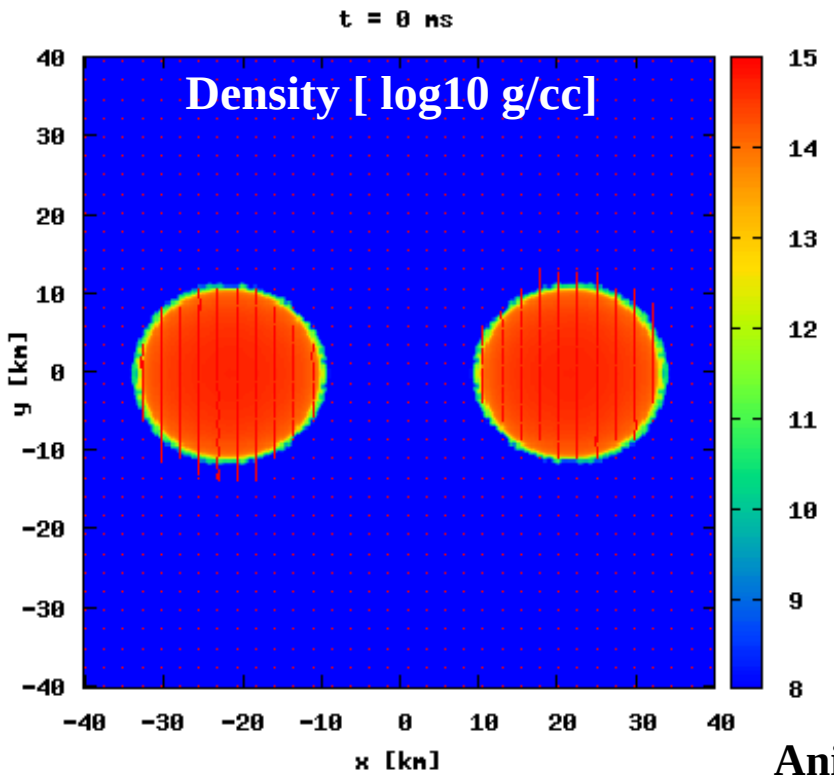

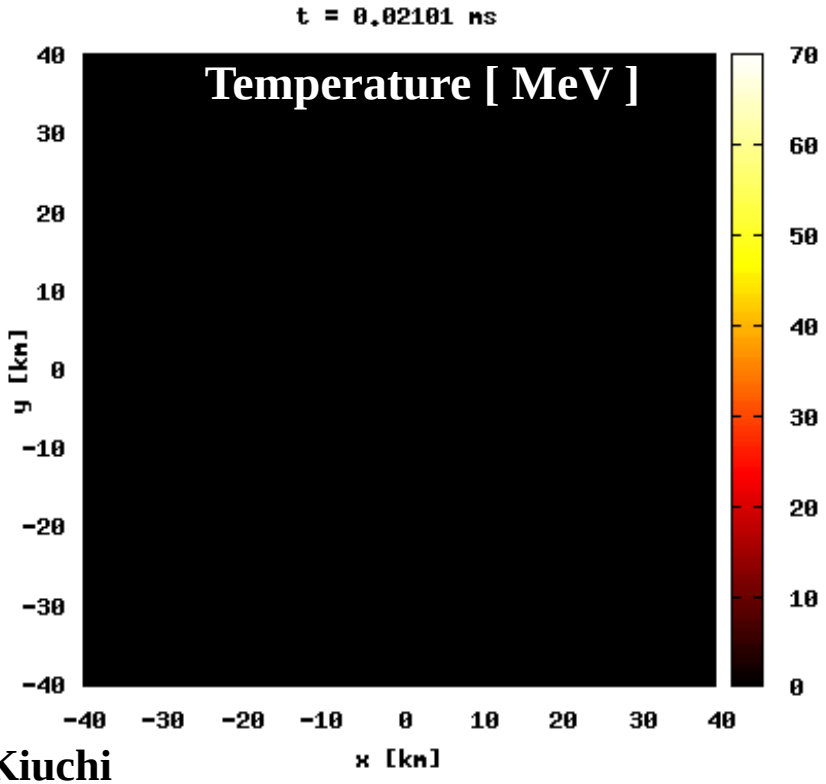

Animation by Kiuchi

Sekiguchi et al. PRL (2011) **107**, 051102; **107**, 211101

Neutrino emission (NS-NS)

- HMNS emits copious neutrinos : $L\nu \sim 3 \times 10^{53}$ erg/s ($E\nu$ = 20-30 MeV)
  - Events within 5 (1) Mpc can be detected by Hyper Kamiokande (SK)
- Large neutrino luminosity of $\sim 10^{53}$ erg/s even after the BH formation

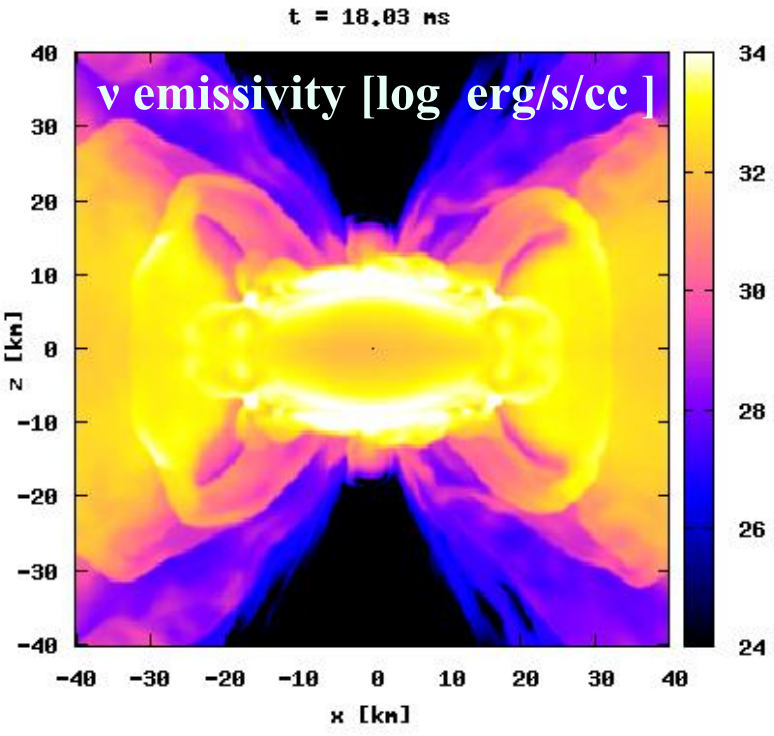

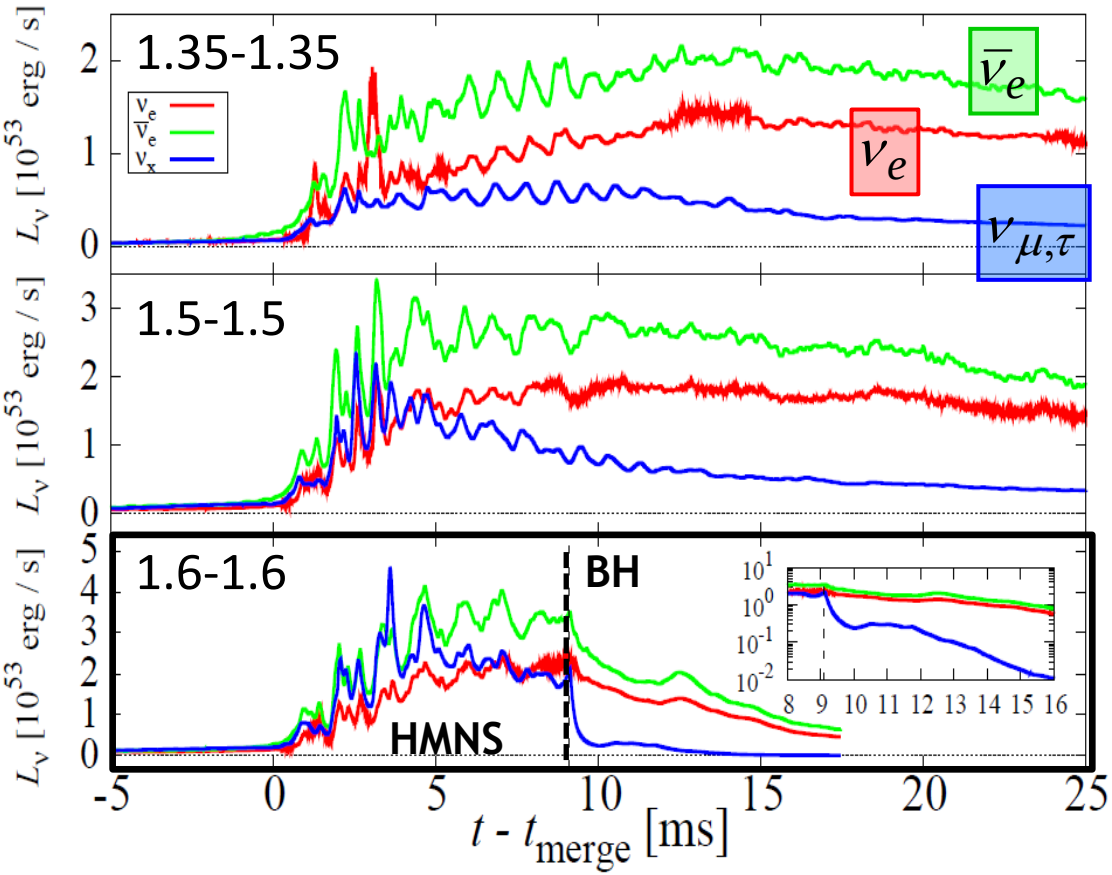

Sekiguchi et al. in prep.

BH-NS merger (4 -1.35 Msolar, a_{BH} = 0.5)

- NS is tidally disrupted and single spiral arm is formed
- The spiral arm interacts with itself and shock wave occur there
- A massive (O(0.1Msolar)) and hot accretion disk eventually forms around the BH

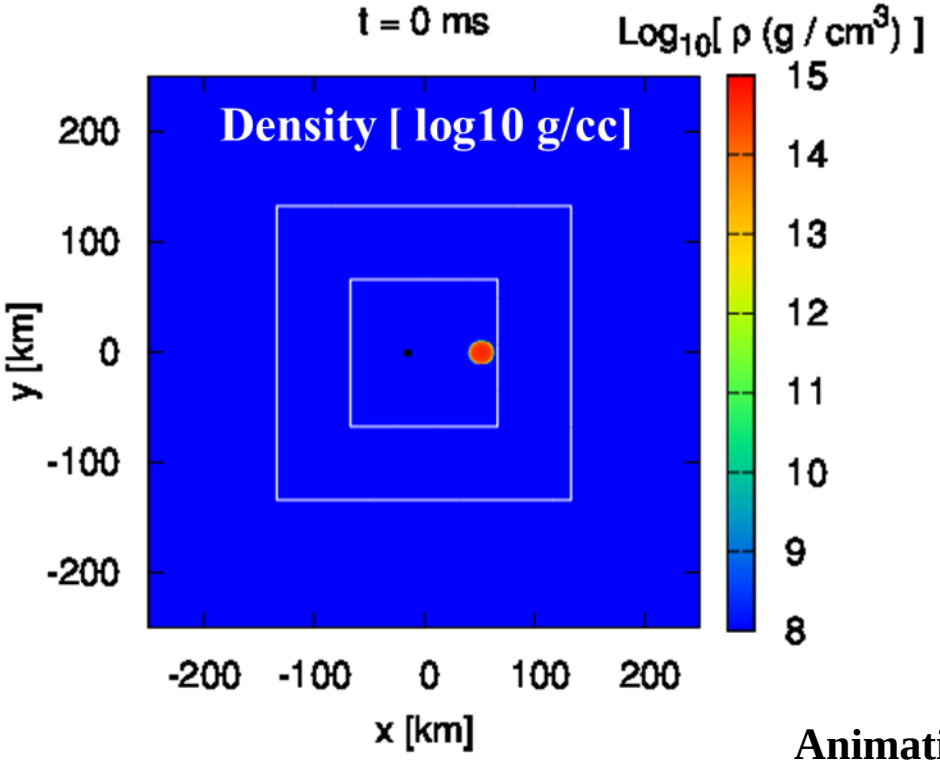

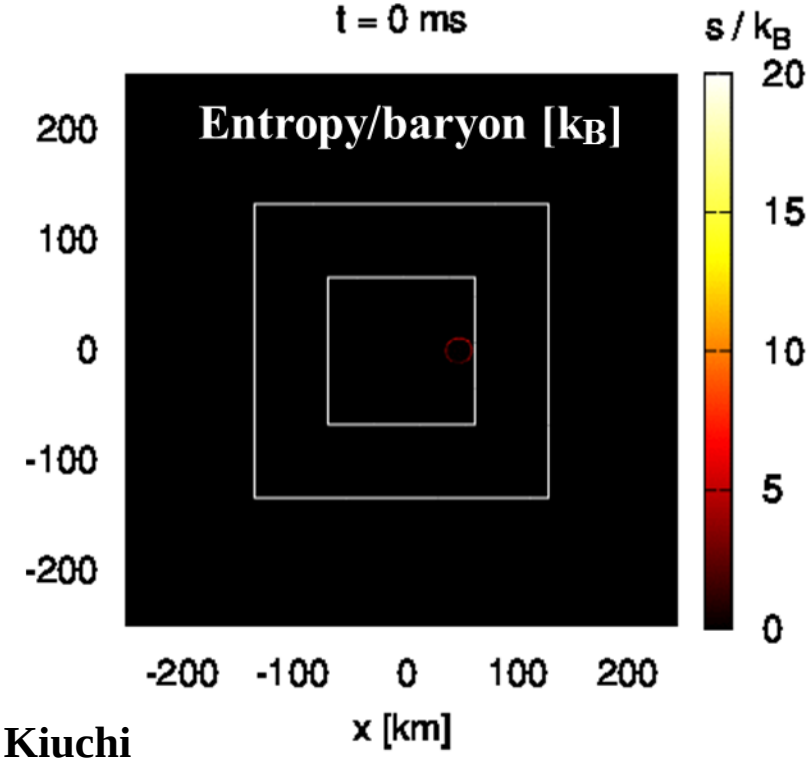

Animation by Kiuchi

Sekiguchi et al. in prep.

BH-NS merger (4 -1.35 Msolar, a_{BH} = 0.5)

- NS is tidally disrupted and single spiral arm is formed
- The spiral arm interacts with itself and shock wave occur there
- A massive (O(0.1Msolar)) and hot accretion disk eventually forms around the BH

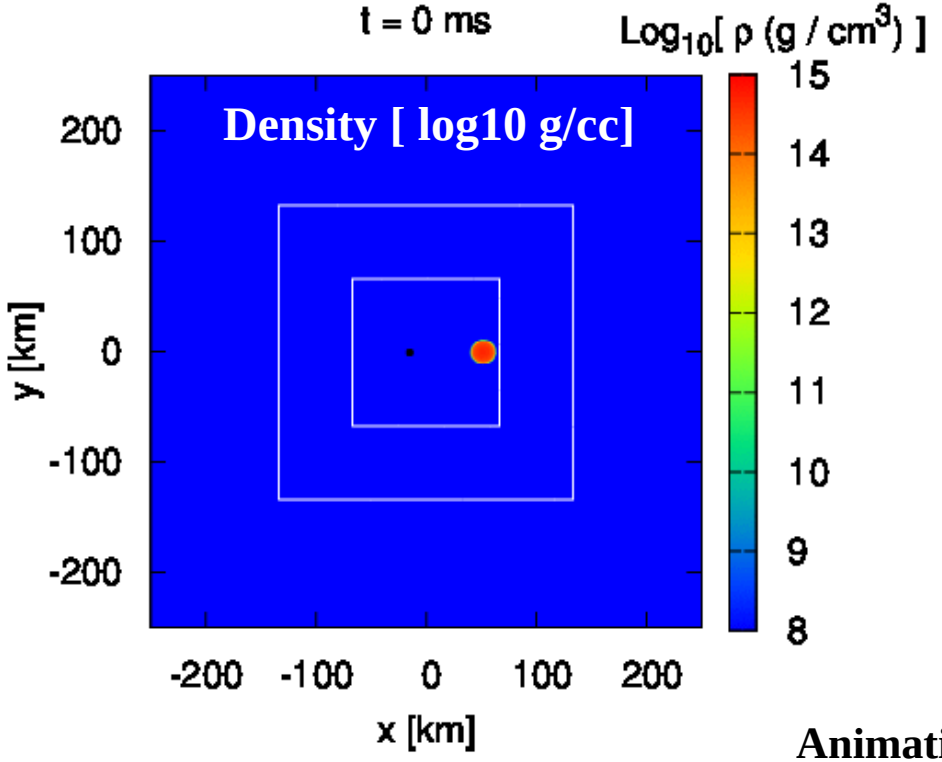

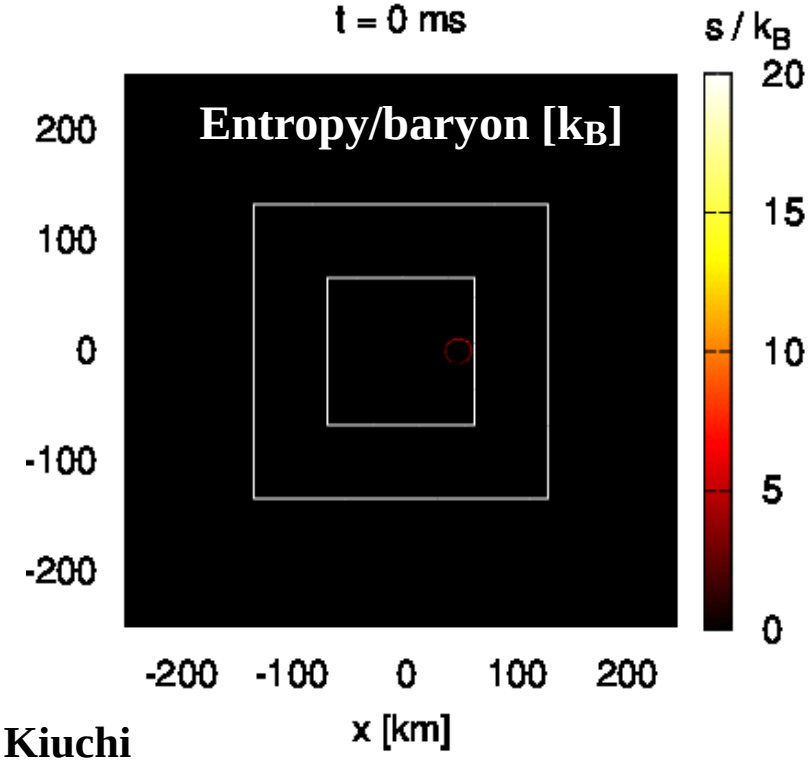

Animation by Kiuchi

Sekiguchi et al. in prep.

Neutrino emission (BH-NS)

- Copious neutrinos (5-8 × 10^{52} erg/s) are emitted from the hot disk
- L_ν is smaller than NS-NS merger case
  - Shock waves are weaker
  - More dense disk : longer diffusion time
- Low density region above BH
  - A potential site for ν-pair annihilation

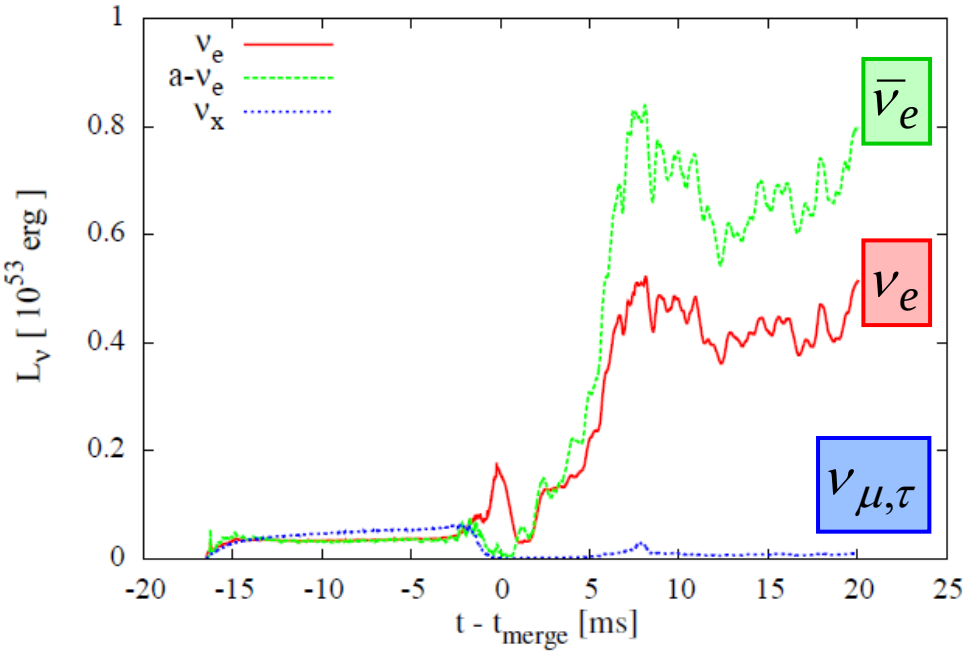

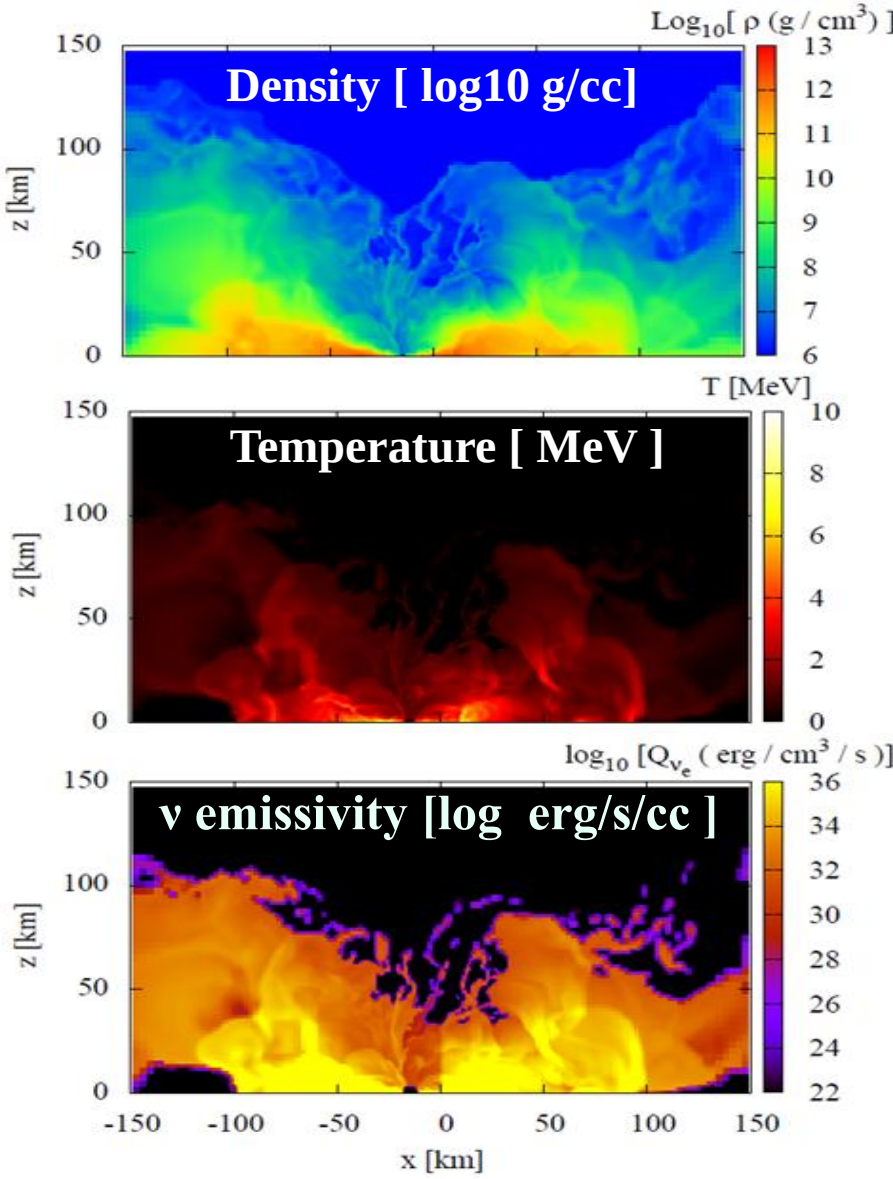

BH formation in stellar core collapse



BH formation and Long GRBs

- Collapse of massive stellar core to BH + Disk
  - Promising theoretical candidate of central engine of **Long Gamma-ray Bursts (LGRBs)**

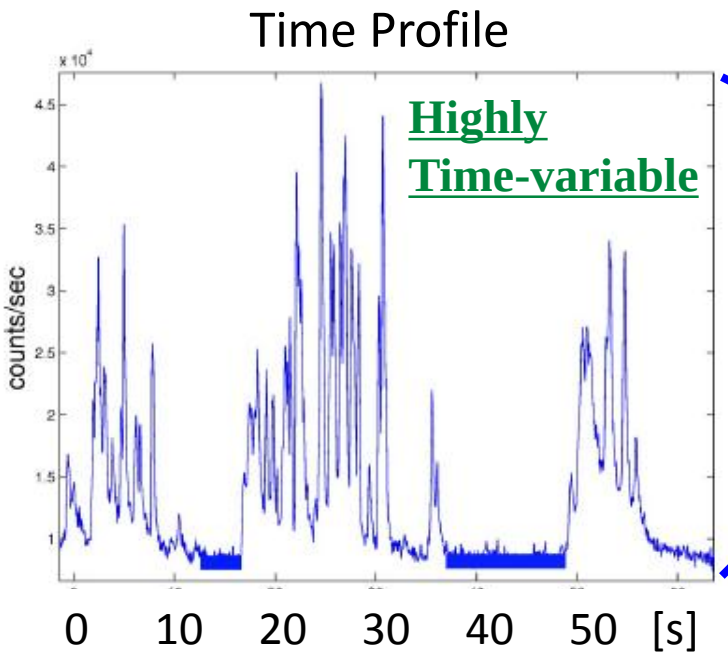

10^{50}erg/s $< L_\gamma < 10^{52}$erg/s

Most violent explosion in the universe

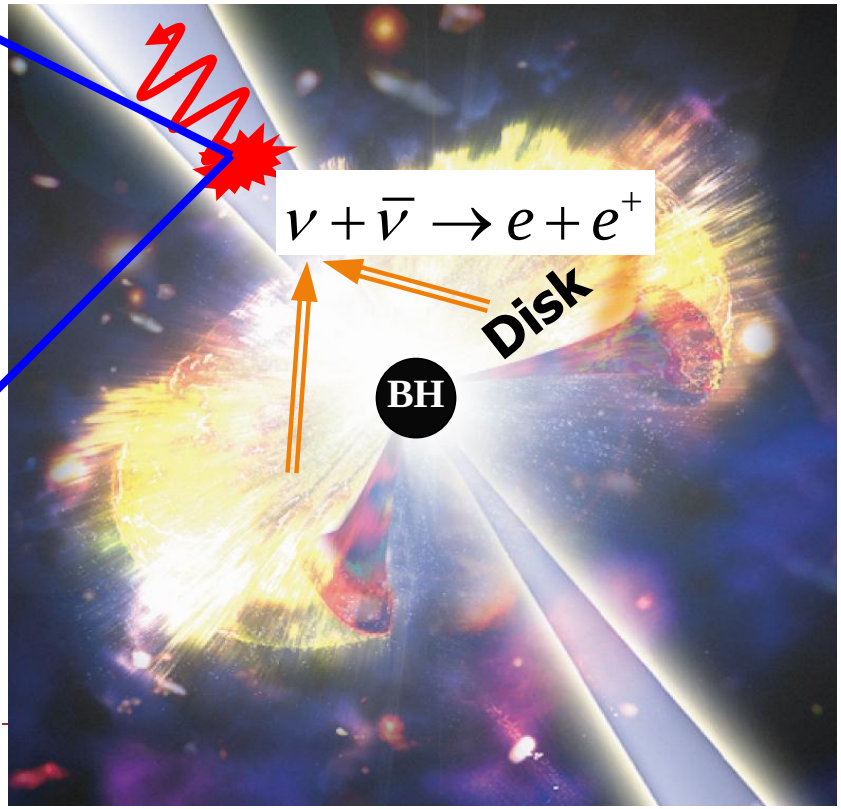

BH formation in 2005

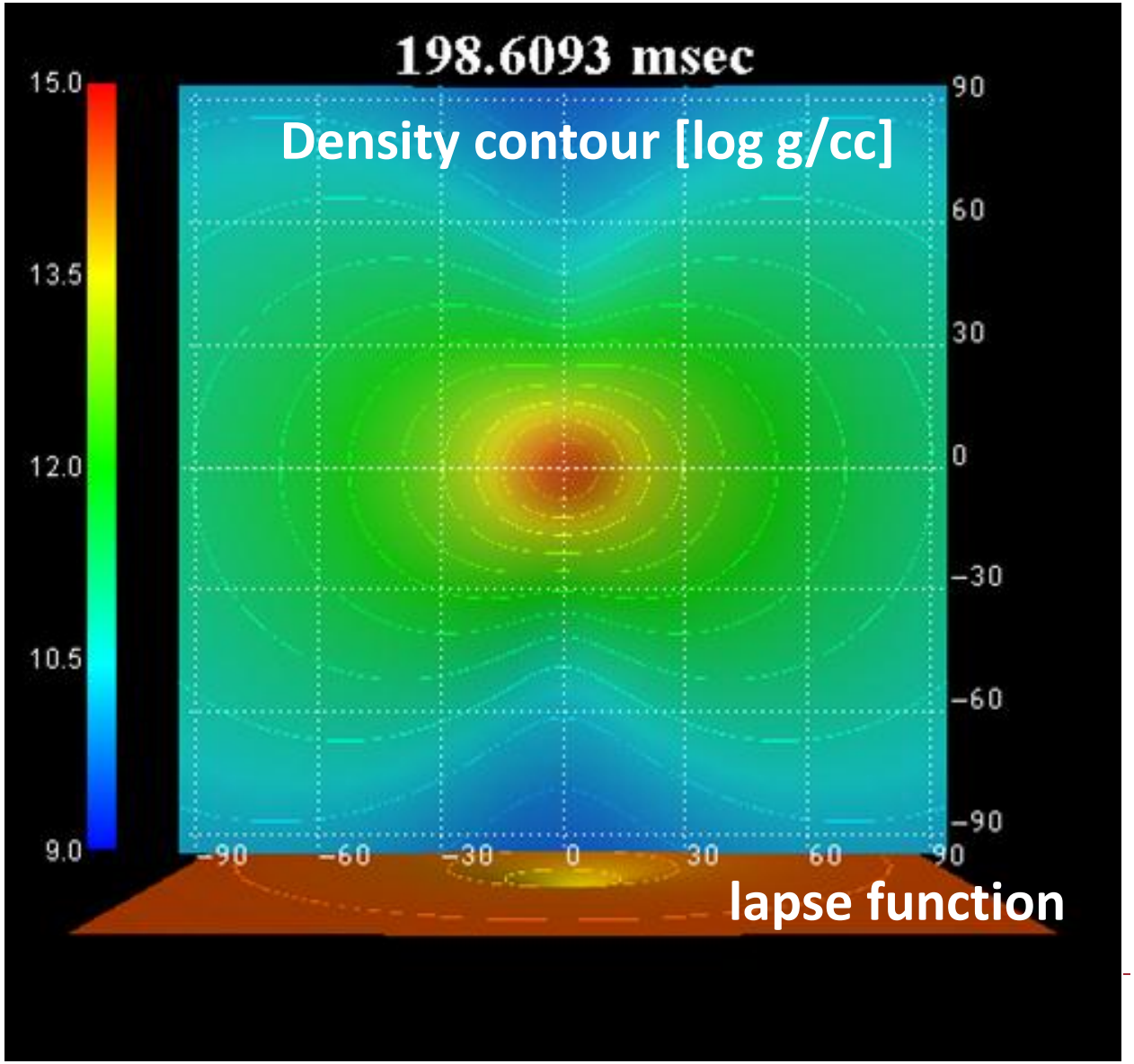

BH formation in 2005

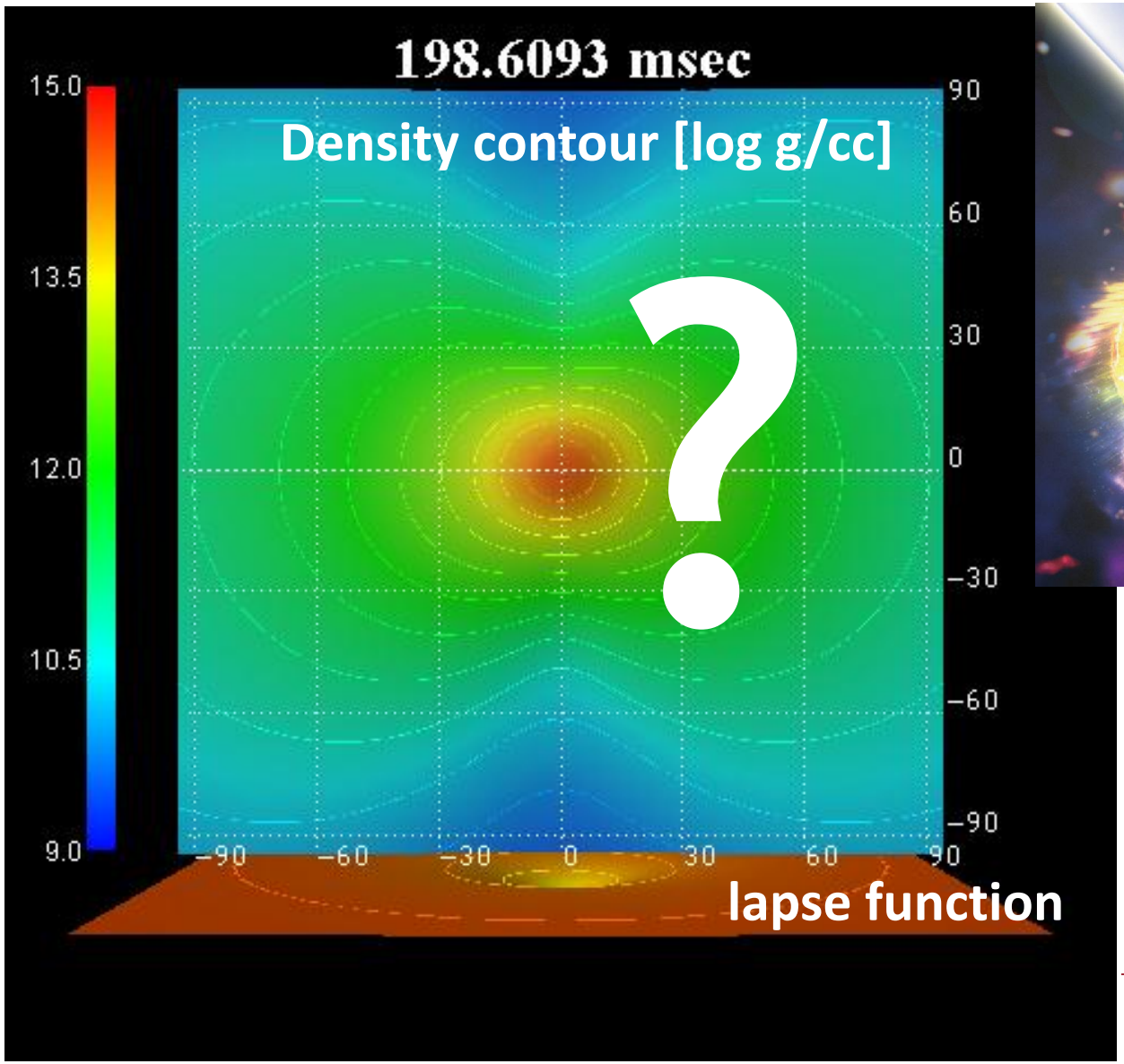

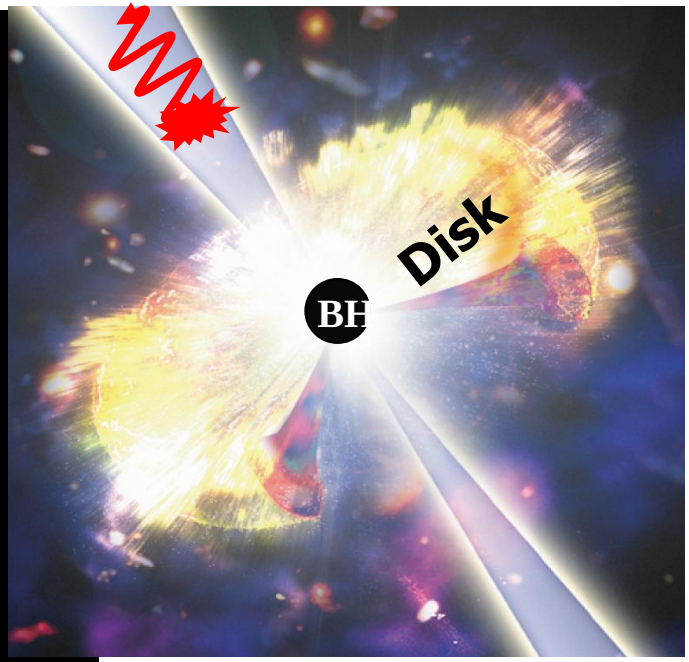

Sekiguchi et al. (2012) Progress of Theoretical & Experimental Physics
Sekiguchi & Shibata ApJ (2011)

BH+Disk formation in stellar core collapse

- 100Msolar model by Umeda & Nomoto (2008) + rotation
- Torus-structured shock : accumulation of matter to the proto-NS
- **Time varying, large (~10^{52} erg/s) neutrino luminosity after BH formation**

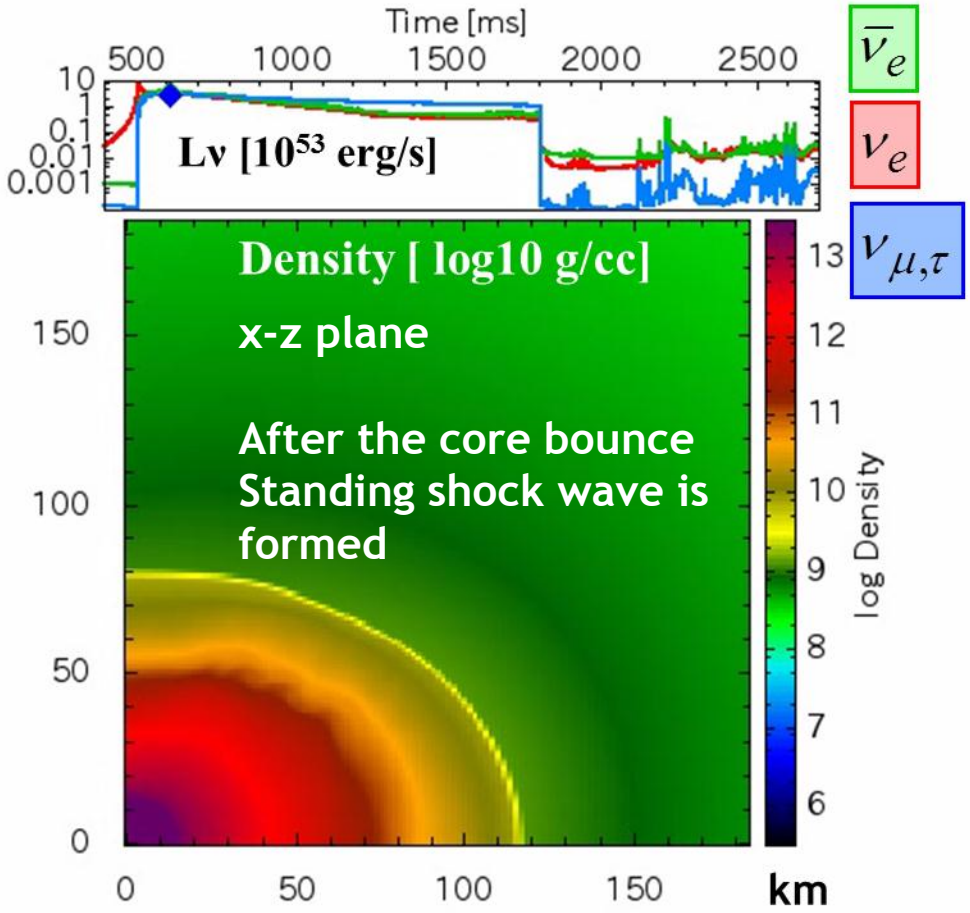

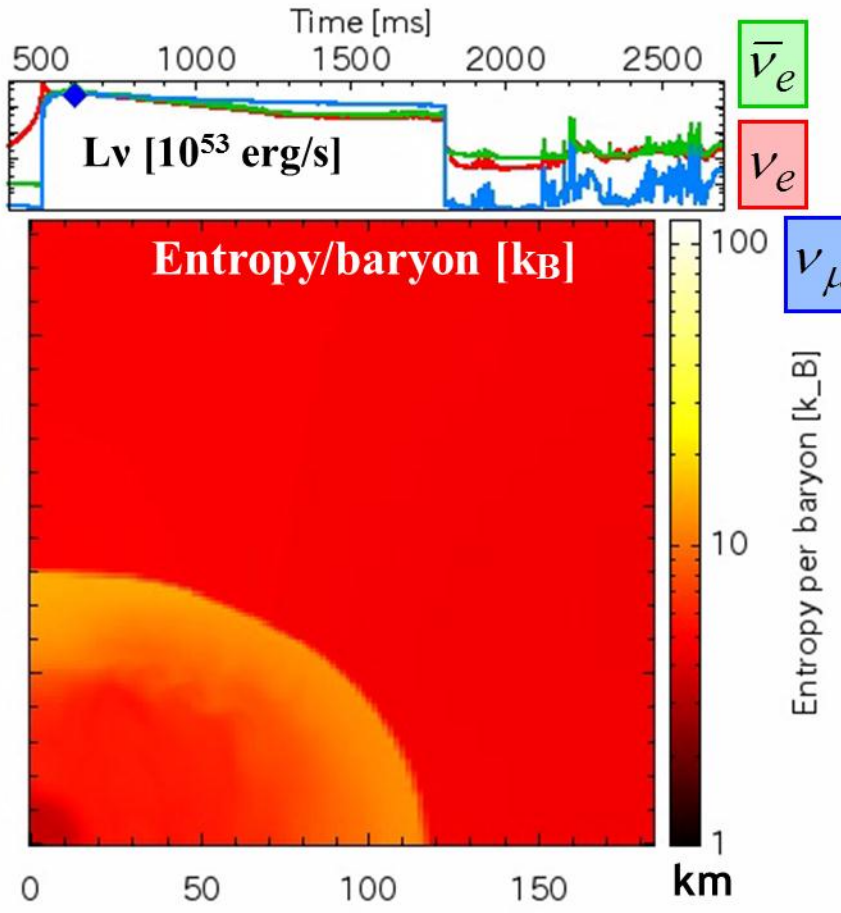

BH+Disk formation in stellar core collapse

- 100Msolar model by Umeda & Nomoto (2008) + rotation
- Torus-structured shock : accumulation of matter to the proto-NS
- **Time varying, large (~10^{52} erg/s) neutrino luminosity after BH formation**

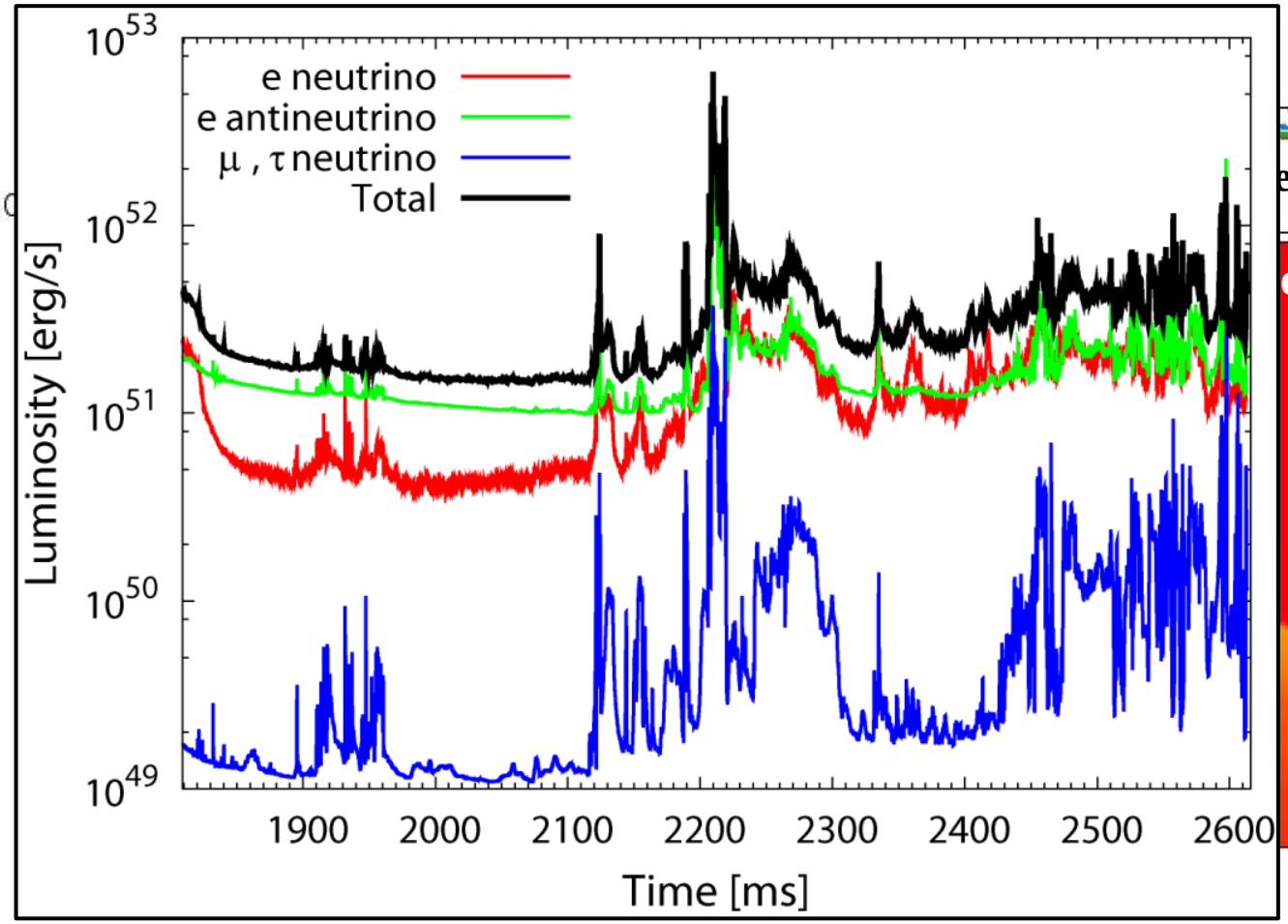

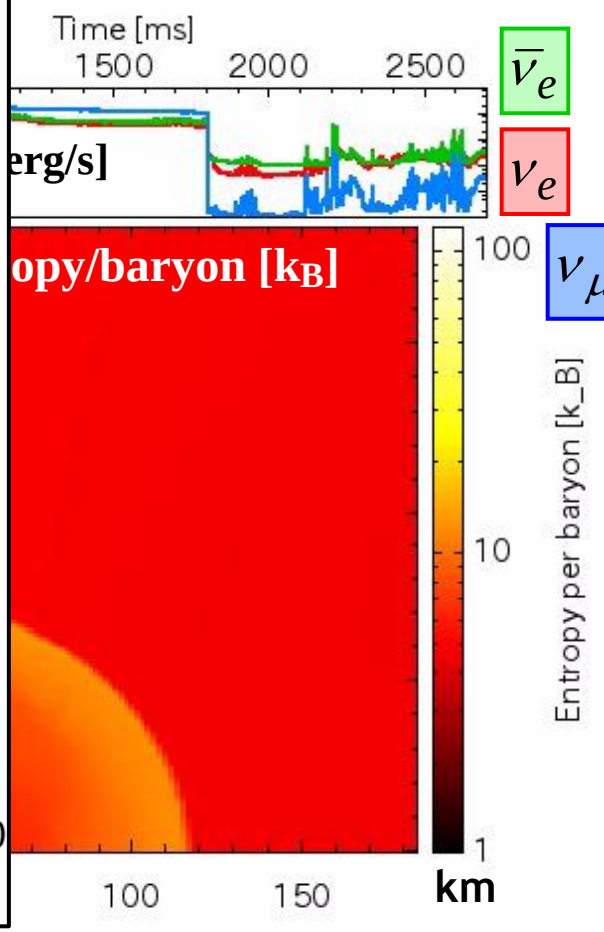

Same model but with Slower Rotation:
Spheroidal configuration, No time variability

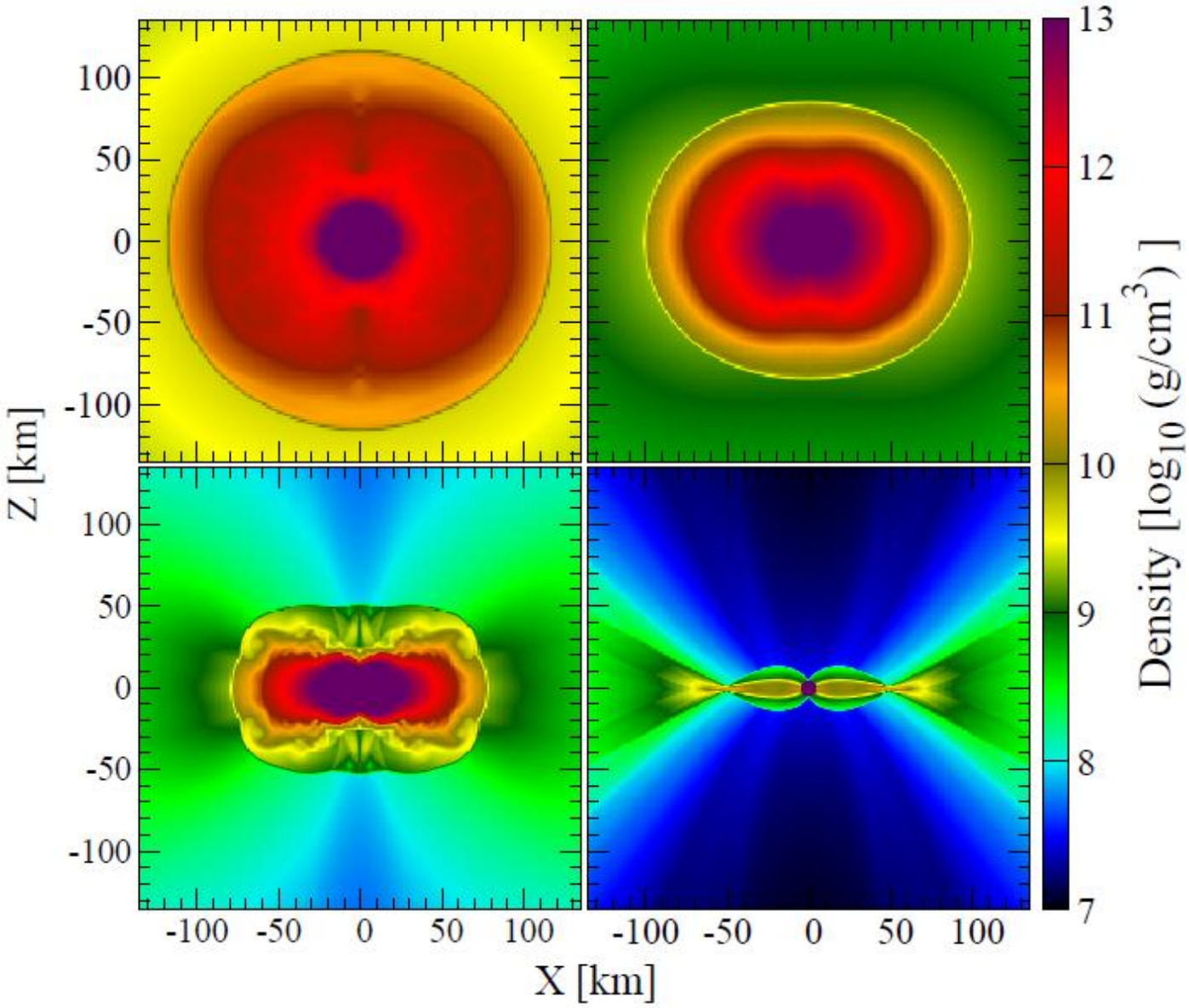

Comparison of Rotational Profile

- Rotational profiles of **Proto-Neutron Star** are similar
- **Small difference in rotational profile of outer region results in large difference in dynamics**

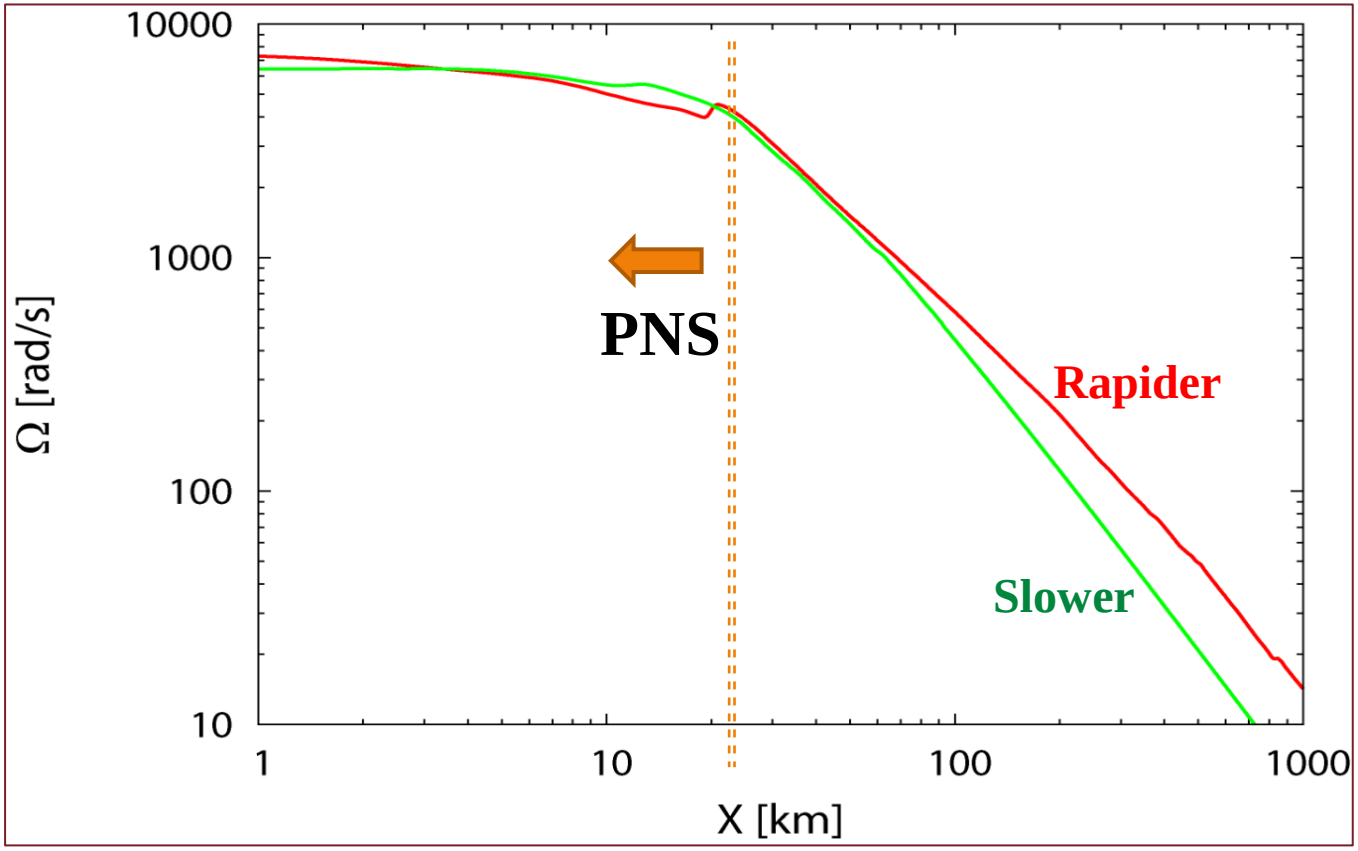

500Msolar-PopIII core collapse:
Outflow appears even when BH is formed directly

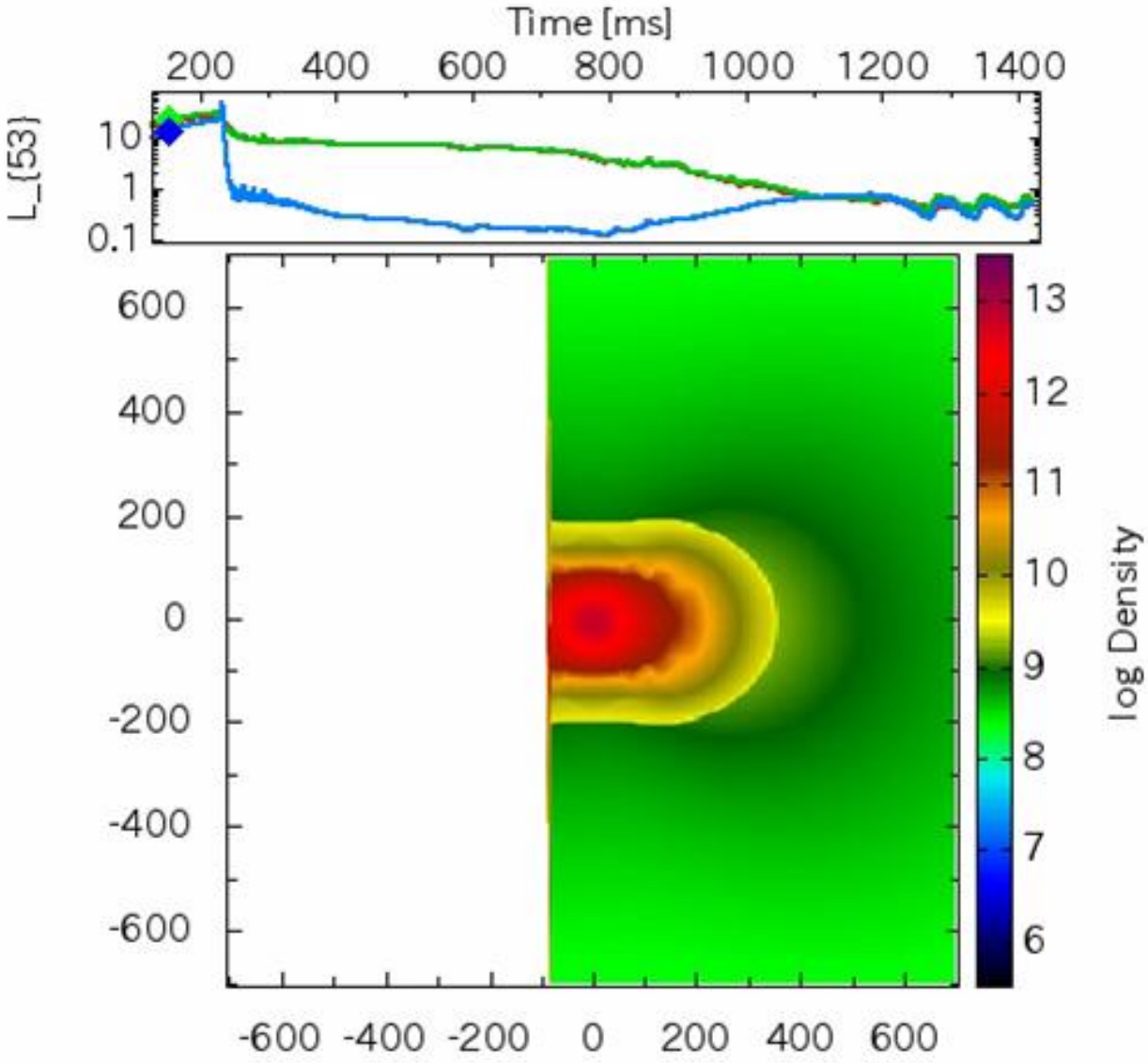

500Msolar-PopIII core collapse:
Outflow appears even when BH is formed directly

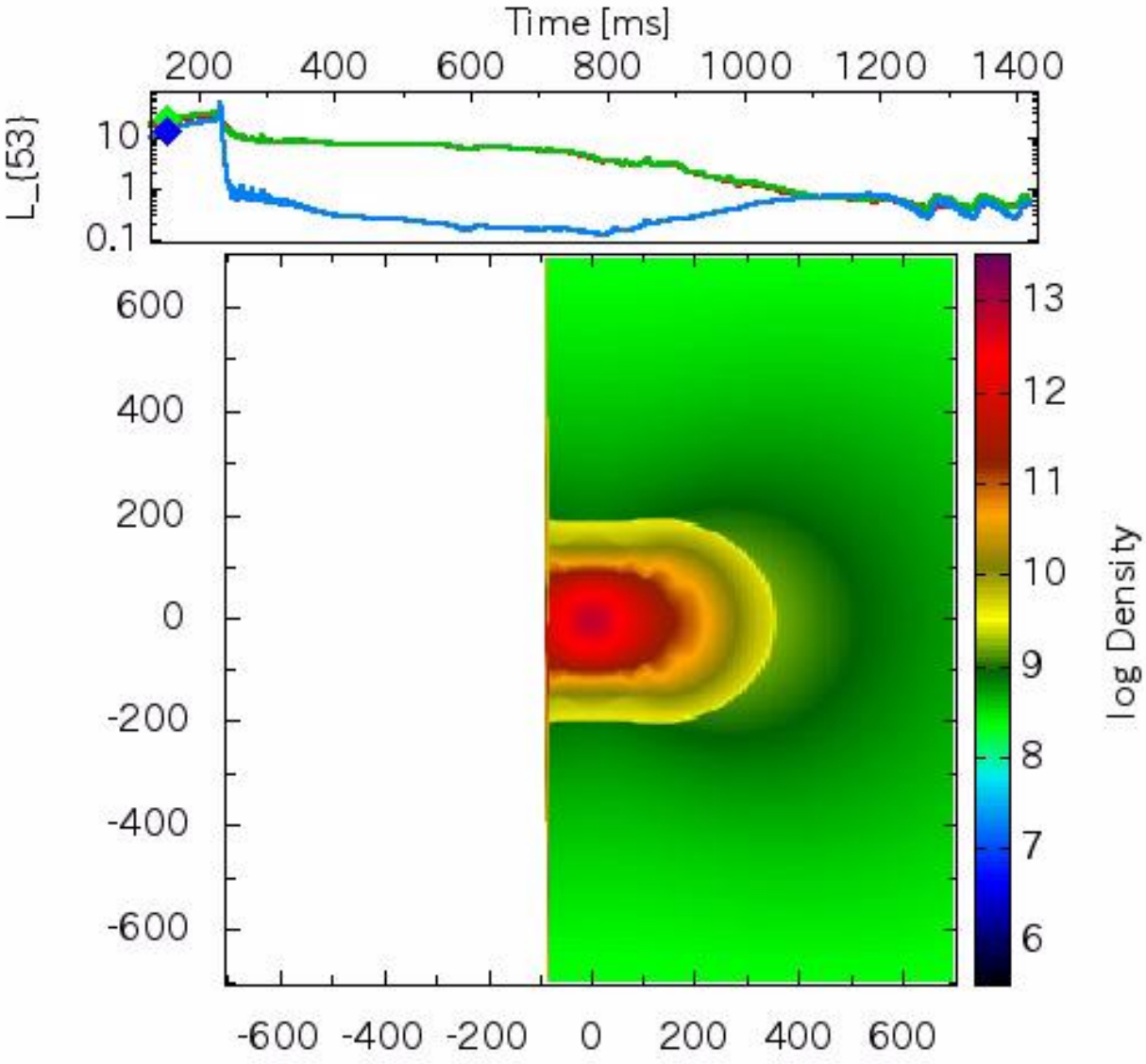

500Msolar-PopIII core collapse:
Outflow appears even when BH is formed directly

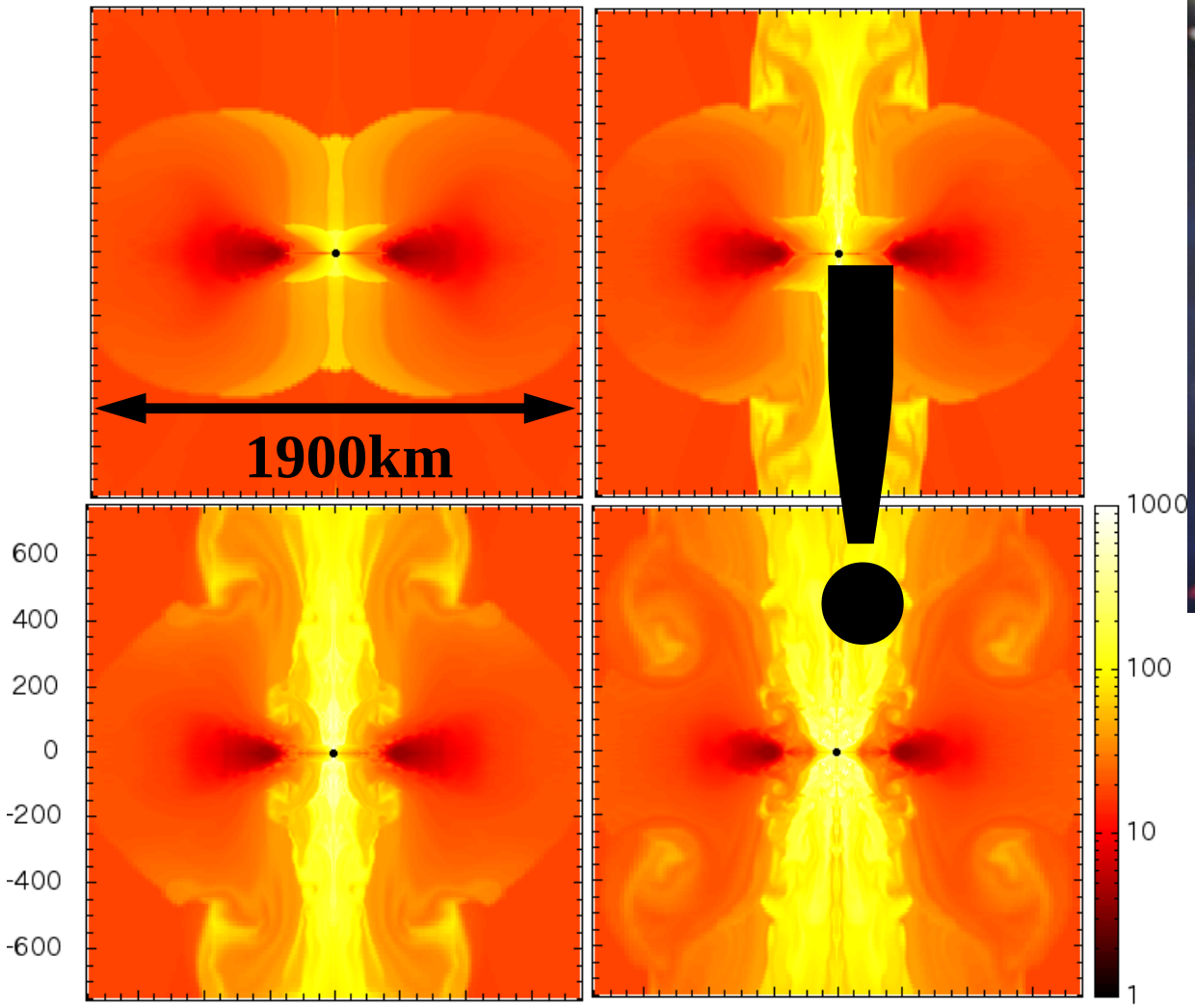

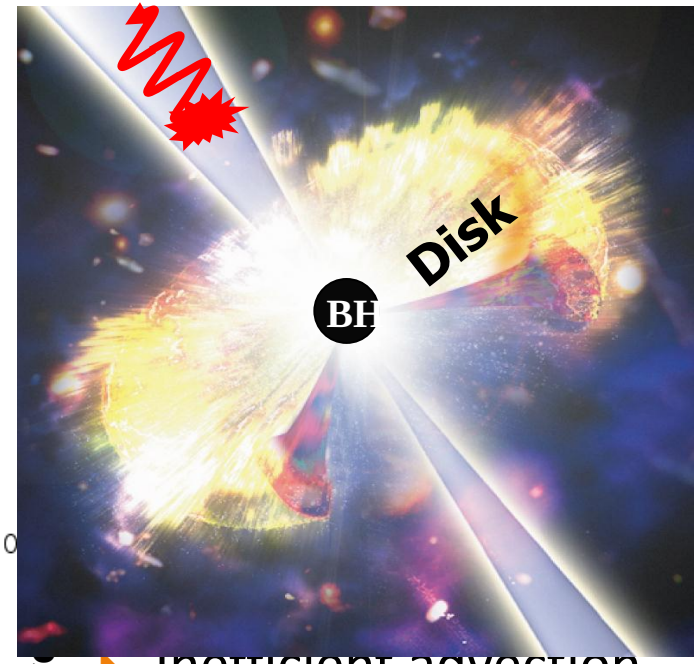

- Inefficient advection cooling
- Thermal energy is stored
- Outflow

Moderate rotation : BH formation zoo

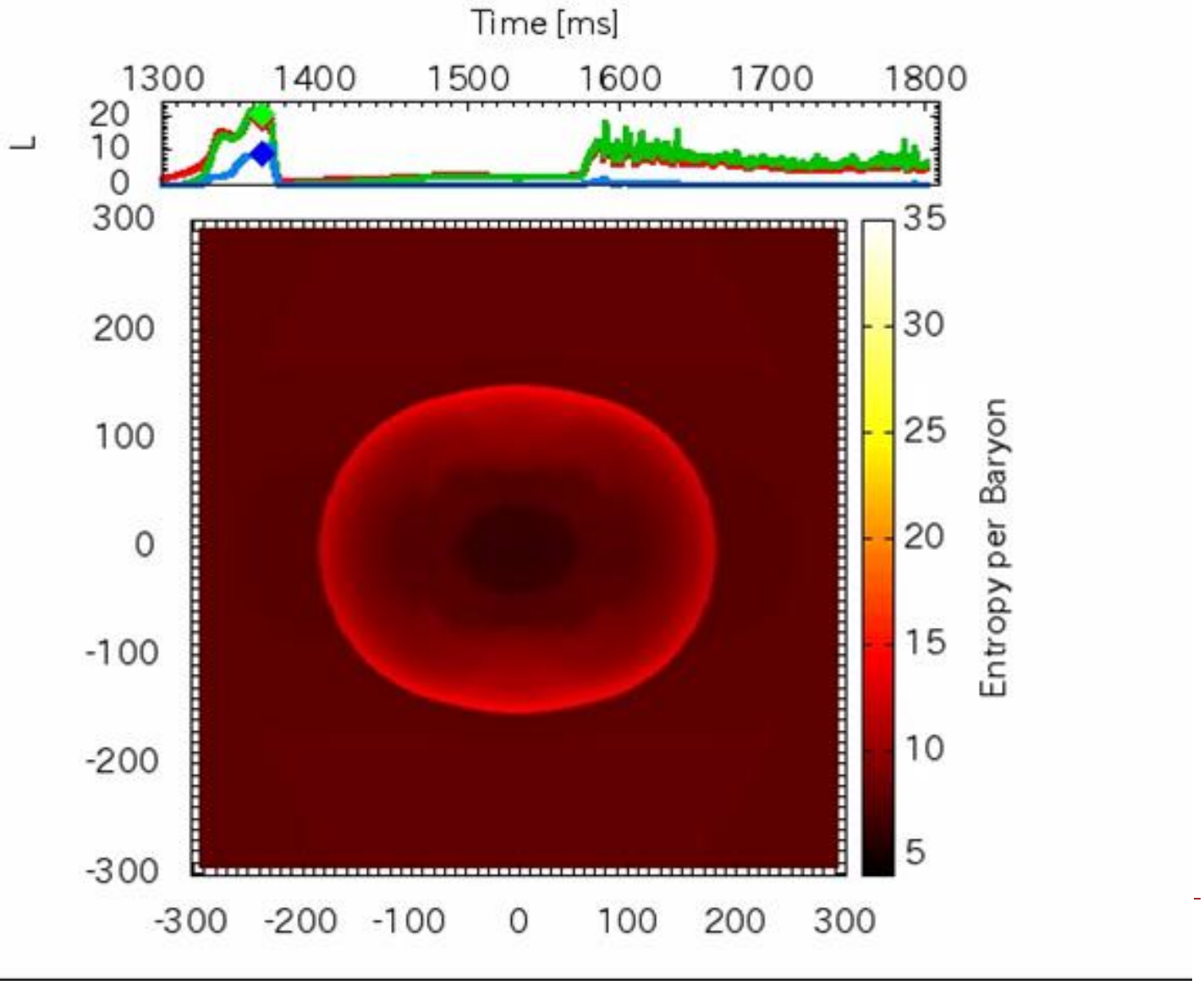

Moderate rotation : BH formation zoo

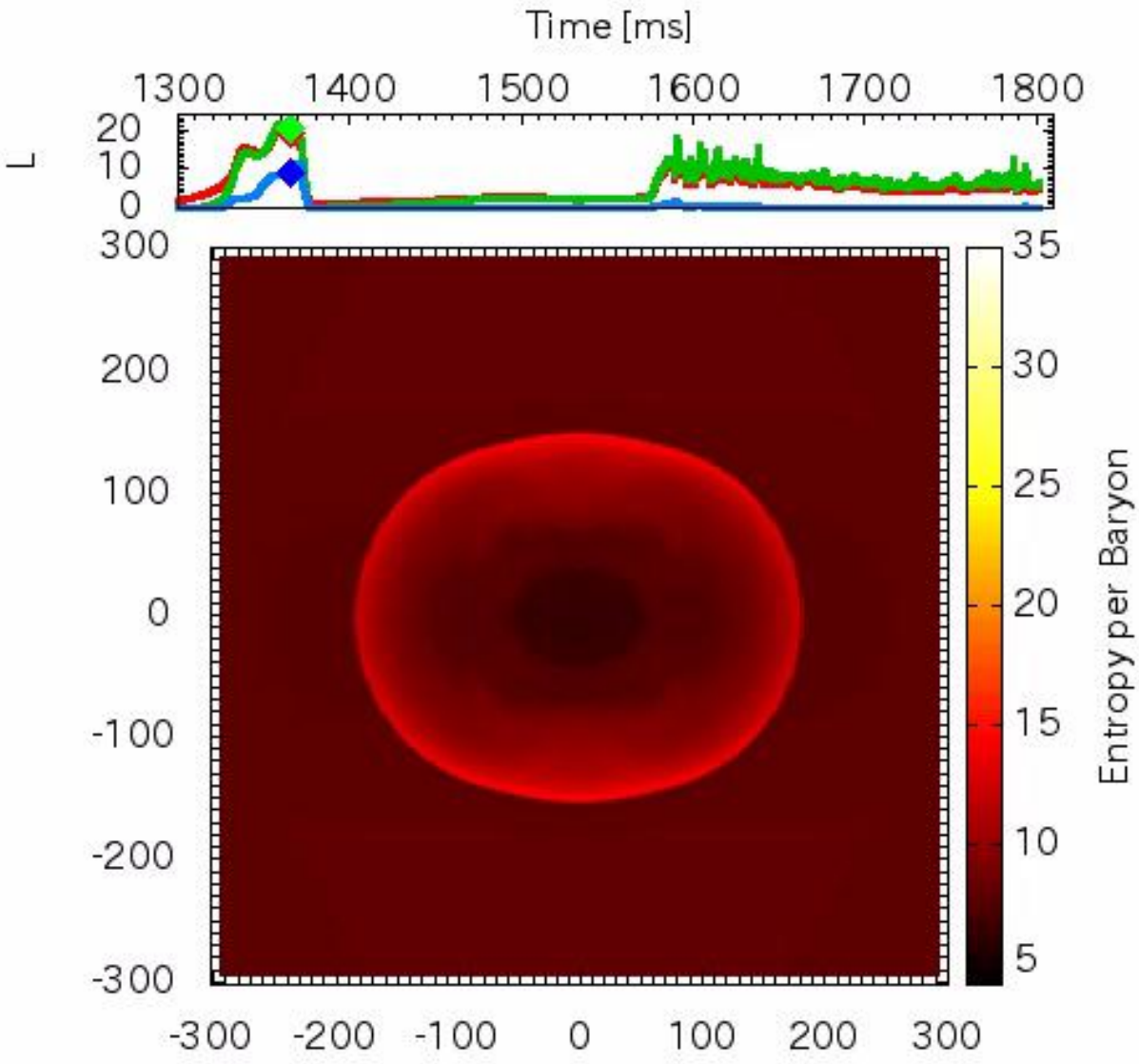

Summary

- Numerical Relativity is the unique tool to study dynamical phenomena in the universe where strong gravity plays a role
  - Recent developments enable us to perform simulations in physical modeling
- NS-NS and BH-NS are very interesting phenomena both in physics and astrophysics
  - Promising sources of ground-based GW detectors
  - As laboratory for exploring physics of dense matter
  - Central engine of SGRB
- BH formation process in stellar core collapse is quite dynamical, accompanying oblique shock, convection, and outflows
  - The dynamics is sensitive to the initial rotational profile
  - The resulting system has preferable features for LGRBs
- More systematic studies with physical modeling will be done in the near future



Appendix



Expected Merger Rate

- Binary Neutron Star (BNS, NS–NS) and ca
  - 6 Binaries with pulsar are expected to merge w
  - Empirical NS–NS merger rate: 3–190 Myr^{-1} /gal
- Merger rate from population synthesis
  - NS–NS : 10–200 Myr^{-1}/gal. (**Kalogera et al. 2004**)
  - BH–NS : 0.1–5 Myr^{-1}/gal. (**Belczynski 2007**)

NS-NS : ~10 - 100 events/yr for advLIGO
BH-NS : ~ 1 - 30 events/yr for advLIGO
Not so rare events !
We can do GW astronomy

$\log_{10}(\tau_g/[\mathrm{yr}])$	7.9	12.4
Masses measured?	Yes	No

	B1820−11	J1829+2456	J1
P [ms]	279.8	41.0	
P_b [d]	357.8	1.18	
e	0.79	0.14	
$\log_{10}(\tau_c/[\mathrm{yr}])$	6.5	10.1	
$\log_{10}(\tau_g/[\mathrm{yr}])$	15.8	10.8	
Masses measured?	No	No	

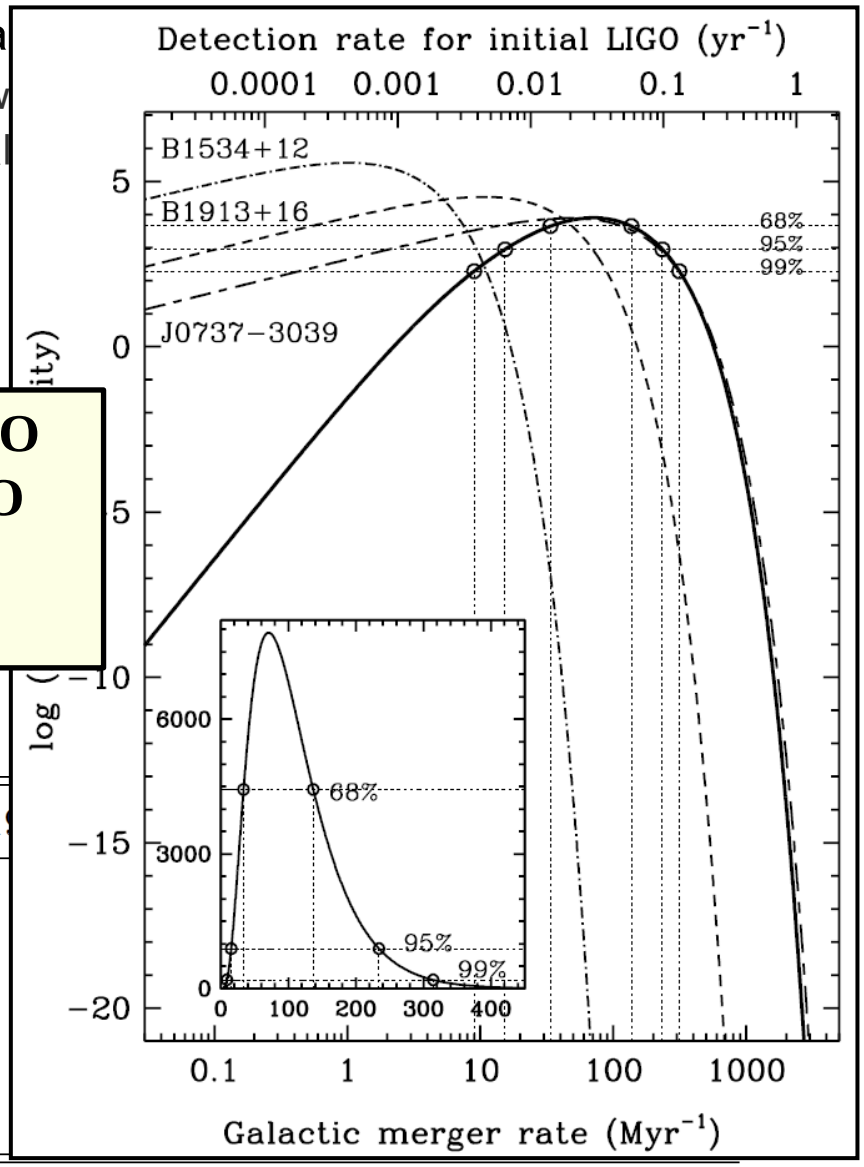

Author	NS-NS		BH-NS		Method
	LIGO	AdLIGO	LIGO	AdLIGO	
Kim et al. [143]	5e-3	27			Empirical
Nakar et al. [198]		~ 2		~ 20.0	SGRBs
Guetta & Stella [128]	7.0e-3	22	7.0e-2	220	SGRBs
Voss & Tauris [323]	6.0e-4	2.0	1.2e-3	4.0	Pop. Synth. – SFR
de Freitas Pacheco et al. [79]	8.0e-4	6.0			Pop. Synth. – SFR
Kalogera et al. [140]	1.0e-2	35	4.0e-3	20	Pop. Synth. – NS-NS
O'Shaughnessy et al. [218]	1.0e-2	10	1.0e-2	10	Pop. Synth. – NS-NS



Why GWs from NS-NS are interesting ?

- **One of most promising source of GWs**
  - Next generation interferometer can see ~ 350Mpc
  - Expected event rate : more than 10/yr
- **Unique window to 'see' inside dense matters**
  - Very small cross section with matter
- **Dynamical response of dense matter**
  - By contrast with static, isolated neutron star
- **Multiple information of equation of state**
  - **Tidal deformation (radius) : relatively low density**
  - Maximum mass : most high density
  - Oscillation :
- **Less uncertain parameters**
  - Inspiral waveform provides information of mass
  - Mass should be determined in isolated neutron star
- **Simple in a complementary sense**
  - Essentially quadrupole formula
  - By contrast with optical observation

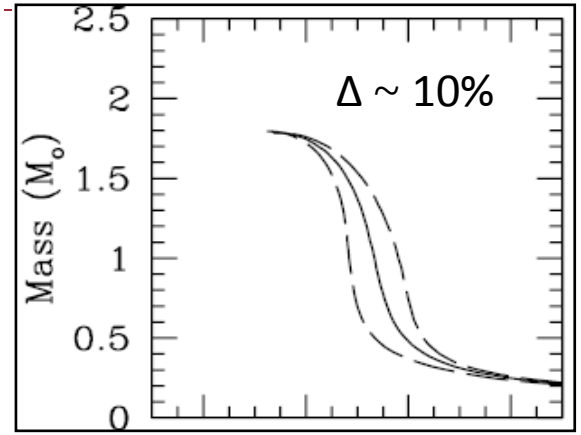

Radius is sensitive to relatively low density parts

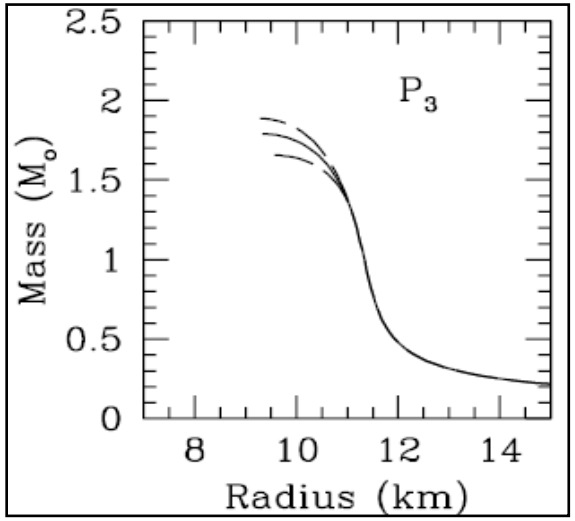

Maximum mass depends on most dense parts

HMNS

- $M_{\rm crit} \approx M_{\rm max,sph.cold.NS} + \Delta M_{\rm rot}^{\rm rigid} + \Delta M_{\rm rot}^{\rm diff} + \Delta M_{\rm thermal}$
  - $M_{\rm max,sph.cold.NS}$: maximum mass of spherical NS at T = 0, depends on EOS
    - Most massive NS accurately observed : 1.97 Msolar (Demorest et al. 2010)
  - $\Delta M_{\rm rot}^{\rm rigid}$: effects of rigid rotation ~ $O(10\%)$
  - $\Delta M_{\rm rot}^{\rm diff}$: effects of differential rotation typically ~ $O(10\%)$
  - $\Delta M_{\rm thermal}$: effects of finite temperature ~ $O(10\%)$
- HMNS formed after the merger is very hot as T ~ O(10MeV)
  - Thermal contribution is not negligible ⇒ Finite temperature EOS
  - Neutrino cooling plays an important role ⇒ Microphysics



Development in Numerical Relativity (1)

- **ADM /3+1decomposition** (Arnowitt, Deser, & Misner 1962; York 1978)
  - General Relativity：Theory on spacetime manifold
    - Time and spatial derivatives appear in equations in a mixed manner
    - It is not clear the type of equation (elliptic, hyperbolic ?)
  - Formulation as an initial (and boundary) problem
- **Basic ideas on coordinate conditions** (Smarr, York, … in 1970's)
  - There is no absolute spacetime and no preferred frame of reference
    - Those who perform simulations must specify coordinate
  - Use this degree of freedom to avoid singularities and to resolve the frame dragging
  - Development of faster conditions (Shibata, Alccubierre, Brugmann, Bona, … ~2000)
- **Some pioneering studies** (Nakamura, Ohara, Teukolsky, …1980's)
    - First full GR simulation of gravitational collapse (Nakamura 1980's)



Development in Numerical Relativity (2)

- **BSSN formalism** (Shibata & Nakamura 1995; Baumgarte & Shapiro 1999)
  - Einstein equation：constrained system
    - Maxwell eq.： Gauss's law, No-monopole condition
    - Einstein eq.： **Hamiltonian(~energy), Momentum constraint equations**
    - **ADM formalism：violation of constraints grows monotonically in time and simulation clash in a short time**
  - Stable, long-term simulations become possible
- **Quasi-equilibrium configurations of NS-NS** (Uryu, Gourgoulhon, Taniguchi, Cook, Shibata, … 90's ~)
    - **The first full GR simulation of NS-NS merger (Shibata & Uryu 2000)**
  - NS-BH initial data (Taniguchi, Shibata, Uryu, Grandclement, Kyutoku, … 2006~)
    - **The first full GR simulation of BH-NS merger (Shibata & Uryu 2006)**



Development in Numerical Relativity (3)

- **Evolving BH spacetime** (Pretorius 2005; Campanelli et al. 2006)
  - **BH excision** : no information from BH interior ⇒ excise and set boundary cond.
    - The first BH-BH merger simulation (Pretorius 2005)
    - Need experienced craftsmanship
  - **BSSN-Puncture** : adopt nice coordinate conditions and variables
    - Easy to implement : most difficult simulation (BH-BH) becomes relatively easier one
    - A large number of BH-BH merger simulations (2006～)
- **(General) Relativistic hydrodynamics** (Font, Marti, Muller, Del Zanna, … 90's~)
- **(General) Relativistic MHD** (Hawley, Komissarov, Anton (Valencia), Duez (Illinoi), Shibata-Sekiguchi, ... 2000~)



Recent development and Future direction

- **Toward more physical modeling**
  - **Numerical Relativity simulations with Microphysics** (Sekiguchi 2010)
    - Nuclear-theory-based finite temperature EOS (Table EOS !)
    - Weak interactions : $e^{\pm}$ capture, neutrino scatterings, neutrino capture
      - $\tau_{\rm weak} << \tau_{\rm dyn}$: Two very different timescales
        $\Rightarrow$ **Numerically, very ' stiff ' source terms**
    - Neutrino cooling : simplified treatment
  - **Towards GR (neutrino)radiation-hydrodynamics**
    - An early attempt : Farris et al. (2008)
    - Covariant formulation based on Thorne's moment formalism : Shibata et al. (2011)
    - The first Full GR radiation-MHD simulation : Shibata & Sekiguchi (2011)
      - Simplified modeling of BH-Disk system
    - 1D core collapse simulation : O'Connor & Ott (2012)
    - An semi-implicit scheme : Roedig et al. (2012)



Why Microphysics ?

- High density (>10^{12} g/cc) and T (> 1-10 MeV) regions
  - $\lambda_\nu >> \lambda_\gamma, \lambda_e$ $\Rightarrow$ neutrinos drive the thermal / chemical evolution
    - 99% of energy released *in stellar core collapse* is carried away by neutrinos
    - **Neutrino : Weak interactions** should be taken into account
    - Strong dependences of weak rates on T $\Rightarrow$ **Finite temperature EOS**
- NS-NS, BH-NS mergers
  - Inspiral : NS is cold ($k_B T/ E_F << 1$) $\Rightarrow$ **zero T EOS**
  - Meger : Compression, shock heating ($k_B T/ E_F \sim O(0.1)$) $\Rightarrow$ **finite T EOS**
  - **Prompt BH formation $\Rightarrow$ hot region quickly swallowed by BH**
    - **Effects of finite temperature would be miner**
  - **HMNS, late time BH, and massive disk formation (more likely)**
    - **Shock heating, neutrino cooling, etc. are important**



Roman Konoplya, JGRG 22(2012)111602

"Stability of black holes: summary of some results for the past 10 years"

RESCEU SYMPOSIUM ON

GENERAL RELATIVITY AND GRAVITATION

JGRG 22

November 12-16 2012

Koshiba Hall, The University of Tokyo, Hongo, Tokyo, Japan

Black holes' stability: A review

R. A. Konoplya

DAMTP, University of Cambridge, UK

Tokyo, Nov. 11 - Nov. 16, 2012
the 60th birthday of T. Futamase, H. Kodama, M. Sasaki

Content:

Recent reviews on stability of BHs:
in $D > 4$ A. Ishibashi, H. Kodama, Prog. Theor. Phys. Suppl. 189 (2011) 165-209
$D \geq 4$ R. A. Konoplya, A. Zhidenko, Rev. Mod. Phys. 83 (2011) 793-836

Introduction

Content:

Recent reviews on stability of BHs:
in $D > 4$ A. Ishibashi, H. Kodama, Prog. Theor. Phys. Suppl. 189 (2011) 165-209
$D \geq 4$ R. A. Konoplya, A. Zhidenko, Rev. Mod. Phys. 83 (2011) 793-836

Introduction

Criteria of stability: analytical vs numerical

Content:

Recent reviews on stability of BHs:
in $D > 4$ A. Ishibashi, H. Kodama, Prog. Theor. Phys. Suppl. 189 (2011) 165-209
$D \geq 4$ R. A. Konoplya, A. Zhidenko, Rev. Mod. Phys. 83 (2011) 793-836

Introduction

Criteria of stability: analytical vs numerical

(In)stability of 3+1 dimensional BHs

Content:

Recent reviews on stability of BHs:
in $D > 4$ A. Ishibashi, H. Kodama, Prog. Theor. Phys. Suppl. 189 (2011) 165-209
$D \geq 4$ R. A. Konoplya, A. Zhidenko, Rev. Mod. Phys. 83 (2011) 793-836

Introduction

Criteria of stability: analytical vs numerical

(In)stability of 3+1 dimensional BHs

Instability of $D > 4$ BHs: Gregory-Laflamme instability and not only

Content:

Recent reviews on stability of BHs:
in $D > 4$ A. Ishibashi, H. Kodama, Prog. Theor. Phys. Suppl. 189 (2011) 165-209
$D \geq 4$ R. A. Konoplya, A. Zhidenko, Rev. Mod. Phys. 83 (2011) 793-836

Introduction

Criteria of stability: analytical vs numerical

(In)stability of 3+1 dimensional BHs

Instability of $D > 4$ BHs: Gregory-Laflamme instability and not only

Potential turbulent instabilities

Content:

Recent reviews on stability of BHs:
in $D > 4$ A. Ishibashi, H. Kodama, Prog. Theor. Phys. Suppl. 189 (2011) 165-209
$D \geq 4$ R. A. Konoplya, A. Zhidenko, Rev. Mod. Phys. 83 (2011) 793-836

Introduction

Criteria of stability: analytical vs numerical

(In)stability of 3+1 dimensional BHs

Instability of $D > 4$ BHs: Gregory-Laflamme instability and not only

Potential turbulent instabilities

Conclusions

We shall discuss *mainly* (but not only) linear dynamical (in)stabilities

Motivations:

Two main motivations to study gravitational stability of black holes:

Motivations:

Two main motivations to study gravitational stability of black holes:

- Criterium of existence (in $D = 4$ for alternative theories of gravity and in $D > 4$ owing to absence of uniqueness)

Motivations:

Two main motivations to study gravitational stability of black holes:

• Criterium of existence (in $D = 4$ for alternative theories of gravity and in $D > 4$ owing to absence of uniqueness)

• gauge-gravity duality (instability corresponds to the phase transition in the dual theory)

Motivations:

Two main motivations to study gravitational stability of black holes:

• Criterium of existence (in $D = 4$ for alternative theories of gravity and in $D > 4$ owing to absence of uniqueness)

• gauge-gravity duality (instability corresponds to the phase transition in the dual theory)

• scenarios with extra dimensions (though experimental data on LHC gives no optimism: no large total transverse energy so far at 8 TEV: CMS collaboration claims that semiclassical BHs with mass below 6.1 TeV are excluded)

From linearized perturbations to a master wave equation

- Step 1: Perturbations can be written in the linear approximation in the form

$$g_{\mu\nu} = g^0_{\mu\nu} + \delta g_{\mu\nu}\,, \tag{1}$$

$$\delta R_{\mu\nu} = \kappa\, \delta \left(T_{\mu\nu} - \frac{1}{D-2} T g_{\mu\nu} \right) + \frac{2\Lambda}{D-2} \delta g_{\mu\nu}\,. \tag{2}$$

Linear approximation means that in Eq. (2) the terms of order $\sim \delta g^2_{\mu\nu}$ and higher are neglected. The unperturbed space-time given by the metric $g^0_{\mu\nu}$ is called the background.

From linearized perturbations to a master wave equation

- Step 1: Perturbations can be written in the linear approximation in the form

$$g_{\mu\nu} = g^0_{\mu\nu} + \delta g_{\mu\nu}\,, \tag{1}$$

$$\delta R_{\mu\nu} = \kappa\, \delta \left(T_{\mu\nu} - \frac{1}{D-2} T g_{\mu\nu} \right) + \frac{2\Lambda}{D-2} \delta g_{\mu\nu}\,. \tag{2}$$

Linear approximation means that in Eq. (2) the terms of order $\sim \delta g^2_{\mu\nu}$ and higher are neglected. The unperturbed space-time given by the metric $g^0_{\mu\nu}$ is called the background.

- Step 2: decomposition of the perturbed space-time into scalar, vector and tensor parts

From linearized perturbations to a master wave equation

- Step 1: Perturbations can be written in the linear approximation in the form

$$g_{\mu\nu} = g^0_{\mu\nu} + \delta g_{\mu\nu}\,, \tag{1}$$

$$\delta R_{\mu\nu} = \kappa\, \delta \left(T_{\mu\nu} - \frac{1}{D-2} T g_{\mu\nu} \right) + \frac{2\Lambda}{D-2} \delta g_{\mu\nu}\,. \tag{2}$$

Linear approximation means that in Eq. (2) the terms of order $\sim \delta g^2_{\mu\nu}$ and higher are neglected. The unperturbed space-time given by the metric $g^0_{\mu\nu}$ is called the background.

- Step 2: decomposition of the perturbed space-time into scalar, vector and tensor parts

- Step 3: using the gauge invariant formalism (or fixing the gauge)

From linearized perturbations to a master wave equation

- Step 1: Perturbations can be written in the linear approximation in the form

$$g_{\mu\nu} = g^0_{\mu\nu} + \delta g_{\mu\nu}, \tag{1}$$

$$\delta R_{\mu\nu} = \kappa\, \delta \left(T_{\mu\nu} - \frac{1}{D-2} T g_{\mu\nu} \right) + \frac{2\Lambda}{D-2} \delta g_{\mu\nu}. \tag{2}$$

Linear approximation means that in Eq. (2) the terms of order $\sim \delta g^2_{\mu\nu}$ and higher are neglected. The unperturbed space-time given by the metric $g^0_{\mu\nu}$ is called the background.

- Step 2: decomposition of the perturbed space-time into scalar, vector and tensor parts

- Step 3: using the gauge invariant formalism (or fixing the gauge)

- Step 4: Reducing the perturbation equations (after separation of angular variables) to a second order partial differential equation, termed *master wave equation*. For example, for static and some stationary BHs the master wave equation has the form:

$$-\frac{d^2 R}{dr_*^2} + V(r, \omega) R = \omega^2 R, \tag{3}$$

Criteria of stability: analytical vs numerical

• If the effective potential V_{eff} in the wave equation (3) is positive definite, the differential operator

$$A = -\frac{\partial^2}{\partial r_*^2} + V_{eff} \tag{4}$$

is a positive self-adjoint operator in the Hilbert space of square integrable functions $L^2(r_*, dr_*)$. Then, there are no negative (growing) mode solutions that are normalizable, i. e., for a well-behaved initial data (smooth data of compact support), all solutions are bounded all of the time.

Criteria of stability: analytical vs numerical

• If the effective potential V_{eff} in the wave equation (3) is positive definite, the differential operator

$$A = -\frac{\partial^2}{\partial r_*^2} + V_{eff} \tag{4}$$

is a positive self-adjoint operator in the Hilbert space of square integrable functions $L^2(r_*, dr_*)$. Then, there are no negative (growing) mode solutions that are normalizable, i. e., for a well-behaved initial data (smooth data of compact support), all solutions are bounded all of the time.

• Yet, in majority of cases A is not positive (negativeness of the effective potential in some regions, dependence of the potential on the complex frequencies ω)

Criteria of stability: analytical vs numerical

• If the effective potential V_{eff} in the wave equation (3) is positive definite, the differential operator

$$A = -\frac{\partial^2}{\partial r_*^2} + V_{eff} \tag{4}$$

is a positive self-adjoint operator in the Hilbert space of square integrable functions $L^2(r_*, dr_*)$. Then, there are no negative (growing) mode solutions that are normalizable, i. e., for a well-behaved initial data (smooth data of compact support), all solutions are bounded all of the time.

• Yet, in majority of cases A is not positive (negativeness of the effective potential in some regions, dependence of the potential on the complex frequencies ω)

• Sometimes the situation can be remedied by the so-called S-deformation of the wave equation to the one with positive definite effective potential, in such a way that the lower bound of the energy spectrum does not change.

Criteria of stability: analytical vs numerical

• If the effective potential V_{eff} in the wave equation (3) is positive definite, the differential operator

$$A = -\frac{\partial^2}{\partial r_*^2} + V_{eff} \tag{4}$$

is a positive self-adjoint operator in the Hilbert space of square integrable functions $L^2(r_*, dr_*)$. Then, there are no negative (growing) mode solutions that are normalizable, i. e., for a well-behaved initial data (smooth data of compact support), all solutions are bounded all of the time.

• Yet, in majority of cases A is not positive (negativeness of the effective potential in some regions, dependence of the potential on the complex frequencies ω)

• Sometimes the situation can be remedied by the so-called S-deformation of the wave equation to the one with positive definite effective potential, in such a way that the lower bound of the energy spectrum does not change.

• Usually, it is difficult to find an ansatz for the S-deformation, so that numerical treatment of the wave equation is necessary.

• The numerical criteria of stability could be the evidence that all the proper oscillation frequencies of the black hole, termed the *quasinormal modes* are damped.

• The numerical criteria of stability could be the evidence that all the proper oscillation frequencies of the black hole, termed the *quasinormal modes* are damped.

• Quasinormal modes are eigenvalues of the master wave equation with appropriate boundary conditions: purely ingoing waves at the horizon and purely outgoing waves at infinity or de Sitter horizon. For AdS BHs boundary condition at infinity is dictated by AdS/CFT and is usually the Dirichlet one $\Psi = 0$, where Ψ is some gauge inv. combination.

• The numerical criteria of stability could be the evidence that all the proper oscillation frequencies of the black hole, termed the *quasinormal modes* are damped.

• Quasinormal modes are eigenvalues of the master wave equation with appropriate boundary conditions: purely ingoing waves at the horizon and purely outgoing waves at infinity or de Sitter horizon. For AdS BHs boundary condition at infinity is dictated by AdS/CFT and is usually the Dirichlet one $\Psi = 0$, where Ψ is some gauge inv. combination.

• Quasinormal modes normally have real and imaginary parts $\omega_{\ell,m,\ldots} = Re\omega + iIm\omega$ and depend on a number of quantum numbers such as multipole number ℓ, azimuthal number m, overtone numbers n. That is, there are infinite countable number of quasinormal modes. Potential difficulties: instability usually occurs at lower multipoles ℓ, but also may happen at high ℓ (Gauss-Bonnet BH), an effective potential may have very cumbersome form, the imaginary part of the unstable mode may be very small, ...

• The numerical criteria of stability could be the evidence that all the proper oscillation frequencies of the black hole, termed the *quasinormal modes* are damped.

• Quasinormal modes are eigenvalues of the master wave equation with appropriate boundary conditions: purely ingoing waves at the horizon and purely outgoing waves at infinity or de Sitter horizon. For AdS BHs boundary condition at infinity is dictated by AdS/CFT and is usually the Dirichlet one $\Psi = 0$, where Ψ is some gauge inv. combination.

• Quasinormal modes normally have real and imaginary parts $\omega_{\ell,m,\ldots} = Re\omega + iIm\omega$ and depend on a number of quantum numbers such as multipole number ℓ, azimuthal number m, overtone numbers n. That is, there are infinite countable number of quasinormal modes. Potential difficulties: instability usually occurs at lower multipoles ℓ, but also may happen at high ℓ (Gauss-Bonnet BH), an effective potential may have very cumbersome form, the imaginary part of the unstable mode may be very small, ...

• How to show that all of the QNMs are damped?

• The numerical criteria of stability could be the evidence that all the proper oscillation frequencies of the black hole, termed the *quasinormal modes* are damped.

• Quasinormal modes are eigenvalues of the master wave equation with appropriate boundary conditions: purely ingoing waves at the horizon and purely outgoing waves at infinity or de Sitter horizon. For AdS BHs boundary condition at infinity is dictated by AdS/CFT and is usually the Dirichlet one $\Psi = 0$, where Ψ is some gauge inv. combination.

• Quasinormal modes normally have real and imaginary parts $\omega_{\ell,m,\ldots} = Re\omega + iIm\omega$ and depend on a number of quantum numbers such as multipole number ℓ, azimuthal number m, overtone numbers n. That is, there are infinite countable number of quasinormal modes. Potential difficulties: instability usually occurs at lower multipoles ℓ, but also may happen at high ℓ (Gauss-Bonnet BH), an effective potential may have very cumbersome form, the imaginary part of the unstable mode may be very small, ...

• How to show that all of the QNMs are damped?

• Ideally, either: to achieve an asymptotic regime in all numbers ℓ, m, etc... and parameters in the *frequency domain* or to perform *time-domain* integration until asymptotic tails. Better - both.

(In)stability of 3+1 dimensional BHs and wormholes

Black hole solution (parameters)	Publication
Schwarzschild (M)	Regge, Wheeler 1957
Reissner-Nordström (M, Q)	Moncrief; Alekseev 1974
exactly extreme Reissner-Nordström (M, Q)	Aretakis 2011
Schwarzschild-dS (M, $\Lambda > 0$)	Mellor, Moss 1989
Schwarzschild-AdS (M, $\Lambda < 0$)	Cardoso, Lemos 2001
Reissner-Nordström-dS (M, Q, Λ)	Mellor 1989
Kerr (M, J)	Press 1973; Teukolsky 1974
exactly extreme Kerr (M, J)	Aretakis 2011; Lucietti, Reall, 2012
Kerr-dS (M, J, $\Lambda > 0$)	Suzuki 1999
Kerr-AdS (M, J, $\Lambda < 0$)	Giammatteo 2005
Kerr-Newmann (M, J, Q)	?
Kerr-Newman-A(dS) (M, J, Q, Λ)	?
Dilaton (M, Q, ϕ)	Holzhey 1991; Ferrari, 2000
Dilaton-axion (M, Q, J, ϕ, ψ)	?
Dilaton-GB (M, ϕ)	Torii 1998, Pani 2009
Born-Infeld (M, Q)	axial only, Fernando 2004
Black universes (M, ϕ)	Bronnikov, Konoplya, Zhidenko 2012
BHs in the Chern-Simons theory (M, β)	Cardoso 2010

(In)stability of 3+1 dimensional BHs and wormholes

- Non extreme four dimensional BHs are usually stable under linear gravitational perturbations, except black universes with the minimal area function and rotating asymptotically AdS BHs (superradiant modes).

(In)stability of 3+1 dimensional BHs and wormholes

- Non extreme four dimensional BHs are usually stable under linear gravitational perturbations, except black universes with the minimal area function and rotating asymptotically AdS BHs (superradiant modes).

- Extreme Kerr and Reissner-Nordstrom BHs space-times are unstable.

(In)stability of 3+1 dimensional BHs and wormholes

- Non extreme four dimensional BHs are usually stable under linear gravitational perturbations, except black universes with the minimal area function and rotating asymptotically AdS BHs (superradiant modes).

- Extreme Kerr and Reissner-Nordstrom BHs space-times are unstable.

- Wormholes and black holes supported by exotic matter, such as phantom fields, are usually unstable.

(In)stability of 3+1 dimensional BHs and wormholes

• Non extreme four dimensional BHs are usually stable under linear gravitational perturbations, except black universes with the minimal area function and rotating asymptotically AdS BHs (superradiant modes).

• Extreme Kerr and Reissner-Nordstrom BHs space-times are unstable.

• Wormholes and black holes supported by exotic matter, such as phantom fields, are usually unstable.

• ...and from
1993 Gregory and Laflamme (black branes)
2003 Ishibashi and Kodama (black holes)

a higher dimensional story starts...

Three types of instability:

• **Gregory-Laflamme instability**. It occurs for black strings at long wavelengthes in the extra dimension z and is connected with inapplicability of the Birkhoff theorem. Gregory and Laflamme 1993. Gubser and Mitra instability (2001) for large highly charged RNdS BHs in $N = 8$ supergravity is of this kind. Developement of black string instability beyond linear order - nonuniform string - thermodynamic arguments and numerical computations by Choptuik and others, 2000th

Three types of instability:

• **Gregory-Laflamme instability**. It occurs for black strings at long wavelengthes in the extra dimension z and is connected with inapplicability of the Birkhoff theorem. Gregory and Laflamme 1993. Gubser and Mitra instability (2001) for large highly charged RNdS BHs in $N = 8$ supergravity is of this kind. Developement of black string instability beyond linear order - nonuniform string - thermodynamic arguments and numerical computations by Choptuik and others, 2000th

• **Superradiant instability of asymptotically AdS rotating BHs**. If

$$\frac{m\Omega}{\omega} > 1, \tag{5}$$

the reflected wave has larger amplitude than the incident one, a superradiance. This effect was predicted by Zeldovich and proved for Kerr BHs by A. Starobinsky in 1974. Super-radiance is connected with extraction of rotational energy of a black hole and occurs at positive ("co-rotating"with a black hole) m. Super-radiance + Dirichlet boundary conditions far from black hole = instability. Therefore, rotating AdS black holes are unstable in the superradiant regime.

Three types of instability:

• **Gregory-Laflamme instability**. It occurs for black strings at long wavelengthes in the extra dimension z and is connected with inapplicability of the Birkhoff theorem. Gregory and Laflamme 1993. Gubser and Mitra instability (2001) for large highly charged RNdS BHs in $N = 8$ supergravity is of this kind. Developement of black string instability beyond linear order - nonuniform string - thermodynamic arguments and numerical computations by Choptuik and others, 2000th

• **Superradiant instability of asymptotically AdS rotating BHs**. If

$$\frac{m\Omega}{\omega} > 1, \tag{5}$$

the reflected wave has larger amplitude than the incident one, a superradiance. This effect was predicted by Zeldovich and proved for Kerr BHs by A. Starobinsky in 1974. Super-radiance is connected with extraction of rotational energy of a black hole and occurs at positive ("co-rotating"with a black hole) m. Super-radiance + Dirichlet boundary conditions far from black hole = instability. Therefore, rotating AdS black holes are unstable in the superradiant regime.

• **"Non-Gregory-Laflamme"instability**. The "other"type of instability which is not connected with the inapplicability of the Birkhoff theorem or superradiance. It happens, for instance, for asymptotically de Sitter highly charged black holes in $D > 6$ space-times.

Instability of RNAdS BHs in supergravity and RNdS instability in EM theory

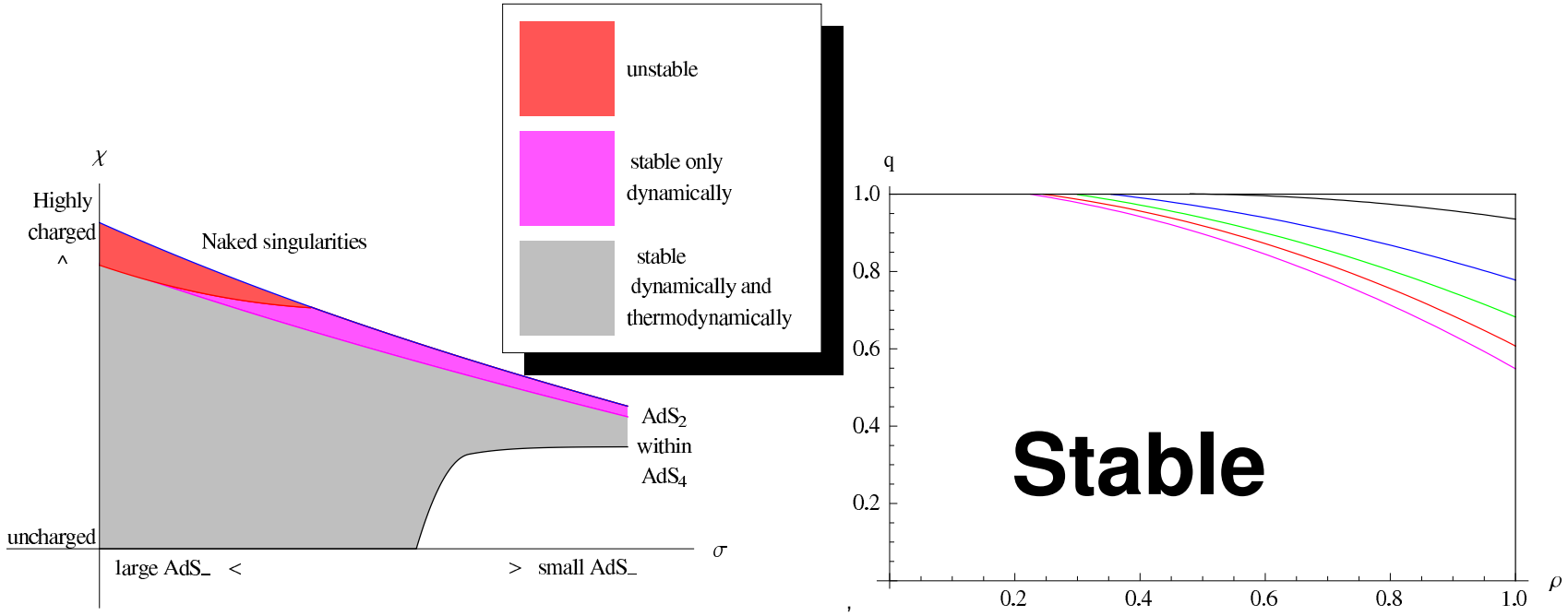

Рис.: **Left:** Gubser-Mitra instability of R-N-AdS in $N = 8$ supergravity; **Right:** R-N-dS instability, Konoplya, Zhidenko PRL, 2009. The parametric region of instability in the right upper corner of the square in the $\rho - q$ "coordinates" for $D = 7$ (top, black), $D = 8$ (blue), $D = 9$ (green), $D = 10$ (red), $D = 11$ (bottom, magenta). The units $r_+ = 1$ are used; $\rho = r_+/r_c = 1/r_c < 1$, r_c is the cosmological horizon. The charge can be normalized by its extremal quantity $q = Q/Q_{ext} < 1$.

Superradiant instability

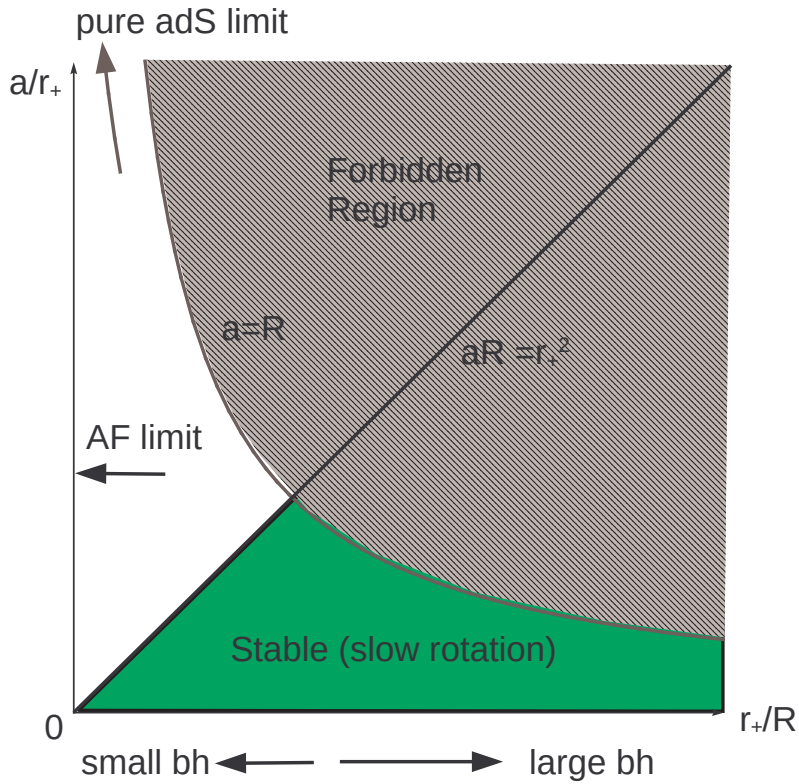

Рис.: The stable region in the parameter plane for the simply rotating higher-dimensional asymptotically AdS black hole. Kodama, Konoplya, Zhidenko 2009. The instability has the tiny growth rate which, apparently, will be suppressed by the intensive Hawking evaporation.

(In)stability of higher-dimensional black holes

Black hole solution (parameters)	Publication
Schwarzschild (M)	Stable for all D Kodama, Ishibashi 2003
non extreme R-N (M, Q)	Stable for $D = 5, 6, \ldots, 11$ K.Z. 2009
Schwarzschild-dS (M, Λ), (M, $\Lambda > 0$)	Stable for $D = 5, 6, \ldots, 11$ K.Z. 2007
Schwarzschild-AdS (M, Λ) (M, $\Lambda < 0$)	Stable in EM theory for $D = 5, 6, \ldots, 11$ K.Z. 2008
R-N -dS (M, Λ) (M, Q, $\Lambda > 0$)	Unstable for $D = 7, 8, \ldots, 11$ K.Z. 2009
R-N -AdS in E-M (M, Λ) (M, Q, $\Lambda < 0$)	stable in E-M K.Z. 2008
R-N -AdS in supergravity (M, Λ) (M, Q, $\Lambda < 0$)	unstable Gubser, Mitra 2000
Gauss-Bonnet (M, α)	Unstable for large α, Dotti 2006
Lovelock (M, α, β, ...)	Unstable for large α, Soda, Takahashi
Myers-Perry and its generalizations (M, J)	? Only particular types of perturbations
Dilaton (M, Q, ϕ)	?
Dilaton-axion (M, Q, J, ϕ, ψ)	?
Dilaton-Gauss-Bonnet (M, ϕ, α)	?
squashed Kaluza-Klein black holes	stable, 2000th Soda, Ishihara and others
black strings and branes	Gregory and Laflamme 1993
black rings, saturns, etc	? (Heuristic arguments and analogies)

K.Z. = Konoplya and Zhidenko

Potential turbulent instability of AdS space-time

- Bizon and Rostworowski (2011) claimed that there is numerical evidence of a weakly turbulent instability of pure AdS space-time

Potential turbulent instability of AdS space-time

• Bizon and Rostworowski (2011) claimed that there is numerical evidence of a weakly turbulent instability of pure AdS space-time

• This claim was supported by some intuitive arguments of O. Dias and collaborators (2011) borrowed from M. T. Anderson (2006): AdS boundary conditions act like a confining box. Any excitation added to the box, after some time, could explore a configuration consistent with the conserved quantities. The conjecture is that an excitation of AdS eventually finds itself inside its Schwarzschild radius and collapses to a black hole .

Potential turbulent instability of AdS space-time

• Bizon and Rostworowski (2011) claimed that there is numerical evidence of a weakly turbulent instability of pure AdS space-time

• This claim was supported by some intuitive arguments of O. Dias and collaborators (2011) borrowed from M. T. Anderson (2006): AdS boundary conditions act like a confining box. Any excitation added to the box, after some time, could explore a configuration consistent with the conserved quantities. The conjecture is that an excitation of AdS eventually finds itself inside its Schwarzschild radius and collapses to a black hole .

• In concordance with this conjecture it was *argued* in a subsequent paper of Dias (2012) that a number of asymptotically AdS space-times including a SdS BH space-time apparently look like non-linearly stable

Potential turbulent instability of AdS space-time

• Bizon and Rostworowski (2011) claimed that there is numerical evidence of a weakly turbulent instability of pure AdS space-time

• This claim was supported by some intuitive arguments of O. Dias and collaborators (2011) borrowed from M. T. Anderson (2006): AdS boundary conditions act like a confining box. Any excitation added to the box, after some time, could explore a configuration consistent with the conserved quantities. The conjecture is that an excitation of AdS eventually finds itself inside its Schwarzschild radius and collapses to a black hole .

• In concordance with this conjecture it was *argued* in a subsequent paper of Dias (2012) that a number of asymptotically AdS space-times including a SdS BH space-time apparently look like non-linearly stable

• By now, in my opinion, there is no clearness in this issue: alternative non-linear computations or possibly higher order perturbative calculations would help...

Conclusions

By now, we know a lot of about various (in)stabilities of black holes and branes in four and higher dimensions in the linear regime, but far from everything....

Conclusions

By now, we know a lot of about various (in)stabilities of black holes and branes in four and higher dimensions in the linear regime, but far from everything....

We know not much about possible nonlinear (in)stabilities in higher dimensions...

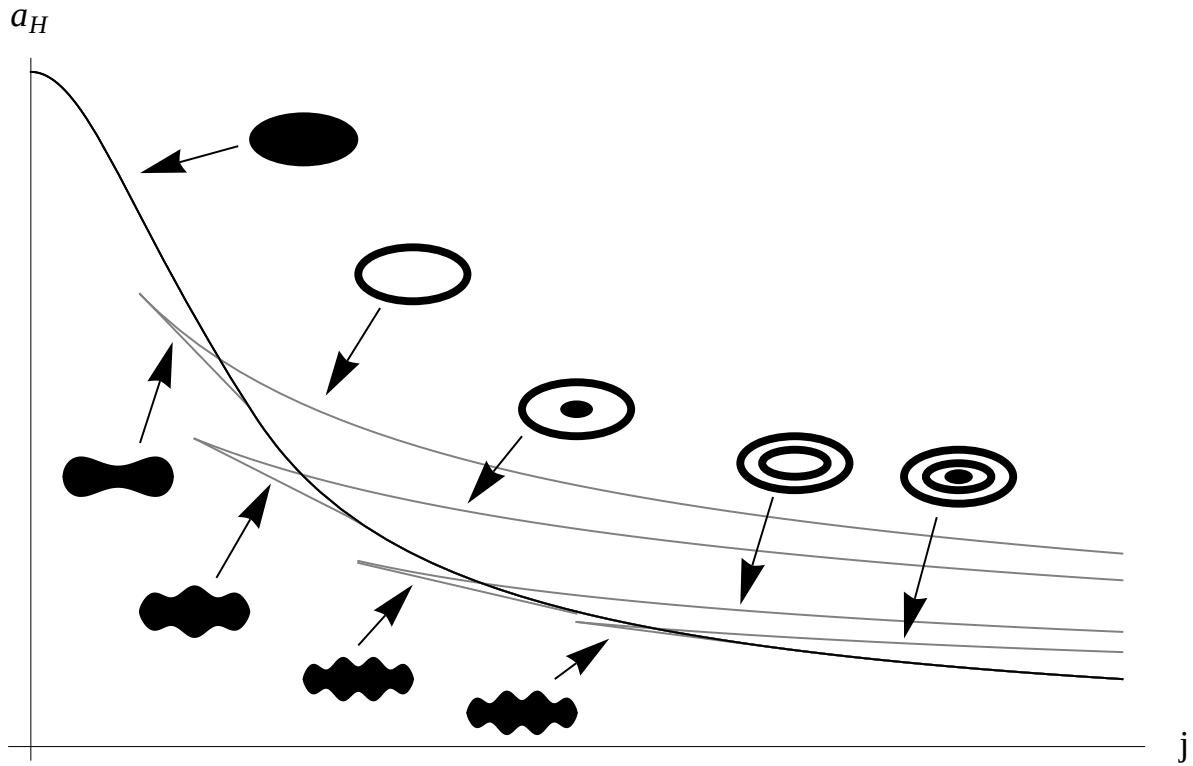

Рис.: The qualitative phase diagram for the black objects in $D \geq 6$ (taken from an Emparan's paper). The horizontal and vertical axes correspond, respectively, to the spin and area of a black object. If thermal equilibrium is not imposed, multirings are possible in the upper region of the diagram.

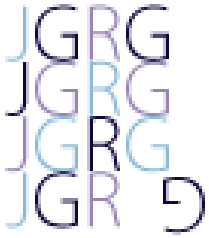

Jaume Garriga, JGRG 22(2012)111603

"Vacuum transitions and the arrow of time"

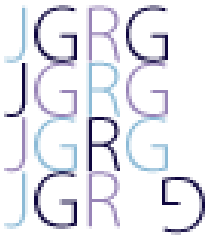

RESCEU SYMPOSIUM ON

GENERAL RELATIVITY AND GRAVITATION

JGRG 22



November 12-16 2012

Koshiba Hall, The University of Tokyo, Hongo, Tokyo, Japan



Vacuum transitions and the arrow of time

Jaume Garriga (U. Barcelona)

ジャウマ ガリガ (Kyoto YITP)

JGRG 2012 Tokyo

Inflationary multiverse:

Gravity coupled to a field theory with several metastable vacua

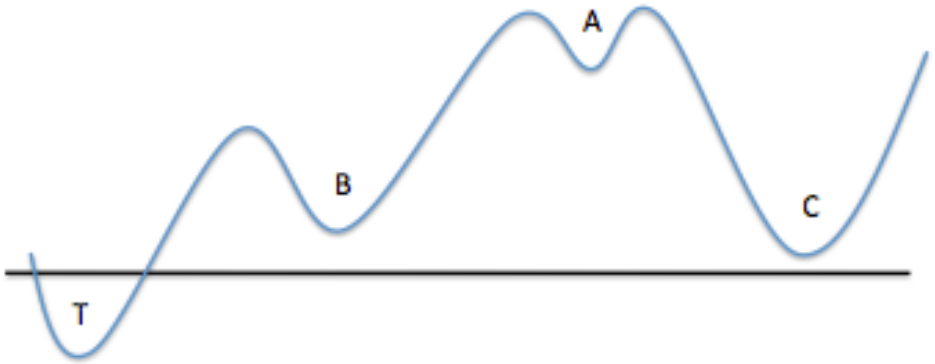

Very interesting dynamics, driven by inflation and vacuum transitions.

Inflationary multiverse:

Gravity coupled to a field theory with several metastable vacua

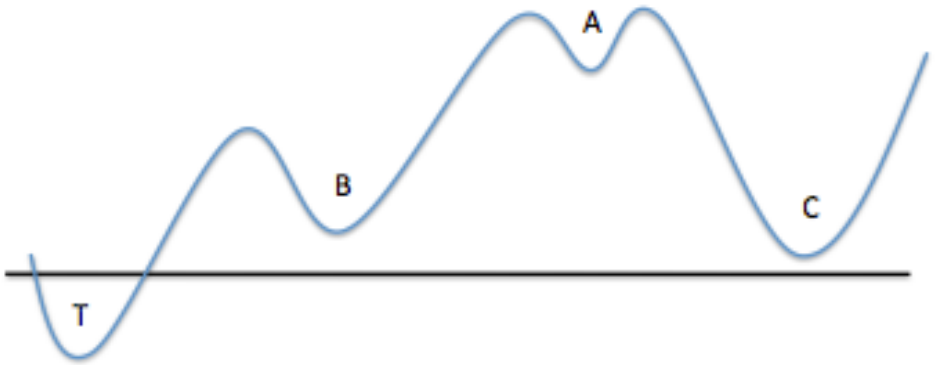

Our universe could well be that system:

- There is some evidence for primordial inflation.

- And some more for cosmic acceleration.

- This scenario may offer a solution of the cc problem
(and all other observed coincidences), given a vast landscape of vacua.

Vacuum transitions:

- **Slow roll**

- **Quantum diffusion**

- **Bubble nucleation**

These are semiclassical mechanisms (there may be other transition mechanisms in a full quantum theory).

Robust features of theories with long lived inflating vacua:

- Inflation is generically **eternal to the future.**

- **All vacua** which are accessible are **eventually populated**. There will be some fraction of the volume of the universe

- The **distribution of vacua [e.g. Vol(\phi,t)] approaches an attractor** at late times.

Bubble formation

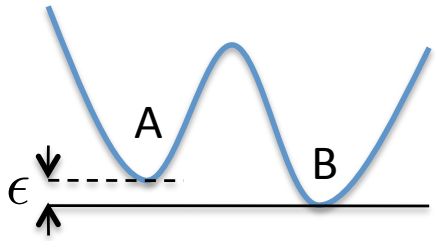

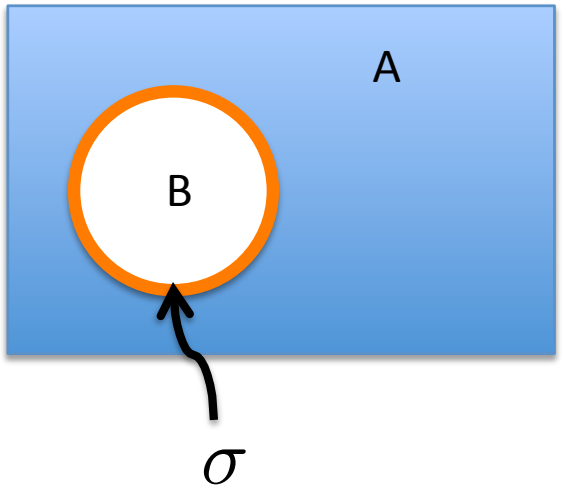

Voloshin, Kobzarev, Okun (75)

$$M(r) = \sigma\ \Omega\ r^{D-2}$$

$$V(r) = \frac{\Omega}{D-1}\ r^{D-1}$$

$$p_r = \gamma M \dot{r}$$

$$\sqrt{p_r^2 + M^2} - \epsilon\ V(r) = 0.$$

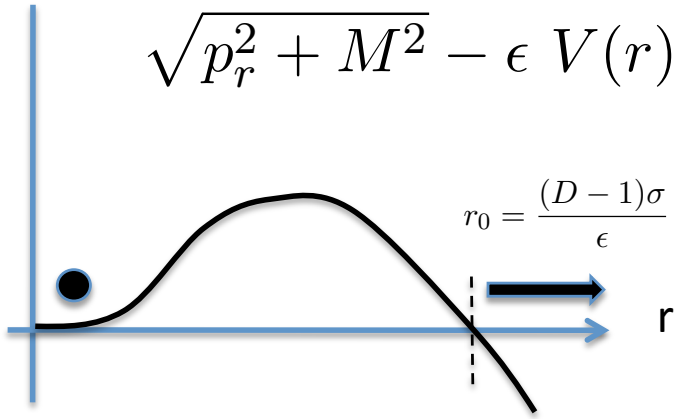

$$\Gamma \sim e^{-\int_{r=0}^{r_0} |p_r| dr}$$

Critical bubble nucleates at rest, and then expands

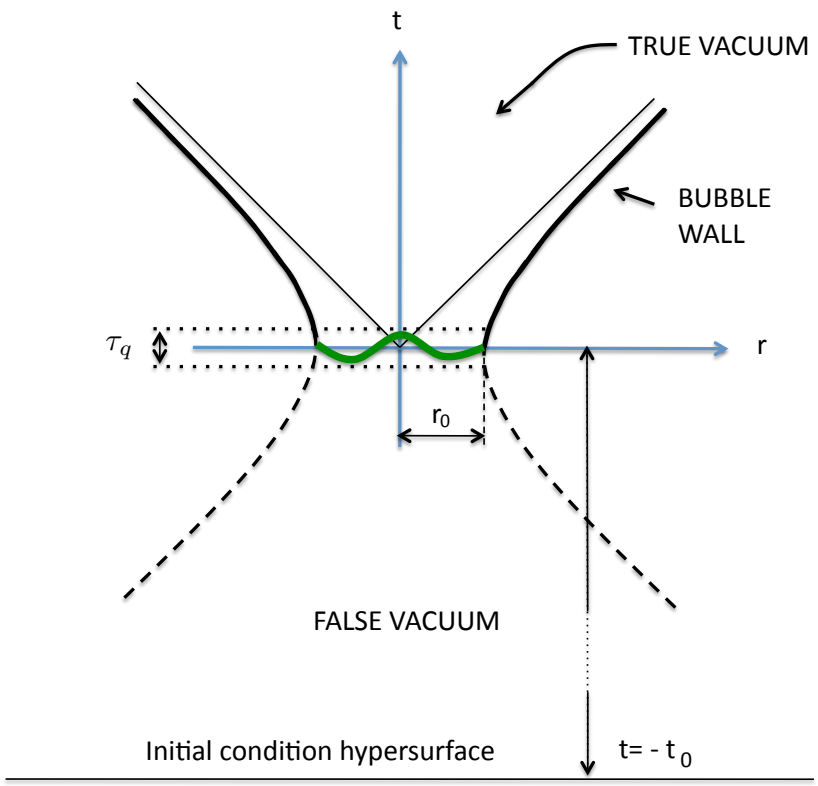

False vacuum approximately Lorentz invariant.

No prefered frame of nucleation.

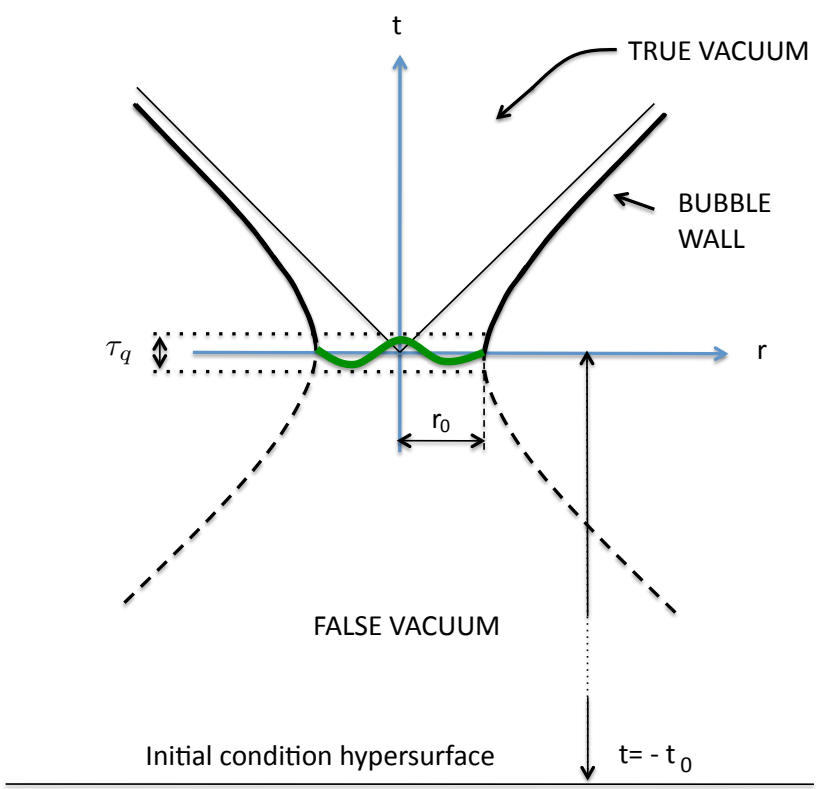

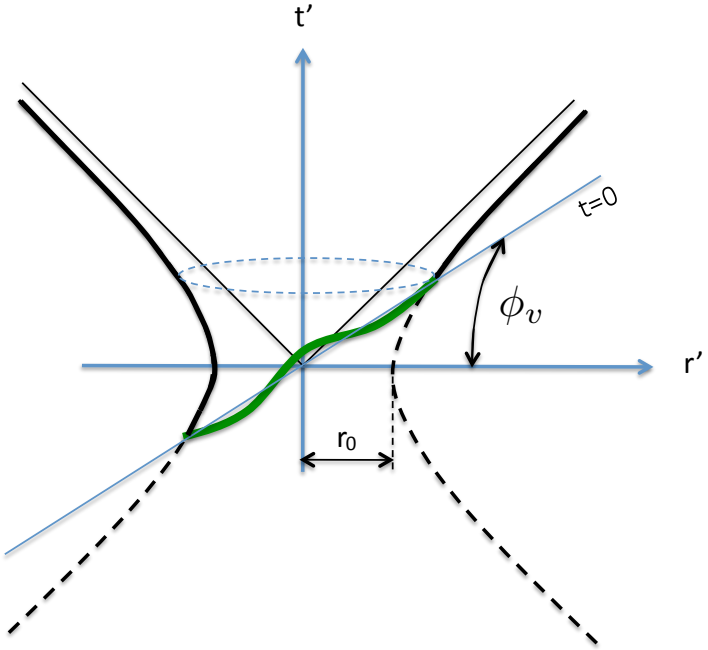

False vacuum approximately Lorentz invariant.

No prefered frame of nucleation.

Integrate over all possible frames? $\Gamma_{total} = \Gamma\ \Omega \int d\phi_v (\sinh \phi_v)^{D-2} = \infty$

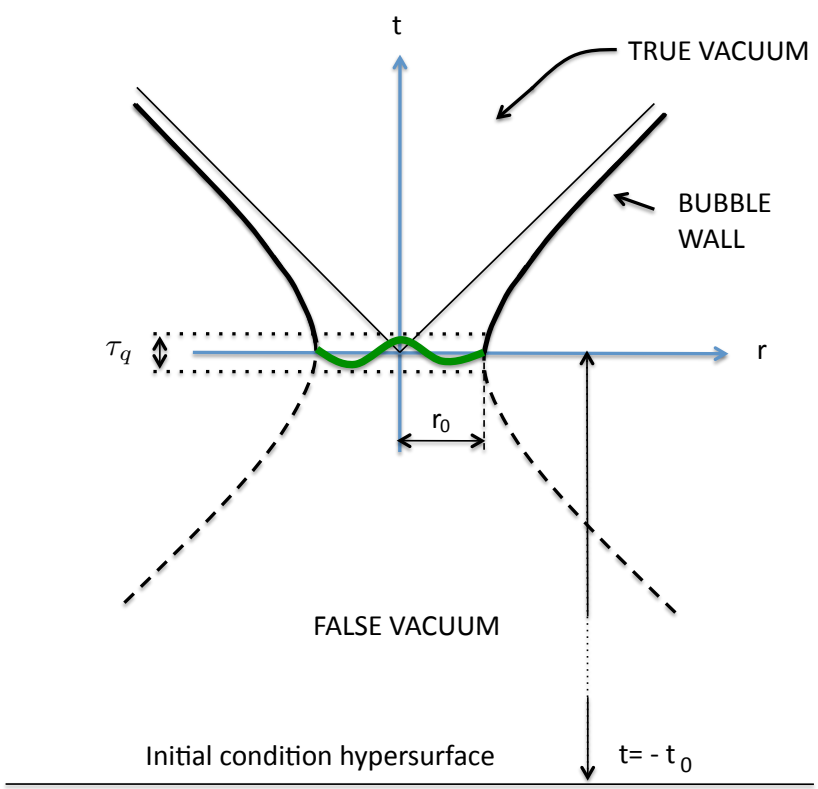

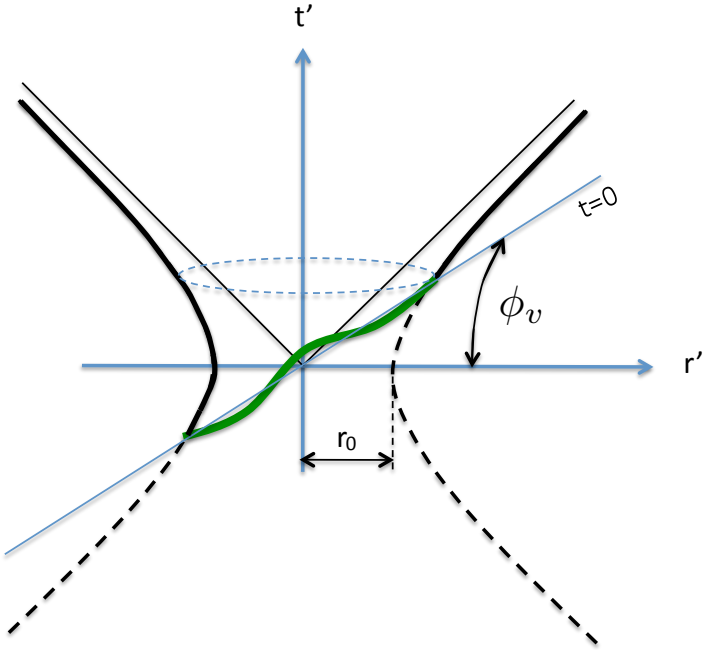

False vacuum approximately Lorentz invariant.

No prefered frame of nucleation.

Integrate over all possible frames? $\Gamma_{total} = \Gamma\ \Omega \int d\phi_v (\sinh \phi_v)^{D-2} = \infty$ $\Gamma = A\ e^{-S_E}$

Coleman (77) showed that the **rate is finite (**integration over rest frame does not play a role)

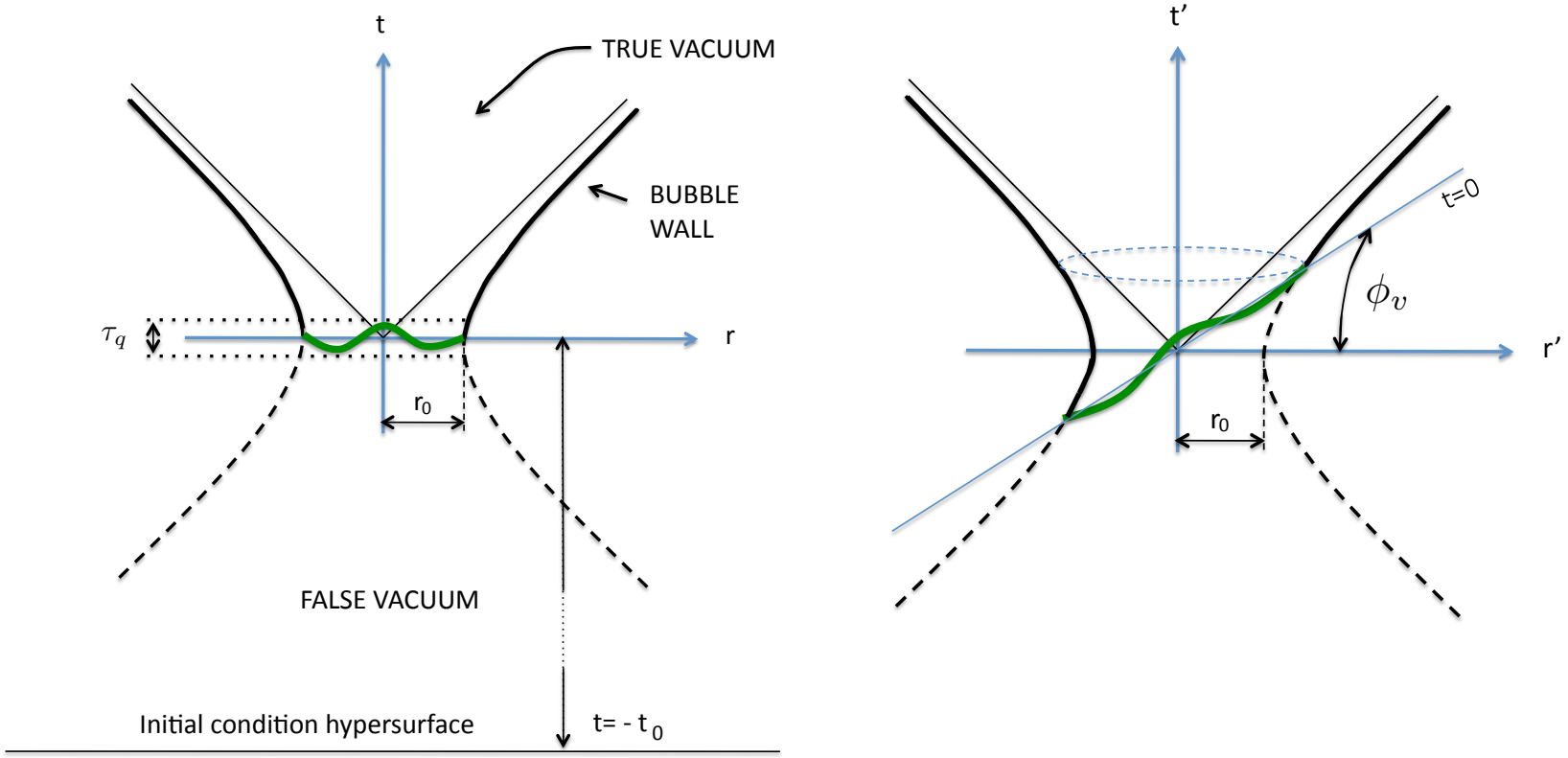

Remaining question: if it is true that the false vacuum approximately Lorentz invariant.

What is it that determines the frame of nucleation?

J.G., Kanno, Sasaki, Soda, Vilenkin (2012)
J.G., Kanno, Tanaka (in preparation).

What is it that determines the frame of nucleation?

The question can be addressed by using a model detector

We need a fully quantum description of bubble nucleation: Schwinger pair production in (1+1)

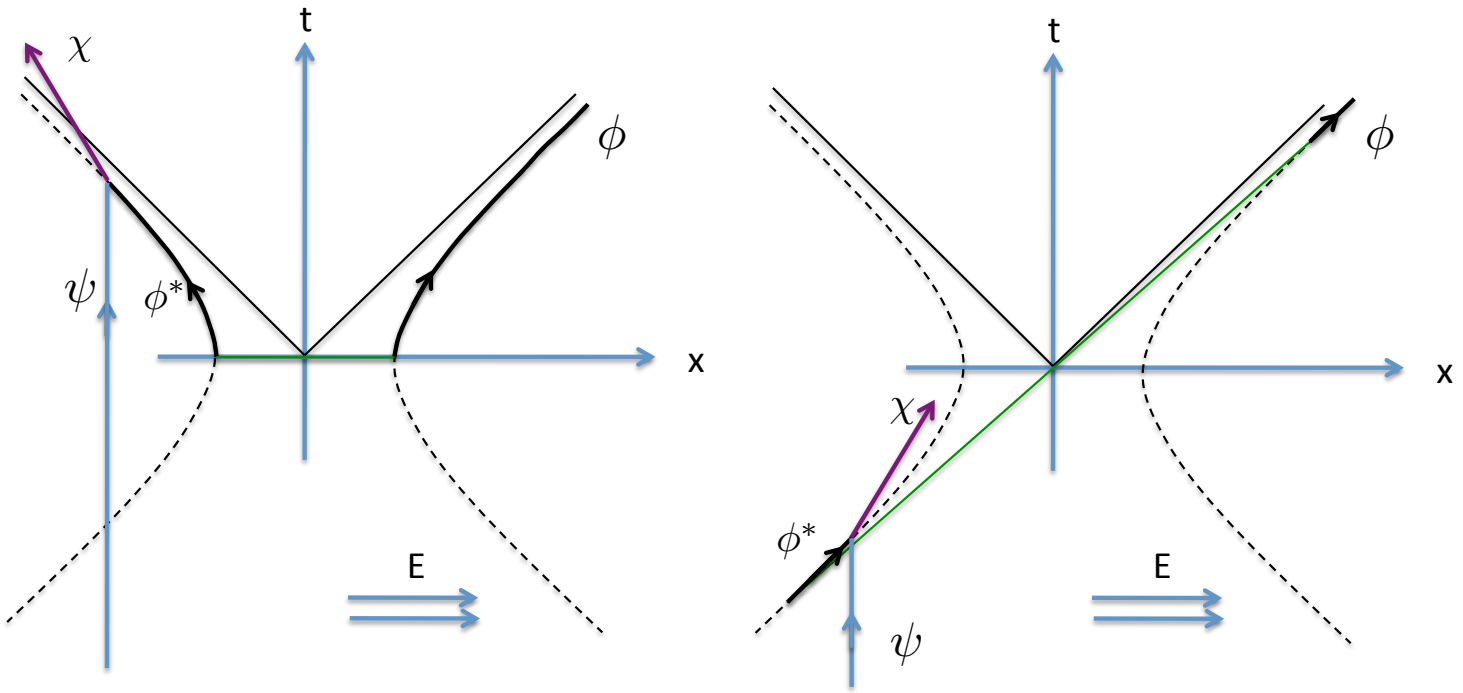

$$g(\phi\psi^*\chi + hc)$$

$$w_\phi + w_\psi = w_\chi$$

Possible outcomes of this "experiment":

(A) - Frame of nucleation is determined by the rest frame of the detector.

(B) - Perhaps the frame of nucleation is not very well determined and the detector can probe part of the contracting branch.

(C) - The frame of nucleation is determined by initial conditions.

$S_E \equiv \pi\lambda \gg 1$ For tunneling to be semiclassical

r_0 Size of the critical bubble

Time-scales:

$\tau_{nuc} \sim r_0$ Timescale of nucleation

$\tau_q \sim \lambda^{-1/3} r_0 \ll r_0$ Quantum fuzziness scale around the turning point

Let us consider $\tau_q \ll r_0 \ll t_0 \to \infty$ (time ellapsed since initial conditions)



This will take care of option (C)

In a constant external electric field

$$\left[\frac{d^2}{dt^2} + m^2 + (k + eEt)^2\right] \phi_k = 0\,.$$

$$k_{\rm phys} = k + eEt.$$

$$\phi_k = \alpha_k\, \phi_k^{\rm out} + \beta_k\, \phi_k^{\rm out*}$$

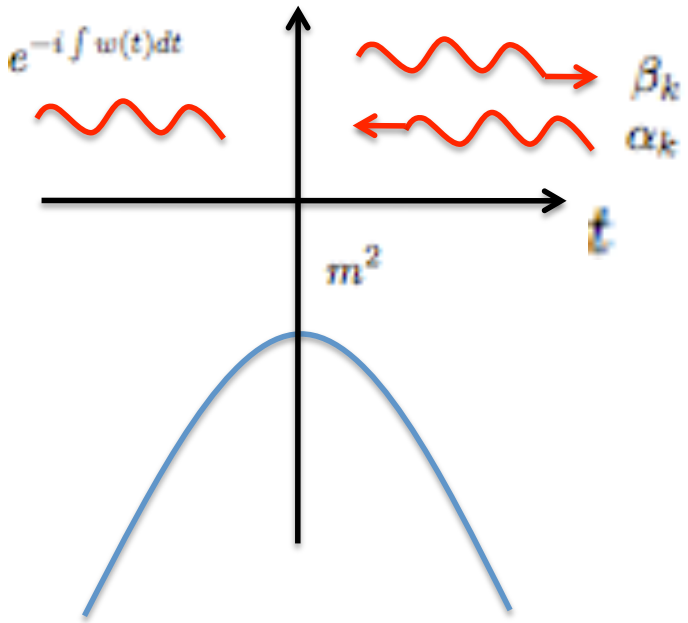

$$|\beta_k|^2 = e^{-\pi\lambda} = e^{-\frac{\pi m^2}{eE}}\,.$$

(Independent of k)

Lorentz invariance of the ``in" vacuum ?

Gauge invariant Wightman function

$$G^+(x^\mu, y^\mu) \equiv {}_{\rm in}\langle\, 0 \,|\, \phi^\dagger(x^\mu)\; e^{-ie\int_x^y A_\nu dx^\nu}\; \phi(y^\mu) \,|\, 0 \,\rangle_{\rm in}\,,$$

$$G^+(\Delta x^\mu) = \frac{|\alpha|^2}{4\pi}\Gamma(-\nu^*)\,\frac{W_{i\lambda/2,\,0}\left(ieE\,\Delta s^2/2\right)}{\sqrt{ieE\,\Delta s^2/2}}\,, \qquad \text{for} \qquad \Delta t - \Delta x > 0$$

$$G^+(\Delta x^\mu) = \frac{|\alpha|^2}{4\pi}\Gamma(-\nu)\,\frac{W_{-i\lambda/2,\,0}\left(-ieE\,\Delta s^2/2\right)}{\sqrt{-ieE\,\Delta s^2/2}}\,, \qquad \text{for} \qquad \Delta t - \Delta x < 0.$$

$$\Delta s^2 = -(\Delta t)^2 + (\Delta x)^2$$

$\Rightarrow$ $|\, 0 \,\rangle_{\rm in}$ translation and boost invariant. .

(Cannot determine the frame of nucleation)

Detector $g(\phi\psi^*\chi + hc)$

$g(t) = g\, e^{-t^2/T^2}$ We connect the interaction for a finite time T

$$\frac{dN_\chi}{dp} \propto |\mathcal{A}_\chi(p; q=0)|^2 \propto \exp\left[-\frac{(p+\omega_p - m_\psi)^2}{(eET)^2}\right]$$

$m_\chi - m_\psi \gg m_\phi$

$T \gg \tau_q$

$$\bar{p} = -\frac{1}{2m_\psi}(m_\chi^2 - m_\psi^2)$$

Negative and in accordance with kinematics

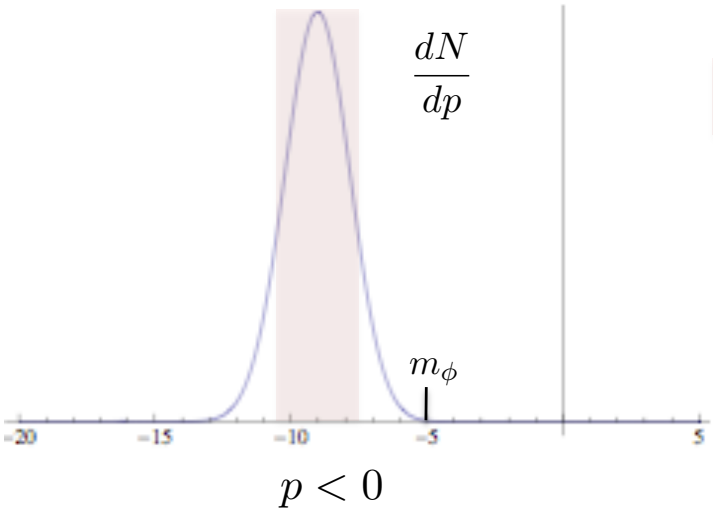

$p < 0$

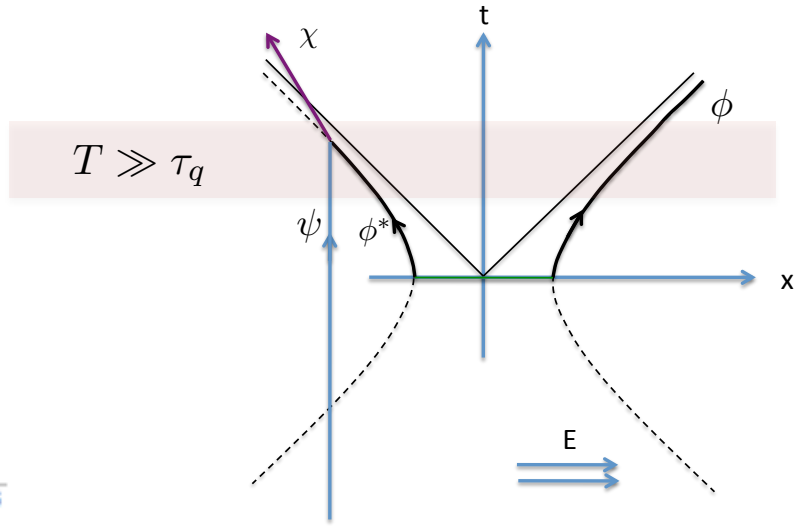

In good agreement with option (A)

De Sitter

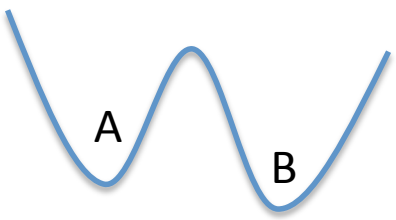

A → B (+)

B → A (-)

Schwinger process in 1+1 de Sitter (J.G. 94)

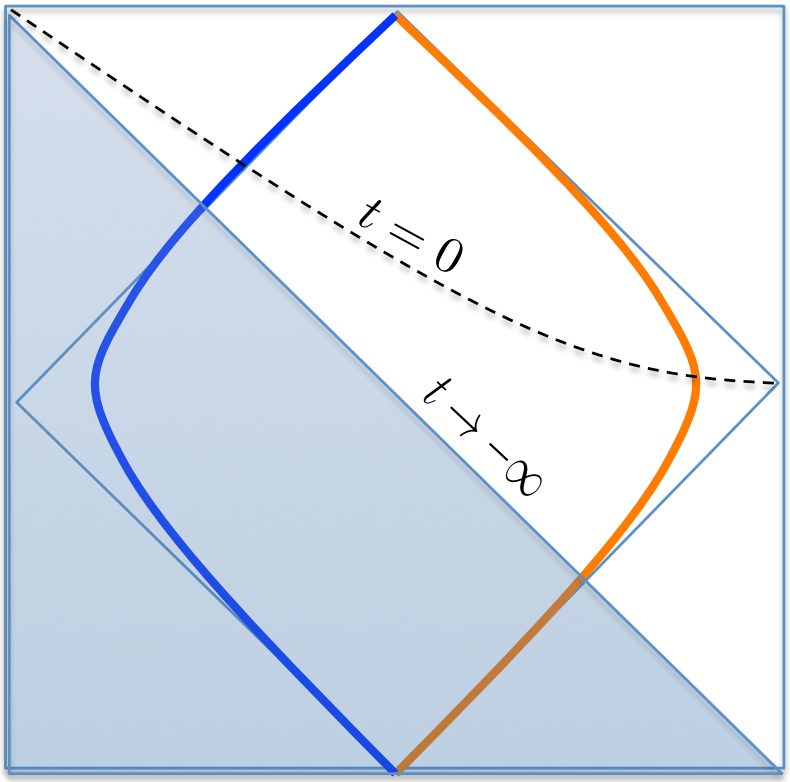

Electric field does not dilute in 1+1

→ $|\beta_k|^2 \approx \exp\left(-\frac{2\pi}{H^2}\left[(\mathcal{M}^2H^2+e^2E_0^2)^{1/2}+eE_0\right]\right),$

→ $|\beta_k|^2 \approx \exp\left(-\frac{2\pi}{H^2}\left[(\mathcal{M}^2H^2+e^2E_0^2)^{1/2}-eE_0\right]\right)$

$|\beta_k|^2 \approx e^{-S_E}$ In agreement with instanton methods.

“in” vacuum state is Hadamard.

Pairs are created at a constant rate, but they are diluted by the expansion. Healthy UV limit.

De Sitter

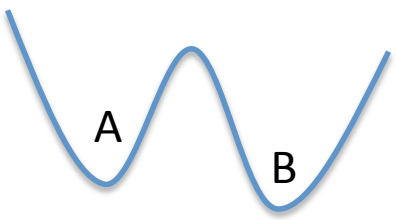

A → B (+)

B → A (-)

Schwinger process in 1+1 de Sitter (J.G. 94)

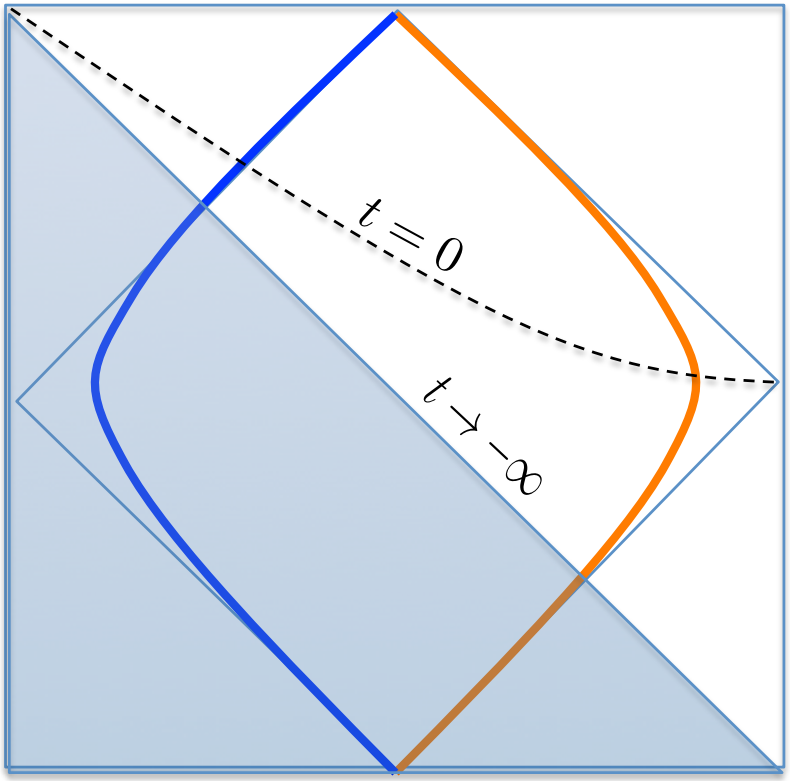

Electric field does not dilute in 1+1

$$|\beta_k|^2 \approx \exp\left(-\frac{2\pi}{H^2}\left[(\mathcal{M}^2H^2+e^2E_0^2)^{1/2}+eE_0\right]\right),$$

$$|\beta_k|^2 \approx \exp\left(-\frac{2\pi}{H^2}\left[(\mathcal{M}^2H^2+e^2E_0^2)^{1/2}-eE_0\right]\right)$$

$|\beta_k|^2 \approx e^{-S_E}$ In agreement with instanton methods.

"in" vacuum state is Hadamard.

Pairs are created at a constant rate, but they are diluted by the expansion. Healthy UV limit.

(GKSSTV 2012) "in" vacuum breaks de Sitter invariance $\langle J_\mu \rangle_{in} = \delta^1_\mu (J^+ - J^-) = \text{finite} \neq 0.$!!

Spontaneous breakdown of dS invariance

Persistent stationary current $\langle J_\mu \rangle \langle J^\mu \rangle = const \neq 0.$

There is no dS invariant Hadamard state in the presence of electric field E

`Arrow of time $t^\mu \propto \epsilon^{\mu\nu} \langle J_\nu \rangle$

determined by the choice of iInitial conditions. It lasts forever.

Discussion:

Is this be related to an arrow of time in the multiverse?

- If we include backreaction, the electric field disappears, and the current disappears.

- However vacuum transitions will continue to occur,

- Bubble nucleation is still **time asymmetric:**

we see expanding bubbles but not contracting ones

- This seems to imply a small deviation from ergodicity even in the case of a dS landscape

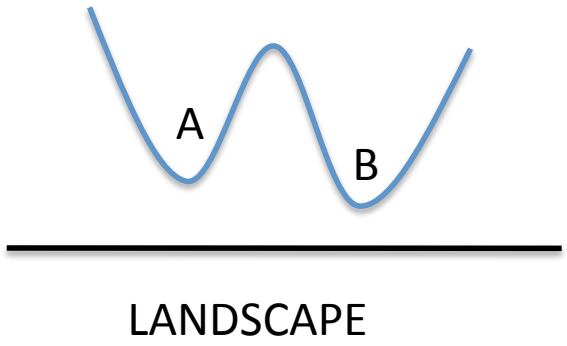

$$\frac{\Gamma_{BA}}{\Gamma_{AB}} = e^{S_B - S_A}$$

Ratio of transition rates per unit volume (from instanton formalism).

$$\frac{\kappa_{BA}}{\kappa_{AB}} = \left(\frac{H_B}{H_A}\right)^{D-1} e^{S_B - S_A}$$

Ratio of transition rates

Slight departure from ergodicity! **Persistent arrow of time.**

(J.G.+ Vilenkin '12)

In real life we need something more drastic

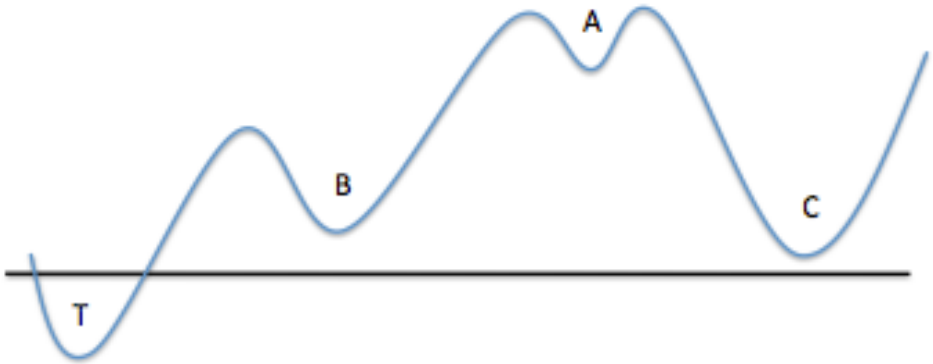

In real life we need something more drastic

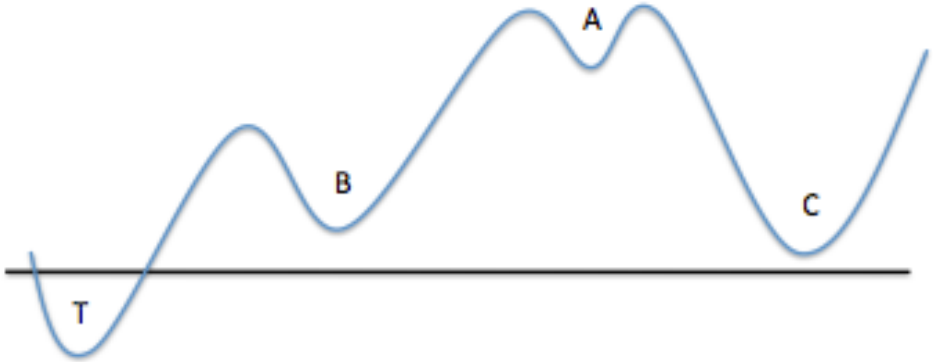

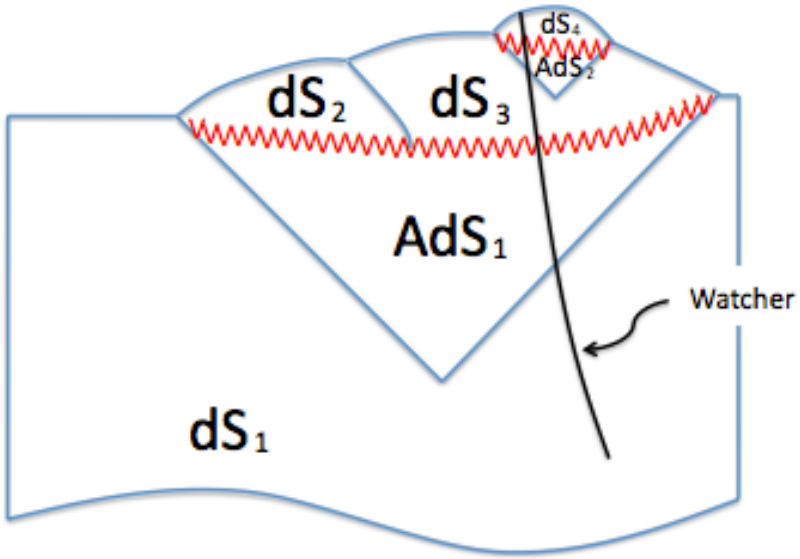

Transitions through crunches, if allowed, are likely to be very far from ergodic.

We expect in this case a very well defined arrow of time.

(J.G.+ Vilenkin ‘12)

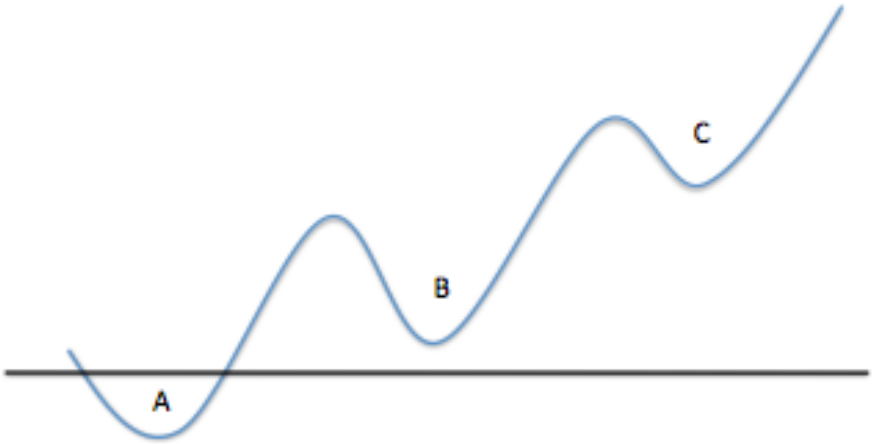

$$f_C/f_B \sim \exp(S_C - S_B)$$ If crunches are terminal

$$f_C/f_B \sim \kappa_{AB}/\kappa_{BC}$$ If we can pass through crunches

Alexei Starobinsky, JGRG 22(2012)111604

"Duration and decay branching ratios of stochastic inflation"

RESCEU SYMPOSIUM ON

GENERAL RELATIVITY AND GRAVITATION

JGRG 22

November 12-16 2012

Koshiba Hall, The University of Tokyo, Hongo, Tokyo, Japan

Duration and Decay Branching Ratios of Stochastic Inflation

Alexei A. Starobinsky

Landau Institute for Theoretical Physics RAS, Moscow and
RESCEU, The University of Tokyo, Tokyo

RESCEU Symposium on General Relativity and Gravitation JGRG22
Celebrating the 60th birthday of Profs. Hideo Kodama, Misao Sasaki and Toshifumi Futamase
Tokyo, Japan, 16.11.2012

Perturbative results

Stochastic slow-roll inflation

Langevin and Fokker-Planck equations

Probabilities to go to different vacua after inflation

Local duration of inflation

Choice of an initial condition

Correlations and joint PDF

Conclusions

Perturbative anomalous growth of light scalar fields in the de Sitter space-time

Background - fixed - de Sitter or, more interestingly, quasi-de Sitter space-time (slow roll inflation).
Occurs for $0 \leq m^2 \ll H^2$ where $H \equiv \frac{\dot{a}}{a}$, $a(t)$ is a FRW scale factor. The simplest and textbook example:
$m = 0$, $H = H_0 = const$ for $t \geq t_0$ and the initial quantum state of the scalar field at $t = t_0$ is the adiabatic vacuum for modes with $k/a(t_0) \gg H_0$ and some infrared finite state otherwise:

$$< \phi^2 >= \frac{H_0^2 N}{4\pi^2} + const$$

Here $N = \ln \frac{a}{a(t_0)} \gg 1$ is the number of e-folds from the beginning of inflation and the constant depends on the initial quantum state (Linde, 1982; Starobinsky, 1982; Vilenkin and Ford, 1982).
Straightforward generalization to the slow-roll case $|\dot{H}| \ll H^2$.

For $0 < m^2 \ll H^2$, the Bunch-Davies equilibrium value

$$< \phi^2 >= \frac{3H_0^4}{8\pi m^2} \gg H_0^2$$

is reached after a large number of e-folds $N \gg \frac{H_0^2}{m^2}$. In the slow-roll case with $\dot{H} \neq 0$, the "instantaneous" value with $H(t)$ instead of H_0 is generically never reached at all! Purely infrared effect - creation of real field fluctuations; renormalization is not important and does not affect it.

For the de Sitter inflation (gravitons only) (AS, 1979):

$$P_g(k) = \frac{16GH_0^2}{\pi}; \quad < h_{ik}h^{ik} >= \frac{16GH_0^2N}{\pi} .$$

The assumption of small perturbations breaks down for $N \gtrsim 1/GH_0^2$. Still ongoing discussion on the final outcome of this effect. My opinion - no screening of the background cosmological constant, instead - stochastic drift through an infinite number of locally de Sitter, but globally non-equivalent vacua. A finite and small shift in H_0 : $\delta H_0 \sim GH_0^3$.

Reason: the de Sitter space-time is *not* the generic late-time asymptote of classical solutions of GR with a cosmological constant Λ both without and with hydrodynamic matter. The generic late-time (expanding) asymptote is (Starobinsky, 1983):

$$ds^2 = dt^2 - \gamma_{ik} dx^i dx^k$$

$$\gamma_{ik} = e^{2H_0 t} a_{ik} + b_{ik} + e^{-H_0 t} c_{ik} + ...$$

where $H_0^2 = \Lambda/3$ and the matrices a_{ik}, b_{ik}, c_{ik} are functions of spatial coordinates. a_{ik} contains two independent physical functions (after 3 spatial rotations and 1 shift in time + spatial dilatation) and can be made unimodular, in particular.

An always larger effect - due to scalar (adiabatic) fluctuations of an inflaton degree of freedom (Mukhanov and Chibisov, 1981; Hawking, 1982; Starobinsky, 1982; Guth and Pi, 1982):

$$P_\zeta(k) = \frac{GH_k^4}{\pi|\dot{H}|_k}$$

where the index k means that the quantity is taken at the moment $t = t_k$ of the Hubble radius crossing during inflation for each spatial Fourier mode $k = a(t_k)H(t_k)$.
The consistency relation for inflaton-driven inflation

$$r \equiv \frac{P_g}{P_\zeta} = \frac{16|\dot{H}_k|}{H_k^2} = 8|n_g| < 0.17$$

(the last inequality - from the most recent observations).
For sufficiently large $N_f = \ln\left(\frac{a_f}{a}\right)$, inhomogeneous fluctuations become larger than 1. Loop corrections proportional to higher powers of h may become important in this regime only.

Beyond small perturbations during slow-roll inflation

Locally – around our world-line – slow-roll inflation has both the beginning and the end.
Globally it has no beginning and no end in the most of interesting cases – in the sense that patches of an approximately de Sitter space-time (not necessarily expanding only) always exist somewhere in space and time (but outside our past and future light cones) - "eternal inflation".
Taking backreaction into account $\Longrightarrow$ quantum background.

Stochastic approach to inflation ("stochastic inflation"):

$$\hat{R}^{\nu}_{\mu} - \frac{1}{2}\delta^{\nu}_{\mu}\hat{R} = 8\pi G\,\hat{T}^{\nu}_{\mu}(\hat{g}_{\alpha\beta})$$

- not as a function of $< \hat{g}_{\alpha\beta} >$!

Leads to QFT in a stochastic background.

Stochastic inflation:

1) can deal with an arbitrary large (though sufficiently smooth) global inhomogeneity;

2) takes backreaction of created fluctuations into account;

3) goes beyond any finite order of loop corrections.

Fully developed in Starobinsky (1984,1986) though the first simplified application (but beyond the one-loop approximation) was already in Starobinsky (1982).

Langevin equation for the large-scale field

The first main idea: splitting of the inflaton field ϕ into a large-scale and a small-scale parts with respect to H. More exactly, the border is assumed to lie at $k = \epsilon a H$ with $\exp\left(-\frac{H^2}{|\dot{H}|}\right) \ll \epsilon \ll 1$.

The second main idea: a non-commutative part of the large-scale field is very small (it is composed from decaying modes), so we may neglect it. Then the remaining part is equivalent (not equal!) to a stochastic c-number (classical) field with some distribution function.

$$\frac{d\phi}{d\tau^{(n)}} = -\frac{1}{3H^{n+1}}\frac{dV}{d\phi} + f \ ,$$

$$< f(\tau_1^{(n)})\, f(\tau_2^{(n)}) >= \frac{H^{3-n}}{4\pi^2}\, \delta(\tau_1^{(n)} - \tau_2^{(n)}) \, .$$

The time-like variables $\tau^{(n)} = \int H^n(t, \mathbf{r})\, dt$, where $H^2 = 8\pi G V(\phi)/3$.

This is not a time reparametrization $t \to f(t)$ in GR. Different $\tau^{(n)}$ describe different stochastic processes and even have different dimensionality. Different "clocks" are needed to measure them:
1) $n = 0$: phase of a wave function of a massive particle ($m \gg H$);
2) $n = 1$: scalar metric perturbations (δN formalism);
3) $n = 3$: dispersion of a light scalar field generated during inflation

$$< \chi^2 >= \frac{1}{4\pi^2} < \int H^3 \, dt >= \frac{< \tau^{(3)} >}{4\pi^2} \, .$$

See F. Finelli *et al.*, Phys. Rev. D **79**, 044007 (2009) for more details.

f describes the flow of small-scale linear field modes through the border $k = \epsilon aH$ to the large-scale region in the course of the universe expansion. In the leading approximation, it is constructed from solutions of the massless scalar field equation in the de Sitter space-time with the adiabatic vacuum initial condition for a given spatial Fourier mode:

$$\phi_k = H_0 \, (2k)^{-1/2} \left(\eta - \frac{i}{k} \right) e^{-ik\eta} \, , \quad \eta = -(a(t) H_0)^{-1}$$

$$f(t, \mathbf{r}) = \frac{\epsilon a H_0^2}{(2\pi)^{3/2}} \int d^3k \, \delta(k - \epsilon a H_0) \, \frac{(-i) H_0}{\sqrt{2} k^{3/2}} \left[a_k e^{-i\mathbf{kr}} - a_k^\dagger e^{i\mathbf{kr}} \right]$$

Though formally an operator, $f(t, \mathbf{r})$ is equivalent to a classical Gaussian white noise.

Applicability conditions – the standard slow-roll ones:

$$V'^2 \ll 48\pi G V^2, \quad |V''| \ll 8\pi G V/3$$

Einstein-Smoluhovsky (Fokker-Planck) equation

$$\frac{\partial \rho}{\partial \tau} = \frac{\partial}{\partial \phi}\left(\frac{V'}{3H^{n+1}}\,\rho\right) + \frac{1}{8\pi^2}\,\frac{\partial^2}{\partial \phi^2}\left(H^{3-n}\rho\right) .$$

Probability conservation: $\int \rho\, d\phi = 1$.

Remarks

- More generally, the last term can be written the form

$$\frac{1}{8\pi^2}\,\frac{\partial}{\partial \phi}\left(H^{(3-n)\alpha}\,\frac{\partial}{\partial \phi}\left(H^{(3-n)(1-\alpha)}\rho\right)\right)$$

  with $0 \leq \alpha \leq 1$.

  $\alpha = 0$ – Ito calculus.

  $\alpha = 1/2$ – Stratonovich calculus.

  However, keeping terms explicitly depending on α exceeds the accuracy of the stochastic approach. Thus, α may put 0.

- All results are independent of the form of a cutoff in the momentum space as far as it occurs for $k \ll aH$ $(\epsilon \ll 1)$.
- Backreaction is taken into account: $\delta T^{\nu}_{\mu} = (V - V_{clas})\,\delta^{\nu}_{\mu}$.
- No necessity in any infrared cutoff. Problems with the so called "volume weighting" arise because quantities like $a^3\rho$ are considered which are not normalizable, thus, they may not be considered as probabilities of anything from the mathematical point of view ("unitarity breaking"). Their physical justification is also flawed since it based on the wrong assumption that all Hubble physical volumes ("observers") emerging from expansion of a previous inflationary patch are clones of each other while it is not so.

- Another possible source of apparent infrared divergences: use of "gauge invariant" (with respect to a background space-time metric) variables like $\zeta(\mathbf{r}, t)$ which are not generally covariant with respect to the full metric and, therefore, not directly observable. In contrast, quantities like $\zeta(\mathbf{r}, t) - \zeta(0, t_0)$ are generally covariant and observable though non-local.
- The accuracy of the stochastic approach is not sufficient for calculating quantities $\sim H^2$ in $< \phi^2 >$ and $\sim H^4$ in EMT average values because of the omission of a contribution from the small-scale part (including the conformal anomaly). However, all larger quantities (if exist) can be calculated quantitatively correctly. Also, the small-scale part is mainly the one-loop correction from a massless minimally coupled scalar field, so it can be added.

Transition to predictions for the post-inflationary evolution

From $\rho(\phi, \tau)$ during inflation to the distribution $w(\tau)$ over the total local duration of inflation:

$$w(\tau) = \lim_{\phi \to \phi_{end}} j = \lim_{\phi \to \phi_{end}} \frac{|V'|}{3H^{n+1}} \rho(\phi, \tau) \, .$$

For the graceful exit to a post-inflationary epoch, the stochastic force should be much less than the classical one during last e-folds of inflation.

The same way to obtain the joint distribution $w(0, \tau_1; \ |\mathbf{r}|, \tau_2)$ from the 2-point joint probability distribution $\rho(\phi_1, 0, \tau_1; \phi_2, |\mathbf{r}|, \tau_2)$ during inflation.

From δN- to N-formalism

Let $n = 1$. When

$$ds^2 = dt^2 - a^2(t)e^{2\zeta(\mathbf{r})}d\mathbf{r}^2 + \text{small terms}$$

after inflation and complete thermalization where

$$\zeta(\mathbf{r}) = N(\mathbf{r}) \equiv \tau^{(1)}(\mathbf{r}) \ .$$

Probabilities to go to different vacua after inflation

Let inflation may end in two vacua: $\phi = \phi_1$ and $\phi = \phi_2$ with $V(\phi_1) = V(\phi_2) = 0$ (to consider a larger number of post-inflationary vacua, ϕ should have more than one-dimensional internal space).

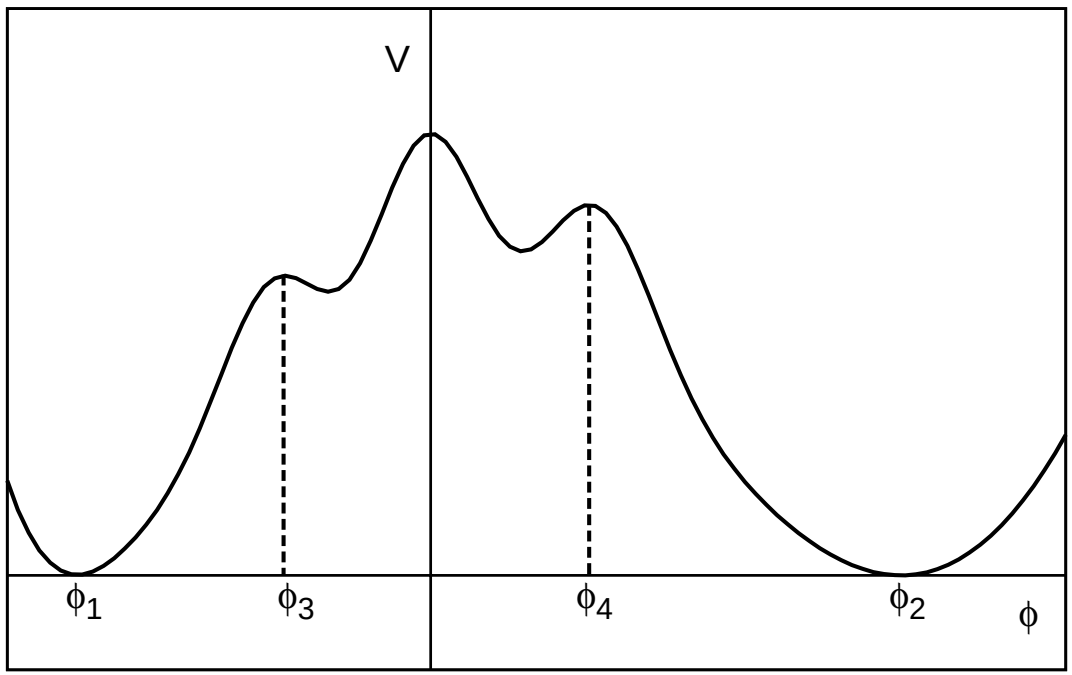

Boundary conditions at the end of inflation:
$\rho(\phi_1, \tau) = \rho(\phi_2, \tau) = 0$.

Method of calculation (Starobinsky (1984,1986)): consider the quantities

$$Q_m(\phi) = \int_0^\infty \tau^m \rho(\phi, \tau)\, d\tau$$

where $\tau = 0$ corresponds to the local beginning of inflation.
$Q_m(\phi_1) = Q_m(\phi_2) = 0$.

By integrating the Fokker-Planck equation over τ, we get for $m = 0$:

$$Q_0(\phi) = \frac{8\pi^2}{H^{3-n}} \exp\left(\frac{\pi}{GH^2(\phi)}\right) \int_{\phi_1}^{\phi} d\psi \exp\left(-\frac{\pi}{GH^2(\psi)}\right) \times$$

$$\left(C_0 - \int_{\phi_1}^{\psi} \rho_0(\psi_1)\, d\psi_1\right),$$

$$C_0 = \frac{\int_{\phi_1}^{\phi_2} d\phi \exp\left(-\frac{\pi}{GH^2(\phi)}\right) \int_{\phi_1}^{\phi} \rho_0(\psi)\, d\psi}{\int_{\phi_1}^{\phi_2} d\phi \exp\left(-\frac{\pi}{GH^2(\phi)}\right)}.$$

$P_1 = C_0$ – the absolute probability to go to the vacuum $\phi = \phi_1$;

$P_2 = 1 - C_0$ – the absolute probability to go to the vacuum $\phi = \phi_2$.

No n dependence in C !

Local duration of inflation

$$Q_1(\phi) = \frac{8\pi^2}{H^{3-n}} \exp\left(\frac{\pi}{GH^2(\phi)}\right) \int_{\phi_1}^{\phi} d\psi \exp\left(-\frac{\pi}{GH^2(\psi)}\right) \times$$

$$\left(C_1 - \int_{\phi_1}^{\psi} Q_0(\psi_1)\, d\psi_1\right),$$

$$C_1 = \frac{\int_{\phi_1}^{\phi_2} d\phi \exp\left(-\frac{\pi}{GH^2(\phi)}\right) \int_{\phi_1}^{\phi} Q_0(\psi)\, d\psi}{\int_{\phi_1}^{\phi_2} d\phi \exp\left(-\frac{\pi}{GH^2(\phi)}\right)}.$$

$$< \tau_1 >= \frac{C_1}{C_0}, \quad < \tau_2 >= \frac{\tilde{C}_1}{1 - C_0},$$

$$< \tau >_{tot} = C_0 < \tau_1 > + (1 - C_0) < \tau_2 >= \int_{\phi_1}^{\phi_2} Q_0(\phi)\, d\phi\,.$$

$\tilde{C}_1$ is C_1 with ϕ_1 and ϕ_2 interchanged.

Some thoughts on the choice of an initial condition

- Static solutions – not normalizable in the inflationary (i.e. unstable) case.
- $\rho_0(\phi) = \delta(\phi - \phi_0)$ – why?
- "Eternal inflation as an initial condition": $\rho_0(\phi) \propto \rho_{E_1}(\phi)$ – the wave function of the lowest energy level of the Schrodinger equation arising through the separation of variables in the Fokker-Planck equation ($E_0 = 0$ due to hidden supersymmetry of the former).
  1) Not possible in the continuum spectrum case.
  2) In the discrete spectrum case, generically $E_2 - E_1 \sim E_1$ – not enough time for relaxation.
  As a whole, "eternal" inflation seems not be eternal enough to fix the initial condition uniquely.

However, if inflation had occurred at all, the dependence of predictions on $\rho_0(\phi)$ is comparatively weak: for almost all $\rho_0(\phi)$ except from the HH-like one $\rho_0(\phi) \propto \exp\left(\frac{\pi}{GH^2(\phi)}\right)$, the main contribution comes from the highest maximum of $V(\phi)$ without any necessity of a "tunneling" initial condition.

On the other hand, if $\rho_0(\phi) \propto \exp\left(\frac{\pi}{GH^2(\phi)}\right)$, there is practically no inflation at all, and final probabilities P_1 and P_2 are equal to the initial ones.

Correlations and joint PDF

Following A.A. Starobinsky and J. Yokoyama, Phys. Rev. D **50**, 6357 (1994).
In the leading approximations, all Green functions and joint n-point probability distributions of the inflaton field can be expressed through solutions of the same Fokker-Planck equation with different initial conditions only. In particular, in the case $H \approx H_0$ during inflation (for simplicity only), the general two-point PDF for 4D-points lying outside each other future light cones in the stochastic approach is:

$$\rho_2[\phi_1(\mathbf{r_1}, t_1), \phi_2(\mathbf{r_2}, t_2)] =$$

$$\int \Pi[\phi_1(\mathbf{r_1}, t_1)|\phi_r(\mathbf{r_1}, t_r)]\Pi[\phi_2(\mathbf{r_2}, t_2)|\phi_r(\mathbf{r_2}, t_r)]\rho_1(\phi_r, t_r)\, d\phi_r$$

where t_r is the time in the past when both corresponding 3D-points were inside one Hubble volume and $\Pi[\phi_1(\mathbf{r}, t_1)|\phi_2(\mathbf{r}, t_2)]$ satisfies the Fokker-Planck equation with respect to both its time and field variables with the initial condition

$$\Pi[\phi_1(\mathbf{r}, t_1)|\phi_2(\mathbf{r}, t_1)] = \delta(\phi_1 - \phi_2)$$

Through the N-formalism - joint probability distributions of a space-time metric after inflation.

Otherwise, if the 4D-points are inside the future light cone of one of them, the spatial points $\mathbf{r_1}$ and $\mathbf{r_2}$ are inside one elementary averaging volume, so they coincide in terms of the stochastic approach. Then, for $t_1 < t_2$,

$$\rho_2[\phi_1(\mathbf{r}, t_1), \phi_2(\mathbf{r}, t_2)] = \Pi[\phi_2(\mathbf{r}, t_2)|\phi_1(\mathbf{r}, t_1)]\rho_1(\phi_1, t_1))$$

Conclusions

- During slow-roll inflation, backreaction of created inflaton fluctuations has to be taken into account for sufficiently long inflation and leads to QFT in a stochastic background.
- No problems of principle in predicting all joint probability distributions for light scalar fields, including the inflaton itself, during and after inflation (N-formalism) in the original (probability conserving) stochastic approach, once an initial condition $\rho_0(\phi)$ is given. No necessity to refer to other universes outside our light cone.
- New "clocks" apart from metric perturbations are probably needed to measure large infrared effects like the total local duration of an inflationary stage in our Universe.

- No satisfactory principle to fix $\rho_0(\phi)$ uniquely.
- Some dependence on $\rho_0(\phi)$ remains in final answers, so a possibility to get some knowledge on it from observational data does not seem hopeless. However, if inflation had occurred at all, the dependence of predictions on $\rho_0(\phi)$ is weak and mainly produced by the region around the highest maximum of $V(\phi)$. For this, no specific "tunneling" initial condition is needed.

Congratulations and best wishes to Kodama-san, Sasaki-san and Futamase-san once more!

Kei-ichi Maeda, JGRG 22(2012)111605

"Conclusion"

RESCEU SYMPOSIUM ON

GENERAL RELATIVITY AND GRAVITATION

JGRG 22

November 12-16 2012

Koshiba Hall, The University of Tokyo, Hongo, Tokyo, Japan

CONCLUSION ?



Kei-ichi Maeda

Waseda University

Research on Gravitation

Gravity Provide Mystery ➡ Big Progress in Physics

motion of planets & falling objects

➡ universal gravitation (Newton)

Dawn of modern physics

⬇

Genral Relativity (Einstein)

gravity=geometry

spacetime becomes a physical object

⤷ cosmology • black holes • GWs

Now

- Microscopic

  Unification of fundamental interactions

  Quantization

  ⟹ gravity is exceptional

- Macroscopic

  Dark energy ?

  Many “modified” gravitational theories are proposed

➤ **new big progress in physics ?**

Research on Gravitation in Japan

Workshop on General Relativity and Gravitation 1974-76

(Uchiyama, Hirakawa, Nariai, Kimura, K. Hayashi, Fujii,....)

Importance of GR

3K CMB (1964) and a pulsar (1967)

JGRG1 (*Tokyo Metropolitan University*, Dec 4- 6 1991)

T. Nakamura and KM

a grant-in-aid for scientific research on **priority areas**,
"gravitational wave astronomy" → TAMA project
(PI: S. Hayakawa →T. Nakamura)

Community (BIG3: **Kodama, Sasaki, and Futamase)**

JGRG1 (*Tokyo Metropolitan University*, Dec 4 - 6 1991)
JGRG2 (*Waseda University*, Jan 18-20 1993)
JGRG3 (*The University of Tokyo*, Jan 17- 20 1994)
JGRG4 (*YITP, Kyoto University*, Nov 28 - Dec 1 1994)
JGRG5 (*Nagoya University*, Jan22-25 1996)
JGRG6 (*Tokyo Institute of Technology*, Dec 2- 5 1996)
JGRG7 (*YITP, Kyoto University*, Oct 27- 30 1997)
JGRG8 (*Niigata University*, 19th Oct - 22nd Oct 1998)
JGRG9 (*Hiroshima University*, 3rd Nov - 6th Nov 1999)
JGRG10 (*Osaka University*, 11th Sep - 14th Sep 2000) International Workshop
JGRG11 (*Waseda University*, 9th Jan - 12th Jan 2002)
JGRG12 (*Komaba, The University of Tokyo*, 25th Nov - 28th Nov 2002)
JGRG13 (*Osaka City University*, 1st Dec - 4th Dec 2003)
JGRG14 (*YITP, Kyoto University*, 29th Nov - 3rd Dec 2004)
JGRG15 (*Tokyo Institute of Technology*, 28th Nov - 2rd Dec 2005)
JGRG16 (*Niigata Prefectural Center*, 27th Nov - 1st Dec 2006)
JGRG17 (*Nagoya University*, 3rd Dec - 7th Dec 2007)
JGRG18 (*Hiroshima University*, 17th-21st Nov 2008)
JGRG19 (*Rikkyo University*, 30th Nov -4th Dec 2009)
JGRG20 (*YITP, Kyoto University*, 21st Sep -25th Sep 2010)
JGRG21 (*Tohoku University*, 26th Sep -29th Sep 2011)
JGRG22 (*Tokyo University*, 26th Sep -29th Sep 2011)

New Project : KAGRA

Although they (Kodama, Sasaki, and Futamase)
have played very important roles in research on gravity,

More important point is the following fact:

The JGRG workshop series have been supported by
active involvement of young postdocs and graduate students.
In turn,
it is hoped that their experience from the JGRG workshop series
will help them grow into world's leading scientists.

From JGRG homepage:http://www-tap.scphys.kyoto-u.ac.jp/jgrg/about.html

So we will continue this series:

Next is

Hirosaki University







We would like to thank

RESQEU group

Jun’ichi Yokoyama (chairperson)
and
Teruaki Suyama, ・・・・